ACTA CHEMICA SCANDINAVICA 27 (1973) 1–4

A New Method for Measuring Ultrasonic Velocity

JØRGEN RASSING* and BO N. JENSEN

Chemical Laboratory III, University of Copenhagen, Denmark

A new cell has been developed for the investigation of ultrasonic velocities. It makes use of a quartz crystal through which a small hole has been bored. The sound velocity in a liquid placed into this hole can be determined by a comparison method from the frequency shift of the resonance peak of the crystal. The test cell has been specially designed for small quantities of liquid (0.2 ml) and to be used at low frequencies (250 kHz).

The ultrasonic relaxation technique has been extensively used to investigate the rates and mechanisms of very fast chemical reactions. Several investigations have been concerned with reactions of biochemical importance, hydrogen bond formation,[1–6] micelle formation,[7,8] and polymer conformation,[9–11] for example, having been studied. A general conclusion of these seems to be that to test a proposed mechanism measurements at low frequencies are desirable.

The resonance technique recently developed [12] can in principle be used to determine sound absorption coefficients and sound velocities at such low frequencies (200 kHz – 1 MHz) and, although there are still certain technical difficulties, the cells designed so far have permitted these determinations to be made. However, measurements at 200 kHz require at least 40 ml of sample, a necessity which, in particular, prohibits the investigation of several synthetic macromolecules which could be studied as models for biological systems.

In this paper a new cell which can be used in the application of the resonance technique is presented. It requires only 0.2 ml of sample and can be used for measurement of ultrasonic velocities at low frequencies.

THEORY

The resonating cavity usually consists of two quartz crystals with the sample between. Standing waves are established in this cavity and a resonance curve is then recorded by measuring the amplitude of the sound wave transported through the cell as a function of its frequency. From this curve the sound absorption coefficient can be obtained. The quality factor, Q, which is

* Present address: Roskilde University Center, Roskilde, Denmark.

obtained from the 3 dB point of the resonance curve, is related to the sound absorption coefficient. The sound velocity is determined from the difference between two successive resonance frequencies.

There are several technical difficulties associated with the construction of satisfactory cells. It is important that the quality factor which is determined is mainly due to the sample. This requires that the two quartz crystals oscillate freely and consequently are not coupled to the cell. Furthermore the interpretation of the measurements is based upon the assumption of plane waves so this imposes certain restrictions on the size of the crystals. A measurement at 200 kHz requires a quartz diameter of at least 6 cm. In the past the problems have been partially overcome by mounting big crystals in the cell with soft

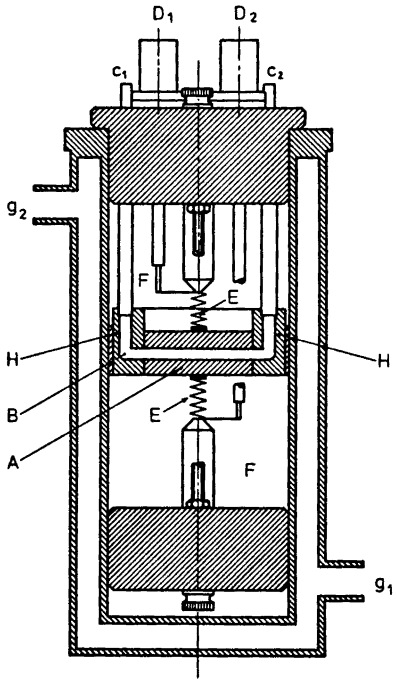

Fig. 1. The resonance cell. A: The x-cut quartz cylinder with a diameter of 3 cm and a basic frequency of 272 kHz. The cylinder is gold plated on both sides. B: The hole (diameter 0.15 cm) which penetrates the crystal and in which the sample is placed. C_1 and C_2: Input and output of sample. D_1 and D_2: Coaxial connections. E: Spring contacts. F: Cavity filled with air. G_1 and G_2: Water jacket.

The resonance frequency of the cell is measured by means of a set up from Wandel und Goltermann, Wobbelmessplatz, WM-50.

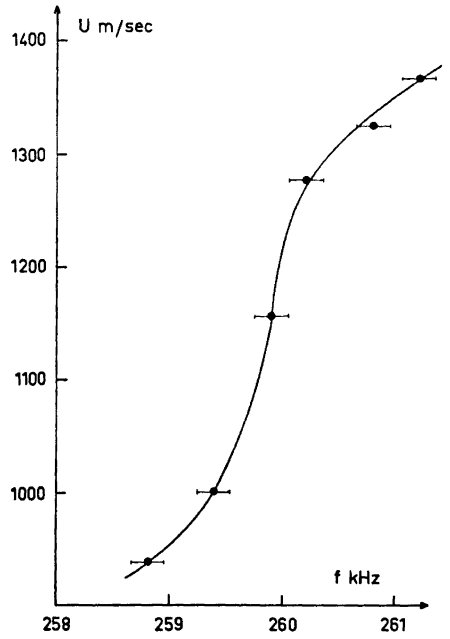

Fig. 2. The relationship between the velocities of the different samples and the resonance frequency of the quartz crystal inside which the samples are placed. The samples used are carbon tetrachloride, chloroform, acetone, cyclohexane, benzene, and dioxane.

glue. Unfortunately, however, the sample is then in close contact with the glue so that several important organic compounds cannot be used as solvents. In addition the size of the crystals necessitates about 40 ml of sample.

THE NEW METHOD

The method proposed here involves the use of a single x-cut quartz crystal. The lowest resonance frequency for this crystal is given by

$$f = U/2l \quad (1)$$

where U is the sound velocity in quartz and l is the thickness of the crystal. A crystal with a lowest resonance frequency of 272 kHz has been successfully used. Through this crystal a small hole perpendicular to the direction of particle motion has been made. This hole decreases the lowest resonance frequency of the crystal in a complicated manner. It is apparent, however, that the observed decrease is related to the velocity of sound in any liquid placed in the hole. A suitable hole requires only 0.2 ml of sample liquid. Fig. 1 shows the detailed cell design. Before use, a calibration curve such as that shown in Fig. 2 must be plotted. By comparing the resonance frequency of the crystal with a sample and a reference liquid placed in the hole, respectively, the velocity of sound for the sample can be calculated. With the cell described it is possible to measure the sound velocity with a reproducibility of 0.5 %; however, the accuracy may be considerably improved by using a differential cell using two identical crystals.

Measurements at higher frequencies (the odd harmonics) may be carried out although the frequency shift observed decreases the higher the odd harmonics used.

CONCLUSION

A new method which permits measurement of the velocity of sound at low frequencies (250 kHz) in very small samples (0.2 ml) has been developed. The method requires a single x-cut quartz crystal in which a small hole containing the sample has been made. This causes a shift in the normal resonance frequency of the quartz crystal. After suitable calibration this shift can be employed to calculate the sound velocity. Further work improving the performance of the cell is in progress.

Acknowledgement. The authors express their appreciation to professor Thor A. Bak for helpful discussions and to *Statens naturvidenskabelige Forskningsråd*, Denmark, for financial support.

REFERENCES

1. Rassing, J. *Acta Chem. Scand.* **25** (1971) 1418.
2. Garland, F., Rassing, J. and Atkinson, F. *J. Phys. Chem.* **75** (1971) 3182.
3. Rassing, J. and Jensen, B. N. *Acta Chem. Scand.* **25** (1971) 3663.
4. Rassing, J. *Advan. Mol. Relaxation Processes* **4** (1972) 55.
5. Rassing, J. *J. Chem. Phys.* **56** (1972) 5225.

6. Hammes, G. G. and Spivey, H. O. *J. Am. Chem. Soc.* **20** (1966) 1621.
7. Graber, E., Lang, J. and Zana, R. *Kolloid Z. Z. Polym.* **238** (1970) 470 and 479.
8. Sams, P., Wyn-Jones, E. and Rassing. J. *Chem. Phys. Lett.* **13** (1972) 233.
9. Rassing, J. *Acta Chem. Scand.* **25** (1971) 1506.
10. Ludlow, W., Wyn-Jones, E. and Rassing, J. *Chem. Phys. Lett.* **13** (1972) 477.
11. Bauer, H. J., Hässler, H. and Immendörfer, M. *Discussions Faraday Soc.* **49** (1970) 238.
12. Eggers, F. *Acustica* **19** (1969) 323.

Received June 15, 1972.

ACTA CHEMICA SCANDINAVICA 27 (1973) 5–14

Crystal Structure of a Cyclisation Product of 6-Chloropyrid-2-thione ($C_{15}H_9N_3S_3$)

P. GROTH

Department of Chemistry, University of Oslo, Oslo 3, Norway

The crystals are monoclinic with space group $P2_1/c$, cell dimensions $a = 14.21_7$ Å, $b = 7.88_5$ Å, $c = 15.20_7$ Å, $\beta = 119.5_7°$, and four molecules in the unit cell. The structure was solved by direct methods and refined by full-matrix least squares technique to an R-value of 2.8 % ($R_w = 3.4$ %) for 1115 reflections recorded on an automatic four circle diffractometer. The molecule has a pseudo mirror plane and the angles between the three ring planes are 66°, 61° and 57°. Average bond distances and angles are: C–S: 1.780 Å, C–N: 1.335 Å, C–C: 1.376 Å, C–S–C: 101.9°, N–C–S: 117.7°, C–C–S: 118.7°, C–N–C: 116.7°, N–C–C: 123.5°, C–C–C: 118.6° with estimated standard deviations of about 0.005 Å and 0.4° in the individual values. The average N–N distance across the ring is 2.941 Å.

Intermolecular reactions of 6-chloropyrid-2-thione have recently been studied by Reistad *et al.*[1] Such reactions will eventually lead to polymerization or to cyclisation at some intermediate stage. NMR evidence for the simplest product is in favour of a cyclic trimeric pyridine with sulphur bridges between the pyridyl 2,6-positions.

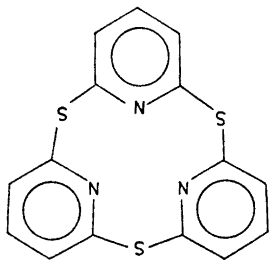

In order to obtain conformational information of this new 12-membered heterocyclic ring system a crystal structure determination has been carried out.

The crystals are monoclinic with space group $P2_1/c$. The cell dimensions, determined by a manual four circle diffractometer, with estimated standard

deviations [2*] are: $a = 14.217(3)$ Å, $b = 7.885(2)$ Å, $c = 15.207(5)$ Å, $\beta = 119.57(2)°$. The unit cell contains four molecules ($\varrho_{calc} = 1.46$ g cm^{-3}, $\varrho_{obs} = 1.47$ g cm^{-3}).

1300 reflections were measured on an automatic four circle diffractometer ($2\theta_{max} = 45°$), using Mo$K\alpha$-radiation and a highly orientated graphite crystal monochromator. With an observed-unobserved cutoff at $2.0\sigma(I)$, 1115 reflections were recorded as observed. No corrections for absorption or secondary extinction effects have been carried out.

The structure was solved by direct methods and refined by full-matrix least squares technique.

Anisotropic temperature factors were introduced for sulphur, nitrogen, and carbon atoms. For hydrogens only positional parameters (having been calculated) were refined. The weights in least squares were obtained from the standard deviations in intensities, $\sigma(I)$, taken as

$$\sigma(I) = [C_T + (0.02\ C_N)^2]^{\frac{1}{2}}$$

where C_T is the total number of counts, and C_N the net count (peak minus background). The R-value arrived at was 2.8 % (weighted value $R_w = 3.4$ %) for 1115 observed reflections. The atomic form factors were those of Hanson *et al.*[3] except for hydrogen.[4]

Final fractional coordinates and thermal parameters with estimated standard deviations are given in Tables 1 and 2. The expression for anisotropic vibration is:

$$\exp\ [-(B_{11}h^2 + B_{22}k^2 + B_{33}l^2 + B_{12}hk + B_{13}hl + B_{22}kl)]$$

Table 1. Fractional atomic coordinates and anisotropic thermal vibration parameters with estimated standard deviations (multiplied by 10^5).*

Atom	x	y	z	B_{11}	B_{22}	B_{33}	B_{12}	B_{13}	B_{23}
S_1	14407	68376	18260	1022	4257	794	1418	1082	1684
	8	16	8	11	37	9	33	17	29
S_2	20921	48265	54471	704	1988	545	267	650	−21
	6	11	6	8	21	6	22	11	19
S_3	40562	16562	36908	1289	1931	1575	692	2131	34
	9	13	9	12	24	13	27	22	28
N_1	16404	59795	36173	611	1870	625	265	659	187
	18	33	18	24	62	21	62	39	60
N_2	30400	30038	46072	615	1608	738	170	673	103
	19	31	19	63	60	22	62	39	61
N_3	28874	43904	27637	640	223	701	−251	835	−391
	20	35	19	24	67	21	67	39	63
C_1	09831	66260	27113	698	1926	651	259	656	318
	25	43	24	31	80	27	81	50	74

* All programs used are included in this reference.

Table 1. Continued.

C_2	−00542	71849	24175	686	2292	744	656	515	648
	29	47	30	30	91	27	87	50	84
C_3	−04227	70658	30919	619	2509	1010	816	765	610
	29	48	30	31	95	35	91	59	94
C_4	02298	63329	40171	664	2102	893	356	967	125
	26	45	28	32	83	31	86	55	87
C_5	12441	57942	42456	601	1428	625	−85	614	−158
	23	39	22	28	66	26	71	46	67
C_6	24538	28969	50687	549	1711	495	27	408	100
	24	39	21	27	76	23	77	43	68
C_7	21353	13827	52978	1286	1971	817	−130	1323	359
	32	48	27	42	86	31	100	63	87
C_8	24332	−00934	50175	1788	1730	1071	−192	1814	243
	39	52	33	52	86	36	113	75	91
C_9	29948	−00204	45040	1424	1308	1018	232	1281	100
	34	45	30	45	76	35	100	67	87
C_{10}	32744	15539	43065	785	1607	741	320	750	−99
	26	43	24	32	76	27	82	51	75
C_{11}	38897	38065	33014	719	2148	787	−82	965	−475
	26	43	25	32	86	29	87	54	82
C_{12}	47976	47690	35451	630	3087	1015	−88	817	478
	29	58	30	32	110	34	101	57	101
C_{13}	46588	63945	32083	719	3514	944	−1200	502	440
	33	61	32	35	123	34	114	59	112
C_{13}	36444	70663	26985	1209	2024	738	−765	964	−32
	34	51	28	42	89	30	101	64	81
C_{14}	27814	60284	25057	926	1948	535	−39	871	−143
	27	45	22	36	78	31	93	59	87

* For numbering of atoms, see Fig. 1.

A comparison between observed and calculated structure factors is presented in Table 3.

The principal axes of the thermal vibration ellipsoids were calculated from the thermal parameters of Table 1. Root mean square amplitudes and the corresponding B-values for the atomic anisotropic thermal vibration along the principal axes together with the components of these axes along the crystal ones are given in Table 4.

Rigid body analysis of translational, librational, and screw motion [5] gave relatively large r.m.s. discrepancy between atomic vibration tensor components calculated from the thermal parameters of Table 1 and those calculated from the rigid body parameters. By including all non-hydrogen

Table 2. Fractional atomic coordinates with e.s.d.'s for hydrogen atoms. The isotropic thermal parameter is 5.0 Å² for all.

Atom	x	y	z
H_2	−.0472	−.7700	−1.802
	23	37	23
H_3	−.1173	−.7493	−.2852
	25	38	21
H_4	−.0008	−.6256	−.4507
	23	38	21
H_7	−.1671	−.1411	−.5651
	22	36	21
H_8	−.2222	−.1243	−.5189
	22	40	20
H_9	−.3213	−.1013	−.4307
	22	39	20
H_{12}	−.5466	−.4308	−.3929
	23	37	21
H_{13}	−.5285	−.7030	−.3381
	25	37	22
H_{14}	−.3505	−.8245	−.2516
	23	39	21

atoms the value obtained was 0.010 Å², which by no means supports the assumption of regarding the molecule as an oscillating rigid body. The coordinates were therefore not corrected for librational motion.

Bond distances and angles and dihedral angles are listed in Tables 5 and 6. The C−S bond lengths, in the range 1.769 Å − 1.790 Å, are not far from a single bond (1.816 Å).[6] The fact that there is little conjugation between the pyridine rings through the sulphur bridges is also indicated by the UV spectra.[1] Similar results have been reported for diphenyl sulphides.[7] As indicated in Fig. 2, the molecule has a pseudo mirror plane through S_2, N_3, C_{13}. The more symmetrical form with a threefold axis of symmetry is thus not preferred. Repulsion between the lone pair electrons on the pyridyl nitrogens may possibly explain this since, in the latter case, the principal direction of all three orbitals would be towards a common point. The bond distances C−S_1 and C−S_3 seem to be somewhat shorter (mean value 1.774 Å) than C−S_2 (1.789 Å). Also the angle at S_2 (101.0°) is apparently significantly smaller than those at S_1 and S_3 (102.1°). However, in view of the fact that S_1 and S_3 (but not S_2) have very large thermal vibration amplitudes (see Table 4), the significance of these differences may be doubted.

Table 3. Observed and calculated structure factors (on 10 times absolute scale).

h	k	l	Fo	Fc
0	0	2	148	-145
0	0	4	509	452
0	0	6	152	158
0	0	8	139	-141
0	0	10	280	-290
0	0	14	104	-102
1	0	-14	140	-142
1	0	-12	262	262
1	0	-8	133	138
1	0	-6	224	229
1	0	-4	569	569
1	0	-2	707	-679
1	0	0	132	128
1	0	2	459	448
1	0	4	344	343
1	0	6	498	-499
1	0	10	150	145
1	0	12	171	-172
2	0	-12	239	236
2	0	-10	172	171
2	0	-8	455	455
2	0	-6	630	620
2	0	-4	1631	-1689
2	0	-2	46	-62
2	0	0	942	-918
2	0	2	1982	-2251
2	0	4	598	-600
2	0	6	454	-454
2	0	8	158	-154
2	0	10	200	196
3	0	-12	176	174
3	0	-10	234	-222
3	0	-6	692	-689
3	0	-4	166	160
3	0	-2	1141	-1166
3	0	2	434	425
3	0	4	573	581
3	0	6	450	-456
3	0	8	295	302
3	0	10	120	110
4	0	-10	130	-129
4	0	-8	231	219
4	0	-6	1327	-1340
4	0	-4	36	-33
4	0	-2	585	589
4	0	0	120	119
4	0	2	674	691
4	0	4	977	1000
4	0	6	500	509
4	0	8	174	171
5	0	-12	371	-387
5	0	-10	79	84
5	0	-8	355	331
5	0	-6	461	438
5	0	-2	351	346
5	0	0	274	281
5	0	2	298	309
5	0	4	473	-476
5	0	10	134	-125
6	0	-14	163	-156
6	0	-12	164	-163
6	0	-10	158	158
6	0	-8	228	-228
6	0	-6	680	662
6	0	-4	605	605
6	0	0	202	201
6	0	2	300	-305
6	0	4	472	-498
6	0	6	321	-333
6	0	8	190	-198
7	0	-12	127	136
7	0	-10	177	184
7	0	-6	166	-160
7	0	-4	530	-533
7	0	-2	457	-475
7	0	0	321	309
7	0	2	344	-348
8	0	-14	111	110
8	0	-12	482	485
8	0	-10	274	-277
8	0	-8	94	-92
8	0	-6	287	287
8	0	-4	513	-517
8	0	-2	562	-568
8	0	0	121	126
8	0	4	277	279
9	0	-14	108	-93
9	0	-8	174	-173
9	0	-6	248	-254
9	0	-2	510	514
9	0	2	207	217
9	0	4	250	247
9	0	6	112	-110
10	0	-16	227	-215
10	0	-12	310	-320
10	0	-10	341	-346
10	0	-8	409	410
10	0	-6	73	-67
10	0	-4	201	-213
10	0	-2	238	254
10	0	0	192	191
10	0	4	174	178
11	0	-8	332	345
11	0	-6	225	-221
11	0	-4	447	430
11	0	-2	304	-312
11	0	0	182	-170
12	0	-14	129	127
12	0	-10	189	189
12	0	-8	528	536
12	0	-6	119	-124
12	0	-4	103	-91
12	0	0	141	-145
13	0	-8	247	-238
13	0	-6	185	179
13	0	-2	258	-248
14	0	-12	92	-104
14	0	-10	140	-134
14	0	-6	223	-215
15	0	-10	222	-219

h	k	l	Fo	Fc
15	0	-6	156	152
0	1	-11	217	-225
0	1	-10	129	127
0	1	-9	80	-79
0	1	-8	142	-142
0	1	-7	228	-234
0	1	-6	92	89
0	1	-5	31	36
0	1	-4	247	237
0	1	-3	349	-346
0	1	-2	417	-400
0	1	-1	494	462
0	1	1	486	462
0	1	2	414	400
0	1	3	350	-346
0	1	4	241	-237
0	1	6	87	-89
0	1	7	224	-234
0	1	8	140	142
0	1	9	72	-79
0	1	10	125	-127
0	1	11	226	-225
1	1	-13	132	-128
1	1	-10	163	158
1	1	-9	113	114
1	1	-8	63	-68
1	1	-7	141	138
1	1	-6	368	-352
1	1	-5	98	-93
1	1	-4	372	368
1	1	-3	1121	1119
1	1	-2	417	-396
1	1	-1	258	-258
1	1	0	266	-257
1	1	1	916	920
1	1	2	1471	-1535
1	1	3	416	-414
1	1	4	385	-391
1	1	5	600	-610
1	1	7	319	-327
1	1	11	106	-113
1	1	12	99	99
2	1	-13	71	76
2	1	-11	304	305
2	1	-10	159	-150
2	1	-9	116	120
2	1	-8	263	-253
2	1	-7	301	315
2	1	-6	533	544
2	1	-5	284	285
2	1	-4	828	-826
2	1	-3	668	-653
2	1	-1	119	-105
2	1	0	1138	1149
2	1	1	423	425
2	1	2	243	-241
2	1	3	202	199
2	1	4	297	-306
2	1	5	218	-216
2	1	10	193	192
2	1	11	138	134
3	1	-12	183	193
3	1	-11	322	327
3	1	-10	68	-77
3	1	-9	330	336
3	1	-8	356	-347
3	1	-7	462	-470
3	1	-5	123	121
3	1	-4	154	151
3	1	-3	553	-544
3	1	-2	136	139
3	1	-1	667	-649
3	1	0	274	271
3	1	1	408	-399
3	1	2	346	334
3	1	3	220	219
3	1	4	740	734
3	1	5	299	306
3	1	7	230	243
3	1	9	98	100
3	1	10	120	122
3	1	11	96	93
4	1	-12	237	250
4	1	-11	149	-148
4	1	-10	277	-297
4	1	-9	309	-316
4	1	-8	733	735
4	1	-7	115	116
4	1	-6	311	-313
4	1	-5	549	-538
4	1	-4	389	-392
4	1	-3	304	-312
4	1	-2	743	733
4	1	-1	136	136
4	1	0	176	-167
4	1	1	286	287
4	1	2	368	-365
4	1	3	191	-190
4	1	4	138	143
4	1	5	346	340
4	1	6	118	-119
5	1	-13	206	-208
5	1	-12	88	85
5	1	-10	151	-148
5	1	-9	417	-441
5	1	-8	147	147
5	1	-7	46	38
5	1	-6	30	37
5	1	-5	178	-175
5	1	-4	308	295
5	1	-3	562	559
5	1	-2	200	186
5	1	-1	318	321
5	1	0	573	-574
5	1	1	124	118
5	1	2	235	243
5	1	3	111	113
5	1	4	258	-252
5	1	6	288	-293
5	1	7	145	-134

h	k	l	Fo	Fc
5	1	9	145	-145
6	1	-12	166	-172
6	1	-11	153	-159
6	1	-10	122	134
6	1	-9	297	304
6	1	-8	245	252
6	1	-7	584	595
6	1	-6	966	-955
6	1	-5	96	96
6	1	-4	174	168
6	1	-3	122	-118
6	1	-2	443	455
6	1	-1	675	677
6	1	0	441	-427
6	1	1	273	-274
6	1	2	113	118
6	1	3	128	-123
6	1	5	247	-238
7	1	-13	231	232
7	1	-9	189	192
7	1	-8	193	190
7	1	-7	129	132
7	1	-5	332	330
7	1	-4	116	-112
7	1	-3	92	-81
7	1	-2	266	-263
7	1	-1	233	-251
7	1	0	72	70
7	1	1	168	-165
7	1	2	212	206
7	1	4	267	-269
7	1	5	218	-216
7	1	6	242	255
8	1	-15	141	136
8	1	-13	85	82
8	1	-11	144	149
8	1	-10	218	214
8	1	-8	322	-312
8	1	-7	219	-234
8	1	-6	97	92
8	1	-5	522	-524
8	1	-4	382	372
8	1	-3	83	-92
8	1	-2	123	115
8	1	-1	152	-156
8	1	1	93	91
8	1	2	117	121
8	1	4	166	-170
9	1	-14	99	-97
9	1	-9	163	-159
9	1	-7	280	-276
9	1	-6	75	71
9	1	-5	70	-71
9	1	-4	282	-280
9	1	-3	131	-131
9	1	-2	95	99
9	1	-1	84	-98
9	1	0	313	303
9	1	1	234	231
9	1	2	81	-82
9	1	3	283	281
10	1	-15	172	-166
10	1	-13	135	-133
10	1	-12	197	191
10	1	-11	89	-87
10	1	-10	105	-114
10	1	-9	77	75
10	1	-8	201	-212
10	1	-7	135	-144
10	1	-6	176	175
10	1	-5	205	216
10	1	-4	97	-93
10	1	-2	92	-94
10	1	-1	267	264
10	1	0	109	-98
11	1	-15	115	-111
11	1	-13	95	-95
11	1	-12	79	91
11	1	-10	150	151
11	1	-9	228	223
11	1	-8	146	147
11	1	-7	218	216
11	1	-6	195	-190
11	1	-5	105	107
11	1	[illegible]	244	244
11	1		68	-77
11	1	3	130	-124
12	1	-14	108	99
12	1	-13	97	92
12	1	-11	88	90
12	1	-10	111	-111
12	1	-8	227	221
12	1	-7	312	315
12	1	-6	88	-78
12	1	-5	128	-130
12	1	-1	128	-126
12	1	1	126	-123
13	1	-6	196	-195
13	1	-3	150	-147
14	1	-12	161	-154
14	1	-11	243	-233
14	1	-8	103	107
15	1	-6	105	106
0	2	-12	131	-119
0	2	-11	110	-98
0	2	-10	243	-240
0	2	-8	68	-58
0	2	-7	136	-134
0	2	-6	141	-141
0	2	-5	152	-155
0	2	-3	212	213
0	2	-2	881	891
0	2	-1	1221	1242
0	2	0	256	-251
0	2	1	1196	-1282
0	2	2	874	881
0	2	3	209	-213
0	2	5	157	154
0	2	6	137	-141
0	2	7	138	134

h	k	l	Fo	Fc
0	2	10	238	-240
0	2	11	182	98
0	2	12	126	-119
1	2	-13	115	109
1	2	-12	132	-130
1	2	-11	149	-146
1	2	-8	243	254
1	2	-7	128	129
1	2	-5	390	-384
1	2	-4	382	374
1	2	-3	128	-126
1	2	-2	599	583
1	2	-1	559	537
1	2	1	216	-210
1	2	2	460	460
1	2	4	615	-620
1	2	5	484	-490
1	2	6	186	-194
1	2	8	127	-126
1	2	9	164	156
1	2	10	168	-172
2	2	-10	272	276
2	2	-9	131	130
2	2	-7	77	-80
2	2	-6	279	279
2	2	-5	32	11
2	2	-4	34	16
2	2	-3	436	433
2	2	-2	425	-416
2	2	-1	231	216
2	2	0	743	-735
2	2	1	312	-314
2	2	2	397	389
2	2	3	229	226
2	2	4	533	-530
2	2	5	107	-96
2	2	6	114	116
2	2	9	115	112
2	2	10	75	77
2	2	11	136	-134
2	2	12	123	121
3	2	-14	115	109
3	2	-11	150	-148
3	2	-10	395	410
3	2	-9	296	305
3	2	-8	309	-314
3	2	-7	402	-415
3	2	-6	130	-130
3	2	-5	89	92
3	2	-4	273	-274
3	2	-3	34	45
3	2	-2	358	-351
3	2	-1	148	145
3	2	0	531	-534
3	2	1	597	609
3	2	2	190	-187
3	2	3	55	-53
3	2	4	121	122
3	2	5	299	-292
3	2	6	285	300
3	2	7	185	182
3	2	8	95	88
3	2	9	92	96
3	2	10	108	106
3	2	11	78	-75
4	2	-13	106	115
4	2	-12	65	-64
4	2	-11	125	122
4	2	-10	174	-179
4	2	-9	151	-151
4	2	-8	174	-167
4	2	-7	291	-282
4	2	-6	92	-90
4	2	-5	161	172
4	2	-4	229	-222
4	2	-2	290	-282
4	2	-1	552	-534
4	2	0	535	533
4	2	1	137	127
4	2	3	216	221
4	2	4	204	206
4	2	5	103	-104
4	2	6	145	142
4	2	7	63	-62
5	2	-14	201	-199
5	2	-13	267	-276
5	2	-11	306	322
5	2	-10	194	-197
5	2	-9	97	87
5	2	-8	222	-235
5	2	-7	171	-169
5	2	-6	146	141
5	2	-5	56	-51
5	2	-4	203	209
5	2	-3	73	63
5	2	-2	685	682
5	2		86	-83
5	2	1	89	-95
5	2	2	241	240
5	2	3	327	-328
5	2	4	98	105
5	2	5	113	111
5	2	8	164	-153
5	2	9	121	-114
6	2	-12	171	-181
6	2	-11	121	-122
6	2	-9	89	-96
6	2	-8	287	290
6	2	-7	314	317
6	2	-6	420	420
6	2	-4	192	-190
6	2	-2	507	495
6	2	-1	157	148
6	2	0	62	-59
6	2	2	144	-143
6	2	3	100	-105
6	2	4	229	-230
6	2	5	88	83
6	2	6	89	-92
7	2	-14	176	177

h	k	l	Fo	Fc
7	2	-13	156	165
7	2	-12	202	204
7	2	-11	148	150
7	2	-8	191	186
7	2	-6	59	-51
7	2	-5	220	-229
7	2	-4	349	338
7	2	-3	120	120
7	2	-2	303	-308
7	2	-1	271	269
7	2	0	302	-318
7	2	1	158	-153
7	2	4	161	-172
7	2	5	120	114
7	2	6	106	-106
8	2	-15	93	100
8	2	-14	140	137
8	2	-11	157	-152
8	2	-10	126	120
8	2	-9	134	130
8	2	-7	297	312
8	2	-6	454	-449
8	2	-5	310	-319
8	2	-4	191	-196
8	2	-2	66	-75
8	2	-1	159	171
8	2	0	118	-117
8	2	2	154	153
8	2	4	100	-109
8	2	5	198	-194
8	2	6	174	178
9	2	-12	182	-186
9	2	-11	124	-129
9	2	-9	221	-224
9	2	-8	431	-437
9	2	-7	117	-127
9	2	-5	101	108
9	2	-4	75	-74
9	2	-3	164	158
9	2	-2	100	-97
9	2	2	309	307
9	2	5	108	-109
10	2	-14	151	-145
10	2	-13	82	-79
10	2	-12	139	-137
10	2	-10	119	123
10	2	-9	200	211
10	2	-8	188	-184
10	2	-7	355	-369
10	2	-5	120	-117
10	2	-4	185	186
10	2	-3	110	112
10	2	-2	152	151
10	2	0	191	196
10	2	1	110	101
11	2	5	103	-103
11	2	-14	99	-95
11	2	-11	89	87
11	2	-10	124	123
11	2	-9	195	192
11	2	-8	141	146
11	2	-6	295	288
11	2	-5	131	125
11	2	-3	111	-110
12	2	-12	142	135
12	2	-11	195	201
12	2	-10	83	91
12	2	-9	98	103
12	2	-7	151	-153
12	2	-6	124	122
12	2	-4	187	-184
12	2	0	149	-149
13	2	-5	94	-92
13	2	-4	168	-166
13	2	-3	159	-161
14	2	-10	112	-107
0	3	-13	110	-108
0	3	-11	100	-104
0	3	-9	251	-240
0	3	-8	84	69
0	3	-6	70	72
0	3	-5	192	-187
0	3	-4	388	373
0	3	-3	277	-266
0	3	-2	274	270
0	3	-1	344	340
0	3	1	358	340
0	3	2	269	-270
0	3	3	272	-266
0	3	4	386	-373
0	3	5	195	-187
0	3	6	62	-72
0	3	8	74	-69
0	3	9	249	-240
0	3	11	102	-114
0	3	13	116	-108
1	3	-9	92	-96
1	3	-8	120	124
1	3	-7	375	372
1	3	-5	808	817
1	3	-4	79	-74
1	3	-3	347	338
1	3	-2	583	553
1	3	-1	238	231
1	3	0	63	68
1	3	1	447	-456
1	3	2	103	-108
1	3	3	40	51
1	3	4	124	-119
1	3	5	60	-60
1	3	7	482	-491
1	3	8	187	196
1	3	9	245	-253
1	3	12	123	114
2	3	-14	136	127
2	3	-13	91	94
2	3	-12	77	66
2	3	-9	244	248
2	3	-8	140	-134
2	3	-7	407	417

h	k	l	Fo	Fc
2	3	-6	81	-83
2	3	-5	220	-224
2	3	-4	292	-283
2	3	-3	382	372
2	3	-2	335	-329
2	3	-1	435	437
2	3	0	308	310
2	3	1	577	-595
2	3	3	189	-189
2	3	4	89	-86
2	3	7	160	162
2	3	8	185	194
2	3	9	134	129
3	3	-13	298	288
3	3	-8	121	-120
3	3	-6	311	-303
3	3	-5	369	-362
3	3	-4	82	79
3	3	-3	697	-675
3	3	-2	323	-321
3	3	-1	566	-571
3	3	0	57	70
3	3	1	414	-418
3	3	2	273	276
3	3	3	394	386
3	3	4	212	-224
3	3	7	116	120
3	3	8	102	-97
3	3	9	286	274
4	3	-11	269	-271
4	3	-9	123	120
4	3	-8	76	-89
4	3	-7	618	-620
4	3	-5	215	-224
4	3	-4	192	183
4	3	-3	238	242
4	3	-2	85	97
4	3	-1	341	-332
4	3	0	185	184
4	3	1	149	-146
4	3	2	129	133
4	3	3	160	164
4	3	4	78	80
4	3	5	84	92
4	3	7	109	108
4	3	8	116	-117
5	3	-13	236	-230
5	3	-11	388	-398
5	3	-10	273	284
5	3	-9	69	-67
5	3	-7	89	-87
5	3	-6	102	101
5	3	-5	305	307
5	3	-4	222	212
5	3	-3	469	454
5	3	-2	107	-105
5	3	-1	188	193
5	3	0	193	191
5	3	1	592	594
5	3	2	171	-171
5	3	4	132	132
5	3	5	124	-119
6	3	-11	215	219
6	3	-10	218	221
6	3	-9	97	91
6	3	-8	58	55
6	3	-7	143	-142
6	3	-6	100	94
6	3	-5	669	666
6	3	-4	113	-102
6	3	-3	296	304
6	3	-1	142	-147
6	3	0	223	-216
6	3	1	121	125
6	3	2	270	-272
6	3	3	148	-158
7	3	-13	88	95
7	3	-11	349	355
7	3	-10	66	-74
7	3	-9	380	392
7	3	-7	115	112
7	3	-4	220	-220
7	3	-3	183	-194
7	3	-1	197	-196
7	3	1	160	-168
7	3	2	162	-168
7	3	3	446	-445
8	3	-11	89	-87
8	3	-10	260	-260
8	3	-9	388	-397
8	3	-8	79	-84
8	3	-6	71	-68
8	3	-5	105	-99
8	3	-3	253	-255
8	3	-1	163	-151
8	3	0	104	96
8	3	2	98	104
8	3	3	114	-115
8	3	5	144	131
9	3	-9	372	-378
9	3	-7	331	-329
9	3	-5	332	-329
9	3	-3	113	116
9	3	-2	108	102
9	3	-1	222	217
9	3	0	127	124
9	3	3	133	137
9	3	5	138	126
10	3	-11	135	-135
10	3	-10	118	117
10	3	-9	115	118
10	3	-7	292	305
10	3	-4	125	129
10	3	-3	110	115
10	3	-1	131	125
10	3	1	102	99
11	3	-11	116	112
11	3	-7	108	108
11	3	-6	130	-136
11	3	-5	290	278

Table 3. Continued.

h	k	l	Fo	Fc	h	k	l	Fo	Fc	h	k	l	Fo	Fc	h	k	l	Fo	Fc	h	k	l	Fo	Fc	h	k	l	Fo	Fc
11	3	-3	290	285	3	4	3	116	120	8	4	-8	91	97	2	5	-1	250	-248	8	5	-7	157	-150	5	6	-6	79	82
11	3	1	110	-101	3	4	4	127	128	8	4	-7	261	-263	2	5	0	325	-331	8	5	-5	202	-203	5	6	-5	98	101
12	3	-9	149	142	3	4	5	196	192	8	4	-6	288	-301	2	5	1	121	-118	8	5	-4	209	-214	5	6	0	131	139
12	3	-7	173	-178	3	4	6	139	127	8	4	-5	120	116	2	5	2	95	104	8	5	-3	94	-97	5	6	1	202	-208
12	3	-5	119	-129	3	4	7	220	-223	8	4	-4	104	-101	2	5	3	318	-327	8	5	1	138	-134	5	6	2	170	152
12	3	-4	219	-216	3	4	8	109	115	8	4	0	86	-80	2	5	4	214	210	9	5	-10	88	-94	5	6	4	99	-85
12	3	-3	101	-92	4	4	-14	111	110	8	4	1	133	135	2	5	5	135	-124	9	5	-9	152	-150	5	6	5	164	-153
13	3	-9	130	-124	4	4	-13	86	-86	8	4	4	135	142	3	5	-12	80	-72	9	5	-8	106	-103	6	6	-6	131	118
13	3	-7	173	-171	4	4	-12	61	56	9	4	-13	65	-82	3	5	-11	88	84	9	5	-5	96	100	6	6	-5	140	132
13	3	-3	165	-164	4	4	-10	223	-217	9	4	-10	219	-215	3	5	-6	80	-81	9	5	-4	226	227	6	6	-4	208	213
0	4	-12	135	-132	4	4	-9	80	-82	9	4	-7	101	104	3	5	-5	191	-194	9	5	1	125	122	6	6	-3	193	-201
0	4	-9	103	110	4	4	-8	153	-152	9	4	-1	182	189	3	5	-4	175	-178	10	5	-8	111	112	6	6	0	118	-110
0	4	-8	78	-88	4	4	-7	233	231	9	4	0	105	106	3	5	-3	109	-108	10	5	-6	131	-131	7	6	-10	212	207
0	4	-5	255	257	4	4	-5	135	-127	10	4	-13	147	134	3	5	-2	68	70	10	5	-3	158	156	7	6	-5	170	-177
0	4	-4	463	455	4	4	-4	134	-138	10	4	-12	101	-106	3	5	-1	57	-57	11	5	-7	130	122	7	6	-4	221	-222
0	4	-3	335	331	4	4	-3	80	74	10	4	-10	145	-142	3	5	0	149	149	11	5	-2	105	-98	7	6	-1	103	-113
0	4	-2	331	320	4	4	-2	72	-75	10	4	-9	132	-128	3	5	2	55	48	0	6	-7	136	131	7	6	0	90	-96
0	4	-1	640	-642	4	4	-1	374	362	10	4	-8	194	-201	3	5	3	205	-213	0	6	-6	98	88	7	6	3	123	122
0	4	0	106	-99	4	4	0	452	451	10	4	-7	195	190	3	5	5	217	231	0	6	-2	199	207	8	6	-9	80	-90
0	4	1	636	641	4	4	2	264	268	10	4	-5	216	212	4	5	-9	343	-335	0	6	0	430	421	8	6	-6	113	108
0	4	2	330	320	4	4	3	122	130	10	4	-4	224	222	4	5	-8	217	-212	0	6	2	200	207	8	6	-4	152	-147
0	4	3	329	-331	4	4	6	187	190	10	4	-2	124	121	4	5	-6	127	131	0	6	6	88	98	8	6	-2	153	-148
0	4	4	451	455	4	4	8	82	91	11	4	-11	89	94	4	5	-4	123	138	0	6	7	129	-131	9	6	-9	67	74
0	4	5	250	-257	5	4	-10	104	-101	11	4	-5	275	-271	4	5	-3	331	-326	0	6	8	77	-65	9	6	-7	119	-120
0	4	8	78	-88	5	4	-8	126	-121	11	4	-3	97	111	4	5	-2	167	-167	1	6	-7	87	89	9	6	-6	87	-78
0	4	9	109	-110	5	4	-7	101	108	12	4	-12	184	182	4	5	-1	215	224	1	6	-6	127	126	9	6	-3	109	109
0	4	12	134	-132	5	4	-6	84	-87	12	4	-10	111	111	4	5	0	72	-70	1	6	-4	174	191	10	6	-8	106	100
1	4	-11	142	137	5	4	-5	134	131	12	4	-5	193	-188	4	5	1	227	224	1	6	-3	167	-166	0	7	-6	131	122
1	4	-6	115	122	5	4	-4	353	355	12	4	-2	106	-99	4	5	2	358	355	1	6	-1	211	-218	0	7	-2	144	-142
1	4	-4	114	111	5	4	-3	105	108	13	4	-6	143	-142	4	5	3	135	141	1	6	0	137	-143	0	7	-1	163	-156
1	4	-3	341	340	5	4	-2	66	-60	0	5	-11	117	-117	4	5	5	92	86	1	6	1	330	-332	0	7	1	158	-166
1	4	-2	189	195	5	4	-1	161	-169	0	5	-10	96	-83	4	5	7	92	91	1	6	2	70	-70	0	7	2	138	142
1	4	-1	51	58	5	4	1	70	-68	0	5	-8	156	149	5	5	-10	135	136	1	6	3	96	-88	0	7	6	124	-122
1	4	0	104	98	5	4	3	218	213	0	5	-5	105	102	5	5	-9	122	-120	1	6	4	127	129	1	7	-5	110	114
1	4	1	77	-71	5	4	4	203	193	0	5	-4	102	103	5	5	-8	98	101	1	6	5	145	-155	1	7	-3	124	117
1	4	2	396	-408	5	4	6	127	-124	0	5	-3	354	350	5	5	-7	100	-96	1	6	6	77	-64	1	7	-1	170	176
1	4	3	301	-307	5	4	8	86	-80	0	5	-2	256	255	5	5	-5	167	178	1	6	8	122	-114	1	7	0	165	-171
1	4	5	162	177	6	4	-14	111	-112	0	5	2	262	-255	5	5	-4	113	-115	2	6	-8	259	251	1	7	2	132	-126
1	4	7	177	174	6	4	-12	93	-82	0	5	3	348	350	5	5	-3	107	104	2	6	-5	76	-78	1	7	5	140	-138
1	4	9	120	-120	6	4	-11	114	111	0	5	4	99	-103	5	5	-2	147	152	2	6	-3	70	-67	2	7	-2	102	-105
1	4	11	161	163	6	4	-10	83	-78	0	5	5	99	102	5	5	-1	209	218	2	6	-2	87	74	2	7	1	166	170
2	4	-11	118	111	6	4	-9	360	357	0	5	6	61	53	5	5	0	125	-130	2	6	0	74	-76	3	7	-6	114	-117
2	4	-10	98	89	6	4	-8	263	267	0	5	8	153	-149	5	5	1	84	-94	2	6	1	99	-103	3	7	-5	149	-147
2	4	-9	166	-164	6	4	-5	63	-71	0	5	10	95	93	5	5	2	118	-120	2	6	2	528	-536	3	7	-1	136	-129
2	4	-6	132	134	6	4	-4	153	152	0	5	11	122	-117	5	5	3	219	231	2	6	3	190	189	3	7	4	198	211
2	4	-4	72	74	6	4	-3	93	93	1	5	-9	104	115	5	5	7	139	-137	2	6	4	187	-195	4	7	-5	84	-80
2	4	-3	691	-692	6	4	-1	209	-206	1	5	-8	120	123	6	5	-7	343	345	3	6	-11	94	-101	4	7	-3	100	-82
2	4	-2	453	-455	6	4	1	239	-228	1	5	-6	89	85	6	5	-6	321	323	3	6	-10	105	-114	4	7	-2	128	128
2	4	-1	58	47	6	4	2	362	-368	1	5	-5	170	160	6	5	-5	60	-63	3	6	-4	131	-128	5	7	-7	126	-124
2	4	0	305	-315	6	4	3	124	-129	1	5	-4	219	-215	6	5	-3	143	153	3	6	-2	74	-78	5	7	-6	152	153
2	4	1	459	470	6	4	6	101	-91	1	5	-3	244	244	6	5	-2	310	-321	3	6	-1	169	159	5	7	1	171	177
2	4	2	324	-328	7	4	-11	173	-178	1	5	-1	160	165	6	5	0	96	97	3	6	1	154	161	6	7	-9	138	139
2	4	3	309	-317	7	4	-6	92	88	1	5	1	140	-140	6	5	1	112	-110	3	6	2	192	195	6	7	-6	89	-99
2	4	4	229	-218	7	4	-5	100	101	1	5	2	187	199	6	5	2	117	-116	3	6	3	241	236	7	7	-7	102	106
2	4	5	75	74	7	4	-4	92	93	1	5	3	211	-211	7	5	-11	137	137	3	6	5	179	178	7	7	-5	91	102
2	4	6	180	-193	7	4	-3	169	-176	1	5	4	72	-91	7	5	-6	198	-205	4	6	-8	180	-191	7	7	-2	127	-121
2	4	8	143	146	7	4	-2	85	-89	1	5	5	113	-112	7	5	-4	103	111	4	6	-6	208	-204	7	7	-1	105	-103
2	4	10	82	-84	7	4	-1	138	-134	1	5	6	93	-90	7	5	-1	217	-226	4	6	-4	121	-127	0	8	-3	112	112
3	4	-11	81	96	7	4	0	194	-185	1	5	9	141	-148	7	5	0	108	-110	4	6	-3	93	91	0	8	-2	90	100
3	4	-9	209	-210	7	4	1	109	114	1	5	10	100	94	7	5	1	213	-216	4	6	-2	185	158	0	8	2	100	100
3	4	-7	54	-55	7	4	2	100	-106	2	5	-10	136	124	7	5	4	145	138	4	6	1	99	109	0	8	3	111	-112
3	4	-5	105	-110	7	4	3	122	-127	2	5	-9	140	139	8	5	-12	71	-66	4	6	2	228	234	2	8	-2	85	-77
3	4	-4	65	-71	8	4	-14	119	120	2	5	-6	116	-116	8	5	-11	102	-104	4	6	4	156	148	2	8	-1	121	-110
3	4	-1	190	-178	8	4	-13	98	-97	2	5	-5	195	136	8	5	-10	120	-115	4	6	6	93	93	2	8	1	127	-129
3	4	0	66	-67	8	4	-10	162	165	2	5	-4	66	58	8	5	-9	192	189	5	6	-9	77	77	4	8	0	104	104
3	4	2	266	-271	8	4	-9	318	-315	2	5	-3	61	-67	8	5	-8	90	89	5	6	-7	143	127					

Table 4. The principal axes of the thermal vibration ellipsoids given by the components of a unit vector in fractional coordinates e_x, e_y, e_z; the corresponding r.m.s. amplitudes, and the B-values.

Atom	e_x	e_y	e_z	$(\overline{u^2})^{\frac{1}{2}}$ Å	B(Å^2)
	.183	.348	.209	.401	12.69
S_1	.257	−.066	.021	.256	5.18
	.070	−.091	.221	.216	3.70
	.137	.225	.020	.259	5.29
S_2	.226	−.088	.183	.227	4.07
	−.049	.064	.173	.212	3.54
	.311	.027	.422	.382	11.51
S_3	.136	.207	−.073	.277	6.04
	−.129	.131	.036	.199	3.13

Table 4. Continued.

	.127	.208	.150	.251	4.99
N_1	.046	−.105	.223	.230	4.16
	.211	−.067	.033	.208	3.40
	.081	.030	.287	.259	5.28
N_2	.124	.196	.007	.230	4.17
	.203	−.107	.063	.210	3.48
	.117	−.228	.182	.279	6.13
N_3	.151	.136	.216	.236	4.39
	−.171	.006	.048	.199	3.12
	.114	.201	.189	.260	5.35
C_1	.155	.057	−.110	.237	4.43
	.186	−.130	.169	.222	3.88
	.086	.218	.226	.294	6.83
C_2	.165	.118	−.118	.272	5.86
	.189	−.104	.150	.202	3.23
	.124	.174	.305	.318	8.01
C_3	.088	.205	−.136	.283	6.34
	.201	−.082	.080	.194	2.96
	.178	.078	.312	.283	6.33
C_4	.028	.239	−.087	.260	5.34
	−.188	.057	.001	.197	3.06
	.082	−.076	.256	.239	4.52
C_5	.211	−.071	.018	.214	3.63
	.102	.185	.086	.208	3.42
	−.095	.153	.115	.237	4.45
C_6	.123	.172	−.046	.229	4.16
	.189	−.031	.207	.202	3.22
	.361	−.012	.220	.317	7.94
C_7	−.016	.212	.157	.269	5.70
	.031	.130	−.150	.213	3.57
	.427	−.016	.251	.373	11.01
C_8	−.025	.120	.236	.276	6.02
	.022	.200	−.084	.222	3.89
	.381	.027	.167	.333	8.75
C_9	.022	.001	.302	.292	6.75
	.019	−.201	.009	.202	3.22
	.092	.121	−.175	.264	5.49
C_{10}	.248	.065	.236	.253	5.03
	−.101	.178	.016	.210	3.47
	.132	−.190	.244	.285	6.42
C_{11}	.189	.167	.165	.245	4.63
	−.143	.060	.074	.200	3.16

	.035	.251	.233	.332	8.72
C_{12}	.095	−.183	.249	.284	6.38
	.233	.026	.056	.213	3.57
	−.132	.290	.154	.381	11.47
C_{13}	.107	−.137	.283	.283	6.34
	.212	.089	.083	.205	3.33
	.320	−.145	.074	.325	8.34
C_{14}	.124	.082	.276	.254	5.10
	.077	.190	−.068	.227	4.08
	.306	−.028	.161	.268	5.67
C_{15}	.031	.244	−.024	.249	4.88
	−.004	.031	.190	.195	3.00

Table 5. Bond distances and angles with e.s.d.'s. (For numbering of atoms, see Fig. 1. H_n is bonded to C_n.)

Distance	Å	Distance	Å
S_3-C_1	1.769(3)	C_6-C_7	1.381(4)
S_1-C_{15}	1.778(4)	C_7-C_8	1.376(5)
S_2-C_5	1.788(3)	C_8-C_9	1.366(5)
S_2-C_6	1.790(3)	C_9-C_{10}	1.381(4)
S_3-C_{10}	1.774(4)	$C_{11}-C_{12}$	1.380(5)
S_3-C_{11}	1.773(4)	$C_{12}-C_{13}$	1.358(5)
N_1-C_1	1.327(4)	$C_{13}-C_{14}$	1.363(5)
N_1-C_5	1.336(4)	$C_{14}-C_{15}$	1.381(5)
N_2-C_6	1.331(4)	C_2-H_2	0.92(3)
N_2-C_{10}	1.333(4)	C_3-H_3	1.00(3)
N_3-C_{11}	1.327(4)	C_4-H_4	0.94(3)
N_3-C_{15}	1.337(4)	C_7-H_7	1.04(3)
C_1-C_2	1.385(5)	C_8-H_8	1.03(3)
C_2-C_3	1.366(5)	C_9-H_9	0.94(3)
C_3-C_4	1.373(5)	$C_{12}-H_{12}$	0.91(3)
C_4-C_5	1.373(4)	$C_{13}-C_{13}$	0.94(3)
		$C_{14}-C_{14}$	0.96(3)

Angle	(°)	Angle	(°)
$C_1-S_1-C_{15}$	102.4(1)	$C_2-C_3-C_4$	118.9(3)
$C_5-S_2-C_6$	101.0(2)	$C_3-C_4-C_5$	118.9(3)
$C_{10}-S_3-C_{11}$	101.8(2)	$C_6-C_7-C_8$	117.6(3)
$N_1-C_1-S_1$	119.4(2)	$C_7-C_8-C_9$	119.8(4)
$N_1-C_5-S_2$	117.9(2)	$C_8-C_9-C_{10}$	118.3(4)
$N_2-C_6-S_2$	118.0(2)	$C_{11}-C_{12}-C_{13}$	118.4(4)
$N_2-C_{10}-S_3$	118.0(2)	$C_{12}-C_{13}-C_{14}$	119.8(4)
$N_3-C_{15}-S_1$	116.8(3)	$C_{13}-C_{14}-C_{15}$	118.0(4)
$N_3-C_{11}-S_3$	117.6(2)	$C_1-C_2-H_2$	121(2)
$C_2-C_1-S_1$	117.3(3)	$H_2-C_2-C_3$	120(2)
$C_4-C_5-S_2$	119.0(3)	$C_2-C_3-H_3$	116(2)
$C_7-C_6-S_2$	118.1(3)	$H_3-C_3-C_4$	125(2)
$C_9-C_{10}-S_3$	118.6(3)	$C_3-C_4-H_4$	121(2)

Table 5. Continued.

$C_{14}-C_{15}-S_1$	119.7(3)	$H_4-C_4-C_5$	120(2)
$C_{12}-C_{11}-S_3$	118.9(3)	$C_6-C_7-H_7$	119(2)
$C_1-N_1-C_5$	117.1(3)	$H_7-C_7-C_8$	123(2)
$C_6-N_2-C_{10}$	117.0(3)	$C_7-C_8-H_8$	120(2)
$C_{11}-N_3-C_{15}$	116.6(3)	$H_8-C_8-C_9$	121(2)
$N_1-C_1-C_2$	123.3(3)	$C_8-C_9-H_9$	121(2)
$N_1-C_5-C_4$	123.1(3)	$H_9-C_9-C_{10}$	120(2)
$N_2-C_6-C_7$	123.8(3)	$C_{11}-C_{12}-H_{12}$	120(2)
$N_2-C_{10}-C_9$	123.3(3)	$H_{12}-C_{12}-C_{13}$	122(2)
$N_3-C_{11}-C_{12}$	123.5(3)	$C_{12}-C_{13}-H_{13}$	117(2)
$N_3-C_{15}-C_{14}$	123.4(3)	$H_{13}-C_{13}-C_{14}$	123(2)
$C_1-C_2-C_3$	118.6(3)	$C_{13}-C_{14}-H_{14}$	123(2)
		$H_{14}-C_{14}-C_{15}$	118(2)

Each of the three 2,6-sulphursubstituted pyridyl groups are planar to within 0.05 Å. The angles between these planes (Fig. 2) are:

$$\angle \text{I,II} : 66.3°, \quad \angle \text{I,III} : 61.0°, \quad \angle \text{II,III} : 57.1°.$$

The average bond distances and angles of the pyridine rings agree within probable limits of error with the micro wave results for pyridine:[8]

	Title compound	Pyridine
C–N	1.335 Å	1.3402 Å
C–C	1.376 Å	1.3945 Å
C–N–C	116.7°	116° 50′
N–C–C	123.5°	123° 53′
C–C–C	118.6°	118° 26′

In fact the C–C distances seem to be somewhat shorter than the pyridine value. However, from Table 4 may be seen that the carbon atoms C_2, C_3, C_4, C_7, C_8, C_9, C_{12}, C_{13} and C_{14} have relatively large thermal vibration amplitudes (in the range 6.3 Å to 11.5 Å). Since no corrections in positional parameters

Table 6. Some dihedral angles with e.s.d.'s.

Angle	(°)
$N_3-C_{15}-S_1-C_1$	64.1 (3)
$N_1-C_1-S_1-C_{15}$	0.0 (3)
$N_3-C_{11}-S_3-C_{10}$	53.5 (3)
$N_2-C_{10}-S_3-C_{11}$	19.1 (3)
$N_1-C_5-S_2-S_6$	53.5 (3)
$N_2-C_6-S_2-C_5$	64.5 (3)

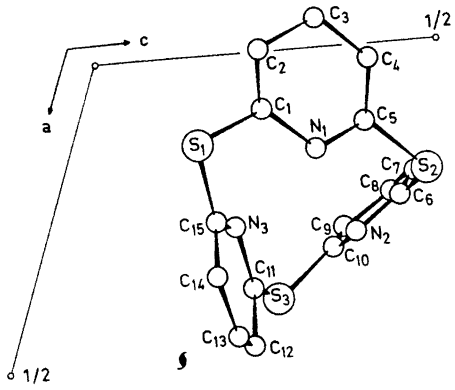

Fig. 1. Schematical drawing of the molecule viewed along [010].

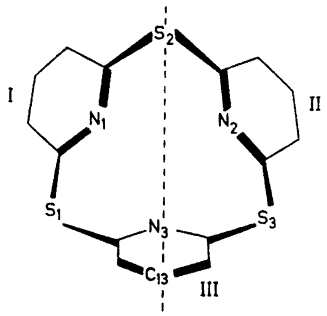

Fig. 2.

for this motion have been made, the difference cannot with confidence be regarded as significant.

The N – N distances across the ring correspond to van der Waals contacts:

$N_1 \cdots N_2$: 2.962 Å; $N_1 \cdots N_3$: 2.945 Å; $N_2 \cdots N_3$: 2.916 Å.

No short *inter*molecular distances have been found.

REFERENCES

1. Reistad, K. R., Groth, P., Lie, R. and Undheim, K. *Chem. Commun.* **1972** 1059.
2. Dahl, T., Gram, F., Groth, P., Klewe, B. and Rømming, Chr. *Acta Chem. Scand.* **24** (1970) 2232.
3. Hanson, H. P., Herman, F., Lea, J. D. and Skillman, S. *Acta Cryst.* **17** (1964) 1040.
4. Stewart, R. F., Davidson, E. R. and Simpson, W. T. *J. Chem. Phys.* **42** (1965) 3175.
5. Schomaker, V. and Trueblood, K. N. *Acta Cryst.* **B 24** (1968) 63.
6. Knobler, C., Baker, C., Hope, H. and McCullough, J. D. *Inorg. Chem.* **10** (1971) 697.
7. *Organic Sulphur Compounds*, Kharasch, N., Ed., Pergamon, Oxford 1971, Vol. 1, p. 57.
8. Bak. B., Hansen-Nygaard, L. and Rastrup-Andersen, J. *J. Mol. Spectry.* **2** (1958) 361.

Received June 28, 1972.

ACTA CHEMICA SCANDINAVICA 27 (1973) 15–20

Molecular Structure of Gaseous Dimethyl-1,2,4-trithia-3,5-diborolane

H. M. SEIP,[a] R. SEIP[a] and W. SIEBERT[b]

[a] *Department of Chemistry, University of Oslo, Oslo 3, Norway.* [b] *Institut für anorganische Chemie der Universität Würzburg, Würzburg, Germany*

Dimethyl-1,2,4-trithia-3,5-diborolane has been shown by electron diffraction to have an at least approximately planar skeleton. The B–S bond distances are nearly equal; the average was found to be 1.803(0.003) Å. Some other important parameters are: r_a(S–S) = 2.076(0.003) Å, r_a(B–C) = 1.569(0.005) Å, ∠BSB = 101.6(0.4)°, ∠SBS = 117.7(0.2)°, ∠BSS = 101.5(0.4)°, and ∠S_4BC = 122.8(1.6)°.

Though considerable π-bond order has been established for B–N,[1] B–O,[2–4] B–F [5] bonds, and probably also for B–Cl bonds,[6,7] there is still doubt about the magnitude of a similar effect in B–S bonds. Siebert *et al.*[8] have proposed that the double bond character of the B–S bonds is of importance for the structure and reactivity of thioboranes, while Vahrenkamp finds that the NMR [9] and vibrational spectra [10] indicate negligible π-bond order. As a contribution to the clarification of this problem we are studying boron-sulphur compounds, and report here our results for two 1,2,4-trithia-3,5-diborolane derivatives,[11] *i.e.* $Me_2B_2S_3$ and $Cl_2B_2S_3$,[12] by electron diffraction.

EXPERIMENTAL

The sample of dimethyl-1,2,4-trithia-3,5-diborolane was synthesized by one of us (W.S.), and the electron-diffraction diagrams were recorded with the Oslo apparatus.[13] The nozzle temperature was about 75°C and the electron wave length 0.06458 Å. Four and five plates were used for the long (48.05 cm) and short (25.06 cm) nozzle-to-plate distance, respectively. The data were treated in the usual way,[14] and the modified molecular intensities were calculated using the modification function [14] $s/(|f_B'||f_S'|)$. The agreement between the observed intensity curves was satisfactory, and most of the calculations were carried out on a composite intensity curve ranging from $s = 2.50$ Å^{-1} to $s = 35.0$ Å^{-1}. The s intervals were 0.125 Å^{-1} for $s < 7.50$ Å^{-1} and 0.250 Å^{-1} for s above this value.

STRUCTURE REFINEMENT

The molecule was assumed to have at least a twofold axis of symmetry, *i.e.* either C_2 or C_{2v} symmetry when the H atoms are not taken into consideration. A C_s model was not considered, since the potential function for rotation

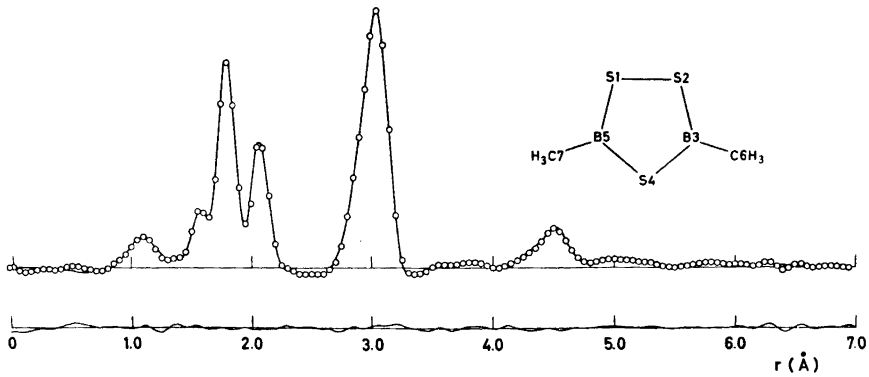

Fig. 1. Experimental (circles) and theoretical radial distribution curves (artificial damping $k = 0.0015$ Å^2). The difference curve is also given.

about the S–S bond has a considerable barrier corresponding to the *syn* form in most molecules (about 9 kcal/mol in H_2S_2 [15]). Models with the methyl groups in fixed positions as well as models with freely rotating groups were tried. It was assumed to be no tilt of these groups. The shrinkage effect [16] was neglected. This approximation seemed justified according to calculations (mainly for the corresponding chloro-compound [12]) by the method described by Stølevik *et al.*[17] using frequencies obtained by Sacher *et al.*[18,19]

The experimental radial distribution (RD) curve (see Fig. 1) calculated by Fourier inversion of the observed intensities (Fig. 2), showed that the B–S bond distances must be nearly equal. Least-squares refinements carried out for various values of the difference, showed that the difference must be less than 0.03 Å. Satisfactory agreement between theoretical and observed intensity and RD curves was obtained assuming a planar ring. The fit was very nearly the same for a model with the methyl groups in fixed positions

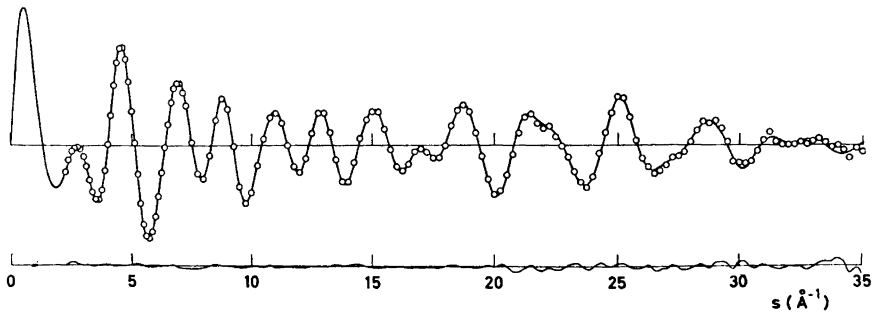

Fig. 2. Experimental (circles) and theoretical intensity curves. The differences between experimental and theoretical curves are also shown.

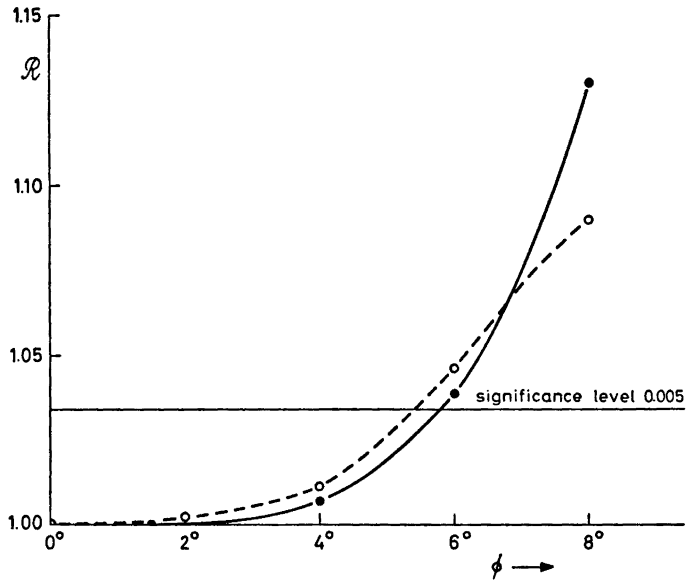

Fig. 3. The relative R factor [20] for various values of the torsional angle $\phi(S_4-B)$ for $Me_2B_2S_3$ (dots) and for $Cl_2B_2S_3$ (open circles). The R values corresponding to $\phi=0$ are put equal to 1 for both compounds.

and a model with freely rotating methyl groups.* However, it seems reasonable to assume that the barrier is low, and most of the subsequent calculations were carried out assuming free rotation.

The torsional angle about S_4-B (ϕ) was then refined as an additional parameter. The result was $\phi=1.4°$ with a standard deviation of 3.7°. Refinements were then carried out for various fixed values of ϕ; the planar arrangement about the boron atoms was kept. Fig. 3 shows a plot of the relative R factor [20] against ϕ for a model with freely rotating methyl groups. The variation in R is very small up to $\phi=4°$. However, a torsional angle of 6° may be rejected at the 0.5 % level. Though one should not take this number too seriously, since the basic assumptions for the test are not fulfilled, the plot shows that the ring must be nearly planar.

The final electron diffraction results are given in Table 1, and the corresponding theoretical RD and intensity curves are compared to the observed values in Figs. 1 and 2. Since the least-squares refinements were carried out using a diagonal weight matrix, the standard deviations were multiplied by [22,23]

$$F = \left(\frac{2a}{\Delta s}\right)^{\frac{1}{2}} \exp\left(-\frac{a^2}{2\pi}R^2\right)$$

with $a=0.5$ Å^{-1}. The uncertainty in the electron wave-length is also included.

* The free rotation was simulated by having each methyl group in 6 different rotational positions.

Table 1. Interatomic distances (r_a[21]), mean amplitudes of vibration (u), and bond angles with estimated standard deviations.

	r_a (Å)	u (Å)
S_4-B_3 S_2-B_3	1.803(0.003)[a]	0.040(0.003)[a]
S–S	2.076(0.003)	0.047(0.003)
B–C	1.569(0.005)	0.045[b]
C–H	1.104(0.012)	0.120(0.012)
S···S	3.086(0.004)	0.054(0.003)
B···S	3.008(0.007)	0.065[b]
B···B	2.795(0.007)	0.065[b]
S_4···C	2.963(0.022)	0.083(0.010)[a]
S_2···C_6	2.916(0.024)	
B···C	4.314(0.012)	0.068[b]
S_1···C_6	4.526(0.008)	0.075[b]
C···C	5.779(0.022)	0.100[b]
	Angles (degrees)	
∠BSB	101.6(0.4)	
∠SBS	117.7(0.2)	
∠BSS	101.5(0.4)	
∠S_4BC	122.8(1.6)	
ϕ(S_4–B)	1.4(3.7)	
∠HCH	108.0[b]	

[a] The parameters were assumed equal. [b] The parameter was not refined simultaneously with the other parameters.

DISCUSSION

The investigation shows that the five-membered ring in dimethyl-1,2,4-trithia-3,5-diborolane is at least nearly planar. The same result is obtained for $Cl_2B_2S_3$.[12] (See Fig. 3.) 1,2,4-Trioxa-3,5-diborolane ($B_2O_3H_2$) is also planar, as has been shown by spectroscopic methods.[24,25] The planarity of this compound in contrast to the puckered 1,2,4-trioxacyclopentane,[26] has been explained by partial π-bond character in the B–O bonds.[3] This is in agreement with the appreciable barriers to rotation about B–O bonds.[4]

It seems difficult to explain the planarity of the B_2S_3 ring without proposing some degree of π-character in the ring bonds. This is in agreement with theoretical calculations by the CNDO/2 method which gives a planar equilibrium conformation of the B_2S_3 ring and a considerable π-bond order for the B–S bonds.[27]

The ring puckering to be expected if the barrier to rotation about the B–S bonds is zero, was estimated using the Westheimer-Hendrickson approach.[28,29] Only torsional and bending contributions to the potential energy were included. The results obtained for three sets of constants are given in Table 2. The potential for rotation about the S–S bond was in the two first calculations taken from the *ab initio* results for the potential in H_2S_2.[15] This ex-

Table 2. Calculated bond angles and torsional angles in the B_2S_3 ring assuming zero barrier about the B–S bonds. "Natural" angles were $\theta°_{SBS}=120°$ and $\theta°_{SSB}=\theta°_{BSB}=100°$ in all the calculations.

	I	II	III
$k_{BSB}=k_{SSB}$ [a]	0.035	0.50	0.050
k_{SBS} [a]	0.035	0.055	0.050
V°(SS) [b]	9.3 [c]	9.3 [c]	5.0 [d]
∠BSB	97.4	97.5	98.0
∠SSB	115.6	116.7	98.0
∠SBS	95.1	96.2	118.0
$\phi(S_4-B)$	17.3	15.6	12.2
$\phi(S_3-B)$	−38.5	−34.6	−26.9
$\phi(S-S)$	41.3	36.9	28.6

[a] In kcal mol^{-1} degree^{-2}. [b] In kcal mol^{-1}. [c] The potential given in Ref. 15 was used. [d] A potential of the form $V(\phi)=\frac{1}{2}V°(1-\cos(2\phi))$ was used.

pression for the potential includes terms up to $\cos(4\phi)$, and gives a barrier of about 9.3 kcal/mol corresponding to the *syn* form. The results in column III were obtained with a simple twofold potential. The bending force constants were similar to those used for tetrahydrothiophene [30] in the first calculation; in the other calculations larger values were used to avoid overestimating the puckering corresponding to a given rotational potential.

The torsional angles in the columns I and II are much too large to be consistent with the electron-diffraction data. Even in column III, corresponding to a considerably reduced barrier about the S–S bond, the puckering is unacceptably large. With the same constants as used in this calculation, but introducing a twofold potential about the B–S bonds, we found that the ring becomes planar when the barrier to rotation about B–S is approximately 2.5 kcal/mol.

Acknowledgements. The authors are grateful to cand.real. A. Almenningen for recording the diffraction diagrams. Financial support from the *Norwegian Research Council for Science and Humanities* is thankfully acknowledged.

REFERENCES

1. Niedenzu, K. and Dawson, J. W. In Muetterties, E. L., Ed., *The Chemistry of Boron and Its Compounds*, Wiley, New York 1967, p. 377, and references cited therein.
2. Coulson, C. A. and Dingle, T. W. *Acta Cryst.* **B 24** (1968) 153.
3. Coulson, C. A. *Acta Cryst.* **B 25** (1969) 807.
4. Lanthier, G. F. and Graham, W. A. G. *Chem. Commun.* **1968** 715.
5. Armstrong, D. R. and Perkins, P. G. *Theor. Chim. Acta* **15** (1969) 413.
6. Lappert, M. F., Litzow, M. R., Pedley, J. B., Riley, P. N. K. and Tweedale, A. *J. Chem. Soc.* **A 1968** 3105.
7. Sawodny, W., Fadini, A. and Ballein, K. *Spectrochim. Acta* **21** (1965) 995.
8. Siebert, W., Gast, E. and Schmidt, M. *J. Organometal Chem.* **23** (1970) 329.

9. Vahrenkamp, H. *J. Organometal Chem.* **28** (1971) 167.
10. Vahrenkamp, H. *J. Organometal Chem.* **28** (1971) 181.
11. Schmidt, M. and Siebert, W. *Chem. Ber.* **102** (1969) 2752.
12. Almenningen, A., Seip, H. M. and Vassbotn, P. *Acta Chem. Scand.* **27** (1973) 21.
13. Bastiansen, O., Hassel, O. and Risberg, E. *Acta Chem. Scand.* **9** (1955) 232.
14. Andersen, B., Seip, H. M., Strand, T. G. and Stølevik, R. *Acta Chem. Scand.* **23** (1969) 3224.
15. Veillard, A. and Demuynck, J. *Chem. Phys. Lett.* **4** (1970) 476.
16. Cyvin, S. J. *Molecular Vibrations and Mean Square Amplitudes*, Universitetsforlaget, Oslo 1968.
17. Stølevik, R., Seip, H. M. and Cyvin, S. J. *Chem. Phys. Lett.* **15** (1972) 263.
18. Miller, F. A., Sacher, R. E. and Siebert, W. *Unpublished results.*
19. Sacher, R. E. *Private communication.*
20. Hamilton, W. C. *Acta Cryst.* **18** (1965) 502.
21. Kuchitsu, K. and Cyvin, S. J. In Cyvin, S. J., Ed., *Molecular Structures and Vibrations*, Elsevier, Amsterdam 1972, Chapter 12.
22. Seip, H. M., Strand, T. G. and Stølevik, R. *Chem. Phys. Lett.* **3** (1969) 617.
23. Seip, H. M. and Stølevik, R. In Cyvin, S. J., Ed., *Molecular Structures and Vibrations*, Elsevier, Amsterdam 1972, Chapter 11.
24. Brooks, W. V. F., Costain, C. C. and Porter, R. F. *J. Chem. Phys.* **47** (1967) 4186.
25. Grimm, F. A. and Porter, R. F. *Inorg. Chem.* **8** (1969) 731.
26. Almenningen, A., Kolsaker, P., Seip, H. M. and Willadsen, T. *Acta Chem. Scand.* **23** (1969) 3398.
27. Gropen, O. and Vassbotn, P. *To be published.*
28. Westheimer, F. H. In Newman, M. S., Ed., *Steric Effects in Organic Chemistry*, Wiley, New York 1956.
29. Hendrickson, J. B. *J. Am. Chem. Soc.* **83** (1961) 4537; **89** (1967) 7036.
30. Náhlovská, Z., Náhlovský, B. and Seip, H. M. *Acta Chem. Scand.* **23** (1969) 3534.

Received June 8, 1972.

ACTA CHEMICA SCANDINAVICA 27 (1973) 21–25

Molecular Structure of Gaseous Dichloro-1,2,4-trithia-3,5-diborolane

A. ALMENNINGEN, H. M. SEIP, and P. VASSBOTN

Department of Chemistry, University of Oslo, Oslo 3, Norway

An electron diffraction investigation of dichloro-1,2,4-trithia-3,5-diborolane showed that the molecule is at least approximately planar. The B – S bond distances must be nearly equal; the average was found to be 1.794(0.005) Å. The other bond distances and angles are: r_a(S – S) = 2.069(0.003) Å, r_a(B – Cl) = 1.756(0.009) Å, ∠BSB = 96.9(0.6)°, ∠SBS = 121.7(0.5)°, ∠BSS = 99.9(0.3)°, and ∠S_4BCl = 120.8(0.5)°.

The investigation of dimethyl-1,2,4-trithia-3,5-diborolane ($Me_2B_2S_3$) discussed in the previous paper,[1] showed that the B – S bond lengths are nearly equal and the five-membered ring is at least approximately planar. It seemed worthwhile to study another compound with the same ring, and we chose dichloro-1,2,4-trithia-3,5-diborolane. Though it was realized that it would not be possible to determine the B – S and B – Cl bond lengths very accurately, small deviations from planarity might be easier to determine in this compound than in the methyl derivative. Possible differences in the ring structures in the two compounds would also be of interest.

EXPERIMENTAL

The sample of dichloro-1,2,4-trithia-3,5-diborolane was kindly synthesized by W. Siebert.[2] The diffraction data were recorded with the Oslo apparatus,[3] the nozzle temperature being about 80°C and the electron wave length 0.06462 Å. Four and five plates were used for the long (48.06 cm) and short (23.05 cm) nozzle-to-plate distances, respectively. The data were treated in the usual way,[4] and the modified molecular intensity were calculated using the modification function [4]

$$s/|f_S'|^2$$

The agreement between the obtained intensity curves was satisfactory, and most of the calculations were carried out on a composite intensity curve ranging from $s = 1.5$ Å^{-1} to 38.0 Å^{-1}. The s intervals were 0.125 Å^{-1} for $s < 10.0$ Å^{-1} and 0.25 Å^{-1} for larger s values.

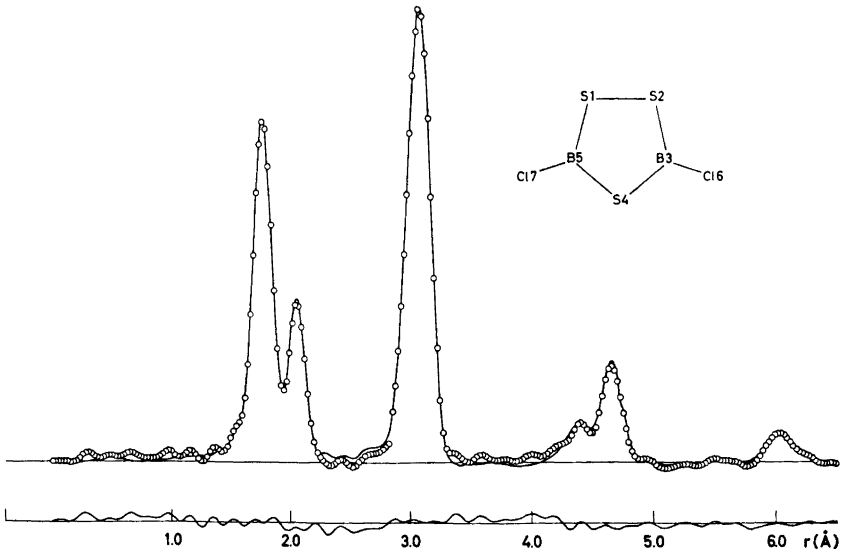

Fig 1. Experimental (circles) and theoretical radial distribution curves (artificial damping $k = 0.001$ Å^2). The differences between experimental and theoretical curves are also shown.

STRUCTURE REFINEMENT

The experimental radial distribution (RD) curve (Fig. 1) calculated by Fourier inversion of the observed intensities (Fig. 2), showed that no appreciable deviations from planarity occur in this molecule. Very satisfactory agreement was obtained by least-squares refinement on the intensity data assuming a planar model (C_{2v} symmetry).

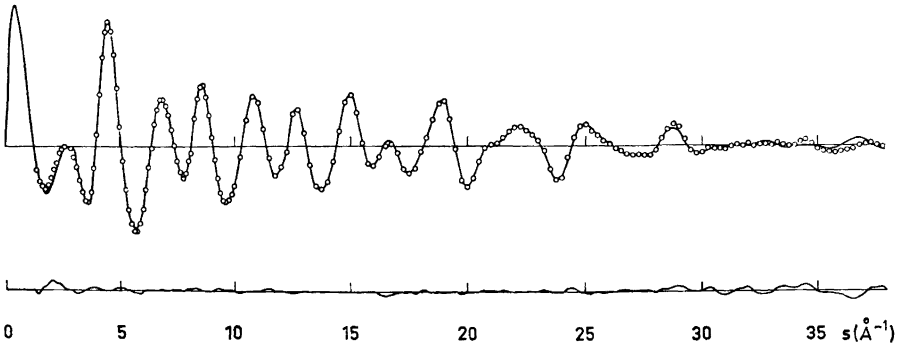

Fig. 2. Experimental (circles) and theoretical intensity curves. The difference curve is also given.

Table 1. Interatomic distances (r_a^s), mean amplitudes of vibration (u^{obs}), and bond angles with estimated standard deviations. Mean amplitudes calculated from spectroscopic data are given as u^{calc}.

	r_a (Å)	u^{obs} (Å)	u^{calc} (Å)
S_4-B_3	1.794(0.005)[a]	0.042(0.005)[a]	0.051
S_2-B_3			0.051
S–S	2.069(0.003)	0.041(0.004)	0.055
B–Cl	1.756(0.009)	0.047(0.007)	0.054
S···S	3.133(0.007)	0.051(0.003)	0.061
B···S	2.962(0.009)	0.057(0.012)	0.074
B···B	2.685(0.017)	0.051[b]	0.077
$S_4\cdots Cl$	3.087(0.007)	0.067(0.006)[a]	0.081
$S_2\cdots Cl_6$	3.035(0.007)		0.083
B···Cl	4.390(0.009)	0.071(0.008)	0.081
$S_1\cdots Cl_6$	4.658(0.006)	0.070(0.003)	0.079
Cl···Cl	6.032(0.010)	0.104(0.007)	0.092
	Angles (degrees)		
∠BSB	96.9(0.6)		
∠SBS	121.7(0.5)		
∠BSS	99.9(0.3)		
$\angle S_4BCl$	120.8(0.5)		

[a] The parameters were assumed equal. [b] The parameter was not refined simultaneously with the other parameters.

The main difficulty in the structure determination lies in the similarity of 3 of the 4 bond distances; only the S–S bond being uniquely identifiable in the RD curve. There is also considerable overlap between the non-bonded distances (see Table 1 and Fig. 1). As in $Me_2B_2S_3$ [1] the B–S bond lengths must be nearly equal, but the possibility of a difference of 0.02 – 0.03 Å cannot be excluded. The results in Table 1 were obtained assuming equal B–S bond lengths, and neglecting the shrinkage effect [5] as for $Me_2B_2S_3$. The standard deviations in Table 1 are based partly on the formula [6,7] used for $Me_2B_2S_3$ [1] and partly on least-squares refinements with a weight matrix of the type discussed in Ref. 6.

Further calculations were carried out for non-planar models (C_2 symmetry) with fixed values for the torsional angle (ϕ) about the S_4-B bond. The plot of the relative R factor is given in Fig. 3 of the previous paper.[1] The minimum in R corresponds to $\phi = 0$, but R increases very slowly for $\phi < 4°$ also for this molecule. For $\phi = 8°$ the relative R value is somewhat smaller for $Cl_2B_2S_3$ than for $Me_2B_2S_3$. However, some of the refined parameters corresponding to this ϕ value were rather unreasonable for the former molecule.

DISCUSSION

The results in Table 1 may be compared to the structure given for $Me_2B_2S_3$ in the previous paper.[1] The B_2S_3 ring is at least nearly planar in both compounds. The bond lengths in the rings are nearly equal, though the average

B – S distance may be slightly shorter in the Cl-compound. The SBS bond angles are somewhat increased and both the BSB and the SSB angles correspondingly decreased in $Cl_2B_2S_3$ compared to $Me_2B_2S_3$, possibly because of the difference in electronegativity between Cl and Me. Theoretical calculations by the CNDO/2 method gave a difference in the charges on Cl and on Me of about 0.14 electrons.[9] A somewhat similar opening of a bond angle is found in fluorobenzene compared to benzene; the CCC angle at fluorine is found to be 123.4°.[10]

The S – S bond distances are in both compounds slightly longer than in H_2S_2 where 2.055 Å has been reported,[11] and approximately the same as found in the somewhat similar ring in the 3,5-diamino-1,2,4-dithiazolium cation ($DADT^+$):

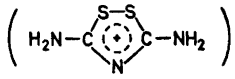

This ring is planar in $DADT^+Cl^-.\frac{1}{2}H_2O$,[12] $DADT^+Br^-$,[13] and $DADT^+I^-$.[14,15] The S – S bond lengths (uncorrected for thermal motion) are 2.063(4) Å, 2.081(8) Å, and 2.083(3) Å, resp. In some other related planar rings the S – S bond may have more π-character as for example in 4-phenyl-1,2-dithiolium chloride, where the S – S bond is 2.021(4) Å.[16]

The B – Cl distance in $Cl_2B_2S_3$ is nearly the same as found in B_2Cl_4 (1.750 (0.005) Å[17]) and slightly longer than in BCl_3 (1.742 (0.004) Å[18]), but the difference is less than two times the standard deviation.

The obtained mean amplitudes (u) are smaller than expected for most distances both in $Cl_2B_2S_3$ and $Me_2B_2S_3$. Using the tentative assignment given by Sacher *et al.*[19,20] and the calculation method described by Stølevik *et al.*[21] the values denoted by u^{calc} in Table 1 were computed. These values are not very accurate, but at least for the bond distances the calculated mean amplitudes seem more reasonable than those obtained by electron diffraction. Likely sources of errors in the mean amplitudes are the "blackness correction"[4] and the applied scattering amplitudes. In the investigations of $Me_2B_2S_3$ and $Cl_2B_2S_3$ plates of rather low density were used, and the blackness correction is therefore small. The scattering amplitudes were calculated in the usual way[4] with Hartree-Fock atomic potentials;[22] a method which usually gives fairly reliable results except perhaps for atoms considerably heavier than chlorine. We have thus at present no explanation for the unusual mean amplitudes. Possible errors in these values should not affect the geometrical parameters in $Me_2B_2S_3$ very much, but may be more serious in $Cl_2B_2S_3$ because of the large number of overlapping distances in the latter compound.

Acknowledgements. The authors are grateful to Dr. W. Siebert for supplying the sample of $Cl_2B_2S_3$ and to Dr. R. E. Sacher for sending his preliminary assignment for the fundamental vibrations of $Cl_2B_2S_3$.

REFERENCES

1. Seip, H. M., Seip, R. and Siebert, W. *Acta Chem. Scand.* **27** (1973) 15.
2. Schmidt, M. and Siebert, W. *Chem. Ber.* **102** (1969) 2752.
3. Bastiansen, O., Hassel, O. and Risberg, E. *Acta Chem. Scand.* **9** (1955) 232.

4. Andersen, B., Seip, H. M., Strand, T. G. and Stølevik, R. *Acta Chem. Scand.* **23** (1969) 3224.
5. Cyvin, S. J. *Molecular Vibrations and Mean Square Amplitudes*, Universitetsforlaget, Oslo 1968.
6. Seip, H. M., Strand, T. G., and Stølevik, R. *Chem. Phys. Lett.* **3** (1969) 617.
7. Seip, H. M. and Stølevik, R. In Cyvin, S. J., Ed., *Molecular Structures and Vibrations*, Elsevier, Amsterdam 1972, Chapter 11.
8. Kuchitsu, K. and Cyvin, S. J. In Cyvin, S. J., Ed., *Molecular Structures and Vibrations*, Elsevier, Amsterdam 1972, Chapter 12.
9. Gropen, O. and Vassbotn, P. *To be published.*
10. Nygaard, L., Bojesen, I., Pedersen, T. and Rastrup-Andersen, J. *J. Mol. Struct.* **2** (1968) 209.
11. Haase, W. *Z. Naturforsch.* **23a** (1968) 56.
12. Hordvik, A. and Sletten, J. *Acta Chem. Scand.* **20** (1966) 1907.
13. Hordvik, A. and Joys, S. *Acta Chem. Scand.* **19** (1965) 1539.
14. Foss, O. and Tjomsland, O. *Acta Chem. Scand.* **12** (1958) 1799.
15. Rodesiler, P. F. and Amma, E. L. *Acta Cryst.* **B 27** (1971) 1687.
16. Grundtvig, F. and Hordvik, A. *Acta Chem. Scand.* **25** (1971) 1567.
17. Ryan, R. R. and Hedberg, K. *J. Chem. Phys.* **50** (1969) 4986.
18. Konaka, S., Murata, Y., Kuchitsu, K. and Morino, Y. *Bull. Chem. Soc. Japan* **39** (1966) 1134.
19. Miller, F. A., Sacher, R. E. and Siebert, W. *Unpublished results.*
20. Sacher, R. E. *Private communication.*
21. Stølevik, R., Seip, H. M. and Cyvin, S. J. *Chem. Phys. Lett.* **15** (1962) 263.
22. Strand, T. G. and Bonham, R. A. *J. Chem. Phys.* **40** (1964) 1686.

Received June 8, 1972.

ACTA CHEMICA SCANDINAVICA 27 (1973) 26–34

The Crystal Structure of Nb_8P_5

SURANG ANUGUL,* CHA-ON PONTCHOUR* and STIG RUNDQVIST

Institute of Chemistry, University of Uppsala, Box 531, S-751 21 Uppsala 1, Sweden

The crystal structure of Nb_8P_5 has been determined by X-ray single crystal methods. The symmetry is orthorhombic, and the unit cell, the dimensions of which are $a = 26.1998$ Å, $b = 9.4652$ Å, $c = 3.4641$ Å, contains 32 niobium atoms and 20 phosphorus atoms. In the refinement of the structure the space group symmetry has been assumed to be *Pbam*. The structure can be described as an array of interconnected Nb_6P triangular prisms, with additional niobium atoms inserted between the prisms.

In previous studies of niobium phosphides,[1–4] several intermediate phases have been prepared by arc-melting mixtures of niobium and NbP. So far, the crystal structures of Nb_3P, Nb_7P_4, and Nb_5P_3 have been determined by X-ray single crystal methods.[2–4] The results from a crystal structure analysis of a compound denoted Nb_8P_5 are reported in the present paper.

EXPERIMENTAL

Preparation. Niobium (Hermann Stark, Berlin, claimed purity 99.3 %) and red phosphorus (purity higher than 99 %) were reacted at about 800°C in evacuated silica tubes to form NbP. Mixtures of niobium and NbP were then arc-melted under purified argon. Attempts were made to obtain as phosphorus-rich products as possible by successive additions of NbP and re-meltings. Powder diffraction examination of the most phosphorus-rich samples obtained in this manner showed the presence of two new phases not previously characterized. Some very small crystals of one of the phases could be picked from the crushed melts and were subsequently used for the single crystal structure determination.

X-Ray diffraction work. Powder diffraction patterns were recorded in a Guinier-Hägg type focussing camera with monochromatic $CrK\alpha_1$ radiation. Silicon ($a = 5.43054$ Å) was used as internal calibration standard. The single crystal studies were performed with a Weissenberg camera using zirconium-filtered MoK radiation. The crystal used for the structure determination was needle-shaped with a rather uniform cross-section of about 0.03 mm. It was rotated about the needle axis, which coincided with the shortest crystallographic axis (the c axis). The small size of the crystal necessitated very long exposures of the Weissenberg films, and the number of reflexions strong enough to be measured

* On leave from the Department of Chemistry, Faculty of Science, Chulalongkorn University, Bangkok, Thailand.

was rather limited. The reflexions were recorded by the multiple-film technique using thin iron foils as absorbers between successive films. The intensities were estimated visually by comparison with an intensity scale prepared from timed exposures of one reflexion from the crystal. The effects of absorption were estimated to be very small and were neglected in the structure refinement.

Calculations. The numerical calculations were made on a CDC 3600 computer using programmes listed in Table 1, Ref. 2.

Table 1. Structure data (and their standard deviations) for Nb_8P_5. Space group *Pbam*. $a = 26.1998(15)$ Å, $b = 9.4652(5)$ Å, $c = 3.4641(2)$ Å.

	x	y	z	B (Å^2)
2 Nb(1) in 2*a*	0	0	0	0.20(14)
4 Nb(2) in 4*g*	0.2164(2)	0.2505(5)	0	0.33(11)
4 Nb(3) in 4*g*	0.3259(2)	0.4137(6)	0	0.16(11)
2 Nb(4) in 4*g*[a]	0.0485(4)	0.5036(10)	0	−0.17(17)
4 Nb(5) in 4*h*	0.4966(2)	0.2444(5)	½	0.38(11)
4 Nb(6) in 4*h*	0.0841(2)	0.0023(6)	½	0.33(10)
4 Nb(7) in 4*h*	0.1208(2)	0.3327(5)	½	0.28(10)
4 Nb(8) in 4*h*	0.2652(2)	0.0029(6)	½	0.08(10)
4 Nb(9) in 4*h*	0.3762(2)	0.1675(5)	½	0.35(11)
4 P (1) in 4*g*	0.0655(6)	0.2079(16)	0	0.32(31)
4 P (2) in 4*g*	0.3388(6)	0.9920(13)	0	−0.38(24)
4 P (3) in 4*g*	0.4272(7)	0.3006(15)	0	0.13(27)
4 P (4) in 4*h*	0.1706(6)	0.1044(14)	½	−0.11(27)
4 P (5) in 4*h*	0.2862(6)	0.2590(15)	½	0.06(28)

[a] Position filled to only 50 %.

STRUCTURE DETERMINATION

The oscillation and Weissenberg films indicated that the symmetry of the new niobium phosphide is orthorhombic. The approximate unit cell dimensions as obtained from the single crystal films were used for indexing the reflexions on the powder films, and accurate cell dimensions were then obtained by a least squares refinement of the powder diffraction data. No significant changes in the unit cell dimensions were observed for different samples. Since the synthetic technique employed makes it very difficult to obtain singlephase samples suitable for chemical analysis (*cf.* Refs. 2 and 4), the composition of the new phosphide could not be determined by ordinary phase-analytical methods. It could only be inferred that the phosphide was intermediate in composition between Nb_5P_3 and NbP. A comparison of the unit cell volume with those for Nb_7P_4, Nb_5P_3, and NbP indicated a cell content of $52 - 54$ atoms.

Inspection of the Weissenberg films showed that $(h0l)$ reflexions with $h = 2n + 1$ and $(0kl)$ reflexions with $k = 2n + 1$ were not visible. If these extinctions are systematic the space group symmetry is either *Pba*2 or *Pbam*. In space group *Pbam*, occupation of positions 8*i*, 4*e*, and 4*f* would lead to unreasonably short interatomic distances, since the *c* axis is only 3.464 Å. Further inspection of the Weissenberg films showed that the intensity ratio between (hkl) and $(hkl + 2)$ reflexions was constant, allowing for the influence

of the Lorentz-polarization factor. This observation indicates that the atoms are confined to two planes perpendicular to the c axis and spaced $c/2$ apart.

It thus seemed reasonable to assume that the structure, at least to a first approximation, should conform to *Pbam* symmetry, with atoms occupying only 4*g*, 4*h*, and $2a-d$ positions. In the Patterson function, all maxima should then appear in the sections $P(uv0)$ and $P(uv\frac{1}{2})$. Accordingly, the Patterson sections mentioned were computed, using the intensity material from the two layer lines ($hk0$) and ($hk1$). Analysis of the Patterson sections by simple superposition methods yielded a partial structure proposal, consisting of one twofold set of niobium atoms in 2*a*, two fourfold sets of niobium atoms in 4*g*, and five fourfold sets of niobium atoms in 4*h*. Signs of the structure factors were calculated on the basis of this partial structure, and the electron density sections $\varrho_o(xy0)$ and $\varrho_o(xy\frac{1}{2})$ were computed. In addition to the expected niobium maxima, new maxima appeared in these sections. Five of these maxima could readily be interpreted as arising from three fourfold sets of phosphorus atoms in 4*g* positions and two fourfold phosphorus sets in 4*h* positions. At this stage only one maximum corresponding to a 4*g* position remained to be interpreted. This maximum was appreciably higher than the maxima corresponding to the phosphorus atoms but had only half the height of the niobium atom maxima. An atom occupying this position would have a coordination, which seemed abnormal for a phosphorus atom but much more reasonable for a niobium atom. However, if the 4*g* position were filled with niobium atoms, one very short interatomic distance would occur between each atom and another atom belonging to the same fourfold set. Such short contacts may be avoided if the fourfold position is occupied to only 50 % or less.

Following these observations it was tentatively assumed that the crucial 4*g* position is occupied by only two niobium atoms. This structure proposal gives a unit cell content of 32 niobium atoms and 20 phosphorus atoms, and accordingly the composition lies between Nb_5P_3 and NbP as required by the phase-analytical results.

A second set of ϱ_o and ϱ_c maps was computed. Since a comparison between the observed and calculated electron densities revealed no further abnormal features it was decided to complete the refinement by the least squares method. The observed 190 ($hk0$) and 176 ($hk1$) reflexions were all included in the refinement. Atomic scattering factors, including dispersion corrections, were taken from the appropriate tables in Ref. 5. Weights of the reflexions were assigned according to the formula $w=1/(A+|F_o|+C|F_o|^2+D|F_o|^3)$ as suggested by Cruickshank *et al.*[6] The constants were adjusted on the basis of weight analyses calculated between each cycle of refinement and were finally given the values $A=80$, $C=0.1$ and $D=0.01$. The following 42 parameters were refined: two scale factors, one for each of the two layer lines, 26 positional parameters and 14 isotropic temperature factors. The refinement converged rapidly, and it was stopped when the parameter shifts were less than one tenth of the calculated standard deviations. The conventional R value for the 366 observed reflexions was then 0.119. The temperature factor values returned by the program were close to zero and even negative for the partially occupied niobium position and for four of the phosphorus positions. The small values of the temperature factors could be a consequence of neglecting absorption correc-

tions, but in the present case the absorption errors were estimated to be much too small for any appreciable influence on the temperature factor values. Extinction errors might be a more likely explanation, and a comparison between observed and calculated structure factors for the strongest low-angle reflexions showed that the observed values were consistently smaller than the calculated ones. It cannot be excluded that this effect might be produced by a systematic error in the visual intensity estimation, but nevertheless a final refinement was made in which the 42 strongest low-angle reflexions were omitted. The R value dropped to 0.109, the temperature factor values increased on average by 0.07 Å^2, while the positional parameters remained practically unchanged.

The results of the refinement indicate that the proposed structure is substantially correct. There are, however, at least two possible ways in which the true space group symmetry might deviate from *Pbam*.

Firstly, the lower space group *Pba*2 leaves the z coordinates as free parameters, and small deviations from the values 0 and $\frac{1}{2}$ cannot be excluded. Previous experience in similar situations (see, *e.g.*, Ref. 7), where only a moderately accurate intensity material is available, shows, however, that it is very difficult to obtain conclusive evidence for minor symmetry deviations by means of ordinary refinement procedures. No attempt to refine the structure assuming *Pba*2 symmetry was therefore made.

Secondly, the assumption of a nearly random partial occupation of one of the niobium positions might be wrong, and a different space group symmetry with fully ordered positions might represent the correct alternative. However, within the accuracy of the available intensity material no violation of the *mmm* Laue symmetry or the *b* or *a* glide plane symmetries could be detected, and no superstructure reflexions (as for instance indicating a larger *c* axis) were observed.

The crystal structure of Nb_8P_5 is accordingly reported with *Pbam* symmetry, and the final structure data are presented in Table 1. Powder data for identification purposes are given in Table 2, and a list of observed and calculated structure factors is given in Table 3.

Table 2. Powder diffraction data for Nb_8P_5. (Guinier-Hägg camera, Cr$K\alpha_1$ radiation, internal calibration standard silicon: $a = 5.43054$ Å.) The sample contained, in addition to Nb_8P_5, an uncharacterized niobium phosphide phase, the diffraction lines of which are not included in the table.

$h\ k\ l$	$\sin^2\theta \times 10^4$ obs	$\sin^2\theta \times 10^4$ calc	I obs	$p\|F\|^2 \times 10^{-4}$	$h\ k\ l$	$\sin^2\theta \times 10^4$ obs	$\sin^2\theta \times 10^4$ calc	I obs	$p\|F\|^2 \times 10^{-4}$
2 0 0		76.4		0.3	2 2 0		661.4		0.5
1 1 0	164.5	165.4	w−	3.0	6 0 0		687.3		0.0
2 1 0		222.7		0.0	3 2 0		757.0		0.0
4 0 0		305.5		0.1	6 1 0	833.9	833.6	w−	1.4
3 1 0		318.1		1.1	4 2 0		890.6		0.1
4 1 0		451.8		0.3	5 2 0		1062.5		1.1
0 2 0		585.2		0.0	7 1 0		1081.8		0.7
1 2 0	603.4	604.2	w−	2.0	0 0 1	1092.2	1092.2	m	9.4
5 1 0		623.6		1.3	2 0 1		1168.6		0.7

Table 2. Continued.

8 0 0	1222.5	1221.9	w	6.3	8 2 1	2900.0	2899.3	m	40.1
1 1 1		1257.6		0.8	10 0 1		3001.4		10.5
6 2 0[a]		1272.5	w−	2.3	6 4 0	3027.9	3027.9	w+	11.1
2 1 1		1314.8		0.0	6 3 1	3096.2	3096.1	m	32.5
1 3 0[b]		1335.7		15.9	10 1 1	3147.0	3147.7	m+	44.9
8 1 0	1368.5	1368.2	w+	6.4	9 2 1		3223.8		1.3
2 3 0	1395.3	1393.0	m	3.3	10 3 0		3225.9		0.2
4 0 1		1397.7		9.1	7 4 0[a]		3276.2	w−	4.3
3 1 1	1409.4	1410.3	m	9.5	12 2 0	3334.1	3334.5	m+	48.0
3 3 0	1487.1	1488.4	w−	0.7	7 3 1		3344.3		0.1
7 2 0	1521.4	1520.7	w−	1.3	13 1 0[a]		3372.9	w	8.9
4 1 1	1545.0	1544.0	w−	1.6	0 4 1		3432.8		0.0
4 3 0	1622.9	1622.1	w+	8.1	1 4 1[c]		3451.9	(m+)	10.6
0 2 1		1677.3		1.6	2 4 1		3509.2		0.0
9 1 0	1696.1	1692.8	m+	12.5	11 1 1		3548.7		5.3
1 2 1		1696.4		16.7	8 4 0		3562.5		1.2
5 1 1	1714.9	1715.8	m	19.4	10 2 1[a]		3586.6	w−	6.1
2 2 1	1753.6	1753.7	st	63.8	3 4 1		3604.6		0.5
6 0 1	1778.8	1779.5	m	15.1	11 3 0	3628.3	3626.8	w	10.9
5 3 0	1794.5	1793.9	m+	31.1	8 3 1		3630.7		0.6
8 2 0	1805.5	1807.1	m	11.5	1 5 0		3676.3		0.4
3 2 1		1849.2		0.2	2 5 0		3733.6		0.0
10 0 0[a]		1909.3	w−	5.3	4 4 1	3739.4	3738.3	w+	18.2
6 1 1	1927.4	1925.8	m	20.4	14 0 0		3742.2		6.6
4 2 1	1983.3	1982.8	w−	2.4	13 2 0		3811.8		2.5
6 3 0	2005.1	2003.9	w−	4.4	3 5 0	3828.7	3829.0	m	32.5
10 1 0[a]		2055.5	w−	2.6	12 0 1		3841.5		0.4
9 2 0[a]		2131.7	w−	1.5	9 4 0		3887.1		0.0
5 2 1	2154.8	2154.7	m	11.2	14 1 0		3888.4		0.4
7 1 1[c]		2174.0	(st)	19.2	5 4 1		3910.1		4.0
7 3 0	2251.8	2252.1	m	26.0	9 3 1[a]		3955.3	w−	4.0
8 0 1	2314.6	2314.1	st	108.2	4 5 0		3962.7		0.1
0 4 0	2340.9	2340.6	m+	46.6	11 2 1	3988.6	3987.5	w+	7.0
1 4 0		2359.7		1.0	12 1 1		3987.8		10.6
6 2 1	2364.1	2364.7	st	224.6	12 3 0		4065.9		0.6
2 4 0		2417.0		2.5	6 4 1		4120.1		5.3
1 3 1	2427.4	2427.9	st	91.3	5 5 0[a]		4134.5	w−	9.7
11 1 0	2457.9	2456.5	st	94.6	10 4 0[a]		4249.9	w−	6.2
8 1 1		2460.4		20.8	10 3 1		4318.0		0.0
2 3 1	2484.3	2485.1	m	31.5	14 2 0[a]		4327.3	w	28.3
10 2 0	2495.6	2494.4	m	22.4	6 5 0		4344.5		0.4
3 4 0		2512.4		0.1	7 4 1		4368.3		6.9
8 3 0		2538.5		0.9	0 0 2	4369.7	4368.7	st+	199.3
3 3 1[c]	2581.2	2580.6	(st)	16.5	12 2 1		4426.7		2.1
7 2 1	2612.3	2612.9	w+	14.7	15 1 0		4442.1		1.3
4 4 0	2646.3	2646.1	st	83.0	2 0 2		4445.1		0.2
4 3 1	2714.2	2714.3	m+	41.3	13 1 1		4465.1		0.1
12 0 0[a]		2749.3	w−	3.6	1 1 2		4534.1		2.5
9 1 1	2784.8	2785.0	m+	49.3	13 3 0[a]		4543.2	w−	10.2
5 4 0[a]		2817.9	w−	2.9	12 1 2		4591.4		0.0
9 3 0	2862.2	2863.1	m	39.8	7 5 0[a]		4592.7	w−	9.5
5 3 1	2886.4	2886.1	st	125.5	11 4 0		4650.8		0.7
11 2 0		2895.4		0.1	8 4 1		4654.7		0.8
12 1 0		2895.6		3.0					

[a] Reflexion too weak for accurate measurement of diffraction angle.
[b] Reflexion overlapped by the silicon (111) reflexion.
[c] Reflexion overlapped by reflexion from uncharacterized niobium phosphide.

Table 3. Observed and calculated structure factors for Nb_8P_5. [a] Reflexion omitted in the final refinement.

	$\lvert F_o\rvert$ ·10	$\lvert F_c\rvert$ ·10		$\lvert F_o\rvert$ ·10	$\lvert F_c\rvert$ ·10		$\lvert F_o\rvert$ ·10	$\lvert F_c\rvert$ ·10		$\lvert F_o\rvert$ ·10	$\lvert F_c\rvert$ ·10		$\lvert F_o\rvert$ ·10	$\lvert F_c\rvert$ ·10		$\lvert F_o\rvert$ ·10	$\lvert F_c\rvert$ ·10
H,K,0			15	[a]2095	2486	9 7	1068	1003	4 15	922	752	24 3	2320	2129	18 7	998	846
			16	962	1044	10 7	628	674	5 15	1093	1292	25 3	1442	1339	20 7	865	965
8 0	1484	1772	21	1144	1250	11 7	2226	2256	6 15	1105	1142	29 3	1990	2351	23 7	912	949
10 0	1390	1628	22	1138	988	12 7	1139	1002	15 15	1789	1775	30 3	934	1100	28 7	1191	1335
12 0	1335	1348	23	2121	2196	13 7	1061	769	0 16	1485	1455	1 4	1114	1150	0 8	1107	679
14 0	1739	1810	24	729	744	15 7	1300	1251	4 16	1252	1486	4 4	1385	1509	1 8	592	514
16 0	1874	1983	25	1469	1432	17 7	2232	2330				5 4	745	710	4 8	1242	937
18 0	[a]3293	3569	26	1268	1040	19 7	721	594	H,K,1			6 4	829	817	5 8	1038	748
20 0	[a]2320	2534	29	1671	1560	21 7	912	1055				7 4	928	927	6 8	1152	897
22 0	[a]1835	1413	33	1659	1878	23 7	862	820	8 0	[a]3897	5202	9 4	435	442	7 8	1169	940
24 0	[a]3947	3803	35	982	852	27 7	926	1051	10 0	1388	1618	10 4	910	866	8 8	632	489
26 0	1260	886	0	[a]4276	4829	0 8	[a]3289	3191	16 0	1640	1808	11 4	494	494	12 8	[a]2638	2962
34 0	1885	1746	2	[a]1558	787	1 8	704	653	18 0	1532	1293	12 4	[a]2721	3244	13 8	979	1082
8 1	1274	1265	4	[a]3704	4556	4 8	[a]2963	3103	20 0	1088	1004	13 4	1011	991	15 8	711	715
9 1	1475	1767	5	786	846	10 8	770	895	24 0	1582	1427	15 4	703	695	18 8	879	1069
10 1	786	814	6	1498	1666	12 8	1527	1623	26 0	2462	2081	17 4	591	673	19 8	827	755
11 1	[a]4332	4864	7	977	1035	14 8	1655	1846	28 0	2589	2504	18 4	1577	1557	1 9	1652	1350
12 1	862	870	8	433	540	16 8	1366	1410	34 0	2136	2060	19 4	996	939	2 9	1384	1164
13 1	1744	1490	10	954	1241	18 8	1308	1250	7 1	1384	1547	22 4	1628	1458	3 9	1664	1644
15 1	810	567	11	432	426	20 8	1485	1405	8 1	1394	1611	1 5	391	309	4 9	1835	1645
17 1	1279	1326	12	[a]1583	1853	21 8	871	961	9 1	[a]2184	2482	2 5	393	368	5 9	2321	2111
18 1	1065	1017	14	[a]2831	3683	22 8	1947	1891	10 1	[a]2094	2369	3 5	559	547	6 9	1416	1128
20 1	586	627	15	499	512	24 8	1446	1139	11 1	858	813	4 5	747	626	13 9	1644	1799
21 1	611	546	16	1115	1224	1 9	1354	1666	12 1	1177	1149	6 5	1316	1274	14 9	880	933
23 1	2115	2007	18	1056	1101	2 9	960	885	16 1	1521	1394	7 5	1019	904	20 9	804	1031
25 1	1146	1066	20	1907	1797	3 9	1250	977	17 1	[a]2872	3426	8 5	1373	1381	21 9	1824	1854
26 1	1188	825	22	2042	1756	4 9	1145	1001	18 1	924	808	9 5	[a]2234	2747	22 9	1079	1146
27 1	783	892	24	910	872	5 9	1826	1806	19 1	1285	1136	10 5	1466	1513	23 9	1187	1446
29 1	1104	1335	25	675	636	7 9	1174	664	20 1	1339	1135	11 5	1509	1451	24 9	1008	1024
30 1	799	805	26	1296	1416	9 9	1205	899	24 1	1212	1159	12 5	577	577	29 9	2047	2144
5 2	505	523	1	691	304	10 9	653	680	29 1	1545	1445	13 5	506	570	0 10	1029	1022
6 2	863	761	3	[a]2543	2852	11 9	1359	1143	5 2	[a]1042	1181	15 5	1327	1319	2 10	2161	2046
7 2	609	576	5	1564	1557	13 9	754	814	6 2	[a]3587	5299	16 5	562	574	6 10	2003	2106
8 2	[a]1714	1693	7	1276	1538	15 9	1609	1604	7 2	1143	1355	17 5	2161	2360	16 10	2180	2166
9 2	665	610	8	946	959	21 9	1917	2015	8 2	1572	1239	18 5	605	552	18 10	1842	1474
10 2	[a]2356	2365	9	485	362	22 9	1605	1401	9 2	399	409	19 5	688	639	3 11	923	1011
12 2	[a]2683	3464	10	549	575	23 9	1628	1530	10 2	843	876	20 5	1599	1507	5 11	785	720
13 2	811	797	11	2144	1964	0 10	1597	1393	11 2	905	935	23 5	1594	1492	6 11	798	778
14 2	2495	2661	12	1009	1025	6 10	758	734	12 2	450	517	25 5	889	963	8 11	796	692
15 2	438	412	13	1590	1499	8 10	1830	1772	13 2	1269	1223	0 6	[a]2177	2713	9 11	1498	1284
16 2	1044	1144	15	[a]2149	2451	10 10	1700	1619	14 2	578	731	2 6	[a]2346	3039	10 11	806	604
18 2	1372	1343	17	[a]2510	2984	12 10	2495	2594	16 2	[a]2396	2751	4 6	[a]1941	2465	11 11	812	638
19 2	531	548	18	656	773	14 10	1053	1080	18 2	[a]2319	2465	6 6	[a]2093	2784	17 11	1916	1735
20 2	663	632	25	895	658	8 11	891	996	19 2	985	878	7 6	473	489	19 11	875	849
22 2	1500	1581	27	1503	1623	9 11	757	687	20 2	1947	1788	8 6	584	639	0 12	1548	1270
26 2	707	633	0	2044	1890	10 11	835	854	21 2	1356	1098	12 6	1760	1474	1 12	828	758
28 2	1819	2063	2	1617	1317	11 11	2877	2852	24 2	1733	2038	14 6	1391	1317	2 12	828	645
30 2	806	606	4	[a]2164	2400	13 11	924	923	27 2	1415	968	18 6	1120	931	4 12	832	704
32 2	2630	2594	6	[a]2942	3050	0 12	4153	4475	1 3	[a]2254	3378	20 6	[a]3109	3860	6 12	1715	1748
34 2	951	838	8	1938	2150	8 12	1495	1479	2 3	1607	1985	28 6	1525	1451	8 12	1888	1794
1 3	1321	1992	10	1620	1393	10 12	885	859	3 3	1364	1434	30 6	1584	1332	16 12	1056	1387
2 3	973	913	12	1044	824	18 12	1609	1676	4 3	1799	2272	1 7	1161	1195	18 12	988	921
3 3	687	423	14	1149	906	20 12	876	801	5 3	[a]2915	3960	5 7	875	575	5 13	883	1040
4 3	1216	1425	16	1394	1470	22 12	1522	1315	6 3	1615	2014	6 7	1111	1010	7 13	1051	1290
5 3	[a]2370	2789	18	1362	1394	24 12	2232	2248	9 3	816	705	7 7	1228	1123	9 13	1267	1148
6 3	972	1053	26	[a]2535	2586	11 13	1460	1541	13 3	1607	1817	8 7	1896	1699	10 13	900	1209
7 3	[a]2293	2549	28	[a]3163	3581	5 14	881	702	14 3	965	762	9 7	[a]2550	3090	17 13	1930	1964
8 3	435	478	1	969	735	6 14	968	905	15 3	1613	1527	10 7	1437	1597	2 14	1206	1288
9 3	[a]2934	3153	3	1794	2136	8 14	889	785	20 3	1504	1607	11 7	2006	1807	6 14	1910	1772
11 3	1724	1652	6	543	502	10 14	982	1013	21 3	2226	2360	13 7	679	491	16 14	1824	1487
12 3	396	395	7	712	459	12 14	1071	1330	22 3	1215	1475	16 7	1515	1276	18 14	1168	1309
13 3	1272	1595	8	957	816	1 15	920	1072	23 3	1636	1331	17 7	1591	1147			

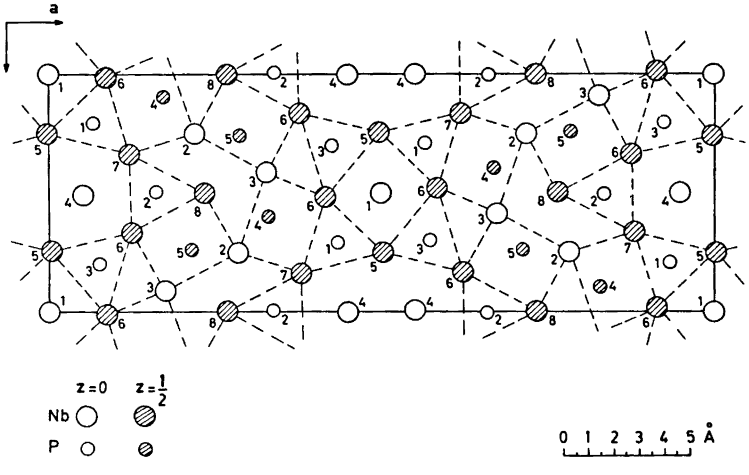

Fig. 1. The structure of Nb_8P_5 projected on (001).

Table 4. Interatomic distances (Å) and their standard deviations ($\times 10^3$) in Nb_8P_5. Distances shorter than 4.0 Å are listed.

Nb(1) –
2 P (1) 2.611(16)
2 P (3) 2.683(16)
4 Nb(6) 2.803(5)
4 Nb(5) 2.977(4)
2 Nb(1) 3.464(0)

Nb(2) –
2 P (5) 2.519(13)
2 P (4) 2.520(11)
1 P (2) 2.704(14)
2 Nb(8) 2.990(6)
2 Nb(7) 3.144(7)
2 Nb(8) 3.181(6)
1 Nb(3) 3.257(8)
1 Nb(3) 3.375(7)
2 Nb(2) 3.464(0)
1 P (1) 3.974(17)

Nb(3) –
2 P (5) 2.495(11)
2 P (4) 2.503(10)
1 P (3) 2.862(18)
2 Nb(6) 3.044(7)
2 Nb(8) 3.067(7)
2 Nb(9) 3.188(6)
1 Nb(2) 3.257(8)
1 Nb(2) 3.375(7)
2 Nb(3) 3.464(0)
1 P (1) 3.981(17)

Nb(4) –
1 Nb(4) 2.544(23)
1 P (1) 2.834(18)
1 P (3) 2.882(18)
1 P (2) 2.955(19)
2 Nb(7) 3.033(10)
2 Nb(9) 3.049(10)
2 Nb(5) 3.097(9)
2 Nb(5) 3.219(10)
2 Nb(4) 3.464(0)

Nb(5) –
2 P (1) 2.543(13)
2 P (3) 2.566(13)
2 Nb(1) 2.977(4)
2 Nb(4) 3.097(9)
2 Nb(4) 3.219(10)
1 Nb(6) 3.229(8)
1 Nb(9) 3.238(8)
1 Nb(6) 3.318(8)
1 Nb(7) 3.334(8)
2 Nb(5) 3.464(0)

Nb(6) –
1 P (4) 2.465(16)
2 P (3) 2.594(12)
2 P (1) 2.651(12)
2 Nb(1) 2.803(5)
2 Nb(3) 2.044(7)
1 Nb(5) 3.229(8)
1 Nb(7) 3.272(8)
1 Nb(5) 3.318(8)
1 Nb(9) 3.335(8)
2 Nb(6) 3.464(0)

Nb(7) –
1 P (4) 2.526(15)
2 P (2) 2.529(10)
2 P (1) 2.548(12)
2 Nb(4) 3.033(10)
2 Nb(2) 3.144(7)
1 Nb(9) 3.170(7)
1 Nb(6) 3.272(8)
1 Nb(5) 3.334(8)
1 Nb(8) 3.395(9)
2 Nb(7) 3.464(0)

Nb(8) –
1 P (5) 2.485(15)
2 P (2) 2.594(12)
1 P (4) 2.656(16)
1 P (5) 2.672(15)
2 Nb(2) 2.990(6)
2 Nb(3) 3.067(7)
2 Nb(2) 3.181(6)
1 Nb(9) 3.299(8)
1 Nb(7) 3.395(9)
2 Nb(8) 3.464(0)

Nb(9) –
1 P (5) 2.513(17)
2 P (3) 2.525(12)
2 P (2) 2.593(10)
2 Nb(4) 3.049(10)
1 Nb(7) 3.170(7)
2 Nb(3) 3.188(6)
1 Nb(5) 3.238(8)
1 Nb(8) 3.299(8)
1 Nb(6) 3.335(8)
2 Nb(9) 3.464(0)

P(1) –
2 Nb(5) 2.543(13)
2 Nb(7) 2.548(12)
1 Nb(1) 2.611(16)
2 Nb(6) 2.651(12)
1 Nb(4) 2.834(18)
2 P (4) 3.398(19)
2 P (1) 3.464(0)
1 P (3) 3.625(24)
1 P (2) 3.677(21)
1 P (3) 3.860(21)
1 Nb(2) 3.974(17)
1 Nb(3) 3.981(17)

P(2) –
2 Nb(7) 2.529(10)
2 Nb(9) 2.593(10)
2 Nb(8) 2.594(12)
1 Nb(2) 2.704(14)
1 Nb(4) 2.955(19)
2 P (5) 3.360(16)
2 P (2) 3.464(0)
1 P (1) 3.677(21)
1 P (3) 3.729(20)

P(3) –
2 Nb(9) 2.525(12)
2 Nb(5) 2.566(13)
2 Nb(6) 2.594(12)
1 Nb(1) 2.683(16)
1 Nb(3) 2.862(18)
1 Nb(4) 2.882(18)
2 P (3) 3.464(0)
1 P (1) 3.625(24)
1 P (2) 3.729(20)
1 P (1) 3.860(21)

P(4) –
1 Nb(6) 2.465(16)
2 Nb(3) 2.503(10)
2 Nb(2) 2.520(11)
1 Nb(7) 2.526(15)
1 Nb(8) 2.656(16)
1 P (5) 3.362(22)
2 P (1) 3.398(19)
1 P (5) 3.460(19)
2 P (4) 3.464(0)

P(5) –
1 Nb(8) 2.485(15)
2 Nb(3) 2.495(11)
1 Nb(9) 2.513(17)
2 Nb(2) 2.519(13)
1 Nb(8) 2.672(15)
2 P (2) 3.360(16)
1 P (4) 3.362(22)
1 P (4) 3.460(19)
2 P (5) 3.464(0)

DESCRIPTION AND DISCUSSION OF THE STRUCTURE

A projection of the structure on the (001) plane is shown in Fig. 1. Interatomic distances are listed in Table 4. Each phosphorus atom is surrounded by six niobium atoms in a triangular prismatic configuration and 1 to 3 additional niobium neighbours situated outside the four-sided faces of the prisms. The Nb_6P prisms are linked into a three-dimensional arrangement in much the same way as in numerous other transition metal phosphide, arsenide, sulphide, and selenide structures. The triangular prisms are indicated by broken lines in Fig. 1.

A feature of particular interest is the coordination about the partially occupied Nb(4) position. Two $Nb_6P(1)$, two $Nb_6P(2)$ and two $Nb_6P(3)$ triangular prisms share edges to form a six-membered ring enclosing a central void. These rings are stacked on top of one another forming infinite tubes in the *c* direction. The void in each ring is in the shape of a twelve-cornered Nb_{12} polyhedron, which can be regarded as composed of two very distorted Nb_8 cubes sharing one face. The Nb(4) atoms are situated at the centres of these distorted cubes. If all cubes were filled with Nb(4) atoms, these atoms would form pairs with an Nb – Nb distance of 2.54 Å, which is more than 0.1 Å shorter than the shortest Nb – Nb distance reported in any previous structure determination. The structure determination of Nb_8P_5 has shown that the Nb(4) position is occupied to only 50 %. It therefore seems most probable that any Nb – Nb contacts of 2.54 Å never occur, but each central void in the six-membered rings contains only one single Nb(4) atom. This atom can, however, occupy any one of the two possible cubic holes in a perfectly random manner.

A similar metal atom arrangement occurs in the Ta_2P-type structure (as represented by Ta_2P,[8] Ti_2S,[9] Hf_2P,[10,11] Ti_2Se, Zr_2S, Zr_2Se,[12] Hf_2As,[13] and Ta_2As[14]). In this case, the two adjoining cubic holes are much less distorted, and both holes are filled with metal atoms having a quite normal distance to one another.

Disregarding the disordered Nb(4) position, the atomic coordination and the interatomic distances in Nb_8P_5 are normal and very similar to those in Nb_7P_4[2] and Nb_5P_3.[4] Although the phosphide Mo_8P_5[15] has the same stoichiometry as Nb_8P_5, the two compounds are not isostructural. The space-filling in the Mo_8P_5 structure is greater than in Nb_8P_5 due to the large voids in the Nb_8P_5 structure at the empty Nb(4) positions.

It may finally be mentioned that there is an isostructural counterpart to Nb_8P_5 in the Zr – As system. A structure determination of Zr_8As_5 is currently being carried out by B. Carlsson at this institute, and the results will be reported in this journal.

Acknowledgements. The authors thank Dr. B. Carlsson for valuable information and discussions. S. A. expresses her gratitude to Dr. R. Hesse and Dr. R. Liminga for receiving a basic introduction to X-ray crystallographic methods. The work has been financially supported by the *Swedish Natural Science Research Council* which is gratefully acknowledged. S. A. and C.-O. P. are indebted to the *International Seminar in Chemistry*, Uppsala, and to the *Swedish International Development Authority* (SIDA) for financial support.

REFERENCES

1. Rundqvist, S. *Nature* **211** (1966) 847.
2. Rundqvist, S. *Acta Chem. Scand.* **20** (1966) 2427.
3. Nawapong, P. C. *Acta Chem. Scand.* **20** (1966) 2737.
4. Hassler, E. *Acta Chem. Scand.* **25** (1971) 129.
5. *International Tables for X-Ray Crystallography*, Kynoch Press, Birmingham 1962, Vol. III.
6. Cruickshank, D. W. J., Philling, D. E., Bujosa, A., Lovell, F. M. and Truter, M. R. *Computing Methods and the Phase Problem*, Pergamon, Oxford 1961, p. 32.
7. Carlsson, B. and Rundqvist, S. *Acta Chem. Scand.* **25** (1971) 1742.
8. Nylund, A. *Acta Chem. Scand.* **20** (1966) 2393.
9. Owens, J. P., Conard, B. R. and Franzen, H. F. *Acta Cryst.* **23** (1967) 77.
10. Lundström, T. and Tansuriwongs, P. *Acta Chem. Scand.* **22** (1968) 704.
11. Lundström, T. and Ersson, N.-O. *Acta Chem. Scand.* **22** (1968) 1801.
12. Franzen, H. F., Smeggil, J. and Conard, B. R. *Mater. Res. Bull.* **2** (1967) 1087.
13. Rundqvist, S. and Carlsson, B. *Acta Chem. Scand.* **22** (1968) 2395.
14. Rundqvist, S., Carlsson, B. and Pontchour, C.-O. *Acta Chem. Scand.* **23** (1969) 2188.
15. Johnsson, T. *Acta Chem. Scand.* **26** (1972) 365.

Received June 16, 1972.

ACTA CHEMICA SCANDINAVICA 27 (1973) 35–46

Pseudomonas Cytochrome *c* Peroxidase

V. Absorption Spectra of the Enzyme and of its Compounds with Ligands. Inhibition of the Enzyme by Cyanide and Azide

RITVA SOININEN and NILS ELLFOLK

Department of Biochemistry, University of Helsinki, SF-00170 Helsinki 17, Finland

A spectrophotometric study of *Pseudomonas* cytochrome *c* peroxidase has been made. Spectra and extinction coefficients of the oxidized and reduced enzyme in sodium phosphate buffer pH = 6.0, $\mu = 0.1$, are given. The effect of pH on the absorption spectra of ferri- and ferroperoxidase has been studied. A pK value of 10.0 was obtained for the transition of ferroperoxidase from the neutral to the alkaline form. Ferroperoxidase reacts with carbon monoxide at pH 6.0; ferri- and ferroperoxidase react with cyanide and ferriperoxidase with azide, the latter reaction being slow at pH 6.0, even at high ligand concentrations. Peroxidase does not react with fluoride. Cyanide inhibits the peroxidatic oxidation of reduced *Pseudomonas* cytochrome *c*-551; the mechanism of the inhibition was found to be of a mixed type (intermediate between competitive and noncompetitive) in respect to hydrogen peroxide; the K_i value is 7.1 μM in sodium phosphate buffer pH = 6.0, $\mu = 0.2$, at a fixed concentration of reduced *Pseudomonas* cytochrome *c*-551 (18.6 μM). Azide inhibition is noncompetitive in respect to hydrogen peroxide, the K_i value being 3.2 mM. No stable hydrogen peroxide-peroxidase compound, similar to hydrogen peroxide-horseradish peroxidase and hydrogen peroxide-yeast cytochrome *c* peroxidase compounds, was detected. The addition of hydrogen peroxide to the enzyme results only in a decrease in the absorbance in the Soret region. At equimolar concentrations of hydrogen peroxide and peroxidase the decrease has two stages: a rapid first-order decrease and an increase to a higher absorbance level is followed by a slow, steady decrease. It appears that during the first stage some kind of hydrogen peroxide-peroxidase compound may be formed, and the second stage is the denaturation of the enzyme by hydrogen peroxide.

Peroxidases like horseradish peroxidase, Japanese radish peroxidase, lactoperoxidase, and yeast cytochrome *c* peroxidase are hemoproteins having non-covalently bound protoheme as the prosthetic group showing typical high-spin spectra.[1–3] *Pseudomonas* cytochrome *c* peroxidase (PsCCP) is a low-spin peroxidase with hemochrome-type spectra and a covalently bound heme *c* as the prosthetic group.[4]

Some plant peroxidases have been classified as low-spin, *b*-type or para-peroxidases.[1,5–7] Recently, the presence of cyanide as a ligand in purified preparations has been demonstrated.[6,7] These low-spin peroxidases can be reversibly converted to high-spin peroxidases by the addition of mercaptide-forming agents.

Thiobacillus cytochrome peroxidase is another low-spin peroxidase which, in addition to PsCCP, has been isolated from bacteria.[8] The spectra of this peroxidase deviate considerably from those of PsCCP, but it is known to contain heme *c* as the prosthetic group.

In this publication the spectra of PsCCP and its oxidized, reduced, and alkaline forms, its reactions with hydrogen peroxide and other ligands, and its inhibition by ligands, are described.

MATERIALS AND METHODS

Pseudomonas cytochrome c *peroxidase (PsCCP)* was prepared by the method previously described,[4] using a slightly modified large scale procedure.[9] The preparation obtained was homogeneous when analysed by disc electrophoresis in 7 % gel pH 8.9 [10] with staining according to Weber and Osborne.[11] The spectral purity of the preparation (A_{407}/A_{280}) was 4.53 and the specific activity 110 – 125 U/mg (method described below). PsCCP concentration was determined spectrophotometrically, using $A(1\ \%,\ 1\ \text{cm}) = 12.1$ at 280 nm;[12] a molecular weight of 43 200, based on the iron content of the enzyme,[12] was assumed.

Peroxidase activity was measured spectrophotometrically at 25°C in sodium phosphate buffer pH 6.0, $\mu = 0.01$, H_2O_2 85 μM, *Pseudomonas* ferrocytochrome *c*-551 (ferro-Ps-cyt-551) 11 μM, unless otherwise stated. The reaction was initiated, after the addition of 2 – 5 μl of enzyme, by rapidly mixing 10 μl H_2O_2 into the reaction mixture (final volume of 2.0 or 2.5 ml), except in the studies of the effect of H_2O_2 on PsCCP when the reaction was initiated by the addition of enzyme which had been incubated with H_2O_2. In the inhibition studies the enzyme was incubated for 20 – 30 sec with the reaction mixture, containing the inhibitor and ferro-Ps-cyt-551, before the addition of H_2O_2. The reaction was followed by recording the oxidation of ferro-Ps-cyt-551 at 551 nm on a Beckman DK-1 A recording spectrophotometer equipped with a thermostated cell compartment. The reaction rates were calculated from (i) the slope of the reaction curve at zero time when the reaction was initiated by adding H_2O_2, or (ii) the final slope after the delay in the reaction [13] when it was initiated by adding enzyme. The peroxidase activity was expressed in terms of arbitrary units (decrease of absorbance at 551 nm per 10 sec) or as initial rates v_0/e (equivalents of electrons transferred per sec per molecule of enzyme).

Pseudomonas cytochrome c*-551 (Ps-cyt-551)* was prepared by the method of Ambler.[14] The spectral purity of the preparations used was 1.06 – 1.16 and their homogeneity was checked by disc electrophoresis as previously described.[13] The concentration of Ps-cyt-551 was determined as previously described.[13] Ferrocytochrome *c*-551 was prepared by anaerobic gel filtration of dithionite-reduced Ps-cyt-551 on Sephadex G-25.[15]

Hydrogen peroxide solutions were prepared from Merck "Perhydrol" (30 % H_2O_2). Peroxide concentration was determined enzymatically with yeast cytochrome *c* peroxidase (prepared according to Ellfolk [16]), using horse heart cytochrome *c* (Type III, Sigma) as substrate.[17]

Potassium cyanide (*p.a.*, Baker) solution was prepared in distilled water and the pH of the solution was adjusted to pH 6.0 with *ortho*-phosphoric acid; its concentration was determined just before use by adding excess ammonia and titrating with standard silver nitrate. Working solution was prepared by diluting stock with buffer. At pH 6.0, KCN is completely (100.0 %) undissociated (pK_a of HCN = 9.31).

Sodium azide (Merck) and *sodium fluoride* (*p.a.*, Merck) solutions were prepared in buffer. At pH 6.0 95.0 % of sodium azide and 100.0 % of sodium fluoride is in the dissociated form (pK_a of $HN_3 = 4.72$ and of HF = 3.17).

Carbon monoxide. The buffer was saturated with carbon monoxide (*purum*, Fluka) before the addition of PsCCP.

Spectrophotometer. Cary 15 instrument, thermostated cell compartments set to 25°C. Absorption spectra were recorded by means of "0 – 1, 1 – 2" slidewires and the absorption maxima were determined from spectra recorded at a scanning speed of 3 – 6 nm/min, the chart scale being 1 nm/division. The wavelength indicator was checked with a mercury lamp. 0.4 ml micro quartz cells with beam masks, or rectangular quartz cells, both with 1.0 cm light path, were used. Most of the spectra were recorded with 4.3 – 6.8 μM PsCCP in a final volume of 210 μl.

Buffers. The following buffers, of ionic strength 0.1, were used for the spectrophotometry: sodium phosphate pH 6.0 – 7.8, tris(hydroxymethyl)aminomethane (TRIS)-HCl pH 7.6 – 8.6, and glycine-NaOH pH 8.9 – 10.9. Enzyme activity measurements were made in pH 6.0 sodium phosphate buffers of ionic strength 0.01 and 0.2. The pH values were measured with a Beckman Zeromatic II pH meter standardized at pH 7.0 with Beckman Standard Buffer No. 3581 and at pH 9.2 with 0.01 M sodium borate.

Chemicals were of analytical grade unless otherwise stated.

RESULTS

Absorption spectra of ferri- and ferro-PsCCP are shown in Fig. 1, and corrected peak wavelengths, extinction coefficients, and relative absorbances in Table 1. The addition of potassium ferricyanide did not alter the spectrum of PsCCP, which shows it to be in the fully oxidized form. The spectrum of ferro-PsCCP was stable for at least 30 min after reduction with sodium dithionite.

Table 1. Spectral characteristics of *Pseudomonas* cytochrome *c* peroxidase.

	Medium	λ of maxima, nm	ε $mM^{-1}cm^{-1}$	Relative absorbances
Ferri-PsCCP	Sodium phosphate buffer pH 6.0, $\mu = 0.1$, 25°C	407	237	$A_{407}(ox.)/A_{280} = 4.53$,[a]
		525	19.6	$A_{407}(ox.)/A_{525}(ox.) = 12.1$
Ferro-PsCCP		420	273	$A_{420}(red.)/A_{407}(ox.) = 1.16$,
		524	27.5	$A_{420}(red.)/A_{557}(red.) =$
		551 (shoulder)	34.2	6.98, $A_{557}(red.)/A_{551}$ (red.) = 1.15
		557	39.2	
Alkaline ferri-PsCCP	0.1 N NaOH, 25°C	410	–[b]	
		535	–[b]	
Alkaline ferro-PsCCP		417	–[b]	$A_{550}/A_{521} \sim 1.7$
		521	–[b]	
		550	–[b]	

[a] $\varepsilon_{280} = 52.3$ mM^{-1} cm^{-1} on a dry weight basis, calculated from $A(1\ \%, 1\ cm) = 12.1$ at 280 nm.[12]
[b] Spectrum unstable.

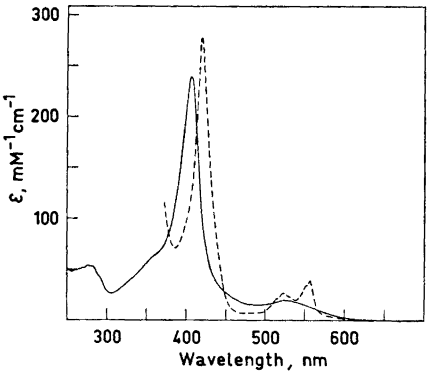

Fig. 1. Absorption spectra of ferri- and ferro-PsCCP in sodium phosphate buffer pH 6.0, $\mu = 0.1$, 25°C. — ferri-PsCCP. - - - - ferro-PsCCP; PsCCP was reduced by the addition of a minimum amount of solid sodium dithionite.

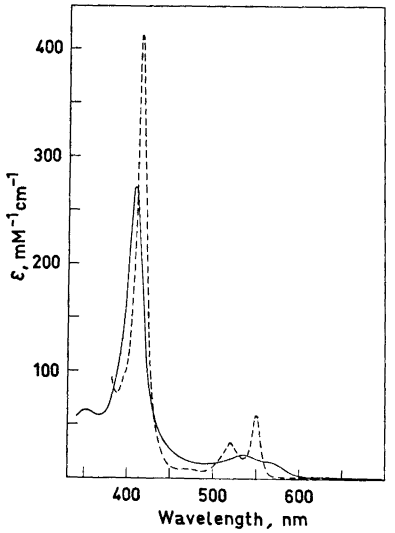

Fig. 2. Absorption spectra of ferri- and ferro-PsCCP in 0.1 N sodium hydroxide, 25°C. — ferri-PsCCP; recorded within 10 min of the mixing PsCCP with sodium hydroxide. - - - - ferro-PsCCP; recorded within 10 min of the reduction of PsCCP in sodium hydroxide with a minimum amount of solid sodium dithionite.

Effect of pH on the absorption spectra of ferri- and ferro-PsCCP. Spectrophotometric titration of ferro-PsCCP in the alkaline pH range. The effect of pH in the range 6.0 – 13.0 on the spectra of PsCCP was studied. With increasing pH the absorbances of the maxima of ferri- and ferro-PsCCP rose (Fig. 2); at the same time the maxima of the ferri-PsCCP spectrum shifted to longer wavelengths, and those of ferro-PsCCP to shorter wavelengths (Table 1). The double α-band disappeared above pH 10, becoming a single maximum at 550 nm (Fig. 3). Ferri-PsCCP was unstable above pH 10.8, the absorbances decreasing slowly ($\Delta\varepsilon_{524-525\ nm}$ less than 5 mM^{-1} cm^{-1} per 10 min) without a concomitant shift in the wavelengths of the maxima; similarly, ferro-PsCCP was unstable above pH 8.9 ($\Delta\varepsilon_{\alpha-band}$ less than 10 mM^{-1} cm^{-1} per 10 min). The pK value for the transition of ferro-PsCCP from the neutral to the alkaline form was determined from the change in absorbance at 550 nm (Fig. 4). A plot of log $[\alpha/(1-\alpha)]$ against pH in the range 7.5 – 10.3 gave straight line of slope 0.32, from which a pK value of 10.0 for the half-dissociated PsCCP was obtained.

Reaction of PsCCP with carbon monoxide, cyanide, azide, and fluoride. That ferro-PsCCP reacts with carbon monoxide at pH 6.0 is indicated by the difference spectrum shown in Fig. 5 A. The Soret band shifted to a shorter wavelength, the difference minimum being at 433 nm and the maximum at 415 nm

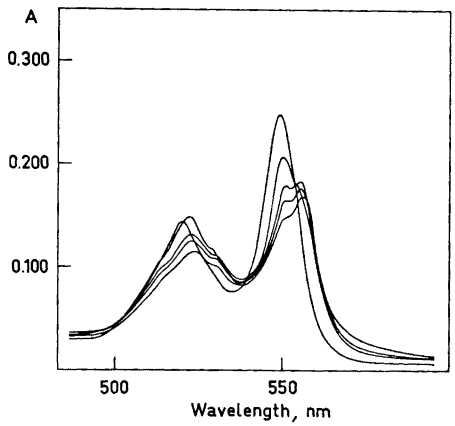

Fig. 3. Effect of pH on the spectrum of ferro-PsCCP in the visible region, $\mu = 0.1$, 25°C. The absorption curves can be distinguished at 550 nm, where the absorbance increases with increasing basicity. Sodium phosphate pH 6.0, TRIS-HCl pH 7.2, and glycine-NaOH pH 8.9 and 10.9 buffers, and 0.1 N NaOH, were used. The spectra were recorded within 5 min of the reduction of 4.3 μM PsCCP with solid sodium dithionite.

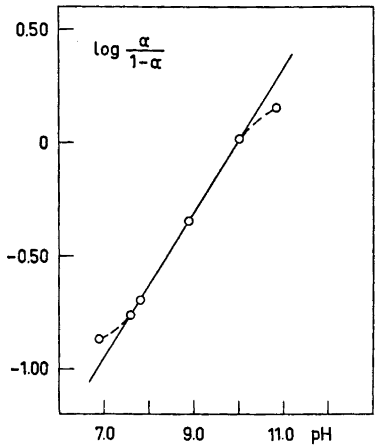

Fig. 4. Graphical determination of pK for the transition of PsCCP from the neutral to the alkaline form. The experimental conditions were identical to those in Fig. 3. $\alpha = (A_{pH\ x} - A_{pH\ 6})/(A_{pH\ 13} - A_{pH\ 6})$, where $A_{pH\ 6}$ is the absorbance at 550 nm of ferro-PsCCP at pH 6.0 (neutral form), $A_{pH\ x}$ the absorbance of ferro-PsCCP at any particular pH value and $A_{pH\ 13}$ the absorbance at pH 13.0 (alkaline form). The pK value obtained was 10.0; the slope of the line is 0.32.

Table 2. Characteristics of the difference spectra of certain compounds of *Pseudomonas* cytochrome *c* peroxidase. Measurements made in sodium phosphate buffer pH 6.0, $\mu = 0.1$, 25°C.

Difference spectrum	λ, nm	$\Delta\varepsilon$, $mM^{-1}cm^{-1}$
CO-ferro-PsCCP *minus* ferro-PsCCP	415 (maximum)	133
	433 (minimum)	59.0
CN-ferri-PsCCP *minus* ferri-PsCCP	~403 (minimum)	not measured
	421 (maximum)	156
CN-ferro-PsCCP *minus* ferro-PsCCP	420 (maximum)	39.6
	436 (minimum)	18.3
N_3-ferri-PsCCP *minus* ferri-PsCCP	402 (minimum)	35.0
	421 (maximum)	83.5

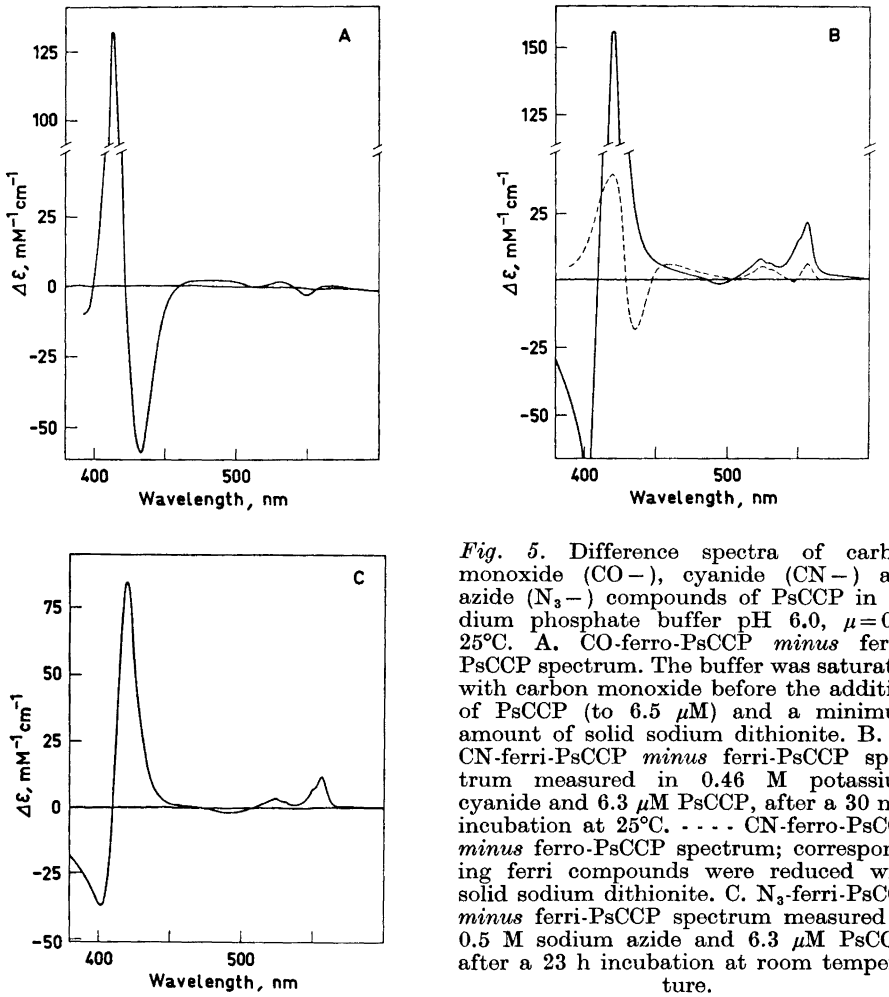

Fig. 5. Difference spectra of carbon monoxide (CO–), cyanide (CN–) and azide (N_3–) compounds of PsCCP in sodium phosphate buffer pH 6.0, $\mu = 0.1$, 25°C. A. CO-ferro-PsCCP *minus* ferro-PsCCP spectrum. The buffer was saturated with carbon monoxide before the addition of PsCCP (to 6.5 μM) and a minimum amount of solid sodium dithionite. B. — CN-ferri-PsCCP *minus* ferri-PsCCP spectrum measured in 0.46 M potassium cyanide and 6.3 μM PsCCP, after a 30 min incubation at 25°C. - - - - CN-ferro-PsCCP *minus* ferro-PsCCP spectrum; corresponding ferri compounds were reduced with solid sodium dithionite. C. N_3-ferri-PsCCP *minus* ferri-PsCCP spectrum measured in 0.5 M sodium azide and 6.3 μM PsCCP, after a 23 h incubation at room temperature.

(Table 2). In the visible region, the absorbance intensified at 520–540 nm and 555–570 nm and decreased at 550 nm. The spectrum was stable for at least 20 min.

Ferro- and ferri-PsCCP were found to react with cyanide at pH 6.0 at high cyanide concentrations (Fig. 5 B, Table 2). The spectra shown in Fig. 5 B are of 6.3 μM PsCCP in 0.46 M potassium cyanide; under these conditions the full difference spectrum of ferri-PsCCP-cyanide was attained in 8 min, and the difference in absorbance at 421 nm after 30 sec was 97 % of the maximum obtained. The difference spectrum was stable for at least 1 h after the maximum absorbances were reached. The cyanide-ferri-PsCCP/ferri-PsCCP difference spectrum shows characteristics of the spectrum of reduced PsCCP, namely the typical α- and β-bands and the shift of the Soret band to a longer wavelength,

although there are differences between the spectra of ferro-PsCCP and cyanide-ferro-PsCCP (Fig. 5 B). With 6.6 μM PsCCP in 4.6 mM potassium cyanide the spectral changes were similar, but the maximal difference absorbance at 421 nm was only about 30 % of that in the presence of 0.46 M potassium cyanide. In 0.1 mM potassium cyanide no changes in the spectrum of ferri-PsCCP were observed.

At pH 6.0 no reaction between ferri-PsCCP (5.5 μM) and azide (5 mM) could be detected during a period of 20 min. 0.5 M azide reacted slowly with ferri-PsCCP (6.3 μM) at room temperature: 20 min after mixing PsCCP and azide the difference absorbance at 421 nm was 30 % of the maximum (measured after 23 h), the proportion being 55 % after 2 h. The spectrum showed the same features of reduced hemochromogen, as was observed after the reaction of ferri-PsCCP with cyanide (Fig. 5 C, Table 2).

There was no reaction between fluoride (5 mM or 0.5 M) and ferri-PsCCP (6.3 μM), the latter being incubated for 23 h in 0.5 M fluoride.

The inhibition by cyanide and azide of the PsCCP-catalyzed peroxidatic oxidation of ferro-Ps-cyt-551 was studied in respect to H_2O_2. The concentration of ferro-Ps-cyt-551 was kept to 18.5 – 18.6 μM, and there were two inhibitor concentrations. Sodium phosphate buffer of pH 6.0 and ionic strength 0.2 was used to avoid changes in ionic strength when the inhibitor was added; such changes affect the initial rate of the reaction.[13] Neither cyanide nor azide was observed to react with the electron donor, as judged from the spectrum of ferro-Ps-cyt-551. The effect of both ligands was determined after a short pre-

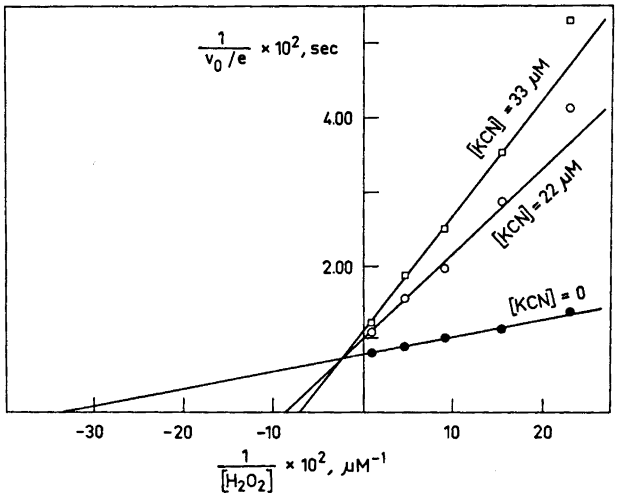

Fig. 6. Lineweaver-Burk plot of the initial rates of the peroxidatic oxidation of ferro-Ps-cyt-551 catalyzed by PsCCP in the presence and absence of cyanide in sodium phosphate buffer pH 6.0, $\mu = 0.2$, 25°C. Concentrations of reactants: 18.6 μM ferro-Ps-cyt-551, 4.4 – 110 μM H_2O_2, 22 and 33 μM KCN and 2.73 nM PsCCP. The following values were obtained: $K_m = 3.0$ μM, $V_m/e = 125$ sec^{-1}, $K_i = 7.1$ μM and α (interaction constant for the effect of the inhibitor on the binding of substrate) = 15 from the abscissa of the intersection of the lines $(-1/\alpha\ K_m)$.

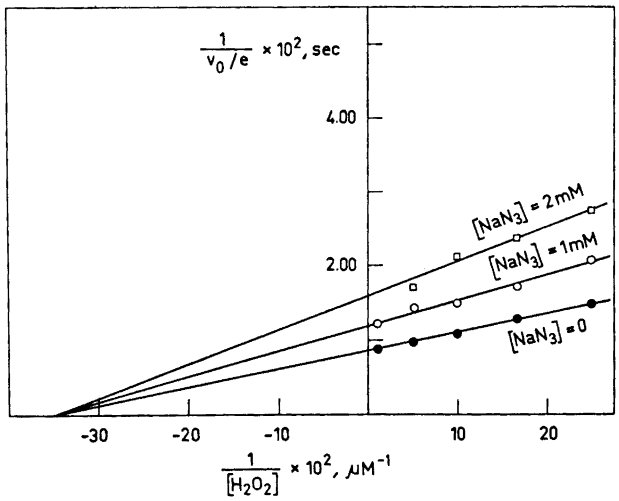

Fig. 7. Lineweaver-Burk plot of the initial rates of the peroxidatic oxidation of ferro-Ps-cyt-551 catalyzed by PsCCP in the presence and absence of azide in sodium phosphate buffer pH 6.0, $\mu = 0.2$, 25°C. Concentrations of reactants: 18.5 μM ferro-Ps-cyt-551, 4 – 100 μM H_2O_2, 1 and 2 mM sodium azide, and 2.66 nm PsCCP. The following values were obtained: $K_m = 3.2$ μM, $V_m/e = 119$ sec^{-1}, and $K_i = 3.1$ mM.

incubation period because the enzyme alone is not stable, for periods of minutes, at the final dilution used in the initial rate measurements. The results are shown in Figs. 6 and 7. The mechanism of the inhibition by cyanide is of a mixed type under these conditions, that is intermediate between competitive and noncompetitive inhibition in respect to H_2O_2. The mean value of the inhibition constant K_i calculated from the slope and the $1/(v_0/e)$ intercept of the plot of $1/(v_0/e)$ against 1/[S] and from the $(v_0/e)/[S]$ intercept of the plot of v_0/e against $(v_0/e)/[S]$ was found to be 7.1 μM. Azide was observed to inhibit the peroxidatic oxidation of ferro-Ps-cyt-551 noncompetitively in respect to H_2O_2; the mean value for K_i was 3.2 mM obtained from the slope and the $1/(v_0/e)$ intercept of the plot of $1/(v_0/e)$ against 1/[S] and from the v_0/e and $(v_0/e)/[S]$ intercepts of the plot of v_0/e against $(v_0/e)/[S]$. In the presence of azide the linear portion of the reaction curve was very short, causing difficulties in the determination of the initial rates.

Reaction of ferri-PsCCP with H_2O_2. When 4.7 – 6.2 μM ferri-PsCCP was incubated with about equimolar H_2O_2 at pH 6.0 there was a decrease in the absorbance in the Soret region, without any detectable change in the wavelength of this maximum or of other features of the spectrum. The time dependence of the change in absorbance at 407 nm after the addition of H_2O_2 to PsCCP is shown in Fig. 8. Two phases of the reaction are observable. During the first minutes the absorbance decreased to a plateau (phase 1), after which there was an increase to a value somewhat below the original followed by a slow, steady decrease (phase 2). For time 0 – 2 min (first phase) the decrease in absorbance of the Soret band was 4 – 6 % of the original absorbance, and

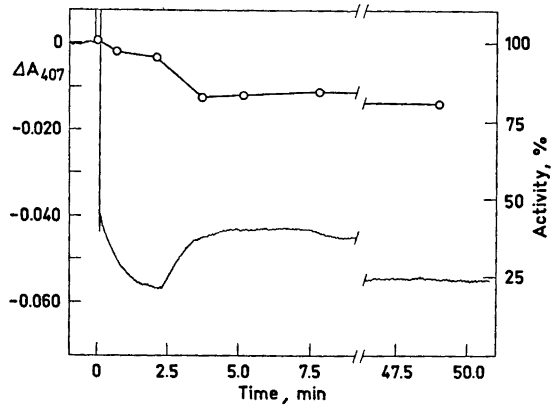

Fig. 5. Time dependence of the reaction of ferri-PsCCP with H_2O_2 in sodium phosphate buffer pH 6.0, $\mu = 0.1$, 25°C, and relative peroxidase activities during the course of the reaction. 5 μl of 1 mM H_2O_2 was added to 200 μl of 4.7 μM PsCCP and the reaction was followed by the difference in absorbance (H_2O_2/ferri-PsCCP *minus* ferri-PsCCP) at 407 nm (the solid line). The absorbance decrease of 0.028 is due to the dilution caused by the addition of H_2O_2. The peroxidase activity was measured in sodium phosphate buffer pH 6.0, $\mu = 0.01$, 25°C, as decribed in the text, and is given as a percentage of the activity of the untreated PsCCP (○).

for the time 6 – 10 min (second phase) the decrease was 2.5 – 4 %. Because H_2O_2 is known to degrade horse heart ferricytochrome *c*,[18,19] the peroxidatic activity of PsCCP during incubation with H_2O_2 was measured (Fig. 8). During the second phase of the reaction of H_2O_2 with PsCCP the activity decreased from 95 % to 80 % of the original. With higher H_2O_2 concentrations the absorbance of the Soret band decreased further without a shift in the position of the absorption maximum. At molar ratios H_2O_2:PsCCP above 3 the reaction was monophasic, the absorbance decreasing almost linearly with time. At a molar ratio of 7 the peroxidase activity of H_2O_2-treated PsCCP was only 15 % of the original, the decrease of the absorbance of the Soret band being less than 5 %.

In a further study of the reaction between H_2O_2 and PsCCP, the addition of potassium ferrocyanide in slight excess after the first phase was found to give no significant increase in the absorbance, as was to be expected if the decrease in absorbance in the first phase were due to the formation of a simple complex between H_2O_2 and the iron in ferri-PsCCP.

DISCUSSION

Two cytochrome peroxidases isolated from bacteria, PsCCP and *Thiobacillus* cytochrome peroxidase, resemble the cytochromes more than the classical peroxidases in having low-spin, hemochrome-type spectra and having heme *c* as the prosthetic group.[4,8] The spectra of *Thiobacillus* peroxidase deviate considerably from the spectra of PsCCP shown in Fig. 1. Characteristics of the spectrum of *Thiobacillus* peroxidase are: with ferriperoxidase Soret band 398

nm, with ferroperoxidase 415 nm, β-band 520 nm and α-band 550 nm without the shoulder characteristic of PsCCP. The functions as cytochromes of PsCCP and *Thiobacillus* peroxidase are not known.

Several bacterial cytochromes *c* with an asymmetric α-band at room temperature have been isolated: *Pseudomonas stutzeri* cytochrome *c*-552,558,[20] *Alcaligenes faecalis* cytochrome *c*-551,557,[21] *Bacillus subtilis* cytochrome *c*-550,554,[22] *Micrococcus* cytochrome *c*-548,554 (="cytochrome b_4"),[23] *Chromatium* strain D cytochrome *c*-550,553,[24] and *Chlorobium thiosulphatophilum* cytochrome *c*-550,555.[25,26] Common features of the bacterial "split α" type cytochromes are a high A_{Soret}(red.)/A_α (red.) ratio, a low A_α (red.)/A_β (red.) ratio, and a low extinction coefficient of the α-band as compared with that of the horse heart type cytochromes *c*.[27] PsCCP, *P. stutzeri* cytochrome *c*-552,558 and *A. faecalis* cytochrome *c*-551,557 deviate from the other bacterial "split α" hemoproteins in being of high molecular weight (43 200 – 74 000) and having two hemes per molecule; they form a sub-group of three similar proteins.

At pH values above 10 the shoulder of the α-band of ferro-PsCCP and *P. stutzeri* ferrocytochrome *c*-552,558 [20] disappears and the α-band:β-band absorbance ratio becomes equal to that of horse heart cytochrome *c* (~ 1.7). Low molecular weight cytochromes of the "split α" type from *Micrococcus* and *Bacillus* are more stable in the alkaline range, being unchanged at pH values up to 13.0 – 13.3.[22,23] The low-spin structure of these cytochromes, that is with internal ligands at the 5th and 6th coordination positions of the iron, are preserved after the alkaline transitions. There is evidently some degradation of PsCCP in the alkaline pH range, as shown by the unstable spectra.

Native mammalian ferrocytochrome *c* does not react with carbon monoxide in the neutral pH-range. Denaturation causes a change of reactivity towards carbon monoxide and this reaction has been widely used as a test for the denaturation of cytochromes.[28] However, several bacterial cytochromes are known to combine in the native form with carbon monoxide,[29] the denatured forms showing modified carbon monoxide spectrum. PsCCP, *P. stutzeri* cytochrome *c*-552,558 [20] and *A. faecalis* cytochrome *c*-551,557 [21] belong to this group of bacterial hemoproteins. The difference spectra of these three hemoproteins, that is of reduced carbon monoxide derivative *minus* reduced hemoprotein, are similar, with a minimum at 430 – 434 nm and a maximum at 415 nm. In contrast, the low molecular weight cytochromes of the "split α" type do not react with carbon monoxide.[22,24] *Thiobacillus* cytochrome peroxidase also combines with carbon monoxide resulting in a shift of the Soret band of the reduced peroxidase to a shorter wavelength.[8]

Ferri- and ferro-PsCCP react with cyanide, and ferri-PsCCP slowly with azide only at high concentrations of these ligands at a neutral pH. *A. faecalis* ferrocytochrome *c*-551,557 combines with cyanide at concentrations comparable with those of our study, and does not react with azide at low concentrations.[21] The reaction of *P. stutzeri* cytochrome *c*-552,558 with cyanide and azide has not been studied.[20] Horse heart cytochrome *c* combines with such ligands in the neutral pH range only when it is in the oxidized form.[27] The reaction of external ligands with the heme iron of horse heart cytochrome *c* requires the replacement of an internal ligand in the axial position relative to the iron and conformational changes of the protein near the heme group.

PsCCP either must have a more open structure in the neighbourhood of the heme, or the 6th internal ligand of the iron must be less firmly bound than in horse heart cytochrome *c* because of the easier reactions with external ligands (carbon monoxide and ferro-PsCCP with cyanide).

Cyanide and azide may also react with secondary groups in the protein as well as with the heme iron. Cyanide can act as reductant, as has been proposed in its reaction with oxidized mammalian cytochrome oxidase; first there is a slow reaction, possibly the reduction of the enzyme at a binding site other than the heme, and then cyanide combines with the reduced heme a_3.[30] The reaction of ferri-PsCCP with cyanide may proceed in a similar way. Azide can also interact with the protein moiety, as has been shown with horseradish peroxidase; it is proposed that azide combines with a methionine residue at the active site of the enzyme.[31] The very slow reaction of ferri-PsCCP with azide may comprise secondary reactions in addition to any direct coordination with the iron.

Cyanide was observed to be an efficient inhibitor of the peroxidatic reaction catalyzed by PsCCP. The inhibition mechanism was of the mixed type, that is intermediate between competitive and noncompetitive in respect to hydrogen peroxide. This seems to indicate that several phenomena are involved in the interaction of the inhibitor with the enzyme. Cyanide competes with hydrogen peroxide, thereby interfering with the binding of the substrate, and to some extent prevents the breakdown of the active complex. The interaction constant α, which is a measure of how much cyanide effects the binding of hydrogen peroxide, was calculated from a Lineweaver-Burk plot (Fig. 6); the value indicates that the affinity of the inhibited enzyme for the substrate is only 1/15th of that of the uninhibited enzyme. The value of the inhibitor constant K_i for cyanide (7.1 μM) is close to the apparent K_m of hydrogen peroxide (6 μM).[13] Using an indirect method for measurement of activity and partially purified PsCCP, Lenhoff and Kaplan found that 0.1 mM cyanide caused a 50 % inhibition.[32] *Thiobacillus* cytochrome peroxidase also is inhibited by cyanide: 39 % inhibition is caused by 1 mM cyanide.[8]

Azide inhibited the peroxidatic reaction noncompetitively, showing that it reacts at a site different from that reacting with hydrogen peroxide. The possibility of irreversible inhibition giving a noncompetitive plot cannot be ruled out on the basis of a kinetic study only. The value of K_i for azide, 3.2 mM, is much greater than that of cyanide. Lenhoff and Kaplan observed a 84.5 % inhibition with 10 mM azide at pH 6.1, the extent of inhibition increasing with decreasing pH.[32]

Hydrogen peroxide did not form a stable, spectrally detectable compound with PsCCP, comparable with that of hydrogen peroxide and plant peroxidases,[1] yeast cytochrome *c* peroxidase,[2] catalase,[1] and myoglobin.[1] A slight decrease in absorbance of the Soret band was observed after the addition of hydrogen peroxide to PsCCP. A similar effect of hydrogen peroxide on mammalian ferricytochrome *c* has been reported by O'Brien [18] and Mochan and Degn.[19] This decrease has been shown to be due to the degradative effect of hydrogen peroxide on the tyrosine residues of the protein moiety.[18] The effect of hydrogen peroxide on PsCCP was found to be biphasic. The first phase may be due to the formation of some kind of PsCCP-hydrogen peroxide

compound, which then decomposes. The nature of the compound could not be elucidated by the present studies. The presence of ferrocyanide did not reduce the oxidizing equivalents of this compound. Such a reduction has been observed with hydrogen peroxide compounds of yeast cytochrome *c* peroxidase (complex ES) and horseradish peroxidase (complexes I and II).[33] This eliminates the possibility of a simple complex formation between hydrogen peroxide and the iron in PsCCP. The second phase of the reaction between hydrogen peroxide and PsCCP is evidently the degradation of PsCCP.

Acknowledgement. This work was supported in part by a grant to one of the authors, R. S., from the *Alfred Kordelin Foundation*, Helsinki, Finland.

REFERENCES

1. Saunders, B. C. *Peroxidase*, Butterworths, London 1964.
2. Yonetani, T. and Ray, G. S. *J. Biol. Chem.* **240** (1965) 4503.
3. Carlström, A. *Acta Chem. Scand.* **23** (1969) 203.
4. Ellfolk, N. and Soininen, R. *Acta Chem. Scand.* **24** (1970) 2126.
5. Morita, Y. and Kameda, R. *Mem. Res. Inst. Food Sci. Kyoto Univ.* **12** (1957) 1.
6. Yamazaki, I., Nakajima, R., Honma, H. and Tamura, M. *Structure and Function of Cytochromes*, University Park Press, Manchester 1968, p. 552.
7. Nakajima, R., Sano, H. and Yamazaki, I. *Biochim. Biophys. Acta* **172** (1969) 578.
8. Yamanaka, T. and Okunuki, K. *Biochim. Biophys. Acta* **220** (1970) 354.
9. Soininen, R. *Acta Chem. Scand.* **26** (1972) 2535.
10. Maurer, H. R. *Disk-Elektrophorese*, Walter de Gruyter, Berlin 1968.
11. Weber, K. and Osborne, M. *J. Biol. Chem.* **244** (1969) 4406.
12. Ellfolk, N. and Soininen, R. *Acta Chem. Scand.* **25** (1971) 1535.
13. Soininen, R. and Ellfolk, N. *Acta Chem. Scand.* **26** (1972) 861.
14. Ambler, R. P. *Biochem. J.* **89** (1963) 341.
15. Yonetani, T. and Ray, G. S. *J. Biol. Chem.* **240** (1965) 3392.
16. Ellfolk, N. *Acta Chem. Scand.* **21** (1967) 175.
17. Yonetani, T. *J. Biol. Chem.* **240** (1965) 4509.
18. O'Brien, P. J. *Biochem. J.* **52** (1952) 511.
19. Mochan, E. and Degn, H. *Biochim. Biophys. Acta* **189** (1969) 354.
20. Kodama, T. and Mori, T. *J. Biochem. (Tokyo)* **65** (1969) 621.
21. Iwasaki, H. and Matsubara, T. *J. Biochem. (Tokyo)* **69** (1971) 847.
22. Miki, K. and Okunuki, K. *J. Biochem. (Tokyo)* **66** (1969) 831.
23. Hori, K. *J. Biochem. (Tokyo)* **50** (1961) 440.
24. Cusanovich, M. A. and Bartsch, R. G. *Biochim. Biophys. Acta* **189** (1969) 245.
25. Yamanaka, T. and Okunuki, K. *J. Biochem. (Tokyo)* **63** (1968) 341.
26. Meyer, T. E., Bartsch, R. G., Cusanovich, M. A. and Mathewson, J. H. *Biochim. Biophys. Acta* **153** (1968) 854.
27. Butt, W. D. and Keilin, D. *Proc. Roy. Soc. (London)* **B 156** (1962) 429.
28. Ben-Gershom, E. *Biochem. J.* **78** (1961) 218.
29. Iwasaki, H. and Shidara, S. *J. Biochem. (Tokyo)* **66** (1969) 775.
30. Antonini, E., Brunori, M., Greenwood, C., Malmström, B. G. and Rotilio, G. C. *Eur. J. Biochem.* **23** (1971) 396.
31. Brill, A. S. and Weinryb, I. *Biochemistry* **6** (1967) 3528.
32. Lenhoff, H. M. and Kaplan, N. O. *J. Biol. Chem.* **220** (1956) 967.
33. Yonetani, T. *J. Biol. Chem.* **241** (1966) 2562.

Received June 5, 1972.

ACTA CHEMICA SCANDINAVICA 27 (1973) 47–56

All Valence-Electron Calculations on *trans*-1-Phenyl-1-propene and its Anion Radical

HENRIK TYLLI and FRANCISKA SUNDHOLM

Department of Chemistry, University of Helsinki, Helsinki, Finland

A series of all valence-electron calculations has been performed for different molecular conformations of *trans*-1-phenyl-1-propene. The various bond lengths and bond angles were kept constant except for the torsional angle between the plane containing the side chain and the plane of the ring. For the neutral molecule the CNDO/2 calculations suggest a nonplanar conformation to be the most stable, the equilibrium torsional angle being 30°. The EHT calculations give unrealistic results. INDO calculations for the anion radical suggest the planar conformation to be the most stable. The hydrogen coupling constants for different torsional angles are also given and the coupling constants after annihilation of the quartet state contaminant are discussed in relation to the experimental results.

Electron resonance data strongly suggest that in anion radicals of compounds with the general formula I, such as 1-phenyl-1-propene,[1] stilbene,[2] and styrene,[3] all the aromatic protons are magnetically inequivalent. In complicated molecules, where deuteration cannot be used as a tool for the assignment of the experimental coupling constants to protons in definite positions

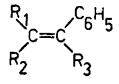

I

of the molecule, the assignment can be made, at least tentatively, by the comparison of experimental data with coupling constants obtained by molecular orbital calculations.

In π-electron calculations of Hückel type, the observed inequivalency of the coupling constants cannot be reproduced, because the geometry of the molecule is not explicitly used and all the overlap integrals between non-neighbours are neglected. Nevertheless HMO calculations have been tried, with variation of either the Coulomb integral [4] ("α-effect") or the resonance

integral [4,5] ("β-effect") to account for the observed inequivalency. The former model implies a repulsion, the latter an imaginary bond between one *ortho*-proton and one ethylenic β-proton. These two empirical approaches have been used with reasonable success in a number of cases.[2,4–8]

Theoretically such calculations are less satisfactory. In addition to the original HMO parametrization and the McLachlan λ, they involve one more parameter, the value of which is chosen to give the best agreement with experiment. One would rather like to have a method with fewer adjustable parameters and which treats directly the core polarization effects leading to the hyperfine interaction. The SCF-MO theory with Intermediate Neglect of Differential Overlap, INDO [9,10] fulfills this requirement. This approximation deals with all the valence electrons on the same basis, and can therefore handle also "σ-radicals" or radicals with σ- and π-fragments within the same framework. Thorough discussions of this and related approximations are given in several texts.[11–17] In addition, in the *trans*-1-phenyl-1-propene molecule the possibility of a nonplanar equilibrium conformation has to be taken into account. Thus this molecule represents a rather complicated dynamic problem. The side chain as a whole performs torsional oscillations about the equilibrium position. The authors therefore found it a further matter of interest to examine the form of the potential function required to describe the torsional oscillations of the side chain in the neutral molecule and in its anion radical. For this purpose MO calculations have been performed for conformations with different angles of torsion around the C_1-C_7 bond (Fig. 1) using the EHT (Extended

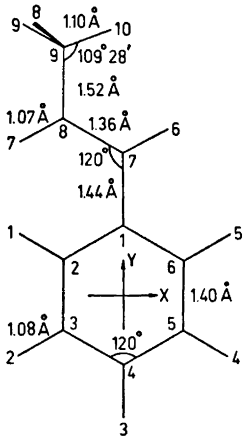

Fig. 1. Bond lengths (Å) and bond angles in *trans*-1-phenyl-1-propene.

Hückel Theory) and the CNDO/2 method (Complete Neglect of Differential Overlap, version 2) for the neutral molecule, and the INDO method for the anion radical. Furthermore the methyl group in the side chain is a slightly hindered rotator. Experimentally it has been shown, however, that the methyl proton splittings are equivalent,[1] indicating that these protons are interconverting rapidly compared with the electron resonance time scale.

PARAMETRIZATION

The Extended Hückel method has been outlined by Hoffmann.[18] The exchange integrals were calculated in terms of the diagonal elements and overlap integrals according to the Wolfsberg – Helmholz formula[19] ($K = 1.75$).[18] The overlap integrals were calculated from Slater orbitals with the usual orbital exponents (1.200 for hydrogen [20] and 1.625 for carbon [21]).

The CNDO/2 and INDO methods have been described by Pople and coworkers.[9–11,22–25] The atomic parameters for these calculations were taken from Ref. 11, pp. 75 – 83.

As no experimental geometry for the *trans*-1-phenyl-1-propene appears to be available, an idealized geometry has been built up for the molecule using fragments from similar molecules.[26–28] The bond lengths and bond angles used are shown in Fig. 1. The programs used in the calculations were all based on programs distributed by the QCPE organisation.[29] The EHT calculations were performed on an IBM 360/50 computer at the State Computer Center in Helsinki using a double precision version of Hoffmann's program,[30] written by L. Backström at the University Computing Center. The CNDO/2 and INDO calculations were carried through on a Burroughs 6500 computer at the Computing Center of the University of Helsinki, using slightly modified versions of the QCPE programs number 91 and 141, written by G. A. Segal and P. A. Dobosh, respectively.[31]

RESULTS AND DISCUSSION

The equilibrium position of the propene side chain. The torsional angle in *trans*-1-phenyl-1-propene and its anion radical is defined as the angle between the plane of the aromatic ring and the plane which contains the methyl group carbon atom and the ethylenic double bond. The electronic energies for different angles of torsion in the neutral molecule were obtained in the EHT calculations. The CNDO/2 calculations for the neutral molecule give the total energies for different torsional angles. Plots of the electronic and the total energy, respectively, *versus* the angle of torsion are shown in Figs. 2 and 3.

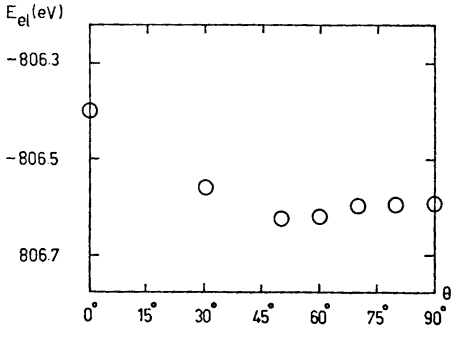

Fig. 2. The total electronic energy of *trans*-1-phenyl-1-propene as a function of torsional angle between the aromatic ring and the plane containing the side chain (EHT).

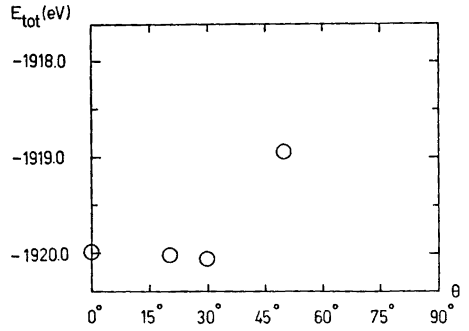

Fig. 3. The total energy of *trans*-1-phenyl-1-propene as a function of torsional angle between the plane of the ring and the plane containing the side chain (CNDO/2).

A nonplanar equilibrium conformation is suggested in both cases. In the EHT calculations the minimum energy for the molecule occurs for a conformation with an angle of torsion of about 50°C. The CNDO/2 calculations suggest a minimum of total energy for a conformation with an angle of torsion of about 30°.* However, the differences between the results obtained from these two approximations are more significant in other respects. The EHT calculations suggest that the planar conformation is less stable than the conformation with a torsional angle of 90° (energy difference 0.233 eV = 22.5 kJ/mol). The CNDO/2 calculations give lower energy for the planar form than for the conformations with torsional angles larger than 30°. The energy difference in this case between the planar and the 30° conformations is 0.097 eV = 9.36 kJ/mol. With increasing angle of torsion the energy increases rapidly, and is 1.13 eV = 109.0 kJ/mol higher for the conformation with a torsional angle of 50° compared with the 30° conformation. No definitive experimentally established geometry seems to exist for *trans*-1-phenyl-1-propene. Suzuki, basing his arguments on the position of the A band in the UV spectrum of substituted styrenes, concluded that the most probable conformation of styrenes with no substituents at hindering positions, is planar or nearly planar in solution.[32]

It is a well established fact that the molecular conformation in radical ions [33] and in excited states [34] may differ significantly from the stable conformation for neutral molecules in the ground state. It is therefore not surprising that the INDO calculations performed for the anion radical of *trans*-1-phenyl-1-propene suggest the minimum of total energy for the planar con-

Table 1. Calculated net charges for *trans*-1-phenyl-1-propene with different torsional angles between the aromatic ring and the plane containing the side chain.

Atom	Net charges (CNDO/2) 0°	20°	30°	50°
C_1	0.041	0.042	0.042	0.039
C_2	−0.014	−0.013	−0.013	−0.014
C_3	0.010	0.010	0.011	0.015
C_4	−0.001	−0.001	−0.002	0.000
C_5	0.010	0.011	0.011	0.015
C_6	−0.013	−0.013	−0.014	−0.016
C_7	−0.018	−0.017	−0.016	−0.015
C_8	−0.001	−0.003	−0.004	−0.006
C_9	−0.011	−0.010	−0.009	−0.007
H_1	−0.004	−0.005	−0.005	−0.005
H_2	−0.007	−0.007	−0.007	−0.006
H_3	−0.007	−0.007	−0.007	−0.007
H_4	−0.007	−0.007	−0.007	−0.007
H_5	−0.006	−0.006	−0.006	−0.006
H_6	0.000	0.002	0.004	0.008
H_7	0.012	0.010	0.008	0.006
H_8	0.007	0.006	0.005	0.003
H_9	0.007	0.008	0.006	0.006
H_{10}	0.012	0.003	0.002	0.002

* *Note added in proof*: Recently Beringhelli *et al.*[46] obtained a torsional angle of 12° using a different semi-empirical approach and a theoretically optimized geometry.

formation. A plot of the total energy *versus* the angle of torsion is shown in Fig. 4. In addition to the prediction of different equilibrium conformations for the neutral molecule and the anion radical, it is seen that the potential energy for the torsional motion is much steeper for the neutral molecule. For the radical the energy difference between the planar and the 50° conformation is only 0.413 eV = 39.8 kJ/mol.

Net charges, dipole moments and bond indices. The net charges for the neutral *trans*-1-phenyl-1-propene obtained in the CNDO/2 calculations with different torsional angles are shown in Table 1. The corresponding values for the anion radical of this parent compound obtained in the INDO calculations are listed in Table 2. The variations in net charge with torsional angle are not large but systematic. With increasing torsional angle the charge difference between the side chain and the aromatic ring decreases in the neutral molecule as well as in the anion radical. This is reflected as a decrease in the calculated

Table 2. Calculated net charges for the anion radical of *trans*-1-phenyl-1-propene with different torsional angles between the aromatic ring and the plane containing the side chain.

Atom	Net charges (INDO) 0°	20°	30°	50°
C_1	−0.010	−0.014	−0.019	−0.046
C_2	−0.062	−0.058	−0.054	−0.043
C_3	0.028	0.026	0.024	0.016
C_4	−0.103	−0.103	−0.104	−0.112
C_5	0.022	0.022	0.022	0.022
C_6	−0.059	−0.059	−0.058	−0.055
C_7	−0.054	−0.050	−0.044	−0.012
C_8	−0.178	−0.176	−0.173	−0.162
C_9	0.107	0.106	0.106	0.103
H_1	−0.051	−0.054	−0.056	−0.065
H_2	−0.077	−0.077	−0.077	−0.078
H_3	−0.073	−0.073	−0.073	−0.075
H_4	−0.078	−0.078	−0.078	−0.080
H_5	−0.066	−0.067	−0.067	−0.070
H_6	−0.072	−0.072	−0.072	−0.078
H_7	−0.038	−0.039	−0.043	−0.042
H_8	−0.087	−0.087	−0.086	−0.083
H_9	−0.087	−0.086	−0.088	−0.083
H_{10}	−0.062	−0.062	−0.061	−0.058

Table 3. Calculated dipole moments for *trans*-1-phenyl-1-propene with different torsional angles between the aromatic ring and the plane containing the side chain (CNDO/2).

Torsional angle	Dipole moment (D)
0°	0.33
20°	0.30
30°	0.25
50°	0.16

dipole moments with increasing angle of torsion. The dipole moments obtained are listed in Table 3. Obviously the decrease in dipole moments with increasing torsional angle is due to the fact that the conjugation between the aromatic ring and the side chain decreases as the torsional angle increases.

The localized bond indices for the neutral molecule in the CNDO/2 approximation and for its anion radical in the INDO approximation were calculated according to Wiberg.[35] The major draw-back of this method is that antibonding interactions are lost in the squaring procedure. Another method of calculating bond indices has recently been introduced by Ehrenson and Seltzer,[36] and the Mulliken population analysis [37] in the CNDO and INDO approximations has been discussed by Kaufman.[38] The calculated bond indices for the *trans*-1-phenyl-1-propene molecule and its anion radical vary systematically as expected with the degree of conjugation between the aromatic ring and the side chain. The variations in the bond indices mean that the equilibrium geometry of the molecule varies continuously as the side chain performs torsional oscillations around its equilibrium position. In fact it has been shown [39–41] that in more accurate calculations of molecular properties, especially torsional barriers, one has to use a flexible geometry for the molecule. In the present case minimization with respect to at least the following parameters should be performed: the C_1-C_7 bond length, the $C_2C_1C_7$ and $C_1C_7C_8$ bond angles, and the torsional angle. The variations in the C_1-C_2, C_1-C_6, and C_7-C_8 bond lengths and the $C_1C_2H_1$, $C_1C_6H_5$, and $C_7C_8H_7$ bond angles

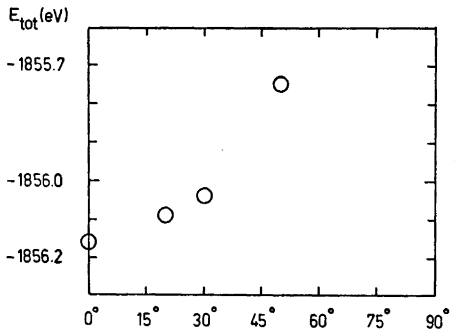

Fig. 4. The total energy of the anion radical of *trans*-1-phenyl-1-propene as a function of torsional angle between the aromatic ring and the plane containing the side chain (INDO).

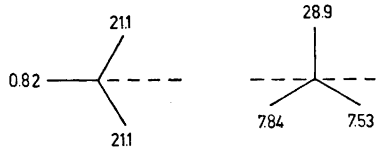

Fig. 5. The two orientations of the methyl group used in the calculation of the methyl hydrogen coupling constants. The indicated coupling constants are those obtained from the INDO calculations without annihilation.

are probably of less significance. However, the authors decided to use the nonflexible model partly because the approximations inherent in the CNDO and INDO methods make accurate calculations impossible, and partly because the flexible model would have required much more computer time.

The hyperfine coupling constants for the anion radical. The hydrogen hyperfine coupling constants were calculated according to the formulas:[11 42]

$$a_H = 539.86\ \varrho_{sHsH} \quad \text{(without annihilation)}$$
$$a_H = 711.25\ \varrho_{sHsH} \quad \text{(with annihilation)}$$

where ϱ_{sHsH}, the diagonal elements of the spin density matrix, indicate the unpaired electronic population of the *s*-orbital of the hydrogen atom under consideration. The hydrogen coupling constants obtained for the anion radical of *trans*-1-phenyl-1-propene are listed in Table 4. The coupling constants are

Table 4. Calculated hydrogen coupling constants for the anion radical of *trans*-1-phenyl-1-propene with different torsional angles between the aromatic ring and the plane containing the side chain (INDO without annihilation).

Hydrogen	Coupling constants 0°	20°	30°	50°
1	−3.84	−3.68	−3.47	−2.93
2	1.85	1.78	1.68	1.28
3	−5.45	−5.50	−5.56	−6.03
4	1.48	1.54	1.60	1.71
5	−3.13	−3.19	−3.24	−3.37
6	−0.92	0.92	3.34	12.0
7	−9.34	−9.04	−8.79	−7.49
8	21.1	19.6	18.2	14.2
9	21.1	21.7	22.3	19.5
10	0.82	0.80	0.77	0.63

found to vary considerably with the torsional angle. An interesting feature is that the coupling constant for the proton H_6 changes sign and increases, while the coupling constant for the proton H_7 decreases with increasing torsional angle.

The methyl group hydrogen hyperfine coupling constants were calculated for two fixed orientations of this group with respect to the plane containing the ethylenic double bond and the aromatic ring (planar conformation). These orientations are indicated in Fig. 5, where also the corresponding splitting constants are shown. As the methyl group rotates through 360° around the C_8-C_9 bond the coupling constant for a particular hydrogen atom varied between 0.82 and 28.9 G. If one assumes entirely free rotation for the methyl group, the effective splitting constant may be calculated as an arithmetic average. This treatment indicates a methyl group hydrogen hyperfine splitting constant of the order of magnitude of 15 G. After annihilation of the quartet state contaminant,[42] the hyperfine splitting constants shown in Fig. 6a are obtained. The experimental splitting constants,[1] and the calculated coupling constants before annihilation also for the planar conformation are shown in Figs. 6b and 6c, respectively. In contrast to earlier findings for other molecules [42] it is seen that the annihilation procedure in this case reduces the calculated coupling constants to about one half their original value. For the methyl group hydrogens, the calculated coupling constant even after annihilation is as high as 12.7 G, which is about three times the one found experimentally,

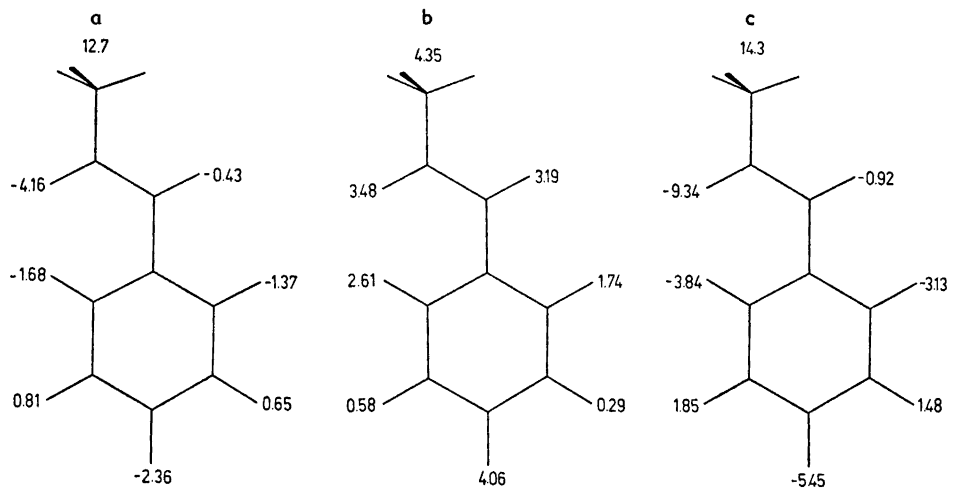

Fig. 6. The hydrogen coupling constants of the anion radical of *trans*-1-phenyl-1-propene. a. Calculated, INDO with annihilation. b. Experimental. c. Calculated, INDO without annihilation.

4.35 G. Obviously this would lead to an electron resonance spectrum with an over all width of at least 30 G. The width of the experimental spectrum was, however, found to be only 23.25 G. This is a serious discrepancy between theory and experiment, especially keeping in mind that good agreement between experiment and theory has been found for, *e.g.*, styrene using the unrestricted Hartree Fock method.[43] The authors wish to point out one possible explanation for this discrepancy. Free rotation was assumed for the methyl group around the C_8-C_9 bond. This is only approximately true. Assuming that the methyl group may be treated as a rigid top bonded to a rigid framework, the potential energy of the reorientation about the threefold symmetry axis of the top may be expressed by the modified Fourier series [41,44]

$$V(\alpha) = \frac{V_3}{2}(1 - \cos 3\alpha) + \frac{V_6}{2}(1 - \cos 6\alpha) + \ldots$$

where V_3 is the height of the threefold potential barrier and so on. In most cases V_6 and higher terms may be neglected. α is the angular coordinate which describes the torsional motion of the top. Substitution of this potential function into the Schrödinger equation leads to the Mathieu equation. The eigenvalues of the Mathieu equation which are lower than V_3 correspond to torsional oscillations, whose eigenfunctions can be approximated with the harmonic oscillator eigenfunctions. For eigenfunctions greater than V_3, the torsional oscillations go over into simple rotation, and the eigenfunctions of this motion can be approximated with the aid of the eigenfunctions for a rigid plane rotator.[45] For higher values of the torsional quantum number the probability distribution for the oscillator resembles that of the classical oscillator. Then one might say that the methyl protons spend a longer time in the plane defined

by the ethylenic double bond, where the calculated splitting has a minimum (0.82 G), than in the plane perpendicular to this plane, where the calculated splitting reaches its maximum (25.4 G annihilated). This would lead to a splitting lower than the arithmetic mean value used. The calculations also give a tenfold splitting for H_7 with respect to H_6, whereas they were assumed to be of the same order of magnitude in the assignment of the experimental spectrum.[1] For the theoretical model this difference is reduced by the torsional oscillations around the equilibrium conformation (Table 4).

Since it is impossible to assign the coupling constants to the proper positions in the molecule without the aid of spectra of deuterated compounds, the possibility that the calculations give the right succession must be taken into account. The simulated spectrum using the coupling constants given in Ref. 1 is also considerably broader than the spectrum obtained experimentally. Although some of the small peaks in the wings of the spectrum may be hidden in the background noise, it seems us that the set of coupling constants given in Table 5 better reproduced the experimental spectrum. Selectively deuterated products of *cis*- and *trans*-1-phenyl-1-propene are in preparation. We therefore hope to return to the problem with the assignment of the coupling constants.

Table 5. Tentative experimental coupling constants of the anion radical of *trans*-1-phenyl-1-propene.

Coupling constant (G)	Number of hyperfine components
4.35	4
4.06	2
2.61	2
1.74	2
1.16	2
0.87	2
0.58	2
0.29	2

Acknowledgements. The authors are indebted to Fil. kand. Lars Backström and Fil. kand. Erkki Vehkamäki at the University Computing Center, Helsinki, for help with the computer programs, and to Dr. Pekka Pyykkö for helpful discussions. One of us (H.T.) is indebted to *Neste Oy* for financial aid.

REFERENCES

1. Sundholm, F. and Tylli, H. *Acta Chem. Scand.* **23** (1969) 1085.
2. Atherton, N. M., Gerson, F. and Ockwell, J. N. *J. Chem. Soc.* **A 1966** 109.
3. Buick, A. R., Kemp, T. J. and Stone, T. J. *J. Phys. Chem.* **74** (1970) 3439.
4. Rieger, P. H. and Fraenkel, G. K. *J. Chem. Phys.* **37** (1962) 2811.
5. Stone, E. W. and Maki, A. H. *J. Chem. Phys.* **38** (1963) 1999.
6. Johnson, C. S., Jr. and Chang, R. *J. Chem. Phys.* **43** (1965) 3183.
7. Buick, A. R., Kemp, T. J., Neal, G. T. and Stone, T. J. *J. Chem. Soc.* **A 1969** 1609.
8. Buick, A. R., Kemp, T. J., Neal, G. T. and Stone, T. J. *J. Chem. Soc.* **A 1970** 2227.
9. Pople, J. A., Beveridge, D. L. and Dobosh, P. A. *J. Chem. Phys.* **47** (1967) 2026.

10. Pople, J. A., Beveridge, D. L. and Dobosh, P. A. *J. Am. Chem. Soc.* **90** (1968) 4201.
11. Pople, J. A. and Beveridge, D. L. *Approximate Molecular Orbital Theory*, McGraw, New York 1970.
12. Dewar, M. J. S. *The Molecular Orbital Theory of Organic Chemistry*, McGraw, New York 1969.
13. Flurry, R. L., Jr. *Molecular Orbital Theories of Bonding in Organic Molecules*, Marcel Dekker, New York 1968.
14. Klopman, G. and O'Leary, B. *Fortschr. Chem. Forsch.* **15** (1970) 445.
15. Kutzelnigg, W., Del Re, G. and Berthier, G. *Fortschr. Chem. Forsch.* **22** (1971) 1.
16. Sinanoglu, O. and Wiberg, K. B. *Sigma Molecular Orbital Theory*, Yale University Press, New Haven 1970.
17. Pople, J. A., Beveridge, D. L. and Ostlund, N. S. *Int. J. Quant. Chem.* **1** (1967) S 293.
18. Hoffmann, R. *J. Chem. Phys.* **39** (1963) 1397.
19. Wolfsberg, M. and Helmholz, L. *J. Chem. Phys.* **20** (1952) 837.
20. Drago, R. S. and Petersen, H., Jr. *J. Am. Chem. Soc.* **89** (1967) 3978.
21. Mulliken, R. S., Rieke, C. A., Orloff, D. and Orloff, H. *J. Chem. Phys.* **17** (1949) 1248.
22. Pople, J. A., Santry, D. P. and Segal, G. A. *J. Chem. Phys.* **43** (1965) 3129.
23. Pople, J. A. and Segal, G. A. *J. Chem. Phys.* **43** (1965) S 136.
24. Pople, J. A. and Segal, G. A. *J. Chem. Phys.* **44** (1966) 3289.
25. Santry, D. P. and Segal, G. A. *J. Chem. Phys.* **47** (1967) 158.
26. Dreuth, W. and Wiebenga, E. H. *Rec. Trav. Chim.* **73** (1954) 218.
27. Robertson, J. M. and Woodward, I. *Proc. Roy. Soc. (London) Ser. A* **162** (1937) 586.
28. Lennard-Jones, J. E. *Proc. Roy. Soc. (London) Ser. A* **158** (1937) 280.
29. *Quantum Chemistry Program Exchange*, Chemistry Department, Indiana University, Bloomington, Indiana.
30. QCPE Program No. 30.
31. The annihilation routine was taken from the FORTRAN 63 version of the CNINDO program, QCPE program No. 142.
32. Suzuki, H. *Electronic Absorption Spectra and Geometry of Organic Molecules*, Academic, New York 1967, pp. 296–299.
33. Herzberg, G. *The Spectra and Structures of Simple Free Radicals*, Cornell University Press, Ithaca 1971.
34. Jaffé, H. H. and Orchin, M. *Theory and Applications of Ultraviolet Spectroscopy*, Wiley, New York 1965, Chapter 7, and references cited therein.
35. Wiberg, K. B. *Tetrahedron* **24** (1968) 1083.
36. Ehrenson, S. and Seltzer, S. *Theor. Chim. Acta* **20** (1970) 17.
37. Mulliken, R. S. *J. Chem. Phys.* **23** (1955) 1833.
38. Kaufman, J. J. *Int. J. Quant. Chem.* **4** (1971) 205.
39. Veillard, A. *Chem. Phys. Letters* **3** (1969) 128.
40. Veillard, A. *Chem. Phys. Letters* **4** (1969) 51.
41. Radom, L. and Pople, J. A. *J. Am. Chem. Soc.* **92** (1970) 4786.
42. Beveridge, D. L. and Dobosh, P. A. *J. Chem. Phys.* **48** (1968) 5532.
43. Ray, N. K. and Sharma, K. K. *Theor. Chim. Acta* **22** (1971) 403.
44. Finch, A., Gates, P. N., Radcliffe, K., Dickson, F. and Bentley, F. F. *Chemical Applications of Far Infrared Spectroscopy*, Academic, New York 1970, pp. 81–97.
45. Allen, H. C. and Cross, P. C. *Molecular Vib-Rotors*, Wiley, New York 1963, pp. 77–84, and references cited therein.
46. Beringhelli, T., Gavezzotti, A. and Simonetta, M. *J. Mol. Struct.* **12** (1972) 333.

Received May 5, 1972.

ACTA CHEMICA SCANDINAVICA 27 (1973) 57–62

Single-Crystal Raman Spectra of Mercurous Bromide, Mercurous Iodide, and Mercuric Iodide

ASTRI ROGSTAD*

Department of Chemistry, University of Southampton, Southampton, England

The Raman active factor-group fundamentals of Hg_2Br_2, Hg_2I_2, and HgI_2 are unambiguously assigned from the single-crystal observations.

The mercurous halides have been extensively investigated by means of both Raman and infrared spectroscopy,[1–9] and several complete vibrational assignments of the fundamentals have been proposed during the last 10 years.

In their study on Hg_2Cl_2 Mathieu *et al.*[1,2] reported a vibrational assignment of the internal modes. Goldstein,[3] however, observed a previously unreported absorption at *ca.* 260 cm^{-1} in a reinvestigation of the far infrared spectrum and a new assignment of the fundamentals was proposed. In more recent works by Durig *et al.*[4] and by Conney *et al.*[5] the vibrational spectra of mercurous bromide and iodide were analysed. The above-mentioned studies were based on a molecular model and insufficient attention was given to the external crystal modes. A single-crystal Raman study on Hg_2Cl_2 by Beattie and Gilson[6] resulted in a revised assignment of the external and internal Raman active modes, and recently Ōsaka[7] measured the infrared absorption spectra of Hg_2X_2 (X = Cl, Br, I) in detail and made an analysis in terms of crystalline solids. In the present work we have obtained single-crystal Raman polarisation data for Hg_2Br_2 and Hg_2I_2 and have attributed the Raman active fundamentals to their respective symmetry classes.

The two mercuric halides $HgCl_2$ and $HgBr_2$ have a linear configuration in all phases, and the crystal lattice is distinctly molecular.[13,14] Mercuric iodide, however, has two modifications.[15,16] The red form that is stable at room temperature undergoes a reversible phase transition to a yellow form at 126°C. The bonding in yellow HgI_2 is apparently molecular, while the red form consists of layers of HgI_4 tetrahedra in the crystal.

A number of vibrational spectroscopic studies have been carried out already on these compounds. The ν_1 and ν_3 stretching frequencies are well

* Present address: Department of Chemistry, University of Oslo, Oslo 3, Norway.

established from gas and melt spectra.[14,17–21] By comparing the ν_1 frequency in passing from vapour [17,18] to melt [19,20] it appears that the frequency shift decreases along the series $HgCl_2$, $HgBr_2$, HgI_2. The bonding forces within HgI_2 are considered as being much less sensitive to environmental effects. The doubly degenerate bending frequency ν_2 is determined from infrared gas [22] and matrix isolation studies.[21] A considerable discrepancy from electronic spectral data [23] was found.

The solid state spectra of $HgCl_2$,[2,24] $HgBr_2$,[24] and HgI_2 [2,25,28] are interpreted on the basis of the symmetry properties of the crystals. Poulet and Mathieu [2] applied vibrational spectroscopy on an $HgCl_2$ single-crystal. While the present work was in progress Adams *et al.*[25] reported the single-crystal Raman spectrum of red mercuric iodide. However, the two translatory modes were unobserved. A crystal of good optical quality was grown and all the Raman active modes appeared. Raman spectra of $HgBr_2$ single-crystal were also obtained. However, the crystals were very imperfect and no meaningful interpretation in terms of crystal structure was possible.

EXPERIMENTAL

The single-crystals of Hg_2Br_2 and Hg_2I_2 were prepared by slow sublimation in a nitrogen atmosphere. The HgI_2 crystal was grown from the vapour phase in an evacuated glass-tube. The spectra were recorded with a Spex 1401 monochromator with a Spectra Physics He/Ne 6328 Å laser excitation of about 50 mW power. Since the mercurous iodide crystal quickly decomposed in the 50 mW laser beam, this crystal was excited with a He/Ne laser of about 0.5 mW power. No decomposition was observed under these conditions.

RESULTS AND DISCUSSION

Previous infrared and Raman data [4,7] of the halides are consistent with the assumption that Hg_2X_2 (X = Cl, Br, I)[11] belong to the same space group as mercurous fluoride,[12] D_{4h}^{17}. The Hg_2X_2 molecules have a fourfold axis in common with the lattice and have consequently D_{4h} site symmetry. Factor group analysis gives four Raman active modes of symmetry type $2a_{1g}+2e_g$, which should arise only in (xx), (yy), (zz), and (xz), (yz) observations, respectively.

The single-crystal observations are summarized in Tables 1 and 2 for Hg_2Br_2 and Hg_2I_2, respectively.

The data enable an unambiguous assignment of the Raman active bands. Our results confirm the interpretation reported by Ōsaka.[7] The weak Raman bands observed at 92 and 65 cm^{-1} for the bromide and iodide, respectively, by Durig *et al.*[4] should clearly be associated with the non-totally symmetric Hg – Hg – X bending mode ν_4, whereas the strong band located at the lowest frequency in the spectra is attributed to the external mode of rotatory origin. Apparent from the (zz), (zx), (yx), and (yz) measurements of the iodide the broad band at *ca.* 68 cm^{-1} consists of two partly overlapping bands, one associated with the ν_4 vibration, while the other might arise from a second-order process.

Table 1. Oriented single-crystal Raman polarisation data [a] for Hg_2Br_2.

ν (cm^{-1})	$I_{x(zz)y}$	$I_{x(zx)y}$	$I_{x(yx)y}$	$I_{x(yz)y}$	$I_{x(zy+zx)z}$ [b]	$I_{x(yy+yx)z}$ [b]	Assignment
221	1.17	0.33	0.06	0.08	0.18	0.07	$\nu_1(a_{1g})$
135	17.04	4.72	0.70	1.25	2.78	0.45	$\nu_2(a_{1g})$
92	0.13	0.42	0.08	0.19	0.18	0.08	$\nu_4(e_g)$
~72							$2\nu_{L_1}=72$
36	2.63	6.95	1.30	3.39	3.19	0.85	$\nu_{L_1}(e_g)$

[a] Peak areas measured in arbitrary units.
[b] Recorded in a different intensity scale.

Table 2. Oriented single-crystal Raman polarisation data [a] for Hg_2I_2.

ν (cm^{-1})	$I_{x(zz)y}$	$I_{x(zx)y}$	$I_{x(yx)y}$	$I_{x(yz)y}$	$I_{z(yz+xz)y}$ [b]	$I_{z(xx+yx)y}$ [b]	Assignment
~223							$2\nu_2=226$ or $\nu_L+\nu_1=224$
193	0.86	0.29	0.04	0.07	0.01	0.03	$\nu_1(a_{1g})$
113	46.2	14.6	1.40	3.44	0.86	0.80	$\nu_2(a_{1g})$
~73	0.06	0.14	0.12	0.29	0.09	0.05	$\nu_4(e_g)$
~64							$2\nu_{L_1}=62$
31	3.94	5.14	2.12	6.70	5.20	1.10	$\nu_{L_1}(e_g)$

[a] Peak areas measured in arbitrary units.
[b] Recorded in a different intensity scale.

Table 3. Oriented single-crystal Raman polarisation data [a] for red HgI_2.

ν (cm^{-1})	$I_{z(y'x')y'}$	$I_{x(y'z)y'}$	$I_{z(x'x')y'}$	$I_{z(x'z)y'}$	$I_{x'(y'z)y'}$ [b]	$I_{x'(y'x')y'}$ [b]	$I_{x'(zz)y'}$ [b]	$I_{x'(zx')y'}$ [b]	Assignment
143.5	10.5	0.5	0	0	0.5	16	0	0	b_{1g}
114.0	24	20	336	68	68	68	219	70	a_{1g}
54.5	2.0	0	0.5	0	0.5	4.8	1.5	0.5	b_{1g}
49.0	0	2.5	0.8	3.0	4.5	0.5	1.5	5.5	e_g
28.5	204	730	114	584	402	201	228	476	e_g
17.5	200	1788	212	1112	745	276	430	88.5	e_g

[a] Peak heights measured in arbitrary units.
[b] Recorded in a different intensity scale.

The crystal structure [16] of red HgI_2 is built up from layers of HgI_4 tetrahedra. It has space symmetry $P4_2/nmc$ (D_{4h}^{15}) ($Z=2$) with I-atoms on sites of symmetry C_{2v}, and Hg-atoms on sites of D_{2d} symmetry. The factor group analysis leads to the irreducible representation.

$$\Gamma_{\text{cryst}} = a_{1g} + a_{2u} + 2b_{1g} + b_{2u} + 3e_g + 2e_u$$

The Raman tensor components are as follows: a_{1g}, $R_{xx}+R_{yy}$, R_{zz}; b_{1g}, $R_{xx}-R_{yy}$; e_g, R_{xz}. To distinguish between a_{1g} and b_{1g} modes we recorded the polarisation measurements at 45° to x- and y-axis. By use of the experimental set of axes (x', y', z) the a_{1g}, b_{1g}, and e_g modes should arise only in ($x'x'$), ($y'y'$), (zz); ($x'y'$); ($x'z$) and ($y'z$) measurements, respectively. The results of the oriented single-crystal measurements are shown in Table 3. The data led to unambiguous assignments of the 6 Raman active modes. Weak bands were previously observed [5,26] in the region 30 – 70 cm^{-1} and attributed to combinations because of lack of single crystal observations. Two of these bands showed apparent orientation effects and are assigned to the two translational modes, ($b_{1g}+e_g$), unobserved by Adams *et al.*[25] In addition two weak bands were observed at 38 and 64 cm^{-1}, which may be due to second-order effects.

Acknowledgements. A *British Council Fellowship* is gratefully acknowledged. I thank professor I. R. Beattie for stimulating discussions and for all facilities placed at my disposal at the University of Southampton during the year 1970 – 71. I am also indebted to Dr. T. R. Gilson for many valuable discussions and help in obtaining the single-crystal Raman spectra.

REFERENCES

1. Hadni, A., Henry, C., Mathieu, J. P. and Polet, H. *Compt. Rend.* **252** (1961) 1585.
2. Poulet, H. and Mathieu, J. P. *J. Chim. Phys.* **60** (1963) 442.
3. Goldstein, M. *Spectrochim. Acta* **22** (1966) 1389.
4. Durig, J. R., Lau, K. K., Nagarajan, G., Walker, M. and Bragin, J. *J. Chem. Phys.* **50** (1969) 2130.
5. Conney, R. P. J., Hall, J. R. and Hooper, M. A. *Aust. J. Chem.* **21** (1968) 2145.
6. Beattie, I. R. and Gilson, T. R. *Proc. Roy. Soc.* **A 307** (1968) 407.
7. Ōsaka, T. *J. Chem. Phys.* **54** (1971) 863.
8. Krishnamurti, P. *Indian J. Phys.* **5** (1930) 113.
9. Gager, H. M., Lewis, J. and Ware, M. J. *Chem. Commun.* **1966** 616.
10. Stammreich, H. and Sans, T. T. *J. Mol. Struct.* **1** (1967 – 68) 55.
11. Havighurst, R. J. *J. Am. Chem. Soc.* **48** (1926) 2113.
12. Ebert, F. and Woitinek, H. *Z. anorg. allgem. Chem.* **210** (1932) 269.
13. Wells, A. F. *Structural Inorganic Chemistry*, Oxford Univ. Press, London 1950.
14. Klemperer, W. and Lindeman, L. *J. Chem. Phys.* **25** (1956) 397.
15. Wyckoff, R. W. G. *Crystal Structures*, Vol. 1, Interscience, New York 1963.
16. Jeffrey, G. A. and Vlasse, M. *Inorg. Chem.* **6** (1967) 396.
17. Braune, H. and Engelbrecht, G. *Z. physik. Chem. (Leipzig)* **B 19** (1932) 303.
18. Beattie, I. R. and Horder, J. R. *J. Chem. Soc.* **A 1970** 2433.
19. Janz, G. J. and James, D. W. *J. Chem. Phys.* **38** (1963) 902.
20. Clarke, J. H. R. and Solomons, C. *J. Chem. Phys.* **48** (1968) 528.
21. Loewenschuss, A., Ron, A. and Schnepp, O. *J. Chem. Phys.* **50** (1969) 2502.
22. Malt'sev, A. A., Selivanov, G. K., Yampolsky, V. I. and Zavalishin, N. I. *Nature Phys. Sci.* **231** (1971) 157.
23. Bell, S. *J. Mol. Spectry.* **23** (1967) 98, and references therein.
24. Mikawa, Y., Jakobsen, R. J. and Brasch, J. W. *J. Chem. Phys.* **45** (1966) 4528, and references therein.

25. Adams, D. M. and Hooper, M. A. *Aust. J. Chem.* **24** (1971) 885.
26. Melveger, A. J., Khanna, R. K., Guscott, B. R. and Lippincott, E. R. *Inorg. Chem.* **7** (1968) 1630.
27. Marqueton, Y., Abba, F., Decamps, E.-A. and Nusimovicic, M.-A. *Compt. Rend.* **B 272** (1971) 1014.
28. Krauzman, N., Krauzman, M. and Poulet, H. *Compt. Rend.* **B 273** (1971) 301.

Received June 9, 1972.

ACTA CHEMICA SCANDINAVICA 27 (1973) 63–70

Infrared Absorption Spectra of Solid Metal Sulfites

BIRGIT NYBERG[a] and RAGNAR LARSSON[b]

[a] *Division of Inorganic Chemistry 2 and* [b] *Division of Inorganic Chemistry 1, Chemical Center, Box 740, S-220 07 Lund 7, Sweden*

The IR spectra of metal sulfites with known structures have been examined. From the spectra it is possible to detect a predominant coordination of the sulfite ion. A general correlation between the average sulfur-oxygen distance and the average stretching frequency in compounds with the SO group has turned out to be valid also for the metal sulfites.

From IR studies Newman and Powell [1] have discussed structural features of some metal sulfites. The fact that the crystal structure of NH_4CuSO_3[2] does not fit into their assumptions initiated this investigation on the IR spectra of compounds with known structures.

EXPECTED VIBRATIONS OF THE SULFITE GROUP IN THE CRYSTALLINE STATE AND CALCULATION OF ν_{SO}

The free sulfite ion has C_{3v} symmetry, giving rise to four infrared and Raman active fundamental modes: ν_1 (symmetric stretch), ν_2 (symmetric bend), ν_3 (asymmetric stretch), and ν_4 (asymmetric bend). The two asymmetric modes are both doubly degenerate.

In the present paper the assignment of vibrational modes for the observed frequencies will follow the work of Evans and Bernstein.[3] From the polarisation effects in the Raman spectrum as well as from the relation between intensities of the Raman and IR spectra these authors concluded that the asymmetric mode γ_3 in sodium sulfite solution occurred at lower frequency than the γ_1 mode.

In the crystalline state there are several factors which affect the sulfite frequencies. The most dominant factors are the effect on the site symmetry of the ion in the structure and the effect of coordination of the ion.

The symmetry of the sulfite ion in a crystal must be C_{3v} or one of the subgroups C_3, C_s, or C_1. Under the site symmetry C_3, C_s, and C_1 the degenerate modes γ_3 and γ_4 split and six vibrations would be expected.

Assuming that the 3*d* orbitals of sulfur participate in bonding, the S – O bond in the sulfite group has at least partial double bond character. Two of the resonance structures of the sulfite ion can be written:

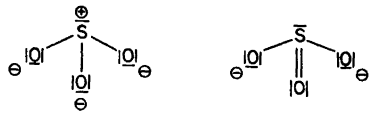

The attachment of oxygen to a positive atom (metal or hydrogen) should favour the former structure, and conversely the attachment of sulfur to a positive atom would support the latter one.

Consequently a decrease in the stretching frequency following the decrease of the bond order would be expected in a compound with oxygen coordination. Furthermore the symmetry of the group is changed to C_s and the number of infrared active fundamentals is increased to six because of the removal of the degeneracy from γ_3 and γ_4.

If the sulfite group is coordinated to metal through sulfur the C_{3v} symmetry is essentially preserved, but the stretching modes should shift to higher frequency compared with the free ion because of the higher bond order.

Lehman [4] has derived an average rule for stretching frequencies of related molecules. The stretching frequency of an isolated AB group is approximately equal to the weighted average (more exactly the root-mean square value) of the symmetric and asymmetric stretching frequencies of a similar AB_x group provided that there is no mixing of the vibrations of the AB_x group and the rest of the molecule.

$$\nu_{AB} = (1/x)\,(\nu_{\mathrm{sym}} + (x-1)\,\nu_{\mathrm{asym}})_{AB_x}$$

This average rule has been applied to the SO_3 group for the metal sulfites under investigation.

EXPERIMENTAL

The IR samples were made by the KBr-pellet technique. The samples showed no reactions with KBr. The spectra were recorded with a Perkin-Elmer 180 spectrometer. X-Ray powder photograms of the compounds were recorded with a Hägg-Guinier camera with Cu$K\alpha_1$ radiation. The compounds were identified with the aid of the known cell-dimensions.

The compound $Na_2[Hg(SO_3)_2]$ was kindly delivered by Professor Bengt Aurivillius. References to earlier IR investigations are listed in Table 2.

RESULTS AND DISCUSSION

For all the examined metal sulfites except sodium sulfite, a schematic drawing of the environment of S and O in the sulfite group is given in Fig. 1. In sodium sulfite the sodium oxygen bonds are weak and there is no hydrogen bonding; its spectrum can therefore be used as a standard for the comparison of the other sulfite spectra. For Na_2SO_3 in the solid state Evans and Bernstein [3] have found the following values of the frequncies in cm^{-1}:

ν_1	ν_3	ν_2	ν_4
1010(m)	961(st)	633(st)	496(st)

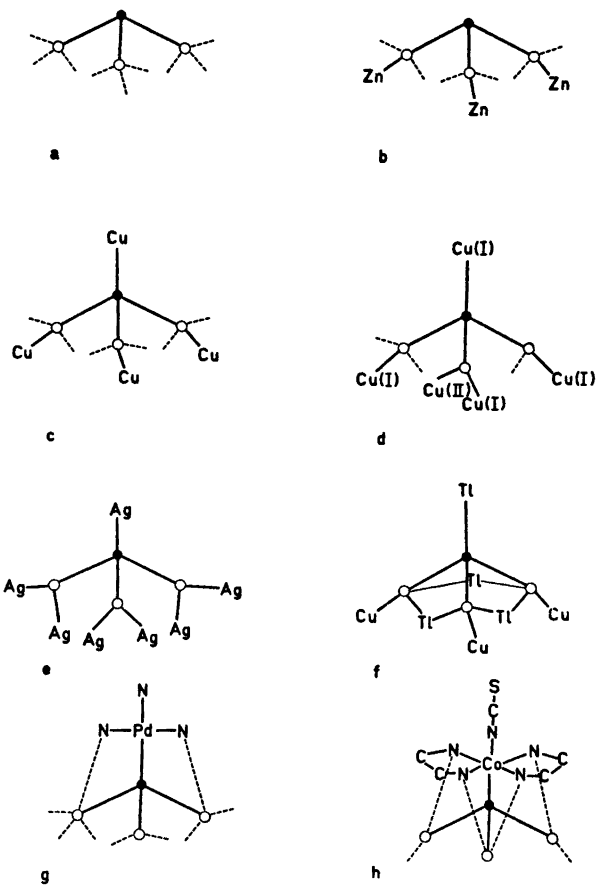

Fig. 1. Schematic drawings showing the environment of the sulfur and the oxygen atoms in the sulfite group. (a) $(NH_4)_2SO_3.H_2O$ and $NiSO_3.6H_2O$; (b) $ZnSO_3.2\frac{1}{2}H_2O$; (c) NH_4CuSO_3; (d) $Cu^{II}[Cu^{I}SO_3]_2.2H_2O$; (e) Ag_2SO_3; (f) $Tl_2[Cu(SO_3)_2]$; (g) $PdSO_3(NH_3)_3$; (h) $Co(en)_2SO_3.NCS.2H_2O$. Open large circles denote oxygen atoms linked to the sulfur atom (small filled circles). Dashed lines indicate possible hydrogen bonds.

Table 1. Vibrational frequencies of the free sulfite ion in cm^{-1}.

	γ_1	γ_2	γ_3	γ_4
Solution (Raman)	967(st)	620(w)	933(m)	469(m)
Solution (IR)	1002(m)	632(w)	954(st)	–

Table 2. Observed frequencies in the region 1100—450 cm^{-1}.

Compound	Observed frequencies (cm^{-1})															
Na_2SO_3 [1,3]			975st								630m				496st	
$(NH_4)_2SO_3.H_2O$				968st	935st					662w	650w	613st	515w		498m	480m
$ZnSO_3.2\frac{1}{2}H_2O$ [5]			984vw		925st					681st		619w	532m		501vw	
$NiSO_3.6H_2O$					960st	870vw				660m					494m	
NH_4CuSO_3 [1,6]				965st						660m	638w	615vw		505w		483m
$Cu^{II}[Cu^{I}SO_3]_2.2H_2O$		1025m	1008m	977m	912m	860w			684w	636m		564m	519w	499w	480w	
$Tl_2[Cu(SO_3)_2]$			981st		894st	860st				670vw		590w		510w	498m	453m
Ag_2SO_3		1035st		970st		908st				665w	632st			500m	494m	478vw
$PdSO_3(NH_3)_3$ [1]	1095st	1077st	989st			840vw	818w			660w	643st		522w	510m	481st	
$Co(en)_2SO_3NCS.2H_2O$ [7,8]	1095st	1089st	1050st	977st	965st	877w	805m	780st	705w	660w	625st	586vw	545vw	510vw	500m	475m

st = strong, m = medium, w = weak, vw = very weak.
The superscript numbers are references to earlier IR investigations.

Table 3. Crystal data, empirical assignments of the sulfite group frequencies and the calculated ν_{SO} for the compounds in this investigation.

Compound	Space group	Sulfite ion site symmetry	r_{S-O} (Å)[a]	ν_1 and ν_3 (cm^{-1})	ν_2 (cm^{-1})	ν_4 (cm^{-1})	ν_{SO}(cm^{-1})	No. in Fig. 2
Na_2SO_3	$P\bar{3}$	C_{3v}	1.504	975	630	496	975	21
$(NH_4)_2SO_3.H_2O$	$P2_1/c$	C_1	1.524	968,935	613	498, 480	946	22
$ZnSO_3.2\frac{1}{2}H_2O$	$P\bar{1}$	C_1	1.54	984,925	681	532, 501	945	23
$NiSO_3.6H_2O$	$R3$	C_3	1.536	960	660	494	960	24
NH_4CuSO_3	$R3m$	C_{3v}	1.514	965	660	483	965	25
$Cu^{II}[Cu^{I}SO_3]_2.2H_2O$	$P2_1/n$	C_1	1.510	1025,977,912[b]	636	499, 480	971	26
$Tl_2[Cu(SO_3)_2]$	$P\bar{1}$	C_1	1.538	981,894,860	670	498, 453	912	27
Ag_2SO_3	$P2_1/c$	C_1	1.516	1035,970,908	632	500, 494	971	28
$PdSO_3(NH_3)_3$	$P2_1/c$	C_1	1.494	1095,1077,989	643	510, 481	1054	29
$Co(en)_2SO_3.NCS.2H_2O$	$P2_1/c$	C_1	1.485	1095,1089,1050	625	500, 475	1078	30

[a] All values without corrections for vibrational motion. [b] Assignments are based on a comparison with Ag_2SO_3.

Here the vibrational modes have frequencies similar to those of the free ion (*cf.* Table 1). In the present investigation ν_1 and ν_3 were not resolved. However, in the investigation of Evans and Bernstein, the average stretching frequency is ν_{SO} 977 cm^{-1} and in this study 975 cm^{-1} (*cf.* Table 3).

From the intensities of the vibrational modes it is difficult to make reliable assignments of the individual stretching frequencies. In Table 3 the symmetric (ν_1) and the asymmetric (ν_3) stretching frequencies are therefore listed together. Fortunately, only in the cases of $(NH_4)_2SO_3.H_2O$[9] and $ZnSO_3.2\frac{1}{2}H_2O$[10] is an assignment necessary for the calculation of ν_{SO}. For these compounds without sulfur coordination the symmetric stretching mode was assumed to have the highest frequency as in sodium sulfite.

The structure of the compounds can be divided into three groups after the sulfite ion coordination.

I. Compounds without sulfur coordination.

II. Compounds with both sulfur and oxygen coordination.

III. Compounds with dominant sulfur coordination.

To group I belong Na_2SO_3,[11] $(NH_4)_2SO_3.H_2O$,[9] $NiSO_3.6H_2O$[12] and $ZnSO_3.2\frac{1}{2}H_2O$.[10] The spectra for these compounds show resemblances with the sodium sulfite spectra, but there is at least one stretching mode at lower frequency in ammonium sulfite and in zinc sulfite. The expected splitting of ν_3 and ν_4 due to the lowering of the symmetry can only be seen in ν_4 for $(NH_4)_2SO_3.H_2O$ and $ZnSO_3.2\frac{1}{2}H_2O$.

The spectrum of NH_4CuSO_3[2] is almost identical with the sodium sulfite spectrum, but the structure has strong copper-sulfur bonds and in addition copper-oxygen bonds and hydrogen bonding. The effect is a sulfite group like the sulfite group in sodium sulfite.

Besides ammonium copper(I) sulfite Ag_2SO_3,[13] $Cu^{II}[Cu^{I}SO_3]_2.H_2O$[14] and $Tl_2[Cu(SO_3)_2]$[15] belong to the second group with both metal-sulfur bonds and metal-oxygen bonds. The spectra of these compounds show stretching frequencies of high intensity above and below 975 cm^{-1}. Analogous shifts have been observed for thiosulfate complexes.[16]

Table 4. r_{SO}, the asymmetric (ν_{as}) and the symmetric (ν_s) stretching frequencies and the calculated ν_{SO} for some metal thiosulfates and sulfates.

Compound	r_{SO}[a] (Å)	ν_{as} (cm^{-1})	ν_s (cm^{-1})	ν_{SO} (cm^{-1})	No. in Fig. 2
$SnSO_4$	1.487 [19]	1183,1064,1031	975 [20]	1063	31
$MgSO_4.7H_2O$	1.471 [21]	1136,1087	981, [20]	1079	32
$FeSO_4.7H_2O$	1.474 [22]	1143,1087	976 [20]	1080	33
$Na_{4n}[Cu(NH_3)_4]_n[Cu(S_2O_3)_{2n}]_n$	1.470 [23]	1177,1137	1012 [16]	1109	34
$Mg\ S_2O_3.6H_2O$	1.468 [24]	1120	998 [16]	1079	35
$BaS_2O_3.H_2O$	1.509 [25]	1120,1105,1075	1007,988 [16]	1066	36
$Na_2S_2O_3$	1.47 [26]	1160,1130	1002	1097	37
$NaAgS_2O_3.H_2O$	1.46 [27]	1150	1018	1106	38

[a] All values without corrections for vibrational motion.

Finally the compounds $PdSO_3(NH_3)_3$ [17] and $Co(en)_2SO_3.NCS.2H_2O$ [8] (en = ethylenediamine) have metal-sulfur bonds and the crystals are composed of discrete molecules held together by hydrogen bonds. The spectra have stretching frequencies above 975 cm^{-1}. The spectra are all consistent with the site symmetry of the anion.

Gillespie and Robinson [18] have applied Lehman's average rule to the SO_x group in various compounds. From the value of ν_{SO} they calculated a force

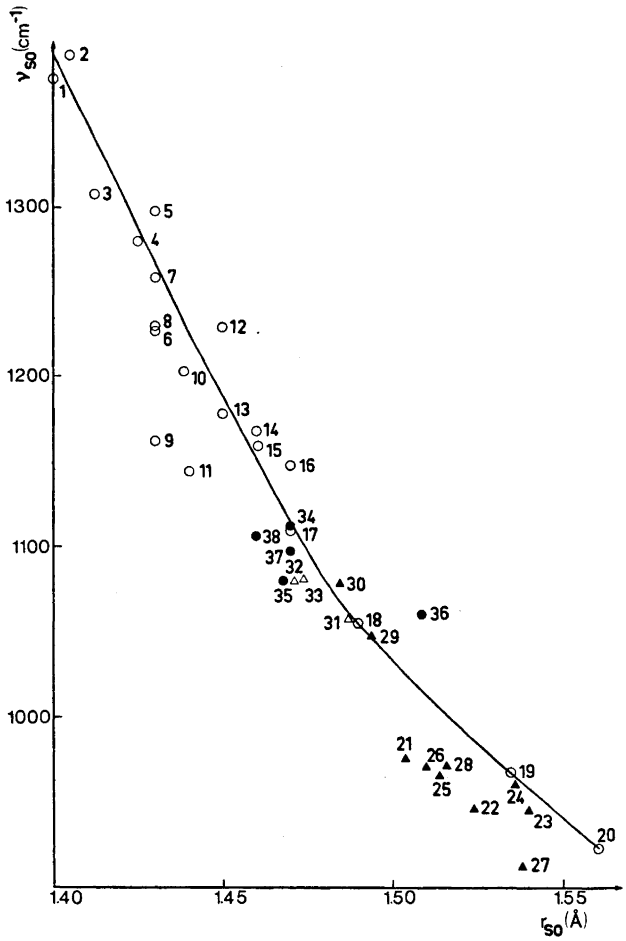

Fig. 2. Plots of ν_{SO} *versus* r_{SO}. The curve is from Gillespie and Robinson and is based on the values (○) 1 – 20. (1) S_3O_9; (2) SO_2F_2; (3) SOF_2; (4) $SO_2(OH)_2$; (5) SO_2Cl_2; (6) $(CH_3)_2SO_2$; (7) SO_2; (8) SO_3; (9) $S_2O_6^{2-}$; (10) $S_2O^{2-}_7$; (11) $NH_2SO_3^-$; (12) $SOCl_2$; (13) $NH(SO_3)^{2-}$; (14) $EtO.SO_3^-$; (15) $CH_2(SO_3)_2^{2-}$; (16) $HO.SO_3^-$; (17) $(CH_3)_2SO$; (18) SO_4^{2-}; (19) $SO_2(OH)_2$; (20) $HO.SO_3^-$, (ν_{SO} calculated for S – O(H)). The following numbers (21 – 38) are explained in Tables 3 and 4. ▲, sulfites. △, sulfates. ●, thiosulfates.

constant of the SO bond and found a linear relationship between log k_{SO} and log r_{SO}, where k_{SO} is the stretching force constant and r_{SO} is the bond length.

Table 3 shows ν_{SO} and r_{SO} for the compounds described in this investigation. Table 4 presents ν_{SO} and r_{SO} for some thiosulfates and sulfates with known structures. In Fig. 2 the values are plotted together with the calculated curve from Gillespie and Robinson.[18] The metal sulfites fit to the curve fairly well, but there is a tendency finding a shorter sulfur-oxygen distance than would be expected from the vibrational frequency using this curve. Nevertheless an average S – O bond length compared to the bond length in sodium sulfite can be suggested from the value of ν_{SO}. However, in the assignments of ν_1 and ν_3 and in the calculation of ν_{SO} and k_{SO} there are several sources of error, so that a proposed bond length from the infrared absorption spectrum has no great accuracy. Robinson [28] has suggested a theoretical value of 1.54 Å for the free sulfite ion in solution on the basis of a proposed relationship between ν_{SO} and bond order. A discussion of bond length in various metal sulfites is given by Kierkegaard et *al.*[29]

The conclusion of this study is that in most metal sulfites the coordination of the sulfite ion can be derived from the infrared absorption spectra. A stretching mode of high intensity above 975 cm^{-1} is an indication of coordination through sulfur. Conversely a mode with high intensity below 960 cm^{-1} is a sign of coordination through oxygen. A spectrum with stretching frequencies around 975 – 960 cm^{-1} can only indicate that the compound is either ionic, *e.g.* sodium sulfite, or has the sulfite group engaged in covalent bonding with bonds to sulfur as well as to oxygen (*cf.* NH_4CuSO_3).

A spectrum of a compound, $Na_2[Hg(SO_3)_2]$, with unknown structure, was also recorded. The observed frequencies in cm^{-1} are 1125(st), 1020(vw), 975(st), 640(st), 520(vw), 510(vw), and 495(st). From the criteria above we propose a structure with a Hg – S bond.

Acknowledgements. The authors are very grateful to Professor Bengt Aurivillius, who intiated this work. We are also indebted to Mrs. Karin Trankéll for running the spectra. Financial support from the *Swedish Natural Science Research Council* is gratefully acknowledged.

REFERENCES

1. Newman, G. and Powell, D. B. *Spectrochim. Acta* **19** (1963) 213.
2. Nyberg, B. and Kierkegaard, P. *Acta Chem. Scand.* **22** (1968) 581.
3. Evans, J. C. and Bernstein, H. J. *Can. J. Chem.* **33** (1955) 1270.
4. Lehman, W. J. *J. Mol. Spectry.* **7** (1961) 261.
5. Pannitier, G., Djega-Mariadassou, G. and Bregeault, J. M. *Bull. Soc. Chim. France* **1964** 1749.
6. Dasent, W. E. and Morrison, D. *J. Inorg. Nucl. Chem.* **24** (1962) 1014.
7. Baldwin, M. E. *J. Chem. Soc.* **1961** 3123.
8. Baggio, S. and Becka, L. N. *Acta Cryst.* **B 25** (1969) 946.
9. Batelle, L. F. and Trueblood, K. N. *Acta Cryst.* **19** (1965) 531.
10. Nyberg, B. *Acta Chem. Scand.* **26** (1972) 857.
11. Larsson, L. O. and Kierkegaard, P. *Acta Chem. Scand.* **23** (1969) 2253.
12. Baggio, S. and Becka, L. N. *Acta Cryst.* **B 25** (1969) 1150.
13. Larsson, L. O. *Acta Chem. Scand.* **23** (1969) 2261.
14. Kierkegaard, P. and Nyberg, B. *Acta Chem. Scand.* **19** (1965) 2189.
15. Hjertén, I. and Nyberg, B. *Unpublished work.*

16. Freedman, A. N. and Straughan, B. P. *Spectrochim. Acta* **A 27** (1971) 1455.
17. Spinnler, M. A. and Becka, L. N. *J. Chem. Soc.* **1967** 1194.
18. Gillespie, R. J. and Robinson, E. A. *Can. J. Chem.* **41** (1963) 2074.
19. Donaldson, J. D. and Puxley, D. C. *Acta Cryst.* **B 28** (1972) 864.
20. Hezel, A. and Ross, S. D. *Spectrochim. Acta* **22** (1966) 1949.
21. Baur, W. H. *Acta Cryst.* **17** (1964) 1361.
22. Baur, W. H. *Acta Cryst.* **17** (1964) 1167.
23. Ferrari, A., Braibanti, A. and Tiripicchio, A. *Acta Cryst.* **21** (1966) 605.
24. Baggio, S., Amzel, L. M. and Becka, L. N. *Acta Cryst.* **B 25** (1969) 2650.
25. Nardelli, M. and Fava, G. *Acta Cryst.* **15** (1962) 477.
26. Sandor, E. and Csordás, L. *Acta Cryst.* **14** (1961) 237.
27. Cavalca, A., Mangia, C., Palmieri, C. and Pelizzi, G. *Inorg. Chim. Acta* **4** (1970) 294.
28. Robinson, E. A. *Can. J. Chem.* **42** (1964) 1494.
29. Kierkegaard, P., Larsson, L. O. and Nyberg, B. *Acta Chem. Scand.* **26** (1972) 218.

Received June 19, 1972.

ACTA CHEMICA SCANDINAVICA 27 (1973) 71–78

MO-Calculations on Nitroxide Radicals

LASSE EFSKIND

Norsk Hydro's Institute for Cancer Research, the Norwegian Radium Hospital, Oslo 3, Norway

Molecular orbital (MO) calculations by the INDO method have been performed for some free nitroxide radicals which might be of importance in cancer therapy.

The calculated order of red/ox potentials was found to be consistent with the order experimentally found.

The spin densities were calculated to be greater on O (70 %) than on N, in contrast to the results deduced from paramagnetic resonance measurements. The INDO calculations also indicate a considerable change in the ratio between total spin density and $2s_N$ spin density on bending the NO-bond. This leads to a possible explanation of the inconsistency between these calculations and the conclusion drawn from paramagnetic resonance measurements.

Nitroxide radicals constitute a group of remarkably stable free radicals. They are hence used for spin labelling of a wide range of compounds.[1] Experiments have demonstrated that this class of free radicals may act as radiosensitizing agents,[2–8] possibly through binding to radiation induced DNA radicals.

The ability of an organic nitroxide radical to react with various compounds will to a large extent depend on the red/ox potentials of the radicals, steric hindrance, and the charge and spin distribution. These properties are also important for the explanation of the reactions between nitroxide radicals and DNA or RNA radicals, as well as for their spin labelling ability.

The present paper gives the results of a semi-empirical MO-calculation for some free nitroxide radicals.

To our knowledge no semi-empirical MO-calculation on nitroxide radicals has previously been published.

METHOD OF CALCULATION

The calculations were performed according to the INDO (Intermediate neglect of differential overlap) method introduced by Pople *et al.*[9–13] All parameter values were chosen according to the original scheme. INDO and the closely related CNDO/2 method include explicitly all valence electrons. INDO gives a better description than does

CNDO/2, of spin densities in open shell systems. This is because it retains all one-center two-electron integrals. The calculations were performed on a CDC 3300 computer.

As to the INDO energy difference ΔE used for comparison with experimental red/ox potentials, ΔE has been used as an approximate value for ΔH, assuming small volume changes. It is further assumed that the ratio between the calculated energy differences can approximately be compared to the ratio between the experimentally found red/ox potentials.

RESULTS AND DISCUSSION

The compounds studied were (Fig. 1): Nitric oxide (I), dihydro nitric oxide II (non-existent), di-*t*-butyl nitroxide (III), 2,2,5,5-tetramethyl-3-carboxamidopyrroline-1-oxyl (IV), 2,2,6,6-tetramethyl-4-piperidone-1-oxyl(V),

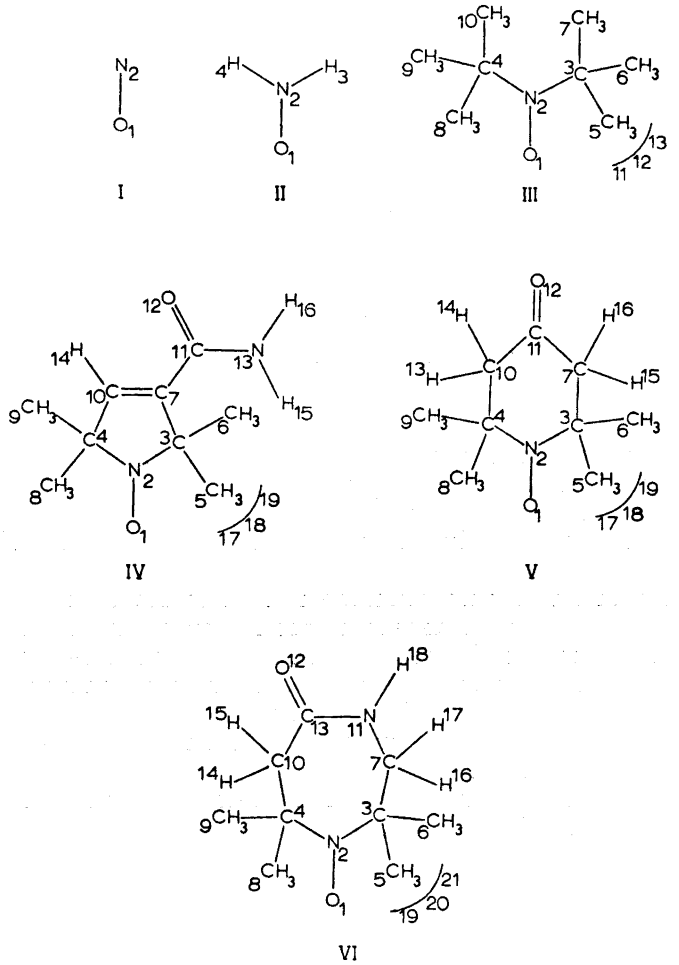

Fig. 1. Numbering of the atoms in the molecules investigated. The numbering refers to the calculations and is not in agreement with standard chemical numbering.

Table 1. Interatomic angles used.

Angles/Molecule (see Fig. 1)	II	III	IV	V	VI
1–2–3	120.0	112.0	123.4	117.0	112.0
1–2–4	120.0	112.0	123.4	117.0	112.0
2–3–5		112.0	112.0	110.0	112.0
2–3–7		112.0	100.0	112.0	112.0
3–5–19		110.0	110.0	110.0	110.0
3–7–11			140.0	112.0	112.0
3–7–10			113.4	–	–
3–7–16			–	110.0	110.0
4–10–7			113.4	–	–
4–10–13			–	110.0	112.0
4–10–14			126.6	110.0	110.0
5–3–6			112.0	110.0	112.0
7–11–10			–	117.0	–
7–11–12			122.0	121.5	–
7–11–13			113.0	–	126.7
10–7–11			100.6	–	–
10–13–11			–	–	120.2
10–13–12			–	–	120.0
11–13–12			–	–	120.0
11–13–16			107.0	–	–

usually called TAN, and 2,2,7,7-tetramethyl-1,4-diazacycloheptan-5-on-1-oxyl (VI).

The angles and distances used are given in Table 1 and 2. Experimental data are not available for all the nitroxide radicals. Standard values are there fore used, constructed from comparison with similar molecules.[15] The radicals

Table 2. Interatomic distances used.

Distances (Å) (see Fig. 1)	I	II	III	IV	V	VI
1–2	1.1500	1.2300	1.2800	1.2800	1.2800	1.2800
2–3		1.0000	1.5120	1.5120	1.5120	1.5120
2–4		1.0000	1.5120	1.5120	1.5120	1.5120
3–5			1.5360	1.5360	1.5360	1.5360
3–7			1.5360	1.5000	1.5360	1.5360
4–8			1.5360	1.5360	1.5360	1.5360
5–19			1.1050	1.1050	1.1050	1.1050
7–10				1.3332	–	–
7–11				1.4800	1.5000	1.4500
7–16				–	1.1050	1.1050
10–14				1.0860	1.1050	1.1050
10–13				–	1.1050	1.5000
11–12				1.2200	1.2200	–
11–13				1.3600	–	1.3213
11–17				–	–	0.8500
12–13				–	–	1.2200
13–16				1.0200	–	–

Table 3. Some quantities comparing the two different configurations of TAN (V), see text.

E_{tot} (a.u.)	$E_{TANH} - E_{TAN}$ (a.u.)	μ_{tot} (D)	Spin N	Spin O	Charge N	Charge O	a_N (gauss)
Standard geometry							
−120.587480	−0.745675	0.607	0.2961	0.7230	0.0015	−0.2359	6.08
Experimental							
−120.597374	−0.750373	1.780	0.2564	0.7408	−0.0035	−0.2285	8.91
Difference							
0.009894	0.004698	1.173	0.0397	−0.0178	0.0050	−0.0074	−2.83

are also assumed to be co-planar in the NO-part, *i.e.* the atoms 1, 2, 3, and 4 (see Fig. 1) constitute one plane (called the NO-plane).

To get a measure of the error introduced by not having an experimentally or energetically optimized configuration, one alternative calculation is performed for TAN (V). In this calculation preliminary results obtained by electron diffraction are used.[19] Not only distances and angles are here different, but also the configuration; a "twisted boat" form (and not co-planar in the NO-part), whereas all the standard configurations are in "chair" form (and co-planar).

From Table 3 it is seen that the dipole moment and the total energy are significantly different in the two cases, whereas predicted charge, spin density, and the red/ox energy differences are more constant. Therefore, a discussion of these last mentioned quantities should be justified without further knowledge of the molecular geometries.

(a) *Relative red/ox potentials.* Consider the reaction

$$NR_1 + NR_2H \rightleftharpoons NR_1H + NR_2$$

where NR is an organic nitroxyl radical and NRH is the corresponding hydroxylamine.

The calculated relative red/ox potentials of the nitroxide radicals are given in Table 6, together with experimental values recently obtained (Tomas, Efskind and Nakken; in press).

The sequence of the red/ox potentials is the same for experimental as for calculated values, VI being the most readily reducible. It is further seen from Table 6 that the relative position of V between the two others is about the same for calculated and for experimental potentials.

It is not relevant to draw more quantitative conclusions (see discussion in Method of calculation).

(b) *Spin and charge distribution.* Nitric oxide (I) was found to have a total spin density of about 70 % on N and 30 % on O. All the other nitroxide radicals have the reverse distribution, *i.e.* 30 % on N and 70 % on O (see Table 5, atoms 1 and 2). Nearly all the spin density originates from $2p_\pi$ atomic orbitals.

In contrast, Stone *et al.*[16] and McConnell *et al.*[1] deduced from paramagnetic resonance measurements that 70 − 90 % of the spin of the nitroxide radicals

Table 4. Atomic charges using standard geometry given in Tables 1 and 2.

Atom	I	II	III	IV	V	VI
1	−0.0407	−0.2085	−0.2533	−0.2399	−0.2359	−0.2440
2	+0.0407	+0.0401	+0.0025	+0.0033	+0.0015	−0.0041
3		+0.0842	+0.1365	+0.1483	+0.1311	+0.1118
4		+0.0842	+0.1365	+0.1228	+0.1311	+0.1118
5			+0.0548	+0.0393	+0.0415	+0.0425
7			+0.0548	−0.1105	−0.0201	+0.1612
8			+0.0548	+0.0475	+0.0415	+0.0425
10			+0.0548	+0.0367	−0.0201	+0.1612
11			−0.01−02	+0.4418	+0.3013	−0.2298
12				−0.4177	−0.3086	−0.4200
13				−0.3073	+0.0022	+0.4270
14				+0.0190	+0.0022	−0.0005
16				+0.1513	−0.0022	−0.0370
17				−0.01−2	−0.01−2	+0.1368
18						−0.01−2
$-E_{tot}$ (a.u.)	28.557414	30.209310	97.682814	130.815825	120.587480	132.449727
μ (debyes)	0.167	2.616	2.641	2.174	0.607	4.363

is located in the $2p_\pi$-atomic orbital on N. This will be further discussed in the next section.

Since the radicals are not planar, there is strictly no σ-π-separation of MO's. However, for the purpose of comparison with the above mentioned results of Stone and McConnell, it is of interest to note that the highest filled MO in the INDO calculations has a nearly 100 % π-character in the NO part.

Table 5. Spin densities (total).

Atom	I	II	III	IV	V	VI
1	+0.3038	+0.7252	+0.7272	+0.7097	+0.7230	+0.7353
2	+0.6962	+0.3197	+0.2919	+0.3118	+0.2961	+0.2845
3		−0.0179	−0.0142	−0.0237	−0.0216	−0.0202
4		−0.0179	−0.0142	−0.0234	−0.0216	−0.0201
5			+0.0021	+0.0093	+0.0102	+0.0091
7			+0.0049	−0.0001	+0.0027	+0.0027
8			+0.0021	+0.0091	+0.0102	+0.0089
10			+0.0049	+0.0002	+0.0027	+0.0028
11			−0.002−10	−0.0008	−0.0025	−0.0005
12				−0.0005	+0.0024	+0.0002
13				−0.0001	−0.0008	−0.0005
14				−0.0001	−0.0008	−0.0007
16				−0.0007	−0.0008	−0.0007
17				−0.0005−12	−0.0003−13	0.0000
18						−0.0001−12

Table 6. The red/ox energy ΔE of the reaction:

$$\text{Radical} + \text{H} \rightleftharpoons \text{Radical} \cdot \text{H}$$

using the INDO hydrogen atom value (0.638730 a.u.). Experimental potentials are taken from Tomas, Efskind and Nakken (in press).

Molecule	IV	V	VI
ΔE (INDO) in a.u.	−0.103128	−0.106945	−0.111013
Experimental red/ox potentials (pH = 7); in V	0.004	0.137	0.252

About 70 % of the spin density contribution from this MO is located on N. Hence, the greater total spin on O is caused by contributions from the lower spin-polarized MO's.

According to our calculations there is hardly any smear-out effect of the spin outside the NO-group, the nearest carbon neighbours (atoms 3 and 4, Table 5) having a small negative spin density.

Nitric oxide (I) has a fairly small charge polarization (Table 4), whereas the oxygen in the NO-part of the nitroxyl radicals has a net charge of −0.20 to −0.25 (atom 1, Table 4). the nitrogen retaining its slightly positive charge unchanged (atom 2, Table 4). The charge on oxygen is mostly compensated by positive charges on the nearest carbon neighbours (atoms 3 and 4, Table 4).

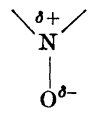

(I)

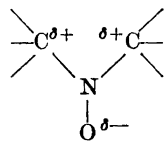

(II)

Stone *et al.*[16] postulate a polar bond structure (I). The present calculation modified this rather to be II leaving the nitrogen neutral.

The carbonyl group in IV, V, and VI is heavily polarized, the oxygen (atom 12, Table 4) being significantly more negative than in the NO-part.

This may be one of the explanations why these radicals react more readily in the carboxyl part than in the free spin part.

(c) *Hyperfine coupling constants for nitrogen.* Stone [16] and McConnell's [1] conclusion of a high spin density on nitrogen is based on observed hyperfine

Table 7. $2s_N$ spin densities and the corresponding hyperfine coupling constants (a_N). The configurations are coplanar in the NO part. Experimental values for a_N are about 15.5 gauss for the nitroxide radicals and about 19.5 for the NH_3^+ ion. The configuration of NH_3^+ ion is taken planar with an NH bond length of 1.02 Å and an H–N–H angle of 120°.

	$NH_3(+)$	II	III	IV	V	VI
$\varrho_{N(2s)}$	0.0537	0.0157	0.0164	0.0176	0.0160	0.0160
$\varrho_{N(2p\pi)}$	1.00	0.29	0.27	0.28	0.27	0.26
$\varrho_{N(total)}$	1.13	0.32	0.29	0.31	0.30	0.28
a_N(gauss)	20.4	5.9	6.2	6.7	6.1	6.1

coupling constants, assuming a proportionality between the large π-electron spin density and the small σ-electron spin density on nitrogen in planar π-electron radicals.

From Table 7 it is seen that the INDO results on radicals, which are coplanar in the NO part, are consistent with this proportionality rule. The NH_3^+ ion is included for comparison as it is a planar system with unity π-electron spin density on nitrogen. In going from NH_3^+ to the nitroxide radicals, the spin density on nitrogen is reduced (according to INDO) to about 0.3. According to the proportionality rule, this gives a value for a_N of about $20 \times 0.3 = 6$ gauss, in good agreement with the calculated values (Table 7).

The coupling constants in Table 7 are calculated according to Pople *et al.*[14] using the $2s_N$ spin density.

Some experimental evidence indicates, however, that the nitroxide radicals are not coplanar in the NO part, giving an angle of 14 – 21° [17–19] between the NO-bond and the plane defined by C(3)–N(2)–C(4). One would expect a larger $2s_N$ spin density for these non-planar radicals where the $\sigma - \pi$ separation is further removed. This is found to hold true by calculating the radicals using an out of plane angle of 20° for the NO-bond (Table 8). The coupling constants

Table 8. Some properties of the bent nitroxide radicals. The NO bond is 20° out of the plane defined by atoms 2, 3, and 4 (see Fig. 1). The bond length of NO is 1.26 Å (1.23 Å for II).

	II	III	IV	V	VI
$\varrho_{total}(N)$	0.2909	0.2917	0.2981	0.2886	0.2819
$\varrho_{total}(O)$	0.7238	0.7173	0.7069	0.7175	0.7275
$\varrho_{2s}(N)$	0.0252	0.0207	0.0233	0.0215	0.0201
a_N(gauss)	9.5	7.9	8.8	8.2	7.6
$-E_{total}$(a.u.)	30.209744	97.684538	130.819521	120.590555	132.451818

* The equilibrium configuration of H_2NO has a total INDO energy of −30.229851 a.u., an NO bond length of 1.23 Å and an NH bond length of 1.07 Å. The angle H–N–H is 113° and the out of the plane angle for the NO bond is 35°. The other radicals would not give such a high out of the plane angle because of the hindrance of the methyl groups.

rise to about 8 gauss as compared to the coplanar values of about 6 gauss. None of the configurations are, however, equilibrium configurations, where one should expect a still higher value. Indeed the coupling constant for the calculated equilibrium configuration of H_2NO^* is 16.3 gauss, as compared to the experimental value of about 15.5 gauss for the nitroxide radicals.

The improved coupling constants for the bent configurations are consistent with the idea that the nitroxide radicals are not, as assumed by Stone and McConnell, coplanar in the NO-part. But even for the bent configurations as calculated by INDO, the total spin density on nitrogen remains as low as 0.3 (Table 8), *i.e.* about the same as for the coplanar configurations (Table 5).

The conclusion of Stone and McConnell, that the value for a_N indicates a large spin density (0.7 – 0.9) on nitrogen, might therefore be erroneous. According to the INDO calculations there is a considerable change in the proportionality between total spin density and $2s_N$ spin density if the NO-bond is bent. It is the bent structure that accounts for the large $2s_N$ spin density and hence the large a_N value, and not a high total spin density. The reservation must be made that this conclusion is completely dependent on the ability of the INDO method to predict spin densities.[13] It may turn out that the small basis set in INDO does not give an adequate description of the spin distribution in this case. *Ab initio* calculations with large basis sets would probably be of importance in deciding this question.

Acknowledgement. The author is indebted to H. Jensen, K. F. Nakken, O. Gropen, P. N. Skancke and A. Pihl for valuable discussions. It is especially a pleasure to thank H. Jensen and K. F. Nakken for help and interest in this work.

REFERENCES

1. Hamilton, C. L. and McConnell, H. M. In Rich and Davidsen, Eds., *Structural Chemistry and Molecular Biology*, Freeman, San Francisco 1968, pp. 115 – 149.
2. Rozantzev, E. G. and Neiman, M. B. *Tetrahedron* **20** (1964) 131.
3. Nofre, C., Cier, A. and Pullman, B., Eds., *Electronic Aspects of Biochemistry*, Academic, New York 1964, p. 397.
4. Emmerson, P. T. and Howard-Flanders, P. *Nature* **204** (1964) 1005.
5. Emmerson, P. T. *Radiation Res.* **30** (1967) 841.
6. Emmerson, P. T. and Willson, R. L. *J. Phys. Chem.* **72** (1968) 3669.
7. Willson, R. L. and Emmerson, P. T. *Radiation Protection and Sensitization*, Proceedings of the Second International Symposium on Radiosensitizing and Radioprotective Drugs, Taylor and Francis, May 1969, pp. 73 – 79.
8. Nakken, K. F., Sikkeland, T. and Brustad, T. *FEBS Letters* **8** (1970) 33.
9. Pople, J. A., Santry, D. P. and Segal, G.A. *J. Chem. Phys.* **43** (1965) 3129.
10. Pople, J. A. and Segal, G. A. *J. Chem. Phys.* **43** (1965) S136.
11. Pople, J. A. and Segal, G. A. *J. Chem. Phys.* **44** (1966) 3289.
12. Santry, D. P. and Segal, G. A. *J. Chem. Phys.* **47** (1967) 158.
13. Pople, J. A., Beveridge, D. L. and Dobosh, P. A. *J. Chem. Phys.* **47** (1967) 2026.
14. Pople, J. A., Beveridge, D. L. and Dobosh, P. A. *J. Am. Chem. Soc.* **90** (1968) 4201.
15. *Tables of Interatomic Distances and Configurations in Molecules and Ions*, The Chemical Society, London 1958.
16. Stone, T. J., Buckman, D., Nordio, P. L. and McConnell, H. M. *Proc. Natl. Acad. Sci. U.S.* **54** (1965) 1010.
17. Lajzerowicz-Bonneteau, P. J. *Acta Cryst.* **B 24** (1968) 196.
18. Boliner, L. J. *Acta Cryst.* **B 26** (1970) 1198.
19. Fredriksen, P. *Thesis*, University of Oslo, Oslo 1972.

Received June 12, 1972.

ACTA CHEMICA SCANDINAVICA 27 (1973) 79–84

The Crystal Structure of $Fe_{.28}Ni_{.28}Te_{.44}$

GUNVOR ÅKESSON and ERLING RØST

Kjemisk institutt, Universitetet i Oslo, Oslo 3, Norway

The crystal structure of $Fe_{.28}Ni_{.28}Te_{.44}$, quenched from 650°C, has been determined by X-ray single crystal methods. The structure is rhombohedral with lattice constants $a = 7.157$ Å and $\alpha = 32.22°$ (in hexagonal setting $a = 3.972$ Å and $c = 20.34$ Å). The space group is $R3m$, and all atoms are situated on three-fold axis in position $3a$ (hexagonal setting). The z parameters are 0 and 0.483 for tellurium, and 0.236, 0.870, and 0.609 for metal atoms. Reduced occupancy is assumed for the metal atoms.

The structure is a layer structure. Hexagonal tellurium layers are stacked in the sequence ABCABC. Every second space between the tellurium layers is open, whereas metal atoms occupy both the octahedral and the tetrahedral positions in the other spaces.

A phase with approximate composition $Ni_{1.5}Fe_{1.5}Te_2$ and rhombohedral crystal structure has been reported by Stevels.[1] The lattice constants are given as $a = 7.213$ Å, $\alpha = 30°50'$ or, in hexagonal setting, $a = 3.981$ Å, $c = 20.510$ Å. The metal/tellurium ratio in this phase can vary within certain limits. A crystal structure was suggested for this phase, based on the space group $R\bar{3}m$. Referring to hexagonal indexing of the structure, the tellurium atoms are situated in position $6(c)$ with $z = 0.254$ and the metal atoms distributed over the position $3(a)$, and $6(c)$ with $z = 0.129$. The structure determination was based on powder diffraction data, and the agreement between observed and calculated intensities is reported to be "not very satisfactory for a number of weak reflections". Stevels [1] also found that a certain change in the structure takes place at 140°C. For the high temperature phase he suggested the positions: Me_I in $3(a)$, Me_{II} in $18(h)$ with $x = 0.064$, $z = 0.131$ and with Te in position $6(c)$ with $z = 0.249$. Also this structure was referred to space group $R\bar{3}m$.

The existence of the phase with rhombohedral structure has been confirmed by Røst and Åkesson.[2] At 600°C the phase extends within the following composition ranges: 17 – 32 at. % Fe, 24 – 41 at. % Ni, and 41 – 45 at. % Te. The lattice constants of the phase increase with decreasing tellurium content, possibly due to varying population of partly occupied metal sites in the structure.

EXPERIMENTAL

The procedure for preparing the samples and the methods for X-ray examination and density measurement of powdered samples are described elsewhere.[2] Single crystals were obtained at about 650°C by heating powdered samples of $Fe_{.28}Ni_{.28}Te_{.44}$ in evacuated and sealed silica tubes in an oven with a certain temperature gradient. Small amounts of iodine were added as transport agent. The crystals were quenched into water. Single crystal photographs were obtained in an integrating Weissenberg camera of 53.3 mm diameter using Mo$K\alpha$-radiation, and multiple film technique was used with Sn-foils between the films. The intensities were estimated photometrically, the weak ones also visually. The crystal used for single crystal photographs was 0.05 mm long by 0.02 mm. Corrections for X-ray absorption were made assuming the crystal to be cylindrical.

The structure determination was carried out by three-dimensional Patterson and Fourier syntheses and by a full-matrix least squares programme.[3] In the calculations no attempt was made to distinguish between Fe and Ni, and the mean values of the atomic form factors were used for the metal positions. Unobserved reflections were omitted in the final calculations.

CRYSTAL DATA

$Fe_{.28}Ni_{.28}Te_{.44}$
Hexagonal setting: $a = 3.972 \pm 0.001$ Å, $c = 20.34 \pm 0.01$ Å, unit cell volume = 277.9 Å^3.
Rhombohedral setting: $a = 7.157$ Å, $\alpha = 32.22°$.
Observed density: 7.13 g cm^{-3}.
Unit cell content: 13.52 atoms (hexagonal cell), *i.e.* 5.94 (6) Te atoms and 7.58 metal atoms (Fe+Ni).
Reflections present: $-h+k+l=3n$
Possible space groups: $R3$, $R\bar{3}$, $R32$, $R3m$, $R\bar{3}m$.

RESULTS AND DISCUSSION

The stoichiometric composition of the crystal used for the X-ray investigation is not necessarily equal to that of the main sample. The variation of the tellurium/metal ratio of the phase is, however, rather limited, and a small variation of the Fe/Ni ratio would not seriously affect the X-ray results.

Table 1. Positional parameters (z), temperature factors assuming isotropy (B) and anisotropy (b_{ij}), and reliability factors (R). Estimated deviations are given in parenthesis. For the metal positions 84.2 % occupancy is assumed.

		Te1	Te2	Me3	Me4	Me5	R %
	z	0	0.4830 (3)	0.236 (3)	0.870 (1)	0.609 (2)	
sotropic							8.9
	B	0.56 (6)	2.0 (2)	5.6 (8)	1.8 (4)	1.7 (3)	
	z	0	0.4825 (2)	0.231 (1)	0.868 (1)	0.607 (1)	
ınisotropic	$b_{11}=b_{22}=b_{12}$	0.012 (2)	0.030 (3)	0.12 (1)	0.037 (8)	0.041 (7)	6.5
	b_{33}	0.0004 (1)	0.0021 (3)	0.0013 (6)	0.0009 (6)	0.0003 (3)	

Table 2. Observed and calculated structure factors assuming isotropic temperature factors. The columns contain k, l, $|F_o|$, and $|F_c|$, respectively.

$h=0$				3	18	75	65	1	6	149	142	5	8	66	65	3	14	45	45	3	15	54	53
k	l			3	21	69	67	1	9	80	77					3	17	57	50	4	2	48	53
0	6	162	167	4	2	99	104	1	12	86	80	$h=2$				3	23	60	58	4	5	22	26
0	9	106	104	4	5	52	53	1	15	139	137	k	l			4	4	58	53	4	8	56	54
0	12	98	99	4	8	116	117	1	18	82	86	0	2	170	177	4	7	29	40				
0	15	162	162	4	11	20	25	1	21	86	86	0	5	121	123	4	10	60	57	$h=4$			
0	18	94	101	4	14	48	48	1	24	28	34	0	8	240	247	4	13	49	44	k	l		
0	21	96	100	4	17	59	55	1	27	38	43	0	14	65	68	4	16	55	43	0	4	69	76
0	27	47	49	4	23	53	63	2	2	149	152	0	17	85	89	5	0	61	59	0	7	67	61
1	2	210	215	5	4	61	57	2	5	99	96	0	23	98	98	5	6	46	45	0	10	95	84
1	5	198	178	5	10	64	62	2	8	211	197	1	4	119	114					0	13	56	66
1	8	353	324	5	13	55	48	2	14	60	62	1	7	90	91	$h=3$				0	16	56	64
1	14	66	77	5	16	55	47	2	17	78	77	1	10	124	122	k	l			0	19	45	35
1	17	99	106	5	22	56	27	2	23	88	87	1	13	97	103	1	2	121	117	0	25	54	47
1	23	117	113	6	0	56	65	2	29	30	38	1	16	99	99	1	5	55	62	2	2	75	69
2	4	146	141	6	6	40	48	3	4	83	86	1	19	49	41	1	8	134	136	2	8	72	72
2	7	101	107					3	7	64	69	1	25	66	61	1	11	26	24	2	14	29	37
2	10	138	141	$h=1$				3	10	88	95	1	31	56	52	1	14	51	52	2	17	30	39
2	13	129	126	k	l			3	13	79	76	2	0	183	179	1	17	59	61	3	4	37	43
2	16	127	119	0	4	221	182	3	16	77	73	2	6	100	99	1	23	67	70	3	7	30	32
2	19	47	43	0	7	129	130	3	19	30	37	2	9	47	45	2	4	67	69	3	10	49	44
2	25	63	68	0	10	169	166	3	25	44	51	2	12	57	56	2	7	60	55				
2	31	58	58	0	13	158	158	4	0	109	113	2	15	91	90	2	10	83	76	$h=5$			
3	0	219	216	0	16	148	148	4	6	72	73	2	18	57	58	2	13	54	59	k	l		
3	3	28	30	0	19	50	48	4	9	30	34	2	21	66	60	2	16	59	57	0	2	81	76
3	6	113	111	0	25	64	76	4	12	42	44	2	24	27	28	2	19	37	33	0	8	70	80
3	9	53	52	0	31	65	64	4	15	61	65	2	27	29	34	2	25	42	43	0	14	36	39
3	12	65	62	1	0	426	349	4	21	43	46	3	2	101	93	3	0	92	89	1	4	45	49
3	15	97	103	1	3	66	70	5	2	64	63	3	5	49	46	3	6	63	61	1	7	44	37
												3	8	106	102	3	12	34	39	1	10	61	52

Refinements of the structure assuming the space group $R\bar{3}m$ were tried, but no acceptable accordance was obtained between observed and calculated intensities. Acceptable results were, however, obtained assuming the space group $R3m$ which represents a lower symmetry. Successive structure refinements led to the atomic positions referred to in Table 1. All the atoms are placed on three-fold axis in the three-fold positions 3(*a*): $0,0,z,+(0,0,0;\ \frac{1}{3},\ \frac{2}{3},\ \frac{2}{3};\ \frac{2}{3},\ \frac{1}{3},\ \frac{1}{3})$. This means that reduced occupancy must be assumed for the metal positions. Refinements assuming isotropic temperature factors and equal occupancy (84.2 %) of all three metal positions led to a reliability factor * of 0.089. Least squares refinements assuming anisotropic temperature factors gave a reliability factor of 0.065. The differences in atomic position compared to those referring to isotropic temperature factors are, however, insignificant. Observed and calculated structure factors given in Table 2 refer to the calculations assuming isotropic temperature factors. The atomic positions are denoted Te1, 2, and Me3, 4, 5. The temperature factor of the metal atom Me3 is rather great compared with those of the other atoms. This may indicate that the position Me3 is less populated than the other metal positions. Refinements were therefore carried out under this assumption, but a significantly better solution of the structure was not obtained.

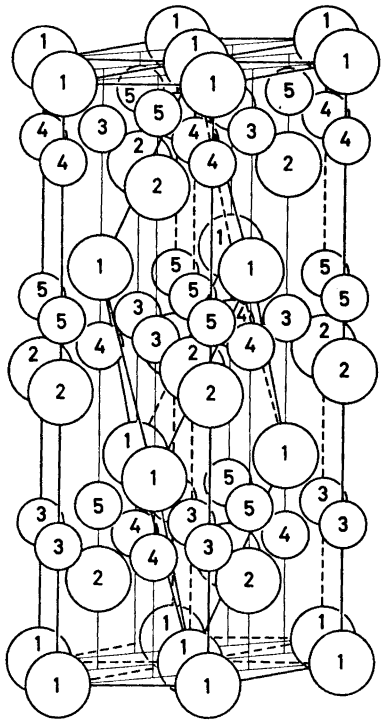

Fig. 1. The crystal structure of $Fe_{.28}Ni_{.28}Te_{.44}$. Large circles represent tellurium atoms and small ones are metal atoms. All atoms are situated on the 3-fold axes which are indicated by lines parallel to the *c*-axis. Both the hexagonal and the rhombohedral cells are indicated.

* Reliability factor $R=\sum||F_o|-|F_c||/\sum|F_o|$

A perspective view of the structure is given in Fig. 1. The greater circles represent tellurium, and the smaller ones represent metal atoms. All the atoms are placed on three-fold axis which are indicated in the figure by lines parallel to the *c*-axis. The rhombohedral unit cell is also indicated. This structure is a marked layer structure with the tellurium atoms arranged in hexagonal layers perpendicular to the trigonal axis. The tellurium atoms are stacked in the sequence ABCABC, which is the same sequence as in a close-packed cubic arrangement. The interplanar distances are, however, alternating between 3.05 and 3.72 Å. The metal atoms occupy both the octahedral and tetrahedral positions in every second intermediate space between the tellurium layers, whereas every second interval is quite empty. According to the stoichiometric composition of the sample the average occupancy of the metal positions is 82.4 %.

Table 3. Interatomic distances for $Fe_{.28}Ni_{.28}Te_{.44}$. Number of equal distances are given in parentheses.

Te1 – Te1	3.97	(6)	Me3 – Te1	3.10	(3)
– Te2	3.80	(3)	– Te2	3.82	(3)
– Me3	3.10	(3)	– Me4	2.37	(3)
– Me4	2.69	(1)	– Me5	2.45	(3)
– Me5	2.60	(3)			
			Me4 – Te1	2.69	(1)
Te2 – Te1	3.80	(3)	– Te2	2.53	(3)
– Te2	3.97	(6)	– Me3	2.37	(3)
– Me3	2.83	(3)	– Me5	2.72	(3)
– Me4	2.53	(3)			
– Me5	2.53	(1)	Me5 – Te1	2.60	(3)
			– Te2	2.53	(1)
			– Me3	2.45	(3)
			– Me4	2.72	(3)

Interatomic distances in the structure are given in Table 3. In the plane perpendicular to the trigonal axis each Te atom is coordinated to six other Te atoms at a distance of 3.97 Å (the *a*-axis). At one side of this plane the Te atoms are coordinated to three Te atoms at 3.80 Å, and at the other side to four metal atoms at distances shorter than 2.70 Å.

The metal atoms are rather closely packed. The position Me3 is octahedrally coordinated by Te atoms whereas a tetrahedral coordination was found for Me4 and Me5. In addition, the metal atoms are surrounded by six metal atoms with bond distances varying from 2.37 Å to 2.72 Å. The distance 2.37 Å which was found between Me3 and Me4 is surprisingly short. This may indicate that position Me3 has a lower degree of occupancy than the other metal positions. The relatively high temperature factor found for Me3 (see Table 2) supports this assumption. However, calculations assuming varying degree of occupancy for the metal positions have been carried out, but a definite solution of this problem was not found.

The present structure is a layer structure with bonds of van der Waals type between the layers. The length of these Te – Te distances are 3.80 Å. Such a structure with weak interplane bonds is in good accordance with the behav-

iour of the sample which is graphite-like when crushed in a mortar. Layer structure formation occurs frequently among ditellurides of transition elements, especially those with $Cd(OH)_2$-type structure and related structures. The Te–Te distances between the layers vary from about 3.4 to 4.0 Å. Also more metal-rich tellurides with layer structures have been described. In CuTe (orthorhombic) the Te–Te distances between layers are 3.98 Å,[4] and in $FeTe_{0.9}$(tetragonal) the corresponding distances are 3.82 Å.[5] Both these phases are reported to form plate-like crystals. In the phase $FeTe_{0.9}$ nickel can be partly substituted for iron.[1,2] This leads to an increase of the metal to tellurium ratio, and the cleavage tendency of the phase disappears successively. When about half of the iron is replaced with nickel, however, the structure changes to the rhombohedral layer structure described in the present investigation.

Acknowledgement. The authors want to thank Dr. Chr. Rømming for valuable discussions concerning the X-ray methods.

REFERENCES

1. Stevels, A. L. N. *Thesis*, Groningen 1969; *Philips Res. Reports Suppl. No. 9* (1969).
2. Røst, E. and Åkesson, G. *Acta Chem. Scand.* **26** (1972) 3662.
3. Dahl, T., Gram, F., Groth, P., Klewe, B. and Rømming, C. *Acta Chem. Scand.* **24** (1970) 2232.
4. Anderko, K. and Shubert, K. *Z. Metallk.* **45** (1954) 371.
5. Grønvold, F., Haraldsen, H. and Vihovde, J. *Acta Chem. Scand.* **8** (1954) 1929.

Received June 8, 1972.

ACTA CHEMICA SCANDINAVICA 27 (1973) 85–95

A Neutron Diffraction Refinement of the Crystal Structure of Telluric Acid, $Te(OH)_6$(mon)

OLIVER LINDQVIST[a] and MOGENS S. LEHMANN[b]

[a] *Department of Inorganic Chemistry, Chalmers University of Technology and the University of Göteborg, P.O. Box, S-402 20 Göteborg 5, Sweden, and* [b] *Department of Inorganic Chemistry, University of Århus, DK-8000 Århus, Denmark*

A neutron diffraction analysis of the monoclinic modification of telluric acid has been carried out in order to obtain the hydrogen positions with high precision and accuracy, thus complementing the earlier X-ray work. Full matrix least squares refinement based on 591 observed reflections gave a final R value of 0.024.

The Te–O and O–H bonds have been determined with a precision of 0.001 and 0.003 Å, respectively. The O–H bonds range from 0.977 to 0.990 Å, with a mean value of 0.985 Å. The mean O–H···O angle in the hydrogen bonds is 173.6°.

The scattering length of tellurium was refined to the value $b_{Te} = 5.80 \pm 0.05$ F, to be compared with 5.6 F given by The Neutron Diffraction Commission.

The crystal structure of the monoclinic modification of telluric acid, $Te(OH)_6$(mon), has recently been determined by Lindqvist [1] using X-ray diffraction methods. Owing to the fact that the tellurium atoms did not contribute to more than one quarter of the possible reflections, five of the six independent hydrogen positions in the unit cell could be located from electron density calculations. However, the precision of the hydrogen parameters was not high, and in order to obtain more information concerning the hydrogen bonding network in $Te(OH)_6$, it was decided to carry out a neutron diffraction study.

EXPERIMENTAL

Crystal growth. The crystal used for the neutron diffraction work was obtained from a saturated solution sealed in a cell at room temperature to prevent too rapid evaporation. The temperature of the solution was gradually lowered by a total amount of 5°C over a period of 20 h in order to obtain supersaturation. After a week at the lower temperature, a single crystal of suitable size for neutron diffraction measurements had formed. The crystal, which showed some well-developed faces, while others were more irregular in shape (*cf.* Fig. 1), had a maximum linear dimension of 7 mm.

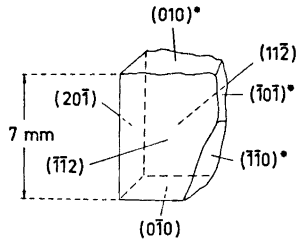

Fig. 1. The morphology of the crystal used for data collection.

Data collection. The intensity measurements were carried out on a Hilger-Ferranti automatic four circle diffractometer located at the Danish Atomic Energy Research Establishment, Risø. The moving crystal and fixed detector technique (ω scan) was used in the measurements with a neutron wave length of 1.025 Å. The monochromatic neutron beam was uniform within ± 3 % for the area ranging over the crystal.

The crystal was mounted with the b axis along the ϕ axis of the instrument. In measuring the reflections the crystal was rotated $\pm 3°$ alternately about the diffraction vector from the A-setting position, thereby at least avoiding simultaneous reflection from $0k0$ and $h0l$, when hkl was recorded.

A total of 1440 reflections with $k \geq 0$ and $\sin\theta/\lambda < 0.55$ Å^{-1} were measured in increasing order of $\sin\theta/\lambda$. A standard reflection, $\bar{1}12$, was measured at intervals of 15. Step scan measurements were used, and counts for each step were recorded. The total scan interval was 4°, and the size of the step was 0.08°. The space group is $P2_1/n$, and the space group extinctions $0k0$ for k odd, and $h0l$ for $h+l$ odd were included in the reflections measured.

Data reduction. The unit cell determined by the X-ray work,[1] *i.e.* $a = 6.495$, $b = 9.320$, $c = 11.393$ Å and $\beta = 133.88°$, was used.

The reflection profiles were reduced to structure factors using a method which determines the points of division between the peak and the background so that $\sigma(I)/I$ is minimized,[2] where I is the integrated intensity and $\sigma(I)$ its standard deviation based on counting statistics.

The reflections were corrected for drift in the experimental conditions as reflected by the variation of the intensity of the standard reflection. This variation was of the order of 2 % within the measuring period.

An absorption correction was performed using the program DATAPH.[3] The calculated linear absorption coefficient is $\mu = 1.90$ cm^{-1}, assuming the incoherent scattering cross-section of the hydrogen atom to be 38 b. The poorly developed faces of the crystal were approximated to crystallographic planes as shown in Fig. 1, the distances to the boundary planes from an internal origin being given in Table 1. The distances to the planes

Table 1. Crystal dimension. The distances from an internal origin to the boundary planes are given. Those planes marked with an asterisk are approximations (*cf.* Fig. 1).

Plane	d (mm)
(0$\bar{1}$0)*	2.7
(0$\bar{1}$0)	2.7
(11$\bar{2}$)	1.0
($\bar{1}\bar{1}$2)	1.0
(20$\bar{1}$)	1.7
($\bar{1}$0$\bar{1}$)*	1.8
($\bar{1}\bar{1}$0)*	1.2

Crystal volume = 40.3 mm^3

$(\bar{1}0\bar{1})$* and $(\bar{1}\bar{1}0)$* were obtained after small adjustments giving an absorption correction which accounted for the intensity variation of the 020 reflection as a function of ϕ. The crystal was divided into $6 \times 8 \times 4$ Gaussian points along the a, b, and c directions, respectively. The calculated transmission factors varied between 0.52 and 0.68.

The symmetry related reflections were averaged, and 591 reflections having $F^2 > 4\sigma(F^2)$ were used for the refinement of the structure.

REFINEMENT OF THE STRUCTURE

The positions of the hydrogen atoms were determined from a nuclear density summation, starting from the tellerium and oxygen parameters obtained in the X-ray work.[1] Minima corresponding to all hydrogen atoms in the cell were clearly resolved.

The refinement of the structure was performed with the least squares program LINUS,[4] and the neutron scattering lengths for the different atoms were $b_H = -3.72$ F, $b_{Te} = 5.6$ F (The Neutron Diffraction Commission [5]) and $b_O = 5.88$ F (Brown and Chidambaram [6]). The quantity minimized was $\sum w||F_o| - |F_c||^2$.

The weights initially used were based on the standard deviations of the structure factors modified as $\sigma_{mod} = (\sigma(F^2) + 1.025F^2)^{\frac{1}{2}} - |F|$. Since this procedure tended to overweight the weak reflections, an artificial weighting

$$w^{-\frac{1}{2}} = \sigma_{art} = \begin{cases} [c - (F-a)^{\frac{1}{2}}]^{\frac{1}{2}}, & F > a \\ (c \times a/F)^{\frac{1}{2}}, & F \leq a \end{cases}$$

scheme was used. When $a = 20.6$ and $c = 33.3$ a more reasonable weighting was obtained (*cf.* Table 2).

Table 2. Agreement analyses using weights based on (a) σ_{mod} and (b) σ_{art}. $R = \sum||F_o| - |F_c||/\sum F_o$, $R_w = (\sum w|F_o - |F_c||^2/\sum wF_o^2)^{\frac{1}{2}}$ and $w\Delta^2$ are normalized quantities $\sum w|F_o - |F_c||^2/N$, where N is the number of reflections in the relevant F_o interval.

F_o interval	N	(a) $w\Delta^2$	(b) $w\Delta^2$
0.0 – 6.8	45	2.85	1.97
6.8 – 9.3	63	2.45	1.78
9.3 – 12.2	64	1.12	0.90
12.2 – 16.1	66	0.71	0.55
16.1 – 20.7	74	0.66	0.60
20.7 – 25.3	68	0.38	0.39
25.3 – 30.6	44	0.56	0.54
30.6 – 42.5	72	0.71	1.41
42.5 – 59.4	52	0.54	1.13
59.4 – 110.0	43	0.25	0.95
		$R = 0.025$	$R = 0.024$
		$R_w = 0.033$	$R_w = 0.019$

Although the weak reflections were given low weight in the refinement, the $w\Delta^2$ values are highest for these data, as is seen in Table 2. The F_c values are often too small, which, in some cases may be due to multiple reflection

effetcs, or merely a result of the fact that, among the reflections just above the limit of acceptance, the statistical counting errors do not conform to the normal distribution curve.

The final atomic parameters are given in Table 3 and observed and calculated structure factors are compared in Table 4.

Table 3. Final neutron diffraction parameters in $Te(OH)_6$. The anisotropic temperature factor is $\exp[-2\pi^2(h^2a^{*2}U_{11}+k^2b^{*2}U_{22}+l^2c^{*2}U_{33}+hka^*b^*U_{12}+hla^*c^*U_{13}+klb^*c^*U_{23})]$. The numbers in parentheses are the e.s.d.'s calculated by the least squares program.

Atom	x	y	z
Te_1	0	0	0
Te_2	0	0	$\frac{1}{2}$
O_1	0.7324(2)	0.1543(2)	0.8943(2)
O_2	0.1252(3)	0.0486(1)	0.2038(2)
O_3	0.7741(3)	0.3751(2)	0.5378(2)
O_4	0.6921(2)	0.0968(2)	0.4545(2)
O_5	0.3251(3)	0.4511(1)	0.7850(2)
O_6	0.7193(3)	0.3270(1)	0.0789(2)
H_1	0.2397(5)	0.2864(3)	0.4688(3)
H_2	0.3306(6)	0.0695(3)	0.2913(3)
H_3	0.4720(6)	0.0931(3)	0.1246(3)
H_4	0.7337(5)	0.1989(3)	0.4873(3)
H_5	0.9476(5)	0.0359(3)	0.2638(3)
H_6	0.8983(6)	0.3332(3)	0.1941(3)

	$U_{11}\times10^4$	$U_{22}\times10^4$	$U_{33}\times10^4$	$U_{12}\times10^4$	$U_{13}\times10^4$	$U_{23}\times10^4$
Te_1	62(10)	119(10)	74(10)	34(10)	74(17)	28(13)
Te_2	85(10)	105(10)	98(11)	−18(12)	124(17)	3(13)
O_1	128(6)	163(7)	135(7)	86(10)	114(11)	16(12)
O_2	109(9)	324(9)	105(7)	−16(17)	131(15)	−89(11)
O_3	105(8)	191(7)	225(7)	35(11)	170(14)	−120(11)
O_4	117(7)	191(10)	194(7)	−13(10)	200(14)	−80(12)
O_5	104(7)	322(8)	118(7)	−34(10)	140(12)	−91(11)
O_6	141(8)	146(6)	145(9)	92(10)	133(16)	1(11)
H_1	285(12)	258(13)	271(13)	−117(19)	363(22)	30(23)
H_2	212(17)	442(14)	199(12)	−57(22)	226(18)	−152(22)
H_3	153(16)	359(14)	274(13)	8(21)	237(26)	110(22)
H_4	273(12)	236(17)	346(13)	4(21)	405(22)	−124(23)
H_5	262(13)	442(15)	222(12)	35(21)	389(22)	40(20)
H_6	225(14)	278(13)	214(16)	83(19)	177(28)	46(19)

In addition to atomic coordinates and anisotropic thermal vibration parameters, an isotropic secondary extinction parameter and the scattering length of tellurium were allowed to vary in the refinement. The extinction effect was unusually small, resulting in a maximum correction to the intensities of less than 3 %.

The tellurium scattering length was refined since the tabulated values are of low precision. Starting from $b_{Te}=5.6$ F [6] for both Te atoms, the b values of Te_1 and Te_2 were refined independently, giving $b_{Te_1}=5.79\pm0.06$ F and

Table 4. Observed and calculated structure factors. The columns are h, k, l, $10F_o$ and $10F_c$. Those reflections with $F_o = 0$ were not included in the refinement.

7	0	-9	265	268	5	4	-4	138	-137	4	6	-8	0	24	3	5	-5	523	532
7	0	-7	273	-273	5	4	-3	109	-95	4	6	-7	347	349	3	5	-4	389	395
7	1	-10	220	214	5	4	-2	142	-131	4	6	-6	175	-169	3	5	-3	184	-193
7	1	-9	129	121	5	5	-10	189	-187	4	6	-5	60	-41	3	5	-2	0	-34
7	1	-8	176	175	5	5	-9	184	-182	4	6	-4	331	-323	3	5	-1	247	245
7	1	-7	268	-272	5	5	-8	180	-183	4	6	-3	198	-189	3	5	0	249	-250
6	0	-10	138	-105	5	5	-7	268	270	4	6	-2	0	32	3	5	1	614	-620
6	0	-8	105	100	5	5	-6	88	-87	4	6	-1	0	20	3	5	2	112	-113
6	0	-6	97	-90	5	5	-5	698	-705	4	6	0	592	596	3	5	3	395	389
6	0	-4	679	689	5	5	-4	318	324	4	7	-9	126	120	3	6	-9	330	-330
6	1	-12	83	65	5	5	-3	92	85	4	7	-8	0	17	3	6	-8	0	15
6	1	-11	0	-26	5	5	-2	684	689	4	7	-7	0	17	3	6	-7	120	-112
6	1	-10	104	104	5	6	-9	206	210	4	7	-6	0	80	3	6	-6	188	-198
6	1	-9	181	185	5	6	-8	50	40	4	7	-5	92	98	3	6	-5	117	-109
6	1	-8	296	308	5	6	-7	144	-145	4	7	-4	276	274	3	6	-4	159	166
6	1	-7	0	16	5	6	-6	100	115	4	7	-3	150	151	3	6	-3	98	93
6	1	-6	0	-34	5	6	-5	212	208	4	7	-2	212	-207	3	6	-2	335	-333
6	1	-5	118	-119	5	6	-4	122	-125	4	7	-1	258	255	3	6	-1	247	245
6	1	-4	75	-48	5	6	-3	85	-80	4	8	-7	106	111	3	6	0	87	67
6	1	-3	71	45	5	7	-7	45	28	4	8	-6	509	532	3	6	1	153	151
6	2	-11	238	237	5	7	-6	438	446	4	8	-5	0	30	3	6	2	217	-214
6	2	-10	148	142	5	7	-5	345	-344	4	8	-4	601	598	3	7	-9	134	130
6	2	-9	407	410	4	0	-12	605	607	4	8	-3	158	160	3	7	-8	109	93
6	2	-8	223	226	4	0	-10	183	183	3	0	-11	164	-166	3	7	-7	0	-31
6	2	-7	526	525	4	0	-8	399	404	3	0	-9	126	124	3	7	-6	0	2
6	2	-6	330	-331	4	0	-6	111	-101	3	0	-7	0	4	3	7	-5	209	208
6	2	-5	252	-251	4	0	-4	125	120	3	0	-5	321	319	3	7	-4	152	147
6	2	-4	129	125	4	0	-2	641	644	3	0	-3	677	-673	3	7	-3	63	-48
6	2	-3	360	-361	4	0	0	286	282	3	0	-1	538	533	3	7	-2	267	-261
6	3	-11	80	-66	4	0	2	285	286	3	0	1	88	-80	3	7	-1	791	797
6	3	-10	127	-129	4	1	-12	89	-79	3	0	3	74	64	3	7	0	425	426
6	3	-9	95	82	4	1	-11	0	-31	3	1	-11	567	571	3	7	1	199	201
6	3	-8	196	197	4	1	-10	0	23	3	1	-10	321	-312	3	8	-7	66	51
6	3	-7	90	-71	4	1	-9	47	37	3	1	-9	144	145	3	8	-6	201	-196
6	3	-6	60	53	4	1	-8	145	-144	3	1	-8	406	401	3	8	-5	224	-226
6	3	-5	117	126	4	1	-7	144	-140	3	1	-7	282	-281	3	8	-4	60	-39
6	3	-4	48	-48	4	1	-6	198	-201	3	1	-6	253	255	3	8	-3	0	-10
6	4	-10	333	334	4	1	-5	86	-85	3	1	-5	288	-286	3	8	-2	93	89
6	4	-9	180	-176	4	1	-4	67	-47	3	1	-4	413	-419	3	8	-1	256	-265
6	4	-8	551	551	4	1	-3	180	166	3	1	-3	618	-621	3	8	0	198	198
6	4	-7	149	-137	4	1	-2	147	-152	3	1	-2	554	557	3	9	-5	0	-36
6	4	-6	309	312	4	1	-1	250	251	3	1	-1	127	126	3	9	-4	453	450
6	4	-5	484	-490	4	1	0	0	-27	3	1	0	54	-37	3	9	-3	0	-40
6	4	-4	456	456	4	1	1	217	-215	3	1	1	67	63	3	9	-2	280	281
6	5	-7	169	-169	4	1	2	131	-130	3	1	2	1075	1090	2	0	-10	203	198
6	5	-8	76	-72	4	2	-12	406	400	3	1	3	75	56	2	0	-8	0	-50
6	5	-7	61	65	4	2	-11	0	-23	3	1	4	190	194	2	0	-6	954	975
6	5	-6	125	119	4	2	-10	187	-181	3	2	-11	60	-67	2	0	-4	0	38
5	0	-11	0	4	4	2	-9	713	-717	3	2	-10	167	-171	2	0	-2	377	372
5	0	-9	195	-195	4	2	-8	602	606	3	2	-9	244	242	2	0	0	657	-659
5	0	-7	285	283	4	2	-7	398	-397	3	2	-8	180	181	2	0	4	847	844
5	0	-5	161	156	4	2	-6	388	384	3	2	-7	173	-174	2	0	6	467	460
5	1	-12	521	525	4	2	-5	298	-299	3	2	-6	170	-164	2	1	-10	108	113
5	1	-11	336	-341	4	2	-4	669	670	3	2	-5	172	168	2	1	-9	96	-88
5	1	-10	0	-9	4	2	-3	323	334	3	2	-4	121	111	2	1	-8	65	65
5	1	-9	251	-234	4	2	-2	622	604	3	2	-3	380	-380	2	1	-7	237	-242
5	1	-8	699	696	4	2	-1	717	706	3	2	-2	258	-265	2	1	-6	221	226
5	1	-7	348	348	4	2	0	62	-46	3	2	-1	74	68	2	1	-5	267	268
5	1	-6	241	-243	4	2	1	0	-28	3	2	0	183	-184	2	1	-4	170	166
5	1	-5	423	430	4	2	2	422	418	3	2	1	244	-243	2	1	-3	89	-80
5	1	-4	564	569	4	3	-10	169	172	3	2	2	317	-319	2	1	-2	53	40
5	1	-3	483	481	4	3	-9	121	-114	3	2	3	84	69	2	1	-1	94	85
5	1	-2	138	-107	4	3	-8	87	88	3	2	4	332	-332	2	1	0	339	330
5	1	-1	229	-227	4	3	-7	84	-77	3	3	-11	372	366	2	1	1	249	-253
5	1	0	84	58	4	3	-6	0	-29	3	3	-10	0	-25	2	1	2	244	-240
5	2	-12	61	72	4	3	-5	0	15	3	3	-9	343	-341	2	1	3	106	103
5	2	-11	0	-28	4	3	-4	115	-126	3	3	-8	94	-88	2	1	4	248	-242
5	2	-10	68	-46	4	3	-3	447	-457	3	3	-7	173	-171	2	1	5	88	93
5	2	-9	138	-105	4	3	-2	0	-20	3	3	-6	306	308	2	1	6	292	-291
5	2	-8	206	-210	4	3	-1	0	-34	3	3	-5	0	-1	2	2	-10	437	431
5	2	-7	218	219	4	3	0	53	43	3	3	-4	221	219	2	2	-9	734	733
5	2	-6	367	370	4	3	1	176	-197	3	3	-3	734	-729	2	2	-8	160	-164
5	2	-5	131	-126	4	3	2	374	-381	3	3	-2	928	932	2	2	-7	509	507
5	2	-4	0	9	4	4	-11	168	158	3	3	-1	105	107	2	2	-6	119	112
5	2	-3	123	125	4	4	-10	184	-177	3	3	0	81	-66	2	2	-5	235	237
5	2	-2	53	28	4	4	-8	262	260	3	3	1	478	-477	2	2	-4	416	-415
5	2	-1	219	221	4	4	-7	356	364	3	3	2	0	-37	2	2	-3	228	-231
5	2	0	219	215	4	4	-6	0	-12	3	3	3	282	292	2	2	-2	198	200
5	3	-11	176	175	4	4	-5	0	7	3	3	4	91	-71	2	2	-1	173	-174
5	3	-10	108	108	4	4	-4	103	-83	3	4	-11	114	117	2	2	0	63	-48
5	3	-9	141	-142	4	4	-3	214	-212	3	4	-10	0	-39	2	2	1	182	-186
5	3	-8	603	610	4	4	-2	261	-263	3	4	-9	119	113	2	2	2	160	162
5	3	-7	668	673	4	4	-1	143	144	3	4	-8	147	138	2	2	3	126	-123
5	3	-6	101	90	4	4	0	292	-296	3	4	-7	135	-135	2	2	4	96	83
5	3	-5	82	71	4	4	1	74	48	3	4	-6	75	56	2	2	5	229	-231
5	3	-4	258	259	4	5	-10	64	-49	3	4	-5	224	221	2	2	6	0	-3
5	3	-3	466	471	4	5	-9	143	130	3	4	-4	624	628	2	3	-9	141	137
5	3	-2	213	-215	4	5	-8	112	112	3	4	-3	217	224	2	3	-8	84	86
5	3	-1	168	-173	4	5	-7	219	213	3	4	-2	199	-203	2	3	-7	207	205
5	3	0	0	319	4	5	-6	89	79	3	4	-1	91	96	2	3	-6	265	-267
5	3	1	0	-49	4	5	-5	223	232	3	4	0	543	545	2	3	-5	134	137
5	3	2	405	402	4	5	-4	148	-150	3	4	1	235	-240	2	3	-4	63	-44
5	4	-11	88	-83	4	5	-3	95	-86	3	4	2	210	197	2	3	-3	64	-51
5	4	-10	74	-67	4	5	-2	0	-33	3	4	3	0	-10	2	3	-2	98	-96
5	4	-9	0	-35	4	5	-1	0	18	3	5	-10	670	672	2	3	-1	421	428
5	4	-8	405	-406	4	5	0	208	212	3	5	-9	446	-446	2	3	0	381	342
5	4	-7	143	-141	4	5	1	164	-163	3	5	-8	634	632	2	3	1	150	-145
5	4	-6	121	-134	4	6	-10	348	347	3	5	-7	237	236	2	3	2	0	-16
5	4	-5	288	-291	4	6	-9	127	-120	3	5	-6	505	509	2	3	3	0	-8
2	3	4	155	151
2	3	5	0	20
2	4	-10	273	272
2	4	-9	0	32
2	4	-8	159	156
2	4	-7	498	-507
2	4	-6	405	407
2	4	-5	396	400
2	4	-4	243	243
2	4	-3	61	-45
2	4	-2	868	875
2	4	-1	473	467
2	4	0	851	862
2	4	1	320	-319
2	4	2	625	624
2	4	3	564	-564
2	4	5	63	50
2	5	-9	119	113
2	5	-8	0	-20
2	5	-7	193	-195
2	5	-6	326	-330
2	5	-5	163	-158
2	5	-4	119	121
2	5	-3	232	-235
2	5	-2	87	-75
2	5	-1	0	1
2	5	0	50	36
2	5	1	291	298
2	5	2	0	-38
2	5	3	0	18
2	5	4	135	133
2	6	-9	0	-15
2	6	-8	326	323
2	6	-7	500	-500
2	6	-6	742	743
2	6	-5	206	221
2	6	-4	460	469
2	6	-3	317	-320
2	6	-2	352	363
2	6	-1	0	240
2	6	0	0	19
2	6	1	61	23
2	6	2	144	144
2	6	3	190	187
2	6	4	293	293
2	7	-8	73	-60
2	7	-7	51	-48
2	7	-6	95	78
2	7	-5	0	-11
2	7	-4	197	202
2	7	-3	163	-170
2	7	-2	187	-193
2	7	-1	427	-434
2	7	0	143	136
2	7	1	80	-52
2	7	2	146	-132
2	7	3	71	-49
2	8	-7	120	-117
2	8	-6	272	-265
2	8	-5	74	57
2	8	-4	64	34
2	8	-3	515	-510
2	8	-2	266	-260
2	8	-1	67	-55
2	8	0	81	68
2	8	1	256	259
2	8	2	170	170
2	9	-5	0	-22
2	9	-4	69	62
2	9	-3	145	145
2	9	-2	246	-239
2	9	-1	0	15
2	9	0	106	-91
2	9	1	127	-122
1	0	-9	121	120
1	0	-7	0	-7
1	0	-5	387	-384
1	0	-3	72	-55
1	0	-1	0	13
1	0	1	105	106
1	0	3	0	14
1	0	5	203	201
1	0	7	166	164
1	1	-10	707	714
1	1	-9	239	-239
1	1	-8	221	-225
1	1	-7	0	-5
1	1	-6	890	902
1	1	-5	677	691
1	1	-4	198	194
1	1	-3	91	95
1	1	-2	524	512
1	1	-1	0	-3
1	1	0	521	514
1	1	1	0	19
1	1	2	551	-543
1	1	3	69	56
1	1	4	88	76
1	1	5	421	423

Table 4. Continued.

1	1	6	237	-233	1	4	-6	89	-85	1	6	-2	317	321	1	9	1	0	-8
1	1	7	207	-197	1	4	-7	143	-142	1	6	-1	0	39	1	9	2	562	561
1	2	-9	0	29	1	4	-8	136	131	1	6	0	217	218	1	10	-2	124	131
1	2	-8	0	-13	1	4	-2	122	114	1	6	1	443	-441	1	10	-1	67	-37
1	2	-7	71	-59	1	4	-4	383	-391	1	6	2	179	176	1	10	0	219	219
1	2	-6	98	98	1	4	-3	149	-160	1	6	3	67	70	0	0	-8	223	-231
1	2	-5	114	106	1	4	-2	386	-397	1	6	4	135	-119	0	0	-6	228	-229
1	2	-4	246	246	1	4	-1	169	-171	1	7	-7	186	-179	0	0	-4	91	84
1	2	-3	0	-1	1	4	0	475	-478	1	7	-6	91	87	0	0	-2	514	510
1	2	-2	95	94	1	4	1	60	44	1	7	-5	244	244	0	1	-8	163	-162
1	2	-1	0	22	1	4	2	296	-296	1	7	-4	685	685	0	1	-7	90	-80
1	2	0	69	-47	1	4	3	78	68	1	7	-3	405	-422	0	1	-6	351	-362
1	2	1	230	247	1	4	4	236	-241	1	7	-2	444	450	0	1	-5	324	330
1	2	2	625	621	1	4	5	112	113	1	7	-1	457	-458	0	1	-4	282	-279
1	2	3	201	-214	1	4	6	0	28	1	7	0	0	27	0	1	-3	187	-185
1	2	4	150	147	1	4	7	112	-116	1	7	1	546	-536	0	1	-2	66	52
1	2	5	0	14	1	5	-8	364	-363	1	7	2	114	112	0	2	-8	0	12
1	2	6	98	84	1	5	-7	564	-568	1	7	3	443	-447	0	2	-7	773	-772
1	2	7	99	-86	1	5	-6	273	-273	1	7	4	243	-242	0	2	-6	586	581
1	3	-9	223	213	1	5	-5	0	-7	1	7	5	399	400	0	2	-5	350	-361
1	3	-8	236	238	1	5	-4	148	155	1	8	-6	236	-239	0	2	-4	638	648
1	3	-7	345	-349	1	5	-3	198	-213	1	8	-5	250	247	0	2	-3	248	252
1	3	-6	542	543	1	5	-2	236	242	1	8	-4	179	182	0	2	-2	259	254
1	3	-5	633	647	1	5	-1	59	45	1	8	-3	147	148	0	2	-1	0	-8
1	3	-4	418	-415	1	5	0	229	232	1	8	-2	0	25	0	2	0	528	512
1	3	-3	92	86	1	5	1	576	571	1	8	-1	175	169	0	3	-8	127	136
1	3	-2	0	-19	1	5	2	472	466	1	8	0	65	-48	0	3	-7	195	-195
1	3	-1	123	133	1	5	3	499	-491	1	8	1	136	-141	0	3	-6	110	-118
1	3	0	167	168	1	5	4	457	453	1	8	2	0	29	0	3	-5	109	-93
1	3	1	621	626	1	5	5	0	-27	1	8	3	198	-204	0	3	-4	392	361
1	3	2	520	526	1	5	6	637	649	1	8	4	82	-83	0	3	-3	0	18
1	3	3	76	-59	1	6	-8	146	126	1	9	-5	93	87	0	3	-2	202	206
1	3	4	868	829	1	6	-7	79	75	1	9	-4	120	114	0	3	-1	135	-106
1	3	5	281	268	1	6	-6	85	-93	1	9	-3	63	51	0	4	-8	215	219
1	3	6	58	-49	1	6	-5	135	135	1	9	-2	0	0	0	4	-7	0	8
1	3	7	373	-383	1	6	-4	0	25	1	9	-1	85	74	0	4	-6	372	372
1	4	-9	56	-49	1	6	-3	101	104	1	9	0	61	-52	0	4	-5	245	-242
0	4	-4	96	88															
0	4	-3	285	-291															
0	4	-2	412	-419															
0	4	-1	191	-203															
0	4	0	293	-286															
0	5	-7	144	146															
0	5	-6	0	42															
0	5	-5	0	36															
0	5	-4	367	375															
0	5	-3	95	-84															
0	5	-2	143	-150															
0	5	-1	68	62															
0	6	-7	151	149															
0	6	-6	179	-179															
0	6	-5	259	260															
0	6	-4	236	-244															
0	6	-3	223	228															
0	6	-2	298	309															
0	6	-1	184	-188															
0	6	0	360	367															
0	7	-6	57	-66															
0	7	-5	156	-152															
0	7	-4	213	-211															
0	7	-3	82	78															
0	7	-2	167	-174															
0	7	-1	343	351															
0	8	-5	268	264															
0	8	-4	352	359															
0	8	-3	506	508															
0	8	-2	486	485															
0	8	-1	0	-45															
0	8	0	312	312															
0	9	-4	69	-51															
0	9	-3	201	207															
0	9	-2	0	6															
0	9	-1	91	-92															
0	10	-1	133	-126															
0	10	0	178	-183															

$b_{Te_2} = 5.81 \pm 0.06$ F. The resulting value, $b_{Te} = 5.80$ F, is probably more reliable than the lower value determined previously, since it is based on the more accurately known scattering lengths of hydrogen [5] and oxygen.[6]

DISCUSSION

The Te – O_6 octahedra. The higher precision of the neutron diffraction data has enabled the molecular dimensions of $Te(OH)_6$ to be determined with appreciably better precision than was obtained in the previous X-ray investigation. However, the improvement in the Te – O bond determination can also be ascribed to the fact that the Te – O distances are determined solely by the oxygen positions, since all tellurium parameters are fixed by the symmetry.

Table 5. Distances and angles within the two tellurium-oxygen coordination polyhedra. The angles listed are those indicated in Fig. 4, where Te_1 corresponds to the tellurium atom at the origin in Fig. 3. E.s.d.'s are given in parentheses. No distances have been corrected for thermal motion.

Distances		Angles	
$Te_1 - O_1$	1.907(1)Å	$O_1 - Te_1 - O_2$	88.69(7) °
$Te_1 - O_2$	1.908(1)	$O_1 - Te_1 - O_3$	91.07(6)
$Te_1 - O_3$	1.910(1)	$O_2 - Te_1 - O_3$	92.08(7)
$Te_2 - O_4$	1.908(1)	$O_4 - Te_2 - O_5$	87.60(6)
$Te_2 - O_5$	1.908(1)	$O_4 - Te_2 - O_6$	88.38(6)
$Te_2 - O_6$	1.914(1)	$O_5 - Te_2 - O_6$	90.71(7)

The tellurium – oxygen bond distances and angles are given in Table 5, and stereoscopic drawings, obtained with the program ORTEP,[7] are shown in Figs. 2 and 3.

The average Te – O bond distance of 1.909 ± 0.001 Å is in good agreement with the X-ray value of 1.916 ± 0.005 Å. In both the neutron and X-ray investigations, it has been found that the $Te_2 - O_6$ bond is slightly longer than

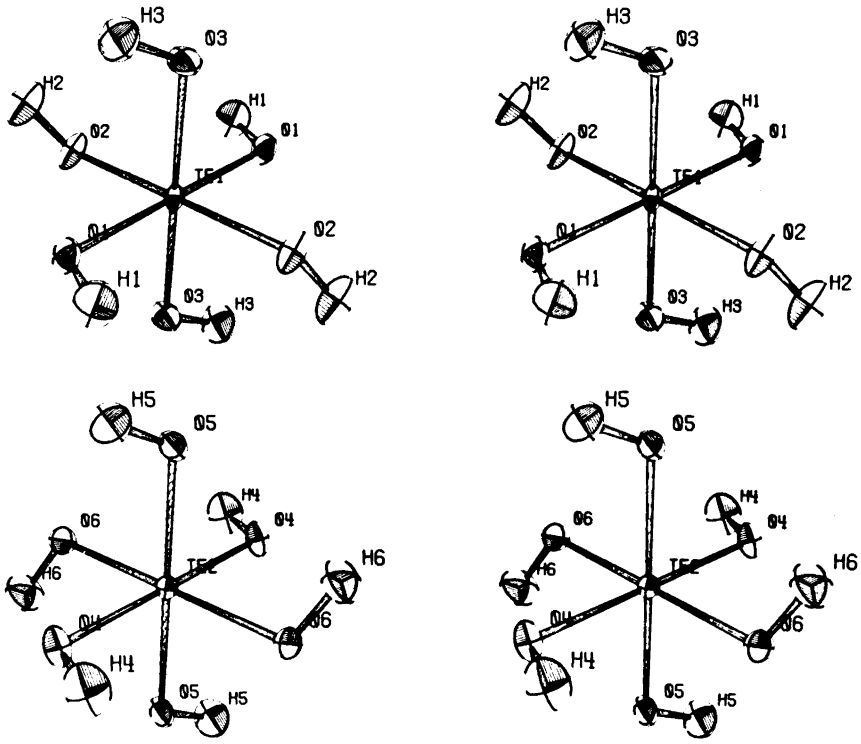

Fig. 2. Stereoscopic pictures [7] of the two independent $Te(OH)_6$ molecules. The thermal ellipsoids enclose areas with an atomic probability density greater than 50 %.

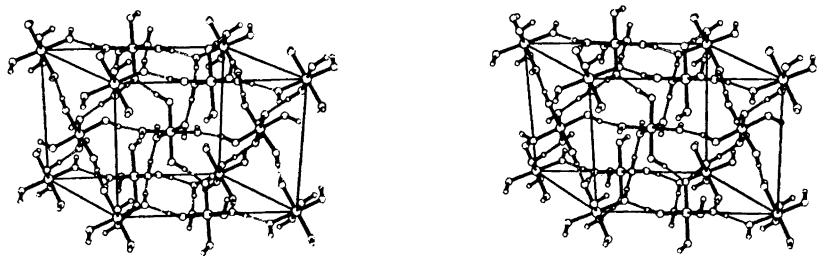

Fig. 3. Stereoscopic picture [7] showing all atoms bonded to tellurium atoms within one unit cell. The cell is viewed along the a^* direction.

the other Te – O bonds, and, according to the neutron diffraction results, this bond may be significantly longer than the $Te_2 - O_4$ and $Te_2 - O_5$ bonds. There seems to be no obvious reason for this effect, but it is possible that the hydrogen bonds in the structure may cause deviations from the ideally octahedral oxygen coordination around tellurium. That this is the case is clearly indicated in the significant deviations of the O – Te – O angles from 90°, as discussed below.

A comparison of the Te – O coordination in $Te(OH)_6$ with that in other tellurates was given in the previous paper.[1]

Hydrogen bonds. The hydrogen positions determined in the X-ray investigation have been shown to be reasonable, and thus the hydrogen bonding network indicated in Fig. 2 and Table 8 of Ref. 1 is correct. However, no detailed discussion of the hydrogen bonds was possible at that stage, since the e.s.d.'s of the hydrogen positions were as high as 0.1 Å. The neutron diffraction results are given in Table 6.

Table 6. Hydrogen bonding in telluric acid.

	O – O	O – H	H···O	∠O – H···O	∠Te – O – H	∠H···O – Te
$Te_1 - O_1 - H_1 \cdots O_6 - Te_2$	2.695(2) Å	0.989(3) Å	1.711(3) Å	173.4(3)°	113.6(2°)	129.7(1)°
$Te_1 - O_2 - H_2 \cdots O_4 - Te_2$	2.709(2)	0.983(3)	1.727(3)	175.3(3)	114.5(2)	129.4(1)
$Te_1 - O_3 - H_3 \cdots O_5 - Te_2$	2.696(2)	0.977(3)	1.720(3)	175.8(3)	114.2(2)	127.8(1)
$Te_2 - O_4 - H_4 \cdots O_3 - Te_1$	2.685(2)	0.990(3)	1.698(3)	174.5(2)	113.1(2)	127.6(1)
$Te_2 - O_5 - H_5 \cdots O_2 - Te_1$	2.676(2)	0.987(3)	1.704(3)	167.2(3)	115.0(2)	126.2(1)
$Te_2 - O_6 - H_6 \cdots O_1 - Te_1$	2.730(2)	0.983(3)	1.750(3)	175.1(3)	112.6(2)	127.0(1)
$\angle H_6 \cdots O_1 - H_1$		111.1(2)°		$\angle H_2 \cdots O_4 - H_4$	111.1(2)	
$\angle H_5 \cdots O_2 - H_2$		115.3(2)		$\angle H_3 \cdots O_5 - H_5$	118.4(2)	
$\angle H_4 \cdots O_3 - H_3$		114.9(2)		$\angle H_1 \cdots O_6 - H_6$	113.3(2)	

The O – H···O distances, ranging from 2.676 Å to 2.730 Å with a mean value of 2.699 Å, indicate rather strong hydrogen bonding in the structure. The complex three-dimensional hydrogen bond network is of (12,8) type (*cf.* the monograph by Hamilton and Ibers,[8] p. 21), *i.e.* each molecule is involved in twelve hydrogen bonds to eight neighbouring molecules (*cf.* Fig. 3). Six of these bonds are directed octahedrally towards six other molecules, a three-dimensional network thus being formed. The remaining six all extend approximately along the [102] direction, making three connections to each of the two adjacent molecules, thus in this direction resulting in the formation of chains running through the structure (*cf.* Fig. 4).

There is no hydrogen bonding between symmetry related $Te(OH)_6$ molecules. The main difference between the two independent molecules in the cell is that the Te_1 molecule supplies four hydrogen atoms to the chain bonds and only two to the octahedral bonds, while these numbers are reversed for Te_2 (*cf.* Fig. 3).

None of the O – H bonds are significantly different from the average value 0.985 Å, but there are small differences among the H···O bonds. Hamilton and Ibers [8] have investigated the correlation between the O – H

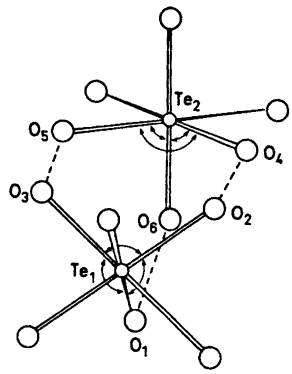

Fig. 4. Schematic drawing indicating the angles listed in Table 5. The unmarked angles are given from symmetry (Te_1 and Te_2 at $\bar{1}$).

bond length and the O – H···O and H···O distances, respectively. In the present investigation, the average H···O bond distance is 1.718 Å, and, according to the empirical curve given by Hamilton and Ibers, this value should correspond to an O – H bond length of 0.99 Å. This is in good agreement with the value of 0.985 Å actually found in $Te(OH)_6$.

The O – H···O angles are close to 175° (except for angle $O_5 - H_5 \cdots O_2$ which is 167.2°) and they are slightly smaller than in the other pure hydroxy-acid known, orthoboric acid. In a neutron diffraction study of D_3BO_3 these angles were found to range from 175.5° to 179.4°.[9] In both compounds, the hydrogen atom is closer to the centre of the molecule than it would have been if the hydrogen bonds had been linear (exception: D_4 in D_3BO_3). In the similar compound H_5IO_6,[10] the range 171 – 178° has been found.

The Me – O – H and H···O – Me angles are of the same magnitudes in D_3BO_3, H_5IO_6, and $Te(OH)_6$, whereas the average H···O – H angle in $Te(OH)_6$ is 114.0° compared to 119.8° for D···O – D in D_3BO_3. In orthoboric acid, the arrangements of atoms around the oxygen atoms is approximately planar, while in telluric acid the oxygen atom is significantly tilted out of the corresponding plane permitting a smaller O···H – O angle. An assumption of sp^2 hybridization of the oxygen atoms and double $\sigma\pi$ Te – O bonds (according to the Te – O bond length) seems reasonable as a first approximation. However, it is difficult to quantitatively discuss the deviations from 120° of the angles subtended at the oxygen atoms.

In a recent powder neutron diffraction investigation of cubic telluric acid the hydrogen atoms were found to be statistically distributed.[11] A detailed comparison of the hydrogen bonds in the two modifications is therefore not possible. It would appear that the more stable monoclinic phase, with its localized hydrogen positions, can be described as being slightly distorted from cubic symmetry.

When hydrogen bonds are formed changes occur in the parts of the molecules involved. In telluric acid the molecules are connected solely through hydrogen bonds and all hydrogen atoms participate, moreover, in similar hydrogen bonds. It ought therefore to be possible to see what influence the hydrogen bonds have on the tellurium coordination and thus obtain some

indications as to how they arise. Assuming that in a free $Te(OH)_6$ molecule the oxygen atoms form a regular octahedron around Te, the main distortion caused by the hydrogen bonding in the $Te(OH)_6$ crystal is that the O – Te – O angles are no longer 90°. One might except to find decreased angles as a result of the O – H···O attractions where two molecules are connected over three hydrogen bonds (*cf.* Fig. 4). This is not, however, the case. Nor is it possible to explain the deviations in terms of strains caused by the preference of any particular Te – O – H angle. There is, moreover, no correlation between hydrogen to hydrogen repulsion and the O – Te – O angles (*cf.* Fig. 5). The

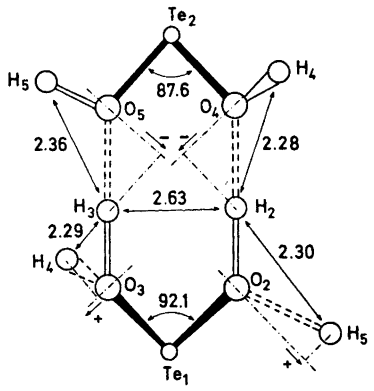

Fig. 5. Schematic drawing showing the effect of the hydrogen bonds on the O – Te – O angles.

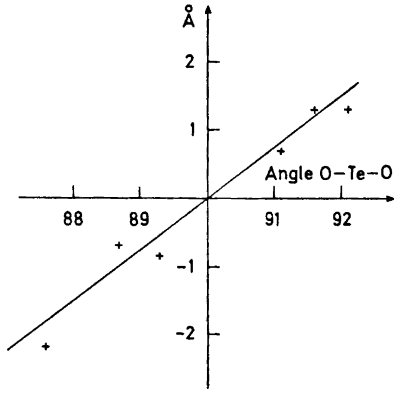

Fig. 6. Correlation between acceptor directions in the hydrogen bonds and the deviations of the O – Te – O angles from 90°. For each angle, the sum of the two H···O projections (*cf.* Fig 5) has been plotted.

deviations of the oxygen atoms from their ideal octahedral positions might, however, be attributable to their role as acceptors in the hydrogen bonds. In order to examine this effect more quantitatively, the acceptor bonds O_a···H and O_b···H were projected on lines in the plane of the $O_a – Te – O_b$ angle under consideration. These lines were perpendicular to the $Te – O_a$ and $Te – O_b$ bonds, respectively, and their positive directions were defined as indicated in Fig. 5. From Fig. 6, in which the sum of the two O_a···H and O_b···H projections for each of the six independent $O_a – Te – O_b$ angles has been plotted against the value of the angle, it is evident that there is a correlation, indicated by a straight line through the origin. The method of just adding the two components for each angle may be crude, and some of the effects mentioned above might also affect the positions of the points in the diagram. The rotation of the O – H bond around the Te – O bond, necessary for the formation of the hydrogen bond network, might also disturb the Te – O $\sigma\pi$ bonding system.

The correlation between the direction of the lone pair of the acceptor oxygen atoms, which is presumably near the hydrogen bond direction, and

the O – Te – O angles (*cf.* Fig. 6) indicates that the increased electron density in the direction towards the H – O donor is large enough to cause the accceptor oxygen nucleus to shift its equilibrium position in this direction. Thus, when hydrogen bonds are formed in $Te(OH)_6$, the main change in the system seems to be concentrated in the accepting lone pair.

As discussed above, the donor O – H bond length is increased by formation of hydrogen bond. In $Te(OH)_6$, this lengthening may partly be regarded as a result of a decreased electron density in the O – H bond caused by transfer of electron density towards the oxygen lone pair directed towards a hydrogen atom in a neighbouring molecule.

The authors thank Professors G. Lundgren and S. E. Rasmussen for encouraging this work. They are also indebted to Professor N.-G. Vannerberg for interesting discussions of the results. Ing. M. H. Nielsen and Ing. E. Andersson are thanked for valuable technical assistance, and Dr. S. Jagner for revising the English text. This work has been finanacially supported by the *Swedish Natural Science Research Council* (*NFR*, Contract No. 2318).

REFERENCES

1. Lindqvist, O. *Acta Chem. Scand.* **24** (1970) 3178.
2. Lehmann, M. S, Hamilton, W. C. and Larsen, F. K. *American Crystallographic Association Meeting Abstracts*, 1972, Albuquerque, New Mexico.
3. *DATAPH*. In use at Dept. of Inorg. Chem., Göteborg. Originally written by Coppens, P., Leiserowitz, L. and Rabinowich, D. and modified by Hamilton, W. C.
4. *LINUS*. In use at Dept. of Inorg. Chem., Göteborg. Originally written by Busing, W. R., Martin, K. O. and Levy, H. A. and modified by Hamilton, W. C. and by Ibers, J. A.
5. The Netron Diffraction Commission, *Acta Cryst.* **A 25** (1969) 391.
6. Brown, G. M. and Chidambaram, R. *Acta Cryst.* **B 25** (1969) 676.
7. Johnson, C. K. *ORNL-3794*, Oak Ridge National Laboratory, Oak Ridge 1965.
8. Hamilton, W. C. and Ibers, J. A. *Hydrogen Bonding in Solids*, W. A. Benjamin, New York 1968.
9. Craven, B. M. and Sabine, T. M. *Acta Cryst.* **20** (1966) 214.
10. Feikema, Y. D. *Acta Cryst.* **20** (1966) 765.
11. Cohen-Addad, C. *To be published.*

Received May 13, 1972.

ACTA CHEMICA SCANDINAVICA 27 (1973) 96–106

Fluoroalcohols

Part 17.[1] Infrared and Raman Spectra of the Perhalogenated *t*-Butyl Alcohols $CCl_3C(CF_3)_2OH$ and $CCl_3C(CF_3)_2OD$

JUHANI MURTO, ANTTI KIVINEN,* KARI KAJANDER, JOUKO HYÖMÄKI and JOUKO KORPPI-TOMMOLA

Department of Physical Chemistry, University of Helsinki, Meritullinkatu 1 C, Helsinki 17, Finland

Infrared spectra of gaseous and liquid and Raman spectra of liquid $CCl_3C(CF_3)_2OH$ and $CCl_3C(CF_3)_2OD$ have been studied. Raman spectra of solutions of the former alcohol in carbon tetrachloride and dimethyl sulphoxide and the IR spectrum in carbon tetrachloride are reported. A vibrational assignment is made. The liquid alcohols are only little associated. The multiplicity of the OH stretching band indicates that three conformers are present in appreciable amounts in the vapour and at least two conformers in the neat liquid and in solutions of the alcohols in CCl_4. Combination bands $\nu OH \pm \tau OH$ relating to only one conformer occur in the vapour spectra.

In connection with a study of the IR and Raman spectra of perfluorinated *t*-butyl alcohol (PFTB),[2] we synthesized 2-trichloromethyl-1,1,1,3,3,3-hexafluoro-2-propanol ($CCl_3C(CF_3)_2OH$, TCHFB). This alcohol is quite acidic; its pK_a is only 5.1 at 25°.[3] We have recorded the IR and Raman spectra of TCHFB and its deuterated analogue $CCl_3C(CF_3)_2OD$ (TCHFB-*d*), mainly because it is one of the few alcohols containing a trichloromethyl group that can be studied both as a vapour and as a liquid at room temperature. The results are reported below.

EXPERIMENTAL

TCHFB was synthesized according to Dear [4] by ultraviolet photochemical chlorination of 2-methyl-1,1,1,3,3,3-hexafluoro-2-propanol in a Hanovia 1-litre photochemical reactor equipped with a 100 W medium pressure mercury lamp. The progress of the chlorination was followed with the aid of a Varian 1520 – 1B gas chromatograph equipped with a dinonyl phthalate column and a hydrogen flame ionisation detector. The product was very hygroscopic and was dried first with sodium sulphate and then with a large

* Department of Pharmacy, University of Helsinki, Fabianinkatu 35, Helsinki 17, Finland.

quantity of molecular sieves (type 4A). The product boiled at 139 – 140° and melted at −2°. The chemical shift δ of the hydroxyl proton in the NMR spectrum of the neat liquid at a temperature of 39° was 3.90 ppm relative to tetramethylsilane. The purity of the compound exceeded 95 % as deduced from the NMR spectrum and the gas chromatogram, the main impurity being 2-dichloromethyl-1,1,1,3,3,3-hexafluoro-2-propanol.

TCHFB-*d* was obtained by shaking TCHFB several times with deuterium oxide, distilling and drying.

Dimethyl sulphoxide (DMSO) was purified by fractional crystallization, and carbon tetrachloride was dried with molecular sieves (type 4A).

The IR spectra were recorded with a Perkin-Elmer 621 spectrometer equipped with an air drying unit. The frequency scale of the spectrometer was calibrated with atmospheric moisture and carbon dioxide. The vapour spectra were measured after injecting liquid alcohol into an evacuated Perkin-Elmer variable temperature cell (KBr windows, path length 5 cm) or a 1 m path length cell with CsI windows. When the spectrum of a liquid was recorded, the liquid was between window plates or in a sealed cell FH-01K (RIIC). Some spectra of the compounds in CCl_4 were recorded also with a Beckman DK-2A spectrophotometer.

The Raman spectra were measured with a Jarrell-Ash 25 – 305 spectrometer equipped with an Orlando Ar/Kr ion laser (model 400 MG) of 2 W total efficiency. The exciting line was the 488 nm line of argon; its intensity at the sample was about 200 mW. The spectra were taken using 90° excitation from above. A half-wave plate, analyser and scrambler were always in the light path; polarization measurements were made after turning the analyser 90°. A slit servo system kept the spectral slit width constant at about 2 cm^{-1}, which permitted the evaluation of relative band intensities. A liquid multipass cell of 2.5 ml capacity was used. We found that by using a screen that allows scattered light only from the liquid and not from the glass of the cell to enter the entrance slit, one can get about 10 cm^{-1} closer to the exciting line.

The reported positions of sharp IR and Raman bands are believed to be accurate to ± 2 cm^{-1}. The non-SI units used are 1 Å $= 10^{-10}$ m and 1 amu $= 1.660 \times 10^{-21}$ g.

RESULTS AND DISCUSSION

A TCHFB molecule has 39 fundamental vibrational modes, of which, assuming C_s symmetry as the CCl_3, CF_3, and OH groups are relatively freely rotating, 22 are of species a' and 17 of species a''. A complete assignment would therefore be difficult and is not attempted here.

The principal axes and moments of inertia of TCHFB and TCHFB-*d* were computed using the programme CART written by Schachtschneider.[5] The values of the structural parameters used were the same as in the case of PFTB with the additions that the carbon-chlorine bond length was taken as 1.76 Å and that the angles Cl – C – Cl and C – C – Cl were assumed tetrahedral. The isotopic masses were used (for chlorine, the mass of ^{35}Cl).

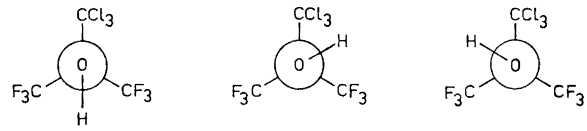

I (c_s) II_a (c_1) II_b (c_1)

Fig. 1. Staggered conformers of TCHFB. Conformers II_a and II_b are spectroscopically equivalent.

Table 1. IR and Raman spectra (values of ν/cm^{-1}) of $CCl_3C(CF_3)_2OH$ (TCHFB) and its solutions (excluding the region 1400–3200 cm^{-1}). Relative Raman intensities are given in parentheses (the intensity of the band at 410 cm^{-1} = 100). P = polarized, DP = depolarized band; the figures after these are the depolarization ratios. ν = stretching, δ = bending, ϱ = rocking, and τ = torsion; sh = shoulder. Subscript s = symmetric, a = antisymmetric vibration.

Vapour	Liquid				Solution			
IR	IR	Raman			0.2 M in CCl_4 IR	37.7 wt. % in CCl_4 Raman	38.7 wt. % in DMSO Raman	Assignment
					3824 br, vw			3580+268
3852 vvw	3835 vvw							
	3667 vw							ν_sOH, conf.(i)
3625 vw	3585 sh	3582 sh	P	0.1	3580 sh			ν_sOH, conf.(ii)
3603 m	3563 m	3564 (3)	P	0.1	3553 br, s	3560 P		ν_sOH, conf.(iii)
3580 w								3580–268
3304 vvw								δ_sOH
1370 m	1363 m	1365 (1)	P	0.6	1364 w	1365 DP?	*b*	
1325 vw[a]	1335 sh[a]	1338 sh[a]			1332 sh[a]			
1269 vvs	1269 vvs	1269 (2)	DP	0.8	1265 vs	1270 DP	1270 DP	ν_aCF_3
1243 vvs		1238 (3)	P	0.6	1234 vvs	1238 P	1238 sh	ν_sCF_3
1227 sh	1225 vvs	1227 (3)	P	0.6		1228 P	1220 sh	ν_sCF_3
1217 vvs		1212 (3)	P?	0.7	1212 vs	1213		ν_aCF_3
	1195 sh?	1192 sh	DP?				1153*a*	
1165 w[a]	1155 sh[a]	1158 (< 1)	DP	0.8[a]	1161 w[a]			ν_aCF_3
1147 vs	1136 vs	1140 (< 1)	DP		1142 vs			ν_sCF_3
1100 sh					1090 vvw		*c*	
1026 w	1022 w	1022 (3)	P	0.5	1023 w	1020 P	1020 sh P	$\nu_s$skel.
1000 sh							*b*	$\nu_a$skel.
956 w	952 m	952 (1)	DP	0.7	953 w	952 DP	840 DP	ν_aCCl_3
850 m	842 m	845 (2)	DP	0.8	846 m	846 DP	789 DP	ν_sCCl_3
790 m	787 m	788 (6)	P	0.6	*b*	*b*		
726 s	722 s	724 (44)	P	0.1	723 s	724 P	726 P	ν_s skel.
724 sh							*b*	
711 s	708 s	708 (1)	DP?		709 s			δ_aCF_3

620 vvw	624 vvw	624	(5)	P	0.7	624 vvw	624 DP	624 DP		$\delta_s CF_3$
563 vvw	564 vvw	565	(1)	DP	0.8	564 vvw	567 DP			$\delta_a CF_3$
540 w	548 w	542	(2)	DP	0.7	540 vw	541 DP	~ 545		$\delta_s CF_3$, $\varrho_a CF_3$
490 vw	491 w	493	(19)	P	0.1	490 vw		494 P		δ_s skel.
409 vvw	409 vvw	410	(100)	P	0.01	409 vvw		410 P		$\nu_s CCl_3$
360 vvw	359 vvw	355	(7)	DP	0.7	360 vvw				δ_a skel.
	328 vvw	328	(15)	P	< 0.1					δ_s skel.
		317	(15)	DP	0.7					$\varrho_a CF_3$
295 vw	294 vw	292	(24)	DP	0.8			292 sh[b]		$\delta_a CCl_3$, $\delta_a CF_3$
287 vvw		285	sh	DP						
268 w	273 vw									$\tau_a OH$
	257 vw	256	(17)	P	0.4			256 P		$\delta_s CCl_3$
	217 vvw	222	(16)	P	0.5			225 P		$\varrho_s CF_3$
209 vvw		209	(16)	P	0.7			210 DP		$\delta_s CCl_3$
		192	(3)	DP	0.8					$\varrho_s CCl_3$, $\varrho_a CCl_3$
		169	(6)	P	0.7		170			$\varrho_s CF_3$
		70br	(1)	DP	0.8?			170		τCF_3, τCCl_3

[a] The band may also be due to the dichloro compound. [b] Solvent bands may be present in this region. [c] The SO stretching band of pure DMSO is at 1045 cm^{-1} In spectra of its mixtures with TCHFB, the band is at 1050 cm^{-1} and is slightly broader. Also the broad shoulder at 1020 cm^{-1} may in part be due to SO stretching (*cf.* HFP [18] and PFTB[2]).

TCHFB should have only two different conformers with respect to rotation of the hydroxyl group around the C–O bond if we accept only conformers where the O–H bond is staggered with respect to the C–C bonds (conformers I and II in Fig. 1; the structures II_a and II_b are spectroscopically equiv-

Table 2. IR and Raman spectra of $CCl_3C(CF_3)_2OD$ (TCHFB-*d*). Above 1500 cm^{-1}, only bands associated with OD stretching are given.

Vapour IR	IR	Liquid Raman[a]			Assignment
2850 vvw	2830 vvw				2644 + 205
	2730 vvw				
2672 sh					ν_sOD, conf. (i)
2660 m	2632 m	2640	P	0.2	ν_sOD, conf. (ii)
2644 w		2610 sh?	P		ν_sOD, conf. (iii)
2440 vvw					2644 – 205
1367 vw[b]					
1318 sh	1318 sh				
1290 vs	1284 vs	1289 (2)	P	0.7	$\nu_s CF_3$
1267 vvs	1258 vvs	1262 (2)	DP	0.8	$\nu_a CF_3$
1243 vvs		1243	P?		$\nu_s CF_3$
	1228 vvs	1230 (2)			$\nu_a CF_3$
1218 sh[b]					
	1200 sh	1200 (< 1)	DP		
1168 m	1163 sh	1162 (1)	P		$\nu_s CF_3$
1151 s	1150 s	1152 (1)	DP	0.8	$\nu_a CF_3$
		1110 (1)	P	< 0.3	
1075 m	1070 m	1070 (1)	P	0.5	δ_sOD
1008 m	1007 m	1007 (2)	P	0.4	ν_s skel.
	973 vvw				
953 vw[b]	952 vvw[b]				
882 sh?	877 m	878 (2)	DP?		ν_a skel.
878 m					
845 m	838 m	837 (3)	DP	0.7	$\nu_a CCl_3$
793 m	789 m	789 (8)	P	0.5	$\nu_s CCl_3$
726 s	724 s	725 (32)	P	0.04	ν_s skel.
705 m	699 m	700 (2)	P		$\delta_a CF_3$
617 vvw	617 vw	619 (5)	P	0.5	$\delta_s CF_3$
	564 vvw	566 (1)	DP		$\delta_a CF_3$
537 w	539 w	542 (2)	P	0.6	$\delta_s CF_3$, $\delta_a CF_3$
487 w	487 w	489 (20)	P	0.1	δ_s skel.
		433 sh(1)	P	0.1	
	409 vvw	409 (100)	P	0.03	ν_s CCl_3
		355 (6)	DP	0.8	δ_a skel.
		329 (16)	P	0.2	δ_s skel.
		319 (15)	DP	0.7	$\varrho_a CF_3$
		292 (22)	DP	0.8	$\delta_a CCl_3$, $\varrho_a CF_3$
		258 (13)	P	0.4	$\delta_s CCl_3$
		224 (16)	P	0.5	$\varrho_s CF_3$
		210 (15)	DP	0.7	$\delta_s CCl_3$
		193 (2)	P	0.6	$\varrho_s CCl_3$, $\varrho_a CCl_3$
		170 (5)	DP?		$\varrho_s CF_3$
		70 br	P?		τCF_3, τCCl_3

[a] The data in the region 1000–1400 cm^{-1} are incomplete because of the low intensities of the bands. [b] This band may be due to the undeuterated compound.

alent). The principal moments of inertia vary very little from conformer to conformer. For structure I (denoted by (i) in the tables; see below) we obtained the values $I_A = 789.7$ (794.6), $I_B = 885.7$ (892.2), and $I_C = 1111.3$ (1113.0) amu Å^2 (the values in parentheses are those obtained for the deuterated compound). The principal axes A and C are in the plane defined by the O–H, C–O and C–CCl_3 bonds and the C axis is almost parallel to the C–O bond and *ca.* 0.3 Å towards the CCl_3 group. The A and B axes lie almost in the plane of the three carbon atoms of the trihalogenomethyl groups.

Band contours in the vapour spectra and moments of inertia give relatively little information because of the large moments of inertia and relatively high boiling points of the compounds. Only the band at 490 cm^{-1} has a comparatively well-defined contour (Fig. 2B), which is similar to the "perpendicular" OH stretching band of PFTB.[2] Also the band at 726 cm^{-1} seems to be somewhat similar in shape. The bands at 852, 623, and 360 cm^{-1} seem to be triangular.

OH (OD) stretching. Chloroalcohols usually show marked splitting of the OH stretching band due to conformational heterogeneity.[6–8] The OH stretching band in the vapour spectrum of TCHFB is a triplet with maxima at 3625, 3603, and 3580 cm^{-1} (Figs. 2 and 4). The value 3625 cm^{-1} is about the same as that found for the C_s conformer of hexafluoro-2-propanol (HFP);[9] also gaseous hexafluoro-*t*-butyl alcohol (HFTB) has a band at this wavenumber.[10] We thus assign the band at 3625 cm^{-1} to a symmetric conformer, type I in Fig. 1 (denoted by (i) in the tables). This band of TCHFB was not well resolved if moisture was present. In carbon tetrachloride solution this conformer absorbs obviously at 3580 cm^{-1}, and thus the frequency shift when going from the vapour to CCl_4 solution is similar for HFP, HFTB, and TCHFB.[9,10]

As the wavenumbers of the other two bands are low, these bands obviously belong to conformers where there is intramolecular influence of the CCl_3 group. As these we propose (ii) a conformer where the OH group lies within

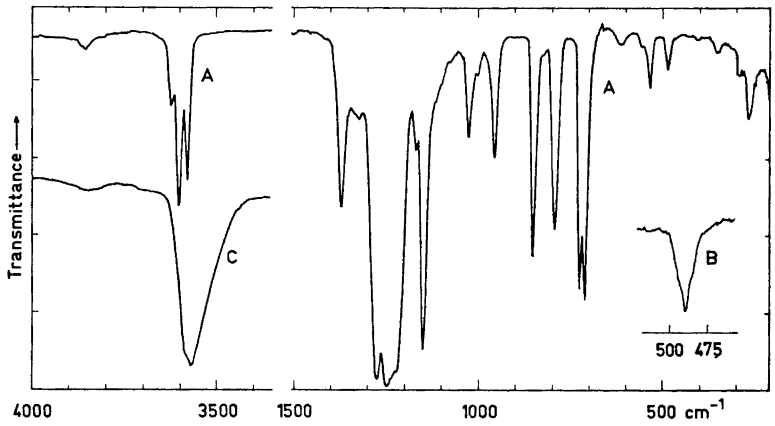

Fig. 2. Infrared spectra of $CCl_3C(CF_3)_2OH$. A, vapour, 1 m cell with CsI windows, pressure about 1 mmHg; B, vapour, path length 1 m, pressure 4 mmHg; C, liquid, between KBr plates.

a $CF_3-C-CCl_3$ angle and interacts mostly with the CF_3 group and (iii) a conformer where the OH group lies also within a $CF_3-C-CCl_3$ angle, but the interaction is mostly with the CCl_3 group. If the conformer (iii) is close to an eclipsed one, it can be stabilised only by strong OH···Cl interaction. In spectra of solutions of TCHFB in CCl_4 a broad band that obviously belongs to conformers (ii) and (iii) is centred at 3553 cm^{-1}. For comparison, it may be mentioned that in CCl_4 solution trichloroethanol has one band at 3599 cm^{-1} (gauche conformer),[6] chloral hydrate two bands, at 3605 and 3578 cm^{-1},[8] $CCl_3C(CH_3)_2OH$ one band at 3584 cm^{-1},[8] and $(CCl_3)_2CHOH$ two bands, at 3591 and 3537 cm^{-1}.[8]

A pair of "satellite" bands are present at 3852 and 3304 cm^{-1} (Fig. 4) in the vapour spectrum of TCHFB (see also the following paper [2]). These are obviously $3580 \pm \tau OH$ bands and give for the OH torsion τOH the value 274 cm^{-1} (the directly measured value is 268 cm^{-1}). The intensity of the sum band is about three times that of the difference band (the theoretical ratio is 3.6). Small amounts of water influence the intensity ratio somewhat; water vapour has a strong absorption band at about 3850 cm^{-1}. The TCHFB-water complex absorbs at about 3360 cm^{-1} (vapour phase).

The contour of the OD stretching band of gaseous TCHFB-*d* is similar to that of the OH stretching band of TCHFB (Fig. 3). The triplet is between 2600 and 2700 cm^{-1} in the spectrum of the deuterated compound. The value of the ratio $\nu OH/\nu OD$ is 1.35 as in the case of HFP[9] and PFTB.[2]

The satellite bands are at 2850 and 2440 cm^{-1} in the vapour spectrum of TCHFB-*d*, and thus $\tau OD = 205$ cm^{-1}. However, in addition to bands due to possible moisture, the overtone bands of the C–F stretching vibrations at 2300 – 2500 cm^{-1} make the determination of the position of the 2440 cm^{-1} band somewhat uncertain.

The spectra of the liquid alcohols indicate that the extent of association is small. The IR (Fig. 2) and Raman (Fig. 3b in the following paper [2]) bands of

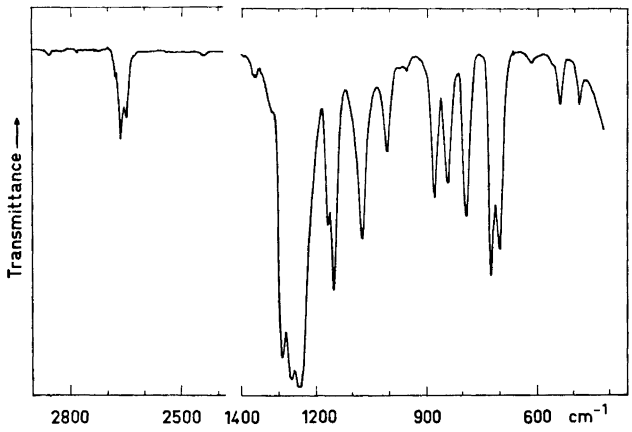

Fig. 3. Infrared spectrum of $CCl_3C(CF_3)_2OD$. Vapour, 5 cm cell, KBr windows, pressure about 10 mmHg, temperature somewhat above the room temperature.

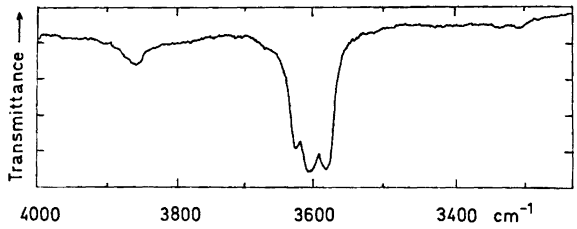

Fig. 4. OH stretching band of $CCl_3C(CF_3)_2OH$. Vapour, 1 m cell with CsI windows.

the liquids have similar contours; obviously only two bands corresponding to unassociated alcohol are present. One of these (at 3585 cm^{-1}) may be due to conformer (i), the other (at 3563 cm^{-1}) to conformers (ii) and (iii). However, the recorded OH stretching bands are broad and asymmetric as there seems to be an additional band on the low-frequency side. This asymmetry may be due to a dimer. If this is true, then the monomer-dimer shift (about 80 cm^{-1} as in the case of PFTB[2]) would be exceptionally small. The vapour-liquid shift of the OH stretching band of the monomer seems to be about normal.

COH bending. The band of the OH in-plane bending (δOH) is at 1330 cm^{-1} in the vapour spectrum [11] and at 1380 cm^{-1} in the liquid spectrum [12,13] of *t*-butyl alcohol. Fluorination seems to increase the OH bending frequency in the vapour as the band is at 1350 cm^{-1} in the spectrum of trifluoro-*t*-butyl alcohol, at 1367 cm^{-1} in the spectrum of HFTB, and at 1381 cm^{-1} in the spectrum of PFTB.[2,10] The increase may in part be due to intramolecular interaction. This band is obviously at 1370 cm^{-1} in the spectrum of TCHFB, for it disappears on deuteration and a similar new band appears at 1075 cm^{-1}. A similar shift occurs in the spectrum of PFTB.[2]

C–F stretchings. According to C_s symmetry, there should be six C–F stretching fundamental bands ($3a' + 3a''$) in the spectra of TCHFB. The C–F stretching bands are usually found between 1100 and 1350 cm^{-1} and are weak in Raman spectra and very strong in IR spectra. Fig. 5a shows that the depolarization ratios of these bands are always relatively high. The most intense Raman C–F stretching band, which also has the lowest depolarization ratio, is that at 1227 cm^{-1}; this obviously arises from the symmetric vibration where all C–F bonds stretch in concert. The maximum C–F stretching intensity occurs at about 1290 cm^{-1} in the Raman spectrum of TCHFB-*d*. The most intense IR band is at 1243 cm^{-1} in the spectra of gaseous TCHFB and TCHFB-*d*.

C–Cl stretchings. Three C–Cl stretching fundamentals are expected. Two of them are found between 650 and 850 cm^{-1} and the third at about 440 cm^{-1} in the spectra of CCl_3NO_2 [14] and CCl_3CHO.[15] The last-mentioned fundamental gives rise to the most intense and highly polarized band in the Raman spectrum; this band is weak in the IR spectrum. The same applies to the band at 410 cm^{-1} in the spectra of liquid TCHFB. However, Holmes and Fild [16] assign a similar band at 409 cm^{-1} in the spectrum of CCl_3PF_4 to a CCl_3 defor-

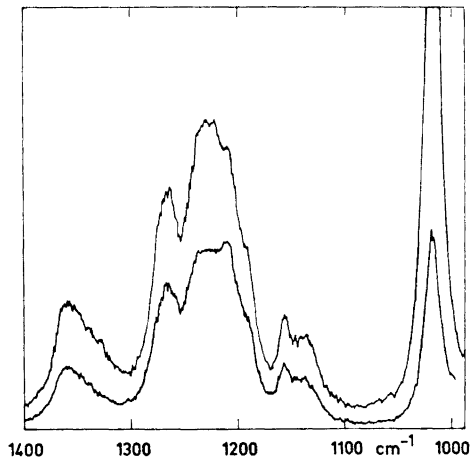

Fig. 5. a. The region 1400 – 1000 cm^{-1} in the Raman spectrum of liquid $CCl_3C(CF_3)_2OH$. The sensitivity of the detector was five times greater than the sensitivity when the spectra in *b* and *c* were recorded. *b.* The region 1050 – 450 cm^{-1} in the Raman spectrum of liquid $CCl_3C(CF_3)_2OH$. *c.* The region 450 – 50 cm^{-1} in the Raman spectrum of liquid $CCl_3C(CF_3)_2OH$. When the band at 410 cm^{-1} was recorded, the sensitivity was one fifth of that when the other bands were recorded.

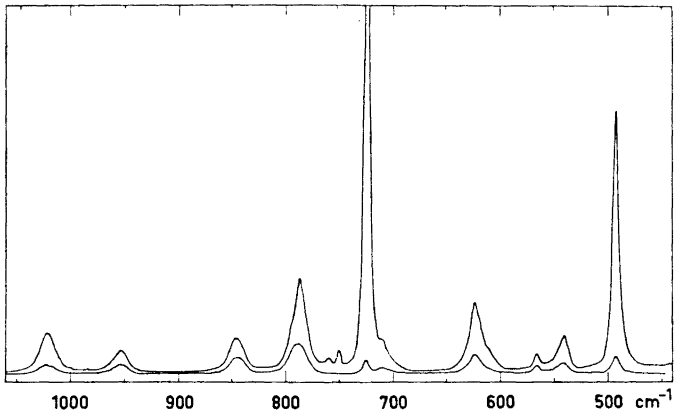

Fig. 5b.

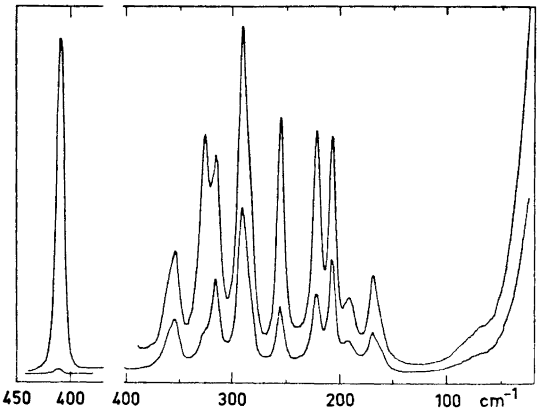

Fig. 5c.

mation vibration. The band of TCHFB at 850 cm^{-1}, which we interpret as a C – Cl stretching band, may also be due to skeletal stretch.

Skeletal vibrations. TCHFB should have four skeletal stretching ($3a' + a''$) and five skeletal bending vibrations ($3a' + 2a''$). It is, however, well known [12,17] that these vibrations are sometimes difficult to identify because of strong coupling effects. This is true also for the C – O stretching vibration band, which may be at 1026 cm^{-1} in the vapour spectrum of TCHFB; this is a polarized band and shifts to 1008 cm^{-1} on deuteration.

There is a band due to the most symmetric skeletal stretching between 700 and 800 cm^{-1} in the spectra of highly fluorinated alcohols. It is intense and highly polarized in the Raman spectra and weaker in the IR spectra. This band is at 725 cm^{-1} in the spectrum of TCHFB.

The band at about 950 cm^{-1} in the spectra of TCHFB is obviously also a skeletal stretching band. On deuteration, it seems to shift to 880 cm^{-1}. A similar shift occurs also in the spectra of PFTB [2] and HFTB.[10]

We assign the band at about 328 cm^{-1} in the spectra of TCHFB and TCHFB-*d* to the $CF_3 - C - CF_3$ bending (*cf.* also Refs. 2, 9, and 10). The band at 490 cm^{-1} is obviously a skeletal bending band, but it is uncertain whether it is to be ascribed mainly to C – O bending or to the most symmetric bending of the C_3CO skeleton.

CF_3 bendings. There should be six CF_3 bending bands ($3a' + 3a''$), but a smaller number is found. By analogy with HFP, we consider the bands at 711, 623, 563, and 541 cm^{-1} to be CF_3 bending bands. It is possible that the band at 541 cm^{-1} corresponds to two superimposed fundamentals and the sixth band is too weak to be seen.

The region below 320 cm^{-1}. In this region there are probably three CCl_3 bending, two CCl_3 rocking, four CF_3 rocking, and two CF_3 torsion bands. Furthermore there are one OH (OD) torsion and one CCl_3 torsion band.

There is a CF_3 rocking band at about 170 cm^{-1} in the Raman spectra of HFP,[9] HFTB,[10] and PFTB,[2] and thus we assign the band at 170 cm^{-1} in the Raman spectrum of TCHFB to CF_3 rocking. The band at 295 cm^{-1} has a shoulder at about 287 cm^{-1} (Fig. 5c); the latter is due either to a fundamental or to the isotope effect of chlorine. In the latter case, the bands must be due to a CCl_3 bending fundamental. However, it is probable (*cf.* HFP[9] and PFTB[2]) that one CF_3 rocking band is at about 290 cm^{-1}.

The OH and OD torsion (out-of-plane bending) bands were discussed already in connection with the OH stretching.

The weak, broad Raman band at 70 cm^{-1} may possibly be due to $CHal_3$ torsions.

Acknowledgements. We gratefully acknowledge financial support from the *Jenny and Antti Wihuri Foundation* (for the purchase of chemicals) and from the *Finnish National Research Council for Sciences.* Dr. A. J. Barnes (University College of Swansea, Wales) is thanked for helpful suggestions, and Miss Rea Viitala, Ph. M., for recording some of the spectra.

REFERENCES

1. Murto, J., Kivinen, A. and Strandman, L. *Suomen Kemistilehti* **B 44** (1971) 308. (Part 16.)
2. Murto, J., Kivinen, A., Korppi-Tommola, J., Viitala, R. and Hyömäki, J. *Acta Chem. Scand.* **27** (1973) 107.
3. Filler, R. and Schure, R. M. *J. Org. Chem.* **32** (1967) 1217.
4. Dear, R. E. A. *Synthesis* **7** (1970) 361.
5. Schachtschneider, J. H. *Technical Report No. 231–64*, Shell Development Co.
6. Krueger, P. J. and Mettee, H. D. *Can. J. Chem.* **42** (1964) 340.
7. Novak, A. and Whalley, E. *Spectrochim. Acta* **16** (1960) 521.
8. Khairetdinova, A. K. and Perelygin, I. S. *Opt. Spectrosc.* **24** (1968) 497.
9. Murto, J., Kivinen, A., Viitala, R. and Hyömäki, J. *Spectrochim. Acta. To be published.*
10. Korppi-Tommola, J. *To be published.*
11. Tanaka, C. *Nippon Kagaku Zasshi* **81** (1960) 1042; **83** (1962) 398.
12. Pritchard, J. G. and Nelson, H. M. *J. Phys. Chem.* **64** (1960) 795.
13. Stuart, A. V. and Sutherland, G. B. B. M. *J. Chem. Phys.* **24** (1956) 559.
14. Mason, J. and Dunderdale, J. *J. Chem. Soc.* **1956** 754.
15. Lucazeau, G. and Novak, A. *Spectrochim. Acta* **A 25** (1969) 1615; Hagen, G. *Acta Chem. Scand.* **25** (1971) 813.
16. Holmes, R. R. and Fild, M. *J. Chem. Phys.* **53** (1970) 4161.
17. Simpson, D. M. and Sutherland, G. B. B. M. *Proc. Roy. Soc. (London)* **A 199** (1949) 169.
18. Murto, J., Kivinen, A., Näsäkkälä, M., Viitala, R. and Hyömäki, J. *Suomen Kemistilehti. To be published.*

Received June 15, 1972.

ACTA CHEMICA SCANDINAVICA 27 (1973) 107–120

Fluoroalcohols

Part 18.[1] Infrared and Raman Spectra of the Perfluorinated *t*-Butyl Alcohols $(CF_3)_3COH$ and $(CF_3)_3COD$

JUHANI MURTO, ANTTI KIVINEN*, JOUKO KORPPI-TOMMOLA, REA VIITALA and JOUKO HYÖMÄKI

Department of Physical Chemistry, University of Helsinki, Meritullinkatu 1 C, Helsinki 17, Finland

The infrared spectra of gaseous, liquid and solid perfluoro-*t*-butyl alcohol, $(CF_3)_3COH$, and of its gaseous and liquid deuterated analogue have been recorded, the spectrum of the former alcohol also in an argon matrix. Raman spectra of the liquid compounds have been studied. A spectral assignment is made. Raman spectra of solutions of $(CF_3)_3COH$ in carbon tetrachloride and dimethyl sulphoxide and the IR spectrum in carbon tetrachloride are reported. Only one conformer seems to be present to a significant extent in perfluoro-*t*-butyl alcohol. The extent of association is relatively small even in the neat liquids. In the spectrum of gaseous $(CF_3)_3COH$, there are two satellite bands displaced by ± 255 cm^{-1} from the OH stretching band; these are due to combinations with OH torsion. No association band of OH bending was found.

Perfluorinated *t*-butyl alcohol, $(CF_3)_3COH$ (PFTB), is an interesting compound as it is the most highly fluorinated aliphatic alcohol (perfluorinated primary and secondary alcohols are not stable compounds) and also as its pK_a is about 5.4 at 25°,[2] *i.e.*, the alcohol is almost as strong an acid as acetic acid. We have measured its infrared and Raman spectra together with those of the other highly fluorinated alcohols hexafluoro-2-propanol (HFP) [3,4] and 2-trichloromethyl-1,1,1,3,3,3-hexafluoro-2-propanol (TCHFB).[1] The results are reported in the present paper together with data for $(CF_3)_3COD$ (PFTB-*d*). A study of the less fluorinated *t*-butyl alcohols, trifluoro-*t*-butyl alcohol and hexafluoro-*t*-butyl alcohol (HFTB), is in progress.[5]

PFTB was first synthesized by Knunyants and Dyatkin.[6] Dear *et al.*[7] studied its lithium, sodium, and potassium salts and Sherry [8] investigated by calorimetric methods its complex formation with various proton acceptors.

* Department of Pharmacy, University of Helsinki, Fabianinkatu 35, Helsinki 17, Finland.

Table 1. IR and Raman spectra (values of ν/cm^{-1}) of $(CF_3)_3COH$ (PFTB). Relative Raman intensities are given in parentheses (the intensity of the band at 770 cm^{-1} = 100). P = polarized (depolarization ratio $\lesssim 0.7$) and DP = depolarized band; the figures after these are the depolarization ratios. ν = stretching, δ = bending, ϱ = rocking and τ = torsion; sh = shoulder. Subscript s = symmetric, a = antisymmetric vibration.

Vapour IR	Liquid IR	Liquid Raman			Solid 200 K	Solid 20 K, Ar matr.[a]	Assignment[b]
7120 vvw							2×3630
3988 vvw							3630+357
3956 vvw							3630+328
3885 vw	3864 vw						3630+252
3691 vvw							3630+70; 3×1260
3634 sh[c]							
3630 s	3616 m	3616 (3)	P	0.1		3608 m	ν_sOH, monomer
3626 sh[c]							
	~3600 sh	3604 sh (1)	P	0.1	3585 vvw		ν_sOH, linear dimer end group
3570 sh?							3630−70, 3×1209
	3530 w	3535 (0.7)	P	0.2		3490 w	ν_sOH, dimer
					3425 br,m		ν_sOH, oligomer
3375 vvw							3630−252
2750 vvw	2750 vvw						2×1381
2574 vvw	2564 vvw						2×1313
2521 vvw	2515 vvw						2×1288
2457 vw	2444 vw						2×1260
2369 vw	2359 vw						2×1209
2338 vvw	2345 sh						1157+1209
2287 vvw	2280 vvw						2×1157
2175 vvw	2170 vvw						979+1209
2125 vvw	2115 vvw						955+1157
2090 vvw	2082 vvw						771+1313
2026 vvw	2030 br, vvw						771+1260
1925 vw	1918 vvw						2×979
1875 vvw	1871 vvw						2×955
1810 vvw	1800 vvw						488+1313
1780 vvw	1765 vvw						535+1260
1725 vvw	1720 vvw						955+771
1640 vvw	1634 vvw						357+1313
1615 vvw	1590 vvw						488+1157
1535 vvw	1535 vvw						535+979
1462 vvw	1455 vvw						2×771
1381 m	1380 m	1380 (0.6)	P	0.4	1381 m	1382 m	δ_sOH
1340 sh					1340 vw		357+979
						1319 s	
1313 vs	1312 vs	1316 (2)	P	0.35	1311 s	1312 s	$\nu_s CF_3$
		1298	P			1303 m	328+979
1288 sh	1282 sh				1281 sh,s	1292 vvs	$\nu_a CF_3$
						1280 m	2×650
						1272 vs	
1270 sh	1270 sh	1270	P	0.5	1266 sh	1269 vvs	$\nu_s CF_3$
						1261 vs	
						1257 vs	
1260 vvs	1250 vvs	1250 (1)	P	0.5	1251 vvs	1254 vvs	$\nu_s CF_3$
					1217 sh	1227 w	488+730
						1209 w	
1209 m	1205 m	1210 (0.6)	DP	0.7	1200 sh	1207 m	$\nu_a CF_3$
						1199 w	

Table 1. Continued.

					1186 w	
1157 vs	1147 vs	1144 (0.3)	DP 0.7	1151 sh	1155 vvs	$\nu_s CF_3$
1145 sh?	1134 vs			1136 s	1145 w	
					1133 vw	2×572
1060 vvw					1060 m	2×535
					984 sh	ν_a skel., assoc.?
979 s	978 s	975 (0.1)	DP	981 s	981 vs	ν_a skel.
958 sh	957 s	960 (0.2)	P 0.4	965 s	960 br,w	ν_s skel., assoc.?
955 s					954 s	ν_s skel.
854 vw	852 vw				857 vw	ν_s skel.? [d]
776						
771 vw	770 w	770 (100)	P 0.01	771 w	769 vw	ν_s skel.
766						
733 sh						
730 s	729 s	730 (0.1)		729 s	727 s	$\delta_a CF_3$
727 sh						
650 vw	649 vw	650 (4)	P 0.4	650 vvw		$\delta_s CF_3$
572 vvw	571 vvw	572 (0.6)	DP 0.8			$\delta_a CF_3$
540 sh	537 m	536 (3)	DP 0.7	535 w		$\delta_s CF_3$
535 w						$\delta_a CF_3$
488 w	488 w	489 (2)	P 0.01			δ_s skel.
		440 (0.2)	P 0.1			δ_s skel.?
357 vw	362 [f]	357 (8)	DP 0.8			δ_a skel.
328 vvw	330 [f]	325 (20)	P 0.3			δ_s skel.
316 vvw	318 vvw [f]	[e]				$\varrho_a CF_3$?
285 sh	288 [f]	292 sh	P			$\varrho_s CF_3$
273 sh	[f]	280 (0.1)	DP			$\varrho_a CF_3$
252 w,br	[f]					$\tau_a OH$
		242 (0.1)	P 0.2			$\varrho_s CF_3$
195 vvw		199 (0.5)	P ~0.01			$\varrho_s CF_3$
165 sh		170 (0.4)	DP 0.8			$\varrho_a CF_3$
		~70 (0.1)				τCF_3?

[a] M/A ratio 1000, 2 μmol of PFTB deposited. All weak bands are not given as the alcohol possibly contained some of the decomposition product. [b] The wavenumbers refer to the vapour. [c] These shoulders were seen when the cell was cooled with Dry Ice. [d] This band may be due to the decomposition product. [e] A band may be superimposed by the band at 325 cm^{-1}. [f] It was difficult to obtain reliable IR data below 400 cm^{-1} because of the great volatility of PFTB.

EXPERIMENTAL

Chemicals. PFTB was synthesized by fluorination of TCHFB with SbF_5 according to Dear.[9] It boiled between 45 and 47° and melted at −17°. The ^{19}F NMR singlet was at 74.4 ppm relative to $CFCl_3$ ($CFCl_2CF_2Cl$ as internal standard); Dear reported the value 74.5 ppm.

It was found that PFTB decomposes slowly on standing and that the decomposition product has a higher boiling point. The vapour of the distillation residue of a sample that had stood about half a year at room temperature gave new IR bands at 3592, 1180 sh, 1090, 1035, 915, 850 (also PFTB may have a weak band at about 850 cm^{-1}) and 755 cm^{-1} (the depolarization ratio of the last-mentioned band in the Raman spectrum was 0.01). Of the new bands, those at 1035, 850, and 755 cm^{-1} were the most intense ones (possible new bands between 1200 and 1300 cm^{-1} were not seen because of strong absorption by PFTB). All spectra except the matrix isolation spectrum were recorded on freshly distilled samples.

PFTB is completely miscible with CCl_4 at room temperature. The cloud point of a 33.6:66.4 (w/w) mixture of PFTB and CCl_4 is 6.3°.

Table 2. IR and Raman spectra of $(CF_3)_3COH$ in solutions in dimethyl sulphoxide (DMSO) and CCl_4. All fundamentals are not included because of solvent bands.

IR	Raman				
6.9 wt. % in CCl_4	35 wt. % in CCl_4		41 wt. % in DMSO		Assignment [a]
3610 m [b]	3606 sh	P	[c]		νOH, monomer
3574 m	3578	P	[c]		νOH, monomer
3500 sh (asym.)					νOH, dimer
1452 vvw					2×771
1376 m	1376	P	[d]		δ_sOH
1341 sh					$357 + 979$
1309 vs	1313	P	[d]		$\nu_s CF_3$
	1300	P	1296 sh	P	
1278 sh	1275 br	DP	1275	DP	$\nu_a CF_3$
1256 vvs	1256	P	1241		$\nu_s CF_3$
			1226		$488 + 730$
1203 m	1208	DP	1179	DP	$\nu_a CF_3$
1195 sh					
1151 vs	1143	DP	1138	DP	$\nu_s CF_3$
1140 sh					
			[e]		
976 s					ν_a skel.
953 s					ν_s skel.
849 vw [d]	[d]		[d]		ν_s skel.?
727 vs [d]	[d]		[d]		$\delta_a CF_3$
647 vw	649	P	[d]		$\delta_s CF_3$
	572	DP	573		$\delta_a CF_3$
536 w	538	DP			$\delta_s CF_3$, $\delta_a CF_3$
487 vw	[d]		488		δ_s skel.
			205		$\varrho_s CF_3$
	170		[d]		$\varrho_a CF_3$

[a] Vapour frequencies. [b] Not seen in a 0.9 M solution, is seen as a shoulder in a 1.8 M solution, and is the most intense OH stretching band in a 3.6 M solution. [c] In DMSO, the OH stretching band is very broad without any definite maximum. [d] Solvent bands may be present in this region. [e] The SO stretching band (which is at 1045 cm^{-1} in pure DMSO) has split into a doublet with components at 1059 and 1020 cm^{-1} (see also spectra of HFP [3] and TCHFB [1]).

As the solubility of PFTB in water is very low (a few per cent at most at 100°), deuteration of the hydroxyl group was carried out by shaking PFTB several times with D_2O and finally distilling.

Recording of spectra. The experimental conditions were similar to those employed previously.[1] Most IR spectra were recorded with a Perkin-Elmer 621 spectrometer (the overtone band of OH stretching was measured with a Beckman DK-2A spectrophotometer and some low-frequency gas spectra with a Perkin-Elmer Model 180 spectrometer at the University of Turku, Finland). A 10 cm gas cell, a 5 cm variable temperature gas cell, both with KBr windows, or a 1 m gas cell with CsI windows was used when recording the vapour spectra. The cells were filled to a suitable pressure using a vacuum line. In some cases, the cells were cooled with Dry Ice.

Liquid and solid spectra were recorded employing sealed cells of type FH-01K (RIIC). The spectrum of solid PFTB was obtained with a variable temperature unit VLT 2 (from RIIC) equipped with NaCl windows. The cell containing the liquid was cooled with a mixture of Dry Ice and acetone and the spectrum was recorded without annealing the sample. The matrix isolation spectrum was kindly recorded by Dr. A. J. Barnes at the University College of Swansea (see Ref. 10 for experimental details).

Table 3. The most important bands in the IR and Raman spectra of $(CF_3)_3COD$ (PFTB-*d*). Relative Raman intensities are given in parentheses.

Vapour IR	Liquid IR	Liquid Raman			Assignment
2860 vvw					2680 + 188
2684 sh, 2680, 2676 sh } s	2668 m	2668	P	0.1	ν_sOD, monomer
	2658 sh	2658 sh	P	0.1	ν_sOD, linear dimer end group
	2610 br	2600 br	P		ν_sOD, dimer
		1326 (3)	P	0.6	$\nu_s CF_3$
1313 vvs	1311 vs	1305 sh			$\nu_s CF_3$
1296 vs	1288 vs	1295 sh	DP		$\nu_a CF_3$
1268 vs	1256 vvs	1260 (1)	P		$\nu_s CF_3$
1245 sh					
1196 s		1195	DP		$\nu_a CF_3$
1169 vs	1165 vs	1145 (0.4)			$\nu_s CF_3$
1063 vs	1058 vs	1060 (0.2)			δ_sOD
979 vs	978 s				ν_a skel.
958 sh [a]					ν_s skel.?
864 m	860 m				ν_s skel.
775, 771, 765 } vw	770 w	770 (100)	P	0.01	ν_s skel.
733 sh, 730, 727 sh } vs	725 vs	725 (0.1)		> 0.5	$\delta_a CF_3$
641 vw	643 vw	643 (5)	P	0.4	$\delta_s CF_3$
570 vvw		574 (1)	DP	0.8	$\delta_a CF_3$
540 sh					$\delta_s CF_3$
535 w	534 w	540 (4)	DP	0.7	$\delta_a CF_3$
483 w	483 w	489 (3)	P	0.01	δ_s skel.
356 vw		359 (8)	DP	0.8	δ_a skel.
328 vvw		330 (20)	P	0.3	δ_s skel.
318 vvw		[b]			$\varrho_a CF_3$?
273 vw		280 (0.1)	DP	0.7	$\varrho_a CF_3$
					$\varrho_s CF_3$
		199 (0.5)	P	0.1	$\varrho_s CF_3$
188 w,br					τ_aOD
165 sh?		169 (0.5)	DP	0.8	$\varrho_a CF_3$
		70			τCF_3?

[a] The band may be due also to the undeuterated compound. [b] Possible band not seen because of the band at 330 cm^{-1}.

The Raman spectra were measured with a Jarrell-Ash 25 – 305 spectrometer equipped with an Orlando Model 400 MG Ar/Kr ion laser of 2 W total efficiency. The exciting line used was the 488 nm line of argon. A slit servo system kept the spectral slit width constant at about 2 cm^{-1} and thus permitted the evaluation of relative band intensities. A liquid multipass cell was used in most cases.

The positions of sharp IR and Raman bands are believed to be accurate to ± 2 cm^{-1}. The non-SI units used are 1 Å = 10^{-10} m and 1 amu = 1.660×10^{-24} g.

RESULTS AND DISCUSSION

The PFTB molecule has 39 normal vibrations, 22 of species a' and 17 of species a'' (point group C_s), similarly as t-butyl alcohol (the symmetry coordinates of the latter have been published by Tanaka [11]). However, the hydroxyl proton would be expected to perturb the $(CF_3)_3CO$ group (symmetry C_{3v}) only slightly (*cf.* Ref. 12). Thus the PFTB molecule can be considered to give rise to 24 fundamentals based on the C_{3v} symmetry and three additional fundamentals that are due to the OH proton. The spectrum of PFTB is indeed much simpler and the number of found fundamentals less than in the spectrum of TCHFB,[1] where we expect to find all 39 fundamentals. All vibrations of point groups C_s and C_{3v} are IR and Raman active, except those of species a_2 (C_{3v}) which are inactive in both cases.

The principal axes and moments of inertia were computed by the programme CART written by Schachtschneider.[13] The following values of structural parameters were used: $r(C-F)=1.33$ Å, $r(C-C)=1.53$ Å, $r(C-O)=1.42$ Å, $r(O-H)=0.98$ Å, $\angle COH=106°$, all other angles tetrahedral. These values were chosen on the basis of Refs. 14–16 as there are no reports on the structure of PFTB. As the angles C–C–F were within $\pm 2°$ of the tetrahedral in all references quoted, the tetrahedral angle was used. The angles C–C–C are possibly slightly greater than tetrahedral, but the angle was taken to be tetrahedral also in these cases. After this work had been completed, a report on the structure of the compound $(CF_3)_3CH$ was published.[17]

If we assume, in the first place, that the CF_3 groups are fixed with one C–F bond parallel to the C–O bond, there are six fluorine atoms in a plane, and we could consider two types of conformers: (i) one type where the O–H and C–C bonds are eclipsed (conformers of this type are usually energetically less favoured; see Ref. 18 concerning t-butyl alcohol) and (ii) another type where the O–H and C–C bonds are staggered. The intramolecular distance from the hydrogen atom to the nearest two fluorine atoms is 2.35 Å in the former and 2.39 Å in the latter case, *i.e.*, the distances are practically equal. However, an electron-diffraction study of the $(CF_3)_3CH$ molecule shows that the CF_3 groups are engaged in a rather large libration type of motion around the C–C bonds, and the mean angle of torsion is 18°. Two more factors operate in PFTB than in $(CF_3)_3CH$, *viz.*, intramolecular OH···F attraction and the repulsion between the fluorine atoms and the lone electron pairs of oxygen. The energetically most favoured conformer of PFTB may be somewhat similar to type (ii) with slightly rotated CF_3 groups.

The principal moments of inertia are $I_A=598.0$, $I_B=598.9$, and $I_C=817.0$ amu Å^2 for both possible conformers of PFTB, and $I_A=602.6$, $I_B=604.4$, and $I_C=818.0$ amu Å^2 for PFTB-*d*. The molecules are thus very nearly oblate symmetric tops. The C axis is very close to and almost parallel with the C–O bond axis.

As the molecules are almost symmetric tops, "parallel" and "perpendicular" bands are expected to occur in the vapour spectra. The formulae of Gerhard and Dennison [19] give for the P–R separation of parallel bands of PFTB the value 10.6 cm^{-1} (at 300 K). The band at 771 cm^{-1} (Fig. 4D) is unquestionably of this type; the P–R separation is 10 cm^{-1}. The OH stretching is obviously

an example of a nearly perpendicular vibration; the band is seen in Fig. 4A. The band at 730 cm^{-1} has a similar countour. The band at 1157 cm^{-1} is almost triangular (however, it is a doublet in the IR spectrum of the liquid).

OH (OD) stretching. In agreement with the above discussion, there was experimental evidence that only one conformer predominates in the vapour. The OH stretching band is at 3630 cm^{-1} (HFP [3] has a band at 3626 cm^{-1} and HFTB [5] at 3623 cm^{-1}) and the OD stretching band at 2680 cm^{-1}; the ratio of these wavenumbers is 1.35. On each side of the OH stretching band and $\pm$ 255 cm^{-1} away from it there are two prominent satellite bands (Fig. 5). These are found also in spectra taken employing a 100 m path length cell (pressure of PFTB 0.15 mmHg) and must thus be due to the monomer. They are obviously the sum and difference combinations of OH stretching with a fundamental at about 255 cm^{-1}; the latter must be the OH torsion. The in-

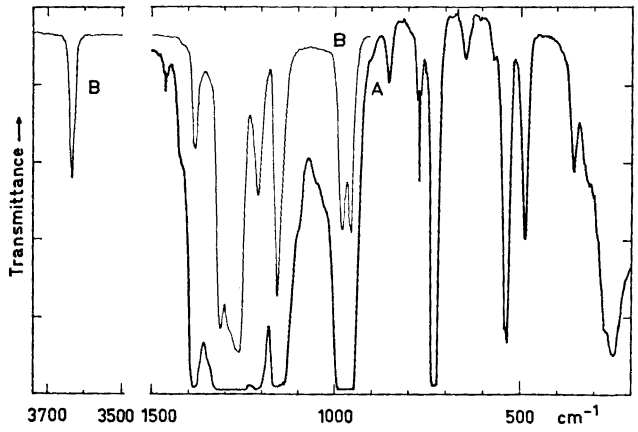

Fig. 1a. IR spectra of gaseous $(CF_3)_3COH$. A, 1 m cell, pressure 6 mmHg. B, 10 cm cell, pressure 4 mmHg.

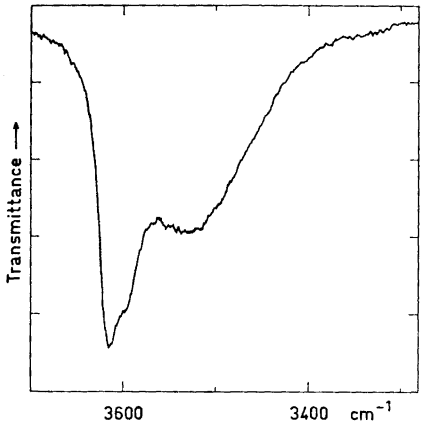

Fig. 1b. IR spectrum of liquid $(CF_3)_3COH$ in the OH stretching region. Cell thickness 0.02 mm.

tensity of the sum band is about 2.5 times that of the difference band; the theoretical ratio is 3.3. Small amounts of water present may influence the difference band; the spectrum of a gaseous PFTB – water mixture showed an intense complex band at about 3360 cm^{-1}. It is interesting that only one pair of prominent satellite bands is observed in the spectrum of PFTB, as there are usually several such pairs in the spectra of other alcohols (this is seen clearly in the vapour spectra of 2,2,2-trifluoroethanol [20] and HFP [3]). The other satellite bands around the OH stretching band in the spectrum of PFTB are much weaker.

The OD stretching band (Fig. 2) is in the region of C – F stretching overtones and it is thus more difficult to locate the satellite bands in this case. There are

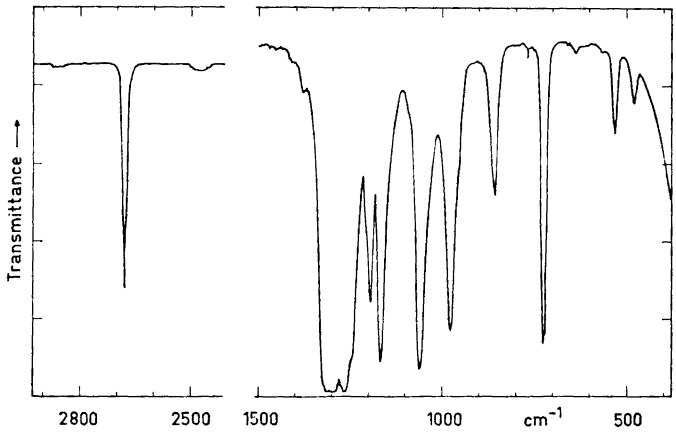

Fig. 2. IR spectrum of gaseous $(CF_3)_3COD$, 10 cm cell, pressure 10 mmHg.

bands ± 180 cm^{-1} ($255/\sqrt{2} = 180$) from the OD stretching band that might be the $\nu OD \pm \tau OD$ bands (from the far-infrared spectrum of gaseous PFTB-*d* we obtain the value 188 cm^{-1} for the OD torsion band).

Inspection of the IR and Raman spectra of the neat liquids (Figs. 1b and 3b) reveals that the extent of association of PFTB is relatively small when compared with that of, *e.g.*, *t*-butyl alcohol, but clearly greater than that of TCHFB. We estimate that roughly 70 – 80 % of PFTB is in the monomeric form. The dimerization constant cannot be measured by the method used previously,[21] as this presupposes that the molar absorption coefficient of the monomer remains constant with increasing alcohol content of the solution, which is true only in dilute solutions. It has been found previously [22] that the dimerization constant of fluorinated *t*-butyl alcohols decreases with increasing number of fluorine atoms in the molecule.

The value of the monomer-dimer shift, about 80 cm^{-1}, is relatively small.[22] There is a shoulder on the low-frequency side of the monomer band in the spectra of liquid PFTB (Figs. 1b and 3b) that probably is due to a terminal OH group of a linear dimer.

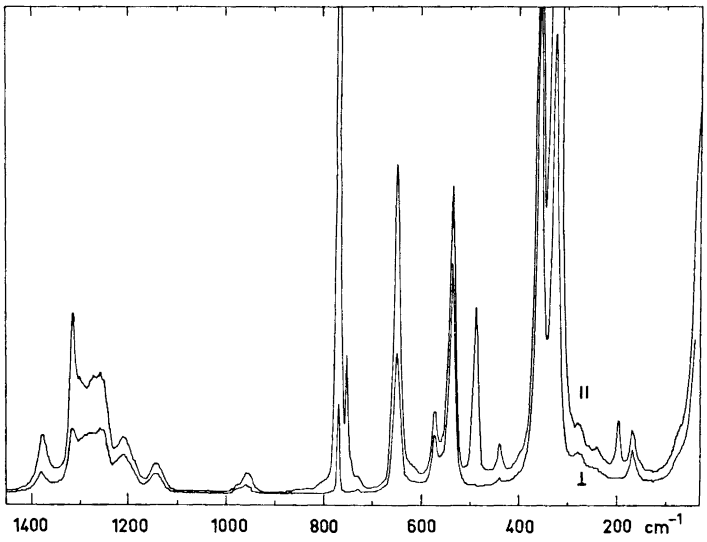

Fig. 3a. Raman spectrum of liquid $(CF_3)_3COH$, region 1400 – 0 cm^{-1}.

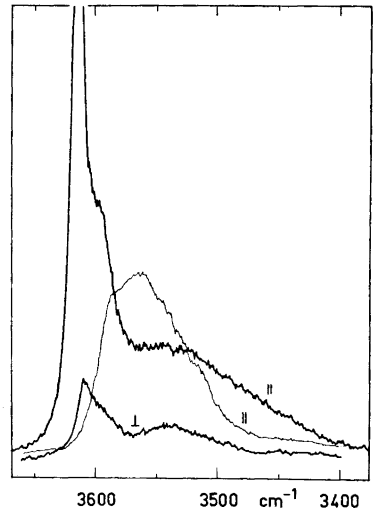

Fig. 3b. Raman spectra in the OH stretching region of liquid $(CF_3)_3COH$ (thick line) and liquid $CCl_3C(CF_3)_2OH$ (thin line). The sensitivity was five times greater than the sensitivity when Fig. 3a was recorded.

In the spectrum of a dilute solution of PFTB in CCl_4, the OH stretching band is at 3574 cm^{-1}; with increasing concentration a shoulder appears at 3610 cm^{-1}. This cannot be due to a terminal OH group as the extent of dimer formation must still be low. This concentration dependence of the bands is exceptional and indicates a specific interaction between PFTB and CCl_4 molecules. Tamborski *et al.*[23] found a similar effect in spectra of aromatic

perfluorinated *t*-butyl alcohols in CCl_4. Also Sherry [8] proposed a specific interaction to occur between PFTB and CCl_4 to explain his calorimetric results.

No "fingers" are found on the low-frequency side of the OH stretching band of liquid and solid PFTB and liquid TCHFB; such intense bands have been observed in spectra of phenol [24] and HFP [3] and they are absent from the vapour spectra.

Only one conformer seems to dominate also in the argon matrix.

OH (OD) bending. The δOH band of tertiary alcohols is usually above 1300 cm^{-1}.[25] It is obviously at 1381 cm^{-1} in the spectrum of gaseous PFTB as it shifts to 1063 cm^{-1} on deuteration (simultaneously it gains in intensity). The frequency ratio is thus 1.30. In the vapour spectrum of TCHFB the OH bending band was at 1370 cm^{-1} and on deuteration it shifted to 1075 cm^{-1}.[1] Fluorination of *t*-butyl alcohol increases the value of the OH bending frequency.[5,1] The OH and OD bending bands seem not to be influenced by aggregation, as no characteristic new association bands were found in the spectra of solid and liquid PFTB (although the OH stretching region of the solid indicated

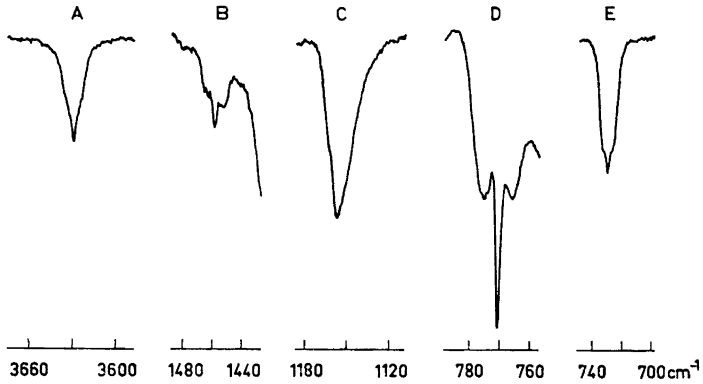

Fig. 4. Band contours in IR spectra of gaseous $(CF_3)_3COH$. Bands A, C, and E, 5 cm cell, pressure 5 mmHg. Bands B and D, 1 m cell, pressure 30 mmHg.

only associated PFTB). The situation was similar in the case of the OD bending band of $(CF_3)_2CHOD$ at about 1000 cm^{-1}; the obvious reason for this kind of behaviour is coupling with other vibrations (two OH association bands are seen in the spectra of liquid HFP [3]). Unfortunately, the OH bending band of PFTB in DMSO could not be seen in the Raman spectrum because of the solvent bands.

C–F stretchings. The representation of the C–F stretching vibrations is $5a' + 4a''$ in point group C_s and $2a_1 + a_2 + 3e$ in point group C_{3v}. As it is expected that the splitting of the degenerate fundamentals is small, there should be six bands due to C–F stretching vibrations in the IR and Raman spectra of PFTB (one of these may be weak in both spectra, as a fundamental of species a_2 is inactive in both cases). The splitting could not be verified even

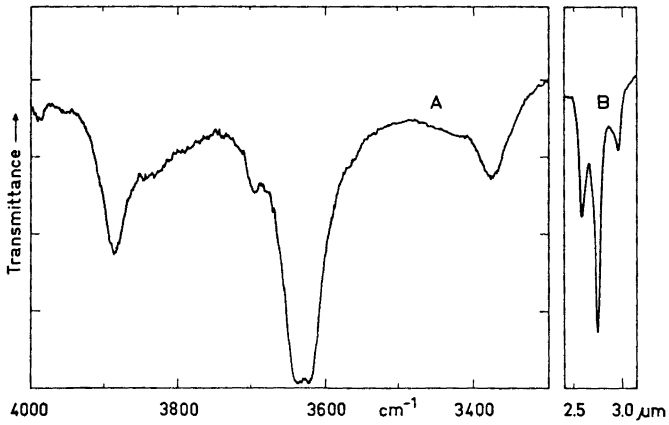

Fig. 5. IR spectrum of gaseous $(CF_3)_3COH$ in the OH stretching region showing the satellite bands. A, 1 m cell, pressure 32 mmHg. B, 100 m cell, pressure 0.15 mmHg.

in the matrix spectrum, as there were very many bands in the region in question (Fig. 7).

C–F stretching bands are usually found between 1100 and 1350 cm^{-1} (see, however, Ref. 26). The highest Raman intensity and the lowest depolarization ratio in this region is at 1316 cm^{-1} for PFTB; this band is probably due

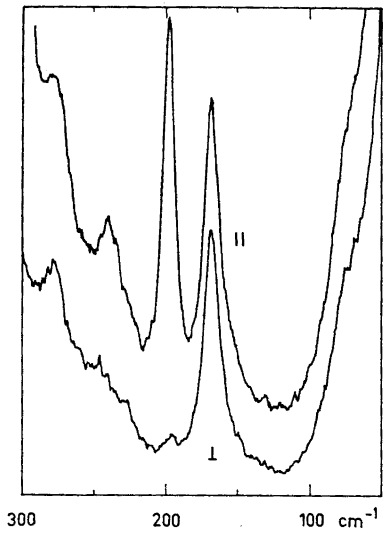

Fig. 6. Raman spectrum of liquid $(CF_3)_3COH$ in the low-frequency region.

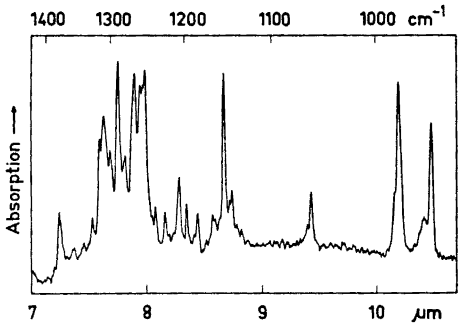

Fig. 7. Part of the IR spectrum of $(CF_3)_3COH$ in an argon matrix. M/A = 1000, 2 μmol of the alcohol deposited.

to the vibration where all C–F bonds stretch in concert. In the Raman spectrum of PFTB-*d* this band is at 1326 cm^{-1} (no IR band is seen at this position). As usual, the CF_3 stretching Raman bands are weak, and as they are also close together, accurate band positions and depolarization ratios were not obtained.

The wavenumbers of the overtones of many vibrations of PFTB are about 1.96 times those of the fundamentals (this is true also for the OH stretching).

Skeletal stretchings. The representation of the skeletal stretching vibrations is $3a'+a''$ (C_s) or $2a_1+e$ (C_{3v}). Because of coupling of vibrations in compounds of type $(CX_3)_3CO$, it is difficult to find a band that relates essentially to C–O stretching.[12,27] In the case of PFTB, the band at 771 cm^{-1} (Fig. 4D) can be unequivocally assigned to a symmetric skeletal stretching vibration. It is the most intense band in the Raman spectrum (it is five times as intense as any other band; it gave 10^5 counts s^{-1} with the FW-130 photomultiplier tube and multipass cell and dead-time effects of the detector begin to become significant at such high intensities). It is also completely polarized. There is a similar weak band at 1462 cm^{-1} in the vapour spectrum (Figs. 1 and 4B) that obviously is the overtone band of the symmetric skeletal stretching vibration. The vibration is thus very anharmonic (1462/771 = 1.896; the intensity of the 1462 cm^{-1} band is about one fifth of that of the 771 cm^{-1} band). The band (at 770 cm^{-1}) is very sharp in the IR spectrum of the liquid, and the same is true regarding the overtone.

The bands at 955 and 979 cm^{-1} are obviously also skeletal stretching bands. The band at 955 cm^{-1} shifts to 864 cm^{-1} on deuteration. A shift of this kind seems to be characteristic of fluorinated *t*-butyl alcohols.[1,5] The fourth skeletal stretching band was not found with certainty; the band may also be obscured by the intense C–F stretching bands.

CF_3 bendings. The representation of these is similar to that of the C–F stretchings, and the bands are usually between 500 and 750 cm^{-1}. There are four bands in this region in the spectrum of PFTB that can be assigned with a high degree of certainty as CF_3 bending bands. The assignment is supported by analogy with HFP,[3] TCHFB [1] and other compounds.[15,16] It is possible that two fundamentals may occur at about the same wavenumber, and we consider the shoulder at 540 cm^{-1} in the vapour spectrum to be the fifth bending fundamental band.

Skeletal bendings. Their representation is $3a'+2a''$ (C_s) or a_1+2e (C_{3v}). Three of the bands (at 488, 357, and 328 cm^{-1}) can be assigned by analogy with HFP, TCHFB and other compounds with a relatively high degree of certainty. The band at 328 cm^{-1} is obviously due to deformation of the CF_3-C-CF_3 angle; its position is relatively insensitive to structure.[1,3,16] The band at 488 cm^{-1} is assigned to the most symmetric (a_1 type) deformation.

CF_3 rockings. The representation is $3a'+3a''$ (C_s) or a_1+a_2+2e (C_{3v}). The band at 199 cm^{-1} (Raman, liquid; Figs. 3a and 6) obviously relates to the most symmetric rock (a_1 type) as it is completely polarized and no such band is seen in spectra of HFTB and HFP. The assignment of the band at 170 cm^{-1} as a rocking band is also on a firm basis (*cf.* Refs. 1 and 3). The assignments of the bands at 291 and 316 cm^{-1} are the least certain.

OH (OD) torsion (out-of-plane bending). The broad torsion band is seen at 252 cm^{-1} in the IR spectrum of gaseous PFTB; the OD torsion band is at

188 cm^{-1} in the spectrum of gaseous PFTB-*d*. The ratio $\tau OH/\tau OD$ is thus 1.34. No association band of the torsions was seen, as is usual with highly fluorinated alcohols.[3,5]

CF_3 torsions. These bands are obviously at about 50 – 70 cm^{-1} (*cf.* Ref. 15). The shoulder at about 70 cm^{-1} on the Rayleigh band in the Raman spectra of liquid PFTB and PFTB-*d* may possibly be due to these.

The *t*-perhalogenobutanols will be discussed further by one of us (J. K.-T.) later.

Acknowledgements. Dr. A. J. Barnes (University College of Swansea, Wales) is thanked for the recording of the matrix isolation spectrum and for helpful suggestions, Mr. J. Corbett (Royal Ordinance Laboratory, Bridgwater, England) for recording the gas spectrum with a 100 m path length cell (this was proposed and kindly arranged by Dr. H. E. Hallam, University College of Swansea), Dr. W. A. Thomas (University College of Swansea) for recording the ^{19}F NMR spectrum, and Dr. J. Kankare (University of Turku, Finland) for checking the wavenumbers of the low-frequency vapour bands with a Perkin-Elmer Model 180 Spectrometer. We gratefully acknowledge financial support from the *Jenny and Antti Wihuri Foundation* (to purchase chemicals) and from the *Finnish National Research Council for Sciences*.

REFERENCES

1. Murto, J., Kivinen, A., Kajander, K., Hyömäki, J. and Korppi-Tommola, J. *Acta Chem. Scand.* **27** (1973) 96. (Part 17.)
2. Dyatkin, B. L., Mochalina, E. P. and Knunyants, I. L. *Tetrahedron* **21** (1965) 2991; Filler, R. and Schure, R. M. *J. Org. Chem.* **32** (1967) 1217.
3. Murto, J., Kivinen, A., Viitala, R. and Hyömäki, J. *Spectrochim. Acta. To be published.*
4. Barnes, A. J. and Murto, J. *J. Chem. Soc. Faraday Trans. 2* **1972**. *In press.*
5. Korppi-Tommola, J. *To be published.*
6. Knunyants, I. L. and Dyatkin, B. L. *Izv. Akad. Nauk SSSR Ser. Khim.* **1964** 923.
7. Dear, R. E. A., Fox, W. B., Fredericks, R. J., Gilbert, E. E. and Huggins, D. K. *Inorg. Chem.* **9** (1970) 2590.
8. Sherry, A. D. *Diss. Abstr.* **B 32** (1971) 3288; *Ph. D. Thesis*, Kansas State University 1971, p. 68; Sherry, A. D. and Purcell, K. F. *J. Am. Chem. Soc.* **94** (1972) 1853.
9. Dear, R. E. A. *Synthesis* **7** (1971) 361.
10. Barnes, A. J., Hallam, H. E. and Scrimshaw, G. F. *Trans. Faraday Soc.* **65** (1969) 3150.
11. Tanaka, C. *Nippon Kagaku Zasshi* **83** (1962) 398.
12. Pritchard, J. G. and Nelson, H. M. *J. Phys. Chem.* **64** (1960) 795.
13. Schachtschneider, J. H. *Technical Report No. 231–64*, Shell Development Co.
14. Boulet, G. A. *Diss. Abstr.* **25** (1964) 3283; Hildebrandt, R. L., Andreassen, A. L. and Bauer, S. H. *J. Phys. Chem.* **74** (1970) 1586; Aziz, N. E. A. and Rogowski, F. *Z. Naturforsch.* **19b** (1964) 967; Buckton, K. S. and Azrak, R. G. *J. Chem. Phys.* **52** (1970) 5652; Prater, B. G. L. *Diss. Abstr.* **B 30** (1970) 5454; Andreassen, A. L., Zebelman, D. and Bauer, S. H. *J. Am. Chem. Soc.* **93** (1971) 1148; Andreassen, A. L. and Bauer, S. H. *J. Chem. Phys.* **56** (1972) 3802.
15. Berney, C. V. *Spectrochim. Acta* **21** (1965) 1809.
16. Miller, F. A. and Kiviat, F. E. *Spectrochim. Acta* **A 25** (1969) 1577.
17. Stølevik, R. and Thom, E. *Acta Chem. Scand.* **25** (1971) 3205.
18. Reece, I. H. and Werner, R. L. *Spectrochim. Acta* **A 24** (1968) 1271.
19. Gerhard, S. L. and Dennison, D. M. *Phys. Rev.* **43** (1933) 197.
20. *E.g.*, Jones, D. *Ph. D. Thesis*, University College of Swansea, University of Wales 1965.
21. Kivinen, A. and Murto, J. *Suomen Kemistilehti* **B 40** (1967) 6.
22. Kivinen, A., Murto, J., Korppi-Tommola, J. and Kuopio, R. *Acta Chem. Scand.* **26** (1972) 904.

23. Tamborski, C., Burton, W. H. and Breed, L. W. *J. Org. Chem.* **31** (1966) 4229.
24. Evans, J. C. *Spectrochim. Acta* **16** (1960) 1382.
25. Stuart, A. V. and Sutherland, G. B. B. M. *J. Chem. Phys.* **24** (1956) 559.
26. Tuazon, E. C., Fateley, W. G. and Bentley, F. F. *Appl. Spectrosc.* **25** (1971) 374.
27. Simpson, D. M. and Sutherland, G. B. B. M. *Proc. Roy. Soc. (London)* **A 199** (1949) 169.

Received June 15, 1972.

ACTA CHEMICA SCANDINAVICA 27 (1973) 121–126

The Effect of Anions on the Oxidase Activity of Rat Ceruloplasmin

ROLF A. LØVSTAD* and EARL FRIEDEN

Department of Chemistry, Florida State University, Tallahassee, Florida 32306, USA, and Institute for Medical Biochemistry, University of Oslo, Oslo, Norway

The oxidation of DPD and PPD by rat ceruloplasmin was studied. With DPD as substrate the double reciprocal plots ($1/V$ *vs.* $1/[S]$) were non-linear, indicating two different, active sites. Recent investigations, however, suggest that the non-linearity is due to the complex interaction between ceruloplasmin, DPD and oxidation products of DPD.

When PPD acted as substrate in the presence of NADH, straight lines were obtained in double reciprocal plots, indicating only one type of active site.

The kinetics of inhibition of the PPD oxidase activity by some monovalent anions were studied, and the order of inhibition was found to be $F^- > I^- > NO_3^- > Br^- > Cl^-$. The inhibitory power of Cl^-, Br^-, NO^-_3 and I^- followed the lyotropic series, the effect being inversely proportional to the radius of the hydrated anion. Kinetic studies revealed a non-competitive inhibition mechanism in the case of Cl^-, Br^-, NO_3^- and I^-, while F^- gave a "mixed type" inhibition pattern. The results suggest that F^- and the other anions investigated bind to different sites on the enzyme molecule. The effect of anions on rat ceruloplasmin was compared with their effect on human ceruloplasmin.

Ceruloplasmin (E.C.1.12.3) is a blue serum protein, containing copper atoms, and having oxidase activity against several aromatic diamines and diphenols.[1–4] The blue color and oxidase activity can be attributed to protein bound cupric ions.[5] During reaction electrons are transferred from substrate to cupric ions, reducing them to cuprous. The latter are reoxidized by molecular oxygen.

Holmberg and Laurell [6] found that human ceruloplasmin was strikingly sensitive to monovalent anion inhibition. The kinetics of anion inhibition were further investigated by Curzon and Speyer,[7,8] who reported that the order of inhibitory effect of halide ions was $F^- > I^- = Cl^- > Br^-$.

Although the kinetics of human ceruloplasmin have been extensively studied,[1–8,10–12] little work has been done on ceruloplasmin from other sources.

* Present address: Institute for Medical Biochemistry, University of Oslo, Oslo, Norway.

This paper describes the kinetic properties of rat ceruloplasmin and the effect of some monovalent anions on the oxidase activity of the enzyme. The results have been compared with those reported for human ceruloplasmin.

EXPERIMENTAL

Materials. DPD.HCl,* PPD, and NADH were purchased from Sigma Chemical Company and Desferal from Ciba Pharmaceutical Company. All other reagents were of the purest grade available commercially. Aqueous solutions were prepared in deionized, glass distilled water.

Ceruloplasmin was purified from serum obtained from female Wistar rats (250 – 300 g). Rat serum (50 ml) was diluted ten times with 0.05 M potassium phosphate buffer, pH 6.8, containing 0.1 M KCl, and placed on a DEAE-Sephadex A-50 column (1.6 cm × 15 cm), equilibrated with 0.05 M potassium phosphate buffer, pH 6.8, in 0.1 M KCl. The purification was carried out in the cold room (4°). Ceruloplasmin formed a blue band on the top of the column, which was thoroughly washed with 0.05 M potassium phosphate buffer, pH 6.8, in 0.1 M KCl. The enzyme was eluted with 0.5 M potassium phosphate buffer, pH 6.8, in 0.1 M KCl. The ratio between the absorbances at 610 mμ and 280 mμ was 0.011.

The enzyme solution was 40 % saturated with ammonium sulfate and centrifuged for 20 min at 12 300 *g* and 0°. The supernatant, containing ceruloplasmin, was 50 % saturated with ammonium sulfate, and 70 % of the total ceruloplasmin content was found in the precipitate after centrifugation for 20 min at 12 300 *g* and 0°. The rest of the ceruloplasmin precipitated at 60 % saturation with ammonium sulfate. The ceruloplasmin-containing precipitates were dissolved in 0.6 M sodium acetate buffer, pH 6.0. The ratio between the absorbances at 610 mμ and 280 mμ was 0.015 for both samples.

Oxidase activity measurements. The activity of rat ceruloplasmin was determined as the rate of formation of the red colored radical, DPD^+, an oxidation product of DPD. DPD^+ has an absorption maximum at 552 mμ ($\varepsilon = 9800\ M^{-1}\ cm^{-1}$). [1,3] A lag period occurred when the absorbance at 552 mμ was recorded, the rate increasing during the first 1 – 2 min. After the lag period the 552 mμ absorption increased linearly and the activity was determined from the linear part of the curve.[1] An iron chelating agent, Desferal, was added to all reaction mixtures in order to prevent the activating effect of iron ions on the ceruloplasmin catalyzed oxidation.[1] DPD was dissolved in 25 μM EDTA immediately before use, and stored in an ice bath. The Cl^- concentration in the reaction mixtures was kept at 2.0 mM by adding NaCl, since DPD in the monohydrochloride form was used.

The ceruloplasmin catalyzed oxidation of PPD in the presence of NADH was also investigated. In this case the oxidation product of PPD was reduced to PPD by NADH, and the activity was determined spectrophotometrically at 340 mμ as the rate of NADH oxidation ($\varepsilon = 6220\ M^{-1}\ cm^{-1}$). No initial lag period was observed with this system. It was necessary to correct for a slight non-enzymic oxidation of NADH.

Anion inhibitors were incubated with rat ceruloplasmin for 10 min at 30° before adding substrate. Incubation of enzyme with inhibitor for 2 h resulted in the same degree of inhibition as noted when the rates were measured after 10 min incubation.

A Beckman DK-1 recording spectrophotometer, equipped with a thermocell (1 cm light path), was used and the temperature was kept at 30 ± 0.3° in all experiments except one.

RESULTS AND DISCUSSION

The effect of enzyme concentration on the initial rate of PPD and DPD oxidation was investigated, and as shown in Fig. 1, the activity increased

* Abbreviations: PPD, *p*-phenylenediamine; DPD, *N,N*-dimethyl-*p*-phenylenediamine, DPD^+, *N,N*-dimethyl-*p*-phenylenediamine radical, Desferal, deferoxamine B-methane sulfonate, NADH, dihydronicotinamide adenine dinucleotide, EDTA, ethylenediaminetetraacetic acid.

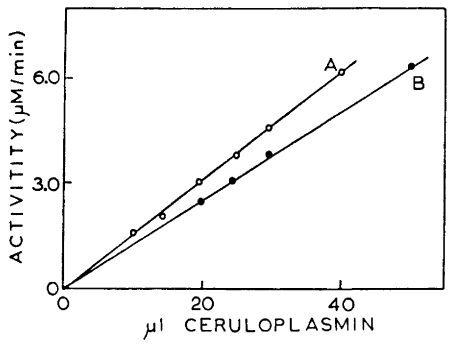

Fig. 1. Effect of rat ceruloplasmin concentration on the oxidase activity at 30°. When PPD (A) acted as substrate the reaction mixture contained 10 – 40 μl ceruloplasmin ($E_{610}=0.10$) (total volume 1.0 ml), 0.5 mM Desferal, 0.24 mM NADH, and 4.0 mM PPD in 0.10 M sodium acetate buffer, pH 5.5. In the presence of DPD (B) the reaction mixture contained 20 – 50 μl ceruloplasmin ($E_{610}=0.03$) (total volume 1.0 ml), 0.5 mM Desferal and 1.0 mM DPD in 0.10 M sodium acetate buffer, pH 5.3.

linearly with enzyme concentration when substrate concentration was kept constant. The pH optimum of rat ceruloplasmin was 5.6 with PPD as substrate and 5.0 with DPD at 30°.

Fig. 2a shows a non-linear relationship between rat ceruloplasmin activity and DPD concentration in a double reciprocal plot ($1/V$ *vs.* 1/[S]) at 30° and

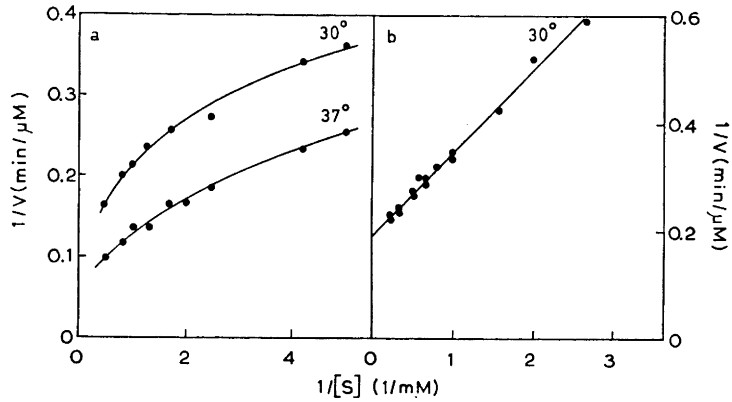

Fig. 2. a. The reciprocal rate of DPD oxidation plotted against the reciprocal DPD concentration. The reaction mixture contained 25 μl rat ceruloplasmin ($E_{610}=0.07$) (total volume 1.0 ml), 0.5 mM Desferal, 2.0 mM Cl^- and DPD (0.2 mM – 2.0 mM) in 0.1 M sodium acetate buffer, pH 5.5. b. The reciprocal rate of PPD oxidation in the presence of NADH plotted against the reciprocal PPD concentration. The reaction mixture contained 25 μl rat ceruloplasmin ($E_{610}=0.10$) (total volume 1.0 ml), 0.5 mM Desferal, 0.24 mM NADH and PPD (0.38 mM – 5.0 mM) in 0.1 M sodium acetate buffer, pH 5.5.

37°. A similar result has been reported for human [1,3] and porcine [9] ceruloplasmin. Curzon [1] and Walaas *et al.*[3] interpreted the non-linear plots in terms of two different active sites acting on the same substrate. However, kinetic studies by Pettersson and Pettersson [10,11] demonstrated that the kinetics observed could be explained by the fact that the first oxidation product of DPD, DPD^+, interacts with ceruloplasmin as reported by Walaas *et al.*,[3] and

that there exists a non-enzymic equilibrium between DPD and its oxidation products, DPD^+ and DPD^{2+}. Kinetic experiments by Curzon,[12] using a DPD-ascorbate coupled system, confirmed the results of Pettersson and Pettersson.

When PPD acted as substrate for rat ceruloplasmin in the presence of NADH, a straight line was obtained in a double reciprocal plot (Fig. 2b), indicating that PPD reacts with only one type of active site. This is in accordance with the observation of Curzon.[12] The apparent Michaelis constant (K_m) for PPD was estimated to 1.0 mM. In the following kinetic studies the PPD-NADH coupled system was used, since the complex mechanism of DPD-ceruloplasmin interaction gives rise to the non-linearity shown in the double reciprocal plots in Fig. 2a.

Monovalent anions of the Hofmeister or lyotropic series [13] had an inhibitory effect on the rat ceruloplasmin catalyzed oxidation of PPD (Fig. 3). The order

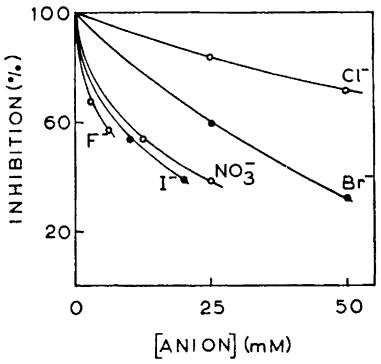

Fig. 3. Inhibitory effect of anions on the maximum rate (V_{max}) of the ceruloplasmin catalyzed oxidation of PPD, as calculated from Fig. 4.

of effectiveness was $F^- > I^- > NO_3^- > Br^- > Cl^-$. The same order of inhibition was observed when DPD acted as substrate. Except for F^- the order of inhibitory power conforms to the lyotropic series as shown for several enzymes ($I^- > Br^- > Cl^- > F^-$).[14–16] The unusually strong binding of F^- to copper enzymes like tyrosinase,[17] laccase,[18] and human ceruloplasmin [7] suggests that F^- binds to protein copper. Studies by Andréasson and Vänngård,[19] made with the electron paramagnetic resonance technique, demonstrated that F^- binds to the type 2 Cu(II) on the human ceruloplasmin molecule.

The order of inhibition of rat ceruloplasmin by halide ions differs somewhat from the order reported by Curzon and Speyer [7] for human ceruloplasmin ($F^- > I^- = Cl^- > Br^-$). I^- is a much better inhibitor than Cl^- and Cl^- inhibits less than Br^- compared to human ceruloplasmin.

The order of inhibitory power of the anions could not be attributed to differences in anionic size in the case of rat ceruloplasmin. However, the degree of inhibition was found to decrease with increasing radius of the hydrated anion (r_s),[20] indicating that the size of the hydrated anion may strongly affect the anion-protein interaction (Fig. 5). F^- did not fit into the plot in Fig. 5 being heavily hydrated ($r_s = 3.06$ Å) and would be expected to be the weakest inhibitor among the anions investigated, as is usually the case.[14–16] It is therefore probable that F^- binds to another site on the enzyme molecule.

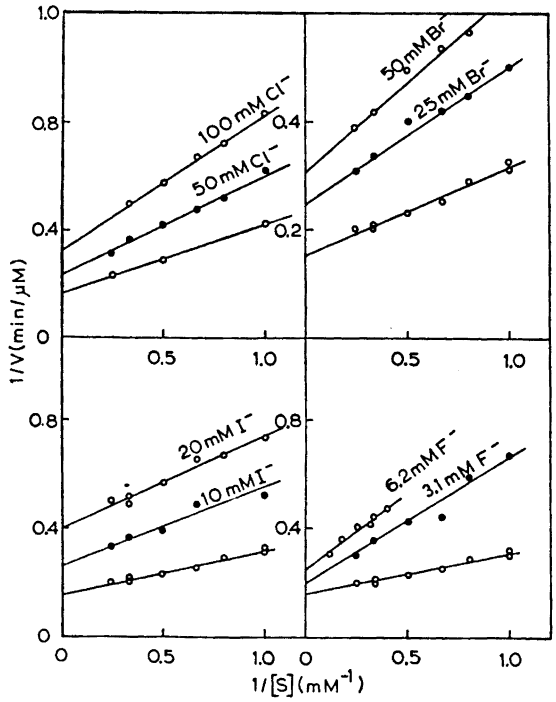

Fig. 4. Effect of anions on the PPD oxidase activity of rat ceruloplasmin at 30°. The reaction mixture contained 25 μl rat ceruloplasmin ($E_{610}=0.10$) (total volume 1.0 ml), 0.5 mM Desferal, 0.24 mM NADH and PPD (1.0 mM – 4.0 mM) in 0.1 M sodium acetate buffer, pH 5.5.

Fig. 4 shows the effect of several inhibitor and substrate concentrations on the oxidase activity of rat ceruloplasmin. The straight lines obtained in the double reciprocal plots intersect very close to the abscissa in the case of Cl^-,

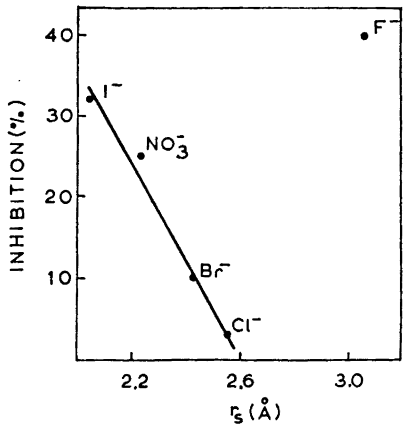

Fig. 5. The inhibitory effect of anions (5.0 mM) on the maximum PPD oxidase activity (V_{max}) of rat ceruloplasmin plotted against the radius of the hydrated anions. Experimental conditions as described in the legend to Fig. 4.

Br^-, NO_3^-, and I^-. This non-competitive mechanism of inhibition indicates that these anions bind to another site on the enzyme than the substrate, and may affect the reaction by inducing a change at the active site or by preventing a possible electron transport on the protein molecule. Ceruloplasmin is reoxidized by molecular oxygen after reduction by substrate and has to store four electrons in order to reduce one molecule of oxygen to water. A transport of electrons from the active site to other parts of the enzyme may therefore take place.

Cl^-, Br^-, NO_3^-, and I^- probably bind to the same site on the enzyme, since the inhibitory mechanism is the same for all of them (Fig. 4), and the order of inhibition follows the lyotropic series.

The mechanism of F^- inhibition is somewhat different as demonstrated in Fig. 4. The lines obtained intersect much closer to the ordinate, suggesting a "mixed type" of inhibition,[21] the effect of F^- being reduced by increasing substrate concentration. This mechanism of inhibition is generally explained by assuming that the inhibitor and substrate bind to different sites on the protein molecule, the inhibitor affecting both the substrate affinity of the enzyme and the rate of product formation.[21]

Acknowledgements. We thank Professor O. Walaas, Dosent E. Walaas and Dr. S. Osaki for their help and interest and Mrs. A. Horn for technical assistance. This work was supported in part by the *U.S. Public Health*, Grant HE 08344.

R. Løvstad was a recipient of U.S. Int. Public Health Service Research Fellowship 1-FO-5-TW-1430-01.

Paper No. 36 in a series from Department of Chemistry, Florida State University, Tallahassee, Florida 32306, USA, on copper biosystems.

REFERENCES

1. Curzon, G. *Biochem. J.* **103** (1967) 289.
2. Peisach, J. and Levine, W. G. *Biochim. Biophys. Acta* **77** (1963) 615.
3. Walaas, E., Løvstad, R. A. and Walaas, O. *Arch. Biochem. Biophys.* **121** (1967) 480.
4. Løvstad, R. A. *Acta Chem. Scand.* **25** (1971) 3144.
5. Broman, L., Malmström, B. G., Aasa, R. and Vänngård, T. *J. Mol. Biol.* **5** (1963) 301.
6. Holmberg, C. G. and Laurell, C. B. *Acta Chem. Scand.* **5** (1951) 921.
7. Curzon, G. and Speyer, B. E. *Biochem. J.* **105** (1967) 243.
8. Curzon, G. and Speyer, B. E. *Biochem. J.* **109** (1968) 25.
9. Sekiguchi, T. and Nosoh, Y. *Arch. Biochem. Biophys.* **138** (1970) 319.
10. Pettersson, G. and Pettersson, I. *Acta Chem. Scand.* **23** (1969) 3235.
11. Pettersson, G. *Acta Chem. Scand.* **23** (1969) 2317.
12. Curzon, G. *Abstract, 8th International Congress of Biochem.*, Switzerland 1970.
13. Alexander, J. *Colloid Chemistry*, Van Nostrand, New York 1937, p. 143.
14. Pocker, Y. and Stone, J. T. *Biochemistry* **6** (1967) 668.
15. Fridovich, I. *J. Biol. Chem.* **238** (1963) 592.
16. Massey, V. *Biochem. J.* **53** (1953) 67.
17. Krueger, R. C. *Arch. Biochem. Biophys.* **57** (1955) 52.
18. Peisach, J. and Levine, W. G. *J. Biol. Chem.* **240** (1965) 2284.
19. Andréasson, L.-E. and Vänngård, T. *Biochim. Biophys. Acta* **200** (1970) 247.
20. Padova, J. *J. Chem. Phys.* **40** (1964) 691.
21. Dixon, M. and Webb, E. C. *Enzymes*, Longmans, London 1964, p. 324.

Received June 14, 1972.

ACTA CHEMICA SCANDINAVICA 27 (1973) 127–140

Gaschromatographische Analyse von Ligninoxydationsprodukten. VII.* Ein verbessertes Verfahren zur Charakterisierung von Ligninen durch Methylierung und oxydativen Abbau

MAGNUS ERICKSON, SAM LARSSON und GERHARD E. MIKSCHE

Institutionen för organisk kemi, Chalmers Tekniska Högskola och Göteborgs Universitet, Fack, S-402 20 Göteborg 5, Schweden

Ein verbessertes Verfahren zur strukturellen Charakterisierung von Ligninen durch Methylierung und oxydativen Abbau wird beschrieben. Die Methylierung der phenolischen Hydroxylgruppen wird mit Dimethylsulfat – KOH in Dimethoxyäthan – Methanol – H_2O (35:35:30) bei pH 11 durchgeführt. Das methylierte Lignin wird zuerst bei 82° mit $KMnO_4$ – $NaJO_4$ in verdünnter Natronlauge, die 15 % *tert.*-Butanol enthält, dann mit H_2O_2 bei pH 9 – 10 (50°) abgebaut. Die so erhaltenen aromatischen Carbonsäuren werden mit Diazomethan methyliert und die Hauptkomponenten des Estergemisches auf gaschromatographischem Wege quantitativ bestimmt. Die Ausbeuten an diesen Estern sind für die Struktur des Lignins charakteristisch. Beispiele für den oxydativen Abbau von Ligninen, die mit natriumsulfidhaltiger Natronlauge aufgeschlossen worden waren («Sulfatlignine«), und von Ligninmodellen werden angegeben.

In einer vorangehenden Arbeit dieser Reihe ist ein zweistufiger Abbau von methylierten Ligninpräparaten beschrieben worden.[1b] Zunächst wurde das Lignin mit $KMnO_4$ bei pH 11 – 12 oxydiert; dabei entstand ein Gemisch von Arylcarbonsäuren und Arylglyoxylsäuren. In einem zweiten Oxydationsschritt wurden letztere mit H_2O_2 bei pH 9 – 10 in die entsprechenden Arylcarbonsäuren übergeführt. Die mit Diazomethan erhaltenen Methylester dieser Abbausäuren wurden gaschromatographisch getrennt und massenspektrometrisch identifiziert (Kombination Gaschromatograph – Massenspektrometer). Die wichtigsten Abbausäuren (*1* – *9*) konnten auch quantitativ bestimmt werden.[1c]

Das hier skizzierte Abbauverfahren ist in der Chemie des Lignins und verwandter Naturstoffe vielseitig anwendbar. Eine dieser Anwendungsmöglichkeiten ist der chemotaxonomische Vergleich von Ligninen verschiedenen Ursprungs. Hierfür wird zunächst das Lignin zweckmässig durch Erhitzen des Pflanzenmaterials mit natriumsulfidhaltiger Natronlauge («Sulfatauf-

* VI. Mitteilung siehe Lit. 1a.

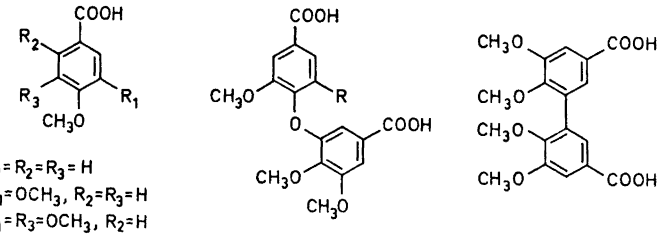

1 $R_1=R_2=R_3=H$
2 $R_1=OCH_3$, $R_2=R_3=H$
3 $R_1=R_3=OCH_3$, $R_2=H$
4 $R_1=OCH_3$, $R_2=H$, $R_3=COOH$
5 $R_1=OCH_3$, $R_2=COOH$, $R_3=H$
6 $R_1=R_3=OCH_3$, $R_2=COOH$

7 R = H
8 $R=OCH_3$

9

schluss«) herausgelöst. Methylierung und oxydativer Abbau des so erhaltenen Sulfatlignins, gefolgt von einer quantitativen Bestimmung der Methylester der wichtigsten Abbausäuren, führt zu einem für das betreffende Lignin charakteristischen Ausbeutenverhältnis der Methylester (vergl. Tab. 2). Dieses Ausbeutenverhältnis spiegelt die Anteile der Guajacyl-, Syringyl- und *p*-Hydroxyphenylpropanstrukturen am Aufbau des betreffenden Lignins wider.[1c] Das zur gleichen Aussage früher herangezogene Verfahren der Nitrobenzoloxydation von Ligninen (für eine kritische Übersicht siehe Lit. 2) ist dem zweistufigen oxydativen Abbau unter anderem darin unterlegen, dass es nur die nicht-kondensierten Arylpropaneinheiten berücksichtigt.

Beim Vergleich der an Ligninen verschiedener Herkunft erhaltenen Ergebnisse ist eine gute Reproduzierbarkeit der quantitativen Bestimmung der Abbausäuren von wesentlicher Bedeutung. Um diese zu gewährleisten, wurden die Versuchsbedingungen für die Methylierung und für den oxydativen Abbau weiter ausgearbeitet. Die Beschreibung der nun eingeführten Verbesserungen, sowie die Anwendung des Verfahrens auf einige Sulfatlignine und eine Anzahl von Ligninmodellen, bildet den Gegenstand der vorliegenden Mitteilung.

Methylierung

Bisher wurde die Methylierung der phenolischen Hydroxylgruppen des Lignins in der üblichen Weise, nämlich durch wechselweise Zugabe von Dimethylsulfat und Natronlauge zu einer Lösung des Ligninpräparats in wässrigem Dioxan, durchgeführt.[1b] Der Wirkungsgrad dieses Verfahrens ist – im Hinblick auf die dabei verbrauchten erheblichen Mengen von Dimethylsulfat und Lauge – gering. Durch den zeitweilig grossen Überschuss an Hydroxylion wird die unerwünschte Hydrolyse des Dimethylsulfats begünstigt; die wechselweise Zugabe von Lauge und Dimethylsulfat ist ausserdem nur mit grösserem Arbeitsaufwand reproduzierbar zu gestalten. Es erschien daher wünschenswert, die Methylierung unter optimalen Bedingungen, d.h. bei möglichst vollständiger Ionisierung der phenolischen Hydroxylgruppen und möglichst geringer Konzentration an Hydroxylionen, durchzuführen. Diese Bedingungen sind dann gegeben, wenn der pH-Wert bei der Methylierung in der Grössenordnung des pK-Wertes (etwa 10) der phenolischen Hydroxylgruppen des Lignins liegt.

Die Konstanthaltung des pH-Wertes bei der Methylierung wurde durch Laugenzugabe mittels eines Magnetventils erzielt, das durch eine mit einem pH-Kontrollgerät gekoppelte Glas-Kalomel-Kombinationselektrode gesteuert wird. Das gesamte Dimethylsulfat wird am Beginn der Methylierung zugegeben und der pH-Wert bei 11 gehalten. Als Lösungsmittel für die Methylierung von Ligninpräparaten und Modellen erwies sich ein Gemisch aus Dimethoxyäthan – Methanol – Wasser (35:35:30) als geeignet. Die Methylierung ist bei 25° nach etwa 24 Stunden beendet.

Der Vorteil dieses Verfahrens gegenüber dem früher angewendeten liegt auch in den sehr milden Bedingungen der Methylierung phenolischer Hydroxylgruppen. Die Vollständigkeit der Methylierung wurde durch Methylierung von Modellverbindungen nachgeprüft.

Modellversuche zur Methylierung

Die phenolischen Modelle *10*, *12* und *14* wurden, wie eben für Lignin beschrieben, bei Zimmertemperatur und pH 11 methyliert. Die erwarteten Methyläther *11*, *13* und *15* wurden in hohen Ausbeuten isoliert. Die einzige Nebenreaktion dürfte die Methylierung eines geringen Teils der alkoholischen Hydroxylgruppen der Modelle *10* und *12* sein; in den Reaktionsprodukten der Methylierung von *12* und *14* konnten nur Spuren von Ausgangsmaterial ($\leq 0{,}5$ %) nachgewiesen werden (Gaschromatographie und Dünnschichtchromatographie), bei dem Produkt aus der Methylierung von *10* lag die Menge von vorhandenem Ausgangsmaterial unter der Nachweisgrenze. Die vollständige Methylierung der beiden *o,o*-disubstituierten Modelle *12* und *14* unter diesen schonenden Bedingungen ist bemerkenswert. Das Verfahren besitzt auch präparativen Wert für die Darstellung von Methyläthern empfindlicher Phenole. Mit einem etwas abgeänderten Verfahren können phenolische Hydroxylgruppen auch mit Carbonsäureanhydriden acyliert und Carboxylgruppen mit Dimethylsulfat verestert werden.[3]

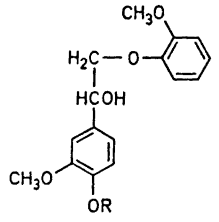

10 R = H
11 R = CH_3

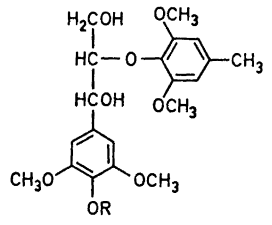

12 R = H
13 R = CH_3

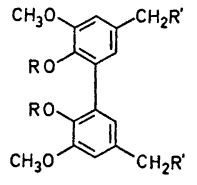

14 R = R' = H
15 R = CH_3, R' = H
16 R = H, R' = CH_2CH_3
17 R = CH_3, R' = CH_2CH_3

Oxydativer Abbau

Früher wurde der erste Schritt des oxydativen Abbaus so durchgeführt, dass eine verdünnte Lösung von Permanganat langsam zur Suspension des

methylierten Lignins in 1-proz. Sodalösung getropft wurde (Reaktionstemperatur für Gymnospermenlignine 100°,[1b] für Angiospermenlignine 80° [1c]).[1b] Eine 10 Min nach der letzten Zugabe von $KMnO_4$ bestehende Violettfärbung zeigte das Ende der Oxydation an. Bei diesem Verfahren mussten die Zutropfgeschwindigkeit und die Reaktionsdauer (etwa 6 Stunden) dem Verbrauch von Permanganat durch das Ligninpräparat angepasst werden, was eine fortlaufende Überwachung der Oxydation erforderte. Die Reproduzierbarkeit dieses Reaktionsschrittes wird beeinträchtigt durch die Schwierigkeit, den jeweils in der Lösung vorhandenen Überschuss an $KMnO_4$ und damit die optimale Zutropfgeschwindigkeit zu beurteilen. Auch können die bei der Reaktion entstehenden grösseren Mengen MnO_2 unter Umständen nicht gelöstes Lignin adsorbieren oder einschliessen.

Eine Standardisierung des Zugabeverfahrens von $KMnO_4$ erschien daher, ebenso wie die Vermeidung der Bildung grösserer Mengen von MnO_2, als wünschenswert. Beides wurde durch die nachfolgend beschriebene Abänderung des Abbauverfahrens erzielt. Der zweite Abbauschritt mit H_2O_2 in schwach alkalischer Lösung wurde unverändert beibehalten.

In alkalischer Lösung oxydiert JO_4^- Manganat (V) oder (VI) zu MnO_4^-. Auf diese Reaktion gründet sich das Verfahren von Lemieux und von Rudloff, mit einer schwach alkalischen Lösung von $NaJO_4$ in Gegenwart katalytischer Mengen von $KMnO_4$ olefinische Doppelbindungen oxydativ zu spalten.[4] Das Lemieux-von Rudloff'sche Verfahren hat inzwischen Verwendung für die selektive Oxydation von Doppelbindungen gefunden.

Wir haben nun die Permanganatoxydation im ersten Schritt des oxydativen Abbaus durch eine Behandlung des methylierten Lignins mit $KMnO_4$-$NaJO_4$ in verdünnter Natronlauge bei 82° ersetzt. Dadurch konnte die Ausführung dieses Abbauschrittes erheblich vereinfacht und die Bildung von MnO_2 während der Oxydation verhindert werden; die Permanganatkonzentration ist nun während der gesamten Reaktionszeit konstant. Eine Voraussetzung für das Gelingen des oxydativen Abbaus mit Permanganat-Perjodat ist die Verwendung von *tert.*-Butanol (15 %) als Lösungsmittelzusatz. Unterbleibt dieser Zusatz, so werden stark verminderte Ausbeuten (allerdings schlecht reproduzierbar) an sämtlichen Abbausäuren erhalten. In Versuchen über die Einwirkung von $KMnO_4$ und/oder $NaJO_4$ auf einige Abbausäuren wurde gezeigt, dass diese in Abwesenheit von *tert.*-Butanol abgebaut werden (Tab. 1). In Gegenwart von *tert.*-Butanol sind sie hingegen weitgehend stabil; nach einer Reaktionsdauer von 6 Stunden wurde ein messbarer Angriff nur bei Trimethylgallussäure (*3*) und Metahemipinsäure (*5*) festgestellt.

Die Ursache für die Stabilisierung der Abbausäuren in Gegenwart von *tert.*-Butanol ist vielleicht darin zu suchen, dass der Alkohol als Abfangmittel für Hydroxylradikale oder andere stark oxydierende Zwischenprodukte wirkt. Hydroxylradikale wurden als Produkte der Oxydation von Hydroxylion durch MnO_4^- postuliert.[5] Nach anderen Autoren ist für die Reduktion von MnO_4^- in Natronlauge die Gegenwart von Übergangsmetallkationen (Co^{2+}, Ni^{2+}, hier wahrscheinlich in Spuren vorhanden) erforderlich.[6] In deren Abwesenheit ist Permanganat auch in stark alkalischer Lösung stabil.[6,7]

Ein weiterer Vorteil der Verwendung von *tert.*-Butanol als Lösungsmittelzusatz [8] ist die erhöhte Löslichkeit des zu oxydierenden Ligninpräparats in

Tab. 1. Stabilität der Abbausäuren unter den Bedingungen des oxydativen Abbaus (6 Stunden bei 82°).

c_{KMnO_4} (mMol/l)	c_{NaJO_4} (mMol/l)	$c_{tert.\text{-Butanol}}$ (Vol-%)	c_{Alkali} (Mol/l)	wiedergewonnene Abbausäuren [a] (in % d. Th.)					
				2	*3*	*4*	*5*	*7*	*9*
3	30	0	0,1 [b]	0	0	30	–	–	–
0	30	0	0,1 [b]	31	30	–	–	–	–
0	30	0	0,14 [c]	30	28	59	–	–	–
3	30	0	0,1 [c]	38	31	70	–	–	–
3 [d]	0	0	0,1 [c]	83	61	97	–	–	–
3	30	15	0,1 [c]	96	86	103	–	95	95
3	30	15	0,1 [c]	98	86	99	83	93	95

[a] Gaschromatographisch als Methylester bestimmt. [b] Na_2CO_3. [c] NaOH. [d] Niederschlag von MnO_2 während der Oxydation.

dem erhaltenen Gemisch; in den meisten beobachteten Fällen war die Oxydationslösung schon von Beginn der Oxydation an oder nach kurzer Oxydationsdauer homogen.

Die mit dem neuen Verfahren bei einer Reaktionstemperatur von 82° und einer Reaktionszeit von 6 Stunden erhaltenen Gesamtausbeuten an den wichtigsten aromatischen Abbausäuren liegen etwas über den mit dem früheren

Tab. 2. Oxydativer Abbau einiger Sulfatlignine.

Lignin	Ester der Abbausäuren (mg Ester per 100 mg Björkman-Lignin oder 400 mg Holzmehl)								
	1	*2*	*3*	*4*	*5*	*6*	*7*	*8*	*9*
Picea abies (Björkman-Lignin)	0,5	21,4	0,15	6,1	0,55	–	1,75	–	3,6
	0,5	20,6	0,15	6,0	0,55	–	1,75	–	3,9
	0,5	21,1	0,15	5,8	0,55	–	1,6	–	4,0
Picea abies (Holzmehl)	0,5	21,3	0,45	5,9	0,6	–	1,65	–	3,4
Torreya nucifera (Holzmehl)	0,7	23,6	–	6,8	0,7	–	2,9	–	5,9
	0,7	23,1	–	6,7	0,5	–	2,6	–	5,9
Taxus baccata (Holzmehl)	0,6	20,1	–	5,9	0,6	–	2,4	–	5,8
	0,5	21,0	–	6,2	0,5	–	2,5	–	5,9
Quercus robur (Holzmehl)	–	5,8	15,8	1,0	0,2	0,25	0,25	0,95	0,45
Syringa vulgaris (Holzmehl)	–	5,7	11,6	1,2	0,15	0,15	0,3	1,4	0,75

Falls die Ausbeute nicht angegeben wurde, bedeutet dies, dass sie unter der Bestimmungsgrenze (0,1 mg per 100 mg Björkman-Lignin oder 400 mg Holzmehl) liegt. Ausbeuten unter 2 mg per 100 mg Björkman-Lignin wurden auf 0,05 mg genau, Ausbeuten über 2 mg per 100 mg Björkman-Lignin auf 0,1 mg genau angegeben; entsprechendes gilt für die Ausbeuten aus Holzmehl (per 400 mg).

Verfahren [1b] erhaltenen. In hier nicht weiter beschriebenen Abbauversuchen an methyliertem Sulfatlignin von Birke (*Betula verrucosa*), erhalten durch Sulfatkochung von Björkman-Lignin, wurde gefunden, dass der oxydative Abbau dieses Lignins im wesentlichen schon nach einer Reaktionsdauer von 4 Stunden abgeschlossen ist; bei verlängerter Reaktionszeit – 5 und 6 Stunden – erhöhten sich die Ausbeuten an Abbausäuren nur unwesentlich.

In Tab. 2 sind einige Ergebnisse des oxydativen Abbaus von Sulfatligninen, die mit dem verbesserten Methylierungs- und Abbauverfahren erhalten wurden, angeführt. Die Sulfatlignine wurden durch Sulfatkochung von Björkman-Lignin (Fichte) und von dem extrahierten Holzmehl (s. exp. Teil) einiger Gymnospermen und Angiospermen erhalten. In einigen Fällen wurden Doppel- und Dreifachbestimmungen durchgeführt; aus diesen Versuchen geht die Reproduzierbarkeit der mit diesem Abbauverfahren erhaltenen Ergebnisse hervor.

Modellversuche zum oxydativen Abbau

Um das Verhalten der wichtigsten Strukturtypen des Lignins genauer kennenzulernen, wurde eine Reihe von Modellverbindungen, die für diese Strukturen repräsentativ sind, dem oxydativen Abbau mit alkalischem $KMnO_4$-$NaJO_4$, gefolgt von der Behandlung mit H_2O_2, unterworfen. Modelle mit freien phenolischen Hydroxylgruppen wurden, mit Ausnahme von Modell *26*, vor dem Abbau mit Dimethylsulfat bei pH 11 methyliert. Die gaschromatographisch bestimmten Ausbeuten an den Methylestern der Abbausäuren *2*, *3*, *4* und *9* sind in Tab. 3 angegeben.

Modelle vom Guajacylpropantyp gaben durchschnittlich etwas höhere Ausbeuten als solche vom Syringylpropantyp. Dies dürfte, wie schon erwähnt, auf den langsamen Abbau von Trimethylgallussäure (*3*) beim oxydativen

Tab. 3. Oxydativer Abbau von Ligninmodellen. Ausbeuten (in % d. Th.) an den Methylestern der Abbausäuren *2*, *3*, *4* und *9* (gaschromatographisch bestimmt).

Modell	*13*	*17*		*19*	*21*	*23*	*23*	*25*
Abbausäure	*3*	*9*	*4*	*3*	*2*	*3*	*3*	*3*
Ausbeute an Methylester	74	66	2	78	65	68	70	77

Modell	*26*		*28*	*31*	*33*	*35*	*37*		*39*
Abbausäure	*4*	*9* [a]	*2*	*2*	*2*	*2*	*2*	*4*	*3*
Ausbeute an Methylester	70	2	60	86	86	91	89	76	75

[a] wahrscheinlich gebildet aus einer Verunreinigung von *26* durch 5,5′-Dehydro-diveratrumaldehyd (*27*).

Abbau zurückzuführen sein. Modelle mit benzylischer Sauerstoffunktion oder kernkonjugierter Doppelbindung (*13*, *19*, *25*, *26*, *31*, *33*, *35*, *37* und *39*) wurden in sehr guten Ausbeuten zu den entsprechenden Carbonsäuren oxydiert. Modelle ohne benzylische Sauerstoffunktion (CH_2-Gruppe), die Verbindungen *17*, *21*, *23* und *28*, gaben die erwarteten Abbausäuren in geringeren, aber ebenfalls noch als gut zu bezeichnenden Ausbeuten.

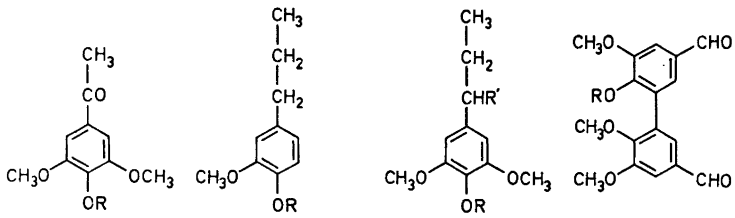

18 R = H
19 R = CH_3

20 R = H
21 R = CH_3

22 R = H, R' = H
23 R = CH_3, R' = H
24 R = H, R' = OH
25 R = CH_3, R' = OH

26 R = H
27 R = CH_3

Im 5,5'-Dehydro-divanillin-monomethyläther (*26*) wurde der unverätherte Ring vollständig aufoxydiert; das gleiche sollte bei Kernen des Lignins der Fall sein, deren phenolische Hydroxylgruppe als Aroxylrest in Arylglycerin-β-arylätherstrukturen (Typ des Modells *12*) veräthert vorliegt.

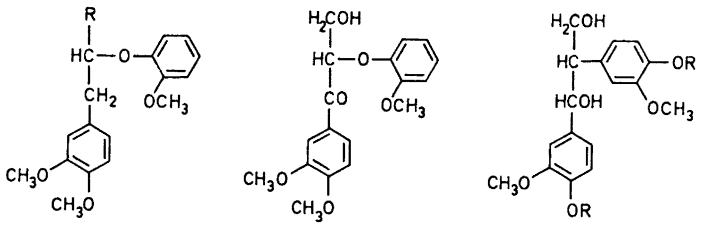

28 R = CH_2OH
29 R = COOH
30 R = $COOCH_3$

31

32 R = H
33 R = CH_3

Während die C_2-Brücke im Diphenyläthan *33* und im Stilben *37* beim oxydativen Abbau gespaltet wird, wobei die entsprechenden Abbausäuren in guten Ausbeuten erhalten wurden, ist die C_1-Brücke in Diphenylmethanstrukturen – sofern die phenolischen Hydroxylgruppen in den beiden Kernen als Methyläther vorliegen – unter den Bedingungen des oxydativen Abbaus weitgehend stabil. Die Ligninmodelle mit Diphenylmethanstruktur (*40*, *44*, *48* und *54*) lieferten die Abbausäuren *2* und *4*, beziehungsweise *2* und *5*, nur in geringen Mengen (Tab. 4). Dies ist darauf zurückzuführen, dass diese Abbausäuren nur durch vollständigen oxydativen Abbau eines der beiden Kerne gebildet werden können.

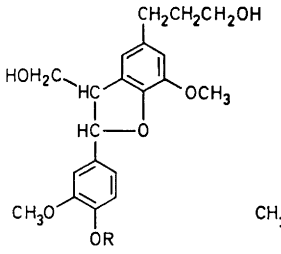

34 R = H
35 R = CH_3

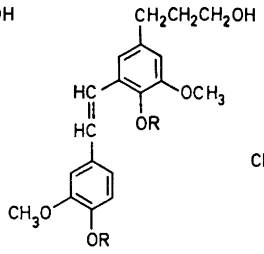

36 R = H
37 R = CH_3

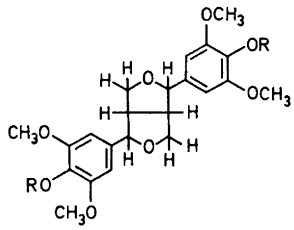

38 R = H
39 R = CH_3

Tab. 4. Oxydativer Abbau von Ligninmodellen mit Diphenylmethanstruktur. Ausbeuten (in % d. Th.) an den Methylestern der Abbausäuren *2*, *4* und *5* (gaschromatographisch bestimmt).

Modell	*40*		*44*		*48*		*54*
Abbausäure	*2*	*5*	*2*	*4*	*2*	*5*	*4*
Ausbeute an Methylester	8	4,5	10	13	7	10	6,5

Das Gemisch der Abbauprodukte der Modelle *40* und *44* zeigte nach Methylierung mit Diazomethan im Gaschromatogramm neben geringen Mengen der Methylester der Abbausäuren *2*, *4* und *5* mehrere schwerer flüchtige Komponenten, unter denen jeweils eine (*42*, Ausbeute *ca.* 30 %; *46*, Ausbeute *ca.* 60 %) überwog. Es sind dies die Methylester der Monocarbonsäuren *41* und *45*, die durch den Abbau der Propylseitenketten in *40* und *44* entstanden waren; in beiden Fällen blieb der Äthylrest am Brückenkohlenstoff intakt. Weiters wurden 6-Veratroyl-veratrumsäure (*49*, aus *40*; Ausbeute *ca.* 5 %), das Lacton *59* (aus *40*; Ausbeute etwa 10 %) und 5-Veratroyl-veratrumsäure

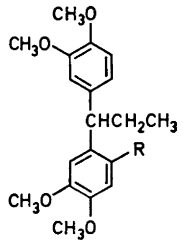

40 R = $CH_2CH_2CH_3$
41 R = COOH
42 R = $COOCH_3$

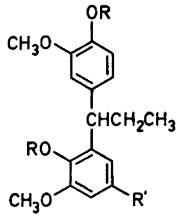

43 R = H, R' = $CH_2CH_2CH_3$
44 R = CH_3, R' = $CH_2CH_2CH_3$
45 R = CH_3, R' = COOH
46 R = CH_3, R = $COOCH_3$

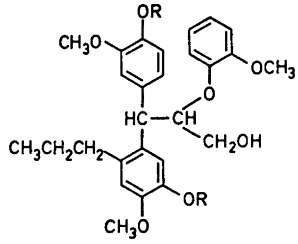

47 R = H
48 R = CH_3

(*51*, aus *44*; Ausbeute *ca.* 5 %) aufgefunden; daneben waren in beiden Fällen noch mehrere, nicht identifizierte Abbausäuren in kleineren Mengen gebildet worden. Auch aus dem durch Methylierung des Modells *47* erhaltenen rohen Dimethyläther *48* entstanden neben den Methylestern von *2*, *5* und *49* mehrere, schwerer flüchtige Abbauprodukte, die aber nicht weiter untersucht wurden.

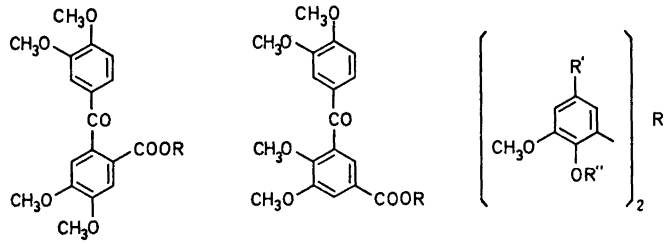

49 R = H
50 R = CH_3

51 R = H
52 R = CH_3

53 R = CH_2, R' = $CH_2CH_2CH_3$, R'' = H
54 R = CH_2, R' = $CH_2CH_2CH_3$, R'' = CH_3
55 R = CH_2, R' = COOH, R'' = CH_3
56 R = CH_2, R' = $COOCH_3$, R'' = CH_3
57 R = CO, R' = COOH, R'' = CH_3
58 R = CO, R' = $COOCH_3$, R'' = CH_3

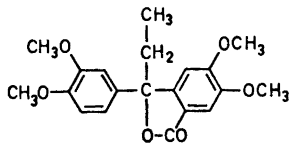

59

Die Verbindung *53* ist ein Modell für die beim alkalischen Abbau des Lignins durch Kondensation von Guajacylpropanstrukturen mit Formaldehyd gebildeten Diphenylmethanstrukturen. Sein Methyläther *54* gab die erwartete Isohemipinsäure (*4*) in geringer Ausbeute, unter den Abbauprodukten überwogen die unvollständig abgebauten Säuren *55* und *57* (Hauptprodukt).

Es ist anzunehmen, dass zumindestens ein Teil der Iso- (*4*) und im besonderen der Metahemipinsäure (*5*), sowie der hier nicht weiter behandelten 3,4,5-Trimethoxy-phthalsäure (*6*) liefernden Einheiten des Lignins als Strukturen von Typ der Verbindungen *40* und *44* vorliegen. Aus diesem Grund sind die über diese Abbausäuren berechneten Werte für die entsprechend kondensierten Strukturen im Lignin als untere Grenzwerte anzusehen (vergl. Lit. 1c).

Beim oxydativen Abbau des Modells *28* wurde neben Veratrumsäure (*2*, s. Tab. 3) die Carbonsäure *29* in einer Ausbeute von etwa 25 % gebildet. In Verbindung mit dem oben angeführten Nachweis der Bildung der Säuren *41*, *45* und *55* aus den Modellen *40*, *44* und *54* weist dieser Befund darauf hin, dass der oxydative Abbau der aliphatischen Seitenketten in Modellen und auch im Lignin gegebenenfalls einer sterischen Hinderung unterliegt. Die Propylseitenketten in den Modellen *21* und *23*, die dem Angriff des Oxydationsmittels frei zugänglich sind, wurden vollständig abgebaut. Der Abbau von abgesättigten Alkylresten setzt wahrscheinlich durch Hydroxylierung des

benzylischen C-Atoms durch MnO_4^- ein (vergl. Lit. 7); dieser Abbauweg wird durch den massenspektrometrischen Nachweis des Lactons *59* als Abbauprodukt von *40* gestützt.

Die Struktur der Abbausäuren *29*, *41*, *45*, *49*, *51*, *55* und *57* wurde aus den Massenspektren der entsprechenden Methylester (*30*, *42*, *46*, *50*, *52*, *56* und *58*) abgeleitet.

EXPERIMENTELLER TEIL

Methylierung

Aufbereitung des Pflanzenmaterials. Sulfatkochung. Das getrocknete, grob zerkleinerte Pflanzenmaterial wurde, suspendiert in Toluol, in einer Kleinschwingmühle der Fa. McCrone, Research Associates, London, feingemahlen. Mahldauer 30 Min bei Raumtemperatur, Mahlkörper aus Sinterkorund, Mahlgefäss aus Polypropylen. Das Mahlgut wurde im Soxhlet je 24 Stunden mit Benzol-Äthanol 2:1 und mit 95-proz. Äthanol extrahiert. Dann wurde es ausgesiebt; nur ein geringer Teil wurde von einem 45-mesh Sieb zurückgehalten. Die feingemahlene Hauptmenge wurde zum Sulfataufschluss verwendet. Sulfataufschluss siehe Lit. 1c.

Methylierung. Die Methylierung wird in einem Gefäss aus Pyrex-Glas vorgenommen, dessen unterer Teil so geformt ist, dass bei einer Flüssigkeitsmenge von 10 ml der Elektrodenkopf ausreichend in die mittels eines Magnetstäbchens (Teflon) durchmischte Flüssigkeit eintaucht. Die Kombinationselektrode (Glas-Kalomelelektrode Nr. GK 2302 der Fa. Radiometer, Kopenhagen) wird durch ein seitlich schräg angesetztes Rohr eingeführt, für die anderen Einlässe sorgt ein aufgesetzter Flanschdeckel mit 4 Durchführungen, und zwar für Inertgas (N_2), Laugenzufluss, Dimethylsulfatzugabe und Druckausgleich. Die Laugenzugabe erfolgt mittels eines Magnetventils (MNV 1, Radiometer), das durch ein mit der Elektrode gekoppeltes pH-Kontrollgerät (TTT 1 oder TTT 2, Radiometer) gesteuert wird. Die Schlauchzuführungen für die Lauge, die sich in einer 50 ml Messbürette befindet, sind aus Teflon (Innendurchmesser 1 mm), mit Ausnahme eines kurzen Schlauchstücks aus Naturgummi für das Magnetventil. Die Austrittsöffnung für die Lauge muss unter der Flüssigkeitsoberfläche nahe am Elektrodenkopf liegen, um eine geringe pH-Bandbreite bei einem unteren pH-Grenzwert von 11 zu gewährleisten.

In die mit Stickstoff gefüllte Apparatur wird die Lösung von 80 mg Björkman-Lignin (bzw. Sulfatlignin aus 50 mg Björkman-Lignin oder 200 mg Holzmehl, 25 mg der Modellverbindungen, im Falle des Modells *47* 10 mg; alle Einwaagen, mit Ausnahme der Einwaage des Holzmehls, auf 0,01 mg genau) in 8 ml eines Gemisches von 1,2-Dimethoxyäthan – Methanol – H_2O (35:35:30, «Methylierungsgemisch«) eingebracht; Nachwaschen mit 3 × 1 ml desselben Gemisches. Nach Einschalten des Magnetrührers wird die Laugenzufuhr in Gang gesetzt und 1 ml Dimethylsulfat mittels einer Pipette zugegeben. Als Lauge wird eine etwa 15-proz. Lösung von KOH im Methylierungsgemisch verwendet. Der Laugenverbrauch kommt nach 18 – 24 Stunden zum Stillstand. Darauf wird die Laugenzufuhr unterbrochen und die Lösung mit 2 M H_3PO_4 auf pH 4 angesäuert. Dann wird der Gefässinhalt in einen Scheidetrichter übergeführt; Nachwaschen mit insgesamt 35 ml Aceton – H_2O 6:1. Nach Zugabe von 30 ml $CHCl_3$ wird durchgeschüttelt und die Phasen werden getrennt. Die wässrige Phase wird noch zweimal mit je 60 ml Aceton – $CHCl_3$ 1:1 ausgeschüttelt. Die vereinigten Extrakte werden mit 5 ml H_2O gewaschen und bei Raumtemperatur in dem später für den oxydativen Abbau verwendeten 250 ml Dreihals-Rundkolben zur Trockene gebracht. Dann werden 10 ml *tert.*-Butanol zugesetzt und das Lösungsmittel wird nochmals abgedampft. Der Rückstand wird, wie unten beschrieben, oxydativ abgebaut. Für das Gelingen der Oxydation ist die vollständige Entfernung von Acetonresten Voraussetzung.

1-(3,4-Dimethoxyphenyl)-2-(2-methoxy-phenoxy)-äthanol (11). Aus 200 mg 1-(4-Hydroxy-3-methoxyphenyl)-2-(2-methoxy-phenoxy)-äthanol [9] (*10*) wurden nach Methylierung bei pH 11 aus Essigester – Hexan 173 mg *11* vom Schmp. 130 – 131° erhalten (Lit.[9] Schmp. 133 – 134°). Die Mutterlauge enthielt in der Hauptsache Verbindung *11* (Dünnschicht auf Kieselgel HF_{254}, Merck; Laufmittel Aceton – Hexan 1:3, zweimal entwickelt).

2,2',3,3'-Tetramethoxy-5,5'-dimethyl-biphenyl (15). Durch Methylierung von 200 mg 2,2'-Dihydroxy-3,3'-dimethoxy-5,5'-dimethyl-biphenyl [10] (*14*) bei pH 11 und Kristallisation aus Essigester – Hexan wurde *15* in farblosen Kristallen vom Schmp. 103 – 105° erhalten, Ausbeute 183 mg. Die Verbindung *15* ist in der Literatur als Öl beschrieben.[10]

Gaschromatographische Untersuchung des Reaktionsprodukts aus dem voranstehenden Versuch. Bedingungen: siehe quantitative Bestimmung der Methylester der Abbausäuren. *Silylierung des Reaktionsprodukts:* 5 µl einer etwa 10-proz. Lösung des Reaktionsprodukts in $CHCl_3$ wurde mit 5 µl Bis-(trimethylsilyl)-trifluor acetamid (BSTFA, Pierce) und 5 µl Pyridin in einer Kapillare 5 Min auf 120° erhitzt. 1 µl dieser Lösung wurde für die gaschromatographische Untersuchung verwendet. *Retentionszeiten* (Min): Bis-(trimethylsilyl)-äther von *14*, 7,0; *15*, 11,8. Das Produkt (*15*) war gaschromatographisch rein; Ausgangsmaterial konnte nicht mit Sicherheit nachgewiesen werden.

threo-*3,4,5-Trimethoxy-phenylglycerin-β-(2,6-dimethoxy-4-methylphenyl)-äther (13).* Aus 102 mg *threo*-3,5-Dimethoxy-4-hydroxy-phenylglycerin-β-(2,6-dimethoxy-4-methylphenyl)-äther (*12*)[25] wurden durch Methylierung bei pH 11 91 mg der Verbindung *13* nach einer Umkristallisation rein erhalten; Schmp. 79 – 81° (Essigester – Hexan). Die dünnschichtchromatographische Untersuchung des Reaktionsprodukts (Kieselgel G, Merck; Aceton – Hexan 1:1, Sprühreagens H_2SO_4 – Formalin 9:1) zeigte neben *12* nur Spuren von schneller laufendem, wahrscheinlich durch Methylierung der alkoholischen Hydroxylgruppen entstandenem Material an.

Gaschromatographische Untersuchung des Reaktionsprodukts aus dem voranstehenden Versuch. Gerät: Perkin-Elmer Modell 900. *Trennsäule:* aus nichtrostendem Stahl, 1 m lang, äusserer Durchmesser 0,3 cm. *Trägermaterial:* Chromosorb G, 80 – 100 mesh, gewaschen mit Säure, behandelt mit Dimethyl-dichlorsilan. *Stationäre Phase:* Silikonelastomer SE-30 (5 Gew.-% des Trägermaterials). *Arbeitstemperaturen:* Injektor 270°, Trennsäule 230°. *Trägergas:* N_2; Strömungsgeschw. 30 ml per Min. *Retentionszeiten* (Min): Bis-(trimethylsilyl)-äther von *13*, 12,0; Tris-(trimethylsilyl)-äther von *12*, 13,8. Nach Silylierung der Mutterlauge mit BSTFA – Pyridin (siehe oben) konnten gaschromatographisch nur Spuren von Ausgangsmaterial nachgewiesen werden.

Oxydativer Abbau

Ausführung. Zu der in 40 ml *tert.*-Butanol – H_2O 3:1 (Merck, *p.a.*) gelösten, methylierten Probe werden 40 ml 0,5 M NaOH zugegeben, weiters (in dieser Reihenfolge) 100 ml 0,06 M $NaJO_4$ und 20 ml 0,03 M $KMnO_4$. Der Kolben wird unter gutem Rühren im thermostatierten Wasserbad auf 82° erwärmt und 6 Stunden bei dieser Temperatur gehalten. Dann werden 5 ml Äthanol zugesetzt und nach 10 Min wird das gebildete MnO_2 durch eine Schicht von Kieselgur abgesaugt und der Rückstand mit wenig 1-proz. Natriumcarbonatlösung gewaschen. Nach Abkühlen wird 2 × mit je 50 ml Äther ausgeschüttelt und die vereinigten Ätherauszüge werden mit 15 ml 1-proz. Sodalösung gewaschen; letztere wird mit der wässrigen Phase vereinigt.

Die wässrige Lösung wird mit 1 M H_2SO_4 neutralisiert und auf 30 ml eingeengt. Zu dieser Lösung werden 0,9 g Na_2CO_3 (wasserfrei) und 5 ml 30 – 35-proz. H_2O_2 zugesetzt. Der Kolbeninhalt wird 10 Min auf 50° erwärmt. Dann werden 100 mg aktives MnO_2 zugegeben und nach Aufhören der Gasentwicklung (Kontrolle durch nochmaligen Zusatz von wenig MnO_2) wird der Braunstein abfiltriert. Mit 10 ml H_2O wird nachgewaschen. Das Filtrat wird mit konz. H_3PO_4 auf pH 2 angesäuert und 3 × mit dem 1,5-fachen Volumen Aceton – $CHCl_3$ (1:1) ausgeschüttelt. Die vereinigten Auszüge werden über Na_2SO_4 getrocknet und das Lösungsmittel wird abgedampft. Dann wird in 10 ml Methanol aufgenommen und das gleiche Volumen einer etwa 2-proz. ätherischen Lösung von Diazomethan zugegeben. Nach 30 Min wird das Lösungsmittel abermals vertrieben und der Rückstand in 1 ml einer 5,00 mg per ml Pyromellitsäure-tetramethylester (innerer Standard für die Gaschromatographie) enthaltenden $CHCl_3$-Lösung zugesetzt. Zur gaschromatographischen Bestimmung der Methylester wird 1 µl dieser Lösung verwendet.

Gaschromatographische Bestimmung der Methylester. Gerät: Perkin-Elmer Modell 900 mit doppeltem Flammenionisationsdetektor. *Trennsäule:* aus nichtrostendem Stahl, 1,75 m lang, äusserer Durchmesser 0,3 cm. *Trägermaterial:* Chromosorb G, 80 – 100 mesh, gewaschen mit Säure, behandelt mit Dimethyldichlorsilan. *Stationäre Phase:* Silikone-

lastomer OV-17 (1,5 Gew.-% des Trägermaterials). *Arbeitstemperaturen:* Injektor 300°, Trennsäule 160 – 255°, 5°/Min, dann isotherm. *Trägergas:* N_2; Strömungsgeschw. 25 ml per Min. Die Auswertung der Chromatogramme erfolgte auf graphischem Weg (Spitzenhöhe × Spitzenbreite in halber Spitzenhöhe). Die angegebenen Ausbeuten sind Mittelwerte von in der Regel drei gaschromatographischen Bestimmungen. Die durch Analyse von Estergemischen bekannter Zusammensetzung ermittelten Korrekturfaktoren für die einzelnen Ester sind häufig nachzuprüfen. Es ist weiters notwendig, die Trennsäule von Zeit zu Zeit durch Injektion von 1 µl Polyglykol (mittleres Molekulargewicht 300) und Durchlauf unter obigen Bedingungen aufzufrischen.

Oxydativer Abbau von Modellverbindungen. Literaturhinweise für die Darstellung der Modelle: 2,2′-Dihydroxy-3,3′-dimethoxy-5,5′-dipropyl-biphenyl [10] (*16*); 3,5-Dimethoxy-4-hydroxy-acetophenon [11] (*18*); 2,6-Dimethoxy-4-propyl-phenol [12] (*22*); 1-(3,5-Dimethoxy-4-hydroxyphenyl)-1-propanol [13] (*24*); 6-Hydroxy-5,5′,6′-trimethoxy-biphenyl-3,3′-dicarbaldehyd [14] (*26*); 1-(2-Methoxy-phenoxy)-2-(3,4-dimethoxyphenyl)-1-propanol [15] (*28*); 1-(3,4-Dimethoxyphenyl)-2-(2-methoxyphenoxy)-3-hydroxy-1-propanon [16] (*31*); *erythro*-1,2-Bis[4-hydroxy-3-methoxyphenyl]-1,3-propandiol [17] (*32*); Dihydro-dehydro-diconiferylalkohol [18] (*34*); *trans*-2,4′-Dihydroxy-3,3′-dimethoxy-5-(3-hydroxypropyl)-stilben [19] (*36*); D,L-Syringaresinol [20] (*38*); 2-(2-Methoxy-phenoxy)-3-(5-hydroxy-4-methoxy-2-propylphenyl)-3-(4-hydroxy-3-methoxyphenyl)-1-propanol [15] (*47*).

Die Modellverbindungen mit freien phenolischen Hydroxylgruppen wurden, mit Ausnahme des 5,5′-Dehydro-divanillin-monomethyläthers (*26*), vor dem oxydativen Abbau methyliert. Die so erhaltenen Methyläther wurden ohne weitere Reinigung oxydativ abgebaut. Beim Abbau der Methyläther *21* und *23* wurde die Neutralfraktion der Abbauprodukte gaschromatographisch untersucht; sie wog in beiden Fällen *ca.* 1 mg. Ausgangsmaterial (*21* und *23*) konnte nur in Spuren aufgefunden werden.

Die Methylester aus dem Abbau der Modelle *28*, *40*, *44* und *54* wurden in Mikrogrammen gaschromatographisch getrennt und in Kapillaren aufgefangen. Zu diesem Zweck wurde ein Perkin-Elmer Modell 880 Gaschromatograph verwendet.

Gaschromatographie: Bedingungen siehe Untersuchung der Methylierung von *12*. Strömungsgeschw. des Trägergases 25 ml/Min. *Retentionszeiten* (relativ zu 5,5′-Dehydrodiveratrumsäure-dimethylester, $t = 19{,}8$ Min): *30*, 0,41; *40*, 0,43; *42*, 0,65; *44*, 0,40; *46*, 0,67; *50*, 1,00; *52* 1,01; *54*, 0,46; *56*, 1,32; *58*, 1,86; *59*, 1,14.

Massenspektren. Gerät: AEI MS 902. *Elektronenenergie:* 70 eV. *Ionenquellentemperatur:* 170°. Teilmassenspektren; nur Ionen der Massenzahlen > 100 wurden beachtet.

2-(2-Methoxy-phenoxy)-3-(3,4-dimethoxyphenyl)-propionsäure-methylester (30). m/e, relative Intensität (≥ 10 %): 346, 59; 223, 98; 222, 12; 191, 16; 181, 26; 164, 19; 163, 40; 151, 100; 149, 14. Die Masse des Molekülions wurde zu 346, 1416 bestimmt. (ber. für $C_{19}H_{22}O_6$: 346,1416).

1-(2-Carbomethoxy-4,5-dimethoxyphenyl)-1-(3,4-dimethoxyphenyl)-propan (42). m/e, rel. Int. (≥ 5 %): 374, 42; 345, 100; 341, 19; 327, 11; 314, 8; 313, 16; 299, 7. (Masse des Molekülions. Gef.: 374,1741. Ber. für $C_{21}H_{26}O_6$: 374,1729.)

1-(3-Carbomethoxy-5,6-dimethoxyphenyl)-1-(3,4-dimethoxyphenyl)-propan (46). m/e, rel. Int. (≥ 5 %): 374, 50; 345, 83; 157, 8; 151, 100. (Masse des Molekülions. Gef.: 374,1712. Ber. für $C_{21}H_{26}O_6$: 374,1729.)

3′,4,4′,5-Tetramethoxy-benzophenon-2-carbonsäuremethylester (50). Synthetisch erhaltenes Präparat.[21] *m/e*, rel. Int. (≥ 10 %): 360, 100; 329, 10; 223, 61; 165, 83.

3′,4′,5,6-Tetramethoxy-benzophenon-3-carbonsäuremethylester (52). m/e, rel. Int. (≥ 10 %): 360, 100; 345, 14; 343, 21; 329, 24; 223, 31; 209, 93; 165, 74; 151, 46; 137, 14. (Masse des Molekülions. Gef.: 360,1215. Ber. für $C_{19}H_{20}O_7$: 360,1209.)

5,5′,6,6′-Tetramethoxy-diphenylmethan-3,3′-dicarbonsäure-dimethylester (56). Die Verbindung kristallisierte beim Auffangen in der Glaskapillare; Schmp. 102 – 103°. *m/e*, rel. Int. (< 10 %): 404, 100; 373, 41; 372, 37; 344, 27; 341, 19; 313, 21; 312, 12; 209, 45; 195, 31; 179, 18; 171, 13; 163, 11; 151, 19; 149, 10. (Masse des Molekülions. Gef.: 404,1486. Ber. für $C_{21}H_{24}O_8$: 404,1471.)

5,5′,6,6′-Tetramethoxy-benzophenon-3,3′-dicarbonsäure-dimethylester (58). m/e, rel. Int. (≥ 10 %): 418, 100; 387, 44; 369, 13; 358, 15; 357, 10; 223, 88; 209, 90; 180, 14; 178, 17; 149, 15; 135, 10. (Masse des Molekülions. Gef.: 418,1256. Ber. für $C_{21}H_{22}O_9$: 418,1264.)

3-Äthyl-3-(3,4-dimethoxyphenyl)-5,6-dimethoxy-phthalid (59). m/e, rel. Int. (≥ 5 %): 358, 18; 329, 100; 165, 6; 164,5, 5. (Masse des Molekülions. Gef.: 358,1397. Ber. für $C_{20}H_{22}O_6$: 358,1416.)

Synthesen

1-(2-Hydroxy-3-methoxy-5-propylphenyl)-1-(4-hydroxy-3-methoxyphenyl)-propan (43). Eine Lösung von 2,0 g 1-(4-Hydroxy-3-methoxyphenyl)-1-propanol [22] und 8 g 4-Propylguajakol (*20*) in 30 ml 10-proz. NaOH wurde in einem Stahlautoklaven unter Stickstoff 2 Stunden auf 140° erhitzt. Nach Ansäuern auf pH 2 wurde die wässrige Lösung mit $CHCl_3$ ausgeschüttelt und der nach Verdampfen des Lösungsmittels verbleibende Rückstand im Kugelrohr destilliert. Bei 0,01 Torr/140 – 150° gingen 1,41 g eines farblosen, zähen Öls über, das in 50 ml abs. Äthanol aufgenommen und nach Zusatz von 150 mg 10 % Pd/C bei Normaldruck hydriert wurde; es nahm nur wenig H_2 auf. Die Verbindung *43* konnte nicht zur Kristallisation gebracht werden. (Gef.: C 72,37, H 8,02. Ber. für $C_{20}H_{26}O_4$ (330,43): C 72,70; H 7,93.)

1-(2,3-Dimethoxy-5-propylphenyl)-1-(3,4-dimethoxyphenyl)-propan (44). Wurde durch Methylierung von *43* mit Dimethylsulfat – KOH erhalten. Farbloses Öl, Kp. 135 – 140°/0,01 Torr (Kugelrohr). (Gef.: C 73,67; H 8,44. Ber. für $C_{22}H_{30}O_4$ (358,48): C 73,71; H 8,44). NMR (60 MHz, 10 % in $CDCl_3$, Tetramethylsilan als innerer Standard). δ-Werte: 0,89 (3) t, C-CH_3; 0,92 (3) t, C-CH_3; 1,62 (2) m, CH_2-CH_2-CH_3; 1,99 (2) m, CH-CH_2-CH_3; 2,61 (2) t, Ar-CH_2; 3,61 (3) s, OCH_3; 3,78 (9) s, 3 OCH_3; 4,20 (1) t, Ar-CH; 6,54 (1) d, H_4 oder H_6; 6,64 (1) d, H_4 oder H_6; 7,20 (3) m, Protonen am trisubstituierten Ring. $J_{4,6} = 2{,}0$ Hz; $J_{CHCH_3} = 7{,}8$ Hz. Bei den Multipletts der Protonen der Propylseitenketten wurden die Mittelpunkte (nicht Schwerpunkte) angegeben.

2,2'-Dihydroxy-3,3'-dimethoxy-5,5'-dipropyl-diphenylmethan (53). Eine Lösung von 1,0 g 2-Methoxy-4-propylphenol (*20*), 980 mg 2-Hydroxy-3-methoxy-5-propylbenzylalkohol [23] und 0,5 g NaOH in 14 ml Äthylenglykol-monomethyläther wurden in einem Stahlautoklaven unter N_2 3 Stunden auf 170° erhitzt. Aus Äther – Hexan wurden nach Aufarbeitung in üblicher Weise 0,8 g *53* in Form farbloser sechseckiger Blättchen vom Schmp. 100 – 101° erhalten. Für *53* ist in der Lit. ein Schmp. von 76 – 77° angegeben.[24] (Gef.: C 73,11; H 8,05. Ber. für $C_{21}H_{28}O_4$ (344,45): C 73,23; H 8,19.)

2,2',3,3'-Tetramethoxy-5,5'-dipropyl-diphenylmethan (54). Aus *53* mit Dimethylsulfat – NaOH. Farbloses Öl, gaschromatographisch einheitlich. NMR (60 MHz, 10 % in $CDCl_3$, Tetramethylsilan als innerer Standard). δ-Werte: 0,88 (6) t, 2 C-CH_3; 1,57 (4) m, 2 C-CH_2-C; 2,47 (4) t, 2 Ar-CH_2-C; 3,70 (6) s, 2 OCH_3; 3,80 (6) s, 2 OCH_3; 3,95 (2) s, Ar-CH_2-Ar; 6,48 (2) d, 2 H_4 oder H_6; 6,55 (2) d, 2 H_4 oder H_6. $J_{4,6} = 2{,}0$ Hz. Bei den Multipletts der Protonen der Propylseitenketten wurden die Mittelpunkte (nicht Schwerpunkte) angegeben.

Herrn Prof. Dr. E. Adler sind wir für wertvolle Diskussionen zu Dank verpflichtet. Frau Ing. I. Somfai danken wir für experimentelle Mitarbeit.

Diese Arbeit wurde von der Westvaco Corp., New York, unterstützt.

LITERATUR

1. a. Larsson, S. und Miksche, G. E. *Acta Chem. Scand.* **26** (1972) 2031; b. *Ibid.* **23** (1969) 917; c. *Ibid.* **25** (1971) 647; d. *Ibid.* **23** (1969) 3337.
2. Sarkanen, K. V. und Hergert, H. L. In Sarkanen, K. V. und Ludwig, C. H. *Lignins*, Wiley-Interscience, New York 1971, S. 54 – 89; Chang, H.-M. und Allan, G. G. *Ibid.* S. 434 – 444.
3. Miksche, G. E. *Unveröffentlicht.*
4. Lemieux, R. V. und von Rudloff, E. *Can. J. Chem.* **33** (1955) 1701; **33** (1955) 1710.
5. Symons, M. C. R. *J. Chem. Soc.* **1953** 3956; Landsberg, R. und Heckner, K. H. *Z. physik. Chem. (Leipzig)* **221** (1962) 211; **230** (1965) 63; Landsberg, R., Heckner, K. H. und Dalchau, S. *Ber. Bunsenges. Phys. Chem.* **72** (1968) 649.
6. Veprek-Siska, J. und Ettel, V. *J. Inorg. Nucl. Chem.* **31** (1969) 789; Veprek-Siska, J., Ettel, V. und Regner, A. *Ibid.* **26** (1964) 1476.
7. Brauman, J. I. und Pandell, A. J. *J. Am. Chem. Soc.* **92** (1970) 329.
8. von Rudloff, E. *Can. J. Chem.* **34** (1956) 1413; Gunstone, F. D. und Morris, L. J. *J. Chem. Soc.* **1959** 2127.
9. Gierer, J. und Norén, I. *Acta Chem. Scand.* **16** (1962) 1713.
10. Richtzenhain, H. *Chem. Ber.* **82** (1949) 447.

11. Mauthner, F. *J. prakt. Chem.* **121** (1929) 255.
12. Mauthner, F. *J. prakt. Chem.* **102** (1921) 36.
13. Richtzenhain, H. *Chem. Ber.* **81** (1948) 260.
14. Galland, J. M. und Hopton, G. U. *J. Chem. Soc.* **1932** 439.
15. Johansson, B. und Miksche, G. E. *Acta Chem. Scand.* **26** (1972) 289.
16. Adler, E., Lindgren, B. O. und Saedén, U. *Svensk Papperstid.* **55** (1952) 563.
17. Lundquist, K. und Miksche, G. E. *Tetrahedron Letters* **1965** 2131.
18. Freudenberg, G. und Hübner, H. H. *Chem. Ber.* **85** (1952) 1181.
19. Adler, E., Marton, J. und Falkehag, I. *Acta Chem. Scand.* **18** (1964) 1311; Miksche, G. E. *Ibid.* **26** (1972) 3269.
20. Freudenberg, K., Kraft, R. und Heimberger, W. *Chem. Ber.* **84** (1951) 472.
21. Vanzetti, B. L. und Dreyfuss, P. *Gazz. chim. Ital.* **64** (1934) 381.
22. Roberti, P. C., York, R. F. und MacGregor W. S. *J. Am. Chem. Soc.* **72** (1950) 5760.
23. Marton, J., Marton, T., Falkehag, I. und Adler, E. *Advan. Chem. Ser.* **59** (1966) 125.
24. Pala, G., Crescenzi, E. und Sekules, G. *Farmaco, Ed. Sci.* **18** (1963) 169, zitiert in *Chem. Abstr.* **59** (1963) 12681.
25. Miksche, G.E. *Acta Chem. Scand.* **27** (1973). *Im Druck.*

Eingegangen am 3. Juli 1972.

ACTA CHEMICA SCANDINAVICA 27 (1973) 141–145

Ylide Reactions of Triphenylarsine Phenylimine

PAUL FRØYEN

Chemical Institute, University of Bergen, N-5000 Bergen, Norway

Triphenylarsine phenylimine reacts with aldehydes, ketones, isocyanates, isothiocyanates, nitroso compounds, quinones, carbon disulfide, sulfur dioxide, dimethyl acetylenedicarboxylate, and nitrile oxides. The compound also easily undergoes alkylation and protonation. The reaction with ketones and aldehydes leads to ketimines and aldimines. In the reaction with nitrile oxides and dimethyl acetylenedicarboxylate 1 : 1 adducts are formed.

Some time ago the present author reported that treatment of certain isocyanates and *N*-sulfinyl amides with triphenylarsine oxide leads to the corresponding triphenylarsine imines in high yield.[1]

Almost no chemical studies have been reported for arsine imines, and an examination of their properties seemed to be of importance. The only members of this class of compounds known so far are a series of carbonyl- and sulfonyl-stabilized derivatives where the powerful electron withdrawal effect of the carbonyl resp. sulfonyl group strongly decreases the electron density on the nitrogen atom, thereby making these compounds very poor nucleophiles. In a preliminary experiment the present author tried to react *p*-nitrobenzaldehyde with triphenylarsine *N*-*p*-toluenesulfonylimine in boiling benzene. The reactants were recovered unchanged. In spite of this negative result, arsine imines were assumed to be more reactive than the corresponding phosphine imines since the basicity sequence for the imines is As>P.[2] The lack of reactivity in the above-mentioned experiment is attributed to the low nucleophilicity of the imine nitrogen due to delocalization of the negative charge onto the *p*-toluenesulphonyl group. Accordingly, it was decided to prepare some arsine imines where delocalization of the negative charge through the carbon portion of the ylide is less effective. Attempts to prepare triphenylarsine *N*-methylimine was unsuccessful, but the more stable *N*-phenyl and *N*-α-naphthyl derivatives were easily prepared.

Reactions with carbonyl compounds. It is assumed that the mechanism of the reactions between triphenylarsine phenylimine and carbonyl compounds parallels that of the Wittig reaction. If this is so, the first step is a nucleophilic attack by the nitrogen atom of the imine on the carbonyl carbon synchronized

with an attack by the oxygen of the carbonyl group on arsenic (Scheme 1). The intermediate thus formed is then converted to triphenylarsine oxide and a Schiff base.

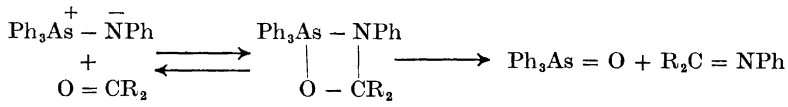

Scheme 1.

This route is probably also followed in the reactions between phosphine imines and carbonyl compounds.[3,4] There is, however, a marked difference in the reactivity between triphenylarsine phenylimine and its phosphorus analogue. The phosphine imine is reported to react with benzophenone only when heated at 150° for 22 h.[5] Triphenylarsine phenylimine, however, gives an excellent yield of diphenylmethylidene aniline when heated for a few minutes with benzophenone in boiling benzene.

The enhanced reactivity of the triphenylarsine phenylimine is also demonstrated by its reaction under mild conditions with quinones and nitroso compounds.[6] The difference in reactivity between triphenylarsine resp. triphenylphosphine phenylimine in these reactions must be attributed to a much higher reactivity of the former in the first step (Scheme 1). The increased nucleophilicity of the arsenic compound indicates that the ionic structure $Ph_3\overset{+}{As}-\overline{N}Ph$ contributes more to the actual structure, $Ph_3\overset{+}{As}-\overline{N}Ph \longleftrightarrow Ph_3As=NPh$, than does $\overset{+}{P}h_3P-\overline{N}Ph$ in the analogous phosphorus case. This conclusion is in accordance with that expressed by Johnson on the basis of studies of arsonium resp. phosphonium fluorenylides that arsenic is less capable than phosphorus of stabilizing the negative charge on the adjacent carbanion by valence shell expansion.[7] Triphenylarsine phenylimine is less reactive, however, than its phosphorus analogue in the reaction with carbon dioxide and phenyl isocyanate. In an attempt to react the compound with carbon dioxide the triphenylarsine phenylimine was recovered unchanged when carbon dioxide had been bubbled through a solution of the compound in boiling benzene for 14 h. The low reactivity against phenyl isocyanate is also remarkable, since triphenylphosphine phenylimine reacts very rapidly with this compound, even at low temperatures. As demonstrated by its fast reaction with carbonyl compounds, it is evident that triphenylarsine phenylimine is a far better nucleophile than its phosphorus analogue. It is possible, however, that the rate of the second step of the reaction is decreased when phosphorus is replaced with arsenic, and that the decomposition of the penta-covalent cyclic intermediate in certain cases becomes rate controlling. This may be the reason why the arsenic compound shows decreased reactivity towards phenyl isocyanate and carbon dioxide as compared to its phosphorus analogue. It should be mentioned, however, that the failure of triphenylarsine phenylimine to react with carbon dioxide may be

partly ascribed to the low concentration of this compound in the reaction mixture, as the reaction was carried out in boiling benzene.

The reaction with dimethyl acetylenedicarboxylate. Triphenylarsine phenylimine reacts with dimethyl acetylenedicarboxylate under formation of a 1 : 1 adduct, m.p. 177°C. IR spectra show two different carbonyl groups at 1734 and 1658 cm^{-1}. It seems, therefore, that the reaction with acetylenes is strictly analogous to that of phosphine imines: [8]

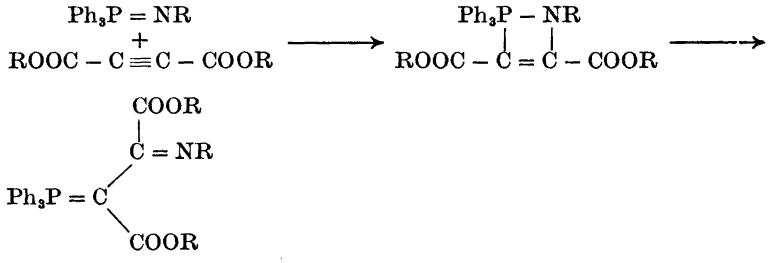

The reaction with triphenylacetonitrile N-*oxide.* Recently several workers have been concerned with the reactions of phosphorus ylides with 1.3 dipoles, especially nitrile oxides.[9–11]

In the reaction between triphenylarsine phenylimine and triphenylacetonitrile *N*-oxide a 1 : 1 adduct is formed

(1)

The structure assigned to the product 1,2,4,5-As^{V}-oxadiaza-arsole (1) is based on the analogous reaction of methylene triphenylphosphorane with benzonitrile *N*-oxide where the product is shown to be the 4,5-dihydro-1,2,5 P^{V}-oxazaphosphole (2).[12]

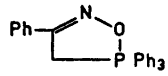

(2)

EXPERIMENTAL

4-Nitrobenzylidene aniline. In a four-necked flask fitted with a stirrer, dropping funnel, nitrogen inlet, and a condenser with a drying tube, 2.4 g of triphenylarsine oxide dissolved in dry benzene was placed. 0.89 g of phenyl isocyanate dissolved in benzene was added dropwise. The temperature of the reaction mixture was held at 5 – 6° during the addition. 1.0 g of *p*-nitrobenzaldehyde dissolved in absolute benzene was then added and most of the benzene was distilled off. The product was dissolved in ether and recrystallized; yield 0.7 g. The infrared spectrum of the compound was identical with that of an authentic sample of 4-nitrobenzylidene aniline, m.p. 93°, lit.[13] 93°.

Diphenylmethylidene aniline. To a solution of triphenylarsine phenylimine prepared from 1.6 g triphenylarsine oxide and 0.58 g phenyl isocyanate a solution of 0.9 g benzophenone in dry benzene was added. The reaction mixture was heated for 1 hour after the addition was completed. Most of the benzene was distilled off and the product was freed from triphenylarsine oxide by treatment with ether; yield 0.9 g. The melting point after recrystallization from ethanol was 112°. Lit. [14] 116°. The product was shown by mixture melting point and thin layer chromatography to be identical with a sample prepared by the method of Reddelien.[15]

N,N'-*Diphenyl* p-*benzoquinone diimine.* To a solution of 0.01 mol of triphenylarsine phenylimine prepared as previously described, 0.005 mol of benzoquinone was added. The resulting deep red solution was concentrated in vacuum. After addition of ether to the concentrated solution most of the triphenylarsine oxide was filtered off. The ether soluble product was recrystallized from absolute ethanol, m.p. 180°, undepressed by admixture of an authentic sample. The product was also identified by its infrared spectrum.

N-*Phenyl* p-*benzoquinone imine.* A benzene solution of triphenylarsine phenylimine was prepared from 1.5 g phenyl isocyanate and 4.1 g triphenylarsine oxide. Benzoquinone (0.9 g) was added and it was observed that the yellow colour of the arsine imine solution was discharged immediately, producing the intense red colour of the benzoquinone imine. Most of the benzene was distilled off and the product recrystallized from ligroin. Yield 1.2 g, m.p. 101°, lit.[16] 100 – 101°. The infrared spectrum of the compound was identical with that of an authentic sample.

N,N'-*Diphenyl 1,4-naphthoquinone diimine* was synthesized in an analogous way from triphenylarsine phenylimine and 1,4-naphthoquinone. The product was crystallized from ether. M.p. 185°, lit.[17] 187°. For further identification 0.2 g of the product was dissolved in 3 ml 48 % sulfuric acid. The solution was allowed to stand a few minutes, whereafter 3 ml of water were added. The mixture was then partially neutralized with 0.1 N sodium hydroxide solution, and the product was extracted with ether. Most of the ether was distilled off and the residue was dissolved in ethanol and recrystallized several times, m.p. 123°. An authentic sample of 1,4-naphthoquinone had m.p. 120 – 124°. The infrared spectra of the two compounds were identical. The aqueous solution was made alkaline with sodium hydroxide solution and extracted with benzene. The benzene solution was dried, whereafter 6 ml acetic anhydride were added. The solvent was evaporated at reduced pressure and the residue recrystallized, m.p. 113°, undepressed by admixture of an authentic sample of acetanilide.

Diphenylcarbodiimide. To a solution of 0.01 mol of triphenylarsine phenylimine in benzene 0.01 mol of phenyl isothiocyanate was added. The reaction mixture was heated for 2 h. The product was identified by its infrared spectrum without isolation. The infrared spectra showed a quantitative transformation of the isothiocyanate into diphenylcarbodiimide. 1.9 g of triphenylarsine sulphide was separated before running the infrared spectra. M.p. 160 – 162°, lit.[18] 162°.

Phenyl isothiocyanate. A solution of 0.01 mol of triphenylarsine phenylimine in benzene was prepared as previously described. Excess of carbon disulphide was added and the reaction mixture was heated for 2 – 3 h. Most of the benzene was distilled off and 2.7 g of triphenylarsine sulphide was filtered away. The filtrate was shown to be a mixture of phenyl isothiocyanate and diphenylcarbodiimide by its infrared spectrum.

N-*Sulfinyl aniline.* 0.01 mol of triphenylarsine phenylimine was dissolved in 100 ml benzene and dry sulphur dioxide was bubbled through the warm solution. Gas chromatographic analysis of the reaction mixture showed the presence of *N*-sulfinyl aniline.

Adduct from dimethyl acetylenedicarboxylate and triphenylarsine phenylimine. 1.3 g of the ester was added to an equivalent amount of triphenylarsine phenylimine prepared as previously described. The solvent was removed and the resulting oil was triturated with ether until it solidified.

The product was recrystallized two times from chloroform-ether. The adduct, 2.5 g, had m.p. 177°C (Found: C 67.06; H 4.96; N 2.83. Calc. for $C_{30}H_{26}AsNO_4$: C 66.8; H 4.86; N 2.60). IR spectrum: peaks (strong) at 1734 cm^{-1} (ester carbonyl) and 1658 cm^{-1} (ester carbonyl, the frequency of the stretching vibration is displaced downwards due to a strong contribution from the enolate structure in the resonance hybrid.) The PMR spectrum exhibited singlets at δ 3.24 (3H) and 3.60 (3H) and multiplets at δ 6.15 – 7.80 (20H).

Adduct from triphenylacetonitrile N-oxide and triphenylarsine phenylimine. 1.2 g of triphenylacetonitrile *N*-oxide was added to the warm solution of an equivalent quantity of the arsine imine in benzene. The reaction mixture was heated for 2 h with stirring, whereafter most of the benzene was distilled off. Ether was added and the product crystallized after several days. Recrystallization from benzene + ether yielded 0.7 g of a white solid, m.p. 182°. IR spectrum: Peak at 1690 cm^{-1} (strong), probably: C=N. The spectrum also indicated the presence of water of crystallization. (Found: C 75.35; H 5.30; N 3.80. Calc. for $C_{44}H_{35}AsN_2O.H_2O$: C 75.41; H 5.32; N 3.99.) The mass spectrum showed no parent molecular ion peak M at *m/e* 700. The ready expulsion of triphenylarsine oxide accounts for the total absence of M in the spectrum and represents just what one would have expected of a molecule of the proposed structure. The principal high mass peaks occurred at *m/e* 378 ($M-Ph_3AsO$) 321, 243 ($Ph_3\overset{+}{C}$), 229, 227 and a series of other skeletal rearrangement products from triphenylarsine.

Reaction with methyl iodide. The triphenylarsine phenylimine was heated a short time with a large excess of methyl iodide in boiling benzene. Most of the solvent was removed and the product washed several times with hot benzene. The resulting red oil was characterized by its PMR spectrum which, besides the low field part of the spectrum due to the phenyl groups, shows a high field signal at 2.82 ppm. The signals due to the methyl and phenyl groups, respectively, are in the ratio 3 : 20 to each other.

REFERENCES

1. Frøyen, P. *Acta Chem. Scand.* **25** (1971) 983.
2. Frøyen, P. *Unpublished results.*
3. Johnson, A. W. and Wong, S. C. K. *Can. J. Chem.* **44** (1966) 2793.
4. Frøyen, P. *Acta Chem. Scand.* **26** (1972) 1777.
5. Staudinger, H. and Hauser, E. *Helv. Chim. Acta* **4** (1921) 861.
6. Frøyen, P. *Acta Chem. Scand.* **25** (1971) 2781.
7. Johnson, A. W. *J. Org. Chem.* **25** (1960) 183.
8. Brown, G. W. *J. Chem. Soc.* **C 1967** 2018.
9. Bestmann, H. J. and Kunstmann, R. *Chem. Ber.* **102** (1969) 1816.
10. Huisgen, R. and Wulff, J. *Chem. Ber.* **102** (1969) 1833.
11. Wulff, J. and Huisgen, R. *Chem. Ber.* **102** (1969) 1841.
12. Huisgen, R. and Wulff, J. *Tetrahedron Letters* **1967** 917.
13. Fischer, O. *Ber.* **14** (1881) 2525.
14. Dimroth, O. and Zoeppritz, R. *Ber.* **35** (1902) 984.
15. Reddelien, G. *Ber.* **42** (1909) 4759.
16. Willstätter, R. and Moore, C. W. *Ber.* **40** (1907) 2665.
17. Fischer, O. and Hepp, E. *Ann.* **256** (1890) 255.
18. La Coste, W. and Michaelis, A. *Ann.* **201** (1880) 244.
19. Appel, R. and Wagner, D. *Angew. Chem.* **72** (1960) 209.
20. Mann, F. C. and Chaplin, E. J. *J. Chem. Soc.* **1937** 527.

Received October 20, 1970.

ACTA CHEMICA SCANDINAVICA 27 (1973) 146–152

Lanthanoid Hexaoxoiodates(VII)

IV. Cerium(IV) Hexaoxoiodate(VII)

ARI H. J. LOKIO*

Department of Chemistry, University of Oulu, Oulu, Finland

The reactions of cerium(III) and cerium(IV) with periodic acid and with alkali metal hexaoxoiodates(VII) were studied. In acid conditions, the product formed was $CeHIO_6.3H_2O$ irrespective of the oxidation number of cerium. This was confirmed by magnetic measurements. By heating this compound, $Ce_2I_2O_{11}$ and $Ce_2I_2O_9$ were prepared. The infrared spectra of the compounds were recorded and interpreted and the thermal decomposition of the compounds was studied by TGA and DSC.

The lanthanoid hexaoxoiodate most frequently mentioned in the literature is cerium periodate. In 1939 Bahl and Singh [1] reported that they had prepared $CeIO_5.4H_2O$ in two different ways. A yellow compound precipitated when an aqueous $Na_2H_3IO_6$ suspension was added to an aqueous solution of cerium nitrate, but a white compound that gradually turned yellow was obtained when H_5IO_6 was used as the precipitating reagent. Two years later, Choudhury published articles dealing with several new M(IV) periodates in which he mentioned, among other compounds, a yellow $CeHIO_6.H_2O$ that he had synthetized by allowing $Na_3H_2IO_6$ to react with ammonium cerium nitrate.[2,3] The first measurements to determine the structure of the compound were made by Sahney *et al.*[4] On the basis of magnetic measurements, they reported the value $\mu_B = 2.356$ for the magnetic moment of the compound $CeIO_5.4H_2O$ at room temperature. They concluded that the compound is a true salt and not a complex salt of periodic acid.

The first attempt to determine cerium analytically as a periodate was made in 1949. It was found that cerium(IV) could be separated from other lanthanoids or thorium by precipitating it with potassium metaperiodate as $CeHIO_6.H_2O$ at a carefully adjusted pH.[5] Venugopalan and George [6] determined cerium(IV) by precipitating it with an excess of potassium metaperiodate. Puzdrenkova *et al.*[7] used the same precipitating reagent in acid

* Present address: Rikkihappo Oy, Oulu, Finland.

solution and obtained the product $CeHIO_6.3H_2O$, which was decomposed to $CeHIO_6$ by drying at 130°C. Alimarin and Puzdrenkova [8] studied periodate complexes of lanthanoids in alkaline solution and observed that the stabilities of the complexes increase in the order:

$$La^{3+} < Pr^{3+} < Er^{3+} < Ce^{4+} \approx Th^{4+} < Fe^{3+}$$

Alimarin *et al.*[9] also synthetized the complex salt $Na_6[Ce(IO_6)_2]$.

Table 1. Analytical data for compounds I–VIII.

Synthetized compound		Ce		I		H_2O		Weight loss on heating	
		obs.	calc.	obs.	calc.	obs.	calc.	obs.	calc.
I	$CeHIO_6.3H_2O$	33.19	33.52	32.84	30.36	12.2	12.92		
II	»	33.50		33.30		12.4			
III	»	33.13		33.29					
IV	»	33.84		33.19					
V	»	33.41		33.33		12.0			
VI	»	33.55		30.25		12.6			
VII	$Ce_2I_2O_{11}$	39.47	39.45	37.45	35.75			15.3	15.07
VIII	$Ce_2I_2O_9$	41.66	41.33	37.48	37.43			21.1	18.90

In the present work the reactions of cerium(III) nitrate and cerium(IV) sulphate with H_5IO_6, $Na_2H_3IO_6$, and $Na_3H_2IO_6$ in acid solution were studied. The compound $CeHIO_6.3H_2O$ was obtained despite the oxidation level of cerium, but some iodate precipitated as an impurity when cerium(III) salt was used. Magnetic measurements showed that $CeHIO_6.3H_2O$ was only slightly paramagnetic. This suggests that the oxidation number of cerium is four. Since no other investigations on the structures of the lanthanoid periodates have been made, their structures were studied by infrared spectroscopy and by TGA and DSC. The magnetic measurements were made by the Gouy method. No diffraction maxima clearly distinguishable from the background noise were observed in the powder diagrams.

Table 2. Magnetic susceptibilities of preparations I–VI.

Compound	Temperature (K)		$\chi_g \times 10^6$		$\chi_M \times 10^6$	
	T_1	T_2	T_1	T_2	T_1	T_2
I	196	296.2	0.126	0.202	52.7	85.7
II	196	296.7	0.152	−0.046	63.4	−19.2
III	196	296.0	0.110	0.139	46.0	58.1
IV	196	295.9	0.209	0.159	87.4	66.5
V	196	296.0	0.279	0.237	116.7	99.1
VI [a]	77	293.0	−0.074	−0.076	−30.7	−31.9

[a] Mean of three determinations.

EXPERIMENTAL

$Ce(NO_3)_3$ ("reinst") and $Ce(SO_4)_2.4H_2O$ (*p.a.*) were obtained from E. Merck AG, Darmstadt. The other reagents used were the same as described in Part I.[10]

Synthesis I. 0.02198 mol of H_5IO_6 was dissolved in 150 ml of distilled water and added to an equimolar amount of $Ce(NO_3)_3$ in aqueous solution at 60°C and the pH adjusted to 1.8. The yellow precipitate that formed was collected on a No. 3 sintered glass filter, washed thoroughly and dried under a pressure of 20 mmHg in a vacuum oven at 39°C. The product was a yellow powder.

Synthesis II. The molar ratio of cerium(III) nitrate and periodic acid was 1:2 and the pH of the solution was adjusted to 1.9. In other details, the procedure was the same as for compound I.

Synthesis III. The molar ratio of cerium(III) nitrate and periodic acid was 2:3. In other details, the procedure was the same as for compound I.

Synthesis IV. An aqueous $Na_2H_3IO_6$ solution made slightly acidic with nitric acid was allowed to react with an equimolar amount of $Ce(NO_3)_3$ at pH 1.9. After this, the procedure was the same as for compound I.

Synthesis V. An aqueous $Na_3H_2IO_6$ solution made slightly acidic with nitric acid was allowed to react with an equimolar amount of $Ce(NO_3)_3$ at pH 2.5. After this, the procedure was the same as for the compound I.

Synthesis VI. An aqueous $Ce(SO_4)_2$ solution made slightly acidic with sulfuric acid was added to an equimolar amount of H_5IO_6 in water at pH 1.5. After this, the procedure was the same as for compound I.

Synthesis VII. The dry product of synthesis IV was heated from room temperature to 355°C during 70 min.

Synthesis VIII. The dry product of synthesis II was heated from room temperature to 365°C during 79 min.

DISCUSSION

Bahl and Singh [1] reported that they had synthetized the compound $CeIO_5.4H_2O$. Sahney *et al.*[4] measured the magnetic moment of cerium in this salt and reported the value $\mu_B = 2.356$. On that basis the same formula was proposed. The product was reported to change colour from white to yellow in the course of the reaction. This suggests that cerium(III) was oxidized to cerium(IV). In addition, the products were of the same color as cerium(IV) periodates prepared later under similar conditions.[2,3] For this reason, cerium hydrogen hexaoxoiodates(VII) were synthetized in the present work by varying the ratio of cerium salt to periodic acid and the pH. It was observed that Ce(III) and Ce(IV) were precipitated in the form of $CeHIO_6.3H_2O$ at pH values from 1.5 to 3. A weak paramagnetism was found in compounds I – V when the cerium(III) salt was used as starting material. This may be explained by assuming that some cerium(III) iodate precipitates when iodine(VII) is reduced and this increases the paramagnetism of the compound. This interpretation is corroborated by the observation that the compound II in which the atomic ratio Ce:I was 1:2 had the lowest susceptibility at room temperature. A diamagnetic compound was obtained when a Ce(IV) salt was the initial reactant.

Iodine analyses revealed that there was more iodine in products I – V than the formula of the compound implies. According to the assumption presented above, even a small amount of cerium(III) iodate present will increase the iodine content of the compound. Therefore, cerium must be oxidized when it is to be determined as $CeHIO_6$. Also Puzdrenkova *et al.*[7] considered

Table 3. Thermal decomposition of preparations I—VI.

Reaction	Δm, % calc.	I TGA, °C	I Δm, %	I DSC, °C	II TGA, °C	II Δm, %	II DSC, °C	III DSC, °C	IV DSC, °C	V TGA, °C	V Δm, %	V DSC, °C	VI TGA, °C	VI Δm, %	VI DSC, °C
$CeHIO_6.3H_2O \rightarrow$	12.92	95—	12.2	113	95—	12.4	119	110	123	95—	12.0	108	90—	12.6	102
$CeHIO_6 + 3H_2O$		270		155	260		162	156		260		155	260		176
$CeHIO_6$		270—			260—					260—			260—		
		330			335					325			280		
$2CeHIO_6 \rightarrow$	2.15	330—	2.4	313	335—	2.0	311	309	303	325—	2.1	298	280—	2.5	308
$Ce_2I_2O_{11} + H_2O$		345			350					345			320		
$Ce_2I_2O_{11}$		345—			350—					345—			320—		
		370			370					375			340		
$Ce_2I_2O_{11} \rightarrow$	43.76	370—	44.8	491	375—	46.0	492	494	489	375—	45.2	485	340—	2.7	367
													380		
$2CeO_2 + I_2 +$		490		498	480		500	499	499	490		497	390—	40.8	448
$3\frac{1}{2}H_2O$													490		456
CeO_2 (residue)		490—			480—					490—			490—		
		1000			1000					1000			1000		
Total weight loss	58.83		59.4			60.4					59.3			58.6	

the oxidation important after observing that precipitation of Ce(III) required a fivefold excess of the reagent. We have also prepared other cerium hexaoxoiodates in acid conditions on which further studies are in progress.

The infrared spectra also corroborated the structure $CeHIO_6.3H_2O$ because a weak δ(IOH) absorption band at 1154 – 1176 cm^{-1} was detected in spectra of some of the synthetized products. The strongest absorption band in the spectra of compounds I – VI that can be interpreted as a ν(IO) vibration was found at 720 – 724 cm^{-1}. This band was at 780 cm^{-1} in the spectra of products VII and VIII. Assignments of bands in the infrared spectra are presented in Table 4.

Table 4. Infrared bands of preparations I – VIII.

Assignment	$CeHIO_6.3H_2O$ I	II	III	IV	V	VI	$Ce_2I_2O_{11}$ VII	$Ce_2I_2O_9$ VIII
ν(OH)	3500 s,b	3600–	3600–	3600–	3570 s,b	3580 s,b		
		3400 s,b	3400 s,b	3300 s,b	3420 s,b	3440 s,b		
2δ(IOH)					2356 w	2368 w		
$\delta(H_2O)$	1639 m	1642 m	1644 m	1644 m	1638 m	1642 m		
			1156 w,b	1176 w,b	1155 m,b	1154 m,b		
δ(IOH)			1072 w	1072 w	1071 w	1072 w		
ν(IO)	720 s	724 s	724 s	724 s	721 s	720 s	781 s	780 s
	592 sh	588 sh	587 sh	591 sh	592 sh	588 sh	494 sh	494 sh
δ(OIO)	461 ms	462 ms	464 ms	464 ms	464 ms	464 ms	450 s	430 s

s = strong. m = medium. w = weak. b = broad. sh = shoulder.

Thermal decomposition of the compound $CeHIO_6.3H_2O$ was followed by TGA and DSC. The decomposition was observed to proceed in the following way:

	TGA (°C)	DSC (°C)
$CeHIO_6.3H_2O \rightarrow CeHIO_6.H_2O + 2H_2O$	95 –	102 – 119
$CeHIO_6.H_2O \rightarrow CeHIO_6 + H_2O$	270	155 – 176
$CeHIO_6$	260 – 330	
$2CeHIO_6 \rightarrow Ce_2I_2O_{11} + H_2O$	280 – 345	308 – 313
$Ce_2I_2O_{11} \rightarrow Ce_2I_2O_9 + O_2$	340 – 375	347 – 368
$Ce_2I_2O_9 \rightarrow 2CeO_2 + I_2 + 2\frac{1}{2}O_2$	370 – 490	448 – 484
		456 – 500
Residue CeO_2	490 –	

Although it has been reported earlier that cerium can be determined gravimetrically by precipitation with periodate and subsequent decomposition of the product to $CeHIO_6.H_2O$ by drying at 100 – 110°C,[5] the thermogram shows that $CeHIO_6$ is a more stable form. Puzdrenkova *et al.*[7] also came to the same conclusion. According to the thermogram, the three molecules of water of crystallization seem to be released as a continuous process over the temperature range from 95 to 270°C. However, the DSC reveals that the reaction proceeds in two stages and is endothermic. The third endothermic peak is associated with the release of water that leads to formation of $Ce_2I_2O_{11}$.

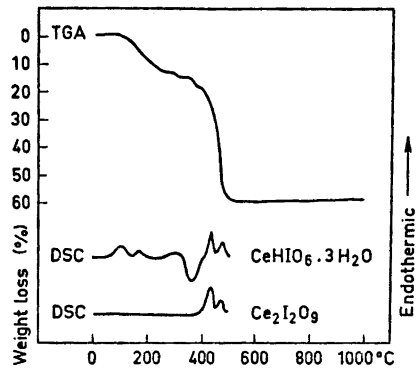

Fig. 1. TGA and DSC diagrams of compound $CeHIO_6.3H_2O$ and the DSC diagram of compound $Ce_2I_2O_9$.

The synthesis of this compound was successful only after several attempts, in which the temperature and the time of heating were varied, because the exothermic reaction involving release of oxygen and simultaneous reduction of iodine begins very soon after the release of water. The excess of iodine found in the compound on analysis may be due to iodate present as an impurity in the product as suggested above. The resulting compound $Ce_2I_2O_9$ decomposes endothermically in the temperature range 370 – 490°C and the reaction proceeds in at least two steps. In their studies on copper hexaoxoiodates, Näsänen *et al.*[11] came to the same conclusion with respect to the decomposition mechanism and suggested that the compound $Cu_2(OH)(H_2IO_6).H_2O$, for which Siebert has later presented the formula $Cu_2HIO_6.H_2O$,[12] decomposes to $Cu_4I_2O_{11}$ at 300°C. The decomposition reaction suggested in the present paper is corroborated by the observation that there were only two endothermic peaks at 489 and 499°C in the DSC diagram of the compound $Ce_2I_2O_9$.

All absorption bands at higher wavenumbers were absent from the infrared spectra of the compounds $Ce_2I_2O_{11}$ and $Ce_2I_2O_9$. The ν(IO) vibration band had moved 60 cm^{-1} to 780 cm^{-1} and the δ(OIO) band to 450 and 430 cm^{-1}, respectively. These shifts indicate that rearrangement had taken place when these compounds were produced.

Acknowledgements. The author expresses his thanks to Professor T. Nortia, University of Turku, Turku, for conducting the magnetic measurements, and to Rikkihappo Oy, Oulu, for the opportunity to perform the thermogravimetric analyses in the Research Laboratory of Rikkihappo Oy. The author thanks also Professor J. Kyrki for many valuable discussions.

REFERENCES

1. Bahl, R. K. and Sigh, S. *J. Indian Chem. Soc.* **16** (1939) 375.
2. Choudhury, P. C. R. *Sci. Cult. (Calcutta)* **7** (1941) 57.
3. Choudhury, P. C. R. *J. Indian Chem. Soc.* **18** (1941) 335.
4. Sahney, R. C., Aggarwal, S. L. and Singh, M. *J. Indian Chem. Soc.* **24** (1947) 193.
5. Venkataramaniah, M. and Baghavarao, Bh. S. V. *Current Sci. India* **18** (1949) 248.
6. Venugopalan, M. and George, K. F. *Naturwiss.* **43** (1956) 348.
7. Puzdrenkova, I. V., Alimarin, I. P. and Frolkina, V. A. *Vestn. Mosk. Univ. Ser. Mat. Mekhan. Astron. Fiz. i Khim.* **13** (1958) 183.

8. Alimarin, I. P. and Puzdrenkova, I. V. *Vestn. Mosk. Univ. Ser. Mat. Mekhan. Astron. Fiz. i Khim.* **14** (1959) 213.
9. Alimarin, I. P., Puzdrenkova, I. V. and Shiryaeva, O. A. *Vestn. Mosk. Univ. Ser. II Khim.* **17** (1962) 61.
10. Kyrki, J. R. and Lokio, A. H. J. *Suomen Kemistilehti* **B 44** (1971) 105.
11. Näsänen, R., Uggla, R. and Hirvonen, Y. *Suomen Kemistilehti* **B 30** (1957) 31.
12. Siebert, H. *Fortschr. Chem. Forsch.* **8** (1967) 470.

Received May 29, 1972.

ACTA CHEMICA SCANDINAVICA 27 (1973) 153–163

Electrophilic Attack on the Furan Ring

Acid-Catalysed Protodedeuteriation, Protodetritiation, Deuteriodeprotonation, and Deuteriodetritiation at the α-Position. Hydrolytic Cleavage of the Ring

PENTTI SALOMAA, ALPO KANKAANPERÄ, EEVA NIKANDER, KAISLI KAIPAINEN and RIITTA AALTONEN

Department of Chemistry, University of Turku, Turku, Finland

Rates of acid-catalysed α-hydrogen exchange reactions in 2-methylfuran have been measured. Both the observed isotope effects and the activation parameters display all the characteristics of the $A\text{-}S_E2$ mechanism of aromatic hydrogen exchange. The subsequent acid-catalysed decomposition reactions were nearly two powers of ten slower than the α-hydrogen exchange reactions.

The possible mechanisms of the ring cleavage are discussed. Experiments conducted with furan, 2-methylfuran, and 2,5-dimethylfuran revealed that, with the exception of 2,5-dimethylfuran, polymeric products are formed in subsequent reactions almost exclusively. Evidence was also collected which showed that these polymer-forming reactions occurred predominantly prior to hydrolytic cleavage of the ring. The latter reaction, which is significant in the case of 2,5-dimethylfuran only, could be best explained in terms of a rate-determining protonation at the β-position.

Acid-catalysed exchange of the isotopes of hydrogen in aromatic systems provides the most elementary model of electrophilic aromatic substitution.[1–5] In all cases studied hitherto, the aromatic systems have not undergone further reactions. This has been a great advantage for the study of the isotope effects themselves and for drawing general conclusions about the nature of electrophilic aromatic substitution. Similar detailed studies of less stable π-electron systems have not been reported. Apart from their interest for permitting comparisons with systems of high stability, they may be expected to give some mechanistic information about the subsequent decomposition of the ring systems.

Our particular system of interest is the furan ring. Furan and its derivatives, although stabilized by their aromaticity, undergo acid-catalysed decomposition reactions much more readily than their sulphur analogues, the

thiophens.[3,6] It was found in a preliminary study of the protodedeuteriation of 2-methylfuran by dilute perchloric acid [7] that this compound exchanges its α-hydrogen at a rate that is roughly two powers of ten higher than that of the subsequent reaction. Similar results have been reported for unsubstituted furan [8] in 4.6 to 7.2 M perchloric acid solutions, although under these conditions the protodedeuteriation rate was only 7 times higher.

The above results [6–8] demonstrate that the rate-determining stage in the hydrolytic cleavage of the furan ring cannot be proton transfer from the catalyst acid to the α-carbon atom of the ring as originally proposed by Stamhuis *et al.*[9] In contrast to the conclusions drawn by Unverferth and Schwetlick,[8] we do not see any argument by which the above results excluded the possibility of a mechanism involving a rate-determining β-protonation in the cleavage of the ring. The only relevant observation (agreeing with ours) was that no β-hydrogen exchange was detected *prior* to further reactions. The nature of the further reactions had not been studied in detail. The only kinetic quantity thus far measured for these reactions has been the rate of decrease of the concentration of the initial reactant, the furan. Possible side reactions competing with the hydrolytic cleavage of the ring have not been discussed.

2-Methylfuran was chosen as the model compound for the isotope exchange studies because this compound has only one exchangeable α-hydrogen atom, that present at the 5-position. Furthermore, a comparison of our earlier results [7] and those obtained for unsubstituted furan [8] revealed that 2-methylfuran is more suitable for these studies, as the subsequent reactions are relatively much slower for this compound and do not thus interfere with the isotope exchange measurements. In addition, the decomposition reactions of furan, 2-methylfuran, and 2,5-dimethylfuran were studied under various conditions by performing kinetic measurements and analysing the reaction products.

EXPERIMENTAL

Materials. Furan, 2-methylfuran, and 2,5-dimethylfuran were purified as described earlier.[6,7]

The α-deuteriated form of 2-methylfuran, 2-methylfuran-5-*d*, was prepared by two methods, both of which yielded identical products. In the first method, 32 g of nondeuteriated 2-methylfuran was dissolved in 200 ml of deuterium oxide – dimethyl sulphoxide solvent in which the mol fraction of each component was 0.5 and which contained 0.04 mol of perchloric acid as catalyst and a small amount of hydroquinone to prevent polymerization. The mixture was kept at 100°C and the progress of the α-deuteriation reaction was followed by PMR spectroscopy. Equilibrium was attained in about 2 h, when about 85 % of the α-protons had been replaced by deuterons. No deuteriation at the β-position was detected. The crude product, which still contained a substantial proportion of the α-protium compound, was then extracted with five 30 ml portions of pentane. The combined extract, to which a small amount of hydroquinone had been added to prevent polymerization, was dried with anhydrous potassium carbonate. After the solution had been separated from the drying agent by filtration, the solvent was distilled off through an efficient column.

The above procedure was then repeated, but using the crude 2-methylfuran-5-*d* as starting material. This treatment yielded a product in which 95 % of the α-protons had been replaced by deuterons. Further deuteriation was not considered to be justified economically, for the initial hydrogen isotope composition in the α-position was actually immaterial in kinetic studies of the dedeuteriation reaction, except that the deuterium content had to be sufficiently high in order that significant changes in the α-D/α-H ratio

could be measured during the course of the reaction. The 95 % deuteriated product was fractionally distilled. The physical constants recorded for the purified product were b.p. 62.0°/760 torr, n_D^{20} 1.4324, d_4^{20} 0.9277. The PMR spectrum of a 10 % solution of the product in carbon tetrachloride containing tetramethylsilane as internal standard showed: 1 H at δ 5.85 ppm (3-hydrogen), 1 H at δ 6.13 ppm (4-hydrogen), and 3 H at δ 2.27 ppm (2-methyl protons). A trace of a peak of 5-protons was observed at δ 7.18 ppm, and it was calculated from the area of this peak that the ratio of the 5-protons to the total number of 5-hydrogens was about 0.05. The IR spectrum of the purified product was also recorded using carbon tetrachloride again as solvent. When this spectrum was compared with that of the corresponding protocompound, 2-methylfuran-5-*h*, strong peaks were observed at 730, 920, and 1150 cm^{-1} in the spectrum of the latter compound, but only traces of these peaks could be seen in the spectrum of 2-methylfuran-5-*d*. In the spectrum of the deuteriocompound, the corresponding peaks had been shifted at frequencies that were lower by factors of about 1.4.

The second method by which 2-methylfuran-5-*d* was prepared was to use a two-phase system consisting of 2-methylfuran and heavy water. The volume of the aqueous phase, which was about 1 M in deuterochloric acid, was approximately ten times that of the organic phase. Hydroquinone was added as before. The reaction vessel was placed in a bath at 50°C and agitated vigorously by means of a mechanical arrangement. At suitable intervals, the agitation was discontinued and the phases were allowed to separate. A sample of the furan phase was then analysed by PMR spectroscopy. It was found that under the chosen conditions, the α-hydrogen exchange had reached equilibrium in 2 to 3 h. The crude product was then separated, and the procedure was repeated as in the first method. The product thus obtained was dried and purified by fractional distillation. The physical constants of the purified compound were almost equal to those obtained for the product prepared by the first method. Furthermore, no significant differences were found in kinetic quantities for the two preparations.

2-Methylfuran which was tritium-labelled at the α-position was prepared by the second method described above as this was found to be somewhat more convenient. The water phase consisted of 200 ml of 1 M hydrochloric acid in ordinary water to which about 20 mCi of tritiated water had been added. The product, after purification by repeated fractional distillation, had the same physical constants (and gave the same PMR and IR spectra) as the unlabelled 2-methylfuran.

The deuterium oxide used was supplied by Norsk Hydro-Elektrisk Kvaelstofaktieselskab, Norway. It was of the same batch as that used in a study of the solubilities of some salts in heavy water.[10] The deuterium atom fraction determined by a method described earlier [11] was 0.9982. Tritium-labelled water was supplied by The Radiochemical Centre, Amersham, England. Dimethyl sulphoxide was a product of E. Merck AG, Darmstadt, West Germany, which was purified by boiling under reflux over calcium hydride for 12 h, by fractional distillation under reduced pressure and by repeated recrystallization.

Kinetic measurements. Depending on the isotopes of hydrogen which participated in the α-hydrogen exchange reaction of 2-methylfuran, different methods were used to follow the progress of the reactions. The rates of the protodedeuteriation and deuteriodeprotonation reactions were in most cases followed by a PMR method based on measuring the rate of appearance or disappearance of the 5-proton signals. The PMR spectra were recorded on a Perkin-Elmer R10 60 MHz spectrometer at 33.5°C. In some control experiments, which gave consistent results, an IR method was employed to study the protium-deuterium exchange at the 5-position. The IR spectra were measured with a Perkin-Elmer Grating Infrared Spectrometer. In the study of the detritiation reactions a Wallac Decem-NTL-314 liquid scintillation counter was used.

When the PMR method was used, the intensity of the signal of the 5-protium atom was measured at suitable intervals. To eliminate the effect of possible fluctuations in the recorded intensities, the intensities were always compared with the intensity of a standard signal. In the present case, it was found that the signal of the 4-proton was an excellent standard, because this proton remained unaffected during the isotope exchange. The signal of the 4-proton is also in the same region of the magnetic field (see above) as that of the 5-proton whose appearance or disappearance was being followed. Thus the ratio of the peak areas for the 5- and 4-protons was proportional to the progress of the dedeuteriation or deprotonation reaction. A further advantage was that, even if some decom-

position of the furan occurred during the isotope exchange measurements (which decomposition was very slow indeed, as shown below), the kinetic quantities measured in this way were independent of whether subsequent reactions took place or not.

Owing to the low solubilities of the furans, the kinetic experiments were run in mixtures of dimethyl sulphoxide and protium or deuterium oxide in which the mol fraction of each component was always 0.500. The concentration of the catalyst perchloric acid varied from 0.180 to 0.190 M in different experiments. After the 2-methylfuran had dissolved in the solvent, aliquots of the reaction mixture were sealed in 10 to 15 PMR sample tubes. The tubes were immersed simultaneously in an oil bath which was held at the desired temperature (70 to 100°C). The first sample was taken after about 15 min, and subsequent samples at intervals during the period when 10 to 80 % change occurred. The final samples were taken after about 8 to 10 times the half-lives of the reactions. All sample tubes were stored in an ice-water bath until the last sample had been taken and were then analysed in close succession. The reactions followed simple first-order kinetics.

When the reactions were followed by the IR method, 5 ml samples of the initial reaction mixture were sealed into glass vials, which were then kept at a constant temperature in a thermostat. The samples were analysed as follows. After a vial had been opened, its contents were carefully rinsed into a separatory funnel using always the same volume (0.6 ml) of water. Ten ml of hexane was added, whereupon the 2-methylfuran present distributed itself between the hexane and water-dimethyl sulphoxide phases. The hexane layer was dried with anhydrous magnesium sulphate and analysed. The IR spectra were recorded in sodium chloride cells. The reference cell was filled with hexane. The progress of the reaction was followed by measuring peak heights at 730, 920, and 1150 cm^{-1} (see above) using reference standard solutions prepared by dissolving weighed quantities of 2-methylfuran-5-*h* in known volumes of hexane.

In the detritiation studies, the procedure was similar to that described above except for the analyses, for which 2 ml samples of the hexane layers were pipetted into the vials of the liquid scintillation counter. The scintillation liquid comprised 4 g of diphenyloxazole and 100 mg of *p*-bis-(*o*-methylstyryl)-benzene dissolved in 1 l of toluene. The volume of the scintillation liquid added to each sample was 8 ml. First-order rate coefficients were calculated from the measured activities of the samples. A small empirical correction (about 3 % of the overall activity change measured during the reaction) was applied to the final samples taken after ten half-lives. Unlike the samples taken in the earlier stages of the reaction, the final samples and also their hexane extracts were light yellow. This caused a slight quenching, which had to be corrected for in the liquid scintillation analysis in order to obtain as accurate values as possible. The empirical correction for this colour quenching was determined by running a reaction with nontritiated 2-methylfuran under the same conditions. Equal amounts of tritiated 2-methylfuran were added to the hexane extracts and the counts per minute were recorded.

Decomposition of the furan ring and product analyses. The rates of subsequent reactions that followed the relatively fast α-hydrogen exchange reactions were also measured under identical conditions. Similar kinetic experiments were also run with 2,5-dimethylfuran. Regardless of the particular nature of the reaction, the rate of decrease of the concentration of the furan in question could be easily measured by the PMR techniques described above, by following the disappearance of the signal of the 5-proton (in case of 2-methylfuran) or of the signals of 3- and 4-protons (in case of 2,5-dimethylfuran). In most experiments, a protium oxide-dimethyl sulphoxide (mol fraction 0.500) mixture was used as solvent. The concentration of the catalyst perchloric acid was the same, about 0.2 M, as in the isotope exchange studies. Samples taken at suitable intervals were analysed as follows. The unchanged furan and the soluble reaction products were extracted into carbon tetrachloride, to which 0.4 vol. % of tetramethylsilane had been added as an internal standard for the PMR analyses. In separate experiments, it was established by gas chromatography that at least 98 % of the unchanged furan was extracted from the sample solution. The peak areas in the PMR spectra were then compared with those of the internal standard and the first-order rate coefficients were calculated.

In the case of 2-methylfuran, no hydrolysis products were detected by PMR or by gas chromatographic analyses. The only product of the reaction was a polymeric compound which was insoluble in the solvents employed. In contrast, acetonylacetone was formed almost quantitatively from 2,5-dimethylfuran under the experimental con-

ditions. Thus the rate of formation of acetonylacetone could be measured (from the PMR spectrum) simultaneously with the rate of decomposition of 2,5-dimethylfuran; both rates were almost equal.

Similar product analyses were also made using other solvents. For example, the reactions of furan and 2-methylfuran in water containing 0.2 mol of perchloric acid per litre as catalyst were studied. No traces of nonpolymeric reaction products were detected in either case.

For the applications to be discussed below, it was of interest to carry out some experiments that would indicate at what stage of the acid-catalysed solvolytic decomposition of the furan ring the polymerization actually takes place. If the polymerization occurred only *after* the cleavage of the ring, the overall rate of disappearance could be set equal to the rate of the ring cleavage. In contrast, if the polymerization (or, at least, a significant part of it) were a side reaction competing with the cleavage reaction, then the rate of the latter reaction would be but a small fraction of the overall rate. A solvent in which this distinction could be made was ethanol. The products of ring cleavage in this solvent are α,δ-diacetals, which, unlike the α,δ-dicarbonyl compounds formed in water, cannot undergo further reactions in this solvent. In these experiments, furan, 2-methylfuran, and 2,5-dimethylfuran were dissolved in ethanol which contained 0.2 mol of perchloric acid per litre. The reaction mixtures were sealed in glass vials and held at 100°C. The samples were analysed by gas chromatography. It was found that, while 2,5-dimethylfuran yielded the respective diacetal at the same rate at which its concentration decreased with time, only traces of diacetals (less than 2 % of the amounts of substrate that had reacted) were detected among the reaction products formed from furan and 2-methylfuran. Thus it could be concluded that the main route to polymeric products in the ethanolysis was *via* side reactions *prior* to ring cleavage and that the polymerization was much more marked with unsubstituted furan and 2-methylfuran than with 2,5-dimethylfuran. Similar conclusions can be drawn about the reactions in aqueous solvents, for, as shown above, the tendencies of different furans to polymerize under acidic conditions in various solvents are very similar. Quite naturally, the (probably very small amounts of) dicarbonyl compounds first formed by the cleavage of furan or 2-methylfuran in the latter solvents may polymerize later.

RESULTS AND DISCUSSION

Acid-catalysed exchange of the isotopes of hydrogen. The isotopically different systems studied were similar to those Kresge and Chiang [12] employed in their investigation of hydrogen exchange in 1,3,5-trimethoxybenzene. The initial compositions were: *A*, $FuD + HClO_4$ in H_2O; *B*, $FuT + HClO_4$ in H_2O; *C*, $FuH + DClO_4$ in D_2O; *D*, $FuT + DClO_4$ in D_2O; here Fu denotes the radical derived from 2-methylfuran by removal of the α-hydrogen atom. Owing to the low solubility of 2-methylfuran in water, the kinetic experiments were run in water-dimethyl sulphoxide mixtures in which the mol fractions of water were 0.500. The concentration of the catalyst perchloric acid was about 0.2 M throughout. The first-order rate law yielding rate coefficients proportional to the molar concentration of the catalyst acid was accurately obeyed at the concentrations used.

The average values of the rate coefficients are collected in Table 1. As described in the experimental section, the slow subsequent reactions did not interfere with the measurement of the rate coefficients for the α-hydrogen exchange reactions. Most of the values in the table are average values from several replicate runs. The values for the detritiation reactions derived by the liquid scintillation counting method were the most accurate. The relative standard errors of these values usually did not exceed 1 %, whereas those for

Table 1. Second-order rate coefficients for the acid-catalysed exchange of the isotopes of hydrogen at the α-position in 2-methylfuran.

Substrate	Reaction	t °C	$10^3 \times k(M^{-1} s^{-1})$
2-Methylfuran-5-*d*	Protodedeuteriation	70	0.196
		80	0.423
		90	0.950
		100	2.86
2-Methylfuran-5-*t*	Protodetritiation	70	0.117
		80	0.290
		90	0.817
		100	1.95
2-Methylfuran-5-*h*	Deuteriodeprotonation	70	0.483
		80	1.18
		90	2.68
		100	6.27
2-Methylfuran-5-*t*	Deuteriodetritiation	70	0.171
		80	0.445
		90	1.092
		100	2.55

the deprotonation and dedeuteriation reactions that were followed by PMR or IR techniques were in the worst cases as large as 4 %.

The plots of the logarithms of the rate coefficients against reciprocal temperature are shown in Fig. 1. Except for the protodedeuteriation of 2-methylfuran-5-*d*, the Arrhenius equation seems to be satisfactorily obeyed. However, owing to the similar nature of the reactions studied, there is no reason to believe that the apparent deviation from the Arrhenius equation is real – it is more likely due to experimental errors. In fact, the experimental data for

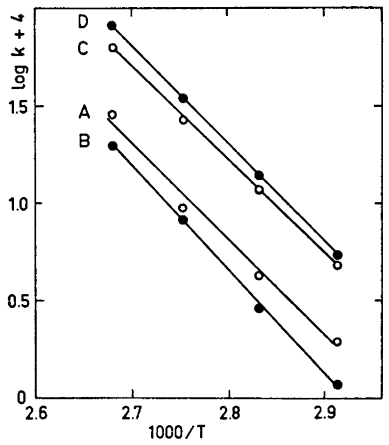

Fig. 1. Arrhenius plots for the acid-catalysed exchange of isotopes of hydrogen in 2-methylfuran. (A) Protodedeuteriation, (B) protodetritiation, (C) deuteriodeprotonation, (D) deuteriodetritiation (log $k + 4.5$).

the dedeuteriation reaction were the least accurate of the data for the four reactions investigated.

The parameters of activation calculated by the method of least squares on the assumption that the Arrhenius equation is valid are given in Table 2. The last column of the table gives the values and standard errors of the rate coefficients at 70°C as calculated by the least squares method.

Table 2. Activation parameters and rate coefficients at 70°C for α-hydrogen exchange in 2-methylfuran.

Reaction	E(kcal/mol)	$\Delta S^{\ddagger}$(cal K^{-1} mol^{-1})	$10^3 \times k^{70}(M^{-1} s^{-1})$
Protodedeuteriation	22.5 ± 1.8	−12.5 ± 5.1	0.179 ± 0.024
Protodetritiation	24.1 ± 0.6	− 8.6 ± 1.7	0.1134 ± 0.0030
Deuteriodeprotonation	21.7 ± 0.2	−12.9 ± 0.7	0.479 ± 0.009
Deuteriodetritiation	22.9 ± 0.0	−11.3 ± 0.1	0.1713 ± 0.0004

Extensive studies of the acid-catalysed exchange of hydrogen atoms attached to aromatic nuclei indicate that the exchange mechanism is a simple two-step A-S_E2 mechanism.[12,13] As exemplified by the protodetritiation, this mechanism may be written for the furan system as follows:

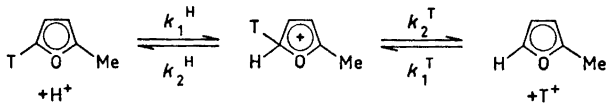

(I)

As the solvent hydrogens (protons or deuterons) are always present in great excess, the reversal of the second step need not be considered. As the reaction intermediate is an unstable species that is present in very low concentration, the steady state principle is applicable. This gives

$$(k_{obs})^{HT} = k_1{}^{H}/(1 + k_2{}^{H}/k_2{}^{T}) \quad (1)$$

for the protodetritiation reaction. Similar equations can be written for the other three exchange systems studied. The four equations thus obtained contain four unknown quantities, $k_1{}^{H}$, $k_1{}^{D}$, $k_2{}^{H}/k_2{}^{D}$, and $k_2{}^{H}/k_2{}^{T}$. An exact solution is therefore possible.

The above analysis does not take into account secondary isotope effects.[12,14] Several methods, all of which give only approximate results, have been proposed. In their study of 1,3,5-trimethoxybenzene, Kresge and Chiang [12] made use of the Swain relations [15] to reduce the number of unknown quantities in the equations that resulted when the secondary effects were taken into account. Owing to the low precision of our values for the dedeuteriation reaction, a

similar method would give but very crude approximations. Gold [16] and Streitwieser and Van Sickle [17] proposed values from 1.15 to 1.17 as appropriate multipliers to calculate values of k_2^H/k_2^D from experimental ones, and Bell [18] proposed a factor of 1.25 for the corresponding secondary effect in k_2^H/k_2^T.

As an explicit consideration of the secondary isotope effects would require experimental values of a very high level of accuracy, no attempt is made here to determine their absolute magnitudes. Instead, uncorrected values for the isotope effects are calculated from eqn. (1) and similar equations for the other systems studied and compared then with similar uncorrected values determined for other aromatic systems. Such a comparison is possible in Table 3.

Table 3. Kinetic isotope effects in aromatic hydrogen exchange reactions.

Substrate	k_1^H/k_1^D	k_2^H/k_2^D	k_2^H/k_2^T	Ref.
1,3,5-Trimethoxybenzene	2.9	6.7		19
Azulene	4.3	9.2		13
Guaiazulene		6.0	14	14
4,6,8-Trimethylazulene		9.6	26	14
Guaiazulene-2-sulphonate		7.4	18	14
2-Methylfuran	3.1	6.2	14	This work

The calculations indicated that much more accurate values could be derived for the isotope effects if only three of the equations of type (1) were used, namely one for deuteriodeprotonation, one for deuteriodetritiation, and one for protodetritiation, for which the most accurate experimental values were available. This method of calculation necessitated the use of the Swain relations [15]

$$k^H/k^T = (k^H k^D)^{1.442};\ k^D/k^T = (k^H/k^D)^{0.442} \qquad (2)$$

The justification of this procedure could be studied by calculating a value for the rate coefficient of the protodedeuteriation reaction and comparing this calculated value with the experimentally measured value. Values at 70°C obtained in this way are:

$k_1^H = (1.71 \pm 0.10) \times 10^{-3}\ M^{-1} s^{-1};\ k_1^D = (0.556 \pm 0.011) \times 10^{-3}\ M^{-1} s^{-1}$
$k_2^H/k^D = 6.25 \pm 0.25;\ k_2^H/k_2^D = 14.1 \pm 0.8$

When these values were used to calculate the rate coefficient for the protodedeuteriation reaction,

$$k^{HD} = k_1^H/(1 + k_2^H/k_2^D)$$

the result was $k^{HD} = (0.236 \pm 0.016) \times 10^{-3}\ M^{-1} s^{-1}$. In view of the low accuracy of the dedeuteriation data, this value agrees satisfactorily with the value in Table 2. The agreement would have been excellent, as shown by calculations, if the rate coefficient for the dedeuteriation at 70°C had been omitted when making the least squares analysis. However, there was no justification for

doing this, for the rate coefficients at the different temperatures had similar standard errors.

It can be seen from Table 3 that the kinetic isotope effects calculated for the furan system resemble closely those derived for other aromatic systems. It should be noted that the present values refer to a temperature of 70°C, whereas the other values given in the table were measured at 25°C. Calculations based on furan data at temperatures below 70°C indicated slightly greater isotope effects, although the extrapolation to temperatures outside the range where the actual measurements were performed made the calculated standard errors of the rate coefficients much larger than those in Table 2.

Table 4 contains values of the parameters of activation for various aromatic hydrogen exchange reactions. It will be seen that the lower reactivity of furan

Table 4. Parameters of activation for various aromatic protodetritiation reactions.

Substrate	$\Delta H^{\ddagger}$(kcal/mol)	$\Delta S^{\ddagger}$(cal K^{-1} mol^{-1})	Ref.
Azulene-1,3-*t*	15.4	−10.1	20
1,3,5-Trimethoxybenzene-2-*t*	15.6	−16.3	21
1,3-Dimethoxybenzene-4-*t*	21.5	− 9.7	21
Thiophene-2-*t*	17.0	−14.6	3
2-Methylfuran-5-*t*	23.4	− 8.6	This work

as compared with its sulphur analogue, thiophen, is primarily due to the relatively high enthalpy of activation. Thiophen also exchanges its β-hydrogens [3] at rates that are lower than the α-hydrogen exchange by factors from 440 to 1200, depending on temperature and the acidity of the reaction solution. As described in the experimental section, similar β-hydrogen exchange without the occurrence of other reactions was not observed in the furans.

Subsequent decomposition reactions of the furan ring. The overall rates of disappearance of 2-methylfuran and 2,5-dimethylfuran in 50 mol % water-dimethyl sulphoxide solvent are given in Table 5.

Table 5. Rate coefficients for the decomposition of furans in water-dimethyl sulphoxide solvent (mol fraction of water = 0.500).

Substrate	°C	$10^5 \times k(M^{-1} s^{-1})$
2-Methylfuran	80	3.10
	90	6.12
	100	10.6
2,5-Dimethylfuran	70	4.46
	80	11.05
	90	27.6

As shown in the experimental section, polymerization reactions predominate over hydrolytic cleavage reactions with furan and 2-methylfuran, whereas only with 2,5-dimethyl furan is the overall decomposition rate approximately equal to the rate of formation of the cleavage product, acetonylacetone. Some experiments described above indicate also that these polymerization reactions are predominantly side reactions rather than reactions following cleavage of the ring. Another piece of evidence that these reactions are side reactions comes from the observation made earlier [6] that the rates of these reactions were enhanced when the reaction mixtures were exposed to ultraviolet light. It was found that if the reactions were carried out in the cell of an UV spectrophotometer, the decomposition rates increased by factors of 2 to 50 from the values measured when the reaction mixtures were kept in the dark. A normal type of acid-catalysed cleavage of the ring (by the A-1, A-2, or A-S_E2 mechanism) would be hardly expected to be affected by light.

Our results are in harmony with experience in preparing α,δ-dicarbonyl compounds by the hydrolysis of furans.[22,23] Only 2,5-dimethylfuran, when treated under relatively mild conditions, gives good yields of the α,δ-dicarbonyl compound, whereas less substituted furans yield only polymeric products.

From the above results it can be concluded that the rate of hydrolytic cleavage of 2-methylfuran hardly exceeds 1 % of the overall decomposition rate. As the latter is lower by a factor of nearly 10^{-2} than the rate of the α-hydrogen exchange reaction, the cleavage rate is some 10^{-4} times lower than the rate of α-hydrogen exchange. A rate of about this magnitude would be what one would expect for the β-protonation of the furan ring in view of the fact that the relative electrophilic reactivities of the α- and β- positions differ more in the furan ring than in its sulphur analogue, the thiophen ring.[24–26]

Explanations based on ring cleavage following α-protonation [8,9] have other difficulties to meet, whereas those based on β-protonation have not. In the latter case, irrespective of the particular mechanism of the cleavage reaction (be it A-1, A-2, or A-S_E2), the β-protonated substrate is an oxonium-carbonium ion, which hydrolyses *via* a hemiacetal [27] to the α,δ-dicarbonyl compound. In the case of 2,5-dimethylfuran, the sequence of the reactions is

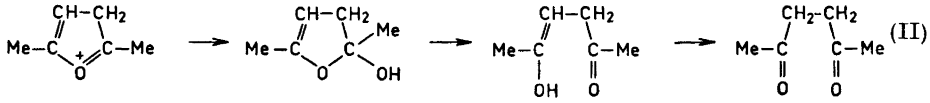

(II)

Similar reactions starting from the β-protonated substrate, which are assumed to be operative in the mechanisms proposed by Stamhuis *et al.*[9] and by Unverferth and Schwetlick,[8] would first lead to an unsaturated keto-alcohol,

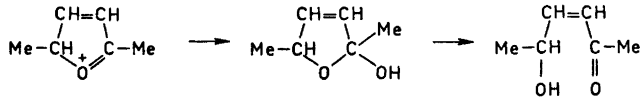

(III)

If the ring cleavage really occurred by the last-mentioned route, one would have to postulate that the unsaturated keto-alcohol first formed rearranges

very rapidly to give the α,δ-dicarbonyl compound, acetonylacetone in the case in question. However, no definite examples of such rapid rearrangements of keto-alcohols of this type are found in the literature. Furthermore, the solvolytic cleavage of 2,5-dimethylfuran in ethanol gives definitely the diacetal of acetonylacetone, which is well understood to result from a reaction route similar to (II), but not if the reaction occurred *via* α-protonation.

The slowness of hydrolytic decomposition reactions of alkylsubstituted furans renders the establishment of general acid catalysis experimentally difficult. However, in the case of a more reactive furan derivative, 2-methoxyfuran, involvement of general acid catalysis has been recently demonstrated.[28]

REFERENCES

1. Kresge, A. J., Onwood, D. P. and Slae, S. *J. Am. Chem. Soc.* **90** (1968) 6982.
2. Longridge, J. F. and Long, F. A. *J. Am. Chem. Soc.* **90** (1968) 3088.
3. Butler, A. R. and Hendry, J. B. *J. Chem. Soc.* **B 1970** 852.
4. Gold, V., Lee, J. R. and Gitter, A. *J. Chem. Soc.* **B 1971** 32.
5. For references to the earlier literature, see Refs. 1–4.
6. Kankaanperä, A. and Salomaa, P. *Acta Chem. Scand.* **21** (1967) 575.
7. Kankaanperä, A. and Kleemola, S. *Acta Chem. Scand.* **23** (1969) 3607.
8. Unverferth, K. and Schwetlick, K. *J. prakt. Chem.* **312** (1970) 882.
9. Stamhuis, E. J., Drenth, W. and van den Berg, H. *Rec. Trav. Chim.* **83** (1964) 167.
10. Salomaa, P. and Mattsén, M. *Acta Chem. Scand.* **25** (1971) 361.
11. Salomaa, P. *Acta Chem. Scand.* **20** (1966) 1263.
12. Kresge, A. J. and Chiang, Y. *J. Am. Chem. Soc.* **89** (1967) 4411.
13. Gruen, L. C. and Long, F. A. *J. Am. Chem. Soc.* **89** (1967) 1287; numerous references to the pertinent literature are given in this article.
14. Longridge, J. L. and Long, F. A. *J. Am. Chem. Soc.* **89** (1967) 1292.
15. Swain, C. G., Stivers, E. C., Reuwer, Jr., J. F. and Schaad, L. J. *J. Am. Chem. Soc.* **80** (1958) 5885.
16. Gold, V. *Discussions Faraday Soc.* **39** (1965) 94.
17. Streitwieser, Jr., A. and Van Sickle, D. E. *J. Am. Chem. Soc.* **84** (1962) 254.
18. Bell, R. P. *Discussions Faraday Soc.* **39** (1965) 16, 94.
19. Kresge, A. J. and Chiang, Y. *J. Am. Chem. Soc.* **84** (1962) 3976.
20. Schulze, J. and Long, F. A. *J. Am. Chem. Soc.* **86** (1964) 331.
21. Kresge, A. J., Chiang, Y. and Sato, Y. *J. Am. Chem. Soc.* **89** (1967) 4418.
22. Dunlop, A. P. and Peters, F. N. *The Furans*, Reinhold, New York 1953, Chapter 14.
23. Young, D. M. and Allen, C. F. H. *Org. Syn.* **2** (1955) 219.
24. Taylor, R. *J. Chem. Soc.* **B 1970** 1364.
25. Clementi, S., Linda, P. and Marino, G. *J. Chem. Soc.* **B 1971** 79.
26. Sappenfield, D. S. and Kreevoy, M. *Tetrahedron* **19** (1963) 157.
27. Ingold, C. K. *Structure and Mechanism in Organic Chemistry*, 2nd Ed., Cornell University Press, Ithaca and London 1969, pp. 447–448.
28. Kankaanperä, A. and Aaltonen, R. *Acta Chem. Scand.* **26** (1972) 2537.

Received June 22, 1972.

ACTA CHEMICA SCANDINAVICA 27 (1973) 164–176

The Structure of L-Mimosine, an L-DOPA Analogue

ARVID MOSTAD,[a] CHRISTIAN RØMMING[a] and EINAR ROSENQVIST[b]

[a] *Department of Chemistry and* [b] *Institute of Pharmacy, University of Oslo, Oslo 3, Norway*

The crystal structure of L-mimosine, β-*N*-(3-hydroxy-4-pyridone)-α-amino propionic acid, has been determined by X-ray methods using 1729 observed reflections collected by counter methods. The crystals are orthorhombic, space group $P2_12_12_1$, with unit cell dimensions $a = 20.45_3$ Å; $b = 9.48_5$ Å; $c = 8.50_0$ Å. The asymmetric unit consists of two independent molecules. The refinements yielded a conventional *R*-factor of 0.064; estimated standard deviations are about 0.005 Å in bond lengths and 0.3° in angles. The conformation of the two non-equivalent molecules is nearly identical and is similar to that found in L-DOPA. The pyridone ring has a pronounced quinoid character.

Mimosine, β-*N*-(3-hydroxy-4-pyridone)-α-amino propionic acid, leucenol, is a naturally occurring amino acid found in certain plants.[1] Its notable biological properties have been described by several authors and summarized by Owen.[2] Hegarthy *et al.*[3] point out that inhibition of mitosis in the hair follicle is the reason for hair loss in sheep by mimosine intoxication, Hylin and Lichton [4] report the loss of fertility in female rats by ingestion of mimosine, and Prabhakaran *et al.*[5] found that injection of the compound inhibit the development of melanoma in mice.

Thompson *et al.*[1] have reviewed various theories for the mechanisms of the toxic action of mimosine in animals. One of these depends on the structural similarity between mimosine and DOPA; mimosine may thus interact with the enzymes concerned with the DOPA metabolism.

The chemical formula for mimosine is usually written as I. Several authors [6–8] have, however, indicated II as an important contributor to the electronic structure. It may be seen that III, the protonized form of II, is isoelectronic with DOPA.

The absolute configuration of L-mimosine has been investigated by chemical methods [9] and shown to belong to the *S*-series.

After the publication of the X-ray structure analysis of L-DOPA,[10] Dr. Hegarthy pointed out for us the analogy between this compound and mimosine and suggested a structure analysis of the latter compound; he also kindly supplied a sample of pure L-mimosine.

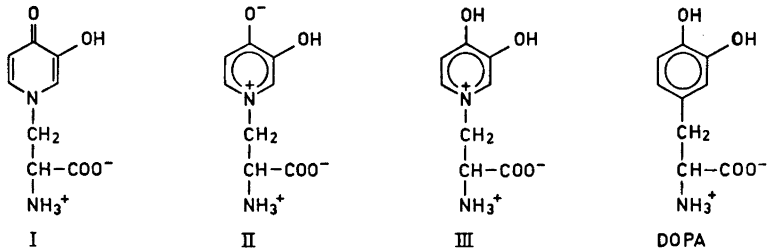

EXPERIMENTAL

A hot saturated solution of L-mimosine was cooled to room temperature during a period of 2 – 3 days. Single crystals in the form of thin, needle-formed very brittle plates separated; a crystal roughly cut to the dimensions $0.13 \times 0.21 \times 0.06$ mm^3 was used for the X-ray experiments.

Oscillation and Weissenberg photographs indicated orthorhombic symmetry; systematically absent reflections determined the space group to be $P2_12_12_1$.

Unit cell parameters were determined from diffractometer measurements on 62 reflections using a manual Picker diffractometer with a copper tube ($\lambda_\beta = 1.3922$ Å, $\lambda_{\alpha_1+\alpha_2} = 1.5418$ Å). The take-off angle was 1.0°. The computer program employed in the least-squares calculation of cell parameters as well as the programs applied during the structure investigation are described in Ref. 11.

Three-dimensional intensity data were recorded on an automatic Picker four-angle diffractometer using graphite crystal monochromated MoK radiation. The take-off angle was 4°. Intensities of 2640 reflections with $2\theta < 60°$ were measured using the $\omega - 2\theta$ scanning mode with a 2θ scanning speed of 1° min^{-1}. Background counts were taken for 20 sec at each of the scan range limits. Three standard reflections measured after every 100 reflections showed a variation of up to 10 % during the run; the intensity data were accordingly adjusted. Estimated standard deviations in the intensities were taken as the square root of the total counts with a 2.5 % addition to allow for the uncertainty in the adjustments.

The 1729 reflections with intensity larger than 2σ (I) were considered to be observed; the rest were regarded as unobserved and excluded from the refinement procedure. Lorentz and polarization corrections were applied to the intensity data.

Atomic form factors used were those of Hanson *et al.*[12] for oxygen, nitrogen, and carbon, and of Stewart *et al.*[13] for hydrogen.

CRYSTAL DATA

S-β-N-(3-hydroxy-4-pyridone)-α-amino propionic acid (L-mimosine, leucenol), $C_8H_{10}N_2O_4$, orthorhombic. $a = 20.453(0.002)$ Å, $b = 9.485(0.001)$ Å; $c = 8.500(0.001)$ Å. Figures in parentheses are estimated standard deviations. $V = 1648.9$ Å^3; $M = 198.18$; F (000) = 832; $Z = 8$; $D_{obs} = 1.59$ g cm^{-3} (flotation); $D_{calc} = 1.595$ g cm^{-3}. Absent reflections: (h00) for h odd, (0k0) for k odd, (00l) for l odd; space group $P2_12_12_1$.

STRUCTURE DETERMINATION

The data were put on an absolute scale by Wilson's statistical method and normalized structure amplitudes were calculated. Eight sets of phases for 250 structure amplitudes were obtained by the application of the symbolic

Table 1. Observed and calculated structure factors. The columns are h, k, l, 10 F_o, and $10|F_c|$.

2	0	0	257	266	21	4	0	71	88	7	11	0	59	71	9	6	1	156	158	6	2	1	318	310
4	0	0	666	675	22	4	0	71	61	5	11	0	91	89	7	6	1	282	285	5	2	1	479	475
6	0	0	787	813	23	4	0	61	47	3	11	0	78	78	6	6	1	113	124	4	2	1	440	432
8	0	0	655	657	25	4	0	75	58	1	11	0	95	115	5	6	1	124	133	3	2	1	675	641
10	0	0	275	273	26	4	0	124	125	0	12	0	107	90	4	6	1	63	62	2	2	1	1556	1525
12	0	0	610	626	27	4	0	90	79	6	12	0	96	88	3	6	1	100	99	1	2	1	354	344
14	0	0	384	395	25	5	0	94	95	9	12	0	71	58	2	6	1	66	68	0	2	1	116	112
16	0	0	506	540	23	5	0	76	69	4	13	1	101	88	1	6	1	207	210	0	1	1	116	115
18	0	0	1045	1137	21	5	0	104	122	11	12	1	141	133	0	6	1	303	317	1	1	1	430	418
20	0	0	89	92	17	5	0	175	186	10	12	1	81	52	0	5	1	92	95	2	1	1	494	515
22	0	0	183	185	16	5	0	69	57	9	12	1	115	115	1	5	1	232	233	3	1	1	104	110
24	0	0	176	166	15	5	0	86	83	7	12	1	88	97	2	5	1	124	141	4	1	1	341	354
26	0	0	183	173	14	5	0	164	180	6	12	1	110	116	3	5	1	162	157	5	1	1	270	270
28	0	0	172	177	12	5	0	68	84	0	12	1	73	53	4	5	1	210	223	6	1	1	482	463
27	1	0	68	52	11	5	0	75	81	2	11	1	84	76	6	5	1	175	179	7	1	1	520	508
22	1	0	126	119	10	5	0	334	349	3	11	1	97	76	7	5	1	138	143	8	1	1	419	403
20	1	0	162	170	9	5	0	46	61	6	11	1	115	132	8	5	1	658	667	9	1	1	461	446
19	1	0	221	225	8	5	0	84	81	7	11	1	94	88	9	5	1	155	157	10	1	1	316	310
17	1	0	155	158	7	5	0	216	226	8	11	1	274	286	10	5	1	353	363	11	1	1	225	221
16	1	0	213	235	6	5	0	223	232	10	11	1	188	198	12	5	1	188	185	12	1	1	100	112
15	1	0	292	312	4	5	0	257	261	11	11	1	130	129	13	5	1	85	75	13	1	1	142	145
14	1	0	95	105	3	5	0	357	369	15	11	1	69	61	14	5	1	100	92	16	1	1	288	306
13	1	0	166	177	2	5	0	297	313	16	10	1	113	110	15	5	1	143	137	17	1	1	248	268
12	1	0	181	180	1	5	0	502	531	11	10	1	126	125	16	5	1	241	252	18	1	1	345	363
10	1	0	382	381	0	6	0	924	993	10	10	1	82	83	17	5	1	183	183	19	1	1	113	116
8	1	0	303	321	2	6	0	380	388	9	10	1	131	140	18	5	1	142	144	20	1	1	88	97
7	1	0	87	83	3	6	0	255	270	8	10	1	121	103	20	5	1	56	69	21	1	1	66	62
6	1	0	65	81	5	6	0	146	151	7	10	1	158	167	23	5	1	70	48	22	1	1	122	124
5	1	0	48	25	6	6	0	194	206	6	10	1	120	131	24	5	1	118	108	24	1	1	133	146
4	1	0	292	313	7	6	0	57	41	4	10	1	76	83	26	5	1	76	58	26	1	1	64	62
2	1	0	223	228	8	6	0	100	108	0	10	1	56	48	27	4	1	75	46	27	1	1	142	124
1	1	0	83	124	9	6	0	142	149	0	9	1	135	131	26	4	1	108	105	28	1	1	122	113
0	2	0	1298	1382	10	6	0	105	113	1	9	1	261	267	25	4	1	103	111	25	0	1	80	82
1	2	0	52	50	11	6	0	145	167	2	9	1	123	123	24	4	1	59	52	24	0	1	63	78
2	2	0	337	366	12	6	0	129	143	3	9	1	165	161	22	4	1	68	69	23	0	1	110	92
3	2	0	69	63	13	6	0	153	168	4	9	1	136	130	20	4	1	54	48	22	0	1	62	50
4	2	0	129	133	15	6	0	145	156	5	9	1	89	81	19	4	1	77	91	21	0	1	63	66
5	2	0	44	34	16	6	0	253	267	6	9	1	136	136	18	4	1	144	151	20	0	1	90	104
6	2	0	81	70	18	6	0	204	220	7	9	1	123	116	17	4	1	72	77	18	0	1	221	225
7	2	0	90	88	19	6	0	124	121	8	9	1	277	292	16	4	1	253	268	17	0	1	194	195
8	2	0	336	341	20	6	0	119	128	10	9	1	147	153	15	4	1	97	106	16	0	1	84	86
9	2	0	44	56	24	6	0	107	105	12	9	1	79	77	14	4	1	80	84	14	0	1	189	197
10	2	0	354	359	20	7	0	61	101	13	9	1	75	63	12	4	1	146	149	12	0	1	154	152
11	2	0	64	70	19	7	0	181	182	14	9	1	81	69	11	4	1	105	114	11	0	1	89	95
12	2	0	70	84	16	7	0	87	91	15	9	1	66	72	10	4	1	57	64	9	0	1	279	284
13	2	0	84	91	15	7	0	161	166	16	9	1	66	80	9	4	1	351	351	7	0	1	248	246
14	2	0	126	127	14	7	0	65	67	17	9	1	119	105	8	4	1	173	173	6	0	1	135	122
15	2	0	163	173	13	7	0	150	158	18	9	1	82	78	7	4	1	176	184	5	0	1	188	190
16	2	0	214	232	12	7	0	75	91	19	9	1	88	71	6	4	1	262	261	4	0	1	51	38
18	2	0	350	364	11	7	0	126	137	22	8	1	79	77	5	4	1	144	148	3	0	1	53	60
19	2	0	185	200	10	7	0	58	49	18	8	1	115	120	4	4	1	261	259	2	0	1	94	85
20	2	0	76	73	9	7	0	93	101	17	8	1	90	101	3	4	1	301	297	1	0	1	52	77
21	2	0	79	90	8	7	0	83	90	16	8	1	177	185	2	4	1	178	174	0	0	2	1494	1619
22	2	0	104	114	7	7	0	53	62	15	8	1	91	86	1	4	1	181	172	1	0	2	533	536
23	2	0	93	74	6	7	0	57	62	14	8	1	75	62	0	4	1	304	312	2	0	2	86	73
26	2	0	100	101	5	7	0	83	78	13	8	1	62	78	0	3	1	232	224	3	0	2	500	524
27	2	0	100	76	4	7	0	53	56	12	8	1	52	41	1	3	1	1529	1477	4	0	2	378	385
26	3	0	175	164	3	7	0	215	214	11	8	1	143	154	2	3	1	274	273	5	0	2	442	444
24	3	0	72	65	2	7	0	63	61	9	8	1	87	99	3	3	1	168	164	6	0	2	524	501
21	3	0	154	157	1	7	0	379	404	8	8	1	64	63	4	3	1	218	218	7	0	2	251	248
19	3	0	359	381	0	8	0	70	81	7	8	1	80	84	5	3	1	276	275	8	0	2	652	637
18	3	0	100	104	2	8	0	62	59	6	8	1	103	106	6	3	1	142	145	9	0	2	839	808
17	3	0	194	207	4	8	0	94	97	5	8	1	93	97	7	3	1	425	422	10	0	2	606	604
15	3	0	261	272	6	8	0	109	117	3	8	1	147	145	8	3	1	348	348	13	0	2	130	130
14	3	0	318	338	7	8	0	94	83	2	8	1	50	67	9	3	1	176	180	15	0	2	49	51
13	3	0	64	56	8	8	0	56	45	1	8	1	125	132	10	3	1	347	349	16	0	2	227	224
12	3	0	298	305	9	8	0	101	105	0	8	1	383	405	11	3	1	56	58	18	0	2	247	257
11	3	0	332	351	12	8	0	88	89	0	7	1	46	41	12	3	1	157	161	19	0	2	99	92
10	3	0	548	531	14	8	0	62	62	1	7	1	192	200	13	3	1	236	246	20	0	2	63	73
9	3	0	246	256	16	8	0	91	98	2	7	1	134	142	14	3	1	76	86	21	0	2	92	96
8	3	0	546	552	17	8	0	58	62	3	7	1	73	63	15	3	1	291	303	23	0	2	69	49
7	3	0	107	107	18	8	0	140	127	4	7	1	84	93	16	3	1	182	194	25	0	2	151	141
6	3	0	683	688	20	9	0	70	44	6	7	1	93	97	17	3	1	286	295	26	0	2	107	103
5	3	0	160	164	18	9	0	83	84	7	7	1	74	67	18	3	1	160	166	27	0	2	87	67
4	3	0	152	150	17	9	0	122	119	8	7	1	213	218	19	3	1	257	265	28	0	2	152	153
3	3	0	473	487	14	9	0	87	88	9	7	1	145	147	20	3	1	72	84	27	1	2	72	62
2	3	0	467	480	12	9	0	179	180	10	7	1	163	166	22	3	1	86	92	26	1	2	83	59
1	3	0	593	591	11	9	0	60	55	11	7	1	90	90	25	3	1	144	135	25	1	2	96	110
0	4	0	92	95	10	9	0	311	326	12	7	1	103	105	26	3	1	88	81	23	1	2	176	165
1	4	0	45	35	9	9	0	83	104	13	7	1	83	96	27	3	1	73	71	21	1	2	112	122
2	4	0	569	583	8	9	0	133	131	14	7	1	76	72	27	2	1	97	93	19	1	2	105	120
3	4	0	146	143	7	9	0	66	37	15	7	1	86	97	26	2	1	141	153	17	1	2	318	322
4	4	0	388	391	6	9	0	296	305	16	7	1	123	134	25	2	1	95	84	16	1	2	187	192
5	4	0	231	226	3	9	0	66	72	17	7	1	63	65	22	2	1	81	84	15	1	2	92	97
6	4	0	261	270	2	9	0	119	113	25	6	1	114	95	21	2	1	61	68	14	1	2	85	95
7	4	0	210	218	1	9	0	162	173	24	6	1	71	78	20	2	1	144	138	13	1	2	70	77
8	4	0	129	123	0	10	0	71	85	21	6	1	78	73	19	2	1	164	161	12	1	2	83	86
9	4	0	376	391	2	10	0	63	75	20	6	1	127	125	18	2	1	144	147	11	1	2	252	262
10	4	0	157	155	6	10	0	110	98	19	6	1	74	72	16	2	1	526	544	10	1	2	349	335
11	4	0	150	148	8	10	0	58	35	18	6	1	185	185	15	2	1	293	300	9	1	2	99	105
12	4	0	112	111	9	10	0	157	160	17	6	1	86	85	14	2	1	88	76	8	1	2	647	623
13	4	0	163	166	10	10	0	141	156	16	6	1	94	96	13	2	1	181	186	7	1	2	151	145
14	4	0	309	330	13	10	0	115	122	15	6	1	121	128	12	2	1	145	146	6	1	2	264	258
15	4	0	49	80	15	10	0	61	77	14	6	1	55	66	11	2	1	214	221	5	1	2	667	642
16	4	0	320	335	18	10	0	79	94	13	6	1	83	88	10	2	1	113	103	4	1	2	408	391
17	4	0	85	103	15	11	0	92	87	12	6	1	96	97	9	2	1	508	491	3	1	2	817	817
18	4	0	129	132	13	11	0	104	93	11	6	1	246	252	8	2	1	266	255	2	1	2	219	222
20	4	0	140	141	8	11	0	63	57	10	6	1	159	163	7	2	1	530	508	1	1	2	844	850

Table 1. Continued.

0	1	2	209	219	6	6	2	247	248	1	8	3	137	144	20	2	3	58	69	5	2	4	207	211
0	2	2	2085	2099	7	6	2	109	118	0	8	3	47	37	19	2	3	51	36	6	2	4	181	187
1	2	2	251	253	8	6	2	54	57	0	7	3	74	77	18	2	3	162	173	7	2	4	339	342
2	2	2	726	722	9	6	2	134	131	1	7	3	130	116	17	2	3	123	144	8	2	4	160	169
3	2	2	332	328	10	6	2	46	45	3	7	3	75	84	16	2	3	91	106	9	2	4	255	259
4	2	2	270	255	11	6	2	146	147	4	7	3	68	70	14	2	3	89	97	10	2	4	280	279
5	2	2	463	435	12	6	2	115	116	5	7	3	74	71	13	2	3	113	111	12	2	4	44	43
6	2	2	549	537	13	6	2	44	42	6	7	3	174	183	12	2	3	113	102	13	2	4	94	109
7	2	2	625	592	14	6	2	93	82	7	7	3	49	51	11	2	3	136	132	14	2	4	128	136
8	2	2	293	285	16	6	2	54	51	8	7	3	339	342	10	2	3	121	121	15	2	4	95	97
9	2	2	536	521	17	6	2	57	44	9	7	3	180	191	9	2	3	386	382	16	2	4	113	114
10	2	2	275	256	18	6	2	97	103	10	7	3	251	258	8	2	3	367	373	17	2	4	141	148
11	2	2	228	229	22	6	2	59	68	11	7	3	76	56	7	2	3	440	414	18	2	4	187	196
12	2	2	163	168	24	6	2	80	76	13	7	3	111	113	6	2	3	187	185	19	2	4	65	76
13	2	2	148	151	21	7	2	65	41	15	7	3	59	71	5	2	3	87	85	20	2	4	65	62
14	2	2	172	172	20	7	2	55	51	16	7	3	105	117	4	2	3	95	90	21	2	4	136	131
15	2	2	77	75	19	7	2	60	66	18	7	3	60	64	3	2	3	96	102	23	2	4	68	82
16	2	2	415	420	17	7	2	79	77	19	7	3	84	56	2	2	3	361	366	24	2	4	79	67
17	2	2	215	222	16	7	2	59	46	22	7	3	117	83	1	2	3	60	60	25	2	4	119	111
18	2	2	487	497	15	7	2	90	98	24	6	3	89	85	0	2	3	572	557	23	3	4	102	101
19	2	2	161	166	14	7	2	89	92	20	6	3	66	58	0	1	3	111	118	22	3	4	81	75
20	2	2	101	95	13	7	2	79	77	19	6	3	61	77	1	1	3	514	514	21	3	4	109	98
21	2	2	120	134	12	7	2	155	145	18	6	3	143	146	3	1	3	261	268	20	3	4	57	49
23	2	2	65	81	11	7	2	110	105	17	6	3	144	150	4	1	3	313	308	19	3	4	63	56
24	2	2	77	81	10	7	2	356	365	16	6	3	162	175	5	1	3	511	507	18	3	4	92	86
26	2	2	101	92	9	7	2	143	148	15	6	3	99	102	6	1	3	511	495	17	3	4	121	125
27	2	2	104	108	8	7	2	256	261	14	6	3	139	122	7	1	3	208	210	16	3	4	104	96
26	3	2	122	110	7	7	2	217	215	13	6	3	74	65	8	1	3	180	175	13	3	4	50	63
25	3	2	162	161	6	7	2	294	297	11	6	3	127	135	9	1	3	434	426	11	3	4	157	157
24	3	2	95	85	5	7	2	108	106	10	6	3	135	132	10	1	3	232	229	10	3	4	92	96
23	3	2	100	93	4	7	2	201	207	9	6	3	99	100	11	1	3	54	51	9	3	4	67	73
21	3	2	104	107	3	7	2	111	114	8	6	3	101	105	13	1	3	292	295	8	3	4	222	224
20	3	2	68	67	2	7	2	134	140	7	6	3	132	130	14	1	3	158	162	7	3	4	72	56
19	3	2	83	76	1	7	2	150	147	5	6	3	154	154	15	1	3	151	153	6	3	4	74	80
18	3	2	154	160	0	8	2	99	93	4	6	3	144	145	16	1	3	195	200	5	3	4	122	127
17	3	2	272	270	1	8	2	44	28	3	6	3	93	97	17	1	3	154	158	4	3	4	190	190
16	3	2	74	80	2	8	2	115	117	2	6	3	184	177	18	1	3	80	76	3	3	4	193	200
15	3	2	142	145	4	8	2	54	58	1	6	3	257	256	19	1	3	133	135	2	3	4	333	331
14	3	2	209	205	7	8	2	315	326	0	6	3	343	335	20	1	3	114	116	1	3	4	176	186
13	3	2	175	174	8	8	2	138	132	0	5	3	156	164	21	1	3	126	127	0	3	4	416	425
12	3	2	110	115	9	8	2	310	316	1	5	3	475	491	23	1	3	137	135	0	4	4	374	371
11	3	2	232	230	11	8	2	133	144	3	5	3	196	210	24	1	3	98	91	1	4	4	166	152
10	3	2	172	170	12	8	2	110	102	4	5	3	148	154	27	1	3	245	226	2	4	4	378	369
9	3	2	298	303	18	8	2	85	84	5	5	3	137	125	26	0	3	168	169	3	4	4	111	111
8	3	2	199	192	20	8	2	73	80	7	5	3	149	155	25	0	3	118	105	4	4	4	88	89
7	3	2	289	287	19	9	2	96	94	8	5	3	162	159	23	0	3	120	111	5	4	4	84	79
6	3	2	185	178	18	9	2	80	74	9	5	3	80	68	16	0	3	112	111	6	4	4	72	66
5	3	2	121	115	15	9	2	79	90	10	5	3	70	85	15	0	3	80	85	7	4	4	222	223
4	3	2	225	210	10	9	2	127	128	11	5	3	66	67	14	0	3	154	158	8	4	4	81	82
3	3	2	303	298	9	9	2	90	92	12	5	3	138	144	12	0	3	48	35	9	4	4	304	303
2	3	2	417	413	8	9	2	90	88	13	5	3	70	72	11	0	3	134	141	10	4	4	174	175
1	3	2	221	223	7	9	2	90	98	14	5	3	87	73	10	0	3	63	64	11	4	4	151	151
0	3	2	104	106	3	9	2	58	58	15	5	3	165	170	9	0	3	61	56	12	4	4	45	47
0	4	2	841	826	2	9	2	61	56	16	5	3	56	67	8	0	3	70	62	13	4	4	143	155
1	4	2	95	96	1	9	2	114	113	17	5	3	241	240	7	0	3	141	142	14	4	4	122	110
2	4	2	432	425	2	10	2	71	56	18	5	3	83	84	6	0	3	133	135	15	4	4	126	125
3	4	2	74	85	4	10	2	93	87	19	5	3	199	196	5	0	3	434	435	16	4	4	199	196
4	4	2	149	141	5	10	2	56	52	22	5	3	71	64	4	0	3	319	327	17	4	4	201	202
5	4	2	331	340	6	10	2	57	63	23	5	3	69	80	3	0	3	278	292	18	4	4	143	145
6	4	2	258	255	7	10	2	77	92	25	5	3	137	127	2	0	3	257	270	19	4	4	74	91
7	4	2	207	206	8	10	2	58	52	26	4	3	136	125	1	0	3	61	73	20	4	4	192	189
8	4	2	86	91	9	10	2	72	70	24	4	3	75	85	0	0	4	184	183	23	4	4	82	56
9	4	2	62	45	10	10	2	98	100	23	4	3	71	55	1	0	4	267	273	25	4	4	77	96
10	4	2	152	152	14	11	2	76	70	20	4	3	86	75	2	0	4	226	248	24	5	4	203	177
11	4	2	110	115	13	11	2	81	74	18	4	3	230	224	3	0	4	615	648	23	5	4	85	84
12	4	2	176	171	10	11	2	70	63	17	4	3	95	105	5	0	4	49	63	21	5	4	112	117
13	4	2	217	224	6	11	2	82	90	16	4	3	378	388	6	0	4	68	57	20	5	4	91	94
14	4	2	54	66	4	11	2	62	84	15	4	3	226	234	7	0	4	622	630	19	5	4	112	109
15	4	2	237	242	3	11	2	75	65	14	4	3	124	118	8	0	4	189	190	18	5	4	197	184
16	4	2	260	265	2	11	2	67	58	13	4	3	115	125	9	0	4	631	638	17	5	4	132	118
17	4	2	164	172	1	11	2	69	63	12	4	3	149	157	10	0	4	212	210	16	5	4	72	53
18	4	2	204	215	0	12	2	88	95	11	4	3	98	95	11	0	4	455	453	14	5	4	112	125
19	4	2	142	142	6	12	2	62	38	10	4	3	156	155	12	0	4	54	56	12	5	4	161	172
20	4	2	64	65	8	12	3	75	25	9	4	3	297	309	13	0	4	104	116	11	5	4	81	84
21	4	2	83	84	6	12	3	65	33	8	4	3	142	145	15	0	4	282	290	10	5	4	445	455
22	4	2	116	124	3	12	3	64	64	7	4	3	156	161	17	0	4	93	77	8	5	4	452	472
23	4	2	86	67	0	11	3	126	131	6	4	3	189	193	18	0	4	142	143	7	5	4	204	202
24	4	2	119	117	1	11	3	169	165	5	4	3	117	117	19	0	4	222	227	6	5	4	297	295
26	4	2	67	63	3	11	3	114	117	4	4	3	248	256	21	0	4	153	161	5	5	4	125	123
24	5	2	82	73	15	10	3	116	108	3	4	3	248	243	25	0	4	150	144	4	5	4	208	213
20	5	2	89	96	8	10	3	65	43	2	4	3	802	777	26	1	4	74	77	3	5	4	238	236
18	5	2	77	73	2	10	3	68	64	1	4	3	163	167	25	1	4	102	97	2	5	4	147	151
17	5	2	186	185	1	10	3	73	68	0	4	3	719	709	19	1	4	79	60	1	5	4	250	256
16	5	2	170	178	0	10	3	67	56	0	3	3	63	58	18	1	4	102	84	0	5	4	66	53
15	5	2	181	185	0	9	3	58	66	1	3	3	481	490	17	1	4	162	164	0	6	4	185	192
14	5	2	136	146	1	9	3	68	77	2	3	3	147	153	16	1	4	137	127	1	6	4	99	104
13	5	2	61	65	2	9	3	130	118	3	3	3	138	134	15	1	4	117	126	3	6	4	100	77
12	5	2	177	173	4	9	3	72	63	4	3	3	128	125	14	1	4	111	112	4	6	4	119	133
11	5	2	148	153	5	9	3	71	68	5	3	3	219	216	13	1	4	63	65	5	6	4	46	56
10	5	2	134	137	6	9	3	96	103	6	3	3	161	161	12	1	4	186	184	7	6	4	338	342
9	5	2	173	176	7	9	3	130	125	7	3	3	141	138	11	1	4	99	100	8	6	4	141	145
8	5	2	140	142	8	9	3	281	284	8	3	3	161	157	10	1	4	109	105	9	6	4	304	303
7	5	2	251	250	10	9	3	178	175	9	3	3	170	169	9	1	4	216	219	10	6	4	114	116
6	5	2	298	291	16	9	3	86	77	10	3	3	175	170	8	1	4	270	265	11	6	4	252	244
5	5	2	265	267	19	8	3	90	74	12	3	3	192	202	7	1	4	111	114	12	6	4	72	69
4	5	2	222	225	17	8	3	70	68	13	3	3	198	195	6	1	4	183	195	13	6	4	101	97
3	5	2	140	133	16	8	3	58	60	14	3	3	258	262	5	1	4	67	56	15	6	4	111	108
2	5	2	159	162	12	8	3	74	70	15	3	3	225	235	3	1	4	146	150	16	6	4	113	115
1	5	2	454	447	9	8	3	155	160	16	3	3	102	93	2	1	4	117	120	17	6	4	143	145
0	5	2	36	45	8	8	3	84	82	17	3	3	169	171	1	1	4	511	524	19	6	4	88	80
0	6	2	201	208	7	8	3	114	115	18	3	3	230	235	0	1	4	165	168	20	6	4	60	65
1	6	2	65	60	6	8	3	150	160	24	3	3	99	93	0	2	4	512	524	22	6	4	64	66
2	6	2	148	145	5	8	3	69	65	25	3	3	100	92	1	2	4	358	368	17	7	4	123	115
3	6	2	144	147	4	8	3	86	87	26	2	3	101	88	2	2	4	215	217	16	7	4	85	101
4	6	2	131	135	3	8	3	82	101	23	2	3	107	116	3	2	4	253	258	15	7	4	73	92
5	6	2	101	95	2	8	3	83	86	21	2	3	63	64	4	2	4	112	113	11	7	4	50	31

Table 1. Continued.

10	7	4	149	148	5	5	5	129	137	6	0	5	122	128	12	5	6	153	141	14	4	7	103	84
9	7	4	162	160	6	5	5	162	160	5	0	5	141	143	10	5	6	221	217	13	4	7	115	98
8	7	4	141	139	7	5	5	182	177	4	0	5	163	175	9	5	6	57	64	12	4	7	69	67
7	7	4	81	78	9	5	5	100	101	3	0	5	122	125	8	5	6	290	292	11	4	7	111	115
6	7	4	168	163	10	5	5	76	80	2	0	5	260	265	6	5	6	125	128	9	4	7	86	80
5	7	4	66	51	11	5	5	127	133	0	0	6	190	197	5	5	6	93	94	8	4	7	60	67
4	7	4	96	98	12	5	5	94	101	1	0	6	123	125	4	5	6	113	115	7	4	7	147	158
2	7	4	47	30	13	5	5	111	102	2	0	6	340	342	3	5	6	131	140	6	4	7	255	257
1	7	4	207	206	14	5	5	154	154	3	0	6	107	105	1	5	6	49	65	5	4	7	125	137
0	8	4	268	274	15	5	5	82	93	4	0	6	44	46	0	6	6	78	88	4	4	7	118	129
1	8	4	180	181	16	5	5	75	61	5	0	6	142	145	3	6	6	99	107	2	4	7	128	135
2	8	4	141	148	17	5	5	78	75	6	0	6	78	89	4	6	6	88	94	1	4	7	67	58
3	8	4	81	70	19	5	5	107	99	7	0	6	83	89	6	6	6	73	60	0	4	7	188	203
4	8	4	66	54	21	5	5	63	48	8	0	6	49	46	8	6	6	118	106	0	3	7	89	92
5	8	4	77	71	20	4	5	71	60	9	0	6	355	378	9	6	6	119	131	1	3	7	173	166
6	8	4	66	48	19	4	5	70	63	10	0	6	344	363	12	6	6	56	45	3	3	7	160	171
7	8	4	78	79	17	4	5	85	81	11	0	6	183	186	13	6	6	78	50	5	3	7	141	155
9	8	4	100	95	16	4	5	69	73	12	0	6	119	119	15	6	6	67	48	6	3	7	138	139
10	8	4	109	102	15	4	5	82	65	13	0	6	75	70	16	6	6	71	71	7	3	7	109	119
14	8	4	62	47	14	4	5	92	90	14	0	6	70	74	18	6	6	128	122	8	3	7	153	161
16	8	4	160	144	12	4	5	64	46	16	0	6	91	96	19	6	6	72	55	9	3	7	79	75
18	8	4	160	150	11	4	5	167	175	17	0	6	66	43	19	7	6	67	81	10	3	7	121	127
19	8	4	101	71	10	4	5	106	108	18	0	6	145	148	18	7	6	69	45	11	3	7	51	49
12	9	4	68	40	9	4	5	116	114	19	0	6	96	107	17	7	6	80	88	12	3	7	105	101
10	9	4	67	42	8	4	5	166	165	20	0	6	100	93	16	7	6	96	94	13	3	7	64	56
7	9	4	123	113	7	4	5	127	127	22	0	6	118	108	14	7	6	63	36	14	3	7	54	43
6	9	4	85	94	6	4	5	84	92	23	0	6	104	86	13	7	6	110	79	15	3	7	57	55
4	9	4	72	43	5	4	5	48	46	24	0	6	91	80	12	7	6	68	56	16	3	7	86	78
2	9	4	62	51	3	4	5	127	128	24	1	6	81	75	11	7	6	93	78	17	3	7	136	125
1	9	4	75	85	2	4	5	60	50	19	1	6	108	111	10	7	6	85	70	18	3	7	70	75
4	10	4	67	55	1	4	5	63	53	17	1	6	103	88	9	7	6	114	101	21	3	7	82	70
7	10	4	109	104	0	4	5	131	136	16	1	6	78	65	8	7	6	107	106	20	2	7	113	93
9	10	4	74	64	0	3	5	139	144	15	1	6	67	68	7	7	6	108	94	16	2	7	185	166
11	10	4	132	131	1	3	5	64	73	13	1	6	72	73	3	7	6	142	152	15	2	7	88	100
15	10	4	67	54	2	3	5	221	227	12	1	6	96	108	1	7	6	157	179	14	2	7	84	89
10	11	4	100	75	3	3	5	71	69	11	1	6	97	96	0	7	6	87	102	13	2	7	126	122
7	11	4	104	95	4	3	5	93	104	10	1	6	246	254	0	8	6	213	218	12	2	7	88	91
3	11	4	89	65	5	3	5	169	172	8	1	6	207	214	1	8	6	84	71	11	2	7	149	142
6	11	5	81	64	6	3	5	236	244	7	1	6	157	166	2	8	6	74	75	10	2	7	66	73
8	11	5	82	74	7	3	5	84	73	6	1	6	129	142	6	8	6	143	134	8	2	7	58	71
10	11	5	94	82	8	3	5	636	647	5	1	6	78	73	7	8	6	205	192	7	2	7	250	253
13	10	5	66	41	9	3	5	257	260	4	1	6	92	95	11	8	6	176	152	6	2	7	47	54
11	10	5	102	88	10	3	5	467	473	3	1	6	42	52	12	8	6	70	42	5	2	7	165	174
10	10	5	70	47	12	3	5	179	188	1	1	6	58	66	16	8	6	101	95	3	2	7	105	106
8	10	5	71	78	13	3	5	151	155	0	1	6	81	83	17	8	6	90	62	2	2	7	208	215
7	10	5	86	95	16	3	5	133	130	0	2	6	116	133	14	9	6	84	92	1	2	7	64	68
4	10	5	85	79	18	3	5	126	120	1	2	6	81	78	8	9	6	177	166	1	1	7	71	76
2	10	5	99	95	19	3	5	61	49	2	2	6	69	61	5	9	6	59	57	2	1	7	103	104
0	10	5	151	148	20	3	5	111	93	3	2	6	196	205	3	9	6	129	130	3	1	7	105	120
0	9	5	94	96	21	3	5	129	123	4	2	6	133	136	2	9	6	84	94	4	1	7	64	60
1	9	5	126	127	23	3	5	66	56	5	2	6	55	54	1	9	6	111	102	5	1	7	100	115
4	9	5	66	50	24	3	5	148	116	6	2	6	67	56	0	9	6	72	63	6	1	7	216	227
5	9	5	99	98	25	2	5	104	110	7	2	6	260	278	0	10	6	152	150	8	1	7	592	621
8	9	5	57	53	24	2	5	68	87	8	2	6	61	57	2	10	6	112	103	10	1	7	338	347
9	9	5	60	42	22	2	5	69	72	9	2	6	390	406	7	10	6	66	81	12	1	7	121	126
11	9	5	60	58	20	2	5	103	99	10	2	6	177	188	9	10	6	85	56	13	1	7	96	86
12	9	5	67	60	19	2	5	79	94	11	2	6	188	188	11	10	6	79	66	14	1	7	82	71
13	9	5	85	73	18	2	5	134	122	12	2	6	52	43	5	10	7	70	70	15	1	7	56	75
19	8	5	111	107	17	2	5	145	147	13	2	6	65	84	2	10	7	161	142	16	1	7	115	98
15	8	5	85	78	16	2	5	50	55	14	2	6	85	76	1	9	7	84	107	19	1	7	72	74
14	8	5	71	68	15	2	5	117	133	15	2	6	101	107	2	9	7	68	74	20	1	7	115	112
9	8	5	106	97	14	2	5	98	85	17	2	6	140	142	3	9	7	77	82	22	0	7	77	78
4	8	5	79	91	13	2	5	67	69	18	2	6	60	36	7	9	7	62	47	20	0	7	62	50
3	8	5	78	66	12	2	5	176	188	19	2	6	55	40	15	8	7	75	70	18	0	7	84	90
2	8	5	103	106	11	2	5	225	223	21	2	6	61	36	13	8	7	70	77	12	0	7	80	71
1	8	5	75	83	10	2	5	147	137	24	2	6	69	46	10	8	7	114	90	11	0	7	71	68
0	7	5	162	174	9	2	5	125	124	18	3	6	101	88	9	8	7	75	64	9	0	7	71	69
1	7	5	329	338	8	2	5	202	209	17	3	6	98	87	7	8	7	79	66	7	0	7	89	96
2	7	5	145	154	7	2	5	145	140	16	3	6	69	75	5	8	7	87	76	6	0	7	63	71
3	7	5	77	83	6	2	5	324	346	15	3	6	55	52	3	8	7	62	66	5	0	7	61	69
6	7	5	62	60	5	2	5	169	172	12	3	6	57	42	2	8	7	114	124	4	0	7	65	95
7	7	5	66	67	4	2	5	145	156	10	3	6	251	251	1	8	7	58	55	3	0	7	53	72
8	7	5	156	155	3	2	5	206	205	9	3	6	147	157	1	7	7	149	169	0	0	8	79	75
9	7	5	95	99	2	2	5	146	151	8	3	6	234	244	4	7	7	76	60	2	0	8	46	42
10	7	5	86	98	1	2	5	118	123	7	3	6	153	164	5	7	7	98	98	3	0	8	60	70
11	7	5	92	77	0	2	5	383	385	6	3	6	301	304	6	7	7	65	56	4	0	8	95	114
12	7	5	73	91	0	1	5	521	537	5	3	6	138	135	7	7	7	80	74	5	0	8	139	151
15	7	5	107	118	1	1	5	500	496	4	3	6	138	141	8	7	7	119	118	6	0	8	85	92
16	7	5	83	84	2	1	5	322	340	3	3	6	180	172	10	7	7	148	144	7	0	8	87	90
17	7	5	164	173	3	1	5	185	191	2	3	6	125	142	16	7	7	63	51	8	0	8	156	155
18	7	5	84	84	4	1	5	82	87	1	3	6	84	90	14	6	7	74	54	9	0	8	168	177
19	7	5	175	173	5	1	5	225	244	0	3	6	119	120	13	6	7	70	50	10	0	8	126	148
20	7	5	74	57	7	1	5	121	125	0	4	6	174	174	12	6	7	78	71	11	0	8	180	195
22	6	5	99	75	8	1	5	288	300	1	4	6	115	120	11	6	7	109	98	13	0	8	146	157
20	6	5	134	128	9	1	5	148	147	2	4	6	79	95	10	6	7	76	72	14	0	8	95	93
19	6	5	111	95	11	1	5	49	44	3	4	6	147	143	7	6	7	160	166	15	0	8	96	84
18	6	5	137	129	12	1	5	62	66	4	4	6	114	117	6	6	7	51	47	16	0	8	75	51
17	6	5	87	86	13	1	5	121	127	5	4	6	178	186	5	6	7	80	67	19	1	8	91	57
16	6	5	213	200	14	1	5	55	76	6	4	6	126	126	1	6	7	51	54	18	1	8	122	95
14	6	5	127	118	15	1	5	181	184	7	4	6	120	121	0	5	7	99	94	16	1	8	66	63
13	6	5	73	67	16	1	5	79	75	8	4	6	182	173	1	5	7	93	103	15	1	8	77	74
12	6	5	64	56	17	1	5	175	179	9	4	6	507	523	2	5	7	85	97	14	1	8	136	137
11	6	5	80	93	18	1	5	86	73	10	4	6	96	91	4	5	7	118	113	12	1	8	65	71
10	6	5	159	155	19	1	5	184	181	11	4	6	95	92	6	5	7	97	95	10	1	8	209	210
9	6	5	75	61	20	1	5	119	131	13	4	6	67	83	7	5	7	51	50	9	1	8	97	116
8	6	5	103	97	23	1	5	102	85	14	4	6	85	91	8	5	7	191	191	8	1	8	228	244
7	6	5	306	301	24	1	5	71	64	15	4	6	127	115	10	5	7	142	134	7	1	8	86	91
5	6	5	51	41	25	1	5	75	64	16	4	6	121	117	12	5	7	59	65	6	1	8	177	184
3	6	5	49	65	23	0	5	66	55	17	4	6	101	95	14	5	7	81	82	3	1	8	111	112
2	6	5	330	327	18	0	5	104	118	18	4	6	89	86	15	5	7	67	64	2	1	8	122	118
1	6	5	329	326	17	0	5	106	101	21	4	6	80	75	16	5	7	113	110	1	1	8	114	116
0	6	5	229	242	14	0	5	83	82	21	5	6	83	67	18	5	7	97	67	0	1	8	112	142
0	5	5	111	107	13	0	5	110	110	20	5	6	86	65	19	5	7	101	85	1	2	8	112	95
1	5	5	179	175	12	0	5	179	180	18	5	6	96	77	20	4	7	94	81	2	2	8	81	90
2	5	5	178	186	10	0	5	153	155	17	5	6	84	94	18	4	7	136	128	3	2	8	53	56
3	5	5	161	170	9	0	5	146	140	16	5	6	72	50	15	4	7	90	74	9	2	8	84	101

Table 1. Continued.

10	2	8	65	93	6	7	9	67	42	4	0	9	54	21	5	5	0	35	25*	14	3	4	46	38*
11	2	8	66	62	13	6	9	65	40	0	0	10	69	54	1	6	0	37	22*	12	3	4	41	25*
12	2	8	53	48	2	6	9	75	56	1	0	10	71	72	4	6	0	37	10*	13	5	4	46	4*
14	2	8	60	48	0	6	9	82	85	2	0	10	125	119	14	6	0	46	5*	9	5	4	43	17*
15	2	8	58	60	1	5	9	81	86	4	0	10	91	97	1	8	0	44	1*	2	6	4	41	36*
19	2	8	63	42	6	5	9	69	49	5	0	10	108	42	3	8	0	44	16*	6	6	4	44	38*
15	3	8	117	105	7	5	9	76	61	7	0	10	87	105	5	8	0	45	2*	3	7	4	45	27*
13	3	8	118	105	8	5	9	127	135	9	0	10	65	50	5	5	0	48	2*	0	7	4	44	24*
11	3	8	84	75	10	5	9	75	55	12	1	10	95	77	4	9	0	47	31*	4	7	5	49	54*
10	3	8	75	74	11	5	9	80	44	10	1	10	70	53	10	8	1	48	41*	5	7	5	49	47*
8	3	8	154	155	13	5	9	75	76	9	1	10	71	60	4	8	1	47	72*	6	6	5	46	25*
6	3	8	101	108	14	4	9	72	59	8	1	10	109	114	5	7	1	40	21*	4	6	5	45	18*
5	3	8	52	40	11	4	9	67	53	2	1	10	61	48	8	6	1	44	45*	4	5	5	42	35*
4	3	8	83	90	10	4	9	86	91	0	1	10	100	98	5	5	1	35	23*	8	5	5	47	25*
3	3	8	88	101	9	4	9	107	108	1	2	10	72	66	11	5	1	39	21*	13	4	5	48	23*
1	3	8	82	104	7	4	9	109	105	2	2	10	98	84	13	4	1	39	5*	4	4	5	38	18*
0	4	8	266	274	6	4	9	73	75	7	2	10	99	85	17	2	1	45	11*	11	3	5	43	30*
1	4	8	102	104	5		9	56	51	8	2	10	61	75	14	1	1	38	50*	14	3	5	48	52*
3	4	8	65	55	2		9	87	86	12	2	10	64	61	15	1	1	40	36*	6	1	5	35	15*
4	4	8	75	80	1	4	9	90	87	8	3	10	86	75	19	0	1	45	5*	10	1	5	40	48*
6	4	8	60	48	0	3	9	91	97	3	3	10	83	64	15	0	1	38	20*	15	0	5	44	6*
7	4	8	53	55	1	3	9	95	99	1	3	10	57	80	13	0	1	36	7*	11	0	5	41	40*
11	4	8	60	46	2	3	9	82	90	6	4	10	82	66	10	0	1	34	27*	8	0	5	35	2*
14	4	8	94	89	4	3	9	66	87	7	4	10	117	125	8	0	1	33	33*	7	0	5	35	12*
15	4	8	57	45	6	3	9	79	72	9	4	10	77	69	11	0	2	35	13*	1	0	5	34	46*
16	4	8	85	78	7	3	9	73	81	10	5	10	109	107	12	0	2	35	2*	2	1	6	37	45*
18	4	8	129	125	8	3	9	114	120	8	5	10	141	136	14	0	2	39	17*	11	3	6	47	43*
14	5	8	106	108	9	3	9	97	90	7	5	10	69	45	17	0	2	44	24*	7	5	6	46	57*
13	5	8	59	63	10	3	9	179	171	6	5	10	95	92	18	1	2	47	51*	2	5	6	47	45*
12	5	8	61	53	12	3	9	103	109	2	5	10	70	53	0	7	2	40	3*	0	5	6	43	24*
7	5	8	87	84	16	3	9	68	72	1	5	10	102	67	3	8	2	43	25*	1	6	6	45	14*
5	5	8	113	115	12	2	9	76	87	0	4	11	74	55	5	8	2	43	21*	2	6	6	46	35*
2	5	8	109	107	11	2	9	172	174	0	3	11	64	61	6	8	2	48	26*	5	6	6	48	20*
0	5	8	69	90	9	2	9	133	145	4	3	11	81	62	0	9	2	46	12*	3	4	7	47	63*
0	6	8	168	173	8	2	9	63	45	5	3	11	81	64	12	6	3	47	25*	2	3	7	43	36*
2	6	8	150	152	7	2	9	167	165	6	3	11	103	118	6	6	3	40	26*	4	3	7	43	16*
4	6	8	79	66	6	2	9	80	66	8	3	11	137	136	2	5	3	37	20*	9	2	7	45	5*
5	6	8	96	86	1	2	9	86	84	8	2	11	78	73	6	5	3	38	24*	0	2	7	41	15*
8	6	8	102	112	0	2	9	191	187	5	2	11	62	39	11	3	3	38	16*	0	1	7	40	7*
9	6	8	78	67	1	1	9	92	111	4	2	11	63	61	15	2	3	43	25*	7	1	7	46	33*
11	6	8	103	88	2	1	9	78	77	1	1	11	114	125	2	1	3	31	10*	9	1	7	47	26*
13	6	8	72	78	5	1	9	106	101	6	1	11	105	75	12	1	3	37	20*	10	0	7	47	35*
15	6	8	69	47	6	1	9	88	107	9	1	11	82	61	18	0	3	48	14*	8	0	7	45	5*
16	6	8	111	116	8	1	9	273	282	10	1	0	49	25*	17	0	3	42	5*	2	0	7	42	30*
10	7	8	112	111	10	1	9	155	163	11	1	0	35	27*	13	0	3	37	8*	1	0	7	40	32*
8	7	8	181	163	14	1	9	63	52	9	1	0	33	10*	4	0	4	32	41*	1	0	8	45	23*
6	7	8	84	78	16	1	9	89	70	3	1	0	32	1*	14	0	4	43	43*	5	1	8	46	41*
2	9	8	69	45	17	1	9	135	113	17	2	0	47	21*	16	0	4	48	61*	4	1	8	48	40*
1	9	8	87	93	18	1	9	68	58	16	3	0	45	50*	11	2	4	39	33*	0	2	8	45	10*
2	8	9	93	76	11	0	9	71	88	13	5	0	41	19*	15	3	4	45	37*	4	2	8	47	46*
1	7	9	71	75	5	0	9	88	72															

addition procedure and the tangent formula.[14,15] In one of the corresponding eight *E*-maps the atoms of the two non-equivalent pyridone rings and also the atoms bonded directly to the rings could be located. A Fourier map based on phases calculated from these atomic positions including all observed structure factors yielded information on the positions of all non-hydrogen atoms.

Preliminary refinements were carried out by the minimum residual method [16] using the 300 largest structure factors. A couple of full-matrix least-squares refinement cycles with isotropic thermal parameters yielded a conventional *R*-factor of 0.125; introduction of anisotropic thermal parameters followed by some cycles of block-diagonal least-squares refinement gave an *R*-factor of 0.084. At this point a difference Fourier map was calculated and from this it was possible to establish the position of the hydrogen atoms. New series of block-diagonal least-squares calculations with refinement of positional parameters of all atoms and anisotropic thermal parameters of the nonhydrogen atoms (the isotropic thermal parameters for the hydrogen atoms were kept constant at 2.2 Å^2) resulted in a final *R*-value of 0.064 ($R_w = 0.047$). The overdetermination ratio was only 5.5, 313 parameters being refined on the basis of 1729 observed reflections with $\sin\theta/\lambda < 0.7$ Å^{-1}. No rigid-body thermal analysis was carried out.

A comparison of observed and calculated structure factors is given in Table 1; the final parameters for non-hydrogen atoms are listed in Table 2 and for

Table 2. Fractional atomic coordinates and thermal parameters with estimated standard deviations ($\times 10^5$). The temperature factor is given by $\exp-(B_{11}h^2+B_{22}k^2+B_{33}l^2+B_{12}hk+B_{13}hl+B_{23}kl)$.

Atom	x	y	z	B_{11}	B_{22}	B_{33}	B_{12}	B_{13}	B_{23}
O1	−7615	17176	45274	119	894	1001	142	189	−59
	11	29	31	7	38	46	26	30	76
O2	−7809	−13723	20360	81	1251	1364	−70	19	−968
	11	30	35	6	42	49	28	31	85
O3	25216	−14133	−1473	131	1201	902	−157	204	−408
	12	31	31	7	41	42	30	32	81
O4	30325	−11327	21311	85	1729	1122	−162	−11	43
	12	34	33	6	50	47	30	33	91
N1	9439	4982	24697	86	504	836	78	−6	−121
	14	31	35	7	36	50	27	33	81
N2	19650	−12695	38617	108	895	986	32	62	218
	15	36	39	7	45	52	34	37	94
C1	3591	−446	19485	101	493	702	36	−15	−155
	16	38	44	8	45	56	33	40	91
C2	−2112	3666	26290	96	487	711	−70	−33	308
	16	38	43	8	46	57	33	41	95
C3	−2284	13308	39214	108	504	714	39	95	203
	17	41	43	9	45	58	35	41	97
C4	3945	17919	44271	140	609	810	−11	−107	−375
	18	42	46	9	51	64	38	43	102
C5	9514	14018	36823	98	545	1254	36	−152	−171
	18	41	50	9	46	70	37	45	106
C6	15559	1541	16361	87	814	799	18	56	−29
	17	41	45	8	54	63	38	41	105
C7	18674	−12397	21462	74	691	839	−30	1	16
	16	41	46	8	48	60	35	40	103
C8	25402	−12829	13021	96	552	918	15	206	6
	17	41	46	9	46	58	37	42	99
O1*	−8862	32200	93725	102	939	1014	−153	253	−271
	12	28	31	6	39	46	27	29	76
O2*	−8171	50870	68492	87	1325	1044	165	46	376
	11	29	32	6	44	45	30	30	85
O3*	29816	47919	69112	74	1116	2469	212	111	114
	12	31	41	6	44	65	28	39	103
O4*	26465	68867	59996	161	868	1360	−94	273	449
	13	30	34	7	39	51	27	35	82

Table 2. Continued.

N1*	8818	43544	75614	66	546	918	−32	12	−299
	14	31	36	7	36	51	27	33	80
N2*	16380	69677	81156	90	708	768	−116	81	−368
	13	32	37	7	40	50	30	35	85
C1*	3193	49011	69395	98	502	699	25	−24	133
	16	38	44	8	45	56	33	40	91
C2*	−2749	45594	75628	89	560	768	45	−23	−34
	16	39	43	9	46	59	34	41	98
C3*	−3261	36160	88501	116	514	765	−34	81	−471
	17	41	44	9	46	59	37	42	98
C4*	2738	31479	94992	135	574	983	−101	−31	95
	18	42	48	10	49	67	38	47	104
C5*	8554	35107	88238	111	401	1068	−23	−142	273
	17	38	49	9	44	66	36	44	99
C6*	15116	46747	67810	84	623	899	−19	172	−352
	17	41	47	8	48	63	34	41	106
C7*	19556	55957	77694	77	638	676	2	53	−83
	17	40	42	8	46	56	34	39	97
C8*	25944	58040	68153	74	880	903	−107	−41	−368
	17	42	46	8	55	61	36	43	107

hydrogen atoms in Table 3. Standard deviations were calculated from the correlation matrix from the block-diagonal least-squares calculations ignoring the standard deviations in cell parameters.

Table 3. Fractional atomic coordinates ($\times 10^4$) with estimated standard deviations for hydrogen atoms.

Atom	x	y	z	Atom	x	y	z
H1	408	−773	1224	H1*	351	5508	6099
	16	36	40		16	37	40
H4	426	2424	5319	H4*	276	2533	10496
	16	37	42		16	36	39
H5	1353	1658	3913	H5*	1310	3243	9242
	16	36	40		16	36	38
H61	1844	924	1915	H61*	1394	5129	5742
	16	34	40		16	34	40
H62	1461	56	610	H62*	1716	3772	6593
	16	33	40		16	36	40

Table 3. Continued.

H7	1600	−2043	1891	H7*	2071	5108	8759
	15	34	41		16	34	39
H1N	2147	−308	4183	H1N*	1285	6796	8961
	16	36	38		16	35	39
H2N	1479	−1352	4436	H2N*	1459	7400	6248
	16	36	40		16	34	40
H3N	2259	−2108	4037	H3N*	1947	7601	9609
	16	36	40		17	34	41
HO2	−1098	78	2530	HO2*	−1126	5073	7544
	16	35	38		16	35	38

DISCUSSION

A drawing of the two molecules (I and II) in the asymmetric unit is presented in Fig. 1; the numbering of the atoms is indicated, as are the bond lengths and angles arrived at in the structure analysis. Interatomic distances and bond angles are also given in Table 4 together with their standard deviations. The latter values might be somewhat underestimated, however, since possible correlations between positional parameters of different atoms are disregarded in the computing procedure.

The crystals of L-mimosine offer the opportunity to study two non-equivalent molecules in different environment. However, the different surroundings seem to have only minor influence on the molecular structure as the bond lengths and angles as well as the conformation of the two molecules are nearly equal.

The molecular conformation. Both of the molecules in the asymmetric unit have a conformation similar to the one found in L-DOPA.[10] The dihedral angle C1 – N – C6 – C7 is 275° and C1*N* – C6* – C7* 113°, the side chain is thus situated on opposite sides of the ring plane in the two molecules, and the molecule II (*) is the one corresponding to L-DOPA.

The carboxyl groups are in *trans* position relative to the phenyl rings with respect to the Cα – Cβ bond; the dihedral angles N – C6 – C7 – C8 and N* – C6* – C7* – C8* are 172° and 178°, respectively, as compared to 175° for the corresponding angle in L-DOPA.

The alanine part. The zwitterionic character of the molecule is apparent in the present structure as usual for such compounds. The four C – O bonds of the carboxy groups are equal, mean bond length 1.242 Å, with a calculated standard deviation equal to the estimated standard deviation of each bond, 0.005 Å. The C – NH_3^+ bonds, 1.472 and 1.484 Å, are possibly on the short side of the expected value 1.49 Å, as found in L-DOPA [10] and L-tyrosine.[17] The C6 – C7 bonds (1.530 and 1.515) are found to be slightly shorter than the C7 – C8 bonds (1.552 and 1.550 Å). The α carbon atom is within the experimental accuracy situated in the plane of the carboxy group in both molecules. The dihedral angle N2 – C7 – C8 – O4 is 350.1° (in clock-wise direction) and the N2* – C7* – C8* – O4* angle is 334.8° (e.s.d. 0.5°), both being within the limits

Table 4. Interatomic distances (Å) and bond angles (°). Estimated standard deviations are 0.005 Å and 0.3°, respectively.

Bond	Molecule I	Molecule II(*)
O1–C3	1.261	1.285
O2–C2	1.357	1.360
O3–C8	1.239	1.247
O4–C8	1.237	1.244
N2–C7	1.472	1.484
N1–C1	1.375	1.368
N1–C5	1.341	1.340
N1–C6	1.475	1.480
C1–C2	1.359	1.365
C2–C3	1.430	1.417
C3–C4	1.414	1.416
C4–C5	1.355	1.364
C6–C7	1.530	1.515
C7–C8	1.552	1.550

Bond angle	Molecule I	Molecule II
O1–C3–C4	124.4	123.1
O1–C3–C2	121.4	121.2
O2–C2–C3	119.3	121.1
O2–C2–C1	118.5	117.8
C1–C2–C3	122.1	121.0
C2–C3–C4	114.2	115.7
C3–C4–C5	122.1	120.9
C4–C5–N1	121.6	121.5
C5–N1–C1	119.8	120.1
N1–C1–C2	120.1	120.6
C1–N1–C6	120.0	118.7
C5–N1–C6	120.1	121.1
N1–C6–C7	114.1	113.1
C6–C7–N2	110.7	110.7
C6–C7–C8	105.1	106.8
N2–C7–C8	109.7	111.2
C7–C8–O3	115.8	113.8
C7–C8–O4	117.1	118.0
O3–C8–O4	127.1	128.2

Hydrogen bond lengths

O1–N2*(−x, $-\frac{1}{2}+y$, $\frac{3}{2}-z$)	2.699
O2–O3*($\frac{1}{2}-+x$, $\frac{1}{2}-y$, 1−z)	2.704
O3–N2 ($\frac{1}{2}-x$, −y, $-\frac{1}{2}+z$)	2.880
O3–N2*(x, −1+y, −1+z)	2.793
O4–O2*($\frac{1}{2}+x$, $\frac{1}{2}-y$, 1−z)	2.696
N2–O1*(−x, $-\frac{1}{2}+y$, $\frac{3}{2}-z$)	2.713
N2–O4*(x, −1+y, z)	2.882
O1*–N2*(−x, $-\frac{1}{2}+y$, $\frac{3}{2}-z$)	2.872

Other intermolecular distances (*cf.* Fig. 2)

O1–N1*	3.348
O1–C1*	3.578
O1–C5*	3.355
O1*–N1	3.448
O1*–C1	3.694
O1*–C5	3.690

reported for amino acids.[18] In both molecules the hydrogen atoms are tetrahedrally arranged about the nitrogen atom; their positions correspond to a 10–15° rotation about the C–N bond relative to a strictly staggered conformation.

The hydroxypyridone part. The six-membered rings are nearly planar, the deviations of the atoms from a least-squares plane being less than 0.03 Å. The non-hydrogen atoms attached to the rings are situated from 0.05 to 0.12 Å out of the ring planes.

Except for the C3–O1 and the C3*–O1* bond lengths the two hydroxypyridone moieties are identical. An estimate of the relative contribution to the structure from the formulae I and II indicated in the introduction may be based on several features in the geometry. The mean value of the C1–C2, C4–C5, C1*–C2*, and the C4*–C5* bonds is 1.361 Å (e.s.d. 0.005 Å) as compared to the mean value for C2–C3, C3–C4, C2*–C3* and C3*–C4* of 1.419 Å (e.s.d. 0.007 Å). The corresponding bond lengths in quinone are 1.322 Å and 1.477 Å,[19] and in quinone in the quinone-resorcinal complex 1.330 Å and 1.468 Å,[20] respectively. The C–C bond length to be expected for

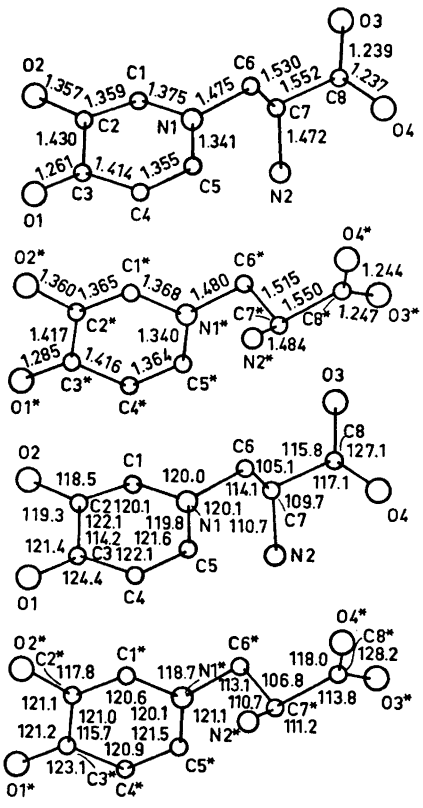

Fig. 1. Bond lengths (Å) and angles (°) observed in L-mimosine.

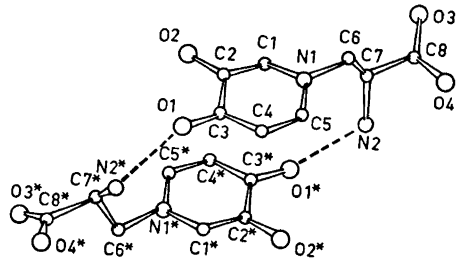

Fig. 2. The dimeric arrangement of the two crystallographically independent molecules of L-mimosine.

an aromatic model is 1.397 Å; the contributions from the two extreme structures appear thus to be about equal. This feature is also indicated by the C3 – O1 and C3* – O1* bonds of 1.261 Å and 1.285 Å, these being close to the mean length of the quinone C = O bond (1.22 Å) and the phenolic C – O bond (1.36 – 1.38 Å).

From these results one might expect the C – N bond lengths to be somewhere between the values reported for pyrrol, 1.374 [21] ("quinoid" case) and for pyridine, 1.339 [22] ("aromatic" case). In the present structure determination both of these values were found for the C – N bonds, the C1 – N1 bond being the longer in both molecules. The difference between the two C – N bonds in each of the two independent molecules is significant according to normal standards of structure analysis; we find no obvious explanation for this difference, however.

The two phenolic C – O bonds are equal in the two molecules, 1.357 and 1.360 Å, respectively.

The bond between the hydroxypyridone and the alanine moieties, N1 – C6, is found equal to 1.475 and 1.480 Å. The $N_{sp^3}-C_{sp^3}$ bond length to be expected is somewhat shorter than the aliphatic N – C of 1.47 Å; the relative lengthening in the present case may be attributed to the positive charge on the nitrogen atom in analogy with the bond length in $C_{sp^3}-\overset{+}{N}H_3$ of 1.49 Å.

The crystal structure. Packing and hydrogen bonding. The high values for the melting point (decomp. 227 – 228°C) and density (1.59 g cm^{-3}) indicate strong intermolecular forces and a close packing of the molecules in the crystal. The packing coefficient [23] estimated from data given by Bondi [24] is as high as 0.82 as compared with the one calculated for L-DOPA of 0.79 and L-tyrosine of 0.75, whereas a normal value for benzene derivatives is given by Kitaigorodskii [23] to be 0.69. It seems reasonable to relate the high values to the zwitterionic character of the molecules, especially for L-mimosine. From the partial quinoid structure it may be deduced that the nitrogen atom in the ring is positively and the keto ozygen atom negatively charged. This also seems reasonable from the way pairs of crystallographically independent molecules are forming dimers in the crystals. The asymmetric unit may be represented as visualized in Fig. 2. The two molecules are linked together by two hydrogen bonds, O1 – N2* (2.699 Å) and O1* – N2 (2.872 Å). The planes of the pyridone moieties are nearly parallel, the interplanar separation being 3.4 Å. The shortest distances between atoms from each molecule apart from the hydrogen bonded atoms are N1 – O1* of 3.448 Å and N1* – O1 of 3.348 Å. This may indicate

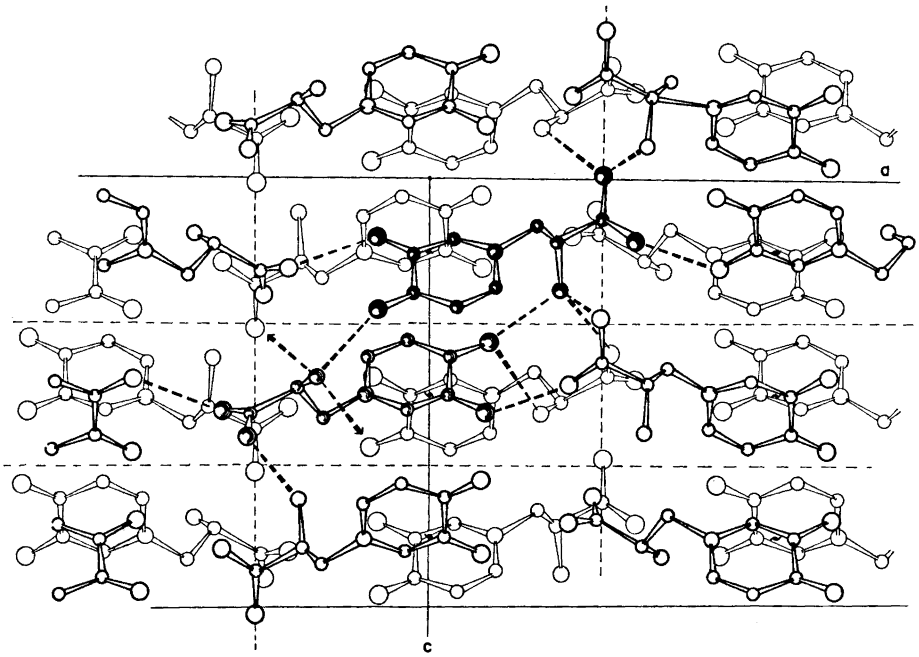

Fig. 3. The crystal structure as seen along the *b*-axis. Hydrogen bonds from one dimer (shaded) are indicated by broken lines.

an electrostatic interaction between the two ring systems owing to their zwitterionic character, and results in a pseudo centre of symmetry between the planar parts of the molecules.

The hydrogen bond system in the crystal is shown in Fig. 3, the hydrogen bond lengths are listed in Table 4. All hydrogen atoms bonded to hetero atoms are engaged in hydrogen bonds, each molecule being involved in eight hydrogen bonds to seven different neighbouring molecules. There is some difference in hydrogen bonding for the two crystallographically independent molecules in that the carbonyl oxygen atom (O1) in the pyridone part is hydrogen acceptor for only one ammonium group, whereas the corresponding oxygen atom (O1*) of the other molecule act as an acceptor of two such hydrogen bonds. Correspondingly, one of the oxygen atoms of the carboxyl group (O3) is acceptor for two ammonium hydrogen atoms and O3* for only one. The nitrogen atom N2 is engaged in hydrogen bonds to two carboxyl oxygen atoms (O3 and O4*) and one carbonyl oxygen atom (O1*); N2* is hydrogen bonded to one carboxyl (O3) and two carbonyl (O1 and O1*) oxygen atoms.

The molecules of type II (*) related by a screw axis in the *b* direction are connected through the hydrogen bonds between O1* and N2*. Similarly, molecules of type I related by a screw axis along *a* are forming chains by means of hydrogen bonds between N2 and O3. Both types of molecules are involved in the hydrogen bonded helix about the screw axis along the *c* direction through the hydrogen bonds O2 – O3* and O4* – N2.

REFERENCES

1. Thompson, J. F., Morris, C. T. and Smith, I. K. *Ann. Rev. Biochem.* **38** (1969) 137.
2. Owen, L. N. *Vet. Rec.* **70** (1958) 454.
3. Hegarthy, M. P., Schinckel, P. G. and Court, R. D. *Austr. J. Agric. Res.* **15** (1964) 153.
4. Hylin, T. W. and Lichton, I. T. *Biochem. Pharmacol.* **14** (1965) 1167.
5. Prabhakaran, K., Harris, E. B. and Kirchheimer, W. F. *Cytobios* **A 1** (1969) 3.
6. Kleipool, R. T. C. and Wibaut, T. P. *Rec. Trav. Chim.* **69** (1960) 37.
7. Bonting, S. L. and Schapman, F. R. *Rec. Trav. Chim.* **69** (1950) 1007.
8. Spencer, I. D. and Notation, A. D. *Can. J. Chem.* **40** (1962) 1374.
9. Beyerman, H. C., Maat, L. and Hegarthy, M. P. *Rec. Trav. Chim.* **83** (1964) 1078.
10. Mostad, A., Ottersen, T. and Rømming, C. *Acta Chem. Scand.* **24** (1970) 1864.
11. Dahl, T., Gram, F., Groth, P., Klewe, B. and Rømming, C. *Acta Chem. Scand.* **24** (1970) 2232.
12. Hanson, H. P., Herman, F., Lea, T. D. and Skillman, S. *Acta Cryst.* **17** (1964) 1040.
13. Stewart, R. F., Davidson, E. R. and Simpson, W. T. *J. Chem. Phys.* **42** (1965) 3175.
14. Karle, J. and Karle, I. L. *Acta Cryst.* **21** (1966) 849.
15. Karle, J. and Hauptman, M. *Acta Cryst* **9** (1956) 635.
16. Stanley, E. *Acta Cryst.* **17** (1964) 1028.
17. Mostad, A., Nissen, H. M. and Rømming, C. *Tetrahedron Letters* **24** (1971) 2131; *Acta Chem. Scand.* **26** (1972) 3819.
18. Sundaralingam, M. and Putkey, E. F. *Acta Cryst.* **B 26** (1970) 790.
19. Trotter, T. *Acta Cryst.* **13** (1960) 86.
20. Ito, T., Minobe, M. and Sakurai, T. *Acta Cryst.* **B 26** (1970) 1145.
21. Potts, W. T. *J. Chem. Phys.* **23** (1955) 73.
22. Pariser, R. *J. Chem. Phys.* **24** (1956) 250.
23. Kitaigorodskii, A. I. *Organic Chemical Crystallography*, Consultants Bureau, New York 1955, p. 106.
24. Bondi, A. *Physical Properties of Molecular Crystals, Liquids and Gases*, Wiley, New York 1968, p. 453.

Received June 30, 1972.

ACTA CHEMICA SCANDINAVICA 27 (1973) 177–190

The Crystal Structure of $Zr_4(OH)_6(CrO_4)_5H_2O$

WANDA MARK

Department of Inorganic Chemistry, Chalmers University of Technology and the University of Göteborg, P.O. Box, S-402 20 Göteborg 5, Sweden

A re-investigation of the crystal structure of a zirconium chromate phase with the approximate composition $Zr_4(OH)_6(CrO_4)_5(H_2O)_x$ has been performed. In this investigation x was approximately 1, but in an earlier crystal structure determination,[2] x was given as 2.

$Zr_4(OH)_6(CrO_4)_5H_2O$ forms orthorhombic crystals, belonging to the space group *Pnnm* with the cell parameters $a = 11.629$, $b = 13.563$, and $c = 6.882$ Å. X-Ray intensity data were collected with an automatic single crystal diffractometer, and the positions of the atoms were determined by means of three-dimensional Patterson and Fourier syntheses. Using a total of 1679 independent reflexions, least squares full matrix refinements yielded a final R value of 0.038.

The structure consists of infinite chains with the approximate composition $[Zr_4(OH)_6CrO_4]_n^{8n+}$, which are joined in two directions by chromate groups. Zirconium exhibits sevenfold coordination, the coordinated oxygen atoms being situated at the vertices of somewhat distorted pentagonal bipyramids. The Zr–O distances range from 2.069 Å to 2.216 Å.

In connection with an investigation of the $ZrO_2-CrO_3-H_2O$ system, the crystal structures of two different phases in the system have been determined. The OD-structure of $Zr(OH)_2CrO_4$ ($ZrO_2.CrO_3.H_2O$) has been published earlier,[1] while the structure of a zirconium chromate with the approximate composition $4ZrO_2.5CrO_3.4H_2O$ is presented in this paper.

Some years ago, Lundgren[2] reported the crystal structure of $4ZrO_2.5CrO_3.5H_2O$. Due to a lower temperature during its preparation, this product had a higher content of water of crystallization than the product described in the present paper. In spite of this, both products constitute the same phase. A re-investigation of the crystal structure of this phase was undertaken since the rather poor data set, that the earlier determination was based on, yielded some discrepancies between observed and calculated structure factors.

PREPARATION AND ANALYSIS

A solid, amorphous zirconium chromate, "$ZrOCrO_4$", was obtained by adding an aqueous solution of zirconium nitrate to a potassium dichromate solution.[3] After the

amorphous product had been washed and dried, it was dissolved in an aqueous chromium trioxide solution, sealed in Pyrex glass tubes and heated for several days. By varying the Cr : Zr ratio, the acidity and the temperature, products with different chromium and water contents were obtained. Apart from $Zr(OH)_2CrO_4$, which is formed at low acidities in the temperature range 140 – 190°C, the structures of the products prepared in the temperature range 100 – 190°C proved to be nearly identical, according to Guinier powder photographs.

The sample investigated was formed in 10 M CrO_3, after ten days at 167°C. The chromium content was determined by atomic absorption spectroscopy and the water content by Penfield's method.[4] The product was heated to 1200°C in a Mettler thermo-balance in order to obtain the $ZrO_2 + Cr_2O_3$ content, and the density was determined by the flotation method. According to the results obtained (shown below) the product has the approximate formula $4ZrO_2.5CrO_3.4H_2O$, while its actual composition, calculated on the basis of the analysis, is $4ZrO_2.4.9CrO_3.3.7H_2O$.

	% Cr	% ($ZrO_2 + Cr_2O_3$)	% H_2O	Density (g cm^{-3})
Found	24.3	82.5	6.3	3.18
Calculated for $4ZrO_2.5CrO_3.4H_2O$	24.4	82.0	6.8	3.234 (*cf.* below)
Calculated for $4ZrO_2.4.9CrO_3.3.7H_2O$	24.3	82.5	6.4	3.188 (*cf.* below)

UNIT CELL AND SPACE GROUP

Preliminary cell dimensions were obtained from rotation and Weissenberg photographs. To obtain accurate cell dimensions, 43 reflexions were indexed on Guinier powder photographs, which were taken with Cu$K\alpha_1$ radiation using lead nitrate as an internal standard ($a_{Pb(NO_3)_2} = 7.8566$ Å at 21°C). Least squares refinement of the cell parameters yielded the results:

$a = 11.6290 \pm 0.0012$ Å, $b = 13.6534 \pm 0.0014$ Å, $c = 6.8818 \pm 0.0007$ Å, $V = 1092.7$ Å^3.

Observed and calculated $\sin^2\theta$ values are listed, together with calculated structure factors, in Table 1.

In accordance with the cell dimensions and the experimental density, the unit cell contains two formula units.

From Weissenberg photographs taken with Cu$K\alpha$ radiation the structure was seen to be orthorhombic, the following reflexions being systematically absent:

$h0l$ with $h+l=2n+1$; $0kl$ with $k+l=2n+1$.

These extinctions are characteristic for space groups Nos. 34, *Pnn*2, and 58, *Pnnm*.[5]

COLLECTION AND PROCESSING OF DATA

The compound $4ZrO_2.5CrO_3.4H_2O$ crystallizes as bright red truncated pyramids, and the crystal chosen for the structure determination had a basal plane with the dimensions 0.13×0.21 mm^2 (y and z directions) and a height of 0.12 mm. It was mounted along the b axis in an automatic single crystal diffractometer (Philips Pailred) and reflexions hkl and $\bar{h}kl$ were registered with Mo$K\alpha$ radiation from the layer lines $h0l - h18l$ with $k = 2n$ and

Table 1. Guinier powder photograph of $\sim 4ZrO_2 . 5CrO_3 . 4H_2O$. $\lambda(CuK\alpha_1) = 1.54050$ Å.

h k l	$10^5 \sin^2\theta$ obs	$10^5 \sin^2\theta$ calc	*F* calc	*I* obs
1 1 0	751	757	37	vvw
1 0 1	1689	1691	182	st
1 2 0	1711	1712	191	st
2 0 0	1755	1755	188	st
2 1 0	2070	2073	51	vvw
1 3 0	3309	3303	59	vvw
0 3 1	4118	4117	116	w
3 1 0	4272	4267	93	vw
2 2 1		4281	54	
1 3 1	4553	4556	88	w
2 3 0	4622	4619	90	vvw
0 0 2	5005	5011	557	vst
0 4 0	5088	5092	–	st
3 0 1	5214	5201	254	vst
3 2 0		5221	327	
3 1 1	5516	5519	72	vvw
1 2 2	6722	6723	138	w
1 4 1	6780	6784	110	w
2 4 0	6847	6847	137	vw
4 0 0	7013	7019	104	vvw
2 1 2	7078	7084	59	vvw
3 1 2	9271	9278	76	vvw
4 2 1	9542	9545	191	m
0 4 2	10102	10103	219	m
3 2 2	10233	10232	128	w
3 4 1	10292	10293	152	w
2 5 1	10969	10964	40	vvw
4 3 1	11130	11136	87	vvw
1 0 3	11711	11713	230	m
1 6 0	11899	11896	165	w
3 5 0		11905	86	
4 0 2	12027	12030	118	vw
4 4 0	12109	12112	120	vw
5 2 0	12246	12241	208	w
3 5 1	13156	13158	85	vvw
2 6 1	14465	14465	96	vvw
5 3 1	15082	15085	83	vvw
3 0 3	15224	15223	227	w
3 6 0	15408	15406	306	w
6 0 0	15801	15794	112	vvw
1 4 3	16798	16805	174	w
1 6 2	16913	16907	124	w
3 5 2		16916	79	
4 4 2	17127	17122	75	vvw
6 2 1	18305	18319	270	m
4 2 3	19562	19567	253	w
4 6 1	19739	19729	225	w
0 0 4	20051	20044	469	vw
3 4 3	20308	20315	153	vw
0 8 0	20358	20369	–	vw
3 6 2	20411	20417	164	vw

from $h0l-h7l$ with $k=2n+1$. It could be seen from the Weissenberg photographs, that those reflexions with $k=2n+1$ were much weaker than those with $k=2n$, and the scanning speed was therefore set to 2.5°/min for layer lines with k even, and to 0.5°/min for layer lines with k odd. The intensities were corrected for Lorentz, polarization and absorption effects, the linear absorption coefficient being 44 cm^{-1}. The preliminary data set thus obtained consisted of 1844 reflexions with k even, and 1485 reflexions with k odd.

DETERMINATION AND REFINEMENT OF THE STRUCTURE

Owing to the somewhat different composition of the product, whose structure was investigated by Lundgren, the crystal structure of $4ZrO_2.5CrO_3.4H_2O$ was determined independently of the previous results. In order to facilitate a comparison between the results of the two determinations, the crystal axes of $4ZrO_2.5CrO_3.4H_2O$ were chosen in accordance with those of $4ZrO_2.5CrO_3.5H_2O$.

From a three-dimensional Patterson synthesis the positions of the Zr_1, Zr_2, Cr_1, and Cr_2 atoms were obtained. A third chromium atom, Cr_3, was also located, but it could not on the basis of the heights of the peaks be unambiguously differentiated from an oxygen atom, and therefore it was not taken into consideration at this stage of the investigation. The atomic parameters were refined and a three-dimensional Fourier synthesis, based on the refined parameters, revealed the positions of Cr_3 and two oxygen atoms, O_5 and O_6. The atoms were assumed to occupy the general position 4(*c*) of space group *Pnn*2, and after two more refinements and subsequent Fourier syntheses it was possible to locate all the remaining atoms, *i.e.* O_1-O_4 and O_7-O_{12}.

The special positions 2(*a*) and 2(*b*) in *Pnn*2 are not possible for the two Cr_3 atoms, since the Patterson calculation shows no peaks corresponding to vectors between Zr in 4(*c*) and Cr in 2(*a*) or 2(*b*). Accordingly, the Cr_3 atoms must be statistically distributed between four equivalent positions. The oxygen atoms O_{11} are coordinated to Cr_3 and, consequently, they must also be arranged statistically. The electron density of the oxygen atom O_{12} in the Fourier synthesis is about half that of the other oxygen atoms and the approximately two O_{12} were therefore assumed to be randomly distributed between four equivalent positions. To be more consistent with the structure, in the following the approximate formula will be written $Zr_4(OH)_6(CrO_4)_5H_2O$. This is in agreement with the electron density found for O_{12}, which ought to correspond to water of crystallization.

Preliminary refinements of the scale factors between the layers and the atomic parameters were carried out, assuming the atoms to be situated in the general position 4(*c*) of space group *Pnn*2. The *z* coordinates of all atoms, with the exception of O_1, O_2, and O_{11}, turned out to be very nearly zero, and as the *R* value did not continue to converge after a few cycles of refinement, the space group *Pnn*2 was abandoned in favour of the centro-symmetric *Pnnm*. Atoms with *z* coordinates almost zero were assumed to occupy the special positions 4(*g*) (*xy*0), while the remaining atoms (O_1, O_2, O_{11}) were assumed to be situated in the general position 8(*h*). Refinement of the following parameters was performed with the program LINUS:[6] scale factors, atomic param-

Table 2. Observed and calculated structure factors for $Zr_4(OH)_6(CrO_4)_5H_2O$. (The columns are h, F_o, F_c, and the phase angles, respectively.)

	H 0 0			2	57	53	0.04	20	30	34	-3.09	13	29	26	0.07		H 2 5		
2	186	188	0.02	4	30	31	-3.05	21	22	19	0.10	15	36	33	0.08	2	41	45	0.06
4	117	104	-3.11	10	66	66	-3.07	22	36	39	-3.07	20	15	19	-3.07	4	115	114	-3.08
6	117	112	3.13	12	77	77	-3.06	23	20	22	-3.04					6	169	170	-3.10
8	65	59	3.14					24	15	16	-3.04		H 1 9			8	52	52	-3.11
10	155	153	-3.11		H 0 9							3	20	17	-3.06	12	19	20	0.02
12	130	129	-3.08	1	59	58	0.02		H 1 3			6	30	24	-3.08	16	76	79	0.07
16	35	32	0.10	3	83	84	0.07	0	26	24	3.14	7	30	29	0.07	18	31	36	0.08
20	30	34	0.04	5	34	35	0.10	1	23	24	3.13	8	22	20	-3.07				
22	40	41	0.07	7	93	94	-3.07	3	44	45	-3.10	10	17	17	0.11		H 2 6		
9	58	58	-3.06	5	22	21	0.01	13	20	17	0.07	1	86	86	-3.10				
	H 0 1			13	37	35	-3.07	6	65	64	-3.11	16	36	34	0.08	3	152	151	-3.09
1	184	182	0.01	15	37	39	-3.07	7	80	75	0.04	18	18	17	0.10	5	90	88	-3.13
3	255	254	0.03	19	33	33	0.10	8	51	48	-3.10	19	36	33	-3.04	7	59	58	-3.12
5	42	47	0.10					9	16	13	0.02					9	111	111	-3.08
7	256	251	-3.11		H 0 10			10	44	42	0.06		H 1 10			11	24	27	0.03
9	97	93	-3.08	0	177	174	0.05	11	33	31	0.02	3	24	22	-3.07	13	82	81	0.07
13	68	68	-3.09	2	63	62	0.03	12	26	24	0.01	9	17	14	-3.06	15	50	51	0.04
15	77	75	-3.10	4	20	19	-3.00	13	29	28	0.05	10	35	32	0.07				
19	48	52	0.08	6	22	22	3.11	14	17	18	0.00	12	29	27	0.08		H 2 7		
21	33	35	0.05	8	30	27	3.13	15	20	19	0.08	13	30	27	0.06	4	145	147	-3.10
				10	68	69	-3.08	16	65	61	0.05	14	18	11	-3.02	6	161	161	-3.10
	H 0 2			12	67	64	-3.05	17	22	22	-3.10	15	31	31	0.08	8	49	47	-3.11
0	552	557	0.02	16	23	24	0.10	18	18	19	0.11					10	31	30	0.09
2	70	77	0.04					19	55	56	-3.07		H 1 11			12	35	34	0.01
4	125	118	-3.11		H 0 11			21	22	23	-3.12	6	26	19	-3.07	16	65	67	0.08
6	21	15	3.07	1	41	38	0.03	22	24	28	-3.06	7	23	21	0.09	18	26	27	0.10
10	106	107	-3.09	3	61	63	0.08					8	18	15	-3.06				
12	121	118	-3.08	5	23	26	0.11		H 1 4			16	27	25	0.09		H 2 8		
14	27	24	3.10	7	64	68	-3.06	1	23	23	0.03					1	60	51	-3.08
20	34	33	0.04	9	43	46	-3.06	2	34	32	0.04		H 1 12			3	87	86	-3.06
22	38	40	0.07	13	26	26	-3.06	3	61	59	-3.10	3	17	14	-3.04	5	48	45	-3.13
				15	30	29	-3.06	4	23	20	-3.11	10	21	19	0.10	7	37	34	-3.11
	H 0 3							5	12	12	3.12	12	23	19	0.10	9	89	91	-3.07
1	231	230	0.01		H 0 12			8	15	15	-0.00					13	56	57	0.09
3	221	227	0.03	0	99	98	0.08	9	36	34	-3.10		H 1 13			15	33	34	0.05
5	38	40	0.11	2	26	27	0.07	10	59	56	0.05	6	19	15	-3.07				
7	273	267	-3.11	10	36	38	-3.05	12	46	43	0.07	7	19	19	0.08		H 2 9		
9	117	114	-3.09	12	49	49	-3.04	13	47	47	0.05					4	92	91	-3.08
11	23	24	3.09					15	56	53	0.06		H 2 0			6	109	108	-3.08
13	56	55	-3.08		H 0 13			20	27	31	-3.09	1	184	191	-3.12	8	39	36	-3.11
15	61	60	-3.09	3	52	53	0.08	22	32	34	-3.06	3	331	327	-3.12	16	53	55	0.08
17	23	23	0.03	7	60	62	-3.06	23	21	23	-3.05	5	220	208	-3.14	18	24	26	0.10
19	49	53	0.08	9	42	44	-3.06					6	15	17	0.03				
21	32	31	0.05						H 1 5			7	101	100	-3.13		H 2 10		
					H 0 14			2	15	13	-3.11	9	167	165	-3.10	1	54	55	-3.08
	H 0 4			0	80	80	0.09	3	42	39	-3.10	11	57	58	0.02	3	102	101	-3.08
0	469	469	0.03	2	28	27	0.06	4	13	14	0.02	13	120	121	0.05	5	58	57	-3.13
2	112	114	0.02					5	17	15	0.02	15	72	73	0.03	7	40	39	-3.12
4	70	70	-3.09		H 1 0			6	45	43	-3.10	17	19	17	0.02	9	60	62	-3.05
6	47	45	3.12	1	26	37	0.02	7	44	41	0.06	21	27	25	0.11	11	22	21	0.02
8	33	30	3.14	2	44	51	0.03	8	35	34	-3.09					13	58	60	0.07
10	118	117	-3.10	3	87	93	-3.12	10	26	25	0.09		H 2 1			15	30	33	0.06
12	107	109	-3.07	4	15	19	-3.10	11	20	20	0.03	2	56	54	0.06				
16	26	27	0.12	5	41	37	3.13	13	28	26	0.05	4	185	191	-3.10		H 2 11		
20	22	29	0.04	8	40	38	-0.00	15	31	30	0.05	6	271	270	-3.11	4	66	65	-3.07
22	33	36	0.08	9	50	49	-3.11	16	50	49	0.06	8	77	75	-3.12	6	81	81	-3.07
				10	71	68	3.06	18	22	25	-3.08	10	20	20	0.15	8	24	22	-3.09
	H 0 5			12	52	51	0.06	19	40	43	-3.05	12	39	40	0.01	16	41	41	0.10
1	76	73	0.02	13	61	60	0.04	21	22	22	-3.12	16	95	95	0.06				
3	142	140	0.05	14	14	12	-3.00	22	21	18	-3.03	18	34	39	0.08		H 2 12		
5	54	53	0.08	15	67	65	0.05									1	36	32	-3.05
7	141	142	-3.09	20	33	36	-3.10		H 1 6				H 2 2			3	52	52	-3.04
9	68	70	-3.07	22	35	35	-3.06	1	12	12	0.06	1	126	138	-3.11	5	19	17	-3.11
13	56	59	-3.09	23	27	27	-3.06	2	20	18	0.06	3	121	128	-3.08	9	52	54	-3.05
15	64	64	-3.09					3	41	39	-3.09	5	102	94	-3.13	13	33	34	0.12
19	39	43	0.09		H 1 1			4	15	11	-3.08	7	46	49	-3.12				
21	26	29	0.05	2	23	20	-3.11	8	15	16	-0.00	9	176	175	-3.10		H 2 13		
				3	73	72	-3.12	9	30	28	-3.09	11	32	16	0.05	4	63	62	-3.07
	H 0 6			4	31	28	0.01	10	46	45	0.06	13	92	91	0.06	6	67	69	-3.06
0	331	323	0.04	5	37	36	0.01	12	42	39	0.07	15	53	56	0.04				
2	87	87	0.03	6	74	74	-3.12	13	38	39	0.05	17	24	23	0.02		H 2 14		
4	38	38	-3.06	7	73	69	0.04	15	48	46	0.06	21	28	33	0.09	1	30	29	-3.05
6	34	32	3.11	8	53	52	-3.10	20	25	26	-3.09					3	48	48	-3.05
8	31	29	3.14	10	44	41	0.06	22	23	29	-3.05		H 2 3						
10	95	98	-3.09	11	31	30	0.03					2	17	11	2.86		H 3 0		
12	100	98	-3.07	13	31	31	0.04		H 1 7			4	250	253	-3.11	1	55	59	0.03
16	23	24	0.13	15	33	31	0.05	3	27	26	-3.08	6	264	261	-3.11	2	87	90	-3.12
20	25	23	0.04	16	65	62	0.05	6	39	37	-3.10	8	83	81	-3.12	3	26	22	-3.12
22	27	32	0.08	17	20	18	-3.08	7	47	43	0.05	10	42	45	0.07	5	11	10	-0.18
				18	26	25	0.08	8	33	29	-3.09	12	53	51	0.01	6	73	74	0.04
	H 0 7			19	54	53	-3.06	10	28	27	0.08	14	24	24	-0.04	7	77	78	0.04
1	110	111	0.01	21	23	27	-3.12	11	22	22	0.03	16	87	90	0.06	9	47	46	0.05
3	125	124	0.05	22	23	24	-3.05	13	21	18	0.07	18	35	34	0.09	10	30	31	0.00
5	32	31	0.12					15	20	15	0.09					11	68	65	-3.10
7	148	147	-3.09		H 1 2			16	42	43	0.07		H 2 4			12	89	86	0.05
9	90	90	-3.09	1	34	36	0.02	18	17	17	0.11	1	121	125	-3.11	13	49	49	-3.10
11	21	18	3.08	2	59	59	0.02	19	42	42	-3.05	3	183	184	-3.10	15	42	43	-3.11
13	40	40	-3.07	3	76	76	-3.11					5	122	119	-3.13	16	43	42	-3.09
15	44	41	-3.07	4	29	30	-3.12		H 1 8			7	67	66	-3.12	18	31	31	-3.10
19	41	41	0.09	9	42	42	-3.11	2	15	14	0.07	9	135	136	-3.09	19	20	19	-3.04
21	26	23	0.06	10	60	58	0.05	3	29	27	-3.07	11	32	33	0.03	22	18	22	-3.05
				12	44	42	0.07	9	21	20	-3.08	13	98	97	0.06	23	33	33	0.10
	H 0 8			13	49	46	0.05	10	36	34	0.07	15	53	57	0.04	24	20	22	-3.03
0	192	188	0.06	15	52	53	0.06	12	32	30	0.08	21	22	26	0.10				

Table 2. Continued.

	H 3 1		
0	113	116	-3.11
1	88	88	0.03
2	40	37	0.03
3	13	13	0.03
4	86	87	0.04
5	85	83	-3.11
6	16	18	0.03
7	30	29	0.04
9	66	66	0.05
11	56	56	0.03
14	37	38	-3.09
15	20	17	0.07
16	69	68	-3.07
19	49	47	-3.05
21	26	28	-3.07
	H 3 2		
1	43	45	0.03
2	63	64	-3.11
3	26	22	-3.12
5	28	26	-3.07
6	68	66	0.05
7	79	76	0.04
8	22	21	-3.09
9	44	41	0.05
10	21	23	0.00
11	42	38	-3.07
12	79	75	0.06
13	40	36	-3.08
15	30	32	-3.11
16	33	30	-3.07
18	19	21	-3.08
19	27	28	-3.07
22	22	25	-3.07
23	28	28	0.11
24	24	26	-3.05
	H 3 3		
0	70	72	-3.09
1	51	51	0.05
2	20	19	0.05
3	18	18	0.02
4	96	93	0.03
5	75	70	-3.10
6	20	21	0.03
7	39	39	0.03
9	71	69	0.04
10	17	16	-3.09
11	55	54	0.03
14	40	40	-3.10
16	70	67	-3.08
19	50	50	-3.06
21	24	25	-3.06
	H 3 4		
1	34	35	0.04
2	52	53	-3.10
6	58	57	0.05
7	67	65	0.05
9	37	35	0.06
10	26	25	0.00
11	48	45	-3.08
12	75	70	0.06
13	41	40	-3.09
15	32	33	-3.11
16	34	32	-3.08
18	26	24	-3.09
19	22	21	-3.05
22	18	21	-3.05
23	25	28	0.11
	H 3 5		
0	66	66	-3.09
1	50	50	0.05
2	22	22	0.04
4	51	49	0.06
5	51	49	-3.09
6	17	14	0.04
7	15	16	0.07
9	47	46	0.06
11	40	39	0.04
12	15	14	0.12
14	29	27	-3.08
15	18	19	0.06
16	57	56	-3.07
19	38	39	-3.04
21	18	25	-3.07
	H 3 6		
1	25	27	0.05
2	38	38	-3.09
6	40	41	0.07
7	50	49	0.06
9	34	31	0.06
10	20	18	0.00
11	41	39	-3.08
12	62	60	0.07
13	34	34	-3.08
15	28	28	-3.11
16	29	27	-3.07
18	19	21	-3.09
19	18	18	-3.04
22	17	18	-3.05
	H 3 7		
0	41	42	-3.07
1	29	28	0.08
2	13	14	0.06
4	51	48	0.06
5	39	36	-3.08
6	20	18	0.03
7	25	22	0.04
9	47	46	0.06
11	36	36	0.04
14	32	31	-3.09
16	48	50	-3.06
19	33	38	-3.05
	H 3 8		
1	17	18	0.08
2	26	26	-3.07
5	14	13	-3.02
6	32	31	0.08
7	41	39	0.07
9	26	24	0.07
10	16	12	0.01
11	20	22	-3.04
12	48	46	0.08
13	25	23	-3.06
15	19	17	-3.09
16	21	18	-3.04
19	21	20	-3.06
	H 3 9		
0	32	30	-3.05
1	22	21	0.10
4	36	33	0.07
5	29	26	-3.06
7	18	13	0.06
9	35	32	0.08
11	25	24	0.05
16	42	41	-3.05
19	28	30	-3.04
	H 3 10		
2	21	22	-3.06
6	26	26	0.09
7	32	32	0.08
9	19	18	0.09
10	20	13	0.01
11	28	27	-3.07
12	39	38	0.08
13	28	26	-3.07
16	17	20	-3.06
	H 3 11		
0	25	25	-3.05
1	16	17	0.10
4	26	24	0.09
5	21	20	-3.05
9	28	24	0.09
16	28	31	-3.04
	H 3 12		
6	17	18	0.11
7	19	22	0.10
11	16	14	-3.02
12	28	28	0.10
	H 3 13		
4	23	21	0.09
9	23	22	0.09
	H 4 0		
2	134	137	-3.12
4	128	120	3.13
6	62	53	-0.01
7	13	16	-3.07
8	111	112	0.02
10	165	166	0.03
11	20	24	0.07
12	136	133	0.05
16	52	52	-3.10
20	19	19	-3.05
22	20	25	-3.05
	H 4 1		
1	106	110	-3.11
3	159	152	-3.11
4	13	16	-3.10
5	136	137	-3.12
7	127	121	0.05
9	139	142	0.03
11	84	83	0.00
12	18	21	-3.07
13	54	55	0.06
15	29	26	0.07
17	22	21	-3.11
19	33	33	-3.05
21	24	23	-3.06
	H 4 2		
0	202	219	-3.09
2	52	56	-3.09
4	86	75	3.12
6	25	21	-3.12
7	17	17	-3.08
8	47	46	0.04
10	121	122	0.04
11	20	24	0.07
12	125	121	0.05
14	24	22	-0.00
16	36	37	-3.08
20	18	19	-3.05
22	28	25	-3.05
	H 4 3		
1	169	174	-3.12
3	153	153	-3.11
5	104	103	-3.11
7	163	159	0.04
9	147	148	0.03
11	93	91	0.00
12	19	19	-3.07
13	45	45	0.07
15	21	17	0.11
17	30	29	-3.12
19	35	35	-3.05
21	22	21	-3.06
	H 4 4		
0	249	260	-3.10
2	93	94	-3.11
4	57	54	3.12
6	17	16	-0.02
7	14	15	-3.07
8	71	70	0.02
10	128	126	0.03
12	109	109	0.05
16	43	41	-3.09
22	21	23	-3.04
	H 4 5		
1	60	60	-3.09
3	101	99	-3.09
5	84	85	-3.11
7	79	78	0.08
9	90	94	0.05
11	51	53	0.01
13	52	51	0.06
15	27	28	0.07
19	31	27	-3.04
21	22	20	-3.06
	H 4 6		
0	203	209	-3.10
2	77	76	-3.11
4	42	36	3.11
6	17	14	-0.02
8	58	57	0.03
10	104	105	0.04
12	97	94	0.06
15	17	17	-3.04
16	28	33	-3.08
19	17	17	0.11
22	21	21	-3.04
	H 4 7		
1	99	101	-3.11
3	100	97	-3.10
5	46	48	-3.08
7	101	103	0.05
9	101	101	0.04
11	52	54	0.01
13	32	36	0.08
14	17	12	0.10
17	19	21	-3.12
19	30	27	-3.04
	H 4 8		
0	122	126	-3.07
2	49	48	-3.09
8	25	26	0.05
10	67	70	0.05
12	75	72	0.07
	H 4 9		
1	59	56	-3.10
3	68	66	-3.08
5	44	42	-3.08
7	65	66	0.08
9	62	63	0.06
11	34	34	0.01
13	32	33	0.08
19	26	22	-3.03
	H 4 10		
0	138	132	-3.08
2	59	58	-3.10
6	20	15	-0.02
8	40	41	0.03
10	71	69	0.05
12	56	58	0.08
16	24	25	-3.07
	H 4 11		
1	45	39	-3.09
3	46	50	-3.07
5	27	28	-3.06
7	46	49	0.09
9	45	47	0.07
11	22	19	0.01
13	25	25	0.09
	H 4 12		
0	71	73	-3.05
2	25	25	-3.06
10	37	38	0.08
12	44	43	0.09
	H 4 13		
1	38	40	-3.10
3	44	43	-3.07
7	41	48	0.08
9	42	43	0.07
	H 4 14		
0	62	63	-3.05
2	25	26	-3.07
	H 5 0		
1	43	49	-3.08
2	53	59	-3.08
3	80	86	0.05
4	21	26	0.06
5	67	68	0.02
6	23	23	0.09
7	17	12	-3.00
8	43	44	-3.11
10	102	109	-3.10
11	16	14	0.16
12	40	39	-3.11
13	24	23	-3.10
14	33	32	0.08
15	76	77	-3.08
17	23	24	-3.13
20	36	39	0.08
22	16	22	0.10
23	20	21	0.04
	H 5 1		
0	8	13	0.22
2	41	40	0.01
3	85	85	0.04
4	48	49	-3.08
5	38	40	-3.07
6	44	47	0.05
7	71	67	-3.09
8	75	71	0.06
9	14	8	0.27
10	29	27	-3.04
11	37	36	-3.11
12	43	40	-3.08
13	50	48	-3.07
16	35	37	-3.10
17	41	38	0.06
18	37	39	-3.07
19	31	36	0.08
20	18	19	-3.09
22	29	34	0.08
	H 5 2		
1	46	50	-3.09
2	66	70	-3.09
3	79	79	0.05
4	36	36	0.04
5	39	39	0.04
6	25	25	0.08
7	12	11	-2.99
8	15	13	-3.03
10	91	89	-3.09
11	34	32	0.07
12	33	30	-3.10
14	21	18	0.14
15	67	66	-3.07
17	24	25	-3.13
20	34	36	0.08
22	23	27	0.08
23	17	17	0.06
	H 5 3		
0	29	31	0.09
1	21	25	0.07
2	19	22	0.01
3	60	62	0.05
4	30	29	-3.04
5	35	35	-3.07
6	48	46	0.04
7	77	73	-3.10
8	72	67	0.07
10	33	31	-3.06
11	39	37	-3.11
12	49	47	-3.09
13	47	45	-3.07
16	35	37	-3.10
17	41	41	0.06
18	33	32	-3.06
19	38	39	0.08
22	35	36	0.07
	H 5 4		
1	43	44	-3.08
2	56	55	-3.07
3	70	71	0.06
4	28	28	0.05
5	41	42	0.04
6	18	19	0.10
8	25	27	-3.09
10	85	82	-3.09
11	20	20	0.10
12	31	29	-3.13
13	20	19	-3.09
14	28	23	0.11
15	67	65	-3.07
17	20	21	-3.13
20	31	34	0.09
22	19	22	0.10
	H 5 5		
0	23	22	0.12
1	12	11	0.15
2	20	19	0.02
3	55	55	0.05
4	42	40	-3.07
5	35	33	-3.07
6	37	36	0.05
7	43	42	-3.07
8	56	55	0.08
9	16	12	0.17
10	21	21	-3.02
11	25	26	-3.10
12	35	28	-3.05
13	45	42	-3.07
16	28	29	-3.10
17	28	29	0.08
18	36	35	-3.07
19	23	29	0.10
20	17	17	-3.09
22	22	26	0.09
	H 5 6		
1	34	33	-3.06
2	45	43	-3.05
3	58	55	0.07
4	18	19	0.07
5	35	34	0.04
6	20	19	0.10
8	27	27	-3.09
10	67	66	-3.08
11	19	16	0.13
12	28	25	-3.13
13	15	17	-3.08
14	24	21	0.11
15	59	57	-3.06
17	19	17	-3.12
20	27	31	0.09
	H 5 7		
0	26	23	0.11
1	17	19	0.09
3	40	39	0.07
4	28	23	-3.03
5	29	27	-3.06
6	36	35	0.05
7	48	45	-3.08
8	51	48	0.08
10	26	24	-3.04
11	26	26	-3.11
12	33	34	-3.08
13	34	33	-3.06
16	25	25	-3.09
17	32	32	0.07
18	27	26	-3.05
19	27	29	0.09
	H 5 8		
1	28	28	-3.06
2	40	37	-3.05
3	45	43	0.08
4	17	18	0.07
5	22	21	0.07
6	15	17	0.11
10	51	50	-3.07
11	24	21	0.09
12	18	17	-3.09
15	47	44	-3.05
20	25	25	0.10
	H 5 9		
0	23	22	0.10
1	16	16	0.10
3	30	28	0.09
4	28	21	-3.03
5	25	22	-3.04
6	26	25	0.07
7	32	31	-3.06
8	40	37	0.09
10	18	17	-3.02
11	18	17	-3.10

Table 2. Continued.

12	26	23	-3.06
13	32	30	-3.05
16	19	19	-3.09
17	23	22	0.09
18	24	23	-3.05
19	23	23	0.10
	H	5	10
1	23	22	-3.05
2	28	27	-3.03
3	38	36	0.09
5	24	22	0.06
8	22	21	-3.09
10	43	44	-3.07
11	16	10	0.16
13	15	15	-3.09
14	19	17	0.11
15	40	40	-3.05
	H	5	11
0	19	16	0.13
3	25	23	0.09
4	22	19	-3.03
6	23	20	0.08
7	24	23	-3.04
8	32	31	0.10
13	25	23	-3.04
	H	5	12
2	21	23	-3.03
3	30	26	0.10
5	18	13	0.09
10	30	28	-3.04
	H	5	13
0	20	15	0.12
4	20	13	-3.00
6	21	16	0.08
7	21	21	-3.05
8	23	24	0.11
	H	5	14
3	22	20	0.11
	H	6	0
1	167	165	0.01
3	311	306	0.02
5	209	205	0.02
6	20	19	-3.08
7	77	72	0.04
9	80	80	0.05
10	26	26	0.07
11	56	54	-3.11
13	55	55	-3.09
14	20	21	-3.05
15	55	55	-3.10
17	52	52	-3.09
19	21	18	-3.12
	H	6	1
2	106	96	0.01
4	223	225	0.03
5	19	21	0.05
6	157	153	0.03
8	32	28	0.11
9	19	21	-3.06
12	27	25	-3.06
13	22	25	0.09
14	19	20	-3.09
16	79	79	-3.09
18	39	37	-3.09
21	25	24	0.10
	H	6	2
1	120	124	0.01
2	9	8	0.05
3	166	164	0.03
5	131	126	0.03
6	14	15	-3.07
7	39	37	0.07
9	94	91	0.04
10	24	26	0.07
11	19	20	-3.07
12	17	18	-3.07
13	34	32	-3.05
14	18	21	-3.05
15	39	41	-3.08
17	58	55	-3.10
19	25	23	-3.12
	H	6	3
2	119	116	0.01
4	245	251	0.03
5	18	19	0.06
6	163	157	0.03
8	46	44	0.07
12	38	38	-3.09
14	31	33	-3.11
16	78	74	-3.09
17	23	25	-3.04
18	33	31	-3.08
21	21	23	0.11
	H	6	4
1	98	100	0.01
3	178	179	0.03
5	140	142	0.03
6	14	14	-3.07
7	56	56	0.05
9	70	69	0.06
10	21	23	0.07
11	33	33	-3.10
13	43	43	-3.07
15	45	44	-3.09
17	47	47	-3.09
19	24	17	-3.11
20	19	19	-3.04
	H	6	5
2	45	46	0.02
4	129	129	0.05
6	101	101	0.04
8	34	33	0.08
10	23	19	-0.01
13	20	21	0.10
16	68	64	-3.08
18	34	32	-3.09
21	19	21	0.11
	H	6	6
1	63	64	0.02
3	138	139	0.04
5	112	113	0.03
6	13	13	-3.06
7	55	54	0.04
9	59	58	0.06
10	19	19	0.08
11	26	28	-3.09
13	40	38	-3.07
14	19	16	-3.04
15	43	41	-3.09
17	40	38	-3.08
	H	6	7
2	65	66	0.01
4	142	143	0.04
6	105	105	0.04
8	37	37	0.07
12	31	32	-3.09
14	25	24	-3.10
16	51	53	-3.08
17	18	21	-3.03
18	23	23	-3.07
	H	6	8
1	36	40	0.03
3	76	78	0.06
5	70	71	0.05
7	36	35	0.06
9	48	50	0.07
10	17	16	0.09
13	25	23	-3.03
15	24	28	-3.07
17	35	32	-3.08
	H	6	9
2	34	34	0.02
4	87	89	0.06
6	47	48	0.06
8	33	33	0.07
16	44	42	-3.07
18	25	21	-3.07
	H	6	10
1	36	36	0.03
3	85	86	0.05
5	75	76	0.04
7	40	40	0.05
9	28	32	0.09
13	36	32	-3.07
15	35	28	-3.08
	H	6	11
2	24	23	0.03
4	60	62	0.07
6	50	51	0.07
8	22	23	0.09
	H	6	12
3	40	41	0.09
5	36	35	0.07
7	22	22	0.08
9	29	30	0.08
	H	6	13
2	26	24	0.03
4	57	57	0.06
6	43	45	0.07
8	22	20	0.09
	H	6	14
3	37	37	0.08
	H	7	0
1	64	75	-3.11
2	106	109	0.04
3	36	35	0.05
5	11	10	0.21
6	91	89	-3.09
7	83	81	-3.08
9	32	32	-3.10
11	81	76	0.05
12	73	70	-3.08
13	18	22	0.04
14	27	24	-3.05
15	27	27	0.01
16	23	24	0.07
17	30	28	0.05
18	41	42	0.07
19	32	31	0.08
23	33	38	-3.06
	H	7	1
0	91	100	0.05
1	71	76	-3.09
2	36	36	-3.10
3	31	33	-3.09
4	103	103	-3.10
5	89	86	0.04
6	16	12	0.04
7	16	16	3.12
8	21	20	0.07
9	68	65	-3.08
11	59	59	-3.09
12	25	24	-3.07
13	19	16	0.12
14	52	52	0.07
16	66	64	0.06
19	36	34	0.08
21	35	40	0.07
24	17	18	-3.07
	H	7	2
1	58	62	-3.10
2	89	91	0.04
3	38	35	0.05
5	33	32	0.06
6	86	82	-3.09
7	83	80	-3.08
9	29	28	-3.09
11	55	53	0.07
12	64	62	-3.08
13	16	12	0.08
14	31	32	-3.08
15	17	18	0.02
17	35	31	0.04
18	33	33	0.08
19	36	37	0.06
23	29	33	-3.05
	H	7	3
0	70	72	0.06
1	53	55	-3.08
2	26	24	-3.08
3	30	32	-3.09
4	104	103	-3.10
5	80	76	0.05
7	22	22	3.13
8	16	16	0.09
9	70	68	-3.08
11	59	58	-3.09
13	17	16	0.12
14	53	53	0.06
16	65	63	0.06
19	35	36	0.07
21	39	36	0.08
	H	7	4
1	49	49	-3.10
2	75	76	0.05
3	25	24	0.07
5	17	16	0.11
6	71	71	-3.08
7	73	70	-3.08
9	26	24	-3.09
11	61	56	0.07
12	60	58	-3.08
13	19	18	0.05
14	27	25	-3.06
15	19	20	0.01
16	19	19	0.09
17	24	25	0.05
18	36	35	0.07
19	28	30	0.07
23	28	32	-3.05
	H	7	5
0	71	68	0.06
1	52	51	-3.07
2	26	25	-3.09
3	22	21	-3.07
4	66	64	-3.08
5	59	58	0.06
8	16	15	0.09
9	51	50	-3.07
10	14	11	-3.09
11	45	46	-3.08
12	24	22	-3.07
14	39	40	0.08
16	50	52	0.07
19	25	27	3.09
21	30	35	0.08
	H	7	6
1	38	38	-3.08
2	59	58	0.06
3	21	18	0.08
5	14	13	0.18
6	57	56	-3.07
7	58	56	-3.07
9	23	22	-3.08
11	51	50	0.07
12	52	51	-3.07
14	21	21	-3.05
16	18	17	0.09
17	20	22	0.06
18	33	31	0.08
19	24	25	0.08
	H	7	7
0	50	47	0.09
1	35	35	-3.05
2	20	18	-3.07
3	16	16	-3.05
4	63	59	-3.08
5	49	45	0.07
9	50	49	-3.07
11	41	42	-3.08
14	43	41	0.07
16	43	45	0.08
19	26	27	0.09
21	26	28	0.09
	H	7	8
1	26	26	-3.06
2	43	43	0.08
3	13	15	0.10
5	18	14	0.11
6	45	43	-3.05
7	48	46	-3.06
9	16	16	-3.07
11	33	32	0.10
12	40	40	-3.06
14	23	22	-3.06
17	17	19	0.06
18	19	23	0.10
19	23	24	0.08
	H	7	9
0	37	36	0.10
1	28	27	-3.04
2	15	12	-3.05
3	16	14	-3.05
4	45	42	-3.06
5	36	34	0.08
9	39	37	-3.06
11	30	31	-3.07
14	29	30	0.09
16	37	36	0.08
	H	7	10
1	23	21	-3.05
2	36	35	0.09
6	36	36	-3.05
7	40	38	-3.05
9	15	12	-3.05
11	35	35	0.08
12	30	33	-3.06
13	17	15	0.06
14	16	14	-3.02
	H	7	11
0	34	31	0.10
1	25	22	-3.03
4	32	31	-3.05
5	28	27	0.09
9	29	29	-3.04
11	25	24	-3.06
14	25	23	0.10
	H	7	12
2	28	26	0.10
6	26	27	-3.03
7	30	28	-3.03
11	23	21	0.12
12	24	24	-3.04
	H	7	13
0	24	23	0.12
1	17	17	-3.01
4	25	27	-3.05
5	20	20	0.11
9	25	25	-3.04
	H	7	14
2	22	21	0.11
	H	8	0
2	132	131	0.03
4	103	102	0.03
6	77	74	-3.13
8	142	141	-3.10
10	99	101	-3.12
12	71	70	-3.10
14	33	33	-3.08
18	21	21	0.03
20	36	36	0.08
	H	8	1
1	190	189	0.03
3	74	66	3.02
4	17	17	0.04
5	22	19	0.05
7	80	74	-3.11
8	20	22	-3.07
9	81	79	-3.10
11	94	93	-3.10
12	21	24	0.08
13	66	64	-3.08
21	28	31	0.07
	H	8	2
0	172	177	0.03
2	83	82	0.04
3	13	13	-3.10
4	83	80	0.04
6	25	24	-3.10
7	21	23	0.06
8	96	93	-3.08
10	72	71	-3.11
11	24	29	-3.08
12	69	63	-3.09
14	49	45	-3.10
19	23	25	-3.04
20	36	36	0.08
	H	8	3
1	235	213	0.03
3	75	71	0.02
4	13	11	0.06
5	17	12	0.07
7	104	99	-3.12
8	21	22	-3.07
9	91	90	-3.10
11	100	100	-3.10
13	57	54	-3.08
21	27	29	0.08
	H	8	4
0	183	189	0.03
2	97	99	3.03
4	73	73	0.04
6	44	43	-3.12
7	15	18	0.07
8	107	105	-3.09
10	81	78	-3.11
11	25	26	-3.07
12	62	58	-3.09
14	38	35	-3.09
19	20	23	-3.04
20	30	33	0.08
	H	8	5
1	115	119	0.05
3	43	42	0.03
5	23	19	0.04
7	43	41	-3.09
8	15	18	-3.05
9	57	56	-3.08
11	68	70	-3.09
12	22	20	0.08
13	55	56	-3.08
21	23	25	0.08
	H	8	6
0	146	150	0.03
2	79	80	0.04
4	65	61	0.05
6	35	35	-3.12
8	90	88	-3.09
10	67	66	-3.11
12	54	52	-3.09
14	30	29	-3.08
15	21	19	0.11
20	23	28	0.09
	H	8	7
1	129	132	0.04
3	49	48	0.02
7	62	61	-3.11
9	67	68	-3.10
11	66	70	-3.09
13	40	41	-3.07
21	20	22	0.09
	H	8	8
0	84	85	0.05
2	53	53	0.05
4	41	43	0.06
8	55	56	-3.05
10	49	42	-3.09

Table 2. Continued.

12	40	39	-3.08
14	29	29	-3.09
19	22	19	-3.03
20	23	23	0.09
	H 8 9		
1	85	85	0.06
3	31	29	0.03
7	36	34	-3.09
9	41	42	-3.08
11	50	51	-3.08
13	34	36	-3.06
	H 8 10		
0	95	91	0.04
2	59	58	0.04
4	34	36	0.06
6	26	26	-3.11
8	62	63	-3.08
10	46	45	-3.10
12	32	32	-3.07
	H 8 11		
1	61	61	0.07
3	21	21	0.04
7	26	22	-3.07
9	28	32	-3.07
11	34	36	-3.06
13	27	27	-3.05
	H 8 12		
0	46	44	0.08
2	32	28	0.08
4	26	25	0.08
8	30	32	-3.03
10	24	22	-3.06
12	26	23	-3.06
	H 8 13		
1	54	55	0.07
7	24	24	-3.09
9	28	30	-3.07
	H 8 14		
0	32	38	0.07
2	29	26	0.08
	H 10 0		
1	41	42	0.05
3	78	75	-3.10
5	239	236	-3.11
7	140	138	-3.11
9	36	36	-3.13
10	21	21	-3.07
11	53	56	0.04
13	44	40	-0.01
15	65	62	0.04
17	55	52	0.09
	H 10 1		
2	111	109	-3.09
4	95	94	-3.09
6	77	75	-3.13
8	131	126	-3.11
9	16	16	0.08
10	62	60	-3.09
12	92	86	0.04
14	65	63	0.05
16	36	38	0.05
	H 10 2		
1	46	47	0.04
3	16	14	-2.94
5	188	184	-3.10
7	112	110	-3.10
9	44	44	-3.14
11	33	32	0.07
13	23	23	-0.01
15	51	50	0.04
17	55	55	0.09
	H 10 3		
2	117	119	-3.10
4	125	125	-3.10
6	83	83	-3.13
8	125	121	-3.11
10	44	41	-3.07
12	91	88	0.04
14	73	69	0.05
16	38	36	0.05
17	20	19	0.11
	H 10 4		
1	25	25	0.08
3	51	50	-3.09
5	175	178	-3.10
7	105	107	-3.10
9	30	32	-3.13
11	39	40	0.05
13	29	29	-0.01
15	46	49	0.04
17	46	49	0.09
	H 10 5		
2	69	74	-3.07
4	69	68	-3.07
5	14	13	-3.08
6	49	51	-3.13
8	90	92	-3.10
10	55	54	-3.09
12	62	61	0.06
14	45	47	0.07
16	31	32	0.06
	H 10 6		
1	15	18	0.10
3	49	51	-3.09
5	139	143	-3.09
7	88	91	-3.10
9	23	26	-3.13
11	33	35	0.06
13	20	23	-0.01
15	45	43	0.05
17	41	44	0.10
	H 10 7		
2	81	82	-3.08
4	91	91	-3.09
6	56	58	-3.13
8	73	76	-3.09
10	31	30	-3.05
12	60	62	0.05
14	49	50	0.06
16	24	27	0.06
	H 10 8		
3	24	25	-3.05
5	97	99	-3.08
7	63	63	-3.09
9	23	22	-3.14
11	19	19	0.09
15	29	29	0.06
17	39	39	0.10
	H 10 9		
2	51	54	-3.06
4	58	60	-3.07
6	35	34	-3.13
8	56	58	-3.08
10	27	30	-3.06
12	37	40	0.07
14	38	36	0.08
16	21	21	0.07
	H 10 10		
3	42	42	-3.10
5	86	93	-3.08
7	56	57	-3.09
11	32	26	0.06
15	29	26	0.06
	H 10 11		
2	42	42	-3.05
4	42	43	-3.06
6	21	23	-3.12
8	39	40	-3.07
10	26	24	-3.05
12	29	30	0.09
14	25	26	0.09
	H 10 12		
5	52	54	-3.05
7	33	36	-3.06
	H 10 13		
2	42	39	-3.06
4	44	42	-3.07
6	23	21	-3.12
8	27	30	-3.06
	H 12 0		
2	113	113	-3.11
4	112	110	-3.09
6	73	71	0.03
8	151	146	0.05
10	58	56	0.02
12	35	33	0.03
14	51	47	0.07
16	29	30	-3.07
20	42	41	-3.06
	H 12 1		
1	185	192	-3.10
3	16	10	2.98
5	22	21	0.04
7	28	26	-0.02
9	56	52	0.05
11	104	100	0.06
13	59	58	0.06
21	35	33	-3.07
	H 12 2		
0	96	98	-3.12
2	85	86	-3.10
4	100	98	-3.08
6	40	42	0.04
8	122	116	0.07
10	40	37	0.03
12	29	29	0.03
14	57	56	0.06
20	41	40	-3.06
	H 12 3		
1	187	198	-3.10
3	19	17	3.05
5	24	21	0.04
7	44	43	-0.01
9	62	60	0.04
11	110	104	0.06
13	54	51	0.07
	H 12 4		
0	106	108	-3.13
2	87	91	-3.10
4	89	90	-3.08
6	49	50	0.04
8	117	118	0.06
10	46	44	0.02
12	30	27	0.03
14	48	46	0.07
18	28	24	-3.06
20	34	36	-3.06
	H 12 5		
1	131	136	-3.09
9	38	38	0.06
11	81	81	0.07
13	53	51	0.07
	H 12 6		
0	85	88	-3.12
2	71	75	-3.10
4	78	79	-3.07
6	40	42	0.04
8	103	102	0.07
10	36	38	0.02
12	30	24	0.03
14	42	39	0.08
18	22	23	-3.06
20	31	32	-3.05
	H 12 7		
1	128	135	-3.09
7	32	25	-0.02
9	45	47	0.04
11	80	77	0.07
13	40	39	0.08
	H 12 8		
0	45	47	-3.11
2	54	53	-3.08
4	60	61	-3.06
8	74	73	0.09
14	40	37	0.08
	H 12 9		
1	94	94	-3.07
9	30	29	0.06
11	62	61	0.08
13	38	33	0.08
	H 12 10		
0	56	53	-3.12
2	53	52	-3.09
4	49	52	-3.05
6	27	29	0.05
8	71	72	0.08
14	24	24	0.10
	H 12 11		
1	71	70	-3.06
11	46	46	0.10
	H 12 12		
0	23	20	-3.10
2	27	28	-3.06
4	42	40	-3.04
8	43	44	0.11
	H 12 13		
1	61	59	-3.06
	H 14 0		
3	97	99	0.02
5	173	172	0.05
7	87	86	0.05
11	41	40	-3.08
15	39	39	-3.09
17	70	68	-3.06
	H 14 1		
2	129	128	0.05
4	117	117	0.04
6	33	33	-0.03
8	58	60	0.08
10	55	53	0.08
12	51	47	-3.05
14	54	49	-3.06
16	30	31	-3.11
	H 14 2		
3	60	63	0.02
5	149	145	0.06
7	75	71	0.06
11	24	25	-3.05
15	29	31	-3.07
17	72	69	-3.06
	H 14 3		
2	127	130	0.05
4	121	126	0.03
6	38	38	-0.02
8	65	62	0.07
10	43	41	0.10
12	55	51	-3.06
14	56	53	-3.07
16	31	29	-3.11
	H 14 4		
3	70	70	0.02
5	142	143	0.06
7	74	72	0.06
11	25	30	-3.07
15	32	32	-3.08
17	67	62	-3.06
	H 14 5		
2	93	97	0.06
4	81	82	0.05
6	21	20	-0.04
8	53	52	0.08
10	50	49	0.08
12	42	38	-3.04
14	40	39	-3.05
16	26	25	-3.10
	H 14 6		
3	58	59	0.02
5	125	123	0.06
7	64	64	0.06
11	26	26	-3.06
15	27	30	-3.08
17	58	54	-3.05
	H 14 7		
2	94	94	0.06
4	85	86	0.04
6	27	26	-0.03
8	45	49	0.08
10	31	33	0.11
12	45	43	-3.06
14	44	41	-3.06
	H 14 8		
3	32	32	0.04
5	95	92	0.08
7	50	48	0.08
17	47	46	-3.05
	H 14 9		
2	68	68	0.08
4	54	57	0.06
8	42	41	0.09
10	34	32	0.10
12	31	31	-3.03
14	35	32	-3.04
	H 14 10		
3	39	37	0.03
5	86	85	0.07
7	46	45	0.08
	H 14 11		
2	53	53	0.09
4	46	40	0.07
8	28	31	0.10
10	29	27	0.11
12	28	25	-3.03
	H 14 12		
5	57	55	0.10
7	34	30	0.10
	H 14 13		
2	45	45	0.09
4	36	35	0.07
	H 16 0		
2	76	78	0.04
4	116	116	0.05
6	29	28	-3.08
8	121	120	-3.08
10	58	58	-3.13
12	44	41	-3.12
14	37	33	-3.05
18	30	27	0.07
	H 16 1		
1	119	122	0.06
9	67	66	-3.11
11	139	135	-3.09
13	41	43	-3.07
15	38	31	0.09
21	23	19	0.12
	H 16 2		
0	28	29	0.06
2	64	64	0.05
4	105	105	0.05
8	104	101	-3.07
10	48	46	-3.12
12	40	37	-3.12
14	38	38	-3.06
18	28	22	0.09
	H 16 3		
1	123	127	0.06
9	59	57	-3.11
11	105	104	-3.09
13	43	39	-3.06
15	33	32	0.08
	H 16 4		
0	39	42	0.04
2	63	66	0.05
4	92	94	0.06
6	22	20	-3.06
8	99	100	-3.07
10	46	47	-3.12
12	34	33	-3.12
14	30	32	-3.05
18	22	23	0.08
	H 16 5		
1	89	95	0.07
9	47	48	-3.10
11	80	84	-3.08
13	37	39	-3.06
	H 16 6		
0	40	40	0.03
2	55	55	0.05
4	77	79	0.06
8	85	86	-3.07
10	39	39	-3.12
12	28	28	-3.11
14	26	28	-3.04
	H 16 7		
1	87	95	0.07
9	48	47	-3.10
11	73	74	-3.07
13	30	31	-3.05
15	28	25	0.10
	H 16 8		
0	22	22	0.05
2	41	41	0.07
4	61	61	0.07
8	66	65	-3.05
10	27	26	-3.11
	H 16 9		
1	69	70	0.08
9	26	31	-3.09
11	57	58	-3.05
13	27	27	-3.05
	H 16 10		
0	38	30	0.03
2	38	40	0.06
4	46	49	0.08
8	58	60	-3.06
10	24	25	-3.11
	H 16 11		
1	54	54	0.10
11	41	43	-3.05
	H 16 12		
2	25	23	0.10
4	35	37	0.10
8	37	39	-3.03
	H 18 0		
3	67	67	-3.11
5	119	119	-3.09
7	69	69	-3.39
11	29	25	0.07
15	28	34	0.06
17	44	43	0.09
	H 18 1		
2	75	76	-3.08
4	81	80	-3.09
6	40	41	-3.13
8	59	59	-3.08
10	32	30	-3.06
12	40	41	0.08
14	35	35	0.07

Table 2. Continued.

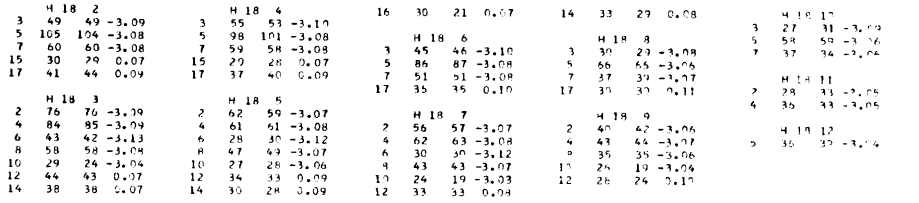

eters including isotropic thermal vibrations, the occupation number of Cr_3 and an isotropic extinction coefficient. An R value of 0.063, based on the total data set (hkl and $\bar{h}kl$) was obtained when correction was made for anomalous dispersion and secondary extinction during the refinements. Since the crystal was very symmetric, the values of the average path lengths in the crystal, used to calculate the extinction correction, are approximately the same for reflexions hkl and $\bar{h}kl$. Hence, mean values of F_{hkl} and $F_{\bar{h}kl}$ could be calculated, giving a final data set consisting of 1679 independent reflexions. After one more cycle of refinement, the R value dropped to 0.052. Anisotropic temperature coefficients were calculated and a few cycles of refinement were performed in which these coefficients were varied together with the atomic coordinates, the occupation number of Cr_3 and the extinction coefficient, while the scale factors were held constant. The shifts of the parameters were then less than 10 % of the standard deviations and the R value had dropped to 0.038. A weighting scheme according to Cruickshank was used in the refine-

Table 3. Atomic coordinates, expressed as fractions of the cell edges. Standard deviations are given within parentheses.

Atom	Occupation number	x	y	z
Zr_1	1	0.05643(5)	0.12439(14)	0
Zr_2	1	0.04063(5)	0.62585(14)	0
Cr_1	1	0.37323(10)	0.16138(15)	0
Cr_2	1	0.36038(9)	0.59065(16)	0
Cr_3	0.475	0.1958(2)	0.8730(4)	0
O_1	1	0.0691(3)	0.1257(7)	0.2998(5)
O_2	1	−0.0528(3)	0.3736(8)	0.3015(5)
O_3	1	0.2442(5)	0.1119(8)	0
O_4	1	0.2307(4)	0.6376(10)	0
O_5	1	0.3573(8)	0.2767(9)	0
O_6	1	0.3449(8)	0.4769(10)	0
O_7	1	0.1044(6)	0.2772(7)	0
O_8	1	0.0886(6)	0.7794(8)	0
O_9	1	0.0956(7)	0.9689(8)	0
O_{10}	1	0.0990(7)	0.4759(8)	0
O_{11}	0.475	0.2755(8)	0.8710(15)	0.1843(15)
O_{12}	0.300	−0.3078(14)	0.1241(38)	0

ments, yielding a weighted R value of 0.046. The final R value based on the comparatively weak structure factors $F_{k=2n+1}$ (685) was 0.052 whereas that based on the stronger structure factors $F_{k=2n}$ (994) was 0.033. In the final cycles of refinement the occupation number of Cr_3 was 0.476 and O_{11} was assigned the same value. Moreover, the occupation number of O_{12} (water of crystallization) was assigned the value 0.30, corresponding to the results of the water analysis. The contributions from these oxygen atoms to the structure factors are small and, accordingly, a refinement of their occupation numbers would have been arbitrary.

In Table 2 the observed and calculated structure factors and the phase angles of the reflexions are listed. The resulting atomic coordinates, together with the standard deviations, and the anisotropic temperature coefficients are given in Tables 3 and 4, respectively.

Table 4. Anisotropic thermal parameters for $Zr_4(OH)_6(CrO_4)_5H_2O$. The temperature factor is $\exp[-(h^2\beta_{11}+k^2\beta_{22}+l^2\beta_{33}+hk\beta_{12}+hl\beta_{13}+kl\beta_{23})]$. Standard deviations are given within parentheses.

Atom	β_{11}	β_{22}	β_{33}	β_{12}	β_{13}	β_{23}
Zr_1	0.00173(3)	0.00083(5)	0.00313(7)	0.00000(6)	0	0
Zr_2	0.00104(2)	0.00070(4)	0.00317(7)	0.00009(5)	0	0
Cr_1	0.00122(5)	0.00114(10)	0.00273(15)	−0.00011(5)	0	0
Cr_2	0.00115(5)	0.00127(10)	0.00298(15)	0.00000(5)	0	0
Cr_3	0.00094(9)	0.00097(12)	0.00465(26)	−0.00009(15)	0	0
O_1	0.0025(2)	0.0037(4)	0.0028(4)	0.0008(3)	−0.0004(2)	0.0009(6)
O_2	0.0024(2)	0.0034(3)	0.0032(4)	−0.0004(3)	0.0006(2)	−0.0001(7)
O_3	0.0015(2)	0.0005(7)	0.0090(9)	−0.0003(3)	0	0
O_4	0.0010(2)	0.0014(8)	0.0114(11)	0.0006(3)	0	0
O_5	0.0043(5)	0.0003(7)	0.0216(24)	−0.0007(4)	0	0
O_6	0.0036(5)	0.0019(9)	0.0203(23)	−0.0002(5)	0	0
O_7	0.0011(3)	0.0006(7)	0.0124(19)	0.0002(3)	0	0
O_8	0.0008(3)	0.0002(6)	0.0139(20)	0.0005(3)	0	0
O_9	0.0020(4)	0.0013(8)	0.0099(17)	−0.0001(4)	0	0
O_{10}	0.0019(3)	0.0009(7)	0.0101(16)	0.0003(4)	0	0
O_{11}	0.0032(5)	0.0037(7)	0.0122(17)	0.0003(7)	−0.0039(8)	−0.0013(16)
O_{12}	0.0003(7)	0.0051(19)	0.0270(74)	−0.0005(16)	0	0

DESCRIPTION OF THE STRUCTURE AND DISCUSSION

The most important distances and angles in $Zr_4(OH)_6(CrO_4)_5H_2O$ are to be found in Table 5. The zirconium atoms Zr_1 and Zr_2 constitute together with the coordinated oxygen atoms O_7, O_8, O_9, and O_{10} infinite chains lying in the xy plane and running along the b axis.

The sequence of zirconium atoms in the chains is Zr_1, Zr_1, Zr_2, Zr_2 . . . , these atoms being joined by double oxygen or hydroxide bridges in the same way as in the structures of $Zr(OH)_2CrO_4$[1] and $Hf(OH)_2SO_4H_2O$.[7] In the same plane as the chains, and at coordination distances from Zr_1 and Zr_2, there are two further oxygen atoms, O_3 and O_4. These oxygen atoms are coordinated to Cr_1 and Cr_2, respectively, and, together with the oxygen atoms mentioned

Table 5. Distances (in Å) and angles in $Zr_4(OH)_6(CrO_4)_5H_2O$. Standard deviations are given within brackets.

Within the ZrO_7 pentagonal bipyramids				
axial oxygens:	Zr_1-2O_1	2.069(3)	Zr_2-2O_2	2.079(3)
equatorial oxygens:	Zr_1-O_3	2.191(5)	Zr_2-O_4	2.216(5)
	Zr_1-O_7	2.160(10)	Zr_2-O_7	2.144(8)
	Zr_1-O_8	2.138(8)	Zr_2-O_8	2.169(10)
	Zr_1-O_9	2.172(11)	Zr_2-O_{10}	2.157(10)
	Zr_1-O_9'	2.179(9)	Zr_2-O_{10}'	2.137(9)
	$O_1-Zr_1-O_1$	171.8(2)°	$O_2-Zr_2-O_2$	172.2(2)°
	$O_3-Zr_1-O_7$	79.5(4)°	$O_4-Zr_2-O_8$	70.9(4)°
	$O_7-Zr_1-O_8$	67.1(3)°	$O_8-Zr_2-O_7$	66.8(3)°
	$O_8-Zr_1-O_9'$	73.7(4)°	$O_7-Zr_2-O_{10}$	78.7(4)°
	$O_9'-Zr_1-O_9$	66.4(4)°	$O_{10}-Zr_2-O_{10}$	67.8(4)°
	$O_9-Zr_1-O_3$	73.4(4)°	$O_{10}'-Zr_2-O_4$	75.8(4)°
ax.–eq.:	O_1-O_3	2.905(5)	O_2-O_4	2.934(5)
	O_1-O_7	2.950(10)	O_2-O_7	3.062(8)
	O_1-O_8	3.049(8)	O_2-O_8	2.972(11)
	O_1-O_9	2.990(11)	O_2-O_{10}	2.970(11)
	O_1-O_9'	3.097(8)	O_2-O_{10}'	3.062(9)
eq.–eq.:	O_3-O_7	2.781(13)	O_4-O_8	2.545(14)
	O_7-O_8	2.374(10)	O_8-O_7	2.374(10)
	O_8-O_9'	2.588(15)	O_7-O_{10}'	2.714(14)
	$O_9'-O_9$	2.381(17)	$O_{10}'-O_{10}$	2.395(16)
	O_9-O_3	2.608(13)	$O_{10}-O_4$	2.687(15)
Within the CrO_4 tetrahedra sharing vertices with ZrO_7				
	Cr_1-2O_2	1.683(4)	Cr_2-2O_1	1.673(4)
	Cr_1-O_3	1.645(7)	Cr_2-O_4	1.638(7)
	Cr_1-O_5	1.585(12)	Cr_2-O_6	1.564(14)
	$O_2-Cr_1-O_2$	108.5(4)°	$O_1-Cr_2-O_1$	110.8(4)°
	$O_2-Cr_1-O_3$	110.5(3)°	$O_1-Cr_2-O_4$	109.8(3)°
	$O_3-Cr_1-O_5$	107.5(5)°	$O_4-Cr_2-O_6$	106.4(6)°
	$O_5-Cr_1-O_2$	109.9(4)°	$O_6-Cr_2-O_1$	109.9(4)°
Within the CrO_4 tetrahedra sharing an edge with ZrO_7				
	Cr_3-O_8	1.786(10)	$O_8-Cr_3-O_9$	94.0(4)°
	Cr_3-O_9	1.752(10)	$O_9-Cr_3-O_{11}$	113.9(7)°
	Cr_3-2O_{11}	1.571(10)	$O_{11}-Cr_3-O_8$	113.5(7)°
			$O_{11}-Cr_3-O_{11}$	107.7(7)°
Other distances				
	$O_{12}(H_2O)-O_8$	2.87(3)		
	$O_{12}(H_2O)-O_9'$	2.77(3)		
	Zr_1-Zr_1	3.641(3)		
	Zr_1-Zr_2	3.592(3)		
	Zr_2-Zr_2	3.564(4)		

earlier, they form planar five-membered rings around the zirconium atoms. In addition there are two further oxygen atoms, O_1, and O_2, which are coordinated to both zirconium and chromium (Cr_1, Cr_2), situated in axial positions

with respect to the five-membered oxygen rings. All the zirconium atoms are thus sevenfold coordinated. The coordination polyhedra are pentagonal bipyramids, which have the ideal symmetry D_{5h}. The chains, which are related to each other by an n glide plane perpendicular to the y axis, are connected in the x and z directions through the chromate groups (Cr_1, $2O_2$, O_3, O_5) and (Cr_2, $2O_1$, O_4, O_6). Two chains of condensed pentagonal bipyramids, connected in the z direction by chromate tetrahedra, are outlined in perspective in Fig. 1.

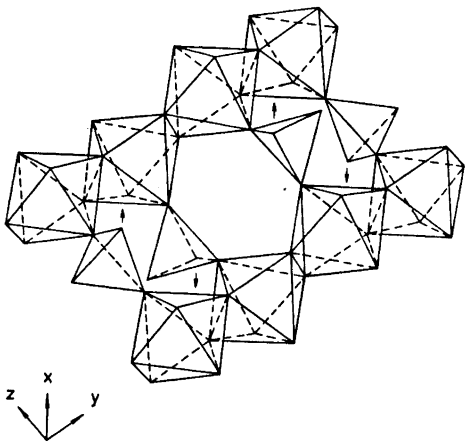

Fig. 1. Connection of the pentagonal bipyramids in two Zr–O chains by Cr–O tetrahedra. Only the oxygen atoms are depicted. The arrows indicate in which way the chains are connected to other chains in the x direction.

The two chains are connected to other chains through the O_3 and O_4 atoms in the chromate tetrahedra, in the directions indicated by the arrows. The chain-connecting chromate tetrahedra thus share three vertices with ZrO_7 bipyramids belonging to three different chains.

The chromate groups corresponding to the remaining chromium atoms, Cr_3, have two oxygen atoms, O_8 and O_9, in common with a bipyramid (Zr_1). They share an edge with the Zr_1 polyhedron, and do not take part in chain-connection, since the O_{11} atoms are coordinated only to Cr_3. The infinite chains can therefore be formulated approximately as $[Zr_4(OH)_6CrO_4]_n^{8n+}$, which is in accordance with the results obtained by Lundgren.[2] A formula unit of $Zr_4(OH)_6(CrO_4)_5H_2O$ is shown in Fig. 2, the interatomic distances being indicated. In order to complete the oxygen coordination around all the zirconium atoms, two additional O_9 atoms have been included in the figure. The condensed chromate tetrahedra (Cr_3) and the water molecules (O_{12}) are situated above or below Zr_1 in the x direction. They are situated in holes in the structure and are randomly distributed between these holes. As a consequence, Zr_1 is not structurally equivalent to Zr_2.

The pentagonal bipyramids in $Zr_4(OH)_6(CrO_4)_5H_2O$, as well as in $Zr(OH)_2CrO_4$, deviate from the ideal D_{5h} symmetry mainly because of two reasons: One is that the double oxygen bridges, which four of the oxygen atoms in the five-membered ring take part in, cause a compression of the ring.

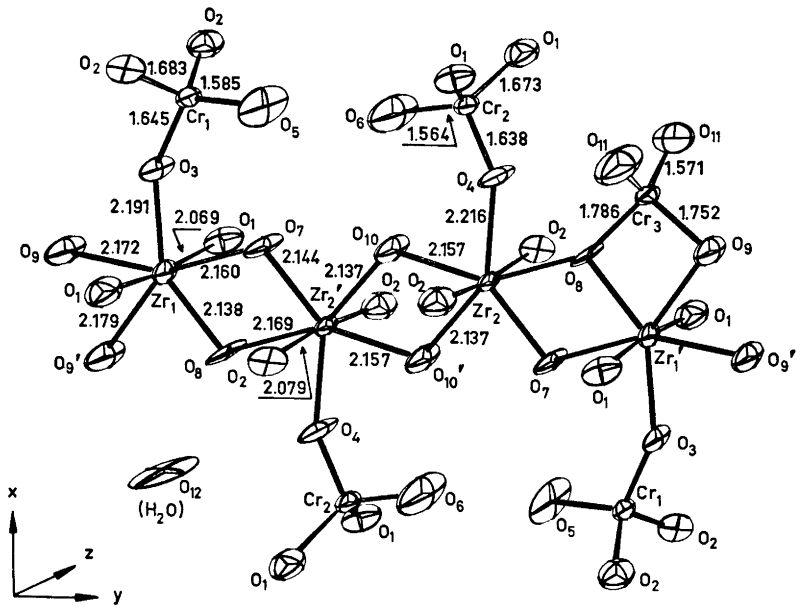

Fig. 2. One formula unit of $Zr_4(OH)_6(CrO_4)_5(H_2O)$. Distances are given in Å and the anisotropic thermal vibrations are outlined.

The other reason is that the axially situated oxygen atoms are involved in chain-connection, resulting in a distortion of the bipyramids due to packing restrictions.

The short distances between the bridging oxygen atoms (O_7, O_8, O_9, O_{10}), 2.37 – 2.40 Å, are in agreement with the corresponding distances in $Zr(OH)_2CrO_4$ (2.35 Å), $Hf(OH)_2SO_4H_2O$ (2.33 Å) and $Zr_2(OH)_2(SO_4)_3(H_2O)_4$ (2.34 Å).[8] The distances between zirconium and the non-bridging oxygen atoms in the five-membered rings (2.19 and 2.22 Å) are longer than the other equatorial oxygen – zirconium distances (*cf.* Table 5), although they are shorter than the corresponding distance (2.26 Å) in $Zr(OH)_2CrO_4$. This fact might be explained by the enhanced packing restrictions that are imposed by the more complicated structure of $Zr(OH)_2CrO_4$.

As can be seen from Table 5, the differently connected chromate tetrahedra are also distorted, the extent of distortion being less for those sharing three vertices with ZrO_7 polyhedra. The shortest Cr – O distances (1.56 and 1.59 Å) are between chromium and those oxygen atoms that are not connected to zirconium atoms. In the tetrahedra that share an edge with a polyhedron, two very long distances of 1.79 and 1.75 Å are found between chromium (Cr_3) and the shared oxygen atoms (O_8, O_9). Moreover, the $O_8 - Cr_3 - O_9$ angle is 94.0°. This large deviation from the tetrahedral angle, together with the long Cr – O distances, can be explained by the fact that the O_8 and O_9 oxygen atoms are each coordinated to two zirconium atoms as well as to one chromium atom.

The same is noted in $Zr(OH)_2CrO_4$, where the corresponding distance and angle are 1.76 Å and 99.2°, respectively.

The distances between O_{12} (water of crystallization) and two hydroxide oxygen atoms in the ZrO_7 pentagonal bipyramid are 2.77 and 2.87 Å, which imply hydrogen bonding (*cf.* Table 5).

The analyses of different products in the $ZrO_2 - CrO_3 - H_2O$ system show that the chromium and water content can vary slightly without changing the structure. This will be discussed in a forth-coming paper on the above-mentioned system.

The author would like to thank Professor Georg Lundgren for his support and great interest in this work. She is also indebted to Dr. Susan Jagner for revising the English text. Financial support, provided by the *Swedish Natural Science Research Council* (NFR, Contract No. 2318) and by *Chalmers University of Technology*, the latter to cover the costs of the computer work, is gratefully acknowledged.

REFERENCES

1. Mark, W. *Acta Chem. Scand.* **26** (1972) 3744.
2. Lundgren, G. *Arkiv Kemi* **13** (1958) 59.
3. Briggs, S. H. C. *J. Chem. Soc.* **1929** 242.
4. Kolthoff, I. M. and Sandell, E. B. *Textbook of Quantitative Inorganic Analysis*, 3rd Ed., McMillan, New York 1952, p. 717.
5. *International Tables for X-Ray Crystallography*, 2nd Ed., Kynoch Press, Birmingham 1965, Vol. I.
6. Lindgren, O. *Computer Programmes in Use at the Department of Inorganic Chemistry, Göteborg. To be published.*
7. Hansson, M. *Acta Chem. Scand.* **23** (1969) 3541.
8. McWhan, D. B. and Lundgren, G. *Inorg. Chem.* **5** (1966) 284.

Received June 20, 1972.

ACTA CHEMICA SCANDINAVICA 27 (1973) 191–196

Base Catalysis and Element Effect in Nucleophilic Aromatic Substitution with *p*-Anisidine

BO LAMM and JÖRGEN LAMMERT

Department of Organic Chemistry, University of Göteborg and Chalmers Institute of Technology, Fack, S-402 20 Göteborg 5, Sweden

The reaction between *p*-anisidine and 1-X-2,4-dinitrobenzenes, X being chlorine, bromine, methylsulphonyl, and phenylsulphonyl, has been studied kinetically in benzene at 25°C. The rates were determined spectrophotometrically. Base catalysis by DABCO (1,4-diaza[2.2.2]-bicyclooctane) was observed with all four leaving groups, in the case of chlorine confirming the result obtained by other workers. The specific rate for the DABCO-catalyzed reaction was found to vary within a factor of 9 between the most reactive compound (phenylsulphonyl derivative) and the least reactive one (chlorine derivative).

The absence of an "element effect" in nucleophilic aromatic substitution was demonstrated by Bunnett and his coworkers in 1957.[1] The specific rates of reaction with a common nucleophile, piperidine, were determined in methanol at different temperatures for a series of 1-X-2,4-dinitrobenzenes, in which X denotes 9 different substituents. Both the enthalpy and entropy of activation were found to be constant within a group of 6 compounds representing 6 different leaving groups X. The conclusion was therefore drawn that the reaction takes place *via* a rate-determining bond formation, followed by a fast bond breaking.

To be able to judge the full validity of the "absence of element effect" criterion one would like to know the magnitude of the element effect to be expected if the second reaction step, involving cleavage of the C–X bond, were actually rate-determining. In their original paper,[1] Bunnett and coworkers refer to an article by Cooper and Hughes,[2] in which solvolytic rates for the different *tert*-butyl halides (F, Cl, Br, I) have been determined in 80 % by volume aqueous ethanol. At 25°C, they are in the ratios 10^{-3} (appr.):1:41:99 in order from F to I.

Although the second step in nucleophilic aromatic substitution and the first step in the solvolysis of the *tert*-butyl halides involve the same kind of rehybridization of the central carbon atom, $sp^3 \rightarrow sp^2$, they are energetically very different. The first case represents a very exothermic reaction, which is

expected to have an "early" transition state,[3] whereas the rate-determining step in the solvolysis reaction is very endothermic and will have a "late", *i.e.*, product-like, transition state. In view of this difference, one can *a priori* suspect the differences between, *e.g.*, chlorine and bromine to be rather small in the aromatic reaction. In such a case, the usefulness of the "absence of element effect" criterion would be somewhat limited.

It was therefore thought to be of interest to investigate the element effect for some representative leaving groups in a case for which the second step is independently known to be the rate-determining one, namely, the reaction of 1-X-2,4-dinitrobenzenes with *p*-anisidine in benzene solution. For X = chlorine and fluorine, this system has been investigated by Bernasconi and Zollinger.[4] These workers found that both reactions were catalyzed by the non-nucleophilic bases DABCO (1,4-diaza[2.2.2]bicyclooctane) and pyridine. In the present work, the reaction between *p*-anisidine and some 1-X-2,4-dinitrobenzenes has been kinetically studied at 25°C using a direct spectrophotometric technique. DABCO was used as a catalyst, and chlorine, bromine, methylsulphonyl, phenylsulphonyl, and nitro were chosen as the leaving-group X. No quantitative data could be obtained for the nitro group, however.

EXPERIMENTAL

General. When not otherwise stated, melting points agree with those found in *Beilstein's Handbuch.*

Materials. 2,4-Dinitrochlorobenzene and 2,4-dinitrobromobenzene (from Fluka AG) were recrystallized twice from absolute ethanol. The purity was checked by NMR and GLC. M.p. 53.0 and 73.5°C, respectively.

1,2,4-Trinitrobenzene was prepared by Borsche's method [5] and recrystallized from methanol to constant melting point. The purity was checked by NMR and TLC. M.p. 60.0°C.

2,4-Dinitrophenylmethylsulphone and 2,4-dinitrodiphenylsulphone were prepared according to Bost *et al.*'s method,[6] recrystallized once from absolute ethanol and then from tetrahydrofuran. The purity was checked by NMR and TLC. M.p. 189.5 and 160.0°C, respectively.

p-Anisidine (Riedel-de Haën, chromatographic purity) was purified by recrystallization from 80 % aqueous ethanol in the presence of a slight amount of sodium dithionite to remove oxidation products and then from 80 % aqueous ethanol after treatment with activated charcoal. The purity was checked by TLC. M.p. 57.2°C. The purified *p*-anisidine was stored under argon.

DABCO (1,4-diaza[2.2.2]bicyclooctane) (Fluka, *purum* quality) was recrystallized from benzene. M.p. 157.0°C.

Benzene (Riedel-de Haën, chromatographic purity) was distilled in a Claisen column and stored over Molecular Sieves 4 A. B.p. 78.1°C (760 mmHg).

Identification of the reaction product. The reaction product from 2,4-dinitrobromobenzene and *p*-anisidine was identified by NMR spectroscopy to be *N*-(2,4-dinitrophenyl)-*p*-anisidine. The products from the reaction with the other substrates were isolated and found to be identical with the product above by use of the mixed melting point method.

Kinetic procedure. The kinetic measurements were performed at 25.00 ± 0.05°C and at a wavelength of 420 nm in 1 cm cells in a Beckmann DU spectrophotometer, equipped with a thermostated water bath in the beam path. The initial concentrations of the different reactants in each kinetic run were 1.00×10^{-3} M for the substrates, 0.200 M for *p*-anisidine, and 0 – 0.05 M for DABCO. The measurements were performed in the following manner. Solutions containing suitable concentrations of the different reactants were pre-thermostated and mixed in the cell, *p*-anisidine being added last. Zero time was recorded at this moment. Absorbance values were determined at regular intervals. For

each run 20 measurements were made. Three different runs were performed for each substrate at each DABCO concentration.

Due to the precipitation of anisidinium salts in some of the reactions, no infinity value was directly measurable, nor could the Guggenheim [7] treatment be applied since the precipitate appeared already after the first half-life. A "synthetic" infinity value was obtained by making a 1.00×10^{-3} M solution of independently prepared *N*-(2,4-dinitrophenyl)-*p*-anisidine in benzene, which also contained 0.198 mol/l of *p*-anisidine. An absorbance value of 2.780 was recorded at 420 nm. This value did not show any variation with addition of *p*-anisidine hydrochloride up to the point of precipitation.

No kinetic runs were allowed to proceed beyond the point of precipitation. The runs with 1,2,4-trinitrobenzene were so rapid under the given conditions that no rate constant could be evaluated. Visual observation showed, however, that the uncatalyzed reaction was completed (no further colour change) in about 3 min, and the catalyzed one in about 20 sec. This indicates, qualitatively, base catalysis.

Treatment of data. From the kinetic measurements, values of A_t, *i.e.*, the absorbance A at time t, were obtained. These values were subtracted from the "synthetic" infinity value A_∞. The function $\ln(A_\infty - A_t)$ was plotted against time, and the slope of the curve was calculated by the least-squares method. The pseudomonomolecular rate constants thus obtained were plotted against DABCO concentration, and the slopes were again calculated by the least-squares method.

All calculations were performed on an Olivetti Programma 101 electronic desk-top computer.

RESULTS AND DISCUSSION

The first-order rate constants, obtained under strictly first-order conditions, are given in Table 1. The standard deviation in each separate run, typically 3 %, is seen to be larger than the deviations between different runs, less than 1 %, indicating good reproducibility. The average values of the first-order rates are plotted *versus* DABCO concentration in Fig. 1.

The detailed description of the reaction between 2,4-dinitro-1-X-benzene and *p*-anisidine is illustrated in Fig. 2. The designations of the rate constants are identical with those used by Bernasconi and Zollinger.[4]

Table 1. First-order rate constants for the DABCO-catalyzed nucleophilic aromatic substitution of 2,4-dinitro-1-X-benzene by *p*-anisidine. Concentration of *p*-anisidine 0.200 M. Errors are standard deviations.

[DABCO] × 10^2	Leaving group X. $k_{obs} \times 10^6$ sec^{-1}			
	Cl	Br	CH_3SO_2	$C_6H_5SO_2$
0	0.85 ± 0.03	1.54 ± 0.06	0.38 ± 0.09	1.40 ± 0.03
	0.83 ± 0.04	1.53 ± 0.05	0.39 ± 0.05	1.41 ± 0.02
	0.82 ± 0.01	1.51 ± 0.05	0.38 ± 0.06	1.40 ± 0.02
2.5	2.20 ± 0.10	3.98 ± 0.09	7.69 ± 0.14	17.26 ± 0.49
	2.18 ± 0.10	3.98 ± 0.12	7.69 ± 0.12	17.24 ± 0.61
	2.21 ± 0.09	3.94 ± 0.08	7.69 ± 0.19	17.25 ± 0.61
5.0	4.16 ± 0.16	7.02 ± 0.17	14.69 ± 0.33	31.29 ± 0.56
	4.14 ± 0.11	6.99 ± 0.25	14.70 ± 0.33	31.30 ± 0.80
	4.14 ± 0.10	6.99 ± 0.19	14.67 ± 0.67	31.33 ± 0.57

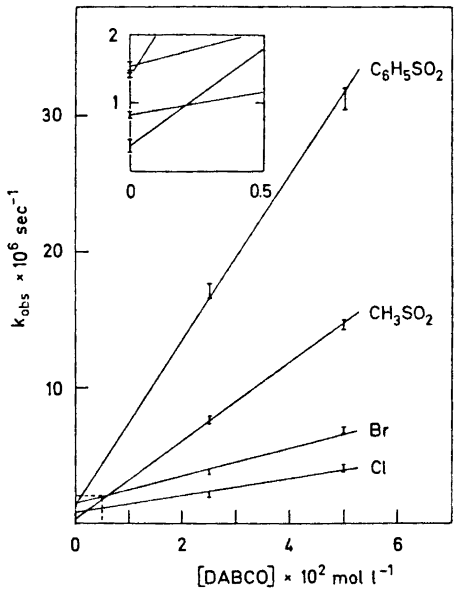

Fig. 1. Plot of the pseudomonomolecular rate constants *versus* DABCO concentration. The errors are calculated as "errors of the mean".[8]

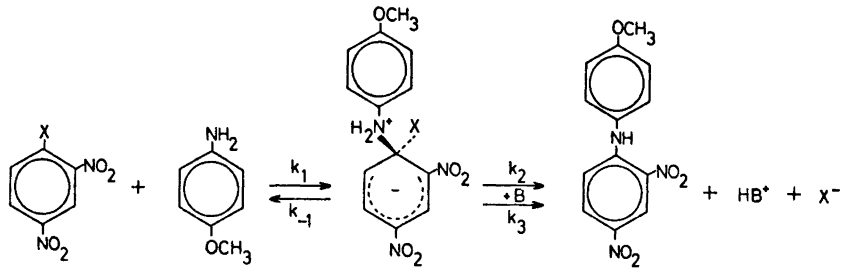

Fig. 2. Reaction scheme for nucleophilic substitution of 2,4-dinitro-1-X-benzene by *p*-anisidine.

The collapse of the intermediate may take place both *via* a base-catalyzed and a non-catalyzed path. Making the usual steady-state approximation, the following expression is obtained for the specific rate of the forward reaction:

$$k_{obs} = k_1 \frac{k_2 + k_3[B]}{k_{-1} + k_2 + k_3[B]} \quad (1)$$

Whether base catalysis is observed or not depends on the relative magnitude of k_{-1} *vs.* $k_2 + k_3[B]$, and, if $k_{-1} \gg k_2 + k_3[B]$, on that of $k_3[B]$ *vs.* k_2.

With good leaving groups like chlorine and bromine, most nucleophilic reagents cause the second reaction step to be much faster than the reversal of the first, and no base catalysis is observed. However, the weak nucleophile

p-anisidine causes the reversal of the first step to be faster than the second step even in the presence of base, and catalysis by the latter is observed. That the rate acceleration is genuine base catalysis and not merely a medium effect has been convincingly proved by Bernasconi and Zollinger.[4]

The approximation $k_{-1} \gg k_2 + k_3[B]$ allows eqn. (1) to be rewritten in the form

$$k_{obs} = \frac{k_1}{k_{-1}} k_2 + \frac{k_1}{k_{-1}} k_3[B] \quad (2)$$

or, for the sake of brevity,

$$k_{obs} = k_0 + k_B[B] \quad (3)$$

Since *p*-anisidine can act both as a nucleophile and as a base, eqn. (3) applies in the absence of DABCO also, and when two bases, A and B, are present simultaneously, we have

$$k_{obs} = k_0 + k_A[A] + k_B[B] \quad (4)$$

With 2,4-dinitro-1-chlorobenzene, Bernasconi and Zollinger [4] were able to verify eqn. (4) using *p*-anisidine and pyridine as bases A and B. A slight deviation, ascribed to mutual medium effects of the two bases, was found, however. Our values for the chlorine compound are roughly twice as large as those obtained by Bernasconi and Zollinger [4] for the same reaction, and we can offer no explanation for this difference.

It is apparent from Fig. 1 that the observed specific rates at different concentrations of DABCO fit eqn. (3). The intercept for each line in Fig. 1 at [B] = 0 represents the contribution to the rate which is unaffected by DABCO, and the slope represents k_B in eqn. (3). It is quite remarkable that some of the lines cross each other. This means that for the DABCO-catalyzed part of the reaction the relative mobility of the leaving groups is different from that for the remaining part of the reaction. However, the latter part is again a sum

Table 2. Termolecular rate constants for the DABCO-catalyzed reaction of 2,4-dinitro-1-X-benzene and *p*-anisidine in benzene at 25°C, together with Bunnett's original values for the related reaction of Ref. 1, recalculated relative to Cl = 1.

Leaving group	Our values		Values from Ref. 1.
	$k_3 \times 10^3$ [a]	Rel. value	Rel. value
F	–	–	767
NO_2	–	–	207
$OSO_2C_6H_4CH_3$-*p*	–	–	23.3
SOC_6H_5	–	–	1.1
Br	0.55	1.65	1.0
Cl	0.33	1.00	1.0
$SO_2C_6H_5$	2.99	9.02	0.7
SO_2CH_3	1.43	4.31	–
$OC_6H_4NO_2$-*p*	–	–	0.7
I	–	–	0.2

[a] $l^2\ mol^{-2}\ sec^{-1}$.

of a *p*-anisidine-catalyzed route and an uncatalyzed one. For the chlorine compound, Bernasconi and Zollinger's data [4] indicate that these two parts of the reaction are of comparable magnitude at the concentration of *p*-anisidine chosen in the present study, 0.2 M. A similar situation probably exists with the other leaving groups. The intercepts in Fig. 1 therefore do not represent a single reaction path. Thus this point was not further pursued but may well deserve further study.

The termolecular rate constants for the DABCO-catalyzed part of the reaction, which at high DABCO concentrations represents the main route, were calculated by dividing the slopes of the lines in Fig. 1 by the *p*-anisidine concentration. The values are given in Table 2.

Qualitatively, the relative order is quite as expected, assuming that bond-breaking between carbon and the leaving group is kinetically significant. Quantitatively, the differences are not particularly impressive compared with those obtained for solvolysis of *t*-butyl halides,[2] where the Br/Cl ratio is 41:1. In Table 2, the values obtained in the present study are compared with Bunnett's original values [1] (recalculated relative to Cl = 1). The similarity between Br and Cl is striking. In our work, NO_2 as a leaving group was found to give too high a rate, even in the absence of DABCO, to allow measurements at 25°C.

The most straightforward explanation of the weak "element effect" found in the present work is that bond-breaking has made very little progress in the rate-determining transition state. Since the second reaction step is a very exothermic process, this follows from Hammond's postulate.[3]

A final point to discuss is the influence of the solvent on the rate ratios. Since the present work was carried out in benzene solution, one might expect that the poor solvating properties of this medium should retard the Cl reaction more than the Br reaction. A change to the solvent used by Bunnett and coworkers,[1] methanol, would certainly not have reversed the situation so as to make Cl faster than Br (*cf.* *t*-butyl halides [2]). They might just have become more equal.

Acknowledgement. Our thanks are directed to Professor Lars Melander for his constructive criticism.

REFERENCES

1. Bunnett, J. F., Garbisch, E. W., Jr. and Pruitt, K. M. *J. Am. Chem. Soc.* **79** (1957) 385.
2. Cooper, K. A. and Hughes, E. D. *J. Chem. Soc.* **1937** 1183.
3. Hammond, G. S. *J. Am. Chem. Soc.* **77** (1955) 334.
4. Bernasconi, C. F. and Zollinger, H. *Helv. Chim. Acta* **49** (1966) 2570.
5. Borsche, W. *Ber.* **56** (1923) 1494.
6. Bost, R. W., Turner, J. O. and Norton, R. D. *J. Am. Chem. Soc.* **54** (1932) 1985.
7. Frost, A. and Pearson, R. *Kinetics and Mechanism*, 2nd Ed., Wiley, New York and London 1963, p. 49.
8. Davies, O. L. *Statistical Methods in Research and Production*, 3rd Ed., Oliver and Boyd, London and Edinburgh 1961.

Received July 5, 1972.

ACTA CHEMICA SCANDINAVICA 27 (1973) 197–208

Sterol and Phospholipid Biosynthesis in Phytohemagglutinin Stimulated Human Lymphocytes

LARS LILJEQVIST, JOSEF GÜRTLER and ROLF BLOMSTRAND

Department of Clinical Chemistry, Serafimerlasarettet, Karolinska Institutet, S-112 83 Stockholm 12, Sweden

The incorporation of acetate-1-^{14}C into sterols and phospholipids of PHA-stimulated * human lymphocytes was studied *in vitro* in lymph samples from a thoracic duct cannulated patient.

The PHA-stimulated lymphocytes incorporated more radioactivity into sterols and phospholipids than the control lymphocytes.

The cholesterol was labelled in both groups of lymphocytes and to a significantly greater extent in the PHA-stimulated lymphocytes. However, the highest specific radioactivity was located in the lathosterol fraction of the PHA-stimulated cells.

Among the phospholipids the phosphatidyl inositol and sphingomyelin exhibited the most pronounced increase of radioactivity.

Many biological membranes contain an appreciable quantity of cholesterol in addition to phospholipids, proteins, *etc.* The interaction of cholesterol with phospholipids is of considerable biological importance and many studies have been made to gain an understanding of the function of cholesterol in biological membranes. As early as in 1908 [1] it was suggested that the cholesterol present in animal tissues was in some way associated with the phospholipids in a liquid crystalline structure. For recent reviews of the interaction of cholesterol and phospholipids in biological systems, see Ref. 2. In recent work on phospholipids and steroids, Van Deenen [3] attempted to correlate phospholipid monolayer characteristics with specific biomembrane function.

The composition of the lipid core in a given membrane is biogenetically determined to a certain extent, but also a number of environmental factors are known to influence the lipid composition of normal interface. In our earlier studies, a pronounced influence on the phospholipid biosynthesis was observed in lymphocytes after treatment with phytohemagglutinin.[4] In the

* *List of abbreviations.* BSTFA, bis-(trimethylsilyl)-trifluoro-acetamide; DCDMS, dichlorodimethylsilane; dimethyl-POPOP, 1,4-bis-2-(4-methyl-5-phenyloxazolyl)benzene; FFA, free fatty acids; PEGS, polyethyleneglycolsuccinate; PHA, phytohemagglutinin; PPO, 2,5-diphenyloxazole; QF-1, fluorosilicone; Se-30, methylsilicone; TMCS, trimethylchlorosilane; TMS, trimethylsilyl.

present investigation, we have searched for alterations both in sterols and phospholipid biosynthesis in the lymphocytes after treatment with PHA. It was found that striking variations can be induced in these membraneous lipids, indicating that PHA-stimulated lymphocytes might be used as a relevant model system for improving our insight into the relations between the structure and function of the lipids present in natural membranes. Sterol biosynthesis of PHA-stimulated and non-stimulated lymphocytes has been compared. In addition, an analysis of the biosynthesized sterols has been carried out with the aid of gas chromatography and mass spectrometry.

EXPERIMENTAL

Lymphocytes and incubation procedure. Cannulation of the thoracic duct was performed in a 36-year-old woman suffering from *myasthenia gravis* in order to deprive the patient of lymph. Details of the treatment of this patient with a therapeutic lymph cannulation are described elsewhere.[5] The first 1000 ml of lymph were collected under sterile conditions into bottles kept at +4°C, while the patient was fasting. 2 IU heparin (Vitrum, Sweden) per ml lymph were added. The lymph contained 10 000 lymphocytes, 100 granulocytes, and 7000 erythrocytes per μl.

After thorough mixing, the lymph was divided into two equal portions. The lymph portions were transferred to two sterile culture vessels (Fernbach, diam. 200 mm. Grave, Sweden). The depth of the lymph in each vessel was 18 mm. 25 000 IU benzylpenicillin (Kabi, Sweden) were added to each vessel and 0.01 ml phytohemagglutinin (Wellcome Foundation, England) per ml lymph was added to one of the lymph portions. The culture vessels were closed with rubber stoppers equipped with needles for gas exchange. The lymph portions were then incubated for 18 h at +37°C in a shaking water bath. During the incubation the lymph portions were flushed with 5 % CO_2 in O_2. After 12 h, 2 μC acetate-1-^{14}C (specific activity 61 mCi/mM, The Radiochemical Centre, Amersham, England) per ml lymph were added to both lymph portions, and the incubations continued as before for 6 h. The cells were isolated by mild centrifugation at about 150 *g* for 10 min. The erythrocytes were hemolyzed by exposure to 0.3 % saline for 20 sec. The lymphocytes were then washed three times with 0.9 % saline. The lymphocytes were isolated from the saline by centrifugation at 150 *g* for 5–10 min. All centrifugations were performed at +4°C.

Extraction and silicic acid separation. The separated and washed lymphocytes were resuspended in saline and disrupted by freezing and thawing. The lipids were extracted according to Folch *et al.*[6] Aliquots of the total lipids were weighed and measured for radioactivity. Silicic acid (SiO_2) separations were carried out on HCl, water, chloroform and methanol washed Silicar 200–325 mesh (Mallinckrodt). Three fractions were eluted: (1) pentane:benzene 85:15 containing hydrocarbons and cholesterol esters; (2) chloroform containing glycerides, free cholesterol, and free fatty acids; and (3) methanol which elutes phospholipids and other polar lipids. Aliquots of these separated lipids were also weighed and measured for ^{14}C.

Thin layer chromatography. The plates were prepared with an automatic TLC-coater (Camag, Muttenz, Switzerland). Air-dried Silica Gel G (Merck, Darmstadt, Germany) plates (0.25 mm layer thickness) were heated for 2 h at 110° before use. The cholesterol ester and free cholesterol fractions from the silicic acid separation were chromatographed with pentane:ether 9:1 (system 1). The phospholipids were chromatographed with chloroform:methanol:13 N ammonia 14:6:1. The detection reagent was $(NH_4)_2SO_4$ 100 g and H_2SO_4 5 ml made up to a volume of 500 ml with water. The plates were charred 90 min at 180°C. Transmission densitometry was performed on a Vitraton TLD 100 densitometer (Vitatron, Dieren, Holland). Conditions and quantitative evaluations will be described elsewhere.[7] Alumina–$AgNO_3$ plates were prepared by mixing 35 g Alumina Woelm neutral (M. Woelm-Eschwege, Germany) with a solution of 10.5 g $AgNO_3$ in 30 ml water and spreading it on three 20 × 20 cm glass plates to a thickness of 0.25 mm. The plates were air-dried in darkness and activated at 120°C for 30 min just prior to

sample application. The developing phase was chloroform:acetone 65:35 (system 2). The spots were visualized by charring. The R_F values relative to cholestane were 0.44 for cholesterol and 0.69 for lathosterol. Squalene and 7-dehydrocholesterol remained at the start.

Water was used as a detection reagent on the TLC plates (white spots on a semi-translucent background) and the lipids were isolated by scraping off the marked areas with a razor blade into centrifuge tubes and extracted after shaking vigorously with 5 ml developing phase. The tubes were centrifuged and the procedure repeated 5 times. The evaporated combined extracts were reextracted with hexane or chloroform and filtered through HCl and methanol washed mineral fibres (1 μ, Bilsom International AB, Billesholm, Sweden).

Assay of radioactivity. Detection and assay of the radioactivity on the thin layer plates were carried out with a Berthold Thin-Layer Scanner II from Berthold Laboratorium, Wildbad, Germany. The weights of lipid fractions and sterols were determined by weighing aliquots of solutions with a Cahn Microbalance or a Mettler Ultra Microbalance UM 7 (Greifensee-Zürich, Switzerland). A Packard Tri-Carb liquid scintillation spectrometer model 3003 with an external standard was used for the assay of the radioactivity of aliquots of the lipid solutions. The scintillator mixture used consisted of 3.5 g PPO, 0.210 g POPOP, and 700 ml toluene.

Radio gas chromatography. The separation of labelled sterols was carried out on an F & M Biomedical Model 400 gas chromatograph equipped with an RGC 170 hydrocracking continuous-flow reaction tube with a proportional counter tube and a radiation measurement set-up (LB 2411) from Berthold Laboratorium, Wildbad, Germany. We have described a modified apparatus and the technique used elsewhere.[8] The U-shaped glass columns were 2 m × 3 mm, washed with conc. HCl and siliconized with 5 % DCDMS in toluene for 2 h. Acid-washed Chromosorb W, 80 – 100 mesh, was treated with 5 % DCDMS and 3 % TMCS in toluene for 12 h, washed with methanol and heated at 150°C for 12 h. The stationary phases used were QF-1 (4 % w/w) at 220°C, Se 30 (3 % w/w) at 250°C, and PEGS (14 % w/w) at 200°C. The gas flow conditions were the same as for fatty acid methylesters as described elsewhere.[8] The retention times relative to cholestane of some sterols are listed in Table 6. The TMS derivatives were prepared with BSTFA as described earlier.[9]

GLC-mass spectrometry. A QF-1 and an Se 30 column were prepared in the same way as described for radio gas chromatography, checked for separation behavior and used in the combined GLC – MS instrument LKB 9000. Operating conditions: Column 220 and 250°C, molecule separator 250°, ion source 270° and electron energy 70 eV.

Chemicals. Cholestane, cholesterol, squalene, and cholestanol were obtained from Koch-Light Laboratories, Ltd., Colnbrook, England. Lathosterol from Calbiochem, California Corporation, and 7-dehydrocholesterol from Mann Research Laboratories, Inc., New York. BSTFA was obtained from Pierce Chem. Co., Rockford, Ill. Solvents were of analytical grade and distilled with Vigreux columns before use.

RESULTS

In Table 1 are shown the results obtained from silicic acid and thin layer chromatograms of the lipids extracted from lymphocytes incubated with or without PHA for 18 h and to which acetate-1-^{14}C was added during the last 6 h of incubation. The total incorporation of radioactivity into the lipids of the stimulated lymphocytes was about 5 times higher that in the control experiment. In the control experiment the main part of the activity was found in the phospholipid fraction. The stimulated lymphocytes showed a considerably higher incorporation of label into the sterols in comparison with the control experiment. This sterol fraction, which was eluted together with the glycerides and FFA from the silicic acid column, was rechromatographed on silica gel G plates, and the sterols were isolated from the thin layer, hydrolyzed and separated from acidic components.

Table 1. Mass and radioactivity distribution among lipid classes from PHA stimulated and non-stimulated lymphocytes.

	Control			PHA-stimulated		
	Mass %	Radioactivity dpm × 10^3	%	Mass %	Radioactivity dpm × 10^3	%
Hydrocarbons [a]	1.5	70	1.1	3.0	518	1.5
Cholesterol esters [b]	3.5	83	1.3	2.8	794	2.3
Monoglycerides [c]	3.6	665	10.4	4.6	3 487	10.1
Cholesterol [d]	7.8	1087	17.0	8.0	11 427	33.1
FFA	1.2	364	5.7	1.1	1 519	4.4
Triglycerides	5.4	748	11.7	11.4	6 387	18.5
Phospholipids	77.0	3375	52.8	69.1	10 391	30.1
Total lipids	100.0	6392	100.0	100.0	34 523	100.0

[a] Front fraction from TLC, containing squalene and other non-polar compounds. [b] Also containing other sterol esters. [c] Not completely separated and identified. [d] Also containing other sterols.

The pentane-benzene fraction from the silicic acid column was separated into sterol esters and hydrocarbons on a silica gel G plate using solvent system 1. The sterol esters and the hydrocarbon fraction of the PHA-stimulated lymphocytes exhibited an increased labelling compared to the non-stimulated controls (Table 1 and Fig. 4). Fig. 4C also shows a sterol ester fraction from lymphocytes stimulated with PHA for 42 h and then incubated with PHA and acetate-1-^{14}C for 6 h. The incorporation of label into the hydrocarbon fraction had risen, whereas the radioactivity of the sterol esters had nearly disappeared.

The mass of the total sterols was esterified to about 20 % in the control lymphocytes. Similar results have been obtained by d'Hollander and Chevallier [10] studying sterol biosynthesis and esterification of different rat

Table 2. Total number of dpm × 10^3 incorporated by human thoracic duct lymphocytes into sterols after incubation with acetate-1-^{14}C.

	Control	PHA-stimulated
Free sterols	1087	11 427
Sterol esters	21 [a]	413 [a]
Free sterols		
Cholesterol	559	7 153
Lathosterol	528	2 925
Esterified sterols		
Cholesterol	5	263
Lathosterol	13	109

[a] Expressed as the activity in the sterol moiety.

tissues. The stimulated lymphocytes exhibited a similar esterification (16 %). The mass of the total lipids increased about 25 % by stimulation. The triglycerides were mainly responsible for this increase. The mass of the free sterols, however, also increased by about 25 % compared with the non-stimulated lymphocytes. The total incorporation of activity into the free sterol pool increased 10 times by PHA-stimulation and was distributed between cholesterol and lathosterol in a ratio of 2:1 (Table 2). After subtraction of the activity found in the fatty acid moiety, the sterol esters exhibited an increase of incorporation by 20 times. This increase was more pronounced for cholesterol (50 times) than for lathosterol (9 times).

None-sterified sterols. The radioactive free sterols from stimulated and non-stimulated lymphocytes isolated from thin layer plates (solvent system 1) were purified by alkaline hydrolysis, silylated with BSTFA and rechromatographed with the same TLC system. All activity moved according to the R_F of the TMS derivative of cholesterol. Radio gas chromatographic analysis with a QF-1 column demonstrated that the main part of the radioactive TMS derivatives exhibited the retention time of cholesterol TMS ether. A minor part of the activity appeared as a tail of the cholesterol peak. No other radioactive peaks were obtained.

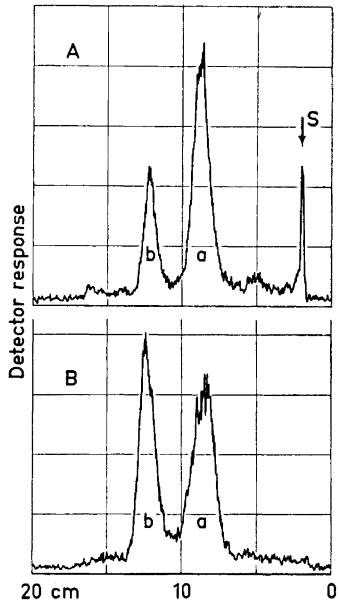

Fig. 1. Thin layer radio scan of the free sterols separated on silver nitrate coated plates. A, PHA-stimulated, and B, non-stimulated lymphocytes. Cholesterol, a; and lathosterol, b. S indicates the start point. The plates were developed in chloroform:acetone 65:35.

Fig. 1 shows radioactivity scans of the free sterols separated on an alumina-$AgNO_3$ thin-layer plate: A, from stimulated lymphocytes, and B, from the control lymphocytes. Peak a has the retention factor of cholesterol. The two radioactive compounds were isolated from the thin layer, and peak

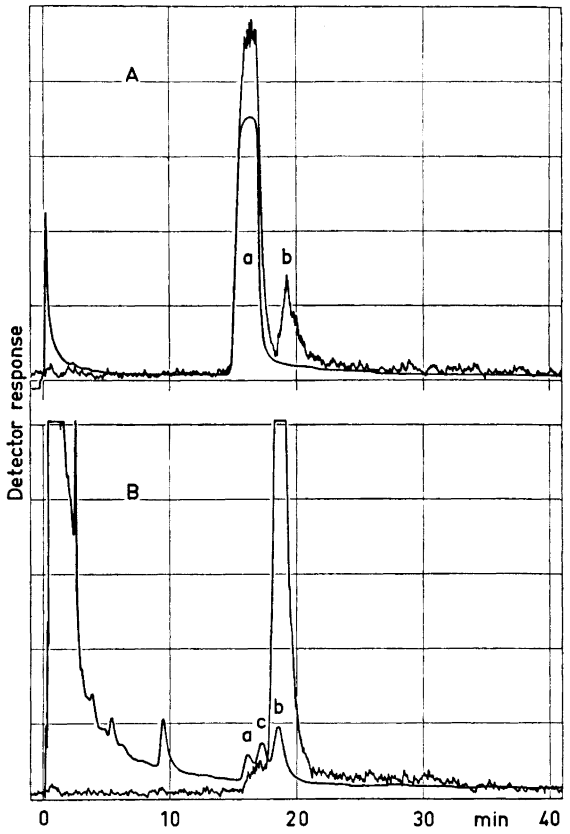

Fig. 2. Radio gas chromatograms of TMS derivatives of the free sterols from stimulated lymphocytes which were isolated from $AgNO_3$ TLC plates. A corresponds to peak a, and B to peak b in Fig. 1A. Peak a has been identified as cholesterol, b as lathosterol, and c as cholestanol. A QF-1 column was used. Conditions, see text.

a (Fig. 1A) had about 99 % of the mass with a specific activity of 3027×10^3 dpm/mg (Table 4). The small amount of compound b (Fig. 1A) and the presence of contaminants did not permit accurate weight determination. Fig. 2A shows a radio gas chromatogram of the TMS derivative of compound a (Fig. 1A). A QF-1 column, which separates cholesterol from cholestanol, was used. The main peak had the retention time of cholesterol TMS ether. The radioactive peak b originates from an incomplete separation on the alumina-$AgNO_3$ plate. Compound a (Fig. 1A) was subjected to GLC-mass spectrometric examination using a QF-1 column with chromatographic behavior identical to the column on the radio gas chromatograph. Cholesterol TMS ether could be identified. No other ions which would refer to additional TMS derivatives were found in the mass spectra. Finally, Fig. 2B shows the radio gas chromatogram of compound b TMS derivatives (Fig. 1A). It is obvious from the figure that compound b, with the retention time of lathosterol TMS ether,

carries the label. The retention time of compound c coincides with that of cholestanol TMS ether. Compound a, cholesterol TMS ether, originated from the incomplete separation on the alumina-$AgNO_3$ plate. All three compounds were identified by GLC-mass spectrometry.

The material remaining at the origin on the TLC plate shown in Fig. 1A was analyzed by TLC and radio gas chromatography. The results suggested that the fraction contained a labelled sterol with hydroxyl function. The preliminary data suggested the presence of 7-dehydrocholesterol, a common precursor in the 24-dihydro series.

Esterified sterols. The sterol esters from the stimulated lymphocytes (Fig. 4A, a) were hydrolyzed with 5 % KOH in 95 % ethanol for 1 h on a boiling water bath under nitrogen. 52 % of the activity was found in the sterol moiety. The residual activity consisted of acidic components and was analyzed

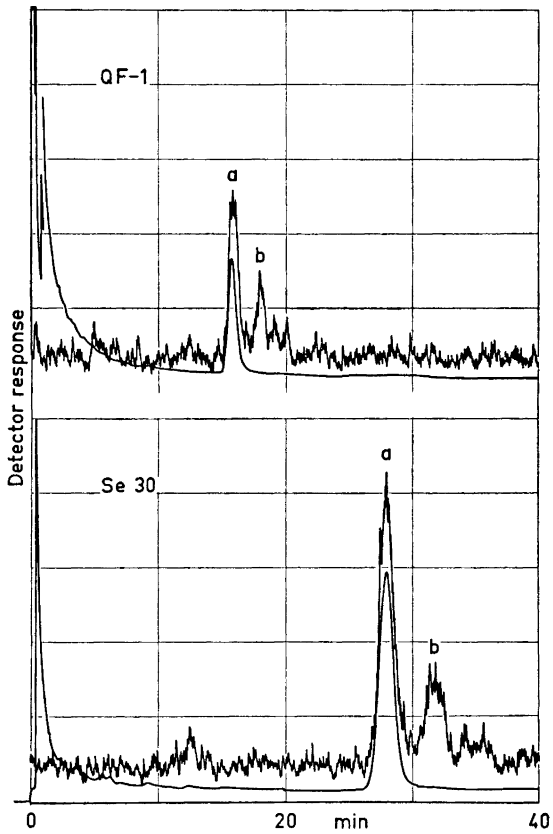

Fig. 3. Radio gas chromatograms of the esterified sterols on two different columns. The TMS derivatives were prepared after alkaline hydrolysis of the sterol esters from the stimulated lymphocytes. a, identified as cholesterol, and b, compound with chromatographic behavior of lathosterol. Column conditions, see text.

Table 3. Percentage distribution of radioactivity incorporated by human thoracic duct lymphocytes into cholesterol and lathosterol after incubation with acetate-1-^{14}C.

	Free sterols		Esterified sterols	
	Cholesterol	Lathosterol	Cholesterol	Lathosterol
Control	51.4 [a]	48.6 [a]	22.2 [a]	59.2 [a]
PHA-stimulated	62.6 [a]	25.6 [a]	63.6 [a]	26.5 [b]

[a] Value obtained by TLC radioscanning. [b] Value obtained by radio gas chromatography.

by radio gas chromatography in respect to fatty acids. These results will be published later.[4] After silylation, the sterols were subjected to radio gas chromatography. Fig. 3 shows chromatograms on two different columns. Compound a (cholesterol TMS ether), which is responsible for 63.6 % of the activity and 99 % of the mass (Table 3), was also identified by mass spectrometry. The extremely small amount of compound b did not allow mass spectrometric identification but the retention time on two different GLC columns coincided with that of lathosterol. Two other radioactive sterols can be seen on the chromatograms. These are responsible for about 10 % of the activity.

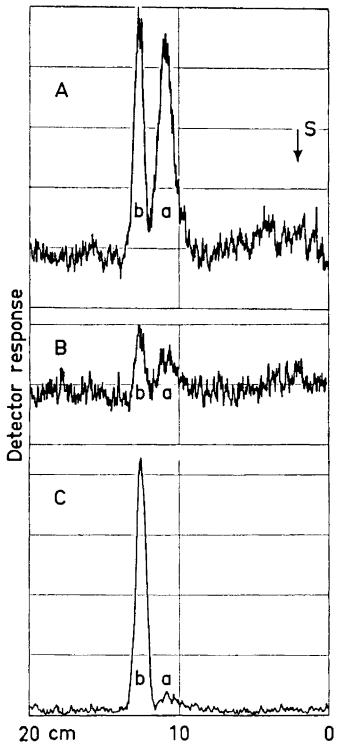

Fig 4. Thin layer radio scan of the cholesterol ester fraction obtained from SiO_2 chromatography. The silica gel G plates were developed with pentane:ether 9:1. A, stimulated lymphocytes; B, non-stimulated lymphocytes; C, lymphocytes incubated 48 h with PHA and with acetate-1-^{14}C added during the last 6 h of incubation. a, sterol esters, and b, hydrocarbons. The label of b has the chromatographic behavior of squalene.

No further attempt was made to identify these sterols, because additional material was not available. The sterol esters from the non-stimulated lymphocytes were also analyzed (Fig. 4B, a). The sterols obtained after alkaline hydrolysis contained 26 % of the radioactivity and were separated on an alumina-$AgNO_3$ plate. According to the radio scan (not shown) recorded from the plate, three radioactive compounds were present: a start fraction containing 18.6 % of the activity (not further analyzed), cholesterol with only 22.2 % of the activity (see Table 3) and lathosterol with 59.2 %. The lathosterol was submitted to radio gas chromatography as the TMS derivate on an Se 30 column. Only one ^{14}C-peak appeared with the retention time of lathosterol TMS ether. The cholesterol isolated from the alumina plate was identified by mass spectrometry. The specific activity was too low for radio gas chromatographic analysis. The identification of esterified lathosterol could only be performed with the aid of radio gas chromatography and radioactivity scanning of thin layer chromatograms.

Hydrocarbons. The hydrocarbon fraction (TLC front fraction) obtained from the silicic acid and TLC chromatograms (Fig. 4, A – C) was alkaline hydrolyzed and the non-saponifiable lipids, containing 96 – 100 % of the radioactivity, were analyzed in respect to the label. It was found that the mass associated with the radioactivity was very small and mass spectral identification could not be performed. The retention factor of the major activity agreed with that of squalene in TLC systems 1 and 2. The label was further analyzed on 3 different radio gas chromatographic columns with QF-1, Se 30, and polyethyleneglycol succinate as the liquid phase. A silylated sample was analyzed on QF-1 and Se 30 columns. The latter column would lengthen the retention time of TMS derivatives and the former shorten it in respect to the parent compound. About 10 % of the label was found to be non-identical with squalene according to the identification methods used, but rather consisted of at least 3 other compounds. No difference in composition of the label was found between the lipids of the stimulated and non-stimulated lymphocytes.

Phospholipids. In Table 5 the distribution of mass and radioactivity among the individual phospholipids from the PHA-stimulated and the non-stimulated lymphocytes is given. The method used for the determination of mass and activity of the individual phospholipids separated on thin layer

Table 4. Specific activity of cholesterol biosynthesized by human thoracic duct lymphocytes after incubation with acetate-1-^{14}C.

	Control dpm × 10^3/mg	PHA-stimulated dpm × 10^3/mg
Free cholesterol	119	3027
Esterified [a] cholesterol	13	471

[a] Expressed as the activity found in the sterol moiety after alkaline hydrolysis.

Table 5. Mass and radioactivity distribution among phospholipids from PHA stimulated and non-stimulated lymphocytes.

	Control		PHA-stimulated	
	Mass %	Radioactivity dpm × 10^3	Mass %	Radioactivity dpm × 10^3
Start fraction	5.9	118	7.1	468
Phosphatidic acid	5.8	145	5.9	436
Phosphatidyl serine	6.3	152	5.6	436
Phosphatidyl inositol	9.7	219	9.8	1 205
Sphingomyelin	17.4	314	15.4	1 309
Phosphatidyl choline	36.4	1 525	37.0	4 146
Phosphatidyl ethanolamine	15.0	537	14.7	1 746
Cardiolipin	0.4	44	0.5	94
Cerebrosides	3.1	321	4.0	551
Total phospholipids	100.0	3 375	100.0	10 391

plates will be discussed elsewhere.[7,11] The total incorporated radioactivity in the phospholipids of the stimulated lymphocytes was about 3 times higher than that of the control experiment (Table 5). A more pronounced increase of radioactivity was found for phosphatidyl inositol and sphingomyelin. After hydrolysis of the phospholipids isolated from the thin-layer plates, almost 100 % of the label was found in the fatty acid moiety.[4]

DISCUSSION

The present report deals with data obtained from studies on sterol and phospholipid biosynthesis in human lymphocytes. Because there are few data available on the composition and synthesis of the different lipid classes in human lymphocytes,[12] we have analyzed the sterols and phospholipids rather extensively. This approach can help to explain the interrelationships among different types of cellular lipids and also elucidate the metabolic functions of lipids.

In a recent investigation from this laboratory,[7] the lipid composition and synthesis in human lymphocytes and thymocytes has been compared. A great

Table 6. GLC retention times of some sterols relative to cholestane.

Compound	Se 30 250°C	QF-1 210°C	PEGS 200°C
Cholestane	1.00	1.00	1.00
Squalene	1.00	0.66	0.90
Cholesterol TMS ether	1.81	2.09	–
Cholestanol TMS ether	1.81	2.27	–
Δ^7-Cholesten-3β-ol TMS ether	2.01	2.74	–
$\Delta^{5,7}$-Cholestadien-3β-ol TMS ether	2.11		

similarity in the lipid composition and metabolism was found in these two types of lymphocytes, although minor differences were observed.

From Tables 1 and 5 can be seen that from a qualitative point of view, non-stimulated and PHA-stimulated lymphocytes have a very similar lipid composition.

This investigation further confirmed the results of our previous investigations that human lymphocytes have a very active lipid synthesis [7,13] and that lipid synthesis is stimulated by PHA.[14]

With regard to the sterol synthesis the data in Tables 2 and 3 indicate that more acetate-1-^{14}C is incorporated into the cholesterol of the PHA-stimulated cells than into other sterols. The specific activity of free lathosterol in the stimulated lymphocytes was, however, about 200 times higher than that of cholesterol as calculated from Fig. 2 (the sensitivity of mass detector was 20 times less in Fig. 2A than in Fig. 2B). The specific activity of lathosterol in the control experiment could not be estimated.

From Table 4 it is obvious that the specific activity of free cholesterol was considerably higher than that of ester cholesterol but in both sterol pools the incorporation of label was increased after PHA-stimulation.

Table 2 shows the total incorporation of label into sterols. It is obvious from the control experiment that in the free sterol pool about the same amount of radioactivity was incorporated into cholesterol and lathosterol, but in the esterified sterol pool lathosterol was labelled 2.5 times as much as cholesterol. In the stimulated lymphocytes, more radioactivity was incorporated into cholesterol than into lathosterol both according to the free and esterified sterol pools. The results suggest a proportionally larger synthesis and esterification of cholesterol in PHA-stimulated lymphocytes.

It is known that PHA stimulates the growth and cell division of lymphocytes.[15] The preferential labelling of the free cholesterol in comparison with the ester cholesterol may be due to a compartmentalization of the lymphocytic sterols.[16] It is also possible that the synthesized sterols are preferentially used for membrane formation as it is generally assumed that cholesterol serves as a structural unit in cellular membranes [2,17] and that it seems to undergo little or no change in tissue culture cells.[18] The incorporation into membranes of lathosterol, 7-dehydrocholesterol, Δ^4-cholesten-3-one, and coprostanol has been reported by Rothblat and Buchko.[19]

The accelerated sterol synthesis of PHA-stimulated lymphocytes also supports the hypothesis of Chevallier and Lutton [20] that only during the formation of cells is there an active cholesterol synthesis.

Besides cholesterol and proteins, phospholipids are the main constituents of the cell membranes. From Table 5 it is obvious that PHA induced an increased phospholipid synthesis. Phosphatidyl inositol and sphingomyelin exhibited the most pronounced increase of radioactivity. The increased synthesis of the latter is of special interest because sphinomyelin seems to be preferentially associated with the plasma membrane.[21] A more detailed description of the influence of PHA on the lymphocyte phospholipids will be given elsewhere.[4]

The present results and those obtained earlier [4] clearly indicate that sterol and phospholipid biosynthesis from acetate-1-^{14}C is stimulated in the

presence of PHA. The observations on the increased incorporation of label into squalene and lathosterol after PHA-stimulation may indicate that PHA influences different steps in the synthesis of cholesterol. The exact nature of the mechanism involved in the PHA-stimulation of lymphocytes is unknown at present. It is possible, however, that the use of PHA as a stimulant of biosynthetic processes in lipid metabolism could be valuable as a tool for the elucidation of the sequences involved in membrane synthesis of lymphocytes.

Acknowledgement. This work was supported by grants from the *Swedish Cancer Society*, the *Swedish Society of Medical Sciences*, and *Reservationsanslaget, Karolinska Institutet.*

REFERENCES

1. White, C. P. *Med. Chron.* **48** (1908) 365.
2. Williams, R. M. and Chapman, D. *Progr. Chem. Fats Other Lipids* **11** (1970) 3.
3. Van Deenen, L. L. M. *Progr. Chem. Fats Other Lipids* **8** (1965) 1.
4. Liljeqvist, L. *Ann. Clin. Res.* (1973). *To be published.*
5. Bergström, K., Franksson, C., Matell, G. and von Reis, G. *To be published.*
6. Folch, J., Lees, M. and Sloane Stanley, G. H. *J. Biol. Chem.* **226** (1957) 497.
7. Liljeqvist, L. *Acta Chem. Scand.* **27** (1973). *To be published.*
8. Blomstrand, R., Gürtler, J., Liljeqvist, L. and Nyborg, G. *Anal. Chem.* **44** (1972) 277.
9. Gürtler, J. and Blomstrand, R. *Int. J. Vitam. Nutr. Res.* **41** (1971) 204.
10. d'Hollander, F. and Chevallier, F. *Biochim. Biophys. Acta* **176** (1969) 146.
11. Liljeqvist, L., Aronson, P. and Nyberg, G. *To be published.*
12. Gottfried, E. L. *J. Lipid Res.* **8** (1967) 321.
13. Blomstrand, R. *Acta Chem. Scand.* **20** (1966) 1122.
14. Blomstrand, R. and Liljeqvist, L. *Acta Chem. Scand.* **26** (1972) 397.
15. Yoffey, J. M., Winter, G. C. B., Osmond, D. G. and Meek, E. S. *Brit. J. Haematol.* **11** (1965) 488.
16. Jungman, R. A. and Schweppe, J. S. *Steroids* **17** (1971) 541.
17. O'Brien, J. S. *J. Theor. Biol.* **15** (1967) 307.
18. Rothblat, G. H. *Advan. Lipid Res.* **7** (1969) 135.
19. Rothblad, G. H. and Buchko, M. K. *J. Lipid Res.* **12** (1971) 647.
20. Chevallier, F. and Lutton, C. *Rev. Éur. Étud. Clin. Biol.* **16** (1971) 16.
21. Stoffel, W. *Arzneim. Forsch.* **19** (1969) 253.

Received May 26, 1972.

ACTA CHEMICA SCANDINAVICA 27 (1973) 209–217

The Thione-Thiol Tautomerism in Simple Thioamides

G. KJELLIN and J. SANDSTRÖM

AB Draco, P.O.B., S-221 01 Lund, and Division of Organic Chemistry 1, Chemical Center, University of Lund, P.O.B. 740, S-220 07 Lund 7, Sweden*

The thioamide/imidothiol ratios found (K_T) in thioacetamide and thiobenzamide and their mono-*N*-methyl derivatives have been measured by the basicity method. pK_T was found to be −8.6 for thioacetamide, −9.6 for *N*-methylthioacetamide, −8.3 for thiobenzamide and −8.9 for *N*-methylthiobenzamide. The thioamides were found to deviate from ideal Hammett base behaviour in aqueous sulphuric acid. pK_T values and ultraviolet spectra are discussed in relation to HMO and PPP calculations.

The concept of a thione-thiol tautomerism (I ⇌ II) in thioamides is one of long standing, and the thiol form has often been invoked to explain *S*-alkylations and *S*-acylations of thioamides. The complete dominance of the

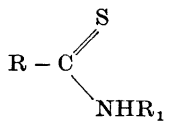

I

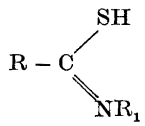

II

thiol form has been advocated on the grounds that carbon and sulphur atoms have a low tendency to form double bonds.[1] However, as early as in 1931, Hantzsch [2] showed that the thione form must dominate in thioacetamide, by comparing the ultraviolet spectra of thioacetamide, thioacetpiperidide, and ethyl thioacetimidate, and it can be stated quite generally that chemical reactivity is a poor guide for judging the position of a tautomeric equilibrium. We have found it desirable to attempt an estimation of the tautomeric ratio in some simple thioamide systems to provide a basis for a more detailed discussion of the factors influencing the tautomerism in different cyclic systems showing a similar type of equilibrium.

A quantitative estimation of the tautomeric ratio is hampered by the low concentration of the imidothiol form II, which precludes a direct measurement

* Subsidiary to AB Astra, Sweden.

by normal physical methods. Claims have recently been made for a large proportion of thiol form in thionicotinic and thioisonicotinic amides based on infrared absorption bands in the S – H stretching region,[3,4] but these claims have been refuted by X-ray crystallographic [5,6] and infrared spectroscopic [6] arguments. In previous quantitative studies of thione-thiol tautomerism in thiopyridones [7,8] and azoline-2-thiones [9] the basicity method has been used. This method is thoroughly discussed in Ref. 10, but to aid the discussion a brief derivation is given as follows, with AH and HA denoting the tautomeric forms I and II:

$$AH + H^+ \rightleftharpoons HAH^+ \rightleftharpoons HA + H^+ \quad (1)$$

$$K_{aI} = [H^+]\,[AH]/[HAH^+] \quad (2a)$$

$$K_{aII} = [H^+]\,[HA]/[HAH^+] \quad (2b)$$

$$K_{obs} = \frac{[H^+]\,([AH] + [HA])}{[HAH^+]} = K_{aI} + K_{aII} \quad (2c)$$

$$K_T = [AH]/[HA] = K_{aI}/K_{aII} \quad (3)$$

Instead of the non-isolable forms I and II, the corresponding *N*- and *S*-methyl derivatives III and IV can be used under the assumption that methylation does not seriously affect the basicity. Since $K_{aI} \gg K_{aII}$, K_{obs} can be

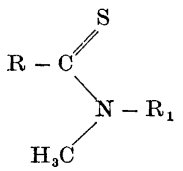

III

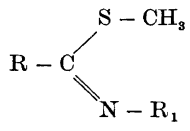

IV

substituted for K_{aI} in (3), thus obviating the effect of methylation on this form. Another problem is posed by the observation [11,12,9] that thioamides in general do not behave as ideal Hammett bases.

EXPERIMENTAL

Thioacetamide was a commercial sample, and *N*-methylthioacetamide, *N*,*N*-dimethylthioacetamide and the analogous thiobenzamides were prepared by standard procedures. The thioacetamides were purified by vacuum sublimation, followed by recrystallization, and the thiobenzamides by recrystallization only. The methyl thiolacetimidates and -benzimidates were obtained as hydroiodides by reaction of the corresponding thioamides with methyl iodide in dry acetone. These compounds were fairly labile and were used for measurement immediately after isolation and drying.

The pK_a values of the thioamides were measured as described in Ref. 9. The thiolimidate hydroiodides were dissolved in water and immediately the pH measured by potentiometric titration with 0.01 N sodium hydroxide and with a total base concentration of less than 2×10^{-3} M, using a Radiometer pH meter Model 25 with scale expander. Titration of the thiolimidate hydroiodides with standard alkali and back-titration with standard acid within a few minutes followed the same curve, indicating that hydrolysis of the thiolimidates was without importance. The glass electrode was attached to a Radiometer titrator Type TTT 1c and the curve was recorded on a Radiometer titrigraph Model SBR 2c.

The pK_a and pK_T values are given in Table 1, and literature values of thioamide and thiolimidate basicities in Table 2. Ultraviolet spectra have been recorded with a Beckman DK-2 spectrophotometer. The absorption maxima of the thioamides, the thiolimidates and their protonated forms are given in Table 3.

DISCUSSION

One fundamental assumption made in using the basicity method, *viz.* that the basicity of the thiocarbonyl sulphur atom is not seriously affected by *N*-methylation, is justified by the data in Table 1. Since sulphur is only a moderately efficient transmitter of electronic effects, *S*-methylation should be expected to influence the basicity of the nitrogen atoms of thiolimidates even less. *N*-Methylation, on the other hand, raises the basicity by 0.6 – 1.0 pK units.

The pK_T values found for these thioamides show a dominance of thione over thiol form which is greater than in the previously studied systems, where the thioamide group forms part of a heterocyclic ring. From the literature data (Table 2) a pK_T value of -11.0 can be obtained for thiourea, and this seems to be the highest ever reported for a thioamide.

The dominance of the thione form in these compounds is due to a combination of different effects, which can be divided into two groups:

1. *Electronic effects.* Here, the difference in π-electron stabilization should be the dominant effect, though the importance of inductive and/or hyperconjugative effects is shown by the basicity increases in the thiolimidates caused by N-alkylation.

Table 1. pK_a and pK_T values for thioamides (A) and thiolimidates (B) in water (H_2SO_4) at +25°C.

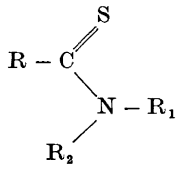

A

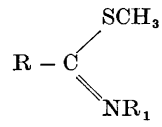

B

R	R_1	R_2	pK_a A	pK_a B	pK_T
CH_3	H	H	-1.9 ± 0.2	6.71 ± 0.01	-8.6 ± 0.2
CH_3	CH_3	H	-1.9 ± 0.2	7.71 ± 0.01	-9.6 ± 0.2
CH_3	CH_3	CH_3	-1.6 ± 0.2	–	–
Ph	H	H	-2.5 ± 0.2	5.83 ± 0.01	-8.3 ± 0.2
Ph	CH_3	H	-2.5 ± 0.3	6.42 ± 0.02	-8.9 ± 0.3
Ph	CH_3	CH_3	-2.3 ± 0.2	–	–

Table 2. Collection of pK_a values from the literature.

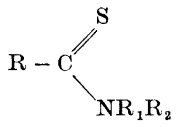

A

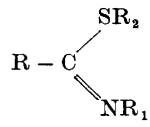

B

R	R_1	R_2	pK_a A	Ref.	pK_a B	Ref.
CH_3	H	H	−1.76[a]	13		
CH_3	H	C_2H_5			6.9	14
CH_3	CH_3	CH_3	−1.53	15		
CH_3	C_2H_5	CH_3			7.75[b]	16
CH_3	H	C_2H_5			6.97[b]	17
Ph	H	C_2H_5			5.86[b]	17
H_2N	H	H	−1.26	18		
H_2N	H	H	−1.19	15		
H_2N	H	CH_3			9.83	19

[a] With hydrochloric acid: no temperature given.
[b] At 30°C in 10 % aqueous acetonitrile.

2. *Solvation and entropy effects.* The solvation energies of the thione and thiol forms depend on their polarities and their capacity to take part in hydrogen bonding. This capacity is determined by the power of the NH and SH groups to act as proton donors in basic solvents, and of the thiocarbonyl sulphur atom and the thiolimidate nitrogen atom to act as proton acceptors in protic solvents. Reasoning by analogy from pyridones, one would conclude that the thione form is generally favoured by the solvation effects, since Beak and Bonham [22] have found that *N*-methyl-2-pyridone and *N*-methyl-4-pyridone are more stabilized relative to the corresponding methoxypyridines in the condensed than in the gaseous phase.

The π-electron effect is probably responsible for the increase of pK_T in the order thiopyridone, azolinethione, acyclic thioamide. In the cyclic compounds, the thiol form gains an extra stabilization by its superior aromatic resonance, and this effect is probably more important in the thiopyridones than in the azolinethiones. These differences have been qualitatively reproduced by MO calculations with an HMO method with α,β-variation.[23,9] Katritzky *et al.*[24] have recently shown that the aromatic resonance in 2-thiopyridone is *ca.* 5.3 kcal/mol less efficient than in pyridine. On the other hand, pyridine-2-thiol can be expected to have a greater resonance energy than pyridine.

Calculations similar to those described in Ref. 9 have been performed for the simple thioamide, thiobenzamide, thiourea, and for the corresponding iminothiol forms. The calculations described in Ref. 9 were performed using parameter set 3 of Ref. 23. However, an inspection of the transition energies reveals that set 3 is not quite suitable to reproduce UV spectra. Therefore,

Table 3. Ultraviolet spectra of thioamides, $R-CS-NR_1R_2$ (A), thiolimidates, $R-C(SCH_3)=NR_1$ (B), protonated thioamides (C), and protonated thiolimidates (D). Spectra of A, B, and D in water, and of C in sulphuric acid.

R	R_1	R_2	System	λ_{max} nm	ε_{max}
CH_3	H	H	A	262	13 800
CH_3	H	–	B	226	15 700
CH_3	H	H	C	234	10 400
CH_3	H	–	D	228	26 000
CH_3	CH_3	H	A	255	16 100
CH_3	CH_3	–	B	226	19 100
CH_3	CH_3	H	C	230	9 600
CH_3	CH_3	–	D	228	25 000
CH_3	CH_3	CH_3	A	264	18 000
CH_3	CH_3	CH_3	C	237	13 000
Ph	H	H	A	287	8 700
Ph	H	–	B	239	27 000
Ph	H	H	C	271	16 000
Ph	H	–	D	258	17 800
Ph	CH_3	H	A	275	17 600
Ph	CH_3	–	B	226	21 000
Ph	CH_3	H	C	264	27 600
Ph	CH_3	–	D	257	16 800
Ph	CH_3	CH_3	A	271	6 500
Ph	CH_3	CH_3	C	249	6 600
H_2N	H	H	A	235[a]	11 200[a]
H_2N	H	–	B	238[b]	38 100[b]
H_2N	H	H	C	End absorption[a]	–[a]
H_2N	H	–	D	220[b]	5 500[b]

[a] Ref. 20. [b] Ref. 21.

the same calculations were performed with parameter set 1, which has previously been found to give good correlations between calculated and experimental transition energies for a large number of simple thiones.[25]

For comparison, calculations have also been performed by the Pariser-Parr-Pople method,[26] with the two-center repulsion integrals calculated according to the Nishimoto-Mataga scheme,[27] and with the parameters proposed by Fabian.[28] All parameters are collected in Table 4. An idealized geometry was

Table 4. Parameters for HMO (α,β variation) [23] and PPP [28] calculations.

Atom	h_x Set 1	h_x Set 3	U_x eV	γ_{xx} eV	Bond	k_{xy} Set 1	k_{xy} Set 3	β_{xy} eV
C	0	0	−11.42	10.84	C–C	1.0	0.75	−2.318
$\dot{N}$	0.5	0.5	−14.12[a]	12.34[a]	C–N	1.2	0.8	−2.318
$\dot{N}$	1.5	1.5	−23.13	12.98	C–S	0.6	0.4	−1.159
S	0.5	0.5	−12.86	9.92	C=S	0.6	0.4	−1.623
S	1.0	1.0	−21.00	10.84				

[a] From Ref. 29.

Table 5. Total π-electron energies ($\sum E_\pi$) and energies of first $\pi \rightarrow \pi^*$ transition ($\Delta E_{\pi \rightarrow \pi^*}$) in units of $-\beta$ for $R-CSNH_2$ (A), $R-C(SH)=NH$ (B), and $[R-C(SH)=NH_2]^+$ (C).

R	System	Set 1		Set 3	
		$\sum E_\pi$	$\Delta E_{\pi \rightarrow \pi^*}$	$\sum E_\pi$	$\Delta E_{\pi \rightarrow \pi^*}$
CH_3	A	6.4171	1.5967	5.1871	1.1025
CH_3	B	6.3154	2.6173	4.7605	1.7633
	$E(A)-E(B)$	0.1017	–	0.4266	–
CH_3	C	–	2.1814	–	–
Ph	A	17.4092	1.1598	13.4702	0.8332
Ph	B	17.2496	1.9394	12.9961	1.3412
	$E(A)-E(B)$	0.1596	–	0.4741	–
Ph	C	–	1.7253	–	–
H_2N	A	10.2444	1.6982	8.5736	1.0896
H_2N	B	9.9885	2.7845	8.0875	1.7759
	$E(A)-E(B)$	0.2589	–	0.4860	–
H_2N	C	–	2.5976	–	–

assumed with all bond angles equal to 120°. The bond lengths of thioacetamide and thiobenzamide were taken from the X-ray structure determination of thioacetamide by Truter.[5] The length of the Ph–C bond in thiobenzamide and the corresponding thiolimidate was assumed to be 1.48 Å. The bond lengths in thiourea were taken from the work of Kunchur and Truter,[30] and the C=N (1.32 Å) and C–S (1.73 Å) bond lengths in all thiolimidates from the work of Flippen and Karle.[31]

The total π-electron energies and the energies of the first $\pi \rightarrow \pi^*$ transitions obtained by the HMO method are collected in Table 5. For comparison with UV spectra, transition energies for the protonated thiolimidates (C and D) have been calculated with parameter set 1 and with the PPP method.

With parameter set 3, the difference in π-electron energy between thione and thiol form, ΔE_π, was -0.046 β for 2-thiopyridone, -0.064 β for 4-thiopyridone, and between -0.289 β and -0.375 β for the azoline thiones.[9] It is apparent that the values given in Table 5 reproduce the higher pK_T values for the acyclic thioamides, although the ΔE_π value obtained for thiobenzamide is too high. The high pK_T for thiourea is reproduced by both parameter sets.

The total π-electron energies obtained by the PPP method are found in Table 6. It appears that the thione forms generally show the higher π-electron

Table 6. Total π-electron energies (E_π) and differences in core repulsion energies (ΔE_{core}) in eV for $R-CS-NH_2$ (A) and $R-C(SH)=NH$ (B).

R	$E_{\pi,A}$	$E_{\pi,B}$	$\Delta E_{core,I}$	$\Delta E_{\pi,I}$	$\Delta E_{core,II}$	$\Delta E_{\pi,II}$
CH_3	−83.103	−81.445	2.613	0.955	1.311	−0.347
Ph	−300.272	−296.709	5.277	1.714	2.193	−1.370
H_2N	−153.907	−150.445	5.876	2.414	3.227	−0.235

Table 7. Calculated π-electron densities (q) and π-bond orders (p) in $R-CS-NH_2$ (A) and $R-C(SH)=NH$ (B)

R	Atom	Set 1		Set 3		PPP	
		A	B	A	B	A	B
CH_3	q (S)	1.471	1.932	1.332	1.939	1.422	1.918
	q (C)	0.839	0.916	0.834	0.885	0.844	0.757
	q (N)	1.690	1.152	1.834	1.176	1.734	1.324
Ph	q (S)	1.449	1.936	1.341	1.954	1.432	1.926
	q (C)	0.861	0.925	0.862	0.901	0.858	0.782
	q (N)	1.722	1.164	1.858	1.196	1.754	1.354
H_2N	q (S)	1.658	1.947	1.394	1.949	1.557	1.944
	q (C)	0.823	0.908	0.823	0.880	0.858	0.806
	q (N)	1.760	1.319	1.858	1.279	1.793	1.480
	Bond						
CH_3	p (C–S)	0.783	0.271	0.882	0.260	0.817	0.318
	p (C–N)	0.600	0.959	0.407	0.986	0.555	0.916
Ph	p (C–S)	0.725	0.256	0.790	0.239	0.858	0.292
	p (C–N)	0.552	0.908	0.395	0.889	0.519	0.853
	p (C–Ph)	0.373	0.316	0.427	0.365	0.357	0.349
H_2N	p (C–S)	0.635	0.242	0.796	0.240	0.711	0.259
	p (C–N)	0.532	0.862	0.409	0.898	0.487	0.788
	p (C–NH_2)	0.532	0.436	0.409	0.347	0.487	0.524

stabilization. However, the difference $E_A - E_B$ must be corrected for the difference in core repulsion energy (E_{core}) between thione and thiol form. Two models have been used to calculate this contribution, *viz.* the point charge model [32] (I) and the orbital-like positive hole model [33] (II). The differences in E_{core} calculated by the two models are given in Table 6. It appears that E_{core} is larger for the thiones than for the thiols here, thus reducing the greater π-stabilization of the thiones. With model I, the thiones become less stable than the thiols. Del Re *et al.*[34] have recently studied the two models and come to the conclusion that model II is most adequate for SCF π-electron calculations. However, the precise value of ΔE_{core} depends strongly on the geometry of the systems, and therefore the $\Delta E_{\pi,II}$ values in Table 6 must be regarded as very approximate. The values for thioacetamide and thiourea are of the right order of magnitude, and the less negative value for thiourea need not be in error. As can be seen in Table 7, the thione sulphur atom has a very high π electron density, which should give extra stabilization to the thione form in water solution.

Calculated π-electron charges and π-bond orders are shown in Table 7. All three models give qualitatively the same relations between charges and bond orders in the different systems, and the agreement between the results from set 1 and the PPP calculations is in most cases remarkably close.

Table 8. Experimental and calculated transition energies for $R-CS-NH_2$ (A), $R-C(SH)=NH$ (B) and $[R-C(SH)=NH_2]^+$ (C) in eV.

R	System	Calc.		Exp.	
		$\Delta E_{\pi\rightarrow\pi^*}$	f	$\Delta E_{\pi\rightarrow\pi^*}$	ε
CH_3	A	4.883	0.479	4.73	13 800
	B	4.898	0.165	5.49	15 700
	C	6.563	0.272	5.41	17 800
Ph	A	3.888	0.409	4.32	8 700
	B	4.795	0.446	5.19	27 000
	C	3.468	0.658	4.63	11 400
H_2N	A	4.643	0.392	5.28	11 200
	B	5.470	0.201	5.21	38 100
	C	6.202	0.265	5.64	5 500

Ultraviolet spectra. An inspection of Table 3 shows that in general the $\pi\rightarrow\pi^*$ transition energies are lower for the thioamides than for the thiolimidates or for the protonated species. This relation is somewhat obscured by the solvents employed, which causes considerable hypsochromic shifts of the thioamide absorption bands. The transition energies calculated by set 1 and set 3 in Table 5 show the same relation, but with set 3 the transition energy for thiourea is smaller than for thioacetamide, whereas the experimental results come in the opposite order. In the thioacetamides and thiobenzamides, the protonated species C and D absorb at longer wavelengths than the thiolimidates B, and this order is reproduced with set 1. The same order is predicted for thiourea, but it is not found experimentally. The differences observed in absorption between forms C and D, which have the same chromophoric system, is partly due to the effects of *N*- and *S*-methyl groups and partly to solvent effects, since the protonated thioamides (C) had to be measured in fairly strong sulphuric acid solution (8 – 9 M).

The transition energies calculated by the PPP method with configuration interaction including all singly excited configurations are given in Table 8 together with pertinent experimental values. The agreement is not very satisfactory, especially not with the protonated forms, and it is probable that the parametrization needs revision.

Non-ideal Hammett behaviour. All thioamides studied give linear plots of $\log([BH^+]/[B])$ *versus* H_0, but the slopes are in the range 1.2 – 1.7 instead of unity, as required by simple theory. Similar behaviour has previously been observed for *N*,*N*-dimethylthioamides,[12] thiolactams,[11] and azolinethiones,[9] and the slopes of the $\log([BH^+]/[B])$ *versus* H_0 plots vary between 1.25 and 2.0. This large variation precludes the introduction of a new acidity scale for thioamides, as has been done for amides by Katritzky *et al.*[35] However, it is evident that the use of an appropriate acidity function would have given higher pK_a values for the thioamides and thus higher pK_T values. Still, one can safely assume that the pK_a values are about equally affected and that the pK_T values fall in the right order.

Acknowledgements. We are grateful to AB Draco for permission to use equipment, and to the *Swedish Natural Science Research Council* for financial support.

REFERENCES

1. Klages, F. *Lehrbuch der organischen Chemie*, de Gruyter, Berlin 1959, Band I, p. 373.
2. Hantzsch, A. *Ber.* **64** (1931) 661.
3. Jensen, K. A. and Nielsen, P. H. *Acta Chem. Scand.* **20** (1966) 597.
4. Sohàr, P. and Nemes, A. *Acta Chim. Acad. Sci. Hung.* **56** (1968) 25.
5. Truter, M. R. *J. Chem. Soc.* **1960** 997.
6. Walter, W., Kubersky, H. P. and Ahlqvist, D. *Ann.* **733** (1970) 170.
7. Jones, R. A. and Katritzky, A. R. *J. Chem. Soc.* **1958** 3610.
8. Albert, A. and Barlin, G. B. *J. Chem. Soc.* **1959** 2384.
9. Kjellin, G. and Sandström, J. *Acta Chem. Scand.* **23** (1969) 2888.
10. Katritzky, A.R. and Lagowski, J. M. *Advan. Heterocycl. Chem.* **1** (1963) 396.
11. Edward, J. T. and Stollar, H. *Can. J. Chem.* **41** (1963) 721.
12. Janssen, M. J. *Rec. Trav. Chim.* **82** (1963) 1197.
13. Rosenthal, D. and Taylor, T. I. *J. Am. Chem. Soc.* **79** (1957) 2684.
14. Lienhard, G. E. and Jencks, W. P. *J. Am. Chem. Soc.* **87** (1965) 3863.
15. Janssen, M. J. *Rec. Trav. Chim.* **81** (1962) 650.
16. Chaturvedi, R. K. and Schmir, G. L. *J. Am. Chem. Soc.* **91** (1969) 737.
17. Chaturvedi, R. K., MacMahon, A. E. and Schmir, G. L. *J. Am. Chem. Soc.* **89** (1967) 6984.
18. Zahradnik, R. *Collection Czech. Chem. Commun.* **24** (1959) 3678.
19. Albert, A., Goldacre, R. and Phillips, J. *J. Chem. Soc.* **1948** 2240.
20. Janssen, M. J. *Thesis*, Utrecht 1959.
21. Mason, S. F. *J. Chem. Soc.* **1954** 2071.
22. Beak, P. and Bonham, J. *Chem. Commun.* **1966** 631.
23. Janssen, M. J. and Sandström, J. *Tetrahedron* **20** (1964) 2339.
24. Cook, M. J., Katritzky, A. R., Linda, P. and Tack, R. D. *Chem. Commun.* **1971** 510.
25. Janssen, M. J. *Rec. Trav. Chim.* **79** (1960) 1066.
26. Dewar, M.J.S. *The Molecular Orbital Theory of Organic Chemistry*, McGraw, New York 1969, p. 156.
27. Mataga, N. and Nishimoto, K. *Z. physik. Chem. (Frankfurt)* **13** (1957) 140.
28. Fabian, J. *Theor. Chim. Acta* **12** (1968) 200.
29. Hinze, J. and Jaffé, H. H. *J. Am. Chem. Soc.* **84** (1962) 540.
30. Kunchur, N. R. and Truter, M. R. *J. Chem. Soc.* **1958** 2551.
31. Flippen, J. L. and Karle, I. L. *J. Phys. Chem.* **74** (1970) 769.
32. Parr, R. G. and Mulliken, R. S. *J. Chem. Phys.* **18** (1950) 1338.
33. Parr, R. G. and Pariser, R. *J. Chem. Phys.* **23** (1955) 711.
34. Del Re, G., Momicchioli, F. and Rastelli, A. *Theor. Chim. Acta* **23** (1972) 316.
35. Katritzky, A. R., Waring, A. J. and Yates, K. *Tetrahedron* **19** (1963) 465.

Received June 21, 1972.

ACTA CHEMICA SCANDINAVICA 27 (1973) 218–228

The Crystal and Molecular Structures of Two Forms of a *trans* Square-Planar Complex of Tellurium Dimethanethiosulphonate with Ethylenethiourea

OLAV FOSS, NILS LYSSANDTRÆ, KNUT MAARTMANN-MOE and MAGNE TYSSELAND

Chemical Institute, University of Bergen, N-5000 Bergen, Norway

The complex, *trans*-dimethanethiosulphonatobis(ethylenethiourea)tellurium(II), $Te(etu)_2(S_2O_2CH_3)_2$, crystallizes in two forms: a triclinic one (I), space group $P\bar{1}$ (No. 2) with $Z=1$, $a=9.519(2)$ Å, $b=10.210(2)$ Å, $c=5.385(1)$ Å, $\alpha=98.88(2)°$, $\beta=105.54(2)°$, $\gamma=98.89(2)°$; and a monoclinic one (II), space group $P2_1/c$ (No. 14) with $Z=2$, $a=9.616(4)$ Å, $b=10.850(6)$ Å, $c=10.672(4)$ Å, $\beta=119.21(4)°$. In both forms, the tellurium atoms lie in centres of symmetry.

The crystal and molecular structures of both forms have been determined by three-dimensional X-ray methods, and refined by least squares procedures based on 912 independent, observed reflections for I and 800 for II.

The centrosymmetric, square-planar TeS_4 coordination groups are very like in the two dimorphs: Te–S(etu) = 2.663(6) Å in I and 2.687(5) Å in II, Te–S(thiosulphonate) = 2.694(6) Å in I and 2.685(4) Å in II, ∠ S–Te–S = 91.6(2)° in I and 92.6(2)° in II. The methanethiosulphonate S–S bond is 2.014(9) Å in I and 2.015(7) Å in II, ∠ Te–S–S = 103.9(3)° in I and 102.3(2)° in II. There are, from one dimorph to the other, some small differences in the rotational positions of the ligand groups.

Complexes of tellurium dimethanethiosulphonate,[1,2] $Te(S_2O_2CH_3)_2$, with thiourea and substituted thioureas as ligands were reported in 1961.[3,4] The crystal and molecular structure of the square-planar *trans* thiourea complex, $Te(tu)_2(S_2O_2CH_3)_2$, has been determined.[5] This paper reports the structures of two crystalline forms of the corresponding ethylenethiourea complex.

CRYSTAL DATA

The triclinic dimorph (I) of *trans*-dimethanethiosulphonatobis(ethylenethiourea)tellurium(II), $Te(etu)_2(S_2O_2CH_3)_2$, occurs as prisms extended along the *c* axis, bounded by {100} and {010} and terminated by {01$\bar{1}$}. This

dimorph was earlier,[3] due to twinning, erroneously described as *C*-centered monoclinic. It appears to be unstable, judging from extraneous reflections appearing on X-ray photographs of samples kept for a year in a refrigerator. The unit cell dimensions are, $a = 9.519(2)$ Å, $b = 10.210(2)$ Å, $c = 5.385(1)$ Å, $\alpha = 98.88(2)°$, $\beta = 105.54(2)°$, $\gamma = 98.89(2)°$. The space group is $P\bar{1}$ (No. 2) and there is one molecule per unit cell; density, calc. 1.89, found [3] 1.89 g/cm³. Cell volume, 487.6 Å³.

The monoclinic dimorph (II) occurs as plates {100} with edges along the *bc* diagonals, and with $a = 9.616(4)$ Å, $b = 10.850(6)$ Å, $c = 10.672(4)$ Å, $\beta = 119.21(4)°$. The space group is $P2_1/c$ (No. 14) and there are two molecules per unit cell; density, calc. 1.89, found [3] 1.89 g/cm³. Cell volume, 971.9 Å³, or 486.0 Å³ per molecule.

EXPERIMENTAL

The procedure used [3] for the preparation of the compound was modified slightly. 1.30 g of tetrakis(ethylenethiourea)tellurium(II) dichloride dihydrate [6] and 0.68 g (a slight excess) of sodium methanethiosulphonate monohydrate were dissolved in 10 ml of dimethylformamide at room temperature. The solution was filtered, and 10 ml of methanol was added to the filtrate under gentle swirling. On standing at room temperature, the product crystallized. After an hour or two, the crystals were filtered off, and washed with methanol, and then with ether. Yield, about 0.85 g, or 76 %.

The product consisted of a mixture of the two dimorphs. The crystals of the two forms could be readily distinguished and picked out under a microscope, on the basis of their different shapes. The colour is the same for both dimorphs, greenish-yellow.

Unit cell dimensions, as given above, were determined from high-order reflections on zero-layer Weissenberg photographs, $\lambda(CuK\alpha_1) = 1.5405$ Å, and evaluated by means of a least squares procedure, from 68 observed 2θ values for I and 34 for II.

Intensities were estimated visually from multiple-film, integrated, equi-inclination Weissenberg photographs taken with Ni-filtered $CuK\alpha$ radiation, except for the *hk*0 data of I which were estimated from a non-integrated film set. The following layers were photographed and used: 0*kl*, 1*kl*, 2*kl*, *hk*0, and *hk*1 for I, and *h*0*l*, *h*1*l*, *h*2*l*, *hk*0, *hk*1, and *hk*2 for II. This gave 1006 independent, accessible reflections for both dimorphs, of which 912 and 800, respectively, were observed with measurable intensities. The crystals used for the intensity photographs had cross-sections 0.08×0.07 mm for the *a*-axis photographs and 0.10×0.07 mm for the first-layer *c*-axis photographs of I, and 0.11×0.08 mm for the *b*-axis photographs and 0.10×0.09 mm for the *c*-axis photographs of II. In the case of the zero-layer *c*-axis photographs of I, a crystal with a slightly smaller cross-section than for the first-layer photographs was used. No corrections for absorption were made ($\mu = 186$ cm^{-1} for I and 187 cm^{-1} for II).

The calculated structure factors were based on the scattering curves listed in *International Tables* (Ref. 7, pp. 202, 211). The tellurium scattering curve, and in the case of II also the sulphur scattering curve, were corrected for anomalous dispersion using the $\Delta f'$ and $\Delta f''$ values given by Cromer,[8] by taking the amplitude of f as the corrected value.

Least squares refinement was in the case of I first carried out on an IBM 1620 computer using a program designed by Mair.[9] The refinement of II, and the final refinement of I, were carried out on an IBM 360/50 H computer with a full-matrix least squares program minimizing the function

$$r = \sum W(|F_o| - K|F_c|)^2$$

where K is a scale factor. The weight is defined by $W = 1/\sigma^2(F_o)$, where $\sigma(F_o)$ is the estimated standard deviation in F_o. Non-observed reflections for which $K|F_c|$ exceeds the observable limit, are included in the refinement with $|F_o|$ equal to the observable limit.

Most of the IBM 360/50 H computer programs were made available by the Chemical Department of X-Ray Crystallography, Weizmann Institute of Science, Rehovoth, Israel, and modified for use on the IBM 360/50 H computer by Dr. D. Rabinovich.

Table 1. Atomic coordinates for triclinic dimorph, in fractions of cell edges. Standard deviations from least squares are given in parentheses. Isotropic thermal parameters (Å²) in the form $\exp[-8\pi^2 U(\sin^2\theta/\lambda^2)]$.

	x	y	z	U
Te	0	0	0	
S_1	0.2381(7)	0.1861(5)	0.0372(14)	
C_1	0.2417(26)	0.3045(19)	0.3084(44)	0.0725
N_1	0.1248(24)	0.3492(17)	0.3406(40)	0.0452
C_2	0.1627(31)	0.4509(24)	0.5947(51)	0.0948
C_3	0.3373(30)	0.4525(23)	0.7044(50)	0.0890
N_2	0.3674(24)	0.3587(18)	0.5015(40)	0.0474
S_2	−0.1672(7)	0.0845(6)	−0.4088(10)	
S_3	−0.2682(6)	0.2163(5)	−0.2395(10)	
C_4	−0.3930(30)	0.1257(23)	−0.1146(51)	0.0942
O_1	−0.3586(19)	0.2701(14)	−0.4480(31)	0.0623
O_2	−0.1612(21)	0.3160(16)	−0.0235(34)	0.0724

STRUCTURE ANALYSIS

The tellurium atoms lie in centres of symmetry in both dimorphs. In the space group $P\bar{1}$ of I, tellurium contributes to all reflections, whereas in the space group $P2_1/c$ of II, it contributes only to reflections with $k+l$ even. The structures were solved in projections, along the c and a axes of I and along the b and c axes of II, through Fourier summations of all but the weakest reflections, with positive signs. In the c-axis projection of II, the $k+l$ odd reflections were not included in the first Fourier synthesis. The sulphur atoms were located from the first Fourier maps, and the lighter atoms from later maps.

Table 2. Atomic coordinates for monoclinic dimorph, in fractions of cell edges. Standard deviations from least squares are given in parentheses. Isotropic thermal parameters (Å²) in the form $\exp[-8\pi^2 U(\sin^2\theta/\lambda^2)]$.

	x	y	z	U
Te	0	0	0	
S_1	−0.0446(5)	0.1260(5)	0.1943(5)	
C_1	−0.1336(17)	0.2576(18)	0.1041(17)	0.0372
N_1	−0.0960(17)	0.3197(17)	0.0144(17)	0.0481
C_2	−0.1930(18)	0.4284(18)	−0.0481(18)	0.0429
C_3	−0.3044(20)	0.4263(20)	0.0219(20)	0.0489
N_2	−0.2527(14)	0.3143(14)	0.1095(14)	0.0396
S_2	0.3177(4)	0.0274(4)	0.1506(5)	
S_3	0.3506(4)	0.1903(4)	0.0782(5)	
C_4	0.3315(21)	0.1646(22)	−0.0967(21)	0.0556
O_1	0.5110(13)	0.2298(14)	0.1744(13)	0.0516
O_2	0.2279(12)	0.2767(12)	0.0576(12)	0.0473

Table 3. Anisotropic thermal parameters (Å²) in the form $\exp[-2\pi^2(h^2a^{-2}U_{11}+\cdots+2hka^{-1}b^{-1}U_{12}+\cdots)]$. All values have been multiplied by 10^4.

	U_{11}	U_{22}	U_{33}	U_{12}	U_{23}	U_{13}
			Triclinic dimorph			
Te	346	379	416	140	52	87
S_1	543	590	859	115	78	380
S_2	587	886	432	385	124	125
S_3	371	617	506	216	158	31
			Monoclinic dimorph			
Te	394	229	431	−2	9	192
S_1	698	449	522	54	65	362
S_2	445	340	603	2	100	194
S_3	391	348	587	−8	−29	277

In all but the *c*-axis projection of I, some overlapping occurred, and in order to locate the carbon and nitrogen atom of the ethylenethiourea groups, use was also made of models based on known distances and angles.

Three-dimensional least squares refinement was started with coordinates derived from the projections. At first, only the tellurium and sulphur parameters were allowed to vary, and later also the parameters of the lighter atoms. Anisotropic thermal parameters for tellurium and sulphur were introduced at later stages. The last refinement cycles gave shifts which were insignificant relative to the standard deviations. The final value of the conventional *R* factor was 0.091 for I and 0.068 for II.

The final atomic coordinates are listed in Tables 1 and 2, anisotropic thermal parameters in Table 3, and observed and calculated structure factors in Tables 4 and 5.

RESULTS

Bond lengths and angles involving the TeS_4 coordination groups, from the coordinates of Tables 1 and 2, are listed in Table 6. The tellurium atoms being located in crystallographic centres of symmetry, the TeS_4 coordination groups are exactly planar in both dimorphs.

Bond lengths and angles are very like in the two dimorphs. The values of Table 6 differ significantly only in three instances: Te−S(ethylenethiourea) = 2.663(6) Å in I and 2.687(5) Å in II, $\Delta = 3.1\ \sigma(\Delta)$; ∠ S−Te−S = 91.6(2)° in I and 92.6(2)° in II, $\Delta = 3.5\ \sigma(\Delta)$; ∠Te−S−S = 103.9(3)° in I and 102.3(2)° in II, $\Delta = 4.4\ \sigma(\Delta)$.

For the thiourea complex, *trans*-dimethanethiosulphonatobis(thiourea)tellurium(II), the following bond lengths and angles were found:[5] Te−S(thiourea) = 2.667(15) Å, Te−S(thiosulphonate) = 2.684(15) Å, ∠S−Te−S = 90.6(5)°, S−C = 1.76(6) Å, S−S = 2.024(18) Å, ∠ Te−S−C = 100.7(2.1)°,

Table 4. Observed and calculated structure factors (× 10) for triclinic dimorph. Unobserved reflections are indicated by a minus sign on $F(O)$ and included at the threshold values.

H	K	L	F(O)	F(C)	H	K	L	F(O)	F(C)	H	K	L	F(O)	F(C)	H	K	L	F(O)	F(C)	H	K	L	F(O)	F(C)
0	1	0	433	524	0	2	4	113	-26	1	-2	3	135	138	1	-6	-3	218	203	2-10	2	177	166
0	2	0	73	-23	0	3	4	115	126	1	-1	3	252	252	1	-5	-3	150	121	2	-9	2	327	310
0	3	0	316	264	0	4	4	226	200	1	0	3	241	242	1	-4	-3	-61	19	2	-8	2	321	319
0	4	0	315	357	0	5	4	219	209	1	1	3	71	56	1	-3	-3	346	312	2	-7	2	89	82
0	5	0	337	293	0	6	4	116	126	1	2	3	114	106	1	-2	-3	415	361	2	-6	2	-65	51
0	6	0	264	286	0	7	4	59	75	1	3	3	336	344	1	-1	-3	480	535	2	-5	2	305	303
0	7	0	76	91	0	8	4	62	93	1	4	3	362	336	1	0	-3	527	535	2	-4	2	192	179
0	8	0	63	75	0-10	5	57	68	1	5	3	288	258	1	1	-3	258	243	2	-3	2	132	155
0	9	0	232	220	0	-9	5	73	86	1	6	3	152	157	1	2	-3	243	226	2	-2	2	267	239
0	10	0	168	175	0	-8	5	99	111	1-11	4	51	38	1	3	-3	332	339	2	-1	2	261	284
0	11	0	142	152	0	-7	5	60	65	1-10	4	-51	39	1	4	-3	187	185	2	0	2	478	481
0	12	0	56	75	0	-6	5	-59	36	1	-9	4	80	97	1	5	-3	-57	17	2	1	2	567	515
0-12	1	76	104	0	-5	5	75	663	1	-8	4	162	153	1	6	-3	174	195	2	2	2	358	376
0-11	1	81	72	0	-4	5	125	110	1	-7	4	132	147	1	7	-3	134	128	2	3	2	416	371
0-10	1	148	154	0	-3	5	134	135	1	-6	4	-67	35	1	8	-3	168	157	2	4	2	233	203
0	-9	1	163	172	0	-2	5	148	160	1	-5	4	96	91	1	9	-3	127	121	2	5	2	149	136
0	-8	1	208	225	0	-1	5	148	140	1	-4	4	278	281	1	-8	-4	106	102	2	6	2	123	152
0	-7	1	342	329	0	0	5	209	211	1	-3	4	385	388	1	-7	-4	155	147	2-10	3	-79	22
0	-6	1	440	463	0	1	5	244	265	1	-2	4	321	306	1	-6	-4	201	188	2	-9	3	153	175
0	-5	1	301	267	0	2	5	133	122	1	-1	4	225	217	1	-5	-4	165	165	2	-8	3	303	272
0	-4	1	526	540	0	3	5	80	67	1	0	4	150	157	1	-4	-4	218	193	2	-7	3	257	241
0	-3	1	74	63	0	4	5	112	122	1	1	4	245	244	1	-3	-4	232	207	2	-6	3	118	134
0	-2	1	132	-113	0	5	5	103	103	1	2	4	153	140	1	-2	-4	164	157	2	-5	3	176	186
0	-1	1	335	335	0	6	5	61	65	1	3	4	-67	16	1	-1	-4	113	113	2	-4	3	491	492
0	0	1	290	282	0	-7	6	106	115	1	4	4	116	114	1	0	-4	143	140	2	-3	3	442	424
0	1	1	815	883	0	-6	6	106	132	1	5	4	110	119	1	1	-4	210	204	2	-2	3	152	170
0	2	1	404	-401	0	-5	6	79	72	1	6	4	98	77	1	2	-4	127	93	2	-1	3	-65	9
0	3	1	195	217	0	-4	6	59	49	1-10	5	39	44	1	3	-4	129	130	2	0	3	81	80
0	4	1	230	194	0	-3	6	104	131	1	-9	5	85	84	1	4	-4	123	134	2	1	3	233	238
0	5	1	640	696	0	-2	6	89	91	1	-8	5	151	163	1	5	-4	277	263	2	2	3	368	314
0	6	1	458	448	0	-1	6	-48	32	1	-7	5	167	147	1	6	-4	318	323	2	3	3	93	91
0	7	1	215	186	0	0	6	-46	33	1	-6	5	117	107	1	7	-4	290	283	2	4	3	110	103
0	8	1	74	23	0	1	6	-42	36	1	-5	5	-63	36	1	8	-4	-79	32	2	5	3	214	204
0	9	1	120	121	0	2	6	64	84	1	-4	5	-63	-23	1	9	-4	107	91	2	6	3	168	155
0	10	1	173	167	1-12	0	131	157	1	-3	5	116	129	1	10	-4	143	143	2-10	4	82	89
0	11	1	76	102	1-11	0	110	107	1	-2	5	212	210	1	-6	-5	67	67	2	-9	4	83	62
0	12	1	36	53	1-10	0	80	95	1	-1	5	-65	52	1	-5	-5	98	91	2	-8	4	127	144
0-12	2	134	131	1	-9	0	134	202	1	0	5	93	81	1	-4	-5	102	89	2	-7	4	108	118
0-11	2	151	160	1	-8	0	258	227	1	1	5	143	150	1	-3	-5	78	58	2	-6	4	95	76
0-10	2	75	63	1	-7	0	408	393	1	2	5	194	199	1	-2	-5	81	60	2	-5	4	-77	77
0	-9	2	-67	18	1	-6	0	294	265	1	3	5	170	192	1	-1	-5	151	141	2	-4	4	-75	80
0	-8	2	124	128	1	-5	0	84	93	1	4	5	106	101	1	0	-5	306	312	2	-3	4	262	240
0	-7	2	255	254	1	-4	0	61	31	1	-7	6	72	94	1	1	-5	275	274	2	-2	4	397	366
0	-6	2	342	305	1	-3	0	575	614	1	-6	6	113	139	1	2	-5	119	102	2	-1	4	182	176
0	-5	2	345	363	1	-2	0	151	166	1	-5	6	89	92	1	3	-5	84	87	2	0	4	95	74
0	-4	2	140	111	1	-1	0	353	407	1	-4	6	95	97	1	4	-5	187	202	2	1	4	348	302
0	-3	2	485	557	1	0	0	410	530	1	-3	6	97	109	1	5	-5	184	191	2	2	4	266	263
0	-2	2	491	516	1	1	0	624	632	1	-2	6	103	115	1	6	-5	80	90	2	3	4	171	165
0	-1	2	487	539	1	2	0	906	893	1	-1	6	94	114	1	7	-5	-61	25	2	4	4	-71	55
0	0	2	516	557	1	3	0	398	383	1	0	6	-41	36	1	8	-5	-55	28	2	-9	5	80	95
0	1	2	344	373	1-12	1	123	137	1	1	6	-37	4	1	-9	-6	66	73	2	-8	5	80	84
0	2	2	162	180	1-11	1	139	140	1	2	6	-27	46	1	-8	-6	91	93	2	-7	5	134	127
0	3	2	258	235	1-10	1	70	24	1-12	-1	71	90	1	-7	-6	152	162	2	-6	5	166	180
0	4	2	215	201	1	-9	1	73	44	1-11	-1	77	109	1	0	-6	107	121	2	-5	5	158	156
0	5	2	78	69	1	-8	1	269	258	1-10	-1	107	93	1	1	-6	-55	14	2	-4	5	89	76
0	6	2	257	260	1	-7	1	421	406	1	-9	-1	96	85	1	2	-6	-55	16	2	-3	5	-67	78
0	7	2	210	205	1	-6	1	463	453	1	-8	-1	165	163	1	3	-6	79	55	2	-2	5	-67	98
0	8	2	126	123	1	-5	1	367	372	1	-7	-1	114	120	1	4	-6	77	84	2	-1	5	89	94
0	9	2	135	105	1	-4	1	305	297	1	-6	-1	400	370	1	5	-6	73	97	2	0	5	87	79
0	10	2	122	142	1	-3	1	422	434	1	-5	-1	506	452	1	6	-6	67	72	2	1	5	-67	47
0	11	2	99	128	1	-2	1	874	1099	1	-4	-1	353	402	1	7	-6	71	88	2	2	5	127	121
0-12	3	65	82	1	-1	1	221	245	1	-3	-1	531	486	2-12	0	114	124	2	3	5	157	162
0-11	3	149	137	1	0	1	116	-112	1	-2	-1	391	367	2-11	0	102	113	2	-4	6	103	142
0-10	3	185	174	1	1	1	183	-164	1	-1	-1	560	583	2-10	0	99	99	2	-3	6	129	86
0	-9	3	125	130	1	2	1	233	234	1	0	-1	859	1036	2	-9	0	186	188	2	-2	6	57	90
0	-8	3	-61	31	1	3	1	548	535	1	1	-1	504	509	2	-8	0	434	409	2	-1	6	76	107
0	-7	3	269	249	1	4	1	487	466	1	2	-1	713	-753	2	-7	0	391	379	2	0	6	76	104
0	-6	3	468	463	1	5	1	245	238	1	3	-1	506	546	2	-6	0	302	264	2	1	6	51	73
0	-5	3	208	187	1	6	1	210	220	1	4	-1	567	517	2	-5	0	206	203	2-12	-1	98	124
0	-4	3	83	-49	1-12	2	138	112	1	5	-1	292	267	2	-4	0	66	41	2-11	-1	100	102
0	-3	3	-50	44	1-11	2	147	149	1	6	-1	246	200	2	-3	0	386	374	2-10	-1	93	99
0	-2	3	264	251	1-10	2	183	170	1	7	-1	122	135	2	-2	0	729	842	2	-9	-1	172	171
0	-1	3	332	274	1	-9	2	146	116	1-11	-2	93	96	2	-1	0	355	458	2	-8	-1	312	274
0	0	3	433	424	1	-8	2	82	60	1-10	-2	126	137	2	0	0	397	-480	2	-7	-1	207	201
0	1	3	254	228	1	-7	2	194	182	1	-9	-2	159	146	2	1	0	270	264	2	-6	-1	123	106
0	2	3	248	239	1	-6	2	364	381	1	-8	-2	64	80	2	2	0	689	745	2	-5	-1	148	-107
0	3	3	443	356	1	-5	2	84	108	1	-7	-2	322	276	2	3	0	711	768	2	-4	-1	367	372
0	4	3	417	400	1	-4	2	103	-80	1	-6	-2	530	492	2	4	0	381	372	2	-3	-1	886	916
0	5	3	218	207	1	-3	2	389	433	1	-5	-2	363	329	2-12	1	71	72	2	-2	-1	912	985
0	6	3	110	105	1	-2	2	678	777	1	-4	-2	-82	37	2-11	1	87	100	2	-1	-1	201	187
0	7	3	106	90	1	-1	2	584	630	1	-3	-2	246	-175	2-10	1	145	145	2	0	-1	413	478
0	8	3	73	82	1	0	2	417	432	1	-2	-2	434	413	2	-9	1	184	162	2	1	-1	486	521
0	9	3	79	99	1	1	2	359	327	1	-1	-2	455	397	2	-8	1	124	126	2	2	-1	502	530
0	10	3	46	72	1	2	2	77	78	1	0	-2	333	394	2	-7	1	230	208	2	3	-1	311	329
0-11	4	62	59	1	3	2	524	414	1	1	-2	144	157	2	-6	1	348	324	2	4	-1	239	131
0-10	4	83	64	1	4	2	467	478	1	2	-2	407	384	2	-5	1	326	306	2	5	-1	233	238
0	-9	4	81	96	1	5	2	77	112	1	3	-2	353	334	2	-4	1	308	270	2	6	-1	165	147
0	-8	4	87	73	1-12	3	50	64	1	4	-2	669	730	2	-3	1	613	659	2	7	-1	221	197
0	-7	4	90	96	1-11	3	67	59	1	5	-2	479	473	2	-2	1	780	912	2-10	-2	81	73
0	-6	4	248	243	1-10	3	109	101	1	6	-2	71	56	2	-1	1	395	542	2	-9	-2	184	166
0	-5	4	365	332	1	-9	3	203	217	1	7	-2	155	174	2	0	1	213	267	2	-8	-2	265	252
0	-4	4	327	307	1	-8	3	252	240	1	8	-2	165	159	2	1	1	268	265	2	-7	-2	281	245
0	-3	4	139	157	1	-7	3	191	167	1	9	-2	206	182	2	2	1	137	119	2	-6	-2	173	157
0	-2	4	130	116	1	-6	3	242	254	1-10	-3	39	75	2	3	1	225	206	2	-5	-2	486	443
0	-1	4	333	313	1	-5	3	344	322	1	-9	-3	53	39	2	4	1	447	425	2	-4	-2	426	371
0	0	4	292	279	1	-4	3	211	212	1	-8	-3	77	81	2	5	1	105	95	2	-3	-2	428	419
0	1	4	-59	11		-3	3	159	153	1	-7	-3	203	181	2-11	2	83	77	2	-2	-2	440	364

Table 4. Continued.

H	K	L	F(o)	F(c)	H	K	L	F(o)	F(c)	H	K	L	F(o)	F(c)	H	K	L	F(o)	F(c)	H	K	L	F(o)	F(c)
2	-1	-2	105	101	-7	2	0	194	189	-5	8	0	244	242	7	3	1	100	81	-2	12	1	70	124
2	0	-2	163	162	-6	2	0	611	560	-4	8	0	83	75	8	3	1	-74	21	-1	12	1	65	93
2	1	-2	136	135	-5	2	0	572	565	-3	8	0	185	179	9	3	1	103	120	-3	12	1	592	634
2	2	-2	-64	22	-4	2	0	115	131	-2	8	0	416	409	-10	4	1	-75	34	3	-1	1	261	300
2	3	-2	308	295	-3	2	0	63	102	1	8	0	-46	73	-9	4	1	142	124	4	-1	1	311	349
2	4	-2	700	757	3	2	0	396	376	2	8	0	269	239	-8	4	1	241	228	5	-1	1	424	428
2	5	-2	237	227	4	2	0	72	59	3	8	0	276	287	-7	4	1	305	306	6	-1	1	219	203
2	6	-2	248	237	5	2	0	142	162	4	8	0	-55	72	-6	4	1	359	333	7	-1	1	-81	28
2	7	-2	220	214	6	2	0	362	369	5	8	0	-48	47	-5	4	1	350	343	8	-1	1	175	143
2	8	-2	190	160	7	2	0	229	216	6	8	0	111	136	-4	4	1	311	297	9	-1	1	297	280
2	-10	-3	92	105	8	2	0	106	115	7	8	0	70	84	-3	4	1	125	123	10	-1	1	171	175
2	-9	-3	127	140	9	2	0	147	139	-9	9	0	36	59	3	4	1	148	130	-4	-2	1	272	291
2	-8	-3	127	114	10	2	0	95	93	-8	9	0	222	227	4	4	1	93	100	-3	-2	1	922	1045
2	-7	-3	144	128	-11	3	0	120	126	-7	9	0	310	286	5	4	1	244	262	3	-2	1	432	377
2	-6	-3	264	252	-10	3	0	124	143	-6	9	0	100	102	6	4	1	263	253	4	-2	1	174	192
2	-5	-3	130	107	-9	3	0	256	224	-5	9	0	-55	15	7	4	1	-77	83	5	-2	1	249	277
2	-4	-3	-71	-4	-8	3	0	156	144	-4	9	0	163	164	8	4	1	-66	33	6	-2	1	225	214
2	-3	-3	207	175	-7	3	0	149	132	-3	9	0	238	232	-9	5	1	197	169	7	-2	1	-81	29
2	-2	-3	363	353	-6	3	0	373	355	1	9	0	149	150	-8	5	1	299	307	8	-2	1	227	221
2	-1	-3	530	504	-5	3	0	312	337	2	9	0	86	85	-7	5	1	192	176	9	-2	1	332	308
2	0	-3	215	195	-4	3	0	292	338	3	9	0	88	76	-6	5	1	186	183	10	-2	1	111	102
2	1	-3	284	320	-3	3	0	283	290	4	9	0	91	108	-5	5	1	251	283	-4	-3	1	368	369
2	2	-3	330	316	3	3	0	271	265	5	9	0	115	118	-4	5	1	504	480	-3	-3	1	497	463
2	3	-3	436	458	4	3	0	163	-113	6	9	0	68	91	-3	5	1	244	232	3	-3	1	204	218
2	4	-3	403	424	5	3	0	265	239	-8	10	0	123	121	3	5	1	186	178	4	-3	1	300	294
2	5	-3	266	276	6	3	0	398	372	-7	10	0	251	229	4	5	1	213	204	5	-3	1	294	297
2	6	-3	133	-64	7	3	0	206	211	-6	10	0	91	120	5	5	1	144	163	6	-3	1	169	154
2	7	-3	-75	27	8	3	0	111	100	-5	10	0	50	65	6	5	1	151	133	7	-3	1	403	358
2	8	-3	245	233	9	3	0	93	93	-4	10	0	199	203	7	5	1	126	144	8	-3	1	293	291
2	9	-3	150	143	10	3	0	111	134	-3	10	0	194	191	8	5	1	83	104	9	-3	1	-77	83
2	-8	-4	79	102	-11	4	0	219	190	1	10	0	194	187	-10	6	1	117	147	10	-3	1	78	90
2	-7	-4	164	183	-10	4	0	118	100	2	10	0	-48	52	-9	6	1	-77	74	11	-3	1	107	109
2	-6	-4	216	176	-9	4	0	174	156	3	10	0	-48	40	-8	6	1	175	147	-5	-4	1	363	365
2	-5	-4	155	148	-8	4	0	265	252	4	10	0	124	139	-7	6	1	293	294	-4	-4	1	396	379
2	-4	-4	156	144	-7	4	0	84	106	5	10	0	81	112	-6	6	1	196	197	-3	-4	1	84	42
2	-3	-4	293	253	-6	4	0	-51	58	-7	11	0	91	104	-5	6	1	372	369	3	-4	1	641	632
2	-2	-4	445	426	-5	4	0	396	394	-6	11	0	181	179	-3	6	1	121	99	4	-4	1	327	299
2	-1	-4	228	217	-4	4	0	731	746	-5	11	0	138	148	2	6	1	-77	-7	5	-4	1	111	-126
2	0	-4	124	131	-3	4	0	491	499	-4	11	0	48	66	3	6	1	198	193	6	-4	1	122	104
2	1	-4	-85	-11	1	4	0	538	543	-3	11	0	-32	102	4	6	1	293	291	7	-4	1	471	456
2	2	-4	124	94	3	4	0	384	396	1	11	0	100	112	5	6	1	115	101	8	-4	1	292	270
2	3	-4	304	321	4	4	0	226	221	2	11	0	48	70	6	6	1	-75	78	9	-4	1	75	41
2	4	-4	183	203	5	4	0	73	58	3	11	0	32	70	7	6	1	110	135	10	-4	1	77	80
2	5	-4	-75	26	6	4	0	199	209	-6	12	0	122	126	8	6	1	76	107	11	-4	1	150	130
2	6	-4	110	114	7	4	0	235	209	-5	12	0	131	145	-10	7	1	220	241	-5	-5	1	457	459
2	7	-4	214	210	8	4	0	115	108	-4	12	0	41	70	-9	7	1	103	95	-4	-5	1	414	387
2	8	-4	169	153	9	4	0	77	95	-3	12	0	35	37	-8	7	1	-98	-21	-3	-5	1	-86	13
2	9	-4	135	144	10	4	0	72	93	1	12	0	-28	50	-7	7	1	117	143	3	-5	1	505	497
2	-7	-5	99	133	-11	5	0	131	143	-8	0	1	316	346	-6	7	1	413	402	4	-5	1	294	274
2	-6	-5	99	104	-10	5	0	174	150	-7	0	1	93	89	-5	7	1	342	342	5	-5	1	74	76
2	-5	-5	77	51	-9	5	0	115	128	-6	0	1	83	-30	-4	7	1	157	132	6	-5	1	317	314
2	-4	-5	-70	48	-8	5	0	319	280	-5	0	1	420	461	-3	7	1	210	191	7	-5	1	255	205
2	-3	-5	128	121	-7	5	0	342	280	-4	0	1	556	639	1	7	1	304	304	8	-5	1	153	149
2	-2	-5	106	112	-6	5	0	-93	-3	-3	0	1	172	155	2	7	1	272	277	9	-5	1	166	155
2	-1	-5	-75	00	-5	5	0	118	114	3	0	1	515	564	3	7	1	144	152	10	-5	1	95	110
2	0	-5	95	72	-4	5	0	550	591	4	0	1	571	615	4	7	1	-81	87	-5	-6	1	201	207
2	1	-5	142	143	-3	5	0	527	571	5	0	1	159	155	5	7	1	-76	75	-4	-6	1	175	162
2	2	-5	253	249	1	5	0	443	419	6	0	1	132	119	6	7	1	93	85	-3	-6	1	227	204
2	3	-5	192	178	2	5	0	170	165	7	0	1	290	269	-10	8	1	167	209	3	-6	1	84	23
2	4	-5	156	150	3	5	0	296	276	8	0	1	100	112	-9	8	1	139	173	4	-6	1	89	-5
2	5	-5	133	140	4	5	0	425	424	9	0	1	136	120	-8	8	1	-75	24	5	-6	1	453	404
2	6	-5	139	123	5	5	0	170	162	10	0	1	145	161	-7	8	1	113	113	6	-6	1	408	372
2	7	-5	86	94	6	5	0	-55	25	-9	1	1	151	161	-6	8	1	208	205	7	-6	1	155	153
2	-4	-6	74	88	7	5	0	-55	79	-8	1	1	280	279	-5	8	1	144	162	8	-6	1	160	155
2	-3	-6	95	106	8	5	0	145	161	-7	1	1	274	266	-4	8	1	116	142	9	-6	1	125	104
2	-2	-6	97	109	9	5	0	106	127	-6	1	1	286	251	-3	8	1	252	256	10	-6	1	68	75
2	-1	-6	122	136	-11	6	0	57	63	-5	1	1	332	308	1	8	1	185	181	-4	-7	1	116	104
2	0	-6	130	170	-10	6	0	188	199	-4	1	1	304	343	2	8	1	303	307	-3	-7	1	298	284
2	1	-6	102	138	-9	6	0	321	253	-3	1	1	406	469	3	8	1	-81	83	3	-7	1	73	-21
2	2	-6	-65	32	-8	6	0	179	172	3	1	1	662	731	4	8	1	-75	25	4	-7	1	234	211
2	3	-6	-84	36	-7	6	0	167	145	4	1	1	386	401	5	8	1	113	110	5	-7	1	476	422
2	4	-6	78	83	-6	6	0	215	206	5	1	1	138	193	6	8	1	89	109	6	-7	1	176	166
2	5	-6	74	87	-5	6	0	124	142	6	1	1	96	69	-9	9	1	117	136	7	-7	1	100	105
3	0	0	226	233	-4	6	0	276	268	7	1	1	231	193	-8	9	1	150	109	8	-7	1	233	200
4	0	0	260	314	-3	6	0	436	431	8	1	1	222	211	-7	9	1	-75	75	9	-7	1	104	124
5	0	0	422	422	1	6	0	230	277	9	1	1	87	62	-6	9	1	-79	74	-5	-8	1	203	190
6	0	0	239	247	2	6	0	210	215	10	1	1	76	91	-5	9	1	223	218	-2	-8	1	173	170
7	0	0	276	269	3	6	0	129	115	-9	2	1	117	122	-4	9	1	226	221	-1	-8	1	179	155
8	0	0	330	315	4	6	0	301	283	-8	2	1	231	218	-3	9	1	203	211	5	-8	1	179	163
9	0	0	63	67	5	6	0	201	211	-7	2	1	417	406	1	9	1	139	137	6	-8	1	301	269
10	0	0	-48	25	6	6	0	-55	23	-6	2	1	321	332	2	9	1	134	148	5	-9	1	203	201
11	0	0	129	139	7	6	0	102	94	-5	2	1	-58	44	3	9	1	131	133	6	-8	1	193	190
-11	1	0	113	133	8	6	0	134	157	-4	2	1	141	-56	4	9	1	77	65	7	-8	1	193	197
-10	1	0	234	224	-10	7	0	154	156	-3	2	1	628	604	5	9	1	70	76	-3	-9	1	99	79
-9	1	0	136	116	-9	7	0	310	276	3	2	1	337	365	-8	10	1	93	142	-2	-9	1	203	173
-8	1	0	-55	19	-8	7	0	113	114	4	2	1	401	408	-7	10	1	111	119	-1	-9	1	327	277
-7	1	0	233	196	-7	7	0	-55	58	5	2	1	351	329	-6	10	1	71	33	2	-9	1	203	162
-6	1	0	305	324	-6	7	0	237	275	6	2	1	99	123	-5	10	1	129	139	3	-9	1	275	244
-5	1	0	532	540	-5	7	0	296	279	7	2	1	117	115	-4	10	1	211	233	4	-9	1	144	152
-4	1	0	561	484	-4	7	0	129	126	8	2	1	184	172	-3	10	1	136	160	5	-9	1	116	105
-3	1	0	188	169	-3	7	0	197	223	9	2	1	94	96	1	10	1	101	123	6	-9	1	210	218
3	1	0	317	357	1	7	0	-55	6	10	2	1	79	75	2	10	1	81	76	7	-9	1	224	226
4	1	0	511	477	2	7	0	310	305	-10	3	1	187	177	3	10	1	81	104	-2	-10	1	134	128
5	1	0	258	241	3	7	0	200	274	-9	3	1	101	90	4	10	1	61	84	-1	-10	1	283	239
6	1	0	111	124	4	7	0	113	131	-8	3	1	-82	70	-7	11	1	84	113	2	-10	1	163	143
7	1	0	321	304	5	7	0	113	122	-7	3	1	451	451	-6	11	1	-56	43	3	-10	1	236	214
8	1	0	332	298	6	7	0	104	118	-6	3	1	431	515	-5	11	1	77	69	4	-10	1	159	128
9	1	0	-164	85	7	7	0	102	96	-5	3	1	220	201	-4	11	1	132	175	5	-10	1	171	153
10	1	0	-46	1	8	7	0	48	63	-4	3	1	96	-61	-3	11	1	117	147	6	-10	1	159	163
11	1	0	88	87	-10	8	0	70	70	-3	3	1	199	167	-1	11	1	149	109	-2	-11	1	81	100
-11	2	0	93	92	-9	8	0	149	151	3	3	1	78	72	1	11	1	69	96	-1	-11	1	30	35
-10	2	0	298	263	-8	8	0	285	241	4	3	1	200	177	-5	12	1	61	93	2	-11	1	91	100
-9	2	0	172	163	-7	8	0	142	155	5	3	1	397	359	-4	12	1	59	65	3	-11	1	90	87
-8	2	0	120	-66	-6	8	0	133	146	6	3	1	412	355	-3	12	1	70	100	4	-11	1	229	206
																				5	-11	1	175	184

Table 5. Observed and calculated structure factors (× 10) for monoclinic dimorph. Unobserved reflections are indicated by a minus sign on $F(O)$ and included at the threshold values.

H	K	L	F(O)	F(C)	H	K	L	F(O)	F(C)	H	K	L	F(O)	F(C)	H	K	L	F(O)	F(C)	H	K	L	F(O)	F(C)
1	0	0	885	968	7	0-10	326	323	0	1 11	207	239	4	1 -9	723	666	0	2 8	527	511				
2	0	0	273	298	8	0-10	542	523	1	1 11	201	206	5	1 -9	665	641	1	2 8	-80	91				
3	0	0	1513	1626	9	0-10	-69	61	1	1 -1	1147	1072	6	1 -9	285	298	2	2 8	380	396				
4	0	0	724	701	10	0-10	-61	18	2	1 -1	571	470	7	1 -9	537	511	3	2 8	312	324				
5	0	0	193	177	11	0-10	236	277	3	1 -1	1025	1052	8	1 -9	440	437	0	2 9	177	204				
6	0	0	861	849	1	0-12	87	-107	4	1 -1	706	721	9	1 -9	125	162	1	2 9	-75	86				
7	0	0	127	94	2	0-12	155	172	5	1 -1	170	157	10	1 -9	330	335	2	2 9	-68	59				
8	0	0	250	210	3	0-12	230	243	6	1 -1	439	489	11	1 -9	305	293	3	2 9	-56	90				
9	0	0	306	405	4	0-12	109	-89	7	1 -1	429	411	1	1-10	134	173	0	2 10	-71	95				
10	0	0	133	111	5	0-12	91	99	8	1 -1	181	176	2	1-10	103	88	1	2 10	201	161				
0	0	2	1433	1416	6	0-12	248	293	9	1 -1	247	262	3	1-10	-66	-60	2	2 10	258	266				
1	0	2	330	338	7	0-12	-62	-4	10	1 -1	234	238	4	1-10	132	123	0	2 11	-56	43				
2	0	2	822	774	8	0-12	252	272	11	1 -1	105	117	5	1-10	148	153	1	2 11	85	-90				
3	0	2	927	862	9	0-12	256	236	1	1 -2	276	-244	6	1-10	104	-111	1	2 -1	641	-556				
4	0	2	135	155	1	1 0	169	-158	2	1 -2	360	275	7	1-10	165	201	2	2 -1	890	880				
5	0	2	936	937	2	1 0	991	1109	3	1 -2	94	89	8	1-10	-63	54	3	2 -1	449	436				
6	0	2	331	377	3	1 0	359	363	4	1 -2	-41	-16	9	1-10	-58	41	4	2 -1	242	-239				
7	0	2	145	158	4	1 0	-44	-12	5	1 -2	250	-211	10	1-10	174	189	5	2 -1	333	343				
8	0	2	502	523	5	1 0	529	511	6	1 -2	134	-206	11	1-10	-40	0	6	2 -1	214	209				
9	0	2	404	381	6	1 0	186	-156	7	1 -2	434	-377	1	1-11	176	213	7	2 -1	189	-170				
0	0	4	238	239	7	1 0	-65	-38	8	1 -2	237	198	2	1-11	336	352	8	2 -1	-80	55				
1	0	4	878	811	8	1 0	270	253	9	1 -2	130	-118	3	1-11	208	200	9	2 -1	-76	-37				
2	0	4	841	775	9	1 0	-67	-31	10	1 -2	175	-179	4	1-11	117	138	10	2 -1	-62	-71				
3	0	4	125	103	10	1 0	-46	-34	11	1 -2	-42	32	5	1-11	380	370	1	2 -2	1168	1188				
4	0	4	536	503	0	1 1	1048	1158	1	1 -3	1037	969	6	1-11	197	194	2	2 -2	1241	1243				
5	0	4	443	407	1	1 1	357	303	2	1 -3	889	772	7	1-11	-60	12	3	2 -2	439	405				
6	0	4	166	-156	2	1 1	1415	1458	3	1 -3	455	385	8	1-11	215	231	4	2 -2	1071	1129				
7	0	4	200	184	3	1 1	1502	1465	4	1 -3	1206	1176	9	1-11	138	145	5	2 -2	607	655				
8	0	4	268	256	4	1 1	355	364	5	1 -3	962	948	10	1-11	-44	57	6	2 -2	223	199				
0	0	6	654	633	5	1 1	705	691	6	1 -3	367	350	11	1-11	211	209	7	2 -2	657	707				
1	0	6	591	543	6	1 1	835	843	7	1 -3	566	567	1	1-12	-39	17	8	2 -2	415	443				
2	0	6	586	593	7	1 1	264	273	8	1 -3	682	669	2	1-12	123	129	9	2 -2	-78	45				
3	0	6	527	536	8	1 1	322	333	9	1 -3	348	361	3	1-12	-51	-64	10	2 -2	392	403				
4	0	6	695	683	9	1 1	384	369	10	1 -3	219	251	4	1-12	-54	-48	11	2 -2	277	263				
5	0	6	174	188	10	1 1	93	94	11	1 -3	317	306	5	1-12	-55	27	1	2 -3	510	-463				
6	0	6	208	202	0	1 2	1316	-1396	1	1 -4	-39	-36	6	1-12	162	-153	2	2 -3	540	-517				
0	0	8	193	127	1	1 2	184	-159	2	1 -4	1044	-913	7	1-12	-52	-37	3	2 -3	561	-440				
1	0	8	163	158	2	1 2	272	275	3	1 -4	445	379	8	1-12	-49	32	4	2 -3	646	-593				
2	0	8	152	155	3	1 2	181	-170	4	1 -4	-43	-36	9	1-12	172	-173	5	2 -3	184	-176				
3	0	8	214	201	4	1 2	168	-130	5	1 -4	129	-93	10	1-12	-33	-26	6	2 -3	-66	29				
4	0	8	118	145	5	1 2	-60	48	6	1 -4	-54	50	3	1-13	175	191	7	2 -3	261	-238				
5	0	8	49	47	6	1 2	336	-286	7	1 -4	-60	40	4	1-13	116	123	8	2 -3	-79	-49				
0	0	10	295	314	7	1 2	-66	44	8	1 -4	-65	71	5	1-13	146	155	9	2 -3	-79	46				
1	0	10	367	453	8	1 2	-60	-32	9	1 -4	155	164	6	1-13	274	274	10	2 -3	-71	3				
2	0	10	214	230	9	1 2	150	-131	10	1 -4	115	-107	7	1-13	154	175	11	2 -3	-55	67				
1	0	-2	1271	1214	0	1 3	245	-188	11	1 -4	71	92	8	1-13	165	176	1	2 -4	288	267				
2	0	-2	924	-923	1	1 3	461	433	1	1 -5	701	657	0	2 2	487	448	2	2 -4	1293	1263				
3	0	-2	497	393	2	1 3	943	919	2	1 -5	1217	1061	1	2 2	348	382	3	2 -4	690	615				
4	0	-2	468	491	3	1 3	191	149	3	1 -5	937	865	2	2 2	977	944	4	2 -4	441	432				
5	0	-2	96	91	4	1 3	245	233	4	1 -5	928	839	3	2 2	408	483	5	2 -4	858	803				
6	0	-2	595	577	5	1 3	648	664	5	1 -5	934	811	4	2 2	552	563	6	2 -4	471	456				
7	0	-2	526	524	6	1 3	207	159	6	1 -5	523	505	5	2 2	512	501	7	2 -4	238	244				
8	0	-2	102	207	7	1 3	267	234	7	1 -5	306	297	6	2 2	586	622	8	2 -4	833	806				
9	0	-2	333	361	8	1 3	426	405	8	1 -5	434	390	7	2 2	299	282	9	2 -4	195	211				
10	0	-2	338	341	9	1 3	140	111	9	1 -5	306	372	8	2 2	188	197	10	2 -4	-73	90				
11	0	-2	252	261	0	1 4	68	-104	10	1 -5	98	126	9	2 2	224	221	11	2 -4	323	336				
1	0	-4	1402	1449	1	1 4	246	242	11	1 -5	116	123	0	2 3	240	196	1	2 -5	216	198				
2	0	-4	1378	1290	2	1 4	254	289	12	1 -5	205	222	1	2 3	233	213	2	2 -5	188	-131				
3	0	-4	765	695	3	1 4	-57	34	1	1 -6	418	369	2	2 3	161	-181	3	2 -5	174	142				
4	0	-4	675	723	4	1 4	392	372	2	1 -6	-50	-24	3	2 3	341	-305	4	2 -5	224	206				
5	0	-4	1178	1285	5	1 4	124	-125	3	1 -6	463	418	4	2 3	-71	82	5	2 -5	382	314				
6	0	-4	900	905	6	1 4	-65	40	4	1 -6	420	360	5	2 3	190	-177	6	2 -5	448	410				
7	0	-4	673	674	7	1 4	89	130	5	1 -6	121	-90	6	2 3	266	-255	7	2 -5	129	137				
8	0	-4	233	267	8	1 4	114	-127	6	1 -6	274	256	7	2 3	-75	13	8	2 -5	112	110				
9	0	-4	535	468	0	1 5	671	667	7	1 -6	-62	-41	8	2 3	-62	-52	9	2 -5	265	247				
10	0	-4	312	356	1	1 5	1058	1015	8	1 -6	341	-319	0	2 4	737	753	10	2 -5	-74	-40				
11	0	-4	220	229	2	1 5	564	571	9	1 -6	132	134	1	2 4	953	958	11	2 -5	-61	13				
1	0	-6	846	777	3	1 5	319	288	10	1 -6	-62	-65	2	2 4	275	237	1	2 -6	150	126				
2	0	-6	1016	962	4	1 5	539	564	11	1 -6	91	-120	3	2 4	313	301	2	2 -6	332	296				
3	0	-6	231	215	5	1 5	306	297	12	1 -6	50	72	4	2 4	593	594	3	2 -6	1333	1256				
4	0	-6	410	356	6	1 5	138	143	1	1 -7	382	341	5	2 4	339	343	4	2 -6	179	159				
5	0	-6	-63	23	7	1 5	301	306	2	1 -7	174	126	6	2 4	280	292	5	2 -6	556	521				
6	0	-6	506	490	0	1 6	240	-244	3	1 -7	454	411	7	2 4	316	316	6	2 -6	625	776				
7	0	-6	323	306	1	1 6	132	126	4	1 -7	664	592	8	2 4	207	205	7	2 -6	338	344				
8	0	-6	-77	-51	2	1 6	278	-298	5	1 -7	236	199	0	2 5	84	87	8	2 -6	347	352				
9	0	-6	268	267	3	1 6	-66	10	6	1 -7	366	317	1	2 5	268	262	9	2 -6	472	493				
10	0	-6	490	476	4	1 6	-56	66	7	1 -7	527	491	2	2 5	-71	-21	10	2 -6	-74	30				
11	0	-6	-62	-7	5	1 6	-60	-38	8	1 -7	239	189	3	2 5	179	149	11	2 -6	231	214				
12	0	-6	227	226	6	1 6	-49	84	9	1 -7	253	281	4	2 5	226	224	12	2 -6	245	267				
1	0	-8	535	503	0	1 7	473	446	10	1 -7	417	443	5	2 5	-79	-43	1	2 -7	152	123				
2	0	-8	328	315	1	1 7	306	305	11	1 -7	182	166	6	2 5	111	111	2	2 -7	139	-103				
3	0	-8	252	200	2	1 7	318	319	12	1 -7	170	179	7	2 5	122	103	3	2 -7	-69	29				
4	0	-8	519	427	3	1 7	336	365	1	1 -8	128	132	0	2 6	925	909	4	2 -7	-69	15				
5	0	-8	328	338	4	1 7	244	241	2	1 -8	117	-94	1	2 6	609	625	5	2 -7	309	-270				
6	0	-8	235	227	5	1 7	219	219	3	1 -8	231	-228	2	2 6	-77	28	6	2 -7	-75	37				
7	0	-8	530	447	0	1 8	134	83	4	1 -8	87	60	3	2 6	589	556	7	2 -7	110	-106				
8	0	-8	536	503	1	1 8	162	169	5	1 -8	388	-342	4	2 6	294	302	8	2 -7	264	-263				
9	0	-8	264	261	2	1 8	192	-98	6	1 -8	-64	-61	5	2 6	124	156	9	2 -7	-79	-14				
10	0	-8	334	351	3	1 8	-59	-11	7	1 -8	134	144	6	2 6	287	275	10	2 -7	126	-129				
11	0	-8	248	274	4	1 8	-50	-49	8	1 -8	336	-301	7	2 6	-28	177	11	2 -7	178	-170				
12	0	-8	74	94	0	1 9	219	217	9	1 -8	-65	57	0	2 7	247	-215	12	2 -7	84	79				
1	0	-10	332	353	1	1 9	217	218	10	1 -8	230	201	1	2 7	157	-130	1	2 -8	426	379				
2	0	-10	587	622	2	1 9	270	277	11	1 -8	131	-138	2	2 7	196	-184	2	2 -8	162	173				
3	0	-10	366	394	3	1 9	117	123	12	1 -8	99	89	3	2 7	-79	-62	3	2 -8	612	602				
4	0	-10	236	235	0	1 10	112	109	1	1 -9	497	498	4	2 7	102	-134	4	2 -8	632	640				
5	0	-10	505	526	1	1 10	-54	4	2	1 -9	436	407	5	2 7	84	-114	5	2 -8	247	206				
6	0	-10	211	210	2	1 10	-44	77	3	1 -9	312	301	6	2 7	-36	14	6	2 -8	586	569				

Table 5. Continued.

H	K	L	F(O)	F(C)
7	2	-8	432	402
8	2	-8	179	183
9	2	-8	288	302
10	2	-8	200	229
11	2	-8	131	160
12	2	-8	199	216
1	2	-9	-80	-127
2	2	-9	164	-158
3	2	-9	186	-178
4	2	-9	5	0
5	2	-9	-80	-97
6	2	-9	-80	23
7	2	-9	277	250
8	2	-9	-79	24
9	2	-9	-75	37
10	2	-9	141	168
11	2	-9	-54	18
1	2	-10	386	365
2	2	-10	322	330
3	2	-10	210	221
4	2	-10	478	450
5	2	-10	355	348
6	2	-10	286	270
7	2	-10	253	223
8	2	-10	184	231
9	2	-10	225	270
10	2	-10	235	222
11	2	-10	140	144
1	2	-11	112	96
2	2	-11	221	215
3	2	-11	-73	14
4	2	-11	106	120
5	2	-11	237	223
6	2	-11	-74	-6
7	2	-11	102	110
8	2	-11	-68	72
9	2	-11	131	-136
10	2	-11	-52	-15
1	2	-12	174	212
2	2	-12	231	232
3	2	-12	238	221
4	2	-12	201	203
5	2	-12	210	233
6	2	-12	170	169
7	2	-12	201	153
8	2	-12	100	124
9	2	-12	269	283
10	2	-12	173	191
3	2	-13	63	-102
4	2	-13	122	-123
5	2	-13	-48	-2
6	2	-13	96	-106
7	2	-13	103	-124
0	2	C	188	162
1	2	C	516	564
2	2	C	648	626
3	2	C	1141	1142
4	2	C	657	671
5	2	C	539	476
6	2	C	573	572
7	2	C	648	642
8	2	C	-58	4
9	2	C	235	242
10	2	C	350	362
1	3	C	349	297
2	3	C	-33	64
3	3	C	-38	-21
4	3	C	-43	65
5	3	C	185	148
6	3	C	337	379
7	3	C	-58	75
8	3	C	-57	-4
9	3	C	-50	49
10	3	C	-37	-26
0	4	C	964	1032
1	4	C	240	150
2	4	C	279	293
3	4	C	469	437
4	4	C	543	552
5	4	C	255	284
6	4	C	641	610
7	4	C	402	407
8	4	C	327	334
9	4	C	347	367
10	4	C	252	266
1	5	C	125	-129
2	5	C	101	-56
3	5	C	-45	23
4	5	C	293	-256
5	5	C	266	-261
6	5	C	82	-43
7	5	C	92	-84
8	5	C	-34	-53
9	5	C	-44	59
C	6	C	780	883
1	6	C	542	531
2	6	C	486	470
3	6	C	1037	1042
4	6	C	322	323
5	6	C	336	337
6	6	C	437	464
7	6	C	217	223
8	6	C	226	242
9	6	C	338	365
1	7	O	381	-386
2	7	O	365	362
3	7	O	177	-173
4	7	O	403	-358
5	7	O	254	263
6	7	O	-58	-43
7	7	O	281	-265
8	7	O	73	73
9	7	O	-32	-32
0	8	O	418	409
1	8	O	754	772
2	8	O	726	811
3	8	O	358	350
4	8	O	603	592
5	8	O	344	361
6	8	O	244	251
7	8	O	372	376
8	8	O	190	166
1	9	O	115	-95
2	9	O	-58	44
3	9	O	242	251
4	9	O	-58	-16
5	9	O	-56	-25
6	9	O	198	201
7	9	O	-43	-17
8	9	O	-29	-19
0	10	O	494	469
1	10	O	292	317
2	10	O	306	327
3	10	O	429	453
4	10	O	246	261
5	10	O	291	304
6	10	O	264	259
7	10	O	134	124
1	11	O	227	-221
2	11	O	174	166
3	11	O	-53	76
4	11	O	-49	-73
5	11	O	185	174
6	11	O	54	70
0	12	O	195	181
1	12	O	263	260
2	12	O	249	240
3	12	O	134	143
4	12	O	221	212
5	12	O	222	225
0	2	1	653	-672
1	2	1	1120	-1074
2	2	1	-45	-28
3	2	1	290	-275
4	2	1	241	-231
5	2	1	311	294
6	2	1	-79	-75
7	2	1	-83	63
8	2	1	219	226
9	2	1	-46	27
10	2	1	-49	43
0	3	1	739	838
1	3	1	859	906
2	3	1	599	543
3	3	1	401	338
4	3	1	511	476
5	3	1	284	254
6	3	1	278	247
7	3	1	293	281
8	3	1	174	174
9	3	1	314	318
10	3	1	-36	210
0	4	1	217	-187
1	4	1	-50	-6
2	4	1	206	157
3	4	1	244	240
4	4	1	-69	95
5	4	1	132	-83
6	4	1	164	136
7	4	1	165	-181
8	4	1	-75	-36
9	4	1	146	124
0	5	1	745	928
1	5	1	236	-170
2	5	1	597	609
3	5	1	856	827
4	5	1	-73	-35
5	5	1	379	400
6	5	1	570	611
7	5	1	-31	98
8	5	1	219	220
9	5	1	260	251
0	6	1	-62	-50
1	6	1	143	125
2	6	1	425	423
3	6	1	217	-198
4	6	1	134	-152
5	6	1	328	328
6	6	1	202	-237
7	6	1	110	-105
8	6	1	-65	86
9	6	1	120	-105
0	7	1	834	827
1	7	1	691	731
2	7	1	401	410
3	7	1	580	611
4	7	1	691	659
5	7	1	376	420
6	7	1	355	397
7	7	1	339	341
8	7	1	222	191
0	8	1	142	-133
1	8	1	134	-181
2	8	1	210	226
3	8	1	-82	-94
4	8	1	-83	-65
5	8	1	-82	51
6	8	1	-76	-25
7	8	1	-64	-89
8	8	1	112	105
0	9	1	435	483
1	9	1	538	549
2	9	1	545	520
3	9	1	411	411
4	9	1	404	453
5	9	1	325	359
6	9	1	296	301
7	9	1	285	263
0	10	1	256	-264
1	10	1	-83	85
2	10	1	-82	-26
3	10	1	127	-127
4	10	1	-76	-93
5	10	1	153	145
6	10	1	-56	57
7	10	1	-34	-25
0	11	1	323	302
1	11	1	185	209
2	11	1	195	255
3	11	1	240	249
4	11	1	140	145
5	11	1	238	227
6	11	1	164	182
0	12	1	100	-112
1	12	1	98	-96
2	12	1	208	216
3	12	1	104	-121
4	12	1	-51	-17
5	12	1	-32	103
0	13	1	80	102
1	13	1	345	370
2	13	1	192	188
3	13	1	68	83
1	3	-1	1266	1367
2	3	-1	591	573
3	3	-1	629	547
4	3	-1	1299	1233
5	3	-1	605	557
6	3	-1	253	223
7	3	-1	915	861
8	3	-1	385	376
9	3	-1	187	185
10	3	-1	445	444
1	4	-1	2226	2245
2	4	-1	514	-506
3	4	-1	430	392
4	4	-1	392	309
5	4	-1	305	-264
6	4	-1	-77	47
7	4	-1	-82	-10
8	4	-1	259	-249
9	4	-1	201	201
10	4	-1	-57	24
1	5	-1	646	621
2	5	-1	428	425
3	5	-1	1210	1122
4	5	-1	731	688
5	5	-1	374	371
6	5	-1	931	913
7	5	-1	405	422
8	5	-1	226	227
9	5	-1	359	361
10	5	-1	245	217
1	6	-1	849	-901
2	6	-1	-64	-52
3	6	-1	-68	-49
4	6	-1	557	-517
5	6	-1	-78	-15
6	6	-1	233	221
7	6	-1	154	-162
8	6	-1	-76	34
9	6	-1	-63	87
10	6	-1	-39	24
1	7	-1	754	695
2	7	-1	319	304
3	7	-1	345	352
4	7	-1	480	449
5	7	-1	383	371
6	7	-1	203	208
7	7	-1	338	337
8	7	-1	141	140
9	7	-1	150	143
1	8	-1	178	-136
2	8	-1	109	-83
3	8	-1	238	247
4	8	-1	116	-116
5	8	-1	117	-80
6	8	-1	-81	94
7	8	-1	-75	15
8	8	-1	-63	-34
9	8	-1	103	94
1	9	-1	478	445
2	9	-1	501	483
3	9	-1	339	328
4	9	-1	347	353
5	9	-1	181	189
6	9	-1	186	206
7	9	-1	263	239
8	9	-1	197	178
1	10	-1	242	181
2	10	-1	117	99
3	10	-1	183	190
4	10	-1	113	108
5	10	-1	-75	-64
6	10	-1	177	166
7	10	-1	-54	-12
8	10	-1	-26	-137
1	11	-1	333	324
2	11	-1	283	278
3	11	-1	451	415
4	11	-1	284	247
5	11	-1	394	380
6	11	-1	408	386
7	11	-1	-33	168
1	12	-1	229	-201
2	12	-1	-69	44
3	12	-1	113	134
4	12	-1	228	-197
5	12	-1	-49	6
6	12	-1	-26	48
1	13	-1	228	196
2	13	-1	435	428
3	13	-1	204	186
4	13	-1	227	256
0	0	2	1308	1419
1	0	2	420	338
2	0	2	780	774
3	0	2	868	862
4	0	2	236	195
5	0	2	930	937
6	0	2	415	377
7	0	2	212	108
8	0	2	558	523
9	0	2	426	381
0	3	2	324	297
1	3	2	196	170
2	3	2	392	-370
3	3	2	627	-607
4	3	2	-104	-110
5	3	2	-115	-69
6	3	2	-122	-28
7	3	2	-120	-39
8	3	2	-106	57
9	3	2	-78	-7
0	4	2	862	912
1	4	2	681	707
2	4	2	692	957
3	4	2	649	701
4	4	2	266	217
5	4	2	511	505
6	4	2	245	209
7	4	2	-118	95
8	4	2	293	254
9	4	2	224	218
0	5	2	243	-242
1	5	2	421	457
2	5	2	-95	102
3	5	2	-103	47
4	5	2	255	221
5	5	2	210	167
6	5	2	-122	-74
7	5	2	-113	73
8	5	2	-93	80
0	6	2	634	643
1	6	2	402	406
2	6	2	791	847
3	6	2	433	406
4	6	2	206	195
5	6	2	514	503
6	6	2	396	386
7	6	2	-106	112
8	6	2	349	306
0	7	2	257	-236
1	7	2	323	318
2	7	2	463	472
3	7	2	278	-270
4	7	2	193	181
5	7	2	243	246
6	7	2	161	-139
7	7	2	-96	72
0	8	2	-114	72
1	8	2	449	490
2	8	2	379	370
3	8	2	419	431
4	8	2	442	459
5	8	2	274	244
6	8	2	359	333
7	8	2	377	374
0	9	2	-121	-109
1	9	2	-122	-65
2	9	2	245	-219
3	9	2	-122	-43
4	9	2	-117	-46
5	9	2	-107	-58
6	9	2	-90	-67
0	10	2	468	485
1	10	2	244	246
2	10	2	414	409
3	10	2	355	335
4	10	2	237	216
5	10	2	325	340
6	10	2	239	223
0	11	2	273	-261
1	11	2	-114	-10
2	11	2	-109	54
3	11	2	238	-230
4	11	2	-89	0
5	11	2	-69	43
0	12	2	390	399
1	12	2	404	426
2	12	2	251	221
3	12	2	291	248
4	12	2	251	257
1	3	-2	618	644
2	3	-2	202	-189
3	3	-2	161	113
4	3	-2	193	-103
5	3	-2	282	-241
6	3	-2	-107	-87
7	3	-2	203	158
8	3	-2	407	-346
9	3	-2	-118	-84
10	3	-2	-100	51
11	3	-2	-67	-56
1	4	-2	1483	1614
2	4	-2	627	645
3	4	-2	732	737
4	4	-2	1120	1169
5	4	-2	822	868
6	4	-2	526	492
7	4	-2	600	595
8	4	-2	387	333
9	4	-2	198	170
10	4	-2	258	237
11	4	-2	151	140
1	5	-2	-82	-80
2	5	-2	338	-300
3	5	-2	-90	63
4	5	-2	276	211
5	5	-2	353	-326
6	5	-2	284	257
7	5	-2	344	290
8	5	-2	-121	12
9	5	-2	-109	90
10	5	-2	172	129
1	6	-2	698	671
2	6	-2	648	575
3	6	-2	782	759
4	6	-2	582	594
5	6	-2	-114	166
6	6	-2	351	339
7	6	-2	388	372
8	6	-2	351	310
9	6	-2	304	292
10	6	-2	221	194
1	7	-2	254	-202
2	7	-2	182	-163
3	7	-2	467	420
4	7	-2	-114	-19
5	7	-2	169	88
6	7	-2	174	145
7	7	-2	-120	-17
8	7	-2	-110	9
9	7	-2	-10	58
1	8	-2	340	296
2	8	-2	460	431
3	8	-2	-117	33
4	8	-2	390	356
5	8	-2	519	533
6	8	-2	-121	113
7	8	-2	370	318
8	8	-2	337	347
9	8	-2	118	114
1	9	-2	191	153
2	9	-2	192	-156
3	9	-2	-122	-37
4	9	-2	-123	99
5	9	-2	331	-296
6	9	-2	-115	25
7	9	-2	-103	116
8	9	-2	230	-219
1	10	-2	491	427
2	10	-2	335	278
3	10	-2	530	526
4	10	-2	376	352
5	10	-2	160	168
6	10	-2	394	362
7	10	-2	222	214
8	10	-2	203	162
1	11	-2	-117	-120
2	11	-2	-116	-124
3	11	-2	253	160
4	11	-2	-108	-46
5	11	-2	-99	-75
6	11	-2	-85	43
1	12	-2	326	281
2	12	-2	430	409
3	12	-2	398	376
4	12	-2	268	252
5	12	-2	333	309
6	12	-2	240	285

Table 6. Dimensions of the coordination group in *trans*-$Te(etu)_2(S_2O_2CH_3)_2$. Standard deviations in parentheses.

	Triclinic dimorph	Monoclinic dimorph
∠ S–Te–S	91.6(2)°	92.6(2)°
Ethylenethiourea ligand		
Te–S	2.663(6) Å	2.687(5) Å
S–C	1.736(22)	1.701(18)
∠ Te–S–C	101.0(8)°	102.5(7)°
Methanethiosulphonate ligand		
Te–S	2.694(6) Å	2.685(4) Å
S–S	2.014(9)	2.015(7)
∠ Te–S–S	103.9(3)°	102.3(2)°

∠Te–S–S = 101.2(7)°. The only significant differences between these values and those of Table 6 occur in the S–Te–S angle relative to the angle in the monoclinic dimorph, and in the Te–S–S angle relative to the angle in the triclinic dimorph. Even these differences are not large.

As in the thiourea complex,[5] the methanethiosulphonate S–S bond length, 2.014(9) Å and 2.015(7) Å, is closer to the length in ionic sodium methanethio-

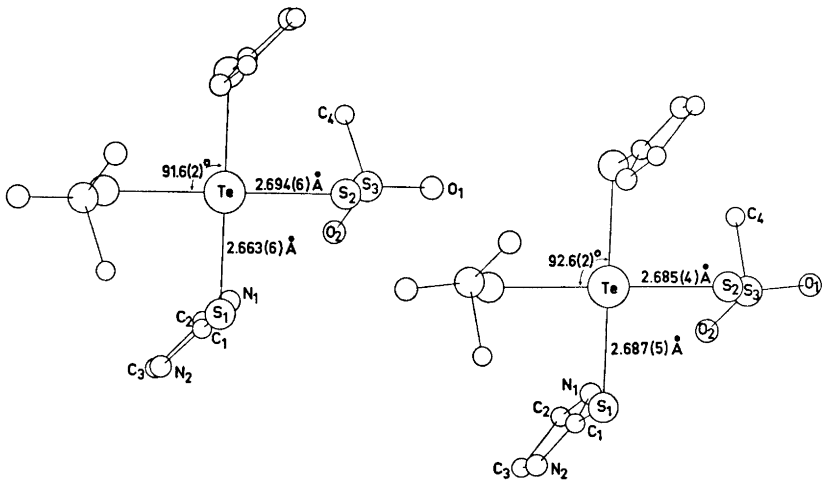

Fig. 1. *trans*-Dimethanethiosulphonatobis(ethylenethiourea)tellurium(II), as seen normal to the TeS_4 coordination group. Left: triclinic dimorph; right: monoclinic dimorph. Tellurium atoms in centres of symmetry.

Table 7. Bond lengths and angles in the ligand groups. Standard deviations in parentheses.

	Triclinic dimorph	Monoclinic dimorph
Ethylenethiourea ligand		
C_1-N_1	1.308(35) Å	1.356(28) Å
C_1-N_2	1.331(26)	1.326(24)
N_1-C_2	1.504(30)	1.449(25)
N_2-C_3	1.456(35)	1.464(25)
C_2-C_3	1.604(39)	1.577(33)
$\angle S_1-C_1-N_1$	124.0(1.3)°	125.6(1.5)°
$\angle S_1-C_1-N_2$	121.5(1.7)°	124.9(1.6)°
$\angle N_1-C_1-N_2$	114.5(1.8)°	109.5(1.6)°
$\angle C_1-N_1-C_2$	111.8(1.8)°	113.3(1.8)°
$\angle C_1-N_2-C_3$	109.7(2.0)°	112.8(1.7)°
$\angle N_1-C_2-C_3$	99.4(1.9)°	101.7(1.6)°
$\angle N_2-C_3-C_2$	104.7(1.8)°	102.6(1.5)°
Methanethiosulphonate ligand		
S_3-O_1	1.457(17) Å	1.439(11) Å
S_3-O_2	1.451(15)	1.437(13)
S_3-C_4	1.732(30)	1.807(24)
$\angle S_2-S_3-O_1$	107.5(0.8)°	107.6(0.6)°
$\angle S_2-S_3-O_2$	111.2(0.9)°	111.1(0.6)°
$\angle S_2-S_3-C_4$	107.9(0.9)°	107.8(0.6)°
$\angle O_1-S_3-O_2$	115.8(0.9)°	115.4(0.8)°
$\angle O_1-S_3-C_4$	105.7(1.2)°	108.4(0.9)°
$\angle O_2-S_3-C_4$	108.3(1.1)°	106.3(0.8)°

sulphonate monohydrate [10] than in the parent substance, tellurium dimethanethiosulphonate.[2]

The values derived for bond lengths and angles in the ethylenethiourea and methanethiosulphonate ligands, other than those associated with the coordinating atoms, are listed in Table 7. In neither dimorph, within the rather large uncertainties, do they differ significantly from values found for these groups in other compounds.

The ethylenethiourea groups are planar within the errors. The largest deviation of the atoms from the least-squares planes of the groups, with the sulphur coordinates, in the calculations of the planes, given three times the weight of the carbon and nitrogen coordinates, are 0.024 Å for C_1 in I and 0.010 Å for C_3 and N_2 in II.

There are some small differences in the rotational positions of the ligand groups, *cf.* Fig. 1 which shows, for the two dimorphs, the molecule projected on to the plane of the TeS_4 coordination group. The plane through the tellurium atom and the two sulphur atoms of the methanethiosulphonate groups makes an angle of 85.2° with the TeS_4 plane in I and 92.8° in II, and the least-squares

plane of the ethylenethiourea group makes an angle of 91.9° with the TeS_4 plane in I and 98.6° in II.

The N–H atoms of the ethylenethiourea groups form hydrogen bonds to oxygen atoms of the methanethiosulphonate groups. One such contact occurs within the molecule: $N_1-H\cdots O_2 = 2.83$ Å in I and 2.95 Å in II, $\angle C_1-N_1\cdots O_2 = 130°$ in I and 116° in II. Another occurs between molecules: $N_2-H\cdots O_1' = 2.85$ Å in I and 2.83 Å in II, $\angle C_1-N_2\cdots O_1' = 125°$ in I and 132° in II, where O_1' is located at $(1+x,y, 1+z)$ relative to O_1 in I and at $(x-1,y,z)$ relative to O_1 in II. All four nitrogen atoms, and all four oxygen atoms of the centrosymmetric molecules, thus engage in hydrogen bonding.

REFERENCES

1. Foss, O. *Acta Chem. Scand.* **5** (1951) 115.
2. Foss, O. and Vihovde, E. H. *Acta Chem. Scand.* **8** (1954) 1032.
3. Foss, O. and Johannessen, I.-J. *Acta Chem. Scand.* **15** (1961) 1943.
4. Foss, O. and Marøy, K. *Acta Chem. Scand.* **15** (1961) 1946.
5. Foss, O., Marøy, K. and Husebye, S. *Acta Chem. Scand.* **19** (1965) 2361.
6. Foss, O. and Fossen, S. *Acta Chem. Scand.* **15** (1961) 1620.
7. *International Tables for X-Ray Crystallography*, Kynoch Press, Birmingham 1962, Vol. 3.
8. Cromer, D. T. *Acta Cryst.* **18** (1965) 17.
9. Mair, G. A. *Structure Factor and Least Squares Programs for the IBM 1620*, National Research Council, Ottawa, Canada 1963.
10. Foss, O. and Hordvik, A. *Acta Chem. Scand.* **18** (1964) 619.

Received July 11, 1972.

ACTA CHEMICA SCANDINAVICA 27 (1973) 229–238

Structures of Linear Multisulphur Systems

III. The Crystal and Molecular Structure of 2-(2-*p*-Methoxyphenyl-2-methylthiovinyl)-3,4-trimethylene-5-methylthio-1,6,6a-thiathiophthene

JORUNN SLETTEN

Chemical Institute, Universty of Bergen, N-5000 Bergen, Norway

The structure of $C_{19}H_{20}OS_5$ has been determined by X-ray diffraction methods. The crystals are monoclinic, space group $P2_1/c$, with cell dimensions $a=12.104(7)$ Å, $b=21.717(5)$ Å, $c=7.561(1)$ Å, $\beta=102.23(4)°$. Data were collected on an off-line automatic diffractometer. The structure was solved by the symbolic addition procedure and refined by full-matrix least-squares to an R of 0.029. Four sulphur atoms are arranged approximately in a linear row with interatomic distances S(1)–S(2)=3.0021(8) Å, S(2)–S(3)=2.1563(7) Å, and S(3)–S(4)=2.5510(7) Å. The S(2)–S(3), and S(3)–S(4) distances resemble the sulphur–sulphur distances in some of the unsymmetrically substituted thiathiophthenes.

The present structure determination is part of a program of X-ray crystallographic investigations of linear multisulphur compounds. A special feature of this type of compound is the occurrence of sulphur-sulphur bonds in the region single bond – van der Waals distance. A number of linear four- and five-sulphur compounds have been synthesized by Stavaux and Lozac'h [1] and by Klingsberg.[2] In addition to the present structure, the structures of three other four-sulphur compounds and two five-sulphur compounds have been determined by X-ray crystallographic methods.[3–7]

EXPERIMENTAL

The compound, 2-(2-*p*-methoxyphenyl-2-methylthiovinyl)-3,4-trimethylene-5-methylthio-1,6,6a-thiathiophthene, was supplied by Stavaux and Lozac'h.

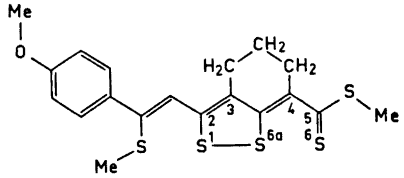

(I)

Different procedures for growing crystals were tried. The best results were obtained by slow evaporation from a carbon disulphide solution. Several crystals were tested before a satisfactory single crystal was found. Space group and initial cell dimensions were determined from Weissenberg photographs. Later, final unit cell dimensions were derived from θ, χ, and ϕ measurements of 21 reflections on the diffractometer.

CRYSTAL DATA

$C_{19}H_{20}OS_5$ M.w. = 424.69
Monoclinic, systematic extinctions: $h0l$ when $l = 2n+1$; $0k0$ when $k = 2n+1$

Space group $P2_1/c$
$a = 12.104(7)$ Å, $b = 21.717(5)$ Å, $c = 7.561(1)$ Å, $\beta = 102.23(4)°$
$V = 1942$ Å^3
$D_m = 1.453$ g cm^{-3}, $D_x = 1.465$ g cm^{-3}
$Z = 4$
$\mu_{MoK\alpha} = 5.87$ cm^{-1}

The crystal used for all X-ray measurements had dimensions 0.90 mm × 0.80 mm × 0.17 mm, and was mounted along the a-axis. Intensity data were collected on a Siemens automatic off-line four-circle diffractometer with niobium filtered Mo$K\alpha$ radiation. 3421 unique reflections with $2\theta \leqslant 50°$ were measured using the moving crystal-moving counter technique. A "five value" measurement was employed. By this procedure the background is measured both on high and low 2θ sides and the integrated intensity of the peak is determined twice, once by scanning the two halves of the peak, on low and high 2θ sides, respectively, and once by scanning the total peak. Scan ranges for low and high 2θ sides of the peaks were calculated according to the tangent relationship of Alexander and Smith,[8] $\Delta\theta_1 = A_1 + B_1 \tan\theta$, $\Delta\theta_2 = A_2 + B_2 \tan\theta$. Before the measurements of each reflection the count rate at the top of the peak is measured. Based on the value obtained, the instrument automatically selects scan rate and, if necessary, attenuators so as to obtain similar counting statistics for all reflections, except the very weakest. Due to the use of attenuators the coincidence loss is negligible even for the strongest reflections.

The net count of each reflection is calculated as $N_{net} = N_{Pk} - N_{Bg}$, where N_{Pk} is the total number of counts in the peak scans, and N_{Bg} is the total background count. The estimated error in net count due to counting statistics is $\sigma_c = (N_{Pk} + N_{Bg})^{\frac{1}{2}}$. Three reference reflections were monitored throughout the data collection, and these measurements were used to scale the data. Also, scale factors according to scan time and attenuators used were applied to bring the data on the same relative scale.

Of the 3421 reflections 376 were less than twice the estimated error in measurement. These reflections were coded unobserved and were given the value $2\sigma_c$. The standard deviations in intensities were calculated as $\sigma_I = k[\sigma_c^2 + (SN_{net})^2]^{\frac{1}{2}}$, where k is the appropriate scale factor and S is an "instability factor" estimated from the variation in intensities of the reference reflections. In this case S was set equal to 0.02. Standard deviations in structure factors were calculated as $\sigma_F = \sigma_I / 2(I\ Lp)^{\frac{1}{2}}$. The data were corrected in

the usual way for Lorentz and polarization effects. Also an absorption correction was applied using the Gaussian integration method described by Busing and Levy.[9]

SOLUTION AND REFINEMENT OF THE STRUCTURE

The structure factors were converted to normalized structure factors using a program written by Shiono.[10] The Wilson method [11] was used to bring the data on absolute scale and to find an overall temperature factor. Three origin determining reflections and three reflections with variable signs were chosen, and a symbolic addition program written by Long [12] was used to calculate the 8 possible sets of signs using Sayre's equation $S(E_h) = S(\sum_{h'} E_{h-h'} E_{h'})$. The 258 reflections with E-values greater than 1.70 were included in this calculation. For each set of signs the consistency index, C, was calculated as

$$C = \frac{\langle |E_h \sum_{h'} E_{h-h'} E_{h'}| \rangle}{\langle |E_h| \sum_{h'} |E_{h-h'}| |E_{h'}| \rangle}.$$

The consistency indexes for the eight sets of signs ranged from 0.44 to 0.97. The set with the highest consistency index was used to calculate an E-map,[13] which clearly revealed peaks corresponding to all non-hydrogen atoms. The successful refinement showed that this was the correct solution.

Structure factor calculation based on atomic positions from the E-map gave an agreement factor of 0.32 ($R = \sum ||F_o| - |F_c|| / \sum |F_o|$). The structure was refined by full-matrix least-squares procedure adjusting scale factor, coordinates and isotropic thermal parameters. At an R of 0.14, anisotropic temperature factors were introduced. All of the 20 hydrogen atoms were located in a three-dimensional difference map and included in the refinement varying positional and isotropic thermal parameters. The refinement converged at an R of 0.029.

The function minimized in the refinement was $\sum w(|F_o| - |F_c|)^2$ where $w = 1/\sigma_F^2$. The scattering factors used were for sulphur those of Dawson,[14] for oxygen and carbon those of Berghuis *et al.*[15] and for hydrogen those of Stewart *et al.*[16]

Table 1a. Final positional parameters with the corresponding standard deviations in parentheses.

	X/a	Y/b	Z/c
S(1)	0.82082(5)	0.10824(3)	0.11360(7)
S(2)	0.65196(4)	0.01317(2)	0.17159(6)
S(3)	0.53130(4)	−0.05403(2)	0.22257(6)
S(4)	0.38468(4)	−0.13069(2)	0.28569(6)
S(5)	0.40285(4)	−0.17868(2)	0.66284(7)
O(1)	1.24864(12)	0.23830(6)	0.68665(18)

Table 1a. Continued.

C(1)	0.87627(15)	0.09468(9)	0.34501(23)
C(2)	0.82411(15)	0.05701(8)	0.44309(23)
C(3)	0.72896(14)	0.01550(8)	0.39136(22)
C(4)	0.69422(14)	−0.02378(8)	0.51160(21)
C(5)	0.59626(14)	−0.06113(8)	0.45106(20)
C(6)	0.55343(14)	−0.10102(8)	0.56618(22)
C(7)	0.45372(15)	−0.13428(8)	0.50258(23)
C(8)	0.94458(27)	0.10630(19)	0.01640(38)
C(9)	0.97638(15)	0.13081(8)	0.43375(23)
C(10)	0.98964(17)	0.19263(9)	0.38891(27)
C(11)	1.07964(17)	0.22646(9)	0.47596(26)
C(12)	1.16260(15)	0.20053(8)	0.60961(23)
C(13)	1.33972(21)	0.21292(13)	0.81693(39)
C(14)	1.15270(16)	0.13880(9)	0.65442(25)
C(15)	1.06029(16)	0.10523(9)	0.56697(24)
C(16)	0.75736(17)	−0.02964(9)	0.70643(23)
C(17)	0.73993(16)	−0.09252(10)	0.78391(25)
C(18)	0.61542(16)	−0.10656(10)	0.76071(24)
C(19)	0.29184(21)	−0.22274(12)	0.52655(35)
H(2)	0.8512(15)	0.0598(9)	0.5692(26)
H(81)	0.9939(27)	0.1336(15)	0.0689(43)
H(82)	0.9704(31)	0.0604(19)	0.0395(44)
H(83)	0.9240(26)	0.1311(14)	−0.0907(46)
H(10)	0.9378(19)	0.2110(11)	0.2998(28)
H(11)	1.0865(18)	0.2669(11)	0.4432(27)
H(131)	1.3950(20)	0.2476(11)	0.8613(31)
H(132)	1.3763(26)	0.1825(16)	0.7503(43)
H(133)	1.3155(24)	0.1964(13)	0.9216(40)
H(14)	1.2042(17)	0.1217(9)	0.7398(27)
H(15)	1.0536(15)	0.0617(9)	0.5928(23)
H(161)	0.7301(17)	0.0012(9)	0.7765(28)
H(162)	0.8396(18)	−0.0229(9)	0.7143(24)
H(171)	0.7739(17)	−0.1244(9)	0.7198(26)
H(172)	0.7797(16)	−0.0941(9)	0.9115(26)
H(181)	0.6017(17)	−0.1447(11)	0.8029(28)
H(182)	0.5821(15)	−0.0780(9)	0.8334(24)
H(191)	0.3292(27)	−0.2486(14)	0.4534(42)
H(192)	0.2347(21)	−0.1939(12)	0.4534(33)
H(193)	0.2640(23)	−0.2450(12)	0.6064(34)

Table 1b. Thermal parameters with the corresponding standard deviations in parentheses. The anisotropic thermal parameters are defined by the expression $T_i = \exp[-2\pi^2(U_{11}h^2a^{*2} + U_{22}k^2b^{*2} + U_{33}l^2c^{*2} + 2U_{12}hka^*b^* + 2U_{13}hla^*c^* + 2U_{23}klb^*c^*)]$ and the isotropic parameters by $T_i = \exp[-8\pi^2 U \sin^2\theta/\lambda^2]$. For non-hydrogen atoms the values are multiplied by a factor of 10^4, for hydrogen atoms by 10^3.

	U_{11}	U_{22}	U_{33}	U_{12}	U_{23}	U_{13}
S(1)	498(3)	851(4)	398(3)	−136(3)	210(3)	7(2)
S(2)	489(3)	496(3)	277(2)	−64(2)	59(2)	1(2)
S(3)	464(3)	439(3)	283(2)	−17(2)	11(2)	−22(2)
S(4)	449(3)	496(3)	407(3)	−85(2)	14(2)	−9(2)
S(5)	461(3)	511(3)	462(3)	−65(2)	50(2)	109(2)
O(1)	568(8)	447(8)	588(8)	−118(7)	−13(6)	97(7)
C(1)	396(10)	432(10)	369(10)	60(8)	50(8)	76(8)

Table 1b. Continued.

C(2)	400(9)	378(10)	313(9)	27(8)	6(7)	38(7)
C(3)	384(9)	365(9)	290(9)	63(8)	−1(7)	40(7)
C(4)	353(9)	350(9)	281(9)	51(7)	−9(7)	44(7)
C(5)	366(9)	343(9)	271(8)	66(7)	−19(7)	36(7)
C(6)	361(9)	354(9)	338(9)	38(7)	−8(7)	62(7)
C(7)	382(9)	336(9)	407(10)	41(8)	−9(7)	88(8)
C(8)	783(19)	1114(26)	509(15)	−207(19)	−36(17)	240(13)
C(9)	388(10)	402(10)	359(9)	33(7)	28(8)	107(7)
C(10)	487(11)	437(11)	457(11)	54(9)	98(9)	115(9)
C(11)	560(12)	338(10)	523(11)	11(9)	66(8)	189(9)
C(12)	456(10)	394(10)	413(9)	−32(8)	−28(8)	186(8)
C(13)	517(13)	600(15)	754(17)	−102(12)	−21(13)	15(12)
C(14)	435(10)	412(10)	379(10)	22(8)	29(8)	75(8)
C(15)	458(10)	323(10)	418(10)	4(8)	30(8)	120(8)
C(16)	435(11)	460(11)	297(9)	−32(9)	25(8)	13(8)
C(17)	446(10)	537(12)	309(9)	47(9)	86(8)	1(8)
C(18)	466(11)	475(12)	328(9)	−37(9)	49(9)	61(8)
C(19)	556(13)	517(14)	633(14)	−130(11)	14(12)	145(12)

	U		*U*		*U*
H(2)	46(5)	H(131)	70(7)	H(171)	51(6)
H(81)	102(11)	H(132)	121(12)	H(172)	48(5)
H(82)	133(14)	H(133)	99(10)	H(181)	61(6)
H(83)	108(11)	H(14)	48(5)	H(182)	40(5)
H(10)	64(6)	H(15)	40(5)	H(191)	106(10)
H(11)	59(6)	H(161)	56(6)	H(192)	81(7)
		H(162)	44(5)	H(193)	82(8)

Table 2. Bond lengths with the corresponding standard deviations in parentheses. Bond lengths corrected for rigid body motion are listed in brackets.

Bond	Distance, Å	Bond	Distance, Å
S(1)−S(2)	3.0021(8)	O(1)−C(13)	1.425(3)
S(1)−C(1)	1.761(2)	C(14)−C(15)	1.381(3)[1.386]
S(1)−C(8)	1.803(4)	C(16)−C(17)	1.518(3)
S(2)−S(3)	2.1563(7)[2.1584]	C(17)−C(18)	1.511(3)
S(2)−C(3)	1.725(2)[1.732]	C(2)−H(2)	0.94(2)
S(3)−S(4)	2.5510(7)[2.5534]	C(8)−H(81)	0.87(3)
S(3)−C(5)	1.747(1)[1.754]	C(8)−H(82)	1.05(4)
S(4)−C(7)	1.677(2)[1.684]	C(8)−H(83)	0.96(3)
S(5)−C(7)	1.759(2)	C(10)−H(10)	0.91(2)
S(5)−C(19)	1.788(2)	C(11)−H(11)	0.92(2)
C(1)−C(2)	1.348(3)	C(13)−H(131)	1.02(2)
C(1)−C(9)	1.480(2)	C(13)−H(132)	0.99(4)
C(2)−C(3)	1.450(2)	C(13)−H(133)	0.97(3)
C(3)−C(4)	1.376(2)[1.378]	C(14)−H(14)	0.88(2)
C(4)−C(5)	1.430(2)[1.432]	C(15)−H(15)	0.97(2)
C(4)−C(16)	1.514(2)	C(16)−H(161)	0.96(2)
C(5)−C(6)	1.403(3)[1.405]	C(16)−H(162)	1.00(2)
C(6)−C(7)	1.401(2)[1.404]	C(17)−H(171)	0.98(2)
C(6)−C(18)	1.508(2)	C(17)−H(172)	0.98(2)
C(9)−C(10)	1.402(3)[1.412]	C(18)−H(181)	0.92(2)

Table 2. Continued.

C(9) – C(15)	1.386(2)[1.396]	C(18) – H(182)	0.97(2)
C(10) – C(11)	1.362(3)[1.368]	C(19) – H(191)	0.97(3)
C(11) – C(12)	1.384(2)[1.394]	C(19) – H(192)	1.01(2)
C(12) – O(1)	1.356(2)	C(19) – H(193)	0.89(3)
C(12) – C(14)	1.394(3)[1.404]		

Table 3. Intramolecular bond angles. The corresponding standard deviations are listed in parentheses.

Angle	°	Angle	°
S(2) – S(1) – C(1)	82.40(7)	C(10) – C(11) – C(12)	121.0(2)
S(2) – S(1) – C(8)	133.9(1)	C(10) – C(11) – H(11)	120(1)
C(1) – S(1) – C(8)	103.1(1)	C(12) – C(11) – H(11)	119(1)
S(1) – S(2) – S(3)	178.05(2)	C(11) – C(12) – C(14)	118.8(1)
S(1) – S(2) – C(3)	82.81(6)	C(11) – C(12) – O(1)	116.1(1)
S(3) – S(2) – C(3)	95.50(6)	C(14) – C(12) – O(1)	125.1(1)
S(2) – S(3) – S(4)	178.14(3)	C(12) – O(1) – C(13)	118.3(2)
S(2) – S(3) – C(5)	93.25(6)	O(1) – C(13) – H(131)	108(1)
S(4) – S(3) – C(5)	86.71(6)	O(1) – C(13) – H(132)	106(2)
S(3) – S(4) – C(7)	89.49(7)	O(1) – C(13) – H(133)	113(2)
C(7) – S(5) – C(19)	103.1(1)	H(131) – C(13) – H(132)	109(2)
S(1) – C(1) – C(2)	121.6(1)	H(131) – C(13) – H(133)	107(2)
S(1) – C(1) – C(9)	117.7(1)	H(132) – C(13) – H(133)	115(3)
C(2) – C(1) – C(9)	120.4(1)	C(12) – C(14) – C(15)	119.6(1)
C(1) – C(2) – C(3)	131.8(1)	C(12) – C(14) – H(14)	120(1)
C(1) – C(2) – H(2)	115(1)	C(15) – C(14) – H(14)	120(1)
C(3) – C(2) – H(2)	114(1)	C(9) – C(15) – C(14)	122.1(2)
S(2) – C(3) – C(2)	121.0(1)	C(9) – C(15) – H(15)	117(1)
S(2) – C(3) – C(4)	116.1(1)	C(14) – C(15) – H(15)	121(1)
C(2) – C(3) – C(4)	122.9(1)	C(4) – C(16) – C(17)	111.6(1)
C(3) – C(4) – C(5)	119.3(1)	C(4) – C(16) – H(161)	109(1)
C(3) – C(4) – C(16)	122.2(1)	C(4) – C(16) – H(162)	110(1)
C(5) – C(4) – C(16)	118.5(1)	C(17) – C(16) – H(161)	109(1)
S(3) – C(5) – C(4)	115.8(1)	C(17) – C(16) – H(162)	109(1)
S(3) – C(5) – C(6)	121.3(1)	H(161) – C(16) – H(162)	109(2)
C(4) – C(5) – C(6)	122.8(1)	C(16) – C(17) – C(18)	110.7(2)
C(5) – C(6) – C(7)	120.7(1)	C(16) – C(17) – H(171)	110(1)
C(5) – C(6) – C(18)	118.8(1)	C(16) – C(17) – H(172)	109(1)
C(7) – C(6) – C(18)	120.5(1)	C(18) – C(17) – H(171)	108(1)
S(4) – C(7) – C(6)	121.7(1)	C(18) – C(17) – H(172)	112(1)
S(4) – C(7) – S(5)	121.63(8)	H(171) – C(17) – H(172)	107(2)
S(5) – C(7) – C(6)	116.6(1)	C(6) – C(18) – C(17)	112.0(1)
S(1) – C(8) – H(81)	110(2)	C(6) – C(18) – H(181)	109(1)
S(1) – C(8) – H(82)	102(2)	C(6) – C(18) – H(182)	109(1)
S(1) – C(8) – H(83)	104(2)	C(17) – C(18) – H(181)	113(1)
H(81) – C(8) – H(82)	115(3)	C(17) – C(18) – H(182)	109(1)
H(81) – C(8) – H(83)	92(3)	H(181) – C(18) – H(182)	105(2)
H(82) – C(8) – H(83)	134(3)	S(5) – C(19) – H(191)	105(2)
C(1) – C(9) – C(10)	121.5(1)	S(5) – C(19) – H(192)	109(1)
C(1) – C(9) – C(15)	121.4(1)	S(5) – C(19) – H(193)	104(2)
C(10) – C(9) – C(15)	117.1(1)	H(191) – C(19) – H(192)	113(2)
C(9) – C(10) – C(11)	121.4(2)	H(191) – C(19) – H(193)	111(3)
C(9) – C(10) – H(10)	120(1)	H(192) – C(19) – H(193)	113(2)
C(11) – C(10) – H(10)	118(1)		

RESULTS AND DISCUSSION

Positional and thermal parameters are listed in Tables 1a and 1b. Bond lengths and angles are given in Tables 2 and 3. The standard deviations in bond lengths calculated from the inverse least-squares matrix are as follows: 0.0008 Å in S–S bonds, 0.002 Å in S–C bonds, 0.002–0.003 Å in C–C and C–O bonds, and 0.02–0.04 Å in C–H bonds. A more realistic estimate of the accuracy of the results is probably obtained by multiplying the above calculated standard deviations by a factor of two.[17]

A drawing of the molecule with pertinent bond lengths and angles is shown in Fig. 1. The row of sulphur atoms S(1) to S(4) is found to be approximately

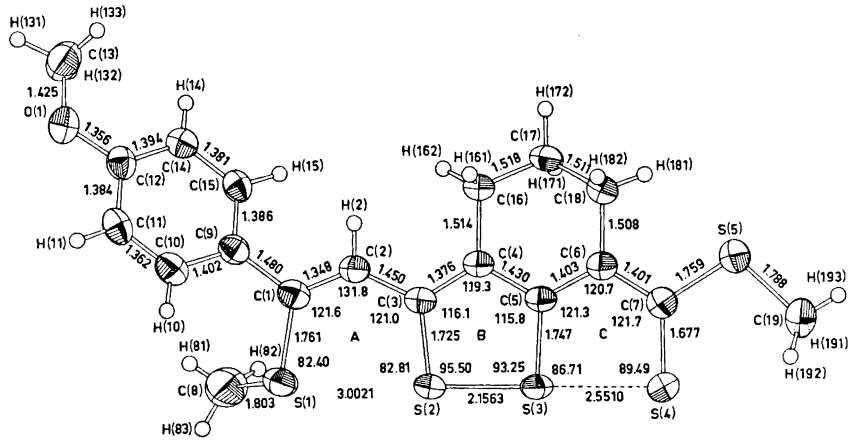

Fig. 1. ORTEP plot [21] of one molecule showing thermal ellipsoids at the 50 % probability level. Hydrogen atoms are plotted with a fixed radius. The most important bond lengths and angles are also shown.

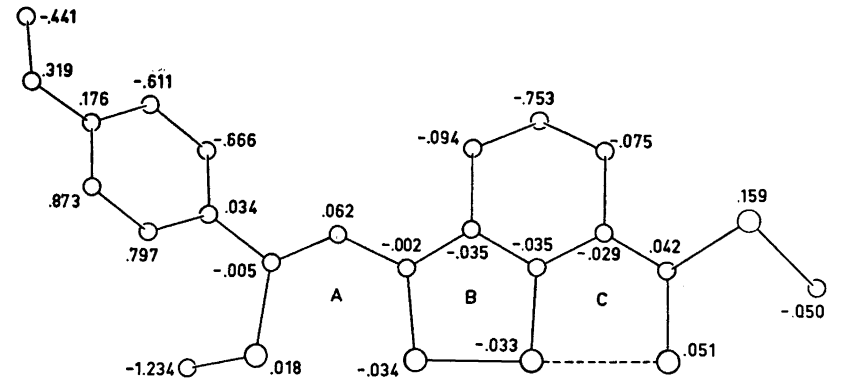

Fig. 2. Atomic deviations from a least-squares plane fitted to the 11 atoms of rings A, B, and C [S(1)–S(4), C(1)–C(7)]. The equation of the plane is $-7.7493\,x+15.9482\,y+2.6913\,z+4.3468=0$. x, y, z are fractional coordinates.

linear. The methyl carbon C(8) deviates from this line, the angle S(2) – S(1) – C(8) being 133.9°. A least-squares plane was fitted to the atoms of rings A, B, and C. This part of the molecule is almost planar with a maximum atomic deviation of 0.06 Å (Fig. 2). C(8) deviates 1.23 Å from this plane. The aromatic ring of the methoxyphenyl group makes an angle of 38° with the ABC plane. The methylthio group S(5)C(19) is slightly twisted out of the plane with a dihedral angle S(4)C(7)S(5)/C(7)S(5)C(19) of 10.5°.

The intramolecular sulphur – sulphur distances in the present compound, I, may be compared with those in the already known linear four-sulphur molecules II, III, and IV.[3–5]

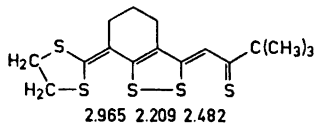

(II)

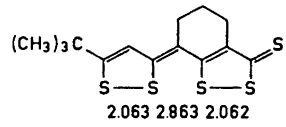

(III)

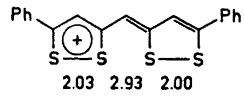

(IV)

The bonding scheme of the sulphur atoms in I and II differs markedly from that in III and IV. Molecules I and II both contain a three-sulphur sequence analogous to those found in several isolated thiathiophthenes. The four-sulphur sequences in III and IV may more adequately be described in terms of two separate disulphide systems with terminal S – S bonds of the same lengths as those found in cyclic five-membered disulphides.[18,5] The interaction across the long central S···S distance is apparently too weak to significantly influence the lengths of these bonds. Similarly there is no indication that the S···S interaction across the distances of 3.002 Å and 2.965 Å, in I and II, respectively, perturbs the sulphur – sulphur bonding in the thiathiophthene part of these molecules. Hence, the structural data obtained so far of compounds containing a linear four-sulphur sequence do not give a clear evidence of a delocalized σ-system extending across the four sulphur atoms. In the two known five-sulphur structures,[6,7] on the other hand, the molecular dimensions indicate the presence of an extended thiathiophthene bonding scheme.

The shortest intramolecular H···H and S···H distances are H(2)···H(15), H(2)···H(162) and S(5)···H(181), 2.41 Å, 2.13 Å and 2.53 Å, respectively. The packing of molecules in the unit cell is shown in Fig. 3. Intermolecular sulphur – sulphur close contacts appear between molecules related by a center of symmetry. The distances S(1)···S(4′) and S(2)···S(3′) are 3.515 Å and 3.433 Å, respectively. The unprimed atoms are located in the reference molecule, while primed atoms refer to its inversion at $\frac{1}{2},0,0$. The reference molecule and its inversion at $\frac{1}{2},0,\frac{1}{2}$ overlap considerably with an interplanar spacing of 3.64 Å.

Thermal ellipsoids at the 50 % probability level are illustrated in Fig. 1. The thermal parameters of the atoms were analyzed in terms of rigid body mo-

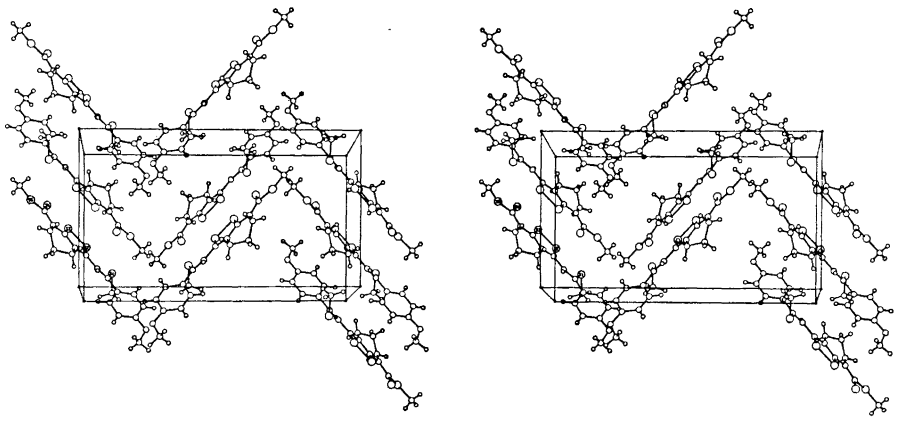

Fig. 3. Stereoview down the c^*-axis. The drawing was done using the ORTEP plotting program.[21]

tion using the method of Schomaker and Trueblood.[19] The results indicate that the whole molecule cannot be regarded as a rigid body. However, the 8 atoms in the thiathiophthene part of the molecule are described reasonably well by the rigid body approximation, the r.m.s. ΔU_{ij} being 0.0012 Å^2. Likewise, the aromatic ring of the methoxyphenyl group may be described as a rigid body. For these atoms the r.m.s. ΔU_{ij} is 0.0015 Å^2. The bond lengths in these parts of the molecule have been corrected for rigid body motion according to Cruickshank's method,[20] and are listed in Table 2 together with the uncorrected bond lengths.

Lists of observed and calculated structure factors may be obtained from the author.

Acknowledgement. The author wishes to thank Drs. M. Stavaux and N. Lozac'h for supplying a sample of the compound.

REFERENCES

1. Stavaux, M. and Lozac'h, N. *Bull. Soc. Chim. France* **1967** 3557; **1968** 4273; **1969** 4184.
2. Klingsberg, E. *J. Heterocycl. Chem.* **3** (1966) 243; *Chem. Ind. (London)* **1968** 1813.
3. Hordvik, A. *Acta Chem. Scand.* **19** (1965) 1253; Hordvik, A., Sletten, E. and Sletten, J. Paper given at the *6th Nordic Structure Chemistry Meeting in Århus*, Denmark, Jan. 1967.
4. Sletten, J. *Chem. Commun.* **1969** 688; *Acta Chem. Scand.* **25** (1971) 3577.
5. Sletten, J. *Acta Chem. Scand.* **26** (1972) 873.
6. Sletten, J. *Acta Chem. Scand.* **24** (1970) 1464.
7. Kristensen, R. and Sletten, J. *Acta Chem. Scand.* **25** (1971) 2366.
8. Alexander, L. E. and Smith, G. S. *Acta Cryst.* **17** (1964) 1195.
9. Busing, W. R. and Levy, H. A. *Acta Cryst.* **10** (1957) 180.
10. Shiono, R. *Normalized Structure Factors Program*, The Crystallography Laboratory, University of Pittsburgh, Pittsburgh 1966.
11. Wilson, A. J. C. *Nature* **150** (1942) 151.
12. Long, R. E. *Ph. D. Diss.*, University of California, Los Angeles 1965.
13. Karle, I. L., Hauptman, H., Karle, J. and Wing, A. B. *Acta Cryst.* **11** (1958) 257.

14. Dawson, B. *Acta Cryst.* **13** (1960) 403.
15. Berghuis, J., Haanappel, I. J. M., Potters, M., Loopstra, O., MacGillavry, C. H. and Veenendaal, A. L. *Acta Cryst.* **8** (1955) 478.
16. Stewart, R. F., Davidson, E. R. and Simpson, W. T. *J. Chem. Phys.* **42** (1965) 3175.
17. Hamilton, W. C. and Abrahams, S. C. *Acta Cryst.* **A 26** (1970) 18.
18. Hordvik, A. *Quart. Rep. Sulphur Chem.* **5** (1970) 21.
19. Schomaker, V. and Trueblood, K. N. *Acta Cryst.* **B 24** (1968) 63.
20. Cruickshank, D. W. J. *Acta Cryst.* **9** (1956) 757.
21. Johnson, C. K. *ORTEP* Report ORNL-3794, Oak Ridge National Laboratory, Oak Ridge, Tennessee.

Received July 10, 1972.

ACTA CHEMICA SCANDINAVICA 27 (1973) 239–250

Studies on Intermediates Involved in the Syntheses of Pentaerythritol and Related Alcohols. III.* Syntheses of α-Hydroxymethyl-substituted Aldehydes

JAN-ERIK VIK**

Department of Organic Chemistry, Chalmers University of Technology and University of Göteborg, Fack, S-402 20 Göteborg 5, Sweden

Methods for the preparation of the α-hydroxymethyl-substituted aldehydes postulated as intermediates in the production of the polyalcohols pentaerythritol, trimethylolethane, and trimethylolpropane are reported. These syntheses involve as their key steps the $LiAlH_4$-reduction of the corresponding acetal esters. The acetals obtained are stable substances, from which the free aldehydes can be generated rather free from by-products in dilute aqueous solution. On attempted concentration, however, those aldehydes, which have α-hydrogens, tend to loose water under formation of unsaturated aldehydes. All the aldehydes have been characterized as 2,4-dinitrophenylhydrazones and as acetals but only two of them as free aldehydes.

Three mass produced polyalcohols, namely 2,2-bis(hydroxymethyl)-1,3-propanediol (pentaerythritol, VI), 2-hydroxymethyl-2-methyl-1,3-propanediol (trimethylolethane, TME, X) and 2-ethyl-2-hydroxymethyl-1,3-propanediol (trimethylolpropane, TMP, XIV) are prepared *via* crossed aldol condensations with formaldehyde (I) followed by crossed Cannizzaro reactions with this aldehyde. The postulated reaction sequences involve as intermediates the hydroxyaldehydes 3-hydroxypropanal (monomethylolacetaldehyde, hydracrolein, III), 3-hydroxy-2-hydroxymethylpropanal (dimethylolacetaldehyde, IV), 3-hydroxy-2,2-bis(hydroxymethyl)-propanal (trimethylolacetaldehyde, V), 3-hydroxy-2-methylpropanal (monomethylolpropionaldehyde, VII), 3-hydroxy-2-hydroxymethyl-2-methylpropanal (dimethylolpropionaldehyde, IX), 2-ethyl-3-hydroxypropanal (monomethylolbutyraldehyde, XII), and 2-ethyl-3-hydroxy-2-hydroxymethylpropanal (dimethylolbutyraldehyde, XIII) as shown in Scheme 1.

* Part II: *Acta Chem. Scand.* **26** (1972) 3165.

** Present address: Perstorp AB, S-284 00 Perstorp, Sweden.

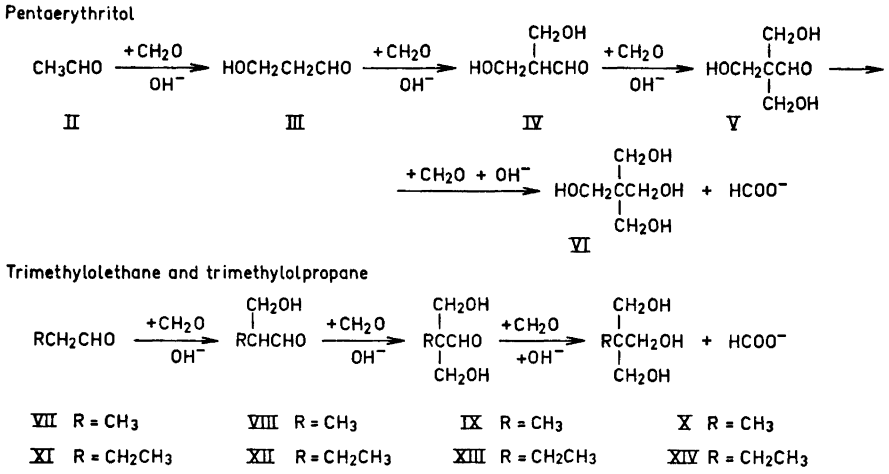

Scheme 1.

Of these hydroxyaldehydes III,[1] V,[2] IX,[3] and XIII [4] have been obtained in a more or less pure state by means of direct condensation of I with acetaldehyde (II), propionaldehyde (VII), and butyraldehyde (XI), respectively. Compound III has also been obtained by acid-catalyzed hydration of 2-propenal.[5] In all these cases the reaction mixtures are difficult to work up, and our attempts to repeat these condensations failed to give pure products. The procedures for the preparation of IX[3] and XIII [4] call for the use of stoichiometric amounts of I with K_2CO_3 as the condensing agent. Thin layer chromatography of the products obtained indicated the formation in both cases of at least three compounds, neither of which was identical with those obtained by the procedures described below. The use of an excess of I to avoid formation of the less hydroxymethyl-substituted aldehydes IV, VIII, and XII gives products, which are difficult to free completely from I. Armour *et al.*[2] successfully used a chromatographic method to perform this task in the case of V, but we did not succeed in repeating this separation.

In connection with work on the detailed kinetics and mechanism of the pentaerythritol synthesis, methods for the preparation of V and the previously unknown IV were sought for. It was found that both substances could be obtained *via* extensions of the synthesis of diethyl diethoxymethylmalonate (XVII) described by Fuson *et al.*[6] as outlined in Schemes 2 and 4. The same general synthetic route has been used for the syntheses of IX and XIII (Scheme 5) and of VIII and XII (Scheme 6). In addition, further extensions of the same general principle have made accessible the aldehydes III (Scheme 8) and the previously unknown dehydration product of IV, 2-hydroxymethyl-2-propenal (XXI, Scheme 3).

The first step in the synthesis of IV is a modification [7] of the original procedure of Claisen [8] for the synthesis of XVI. The mechanism is not known with certainty, but the reaction is thought to involve XVII as an intermediate.[7]

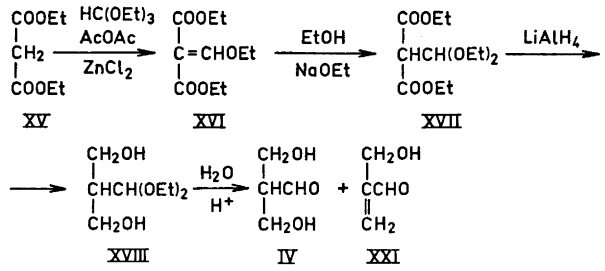

Scheme 2.

Work by Post and Erickson [9] indicated that the reagent actually effecting the diethoxymethylation is acetoxydiethoxymethane (XXII). This compound is formed in a reaction between the orthoformate and acetic anhydride. A probable route to the proposed intermediate XVII then seems to involve electrophilic attack by the diethoxymethyl cation on the double bond of the enol of the malonate ester. The function of the zinc chloride probably is to catalyze the enolization of the diethyl malonate and to effect fission of XXII by complexing with the acetoxyl group. The catalyst is not necessary for the reaction to occur, but it does improve the yield. The analogous condensations with XXVI and XXIX (Scheme 5) show that only one active hydrogen is needed for the reaction to occur, but the lower yields obtained in these cases indicate steric hindrance. In these cases the acetyl-substituted malonic esters, which could be formed in analogous reactions with acetic anhydride, were identified as minor by-products by means of vapour phase chromatography in combination with mass spectrometry.

The intermediate ester XVII (Scheme 2) then undergoes acid-catalyzed elimination of ethanol giving XVI. As the next step in the synthetic sequence shows, the ester XVII actually is the more stable one at lower temperatures, but the high temperature used and the continuous removal of ethanol as ethyl acetate from the reaction mixture force the elimination to completion. Base-catalyzed addition of ethanol to XVI then gives XVII, which on reduction with $LiAlH_4$ provides the diethyl acetal of IV (XVIII) in excellent yield and purity.

The hydrolysis of this acetal turned out to be complicated, since it was found, that IV very easily undergoes dehydration, especially in the presence of bases. Thus, the slightest excess of base, remaining after neutralization of an acid hydrolysis reaction mixture, is likely to cause extensive dehydration of IV giving XXI. This latter aldehyde then can react further in different ways, which is the subject of a separate study. It was found, however, that brief passage of XVIII through an H^+-saturated cation exchanger with water as eluent gives IV in a rather pure state in aqueous solution.

For a study of the equilibrium between IV and its dehydration product XXI[10] a way to prepare this latter aldehyde was needed. Base-catalyzed dehydration of IV did not give a sufficiently pure product. Instead the utilization of a reaction observed by Searles *et al.*[11] in connection with work on the

synthesis of oxetanes led to a convenient route for the preparation of XXI. These authors found that on pyrolysis, in the presence of alkaline catalysts, of 2-oxo-1,3-dioxanes, those carrying a 5-hydrogen gave as main products allylic alcohols instead of oxetanes. When this method was applied to the 2-oxo-1,3-dioxane XIX, the allyl alcohol XX was obtained in about 55 % yield, based on XVIII, and mild acid hydrolysis of XX, preferably brought about by means of brief passage through an acid ion exchanger, gave XXI (Scheme 3).

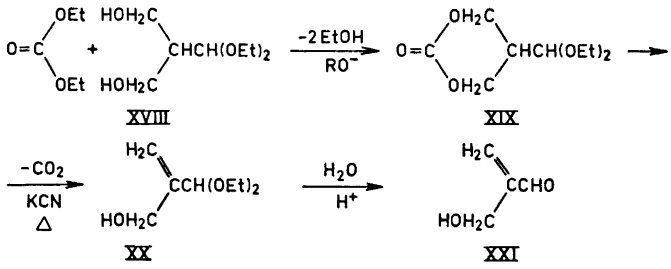

Scheme 3.

Attempts were made to synthesize trimethylolacetaldehyde (V) with trimethyl methanetricarboxylate as starting material. The expected product from the first step, trimethyl diethoxymethylmethanetricarboxylate, was only formed in a very low yield, however, irrespective of whether the condensation with triethyl orthoformate was brought about with zinc chloride or other Lewis acids as catalysts or *via* the sodium or ethoxymagnesium derivative of trimethyl methanetricarboxylate in Grignard-type reactions.

Other possible routes were therefore examined. Base-catalyzed reaction of XVI with methanol gave XXIII. This ester, on base-catalyzed reaction with formaldehyde, gave the crystalline hydroxymethyl-substituted ester XXIV (Scheme 4; *cf.* Böhme and Teltz [12]).

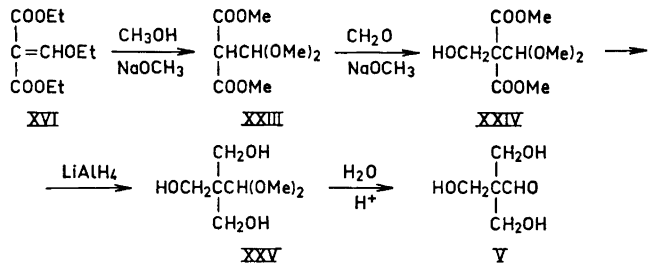

Scheme 4.

Substitution of methoxy groups for the ethoxy groups was found suitable since XXIV was found to be crystallizable and therefore more easily purified than the corresponding liquid ethyl ester.

Reduction of XXIV with $LiAlH_4$ gave XXV, but only in an impure state and in a low yield (about 5 %) when the mixture was worked up in the manner used for XVIII. This method involved destruction of unreacted $LiAlH_4$ with a moderate excess of water, followed by hydrolysis of the salts by treatment with carbon dioxide. Other conventional methods were equally unsatisfactory, apparently because of formation during the reduction of difficultly hydrolyzable complex aluminium salts. Destruction of excess $LiAlH_4$ with aqueous KOH followed by precipitation of the aluminium as phosphate gave a somewhat more satisfactory result, even if the yields varied from 25 to 65 % in different runs. The resulting dimethyl acetal XXV then could be purified by crystallization.

The hydroxyaldehydes IX and XIII were prepared in the same manner as IV. Condensation of the appropriate alkyl-substituted malonic esters with triethyl orthoformate gave the esters XXVII and XXX in moderate yields and the remaining steps were straightforward (Scheme 5).

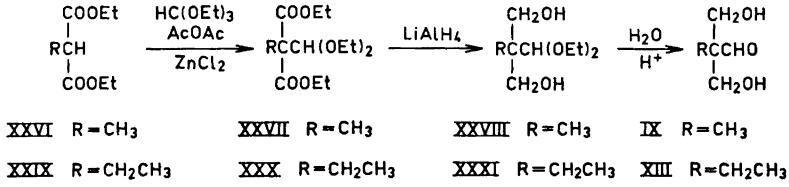

Scheme 5.

The corresponding monohydroxymethyl-substituted aldehydes VIII and XII were obtained starting from the esters XXVII and XXX, respectively. The esters were saponified and with remarkable ease decarboxylated to the corresponding monobasic acids. Esterification with diazomethane without isolation of the acids was followed by reduction to give the acetals of VIII (XXXII) and of XII (XXXIII), respectively (Scheme 6).

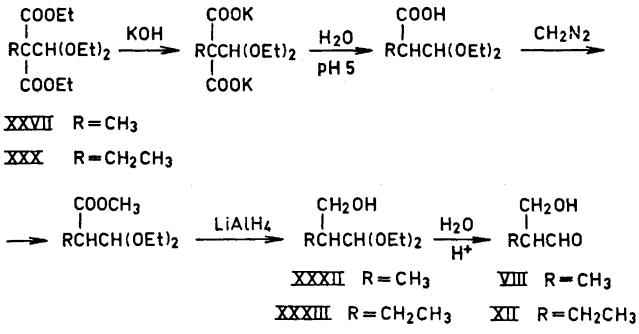

Scheme 6.

The decarboxylation was complicated by subsequent partial elimination of ethanol resulting in formation of the corresponding β-ethoxy α,β-unsaturated acids. On the other hand no significant hydrolysis of the acetal groups was observed. The acetals XXXII and XXXIII were obtained in a rather pure state, although the esters to be reduced were contaminated with the corresponding unsaturated esters. These latter probably are converted into products with completely reduced enol ether groups, in analogy with what was found on reduction of XVI (Scheme 7). This compound gave XXVI as the only isolated product in 25 % yield.

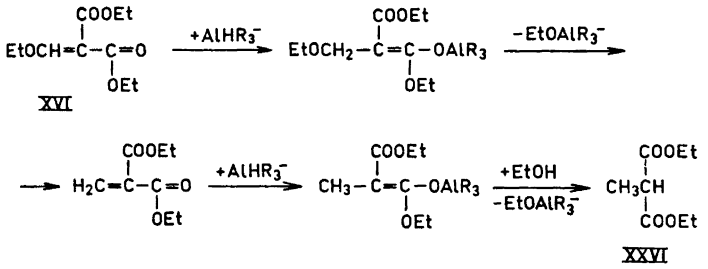

Scheme 7.

The analogous preparation of aldehyde III involved reduction of the ester acetal XXXIV, prepared by the method of Croxall and Schneider,[13] to the corresponding acetal XXXV (Scheme 8).

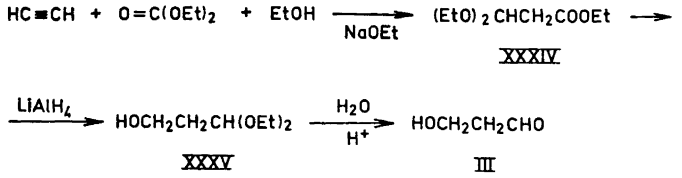

Scheme 8.

The product (XXXV) showed a tendency to form polymeric acetals of the probable type $H(-OCH_2CH_2CH(OEt)-)_n-OEt$ by elimination of ethanol, possibly catalyzed by acid impurities. The distilled product proved to be stable.

Thus it has been found possible to prepare all of the intermediate hydroxymethyl-substituted aldehydes sought for *via* reduction of the corresponding ester acetals. The acetals obtained are stable substances, from which the free aldehydes can be generated by hydrolysis. All of the aldehydes were characterized as 2,4-dinitrophenylhydrazones. The majority of the aldehydes, carrying α-hydrogens, were found to dehydrate so easily that they only could be obtained slightly contaminated with their dehydration products in dilute aqueous

solution. These solutions were sufficiently pure, however, to allow kinetic investigations of some of the reactions, which these aldehydes can undergo in alkaline solutions. These investigations will be reported in forthcoming publications.

EXPERIMENTAL

The organic chemicals used were of the purest grades commercially available (most of them obtained from Fluka AG) and were used without further purification. The purity of starting materials and products were generally tested by vapour phase chromatography on a Perkin-Elmer 800 instrument. IR-spectra were recorded on a Beckman IR-9 instrument and NMR-spectra on a Varian A-60 instrument. Elemental analyses were performed at the Microanalytical Laboratory at the Institute of Physical Chemistry, University of Vienna. Melting and boiling points are uncorrected.

Diethyl ethoxymethylenemalonate (*XVI*) was prepared by the method reported in *Org. Syn.*[7] B.p.$_{1.2}$ 122–123°C. Yield 55 to 60 %. IR-spectrum with strong, slightly split carbonyl peak at 1733 and 1715 cm^{-1} and strong conjugated C=C peak at 1638 cm^{-1}.

Diethyl diethoxymethylmalonate (*XVII*) was prepared by the method of Fuson *et al.*[6] B.p.$_{1.2}$ 111–112°. Yield 80 to 85 %. IR-spectrum with strong, split carbonyl peak at 1740 and 1758 cm^{-1}.

3-Hydroxy-2-hydroxymethylpropanal diethyl acetal (*XVIII*). To a slurry of 57 g of $LiAlH_4$ (1.5 mol) in 1 l of ether kept under a slow stream of N_2 a solution of 131 g of XVII (0.5 mol) was added dropwise at a rate sufficient to keep the ether refluxing. After the first vigorous reaction had subsided the reaction mixture was heated under reflux overnight. The excess $LiAlH_4$ was destroyed by careful addition of 250 ml of water and then carbon dioxide was bubbled through the slurry for 2 h to hydrolyze the salts. The slurry was filtered and the salts washed repeatedly with ether and ethanol. The collected filtrates were freed from solvents by evaporation and the residual oil distilled under high vacuum in a "Kugelrohr". Yield 76.8 g (86 %) of b.p.$_{0.04}$ 120–140°. (Found: C 53.91; H 10.36. Calc. for $C_8H_{18}O_4$: C 53.91; H 10.17.) The IR-spectrum, which bears a strong resemblance to those of the other hydroxyaldehyde acetals, is given in Fig. 1.

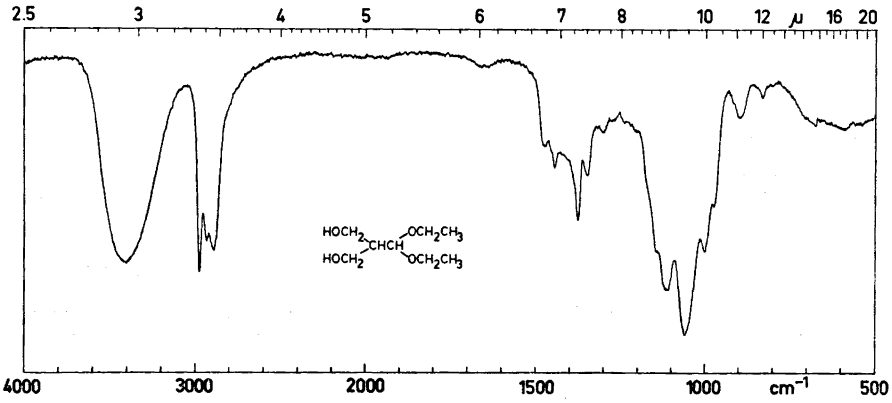

Fig. 1. IR-spectrum of 3-hydroxy-2-hydroxymethylpropanal diethyl acetal.

3-Hydroxy-2-hydroxymethylpropanal (*IV*). A solution of 0.5 g of XVIII in 10 ml of water was passed through a carefully washed, H^+-saturated ion exchange column, 80 × 1 cm, with water as eluent. The eluent was evaporated under reduced pressure and the residual oil dried over P_2O_5 under vacuum. The oil, which was soluble in water, gave

a correct analysis. (Found: C 46.02; H 7.87. Calc. for $C_4H_8O_3$: C 46.15; H 7.75.) However, this may be incidental, since the experience with the other hydroxyaldehydes was, that the extent of drying was decisive for the results obtained. Incomplete drying of course gave too low carbon contents, while extended drying gave too high carbon contents, probably because of dehydration or acetal formation with consequent loss of water. The IR-spectrum had no carbonyl peak, which indicates extensive formation of hemiacetals.

2,4-Dinitrophenylhydrazone of IV. To a solution of 840 mg of 2,4-dinitrophenylhydrazine (DNPH) in 20 ml of diethyleneglycol dimethyl ether (diglym) and 3 ml of acetic acid 810 mg of XVIII was added (*cf.* method of Shine [14]). After addition of 10 ml of water the solution was kept at 30° for 40 h. The yellow crystals formed were recrystallized twice from water – diglym 1 : 4 and dried over P_2O_5. M.p. 149 – 151°. (Found: C 42.35; H 4.15; N 19.77. Calc. for $C_{10}H_{12}N_4O_6$: C 42.26; H 4.26; N 19.71.) Generally it was found, that when the dinitrophenylhydrazones of the hydroxyaldehydes were recrystallized, the presence of solvents with six-membered ring molecules like benzene, cyclohexane and dioxane had to be avoided, since these solvents crystallized together with the aldehyde derivatives as evidenced by NMR-spectra and elemental analyses.

2-Hydroxymethyl-2-propenal diethyl acetal (XX). A mixture of 30 g of XVIII, 29.8 g of diethyl carbonate and 0.1 g of Na was kept at 50° in a flask, equipped with column and condenser, until all the metal had reacted and was then heated to boiling. The ethanol formed was distilled off and the residue was taken up in an equal volume of benzene, washed with 5 ml of brine and then dried over Na_2SO_4. 5-Diethoxymethyl-3-oxo-1,3-dioxane (XIX) could be obtained by distillation of this solution, but since a considerable amount of the carbonic ester formed seems to be present in oligomeric or polymeric form, a higher yield of XX is obtained in the following step if the crude product from the first step is used. After evaporation of the benzene an oil (33.8 g) was obtained, which was mixed with 6.5 g of KCN and gradually heated to 200° in a small flask, equipped with column and condenser. The acetal XX distilled off, carried by a slow stream of N_2. The crude distillate, which contained, among other impurities, a small amount of diethyl carbonate, was purified by vacuum distillation. Yield 15.4 g (57 %) of b.p.$_7$ 88°. (Found: C 59.67; H 10.20. Calc. for $C_8H_{16}O_3$: C 59.97; H 10.07.)

2-Hydroxymethyl-2-propenal (XXI). Hydrolysis of 3.6 g of XVIII in 10 ml of 0.05 M H_2SO_4 for 2 h gave a mixture which was carefully neutralized to pH 7.0 (measured with a pH-meter) with saturated aqueous $Ba(OH)_2$. The resulting solution was chromatographed on a silica gel column with acetone as eluent. The hydrolysis product IV lost water during the passage through the column and the fractions containing XXI were collected and evaporated. About 1 g of a colorless liquid, which gave an NMR-spectrum consistent with a monomeric structure but showing also the presence of a small amount of acetone as impurity, was obtained. When kept for a few hours, even at low temperature, the compound polymerized to give a clear resin, which gave an almost correct analysis. (Found: C 55.15; H 7.07; O 37.58. Calc. for $(C_4H_6O_2)_n$: C 55.81; H 7.03; O 37.17.) Dilute aqueous solutions of XXI were obtained by acid hydrolysis of XX. The carbon dioxide in the air was sufficient to cause complete hydrolysis over a week in a solution which was kept at room temperature. In kinetic runs the formation of XXI in solutions of XX in 10^{-4} M H_2SO_4 was followed by measuring the UV-absorbance maximum of the hydrolysis product (213.5 nm). The pseudo first order rate constant at 25.00° was obtained from a plot of $\log(\alpha_\infty - \alpha_t)$ against time. After dividing by the hydronium ion concentration, the second order rate constant 22.2 l sec^{-1} mol^{-1} was obtained. The absorbancy of XXI at 213.5 nm was determined to $10\,130 \pm 160$ l mol^{-1} cm^{-1}.

2,4-Dinitrophenylhydrazone of XXI. A solution of 2 g of XX in 15 ml of water was added to a solution of 5.1 g of DNPH in 80 ml of 65 % phosphoric acid. The crystals obtained after 30 min were filtered off and washed with water. Preparative thin layer chromatography on silica gel with $CH_3NO_2 - CH_3OH$ 20 : 1 as eluent gave red crystals of m.p. 181 – 183°. (Found: C 44.95; H 3.72; N 21.09. Calc. for $C_{10}H_{10}N_4O_5$: C 45.12; H 3.79; N 21.05.) This compound was obtained in the same manner from XVIII, but the crude product in this case contained a considerably larger proportion of the DNPH-derivative of IV.

Dimethyl dimethoxymethylmalonate (XXIII). To 500 ml of methanol 54 g of XVI and 1 g of Na were added. After stirring for 2 h at 50° the solution was neutralized with glacial acetic acid. The solvent was evaporated and the residue taken up in $CHCl_3$ and washed twice with water. After drying over Na_2SO_4 the solvent was evaporated and the

residual oil examined by VPC and NMR. The product was a mixture of about 75 % of XXIII and 25 % of compounds with one remaining ethoxy group. The treatment was repeated twice, after which the proportion of XXIII was over 98 % and the yield 45.8 g (89 %).

Dimethyl dimethoxymethylhydroxymethylmalonate (*XXIV*). A mixture of 175 g of ester XXIII, 34 g of dry paraformaldehyde (99 % CH_2O) and 10 g of K_2CO_3 in 600 ml of DMSO was stirred for 48 h at room temperature and then taken up in water. Repeated extraction with $CHCl_3$ gave a solution of XXIV, which was washed several times with water to remove the DMSO. After drying over $CaSO_4$ and evaporation of the solvent an oil (139 g; yield 70 %) was obtained, which slowly crystallized. Recrystallization from diisopropyl ether gave white crystals of m.p. 45 – 47°. (Found: C 45.76; H 6.74. Calc. for $C_9H_{16}O_7$: C 45.76; H 6.83.) NMR-spectrum (in $CDCl_3$) showed peaks at 2.93 – 3.15 ppm (triplet; CH_2OH), 3.60 ppm ($CH(OCH_3)_2$), 3.76 ppm ($COOCH_3$), 4.12 – 4.23 ppm (doublet; CH_2OH) and 4.98 ppm ($CH(OR)_2$).

2,2-Bis(hydroxymethyl)-3-hydroxypropanal dimethyl acetal (*XXV*). An ether solution of 11.8 g of XXIV was added dropwise to 4.75 g of $LiAlH_4$ in 1 l of ether. After reflux overnight excess $LiAlH_4$ was destroyed by careful addition of 20 g of KOH in 500 ml of water. After further addition of 14.8 g of K_2HPO_4 and 11.6 g of KH_2PO_4 in 50 ml of water, the resultant slurry was stirred for 2 h on a water bath at 50° whereafter most of the ether had distilled off. The mixture was neutralized with acetic acid, filtered and the filtrate evaporated to dryness under reduced pressure. The residue was extracted five times with acetone and the combined extracts on evaporation gave 5.5 g of an oil, which slowly crystallized (crude yield 62 %). Recrystallization from acetone – benzene 5 : 1 gave white crystals of m.p. 109 – 110°. (Found: C 46.70; H 8.90. Calc. for $C_7H_{16}O_5$: C 46.66; H 8.95.) NMR-spectrum showed singlets at (ppm upfield from the OH-peak) 0.00 ppm (OH), 0.21 ($CH(OCH_3)_2$), 1.03 (CH_2OH) and 1.13 ($CH(OCH_3)_2$) in D_2O.

2,2-Bis(hydroxymethyl)-3-hydroxypropanal (*V*). A solution of 1 g of XXV in 25 ml of 0.05 M H_2SO_4 was stirred at room temperature for 2 h and was then carefully neutralized to pH 7.0 with aqueous $Ba(OH)_2$. The resulting solution was filtered and evaporated under reduced pressure. The residual oil was crystallized from benzene – methanol 1 : 1. Recrystallization gave 410 mg of colorless crystals of m.p. 138 – 139° (lit.[2] 132 – 134°). (Found: C 44.54; H 7.53. Calc. for $C_5H_{10}O_4$: C 44.77; H 7.51.) Spectral data were in agreement with those reported [2] and showed that the free aldehyde is present only to a minor extent in D_2O-solution and not at all in the crystalline state.

2,4-Dinitrophenylhydrazone of V. A solution of 1 g of XXV in 25 ml of methanol – water 1 : 1 was added to 25 ml of a 0.25 M solution of DNPH in 85 % phosphoric acid – methanol 3 : 2. After 1 h the crystals obtained were filtered off and washed with methanol – water 1 : 1. Recrystallization from water gave yellow needles of m.p. 194 – 195° (lit.[2] 198 – 199°). (Found: C 42.04; H 4.50; N 17.92. Calc. for $C_{11}H_{14}N_4O_7$: C 42.04; H 4.49; N 17.83.)

Diethyl diethoxymethylmethylmalonate (*XXVII*). This compound was prepared in analogy with XVI from 1000 g of XXVI as starting material. Yield 472 g (30 %) of b.p.$_{0.03}$ 84°. (Found: C 56.35; H 8.82. Calc. for $C_{13}H_{24}O_6$: C 56.51; H 8.75.) About 60 % of the starting material was recovered unchanged.

3-Hydroxy-2-hydroxymethyl-2-methylpropanal diethyl acetal (*XXVIII*). The reduction of the ester XXVII was carried out in the same way as the reduction of XVII. Yield 86.2 g from 134.8 g of XXVII (92 %). (Found: C 56.31; H 10.69. Calc. for $C_9H_{20}O_4$: C 56.23; H 10.49.)

3-Hydroxy-2-hydroxymethyl-2-methylpropanal (*IX*) was prepared in the same way as V and was crystallized from benzene – methanol. The colorless crystals of m.p. 107 – 109° were obtained first after several weeks standing. (Found: C 50.77; H 8.48. Calc. for $C_5H_{10}O_3$: C 50.83; H 8.53.) The spectral properties were similar to those of V.

2,4-Dinitrophenylhydrazone of IX. This derivative was prepared in the same way as that of IV. Yellow crystals of m.p. 167 – 168°. (Found: C 44.40; H 4.83; N 18.77. Calc. for $C_{11}H_{14}N_4O_6$: C 44.30; H 4.73; N 18.78.) The IR-spectrum, which is representative for those of all of the DNPH-derivatives, is shown in Fig. 2.

Diethyl diethoxymethylethylmalonate (*XXX*). The preparation was analogous with that of XVI. Yield 238 g from 1000 g of XXIX (15 %). B.p.$_{0.03}$ 106°. (Found: C 58.17; H 9.09. Calc. for $C_{14}H_{26}O_6$: C 57.91; H 9.03.) More than 75 % of the starting material was recovered unchanged. NMR-spectrum is shown in Fig. 3.

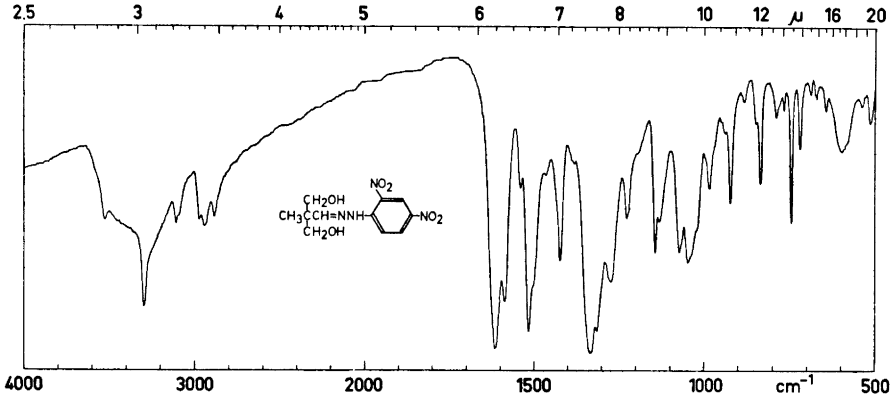

Fig. 2. IR-spectrum of 3-hydroxy-2-hydroxymethyl-2-methylpropanal 2,4-dinitrophenylhydrazone.

2-Ethyl-3-hydroxy-2-hydroxymethylpropanal diethyl acetal (*XXXI*). The reduction of XXX was carried out in the same way as that of XVII. Yield 60.5 g from 104 g of XXX (82 %). (Found: C 58.37; H 10.92. Calc. for $C_{10}H_{22}O_4$: C 58.23; H 10.75.) Attempts to obtain crystalline aldehyde XIII in the same way as V was obtained from XXV have failed so far.

2,4-Dinitrophenylhydrazone of XIII. This derivative was prepared in the same way as that of IV. Yellow crystals of m.p. 151 – 152° (lit.[4] 146 – 148°). (Found: C 46.25; H 5.16; N 17.94. Calc. for $C_{12}H_{16}N_4O_6$: C 46.15; H 5.16; N 17.94.)

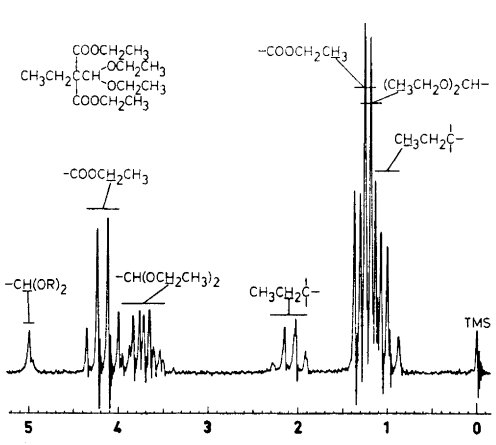

Fig. 3. NMR-spectrum of diethyl diethoxymethylethylmalonate.

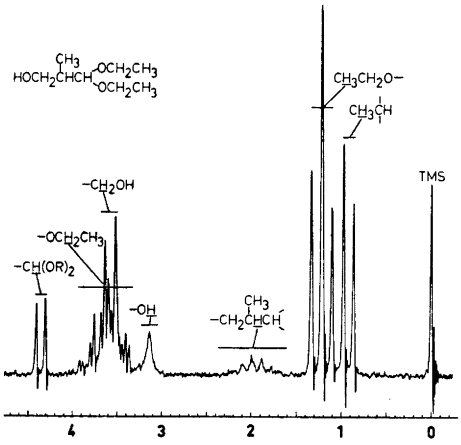

Fig. 4. NMR-spectrum of 3-hydroxy-2-methylpropanal diethyl acetal.

3-Hydroxy-2-methylpropanal diethyl acetal (*XXXII*). A stirred solution of 55.2 g of XXVII (0.2 mol) and 33.6 g of KOH (0.6 mol) in 1000 ml of 70 % ethanol was refluxed overnight. The bulk of the ethanol was then evaporated and replaced by water. Acidification to pH 5.0 with phosphoric acid caused evolution of CO_2 at room temperature. During

3 h N_2 was bubbled through the solution, which was then repeatedly extracted with $CHCl_3$. The combined extracts were washed once with a small amount of water and then dried over $CaSO_4$. Diazomethane in ether was added until the yellow colour of the reagent no longer vanished. Evaporation of the resulting solution gave 30.8 g of an oil, which was shown by VPC and NMR to contain about 90 % of methyl 3,3-diethoxy-2-methylpropionate. Reduction of this oil in the manner used for XVII gave 22.1 g of redistilled XXXII. Yield based on XXVII 68 %. (Found: C 59.43; H 11.37. Calc. for $C_8H_{18}O_3$: C 59.23; H 11.18.) NMR-spectrum is shown in Fig. 4.

2,4-Dinitrophenylhydrazone of VIII. This derivative was prepared in the same way as that of IV. Yellow crystals of m.p. 165–167°. (Found: C 44.71; H 4.51; N 20.99. Calc. for $C_{10}H_{12}N_4O_5$: C 44.78; H 4.51; N 20.89.) NMR-spectrum is shown in Fig. 5.

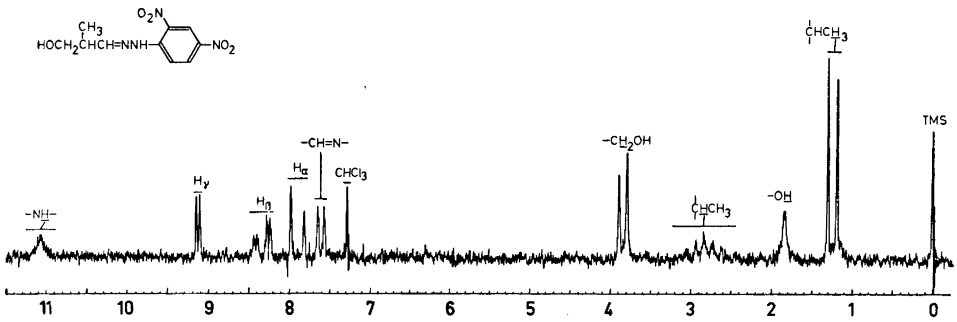

Fig. 5. NMR-spectrum of 3-hydroxy-2-methylpropanal 2,4-dinitrophenylhydrazone.

2-Ethyl-3-hydroxypropanal diethyl acetal (XXXIII). This compound was prepared in the manner used for XXXII from 25 g of XXX. Yield 10.8 g (71 %). (Found: C 61.18; H 11.28. Calc. for $C_9H_{20}O_3$: C 61.33; H 11.44.)

2,4-Dinitrophenylhydrazone of XII. This derivative was prepared in the same way as that of IV. Yellow crystals of m.p. 114–116°. (Found: C 46.73; H 4.98; N 19.56. Calc. for $C_{11}H_{14}N_4O_5$: C 46.81; H 5.00; N 19.85.)

Reduction of XVI. A solution of 54 g of the ester in 200 ml of ether was added to a solution of 10 g of $LiAlH_4$ in 800 ml of ether at room temperature. After 18 h stirring the mixture was worked up in a manner analogous to that used in the reduction of XVII. An oil was obtained (16.2 g), which on distillation gave 11.1 g of a compound identified by VPC and NMR as the ester XXVI. Yield 25 %.

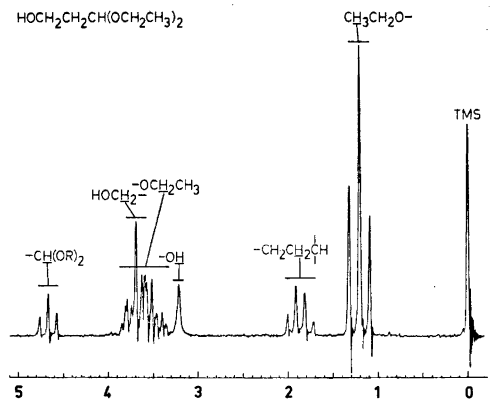

Fig. 6. NMR-spectrum of 3-hydroxypropanal diethyl acetal.

Ethyl 3,3-diethoxypropionate (XXXIV). This ester was prepared from acetylene and diethyl carbonate with sodium methoxide as condensing agent.[13] The crude mixture of XXXIV and the corresponding unsaturated ester, ethyl 3-ethoxy-2-propenoate, obtained was treated with sodium ethoxide in ethanol at 40°. After equilibration the mixture contained about 90 % of XXXIV as compared with about 50 % before this treatment. Pure XXXIV of $b.p._{0.6}$ 53° was obtained by distillation under vacuum.

3-Hydroxypropanal diethyl acetal (XXXV) was prepared by reduction of XXXIV (86.8 g) with 17.4 g of $LiAlH_4$ in 2 l of ether. The reaction mixture was worked up in analogy with the preparation of XVIII from XVII. Yield 61.0 g (90 %) of $b.p._{10}$ 90–92°. (Found: C 56.57; H 10.67. Calc. for $C_7H_{16}O_3$: C 56.73; H 10.88.) The compound has been reported earlier but not characterized.[15] NMR-spectrum is shown in Fig. 6. A preparation of crude acetal lost ethanol on standing under formation of a viscous, polymeric acetal, as indicated by NMR-spectrum of the residue after removal of distillable material. The monomeric acetal could be recovered, however, by treatment of the viscous polymer with ethanol, containing p-TsOH as catalyst, followed by careful neutralization and distillation.

2,4-Dinitrophenylhydrazone of III. This derivative was prepared in the same way as that of IV. Yellow crystals of m.p. 137–138°. (Found: C 42.26; H 3.94; N 21.94. Calc. for $C_9H_{10}N_4O_5$: C 42.53; H 3.97; N 22.04.)

Acknowledgements. This work has been financially supported by Perstorp AB, Perstorp, Sweden, which is gratefully acknowledged. Prof. Erich Adler is thanked for his kind help and interest and Dr. Gerhard Miksche for many helpful suggestions. My thanks are also due to Mrs. Marianne Frantsi, who skilfully carried out most of the experimental work.

REFERENCES

1. Ogata, Y., Kawasaki, A. and Yokoi, K. *J. Chem. Soc.* **B 1967** 1013.
2. Armour, C. A., Bonner, T. G., Bourne, E. J. and Butler, J. *J. Chem. Soc.* **1964** 301.
3. Koch, H. and Zerner, T. *Monatsh.* **22** (1901) 443.
4. Neunhoffer, O. and Neunhoffer, H. *Chem. Ber.* **95** (1962) 102.
5. Hall, R. H. and Stern, E. S. *J. Chem. Soc.* **1950** 490.
6. Fuson, R. C., Parham, W. E. and Reed, L. J. *J. Org. Chem.* **11** (1946) 194.
7. *Org. Syn. Coll. Vol.* **3** (1955) 395.
8. Claisen, L. *Ber.* **26** (1893) 2729; *Ann.* **297** (1897) 76.
9. Post, H. W. and Erickson, E. R. *J. Org. Chem.* **2** (1937) 260.
10. Vik, J.-E. *Acta Chem. Scand.* **27** (1973) 251.
11. Searles, S., Hummel, D. G., Nukina, S. and Throckmorton, P. E. *J. Am. Chem. Soc.* **82** (1960) 2928.
12. Böhme, H. and Teltz, H.-P. *Arch. Pharm.* **288** (1955) 343.
13. Croxall, W. J. and Schneider, H. J. *J. Am. Chem. Soc.* **71** (1949) 1257.
14. Shine, H. J. *J. Org. Chem.* **24** (1959) 1790.
15. McGinnis, N. A. and Robinson, R. *J. Chem. Soc.* **1941** 404.

Received July 20, 1972.

ACTA CHEMICA SCANDINAVICA 27 (1973) 251–257

Studies on Intermediates Involved in the Syntheses of Pentaerythritol and Related Alcohols. IV* The Kinetics of Base-catalyzed Addition of Water to Some 2-Propenals

JAN-ERIK VIK**

Department of Organic Chemistry, Chalmers University of Technology and University of Göteborg, Fack, S-402 20 Göteborg 5, Sweden

The formation of ethers in the syntheses of the industrially important polyalcohols pentaerythritol, trimethylolethane, and trimethylolpropane is believed to involve 2-propenals as intermediates. These aldehydes can be assumed to be formed by reversible dehydration of the corresponding α-hydroxymethyl-substituted aldehydes, present as intermediates in the reaction mixtures. In order to examine the probability of this reaction route, the rates and equilibria of these dehydration-hydration reactions have been studied. The reactions were found to be very efficiently catalyzed by hydroxide ion.

Two alternative mechanisms have been proposed in order to explain the formation of by-products containing ether linkages in the synthesis of pentaerythritol.[1,2] In a previous study,[3] one of these mechanisms [2] was found to be highly improbable. The other mechanism, originally proposed by Wawzonek and Rees,[1] involves the formation of α,β-unsaturated aldehydes *via* base-catalyzed dehydration of α-hydroxymethyl-substituted aldehydes occurring as reaction intermediates. Base-catalyzed addition of alcohols to these unsaturated aldehydes then results in the formation of α-alkoxymethyl-substituted aldehydes, which contain the ether linkage present in the ultimate products of these side-reactions.

Of the α-hydroxymethyl-substituted aldehydes occurring as intermediates in the synthesis of pentaerythritol from acetaldehyde and formaldehyde, both 3-hydroxypropanal (I, hydracrolein, monomethylolacetaldehyde) and 3-hydroxy-2-hydroxymethylpropanal (III, dimethylolacetaldehyde) can undergo dehydration, leading to propenal (II, acrolein) and 2-hydroxymethylpropenal (IV, α-methylolacrolein), respectively. In the analogous syntheses of trimethylolethane from propionaldehyde and formaldehyde and of trimethylol-

* Part III: *Acta Chem. Scand.* **27** (1973) 239.

** Present address: Perstorp AB, S-284 00 Perstorp, Sweden.

propane from butyraldehyde and formaldehyde, the corresponding monohydroxymethyl-substituted aldehydes 3-hydroxy-2-methylpropanal (V, monomethylolpropionaldehyde) and 2-ethyl-3-hydroxy-propanal (VII, monomethylolbutyraldehyde) similarly can undergo dehydration to give 2-methylpropenal (VI, methacrolein) and 2-ethylpropenal (VIII), respectively. Since synthetic routes to the aldehydes III, IV, V, and VII have now been worked out,[4] it has become possible to study all these equilibrium reactions.

It is well known, that II, in the presence of acids but also in neutral aqueous solution, reaches a state of equilibrium with I.[5–7] The kinetics of the acid-catalyzed hydration of II has been studied by Pressman and Lucas [6] and by Hall and Stern,[7] but so far the base-catalyzed reaction, though more or less recognized,[1,8] has received considerably less attention. This is probably due to the fact, that the base-catalyzed hydration in more concentrated solutions is accompanied by several side-reactions and therefore lacks preparative interest.

It has now been found, however, that the base-catalyzed hydration of II conveniently can be followed by means of UV-spectrophotometric measurements in 10^{-3} to 10^{-4} M solutions of II. By the same method, it is also possible to follow the dehydration reactions of III, V, and VII, which also lead to equilibria between saturated and unsaturated aldehydes.

The overall reactions follow eqn. (1):

$$H_2O + H_2C{=}CRCHO \underset{k_{-1}}{\overset{k_1}{\rightleftharpoons}} HOCH_2CHRCHO \qquad (1)$$

As previously has been shown for the acid-catalyzed hydration of II, the equilibrium in this case lies well to the right at room temperature with about 90 % of the aldehyde mixture present as I.[6,7] Preliminary experiments with the aldehydes IV, VI, and VIII showed, however, that in these cases the equilibria lie equally well to the left. In order to be able to determine the rate constants with any precision, one therefore has to follow these reactions from the right to the left.

When the hydration of II is followed in aqueous solution, where water is present in large excess and with hydroxide ion acting as catalyst, the reaction follows the rate expression:

$$-\frac{\mathrm{d}(a(1-x))}{\mathrm{d}t} = k_1'\, a\,(1-x) - k_{-1}'a\,x \qquad (2)$$

where the initial concentration of II is denoted a and the concentration at time t is $a\,(1-x)$. The rate constants k_1' and k_{-1}' are pseudo first-order constants for the forward and reversed reactions, respectively.

After substitution of ε for x_∞ and of k' for $(k_1' + k_{-1}')$ the following integrated rate expression is obtained:

$$\ln\frac{\varepsilon}{\varepsilon - x} = k't = \ln\frac{\alpha_0 - \alpha_\infty}{\alpha_t - \alpha_\infty} \qquad (3)$$

The latter equality is obtained when UV-absorbance units are substituted for the concentration units used previously.

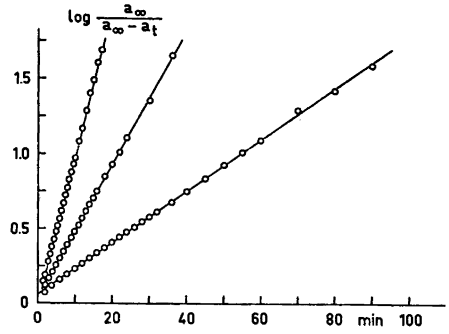

Fig. 1. Dehydration of dimethylolacetaldehyde in water, catalyzed by 0.00100 M OH^- at 15.0, 25.0 and 35.0°C, respectively.

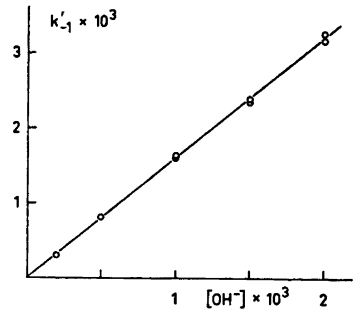

Fig. 2. The pseudo first order rate constant for the dehydration of dimethylolacetaldehyde as a function of the catalyst concentration.

In an analogous manner eqn. (4) is obtained for the case where the dehydration of the saturated aldehyde is followed by measuring the increasing UV-absorption of the product:

$$\ln \frac{\alpha_\infty}{\alpha_\infty - \alpha_t} = k' t \tag{4}$$

As the example given in Fig. 1 shows, the reactions followed these rate expressions with good precision at least to between four and five half-lives, that is to about 95 % completion. The constants k' for the different reactions were found, as expected, to be linearly dependent on the catalyst concentration (see Fig. 2) and it is therefore possible to define second order rate constants:

$$k' = k[OH^-] = (k_1 + k_{-1})[OH^-] \tag{5}$$

Depending on the mechanism of the reactions either k_1 or k_{-1} must be a function of the concentration of water since:

$$K = \frac{[HOCH_2CHRCHO]}{[H_2C{=}CRCHO][H_2O]} = \frac{1}{[H_2O]} K_{exp} = \frac{1}{[H_2O]} \frac{k_1}{k_{-1}} \tag{6}$$

The equilibrium constants for the reactions could not be obtained directly from the kinetic experiments except for the case of hydration of II, since this is the only case where the relative concentrations of the saturated and the unsaturated aldehyde can be obtained directly from the UV-measurements. In the other cases an accurate knowledge of the absorptivity of the unsaturated aldehydes coupled with an equally accurate knowledge of the initial concentrations of the saturated aldehydes would, in principle, allow calculation of the equilibrium constants from the kinetic experiments. In practice, however, the uncertainties in the experimentally determined absorptivities are of the same order of magnitude as the fraction of saturated aldehyde at equilibrium. In these cases, therefore, the equilibrium constants had to be determined from

separate experiments, where the hydration reactions of the unsaturated aldehydes were followed.

The rate and equilibrium constants, calculated from the experimental data as defined by the equations given, are shown in Table 1.

Table 1. Rate constants and activation energies.

Reactant	Temp °C	k $\frac{l}{mol\ sec}$	k_1 $\frac{l}{mol\ sec}$	E_A hydration kcal/mol	k_{-1} $\frac{l}{mol\ sec}$	E_A dehydration kcal/mol	K_{exp}	% conversion at eq.
	15.00	0.153	0.143		0.0101		14.2	93.4
II	25.00	0.335	0.305	12.7	0.0301	18.5	10.1	91.0
	35.00	0.688	0.607		0.082		7.39	88.1
	15.00	0.689	0.059		0.630		0.094	91.4
III	25.00	1.71	0.114	11.2	1.60	15.8	0.072	93.3
	35.00	3.97	0.212		3.76		0.056	94.7
	20.00	0.172	0.0089		0.163		0.054	94.8
V	30.00	0.424	0.016	10.3	0.408	16.2	0.039	96.3
	40.00	0.986	0.027		0.959		0.029	97.2
	20.00	0.171	0.0045		0.167		0.027	97.4
VII	30.00	0.382	0.0068	7.2	0.375	14.3	0.018	98.2
	40.00	0.808	0.0099		0.798		0.012	98.8

At the high conversions experimentally observed, it has to be noted, that even small errors in the absorbance measurements and thereby the concentration determinations lead to relatively large errors in the determinations of K_{exp} and consequently also in the values given for k_{-1} in the case of the equilibrium between I and II and for k_1 in the other cases. The same is true for the values given for the corresponding activation energies. The rate constants given for the reverse reactions, on the other hand, are only to a minor degree affected by these experimental errors, and the values of the corresponding activation energies are therefore much more reliable.

Values for the changes in free energy, enthalpy, and entropy associated with the hydration reactions at 25.0°C have been calculated from the data presented in Table 1 and are given in Table 2. As seen, the negative enthalpy changes associated with the formation of saturated systems are balanced by the loss of entropy connected with the formation of a larger molecule from two smaller.

In the case of the equilibrium between I and II the values of K_{exp} are in excellent agreement with the values given by Pressman and Lucas.[6] The value of $\Delta H°_{298}$, calculated from a plot of log K_{exp} against $1/T$, therefore is the same, -5.8 kcal/mol, as that given by them. The rate constants for the base-catalyzed reactions, however, differ by several orders of magnitude from the rate

Table 2. Changes in free energy, enthalpy and entropy for the hydration reactions at 25.0°C.

Reactant	$\Delta F°_{298}$ kcal/mol	$\Delta H°_{298}$ kcal/mol	$\Delta S°_{298}$ cal/°C, mol
II	+1.0	−5.8	−23
IV	+3.9	−4.6	−29
VI	+4.2	−5.9	−34
VIII	+4.6	−7.1	−39

constants for the acid-catalyzed reactions. Thus, at 25.0°, hydroxide ion is about 5000 times as effective a catalyst as hydronium ion.

When comparing the rate constants for the different aldehydes, it is seen, that at 25.0° II is hydrated about twice as fast as IV, whereas III is dehydrated fifty times as fast as I. The two aldehydes V and VII are dehydrated about eight times as fast as I, while of the corresponding unsaturated aldehydes II is hydrated more than twenty times as fast as VI and almost fifty times as fast as VIII. The effectiveness of the α-substituents, as compared with hydrogen, in promoting the dehydration reaction thus is in the order $CH_2OH > CH_3 \approx CH_2CH_3$, whereas they retard the hydration reactions of the 2-propenals in the order $CH_2CH_3 > CH_3 > CH_2OH$.

The Arrhenius activation energies for the forward and reverse reactions of the different aldehydes are roughly comparable and so are the values for the changes in the other thermodynamic functions. The small differences in these values, however, cause relatively large differences in the equilibria between I and II on one hand and between the other aldehydes on the other hand (Tables 1 and 2).

The hydration of II was studied also at increased ionic strength of the medium. By means of added sodium chloride experimental runs were made at the ionic strengths 0.050 N, 0.100 N, and 0.250 N, respectively, but neither the rates nor the equilibria were significantly altered within the temperature range 15.0° to 35.0°. The use of phosphate buffer solutions influenced the observed rates, but since the mechanism of the hydration reaction involves nucleophilic attack by hydroxide ion on the β-carbon atom (eqns. 7 and 8), "direct" catalysis by other bases actually should give different products (eqns. 7a and 8a):

$$HO^- + H_2C{=}CRCHO \rightleftharpoons [HOCH_2\bar{C}RCHO \leftrightarrow HOCH_2CR{=}CHO^-] \quad (7)$$

$$[HOCH_2\bar{C}RCHO \leftrightarrow HOCH_2CR{=}CHO^-] + H_2O \rightleftharpoons HOCH_2CHRCHO + OH^- \quad (8)$$

$$B^- + H_2C{=}CRCHO \rightleftharpoons [B\bar{C}H_2CRCHO \leftrightarrow BCH_2CR{=}CHO^-] \quad (7a)$$

$$[B\bar{C}H_2CRCHO \leftrightarrow BCH_2CR{=}CHO^-] + HB \rightleftharpoons BCH_2CHRCHO + B^- \quad (8a)$$

General base catalysis is therefore only possible in a concerted "indirect" reaction involving base equilibration. The question whether such general base catalysis (eqns. 7b and 8b) occurs cannot be answered at present.

$$B^- + H_2O + H_2C{=}CRCHO \rightleftharpoons [HOCH_2\bar{C}RCHO \leftrightarrow HOCH_2CR{=}CHO^-] + HB \quad (7b)$$

$$[HOCH_2\bar{C}RCHO \leftrightarrow HOCH_2CR{=}CHO^-] + HB \rightleftharpoons HOCH_2CHRCHO + B^- \quad (8b)$$

EXPERIMENTAL

The acrolein and methacrolein were commercial pract. grade chemicals and were freshly distilled each day before use. 2-Ethylpropenal was prepared by the method of Marvel *et al.*[9] and was also redistilled before use. The other aldehydes used, 2-hydroxymethylpropenal, 3-hydroxy-2-hydroxymethylpropanal, 3-hydroxy-2-methylpropanal, and 2-ethyl-3-hydroxypropanal, were synthesized in the form of their diethyl acetals.[4] The free aldehydes were prepared when needed (see General procedure) and the stock solutions prepared were never used for more than five days although they were found to be reasonably stable for longer periods. At room temperature a slow approach to the hydration-dehydration equilibrium was found to occur in such solutions, but the rates were several orders of magnitude lower than for the base-catalyzed reactions. Sodium hydroxide stock solutions were freshly prepared each week from Merck Titrisol ampoules. These and all other aqueous solutions were made up with boiled carbon dioxide-free distilled water. The UV-measurements were made using a Beckman DU instrument with the cell compartment thermostatted by circulating water from a thermostatted bath of type Lauda. The temperatures in the cuvettes were checked in separate experiments to be within $\pm 0.05°$ from the temperature wanted.

General procedure. The following aqueous stock solutions were prepared: Of 2-propenal (II) 10^{-2} and 10^{-3} M solutions, of the aldehydes III to VIII 10^{-3} M, and of sodium hydroxide 0.100 and 0.010 M solutions.

The stock solutions of the aldehydes III, IV, V, and VII were prepared in the following way. About 0.25 mmol of their respective diethyl acetal was weighed on an analytical balance and then dissolved in about 15 ml of water. This solution was then passed through an H^+-saturated, carefully washed ion exchange column, 80 × 1 cm, filled with analytical grade Amberlite IR 120 resin. With water as eluent 250 ml of eluate was collected in a volumetric flask. The whole operation was made under exclusion of carbon dioxide from the air.

In the kinetic runs with the aldehydes II, III, V, and VII, respectively, 10 ml of the stock solution was added to 70 to 80 ml of distilled water in a 100 ml volumetric flask, which was then immersed in a thermostatted bath for adjustment to the proper temperature. After about half an hour the reactions were started by means of addition of the proper amount of catalyst and the solutions were diluted to the mark and thoroughly shaken. Then a quartz cell with 1.000 cm optical path length and equipped with a teflon plug was filled with the reaction solution and inserted in the cell compartment. A cell filled with an equally concentrated catalyst solution was used as reference. With the more concentrated solution of II a 0.100 cm cell was used instead. The first absorbance reading could normally be taken about 90 sec after the start of the reaction as measured after addition of about half of the amount of sodium hydroxide. When the kinetic runs were performed more than 5° from ambient temperature the rates during the first 5 min deviated slightly from the rates during the remainder of the runs due to temperature deviations in the solutions caused by the mixing and filling procedures.

The determinations of the equilibrium constants with the help of the aldehydes IV, VI, and VIII, respectively, were performed in an analogous way, except that only 4 to 5 ml of the stock solutions were used in order to keep the absorbance between 0.3 to 0.5 where the accuracy is best. In these cases the starting value for the absorbance was obtained by means of graphical extrapolation of the expression log $(\alpha_t - \alpha_\infty)$ as plotted against time.

The absorbance measurements were made at 210 nm for II, at 213.5 nm for IV, at 218.5 nm for VI, and at 220 nm for VIII. Even if the absorbance of II was found to have its maximum nearer 208 nm the measurements thus were made at 210 nm, since the background absorbance of the alkaline solutions rises rapidly below 210 nm and therefore

necessitates excessively wide slits at lower wavelengths. This could partly be overcome in the experiments with the more concentrated solution of II where the shorter path length was used. The observed rates, however, were the same within experimental error.

Acknowledgements. This work was performed in part at the Department of Organic Chemistry at Chalmers University of Technology, Göteborg, and in part at Perstorp AB, Perstorp, Sweden. The work has in its whole been financially supported by Perstorp AB, which is gratefully acknowledged. My thanks are also due to Professor Erich Adler for his kind interest in this work and to Mrs. Marianne Frantsi, Mrs. Ulla-Britt Persson and Mr. Kurt Johnson for skilful laboratory assistance.

REFERENCES

1. Wawzonek, S. and Rees, D. A. *J. Am. Chem. Soc.* **70** (1948) 2433.
2. Berlow, E., Barth, R. H. and Snow, J. E. *The Pentaerythritols*, Am. Chem. Soc. Monograph Series No. 136, Reinhold, New York 1958, p. 5.
3. Bertilsköld, H. and Vik, J.-E. *Acta Chem. Scand.* **25** (1971) 2211.
4. Vik, J.-E. *Acta Chem. Scand.* **27** (1973) 239.
5. Nef, J. U. *Ann.* **335** (1904) 191.
6. Pressman, D. and Lucas, H. J. *J. Am. Chem. Soc.* **64** (1942) 1953.
7. Hall, R. H. and Stern, E. S. *J. Chem. Soc.* **1950** 490.
8. Ingold, C. K. *Structure and Mechanism in Organic Chemistry*, G. Bell and Sons, London 1953, pp. 694–695.
9. Marvel, C. S., Myers, R. L. and Saunders, J. H. *J. Am. Chem. Soc.* **70** (1948) 1694.

Received July 20, 1972.

ACTA CHEMICA SCANDINAVICA 27 (1973) 258–270

Studies of Polarised Ethylenes

Part V.* Ultraviolet Spectra; Experimental Results and PPP Calculations

INGEGERD WENNERBECK

Division of Organic Chemistry 1, Chemical Center, University of Lund, P.O. Box 740, S-220 07 Lund 7, Sweden

The ultraviolet spectra of a number of ethylenes with push-pull substituents have been measured and interpreted with the aid of two modifications of Pariser-Parr-Pople SCF-MO calculations. Solvent effects are discussed from both experimental and theoretical points of view. The electronic absorption spectra of the anions of methylene active compounds with the same electron-accepting groups as the ethylenes were recorded. The charge distributions and bond orders in four compounds are discussed in relation to experimental data.

Ethylenes with both electron-donating and electron-accepting groups exhibit absorption bands in the near ultraviolet region characteristic of the delocalisation of the π-electrons throughout the molecule. Nagakura [1] has studied ethylenes with a nitro or carbonyl group as the electron-accepting group, and has assigned the absorption bands in these compounds to charge-transfer transitions. Loos *et al.*[2] have also studied intramolecular charge-transfer absorption in nitroethylenes from both experimental and theoretical points of view.

Investigations of the restricted internal rotation in ethylenes with push-pull substituents have been reported in previous parts [3–5] of this series. The present work was performed in order to study the ultraviolet spectra of these ethylenes both qualitatively and quantitatively. A UV study of the polarised ethylenes *1A*, *B*, *C*, *D* – *10A*, *B*, *C*, *D* (see below) was therefore undertaken. To obtain a more quantitative understanding of the nature of the electronic transitions in these ethylenes, molecular orbital calculations were carried out on compounds *1A* – *1D*, *3A* – *3D*, *8A* – *8D*, and *10A* – *10D* using the semi-empirical Pariser-Parr-Pople LCAO-SCF-MO method.[6] Furthermore a UV study of the tetrabutylammonium (Q) salts (*E*) or sodium salts of some of the active methylene compounds $X-CH_2-Y$ was carried out.

* Part IV, see Ref. 5.

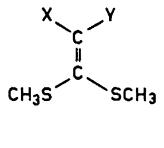

A

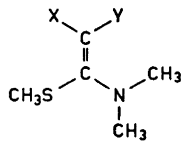

B

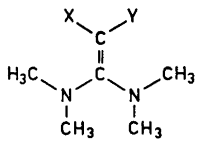

C

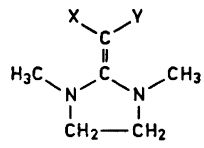

D

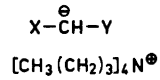

E

	X	Y		X	Y
1.	CH_3OCO	CN	*6.*	Ph	$COCH_3$
2.	PhCO	CN	*7.*	PhCO	$COCH_3$
3.	CN	CN	*8.*	CH_3CO	$COCH_3$
4.	*p*-$NO_2C_6H_4$	CN	*9.*	CH_3CO	CO_2CH_3
5.	Ph	CN	*10.*	CH_3OCO	CO_2CH_3

EXPERIMENTAL

Compounds *1A, C, D – 10A, C, D* were prepared as previously described.[3,7] Gompper and Töpfl [8] have described the preparation of *1B*, and the preparation of *2B*, *3B*, *4B*, *5B*, *6B*, *7B*, and *10B* will be published in a forthcoming paper in this series. Compounds *8B* and *9B* were synthesized according to Ref. 9.

Table 1. Ultraviolet spectra of the anions $X-\overset{\ominus}{C}H-Y$ (E).

X	Y	λ_{max} nm	ε
1. CH_3OCO	CN	246 [b]	12600
2. C_6H_5CO	CN	242	6000
		251	4400
		317 [a]	7300
3. CN	CN	244 [a]	2800 [c]
4. *p*-$NO_2C_6H_4$	CN	264	9100
		462	4600
		596 [a]	4800
7. PhCO	$COCH_3$	248	6100
		310 [a]	12600
8. CH_3CO	$COCH_3$	245	2600
		274 [a]	9000
9. CH_3CO	CO_2CH_3	272 [b]	18000
10. CH_3OCO	CO_2CH_3	258 [b]	3200

[a] Tetrabutylammonium salt in $CHCl_3$.
[b] Sodium salt in ethanol.
[c] Very approximate due to the hygroscopic nature of the salt.

Table 2. The observed wavelengths and molar extinction coefficients for compounds *A*, *B*, *C*, *D* in absolute ethanol.

		A		*B*		*C*		*D*	
X	Y	λ_{max} nm	ε	λ_{max} nm	ε	λ_{max} nm	ε	λ_{max} nm	ε
1. CH_3OCO	CN	307	14 500	265	4 200	251	8 800	232 (sh)	10 400
				318	11 400	284	18 600	276	14 200
2. PhCO	CN	263	9 700	252	11 900	253 (sh)	12 200	251 (sh)	9 600
		349	11 100	346	13 600	320	14 400	310	12 000
3. CN	CN	300 (sh)	9 000	268 (sh)	6 000	243	9 400	240 (sh)	8 000
		330	13 900	307	15 500	276	18 200	262	15 700
4. *p*-$NO_2C_6H_4$	CN	258	10 000	260	8 300	231	16 000	233	14 800
		292	9 000	287	8 800	290	10 800	294	7 800
		362	11 100	401	16 800	418	22 000	435	22 800
5. Ph	CN	234	8 200	230	9 600	235	13 400	229	12 700
		322	10 900	261	8 200	247	15 100	277 (sh)	8 400
				326	14 400	257 (sh)	11 800	317	16 600
						318	17 400		
6. Ph	$COCH_3$	220 (sh)	9 300	227	7 200	225	7 800	235	6 600
		294	6 300	274	9 300	270 (br)	13 500	292	12 600
				357	8 800	340	13 800	318 (sh)	9 200
7. PhCO	$COCH_3$	253	11 400	233	11 200	241	13 100	234	13 800
		318	8 700	271 (sh)	12 000	272 (sh)	12 400	290	14 400
				287	12 800	297	15 600		
				345	3 800				
8. CH_3CO	$COCH_3$	223	5 800	268	18 800	257	17 400	253	12 400
		317	8 200	272 (sh)	18 000	275	16 200	277	21 600
				350	1 400	292 (sh)	11 600		
9. CH_3CO	CO_2CH_3	317	9 000	257	22 800	247	19 200	252	24 800
				345	2 800	299	7 500		
10. CH_3OCO	CO_2CH_3	311	10 300	241	12 000	237	18 600	240	25 200
				265	7 000	293	12 400	274	6 200
				331	6 800				

sh = shoulder. br = broad.

Table 3. Experimental [a] and calculated ultraviolet spectra of compounds *1A – 1D, 3A – 3D, 8A – 8D, 10A – 10D.*

	Experimental		Calculated [b]		Calculated [c]	
Compound	λ_{max} nm	ε	λ_{max} nm	f	λ_{max} nm	f
1A	300 (sh)	8 400	302.2	0.114	244.3	0.215
	327	12 200	319.1	0.215	273.7	0.359
1B I	265	5 600	235.3	0.187	228.5	0.173
	319	14 500	283.1	0.320	279.9	0.577
1B II			234.9	0.348	219.4	0.213
			292.5	0.237	272.1	0.510
1C	249	6 200	212.2	0.232	224.2	0.212
	290	15 800	266.2	0.486	281.5	0.590
1D	229 (sh)	7 700	213.8	0.244	225.1	0.265
	284	13 700	266.6	0.496	285.1	0.632
3A	292 (sh)	9 000	315.7	0.048	223.9	0.029
	324	13 200	330.5	0.263	265.3	0.554
3B	262	6 000	242.3	0.215	244.4	0.246
	310	13 300	298.4	0.280	279.6	0.663
3C	239	9 400	233.8	0.302	237.9	0.293
	282	19 200	275.6	0.472	282.5	0.689
3D	225 (sh)	8 700	231.9	0.311	239.7	0.323
	274	15 600	275.4	0.481	285.2	0.737
$8A_{E-Z}$	309	7 400	321.4	0.111	261.7	0.175
			345.9	0.161	314.0	0.388
$8A_{Z-Z}$			223.2	0.251	220.6	0.494
			337.3	0.044	288.3	0.036
			348.6	0.165	322.6	0.365
$8B_{E-Z}$III	246 (sh)	8 400	218.7	0.289	219.5	0.585
	264	14 400	241.8	0.286	243.0	0.052
	333 (sh)	5 400	312.9	0.168	297.1	0.560
	352 (br)	5 200				
$8B_{E-Z}$IV			216.6	0.373	226.6	0.246
			244.1	0.121	279.3	0.567
			296.0	0.242		
$8B_{Z-Z}$			222.3	0.353	220.0	0.548
			249.7	0.109	251.7	0.079
			312.5	0.142	309.4	0.402
$8C_{E-Z}$	254	15 800	222.9	0.320	238.2	0.289
	264 (sh)	9 800	272.3	0.369	295.6	0.509
	315	8 400				
$8C_{Z-Z}$			228.8	0.313	252.3	0.239
			278.8	0.236	302.3	0.360
$8D_{E-Z}$	252 (sh)	8 800	224.3	0.336	236.7	0.313
	270	13 200	272.0	0.376	293.1	0.544
	302 (sh)	3 000				
$8D_{Z-Z}$			229.9	0.333	249.5	0.278
			278.2	0.241	300.2	0.383
10A	307	9 800	295.3	0.127	233.4	0.258
			327.1	0.144	303.1	0.332
10B V	279 (sh)	4 800	231.2	0.136	227.0	0.164
	313	11 000	275.2	0.248	295.1	0.493
10B VI			233.2	0.256	219.0	0.127
			298.3	0.160	279.3	0.450
10C	247 (sh)	8 200	202.4	0.180	235.6	0.177
	293	14 400	260.2	0.363	291.5	0.489
10D	232	17 400	203.8	0.203	235.1	0.232
	292	9 100	260.1	0.374	294.8	0.529

[a] In cyclohexane with 0.2 % dichloromethane. [b] Method 1. [c] Method 2. sh = shoulder. br = broad.

The preparation of the Q salts of the active methylene compounds was carried out according to the method of ion pair extraction described by Brändström *et al.*[10] The salt *3E* was very hygroscopic and had to be manipulated in a dry box. The identities of the anions were verified by NMR and by adding sulfuric acid to a water solution of the salt and recovering the active methylene compound, the identity of which was verified by IR. Unfortunately not all the desired Q salts (*1E*, *5E*, *6E*, *9E*, *10E*) could be prepared due to secondary reactions or insufficient acidity of the methylene compound. Therefore the UV spectra of the sodium salts of compounds *1E*, *9E*, and *10E* were recorded. The UV spectra of the anions are listed in Table 1.

All the UV spectra were recorded on a Unicam Model SP 800 spectrometer. Absolute ethanol was used as solvent for compounds *1A*, *B*, *C*, *D* – *10A*, *B*, *C*, *D*. The spectra of the compounds used for comparison of calculated and experimental transition energies were also recorded in cyclohexane with 0.2 % dichloromethane. The peak wavelengths (nm) and molar extinction coefficients for all compounds in absolute ethanol are listed in Table 2. Experimental and calculated wavelengths (nm), molar extinction coefficients and oscillator strengths are tabulated in Table 3.

For all compounds *1* two conformations of the ester group are possible and NMR studies [5] of *9C* (X = CO_2CH_3, Y = $COCH_3$) show that the conformation with the ester carbonyl group E [11] to the C=C bond is the most probable one. Assuming this to be valid also for compounds *1*, two conformations (I and II) can be formulated for *1B*.

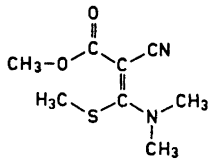

I

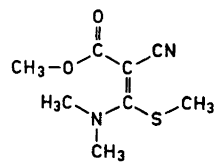

II

In the calculations these two conformations can be taken into account (see Table 3).

The acetyl groups in compounds *8* can have an E – Z arrangement, a Z – Z arrangement or an E – E arrangement with respect to the C – C=O bond. The E – E arrangement is not very likely because of strong dipolar repulsion between the carbonyl groups. Furthermore, NMR studies [5] of *8C* show that the conformation with the acetyl groups in an E – Z arrangement is dominant, but NMR studies of *8D* show that the conformation with Z – Z arrangement also exists. The conformation of *8B* which is E – Z with respect to the C – C=O bond can exist in conformations III and IV with respect to the C=C bond.

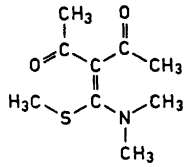

III

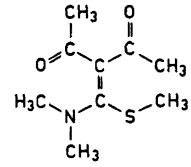

IV

This can be taken into account in the calculations. In Table 3 the conformation with respect to the C – C=O bond is indicated with the indices E – Z and Z – Z, respectively.

For compound *10C*, only the E – Z conformation has been observed [5] and it is assumed to be at least the dominant one for *10A*, *B*, and *D* as well. Two forms, V and VI, must be considered for compound *10B*.

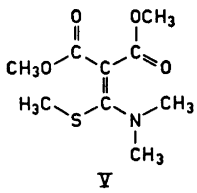

V

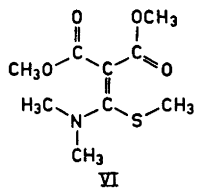

VI

MOLECULAR ORBITAL CALCULATIONS

The calculations have been performed by two somewhat different PPP methods. In all PPP methods the elements of the Fock matrix are given by

$$F_{\mu\mu} = H_{\mu\mu}^{\text{core}} - \tfrac{1}{2}\, q_\mu\, \gamma_{\mu\mu} + \sum_{\nu \neq \mu} q_\nu\, \gamma_{\mu\nu}$$

$$F_{\mu\nu} = \beta_{\mu\nu}^{\text{core}} - \tfrac{1}{2}\, p_{\mu\nu}\, \gamma_{\mu\nu}$$

The difference between the two PPP methods used in this work lies in the evaluation of the integrals.

Method 1. In this method the following expressions are used for the evaluation of the various integrals. The one-center repulsion integrals

$$\gamma_{\mu\mu} = I_\mu - A_\mu$$

where I_μ and A_μ are the valence state ionization potential and electron affinity of atom μ. The two-center repulsion integrals are calculated according to the approximation given by Mataga and Nishimoto [12]

$$\gamma_{\mu\mu} = 14.40/(R_{\mu\nu} + k_{\mu\nu}) \text{ eV}$$

where $R_{\mu\nu}$ is the internuclear distance between atoms μ and ν, and $k_{\mu\nu}$ is defined by

$$k_{\mu\nu} = 14.40/[\tfrac{1}{2}(I_\mu - A_\mu) + \tfrac{1}{2}(I_\nu - A_\nu)]$$

The core Coulomb integrals are calculated according to Goeppert-Mayer and Sklar [13]

$$H_{\mu\mu}^{\text{core}} = W_{\mu\mu} - (n_\mu - 1)\gamma_{\mu\mu} - \sum_{\nu \neq \mu} n_\nu \gamma_{\mu\nu}$$

where n_ν is the number of electrons contributed to the delocalized π-system by the ν atom.

In this method the expression

$$W_{\mu\mu} - (n_\mu - 1)\gamma_{\mu\mu}$$

is approximated by the ionization potential (I_μ) of the atom μ.

The core resonance integrals $\beta_{\mu\nu}^{\text{core}}$ are treated in some cases (see Table 4) as empirical parameters, the values of which have been determined to give a good fit between the experimental and calculated UV data, and in some cases by the expression first proposed by Mulliken [14] and then modified to a relationship of the type [15]

Table 4. Parameters used in PPP method 1.

Atom	$W_{\mu\mu}$ eV	$\gamma_{\mu\mu}$ eV	Ref.	Bond	Bond length Å	$\beta_{\mu\nu}$ eV
C	−11.42	10.84	17	C−C	1.39 [d]	−2.24
$\dot{S}$	−20.40	10.84	17	C−C	1.44 [e]	−2.12
$\ddot{O}$	−26.73	14.58	17	C−C	1.45 [e]	−2.05
				C−$\ddot{S}$	1.74 [d]	−0.90 [a]
$\dot{O}$	−16.86	15.23	18, 19	C−$\dot{N}$ [b]	1.33 [d]	−2.73 [a]
$\dot{N}$	−28.71	16.75	19	C−$\dot{N}$ [c]	1.33 [d]	−2.90 [a]
C (nitril)	−11.19	11.09	19	C−$\dot{N}$	1.14 [d]	−2.95 [a]
				C−$\dot{O}$	1.25 [e]	−3.49
$\dot{N}$ (nitril)	−14.18	12.52	19	C−$\ddot{O}$	1.28 [f]	−3.09

[a] Adjusted values. [b] Compounds *C*. [c] Compounds *D*. [d] Taken from X-ray structure.[20] [e] Evaluated from HMO calculations with α,β-variation. [f] Evaluated from PPP calculations.

$$\beta_{\mu\nu} = -\frac{S_{\mu\nu}}{1+S_{\mu\nu}} \cdot \frac{I_\mu + I_\nu}{2}$$

where $S_{\mu\nu}$ are the overlap integrals, evaluated according to Mulliken *et al.*[16]

The parameters used in this method are tabulated in Table 4. An idealized geometry was assumed, with all bond angles equal to 120° except for the compounds *D* where the N−C−N bond angle was taken to be 110° according to an X-ray crystallographic examination[20] of 1,3-dimethyl-2-(*p*-bromo-benzoyl-cyanomethylene)-imidazolidine. Some of the bond lengths (see Table 4) were estimated according to the expression formulated by Coulson[21] using the values of bond orders obtained from HMO calculations with α,β-variation[22] and PPP calculations, and some of the bond lengths were taken from the X-ray structure determination[20] of the *p*-bromo analogs of *2A* and *2D*.

Method 2. This method is a modified PPP approximation proposed by Roos and Skancke.[23] Evaluation of the integrals is performed in conformity with the following expressions. The one-electron core integrals $W_{\mu\mu}$ are assumed to depend on the environment of atom μ and this gives

$$H_{\mu\mu}^{\text{core}} = W_{\mu\mu} - (n_\mu - 1)\gamma_{\mu\mu} - \sum_{\nu \neq \mu} n_\nu \gamma_{\mu\nu}$$

$$W_{\mu\mu} = W_{\mu\mu}^\circ + \sum_\nu [\Delta W_\mu^\circ(\nu) + \delta\mu\nu^W(R_{\mu\nu} - R_0)]$$

where the summing is over all neighbours to atom μ. $\Delta W_\mu^\circ(\nu)$ is the correction due to the replacement of a hydrogen atom by the atom ν. $R_{\mu\nu}$ is the internuclear distance between atoms μ and ν, and R_0 is a suitably chosen standard length of the bond $\mu\nu$.

The core resonance integrals, $\beta_{\mu\nu}$, and the two-center repulsion integrals, $\gamma_{\mu\nu}$, between nearest neighbours also depend on the bond lengths, and linear relationships are assumed:

$$\beta_{\mu\nu} = \beta_{\mu\nu}^{\circ} + \delta_{\mu\nu}^{\beta}(R_{\mu\nu} - R_0) \text{ and}$$
$$\gamma_{\mu\nu} = \gamma_{\mu\nu}^{\circ} + \delta_{\mu\nu}^{\gamma}(R_{\mu\nu} - R_0)$$

The one-center repulsion integrals, $\gamma_{\mu\mu}$, have been estimated from spectral data,[24] and the ball approximation [25] has been used for calculating the two-electron two-center repulsion integrals, $\gamma_{\mu\nu}$, for non-neighbours.

Table 5. Parameters used in PPP method 2.

Atom	$W_{\mu\mu}^{\circ}$	$\gamma_{\mu\mu}$	Bond $\mu\nu$	$\beta_{\mu\nu}^{\circ}$	$\gamma_{\mu\nu}^{\circ}$	$\delta_{\mu\nu}^{W}$	$\delta_{\mu\nu}^{\beta}$	$\delta_{\mu\nu}^{\gamma}$	$\Delta W_{\mu\nu}^{\circ}$	$\Delta W_{\mu\nu}^{\circ}$	R_0 Å	Ref.
C	−9.84	11.97	C−C	−2.42	6.91	9.22	3.05	−3.99	0.07	0.07	1.397	26
S̈	−10.62	9.58	C−S̈	−1.37	7.28	9.22	3.05	−3.99	−0.70	0	1.714	27
Ṅ	−12.57	15.44	C−Ṅ	−2.72	7.16	5.6	2.6	−3.99	0.03	0.14	1.338	28
N̈	−8.52	15.44	C−N̈	−2.25	6.34	5.6	2.6	−3.99	0.03	0.14	1.338	28
Ȯ	−19.60	18.89	C−Ȯ	−2.46	9.33	0	0	0	−0.71	0	1.22	29
Ö	−11.18	18.89	C−Ö	−1.80	6.20	0	0	0	−0.09	1.51	1.35	30

The parameters used in this method are listed in Table 5. The geometries are the same as in method 1. The C≡N group is not parametrized in this method, and therefore the parameters used for the nitrile nitrogen are those estimated for nitrogen of pyridine character.

RESULTS AND DISCUSSION

General aspects on the experimental UV data. The long wavelength absorption bands recorded in Table 2 have in most cases extinction coefficients higher than 6000 and should be ascribed to $\pi \rightarrow \pi^*$ transitions. The only doubtful case is *8B*, for which the band at 350 nm ($\varepsilon = 1400$) could have been due to an $n \rightarrow \pi^*$ transition in the carbonyl groups. However, the position of this band is hardly affected by changing the solvent from ethanol to cyclohexane (Table 3) which is contrary to the general behaviour of $n \rightarrow \pi^*$ bands.

A certain analogy can be expected between the UV spectra of the compounds studied here and those of analogous thiocarbonyl compounds because of the resemblance in electronic effects between the group X−C−Y and the sulphur atom. However, this analogy cannot be stretched too far, since, when the groups X and Y have large π-electron systems, their influence on the light absorption will tend to overshadow that of the electron-donating groups. The thiocarbonyl compounds analogous to *A*−*C* are VII−IX, for which the $\pi \rightarrow \pi^*$ λ_{max} values [31] are given below the formulas.

The order of λ_{max}, decreasing with increasing electron-donating effect of the substituents at the thiocarbonyl group, is contrary to the qualitative resonance

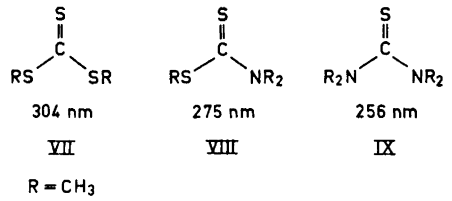

picture but is well supported by quantum chemical calculations.[32] In the series with X = CN, Y = CN (3) and X = PhCO, Y = CN (2) the same order of the wavelength maxima is observed. In all other series except 4 (X = *p*-$NO_2C_6H_4$, Y = CN) and 6 (X = Ph, Y = CN) the wavelengths increase in the order $D < C < A < B$.

It has been shown by NMR lineshape studies [4] and for one of the compounds (*2D*) also by X-ray crystallography [20] that the compounds *D* are twisted around the double bond in the ground state. This must affect the ultraviolet absorption spectra, and generally one should expect the absorption of the cyclic compounds *D* to be shifted further in the direction of the anions $(X-CH-Y)^-$ than those of *C*. To test this hypothesis, the Q salts or sodium salts of some of the active methylene compounds $X-CH_2-Y$ were prepared and their spectra recorded in chloroform or ethanol solution, respectively (Table 1). In the series *1*, *3*, *4*, *8*, *10*, the above assumption is verified, whereas in *2* the spectra of *C*, *D*, and the anion are so similar that no trend can be observed. In *7* and *9* the cyclic diamines *D* absorb at shorter wavelength than both *C* and the anions. In *9D*, however, the spectrum in chloroform shows a shoulder at 279 nm, and a corresponding band is probably present under the broad band at 252 nm in ethanol solution.

Solvent effects. If the degree of interaction between solvent and solute is relatively small there will be a bathochromic shift with increasing polarisibility of the solvent.[33,34] In the following the shifts considered are those which occur on changing the solvent from cyclohexane to ethanol. Comparison of the UV spectra of compounds *1A – 1D*, *3A – 3D*, *8A – 8D*, and *10A – 10D* recorded in absolute ethanol and cyclohexane shows that 1,1-bis-alkylthioethylenes (*A*) and the solvent have the least interaction, except in compound *1A* (X = CN, Y = CO_2CH_3), where there is a hypsochromic shift. *1B*, *3B*, and *8B* are not affected by changing the solvent. However, in *10B* there is a strong bathochromic shift. The compounds *C* and *D* absorb at shorter or the same wavelength when changing to a more polar solvent.

These results can be interpreted in the following way. The hypsochromic shifts and also the lack of shift in some compounds indicate that the polarity is decreased or reversed by the electronic transition, thereby weakening the interaction with polar solvents. In such cases the term charge – transfer band does not apply. The bathochromic shifts in some compounds of type *A* indicate some increase in polarity, but a change depicted as below evidently does not give a good description of the excitation mechanism. The only compound that shows a real charge transfer absorption is *10B*, for which a bathochromic shift

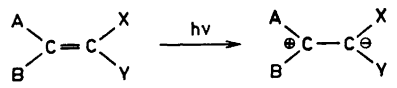

of 18 nm is observed. Calculated charge densities (Table 6) for the ground state and the excited state for atoms 2 and 4 in compound *3A* show that there is a slight increase of the polarity in the excited state, which confirms the

Table 6. Calculated [a] π-electron charges on the various atoms in compounds *3A* and *3C* in the ground and excited states.

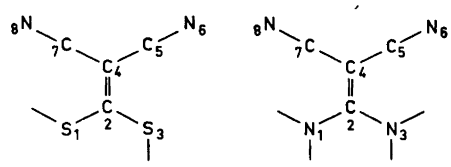

3A *3C*

	q_1	q_2	q_3	q_4	q_5	q_6
A Ground state	+0.046	−0.228	+0.046	+0.176	+0.114	−0.133
Excited state	+0.293	−0.373	+0.293	+0.151	+0.039	−0.220
C Ground state	+0.136	+0.047	+0.136	−0.312	+0.089	−0.182
Excited state	+0.228	−0.234	+0.228	+0.211	+0.002	−0.215

[a] PPP method 2.

above prediction. In compound *3C* a reversed polarity at atoms 2 and 4 is found on going from the ground state to the excited state, and this is in agreement with the observed hypsochromic shift.

Discussion of PPP calculations. The agreement between calculated and observed absorption maxima is at best fair. With systems *1* and *3*, method 1 gives reasonable agreement and also the correct order: $\lambda\ (A) > \lambda\ (B) > \lambda\ (C)$. In the other systems no reasonable trend can be observed. Generally method 2 gives larger discrepancies than method 1, which may be due to the fact that the former method has not been parametrized for the present systems. Especially for systems *C* and *D*, steric effects, which have not been taken into account in the calculation, may contribute to some of the observed discrepancies. This does not apply to systems *3A*, *3B*, *3D*, which should be free from steric effects.

Discussion of π-electron charges and bond orders. The charge and bond order diagrams (Fig. 1) are rather similar in the two methods of calculation. The main differences are the electron densities and bond orders in the C=O and C≡N groups. These differences can be ascribed to the rather different $W_{\mu\mu}$

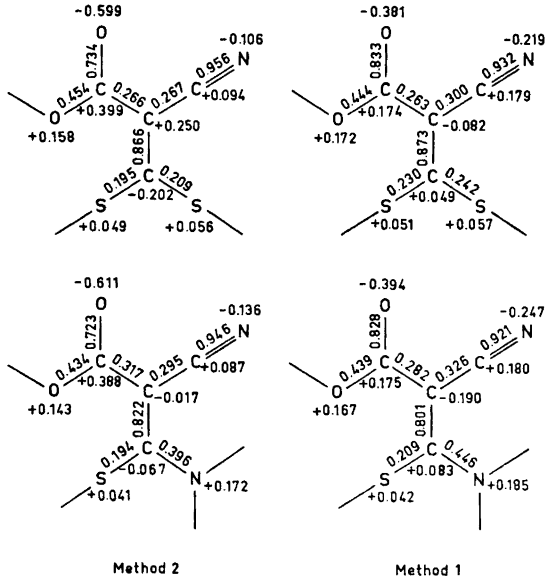

Fig. 1. π-Electron distributions and bond orders for the ground state of compounds *1A* and *1B I* calculated with both PPP methods (see text).

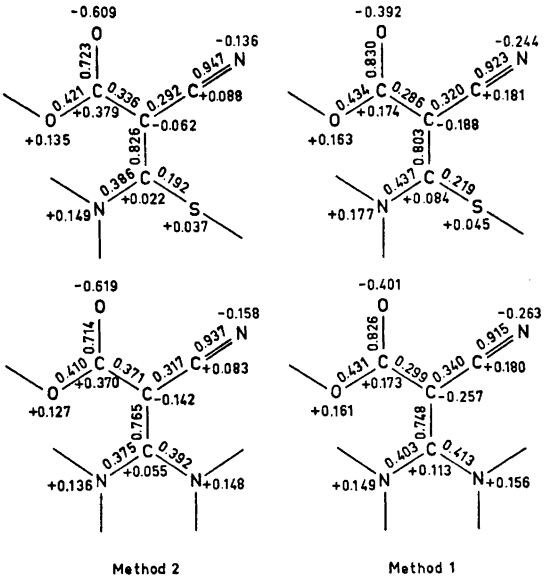

Fig. 2. π-Electron distributions and bond orders for the ground state of compounds *1B II* and *1C* calculated with both PPP methods (see text).

values for oxygen and nitrogen used in the two methods. It is also notable that method 2 gives a greater difference between the E and Z forms of *1B*. Otherwise, both series of diagrams show the expected increase in conjugation effects in the sequence *A*, *B*, *C*. The total positive charge on the electron-donating heteroatoms increases in this series, as does the negative charge on the electron-attracting oxygen and nitrogen atoms, whereas the bond order of the carbon-carbon double bond decreases. With method 1, the "local" dipole moment of the carbon – carbon double bond is always directed with the negative end towards the electron-attracting part of the molecule, whereas with method 2 the double bond in *1A* is quite strongly polarised in the opposite direction. In *1B* the E and Z forms have small polarities in opposite directions, and the double bond polarity in *1C* is in the direction of the overall dipole moment. The same charge relations are observed with compounds *3A* and *3C* (see Table 6 for results with method 2). Which set of results is the more realistic cannot be decided at present, since the dipole moments reveal only the sum of all charge displacements.

Acknowledgements. The author thanks professor Jan Sandström for his stimulating interest in this work and for valuable comments on the manuscript. Thanks are also due to Ingenjör Arne Rosdahl for experimental assistance. Financial support by the *Swedish Natural Science Research Council*, *Kungliga Fysiografiska Sällskapet i Lund*, and by *Fonden för ograduerade forskares vetenskapliga verksamhet* of the University of Lund is gratefully acknowledged.

REFERENCES

1. Nagakura, S. *J. Chem. Phys.* **23** (1955) 1441.
2. Loos, K. R., Wild, P. and Günthard, H. H. *Spectrochim. Acta* **25** (1969) 275.
3. Sandström, J. and Wennerbeck, I. *Acta Chem. Scand.* **24** (1970) 1191.
4. Sandström, J. and Wennerbeck, I. *Chem. Commun.* **1971** 1088.
5. Wennerbeck, I. and Sandström, J. *Org. Magn. Resonance. To be published.*
6. Dewar, M. J. S. *The Molecular Orbital Theory of Organic Chemistry*, McGraw, New York 1969, p. 156.
7. Eriksson, E., Sandström, J. and Wennerbeck, I. *Acta Chem. Scand.* **24** (1970) 3102.
8. Gompper, R. and Töpfl, W. *Chem. Ber.* **95** (1962) 2871.
9. Liljefors, T. and Sandström, J. *Acta Chem. Scand.* **24** (1970) 3109.
10. Brändström, A., Berntsson, P., Carlsson, S., Djurhuus, A., Gustavii, K., Junggren, U., Lamm. B. and Samuelsson, B. *Acta Chem. Scand.* **23** (1969) 2202.
11. Blackwood, J. E., Gladys, C. L., Loening, K. L., Petrarca, A. E. and Rush, J. E. *J. Am. Chem. Soc.* **90** (1968) 509.
12. Mataga, N. and Nishimoto, K. *Z. physik. Chem. (Frankfurt)* **13** (1957) 140.
13. Goeppert-Mayer, M. and Sklar, A. L. *J. Chem. Phys.* **6** (1938) 645.
14. Mulliken, R. S. *J. Phys. Chem.* **56** (1952) 292.
15. Rasch, G. *Z. Chem.* **2** (1962) 347.
16. Mulliken, R. S., Rieke, C. A., Orloff, D. and Orloff, H. *J. Chem. Phys.* **17** (1949) 1248.
17. Fabian, J. *Theor. Chim. Acta* **12** (1968) 200.
18. Forsén, S. and Skancke, P. N. *Selected Topics in Structure Chemistry*, Universitetsforlaget, Oslo 1967, p. 229.
19. Hinze, J. and Jaffé, H. H. *J. Am. Chem. Soc.* **84** (1962) 540.
20. Abrahamsson, S., Rehnberg, G., Liljefors, T. and Sandström, J. *To be published.*
21. Coulson, C. A. *Proc. Roy. Soc. (London)* **A 169** (1939) 413.
22. Janssen, M. J. and Sandström, J. *Tetrahedron* **20** (1964) 2339.
23. Roos, B. and Skancke, P. N. *Acta Chem. Scand.* **21** (1967) 233.

24. Fischer-Hjalmars, I. In Löwdin, P. O. and Pullman, B., Eds., *Molecular Orbitals in Chemistry, Physics and Biology*, Academic, New York 1964, p. 361.
25. Parr, R. G. *J. Chem. Phys.* **20** (1952) 1499.
26. Roos, B. *Acta Chem. Scand.* **21** (1967) 2318.
27. Skancke, A. and Skancke, P. N. *Acta Chem. Scand.* **24** (1970) 23.
28. Fischer-Hjalmars, I. and Sundbom, M. *Acta Chem. Scand.* **22** (1968) 607.
29. Jensen, H. and Skancke, P. N. *Acta Chem. Scand.* **22** (1968) 2899.
30. Höjer, G. *Acta Chem. Scand.* **23** (1969) 2589.
31. Janssen, M. J. *Rec. Trav. Chim.* **79** (1960) 464.
32. Janssen, M. J. *Rec. Trav. Chim.* **79** (1960) 1066.
33. Bayliss, N. S. *J. Chem. Phys.* **18** (1950) 292.
34. Longuet-Higgins, H. C. and Pople, J. A. *J. Chem. Phys.* **27** (1957) 192.

Received June 21, 1972.

ACTA CHEMICA SCANDINAVICA 27 (1973) 271–275

Seven-membered Heterocyclic Rings

III. Thermolysis and Hydrolysis of 2,4,5,7-Tetraphenyl-1,3-oxazepine. Pyrrole Formation[1]

CHRISTIAN L. PEDERSEN and OLE BUCHARDT

Chemical Laboratory II, University of Copenhagen, The H. C. Ørsted Institute, Universitetsparken 5, DK-2100 Copenhagen Ø, Denmark

The thermolysis of 2,4,5,7-tetraphenyl-1,3-oxazepine (I) results in an almost quantitative rearrangement to 2,4,5-triphenyl-3-benzoylpyrrole (II), whereas acid hydrolysis leads to II, *N*-benzoyl-2,3,5-triphenylpyrrole (III), 2,3,5-triphenylpyrrole (IV), and 1,2,4-triphenyl-1,4-butanedione (V). Hydrolysis under basic conditions gives compounds II and V.

The chemistry of seven-membered rings has been the subject of an increasing number of investigations,[2] and this has led to the observation of many novel and interesting reactions.

We therefore found it of interest to examine some of the chemistry of the new heterocyclic system 1,3-oxazepine. Compounds containing this system can be obtained in high chemical yield ($\sim 70-90$ %) as well as high quantum yield ($\sim 10-20$ %) from pyridine *N*-oxides upon irradiation,[3,4] but appear only to be stable when they are highly substituted with phenyl [3,4] or cyano [5] groups. Thus we decided to concentrate our studies on 2,4,5,7-tetraphenyl-1,3-oxazepine (I).

RESULTS

2,4,5,7-Tetraphenyl-1,3-oxazepine upon heating to 240°C in the pure state rearranged in almost quantitative yield to give an isomeric product which was identified as 2,4,5-triphenyl-3-benzoylpyrrole (II).

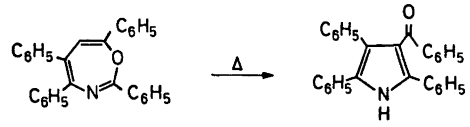

I II

Acid hydrolysis of I in aqueous ethanol gave a mixture of four compounds, which were identified as 2,4,5-triphenyl-3-benzoylpyrrole (II), *N*-benzoyl-2, 3,5-triphenylpyrrole (III), 2,3,5-triphenylpyrrole (IV), and 1,2,4-triphenyl-1, 4-butanedione (V), whereas basic hydrolysis in aqueous ethanol gave a mixture of II and V.

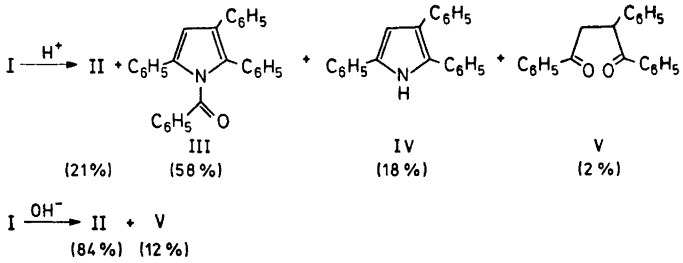

IDENTIFICATION OF PRODUCTS

Compounds II – V all showed the expected spectral characteristics (Table 1), but the spectra do not permit their identification. However, compound IV and V were shown to be identical (IR, mixed m.p.) with authentic samples.[6,7] The remaining compounds were identified by the following chemical reactions.

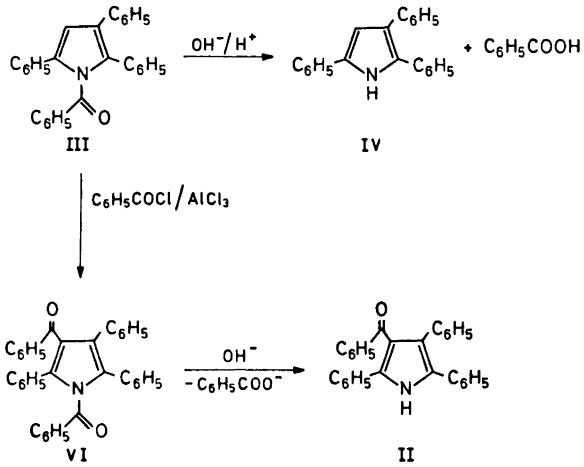

Mild basic hydrolysis of compound III gives in almost quantitative yield 2,3,5-triphenylpyrrole (IV) and benzoic acid. The *N*-benzoyltriphenylpyrrole (III) could be converted to 2,4,5-triphenyl-3-benzoylpyrrole (II) by treatment with benzoyl chloride and aluminium chloride followed by hydrolysis of the product (VI).*

*In view of the mild conditions under which these reactions were performed, it seems unlikely that any rearrangements could occur. The chemistry combined with the spectroscopy is regarded as ample evidence for the structural identifications.

A kinetic study of the rearrangement of I to II in nitrobenzene-d_5, using NMR spectroscopy, showed that the reaction was first order with a rate constant of 4.6×10^{-4} sec^{-1} at 204°C.

DISCUSSION

By analogy with what was proposed for the related reaction of benz[d] [1,3]-oxazepines [8] we suggest that the thermal rearrangement of compound I may be concerted. The formation of compound II in the hydrolytic experiments was shown to be acid or base catalyzed and not due to the thermal rearrangement. The reaction under acid conditions to give compounds III, IV, and V is believed to be due to hydrolysis of the oxazepine (I). The latter can be formulated as an imidoester of an enol which is expected to hydrolyze to give compound VII, which can react as shown in the scheme below. Again these reactions are analogous to what has been found for benz[d] [1,3]oxazepines;[9-11] however, for the latter compounds intermediates analogous to VII and VIII could be isolated and characterized.

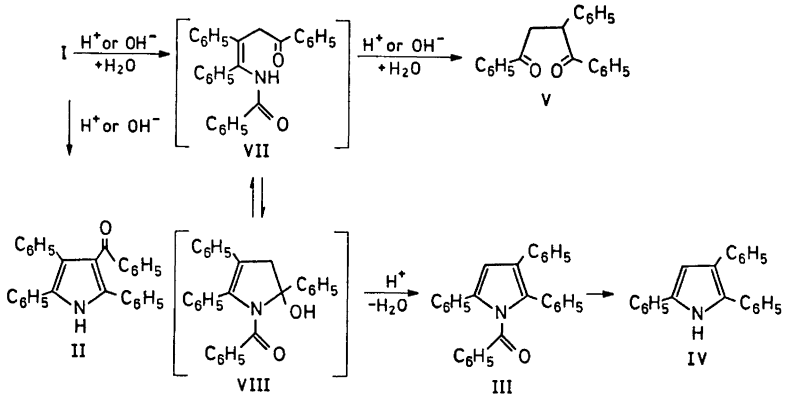

The difference in product distribution in the experiments under acid and basic conditions is presumably due to acid catalysis of the dehydration of VIII.

EXPERIMENTAL

Microanalysis were performed in the microanalysis department of this laboratory.

Melting points (uncorr.) were determined on a Reichert melting point microscope.

Infrared spectra were recorded on a Perkin-Elmer Model 337 grating infrared spectrophotometer. Ultraviolet spectra were recorded on a Unicam SP 1800 Ultraviolet spectrophotometer.

Nuclear magnetic resonance spectra were recorded on a Varian A60A spectrometer.

Preparative layer chromatography (PLC) was performed using 20×100 cm plates with a 2.5 mm thick layer of silica gel (Merck $PF_{254+366}$). The plates were developed 2 – 3 times. The fractions were isolated by continuous extraction with chloroform in a Soxhlet apparatus.

Thermolysis of 2,4,5,7-tetraphenyl-1,3-oxazepine (I). Compound I (1.00 g) was thermolyzed without solvent at 240°C for 12 min. After cooling the melt was dissolved in benzene,

Table 1. Characteristic IR and UV absorptions, and NMR spectra of compounds II, III, and VI.

	UV						IR (in KBr)	NMR[a] (in $CDCl_3$)	
	λ_{max} nm	log ε	λ_{max} nm	log ε	λ_{max} nm	log ε	cm^{-1}	aromatic τ	other τ
II[b]	207	4.57	243	4.35	283	4.32	3270 (N−H), 1625 (C=O)	2.23−3.15 (20 H)	1.42 (1 H) broad[d]
III[b]	206	4.55	257	4.41	273sh	4.36	1710 (C=O)	2.42−3.03 (20 H)	3.38 (1 H)
VI[c]	210	4.73	259	4.63	280	4.46	1705, 1656 (C=O)	2.23−3.20	

[a] Spectra recorded at 60 MHz with tetramethylsilane as interna l reference. Relative intensities are given in parantheses. [b] Absolute ethanol. [c] 96 % ethanol. [d] Singlet disappeared by shaking with D_2O.

and petroleum ether was added until crystallization began. After cooling the crystals were isolated by filtration (0.96 g, ~96 %). (Found: C 87.50; H 5.67; N 2.90. Calc. for $C_{29}H_{21}NO$: C 87.19; H 5.30; N 3.51.) M.p. 200–201° from benzene/petroleum ether.

Acid catalyzed hydrolysis of I. Compound I (1.003 g) was dissolved in ethanol (100 ml, 96 %) and hydrochloric acid (10 ml, 2 N) was added. The mixture was refluxed for 75 min. After cooling *N*-benzoyl-2,3,5-triphenylpyrrole (III) crystallized out. After filtration of the crystals (551 mg), the mother liquor was separated by PLC (developant, benzene/petroleum ether 1:1) into 2,3,5-triphenylpyrrole (IV) (131 mg, ~18 %), *N*-benzoyl-2,3,5-triphenylpyrrole (III) (28 mg, total yield 58 %). (Found: C 87.30; H 5.30; N 3.29. Calc. for $C_{29}H_{21}NO$: C 87.19, H 5.30; N 3.51.) M.p. 154–155° from hexane), 1,2,4-triphenyl-1,4-butanedione (V) (19 mg ~2 %), and 3-benzoyl-2,4,5-triphenylpyrrole (II) (212 mg, ~21 %).

Base catalyzed hydrolysis of I. Compound I (501 mg) was dissolved in ethanol (50 ml, 96 %) and sodium hydroxide (5 ml, 2 N) was added. The mixture was refluxed for 42 h. After evaporation the residue was separated by PLC (developant, toluene/petroleum ether/acetone 7:7:1) into 1,2,4-triphenyl-1,4-butanedione (V) (46 mg, ~12 %) and 3-benzoyl-2,4,5-triphenylpyrrole (II) (422 mg, ~84 %).

Basic hydrolysis of III. Compound III (132 mg) was dissolved in ethanol (25 ml, 96 %) and sodium hydroxide (2 ml, 2 N) was added. The mixture was refluxed for 25 h and evaporated to dryness. Extraction with chloroform followed by evaporation gave 2,3,5-triphenylpyrrole (IV) (97 mg, ~99 %). The residue was acidified with dilute hydrochloric acid and extracted with chloroform. The extract after evaporation yielded benzoic acid.

Benzoylation of III. Compound III (1.00 g) was dissolved in carbon disulfide (20 ml). Benzoyl chloride (0.37 g) and aluminium chloride (1.00 g) were added. The mixture was stirred at room temperature for 14 h and refluxed on a steam bath for 3 h. The reaction mixture was poured on ice and hydrochloric acid, and extracted twice with chloroform. The extract was separated by PLC (developant, toluene/petroleum ether/acetone 7:7:1) into starting material (458 mg) and 1,3-dibenzoyl-2,4,5-triphenylpyrrole (VI) (586 mg, ~86 %, calculated from reacted starting material). (Found: C 85.86; H 5.31; N 2.59. Calc. for $C_{36}H_{25}NO_2$: C 85.86; H 5.00; N 2.78.) M.p. 177–178° from benzene/petroleum ether.

Basic hydrolysis of VI. Compound VI (100 mg) was dissolved in ethanol (10 ml, 96 %) and sodium hydroxide (1 ml, 2 N) was added. The mixture was refluxed for 40 min and evaporated to dryness. Extraction with chloroform gave 3-benzoyl-2,4,5-triphenylpyrrole (III) (78 mg, ~99 %).

REFERENCES

1. For the previous paper in this series, see Svanholm, U. *Acta Chem. Scand.* **25** (1971) 640.
2. *Ann. Repts. on Progr. Chem. (Chem. Soc. London)* **66** (1969) 460; **67** (1970) 460; Spence, G. G., Taylor, E. C. and Buchardt, O. *Chem. Rev.* **70** (1970) 231.
3. Kumler, P. L. and Buchardt, O. *Chem. Commun.* **1968** 1321.
4. Buchardt, O., Pedersen, C. L. and Harrit, N. *J. Org. Chem.* **37** (1972) 3592.
5. Ishikawa, M., Kaneko, C., Yokoe, I. and Yamada, S. *Tetrahedron* **25** (1969) 295.
6. Angelico, F. and Calvello, E. *Gazz. Chim. Ital.* **31** (1901) 4.
7. Smith, A. *J. Chem. Soc.* **57** (1890) 643.
8. Buchardt, O., Kumler, P. L. and Lohse, C. *Acta Chem. Scand.* **23** (1969) 2149.
9. Buchardt, O., Kumler, P. L. and Lohse, C. *Acta Chem. Scand.* **23** (1969) 159.
10. Buchardt, O., Becker, J., Lohse, C. and Møller, J. *Acta Chem. Scand.* **20** (1966) 262.
11. Buchardt, O., Becker, J. and Lohse, C. *Acta Chem. Scand.* **20** (1966) 2467.

Received July 4, 1972.

ACTA CHEMICA SCANDINAVICA 27 (1973) 276–286

On the Infrared Absorption Intensity of the N—N Stretching Vibration in Some Iridium and Rhenium Dinitrogen Complexes

BÖRJE FOLKESSON

Division of Inorganic Chemistry, Chemical Center, University of Lund, Box 740, S-220 07 Lund 7, Sweden

The infrared absorption intensity of the N – N stretching vibration has been measured for the complexes

$IrClN_2(PPh_3)_2$, $IrClN_2(C_8H_{12}O_4)(PPh_3)_2$,
$ReClN_2(Ph_2PCH_2PPh_2)_2$, $ReClN_2[Ph_2P(CH_2)_2PPh_2]_2$,
$ReClN_2(Ph_2PCH=CHPPh_2)_2$, $ReClN_2(PMe_2Ph)_4$ and
$ReClN_2(PPh_2Me)_4$

in the solid state and in solution. It has been found that the intensity (A_{NN}) increases with decreasing frequency (ν_{NN}), which is in agreement with a model of $d\pi - p\pi^*$ back donation. The generalization given before [1] has now been extended to cover a greater frequency range. It is concluded that as A_{NN} is greater for Re than for Ir complexes, the degree of backbonding increases from Ir to Re. From the obtained intensities (A_{NN}) in chloroform solution for some of the complexes, the dipole moment derivative $d\mu/dr$, has been calculated. From this quantity and the effective charges on the nitrogen atoms, it was possible to get an approximate value of the variation of charge with interatomic distance dq/dr. An estimation of dq/dr has also been performed from experimentally determined charges on the nitrogen atoms and N – N distances calculated from Badger's rule. By comparison between the dq/dr values obtained in different ways, it has been possible to find out which nitrogen atom that carries which charge. Thus, it has been concluded that the terminal nitrogen atom in the complexes carries the smallest negative charge and that the inner nitrogen atom is the most negative one.

The results of this and the earlier [1] investigation are compared with the result of an infrared study of chemisorbed dinitrogen on nickel by Eischens and Jacknow. The similarities between metal dinitrogen complexes and the adsorbed dinitrogen nickel complex are discussed.

In a previous paper,[1] infrared absorption intensities of the N – N stretching vibration in dinitrogen complexes of ruthenium and osmium have been reported. It was found [1] that the intensity of the N – N stretching vibration (A_{NN}) increases with decreasing frequency (ν_{NN}), which is in agreement with a model of $d\pi - p\pi^*$ back donation. It was concluded that the lower the ν_{NN}

and the higher the A_{NN}, the greater was the disturbance of the dinitrogen molecule. It would therefore be of interest to investigate other dinitrogen complexes both with lower and higher frequencies ν_{NN} in order to cover a great frequency range. Therefore, this infrared study will deal with iridium and rhenium dinitrogen complexes. Collman *et al.*[2–4] have reported the preparation and properties of two iridium dinitrogen complexes, *viz.* $IrClN_2(PPh_3)_2$ and $IrClN_2(C_8H_{12}O_4)(PPh_3)_2$, which show quite different frequencies (ν_{NN}). The infrared absorption intensity of the N–N stretching vibration in these two iridium dinitrogen complexes has been measured in the present investigation. Of special interest are rhenium dinitrogen complexes, which recently have been prepared by Chatt *et al.*[5] These authors find that in some of these complexes, the frequency ν_{NN} is as low as 1922 cm^{-1}. This fact indicates a strong perturbation of the dinitrogen molecule and consequently the metal-dinitrogen bond must be stronger in these complexes than in the previously investigated ruthenium and osmium dinitrogen complexes. Intensity measurements on some rhenium dinitrogen complexes are presented here.

Triphenylphosphine and the other phosphines used show strong absorption in the frequency range 600 – 400 cm^{-1}. This fact makes it impossible to observe the weak band corresponding to the M – N_2 stretching vibration in the complexes. This investigation is therefore limited to intensity measurements on the N–N stretching vibration in the complexes.

EXPERIMENTAL

Preparation of iridium dinitrogen complexes. $IrClN_2(PPh_3)_2$ was commercially obtained from Strem Chemicals Inc. as a pure crystalline compound. Its purity was confirmed by elemental analysis of carbon, hydrogen and nitrogen. (Found: C 53.4; H 4.23; N 3.20. Calc.: C 55.4; H 3.88; N 3.58.) The obtained analysis value of nitrogen is about 10 % lower than the calculated one, which may be because the compound is not quite pure or due to difficulties of obtaining a correct analysis value when such an instable compound is analysed. It is thus quite reasonable that the measured intensity value (A_{NN}) is somewhat too low. As this complex has been prepared according to Collman *et al.*[4] from Vaska's [6] iridium complex and α-furoyl azide, the absence of carbonyl absorption in the infrared spectrum has been checked. $IrClN_2(C_8H_{12}O_4)(PPh_3)_2$ was prepared from the dinitrogen complex above and diethyl maleate according to Collman *et al.*[4] Its purity was checked by the infrared spectrum and by elemental analysis. (Found: C 55.9; H 5.34; N 2.37. Calc.: C 55.5; H 4.41; N 2.94.) For this iridium complex also the analysis value of nitrogen is lower than the calculated one. For the same reasons as above for $IrClN_2(PPh_3)_2$, it is reasonable that the obtained intensity value (A_{NN}) for the diethyl maleate dinitrogen complex can be about 10 % too low.

The two iridium dinitrogen complexes above are not stable in air, but must be kept in a nitrogen atmosphere.

Preparation of rhenium dinitrogen complexes. The starting chemicals, rhenium metal and triphenylphosphine, were of *purissimum* quality. From these chemicals, $ReOCl_3(PPh_3)_2$ was prepared by a minor modification of the method given by Chatt and Rowe.[7] Monobenzoyl hydrazine was prepared from ethyl benzoate and hydrazine hydrate according to a method given by Dilworth.[8] Ethyl benzoate and hydrazine hydrate were of *purum* quality. Then the intermediate chelated benzoylazo complex of rhenium(III) was prepared.[8] Rhenium dinitrogen complexes with various phosphines could then be prepared according to Chatt *et al.*[5,8] The phosphines used, bis(1,2-diphenylphosphino)methane, bis(1,2-diphenylphosphino)ethane, *cis*-bis(1,2-diphenylphosphino)ethylene and methyldiphenylphosphine, were obtained from Strem Chemicals Inc. Dimethylphenylphosphine was obtained from K & K Laboratories Inc. The phosphines were used without further treatment. The following rhenium dinitrogen complexes have been

prepared: $ReClN_2(Ph_2PCH_2PPh_2)_2$ (I), $ReClN_2[Ph_2P(CH_2)_2PPh_2]_2$ (II), $ReClN_2(Ph_2PCH=CHPPh_2)_2$ (III), $ReClN_2(PMe_2Ph)_4$ (IV) and $ReClN_2(PPh_2Me)_4$ (V). In the formulas above, Me and Ph stand for methyl and phenyl. The purity of the prepared complexes has been checked only by infrared spectra, *viz.* if the complexes give strong N – N absorption and if the intensity (A_{NN}) of the N – N bands is of about the same order of magnitude as the intensity (A_{NN}) measured for the ruthenium and osmium dinitrogen complexes,[1] then the complexes are assumed to be pure. Only compound V was found to be impure and intensity values for this complex could therefore not be used. The rhenium dinitrogen complexes are generally very stable. They are much more stable than the above mentioned iridium dinitrogen complexes, and can therefore be kept in air for a long time without decomposition.

Infrared spectral measurements. The infrared spectra were recorded with a Perkin Elmer Spectrophotometer Model 521 equipped with a linear absorbance potentiometer. All spectra on the N – N stretching vibration were recorded with a wavenumber scale expansion, so that 1 cm on the chart corresponded to 25 cm^{-1}. The wavenumber readings of the spectrophotometer were checked by recording spectra of carbon monoxide. Measurements on the dinitrogen complexes have been performed both in the solid state and in solution. The solid samples were examined in KBr disks. Chloroform, benzene, and tetrahydrofuran (THF) were used as solvents. Chloroform and benzene were of spectroscopic grade and tetrahydrofuran of analytical grade. The solvents were dried by shaking with molecular sieves 5 Å for a few minutes before use. Cells with CaF_2-windows and 0.2 mm teflon spacers were used. The exact cell-thicknesses were determined interferometrically.

Intensity measurements were performed on at least two preparations of each dinitrogen complex and at a number of concentrations. Linear Beer's law plots were observed for all the complexes in all solvents. A representative example is given in Fig. 1. The measurements on iridium and rhenium dinitrogen complexes in solution were performed rapidly, since it was found that the complexes were not stable in solution. Spectra were recorded immediately after complete dissolution of the compounds. Two or three spectra were recorded after each other, and a small decrease in absorbance for each spectrum was found. The decrease in intensity was, however, very small for spectra recorded in this way after each other. Reported intensity values are generally those calculated from the first recorded spectrum. Only $IrClN_2(C_8H_{12}O_4)(PPh_3)_2$ was found to decompose more rapidly than the other complexes investigated. This complex shows an N – N band at 2105 cm^{-1} in the infrared spectrum of the chloroform solution besides the N – N band at 2200 cm^{-1}. This fact indicates that the complex decomposes and also gives the complex from which it has been prepared. As $IrClN_2(PPh_3)_2$ has been measured before, it was possible to determine its concentration and thereby also the concentration of the iridium diethylmaleate dinitrogen complex, which gives the band at 2200 cm^{-1}. The intensity of the band at 2200 cm^{-1} was found to decrease with time. The reported intensity value on this iridium complex has been obtained through extrapolation to zero time. It was also found that the decrease in absorbance of the N – N band at 2105 cm^{-1} was greater than when $IrClN_2(PPh_3)_2$ alone was measured. When the two N – N bands at 2105 cm^{-1} and 2200 cm^{-1} decrease in absorbance and intensity with time a new band at 2250 cm^{-1} appears. This band increases in intensity with time, and can probably be assigned to a common decomposition product of the two iridium dinitrogen complexes.

The areas under the bands were determined with a planimeter. The values obtained were then multiplied with ln 10 to get integrated absorption intensities relating to Beer's law. The reported intensity values are the mean values of the intensities determined at different concentrations. The error limits give the maximum deviation from the mean value.

RESULTS

The results of the intensity measurements on the iridium dinitrogen complexes are given in Table 1. The good agreement of the intensity values (A_{NN}) determined in various dispersion media for the complex $IrClN_2(PPh_3)_2$ shows that the intensity is not dependent on the medium. The agreement of the intensity values for $IrClN_2(C_8H_{12}O_4)(PPh_3)_2$ is not so good, probably depending

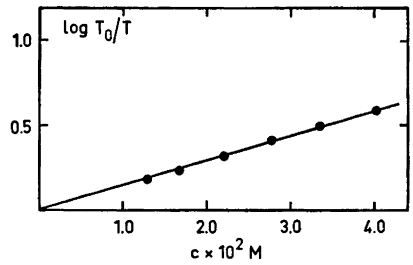

Fig. 1. The Beer's law plot of the absorption of the N–N stretching vibration at 2105 cm^{-1} in $IrClN_2(PPh_3)_2$ in chloroform solution.

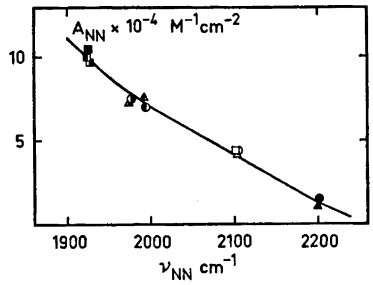

Fig. 2. The correlation between intensity A_{NN} and frequency ν_{NN} for the iridium and rhenium dinitrogen complexes. $IrClN_2(PPh_3)_2$ in KBr (○), $CHCl_3$ (△) and C_6H_6 (□). $IrClN_2(C_8H_{12}O_4)(PPh_3)_2$ in KBr (●) and $CHCl_3$ (▲). $ReClN_2(Ph_2PCH_2PPh_2)_2$ in KBr (◐) and $CHCl_3$ (◭). $ReClN_2[Ph_2P(CH_2)_2PPh_2]_2$ in KBr (◑) and $CHCl_3$ (◮). $ReClN_2(PMe_2Ph)_4$ in KBr (■), $CHCl_3$ (◧) and C_6H_6 (◨).

on the instability of this complex in solution and thereby the difficulty of obtaining a correct intensity value. The frequencies (ν_{NN}) in the two iridium dinitrogen complexes are quite different. In the diethylmaleate complex, the frequency (ν_{NN}) is about 100 cm^{-1} higher than in $IrClN_2(PPh_3)_2$. This fact indicates a reduction of the $d\pi - p\pi^*$ back donation, which is as expected since the olefin competes with dinitrogen for the available d-electrons. A corresponding decrease in the absorption intensity is to be expected and is also found.

The results of the infrared absorption intensity measurements on the rhenium dinitrogen complexes are collected in Table 2. It can immediately be seen that there is a good agreement in the measured intensity values (A_{NN}) for different dispersion media. The intensity is thus apparently not dependent on the medium. The complexes I and II show in the infrared spectrum in the solid state (KBr) two bands assigned to the N–N stretching vibration. This fact indicates a crystal effect, since in solution only one N–N band is found.

Table 1. The results of the absorption intensity measurements on the iridium dinitrogen complexes.

Metal complex	Dispersion medium	ν_{NN} cm^{-1}	ε_{NN} M^{-1} cm^{-1}	$A_{NN} \times 10^{-4}$ M^{-1} cm^{-2}
$IrClN_2(PPh_3)_2$	KBr	2103	690 ± 25	4.2 ± 0.3
	$CHCl_3$	2105	725 ± 25	4.2 ± 0.3
	C_6H_6	2103	925 ± 25	4.4 ± 0.3
	THF	2103	900 ± 25	4.2 ± 0.3
$IrClN_2(C_8H_{12}O_4)(PPh_3)_2$	KBr	2202	340 ± 40	1.5 ± 0.2
	$CHCl_3$	2200	200 ± 20	1.1 ± 0.1

Table 2. The results of the absorption intensity measurements on the rhenium dinitrogen complexes.

	Metal complex	Dispersion medium	ν_{NN} cm^{-1}	ε_{NN} $M^{-1}\,cm^{-1}$	$A_{NN} \times 10^{-4}$ $M^{-1}\,cm^{-2}$
I.	$ReClN_2(Ph_2PCH_2PPh_2)_2$	KBr	1973	870 ± 50	7.0 ± 0.7
			1995	800 ± 50	
		$CHCl_3$	1993	1350 ± 50	7.6 ± 0.4
II.	$ReClN_2[Ph_2P(CH_2)_2PPh_2]_2$	KBr	1978	1350 ± 100	7.5 ± 0.4
			1930	500 ± 50	
		$CHCl_3$	1975	1000 ± 50	7.3 ± 0.3
III.	$ReClN_2(Ph_2PCH=CHPPh_2)_2$	KBr	1965	700 ± 50	6.0 ± 0.4
		$CHCl_3$	1970	850 ± 50	5.7 ± 0.3
IV.	$ReClN_2(PMe_2Ph)_4$	KBr	1925	1600 ± 150	10.5 ± 0.5
		$CHCl_3$	1924	1600 ± 50	10.0 ± 0.3
		C_6H_6	1928	2600 ± 100	9.7 ± 0.3
V.	$ReClN_2(PPh_2Me)_4$	KBr	1928		
		$CHCl_3$	1922		
		C_6H_6	1925		

The complex III gives a somewhat lower intensity value than the complexes I and II, even though the frequency ν_{NN} is lower in complex III than in the complexes I and II. This is probably because the complex III is not quite pure. The frequencies ν_{NN} in the rhenium dinitrogen complexes are generally lower than in the iridium dinitrogen complexes investigated above. Consequently, the intensities (A_{NN}) are found to be higher in the rhenium complexes than in the iridium complexes. The highest intensity is found for complex IV, which also shows the lowest N – N stretching frequency. In accordance with the results given before,[1] the degree of $d\pi - p\pi^*$ back donation must be greater in the rhenium than in the iridium dinitrogen complexes. It will also mean that the disturbance of the dinitrogen molecule and the decrease in the N – N bond order must be greater in the rhenium than in the iridium dinitrogen complexes. A high intensity value of the N – N stretching vibration also gives indication of a strong metal – dinitrogen bond. In agreement with this, it may be noted that the rhenium dinitrogen complexes are more stable to chemical attack than the corresponding iridium complexes both in the solid state and in solution. In Fig. 2, the intensities A_{NN} are plotted against the frequency ν_{NN} for the rhenium and the iridium dinitrogen complexes. The generalization found before,[1] *viz.* the lower the frequency the higher the intensity, is found also for the rhenium and the iridium complexes. This correlation now covers a larger frequency range than before when only osmium and ruthenium dinitrogen complexes were available. It is evident from Fig. 2 that the intensity (A_{NN}) approaches zero, when the frequency (ν_{NN}) approaches the limiting value for the free dinitrogen molecule, *i.e.* 2331 cm^{-1} (*cf.* Ref. 9, p. 72). The previously [1] determined intensities (A_{NN}) for the ruthenium and osmium dinitrogen complexes are not given in Fig. 2, but on comparison with Figs. 2 and 4 in Ref.

1, it is obvious that these intensity values (A_{NN}) fall on this curve. The only exceptions are the intensity values for $Os(NH_3)_5N_2I_2$ dissolved in DMSO and DMF, which are higher than the highest intensity value for the rhenium dinitrogen complexes. The present results thus give further support for the theory that some special effect, *e.g.* a charge-transfer association of outer-sphere ligands, causes the high intensity of the N–N stretching vibration in $Os(NH_3)_5N_2I_2$ dissolved in DMSO and DMF.

To get approximate information about the polarity of the N–N bond, the fixed charge model has been applied. The complexes are considered as two-atomic molecules, *viz.* consisting of, *e.g.*, $(PhMe_2P)_4ClReN$ and N. For a two-atomic molecule, the absorption intensity is related to the dipole moment of the molecule by the formula (*cf.* Refs. 1 and 10)

$$A = \frac{\pi \cdot N}{3c^2 \times 10^3 \times \mu_{red}} \left(\frac{d\mu}{dr}\right)^2 \quad (1)$$

Here N and c stand for the Avogadro number and the velocity of light. μ_{red} is the reduced mass and has thus in the present case been calculated from the above mentioned molecular fragments. μ is the dipole moment and r the interatomic distance. In the calculation of $d\mu/dr$, intensities of the N–N stretching vibration measured in chloroform solution were used. Calculations have been performed on $IrClN_2(PPh_3)_2$ and on three of the rhenium dinitrogen complexes, *viz.* complex I, II, and IV (those which were obtained in pure form). If it is assumed that the charges on the molecular fragments are $+q$ and $-q$ (atomic units), the dipole moment is

$$\mu = rq \quad (2)$$

If, as stated in the fixed charge model, it is assumed that q does not change with r, it follows that

$$d\mu/dr = q \quad (3)$$

If, on the other hand, there is a variation of charge with interatomic distance, a term relating to this, *viz.* dq/dr, is easily derived from eqn. (2), *i.e.*

$$d\mu/dr = q + r dq/dr \quad (4)$$

Table 3. Calculated values of $d\mu/dr$ and the experimentally obtained charges on the nitrogen atoms (M–N_1–N_2) in the dinitrogen complexes of iridium and rhenium.

Metal complex	$\lvert d\mu/dr \rvert$ a.u.	Extended Hückel		CNDO		*Ab initio* SCF MO	
		$-q_{N_1}$ a.u.	$-q_{N_2}$ a.u.	$-q_{N_1}$ a.u.	$-q_{N_2}$ a.u.	$-q_{N_1}$ a.u.	$-q_{N_2}$ a.u.
$IrClN_2(PPh_3)_2$	2.43	0.90	0.20	0.40	0.23	0.47	0.27
$ReClN_2(Ph_2PCH_2PPh_2)_2$	3.30	1.20	0.25	0.47	0.24	0.56	0.28
$ReClN_2[Ph_2P(CH_2)_2PPh_2]_2$	3.24	1.20	0.25	0.47	0.24	0.56	0.28
$ReClN_2(PMe_2Ph)_4$	3.78	1.30	0.30	0.50	0.25	0.60	0.30

Calculated values of $d\mu/dr$ from eqn. (1) are given in Table 3. The values are relatively high, so it is reasonable to suppose that the charge varies with the interatomic distance. To determine dq/dr, the charges on the nitrogen atoms and the interatomic distance r must be known. The charges on the nitrogen atoms have been determined from ESCA measurements.[11] Nitrogen 1*s* electron spectra of the above mentioned dinitrogen complexes show two peaks indicating [12] different effective charges on the nitrogen atoms. ESCA measurements have also been performed on a number of nitrogen compounds and the obtained nitrogen 1*s* binding energies plotted against calculated charge on nitrogen atoms to get a correlation diagram. As different methods of charge calculation give different results, *viz.*, *e.g.*, extended Hückel, CNDO, and *ab initio* SCF MO calculations, three different correlation diagrams have been made. The charges on the nitrogen atoms in the dinitrogen complexes can thus be obtained if the measured nitrogen 1*s* binding energies are compared with the correlation diagrams. This will be presented in more detail in a subsequent paper.[11] The charges obtained on the nitrogen atoms in the various dinitrogen complexes are given in Table 3. The error in the determined charges is of course dependent on the error in the measured binding energies, which amounts to ± 0.1 eV. The error in the charges from extended Hückel calculations amounts then to about ± 0.05 a.u. In the other two methods of charge calculation, the error in the obtained charges is about ± 0.01 a.u.

When $d\mu/dr$ is calculated from eqn. (1), the absolute value of this quantity is obtained. Since the negative charge on the terminal nitrogen atom (q) increases from the iridium dinitrogen complex to the rhenium dinitrogen complexes (*cf.* Table 3), as does the N–N distance calculated from Badger's rule [13] (see below), it follows that $dq/dr < 0$. Further, as also $q < 0$, both the terms on the right side of eqn. (4) get a negative sign and thus the negative sign on $d\mu/dr$ must be used in the calculations from eqn. (4).

The value of the distance r is more difficult to obtain, as it is the distance between two charge centers and it is difficult to know where the charge center on the big molecular fragment of the complex (*cf.* p.281) should be placed. To use the N–N distance in eqn. (4) to obtain a value of dq/dr is thus not correct. If one uses the N–N distance in eqn. (4), a limit for the highest possible value of $-dq/dr$ is obtained. Similarly, a limit for the least possible value of $-dq/dr$ is obtained if the M-terminal N distance is used in the calculation. As an example, the complex $ReClN_2(PMe_2Ph)_4$ is considered. A calculation of $-dq/dr$ on this complex ($M-N_1-N_2$) from eqn. (4), using the distances [14] $r_{N_1-N_2}$ and r_{M-N_2} and under the assumption that the terminal nitrogen atom carries the greatest negative charge (CNDO calculated charges are used), yields the values 1.55 a.u. and 0.54 a.u., respectively. If the terminal nitrogen atom carries the smallest negative charge, the $-dq/dr$ values become 1.67 a.u. and 0.58 a.u., respectively. A corresponding calculation of $-dq/dr$ from *ab initio* SCF MO calculated charges gives the same values as those above. A true value of $-dq/dr$ is thus difficult to obtain, but probably this lies closer to the smallest than the highest of the two calculated values above. Calculations on the other dinitrogen complexes are more difficult to perform, since interatomic distances are not known. On the other hand, it is expected that the values of $-dq/dr$ do not deviate much from those obtained above for $ReClN_2(PMe_2Ph)_4$.

From the example above it can also be seen that there is only a small difference in $-dq/dr$, when the terminal nitrogen atom carries the greatest or the smallest negative charge.

A way to obtain a more accurate value of the charge parameter dq/dr is from experimentally determined charges on the nitrogen atoms and interatomic distances calculated from Badger's rule.[13] This rule is used in the following form:

$$r_e = \left(\frac{c_{ij}}{k_e}\right)^{1/3} + d_{ij} \qquad (5)$$

Here r_e is the equilibrium interatomic distance in Ångström units and k_e is the force constant in megadynes per centimeter. c_{ij} and d_{ij} are constants characteristic of all diatomic molecules made up of one element in the ith row and one in the jth row of the periodic system. The force constants of the N–N bond in the dinitrogen complexes have been determined from the formula (*cf.*, *e.g.*, Ref. 9, p. 8)

$$\bar{\nu} = \frac{1}{2\pi c}\sqrt{\frac{k_e}{\mu_{red}}} \qquad (6)$$

μ_{red} is the reduced mass and has been calculated from the above mentioned molecular fragments (*cf.* p. 281) of the dinitrogen complexes. Then the interatomic distances could be determined from eqn. (5). The result is presented in Table 4. The charge on the nitrogen atoms in the various complexes is then

Table 4. The N–N distances in the dinitrogen complexes of iridium and rhenium calculated from Badger's rule.

Metal complex	ν_{NN} cm^{-1} in chloroform	k_{N-N} megadyn/cm	r_{N-N} Å
$IrClN_2(PPh_3)_2$	2105	3.61	1.052
$ReClN_2(Ph_2PCH_2PPh_2)_2$	1993	3.25	1.065
$ReClN_2[Ph_2P(CH_2)_2PPh_2]_2$	1975	3.19	1.068
$ReClN_2(PMe_2Ph)_4$	1924	3.01	1.075

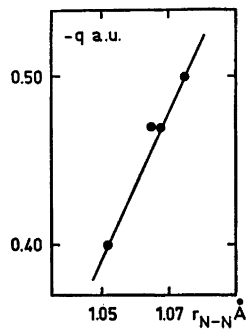

Fig. 3. A plot of CNDO calculated charges on the nitrogen atoms against N–N distances from Badger's rule.

plotted against the N–N distance determined from eqn. (5) and dq/dr is obtained from the slope of the straight line. A typical plot is given in Fig. 3. dq/dr has been determined both when the terminal nitrogen atom has the largest and the smallest negative charge. The result is presented in Table 5.

Table 5. The variation of charge with interatomic distance (dq/dr) determined from the obtained charges on the nitrogen atoms and the interatomic distances from Badger's rule.

Method of charge calculation	$-dq/dr$ a.u. Terminal nitrogen atom carrying the largest negative charge	$-dq/dr$ a.u. Terminal nitrogen atom carrying the smallest negative charge
Extended Hückel	8.5 ± 2.0	2.0 ± 1.0
CNDO	2.2 ± 0.4	0.5 ± 0.3
Ab initio SCF MO	2.8 ± 0.4	0.7 ± 0.3

It can be seen that the $-dq/dr$ values vary with the method of charge calculation. On the other hand, the largest values of $-dq/dr$ are obtained if the terminal nitrogen atom carries the largest negative charge. The error in the $-dq/dr$ values is about 25 %. Considerably smaller values of $-dq/dr$ are obtained if it is assumed that the terminal nitrogen atom carries the smallest negative charge. As the charge on the nitrogen atom in this case does not vary very much from one complex to another (*cf.* Table 3), the error in the $-dq/dr$ values is about 50 %. Nevertheless, as these last values of $-dq/dr$ are more in agreement with those obtained from infrared intensity data (*cf.* the example given above), it is concluded that the terminal nitrogen atom carries the smallest negative charge.

DISCUSSION

Recently, infrared intensity measurements of the N–N and C–O stretching vibrations in iridium(I) complexes have been reported by Darensbourg and Hyde.[15] These authors find that more meaningful conclusions about the π^*-acceptor ability of the dinitrogen and carbonyl ligands can be obtained from intensity measurements than in any other of the earlier investigations [4,16,17] based only on frequency data. It has been found [15] that the intensity of the N–N stretching vibration in $IrClN_2(PPh_3)_2$ is much smaller than the intensity of the C–O stretching vibration in $IrCl(CO)(PPh_3)_2$. From this fact it was concluded that the acceptor ability of the dinitrogen π^*-orbital is much smaller than that of carbonyl. This interpretation is in accordance with the result of the present investigation, *viz.* the higher the intensity of the N–N stretching vibration the greater the degree of $d\pi - p\pi^*$ back donation (measured by the effective charges on the nitrogen atoms determined with ESCA [11]). The intensity value (A_{NN}) obtained by Darensbourg and Hyde [15] is about 25 % lower than that obtained in the present investigation. Probably their compound $IrClN_2(PPh_3)_2$ was not pure. One preparation of $IrClN_2(PPh_3)_2$

obtained from Strem Chemicals Inc. by the present author gave the same intensity value A_{NN} as that reported in Ref. 15 and this compound was found impure. A further proof that the complex $IrClN_2(PPh_3)_2$, used by Darensbourg and Hyde,[15] probably was impure, is that intensity measurements of the C–O stretching vibration in $IrCl(CO)(PPh_3)_2$ by the present author gave the same intensity value as that reported by Darensbourg and Hyde,[15] *viz.* 8.7×10^4 M^{-1} cm^{-2}.

An essential result of the present investigation is that, through a combination of infrared intensity data with experimentally determined charges on atoms, it was possible to determine the variation of charge with interatomic distance (dq/dr). This quantity gives increased characterisation of the electronic structure of a molecule by indicating the degree of mobility of charges over the bond in question. In the estimation of dq/dr it was also found possible to elucidate which nitrogen atom that carries which charge. In a recent paper by Leigh *et al.*[18] on ESCA measurements of two rhenium dinitrogen complexes, the smallest nitrogen 1*s* binding energy was assigned to the terminal nitrogen atom and consequently this is the most negative one. In the present work it has been shown rather that the terminal nitrogen atom carries the smallest negative charge.

It is also of interest to compare the result of the present investigation and the earlier results [1] of intensity measurements with an investigation of chemisorbed dinitrogen on nickel performed by Eischens and Jacknow.[19] It has been found [19] that dinitrogen chemisorbed on nickel gives rise to strong infrared absorption at 2202 cm^{-1}. This band has been assigned to the N–N stretching vibration in the structure $Ni-N\equiv N^+$. Further evidence for a linear structure is given by Chernikov *et al.*[20] The integrated absorption intensity of this N–N band has been calculated [21] to 3.96×10^4 M^{-1} cm^{-2}. This value is, however, somewhat uncertain, depending on the calculation procedure used. The frequency (ν_{NN}) of chemisorbed dinitrogen is the same as that obtained for the iridium diethylmaleate dinitrogen complex (*cf.* Table 1). The intensity value is somewhat higher, but still of the same order of magnitude (3.96×10^4 compared with 1.5×10^4). An estimation of the charge separation between Ni and N_2 has also been made in the following way. The intensity values of the $M-N_2$ stretching vibration in the ruthenium and osmium dinitrogen complexes (*cf.* Table 1, Ref. 1) are plotted against the N–N stretching frequency. The curve is drawn so that it passes through the point (0,2331), *i.e.* the limiting value for the free dinitrogen molecule (*cf.* Ref. 9, p. 72). This gives a maximum value of A_{M-N_2} at 2202 cm^{-1} of about 0.6×10^3 M^{-1} cm^{-2}, which can be seen in Fig. 4.

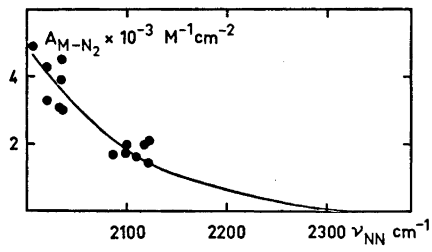

Fig. 4. An estimation of the intensity of the $Ni-N_2$ stretching vibration in the adsorbed dinitrogen complex from intensities (A_{M-N_2}) of ruthenium and osmium dinitrogen complexes (Table 1, Ref. 1) plotted against the N–N stretching frequency.

Then $d\mu/dr$ is calculated from eqn. (1) and the value 0.35 a.u. is obtained. This value can be compared with the corresponding values of charge separation calculated for the ruthenium and osmium dinitrogen complexes in a previous paper.[1] This illustrates the similarities between metal dinitrogen complexes and dinitrogen chemisorbed on a metal surface. It is therefore of great interest to perform ESCA measurements on gases adsorbed on metal surfaces and especially dinitrogen adsorbed on metal surfaces to get more information about the electronic structure of adsorbed species.

This work has been financially supported by the *Swedish Board for Technical Development (Styrelsen för teknisk utveckling)* and by the *Faculty of Science*, Lund, which support is gratefully acknowledged. The author also wishes to thank Dr. R. Larsson for his stimulating and helpful interest and Dr. A. Miezis for valuable comments on this work.

REFERENCES

1. Folkesson, B. *Acta Chem. Scand.* **26** (1972) 4008.
2. Collman, J. P. and Kang, J. W. *J. Am. Chem. Soc.* **88** (1966) 3459.
3. Collman, J. P., Kubota, M., Sun, J. Y. and Vastine, F. *J. Am. Chem. Soc.* **89** (1967) 169.
4. Collman, J. P., Kubota, M., Vastine, F. D., Sun, J. Y. and Kang, J. W. *J. Am. Chem. Soc.* **90** (1968) 5430.
5. Chatt, J., Dilworth, J. R. and Leigh, G. J. *Chem. Commun.* **1969** 687.
6. Vaska, L. and DiLuzio, J. W. *J. Am. Chem. Soc.* **83** (1961) 2784.
7. Chatt, J. and Rowe, G. A. *J. Chem. Soc.* **1962** 4019.
8. Dilworth, J. R. *Personal communication.*
9. Nakamoto, K. *Infrared Spectra of Inorganic and Coordination Compounds*, Wiley, New York 1963.
10. Barrow, G. M. *Introduction to Molecular Spectroscopy*, McGraw, New York 1962.
11. Folkesson, B. *Acta Chem. Scand.* **27** (1973). *To be published.*
12. Siegbahn, K., Nordling, C., Fahlman, A., Nordberg, R., Hamrin, K., Hedman, J., Johansson, G., Bergmark, T., Karlsson, S-E., Lindgren, I. and Lindberg, B. *ESCA – Atomic, Molecular and Solid State Structure Studied by Means of Electron Spectroscopy*, Almqvist and Wiksell, Uppsala 1967.
13. Badger, R. M. *J. Chem. Phys.* **2** (1934) 128; **3** (1935) 710.
14. Davis, B. R. and Ibers, J. A. *Inorg. Chem.* **10** (1971) 578.
15. Darensbourg, D. J. and Hyde, C. L. *Inorg. Chem.* **10** (1971) 431.
16. Chatt, J., Melville, D. P. and Richards, R. L. *J. Chem. Soc.* **A 1969** 2841.
17. Purcell, K. F. *Inorg. Chim. Acta* **3** (1969) 540.
18. Leigh, G. J., Murrell, J. N., Bremser, W. and Proctor, W. G. *Chem. Commun.* **1970** 1661.
19. Eischens, R. P. and Jacknow, J. *Proc. 3rd Int. Congr. on Catalysis, Amsterdam 1964*, North Holland, Amsterdam 1964.
20. Chernikov, S. S., Kuz'min, S. G. and Borod'ko, Yu. G. *Russ. J. Phys. Chem.* **42** (1968) 1071.
21. Little, L. H. *Infrared Spectra of Adsorbed Species*, Academic, London 1966, pp. 401 – 402.

Received July 10, 1972.

ACTA CHEMICA SCANDINAVICA 27 (1973) 287–302

ESCA Studies on the Charge Distribution in Some Dinitrogen Complexes of Rhenium, Iridium, Ruthenium, and Osmium

BÖRJE FOLKESSON

Division of Inorganic Chemistry, Chemical Center, University of Lund, Box 740, S-220 07 Lund 7, Sweden

Nitrogen 1*s* electron spectra have been recorded on the following rhenium dinitrogen complexes, *viz.* $ReClN_2(Ph_2PCH_2PPh_2)_2$, $ReClN_2[Ph_2P(CH_2)_2PPh_2]_2$, $ReClN_2(Ph_2PCH=CHPPh_2)_2$, $ReClN_2(PMe_2Ph)_4$ and $ReClN_2(PPh_2Me)_4$ and on $IrClN_2(PPh_3)_2$. Two peaks in the N1*s* electron spectra show that the dinitrogen ligand has an appreciable polarity. It has been found that both the nitrogen atoms in the complexes carry a negative charge. The total charge on the dinitrogen group was found to be about 0.7 – 0.9 a.u. A connection between the magnitude of the shift in nitrogen 1*s* binding energy and the N – N stretching frequency has been found, *viz.* the lower the N – N stretching frequency the larger the chemical shift in binding energy. This means that the more disturbed the dinitrogen molecule is, indicated by a low N – N stretching frequency, the larger is the charge separation on the nitrogen atoms.

Nitrogen 1*s* electron spectra have also been recorded on dinitrogen complexes of ruthenium and osmium, *viz.* $Ru(NH_3)_5N_2X_2$ and $Os(NH_3)_5N_2X_2$, where X = Cl, Br, I. As these complexes also contain ammonia, the N1*s* electron spectra were found to be broad and of high intensity. So far, no resolution of the spectra into components has been successful, and consequently no information about the charge distribution on the dinitrogen ligand in the ruthenium and the osmium complexes is yet available. Work on this subject is in progress.

Besides nitrogen 1*s* electron spectra, some metal electron spectra have also been recorded on the dinitrogen complexes and on some other compounds of various formal oxidation states of the metal. Thereby, it was possible to get an idea about the charge on the metal atom in the dinitrogen complexes. Thus, it was found that the metal atom in the dinitrogen complexes of rhenium and iridium carries a small positive charge only, while the metal atom in the dinitrogen complexes of ruthenium and osmium was considerably more positive.

The binding energies of the atomic core electrons depend on the chemical surroundings of the atom. Recent developments in photoelectron spectroscopy (ESCA) have made possible the measurements of chemical shifts of inner-electron binding energies.[1] Correlations have been established between measured electron binding energies and formal oxidation state in sulphur [1,2]

and chlorine [1,3] compounds and with fractional atomic charges (calculated by a modification of Pauling's method [4]) in sulphur,[1] nitrogen,[5] and carbon [6] compounds. Also, more elaborate theoretical calculations, *e.g.* CNDO calculations,[7] of the charge distribution in molecules have been performed and correlated with ESCA data.[8–11] Atomic charges from extended Hückel calculations [12] have also been correlated with electron binding energies in nitrogen [13] and phosphorus [14] compounds.

Recently, Leigh *et al.*[15] reported nitrogen 1*s* electron spectra on two rhenium dinitrogen complexes. In one of these complexes, a chemical shift in the nitrogen 1*s* binding energy of about 2 eV was found. This shift was found to correspond to a difference in charge on the two nitrogen atoms of 0.4 a.u. based on Pauling charges from the correlation diagram given by Nordberg *et al.*[5] It was thus shown that the N–N bond has an appreciable polarity.

Earlier, infrared spectroscopic investigations by the present author [16,17] on metal dinitrogen complexes have given approximate information about the polarity of the N–N bond. Increased information about the charge distribution in the dinitrogen complexes is to be expected by applying the ESCA method on these complexes. Nitrogen 1*s* electron spectra have therefore been recorded on the following metal dinitrogen complexes: $Ru(NH_3)_5N_2X_2$, $Os(NH_3)_5N_2X_2$, where X = Cl, Br and I; $IrClN_2(PPh_3)_2$ and some rhenium dinitrogen phosphino complexes. The N–N stretching frequency in the above mentioned complexes varies between 1900 cm^{-1} and 2100 cm^{-1}, and perhaps there is a connection between the magnitude of the ESCA shift in binding energy and the N–N stretching frequency. Nitrogen 1*s* electron spectra have also been redetermined for a number of ionic nitrogen compounds. The measured nitrogen 1*s* binding energies have been plotted against calculated charges on nitrogen atoms given in the literature. The correlation diagrams thus obtained have been used in the determination of the charges on the nitrogen atoms in the dinitrogen complexes.

Electron spectra have also been recorded on pure metals of ruthenium, osmium, iridium, and rhenium and on some oxides and chlorides of the metals to compare the binding energies of some of the metal core electrons with the corresponding binding energies for the dinitrogen complexes. Thereby, some information about the charge on the metal atom in the dinitrogen complexes is to be expected.

EXPERIMENTAL

Chemicals. The same preparations of the dinitrogen complexes as those used in the earlier work [16,17] were used in this investigation. The ionic nitrogen compounds used to construct the correlation diagrams were of analytical grade. The metals, the metal oxides, and the metal chlorides were of lower purity.

Experimental techniques. The measurements were performed with an AEI ES 100 electron spectrometer. This is equipped with a hemispherical electrostatic analyzer and uses a preretardation field. Oil diffusion pumps fitted with cold traps produce a vacuum of 10^{-7} torr during the measurements. All spectra were obtained with Al$K\alpha$-radiation (1486.6 eV). The instrumental resolution for gold $4f_{7/2}$ electrons is 1.30 eV under the experimental conditions in this work. The electron binding energy E_b can be obtained [1] from the following expression:

$$E_b = h\nu - E_{kin} - \phi_{spec} \quad (1)$$

where $h\nu$ is the quantum energy of the characteristic X-rays used to eject the electrons and E_{kin} is the measured kinetic energy of the electrons. ϕ_{spec} is a constant including the work function of the spectrometer. According to the calibration,[18] it has been found that electron binding energies can be obtained from the following equation, when $AlK\alpha$-radiation is used, *viz.*

$$E_b = 1476.9 - E_{kin} \quad (2)$$

As ESCA is a surface method, it is of importance how the surface is constituted during the measurements. Therefore, the following preparation procedure was used. The dinitrogen complexes were dissolved in a suitable solvent; the iridium and rhenium dinitrogen complexes were dissolved in chloroform, the other dinitrogen complexes in water. The ionic nitrogen compounds were partly dissolved in water-ethanol. One or two drops of the solution or suspension were immediately placed on a platinum foil. A thin film of the compound was obtained on the foil after evaporation of the solvent. Through this preparation procedure no surface charging effects were obtained during the measurements. Charging effects depending on sample thickness have recently been investigated by Johansson *et al.*[19] Their results are in agreement with our findings. If the film was not too thick, it was possible to register platinum signals and thus refer measured binding energies to a fixed platinum peak. As reference peak, that of $Pt4f_{7/2}$ electrons has been chosen, which was found to have $E_{kin} = 1405.8$ eV. The binding energy of $Pt4f_{7/2}$ electrons is thus from eqn. (2) 71.1 eV, a value in good agreement with the literature.[20] Two or sometimes three measurements were made on each sample except for the dinitrogen complexes, for which nitrogen 1*s* electron spectra were recorded at least five times. After each recording, the $Pt4f_{7/2}$ electron peak from the backing platinum foil was also recorded. All reported binding energy values are consequently referred to the binding energy of $Pt4f_{7/2}$ electrons. The reproducibility of the photoelectron peaks was within 0.1 eV.

RESULTS AND DISCUSSION

Rhenium and iridium dinitrogen complexes. Nitrogen 1*s* electron spectra have been recorded on five rhenium dinitrogen complexes, *viz.* the complexes I–V in Table 1. Fig. 1 shows the nitrogen 1*s* electron spectrum of $ReClN_2(Ph_2PCH_2PPh_2)_2$. It is evident that the 1*s* electrons of coordinated dinitrogen give rise to two peaks separated by 1.9 eV. The 1*s* electrons of the two nitrogen atoms have thus different binding energies, which indicates [1] different effective charges on the nitrogen atoms. Compound II gave an identical nitrogen 1*s* electron spectrum, but the intensity of the N1*s* electron peaks was smaller, probably depending on lower crystallinity of this complex. Compound III, on the other hand, gave also the same nitrogen 1*s* electron spectrum as compounds I and II, but the N1*s* electron peaks were not at the same binding energy between different recordings. This fact can indicate surface charging or decomposition effects. It was found previously [17] that complex III was probably not quite pure. Surface charging or decomposition effects can probably occur as a result of the impurity of complex III. Even the positions of the C1*s* and Re electron peaks were found to change with time. The shift in binding energy of the N1*s* electrons was, however, constant and equal to that found for complexes I and II. The first recorded spectrum of complex III gave the same N1*s* binding energies as complexes I and II. In Fig. 2, the nitrogen 1*s* electron spectrum of complex IV is shown. It can be seen that the difference in N1*s* binding energy for the two nitrogen atoms is somewhat larger (about 2.1 eV) than for complex I (*cf.* Fig. 1). This fact indicates a larger charge separation on the nitrogen atoms. Complex V, *viz.* $ReClN_2(PPh_2Me)_4$, gave

Table 1. Measured nitrogen 1*s* binding energies (E_b) and obtained charges on the nitrogen atoms ($M-N_1-N_2$) in the dinitrogen complexes of rhenium and iridium.

Metal complex	E_b eV $N_1 1s$	$N_2 1s$	Shift eV	Extended Hückel $-q_{N1}$ a.u.	$-q_{N2}$ a.u.	CNDO $-q_{N1}$ a.u.	$-q_{N2}$ a.u.	*Ab initio* SCF MO $-q_{N1}$ a.u.	$-q_{N2}$ a.u.	$\nu_{NN}(CHCl_3)$ cm^{-1}
I. $ReClN_2(Ph_2PCH_2PPh_2)_2$	398.5	400.4	1.9±0.1	1.20	0.25	0.47	0.24	0.56	0.28	1993
II. $ReClN_2[Ph_2P(CH_2)_2PPh_2]_2$	398.5	400.4	1.9±0.1	1.20	0.25	0.47	0.24	0.56	0.28	1975
III. $ReClN_2(Ph_2PCH=CHPPh_2)_2$	398.5	400.4	1.9±0.1	1.20	0.25	0.47	0.24	0.56	0.28	1970
IV. $ReClN_2(PMe_2Ph)_4$	398.2	400.3	2.1±0.1	1.30	0.30	0.50	0.25	0.60	0.30	1924
V. $ReClN_2(PPh_2Me)_4$	–	–	2.1±0.1	1.30	0.30	0.50	0.25	0.60	0.30	1922
$IrClN_2(PPh_3)_2$	399.1	400.5	1.4±0.2	0.90	0.20	0.40	0.23	0.47	0.27	2105

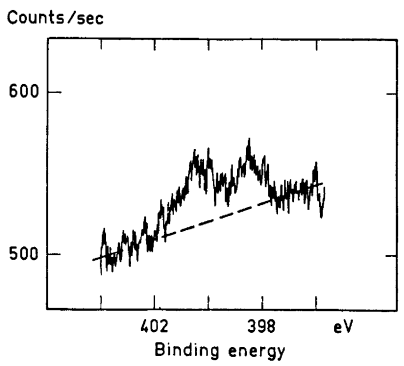

Fig. 1. Nitrogen 1*s* electron spectrum of $ReClN_2(Ph_2PCH_2PPh_2)_2$.

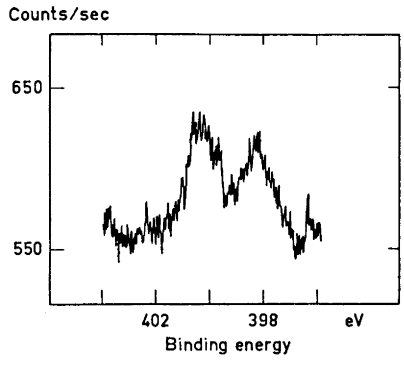

Fig. 2. Nitrogen 1*s* electron spectrum of $ReClN_2(PMe_2Ph)_4$.

also two N1*s* electron peaks, but the position of the peaks in the spectrum was found to be different between different recordings. The difference in N1*s* binding energy for the two nitrogen atoms was, however, the same as for complex IV. Complex V has earlier[17] been found to be impure and infrared intensity measurements could not be performed on this complex. As suggested above, surface charging or decomposition is probably related to the impurity of the compounds. The measurements on complex V have been omitted, as accurate N1*s* binding energy values could not be determined and the infrared intensity value (A_{NN}) was not available. Nitrogen 1*s* electron spectra have also been recorded on $IrClN_2(PPh_3)_2$. The intensity of the two N1*s* electron peaks was, however, small and therefore it was more difficult to determine the exact position of the two peaks. The magnitude of the shift in N1*s* binding energy was, however, found to be smaller than the corresponding shift for the rhenium dinitrogen complexes. The error in the measured binding energy is as mentioned above ± 0.1 eV, but for $IrClN_2(PPh_3)_2$ the error in the measured N1*s* binding energy was found to be ± 0.2 eV. The measured nitrogen 1*s* binding energies for the complexes described so far are given in Table 1.

To obtain the charges on the nitrogen atoms in the dinitrogen complexes, the measured binding energies can be compared with correlation diagrams given in the literature.[5,13] Because of various preparation techniques and different ways of referring measured binding energies (*e.g.* with the C1*s* electron peak as a reference [1]), a direct comparison with earlier measurements seems to be uncertain. Therefore, nitrogen 1*s* electron spectra have been recorded on a number of ionic nitrogen compounds, *i.e.* such compounds which have been measured before [13] and for which the charge on the nitrogen atoms has been calculated. The N1*s* binding energies measured by the present author are given in Table 2 together with the effective charge on the nitrogen atoms calculated by Hendrickson *et al.*[13] Recently, Wyatt *et al.*[21] have presented charges on the nitrogen atoms in the salts KN_3, KNO_2, and KNO_3 from *ab initio* SCF

Table 2. Nitrogen 1*s* binding energies and calculated charges.

Compound No.	Compound	Half-width eV	Nitrogen 1*s* binding energy	Calculated nitrogen atom charge a.u.		
				Extended Hückel [13]	CNDO [13]	*Ab initio* SCF MO [21]
1	$NaNO_3$	1.7	407.3	+2.557	+0.429	+0.66
2	$NaNO_2$	1.7	403.3	+1.273	+0.100	+0.20
3	NaN_3	1.8	403.0	+1.066	+0.096	+0.14
3	NaN_3	1.9	398.6	−1.033	−0.548	−0.57
4	$N_2H_6SO_4$	2.0	401.7	+0.184	+0.094	
5	KCN	1.9	398.1	−1.181	−0.518	
6	KOCN	2.2	397.9	−1.572	−0.550	
7	NaSCN	1.6	397.8	−1.672		
8	NH_4NO_3	1.8	406.0	+2.557	+0.429	
8	NH_4NO_3	2.1	400.9	−0.145	+0.039	
9	$NH_2OH.HCl$	2.7	401.4	+0.612	+0.219	

MO calculations and these charges are also included in Table 2. On comparison between the binding energies measured by the present author and those measured by Hendrickson *et al.*[13] and by Wyatt *et al.*[21], a fairly good agreement is obtained. The binding energies are then plotted against calculated charge. In this way, three different correlation diagrams are obtained (Figs. 3–5). The correlation between nitrogen 1*s* binding energy and calculated charge seems to be linear in all diagrams. This was also the case from the

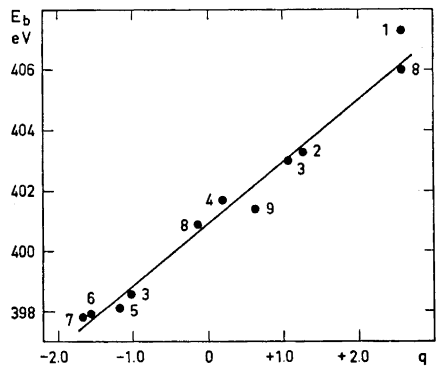

Fig. 3. Plot of nitrogen 1*s* binding energies (E_b) against extended Hückel calculated charges (q) on nitrogen atoms. The numerals refer to those used in Table 2.

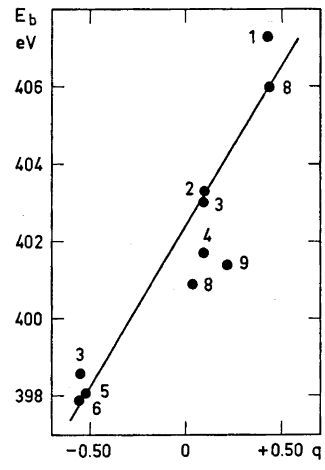

Fig. 4. Plot of nitrogen 1*s* binding energies (E_b) against CNDO calculated charges (q) on nitrogen atoms. The numerals refer to those used in Table 2.

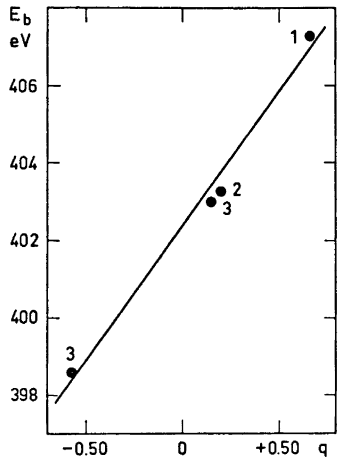

Fig. 5. Plot of nitrogen 1*s* binding energies (E_b) against *ab initio* SCF MO calculated charges (q) on nitrogen atoms. The numerals refer to those used in Table 2.

results of Hendrickson *et al.*[13] It can also be seen from Table 2 that the nitrogen atom charges obtained from extended Hückel calculations range from -1.7 to almost $+2.6$. Much smaller charge variation is obtained from CNDO calculations. It is also of interest to see that the charges obtained from CNDO and *ab initio* SCF MO calculations are almost the same.

The charges on the nitrogen atoms in the dinitrogen complexes can now be estimated by comparison between measured N1*s* binding energies and the correlation diagrams. The result is given in Table 1. It can be seen that both the nitrogen atoms are found to be negatively charged. This fact indicates an increase of the electron density over the dinitrogen ligand caused by $d\pi - p\pi^*$ back donation from filled metal *d*-orbitals to antibonding π-orbitals of dinitrogen. This result thus confirms and strengthens the earlier results from the infrared intensity measurements.[16,17] The total negative charge on the dinitrogen ligand is found to be greatest for $ReClN_2(PMe_2Ph)_4$ and smallest for $IrClN_2(PPh_3)_2$. This result is completely in accordance with the infrared intensity measurements,[17] for the intensity (A_{NN}) for $ReClN_2(PMe_2Ph)_4$ was found to be larger than the intensity (A_{NN}) for $IrClN_2(PPh_3)_2$. It seems, however, difficult to decide [22] which nitrogen atom should carry which charge. Leigh *et al.*[15] assign the smallest N1*s* binding energy to the terminal nitrogen atom, which thus gets the largest negative charge. It has been concluded earlier,[17] through a combination of infrared intensity data and the charges on the nitrogen atoms determined in this investigation, that the terminal nitrogen atom is the least negative one. Therefore, the largest nitrogen 1*s* binding energy is assigned to the terminal nitrogen atom. The difference in charge on the two nitrogen atoms is about 1 a.u. from the extended Hückel method. From the CNDO method and the *ab initio* SCF MO method the difference in charge on the nitrogen atoms is about 0.2 to 0.3 a.u., respectively. The charge separation varies, however, from one complex to another. The

greatest difference in charge on the nitrogen atoms is observed for $ReClN_2(PMe_2Ph)_4$ and the smallest for $IrClN_2(PPh_3)_2$. It was mentioned above that surface charging effects probably occur on the measurements on $ReClN_2(PPh_2Me)_4$, which made it impossible to get accurate N1*s* binding energies. The charges on the nitrogen atoms in this complex are, however, assumed to be the same as those in $ReClN_2(PMe_2Ph)_4$, as the magnitude of the shift in N1*s* binding energy is the same for both the complexes. Further support for this suggestion is that the N–N stretching frequency is the same in the two complexes (*cf.* Table 1).

It is of interest to compare the magnitude of the shift in N1*s* binding energy with the N–N stretching frequency in the dinitrogen complexes (*cf.* Table 1). The largest shift in N1*s* binding energy is found for the complexes $ReClN_2(PMe_2Ph)_4$ and $ReClN_2(PPh_2Me)_4$. Thus, the lower the N–N stretching frequency the larger is the shift in binding energy. This means that when the disturbance of the dinitrogen molecule is large, *i.e.* low ν_{NN}, the charge separation on the nitrogen atoms is large. When the disturbance of the dinitrogen molecule is considerable, there will be a decrease in the N–N bond order. It then follows [16,17] that the $M-N_2$ bond will be stronger. The conclusion above can thus be expressed in another way, *viz.* the stronger the dinitrogen ligand is bound to the metal, the more pronounced is the charge separation on the nitrogen atoms. The smallest shift in N1*s* binding energy is found for $IrClN_2(PPh_3)_2$, which complex also shows the highest N–N stretching frequency. The charge separation on the nitrogen atoms in this complex is thus smaller than the charge separation on the nitrogen atoms in the rhenium complexes. The smallest N1*s* binding energy is found for the inner nitrogen atom in $ReClN_2(PMe_2Ph)_4$, and thus this nitrogen atom is the most negative one. In the other rhenium dinitrogen complexes and in $IrClN_2(PPh_3)_2$, the corresponding binding energy is higher and thereby the inner nitrogen atom is less negative. The difference in N1*s* binding energy of the terminal nitrogen atom for the various complexes is not so pronounced (*cf.* Table 1) and consequently, the charges on the terminal nitrogen atoms are more similar than the charges on the inner nitrogen atoms.

To get an idea about the charge on the metal atom in the complexes some metal core electron spectra have also been recorded. Table 3 shows the binding energies of $Re4f_{5/2}$ and $Re4f_{7/2}$ electrons in the dinitrogen complexes together with the corresponding binding energies for Re metal and $ReOCl_3(PPh_3)_2$. A representative example of a Re4*f* electron spectrum of a rhenium dinitrogen complex is given in Fig. 6. For $IrClN_2(PPh_3)_2$, the $Ir4f_{5/2}$ and $Ir4f_{7/2}$ electron peaks have been registered and the binding energies are compared with the corresponding binding energies for Ir metal and $IrCl_3$. These binding energies are included in Table 3. It is evident that the $Re4f_{5/2}$ and $Re4f_{7/2}$ electron binding energies are practically constant from one rhenium dinitrogen complex to another. These binding energies are also about the same as those measured for Re metal. This indicates a low positive charge on the metal atom. On the other hand, it is expected that the π^*-acceptor ability of the dinitrogen ligand should cause a lower electron density around the metal atom and consequently a higher binding energy and thereby a positive charge on the rhenium atom. Probably the increased positive charge is partly reduced by the σ-bond from

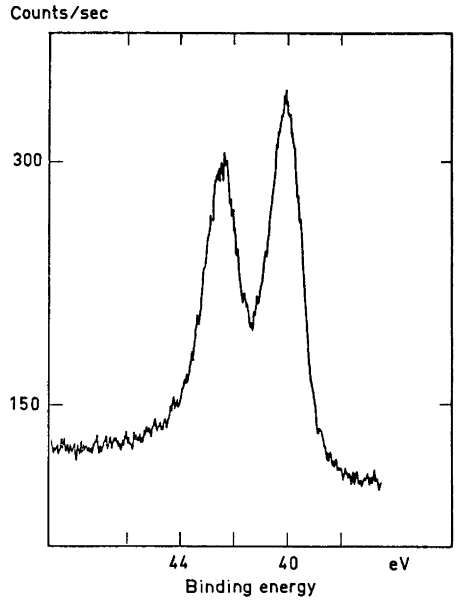

Fig. 6. Rhenium 4*f* electron spectrum of $ReClN_2(Ph_2PCH_2PPh_2)_2$.

the dinitrogen ligand to the metal. Depending on the various degree of π-backbonding in the different complexes, there should be a slight difference in electron density around the metal atom and consequently a difference in binding energy. This has, however, not been found. It must be pointed out that also the σ-donor and π-acceptor ability of the phosphine ligands can influence the charge on the metal atom and certainly do so, but this effect has not been investigated. Probably this balance of σ- and π-bonding can serve to keep the electron density around the rhenium atom fairly constant, as observed. It is, however, evident that the σ-donor ability of the phosphine ligands can be the most pronounced, and thus cause an increase of the electron

Table 3. The binding energies of $M4f_{5/2}$ and $M4f_{7/2}$ electrons in the dinitrogen complexes of rhenium and iridium and in some other rhenium and iridium compounds. M stands for Re and Ir.

Compound	E_b eV	
	$M4f_{5/2}$	$M4f_{7/2}$
Re metal	42.5	40.1
$ReClN_2(Ph_2PCH_2PPh_2)_2$	42.5	40.1
$ReClN_2[Ph_2P(CH_2)_2PPh_2]_2$	42.4	40.1
$ReClN_2(PMe_2Ph)_4$	42.6	40.2
$ReOCl_3(PPh_3)_2$	46.2	43.7
Ir metal	63.2	60.3
$IrClN_2(PPh_3)_2$	63.5	60.7
$IrCl_3$	65.4	62.7

density around the metal atom and thereby reduce the positive charge caused by π-backbonding to the dinitrogen ligand. The suggestions above can thus explain the low and equal Re4*f* electron binding energies measured for the rhenium dinitrogen complexes. The effect of σ-donor and π-acceptor ability of phosphine ligands has been discussed in connection with ESCA measurements by Blackburn *et al.*[23] on some metal phosphine complexes and by Cook *et al.*[24] on some platinum phosphine complexes. These authors [23,24] find that the P2*p* electron binding energies are practically constant from one complex to another, which indicates that there might be a balance between the P→M σ-bonding and the M→P π-bonding. The effect of σ- and π-bonding in some palladium phosphine complexes has recently been discussed by Kumar *et al.*,[25] supporting the suggestions above on the rhenium dinitrogen phosphino complexes.

In the compound $ReOCl_3(PPh_3)_2$, the $Re4f_{5/2}$ and $Re4f_{7/2}$ electron binding energies are higher than the corresponding binding energies in the rhenium dinitrogen complexes, which is also to be expected, as the formal oxidation state on the rhenium atom is greater. It must, however, be pointed out that the Re4*f* electron binding energies measured in this investigation are about 5 eV lower than those given by Siegbahn *et al.*[1] In the electron spectrum of Re metal, small peaks were obtained at binding energies about 5 eV higher than the main peaks, so the binding energies given by Siegbahn *et al.*[1] probably are assigned to Re of a higher formal oxidation state. Recently, Nefedow [26] reported binding energies of Re in good agreement with those measured in this work.

The degree of $d\pi - p\pi^*$ back donation from metal *d*-orbitals to π-orbitals of dinitrogen has earlier [17] been found to be smaller in the iridium dinitrogen complex, $IrClN_2(PPh_3)_2$, than in the rhenium dinitrogen complexes. It is thus to be expected that the iridium atom is less positive than the rhenium atom in the dinitrogen complexes. But the $Ir4f_{5/2}$ and $Ir4f_{7/2}$ electron binding energies in $IrClN_2(PPh_3)_2$ are somewhat higher than the corresponding binding energies in Ir metal, which indicates a small positive charge on the iridium atom. This is to be compared with the rhenium complexes above, where the $Re4f_{5/2}$ and $Re4f_{7/2}$ electron binding energies were found to be equal to those measured for Re metal. The influence of the phosphine ligands on the charge of the iridium atom has not been investigated. In an investigation by Chatt *et al.*[27] on iridium dinitrogen complexes containing various phosphine ligands, it was found that the more aliphatic phosphine complexes tend to have slightly lower N–N stretching frequencies. The more aliphatic phosphines are the more basic ones and so they should consequently increase the electron density around the metal atom. It is thus quite reasonable that the σ-bond from the phosphorus in triphenylphosphine to the metal is weaker in the iridium complex than in the more aliphatic phosphino rhenium complexes above. Consequently, the iridium atom can be more positive than the rhenium atom in the dinitrogen complexes, which is shown by the results reported here.

The $Ir4f_{5/2}$ and $Ir4f_{7/2}$ electron binding energies in $IrClN_2(PPh_3)_2$ are, however, found to be smaller than the corresponding binding energies in $IrCl_3$, which also is to be expected, as the formal oxidation state on the metal atom is smaller in $IrClN_2(PPh_3)_2$ than in $IrCl_3$.

Table 4. Measured nitrogen 1*s* binding energies (E_b) and half-widths of the N1*s* electron peaks in the dinitrogen complexes of ruthenium and osmium.

Metal complex	E_b eV	Half-width eV
$Ru(NH_3)_5N_2Cl_2$	399.6	2.0
$Ru(NH_3)_5N_2Br_2$	399.4	2.2
$Ru(NH_3)_5N_2I_2$	399.6	1.8
$Os(NH_3)_5N_2Cl_2$	399.5	2.2
$Os(NH_3)_5N_2Br_2$	399.7	2.0
$Os(NH_3)_5N_2I_2$	399.6	1.9

Ruthenium and osmium dinitrogen complexes. Nitrogen 1*s* electron spectra have also been recorded on the ruthenium and osmium dinitrogen complexes, which were investigated earlier [16] by infrared spectroscopy. As these complexes also contain ammonia, the nitrogen 1*s* electron spectrum shows a quite symmetrical N1*s* electron peak arising from the nitrogen in ammonia and the nitrogen in the dinitrogen ligand. The expected two N1*s* electron peaks from coordinated dinitrogen are overlapped by the peak from nitrogen in ammonia. A typical nitrogen 1*s* electron spectrum for this kind of dinitrogen complex is given in Fig. 7. In Table 4, measured N1*s* binding energies of the ammonia nitrogen in the various dinitrogen complexes of ruthenium and osmium are given together with the half-widths of the N1*s* electron peaks. The half-widths of the peaks are about the same as those found for the ionic nitrogen compounds (*cf.* Table 2), and consequently no indication that the peaks can consist of several components is observed. It is evident from the correlation diagrams (Figs. 3 – 5) that the ammonia nitrogen in the dinitrogen complexes carries a negative charge. The negative charge on the ammonia nitrogen is about the same for all the complexes. The N1*s* binding energies measured for the ammonia nitrogen lie between those measured for the two nitrogen atoms in the rhenium and iridium dinitrogen complexes (*cf.* Table 1). It is thus reasonable that the N1*s* electron peaks corresponding to coordinated dinitrogen are located on either side of the maximum of the large N1*s* electron peak. This conclusion is also supported by the connection between the magnitude of the shift in N1*s* binding energy and the N – N stretching frequency, which has been found for Re and Ir complexes, and also applied to these complexes. Work is in progress to resolve the N1*s* electron peaks into components, but as the peaks are quite symmetrical, it is uncertain if this will be successful. The N1*s* electron spectra of the osmium dinitrogen complexes are particularly complicated to analyse, as these compounds also contain a bisdinitrogen complex.[16] N1*s* electron spectra on which resolution calculations are in progress have been obtained through measurements with better statistics. If it is possible to resolve the N1*s* electron spectra of these dinitrogen complexes, the results will be presented later.

To get some information about the charge on the metal atom in the dinitrogen complexes, some metal core electron spectra have also been recorded. It has been found that the Ru3$p_{3/2}$ and Ru3$d_{5/2}$ electron levels give the highest

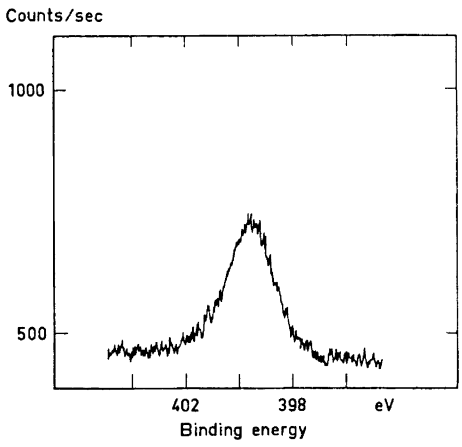

Fig. 7. Nitrogen 1*s* electron spectrum of $Os(NH_3)_5N_2I_2$.

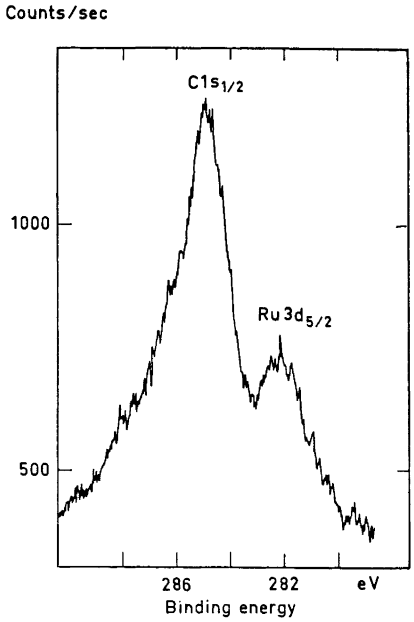

Fig. 8. Electron spectrum of $Ru(NH_3)_5N_2I_2$ in the carbon 1*s* region.

intensity of the peaks. The Ru3$d_{3/2}$ electrons have about the same binding energy as C1*s* electrons and, as a carbon peak arising from the pump oil contamination is always obtained, it is difficult to separate the Ru3$d_3/_2$ electron peak from the carbon 1*s* electron peak. This is demonstrated in Fig. 8, which shows the electron spectrum of $Ru(NH_3)_5N_2I_2$ in the carbon 1*s* region. Therefore, the Ru3$p_{3/2}$ electron peak has been studied instead of the Ru3$d_3/_2$ electron peak. Electron spectra have also been recorded on Ru metal, $RuCl_3$, and RuO_2 and the binding energies of the Ru3$p_{3/2}$ and Ru3$d_{5/2}$ electron levels determined. The results are given in Table 5. The binding energies measured for

Table 5. Binding energies (E_b) of Ru3$p_{3/2}$ and Ru3$d_{5/2}$ electrons in the ruthenium dinitrogen complexes and in some other ruthenium compounds.

Compound	E_b eV	
	Ru3$p_{3/2}$	Ru3$d_{5/2}$
Ru metal	462.2	279.9
$Ru(NH_3)_5N_2Cl_2$	463.3	282.5
$Ru(NH_3)_5N_2Br_2$	462.2	280.5
$Ru(NH_3)_5N_2I_2$	463.5	282.2
$RuCl_3$	463.3	281.8
RuO_2	463.2	282.1

Ru metal are about 1 eV higher than those given by Siegbahn *et al.*[1] It is evident that the binding energies measured for the dinitrogen complexes are close to those for $RuCl_3$ and RuO_2. The binding energies are also higher than the corresponding binding energies for Ru metal. The only exception is the ruthenium bromide. The high binding energy values indicate a high positive charge on the metal atom in the dinitrogen complexes. This result can be compared with the results for the rhenium and iridium dinitrogen complexes, where the binding energies of the metal electrons were close to those of the pure metals, indicating a low positive charge on the metal atom. The reason for the high positive charge on the metal atom in the dinitrogen complexes of ruthenium is, besides the $d\pi - p\pi^*$ back donation from metal to the dinitrogen ligand, that the metal atoms are surrounded by strongly electronegative halide ions.

The ruthenium bromide, on the other hand, shows Ru$3p_{3/2}$ and Ru$3d_{5/2}$ electron binding energies which are considerably smaller than the corresponding binding energies for the chloride and iodide. This fact could indicate a low positive charge on the metal atom in the bromide complex. But a more reasonable explanation of the low binding energies of this complex is that the bromide complex contains an impurity. During the preparation procedure [16] of the dinitrogen complex, the initial azide complex $Ru(NH_3)_5N_3^{2+}$ decomposes to $Ru(NH_3)_5N_2^{2+}$. The infrared N – N stretching vibration band of the ruthenium bromide in the solid state showed a small shoulder at the low frequency side of the spectrum, indicating [28] an azide impurity. The N1*s* electron peak is somewhat broader in the bromide complex than in the chloride and iodide complexes (*cf.* Table 4). It can also be mentioned that the Ru$3p_{3/2}$ electron peak of the bromide complex is broader than the corresponding peak for the other complexes. The same is also the case for the Ru$3d_{5/2}$ electron peak. It is evident that there is probably an impurity in the bromide complex, and in such a case the measured binding energy values are uncertain (*cf.* the rhenium dinitrogen complexes above).

Metal core electron spectra have also been recorded for the osmium dinitrogen complexes and compared with the corresponding spectra of some other osmium compounds. The Os$4f_{5/2}$ and Os$4f_{7/2}$ electron peaks were chosen as suitable electron peaks. Fig. 9 shows the Os4*f* electron spectrum of $Os(NH_3)_5N_2Br_2$. The measured binding energy values are collected in Table 6. Like the binding energies of Ru metal, the binding energies for Os metal are found to be 1 eV higher than those given by Siegbahn *et al.*[1] It can be seen from Table 6 that the binding energies measured for the osmium dinitrogen complexes are higher than those measured for Os metal. The metal atom in the complexes thus carries a positive charge, which is expected for the same reasons as were mentioned for the ruthenium complexes above. The difference in binding energy between the Os$4f_{5/2}$ and Os$4f_{7/2}$ electron levels is found to be 2.0 – 2.4 eV for the dinitrogen complexes with the exception of $Os(NH_3)_5N_2I_2$. In this latter complex, the difference is 3.0 eV. The reason for this is that the Os$4f_{7/2}$ electron binding energy value is somewhat uncertain, as the Os$4f_{7/2}$ electron peak is overlapped by the I4*d* electron peak. The Os$4f_{5/2}$ and Os$4f_{7/2}$ electron binding energies for OsO_2 and K_2OsCl_6 are somewhat greater than the corresponding binding energies in the dinitrogen complexes. Consequently, the

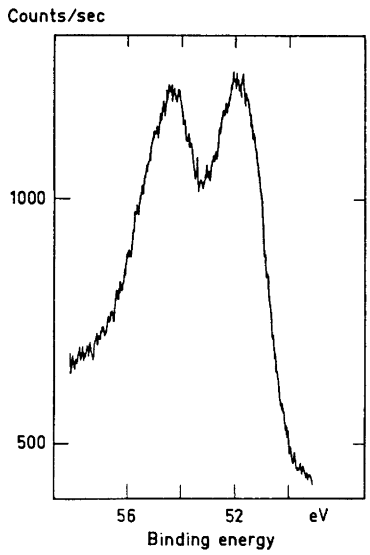

Fig. 9. Osmium 4*f* electron spectrum of $Os(NH_3)_5N_2Br_2$

positive charge on the osmium atom is greater in OsO_2 and K_2OsCl_6 than in the osmium dinitrogen complexes.

It was suggested before,[16] that a reasonable explanation of the different influence of dimethyl sulfoxide on the mono- and bisdinitrogen osmium complexes could be that the charge on the metal ion was smaller in the bisdinitrogen complex than in the monodinitrogen complex. The same suggestion was used to explain the stability of the bisdinitrogen complex in alkaline solution.[29] This suggestion can easily be checked with the ESCA method. As only one preparation of the pure bisdinitrogen complex, *viz.* $Os(NH_3)_4(N_2)_2Br_2$, was available, the binding energies could be measured only for this complex. It can be seen from Table 6 that the $Os4f_{5/2}$ and $Os4f_{7/2}$ electron binding energies of the bisdinitrogen complex are about 0.5 eV smaller than the corresponding

Table 6. Binding energies (E_b) of $Os4f_{5/2}$ and $Os4f_{7/2}$ electrons in the osmium dinitrogen complexes and some other osmium compounds.

Compound	E_b eV	
	$Os4f_{5/2}$	$Os4f_{7/2}$
Os metal	53.3	50.6
$Os(NH_3)_5N_2Cl_2$	54.2	52.2
$Os(NH_3)_5N_2Br_2$	54.4	52.0
$Os(NH_3)_5N_2I_2$	53.9	50.9
$Os(NH_3)_4(N_2)_2Br_2$	53.9	51.6
OsO_2	55.0	52.7
K_2OsCl_6	55.7	53.0

binding energies for the monodinitrogen complex. This fact indicates that the positive charge on the metal ion is smaller in the bisdinitrogen complex than in the monodinitrogen complex and the suggestion presented before [16,29] is thus well supported.

CONCLUSIONS

The results of the ESCA measurements for the rhenium and the iridium dinitrogen complexes give direct evidence of the charge carried by a dinitrogen molecule in the complexes. Furthermore, from the recorded metal core electron spectra for the dinitrogen complexes and the other metal compounds, it has been possible to get an idea about the charge on the metal atom in the dinitrogen complexes. ESCA spectra thus seem to be capable of providing some information on bonding between the atoms in the dinitrogen complexes. Thus it is possible to get more detailed information from ESCA data about the charge distribution in the dinitrogen complexes than from infrared intensity measurements (*cf.* Refs. 16 and 17). The combination of infrared intensity data with ESCA data seems to be able to provide increased knowledge about the electronic structure of molecules (*cf.* Ref. 17).

The question of homolytic and heterolytic splitting of a diatomic molecule is of major interest when considering the activation of the dinitrogen molecule. On homolytic splitting of a diatomic molecule, the electronic structure around each atom will be the same, while on heterolytic splitting the electronic structure will be different. From the present investigation it is evident that the electronic structure around the two nitrogen atoms is different, as the difference in N1*s* binding energy of the two nitrogen atoms corresponds to different effective charges on the nitrogen atoms. If the charge separation on the nitrogen atoms is considered as a splitting, this is both homolytic and heterolytic; homolytic, since both the nitrogen atoms are negatively charged and heterolytic since there is a small difference in charge on the two nitrogen atoms. This fact is of importance when contemplating the choice of suitable reagents capable of reducing the dinitrogen group.

Ever since the dinitrogen complexes have been known, they have been considered as possible models for nitrogen-fixing enzymes or as models for surface adsorption complexes, which are intermediates in the technical catalytic production of ammonia. For a complete model system one must be able to show the possibility of reduction of the dinitrogen ligand to ammonia. This subject has been attacked earlier,[30–32] unsuccessfully. Now, since the charge distribution on the dinitrogen ligand is known, the problem of reducing the dinitrogen group probably can be resolved. Recently, Vol'pin *et al.*[33] have shown that it is possible to reduce dinitrogen in $CoHN_2(PPh_3)_3$ under mild conditions in the presence of compounds of transition metals of Groups IV – VI of the periodic system. Such work is also planned at this laboratory.

The financial support for this work from the *Swedish Board for Technical Development* and the *Bank of Sweden Tercentenary Fund* is gratefully acknowledged. The author thanks Dr. G. Schön for help in introducing him to the ESCA technique and Dr. R. Larsson for kind interest and valuable discussions during this work. The author is indebted to Dr. C.-E. Boman for the gift of some of the ruthenium and osmium compounds investigated.

REFERENCES

1. Siegbahn, K., Nordling, C., Fahlman, A., Nordberg, R., Hamrin, K., Hedman, J., Johansson, G., Bergmark, T., Karlsson, S.-E., Lindgren, I. and Lindberg, B. *ESCA – Atomic, Molecular and Solid State Structure Studied by Means of Electron Spectroscopy*, Almqvist and Wiksell, Uppsala 1967.
2. Fahlman, A., Hamrin, K., Hedman, J., Nordberg, R., Nordling, C. and Siegbahn, K. *Nature* **210** (1966) 4.
3. Fahlman, A., Carlsson, R. and Siegbahn, K. *Arkiv Kemi* **25** (1966) 301.
4. Pauling, L. *The Nature of the Chemical Bond*, 3rd Ed., Cornell University Press, Ithaca 1960.
5. Nordberg, R., Albridge, R. G., Bergmark, T., Ericson, U., Hedman, J., Nordling, C., Siegbahn, K. and Lindberg, B. J. *Arkiv Kemi* **28** (1968) 257.
6. Nordberg, R., Gelius, U., Hedén, P. F., Hedman, J., Nordling, C., Siegbahn, K. and Lindberg, B. J. *Phys. Scr.* **2** (1970) 70.
7. Pople, J. A., Santry, D. P. and Segal, G. A. *J. Chem. Phys.* **43** (1965) S130.
8. Lindberg, B. J., Hamrin, K., Johansson, G., Gelius, U., Fahlman, A., Nordling, C. and Siegbahn, K. *Phys. Scr.* **1** (1970) 286.
9. Siegbahn, K., Nordling, C., Johansson, G., Hedman, J., Hedén, P. F., Hamrin, K., Gelius, U., Bergmark, T., Werme, L. O., Manne, R. and Baer, Y. *ESCA Applied to Free Molecules*, North Holland, Amsterdam 1969.
10. Hollander, J. M., Hendrickson, D. N. and Jolly, W. L. *J. Chem. Phys.* **49** (1968) 3315.
11. Hendrickson, D. N., Hollander, J. M. and Jolly, W. L. *Inorg. Chem.* **9** (1970) 612.
12. Hoffmann, R. *J. Chem. Phys.* **39** (1963) 1397.
13. Hendrickson, D. N., Hollander, J. M. and Jolly, W. L. *Inorg. Chem.* **8** (1969) 2642.
14. Pelavin, M., Hendrickson, D. N., Hollander, J. M. and Jolly, W. L. *J. Phys. Chem.* **74** (1970) 1116.
15. Leigh, G. J., Murrell, J. N., Bremser, W. and Proctor, W. G. *Chem. Commun.* **1970** 1661.
16. Folkesson, B. *Acta Chem. Scand.* **26** (1972) 4008.
17. Folkesson, B. *Acta Chem. Scand.* **27** (1973). *To be published.*
18. Schön, G. *To be submitted to J. Electron Spectr.*
19. Johansson, G., Hedman, J., Berndtsson, A., Klasson, M. and Nilsson, R. *UUIP-769*, 1972.
20. Karlsson, S.-E., Norberg, C. H., Nilsson, Ö., Högberg, S., El-Farrash, A. H., Nordling, C. and Siegbahn, K. *Arkiv Fysik* **38** (1968) 341.
21. Wyatt, J. F., Hillier, I. H., Saunders, V. R., Connor, J. A. and Barber, M. *J. Chem. Phys.* **54** (1971) 5311.
22. Leigh, G. J. *Int. Symp. on X-Ray Photoelectron Spectroscopy*, Zürich, Switzerland, Oct. 4 – 6, 1971.
23. Blackburn, J. R., Nordberg, R., Stevie, F., Albridge, R. G. and Jones, M. M. *Inorg. Chem.* **9** (1970) 2374.
24. Cook, C. D., Wan, K. Y., Gelius, U., Hamrin, K., Johansson, G., Olsson, E., Siegbahn, H., Nordling, C. and Siegbahn, K. *UUIP-717*, 1970.
25. Kumar, G., Blackburn, J. R., Albridge, R. G., Moddeman, W. E. and Jones, M. M. *Inorg. Chem.* **11** (1972) 296.
26. Nefedow, W. I. *Int. Symp. on X-Ray Photoelectron Spectroscopy*, Zürich, Switzerland, Oct. 4 – 6, 1971.
27. Chatt, J., Melville, D. P. and Richards, R. L. *J. Chem. Soc.* **A 1969** 2841.
28. Allen, A. D., Bottomley, F., Harris, R. O., Reinsalu, V. P. and Senoff, C. V. *J. Am. Chem. Soc.* **89** (1967) 5595.
29. Folkesson, B. *Acta Chem. Scand.* **26** (1972) 4157.
30. Chatt, J., Richards, R. L., Fergusson, J. E. and Love, J. L. *Chem. Commun.* **1968** 1522.
31. Chatt, J., Fergusson, J. E., Richards, R. L. and Sanders, J. R. *Nature* **221** (1969) 551.
32. Chatt, J., Nikolsky, A. B., Richards, R. L., Sanders, J. R., Fergusson, J. E. and Love, J. L. *J. Chem. Soc.* **A 1970** 1479.
33. Vol'pin, M. E., Lenenko, V. S. and Shur, V. B. *Izv. Akad. Nauk SSSR, Ser. Khim.* **2** (1971) 463.

Received July 10, 1972.

ACTA CHEMICA SCANDINAVICA 27 (1973) 303–314

Kinetic Studies of Lanthanoid Carboxylate Complexes

III. The Dissociation Rates of Praseodymium, Neodymium, Europium, and Erbium EDTA Complexes

TORSTEN RYHL

Division of Physical Chemistry, Chemical Center, University of Lund, P.O.B. 740, S-220 07 Lund 7, Sweden

The dissociation rates of praseodymium, neodymium, europium, and erbium EDTA complexes in a slightly acid medium have been investigated. The rate constants of these dissociations were determined from reactions in which the ligand is exchanged between two different metal ions. The measurements were made at 25.0°C and at an ionic strength of 0.5 M, using potassium chloride as neutral salt. The solutions were buffered with 12.5 mM sodium acetate and varying amounts of acetic acid. The dissociation was found to be catalyzed by hydrogen ions, according to the equation $f = k_0 + \bar{k}_1[H^+] + \bar{k}_2[H^+]^2$ for the rate constant f.

In a preceding paper [1] rate constants for the dissociation of lanthanum, erbium, ytterbium, and copper EDTA complexes in a slightly acid medium were reported. The dissociation rate of the lanthanum EDTA complex in a slightly alkaline medium and measurements of the labilities of the coordinative bonds in lanthanoid EDTA complexes were published in a second paper.[2] The present work is an investigation of the dissociation rates of the praseodymium, neodymium, europium, and erbium EDTA complexes by means of exchange reactions in a slightly acid medium: $LA + M \rightleftharpoons L + MA$.

EXPERIMENTAL

Chemicals. All chemicals were of analytical grade. Standard solutions of $PrCl_3$, $NdCl_3$, $EuCl_3$, $ErCl_3$, and $CuCl_2$ were prepared by dissolving the corresponding oxides (from Potash & Chemical Corp.) in hydrochloric acid. The solutions were standardized as previously described.[1] Solutions of EDTA, potassium chloride, and acetate buffer were prepared as described in Ref. 1.

Measurements. All measurements were made at 25.0 ± 0.1°C and at the ionic strength 0.5 M. The solutions were buffered with 12.5 mM sodium acetate and varying amounts of acetic acid. The ionic strength for each of the solutions S and T (see below) was adjusted to 0.5 M by potassium chloride.

The reactions were performed by mixing two solutions, and the hydrogen ion concentration of the resulting solution was measured as described in Ref. 1.

The praseodymium and neodymium systems. Copper was used as the second metal, M, for both these systems. The reaction rates were studied by a Durrum-Gibson stopped-flow spectrophotometer, using a wavelength range of 600 – 820 nm. To verify the absence of photochemical effects, some of the solutions were studied at different wavelengths and slitwidths. No differences in the observed rate constants could be detected.

The two solutions, S and T, which were mixed in equal volumes, had the following compositions:

S: $2\,C_L^\circ$ $PrCl_3$ or $NdCl_3$; $2\,C_A^\circ$ Na_2H_2EDTA; buffer; $I = 0.5$ M (KCl)

T: $2\,C_M^\circ$ $CuCl_2$; buffer; $I = 0.5$ M (KCl)

To remove dissolved air, the solutions were boiled at decreased pressure at room temperature for 2 min before mixing.

The reactions were followed during approximately three half-lives. The data in Tables 1 and 2 are averages of three independent measurements.

The europium system. In the aforementioned exchange reactions, copper was used together with one of the lanthanoids. In the europium system, however, ytterbium was used as the second metal, M, in order to investigate if the over-all reaction proceeds to a measurable extent with direct substitution, path II (see Ref. 1), when both the metals are lanthanoids.

Because of the small absorption coefficients of the *f-f* spectra and the nearly identical UV spectra for different lanthanoid complexes containing the same ligand, the reaction between ytterbium ions and the europium EDTA complex is difficult to follow by spectrophotometric methods. Therefore the system was studied polarographically.

The polarographic half-wave potentials of the free europium ion and its EDTA complex are well separated both from one another and from the corresponding potentials of the other lanthanoid ions.[3] Hence, it is possible to follow the exchange reaction by measuring the diffusion current of the free europium ion when the reaction rate is suitable.

Table 1. Rate data for the praseodymium system. L = Pr and M = Cu.

$[H^+] \times 10^5$/M, $k_{obs} \times 10$/s^{-1}, $100(k_{obs} - k_{calc})/k_{calc}$, $f_{LA,exp} \times 10$/s^{-1};

$C_L^\circ = 6.20 \times 10^{-4}$ M, $C_A^\circ = 6.00 \times 10^{-4}$ M, $C_M^\circ = 1.50 \times 10^{-3}$ M: 9.00, 1.43, 5.5, 1.68; 12.9, 2.11, 8.6, 2.49; 24.6, 4.12, 7.0, 4.89; 32.8, 5.54, 5.0, 6.64;

$C_L^\circ = 3.10 \times 10^{-4}$ M, $C_A^\circ = 3.00 \times 10^{-4}$ M, $C_M^\circ = 4.99 \times 10^{-3}$ M: 6.60, 1.08, −4.3, 1.12; 21.2, 3.73, 3.8, 4.01;

$C_L^\circ = 3.10 \times 10^{-4}$ M, $C_A^\circ = 3.00 \times 10^{-4}$ M, $C_M^\circ = 9.98 \times 10^{-3}$ M: 3.21, 0.616, 4.0, 0.626; 4.34, 0.759, −1.8, 0.774; 16.5, 2.88, 3.2, 3.04; 20.0, 3.51, 3.2, 3.74; 29.6, 5.03, −1.8, 5.50; 40.1, 7.61, 7.4, 8.56;

$C_L^\circ = 3.10 \times 10^{-4}$ M, $C_A^\circ = 3.00 \times 10^{-4}$ M, $C_M^\circ = 1.50 \times 10^{-2}$ M: 4.81, 0.850, 0.0, 0.866; 8.09, 1.32, −4.5, 1.36; 11.9, 1.98, −2.0, 2.06; 14.6, 2.41, −2.2, 2.52; 17.9, 2.96, −2.5, 3.13; 20.2, 3.56, 3.3, 3.79; 23.7, 4.18, 2.9, 4.49; 27.4, 4.63, −1.9, 5.02; 31.5, 5.38, −1.7, 5.90; 37.5, 6.45, 2.3, 7.19; 46.1, 8.23, −0.4, 9.39; 53.7, 9.66, −1.1, 11.2; 60.7, 10.9, −2.6, 12.9;

$C_L^\circ = 3.10 \times 10^{-4}$ M, $C_A^\circ = 3.00 \times 10^{-4}$ M, $C_M^\circ = 2.00 \times 10^{-2}$ M: 10.3, 1.62, −7.5, 1.68; 26.5, 4.47, −2.1, 4.84;

$C_L^\circ = 6.20 \times 10^{-4}$ M, $C_A^\circ = 3.00 \times 10^{-4}$ M, $C_M^\circ = 2.00 \times 10^{-2}$ M: 3.97, 0.727, 1.8, 0.741; 11.9, 1.98, −1.9, 2.06; 19.9, 3.40, 0.6, 3.62; 27.9, 4.81, 0.1, 5.23; 35.8, 5.99, −4.6, 6.66.

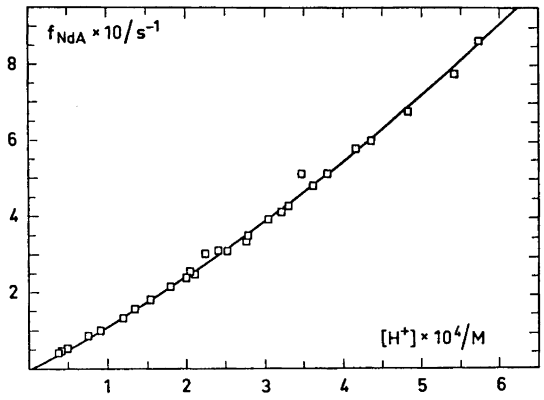

Fig. 1. The dissociation rate constant of the neodymium EDTA complex, f_{NdA}, as a function of the hydrogen ion concentration. The fulldrawn curve has been calculated from the rate constants obtained in this work.

Table 2. Rate data for the neodymium system. L = Nd and M = Cu.

$[H^+] \times 10^5/M$, $k_{obs} \times 10/s^{-1}$, $100(k_{obs} - k_{calc})/k_{calc}$, $f_{I,A,exp} \times 10/s^{-1}$;

$C_L^\circ = 6.78 \times 10^{-4}$ M, $C_A^\circ = 6.40 \times 10^{-4}$ M, $C_M^\circ = 4.99 \times 10^{-3}$ M: 22.4, 2.77, 9.8, 3.07;

$C_L^\circ = 6.78 \times 10^{-4}$ M, $C_A^\circ = 6.40 \times 10^{-4}$ M, $C_M^\circ = 9.98 \times 10^{-3}$ M: 4.11, 0.445, −0.1, 0.459; 7.57, 0.862, 3.9, 0.865; 20.5, 2.40, 2.5, 2.59; 34.7, 4.58, 11.3, 5.15; 41.6, 5.07, 1.1, 5.80; 57.4, 7.22, 0.6, 8.61;

$C_L^\circ = 3.39 \times 10^{-4}$ M, $C_A^\circ = 3.20 \times 10^{-4}$ M, $C_M^\circ = 1.50 \times 10^{-2}$ M: 4.90, 0.539, 0.1, 0.551; 9.06, 0.983, −2.0, 1.02; 12.1, 1.31, −3.6, 1.37; 13.4, 1.51, 0.2, 1.59; 15.5, 1.73, −1.2, 1.83; 18.0, 2.06, 0.3, 2.20; 21.0, 2.36, −2.6, 2.53; 25.2, 2.86, −2.4, 3.11; 27.9, 3.24, −1.2, 3.54; 33.0, 3.87, −1.1, 4.31; 38.0, 4.58, −0.1, 5.15; 43.6, 5.26, −1.2, 6.01; 48.3, 5.83, −1.9, 6.76; 54.3, 6.60, −2.7, 7.76; 60.8, 7.88, 2.7, 9.45;

$C_L^\circ = 6.78 \times 10^{-4}$ M, $C_A^\circ = 3.20 \times 10^{-4}$ M, $C_M^\circ = 1.50 \times 10^{-2}$ M: 3.78, 0.423, 2.6, 0.433; 11.9, 1.30, −2.5, 1.36; 20.0, 2.25, −1.5, 2.42; 24.0, 2.89, 3.7, 3.14; 32.1, 3.74, −1.7, 4.15; 36.2, 4.30, −0.7, 4.83;

$C_L^\circ = 6.78 \times 10^{-4}$ M, $C_A^\circ = 6.40 \times 10^{-4}$ M, $C_M^\circ = 2.00 \times 10^{-2}$ M: 27.7, 3.08, −5.1, 3.37; 30.5, 3.59, −0.4, 3.96.

Fig. 2 shows the waves of three different solutions, recorded by a Radiometer P04 polarograph with a dropping mercury electrode (dropping time 2.7 s and flow rate 3.39 mg/s) against a saturated calomer electrode, S.C.E., as reference. The half-wave potential *vs.* S.C.E. in the medium used was found to be −0.72 V for free europium ions and −1.03 V for europium EDTA.

The polarograph was equipped with a fast recorder, type Servogor Re 511, in order to record concentration *vs.* time curves. The concentration of uncomplexed europium was followed at a constant voltage of −0.85 V.

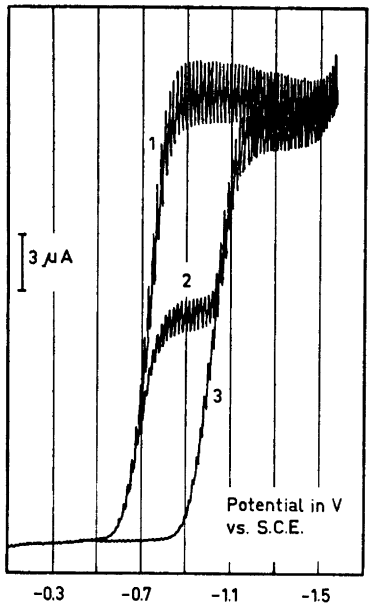

Fig. 2. Polarographic waves for (1) 5.89 mM Eu^{3+}; (2) 5.89 mM Eu^{3+} and 2.9 mM EDTA; and (3) 5.89 mM Eu^{3+} and ~10 mM EDTA. Medium: pH = 4, [NaAc] = 12.5 mM, 0.01 % gelatin, and I = 0.5 M (KCl).

3.00 ml of the thermostated solution S was injected by a syringe into 17.0 ml of solution T, which was thermostated in the reaction vessel. The solutions S and T had the following compositions:

$$\text{S:}\begin{cases} 6.67\ C_L^\circ\ EuCl_3 \\ 6.67\ C_A^\circ\ Na_2EDTA \\ I = 0.5\ M\ (KCl) \end{cases} \qquad \text{T:}\begin{cases} 1.18\ C_M^\circ\ YbCl_3 \\ 1.18 \times 12.5\ mM\ NaAc \\ \text{var. HAc} \\ 1.18 \times 0.01\ \%\ \text{gelatin} \\ I = 0.5\ M\ (KCl) \end{cases}$$

The mixing time was less than 3 s. Before mixing, dissolved oxygen was removed by bubbling nitrogen through the solutions. The reaction was followed during at least three half-lives.

It was not possible to vary the hydrogen ion concentration more than by a factor of 5. Precipitation of hydroxo complexes occurred at low hydrogen ion concentrations. In more acid solutions the reactions became too fast for this method, which is limited to reactions with half-lives longer than 15 s.[4]

From some experiments it was found that moderate changes in the gelatin concentration did not affect the observed rate constants. The data in Table 3 are averages of at least three independent measurements.

The erbium system. The erbium system was investigated with copper as the second metal, M. Two solutions, S and T, were mixed rapidly (mixing time less than 5 s) in a reaction vessel. Samples from this vessel were then taken at different time intervals and measured by a Zeiss PMQ II spectrophotometer, equipped with a Solatron digital voltmeter LM 142.02, from which the transmittance of the copper EDTA complex was read.

Because of the small total concentrations, it was necessary to perform the measurements in the UV region (wave length 280 – 300 nm), where the molar light absorptivity is high. Because of photochemical effects it was necessary to use this sampling technique (see Ref. 1).

Table 3. Rate data for the europium system. L = Eu and M = Yb.

$[H^+] \times 10^5$/M, $k_{obs} \times 10^2/s^{-1}$, $100(k_{obs} - k_{calc})/k_{calc}$, $f_{L,A,exp} \times 10^2/s^{-1}$;

$C_L^\circ = 4.56 \times 10^{-4}$ M, $C_A^\circ = 2.00 \times 10^{-4}$ M, $C_M^\circ = 5.02 \times 10^{-3}$ M: 1.88, 0.701, −6.3, 0.842; 3.59, 1.49, −6.2, 1.77; 5.30, 2.24, −12.9, 2.62; 7.01, 3.65, −1.4, 4.33;

$C_L^\circ = 2.94 \times 10^{-4}$ M, $C_A^\circ = 2.00 \times 10^{-4}$ M, $C_M^\circ = 7.47 \times 10^{-3}$ M: 2.74, 1.28, 3.9, 1.46; 5.73, 3.32, 6.9, 3.65; 7.81, 4.86, 5.1, 5.36;

$C_L^\circ = 2.94 \times 10^{-4}$ M, $C_A^\circ = 2.00 \times 10^{-4}$ M, $C_M^\circ = 1.01 \times 10^{-2}$ M: 2.38, 1.25, 12.6, 1.35; 3.08, 1.59, 6.6, 1.71; 3.38, 1.84, 11.0, 1.99; 4.36, 2.21, −1.8, 2.37; 4.99, 2.75, 3.5, 2.96; 5.37, 3.32, 13.8, 3.59; 5.83, 3.21, −0.6, 3.45; 6.51, 3.64, −2.0, 3.92; 7.24, 4.28, 0.5, 4.62; 8.59, 5.21, −2.4, 5.63;

$C_L^\circ = 2.94 \times 10^{-4}$M, $C_A^\circ = 1.02 \times 10^{-4}$ M, $C_M^\circ = 1.01 \times 10^{-2}$ M: 1.82, 0.801, −2.6, 0.858; 3.42, 1.52, −9.9, 1.62; 5.02, 2.61, −2.7, 2.80; 6.62, 3.80, 0.1, 4.09.

The solutions S and T had the following compositions:

S: $2\ C_L^\circ$ $ErCl_3$; $2\ C_A^\circ$ Na_2H_2EDTA; buffer; $I = 0.5$ M (KCl)

T: $2\ C_M^\circ$ $CuCl_2$; buffer; $I = 0.5$ M (KCl)

Equal volumes of the solutions S and T were mixed. The reactions were followed during approximately three half-lives. The data in Table 4 are averages of three independent measurements.

Table 4. Rate data for the erbium system. L = Er and M = Cu.

$[H]^+ \times 10^5$/M, $k_{obs} \times 10^3/s^{-1}$, $100(k_{obs} - k_{calc})/k_{calc}$, $f_{L,A,exp} \times 10^3/s^{-1}$;

$C_L^\circ = 2.00 \times 10^{-4}$ M, $C_A^\circ = 1.94 \times 10^{-4}$ M, $C_M^\circ = 4.99 \times 10^{-3}$ M: 1.21, 0.126, 4.5, 0.124; 1.67, 0.160, −7.2, 0.157; 2.45, 0.268, 1.1, 0.267; 3.16, 0.368, 3.0, 0.369; 4.68, 0.560, −3.0, 0.568; 6.17, 0.777, −5.5, 0.796; 7.67, 1.17, 6.9, 1.22; 9.22, 1.45, 2.5, 1.52; 10.7, 1.72, −0.9, 1.82; 12.2, 2.10, 0.6, 2.25; 14.0, 2.52, −1.5, 2.72; 15.1, 2.92, 2.1, 3.18; 16.4, 3.20, −0.8, 3.52; 18.0, 3.65, −1.9, 4.05;

$C_L^\circ = 3.19 \times 10^{-4}$ M, $C_A^\circ = 3.12 \times 10^{-4}$ M, $C_M^\circ = 4.99 \times 10^{-3}$ M: 5.44, 0.682, −3.2, 0.689; 6.51, 0.893, 0.7, 0.913; 9.55, 1.50, 1.0, 1.57;

$C_L^\circ = 7.02 \times 10^{-4}$ M, $C_A^\circ = 3.12 \times 10^{-4}$ M, $C_M^\circ = 4.99 \times 10^{-3}$ M: 2.03, 0.208, −4.6, 0.202; 6.12, 0.831, 2.7, 0.859; 10.2, 1.54, −3.9, 1.64; 14.3, 2.45, −5.1, 2.70; 18.5, 4.05, 7.5, 4.66;

$C_L^\circ = 2.00 \times 10^{-4}$ M, $C_A^\circ = 1.94 \times 10^{-4}$ M, $C_M^\circ = 7.48 \times 10^{-3}$ M: 3.38, 0.420, 9.0, 0.425; 7.04, 0.988, 1.6, 1.03; 8.22, 1.16, −3.3, 1.21; 11.4, 1.90, −0.1, 2.03; 13.2, 2.33, 0.1, 2.52; 16.6, 3.32, 0.9, 3.66;

$C_L^\circ = 2.00 \times 10^{-4}$ M, $C_A^\circ = 1.94 \times 10^{-4}$ M, $C_M^\circ = 9.97 \times 10^{-3}$ M: 2.80, 0.322, 4.8, 0.325; 4.00, 0.472, 0.1, 0.480.

CALCULATIONS AND RESULTS

The maximum errors in the observed rate constants were approximately ± 5 % except for the europium system, where they were around ± 8 %. The hydrogen ion concentration was determined with an error of about 1 %.

Table 5. Stability constants used in the calculations.

System	log β	Ref.	log K_{LAH}	Ref.
Pr	15.76	5	2.5	7
Nd	16.05	5	2.5	7
Eu	16.66	5	2.6	7
Er	18.37	5	2.8	7
Yb	18.99	5	2.7	7
Cu	18.68	6	3.0	6

All the k_{obs}-values were calculated from a simple first order equation (see Ref. 1). The stability constants for the lanthanoid EDTA complexes determined by Betts and Dahlinger [5] in 0.1 M potassium chloride were used in the calculations. The stability constant for the copper EDTA complex determined by Schwarzenbach *et al.*[6] was adjusted to 25°C by means of the enthalpy value given by Case and Stavely.[8] The constants for formation of the acid complexes were those of Kolat and Powell [7] for the lanthanoids, and of Schwarzenbach *et al.*[6] for copper. The constants valid in 0.1 M medium have been shown to be good approximations for the values in the 0.5 M medium used.[1] The constants used are given in Table 5.

The observed rate constant, k_{obs}, for the exchange reaction is related to the dissociation rate constants f_{LA} and f_{MA} of the complexes LA and MA according to eqn. (1):

$$k_{obs} = \left(\frac{f_{LA}}{1 + (f_{LA}/f_{MA})\delta_1} + f_D \frac{C_M}{\alpha_M} \right) \delta_2 \quad (1)$$

All notations are defined in Ref. 1.

Copper was used as the second metal, M, in the praseodymium, neodymium, and erbium systems. The dissociation rate constant for the copper EDTA complex f_{MA} is [1]

$$f_{CuA} = [(9.0 \pm 5.1)10^{-5} + (6.5 \pm 1.0)[H^+] + (3.5 \pm 0.3)[H^+]^2/s^{-1}$$

In the europium system, ytterbium was used as the second metal, M. The rate constant for the dissociation of the ytterbium EDTA complex f_{MA} is [1]

$$f_{YbA} = [(0.76 \pm 0.08)[H^+] + (1.43 \pm 0.07)10^4[H^+]^2/s^{-1}$$

The parameters in the expression for the rate constant f in the above systems were computed by a data program written by Ekström and Ryhl.[9] Eqn. (2) described the results from all four systems:

$$f = \bar{k}_0 + \bar{k}_1[H^+] + \bar{k}_2[H^+]^2 \quad (2)$$

Here each $\bar{k}_i$ is a product of the true rate constant and the corresponding equilibrium constant for the association of protons to the lanthanoid EDTA

Table 6. The obtained rate constants of dissociation of lanthanoid EDTA complexes together with the values of other authors. The constants $\bar{k}_{01}$, $\bar{k}_1$, and $\bar{k}_2$ contain the equilibrium constants for the corresponding complexes. The errors given are the confidence limits on the 99 % level.

Ln	k_0/s^{-1}	$\bar{k}_1/s^{-1}\,M^{-1}$	$\bar{k}_2/s^{-1}\,M^{-2}$	t°C	Ref.
La	$(2.0 \pm 1.0)10^{-2}$	$(3.7 \pm 0.3)10^3$	$(1.9 \pm 0.7)10^6$	25	1
	–	7.0×10^3	–	25	22
Ce	–	1.6×10^3	–	20	14
	–	1.8×10^3	–	20	17
	–	3.5×10^3	–	25	23
Pr	$(9.0 \pm 7.5)10^{-3}$	$(1.6 \pm 0.1)10^3$	$(1.0 \pm 0.4)10^6$	25	This work
	–	1.7×10^3	–	25	23
Nd	–	$(1.09 \pm 0.04)10^3$	$(7.0 \pm 1.5)10^5$	25	This work
		6.6×10^2	–	20	17
		1.08×10^3	–	25	22
Eu	–	$(4.3 \pm 0.7)10^2$	$(2.8 \pm 1.5)10^6$	25	This work
		6.0×10^2	–	22	10
Gd	–	87	6.0×10^6	20	17
Tb	–	31	9.5×10^6	20	17
Dy	–	12.3	5.8×10^5	25	22
Ho	–	12.8	–	24	24
Er	–	8.9 ± 0.5	$7.7 \pm 0.7)10^4$	25	This work
Yb	–	0.76 ± 0.08	$(1.43 \pm 0.07)10^4$	25	1
	–	0.70	2.3×10^4	25	22
Lu	–	0.52	5.4×10^3	20	17
	–	0.23	–	25	13
La	$\bar{k}_{01} = (2.0 \pm 0.4)10^8$ $s^{-1}\,M^{-1}$			45	2

complex. f_D, *i.e.* the rate constant for direct substitution, path II, was found to be zero for all these systems. The results are given in Table 6.

DISCUSSION

The following discussion of the dissociation of the lanthanoid EDTA complexes is based on the results from this and two previous papers.[1,2]

The rate law of exchange reactions. The rate law for the gross reaction

$$LA + M \rightleftharpoons L + MA \qquad (3)$$

can be described fairly well by the proposed model.[1] The gross reaction is considered to consist of two parallel sets of reactions, *viz.* (i) path I, a primary dissociation of the complex LA, followed by an association of the ligand A to the metal ion M, and (ii) path II, a direct substitution between M and the complex LA to give the products L and MA.

The expression for the observed rate constant [1] can be rearranged in two different ways:

(i) If the dissociation of LA is rate determining, which is the case for $f_{LA}C_L/\alpha_L \ll (f_{MA}\beta_M/\beta_L)C_M/\alpha_M$

$$k_{obs} = \left(\frac{f_{LA}}{(1 + (f_{LA}/f_{MA})\delta_1} + f_D \frac{C_M}{\alpha_M} \right) \delta_2 \quad (4)$$

$$\delta_1 = \frac{\beta_L C_L \alpha_M}{\beta_M C_M \alpha_L}$$

$$\delta_2 = \frac{1}{\alpha_{LA}} \left(1 + \frac{C_{LA}}{C_M} + \frac{\beta_L}{\beta_M} \cdot \frac{C_L + C_{MA}}{C_M} \cdot \frac{\alpha_M \alpha_{LA}}{\alpha_L \alpha_{MA}} \right)$$

In this case, f_{LA} can be determined from eqn. (4).

(ii) If the association of A to M is rate determining, which is the case for $f_{LA} C_L/\alpha_L \gg (f_M \beta_M/\beta_L) C_M/\alpha_M$

$$k_{obs} = \left(\frac{f_{MA}}{(1 + (f_{MA}/f_{LA})\delta_1'} + \frac{\beta_L}{\beta_M} f_D \frac{C_L}{\alpha_L} \right) \delta_2'$$

$$\delta_1' = \frac{\beta_M C_M \alpha_L}{\beta_L C_L \alpha_M}$$

$$\delta_2' = \frac{1}{\alpha_{MA}} \left(1 + \frac{C_{MA}}{C_L} + \frac{\beta_M}{\beta_L} \cdot \frac{C_M + C_{LA}}{C_L} \cdot \frac{\alpha_L \alpha_{MA}}{\alpha_M \alpha_{LA}} \right)$$

Here the dissociation rate of the MA complexes, f_{MA}, can be determined from eqn. (5).

If f_{LA} and f_{MA} β_M/β_L are of the same order of magnitude, either f_{LA} or f_{MA} can be determined from reaction (3), depending on the relative values of C_M/α_M and C_L/α_L.

D'Olieslager and Choppin [10] have used a large excess of both lanthanum ions and lanthanum EDTA complex over europium ions in the reaction

$$\text{LaEDTA} + \text{Eu} \rightleftharpoons \text{La} + \text{EuEDTA}$$

which obeys the experimental rate law

$$-\frac{\text{d[Eu]}}{\text{d}t} = k \frac{[\text{H}^+][\text{LaEDTA}]}{[\text{La}]} [\text{Eu}]$$

This is just a special case of the rate law discussed earlier. By dividing their rate constant by the quotient β_{Eu}/β_{La}, almost the same value of the dissociation rate constant of the europium complex is obtained as in the present paper (Table 6).

The rate law has also been checked by the following two experiments: (i) By using large concentrations of both lanthanum ions and lanthanum EDTA complex together with a small concentration of copper ions; and (ii) by using a large excess of ytterbium ions over both copper ions and the copper complex. The rate constants of the dissociation of the copper EDTA complex obtained from the two experiments were in agreement.[1]

The mechanism of dissociation. The dissociation of EDTA from the lanthanoid EDTA complexes is catalyzed both by hydrogen ions and hydroxide ions.[2] The hydrogen ion catalysis proceeds through two parallel path-ways,

viz. via complexes, containing a monoprotonated and a diprotonated ligand, whereas the path catalysed by hydroxide ions proceeds through the hydroxo complex.

$$\mathrm{Ln(OH)EDTA} \xrightarrow{k_{01}} \mathrm{Ln(OH)} + \mathrm{EDTA}$$

$$\mathrm{LnEDTA} \xrightarrow{k_0} \mathrm{Ln} + \mathrm{EDTA}$$

$$\mathrm{Ln(EDTA)H} \xrightarrow{k_1} \mathrm{Ln} + \mathrm{H(EDTA)}$$

$$\mathrm{Ln(EDTA)H_2} \xrightarrow{k_2} \mathrm{Ln} + \mathrm{H_2(EDTA)}$$

The acid and hydroxo complexes are all in rapid equilibria with each other (see below).

According to Lind *et al.*[11] the proton in La(EDTA)H is bound to one of the four non-coordinating carboxylate oxygens. The configuration of the complex makes it impossible for any of the nitrogen atoms to bind a proton. Presumably, this is also the case for the second proton in the diprotonated complex, where both the protons are then bound to carboxylate groups.

The PMR spectra [2] show that the metal-oxygen bonds have short lifetimes both in the rapidly dissociating lanthanum complex and in the much more slowly dissociating lutetium complex. The metal-nitrogen bond has a long lifetime in the lutetium complex, but is labile in the lanthanum complex. Hence, the rate-determining factor of the dissociation seems to be the cleavage of the metal-nitrogen bond. The same conclusion has been drawn by Margerum [12] from exchange reactions of copper and nickel with EDTA and with hydroxyethylethylenediaminetriacetate.

The formation of a protonated complex in solution presumably proceeds *via* the primary association of a proton to the non-coordinated oxygen atom of a carboxylate oxygen, which is probably a very rapid process, followed by a cleavage of the coordinative bond between the metal and the other oxygen atom in the same carboxylate group.

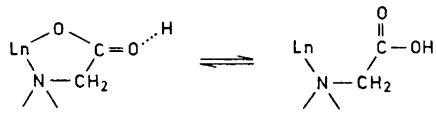

Since the PMR data may be interpreted in support of the view that the cleavage of the metal-nitrogen bond is the rate-determining step of the dissociation, the cleavage of the metal-oxygen bond described above must also be a fast part of the multistep dissociation. One reason for the slower cleavage of the metal-nitrogen bond might be that the nitrogen atom in EDTA is not available for proton attack of the type possible on a carboxylate group, because of its second oxygen atom.

On the other hand, the metal-nitrogen bond is also labilized when the ligand becomes protonated, which is of course the reason why hydrogen ions act as catalyst for the dissociation.

Some authors [10,13,14] have proposed a mechanism in which the association of protons to the complex is a slow process followed by a rapid dissociation of the ligand. This mechanism does not seem to be very probable for reasons given above.

In the hydroxo complex, formed by dispelling one proton from one of the coordinated water molecules, the hydroxide ion is bound directly to the lanthanoid ion. The effective charge of the metal ion is thus reduced which would lead to a labilization of the coordinative bonds. In accordance with this, the rate constant [2] for the path catalysed by hydroxide ions is several orders of magnitude greater than that for the reaction catalysed by hydrogen ions *via* the monoprotonated species.

By substitution of water molecules in the lanthanoid EDTA complex, it is possible to coordinate a second ligand, thus forming a mixed complex. Acetate ions accelerate the dissociation of the EDTA complex to a small extent.[1,14] Brucher and Szilagyi [15] found from exchange reactions with copper that glycolate ions increase the dissociation rate of the terbium EDTA complex to a considerable extent. The affinity of acetate ions for lanthanoid ions is much greater than that of glycolate ions. The concentration of the mixed acetate complex is much smaller than that of the mixed glycolate complex at similar concentrations of acetate and glycolate. Both these ligands are presumably bound directly to the metal ion in the mixed lanthanoid complexes. Their ability to increase the dissociation rates may then be due to a labilization of the metal-nitrogen bonds in the EDTA complex, *i.e.* an effect similar to, but weaker than that of the hydroxide ion.

Variations of the dissociation rates with the ionic radii of the lanthanoid ions. In Table 6, the rate constants from this investigation have been collected together with the values from other authors. The constants given for the pathways catalysed by hydrogen ions and hydroxide ions are products of the constant $K_{\mathrm{LnAH_n}}{}^{1}$ and $K_{\mathrm{LnA(OH)}}{}^{2}$ for the corresponding complex and the true rate constant. Kolat and Powell have reported such constants for almost all the monoprotonated lanthanoid complexes. The logarithm of these constants have values between 2.5 and 2.8. Some tentative values of the stepwise constants $K_{\mathrm{LnAH_2}}/K_{\mathrm{LnAH}}$ for the diprotonated complexes have been reported by Brucher and Szarvas [16,17] to be in the range $(0.1-0.2)$ $\mathrm{M^{-1}}$. It is likely that the constants $K_{\mathrm{LnAH_2}}$ for the diprotonated complexes do not change more than those for the monoprotonated complexes along the lanthanoid series. The constant, $K_{\mathrm{LaA(OH)}}$, for the hydroxo EDTA complex of lanthanum is estimated to be less than 1000 $\mathrm{M^{-1}}$.[18] Because of the lack of accurate values of these constants, no calculations of the true rate constants have been done.

In Fig. 3, $\log \bar{k}_1$ and $\log \bar{k}_2$ have been plotted *vs.* the inverse ionic radius of the lanthanoid ions. In this graph the rate constants valid at 20 or 24°C have been adjusted to 25°C by means of a value of the activation energy, 12 kcal/mol, for the protonated cerium complex, determined by Glentworth *et al.*[14]

Both curves show an irregularity, *viz.* for $\bar{k}_1$ in the region dysprosium to

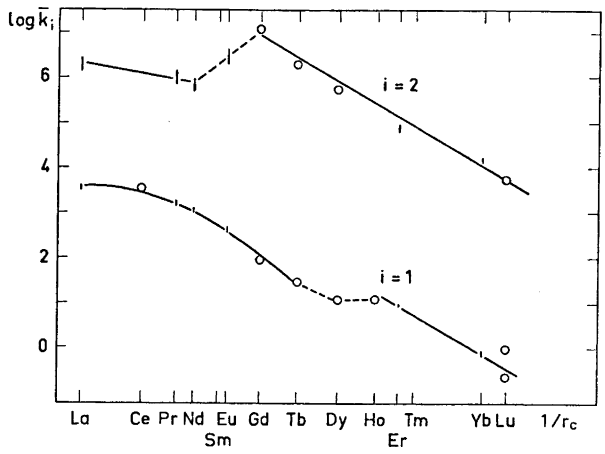

Fig. 3. The logarithm of the dissociation rate constants for the paths with first and second order dependence of the hydrogen ion concentration, as a function of the inverse ionic radius of the lanthanoid ions.

erbium and for $\bar{k}_2$ between neodymium and gadolinium. Geier and Karlen [19] found a corresponding behaviour of the rate constant for the nonprotonated complexes reacting with oxyquinoline-5-sulfonate in the region of samarium to terbium. They have also carried out some spectrophotometric measurements on europium EDTA complexes at varying temperatures.[20] They claim that the temperature dependence of the spectra is due to the existence of two kinds of complexes, *viz.* $Ln(EDTA)(H_2O)_3^-$ and $Ln(EDTA)(H_2O)_2^-$, which are in equilibrium with each other. The one with three water molecules predominates in the beginning of the series, whereas the dihydrated complex is favoured at the end of the series. Ots [21] has found clear evidence for this reaction from calorimetric measurements of the enthalpy of formation of the lanthanoid EDTA complexes at different temperatures. Lind *et al.*[11] have found four water molecules coordinating to the lanthanum ion in the solid $LaH(EDTA)(H_2O)_4$.

On the grounds given above, one may conclude that the two regions with monotonous changes of the rate constants in each of the two curves correspond to complexes with different numbers of coordinated water molecules. Thus, the monoprotonated complexes might have four coordinated water molecules in the beginning of the series and three water molecules at the end.

Acknowledgements. I express my sincere gratitude to Professor Ido Leden, Docent Ingmar Grenthe and Fil. lic. Carl-Gustav Ekström for many invaluable discussions and suggestions. My thanks are also due to Fil. mag. Ingegerd Lind for skilful help with the measurements and to Dr. R. E. Carter for linguistic criticism. The *Swedish Natural Science Research Council* has provided financial support for the stopped-flow measurements.

REFERENCES

1. Ryhl, T. *Acta Chem. Scand.* **26** (1972) 3955.
2. Ryhl, T. *Acta Chem. Scand.* **26** (1972) 4001.
3. Kolthoff, I. M. and Lingane, J. J. *Polarography*, Interscience, New York 1952, Vol. 2, pp. 438–441.
4. Heyrovsky, J. and Kuta, J. *Principles of Polarography*, Academic, New York 1966, pp. 281–282.
5. Betts, R. H. and Dahlinger, O. F. *Can. J. Chem.* **37** (1959) 91.
6. Schwarzenbach, G., Gut, R. and Anderegg, G. *Helv. Chim. Acta* **37** (1957) 937.
7. Kolat, R. S. and Powell, J. E. *Inorg. Chem.* **1** (1962) 485.
8. Case, R. A. and Stavely, L. A. K. *J. Chem. Soc.* **1956** 4571.
9. Ryhl, T. *Studies on Dissociation Rates of Some Lanthanoid EDTA Complexes*, Diss., University, Lund 1971.
10. D'Olieslager, W. and Choppin, G. R. *J. Inorg. Nucl. Chem.* **33** (1971) 127.
11. Lind, M. D., Byunkook, L. and Hoard, J. L. *J. Am. Chem. Soc.* **87** (1965) 1611.
12. Margerum, D. W. *Rec. Chem. Progr.* **24** (1963) 237.
13. Aasano, T., Okada, S., Sakanoto, K., Taniguchi, S. and Kobayashi, Y. *Radioisotopes* **14** (1965) 363; *J. Inorg. Nucl. Chem.* **31** (1969) 2127.
14. Glentworth, P., Wiseall, B., Wright, C. L. and Mahmood, A. J. *J. Inorg. Nucl. Chem.* **30** (1968) 967.
15. Brucher, E. and Szilagyi, M. *Proc. 3rd Symposium Coord. Chem.* Hungary 1970, Vol. 1, p. 323.
16. Brucher, E. and Szarvas, P. *Acta Chim. Acad. Sci. Hung.* **50** (1966) 279.
17. Brucher, E. and Szarvas, P. *Inorg. Chim. Acta* **4** (1970) 632.
18. Merbach, A. and Gnägi, F. *Chimia* **23** (1969) 271.
19. Geier, G. and Karlen, U. *Proc. XIII Intern. Conf. Coord. Chem.*, Crakow-Zakopane 1970, p. 45.
20. Geier, G. and Karlen, U. *Helv. Chim. Acta* **52** (1969) 1967.
21. Ots, H. *Acta Chem. Scand. In press.*
22. Betts, R. H., Dahlinger, O. F. and Munro, D. M. *Radioisotopes in Scientific Research*, Pergamon, New York 1958, Vol. 2, p. 326.
23. Shiokawa, T. and Omori, T. *Bull. Chem. Soc. Japan* **38** (1965) 1892.
24. Makashev, Yu. A., Makasheva, I. E. and Mel'nikov, V. A. *Radiokhimiya* **8** (1966) 371.

Received July 11, 1972.

ACTA CHEMICA SCANDINAVICA 27 (1973) 315–318

Ring Strain in Diiodocyclobutane

STIG SUNNER and CLAUS A. WULFF*

Thermochemistry Laboratory, Chemical Center, University of Lund, S-220 07 Lund 7, Sweden

Bicyclobutane, free of cyclobutene, reacts quantitatively with iodine in a sealed vessel at temperatures between 78 and 100°C. The thermochemistry of this reaction has been studied to provide enthalpies of formation of diiodocyclobutane; $\Delta H_f^\circ = 32._2 \pm 1.5$ and $46._2 \pm 2$ kcal/mol for diiodocyclobutane liquid and gas, respectively. The "strain energy" in the four-carbon ring has been estimated as 32 kcal/mol.

The preparation of small polycyclic molecules in recent years presents an interesting opportunity to obtain thermochemical data for substituted cycloalkanes. In particular, the highly reactive bridgehead bond in bicyclobutane (hereafter BCB) allows the facile addition of I_2 to form 1,3-diiodocyclobutane (hereafter CBI_2). Wiberg *et al.*[1,2] have shown that the reaction gives a single product, albeit a mixture of *cis*- and *trans*-isomers. The thermochemical literature [3,4] indicates that data for CBI_2 would be the first data for an alicyclic diiodide. The addition, the question of iodine-iodine interaction induced excess strain in cyclobutane, seemed to be an interesting problem to attack. The development of a reliable closed-bomb reaction calorimeter [5] permits the handling of a normally volatile material at elevated temperatures. Reported below are enthalpies of reaction for the process $BCB + I_2 = CBI_2$ in CCl_4 solutions.

EXPERIMENTAL

BCB was prepared [1,6] from 3-chlorocyclobutanecarboxylic acid, which, in turn, had been prepared [7] from 1,1-cyclobutanedicarboxylic acid (Aldrich). The initial BCB, admixed with cyclobutane and cyclobutene, was collected in hexane cooled in a dry-ice acetone bath. The BCB was separated from its impurities and the solvent by GLC on a dinonyl phthalate column in a Perkin Elmer F21 preparative scale GLC. The volatile BCB was collected in a Teflon valved glass cylinder maintained in a dry-ice acetone bath. The cylinder was connected to the GLC outlet by a condenser which had chilled acetone circulating through its jacket. Although the purification process provided clean BCB

* Present address: Department of Chemistry, University of Vermont, Burlington, Vt. 05401, U.S.A.

Table 1. The enthalpy of reaction of BCB with I_2.

Temperature, °C	Sample	g I_2[a]	ΔH(kcal/mol)
78	I	0.021301	−14.07
78	I	0.024410	−14.36
99	I	0.021743	−13.91
99	II	0.004943	−13.85
99	II	0.011083	−14.09

[a] Corrected to vacuum.

(as judged by GLC), the total yield was extremely small, *ca.* 0.3 % based on the original diacid. A comparison of results obtained with this material with those obtained for a sample containing some 5 % impurities indicates that for many thermochemical processes the impure material would be satisfactory. (This is particularly true for "strain energy" evaluations, which are themselves an ambiguous quantity.)

The calorimetry was performed in a sealed rotating-bomb reaction calorimeter [5] thermostated in a Hallikainen bath containing silicon oil. Preliminary experiments at 25° and 50°C were unsatisfactory because the reaction proceeded too slowly. At 78°C the reaction went to completion in 30 – 40 min, and at 99°C the reaction was complete in less than 30 min. Completeness of reaction was judged by the absence of the pink color of I_2 (the limiting reagent) in the CCl_4 solution.

Experiments were performed by breaking an ampoule of I_2 crystals (Mallinckrodt, resublimed) into an excess of BCB dissolved in freshly distilled CCl_4. The raw data were corrected for heat effects engendered by the vaporization of the solvent mixture and for the condensation of I_2 vapor in the partially filled ampoules. The corrections were based on results obtained with empty ampoules and literature values for the vapor pressure and enthalpy of sublimation of I_2.[8] Corrected results, based on the thermochemical calorie defined as 1 cal = 4.1840 joules, appear in Table 1 where the samples designations refer to BCB that does (I) or does not (II) contain the cyclobutane and cyclobutene impurities.

DISCUSSION

To obtain a value for the enthalpy of formation of CBI_2 the following scheme was considered

$BCB(g) = BCB(liq)$	ΔH_1°
$BCB(liq) = BCB(soln\ in\ CCl_4)$	ΔH_2°
$BCB(soln\ in\ CCl_4) + I_2(c) = CBI_2(soln\ in\ CCl_4)$	ΔH_3°
$CBI_2(soln\ in\ CCl_4) = CBI_2(liq)$	ΔH_4°
$CBI_2(liq) = CBI_2(g)$	ΔH_5°
$BCB(g) + I_2(c) = CBI_2(g)$	$\Delta H^\circ = \Delta H_f^\circ(CBI_2) - \Delta H_f^\circ(BCB)$

Wiberg *et al.*[1] have determined the vapor pressure of BCB between −21° and +8°C. From the temperature dependence of the vapor pressure they report $\Delta H_1^\circ = -6041$ cal/mol over the temperature range of their experiments. Selecting $\Delta C_p^\circ = 12$ cal/(mol K) for the condensation process, by comparison for data with other simple hydrocarbons,[4] we estimate $\Delta H_1^\circ = -5.6$ kcal/mol at 298 K. Enthalpies of solution (or mixing) for non-polar systems tend to

be small and we have estimated $\Delta H_2^\circ + \Delta H_4^\circ = 0 \pm 0.5$ kcal at 298 K. Our data for ΔH_3° do not permit a reliable estimate for ΔC_p. The quantity is likely to be small, since the reaction does not involve vapors or polar substances, and, accordingly, we choose $\Delta H_3^\circ = -14.1 \pm 1.0$ kcal at 298 K. Enthalpy of vaporization differences between bromo and iodo compounds and an estimate of the enthalpy of vaporization of dibromocyclobutane based on its boiling point [9] and Wadsö's correlations [10] lead to an estimated $\Delta H_5^\circ = 14.0 \pm 1.0$ kcal at 298 K. The same estimate can be obtained by adding the enthalpy of vaporization difference for diiodobenzene-benzene to the enthalpy of vaporization of cyclobutane.[3] Summing ΔH_1° to ΔH_5° we obtain $\Delta H^\circ = -5._7 \pm 2$ kcal/mol for $BCB(g) + I_2(c) = CBI_2(g)$.

The enthalpy of formation of BCB has been determined as $\Delta H_f^\circ = 51.9$ kcal/mol [11] leading to $\Delta H_f^\circ = 46._2 \pm 2$ and $32._2 \pm 1.5$ kcal/mol for CBI_2 in the vapor and liquid phases, respectively.

The evaluation of "strain energy" is, at best, an ambiguous process.[12] Application of a group contribution scheme [3] leads to a predicted enthalpy of formation of 11.8 kcal/mol $CBI_2(g)$. Comparison of this value with our experimental quantity indicates a difference, or "strain energy", of 32 kcal/mol, some 6 kcal/mol greater than that of the parent cyclobutane as derived by the same set of group parameters. The application of group parameters to an alicyclic diiodide has the disadvantage that the group parameter values are derived almost exclusively from data for non-cyclic compounds. A second, probably better, estimate can be derived from the ΔH for the reaction

$$\text{cyclobutane} + \text{"diiodocyclohexane"} = \text{cyclohexane} + CBI_2$$

where "diiodocyclohexane" represents a moiety free of iodine-iodine interactions. The enthalpy of formation of this species can be estimated as $\{2\Delta H_f^\circ(\text{iodocyclohexane}) - \Delta H_f^\circ(\text{cyclohexane})\} = 5.1$ kcal/mol from tabulated data.[3] This hypothetical reaction leads to a "strain energy" estimate of 5 kcal/mol more for CBI_2 than for cyclobutane.

It appears that the four carbon ring in CBI_2 is somewhat more "strained" than it is in cyclobutane. While it is tempting to ascribe the increased strain to an opening of the dihedral angle as a response to iodine-iodine repulsion, there is no supporting evidence. The inter-planar angles in 1,3-dibromo- and 1,3-chlorobromo-cyclobutanes have been reported as $147 \pm 2°$.[13] While this represents a slight opening from the $143 - 146°$ reported for cyclobutane,[14,15] the uncertainties are too large to provide definitive conclusions regarding angle-substitution relationships. Structural information on CBI_2 would be desirable.

Acknowledgements. The authors are grateful in acknowledging the financial support provided by the *Swedish Natural Science Research Council*, and by the *American-Scandinavian Foundation* for their award of a fellowship to C.A.W.

REFERENCES

1. Wiberg, K. B., Lampman, G. M., Ciula, R. P., Connor, D. S., Schertler, P. and Lavanish, J. *Tetrahedron* **21** (1965) 2749.
2. Wiberg, K. B. and Lampman, G. M. *J. Am. Chem. Soc.* **88** (1966) 4429.
3. Cox, J. D. and Pilcher, G. *Thermochemistry of Organic and Organometallic Compounds*, Academic, London 1970.

4. Stull, D. R., Westrum, Jr., E. F. and Sinke, G. C. *The Chemical Thermodynamics of Organic Compounds*, Wiley, New York 1969.
5. Ölofsson, G., Sunner, S., Efimov, M. and Laynez, J. *J. Chem. Thermodynamics. In press.*
6. Lampman, G. M. and Aumiller, J. C. *Org. Syn.* **51** (1971) 55 ff.
7. Nevill, W. A., Frank, D. S. and Trepka, R. D. *J. Org. Chem.* **27** (1962) 422.
8. *JANAF Thermochemical Tables*, Ed. by D. R. Stull, CFSTI, U.S. Dept. of Commerce, Springfield 1965.
9. Abell, P. I. and Chiao, C. *J. Am. Chem. Soc.* **82** (1960) 3610.
10. Wadsö, I. *Acta Chem. Scand.* **22** (1968) 2438.
11. Wiberg, K. B. and Fenoglio, R. A. *J. Am. Chem. Soc.* **90** (1968) 3395.
12. Nelander, B. and Sunner, S. *J. Chem. Phys.* **44** (1966) 2476.
13. Almenningen, A., Bastiansen, O. and Walløe, L. In *Selected Topics in Structure Chemistry*, Universitetsforlaget, Oslo 1967, p. 91; *Chem. Abstr.* **69** (1968) 10046.
14. Dows, D. and Rich, N. *J. Chem. Phys.* **47** (1967) 333.
15. Ueda, T. and Shimanouchi, T. *J. Chem. Phys.* **49** (1968) 470.

Received August 2, 1972.

ACTA CHEMICA SCANDINAVICA 27 (1973) 319–328

Viscosities of Some Binary Mixtures between $MgCl_2$, $CaCl_2$ and AlkCl

D. DUMAS,* B. FJELD, K. GRJOTHEIM and H. A. ØYE

Institutt for uorganisk kjemi, Norges tekniske høgskole, Universitetet i Trondheim, N-7034 Trondheim-NTH, Norway

The viscosity, η, of the following binary molten mixtures has been determined mainly in the temperature range 750° to 850°C by the method of an oscillating sphere: $CaCl_2-NaCl$, $CaCl_2-KCl$, $MgCl_2-CaCl_2$, $MgCl_2-LiCl$, $MgCl_2-NaCl$, $MgCl_2-KCl$, $MgCl_2-RbCl$, and $MgCl_2-CsCl$. Values for the excess Gibbs energy of activation for viscous flow have been calculated according to the equation

$$\Delta G^{E\neq} = RT[\ln \eta - (X_1 \ln \eta_1 + X_2 \ln \eta_2)]$$

The results have been interpreted in terms of bond strength, complex formation, and ionization of the partially covalent $MgCl_2$ liquid lattice. The relevance of the present investigation to the industrial electrowinning of magnesium is discussed.

Experimental determination of the viscosities of binary mixtures between $MgCl_2$, $CaCl_2$, and alkali chlorides were undertaken. This was part of a general study of physico-chemical properties of molten salt systems of interest in magnesium electrolysis. These systems are also of interest in developing a better understanding of the behaviour of ionic mixtures.

The viscosities of the salt mixtures studied are in the range 0.01 – 0.03 poise. In our opinion, the best method for measuring viscosities of these very hygroscopic melts is the torsional pendulum method. The theory and utilization of this method is described in detail by Dumas *et al.*[1]

EXPERIMENTAL

Apparatus. The apparatus was that described by Dumas *et al.*[1] Further trials with thinner torsional wires were conducted in order to increase the period of the pendulum swing, but proved unsuccessful since poor stability resulted even with careful pretreating in a hydrogen atmosphere.[2]

* Present address: Societé des Électrodes et Refractoires Savoie, Savoie, 10, Rue de l'Industrie, (69) Veissieux, France.

Chemicals. The following chemicals were used: *p.a.* NaCl, KCl, RbCl, CsCl, and $MgCl_2$, from Merck, Darmstadt (Germany), and *p.a.* LiCl and $CaCl_2$, from Baker (USA).

The NaCl, KCl, RbCl, and CsCl were dried under vacuum for 12 h, melted under a nitrogen atmosphere and cooled slowly. Only clear crystals were picked out and used for the experiments. Anhydrous $MgCl_2$, $CaCl_2$, and LiCl were treated with HCl gas, melted and filtered.[3]

Procedure. The salt crystals were mixed mechanically in a dry-box. The crystals were then placed in a pyrex container fitted with a valve which allowed the transfer of salt to the viscosity crucible without exposure to air (see Fig. 4 in Ref. 1). This transfer mechanism was also used for adding LiCl, NaCl, and KCl to the first prepared melts in order to change the composition. However, this procedure was found to be unsatisfactory for RbCl and CsCl. When using this procedure, neither salt mixed properly with the firstly prepared melts. This was probably due to the high density of RbCl and CsCl. To obtain proper mixing, therefore, the mixtures were premelted in a quartz ampule obtaining mixing by convective flow caused by uneven heating. For each temperature at least three separate experiments were run to determine the damping of the pendulum. This was done to detect possible erroneous results in the delicate manual apparatus.

Calculation of the viscosity. The method of calculating the viscosity from the measurements was essentially the same as used before.[1]

The amplitude values of both sides were read from a scale for every second period. However, in the present investigation a computer program was used to smooth the amplitude values as a function of the oscillation number. The computer program took into account that each set of opposite readings differed by half a period and discarded automatically all amplitudes which deviated by more than 0.1 cm (about 0.5 % of the maximum amplitude). The typical number of discarded readings were between 1 and 5 out of about 40. The smoothing procedure also gave the arbitrary equilibrium position. This was different for each experiment.

The amplitudes remaining from the smoothing procedure were used to calculate the damping, δ, according to the procedure used by Dumas *et al.*[1]

RESULTS

Control experiments were performed with H_2O, KNO_3 and KCl. The results are given in Table 1. These values deviate less than 0.7 % from the literature values.[1,4,5] The viscosities for the binary mixtures as functions of temperature and composition are given in Figs. 1 – 8. If measurements at 800°C were not performed the curves in Figs. 1 – 8 were extrapolated to this temperature. A comparison between the results at 800°C are given in Figs. 9 and 10.

The platinum sphere of the pendulum had to be remachined after use in LiCl-melts. At the same time minor rearrangements in the apparatus were made.

Table 1. Observed viscosities compared with literature values for H_2O,[9] KNO_3,[10] and KCl.[6]

Compound	Temp. °C	Viscosity, cP	
		This work	Lit. values
H_2O	14.7	1.151	1.152
	17.7	1.078	1.073
	19.6	1.026	1.022
KNO_3	362.0	2.352	2.342
	374.8	2.477	2.487
	397.0	2.106	2.092
KCl	819.7	0.930	0.935

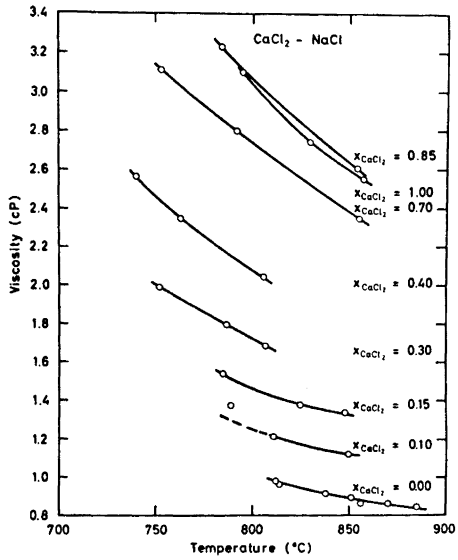
CaCl2 - NaCl
Viscosity (cP)
Temperature (°C)
xCaCl2 = 0.85
xCaCl2 = 1.00
xCaCl2 = 0.70
xCaCl2 = 0.40
xCaCl2 = 0.30
xCaCl2 = 0.15
xCaCl2 = 0.10
xCaCl2 = 0.00

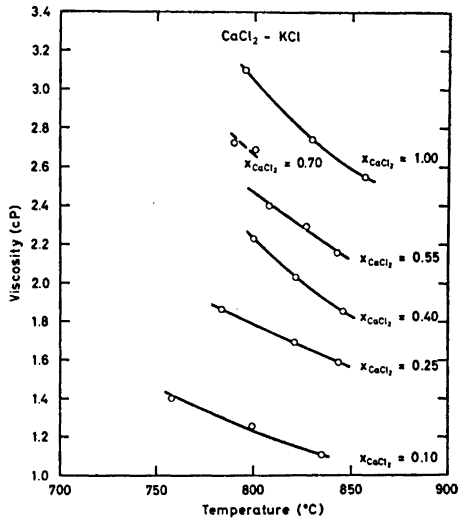
CaCl2 - KCl
Viscosity (cP)
Temperature (°C)
xCaCl2 = 0.70
xCaCl2 = 1.00
xCaCl2 = 0.55
xCaCl2 = 0.40
xCaCl2 = 0.25
xCaCl2 = 0.10

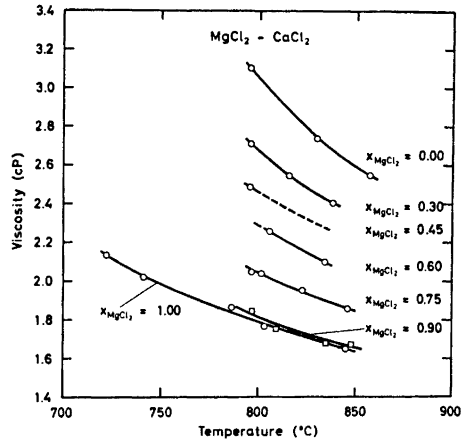
MgCl2 - CaCl2
Viscosity (cP)
Temperature (°C)
xMgCl2 = 0.00
xMgCl2 = 0.30
xMgCl2 = 0.45
xMgCl2 = 0.60
xMgCl2 = 0.75
xMgCl2 = 0.90
xMgCl2 = 1.00

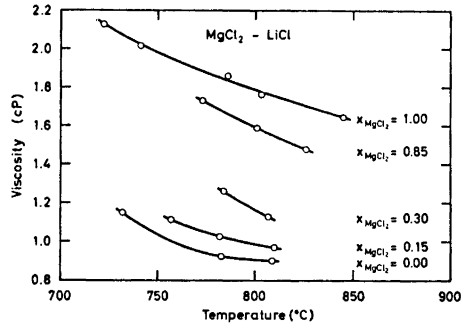
MgCl2 - LiCl
Viscosity (cP)
Temperature (°C)
xMgCl2 = 1.00
xMgCl2 = 0.85
xMgCl2 = 0.30
xMgCl2 = 0.15
xMgCl2 = 0.00

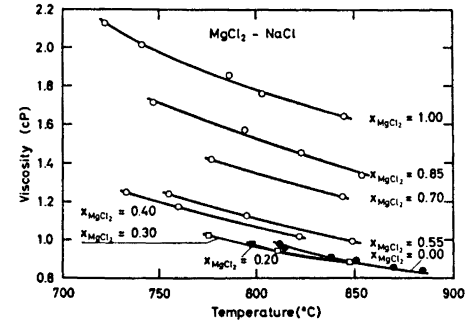
MgCl2 - NaCl
Viscosity (cP)
Temperature (°C)
xMgCl2 = 1.00
xMgCl2 = 0.85
xMgCl2 = 0.70
xMgCl2 = 0.40
xMgCl2 = 0.30
xMgCl2 = 0.55
xMgCl2 = 0.00
xMgCl2 = 0.20

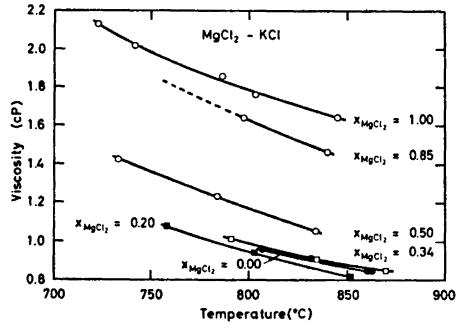
MgCl2 - KCl
Viscosity (cP)
Temperature (°C)
xMgCl2 = 1.00
xMgCl2 = 0.85
xMgCl2 = 0.20
xMgCl2 = 0.50
xMgCl2 = 0.34
xMgCl2 = 0.00

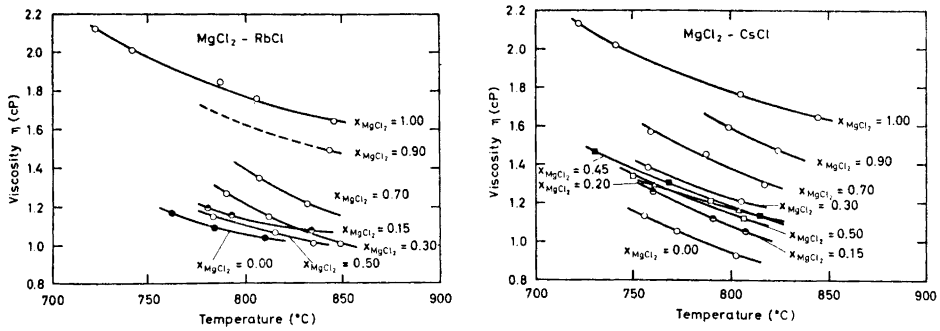

Figs. 1–8. Shear viscosity of the molten binary systems: $CaCl_2-NaCl$, $CaCl_2-KCl$, $MgCl_2-CaCl_2$, $MgCl_2-LiCl$, $MgCl_2-NaCl$, $MgCl_2-KCl$, $MgCl_2-RbCl$ and $MgCl_2-CsCl$.

A general discussion of the sources of error was given by Dumas *et al.*[1] Although some errors have been reduced with the more exact measurement of the sphere dimensions and through computer treatment of the data we still consider ± 2 % to be a reasonable estimate for the standard deviation.

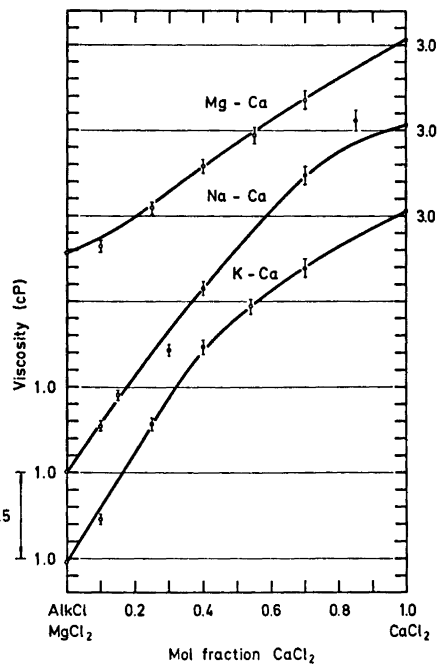

Fig. 9. Viscosities of the binary mixtures $CaCl_2-NaCl$, $CaCl_2-KCl$, and $CaCl_2-MgCl_2$ at 800°C.

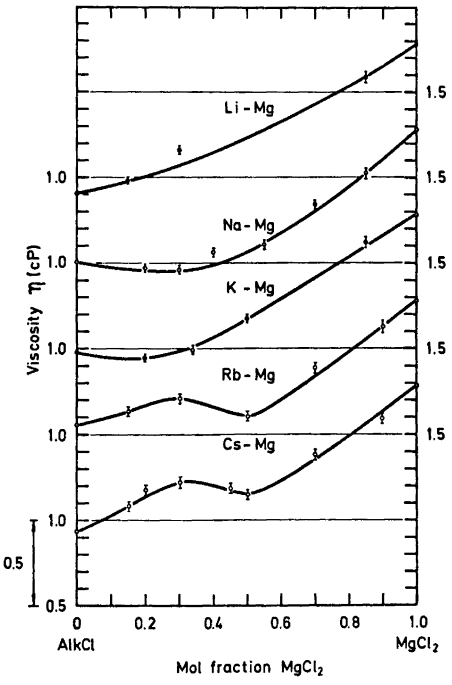

Fig. 10. Viscosities of the systems $MgCl_2$–AlkCl at 800°C.

DISCUSSION

Definition of ideality. Rice *et al.*[6] in their discussion of viscosity of simple liquids define an ideal binary mixture as a mixture where the compounds have the same energy interaction parameter, ε, and the same rigid core diameter, σ. They point out that the Eyring theory [7,8] then leads to linear additivity of the fluidity, $\phi = 1/\eta$. The Rice-Alnatt theory,[9] however, gives linear additivity of the viscosity, while other theories give more complex behaviour.[6]

None of these theories, however, can be used in the present case. For example, our mixtures of molten salts are far from being ideal in this sense since ε and σ are not the same for each component. It is, therefore, necessary to resort to more semi-empirical theories in order to correlate the data we obtained.

The temperature dependence of high-viscosity fluids is often best represented by a Vogel-type equation,[10] involving a temperature parameter T_0 related to the glass transition temperature,[11]

$$\log \eta = a + \frac{b}{T - T_0} \tag{1}$$

where a and b are constants.

For low-viscosity molten salts at temperatures far from the glass-transition temperature, the temperature dependence of the viscosity is best given by an Arrhenius-type function [11]

$$\eta = A\, \mathrm{e}^{B/T} \tag{2}$$

where A and B are constants. This equation follows from the Eyring theory,[7,8]

$$\eta = A\, \mathrm{e}^{\Delta G^{\ddagger}/RT} = A\, \mathrm{e}^{[(\Delta H^{\ddagger}/RT) - (\Delta S^{\ddagger}/R)]} \tag{3}$$

where $\Delta G^{\ddagger}$, $\Delta H^{\ddagger}$, and $\Delta S^{\ddagger}$ are, respectively, the Gibbs energy, the enthalpy, and the entropy of activation for viscous flow.

By introducing $A = Nk/V$, where N is the number of atoms, k is the Boltzmann's constant and V is the volume, we obtain

$$\eta = (Nk/V)\, \mathrm{e}^{\Delta G^{\ddagger}/RT} \tag{4}$$

The temperature dependence of the viscosity given by the Arrhenius function is appropriate for our results.

The viscosity of ideal mixtures, assuming no enthalpy or volume change on mixing, has been studied by several authors.[12] Negative deviations from linear additivity of the viscosity are found. The results are often satisfactorily described by the Arrhenius rule,[13]

$$\ln \eta = X_1 \ln \eta_1 + X_2 \ln \eta_2 \tag{5}$$

where X_1 and X_2 represent mol fractions. Arrhenius originally recommended the use of mass fractions. Use of volume fraction has also been suggested.[14,15] Eqn. (5) can be justified theoretically from the rate theory by assuming the following linear additivity of the interaction parameters

$$\Delta H^{\ddagger} = X_1 \Delta H_1^{\ddagger} + X_2 \Delta H_2^{\ddagger} \tag{6}$$

$$\Delta S^{\ddagger} = X_1 \Delta S_1^{\ddagger} + X_2 \Delta S_2^{\ddagger} \tag{7}$$

and by assuming the pre-exponential factor in eqn. (4) to be equal for the two components. Eqn. (5) can be considered then as the definition of an ideal mixture, but it leads to a different ideality in viscosity than the equations given by Rice *et al.*[6]

Linear additivity of viscosity itself will only be fulfilled in eqn. (5) if $\eta_1 = \eta_2$, and then η is independent of composition. For $\eta_1 \neq \eta_2$ a negative deviation from linear additivity of the viscosity is ideal according to this definition. For example, the deviation for an equimolar mixture is 13 % if the two viscosities differ by a factor of 3.

For non-ideal mixtures a natural expansion of the linear additivity of the interaction parameters must include an excess viscous Gibbs energy of activation:

$$\eta = \frac{Nk}{V} \exp\left(\frac{X_1 \Delta G_1^{\neq} + X_2 \Delta G_2^{\neq} + \Delta G^{E\neq}}{RT}\right) \tag{8}$$

$$\ln \eta = X_1 \ln \eta_1 + X_2 \ln \eta_2 + \frac{\Delta G^{E\neq}}{RT} \tag{9}$$

The excess viscous Gibbs energy of activation, $\Delta G^{E\neq}$, must be zero for X_1 or $X_2 = 0$. The simplest equation in which $\Delta G^{E\neq}$ fulfills this necessary boundary conditions is

$$\Delta G^{E\neq} = X_1 X_2 b^{\neq} \tag{10}$$

This is analogous to the form of ΔG^E for regular solutions

$$\Delta G^E = \Delta H_{mix} = X_1 X_2 b \tag{11}$$

The viscosity can then be given as

$$\ln \eta = X_1 \ln \eta_1 + X_2 \ln \eta_2 + \frac{X_1 X_2 b^{\neq}}{RT} \tag{12}$$

An equation of the type given as eqn. (9) was first proposed by Powell *et al.*[16] However, they unjustifiedly used the thermodynamic excess Gibbs energy. An experimental correlation between the excess parameter $b^{\neq}$ in eqn. (12) and enthalpy has been established experimentally.[17,18] The correlation yields for regular solutions, eqn. (11), a $b^{\neq}$ which is opposite in sign from b in accordance with intuitive reasoning from a bond force concept. Increasing the bond forces in the mixture, $b < 0$, leads to a positive excess viscosity, $b^{\neq} > 0$. This simple concept will, however, break down for large negative deviations caused by the formation of complexes as the viscosity is not expected to be related directly to the bond strength within the complex. In cases with complex formation or association, Bondi recommends interpretation in terms of the complexes formed.[11]

Pure molten chlorides. Our data for LiCl, RbCl, and $CaCl_2$ at 800°C are in agreement with the values reported by Janz *et al.* in a recent National Bureau of Standards Circular.[19] Our value for KCl is 11 % lower and our value for CsCl is 6 % higher than the values they present. For NaCl a severe discrepancy is found; our value is nearly 50 % lower.

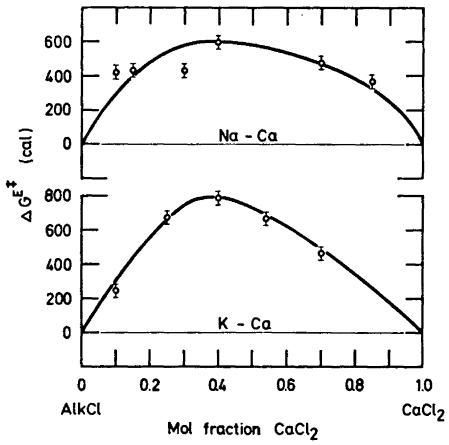

Fig. 11. Excess viscous Gibbs energy of activation, $\Delta G^{E\ddagger}$, from eqn. (9) for the systems: $CaCl_2-NaCl$ and $CaCl_2-KCl$.

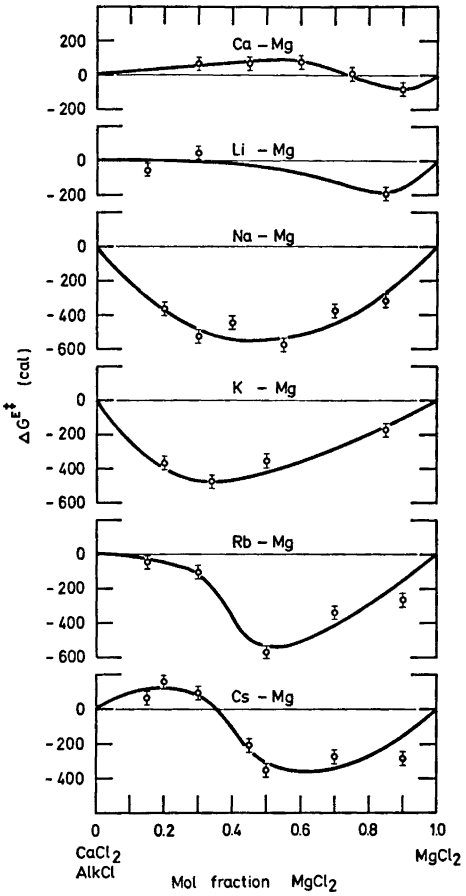

Fig. 12. Excess viscous Gibbs energy of activation, $\Delta G^{E\ddagger}$, from eqn. (9) for the systems: $MgCl_2-CaCl_2$, $MgCl_2-LiCl$, $MgCl_2-NaCl$, $MgCl_2-KCl$, $MgCl_2-RbCl$ and $MgCl_2-CsCl$.

Our measured viscosity for $MgCl_2$ of 1.78 cP at 800°C [1] differs significantly from the often quoted literature value of 4 cP at the same temperature.[20] We also observed that our measured viscosities of the alkali chlorides remained almost constant throughout the series from LiCl to CsCl. The electrical conductivity of the alkali chlorides, however, decreases strongly from LiCl to CsCl.[19] Therefore, the Frenkel correlation [21] between the equivalent conductivity, Λ, and the viscosity, η, given by eqn. (13)

$$\Lambda^n \eta = \text{constant} \qquad (13)$$

is not obeyed. The constant viscosity may be explained as a balance between decreasing bond forces and increasing cation size as one proceeds from LiCl to CsCl.

Binary chloride mixtures. In Figs. 11 and 12 are presented the excess Gibbs energy of activation, for viscous flow, $\Delta G^{E\ddagger}$, calculated from eqn. (9). For the systems $CaCl_2-NaCl$ and $CaCl_2-KCl$ a correlation between $\Delta G^{E\ddagger}$ and the thermodynamic enthalpy of mixing [22] is found. This is similar to what one observes for mixtures of organic liquids.[11] $\Delta G^{E\ddagger}$ and ΔH have opposite signs, and the value of $\Delta G^{E\ddagger}$ increases with an increasing negative ΔH. The correlation between $\Delta G^{E\ddagger}$ and ΔH_{mix} or ΔG^{E} breaks down, however, for systems containing $MgCl_2$. This is particularly true for the systems $MgCl_2-$ NaCl, $-$KCl, $-$RbCl, $-$CsCl where large negative heats of mixing are observed,[23] while the excess Gibbs energy of activation for viscosity is mainly strongly negative.

It is possible to explain the deviation from the "ideal law", eqn. (5), in terms of the following three guiding principles. These three principles were also applied to our studies of conductivity,[3] density,[24] and surface tension.[25]

(i) For minor structural changes the interaction between the next nearest neighbours results in an exothermic mixing reaction (negative excess Gibbs energy of mixing) and a strengthening of the bond forces.

(ii) When cations with strong field strengths are present, the polarization of anions leads to the strengthening of bonds between this cation and the nearest neighbour anions at the cost of the other short-range cation-anion bonds. In the extreme case, complex formations result; for example, $MgCl_4^{2-}$.

(iii) Structural breakdown of the melts with partly covalent character occurs; for example for $MgCl_2$, resulting in the ionization of the lattice.

As already pointed out, the deviation from logarithmic additivity for the systems $CaCl_2-NaCl$ and $CaCl_2-KCl$ is explained by the bond strength concept in (i). An increasing negative ΔH_{mix} leads to an increasingly positive excess viscosity. A polarization of Cl^- by Ca^{2+} might also be operative.[26] The near ideal viscosity behaviour of the systems $MgCl_2-CaCl_2$ and $MgCl_2-NaCl$ for $CaCl_2$ and NaCl rich mixtures is explained by a small ΔH_{mix} [22,26] causing small changes in the bond forces during mixing.

The breakdown of the covalent structure of magnesium chloride, (iii), is demonstrated by the slightly negative deviations in viscosity from eqn. (5) for the systems $MgCl_2-CaCl_2$ and $MgCl_2-LiCl$, and the stronger, nearly constant, negative deviations in viscosity for the systems $MgCl_2-NaCl$, $-KCl$, $-RbCl$, and $-CsCl$ for $MgCl_2$ rich mixtures.

The system $MgCl_2-CsCl$ has the largest negative enthalpy of mixing [23] and the most pronounced tendency to form $MgCl_4^{2-}$. For the CsCl-rich mixtures a positive deviation from logarithmic additivity in viscosity is exhibited with a maximum near the stoichiometric composition Cs_2MgCl_4. The system $MgCl_2-$ RbCl tends toward a positive deviation in viscosity near the stoichiometric composition Rb_2MgCl_4. This disappears for the systems $MgCl_2-KCl$ and $MgCl_2-NaCl$. Since formation of the stable entity $MgCl_4^{2-}$ is expected to lead to increased viscosity, it is surprising that this is not manifested by an excess positive viscosity for the KCl melts. Raman spectroscopy and previous thermodynamic studies have indicated $MgCl_4^{2-}$ formation in these melts.[28] The dif-

ference in behaviour between the NaCl and KCl systems in contrast with the RbCl and CsCl systems might give a clue to understanding of the kinetic stability of $MgCl_4^{2-}$. The relaxation time of $MgCl_4^{2-}$ may be so much shorter in the NaCl and KCl systems that it is not manifested in the viscosity.

Relevance of the present studies to the electrowinning of magnesium. One of the main objectives of this study was to clarify the effect of a change in composition and temperature on the viscosity of the industrially important magnesium electrolyte. Although the present study includes only binary systems, we can predict the viscosity behaviour of quaternary industrial electrolytes such as the mixture $MgCl_2-CaCl_2-NaCl-KCl$.

As mentioned above, the high viscosity of $MgCl_2$ reported in earlier literature [20] has been disproved. The viscosities we measured do not seem to be sensitive to structure. No sharp viscosity maximum as function of composition is found here as reported by Strelets *et al.*[20]

Although the viscosity of $MgCl_2$ is somewhat higher than that for NaCl and KCl, an increase of the $MgCl_2$ content in the industrially interesting range (5 to 15 mol %) actually results in a small lowering of the viscosity (Fig. 10).

Exchange of NaCl for KCl in an $MgCl_2-CaCl_2-NaCl-KCl$ mixture is expected to result only in very small changes in viscosity. This is due to the nearly equal viscosities of the pure salts and the similarities between the viscosity curves for the $MgCl_2-NaCl$ and $MgCl_2-KCl$ systems and for the $CaCl_2-NaCl$ and $CaCl_2-KCl$ systems (Figs. 9 and 10).

An increase in the $CaCl_2$ content of the quaternary mixture $MgCl_2-CaCl_2-NaCl-KCl$ is always expected to result in an increase in viscosity as shown in Fig. 9. The viscosity of pure $CaCl_2$ at 800°C is 3.03 cP. A lowering of the temperature by 50°C from 800 to 750°C will result in a viscosity increase of about 10 to 15 % for the melts studies (Figs. 1–8). One would, therefore, expect the $MgCl_2-CaCl_2-NaCl-KCl$ system to exhibit a similar behaviour.

We might conclude that the change in viscosity as a function of composition and temperature in the presently studied mixtures is relatively modest compared with viscosity changes in other important industrial liquids as for instance oils and high-polymer solutions.

Acknowledgement. We are indebted to Ing. Harry Sagen for technical assistance with salt preparations, and to Avd. ing. Rolf Dehli and the *Institutt for maskinteknisk fabrikkdrift og verktøymaskiner* for valuable help in remachining and measuring the Pt-sphere. Support from *Norsk Hydro a.s.* and *Norges Teknisk-Naturvitenskapelige Forskningsråd* is gratefully acknowledged.

REFERENCES

1. Dumas, D., Grjotheim, K., Høgdahl, B. and Øye, H. A. *Acta Chem. Scand.* **24** (1970) 510.
2. Bearden, J. E. *Phys. Rev.* **56** (1939) 1023.
3. Grjotheim, K., Nikolic, R. and Øye, H. A. *Acta Chem. Scand.* **24** (1970) 489.
4. Landolt-Børnstein, *Zahlenwerte und Funktionen*, 6. Auflage, IV. Band, 1. Teil, Springer, Berlin 1955.
5. Kleinschmit, P. *Thesis*, Techn. Hochschule, Hannover 1968.
6. Rice, S. A., Boon, J. P. and Davis, H. T. *Comments on the Experimental and Theoretical Study of Transport Phenomena in Simple Liquids*, In Frisch, H. L. and Salsburg, S. W., Eds., *Simple Dense Fluids*, Academic, New York 1968, p. 251.

7. Glasstone, S., Laidler, K. J. and Eyring, H. *The Theory of Rate Processes*, McGraw, New York 1941.
8. Kincaid, J. F., Eyring, H. and Stearn, A. E. *Chem. Rev.* **28** (1941) 301.
9. Rice, S. A. and Alnatt, A. R. *J. Chem. Phys.* **34** (1961) 409.
10. Vogel, H. *Physik Z.* **22** (1921) 645.
11. Bondi, A. *Physical Properties of Molecular Crystals, Liquids, and Glasses*, Wiley, New York 1968, p. 337, and references therein.
12. Bretsznajder, S. *Prediction of Transport and Other Physical Properties of Fluids*, Pergamon, Oxford 1971, p. 207.
13. Arrhenius, S. A. *Z. Phys. Chem. (Leipzig)* **1** (1887) 285.
14. Tamura, M. and Kurata, M. *Bull. Chem. Soc. Japan* **25** (1952) 32.
15. Tamura, M., Kurata, M. and Sata, S. *Bull. Chem. Soc. Japan* **25** (1952) 124.
16. Powell, R. E., Roseveare, W. E. and Eyring, H. *Ind. Eng. Chem.* **33** (1941) 430.
17. Greenberg, L. and Nissan, A. H. *Nature* **164** (1949) 799.
18. Fort, R. J. and Moore, W. R. *Trans. Faraday Soc.* **62** (1966) 1112.
19. Janz, G. J., Dampier, F. W., Lakshminarayanan, G. R., Lorenz, P. K. and Tomkins, R. P. T. *Molten Salts, Vol. 1. Electrical Conductance, Density, and Viscosity Data.* NSRDS-NBS 15 Wash. 1968.
20. Strelets, Kh. L., Jaiz, A. J. and Gulpantizki, B. *Metallurgie des Magnesiums*, Verlag Technik, Berlin 1953.
21. Frenkel, J. *Kinetic Theory of Liquids*, Oxford University Press, London 1946.
22. Østvold, T. *Thesis*, University of Trondheim, Trondheim-NTH 1971.
23. Kleppa, O. J. and McCarty, F. G. *J. Phys. Chem.* **70** (1966) 1249.
24. Grjotheim, K., Holm, J. L., Lillebuen, B. and Øye, H. A. *Trans. Faraday Soc.* **67** (1971) 640.
25. Grjotheim, K., Holm, J. L., Lillebuen, B. and Øye, H. A. *Acta Chem. Scand.* **26** (1972) 2050.
26. Tørklep, K. E. and Øye, H. A. *To be published.*
27. Papatheodorou, G. N. and Kleppa, O. J. *J. Chem. Phys.* **47** (1967) 2014.
28. Maroni, V. A., Hathaway, E. J. and Cairns, E. J. *J. Phys. Chem.* **75** (1971) 155, and references therein.

Received June 26, 1972.

ACTA CHEMICA SCANDINAVICA 27 (1973) 329–335

Direct Cyanation of Aromatic Compounds

II.[1] A Comparison of Isomer Distributions from Different Cyanation Methods

SVEN NILSSON

Division of Organic Chemistry 1, Chemical Center, University of Lund, P.O. Box 740, S-220 07 Lund 7, Sweden

The isomer distributions of aromatic nitriles formed in five direct cyanation reactions have been determined and are discussed in terms of the possible reaction mechanisms. The reactions investigated are anodic cyanation, photolysis of aromatic compounds in cyanide solution, photolysis of halogen cyanide, diazotation of cyanamide in the presence of aromatic compounds, and cyanation of aromatic compounds with cyanogen chloride/aluminium chloride. In the first two of these reactions the cyano group attacks the aromatic ring as a nucleophile, the two following are radical reactions, whereas the last reaction is best described as an electrophilic aromatic substitution reaction.

RESULTS AND DISCUSSION

Anodic cyanation was first described by Koyama *et al.*[2] in 1965 and has been the subject of numerous investigations since then. The fact that cyanide ions are oxidixed at a lower potential than most aromatics made it theoretically possible that cyanide ions were oxidized to cyano radicals which reacted with aromatic compounds in the solution *via* a homolytic mechanism. Evidence from controlled potential experiments,[3,4] isomer distribution determination of aromatic nitriles formed [4] and the observation that cyanide ion has a high overpotential on platinum due to formation of cyanide compounds as a film on the electrode surface [5] have ruled out this mechanism. Anodic cyanation is now best described as a nucleophilic attack by cyanide ion on a cation radical formed by an initial one-electron transfer from the substrate to the anode (see Scheme 1). The isomer distribution of nitriles formed in anodic cyanation reaction with some selected aromatic compounds are shown in Table 1.

Photolysis of aromatic compounds in the presence of cyanide ions. In 1961, Havinga published some interesting results on the hydrolysis of phosphate esters of nitrophenols.[6] The hydrolysis rate was strongly enhanced when an

Table 1. Isomer distributions of aromatic nitriles formed in anodic cyanation.

Compound	Isomer distributions of nitriles, % *ortho* or α-	*meta* or β-	*para*
Anisole	53	0.1	47
Chlorobenzene	50	0.5	50
Biphenyl	24	0.4	76
Toluene	40	8	52
Isopropylbenzene	4	9	87
t-Butylbenzene	41	13	46
Naphthalene	90	10	

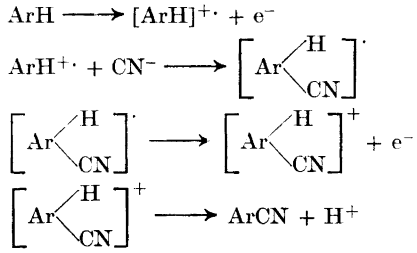

Scheme 1.

alkaline solution of the ester was placed in the sunlight.[7,8] This observation was during the 60's followed by others which can be collected under the heading "Light Induced Heterolytic Reactions in Solution". The reactions follow the general equation:

$$ArX + Y^- \xrightarrow{h\nu} ArY + X^-$$

where X^- is OPO_3^-, OCH_3^-, *etc.*, and Y^- is OH^-, $NHCH_3^-$, CN^-, *etc.* Thus Letsinger and McCain [8] reported that photolysis of aromatic nitro compounds in cyanide solution gave 3-nitrobenzonitriles. We have independently found that aromatics (not necessarily nitroaromatics) can be cyanated in this way.* The isomer distributions from some of these reactions are shown in Table 2.

Table 2. Isomer distributions of aromatic nitriles formed in photolysis of aromatic compounds in the presence of cyanide ions.

Compound	Isomer distributions of nitriles, % *ortho* or α-	*meta* or β-	*para*
Anisole	53	0.2	47
Biphenyl	30	3	67
Naphthalene	90	10	

* This reaction was also reported recently by Vink, J. A. J., Lok, C. M., Cornelisse, J. and Havinga, E. *Chem. Commun.* **1972** 710.

The reaction mechanisms for these light induced reactions are not known with certainty. Havinga [9] proposed a mechanism for the hydrolysis of nitrophenolate esters that proceeds *via* the singlet state:

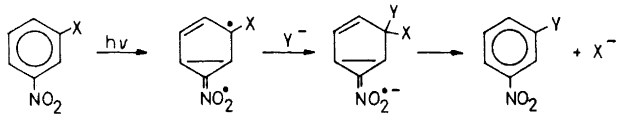

This mechanism may be valid when X^- is a good leaving group and the singlet state (that here is written as a diradical according to Bryce-Smith and Gilbert [10]) is stabilized by a substituent like the nitro group. When the leaving grouop is H^- (as in direct cyanation) it appears more probable that the reaction starts with a photoionisation of the aromatic compound. The reaction sequence would then be (Scheme 2):

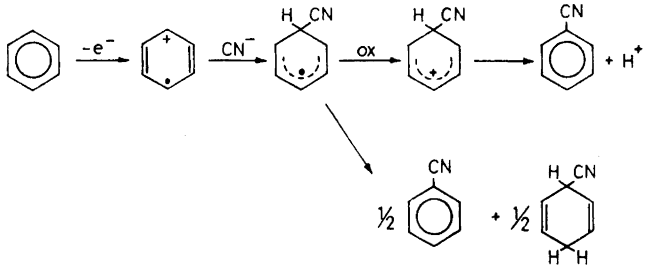

Scheme 2.

The second oxidation to a Wheland-type intermediate may occur with oxygen.[8] The other possibility is disproportionation to an aromatic nitrile and a dihydro compound. In the photolysis of naphthalene we actually found a dihydro compound, 1,4-dihydro-1-cyanonaphthalene, which may have been formed in this way. It is, however, possible that this compound has been formed from reaction between 1-cyanonaphthalene and solvated electrons. 1-Cyanonaphthalene reacts faster than naphthalene with solvated electrons [11] by a factor of 4.

Photolysis of halogen cyanide in the presence of aromatic compounds. Photolysis of iodine, bromine, and chlorine yields free halogen radicals. It is not possible to get cyano radicals in the same way from cyanogen due to its instability and tendency to polymerize. A homolytic dissociation of a halogen cyanide depends on the bond strength and polarity of the carbon-halogen bond. The determination of bond lengths [12] and bond energy [12–14] (dissociation energy) of different halogen cyanides together with determination of the ionisation potential of the cyano group [15] and calculations of the electronegativity of the cyanide ion [16,17] and the electron affinity of the cyano radical [17–19] make it possible to arrange the cyano group in these respects in a series of halogens

and pseudo-halogens: F, ONC, OCN, Cl, Br, CN, SCN, ClO_2, I. The names of the halogen cyanides should according to this be cyanogen fluoride, cyanogen chloride, cyanogen bromide, and iodine cyanide. The first three of them should give a positive cyano ion and a halogenide ion while iodine cyanide should give iodonium ion and cyanide ion when subjected to heterolytic dissociation. This prediction is confirmed by the results from hydrolysis of halogen cyanides.[20] A homolytic dissociation should give cyano and halogen radicals and should be easiest to perform with cyanogen bromide or iodine cyanide.

When a solution of iodine cyanide and an aromatic compound in carbon tetrachloride or methanol was photolysed, a mixture of aromatic nitriles was formed. The isomer distributions (Table 3) indicate that the reaction starts

Table 3. Isomer distributions of aromatic nitriles formed in photolysis of iodine cyanide in the presence of aromatic compounds.

Compound	Solvent	Isomer distributions of nitriles, % *ortho* or α-	*meta* or β-	*para*
Anisole	CH_3OH	58	14	28
Anisole	CCl_4	51	16	33
Chlorobenzene	CCl_4	27	27	46
Nitrobenzene	CCl_4	22.5	63	14.5
Biphenyl	CH_3OH	44	28	28
Toluene	CH_3OH	47.5	31.5	21
Naphthalene	CH_3OH	61	39	

with homolytic dissociation of iodine cyanide and that the cyano radical attacks the aromatic ring (Scheme 3). The intermediate radical looses a hydrogen radical either by oxidation, disproportionation, or by a second attack by another cyano radical. The iodine radicals dimerize to iodine which is observed by its colour. Aromatic iodination could not be detected. It is, however, possible that aromatic iodides formed in this reaction were destroyed during the photolysis.[21]

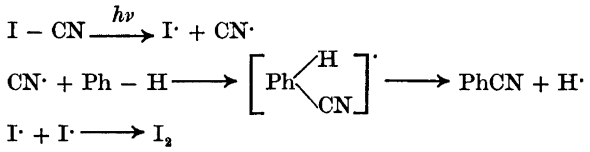

Scheme 3.

Diazotation of cyanamide in the presence of aromatic compounds. When photolysis of halogen cyanide is used as a source of cyano radicals, the result may become complicated due to photorearrangement. In Part I of this series [1] a thermal method of generating cyano radicals is described. The reaction mech-

anism discussed therein (Scheme 4) implies a radical attack on the aromatic ring, and the isomer distributions of aromatic nitriles formed in the reaction are in accordance with this mechanism (Table 4).

Table 4. Isomer distributions of aromatic nitriles formed by diazotation of cyanamide in the presence of aromatic compounds.

Compound	Isomer distributions of nitriles, %		
	ortho or α-	*meta* or β-	*para*
Anisole	44	13	43
Chlorobenzene	41	9	50
Biphenyl	54	29	17
Toluene	50	27	23
Ethylbenzene	14	10	76
Isopropylbenzene	29	0	71
Naphthalene	60	40	

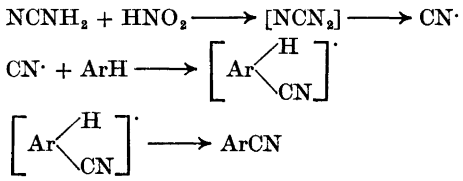

Scheme 4.

Cyanation of aromatic compounds with cyanogen chloride/aluminium chloride. Cyanogen chloride or bromide reacts with aromatic compounds in the presence of aluminium chloride to give aromatic nitriles. The method has been known since the end of the last century [22,23] but has not received wide attention due to side reactions. In the light of the earlier discussion, it is evident that a heterolytic dissociation of cyanogen chloride would give a cyano cation and a chloride ion. The cyanation reaction has also been described to proceed *via* formation of cyanogen cations [24,25] (Scheme 5).

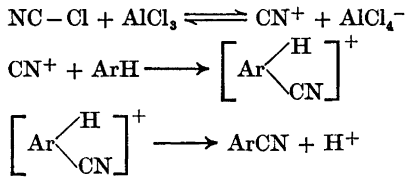

Scheme 5.

It is, however, not necessary to postulate "free" cyano cations. An investigation of the infrared spectra of adducts of antimony(V) chloride and cyanogen halogenides [26] makes it probable that these have a structure like

$X-\dot{\overset{+}{C}}=N \longrightarrow \bar{S}bCl_5$. The infrared spectrum of cyanogen chloride also changes when aluminium chloride is added but the bathochromic shifts of the frequencies of the nitrile group and the carbon-halogen bond are less pronounced. From these facts it is possible to propose a modified mechanism for this Friedel-Crafts resembling reaction (Scheme 6).

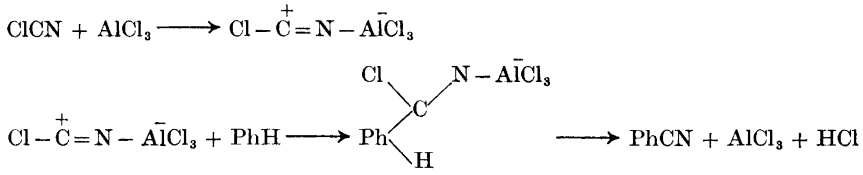

Scheme 6.

Both of the mechanisms are in accordance with the isomer distributions observed in the reaction (Table 5).

Table 5. Isomer distributions of aromatic nitriles formed in reaction with cyanogen chloride/aluminium chloride.

Compound	Isomer distributions of nitriles, %		
	ortho or α-	*meta* or β-	*para*
Anisole	11	0	89
Toluene	28	0	72
Naphthalene	92	8	

As is evident from the preceding discussions and can be seen in the experimental part it is possible to introduce a cyano group into an aromatic ring under very different reaction conditions. Heterolytic cyanation can take place at the electrode surface in an anodic cyanation reaction, under influence of ultraviolet light in solution or in the presence of a strong Lewis acid. The isomer distributions of nitriles formed follow the same general pattern. The reaction conditions of the two radical cyanations are very much different. In one of them, ultraviolet light is used, in the other, diazotation in acid solution generates the cyano radical. Here too the isomer distributions are similar although not identical. The preparative possibilities of the reactions are promising but not fully investigated yet.

EXPERIMENTAL

General. Solvents and starting materials were purified and checked before use by VPC. Reference substances were prepared by standard methods if not commercially available (see Part I [1]). Analyses were made with VPC (Perkin-Elmer 880 equipped with 5 % neopentylglycol succinate on Chromosorb P) and the retention times of the products from

the reactions were compared with reference substances. In some cases IR, UV, NMR, and mass spectra were used as additional proof of the structures.

Anodic cyanation. A solution of 0.1 mol aromatic compound and 0.2 mol sodium cyanide in 300 ml methanol was electrolysed af the half-wave potential of the aromatic compound. After 10 % of the theoretically calculated amount of charge had passed, the electrolyte was evaporated, extracted with ether and the ether solution analysed by VPC.

Photolysis of aromatic compounds in cyanide solution. A solution of 0.1 mol aromatic compound and 0.2 mol sodium cyanide in 120 ml methanol was photolysed for 50 min with a high pressure mercury lamp mounted in the reaction flask. The solution was worked up as before.

Photolysis of iodine cyanide in the presence of aromatic compounds. A solution of 0.1 mol aromatic compound and 0.5 g iodine cyanide in 120 ml methanol was photolysed as described. Use of the less polar solvent carbon tetrachloride gave approximately the same results.

Diazotation of cyanamide in the presence of aromatic compounds. See Part I.[1]

Cyanation with cyanogen chloride/aluminium chloride. A solution of 0.01 mol aromatic compound and 1.0 g aluminium chloride in 50 ml carbon disulfide was stirred during inlet of cyanogen chloride in the cold. After reflux for 15 min and distillation the rest was poured on ice and extracted. A preparative run with 0.5 mol toluene and equivalent amount of cyanogen chloride (precondensed in a cooling trap) gave a yield of 39 % tolunitriles.

REFERENCES

1. Eberson, L., Nilsson, S. and Rietz, B. *Acta Chem. Scand.* **26** (1972) 3870.
2. Koyama, K., Susuki, T. and Tsutsumi, S. *Tetrahedron Letters* **1965** 627.
3. Parker, V. D. and Burgert, B. E. *Tetrahedron Letters* **1965** 4065.
4. Eberson, L. and Nilsson, S. *Discussions Faraday Soc.* **45** (1968) 242.
5. Sawyer, D. T. and Day, R. J. *J. Electroanal. Chem.* **5** (1963) 195.
6. Havinga, E. *Koninkl. Ned. Akad. Wetenschap., Verslag Gewone Vergader. Afdel. Nat.* **70** (1961) 52.
7. Havinga, E., de Jongh, R. O. and Kronenberg, M. E. *Helv. Chim. Acta* **50** (1967) 2550.
8. Letsinger, R. and McCain, J. H. *J. Am. Chem. Soc.* **88** (1966) 2884.
9. Havinga, E. In *Reactivity of the Excited Organic Molecule*, Interscience, New York 1965, p. 201.
10. Bryce-Smith, D. and Gilbert, A. *Chem. Commun.* **1967** 240.
11. Hart, E. J. and Anbar, M. *The Hydrated Electron*, Wiley–Interscience, New York 1970, Table XG1 and XG2.
12. Glockner, G. *J. Phys. Chem.* **63** (1959) 828.
13. Goldfinger, P. *Bull. Soc. Chim. Belges* **56** (1947) 282.
14. Errede, L. A. *J. Phys. Chem.* **64** (1960) 1031.
15. Neale, R. S. *J. Phys. Chem.* **68** (1964) 143.
16. Clifford, A. F. *J. Phys. Chem.* **63** (1959) 1227.
17. Wilmshurst, J. K. *J. Chem. Phys.* **28** (1958) 733.
18. Morris, D. F. C. *Acta Cryst.* **14** (1961) 547.
19. Napper, R. and Page, F. M. *Trans. Faraday Soc.* **59** (1963) 1086.
20. Kikindai, T. *Bull. Soc. Chim. France* **1951** 799.
21. Kharasch, N. and Göthlich, L. *Angew. Chem.* **74** (1962) 651.
22. Merz, V. and Weith, W. *Ber.* **10** (1877) 746.
23. Friedel, C. and Crafts, J.-M. *Ann. Chim. Phys.* **1** (1884) 449.
24. Woolf, A. A. *Chem. Ind. (London)* **1953** 868.
25. Woolf, A. A. *J. Chem. Soc.* **1954** 252.
26. Allenstein, E. and Schmidt, A. *Chem. Ber.* **97** (1964) 1286.

Received July 10, 1972.

ACTA CHEMICA SCANDINAVICA 27 (1973) 336–344

Incorporation of ^{3}H-Leucine into Insoluble Proteins of Neuronal and Glial Cell Fractions *in Vitro*

KARI HEMMINKI

Department of Medical Chemistry, University of Helsinki, Helsinki, Finland

Rat brain cerebral cortex was dispersed by collagenase-hyaluronidase digestion and neurons and glia were separated by gradient centrifugation. The cell fractions obtained were studied by electron microscopy and incubated with ^{3}H-leucine following uptake and incorporation into soluble and insoluble proteins. Insoluble proteins were separated by polyacrylamide gel electrophoresis and specific radioactivities of individual protein bands were determined. (a) Uptake of ^{3}H-leucine proceeds more rapidly in glia reaching maximal radioactivity at 20 min. (b) Incorporation of ^{3}H-leucine into protein is 7 fold higher in neurons compared to glia at 20 min but the ratio increases up to 2 h. In both cell fractions the insoluble protein reaches around 5 times higher specific radioactivity than the soluble protein. In neurons the radioactivity increases up to 2 h while in glia a plateau is reached at 20 min. (c) Electrophoretic patterns of the proteins of the cell fractions differ only slightly. The highest specific radioactivities are found in the slowly moving neuronal bands.

Advances in preparative and analytical techniques have opened new aspects of brain protein metabolism in recent years. Extraction of brain tissue with aqueous media leaves a bulky residue containing 98 to 50 % of the total brain protein depending on the media used.[1,2] The insoluble residue, including largely membrane proteins, has been shown to label rapidly with radioactive precursors motivating a detailed study of the insoluble protein. Polyacrylamide gel electrophoresis introduced by Ornstein and Davis [3] can be adapted to separation of insoluble proteins by performing electrophoresis in the presence of detergents in acidic,[4,5] basic,[6] or neutral milieu.[7] Such techniques have been applied for analysing patterns of insoluble proteins from myelin,[6–8] synaptosomes,[9,10] and mitochondria.[11]

In this paper insoluble proteins of neuronal and glial cell fractions are characterized. The fractions obtained by collagenase-hyaluronidase digestion and gradient centrifugation [12,13] are incubated for various times with radioactive leucine *in vitro* and incorporation into protein is determined. Insoluble proteins are separated by polyacrylamide gel electrophoresis and specific radioactivities of stained protein discs are measured.

MATERIALS AND METHODS

Preparation of neuronal and glial fractions. Cerebral cortices from 8 rats, six weeks old, were used for each experiment. Tissue was digested in a collagenase-hyaluronidase incubation medium for 60 min and cells separated by gentle sieving on a ball vibrator as previously described.[12] Neuronal and glial fractions were separated in a Ficoll-sucrose gradient by centrifuging in the Spinco SW-25.1 rotor at 63 000 *g* for 90 min.[13] The neuronal fraction containing about 4.5 mg of protein was collected at the 30 % Ficoll-2 M sucrose interphase and the glial fraction containing 5.5 mg of protein at the 10 – 20 % Ficoll interphase. The morphology of the cells and purity of the fractions was characterized by light microscopy as described recently.[13] For electron microscopy the cell fractions were fixed in 2.5 % glutaraldehyde in 0.32 M sucrose and 0.2 M phosphate buffer, pH 7.2 for 90 min and sedimented at 800 *g*. The pellet was prepared according to Sabatini *et al.*[14]

Incorporation of ^{3}H-leucine

The cell fractions obtained from the gradient were repeatedly washed with buffer sedimenting at 300 *g*. Finally 2 ml of Krebs-Ringer phosphate buffer, pH 7.4, containing 10 mM glucose was added. Aliquots containing 0.5 ml of the cell suspensions were shaken at a rate of 60/min on a water bath at 37° for 10 min. After the preincubation 10 μCi 4,5-^{3}H-leucine (specific activity 17 Ci/mmol, Amersham) in a volume of 10 μl was added into each tube and incubation was continued for various times (1, 5, 20, and 120 min) under air.

Stopping incubation. At the end of the incubation the cell suspensions were rapidly poured into 100 ml cold Krebs-Ringer phosphate buffer and sedimented for 3 min.[13] The supernatants were decanted and the walls of the tubes were carefully wiped with paper, holding the tubes upsidedown. 2 ml of cold 10 mM Tris buffer, pH 7.0, was added and the cellular pellets were collected with a Pasteur pipette for homogenization in a Potter-Elvehjem homogenizer about 5 min after stopping the incubation.

The homogenate was frozen and thawed three times and centrifuged at 100 000 *g* for 30 min. By definition the proteins recovered in the 100 000 *g* pellet were called insoluble and those recovered in the supernatant were called soluble.

TCA-soluble fraction and soluble proteins. The 100 000 *g* supernatant was mixed with an equal volume of cold 12 % TCA and the solution centrifuged. An aliquot of the supernatant was added to Bray's scintillation fluid to determine the TCA-soluble radioactivity representing intracellular ^{3}H-leucine. Results for TCA soluble radioactivity were expressed per unit protein summing the soluble and insoluble protein. The TCA-precipitate was washed three times with 6 % TCA, twice with ethanol and once with ethanol-chloroform, ethanol-ether, and ether. The residue was dissolved in 0.5 N NaOH. Protein content of this alkaline solution was measured according to Lowry *et al.*[15] The remaining NaOH solution was added into Bray CAB-O-SIL gel for determination of radioactivity of the soluble protein.

Insoluble proteins. The 100 000 *g* pellet containing the insoluble proteins was extracted twice with Tris buffer to wash the soluble radioactivity away. The resulting pellet was dissolved by repeated freeze-thawing in 250 μl of the sample solvent containing 50 mM K_2SO_3, 8 M urea, 10 % mercaptoethanol and 5 % Triton X-100, pH 9 – 10.[5] A 100 μl aliquot of this solution was precipitated by 6 % TCA and protein and radioactivity were determined as above. The remaining 150 μl were saved for electrophoresis.

Polyacrylamide gel electrophoresis of insoluble proteins

Polyacrylamide gel electrophoresis was performed according to Lim and Tadayyon [5] by replacing *N,N'*-methylene bisacrylamide by ethylene diacrylate (Borden Chemical Co.) in the small pore solution to make the gel alkali labile.[16] Tubes 15 cm long were used with a current of 2.5 mA/tube until the methyl green dye had reached the

cathode end of the gel. Protein (400 – 600 μg) was applied in a volume of 150 μl onto each gel for electrophoresis. Staining was performed in a solution containing 1 % amido black, 10 % acetic acid, and 10 % methanol for 15 min. For destaining the gels were floated in acetic acid-methanol solution for several days. Relative mobilities of the bands were calculated in relation to the methyl green front.

Determination of specific radioactivities of proteins in gels. The protein discs developed in the gels were cut out on an apparatus set for slices of 2 mm by thickness. 8 gels were cut at a time carefully checking that each disc was entirely contained in a slice. The slices were depolymerized in 0.5 ml of 0.5 N NaOH. Optical density of amido black was measured at 625 nm for protein [17] and 10 ml Bray CAB-O-SIL was added for liquid scintillation counting. External standardization was used to correct for quenching. Results are expressed as dpm/mg of protein. The technique for determination of specific radioactivities of protein discs has been shown to be reproducible [18] within standard errors of less than 10 %. Soluble and insoluble brain protein separated by electrophoresis and stained were cut out of the gel and amido black measurement was followed by protein measurement using Lowry's method. A linear relationship between protein content and binding of amido black was demonstrated, parallelling the findings of Davies [17] for serum albumin.

RESULTS

Integrity of cell structure as interpreted by electron microscopy. The neuronal fraction (Figs. 1 and 2) contained cells with relatively abundant cytoplasm and rich Nissl substance surrounded by a plasma membrane, frequently discontinuous. Conforming well to criteria established *in situ*,[19] these cells were identified as neurons. A small number of glial cells and endothelial cells were also present. Cells in the glial fraction (Figs. 3 and 4) could be classified at least in two groups: One containing cells with long, thin processes, a uniformly dense nucleus and mitochondria as the most prominent cytoplasmic organelle (Fig. 3); the other consisted of round cells with a thin rim of cytoplasm and a nucleus with dense islands of chromatin (Fig. 4). These cell types closely resemble those described by Raine *et al.*[20] and accordingly the former is suggested to be astroglia and the latter oligodendroglia. Plasma membrane interruptions were also encountered in these cells.

Accumulation of ^{3}H-leucine into the TCA-soluble pool and cellular protein. Uptake of radioactive leucine by the neuronal and glial fractions (Fig. 5a) proceeded rapidly to a level characteristic of the cell type. The neurons accumulated radioactive leucine maximally at 270 000 dpm/mg protein compared to 430 000 dpm/mg protein of the glia. Maximal labelling of the intracellular precursor pool occurred at 20 min in glia and later, though not precisely determined, in neurons. Incorporation of radioactive leucine into neuronal proteins (Fig. 5b) increased up to 2 h. The specific radioactivity of the insoluble protein was on average 5 times higher than that of the soluble protein. As the dilute buffer used to extract soluble proteins dissolved 20 % of the neuronal protein, the total radioactivity present in the soluble protein fraction is only 4 %.

The glial incorporation (Fig. 5c) differed in two respects from the neuronal. First, incorporation into the insoluble protein reached a maximum at 20 min; second, the rate of incorporation is initially only 35 % of the neuronal incorporation dropping to 15 % at 20 min. The proportion of radioactivity incorporated into the glial soluble protein is, like in neurons, around 20 % of the total. The amount of extractable protein is higher in the glia, *i.e.* 35 %.

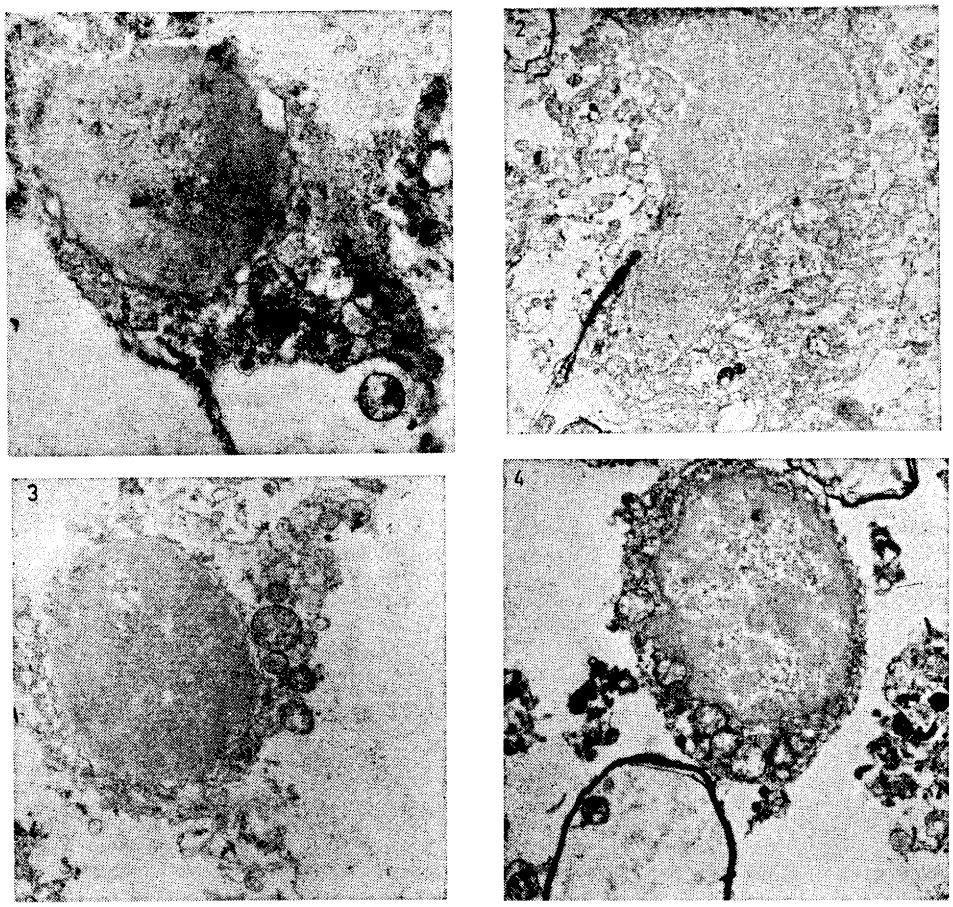

Figs. 1 to 4. Electron micrographs of neuronal and glial pellets fixed in 2.5 % glutaraldehyde. *Fig. 1.* A single cell from a neuronal pellet, 4000 ×, showing some mitochondria, plasma membrane and a synapse. *Fig. 2.* A neuron 2300 ×, with typically prominent rough endoplasmic reticulum. *Fig. 3.* A cell from a glial pellet identified as astroglia, 4000 ×, with processes, prominent mitochondria, very little rough reticulum and a nucleus with dense chromatin. *Fig. 4.* A cell from a glial pellet identified as oligodendroglia, 4000 × with narrow but dense cytoplasm and a nucleus with chromatin islands.

Patterns of insoluble proteins in polyacrylamide gels. Gel electrophoretic patterns of the neuronal and glial insoluble proteins (Fig. 6) appear to show both quantitative and qualitative differences. Bands N2 to N6 seem to be unique for the neuronal fraction while glial band G13 cannot be detected in the neuronal gel. The intensities of bands N2 to N5 in the neuronal fraction varied from one gel to another and by electrophoretic mobility they were concluded to originate from erythrocytes contaminating the neuronal fraction by 6 %.[13] The patterns of the slowly moving proteins in the two gels, G16 to G22 and N8 to N12, are on the other hand roughly similar.

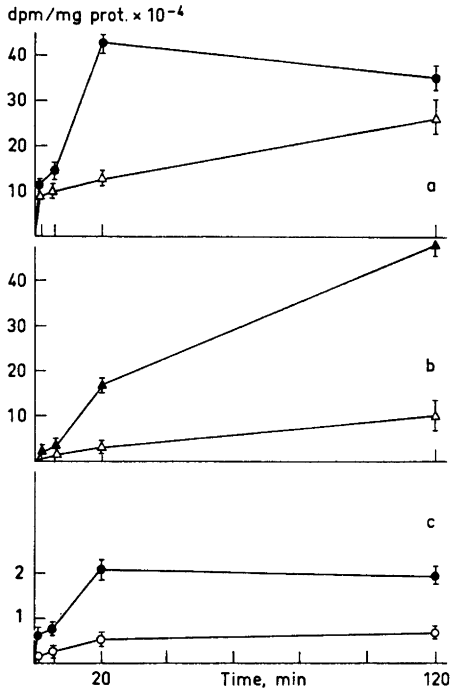

Fig. 5. Uptake and incorporation of[^{3}H]-leucine by the neuronal and glial cell fractions. Cells were incubated in 0.5 ml with 10 μCi [4,5-^{3}H]leucine for various times. (a) TCA-soluble radioactivity of neurons △ and glia ●. (b) TCA-precipitable radioactivity of neurons; insoluble proteins ▲, soluble proteins △. (c) TCA-precipitable radioactivity of glia; insoluble proteins ●, soluble proteins ○. Means of two experiments, ranges indicated.

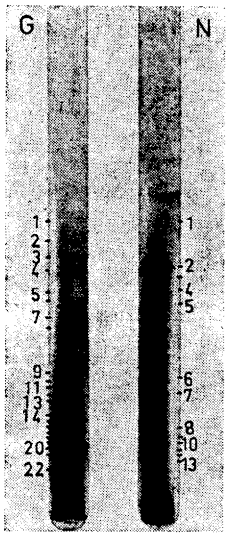

Fig. 6. Polyacrylamide gels of neuronal (N) and glial (G) insoluble proteins prepared according to Lim and Tadayyon.[5] Origin is at the bottom. Numbering refers to Tables 1 and 2 listing specific radioactivities of the individual bands.

Specific radioactivities of the protein discs. Specific radioactivities of the most prominent bands seen and numbered in Fig. 6 are shown in Tables 1 and 2. Specific radioactivities of the neuronal and glial proteins follow the labelling of the total insoluble fractions quoted in Fig. 5. The highest specific activities in the neuronal fraction are detected in the bands moving slowest. The difference between the smallest and the largest specific activity is only 7 fold indicating that all insoluble proteins analysed incorporate ^{3}H-leucine at a rather uniform rate. Radioactivities determined for glial discs also follow kinetics determined by the radioactivity of the precursor pool, most of the bands labelling maximally at 20 min.

Table 1. Relative mobilities and specific radioactivities of individual insoluble proteins of the neuronal fraction after polyacrylamide gel electrophoresis. Cell fractions were incubated with 10μCi of [4,5-^{3}H]leucine. Results are expressed as means of two experiments.

Disc No.	Relative mobility	Specific radioactivity (dpm/mg of protein) × 10^3 at various times (min)		
		5	20	120
N1	0.55	23.6	37.6	173
N2	0.47	5.3	27.8	98.5
N3	0.44	4.4	41.8	100.3
N4	0.42	5.1	30.7	97.4
N5	0.39	11.7	45.0	97.1
N6	0.26	11.3	50.3	144
N7	0.23	11.9	44.0	188
N8	0.16	9.4	55.3	268
N9	0.15	14.2	119	418
N10	0.14	23.6	109	690
N11	0.12	20.6	137	465
N12	0.11	18.2	198	422
N13	0.10	27.0	196	640

Table 2. Relative mobilities and specific radioactivities of individual insoluble proteins of the glial fraction. Results are expressed as means of two experiments.

Disc No.	Relative mobility	Specific radioactivity (dpm/mg of protein) × 10^3 at various times (min)		
		5	20	120
G1	0.53	15.2	15.6	13.4
G2	0.51	9.6	13.6	14.0
G3	0.48	8.3	15.6	12.6
G4	0.45	28.3	26.1	10.5
G5	0.41	16.4	35.1	15.3
G6	0.40	10.2	30.0	20.9
G7	0.36	18.2	25.5	31.1
G8	0.34	14.9	22.7	19.4
G9	0.26	21.8	48.8	30.8
G10	0.25	23.3	23.1	17.1
G11	0.23	5.2	29.0	18.6
G12	0.22	34.0	30.7	26.8
G13	0.21	10.2	23.6	22.3
G14	0.19	7.1	24.5	19.5
G15	0.17	18.1	22.4	24.3
G16	0.16	15.1	35.1	25.4
G17	0.15	10.6	27.9	16.3
G18	0.14	21.4	16.5	24.1
G19	0.14	11.9	69.0	22.9
G20	0.12	9.9	38.8	21.1
G21	0.11	6.2	24.3	25.3
G22	0.08	7.9	28.1	28.9

DISCUSSION

Electron microscopy of brain cell fractions has been presented by several authors [21–23] but satisfactory morphology and cell classification has been published only by Raine *et al.*[20] after careful examination of the preparative procedures. In this paper we show cells essentially similar to those of Raine *et al.*[20] using standard electron microscopic preparation. Comparing the fractions shown here to preparations *in situ* [19,24] it is evident that the separation procedure has affected the cells; membranes are frequently discontinuous and organelles show swelling and rarefaction. This must be kept in mind when considering the data presented. They primarily describe the function of organelles associated with glia and neurons, respectively, and they can be extrapolated to the level of intact cells only with extreme caution. For comparison it is necessary to obtain similar data on the function of isolated organelles and such work is indeed being carried out in our laboratory.

The glial cell fraction accumulates ^{3}H-leucine from the incubation medium more rapidly than the neuronal, reaching three times higher radioactivity. At 20 min the precursor has freely mixed with the endogenous amino acid pool in glia, while a longer time is needed for neurons. These results are in agreement with our earlier observations [13] quoting two times higher TCA-soluble radioactivity for glia after one hour incubation. Similarly Hamberger [25] has recently reported a higher glial capacity for accumulation of a number of amino acids. Rose [26] has found that the glial amino acid pool is more rapidly metabolized than the neuronal, although smaller. Kinetically the uptake of labelled amino acids by brain slices is largely analogous to the cell suspension equilibrating with the endogenous pool at 30 min.[27–29]

Incorporation of amino acids into protein is close to linear up to 20 min in the cell suspension. Neuronal proteins and glial soluble proteins continue incorporation at a decreasing rate up to 2 h bearing analogy to brain slices. By contrast, incorporation into the glial insoluble protein reaches a maximum at a level of 25 000 dpm/mg protein showing rapid degradation or decreased protein synthesis. Interestingly much of the brain proteolytic activity has been found in membraneous fractions [11] and particularly in grey matter and myelin [30] closely related to glia. Yet no exceptional *in vivo* turnover of the glial protein has been observed by Blomstrand and Hamberger.[31]

The early leveling of glial incorporation curve suggests a relatively more dominant role for mitochondrial protein synthesis in glia compared to neurons. Incorporation of isolated mitochondria usually levels off at around 20 min while brain polysomes incorporate in a linear fashion for some hours.[32,33] Such an observation is further supported by electron microscopy showing an abundance of mitochondria compared to rough endoplasmic reticulum in isolated glia (Figs. 3 and 4). Additionally, higher specific radioactivities are measured in glial than in neuronal mitochondria after *in vitro* incubation.[34]

The radioactivities of the individual neuronal protein bands (Table 1) constantly increase with time indicating net deposition of radioactive protein. Judged by electrophoretic controls of isolated subcellular organelles (Hemminki, in preparation) the slowly moving bands (Fig. 6) most likely originate from microsomal and mitochondrial membrane structures. The rapid labelling

of these proteins parallels our finding *in vivo* (Hemminki, in preparation) accentuating the active metabolism of membrane proteins in brain. Most of the glial proteins on the other hand label maximally at 20 min showing an equilibrium between protein synthesis and degradation. Whether the apparently different maxima of some proteins (Table 2) imply existence of protein pools with unique incorporation kinetics cannot be estimated with the present accuracy of the technique. Although the rate of incorporation into neuronal and glial proteins is strikingly different, the protein patterns are largely similar in gel electrophoresis (Fig. 6). The few bands, probably unique for the cell fraction, show no exceptional incorporation features. Packmann *et al.*[35] reported analogous results for neuronal and glial soluble proteins.

Quantitative differences of the neuronal and glial protein incorporation *in vitro* have been a subject of several studies [26,36,37, 13] generally quoting 2 to 5 times higher incorporation into the neuronal fraction. In this study the difference is found to depend on the incubation time. If the 20 min values are taken for comparison the difference is 7 fold. As the specific activity of the precursor is probably much lower in the neuronal fraction, the efficiency of incorporation may be at least 15 times higher in neurons. The actual rate of protein synthesis in the two cell types cannot be derived from these data because the specific radioactivity of the precursor is not known and rapid degradation of protein may very much obscure the estimation.

For comparison some approximations can be given. The rate of incorporation of labelled leucine is around 8 pmol (mg protein h)$^{-1}$ for the neuronal insoluble protein and 0.5 pmol (mg protein h)$^{-1}$ for the glial insoluble protein. To derive the absolute rate of incorporation the specific activity of the precursor pool should be known. The concentration of labelled leucine was 1.2 μM and around 1 mg protein was in each incubation vessel. Arbitrarily taking the data of Jones and McIlwain [29] on tissue amino acid pools, we can very approximately calculate that for absolute incorporation the above rates should be multiplied by around four, and yet no provision is made for the rapid release of amino acids during the incubation as described by Jones and McIlwain.[29] Tiplady and Rose [37] presented similar data quoting an incorporation of 4 to 11 pmol (mg protein h)$^{-1}$ for labelled lysine.

At least two principal techniques are currently available for preparing cell suspensions from brain tissue. One introduced by Rose [21] based on mechanical sieving, has been characterized by light and electron microscopy and by enzymatic and metabolic studies [21,38,22] and is now used in several modifications.[31,23] The other is based on enzymatic digestion with trypsin [39] or with collagenase-hyaluronidase.[12] The cells prepared by collagenase-hyaluronidase incubation have been characterized by light and electron microscopy and their ability to accumulate amino acids and potassium, to consume oxygen and to incorporate radioactive amino acids in protein.[13] In this study electron microscopic findings are presented to show the relatively well preserved structural organisation of the preparation. Uptake and incorporation of ^{3}H-leucine by the neuronal and glial cell fractions largely follows kinetics quoted for brain slices. High specific radioactivities incorporated into protein and relatively large yields of material obtained recommend collagenase – hyaluronidase preparation even for detailed studies of individual proteins.

Acknowledgements. This work was supported by the *Sigrid Jusélius Foundation* and the *National Research Council for Medical Sciences*, Finland. Electron microscopy was performed in the Electron Microscope Laboratory, Helsinki.

The author is grateful to Professor J. Järnefelt and to Professor A. Raina for critical evaluation of the manuscript. The skilled technical assictance of Mrs. Kirsti Salmela is appreciated.

REFERENCES

1. Lajtha., A. *Intern. Rev. Neurobiol.* **6** (1964) 1.
2. Gaitonde, M. K. and Martenson, R. E. *J. Neurochem.* **17** (1970) 551.
3. Ornstein, L. and Davis, B. J. *Ann. N. Y. Acad. Sci.* **121** (1964) 321.
4. Takayama, K., MacLennan, D. H., Tzagoloff, A. and Stoner, C. D. *Arch. Biochem. Biophys.* **114** (1966) 223.
5. Lim, R. and Tadayyon, E. *Anal. Biochem.* **34** (1970) 9.
6. Martenson, R. E. and Gaitonde, M. K. *J. Neurochem.* **16** (1969) 333.
7. Waehneldt, T. V. and Mandel, P. *FEBS Lett.* **9** (1970) 209.
8. Agrawal, H. C., Banik, N. L., Bone, A. H., Davidson, A. N., Mitchell, R. F. and Spohn, M. *Biochem. J.* **120** (1970) 635.
9. Cotman, C. W. and Mahler, H. R. *Arch. Biochem. Biophys.* **120** (1967) 384.
10. Bosmann, H. B., Case, R. and Shea, M. B. *FEBS Lett.* **11** (1970) 261.
11. D'Monte, B., Marks, N., Datta, R. K. and Lajtha, A. *Protein Metabolism of the Nervous System*, Plenum Press, New York 1970, p. 185.
12. Hemminki, K. *FEBS Lett.* **9** (1970) 290.
13. Hemminki, K. and Holmila, E. *Acta Physiol. Scand.* **82** (1971) 135.
14. Sabatini, D. D., Bensch, K. and Barnett, R. J. *J. Cell. Biol.* **17** (1963) 19.
15. Lowry, O. H., Rosebrough, N. J., Farr, A. L. and Randall, R. J. *J. Biol. Chem.* **193** (1951) 265.
16. Cain, D. F. and Pitney, R. E. *Anal. Biochem.* **22** (1969) 11.
17. Davies, W. E. *J. Neurochem.* **17** (1970) 297.
18. Hemminki, K. *Acta Chem. Scand.* **25** (1971) 3887.
19. Hydén, H. *The Cell*, Academic, New York 1961, Vol. 4, p. 215.
20. Raine, C. S., Poduslo, S. E. and Norton, W. T. *Brain Res.* **27** (1971) 11.
21. Rose, S. P. R. *Biochem. J.* **102** (1967) 33.
22. Flangas, A. L. and Bowman, R. E. *J. Neurochem.* **17** (1970) 1237.
23. Johnson, D. E. and Sellinger, O. Z. *J. Neurochem.* **18** (1971) 1445.
24. Mugnaini, E. and Walberg, F. *Ergeb. Anat. Entwick.-Gesch.* **37** (1964) 194.
25. Hamberger, A. *Brain Res.* **31** (1971) 109.
26. Rose, S. P. R. *J. Neurochem.* **15** (1968) 1415.
27. Järnefelt, J. and Huttunen, M. O. *Regulatory Functions of Biological Membranes*, Elsevier, Amsterdam 1968, p. 208.
28. Huttunen, M. O. *Protein and Ribonucleic Acid Metabolism in Rat Brain Cortex Slices*, Diss., University, Helsinki 1969.
29. Jones, D. A. and McIlwain, H. *J. Neurochem.* **18** (1971) 41.
30. Palladin, A. V. and Belik, Ya. V. *Protein Metabolism of the Nervous System*, Plenum Press, New York 1970, p. 77.
31. Blomstrand, C. and Hamberger, A. *J. Neurochem.* **16** (1969) 1401.
32. Hemminki, K. *J. Neurochem.* **19** (1972) 2699.
33. Campbell, M. K., Mahler, H. R., Moore, W. J. and Tewari, S. *Biochemistry* **5** (1966) 1174.
34. Blomstrand, C., Hamberger, A. and Yanagihara, T. *J. Neurochem.* **18** (1971) 1469.
35. Packman, P. M., Blomstrand, C. and Hamberger, A. *J. Neurochem.* **18** (1971) 1.
36. Blomstrand, C. and Hamberger, A. *J. Neurochem.* **17** (1970) 1187.
37. Tiplady, B. and Rose, S. P. R. *J. Neurochem.* **18** (1971) 549.
38. Rose, S. P. R. and Sinha, A. K. *J. Neurochem.* **16** (1969) 1319.
39. Norton, W. T. and Poduslo, S. E. *Science* **167** (1970) 1144.

Received July 3, 1972.

ACTA CHEMICA SCANDINAVICA 27 (1973) 345–356

The Crystal Structure of $Tl_2[Cu(SO_3)_2]$

INGER HJERTÉN and BIRGIT NYBERG

Institute of Inorganic and Physical Chemistry, University of Stockholm, S-113 86 Stockholm, and Division of Inorganic Chemistry 2, Chemical Center, Box 740, S-220 07 Lund 7, Sweden

The crystal structure of thallium(I) copper(II) disulfite has been determined and refined from three dimensional X-ray film and diffractometer data. The structure is triclinic with the space group $P\bar{1}$. The unit cell, which contains one formula unit, has the dimensions

$a = 5.4738(3)$ Å, $b = 7.3290(4)$ Å, $c = 5.4717(5)$ Å, $\alpha = 111.638(7)°$, $\beta = 123.570(4)°$, $\gamma = 88.019(7)°$.

The structure consists of trigonal pyramids of SO_3^{2-} and somewhat distorted CuO_6 octahedra. The six oxygen atoms around Cu belong to six different SO_3^{2-} groups. The CuO_6 octahedra and the SO_3^{2-} pyramids form $Cu(SO_3)_2^{2-}$ layers extending almost parallel to the *ac* plane. These layers are held together by thallium atoms. The average bond distances in the sulfite group are S – O = 1.54 Å and O – O = 2.43 Å. The average value of the angle O – S – O is 104.5°.

During the last years the crystal structures of a series of different metal sulfites have been studied. Reports on the structures of $Cu_2SO_3.CuSO_3.2H_2O$,[1] NH_4CuSO_3,[2] and Ag_2SO_3,[3] as well as a report on a structural refinement of Na_2SO_3,[4] have been published. In connection with the crystal structure studies of the copper sulfites the compound thallium(I) copper(II) sulfite was investigated.

EXPERIMENTAL

Preparation of the crystals. When synthesizing $Tl_2[Cu(SO_3)_2]$ a method according to Canneri [5] was used. To a saturated aqueous solution of $CuSO_4.5H_2O$ an equivalent amount of Tl_2CO_3 was added, the latter also as a saturated aqueous solution. SO_2 was passed through the solution, and after a few minutes a yellow crystalline precipitate was obtained. After washing with water the crystals were dried in a nitrogen atmosphere. Microscopic investigation revealed thin yellow transparent plates.

Analysis. A small sample of $Tl_2[Cu(SO_3)_2]$ was ignited, and the SO_2 formed was converted to H_2SO_4 in an H_2O_2-solution, whereupon the amount of sulfur was determined by titration with alkali. The amount of copper was determined by atomic absorption spectroscopy. (Found: Cu 10.22 ± 0.5; S 8.93 ± 0.25. Calc. for $Tl_2[Cu(SO_3)_2]$: Cu 10.05; S 10.14.)

Infrared absorption spectrum. The infrared spectrum of a sample of $Tl_2[Cu(SO_3)_2]$ was recorded with a Perkin-Elmer 180 spectrophotometer, using the KBr-pellet technique.

The maxima of absorption were observed at the following frequencies (cm^{-1}) and intensities: 980 (st), 895 (st), 860 (st), 670 (m), 590 (w), 500 (st) and 455 (m). The frequencies are in good agreement with the values reported in the literature.[6]

X-Ray diffraction data and computing methods. The unit cell parameters were calculated by least squares refinement from a powder photograph taken with strictly monochromatized Cu$K\alpha_1$ radiation ($\lambda = 1.54050$ Å) in a Guinier-Hägg focusing camera. Potassium chloride ($a = 6.29228$ Å) [7] was used as an internal standard. The powder pattern was completely indexed (Table 1) on the basis of the following triclinic cell (25°C).

a	= 5.4738(3) Å	α	= 111.638(7)°
b	= 7.3290(4) Å	β	= 123.570(4)°
c	= 5.4717(5) Å	γ	= 88.019(7)°
V	= 165.895 Å^3		

Table 1. X-Ray powder pattern for $Tl_2[Cu(SO_3)_2]$. Cu$K\alpha_1$-radiation ($\lambda = 1.54050$ Å).

h k l	$10^5 \sin^2\theta$ obs	$10^5 \sin^2\theta$ calc	I_{obs}
0 1 0	1341	1342	m
−1 0 1	2713	2713	m
1 0 0	2997	2995	
0 −1 1		2996	st
−1 −1 1	3121	3121	st
−1 1 0	3464	3451	
0 0 1		3465	v st
−1 1 1	4985	4990	m
0 −2 1	5213	5212	m
1 1 0		5214	
−1 −2 1	6210	6215	v st
−1 2 0	6613	6611	v v st
0 1 1		6618	
−1 −1 2	7960	7959	v v st
1 −1 1	8859	8862	v v st
−2 −1 1	9231	9237	m
−2 1 1	9354	9352	m
−1 2 1	9951	9952	m
0 −3 1	10112	10114	m
1 2 0		10118	
1 −2 1	10199	10201	m
−2 −1 2	10323	10328	m
−2 0 2	10845	10845	st
−2 1 0	11577	11570	v w
0 −1 2		11581	
2 0 0	11982	11981	st
0 −2 2		11986	
−1 −3 1		11993	
−2 −2 2	12481	12487	w
−2 −2 1	13207	13207	w
−1 −3 2		13208	
−2 2 1	13440	13437	v v w (d)
−1 1 2		13450	
−2 2 0	13850	13844	m
0 0 2		13860	
−2 1 2	14067	14065	m
1 −3 1	14223	14226	v w
0 −3 2	15074	15076	st
2 1 0		15077	

Table 1. Continued.

−2 −3 2	17333	17331	w (d)
−1 3 1	17603	17599	v v w (d)
0 −4 1	17698	17700	w (d)
1 3 0		17708	
−3 0 2	18340	18337	v w
−2 −1 3		18349	
−3 −1 2	18679	18688	w
−2 3 0	18805	18802	w
−3 0 1	19182	19182	w
−3 1 1	19710	19705	m
−1 −4 2	19869	19860	v w (d)
−2 −3 1		19862	
−2 3 1	20213	20207	w (d)
−1 2 2		20223	
−3 1 2	20681	20671	w (d)
−2 0 3		20686	
1 −4 1	20944	20935	w (d)
1 2 1		20953	
2 −2 1	21178	21180	w
0 4 0	21479	21479	v v w (d)
−3 −2 2	21725	21723	m
−2 −3 3		21730	
1 −3 2	22935	22935	st
2 0 1		22940	
−1 0 3		22941	
−3 −2 3	24189	24187	v w (d)
2 −3 1	24339	24328	m
1 0 2		24350	
−2 −4 2	24859	24860	v w (d)
−3 1 0	25672	25670	st
−3 −2 1	26191	26191	m
−1 −4 3		26195	

The powder photograph was measured and interpreted to $\sin^2\theta = 0.47$.

A powder photograph without any internal standard showed that no reaction had occurred between $Tl_2[Cu(SO_3)_2]$ and KCl.

The unit cell is not reduced according to Buerger [8] or to Delaunay [9] on account of similarities in cell dimensions and structure with the earlier investigated structure of NH_4CuSO_3.[2] The unit cell reduced according to Buerger [8] as well as to Delaunay [9] should have the following dimensions

a	= 5.4717 Å	α	= 110.660°
b	= 7.3275 Å	β	= 118.195°
c	= 5.1748 Å	γ	= 92.014°

The observed density of $Tl_2[Cu(SO_3)_2]$, determined from the apparent loss of weight in chloroform, is 5.98 ± 0.10 g/cm³. Assuming one formula unit in the unit cell gives the calculated density = 6.33 g/cm³. The rather big difference between the values could depend on the fact that the determination was made in an early stage when the preparation was not quite pure.

554 independent reflections were recorded, using Weissenberg multiple film technique, with Ni-filtered CuK radiation. Two crystals were investigated, and the relative intensities were visually estimated by comparison with an intensity scale obtained by photographing one reflection with different exposure times. In spite of the great tendency of twinning, the crystals did not show any such effect. The space group was assumed to be $P\bar{1}$.

The accuracy of the structure determination based upon the film data, especially in the case of the S – O distances, was not as good as wanted, so a new set of three dimensional intensity data was collected. A crystal [an irregular triangular plate, volume = 1.2×10^{-4} mm^3, thickness = 0.011 mm (b^* direction)], without satellites or any twinning tendency was selected by means of Weissenberg technique. A Siemens automatic X-ray diffractometer equipped with a scintillation counter with pulse height discrimination was used. The 5-values measuring technique was applied and 1048 independent reflections up to $\theta = 34°$ were measured, using Nb-filtered MoK radiation. The value of $\sigma(I_0)/I_0$ was then ≤ 0.3. Three standard reflections were measured with a period of 40 reflections.

Corrections were made for Lorentz, polarization and absorption effects, with the linear absorption coefficient value,[10] $\mu = 526.6$ cm^{-1}. The calculations were performed on the electronic computers CD 3600, IBM 1800, and IBM 360/75. A list of the programs used in the calculations is given in Table 2.

Table 2. Computer programs used for the crystallographic calculations. All the programs are written in FORTRAN IV.

Program name and function	Authors
ABS. Absorption, extinction and Lp-factors.	P. E. Werner and M. Leijonmarck, Stockholm, Sweden.
DATA. Reflection data handling including storing on disk, correction of erroneous reflections or inclusions of new ones in a data set stored on disk; index transformation.	B. G. Brandt, Stockholm, Sweden.
DRF. Fourier summations and structure factor calculations.	A. Zalkin, Berkeley, USA. Modified by R. Liminga and J.-O. Lundgren, Uppsala, Sweden. Further modified by O. Lindgren, Göteborg and by A. G. Nord and B. G. Brandt, Stockholm, Sweden.
LALS. Full matrix least-squares refinement of positional and thermal parameters and of scale factors.	P. K. Gantzel, R. A. Sparks and K. N. Trueblood, Los Angeles, USA. Modified by A. Zalkin, Berkeley, USA, and by J.-O. Lundgren, R. Liminga and C.-I. Brändén, Uppsala, Sweden. Further modified by O. Lindgren, Göteborg and by B. G. Brandt and A. G. Nord, Stockholm, Sweden.
DISTAN. Calculation of interatomic distances and bond angles with estimated standard deviations.	A. Zalkin, Berkeley, USA. Modified by A. G. Nord and B. G. Brandt, Stockholm, Sweden.
LAZY. Calculation of $\sin^2\theta$ and d-values from the measured reflection sites of a Guinier powder photograph after internal standard correction.	A. G. Nord, Stockholm, Sweden.
PIRUM, PURUM. Indexing of powder photographs and determination or refinement of unit cell parameters from powder or diffraction data by the method of least squares.	P.-E. Werner, Stockholm, Sweden.

Table 2. Continued.

TRICL. Calculation of direct and reciprocal cell parameters, the constants in the quadratic formula and tests for reducibility according to Delauny and Buerger.	L. Kihlborg, Stockholm, Sweden.
VIP. Angle settings for three circle diffractometers.	R. Norrestam, Stockholm, Sweden.
SIP. Generation of steering paper tape for Siemens AED.	R. Norrestam, Stockholm, Sweden.
SIMSA. Interpretation of output on paper tape from Siemens AED and evaluation of intensities.	R. Norrestam, Stockholm, Sweden.
EXTDATA. Calculation of the factor C in Zachariasen's 1963-formula for extinction correction. Application of the correction.	B. G. Brandt, Stockholm, Sweden.
ORTEP. Thermal ellipsoid plot. For crystal structure illustration.	C. K. Johnsson, Oak Ridge, USA. Modified by I. Carlbom, Stockholm, Sweden.

STRUCTURE DETERMINATION

In the space group $P\bar{1}$ eight special point positions and the general position $2(i)$: $\pm(x,y,z)$ exist. By placing the only copper atom in the position $1(h)$: $\frac{1}{2},\frac{1}{2},\frac{1}{2}$ the origin was fixed. The two thallium atoms could be situated either in two special positions or in the general twofold position $2(i)$. From the absence of any high peak in the Patterson projections $P(p\ v\ w)$ and $P(u\ p\ w)$ at u, v or $w=\frac{1}{2}$ it was concluded that the position $2(i)$ was the only one available for thallium. The parameters could be derived, and the electron density projections $\varrho(p\ y\ z)$ and $\varrho(x\ p\ z)$ were calculated using the signs of $F(0kl)$ and $F(h0l)$ obtained from the thallium and copper contributions. The positions of the two sulfur atoms and the six oxygens atoms, all in position $2(i)$, could then be obtained.

A refinement of the coordinates was performed by means of the least-squares method. Anisotropic temperature factors were used for all the atoms, and it was evident that using the atomic scattering curves for neutral atoms given by Cromer and Waber,[11] with the real part of the anomalous dispersion correction [12] applied, gave the best results. When a correction for secondary extinction was made according to Zachariasen,[13] the R-value from the refinement including all the reflections was down to 3.12%. The weighting function used was that of Cruickshank, $w = (A + |F_{obs}| + C|F_{obs}|^2 + D|F_{obs}|^3)^{-1}$, with the following final values for the parameters: $A = +60$, $C = +0.007$, $D = +0.001$. No unobserved reflections were introduced, and a three dimensional difference synthesis showed no peak heights above 15% of the oxygen peak height. The results thus obtained are good enough to leave the possibility of the lower symmetry out of consideration.

The final values of the atomic parameters, the anisotropic temperature factors of all the atoms and their standard deviations are given in Table 3. A list of observed and calculated structure factors is presented in Table 4. A weight analysis obtained in the last cycle is given in Table 5.

Table 3. The structure of $Tl_2[Cu(SO_3)_2]$.

Space group: $P\bar{1}$.
Unit cell dimensions: $a = 5.4738$ (3) Å
$b = 7.3290$ (4) Å
$c = 5.4717$ (5) Å
$\alpha = 111.638$ (7)°
$\beta = 123.570$ (4)°
$\gamma = 88.019$ (7)°

Cell content: 1 $[Tl_2[Cu(SO_3)_2]]$
Arrangement of atoms: 1 Cu in 1(h): $(\frac{1}{2}, \frac{1}{2}, \frac{1}{2})$
2 Tl, 2 S, 6 O(1)–(3) in 2(i): $\pm(x, y, z)$

Fractional atomic coordinates with e.s.d.'s. as calculated from the least-squares refinement, in parentheses.

Atom	x	y	z
Tl	0.70128(7)	0.12150(4)	0.92013(8)
Cu	$\frac{1}{2}$	$\frac{1}{2}$	$\frac{1}{2}$
S	0.87579(34)	0.60292(20)	0.22741(38)
O(1)	0.7750(13)	0.7152(8)	0.4390(14)
O(2)	0.2191(11)	0.6866(7)	0.4386(13)
O(3)	0.2506(11)	0.3124(7)	0.0316(13)

Anisotropic thermal parameters, β_{ij} with e.s.d.'s.
The β values refer to the temperature factor

$$\exp(-(\beta_{11}h^2 + \beta_{22}k^2 + \beta_{33}l^2 + \beta_{12}hk + \beta_{13}hl + \beta_{23}kl)).$$

Atom	β_{11}	β_{22}	β_{33}	β_{12}	β_{13}	β_{23}
Tl	0.0217 (2)	0.0079 (1)	0.0227 (2)	0.0060 (1)	0.0206 (3)	0.0097 (1)
Cu	0.0095 (4)	0.0059 (2)	0.0082 (5)	0.0055 (4)	0.0070 (8)	0.0059 (5)
S	0.0096 (6)	0.0047 (2)	0.0092 (7)	0.0020 (5)	0.0073 (11)	0.0059 (6)
O(1)	0.018 (2)	0.011 (1)	0.016 (3)	0.012 (2)	0.025 (4)	0.013 (2)
O(2)	0.007 (2)	0.007 (1)	0.016 (3)	0.006 (2)	0.009 (4)	0.008 (2)
O(3)	0.012 (2)	0.007 (1)	0.012 (2)	0.005 (2)	0.007 (4)	0.009 (2)

R.m.s. components of thermal displacement (in Å) along the principal axes of the ellipsoid of thermal vibration.

Atom	R(1)	R(2)	R(3)
Tl	0.1322	0.1391	0.1670
Cu	0.0794	0.1019	0.1277
S	0.0858	0.1025	0.1145
O(1)	0.0939	0.1251	0.1636
O(2)	0.0762	0.1211	0.1472
O(3)	0.0884	0.1205	0.1390

Table 4. The observed and calculated structure factors of $Tl_2[Cu(SO_3)_2]$. Each group of three columns contains k, 10 $|F_o|$ and 10 $|F_c|$. It is headed by the values h and l common to the group.

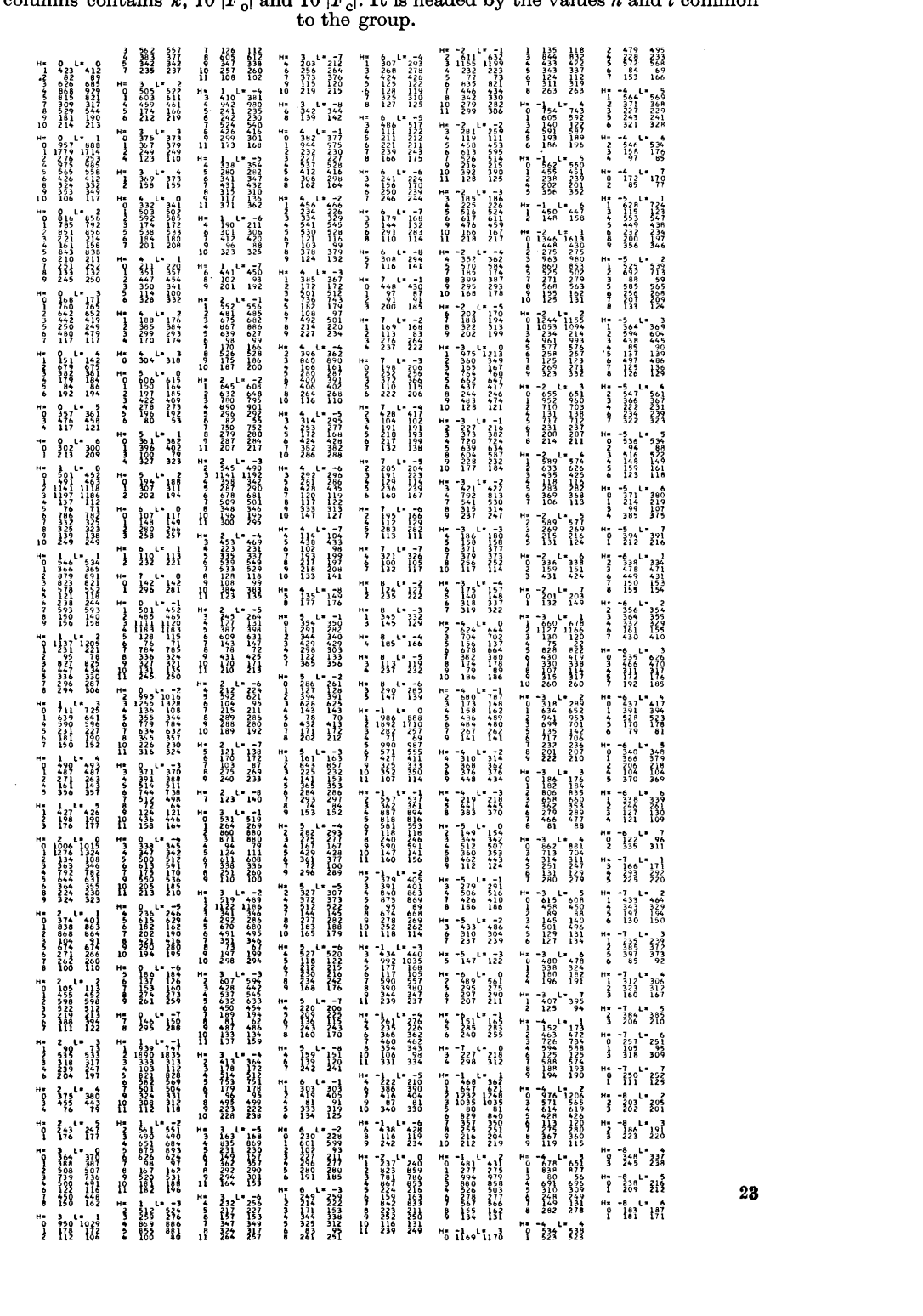

Table 5. Weight analysis obtained in the final cycle of the least-squares refinement of $Tl_2[Cu(SO_3)_2]$. w = weighting factor. $\Delta = |F_o| - |F_c|$.

Interval $\sin\theta$	Number of independent reflections	$\overline{w\Delta^2}$	Interval F_o	Number of independent reflections	$\overline{w\Delta^2}$
0.0 – 0.269	134	2.44	0.0 – 11.9	104	1.62
0.269 – 0.339	122	0.95	11.9 – 15.7	105	1.34
0.339 – 0.388	114	0.93	15.7 – 19.7	105	0.71
0.388 – 0.427	110	0.68	19.7 – 23.5	105	0.69
0.427 – 0.460	117	0.41	23.5 – 28.7	105	0.56
0.460 – 0.489	99	0.98	28.7 – 34.3	104	0.51
0.489 – 0.515	99	0.91	34.3 – 42.1	105	0.52
0.515 – 0.538	107	0.65	42.1 – 52.0	105	1.30
0.538 – 0.560	105	0.72	52.0 – 67.8	105	0.89
0.560 – 0.580	41	1.14	67.8 – 189.2	105	1.86

DESCRIPTION AND DISCUSSION OF THE STRUCTURE

The structure of $Tl_2[Cu(SO_3)_2]$ may be described as consisting of layers of trigonal pyramids of SO_3^{2-} and somewhat distorted CuO_6 octahedra linked together by corner sharing. A projection of the structure is given in Fig. 1, and a stereoscopic view of a part of the structure is shown in Fig. 2.

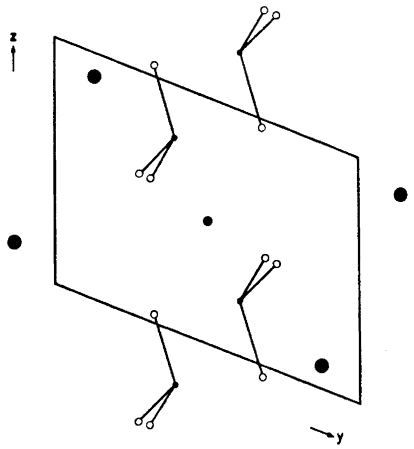

Fig. 1. Projection along the *a* axis on to the *bc* plane of the crystal structure of $Tl_2[Cu(SO_3)_2]$. The sulfite groups are indicated by full lines. Open circles denote oxygen atoms, small filled circles sulfur, medium filled circles copper, and large filled circles denote thallium atoms.

The composition of a layer can be represented by the formula $[Cu(SO_3)_2^{2-}]_n$. The layers are almost parallel to the *ac* plane and are held together by thallium atoms. The function of the thallium atoms is similar to that of the ammonium ions in NH_4CuSO_3.[2]

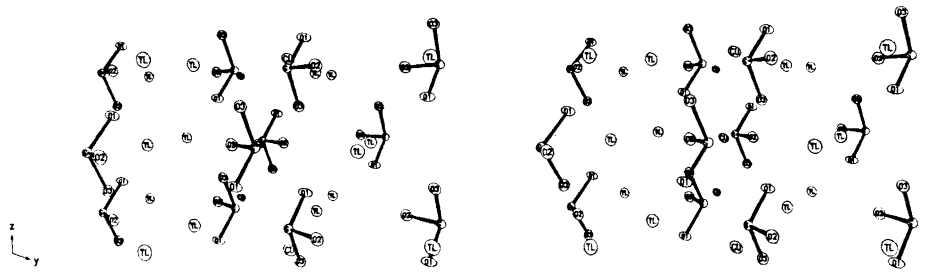

Fig. 2. A stereoscopic view of the structure of $Tl_2[Cu(SO_3)_2]$ showing the linking in the b* direction of the $[Cu(SO_3)_2^{2-}]_n$ layers and the thallium atoms. The *ac* plane is vertical and perpendicular to the paper plane. The atoms are represented by the boundary "thermal ellipsoid" scaled to include 50 % of the probability distribution.

A bounded straight projection (along b^*) of a part of a layer together with the nearest thallium atoms is given in Fig. 3.

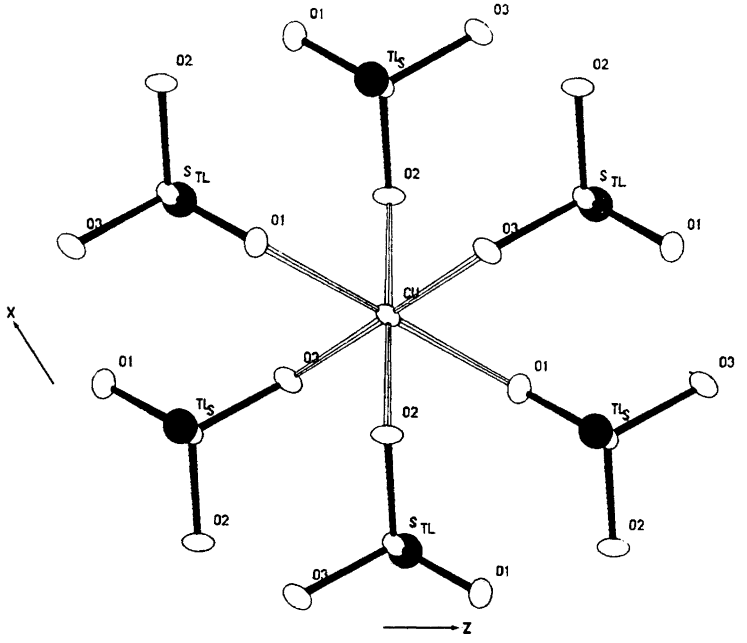

Fig. 3. A bounded straight projection on the *ac* plane of the environment of the copper atom.

Thallium is coordinated to one sulfur atom and to six oxygen atoms from three different sulfite groups in one layer and to three oxygen atoms from three different sulfite groups in the next layer (Fig. 4, Fig. 5b).

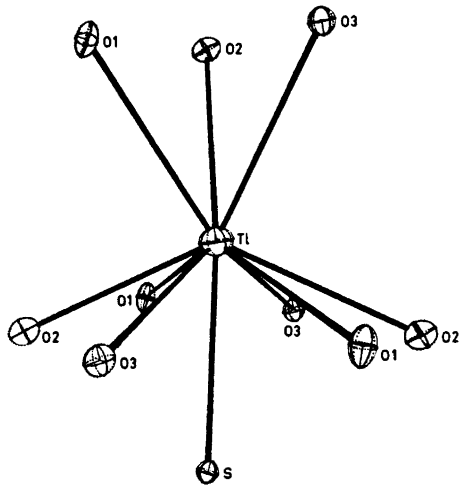

Fig. 4. A view of the environment of the thallium atom in $Tl_2[Cu(SO_3)_2]$. The atoms are represented by "thermal ellipsoids" scaled to include 50 % of the probability distribution.

The interatomic distances and angles with standard deviations are given in Table 6.

The mean value of the S – O distances in the sulfite ion is 1.538 Å, well corresponding to the theoretical value of 1.54 Å suggested by Gillespie and Robinson.[14] The dimensions of the SO_3^{2-} group are also consistent with the values found in $(NH_4)_2SO_3.H_2O$,[15] $NiSO_3.6H_2O$,[16] and $ZnSO_3.2\frac{1}{2}H_2O$.[17] In these com-

Table 6. Interatomic distances (Å) and angles (°) and their e.s.d.'s in $Tl_2[Cu(SO_3)_2]$. The distances are uncorrected for thermal motion.

S – O(1)	1.515 (6)	O(1) – S – O(2)	105.22 (30)
S – O(2)	1.549 (5)	O(1) – S – O(3)	104.89 (29)
S – O(3)	1.551 (5)	O(2) – S – O(3)	103.51 (28)
O(1) – O(2)	2.434 (7)		
O(1) – O(3)	2.431 (8)		
O(2) – O(3)	2.435 (7)		
Cu – 2O(1)	2.444 (6)	O(1) – Cu – O(2)	86.45 (19)
Cu – 2O(2)	1.992 (5)	O(1) – Cu – O(3)	86.34 (20)
Cu – 2O(3)	1.996 (5)	O(2) – Cu – O(3)	86.80 (21)
Tl – O(1)	2.818 (6)	Tl – S	3.205 (1)
Tl – O(1)	2.823 (6)		
Tl – O(2)	3.008 (5)	Tl – O(1)	3.357 (6)
Tl – O(2)	3.032 (5)	Tl – O(2)	3.281 (5)
Tl – O(3)	3.001 (5)	Tl – O(3)	3.277 (5)
Tl – O(3)	3.035 (5)		
		Tl – Tl	3.492 (1)
		Tl – Tl	3.495 (1)
		Tl – Tl	3.513 (1)

pounds the sulfite oxygen atoms are affected by hydrogen bonding or metal bonding, and the S – O distances and angles are slightly different from the values found in Na_2SO_3.[4]

In $Tl_2[Cu(SO_3)_2]$ the individual S – O distances in the sulfite group can be correlated to the length of the bond between oxygen and copper. When the oxygen atom is found at a short distance (2.00 Å) from the copper atom its distance to the sulfur atom is long (1.55 Å), while a long Cu – O distance (2.44 Å) corresponds to a short S – O distance (1.52 Å).

As could be seen in the discussion of various sulfites performed by Kierkegaard *et al.*[18] there is a rather regular variation of the O – S – O angle with the S – O distance, which is also consistent with $Tl_2[Cu(SO_3)_2]$. The distorted octahedron CuO_6 has dimensions very similar to those found for divalent copper in $Cu_2SO_3.CuSO_3.2H_2O$.[1]

The coordination around thallium can hardly be described in terms of a regular polyhedron, but there are similarities with half a cuboctahedron (Fig. 5a, b).

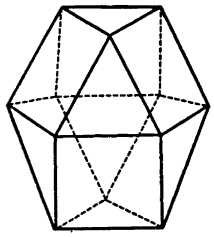

Fig. 5a. An ideal cuboctahedron.

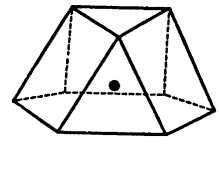

Fig. 5b. An idealization of the environment of Tl (I) in $Tl_2[Cu(SO_3)_2]$. The small full circle denotes the sulfur atom and the large filled circle denotes the thallium atom. The nine oxygen atoms are to be found at the corners of the indicated coordination polyhedron.

The Tl – S distance (3.21 Å) is below the value found in the ionic compound Tl(I)Tl(III)S_2 (Tl(I) – 8 S: 3.32 Å).[19] According to Shannon and Prewitt [20] the sum of the ionic radii for Tl^+ and S^{2-} with a coordination number of eight is 3.44 Å (1.60 Å + 1.84 Å). The values of the ionic radii are somewhat uncertain, but with regard to the distribution of the atoms around Tl and the relatively short Tl – S distance, a covalent bond may be assumed. The six nearest oxygen atoms, all belonging to the same layer, have a mean distance to the thallium atom of 2.95 Å. The sum of the ionic radii of Tl^+ and O^{2-} is 3.00 Å (1.60 + 1.40 Å).[20] Three additional bond distances from the thallium atom to oxygen atoms in another layer have a mean value of 3.30 Å. The shortest distance between two thallium atoms is 3.492 Å, which may be compared to the Tl – Tl metal distance: 3.408 Å.[21]

In this compound the inert pair of electrons in thallium (I) is not very stereochemically active. In the compounds Tl_2SO_4[22] and $TlNO_3.4TU$ [23] (TU = thiourea) thallium(I) is stereochemically inactive.

Further studies of metal sulfites are in progress to gain more information of the sulfite group.

Acknowledgements. The authors thank Professors Peder Kierkegaard, Arne Magnéli and Bengt Aurivillius for encouraging interest and for all facilities placed at their disposal. Thanks are also due to Dr. Sven Westman for his correction of the English of this paper.

This investigation has been performed with financial support from the *Swedish Natural Science Research Council* and from the *Tri-Centennial Fund of the Bank of Sweden.*

REFERENCES

1. Kierkegaard, P. and Nyberg, B. *Acta Chem. Scand.* **19** (1965) 2189.
2. Nyberg, B. and Kierkegaard, P. *Acta Chem. Scand.* **22** (1968) 581.
3. Larsson, L. O. *Acta Chem. Scand.* **23** (1969) 2261.
4. Larsson, L. O. and Kierkegaard, P. *Acta Chem. Scand.* **23** (1969) 2253.
5. Canneri, G. *Gazz. Chim. Ital.* **52** (1922) 266.
6. Newman, G. and Powell, D. B. *Spectrochim. Acta* **19** (1963) 213.
7. Hambling, P. G. *Acta Cryst.* **6** (1953) 98.
8. Buerger, M. J. *X-Ray Crystallography*, Wiley, New York 1962, p. 364.
9. *International Tables for X-Ray Crystallography*, Kynoch Press, Birmingham 1962, Vol. I, p. 530.
10. *International Tables for X-Ray Crystallography*, Kynoch Press, Birmingham 1962, Vol. III, p. 162.
11. *International Tables for X-Ray Crystallography*, Vol. IV, in manuscript.
12. *International Tables for X-Ray Crystallography*, Kynoch Press, Birmingham 1962, Vol. III, p. 215.
13. Zachariasen, W. H. *Acta Cryst.* **16** (1963) 1141.
14. Gillespie, R. J. and Robinson, E. A. *Can. J. Chem.* **41** (1963) 2074.
15. Batelle, L. F. and Trueblood, K. N. *Acta Cryst.* **19** (1965) 531.
16. Baggio, S. and Becka, L. N. *Acta Cryst.* **B 25** (1969) 1150.
17. Nyberg, B. *Acta Chem. Scand.* **26** (1972) 857.
18. Kierkegaard, P., Larsson, L. O. and Nyberg, B. *Acta Chem. Scand.* **26** (1972) 218.
19. Hahn, H. and Klingler, W. *Z. anorg. Chem.* **260** (1949) 110.
20. Shannon, R. D. and Prewitt, C. T. *Acta Cryst.* **B 25** (1969) 925.
21. *Tables of Interatomic Distances and Configuration in Molecules and Ions*, The Chemical Society, London 1958.
22. Pannetier, G. and Gaultier, M. *Compt. Rend. Acad. Sci. Ser. C.* **263** (1966) 132.
23. Boeyens, J. C. A. and Herbstein, F. H. *Inorg. Chem.* **6** (1967) 1408.

Received July 24, 1972.

ACTA CHEMICA SCANDINAVICA 27 (1973) 357–382

Short Communications

Analysis of the PMR Spectra of the 2-Methoxy- and 2-Methylthio-1,3,2-Oxathiaphospholanes

KNUT BERGESEN and MALVIN BJORØY

Chemical Institute, University of Bergen, N-5000 Bergen, Norway

In an earlier paper [1] an analysis of the PMR spectra of 2-chloro-, 2-phenyl-, and 2-phenoxy-1,3,2-oxathiaphospholanes has been reported. As a continuation of this work the PMR spectra of the ring protons of 2-methoxy- and 2-methylthio-1,3,2-oxathiaphospholanes, I and II, have been investigated. The spectra were analysed on the basis of ABXYP spin-system, and a good fit between theoretical and experimental spectra were obtained, Figs. 1 and 2. The spectral parameters are listed in Table 1. The preferred conformations of the five-membered ring is proposed on the basis of the chemical shifts and coupling constants.

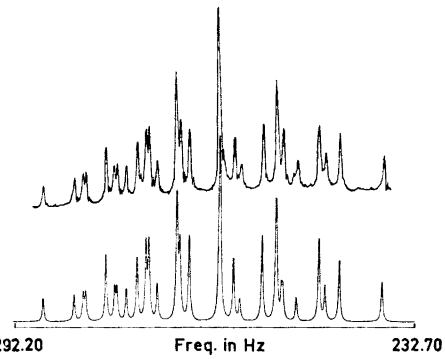

Fig. 1. 60 MHz spectrum of the X and Y protons in 2-methoxy-1,3,2-oxathiaphospholane. *Upper:* Observed spectrum. *Lower:* Calculated spectrum.

Table 1. Chemical shift data for I and II. Chemical shift in ppm from TMS.

Compound	A	B	X	Y
I	4.55	4.22	3.05	2.93
II	4.58	4.16	3.15	2.72

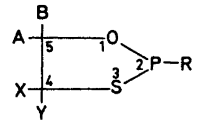

I: R = OCH_3, II: R = SCH_3.

The 60 MHz PMR spectra of I and II show a rather complex, but well resolved pattern. The spectrum can be divided into two bands, and the separation between them is large compared to the coupling constants involved. The band at low field is assigned to the AB protons at carbon 5 and the high field band to the XY protons at carbon 4. The lower field resonance of the AB protons compared to the XY protons is due to the more deshielding effect of the ring oxygen atom as compared to the sulfur atom.

The geminal coupling constants, J_{AB} and J_{XY}, in the oxathiaphospholanes I and II are found to be in the expected ranges,[1–5] −8.0 to −9.6 and −10.5 to −12.5, respectively. The smaller (more negative) geminal coupling constant for the XY protons compared to the AB protons is caused by the different size and electronegativity of the sulfur atom as compared to the oxygen atom.

Table 2. Spin-spin coupling constants (in Hz) for I and II.

Compound	$^2J_{AB}$	$^3J_{AX}$	$^3J_{AY}$	$^3J_{AP}$	$^3J_{BX}$	$^3J_{BY}$	$^3J_{BP}$	$^2J_{XY}$	$^3J_{XP}$	$^3J_{YP}$
I	−9.35	5.99	6.12	4.40	6.88	6.02	8.64	−11.09	−2.11	3.17
II	−9.52	2.28	5.90	14.13	5.23	10.66	3.38	−10.50	1.70	0.25

The internal shift difference of the AB protons at carbon 5 and the XY protons at carbon 4 in I is 19.7 and 7.0 Hz, respectively, while the difference in II is equal, 25.6 Hz. The larger shift difference values for the AB protons as compared to the XY protons in I have also been found in the 2-phenyl- and 2-phenoxy-1,3,2-oxathiaphospholanes.[1] The reverse order is observed for the 2-chloro-1,3,2-oxathiaphospholane[1] and 2-chloro-1,3,2-oxathiarsolane.[6] Due to a rapid chlorine-exchange process resulting in inversion at phosphorus and arsenic at room temperature, the spectra of the latter compounds were observed at −40°C and −35°C, respectively.

The small differences between the *cis* and *trans* coupling constants in I, J_{AY}, J_{BX} and J_{AX}, J_{BY}, probably indicate that the oxathiaphospholane ring with the methoxy group attached to the phosphorus atom exists in an equlibrium between two envelope conformations A and B, where the carbon atom in position 5 is out of the ring plane.

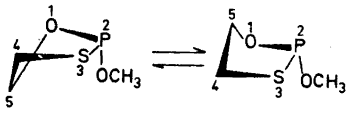

A B

The magnitude of the phosphorus-proton coupling constants is in agreement with the above assumption. However, in the 2-methylthio compound II the observed *cis* and *trans* coupling constants are quite different, which probably indicates that one conformation predominates. The phosphorus proton coupling constants observed for the AB protons in the oxygen part of the ring are found to be 14.1 and 3.4 Hz, corresponding to dihedral angles of 180° and 90°, are in agreement with the fixed conformation C.

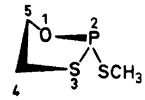

C

The reason for the fixed conformation of II is probably a combination of a smaller negative inductive effect of the methylthio group as compared to the methoxy group[7] and the postulated "anomeric effect",[8,9] which involved the repulsion between lone-pair orbitals of the ring sulfur atom and the sulfur atom in the axial methylthio group.

The O−C−C−S torsional angle in I and II has been calculated from the vicinal coupling constants of the CH_2-CH_2 moiety using the *R*-value method due to

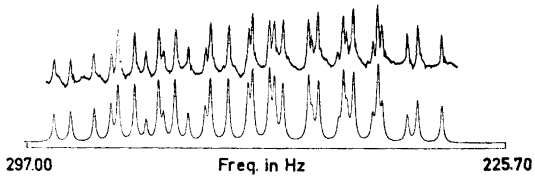

Fig. 2. 60 MHz spectrum of the A and B protons in 2-methylthio-1,3,2-oxathiaphospholane. *Upper:* Observed spectrum. *Lower:* Calculated spectrum.

Lambert [10] and Buys.[11] The calculated torsional angles are approx. 44° and 48° for I and II, respectively. Similar values have been found for 2-chloro-, 2-phenyl-, and 2-phenoxy-1,3,2-oxathiaphospholanes[1].

Experimental. *2-Methoxy-1,3,2-oxathiaphospholane* (I) was prepared from 2-chloro-1,3,2-oxathiaphospholane[1] and methanol in ether solution using triethylamin as base, $b.p._{0.1}$ 34°.

2-Methylthio-1,3,2-oxathiaphospholane (II) was prepared from 2-chloro-1,3,2-oxathiaphospholane and methanethiol in ether solution using triethylamin as base, $b.p._{0.1}$ 62°.

The PMR spectra were measured at 28°C in 50 % solution of I and II in $CDCl_3$ and were recorded on a 60 MHz, JEOL, C-60H instruments. The line positions were taken as an average of several spectra. The computation was carried out using an IBM 360/50 computer. The magnitudes of the chemical shifts and coupling constants involved have been determined by the iterative computer program LAOCN3.[12] The final RMS error observed was 0.05, when all parameters were allowed to vary.

1. Bergesen, K., Bjorøy, M. and Gramstad, T. *Acta Chem. Scand.* **26** (1972) 2156.
2. Bergesen, K., Bjorøy, M. and Gramstad, T. *Acta Chem. Scand.* **26** (1972) 3037.
3. Peake, S. C., Field, M., Schmutzler, R., Harris, R. K., Nichols, J. M. and Rees, R. G. *J. Chem. Soc. Perkin Trans. 2* **1971** 380.
4. Devillers, J., Navech, J. and Albrand, J. P. *Org. Magn. Resonance* **3** (1971) 177.
5. Haake, P., McNeal, J. P. and Golsmith, E. *J. Am. Chem. Soc.* **90** (1968) 715.
6. Aksnes, D. W. and Vikane, O. *Acta Chem. Scand. In press.*
7. March, J. *Advanced Organic Chemistry: Reactions, Mechanisms and Structure*, McGraw, New York 1968, p. 21.
8. Eliel, E. L. and Giza, C. A. *J. Org. Chem.* **33** (1968) 3754.
9. a. Lemieux, R. U. In de Mayo, P., Ed., *Molecular Rearrangements*, Interscience, New York 1964, Chapter 12; b. Angyal, S. J. J. *Angew. Chem.* **81** (1969) 172.
10. Lambert, J. B. *Accounts Chem. Res.* **4** (1971) 87.
11. Buys, H. R. *Rec. Trav. Chim.* **88** (1969) 1003.
12. Castellano, S. and Bothner-By, A. A. *J. Phys. Chem.* **41** (1964) 3863.

Received December 21, 1972.

Electrophilic Bromination of 2-Methyl-4-carbethoxy-1,3,6,7-tetraazacycl[3.3.3]azine

OLOF CEDER and KENNETH ROSÉN

Department of Organic Chemistry, University of Göteborg and Chalmers Institute of Technology, Fack, S-402 20 Göteborg 5, Sweden

The preparation of 2-methyl-4-carbethoxy-1,3,6,7-tetraazacycl[3.3.3]azine, *1*, has recently been described.[1] Simple HMO calculations suggested[1] that *1* should be electrophilically substituted at C-9. (*cf.* Fig. 1).

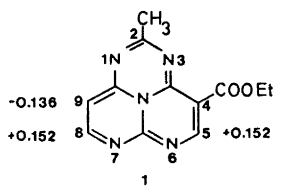

1

Fig. 1. Charge densities at C-5, C-8, and C-9 in 2-methyl-4-carbethoxy-1,3,6,7-tetraazacycl[3.3.3]azine.

In order to verify the theoretical predictions, *1* was treated with *N*-bromosuccinimide in chloroform at room temperature.[2,3] A 60 % yield of 9-bromo-4-carbethoxy-2-methyl-1,3,6,7-tetraazacycl[3.3.3]azine, *2*, was isolated. The mass spectrum shows molecular ion peaks at $m/e = 335$ and 337 m.u. (intensity 1:1) in agreement with the formula $C_{12}H_{10}N_5O_2Br$. The fragmentation pattern of *2* is entirely analogous with that of the 9-bromo derivative of *3*.[3] In the NMR spectrum of *1*[4] the H-8 and H-9 signals appear as two doublets centered at 7.75 and 5.75 ppm, respectively. In the spectrum of *2*, the signal at higher field has vanished and the lower-field signal remains as a singlet at 8.00 ppm. Therefore, substitution has occurred at C-9. The H-5 singlet is found at 8.30 ppm.

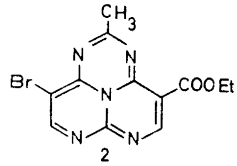

2

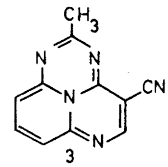

3

Lambert [10] and Buys.[11] The calculated torsional angles are approx. 44° and 48° for I and II, respectively. Similar values have been found for 2-chloro-, 2-phenyl-, and 2-phenoxy-1,3,2-oxathiaphospholanes[1].

Experimental. *2-Methoxy-1,3,2-oxathiaphospholane* (I) was prepared from 2-chloro-1,3,2-oxathiaphospholane[1] and methanol in ether solution using triethylamin as base, $b.p._{0.1}$ 34°.

2-Methylthio-1,3,2-oxathiaphospholane (II) was prepared from 2-chloro-1,3,2-oxathiaphospholane and methanethiol in ether solution using triethylamin as base, $b.p._{0.1}$ 62°.

The PMR spectra were measured at 28°C in 50 % solution of I and II in $CDCl_3$ and were recorded on a 60 MHz, JEOL, C-60H instruments. The line positions were taken as an average of several spectra. The computation was carried out using an IBM 360/50 computer. The magnitudes of the chemical shifts and coupling constants involved have been determined by the iterative computer program LAOCN3.[12] The final RMS error observed was 0.05, when all parameters were allowed to vary.

1. Bergesen, K., Bjorøy, M. and Gramstad, T. *Acta Chem. Scand.* **26** (1972) 2156.
2. Bergesen, K., Bjorøy, M. and Gramstad, T. *Acta Chem. Scand.* **26** (1972) 3037.
3. Peake, S. C., Field, M., Schmutzler, R., Harris, R. K., Nichols, J. M. and Rees, R. G. *J. Chem. Soc. Perkin Trans. 2* **1971** 380.
4. Devillers, J., Navech, J. and Albrand, J. P. *Org. Magn. Resonance* **3** (1971) 177.
5. Haake, P., McNeal, J. P. and Golsmith, E. *J. Am. Chem. Soc.* **90** (1968) 715.
6. Aksnes, D. W. and Vikane, O. *Acta Chem. Scand. In press.*
7. March, J. *Advanced Organic Chemistry: Reactions, Mechanisms and Structure*, McGraw, New York 1968, p. 21.
8. Eliel, E. L. and Giza, C. A. *J. Org. Chem.* **33** (1968) 3754.
9. a. Lemieux, R. U. In de Mayo, P., Ed., *Molecular Rearrangements*, Interscience, New York 1964, Chapter 12; b. Angyal, S. J. J. *Angew. Chem.* **81** (1969) 172.
10. Lambert, J. B. *Accounts Chem. Res.* **4** (1971) 87.
11. Buys, H. R. *Rec. Trav. Chim.* **88** (1969) 1003.
12. Castellano, S. and Bothner-By, A. A. *J. Phys. Chem.* **41** (1964) 3863.

Received December 21, 1972.

Electrophilic Bromination of 2-Methyl-4-carbethoxy-1,3,6,7-tetraazacycl[3.3.3]azine

OLOF CEDER and KENNETH ROSÉN

Department of Organic Chemistry, University of Göteborg and Chalmers Institute of Technology, Fack, S-402 20 Göteborg 5, Sweden

The preparation of 2-methyl-4-carbethoxy-1,3,6,7-tetraazacycl[3.3.3]azine, *1*, has recently been described.[1] Simple HMO calculations suggested[1] that *1* should be electrophilically substituted at C-9. (*cf.* Fig. 1).

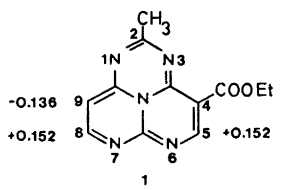

1

Fig. 1. Charge densities at C-5, C-8, and C-9 in 2-methyl-4-carbethoxy-1,3,6,7-tetraazacycl[3.3.3]azine.

In order to verify the theoretical predictions, *1* was treated with *N*-bromosuccinimide in chloroform at room temperature.[2,3] A 60 % yield of 9-bromo-4-carbethoxy-2-methyl-1,3,6,7-tetraazacycl[3.3.3]azine, *2*, was isolated. The mass spectrum shows molecular ion peaks at $m/e = 335$ and 337 m.u. (intensity 1:1) in agreement with the formula $C_{12}H_{10}N_5O_2Br$. The fragmentation pattern of *2* is entirely analogous with that of the 9-bromo derivative of *3*.[3] In the NMR spectrum of *1*[4] the H-8 and H-9 signals appear as two doublets centered at 7.75 and 5.75 ppm, respectively. In the spectrum of *2*, the signal at higher field has vanished and the lower-field signal remains as a singlet at 8.00 ppm. Therefore, substitution has occurred at C-9. The H-5 singlet is found at 8.30 ppm.

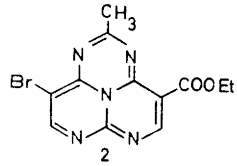

2

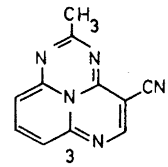

3

On a TLC plate and in the dry state, *2* is destroyed when not protected from air and light. In chloroform solution at −20°, *2* seems to be stable.

The conditions necessary to monobrominate *1* were somewhat more vigorous than those needed to produce the 9- or 7-bromo derivatives of the 1,3,6-triazacycl-[3.3.3]azine *3*.[3]

Efforts to prepare *2*, by treating *1* with bromine in glacial acetic acid were unsuccessful since *1* is unstable in this medium.

Attempts to decarboxylate *1* by the method used to prepare *4* [5,6] from its 4-carbethoxy derivative (diphenyl ether, traces of *p*-toluenesulphonic acid,[6] 100–258°) in order to obtain the symmetrical system *5* failed, since *1* was unstable under these conditions.

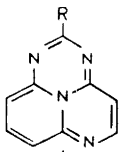

4

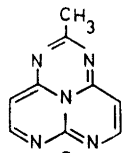

5

R = CH_3 and H

The observations reported above thus indicate that the 1,3,6,7-tetraazacycl[3.3.3]-azine system *1* is less susceptible to electrophilic substitution and, at least in some respects, chemically more unstable than the corresponding 1,3,6-analog *3*.

Experimental. General. Nuclear magnetic resonance (NMR) spectra were determined in $CDCl_3$ with a Varian Model A-60 spectrometer, using tetramethylsilane as internal reference. Mass spectra were recorded with a GEC-AEI MS 902 instrument at the Department of Medical Biochemistry, University of Göteborg. Thin-layer chromatography (TLC) was performed on Silica Gel GF_{254} (Merck) according to Stahl and the spots were visualized by means of short-wave ultraviolet light. For column chromatography, silica gel, 0.05–0.2 mm (Merck), was used.

Bromination of 1 with NBS. A mixture of 45 mg of *1* and 135 mg of *N*-bromosuccinimide in 9 ml of chloroform was stirred at *ca.* 25°. The formation of *2* was followed by TLC (EtOAc). After 6 h the starting material had vanished and red-violet *2* was present (R_F = 0.68). The volume of the reaction solution was reduced to *ca.* 5 ml and succinimide and unreacted NBS, which then precipitated, were removed by filtration. The filtrate was poured on to a column of silica gel (25 × 2.5 cm) and the red-violet band was eluted with chloroform–ethylacetate (1:1). After careful evaporation under reduced pressure at *ca.* 30° 36 mg (60 %) of *2* was obtained. It was immediately dissolved in chloroform and kept in the dark in a Dewar vessel together with dry ice.

Acknowledgements. We are indebted to the *Swedish Natural Science Research Council* for financial support, to *Stiftelsen Bengt Lundqvists Minne* for a fellowship (to K.R.), and to Miss Gun Myrne for technical assistance.

1. Ceder, O. and Witte, J. F. *Acta Chem. Scand.* **26** (1972) 635.
2. Paudler, W. W. and Blewitt. *J. Org. Chem.* **30** (1965) 4081.
3. Ceder, O., Andersson, J. E. and Johansson, L. E. *Acta Chem. Scand.* **26** (1972) 624.
4. *Cf.* Ref. 1, p. 640.
5. Ceder, O. and Andersson, J. E. *Acta Chem. Scand.* **26** (1972) 596.
6. Ceder, O. and Samuelsson, M. L. *To be published.*

Received December 16, 1972.

The Structure of 3,4-Dimethyl-6a-selenathiophthene

ASBJØRN HORDVIK, TOR S. RIMALA and LEIF J. SÆTHRE

Chemical Institute, University of Bergen, N-5000 Bergen, Norway

So far X-ray structure determinations of two 6a-selenathiophthenes have been reported.[1,2] The Se–S bonds in 6a-selenathiophthene (I) [1] were found to be 2.446(5) Å, and the Se–S bonds in 2,5-diphenyl-6a-selenathiophthene (II) [2] were found to be 2.433(3) Å and 2.419(3) Å, respectively.

A structure investigation of 3,4-dimethyl-6a-selenathiophthene (III) has been carried out in order to obtain further information about the bonding in the 6a-

On a TLC plate and in the dry state, *2* is destroyed when not protected from air and light. In chloroform solution at −20°, *2* seems to be stable.

The conditions necessary to monobrominate *1* were somewhat more vigorous than those needed to produce the 9- or 7-bromo derivatives of the 1,3,6-triazacycl-[3.3.3]azine *3*.[3]

Efforts to prepare *2*, by treating *1* with bromine in glacial acetic acid were unsuccessful since *1* is unstable in this medium.

Attempts to decarboxylate *1* by the method used to prepare *4* [5,6] from its 4-carbethoxy derivative (diphenyl ether, traces of *p*-toluenesulphonic acid,[6] 100–258°) in order to obtain the symmetrical system *5* failed, since *1* was unstable under these conditions.

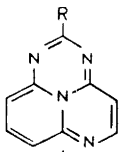

4

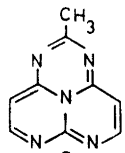

5

R = CH_3 and H

The observations reported above thus indicate that the 1,3,6,7-tetraazacycl[3.3.3]-azine system *1* is less susceptible to electrophilic substitution and, at least in some respects, chemically more unstable than the corresponding 1,3,6-analog *3*.

Experimental. General. Nuclear magnetic resonance (NMR) spectra were determined in $CDCl_3$ with a Varian Model A-60 spectrometer, using tetramethylsilane as internal reference. Mass spectra were recorded with a GEC-AEI MS 902 instrument at the Department of Medical Biochemistry, University of Göteborg. Thin-layer chromatography (TLC) was performed on Silica Gel GF_{254} (Merck) according to Stahl and the spots were visualized by means of short-wave ultraviolet light. For column chromatography, silica gel, 0.05–0.2 mm (Merck), was used.

Bromination of 1 with NBS. A mixture of 45 mg of *1* and 135 mg of *N*-bromosuccinimide in 9 ml of chloroform was stirred at *ca.* 25°. The formation of *2* was followed by TLC (EtOAc). After 6 h the starting material had vanished and red-violet *2* was present (R_F = 0.68). The volume of the reaction solution was reduced to *ca.* 5 ml and succinimide and unreacted NBS, which then precipitated, were removed by filtration. The filtrate was poured on to a column of silica gel (25 × 2.5 cm) and the red-violet band was eluted with chloroform–ethylacetate (1:1). After careful evaporation under reduced pressure at *ca.* 30° 36 mg (60 %) of *2* was obtained. It was immediately dissolved in chloroform and kept in the dark in a Dewar vessel together with dry ice.

Acknowledgements. We are indebted to the *Swedish Natural Science Research Council* for financial support, to *Stiftelsen Bengt Lundqvists Minne* for a fellowship (to K.R.), and to Miss Gun Myrne for technical assistance.

1. Ceder, O. and Witte, J. F. *Acta Chem. Scand.* **26** (1972) 635.
2. Paudler, W. W. and Blewitt. *J. Org. Chem.* **30** (1965) 4081.
3. Ceder, O., Andersson, J. E. and Johansson, L. E. *Acta Chem. Scand.* **26** (1972) 624.
4. *Cf.* Ref. 1, p. 640.
5. Ceder, O. and Andersson, J. E. *Acta Chem. Scand.* **26** (1972) 596.
6. Ceder, O. and Samuelsson, M. L. *To be published.*

Received December 16, 1972.

The Structure of 3,4-Dimethyl-6a-selenathiophthene

ASBJØRN HORDVIK, TOR S. RIMALA and LEIF J. SÆTHRE

Chemical Institute, University of Bergen, N-5000 Bergen, Norway

So far X-ray structure determinations of two 6a-selenathiophthenes have been reported.[1,2] The Se–S bonds in 6a-selenathiophthene (I) [1] were found to be 2.446(5) Å, and the Se–S bonds in 2,5-diphenyl-6a-selenathiophthene (II) [2] were found to be 2.433(3) Å and 2.419(3) Å, respectively.

A structure investigation of 3,4-dimethyl-6a-selenathiophthene (III) has been carried out in order to obtain further information about the bonding in the 6a-

selenathiophthene system. The preliminary results are given here.

The 3,4-dimethyl-6a-selenathiophthene molecule lies with the Se–C bond on a crystallographic two-fold axis, and the two halves of the molecule are therefore

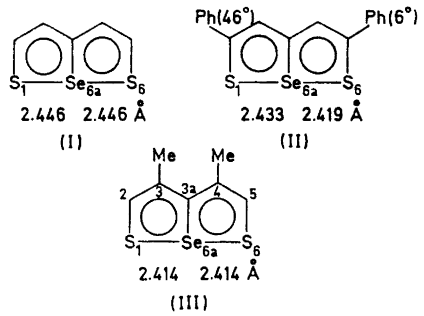

exactly equal. The Se–S distances are 2.414(1) Å with the S–Se–S angle equal to 176.2(1)°. Other bond lengths in the molecule are, S(1)–C(2) = 1.691(3) Å, C(2)–C(3) = 1.375(4) Å, C(3)–C(3a) = 1.420(3) Å, and Se(6a)–C(3a) = 1.917(3) Å.

A sample of III was generously supplied by Reid.[3] The crystals are deep red and belong to the monoclinic space group $C2/c$ with the cell dimensions $a = 15.913(2)$ Å, $b = 7.503(1)$ Å, $c = 7.280(2)$ Å, and $\beta = 99.79(2)°$. There are four molecules per unit cell; $D_c = 1.824$ g/cm³, $D_m = 1.83$ g/cm³.

The structure analysis is based on X-ray data collected on a paper-tape controlled Siemens AED diffractometer using Mo$K\alpha$ radiation. 1874 reflections were observed within $\theta = 35°$.

The structure was solved by the heavy atom method and refined by full matrix least squares. The final R factor is 0.041.

We thank Dr. D. H. Reid, Department of Chemistry, The University, St. Andrews, Scotland, for a sample of 3,4-dimethyl-6a-selenathiophthene.

1. Hordvik, A. and Julshamn, K. *Acta Chem. Scand.* **25** (1971) 1895.
2. Hordvik, A., Rimala, T. S. and Sæthre, L. J. *Acta Chem. Scand.* **26** (1972) 2139, and *to be published*.
3. Reid, D. H. *J. Chem. Soc.* **C 1971** 3187.

Received December 13, 1972.

The Enthalpies of Formation of the Solid Compounds K_2MgCl_4, Rb_2MgCl_4, Cs_2MgCl_4, and $KMgCl_3$, $RbMgCl_3$, $CsMgCl_3$

JAN LÜTZOW HOLM

Institute of Physical Chemistry, The University of Trondheim, N-7034 Trondheim, Norway

It is well-known that compounds of the type A_2MgCl_4 and $AMgCl_3$ (A = K, Rb, and Cs) are found in the systems ACl-$MgCl_2$. For instance, the phase diagram of the system KCl-$MgCl_2$ has recently been examined by Grjotheim, Holm and Rønes.[1] They found two congruently melting compounds, K_2MgCl_4 and $KMgCl_3$, in this system. In the case of the two systems RbCl-$MgCl_2$ and CsCl-$MgCl_2$, phase diagram examinations by Markov and Panchenko [2] show the existence of the following four congruently-melting compounds: Rb_2MgCl_4 and $RbMgCl_3$ in the former system, and Cs_2MgCl_4 and $CsMgCl_3$ in the latter. In Table 1 are given the structures and melting points of the six compounds. The structures have been determined by Svedahl.[3]

Table 1. Structures and melting temperatures for alkali chloride-magnesium chloride compounds.

Compound	Structure [3]	T_f/K
K_2MgCl_4	tetragonal	705[1]
Rb_2MgCl_4	tetragonal	740[2]
Cs_2MgCl_4	orthorhombic	813[2]
$KMgCl_3$	hexagonal	755[1]
$RbMgCl_3$	hexagonal	825[2]
$CsMgCl_3$	hexagonal	883[2]

While the enthalpies of mixing in the liquid state have been determined,[4] the enthalpies of reaction between the solid compounds are not known. These enthalpies can, however, be calculated from enthalpy data as shown by the following two cycles.

selenathiophthene system. The preliminary results are given here.

The 3,4-dimethyl-6a-selenathiophthene molecule lies with the Se–C bond on a crystallographic two-fold axis, and the two halves of the molecule are therefore

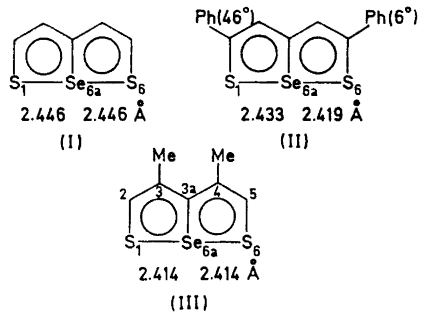

exactly equal. The Se–S distances are 2.414(1) Å with the S–Se–S angle equal to 176.2(1)°. Other bond lengths in the molecule are, S(1)–C(2) = 1.691(3) Å, C(2)–C(3) = 1.375(4) Å, C(3)–C(3a) = 1.420(3) Å, and Se(6a)–C(3a) = 1.917(3) Å.

A sample of III was generously supplied by Reid.[3] The crystals are deep red and belong to the monoclinic space group $C2/c$ with the cell dimensions $a = 15.913(2)$ Å, $b = 7.503(1)$ Å, $c = 7.280(2)$ Å, and $\beta = 99.79(2)°$. There are four molecules per unit cell; $D_c = 1.824$ g/cm³, $D_m = 1.83$ g/cm³.

The structure analysis is based on X-ray data collected on a paper-tape controlled Siemens AED diffractometer using Mo$K\alpha$ radiation. 1874 reflections were observed within $\theta = 35°$.

The structure was solved by the heavy atom method and refined by full matrix least squares. The final R factor is 0.041.

We thank Dr. D. H. Reid, Department of Chemistry, The University, St. Andrews, Scotland, for a sample of 3,4-dimethyl-6a-selenathiophthene.

1. Hordvik, A. and Julshamn, K. *Acta Chem. Scand.* **25** (1971) 1895.
2. Hordvik, A., Rimala, T. S. and Sæthre, L. J. *Acta Chem. Scand.* **26** (1972) 2139, and *to be published*.
3. Reid, D. H. *J. Chem. Soc.* **C 1971** 3187.

Received December 13, 1972.

The Enthalpies of Formation of the Solid Compounds K_2MgCl_4, Rb_2MgCl_4, Cs_2MgCl_4, and $KMgCl_3$, $RbMgCl_3$, $CsMgCl_3$

JAN LÜTZOW HOLM

Institute of Physical Chemistry, The University of Trondheim, N-7034 Trondheim, Norway

It is well-known that compounds of the type A_2MgCl_4 and $AMgCl_3$ (A = K, Rb, and Cs) are found in the systems ACl-$MgCl_2$. For instance, the phase diagram of the system KCl-$MgCl_2$ has recently been examined by Grjotheim, Holm and Rønes.[1] They found two congruently melting compounds, K_2MgCl_4 and $KMgCl_3$, in this system. In the case of the two systems RbCl-$MgCl_2$ and CsCl-$MgCl_2$, phase diagram examinations by Markov and Panchenko [2] show the existence of the following four congruently-melting compounds: Rb_2MgCl_4 and $RbMgCl_3$ in the former system, and Cs_2MgCl_4 and $CsMgCl_3$ in the latter. In Table 1 are given the structures and melting points of the six compounds. The structures have been determined by Svedahl.[3]

Table 1. Structures and melting temperatures for alkali chloride-magnesium chloride compounds.

Compound	Structure [3]	T_f/K
K_2MgCl_4	tetragonal	705[1]
Rb_2MgCl_4	tetragonal	740[2]
Cs_2MgCl_4	orthorhombic	813[2]
$KMgCl_3$	hexagonal	755[1]
$RbMgCl_3$	hexagonal	825[2]
$CsMgCl_3$	hexagonal	883[2]

While the enthalpies of mixing in the liquid state have been determined,[4] the enthalpies of reaction between the solid compounds are not known. These enthalpies can, however, be calculated from enthalpy data as shown by the following two cycles.

Cycle I:

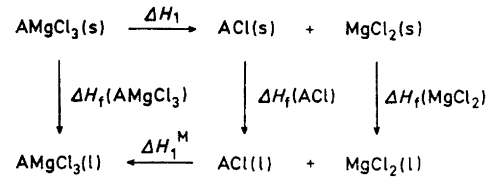

gives

$$\Delta H_1 = \Delta H_f(AMgCl_3) - \Delta H_1^M - \Delta H_f(ACl) - \Delta H_f(MgCl_2) \quad (1)$$

Cycle II:

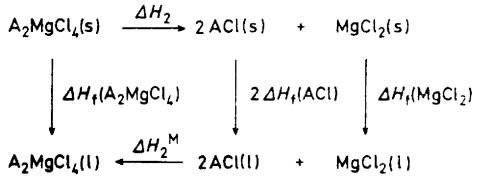

gives

$$\Delta H_2 = \Delta H_f(A_2MgCl_4) - \Delta H_2^M - 2\Delta H_f(ACl) - \Delta H_f(MgCl_2) \quad (2)$$

In the following the enthalpies ΔH_1 and ΔH_2 are calculated at 700 K, a temperature which is below the melting points of all six compounds.

The enthalpies of fusion and of mixing used in the calculation are summarized in Tables 2 and 3. The enthalpies of mixing for the compounds were measured by Kleppa and McCarty [4] at 1073 K and 993 K. The values at 700 K have been calculated by use of their data and the heat capacities given by Holm *et al.*[5] The enthalpies of fusion of the alkali chlorides are those given by Dworkin and Bredig.[6]

Table 2. Enthalpies of fusion at 700 K used in the calculations.

Compound	ΔH_f / kcal mol^{-1}	Ref.
KCl	6.0	6, 7
RbCl	5.4	6, 7
CsCl	4.6	6, 7
$MgCl_2$	9.1	8
$KMgCl_3$	10.1	5
$RbMgCl_3$	12.1	5
$CsMgCl_3$	13.5	5
K_2MgCl_4	10.7	5
Rb_2MgCl_4	11.9	5
Cs_2MgCl_4	8.8	5

Table 3. Enthalpies of mixing of $2ACl(l) + MgCl_2(l) = A_2MgCl_4(l)$ (ΔH_2^M) and $ACl(l) + MgCl_2(l) = AMgCl_3(l)$ (ΔH_1^M) at 700 K.

Mixing process	ΔH^M / kcal mol^{-1}	Ref.
$2KCl + MgCl_2$	−16.2	4, 5
$2RbCl + MgCl_2$	−17.7	»
$2CsCl + MgCl_2$	−19.5	»
$KCl + MgCl_2$	−8.4	»
$RbCl + MgCl_2$	−9.2	»
$CsCl + MgCl_2$	−10.2	»

The enthalpies of formation from the simple chlorides

$$2ACl(s) + MgCl_2(s) = A_2MgCl_4(s)$$

and

$$ACl(s) + MgCl_2(s) = AMgCl_3(s)$$

have been calculated directly from the cycles at 700 K and the enthalpies transferred to 298.15 K by use of enthalpy increment data for KCl, RbCl, and CsCl given in JANAF [9] and for the complex compounds given by Holm *et al.*[5] The results are given in Table 4. In Table 5 are given the enthalpies of the reactions

$$2AMgCl_3(s) = A_2MgCl_4(s) + MgCl_2(s)$$

for A = K, Rb, and Cs. As can be seen from this table the stability of $AMgCl_3$ increases

Table 4. Enthalpies of reaction of $ACl(s) + MgCl_2(s) = AMgCl_3(s)$ and $2ACl(s) + MgCl_2(s) = A_2MgCl_4(s)$ at 298.15 K and 700 K (estimated uncertainties ± 1 kcal).

Compound	ΔH/kcal mol^{-1} 700 K	298.15 K
$KMgCl_3$	−3.4	−3.7
$RbMgCl_3$	−6.8	−6.8
$CsMgCl_3$	−10.0	−10.0
K_2MgCl_4	−5.5	−8.5
Rb_2MgCl_4	−9.7	−12.3
Cs_2MgCl_4	−10.0	−12.0

Table 5. Enthalpies of disproportionation $2AMgCl_3(s) = A_2MgCl_4(s) + MgCl_2(s)$, (estimated uncertainties ± 1 kcal).

Reaction	ΔH_{700} / kcal mol^{-1}	$\Delta H_{298.15}$ / kcal mol^{-1}
$2KMgCl_3(s) = K_2MgCl_4(s) + MgCl_2(s)$	+1.3	−1.1
$2RbMgCl_3(s) = Rb_2MgCl_4(s) + MgCl_2(s)$	+3.9	+1.3
$2CsMgCl_3(s) = Cs_2MgCl_4(s) + MgCl_2(s)$	+10.0	+8.0

considerably from the potassium to the cesium compound.

Acknowledgement. Thanks are due to Docent Fr. Grønvold for his kind permission to use the drop calorimeter.

1. Grjotheim, K., Holm, J. L. and Rønes, M. *Acta Chem. Scand.* **26** (1972) 3802.
2. Markov, B. F. and Panchenko, I. D. *Zh. Obshch. Khim.* **35** (1955) 2083.
3. Svedahl, G. M.Sc. Thesis, Institute of Inorganic Chemistry, The University of Trondheim, Dec. 1969.
4. Kleppa, O. J. and McCarty, F. G. *J. Phys. Chem.* **70** (1966) 1249.
5. Holm, J. L., Jenssen Holm, B., Rinnan, B. and Grønvold, F. *J. Chem. Thermodynamics* **5** (1973) 97.
6. Dworkin, A. S. and Bredig, M. A. *J. Phys. Chem.* **64** (1960) 269.
7. Kelley, K. K. *Contributions to the Data on Theoretical Metallurgy*, XIII, Bull. 584, U.S. Bur. Mines 1960.
8. Holm, J. L. and Grønvold, F. *Acta Chem. Scand.* **27** (1973) 370.
9. *JANAF Thermochemical Tables*, Clearinghouse, Springfield, Virginia 1972.

Received November 27, 1972.

Calculation of C=C and C—F Bond Lengths in CH_2=CH_2, CH_2=CHF, *cis*-CHF=CHF, and CH_2=CF_2

BØRGE BAK, CECILIA KIERKEGAARD, JAN PAPPAS* and STEEN SKAARUP

Chemical Laboratory V, The H. C. Ørsted Institute, University of Copenhagen, DK-2100 Copenhagen, Denmark

Experimental observations of C=C and C−F bond lengths in ethylene and fluorinated ethylenes (Table 1) indicate decreasing lengths with progressing fluorination. Earlier "resonance" structures such as $\bar{C}H_2-CH=\overset{+}{F}$ would seem to connect increasing C=C length with decreasing C−F length. This communication reports results of *ab initio* calculations of the molecules of Table 1 in which the molecular energy was separately minimized with respect to the C=C and C−F bond(s) in that order, taking remaining geometrical parameters from Refs. 1−3. A relatively small, Gaussian basis set [4] (*s,p* = 7,3 contracted to 4,2) was used. The set was tested to see how well the experimental carbon-carbon distances in ethane (r_z = 1.532 Å),[5] in ethylene (r_z = 1.335 Å),[1] and in acetylene (r_e = 1.203 Å)[6] were reproduced. The results (r_e) were 1.554, 1.314, and 1.188 Å, respectively. Obviously, to assign significance to what follows one must assume that somehow the molecules of Table 1 are more "related" than C_2H_6, C_2H_4, and C_2H_2.

The results of Table 2 are a minor part of a more comprehensive investigation.[7] To the best of our knowledge only one paper [8] based on the experimental structure of CH_2=CHF (Table 1) has appeared earlier. At the present level of approximation the calculated bond lengths of Table 2 show the same trends as the experiments. The computed gross atomic charges show that carbon in ethylene, when binding fluorine instead of hydrogen, donates *ca.* 0.6 e (~ 6.3965 (col. 1) − 5.7818 (col.2) ~ 6.3965 − 5.8433 (col.3) ~ 0.5(6.3965 − 5.2163) (col.4)) to fluorine, the hydrogen gross electronic charges (not quoted) being practically constant (0.8 e). Unsubstituted C prac-

* On leave of absence from the Department of Physics, University of Oslo, Oslo 3, Norway.

Table 5. Enthalpies of disproportionation $2AMgCl_3(s) = A_2MgCl_4(s) + MgCl_2(s)$, (estimated uncertainties ± 1 kcal).

Reaction	ΔH_{700} / kcal mol^{-1}	$\Delta H_{298.15}$ / kcal mol^{-1}
$2KMgCl_3(s) = K_2MgCl_4(s) + MgCl_2(s)$	+1.3	−1.1
$2RbMgCl_3(s) = Rb_2MgCl_4(s) + MgCl_2(s)$	+3.9	+1.3
$2CsMgCl_3(s) = Cs_2MgCl_4(s) + MgCl_2(s)$	+10.0	+8.0

considerably from the potassium to the cesium compound.

Acknowledgement. Thanks are due to Docent Fr. Grønvold for his kind permission to use the drop calorimeter.

1. Grjotheim, K., Holm, J. L. and Rønes, M. *Acta Chem. Scand.* **26** (1972) 3802.
2. Markov, B. F. and Panchenko, I. D. *Zh. Obshch. Khim.* **35** (1955) 2083.
3. Svedahl, G. M.Sc. Thesis, Institute of Inorganic Chemistry, The University of Trondheim, Dec. 1969.
4. Kleppa, O. J. and McCarty, F. G. *J. Phys. Chem.* **70** (1966) 1249.
5. Holm, J. L., Jenssen Holm, B., Rinnan, B. and Grønvold, F. *J. Chem. Thermodynamics* **5** (1973) 97.
6. Dworkin, A. S. and Bredig, M. A. *J. Phys. Chem.* **64** (1960) 269.
7. Kelley, K. K. *Contributions to the Data on Theoretical Metallurgy*, XIII, Bull. 584, U.S. Bur. Mines 1960.
8. Holm, J. L. and Grønvold, F. *Acta Chem. Scand.* **27** (1973) 370.
9. *JANAF Thermochemical Tables*, Clearinghouse, Springfield, Virginia 1972.

Received November 27, 1972.

Calculation of C=C and C—F Bond Lengths in CH_2=CH_2, CH_2=CHF, *cis*-CHF=CHF, and CH_2=CF_2

BØRGE BAK, CECILIA KIERKEGAARD, JAN PAPPAS* and STEEN SKAARUP

Chemical Laboratory V, The H. C. Ørsted Institute, University of Copenhagen, DK-2100 Copenhagen, Denmark

Experimental observations of C=C and C−F bond lengths in ethylene and fluorinated ethylenes (Table 1) indicate decreasing lengths with progressing fluorination. Earlier "resonance" structures such as $\bar{C}H_2-CH=\overset{+}{F}$ would seem to connect increasing C=C length with decreasing C−F length. This communication reports results of *ab initio* calculations of the molecules of Table 1 in which the molecular energy was separately minimized with respect to the C=C and C−F bond(s) in that order, taking remaining geometrical parameters from Refs. 1−3. A relatively small, Gaussian basis set [4] (*s,p* = 7,3 contracted to 4,2) was used. The set was tested to see how well the experimental carbon-carbon distances in ethane (r_z = 1.532 Å),[5] in ethylene (r_z = 1.335 Å),[1] and in acetylene (r_e = 1.203 Å)[6] were reproduced. The results (r_e) were 1.554, 1.314, and 1.188 Å, respectively. Obviously, to assign significance to what follows one must assume that somehow the molecules of Table 1 are more "related" than C_2H_6, C_2H_4, and C_2H_2.

The results of Table 2 are a minor part of a more comprehensive investigation.[7] To the best of our knowledge only one paper [8] based on the experimental structure of CH_2=CHF (Table 1) has appeared earlier. At the present level of approximation the calculated bond lengths of Table 2 show the same trends as the experiments. The computed gross atomic charges show that carbon in ethylene, when binding fluorine instead of hydrogen, donates *ca.* 0.6 e (~ 6.3965 (col. 1) − 5.7818 (col.2) ~ 6.3965 − 5.8433 (col.3) ~ 0.5(6.3965 − 5.2163) (col.4)) to fluorine, the hydrogen gross electronic charges (not quoted) being practically constant (0.8 e). Unsubstituted C prac-

* On leave of absence from the Department of Physics, University of Oslo, Oslo 3, Norway.

Table 1. Experimental geometric parameters of ethylene and three fluorinated ethylenes as taken from Refs. 1–3. Distances in Å.

Molecule	$R_{C=C}$ [a]	R_{C-F} [a]	Reference
$CH_2=CH_2$	1.335±0.003		1
$CH_2=CHF$	1.329±0.006	1.347±0.009	2
$CHF=CHF$ (*cis*)	1.324±0.004	1.335±0.004	3
$CH_2=CF_2$	1.315±0.002	1.325±0.002	3

[a] Largely R_z parameters.

Table 2. Calculated equilibrium distances, σ- and π-overlap charges and σ- and π-gross atomic charges for $CH_2=CH_2$, $C(2)H_2=C(1)HF$, *cis*-$C(2)HF=C(1)HF$, and $C(2)H_2=C(1)F_2$. Distances in Å, charges in units of electronic charge.

	$CH_2=CH_2$	$CH_2=CHF$	*cis*-$CHF=CHF$	$CH_2=CF_2$
C=C distance	1.315	1.306	1.305	1.300
σ-Overlap	0.6286	0.5404	0.3612	0.4205
π-Overlap	0.5300	0.5114	0.4974	0.4850
$\sigma+\pi$-Overlap	1.1585	1.0518	0.8586	0.9055
C(1), σ-gross	5.3965	4.7805	4.7798	4.2644
C(1), π-gross	1.0000	1.0013	1.0635	1.0019
$(\sigma+\pi)$-Gross	6.3965	5.7818	5.8433	5.2163
C(2), σ-gross	5.3965	5.4093	4.7798	5.3839
C(2), π-gross	1.0000	1.0639	1.0635	1.1342
$(\sigma+\pi)$-Gross	6.3965	6.4732	5.8433	6.5103
C–F distance		1.370	1.357	1.350
σ-Overlap		0.4123	0.4216	0.4682
π-Overlap		0.0115	0.0102	0.0300
$\sigma+\pi$-Overlap		0.4238	0.4318	0.4982
F, σ-gross		7.4789	7.4576	7.4530
F, π-gross		1.9348	1.9365	1.9320
$(\sigma+\pi)$-Gross		9.4137	9.3941	9.3850

tically retains its gross charge (6.3965 compared to 6.4732 and 6.5103). The role of fluorine as a donor to the "conjugated" π-system is rather modest (2.00 – 1.93 = 0.07 e). If the overlap charges of the C=C and C–F bonds were the main factors determining bond lengths our calculations would be contradictory. However, other factors may probably be important emerging, perhaps, when a larger basis set is applied.

Acknowledgements. We are indebted to the Danish computing centre NEUCC for access to their IBM 360/75 computer and to Helge Johansen, Chem. Lab. IV of this institute for helpful advice.

1. Kuchitsu, K. *J. Chem. Phys.* **44** (1966) 906.
2. Lide, D. R. and Christensen, D. *Spectrochim. Acta* **17** (1961) 665.
3. Laurie, V. W. and Pence, D. T. *J. Chem. Phys.* **38** (1963) 2693.
4. Roos, B. and Siegbahn, P. *Theor. Chim. Acta* **17** (1970) 209.
5. Kuchitsu, K. *J. Chem. Phys.* **49** (1968) 4456.
6. Fast, H. and Welsh, H. L. *J. Mol. Spectry.* **41** (1972) 203.
7. Pappas, J. *A Quantum Mechanical Study of Variations in the Geometry of Organic Molecules by Fluorine Substitution*, University of Oslo, Dept. of Physics, Thesis 1972 (in Norwegian).
8. Meza, S. and Wahlgren, U. *Theor. Chim. Acta* **21** (1971) 323.

Received December 12, 1972.

Acidolytic Formation of Methanol from Quinones and Quinonoid Compounds Related to Lignin

LENNART HEMRÅ and
KNUT LUNDQUIST

Department of Organic Chemistry, Chalmers University of Technology and University of Göteborg, Fack, S-402 20 Göteborg 5, Sweden

Quinone and quinonoid units may be important chromophoric groups in lignin.[1-3] In a previous paper, support for the presence of quinone and quinonoid units in lignin was given by the formation of methanol during acidolysis [heating with 0.2 M HCl in dioxan-water (9:1) at reflux temperature] of lignin and model compounds.[4] In this report, additional results obtained by studies of the formation of methanol on acidolysis are presented. Acidolysis and determination of methanol was made as described in Ref. 4.

Results obtained with a number of quinones and quinonoid compounds are summarized in Table 1. The formation of methanol from compound I may occur in analogy with the reaction route suggested by Hewgill and Middleton [5] for the formation of methanol from a methoxyl containing *p*-quinol ether on acid treatment.

Table 1. Yields of methanol on acidolysis (given in mol/mol).

Compound [a]	Time of acidolysis (h) 0.25	4
I	0.66	0.81
II	0.02	0.08
III	0.16	1.7
IV	0.12	0.80
V	0.22	0.34
VI	1.0	–
VII	1.7	–
VIII	0.9	–
IX	0.00	0.00

[a] Gifts of compounds from Prof. E. Adler (compound VIII) and from Dr. H.-D. Becker (compounds I, VI and IX) are gratefully acknowledged.

However, other routes, *e.g. via* an *o*-diphenoquinone (*cf.* Ref. 6), also seem possible. In the course of the examination of model compounds representative of major lignin structures (which merely contain methoxyl groups linked to aromatic rings) it was found that model compounds of the biphenyl type gave small amounts of methanol on acidolysis.[4] Further studies showed that clearly larger amounts of methanol were obtained from biphenyl model compounds prepared by dehydrogenation of phenols, if the biphenyls were not carefully purified. It therefore seems possible that methanol obtained from model compounds of the biphenyl type is produced from contaminants with structural resemblance to compound I.

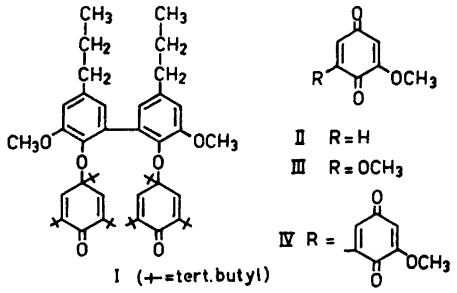

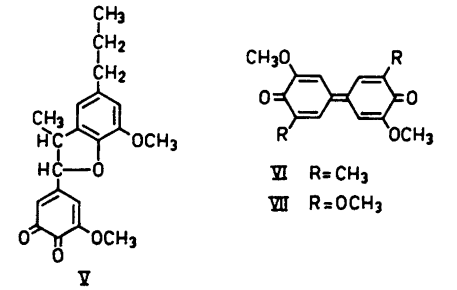

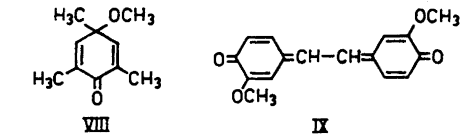

Compounds of the same type as compound I (aromatic *p*-quinol ethers) have been found to be in equilibrium with free radicals.[7] Thus there may be a connection between the fact that various lignin prep-

arations have been found to contain minor amounts of free radicals [8] and the occurrence of quinonoid structures in lignin.

The formation of methanol from methoxyquinones II – VII (concerning the preparation of IV and V, see Ref. 9) can be understood as a hydrolysis of vinylogous esters. The occurrence of lignin structures corresponding to compounds VI and VII, *i.e.* *p*-diphenoquinone structures, does not seem very likely. However, in recent studies on enzymatic oxidation of lignin model compounds a product has been obtained which possibly is a *p*-diphenoquinone.[2] The formation of methanol from compound VIII does not directly apply to formation of methanol from lignin, since methoxyl groups cannot be expected to be linked to lignin units in this position. However, the reaction is of interest as an example of a hydrolysis of a *p*-quinol ether on acidolysis. Although the stilbenequinone IX can be considered as an extended vinylogous ester, no methanol was formed on acidolysis. Possibly this compound, containing "quinone methide groupings" reacts under addition of water to these groupings. Stilbenequinone structures are not expected to occur in native lignin, but may occur in lignin preparations obtained on various hydrolytic treatments of lignin (*e.g.* kraft cooking) due to autoxidation of stilbene structures formed during the hydrolysis.

Relatively larger amounts of methanol were obtained from wood meal and lignin carbohydrate complex [10] from spruce (about 0.05 mol/OCH_3 on 4 h acidolysis) than from Björkman lignin from spruce (0.018 mol/OCH_3 on 4 h acidolysis [4]). It is unclear if this result reflects a difference in content of quinone and quinonoid units, since 4-*O*-methylglucuronic acid units can be expected to give rise to a substantial portion of the methanol obtained from wood meal and lignin carbohydrate complex (see Ref. 4).

The formation of methanol from borohydride treated lignin was studied in connection with attempts to characterize quinone and quinonoid units in Björkman lignin from spruce. Methanol was formed but experimental difficulties did not permit any closer quantitative evaluation of the results. However, it appeared that some groups were formed on borohydride reduction which very rapidly gave methanol on acidolysis. Analogy with this behaviour was found in experiments with model compounds. The *o*-quinol ether model 6-methoxy - 5,6 - dimethyl - 2,4 - cyclohexadienone has been found to give methanol slowly on acidolysis;[4] however, after borohydride reduction, the reduced product rapidly gave high yield of methanol on acidolysis.

Treatment of lignin in dioxan-water solution with sulphur dioxide decreases the absorbance in the ultraviolet and the visible range. With methoxy-*p*-benzoquinone as reference compound ($\lambda_{max} = 359$ nm, ε 1450) the decrease in absorbance corresponded to 1 – 2 % units of quinone type of the total number of units. The decrease in absorption caused by sulphur dioxide treatment was only about 10 % of the decrease caused by borohydride reduction.

Acknowledgements. The authors thank Prof. E. Adler and Prof. M. Nilsson for their kind interest in this work. Financial support from *Cellulosaindustriens stiftelse för teknisk och skoglig forskning samt utbildning* is gratefully acknowledged.

1. Pew, J. C. and Connors, W. J. *Tappi* **54** (1971) 245.
2. Connors, W. J., Ayers, J. S., Sarkanen, K. V. and Gratzl, J. S. *Tappi* **54** (1971) 1284.
3. Imsgard, F., Falkehag, S. I. and Kringstad, K. P. *Tappi* **54** (1971) 1680.
4. Lundquist, K. and Ericsson, L. *Acta Chem. Scand.* **25** (1971) 756.
5. Hewgill, F. R. and Middleton, B. S. *J. Chem. Soc.* **C 1967** 2316.
6. Hewgill, F. R. and Kennedy, B. R. *J. Chem. Soc.* **C 1966** 362; Hewgill, F. R. and Hewitt, D. G. *J. Chem. Soc.* **C 1967** 723.
7. Becker, H.-D. *J. Org. Chem.* **30** (1965) 982; Brunow, G. *Acta Chem. Scand.* **23** (1969) 2537.
8. Ludwig, C. H. In Sarkanen, K. V. and Ludwig, C. H., Eds., *Lignins*, Wiley, New York 1971, p. 299.
9. Adler, E. and Lundquist, K. *Acta Chem. Scand.* **15** (1961) 223.
10. Björkman, A. *Svensk Papperstid.* **60** (1957) 243.

Received December 12, 1972.

A Quinol Glucoside Isolated from *Cornus* Species

S. ROSENDAL JENSEN, A. KJÆR and B. JUHL NIELSEN

Department of Organic Chemistry, Technical University of Denmark, DK-2800 Lyngby, Denmark

A glucoside, with a chemical structure novel in type to constituents of higher plants, has been isolated by column chromatography from an aqueous, flavonoid-free extract of autumn foliage of the North American dogwood *Cornus femina* Miller. The non-crystalline glucoside, $C_{14}H_{20}O_8$, has been assigned the structure *1* on the following evidence.

UV, [λ_{max} (EtOH) 227 nm (ε 9400)]; IR, [λ_{max} (KBr) 1618, 1663 cm^{-1}], and ^1H NMR data (see Experimental) were

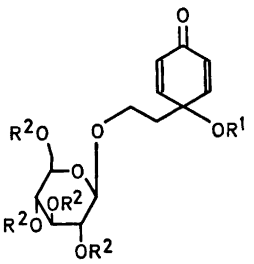

1 $R^1 = R^2 = H$

2 $R^1 = H, R^2 = Ac$

3 $R^1 = R^2 = Ac$

all in accord with those expected for structure *1*.* Acetylation, with Ac_2O in pyridine, afforded a tetraacetate *2*, and a pentaacetate *3*, both syrupy, exhibiting, as parts of their ^1H spectra, signals virtually coinciding with those of methyl tetra-*O*-acetyl-β-D-glucopyranoside, save for the anomeric proton. Emulsin-catalyzed hydrolysis of *1* proceeded easily to give glucose and the aglucone, isolated as the non-crystalline diacetate *4*, exhibiting the expected NMR signals.

Additional chemical evidence in support of structure *1* was provided by BF_3-induced rearrangement [2] of *2* to give, after acetylation, the expected hydroquinone glucoside acetate *5*, as colourless crystals. Similarly, acid-catalyzed hydrolysis of *1*,

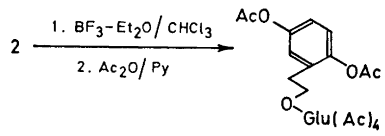

5

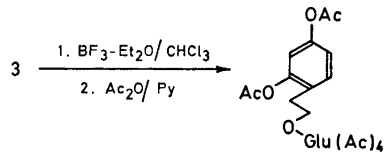

7

followed by acetylation, afforded homogentisyl triacetate *6* as the major product. On treatment with BF_3-etherate in $CHCl_3$, *3* underwent quinol ester-phenol rearrangement [2] to give, after acetylation, the resorcinol glucoside acetate *7*.

The genus *Cornus* (*sensu* Wangerin) comprises 46 species, 32 of which compose the subgenus *Thelycrania* Endl.[3] In the present work, 17 of the latter were studied and invariably found to contain *1*. Conversely, none of 7 studied species, belonging to 4 other subgenera,[3] contained *1* in detectable amounts. Taxonomically interesting, the occurrence of *1* and of iridoid glucosides, studied in parallel on the 24 *Cornus* species, appears to be mutually exclusive.

Salidroside, *8*, formerly known from species of *Salix* [4] and several other genera,

* 4-Hydroxy-4-methyl-cyclohexa-2,5-dienone exhibits absorption maxima at λ 226 nm (ε 17 760) (EtOH) in the UV,[1] and at 1617 and 1673 cm^{-1} ($CHCl_3$) in the IR region.[2]

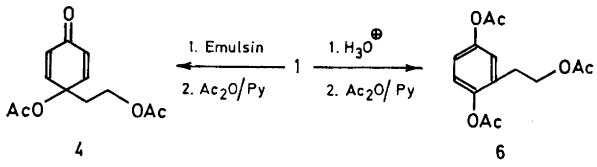

4 6

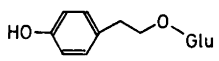

8

was consistently encountered as a minor congener of *1*.

A full account of the distribution of *1* and iridoids within the *Cornus* group will appear elsewhere.

Experimental. Ultraviolet spectra were measured in EtOH; ^{1}H NMR spectra were recorded on a Varian HA-100 instrument in $CDCl_3$-solution with TMS as an internal reference, when not otherwise indicated. For TLC, silica gel PF_{254} (Merck) was employed; preparative separations were performed on 20 × 40 cm plates, coated with 1 mm thick layers of silica gel. Detection in UV light.

Isolation of glucoside 1. Frozen foliage (350 g) of *C. femina* (collected in September 1971 and stored at −28° in polyethylene bags) was homogenized in ethanol (1.0 l). After filtration, the filter cake was treated similarly with another 0.5 l portion of ethanol. The combined filtrates were concentrated *in vacuo* to 150 ml. The remaining solution was extracted with two 500 ml portions of ether. The ether solutions were discarded. The aqueous phase was filtered through a column of alumina (300 g),[5] followed by washing of the column with water (1 l). The combined filtrates were passed through a filter bed of charcoal (175 g) and Celite (200 g), placed in a 22 cm Büchner funnel. The adsorbed glycosides were washed free of carbohydrates with 4 l of water. Elution with 50 % EtOH (2 l) and then 66 % EtOH (0.75 l), followed by concentration of the eluates *in vacuo*, afforded a crude glycoside fraction (5.7 g).

Repeated column chromatography on silica gel, with BuOH:MeOH:H_2O (7:1:3) as the mobile phase, yielded a fast-running glycoside (fraction a, see below) in addition to the sirupy, chromatographically homogeneous glycoside *1* (3 g). After thorough drying (over P_2O_5), the material was used for further characterization: $[\alpha]_D^{22}$ − 23° (*c* 1.6, EtOH); the ^{1}H NMR spectrum (in D_2O, TMS as external reference) exhibited signals at: 7.44 and 6.59 (4H, vinylic, composing an AA'BB' system; J_{AB} 10.5 Hz), 4.71 (1H, anomeric proton H-1', d, *J* 7 Hz), 2.48 (2H, t, *J* = 7 Hz), and 3.40 − 4.50 ppm (8H, consisting of 2H from the aglucone, and the 6 non-anomeric, carbon-bound protons of the glucose moiety).

Acetates of 1. Acetylation of *1* (1.0 g) was performed in pyridine (10 ml) with acetic anhydride (5 ml) at room temperature. After 18 h, work-up in the usual way yielded a mixture of two acetates (1.39 g), separated on chromatography (in ether) into a slow- and a faster-running component.

The former, consisting of *2* (203 mg), was thoroughly dried before analysis. (Found: C 52.35; H 6.20. Calc. for $C_{22}H_{28}O_{12}$: C 52.17; H 6.13). $[\alpha]_D^{22}$ − 26° (*c* 3.6; EtOH); λ_{max} 227 nm (ε 10 600); NMR-data: 6.92 and 6.16 (2 × 2H, vinylic), 5.40 − 4.90 (3H; H-2', H-3', H-4'), 4.56 (1H, H-1', d, *J* 7.5 Hz), 4.27 and 4.23 (2H, H-6'), 4.08 and 3.71 (2 × 1H; A and B part of an ABX_2-system), *ca* 3.75 (1H, H-5'), 3.37 (1H, O*H*), and 2.13 − 2.00 ppm (14H, 4 OAc plus CH_2).

The pentaacetate, *3* (532 mg), was analyzed after drying. (Found: C 54.57; H 5.59. Calc. for $C_{24}H_{30}O_{13}$: C 54.75; H 5.74). $[\alpha]_D^{22}$ − 18.0° (*c* 2.0; EtOH); λ_{max} 239 nm (ε 9800). NMR-data: 6.90 and 6.28 (4H, vinylic), 5.35 − 4.85 (3H; H-2', H-3', H-4'), 4.52 (1H, H-1', d, J 7.5 Hz), 4.28 and 4.23 (2H, H-6'), 3.99 and 3.61 (each 1H; A and B part of an ABX_2-system, J_{AB} 10.5 Hz, $J_{AX} = J_{BX} = 6$ Hz), *ca.* 3.75 (1H, H-5'), 2.18 (2H, t, X_2-part of an

ABX_2-system), and 2.15–2.03 ppm (15H; 5 OAc).

Enzymic hydrolysis of 1. A mixture of *1* (408 mg), emulsin (190 mg), and water (10 ml) was stirred overnight at room temperature. The filtered solution was extracted with three 10 ml portions of BuOH; the solvent was removed *in vacuo*, and the residue was subjected to acetylation (with Ac_2O in pyridine). From the resulting product mixture (175 mg), a homogeneous, non-crystalline product, consisting of *4*, was isolated by chromatography with C_6H_6:Et_2O (1:1) as the mobile phase. (Found: C 60.38; H 5.82. Calc. for $C_{12}H_{14}O_5$: C 60.50; H 5.92.) λ_{max} 239 nm (ε 7100); NMR-data: 6.88 and 6.28 (each 2H, composing an AA'BB'-system), 4.18 (2H, t, *J* 6.5 Hz), 2.19 (2H, t, *J* 6.5 Hz), 2.08 and 2.03 ppm (2×3H; 2 OAc).

In the above aqueous solution, the presence of glucose was demonstrated by paper-chromatographic analysis and comparison with an authentic specimen, in (i) BuOH:EtOH:H_2O (4:1:3), and (ii) BuOH:Py:H_2O (6:4:3).

Rearrangement of 2. A solution of the tetra-acetate *2* (250 mg) in $CHCl_3$ (5 ml) was treated with BF_3,Et_2O (150 mg) for 3 h at room temperature. An excess of $NaHCO_3$-solution was added, and the mixture was extracted with $CHCl_3$. The crude reaction product (270 mg) was purified by chromatography (ether as an eluent) to give the rearranged product (131 mg). Acetylation, with Ac_2O in pyridine, afforded the hexaacetate *5* (157 mg), which was recrystallized from MeOH, m.p. 136–137.5°. (Found: C 54.94; H 5.76. Calc. for $C_{26}H_{32}O_{14}$: C 54.92; H 5.67) $[\alpha]_D^{22}$ −16.0° (*c* 3; $CHCl_3$). λ_{max} 267 (ε 600) and 272 nm (ε 560). NMR-data: 7.0 (3H, s, arom.), 2.81 (2H, t, *J* 7 Hz, benzylic CH_2), 2.31 and 2.29 (2×3H, phenolic OAc); 2.09, 2.02, 1.99, and 1.96 ppm (4×3H, aliphatic OAc).

Rearrangement of 3. The pentaacetate *3* (129 mg) was dissolved in CH_2Cl_2 (10 ml), and two drops of BF_3,Et_2O were added. After 5 min at room temperature, the solution was washed with two 5 ml portions of a $NaHCO_3$-solution. After drying, and concentration to dryness, the residue was reacetylated (Ac_2O in pyridine) to give a mixture of products (99 mg), from which *7* was isolated as the major product (66 mg) by chromatography in Et_2O. (Found: C 55.01; H 5.55. Calc. for $C_{26}H_{32}O_{14}$: C 54.93; H 5.67.) $[\alpha]_D^{22}$ −11° (*c* 2.1, EtOH); λ_{max} 266 (ε 560) and 271 nm (ε 580). NMR-data: 7.26 (1H, dd, *J* 9 Hz and *ca.* 1 Hz, arom.), 7.01–6.88 (2H, arom.), 2.83 (2H, t, *J* 6.5 Hz, benzylic CH_2), 2.32 and 2.27 (2×3H, phenolic OAc), and 2.10–1.95 ppm (4×3H, aliphatic OAc).

Acid hydrolysis of 1. The glucoside *1* (138 mg) was dissolved in 3 % H_2SO_4 (5.5 ml) and heated on a steam-bath for 48 h. Ether extraction (5×10 ml) afforded the aglucone (34 mg), which was subjected to acetylation (Ac_2O in pyridine) for 2 h at r.t. and worked up in the usual way to give a crude product (43 mg), which was purified by chromatography (pentane-ether, 5:2) to give a homogeneous specimen (30 mg) of homogentisyl acetate *6*. (Found: C 60.08; H 5.76. Calc. for $C_{14}H_{16}O_6$: C 59.99; H 5.75.) λ_{max} 217 (ε 5500), 268 (ε 575), and 273 nm (ε 550). NMR-data: 7.09 (3H, s, arom.), 4.28 (2H, t, *J* 7.5 Hz), 2.89 (2H, t, *J* 7.5 Hz, benzylic CH_2), 2.34 and 2.29 (2×3H, phenolic OAc), and 2.04 ppm (3H, aliphatic OAc).

Isolation of salidroside, 8. Fraction a, from the glucoside isolation, was freed of less polar contaminants by extraction with three 50 ml portions of EtOAc. The aqueous solution was taken to dryness *in vacuo*, and the residue was subjected to acetylation (Ac_2O, pyridine, 2 days). Repeated chromatography (Et_2O as the eluent) gave a fraction (98 mg) which, according to NMR analysis, was rich in salidroside acetate. Deacetylation, with NH_3 in MeOH, yielded a crude glucoside, which was purified by chromatography (in $CHCl_3$:MeOH, 4:1) to give a homogeneous fraction. On trimethylsilylation a product was formed, possessing an NMR-spectrum, indistinguishable from that of persilylated salidroside.[6]

We thank Dr. E. Hartmann, The Arboretum, Hørsholm, Denmark, and Dr. N.-G. Treschow, The Botanic Garden of the University of Copenhagen, for supplying the plant material used in the present study. Authentic specimens of help in identifying salidroside were kindly provided by Professor H. Thieme, Leipzig, and Professor L. Birkofer, Düsseldorf.

1. Derkosch, J. and Kaltenegger, W. *Monatsh.* **88** (1957) 778.
2. Goodwin, S. and Witkop, B. *J. Am. Chem. Soc.* **79** (1957) 179.
3. Wangerin, W. In Engler, A. and Engelmann, W., Eds., *Das Pflanzenreich*, Leipzig 1910, IV. 229, p. 43.
4. Thieme, H. *Naturwiss.* **51** (1964) 360.
5. Sticher, O. *Helv. Chim. Acta* **53** (1970) 2010.
6. Birkofer, L., Kaiser, C. and Thomas, U. *Z. Naturforsch.* **23b** (1968) 1951.

Received December 22, 1972.

The Enthalpy of Fusion of Magnesium Chloride

JAN LÜTZOW HOLM[a] and FREDRIK GRØNVOLD[b]

[a] *Institute of Physical Chemistry, The Technical University of Norway, N-7034 Trondheim-NTH, Norway.* [b] *Institute of Chemistry, The University of Oslo, Blindern, Oslo 3, Norway*

The enthalpy of fusion of $MgCl_2$ has been redetermined by means of a high precision drop calorimeter with adiabatic shields.

The drop experiments were carried out by using the same method and technique as described by Grønvold [1] and used for the enthalpy of fusion determinations on the alkali magnesium chlorides, K_2MgCl_4, Rb_2MgCl_4, Cs_2MgCl_4, $KMgCl_3$, $RbMgCl_3$, and $CsMgCl_3$, by Holm, Jenssen Holm, Rinnan, and Grønvold.[2]

Anhydrous magnesium chloride was prepared by the same method as described before.[2] Chemical analysis showed the purified product to contain 99.5 mol % $MgCl_2$.

The results from the drop experiments are given in Table 1 and plotted in Fig. 1.

Table 1. Enthalpy increments for solid and liquid $MgCl_2$ ($cal_{th} = 4.1847$).

T/K	$H_T - H_{298.15}$ / $cal_{th}mol^{-1}$	
	exp	calc
906.1	11586	11553
918.0	11853	11802
922.6	11951	11898
929.3	11903	12038
942.2	12236	12308
948.3	12493	12436
953.6	12450	12547
964.8	12891	12781
997.7	19638	—
1002.2	23035	23061
1004.6	23077	23115
1015.5	23292	23356
1019.0	23478	23434
1024.2	23518	23549
1027.9	23718	23631
1035.1	23861	23791
1040.4	23951	23908
1048.1	24100	24079
1056.9	24200	24274
1072.0	24578	24609

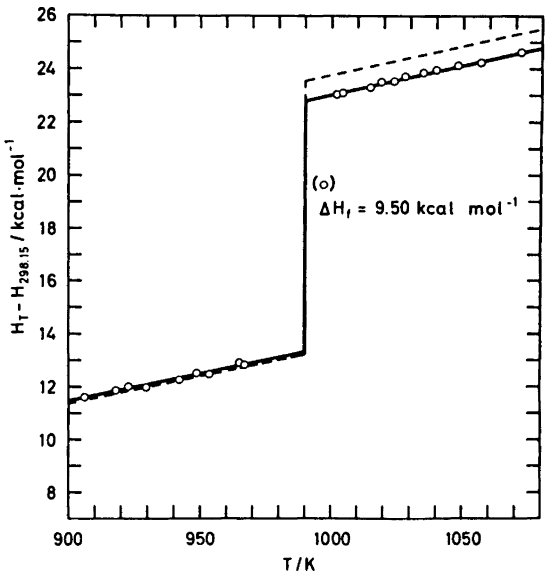

Fig. 1. Enthalpy curve, $H_T - H_{298.15}$ for $MgCl_2$. Results from this work, O; from literature (Ref. 3) – – –.

The data were fitted by a least squares treatment to equations of the type

$$H_T - H_{298.15} = a + b \times T$$

where b corresponds to the assumed constant heat capacity of the solid or the liquid over the limited temperature ranges in question; (*cf.* Table 1). The following equations were obtained:

solid $MgCl_2$: $H_T - H_{298.15} = 7407 + 20.92T$ $cal_{th}mol^{-1}$ ($\sigma = 96$)
liquid $MgCl_2$: $H_T - H_{298.15} = +837 + 22.18T$ $cal_{th}mol^{-1}$ ($\sigma = 58$) corresponding to

$$\Delta H_f(MgCl_2) = 8244 + 1.26T cal_{th}mol^{-1}$$

At the melting point 980 K this corresponds to an enthalpy of fusion

$$\Delta H_f(MgCl_2) = 9500 cal_{th}mol^{-1}$$

with an estimated uncertainty of 200 $cal_{th}mol^{-1}$. This value should be compared with the value given by Moore [3] and adopted by Kelley,[4] $\Delta H_f = 10\ 300$ $cal_{th}mol^{-1}$.

The agreement between the literature values and ours are excellent for solid $MgCl_2$,[3,4], while our data are about 4 % lower than those given for liquid $MgCl_2$.

Our heat capacity value for liquid $MgCl_2$, 22.17 $cal_{th}K^{-1}$ mol^{-1} is, however, in good agreement with the value reported in literature,[4] 22.1 $cal_{th}K^{-1}$ mol^{-1}.

Acknowledgements. Financial support from *Norges Almenvitenskapelige Forskningsråd* and from *Kaltenborn Griegs Stipendiefond* (to Jan Lützow Holm) is gratefully acknowledged.

1. Grønvold, F. *Acta Chem. Scand.* **26** (1972) 2216.
2. Holm, J. L., Jenssen Holm, B., Rinnan, B. and Grønvold, F. *J. Chem. Thermodynamics* **5** (1973) 97.
3. Moore, G. E., *J. Am. Chem. Soc.* **65** (1943) 1700.
4. Kelley, K. K, *Contributions to the Data on Theoretical Metallurgy*, XIII, Bull. 584, U.S. Bur. Mines 1960.

Received November 23, 1972.

The Structure of Molten Sodium Tetrafluoro Aluminate, $NaAlF_4$

JAN LÜTZOW HOLM

Institute of Physical Chemistry, The University of Trondheim, The Technical University of Norway N-7034 Trondheim-NTH, Norway

The use of the term "complex" in ionic molten salt mixtures has been questioned on several occasions. Critic has been raised mainly because formation of complexes has been postulated in several molten salt solutions without reference to properties like the symmetry of the complex, its life time, *etc.* Despite these objections it has generally been accepted that complex ions may be formed in binary charge unsymmetrical mixtures like $AX\text{-}BX_2$, $AX\text{-}CX_3$ *etc.* The strong negative deviation from ideality which has often been found in certain concentration ranges in ionic mixtures of, for instance, $KF\text{-}BeF_2$, $RbF\text{-}BeF_2$,[1] and in certain $AlkCl\text{-}MgCl_2$ mixtures,[2] may very well justify the use of the term complex, despite the fact that important structural properties are not known. The term "complex" does not always mean the same thermodynamically as it does spectroscopically. This is because in spectroscopy one looks for interactions between the atoms in the complex, while the thermodynamical stability of the complex depends on the surroundings as well. This is particularly the case when dealing with ionic liquids or molten salts with a "lattice-like" structure.

In this paper the thermodynamic stability of the rather controversial AlF_4^-ion will be discussed. This ion has for some time been assumed to be a stable complex ion in mixtures of molten sodium fluoride and aluminium fluoride.[3] The present author has shown [4,5] how the degree of dissociation, or stability, of ionic complex ions can be calculated using enthalpy of mixing data. The equation.

$$\Delta H_C^M = \Delta H^{Diss} N_0(\alpha_1 - \alpha_0) \qquad (1)$$

where ΔH^{Diss} is the enthalpy of dissociation of the pure complex, N_0 is the weighed-in mol fraction of the complex, and α_0 and α_1 are the degrees of dissociations in the pure complex and in the mixture, respectively, was used to calculate the dissociation of cryolite, Na_3AlF_6, in molten $NaF\text{-}Na_3AlF_6$ mixtures.

The data were fitted by a least squares treatment to equations of the type

$$H_T - H_{298.15} = a + b \times T$$

where b corresponds to the assumed constant heat capacity of the solid or the liquid over the limited temperature ranges in question; (*cf.* Table 1). The following equations were obtained:

solid $MgCl_2$: $H_T - H_{298.15} = 7407 + 20.92T$ $cal_{th}mol^{-1}$ ($\sigma = 96$)
liquid $MgCl_2$: $H_T - H_{298.15} = +837 + 22.18T$ $cal_{th}mol^{-1}$ ($\sigma = 58$) corresponding to

$$\Delta H_f(MgCl_2) = 8244 + 1.26T cal_{th}mol^{-1}$$

At the melting point 980 K this corresponds to an enthalpy of fusion

$$\Delta H_f(MgCl_2) = 9500 cal_{th}mol^{-1}$$

with an estimated uncertainty of 200 $cal_{th}mol^{-1}$. This value should be compared with the value given by Moore [3] and adopted by Kelley,[4] $\Delta H_f = 10\ 300$ $cal_{th}mol^{-1}$.

The agreement between the literature values and ours are excellent for solid $MgCl_2$,[3,4], while our data are about 4 % lower than those given for liquid $MgCl_2$.

Our heat capacity value for liquid $MgCl_2$, 22.17 $cal_{th}K^{-1}$ mol^{-1} is, however, in good agreement with the value reported in literature,[4] 22.1 $cal_{th}K^{-1}$ mol^{-1}.

Acknowledgements. Financial support from *Norges Almenvitenskapelige Forskningsråd* and from *Kaltenborn Griegs Stipendiefond* (to Jan Lützow Holm) is gratefully acknowledged.

1. Grønvold, F. *Acta Chem. Scand.* **26** (1972) 2216.
2. Holm, J. L., Jenssen Holm, B., Rinnan, B. and Grønvold, F. *J. Chem. Thermodynamics* **5** (1973) 97.
3. Moore, G. E., *J. Am. Chem. Soc.* **65** (1943) 1700.
4. Kelley, K. K, *Contributions to the Data on Theoretical Metallurgy*, XIII, Bull. 584, U.S. Bur. Mines 1960.

Received November 23, 1972.

The Structure of Molten Sodium Tetrafluoro Aluminate, $NaAlF_4$

JAN LÜTZOW HOLM

Institute of Physical Chemistry, The University of Trondheim, The Technical University of Norway N-7034 Trondheim-NTH, Norway

The use of the term "complex" in ionic molten salt mixtures has been questioned on several occasions. Critic has been raised mainly because formation of complexes has been postulated in several molten salt solutions without reference to properties like the symmetry of the complex, its life time, *etc.* Despite these objections it has generally been accepted that complex ions may be formed in binary charge unsymmetrical mixtures like $AX\text{-}BX_2$, $AX\text{-}CX_3$ *etc.* The strong negative deviation from ideality which has often been found in certain concentration ranges in ionic mixtures of, for instance, $KF\text{-}BeF_2$, $RbF\text{-}BeF_2$,[1] and in certain $AlkCl\text{-}MgCl_2$ mixtures,[2] may very well justify the use of the term complex, despite the fact that important structural properties are not known. The term "complex" does not always mean the same thermodynamically as it does spectroscopically. This is because in spectroscopy one looks for interactions between the atoms in the complex, while the thermodynamical stability of the complex depends on the surroundings as well. This is particularly the case when dealing with ionic liquids or molten salts with a "lattice-like" structure.

In this paper the thermodynamic stability of the rather controversial AlF_4^-ion will be discussed. This ion has for some time been assumed to be a stable complex ion in mixtures of molten sodium fluoride and aluminium fluoride.[3] The present author has shown [4,5] how the degree of dissociation, or stability, of ionic complex ions can be calculated using enthalpy of mixing data. The equation.

$$\Delta H_C^M = \Delta H^{Diss} N_0(\alpha_1 - \alpha_0) \qquad (1)$$

where ΔH^{Diss} is the enthalpy of dissociation of the pure complex, N_0 is the weighed-in mol fraction of the complex, and α_0 and α_1 are the degrees of dissociations in the pure complex and in the mixture, respectively, was used to calculate the dissociation of cryolite, Na_3AlF_6, in molten $NaF\text{-}Na_3AlF_6$ mixtures.

Table 1. The degree of dissociation of AlF_6^{3-} and the composition of different melts in the Na_3AlF_6-AlF_3 system.

Composition mol fraction AlF_3	ΔH^M cal mol^{-1}	α	Mol fractions AlF_6^{3-}	"AlF_3"	F^-
0	0	0.31	0.36	0.16	0.48
0.100	−200	0.30	0.35	0.20	0.45
0.445	+1000	0.39	0.21	0.40	0.39
0.575	+2600	0.59	0.10	0.47	0.43
0.667	+4100	0.87	0.02	0.51	0.47

The two most probable dissociation schemes for molten cryolite

(I) $Na_3AlF_{6(l)} = 3NaF_{(l)} + "AlF_{3(l)}"$

(II) $Na_3AlF_{6(l)} = 2NaF_{(l)} + NaAlF_{4(l)}$

were discussed. It was concluded that scheme II is of minor importance on the *NaF-side* of the system. The main species present in basic (NaF-rich) melts will be:

Na^+, AlF_6^{3-}, F^-, and "AlF_3"

In this dissociation scheme "AlF_3" is not supposed to be a separate species, but rather the inner and most stable part of the distorted AlF_6^{3-}-complex.

Here eqn. (1) will be used to calculate the dissociation of Na_3AlF_6 according to scheme I in molten mixtures of cryolite and aluminium fluoride.

Calculations. The weighed-in mol fractions are $N_0(Na_3AlF_6)$ and $N_1(AlF_3)$, and the degree of dissociation of Na_3AlF_6 in the mixture is α_1. The mol fractions of the three main species assumed to be present are then given by

$$X_{AlF_6^{3-}} = \frac{N_0(1-\alpha_1)}{1+3N_0\alpha_1} \qquad (2a)$$

$$X_{AlF_3} = \frac{N_1+N_0\alpha_1}{1+3N_0\alpha_1} \qquad (2b)$$

$$X_{F^-} = \frac{3N_0\alpha_1}{1+3N_0\alpha_1} \qquad (2c)$$

These ionic fractions are given in Table 1 as a function of N_1, together with the enthalpies of mixing measured in the system Na_3AlF_6-AlF_3 by Holm.[6] On the NaF side of the system NaF-AlF_3 the best value for the heat of dissociation of cryolite was found to be $\Delta H^{Diss} = 22\,000$ cal mol^{-1}.[4,6] By adopting this value on the AlF_3 side too, and using the experimental ΔH^M values, the degree of dissociation, α_1, was calculated. The results are given in Table 1.

Discussion. From the ΔH^M values given in Table 1 it is clear that the interactions between F^- and AlF_3 in a 1:1 NaF-AlF_3 mixture are weak, with ΔH^M for a mixture of $0.5NaF + 0.5AlF_3$ equal to -1700 cal mol^{-1}.[6] The present author has shown [5,6] that the equilibrium

(III) $Na_3AlF_{6(l)} + 2AlF_{3(l)} = 3NaAlF_{4(l)}$

is shifted to the left, with $\Delta H = 12$ kcal mol^{-1}, $\Delta S \simeq 0$ cal K^{-1} mol^{-1}.

Hence, when the AlF_3 content in the melt is increased beyond the cryolite composition, the result will be an increased dissociation of AlF_6^{3-} to "AlF_3" and F^- according to

$$AlF_6^{3-} \rightarrow "AlF_3" + 3F^-$$

and not any formation of a strong AlF_4^- complex. A melt of the $NaAlF_4$ composition consists of 0.02 mol Na_3AlF_6, 0.51 mol "AlF_3", and 0.47 mol NaF (Table 1). In this melt the solvated aluminium fluoride, "AlF_3," can formally be treated as an AlF_4^- complex. The bond between the solvated AlF_3 and the fourth fluoride ion must, however, be a weak one as the low ΔH^M indicates. The AlF_4^--complex can be illustrated by $^-F\ldots\ldots AlF_3$. From this one can conclude that in a melt of the $NaAlF_4$ composition, "AlF_3" exists in a weak distorted *tetrahedral* field:

$AlF_4^- = (AlF_3)F^-$(distorted tetrahedral)

This is different from a pure cryolite melt, where, as it has previously been shown,[5] "AlF_3" most probably will be present in a somewhat distorted *octahedral* field:

$AlF_6^{3-} = (AlF_3)3F^-$(distorted octahedral)

1. Holm, J. L. and Kleppa, O. J. *Inorg. Chem.* **8** (1969) 207.
2. Kleppa, O. J. and McCarty, F. G. *J. Phys. Chem.* **70** (1966) 1249.
3. Grjotheim, K. *Contributions to the Theory of the Aluminium Electrolysis, Kgl. Norske Videnskap. Selskabs, Skrifter* **1956**, No. 5.
4. Holm, J. L. *Thermodynamic Properties of Molten Cryolite and Other Fluoride Mixtures*, Dr. Thesis. The University of Trondheim, NTH 1971.
5. Holm, J. L. *Inorg. Chem. To be published.*
6. Holm. J. L. *High Temperature Science. To be published.*

Received December 5, 1972.

The Crystal and Molecular Structure of Methyl 3,6-Anhydro-α-D-glucopyranoside

BÖRJE LINDBERG,[a] BENGT LINDBERG[b] and SIGFRID SVENSSON[b]

[a]*Institute of Inorganic and Physical Chemistry, University of Stockholm, S-104 05 Stockholm, Sweden.* [b]*Institute of Organic Chemistry, University of Stockholm, Sandåsgatan 2, S-113 27 Stockholm, Sweden*

The pyranose rings in methyl 3,6-anhydro-α-D-glucopyranoside (I) and 1,6-anhydro-β-D-glucopyranose (II) are forced into the $^1C_4$ conformation and should be considerably distorted as a result of the strain caused by the *cis*-fused 5-membered ring. The distance between the axial oxygen atoms, O-2 and O-4, should therefore be longer in (II) and shorter in (I) than in a corresponding unstrained system. A recent X-ray diffraction study of II [1] demonstrated, *inter alia*, that the distance between O-2 and O-4 was 3.30 Å. A similar study of methyl 3,6-anhydro-α-D-galactopyranoside [2] demonstrated the distortion of the pyranose ring.

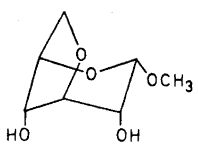

I

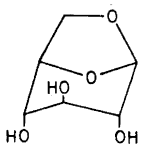

II

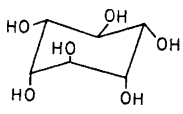

III

That the distance between O-2 and O-4 in I is exceptionally short was indicated by two observations. Firstly the β-anomer of I, which should have a similar structure, showed unexpectedly high mobilities on paper electrophoresis in borate and sulphonated phenyl boronic acid buffers.[3] The complex formation with boron, which requires an O–O distance of approximately 2.4 Å,[4] can only take place between the axially disposed oxygen atoms O-2 and O-4.

Secondly Schwarz and Totty [5,6] observed that I was a considerably stronger acid (K_a 62.3×10^{-14}) than, *e.g.*, the unstrained *muco*-inositol (III, K_a 7.10×10^{-14}). 1,6-Anhydro-β-D-glucopyranose is even weaker (K_a 2.96×10^{-14}). These results were explained in terms of a hydrogen bridge between O-2 and O-4 in the corresponding anions. The distance between these atoms in III is about 2.89 Å and should consequently be considerably smaller in I.

We now report an X-ray diffraction study of I. The compound crystallized in space group $P2_12_12_1$; **a** = 8.210 (1), **b** = 17.764 (3), **c** = 5.555 (1), $Z = 4$. The crystals decomposed on X-ray irradiation. From equi-inclination Weissenberg photographs, taken using Cu$K\alpha$ radiation, 335 data were collected. The phase determinations were carried out by a computerized application

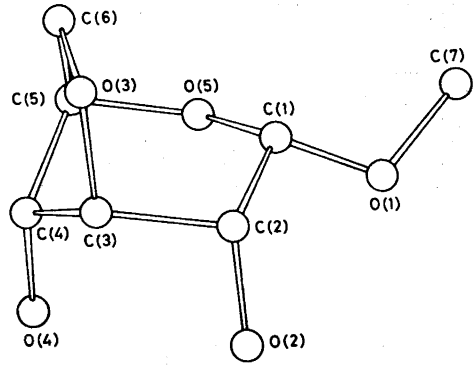

Fig. 1. The molecular structure of methyl 3,6-anhydro-α-D-glucopyranoside.

1. Holm, J. L. and Kleppa, O. J. *Inorg. Chem.* **8** (1969) 207.
2. Kleppa, O. J. and McCarty, F. G. *J. Phys. Chem.* **70** (1966) 1249.
3. Grjotheim, K. *Contributions to the Theory of the Aluminium Electrolysis, Kgl. Norske Videnskap. Selskabs, Skrifter* **1956**, No. 5.
4. Holm, J. L. *Thermodynamic Properties of Molten Cryolite and Other Fluoride Mixtures*, Dr. Thesis. The University of Trondheim, NTH 1971.
5. Holm, J. L. *Inorg. Chem. To be published.*
6. Holm. J. L. *High Temperature Science. To be published.*

Received December 5, 1972.

The Crystal and Molecular Structure of Methyl 3,6-Anhydro-α-D-glucopyranoside

BÖRJE LINDBERG,[a] BENGT LINDBERG[b] and SIGFRID SVENSSON[b]

[a]*Institute of Inorganic and Physical Chemistry, University of Stockholm, S-104 05 Stockholm, Sweden.* [b]*Institute of Organic Chemistry, University of Stockholm, Sandåsgatan 2, S-113 27 Stockholm, Sweden*

The pyranose rings in methyl 3,6-anhydro-α-D-glucopyranoside (I) and 1,6-anhydro-β-D-glucopyranose (II) are forced into the $^1C_4$ conformation and should be considerably distorted as a result of the strain caused by the *cis*-fused 5-membered ring. The distance between the axial oxygen atoms, O-2 and O-4, should therefore be longer in (II) and shorter in (I) than in a corresponding unstrained system. A recent X-ray diffraction study of II [1] demonstrated, *inter alia*, that the distance between O-2 and O-4 was 3.30 Å. A similar study of methyl 3,6-anhydro-α-D-galactopyranoside [2] demonstrated the distortion of the pyranose ring.

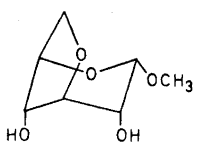

I

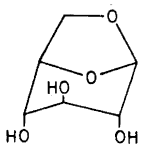

II

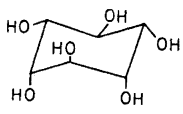

III

That the distance between O-2 and O-4 in I is exceptionally short was indicated by two observations. Firstly the β-anomer of I, which should have a similar structure, showed unexpectedly high mobilities on paper electrophoresis in borate and sulphonated phenyl boronic acid buffers.[3] The complex formation with boron, which requires an O–O distance of approximately 2.4 Å,[4] can only take place between the axially disposed oxygen atoms O-2 and O-4.

Secondly Schwarz and Totty [5,6] observed that I was a considerably stronger acid (K_a 62.3×10^{-14}) than, *e.g.*, the unstrained *muco*-inositol (III, K_a 7.10×10^{-14}). 1,6-Anhydro-β-D-glucopyranose is even weaker (K_a 2.96×10^{-14}). These results were explained in terms of a hydrogen bridge between O-2 and O-4 in the corresponding anions. The distance between these atoms in III is about 2.89 Å and should consequently be considerably smaller in I.

We now report an X-ray diffraction study of I. The compound crystallized in space group $P2_12_12_1$; **a** = 8.210 (1), **b** = 17.764 (3), **c** = 5.555 (1), $Z = 4$. The crystals decomposed on X-ray irradiation. From equi-inclination Weissenberg photographs, taken using Cu$K\alpha$ radiation, 335 data were collected. The phase determinations were carried out by a computerized application

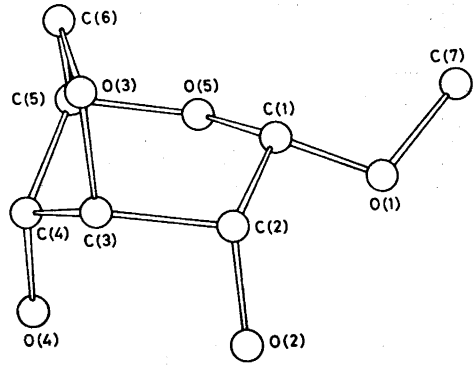

Fig. 1. The molecular structure of methyl 3,6-anhydro-α-D-glucopyranoside.

of direct methods using the weighted phase-sum formula.[7] Several cycles of full-matrix least-squares refinement (only isotropic non-hydrogen atoms included) gave an R-value of 0.136. The molecular structure is shown in Fig. 1. Intramolecular distances and angles are listed in Table 1. Full details

Table 1. Intramolecular distances and angles. Estimated standard deviations in parentheses.

C(1)–C(2)	1.50(3) Å	C(1)–C(2)–C(3)	108(2)°
C(2)–C(3)	1.57(3)	C(2)–C(3)–C(4)	118(2)
C(3)–C(4)	1.41(4)	C(3)–C(4)–C(5)	100(2)
C(4)–C(5)	1.56(3)	C(4)–C(5)–O(5)	109(2)
C(5)–C(6)	1.53(4)	C(5)–O(5)–C(1)	116(2)
C(1)–O(1)	1.38(2)	O(5)–C(1)–C(2)	116(2)
C(2)–O(2)	1.50(2)	C(1)–O(1)–C(7)	115(2)
C(3)–O(3)	1.50(3)	O(1)–C(1)–C(2)	108(2)
C(4)–O(4)	1.46(3)	O(1)–C(1)–O(5)	108(2)
C(5)–O(5)	1.49(2)	C(1)–C(2)–O(2)	108(2)
C(1)–O(5)	1.40(3)	O(2)–C(2)–C(3)	103(2)
C(6)–O(3)	1.44(3)	C(2)–C(3)–O(3)	104(2)
C(7)–O(1)	1.47(3)	C(3)–C(3)–C(4)	104(2)
		C(3)–C(4)–O(4)	120(2)
		O(4)–C(4)–C(5)	111(2)
		C(4)–C(5)–C(6)	97(2)
		C(6)–C(5)–O(5)	111(2)
		C(3)–O(3)–C(6)	105(2)
		O(3)–C(6)–C(5)	107(2)

of the X-ray diffraction investigation wil be published elsewhere.

As expected, the distance between O-2 and O-4 is short, 2.76 Å, in accordance with the observed chemical properties. Furthermore, although the hydrogens have not been located, the packing of the molecules would suggest an intramolecular hydrogen bond between O-2 and O-4 in the crystalline state.

Acknowledgement. We are grateful to Dr. J. C. P. Schwarz, Edinburgh, for information on unpublished results. We are also indebted to Professor Peder Kierkegaard for his interest. The investigation has been financially supported by the *Tri-Centennial Fund of the Bank of Sweden* and the *Swedish Natural Science Research Council.*

1. Park, J. Y., Kim, H. S. and Jeffrey, G. A. *Acta Cryst.* **B 27** (1971) 220.
2. Campell, J. W. and Harding, M. M. *J. Chem. Soc. Perkin Trans. 2* **1972** 1721.
3. Theander, O. *Acta Chem. Scand.* **18** (1964) 1297.
4. Weigel, H. *Advan. Carbohyd. Chem.* **18** (1963) 61.
5. Schwarz, J. C. P. and Totty, R. N. *Unpublished results.*
6. Totty, R. N. *Ph. D. Thesis*, Edinburgh 1968.
7. Norrestam, R. *Acta Cryst.* **A 28** (1972) 303.

Received December 29, 1972.

Stereoselective Cyclopropane Ring Opening Reactions of Nortricyclene Hydrocarbons in Formic Acid I. Reactions of Nortricyclene, Norbornene and Tricyclene

JAAKKO PAASIVIRTA

Department of Chemistry, University of Jyväskylä, Jyväskylä, Finland

During the study of the stereochemistry of the nortricyclene compounds and their cyclopropane ring opening products in our laboratory, the course of the reactions of nortricyclene hydrocarbons in formic acid has been examined.[1,2] The protonation of the cyclopropane ring in this system apparently leads to the same cationic intermediates as are found in the SN_1 solvolyses and E_1 eliminations of 2-norbornyl derivatives.[3,4] The aim in the present series is to connect kinetic data with the intermediate and final product analysis.

The addition of formic acid to nortricyclene (I) or norbornene (III) has norbornyl-2-*exo*-formate (II) as the sole main product.[5,6] This was confirmed in the present study. The hydrocarbon III from I, or I from III, occurred as a minor side product of the reaction, leading to the following overall picture:

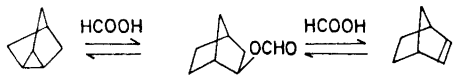

I II III

Only one ester product, isobornyl formate (V), was found from tricyclene (IV); the only hydrocarbon byproduct present

of direct methods using the weighted phase-sum formula.[7] Several cycles of full-matrix least-squares refinement (only isotropic non-hydrogen atoms included) gave an R-value of 0.136. The molecular structure is shown in Fig. 1. Intramolecular distances and angles are listed in Table 1. Full details

Table 1. Intramolecular distances and angles. Estimated standard deviations in parentheses.

C(1)–C(2)	1.50(3) Å	C(1)–C(2)–C(3)	108(2)°
C(2)–C(3)	1.57(3)	C(2)–C(3)–C(4)	118(2)
C(3)–C(4)	1.41(4)	C(3)–C(4)–C(5)	100(2)
C(4)–C(5)	1.56(3)	C(4)–C(5)–O(5)	109(2)
C(5)–C(6)	1.53(4)	C(5)–O(5)–C(1)	116(2)
C(1)–O(1)	1.38(2)	O(5)–C(1)–C(2)	116(2)
C(2)–O(2)	1.50(2)	C(1)–O(1)–C(7)	115(2)
C(3)–O(3)	1.50(3)	O(1)–C(1)–C(2)	108(2)
C(4)–O(4)	1.46(3)	O(1)–C(1)–O(5)	108(2)
C(5)–O(5)	1.49(2)	C(1)–C(2)–O(2)	108(2)
C(1)–O(5)	1.40(3)	O(2)–C(2)–C(3)	103(2)
C(6)–O(3)	1.44(3)	C(2)–C(3)–O(3)	104(2)
C(7)–O(1)	1.47(3)	C(3)–C(3)–C(4)	104(2)
		C(3)–C(4)–O(4)	120(2)
		O(4)–C(4)–C(5)	111(2)
		C(4)–C(5)–C(6)	97(2)
		C(6)–C(5)–O(5)	111(2)
		C(3)–O(3)–C(6)	105(2)
		O(3)–C(6)–C(5)	107(2)

of the X-ray diffraction investigation wil be published elsewhere.

As expected, the distance between O-2 and O-4 is short, 2.76 Å, in accordance with the observed chemical properties. Furthermore, although the hydrogens have not been located, the packing of the molecules would suggest an intramolecular hydrogen bond between O-2 and O-4 in the crystalline state.

Acknowledgement. We are grateful to Dr. J. C. P. Schwarz, Edinburgh, for information on unpublished results. We are also indebted to Professor Peder Kierkegaard for his interest. The investigation has been financially supported by the *Tri-Centennial Fund of the Bank of Sweden* and the *Swedish Natural Science Research Council.*

1. Park, J. Y., Kim, H. S. and Jeffrey, G. A. *Acta Cryst.* **B 27** (1971) 220.
2. Campell, J. W. and Harding, M. M. *J. Chem. Soc. Perkin Trans. 2* **1972** 1721.
3. Theander, O. *Acta Chem. Scand.* **18** (1964) 1297.
4. Weigel, H. *Advan. Carbohyd. Chem.* **18** (1963) 61.
5. Schwarz, J. C. P. and Totty, R. N. *Unpublished results.*
6. Totty, R. N. *Ph. D. Thesis*, Edinburgh 1968.
7. Norrestam, R. *Acta Cryst.* **A 28** (1972) 303.

Received December 29, 1972.

Stereoselective Cyclopropane Ring Opening Reactions of Nortricyclene Hydrocarbons in Formic Acid I. Reactions of Nortricyclene, Norbornene and Tricyclene

JAAKKO PAASIVIRTA

Department of Chemistry, University of Jyväskylä, Jyväskylä, Finland

During the study of the stereochemistry of the nortricyclene compounds and their cyclopropane ring opening products in our laboratory, the course of the reactions of nortricyclene hydrocarbons in formic acid has been examined.[1,2] The protonation of the cyclopropane ring in this system apparently leads to the same cationic intermediates as are found in the SN_1 solvolyses and E_1 eliminations of 2-norbornyl derivatives.[3,4] The aim in the present series is to connect kinetic data with the intermediate and final product analysis.

The addition of formic acid to nortricyclene (I) or norbornene (III) has norbornyl-2-*exo*-formate (II) as the sole main product.[5,6] This was confirmed in the present study. The hydrocarbon III from I, or I from III, occurred as a minor side product of the reaction, leading to the following overall picture:

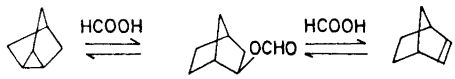

I II III

Only one ester product, isobornyl formate (V), was found from tricyclene (IV); the only hydrocarbon byproduct present

Table 1. The first-order rate coefficients and Arrhenius parameters of the reactions of nortricyclene (I), norbornene (III), and tricyclene (IV) in formic acid-methylene chloride 1:1 mixture.

Compound	Temp. °C	$k \times 10^5$ sec^{-1}	E kcal/mol	log A	Corr. factor R
I	0.	0.330			
	14.9	1.936			
	22.8	3.229	18.10± 1.20	8.98± 0.90	−0.9957
	40.0	24.99			
III	14.9	0.791			
	22.8	2.100			
	30.0	3.714	21.44± 1.59	11.13± 1.15	−0.9918
	35.5[a]	8.908			
	40.0	17.32			
IV	0.	0.594			
	26.0	7.281	15.93± 0.31	7.52± 0.23	−0.9998
	37.2	20.34			

[a] Rate determination by NMR.[1] The other measurements were made by gas chromatography.

was bornylene (VI). The absence of camphene (IX) and the camphene hydrate formates (VII and VIII) in the reactions mixture was confirmed by gas chromatography using authentic reference samples. The formation of tertiary intermediate products was prevented possibly because of steric repulsions hindering the attack of the nucleophile ($HCOO^-$ or HCOOH).

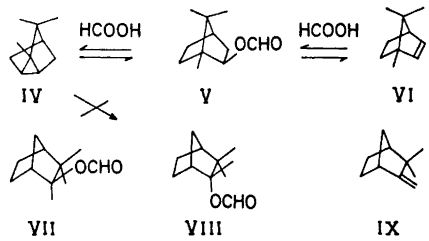

The reaction rates were difficult to determine in pure formic acid owing to the slow solubility of the hydrocarbons I, III, and IV. However, the hydrocarbons dissolved quickly when a formic acid-methylene chloride 1:1 (w/w) mixture was used. Methylene chloride retarded the reaction rates, but did not influence the product ratios. The mixture was taken for general use in this series. The reactions were followed mainly by gas chromatography, and in some cases also with NMR spectrometry.[1]

The rate coefficients and Arrhenius parameters obtained are collected in Table 1. The termodynamic data of activation at 25 and 105°C were calculated using the theory of absolute reaction rates and are collected in Table 2.

The free energy difference between nortricyclene (I) and norbornene (III) is small; 0.9 kcal/mol at 105°C according to Schleyer.[7] The closely similar values of the free energies of activation for the reactions of I and III (see Table 2) thus indicate that both reactions proceed through equivalent transition states to the same product, II. Such a transition state is formed from an intermediate carbonium ion, the structure of which could also be presented as being the same from both I and III. This interpretation is supported by the distribution of deuterium in the products of DX additions to I and III,[8,9] and in the products of different electrophilic additions to 5,6-dideuterionorbornenes.[10] The intermediate is to be "asymmetrically bridged": either the nonclassical 6-norbornonium ion (X) [1,11,12] or an equilibrium mixture of classical 2-norbornyl cations.[13,14] This intermediate involves the Wagner-Meerwein rearrangement. The nonclassical structure X has additionally been supported by spectral studies from superacid solutions at low tempera-

Table 2. Thermodynamic parameters for the reactions of nortricyclene (I), norbornene (III), and tricyclene (IV) with formic acid calculated from the results of the kinetic measurements.

Reaction	Temp. °C	ΔH^* kcal/mol	ΔS^* cal/degr. mol	ΔG^* kcal/mol
I in formic acid-CH_2Cl_2	25	17.51	−19.41	23.30
III in formic acid-CH_2Cl_2	105	17.35	−19.89	24.87
	25	20.84	− 9.57	23.70
III in pure formic acid [a]	105	20.68	−10.04	24.48
	25	14.17	−25.35	21.73
IV in formic acid-CH_2Cl_2	105	14.01	−25.82	23.78
	25	15.34	−26.11	23.13
	105	15.18	−26.58	25.23

[a] Calculated from the data in Table 5 of Ref. 1. The other results are calculated from the data in Table 1 of the present paper.

tures.[15,16] Another intermediate, C-nortricyclonium ion (XI),[12] which is somewhat less stable than X, might be the route of 1,2,6-hydrogen shifts during the reactions if the conditions allow the cations a longer lifetime. The cyclopropane ring opening, of I and IV could also, at least partly, proceed via this XI-type of edge-protonated nortricyclene structure.

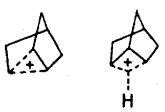

X XI

Acknowledgement. The author is grateful to Mrs. Tellervo Laasonen and Mr. Reijo Kauppinen for their skilful assistance with the experimental work, which has been financially supported by the *National Research Council for Sciences (Valtion Luonnontieteellinen Toimikunta)*.

1. Paasivirta, J. *Acta Chem. Scand.* **22** (1968) 2200.
2. Paasivirta, J. Resuméer av Sektionsföredrag, 14:e Nordiska Kemistmötet, Umeå 1971, 197.
3. Collins, C. J. *Chem. Rev.* **69** (1969) 543.
4. Lee, C. C. *Progr. Org. Chem.* **7** (1970) 129.
5. Pulkkinen, E. *Suomen Kemistilehti* **A 27** (1954) 26.
6. Kleinfelter, D. C. and Schleyer, P. von R. *Org. Syn.* **42** (1963) 79.
7. Schleyer, P. von R. *J. Am. Chem. Soc.* **80** (1958) 1700.
8. Nickon, A. and Hammons, J. H. *J. Am. Chem. Soc.* **86** (1964) 3322.
9. Brown, J. M. and McIvor, M. C. *Chem. Commun* **1969** 238.
10. Werstiuk, N. H. and Vancas, I. *Can. J. Chem.* **48** (1970) 3963.
11. Winstein, S. and Trifan, D. S. *J. Am. Chem Soc.* **71** (1949) 2953; **74** (1952) 79.
12. Olah, G. A. *J. Am. Chem. Soc.* **94** (1972) 808.
13. Brown, H. C. *The Transition State, Chem. Soc. Special Publ. 1962, No. 16* 140, 174; *Chem. & Eng. News.* (1967) 87.
14. Brown, H. C., Kawamaki, J. H. and Liu, K.-T. *J. Am. Chem. Soc.* **92** (1970) 5536.
15. Olah, G. A. and White, A. M. *J. Am. Chem. Soc.* **91** (1969) 3956.
16. Olah, G. A., White, A. M., DeMember, J. R., Commeyras, A. and Lui, C. Y. *J. Am. Chem. Soc.* **92** (1970) 4627.

Received November 30, 1972.

H_3O^+ Used as Terminating Ion in Isotachophoresis

ANDERS VESTERMARK

Department of Biochemistry, University of Stockholm, S-113 82 Stockholm, Sweden

In 1908 W. Lash Miller discussed the moving boundary method for determination of transport numbers.[1] Miller stressed that to ensure a sharp meniscus in such experiments the direction of the field had to be chosen so that the "specifically slower" ion species moved behind the "specifically faster species". A stable meniscus between water solutions of acetic acid and sodium acetate could according to Miller be expected if the positive current was arranged to move from the acetic acid to the sodium acetate. This idea was confirmed by experiments carried out by Dawson and Graham in Miller's laboratory. The net mobility [2] of the hydrogen ion was evidently under the conditions used lower than that of the sodium ion.

The aim of the work presented here has been to demonstrate that the hydrogen ion can be used as terminating ion in isotachophoretic experiments and that the net mobility of the hydrogen ion can be changed by employing different counterions or mixtures of counterions.

Experimental. One series of experiments was performed in sucrose gradients (from 10 to 50 % sucrose) in vertical U-tubes, 0.9 cm i.d.[3] 0.1 M solutions of acetic acid, formic acid, monochloroacetic acid or trichloroacetic acid were used as terminating electrolytes. 0.1 M solutions (pH about 7) of the potassium salts of the acids were used as leading electrolytes. In some experiments, mixtures of acetic acid and trichloroacetic acid were used as terminating electrolytes and mixtures of the corresponding potassium salts as leading electrolytes. One ml of a 0.5 M pyridinium salt solution of pH 5.2 was used as sample. The counterion in the pyridinium salt solution was the same as that in the leading electrolyte.

The voltage was adjusted to give a downward movement of the pyridinium zone of about 15 cm in 15 to 20 h. The pH and UV-absorption (256 nm) in the eluate of the contents of the anodic part of the U-tube was determined. The presence of potassium was determined by the flame reaction.

For another series of experiments a cooled glass plate apparatus of the Crestfield and Allen type was employed.[4] Cellulose acetate strips 1 × 20 cm (Machery-Nagel & Co., Düren, Germany) were used as anticonvectional medium. The strips moistened with the leading electrolyte were placed with one end in contact with the wick of the leading electrolyte. A piece of filterpaper moistened with the sample was placed in contact with the other end of the strip and the wick of the terminating electrolyte. In some experiments 0.5 M solutions of copper, cobalt or ferric sulphate were employed as samples. In other experiments histidine or glycine acted as samples together with small amounts of a mixture of malachite green and toluyleneblue. The two dyes contained impurities which indicated the limits of the amino acid zones developed during the experiments.

The isotachophoretic experiments on strips were run at a tension of 600 to 1000 V and lasted for 1 h.

Results. In the density gradient experiments with acetic, formic and monochloroacetic acids a pH shelf developed between pH 4 and 5 (Fig. 1). The position of a UV

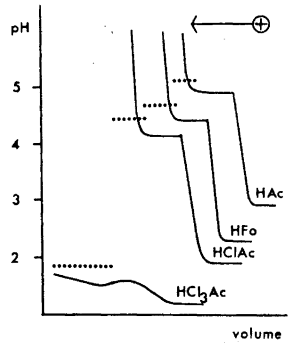

Fig. 1. pH determinations in experiments with acids as terminating and their corresponding potassium salts as leading electrolytes. The arrow indicates the direction of the positive current. The dotted line denotes presence of potassium. Well collected UV-absorbing zones, coinciding with the pH shelves were found in the experiments with acetic (HAc), formic (HFo) and monochloroacetic (HClAc) acids. To make the figure simpler the UV-zones have been left out. They were all of the same shape as the one shown in the experiment with 100 % HAc in Fig. 2. In the experiment with trichloroacetic acid (HCl_3Ac) no pH shelf developed.

absorbing zone coincided with the shelf. In front of this zone (to the left in Fig. 1) potassium ions were found. In the main part of the potassium-region (outside Fig. 2) pH reached a level of 7 or higher. Behind the shelf pH was low. These findings indicate that the order of the net mobilities of the positive ions in the experiments was potassium > pyridinium > hydrogen. When trichloroacetic acid was employed, no pH shelf developed (Fig. 1). During the experiment, H_3O^+ ions moved from the terminating solution through the pyridinium zone into the leading electrolyte. The resulting pH in the now zone-electrophoretically moving pyridinium zone was 3 – 4 units below the pK_a value, 5.2, of the pyridinium ion. No pH shelf could be expected. The order of the net mobilities of the positive ions was obviously in this experiment hydrogen > potassium > pyridinium.

In all the experiments with mixtures of acetic and trichloroacetic acids the front boundary was sharp (Fig. 2). Also the rear boundary was sharp in the experiments with mixtures containing 70 % acetic acid or more. At lower concentrations of acetic acid a sharp boundary did not develop on the terminating side of the pyridinium zone.

The net mobility of the hydrogen ion and the pyridinium ion increases when the content of the stronger acid in the terminating acid mixture increases. The difference in net mobility between the pyridinium ion and the hydrogen ion decreases. This difference has evidently in the experiments with 50 or 60 % acetic acid been too small to produce a sharp boundary between the pyridinium and hydrogen ions. For the development of such a boundary a longer migration distance would have been necessary.

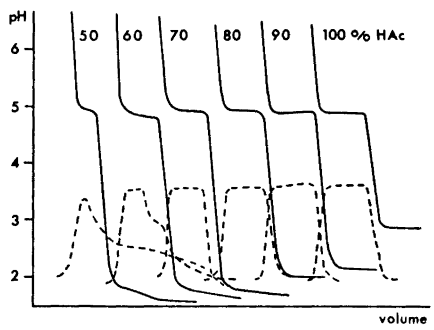

Fig. 2. pH determinations in experiments with mixtures of acetic and trichloroacetic acids as terminating and mixtures of the corresponding potassium salts as leading electrolytes. The broken line indicates the absorption at 256 nm (arbitrary units). The leading boundary of the pyridinium zone was sharp in all experiments. Potassium ions were present in about the same region as in the corresponding experiment in Fig. 1. In the experiments with 50 and 60 % acetic acid a sharp rear boundary did not develop.

The experiments in Fig. 1 illustrate that the net mobility of the hydrogen ion can be changed stepwise by changing the counter ion species. The experiments in Fig. 2 indicate that the net mobility of the hydrogen ion can be modified in a continuous manner by changing the ratio of the components in the counter ion mixture.

In the experiments on cellulose acetate strips cobalt, copper, and iron formed nice zones when acetic acid was used as terminating solution. In one experiment a mixture of the three metal ions produced three consecutive zones, each one centimeter long, with no observable overlapping. Histidine also formed a zone in the acetic acid system. Glycine could not be shown to move isotachophoretically under these conditions. The ferric ions moved immediately behind the hydrogen ion front in the formic acid system in a non-isotachophoretic manner. The other four ions developed isotachophoretically moving zones in this system as well as in the monochloroacetic acid system. The two amino acids gave when run together two distinct zones, the glycine zone moving behind that of histidine. None of the five ions tested developed distinct zones when trichloroacetic acid was used as terminator.

By the experiments on cellulose acetate it has been demonstrated that the hydrogen ion can be used as terminating ion in isotachophoretic systems for the separation of metal ions. The fact that the pH is low in the terminating electrolyte is of special interest when the isotachophoretic procedure is used for extraction [5] of say metal ions from biological materials. The low pH counteracts binding of metals to carboxyl groups in the biological material.

H_3O^+ acts not only as a terminating ion, the mobility of which can be easily controlled, but also as a source of positive charges for amino acids and other amines. Protons seem to be ideal terminating ions for the isotachophoretic separation of amino acids.

1. Miller, W. L. *Z. physik. Chem. (Leipzig)* **69** (1909) 436.
2. Consden, R., Gordon, A. H. and Martin, A. J. P. *Biochem. J.* **40** (1946) 33.
3. Vestermark, A. *Sci. Tools* **17** (1970) 24.
4. Crestfield, A. M. and Allen, F. W. *Anal. Chem.* **216** (1955) 67.
5. Vestermark, A. and Sjödin, B. *J. Chromatog.* **73** (1972) 211.

Received November 27, 1972.

The Structure of 2,5-Diphenyl-3,4-dimethyl-6a-thiathiophthene

ASBJØRN HORDVIK, ODDVAR SJØLSET and LEIF J. SÆTHRE

Chemical Institute, University of Bergen, N-5000 Bergen, Norway

The structure study of 2,5-diphenyl-3-methyl-6a-thiathiophthene (I)[1] showed that the sulphur-sulphur bonds there are unequal, *i.e.* S(1) – S(6a) = 2.255(1) Å and S(6a) – S(6) = 2.398(1) Å.

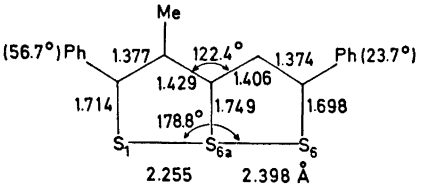

(I)

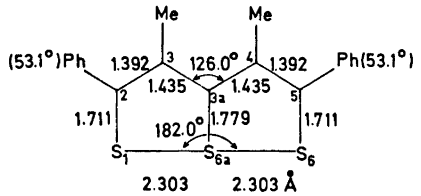

(II)

This agrees with the results from CNDO/2 calculations of mono-methyl and mono-phenyl substituted 6a-thiathiophthenes.[2]

A structure investigation of 2,5-diphenyl-3,4-dimethyl-6a-thiathiophthene (II) has been carried out in order to obtain further information about the degree to which methyl and phenyl substituents affect the S – S bonding in 6a-thiathiophthenes; the preliminary results are given.

The S(6a) – C(3a) bond in II lies along a crystallographic two-fold axis, and the two halves of the molecule are therefore exactly equal. The bond lengths in the 6a-thiathiophthene system of II are, S(1) – S(6a) = 2.303(1) Å, S(1) – C(2) = 1.711(4) Å, S(6a) – C(3a) = 1.779(4) Å, C(2) – C(3) = 1.392(4) Å, and C(3) – C(3a) = 1.435(4) Å. The phenyl groups are twisted 53.1° about the connecting bonds.

The S(6a) – C(3a) bond in II is 0.03 Å longer than that in I, and it is in fact the longest S(6a) – C(3a) bond which so far has been found in 6a-thiathiophthenes.

A sample of 2,5-diphenyl-3,4-dimethyl-6a-thiathiophthene was generously supplied by M. Stavaux.[3] The crystals are dark red and belong to the orthorhombic space group *Aba*2. The cell dimensions are a = 7.7023(17) Å, b = 29.6436(32) Å, and c = 7.2417(8) Å. There are four molecules per unit cell; density, calculated 1.367 g/cm³, found 1.362 g/cm³.

The structure analysis is based on X-ray data collected on a paper-tape controlled Siemens AED diffractometer using Mo$K\alpha$ radiation. 800 reflections were observed within $\theta = 28°$.

The structure was solved by the heavy atom (S) method and refined by full matrix least squares. The final R factor is 0.033.

The authors are indebted to Dr. M. Stavaux, Faculté des Science de Cáen, France, for providing a sample of 2,5-diphenyl-3,4-dimethyl-6a-thiathiophthene.

1. Hordvik, A., Sjølset, O. and Sæthre, L. J. *Acta Chem. Scand.* **26** (1972) 1297; and *to be published.*
2. Hansen, L. K., Hordvik, A. and Sæthre, L. J. *Chem. Commun.* **1972** 222.
3. Stavaux, M. and Lozac'h, N. *Bull. Soc. Chim. France* **1967** 2082.

Received December 13, 1972.

The Crystal and Molecular Structure of Methyl 6-*O*-Acetyl-*β*-D-galactopyranoside

BÖRJE LINDBERG,[a] PER J. GAREGG[b] and CARL-GUNNAR SWAHN[b]

[a]*Institute of Inorganic and Physical Chemistry, University of Stockholm, S-104 05 Stockholm, Sweden.* [b]*Institute of Organic Chemistry, University of Stockholm, S-104 05 Stockholm, Sweden*

In the course of studies of the circular dichroism of *O*-acetylated glycopyranosides[1,2] differential dichroic absorption was observed for glycosides with an *O*-acetyl group in the 6-position. On the basis of NMR studies, Hall and Manville have concluded that, in solution, conformation A predominates for D-*threo*-hexopyranoses, while that of B predominates for D-*erythro*-hexopyranoses.[3] Lemieux and co-workers, on the basis of NMR studies as well as from studies of optical rotation, have concluded that at least for D-*erythro*-hexopyranoses, conformation C predominates in solution.[4,5]

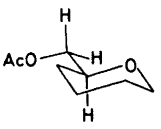

A

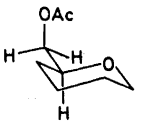

B

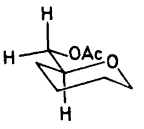

C

It was therefore considered of interest to determine the conformation in the solid state of a 6-*O*-acetylhexopyranoside by means of X-ray crystallography in order to see if this conformation would correlate with the observed dichroism. Due to its crystalline properties, methyl 6-*O*-acetyl-*β*-D-galactopyranoside[6] was selected for the study.

The compound crystallized in space group $P2_12_12_1$, **a** = 26.230, **b** = 9.196, **c** = 4.718, Z = 4. The X-ray data were obtained

Table 1. Intramolecular nonhydrogen bond distances and angles. Estimated standard deviations are given in parentheses.

C(1)–C(2)	1.519 (6) Å	C(1)–O(2)–C(3)	111.0 (4)°
C(2)–C(3)	1.518 (6)	C(2)–C(3)–C(4)	109.9 (4)
C(3)–C(4)	1.523 (6)	C(3)–C(4)–C(5)	109.6 (4)
C(4)–C(5)	1.504 (7)	C(4)–C(5)–O(5)	110.9 (4)
C(5)–C(6)	1.518 (7)	C(5)–O(5)–C(1)	112.6 (3)
C(8)–C(9)	1.465 (10)	O(5)–C(1)–C(2)	110.3 (4)
C(1)–O(1)	1.374 (6)	C(4)–C(5)–C(6)	114.7 (4)
C(7)–O(1)	1.428 (7)	O(5)–C(5)–C(6)	105.1 (4)
C(2)–O(2)	1.421 (5)	C(5)–C(6)–O(6)	106.8 (5)
C(3)–O(3)	1.416 (5)	C(1)–O(1)–C(7)	114.4 (5)
C(4)–O(4)	1.431 (5)	C(6)–O(6)–C(8)	117.9 (4)
C(1)–O(5)	1.437 (5)	O(6)–C(8)–C(9)	114.5 (5)
C(5)–O(5)	1.427 (6)	O(6)–C(8)–O(7)	121.1 (5)
C(6)–O(6)	1.445 (7)	C(9)–C(8)–O(7)	124.1 (5)
C(8)–O(6)	1.285 (5)	O(1)–C(1)–O(5)	107.3 (4)
C(8)–O(7)	1.181 (8)	O(1)–C(1)–C(2)	108.7 (4)
		C(1)–C(2)–O(2)	109.9 (4)
		C(3)–C(2)–O(2)	110.0 (4)
		C(2)–C(3)–O(3)	113.7 (4)
		C(4)–C(3)–O(3)	111.4 (4)
		C(3)–C(4)–O(4)	109.5 (4)
		C(5)–C(4)–O(4)	109.9 (4)

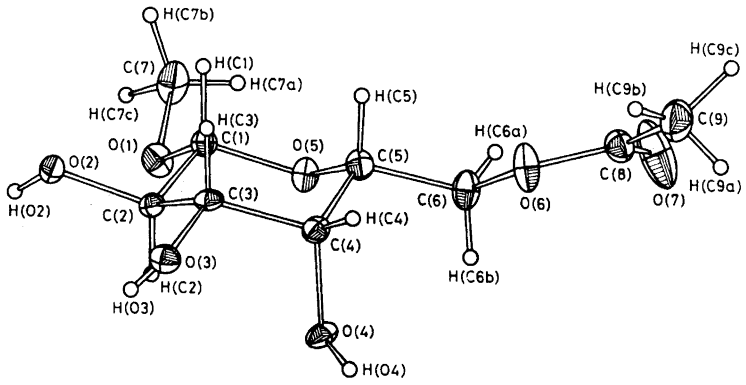

Fig. 1.

on a Philips PW 1100 computer-controlled single-crystal diffractometer with graphite monochromatized Cu$K\alpha$ radiation. The phase determinations were carried out by a computerized application of direct methods using the weighted phase-sum formula described by Norrestam.[7] Several cycles of full-matrix least-squares refinement (anisotropic nonhydrogen and fixed isotropic hydrogen temperature parameters) gave an R-value of 0.044. The molecular structure is shown in Fig. 1. Intramolecular distances and angles are listed in Table 1. Full details of the X-ray diffraction investigation will be published elsewhere.

The conformation found agrees with that suggested by Hall and Manville [3] for D-*threo*-hexopyranoses (A). In this conformation the acetoxy group and the ring oxygen are *trans*-oriented (D). As discussed elsewhere [1,2] the Cotton effect associated with an $n \rightarrow \pi^*$ transition of an acetoxy carbonyl group situated near a chiral centre in a pyranose ring most probably is determined by the dihedral angle of the acetoxy group and a neighbouring oxygen or oxymethylene function.

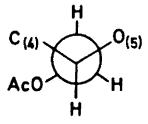

D

By this argument, D would not be expected to give rise to a Cotton effect. As discussed in another paper,[2] the CD band observed for the title compound most likely is caused by the presence, in solution, of molecules in conformation C.

Acknowledgement. The authors are indebted to Professor Peder Kierkegaard and to Professor Bengt Lindberg for their interest. The investigation received financial support from *Riksbankens Jubileumsfond*, *Hierta Retzius stipendiefond*, *Wallenbergsstiftelsens jubileumsanslag för befordrande av vetenskapligt arbete* samt *Statens Naturvetenskapliga Forskningsråd*.

1. Borén, H. B., Garegg, P. J., Kenne, L., Maron, L. and Svensson, S. *Acta Chem. Scand.* **26** (1972) 644.
2. Borén, H. B., Garegg, P. J., Kenne, L., Pilotti, Å., Svensson, S. and Swahn, C.-G. *Acta Chem. Scand.* **27** (1973). *In press.*
3. Hall, L. D. and Manville, J. F. *Can. J. Chem.* **47** (1969) 1.
4. Lemieux, R. U. and Stevens, J. D. *Can. J. Chem.* **43** (1965) 2059.
5. Lemieux, R. U. and Martin, J. C. *Carbohyd. Res.* **13** (1970) 139.
6. Garegg, P. J. and Swahn, C.-G. *Acta Chem. Scand.* **26** (1972) 3895.
7. Norrestam, R. *Acta Cryst.* **A 28** (1972) 303.

Received December 14, 1972.

The Structure of 2,5-Diphenyl-3,4-dimethylene-6a-thia-thiophthene

BJØRN BIRKNES, ASBJØRN HORDVIK and LEIF J. SÆTHRE

Chemical Institute, University of Bergen, N-5000 Bergen, Norway

2,5-Diphenyl-3,4-dimethylene-6a-thia-thiophthene (II) possesses intramolecular strain caused by the presence of the dimethylene bridge. A structure analysis of II has been carried out in order to find the degree to which the intramolecular strain affects the bonding in the 6a-thiathiophthene system of II relative to the bonding in the 6a-thiathiophthene system of 2,5-diphenyl-3,4-trimethylene-6a-thiathiophthene (I).[1] The preliminary results from this study are given.

The 2,5-diphenyl-3,4-dimethylene molecules lie across crystallographic mirror planes, and the two halves of the molecule

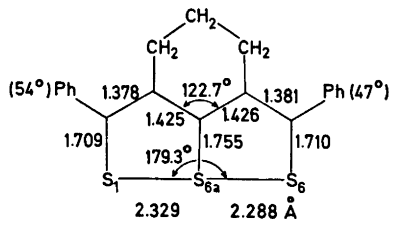

(I)

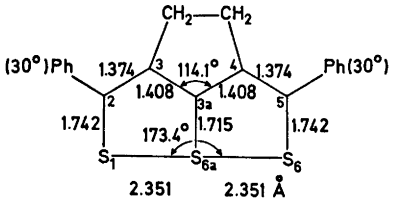

(II)

are therefore exactly equal. The bond lengths in the 6a-thiathiophthene system of II are, S(1)–S(6a) = 2.351(1) Å, S(1)–C(2) = 1.742(4) Å, S(6a)–C(3a) = 1.715(5) Å, C(2)–C(3) = 1.374(5) Å, and C(3)–C(3a) = 1.408(4) Å. The twist angles of the phenyl groups about the respective connecting bonds are 30°.

The central C–S bond in II is shorter than the terminal C–S bonds. This is opposite to what so far has been found for the C–S bonds in 6a-thiathiophthenes.[2] Furthermore, the dimethylene bridge has caused a lengthening of about 0.1 Å of the three-sulphur sequence in II relative to that in I.

A sample of 2,5-diphenyl-3,4-dimethylene-6a-thiathiophthene was generously supplied by M. Stavaux.[3] The crystals are very dark red and belong to the orthorhombic space group *Pnma*. The cell dimensions are, $a = 7.165(1)$ Å, $b = 29.704(4)$ Å, and $c = 7.372(3)$ Å. There are four molecules per unit cell; $D_c = 1.433$ g/cm³, $D_m = 1.427$ g/cm³.

The structure analysis is based on X-ray data collected on a paper-tape controlled Siemens AED diffractometer using Mo$K\alpha$ radiation. 812 reflections were observed within $\theta = 27°$.

The structure was solved by the heavy atom method and refined by full matrix least squares. The final R factor is 0.037.

We thank Dr. M. Stavaux, Departement de Chimie, Université de Caen, France, for a sample of 2,5-diphenyl-3,4-dimethylene-6a-thiathiophthene.

1. Birknes, B., Hordvik, A. and Sæthre, L. J. *Acta Chem. Scand.* **26** (1972) 2141.
2. Hansen, L. K. and Hordvik, A. *Acta Chem. Scand.* **27** (1973). *In press.*
3. Stavaux, M. and Lozac'h, N. *Bull. Soc. Chim France* **1967** 2082.

Received December 13, 1972.

ACTA CHEMICA SCANDINAVICA 27 (1973) 383–390

Quaternization Reactions

IV. Quaternization of 3,6-Dialkylpyridazines

HENNING LUND and VIGGO LUND

Department of Organic Chemistry, University of Aarhus, DK-8000 Aarhus C, Denmark

A series of 3,6-dialkylpyridazines has been quaternized with methyl iodide and the product distribution analyzed by NMR-spectroscopy. The product distribution is kinetically controlled under the present reaction conditions, and it is independent of the nature of the solvent, except in ethers. The product distribution is only moderately dependent on the electrical properties of substituents, but much more on steric factors.

The alkylation of tertiary amines has been used in several cases [1–9] to throw light on the steric influence of substituents on reaction rates; the quaternization of some 3,6-disubstituted pyridazines [3] has previously been studied in this context; in the present investigation a series of unsymmetrically substituted 3,6-dialkylpyridazines has been included.

On quaternization of such pyridazines two products are obtained, one quaternized at N-1 (QN1) and one at N-2 (QN2), and the product distribution QN1/QN2 is the measured quantity. This is evaluated from the NMR-spectrum of the reaction mixture from which the reaction medium, usually acetonitrile, has been removed. The ratio QN1/QN2 is of interest if the reaction is kinetically controlled as QN1/QN2 then is equal to the ratio of the rate constants k_{N1}/k_{N2}, where k_{N1}, resp. k_{N2}, are the rate constants of the reaction at N1, resp. N2.

RESULTS AND DISCUSSION

The value of the data is critically dependent upon whether the reaction is kinetically or thermodynamically controlled. The previous data [3] suggested kinetic control and this has been confirmed in two ways.

A kinetic control requires that the reverse reaction is negligible under the employed reaction conditions. This was tested by treating 1-ethyl-3,6-dialkylpyridazinium iodides with a great excess of methyl iodide in acetonitrile under various conditions (Table 1).

Table 1. Reaction between 1-ethyl-3,6-dialkylpyridazinium iodide and methyl iodide in acetonitrile under various conditions.

R-3	R-6	Reaction time (days)	Temperature	Exchange %
CH_3	CH_3	7	110°	0
$C(CH_3)_3$	$C(CH_3)_3$	1	65°	0
»	»	4	65°	0
»	»	14	65°	15
»	»	5	80°	50

An attack of iodide on the quaternized compound would yield ethyl iodide and the pyridazine which would quaternize with the excess of methyl iodide. An exchange of the ethyl group with a methyl group would be easily detectable in the NMR-spectrum of the reaction mixture.

Whereas even forced conditions (110°, 7 days) failed to produce detectable products of the reverse reaction of 1-ethyl-3,6-dimethylpyridazinium iodide, prolonged heating at a more moderate temperature (65°, 14 days) of the sterically very crowded 1-ethyl-3,6-di-*tert*-butylpyridazinium iodide did, in fact, give some 1-methyl-3,6-di-*tert*-butylpyridazinium iodide. The rate of the reverse reaction was, however, far too small to influence the product distribution under the usually employed experimental conditions (50°C, 24 h).

Quaternization of 3-*tert*-butyl-6-dimethylaminopyridazine with methyl iodide in CD_3CN could be followed in the NMR-spectrometer. The results (Table 2) shows that the ratio between the two products quaternized at N-1

Table 2. Product distribution during reaction between methyl iodide and 3-*tert*-butyl-6-dimethylaminopyridazine in CD_3CN.

Reaction time	Temp.	% Reaction	k_{N1}/k_{N2}	% quat. at NMe_2
1 h 10′	35°	10	64/36	15
2 h 40′	35°	20	62.2/37.8	15
5 h 15′	35°	40	62.6/37.4	15
24 h	35°	90	61.5/38.5	15
4 days	35°	> 99	63/37	8
6 days	35°	> 99		5
2 days	60°	> 99	62.8/37.2	0

and N-2 was constant during the reaction; a certain amount of product quaternized at the dimethylamino group was formed during the reaction, but as this reaction is reversible under these conditions (*vide infra*), the exo-quaternized product disappeared at the end of the reaction.

3,6-Bis(dimethylamino)pyridazine with methyl iodide quaternizes at 35°C to the iodide of 3-dimethylamino-6-trimethylammonium pyridazine. Heating a solution of this compound in acetonitrile with equimolar amounts

of 3,6-dimethylpyridazine gives a mixture of 1,3,6-trimethylpyridazinium iodide and 1-methyl-3,6-bis(dimethylamino)pyridazinium iodide together with some of the unquaternized pyridazines. The amount of quaternized product is somewhat smaller than corresponding to the starting material. The exo-quaternized compound is attacked by iodide and some of the methyl iodide thus formed is lost, whereas the remaining part quaternizes the ring-nitrogens in the usual manner.

Influence of solvent. Solvation of reaction partners is one of the most important factors in reactions in solution. The influence of an *o*-substituent could conceivably work through a change in the solvation of the reaction centre.

Previously the quaternization of 3-chloro-6-methylpyridazine has been investigated in acetonitrile and benzene and no difference in product distribution was found. In order to test this apparent independence of solvent a pyridazine, 3-*tert*-butyl-6-dimethylaminopyridazine, having a polar group (dimethylamino) and a non-polar group (*tert*-butyl) near the two reaction centres was quaternized in different solvents with dielectric constants ranging from 1.9 to 35 and dipole moments from 0 to 3.9 Debye (Table 3).

Table 3. Product distribution in the reaction between methyl iodide and 3-*tert*-butyl-6-dimethylaminopyridazine in various solvents.

Solvent	% quat. at N-1	% quat. at N-2
Hexane	62.6	37.4
Benzene	62.8	37.2
Carbon tetrachloride	62	38
Acetone	62.8	37.2
Acetonitrile	63	37
Dimethoxyethane	79	21
Tetrahydrofuran	84	16

From Table 3 it is evident that most solvents, both polar and non-polar ones, do not influence the product distribution, that is, they influence the two rate constants in the same manner. Ethers, however, differ from most other solvents. This effect, albeit smaller, is also found in the quaternization of 3-methyl-6-isopropylpyridazine with methyl iodide in acetonitrile (QN-2/QN-1 = 81.5/18.5), tetrahydrofuran (QN-2/QN-1 = 85.5/14.5), and diethyl ether (QN-2/QN-1 = 85/15). The reason for this anomaly is not known; one could imagine that the methylating agent in ethers was an oxonium compound having other steric requirements than methyl iodide. Although it has previously been found that replacement of methyl iodide with a larger alkyl iodide (ethyl or isopropyl iodide) changed the product distribution in the same manner as ethers do, it has not been demonstrated that QN-2/QN-1 in the methylation reaction was dependent on the leaving group of the methylating reagent.

Electrical influence of substituents. In a previous investigation [3] it was concluded that the most important factor in determining the product distribu-

tion in quaternization of pyridazines was the steric influence of the substituents adjacent to the reaction centre. In order to test that, a few 4-substituted pyridazines, unsubstituted in the 3- and 6-positions, were quaternized with methyl iodide (Table 4).

Table 4. Product distribution in quaternization of various 4-substituted pyridazines with methyl iodide in acetonitrile.

R-4	% quat. at N-1	% quat. at N-2
CH_3	~50	~50
tert-C_4H_9	~50	~50
$N(CH_3)_2$	75	25

The results show that alkyl groups, in accordance with previous findings, did not have any detectable effect within the experimental error of the method; the dimethylamino group had, however, a noticeable effect. In a Hammett equation the observed difference in the rate of quaternization at the *meta* and *para* positions would correspond to a value of the reaction constant ϱ of approximately -0.2, assuming it valid to use σ_p^+ and σ_m^+; the validity of this assumption is questionable.

At present no quantitative correlation is attempted and we shall here only argue that the electrical influence of 4-substituents on the product distribution is small. The "normal" electrical effect of a substituent *ortho* to the reaction centre is better represented by σ_p than by σ_m, but the electrical effect of an *o*-substituent on reactions involving the lone pair electrons of the nitrogen atom in pyridine, quinoline, and isoquinoline is "abnormal" and is better represented by the σ_I- or σ_m-substituent constant than by σ_p.[10] In this connection it is of interest that it was found that 4-methylpyrimidine quaternized 80 % at N-1 and 20 % at N-3, whereas 3-methylpyridazine quaternizes 72 % at N-2.

A substituent in the 3- or 6-position is *ortho* and *meta* to the reaction centres, and if it is assumed that the "abnormal" behaviour in the pyridine and quinoline series also would be found in the pyridazine series for reactions involving the lone pair electrons, the electrical influence of a substituent in the 3- (or 6)-position would be proportional to $\sigma_m - \sigma_o$ which would be small. As the reaction constant for the quaternization of pyridazines is fairly small, it may be concluded that the electrical influence of substituents is small. Alkyl groups have, furthermore, only a small electrical effect, and in pyridazines substituted in both the 3- and 6-positions with alkyl groups the difference in electrical effect on the two reaction centres would be very small indeed.

The results from the quaternization of a series of 3,6-dialkylpyridazines are shown in Table 5. In Fig. 1 the abscissa is log k_{alkyl}/k_{Me} for pyridazines and the ordinate log k_{alkyl}/k_{Me} for 2-alkylated pyridines;[11] the plot shows that the effect exhibited by alkyl groups *ortho* to the nitrogen in pyridazines parallels that found in pyridines. The steric effect of a given alkyl group is, however, slightly smaller in the pyridazine series than in the pyridine series.

Table 5. Product distribution in reaction between methyl iodide and unsymmetrically substituted 3-R-6-R′-pyridazines in acetonitrile.

	R (3)	R′ (6)	% quat. at N-1	% quat. at N-2	log k_{N2}/k_{N1}
I	H	CH_3	28	72	0.41
II	CH_3	CH_3	(50)	(50)	0
III	C_2H_5	CH_3	65	35	−0.27
IV	$CH(CH_3)_2$	CH_3	81.5	18.5	−0.64
V	$C(CH_3)_3$	CH_3	> 99	< 1	(~ −2.6)[a]
VI	$CH(CH_3)_2$	C_2H_5	68	32	−0.33
VII	$C(CH_3)_3$	C_2H_5	> 99	< 1	
VIII	$C(CH_3)_3$	$CH(CH_3)_2$	~ 99	~ 1	~ −2

[a] Calculated.

In Fig. 1 the point indicating the *tert*-butyl group does not correspond to a measurement in the pyridazine series, but is calculated from the data of 3-isopropyl-6-*tert*-butylpyridazine and 3-methyl-6-isopropylpyridazine (Table 5) on the assumption that $Q_AN\text{-}1/Q_CN\text{-}2 = (Q_AN\text{-}1/Q_BN\text{-}2)\ (Q_BN\text{-}1/Q_CN\text{-}2)$ where Q_AN, Q_BN, and Q_CN are proportional to the rate of quaternization at a nitrogen *ortho* to a methyl, isopropyl, or *tert*-butyl group, respectively.

The geometry of the pyridine [12,13] and pyridazine [14] nuclei differs only slightly and whether these small differences could explain the results seems doubtful. It might rather be that the $N-N-CH_3$ ($-I$) angle in the transition state in pyridazines were smaller than 120° and that the higher double bond character of the N(2)−C(3) bond compared to the N(1)−N(2) bond was of importance in this connection.

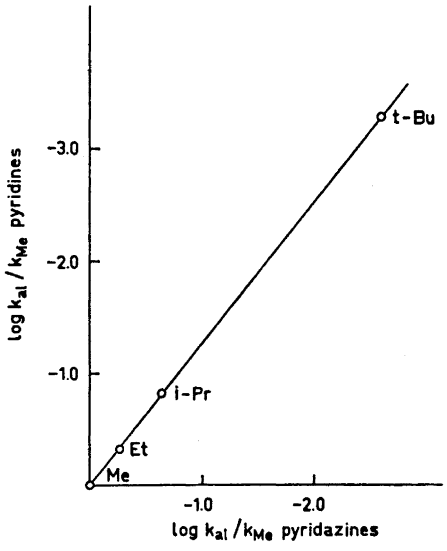

Fig. 1. Comparison of the influence of alkyl groups on the rate of quaternization at an adjacent ring nitrogen in the pyridazine and pyridine series. Abscissa: log $k_{6\text{-alkyl}}/k_{3\text{-methyl}}$ of pyridazines; ordinate: log $k_{2\text{-alkyl}}/k_{2\text{-methyl}}$ of pyridines.

The lower reaction rate of *o*-substituted pyridazines is caused by steric strain in the transition state, and in evaluating this strain all possible conformations must be considered; the great difference in steric influence between the *tert*-butyl group and the isopropyl group is due to the possibility of having a conformation of the isopropyl group in which a proton rather than a methyl group points towards the attacking reagent.

Table 6. Product distribution in quaternization of some 3,4,6-trisubstituted pyridazines with methyl iodide in acetonitrile.

	R-3	R′-4	R″ 5	R‴ 6	% quat. at N-1	% quat. at N-2
IX	CH_3	*tert*-C_4H_9	H	CH_3	67	33
X	CH_3	H	H	C_6H_5	8	92
XI	CH_3	*tert*-C_4H_9	H	C_6H_5	20	80
XII	CH_3	H	*tert*-C_4H_9	C_6H_5	62	38
XIII	C_6H_5	*tert*-C_4H_9	H	C_6H_5	5	95

In Table 6 are presented data showing an effect which may mainly be due to the different steric requirements of a phenyl group in two different positions with regard to the pyridazine ring. In one situation the angle between the planes of the phenyl and pyridazine rings in the most stable conformation is small, whereas in the other situation the angle between the planes is forced by an *ortho*-substituent in the pyridazine ring to be approximately 90°.

In the quaternization of 4-*tert*-butyl-6-methyl-3-phenylpyridazine (XII) the steric effect of a phenyl ring perpendicular to the pyridazine ring, the "thickness" of a phenyl ring, is compared to that of a methyl group. The observed effect of the phenyl ring may include a "buttressing effect" induced by the bulky *tert*-butyl group, which adds to the apparent "thickness" of the phenyl ring. The finding that the steric requirements of the phenyl group under these conditions is slightly smaller than that of a methyl group is in accordance with the generally accepted idea of the shape of a phenyl group.

The magnitude of the "buttressing effect" may be estimated from the quaternization of 4-*tert*-butyl-3,6-dimethylpyridazine (IX). This result suggests that in the absence of a "buttressing effect" the reaction mixture of XII would probably have the composition 75:25 rather than 62:38 found experimentally.

The quaternizing reagent also influences the product distribution (Table 7); going from methyl iodide through ethyl iodide to isopropyl iodide the percentage of the major compound has been found to increase. Although other than steric factors may operate and the change is not dramatic it is worth noting that the direction of the effect is that which would be expected from steric influence of the substituents. Such an influence would come more into play when a larger reagent attacks.

Other diazaheterocyclic systems, such as 1,3,4-thiadiazoles,[15] quinoxalines, and 1,8-naphthyridines [16] may be investigated similarly, and a more thorough

Table 7. Product distribution in quaternization of some 3,6-substituted pyridazines in acetonitrile with different alkyl iodides RI.

R'-3	R''-6	R	% quat. at N-1	% quat. at N-2	log k_{N1}/k_{N2}
CH_3	H	CH_3	72	28	0.41
CH_3	H	C_2H_5	80	20	0.60
CH_3	H	i-C_3H_7	90	10	0.95
CH_3	C_2H_5	CH_3	35	65	−0.27
CH_3	C_2H_5	C_2H_5	31	69	−0.35
CH_3	C_2H_5	i-C_3H_7	30	70	−0.37
CH_3	i-C_3H_7	CH_3	18.5	81.5	−0.64
CH_3	i-C_3H_7	C_2H_5	18	82	−0.66
CH_3	i-C_3H_7	i-C_3H_7	16	84	−0.72
t-C_4H_9	$N(CH_3)_2$	CH_3	63	37	0.23
t-C_4H_9	$N(CH_3)_2$	C_2H_5	70	30	0.37
t-C_4H_9	$N(CH_3)_2$	i-C_3H_7	80	20	0.60

discussion will be postponed until more results are available. A preliminary conclusion is, however, that a major influence of a substituent on the rate of the quaternization reaction in pyridazines is of steric origin, which may include steric hindrance of the attack of the reagent on the reaction site, steric strain in the transition state, steric control of the reacting conformation, steric hindrance of solvation, and steric inhibition of resonance.

EXPERIMENTAL

Materials. The dialkylpyridazines were made according to Levisalles and Baranger.[17] 3-*tert*-Butyl-6-isopropylpyridazine, m.p. 136–137°. (Found: C 74.31; H 10.15; N 15.61. Calc. for $C_{11}H_{18}N_2$: C 74.11; H 10.18; N 15.71.) 3-*tert*-Butyl-6-dimethylamine pyridazine was prepared from 3-*tert*-butyl-6-chloropyridazine and an alcoholic solution of dimethylamine at 80°C in a closed vessel. M.p. 95–97°. (Found: C 67.13; H 9.56; N 23.31. Calc. for $C_{10}H_{17}N_3$: C 67.00; H 9.56; N 23.44.) 4-*tert*-Butyl-3,6-diphenylpyridazine, 4-*tert*-butyl-3,6-dimethylpyridazine, 4- and 5-*tert*-butyl-3-methyl-6-phenylpyridazine were made by addition of *tert*-butylmagnesium chloride to the appropriate pyridazines and oxidizing the dihydro compounds according to Avellén and Crossland.[18]

Quaternization was performed in a closed vessel as previously described; reaction temperature 50°C, reaction time 24 h.

The analysis of the reaction mixture was performed with a Varian A 60 NMR-spectrophotometer as described previously.[3] The reproducibility of the determinations was generally better than 2 % and often better than 1 % when the intensity of two singlets were compared; the results from the quaternizations with ethyl iodide and isopropyl iodide were less reproducible (within 5 %). The results given are the average of at least 3 quaternizations.

REFERENCES

1. Brown, H. C. *J. Chem. Educ.* **36** (1959) 424.
2. Brown, H. C. and McDonald, G. J. *J. Am. Chem. Soc.* **88** (1966) 2514.
3. Lund, H. and Lunde, P. *Acta Chem. Scand.* **21** (1967) 1067.
4. Gallo, R. *Thesis*, Université de Provence 1971.
5. Deady, L. W. and Zoltewicz, J. A. *J. Org. Chem.* **37** (1972) 603.

6. Zoltewicz, J. A. and Deady, L. W. *J. Am. Chem. Soc.* **94** (1972) 2765.
7. Bare, T. M., Hershey, N. D., House, H. O. and Swain, C. G. *J. Org. Chem.* **37** (1972) 997.
8. Swain, C. G. and Hershey, N. D. *J. Am. Chem. Soc.* **94** (1972) 1901.
9. Chanon, M., Gallo, R., Lund, H. and Metzger, J. *Tetrahedron Letters* **1972** 3857.
10. Charton, M. *J. Am. Chem. Soc.* **86** (1964) 2033.
11. Brown, H. C. and Cahn, A. *J. Am. Chem. Soc.* **77** (1955) 1715.
12. Bak, B., Hansen, L. and Rastrup-Andersen, J. *J. Chem. Phys.* **22** (1954) 2013.
13. Almenningen, A., Bastiansen, O. and Hansen, L. *Acta Chem. Scand.* **9** (1955) 1306.
14. Innes, K. K. and Lucas, R. M. *J. Mol. Spectry.* **24** (1967) 247.
15. Lund, H. *Acta Chem. Scand.* **27** (1973) 391.
16. Jones, R. A. Y. and Waystaff, N. *Chem. Commun.* **1969** 56.
17. Levisalles, J. and Baranger, P. *Compt. Rend.* **242** (1956) 1336.
18. Avellén, L. and Crossland, I. *Acta Chem. Scand.* **23** (1969) 1887.

Received August 8, 1972.

ACTA CHEMICA SCANDINAVICA 27 (1973) 391–395

Quaternization Reactions

V. Quaternization of 1,3,4-Thiadiazoles

HENNING LUND

Department of Organic Chemistry, University of Aarhus, DK-8000 Aarhus C, Denmark

A series of 2,5-disubstituted 1,3,4-thiadiazoles has been quaternized with methyl iodide. The influence of alkyl substituents on product distribution is smaller in the thiadiazole series than in the pyridazine series. The difference in geometry of the 5- and 6-membered rings may be responsible for the observed difference between the two series.

Certain diazaheteroaromatic compounds, such as pyridazines, their benzo-derivatives, and 1,3,4-thiadiazoles, are well suited for the study of steric influence on the quaternization reaction, as they are planar molecules and possess two reaction centres which are symmetrically situated with respect to the ring. Each half of the ring may be considered independently, and the reaction rate at one nitrogen atom may to a first approximation be assumed to be dependent only on the adjacent substituent.

The quaternization of some pyridazines,[1,2] cinnolines,[3,4] and naphthyridines[5] has been investigated by this method and the results compared to the kinetic results from the quaternization of pyridines. In the present investigation, 1,3,4-thiadiazoles have been quaternized with methyl iodide; kinetic results from quaternization of thiazoles are of interest in this connection.[6,7]

RESULTS AND DISCUSSION

The quaternization of the 1,3,4-thiadiazoles was performed under conditions where the reaction is practically irreversible and the product distribution thus kinetically controlled; the thiadiazoles were quaternized at 50° for 20 h, and as treatment of 3-ethyl-2,5-dimethyl-1,3,4-thiadiazolium iodide with methyl-iodide at 80° for 10 days did not produce any detectable amount of the 2,3,5-trimethyl derivative, the loss of an alkyl group from a quaternized ring nitrogen is too slow to influence the product distribution even at the higher temperature.

In Table 1 is given the product distribution of the quaternization with methyl iodide of some 2,5-unsymmetrically substituted 1,3,4-thiadiazoles, where the alkyl substituents are methyl groups in which some of the hydrogen atoms are replaced by methyl groups.

Table 1. Product distribution in the quaternization of some 1,3,4-thiadiazoles with methyl iodide in acetonitrile at 50°C.

R-2	R-5	% quat. at N-3	% quat. at N-4	log k_{N3}/k_{N4}
H	CH_3	55	45	+0.09
CH_3	CH_3	(50)	(50)	0
CH_3CH_2	CH_3	43.5	56.5	−0.11
$(CH_3)_2CH$	CH_3	26	74	−0.45
$(CH_3)_3C$	CH_3	2.5	97.5	−1.60
$(CH_3)_2CH$	C_2H_5	38	62	−0.21
$(CH_3)_3C$	C_2H_5	4.5	95.5	−1.33
$(CH_3)_3C$	$CH(CH_3)_2$	8.5	91.5	−1.03

The product distribution of the quaternization of some unsymmetrically substituted 1,3,4-thiadiazoles, in which R-2 is ethyl, propyl, isobutyl, neopentyl, or benzyl and R-5 is methyl, ethyl, or isopropyl, is given in Table 2.

Table 2. Product distribution in the quaternization of some 1,3,4-thiadiazoles with methyl iodide in acetonitrile at 50°C.

R-2	R-5	% quat. at N-3	% quat. at N-4	log k_{N3}/k_{N4}
HCH_2CH_2	CH_3	43.5	56.5	−0.11
$CH_3CH_2CH_2$	CH_3	42	58	−0.14
$(CH_3)_2CHCH_2$	CH_3	39	61	−0.19
$(CH_3)_3CCH_2$	CH_3	33	67	−0.30
$C_6H_5CH_2$	CH_3	40	60	−0.18
$CH_3CH_2CH_2$	C_2H_5	47	53	−0.05
$(CH_3)_2CHCH_2$	C_2H_5	45.5	54.5	−0.08
$(CH_3)_3CCH_2$	C_2H_5	43.5	56.5	−0.11
$C_6H_5CH_2$	C_2H_5	48	52	−0.04
$CH_3CH_2CH_2$	$CH(CH_3)_2$	57	43	0.12
$(CH_3)_2CHCH_2$	$CH(CH_3)_2$	57	43	0.12
$(CH_3)_3CCH_2$	$CH(CH_3)_2$	56	44	0.10

In Table 3 are given the results from quaternization of some 1,3,4-thiadiazoles containing other substituents than alkyl groups.

Table 3. Product distribution in the quaternization of some derivatives of amino-1,3,4-thiadiazoles with methyl iodide in acetonitrile.

R-2	R-5	% quat. at N-3	% quat. at N-4
H	NH_2	27	73
CH_3	NH_2	24	76
H	$NHCOCH_3$	68	32
CH_3	$NHCOCH_3$	63	37

5-Amino-2-methyl-1,3,4-thiadiazole has been reported [8] to quaternize with ethyl iodide at N-3; the assignment was made on the ground that the product has an active methyl group. The results with methyl iodide show that the major product is 5-amino-2,4-dimethyl-1,3,4-thiadiazolium iodide and suggest that ethyl iodide also would quaternize at the nitrogen adjacent to the amino group. This emphasizes that assignment of products in the quaternization of diazaheterocyclic compounds, based solely upon chemical data, must be treated with care.

Compared to the results obtained in the pyridazine series, the effect of the *ortho*-substituents in 1,3,4-thiadiazoles is smaller. As for the pyridazines, the main influence of the substituents is assumed to be of steric origin, including steric hindrance of the attack of the reagent on the reaction site, steric strain in the transition state, steric control of the reacting conformation, steric hindrance of solvation, and steric inhibition of resonance.

From a statistical investigation of equilibrium and rate constants of *ortho*-substituted aromatic compounds, it has been concluded [9,10] that in the majority of cases the influence of *ortho*-substituents could be expressed in terms of inductive and resonance effects and that it was not necessary to include steric effects, except for very bulky groups, such as the *tert*-butyl group.

The equilibrium constants involving proton transfer to monosubstituted benzenes or heteroaromatic compounds are not likely to be dependent on steric hindrance; the rate constants considered [9,10] are for reactions which take place at an atom outside the ring and which in most cases allow an attack of the reagent perpendicular to the plane of the ring, as only one *ortho*-substituent is present. Neither the equilibrium constants nor the rate constants considered would thus be expected to show serious complications due to steric hindrance.

The direction of the attack of the reagent and thus the geometry of the transition state is important for the discussion of steric effects; the addition of the bulky *tert*-butylmagnesium chloride to unsymmetrically substituted pyridazines [11] is much less dependent on the size of the substituents than the quaternization reaction; in the former case, the reagent attacks nearly perpendicular to the plane of the pyridazine ring, whereas the quaternizing reagent attacks along a path which deviates only slightly from a line passing through the centre of the ring and the nitrogen atom; the attacking reagent and the *ortho*-substituents is thus situated in the same plane (or nearly so) which makes the steric strain in the transition state important.

The influence of an alkyl group on the rate of quaternization at an adjacent centre is very nearly the same in the 1,3,4-thiadiazole and the thiazole series,[6,7] but it is smaller than in the pyridine or pyridazine series.

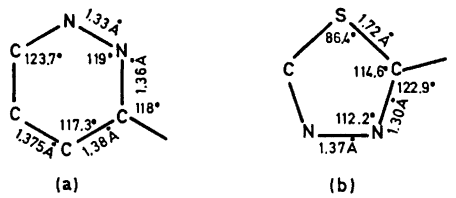

Fig. 1. Molecular shape of pyridazine [12] (a) and 1,3,4-thiadiazole [13] (b).

In Fig. 1 the geometry of the pyridazine and the 1,3,4-thiadiazole rings are shown. For the steric strain in the transition state of the quaternization reaction, the angles N2-C3-subst. and N3-C2-subst. of the pyridazine, resp. 1,3,4-thiadazole ring are important; the greater the angle, the further removed from the reaction centre is the substituent and thus the smaller is its steric influence. The steric influence of an *ortho*-substituent in a five-membered ring would thus be expected to be smaller than in a six-membered ring which is in accordance with the experimental results.

EXPERIMENTAL

Materials. The 1,3,4-thiadiazoles were obtained by treatment of the appropriate diacylhydrazines with recrystallized P_2S_5. The NMR-spectra are given in Table 4. Before quaternization the material was purified by preparative GLC on a column of 20 % SE 30 on Chromosorb W.

Table 4. Chemical shifts in the NMR-spectra of 2,5-dialkyl-1,3,4-thiadiazoles.

R-2	R-5	C (2) 2^2	C (1) 2^1	C (1) 5^1	C (2) 5^2	C (3) 5^3	Solvent
CH_3	CH_3		2.72	2.72			$CDCl_3$
CH_3	C_2H_5		2.72	3.08	1.39		none
CH_3	$CH(CH_3)_2$		2.70	3.37	1.34		»
CH_3	$C(CH_3)_3$		2.70		1.41		»
CH_3	$CH_2CH_2CH_3$		2.69	3.02	1.78	0.96	»
CH_3	$CH_2CH(CH_3)_2$		2.70	2.92	1.99	0.95	»
CH_3	$CH_2C(CH_3)_3$		2.75	2.97		1.02	»
CH_3	$CH_2C_6H_5$		2.62	4.32	7.25		$CDCl_3$
C_2H_5	$CH(CH_3)_2$	1.36	3.07	3.27	1.38		none
C_2H_5	$C(CH_3)_3$	1.40	3.11		1.48		»
C_2H_5	$CH_2CH_2CH_3$	1.40	3.10	3.02	1.81	1.02	$CDCl_3$
C_2H_5	$CH_2CH(CH_3)_2$	1.40	3.12	2.95	2.08	1.01	none
C_2H_5	$CH_2C(CH_3)_3$	1.41	3.11	2.96		1.03	»
C_2H_5	$CH_2C_6H_5$	1.31	3.00	4.32	7.27		$CDCl_3$
$CH(CH_3)_2$	$C(CH_3)_3$	1.43	3.42		1.48		none
$CH(CH_3)_2$	$CH_2CH_2CH_3$	1.37	3.38	3.02	1.79	0.98	»
$CH(CH_3)_2$	$CH_2CH(CH_3)_3$	1.42	3.41	2.93	2.0	1.01	»
$CH(CH_3)_2$	$CH_2C(CH_3)_3$	1.46	3.41	2.95		1.02	»

The *quaternization* was made by treating a solution (1 %) of the thiadiazole in acetonitrile with a ten-fold excess of methyl iodide at 50°C for 20 h in a closed vessel. After removal of the solvent and excess methyl iodide, the residue was dissolved in deuterated chloroform and the NMR-spectra recorded.

The *analysis* of the reaction mixture was performed with a Varian A 60 NMR-spectrophotometer as described previously.[1,2] The reproducibility of the determinations was generally better than 2 % and often better than 1 % when the intensity of two singlets were compared; the results from the quaternizations with ethyl iodide and isopropyl iodide were less reproducible (within 5 %). The results given are the average of at least 3 quaternizations.

REFERENCES

1. Lund, H. and Lunde, P. *Acta Chem. Scand.* **21** (1967) 1067.
2. Lund, H. and Lund, V. *Acta Chem. Scand.* **27** (1973) 383.
3. Ames, D. E., Novitt, B., Waite, D. and Lund, H. *J. Chem. Soc.* **C 1969** 796.
4. Palmer, M. H. and McIntyre, P. S. *Tetrahedron* **27** (1971) 2913.
5. Jones, R. A. Y. and Wagstaff, N. *Chem. Commun.* **1969** 56.
6. Gallo, R. *Thesis*, Université de Provence 1971.
7. Chanon, M., Gallo, R., Lund, H. and Metzger, J. *Tetrahedron Letters* **1972** 3857.
8. Anish, A. W. and Clark, C. A. U. S. Pat. 2 500 112 (1950); *Chem. Abstr.* **44** (1950) 5741.
9. Charton, M. *J. Org. Chem.* **36** (1971) 882.
10. Charton, M. *Progr. Phys. Org. Chem.* **8** (1971) 235.
11. Avellén, L. and Crossland, I. *Acta Chem. Scand.* **23** (1969) 1887.
12. Innes, K. K. and Lucas, R. M. *J. Mol. Spectry.* **24** (1967) 247.
13. Bak, B., Nygaard, L. and Rastrup-Andersen, J. *J. Mol. Spectry.* **19** (1966) 283.

Received August 8, 1972.

ACTA CHEMICA SCANDINAVICA 27 (1973) 396–400

Determinations of the Thermodynamic Functions of NaBr in NaBr-KBr Mixtures from Concentration Cell Measurements

VIOLETTE SABET* and TERJE ØSTVOLD

Institute of Physical Chemistry, Technical Institute of Norway, The University of Trondheim, N-7034 Trondheim, Norway

The partial Gibbs energies of mixing of NaBr in liquid mixtures with KBr have been determined by emf measurements of the following cell:

$$C(s)Br_2(g)\,|\,NaBr(l)\,|\,Na\text{-}K\ glass\,|\,NaBr(l)KBr(l)\,|\,Br_2(g)C(s)$$

and measurements of transport number of the alkali ion in the Na-K glass membrane used to separate the two half cells in the above concentration cell.

From the values obtained for the partial free energies of mixing of NaBr, the Gibbs energies of mixing in the NaBr-KBr system were determined, and the excess Gibbs energies of mixing and excess entropies of mixing calculated. The results indicate small excess entropies of mixing.

In the present work the change in the chemical potentials of mixing of NaBr in molten NaBr-KBr mixtures were obtained using a concentration cell with Na-K glass membrane. The emf of this cell is dependent upon the transport properties in the membrane, *i.e.* "the liquid junction potential". Therefore the transport numbers of the two alkali ions in the glass were determined.

The following galvanic cell was studied:

$$C(s)Br_2(g)\,|\,NaBr(l)\,|\,Na\text{-}K\ glass\,|\,NaBr(l)KBr(l)\,|\,Br_2(g)C(s)$$

The electrolyte consisted of a fused mixture of NaBr and KBr on the right hand side, and pure fused NaBr on the left hand side of the glass membrane. The membrane is a cation exchange membrane and it contains the two mobile ions Na^+ and K^+. The bromine over graphite electrodes are reversible to the Br^+ ions only.

* Present address: Chemistry Dept., Faculty of Science, Moharam Bey, Alexandria University, Egypt.

EXPERIMENTAL

The cell used in the present investigation is similar to the one described in previous papers.[1,2] The composition of the glass was 80 mol % SiO_2, 10 mol % Al_2O_3, 5 mol % Na_2CO_3 and 5 mol % K_2CO_3. All the components of the glass, obtained from E. Merck, Germany, were ground together and melted. The glass was then crushed and remelted to assure uniform composition. The emf of the above cell was investiged over a concentration range $x_{NaBr}=0.06$ to $x_{NaBr}=0.8$ at 800°C. The temperature and emf were recorded on a dual channel Philips recorder (type PR 2212A/00). Both were compensated by bucking potentials supplied from a thermostatically housed reference voltage supply and divider built by Sintef, Norway. These were calibrated daily against a Tinsley "Thermoelectric Free" potentiometer. The analytical reagent grade salts, NaBr and KBr, obtained from E. Merck, Germany, were melted before use in order to remove moisture and crushed into suitable fragments before weighed out to give the wanted compositions.

The above cell was also used for the determination of the transport numbers of K^+ and Na^+ ions in the glass membrane. The course of a typical experiment was as follows. The cathode compartment, containing the glass membrane at the bottom, was filled with about 6 g of pure NaBr and then immersed in the fused NaBr-KBr mixture. Bromine gas was bubbled over the graphite electrodes and a positive current of about 10 mA passed through the cell from the mixture to the pure salt for about 8 h. The amount of charge passing through the cell was measured with a digital coulombmeter. The amount of potassium which had migrated into the cathode compartment through the glass membrane was determined by flame photometry.

RESULTS AND DISCUSSION

The emf as function of composition of the galvanic cell

$$C(s)Br_2(g)\,|\,NaBr(l)\,|\,Na\text{-}K\ glass\,|\,NaBr(l)KBr(l)\,|\,Br_2(g)C(s)$$

is shown in Fig. 1. The emf is related to the change in Gibbs energy for the cell reaction by the equation [3]

$$\Delta G = -EF = \Delta\bar{G}_{NaBr} - \int_1^2 t_{K^+}\mathrm{d}(\bar{G}_{Na\text{-}sil.} - \bar{G}_{K\text{-}sil.}) \qquad (1)$$

over membrane

Using Gibbs-Duhem equation one obtains

$$\Delta G = -EF = \Delta\bar{G}_{NaBr} - \int_1^2 \frac{t_{K^+}}{x_{K\text{-}sil.}}\,\mathrm{d}\bar{G}_{Na\text{-}sil.} \qquad (2)$$

over membrane

where $\Delta\bar{G}_{NaBr}=\bar{G}_{NaBr}-G^\circ_{NaBr}$ is the change in chemical potential on mixing, t_{K^+} is the transport number of potassium in the glass membrane and $x_{K\text{-}sil.}$ is the mol fraction of K^+ ions in the glass.

Since the emf and the Gibbs energy changes for the cell reaction are dependent on the transport properties of the ions in the glass membrane separating the two half cells, one has to know the value of the integral in eqn. (2) before the partial quantities of mixing can be calculated. For this reason the transport number of the K^+ ions in the glass membrane was measured at 800°C.

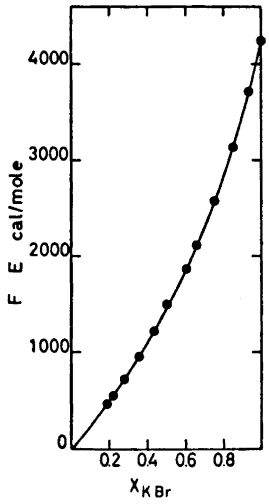

Fig. 1. Variation of emf with composition of NaBr-KBr melt at 800°C for the galvanic cell:

C(s)Br_2(g)|NaBr(l)|Na-K glass|NaBr(l) KBr(l)|Br_2(g)C(s).

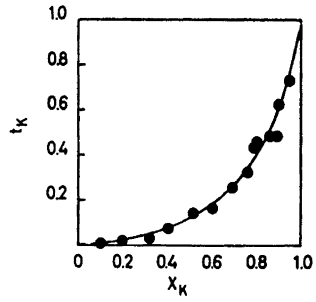

Fig. 2. Dependence of transport numbers in Na-K glass with composition of NaBr-KBr melt at 800°C.

From the concentration of KBr in the pure NaBr melt after electrolysis, the transport number of K^+ ions in the glass membrane can be calculated from eqn. (3):

$$t_{K^+} = \frac{n_{KBr}}{\Delta Q/F} \tag{3}$$

where n_{KBr} is the number of equivalent of KBr found in the pure NaBr melt after electrolysis and ΔQ is the amount of charge transferred through the cell measured in Coulomb.

The concentration dependence of the transport number is shown in Fig. 2.

In the above cell the pure NaBr in the left hand side compartment is used as the standard state for NaBr in the mixture. Therefore, for a small change in composition of the NaBr-KBr mixture the change in emf of the cell is given by

$$F\mathrm{d}E = -\mathrm{d}\bar{G}_{NaBr} + t_{K^+}\mathrm{d}(\bar{G}_{Na\text{-}sil.} - \bar{G}_{K\text{-}sil.}) \tag{4}$$

Equilibrium is assumed at the interface between Na^+ and K^+ ions in solution and Na^+ and K^+ ions in the silicate. For a small change in composition of the NaBr-KBr mixture the change in the equilibrium conditions is described by the following equation:

$$\mathrm{d}\bar{G}_{NaBr(2)} + \mathrm{d}\bar{G}_{K\text{-}sil.(2)} = \mathrm{d}\bar{G}_{KBr(2)} + \mathrm{d}\bar{G}_{Na\text{-}sil.(2)} \tag{5}$$

Combining eqns. (4) and (5) one obtains

$$F\mathrm{d}E = -\mathrm{d}\bar{G}_{\mathrm{NaBr}} + t_{\mathrm{K}^+}\mathrm{d}(\bar{G}_{\mathrm{NaBr}} - \bar{G}_{\mathrm{KBr}}) = -t_{\mathrm{Na}^+}\mathrm{d}\bar{G}_{\mathrm{NaBr}} - t_{\mathrm{K}^+}\mathrm{d}\bar{G}_{\mathrm{KBr}} \quad (6)$$

Using the Gibbs-Duhem equation, eqn. (6) takes the form

$$\Delta\bar{G}_{\mathrm{NaBr}} = F\int_1^2 \frac{x_{\mathrm{KBr}}}{t_{\mathrm{K}^+} - x_{\mathrm{KBr}}}\,\mathrm{d}E \quad (7)$$

where x_{KBr} is the mol fraction of KBr in the mixture. A similar equation has been derived by Førland and Thulin [4] for a similar system. For a given composition of the mixture NaBr-KBr, one can measure the emf, E, of the cell and the transport number of K^+ ions in the glass, t_{K^+}, in equilibrium with the bromide mixture. By plotting corresponding values of $x_{\mathrm{KBr}}/(t_{\mathrm{K}^+} - x_{\mathrm{KBr}})$ and FE, the change in chemical potential of NaBr on mixing, ΔG_{NaBr}, is obtained as the area under the curve.

Hersh and Kleppa [5] give the following equation for the molar enthalpies of mixing in the liquid mixture of KBr and NaBr at 770°C:

$$\Delta H_{\mathrm{mix}} = x_1x_2(-510 - 60x_1) \quad (8)$$

where x_1 and x_2 are the mol fractions of NaBr and KBr, respectively. The enthalpy of mixing measured by Hersh and Kleppa were performed at lower temperatures than the emf measurements presented in this work. The enthalpy of mixing for simple alkaili halides and nitrates is not much temperature dependent. The entropies of mixing calculated by using Gibbs energies and enthalpies measured at different temperatures are therefore quite reliable.

From the values obtained for $\Delta\bar{G}_{\mathrm{NaBr}}$, $\Delta\bar{G}_{\mathrm{KBr}}$ was calculated using the Gibbs-Duhem equation and ΔG_{mix} could thus be determined by the equation

$$\Delta G_{\mathrm{mix}} = x_{\mathrm{NaBr}}\Delta\bar{G}_{\mathrm{NaBr}} + (1 - x_{\mathrm{NaBr}})\Delta\bar{G}_{\mathrm{KBr}} \quad (9)$$

Differences between experimentally observed quantities and quantities to be expected for a Temkin [6] mixture or ideal mixture are given by the excess quantities:

$$\Delta G^{\mathrm{E}}{}_{\mathrm{mix}} = \Delta G^{\mathrm{obs}}{}_{\mathrm{mix}} - \Delta G^{\mathrm{id}} \quad (10)$$

Table 1. Thermodynamic data for the NaBr-KBr mixtures calculated from emf and transport number measurements at 1073 K.

x_{KBr}	t_{K^+}	FE cal/mol	$\Delta\bar{G}_{\mathrm{KBr}}$ cal/mol	$\Delta\bar{G}_{\mathrm{NaBr}}$ cal/mol	ΔG_{mix} cal/mol	$\Delta G^{\mathrm{E}}{}_{\mathrm{mix}}$ cal/mol	ΔH_{mix} cal/mol	$\Delta S^{\mathrm{E}}{}_{\mathrm{mix}}$ cal/deg. mol
0.1	0.01	190	−230	−5460	−753	−59	−50.8	0.01
0.2	0.02	470	−500	−3852	−1170	−103	−89.3	0.01
0.3	0.04	760	−825	−2874	−1440	−137	−115.9	0.02
0.4	0.07	1090	−1225	−2164	−1601	−166	−131.0	0.03
0.5	0.12	1450	−1650	−1613	−1632	−154	−135.0	0.02
0.6	0.18	1850	−2225	−1169	−1591	−156	−128.2	0.03
0.7	0.27	2280	−2875	−800	−1423	−120	110.9	0.01
0.8	0.40	2810	−3850	−496	−1167	−100	−83.5	0.02
0.9	0.60	3450	−5375	−230	−745	−51	−46.4	0.00

The excess entropy of mixing and the excess enthalpy of mixing are defined in an analogous way.

The data of the excess quantities together with the transport numbers and emf's as function of composition are listed in Table 1.

The results indicate that there are small excess entropies of mixing which means that the deviation from regular solution behaviour for the NaBr-KBr mixture is very small.

REFERENCES

1. Robbins, G. D., Førland, T. and Østvold, T. *Acta Chem. Scand.* **22** (1968) 3002.
2. Thulin, L. U. *Acta Chem. Scand.* **36** (1972) 225.
3. Førland, T. and Østvold, T. *Acta Chem. Scand.* **20** (1966) 2086.
4. Førland, T. and Thulin, L. U. *Acta Chem. Scand.* **22** (1968) 3023.
5. Hersh, L. S. and Kleppa, O. J. *J. Chem. Phys.* **42** (1965) 1309.
6. Temkin, H. *Acta Physicochim. USSR* **20** (1945) 411.

Received August 17, 1972.

ACTA CHEMICA SCANDINAVICA 27 (1973) 401–410

Crystal Structure of DL-Tyrosine

ARVID MOSTAD and CHRISTIAN RØMMING

Department of Chemistry, University of Oslo, Oslo 3, Norway

The crystal structure of DL-tyrosine has been determined by X-ray methods using 1180 observed reflections collected by counter methods. The crystals are orthorhombic, space group $Pna2_1$, with unit cell dimensions $a = 20.83_6$ Å, $b = 6.81_0$ Å, and $c = 5.90_5$ Å. The structure was solved by direct methods and refined to a conventional R-factor of 0.037; estimated standard deviations in bond lengths not involving hydrogen are 0.003 Å and in angles 0.2°. The molecular dimensions are found to be nearly identical with those found for L-tyrosine. The difference in crystal packing between the L and the DL form is discussed.

The preferred conformation of tyrosine is of interest in several biochemical relations and has frequently been discussed. Information on the structure of the molecule in solution is difficult to obtain; one approach to the problem is to examine the molecular structure in various crystal modifications in order to study the influence of the environment on the conformation. For an optically active compound crystals of the active and racemic forms may both be examined.

The conformation of tyrosine in the crystals of L-tyrosine [1] is different from that in L-tyrosine hydrochloride [2] but is the same as the one reported for L-phenylalanine hydrochloride [3] and potassium L-tyrosine-*o*-sulphate dihydrate.[4] We have now investigated the crystal structure of DL-tyrosine in which the molecular packing necessarily is different from that in L-tyrosine. Furthermore, as the crystal data on L-tyrosine were found to be different from those derived from powder data,[5] we felt that the crystal data on DL-tyrosine arrived at from powder photographs [6] ought to be checked against single crystal results.

EXPERIMENTAL

DL-Tyrosine was recrystallized following the same procedure as the one worked out for L-tyrosine.[7] A single crystal with approximate dimensions $0.2 \times 0.25 \times 0.35$ mm^3 was mounted with the direction of the largest dimension (c) along the goniometer head axis and used in all the X-ray experiments.

Precession photographs indicate orthorhombic symmetry; space group extinctions are $(0kl)$ for $k+l$ odd and $(h0l)$ for h odd. The absence of centers of symmetry was proved by Wilson statistics; the space group is thus $Pna2_1$.

Unit cell dimensions were determined from diffractometer measurements on 30 general reflections using Mo$K(\alpha_1+\alpha_2)$ radiation ($\lambda=0.71069$ Å). It may be noted that one axis (6.810 Å) has half the length of that derived from powder data (13.68 Å).[6]

The intensity data were recorded with the use of a SYNTEX P$\bar{1}$ diffractometer with graphite crystal monochromated MoK radiation for 1369 independent reflections with $2\theta < 60°$ using the $\omega-2\theta$ scanning mode with scan speed varying from 2 to 12° min^{-1} dependent on the intensity. The scan range was from 1° below 2θ (α_1) to 1° above 2θ (α_2) and background counts were taken for half the scan time at each of the scan range limits. Three standard reflections measured after every 50 reflections showed no systematic fluctuation during the experiment. The 1180 reflections greater than $2.5\sigma(I)$ were considered to be observed; the remaining 189 were excluded from the structure refinement procedure.

The structure determination was based on the program MULTAN written by P. Main, M. M. Woolfson and G. Germain. All other computer programs applied are described in Ref. 10.

Atomic form factors used were those of Doyle and Turner [8] for oxygen, nitrogen, and carbon atoms and of Stewart, Davidson and Simpson [9] for hydrogen.

CRYSTAL DATA

DL-4-Hydroxyphenylalanine (DL-tyrosine) $C_9H_{11}O_3N$, orthorhombic. $a=20.836$ (0.0008) Å; $b=6.810$ (0.002) Å; $c=5.905$ (0.002) Å. $V=837.9$ Å^3, $M=181.19$, $F(000)=384$, $Z=4$, $D_{calc}=1.435$ g cm^{-3}. Absent reflections: $(0kl)$ for $k+l$ odd, $(h0l)$ for h odd. Space group $Pna2_1$.

STRUCTURE DETERMINATION

The intensity data were put on an absolute scale by Wilson's statistical method and normalized structure amplitudes were calculated. The 154 of these with E-values larger than 1.50 were used as input in the program assembly MULTAN.[11] Of the solutions obtained the one with the highest figure of merit was used as the basis for an E-map which readily indicated the positions of all non-hydrogen atoms. Initial least-squares refinement included the thirteen heavy atoms with isotropic, then anisotropic temperature factors. When the R-factor reached 0.05 all hydrogen atoms were assigned coordinates from stereochemical considerations and were included in the further least-squares calculations with individual isotropic thermal parameters. After five cycles the shifts in the parameters were negligible compared to the corresponding standard deviations. The final conventional R-factor was 0.037 and the weighted R was 0.055. A comparison of observed and calculated structure factors is given in Table 1; the final parameters for non-hydrogen atoms are listed in Table 2 and for hydrogen atoms in Table 3.

Magnitudes and directions of the principal axes of the ellipsoids of vibrations are given in Table 4. An analysis of the thermal parameters showed that the phenol and alanine parts may each be regarded as rigid bodies. The phenol part has the axis of the largest oscillation (4.6°) nearly parallel to the O1 – C4 – C1 – C7 direction; the alanine part has the corresponding axis (7.9°) parallel to the C8 – O3 direction. The bond lengths were corrected for librational effects according to this model.

Table 1. Observed and calculated structure factors. The columns are h, k, l, $10|F_o|$ and $10|F_c|$.

2 0 0	55	55	11 4 0	33	29	24 0 1	23	20	18 4 1	53	52	18 0 2	61	62	12 4 2	102	101
4 0 0	353	353	12 4 0	110	111	26 0 1	79	76	19 4 1	29	29	20 0 2	29	21	13 4 2	201	202
6 0 0	292	286	13 4 0	183	190	28 0 1	82	74	20 4 1	36	36	22 0 2	20	26	14 4 2	144	146
8 0 0	555	558	14 4 0	141	135	0 1 1	1022	1008	21 4 1	47	43	24 0 2	71	70	15 4 2	42	44
10 0 0	616	603	16 4 0	43	43	1 1 1	144	131	22 4 1	52	52	26 0 2	87	87	16 4 2	114	113
12 0 0	18	16	17 4 0	68	67	2 1 1	415	417	23 4 1	65	62	28 0 2	83	80	17 4 2	126	129
13 0 0	22	8	18 4 0	88	90	3 1 1	249	241	24 4 1	32	26	1 1 2	190	179	18 4 2	36	32
14 0 0	38	36	19 4 0	36	38	4 1 1	243	233	25 4 1	40	40	2 1 2	386	375	19 4 2	35	35
16 0 0	74	67	20 4 0	121	118	5 1 1	243	233	0 5 1	37	39	3 1 2	399	394	20 4 2	29	33
18 0 0	159	178	21 4 0	48	50	6 1 1	257	248	1 5 1	182	181	4 1 2	478	455	21 4 2	53	53
20 0 0	185	196	22 4 0	41	42	7 1 1	196	188	2 5 1	93	98	5 1 2	325	321	22 4 2	66	64
22 0 0	57	53	23 4 0	42	43	8 1 1	126	123	3 5 1	93	90	6 1 2	96	84	23 4 2	31	28
24 0 0	49	87	24 4 0	48	50	9 1 1	72	73	4 5 1	48	43	7 1 2	150	161	25 4 2	41	42
26 0 0	73	73	25 4 0	22	24	10 1 1	297	286	5 5 1	20	19	8 1 2	188	182	1 5 2	78	77
28 0 0	25	18	26 4 0	35	37	11 1 1	73	72	6 5 1	114	110	9 1 2	202	202	2 5 2	89	88
1 1 0	203	202	2 5 0	190	184	12 1 1	156	161	7 5 1	142	138	10 1 2	96	87	3 5 2	45	43
2 1 0	327	338	3 5 0	96	89	13 1 1	174	170	8 5 1	27	30	11 1 2	150	149	4 5 2	229	228
3 1 0	648	666	5 5 0	29	31	14 1 1	204	201	9 5 1	114	110	12 1 2	73	71	5 5 2	204	200
4 1 0	268	277	6 5 0	99	108	15 1 1	29	34	10 5 1	62	64	13 1 2	107	106	6 5 2	118	124
5 1 0	698	722	7 5 0	126	129	16 1 1	96	96	11 5 1	48	50	14 1 2	160	170	7 5 2	85	84
6 1 0	443	435	8 5 0	39	42	17 1 1	65	69	12 5 1	66	69	15 1 2	132	137	8 5 2	25	25
7 1 0	363	380	9 5 0	90	95	18 1 1	51	57	13 5 1	95	96	16 1 2	155	154	9 5 2	44	43
8 1 0	399	383	10 5 0	37	31	19 1 1	78	78	14 5 1	143	145	18 1 2	191	195	10 5 2	73	71
9 1 0	111	114	11 5 0	125	125	20 1 1	121	123	15 5 1	120	122	19 1 2	40	39	11 5 2	27	31
10 1 0	205	188	12 5 0	48	46	21 1 1	42	46	16 5 1	66	68	20 1 2	50	52	12 5 2	60	61
12 1 0	351	355	13 5 0	79	79	23 1 1	26	28	17 5 1	75	74	21 1 2	27	31	14 5 2	37	37
13 1 0	206	207	14 5 0	34	33	24 1 1	22	25	18 5 1	69	74	22 1 2	85	83	15 5 2	126	124
14 1 0	151	145	15 5 0	99	101	25 1 1	43	39	19 5 1	34	35	23 1 2	37	36	17 5 2	47	44
15 1 0	107	104	16 5 0	46	42	26 1 1	74	71	20 5 1	44	41	24 1 2	77	76	18 5 2	91	89
16 1 0	144	136	17 5 0	40	42	28 1 1	73	64	21 5 1	28	29	25 1 2	29	38	19 5 2	29	38
17 1 0	112	112	18 5 0	80	81	1 2 1	443	425	22 5 1	54	57	26 1 2	63	59	21 5 2	27	25
18 1 0	50	51	19 5 0	31	28	2 2 1	223	216	24 5 1	38	35	27 1 2	54	54	22 5 2	52	46
19 1 0	54	52	20 5 0	74	74	3 2 1	382	372	1 6 1	25	19	28 1 2	55	56	23 5 2	24	22
20 1 0	124	133	21 5 0	24	12	4 2 1	216	214	2 6 1	109	109	0 2 2	446	431	0 6 2	170	176
22 1 0	27	28	22 5 0	81	85	5 2 1	36	30	3 6 1	148	149	1 2 2	198	190	1 6 2	117	121
23 1 0	31	28	23 5 0	53	52	6 2 1	193	184	4 6 1	187	184	2 2 2	303	300	2 6 2	195	200
25 1 0	40	40	0 6 0	131	136	7 2 1	211	200	6 6 1	38	38	3 2 2	121	120	3 6 2	75	76
26 1 0	32	35	2 6 0	33	34	8 2 1	98	101	7 6 1	70	69	4 2 2	223	207	4 6 2	70	73
27 1 0	51	54	3 6 0	49	45	9 2 1	207	206	8 6 1	46	48	5 2 2	195	188	5 6 2	45	42
28 1 0	74	71	4 6 0	134	135	10 2 1	237	223	9 6 1	46	45	6 2 2	103	97	6 6 2	75	76
1 2 0	75	72	5 6 0	25	22	11 2 1	140	132	10 6 1	84	79	7 2 2	126	122	7 6 2	36	40
2 2 0	721	732	6 6 0	47	43	12 2 1	139	134	11 6 1	47	46	8 2 2	145	142	8 6 2	69	72
3 2 0	544	543	7 6 0	104	102	13 2 1	171	170	12 6 1	70	70	9 2 2	72	73	9 6 2	76	81
4 2 0	58	47	10 6 0	88	90	14 2 1	40	40	13 6 1	46	53	10 2 2	195	196	10 6 2	77	76
5 2 0	320	308	11 6 0	96	96	15 2 1	47	88	14 6 1	40	38	11 2 2	31	28	12 6 2	53	51
6 2 0	329	319	12 6 0	25	25	16 2 1	156	159	15 6 1	39	37	12 2 2	90	96	13 6 2	29	32
7 2 0	144	135	13 6 0	97	100	17 2 1	145	148	16 6 1	41	37	13 2 2	141	148	14 6 2	31	31
8 2 0	231	223	14 6 0	203	200	18 2 1	64	68	17 6 1	67	70	14 2 2	195	199	15 6 2	28	32
9 2 0	72	68	15 6 0	77	81	20 2 1	30	34	18 6 1	67	66	15 2 2	42	44	16 6 2	40	41
10 2 0	44	41	16 6 0	50	51	21 2 1	32	31	19 6 1	35	35	16 2 2	161	167	17 6 2	57	61
11 2 0	323	313	17 6 0	45	44	23 2 1	42	43	20 6 1	36	34	17 2 2	44	45	19 6 2	26	26
12 2 0	47	47	18 6 0	66	65	24 2 1	37	37	22 6 1	27	24	18 2 2	123	122	20 6 2	45	41
13 2 0	414	408	19 6 0	49	47	25 2 1	24	23	0 7 1	58	61	19 2 2	103	106	1 7 2	79	80
15 2 0	67	70	22 6 0	47	42	26 2 1	29	33	1 7 1	86	89	20 2 2	72	71	2 7 2	22	22
16 2 0	142	143	1 7 0	74	76	28 2 1	42	43	2 7 1	49	48	22 2 2	24	31	3 7 2	52	54
18 2 0	145	132	2 7 0	145	150	0 3 1	354	342	3 7 1	49	48	23 2 2	37	36	4 7 2	75	74
19 2 0	131	135	3 7 0	47	49	1 3 1	327	323	4 7 1	29	24	24 2 2	43	42	7 7 2	99	100
20 2 0	52	60	4 7 0	36	35	2 3 1	249	242	5 7 1	28	25	25 2 2	39	37	8 7 2	27	25
21 2 0	43	36	5 7 0	26	22	3 3 1	330	320	6 7 1	63	61	26 2 2	44	47	9 7 2	39	38
22 2 0	70	72	6 7 0	77	78	4 3 1	156	152	7 7 1	61	59	27 2 2	81	82	10 7 2	53	53
23 2 0	41	46	9 7 0	112	111	5 3 1	165	158	8 7 1	45	44	1 3 2	130	123	11 7 2	32	33
26 2 0	73	72	10 7 0	36	33	6 3 1	162	162	9 7 1	88	85	2 3 2	260	253	12 7 2	56	55
28 2 0	77	77	14 7 0	24	14	7 3 1	127	133	10 7 1	31	29	3 3 2	200	193	13 7 2	25	25
1 3 0	64	61	16 7 0	79	75	8 3 1	87	81	11 7 1	97	93	4 3 2	94	98	15 7 2	37	35
2 3 0	17	23	17 7 0	79	80	9 3 1	79	81	12 7 1	92	90	5 3 2	260	247	17 7 2	44	40
3 3 0	48	54	18 7 0	57	56	10 3 1	46	49	13 7 1	29	32	6 3 2	108	95	18 7 2	58	58
4 3 0	127	111	0 8 0	63	68	11 3 1	177	176	14 7 1	46	48	7 3 2	161	161	0 8 2	79	79
5 3 0	89	79	1 8 0	48	47	12 3 1	108	109	15 7 1	36	38	8 3 2	192	188	1 8 2	35	38
6 3 0	47	39	3 8 0	30	26	13 3 1	122	129	16 7 1	51	52	9 3 2	201	203	2 8 2	71	72
7 3 0	130	128	4 8 0	36	33	14 3 1	199	198	17 7 1	73	68	10 3 2	17	19	3 8 2	45	49
8 3 0	135	127	5 8 0	28	26	15 3 1	103	104	18 7 1	31	35	11 3 2	98	97	4 8 2	65	66
9 3 0	142	146	6 8 0	42	49	16 3 1	128	132	19 7 1	60	60	12 3 2	58	58	5 8 2	91	90
10 3 0	204	196	7 8 0	51	47	17 3 1	44	46	1 8 1	24	25	13 3 2	115	119	6 8 2	26	26
11 3 0	214	220	8 8 0	37	38	18 3 1	64	68	2 8 1	49	48	14 3 2	33	37	7 8 2	33	33
12 3 0	150	145	9 8 0	26	23	19 3 1	32	27	3 8 1	55	55	15 3 2	234	237	9 8 2	49	50
13 3 0	37	37	10 8 0	46	47	20 3 1	86	86	4 8 1	68	64	16 3 2	143	144	10 8 2	24	23
14 3 0	55	67	11 8 0	77	77	22 3 1	59	61	5 8 1	40	36	17 3 2	93	91	11 8 2	45	48
15 3 0	41	41	12 8 0	76	74	23 3 1	27	33	6 8 1	62	61	18 3 2	73	74	12 8 2	32	29
16 3 0	76	72	13 8 0	55	54	24 3 1	36	40	8 8 1	50	50	19 3 2	60	60	13 8 2	62	59
17 3 0	39	41	14 8 0	65	62	25 3 1	57	50	9 8 1	67	68	20 3 2	35	31	1 9 2	49	49
18 3 0	84	79	15 8 0	40	37	27 3 1	34	32	10 8 1	44	43	21 3 2	32	30	2 9 2	23	30
19 3 0	51	52	16 8 0	28	32	1 4 1	187	186	12 8 1	51	50	22 3 2	75	76	3 9 2	33	32
20 3 0	39	39	1 9 0	51	56	2 4 1	296	295	14 8 1	31	27	23 3 2	41	41	4 9 2	45	41
21 3 0	60	57	2 9 0	34	33	3 4 1	298	295	15 8 1	33	32	25 3 2	67	61	6 9 2	24	22
22 3 0	36	38	3 9 0	24	5	4 4 1	67	64	0 9 1	48	49	26 3 2	39	37	7 9 2	34	37
23 3 0	65	65	4 9 0	30	28	5 4 1	103	100	1 9 1	38	37	27 3 2	54	49	2 0 3	419	404
24 3 0	86	82	9 9 0	82	81	6 4 1	176	168	3 9 1	32	32	0 4 2	129	129	4 0 3	133	127
25 3 0	88	86	2 0 1	219	216	7 4 1	62	53	7 9 1	43	43	1 4 2	142	141	6 0 3	197	187
1 4 0	48	49	4 0 1	453	449	8 4 1	64	58	8 9 1	33	29	2 4 2	154	153	8 0 3	220	210
2 4 0	182	179	6 0 1	200	178	9 4 1	45	46	0 0 2	435	429	3 4 2	177	173	10 0 3	218	220
3 4 0	246	246	8 0 1	75	77	10 4 1	89	88	2 0 2	401	391	4 4 2	86	79	12 0 3	232	233
4 4 0	76	73	10 0 1	366	353	11 4 1	51	52	4 0 2	411	403	5 4 2	150	158	14 0 3	239	245
5 4 0	46	50	12 0 1	90	91	12 4 1	59	57	6 0 2	476	459	6 4 2	21	25	16 0 3	145	142
6 4 0	163	167	14 0 1	94	94	13 4 1	65	69	8 0 2	247	252	7 4 2	26	30	18 0 3	99	84
7 4 0	65	63	16 0 1	106	106	14 4 1	55	57	10 0 2	55	59	8 4 2	112	109	20 0 3	63	65
8 4 0	45	45	18 0 1	134	139	15 4 1	227	232	12 0 2	149	148	9 4 2	113	110	22 0 3	47	50
9 4 0	22	25	20 0 1	76	88	16 4 1	45	48	14 0 2	215	216	10 4 2	40	41	24 0 3	125	123
10 4 0	78	70	22 0 1	54	51	17 4 1	69	66	16 0 2	329	344	11 4 2	128	132	26 0 3	24	32

Table 1. Continued.

0 1 3	229	232	5 5 3	44	42	10 2 4	82	79	14 7 4	31	26	1 5 5	57	53	3 4 6	27	29
1 1 3	133	133	7 5 3	127	127	11 2 4	176	189	0 9 4	76	74	2 5 5	22	26	4 4 6	23	11
2 1 3	341	324	9 5 3	43	44	12 2 4	54	55	1 9 4	29	31	3 5 5	39	37	5 4 6	51	51
3 1 3	34	36	9 5 3	82	91	13 2 4	72	71	2 8 4	31	23	4 5 5	39	37	6 4 6	65	67
4 1 3	109	102	10 5 3	57	66	14 2 4	86	89	3 8 4	25	20	5 5 5	22	25	7 4 6	54	54
5 1 3	156	152	12 5 3	89	90	15 2 4	45	44	8 8 4	32	26	6 5 5	36	37	8 4 6	40	44
6 1 3	170	162	14 5 3	50	51	16 2 4	22	20	2 0 5	290	302	7 5 5	47	50	9 4 6	27	22
7 1 3	125	123	15 5 3	46	44	17 2 4	76	82	4 0 5	171	172	8 5 5	71	74	10 4 6	33	37
8 1 3	82	80	16 5 3	52	49	18 2 4	27	31	6 0 5	221	224	9 5 5	33	34	12 4 6	34	31
9 1 3	95	93	17 5 3	31	35	19 2 4	78	82	8 0 5	217	237	10 5 5	62	61	13 4 6	59	60
10 1 3	68	67	18 5 3	66	62	21 2 4	73	74	10 0 5	82	81	11 5 5	30	30	14 4 6	37	39
11 1 3	33	32	19 5 3	75	76	22 2 4	44	45	12 0 5	30	26	12 5 5	59	55	15 4 6	54	52
12 1 3	178	181	22 5 3	30	30	24 2 4	42	41	14 0 5	137	150	13 5 5	64	65	16 4 6	46	45
13 1 3	81	80	1 6 3	113	113	1 3 4	210	215	16 0 5	60	59	14 5 5	73	73	1 5 6	52	54
14 1 3	153	155	2 6 3	76	76	2 3 4	100	103	18 0 5	111	113	16 5 5	34	36	3 5 6	27	21
15 1 3	95	99	3 6 3	35	33	3 3 4	144	148	20 0 5	85	80	17 5 5	29	25	4 5 6	94	90
16 1 3	259	263	4 6 3	61	57	4 3 4	78	83	22 0 5	66	68	1 6 5	48	51	5 5 6	121	120
18 1 3	67	70	5 6 3	51	48	5 3 4	78	75	0 1 5	213	215	2 6 5	46	48	6 5 6	56	55
19 1 3	96	94	6 6 3	84	83	6 3 4	118	124	1 1 5	213	215	4 6 5	40	43	7 5 6	31	29
20 1 3	23	29	7 6 3	57	61	7 3 4	82	83	2 1 5	182	183	5 6 5	37	36	8 5 6	29	34
24 1 3	82	79	8 6 3	54	49	8 3 4	23	20	3 1 5	111	118	6 6 5	87	86	9 5 6	57	52
26 1 3	50	45	9 6 3	43	43	9 3 4	144	142	4 1 5	201	202	8 6 5	54	53	10 5 6	24	27
27 1 3	50	47	10 6 3	79	83	10 3 4	81	88	5 1 5	68	65	9 6 5	78	78	11 5 6	33	32
1 2 3	218	217	12 6 3	71	68	11 3 4	84	85	6 1 5	34	40	10 6 5	53	58	12 5 6	52	46
2 2 3	173	169	13 6 3	25	26	12 3 4	97	96	7 1 5	125	125	11 6 5	46	48	0 6 6	102	102
3 2 3	151	144	14 6 3	50	48	13 3 4	127	133	8 1 5	117	121	12 6 5	39	34	1 6 6	59	52
4 2 3	327	311	15 6 3	29	25	14 3 4	138	144	9 1 5	125	129	14 6 5	56	51	2 6 6	46	45
5 2 3	132	127	18 6 3	59	61	16 3 4	108	99	10 1 5	57	61	0 7 5	87	87	3 6 6	40	40
6 2 3	121	124	19 6 3	63	61	17 3 4	114	117	11 1 5	107	113	1 7 5	26	29	4 6 6	27	26
7 2 3	157	157	20 6 3	38	35	18 3 4	57	59	12 1 5	89	89	3 7 5	57	52	5 6 6	26	28
8 2 3	177	180	0 7 3	134	136	19 3 4	65	64	13 1 5	63	63	4 7 5	43	39	6 6 6	26	30
9 2 3	62	65	1 7 3	74	74	20 3 4	28	31	14 1 5	159	169	6 7 5	36	39	8 6 6	65	67
11 2 3	101	99	2 7 3	120	120	21 3 4	55	52	15 1 5	52	46	8 7 5	36	35	2 0 7	123	114
12 2 3	180	185	3 7 3	67	69	22 3 4	33	33	16 1 5	65	66	9 7 5	33	27	4 0 7	144	142
13 2 3	105	112	4 7 3	54	53	23 3 4	25	24	18 1 5	47	44	0 0 6	80	79	6 0 7	161	160
14 2 3	89	86	5 7 3	72	74	24 3 4	66	60	19 1 5	51	52	2 0 6	93	83	8 0 7	96	89
15 2 3	122	126	6 7 3	91	87	0 4 4	252	264	20 1 5	78	73	4 0 6	147	151	10 0 7	55	55
16 2 3	136	139	7 7 3	31	32	1 4 4	82	78	21 1 5	47	47	6 0 6	102	103	12 0 7	36	34
17 2 3	88	89	8 7 3	30	29	2 4 4	78	80	22 1 5	38	37	8 0 6	35	42	14 0 7	50	47
18 2 3	89	91	9 7 3	45	44	3 4 4	67	70	23 1 5	47	45	10 0 6	31	32	0 1 7	124	117
19 2 3	77	77	12 7 3	75	73	4 4 4	33	32	1 2 5	72	70	12 0 6	59	57	1 1 7	116	116
20 2 3	35	37	13 7 3	42	40	5 4 4	41	44	2 2 5	145	142	14 0 6	121	123	2 1 7	51	49
21 2 3	96	95	14 7 3	54	55	6 4 4	55	61	3 2 5	104	109	16 0 6	63	63	3 1 7	47	47
22 2 3	39	41	16 7 3	42	42	7 4 4	80	78	4 2 5	153	156	18 0 6	38	41	6 1 7	32	32
23 2 3	82	79	1 8 3	66	68	8 4 4	112	113	5 2 5	131	136	20 0 6	39	36	7 1 7	79	75
25 2 3	27	28	2 8 3	33	34	9 4 4	79	85	6 2 5	95	98	2 1 6	121	121	8 1 7	32	29
26 2 3	64	63	4 8 3	47	44	10 4 4	49	49	7 2 5	95	99	3 1 6	62	61	9 1 7	83	81
0 3 3	98	101	5 8 3	27	29	11 4 4	100	105	8 2 5	93	97	4 1 6	117	120	10 1 7	106	101
1 3 3	209	206	6 8 3	25	28	12 4 4	56	55	9 2 5	50	52	5 1 6	56	56	11 1 7	41	38
2 3 3	70	69	7 8 3	46	47	13 4 4	58	63	11 2 5	89	90	8 1 6	110	118	13 1 7	51	50
3 3 3	154	156	9 8 3	27	20	15 4 4	57	56	12 2 5	101	104	9 1 6	49	48	14 1 7	52	51
4 3 3	43	45	10 8 3	44	45	18 4 4	33	30	13 2 5	50	53	10 1 6	51	52	1 2 7	63	62
5 3 3	98	98	12 8 3	43	39	19 4 4	60	62	14 2 5	43	47	12 1 6	31	31	2 2 7	39	39
6 3 3	164	163	0 0 4	150	162	20 4 4	41	39	15 2 5	38	36	13 1 6	21	12	4 2 7	73	64
7 3 3	98	95	2 0 4	137	145	22 4 4	36	46	16 2 5	55	57	14 1 6	41	41	5 2 7	95	91
8 3 3	17	11	4 0 4	55	48	1 5 4	207	211	17 2 5	69	70	15 1 6	64	60	7 2 7	108	107
9 3 3	109	108	6 0 4	154	154	2 5 4	31	33	18 2 5	66	66	16 1 6	76	69	8 2 7	65	64
10 3 3	80	81	8 0 4	126	135	3 5 4	51	55	19 2 5	35	41	17 1 6	28	29	9 2 7	43	46
11 3 3	133	147	10 0 4	18	22	5 5 4	95	98	20 2 5	43	43	18 1 6	60	57	10 2 7	36	34
12 3 3	160	163	12 0 4	145	150	7 5 4	24	22	21 2 5	41	41	19 1 6	32	30	11 2 7	54	51
13 3 3	122	127	14 0 4	133	129	8 5 4	59	65	0 3 5	109	109	0 2 6	24	27	12 2 7	69	72
14 3 3	63	57	16 0 4	27	28	9 5 4	64	65	1 3 5	59	60	1 2 6	56	57	13 2 7	57	54
15 3 3	110	118	18 0 4	51	54	10 5 4	57	60	2 3 5	79	84	2 2 6	58	60	14 2 7	24	25
16 3 3	59	59	20 0 4	85	81	11 5 4	124	121	3 3 5	110	108	3 2 6	52	55	0 3 7	72	71
17 3 3	107	112	22 0 4	41	40	12 5 4	102	101	4 3 5	41	35	4 2 6	99	97	1 3 7	54	54
18 3 3	88	88	24 0 4	83	81	13 5 4	23	22	5 3 5	40	47	5 2 6	76	76	3 3 7	31	35
19 3 3	64	66	1 1 4	117	117	15 5 4	29	25	6 3 5	55	57	6 2 6	48	45	4 3 7	41	43
20 3 3	89	88	2 1 4	229	230	16 5 4	25	24	9 3 5	22	26	7 2 6	45	49	5 3 7	72	71
21 3 3	99	87	3 1 4	128	133	17 5 4	24	25	10 3 5	77	80	8 2 6	32	34	9 3 7	35	36
22 3 3	26	29	4 1 4	133	107	18 5 4	65	61	11 3 5	130	135	9 2 6	32	37	10 3 7	43	36
23 3 3	45	44	5 1 4	78	70	19 5 4	78	76	12 3 5	31	33	10 2 6	41	42	11 3 7	35	38
24 3 3	24	33	6 1 4	90	91	20 5 4	89	92	13 3 5	62	60	11 2 6	49	50	12 3 7	65	60
25 3 3	28	29	7 1 4	32	32	0 6 4	117	118	14 3 5	51	51	12 2 6	48	50	13 3 7	91	88
1 4 3	159	164	8 1 4	115	122	1 6 4	25	17	15 3 5	54	54	13 2 6	36	38	1 4 7	62	64
2 4 3	43	42	9 1 4	109	105	2 6 4	76	77	17 3 5	113	111	14 2 6	43	45	2 4 7	35	32
3 4 3	65	69	10 1 4	34	33	3 6 4	26	25	18 3 5	53	53	15 2 6	29	34	4 4 7	67	68
4 4 3	169	177	11 1 4	45	49	5 6 4	35	34	19 3 5	49	45	16 2 6	34	32	5 4 7	120	116
5 4 3	106	109	12 1 4	153	155	6 6 4	49	47	20 3 5	29	32	17 2 6	71	72	6 4 7	53	49
6 4 3	151	158	13 1 4	66	63	7 6 4	47	45	21 3 5	40	38	19 2 6	36	36	7 4 7	54	53
7 4 3	128	129	14 1 4	96	99	8 6 4	54	52	1 4 5	96	95	1 3 6	24	20	8 4 7	28	27
8 4 3	81	78	15 1 4	41	46	10 6 4	58	59	2 4 5	48	45	2 3 6	61	60	0 5 7	55	54
9 4 3	91	92	16 1 4	57	57	11 6 4	36	41	3 4 5	56	51	3 3 6	104	108	2 5 7	41	39
10 4 3	127	129	17 1 4	34	33	12 6 4	28	29	4 4 5	55	57	4 3 6	81	83	3 5 7	34	29
11 4 3	60	63	18 1 4	73	73	13 6 4	34	36	5 4 5	94	88	5 3 6	75	75	4 5 7	46	46
12 4 3	46	50	19 1 4	35	31	15 6 4	38	38	6 4 5	41	45	6 3 6	63	66	0 0 8	129	124
13 4 3	21	16	20 1 4	33	31	16 6 4	35	34	7 4 5	62	63	7 3 6	94	91	2 0 8	92	89
14 4 3	85	89	21 1 4	27	32	17 6 4	46	46	8 4 5	47	51	8 3 6	70	68	6 0 8	51	46
15 4 3	89	91	22 1 4	100	99	18 6 4	65	63	9 4 5	74	78	9 3 6	23	16	8 0 8	50	49
16 4 3	37	39	23 1 4	30	26	1 7 4	36	35	11 4 5	116	112	10 3 6	24	21	1 1 8	27	24
17 4 3	35	33	24 1 4	26	27	2 7 4	44	42	12 4 5	82	82	12 3 6	41	43	3 1 8	45	49
18 4 3	97	99	0 2 4	73	72	3 7 4	51	49	13 4 5	43	42	13 3 6	33	37	4 1 8	37	36
19 4 3	88	83	1 2 4	63	64	4 7 4	67	63	14 4 5	35	35	14 3 6	49	48	5 1 9	44	43
20 4 3	43	44	2 2 4	192	205	5 7 4	69	64	15 4 5	80	76	15 3 6	73	74	0 2 8	28	26
21 4 3	60	59	3 2 4	132	139	6 7 4	25	20	16 4 5	64	63	17 3 6	51	59	1 2 8	58	55
0 5 3	97	98	5 2 4	55	56	7 7 4	26	25	17 4 5	37	39	18 3 6	63	57	2 2 8	91	90
1 5 3	159	165	6 2 4	74	69	8 7 4	46	49	18 4 5	37	32	0 4 6	52	50	3 2 8	38	38
2 5 3	200	204	7 2 4	62	60	9 7 4	51	53	19 4 5	32	32	1 4 6	27	25	4 2 8	25	24
3 5 3	79	75	8 2 4	45	45	10 7 4	46	48	20 4 5	59	58	2 4 6	40	48	5 2 8	25	21
4 5 3	34	34	9 2 4	26	18	12 7 4	37	38	0 5 5	132	135						

Table 2. Fractional atomic coordinates and thermal parameters with estimated standard deviations ($\times 10^5$) for non-hydrogen atoms. The temperature factor is given by $\exp-(B_{11}h^2+B_{22}k^2+B_{33}l^2+B_{12}hk+B_{13}hl+B_{23}kl)$.

Atom	x	y	z	B_{11}	B_{22}	B_{33}	B_{12}	B_{13}	B_{23}
O1	−10168	73060	17400	112	2000	1565	−117	−20	273
	7	27		3	39	49	17	22	81
O2	17158	40200	2030	169	1400	1506	−219	−126	−464
	8	24	44	4	31	44	17	22	68
O3	21463	67438	−12859	161	1659	1047	−103	51	30
	8	25	45	4	34	43	18	21	68
N	19866	49323	44313	113	1336	949	36	5	116
	8	26	45	3	35	40	17	21	71
C1	9488	79124	28302	108	933	1319	45	35	−78
	9	27	47	4	34	52	18	26	76
C2	6665	84401	7769	117	1136	1185	39	161	313
	9	30	50	4	37	49	20	26	77
C3	96	82104	4253	122	1182	1284	68	−48	202
	10	31	52	4	36	57	20	28	83
C4	−3696	74333	21334	104	972	1340	−15	31	−252
	9	29	48	4	35	55	19	26	79
C5	−970	68510	41867	122	1119	1247	−13	116	314
	10	31	52	4	35	53	20	26	78
C6	5619	71018	45145	123	1189	1151	117	53	284
	10	30	48	4	37	50	20	27	76
C7	16567	82769	32339	108	1115	1426	−30	18	−331
	9	29	48	4	35	61	19	24	76
C8	20904	65017	27242	87	1181	850	−76	−9	−81
	9	31	47	4	37	45	18	22	74
C9	19741	56741	3502	78	1294	931	54	−58	−460
	8	30	47	3	39	46	18	21	77

Standard deviations in bond lengths and angles were computed from the correlation matrix ignoring standard deviations in cell parameters. For distances and angles the standard deviations were calculated to be 0.003 Å and 0.2°, respectively, except for the bond lengths involving hydrogen where the standard deviation varied from 0.03 to 0.06 Å.

DISCUSSION

A drawing of the molecule is shown in Fig. 1 in which the numbering of the atoms is also indicated. The bond lengths (corrected for thermal effects) and valence angles are given in this figure; interactomic distances and bond angles are also listed in Table 5.

The unit cell dimensions for DL-tyrosine are quite close to those found for L-tyrosine,[1] and it is interesting to note that the same relation exists between the space groups of L- and DL-tyrosine as that reported for L- and DL-alanine,[12] *viz.* $P2_12_12_1$ for the optically active crystals and $Pna2_1$ for the racemate. It has recently been pointed out by Pedone and Benedetti[13] that such relations

Table 3. Fractional coordinates ($\times 10^4$) and isotropic thermal parameters (Å^2) with estimated standard deviations for hydrogen atoms.

Atom	x	y	z	B
H2	984	8954	−479	5.3
	23	69	112	1.2
H3	−202	8587	−1020	2.5
	13	41	75	0.6
H5	−367	6261	5327	2.1
	15	40	72	0.6
H6	721	6847	5787	4.5
	15	53	87	0.8
H71	1744	8652	4920	2.4
	17	49	91	0.9
H72	1773	9259	2367	1.6
	12	41	65	0.6
H8	2511	6857	3006	1.4
	15	41	60	0.6
HO1	−1170	6871	2893	5.1
	18	45	85	0.8
HN1	1668	4558	4428	5.8
	22	65	112	1.2
HN2	2018	5535	5782	4.8
	14	45	65	0.6
HN3	2284	3906	4282	3.4
	13	43	71	0.7

Table 4. R.m.s. amplitudes of vibration $(\overline{u^2})^{\frac{1}{2}}$ and B-values (Å^2) along the principal axes of vibration given by the components of a unit vector **e** in fractional coordinates ($\times 10^3$).

Atom	$(\overline{u^2})^{\frac{1}{2}}$	B	e_x	e_y	e_z
	.219	3.80	−9	143	23
O1	.165	2.15	1	21	−168
	.155	1.89	47	26	6
	.208	3.41	−38	89	3
O2	.181	2.60	20	85	−118
	.143	1.63	21	81	121
	.203	3.26	26	−124	4
O3	.182	2.63	40	79	17
	.135	1.45	5	5	−168
	.178	2.51	9	144	13
N	.157	1.95	−47	28	1
	.129	1.32	0	12	−169
	.158	1.97	41	52	66
C1	.154	1.86	8	79	−140
	.143	1.61	−24	112	68
	.176	2.45	31	86	85
C2	.158	1.98	29	−115	23
	.132	1.37	23	32	−145

Table 4. Continued.

	.173	2.36	29	117	18
C3	.163	2.09	−34	68	91
	.145	1.66	18	−58	142
	.162	2.07	14	−89	124
C4	.150	1.77	45	41	−26
	.144	1.63	−5	109	112
	.171	2.32	33	69	93
C5	.164	2.13	−29	117	13
	.137	1.49	19	56	−141
	.181	2.58	31	107	44
C6	.153	1.85	−37	90	28
	.139	1.53	2	44	−161
	.171	2.32	10	−110	107
C7	.153	1.85	46	1	−52
	.149	1.75	11	98	121
	.169	2.25	13	−141	9
C8	.135	1.45	46	39	−24
	.122	1.18	6	13	167
	.179	2.54	8	138	−51
C9	.132	1.38	−43	39	63
	.120	1.14	21	30	149

may indeed be expected between crystals of the optically active and racemic compounds where virtually identical layers of molecules are packed through the operation of different symmetry elements. This appears to be the case in L- and DL-tyrosine, the layer of molecules between the diagonal glide-planes shown in Fig. 3 is nearly the same in both structures. The layers are differently

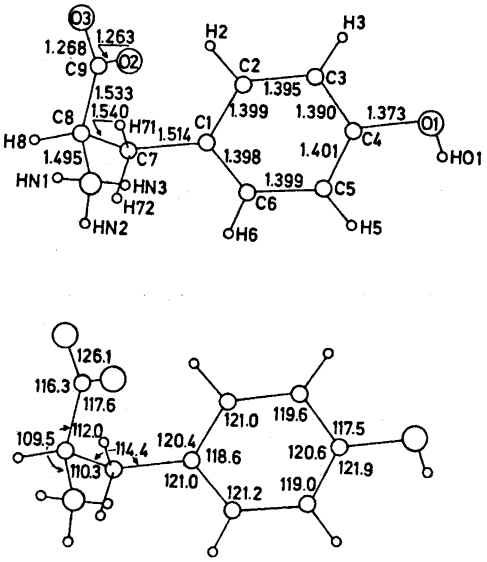

Fig. 1. Bond lengths (Å) corrected for thermal vibration effects and angles (°) in DL-tyrosine.

Table 5. Bond lengths (Å) and bond angles (°) in DL-tyrosine.

	Bond length	Corrected	Bond angle	
C1 – C2	1.395	1.399	C1 – C2 – C3	121.0
C2 – C3	1.393	1.395	C2 – C3 – C4	119.6
C3 – C4	1.386	1.390	C3 – C4 – C5	120.6
C4 – C5	1.396	1.401	C4 – C5 – C6	119.0
C5 – C6	1.397	1.399	C1 – C6 – C5	121.2
C1 – C6	1.394	1.398	C2 – C1 – C6	118.6
C1 – C7	1.513	1.514	C7 – C1 – C2	120.4
C7 – C8	1.540		C7 – C1 – C6	121.0
C8 – C9	1.530	1.533	O1 – C4 – C5	121.9
C8 – N	1.485	1.495	O1 – C4 – C3	117.5
C9 – O2	1.251	1.263	C1 – C7 – C8	114.4
C9 – O3	1.262	1.268	C7 – C8 – C9	112.0
C4 – O1	1.371	1.373	C7 – C8 – N	110.3
O1 – HO1	0.81		N – C8 – C9	109.5
N – H1N	0.70		C8 – C9 – O2	117.6
N – H2N	0.90		C8 – C9 – O3	116.3
N – H3N	0.94		O2 – C9 – O3	126.1
C2 – H2	1.05			
C3 – H3	0.99	Hydrogen bond lengths		
C5 – H5	0.97			
C6 – H6	0.84	O1 – O2($-x$, $1-y$, $\frac{1}{2}+z$)		2.668
C7 – H71	1.04	N – O1 ($-x$, $1-y$, $\frac{1}{2}+z$)		2.875
C7 – H72	0.87	N – O3 (x, y, $1+z$)		2.833
C8 – H8	0.92	N – O3 ($\frac{1}{2}-x$, $-\frac{1}{2}+y$, $\frac{1}{2}+z$)		2.856

packed, however, as may be expected since all layers in L-tyrosine are identical whereas the layers in DL-tyrosine consist alternatingly of D and L forms. The difference in packing is visualized in Figs. 2 (A) and (B) which show the coupling of molecules of different layers through the alanine parts; (A) shows the conditions in L-tyrosine as viewed along the *a*-axis (6.913 Å) and (B) represents the DL-tyrosine structure as viewed down the *b*-axis (6.810 Å). The pertinent symmetry elements responsible for the coupling of layers are screw axes and glide-planes, respectively. The molecular packing is somewhat denser in the racemate, the density being 1.435 g cm^{-3} as compared to 1.414 g cm^{-3} for L-tyrosine.

The bond lengths and angles found in the present investigation are nearly identical to those determined from the study of the L-form. Except for the C9 – O2 bond in the carboxyl group the differences in corresponding bonds are insignificant, 0.008 Å or less; the C9 – O2 bond is found 0.017 Å longer than in L-tyrosine. The differences in corresponding angles are 0.7° or less, the largest dissimilarities are found in the alanine moiety. The conformation in the two structures are also equal; the angle between the phenyl ring plane and the plane defined by the C1 – C7 – C8 atoms is 85.8° (as compared to 85.9° in L-tyrosine), the dihedral angles C1 – C7 – C8 – C9 and C1 – C7 – C8 – N are 52.5° and 290.3, respectively (53.1° and 290.7° in L-tyrosine) whereas the torsional angle N – C8 – C9 – O2 is 11.7°, 2.3° less than the corresponding angle in L-tyrosine.

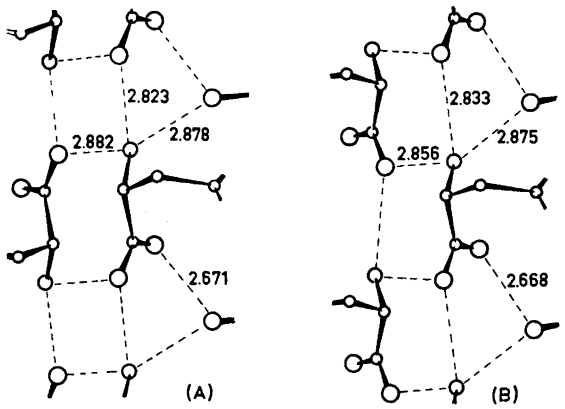

Fig. 2. Molecular arrangement in L-tyrosine (A) and in DL-tyrosine (B) crystals.

The hydrogen bond system in the crystals of DL-tyrosin is shown in Fig. 3. Each molecule is hydrogen donor as well as acceptor in four hydrogen bonds in such a way that one molecule is hydrogen bonded to six neighbouring molecules. The hydrogen bond lengths (given in Table 5) within the layers of molecules of equal chirality are nearly the same as the corresponding bonds in L-tyrosine; the hydrogen bonds linking the layers together are by 0.026 Å shorter in the racemate than in the crystals of the L-form.

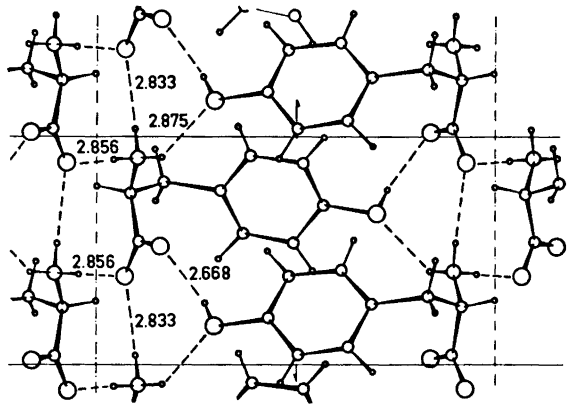

Fig. 3. The crystal structure of DL-tyrosine as viewed along the *b*-axis.

REFERENCES

1. Mostad, A., Nissen, H. M. and Rømming, C. *Acta Chem. Scand.* **26** (1972) 3819.
2. Srinsivasan, R. *Proc. Indian. Acad. Sci.* **A 50** (1959) 19.
3. Vainshtain, B. K. and Gurskaya, G. V. *Dokl. Akad. Nauk. SSSR* **156** (1964) 312.

4. Fries, D. C. and Sundaralingam, M. *Acta Cryst.* **B 27** (1971) 401.
5. Khawas, B. and Krishna Murti. *Acta Cryst.* **B 25** (1969) 1006, 2663.
6. Khawas, B. *Acta Cryst.* **B 26** (1970) 1919.
7. Mostad, A., Nissen, H. M. and Rømming, C. *Acta Chem. Scand.* **25** (1971) 1145.
8. Doyle, P. A. and Turner, P. S. *Acta Cryst.* **A 24** (1968) 390.
9. Stewart, R. F., Davidson, E. R. and Simpson, W. T. *J. Chem. Phys.* **42** (1965) 3175.
10. Dahl, T., Gram, F., Groth, P., Klewe, B. and Rømming, C. *Acta Chem. Scand.* **24** (1970) 2232.
11. Germain, G., Main, P. and Woolfsen, M. M. *Acta Cryst.* **A 27** (1971) 368.
12. Simpson, H. J. and Marsh, R. E. *Acta Cryst.* **20** (1966) 550.
13. Pedone, C. and Benedetti, E. *Acta Cryst.* **B 28** (1972) 1970.

Received August 11, 1972.

ACTA CHEMICA SCANDINAVICA 27 (1973) 411–420

The Crystal and Molecular Structure of 6a-Thiathiophthene

LARS K. HANSEN and ASBJØRN HORDVIK

Chemical Institute, University of Bergen, N-5000 Bergen, Norway

6a-Thiathiophthene crystallizes in the orthorhombic space group *Pnma* with four molecules in a unit cell of dimensions: $a = 7.768(6)$, $b = 15.784(6)$, and $c = 5.385(2)$ Å.

The structure was solved from Patterson and Fourier syntheses, and the atomic parameters were refined by the full-matrix least squares method. The refinement comprises the 1145 independent reflections (Mo$K\alpha$) in the range $10° < \theta < 32°$.

The 6a-thiathiophthene molecule is almost planar, and lies across a crystallographic mirror plane passing through the central carbon and sulphur atoms. The S–S distances are thus exactly equal, 2.363(1) Å, and the S(1)–S(6a)–S(6) angle is 177.93(8)°. Other bond lengths in the molecule are S(1)–C(2) = 1.684(3) Å, S(6a)–C(3a) = 1.748(3) Å, C(2)–C(3) = 1.354(3) Å, and C(3)–C(3a) = 1.409(2) Å.

The S–S, S–C and C–C bond lengths have been corrected for libration.

A number of 6a-thiathiophthene structures has been studied.[1] We carried out the present structure study of 6a-thiathiophthene (I) because we thought that the molecular dimensions of this compound would be of interest

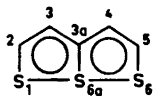

(I)

as a reference when judging the degree to which different substituents perturb the bonding in the 6a-thiathiophthene system.

STRUCTURE DETERMINATION

A brief account of a structure determination of I based on photographic data has been reported,[2] and a more detailed description of a diffractometer study of the compound is given here.

Crystals of 6a-thiathiophthene were generously supplied by Reid.[3] The crystals are orange red and belong to the orthorhombic space group *Pnma*.

The structure analysis is based on X-ray data collected on a paper-tape controlled Siemens AED diffractometer using Mo$K\alpha$ radiation.

The structure was solved by the heavy atom (S) method, and the atomic parameters were refined by full-matrix least squares to a final R factor of 4.0 %.

A rigid body analysis of the 6a-thiathiophthene molecule has been carried out according to the method of Schomaker and Trueblood,[4] and the S–S, S–C, and C–C bond lengths have been corrected for rigid body libration according to Cruickshank's formula.[5] For further details with respect to the structure determination, see Experimental.

STRUCTURE DESCRIPTION

Bond lengths and angles in the 6a-thiathiophthene molecule, together with their standard deviations, are listed in Tables 1 and 2, and shown in Fig. 1.

The 6a-thiathiophthene molecule lies across the crystallographic mirror plane m, which passes through the crystal normal to the b-axis. The dimensions of the two fused rings are therefore exactly equal.

Table 1. Bond lengths (l) and standard deviations in bond lengths $\sigma(l)$ in 6a-thiathiophthene. Bond lengths (l') with corrections for rigid-body libration are given for the S–S, S–C, and C–C bonds.

Bond	l' (Å)	l (Å)	$\sigma(l)$ (Å)
S(1)–S(6a)	2.363	2.350	0.001
S(1)–C(2)	1.684	1.673	0.003
S(6a)–C(3a)	1.748	1.737	0.003
C(2)–C(3)	1.354	1.347	0.003
C(3)–C(3a)	1.409	1.401	0.002
C(2)–H(2)		0.88	0.04
C(3)–H(3)		0.85	0.03

Table 2. Bond angles ∠(ijk) in 6a-thiathiophthene. The standard deviations given in parentheses refer to the last digits of the respective values.

i	j	k	∠(ijk)°
S(1)	S(6a)	S(6)	177.9(1)
C(2)	S(1)	S(6a)	92.0(1)
S(1)	C(2)	C(3)	120.1(2)
C(2)	C(3)	C(3a)	120.3(2)
C(3)	C(3a)	C(4)	123.0(2)
C(3)	C(3a)	S(6a)	118.5(1)
S(1)	S(6a)	C(3a)	89.1(1)
S(1)	C(2)	H(2)	119(2)
H(2)	C(2)	C(3)	121(2)
C(2)	C(3)	H(3)	124(2)
H(3)	C(3)	C(3a)	116(2)

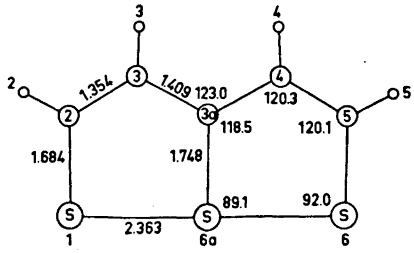

Fig. 1. Bond lengths (Å) and bond angles (°) in 6a-thiathiophthene.

The equation for the least squares plane of the atoms of the rings, with weights inversely proportional to the respective standard deviations in coordinates, is

$$0.82581\ X + 0.56396\ Z = 1.01260$$

with X and Z in Å units. Deviations from the plane for the atoms S(1), S(6a), C(2), C(3), and C(3a) are −0.008, 0.017, −0.009, 0.004, and 0.009 Å, respectively. Thus the 6a-thiathiophthene system is very nearly planar.

Comparison with other 6a-thiathiophthene structures. A comparison of the S−S bond lengths, the sums of the S−S bond lengths, and the C−S bond lengths in the 6a-thiathiophthenes so far studied (compounds I−XII [6–16]), is given in Table 3. One notes from Table 3 that the S−S bond lengths in compounds I−XII lie in the range 2.163(8)−2.561(8) Å, and that equal S−S bond lengths occur in symmetric as well as unsymmetric derivatives, *cf.* compounds I, II, and VI.

Table 3. A comparison of the S−S bond lengths, the sum of the S−S bond lengths, and the C−S bond lengths in different 6a-thiathiophthenes. Values in Å units.

Compound	S(1)–S(6a)	S(6a)–S(6)	∑(S–S)	S(1)–C(2)	S(6a)–C(3a)	S(6)–C(5)	Ref. No.
I	2.363(1)	2.363(1)	4.726(1)	1.684(3)	1.748(3)	1.684(3)	This paper
II [a]	2.358(1)	2.358(1)	4.716(1)	1.701(4)	1.745(4)	1.701(4)	6
III	2.362(3)	2.304(3)	4.666(3)	1.712(6)	1.753(6)	1.703(6)	7
IV [a]	2.232(4)	2.434(4)	4.666(4)	1.664(13)	1.749(13)	1.664(13)	8
V	2.329(1)	2.288(1)	4.617(1)	1.709(3)	1.755(3)	1.710(3)	9
VI	2.348(2)	2.350(2)	4.698(2)	1.705(4)	1.748(3)	1.689(3)	10
VII	2.431(2)	2.308(2)	4.739(2)	1.698(4)	1.763(5)	1.681(5)	11
VIII	2.481(2)	2.242(2)	4.723(2)	1.691(5)	1.751(4)	1.696(5)	12
IX	2.504(3)	2.222(3)	4.726(3)	1.701(5)	1.745(5)	1.673(7)	13
X	2.270(4)	2.375(4)	4.645(4)	1.680(8)	1.759(8)	1.669(10)	14
XI	2.255(1)	2.398(1)	4.653(1)	1.714(2)	1.749(2)	1.698(2)	15
XIIa [a]	2.454(8)	2.168(8)	4.622(8)	1.72(3)	1.70(2)	1.69(2)	16
XIIb [a]	2.561(8)	2.163(8)	4.724(8)	1.68(2)	1.78(2)	1.72(2)	16

[a] The bond lengths have not been corrected for rigid-body libration.

The sum of the S – S bonds varies from one derivative to the next, being as small as 4.617(1) Å in 2,5-diphenyl-3,4-trimethylene-6a-thiathiophthene (V), and as great as 4.739(2) Å in 2-methyl-6a-thiathiophthene (VII).

There is no clear indication that the sum of the S – S bond lengths increases with the asymmetry of the S – S bond lengths. Thus, in the asymmetric structure XIIa the sum of the S – S distances is 4.622(8) Å, while in the symmetric structure I it is 4.726 Å. Furthermore, if one also takes into account that $\sum$(S – S) for XIIb is 4.724(8) Å, it seems likely that changes in $\sum$(S – S) may be caused by intermolecular packing as well as by substituents.

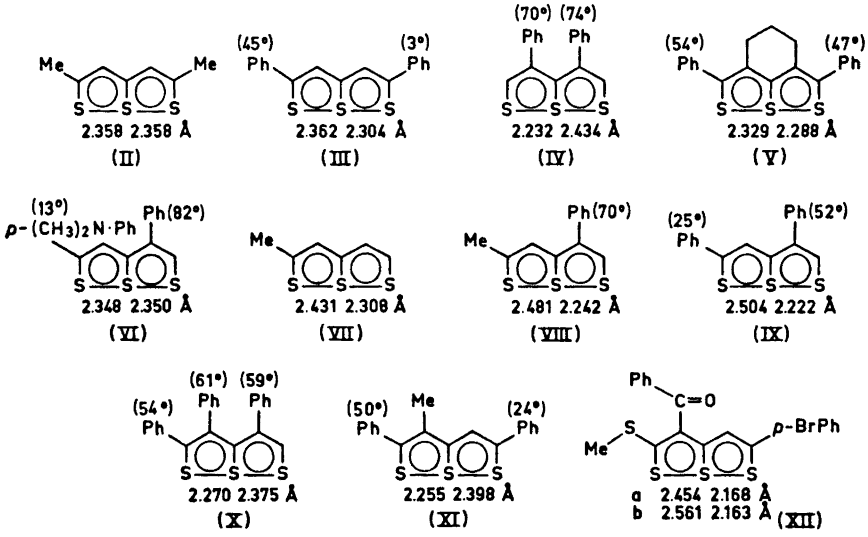

The S(6a) – C(3a) bond length is remarkably constant in different 6a-thiathiophthene derivatives. The first eleven entries in Table 3 vary from 1.745(4) Å for II to 1.763(5) Å for VII, and none of the listed S(6a) – C(3a) bond lengths deviate significantly from the value 1.748(3) Å for the mother compound (I).

The S(1) – C(2) and the S(6) – C(5) bond lengths vary more, the former from 1.664(13) Å in IV to 1.714(2) Å in XI, and the latter from 1.664(13) Å in IV to 1.710 Å in V. Thus, the terminal C – S bonds seem to be more affected by the substituents than is the central C – S bond.

A comparison of the C – C bond lengths in compounds I – XII is given in Table 4. One finds from the values there that for each of the various structures the sum of the C(3) – C(3a) and C(3a) – C(4) bond lengths is greater than the sum of the C(2) – C(3) and C(3) – C(4) bond lengths. In this respect the structure of the 6a-thiathiophthene system resembles that of naphthalene.[17] One should remember that 6a-thiathiophthene and naphthalene are analogous compounds as far as their π-bonding systems are concerned; there is a 10 π-electron system in both. The lengths of the terminal and central C – C bonds

Table 4. A comparison of the C–C bond lengths in the 6a-thiathiophthene system of different 6a-thiathiophthene derivatives.

Compound	C(2)–C(3)	C(3)–C(3a)	C(3a)–C(4)	C(4)–C(5)
I	1.354(3)	1.409(2)	1.409(2)	1.354(3)
II [a]	1.363(4)	1.402(4)	1.402(4)	1.363(4)
III	1.374(9)	1.413(9)	1.391(9)	1.393(8)
IV [a]	1.404(20)	1.450(20)	1.437(20)	1.398(20)
V	1.378(4)	1.425(4)	1.426(4)	1.381(4)
VI	1.388(4)	1.394(4)	1.428(4)	1.360(4)
VII	1.362(7)	1.408(6)	1.428(7)	1.367(7)
VIII	1.387(6)	1.397(6)	1.442(5)	1.366(6)
IX	1.377(11)	1.403(9)	1.451(11)	1.363(9)
X	1.379(12)	1.433(11)	1.414(12)	1.371(12)
XI	1.377(2)	1.429(3)	1.406(2)	1.374(3)
XIIa [a]	1.38(4)	1.45(2)	1.46(4)	1.40(3)
XIIb [a]	1.39(4)	1.42(3)	1.41(4)	1.37(2)

[a] The bond lengths have not been corrected for rigid-body libration.

in the present structure are 1.354(3) and 1.409(2) Å, respectively, and the average lengths of the corresponding bonds in naphthalene are 1.357(5) and 1.420(5) Å.

The arrangement of 6a-thiathiophthene molecules in the unit cell as seen along the *c*-axis is shown in Fig. 2. There are no intermolecular atomic distances shorter than corresponding van der Waals distances.

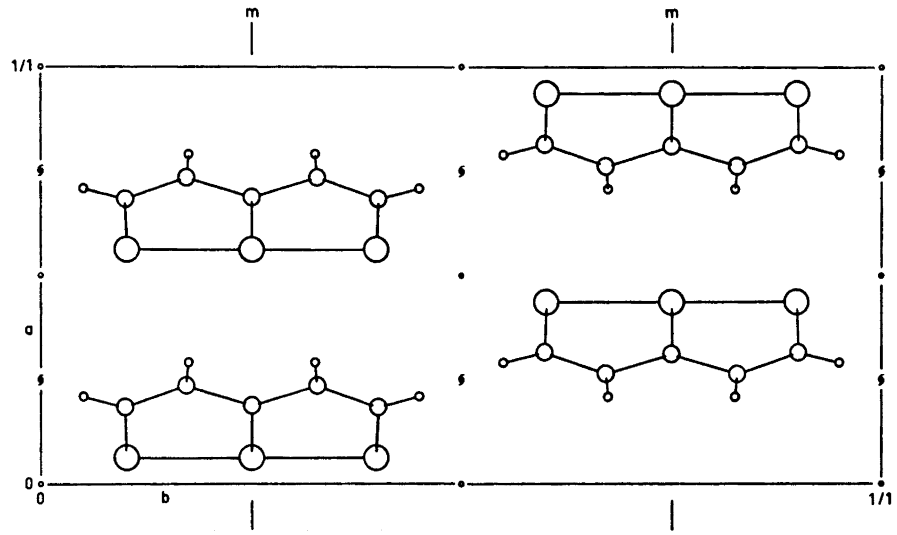

Fig. 2. The arrangement of 6a-thiathiophthene molecules in the unit cell as seen along the *c*-axis.

EXPERIMENTAL

The unit cell dimensions for crystals of 6a-thiathiophthene were determined from the 2θ values for 12 high order reflections. The 2θ values were measured at room temperature, $t = 22°C$, on the diffractometer using Mo$K\alpha$ radiation. A least squares procedure gave $a = 7.768(6)$ Å, $b = 15.784(6)$ Å, and $c = 5.385(2)$ Å.

The molecular weight of the compound ($C_5H_4S_3$) is 160.29, and four molecules per unit cell give a calculated density of 1.612 g/cm³, as compared with the density 1.61 g/cm³ found by flotation.

The intensities of the reflections were measured on the diffractometer by means of the five-value scan technique.[18] Reflections for which the net count was greater than two times the respective standard deviation in the net count were accepted as observed. With this criterion 817 out of 1145 independent reflections in the range $10° < \theta < 32°$ were accepted as observed. Reflections below $\theta = 10°$ were neglected.[19]

A small crystal, with dimensions of about $0.15 \times 0.15 \times 0.15$ mm in the three axial directions, was used for the data collection. Lp corrections were applied, but absorption corrections were considered unnecessary, $\mu_{MoK\alpha} = 9.6$ cm^{-1}.

The scattering factors used for sulphur and carbon were those given in *International Tables*.[20] For hydrogen the scattering factor curve given by Stewart *et al.*[21] was used.

The full-matrix least squares program which was applied minimizes the function

$$D = \sum w(|F_o| - (1/K)|F_c|)^2$$

The weight was taken to be

$$w = 1/\sigma^2(F_o)$$

where

$$\sigma^2(F_o) = F_o^2(I_{total} + I_{background} + (k\, I_{net})^2)/4I^2_{net}$$

In the latter expression k is the relative standard deviation in the scaling curve from the reference reflections. It was estimated to be 0.014 in the present case.

Final atomic coordinates from the least squares refinement are listed in Table 5, and the temperature parameters are listed in Table 6. A pictorial representation of the thermal motion of the sulphur and carbon atoms is given in Fig. 3.[22] The final list of structure factors is given in Table 8.

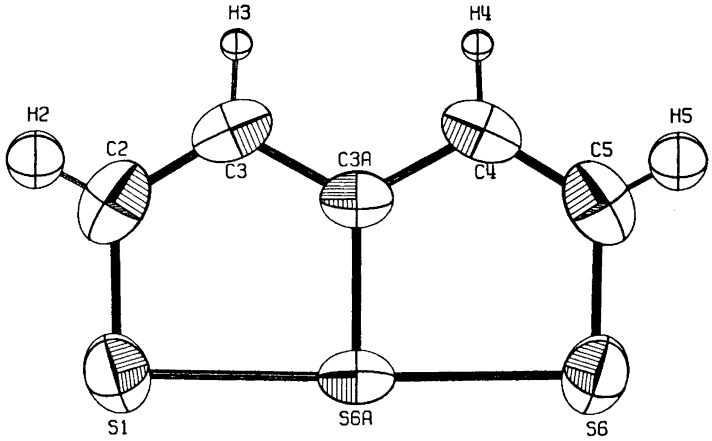

Fig. 3. The thermal ellipsoid plot showing the anisotropic vibration of the sulphur and carbon atoms and the isotropic vibration of the hydrogen atoms. The latter has been scaled down by a factor of 2.

Table 5. Atomic coordinates in fractions of corresponding cell edges. The standard deviations given in parentheses refer to the last digits of the respective values.

Atom	x	y	z
S(1)	0.06293(7)	0.10115(3)	0.19801(12)
S(6a)	0.06296(8)	0.25000(0)	0.20590(11)
C(2)	0.18421(29)	0.09902(16)	−0.05864(48)
C(3)	0.23620(27)	0.17199(14)	−0.16434(39)
C(3a)	0.18825(29)	0.25000(0)	−0.06116(44)
H(2)	0.2096(40)	0.0499(25)	−0.1267(70)
H(3)	0.2920(34)	0.1746(16)	−0.2996(54)

Table 6. Temperature parameters U_{ij} (Å²) for sulphur and carbon, and U (Å²) for hydrogen. The expressions used are $\exp[-2\pi^2(h^2a^{*2}U_{11}+\cdots 2hka^*b^*U_{12}\cdots)]$ and $\exp[-8\pi^2U(\sin^2\theta/\lambda^2)]$. All values are multiplied by 10^4. Standard deviations in parentheses refer to the last digits of the respective values.

Atom	U_{11}	U_{22}	U_{33}	U_{12}	U_{23}	U_{13}
S(1)	563(3)	448(3)	688(4)	−10(2)	84(2)	5(3)
S(6a)	332(3)	609(4)	334(3)	0	0	40(3)
C(2)	555(12)	535(11)	713(15)	99(10)	−143(11)	−47(11)
C(3)	434(9)	663(13)	435(10)	73(10)	−119(10)	37(8)
C(3a)	298(10)	555(14)	335(11)	0	0	−9(9)

Atom	U
H(2)	615(90)
H(3)	335(66)

Table 7. Results from the rigid-body analysis of the 6a-thiathiophthene molecule.

	Eigenvalues	Eigenvectors. Direction cosines $\times 10^4$ relative to a, b, and c, respectively		
Librational tensor, **L**	22.2 (°)²	9750	0	2221
	21.5	0	−10000	0
	13.8	2221	0	−9750
Translational tensor, **T**	0.0472 Å²	0	10000	0
	0.0316	2610	0	−9654
	0.0286	−9654	0	−2610

Symmetrized screw tensor, **S**

$$\begin{bmatrix} 0 & -112 & 0 \\ -112 & 0 & 116 \\ 0 & 116 & 0 \end{bmatrix} \times 10^5 \text{ rad. Å}$$

Center of gravity of the molecule is at $x=0.12120$, $y=0.25000$, $z=0.07705$.
The origin which symmetrizes **S** is at $x=0.11723$, $y=0.25000$, $z=0.06736$.

Table 8. Observed and calculated structure factors for 6a-thiathiophthene. The values given are ten times the absolute values. Unobserved reflections are marked with a minus sign in front of F_o.

H	K	L	F(O)	F(C)	H	K	L	F(O)	F(C)	H	K	L	F(O)	F(C)	H	K	L	F(O)	F(C)	H	K	L	F(O)	F(C)
0	8	C	448	499	10	10	0	-17	-6	5	11	1	-11	4	11	3	1	-14	3	5	1	2	202	193
0	10	0	287	303	10	11	0	18	-5	5	12	1	22	24	11	4	1	-14	6	5	2	2	13	14
0	12	0	372	395	0	9	1	14	-12	5	13	1	70	-66	11	5	1	-15	4	5	3	2	48	49
0	14	0	473	-500	0	11	1	121	-128	5	14	1	20	-23	11	6	1	-15	-17	5	4	2	15	17
0	16	0	103	-100	0	13	1	310	-313	5	15	1	20	22	0	6	2	305	332	5	5	2	44	41
0	18	0	-22	28	0	15	1	90	86	5	16	1	-13	2	0	8	2	222	-231	5	6	2	312	309
0	20	0	169	169	0	17	1	92	92	5	17	1	18	20	0	10	2	106	-112	5	7	2	132	-126
0	22	0	-18	-7	0	19	1	105	105	5	18	1	-13	1	0	12	2	131	-133	5	8	2	168	-165
2	7	0	783	789	0	21	1	91	-88	5	19	1	-14	6	0	14	2	233	239	5	9	2	-12	-3
2	8	0	359	362	0	23	1	36	-35	5	20	1	-15	6	0	16	2	17	18	5	10	2	73	-73
2	9	0	36	40	1	7	1	240	239	5	21	1	-15	-10	0	18	2	35	-31	5	11	2	-12	-10
2	10	0	158	159	1	8	1	151	146	6	0	1	269	-271	0	20	2	69	-73	5	12	2	68	-63
2	11	0	44	-45	1	9	1	35	38	6	1	1	239	234	0	22	2	-14	14	5	13	2	98	94
2	12	C	56	50	1	10	1	102	99	6	2	1	53	53	1	5	2	142	-143	5	14	2	85	87
2	13	0	371	-371	1	11	1	15	21	6	3	1	66	68	1	6	2	159	155	5	15	2	20	-23
2	14	0	146	-146	1	12	1	109	108	6	4	1	15	16	1	7	2	349	350	5	16	2	27	28
2	15	C	93	93	1	13	1	165	-163	6	5	1	176	171	1	8	2	84	-79	5	17	2	22	-22
2	16	0	46	-45	1	14	1	120	-118	6	6	1	247	246	1	9	2	38	39	5	18	2	-14	17
2	17	C	95	93	1	15	1	30	32	6	7	1	336	-339	1	10	2	54	-52	5	19	2	24	-20
2	18	0	-13	-4	1	16	1	43	-42	6	8	1	148	-149	1	11	2	37	-33	5	20	2	55	-54
2	19	C	98	93	1	17	1	34	35	6	9	1	25	27	1	12	2	21	26	6	0	2	351	360
2	20	C	87	90	1	18	1	-13	-6	6	10	1	57	-57	1	13	2	176	-175	6	1	2	172	166
2	21	0	73	-72	1	19	1	34	31	6	11	1	23	22	1	14	2	-13	-11	6	2	2	101	-101
2	22	0	-14	-7	1	20	1	54	52	6	12	1	58	-58	1	15	2	31	30	6	3	2	25	24
2	23	0	33	-30	1	21	1	20	-19	6	13	1	136	132	1	16	2	15	15	6	4	2	20	-20
4	0	0	174	172	1	22	1	-14	4	6	14	1	93	97	1	17	2	49	47	6	5	2	52	51
4	1	0	416	-429	1	23	1	-14	-9	6	15	1	32	-39	1	18	2	18	16	6	6	2	219	-216
4	2	0	101	-101	2	6	1	462	495	6	16	1	17	12	1	19	2	53	53	6	7	2	148	-140
4	3	C	145	-137	2	7	1	440	462	6	17	1	26	-27	1	20	2	23	-20	6	8	2	126	124
4	4	0	45	-47	2	8	1	277	-274	6	18	1	-14	4	1	21	2	29	-31	6	9	2	15	12
4	5	0	190	-190	2	9	1	40	42	6	19	1	53	-49	1	22	2	-14	-4	6	10	2	37	39
4	6	0	151	140	2	10	1	142	-141	7	0	1	156	-159	2	3	2	75	69	6	11	2	-13	2
4	7	0	489	499	2	11	1	12	-12	7	1	1	76	-75	2	4	2	66	65	6	12	2	100	96
4	8	0	72	-65	2	12	1	132	-125	7	2	1	44	42	2	5	2	99	100	6	13	2	81	83
4	9	0	-10	6	2	13	1	327	-332	7	3	1	22	-20	2	6	2	504	535	6	14	2	118	-117
4	10	C	25	-21	2	14	1	203	200	7	4	1	16	17	2	7	2	297	-299	6	15	2	31	-34
4	11	0	64	-66	2	15	1	105	110	7	5	1	73	-72	2	8	2	310	-313	6	16	2	-14	-8
4	12	C	22	31	2	16	1	44	40	7	6	1	87	84	2	9	2	25	24	6	17	2	20	-19
4	13	0	237	-233	2	17	1	82	83	7	7	1	121	121	2	10	2	105	-105	6	18	2	-14	-5
4	14	0	27	-34	2	18	1	-13	-6	7	8	1	55	-54	2	11	2	32	32	6	19	2	-15	-13
4	15	0	78	77	2	19	1	52	53	7	9	1	-13	-8	2	12	2	104	-106	7	0	2	71	-70
4	16	C	16	11	2	20	1	86	-83	7	10	1	13	-12	2	13	2	151	152	7	1	2	91	90
4	17	0	64	63	2	21	1	54	-57	7	11	1	-13	-2	2	14	2	174	176	7	2	2	34	32
4	18	0	19	21	2	22	1	-14	6	7	12	1	45	-43	2	15	2	66	-67	7	3	2	27	32
4	19	0	61	62	2	23	1	23	-22	7	13	1	48	-45	2	16	2	30	33	7	4	2	14	15
4	20	C	15	-13	3	4	1	34	28	7	14	1	51	51	2	17	2	45	-43	7	5	2	79	79
4	21	C	56	-56	3	5	1	106	-105	7	15	1	-14	9	2	18	2	-13	1	7	6	2	14	-17
4	22	C	-14	-3	3	6	1	82	74	7	16	1	15	8	2	19	2	26	-28	7	7	2	139	-141
6	0	0	363	-369	3	7	1	207	195	7	17	1	-14	4	2	20	2	85	-84	7	8	2	-13	11
6	1	0	391	-391	3	8	1	26	-21	7	18	1	-15	-2	2	21	2	39	41	7	9	2	-13	-8
6	2	0	114	113	3	9	1	25	22	8	0	1	27	-20	2	22	2	-15	13	7	10	2	-12	0
6	3	0	75	-74	3	10	1	-10	-3	8	1	1	221	226	3	0	2	629	-671	7	11	2	-13	12
6	4	0	54	54	3	11	1	35	-37	8	2	1	-13	12	3	1	2	319	-300	7	12	2	32	-23
6	5	0	130	-124	3	12	1	38	-36	8	3	1	-12	10	3	2	2	144	135	7	13	2	62	58
6	6	C	148	141	3	13	1	62	-55	8	4	1	14	12	3	3	2	90	-86	7	14	2	24	21
6	7	0	325	324	3	14	1	20	22	8	5	1	78	75	3	4	2	139	133	7	15	2	-14	-9
6	8	0	94	-93	3	15	1	-12	-2	8	6	1	31	-30	3	5	2	79	-79	7	16	2	-14	1
6	9	0	18	-21	3	16	1	-12	5	8	7	1	167	-170	3	6	2	265	255	7	17	2	-14	-9
6	10	0	42	-41	3	17	1	19	17	8	8	1	-14	11	3	7	2	205	202	8	0	2	152	151
6	11	0	-12	4	3	18	1	-13	5	8	9	1	-13	12	3	8	2	131	-124	8	1	2	15	-23
6	12	0	101	-91	3	19	1	35	32	8	10	1	-13	8	3	9	2	-11	6	8	2	2	46	-48
6	13	0	198	-195	3	20	1	-15	-7	8	11	1	15	-12	3	10	2	90	-85	8	3	2	-12	-2
6	14	0	126	123	3	21	1	-15	-13	8	12	1	-14	-6	3	11	2	-11	4	8	4	2	-12	9
6	15	C	63	68	3	22	1	-14	0	8	13	1	116	114	3	12	2	157	-154	8	5	2	-13	1
6	16	0	-14	10	4	0	1	928	-942	8	14	1	-15	5	3	13	2	127	-126	8	6	2	129	-129
6	17	C	42	43	4	1	1	142	137	8	15	1	38	-43	3	14	2	174	171	8	7	2	-14	-2
6	18	0	17	-14	4	2	1	178	170	8	16	1	-14	-1	3	15	2	23	32	8	8	2	93	94
6	19	0	43	41	4	3	1	11	-13	9	0	1	69	-69	3	16	2	45	41	8	9	2	14	7
6	20	0	36	-32	4	4	1	142	140	9	1	1	37	40	3	17	2	32	30	8	10	2	-13	12
8	0	0	335	-347	4	5	1	78	-74	9	2	1	-13	13	3	18	2	-14	-10	8	11	2	-14	10
8	1	C	30	31	4	6	1	560	572	9	3	1	-13	3	3	19	2	34	30	8	12	2	31	33
8	2	0	86	85	4	7	1	80	81	9	4	1	-13	-6	3	20	2	56	-55	8	13	2	-15	-13
8	3	0	13	-8	4	8	1	337	-336	9	5	1	37	38	3	21	2	21	-23	8	14	2	51	-53
8	4	0	14	-9	4	9	1	20	-22	9	6	1	72	75	3	22	2	-15	-2	8	15	2	-14	-1
8	5	0	27	-22	4	10	1	143	-139	9	7	1	62	-63	4	0	2	62	-62	8	16	2	-14	-1
8	6	0	314	314	4	11	1	31	-30	9	8	1	37	-36	4	1	2	516	518	9	0	2	25	30
8	7	0	21	20	4	12	1	196	-192	9	9	1	-14	11	4	2	2	26	26	9	1	2	84	86
8	8	0	193	-197	4	13	1	45	40	9	10	1	15	-13	4	3	2	124	119	9	2	2	-13	-8
8	9	0	-14	6	4	14	1	276	275	9	11	1	-14	-1	4	4	2	24	24	9	3	2	-13	1
8	10	0	36	-36	4	15	1	16	-16	9	12	1	24	-22	4	5	2	241	231	9	4	2	-13	-14
8	11	0	17	-13	4	16	1	49	47	9	13	1	24	23	4	6	2	44	-45	9	5	2	24	20
8	12	0	95	-89	4	17	1	-13	-6	9	14	1	17	22	4	7	2	509	-521	9	6	2	-14	12
8	13	C	26	12	4	18	1	-13	-11	10	0	1	103	113	4	8	2	41	39	9	7	2	53	-51
8	14	0	114	119	4	19	1	-14	10	10	1	1	73	75	4	9	2	21	21	9	8	2	17	-15
8	15	0	-15	-6	4	20	1	108	-105	10	2	1	44	-45	4	10	2	13	-6	9	9	2	-14	8
8	16	C	-15	11	4	21	1	-15	-5	10	3	1	-13	-6	4	11	2	21	24	9	10	2	-14	6
8	17	0	-15	-5	5	0	1	120	109	10	4	1	-14	4	4	12	2	17	-17	9	11	2	15	-14
10	0	C	97	-98	5	1	1	139	-135	10	5	1	55	55	4	13	2	257	254	9	12	2	-15	12
10	1	0	90	96	5	2	1	38	-34	10	6	1	50	-55	4	14	2	-14	11	9	13	2	43	42
10	2	0	36	36	5	3	1	25	-22	10	7	1	92	-94	4	15	2	84	-86	10	0	2	96	95
10	3	C	-14	-4	5	4	1	-10	-6	10	8	1	33	38	4	16	2	-13	-2	10	1	2	40	-43
10	4	0	-14	1	5	5	1	12	4	10	9	1	23	25	4	17	2	49	-50	10	2	2	38	-43
10	5	0	81	81	5	6	1	29	-28	10	10	1	-14	-3	4	18	2	-14	-3	10	3	2	-14	11
10	6	0	53	45	5	7	1	51	53	10	11	1	-14	-5	4	19	2	72	-68	10	4	2	18	15
10	7	0	118	-125	5	8	1	20	20	11	0	1	-15	4	4	20	2	-16	7	10	5	2	34	-35
10	8	0	27	-25	5	9	1	-11	7	11	1	1	23	19	4	21	2	60	59	10	6	2	60	-61
10	9	0	18	18	5	10	1	-11	-10	11	2	1	-14	0	5	0	2	256	-258	10	7	2	53	55

Table 8. Continued.

H	K	L	F(O)	F(C)	H	K	L	F(O)	F(C)	H	K	L	F(O)	F(C)	H	K	L	F(O)	F(C)	H	K	L	F(O)	F(C)
10	8	2	43	44	5	0	3	127	130	1	2	4	31	-27	6	9	4	18	-15	3	10	5	-13	4
10	9	2	19	-18	5	1	3	320	323	1	3	4	78	76	6	10	4	-13	6	3	11	5	16	10
10	10	2	-14	-2	5	2	3	17	-14	1	4	4	-11	4	6	11	4	-13	-4	3	12	5	24	26
11	0	2	39	43	5	3	3	52	52	1	5	4	171	179	6	12	4	-14	1	3	13	5	98	-103
11	1	2	22	21	5	4	3	-11	0	1	6	4	268	-276	6	13	4	-15	-17	3	14	5	44	-45
11	2	2	15	-16	5	5	3	78	79	1	7	4	364	-379	6	14	4	25	24	3	15	5	40	37
11	3	2	-14	-8	5	6	3	158	-157	1	8	4	161	164	6	15	4	20	17	3	16	5	-14	2
11	4	2	-15	12	5	7	3	213	-209	1	9	4	-12	11	6	16	4	-14	-13	3	17	5	-15	16
0	1	3	472	519	5	8	3	79	78	1	10	4	40	41	7	0	4	165	147	4	0	5	65	-59
0	3	3	95	98	5	9	3	18	-17	1	11	4	13	6	7	1	4	134	-134	4	1	5	27	-28
0	5	3	196	203	5	10	3	34	37	1	12	4	60	54	7	2	4	57	-60	4	2	5	43	44
0	7	3	438	-476	5	11	3	18	-22	1	13	4	194	198	7	3	4	-13	5	4	3	5	-13	-9
0	9	3	71	64	5	12	3	42	37	1	14	4	76	-75	7	4	4	-13	8	4	4	5	35	-37
0	11	3	16	13	5	13	3	170	169	1	15	4	59	-57	7	5	4	97	-97	4	5	5	38	37
0	13	3	213	223	5	14	3	48	-45	1	16	4	17	-18	7	6	4	74	-72	4	6	5	64	63
0	15	3	94	-95	5	15	3	45	-44	1	17	4	42	-38	7	7	4	160	163	4	7	5	42	-38
0	17	3	44	-50	5	16	3	-14	-12	1	18	4	-15	-15	7	8	4	41	43	4	8	5	57	-58
0	19	3	49	-48	5	17	3	33	-31	1	19	4	59	-58	7	9	4	28	-28	4	9	5	-14	15
0	21	3	60	62	5	18	3	-15	-13	1	20	4	54	49	7	10	4	-14	2	4	10	5	17	14
1	0	3	527	-550	5	19	3	35	-34	2	0	4	176	162	7	11	4	-14	5	4	11	5	-14	12
1	1	3	247	238	6	0	3	203	199	2	1	4	105	-100	7	12	4	47	47	4	12	5	-14	-9
1	2	3	99	91	6	1	3	94	-91	2	2	4	81	-74	7	13	4	71	-70	4	13	5	-15	-14
1	3	3	34	34	6	2	3	65	-66	2	3	4	18	19	7	14	4	53	-51	4	14	5	30	29
1	4	3	94	88	6	3	3	-12	11	2	4	4	14	-11	8	0	4	71	-72	4	15	5	-15	0
1	5	3	49	-45	6	4	3	-12	4	2	5	4	58	-58	8	1	4	-14	1	4	16	5	-15	-18
1	6	3	339	355	6	5	3	33	-35	2	6	4	32	-30	8	2	4	42	41	5	0	5	84	-87
1	7	3	20	-24	6	6	3	144	-139	2	7	4	107	105	8	3	4	17	-11	5	1	5	177	-176
1	8	3	194	-194	6	7	3	81	81	2	8	4	56	59	8	4	4	19	-12	5	2	5	34	30
1	9	3	23	-21	6	8	3	112	106	2	9	4	29	-30	8	5	4	-14	15	5	3	5	16	20
1	10	3	101	-100	6	9	3	32	-31	2	10	4	14	-19	8	6	4	33	30	5	4	5	18	-13
1	11	3	15	-17	6	10	3	-13	6	2	11	4	-12	2	8	7	4	-15	-12	5	5	5	79	-80
1	12	3	121	-126	6	11	3	-13	6	2	12	4	24	28	8	8	4	27	-29	5	6	5	82	83
1	13	3	101	100	6	12	3	47	42	2	13	4	44	-44	8	9	4	-14	4	5	7	5	145	143
1	14	3	165	166	6	13	3	37	-39	2	14	4	55	-57	8	10	4	-14	12	5	8	5	60	-59
1	15	3	36	-35	6	14	3	69	-71	2	15	4	32	31	8	11	4	-15	2	5	9	5	27	-24
1	16	3	40	41	6	15	3	27	24	2	16	4	-14	10	8	12	4	22	-22	5	10	5	-14	-1
1	17	3	33	-30	6	16	3	-14	4	2	17	4	-14	0	9	0	4	74	-79	5	11	5	-14	14
1	18	3	-13	-2	6	17	3	-14	8	2	18	4	23	19	9	1	4	101	-103	5	12	5	17	-21
1	19	3	-14	0	6	18	3	-15	2	2	19	4	-15	8	9	2	4	34	36	5	13	5	90	-88
1	20	3	72	-69	7	0	3	217	225	2	20	4	-15	9	9	3	4	-14	15	5	14	5	30	32
1	21	3	-15	10	7	1	3	-13	10	3	0	4	396	403	9	4	4	-14	-10	5	15	5	40	41
2	0	3	444	441	7	2	3	61	-61	3	1	4	73	65	9	5	4	48	-43	6	0	5	16	12
2	1	3	139	137	7	3	3	-12	4	3	2	4	117	-112	9	6	4	40	41	6	1	5	68	69
2	2	3	117	-110	7	4	3	20	-20	3	3	4	-11	6	9	7	4	73	73	6	2	5	-14	1
2	3	3	-10	0	7	5	3	47	47	3	4	4	42	-42	9	8	4	25	-25	6	3	5	24	-26
2	4	3	29	-26	7	6	3	119	-120	3	5	4	-12	2	9	9	4	-15	-16	6	4	5	-14	9
2	5	3	53	52	7	7	3	80	-77	3	6	4	200	-203	10	0	4	-15	-9	6	5	5	-14	9
2	6	3	285	-289	7	8	3	68	68	3	7	4	34	-31	10	1	4	32	31	6	6	5	38	-36
2	7	3	146	-138	7	9	3	19	21	3	8	4	109	110	10	2	4	-15	5	6	7	5	22	-17
2	8	3	192	191	7	10	3	-14	17	3	9	4	-12	1	0	1	5	18	-19	6	8	5	-15	11
2	9	3	19	14	7	11	3	-14	12	3	10	4	47	50	0	3	5	41	46	6	9	5	15	17
2	10	3	42	42	7	12	3	70	69	3	11	4	-12	-2	0	5	5	63	65	6	10	5	-14	9
2	11	3	20	23	7	13	3	-15	6	3	12	4	110	113	0	7	5	79	-81	6	11	5	22	-21
2	12	3	84	85	7	14	3	66	-69	3	13	4	28	32	0	9	5	29	-30	6	12	5	-15	8
2	13	3	63	67	7	15	3	-15	-5	3	14	4	132	-131	0	11	5	-13	15	6	13	5	30	30
2	14	3	135	-137	7	16	3	17	-13	3	15	4	16	-12	0	13	5	16	14	7	0	5	130	-132
2	15	3	46	-44	8	0	3	-14	-9	3	16	4	18	-17	0	15	5	24	24	7	1	5	30	-27
2	16	3	-13	-5	8	1	3	138	-140	3	17	4	20	-11	0	17	5	-14	1	7	2	5	58	58
2	17	3	-13	-12	8	2	3	14	9	3	18	4	-14	2	1	0	5	313	307	7	3	5	-14	3
2	18	3	-14	4	8	3	3	21	20	3	19	4	-15	-1	1	1	5	106	-104	7	4	5	22	-20
2	19	3	-14	-10	8	4	3	-13	-7	4	0	4	56	-56	1	2	5	98	-96	7	5	5	17	-25
2	20	3	54	52	8	5	3	81	-80	4	1	4	124	-119	1	3	5	-12	1	7	6	5	85	83
2	21	3	-15	19	8	6	3	-14	7	4	2	4	28	25	1	4	5	-12	7	7	7	5	43	39
3	0	3	220	-218	8	7	3	137	138	4	3	4	21	28	1	5	5	29	-31	7	8	5	59	-55
3	1	3	258	256	8	8	3	19	-11	4	4	4	-12	10	1	6	5	211	-219	7	9	5	-15	-13
3	2	3	29	29	8	9	3	32	-34	4	5	4	37	-36	1	7	5	58	60	7	10	5	-15	4
3	3	3	115	111	8	10	3	-14	8	4	6	4	20	-17	1	8	5	139	138	7	11	5	-15	6
3	4	3	14	12	8	11	3	-14	10	4	7	4	98	95	1	9	5	-13	10	8	0	5	21	24
3	5	3	223	219	8	12	3	-14	-2	4	8	4	-15	7	1	10	5	24	23	8	1	5	22	-26
3	6	3	222	215	8	13	3	71	-68	4	9	4	57	-54	1	11	5	-13	8	8	2	5	-15	-13
3	7	3	421	-425	8	14	3	-15	3	4	10	4	-13	13	1	12	5	75	84	8	3	5	-14	-6
3	8	3	112	-106	9	0	3	84	81	4	11	4	-13	3	1	13	5	56	-55	8	4	5	-14	1
3	9	3	-15	5	9	1	3	-14	-3	4	12	4	23	-23	1	14	5	105	-104	8	5	5	-14	2
3	10	3	50	-50	9	2	3	29	-28	4	13	4	39	-43	1	15	5	21	19	8	6	5	-15	0
3	11	3	43	40	9	3	3	-14	-9	4	14	4	-14	12	1	16	5	-14	-6	8	7	5	-15	0
3	12	3	61	-60	9	4	3	18	21	4	15	4	41	44	1	17	5	-14	4	8	8	5	-15	2
3	13	3	160	159	9	5	3	27	-23	4	16	4	-14	3	1	18	5	-15	-5	9	0	5	61	-64
3	14	3	68	68	9	6	3	92	-93	4	17	4	-14	8	2	0	5	25	25	9	1	5	-15	15
3	15	3	29	-30	9	7	3	33	37	4	18	4	-14	-5	2	1	5	-12	-4	9	2	5	31	31
3	16	3	14	17	9	8	3	57	59	5	0	4	205	201	2	2	5	18	19	0	0	6	54	60
3	17	3	37	-35	9	9	3	-15	-6	5	1	4	59	-54	2	3	5	20	24	0	2	6	18	-4
3	18	3	-14	14	9	10	3	-14	6	5	2	4	50	-47	2	4	5	-12	-15	0	4	6	27	-35
3	19	3	71	-68	9	11	3	-14	-5	5	3	4	-11	-12	2	5	5	66	-64	0	6	6	30	18
3	20	3	34	-35	9	12	3	-16	19	5	4	4	16	13	2	6	5	39	-39	0	8	6	38	-37
3	21	3	43	41	10	0	3	66	-73	5	5	4	-13	5	2	7	5	88	86	0	10	6	22	17
4	0	3	199	196	10	1	3	17	-21	5	6	4	211	-213	2	8	5	-13	-4	0	12	6	26	33
4	1	3	-11	-9	10	2	3	35	36	5	7	4	-13	14	2	9	5	35	-35	0	14	6	18	-10
4	2	3	74	-73	10	3	3	-14	2	5	8	4	141	139	2	10	5	23	25	1	0	6	49	-50
4	3	3	15	5	10	4	3	19	-20	5	9	4	-13	9	2	11	5	15	-14	1	1	6	146	-142
4	4	3	-10	1	10	5	3	-15	-7	5	10	4	24	22	2	12	5	15	19	1	2	6	24	22
4	5	3	19	-16	10	6	3	51	54	5	11	4	-13	6	2	13	5	14	2	1	3	6	25	25
4	6	3	142	-139	10	7	3	-16	16	5	12	4	43	48	2	14	5	-14	-3	1	4	6	-13	0
4	7	3	-12	11	10	8	3	33	-37	5	13	4	29	-28	2	15	5	17	18	1	5	6	74	-78
4	8	3	113	112	0	0	4	132	130	5	14	4	69	-70	2	16	5	-14	-15	1	6	6	23	24
4	9	3	17	10	0	2	4	52	-58	5	15	4	-14	4	2	17	5	-14	-10	1	7	6	131	135
4	10	3	15	18	0	4	4	39	44	5	16	4	-14	-10	2	18	5	19	-11	1	8	6	34	-30
4	11	3	-12	-2	0	6	4	164	-171	5	17	4	15	10	3	0	5	132	119	1	9	6	41	-40
4	12	3	30	34	0	8	4	125	126	6	0	4	50	-44	3	1	5	202	-201	1	10	6	16	10
4	13	3	-13	-7	0	10	4	-12	12	6	1	4	38	-37	3	2	5	59	-41	1	11	6	-14	14
4	14	3	80	-80	0	12	4	16	14	6	2	4	30	31	3	3	5	-12	-5	1	12	6	-14	-11
4	15	3	-14	2	0	14	4	58	-60	6	3	4	-12	14	3	4	5	-13	12	1	13	6	61	-66
4	16	3	-14	7	0	16	4	24	19	6	4	4	29	-33	3	5	5	122	-122	1	14	6	-15	15
4	17	3	-14	-5	0	18	4	-14	-6	6	5	4	32	-32	3	6	5	103	-101	1	15	6	42	35
4	18	3	16	10	0	20	4	28	24	6	6	4	66	67	3	7	5	230	230	2	0	6	-14	16
4	19	3	-15	6	1	0	4	238	229	6	7	4	49	50	3	8	5	77	75	2	1	6	-14	-5
4	20	3	23	24	1	1	4	371	368	6	8	4	59	-60	3	9	5	47	-46	2	2	6	14	11

Table 8. Continued.

H	K	L	F(O)	F(C)	H	K	L	F(O)	F(C)	H	K	L	F(O)	F(C)	H	K	L	F(O)	F(C)	H	K	L	F(O)	F(C)
2	3	6	21	-24	3	13	6	43	-42	5	10	6	16	16	1	0	7	110	-108	3	3	7	30	-28
2	4	6	-14	11	3	14	6	67	64	5	11	6	-15	-13	1	1	7	47	43	3	4	7	-14	-2
2	5	6	-14	6	4	0	6	40	39	5	12	6	39	-44	1	2	7	60	62	3	5	7	30	31
2	6	6	74	-77	4	1	6	34	-34	6	0	6	43	-42	1	3	7	23	-23	3	6	7	-15	6
2	7	6	-14	-2	4	2	6	22	-25	6	1	6	-15	-16	1	4	7	32	-37	3	7	7	55	-50
2	8	6	42	41	4	3	6	16	-11	6	2	6	15	12	1	5	7	46	49	3	8	7	-15	-7
2	9	6	18	21	4	4	6	-14	-3	6	3	6	-14	-5	1	6	7	80	81	3	9	7	30	28
2	10	6	-14	12	4	5	6	33	-33	6	4	6	-14	12	1	7	7	61	-63	4	0	7	62	-62
2	11	6	-14	1	4	6	6	24	19	6	5	6	-15	4	1	8	7	63	-65	4	1	7	-15	8
2	12	6	-14	4	4	7	6	53	53	6	6	6	-16	1	1	9	7	21	21	4	2	7	22	23
2	13	6	-15	-9	4	8	6	-15	-12	6	7	6	-15	-3	1	10	7	-15	16	4	3	7	-15	1
2	14	6	-15	-6	4	9	6	-14	4	6	8	6	-15	6	1	11	7	-15	-2	4	4	7	-15	-6
2	15	6	-15	-12	4	10	6	-14	-6	6	9	6	-15	7	2	0	7	22	-22	4	5	7	-15	-15
3	0	6	174	-170	4	11	6	-15	-1	7	0	6	-15	-11	2	1	7	62	-59	4	6	7	37	39
3	1	6	84	-81	4	12	6	-15	16	7	1	6	60	63	2	2	7	-14	3	4	7	7	24	18
3	2	6	81	79	4	13	6	25	-25	7	2	6	-15	8	2	3	7	-14	7	4	8	7	23	-18
3	3	6	-14	15	5	0	6	135	-137	7	3	6	16	-20	2	4	7	-14	1	5	0	7	-15	16
3	4	6	38	-41	5	1	6	68	66	7	4	6	-14	-7	2	5	7	16	-14	5	1	7	42	42
3	5	6	48	-47	5	2	6	61	63	7	5	6	39	41	2	6	7	20	24	5	2	7	-15	-10
3	6	6	134	135	5	3	6	-15	-19	7	6	6	-15	12	2	7	7	-16	21	5	3	7	24	-25
3	7	6	71	72	5	4	6	23	-27	0	1	7	-14	-14	2	8	7	16	-12	5	4	7	-15	4
3	8	6	94	-92	5	5	6	41	40	0	3	7	-14	-9	2	9	7	-15	4	5	5	7	40	41
3	9	6	15	-15	5	6	6	97	96	0	5	7	31	-32	2	10	7	-15	-6	0	0	8	72	-72
3	10	6	-14	2	5	7	6	57	-56	0	7	7	45	52	3	0	7	19	-13	0	2	8	35	39
3	11	6	16	13	5	8	6	73	-72	0	9	7	-15	-8	3	1	7	77	80	1	0	8	34	36
3	12	6	45	-46	5	9	6	22	14	0	11	7	-15	-4	3	2	7	-15	7	1	1	8	46	43

An analysis of the thermal parameters of the S and C atoms, assuming the molecule to be a rigid body, was carried out according to the method by Schomaker and Trueblood.[4] The rigid-body tensors arrived at are given in Table 7. The r.m.s. difference between observed and calculated U_{ij}'s is 0.0021 Å^2. Bond lengths which have been corrected according to the libration tensor **L** in Table 7 are given in the first column of Table 1.

Acknowledgements. The authors are indebted to Dr. D. H. Reid, Department of Chemistry, The University, St. Andrews, Scotland, for providing a sample of 6a-thiathiophthene. One of us (A.H.) wishes to thank the *Norwegian Research Council for Science and the Humanities* for financial aid.

REFERENCES

1. Hordvik, A. and Sæthre, L. J. *Israel J. Chem.* **10** (1972) 239.
2. Hansen, L. K. and Hordvik, A. *Acta Chem. Scand.* **24** (1970) 2246.
3. Dingwall, J. G., McKenzie, S. and Reid, D. H. *J. Chem. Soc.* **C 1968** 2543.
4. Schomaker, V. and Trueblood, K. N. *Acta Cryst.* **B 24** (1968) 63.
5. Cruickshank, D. W. J. *Acta Cryst.* **9** (1956) 757; **14** (1961) 896.
6. Leung, F. and Nyburg, S. C. *Chem. Commun.* **1969** 137.
7. Hordvik, A. *Acta Chem. Scand.* **25** (1971) 1583.
8. Johnson, P. L. and Paul, I. C. *Chem. Commun.* **1969** 1014.
9. Birknes, B., Hordvik, A. and Sæthre, L. J. *Acta Chem. Scand.* **26** (1972) 2140; and *to be published.*
10. Hordvik, A. and Sæthre, L. J. *Acta Chem. Scand.* **24** (1970) 2261; **26** (1972) 1729.
11. Hordvik, A. and Sæthre, L. J. *Acta Chem. Scand.* **26** (1972) 3114; and *to be published.*
12. Hordvik, A. and Julshamn, K. *Acta Chem. Scand.* **25** (1971) 1835.
13. Hordvik, A., Sletten, E. and Sletten, J. *Acta Chem. Scand.* **23** (1969) 1852.
14. Hordvik, A. *Acta Chem. Scand.* **25** (1971) 1822.
15. Hordvik, A., Sjølset, O. and Sæthre, L. J. *Acta Chem. Scand.* **26** (1972) 1297; and *to be published.*
16. Johnson, S. M., Newton, M. G. and Paul, I. C. *J. Chem. Soc.* **B 1969** 986.
17. Cruickshank, D. W. J. *Acta Cryst.* **10** (1957) 504.
18. Troughton, P. G. H. *Siemens Review* XXXVII (1970), Fourth Special Issue: X-Ray and Electron Microscopy News.
19. Furberg, S. and Jensen, L. H. *Acta Cryst.* **B 26** (1970) 1260.
20. *International Tables for X-Ray Crystallography*, Kynoch Press, Birmingham 1968, Vol. III, p. 202.
21. Stewart, R. F., Davidson, E. R. and Simpson, W. R. *J. Chem. Phys.* **42** (1965) 3175.
22. Johnson, C. K. *A Fortran Thermal Ellipsoid Plot Program for Crystal Structure Illustrations*, ORNL-3794, Oak Ridge National Laboratory, Tennessee 1965.

Received July 20, 1972.

ACTA CHEMICA SCANDINAVICA 27 (1973) 421–428

The Determination of Hydrogen Basicities in Acetonitrile

p-Nitrobenzyl Triphenylphosphonium Perchlorate as Reference Acid

OLAV VIKANE and JON SONGSTAD

Chemical Institute, University of Bergen, N-5000 Bergen, Norway

p-Nitrobenzyl triphenylphosphonium perchlorate is a valuable reference acid for the determination of hydrogen basicities in acetonitrile, due to the intense colour of the conjugate base, the ylide.

This reference acid, with a pK_a of 21.2 in acetonitrile, is well suited for the determination of pK_a values in the range 15 to 21 which includes the protonated form of the usual aliphatic amines.

For several bases tested, including aliphatic amines and small iorganic anions of varying concentrations and basicities, the ylide absorbance was of identical form with constant half-band width, suggesting the ylide to heteroconjugate or homoconjugate with acids present to only a negligible extent.

For acids, making very strong homoconjugates with their corresponding anions and, with largely unknown homoconjugation constants, K_f, only the sum of the pK_a and the pK_f values can be determined by this method. For hydrazoic acid, nitrous acid, hydroisocyanic acid and acetic acid, the sums of pK_a and pK_f are found to be 19.15, 19.25, 20.0, and 22.0, respectively.

p-Nitrobenzyl triphenylphosphonium perchlorate is too strong an acid to be suitable for the determination of $pK_a + pK_f$ for the very basic cyanide ion.

As pointed out by Parker,[1] the chemistry of anions in dipolar aprotic solvents differs greatly from their chemistry in water and other protic solvents. The greater solvation of the anions in protic solvents increases the dissociation of the conjugate acids and causes a decrease in the hydrogen basicity of the anions in protic solvents relative to the aprotic solvents. This decrease is highly dependent upon the size and polarizability of the anions, and there is consequently no correlation between the hydrogen basicity of anions in protic and aprotic solvents.[2] Furthermore, due to the different solvation of the acid, the hydrogen ion, and the anion in different aprotic solvents, one cannot safely calculate the hydrogen basicity of an anion or a base in one solvent from experiments in another solvent, even an isodielectric one.[3]

Some knowledge of the hydrogen basicity of an ion in a solvent is generally required in order to understand the ion's behaviour in the solvent. The fluoride ion, a weak base in water, is a very strong base in dimethyl sulfoxide,[4] and at elevated temperatures formation of the dimethylsulfinyl carbanion occurs and this may complicate the use of the fluoride ion in this solvent.[5] In acetonitrile, on the other hand, where bases generally are less basic than in dimethylformamide and dimethyl sulfoxide,[3] tetraethylammonium fluoride has been found to be a valuable reagent for proton abstraction.[6] For a general review on elimination reactions promoted by the halide ions, see Ref. 7. Likewise, the cyanide ion in dimethyl sulfoxide and dimethylformamide, apart from being a powerful nucleophile toward aliphatic carbon in these solvents,[8] is able to catalyze the dimerization of aromatic Schiff bases.[9] The choice of solvent and reagent may thus alter the ratio of elimination to substitution in either the desired or undesired direction.[10,11] The hydrogen basicity of an eliminating reagent may also affect the steric course in bimolecular elimination reactions.[12] Finally, accurate pK_a values of the conjugate acids of anions and other bases in aprotic solvents are necessary for an experimental test of the Edwards equation [13] in solvents other than the usual protic ones. The need for determination of hydrogen basicities of anions and other bases in non-aqueous solvents is thus apparent.

From the fundamental works of Kolthoff [14] and Coetzee [15] several methods are now available for the determination of hydrogen basicities in non-aqueous solvents.[3] The glass electrode has been found to be a valuable tool since it responds reversibly to changes in hydrogen ion activity over a very wide range both in acetonitrile [15] and dimethyl sulfoxide.[16,17] Titrations of acids in non-aqueous solutions may be carried out with standard solutions of a tetraalkylammonium hydroxide. Since these solutions always contain protic contaminants and as water is formed during the neutralization, the reliability of this method has been questioned.[18] The indicator method, with coloured indicators, has been used successfully.[19]

We wish to report some studies on the determination of the hydrogen basicity of some bases by a method of the indicator type using *p*-nitrobenzyl triphenylphosphonium perchlorate as the reference acid. The acid-base equilibrium between various onium salts and their corresponding ylides is well documented.[20] Several onium salts, where one or several of the groups attached to the central atom contain both highly electronegative substituents and labile hydrogen on the carbon atom alpha to the central atom, are moderately strong acids. From studies on, especially, acyl onium salts, the acidity is known to depend upon the attached groups, the central atom, and the solvent.[21–26]

When one of the attached groups is a *p*-nitrobenzyl group, the corresponding bases or ylides are highly coloured and are stable in non-aqueous solvents not containing carbonyl groups.[27] *p*-Nitrobenzyl onium salts are stable acids which are easily synthesized and purified, and cover a wide range of acidities according to the hetero-atom and substituents present. Most important, the conjugate base, the ylide, is well suited for quantitative determination by means of UV spectroscopy. The relative acidities of carbon-hydrogen acids are far less dependent upon solvents than are oxygen and nitrogen acids.[25]

As the onium cations useful in this method are of rather similar size and structure, the dependence upon the cation of the calculated pK_a values of the anion's conjugate acids is effectively diminished.[28–30] By using tetraphenylarsonium salts as the source of the anions, as in this work, the cations of the acid and the base will be of the same size and of similar structure.

Acetonitrile was chosen as the solvent due to its very large autoprotolysis constant,[31] the length of the relative scale of acidity, and especially its differentiating effect.[32] Furthermore, salts of large ions are known to dissociate very well in acetonitrile.[33,34]

Although acetonitrile is known to form complexes with Pt(II) substrates through the lone pair electrons on nitrogen,[35] and to act as a proton acceptor in hydrogen bond formation with phenol,[36] acetonitrile is an extremely weak base.[37,38] This makes acetonitrile a poor solvating agent for both the undissociated acids [29,39,40] and their anions.[41,42] As a result, homoconjugation between anions and conjugate acids is far more pronounced in acetonitrile than in other more basic isodielectric solvents like dimethyl sulfoxide and dimethylformamide.[3,17,30] As the homoconjugation constants for a large number of bases in acetonitrile are known,[15] the complexities due to homoconjugation which arise when determining hydrogen basicities in acetonitrile can be easily coped with. Acetonitrile is, however, a sufficiently strong base to cause complete dissociation of perchloric acid.[14,43] The perchlorate salt is therefore used as the source of the *p*-nitrobenzyl triphenylphosphonium cation in this work.

In using *p*-nitrobenzyl triphenylphosphonium perchlorate as reference acid, here called PH^+, the procedure is to determine the amount of ylide, P, given by its absorbance at 510 mμ, for different concentrations of reference acid and added base, B. The following two consecutive equilibria will be established:

$$PH^+ + B \overset{K}{\rightleftharpoons} P + BH^+ \quad (1)$$

$$BH^+ + B \overset{K_f}{\rightleftharpoons} B_2H^+ \quad (2)$$

From the concentration of the ylide, calculated by the usual Benesi-Hildebrand method,[44] the equilibrium constants, K, for the reaction between the reference acid and some amines of known hydrogen basicity in acetonitrile could be calculated allowing for the necessary corrections due to homoconjugation.[15] (See experimental part.)

The plot between the logarithms of the calculated equilibrium constants, and the literature [15] pK_a values in acetonitrile of the protonated form of the tested amines, benzylamine, morpholine, triethylamine, and piperidine, was linear with a slope of 1.07 ± 0.03. The proton acceptor power of these amines was thus found to be independent of the type of reference acid used, as required for a general method. The linear plot suggests the following relation for the calculation of unknown pK_a values in acetonitrile from the equilibrium constant K determined by the present method:

$$pK_a = 1.07^{-1} (\log K + 22.7) \quad (3)$$

In the case of the inorganic anions, cyanate, azide, acetate, and cyanide, the homoconjugation constants in acetonitrile, K_f, are very large and mostly

unknown. Salts of $H(NO_2)_2^-$, $H(CN)_2^-$ and $H(OAc)_2^-$ are known to be stable in acetonitrile.[45] The presence of large counter-ions, as used in this work, will further increase the homoconjugation.[46]

The calculation of equilibrium constants confirmed the existence of the homoconjugation equilibria. The 1:2 reaction of hydrogen ion with the cyanate and the azide ion, where the homoconjugated ions appear to be previously unknown, was further confirmed by IR measurements at 2140 cm^{-1} and 2005 cm^{-1}, respectively,[47] using IR liquid cells and reference acid in excess.

When the homoconjugation constant, K_f, is large and unknown, the present method does not allow the calculation of the pK_a of the corresponding acid of an anion. The measured equilibrium constants will be the product of the equilibrium constants K and K_f. For studies on elimination reactions in dipolar aprotic solvents where small inorganic anions are the eliminating reagent, the sum of the pK_a and the pK_f values will be of more importance than the pK_a values alone.

Attempts were made to determine the equilibrium constant for the reaction between *p*-nitrobenzyl triphenylphosphonium perchlorate and the very basic cyanide ion, but in this case the reference acid was found to be too strong. For all combinations of concentrations of the reference acid and tetraphenylarsonium cyanide, the amount of ylide was found to be identical to the concentration of *p*-nitrobenzyl triphenylphosphonium perchlorate. A minimum value of 23 for $pK_a + pK_f$ of hydrocyanic acid is thus suggested. The experiments with the cyanide confirmed the extinction coefficient of the ylide at 510 mμ as calculated for the less basic bases from the Benesi-Hildebrand plot. No attempt was made to obtain the desired ylide pure as previous attempts to purify this compound have failed.[27]

Even the acetate ion was close to being a too strong base in acetonitrile to allow an accurate determination of $pK_a + pK_f$ of acetic acid. The calculated value, 22.0 ± 0.2, is in good agreement with a previously obtained value, 22.3.[3]

Table 1. Equilibrium constants, K, for $PH^+ + B \rightleftharpoons P + BH^+$ and KK_f for $PH^+ + 2B \rightleftharpoons P + B_2H^+$ at an ionic strength of 0.01 M.

Base (B)	K	KK_f	pK_a(AN)	$pK_a + pK_f$(AN)
Morpholine	1.2×10^{-5} [a]		16.61 [b]	17.61 [b]
Benzylamine	1.8×10^{-5} [a]		16.76 [b]	17.94 [b]
Triethylamine	1.3×10^{-3} [a]		18.46 [b]	18.46 [b]
Piperidine	4.0×10^{-3} [c]		18.92 [b]	20.33 [b]
N_3^-		6.3×10^{-3} [d]		19.15 ± 0.1 [e]
NO_2^-		7.6×10^{-3} [d]		19.25 ± 0.1 [e]
OCN^-		4.7×10^{-2} [d]		20.0 ± 0.1 [e]
CH_3COO^-		7.0 [d]		22.0 ± 0.2 [e]
CN^-		> 100 [d]		> 23 [e]
Reference acid			21.2 [f]	

[a] Calculated by eqn. (9). [b] Ref. 15. [c] Calculated by eqn. (7). [d] Calculated by eqn. (11). [e] From eqn. (3). [f] Calculated from pK_a values of the conjugate acids of amines.[15]

The experimentally determined equilibrium constants and the calculated $pK_a + pK_f$ values are listed in Table 1.

For the amines used in these experiments a correction due to homoconjugation was found to be necessary for only the most basic one, piperidine. When applied to amines, the method described in this work for the determination of hydrogen basicities in acetonitrile thus appears to be best suited when the equilibrium constant K is small.

For all the bases tested, the ylide absorbance at 510 mμ was found to be of identical form with a half-band width of approximately 35 mμ. In the case of the cyanate ion, a slight increase of the absorbance was experienced after some time. This effect was due neither to an aging of the solution of ionic cyanate, nor to a possible Wittig reaction between the ylide and the cyanate ion or the hydrogendicyanate ion, as solutions of the reference acid and tetraphenylarsonium cyanate did not yield any trace of triphenylphosphine oxide even after prolonged periods. The increase may be due to some instability of the $H(NCO)_2^-$ ion yielding basic contaminants.

Kolthoff and co-workers [48] have stressed that caution must be observed in the use of acid-base indicators for the spectrophotometric determination of pK_a values in acetonitrile and other aprotic solvents due to homoconjugation and heteroconjugation between species present. Usually, uncharged oxygen acids like substituted phenols have been used as reference acids. These acids are known to homoconjugate strongly with their conjugate bases, the negatively charged phenolate anions, where the homoconjugates have absorbance spectra different from those of both the phenols and the phenolate anions.

The origin of these difficulties is primarily due to the poor ability of dipolar aprotic solvents to solvate negatively charged ions. Positively charged ions are known to be far better solvated by dipolar aprotic solvents than are anions.[49] Homoconjugation between a reference acid and its conjugate base should therefore be far less pronounced when a positively charged acid is applied, as in this work. The large size of the reference acid and its conjugate base, as in the case of *p*-nitrobenzyl triphenylphosphonium perchlorate, will further reduce the difficulties due to homoconjugation. The identical form of the ylide absorbance, regardless the size, the basicity, and the concentration of the added base, as observed in this work, suggests that the ylide is homoconjugating with acids present only to a negligible extent.

The reference acid used in this work, *p*-nitrobenzyl triphenylphosphonium perchlorate, with a calculated pK_a in acetonitrile of 21.2, appears to be well suited for the determination of pK_a values ranging from 15 to 21. In other, more basic dipolar aprotic solvents where the homoconjugation between small anions and their conjugate acids is far less pronounced,[48] this method may allow the direct determination of the pK_a values of inorganic acids in these solvents. Further applications of this method are being investigated in this laboratory.

EXPERIMENTAL

Acetonitrile was purified with P_2O_5 and CaH_2 as earlier.[47] *Benzylamine*, *morpholine*, *pyridine*, and *triethylamine* were purified according to Coetzee and Padmanabhan.[15]

Tetraphenylarsonium cyanide, *cyanate*, *azide*, and *acetate* were prepared according to the procedure described previously,[47] and were dried to constant weight prior to use.

Tetraphenylarsonium perchlorate was prepared as described by Springer *et al.*[50]

Tetraphenylarsonium nitrite was made by adding a concentrated solution of potassium nitrite to an aqueous solution of tetraphenylarsonium chloride. Tetraphenylarsonium nitrite precipitated immediately. A near quantitative yield was obtained after leaving the reaction mixture in the refrigerator overnight. The solid was washed repeatedly with benzene and ether, dried in vacuum, dissolved in acetonitrile, filtered, and precipitated with ether. The product was finally recrystallized from acetone and dried to constant weight prior to use.

p-*Nitrobenzyl triphenylphosphonium perchlorate* was made from the corresponding bromide by adding an equivalent amount of lithium perchlorate in a water/ethanol mixture. A quantitative amount of the perchlorate precipitated immediately. The salt was washed several times with cold water, then with cold acetone and finally recrystallized twice from acetonitrile. The salt was dried to constant weight prior to use. M.p. 196–197°C.

Stock solutions of the tetraphenylarsonium salts and *p*-nitrobenzyl triphenylphosphonium perchlorate were prepared by weighing the salts immediately after drying, adding acetonitrile and diluting to desired volume. Stock solutions of the amines were made with care to avoid contamination by atmospheric moisture.

Equilibrium mixture of acids and bases were prepared by pipetting from the stock solutions and diluting in volumetric flasks. In the runs where the reference acid was in excess, the concentration of this acid was 1×10^{-2} M. In other cases where the total ionic strength due to the reference acid and the ionic bases was less then 1×10^{-2} M, the necessary amount of tetraphenylarsonium perchlorate was added. The concentrations of both acid and bases were in the 5×10^{-5} M to 1×10^{-2} M range.

The measurements were performed at the absorption maximum of the *p*-nitrobenzyl triphenylphosphonium ylide at 510 mμ. This was the only species in the reaction mixtures absorbing at this wavelength. The method of Benesi and Hildebrand [44] was used to determine the extinction coefficient of the ylide. The calculated extinction coefficient for the ylide from all measured bases and inorganic anions was identical. The UV measurements were performed with a Beckman DB-GT Spectrophotometer using 1 cm quartz cells and cell compartments thermostated at 25 ± 0.3°C.

CALCULATIONS

For the reaction between a base, B, and *p*-nitrobenzyl triphenylphosphonium perchlorate, PH^+, in acetonitrile, the following two consecutive equilibria will be established:

$$PH^+ + B \overset{K}{\rightleftharpoons} P + BH^+ \quad (1)$$

$$BH^+ + B \overset{K_f}{\rightleftharpoons} B_2H^+ \quad (2)$$

K is the equilibrium constant and K_f is the homoconjugation constant as defined by Coetzee and Padmanabhan.[15] P is the ylide. By applying the following relations:

$$[PH^+]_0 = [PH^+] + [P] \quad (4)$$

$$[B]_0 = 2[B_2H^+] + [BH^+] + [B] \quad (5)$$

$$[P] = [BH^+] + [B_2H^+] \quad (6)$$

the following expression for the equilibrium constant K is obtained:

$$K = \frac{[B]_0 - [B]}{[PH^+]_0 - [P]} \quad \frac{[P]}{(2K_f[B] + 1)[B]} \tag{7}$$

where [B] is obtained by solving the equation:

$$K_f[B]^2 + (1 + 2K_f[P] - K_f[B]_0)B - ([B]_0 - [P]) = 0 \tag{8}$$

For small values of K_f, the homoconjugation equilibrium (2) can be neglected, and the combined expressions (7) and (8), by putting $K_f = 0$, reduce to:

$$K = \frac{[P]^2}{([PH^+]_0 - [P])[(B]_0 - [P])} \tag{9}$$

Eqn. (9) was used for all amines except for piperidine, where eqns. (7) and (8) were used.

In the case of the inorganic anions, the 1:2 reaction gives the following equilibrium:

$$PH^+ + 2B \overset{KK_f}{\rightleftharpoons} P + B_2H^+ \tag{10}$$

where KK_f is given by:

$$KK_f = \frac{[P]^2}{([PH^+]_0 - [P])([B]_0 - 2[P]^2)} \tag{11}$$

The equilibrium constants listed in Table 1 are the average values from 4 to 8 measurements with varying concentrations of both the reference acid and the base.

Acknowledgement. The authors are indebted to Dr. O. Foss for valuable suggestions.

REFERENCES

1. Parker, A. J. *Quart. Rev. Chem. Soc.* **16** (1962) 162.
2. Janz, G. J. and Danyluk, S. S. *Chem. Rev.* **60** (1960) 209.
3. Demange-Guerin, G. *Talanta* **17** (1970) 1099.
4. Le Goff, E. *J. Am. Chem. Soc.* **84** (1962) 3975.
5. Corey, E. J. and Chaykovsky, M. *J. Am. Chem. Soc.* **87** (1965) 1345.
6. Hayami, J., Ono, N. and Kaji, A. *Tetrahedron Letters* **1968** 1385.
7. Banthorpe, D. V. *Elimination Reactions*, Elsevier, London 1963, p. 33.
8. Friedman, L. and Shechter, H. *J. Org. Chem.* **25** (1960) 877.
9. Becker, H. D. *J. Org. Chem.* **35** (1970) 2099.
10. McLennan, D. J. *Quart. Rev. Chem. Soc.* **21** (1967) 490.
11. Zook, H. D., Kelly, W. L. and Posey, I. Y. *J. Org. Chem.* **33** (1968) 3477.
12. Zavada, J. and Svoboda, M. *Tetrahedron Letters* **1972** 23.
13. Edwards, J. O. *J. Am. Chem. Soc.* **76** (1954) 1540.
14. Kolthoff, I. M., Bruckenstein, S. and Chantooni, M. K., Jr. *J. Am. Chem. Soc.* **83** (1961) 3927.
15. Coetzee, J. F. and Padmanabhan, G. R. *J. Am. Chem. Soc.* **87** (1965) 5005.
16. Ritchie, C. D. and Uschold, R. E. *J. Am. Chem. Soc.* **89** (1967) 1721.
17. Kolthoff, I. M. and Chantooni, M. K., Jr. *J. Am. Chem. Soc.* **90** (1968) 5961.
18. Kolthoff, I. M. and Chantooni, M. K., Jr. *J. Am. Chem. Soc.* **91** (1969) 25.
19. Clare, B. W., Cook, D., Ko, E. C. F., Mac, Y. C. and Parker, A. J. *J. Am. Chem. Soc.* **88** (1966) 1911.

20. Johnson, A. W. *Ylid Chemistry*, Academic, New York 1966.
21. Issleib, K. and Linden, K. *Ann.* **707** (1967) 120.
22. Bestmann, H. J. *Angew. Chem.* **77** (1965) 609.
23. Johnson, A. W. and Amel, R. T. *Can. J. Chem.* **46** (1968) 461.
24. Aksnes, G. and Songstad, J. *Acta Chem. Scand.* **18** (1964) 655.
25. Mastryukova, T. A., Alajeva, I. M., Suerbayev, H. A., Matrosov, Y. I. and Petrovsky, P. V. *Phosphorus* **1** (1971) 159.
26. Lloyd, D. and Singer, M. I. C. *Chem. Ind. (London)* **1968** 1277.
27. Kröhnke, F. *Chem. Ber.* **83** (1950) 291.
28. Courtot-Coupez, J. and Le Demezet, M. *Bull. Soc. Chim. France* **1969** 1033.
29. Kolthoff, I. M. and Reddy, T. B. *Inorg. Chem.* **2** (1962) 189.
30. Kolthoff, I. M., Chantooni, M. K., Jr. and Bhowmik, S. *J. Am. Chem. Soc.* **90** (1968) 23.
31. Kolthoff, I. M. and Chantooni, M. K., Jr. *J. Phys. Chem.* **72** (1968) 2270.
32. Kreshkov, A. P. *Talanta* **17** (1970) 1029.
33. Coetzee, J. F. and Cunningham, G. P. *J. Am. Chem. Soc.* **87** (1965) 2529.
34. Kay, R. L., Evans, D. F. and Cunningham, G. P. *J. Phys. Chem.* **73** (1969) 3322.
35. Weil, T., Spaulding, L. and Orchin, M. *J. Coord. Chem.* **1** (1971) 25.
36. Gramstad, T. and Sandstrøm, J. *Spectrochim. Acta* **A 25** (1969) 31.
37. Agami, C. and Caillot, M. *Bull. Soc. Chim. France* **1969** 1990.
38. Agami, C. *Bull. Soc. Chim. France* **1969** 2183.
39. Parker, A. J. *Austr. J. Chem.* **16** (1963) 585.
40. Le Demezet, M. *Bull. Soc. Chim. France* **1970** 4550.
41. Joesten, M. D. and Drago, R. S. *J. Am. Chem. Soc.* **84** (1962) 2696.
42. Lindberg, J. J. and Majami, C. *Suomen Kemistilehti* **B 37** (1964) 21.
43. Coetzee, J. F. and Kolthoff, I. M. *J. Am. Chem. Soc.* **79** (1957) 6110.
44. Benesi, J. A. and Hildebrand, J. H. *J. Am. Chem. Soc.* **71** (1949) 2703.
45. Tuck, D. G. *Progr. Inorg. Chem.* **9** (1968) 161.
46. Basolo, F. *Coord. Chem. Rev.* **3** (1968) 213.
47. Austad, T., Songstad, J. and Åse, K. *Acta Chem. Scand.* **25** (1971) 331.
48. Kolthoff, I. M., Chantooni, M. K., Jr. and Bhowmik, S. *J. Am. Chem. Soc.* **88** (1966) 5430.
49. Yamdagni, R. and Kebarle, P. *J. Am. Chem. Soc.* **94** (1972) 2940.
50. Springer, C. H., Coetzee, J. F. and Kay, R. L. *J. Phys. Chem.* **73** (1969) 471.

Received July 20, 1972.

ACTA CHEMICA SCANDINAVICA 27 (1973) 429–432

Initial Thermoelectric Powers of the Quinhydrone-Electrode in Ethanol-Water and Acetonitrile-Water Mixtures

H. HOLTAN and S. ELIASSEN

The University of Trondheim, Norwegian Institute of Technology, Department of Industrial Electrochemistry, N-7034 Trondheim-NTH, Norway

Initial thermoelectric powers of the quinhydrone-electrode were measured in solvent mixtures of ethanol – water and acetonitrile – water. Two different acids, 0.1 M HCl and 0.1 M $HClO_4$, were used as electrolytes. The results show the great influence of the solvent on the initial thermoelectric power. In the acetonitrile – water system the initial thermoelectric power even changes its sign at about 65 wt. % of acetonitrile.

The measurement of the thermoelectric power (ε_0) in an electrolytic thermocell when the Soret effect is hindered is relatively simple and has been carried out for a number of systems. The quinhydrone-electrode has been used by several authors with aqueous solutions of strong acids.[1–5] Measurements in nonaqueous solvents, however, have only been carried out in a few systems. Haase and Jansen [6] have used the silver-silverhalide electrode in pure methanol and *N*-methylformamid, Lin and de Haven [7] have used the hydrogen electrode in ethanol – water mixtures, and Lin [5] has used the quinhydrone-electrode in ethanol – water mixtures.

Studies of the solvent effects on the thermoelectric properties of thermocells may reveal interesting information concerning the structure of the solvent system and the mechanism of hydrogen ion transfer across a temperature-gradient. Lin [5] has suggested that thermoelectric studies on electrolytes in the mixed solvent system should be useful in elucidating such phenomena as ion-ion, ion-solvent, and solvent-solvent interaction. In this connection the initial thermoelectric power was measured using the quinhydrone-electrode with the strong acids HCl and $HClO_4$ in ethanol – water and acetonitrile – water mixtures.

The quinone – hydroquinone (Q – QH_2) system has been considered as the classical organic reversible redox reaction:

$$\tfrac{1}{2}Q - \tfrac{1}{2}QH_2 + H^+ + e^- = 0 \qquad (1)$$

The general equation for the initial thermoelectric power for an electrolytic thermocell containing two kinds of charged particles is given by Holtan.[8]

$$F\,\varepsilon_0 = -\frac{t_-}{z^-}S_a^* - \frac{t_+}{z^+}S_c^* - S_{el}^* - \Delta S + \frac{t_+}{z^+}S_c + \frac{t_-}{z^-}S_a + \Delta N\,S_{solv} + S_{el} \qquad (2)$$

where F is the Faraday, ε_0 the initial thermoelectric power, t the ionic transport number, z the charge, S_a^* and S_c^* are the entropy of transport of the solvated anion and cation, respectively, S_{el}^* and S_{el} the entropy of transport and the molar entropy for the electron, S_c and S_a the partial molar entropy of the cation and anion, ΔS is the entropy change for the electrode reaction, ΔN the number of moles of solvent carried from anode to cathode compartment when one Faraday of electricity has passed through the solution, and S_{solv} is the partial molar entropy of the solvent.

For the thermocell

$$\underset{T_1}{Pt|Q-QH_2|solution|}\underset{T_2}{Q-QH_2|Pt}$$

the solution being a mixture of ethanol – water or acetonitrile – water containing 0.1 m HCl or 0.1 M $HClO_4$, the initial thermoelectric power is given, using eqn. (2), as:

$$F\,\varepsilon_0 = \tfrac{1}{2}(S_{QH_2} - S_Q) - t_{A^-}S_{HA} - S_{el}^* - t_{H^+}S_{H^+}^* + t_{Cl^-}S_{Cl^-}^* + \Delta N_{H_2O}S_{H_2O} + \Delta N_2 S_2 \quad (3)$$

the number 2 referring to the nonaqueous solvent.

Expressions similar to (2) are given by Haase,[9] Agar [10] and Tyrell.[11] Haase [9] has discussed transport numbers and found that using water as frame of reference, the term containing transport of solvent falls out.

EXPERIMENTAL

The cell used for measuring the initial thermoelectric power in this work is earlier described by Tyrell and Hollis [12] and Haase and Schönert.[13]

The reagents used were Merck preparations of *p.a.* quality, distilled water and commercial, redistilled ethanol.

The electrodes consisted of a platinum net dipping into the solution containing 3 g of quinhydrone per liter. This gives an unsaturated solution in water at 298 K and in the solvent mixtures. According to Breck,[3] solutions unsaturated with respect to quinhydrone are the most desireable. The solutions were made by mixing proper amounts of the concentrated acids (HCl and $HClO_4$) with destilled water and acetonitrile or ethanol.

Oxygen was removed by bubbling pure nitrogen through the solution. The quinhydrone was washed with the acidic solution before its addition to the cell.

After filling the cell with the solution there was always a small isothermal emf due to some slight difference in the solutions or electrodes. If the isothermal emf was greater than 50 μV the solution was replaced by a new solution with an isothermal emf lower than 50 μV.

Measurements of emf were made using a potentiometer with a sensitive galvanometer of high resistance. The mean temperature was 298 K and the temperature difference was 10 K.

RESULTS AND DISCUSSION

The cell emf is considered positive when the hot electrode is positive.

Ethanol – water mixtures. The measured initial thermoelectric powers ε_0 are given in Fig. 1. ε_0 is plotted against the weight percent of ethanol. The results are compared with the results previously obtained [5] in 0.01 N HCl.

It has been reported [14] that hydrochloric acid has a tendency to chlorinate quinone and give less reproducible results. In nonaqueous solvents the chlorination should be more prominent. In the present study, however, we have found that the electrode systems are quite stable and that reproducible results are obtained. This has also been noticed by several authors.[5,15]

The entropy of mixing in the water–ethanol system given by Franks and Ives [16] shows a minimum value at about 20 wt. % of ethanol. Lin [5] has compared his results with the entropy of mixing and found a maximum value for the transport number t_{H^+} at about 20 wt. %. The initial thermoelectric power shows no minimum at 20 wt. % but at about 40 wt. %. Other factors than mixing effects must therefore be considered.

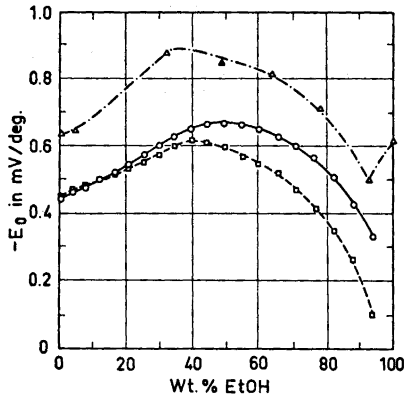

Fig. 1. Initial thermoelectric powers of the quinhydrone-electrode in the ethanol–water system. ○, 0.1 M HCl. □, 0.1 M $HClO_4$. △, 0.01 M HCl taken from Ref. 5.

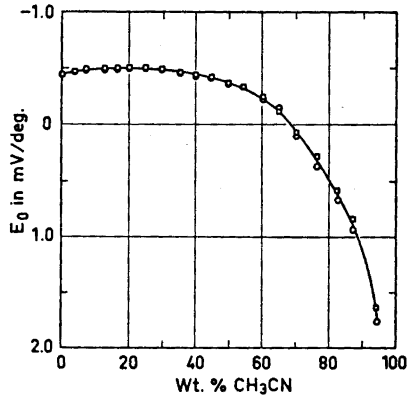

Fig. 2. Initial thermoelectric powers of the quinhydrone-electrode in the acetonitrile–water system. ○, 0.01 m HCl. □, 0.1 M $HClO_4$.

Wear *et al.*[17] have measured the number of grams of solvent transported from the anode to the cathode compartment per Faraday in the ethanol–water system with 0.2 N HCl, using the method first described by Buchböck.[18] The results are unfortunately not of high accuracy but they found that larger increasing amounts of solvent were transported with increasing concentration of ethanol.

Acetonitrile–water mixtures. This system is more complicated than the ethanol–water system. Polarographic investigations of the quinhydrone–electrode [19–20] in pure acetonitrile have showed that the electrode is not reversible. A small addition of water, however, arises the reversibility.[20]

It was therefore surprising to see how reproducible the results were. The measured thermoelectric powers are given in Fig. 2. ε_0 is plotted against wt. % of acetonitrile. The continuous curve is very interesting showing that the initial thermoelectric power changed the sign at about 65 wt. % of acetonitrile.

REFERENCES

1. Khoroshin, A. B. and Temkin, M. N. *Zh. Fiz. Khim.* **26** (1952) 773.
2. Lohonyai, N. and Proszt, J. *Magy, Kem. Folyoirat* **66** (1960) 423.
3. Breck, W. G. *Trans. Faraday Soc.* **59** (1963) 729.
4. Breck, W. G., Gadenhead, G. and Hamnerli, M. *Trans. Faraday Soc.* **61** (1965) 37.
5. Lin, J. *J. Electrochem. Soc.* **116** (1969) 1708.
6. Haase, R. and Jansen, H. J. *Z. physik. Chem. (Frankfurt)* **61** (1968) 310.
7. Lin, J. and de Haven, J. J. *J. Electrochem. Soc.* **116** (1969) 805.
8. Holtan, H. *Electric Potentials in Thermocouples and Thermocells, Thesis,* Utrecht 1953, p. 42.
9. Haase, R. *Thermodynamics of Irreversible Processes*, Addison-Wesley, Reading 1969.
10. Agar, J. N. *Advan. Electrochem. Electrochem. Eng.* **3** (1963) 31.
11. Tyrell, H. J. V. *J. Chem. Soc.* **1963** 3739.
12. Tyrell, H. J. V. and Hollis, G. L. *Trans. Faraday Soc.* **48** (1952) 893.
13. Haase, R. and Schönert, H. *Z. physik. Chem. (Frankfurt)* **25** (1960) 193.
14. Ebert, L. *Ber.* **58** (1925) 175.
15. Ives, D. J. G. and Janz, D. G. *Reference Electrodes*, Academic, New York 1961, p. 302.
16. Franks, F. and Ives, D. J. G. *Quart. Rev. Chem. Soc.* **20** (1966) 1.
17. Wear, J. O., Curtis, J. I. and Amis, E. S. *J. Inorg. Nucl. Chem.* **24** (1962) 93.
18. Buchböck, G. *Z. physik. Chem. (Leipzig)* **55** (1906) 563.
19. Eggins, B. R. and Chambers, J. Q. *J. Electrochem. Soc.* **117** (1970) 186.
20. Wawzonek, S., Berkey, R., Blaha, E. W. and Runner, M. E. *J. Electrochem. Soc.* **103** (1956) 456.

Received June 29, 1972.

ACTA CHEMICA SCANDINAVICA 27 (1973) 433–438

Studies on Orchidaceae Alkaloids

XXXI.* Synthesis of 1-Ethoxycarbonyl-$\Delta^{1,8}$-dehydropyrrolizidine and Some Other Pyrrolizidine Derivatives

SVANTE BRANDÄNGE, BJÖRN LÜNING and CLAES LUNDIN

Department of Organic Chemistry, University of Stockholm, Sandåsgatan 2, S-113 27 Stockholm, Sweden

The UV absorption band at 290 nm previously ascribed to the alkaloid chysin (I) has been shown to be due to the presence of small amounts of 1-methoxycarbonyl-$\Delta^{1,8}$-dehydropyrrolizidine (II), formed by dehydrogenation of I during preparative GLC. The homologous ethyl ester (VI) has been synthesised from the corresponding saturated ester (III). VI has been shown not to be a major product from the dehydration of 1-hydroxy-1-ethoxycarbonylpyrrolizidine (V) with phosphoryl chloride and pyridine. *Exo*- and *endo*-2- and 3-methoxycarbonylpyrrolizidine have been prepared, the 3-isomers by using a trichloroacetylation of the pyrrole XIV as the key step.

The alkaloid chysin (I), characterised in 1968 by Lüning and Tränkner,[2] showed an unaccounted for UV absorption band at 290 nm (ε 40, hexane) which in ethanol [3] shifted to 302 nm. The band disappeared on acidification and was absent in the spectrum of the corresponding sodium carboxylate. It was not possible to demonstrate any Cotton effect associated with the absorption band. The material used in these investigations had been purified by preparative GLC.

In a recent paper [4] we described the synthesis of the racemic ethyl homologue of I (III). After a thorough hydrogenation and purification *via* its picrate, III showed no absorption band in the 300 nm region, which implies that the natural material had been contaminated.

From the spectral results given above, it seemed probable that the contaminating compound was the $\Delta^{1,8}$-dehydroester (II). The UV spectrum obtained is similar to those reported [5] for β-amino acrylic esters. Furthermore, it was possible to remove the absorption band by reduction with sodium tetrahydridoborate in methanol. 1-Ethoxycarbonyl-$\Delta^{1,10}$-dehydroquinolizidine (IV) has previously been transformed into its corresponding saturated ester by the same reagent.[6,7]

* Part XXX, see Ref. 1.

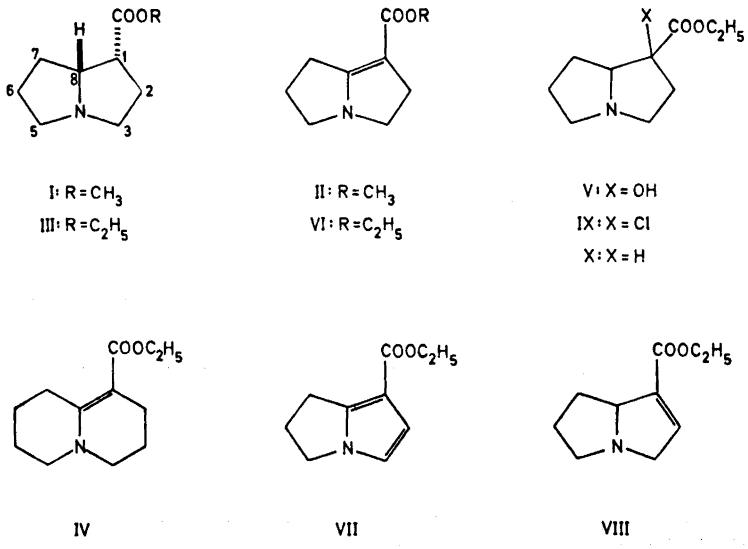

Fig. 1. Only one enantiomer from the racemate III is depicted.

To obtain more convincing evidence for the presence of II in the chysin sample we needed the UV absorption spectrum of II or VI. The latter compound was considered by Kochetkov *et al.* to be an intermediate in their synthesis of (±)-isoretronecanol.[8] In the synthesis, 1-hydroxy-1-ethoxycarbonylpyrrolizidine (V) was treated with phosphoryl chloride and pyridine and the resulting distilled product was considered (no spectral data were given) to be the $\Delta^{1,8}$-dehydroester because its lithium tetrahydridoaluminate reduction product behaved like an enamine.[8,9] In our hands, however, V on treatment with phosphoryl chloride and pyridine yielded after distillation a six-component mixture, the two main components of which were isolated by preparative GLC and characterised by IR, NMR, and mass spectrometry. These two products were identified as the 1-chloroester (IX) and the $\Delta^{1,2}$-dehydroester (VIII). Minor components were the starting material, the $\Delta^{1,8}$-dehydroester (VI), the pyrrolic ester (VII) and another compound, probably the saturated ester (X). The two latter compounds were shown to be disproportionation products from heating the $\Delta^{1,2}$-dehydroester. The main spectral characteristics of our $\Delta^{1,2}$-dehydroester agree with those reported [10] (see also Ref. 11) for 1-methoxycarbonyl-$\Delta^{1,2}$-dehydropyrrolizidine, synthesised by a different route.

Other routes to VI were then investigated. III [4] was transformed into its *N*-oxide (XIX) by reaction with *m*-chloroperbenzoic acid according to the general method of Cymerman Craig and Purushothaman.[12] XIX was then reacted with trifluoroacetic anhydride,[13] a reagent known to favour elimination of a tertiary hydrogen adjacent to nitrogen.[14] In the present case this reaction directly led to the unsaturated ester VI. The *N*-oxide was less suc-

cessfully treated with potassium chromate in water solution, a method for converting *N*-oxides into carbinolamines,[15] favouring elimination of a primary hydrogen adjacent to nitrogen.[16] Other ways to VI were attempted without success. Thus manganese dioxide oxidation of III yielded in excellent yield the pyrrolic compound VII (*cf.* Ref. 17), and treatment of III with triphenylmethyl perchlorate [18] gave no reaction (*cf.* Ref. 19). Compound VI showed a UV absorption maximum at the same wavelength as the sample of chysin, which had been purified by GLC. Based on extinction calculations, the amount of II present in the chysin sample was less than 1 %.

As the chysin sample on which the UV measurement was performed was obtained by preparative gas chromatography and as the separation between III and VI, and hence between I and II, was good, the effect of preparative gas chromatography on III was investigated. When III, which after treatment with sodium tetrahydridoborate showed no absorption band at 303 nm, was subjected to preparative GLC (one injection, col. 160°, det. 180°) an absorption peak (ε 6) was obtained in the spectrum of the collected material. This absorption peak (ε 25) was also obtained when III was stored in chloroform (ethanol-stabilised) solution in the dark at room temperature for eleven days. The mechanism of this reaction might be similar to that proposed for the reaction between tertiary amines and carbon tetrachloride,[20] or might alternatively be an autoxidative attack at H-8 followed by elimination.

In this connexion we also wish to report the syntheses and properties of the 2- and 3-isomers of methoxycarbonylpyrrolizidine. 6-Methoxycarbonyl-3H-pyrrolizine (XI), prepared [21] from methyl 3-(2′-formyl-*N*-pyrryl)propionate, was hydrogenated to *endo*-2-methoxycarbonylpyrrolizidine (XII). Treatment

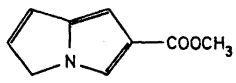

XI

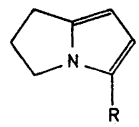

XIV: R=H
XV: R=COCCl$_3$
XVI: R=COOCH$_3$

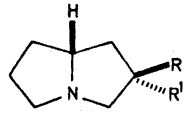

XII: R=H, R^1=COOCH$_3$
XIII: R=COOCH$_3$, R^1=H

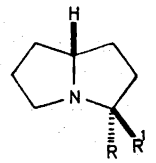

XVII: R=COOCH$_3$, R^1=H
XVIII: R=H, R^1=COOCH$_3$

Fig. 2. Only one enantiomer from each of the racemates XII, XIII, XVII and XVIII is depicted.

of XII with sodium methoxide in methanol gave only a partial epimerisation to the *exo* compound (XIII). Both XII and the mixture of XII and XIII showed after preparative GLC a shoulder around 300 nm (ε 3) which disappeared on acidification. By dehydrogenation of these compounds, it is possible to obtain a $\Delta^{2,3}$-dehydroester. The 3-esters were prepared from 1,2-dihydro-3H-pyrrolizine[22] (XIV), which was acylated in 92 % yield with trichloroacetyl chloride and pyridine at $-80°$ to 1,2-dihydro-5-trichloroacetyl-3H-pyrrolizine (XV). Treatment of XV with sodium methoxide yielded, in analogy with the findings of Houben and Fischer,[23] the methyl ester XVI, which upon hydrogenation was converted to *endo*-3-methoxycarbonylpyrrolizidine (XVII). Epimerisation of XVII with sodium methoxide gave XVII and the corresponding *exo* compound (XVIII) in the ratio 2:98. 3-Methoxycarbonylpyrrolizidine of unknown stereochemistry has previously been synthesised by Seiwerth and Djokic.[24]

EXPERIMENTAL

Melting points are corrected. NMR spectra were recorded on a Varian A-60A, UV spectra on a Beckman DK2 and IR spectra on a Perkin-Elmer 257 spectrometer. Mass spectra were measured on an LKB 9000 instrument equipped with a GLC inlet system (2.8 m 1 % SE-30). Preparative GLC operations were carried out with helium as carrier gas using 20 % SE-52 on Chromosorb AW DMCS in a metal column (0.8 × 240 cm) mounted in an Aerograph A-90-P chromatograph with a hot wire detector, through which the whole sample had to pass. For analytical GLC a Perkin-Elmer 900 instrument was used with a 20 % SE-52 on Chromosorb AW DMCS column (0.2 × 190 cm) and nitrogen as carrier gas.

Dehydration of 1-ethoxycarbonyl-1-hydroxypyrrolizidine (V). The title compound V (6.4 g), on treatment with phosphoryl chloride as described by Kochetkov *et al.*,[8] yielded a mixture (2.85 g), b.p. 59 – 64°/0.5 mm, consisting (GLC, 174°) of six compounds, V – X: *1-Ethoxycarbonyl-$\Delta^{1,2}$-dehydropyrrolizidine (VIII)*, ret. time 3.3 min, nearly 50 % of the total yield. NMR ($CDCl_3$): τ 3.27 (q, 1H). UV (EtOH): 212 nm (ε 7700). IR (CCl_4): 1726 (s) and 1643 (m) cm^{-1}. MS: $M^+ = 181$ (52), 136 (100), 108 (36), 80 (53). Lit.[10] values for the corresponding methyl ester. NMR: τ 3.40 (q, 1H). UV (EtOH): 214 nm (ε 7375). IR (film): 1727 (s), 1645 (m) cm^{-1}. *1-Ethoxycarbonyl-1-chloropyrrolizidine (IX)*, ret. time 4.8 min, nearly 50 % of the total yield. (Found: C 54.9; H 7.34; Cl 16.1; N 6.43; O 14.9. Calc. for $C_{10}H_{16}ClNO_2$: C 55.2; H 7.71; Cl 16.3; N 6.44; O 14.7.) IR (CCl_4): 1743 (s) cm^{-1}. MS: $M^+ = 219$ (2) and 217 (5), 83 (100). *1-Ethoxycarbonyl-$\Delta^{1,8}$-dehydropyrrolizidine (VI)*, ret. time 6.4 min. Its mass spectrum and ret. time were identical with those of the synthetic sample described below. *7-Ethoxycarbonyl-1,2-dihydro-3H-pyrrolizine (VII)*, ret. time 7.1 min. MS: $M^+ = 179$ (37), 150 (70), 134 (100), 106 (47). *1-Ethoxycarbonylpyrrolizidine (X)*, ret. time 3.0 min. (identical with that of III). As this peak appeared only as a shoulder of the much larger peak from the $\Delta^{1,2}$-dehydroester, no mass spectrum was obtained. The shoulder was absent before the distillation. The starting material V had the ret. time 3.9 min.

Disproportionation of 1-ethoxycarbonyl-$\Delta^{1,2}$-dehydropyrrolizidine (VIII). The title compound was heated (200°, 1 h) in a sealed tube. The reaction mixture contained (GLC-MS) large amounts of the pyrrole VII and the saturated ester (X) and smaller amounts of VI and the starting material.

endo-*1-Ethoxycarbonylpyrrolizidine N-oxide (XIX).* A solution of *m*-chloroperbenzoic acid (0.39 g) in chloroform (2.5 ml) was added in portions to a stirred solution of III[4] (0.40 g) in chloroform (2.5 ml). Stirring was continued overnight at room temperature. The concentrated reaction mixture was passed through basic alumina. Chloroform and then methanol-chloroform (1:3) eluted the *N*-oxide, which after evaporation of the solvent, addition of chloroform (100 %), and evaporation and drying in a vacuum de-

siccator weighed 0.36 g (dark oil). Picrate (from EtOH), m.p. 98 – 100°. (Found: C 45.1; H 4.63; N 13.1; O 37.2. Calc. for $C_{16}H_{20}N_4O_{10}$: C 44.9; H 4.71; N 13.1; O 37.4.)

Reaction of XIX with trifluoroacetic anhydride. XIX (40 mg, 0.20 mmol) was dissolved in chloroform (0.5 ml, 100 %) and trifluoroacetic anhydride (72 mg, 0.34 mmol) was added. Water was added after the solution had stood for 30 min, the pH was adjusted to 9 and the chloroform layer was washed twice with water. Most of the Dragendorff-positive material was left in the chloroform layer, which contained (GLC) a mixture of 7 % of VII, 50 % of VI, and approximately 40 % of unidentified products, giving several irreproducible peaks. Pure VI was obtained by preparative GLC (160°). IR (CCl_4): 1679 (s) and 1627 (s) cm^{-1}. UV (hexane): 289 nm (ε 13 000). UV (EtOH): 303 nm (ε 18 000). Retention time on the analytical column, 174°: 6.4 min. MS: $M^+ = 181$ (55), 153 (8) 152 (17), 136 (100), 109 (51), 108 (57).

Reaction of XIX with potassium chromate. XIX (40 mg, 0.20 mmol), dissolved in water (0.5 ml), was mixed with a solution of potassium chromate (58 mg, 0.30 mmol) in water (1.0 ml). The solution was kept at 65° for 15 min and was then cooled and the pH adjusted to 9. Two extractions with chloroform left most of the Dragendorff-positive material in the aqueous layer. The chloroform layer contained (GLC) VI and VII in the ratio 2:1.

Manganese dioxide oxidation of III. A mixture of III [4] (25 mg), active manganese dioxide (Merck, 1.3 g), and methylene chloride (20 ml) was stirred at room temperature for 22 h. The product, which formed a single peak on GLC, was identified (GLC-MS) as VII. The use of 180 mg of MnO_2 and 35 mg of III resulted in approximately 50 % conversion to VII, but no VI was formed.

endo-*2-Methoxycarbonylpyrrolizidine (XII).* The pyrrolizine XI [21] (1.5 g) was hydrogenated over 5 % rhodium on alumina (1.0 g) in acetic acid (25 ml). After 1.5 h the solvent was evaporated, water was added and the solution washed four times with ether. Potassium carbonate was added until pH 9 was reached, XII (contaminated by less than 5 % of the corresponding *exo*-isomer XIII, see below) was extracted with chloroform and was then purified by preparative GLC. (Found: C 63.8; H 8.98; N 8.23; O 19.1. Calc. for $C_9H_{15}NO_2$: C 63.9; H 8.93; N 8.28; O 18.9.)

Epimerisation of XII. XII (50 mg) was added to a solution of sodium methoxide (from 0.1 g of sodium) in methanol (5 ml). The mixture was refluxed for 19 h, after which it was cooled and acetic acid (1 ml) was added. After evaporation of the solvent and addition of water (5 ml), the pH was adjusted to 9 and the aqueous layer extracted with chloroform. Two peaks having approximately the same area were obtained on GLC (116°), ret. times 38.5 min (XII) and 42.5 min (XIII).

1,2-Dihydro-5-trichloroacetyl-3H-pyrrolizine (XV). Pyridine (13.0 g, 0.165 mol), followed by a solution of 1,2-dihydro-3H-pyrrolizine, XIV [22] (5.5 g, 0.051 mol) in methylene chloride (15 ml), were added dropwise to a stirred and cooled solution (– 80°) of trichloroacetyl chloride (9.5 g, 0.052 mol) in methylene chloride (15 ml). The reaction mixture, after being kept cooled (– 80° for 1 h, – 20° for 20 h), was poured onto dilute hydrochloric acid and ice. Extraction with chloroform, washing with water, drying ($MgSO_4$) and evaporation of the solvent left a crystalline residue (11.9 g, 92 %) which could be recrystallised from ether-hexane leaving analytically pure XV, m.p. 84 – 85°. (Found: C 42.9; H 3.23; Cl 42.2; N 5.66; O 6.34. Calc. for $C_9H_8Cl_3NO$: C 42.8; H 3.19; Cl 42.1; N 5.55; O 6.34.) IR (CCl_4): 1672 (s) cm^{-1}.

1,2-Dihydro-5-methoxycarbonyl-3H-pyrrolizine (XVI). XV (11.9 g, 0.047 mol) was dissolved in a solution of sodium methoxide (from 2.0 g of sodium, 0.087 mol) in methanol (200 ml). After 3 h part of the methanol was evaporated and the residue partitioned between hydrochloric acid and chloroform. After drying (Na_2SO_4), the chloroform was evaporated. Distillation at 82 – 84°/0.6 mmHg yielded XVI (5.7 g, 73 %). (Found: C 65.3; H 6.66; N 8.64; O 19.5. Calc. for $C_9H_{11}NO_2$: C 65.4; H 6.71; N 8.48; O 19.4.) IR ($CHCl_3$): 1708 (s) cm^{-1}.

endo-*3-Methoxycarbonylpyrrolizidine (XVII).* The ester XVI (1.0 g) was hydrogenated (23 atm., 25°, 20 h) over 5 % rhodium on alumina in acetic acid (75 ml) and the product was worked up as above, yielding a mixture (0.93 g) consisting (GLC) of XVII (96 %) and the corresponding *exo*-compound (XVIII, 4 %, see below). (Found: C 63.9; H 8.83; N 8.29; O 19.1. Calc. for $C_9H_{15}NO_2$: C 63.9; H 8.93; N 8.28; O 18.9.) IR (CCl_4): 1740 (s) cm^{-1}.

exo-*3-Methoxycarbonylpyrrolizidine (XVIII)*. Treatment of XVII with sodium methoxide in boiling methanol for 4 h afforded (GLC 130°) a mixture of XVIII (98 %) and XVII (2 %). IR (CCl_4): 1748 (s) cm^{-1}.

Acknowledgements. We thank Dr. Ragnar Ryhage for measuring the mass spectra and the *Swedish Natural Science Research Council* for financial support.

REFERENCES

1. Brandänge, S., Lüning, B., Moberg, C. and Sjöstrand, E. *Acta Chem. Scand.* **26** (1972) 2558.
2. Lüning, B. and Tränkner, H. *Acta Chem. Scand.* **22** (1968) 2324.
3. Lüning, B. and Tränkner, H. *Unpublished result.*
4. Brandänge, S. and Lundin, C. *Acta Chem. Scand.* **26** (1971) 2447.
5. Ostercamp, D. L. *J. Org. Chem.* **35** (1970) 1632, and refs. given therein.
6. Goldberg, S. I. and Ragade, I. *J. Org. Chem.* **32** (1967) 1046.
7. Goldberg, S. I. and Lipkin, A. H. *J. Org. Chem.* **35** (1970) 243.
8. Kochetkov, N. K., Likhosherstov, A. M. and Lebedeva, A. S. *Zh. Obshch. Khim.* **31** (1961) 3461; *Chem. Abstr.* **57** (1962) 349e.
9. Kochetkov, N. K. and Likhosherstov, A. M. *Advan. Heterocycl. Chem.* **5** (1965) 337.
10. Tette, J. P., Diss. 1968, State University of New York at Buffalo.
11. Tufariello, J. J. and Tette, J. P. *Chem. Commun.* **1971** 469.
12. Cymerman Craig, J. and Purushothaman, K. K. *J. Org. Chem.* **35** (1970) 1721.
13. Cave, A., Kan-Fan, C., Potier, P. and Le Men, J. *Tetrahedron* **23** (1967) 4681.
14. Michelot, R. *Bull. Soc. Chim. France* **1969** 4377.
15. Bentley, K. W. and Murray, A. W. *J. Chem. Soc.* **1963** 2497, and refs. given therein.
16. Hellman, J. W. *Diss. Abstr.* **B 22** (1962) 2196.
17. Culvenor, C. C. J., Edgar, J. A., Smith, L. W. and Tweeddale, H. J. *Austr. J. Chem.* **23** (1970) 1869, and previous works.
18. Dauben, H. J., Jr., Honnen, L. R. and Harmon, K. M. *J. Org. Chem.* **25** (1960) 1442.
19. Volz, H. and Kiltz, H. H. *Ann. Chem.* **752** (1971) 86.
20. Unger, F. M. *Diss. Abstr.* **B 29** (1969) 2821.
21. Flitsch, W. and Heidhues, R. *Chem. Ber.* **101** (1969) 3843.
22. Schweitzer, E. E. and Light, K. K. *J. Am. Chem. Soc.* **86** (1964) 2963.
23. Houben, J. and Fischer, W. *Chem. Ber.* **64** (1931) 2636.
24. Seiwerth, R. and Djokić, S. *Croat. Chem. Acta* **29** (1957) 403.

Received July 1, 1972.

ACTA CHEMICA SCANDINAVICA 27 (1973) 439–444

Aggregation of Di(isononyl)ammonium Chloride in Chloroform Solution, and Extraction of Zinc Chloride

BJÖRN WARNQVIST

Department of Inorganic Chemistry, Royal Institute of Technology, S-100 44 Stockholm, Sweden

The aggregation of a secondary aliphatic ammonium salt, di(3,5,5-trimethyl)ammonium chloride, $[(CH_3)_3C_6H_{10}]_2NH_2Cl$, "DINAHCl", in dry chloroform has been studied by osmometric measurements. The data indicate that the ammonium salt in this solvent exists as a dimer $(DINAHCl)_2$(org) only. This result is consistent with that of an earlier emf study.[1] Distribution data for a metal ion, Zn^{2+}, between 1 M $(H^+)Cl^-$(aq), and DINAHCl in $CHCl_3$, are in agreement with a constant aggregation number for the ammonium salt.

In a previous communication [1]* the results of a study, mainly by two-phase emf measurements, on the system diisononylamine (=DINA=di(3,5,5-trimethylhexyl)amine)-HCl-$CHCl_3$-H_2O (1 M LiCl) were presented. Within the concentration range and the accuracy of the data practically all the ammonium salt formed in the organic phase was found to be dimeric, $(DINAHCl)_2$. In this paper a further study using osmometry is reported together with some distribution experiments with zinc chloride.

EXPERIMENTAL

Chemicals. For DINA and HCl, see Ref. 1a. Chloroform (Merck, *p.a.*) was shaken 3–4 times with water to remove the ethanol. For osmometry it was desiccated on an alumina column. The amount of water present after desiccation was checked by Karl Fischer titration, and found to be less than 1 mM, close to the detection limit of the method.

DINAHCl(s) was prepared as described previously.[1] It was recrystallized twice from hexane. For the osmometric study it was dried over P_2O_5. Zinc chloride (Merck, *p.a.*) was used without further purification. All aqueous solutions were prepared using doubly distilled water.

Zinc-65 chloride was obtained from Amersham, England, in the form of an 0.0223 M solution in 0.1 M HCl.

* A misprint in Ref. 1a should be corrected: Near the bottom of page 1365, *read* $(Z_{HCl} < 1)$ . . .

Osmometric measurements were made at 25.0°C using a Mechrolab Vapor Pressure Osmometer Model 301A and at 30°, 35° and 40°C using a Hitachi Perkin Elmer Molecular Weight Apparatus, Model 115. The resistance difference, ΔR, between matched thermistors, one with a drop of solution, the other with solvent, was recorded every minute, 2 – 12 min after application of the solution drop. Runs were made at least in duplicate with each solution in order to check reproducibility. Distribution experiments: Solutions in stoppered tubes of $ZnCl_2$ in 1 $M(H^+)Cl^-$ (10.0 ml) were equilibrated with DINAHCl in $CHCl_3$ (10.0 ml) by slow rotation. After centrifugation, aliquots were withdrawn from each phase for γ counting. All experiments were made in a room thermostated at 25 ± 0.5°C.

OSMOMETRIC RESULTS

Solutions of DINA chloride in chloroform were studied, as well as solutions of DINA (base) and of benzil (as standard) in the same solvent.

ΔR values taken at a constant time = 12 min after application of the solution drop were used (ΔR values obtained by extrapolating experimental ΔR *vs.* time curves to time = 0 were found not to produce significantly different final results; *cf.* below). The results are shown in Fig. 1 as a plot of $\Delta R/C$

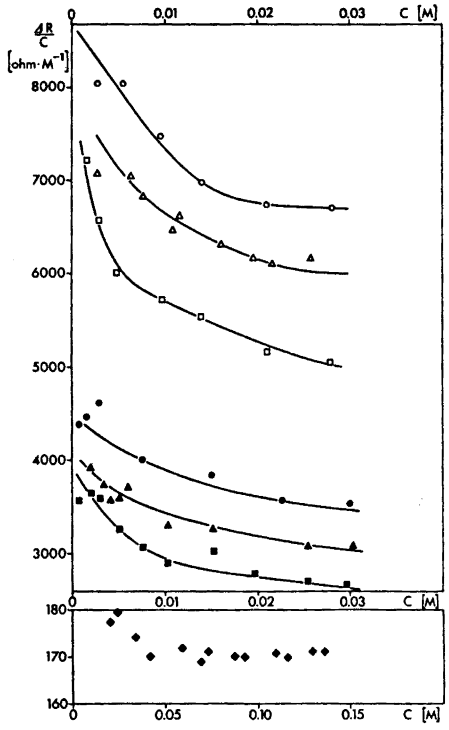

Fig. 1. $\Delta R/C$ plotted *versus* C for DINAHCl (filled symbols) and benzil (open symbols) in chloroform. ■ □, 40°C. ▲ △, 35°C. ● ○, 30°C. ◆, 25°C. ($\Delta R/C$ for DINA at 25°C = 315 ± 3.) Averaged calibration curves drawn through the benzil points. Average curve corresponding to $\bar{n} = 2$ drawn through the DINAHCl points at 30 – 40°C.

vs. C where C is total concentration in M (mol l^{-1}). See also Table 1. The amine base form, DINA, gave very nearly the same results as benzil, *i.e.*, it may be regarded as monomeric in chloroform solution.

Table 1. Osmometric data for DINAHCl in $CHCl_3$, given as C, ΔR.

25°C:	0.1353, 23.14; 0.1280, 21.90; 0.1152, 19.60; 0.1082, 18.48; 0.0922, 15.75; 0.0866, 14.72; 0.0735, 12.55; 0.0693, 11.65; 0.0588, 10.10; 0.0416, 7.06; 0.0333, 5.80; 0.0235, 4.22; 0.0200, 3.55;
30°C:	0.03013, 106.94; 0.02276, 80.94; 0.01506, 57.80; 0.00753, 30.06; 0.00301, 13.90; 0.00151, 6.72; 0.00075, 3.30;
35°C:	0.03038, 94.06; 0.02550, 78.34; 0.01519, 49.74; 0.01020, 33.70; 0.00608, 22.60; 0.00510, 18.32; 0.00409, 14.60; 0.00304, 11.30; 0.00204, 8.00; 0.00127, 6.16;
40°C:	0.02952, 78.70; 0.02538, 69.16; 0.01972, 55.00; 0.01527, 46.10; 0.01026, 29.50; 0.00763, 23.35; 0.00513, 16.74; 0.00305, 10.96; 0.00205, 7.54; 0.00076, 2.72.

The following equations apply:

$$\Delta R = k_{R1}S + k_{R2}S^2 \tag{1}$$

$$S = c + K_2c^2 + \cdots + K_nc^n \tag{2}$$

$$C = c + 2K_2c^2 + \cdots + nK_nc^n \tag{3}$$

$$\bar{n} = C/S \tag{4}$$

where k_{R1} and k_{R2} are proportionality factors, which may usually be considered constant at constant temperature for a given solvent; S is the concentration of solute molecules, in M; c is the concentration of monomeric solute, in M; $\bar{n}$ is the average aggregation number; K_n is the equilibrium constant for the reaction

$$nA \rightleftharpoons A_n$$

where A is the solute. The parameters, k_{R1} and k_{R2}, were evaluated from measurements with benzil (and DINA at 25°C). Preliminary calculations indicated, in agreement with previous results,[1] that $\bar{n} \approx 2$ over the whole concentration range studied and that values of $n > 2$ need not be considered.

In the calculations a version [2c] of the general minimization program LETAGROP [2] was employed. The quantity (error squares sum) minimized was either

$$U_1 = \sum(\Delta R_{calc} - \Delta R)^2 \tag{5a}$$

or

$$U_2 = \sum((\Delta R_{calc} - \Delta R)/\Delta R_{calc})^2 \tag{5b}$$

where the sum was taken over experimental points in the C range $7 \times 10^{-4} - 3 \times 10^{-2}$ at each of the temperatures 30, 35, and 40°C, and in the range 0.02 – 0.15 M at 25°C. ΔR_{calc} was computed using eqns. (3), (2), and (1). These calculations indicated that within accuracy of the data diisononylammonium chloride is dimeric in chloroform, *i.e.* it was found that $K_2 \geq 10^6$ M^{-1} at 30 – 40°C. (The results obtained with the Mechrolab Osmometer in the range $C < 0.02$ M at 25°C suggested some monomer formation.[1b] These data were found to be of lower precision, however, and were not included in the final treatment of the material.)

However, the computer program available [2c] does not, at present, allow a strict evaluation of curved plots of $\Delta R/C$ *vs.* C of the type found experimentally both for benzil and DINAHCl, at 30 – 40°C (*cf.* Fig. 1). Such a case

may be dealt with either by adding higher-order term(s) to the right hand side of eqn. (1), or by fitting an exponential calibration curve.[3]

A third possibility is the evaluation of $\bar{n}$ from

$$\bar{n} = (\Delta R/C)_{\text{ref}}/(\Delta R/C)_{\text{DINAHCl}} \tag{6}$$

at each individual C value; *i.e.*

$$\bar{n} = \frac{k_{R1}(C) + k_{R2}(C)C}{k_{R1}(C)\bar{n}^{-1} + k_{R2}(C)C\bar{n}^{-2}} \tag{7}$$

where it has been indicated that k_{R1} and k_{R2} (obtained from the monomeric calibration substance, *e.g.*, benzil) may vary with C.

Eqn. (7) becomes a simple identity if $k_{R2}(C) = 0$ for all C values, and eqn. (6) may then be applied directly. This was the case for the data at 25°C. Data at the other temperatures were treated by applying eqn. (7) iteratively. The resulting final $\bar{n}$ values have been plotted as a function of C in Fig. 2; it is

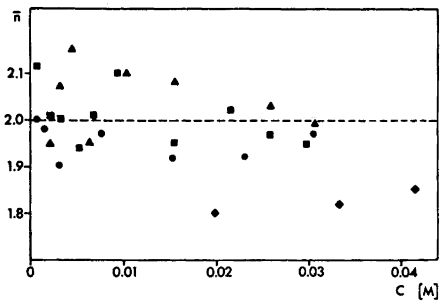

Fig. 2. Mean aggregation number, $\bar{n}$, plotted as a function of C for DINAHCl in chloroform at temperatures 25 – 40°C. Same symbols as in Fig. 1. (Points at 25°C with C values 0.05 – 0.14 M all have $\bar{n}$ values in the range 1.82 – 1.86.)

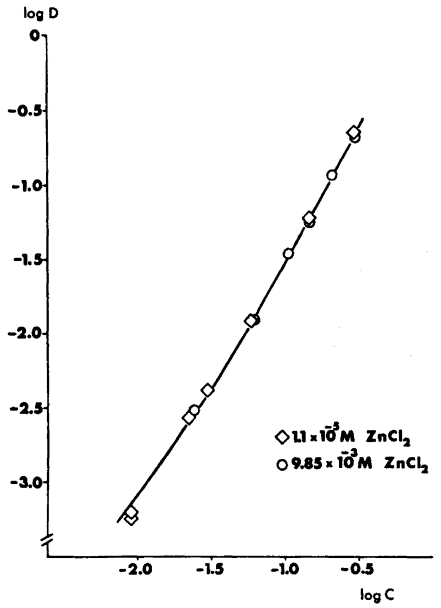

Fig. 3. Log of distribution ratio for $ZnCl_2$ between chloroform and 1 M $(H^+)Cl^-(aq)$ as a function of log C (DINAHCl) at 25.0°C. The curve has been computed using $K_{11}' = 0.1108$ M^{-1} and $K_{12}' = 9.40$ M^{-2}.

seen that, within the limits of error (± 5 % at 30 – 40°C; ± 10 % at 25°C), $\bar{n} = 2$ at all C values and temperatures considered. From the experimental error limits the following lower limits for K_2 can be estimated:

$K_2 \gtrsim 10^5$ M^{-1} at 30 – 40°C ($C \gtrsim 0.001$ M)

and $K_2 \gtrsim 2 \times 10^3$ M^{-1} at 25°C ($C \gtrsim 0.02$ M)

DISTRIBUTION OF $ZnCl_2$

The distribution equilibrium of $ZnCl_2$ between an organic phase, C M DINAHCl in $CHCl_3$, and an aqueous phase, Zn^{2+} in 1.00 M $(H^+)Cl^-$, has been studied. Two different initial concentrations of $ZnCl_2$(aq), 1.1×10^{-5} M and 1×10^{-2} M were used, and C was varied throughout the range 0.01 – 0.3 M. The data have been plotted in Fig. 3 as log D_{Zn} *vs.* log C, where

$$D_{Zn} = \frac{[ZnCl_2(org)]}{[ZnCl_2(aq)]} = \frac{^{65}Zn \text{ activity(org)}}{^{65}Zn \text{ activity(aq)}} \quad (6)$$

See also Table 2.

Table 2. Distribution data for Zn(II) between 1 M $(H^+)Cl^-$ and C M DINAHCl in $CHCl_3$ at 25°C, given as C, D_{Zn}; where D_{Zn} is the average of two determinations (*cf.* Fig. 3).

[Zn(II)] (initial) = 1.11×10^{-5} M: 0.0091, 0.00060; 0.0227, 0.00266; 0.0297, 0.0040; 0.0300, 0.00397; 0.0600, 0.0120; 0.149, 0.0595, 0.298, 0.2222;
[Zn(II)] (initial) = 9.85×10^{-3} M: 0.0242, 0.00294; 0.0605, 0.0118; 0.1059, 0.0337; 0.1482, 0.0568; 0.2117, 0.1150; 0.2965, 0.211.

The experimental points in Fig. 3 all seem to fall on a nearly straight line with slope ≈ 1.7, independent of $ZnCl_2$ concentration. This would suggest that $ZnCl_2$ is extracted in the form of homo-nuclear complexes with n and (mainly) $2n$ DINAHCl units; according to the osmometric results, $n = 2$:

$$ZnCl_2(aq) + (DINAHCl)_2(org) \rightleftharpoons ZnCl_2(DINAHCl)_2(org) \quad (K_{11}') \quad (7a)$$

$$ZnCl_2(aq) + 2(DINAHCl)_2(org) \rightleftharpoons ZnCl_2[(DINAHCl)_2]_2(org) \quad (K_{12}') \quad (7b)$$

In addition, we have the equilibria between Zn^{2+} and Cl^- in the aqueous phase. Since, however, the Cl^-(aq) concentration is constant the proportions of $Zn^{2+} - Cl^-$ complexes in the aqueous phase are constant, and correspond to a constant factor included in K_{11}' and K_{12}'.

A preliminary graphical treatment of the data indicated $K_{11}' = 0.136$ and $K_{12}' = 9.3$. The data were then treated by a special version of the LETAGROP program,[2,4] minimizing the quantity

$$U = \sum(\log D_{Zn}(calc) - \log D_{Zn})^2$$

The full drawn curve in Fig. 3 has been calculated using the following values, obtained in the LETAGROP treatment:

$$K_{11}' = 0.1108 \pm 0.0052 \text{ M}^{-1}$$

$$K_{12}' = 9.40 \pm 0.21 \text{ M}^{-2}$$

(The standard deviations (σ) are quoted.)

It is worth mentioning that as long as the aggregation number is constant the system can be treated formally as a mononuclear one.

DISCUSSION

The dimeric state of DINAHCl in chloroform found in this work is consistent with the previous two-phase emf work [1] at 25°C.

Besides the present work, and Ref. 1, the only published study of secondary ammonium halides in chloroform seems to be that by Casey *et al.*[5] Their two-phase emf titrations and v.p. osmometry data for dilaurylammonium halides, DLAHX, were explained in terms of a monomer-dimer equilibrium; K_2 (*cf.* eqns. (2) and (3)) being 400 ± 100 M^{-1} for $X^- = Cl^-$ at 25°C; lower K_2 values were found for $X^- = Br^-$ and I^-.

The aggregation of long-chain ammonium salts in chloroform does not seem to proceed beyond dimers in the systems studied so far,[6a] and the results in this paper are consistent with these results. A comparison with the results of Casey *et al.* shows that DINAHCl has a larger dimerization constant than DLAHCl. Perhaps the branching of the hydrocarbon chains in DINAHCl permits less interaction with the solvent, thus promoting dimerization.

In the general case the degree of association varies with composition.[6b,7,8] Nevertheless, metal extraction as well as excess acid extraction is often "best" described with mononuclear complexes only, a fact which still remains to be fully understood.

Acknowledgements. I am indebted to the late Professor L. G. Sillén for his interest in this work. Thanks are due to Professor S. Ahrland and to Dr. E. Högfeldt for valuable discussions, to Ing. F. Fredlund for experimental assistance, and to Dr. D. Lewis for revising the English of the paper.

This work has been supported by *Statens Naturvetenskapliga Forskningsråd (Swedish Natural Science Research Council).*

REFERENCES

1. a. Warnqvist, B. *Acta Chem. Scand.* **21** (1967) 1353; b. Warnqvist, B., *Diss.*, KTH, Stockholm 1971.
2. a. Ingri, N. and Sillén, L. G. *Arkiv Kemi* **23** (1964) 97; b. Sillén, L. G. and Warnqvist, B. *Arkiv Kemi* **31** (1969) 315; c. Warnqvist, B. *Chemica Scripta* **1** (1971) 49.
3. van Ooyen, H. and Zangen, M. *Private communication*, 1971.
4. Liem, D. H. *Acta Chem. Scand.* **25** (1971) 1521.
5. Casey, A. T., Catrall, R. W. and Davey, D. E. *J. Inorg. Nucl. Chem.* **31** (1971) 535.
6. Marcus, Y. and Kertes, A. S. *Ion Exchange and Solvent Extraction of Metal Complexes*, Wiley-Interscience, New York 1969, (a) p. 763, (b) p. 790.
7. Högfeldt, E. In Kertes, A. S. and Marcus, Y., Eds., *Solvent Extraction Research*, Wiley, New York 1969, p. 157, and references quoted therein.
8. Kuča, L. and Högfeldt, E. *Acta Chem. Scand.* **22** (1968) 183.

Received August 22, 1973.

ACTA CHEMICA SCANDINAVICA 27 (1973) 445–452

Some Characteristics and Control of Pantothenate Transport in *Escherichia coli* U-5/41

PEKKA MÄNTSÄLÄ

Department of Biochemistry, University of Turku, SF-20500 Turku 50, Finland

Properties and formation of the pantothenate transport system in *Escherichia coli* U-5/41 were investigated. The results in this paper suggest the existence of an active transport process, which is formed constitutively.

Transport activity was inhibited by 2,4-dinitrophenol and sodium azide. The K_m value for pantothenate uptake was approximately 2.5×10^{-5} M. Pantothenate transport was temperature- and pH-dependent, the respective optima being 45 – 50° and 4.0 – 4.5.

Exit was prevented by some monovalent ions and also by glucose ($10^{-2} - 5 \times 10^{-1}$ M) when the cells were precultured for at least 2 h in the glucose minimal medium.

Pantothenate was transported into the cells of *E. coli* without phosphorylation and transport activity was reduced by osmotic shock. Pantothenate-binding activity was demonstrated in the concentrated shock fluid, in the ammonium sulphate precipitate and in the Sephadex G-100 eluate.

Biological transport systems have received much attention during the last few years. Attention has also been paid to the systems by which most vitamins of the B group are taken up by microorganisms.[1–5] It has long been recognized that the transport process is usually not one of passive diffusion but involves the functioning of an active permeation process, which may exhibit general regulatory patterns. Although much has been learned about the specific components and their possible relationships to the transport of carbohydrates,[6,7] little is known of the manner in which charged compounds, including several vitamins, are transported. Kawasaki *et al.*[1] reported that membrane thiamine kinase participated in the uptake of thiamine, a process by which this vitamin is accumulated as thiamine pyrophosphate against a concentration gradient. DiGirolamo and Bradbeer [4] found that *E. coli* has an initial vitamin B_{12}-binding system with a high affinity for vitamin B_{12} coupled with a large B_{12} storage capacity.

In a preliminary report of this work some properties of the pantothenate transport system in *E. coli* were outlined.[8] In the present study this system is further characterized. Evidence is presented that the uptake of pantothenate

is dependent on temperature, pH and energy supply. Furthermore, formation of the uptake system has been shown to be constitutive, and acumulation of pantothenate occurs without phosphorylation. Pantothenate-binding activity was demonstrated in the shock fluid.

EXPERIMENTAL

Materials. [^{14}C]-D-Pantothenate was obtained from the New England Nuclear Corporation, Boston, Mass. All chemicals were from commercial suppliers.

Organism and growth media. The test organism, *Escherichia coli* U-5/41, was cultured in a minimal salt medium [9] containing 0.2 % or 10 mmol of a carbon compound.

Cultivation. Bacteria were grown with aeration at 37° until the exponential phase of growth. In the experiments on the formation of the pantothenate transport system during growth, samples were withdrawn at intervals of 1 h. Growth was estimated from the turbidity measurements made with a Klett-Summerson colorimeter fitted with a No. 62 filter. The cells (about 0.1 mg of dry weight) were collected by centrifugation at 4° and washed with cold minimal salt solution.

Measurement of pantothenate uptake. The samples were preincubated for 3 min at 45° in the presence of chloramphenicol (100 μg/ml) and the uptake process was then initiated by adding 0.1 ml of the preincubated minimal salt solution containing 60 000 cpm of [^{14}C]-D-pantothenate and 0.05 mM D-pantothenate. Initial velocities were measured by stopping incubation at intervals of 30 sec with cold 0.1 M sodium chloride containing 10 mM pantothenate. The cells were filtered on a Millipore membrane filter (0.45 μ pore size) and washed for 3 min with the same cold sodium chloride solution. The filters were removed from the suction apparatus immediately, dried, and placed in counting vials containing 5 ml of toluene-based scintillation fluid. Uptake rates are expressed as nanomoles of labelled compound per milligram of bacteria (dry weight) per minute.

Identification of accumulated compounds. The cells (0.4 mg) were incubated for 2, 4, 10, 20, and 60 min, then deposited on a Millipore filter and washed for 10 min as described above. [^{14}C]-Pantothenate was extracted from the cells by incubating them for 15 min in 50 % ethanol at 25° or for 15 min in 0.01 M sodium acetate buffer, pH 4.5, at 85°. The suspensions were centrifuged at 5 000 *g* and the supernatant was lyophilized and dissolved in 0.1 ml of water. The samples were chromatographed on paper with a 1-butanol : acetic acid : water (25:4:10) developing system.

Exit measurements. The cells (0.1 mg dry weight) from the exponential phase of growth were centrifuged and washed with mineral salt solution. The samples were then incubated at 45° for 30 min in the presence of 0.1 ml of [^{14}C]-pantothenate. After incubation the cells were washed with various salt solutions or with glucose.

Measurement of binding activity. For the preparation of binding material the washed cells were treated by the method of Neu and Heppel [14] with 0.05 M Tris-HCl buffer (pH 7.5), which contained 0.001 M EDTA and 20 % sucrose. The solution was shaken for 10 min at 30°, and the cells, when they had been centrifuged, were osmotically shocked with 5×10^{-4} M $MgCl_2$. The supernatant (15 000 *g*) was lyophilized and the binding activity determined by equilibrium dialysis. The dialysis bags contained 0.2 ml of concentrated shock fluid and this was dialyzed for 24 h at 4° against 0.05 M Tris-HCl buffer (pH 7.5) containing 5000 cpm/ml of [^{14}C]-pantothenate (specific activity 4.75 mCi/mmol). The radioactivity of the samples (0.1 ml) was measured as described above.

Partial purification of the binding material. Unless specified otherwise, purification procedure was carried out at 4 – 6°. The lyophilizate (140 mg) was dissolved in cold 0.05 M potassium phosphate buffer (pH 7.0). Centrifugation of the resulting solution (50 000 *g*, 1 h) was followed by concentration with ammonium sulphate up to 40 % saturation. The insoluble material was discarded. Additional ammonium sulphate (up to 80 % saturation) was added, the pH adjusted to 7.0, and the precipitate collected by centrifugation. The precipitated material was dissolved in 10 ml of potassium phosphate buffer (pH 7.0) and applied to a column of Sephadex G-100, which had been pre-equilibrated with the same buffer. The eluted fractions were tested for binding activity and the active fractions were combined and concentrated by addition of ammonium sulphate. Disc electrophoresis was carried out as described originally by Ornstein and Davies and modified by Chang *et al.*[11]

RESULTS

The time course of the uptake of pantothenate by the cells of strain U-5/41 at various temperatures is shown in Fig. 1. The transport reaction proceeded linearly for at least 10 min under the conditions used. However, cells incubated

Table 1. Effect of 2,4-dinitrophenol and sodium azide on pantothenate uptake.[a]

Compound		Activity (%) Preincubated	Added to the reaction mixture
None		100	
2,4-Dinitrophenol	0.1 mM	94	98
»	0.5 mM	65	85
»	1.0 mM	28	60
Sodium azide	1.0 mM	90	95
»	5.0 mM	70	90
»	10.0 mM	33	82

[a] Experimental conditions are the same as those given in the legend to Fig. 4.

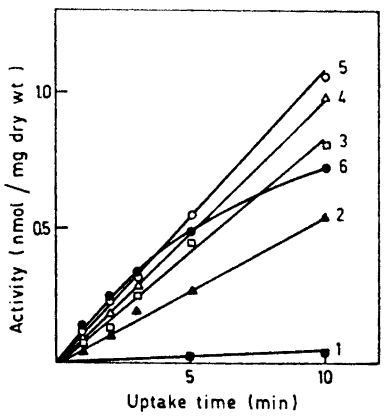

Fig. 1. Effect of temperature on the time course of pantothenate uptake. Cells of *E. coli* U-5/41 were harvested from exponentially growing cultures in glucose minimal medium and resuspended in 0.1 ml of mineral salts solution. The cell suspension (0.1 mg dry weight) was then incubated in the presence of 60 000 cpm of [^{14}C]-D-pantothenate and 0.05 mM D-pantothenate. Initial velocities were measured as described in the text. 1, at 0°; 2, at 30°; 3, at 40°; 4, at 45°; 5, at 50°; 6 at 55°.

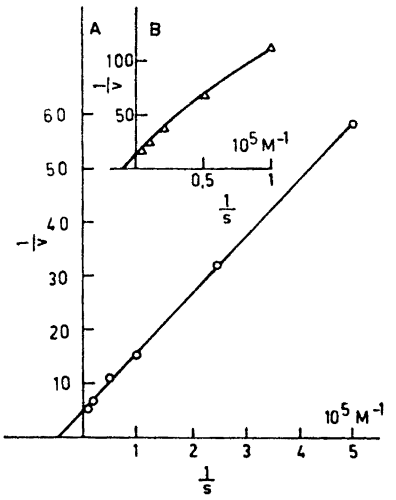

Fig. 2. Concentration dependence of pantothenate transport. Time course curves were obtained for each substrate concentration. Other experimental conditions are described in the text. A, radioactivity taken up at 45°; B, radioactivity taken up at 25°. Activity is expressed as nmol per min per mg dry weight.

for 20 min in the presence of 1 mM 2,4-dinitrophenol or 10 mM sodium azide had only about 30 % of their initial transport activity (Table 1). Thus, the accumulation process depends on metabolic energy. Furthermore, concentration gradients of pantothenate can be produced through transport into the cells of *E. coli* U-5/41. These results suggest the active transport of pantothenate under the conditions used.

In this system, the uptake of pantothenate into the cells of strain U-5/41 followed saturation kinetics. Fig. 2 shows a reciprocal plot of initial rate of uptake *versus* substrate concentration. Initial rates were computed from points taken at intervals of 30 sec during the first 4 min. The concentrations ranged from 2 to 100 μM. A value of 2.5×10^{-5} M for K_m and of 0.3 nmol per min per mg dry weight of cells for V_{max} was obtained. At temperatures below 30° the K_m value for pantothenate transport was approximately 1×10^{-4} M and the uptake system was not inhibited by 1 mM 2,4-dinitrophenol, which suggests that pantothenate was transported into the cells by diffusion.

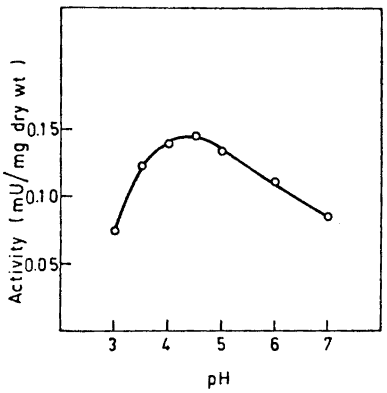

Fig. 3. Uptake of pantothenate as a function of pH. Uptake reactions were carried out in citrate buffers at 45°. Other experimental conditions are the same as in the legend to Fig. 1.

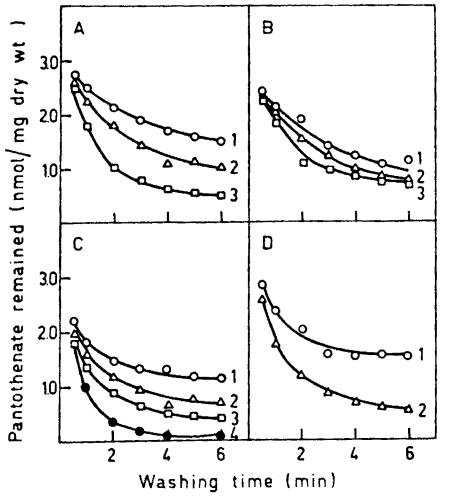

Fig. 4. Effect of temperature and glucose concentration on exit reaction. A. Exit against mineral salts solution 1, at 0°; 2, at 30°; 3, at 45°. B. Exit against glucose solution (20 mM) 1, at 0°; 2, at 30°; 3, at 45°. C. Exit against glucose solution at 30° 1, 50 mM; 2, 20 mM; 3, 10 mM; 4, H_2O. D. Exit against mineral salts solution containing 1 mM iodoacetamide at 0°, 1; at 45°, 2.

The effect of pH on pantothenate uptake was studied in citrate buffers. As shown in Fig. 3, the rate of pantothenate accumulation was maximal at 4.0 – 4.5.

The effect of temperature and various compounds on exit was investigated by allowing the cells to accumulate [^{14}C]-pantothenate at 45° for 10 min and then chilling, harvesting by centrifugation at 4°, and resuspending the bacteria in solutions of different salts with pantothenate added. Fig. 4 shows the results of the experiment. At 45° exit was much more rapid than at 30° and at 30° more rapid than at 4°. When the cells were resuspended in medium containing only 10^{-4} M pantothenate the exit rates were marked even at 4°. Glucose, when added to the pantothenate solution, prevented the exit of [^{14}C]-pantothenate at 45°, 30°, and 4° in cells precultured for at least 2 h in the glucose minimal medium.

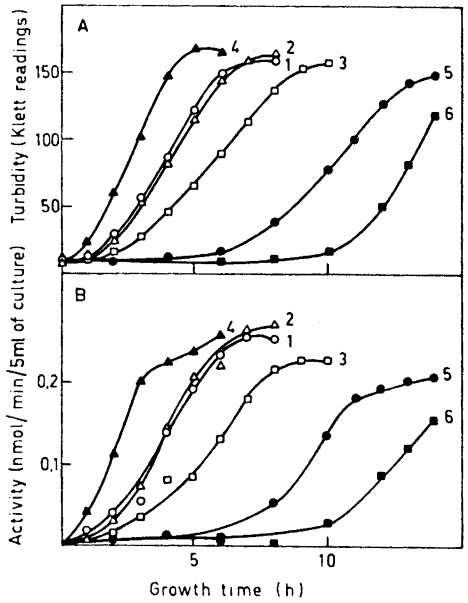

Fig. 5. Formation of the pantothenate transport system during growth of *E. coli* U-5/41 in various media. Experimental conditions are the same as in the legend to Fig. 1. A. Growth 1, on glucose; 2, on glucose + pantothenate; 3, on glycerol; 4, on casamino acids; 5, on succinate; 6, on glutamate. The concentration of carbon compound was 10 mM (casamino acids 0.1 %). B. Activity of the transport system. The symbols are the same as above.

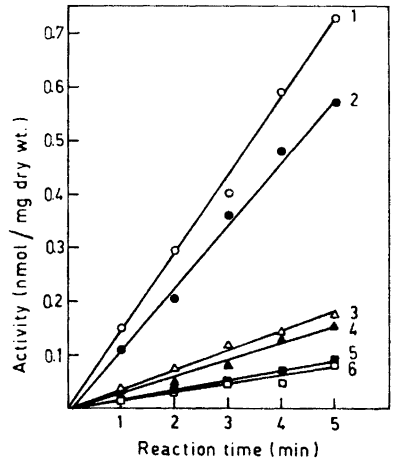

Fig. 6. Effect of shock treatment and freezing and thawing on the time course of pantothenate uptake. Experimental conditions are described in the text. 1, the cells were taken from the early logarithmic phase of growth; 2, the cells were taken from the end of the logarithmic phase of growth; 3, the osmotically shocked cells taken from the early logarithmic phase; 4, the osmotically shocked cells taken from the end of the logarithmic phase of growth; 5, the cells were taken from the early logarithmic phase of growth and disrupted by freezing and thawing; 6, the cells were taken from the end of the logarithmic phase of growth and disrupted by freezing and thawing.

The pantothenate accumulated by the cells was not phosphorylated, because in cells pulsed for a short time at 45° only one radioactive spot identical with [^{14}C]-pantothenate was found on a chromatogram. The presence of pantothenate kinase and absence of pantothenate hydrolase in *E. coli* U-5/41 were demonstrated and when the cells were pulsed for a longer period at 37° various spots were obtained by chromatography.

A pantothenate transport system was formed constitutively in the cells of strain U-5/41. Formation of the transport system on glucose, glucose + pantothenate, glycerol, glutamate, casamino acids, or succinate almost completely paralleled the growth curves, the activities reaching maxima at the end of the exponential phase of growth (Fig. 5).

Transport activity was reduced by osmotic shock or by freezing and thawing. Fig. 6 shows that after osmotic shock approximately equal proportions of the ability to transport pantothenate were lost in cells taken from the early exponential phase and those from the end of the exponential phase of growth. When the shock fluid was concentrated by lyophilization, it was possible to demonstrate binding of pantothenate to the lyophilized material.

Table 2. Partial purification of pantothenate-binding material from *E. coli* U-5/41.

	Protein (mg)	Binding activity (nmol)	Specific activity (nmol/mg protein)
Shock fluid	70	18	0.25
Lyophilizate	71	14	0.20
$(NH_4)_2SO_4$ precipitate (80 % saturation)	41	18	0.44
Sephadex G-100	22	17	0.78

Table 2 shows the results of purification procedures on the binding material. The Sephadex G-100 fractions appeared to be purified only about 3-fold over the shock fluid. Four or five proteins with molecular weights in order of tens of thousands were observed in the active Sephadex G-100 fractions by using disc electrophoresis.

DISCUSSION

From the results described above it is obvious that transport of pantothenate into the cells of *E. coli* U-5/41 is an active process. The results reported here resemble those described in several previous papers,[12–17] except for the low pH and high temperature optima in pantothenate transport. High transport activity at low pH values may indicate weak dependence on ionic attraction for binding of pantothenate and the relatively greater importance of van der Waals forces. The rate of uptake increased with increasing temperature up to 50°, then decreased rapidly at higher temperatures, the later behavior probably being due to partial cell destruction or death. Mandelbaum-Shavit and Grossowicz [18] have found two uptake systems for folinate in

Pediococcus cerevisiae, one of them dependent on temperature, pH and glucose, the other independent of temperature and glucose. No different phases, such as were found in the transport of vitamin B_{12} in *E. coli*,[4] were observed in pantothenate transport. On the other hand, the initial phase of B_{12} uptake was extremely rapid and it may be difficult to demonstrate its counterpart in other systems. Furthermore, the total counts during the initial phase were only about 15 % of the counts during the second phase.

Although the existence of pantothenate kinase in these cells was demonstrated by the method of Ward *et al.*,[19] pantothenate was accumulated without phosphorylation. On the other hand, formation of 4′-phosphopantothenate requires ATP, which is generated by oxidative phosphorylation. Because, although pantothenate was transported without phosphorylation, uptake was inhibited by 2,4-dinitrophenol, energy must be required for some other process involved in the accumulation of pantothenate. It is suggested that energy may be required for passage of pantothenate across the membrane as in the case of β-galactosides in *E. coli*.[20] Thiamine is accumulated as thiamine pyrophosphate in *E. coli* [1] and in this system energy is required for accumulation of thiamine, but not for the passage of thiamine across the membrane. Glucose was found to increase the internal steady-state concentration of pantothenate only if the cells had been grown on glucose for at least 2 h. It is therefore suggested that the effect of glucose in preventing exit is involved in the supply of energy after induction of the pathway of degradation of glucose.

The uptake of pantothenate in *Pseudomonas fluorescens* P-2 is an inducible process.[5] On the other hand, the uptake system in *E. coli* U-5/41 is a constitutive one. Although pantothenate uptake in *P. fluorescens* was controlled by induction and repression [5] and thiamine uptake in *E. coli* by repression and derepression,[21] pantothenate, when added to the growth medium, had no influence upon the growth of *E. coli* and only a slight influence upon pantothenate transport. Rogers and Lichstein [22] reported that the activity of the biotin transport system in *Saccharomyces cerevisiae* was not inhibited by intracellular free biotin pools, although the synthesis of the biotin transport system may be repressed during growth in a medium containing a high concentration of biotin. Although pantothenate, when added to the growth medium at a high concentration, decreased transport activity, this can hardly be regarded as repression of the transport system, because over 10 mM pantothenate was required to achieve a 20 % decrease in transport activity. More likely the intracellular pantothenate pool tends to decrease pantothenate transport. Furthermore, although Iwasima *et al.*[23] found that formation of thiamine-binding protein was repressed by thiamine added to the growth media, no repression of pantothenate-binding material was observed when pantothenate was added to the growth media.

REFERENCES

1. Kawasaki, I., Miyata, I., Esaki, K. and Nose, Y. *Arch. Biochem. Biophys.* **131** (1969) 223.
2. Roth, J. A., McCormick, D. B. and Wright, L. D. *J. Biol. Chem.* **245** (1970) 6264.
3. Cooper, B. A. *Biochim. Biophys. Acta* **208** (1970) 99.
4. DiGirolamo, P. M. and Bradbeer, C. *J. Bacteriol.* **106** (1971) 745.

5. Mäntsälä, P. *Acta Chem. Scand.* **26** (1972) 127.
6. Kaback, H. R. *Ann. Rev. Biochem.* **39** (1970) 561.
7. Pardee, A. B. *Science* **162** (1968) 632.
8. Mäntsälä, P. *Scand. J. Clin. Lab. Invest.* **29** *Suppl.* **122** (1972) 34.
9. Davis, B. D. and Mingioli, E. S. *J. Bacteriol.* **60** (1950) 17.
10. Neu, H. C. and Heppel, L. A. *J. Biol. Chem.* **240** (1966) 3685.
11. Chang, L. O., Srb, A. M. and Steward, E. L. *Nature* **193** (1962) 756.
12. Cowie, D. B. and McClure, F. T. *Biochim. Biophys. Acta* **31** (1959) 236.
13. Kepes, A. and Cohen, G. N. In Gunsalus, I. C. and Stanier, R. Y., Eds., *The Bacteria*, Academic, New York 1962, Vol. 4, p. 179.
14. Kundig, W., Ghosh, S. and Roseman, S. *Proc. Natl. Acad. Sci. U.S.* **52** (1964) 1067.
15. Koch, A. L. *Biochim. Biophys. Acta* **79** (1964) 177.
16. Wong, P. T. S. and Wilson, T. H. *Biochim. Biophys. Acta* **196** (1970) 336.
17. Phibbs, P. V., Jr. and Eagon, R. G. *Arch. Biochem. Biophys.* **138** (1970) 470.
18. Mandelbaum-Shavit, F. and Grossowicz, N. *J. Bacteriol.* **104** (1970) 1.
19. Ward, G. B., Brown, G. M. and Snell, E. E. *J. Biol. Chem.* **213** (1955) 869.
20. Scarborough, G. A., Rumley, M. K. and Kennedy, E. P. *Proc. Natl. Acad. Sci. U.S.* **60** (1968) 951.
21. Kawasaki, I. and Esaki, K. *Arch Biochem. Biophys.* **142** (1971) 163.
22. Rogers, T. O. and Lichstein, H. C. *J. Bacteriol.* **100** (1969) 565.
23. Iwashima, A., Matsuura, A. and Nose, Y. *J. Bacteriol.* **108** (1971) 1419.

Received August 29, 1972.

ACTA CHEMICA SCANDINAVICA 27 (1973) 453–460

Investigation of the Stability of Dioxolanylium Ions Derived from 1,5-Anhydro-D-arabinitol

STEFFEN JACOBSEN, INGE LUNDT and CHRISTIAN PEDERSEN

Department of Organic Chemistry, Technical University of Denmark, DK-2800 Lyngby, Denmark

The relative stabilities of a series of dioxolanylium ions, (V) and (VI), derived from 1,5-anhydro-D-arabinitol, have been measured in hydrogen fluoride solution and in deuterioacetonitrile. The ions (V) and (VI) were prepared by treatment of triacylated 1,5-anhydro-D-arabinitol (III) with anhydrous hydrogen fluoride, or by reaction of 2-*O*-acyl-1,5-anhydro-3,4-*O*-benzylidene-D-arabinitol (IV) with triphenylmethyl fluoroborate in deuterioacetonitrile.

Reaction of *cis*-1,2-diacyloxy-cyclohexanes or cyclopentanes with anhydrous hydrogen fluoride leads to formation of dioxolanylium ions. If two different acyl groups are present two dioxolanylium ions may be formed. It was found that the less stable ion was formed as the main product in a kinetically controlled reaction.[1]

It was of interest to obtain information about the relative stability of variously substituted dioxolanylium ions, and for this purpose the equilibrium

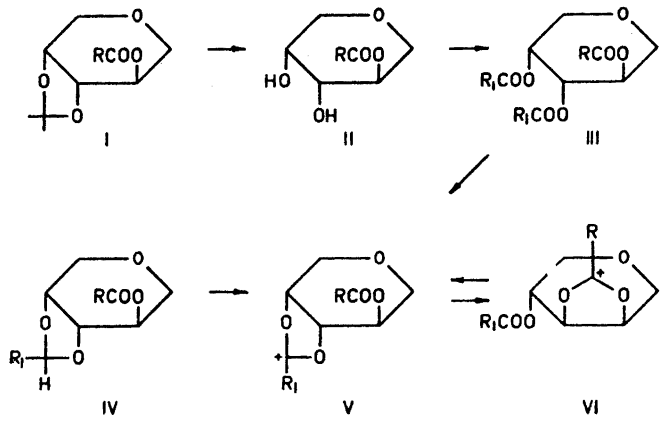

between the isomeric ions (V) and (VI), derived from 1,5-anhydro-D-arabinitol, has been studied. These ions were prepared, either by reaction of the triesters (III) with anhydrous hydrogen fluoride, or by treatment of the benzylidene derivatives (IV) with triphenylmethyl fluoroborate.

Tri-*O*-acetyl-1,5-anhydro-D-arabinitol (III, $R=R_1=CH_3$) contains a pair of *cis*-oriented 1,2-diacyloxy groups and it would therefore be expected to give an acetoxonium ion by treatment with anhydrous hydrogen fluoride.[1-3] It was found that when the triacetate (III) was kept in hydrogen fluoride for *ca.* 5 h at 0°C a quantitative conversion to the acetoxonium ion (V, $R=R_1=CH_3$) took place. This was seen from the NMR spectrum of the hydrogen fluoride solution which showed the presence of one acetoxy group, one equivalent of acetic acid, and one signal at 2.90 ppm corresponding to an acetoxonium ion (Table 1). A similar treatment of the tribenzoate (III, $R=R_1=C_6H_5$) gave the benzoxonium ion (V, $R=R_1=C_6H_5$) in the course of 20 h at room temperature (Table 1).

Paulsen *et al.*[4,5] have investigated similar esters in the cyclohexane and cyclopentane series and on the basis of their results a rapid equilibration would be expected to take place between the ions (V) and (VI). When the triacetate or the tribenzoate (III) are the starting material (V) and (VI) are identical.[3] However, if R is different from R_1 the ions (V) and (VI) are different and the equilibrium between them should give information about their relative stabilities. To obtain this information a number of compounds (III), in which R and R_1 are different, have been prepared and their reactions with hydrogen fluoride have been studied.

When 3,4-di-*O*-acetyl-2-*O*-benzoyl-1,5-anhydro-D-arabinitol (III, $R=C_6H_5$, $R_1=CH_3$) was kept for *ca.* 20 h in anhydrous hydrogen fluoride NMR spectra showed that one equivalent of acetic acid was cleaved off and *ca.* one acetoxy-group was present (Table 1). Besides, a small amount of acetoxonium ion was formed as seen from a signal at 2.90 ppm. This shows that (III, $R=C_6H_5$, $R_1=CH_3$) is converted almost completely into the benzoxonium ion (VI, $R=C_6H_5$, $R_1=CH_3$) by treatment with hydrogen fluoride. The reaction must proceed *via* the acetoxonium ion (V, $R=C_6H_5$, $R_1=CH_3$) which rearranges to (VI) because the latter is the more stable of the two. The small acetoxonium ion signal may arise from a small amount of (V) in equilibrium with (VI). It may, however, also be due to the presence of a small amount of the acetoxonium ion (V, $R=R_1=CH_3$) which could be formed by exchange of the benzoyloxy-group of (III, $R=C_6H_5$, $R_1=CH_3$) with acetic acid, liberated in the first step. This would give (III, $R=R_1=CH_3$) which, in turn, would yield (V, $R=R_1=CH_3$). Exchange reactions of this type were found in the cyclohexane and cyclopentane series[1] and they can also take place in the present type of compounds (see below).

When the diacetate-*p*-methoxybenzoate (III, $R=p$-$MeOC_6H_4$, $R_1=CH_3$) was treated with hydrogen fluoride the product formed almost exclusively was the *p*-methoxy-benzoxonium ion (VI, $R=p$-$MeOC_6H_4$, $R_1=CH_3$). The diacetate-*p*-nitrobenzoate (III, $R=p$-$NO_2C_6H_4$, $R_1=CH_3$), on the other hand, gave the acetoxonium ion (V, $R=p$-$NO_2C_6H_4$, $R_1=CH_3$) as the sole product as seen from the acetoxonium ion signal at 2.90 ppm (Table 1).

Table 1. NMR spectra of dioxolanylium ions (V) and (VI) in anhydrous hydrogen fluoride at 0°C or in deuterioacetonitrile at room temperature. Position of signals are given in ppm relative to $(CH_3)_3SiCH_2CH_2CH_2SO_3Na$ in hydrogen fluoride and relative to tetramethylsilane in acetonitrile. When a mixture of (V) and (VI) is formed only the spectrum of the major product is given.

Product	Solvent	R	R_1	δ-Values [a]								Coupling constants							
				H_1	$H_{1'}$	H_2	H_3	H_4	H_5	$H_{5'}$	CH_3	$J_{11'}$	J_{12}	$J_{1'2}$	J_{23}	J_{34}	J_{45}	$J_{45'}$	$J_{55'}$	J_{15}
V=VI	HF	CH_3	CH_3	4.7	4.28	~6.0		5.6	4.5	3.9	2.3, 2.6 2.9	15	~0.5	~0.5		2.5	6.5	6.5	13	
V=VI	HF	C_6H_5	C_6H_5			~6.3	~6.1	5.0	4.18			15	~0.5	~0.5	8.5	4.5	6.5	7.0	13	
V=VI	CD_3CN	C_6H_5	C_6H_5	4.56	4.19	6.13	6.28	5.66	4.32	3.71		15.2	~0.5	2.1	8.4	4.6	6.6	7.1	12.4	~1
V and VI(1:20)	HF	C_6H_5	CH_3	4.8	4.4	~6.1		5.7	4.55	4.0	2.4, 2.63 2.9	15.5	~0.5	~1			7	7	13	
V	HF	p-$NO_2C_6H_4$	CH_3	4.4–4.9		5.7–6.3		4.6	4.0		2.35, 2.62 2.9									
V and VI(1:6)	HF	p-$MeOC_6H_4$	CH_3	4.8	4.4	~6		~5.6	4.5	4.0	2.4, 2.6 2.9	15	~0.5	~1			6.5	6.5	13	
V and VI(1:3)	HF	p-MeC_6H_4	C_6H_5								2.47, 2.55 2.60									
V and VI(1:3)	CD_3CN	p-MeC_6H_4	C_6H_5	4.54	4.18	6.08	6.23	5.64	4.31	3.71	2.40 2.52	15.0	~0.5	2.0	8.4	4.5	6.4	7.1	12.3	
VI	CD_3CN	p-$MeOC_6H_4$	C_6H_5	4.50	4.15	5.99	6.14	5.59	4.27	3.69	3.99	14.8	~0.5	2.0	8.2	4.6	6.4	7.1	12.5	~1
V	CD_3CN	p-$NO_2C_6H_4$	C_6H_5	4.59	4.22	6.19	6.36	5.71	4.34	3.76		15.0	~0.5	2.2	8.3	4.6	6.8	7.3	12.5	~1
V and VI(1:1)	HF	p-MeC_6H_4	p-$MeOC_6H_4$								2.43, 2.53 2.62									
V and VI(9:1)	CD_3CN	p-MeC_6H_4	p-$MeOC_6H_4$	4.49	4.15	5.98	6.12	5.57	4.27	3.69	2.39, 2.51 3.84, 3.98	14.9	~0.5	2.0	8.2	4.5	6.5	7.0	12.5	~1

[a] In this table (V) and (VI) are numbered in opposite directions in such a manner that H_3 and H_4 are the protons attached to the dioxolanylium ring in both formulas.

The dibenzoate-*p*-toluate (III, R = *p*-$CH_3C_6H_4$, $R_1 = C_6H_5$) gave a 3:1 mixture of the *p*-methylbenzoxonium ion (VI, R = *p*-$CH_3C_6H_4$, $R_1 = C_6H_5$) and the benzoxonium ion (V). This was seen from the signals at 2.47 and 2.60 ppm (Table 1). A signal at 2.55 ppm showed that *p*-toluic acid was present in the hydrogen fluoride solution. This must be due to exchange of *p*-toluyloxy-groups with benzoic acid, as described above, and formation of some of the benzoxonium ion (V, $R = R_1 = C_6H_5$). The hydrogen fluoride solution was hydrolyzed and the product was washed with base to remove acids. Integrated NMR spectra of the product thus obtained showed that 17 % of the toluyloxy-groups were lost. This must correspond to the amount of ester-exchange that has taken place.

The di-*p*-methoxybenzoate-mono-*p*-toluate (III, R = *p*-$CH_3C_6H_4$, R_1 = *p*-$CH_3OC_6H_4$) gave equal amounts of the ions (V) and (VI) (R = *p*-$CH_3C_6H_4$, R_1 = *p*-$CH_3OC_6H_4$). In this case ester-exchange was also a competing reaction, 20 % of *p*-toluic acid being cleaved off.

In order to avoid the complications caused by exchange reactions the ions (V) and (VI) were prepared in a different manner. It is well known that triphenylmethyl fluoroborate can abstract hydride ions from cyclic aldehyde acetals to give dioxolanylium ions.[5,6] By this method the benzylidene derivatives (IV) could be converted to the ions (V) and (VI) by treatment with triphenylmethyl fluoroborate in acetonitrile at room temperature in the course of 1 – 5 h. The reactions were followed by NMR spectroscopy.

In this way the benzoxonium ion (V, $R = R_1 = C_6H_5$) was obtained from the benzylidene compound (IV, $R = R_1 = C_6H_5$) in 3 – 4 h. The NMR spectrum could be completely analyzed at 100 MHz (Table 1); the corresponding spectrum in hydrogen fluoride was less well resolved. When the nitrobenzoate (IV, R = *p*-$NO_2C_6H_4$, $R_1 = C_6H_5$) was treated with triphenylmethyl fluoroborate the benzoxonium ion (V, R = *p*-$NO_2C_6H_4$, $R_1 = C_6H_5$) was formed as the only product in the course of 3 – 5 h. From the spectral data, presented in Table 1, a distinction between the benzoxonium ion (V) and the nitrobenzoxonium ion (VI) could not be made. However, a complex group of signals in the aromatic region clearly showed that a benzoxonium ion was present since the spectra of such ions are known from previous work.[1] The nitrobenzoxonium ion (VI, R = *p*-$NO_2C_6H_4$, $R_1 = C_6H_5$) would contain a benzoyloxy-group and signals corresponding to this could not be found in the aromatic region.

The *p*-methoxybenzoate (IV, R = *p*-$MeOC_6H_4$, $R_1 = C_6H_5$) gave the methoxybenzoxonium ion (VI, R = *p*-$MeOC_6H_4$, $R_1 = C_6H_5$) as the sole product under the same conditions. This was seen from the δ-value of the methoxy-group which was found to be 3.99, in agreement with the value in hydrogen fluoride (Table 1) and in fluorosulfonic acid.[7] The corresponding value for the methoxybenzoate (IV) was 3.80 and a similar value would be expected for the isomeric ion (V, R = *p*-$MeOC_6H_4$, $R_1 = C_6H_5$).

The two toluates (IV, R = *p*-MeC_6H_4, $R_1 = C_6H_5$) and (IV, R = *p*-MeC_6H_4, R_1 = *p*-$MeOC_6H_5$) both gave mixtures of the two isomeric ions (V) and (VI) (Table 1). The products formed could be identified from the signals of the methyl groups. Those of the *p*-methylbenzoxonium ions (VI) were found at 2.52 and 2.51 ppm, respectively, whereas the *p*-toluyloxy-groups in the isomeric ions (V) gave NMR signals at 2.40 and 2.39 ppm (Table 1).

From these results and from the results obtained in hydrogen fluoride it can be concluded that the stabilities of the dioxolanylium ions (V) and (VI) vary in the following way with the groups attached to C-2 of the dioxolanylium ring: *p*-methoxyphenyl > *p*-methylphenyl > phenyl > methyl > *p*-nitrophenyl. This is of course the range of stabilities that would be expected from inductive and resonance effects. It may be noted that whereas the ions (V) and (VI) ($R_1 = p\text{-}MeOC_6H_4$, $R = p\text{-}MeC_6H_4$) were formed in equal amounts in hydrogen fluoride solution the methoxybenzoxonium ion (V) was found to be more stable than the methylbenzoxonium ion (VI) in acetonitrile (Table 1). This is probably due to a partial protonation of the methoxy-group in hydrogen fluoride, a reaction which will destabilize the methoxybenzoxonium ion (V). The low stability of the *p*-nitrobenzoxonium ion is in agreement with the fact that a *p*-nitrobenzoyl-group shows little tendency to exert a neighbouring group effect in solvolysis reactions.[8]

From the order of stabilities found above it is evident that reaction of unsymmetrically acylated 1,2-cyclohexanediols or cyclopentanediols with hydrogen fluoride [1] leads to formation of the thermodynamically less stable of the two possible dioxolanylium ions.

The 1,5-anhydro-D-arabinitol derivatives (III) were prepared from 3,4-*O*-isopropylidene-1,5-anhydro-D-arabinitol,[9] which by acylation yielded the 2-*O*-acyl-derivatives (I). Hydrolysis of (I) gave the 2-*O*-acyl-1,5-anhydro-D-arabinitols (II), and subsequent diacylation furnished the desired products (III).

The benzylidene derivatives (IV) were obtained by acylation of crude 3,4-*O*-benzylidene-1,5-anhydro-D-arabinitol. Two diastereomeric products (*exo* and *endo*) were obtained in all cases due to asymmetry at the benzylic carbon. The diastereomers were separated and their structures were tentatively assigned from their NMR spectra assuming that the *endo* benzylic protons resonate at lower field than the *exo* protons.[10,11] When the pure isomers were treated with triphenylmethyl fluoroborate they were immediately equilibrated to a mixture of the two diastereomers. Hence a separation of the isomeric pairs is unnecessary.

EXPERIMENTAL

Melting points are uncorrected. Thin layer chromatography (TLC) was performed on silica gel PF_{254} (Merck). For preparative TLC 1 mm thick layers on 20 × 40 cm plates were used. NMR spectra were obtained on Varian A-60 and HA-100 instruments. NMR spectra in anhydrous hydrogen fluoride were measured in Teflon sample tubes using $(CH_3)_3SiCH_2CH_2CH_2SO_3Na$ as internal reference.

*1,5-Anhydro-3,4-*O*-isopropylidene-*D*-arabinitol* was prepared according to Hedgley and Fletcher.[8] Alternatively, 1,5-anhydro-D-arabinitol (1.2 g) in acetone (15 ml) was stirred for 20 h with conc. sulfuric acid (0.1 ml) and anhydrous copper sulfate (6 g). Neutralization with barium carbonate, filtration, and evaporation gave the product as a syrup (1.2 g).

*3,4-Di-*O*-acetyl-1,5-anhydro-2-*O*-benzoyl-*D*-arabinitol* (III, $R_1 = CH_3$, $R = C_6H_5$). 1,5-Anhydro-3,4-*O*-isopropylidene-D-arabinitol (3.0 g) was benzoylated with pyridine (10 ml) and benzoyl chloride (2 ml) in the usual way to give 4.1 g of crude (I, $R = C_6H_5$). Crystallization from ethanol gave the pure product (3.34 g), m.p. 101 – 102°C (reported [8] m.p. 102 – 103°C).

The product (553 mg) was suspended in ethanol (10 ml) and 0.8 % sulfuric acid (2 ml). The mixture was then boiled under reflux for 2 h at which time TLC analysis showed that the hydrolysis was complete. The solution was neutralized with barium carbonate, filtered through activated carbon and evaporated. The residue (504 mg) was crystallized from ether-pentane to give pure 1,5-anhydro-2-*O*-benzoyl-D-arabinitol (II, R = C_6H_5), m.p. 96 – 97°C, $[\alpha]_D^{23} = -83.5°$ (*c* 4.0, $CHCl_3$). (Found: C 60.38; H 6.05. Calc. for $C_{12}H_{14}O_5$: C 60.50; H 5.92.)

Acetylation of this product (528 mg) in pyridine (5 ml) with acetic anhydride (1 ml) gave 637 mg of crystalline (III, R = C_6H_5, $R_1 = CH_3$). Recrystallization from ether-pentane gave the pure product, m.p. 92.5 – 93°C, $[\alpha]_D^{23} = -116°$ (*c* 1.5, $CHCl_3$). (Found: C 59.72; H 5.62. Calc. for $C_{16}H_{18}O_7$: C 59.62; H 5.63.)

The other compounds with structures (I), (II), and (III) were prepared by the same procedure. They all gave NMR spectra which were in accordance with their structures.

1,5-Anhydro-3,4-*O*-isopropylidene-D-arabinitol was treated with *p*-nitrobenzoyl chloride in pyridine to give (I, R = *p*-$NO_2C_6H_4$), recrystallized from ether-pentane, m.p. 126 – 127°C. Hydrolysis gave (II, R = *p*-$NO_2C_6H_4$), m.p. 138 – 139°C. Acetylation of this product yielded 3,4-di-*O*-acetyl-1,5-anhydro-2-*O*-*p*-nitrobenzoyl-D-arabinitol (III, R = *p*-$NO_2C_6H_4$, $R_1 = CH_3$) as a syrup which was purified by preparative TLC with ether-pentane (1:2) as eluent, $[\alpha]_D^{23} = -119°$ (*c* 3, $CHCl_3$). (Found: C 52.48; H 4.81. Calc. for $C_{16}H_{17}NO_9$: C 52.31; H 4.67.)

p-Methoxybenzoylation of 1,5-anhydro-3,4-*O*-isopropylidene-D-arabinitol gave (I, R = *p*-$MeOC_6H_4$) which was purified by preparative TLC with ether-pentane (1:1) as eluent; m.p. 68 – 69°C. Hydrolysis as described above yielded (II, R = *p*-$MeOC_6H_4$), m.p. 160 – 161°C. Acetylation finally gave 3,4-di-*O*-acetyl-1,5-anhydro-2-*O*-*p*-methoxybenzoyl-D-arabinitol (III, R = *p*-$MeOC_6H_4$, $R_1 = CH_3$), m.p. 88 – 89°C after recrystallization from ether-pentane, $[\alpha]_D^{23} = -130°$ (*c* 3, $CHCl_3$). (Found: C 58.15; H 5.83. Calc. for $C_{17}H_{20}O_8$: C 57.95; H 5.72.)

Treatment of 1,5-anhydro-3,4-*O*-isopropylidene-D-arabinitol with *p*-toluyl chloride in pyridine gave (I, R = *p*-MeC_6H_4), m.p. 95 – 96°C, after recrystallization from ether-pentane. Hydrolysis gave (II, R = *p*-MeC_6H_4), recrystallized from ether-pentane, m.p. 145 – 147°C. Benzoylation yielded 1,5-anhydro-3,4-di-*O*-benzoyl-2-*O*-*p*-toluyl-D-arabinitol (III, R = *p*-MeC_6H_4, $R_1 = C_6H_5$), crystallized from ether-pentane, m.p. 109 – 110°C, $[\alpha]_D^{23} = -248°$ (*c* 1.6, $CHCl_3$). (Found: C 70.32; H 5.15. Calc. for $C_{27}H_{24}O_7$: C 70.41; H 5.25.)

Treatment of (II, R = *p*-MeC_6H_4) with *p*-methoxybenzoyl chloride in pyridine gave 1,5-anhydro-3,4-di-*O*-*p*-methoxybenzoyl-2-*O*-*p*-toluyl-D-arabinitol (III, R = *p*-MeC_6H_4, R_1 = *p*-$MeOC_6H_4$), m.p. 150 – 151°C, after recrystallization from ethanol, $[\alpha]_D^{23} = -245°$ (*c* 1.3, $CHCl_3$). (Found: C 66.76; H 5.26. Calc. for $C_{29}H_{28}O_9$: C 66.92; H 5.42.)

Benzylidene derivatives (IV). 1,5-Anhydro-D-arabinitol (500 mg), benzaldehyde (400 mg), and *p*-toluenesulfonic acid (10 mg) were dissolved in benzene (25 ml) and heated under reflux with a water-separator until no more water was formed (4 h). The solution was then cooled and neutralized with solid potassium carbonate. Filtration and evaporation gave 900 mg of a colourless syrup which was treated with *p*-toluyl chloride (700 mg) in pyridine (10 ml). Work up in the usual way gave 1.2 g of a product which was separated into two fractions by preparative TLC with ether-pentane (1:1) as eluent. The fast running fraction gave 510 mg (40 %) of a product which was crystallized from ethyl acetate-pentane to give 278 mg (22 %), m.p. 96 – 97°C. The second fraction gave 585 mg (46 %), which was crystallized from ethyl acetate-pentane to give 353 mg (28 %) of a product with m.p. 113 – 114°C. Further data are given in Table 2. The two products are *endo* and *exo* forms of 1,5-anhydro-3,4-*O*-benzylidene-2-*O*-*p*-toluyl-D-arabinitol (IV, R = *p*-$CH_3C_6H_4$, $R_1 = C_6H_5$).

The other products shown in Table 2 were prepared by the same method; they all gave satisfactory NMR spectra.

Reactions with hydrogen fluoride. In order to obtain NMR spectra in hydrogen fluoride solution 150 – 200 mg of the triesters (III) were dissolved in 0.5 – 1.0 ml of anhydrous hydrogen fluoride at 0°C and the solution was poured into a Teflon NMR sample tube. The solutions were kept at 0°C or at room temperature and the spectra were measured at 0°C.

The two esters (III, R = *p*-MeC_6H_4, $R_1 = C_6H_5$) and (III, R = *p*-MeC_6H_4, R_1 = *p*-$MeOC_6H_4$) were kept in hydrogen fluoride solution until no further reactions took place as seen from the NMR spectra (*ca.* 20 h at room temperature). The solutions were then

Table 2. 2-*O*-Acyl-1,5-anhydro-3,4-*O*-benzylidene-D-arabinitols (IV).

Substance R	Substance R_1	*endo* or *exo* H	δ-Value of benzylic proton	M.p. °C	$[\alpha]_D^{21}$ in $CHCl_3$	Analyses C found	Analyses C calc.	Analyses H found	Analyses H calc.	Yield %
C_6H_5	C_6H_5	*endo*	6.29	113–114	−97.3°, *c* 1.5	69.82	69.92	5.43	5.56	30
C_6H_5	C_6H_5	*exo*	5.98	103–104	−134.0, *c* 1.5	70.08	69.92	5.45	5.56	33
C_6H_5	*p*-$NO_2C_6H_4$	*endo*	6.30	92–93	−109.6, *c* 1.6	61.24	61.45	4.65	4.61	13
C_6H_5	*p*-$NO_2C_6H_4$	*exo*	5.97	113–113.5	−147.5, *c* 1.7	61.30	61.45	4.72	4.61	27
C_6H_5	*p*-$MeOC_6H_4$	*endo*	6.28	103–104	−115.3, *c* 1.3	67.26	67.40	5.82	5.66	25
C_6H_5	*p*-$MeOC_6H_4$	*exo*	5.96	114–115	−141.3, *c* 1.6	67.52	67.40	5.72	5.66	33
p-$MeOC_6H_4$	*p*-MeC_6H_4	*endo*	6.25	103–103.5	−99.0, *c* 1.2	67.93	68.09	5.90	5.99	25
p-$MeOC_6H_4$	*p*-MeC_6H_4	*exo*	5.88	128–129	−151.6, *c* 1.1	67.89	68.09	5.97	5.99	22
C_6H_5	*p*-MeC_6H_4	*endo*	6.28	96–97	−109.0, *c* 1.1	70.53	70.57	5.94	5.92	22
C_6H_5	*p*-MeC_6H_4	*exo*	5.89	113–114	−137.7, *c* 1.2	70.58	70.57	6.02	5.92	28

poured onto ice and the products were extracted with methylene chloride. The solutions were washed with aqueous sodium hydrogen carbonate, dried and evaporated. NMR spectra of the products thus obtained showed signals at *ca.* 2 ppm arising from the *p*-toluyloxy-groups. Integration gave information about the amount of ester-exchange that had taken place as described in the discussion.

Reactions in deuterioacetonitrile. The benzylidene esters (IV) (50 – 60 mg) and a 3 – 5 % excess of triphenylmethyl fluoroborate were dissolved in 0.4 ml of deuterioacetonitrile (dried over molecular sieves, 3 Å) in an NMR sample tube which was then closed with a rubber serum cap. The spectra were measured at the probe temperature (*ca.* 33°C).

Analyses were carried out by Dr. A. Bernhardt.

REFERENCES

1. Lundt, I. and Pedersen, C. *Acta Chem. Scand.* **26** (1972) 1938.
2. Pedersen, C. *Tetrahedron Letters* **1967** 511.
3. Hedgley, E. J. and Fletcher, H. G., Jr. *J. Am. Chem. Soc.* **85** (1963) 1615.
4. Paulsen, H. *Advan. Carbohyd. Chem. Biochem.* **26** (1971) 127.
5. Paulsen, H. and Behre, H. *Chem. Ber.* **104** (1971) 1281.
6. Meerwein, H., Hederich, V., Morschel, H. and Wunderlich, K. *Ann. Chem.* **635** (1960) 1.
7. Tomalia, D. A. and Hart, H. *Tetrahedron Letters* **1966** 3389.
8. Glaudemans, C. P. J. and Fletcher, H. G., Jr. *J. Am. Chem. Soc.* **87** (1965) 2456.
9. Hedgley, E. J. and Fletcher, H. G., Jr. *J. Org. Chem.* **30** (1965) 1282.
10. Baggett, N., Buck, K. W., Foster, A. B. and Webber, J. M. *J. Chem. Soc.* **1965** 3401.
11. Inch, T. D. *Carbohyd. Res.* **21** (1972) 37.

Received August 7, 1972.

ACTA CHEMICA SCANDINAVICA 27 (1973) 461–465

Line Broadening in the EPR Spectrum of the Negative Radical Ion of 1,2,3,4-Tetrahydroanthracene

JORMA ELORANTA and KAIJA PASANEN

Department of Chemistry, University of Jyväskylä, Jyväskylä, Finland

The radical anion of tetrahydroanthracene was produced by reduction of the hydrocarbon with potassium in 1,2-dimethoxyethane and by electrolysis in dimethylformamide. Appreciable line broadening is observed with rising temperature in the EPR spectra of the radical ion in 1,2-dimethoxyethane recorded in the range from −90°C to room temperature. The EPR spectra are compared with the spectra of the probable reduction and oxidation products of the tetrahydroanthracene anion.

Conformational change (chair boat) has been found to cause line broadening in the EPR spectra of the radical ions of tetrahydropyrene and hexahydropyrene in solution.[1–3] The radical ions of di-, tetra-, and octahydrophenanthrene have been studied by EPR spectrometry in 1,2-dimethoxyethane.[4–6] Line broadening has been observed by Iwaizumi and Bolton to result from ion pair formation in the EPR spectrum of the radical ion of dihydroanthracene.[7]

1,2,3,4-Tetrahydroanthracene has the structure:

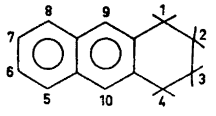

In order to be able to identify the disproportionation products of the radical ion of tetrahydroanthracene, it was necessary to prepare and record the EPR spectra of the radical anions of anthracene, dihydroanthracene, and octahydroanthracene.

EXPERIMENTAL

1,2,3,4-Tetrahydroanthracene was prepared under high pressure by hydrogenating 9,10-dihydroanthracene with the theoretical amount of hydrogen in the presence of Raney nickel. The products were analysed and purified by gas chromatography (Varian

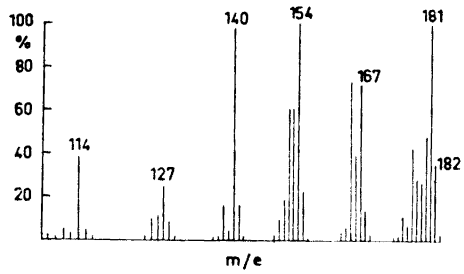

Fig. 1. The mass spectrum of 1,2,3,4-tetrahydroanthracene.

Autoprep 705). Four components were observed. Of these the component, in whose mass spectrum (Perkin-Elmer) the molecular ion peak was located at $M^+ = 182$, (Fig. 1), was collected with the gas chromatograph. The NMR spectrum (Perkin-Elmer) of the purified product showed that addition of hydrogen had occurred at positions 1, 2, 3, and 4.

1,2,3,4,9,10,11,12-Octahydrophenanthrene was prepared by the same method as tetrahydroanthracene. The molecular ion peak of the compound was located at $M^+ = 186$. The IR spectrum of 1,2,3,4,9,10,11,12-octahydrophenanthrene, which is reproduced in Fig. 2, differs clearly from the IR spectrum of symmetric 1,2,3,4,5,6,7,8-octahydrophenanthrene.

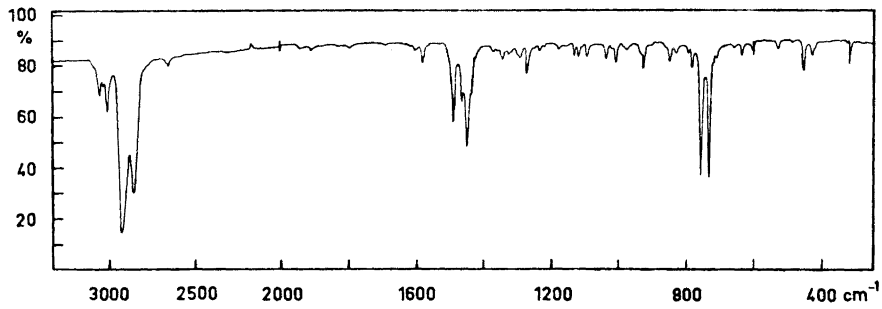

Fig. 2. The IR spectrum of 1,2,3,4,9,10,11,12-octahydrophenanthrene.

9,10-Dihydroanthracene was a commercial product, which was purified by gas chromatography.

The purification of the solvents and the preparation of samples in a high vacuum were carried out as described earlier.[4]

The EPR spectra were measured with a Varian E-12 spectrometer equipped with a Varian temperature regulator.

Molecular orbital, spin density and theoretical EPR spectrum calculations were performed at the Computer Centre of the University of Jyväskylä.

RESULTS AND DISCUSSION

Iwaizumi and Bolton [7] found that there are three quintets in the EPR spectrum of the anion of 9,10-dihydroanthracene in dimethoxyethane at -87°C and that the anion is unstable above -75°C. They did not report what the decomposition products were. It is surprising that all four methylene

protons are equivalent at these low temperatures. In order to obtain a reference spectrum for possible decomposition products of tetrahydroanthracene, we measured the EPR spectrum of the 9,10-dihydroanthracene anion in dimethoxyethane and found it to be identical with the spectrum obtained by Iwaizumi and Bolton. At room temperature the EPR spectrum had changed into the spectrum of the anion of anthracene.

Coupling constants of the radical anion of 1,2,3,4-tetrahydroanthracene in 1,2-dimethoxyethane at -60°C are collected in Table 1. The EPR spectra

Table 1. Coupling constants of the negative radical ion of 1,2,3,4-tetrahydroanthracene in 1,2-dimethoxyethane at -60°C.

Positions	a_H(G)
6, 7	1.69
1, 4	2.56
2, 3	0.16
5, 8	4.72
9, 10	4.90

of aromatic radical anions produced when potassium is used as reductant do not usually contain bands indicating coupling of potassium as signs of ion pair formation. Bands indicative of ion pair formation are not seen in Figs. 3, 4, and 5 (6). However, the variation of line width and intensity with temperature is considerable. The triplet $^3a = 1.69$ G due to the protons in positions 6 and 7 remains sharp at temperatures up to 0°C. The intensities of the lines of the protons at positions 1 and 4 rapidly approach the intensities of the quintet lines as the temperature rises above -60°C and the lines are sharp up to 0°C. When, however, the temperature is lowered below -60°C, the intensities

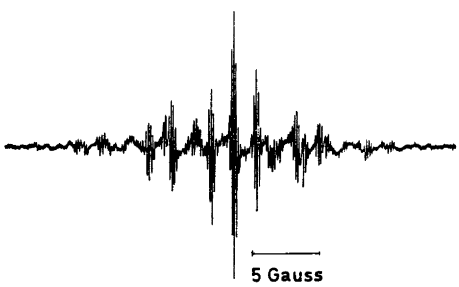

Fig. 3. EPR spectrum at -90°C of the products of the reduction of 1,2,3,4-tetrahydroanthracene with potassium in 1,2-dimethoxyethane.

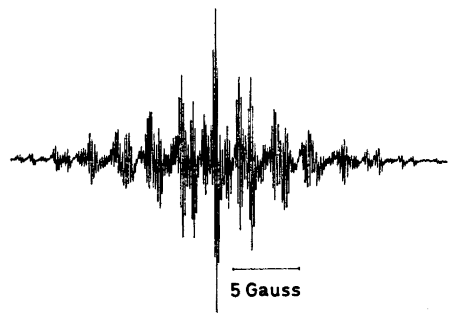

Fig. 4. EPR spectrum at -60°C of the products of the reduction of 1,2,3,4-tetrahydroanthracene with potassium in 1,2-dimethoxyethane.

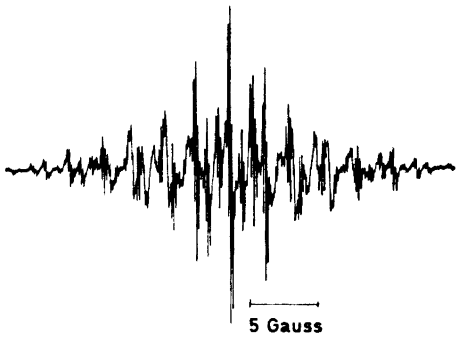

Fig. 5. EPR spectrum at −20°C of the products of the reduction of 1,2,3,4-tetrahydroanthracene with potassium in 1,2-dimethoxyethane.

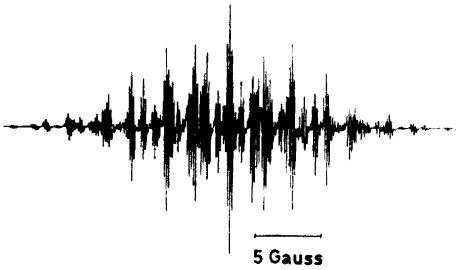

Fig. 6. Calculated spectrum with $^{5}a=4.72$ G, $^{5}a=2.56$ G, $^{3}a=1.69$ G, and $^{5}a=0.16$ G. Line width 0.05 G.

of the lines due to the protons at positions 1 and 4 diminish and the lines broaden.

The coupling constant 2.56 G is hardly visible at −90°C and yet the overall length of the spectrum is the same. 1,2,3,4-Tetrahydroanthracene has two chair and two boat conformations. When the conformational change is slow, the change in the coupling constants of the protons on carbons 1 and 4 leads to the line broadening. This is clearly evident already at −90°C. Because the solvent freezes, it was not possible to reach so low a temperature that the coupling constants of the axial and equatorial protons could be separately determined. When the temperature rises to −60°C, the limit of rapid change is attained and the line becomes sharper with rising temperature. In this respect there is a clear difference compared with tetrahydrophenanthrene, the coupling constants of the axial and equatorial protons of which can be determined using dimethoxyethane as solvent. The conformational change evidently takes place much more easily with tetrahydroanthracene than with tetrahydrophenanthrene.

Conformational changes cannot, however, explain the extremely low intensities of the peaks due to the protons in positions 5, 8 and 9, 10 that are seen in Fig. 4. Though ion-pair coupling cannot be seen in the EPR spectrum of the tetrahydroanthracene anion, it is obvious that the rapid movement of the potassium ion above the plane of the aromatic moiety comes the intensities of the peaks of the protons in positions 5, 8 and 9, 10 to decrease as observed by Iwaizumi and Bolton in the case of the anion of 9,10-dihydroanthracene.[7]

The highest spin densities are observed in the positions 9, 10 and 5, 8 in the anion of tetrahydroanthracene. The potassium ion is located in this region and does not alter the intensities of the peaks of the protons in positions 6 and 7.

By varying the values of the coulombic integrals at positions 1, 4, 4a, and 9a and taking for the resonance integral β_{1-9a} and β_{4-4a} values greater than unity, the highest spin density is obtained for position 9, 10 by Hückel calculations. The tetrahydroanthracene anion is fairly stable and no changes were

seen in the EPR spectrum although the sample was allowed to warm to room temperature and recooled. The anion was produced also electrolytically in dimethylformamide at room temperature. It gave an EPR spectrum that was identical with the spectrum of the anion produced by reduction with potassium.

A radical anion was not obtained when symmetric octahydroanthracene was treated with potassium. Instead of asymmetric octahydroanthracene, we used 1,2,3,4,9,10,11,12-octahydrophenathrene, the EPR spectrum of whose anion evidently must be almost identical with the spectrum of the anion of the corresponding octahydroanthracene.

The EPR spectrum of the anion of 1,2,3,4,9,10,11,12-octahydroanthracene in 1,2-dimethoxyethane at room temperature is shown in Fig. 7. It contains

Fig. 7. EPR spectrum at room temperature of the products of the reduction of 1,2,3,4,9,10,11,12-octahydrophenanthrene with potassium in 1,2-dimethoxyethane.

two triplets with coupling constants $^3a(6,7) = 1.78$ G and $^3a(5,8) = 4.77$ G that are fairly close in value to the corresponding coupling constants of the anion of tetrahydrophenanthrene.

When the EPR spectra of tetrahydroanthracene, anthracene, and 9,10-dihydroanthracene are compared, it is found that lines indicating presence of the last two anions are not present in the spectrum of tetrahydroanthracene. The conclusion is that no disproportionation has taken place. However, one cannot exclude the possibility that the anion of tetrahydroanthracene is reduced to the anion of asymmetric octahydroanthracene, as indicated by the coupling constants of the anion of asymmetric octahydrophenanthrene. The variations of the peak intensities with temperature and the stabilities of the intensities of the peaks of the protons in positions 6 and 7 show, however, that signs due to products of reduction are not either evident in the EPR spectrum of the radical anion of tetrahydroanthracene. As the temperature decreases, the influence of the hydrated ring in the anion of tetrahydroanthracene decreases, for the coupling constant $^5a(5,8,9,10)$ is found to be 4.72 G at -90°C. Its structure then resembles more the structure of the anion of naphthalene than that of 2,3-dimethylnaphthalene.[8]

REFERENCES

1. de Boer, E. and Praat, A. P. *Mol. Phys.* **8** (1964) 291.
2. Iwaizumi, M. and Isobe, T. *Bull. Chem. Soc. Japan* **38** (1965) 1547.
3. Claridge, R. F. C. and Peake, B. M. *Mol. Phys.* **18** (1970) 137.
4. Eloranta, J. and Pasanen, K. *Suomen Kemistilehti* **B 44** (1971) 16.
5. Eloranta, J. and Pasanen, K. *Suomen Kemistilehti* **B 45** (1972) 164.
6. Eloranta, J. and Pasanen, K. *Suomen Kemistilehti* **B 44** (1971) 358.
7. Iwaizumi, M. and Bolton, J. R. *J. Magn. Resonance* **2** (1970) 278.
8. Gerson, F., Weidemann, B. and Heilbronner, E. *Helv. Chim. Acta* **47** (1964) 1951.

Received August 22, 1972.

ACTA CHEMICA SCANDINAVICA 27 (1973) 466–470

The Synthesis of Thiophenes by the Spontaneous Cyclisation of Thionated γ-Diketones

FRITZ DUUS*

Department of Chemistry, Aarhus University, 8000 Aarhus C, Denmark

The acid catalysed reactions of some γ-diketones with H_2S at −35°C are described. The spontaneous intramolecular cyclisation of the primarily formed intermediate enethiols leads to the formation of thiophenes, which were isolated as the main products. A similar cyclisation reaction of transiently formed *gem*-dithiols gives rise to the formation of 2-mercapto-2,3-dihydrothiophenes and 2,5-dimercaptotetrahydrothiophenes, which were isolated as by-products. The structures of the latter compounds are discussed on the basis of the NMR spectra.

In connection with the study of the thione-enethiol tautomerism of β-thioketoesters [1] several α-substituted β-thioketoesters were prepared by the acid catalysed action of H_2S on the corresponding β-ketoesters at low temperatures (−60° to −40°C).[1] Ethyl α-acetonylacetoacetate (Ia), when subjected to these reaction conditions, neither gave the related β-thioketoester, nor the related *gem*-dithiol.[1] Instead two cyclic compounds, IIa and IIIa, were isolated from the reaction mixture by preparative layer chromatography (PLC) in yields of 57 %, and 17 %, respectively. The thiophene IIa was not an unexpected product, as an early known synthetic route to thiophenes in fact is based on the thionation of γ-diketones, and the subsequent, spontaneous cyclisation of the thionated intermediate.[2] The thionation agents generally used are P_2S_3 [3] and P_2S_5.[4] However, according to a recent paper,[5] the action of P_2S_5 on Ia (and, generally, on γ-diketones containing an ester group as in Ia) does not lead to the formation of IIa, but rather to the furanoic thionoester V. Thus, the present ester group evidently promotes the enolization process to such a degree that cyclisation of Ia, through dehydration, occurs prior to thionation. The subsequent conversion of the furanoic ester to the corresponding thionoester is expected under the reaction conditions.[5,6]

* Present address: Department of Chemistry, Odense University, Niels Bohrs Allé, 5000 Odense, Denmark.

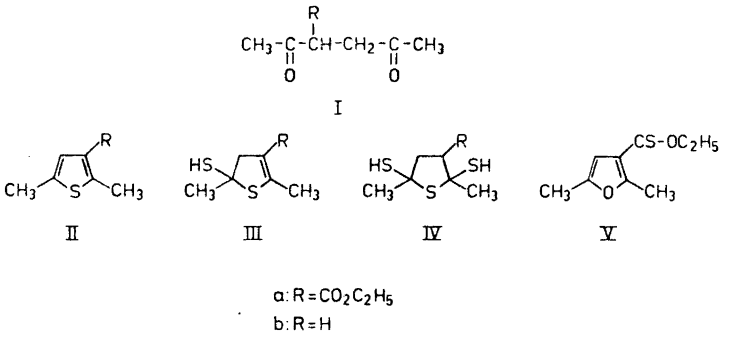

a: R = $CO_2C_2H_5$
b: R = H

Apparently, H_2S has been used as thionation agent only in one case, in which acetonylacetone (Ib) on treatment with H_2S at 325°C in the catalytic presence of Al_2O_3 was reported to give 2,5-dimethylthiophene (IIb) in a yield of 35 %.[7] Consequently, Ib was exposed to treatment with H_2S in acid ethanol at a temperature < -35°C. From the crude reaction product mixture, pure IIb was isolated by simple distillation in a yield of 33 %. A higher boiling fraction contained the hitherto unknown di- and tetrahydrothiophenes IIIb and IVb, which were separated by PLC and isolated in yields of 3.3 % and 15 %, respectively. Thus, the hereby presented experimental method appears to represent a new, useful synthetic route to substituted thiophenes.

Obviously, the mercaptodihydrothiophenes IIIa and IIIb, and the dimercaptotetrahydrothiophene IVb are cyclisation products of intermediately formed *gem*-dithiols. The last named compounds are very often reaction products, when ketones are subjected to the actual reaction conditions and the enethiolisation process of the primarily formed thiones is not especially favourable, or impossible.[1,8,9] IIIa, IIIb, and IVb are all stable compounds which can be distilled at reduced pressure without detectable evolution of H_2S. Moreover, no decomposition occurred when IIIa was kept in acidic ethanol solution at room temperature for 20 h. Reflux of IIIa in the same medium for 4 h resulted only in partial (27 %) conversion to IIa. Therefore, the possibility that the unsaturated heterocycles were formed by stepwise H_2S elimination from the more saturated compounds within the same series (*i.e.* IV→III→II) under the reaction conditions seems most unlikely. Rather, the product distribution reflects the relative stability of the equilibrated, transient open-chain thiones and *gem*-dithiols. The complete absence of IVa among the reaction products is not surprising, as evidently in this special case H_2S elimination is energetically favourable due to the emergence of a carbonyl-conjugated double bond.[10] Further, the successive formation of transient β-thioketo- and especially β,β-dimercaptoesters from Ia is very probably less prevalent due to the enforcing effect of the ester groups on competing enolisation and enethiolisation processes.

Presumably both of the two geometrical isomers of the compounds III were formed. They are, however, NMR-spectroscopically indistinguishable (Table 1). Possessing two chiral centers, IVb can occur in three stereo-isomeric forms of

Table 1. ^{1}H NMR chemical shifts (ppm, δ-values) and coupling constants (Hz, in brackets) of synthesised heterocyclic compounds. The following abbreviations are used: s (singlet), d (doublet), t (triplet), q (quartet), and m (multiplet).[a] Unless stated to the contrary, the solvent is CS_2.

	$CH_3-\overset{\vert}{\underset{\vert}{C}}-$	$-SH$	$-CH_2-$	$CH_3-\overset{\vert}{C}=$	$-CH=$
IIa[b]				2.33 (dq) [1.1/0.5] 2.58 (qd) [0.5/0.25]	6.86 (qq) [1.1/0.25]
IIb				2.34 (m[c])	6.34 (m[c])
IIIa[d]	1.84 (d) [0.85]	2.74 (q) [0.85]	3.24 (qd[e]) [1.8]	2.24 (t) [1.8]	
IIIb	1.83 (d) [0.9]	2.70 (q) [0.9]	2.90 (dq) [2.6/2.1]	1.90 (td) [2.1/1.6]	5.09 (tq) [2.6/1.6]
IVb	1.89[f] (s) 1.77[g] (d) [0.7]	2.51[f] (s) 2.63[g] (q) [0.7]	2.0 – 3.0 (m[h])		
IVb[i]	1.72[f] (s) 1.57[g] (d) [0.7]	2.39[f] (s) 2.57[g] (q) [0.7]	1.8 – 2.8 (m[h])		

[a] In combinations, the first mentioned multiplicity symbol refers to the greater coupling.
[b] Ester group protons: 4.15 (q), and 1.28 (t), $J = 7$ Hz.
[c] The multiplicity of the sharp signal is observable only on the 50 Hz scale, and cannot be further specified without a better resolution.
[d] Ester group protons: 4.06 (q), and 1.24 (t), $J = 7$ Hz.
[e] The doublet reflects the magnetical non-equivalence of the methylene protons (separation ~6 Hz).
[f] Form A≡D,L-form.
[g] Form B≡*meso*-forms.
[h] Two overlapping AA'BB' patterns.
[i] Solvent: C_6D_6.

which the D- and L-forms can be expected to be mutually indistinguishable (by NMR), but distinguishable from the *meso*-form. In fact, the NMR spectrum of IVb shows two distinct methyl signals as well as two mercapto-proton signals. The individual affiliations of the former signals to exclusively one or the other of the latter was unambigously manifested from the signal intensities and existing couplings (Table 1). Although the mercapto-proton signals appear within the complex region of the two overlapping AA'BB' patterns of the methylene protons, they are nevertheless easily extracted due to the characteristic low-field displacements, which occur on replacing the solvent CS_2 by CD_3CN. It is evident that the D,L-forms possess a dipole moment vector different from that of the *meso*-form. According to Ledaal,[11] the preferred or

"average" shape of the collision complex of a solute molecule and a solvent benzene molecule is determined by the aligment of the six-fold symmetry axis of the benzene molecule and the "averted" dipole moment vector of the solute molecule. In a magnetic field, the solute molecule will be exposed to the diamagnetic anisotropy associated with the induced ring currents in the benzene molecule, and shielding (or deshielding) of the solute protons will occur. Based on C_6D_6-induced NMR solvent shifts ($\Delta\delta_{CH_3}$ (A) = +0.17, $\Delta\delta_{SH}$ (A) = +0.12, $\Delta\delta_{CH_3}$ (B) = +0.20, $\Delta\delta_{SH}$ (B) = +0.06 ppm; + denotes upfield shift), the A- and B-form signals (Table 1) are tentatively assigned to the D,L- and the *meso*-form, respectively.

EXPERIMENTAL

^{1}H NMR spectra of 20 % (vol.) solutions were recorded at 60 MHz on a Varian A-60 spectrometer at 37 ± 2°C. TMS was used as internal reference standard. Coupling constants were measured on the 50 Hz scale.

IR spectra were recorded as 5 % solutions in CCl_4 on a Beckman IR 18 spectrophotometer.

PLC was carried out on 20 × 40 cm glass sheets with a 3 mm coating of Kiselgel PF$_{254+366}$ (Merck). Elution was performed with a mixture of ether and light petroleum (1:19). Boiling points are uncorrected. Yields refer to the isolated, pure products. Elemental analyses were carried out on the microanalytical laboratory of Løvens Kemiske Fabrik, Ballerup, Denmark.

2,5-Dimethyl-3-ethoxycarbonylthiophene (*IIa*), and *2,5-dimethyl-2-mercapto-4-ethoxycarbonyl-2,3-dihydrothiophene* (*IIIa*): 18.6 g (0.1 mol) of ethyl α-acetonylacetoacetate (Ia) were dissolved in 225 ml of 99 % ethanol, and the solution was cooled to −50°C. H_2S gas was passed through the solution for 1 h, followed by dry HCl gas also for 1 h, during which the temperature of the solution raised to −35°C. Finally, H_2S gas was passed through the solution at the latter temperature for additionally 3½ h. The reaction mixture was poured into a mixture of light petroleum (200 ml) and ice-water (400 ml) with manual stirring. The layers were separated, and the organic layer was washed with water, and dried ($CaSO_4$). After removed of light petroleum, the remaining oil (17.8 g) was subjected to PLC (13 sheets, 3 elutions). Two bands appeared. The combined 13 upper bands (R_F'' = 0.68) gave, after extraction with ether and subsequent evaporation of the latter, 10.5 g (57 %) of pure IIa, b.p.$_{12}$ 115°, n_D^{25} 1.5128 (lit.[12] b.p.$_8$ 106–109°, $n_D^{20.5}$ 1.5142); IR, ν[C=O]: 1715 cm^{-1} (s); ν[C=C]: 1560 cm^{-1} (m), 1500 cm^{-1} (m). (Found: C 58.72; H 6.57; S 16.82. Calc. for $C_9H_{12}O_2S$: C 58.69; H 6.57; S 17.38.)

Similarly, the 13 lower bands [R_F'' = 0.47) gave 3.7 g (17 %) of pure IIIa, b.p.$_{0.17}$ 82°, n_D^{25} 1.5451; IR, ν[S–H]: 2550 cm^{-1} (w), ν[C=O]: 1710 cm^{-1} (s); ν[C=C]: 1651 cm^{-1} (s). (Found: C 50.00; H 6.51; S 28.79. Calc. for $C_9H_{14}O_2S_2$: C 49.54; H 6.47; S 29.33.)

2,5-Dimethylthiophene (*IIb*), *2,5-dimethyl-2-mercapto-2,3-dihydrothiophene* (*IIIb*), *and 2,5-dimethyl-2,5-dimercaptotetrahydrothiophene* (*IVb*). 17.1 g (0.15 mol) of acetonylacetone were dissolved in 250 ml of 99 % ethanol, and treated with H_2S and HCl as described above (second H_2S-supply: 2½ h). Otherwise following the work-up procedure described above, 14.8 g of a colourless oil were obtained after the removal of light petroleum. Distillation through a Vigreux-column gave three fractions:

(1) 32–38°/12 mmHg, (2) 38–110°/12 mmHg, and (3) 110–112°/12 mmHg.

Redistillation of the first fraction gave 5.7 g (33 %) of pure IIb, b.p. 138°, n_D^{25} 1.5103 (lit.[3] b.p. 135.5–136°, n_D^{19} 1.51418).

The second fraction (~0.5 g) contained mainly IIb, but was not further characterized.

The third fraction (8.2 g) was subjected to PLC (8 sheets, one elution). The combined bands (R_F = 0.65) gave 730 mg (3.3 %) of pure IIIb, b.p.$_{0.6}$ 34–36°; IR, ν[S–H]: 2545 cm^{-1} (w), ν[C=C]: 1640 cm^{-1} (m). (Found: C 49.18; H 6.91; S 43.51. Calc. for $C_6H_{10}S_2$: C 49.31; H 6.90; S 43.79.)

The combined bands (R_F = 0.45) gave 4.1 g (15 %) of pure IVb, b.p.$_{0.6}$ 69°, n_D^{25} 1.5690; IR, ν[S–H]: 2540 cm^{-1} (m). (Found: C 40.13; H 6.83; S 52.84. Calc. for $C_6H_{12}S_3$: C 40.00; H 6.71; S 53.29.)

Attempted elimination of H_2S from IIIa. 1.2 g of IIIa was dissolved in 20 ml of 0.5 N ethanolic HCl, and the solution was refluxed for 4 h. After cooling, the solvent was evaporated, and the remaining oil (0.97 g) was examined by NMR. The spectrum showed the presence of only IIa and IIIa, in percentages of 27, and 73, respectively (calculated from signal integrals).

REFERENCES

1. Duus, F. *Tetrahedron* **28** (1972) 5923.
2. Paal, C. *Ber.* **18** (1886) 551.
3. Buu-Hoi, N. P. and Nguyen-Hoan. *Rec. Trav. Chim.* **67** (1948) 309.
4. Farrar, M. W. and Levine, R. *J. Am. Chem. Soc.* **72** (1950) 4433.
5. Trebaul, C. and Teste, J. *Bull. Soc. Chim. France* **1970** 2272.
6. Trebaul, C. *Bull. Chim. France* **1971** 1102.
7. Yur'ev, Yu. K. and Makarov, N. V. *Zh. Obshch. Khim.* **28** (1958) 885.
8. Demuynck, M. and Vialle, J. *Bull. Soc. Chim. France* **1967** 1213.
9. Bleisch, S. and Mayer, R. *Chem. Ber.* **100** (1967) 93.
10. Duus, F. and Lawesson, S.-O. *Tetrahedron* **27** (1971) 387.
11. Ledaal, T. *Tetrahedron Letters* **1968** 1683.
12. Schulte, K. E., Reisch, J. and Bergenthal, D. *Chem. Ber.* **101** (1968) 1540.

Received July 15, 1972.

ACTA CHEMICA SCANDINAVICA 27 (1973) 471–484

Crystal Structure of DL-Tryptophan Formate

ERIK BYE, ARVID MOSTAD and CHRISTIAN RØMMING

Department of Chemistry, University of Oslo, Oslo 3, Norway

The crystal structure of DL-tryptophan formate has been determined by X-ray methods using 2346 reflections recorded by counter methods. The crystals are monoclinic, space group $P2_1/c$, with unit cell dimensions $a = 11.23_7$ Å; $b = 6.72_8$ Å; $c = 16.01_3$ Å; $\beta = 96.2_9°$. The structure was refined to a conventional R-factor of 0.051; estimated standard deviations are 0.002 – 0.003 Å in interatomic distances and 0.15° in angles.

The 3-indolylmethyl part of the molecule is planar and the alanine moiety exists in the extended form with the acid group *anti* relative to the aromatic part. The crystals are built up by layers of molecules; within each layer there is an extensive network of hydrogen bonds whereas the layers are held together by van der Waals forces.

The crystal structure of tryptophan formate has been determined as part of the series of structure determinations of tyrosine and tryptophan derivatives being carried out in this laboratory. Preliminary results have previously been published.[1] In the present paper a more detailed account of the structure is given.

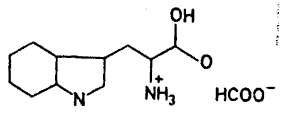

EXPERIMENTAL

Plate formed single crystals were formed by diffusion of diethyl ether into a solution of DL-tryptophan in formic acid.

Oscillation, Weissenberg and precession photographs indicated monoclinic symmetry. Systematically absent reflections were $h0l$ for l odd and $0k0$ for k odd; the space group is thus $P2_1/c$.

Unit cell dimensions were determined from diffractometer measurements on twelve general reflections and their Laue-symmetric equivalents. A manual Picker four-circle diffractometer was used with Cu$K\beta$ radiation ($\lambda = 1.3922$ Å). The computer program applied for the least-squares calculations as well as the computer programs used for the structure investigation are described in Ref. 2.

Three-dimensional intensity data were recorded on an automatic Picker four-circle diffractometer using graphite crystal monochromated Mo$K\alpha$ radiation. The crystal had dimensions $0.50 \times 0.25 \times 0.06$ mm^3 and was mounted with the [302] direction along the diffractometer ϕ-axis. The $\omega - 2\theta$ scanning mode with a 2θ scan speed of 1° min^{-1} was applied through the scan range of 0.5° below $2\theta(\alpha_1)$ to 0.5° above $2\theta(\alpha_2)$. Background counts were taken for 20 sec at each of the scan range limits. The take-off angle was 4° and the temperature was kept constant at 18°C. The intensities of three standard reflections were measured for every 100 reflections of the data set. They showed slow variation and also a small net decrease, and the data was accordingly adjusted. The standard deviations in the intensities were taken as the square root of the total counts with a 2 % addition.

The measurements included 2757 unique reflections with $\sin\theta/\lambda$ less than 0.7; 2346 had net intensity larger than $2\sigma(I)$ and were regarded as observed whereas the remaining reflections were excluded from the further calculations.

The intensity data were corrected for Lorentz and polarization effects.

Atomic form factors used were those of Hanson *et al.*[3] for oxygen, nitrogen, and carbon, and of Stewart *et al.*[4] for hydrogen.

CRYSTAL DATA

DL-Tryptophan formate (DL-α-ammonium-β-indolepropionic acid formate), $C_{11}H_{13}N_2O_2.CHO_2$, monoclinic. $a = 11.237(0.003)$ Å; $b = 6.728(0.002)$ Å; $c = 16.013(0.003)$ Å; $\beta = 96.29(0.01)°$. $V = 1203.4$ Å^3, $M = 250.26$, $F(000) = 528$, $Z = 4$. $D_{obs} = 1.37$ g cm^{-3}, $D_{calc} = 1.381$ g cm^{-3}. Absent reflections: $h0l$ when l is odd, $0k0$ when k is odd, space group $P2_1/c$.

STRUCTURE DETERMINATION

Preliminary scale and isotropic thermal vibration factors were calculated using Wilson's statistical method and unitary structure factors were computed. Three origin defining reflections were given positive sign and three additional reflections were assigned symbolic signs. The symbolic addition procedure[5,6] yielded signs or symbols for nine additional structure factors (acceptance probability 97 %). The fifteen unitary structure factors were now used for sign determination by the application of Sayre's equation[7] for each of the eight sign combinations of the three symbols. Signs for 165 structure factors were evaluated in each case followed by a Fourier synthesis.

In one of the Fourier maps the position of the indole part and the carbon atom directly bonded to it could readily be found and one Fourier refinement based on these atoms yielded information of the coordinates of all non-hydrogen atoms. Further Fourier refinements followed by several cycles of least squares refinement with anisotropic thermal parameters gave a conventional R-factor of 0.08. Most of hydrogen atoms were assigned coordinates from stereochemical considerations, the hydrogen atoms of the hydroxyl and ammonium groups were localized from difference Fourier maps. Final least squares refinement calculations with individual isotropic thermal parameters for hydrogen atoms yielded an R-factor of 0.051 ($R_w = 0.047$). A total difference Fourier map showed no electron density exceeding 0.3 e Å^{-3}.

A comparison of the observed and calculated structure factors is given in Table 1; the parameters for non-hydrogen atoms are listed in Table 2 and for hydrogen atoms in Table 3. The anisotropic temperature factor is given by

Table 1. Observed and calculated structure factors. The columns are $h, k, l, 10|F_o|$ and $10\,F_c$

-15	0	8	92	-81
-15	0	2	86	-81
-14	0	4	52	45
-14	0	6	95	-83
-13	0	14	21	-17
-13	0	12	41	39
-13	0	10	22	25
-13	0	8	62	-57
-13	0	4	27	-27
-13	0	2	35	36
-12	0	2	58	-59
-12	0	4	53	-46
-12	0	8	54	-49
-12	0	10	36	-34
-12	0	12	59	56
-12	0	14	61	-64
-12	0	16	37	33
-11	0	16	40	30
-11	0	12	29	-31
-11	0	8	71	-68
-11	0	6	110	105
-11	0	4	189	-180
-11	0	2	91	-89
-10	0	2	77	75
-10	0	4	74	76
-10	0	8	68	-65
-10	0	10	21	21
-10	0	14	65	66
-10	0	16	21	16
-10	0	18	32	-26
-9	0	12	174	177
-9	0	10	40	41
-9	0	8	77	76
-9	0	6	16	12
-9	0	4	257	247
-9	0	2	19	24
-8	0	2	264	261
-8	0	6	38	-37
-8	0	8	268	264
-8	0	10	22	-14
-8	0	12	17	18
-8	0	14	36	32
-8	0	16	32	-32
-8	0	18	104	96
-8	0	20	27	-39
-7	0	20	29	28
-7	0	18	28	23
-7	0	16	56	-55
-7	0	14	59	58
-7	0	12	224	-228
-7	0	10	116	116
-7	0	8	43	50
-7	0	6	165	-164
-7	0	4	54	-52
-7	0	2	75	79
-6	0	2	387	394
-6	0	4	289	-280
-6	0	6	224	-209
-6	0	8	189	188
-6	0	10	156	-162
-6	0	12	145	-149
-6	0	14	45	44
-6	0	16	189	187
-6	0	18	118	-118
-6	0	20	24	24
-5	0	20	34	32
-5	0	18	103	109
-5	0	16	55	58
-5	0	14	70	78
-5	0	12	19	-21
-5	0	10	184	179
-5	0	8	422	415
-5	0	6	294	-299
-5	0	4	45	48
-5	0	2	409	397
-4	0	2	250	236
-4	0	4	560	552
-4	0	8	100	98
-4	0	10	419	441
-4	0	14	257	265
-4	0	16	115	119
-4	0	20	83	83
-4	0	22	31	27
-3	0	22	23	-22
-3	0	20	78	75
-3	0	18	19	-15
-3	0	16	98	99
-3	0	14	40	43
-3	0	12	26	18
-3	0	10	275	293
-3	0	8	90	90
-3	0	6	183	186
-3	0	4	870	857
-3	0	2	1061	-1078
-2	0	2	674	687
-2	0	4	165	-180
-2	0	6	391	415
-2	0	8	188	-185
-2	0	10	15	5
-2	0	12	157	162
-2	0	14	180	188
-2	0	16	168	-178
-2	0	18	90	-94
-2	0	20	45	49
-1	0	20	61	63
-1	0	18	77	-82
-1	0	12	211	224
-1	0	10	186	-191
-1	0	8	204	211
-1	0	6	765	821
-1	0	4	246	241
-1	0	2	288	302
0	0	2	509	-515
0	0	4	326	-331
0	0	6	578	564
0	0	8	423	429
0	0	10	227	229
0	0	14	18	-9
0	0	16	109	114
0	0	18	58	-55
0	0	20	34	28
0	0	22	67	62
1	0	20	49	-42
1	0	18	31	38
1	0	16	131	129
1	0	14	66	64
1	0	12	258	-262
1	0	10	92	86
1	0	8	61	-51
1	0	6	835	827
1	0	4	334	-339
1	0	2	394	370
1	0	0	518	535
2	0	0	302	-309
2	0	2	42	-50
2	0	4	438	-433
2	0	6	138	-135
2	0	8	173	156
2	0	10	254	-250
2	0	12	63	-62
2	0	14	41	45
2	0	20	49	-49
3	0	18	88	78
3	0	14	201	-215
3	0	12	382	394
3	0	10	72	-70
3	0	8	400	-395
3	0	6	63	-67
3	0	4	307	302
3	0	2	389	376
3	0	0	445	-458
4	0	0	338	330
4	0	2	46	37
4	0	4	69	67
4	0	6	433	416
4	0	8	108	-109
4	0	10	95	100
4	0	12	404	422
4	0	14	88	-94
4	0	16	113	-119
4	0	18	123	114
5	0	18	104	91
5	0	16	59	-63
5	0	12	20	11
5	0	10	173	179
5	0	8	32	-27
5	0	6	226	233
5	0	4	322	315
5	0	2	87	-88
5	0	0	188	190
6	0	0	59	-58
6	0	2	99	-100
6	0	4	118	-127
6	0	6	149	148
6	0	8	69	68
6	0	10	193	-202
6	0	12	48	53
6	0	16	83	-87
6	0	18	77	-59
7	0	16	53	-55
7	0	12	66	-66
7	0	10	249	-262
7	0	8	60	64
7	0	6	40	-39
7	0	4	137	-134
7	0	2	112	113
7	0	0	176	-173
8	0	0	64	69
8	0	2	65	73
8	0	4	51	-48
8	0	6	101	-102
8	0	8	64	63
8	0	10	21	-14
8	0	12	53	-60
8	0	14	34	-50
8	0	16	36	-29
9	0	16	67	55
9	0	12	71	-75
9	0	10	33	26
9	0	8	34	-35
9	0	6	168	-168
9	0	4	212	220
9	0	0	31	-32
10	0	0	232	-237
10	0	4	111	-110
10	0	6	28	-29
10	0	8	78	-76
10	0	10	59	56
10	0	12	81	-77
11	0	8	54	-56
11	0	6	236	-238
11	0	4	66	62
11	0	2	31	31
11	0	0	211	-208
12	0	0	65	67
12	0	2	189	-186
12	0	4	64	55
12	0	6	65	-64
12	0	10	34	44
12	0	12	41	-43
13	0	10	44	43
13	0	6	25	12
13	0	4	69	-77
13	0	2	105	99
14	0	0	36	-41
14	0	2	46	-48
14	0	6	41	42
15	0	2	42	-41
15	0	0	44	45
15	1	2	40	36
15	1	3	31	34
14	1	6	35	34
14	1	5	26	-26
14	1	3	36	36
14	1	2	42	-42
14	1	0	105	97
13	1	0	56	-54
13	1	1	41	39
13	1	3	44	-40
13	1	6	29	25
13	1	9	47	46
12	1	10	40	38
12	1	9	40	40
12	1	8	42	-35
12	1	5	61	-62
12	1	4	106	-101
12	1	2	22	-15
12	1	1	37	45
11	1	0	65	65
11	1	1	31	24
11	1	2	95	-93
11	1	4	138	139
11	1	5	23	-25
11	1	7	28	-29
11	1	8	63	-64
10	1	12	42	38
10	1	11	38	33
10	1	10	43	46
10	1	9	57	-59
10	1	7	43	44
10	1	6	21	13
10	1	5	86	-89
10	1	4	49	49
10	1	3	53	55
10	1	2	170	170
10	1	0	100	102
9	1	0	64	68
9	1	1	51	-43
9	1	2	62	68
9	1	3	102	-100
9	1	4	78	82
9	1	5	175	179
9	1	6	138	143
9	1	7	36	-41
9	1	8	47	51
9	1	9	83	-81
9	1	11	25	32
9	1	12	79	-80
9	1	14	27	25
8	1	16	34	27
8	1	15	69	-58
8	1	12	43	-45
8	1	10	45	45
8	1	9	59	60
8	1	8	78	82
8	1	7	207	-209
8	1	6	79	-79
8	1	5	115	119
8	1	4	122	127
8	1	3	86	88
8	1	2	93	-88
8	1	1	131	-126
8	1	0	224	218
7	1	0	46	44
7	1	1	158	-159
7	1	4	61	58
7	1	5	86	90
7	1	6	117	119
7	1	8	52	54
7	1	9	120	-127
7	1	10	118	126
7	1	11	101	103
7	1	13	84	-84
6	1	18	44	35
6	1	17	72	67
6	1	14	127	123
6	1	13	148	-152
6	1	12	178	183
6	1	11	152	158
6	1	10	88	84
6	1	8	82	83
6	1	7	150	-147
6	1	6	158	153
6	1	5	157	152
6	1	4	153	158
6	1	3	116	111
6	1	2	301	293
6	1	1	32	25
6	1	0	107	104
5	1	0	173	-172
5	1	1	147	147
5	1	2	35	29
5	1	3	26	-28
5	1	4	493	484
5	1	5	81	-85
5	1	6	29	-18
5	1	7	47	50
5	1	8	198	206
5	1	9	201	213
5	1	10	60	64
5	1	11	26	26
5	1	12	103	106
5	1	13	60	-58
5	1	14	101	98
5	1	16	35	34
5	1	17	62	61
5	1	18	42	41
5	1	19	25	20
5	1	20	90	76
4	1	20	30	19
4	1	19	40	30
4	1	18	40	25
4	1	16	35	31
4	1	14	119	128
4	1	13	58	61
4	1	12	108	-115
4	1	11	26	-24
4	1	10	64	68
4	1	9	166	172
4	1	8	122	124
4	1	7	129	-129
4	1	6	299	-287
4	1	5	160	155
4	1	4	76	72
4	1	3	34	-35
4	1	2	139	130
4	1	1	22	23
4	1	0	309	-297
3	1	0	138	-144
3	1	1	423	-413
3	1	2	128	115
3	1	3	87	-84
3	1	4	351	-338
3	1	5	53	56
3	1	6	103	101
3	1	9	142	-150
3	1	10	41	-40
3	1	11	36	-35
3	1	12	36	-28
3	1	13	163	165
3	1	14	51	-52
3	1	15	42	36
3	1	17	119	-114
3	1	18	40	42
3	1	21	96	80
2	1	19	40	35
2	1	17	97	-100
2	1	15	107	112
2	1	14	47	42
2	1	13	75	76
2	1	12	148	155
2	1	11	57	-62
2	1	10	92	-98
2	1	9	332	-341
2	1	8	281	274
2	1	7	193	187
2	1	6	90	79
2	1	5	437	438
2	1	4	23	29
2	1	3	457	-456
2	1	2	849	820
2	1	1	706	-677
2	1	0	917	889
1	1	0	293	-283
1	1	1	42	45
1	1	2	577	551
1	1	3	541	-538
1	1	4	170	171
1	1	5	343	331
1	1	6	555	538
1	1	7	312	293
1	1	8	572	563
1	1	9	170	-169
1	1	10	101	-94
1	1	11	128	-133
1	1	12	102	107
1	1	13	189	191
1	1	14	162	160
1	1	15	41	-39
1	1	16	55	-57
1	1	17	44	-42
1	1	18	66	69
1	1	19	65	70
0	1	21	34	-26
0	1	19	111	101
0	1	18	46	46
0	1	17	45	47
0	1	15	155	-158
0	1	14	66	60
0	1	12	121	126
0	1	11	69	70
0	1	10	81	82
0	1	9	187	187
0	1	7	15	-15
0	1	6	288	271
0	1	5	165	-157
0	1	4	170	158
0	1	3	368	338
0	1	2	332	323
0	1	1	320	316
-1	1	1	307	302
-1	1	2	1074	-1068
-1	1	3	657	637
-1	1	4	302	-298
-1	1	5	279	-268
-1	1	6	65	-63
-1	1	7	43	-44
-1	1	8	107	-101
-1	1	9	296	301
-1	1	10	113	112
-1	1	11	152	-154
-1	1	12	170	176
-1	1	13	88	88
-1	1	14	208	-218
-1	1	15	45	-48
-1	1	16	45	43
-1	1	17	56	-56
-1	1	18	31	26
-1	1	19	54	54
-2	1	22	36	32
-2	1	20	36	-36
-2	1	18	56	54
-2	1	16	59	62
-2	1	15	25	-30
-2	1	14	57	58
-2	1	12	143	140
-2	1	11	86	87
-2	1	10	15	13
-2	1	9	55	-53
-2	1	8	272	-273
-2	1	7	215	217
-2	1	6	118	112
-2	1	5	522	-506
-2	1	4	180	-175
-2	1	3	768	766
-2	1	2	568	554
-2	1	1	279	286
-3	1	1	1108	1122
-3	1	2	74	68
-3	1	3	945	-966
-3	1	4	291	-289
-3	1	6	30	32
-3	1	7	443	437
-3	1	8	130	128
-3	1	9	21	26
-3	1	10	110	105
-3	1	11	78	-78
-3	1	12	80	75
-3	1	13	24	-21
-3	1	14	73	71
-3	1	15	188	183
-3	1	16	72	72
-3	1	18	67	66
-3	1	19	35	-33
-3	1	22	88	80
-4	1	21	50	47
-4	1	19	33	-34

Table 1. Continued.

-4	1	14	57	-	56
-4	1	16	229		228
-4	1	14	27	-	21
-4	1	13	226		228
-4	1	12	131	-	130
-4	1	11	171	-	167
-4	1	10	86	-	83
-4	1	9	72		63
-4	1	8	50		51
-4	1	7	233		228
-4	1	6	45		46
-4	1	5	28		17
-4	1	4	87		82
-4	1	3	187	-	192
-4	1	2	504	-	500
-4	1	1	135		144
-5	1	1	279		269
-5	1	2	338	-	344
-5	1	3	45	-	43
-5	1	4	465	-	479
-5	1	5	425	-	435
-5	1	6	104	-	106
-5	1	7	418		411
-5	1	8	293	-	296
-5	1	9	87	-	87
-5	1	11	67	-	64
-5	1	12	132	-	135
-5	1	13	75		74
-5	1	14	52	-	52
-5	1	15	31		28
-5	1	16	96	-	94
-5	1	17	31		29
-5	1	18	31	-	34
-5	1	19	39	-	33
-5	1	20	28		23
-5	1	21	33		33
-6	1	19	32	-	25
-6	1	16	86	-	80
-6	1	15	55		56
-6	1	14	94	-	93
-6	1	13	62	-	61
-6	1	12	32	-	36
-6	1	10	121	-	121
-6	1	9	79	-	75
-6	1	8	152	-	152
-6	1	7	27	-	25
-6	1	6	46	-	45
-6	1	5	77		79
-6	1	4	104	-	104
-6	1	3	56	-	54
-6	1	2	156	-	155
-6	1	1	129	-	132
-7	1	1	146		139
-7	1	2	182	-	173
-7	1	3	70		72
-7	1	4	291		300
-7	1	5	23	-	10
-7	1	6	32	-	28
-7	1	7	141	-	137
-7	1	8	125	-	128
-7	1	9	70		75
-7	1	10	45		44
-7	1	11	37		37
-7	1	12	69		66
-7	1	13	117	-	118
-7	1	15	31		27
-7	1	16	26		4
-7	1	18	94	-	93
-7	1	20	53		48
-8	1	17	46		40
-8	1	15	38	-	45
-8	1	14	31		26
-8	1	13	68	-	67
-8	1	12	90	-	87
-8	1	11	92		92
-8	1	10	139		144
-8	1	9	85		88
-8	1	7	97	-	101
-8	1	5	83		82
-8	1	4	175		182
-8	1	2	41	-	44
-8	1	1	152		149
-9	1	2	101	-	103
-9	1	3	188		191
-9	1	4	186	-	190
-9	1	6	98	-	103
-9	1	7	28	-	25
-9	1	10	31	-	35
-9	1	11	81		82
-9	1	12	38	-	34
-9	1	14	31	-	30
-9	1	17	34		26
-9	1	19	68	-	58
-10	1	18	33	-	31
-10	1	15	41		37
-10	1	13	29	-	28
-10	1	12	70	-	69
-10	1	11	46		46
-10	1	10	71	-	69
-10	1	7	41	-	48
-10	1	6	211	-	216
-10	1	5	30		35
-10	1	4	86	-	90
-10	1	3	82		78
-10	1	2	99	-	101
-10	1	1	93	-	95

-11	1	2	21		20
-11	1	3	24	-	30
-11	1	4	68	-	70
-11	1	6	96	-	98
-11	1	9	63		61
-11	1	10	132	-	24
-11	1	11	56	-	58
-11	1	12	85	-	86
-11	1	14	75		72
-11	1	15	51		46
-11	1	16	36	-	33
-11	1	17	42		27
-12	1	13	53	-	52
-12	1	11	48		44
-12	1	10	55	-	48
-12	1	9	33		33
-12	1	7	65	-	56
-12	1	6	47		54
-12	1	5	28		26
-12	1	4	24		11
-12	1	3	65	-	66
-12	1	2	24	-	24
-13	1	7	61	-	57
-13	1	9	56		62
-13	1	10	65	-	61
-13	1	12	38		41
-13	1	14	62	-	54
-14	1	9	65	-	64
-14	1	4	35	-	38
-14	1	3	74		66
-14	1	2	38		39
-14	1	1	61	-	54
-15	1	4	35		29
-15	1	5	30		31
-15	2	6	41		47
-15	2	2	43		44
-14	2	10	51		38
-13	2	13	86	-	79
-13	2	12	41		33
-13	2	9	37		30
-13	2	7	61	-	60
-13	2	6	49	-	42
-13	2	5	30		27
-13	2	4	98		93
-13	2	3	44	-	46
-13	2	2	46	-	46
-13	2	1	69		65
-12	2	2	24		16
-12	2	3	37		30
-12	2	4	67		68
-12	2	6	24	-	28
-12	2	9	41	-	46
-12	2	10	75		75
-12	2	12	48	-	37
-11	2	15	34	-	25
-11	2	9	24		18
-11	2	7	100	-	100
-11	2	6	108		109
-11	2	5	29	-	23
-11	2	4	47		46
-11	2	2	83		79
-10	2	1	22		11
-10	2	2	45	-	44
-10	2	3	122	-	125
-10	2	4	23		19
-10	2	6	35		38
-10	2	7	64	-	66
-10	2	9	127	-	128
-10	2	10	33	-	28
-10	2	11	96		92
-10	2	14	40	-	39
-10	2	15	45	-	48
-10	2	16	38		31
-9	2	18	61	-	58
-9	2	17	33		26
-9	2	15	32	-	32
-9	2	12	99	-	98
-9	2	9	106	-	111
-9	2	8	158	-	162
-9	2	7	137		143
-9	2	6	45	-	46
-9	2	4	33		39
-9	2	3	223	-	225
-9	2	2	77	-	79
-9	2	1	36	-	32
-8	2	2	27	-	27
-8	2	3	135	-	142
-8	2	5	47		40
-8	2	6	285	-	298
-8	2	7	164		169
-8	2	8	112		116
-8	2	9	37	-	38
-8	2	11	47	-	44
-8	2	12	97	-	97
-8	2	13	77		70
-8	2	14	27	-	24
-8	2	15	28		25
-8	2	16	23		19
-8	2	17	38	-	41
-8	2	18	42	-	35
-7	2	20	52	-	45
-7	2	19	71	-	64
-7	2	16	45		46
-7	2	17	30	-	21
-7	2	15	33		23
-7	2	13	73		74

-7	2	12	28	-	24
-7	2	11	66	-	63
-7	2	10	75		79
-7	2	9	24	-	8
-7	2	8	34		42
-7	2	7	44		38
-7	2	6	101	-	104
-7	2	5	78		79
-7	2	4	29	-	31
-7	2	3	97		94
-7	2	2	282		283
-7	2	1	35		42
-6	2	1	278		274
-6	2	2	328		330
-6	2	3	81		80
-6	2	4	374	-	369
-6	2	5	363	-	333
-6	2	6	175		180
-6	2	7	95		94
-6	2	8	44		42
-6	2	9	23	-	15
-6	2	10	129		134
-6	2	12	48	-	48
-6	2	13	35	-	32
-6	2	14	105	-	102
-6	2	15	94	-	93
-6	2	16	77		75
-6	2	20	49	-	49
-5	2	21	42	-	39
-5	2	20	43	-	34
-5	2	19	37		36
-5	2	18	95	-	93
-5	2	17	41		43
-5	2	16	34		31
-5	2	15	147	-	144
-5	2	14	112	-	114
-5	2	13	73	-	73
-5	2	12	62	-	59
-5	2	11	83	-	79
-5	2	10	90	-	91
-5	2	9	66		69
-5	2	8	53	-	56
-5	2	7	141	-	139
-5	2	6	278	-	284
-5	2	5	484	-	494
-5	2	4	137		143
-5	2	3	364		371
-5	2	2	245	-	236
-5	2	1	73		69
-4	2	1	230	-	219
-4	2	2	357	-	350
-4	2	3	309	-	319
-4	2	4	91	-	86
-4	2	5	189		189
-4	2	6	199	-	204
-4	2	7	65	-	58
-4	2	9	27	-	25
-4	2	10	212	-	217
-4	2	11	96	-	101
-4	2	12	197	-	207
-4	2	13	52	-	54
-4	2	15	24		29
-4	2	16	117	-	115
-4	2	17	36		34
-4	2	18	83	-	80
-4	2	19	35		39
-4	2	21	51	-	44
-3	2	19	64		65
-3	2	18	22	-	12
-3	2	16	173	-	174
-3	2	14	118		123
-3	2	13	88		86
-3	2	10	174	-	174
-3	2	9	94	-	98
-3	2	8	210	-	208
-3	2	7	105		97
-3	2	5	35	-	37
-3	2	4	293	-	281
-3	2	3	147		139
-3	2	2	389		392
-3	2	1	306	-	297
-2	2	1	769	-	746
-2	2	2	101		97
-2	2	3	216		211
-2	2	4	463	-	454
-2	2	5	121		117
-2	2	6	242		239
-2	2	7	192	-	187
-2	2	8	17		12
-2	2	9	97		91
-2	2	10	198	-	196
-2	2	11	183	-	188
-2	2	12	31		26
-2	2	13	310		320
-2	2	15	55		53
-2	2	16	21		17
-2	2	17	132	-	127
-2	2	18	35	-	33
-2	2	19	62		55
-2	2	20	82		81
-2	2	21	69		55
-1	2	20	40		35
-1	2	18	71	-	67
-1	2	17	53	-	58
-1	2	15	107		106
-1	2	14	28	-	30

-1	2	13	87	-	83
-1	2	12	46		48
-1	2	11	54	-	54
-1	2	10	188	-	196
-1	2	9	263		262
-1	2	6	399	-	370
-1	2	5	320	-	306
-1	2	4	356	-	353
-1	2	3	130	-	125
-1	2	2	287	-	282
-1	2	1	33	-	35
0	2	0	29		35
0	2	2	787	-	774
0	2	3	208		200
0	2	4	663	-	650
0	2	5	196	-	179
0	2	6	196	-	196
0	2	7	126		122
0	2	8	71		67
0	2	9	139		138
0	2	10	183	-	186
0	2	11	68		66
0	2	12	279	-	291
0	2	13	57	-	56
0	2	14	107		107
0	2	15	20	-	14
0	2	16	63	-	64
0	2	19	24	-	27
0	2	20	26	-	24
0	2	21	24		11
1	2	21	28	-	17
1	2	19	56	-	49
1	2	18	25	-	14
1	2	17	25		12
1	2	16	27	-	27
1	2	15	133		131
1	2	13	63	-	67
1	2	11	43	-	54
1	2	10	38	-	39
1	2	9	260		267
1	2	8	35	-	35
1	2	7	121	-	112
1	2	6	37		31
1	2	5	466		455
1	2	4	482	-	479
1	2	3	289		271
1	2	2	205	-	200
1	2	1	55		55
1	2	0	45		53
2	2	0	119		118
2	2	1	35	-	29
2	2	2	236	-	219
2	2	3	74		69
2	2	4	126		118
2	2	5	406		390
2	2	6	318		307
2	2	7	280	-	273
2	2	8	46		51
2	2	9	85		82
2	2	10	84	-	92
2	2	11	179		167
2	2	12	52		50
2	2	13	110	-	115
2	2	14	43		46
2	2	15	25		24
2	2	18	33		28
2	2	19	23		6
2	2	21	46		46
3	2	20	39		43
3	2	16	75	-	66
3	2	14	32	-	28
3	2	12	67		71
3	2	11	21		21
3	2	10	100		104
3	2	9	125	-	126
3	2	8	138	-	144
3	2	7	79	-	82
3	2	6	43	-	45
3	2	5	84		80
3	2	4	134		141
3	2	3	131	-	132
3	2	2	79		83
3	2	1	15		19
3	2	0	228	-	214
4	2	0	214	-	216
4	2	1	203	-	191
4	2	2	374	-	355
4	2	3	373	-	368
4	2	4	202		190
4	2	5	37		30
4	2	6	188	-	187
4	2	7	200		195
4	2	8	107	-	107
4	2	9	130	-	132
4	2	10	205	-	208
4	2	11	62	-	67
4	2	12	84		86
4	2	14	64	-	62
4	2	16	59	-	58
4	2	17	55		49
4	2	20	47		39
5	2	18	79		69
5	2	17	41		40
5	2	16	77	-	68
5	2	15	67		59
5	2	14	57	-	54

5	2	13	45		42
5	2	12	19		13
5	2	11	92		95
5	2	10	102		109
5	2	9	46	-	50
5	2	8	221	-	222
5	2	7	22		12
5	2	6	19	-	22
5	2	5	119		112
5	2	4	119	-	119
5	2	3	132	-	124
5	2	2	250	-	247
5	2	1	309		304
5	2	0	50		50
6	2	0	108	-	104
6	2	1	245		244
6	2	2	18		12
6	2	3	32	-	33
6	2	5	153		152
6	2	6	192		209
6	2	7	97		103
6	2	8	149	-	149
6	2	9	57	-	63
6	2	10	78		84
6	2	11	187		176
6	2	12	39		39
6	2	13	34		33
6	2	14	30		26
6	2	15	32		24
6	2	16	63		63
6	2	17	42		40
6	2	18	37		34
7	2	17	48		43
7	2	16	76		58
7	2	15	54	-	51
7	2	14	22		5
7	2	12	55		57
7	2	11	61		61
7	2	10	41		44
7	2	9	178		180
7	2	8	175		175
7	2	7	31		27
7	2	6	64	-	65
7	2	5	149	-	153
7	2	4	188		191
7	2	3	105		100
7	2	2	211	-	212
7	2	1	190		187
7	2	0	66		60
8	2	0	64	-	67
8	2	1	45	-	48
8	2	2	35	-	34
8	2	3	29		22
8	2	5	101		99
8	2	6	61		66
8	2	7	35		30
8	2	10	51	-	50
8	2	11	24		18
8	2	12	29		36
8	2	14	52		52
8	2	15	32	-	28
9	2	14	37	-	24
9	2	11	27	-	31
9	2	10	61		68
9	2	9	95	-	103
9	2	8	25	-	24
9	2	6	62		63
9	2	4	51	-	50
9	2	1	46		41
9	2	0	70	-	74
10	2	0	74		74
10	2	1	59		59
10	2	2	53		55
10	2	3	72		78
10	2	4	109		111
10	2	5	62		64
10	2	6	50	-	43
10	2	9	27	-	28
10	2	10	81		82
10	2	12	28		25
10	2	13	37		78
11	2	10	88		79
11	2	8	97		100
11	2	6	70	-	69
11	2	5	25	-	19
11	2	4	85		84
11	2	2	142		139
11	2	1	57		53
11	2	0	26	-	18
12	2	2	89		84
12	2	4	24		17
12	2	5	84	-	82
12	2	6	34	-	34
12	2	8	33		25
12	2	9	37		37
13	2	9	50		46
13	2	6	26		17
13	2	5	27	-	41
13	2	4	33	-	36
13	2	3	36		32
14	2	1	52	-	45
14	2	3	52		48
15	2	1	34		28
14	3	1	26		27
13	3	0	36		29
13	3	2	45	-	44

Table 1. Continued.

13	3	7	44	-39
12	3	9	39	44
12	3	6	78	76
12	3	3	25	0
12	3	2	23	19
12	3	0	72	73
11	3	0	92	-91
11	3	3	63	60
11	3	4	52	46
11	3	5	22	16
11	3	6	28	-24
11	3	7	34	29
11	3	8	42	-40
11	3	11	38	26
11	3	12	35	40
10	3	11	35	34
10	3	10	26	-16
10	3	9	36	36
10	3	8	28	-10
10	3	7	39	-46
10	3	6	97	-93
10	3	5	34	26
10	3	4	68	71
10	3	3	146	141
10	3	1	72	-75
10	3	0	160	-159
9	3	0	38	35
9	3	1	80	-83
9	3	2	208	-212
9	3	3	113	117
9	3	4	46	45
9	3	5	67	58
9	3	7	117	-119
9	3	8	67	-65
9	3	9	53	46
9	3	12	28	-34
9	3	13	43	37
8	3	16	67	63
8	3	15	25	23
8	3	13	29	19
8	3	12	64	-65
8	3	9	60	57
8	3	8	30	21
8	3	6	80	76
8	3	4	120	-123
8	3	3	63	66
8	3	1	176	-179
8	3	0	49	48
7	3	0	59	57
7	3	1	77	-73
7	3	2	82	78
7	3	3	64	59
7	3	4	144	-142
7	3	5	71	-64
7	3	6	103	-104
7	3	7	38	32
7	3	8	58	59
7	3	9	46	50
7	3	10	27	22
7	3	11	33	34
7	3	13	22	19
7	3	15	28	32
7	3	16	37	-29
7	3	17	55	53
6	3	17	48	43
6	3	16	26	-27
6	3	15	51	-49
6	3	12	39	-33
6	3	10	119	-120
6	3	9	42	34
6	3	8	20	26
6	3	7	27	26
6	3	6	178	-180
6	3	5	216	-215
6	3	3	45	-44
6	3	2	101	-102
6	3	1	64	63
6	3	0	210	-209
5	3	0	274	-269
5	3	1	25	-31
5	3	2	141	-147
5	3	3	102	-105
5	3	4	69	69
5	3	5	52	-57
5	3	6	87	-85
5	3	7	45	-39
5	3	8	303	-313
5	3	9	255	-264
5	3	12	31	-24
5	3	14	26	18
5	3	15	65	-70
5	3	16	86	-79
5	3	18	48	-48
4	3	15	112	-111
4	3	12	75	-79
4	3	11	26	-24
4	3	10	123	-127
4	3	9	116	-117
4	3	8	143	135
4	3	7	173	-175
4	3	6	24	-27
4	3	5	153	154
4	3	3	217	-203
4	3	2	263	-253
4	3	1	83	-85
4	3	0	62	-59
3	3	0	192	-187
3	3	1	202	-192
3	3	2	233	225
3	3	3	27	29
3	3	4	108	-106
3	3	5	102	112
3	3	6	47	48
3	3	7	214	213
3	3	9	130	-123
3	3	10	109	-118
3	3	11	52	-48
3	3	12	113	110
3	3	13	55	56
3	3	15	99	-94
3	3	17	42	44
3	3	18	43	-35
3	3	20	26	9
2	3	17	51	-45
2	3	16	40	-41
2	3	12	171	-176
2	3	11	208	215
2	3	10	67	69
2	3	9	207	-211
2	3	7	250	247
2	3	6	87	-97
2	3	4	378	-372
2	3	3	81	-81
2	3	2	53	43
2	3	1	312	295
1	3	0	221	-223
1	3	1	260	241
1	3	2	214	-205
1	3	3	616	-593
1	3	5	176	166
1	3	6	163	-161
1	3	8	17	-18
1	3	9	36	-39
1	3	10	334	-338
1	3	11	40	-35
1	3	12	31	36
1	3	14	54	-63
1	3	16	32	-35
1	3	17	50	-49
1	3	20	66	-59
0	3	19	41	-41
0	3	18	49	46
0	3	16	57	-67
0	3	14	131	-132
0	3	13	112	121
0	3	11	125	-130
0	3	10	20	-22
0	3	9	159	-164
0	3	7	79	-78
0	3	6	57	-62
0	3	5	42	-37
0	3	4	306	-293
0	3	3	504	-487
0	3	2	241	233
0	3	1	229	-228
-1	3	1	248	-240
-1	3	2	130	125
-1	3	3	469	-460
-1	3	4	210	207
-1	3	5	166	-160
-1	3	6	60	58
-1	3	7	54	50
-1	3	8	80	-76
-1	3	9	175	-172
-1	3	10	94	96
-1	3	11	51	57
-1	3	12	25	-24
-1	3	13	31	-29
-1	3	16	33	-34
-1	3	18	30	28
-1	3	19	60	57
-1	3	21	37	33
-2	3	21	50	46
-2	3	19	52	45
-2	3	18	94	-91
-2	3	16	40	38
-2	3	14	36	-43
-2	3	13	98	-95
-2	3	12	35	32
-2	3	11	72	77
-2	3	10	61	56
-2	3	9	62	-65
-2	3	8	81	-85
-2	3	7	198	-197
-2	3	6	20	-15
-2	3	5	43	28
-2	3	4	105	102
-2	3	3	133	-133
-2	3	2	108	106
-2	3	1	52	-51
-3	3	1	208	209
-3	3	2	128	-126
-3	3	3	29	25
-3	3	4	193	-197
-3	3	6	212	207
-3	3	7	305	-312
-3	3	8	74	-72
-3	3	10	176	-178
-3	3	11	71	-73
-3	3	13	97	-95
-3	3	14	56	-56
-3	3	16	41	42
-3	3	17	102	-94
-3	3	18	39	-36
-3	3	20	102	-93
-4	3	20	68	-56
-4	3	19	101	-92
-4	3	17	53	-53
-4	3	16	33	25
-4	3	13	122	-122
-4	3	12	94	-96
-4	3	11	199	-202
-4	3	10	66	-67
-4	3	9	22	21
-4	3	8	132	134
-4	3	7	128	-131
-4	3	6	111	116
-4	3	5	120	-119
-4	3	4	280	-284
-4	3	3	52	53
-4	3	2	17	-23
-5	3	1	125	-129
-5	3	2	29	-35
-5	3	3	17	21
-5	3	4	261	271
-5	3	5	145	-145
-5	3	6	19	18
-5	3	7	87	90
-5	3	8	100	105
-5	3	9	158	160
-5	3	10	75	84
-5	3	11	239	-241
-5	3	12	35	-35
-5	3	13	91	-91
-5	3	14	80	83
-5	3	15	107	103
-5	3	16	44	-37
-5	3	17	44	-37
-5	3	19	118	-110
-5	3	20	77	71
-6	3	20	47	43
-6	3	17	74	-69
-6	3	15	84	80
-6	3	14	64	-64
-6	3	12	93	94
-6	3	11	86	-87
-6	3	10	175	181
-6	3	9	184	184
-6	3	8	47	-47
-6	3	7	127	130
-6	3	5	203	-212
-6	3	4	175	180
-6	3	3	118	118
-6	3	2	34	35
-7	3	4	77	80
-7	3	5	81	-85
-7	3	6	232	242
-7	3	7	59	63
-7	3	8	265	-273
-7	3	9	42	41
-7	3	10	52	50
-7	3	12	55	53
-7	3	14	26	-15
-7	3	15	37	39
-7	3	17	56	-52
-7	3	18	27	-14
-8	3	18	27	22
-8	3	17	28	-28
-8	3	13	71	68
-8	3	11	28	-30
-8	3	10	33	-36
-8	3	9	24	-22
-8	3	8	103	95
-8	3	7	210	-223
-8	3	6	161	-170
-8	3	5	79	81
-8	3	4	91	96
-8	3	2	50	54
-8	3	1	87	-85
-9	3	1	187	-196
-9	3	2	65	63
-9	3	3	121	127
-9	3	5	145	-150
-9	3	6	51	47
-9	3	7	70	-65
-9	3	8	157	159
-9	3	11	41	-37
-9	3	12	52	-56
-9	3	14	49	42
-9	3	15	77	-73
-9	3	16	48	43
-9	3	17	48	41
-10	3	17	43	41
-10	3	16	32	21
-10	3	14	72	67
-10	3	13	73	-67
-10	3	12	56	-51
-10	3	11	45	43
-10	3	10	150	156
-10	3	9	63	-66
-10	3	7	29	36
-10	3	5	86	-84
-10	3	4	65	71
-10	3	3	97	95
-10	3	2	30	31
-11	3	1	121	124
-11	3	2	42	-43
-11	3	3	34	31
-11	3	6	30	31
-11	3	7	64	-67
-11	3	8	84	88
-11	3	9	77	85
-11	3	10	46	-44
-11	3	12	25	25
-11	3	13	44	-41
-11	3	15	26	-17
-12	3	14	27	18
-12	3	12	33	30
-12	3	11	31	-32
-12	3	10	30	-40
-12	3	7	35	37
-12	3	6	32	28
-12	3	5	23	8
-12	3	4	51	-53
-12	3	3	29	23
-12	3	2	51	59
-12	3	1	38	38
-13	3	3	29	-20
-13	3	4	29	13
-13	3	7	41	46
-13	3	9	38	-43
-14	3	7	26	17
-14	3	5	40	36
-14	3	4	69	64
-14	3	3	36	-42
-13	4	8	30	13
-12	4	2	51	-51
-12	4	4	98	95
-12	4	5	36	-22
-12	4	8	40	-37
-12	4	9	59	60
-11	4	14	41	-19
-11	4	10	76	86
-11	4	9	58	61
-11	4	6	124	-124
-11	4	4	35	38
-11	4	3	58	64
-11	4	2	90	-97
-11	4	1	59	56
-10	4	1	42	47
-10	4	2	32	-41
-10	4	3	84	96
-10	4	7	128	135
-10	4	8	47	-46
-10	4	11	30	26
-10	4	12	36	-33
-9	4	16	69	66
-9	4	13	32	27
-9	4	12	23	-7
-9	4	10	51	-50
-9	4	9	23	30
-9	4	8	150	156
-9	4	7	33	-39
-9	4	6	46	-46
-9	4	5	135	142
-9	4	4	27	-26
-9	4	3	22	2
-9	4	2	32	-36
-9	4	1	53	55
-8	4	1	76	-84
-8	4	3	29	-26
-8	4	4	63	62
-8	4	5	68	72
-8	4	6	20	-14
-8	4	8	63	-67
-8	4	9	91	-92
-8	4	10	87	86
-8	4	13	29	-29
-8	4	15	43	44
-8	4	16	91	78
-8	4	17	58	-51
-7	4	17	29	-25
-7	4	16	79	77
-7	4	14	62	-65
-7	4	13	46	50
-7	4	12	54	-61
-7	4	11	38	-32
-7	4	10	178	174
-7	4	8	77	-79
-7	4	7	80	-85
-7	4	6	35	34
-7	4	5	29	-24
-7	4	4	109	-116
-7	4	3	66	77
-7	4	2	45	50
-7	4	1	142	-146
-6	4	1	125	133
-6	4	2	169	174
-6	4	3	80	-76
-6	4	5	69	76
-6	4	6	157	-165
-6	4	7	34	35
-6	4	8	76	79
-6	4	9	67	68
-6	4	10	88	88
-6	4	12	40	31
-6	4	13	55	58
-6	4	14	71	-72
-6	4	15	25	24
-6	4	17	35	31
-6	4	18	25	17
-5	4	19	26	-1
-5	4	18	37	34
-5	4	17	77	67
-5	4	16	26	23
-5	4	15	41	40
-5	4	13	30	-25
-5	4	12	64	65
-5	4	11	136	141
-5	4	10	48	-49
-5	4	9	92	90
-5	4	8	90	90
-5	4	7	135	134
-5	4	6	171	173
-5	4	5	91	-90
-5	4	4	60	64
-5	4	3	86	88
-5	4	1	159	166
-4	4	1	116	118
-4	4	2	132	136
-4	4	3	112	-117
-4	4	4	66	-67
-4	4	5	96	95
-4	4	6	256	264
-4	4	7	44	44
-4	4	8	26	17
-4	4	9	70	74
-4	4	10	102	-101
-4	4	11	33	32
-4	4	12	137	137
-4	4	13	72	-71
-4	4	14	34	24
-4	4	15	59	57
-4	4	17	25	17
-4	4	19	37	-36
-3	4	19	83	-74
-3	4	18	58	-49
-3	4	16	86	-79
-3	4	15	25	-26
-3	4	14	104	101
-3	4	13	108	-109
-3	4	11	22	-24
-3	4	10	102	-111
-3	4	9	69	70
-3	4	8	67	63
-3	4	7	66	-70
-3	4	6	23	21
-3	4	5	38	36
-3	4	4	81	-82
-3	4	2	191	187
-3	4	1	52	47
-2	4	1	141	-132
-2	4	2	267	260
-2	4	3	205	235
-2	4	4	315	-316
-2	4	5	201	201
-2	4	6	30	-11
-2	4	7	48	-51
-2	4	8	150	157
-2	4	9	82	-85
-2	4	10	44	-45
-2	4	11	46	-46
-2	4	12	100	-103
-2	4	13	38	32
-2	4	14	91	93
-2	4	15	72	-71
-2	4	17	63	-56
-2	4	18	36	-33
-2	4	20	42	36
-1	4	18	75	67
-1	4	17	32	-24
-1	4	16	31	26
-1	4	15	51	-48
-1	4	12	53	56
-1	4	11	69	68
-1	4	10	116	-122
-1	4	9	119	-121
-1	4	8	301	306
-1	4	7	45	42
-1	4	6	49	51
-1	4	5	21	26
-1	4	4	234	-226
-1	4	3	192	193
-1	4	2	261	251
-1	4	1	71	74
0	4	0	61	62
0	4	1	28	33
0	4	2	33	40
0	4	3	91	-85
0	4	4	292	291
0	4	5	20	16
0	4	6	20	-17
0	4	7	63	-64
0	4	8	158	160
0	4	9	135	-145
0	4	10	89	-88
0	4	12	104	110
0	4	13	62	72
0	4	14	112	109
0	4	15	95	-91
0	4	17	39	31
0	4	18	30	20
0	4	19	25	19
1	4	17	31	-33
1	4	16	62	-64
1	4	15	26	25
1	4	14	95	91
1	4	13	70	-70
1	4	12	79	-75
1	4	11	51	-40

Table 1. Continued.

1	4	10	97	94
1	4	9	72	-61
1	4	8	40	-46
1	4	7	21	-19
1	4	6	85	79
1	4	5	217	-214
1	4	4	155	153
1	4	3	350	-349
1	4	2	66	-61
1	4	1	35	28
2	4	1	113	-116
2	4	2	86	81
2	4	3	161	-167
2	4	4	129	-128
2	4	5	195	-197
2	4	7	67	65
2	4	8	36	-30
2	4	11	130	-134
2	4	12	59	56
2	4	15	27	29
2	4	16	123	-120
2	4	18	26	-23
2	4	19	31	-32
3	4	17	50	-35
3	4	15	33	27
3	4	13	31	31
3	4	11	129	-133
3	4	10	177	-183
3	4	9	178	182
3	4	8	167	169
3	4	7	71	69
3	4	6	70	71
3	4	4	96	91
3	4	3	66	-68
3	4	2	180	-181
3	4	1	64	62
3	4	0	80	78
4	4	0	250	248
4	4	1	80	-85
4	4	2	139	-141
4	4	3	211	211
4	4	4	257	254
4	4	5	39	-43
4	4	7	123	132
4	4	8	62	-63
4	4	9	99	-97
4	4	10	124	122
4	4	11	38	41
4	4	12	34	-45
4	4	17	41	-33
5	4	17	31	-20
5	4	15	115	-99
5	4	13	32	-38
5	4	11	45	-36
5	4	10	58	61
5	4	8	207	-211
5	4	7	117	-116
5	4	5	68	-68
5	4	4	198	199
5	4	3	102	103
5	4	2	37	34
5	4	1	48	-46
5	4	0	38	-37
6	4	0	121	-114
6	4	1	20	-13
6	4	2	36	-32
6	4	3	68	-70
6	4	4	40	-38
6	4	5	51	51
6	4	6	121	-119
6	4	7	249	-252
6	4	8	44	-51
6	4	9	94	-86
6	4	13	64	-66
6	4	14	101	-97
6	4	15	91	-79
6	4	16	42	-34
6	4	17	50	-48
7	4	11	31	-34
7	4	9	37	-35
7	4	8	126	-134
7	4	7	33	-30
7	4	6	32	21
7	4	5	87	-87
7	4	2	186	-187
7	4	1	122	-122
8	4	0	73	73
8	4	1	101	-97
8	4	2	230	-239
8	4	3	62	-61
8	4	4	58	59
8	4	6	125	123
8	4	7	57	-56
8	4	8	80	-85
8	4	11	38	-28
8	4	13	26	26
9	4	13	27	15
9	4	11	52	-45
9	4	9	25	-35
9	4	7	56	51
9	4	6	38	-38
9	4	5	36	-30
9	4	4	33	24
9	4	3	110	-109
9	4	2	31	25
9	4	1	61	-52

10	4	0	74	-74
10	4	1	51	-62
10	4	2	81	80
10	4	3	64	-64
10	4	4	60	-62
10	4	6	31	-34
10	4	7	24	-10
10	4	9	30	-30
10	4	10	40	26
10	4	12	27	-25
11	4	4	99	-95
11	4	3	26	-23
11	4	2	38	33
11	4	1	24	20
12	4	0	41	-32
12	4	3	48	43
12	4	4	39	41
12	4	6	47	-49
12	4	7	53	-45
13	4	5	29	-35
13	4	3	27	32
13	4	2	29	26
13	4	1	35	28
13	4	0	64	-58
14	4	0	38	-32
12	5	9	37	-39
12	5	2	39	32
12	5	0	51	-43
11	5	0	65	-66
11	5	3	40	-35
11	5	4	65	59
11	5	7	35	-28
10	5	7	57	-43
10	5	6	65	60
10	5	4	39	-41
10	5	1	66	-64
10	5	[illegible]	31	-26
9	5	0	47	-47
9	5	3	49	51
9	5	4	50	50
9	5	5	30	-14
9	5	6	27	-23
9	5	7	42	-32
9	5	11	43	34
8	5	11	37	-32
8	5	8	37	28
8	5	7	57	-59
8	5	6	78	-73
8	5	5	57	55
8	5	4	45	-48
8	5	3	24	12
8	5	2	64	64
8	5	1	26	24
7	5	0	37	41
7	5	1	101	-107
7	5	2	50	47
7	5	3	117	111
7	5	4	108	-99
7	5	5	70	-70
7	5	6	71	69
7	5	7	60	-59
7	5	8	73	-75
7	5	12	60	-47
7	5	13	58	-50
7	5	14	81	-70
6	5	15	28	-19
6	5	14	45	-41
6	5	13	48	-39
6	5	11	25	24
6	5	9	31	-36
6	5	8	68	69
6	5	7	65	71
6	5	5	52	-57
6	5	4	94	-95
6	5	3	43	50
6	5	2	136	137
6	5	0	176	175
5	5	0	106	104
5	5	1	147	153
5	5	2	71	73
5	5	3	62	-71
5	5	5	209	212
5	5	6	93	100
5	5	7	31	-33
5	5	8	82	79
5	5	10	43	-45
5	5	11	75	71
5	5	12	55	52
5	5	13	71	62
5	5	16	32	-31
4	5	14	82	80
4	5	13	62	53
4	5	12	56	57
4	5	9	26	-3
4	5	8	116	-111
4	5	7	80	74
4	5	6	186	190
4	5	5	145	144
4	5	4	154	156
4	5	2	147	-147
4	5	1	22	-28
4	5	0	167	167
3	5	1	126	-130
3	5	2	306	-304
3	5	3	23	-27
3	5	4	87	91

3	5	5	31	-33
3	5	6	261	264
3	5	7	119	118
3	5	8	149	-150
3	5	9	90	-103
3	5	10	24	37
3	5	11	23	21
3	5	12	51	52
3	5	15	35	-19
3	5	16	35	34
2	5	18	61	54
2	5	16	37	41
2	5	15	62	-56
2	5	12	35	37
2	5	11	36	27
2	5	10	31	35
2	5	9	73	-74
2	5	6	48	49
2	5	5	22	-20
2	5	3	110	-113
2	5	2	51	-55
2	5	1	100	97
2	5	0	32	-25
1	5	0	93	-89
1	5	1	150	154
1	5	2	113	111
1	5	4	59	58
1	5	5	91	91
1	5	6	215	-221
1	5	8	79	79
1	5	10	164	165
1	5	11	49	47
1	5	12	30	33
1	5	13	25	19
1	5	14	46	-48
1	5	15	39	36
1	5	16	27	30
1	5	17	42	-35
1	5	18	81	77
0	5	17	36	-32
0	5	16	65	69
0	5	15	29	30
0	5	14	33	40
0	5	13	113	106
0	5	12	134	-132
0	5	11	29	-34
0	5	10	224	229
0	5	8	24	-18
0	5	7	102	103
0	5	6	276	-279
0	5	5	245	245
0	5	4	155	155
0	5	3	55	57
0	5	2	91	93
0	5	1	150	153
-1	5	1	165	169
-1	5	2	85	-81
-1	5	4	67	70
-1	5	5	89	93
-1	5	6	95	-92
-1	5	7	126	123
-1	5	10	39	-46
-1	5	11	38	34
-1	5	12	56	-62
-1	5	13	25	29
-1	5	14	42	47
-1	5	15	34	-39
-1	5	17	34	24
-1	5	18	54	-49
-2	5	18	42	-39
-2	5	17	38	-35
-2	5	15	42	42
-2	5	14	37	39
-2	5	13	45	-43
-2	5	12	62	-64
-2	5	11	37	29
-2	5	10	111	-112
-2	5	8	31	31
-2	5	7	148	155
-2	5	6	154	163
-2	5	5	24	-34
-2	5	4	150	-146
-2	5	2	55	49
-2	5	1	19	-16
-3	5	1	97	99
-3	5	2	120	-129
-3	5	3	103	105
-3	5	4	64	67
-3	5	5	29	-37
-3	5	6	49	46
-3	5	8	153	159
-3	5	9	98	98
-3	5	10	68	-73
-3	5	11	38	43
-3	5	12	41	-44
-3	5	13	63	59
-3	5	14	107	107
-3	5	15	50	44
-3	5	16	59	-56
-3	5	17	30	-26
-4	5	17	60	55
-4	5	15	80	75
-4	5	14	34	26
-4	5	13	65	59
-4	5	12	77	83
-4	5	11	47	-50

-4	5	10	23	-21
-4	5	9	197	203
-4	5	8	91	98
-4	5	6	71	-78
-4	5	5	66	74
-4	5	4	124	133
-4	5	3	53	-54
-4	5	2	25	24
-4	5	1	173	170
-5	5	1	51	-50
-5	5	2	55	-47
-5	5	3	117	115
-5	5	4	49	-48
-5	5	5	37	-25
-5	5	6	35	39
-5	5	7	47	52
-5	5	8	76	-82
-5	5	9	42	37
-5	5	10	63	68
-5	5	12	31	29
-5	5	15	111	107
-5	5	16	53	53
-6	5	15	33	30
-6	5	13	48	-44
-6	5	10	23	-10
-6	5	9	26	-12
-6	5	7	57	65
-6	5	6	118	-119
-6	5	5	133	-134
-6	5	2	29	44
-6	5	1	50	55
-7	5	1	55	59
-7	5	2	94	95
-7	5	4	125	-127
-7	5	5	43	39
-7	5	6	75	-79
-7	5	7	34	-37
-7	5	8	25	29
-7	5	11	55	-52
-7	5	12	26	30
-7	5	13	38	29
-7	5	14	32	-24
-8	5	15	31	26
-8	5	14	28	-16
-8	5	10	43	-35
-8	5	9	53	50
-8	5	8	56	-56
-8	5	5	44	34
-8	5	4	44	-36
-8	5	3	123	130
-8	5	2	26	16
-8	5	1	59	-64
-9	5	3	106	104
-9	5	4	72	-69
-9	5	6	60	62
-9	5	8	38	-41
-9	5	9	96	92
-9	5	10	79	-75
-10	5	13	30	-20
-10	5	12	40	-38
-10	5	11	38	39
-10	5	10	54	-54
-10	5	8	31	30
-10	5	6	32	34
-10	5	5	33	-33
-10	5	2	48	-44
-11	5	5	37	-40
-11	5	6	27	24
-11	5	7	46	-34
-11	5	11	54	49
-12	5	6	45	-43
-12	5	1	28	-28
-13	5	5	34	25
-11	6	3	28	-33
-11	6	2	42	28
-11	6	1	35	21
-10	6	1	44	-39
-10	6	2	54	55
-10	6	3	38	-43
-10	6	5	51	-48
-9	6	5	33	-26
-9	6	8	51	43
-9	6	7	62	-56
-9	6	2	42	36
-9	6	1	118	-111
-8	6	1	33	-36
-8	6	4	52	45
-8	6	5	56	51
-8	6	6	30	-13
-8	6	7	36	-37
-8	6	8	45	40
-8	6	9	40	-37
-8	6	12	59	-49
-7	6	14	44	33
-7	6	12	59	-60
-7	6	10	39	-31
-7	6	9	50	46
-7	6	7	53	-49
-7	6	5	26	28
-7	6	4	25	-39
-7	6	2	79	84
-7	6	1	51	-59
-6	6	1	89	-99
-6	6	2	57	50
-6	6	3	55	-55
-6	6	6	55	-51

-5	6	9	28	-34
-6	6	12	40	-44
-6	6	13	62	-51
-6	6	15	42	37
-5	6	14	26	14
-5	6	13	55	-54
-5	6	12	40	-31
-5	6	11	39	-32
-5	6	9	39	-35
-5	6	6	161	-163
-5	6	3	123	-119
-5	6	2	34	34
-4	6	1	165	175
-4	6	2	22	-19
-4	6	3	71	-73
-4	6	5	48	-56
-4	6	6	149	-146
-4	6	7	31	-26
-4	6	8	86	81
-4	6	9	31	40
-4	6	11	24	23
-4	6	12	28	-23
-4	6	13	28	-33
-4	6	14	27	27
-3	6	15	64	55
-3	6	14	50	48
-3	6	13	81	-74
-3	6	11	73	65
-3	6	10	68	73
-3	6	9	26	31
-3	6	8	27	-16
-3	6	6	85	88
-3	6	4	113	-112
-3	6	3	60	56
-3	6	2	40	38
-3	6	1	38	-33
-2	6	1	47	-48
-2	6	2	70	-70
-2	6	3	82	-85
-2	6	5	88	92
-2	6	6	141	139
-2	6	7	71	-71
-2	6	11	38	29
-2	6	15	48	-45
-2	6	16	41	31
-2	6	17	67	66
-1	6	17	38	-23
-1	6	15	46	-42
-1	6	14	27	20
-1	6	13	80	76
-1	6	12	37	-37
-1	6	11	38	50
-1	6	10	46	-51
-1	6	9	163	-163
-1	6	8	45	44
-1	6	7	34	-34
-1	6	5	56	53
-1	6	4	76	77
-1	6	3	57	64
-1	6	2	127	-130
-1	6	1	77	-75
0	6	0	32	40
0	6	1	76	-73
0	6	3	38	43
0	6	6	27	26
0	6	7	76	68
0	6	8	27	21
0	6	9	98	-98
0	6	10	109	-108
0	6	11	73	69
0	6	13	58	57
0	6	16	70	-65
1	6	13	44	47
1	6	11	33	29
1	6	10	60	-64
1	6	9	51	48
1	6	8	27	-20
1	6	7	102	100
1	6	6	94	95
1	6	5	31	29
1	6	4	168	-168
1	6	3	136	-136
1	6	2	44	52
1	6	1	281	282
1	6	0	159	161
2	6	0	46	47
2	6	1	76	80
2	6	3	56	-55
2	6	4	90	-116
2	6	5	76	-71
2	6	6	77	76
2	6	7	197	204
2	6	8	119	-120
2	6	9	65	64
2	6	10	47	50
2	6	11	111	-100
2	6	12	41	37
2	6	14	66	-56
2	6	15	50	46
2	6	16	69	61
3	6	15	87	76
3	6	12	35	36
3	6	11	107	-99
3	6	9	60	65
3	6	7	61	60
3	6	6	49	-50

Table 1. Continued.

3	6	5	113	- 111	11	6	0	43	- 42	1	7	0	85	90	-4	7	1	35	29	0	8	8	39	- 28
3	6	3	68	67	10	7	1	31	30	1	7	1	53	- 55	-5	7	1	36	35	0	8	9	44	41
3	6	2	119	- 120	9	7	0	49	38	1	7	2	56	47	-5	7	3	35	- 43	1	8	11	28	- 25
3	6	1	50	- 44	9	7	1	40	42	1	7	3	38	- 36	-5	7	7	49	- 45	1	8	10	29	- 8
4	6	0	76	- 74	9	7	3	82	- 77	1	7	4	29	24	-5	7	6	32	- 27	1	8	6	43	45
4	6	1	41	37	9	7	4	36	26	1	7	5	52	51	-5	7	9	44	- 42	1	8	5	27	- 22
4	6	2	74	- 69	9	7	5	34	37	1	7	6	34	- 40	-5	7	10	44	- 40	1	8	4	43	- 44
4	6	3	104	103	8	7	6	37	39	1	7	7	67	- 69	-6	7	11	57	53	1	8	1	25	- 26
4	6	4	53	50	8	7	4	28	- 27	1	7	10	54	55	-6	7	10	43	40	2	8	0	37	- 32
4	6	5	22	- 10	8	7	2	48	42	1	7	11	36	- 42	-6	7	9	46	- 46	2	8	1	27	17
4	6	6	44	- 37	8	7	0	28	27	1	7	14	102	- 92	-6	7	4	48	40	2	8	2	58	58
4	6	7	38	- 43	7	7	1	27	- 24	0	7	14	36	- 29	-6	7	2	28	- 15	2	8	4	31	- 26
4	6	8	31	35	7	7	2	33	35	0	7	11	41	- 38	-6	7	1	27	18	2	8	6	45	41
4	6	11	35	34	7	7	3	82	83	0	7	10	39	33	-7	7	2	53	45	2	8	8	27	- 15
4	6	10	36	40	7	7	5	51	45	0	7	9	28	23	-8	7	5	54	60	2	8	9	34	- 24
4	6	13	46	36	7	7	7	33	- 31	0	7	7	112	- 109	-8	7	3	34	- 28	2	8	10	31	16
4	6	14	41	35	6	7	10	57	46	0	7	6	34	- 23	-8	7	1	38	36	3	8	5	36	31
5	6	12	68	58	6	7	8	58	45	0	7	5	77	- 79	-9	7	0	43	- 35	3	8	3	68	- 64
5	6	12	116	106	6	7	7	30	- 36	0	7	2	83	88	-10	7	4	36	- 31	3	8	1	52	45
5	6	11	78	62	6	7	5	48	47	-1	7	1	65	- 61	-10	7	3	37	46	3	8	0	86	75
5	6	9	49	43	6	7	3	35	36	-1	7	2	59	57	-10	7	2	42	- 43	4	8	1	74	69
5	6	8	116	114	6	7	2	32	- 29	-1	7	3	95	100	-7	8	2	58	- 60	4	8	2	66	- 66
5	6	7	137	132	6	7	1	98	- 90	-1	7	5	134	- 132	-6	8	1	79	91	4	8	5	29	- 14
5	6	1	30	23	5	7	1	83	- 76	-1	7	6	44	- 43	-6	8	4	57	46	4	8	6	44	- 36
5	6	0	65	- 63	5	7	2	65	- 61	-1	7	7	73	74	-5	8	6	75	79	5	8	5	29	- 20
6	6	0	32	- 23	5	7	3	57	- 50	-1	7	8	63	47	-5	8	8	66	- 63	5	8	3	42	- 39
6	6	1	88	- 70	5	7	4	46	- 43	-1	7	9	72	- 62	-5	8	3	42	39	5	8	2	52	- 50
6	6	2	102	102	5	7	5	69	59	-1	7	14	54	48	-5	8	2	124	115	5	8	1	44	- 40
6	6	4	39	43	5	7	7	65	- 66	-2	7	13	63	54	-5	8	1	40	19	5	8	0	47	- 40
6	6	5	79	73	4	7	13	45	36	-2	7	12	36	- 26	-4	8	1	27	- 39	6	8	0	69	- 64
6	6	6	144	144	4	7	11	36	- 32	-2	7	11	88	- 80	-4	8	3	52	47	6	8	1	39	- 32
6	6	7	31	- 20	4	7	10	62	- 59	-2	7	7	131	127	-4	8	5	46	- 41	6	8	6	32	23
6	6	8	42	- 39	4	7	8	70	- 67	-2	7	5	100	- 107	-4	8	6	71	- 66	7	8	2	33	31
6	6	9	72	63	4	7	6	27	23	-2	7	4	44	- 33	-4	8	8	35	32	7	8	1	29	- 7
6	6	10	32	26	4	7	4	32	- 38	-2	7	2	87	- 89	-4	8	10	28	25	7	8	0	28	- 28
6	6	11	88	81	4	7	3	138	- 131	-2	7	1	129	138	-3	8	11	35	- 31	4	9	0	42	- 40
6	6	12	54	55	4	7	2	61	- 58	-3	7	1	41	45	-3	8	10	63	59	3	9	1	34	31
7	6	5	99	97	4	7	0	27	20	-3	7	2	103	- 107	-3	8	8	49	- 47	3	9	2	30	29
7	6	4	69	69	3	7	1	41	- 44	-3	7	3	87	- 84	-3	8	7	49	- 41	2	9	4	29	- 27
7	6	2	31	29	3	7	2	27	- 20	-3	7	5	74	- 77	-3	8	6	51	43	2	9	2	38	30
7	6	1	36	- 31	3	7	3	31	- 31	-3	7	7	94	87	-3	8	4	51	- 43	1	9	1	29	19
8	6	4	82	80	3	7	6	29	- 21	-3	7	8	26	- 22	-3	8	2	41	- 32	0	9	0	41	39
8	6	6	99	- 94	3	7	9	36	- 29	-3	7	9	29	31	-3	8	1	33	- 28	0	9	4	29	- 23
8	6	7	27	23	3	7	10	54	- 55	-3	7	10	27	- 27	-2	8	1	28	- 25	0	9	3	43	- 46
9	6	5	29	9	3	7	13	30	36	-3	7	11	84	- 80	-2	8	10	53	- 45	-1	9	1	32	- 21
9	6	5	31	- 15	2	7	13	36	29	-3	7	14	39	31	-1	8	10	64	- 61	-1	9	2	27	27
9	6	4	49	- 40	2	7	12	35	- 31	-4	7	12	32	23	-1	8	2	82	- 78	-1	9	4	52	- 40
9	6	3	44	33	2	7	9	25	- 26	-4	7	11	39	- 36	-1	8	1	27	- 29	-2	9	5	40	- 40
9	6	2	26	30	2	7	7	39	45	-4	7	10	80	- 73	0	8	6	72	76	-2	9	3	31	- 21
10	6	0	54	- 51	2	7	5	50	- 53	-4	7	8	34	- 32	0	8	2	59	- 64	-2	9	2	41	38
10	6	3	33	- 34	2	7	4	53	53	-4	7	5	78	- 71	0	8	4	45	- 54	-3	9	1	42	39
10	6	4	32	27	2	7	3	70	64	-4	7	4	46	- 40	0	8	5	23	31	-4	9	2	62	- 59
10	6	5	87	81	2	7	2	27	- 22	-4	7	3	82	- 84	0	8	6	24	36	-4	9	1	58	55
10	6	6	29	- 32	2	7	1	144	- 146	-4	7	2	42	39	0	8	7	26	- 19					

$$\exp -(B11h^2+B22k^2+B33l^2+B12hk+B13hl+B23kl).$$

Magnitudes and directions of the principal axes of the ellipsoids of vibration are given in Table 4. The analysis of the thermal parameters showed that the methylindole part of the molecule to a good approximation can be regarded as a rigid body. The positional parameters of the atoms of this group were corrected for librational effects. No corrections were performed for the rest of the molecule.

Standard deviations in bond lengths and angles were calculated using the correlation matrix from the last least-squares refinement cycle but ignoring the standard deviations in cell parameters. For distances and angles the standard deviations were found to be 0.002 – 0.003 Å and 0.15°, respectively, except for the bond lengths involving hydrogen where the standard deviation is 0.02 Å.

DISCUSSION

Interatomic distances and bond angles are listed in Table 5; bond lengths and angles are shown in Fig. 1 in which the numbering of the atoms is also indicated. The molecular arrangement and hydrogen bonding system are illustrated in Figs. 2 and 3.

Table 2. Fractional atomic coordinates and thermal parameters with standard deviations ($\times 10^5$) for non-hydrogen atoms.

Atom	x	y	z	$B11$	$B22$	$B33$	$B12$	$B13$	$B23$
N1	24678	50370	27235	842	1459	437	−6	216	−438
	12	20	9	13	35	7	36	15	25
C2	20728	42927	19447	671	1431	391	−198	88	71
	13	24	10	14	40	7	41	16	29
C3	26182	25425	18144	511	1356	298	−396	106	−88
	12	23	9	11	27	6	36	13	26
C4	41920	6009	28133	646	2393	380	486	97	−261
	14	27	10	14	49	8	36	16	34
C5	48286	6908	36010	757	3765	470	1170	−57	−16
	16	34	12	16	69	9	60	19	43
C6	47011	22972	41392	819	4776	338	213	−157	−427
	15	37	10	17	82	8	64	18	44
C7	39342	38305	39079	833	3248	347	−520	154	−833
	15	31	10	16	62	7	55	17	37
C8	32855	37392	31182	751	1815	334	−397	183	−430
	13	25	9	13	42	7	40	15	30
C9	34028	21394	25630	490	1550	300	−251	162	−245
	12	23	9	12	39	6	37	13	27
C10	24047	12857	10433	702	1686	275	−546	90	−79
	13	25	9	14	42	6	42	15	28
C11	16571	−5641	11741	644	1465	221	−290	−2	−2
	13	24	8	13	38	6	39	13	25
C12	13522	−17159	3597	767	1368	235	−453	60	1
	12	23	8	14	39	6	41	14	25
O13	22810	−21321	−197	747	3169	393	−620	209	−1016
	9	19	6	10	40	5	35	12	25
O14	3278	−21431	197	749	2667	312	−882	63	−545
	8	19	6	11	36	5	33	11	22
N15	5117	−321	15104	710	1491	227	−476	71	−80
	10	18	7	11	33	5	33	12	20
C16	12109	3533	36877	717	1641	216	64	101	−87
	13	24	8	14	41	5	41	14	25
O17	6435	13985	31516	732	1533	239	284	87	52
	8	15	5	9	26	4	27	95	18
O18	15775	−13832	35874	1023	1532	286	765	250	127
	10	16	6	11	27	4	30	11	19

Table 3. Fractional coordinates ($\times 10^4$) and isotropic thermal parameters (Å^2) with standard deviations for hydrogen atoms.

Atom	x	y	z	B
H1	2214	6206	2930	4.9
	15	28	11	.4
H2	1500	4998	1508	3.9
	13	24	10	.4
H4	4264	−516	2430	3.3
	13	23	9	.4
H5	5398	−388	3810	5.7
	15	29	12	.5
H6	5099	2371	4721	5.2
	15	29	11	.4
H7	3836	4914	4272	4.7
	14	26	11	.4
H101	3165	791	864	3.7
	13	24	10	.4
H102	1933	2079	556	3.8
	13	25	10	.4
H11	2134	−1452	1592	2.8
	12	22	9	.3
H13	1983	2773	−603	7.4
	17	31	13	.6
H151	672	542	2047	3.6
	13	23	10	.4
H152	17	−1195	1556	4.7
	14	26	10	.5
H153	108	905	1146	3.8
	13	24	10	.4
H16	1389	963	4250	4.0
	13	24	10	.4

The crystal structure is built up by molecular double layers parallel to (100). The layers are connected through van der Waals forces whereas the ions within the layers are bonded together by an extensive hydrogen bond system. Similar arrangements are reported for the tryptophan halides.[8] Dimers of tryptophan ions are formed about centers of symmetry through hydrogen bonds between carboxyl and amino groups (O14 – N15 3.026 Å). These are the only direct hydrogen bonds between two tryptophan molecules. The formate anions link the dimers together with hydrogen bonds to form the layers. All hetero atoms

Table 4. R.m.s. amplitudes of vibration and B-values (Å^2) along the principal axes of vibration given by the components of a unit vector **e** in fractional coordinates ($\times 10^4$).

Atom	$(\overline{u^2})^{\frac{1}{2}}$	B	e_x	e_y	e_z
	0.249	4.90	343	531	558
N1	0.228	4.09	825	310	141
	0.168	2.22	−54	1353	251
	0.226	4.02	−136	236	599
C2	0.208	3.43	839	430	185
	0.177	2.47	280	1403	−44
	0.202	3.22	521	823	412
C3	0.191	2.89	−404	580	470
	0.155	1.90	606	1093	61
	0.252	5.00	303	1217	−267
C4	0.215	3.64	422	415	555
	0.187	2.77	−729	746	126
	0.312	7.70	381	1322	−75
C5	0.250	4.94	−124	367	589
	0.190	2.86	801	−571	204
	0.335	8.88	96	1448	−116
C6	0.245	4.72	−715	302	299
	0.187	2.77	530	145	540
	0.297	6.96	227	−1286	288
C7	0.226	4.02	850	204	110
	0.180	2.55	164	716	548
	0.238	4.46	343	−1000	421
C8	0.184	2.68	−690	215	335
	0.171	2.31	456	1074	324
	0.213	3.59	347	914	456
C9	0.176	2.43	−318	874	429
	0.167	2.21	762	781	53
	0.229	4.13	712	901	53
C10	0.189	2.81	138	307	593
	0.174	2.40	525	1141	201
	0.212	3.54	−770	646	108
C11	0.177	2.48	270	1271	−243
	0.165	2.15	369	420	569
	0.229	4.14	−820	566	16
C12	0.174	2.39	89	−135	626
	0.167	2.19	348	1367	55
	0.305	7.36	230	−1212	342
O13	0.211	3.52	843	136	−137
	0.178	2.50	194	850	509

Table 4. Continued.

	0.274	5.94	428	−1237	208
O14	0.214	3.62	620	241	−391
	0.167	2.21	483	787	446
	0.224	3.96	778	−733	32
N15	0.176	2.45	275	904	−436
	0.165	2.15	348	925	451
	0.213	3.60	882	249	38
C16	0.195	3.00	156	−1425	152
	0.164	2.13	8	339	609
	0.220	3.83	830	554	37
O17	0.183	2.64	−293	1277	223
	0.174	2.38	164	−522	586
	0.267	5.62	822	560	142
O18	0.187	2.75	112	42	−611
	0.171	2.30	338	−1376	39

Table 5. Bond lengths (Å) and bond angles (°) in DL-tryptophan formate.

	Bond length	Corrected	Bond angle	
N1 – C2	1.372	1.376	N1 – C2 – C3	110.53
N1 – C8	1.371	1.377	N1 – C8 – C9	107.43
C2 – C3	1.354	1.360	C2 – N1 – C8	108.68
C3 – C9	1.434	1.440	C2 – C3 – C9	106.43
C3 – C10	1.494	1.498	C3 – C9 – C8	106.92
C4 – C9	1.393	1.400	C3 – C9 – C4	134.01
C4 – C5	1.382	1.386	C9 – C4 – C5	118.67
C5 – C6	1.399	1.404	C4 – C5 – O6	121.22
C6 – C7	1.369	1.375	C5 – C6 – C7	121.29
C7 – C8	1.390	1.395	C6 – C7 – C8	117.68
C8 – C9	1.412	1.418	C7 – C8 – C9	122.07
C10 – C11	1.529		C8 – C9 – C4	119.07
C11 – C12	1.523		C7 – C8 – N1	130.50
C11 – N15	1.492		C2 – C3 – C10	125.81
C12 – O13	1.295		C9 – C3 – C10	127.74
C12 – O14	1.214		C3 – C10 – C11	112.85
C16 – O17	1.232		C10 – C11 – C12	111.85
C16 – O18	1.255		C10 – C11 – N15	111.27
N1 – H1	0.91		C12 – C11 – N15	108.00
C2 – H2	0.95		C11 – C12 – O13	113.24
C4 – H4	0.98		C11 – C12 – O14	121.88
C5 – H5	1.00		O13 – C12 – O14	124.86
C6 – H6	0.99		O17 – C16 – O18	126.46
C7 – H7	0.95			
C10 – H101	0.99		Hydrogen bond lengths	
C10 – H102	1.04		N1 – O18 (x, $1+y$, z)	3.003
C11 – H11	1.01		O13 – O18 (x, $-\frac{1}{2}-y$, $-\frac{1}{2}+z$)	2.492
O13 – H13	1.05		N15 – O14 ($-x$, $-y$, $-z$)	3.026
N15 – H151	0.94		N15 – O17 (x, y, z)	2.787
N15 – H152	0.97		N15 – O17 ($-x$, $-\frac{1}{2}+y$, $\frac{1}{2}-z$)	2.811
N15 – H153	0.94			
C16 – H16	0.99			

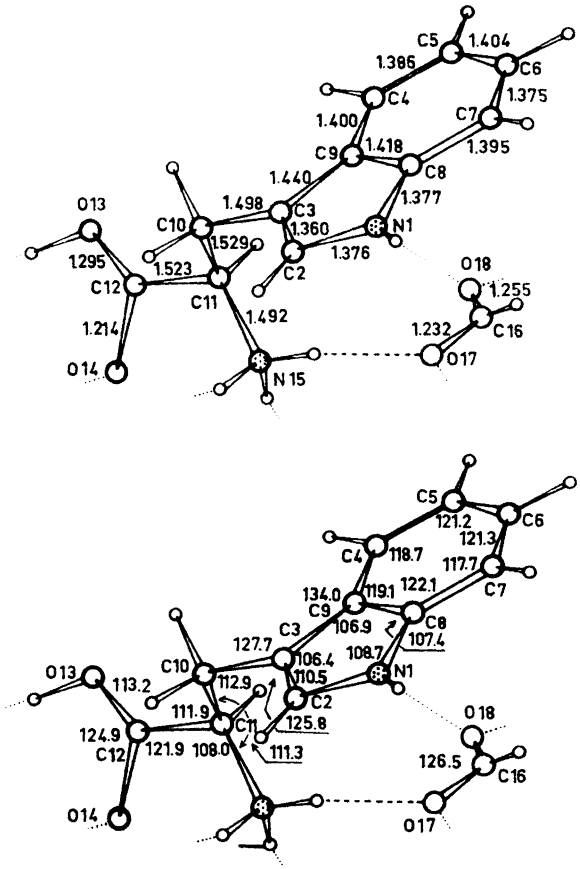

Fig. 1. Bond lengths (Å) and angles (°) in DL-tryptophan formate. Bond lengths in the 3-indolylmethyl-part are corrected for thermal effects.

of the tryptophan molecules are engaged in the hydrogen bond network; each tryptophan molecule is thus donor in five such bonds and acceptor in one. Each formate ion is hydrogen acceptor in four hydrogen bonds involving different tryptophan molecules (N1 – O18 3.003 Å, N15′ – O17 2.787 Å, O13″ – O18 2.492 Å, and N15″ – O17 2.811 Å). The short distance of 2.492 Å between O13″ and O18 indicates a rather strong competition for the proton situated between the carboxy oxygen atoms. The O13 – H bond is found to be relatively long (*cf.* Table 5). The angles O13″ – H···O18 and C16 – O18···H were found to be 179° and 110°, respectively.

The two C – O bond lengths in the formate ion, C16 – C17 1.232 Å and C16 – O18 1.255 Å, are consistent with the ionized state of the molecule. The difference between the two is highly significant, however, and the greater

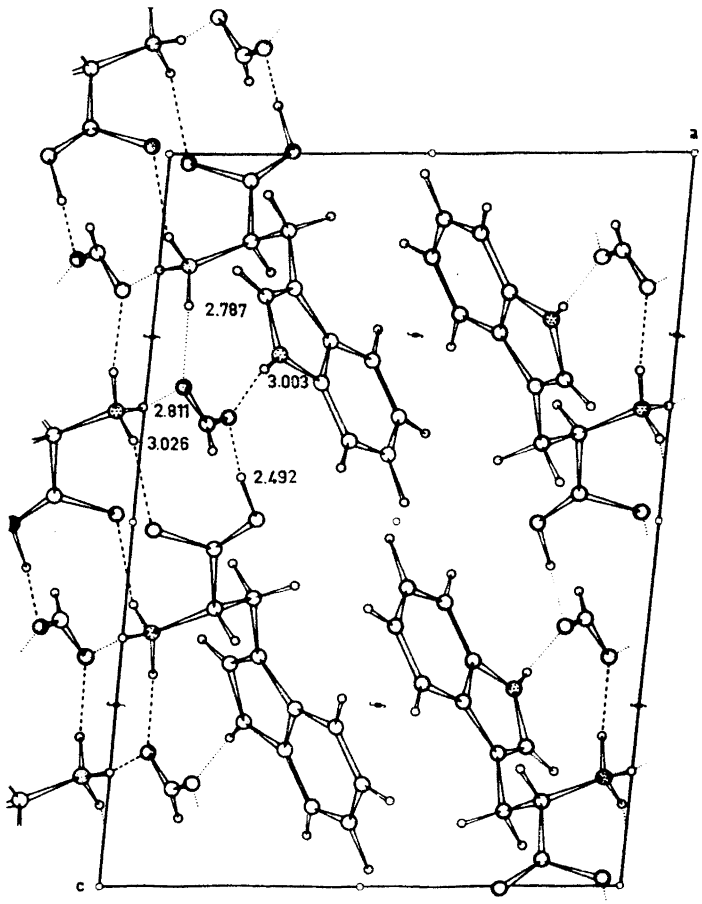

Fig. 2. Molecular arrangement and hydrogen bonds (Å) in the DL-tryptophan formate crystals as seen along the *b*-axis.

length of C16 – C18 is believed to be due to the very strong O18 – O13 hydrogen bond.

In the alanine part of the molecule the two C – O distances agree well with the expected values for a protonized carboxyl group. The slight shortening of the C – OH bond (1.291 Å) relative to the weighted average of such bonds (1.306 Å [9]) is also believed to be a result of the strong hydrogen bond O18 – O13. All other bond lengths and angles in the alanine moiety are in agreement with those reported for other α-amino acids. The dihedral angle N15 – C11 – C12 – O14 is only $-4.3°$ and the N15 atom is thus close to the plane of the carboxyl group.

The atoms of the indole moiety are co-planar, the C10 atom also included. The largest deviation from a least-squares plane through these atoms is 0.008

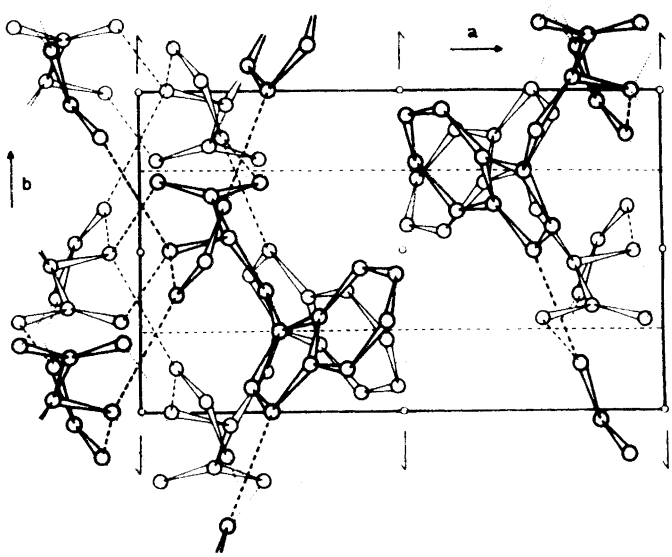

Fig. 3. The crystal structure as seen along the *c*-axis.

Å (C3) The bond lengths and angles in the indole nucleus as given in Table 5 and Fig. 1 are in good agreement with what is found in similar systems, *e.g.* serotonine picrate[10] and 5-methoxy-*N*,*N*-dimethyl tryptamine,[11] and they seem to be typical for such molecules.

The conformation of the tryptophan cation may be described by the torsion angles about the C–C and C–N bonds in the side chain. The dihedral angle C2–C3–C10–C11 is 105.1° and C3–C10–C11–C12 is −174.6°. The C3 atom and the carbon atoms in the alanine part lie thus approximately in a plane which is close to be normal to the indole plane; the carboxyl group is in the *anti* position relative to the indole group. The conformation about the C11–N15 bond is staggered.

REFERENCES

1. Bye, E., Mostad, A. and Rømming, C. *Acta Chem. Scand.* **25** (1971) 364.
2. Dahl, T., Gram, F., Groth, P., Klewe, B. and Rømming, C. *Acta Chem. Scand.* **24** (1970) 2232.
3. Hanson, H. P., Herman, F., Lea, J. D. and Skillman, S. *Acta Cryst.* **17** (1964) 1040.
4. Stewart, R. F., Davidson, E. R. and Simpson, W. T. *J. Chem. Phys.* **42** (1965) 3175.
5. Zachariasen, W. H. *Acta Cryst.* **5** (1952) 68.
6. Karle, J. and Karle I. L. *Acta Cryst.* **21** (1966) 849.
7. Sayre, D. *Acta Cryst.* **5** (1952) 60.
8. Takigawa, T., Ashida, T., Sasada, Y. and Kakudo, M. *Bull. Chem. Soc. Japan* **39** (1966) 2369.
9. Sundaralingam, M. and Putkey, E. F. *Acta Cryst.* **B 26** (1970) 790.
10. Thewalt, U. and Bugg, C. E. *Acta Cryst.* **B 28** (1972) 82.
11. Falkenberg, G. and Carlstrom, D. *Acta Cryst.* **B 27** (1917) 411.

Received Augusti 29, 1972.

ACTA CHEMICA SCANDINAVICA 27 (1973) 485–492

The Crystal and Molecular Structure of 3,4-Trimethylene-6a-selenaselenophthene

ASBJØRN HORDVIK and JAN A. PORTEN

Chemical Institute, University of Bergen, N-5000 Bergen, Norway

3,4-Trimethylene-6a-selenaselenophthene crystallizes in the orthorhombic space group $Pn2_1a$, with unit cell dimensions: $a = 11.437(3)$ Å, $b = 4.860(5)$ Å, and $c = 16.589(4)$ Å. There are four molecules per unit cell.

The structure has been solved by three-dimensional Patterson synthesis, and refined by full-matrix least squares. The refinement comprises 1004 *h0l*–*h4l* reflections, including 101 unobserved.

The atoms of the 6a-selenaselenophthene system and the methylene-carbons C(6) and C(8), bonded to C(3) and C(4), respectively, lie almost in the same plane. The Se-Se bond lengths are Se(1) – Se(6a) = 2.568(3) Å and Se(6a) – Se(6) = 2.554(3) Å, with the angle Se(1) – Se(6a) – Se(6) = 175.2(2)°. The other bond lengths in the selenaselenophthene system are: Se(1) – C(2) = 1.777(23) Å, Se(6a) – C(3a) = 1.906(20) Å, Se(6) – C(5) = 1.817(22) Å, C(2) – C(3) = 1.379(24) Å, C(3) – C(3a) = 1.435(23) Å, C(3a) – C(4) = 1.418(22) Å, and C(4) – C(5) = 1.400(23) Å.

In the crystals, Se(1) of the reference molecule approaches Se(6a) of a screw axis-related molecule at a distance of 3.57 Å.

The present structure investigation of 3,4-trimethylene-6a-selenaselenophthene (I) has been carried out in order to obtain further experimental evidence for the bonding in 6a-selenaselenophthenes.

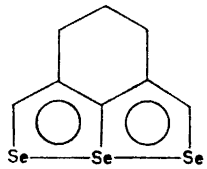

(I)

STRUCTURE DETERMINATION

Crystals of 3,4-trimethylene-6a-selenaselenophthene (I) were generously supplied by Reid.[1] The crystals are very dark purple and belong to the orthorhombic space group $Pn2_1a$.

The structure study is based on photographic data, taken with Weissenberg camera and Cu$K\alpha$ radiation. The data comprise 1004 *h0l–h4l* reflections, including 101 unobserved.

Approximate selenium positions were found from a three-dimensional Patterson map, and the carbon atoms revealed themselves during a subsequent Fourier synthesis.

The structure was refined by a full-matrix least squares procedure (*cf.* Ref. 2). The constants a_1 and a_2 in the weighting scheme were in the present case set equal to 1.0. Unobserved reflections with $K|F_c|$ greater than $F_o^{\text{threshold}}$ were included in the refinement with $F_o = F_o^{\text{threshold}}$. Anisotropic temperature factors were applied to selenium and carbon, and isotropic to hydrogen. Four low order reflections, supposed to be affected by secondary extinction, were excluded from the least squares refinement. The final R factor is 0.076 when unobserved reflections are included, and 0.075 when they are omitted. For further details with respect to the structure determination, see Experimental.

DISCUSSION

Molecular shape and dimensions. Bond lengths and angles in the 3,4-trimethylene-6a-selenaselenophthene molecule, together with their standard deviations, are listed in Tables 1 and 2, and shown in Fig. 1, a and b.

The molecule is presented in Fig. 1, a and b, in a projection on to the least squares plane of the atoms of the 6a-selenaselenophthene system and the methylene carbons C(6) and C(8). The equation for this plane, with weights equal to four for selenium, and one for carbon, is,

$$-0.63748\,X + 0.76127\,Y - 0.11871\,Z = -0.78216$$

with X, Y, and Z in Å units. Deviations from the plane for the selenium and the carbon atoms are given in Fig. 1a. It is seen that the methylene carbons C(6) and C(8) and the atoms of the 6a-selenaselenophthene system lie almost in the same plane.

Table 1. Bond lengths (l) and standard deviations in bond lengths $\sigma(l)$ in 3,4-trimethylene-6a-selenaselenophthene. Bond lengths (l') include corrections for rigid-body libration.

Bond	l' (Å)	l (Å)	$\sigma(l)$ (Å)
Se(1) – Se(6a)	2.568	2.563	0.003
Se(6a) – Se(6)	2.554	2.548	0.003
Se(1) – C(2)	1.777	1.771	0.023
Se(6a) – C(3a)	1.906	1.899	0.020
Se(6) – C(5)	1.817	1.811	0.022
C(2) – C(3)	1.379	1.375	0.024
C(3) – C(3a)	1.435	1.432	0.023
C(3a) – C(4)	1.418	1.414	0.022
C(4) – C(5)	1.400	1.397	0.023
C(3) – C(6)	1.499	1.494	0.028
C(6) – C(7)	1.507	1.503	0.024
C(7) – C(8)	1.564	1.561	0.024
C(8) – C(4)	1.549	1.544	0.030

Table 2. Bond angles ∠(ijk) in 3,4-trimethylene-6a-selenaselenophthene. The standard deviations given in parentheses refer to the last digits of the respective values.

i	j	k	∠(ijk)°
Se(6a)	Se(1)	C(2)	87.7(6)
Se(1)	Se(6a)	C(3a)	87.5(5)
Se(1)	Se(6a)	Se(6)	175.2(2)
Se(6)	Se(6a)	C(3a)	88.0(5)
Se(6a)	Se(6)	C(5)	89.0(5)
Se(1)	C(2)	C(3)	126.7(1.5)
C(2)	C(3)	C(3a)	118.6(1.7)
C(2)	C(3)	C(6)	121.5(1.5)
C(6)	C(3)	C(3a)	119.9(1.4)
Se(6a)	C(3a)	C(3)	119.5(1.2)
Se(6a)	C(3a)	C(4)	119.1(1.3)
C(3)	C(3a)	C(4)	121.4(1.7)
C(3a)	C(4)	C(5)	121.4(1.7)
C(3a)	C(4)	C(8)	119.6(1.4)
C(5)	C(4)	C(8)	118.9(1.4)
Se(6)	C(5)	C(4)	122.5(1.3)
C(3)	C(6)	C(7)	108.8(1.9)
C(6)	C(7)	C(8)	109.8(1.5)
C(4)	C(8)	C(7)	105.8(1.9)

Comparison with related molecules. Fig. 1a shows that the 3,4-trimethylene-6a-selenaselenophthene molecule is nearly symmetric about a plane perpendicular to the molecular plane and passing through Se(6a), C(3a), and C(7).

If one takes the average of corresponding bond lengths (l) in the two halves of 3,4-trimethylene-6a-selenaselenophthene, one gets the values given in Ia.

There are no significant deviations between the C-C and C-Se bond lengths in structure Ia and the corresponding C-C and C-Se bond lengths in the average structure of 6a-selenaselenophthene (II).[2] However, the Se-Se bonds in Ia, 2.556(3) Å, are significantly shorter than the Se-Se bonds in II, 2.583(3) Å, and the shortening of the Se-Se bonds seems to be due to the presence of the 3,4-trimethylene bridge.

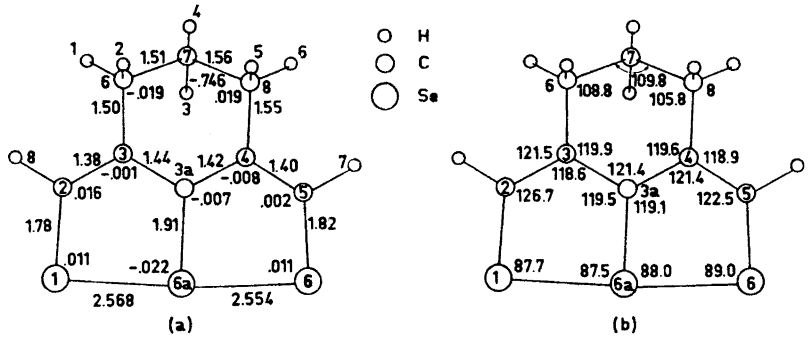

Fig. 1. (a) Bond lengths (Å) in the 3,4-trimethylene-6a-selenaselenophthene molecule, and atomic distances (Å) from the least squares plane of the atoms of the 6a-selenaselenophthene system and carbons C(6) and C(8). (b) Bond angles (°).

Support for this idea derives from a comparison of the structures Ia and II with the structures of 2,5-diphenyl-3,4-trimethylene-6a-thiathiophthene (III)[3] and 2,5-diphenyl-6a-thiathiophthene (IV).[4] The sum of the Se-Se bond lengths in Ia, 5.112 Å, is 0.054 Å shorter than the sum of the Se-Se bond lengths

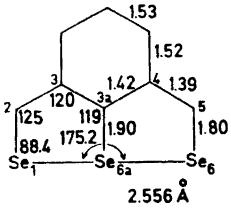

(Ia)

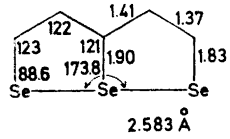

(II)

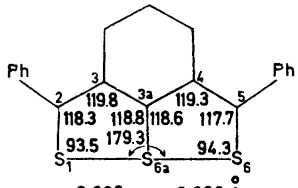

(III)

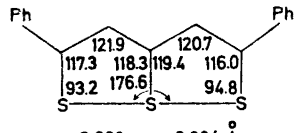

(IV)

in II, 5.166 Å, and similarly the sum of the S-S bond lengths in III, 4.617 Å, is 0.049 Å shorter than the sum of the S-S bond lengths in IV, 4.666 Å.

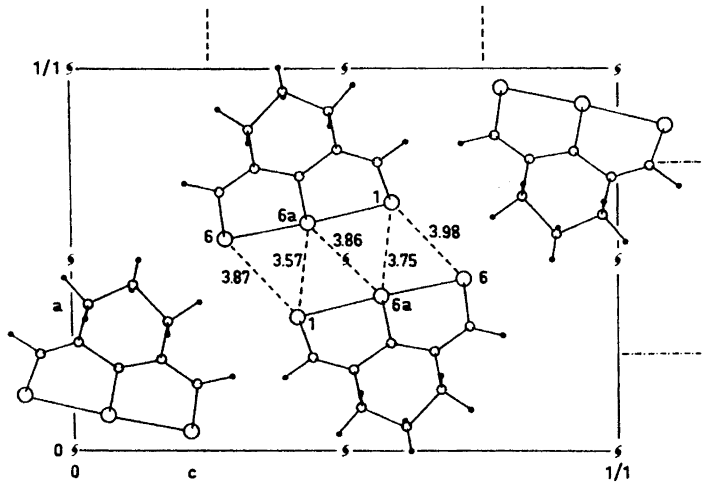

Fig. 2. The arrangement of 3,4-trimethylene-6a-selenaselenophthene molecules in the crystal as seen along the *b*-axis. Atomic distances are given in Å units.

A comparison of bond angles in Ia and II shows that the bond angle at Se(1) is almost the same in the two compounds, while the bond angle at C(2) is greater, and the bond angles at C(3) and C(3a) are smaller in Ia than in II. Similar equalities and differences in bond angles are found for structures III and IV.

The arrangement of 3,4-trimethylene-6a-selenaselenophthene molecules in the unit cell, as seen along the *b* axis, is shown in Fig. 2. Intermolecular atomic distances shorter than corresponding van der Waals distances are given in the figure.

Table 3. Atomic coordinates in fractions of corresponding cell edges. The standard deviations given in parentheses refer to the last digits of the respective values.

Atom	x	y	z
Se(1)	0.14332(17)	0.02769(87)	−0.08708(9)
Se(6a)	0.09320(13)	0.00000	0.06329(9)
Se(6)	0.05284(18)	0.00969(90)	0.2143(11)
C(2)	0.2553(17)	0.2633(55)	−0.0613(11)
C(3)	0.2832(13)	0.3543(43)	0.0148(8)
C(3a)	0.2159(16)	0.2557(47)	0.0816(10)
C(4)	0.2392(14)	0.3435(43)	0.1613(8)
C(5)	0.1726(16)	0.2498(52)	0.2264(9)
C(6)	0.3816(15)	0.5508(56)	0.0289(11)
C(7)	0.4323(15)	0.4980(72)	0.1110(9)
C(8)	0.3378(15)	0.5536(64)	0.1770(10)
H(1)	0.454	0.499	−0.010
H(2)	0.348	0.737	0.025
H(3)	0.430	0.265	0.113
H(4)	0.496	0.520	0.123
H(5)	0.303	0.728	0.176
H(6)	0.384	0.487	0.231
H(7)	0.196	0.317	0.288
H(8)	0.308	0.329	−0.110

Table 4. Temperature parameters U_{ij} (Å²) for selenium and carbon. The expression used is $\exp[-2\pi^2(h^2a^{*2}U_{11} + \cdots + 2hka^*b^*U_{12} + \cdots)]$. All values are multiplied by 10^4. Standard deviations in parentheses refer to the last digits of the respective values. Isotropic temperature factors $\exp[-8\pi^2U(\sin^2\theta/\lambda^2]$ with $U = 0.0375$ Å² were used for the hydrogen atoms.

	U_{11}	U_{22}	U_{33}	U_{12}	U_{23}	U_{13}
Se(1)	446(9)	432(15)	271(6)	82(16)	−92(14)	−68(6)
Se(6a)	300(6)	232(12)	340(7)	−20(12)	−7(12)	−13(6)
Se(6)	500(10)	437(15)	373(8)	−11(18)	28(19)	150(7)
C(2)	415(95)	343(146)	340(95)	133(103)	−19(101)	33(79)
C(3)	299(68)	281(116)	91(56)	32(72)	24(63)	−21(54)
C(3a)	475(94)	74(114)	212(75)	−75(90)	−53(77)	19(66)
C(4)	315(74)	203(119)	104(64)	−99(72)	−37(65)	−52(55)
C(5)	490(95)	402(135)	186(66)	34(100)	−36(84)	−8(72)
C(6)	340(72)	152(147)	484(81)	−49(89)	−8(102)	142(65)
C(7)	403(80)	599(176)	335(77)	−397(142)	252(133)	−58(65)
C(8)	418(86)	445(191)	350(71)	1(121)	−17(120)	76(67)

Table 5. Observed and calculated structure factors for 3,4-trimethylene-6a-selenaselenophthene. The values given are ten times the absolute values. Unobserved reflections are marked with a minus sign.

H	K	L	F(O)	F(C)
2	0	0	364	291
4	0	0	1151	1165
6	0	0	752	763
8	0	0	131	114
10	0	0	370	321
12	0	0	61	63
14	0	0	81	67
0	0	2	723	617
0	0	4	112	76
0	0	6	1555	1546
0	0	8	1393	1327
0	0	10	520	469
0	0	12	277	254
0	0	14	873	880
0	0	16	374	330
0	0	18	103	127
0	0	20	177	176
1	0	2	457	463
1	0	3	422	387
1	0	4	657	617
1	0	5	74	77
1	0	6	931	924
1	0	8	563	462
1	0	9	131	164
1	0	10	420	374
1	0	11	209	180
1	0	12	490	453
1	0	13	614	632
1	0	14	342	270
1	0	15	422	333
1	0	16	127	142
1	0	17	250	150
1	0	18	203	227
1	0	19	140	141
1	0	20	359	420
2	0	1	467	434
2	0	2	657	657
2	0	3	873	915
2	0	4	541	504
2	0	5	500	329
2	0	6	305	282
2	0	7	605	580
2	0	8	254	231
2	0	9	179	180
2	0	10	132	119
2	0	11	271	233
2	0	12	675	605
2	0	13	531	1211
2	0	14	407	373
2	0	15	207	227
2	0	16	-38	31
2	0	17	119	106
2	0	18	247	211
2	0	19	521	510
3	0	1	717	740
3	0	2	736	800
3	0	3	254	240
3	0	4	278	241
3	0	5	1330	1537
3	0	6	1304	1340
3	0	7	409	422
3	0	8	455	420
3	0	9	169	160
3	0	10	290	176
3	0	11	547	562
3	0	12	746	772
3	0	13	436	429
3	0	14	638	526
3	0	15	198	181
3	0	16	-37	67
3	0	17	135	141
3	0	18	122	83
3	0	19	230	223
3	0	20	402	427
4	0	1	1102	1173
4	0	2	866	910
4	0	3	217	214
4	0	4	382	407
4	0	5	859	543
4	0	6	1028	1103
4	0	7	244	207
4	0	8	534	550
4	0	9	666	663
4	0	10	-36	11
4	0	11	-39	23
4	0	12	467	480
4	0	13	430	450
4	0	14	143	115
4	0	15	422	393
4	0	16	-46	22
4	0	17	-63	33
4	0	18	163	153
4	0	19	159	147
4	0	20	31	88
5	0	1	839	874
5	0	2	1137	1274
5	0	3	365	352

H	K	L	F(O)	F(C)
5	0	4	216	214
5	0	5	314	300
5	0	6	405	420
5	0	7	683	711
5	0	8	1033	1199
5	0	9	502	493
5	0	10	96	89
5	0	11	129	111
5	0	12	33	75
5	0	13	357	330
5	0	14	435	399
5	0	15	374	333
5	0	16	384	365
5	0	17	300	244
5	0	18	320	293
6	0	1	312	322
6	0	2	302	255
6	0	3	169	140
6	0	4	357	333
6	0	5	330	296
6	0	6	137	207
6	0	7	233	284
6	0	8	409	451
6	0	9	538	606
6	0	10	499	355
6	0	11	230	201
6	0	12	325	324
6	0	13	-57	10
6	0	14	-49	377
6	0	15	538	536
6	0	16	308	309
6	0	17	170	158
6	0	18	355	375
6	0	19	156	180
7	0	1	103	105
7	0	2	191	192
7	0	3	129	118
7	0	4	799	895
7	0	5	684	707
7	0	6	116	124
7	0	7	239	255
7	0	8	354	407
7	0	9	132	202
7	0	10	420	424
7	0	11	598	540
7	0	12	203	164
7	0	13	-56	7
7	0	14	-65	63
7	0	15	239	223
7	0	16	100	95
7	0	17	272	271
7	0	18	154	160
8	0	1	309	288
8	0	2	614	653
8	0	3	961	1187
8	0	4	330	469
8	0	5	477	526
8	0	6	104	86
8	0	7	113	101
8	0	8	147	133
8	0	9	431	484
8	0	10	146	125
8	0	11	723	697
8	0	12	445	432
8	0	13	-35	60
8	0	14	173	145
8	0	15	-58	15
8	0	16	56	60
8	0	17	234	101
9	0	1	37	67
9	0	2	636	691
9	0	3	238	219
9	0	4	848	949
9	0	5	447	450
9	0	6	183	167
9	0	7	206	174
9	0	8	419	393
9	0	9	622	610
9	0	10	482	444
9	0	11	133	124
9	0	12	307	273
9	0	13	-31	22
9	0	14	159	125
9	0	15	160	129
9	0	16	67	77
10	0	1	186	170
10	0	2	483	494
10	0	3	242	186
10	0	4	-70	49
10	0	5	415	403
10	0	6	-70	73
10	0	7	-69	43
10	0	8	191	139
10	0	9	-67	56
10	0	10	532	566
10	0	11	125	114
10	0	12	-59	23

H	K	L	F(O)	F(C)
10	0	13	73	64
11	0	1	117	93
11	0	2	118	95
11	0	3	438	365
11	0	4	439	368
11	0	5	-63	77
11	0	6	-67	33
11	0	7	-66	68
11	0	8	-64	29
11	0	9	436	384
11	0	10	242	177
11	0	11	218	209
11	0	12	113	110
12	0	1	-62	56
12	0	2	210	180
12	0	3	624	562
12	0	4	108	119
12	0	5	214	180
12	0	6	134	125
12	0	7	-58	71
12	0	8	157	135
12	0	9	229	225
12	0	10	229	201
12	0	11	185	177
13	0	1	165	151
13	0	2	243	242
13	0	3	-33	67
13	0	4	364	404
13	0	5	221	139
14	0	1	-41	30
14	0	2	-40	48
14	0	3	255	313
14	0	4	54	81
14	0	5	138	155
4	1	0	1276	1204
6	1	0	244	209
8	1	0	160	155
10	1	0	109	110
12	1	0	211	188
14	1	0	75	83
0	1	3	1228	1163
0	1	5	1176	1008
0	1	7	602	670
0	1	9	133	122
0	1	11	85	50
0	1	13	1254	1445
0	1	15	241	224
0	1	17	134	119
0	1	19	496	504
0	1	21	207	325
1	1	1	1019	1159
1	1	2	691	824
1	1	3	50	22
1	1	4	451	390
1	1	5	869	829
1	1	6	1393	1419
1	1	7	1329	1361
1	1	8	267	244
1	1	9	-51	48
1	1	10	454	448
1	1	11	204	180
1	1	12	658	667
1	1	13	495	503
1	1	14	513	533
1	1	15	202	176
1	1	16	-70	46
1	1	17	216	187
1	1	18	102	65
1	1	19	-55	25
1	1	20	462	514
2	1	1	1128	1182
2	1	2	737	715
2	1	3	166	136
2	1	4	180	138
2	1	5	702	658
2	1	6	1358	1471
2	1	7	255	203
2	1	8	981	994
2	1	9	535	496
2	1	10	311	302
2	1	11	68	68
2	1	12	270	284
2	1	13	344	378
2	1	14	507	560
2	1	15	384	394
2	1	16	213	192
2	1	17	115	94
2	1	18	-61	16
2	1	19	122	130
2	1	20	123	115
3	1	1	1346	1409
3	1	2	815	818
3	1	3	224	190
3	1	4	214	193
3	1	5	69	51
3	1	6	112	94
3	1	7	1324	1570

H	K	L	F(O)	F(C)
3	1	8	1030	1080
3	1	9	229	214
3	1	10	103	101
3	1	11	224	230
3	1	12	147	136
3	1	13	491	585
3	1	14	360	366
3	1	15	415	377
3	1	16	370	301
3	1	17	-65	25
3	1	18	348	316
3	1	19	163	145
3	1	20	129	141
4	1	1	517	439
4	1	2	488	448
4	1	3	191	169
4	1	4	608	606
4	1	5	153	130
4	1	6	384	415
4	1	7	451	461
4	1	8	530	475
4	1	9	433	487
4	1	10	153	154
4	1	11	352	392
4	1	12	565	526
4	1	13	512	500
4	1	14	574	543
4	1	15	461	445
4	1	16	134	111
4	1	17	-63	46
4	1	18	383	379
4	1	19	330	333
4	1	20	-36	61
5	1	2	587	537
5	1	1	478	403
5	1	3	391	337
5	1	4	692	679
5	1	5	1140	1295
5	1	6	531	517
5	1	7	331	315
5	1	8	146	137
5	1	9	216	237
5	1	10	181	192
5	1	11	657	754
5	1	12	491	531
5	1	13	165	171
5	1	14	284	260
5	1	15	277	271
5	1	16	165	130
5	1	17	186	175
5	1	18	171	155
5	1	19	259	243
6	1	1	828	703
6	1	2	974	972
6	1	3	772	755
6	1	4	615	579
6	1	5	864	674
6	1	6	516	507
6	1	7	-58	54
6	1	8	306	305
6	1	9	549	604
6	1	10	221	233
6	1	11	385	406
6	1	12	602	621
6	1	13	298	295
6	1	14	172	135
6	1	15	238	202
6	1	16	100	102
6	1	17	-55	31
6	1	18	221	225
6	1	19	113	130
7	1	1	417	362
7	1	2	921	962
7	1	3	447	426
7	1	4	616	630
7	1	5	573	564
7	1	6	419	424
7	1	7	145	143
7	1	8	747	835
7	1	9	580	663
7	1	10	238	237
7	1	11	78	58
7	1	12	274	244
7	1	13	163	146
7	1	14	249	241
7	1	15	218	190
7	1	16	206	205
7	1	17	354	330
7	1	18	40	70
8	1	1	611	577
8	1	2	567	521
8	1	3	75	70
8	1	4	192	187
8	1	5	444	403
8	1	6	87	80
8	1	7	110	112
8	1	8	214	215

H	K	L	F(O)	F(C)
8	1	9	270	302
8	1	10	626	625
8	1	11	79	73
8	1	12	110	104
8	1	13	131	106
8	1	14	124	104
8	1	15	402	385
8	1	16	429	426
8	1	17	92	81
9	1	1	90	93
9	1	2	99	94
9	1	3	255	245
9	1	4	701	699
9	1	5	176	166
9	1	6	184	163
9	1	7	-70	65
9	1	8	291	257
9	1	9	445	402
9	1	10	367	330
9	1	11	456	388
9	1	12	-64	29
9	1	13	-60	36
9	1	14	-55	25
9	1	15	155	157
10	1	1	32	48
10	1	2	92	85
10	1	3	952	927
10	1	4	101	65
10	1	5	370	281
10	1	6	-71	65
10	1	7	90	76
10	1	8	-69	65
10	1	9	307	287
10	1	10	164	157
10	1	11	531	486
10	1	12	94	73
10	1	13	149	147
10	1	14	-46	30
10	1	15	63	77
11	1	1	-68	91
11	1	2	451	404
11	1	3	-69	19
11	1	4	807	722
11	1	5	-68	55
11	1	6	-67	25
11	1	7	160	141
11	1	8	-64	35
11	1	9	234	218
11	1	10	519	492
11	1	11	-53	25
11	1	12	194	195
11	1	13	99	105
12	1	1	-61	53
12	1	2	217	190
12	1	3	396	372
12	1	4	-61	71
12	1	5	282	261
12	1	6	132	142
12	1	7	-56	37
12	1	8	168	143
12	1	9	-50	40
12	1	10	297	311
12	1	11	230	251
13	1	1	125	119
13	1	2	114	88
13	1	3	216	222
13	1	4	-50	27
13	1	5	109	109
13	1	6	-46	26
13	1	7	-43	36
13	1	8	109	109
13	1	9	212	261
14	1	1	109	118
14	1	2	201	238
14	1	3	195	227
14	1	4	84	102
14	1	5	88	102
2	2	0	1437	1312
4	2	0	1477	1373
6	2	0	577	565
8	2	0	180	159
10	2	0	232	214
12	2	0	-54	34
0	2	2	332	268
0	2	4	130	114
0	2	6	1336	1273
0	2	8	1003	949
0	2	10	423	414
0	2	12	-67	20
0	2	14	611	597
0	2	16	210	192
0	2	18	-55	87
1	2	1	1184	1150
1	2	2	252	248
1	2	3	245	197
1	2	4	229	217
1	2	5	118	126

Table 5. Continued.

H	K	L	F(O)	F(C)
1	2	6	665	625
1	2	7	1418	1529
1	2	8	467	367
1	2	9	161	161
1	2	10	217	228
1	2	11	145	145
1	2	12	431	398
1	2	13	471	466
1	2	14	610	602
1	2	15	380	353
1	2	16	135	186
1	2	17	143	158
1	2	18	171	148
1	2	19	139	135
2	2	1	259	263
2	2	2	312	285
2	2	3	557	545
2	2	4	566	546
2	2	5	568	519
2	2	6	374	363
2	2	7	620	664
2	2	8	432	383
2	2	9	249	257
2	2	10	-59	59
2	2	11	149	139
2	2	12	367	351
2	2	13	874	931
2	2	14	472	442
2	2	15	261	244
2	2	16	-65	33
2	2	17	-31	41
2	2	18	229	240
2	2	19	375	400
3	2	1	578	562
3	2	2	808	745
3	2	3	444	368
3	2	4	134	147
3	2	5	1041	1080
3	2	4	134	147
3	2	5	1041	1080
3	2	6	552	1001
3	2	7	132	119
3	2	8	315	340
3	2	9	256	261
3	2	10	134	191
3	2	11	481	526
3	2	12	505	563
3	2	13	228	216
3	2	14	301	285
3	2	15	86	70
3	2	16	-64	4
3	2	17	118	135
3	2	18	91	83
3	2	19	136	146
4	2	1	1191	1152
4	2	2	1040	982
4	2	3	217	215
4	2	4	470	439
4	2	5	869	906
4	2	6	855	823
4	2	7	79	96
4	2	8	503	530
4	2	9	616	670
4	2	10	129	132
4	2	11	146	143
4	2	12	565	565
4	2	13	474	430
4	2	14	210	203
4	2	15	393	374
4	2	16	107	115
4	2	17	126	125
4	2	18	100	104
4	2	19	134	154
5	2	1	764	766
5	2	2	926	924
5	2	3	131	138
5	2	4	282	284
5	2	5	385	381
5	2	6	518	547
5	2	7	719	793
5	2	8	860	1082
5	2	9	359	427
5	2	10	-54	28
5	2	11	120	120
5	2	12	226	212
5	2	13	402	393
5	2	14	197	154
5	2	15	244	238
5	2	16	246	234
5	2	17	191	186
5	2	18	176	190
6	2	1	640	589
6	2	2	-58	13
6	2	3	282	264
6	2	4	372	409
6	2	5	212	213
6	2	6	243	258
6	2	7	162	171
6	2	8	238	269
6	2	9	317	355
6	2	10	348	372
6	2	11	378	368
6	2	12	365	360
6	2	13	-66	86
6	2	14	334	294
6	2	15	435	448
6	2	16	238	236
6	2	17	97	88
6	2	18	257	310
7	2	1	34	79
7	2	2	206	195
7	2	3	129	119
7	2	4	795	831
7	2	5	629	695
7	2	6	91	102
7	2	7	192	228
7	2	8	190	210
7	2	9	86	76
7	2	10	348	306
7	2	11	625	584
7	2	12	323	276
7	2	13	-63	45
7	2	14	120	113
7	2	15	215	206
7	2	16	111	109
7	2	17	261	280
8	2	1	163	269
8	2	2	424	436
8	2	3	765	326
8	2	4	270	256
8	2	5	514	480
8	2	6	143	129
8	2	7	69	76
8	2	8	-69	17
8	2	9	298	270
8	2	10	67	93
8	2	11	501	476
8	2	12	338	319
8	2	13	145	154
8	2	14	125	121
9	2	1	108	103
9	2	2	541	543
9	2	3	234	257
9	2	4	700	664
9	2	5	299	277
9	2	6	156	141
9	2	7	169	158
9	2	8	234	246
9	2	9	441	399
9	2	10	369	375
9	2	11	-62	17
9	2	12	223	206
9	2	13	-53	33
9	2	14	135	142
9	2	15	124	123
10	2	1	133	152
10	2	2	377	406
10	2	3	404	274
10	2	4	-69	8
10	2	5	324	295
10	2	6	111	117
10	2	7	-66	20
10	2	8	204	186
10	2	9	152	137
10	2	10	568	510
10	2	11	224	208
10	2	12	-50	52
10	2	13	56	59
11	2	1	110	125
11	2	2	-64	81
11	2	3	263	264
11	2	4	156	161
11	2	5	178	148
11	2	6	-62	60
11	2	7	97	98
11	2	8	81	62
11	2	9	387	398
11	2	10	120	112
11	2	11	137	122
11	2	12	62	68
12	2	1	71	83
12	2	2	225	225
12	2	3	493	514
12	2	4	94	93
12	2	5	151	143
12	2	6	113	103
12	2	7	-48	44
12	2	8	91	90
12	2	9	210	228
13	2	1	121	133
13	2	2	210	231
13	2	3	130	125
13	2	4	384	459
13	2	5	125	159
13	2	6	36	46
2	3	0	1660	1708
4	3	0	898	858
6	3	0	248	240
8	3	0	273	265
10	3	0	146	134
12	3	0	113	118
0	3	1	743	630
0	3	3	632	546
0	3	5	663	597
0	3	7	642	609
0	3	9	235	237
0	3	11	-60	76
0	3	13	925	854
0	3	15	122	118
0	3	17	102	79
1	3	1	959	861
1	3	2	547	439
1	3	3	54	30
1	3	4	254	245
1	3	5	365	341
1	3	6	879	867
1	3	7	705	697
1	3	8	234	253
1	3	9	187	178
1	3	10	240	250
1	3	11	193	203
1	3	12	405	481
1	3	13	403	392
1	3	14	469	388
1	3	15	169	142
1	3	16	-68	45
1	3	17	134	149
2	3	1	600	571
2	3	2	414	382
2	3	3	82	47
2	3	4	202	193
2	3	5	522	494
2	3	6	878	957
2	3	7	149	143
2	3	8	604	727
2	3	9	397	419
2	3	10	137	175
2	3	11	-78	49
2	3	12	161	134
2	3	13	378	376
2	3	14	446	433
2	3	15	192	178
2	3	16	139	132
2	3	17	76	73
3	3	1	772	738
3	3	2	522	501
3	3	3	79	61
3	3	4	171	131
3	3	5	174	172
3	3	6	156	115
3	3	7	982	1106
3	3	8	615	634
3	3	9	119	110
3	3	10	-75	28
3	3	11	228	223
3	3	12	90	101
3	3	13	342	328
3	3	14	308	306
3	3	15	323	327
3	3	16	254	242
3	3	17	-56	30
3	3	18	145	162
4	3	1	414	365
4	3	2	180	170
4	3	3	180	206
4	3	4	455	461
4	3	5	259	254
4	3	6	255	246
4	3	7	221	215
4	3	8	299	309
4	3	9	231	240
4	3	10	108	84
4	3	11	274	251
4	3	12	396	395
4	3	13	393	393
4	3	14	401	363
4	3	15	358	302
4	3	16	100	85
5	3	1	225	197
5	3	2	351	335
5	3	3	272	249
5	3	4	519	502
5	3	5	755	876
5	3	6	396	410
5	3	7	174	197
5	3	8	-75	34
5	3	9	108	96
5	3	10	69	88
5	3	11	500	495
5	3	12	377	326
5	3	13	-74	57
5	3	14	169	168
5	3	15	145	129
5	3	16	-56	34
5	3	17	124	137
6	3	1	551	554
6	3	2	645	735
6	3	3	466	511
6	3	4	305	305
6	3	5	464	553
6	3	6	325	326
6	3	7	88	102
6	3	8	163	155
6	3	9	359	347
6	3	10	154	169
6	3	11	373	347
6	3	12	404	429
6	3	13	196	210
6	3	14	92	76
6	3	15	156	168
6	3	16	108	126
7	3	1	365	372
7	3	2	621	658
7	3	3	253	252
7	3	4	368	376
7	3	5	347	371
7	3	6	287	308
7	3	7	152	143
7	3	8	563	545
7	3	9	494	492
7	3	10	215	212
7	3	11	-73	14
7	3	12	271	262
7	3	13	183	154
7	3	14	132	129
7	3	15	111	107
8	3	1	322	339
8	3	2	308	291
8	3	3	82	75
8	3	4	82	62
8	3	5	340	303
8	3	6	196	194
8	3	7	111	100
8	3	8	207	248
8	3	9	237	235
8	3	10	446	478
8	3	11	97	87
8	3	12	110	111
8	3	13	105	125
8	3	14	84	72
9	3	1	114	112
9	3	2	105	70
9	3	3	254	237
9	3	4	441	424
9	3	5	111	109
9	3	6	126	106
9	3	7	131	146
9	3	8	204	192
9	3	9	271	255
9	3	10	286	293
9	3	11	235	260
9	3	12	88	91
10	3	1	-74	2
10	3	2	-74	56
10	3	3	610	633
10	3	4	128	108
10	3	5	280	272
10	3	6	-71	61
10	3	7	-68	59
10	3	8	-65	7
10	3	9	180	188
10	3	10	89	74
10	3	11	272	313
11	3	1	-63	58
11	3	2	261	270
11	3	3	82	86
11	3	4	498	358
11	3	5	105	132
11	3	6	82	85
11	3	7	95	84
11	3	8	-50	38
11	3	9	88	88
12	3	1	65	74
12	3	2	175	196
12	3	3	239	270
12	3	4	61	66
12	3	5	139	147
12	3	6	82	89
2	4	0	474	448
4	4	0	609	578
6	4	0	425	430
8	4	0	126	141
10	4	0	159	164
0	4	2	243	207
0	4	4	97	85
0	4	6	825	930
0	4	8	717	691
0	4	10	181	185
0	4	12	137	137
0	4	14	487	477
0	4	16	144	172
1	4	1	661	677
1	4	2	130	138
1	4	3	123	111
1	4	4	215	212
1	4	5	58	111
1	4	6	336	320
1	4	7	759	885
1	4	8	251	265
1	4	9	119	138
1	4	10	139	132
1	4	11	138	136
1	4	12	260	244
1	4	13	344	311
1	4	14	226	216
1	4	15	229	232
1	4	16	83	87
2	4	1	317	322
2	4	2	215	202
2	4	3	307	310
2	4	4	254	235
2	4	5	418	446
2	4	6	-75	19
2	4	7	286	281
2	4	8	148	117
2	4	9	158	144
2	4	10	-83	30
2	4	11	127	117
2	4	12	268	250
2	4	13	540	523
2	4	14	173	170
2	4	15	112	110
3	4	1	346	341
3	4	2	426	443
3	4	3	205	168
3	4	4	132	140
3	4	5	498	539
3	4	6	518	608
3	4	7	166	167
3	4	8	81	78
3	4	9	106	99
3	4	10	125	134
3	4	11	279	273
3	4	12	429	380
3	4	13	234	207
3	4	14	247	240
3	4	15	74	66
4	4	1	507	491
4	4	2	415	425
4	4	3	134	120
4	4	4	195	187
4	4	5	376	411
4	4	6	373	394
4	4	7	115	120
4	4	8	273	264
4	4	9	336	317
4	4	10	132	158
4	4	11	129	119
4	4	12	264	236
4	4	13	317	328
4	4	14	155	151
4	4	15	131	140
5	4	1	399	401
5	4	2	421	462
5	4	3	136	107
5	4	4	134	121
5	4	5	196	199
5	4	6	227	242
5	4	7	399	413
5	4	8	529	549
5	4	9	336	331
5	4	10	-79	60
5	4	11	124	123
5	4	12	93	65
5	4	13	174	162
5	4	14	157	166
6	4	1	362	365
6	4	2	178	170
6	4	3	124	148
6	4	4	131	141
6	4	5	175	177
6	4	6	266	288
6	4	7	143	131
6	4	8	312	290
6	4	9	256	255
6	4	10	269	251
6	4	11	177	186
6	4	12	156	162
7	4	1	146	102
7	4	2	-88	73
7	4	3	-88	40
7	4	4	470	449
7	4	5	325	296
7	4	6	-63	90
7	4	7	227	216
7	4	8	194	160
7	4	9	123	81
7	4	10	223	216
7	4	11	254	263
7	4	12	138	134
8	4	1	145	104
8	4	2	325	300
8	4	3	563	575
8	4	4	185	158
8	4	5	388	363
8	4	6	-76	62
8	4	7	-76	62
8	4	8	-72	60
8	4	9	202	204
8	4	10	-51	54
8	4	11	248	321
9	4	1	182	186
9	4	2	385	374
9	4	3	212	208
9	4	4	378	458
9	4	5	242	246
9	4	6	156	156
9	4	7	85	86
9	4	8	156	167
9	4	9	223	235
10	4	1	123	133
10	4	2	237	239
10	4	3	99	96
10	4	4	-59	64
10	4	5	162	155
10	4	6	92	90
11	4	1	73	96
11	4	2	-44	63
11	4	3	124	145

EXPERIMENTAL

The unit cell dimensions for crystals of 3,4-trimethylene-6a-selenaselenophthene were determined from high-order reflections on *h*0*l* and 0*kl* Weissenberg photographs, where lead nitrate powder lines had been superimposed for reference. A least squares procedure on 41 measured 2θ-values gave $a = 11.437(3)$ Å, $b = 4.860(5)$ Å, and $c = 16.589(4)$ Å.

Four molecules per unit cell give a calculated density of 2.456 g/cm^3 as compared with the density 2.45 g/cm^3, found by flotation.

The intensities of the *h*0*l*–*h*4*l* and 0*kl* reflections were estimated visually from Weissenberg photographs taken with Ni-filtered Cu$K\alpha$ radiation ($\mu = 159.4$ cm^{-1}). 0*kl* reflections from the zero layer about *a* were used for scaling only.

Lp corrections and absorption corrections were applied, the latter according to a procedure of Coppens *et al.*[5]

The hydrogen positions were estimated and included in the structure factor calculations, but not refined.

The scattering factors used for selenium, carbon, and hydrogen in the structure factor calculations were those given in the International Tables.[6] The selenium scattering curve was corrected for anomalous dispersion, using the $\Delta f'$ and $\Delta f''$ values given by Cromer.[7]

The final atomic coordinates are listed in Table 3, the temperature parameters in Table 4. The final list of structure factors is given in Table 5.

An analysis of the thermal parameters of the S and C atoms, assuming the molecule a rigid body was carried out according to the method of Schomaker and Trueblood.[8] The Se–Se, Se–C, and C–C bond lengths have been corrected for rigid body libration according to Cruickshank's formula.[9] The corrected bond lengths are listed in the first column of Table 1.

Acknowledgements. We thank Dr. D. H. Reid, Department of Chemistry, The University, St. Andrews, Scotland, for a sample of 3,4-trimethylene-6a-selenaselenophthene.

REFERENCES

1. Jackson, M. G. and Reid, D. H. *Unpublished data*; Jackson, M. G., Ph. D. Thesis, University of St. Andrews 1973.
2. Hordvik, A. and Julshamn, K. *Acta Chem. Scand.* **25** (1971) 2507.
3. Birknes, B., Hordvik, A. and Sæthre, L. J. *Acta Chem. Scand.* **26** (1972) 2140.
4. Hordvik, A. *Acta Chem. Scand.* **25** (1971) 1583.
5. Coppens, P., Leiserowitz, L. and Rabinovich, D. *Acta Cryst.* **18** (1965) 1035.
6. *International Tables for X-Ray Crystallography*, Kynoch Press, Birmingham 1962, Vol. III, p. 202.
7. Cromer, D. T. *Acta Cryst.* **18** (1965) 17.
8. Schomaker, V. and Trueblood, K. N. *Acta Cryst.* **B 24** (1968) 63.
9. Cruickshank, D. W. J. *Acta Cryst.* **9** (1956) 757; **14** (1961) 896.

Received June 29, 1972.

ACTA CHEMICA SCANDINAVICA 27 (1973) 493–502

Automatic Densitometer Measurements of Powder Diffraction Photographs

GUNNAR MALMROS and PER-ERIK WERNER

Institute of Inorganic and Physical Chemistry, University of Stockholm, S-104 05 Stockholm 50, Sweden

The use of an automatic drum densitometer for the evaluation of powder diffraction photographs is described. Computer programs for the calculation of Bragg angles and diffraction intensities from Guinier-Hägg photographs have been constructed. The speed and accuracy of the technique are discussed and illustrated by examples.

Due to the availability of automatic drum film scanners, it is possible to make fast routine determinations of interplanar spacings and diffraction intensities from X-ray powder photographs. Accuracy in low-order lines is of great importance when the high-angle region is too crowded or too weak to be of any use for indexing complicated patterns or measuring lattice constants. A vast number of research problems falls into these categories and it has been found that powder photographs obtained in a focusing camera of the Guinier-Hägg type and measured by a precision method described by Hägg [1] and Westman and Magnéli [2] give results satisfactory for most needs. The use of an internal standard with known cell constants makes it possible in principle to attain a precision limited by the instrumental inaccuracy and the precision of the lattice parameters of the standard. However, the application of the method is often tiresome, and subjective errors in reading and operating may well be introduced. The use of an automatic film scanner offers a possibility of avoiding subjective errors and of giving more satisfactory intensity measurements than the frequently used visual estimations: *v*ery *s*trong, *s*trong, *m*edium, *w*eak, *v*ery *w*eak and *v*ery *v*ery *w*eak. Furthermore in favourable situations, *e.g.* where there are only small orientation effects in the specimen, it may be possible to measure the intensities with an accuracy comparable with that obtained with a single-crystal Weissenberg camera (*cf.* Table 3). It is also well known that fine powders can be ideal subjects for accurate intensity measurements because of the virtual absence of both primary and secondary extinction in most cases.[3]

FILM SCANNER PROCESS

The drum scanner used in the present work is an automatic film scanner SAAB model 2,[4] designed by Abrahamsson.[5] A special film cassette for Guinier photographs was designed. In this cassette the film is mounted with the powder lines perpendicular to the film scanner drum axis. The film is pierced with a needle close to the primary beam streak in order to facilitate the automatic indexing of the lines from the standard. The scanner is connected to an IBM 1800 computer.[6] A block diagram of the film scanner process is given in Fig. 1.

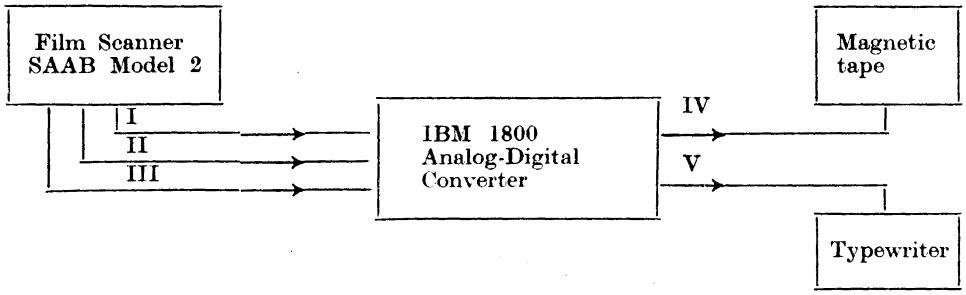

Fig. 1. Film scanner process block diagram. I. Process interrupt (about 3 times/sec). II. Analog output of transmission values. III. Synchronization pulses at each 60 μm film translation. IV. Digital transmission values. V. System messages.

The process programs, written in IBM 1800 Assembler Language,[7] are executed on-line under the IBM 1800 Multiprogramming Executive System, MPX.[8] At the present stage the following equipment is available: a 32 K core memory, a card read-punch station, a line printer, a console typerwriter, a magnetic tape unit and two disk drives. By the use of data-channels the need for central process unit time is reduced to only a few per cent of the total scan time, which latter is about 10 min for the measuring of one Guinier photograph. This means that non-process programs or other programs of lower priorities which do not need the magnetic tape unit may be executed simultaneously without any considerable loss of speed.

It should be noted that the SAAB scanner produces transmission values and not optical densities, contrary to other drum film scanners available on the market. It has been found that the *positions* of the lines are more easily detected and measured on a transmission curve than on an intensity curve (*cf.* Fig. 3).

Each revolution of the film scanner drum corresponds to a translation of 45 μm along the drum axis and produces one magnetic tape record of 266 transmission values, *i.e.* 266×60 μm $= 15.96$ mm on the photograph parallel to the powder lines. By means of the analog digital converter (*cf.* Fig. 1) the transmission values are calculated with a precision of eleven binary digits. Thus a digitized picture of the Guinier photograph is stored on the magnetic tape.

SOFTWARE SYSTEM

In order to calculate interplanar spacings, d, and integrated intensities from the transmission values stored on the magnetic tape, one of us (G. M.) has written the computer program PILT (Powder Intensity and Lattice Tracing) in IBM 1800 Fortran.

In the first step the program evaluates the positions, s, of the lines on the film. The relation between Bragg angles, θ, and s-values is computed by least-squares treatment of the positions of the lines from the standard substance. It has been observed that s as a function of θ is better approximated by a parabolic function (*cf.* Fig. 2 in Ref. 2) than by use of a linear function. This technique is therefore included in the program. In the next step PILT computes integrated intensities and applies the PLG-factors, where P, L, and G, are the polarization, the Lorentz, and the geometric factors.

$$P = [1 + \cos^2(2\alpha)\cos^2(2\theta)]/[1 + \cos^2(2\alpha)]$$

where α is the Bragg angle for the monochromator crystal which is assumed to have an ideal mosaic structure.[9]

$$L = 1/\sin^2\theta \cos\theta$$

and

$$G = 1/\cos(2\theta - \phi)$$

where ϕ is the angle between the normal to the specimen plane and the primary beam.[10] The program also punches data cards for the program PIRUM,[11] which performs indexing of powder patterns and refines cell parameters by the method of least-squares.

In calculation of the line positions two problems arise. The first is to distinguish between the diffraction lines and the background variations and the second is to determine the peak positions. The principles used by PILT will now be summarized.

From each revolution of the film scanner drum, corresponding to a 45 μm translation along the film, the arithmetic mean T_m of the transmission values from a 2 mm broad slit is calculated (*cf.* Fig. 2). The slit corresponds to 34 single readings by the scanner. This procedure reduces the great amount of data on the tape to a vector of less than 2700 integers which can be kept in core memory. Each integer represents the average transmission, T_m, of 45 μm perpendicular to the diffraction lines on the film.

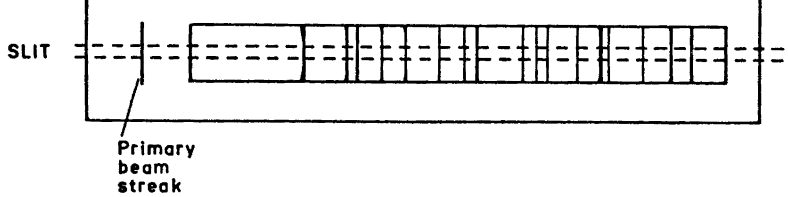

Fig. 2. Schematic drawing of a powder photograph.

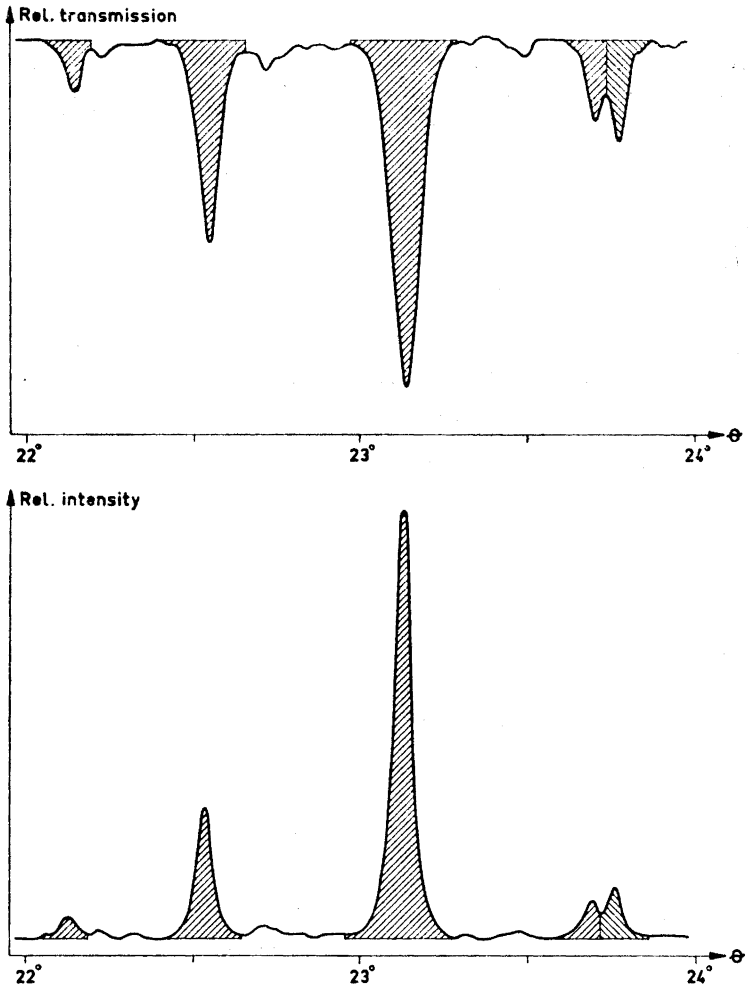

Fig. 3. Parts of corresponding transmission and relative intensity curves derived from a powder photograph of α-Bi_2O_3.

As can be seen from Fig. 3 the weak lines appear much more clearly on the transmission curve than on the intensity curve. Therefore, the positions of the lines are calculated from the transmission values. For each T_m the derivative dT_m/ds is calculated and it is supposed that a line may be present if dT_m/ds exceeds a certain limit. The position of the line is estimated by linear interpolation to the s-value where $dT_m/ds = 0$. If the difference between the minimum transmission and the transmission value 90 μm (*i.e.* 2 revolutions) away is less than 5 %, the assumed line is discarded. Often this procedure eliminates all

spurious lines. If such "lines" occur they can easily be removed by visual inspection of the transmission curve given on the line printer.

In calculating the integrated intensities it is essential to determine a proper background level. The following procedure is used by the program. For each group of 100 T_m values the 10 consecutive ones giving the highest mean transmission are chosen as the background level. The background, T_b, for each point on the curve is then calculated by linear interpolation.

The width of a peak is defined by revolutions r_1 and r_2 where dT_m/ds is zero or changes sign. In Fig. 3 the shadowed areas represent the integrated intensities

$$I = 100 \times \sum_{i=r_1}^{r_2} D_i'$$

where D_i' are corrected relative optical densities calculated from the equations

$$D_i' = D_i \ (1 + kD_i)$$

and

$$D_i = \log \ (T_b/T_m)$$

The correction term kD_i is further discussed in Ref. 12. The value 0.4 is usually suitable for k.

DISCUSSION

The correctness of cell parameters with standard deviations and intensities of powder lines obtained by the technique described above has been tested.

Table 1. Guinier powder pattern of $Pb(NO_3)_2$ Cu$K\alpha_1$ radiation, $\lambda = 1.54051$ Å. $\Delta = 10^5 \times (\sin^2\theta_{obs\ II} - \sin^2\theta_{calc\ II})$.

$\lvert F\rvert^2_{obs}$	$\sum h^2+k^2+l^2$	$\sin^2\theta_{obs\ I} \times 10^5$	$\sin^2\theta_{obs\ II} \times 10^5$	$\sin^2\theta_{calc\ II} \times 10^5$	Δ
1064	3	2875	2875	2884	−8
861	4	3840	3841	3845	−4
187	5	4804	4807	4806	1
153	6	5768	5768	5767	1
1551	8	7688	7690	7690	0
3471	11	10575	10576	10573	2
2043	12	11536	11538	11535	4
1331	16	15387	15386	15380	6
55	18	17305	17312	17302	10
2802	19	18269	18267	18263	4
2682	20	19230	19230	19224	6
2719	24	23078	23076	23069	7
3172	27	25949	25953	25953	0
1808	32	30753	30754	30759	−6
5423	35	33633	33640	33643	−3
2768	36	34605	34600	34604	−4
1434	40	38445	38443	38449	−6
1841	43	41342	41334	41333	1
2175	44	42321	42293	42294	−1

Such tests have been performed by use of photographs from substances of different symmetries.

A powder photograph of $Pb(NO_3)_2$ with Si ($a = 5.4301$ Å)[13] as internal standard was obtained at 25°C by a Guinier-Hägg focusing camera.[1] The photograph was mounted in the film cassette and scanned twice by the drum densitometer. The $\sin^2 \theta$ values derived from the two scans are presented in Table 1. The cell edges with standard deviations of this cubic substance derived by least-squares treatment are 7.8564 (2) Å and 7.8559 (3) Å, respectively. Thus, the reproducibility of the procedure is within two estimated standard deviations. These calculated cell dimensions may also be compared with those obtained by Westman and Magneli,[2] 7.8560 (2) Å at 20°C, and by Swanson *et al.*,[14] 7.8568 Å (no standard deviation given) at 25°C.

As mentioned above the θ values are derived by a least-squares treatment of a parabolic function $s = f(\theta)$. It has been found that if a linear dependence of the line positions, s, as a function of θ is assumed, errors in the calculated cell dimensions with an order of magnitude of several standard deviations may occur.

In Table 2 the cell dimensions of MoO_3 derived from film scanner data are compared with the cell parameters obtained by Westman and Magnéli [2] from careful visual estimation of the same photograph. As can be seen from Table 2

Table 2. Lattice parameters for MoO_3. Radiation used: Cu$K\alpha_1$, $\lambda = 1.54051$ Å.

Present work	Westman and Magnéli[2]
$a = 3.9623$ (3) Å	$a = 3.9628$ (9) Å
$b = 13.858$ (2) Å	$b = 13.855$ (4) Å
$c = 3.6978$ (4) Å	$c = 3.6964$ (8) Å

the standard deviations are significantly diminished by the film scanner technique. It should also be noted that the cumbersome visual estimation of the line positions is reduced to a small number of manual operations of the scanner and that the complete result was achieved within a few minutes after the scan procedure.

The squares of the structure factors derived from a powder specimen of α-Bi_2O_3 are shown in Table 3 together with those calculated from the known structure of the substance. The structure has been determined by X-ray single crystal technique to a conventional R value of 0.09.[15] It may be concluded from this comparison that in favourable situations it is possible to obtain structure factors of considerable accurracy by this technique. No orientation effects are detectable in this powder pattern. On the other hand the overlaps in the pattern make it impossible to resolve the individual structure factors in most cases. An R value defined as $\sum(F^2_{calc} - F^2_{obs})/\sum F^2_{calc}$ was calculated to 0.15. Overlap peaks were included as the sums of their contributions.

Table 3. Guinier powder pattern for α-Bi_2O_3 with observed and calculated intensities. The intensities are corrected for the PLG-factor. Radiation used: Cu$K\alpha_1$, $\lambda = 1.54051$ Å. $\Delta = 10^5$ ($\sin^2\theta_{obs} - \sin^2\theta_{calc}$). p = multiplicity factor.

Lattice parameters:

Present work	Malmros [15]
$a =$ 5.8478 (3) Å	$a =$ 5.8486 (5) Å
$b =$ 8.1673 (6) Å	$b =$ 8.1661 (10) Å
$c =$ 7.5102 (4) Å	$c =$ 7.5097 (8) Å
$\beta = 112.979$ (4)°	$\beta = 113.000$ (10)°

$h\ k\ l$	$\sin^2\theta_{obs} \times 10^5$	$\sin^2\theta_{calc} \times 10^5$	Δ	$\lvert F\rvert^2_{calc}$	$p\lvert F\rvert^2_{calc}$	$\lvert F\rvert^2_{obs}$
011	2129	2130	−1	17	66	71
−111	2934	2933	1	28	164	114
110		2936		13		
020	3558	3558	0	76	152	189
−102	4521	4522	−1	371	741	864
021	4798	4799	−1	20	78	75
002	4962	4964	−2	1095	2190	2337
−112	5414	5412	2	518	3709	3543
111		5422		410		
−121	5600	5601	−1	1086	11831	7690
120		5605		1871		
012	5852	5853	−1	723	2893	3138
−211	7831	7829	2	179	714	727
−122		8080		729		
121	8088	8090	−2	725	5816	5789
−202	8178	8174	4	1669	7369	5404
200		8188		2015		
022	8521	8522	−1	256	1023	1108
−212	9065	9063	2	550	2630	2675
210		9077		108		
031	9245	9246	1	346	1384	1355
102	9500	9500	0	599	1198	1190
−131	10049	10048	1	158	1041	1060
130		10052		102		
−113		10372		230		
112	10384	10389	−5	536	3064	3405
−222	11732	11732	0	289	1162	1386
220		11745		1		
−132		12527		77		
131	12535	12537	−2	182	1037	1331
−213	12782	12780	2	229	1140	1414
211		12807		56		
−123		13040		38		
122	13057	13058	−1	478	2066	2042
040	14228	14231	−3	161	322	291
023	14727	14727	0	429	1715	1999
−223		15448		297		
041	15467	15472	−5	1765	8254	7376
221		15475		2		
−232		16179		92		
230	16190	16193	−3	46	552	569
−141	16276	16274	2	3	855	687
140		16278		211		

Table 3. Continued.

−312		16809		499	2650	2400
−311	16816	16819	−3	163		
−104	16925	16925	0	2137	4274	5349
−133	17496	17488	8	308	2496	2415
132		17505		316		
−114		17815		55		
113	17838	17839	−1	621	2704	2934
−204		18088		16		
202	18124	18129	−5	171	375	326
−142	18749	18753	−4	145	633	589
141		18763		13		
−214		18978		259		
212	19011	19019	−8	775	4136	4340
033	19173	19174	−1	864	3849	3978
042		19195		99		
−322	19481	19477	4	944	7052	6099
−321		19488		819		
−233		19895		430		
231	19913	19922	−9	930	5439	5168
014	20746	20746	0	99	397	538
−241	21169	21171	−2	1739	6957	6182
−224	21651	21646	5	1054	5560	5962
222		21687		336		
−323		21949		97		
320	21979	21980	−1	900	3989	3762
−242	22405	22405	0	123	598	679
240		22419		26		
−304		23345		1468		
024	23397	23414	−17	890	6495	7835
−143	23711	23714	−3	976	4332	4509
142		23731		107		
−314		24235		252		
−151	24277	24279	−2	73	4494	4473
150		24283		96		
311		24286		702		
−134	24935	24930	5	99	596	703
133		24954		50		
043	25414	25400	14	60	241	267
−234		26093		6		
−243		26121		189		
232	26141	26134	7	42	3865	3381
241		26149		729		
−333	26398	26396	2	651	3218	3134
330		26427		154		
−152		26758		172		
151	26769	26768	1	327	1998	1814
104	26885	26881	4	1180	2783	3762
−324		26903		106		
213		27713		93		
−115		27739		62	2726	3256
−402	27750	27759	−9	1055		
114		27770		0		
−412	28658	28649	9	87	348	243
−251	29166	29176	−10	81	323	247
−225	30344	30326	18	662	3999	5318
223		30381		337		
302	30862	30853	9	196	392	306
−144		31156		61		

Table 3. Continued.

143	31180	31180	0	630	2764	2741
−153		31719		303		
152	31733	31736	−3	472	3743	3656
312		31742		161		
015	31914	31915	−1	275	1098	1807
−244	32320	32319	1	135	771	683
242		32360		58		
−343	32634	32622	12	283	1515	2176
340		32653		96		
400	32750	32751	−1	1027	2054	1673
053	33407	33405	2	133	534	428
−414		33585		158		
410	33629	33640	−11	281	1756	1453
−161		34063		958		
160		34067		303		
044	34081	34087	−6	118	7103	6633
−253		34126		397		
025	34587	34583	4	490	1958	2042
233		34828		610		
−135	34843	34855	−12	116	3596	3468
134		34886		173		
−432	35767	35764	3	192	768	577
−424	36255	36253	2	613	2451	2156
−162		36542		30		
161	36556	36552	4	713	3043	2718
062		36984		3		
−433		36991		167		
−431	37019	37019	0	107	1109	1335
204	37999	37999	0	181	363	503
−216		38820		88		
332	38861	38858	3	352	1913	3114
214		38889		39		
153		39185		300		
−106	39226	39257	−31	815	2829	4520
−116		40146		317		
115	40175	40184	−9	201	3041	3146
−262		40194		48		
260		40207		194		
350	40678	40658	20	260	3677	4689
−306		40699		1120		
−434		40701		99		
243		41054		42		
−145	41077	41081	−4	1124	4701	4403
144		41111		10		
−226		41489		645		
−163	41507	41502	5	265	3642	5714
162		41519		1		
−425	42436	42445	−9	602	2407	1701
063		43189		507		
−443	43227	43217	10	287	6839	5522
−441		43245		916		
−263	43915	43910	5	467	2338	1653
261		43937		117		
−513		44565		38		
−512	44581	44582	−1	216	1016	848
−345	45020	45012	8	1252	5008	4964

In Fig. 3 a small part of the transmission curve and the corresponding intensity curve from α-Bi_2O_3 are shown. The integrated areas shadowed in Fig. 3 are denoted by zeros on the corresponding curves produced on the line printer. This makes it possible to judge the integration procedure and the definition of the background level for the various peaks.

At $\theta = 23.7°$ (*cf.* Fig. 3) a double peak corresponding to sin $\theta = 0.1619$ and 0.1628, respectively, is seen. Although the sum of the intensities from these lines may be fairly correct they are not well resolved. It might be possible to resolve the intensities by Fourier techniques in the present case. However, considering the usually occurring orientation effects, overlaps, variation in line profiles with θ *etc.* it does not seem worth-while to include such a procedure at the present stage.

Acknowledgements. The authors are indebted to Professor Peder Kierkegaard for his active interest in this work and for all facilities placed at their disposal. Thanks are also due to Mr. Karl-Erik Johansson for his construction of the film cassette used in this work and to Dr. Don Koenig for his correction of the English of this paper.

This work has received financial support from the *Tri-Centennial Fund of the Bank of Sweden* and from the *Swedish Natural Science Research Council.*

REFERENCES

1. Hägg, G. *Rev. Sci. Instr.* **18** (1947) 371.
2. Westman, S. and Magnéli, A. *Acta Chem. Scand.* **11** (1957) 1587.
3. Klug, H. P. and Alexander, L. E. *X-Ray Diffraction Procedures for Polycrystalline and Amorphous Materials*, Wiley, New York 1954.
4. SAAB. *Film Scanner Manual*, 1967.
5. Abrahamsson, S. *J. Sci. Instr.* **43** (1966) 931.
6. Werner, P.-E. *Arkiv. Kemi* **31** (1969) 505.
7. IBM 1800 *Assembler Language* (Manual 1966).
8. IBM 1800 *Multiprogramming Executive Operating System* (Manual 1972).
9. Arndt, U. W. and Willis, B. T. M. *Single Crystal Diffractometry*, University Press, Cambridge 1966.
10. Sas, W. H. and De Wolff, P. M. *Acta Cryst.* **21** (1966) 826.
11. Werner, P.-E. *Arkiv. Kemi* **31** (1969) 513.
12. Werner, P.-E. *J. Sci. Instr. (J. Physics E)* **4** (1971) 351.
13. Parrish, W. *Acta Cryst.* **13** (1960) 838.
14. Swanson, H. E., Gilfrich, N. T. and Ugrinic, G. M. *Standard X-Ray Diffraction Powder Patterns*, NBS Circular 539, V, **21** (1963) 37.
15. Malmros, G. *Acta Chem. Scand.* **24** (1970) 384.

Received September 1, 1972.

ACTA CHEMICA SCANDINAVICA 27 (1973) 503–509

Electrolysis in Non-nucleophilic Media

Part V.[1] Formation of Mixed Biaryls in the Anodic Oxidation of Naphthalene in the Presence of Alkylbenzenes

KLAS NYBERG

Division of Organic Chemistry, Chemical Center, University of Lund, P.O. Box 740, S-220 07 Lund, Sweden

The anodic oxidation of naphthalene in the presence of alkylbenzenes in 0.1 M $Bu_4NBF_4/CH_3CN/CH_3COOH$ at a platinum anode results in the formation of 1-arylnaphthalenes. The products are assumed to be formed in an electrophilic reaction between naphthalene cation radicals and alkylbenzenes. The relative yield of 1-arylnaphthalenes follows the relative nucleophilicity of the alkylbenzenes. Preparative scale electrolysis was carried out with naphthalene/isodurene and naphthalene/pentamethylbenzene mixtures and gave 1-(2,3,4,6-tetramethylphenyl)-naphthalene and 1-(pentamethylphenyl)-naphthalene in 42 % and 56 % yields, respectively.

In Part IV of this series it was shown that anodic oxidation of naphthalene in an acetic acid/acetonitrile mixture and in the presence of mesitylene gave 1,1′-binaphthyl and 1-mesitylnaphthalene as the only products.[1] On the basis of voltammetric data and the products, it was suggested that the mixed biaryl was formed according to eqns. (1)–(3):

$$ArH \rightarrow ArH^{+\cdot} + e \quad (1)$$

$$ArH^{+\cdot} + Ar'H \rightarrow H-\overset{+}{Ar}-\dot{Ar}'-H \quad (2)$$

$$H-\overset{+}{Ar}-\dot{Ar}'-H \rightarrow Ar-Ar' + e + 2H^{+} \quad (3)$$

ArH = naphthalene, Ar′H = mesitylene

This type of mechanism has also been suggested for the anodic coupling of polymethylbenzenes.[2]

The preparative and mechanistic aspects of the mixed coupling reaction are further investigated in this paper. Anodic oxidation of naphthalene has been carried out in the presence of a number of alkylbenzenes.

RESULTS

Small scale electrolysis was carried out on 50 ml solutions of CH_3CN/CH_3COOH (volume ratio 9:1) containing 0.1 M Bu_4NBF_4, naphthalene and the appropriate alkylbenzene between two platinum electrodes using the saturated calomel electrode as a reference electrode. In general, only two products were formed, 1,1′-binaphthyl (I) and a mixed biaryl (II). In order

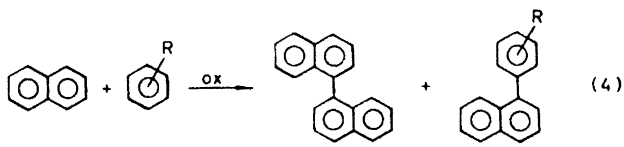

(4)

I II

to reduce further reactions of the products, the current yields of I and II were determined after passage of 0.2 *F*/mol of naphthalene. The results from these experiments are presented in Table 1. The yield of mixed biaryl increases remarkably in going from *m*-xylene to pentamethylbenzene, *i.e.* when the number of methyl groups in the alkylbenzene is increased. An exception is durene, which will be mentioned later.

Table 1. Anodic oxidation of naphthalene (1.0 M) in CH_3CN/CH_3COOH (volume ratio 9:1) containing 0.1 M Bu_4NBF_4 in the presence of alkylbenzenes at a platinum anode. Anode potential 1.4 – 1.5 V.

Alkylbenzene	Conc. (M)	% Yield of 1,1′-binaphthyl	% Yield of mixed biaryl
m-Xylene	3.0	28	0.4
1,2,4-Trimethylbenzene	3.0	24	1.6
Mesitylene [a]	3.0	22	19
Durene	1.0	21	1.1
Isodurene	1.0	10	32
Pentamethylbenzene	1.0	1.6	64
5-Isopropyl-*m*-xylene	3.0	31	8.3
5-*t*-Butyl-*m*-xylene	3.0	36	4.2
1,3,5-Triethylbenzene [b]	1.5	30	6.6

[a] Data from Ref. 1.
[b] Naphthalene conc. 0.5 M.

Durene, isodurene and pentamethylbenzene are oxidized in the same potential region as naphthalene, while the other alkylbenzenes are oxidized at significant higher anode potentials. This means that the latter compounds are not oxidized during the electrolysis, since the working potential was set near the oxidation potential of naphthalene. The mixed biaryl must therefore in these cases be formed from the reaction of oxidized naphthalene, and most

reasonably its cation radical. However, in the case of durene, isodurene, and pentamethylbenzene, one cannot draw the same conclusion by just regarding the difference in oxidation potentials. For this reason anodic oxidation of naphthalene in the presence of isodurene or pentamethylbenzene was carried out at different concentrations of the substrates. The results from these experiments are shown in Tables 2 and 3. Keeping the concentration of naph-

Table 2. Anodic oxidation of naphthalene in CH_3CN/CH_3COOH/0.1 M Bu_4NBF_4 in the presence of isodurene at a Pt anode. Anode potential 1.4 – 1.5 V.

Naphthalene conc. M	Isodurene conc. M	% Yield of binaphthyl	% Yield of mixed biaryl
0.2	1.0	4	29
1.0	0.2	14	8
1.0	1.0	10	32
1.0	2.0	6	36

Table 3. Anodic oxidation of naphthalene in CH_3CN/CH_3COOH/0.1 M Bu_4NBF_4 in the presence of pentamethylbenzene at a Pt anode. Anode potential 1.4 – 1.5 V.

Napthalene conc. M	Pentamethyl-benzene conc. M	% Yield of binaphthyl	% Yield of mixed biaryl
0.2	1.0	–	48
0.5	1.0	1.2	48
1.0	0.2	3.4	21
1.0	0.5	2.7	42
1.0	1.0	1.6	64
1.0	2.0	1.3	62

thalene constant at 1.0 M and increasing the isodurene concentration from 0.2 M to 2.0 M results in a considerable increase in the yield of mixed biaryl. On the other hand there is no significant change in the yield of mixed biaryl when the isodurene concentration is kept constant and that of naphthalene is varied. The same pattern is shown by the results in Table 3, which indicates that only naphthalene is oxidized during the electrolyses.

Two 5-alkylsubstituted *m*-xylenes were also used as substrates. Thus, naphthalene was electrolyzed with 5-isopropyl- and 5-*t*-butyl-*m*-xylene, respectively, but in both experiments only low yields of mixed biaryl were formed, as shown in Table 1. The yields should be compared with that obtained from oxidation of naphthalene in the presence of mesitylene, which is much higher. This behaviour is similar to the one observed from anodic coupling of the same three compounds.[3] Mesitylene affords a biaryl in much higher yield than 5-isopropyl- or 5-*t*-butyl-*m*-xylene.

The preparative use of the mixed coupling reactions was also investigated. The anodic oxidation of naphthalene in the presence of isodurene on a preparative scale produced 1-(2,3,4,6-tetramethylphenyl)-naphthalene (III) in

an isolated current yield of 42 %. Oxidation of naphthalene in the presence of pentamethylbenzene gave 1-(pentamethylphenyl)-naphthalene (IV) in 56 % yield. Although the yields of mixed biaryls from oxidation of naphthalene in the presence of 5-isopropyl-*m*-xylene, 5-*t*-butyl-*m*-xylene, and 1,3,5-triethylbenzene were low, attempts were made to isolate these compounds on a preparative scale. Only in the case of 1,3,5-triethyl-benzene was this practically feasible, the mixed biaryl, 1-(2,4,6-triethylphenyl)-naphthalene, being isolated in a crude state in 2 % current yield.

DISCUSSION

The results presented in this paper clearly support the mechanism proposed for the anodic coupling of aromatic hydrocarbons, *i.e.* eqns. (1) – (3). Mixed biaryls are formed, although only one of the aromatic compounds is electroactive under the conditions used during the electrolysis, which must mean that the cation radical reacts as an electrophile to form the coupled product.

In Part IV of this series,[1] it was demonstrated by current-voltage curves that electrolysis of naphthalene and mesitylene in the system $CH_3CN/CH_3COOH/Bu_4NBF_4$ proceeds by preferential oxidation of naphthalene. If one attempts to apply the same technique to the electrolysis of naphthalene/isodurene or naphthalene/pentamethylbenzene mixtures one does not obtain any useful information, since these three compounds are oxidized at about the same anode potential. Therefore the amount of mixed biaryl and 1,1′-binaphthyl was determined for the electrolysis of the mixtures mentioned under various conditions (Tables 2 and 3). The yields of mixed biaryl increases significantly only when the concentration of the alkylbenzene is increased.

Electrolysis was also carried out in the same medium but in the absence of naphthalene. The products obtained from the anodic oxidation of isodurene or pentamethylbenzene were mainly polymethylbenzyl acetates formed in about 40 % yield, and only small amounts of dehydrodimers, substituted diphenylmethanes, were present.

Further support for an electrophilic reaction is obtained by comparing the relative yields of mixed biaryls with the relative basicity of the alkylbenzenes.[4] The basicity of the alkylbenzenes can also be taken as a measure of their relative nucleophilicity, although some caution should be exercised with the highly substituted benzenes, since steric factors may reduce the nucleophilicity. The data presented in Table 4 show a good correlation between the relative basicity of the alkylbenzenes and the relative yields of mixed biaryls. The latter values were calculated by taking into account the amount of binaphthyl formed at the same concentration level of alkylbenzene. Competitive experiments verified the relation. Electrolysis of naphthalene and durene gave a low yield of mixed biaryl, which certainly is due to the low nucleophilicity of durene. In the presence of the more nucleophilic substrates, mesitylene, isodurene, and pentamethylbenzene, electrolysis of naphthalene gave the highest yields of mixed biaryls.

In connection with the mechanism it is of interest to discuss the observation that naphthalene is the only compound that is oxidized during electrolysis,

Table 4. Relation between the yield of mixed biaryl from anodic oxidation of naphthalene in the presence of alkylbenzenes and the basicity of the alkylbenzenes.

Alkylbenzene	Relative yield of mixed biaryl	Relative basicity
m-Xylene	1	1
1,2,4-Trimethylbenzene	6	3.5
Durene	10	1.4
Mesitylene	61	560
Isodurene	650	5 000
Pentamethylbenzene	7 600	19 000

although the alkylbenzenes are present. If one examines only the oxidation potentials of these compounds, one would expect the alkylbenzenes as well as naphthalene to be oxidized. However, this is obviously not the case. One reason for this behaviour might be a preferential adsorption of naphthalene molecules at the anode surface. This would lead to a blocking of the appropriate alkylbenzene molecules and thereby only oxidation of naphthalene will take place.[5-7]

The synthetic utility of anodic coupling reactions is further demonstrated in this work. Especially the high yield of 1-(pentamethylphenyl)-naphthalene from oxidation of naphthalene in the presence of pentamethylbenzene is remarkable.[8]

However, there are certain limitations in the use of anodic coupling reactions for synthesis of biaryls. Some of these are: firstly, the product should not be oxidizable at a significantly lower anodic potential than the starting materials. Secondly, the substrate should be highly substituted; otherwise further reactions will take place leading to oligomers and polymers. Thirdly, the substrate, or one of the substrates in a mixed coupling, should possess sufficient nucleophilicity to react with the cation radical which is produced. And fourthly, the positive charge density in the cation radical must be large in an unsubstituted position.[2] It is obvious from these restriction that the number of suitable aromatic hydrocarbons, which are available for such coupling, is limited. Experience so far indicates that the anodic coupling of aromatic hydrocarbons will be most useful in the preparation of highly substituted biaryls.

EXPERIMENTAL

The electrolysis cell, potentiostat, and the analytical instruments were the same as previously reported.[1]

Materials. Acetonitrile (Baker, 0.3 %), and acetic acid (*p.a.*) were used as solvents. Bu_4NBF_4 [9] and 1,3,5-triethylbenzene [10] were prepared as previously reported. Isodurene (Aldrich, technical grade) which contains 10 – 15 % durene was purified by treatment with chlorosulphonic acid (an excess of isodurene is necessary in order to avoid the formation of durene sulphonic acid) followed by desulphonation of isodurene sulphonic acid. Thus 1 mol of chlorosulphonic acid dissolved in 100 ml CH_2Cl_2 was added dropwise to a stirred solution of 2 mol of isodurene in 2 l CH_2Cl_2. After the addition, stirring was continued for 30 min and then 2 mol of sodium hydroxide in 1 l water was added drop-

wise. The mixture was filtered and the precipitate was washed with CH_2Cl_2. The precipitate and the water phase were combined and 300 ml concentrated hydrochloric acid was added. This mixture was subjected to steam distillation, the distillate (about 4 l) was extracted with CH_2Cl_2 and the organic phase was dried. After removing the solvent by evaporation *in vacuo*, the residue was distilled at reduced pressure to give isodurene of about 99 % purity (yield 70 – 80 %). All other compounds were of high commercial quality.

Electrolysis. Small scale electrolysis was carried out on 50 ml solutions. All details regarding the amount of materials and the time used for electrolysis are given in the tables. The electrolysis mixtures were worked up by removing the solvents by evaporation *in vacuo*, treating the residue with ether, filtering off the supporting electrolyte and then analyzing the concentrated ether solution by GLC and mass spectrometry. The yields of products were calculated by adding a standard to the ether solutions and then integrating the GLC peak areas. All products except those isolated were identified solely on the basis of their mass spectral fragmentation pattern.

Anodic synthesis of 1-(pentamethylphenyl)-naphthalene. A solution made up of 0.25 mol of naphthalene, 0.25 mol of pentamethylbenzene, 0.025 mol of Bu_4NBF_4, 225 ml acetonitrile and 25 ml acetic acid was electrolyzed between two platinum electrodes at a constant current of 0.5 A until 1 *F*/mol of naphthalene had passed. The solvents were removed by evaporation *in vacuo*, ether was added to the residue and the salt was filtered off (in case the salt does not precipitate, the ether solution was decanted). The ether was distilled off and the residue was distilled up to 115°/12 mm in order to remove naphthalene and pentamethylbenzene. The residue was extracted with 250 ml boiling pentane. The pentane solution was decanted and run through a short alumina column. Another 250 ml pentane was also used as eluent. Pentane was removed from the eluate leaving a white solid, which was recrystallized from a mixture of ethanol (500 ml) and benzene (150 ml) to give 19.3 g of 1-(pentamethylphenyl)-naphthalene, m.p. 119 – 121° (yield 56 %). According to GLC the purity was 98.5 %.

MS: *m/e* 274 (100 % abundance), 259 (51 %), 244 (33 %), 229 (32 %). NMR (CCl_4) δ 1.77 (s, 6, 2,6-CH_3), 2.23 (s, 6, 3,5-CH_3), 2.28 (s, 3, 4-CH_3), 7.03 – 7.87 (m, 7, $C_{10}H_7$).

Anodic synthesis of 1-(2,3,4,6-tetramethylphenyl)-naphthalene. The electrolysis solution consisted of 0.25 mol of naphthalene, 0.50 mol of isodurene, 0,025 mol of Bu_4NBF_4, 225 ml acetonitrile and 25 ml acetic acid. The experiment was performed in the same way as the previous one and work-up procedure was also the same. The white solid obtained after chromatography was recrystallized from 200 ml ethanol to give 13.8 g of 1-(2,3,4,6-tetramethylphenyl)-naphthalene, m.p. 108 – 111° (current yield 42 %). GLC purity 99 %.

MS: *m/e* 260 (100 %), 245 (69 %), 230 (38 %), 229 (42 %), 215 (44 %). NMR (CCl_4) δ 1.78 (s, 6, 2,6-CH_3), 2.20 (s, 3, 3-CH_3), 2.32 (s, 3, 4-CH_3), 6.88 (s, 1, $C_6H(CH_3)_4$), 7.07 – 7.87 (m, 7, $C_{10}H_7$).

Anodic synthesis of 1-(2,4,6-triethylphenyl)-naphthalene. The electrolysis solution consisted of 0.15 mol of naphthalene, 0.45 mol of 1,3,5-triethylbenzene, 0.015 mol of Bu_4NBF_4, 135 ml acetonitrile and 15 ml acetic acid. At a constant current of 0.5 A the electrolysis was continued until 1 *F*/mol of naphthalene had passed. The solvents were removed by evaporation *in vacuo* and ether was added to the residue in order to precipitate the salt. The ether solution was evaporated and the starting materials were then removed by distillation up to 95°/12 mm. Further distillation at 160 – 230°/0.5 mm gave 3.2 g of a liquid. This was dissolved in pentane and chromatographed on an alumina column. After evaporation of pentane 470 mg of a colorless liquid remained which did not solidify. GLC showed one major peak and the peak area corresponded to about 97 % of the total peak areas. This was identified as 1-(2,4,6-triethylphenyl)-naphthalene on the basis of spectral data.

MS: *m/e* 288 (100 %), 273 (28 %), 259 (39 %), 244 (19 %), 229 (17 %) and 215 (41 %). NMR (CCl_4) δ 0.90 (t, 6, 2,6-CH_3CH_2), 1.32 (t, 3, 4-CH_3CH_2), 2.13 (q, 4, 2,6-CH_3CH_2), 2.68 (q, 2, 4-CH_3CH_2), 6.93 (s, 2, $C_6H_2(CH_2CH_3)_3$), 7.17 – 7.83 (m, 7, $C_{10}H_7$).

Acknowledgements. The author gratefully acknowledges valuable discussions with Professor Lennart Eberson. This work was supported by grants from the *Swedish Natural Science Research Council*, *Kungliga Fysiografiska Sällskapet i Lund*, and *Karl Tryggers Stiftelse*. The mass spectrometer was donated by the *Alice and Knut Wallenbergs Stiftelse*.

REFERENCES

1. Part IV, see Nyberg, K. *Acta Chem. Scand.* **25** (1971) 3770.
2. Nyberg, K. *Acta Chem. Scand.* **25** (1971) 2499.
3. Nyberg, K. *Acta Chem. Scand.* **25** (1971) 2983.
4. Perkampus, H. H. *Advan. Phys. Org. Chem.* **4** (1966) 195.
5. Dahms, H. and Green, M. *J. Electrochem. Soc.* **110** (1963) 1075.
6. Bockris, J. O'M., Green, M. and Swinkels, D. A. J. *J. Electrochem. Soc.* **111** (1964) 743.
7. Eberson, L. and Wilkinson, R. G. *Acta Chem. Scand.* **26** (1972) 1671.
8. A simple large scale electrolysis cell has recently been constructed and with that 1-(pentamethylphenyl)-naphthalene has been synthesized in 100 g quantities; see Eberson, L., Nyberg, K. and Sternerup, H. *Chemica Scripta* **3** (1973) 12.
9. Nyberg, K. *Acta Chem. Scand.* **24** (1970) 1609.
10. Norris, J. F. and Rubinstein, D. *J. Am. Chem. Soc.* **61** (1939) 1163.

Received August 30, 1972.

ACTA CHEMICA SCANDINAVICA 27 (1973) 510–520

The Crystal and Molecular Structure of 2,5-Diphenyl-3,4-diaza-6a-thiathiophthene

ASBJØRN HORDVIK and LARS M. MILJE

Chemical Institute, University of Bergen, N-5000 Bergen, Norway

2,5-Diphenyl-3,4-diaza-6a-thiathiophthene crystallizes in the orthorhombic space group $Pc2_1n$, with unit cell dimensions: $a = 12.494(12)$ Å, $b = 4.007(8)$ Å, and $c = 28.185(15)$ Å. There are four molecules per unit cell.

The structure was solved by the heavy atom method, and refined by full matrix least squares. The refinement comprises 1039 $h0l - h3l$ reflections.

The 2- and 5-phenyl groups are twisted 2.0 and 7.0° about the respective connecting bonds, and the lengths of the S(1)–S(6a) and S(6a)–S(6) bonds are 2.319(3) and 2.328(3) Å, respectively, with the angle S(1)–S(6a)–S(6) = 174.3(2)°. The other bond lengths in the central ring system are S(1)–C(2) = 1.692(9) Å, S(6a)–C(3a) = 1.786(8) Å, S(6)–C(5) = 1.698(8) Å, C(2)–N(3) = 1.325(10) Å, N(3)–C(3a) = 1.330(9) Å, C(3a)–N(4) = 1.344(10) Å, and N(4)–C(5) = 1.336(10).

The C–C bonds connecting the phenyl groups to the 3,4-diaza-6a-thiathiophthene system are C(2)–C(12) = 1.515(11) Å and C(5)–C(6) = 1.475(11) Å.

The S–S, S–C, N–C, and C–C bond lengths have been corrected for libration.

There are no intermolecular close contacts between sulphur and neighbouring atoms or groups.

The present structure study of 2,5-diphenyl-3,4-diaza-6a-thiathiophthene (I) has been carried out in order to obtain further experimental evidence for the effect of phenyl substituents on the sulphur-sulphur bonding in 6a-thiathiophthenes.

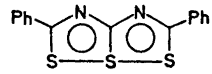

(I)

STRUCTURE DETERMINATION

A brief account of the structure determination has been reported earlier,[1] and a more detailed description is given here.

Compound I was first described by Derocque, Perrier and Vialle.[2] The crystals are orange-red and belong to the orthorhombic space group $Pc2_1n$.

The structure analysis is based on photographic data, taken with Weissenberg camera and Cu$K\alpha$ radiation. 1039 $h0l-h3l$ reflections were observed.

The structure was solved by the heavy atom method and refined by a least squares procedure (see for example Ref. 7). The constants a_1 and a_2 in the weighting scheme were in the present case set equal to 1.0. Unobserved reflections with $K|F_c|$ greater than $F_o^{\text{threshold}}$ were included in the refinement with $F_o = F_o^{\text{threshold}}$. Anisotropic temperature factors were applied to sulphur, nitrogen, and carbon, and isotropic ones to hydrogen. Fourteen low order reflections whose intensities were very difficult to estimate, were excluded from the least squares refinement. The final R factor is 0.068 when unobserved reflections are included, and 0.065 when they are omitted.

A rigid-body analysis of the 2,5-diphenyl-3,4-diaza-6a-thiathiophthene molecule has been carried out according to the method of Schomaker and Trueblood,[3] and the S–S, S–C, N–C, and C–C bond lengths have been corrected for rigid-body libration according to Cruickshank's formula.[4] For further details with respect to the structure determination, see Experimental.

DISCUSSION

Molecular shape and dimensions. Bond lengths and angles in the 2,5-diphenyl-3,4-diaza-6a-thiathiophthene molecule are listed in Tables 1 and 2, and shown in Figs. 1a and 1b. Furthermore, in Fig. 1a the deviations for sulphur, nitrogen, and carbon from the least squares plane of the molecule are given. The equation for this plane, with neglect of hydrogen and triple weight on sulphur, is

$$0.20734X + 0.90184Y - 0.37908Z = -0.65397$$

where X, Y, and Z are in Å units. One notes with respect to the linear sequences C(2)–C(12)–C(15) and C(5)–C(6)–C(9), *cf.* Fig. 1a, that the former lies almost in the plane of the molecule and that the latter points slightly out of it.

The equation for the least squares plane through the atoms of the central ring system with triple weight on sulphur, is

$$0.21283X + 0.90443Y - 0.36974Z = -0.51717$$

and the deviations in Å units from this plane are S(1) 0.006, S(6a) −0.006, S(6) −0.003, C(2) −0.002, N(3) −0.015, C(3a) 0.008, N(4) −0.007, and C(5) 0.023. Thus, the 3,4-diaza-6a-thiathiophthene system is planar within the error.

The twist angle of the 2-phenyl group about C(2)–C(12) is 2.0°. The twist angle was taken as the angle between the plane through S(1), C(2), N(3), and C(12), and the plane through C(2), C(12), C(13), and C(17).

Table 1. Bond lengths (l) and standard deviations in bond lengths $\sigma(l)$ in 2,5-diphenyl-3,4-diaza-6a-thiathiophthene. Bond lengths (l') have been corrected for rigid-body libration.

Bond	l' (Å)	l (Å)	$\sigma(l)$ (Å)
S(1) – S(6a)	2.319	2.316	0.003
S(6a) – S(6)	2.328	2.325	0.003
S(1) – C(2)	1.692	1.691	0.009
S(6a) – C(3)	1.786	1.784	0.008
S(6) – C(5)	1.698	1.697	0.008
C(2) – N(3)	1.325	1.323	0.010
N(3) – C(3a)	1.330	1.328	0.009
C(3a) – N(4)	1.344	1.344	0.010
N(4) – C(5)	1.336	1.333	0.010
C(5) – C(6)	1.475	1.473	0.011
C(6) – C(7)	1.390	1.389	0.012
C(7) – C(8)	1.372	1.372	0.013
C(8) – C(9)	1.410	1.408	0.016
C(9) – C(10)	1.370	1.368	0.013
C(10) – C(11)	1.385	1.383	0.012
C(11) – C(6)	1.413	1.410	0.013
C(2) – C(12)	1.515	1.513	0.011
C(12) – C(13)	1.388	1.387	0.011
C(13) – C(14)	1.396	1.396	0.015
C(14) – C(15)	1.360	1.360	0.017
C(15) – C(16)	1.385	1.385	0.015
C(16) – C(17)	1.393	1.391	0.013
C(17) – C(12)	1.417	1.415	0.012
Bond	l (Å)	Bond	l (Å)
C(7) – H(7)	0.89	C(13) – H(13)	1.13
C(8) – H(7)	1.01	C(14) – H(14)	0.88
C(9) – H(9)	1.07	C(15) – H(15)	1.05
C(10) – H(10)	1.07	C(16) – H(16)	0.96
C(11) – H(11)	0.94	C(17) – H(17)	1.10

Table 2. Bond angles ∠(ijk) in 2,5-diphenyl-3,4-diaza-6a-thiathiophthene. The standard deviations given in parentheses refer to the last digits of respective values.

i	j	k	∠(ijk)°	i	j	k	∠(ijk)°
C(2)	S(1)	S(6a)	91.3(3)	C(5)	C(6)	C(7)	122.6(8)
S(1)	S(6a)	S(6)	174.3(2)	C(5)	C(6)	C(11)	119.9(7)
S(1)	S(6a)	C(3a)	87.1(3)	C(7)	C(6)	C(11)	117.5(9)
S(6)	S(6a)	C(3a)	87.1(3)	C(6)	C(7)	C(8)	122.5(9)
S(6a)	S(6)	C(5)	91.9(3)	C(7)	C(8)	C(9)	118.6(9)
S(1)	C(2)	N(3)	122.2(6)	C(8)	C(9)	C(10)	120.2(9)
S(1)	C(2)	C(12)	121.2(6)	C(9)	C(10)	C(11)	120.6(9)
N(3)	C(2)	C(12)	116.6(7)	C(10)	C(11)	C(6)	120.5(8)
C(2)	N(3)	C(3a)	117.6(7)	C(2)	C(12)	C(13)	120.9(8)

Table 2. Continued.

N(3)	C(3a)	S(6a)	121.6(6)	C(2)	C(12)	C(17)	119.0(7)
N(3)	C(3a)	N(4)	116.8(8)	C(13)	C(12)	C(17)	120.0(8)
N(4)	C(3a)	S(6a)	121.5(6)	C(12)	C(13)	C(14)	118.5(9)
C(3a)	N(4)	C(5)	118.1(7)	C(13)	C(14)	C(15)	122.1(1.1)
N(4)	C(5)	S(6)	121.3(6)	C(14)	C(15)	C(16)	119.9(1.0)
N(4)	C(5)	C(6)	116.8(7)	C(15)	C(16)	C(17)	120.1(1.0)
C(6)	C(5)	S(6)	121.8(6)	C(16)	C(17)	C(12)	119.5(8)

Similarly, the twist angle of the 5-phenyl group about C(5) – C(6) was found to be 7.0°.

Comparison with the structure of 2,5-diphenyl-6a-thiathiophthene. Bond lengths in 2,5-diphenyl-6a-thiathiophthene (II) are given in Fig. 2.[5]

The sulphur-sulphur bonds are almost equal in the present structure where the 2- and 5-phenyl groups are twisted 2.0 and 7.0°, respectively; the bond lengths are S(1) – S(6a) = 2.319(3) Å and S(6a) – S(6) = 2.328(3) Å, *cf.* Fig. 1a.

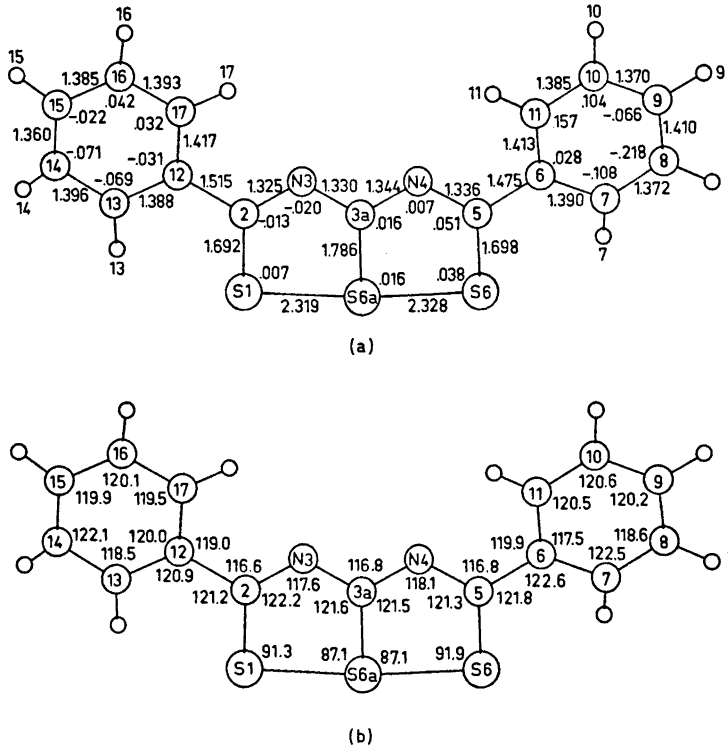

Fig. 1. (a) Bond lengths (Å) in 2,5-diphenyl-3,4-diaza-6a-thiathiophthene, and atomic distances (Å) from the least squares plane of the molecule. (b) Bond angles (°).

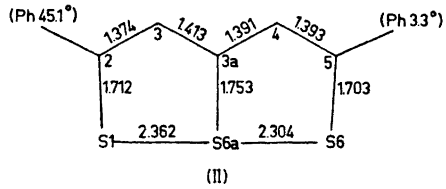

Fig. 2. Bond lengths (Å) in 2,5-diphenyl-6a-thiathiophthene.

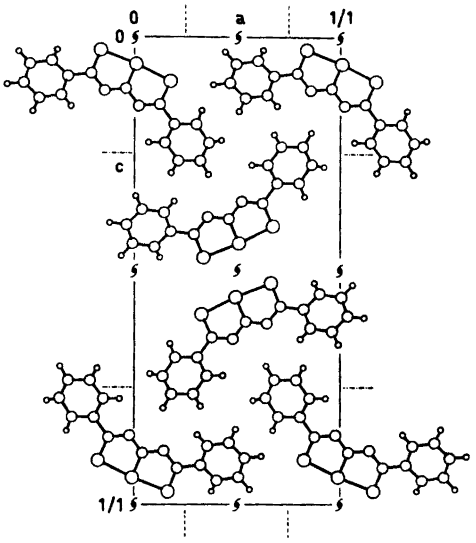

Fig. 3. The arrangement of 2,5-diphenyl-3,4-diaza-6a-thiathiophthene molecules in the crystal as seen along the *b*-axis.

In compound II, however, where the 2- and 5-phenyl groups are twisted 45.1 and 3.3° about the respective connecting bonds, the S – S bonds are significantly different, *i.e.* S(1) – S(6a) = 2.362(3) Å and S(6a) – S(6) = 2.304(3) Å. This agrees with the results from CNDO/2 calculations on phenyl substituted 6a-thiathiophthenes.[6] A 2-phenyl group will, according to the CNDO/2 results, cause a lengthening of the S(1) – S(6a) bond which varies with the twist angle of the phenyl group, being negligible at twist angle 0° and most pronounced at 90°.

The difference between the length of the S(6a) – C(3a) bond in I, 1.786(8) Å, and the length of the S(6a) – C(3a) bond in II, 1.753(6) Å, may be real, and due to the presence of the nitrogen atoms in I. Thus the S(6a) – C(3a) bond lengths in eleven different 6a-thiathiophthene structures are found in the range 1.748 – 1.763 Å,[7] while the S(6a) – C(3a) bond length in 2,5-dianilino-3,4-diaza-6a-thiathiophthene [8] is found to be 1.790(8) Å, in close agreement with the length of the equivalent bond in the present structure.

The lengths of the carbon-nitrogen bonds in I, C(2) – N(3) = 1.325(10) Å, N(3) – C(3a) = 1.330(9) Å, C(3a) – N(4) = 1.344(10) Å, and N(4) – C(5) = 1.336(10) Å, agree with the length of the aromatic C – N bond in pyridine, 1.340 Å,[9] and there is no significant difference between the central and the terminal C – N bond lengths. Also in this respect there seems to be a difference between 3,4-diaza-6a-thiathiophthenes and 6a-thiathiophthenes. The sum of the C(3a) – C(3) and the C(3a) – C(4) bond lengths in the latter is namely always found to be greater than the sum of the C(2) – C(3) and the C(4) – C(5) bond lengths.[7]

The crystal structure of 2,5-diphenyl-3,4-diaza-6a-thiathiophthene as seen along the *b*-axis is shown in Fig. 3. There are no intermolecular atomic distances shorter than the corresponding van der Waals distances.

EXPERIMENTAL

The unit cell dimensions for crystals of 2,5-diphenyl-3,4-diaza-6a-thiathiophthene were determined from high-order reflections on $0kl$ and $h0l$ Weissenberg photographs where lead nitrate powder lines had been superimposed for reference. A least squares procedure on 30 measured 2θ-values gave $a = 12.494(12)$ Å, $b = 4.007(8)$ Å, and $c = 28.185(15)$ Å.

Four molecules per unit cell give a calculated density of 1.480 g/cm³ as compared with the density 1.49 g/cm³ found by flotation.

The intensities of the $h0l - h3l$ reflections were estimated visually from Weissenberg photographs taken with Ni-filtered Cu$K\alpha$ radiation ($\mu = 45.2$ cm^{-1}).

A crystal with dimensions about $0.08 \times 0.7 \times 0.03$ mm in the three axial directions was used for the intensity data collection. Lp corrections, and corrections for extended spots on upper layer Weissenberg films, were applied, but absorption corrections were not applied.

Table 3. Atomic coordinates in fractions of corresponding cell edges. The standard deviations given in parentheses refer to the last digits of respective values.

Atom	*x*	*y*	*z*
S(1)	0.17397(15)	−0.0255(0)	0.09414(7)
S(6a)	0.00714(16)	−0.0127(11)	0.05747(6)
S(6)	−0.16457(18)	0.0279(9)	0.02732(6)
C(2)	0.12310(59)	0.1521(25)	0.14367(29)
N(3)	0.02089(45)	0.2338(21)	0.14743(20)
C(3a)	−0.04169(59)	0.1785(26)	0.11018(24)
N(4)	−0.14522(47)	0.2640(21)	0.11462(22)
C(5)	−0.20977(58)	0.2128(23)	0.07766(26)
C(6)	−0.32299(62)	0.3061(25)	0.08373(27)
C(7)	−0.41122(68)	0.2265(30)	0.05060(32)
C(8)	−0.50760(73)	0.2943(35)	0.05781(34)
C(9)	−0.53728(71)	0.4772(35)	0.09840(36)
C(10)	−0.46174(67)	0.5659(28)	0.13120(30)
C(11)	−0.35525(60)	0.4853(33)	0.12434(27)
C(12)	0.19300(53)	0.2230(23)	0.18632(28)
C(13)	0.30040(68)	0.1357(29)	0.18650(34)
C(14)	0.36122(97)	0.2101(45)	0.22665(38)
C(15)	0.31903(84)	0.3679(32)	0.26502(35)
C(16)	0.21237(79)	0.4620(40)	0.26485(32)
C(17)	0.14814(71)	0.3897(28)	0.22585(29)
H(7)	−0.3762(41)	0.100(17)	0.0271(18)
H(8)	−0.5624(58)	0.250(24)	0.0322(27)
H(9)	−0.5218(79)	0.512(47)	0.1002(36)
H(10)	0.4949(71)	0.710(33)	0.1596(34)
H(11)	0.3048(64)	0.522(40)	0.1484(33)
H(13)	0.3249(62)	0.025(39)	0.1556(32)
H(14)	0.4249(82)	0.119(43)	0.2220(46)
H(15)	0.3591(86)	0.480(61)	0.2937(43)
H(16)	0.1758(61)	0.562(32)	0.2910(29)
H(17)	0.0680(48)	0.522(29)	0.2259(21)

Table 4. Temperature parameters U_{ij} (Å^2) for sulphur, nitrogen and carbon, and U (Å^2) for hydrogen. The expressions used are exp $[-2\pi^2(h^2a^{*2}U_{11}+\cdots 2hka^*b^*U_{12}+\cdots)]$ for sulphur, nitrogen and carbon, and exp $[-8\pi^2U(\sin^2\theta/\lambda^2)]$ for hydrogen. All values are multiplied by 10^4. Standard deviations in parentheses refer to the last digits of the respective values.

	U_{11}	U_{22}	U_{33}	U_{12}	U_{23}	U_{13}
S(1)	941(10)	482(16)	454(9)	118(17)	−75(13)	103(8)
S(6a)	610(11)	299(12)	347(8)	38(13)	−29(12)	153(8)
S(6)	610(11)	475(17)	350(8)	−19(15)	−55(12)	58(8)
C(2)	430(43)	268(55)	539(45)	66(42)	82(42)	88(35)
N(3)	366(33)	381(50)	360(32)	55(34)	−39(33)	30(25)
C(3a)	461(44)	383(56)	325(35)	8(43)	23(39)	21(30)
N(4)	387(34)	440(52)	416(33)	50(35)	34(33)	29(26)
C(5)	488(42)	281(58)	368(38)	−16(43)	80(38)	57(33)
C(6)	458(43)	347(58)	436(41)	−18(45)	52(40)	−40(34)
C(7)	507(51)	487(70)	631(49)	35(49)	−1(50)	−57(40)
C(8)	526(52)	640(76)	651(56)	−8(58)	137(69)	−192(47)
C(9)	593(52)	458(69)	814(60)	44(82)	60(72)	94(48)
C(10)	483(45)	443(75)	553(46)	103(48)	−5(45)	77(36)
C(11)	508(44)	387(58)	491(40)	132(62)	3(53)	−32(33)
C(12)	388(42)	258(58)	432(40)	1(38)	72(37)	60(31)
C(13)	498(50)	535(74)	549(48)	130(47)	−123(50)	−5(39)
C(14)	752(77)	1062(117)	525(56)	−40(89)	−63(69)	−76(52)
C(15)	769(69)	664(94)	487(49)	−155(63)	91(52)	−161(48)
C(16)	688(56)	698(81)	513(45)	−11(76)	−215(64)	−4(41)
C(17)	514(49)	553(81)	490(46)	56(49)	−42(46)	−2(37)

	U		U
H(7)	130	H(13)	494
H(8)	161	H(14)	1072
H(9)	920	H(15)	707
H(10)	557	H(16)	441
H(11)	502	H(17)	99

The scattering factors used for sulphur, nitrogen, carbon and hydrogen in the structure factor calculations were those given in the *International Tables*.[10]

Final atomic coordinates from the least squares refinement are listed in Table 3, and the temperature parameters in Table 4. A pictorial representation of the thermal motion of the atoms is given in Fig. 4.[11]

An analysis of the thermal parameters of the S, N, and C atoms, assuming the whole molecule a rigid body, was carried out according to the method of Schomaker and True-

Table 5. Libration tensor L from the rigid-body analysis.

Eigenvalues		Eigenvectors (Direction cosines × 10^4 relative to *a*, *b*, and *c*, respectively)		
L	5.0 (°)^2	0.8408	0.4491	−0.3023
	3.1	0.0365	0.5017	0.8643
	2.9	0.5401	−0.7366	0.4070

Table 6. Observed and calculated structure factors for 2,5-diphenyl-3,4-diaza-6a-thia-thiophthene. The values given are ten times the absolute values. Unobserved reflections are marked with a minus sign in front of F_o.

H	K	L	F(O)	F(C)	H	K	L	F(O)	F(C)	H	K	L	F(O)	F(C)	H	K	L	F(O)	F(C)	H	K	L	F(O)	F(C)
0	2	6	1274	1321	3	0	14	421	418	6	0	11	-38	42	9	0	18	-47	0	13	0	12	-40	37
0	0	8	-23	21	3	0	15	611	604	6	0	12	-39	17	9	0	19	113	115	13	0	13	-39	25
0	2	10	227	229	3	0	16	149	148	6	0	13	-40	35	9	0	20	-46	41	13	0	14	-38	9
0	0	12	271	264	3	0	17	519	537	6	0	14	148	144	9	0	21	-45	20	13	0	15	-37	15
0	2	14	220	217	3	0	18	-41	30	6	0	15	-42	0	9	0	22	79	83	13	0	16	-35	5
0	0	16	210	205	3	0	19	401	315	6	0	16	192	186	9	0	23	-42	48	13	0	17	-33	10
0	2	18	-39	36	3	0	20	-44	35	6	0	17	-44	0	9	0	24	-41	17	13	0	18	-31	26
0	0	20	-42	31	3	0	21	74	70	6	0	18	68	66	9	0	25	-39	15	13	0	19	-29	12
0	2	22	164	166	3	0	22	-46	35	6	0	19	-46	4	9	0	26	-36	15	13	0	20	-26	35
0	0	24	432	453	3	0	23	-47	19	6	0	20	-47	12	9	0	27	-33	13	14	0	1	-40	40
0	2	26	141	135	3	0	24	-47	35	6	0	21	-47	26	9	0	28	-30	6	14	0	2	-40	37
0	0	28	206	215	3	0	25	-47	41	6	0	22	-47	35	9	0	29	-26	32	14	0	3	45	47
0	2	30	-44	16	3	0	26	-47	42	6	0	23	-47	52	10	0	1	-45	4	14	0	4	69	84
0	0	32	141	153	3	0	27	-47	9	6	0	24	157	216	10	0	2	-45	31	14	0	5	-39	15
0	2	34	237	238	3	0	28	-46	16	6	0	25	-46	2	10	0	3	140	141	14	0	6	-39	11
1	0	2	-14	15	3	0	29	113	112	6	0	26	170	164	10	0	4	90	85	14	0	7	38	68
1	0	3	37	38	3	0	30	-42	12	6	0	27	-43	48	10	0	5	-46	10	14	0	8	38	43
1	0	4	665	907	3	0	31	136	142	6	0	28	173	166	10	0	6	-46	19	14	0	9	73	91
1	0	5	87	83	3	0	32	-37	4	6	0	29	100	91	10	0	7	304	285	14	0	10	93	107
1	0	6	235	198	3	0	33	-34	40	6	0	30	-36	1	10	0	8	431	391	14	0	11	67	79
1	0	7	-22	21	3	0	34	-30	18	6	0	31	-33	41	10	0	9	458	442	14	0	12	48	78
1	0	8	498	481	4	0	1	142	133	6	0	32	157	163	10	0	10	204	188	14	0	13	36	44
1	0	9	138	132	4	0	2	204	215	7	0	1	342	403	10	0	11	71	43	14	0	14	34	49
1	0	10	716	707	4	0	3	206	204	7	0	2	196	208	10	0	12	58	71	14	0	15	-29	1
1	0	11	122	127	4	0	4	171	166	7	0	3	62	63	10	0	13	209	188	14	0	16	94	106
1	0	12	59	53	4	0	5	168	171	7	0	4	62	81	10	0	14	122	96	2	0	0	106	97
1	0	13	-31	31	4	0	6	103	106	7	0	6	-37	15	10	0	15	-47	2	4	0	0	126	121
1	0	14	-33	17	4	0	7	823	809	7	0	7	-38	15	10	0	15	-47	2	8	0	0	99	94
1	0	15	118	119	4	0	8	627	630	7	0	8	273	249	10	0	16	230	209	10	0	0	51	30
1	0	16	36	51	4	0	9	773	761	7	0	9	138	122	10	0	17	124	129	12	0	0	134	131
1	0	17	50	50	4	0	10	410	396	7	0	10	464	478	10	0	18	76	76	14	0	0	-41	41
1	0	18	239	319	4	0	11	49	49	7	0	11	263	242	10	0	19	89	78	0	1	4	717	783
1	0	19	148	152	4	0	12	125	127	7	0	12	-42	12	10	0	20	183	175	0	1	6	1028	1066
1	0	20	106	103	4	0	13	329	323	7	0	13	-43	55	10	0	21	-42	47	0	1	8	204	200
1	0	21	-44	37	4	0	14	235	246	7	0	14	43	59	10	0	22	104	92	0	1	10	53	39
1	0	22	314	303	4	0	15	-38	13	7	0	15	88	87	10	0	23	-39	45	0	1	12	127	131
1	0	23	332	352	4	0	16	456	455	7	0	16	99	110	10	0	24	60	65	0	1	14	304	297
1	0	24	448	473	4	0	17	272	274	7	0	17	-46	2	10	0	25	128	125	0	1	16	128	114
1	0	25	229	217	4	0	18	257	255	7	0	18	184	186	10	0	26	67	69	0	1	18	129	117
1	0	26	-47	39	4	0	19	183	155	7	0	19	58	67	10	0	27	73	76	0	1	20	54	88
1	0	27	-47	17	4	0	20	295	303	7	0	20	-47	8	11	0	2	134	136	0	1	22	324	303
1	0	28	-46	59	4	0	21	-44	16	7	0	21	79	87	11	0	3	-47	17	0	1	24	80	99
1	0	29	-45	27	4	0	22	-46	37	7	0	22	232	247	11	0	4	-47	1	0	1	26	216	205
1	0	30	44	69	4	0	23	186	200	7	0	23	113	122	11	0	5	-47	22	0	1	28	371	348
1	0	31	-41	9	4	0	24	115	124	7	0	24	225	236	11	0	6	82	65	0	1	30	231	224
1	0	32	127	126	4	0	25	243	212	7	0	25	114	129	11	0	7	71	53	0	1	32	218	209
1	0	33	152	143	4	0	26	141	127	7	0	26	-43	22	11	0	9	-47	38	0	1	34	95	99
1	0	34	132	139	4	0	27	86	94	7	0	27	61	73	11	0	10	-47	43	1	1	6	436	438
1	0	35	143	164	4	0	28	-45	38	7	0	28	-35	14	11	0	11	-47	6	1	1	7	251	234
2	0	1	384	357	4	0	29	-43	27	7	0	29	-36	30	11	0	12	-47	42	1	1	8	165	160
2	0	2	697	721	4	0	30	-41	35	7	0	30	57	77	11	0	13	-47	11	1	1	9	317	296
2	0	3	407	424	4	0	31	-38	33	8	0	1	72	85	11	0	14	92	101	1	1	10	427	418
2	0	4	595	585	4	0	32	-35	21	8	0	2	77	82	11	0	15	68	73	1	1	11	179	180
2	0	5	437	424	4	0	33	87	66	8	0	3	110	114	11	0	16	-45	57	1	1	12	223	218
2	0	6	54	61	5	0	1	706	718	8	0	4	-35	27	11	0	17	-44	15	1	1	13	116	107
2	0	7	363	348	5	0	2	82	72	8	0	5	196	209	11	0	18	-43	45	1	1	14	128	118
2	0	8	243	227	5	0	3	317	319	8	0	6	57	66	11	0	19	-41	27	1	1	15	162	162
2	0	9	356	371	5	0	4	355	352	8	0	7	162	154	11	0	20	-40	50	1	1	16	157	150
2	0	10	733	816	5	0	5	143	142	8	0	8	77	71	11	0	21	103	101	1	1	17	-44	53
2	0	11	499	508	5	0	6	212	216	8	0	9	322	300	11	0	22	87	62	1	1	18	-46	49
2	0	12	433	487	5	0	7	331	329	8	0	10	520	495	11	0	23	-33	9	1	1	19	-47	42
2	0	13	289	308	5	0	8	453	520	8	0	11	318	297	11	0	24	74	73	1	1	20	319	304
2	0	14	337	370	5	0	9	180	156	8	0	12	308	285	11	0	25	92	112	1	1	21	155	153
2	0	15	114	108	5	0	10	206	203	8	0	13	190	173	12	0	1	103	99	1	1	22	412	311
2	0	16	417	422	5	0	11	71	78	8	0	14	306	268	12	0	2	242	237	1	1	23	177	199
2	0	17	-38	32	5	0	12	183	190	8	0	15	147	159	12	0	3	202	204	1	1	24	218	199
2	0	18	494	543	5	0	13	38	55	8	0	16	254	245	12	0	4	88	110	1	1	25	202	169
2	0	19	257	262	5	0	14	124	128	8	0	17	71	99	12	0	5	-47	12	1	1	26	107	114
2	0	20	357	389	5	0	15	57	105	8	0	18	334	304	12	0	6	114	99	1	1	27	149	156
2	0	21	-44	31	5	0	16	73	93	8	0	19	-47	52	12	0	7	-47	14	1	1	28	-51	61
2	0	22	134	104	5	0	17	-43	0	8	0	20	91	99	12	0	8	119	116	1	1	29	262	247
2	0	23	341	333	5	0	18	119	119	8	0	21	-47	47	12	0	9	-46	36	1	1	30	47	65
2	0	24	139	104	5	0	19	143	131	8	0	22	46	60	12	0	10	56	43	1	1	31	180	164
2	0	25	371	333	5	0	20	127	132	8	0	23	123	116	12	0	11	-45	12	1	1	32	62	75
2	0	26	230	203	5	0	21	70	82	8	0	24	-44	23	12	0	12	-45	5	1	1	33	72	71
2	0	27	114	102	5	0	22	92	56	8	0	25	133	153	12	0	13	-44	3	1	1	34	49	53
2	0	28	-46	18	5	0	23	71	95	8	0	26	-40	41	12	0	14	48	61	2	1	1	160	158
2	0	29	-45	16	5	0	24	271	263	8	0	27	-38	53	12	0	15	-42	16	2	1	2	277	282
2	0	30	48	61	5	0	25	155	197	8	0	28	-35	31	12	0	16	99	100	2	1	3	166	164
2	0	31	-41	17	5	0	26	98	101	8	0	29	-32	4	12	0	17	-39	28	2	1	4	269	254
2	0	32	-38	14	5	0	27	138	127	8	0	30	56	61	12	0	18	-38	1	2	1	5	658	684
2	0	33	109	94	5	0	28	112	105	9	0	1	161	155	12	0	19	36	48	2	1	6	254	243
2	0	34	38	53	5	0	29	77	69	9	0	2	-42	43	12	0	20	34	45	2	1	7	274	251
2	0	35	79	81	5	0	30	55	55	9	0	3	121	108	12	0	21	39	58	2	1	8	322	315
3	0	1	621	598	5	0	31	40	48	9	0	4	106	102	12	0	22	-29	12	2	1	9	381	369
3	0	2	63	63	5	0	32	117	125	9	0	5	86	87	12	0	23	36	43	2	1	10	372	380
3	0	3	150	150	5	0	33	81	91	9	0	6	225	215	13	0	1	88	94	2	1	11	484	486
3	0	4	-23	25	6	0	1	79	80	9	0	7	-44	39	13	0	2	148	143	2	1	12	546	556
3	0	5	129	122	6	0	2	403	417	9	0	8	-44	6	13	0	3	78	86	2	1	13	272	277
3	0	6	207	154	6	0	3	102	101	9	0	9	289	265	13	0	4	80	94	2	1	14	521	545
3	0	7	94	79	6	0	4	126	127	9	0	11	138	128	13	0	5	-44	14	2	1	15	129	109
3	0	8	238	228	6	0	5	-33	15	9	0	12	447	461	13	0	6	114	129	2	1	16	192	186
3	0	9	641	647	6	0	6	368	375	9	0	13	139	126	13	0	7	-44	48	2	1	17	80	79
3	0	10	-29	28	6	0	7	-34	26	9	0	14	157	163	13	0	8	123	125	2	1	18	189	190
3	0	11	422	426	6	0	8	77	89	9	0	15	403	390	13	0	9	-43	32	2	1	19	345	323
3	0	12	533	522	6	0	9	85	75	9	0	16	71	82	13	0	10	91	101	2	1	20	397	383
3	0	13	173	186	6	0	10	-37	1	9	0	17	171	143	13	0	11	50	53	2	1	21	417	378

Table 6. Continued.

H	K	L	F(O)	F(C)	H	K	L	F(O)	F(C)	H	K	L	F(O)	F(C)	H	K	L	F(O)	F(C)	H	K	L	F(O)	F(C)
2	1	22	228	213	5	1	27	95	105	9	1	8	-51	36	13	1	14	-40	36	3	2	1	173	163
2	1	23	136	117	5	1	28	47	59	9	1	9	58	68	13	1	15	-39	42	3	2	2	80	78
2	1	24	75	89	5	1	29	168	167	9	1	10	258	272	13	1	16	-37	34	3	2	3	166	155
2	1	25	60	65	5	1	30	59	62	9	1	11	327	292	13	1	17	-34	19	3	2	4	41	40
2	1	26	-53	43	5	1	31	138	142	9	1	12	65	91	13	1	18	-32	47	3	2	5	36	42
2	1	27	90	102	5	1	32	34	54	9	1	13	398	401	13	1	19	-28	25	3	2	6	141	141
2	1	28	62	82	5	1	33	-29	46	9	1	14	254	261	13	1	20	40	70	3	2	7	275	269
2	1	29	-49	26	6	1	1	171	175	9	1	15	246	236	14	1	1	-43	9	3	2	8	102	97
2	1	30	-47	39	6	1	2	418	462	9	1	16	242	211	14	1	2	-43	37	3	2	9	441	442
2	1	31	-44	39	6	1	3	93	102	9	1	17	-53	52	14	1	3	-43	30	3	2	10	-39	26
2	1	32	70	78	6	1	4	473	517	9	1	18	-52	54	14	1	4	-43	8	3	2	11	277	290
2	1	33	-36	11	6	1	5	132	135	9	1	19	192	180	14	1	5	76	66	3	2	12	80	85
2	1	34	48	62	6	1	6	348	379	9	1	20	-51	73	14	1	6	51	49	3	2	13	50	60
3	1	1	143	138	6	1	7	221	230	9	1	21	178	167	14	1	7	61	81	3	2	14	105	94
3	1	2	127	125	6	1	8	101	100	9	1	22	68	68	14	1	8	49	66	3	2	15	541	517
3	1	3	350	333	6	1	9	94	90	9	1	23	73	82	14	1	9	-39	36	3	2	16	214	202
3	1	4	64	63	6	1	10	-43	33	9	1	24	-44	10	14	1	10	68	47	3	2	17	717	654
3	1	5	194	184	6	1	11	-44	19	9	1	25	-41	45	14	1	11	-37	45	3	2	18	63	60
3	1	6	-29	22	6	1	12	167	163	9	1	26	-38	26	14	1	12	61	81	3	2	19	258	243
3	1	7	264	258	6	1	13	47	47	9	1	27	49	54	14	1	13	66	51	3	2	20	-53	76
3	1	8	178	171	6	1	14	150	155	9	1	28	-36	42	3	1	0	52	50	3	2	21	107	113
3	1	9	136	133	6	1	15	127	126	10	1	1	78	64	5	1	0	116	113	3	2	22	85	98
3	1	10	316	313	6	1	16	75	70	10	1	2	167	165	7	1	0	116	122	3	2	23	-53	78
3	1	11	528	525	6	1	17	62	64	10	1	3	165	146	9	1	0	69	54	3	2	24	-53	8
3	1	12	129	149	6	1	18	148	138	10	1	4	-52	14	11	1	0	155	168	3	2	25	-51	39
3	1	13	674	734	6	1	19	-53	67	10	1	5	215	190	13	1	0	60	74	3	2	26	-50	3
3	1	14	316	357	6	1	20	-53	40	10	1	6	64	93	0	2	2	407	489	3	2	27	-48	44
3	1	15	441	495	6	1	21	99	27	10	1	7	171	167	0	2	4	239	246	3	2	28	-45	7
3	1	16	214	206	6	1	22	149	149	10	1	8	118	106	0	2	6	563	561	3	2	29	73	78
3	1	17	85	91	6	1	23	-53	43	10	1	9	160	132	0	2	8	49	48	3	2	30	-39	25
3	1	18	146	134	6	1	24	109	85	10	1	10	182	177	0	2	10	47	42	3	2	31	66	87
3	1	19	366	369	6	1	25	-51	60	10	1	11	184	183	0	2	12	198	182	3	2	32	-29	24
3	1	20	97	96	6	1	26	85	98	10	1	12	165	162	0	2	14	201	193	4	2	1	208	216
3	1	21	316	309	6	1	27	-47	64	10	1	13	-53	17	0	2	16	204	192	4	2	2	114	118
3	1	22	-52	23	6	1	28	209	223	10	1	14	188	166	0	2	18	195	193	4	2	3	222	226
3	1	23	233	230	6	1	29	-42	46	10	1	15	-53	35	0	2	20	-52	59	4	2	4	126	121
3	1	24	-53	20	6	1	30	173	193	10	1	16	151	134	0	2	22	93	90	4	2	5	113	114
3	1	25	70	66	6	1	31	83	87	10	1	17	117	116	0	2	24	118	106	4	2	6	227	250
3	1	26	-53	9	6	1	32	106	128	10	1	18	61	65	0	2	26	372	355	4	2	7	462	489
3	1	27	82	99	7	1	1	206	215	10	1	19	73	83	0	2	28	224	225	4	2	8	168	183
3	1	28	-50	43	7	1	2	138	138	10	1	20	100	104	0	2	30	205	199	4	2	9	225	227
3	1	29	72	81	7	1	3	293	329	10	1	21	122	121	0	2	32	181	215	4	2	10	247	248
3	1	30	-46	29	7	1	4	347	356	10	1	22	111	116	1	2	1	326	379	4	2	11	113	130
3	1	31	-47	49	7	1	5	330	342	10	1	23	142	149	1	2	2	208	231	4	2	12	100	106
3	1	32	-39	11	7	1	6	261	277	10	1	24	122	121	1	2	3	585	649	4	2	13	90	94
3	1	33	-35	31	7	1	7	201	203	10	1	25	43	58	1	2	4	491	504	4	2	14	76	76
3	1	34	-30	28	7	1	8	187	192	10	1	26	44	50	1	2	5	202	187	4	2	15	140	127
4	1	1	239	236	7	1	9	220	213	11	1	1	142	131	1	2	6	349	349	4	2	16	308	272
4	1	2	80	87	7	1	10	220	213	11	1	2	65	72	1	2	7	609	604	4	2	17	196	195
4	1	3	331	322	7	1	11	94	109	11	1	3	211	186	1	2	8	557	566	4	2	18	356	328
4	1	4	84	82	7	1	12	171	164	11	1	4	173	150	1	2	9	450	442	4	2	19	166	146
4	1	5	468	450	7	1	13	78	88	11	1	5	230	228	1	2	10	457	424	4	2	20	152	148
4	1	6	190	191	7	1	14	57	57	11	1	6	146	156	1	2	11	170	167	4	2	21	76	88
4	1	7	110	113	7	1	15	116	119	11	1	7	80	83	1	2	12	115	111	4	2	22	-53	51
4	1	8	131	125	7	1	16	158	153	11	1	8	-53	47	1	2	13	42	26	4	2	23	136	138
4	1	9	264	255	7	1	17	-52	57	11	1	9	-53	60	1	2	14	107	103	4	2	24	78	91
4	1	10	329	351	7	1	18	65	63	11	1	10	128	118	1	2	15	-45	23	4	2	25	166	157
4	1	11	248	255	7	1	19	-53	24	11	1	11	-53	44	1	2	16	-47	51	4	2	26	96	98
4	1	12	387	411	7	1	20	178	172	11	1	12	103	114	1	2	17	145	141	4	2	27	117	105
4	1	13	96	99	7	1	21	59	70	11	1	13	63	76	1	2	18	236	229	4	2	28	110	90
4	1	14	366	382	7	1	22	182	177	11	1	14	-51	9	1	2	19	125	119	4	2	29	49	63
4	1	15	-44	35	7	1	23	-52	61	11	1	15	-50	47	1	2	20	101	108	4	2	30	-36	31
4	1	16	277	268	7	1	24	-50	55	11	1	16	-45	35	1	2	21	75	59	4	2	31	55	62
4	1	17	93	76	7	1	25	-49	60	11	1	17	65	86	1	2	22	80	83	5	2	1	317	328
4	1	18	203	192	7	1	26	104	107	11	1	18	-46	49	1	2	23	-54	61	5	2	2	141	124
4	1	19	221	199	7	1	27	-44	45	11	1	19	-44	31	1	2	24	176	162	5	2	3	300	308
4	1	20	245	247	7	1	28	71	77	11	1	20	67	77	1	2	25	184	189	5	2	4	55	65
4	1	21	267	271	7	1	29	137	138	11	1	21	49	54	1	2	26	158	156	5	2	6	323	340
4	1	22	208	191	7	1	30	-34	16	11	1	22	74	95	1	2	27	222	224	5	2	7	173	196
4	1	23	157	185	7	1	31	106	134	11	1	23	99	109	1	2	28	82	94	5	2	8	228	240
4	1	24	92	90	8	1	1	114	121	11	1	24	108	118	1	2	29	74	75	5	2	9	100	110
4	1	25	-53	29	8	1	2	75	64	12	1	1	156	160	1	2	30	72	61	5	2	10	172	176
4	1	26	92	73	8	1	3	79	85	12	1	2	169	166	1	2	31	106	112	5	2	11	-46	22
4	1	27	62	79	8	1	4	-46	55	12	1	3	-52	56	1	2	32	-33	35	5	2	12	103	100
4	1	28	-49	54	8	1	5	252	273	12	1	4	207	210	2	2	1	236	245	5	2	13	91	73
4	1	29	-47	8	8	1	6	142	126	12	1	5	78	83	2	2	2	175	166	5	2	14	136	135
4	1	30	-44	59	8	1	7	250	236	12	1	6	64	72	2	2	3	117	119	5	2	15	-51	48
4	1	31	-41	19	8	1	8	201	194	12	1	7	63	68	2	2	4	117	117	5	2	16	-52	2
4	1	32	-37	42	8	1	9	163	152	12	1	8	-51	56	2	2	5	242	243	5	2	17	-53	48
4	1	33	-32	38	8	1	10	250	225	12	1	9	-51	4	2	2	6	246	226	5	2	18	146	137
5	1	1	254	266	8	1	11	322	294	12	1	10	-50	37	2	2	7	643	658	5	2	19	153	146
5	1	2	300	304	8	1	12	405	381	12	1	11	-50	24	2	2	8	516	500	5	2	20	66	83
5	1	3	678	711	8	1	13	266	249	12	1	12	54	75	2	2	9	303	296	5	2	21	80	86
5	1	4	609	645	8	1	14	258	263	12	1	13	-48	5	2	2	10	84	93	5	2	22	-53	65
5	1	5	458	501	8	1	15	105	109	12	1	14	-47	38	2	2	11	146	140	5	2	23	-52	26
5	1	6	354	374	8	1	16	-53	57	12	1	15	-45	14	2	2	12	-41	36	5	2	24	115	122
5	1	7	131	130	8	1	17	92	101	12	1	16	-44	2	2	2	13	174	177	5	2	25	177	175
5	1	8	92	89	8	1	18	-53	58	12	1	17	-42	16	2	2	14	161	155	5	2	26	138	147
5	1	9	106	109	8	1	19	218	212	12	1	18	45	64	2	2	15	131	115	5	2	27	178	192
5	1	10	318	344	8	1	20	117	136	12	1	19	-38	41	2	2	16	419	402	5	2	28	81	84
5	1	11	-41	43	8	1	21	148	144	12	1	20	-35	22	2	2	17	92	100	5	2	29	-37	43
5	1	12	259	257	8	1	22	72	85	12	1	21	-32	35	2	2	18	209	201	5	2	30	78	87
5	1	13	-44	12	8	1	23	-49	46	12	1	22	-29	29	2	2	19	100	107	6	2	1	-42	25
5	1	14	-45	48	8	1	24	-48	56	13	1	1	-45	37	2	2	20	-53	27	6	2	2	448	453
5	1	15	-47	45	8	1	25	75	74	13	1	2	-49	16	2	2	21	75	63	6	2	3	198	165
5	1	16	-48	37	8	1	26	-43	24	13	1	3	69	60	2	2	22	-54	61	6	2	4	105	105
5	1	17	146	127	8	1	27	-40	58	13	1	4	84	94	2	2	23	89	84	6	2	5	204	213
5	1	18	137	129	8	1	28	-37	38	13	1	5	96	101	2	2	24	-53	34	6	2	6	320	304
5	1	19	-51	19	8	1	29	-33	23	13	1	6	157	160	2	2	25	139	131	6	2	7	-45	33
5	1	20	258	241	9	1	1	134	126	13	1	7	142	133	2	2	26	-51	65	6	2	8	147	135
5	1	21	130	123	9	1	2	-49	45	13	1	8	-47	61	2	2	27	98	86	6	2	9	-47	52
5	1	22	227	204	9	1	3	138	130	13	1	9	-46	29	2	2	28	-46	59	6	2	10	-48	47
5	1	23	182	165	9	1	4	-50	13	13	1	10	-45	52	2	2	29	-44	50	6	2	11	133	120
5	1	24	145	127	9	1	5	-50	63	13	1	11	-44	26	2	2	30	49	59	6	2	12	114	114
5	1	25	90	92	9	1	6	-50	53	13	1	12	71	88	2	2	31	-36	49	6	2	13	-51	45
5	1	26	-51	45	9	1	7	203	174	13	1	13	-42	34	2	2	32	44	48	6	2	14	118	128

Table 6. Continued.

H	K	L	F(O)	F(C)	H	K	L	F(O)	F(C)	H	K	L	F(O)	F(C)	H	K	L	F(O)	F(C)	H	K	L	F(O)	F(C)
6	2	15	-52	20	9	2	25	39	31	0	3	26	-44	46	4	3	7	168	183	7	3	21	61	64
6	2	16	131	121	10	2	1	-54	30	0	3	28	169	195	4	3	8	158	152	7	3	22	-40	34
6	2	17	-53	26	10	2	2	-54	61	1	3	1	103	122	4	3	9	-50	53	7	3	23	-36	16
6	2	18	76	88	10	2	3	122	117	1	3	2	84	87	4	3	10	84	91	8	3	1	103	97
6	2	19	-54	27	10	2	4	-54	17	1	3	3	266	293	4	3	11	209	202	8	3	2	-55	33
6	2	20	80	76	10	2	5	164	151	1	3	4	180	194	4	3	12	364	337	8	3	3	-55	44
6	2	21	59	68	10	2	6	93	89	1	3	5	291	314	4	3	13	243	226	8	3	4	-55	57
6	2	22	63	77	10	2	7	165	145	1	3	6	292	298	4	3	14	260	248	8	3	5	158	153
6	2	23	-50	19	10	2	8	-53	45	1	3	7	153	151	4	3	15	82	89	8	3	6	149	167
6	2	24	68	62	10	2	9	93	92	1	3	8	-40	21	4	3	16	139	120	8	3	7	160	153
6	2	25	-46	56	10	2	10	-53	66	1	3	9	108	113	4	3	17	95	80	8	3	8	82	84
6	2	26	207	215	10	2	11	-52	31	1	3	10	114	120	4	3	18	91	87	8	3	9	-55	16
6	2	27	74	69	10	2	12	-52	48	1	3	11	-47	39	4	3	19	66	49	8	3	10	77	74
6	2	28	128	133	10	2	13	96	94	1	3	12	95	90	4	3	20	122	117	8	3	11	81	98
6	2	29	76	82	10	2	14	-50	8	1	3	13	80	83	4	3	21	186	177	8	3	12	136	113
7	2	1	261	250	10	2	15	110	104	1	3	14	140	132	4	3	22	166	161	8	3	13	91	90
7	2	2	195	194	10	2	16	72	66	1	3	15	112	104	4	3	23	148	126	8	3	14	210	199
7	2	3	236	232	10	2	17	125	119	1	3	16	76	86	4	3	24	106	105	8	3	15	-51	14
7	2	4	210	223	10	2	18	186	175	1	3	17	-55	53	4	3	25	63	72	8	3	16	128	125
7	2	5	103	111	10	2	19	183	183	1	3	18	137	144	4	3	26	54	70	8	3	17	170	159
7	2	6	238	229	10	2	20	98	95	1	3	19	-55	51	4	3	27	41	55	8	3	18	109	98
7	2	7	367	358	10	2	21	-39	8	1	3	20	106	108	5	3	1	127	145	8	3	19	120	121
7	2	8	486	447	10	2	22	62	63	1	3	21	104	100	5	3	2	160	170	8	3	20	129	129
7	2	9	246	228	10	2	23	97	93	1	3	22	91	77	5	3	3	225	240	8	3	21	84	89
7	2	10	259	250	11	2	1	289	304	1	3	23	59	100	5	3	4	87	88	8	3	22	67	73
7	2	11	-51	52	11	2	2	-53	68	1	3	24	92	89	5	3	5	105	96	9	3	1	-55	43
7	2	12	-52	57	11	2	3	-53	34	1	3	25	90	88	5	3	6	118	115	9	3	2	-55	32
7	2	13	74	81	11	2	4	162	148	1	3	26	92	103	5	3	7	113	99	9	3	3	-55	45
7	2	14	113	117	11	2	5	203	206	1	3	27	-40	52	5	3	8	-51	57	9	3	4	-54	33
7	2	15	-53	59	11	2	6	121	129	1	3	28	50	58	5	3	9	78	97	9	3	5	-54	45
7	2	16	80	66	11	2	7	73	85	2	3	1	135	142	5	3	10	145	130	9	3	6	-54	24
7	2	17	66	70	11	2	8	85	84	2	3	2	41	48	5	3	11	-54	76	9	3	7	113	97
7	2	18	56	114	11	2	9	-51	12	2	3	3	110	111	5	3	12	98	104	9	3	8	-53	70
7	2	19	-53	30	11	2	10	-50	52	2	3	4	57	59	5	3	13	-55	46	9	3	9	-53	69
7	2	20	-52	56	11	2	11	-49	13	2	3	5	203	210	5	3	14	83	78	9	3	10	64	74
7	2	21	-51	39	11	2	12	-49	37	2	3	6	240	262	5	3	15	78	52	9	3	11	89	94
7	2	22	82	76	11	2	13	-48	48	2	3	7	284	311	5	3	16	67	62	9	3	12	62	61
7	2	23	-48	41	11	2	14	-46	55	2	3	8	238	259	5	3	17	-55	60	9	3	13	167	144
7	2	24	113	107	11	2	15	-45	39	2	3	9	145	145	5	3	18	89	87	9	3	14	-48	71
7	2	25	80	87	11	2	16	-43	2	2	3	10	222	223	5	3	19	88	67	9	3	15	144	153
7	2	26	90	91	11	2	17	-41	35	2	3	11	261	255	5	3	20	96	88	9	3	16	148	146
7	2	27	73	86	11	2	18	48	47	2	3	12	339	315	5	3	21	83	93	9	3	17	97	89
7	2	28	63	68	11	2	19	90	88	2	3	13	189	187	5	3	22	141	134	9	3	18	40	53
8	2	1	87	90	11	2	20	88	82	2	3	14	335	342	5	3	23	150	159	9	3	19	65	95
8	2	2	-50	43	11	2	21	48	56	2	3	15	98	83	5	3	24	82	83	9	3	20	62	61
8	2	3	141	136	12	2	1	-50	64	2	3	16	-54	75	5	3	25	-39	62	9	3	21	35	88
8	2	4	62	70	12	2	2	113	121	2	3	17	142	135	5	3	26	59	71	10	3	1	101	78
8	2	5	84	80	12	2	3	-49	50	2	3	18	157	159	6	3	1	254	235	10	3	2	78	51
8	2	6	-51	37	12	2	4	69	84	2	3	19	106	85	6	3	2	317	283	10	3	3	119	112
8	2	7	156	177	12	2	5	60	82	2	3	20	160	158	6	3	3	184	175	10	3	4	103	91
8	2	8	257	243	12	2	6	-48	61	2	3	21	159	156	6	3	4	403	388	10	3	5	100	109
8	2	9	168	160	12	2	7	-48	10	2	3	22	122	109	6	3	5	183	172	10	3	6	109	128
8	2	10	128	118	12	2	8	53	60	2	3	23	71	56	6	3	6	272	245	10	3	7	-50	42
8	2	11	102	83	12	2	9	52	63	2	3	24	59	74	6	3	7	65	90	10	3	8	-50	51
8	2	12	-53	80	12	2	10	-49	23	2	3	25	46	66	6	3	8	113	112	10	3	9	92	67
8	2	13	171	164	12	2	11	-44	31	2	3	26	-43	39	6	3	9	66	79	10	3	10	-48	20
8	2	14	54	72	12	2	12	-43	22	2	3	27	75	75	6	3	10	94	110	10	3	11	78	89
8	2	15	218	156	12	2	13	-42	25	2	3	28	41	41	6	3	11	-55	46	10	3	12	85	86
8	2	16	293	276	12	2	14	-40	39	3	3	1	41	48	6	3	12	-55	28	10	3	13	-44	67
8	2	17	-53	83	12	2	15	-38	14	3	3	2	-37	22	6	3	13	-55	36	10	3	14	82	85
8	2	18	101	99	12	2	16	68	65	3	3	3	60	65	6	3	14	-55	48	10	3	15	49	44
8	2	19	77	99	12	2	17	-34	25	3	3	4	64	65	6	3	15	-55	27	10	3	16	71	82
8	2	20	-50	53	12	2	18	-31	27	3	3	5	146	149	6	3	16	-54	36	11	3	1	-48	41
8	2	21	76	73	13	2	1	88	95	3	3	6	-42	24	6	3	17	-53	27	11	3	2	127	122
8	2	22	-46	41	13	2	2	73	66	3	3	7	145	160	6	3	18	101	90	11	3	3	124	121
8	2	23	100	101	13	2	3	-44	41	3	3	8	-45	51	6	3	19	-51	40	11	3	4	57	64
8	2	24	-41	22	13	2	4	53	68	3	3	9	193	202	6	3	20	-49	18	11	3	5	46	65
8	2	25	105	103	13	2	5	-43	60	3	3	10	-48	21	6	3	21	-47	39	11	3	6	-46	44
9	2	1	64	70	13	2	6	-42	6	3	3	11	381	369	6	3	22	89	98	11	3	7	-45	27
9	2	2	64	84	13	2	7	-41	43	3	3	12	99	95	6	3	23	51	60	11	3	8	-44	45
9	2	3	87	101	13	2	8	115	111	3	3	13	320	310	6	3	24	63	90	11	3	9	-43	21
9	2	4	-53	43	13	2	9	56	75	3	3	14	-53	66	6	3	25	-34	45	11	3	10	42	52
9	2	5	-53	52	13	2	10	57	72	3	3	15	222	202	7	3	1	100	105	11	3	11	-40	17
9	2	6	111	97	13	2	11	45	47	3	3	16	147	122	7	3	2	66	68	11	3	12	-38	44
9	2	7	-53	39	13	2	12	35	43	3	3	17	-55	61	7	3	3	187	178	11	3	13	-36	18
9	2	8	-53	80	13	2	13	-33	30	3	3	18	91	71	7	3	4	179	161	11	3	14	-34	32
9	2	9	195	170	2	2	0	49	54	3	3	19	109	95	7	3	5	246	217	12	3	1	81	96
9	2	10	-54	56	4	2	0	88	86	3	3	20	-54	46	7	3	6	191	185	12	3	2	146	159
9	2	11	200	189	6	2	0	461	468	3	3	21	147	135	7	3	7	95	88	12	3	3	-40	50
9	2	12	60	69	8	2	0	61	66	3	3	22	-51	28	7	3	8	-55	59	12	3	4	112	125
9	2	13	118	126	10	2	0	54	68	3	3	23	110	109	7	3	9	-55	45	12	3	5	58	71
9	2	14	92	92	12	2	0	200	216	3	3	24	-47	12	7	3	10	-55	24	12	3	6	-38	41
9	2	15	203	198	0	3	6	354	381	3	3	25	88	93	7	3	11	-55	21	12	3	7	-37	46
9	2	16	73	91	0	3	8	155	153	3	3	26	-41	36	7	3	12	-55	49	12	3	8	-35	36
9	2	17	342	317	0	3	10	132	139	3	3	27	52	62	7	3	13	82	65	12	3	9	-34	16
9	2	18	127	114	0	3	12	129	138	3	3	28	-31	19	7	3	14	66	83	12	3	10	-31	49
9	2	19	199	221	0	3	14	109	115	4	3	1	63	59	7	3	15	65	77	1	3	0	31	45
9	2	20	89	100	0	3	16	81	87	4	3	2	82	91	7	3	16	-52	65	3	3	0	36	31
9	2	21	97	78	0	3	18	83	88	4	3	3	132	130	7	3	17	-51	41	5	3	0	133	148
9	2	22	-42	49	0	3	20	-55	40	4	3	4	73	86	7	3	18	99	93	7	3	0	140	131
9	2	23	-39	31	0	3	22	121	123	4	3	5	159	160	7	3	19	72	77	9	3	0	-55	30
9	2	24	-36	33	0	3	24	98	98	4	3	6	135	127	7	3	20	97	108	11	3	0	67	53

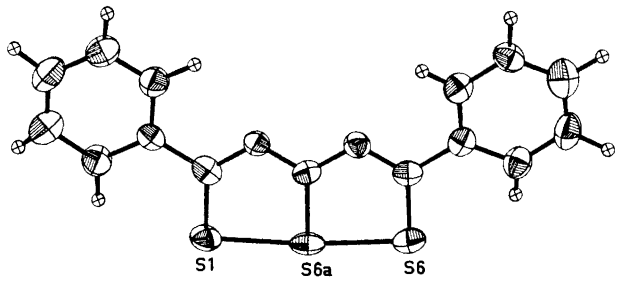

Fig. 4. The thermal ellipsoid plot showing the anisotropic vibration of the non-hydrogen atoms.

blood.[3] The libration tensor **L** arrived at is given in Table 5. Bond lengths, which have been corrected according to the libration tensor L, are listed in the first column of Table 1.

The final list of structure factors is given in Table 6.

Acknowledgements. We thank Professor Hans Behringer, Organisch-Chemisches Institut der Universität München, Germany, for a sample of 2,5-diphenyl-3,4-diaza-6a-thiathiophthene and the *Norwegian Research Council for Science and the Humanities* for financial support (to A. H.).

REFERENCES

1. Hordvik, A. and Milje, L. M. *Chem. Commun.* **1972** 182.
2. Derocque, J. L., Perrier, M. and Vialle, J. *Bull. Soc. Chim. France* **1967** 3079; **1968** 2062.
3. Schomaker, V. and Trueblood, K. N. *Acta Cryst.* **B 24** (1968) 63.
4. Cruickshank, D. W. J. *Acta Cryst.* **9** (1956) 757; **14** (1961) 896.
5. Hordvik, A. *Acta Chem. Scand.* **22** (1968) 2398; **25** (1971) 1583.
6. Hansen, L. K., Hordvik, A. and Sæthre, L. J. *Chem. Commun.* **1972** 222.
7. Hansen, L. K. and Hordvik, A. *Acta Chem. Scand.* **27** (1973) 411.
8. Hordvik, A. and Oftedal, P. *Chem. Commun.* **1972** 543.
9. Bak, B., Hansen-Nygaard, L. and Rastrup-Andersen, J. *J. Mol. Spectry.* **2** (1958) 361.
10. *International Tables for X-Ray Crystallography*, Kynoch Press, Birmingham 1962, Vol. III, p. 202.
11. Johnson, C. K. *A Fortran Thermal Ellipsoid Plot Program for Crystal Structure Illustrations*, ORNL-3794, Oak Ridge National Laboratory, Tennessee 1965.

Received July 20, 1972.

ACTA CHEMICA SCANDINAVICA 27 (1973) 521–527

Approximate Self Consistent Field Molecular Orbital Calculations on the Complexes of Trimethylboron, Boron Trichloride, Trimethylaluminium, Alane and Aluminium Trichloride with Trimethylamine

ODD GROPEN and ARNE HAALAND

Department of Chemistry, University of Oslo, Blindern, Oslo 3, Norway

CNDO/2 calculations have been carried out on the complexes Me_3BNMe_3, Cl_3BNMe_3, Me_3AlNMe_3, H_3AlNMe_3 and Cl_3AlNMe_3. It is found that the amount of charge transferred from donor to acceptor increases as the substituents on the acceptor become more electronegative. The resulting net negative charge on the acceptor is carried by the substituents, the resulting net positive charge on the donor is carried by the methyl groups.

It is well known that the chlorides of boron and aluminium are stronger Lewis acids than trimethylboron and trimethylaluminium: Thus the enthalpy of formation of the gaseous complex from the gaseous components

$$BX_3(g) + \text{pyridine}(g) = X_3B.\text{pyridine}(g)$$

is $\Delta H_f(g) = -17$ kcal/mol for X = Me [1] and $\Delta H_f(g) = -36$ kcal/mol for X = Cl.[2] The B–N bond distance in Cl_3BNMe_3 is 1.575(11) Å,[3] while the B–N bond distance in Me_3BNMe_3 has been estimated to lie in the region 1.70 to 1.90 Å.[4]

Similarly the enthalpy of formation of the gaseous complexes Me_3AlNMe_3 and Cl_3AlNMe_3 from the gaseous monomeric components are -30.7 ± 0.3 kcal/mol [5,6] and -47.5 ± 2.0 kcal/mol,[6,7] respectively. The Al–N bond distance in Cl_3AlNMe_3 is 1.96(1) Å [8] while the Al–N bond distance in Me_3AlNMe_3 is 2.099(10) Å.[6]

This variation of Lewis acid strength has been interpreted as an inductive effect.[9] In order to obtain clues into the manner in which it operates we have performed a series of approximate self consistent field molecular orbital calculations on the complexes of BMe_3, BCl_3, $AlMe_3$, and $AlCl_3$ with NMe_3 and on some related species.

The enthalpy of formation of H_3AlNMe_3 is not known, but the magnitude of the Al–N bond distance, 2.063(11) Å,[10] indicates that the Lewis acid strength of AlH_3 is intermediate between that of $AlMe_3$ and $AlCl_3$. This is indeed to be expected if an inductive effect was dominant, and calculations were therefore performed on this complex and related species as well.

CALCULATIONS

The main structure parameters of the species considered are listed in Table 1. The C–H bond distance and the ∠N–C–H valence angle in free NMe_3 [11] was assumed to remain unaltered in the complexes and in NMe_4^+.

Table 1. Structure parameters of the species NMe_3, NMe_4^+, MX_3, MX_4^- and the complexes X_3MNMe_3.

	R(X–M) (Å)	∠X–M–C_3 (°)	R(M–N) (Å)	∠C_3–N–C (°)	R(N–C) (Å)	Ref.
NMe_3				108.3	1.454	11
NMe_4^+				α	1.499	12
BMe_3	1.578	90				13
BMe_4^-	1.65	α				ass
Me_3BNMe_3	1.60	109.6	1.70	110.8	1.502	ass
BCl_3	1.742	90				14
BCl_4^-	1.81	α				ass
Cl_3BNMe_3	1.831	109.6	1.575	110.8	1.502	3
$AlMe_3$	1.957	90				15
$AlMe_4^-$	2.023	α				16
Me_3AlNMe_3	1.987	102.3	1.099	109.3	1.474	6
AlH_3	1.54	90				ass
AlH_4^-	1.58	α				ass
H_3AlNMe_3	1.560	104.3	2.063	109.0	1.476	10
$AlCl_3$	2.06	90				17
$AlCl_4^-$	2.13	α				18
Cl_3AlNMe_3	2.123	107.0	1.96	110.3	1.50(ass)	8

α = tetrahedral angle; ass = assumed.

Similarly the C–H bond distances and the ∠B–C–H and ∠Al–C–H valence angles of free BMe_3 [13] and $AlMe_3$ [15] were assumed to remain unaltered in the complexes and in BMe_4^+ and $AlMe_4^+$.

The MO calculations were carried out in the CNDO/2 approximation with standard values for all parameters.[19,20] The calculations on species containing Al or Cl were carried out with two bases, one (*sp*) consisting only of valence shell Slater type *s* and *p* atomic orbitals, the other (*spd*) including Slater type 3*d* orbitals on Al and Cl with the same orbital exponent ($Z' = 3.50$ for Al, $Z' = 6.10$ for Cl) as the 3*s* and 3*p* orbitals.

RESULTS AND DISCUSSION

Charge distribution and dipole moment. The atomic charges (in 0.01 electron units) obtained for Me_3BNMe_3 and Cl_3BNMe_3 and related species, the charge transferred from donor to acceptor (q_{transf}) and the dipole moments are displayed in Fig. 1. For the species containing Cl the first number has been obtained with the (*sp*), the second with the (*spd*) basis. The calculated dipole

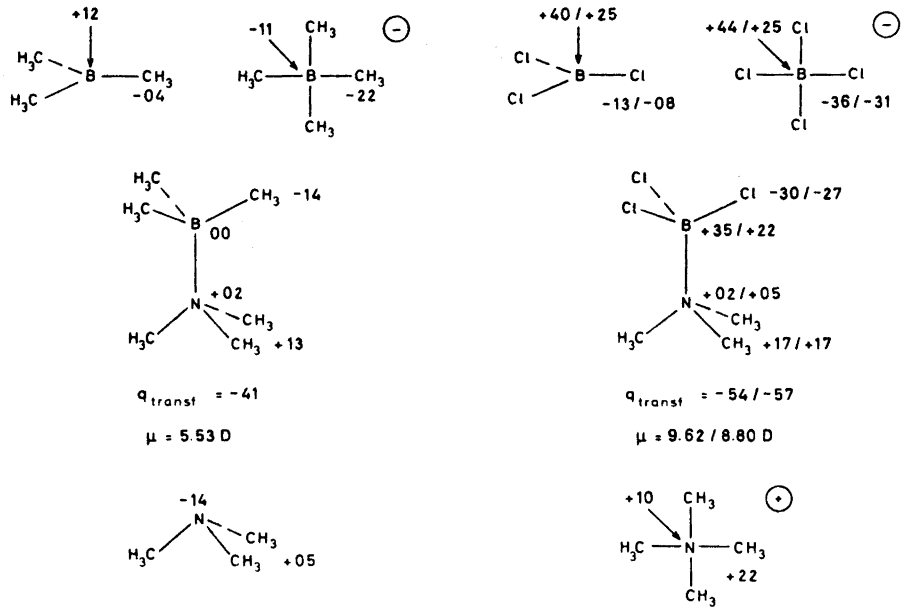

Fig. 1. Atomic charges (in 0.01 electron units) obtained for Me_3BNMe_3 and Cl_3BNMe_3 and related species, the charge transferred from donor to acceptor (q_{transf}) and the dipole moments. For the species containing Cl the first number has been obtained with the (*sp*), the second with the (*spd*) basis.

moments of the complexes are in reasonable agreement with the values obtained by measurement on benzene solutions, 3.92 ± 0.03 D for Me_3BNMe_3 [21] and 6.28 ± 0.02 D for Cl_3BNMe_3.[22]

The empirical parameters used in CNDO calculations have been carefully calibrated for first row elements and hydrogen,[20] while the parameters for second row elements have been obtained by rough approximations.[19] The most reliable results are therefore obtained by calculations on species consisting of first row elements and hydrogen only.

In particular there is uncertainty as to the proper size of the 3*d* orbitals of second row elements, *i.e.* as to the proper magnitude of the orbital exponent. In calculations with the (*sp*) basis the influence of the 3*d* orbitals is neglected altogether. In the (*spd*) basis the 3*d* orbitals have certainly become too compact, and their importance will be overestimated. One may hope therefore that the values computed for various molecular properties by calculations with both bases will bracket the real value.

It is seen that the positive charge on the B atom in BCl_3, BCl_4^-, and Cl_3BNMe_3 decreases with 0.1 to 0.2 electron units when *d*-orbitals are included in the basis. Inspection of the electron density matrix of BCl_3 shows that this is the result of changes both in the σ and π components of the B – Cl bond.

All the charges calculated, and particularly those of the species containing Cl, must be regarded as uncertain. Nevertheless the fact that they are in perfect agreement with the speculations below must be regarded as giving them some weight.

The B atom in BMe_3 carries a small positive charge. Formation of the complex leads to the transfer of 0.4 units of negative charge from the donor. About one fourth of this charge remains located on the B atom, the rest is passed on to the three methyl groups. In the complex, therefore, the boron atom is essentially neutral while the net positive charge on the acceptor is carried by the substituents.

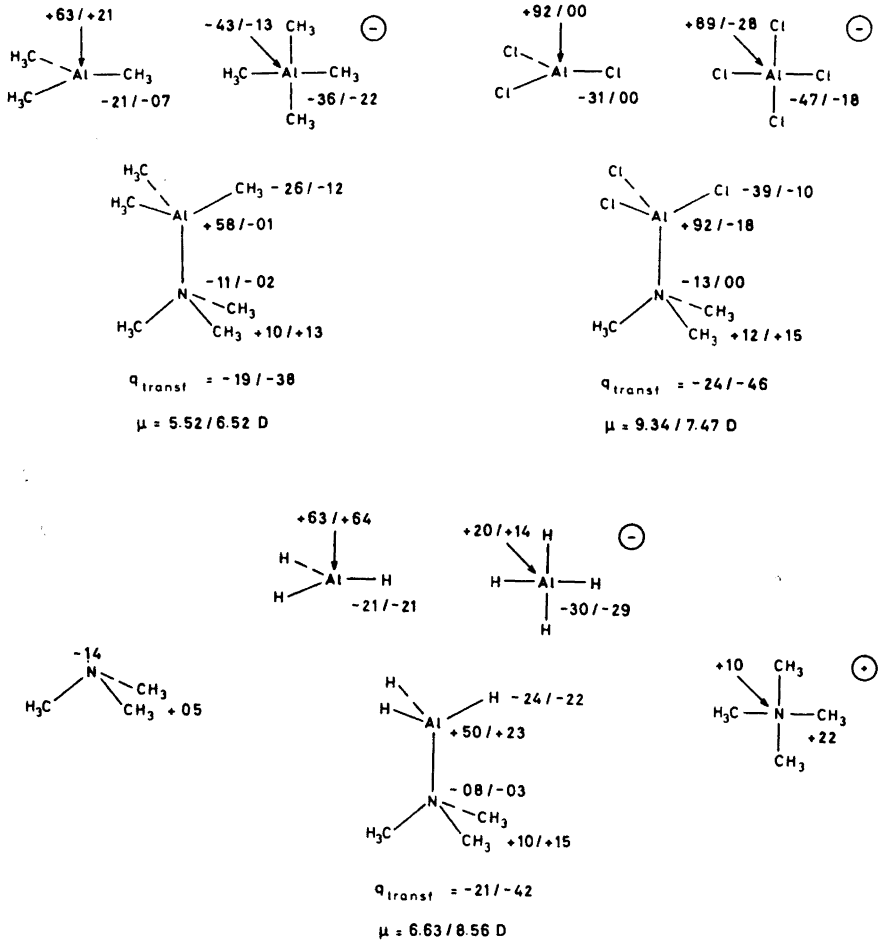

Fig. 2. Atomic charges (in 0.01 electron units) obtained for Me_3AlNMe_3, H_3AlNMe_3, and Cl_3AlNMe_3 and related species, the charge transferred from donor to acceptor (q_{transf}) and the dipole moments. The first number in each case has been obtained with the (*sp*), the second with the (*spd*) basis.

Substitution of the Me groups in BMe_3 by the more electronegative Cl atoms increases the positive charge on B to about 0.3 in BCl_3. The more electronegative Cl atom not only allows more negative charge to be transferred from the donor during complex formation, but also allows the B atom to pass nine tenths of the charge received on to the substituents with the result that it retains its positive charge and that the Cl atoms carry the corresponding negative charge in addition to the net negative charge on the acceptor.

While the N atom in free NMe_3 carries a small negative charge, the transfer of charge during complex formation leaves the N atom essentially neutral in the complexes while the net positive charge on the donor is carried by the Me groups.

The atomic charges of the complexes Me_3AlNMe_3, H_3AlNMe_3, and Cl_3AlNMe_3 are displayed in Fig. 2. The calculated dipole moments of H_3AlNMe_3 are in tolerable agreement with the experimental dipole moment in cyclohexane solution, 4.11 ± 0.08 D.[23] Again the first number in each case has been obtained by calculations with the (*sp*) basis. It is seen that the inclusion of the 3*d* orbitals has a great impact on the charge distribution: The charge on the Al atom in $AlCl_3$, $AlCl_4^-$, and Cl_3AlNMe_3 becomes more negative by about one electron unit, the charge on the Al atom in $AlMe_3$, $AlMe_4^-$, and Me_3AlNMe_3 becomes more negative by half an electron unit, while the charge on Al in H_3AlNMe_3 becomes more negative by a quarter of an electron unit. Only in AlH_3 and AlH^-_4 do the charges remain nearly unaltered.

This is not to say that the Al 3*d* orbitals do not appear with appreciable coefficients in the MO's of AlH_3 and AlH_4^-, they do, but only that the coefficient of the hydrogen 1*s* orbital remains unchanged.

Inspection of the density matrices of $AlMe_3$ and $AlCl_3$ again shows that the variation of the calculated charges is the result of change in both the σ and π components of the Al – Me and Al – Cl bonds.

Clearly the calculated charges for the alane complexes are too uncertain to warrant a detailed discussion. It should nevertheless be noted that they are in agreement with the following general hypotheses:

(i) The amount of charge transferred from donor to acceptor increases as the substituents on the acceptor become more electronegative.

(ii) The acceptor atom remains positively charged or neutral in the complex. The net negative charge is carried by the substituents.

(iii) The N atom in the donor is neutral or carries a small negative charge in the complex. The net positive charge on the donor is carried by the methyl groups.

In all the five complexes that have been studied it has been found that the net negative charge on the acceptor is distributed in such a way that the atomic charges are intermediate between those of the free acceptor and the corresponding "ate" ion, while the atomic charges on the donor are intermediate between those of free NMe_3 and NMe_4^+.

Binding energies. The calculated binding energies of the complexes, defined as the energy of the complex minus the sum of the energies of the free monomeric acceptor and the free donor, are listed in Table 2 along with the observed enthalpies of formation.

Table 2. Calculated binding energies (BE) and observed enthalpies of formation of the gaseous complexes from gaseous monomeric acceptor and donor (in kcal/mol).

	BE(*sp*)	BE(*spd*)	ΔH_f(obs)	Ref.
Me_3BNMe_3	−95		−18	24
Cl_3BNMe_3	−183	−192		
Me_3AlNMe_3	+18	−125	−31	5, 6
H_3AlNMe_3	+12	−159		
Cl_3AlNMe_3	+84	−119	−48	6, 7

It is seen that calculations with the (*sp*) basis fail to predict the stability of the three alane complexes. This does not mean that the 3*d* orbitals necessarily must be included in the basis if stable complexes are to be predicted; very likely this could be achieved through change of one or more empirical parameters. The binding energies of the alane complexes calculated with the (*spd*) basis and those calculated for the borane complexes with either basis grossly overestimate the strength of the complexes.

Equilibrium M−N bond distances. The equilibrium B−N and Al−N bond distances were determined by performing a series of calculations with varying M−N bond distance, but with donor and acceptor geometries unchanged. The results are listed in Table 3.

Table 3. Calculated and observed M−N bond distances (in Å).

	R_{calc}(*sp*)	R_{calc}(*spd*)	R(obs)	Ref.
Me_3BNME_3	1.61	–	1.70−1.90	4
Cl_3BNMe_3	1.55	1.52	1.58	3
Me_3AlNMe_3	Unstable	2.12	2.10	6
H_3AlNMe_3	»	2.06	2.06	10
Cl_3AlNMe_3	»	2.07	1.96	8

In agreement with the results discussed in the preceding section it was found that the energies of the three alane complexes calculated with the (*sp*) basis decreased monotonically as the Al−N distances were increased from 1.60 Å to 2.50 Å. With the (*spd*) basis the Al−N bond distances calculated for the Me_3AlNMe_3 and H_3AlNMe_3 complexes are very close to the experimental values, while the bond distance calculated for Cl_3AlNMe_3 is 0.11 Å too long.

The calculations do predict that the B−N bond distance in Me_3BNMe_3 is longer than in Cl_3BNMe_3, but in both cases the calculated bond distance is too short.

Barriers to internal rotation. The barriers to internal rotation about the M−N bonds were calculated as the energy of the eclipsed molecule minus the energy of the staggered molecule. Hence a positive barrier implies a staggered, a negative barrier an eclipsed equilibrium conformation. Barriers were calculated with the M−N distance fixed at the experimental values with both bases and with the M−N equilibrium distance calculated for the staggered molecule and the (*spd*) basis. The results are shown in Table 4.

Table 4. Calculated and observed barriers to internal rotation about M–N bonds (in kcal/mol).

	$V_0(sp)$	$V_0(spd)$		V_0(obs)	Ref.
	$R=R$(obs)	$R=R_{obs}$	$R=R_{calc}(spd)$		
Me_3BNMe_3	+1.7	–	+2.4		
Cl_3BNMe_3	+6.8	−3.3	−3.8		
Me_3AlNMe_3	+2.0	5.3	5.0	>0	6
H_3AlNM_3	+1.4	3.7	3.7	>0	10
Cl_3AlNMe_3	+2.9	4.2	3.4	>0	25

In every instance it was found that the electronic energy is lowest in the eclipsed conformation while the core repulsion energy is lowest in the staggered conformation. In every instance except Cl_3BNMe_3 with an (*spd*) basis the core repulsion energy dominates, and the calculations predict a staggered equilibrium conformation. More accurate calculations have shown similar conditions to prevail in H_3BNH_3.[26]

The three species for which experimental information is available are indeed staggered in the gas phase.

REFERENCES

1. Brown, H. C. and Barbaras, G. K. *J. Am. Chem. Soc.* **69** (1947) 1137.
2. Greenwood, N. N. and Perkins, P. G. *J. Chem. Soc.* **1960** 1141.
3. Hess, H. *Acta Cryst.* **B 25** (1969) 2338.
4. Lide, R. D., Taft, R. W. and Love, P. *J. Chem. Phys.* **31** (1959) 561.
5. Henrickson, C. H., Duffy, D. and Eyman, D. P. *Inorg. Chem.* **7** (1968) 1047.
6. Anderson, G. A., Forgaard, F. R. and Haaland, A. *Acta Chem. Scand.* **26** (1972) 1947.
7. Eley, D. D. and Watts, H. *J. Chem. Soc.* **1954** 1319.
8. Grant, D. F., Killean, R. C. G. and Lawrence, J. L. *Acta Cryst.* **B 25** (1969) 377.
9. Coates, G. E. and Wade, K. *Organometallic Compounds*, Methuen, London 1967, Vol. 1.
10. Almenningen, A., Gundersen, G., Haugen, T. and Haaland, A. *Acta Chem. Scand. In press.*
11. Beagley, B. and Hewitt, T. G. *Trans. Faraday Soc.* **64** (1968) 2561.
12. McLean, W. J. and Jeffrey, G. A. *J. Chem. Phys.* **47** (1967) 414.
13. Bartell, L. S. and Carroll, B. L. *J. Chem. Phys.* **42** (1965) 3076.
14. Konaka, S., Murata, Y., Kuchitsu, K. and Morino, Y. *Bull. Chem. Soc. Japan* **39** (1966) 1134.
15. Almenningen, A., Halvorsen, S. and Haaland, A. *Acta Chem. Scand.* **25** (1971) 1937.
16. Gerteis, R. L., Dickerson, R. E. and Brown, T. L. *Inorg. Chem.* **3** (1964) 872.
17. Zasorin, E. Z. and Rambidi, N. S. *J. Struct. Chem. (USSR) (Eng. Transl.)* **8** (1967) 347.
18. Baenziger, N. C. *Acta Cryst.* **4** (1951) 216.
19. Santry, D. P. and Segal, G. A. *J. Chem. Phys.* **47** (1967) 158.
20. Pople, J. A. and Beveridge, D. L. *Approximate Molecular Orbital Theory*, McGraw, New York 1970.
21. Abuzov, B. A. and Shavsha, T. G. *Dokl. Akad. Nauk SSSR* **68** (1949) 859.
22. Phillips, G. M., Hunter, J. S. and Sutton, L. E. *J. Chem. Soc.* **1945** 146.
23. Hendricker, D. G. and Heitsch, C. W. *J. Phys. Chem.* **71** (1967) 2683.
24. Brown, H. C., Taylor, M. D. and Gerstein, M. *J. Am. Chem. Soc.* **66** (1944) 431.
25. Almenningen, A., Haugen, T., Haaland, A. and Novak, D. P. *Unpublished result.*
26. Armstrong, D. R. and Perkins, P. G. *J. Chem. Soc.* **A 1969** 1044.

Received August 17, 1972.

ACTA CHEMICA SCANDINAVICA 27 (1973) 528–540

Some 2-(2-Thiazolylazo)-4-methoxyphenol (TAMP) Complex Equilibria. I. Acid-base Properties of TAMP in Water and in Various Mixed Solvents

VLASTIMIL KUBÁŇ[a] and JOSEF HAVEL[b]*

[a] *Department of Analytical Chemistry, J. E. Purkyně University, Brno, Czechoslovakia.*
[b] *Department of Inorganic Chemistry, Royal Institute of Technology, S-100 44 Stockholm 70, Sweden*

The dissociation constant of 2-(2-thiazolylazo)-4-methoxyphenol (TAMP) in 0.1 M KNO_3 at 25.0°C in aqueous solution, as well as in various mixed solvents was determined by means of spectrophotometry. The data were treated by graphical methods as well as by a computer using the general minimizing program LETAGROP-SPEFO. A simple program for evaluation of dissociation constants from spectrophotometric data has also been developed and compared with LETAGROP. The protonation constant of TAMP in water and 30 % ethanol has also been determined.

TAMP and some other dyes of the same group were prepared by Kawase [1] in 1962. He also studied its complexes with some divalent ions [2,3] as well as Co(III).[4] Later Chromý and Vřeštál [5] used TAMP for complexometric determination of Sn(II) in organic compounds. Chromý and Sommer [6] studied TAMP as a complexometric indicator for the determination of some di- and tri-valent metal ions and they worked out several methods for their determination. Sommer, Šepel, and Ivanov [7] showed that TAMP was a very sensitive spectrophotometric reagent for the determination of uranyl ion and deduced composition and some other properties of the complex UO_2R^+ (R = TAMP). Recently Kai [8] used TAMP for the spectrophotometric and complexometric determination of mercury(II) in solution and found two complexes with molar ratios M : R equal to 1 : 1 and 1 : 2. More recently, Chromý and Sommer [9,10] studied complexes of Cu(II) with TAMP, and some of its derivatives in aqueous solution.

* The experimental work and the graphical treatment of the data were carried out by V. K. in Brno, the computer adjustment by J. H. in Stockholm. Permanent address: the same as for V. K.

In order to evaluate the complex formation between TAMP and various metal ions it is necessary to know its acid-base properties in the solvents studied. For that reason we have determined the dissociation constant of TAMP in water as well as several mixed solvents with water as one component.

The solvents studied were: H_2O, 30 % CH_3OH, 30 % DMF, 10, 20, 40, and 50 % C_2H_5OH. The experimental data have been treated with several calculation methods and the results of the calculations compared.

In order to check that the protonation equilibrium of TAMP does not interfere with the complex formation of metal ions down to pH≈1, *e.g.* the complex equilibria with Ni(II),[47] some experiments have been performed at high acidities in H_2O and 30 % C_2H_5OH. The data for the protonation of TAMP and the data for the evaluation of the dissociation constant of TAMP in 20 % and 40 % ethanol were treated by graphical methods only.

EXPERIMENTAL

Reagents and solutions. TAMP was prepared by Svoboda and Bendová [29] (Institute of Pure Chemicals, Lachema, Brno) in a form of bright, darkgreen crystals, sparingly soluble in water but very soluble in dimethylformamide (DMF) and alcohols, giving yellow-orange solutions. It was recrystallized twice from hot ethanol, dried and 99.31 % of the dye was found by elemental analysis of C, H, N in this preparation.

The purity of TAMP was further checked by thin layer chromatography on silica gel (MN-Kieselgel G) using the following mixtures as eluents: 1, 20 ml benzene + 5 ml $CHCl_3$ + 9 ml diethylether + 0.3 ml conc. acetic acid; 2, 33 ml CCl_4 + 18 ml diethylether + 3 ml conc. acetic acid; 3, 35 ml benzene + 4 ml $CHCl_3$ + 4 ml conc. acetic acid. In all cases one spot was found;[30] *i.e.* the dye was chromatographically pure.

A stock solution of TAMP ($c_R = 5 \times 10^{-4} - 1 \times 10^{-3}$ M) was prepared by dissolving the dye in 2.5 ml DMF and 2.5 ml 1 M NaOH and dilution with water up to the mark so that the DMF concentration was not larger than 1 % (*v/v*) in the stock solution and 0.1 (or 0.2 %) (*v/v*) in the others. Traces of heavy metal ions were masked by adding a solution of EDTA.

pH Control. The pH in the solutions used was adjusted by mixing in a nitrogen atmosphere the acid solution of the reagent (pH≈1.1) with an alkaline solution (pH = 11 – 12) containing the same concentration of TAMP. The equipment used permitted continuous measurements of spectrophotometric curves.[31,32] More details about this technique can be found elsewhere.[33] The pH meter (Radiometer, Type S-1001) was calibrated by phosphate (pH = 6.48 at 25°C), phthalate (NBI, pH = 4.01 at 25°C) and tetraborate (NBI, pH = 9.18 at 25°C) buffer solutions. The pH values in mixed solvents were not corrected and we use the symbol pH in all cases.

Ionic strength. Constant ionic strength $I = 0.10$ was maintained during these studies by addition of potassium nitrate (twice recrystallized) or prepared from a mixture of nitric acid and sodium hydroxide.

All other chemicals and solvents were commercial products of *p.a.* purity and purified by recrystallization, distillation *etc.*, before use.

Instruments. All spectrophotometric measurements were made at constant temperature (25.00 ± 0.05°C) on the one beam spectrophotometer SFD-2. Absorption spectra were registered on a UNICAM SP 700 recording spectrophotometer at room temperature. The pH values of the solutions used were measured with a Radiometer PHM-4d pH meter with a precision of ± 0.02 pH unit using glass G 202B and saturated calomel K 401 electrodes (Radiometer).

RESULTS

Table 1a gives a survey of the titrations in the solvents used. Table 1b gives the experimental data for one typical titration in water together with the

Table 1a. Survey of experiments. $t = 25°C$, $I = 0.1$ M (KNO_3).

Set No.	Solvent	C_R M	C_{EDTA} M	pH-range
1	H_2O	5.00×10^{-5}	0	6.26 – 10.30
2	H_2O	5.00×10^{-5}	2×10^{-4}	6.05 – 11.63
3	H_2O	1.00×10^{-4}	4×10^{-4}	6.20 – 9.98
4	H_2O	2.00×10^{-4}	6×10^{-4}	6.09 – 10.04
5	30 % DMF	5.00×10^{-5}	2×10^{-4}	6.20 – 10.34
6	30 % CH_3OH	5.00×10^{-5}	2×10^{-4}	6.20 – 10.15
7	10 % C_2H_5OH	5.00×10^{-5}	2×10^{-4}	6.29 – 9.87
8	50 % C_2H_5OH	5.00×10^{-5}	2×10^{-4}	7.08 – 11.03
9[a]	H_2O	4.50×10^{-5}	0	0 – 1.8
10[a]	H_2O	4.50×10^{-5}	0	0.15 – 1.51
11[a]	30 % C_2H_5OH	4.50×10^{-5}	0	0.03 – 1.92
12[a]	30 % C_2H_5OH	4.50×10^{-5}	0	0.14 – 1.66
13	20 % C_2H_5OH	5.00×10^{-5}	2.00×10^{-4}	5.12 – 11.50
14	40 % C_2H_5OH	5.00×10^{-5}	2.00×10^{-4}	5.20 – 12.00

[a] The ionic strength not constant but varied around 0.1 M.

Table 1b. Experimental data (pH; A_{exp}) for the dissociation of TAMP in water. For all points deviations $\Delta A = 10^3(A_{calc} - A_{exp})$ are given, using the dissociation constants and molar absorptivities determined by LETAGROP-SPEFO (see Tables 2 and 3). $I = 0.10$ M KNO_3; $t = 25°C$. Set No. 1.

pH	A $\lambda=500$	ΔA	A $\lambda=525$	ΔA	A $\lambda=540$	ΔA	A $\lambda=560$	ΔA	A $\lambda=580$	ΔA	A $\lambda=610$	ΔA
6.26	0.276	−4	0.153	−1	0.097	+1	0.057	−2	0.040	+5	0.027	+7
6.40	0.277	−4	0.160	−3	0.103	+1	0.070	−3	0.048	+3	0.033	+5
6.53	0.278	−4	0.167	−4	0.113	−2	0.075	+2	0.056	+3	0.040	+3
6.63	0.278	−4	0.170	−2	0.121	−2	0.085	0	0.066	+1	0.047	+1
6.73	0.279	−3	0.177	−2	0.131	−3	0.096	−1	0.078	−1	0.055	−1
6.87	0.279	−1	0.190	−3	0.147	−3	0.115	+2	0.095	−2	0.065	0
6.96	0.285	−1	0.200	−3	0.160	−3	0.132	−1	0.111	−4	0.075	−1
7.03	0.286	0	0.207	−2	0.170	−2	0.145	+1	0.121	−2	0.084	−3
7.14	0.290	+1	0.222	−1	0.193	−4	0.169	0	0.147	−7	0.099	−4
7.23	0.295	0	0.237	+1	0.210	−2	0.191	0	0.165	−4	0.113	−5
7.35	0.297	4	0.257	+1	0.240	−2	0.224	+1	0.195	−3	0.131	−3
7.42	0.301	4	0.272	1	0.258	−2	0.245	0	0.218	−6	0.146	−5
7.51	0.305	6	0.292	1	0.285	0	0.277	3	0.246	−6	0.163	−4
7.60	0.315	2	0.315	−1	0.313	−2	0.305	2	0.274	−4	0.180	−2
7.70	0.318	6	0.331	8	0.347	5	0.340	4	0.306	−1	0.203	−3
7.79	0.323	7	0.358	4	0.377	5	0.372	1	0.337	1	0.221	−1
7.90	0.330	8	0.382	9	0.415	7	0.415	−2	0.372	6	0.245	0
8.01	0.340	6	0.412	6	0.451	5	0.459	0	0.409	5	0.268	2
8.10	0.349	2	0.430	9	0.480	10	0.488	6	0.440	5	0.290	−2
8.23	0.358	1	0.462	5	0.517	7	0.531	−3	0.480	4	0.314	−1
8.35	0.362	4	0.483	7	0.541	6	0.571	−2	0.512	3	0.336	−3
8.44	0.365	5	0.501	4	0.560	7	0.590	−1	0.529	7	0.345	1
8.51	0.370	3	0.510	5	0.578	3	0.610	−1	0.549	1	0.357	−1
8.63	0.376	1	0.529	1	0.600	1	0.630	0	0.570	2	0.370	−1
8.73	0.380	0	0.540	1	0.610	5	0.651	−1	0.581	5	0.378	0
8.82	0.385	−3	0.550	−1	0.629	−4	0.663	−2	0.598	−1	0.385	0
8.94	0.387	−3	0.558	−1	0.635	2	0.672	0	0.601	−1	0.394	−1
9.12	0.390	−3	0.570	−3	0.652	−2	0.690	3	0.621	2	0.398	4
9.23	0.391	−3	0.575	−3	0.658	−2	0.702	4	0.630	−1	0.404	2
9.38	0.395	−5	0.585	−8	0.672	−9	0.710	7	0.640	−4	0.408	2
9.53	0.396	−4	0.590	−9	0.675	−8	0.712	−1	0.650	−9	0.410	2
9.81	0.400	−5	0.597	−9	0.688	−12	0.725	−4	0.653	−5	0.413	3
10.30	0.422	1	0.603	3	0.692	34	0.738	−2	0.660	21	0.419	0

difference in absorbance $\Delta A = 10^3\ (A_{calc} - A_{exp})$ obtained by LETAGROP using the dissociation constants and molar absorptivities given in Tables 2 and 3.

The full experimental material covering the dissociation of TAMP in the solvents water, 30 % DMF, 30 % methanol, 10, 20, 40, and 50 % ethanol as well as the protonation of TAMP in water and 30 % ethanol can be obtained upon request.

Treatment of data

Within the last decades many numerical and graphical methods have been employed for the determination of equilibrium constants from spectrophotometric data.[11–17] Although the graphical methods are easy to use and give good results as long as the number of parameters to be determined does not exceed three they have the disadvantage of being laborious and time consuming. This can be remedied by letting a computer calculate the normalized functions to be used.[41]

It is difficult, however, to get good estimates for the standard deviations of equilibrium constants and molar extinction coefficients of the complexes under study.

Several computer programs have been developed for the evaluation of spectrophotometric data,[20–24] employing least-squares methods. All these methods suffer from being developed for surprisingly simple special cases such as the formation of a complex AB from A and B.[20] An attempt of a method generally applicable to the formation of mononuclear as well as polynuclear species, even with several ligands, is the program LETAGROP [35,45,46] developed by Sillén and coworkers and applied to many different kinds of equilibria.[42–44] Recently a version called LETAGROP-SPEFO was developed for the treatment of spectrophotometric data.[25,26] A good survey can be found in the literature.[18,19,28,36,37]

In the following the results from graphical as well as the computer programs LETAGROP-SPEFO and PRCEK, the latter one developed by the present writers,[34] are given.

I. Graphical treatment of data. The principles of the graphical methods we have been using for some time may be found elsewhere.[15–17] For the sake of brevity we shall give only the final equations. The transformations are derived from the equation for the equilibrium constant and mass balance equations, combined with the equation for total absorbancy of the solution (validity of Lambert-Beer's law is assumed, of course). After simple rearrangement and elimination of unknowns one obtains for the equilibrium (A) the following transformations:

$$\underset{\varepsilon_1}{RH_x} \rightleftharpoons \underset{\varepsilon_2}{RH_{x-q}} + qH^+ \qquad \text{(A)}$$

$$A = \varepsilon_1 c_R + (\varepsilon_2 c_R - A)[H^+]^{-q} K_x = A_{01} + F_1 K_x \qquad (1)$$

$$A = \varepsilon_2 c_R - (A - \varepsilon_1 c_R) K_x^{-1} [H^+]^q = A_{02} - F_2 K_x^{-1} \qquad (2)$$

$$c_R/A = 1/\varepsilon_1 - (c_R \varepsilon_2 - A)[H^+]^{-q} A^{-1} \varepsilon_1^{-1} K_x = \varepsilon_1^{-1} - Q_1 [H^+]^{-q} \qquad (3)$$

$$c_R/A = 1/\varepsilon_2 + (A - c_R\varepsilon_1)[H^+]^q A^{-1}\varepsilon_2^{-1}K_x^{-1} = \varepsilon_2^{-1} + Q_2[H^+]^q \quad (4)$$

where A is absorbancy, c_R the total reagent concentration, ε_1 and ε_2 are molar absorption coefficients, K_x is the equilibrium constant of the reaction (A), and the other symbols are self-explanatory. K_1 is the dissociation constant of TAMP and K_2 the dissociation constant of its protonated form.

By plotting $A = f(F_1$ or $F_2)$ or $c_R/A = f(Q_1[H^+]^{-q}$ or $Q_2[H^+]^q)$ straight lines are obtained for the right q value. The number of protons liberated in the reaction (A) may thus be evaluated by inserting various values for q. The values for the molar absorptivities and the equilibrium constant can then be obtained from the intercept (ε_1 and ε_2) and from the slope (K). More precise values of K_x and q could be evaluated by using "the graphical logarithmic analysis". The corresponding equation can be derived from any of eqns. (1) – (4) in the form (5)

$$\log \frac{A - \varepsilon_1 c_R}{\varepsilon_2 c_R - A} = \log K_x + q\mathrm{pH} \quad (5)$$

The slope of the plot $\log [(A - A_{01})/(A_{02} - A)] = f(\mathrm{pH})$ gives the value of q, and the value of pH for which $\log [(A - A_{01})/(A_{02} - A)]$ is equal to zero determines the value of pK/q, where $pK = -\log K_x$.

An example of graphical analysis of this type may be found in Figs. 1 and 2. From Figs. 1a and 1b for the protonation of TAMP in H_2O it can be seen, when applying equation (3) (Fig. 1a) that a linear relationship is obtained for $q = 1$. This value is then proved by applying equation (5) as can be seen from the unique slope of the line in Fig. 1b. Similarly, the dissociation constant of TAMP can be found graphically as illustrated in Fig. 2.

The procedure described and illustrated above, was applied separately to each wavelength and from the series of pK_x values mean values were calculated, which are listed in Tables 2 and 6.

Deviations from the mean $p\bar{K}$ values were evaluated using eqn. (6) [40]

$$\sigma(pK) = \left[\frac{1}{N_\lambda}\sum_{n=1}^{N_\lambda}(p\bar{K} - pK_n)^2\right] \quad (6)$$

where $p\bar{K}$ is the mean value calculated from pK values obtained from curves for individual wavelength n, N_λ is the number of wavelengths used. For better comparison with standard deviations computed by PRCEK (*cf.* below) and LETAGROP-SPEFO, the values $3\sigma(pK)$ have been listed, as well.

II. Treatment of the data by linear least-squares method (program PRCEK). In just the same way, as by means of the graphical method discussed in this paper, the "best" lines of transformations (1) and (2) could be found objectively using the linear least-squares method with help of a digital computer. Applying proper formulae one can evaluate standard deviations for molar absorptivities as well as for equilibrium constants. The values of ε_1 or ε_2 show a slight interdependence. Thus, one has to use repeatedly eqns. (1) and (2), until the values of the intercept $\varepsilon_2 c_R$ or $\varepsilon_1 c_R$ and the slopes are not altered significantly or, better, the changes are within certain limits. We did stop the calculations, if two consecutive values differed less than 0.1 rel. percent. By the use of a computer this can be achieved very easily. For the final lines obtained, the standard

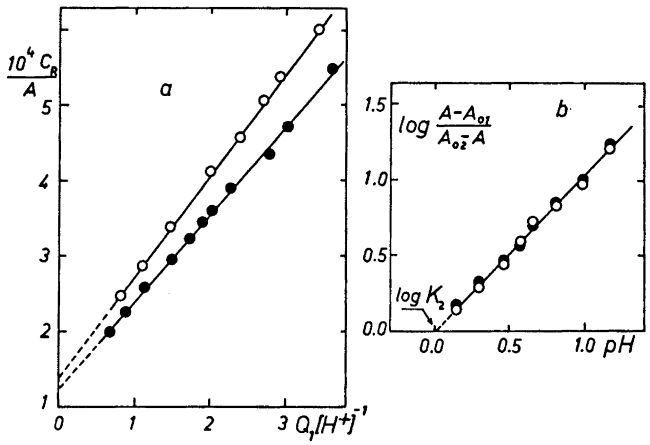

Fig. 1. Graphical analysis of the protonation of TAMP in H_2O. *a.* $10^4\ c_R/A$ plotted against $Q_1[H^+]^{-1}$ for two different wavelengths and $c_R = 4.50 \times 10^{-5}$ M. According to eqn. (3) straight lines correspond to $q = 1$ and the value ε_2 used (ε of RH form in this case) was equal to 800 and 1800. Open symbols correspond to 560 nm, filled symbols to 540 nm. *b.* log $[(A-A_{01})/(A_{02}-A)]$ plotted against pH for the same wavelengths as in Fig. 1a. According to eqn. (5) the extrapolation to $(A-A_{01})/(A_{02}-A) = 0$ gives $-\log K_2$, which should be independent of wavelength. The difference at the two wavelengths used indicates a slight systematic error, smaller than the experimental uncertainty.

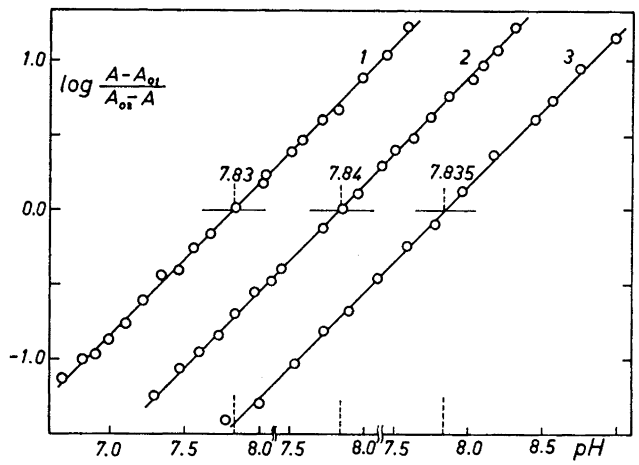

Fig. 2. Graphical determination of the dissociation constant of TAMP in water employing eqn. (5) for wavelength 560 nm. The values for ε_1 and ε_2 were obtained by graphical extrapolation using eqns. (3) and (4).

Curve 1: $c_R = 5.00 \times 10^{-5}$ M, $\varepsilon_1 = 1000$, $\varepsilon_2 = 14\ 520$. Curve 2: $c_R = 1.00 \times 10^{-4}$ M, $\varepsilon_1 = 810$, $\varepsilon_2 = 15\ 350$. Curve 3: $c_R = 2.00 \times 10^{-4}$ M, $\varepsilon_1 = 810$, $\varepsilon_2 = 15\ 350$. The lines have been plotted separately for the sake of clarity.

deviations of molar absorptivities and equilibrium constants were always calculated.

We have written a small Algol program called PRCEK [34] (DWARF in English) to achieve this. It contains some safeguards to avoid possible erratic behaviour. In the program one has to find some starting values for molar absorptivity coefficients, ε_1 in eqn. (1) and ε_2 in eqn. (2). We have taken the values found in a previous graphical analysis but they could be inferred from the graphs $A = f(pH)$, as well.

It is shown elsewhere,[34] that even starting with a quite poor estimate (several times higher or lower) the proper ε values are quickly found after a few successive cycles. The experimental points near the absorbancy value $A_{01} = \varepsilon_1 c_R$ or $A_{02} = \varepsilon_2 c_R$ usually cause trouble due to the fact, that even small experimental errors in absorbancy cause a large scatter of the functions F_1 or F_2. Therefore in the program the points for which the difference $|A - \varepsilon_1 c_R|$ or $|A - \varepsilon_2 c_R|$ was less than 10 (sometimes we have used even 20) % of the $|\varepsilon_1 - \varepsilon_2|\ c_R$ value, were discarded and the "best" lines were calculated from the rest of the experimental data.

The process was repeated for each wavelength and for the final values of K, and $\sigma(K)$, the average numbers were taken. Finally, the error-square sum

$$U = \sum_{N_p} \sum_{N_\lambda} (A_{calc} - A_{exp})^2 \qquad (7)$$

was calculated. N_p is the number of points at each wavelength, N_λ is the number of wavelengths and A_{calc} is the value of absorbancy, calculated from eqn. (8)

$$A_{calc} = (\varepsilon_1 [H^+]^q + \varepsilon_2 K) c_R ([H^+]^q + K)^{-1} \qquad (8)$$

Tables 2 and 3 give some values obtained in this way.

III. Treatment of the data by the program LETAGROP-SPEFO. The values of K found graphically for different media were used as starting values for the LETAGROP refinement.

The program searches for the "best" set of unknown parameters (equilibrium constants) K_1, K_2,...K_N (in our case $N = 1$ or 2 only) and another series of parameters ε_1, ε_2,...ε_N-molar absorptivities of individual species for individual wavelengths. Such a "best" set is defined as the one which gives the minimum value to the error square sum as defined above in eqn. (7).

One can choose by using a value of *val* (1 or 2) the error square sum to be minimized either on $U = \sum (A_{calc} - A_{exp})^2$ (absolute errors, $val = 1$), or $U = \sum [(A_{calc} - A_{exp})/A_{exp}]^2$ (relative errors, $val = 2$). We have used $val = 1$ in all calculations; in this way the experimental points have been given the same weight as with PRCEK, *i.e.* all points have the same weight.

In Table 2 the resulting values of $\log K \pm 3\sigma(\log K)$ are given, where $\sigma(\log K)$ is defined by

$$\sigma(\log K) = \tfrac{1}{2} \log \frac{K + \sigma(K)}{K - \sigma(K)}.$$

Table 2. Dissociation constants of TAMP determined by graphical method, PRCEK and LETAGROP-SPEFO programs. ($I = 0.10$ M KNO_3; $t = 25$°C. The experimental conditions for each set are given in Table 1a).

Set No.	Medium	$-\log K_1$[a] Graph.	$-\log K_1$	$U \times 10^3$ PRCEK	$-\log K_1$	$U \times 10^3$	$\sigma(A) \times 10^3$ LETAGROP	$\Delta \log K_1$[b]
1	H_2O	7.83 ± 0.03	7.830 ± 0.010	9.954	7.815 ± 0.007	3.240	± 4.12	+ 0.015
2	H_2O	7.83 ± 0.03	7.827 ± 0.015	5.395	7.836 ± 0.009	2.880	3.91	− 0.009
3	H_2O	7.84 ± 0.03	7.855 ± 0.013	5.140	7.861 ± 0.010	2.090	4.11	− 0.006
4	H_2O	7.83 ± 0.03	7.859 ± 0.019	13.838	7.858 ± 0.012	7.019	9.14	+ 0.001
Mean value		7.83 ± 0.03	7.846 ± 0.016	–	7.852 ± 0.010	–	–	–
All data together		–	–	–	7.858 ± 0.009	2.619	7.93	–
5	30 % DMF	8.38 ± 0.02	8.382 ± 0.014	10.564	8.386 ± 0.006	2.376	± 3.26	− 0.004
6	30 % CH_3OH	8.16 ± 0.03	8.156 ± 0.011	6.435	8.159 ± 0.006	2.107	3.07	− 0.003
7	10 % C_2H_5OH	7.92 ± 0.04	7.923 ± 0.012	3.298	7.922 ± 0.009	2.467	4.46	+ 0.001
8	50 % C_2H_5OH	8.92 ± 0.03	8.921 ± 0.022	11.389	8.925 ± 0.016	8.576	8.49	− 0.004

[a] Values resulting as a mean from the values calculated for each wavelength using eqn. (5).
[b] $\Delta \log K_1 = -\log K_1$ (PRCEK) + $\log K_1$ (LETAGROP).

Table 3. Molar absorptivities of R^- and RH forms of TAMP determined from the horizontal parts of $A = f(pH)$ curves, by graphical method, and by PRCEK and LETAGROP-SPEFO programs.

Set No.	λ (nm)	$\varepsilon_i = A_{01} i / c_R$[a] $\varepsilon_2(R^-)$	$\varepsilon_1(RH)$	Graphical method[a] ε_2	ε_1	PRCEK $\varepsilon_2 \pm \sigma(\varepsilon_2)$		$\varepsilon_1 \pm \sigma(\varepsilon_1)$		LETAGROP-SPEFO $\varepsilon_2 \pm \sigma(\varepsilon_2)$		$\varepsilon_1 \pm \sigma(\varepsilon_1)$	
1	500	8 010	5 400	7 950	5 450	7 980	± 20	5 485	± 19	7 890	± 21	5 370	± 24
	525	12 040	3 060	11 950	2 950	11 850	24	2 670	23	11 830	27	2 840	28
	540	13 800	1 740	13 700	1 720	13 650	36	1 855	43	13 630	29	1 680	30
	560	14 600	1 140	14 400	940	14 020	35	920	33	14 510	28	900	29
	580	13 100	800	13 150	710	13 030	32	700	44	13 110	30	620	31
	610	8 300	540	8 330	440	8 250	26	350	38	8 430	26	510	27
2	440	2 680	7 000	2 700	7 120	2 690	21	7 230	43	2 660	15	7 190	16
	470	4 120	7 460	4 200	7 550	4 190	11	7 560	21	4 160	14	7 500	14
	510	9 780	4 600	9 720	4 650	9 650	25	4 640	27	9 600	26	4 560	26
	540	14 000	1 880	13 870	1 770	13 720	44	1 830	45	13 740	31	1 780	32
	560	14 880	1 040	14 520	1 000	14 640	58	910	25	14 690	32	930	32
	580	12 800	700	12 700	620	13 160	50	620	41	13 230	31	640	31
	610	8 460	360	8 350	390	8 410	21	450	28	8 530	31	570	31

[a] Standard deviations have not been estimated for molar absorptivities found from horizontal parts of $A = f(pH)$ curves and by graphical methods.

Moreover, $\sigma(A)$ the standard deviation in A is given. Molar absorptivities ε_i together with their standard deviations $\pm\sigma(\varepsilon_i)$ are given in Table 3 for one typical run in water.

The possible existence of the complex $R(RH)^-$. By LETAGROP one can very easily try to introduce a new species and see whether this addition can significantly improve the fit or not. It is made possible in a quite elegant way [35] by a "species selector" in the program.

Table 4. Values of error square sum U_{min}, logarithms of constants K_1 and K_{12} (assuming species R^- and $R(RH)^-$, respectively).

Set No.	10^3U	$\sigma(A)\times 10^3$	pK_1	$10^3\times U$	$\sigma(A)\times 10^3$	pK_1	pK_{12}
	assuming only reaction (A)			assuming reaction (A) and (B)			
1	3.240	±4.12	7.815±0.007	0.930	±2.25	7.98(max 7.76)	4.28±0.20
2	2.880	3.91	7.836±0.009	2.258	3.54	7.88±0.06	4.72±0.21
3	2.090	4.11	7.861±0.010	–	–	7.78±0.20	rejected
4	7.019	9.14	7.858±0.012	–	–	7.88±0.06	rejected
	26.193[a]	7.93	7.858±0.009	–	–	7.87±0.02	rejected
5	2.376	3.26	8.386±0.006	2.336	3.30	8.39±0.01	6.18±0.17
6	2.107	3.07	8.159±0.006	–	–	8.19±0.03	rejected
7	2.467	4.46	7.922±0.009	2.098	4.22	7.92±0.02	4.89(max 4.67)
8	8.576	8.49	8.925±0.016	–	–	–	K < 0; rejected

[a] All data together.

The new species added is accepted, if U_{min} is significantly lower than the previous one and if the constant for the new complex is coming out with a standard deviation $\sigma(K)$, for which the condition $K > F_\sigma \times \sigma(K)$ is fulfilled. F_σ is the value for *Sigfak* in the program. We have used $F_\sigma = 1.5$, *i.e.* the confidence level 93 %.

It was of some interest to test the formation of a species $R(RH)^-$. In series 1 and 2, *i.e.* for $c_R = 5\times 10^{-5}$ M the species was accepted (see Table 4), U_{min} decreased, as well as $\sigma(A)$. It was also accepted for 10 % v/v ethanol with a similar K_{12} value (log $K_{12} \approx -4.5$) and also in 30 % v/v DMF, but rejected in 50 % ethanol and 30 % methanol (see Table 4).

To be quite certain about the existence of this complex the absorbance – pH curves also for two higher c_R values (1×10^{-4} and 2×10^{-4} M TAMP) were measured, where one could expect more of this "dimer". In calculations on these data the species was not accepted and then rejected when treating series 2, 3, and 4 altogether.

A probable explanation of $R(RH)^-$ being accepted in some series is the complex formation of TAMP with some metal impurities in the ionic medium in spite of the presence of EDTA in most of the cases. And really, the best "improvement" in the U value after adding species $R(RH)^-$ was observed for H_2O, $C_{EDTA} = 0$ but no improvement was obtained for series with higher EDTA concentrations. We can therefore imagine, that the acceptance of the hypothetical reaction (B) with the equilibrium constant K_{12} (*cf.* Table 4)

$$R^- + RH \rightleftharpoons R(RH)^- \qquad (B)$$

is rather due to complex formation of TAMP with metal impurities, Me^{z+} such as

$$Me^{z+} + 2\ RH \rightleftharpoons MeR(RH)^{(z-1)} + H^+ \qquad (C)$$

$$\text{or } Me^{z+} + R^- + RH \rightleftharpoons MeR(RH)^{(z-1)+} \qquad (D)$$

The formation of mixed species containing EDTA cannot be excluded, of course. This interfering reaction was hindered by higher EDTA concentrations in the case of series 3 and 4, so that $R(RH)^-$ species was not accepted. The same can be true for the other media as well, thus we can eventually conclude that no "dimer" $R(RH)^-$ is formed during the experimental conditions used in this paper.

CONCLUSIONS

Three optically different species of TAMP exist in aqueous as well as in mixed solvents depending on the pH value. The first orangered species RH_2^+ with absorption maximum 495 – 520 mn predominates down to pH ≈ 1, the second form RH is yellow with maximum 465 – 475 nm, predominating in the pH range 1 – 7 and the violet-blue form R^- ($\lambda_{max} = 560 - 570$ nm) predominates above pH = 7. There are two isosbestic points on the absorption curves – one of them indicates deprotonation of RH_2^+ and the second the deprotonation of RH to yield R^- (see Table 6).

Absorption curves of the reagent measured in the pH region 0 – 11 and in concentrated sulphuric and perchloric acids were found to be in good agreement with Chromý and Sommer.[6] The values of λ_{max} which have been found for the species RH_2^+, RH, and R^- in different media are given in Table 5.

All methods for the determination of dissociation constants, described above, were applied only to the dissociation of TAMP (K_1) in all aqueous as well as in mixed solvents (except 20 and 40 % ethanol) because these data were obtained with an accuracy good enough to justify use of computer methods.

The dissociation constant of the protonated form of TAMP (K_2) was determined for aqueous solutions and for 30 % v/v ethanol by the graphical method by extrapolation of $\log \{(A - A_{01})/(A_{02} - A)\} = f(pH)$ plots for

Table 5. Summary of optical data of TAMP.

Form	Solvent	pH region	λ_{max} (nm) This paper	ε^a	λ_{max} (nm) Lit.	Ref.
RH_2^+	H_2O	1 [b]	510, 381	10 420	523, 380	6
	30 % CH_3OH		495, 382		372	1
	30 % DMF		493, 376			
RH	H_2O	1 – 7	467, 369	7.480	468, 370	6
	30 % CH_3OH		474, 370	8.550	462, 366	1
	30 % DMF		476, 370	8.750	481, 365	38
R^-	H_2O	7	559, 369	15 420	561, 370	6
	30 % CH_3OH		565, 368	15 520	562, 366	1
	30 % DMF		571, 370	16 510		
	10 % C_2H_5OH			15 840		
	50 % C_2H_5OH			17 070		

[a] $\varepsilon_{RH_2^+}$ given for 510 nm, ε_{RH} for 470 nm, ε_{R^-} for 560 nm.
[b] The ionic strength was varied in the range 0.10 – 1.20 (HNO_3 + 0.10 M KNO_3).

Table 6. Final values of the protonation constant of TAMP, determined by graphical method and final values for the dissociation constant as found by LETAGROP-SPEFO. A comparison with literature data.

Equilibrium	Solvent	λ Isosbestic point	This paper ($I=0.10(KNO_3)$	$-\log K$ 25.0°C	Lit.	Ref.
$RH_2^+ \rightleftharpoons RH + H^+$	H_2O	418 nm	0.00 ± 0.04[a]		0.03 ± 0.03	6
	30 % EtOH		0.12 ± 0.05[a]			
	30 % dioxane				0.3	8
$RH \rightleftharpoons R^- + H^+$	H_2O	493 nm	7.858 ± 0.009		8.13 ± 0.02	6
	30 % CH_3OH		8.159 ± 0.006			
	30 % DMF		8.386 ± 0.006			
	10 % EtOH		7.923 ± 0.009			
	20 % EtOH		8.18 ± 0.03[a]			
	30 % EtOH		8.328 ± 0.017			47
	40 % EtOH		8.56 ± 0.06[a]			
	50 % EtOH		8.925 ± 0.016			
	20 % dioxane				8.4	1
	20 % dioxane				8.2	39
	30 % dioxane				7.90	8
	50 % dioxane				9.18	3

[a] Determined by means of the graphical method only.

pH < 1.0. The values of $-\log K_2$ obtained are equal to 0.00 ± 0.04 and 0.12 ± 0.05, respectively. One can see that the protonation of TAMP becomes important only in rather strongly acidic solutions, *i.e.* below pH = 1.

The relevant values of absorption maxima λ_{max}, wavelength of isosbestic points λ_{isosb}, and final values of $-\log K_1$ and $-\log K_2$ and molar absorptivities of all species determined by LETAGROP-SPEFO procedure are listed in Tables 5 and 6.

It deserves to be mentioned that the small amount of DMF used to bring TAMP into solution in the various solvents has a negligible effect on the pK-values obtained.

The difference in pK between 0.1 % DMF solution and that obtained for pure H_2O (calculated from the difference of pK values obtained for H_2O and 30 % DMF in this paper) is about 0.002 pK which is much less than the experiment uncertainty.

From Tables 2 and 3 where the values of $-\log K$ and ε_i are listed one can see, that individual values determined by different procedures are in good agreement, irrespective of the different basic principles of the graphical and least squares method on one hand, and of LETAGROP-SPEFO on the other.

The program PRCEK is useful for the determination of equilibrium constants in cases, where only two absorbing species are present in solution in the pH interval studied. In more complicated cases, if three absorbing species are present, the problem can be solved by dividing the investigated pH interval into regions where only two species absorb. It is the same principle as that one used in solving simultaneous equilibria by graphical methods.

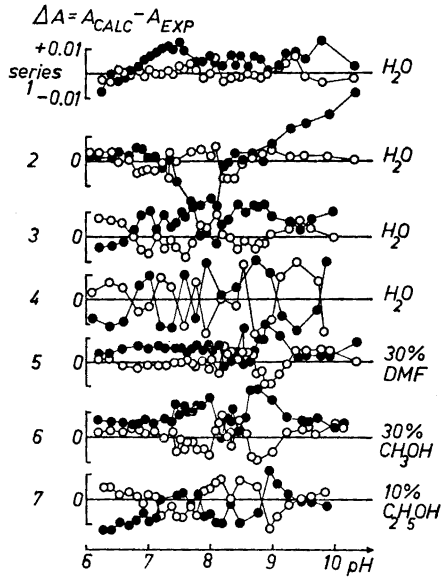

Fig. 3. The deviations $\Delta A = A_{calc} - A_{exp}$ at the arbitrarily chosen wavelength 560 nm as a function of pH for various mixed solvents, determined by PRCEK (open symbols) and LETAGROP-SPEFO (filled symbols). The conditions for each series are given in Table 1a. The data in this figure correspond to ~ 1/6 of all the experimental data.

As seen from Table 2 the program PRCEK gives error square sums about three times as big as LETAGROP. However, the difference in the constants obtained is so small that results with PRCEK are acceptable. The highest deviation between the pK value calculated by means of PRCEK and LETAGROP-SPEFO was for series 1, *i.e.* 0.015 logarithmic units, but the average absolute deviation for all the series was 0.005 logarithmic units, which is quite acceptable (see Table 2).

A comparison of the deviations $\Delta A = A_{calc} - A_{exp}$ calculated by both programs for various mixed solvents is given in Fig. 3 for one of the wavelengths. It may be seen that PRCEK gives slightly higher deviations, but for the present purpose this is not serious.

The final values for the dissociation constants of TAMP are given in Table 6 and are those calculated by LETAGROP-SPEFO, since they are taken as the "best" values obtainable from our experimental data.

Acknowledgements. We thank Professor Lumír Sommer for suggesting this work. Professor Erik Högfeldt is thanked for some helpful suggestion and discussions concerning the presentation of material in this paper. Dr. Diego Ferri is thanked for valuable remarks, as well. Dr. Peter Staples kindly revised the English of the text.

Financial support to part of the work in this paper by the *Swedish Natural Science Research Council* (NFR) is gratefully acknowledged.

REFERENCES

1. Kawase, A. *Bunseki Kagaku* **11** (1962) 621.
2. Kawase, A. *Bunseki Kagaku* **11** (1962) 628.
3. Kawase, A. *Bunseki Kagaku* **13** (1964) 553.
4. Kawase, A. *Bunseki Kagaku* **12** (1963) 903.

5. Chromý, V. and Vřeštál, J. *Chem. Listy* **60** (1966) 1537.
6. Chromý, V. and Sommer, L. *Talanta* **14** (1967) 393.
7. Sommer, L., Šepel, T. and Ivanov, V. M. *Talanta* **15** (1968) 949.
8. Kai, F. *Anal. Chim. Acta* **44** (1969) 242.
9. Chromý, V. and Sommer, L. *Publ. Fac. Sci. Univ. Brno 1970, No. 519*, 407.
10. Chromý, V., Diss, Brno 1969.
11. Benesi, H. A. and Hildebrand, J. H. *J. Am. Chem. Soc.* **71** (1949) 2703.
12. Heller, J. and Schwarzenbach, G. *Helv. Chim. Acta* **34** (1951) 1876.
13. Ågren, A. *Acta Chem. Scand.* **8** (1954) 266.
14. Bent, H. E. and French, C. L. *J. Am. Chem. Soc.* **63** (1941) 568.
15. Sommer, L., Kučerová, J., Procházková, H. and Hniličková, M. *Publ. Fac. Sci. Univ. Brno 1965, No. 464*, 249.
16. Sommer, L., Kubáň, V. and Havel, J. *Folia Fac. Rer. Nat. Univ. Brno* **11** *(Chemica 7)* Part 1 (1970).
17. Rossotti, F. J. C. and Rossotti, H. *The Determination of Stability Constants*, McGraw, New York 1961.
18. Rydberg, J. and Sullivan, J. C. *Acta Chem. Scand.* **13** (1959) 186.
19. Rydberg, J., Sullivan, J. C. and Miller, W. F. *Acta Chem. Scand.* **13** (1959) 2023.
20. Ramette, R. W. *J. Chem. Educ.* **44** (1967) 647.
21. Conrow, K., Johnson, G. D. and Bowen, R. E. *J. Am. Chem. Soc.* **86** (1964) 1025.
22. Wentworth, W. E., Hirsch, W. and Chem, E. *J. Phys. Chem.* **71** (1967) 218.
23. Rabideau, S. W. and Klein, R. J. *J. Phys. Chem.* **64** (1960) 680.
24. Ropars, C. and Viovy, R. *Bull. Soc. Chim. France* **1966** 3637.
25. Sillén, L. G. and Warnqvist, B. *Acta Chem. Scand.* **22** (1968) 3032.
26. Sillén, L. G. and Warnqvist, B. *Arkiv Kemi* **31** (1969) 377.
27. Dyrssen, D., Ingri, N. and Sillén, L. G. *Acta Chem. Scand.* **15** (1961) 695.
28. Dyrssen, D., Jagner, D. and Wengelin, F. *Computer Calculation of Ionic Equilibria and Titration Procedures*, Almqvist & Wiksell, Stockholm 1968.
29. Svoboda, V. and Bendová, L. *Unpublished results.*
30. Toul, J. and Mouková, N. *J. Chromatogr.* **67** (1972) 335.
31. Havel, J. *Chem. Listy* **62** (1968) 1250.
32. Wallin, T. *Arkiv Kemi* **26** (1966) 13.
33. Kubáň, V. Thesis, Univ. Brno 1972.
34. Havel, J. and Kubáň, V. *Scripta Fac. Sci Nat. UJEP Brunensis, Chemica 2*, 1: 87 (1971).
35. Sillén, L. G. and Warnqvist, B. *Arkiv Kemi* **31** (1969) 341.
36. Perrin, D. D. *Talanta* **14** (1967) 833.
37. Childs, C. W., Hallman, P. S. and Perrin, D. D. *Talanta* **16** (1969) 629, 1119.
38. Kawase, A. *Talanta* **12** (1965) 195.
39. Shibata, S. and Isiguro, I. *Rept. Gov. Ind. Res. Inst. Nagoya* **11** (1962) 318.
40. Eckschlager, K. *Chyby chemických rorborů*, SNTL Praha 1961, p. 92.
41. Ferri, D. *Private communication.*
42. Arnek, R., Sillén, L. G. and Wahlberg, O. *Arkiv Kemi* **31** (1969) 353.
43. Brauner, P., Sillén, L. G. and Whiteker, R. *Arkiv Kemi* **31** (1969) 365.
44. Arnek, R. *Arkiv Kemi* **32** (1970) 81.
45. Ingri, N. and Sillén, L. G. *Arkiv Kemi* **23** (1964) 97.
46. Sillén, L. G. and Warnqvist, B. *Arkiv Kemi* **31** (1969) 315.
47. Kubáň, V., Sommer, L. and Havel, J. *To be published.*

Received July 15, 1972.

ACTA CHEMICA SCANDINAVICA 27 (1973) 541–550

Non-enzymatic Ethanol Oxidation in Biological Extracts

HELMUTH W. SIPPEL

Research Laboratories of the State Alcohol Monopoly (Alko), Helsinki 10, Finland

Non-enzymatic ethanol oxidation was found to occur in fresh PCA-precipitated blood and tissue homogenate. The same reaction occurred in ascorbic acid but not in dehydroascorbic acid solutions. Hydrogen peroxide was completely inactive as a direct oxidizing agent in the absence of ascorbic acid. A semidehydroascorbate peroxy radical was hypothesized to act as an electron acceptor in the reaction.

Truitt [1] has found that varying amounts of acetaldehyde are produced when ethanol is added to blood precipitates *in vitro* and the sample is incubated at 55°C for 15 – 20 min. This artificially-produced acetaldehyde interferes with the determination of small amounts of acetaldehyde in biological samples.[1] It has been assumed that the source of the acetaldehyde is a protein from which an acetaldehyde group is split off, or a release of bound acetaldehyde by ethanol.[1–4] On the other hand, von Euler and Hasselquist [5] have assumed that the observed oxidation of ethanol is caused by hydrogen peroxide and is catalyzed by ascorbic acid and dehydroascorbic acid in the presence of ferric ions. The oxidative properties of ascorbic acid in the presence of oxygen have also been reported by other investigators.[6,7]

Fresh blood precipitates always contain small amounts of ascorbic acid and traces of iron ions; in addition, the autoxidation of ascorbic acid produces hydrogen peroxide.[8] Therefore, it is possible that the acetaldehyde found in blood precipitates might have been produced by this ascorbic acid system, rather than being released from a protein or macromolecule. This hypothesis requires that ascorbic acid is able to oxidize ethanol to acetaldehyde in biological extracts. The present studies have been carried out in an attempt to test this possibility.

MATERIALS AND METHODS

Chemicals. All chemicals were of analytical grade. Ethanol (AaS) from Alko, Helsinki, Finland; acetaldehyde, L(+)ascorbic acid, perhydrol, perchloric acid and riboflavin from E. Merck AG, Darmstadt, Germany; dehydro-L(+)-ascorbic acid from Fluka AG, Buchs, Switzerland.

Tissue materials. Rat and mouse livers were quickly removed from the animals after decapitation, then were weighed and homogenized in ice-cold 0.6 N perchloric acid (PCA). The precipitate was centrifuged, and 0.5 ml of the supernatant was incubated and analyzed by gas chromatography. In other experiments fresh bovine liver was used. The extract was filtered and the filtrate analyzed. Rat blood was also obtained by decapitation. The homogenate concentrations in the samples were reported as g tissue or ml blood per 100 ml sample.

Gas chromatography. The quantity of acetaldehyde formed was determined in a Perkin-Elmer automatic F 40 head-space gas liquid chromatograph with a hydrogen flame detector (hydrogen flow rate: 35 ml/min; air flow rate: 300 ml/min). The commercial column (15 % polyethylene glycol on celite 60/100) sold by the manufacturer was used. The column temperature was 75°C, and purified nitrogen was used as carrier gas, flow rate 35 ml/min. 0.5 ml of sample was added to each bottle in which the head-space was produced. The bottles were placed in a thermostatically controlled water bath at 65°C and kept at equilibrium for at least 15 min prior to the automatic analysis of the head-space gas. The highest sensitivity was used. The analytical procedure was standardized with samples of diluted acetaldehyde and ethanol. Standard and unknown samples were determined by identical procedures. 0.2 ‰ *tert*-butanol was used as internal standard in the ethanol determination. The acetaldehyde was determined by using fresh redistilled acetaldehyde (50 nmol/ml) as a reference standard. The acetaldehyde concentration in the standard was checked daily with 0.025 ‰ *tert*-butanol as the internal standard.

Gel filtration. The filtration experiments were done with columns packed with cross-linked polysaccharide Sephadex G-25 (manufactured by Pharmacia, Uppsala, Sweden). The characteristics of the bed material were: water regain = 2.5 g water/g dry gel; wet density = 1.13 g/ml. The packing of the column has been described by Gelotte.[9] V_0 necessary for the calculation of K_d was experimentally determined as the elution volume for bovine albumin (from Armour Pharmaceutical Company Ltd., Eastbourne, England) with 0.05 N NaCl as eluent.

Thin layer chromatography (TLC). Glass plates were coated with a thin layer of Silica Gel G (from E. Merck AG, Darmstadt, Germany) and dried at 110°C for 20 min. Samples of bovine liver extract (pH 5), eluted through Sephadex G-25 with distilled water and shaken with Florisil (magnesium trisilicate, 60 – 100 mesh, from Serva Feinbiochemica GmbH & Co., Heidelberg, Germany), were applied to the plate. The plate was developed in the solvent system 1-butanol : oxalic acid : water (4 : 1 : 5) and sprayed with a molybdate reagent that stains all reducing substances blue.[10]

RESULTS

Acetaldehyde formation in PCA-precipitated liver extract

Non-enzymatic ethanol oxidation was found to occur in biological extracts. The rate is dependent primarily on the homogenate concentration. Thus, it is possible to minimize the formation of acetaldehyde by using very diluted solutions. Compared with blood, liver tissue from rats and mice produced large amounts of acetaldehyde. Fig. 1 contains data which show that the amount of acetaldehyde formed was linearly proportional to the ethanol concentration.

Reaction time. The duration of incubation at 65°C had, as shown in Fig. 2, an obvious effect on the acetaldehyde production in liver extract. Compared with liver, PCA-precipitated blood produced only insignificant amounts of acetaldehyde. Blood cells supplied much more acetaldehyde than plasma in the presence of ethanol, which is in close agreement with the findings of Truitt.[1]

Effect of pH. As shown in Fig. 3 the pH of the analyzed solution had a clear effect on the acetaldehyde formation. At pH 1 the amount of acetaldehyde

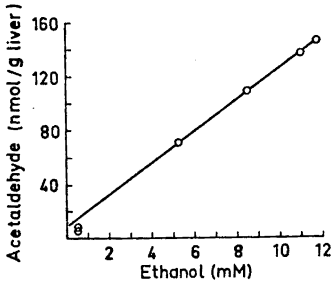

Fig. 1. Non-enzymatic ethanol oxidation in rat liver extract incubated at 65°C for 15 min with ethanol. The liver was homogenized in ice-cold 0.6 N PCA solution containing varying amounts of ethanol, centrifugated, and the supernatant was analyzed immediately. The amount of acetaldehyde formed is reported as nmol per g liver tissue.

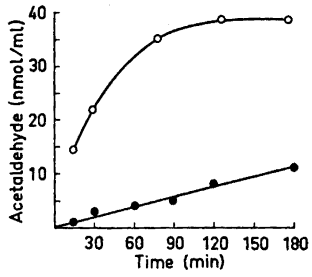

Fig. 2. The acetaldehyde formation in PCA-precipitated blood and liver extracts incubated with ethanol for different lengths of time at 65°C. (○) Rat liver homogenate (conc. 20 %) and (●) rat blood (conc. 25 %). The ethanol concentration was 20 mM in the former and 44 mM in the latter experiment.

formed was only 18 % of the maximal acetaldehyde concentration produced at pH 5.

Fig. 3. Effect of different pH on the acetaldehyde formation in PCA-precipitated bovine liver extract. The pH-value was gradually increased by adding NaOH to the sample; it was checked both before and after the analysis. The dilution of the extract can be disregarded because the homogenate concentration was decreased only about 3 % during the pH change from 1–7. The circles represent mean values obtained in two experiments. The samples were incubated for 60 min at 65°C before the analysis.

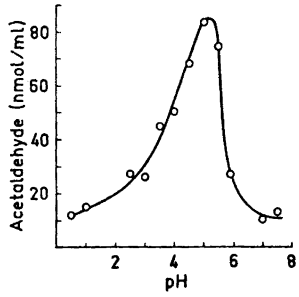

Effect of heating on the acetaldehyde formation. Bovine liver extract was heated in a covered test tube in a water bath at 80°C for different lengths of time. The result of this experiment showed that heating liver extract (pH < 1) in the water bath for 90 min had no effect on the acetaldehyde formation. At higher pH, the heating of the extract before the addition of ethanol greatly reduced the acetaldehyde production.

Effect of the redox system, ascorbic acid – dehydroascorbic acid, on the ethanol oxidation

Ascorbic acid was found to oxidize ethanol to acetaldehyde when a 0.5 mM ascorbic acid solution was incubated in the presence of 20 mM ethanol and Cu^{2+} for 15 min at pH 5 and 7 (Table 1).

Table 1. Ethanol oxidation in ascorbic acid and dehydroascorbic acid solutions. The ethanol concentration was 20 mM and the samples were incubated for 15 min at 65°C. The acetaldehyde formed is given as nmol per ml incubation solution.

Solution	pH	$CuSO_4$ (μM)	Acetaldehyde concentration (nmol/ml)
Ascorbic acid (0.5 nM)	5	10	55
	7	10	15
	5	–	72
Dehydroascorbic acid (0.5 mM)	5	10	0
	7	10	0
	5	–	0
Ascorbic acid (0.25 mM) + dehydroascorbic acid (0.25 mM)	5	10	28
	7	10	4

Ascorbic acid is easily oxidized to dehydroascorbic acid, especially at pH > 4.[11] In order to test if dehydroascorbic acid is also able to oxidize ethanol the same experiment was repeated with the former compound. As Table 1 illustrates, there was no acetaldehyde formed in this case. If equivalent amounts of 0.5 mM ascorbic acid and 0.5 mM dehydroascorbic acid were then mixed together and the mixture was analyzed, there was only a quarter as much acetaldehyde produced at pH 7 as in the first experiment. Even a suspension of dehydroascorbic acid did not produce any acetaldehyde after an incubation time of 15 min.

Effect of varying concentrations of ascorbic acid on the reaction at different pH

As shown in Fig. 4A, the amount of acetaldehyde produced was a direct function of the ascorbic acid concentration. Very little ascorbic acid is needed for the reaction; even a 0.2 mM solution (pH4) produced 50 nmol acetaldehyde per ml after incubation with 20 mM ethanol for 15 min. At pH 7, greater amounts of acetaldehyde were formed only when the ascorbic acid concentration was over 0.6 mM. In a strong acid PCA-solution (pH < 1), an ascorbic acid concentration of 1.2 mM produced only insignificant amounts of acetaldehyde after an incubation time of 15 min (Fig. 4A).

Fig. 4B illustrates that the acetaldehyde formation in a solution of 0.25 mM ascorbic acid and 20 mM ethanol has a maximum at pH 4. No measurable acetaldehyde was formed at pH 7 – 8.

To check if ascorbic acid has the same oxidizing capacity in PCA-precipitated liver homogenate, varying amounts of ascorbic acid were added to liver extract (Fig. 5). Compared with the reaction in a pure ascorbic acid

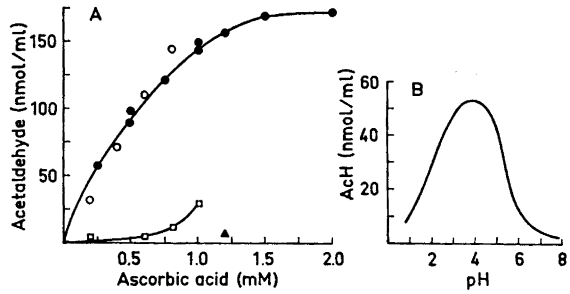

Fig. 4. A. Effect of different ascorbic acid concentrations on the acetaldehyde formation. The ascorbic acid was dissolved in distilled water and the pH of the solution regulated with HCl or NaOH, respectively. The samples were incubated at 65°C in the presence of 20 mM ethanol: (●) 15 min at pH 4, (○) 60 min at pH 4, (□) 60 min at pH 7, and (▲) 15 min at pH < 1 (in the latter experiment, the ascorbic acid was dissolved in a 0.6 N PCA solution). B. Acetaldehyde formed at different pH values. The concentration of the ascorbic acid solution was 0.25 mM and that of the ethanol concentration 20 mM. The samples were incubated for 60 min.

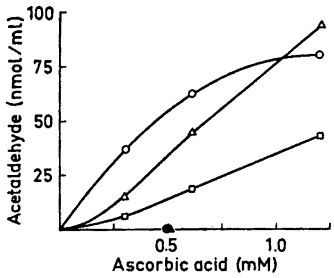

Fig. 5. Effect of ascorbic and dehydroascorbic acid at different pH on the non-enzymatic ethanol oxidation in PCA-precipitated rat liver extract (homogenate conc. 8 %). The samples were incubated for 15 min at 65°C in the presence of 20 mM ethanol before the analysis. Ascorbic acid: (△) ph < 1, (○) pH 5, (□) pH 7; dehydroascorbic acid: (▲) pH < 1, (●) pH 5. pH was regulated with NaOH. The acetaldehyde values given were subtracted from the acetaldehyde formed in a sample without added ascorbic acid at respective pH.

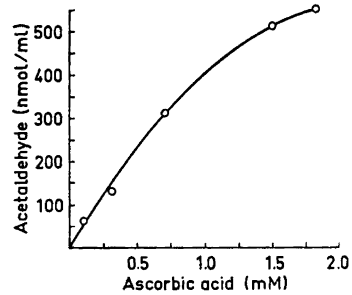

Fig. 6. Effect of hydrogen peroxide and ascorbic acid on the acetaldehyde formation. Varying amounts of ascorbic acid were added to a solution containing 20 mM ethanol and 1 mM H_2O_2. The samples were incubated for 15 min at 65°C and the acetaldehyde formed was analyzed.

solution, the liver extract gave much less acetaldehyde at pH 5, especially at high ascorbic acid concentrations. The reason for this may be that liver extract contains redox compounds such as glutathione and cysteine which have a strong inhibitory effect on the autoxidation of ascorbic acid.[12] On the other hand, in a strong acid solution (pH < 1) a much greater amount of acetaldehyde was

formed in the liver extract than in the pure ascorbic acid solution. When dehydroascorbic acid was added instead of ascorbic acid to the PCA-extract no acetaldehyde was produced.

Effect of hydrogen peroxide on the reaction

Hydrogen peroxide is generated by the autoxidation of ascorbic acid.[8,13] To investigate the effect of H_2O_2 as a direct oxidizing agent on the reaction, varying amounts of hydrogen peroxide were added to a 20 mM ethanol solution and the sample was incubated for 15 min at 65°C. H_2O_2 concentrations up to 1.0 mM gave only insignificant amounts of acetaldehyde (< 5 nmol/ml). If, on the other hand, 1.0 mM hydrogen peroxide was added to a solution containing ascorbic acid and ethanol, the acetaldehyde formation increased considerably (Fig. 6). This catalytic effect of hydrogen peroxide on the non-enzymatic ethanol oxidation on fresh liver extract is illustrated in Fig. 7.

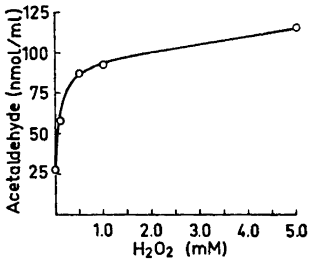

Fig. 7. Effect of hydrogen perioxide on the non-enzymatic ethanol oxidation in rat liver extract (pH < 1). The homogenate concentration was 20 %, and the samples (○) were incubated with 20 mM ethanol for 15 min at 65°C. (●) Control: acetaldehyde formed in extract without added H_2O_2.

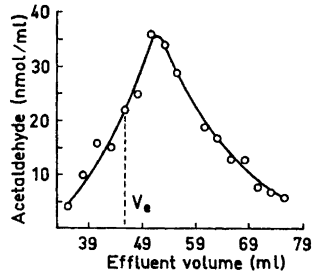

Fig. 8. 2 ml concentrated liver extract (pH 5) was applied on a Sephadex G-25 column and eluted by 0.05 N NaCl. Fractions of 2.5 ml were collected and their activity (capacity for acetaldehyde formation in the presence of ethanol) measured by GLC, after incubation at 65°C for 60 min in the presence of 20 mM ethanol. V_e for the active compound was 46.5 ml.

Ethanol-induced release of "bound" acetaldehyde

In order to determine whether acetaldehyde is liberated from some macromolecules by ethanol the macromolecules in the liver extract were separated by gel filtration. Bovine liver extract was eluted through a Sephadex G-25 column. The effluent volume (V_e) was determined by measuring V_e from the point at which the extract was added to the point at which the activity of the eluted substance was optimal (Fig. 8). There was no activity in the first 16 fractions (no acetaldehyde was formed when ethanol was added to the fractions), but it rapidly increased to maximum at an effluent volume of about 52 – 53 ml. From the data obtained, the distribution coefficient (K_d) of the active compound was calculated to be 0.6. The single maximum found shows

that there was probably only one agent present in the extract capable of oxidizing ethanol to acetaldehyde.

The high K_d-value of the active compound makes it unlikely that the observed acetaldehyde had been released from a macromolecule by ethanol. If riboflavin (Mw 367) is eluted under the same conditions with 0.05 N NaCl, both it and the active compound have the same K_d-value.

The active fractions collected had a strong yellow color. To test whether these pigments have a direct effect on the acetaldehyde production, florisil was added to the fractions and the mixture was shaken until the yellow color was adsorbed on the florisil. The yellow florisil extract had no activity at all, while the colorless liver extract had a high activity. Active, colorless liver extract, analyzed by TLC, showed the presence of ascorbic acid.

DISCUSSION

The results show that ethanol is oxidized to acetaldehyde in the presence of ascorbic acid. This reaction was found to take place also in biological extracts. Ascorbic acid is widely distributed throughout the animal, including the liver.[14] Thus it seems probable that the ascorbic acid present in fresh liver tissue homogenate gave rise to the non-enzymatic acetaldehyde formation in the biological extracts. The results obtained by gel filtration and TLC of liver extract strongly support this hypothesis by showing first that the acetaldehyde is not released from a protein or another macromolecule by ethanol, and then that the active compound contained ascorbic acid.

The heat stability of ascorbic acid in strong acidic solutions is well known.[15] If ascorbic acid is involved in the acetaldehyde formation it would be logical to expect that the active liver extract could be heated without loss of activity. This is, in fact, what happened. It was possible to heat acidic liver extract without any loss of activity. At higher pH (> 3) ascorbic acid loses its heat stability;[12] consistently, the activity of liver extracts at pH > 3 is eliminated by heating.

The fact that the active compound had no absorbancy in the visible area excludes free flavins or other redox pigments, but not ascorbic acid as the actual oxidizing agents.

From the data given in Fig. 2, it was possible to calculate that 1 g fresh liver from a rat could non-enzymatically oxidize 25 nmol of ethanol per min after 15 – 30 min at 65°C. Compared with liver homogenate, blood from the rat gives only insignificant amounts of acetaldehyde (Fig. 2). The low ascorbic acid content in whole blood may be the reasons for this finding.[14]

The maximum pH for acetaldehyde formation in both an ascorbic acid solution (Fig. 4B) and crude liver extract (Fig. 3) are approximately the same. The reason that the pH-maximum is somewhat higher in crude extract may be that ascorbic acid is more stable in it than in a water solution at pH > 6.[11]

The observation that small amounts of hydrogen peroxide were completely inactive as direct oxidizing agents in the absence of ascorbic acid is in agreement with the results obtained by Udenfriend *et al.*[6] and Kersten *et al.*,[7] but contrary to the hypothesis that H_2O_2 itself is the oxidizing agent at physiologi-

cal concentration. In the presence of ascorbic acid, however, the hydrogen peroxide had an obvious effect on the oxidation reaction.[5]

A semiquinone like intermediate between ascorbic acid and dehydroascorbic acid is hypothesized to be the electron acceptor in the ethanol oxidation. The autoxidation of ascorbic acid (I; Scheme 1) to dehydroascorbic acid (VIII) is generally assumed to proceed by a free radical mechanism, and free radicals have also been detected in solutions of ascorbic acid.[16,17] The reaction is catalyzed by Cu^{2+} and Fe^{3+} but also proceeds without a catalyst.[18]

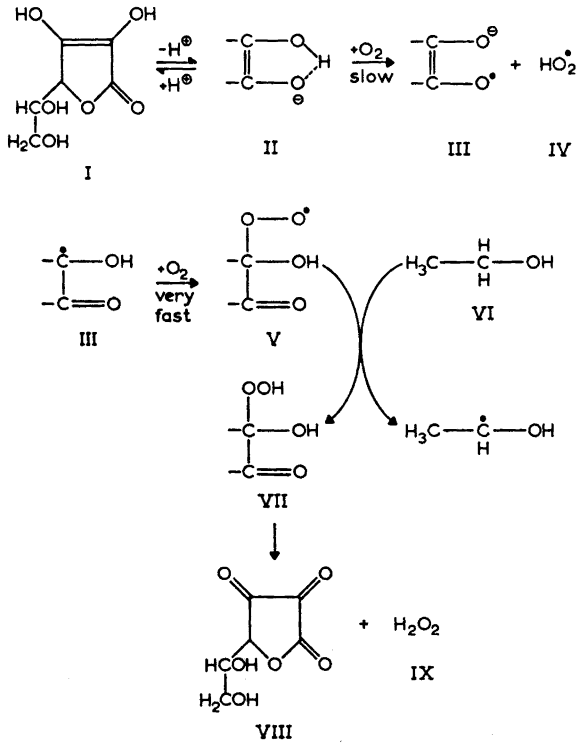

Scheme 1.

An unstable ascorbate-oxygen complex is formed in the presence of molecular oxygen, and the subsequent decomposition of this complex yields a free radical of semiquinone type and a reactive perhydroxyl radical $HO_2^{\cdot}$ (IV). The rate-determining step is the transference of one electron from an ascorbate monoanion (II) to molecular oxygen. This implies that the rate of the reaction is dependent on the pH of the solution (Figs. 3, 4B).

As shown in Scheme 1, the semidehydroascorbate free radical (III) reacts rapidly with molecular oxygen to form a semidehydroascorbate peroxy radical (V)[19] which is able to oxidize ethanol (VI) to acetaldehyde. It is also possible

that the free radical can directly oxidize ethanol to acetaldehyde, and is itself reduced to ascorbic acid.

Khan and Martell [18] have suggested that ascorbic acid at low oxygen concentrations may be directly oxidized by the $HO_2\cdot$ formed. It is possible that, under the same conditions, ethanol can be oxidized by this reactive radical.

The hydrogen peroxide (IX) formed has a catalytic effect on the non-enzymatic acetaldehyde formation (Figs. 6, 7), probably by accelerating the autoxidation of ascorbic acid, or by assisting in the formation of the reactive peroxy radical. In the presence of ferrous and cuprous ions, H_2O_2 decomposes very rapidly, giving $HO_2\cdot$ and a new reactive radical, $OH\cdot$, which is able to oxidize ethanol to acetaldehyde. The existence of such an active semidehydroascorbate radical has been demonstrated by many investigators.[16,20] Schneider and Staudinger [21] have postulated that this radical can be formed by "comproportionation" between ascorbic acid and dehydroascorbic acid.

The oxidation of ethanol into acetaldehyde in the microsomal fraction of liver has been reported by Lieber and De Carli,[22] Lieber *et al.*[23] and Khanna *et al.*[24] The so-called microsomal ethanol oxidizing system (MEOS) which they describe requires NADPH and O_2, and they considered that ADH, the principal ethanol oxidizing enzyme *in vivo*, was not involved in this reaction. A similar ethanol oxidation system was found in adipose tissue from rat.[25]

The activity of the MEOS has been expressed as the acetaldehyde formed per unit of time. Using the method described by Burbridge *et al.*[26] this acetaldehyde concentration has been analyzed by microdiffusion separation and the subsequent spectrophotometric measuring of acetaldehyde semicarbazone formed. Truitt [1] has reported that both the spectrophotometric method of Burbridge *et al.*[26] and the gas chromatographic method developed by Duritz and Truitt [27] produce high levels of non-enzymatically formed acetaldehyde. Thus, it is possible that a part of the acetaldehyde which was thought to have been produced by the MEOS in fact was formed by the ascorbic acid system.

Non-enzymatic ethanol oxidation also occurs at physiological temperature (37°C), but its physiological role has not yet been determined.

Acknowledgement. This investigation was carried out under the guidance of Dr. O. Forsander. I am deeply grateful for the invaluable help which he gave me during all the stages of the work. I wish to thank Dr. D. Sinclair for checking the language and for his helpful criticism of my manuscript.

This work was supported by grants from the *Svenska Kulturfonden*, Helsinki.

REFERENCES

1. Truitt, E. B. *Quart. J. Studies Alc.* **31** (1970) 1.
2. Barker, S. B. *J. Biol. Chem.* **137** (1941) 783.
3. Stotz, E. A. *J. Biol. Chem.* **148** (1943) 585.
4. MacLeod, L. D. *Quart. J. Studies Alc.* **11** (1950) 385.
5. von Euler, H. and Hasselquist, H. *Z. physiol. Chem.* **303** (1956) 176.
6. Udenfriend, S., Clark, C. T., Axelrod, J. and Brodie, B. B. *J. Biol. Chem.* **208** (1954) 731.
7. Kersten, H., Kersten, W. and Staudinger, H. *Biochem. Z.* **328** (1956) 24.
8. Kauffman, H. J. *J. Am. Chem. Soc.* **73** (1951) 4311.
9. Gelotte, B. *J. Chromatog.* **3** (1960) 330.
10. Strohecker, R., Heimann, W. and Matt, F. *Z. Anal. Chem.* **145** (1956) 401.

11. Borsook, H., Davenport, H. W., Jeffreys, C. E. P. and Warner, R. C. *J. Biol. Chem.* **117** (1937) 237.
12. Spanyár, P. and Kevei, E. Z. *Lebensm. Untersuch. Forsch.* **120** (1963) 1.
13. Spanyár, P., Kevei, E. and Blazovich, M. Z. *Lebensm. Untersuch. Forsch.* **126** (1964) 10.
14. Nathani, M. G. and Nath, M. C. *Metab. Clin. Exptl.* **21** (1972) 137.
15. von Euler, H. and Hasselquist, H. *Arkiv Kemi* **4** (1951) 169.
16. Yamazaki, I. *J. Biol. Chem.* **237** (1962) 224.
17. Lagercrantz, C. *Acta Chem. Scand.* **18** (1964) 562.
18. Khan, M. M. T. and Martell, A. E. *J. Am. Chem. Soc.* **89** (1967) 4176.
19. Harper, K. A., Morton, A. D. and Rolfe, E. J. *J. Food Technol.* **4** (1969) 255.
20. von Foerster, G., Weis, W. and Staudinger, H. Z. *physiol. Chem.* **344** (1966) 217.
21. Schneider, W. and Staudinger, H. *Biochem. Biophys. Acta* **96** (1965) 157.
22. Lieber, C. S. and DeCarli, L. M. *J. Biol. Chem.* **245** (1970) 2505.
23. Lieber, C. S., Rubin, E. and DeCarli, L. M. *Biochem. Biophys. Res. Commun.* **40** (1970) 858.
24. Khanna, J. M., Kalant, H. and Lin, G. *Biochem. Pharmacol.* **19** (1970) 2493.
25. Scheig, R. *Biochim. Biophys. Acta* **248** (1971) 48.
26. Burbridge, T. N., Hine, C. N. and Schick, A. F. *J. Lab. Clin. Med.* **35** (1950) 985.
27. Duritz, G. and Truitt, E. B. *Quart. J. Studies Alc.* **25** (1964) 498.

Received August 25, 1972.

ACTA CHEMICA SCANDINAVICA 27 (1973) 551–555

Structures of Some Aliphatic Monoterpenoids Isolated from the Essential Oil of *Ledum palustre* L.

MAX VON SCHANTZ, KARL-GUSTAV WIDÉN and RAIMO HILTUNEN

Department of Pharmacognosy, University of Helsinki, Helsinki, Finland

The elucidation of the structures of 2,6-dimethylene-7-octen-3-one, 2-methylene-6-methyl-5,7-octadien-3-ol, and *trans*-2-methyl-6-methylene-3,7-octadien-2-ol, all three isolated from the essential oil of *Ledum palustre* L., is described.

Two of us [1] reported recently on the composition of the essential oil of *Ledum palustre* L. In this investigation we elucidate and revise the structures of some of the compounds dealt with in the earlier study.

Spectral data for compound 4 (numbering as in the paper of v. Schantz and Hiltunen [1]) are presented in Fig. 1. According to the parent peak in the mass spectrum of the compound, its molecular weight is 150. On carbon skeleton chromatography [2] in combination with mass spectrometry, three different hydrocarbons were produced, namely 2,6-dimethyloctane (90 %), 2,6-dimethylheptane, and 2-methyloctane (the last two together amounting to about 10 %). It is thus very likely that compound *4* has the normal aliphatic head-to-tail monoterpene skeleton [2,6-dimethyloctane or hexahydromyrcene (Fig. 2)]. As its molecular weight is 150, the molecule must have the formula $C_{10}H_{14}O$ and contain four double bonds. The IR spectrum has a strong absorption based at 1679 cm^{-1} which reveals a carbonyl group and hence one double bond. The NMR spectrum contains only one signal of three methyl protons (δ 1.85 ppm). The other three double bonds must hence be vinylidene or vinyl ones. The corresponding six methylene protons give signals at δ 4.99 (4H) and 5.82 ppm (2H) in the NMR spectrum, while the methine proton absorption is centered at δ 6.35 ppm as two pairs of doublets. The position of the keto group is then to be settled. According to the IR spectrum, the compound is α,β-unsaturated (absorption at 1679 cm^{-1}). The UV spectrum corresponds to a monosubstituted butadiene or a ketone with the carbonyl group conjugated with one olefinic double bond [λ_{max} (ethanol) 224 nm]. So C-3 seems a very likely position for the carbonyl group. Hence, the structure of compound *4* is 2,6-dimethylene-7-octen-3-one (Fig. 2).

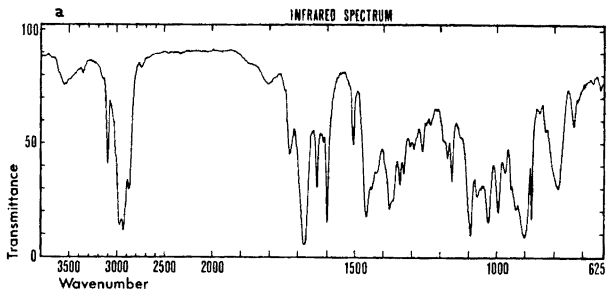

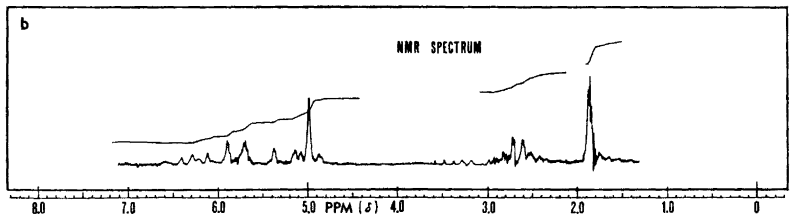

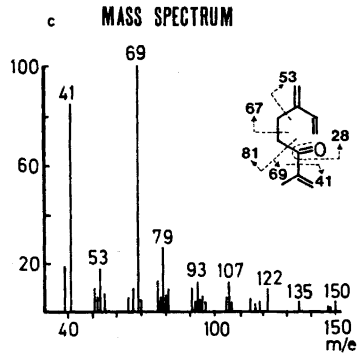

Fig. 1. Spectral data for compound *4*. Solvent residue (CCl_4) absorbs between 740 and 815 cm^{-1} in the IR spectrum.

2,6-DIMETHYL-OCTANE

2,6-DIMETHYLENE-7-OCTEN-3-ONE

COMPOUND 4

trans-2-METHYL-6-METHYLENE-3,7-OCTADIEN-2-OL

COMPOUND 5

2-METHYLENE-6-METHYL-5,7-OCTADIEN-3-OL

COMPOUND 10

Fig. 2.

Further support for this structure is found in the fragmentation pattern of the mass spectrum (Fig. 1). The fragment with $m/e = 79$ probably corresponds to a hexatrienyl ion formed by fission of the bond between C-3 and C-4 and subsequent elimination of hydrogen (*cf.* Ohloff *et al.*[3]). Also the IR spectrum speaks in favour of the structure proposed for compound *4*. The absorption based at 991 cm^{-1} can be attributed to the vinyl double bond, which together with the vinylidene double bonds absorbs also at 3089 and 897 cm^{-1} (broad absorptions). The last mentioned double bonds give absorption bands at 1649 and 1800 cm^{-1}. Finally, the strong band at 1597 cm^{-1} can be attributed to conjugated double bonds.

Spectral data for compound *10* are given in Fig. 3. According to the mass spectrum, the molecular weight is 152. On carbon skeleton chromatography, about 95 % hexahydromyrcene was produced, which fact suggests the same skeleton. The formula $C_{10}H_{16}O$, which implies three double bonds, evolves for compound 10. IR bands at 3400 and 1054 cm^{-1} indicate an alchohol. The NMR spectrum contains a triplet centered at δ 4.03 ppm (1H) which is attributable to a proton attached to the same carbon as the oxygen. The alcohol must hence be a secondary one. On oxidation with chromic acid, a ketone (mol. wt. 150) was obtained whose mass spectrum was practically identical with that of compound 4. As the keto group directs the fragmentation very much, the position of the oxygen atom can now be fixed at C-3 as in compound *4*, and one double bond can tentatively be placed in the isopropyl group, while the other two must be on the other side of C-3. The UV absorption [λ_{max} (ethanol) 224 nm] corresponds to that of a butadiene. The existence of conjugated double bonds is confirmed also by the strong IR absorption band at 1596 cm^{-1}. A band attributable to a vinyl double bond is found in the IR spectrum at 990 cm^{-1}. The NMR spectrum reveals six methyl protons and hence two methyl groups which are attached to double-bonded carbon atoms (signals at δ 1.70 and 1.75 ppm). Taking into consideration the position of the oxygen atom and the spectral data for the double bonds, we must place the two conjugated double bonds in positions five and seven. Probably the trisubstituted double bond absorbs at 834 cm^{-1} in the IR spectrum. One of the two methyl groups revealed by the NMR information has thus been located. The third double bond and the other methyl group must then both be in the isopropyl group. The aliphatic vinylidene double bond gives infrared absorption bands at 1654 and 1800 and, together with the vinyl double bond, also at 3100 and 900 cm^{-1} (broad bands). The structure of compound *10* is then 2-methylene-6-methyl-5,7-octadien-3-ol (Fig. 2). Additional confirmation of this structure is provided by its mass spectrometric fragmentation (Fig. 3). The question whether compound *10* is the *cis* or *trans* isomer in respect of the trisubstituted double bond, we have not been able to decide.

In a similar way as the structures of the above two compounds, the structure *trans*-2-methyl-6-methylene-3,7-octadiene-2-ol could be deduced for compound *5* by analysis of its spectra. However, this compound has been isolated earlier from *Pinus ponderosa* Laws. by Silverstein *et al.*,[4] who also elucidated its structure mainly by spectral methods. As we came to the same conclusion about the structure, we refer to the paper of these authors for spectral details and their interpretation.

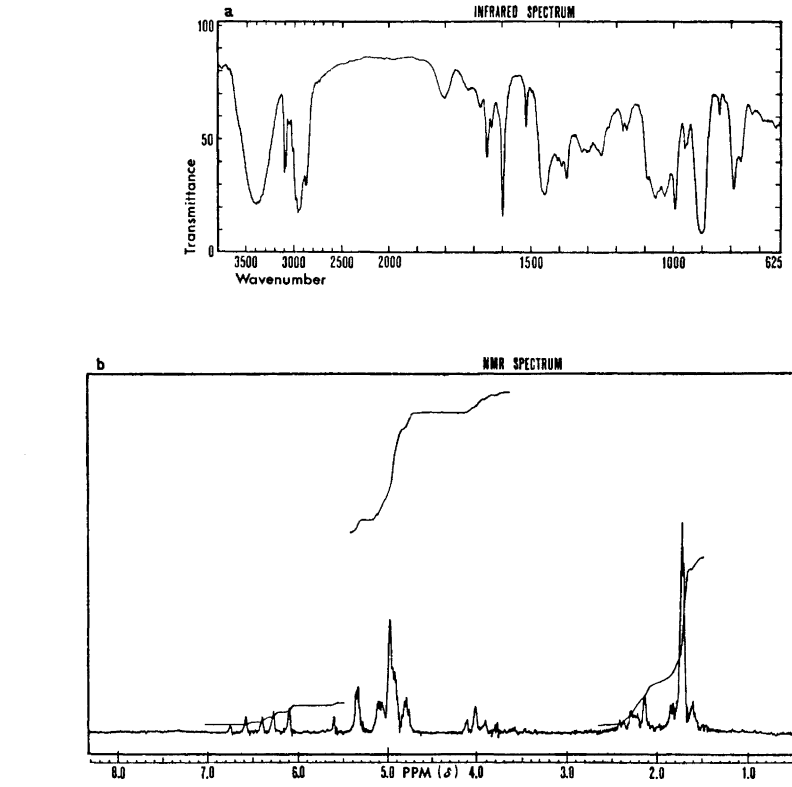

Fig. 3. Spectral data for compound *10*. Solvent residue (CCl_4) absorbs between 740 and 815 cm^{-1} in the IR spectrum.

All three compounds discussed above differ from other known naturally occurring acyclic, oxygenated monoterpenoids in having three olefinic double bonds instead of two.

EXPERIMENTAL

Details about the isolation of the compounds have been reported by v. Schantz and Hiltunen.[1] About 10 mg of each compound was available. They were all greenish liquids.

IR spectra were run on a Pye Unicam SP 1000 instrument (sample as liquid film) and NMR spectra on a Varian A 60 spectrometer operating at 60 Mc/s (with carbon tetrachloride as solvent and tetramethylsilane as internal standard). Mass spectra were recorded on a Perkin-Elmer 270 GC-MS instrument (ion source 190°C, manifold 200°C, electron energy 70 eV, ion source and analyzer pressures about 10^{-6} and 10^{-7} torr, respectively). The UV spectrophotometer used was a Beckman DB-G instrument.

Carbon skeleton chromatography was carried out on-line with the Perkin Elmer 270 GC-MS instrument using 3 % platinum on Chromosorb W as catalyst at 200°C, a 50 m, 0.25 mm i.d., OV-17 WCOT column, and hydrogen as carrier gas (Widén [5]). The reaction products were identified with the aid of the mass spectra.

Oxidation of compound 10 with chromic acid was carried out in the following way. A solution of the compound (10 mg) in ether (2 ml) was stirred with a solution of sodium dichromate dihydrate in sulphuric acid (20 mg) and water (0.3 ml) at room temperature overnight. After addition of water, the product was taken up in ether, washed with 10% sodium bicarbonate solution and dried with sodium sulphate. After evaporation of the solvent, the product was studied by GC-MS and found to be a ketone (amounting to about 90 % of the reaction mixture) with a mass spectrum practically identical with that of compound *4*.

Acknowledgements. We are grateful to Mrs. Eila M. Bernström, M. Sc., for the recording of NMR spectra.

REFERENCES

1. von Schantz, M. and Hiltunen, R. *Sci. Pharm.* **39** (1971) 137.
2. Beroza, M. and Sarmiento, R. *Anal. Chem.* **35** (1963) 1353.
3. Ohloff, G., Seibl, J. and Kovats, E. *Liebigs Ann. Chem.* **675** (1964) 83.
4. Silverstein, R. M., Rodin, J. O., Wood, D. L. and Browne, L. E. *Tetrahedron* **22** (1966) 1929.
5. Widén, K.-G. *Farm. Aikak.* **82** (1973). *In press.*

Received July 11, 1972.

ACTA CHEMICA SCANDINAVICA 27 (1973) 556–560

Synthesis of Methyl 3-*O*-(3,6-Dideoxy-α-D-*ribo*-hexopyranosyl)-α-D-mannopyranoside

GUNNEL ALFREDSSON and PER J. GAREGG

Institutionen för organisk kemi, Stockholms universitet, S-104 05 Stockholm 50, Sweden

The synthesis of methyl 3-*O*-(3,6-dideoxy-α-D-*ribo*-hexopyranosyl)-α-D-mannopyranoside, required for immunological studies, is described. The key step in the synthesis consists in the boron trifluoride catalyzed reaction of 2,3,4,6-tetra-*O*-benzoyl-D-*arabino*-hex-1-enopyranose (I) with methyl 2-*O*-benzyl-4,6-*O*-benzylidene-α-D-mannopyranoside (II).

The repeating unit of the O-specific side-chains of the *Salmonella* serogroup A cell wall lipopolysaccharide may be formulated as follows.[1] α-Par*p*

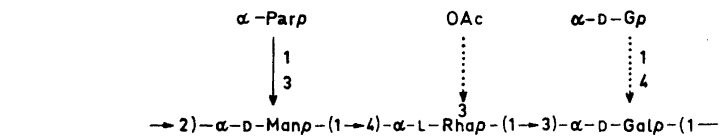

denotes a 3,6-dideoxy-α-D-*ribo*-hexopyranosyl (α-paratosyl) unit. The serological O-factor 2 is thought to be associated with the α-paratosyl unit linked to the 3-position of the α-D-mannose residue. It is of immunological interest to have available di- and oligosaccharides corresponding to the various postulated O-factors. Syntheses of methyl 3-*O*-(3,6-dideoxy-α-D-*arabino*-hexopyranosyl)-α-D- and -β-D-mannopyranosides corresponding to the *Salmonella* O-factors 9 and 46 have previously been communicated from this laboratory.[2,3] In these syntheses, advantage was taken of the orthoester glycosylation method,[4] which produces the required 1,2-*trans* geometry at the 1- and 2-positions in the 3,6-dideoxyhexose moiety. In the corresponding D-*ribo* isomer (paratose), however, this relationship is 1,2-*cis*. Two recent methods of potential value for the synthesis of α-D-glycosides and disaccharides with *cis*-geometry at positions 1 and 2 have been described. One of these, devised by Lemieux and co-workers, uses nitrosyl chloride adducts of glycals.[5] In the other, devised by Ferrier and co-workers, an acylated 2-hydroxyglycal is treated with an alcohol, which may be a suitably protected monosaccharide unit, in benzene

solution, with boron trifluoride as catalyst. A displacement reaction takes place in which the double bond migrates to the 2,3-positions and the acyloxy group at C-3 is expelled.

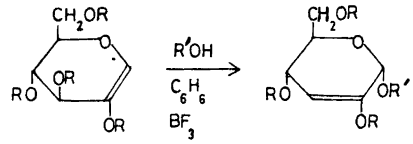

R = $COCH_3$ or COC_6H_5

In 3,6-dideoxyglycoside synthesis, the latter method has the attractive feature of glycosidation occurring with the simultaneous introduction of the 3-deoxy function. This and the high yields generally obtained in the reaction offset the fact that the glycosidation is not stereospecific.

The present paper describes the synthesis, by the Ferrier method [6] of methyl 3-*O*-(3,6-dideoxy-α-D-*ribo*-hexopyranosyl)-α-D-mannopyranoside (VII), required for immunological studies which will be reported elsewhere.

2,3,4,6-Tetra-*O*-benzoyl-1-deoxy-D-*arabino*-hex-1-enopyranose (I) was allowed to react with methyl 2-*O*-benzyl-4,6-*O*-benzylidene-α-D-mannopyranoside (II) in benzene containing a catalytic amount of boron trifluoride. The yield of syrupy III, purified by silica gel column chromatography, was 51 %. A slower-moving fraction which probably contained the impure β-anomer of III was also obtained. The olefinic disaccharide III was dissolved in the

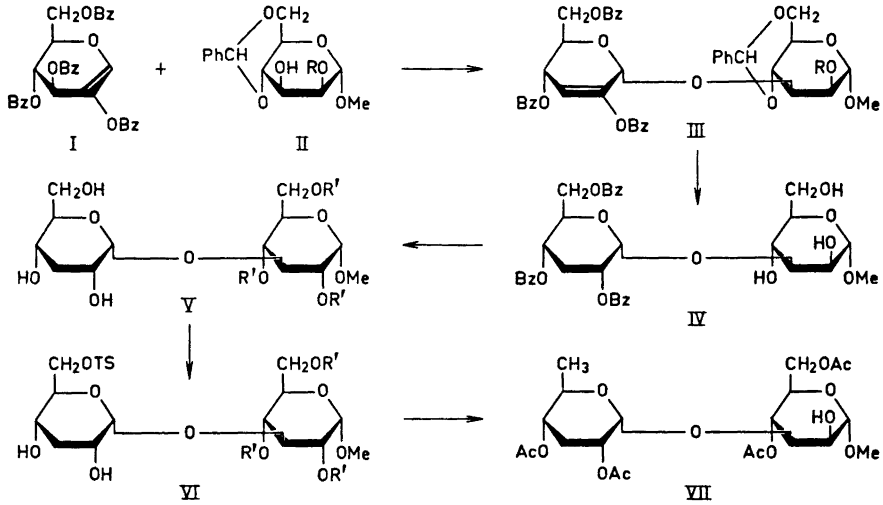

Bz = C_6H_5CO- R = $C_6H_5CH_2$- R' = $CH_3\underset{|}{C}HOEt$

minimum amount of tetrahydrofuran, the solution was diluted with ethanol and hydrogenated with 10 % palladium on charcoal at atmosphere pressure. The choice of solvent was important for the success of the reaction, *i.e.* simultaneous removal of benzyl and benzylidene as well as hydrogenation of the pyranosidic double bond. Chromatographic purification of the product afforded pure, syrupy IV in a 74 % yield. The epimeric isomer of IV containing a 3-deoxy-D-*arabino*-hexosyl unit instead of the 3-deoxy-D-*ribo*-hexosyl unit of IV was present in a minor fraction isolated by chromatography. The 3-deoxy-hexosyl unit of IV was converted into the corresponding 3,6-dideoxy-hexosyl unit by the following route: Acetalization of the three free hydroxyl groups in the mannosyl unit of IV by the acid-catalyzed reaction of IV with ethyl vinyl ether, followed by debenzoylation afforded syrupy V in a 48 % yield. Monotosylation of V at low temperature afforded a 39 % yield of VI in addition to unreacted starting material. Reduction of VI with lithium aluminium hydride introduced the required 6-deoxy group. Careful hydrolysis of the product with 50 % aqueous acetic acid at room temperature removed the 1'-etoxyethyl residues from the disaccharide. Acetylation of the resulting disaccharide and chromatographic purification of the final product afforded pure VII in a yield of 68 % from VI. The product VII gave a correct elemental analysis. The optical rotation is in agreement with the expected anomeric configuration. Further confirmation of the structure of VII was obtained as follows. Deacetylation yielded methyl 3-*O*-(3,6-dideoxy-α-D-*ribo*-hexopyranosyl)-α-D-mannopyranoside. Mild acid hydrolysis of an aliquot of this material, followed by borohydride reduction and acetylation gave methyl 2,3,4,6-tetra-*O*-acetyl-α-D-mannopyranoside and 1,2,4,5-tetra-*O*-acetyl-3,6-dideoxy-α-D-*ribo*-hexitol in the expected proportion. Another aliquot was fully methylated to yield VIII which was examined by GLC, in which a single component was observed, and by MS. The mass spectrum was that expected for the postulated structure. The origin of some of the pertinent fragment is indicated in VIII.

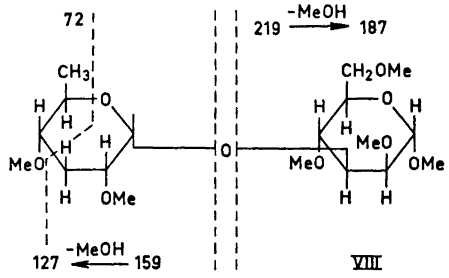

The various fragments obtained and their relative intensities are given in the experimental part. The mass spectrum is consistent with the structure VIII.[7,8] An identical spectrum, apart from minor differences in relative peak intensities, was observed for the corresponding pentamethyl ether of the previously synthesized methyl 3-*O*-(3,6-dideoxy-α-D-*arabino*-hexopyranosyl-β-D-mannopyranoside.

EXPERIMENTAL

General methods. Concentrations were performed at reduced pressure. Optical rotations were determined at room temperature (20–22°) using a Perkin-Elmer 141 polarimeter. NMR spectra (in deuteriochloroform) were recorded with a Varian A-60 A spectrometer with a V 6058 A unit for decoupling experiments. Tetramethylsilane was used as internal reference and chemical shifts (δ) are given in ppm downfield from this reference. Pertinent parts of the various NMR spectra are given in the appropriate sections below, the remainder of the spectra were invariably in accordance with the presumed structures. GLC-MS was run on a Perkin-Elmer 270 instrument at a manifold temperature of 200°, an ionization potential of 70 eV, ionization current of 80 μA and a temperature at the ion source chamber of 80°. TLC was performed on silica gel F_{254} (Merck). Sulphuric acid was used as spray reagent. GLC analyses were performed on a Perkin-Elmer F 11 instrument fitted with glass columns. The carrier gas was nitrogen and the flow rate 30 ml/min. The column packing was 3 % ECNSS-M on Gas Chrom Q unless otherwise stated.

Methyl 3-O-(2,4,6-tri-O-benzoyl-3-deoxy-α-D-glycero-hex-2-enopyranosyl)-2-O-benzyl-4,6-O-benzylidene-α-D-mannopyranoside (III). 2,3,4,6-Tetra-*O*-benzoyl-D-*arabino*-hex-1-enopyranose, I,[9] (1.50 g) and methyl 2-*O*-benzyl-4,6-*O*-benzylidene-α-D-mannopyranoside, II[2], (0.98 g) were dissolved in dry benzene (25 ml). Boron trifluoride etherate (45 %, 1.5 ml) was added and the solution was allowed to stand at room temperature for 25 min. The reaction mixture was neutralized with sodium carbonate, poured into water and the aqueous solution extracted with chloroform. The combined chloroform phases were dried over sodium sulphate, filtered and concentrated. The resulting syrupy product was purified by silica gel column chromatography (solvent, toluene–ethyl acetate 4:1). The yield of syrupy III was 1.11 g. The product III which was chromatographically pure was used directly in the next step. NMR: δ 5.79 (1 H), doublet, $J = 2$ Hz, H-3; δ 5.29 (1 H), singlet, benzylidene methine, δ 4.92 (1 H), singlet, H-1; δ 4.42 (2 H), singlet, benzyl methylene; δ 2.82 (3 H), singlet, methoxyl proton. A slower fraction containing the aglycone II together with another disaccharide component, possibly the β-anomer of III, was also obtained.

Methyl 3-O-(2,4,6-tri-O-benzoyl-3-deoxy-α-D-ribo-hexopyranosyl)-α-D-mannopyranoside (IV). The above product III (3.18 g) was dissolved in the minimum quantity of tetrahydrofuran, diluted with ethanol and hydrogenated with 10 % palladium on charcoal (1.0 g) at atmospheric pressure. The theoretical amount of hydrogen was absorbed after 36 h. The product was purified by TLC (solvent, ethyl acetate) to yield a chromatographically pure syrup (1.71 g). A minor fraction was obtained which upon debenzoylation gave a disaccharide glycoside which on sugar analysis (see below) was shown to contain mannose and 3-deoxy-D-*arabino*-hexopyranose. NMR of IV: δ 7.2–8.2 (15 H) aromatic; no olefinic, methine or methylene protons present (*cf.* III above); δ 3.26 (3 H), singlet, methoxyl. NMR on debenzoylated (see below) and per-trimethylsilylated IV: Two anomeric signals were observed, δ 5.11, $J = 3.5$ Hz; δ 4.57, $J = 2$ Hz, showing α-configuration for the 3-deoxy-D-*ribo*-hexosyl moiety. An aliquot of IV was debenzoylated as described below, hydrolyzed with 0.12 M aqueous sulphuric acid, neutralized with barium carbonate, filtered, concentrated and converted into the corresponding alditol acetate mixture. GLC[10] showed the presence of two components in a ratio 1:1 with retention times indistinguishable from 1,2,4,5,6-penta-*O*-acetyl-3-deoxy-D-glucitol (which has a higher retention time than the corresponding D-mannitol derivative) and 1,2,3,4,5,6-hexa-*O*-acetyl-D-mannitol.

Methyl 3-O-(3-deoxy-6-O-p-tolylsulphonyl-α-D-ribo-hexopyranosyl)-2,4,6-tri-O-(1'-ethoxyethyl)-α-D-mannopyranoside (VI). The above product IV (1.71 g) dissolved in dichloromethane (40 ml) containing 0.4 % hydrogen chloride, was treated with ethyl vinyl ether (4.0 ml) for 96 h, neutralized with sodium carbonate, filtered and concentrated. TLC (solvent, ethyl ether–light petroleum (40–60°) 3:1) showed a major component contaminated by small amounts of faster- and slower-moving materials. The major product was obtained in a chromatographically pure state as a syrup (1.19 g) by TLC. This, without further characterization, was used directly in the next step. The syrup (510 mg) in methanol (50 ml) was treated with barium oxide (100 mg) at reflux temperature for 1 h. The mixture was cooled, filtered and concentrated to yield a syrup which after purification by TLC (solvent, ethyl ether–acetone 1:1) yielded chromatographically

pure material (301 mg). This was dissolved in pyridine (20 ml). *p*-Toluenesulphonyl chloride (134 mg) was added at −30°. After 24 h at this temperature further *p*-toluenesulphonyl chloride (134 mg) was added at the same temperature. After a further 48 h at −30° the solution was poured into ice-water. The mixture was extracted with chloroform. The combined chloroform phases were dried over magnesium sulphate, filtered and concentrated to yield an impure syrup (275 mg) from which the major component (145 mg) was isolated by TLC (solvent, ethyl ether−acetone 1:1). NMR: δ 7.97 (2 H), doublet $J=8$ Hz, aromatic, δ 7.50 (2 H), doublet, $J=8$ Hz, aromatic, $J=8$ Hz; δ 3.45 (3 H), singlet, methoxyl; δ 2.50 (3 H), singlet, toluene methyl protons.

*Methyl 3-O-(3,6-dideoxy-α-D-*ribo*-hexopyranosyl)-α-D-mannopyranoside pentaacetate* (VII). The above monotosylate VI (145 mg) was dissolved in tetrahydrofuran (10 ml). Lithium aluminium hydride (excess) was added and the mixture refluxed for 3 h. The reaction mixture was neutralized with aqueous phosphoric acid, filtered and concentrated to a syrup (140 mg). The latter was hydrolyzed in 50 % aqueous acetic acid at room temperature for 15 min and concentrated to a syrup which was acetylated with acetic anhydride (1 ml) in pyridine (1 ml) at room temperature overnight. The impure product VII was poured onto ice-water and the mixture extracted with chloroform. The combined chloroform phases were dried over magnesium sulphate and concentrated to yield a syrup (119 mg) which was purified by TLC (toluene−ethyl acetate 3:2) to yield chromatographically pure VII (80 mg), $[\alpha]_D$ +85°. (Found: C 51.7; H 6.53. $C_{23}H_{34}O_{14}$ requires: C 51.7; H 6.41.) An aliquot of VII was deacetylated with 1.67 % ammoniacal methanol. Part of the deacetylated VII was subjected to mild acid hydrolysis (0.125 M aqueous sulphuric acid, for 1 h at 100°), the hydrolysate was neutralized with barium carbonate and worked up. The mixture was reduced with sodium borohydride and per-acetylated. Examination by GLC-MS [11,12] revealed the presence of methyl α-D-mannoside tetraacetate, indistinguishable from authentic material and also 1,2,4,5-tetra-*O*-acetyl-3,6-dideoxy-α-D-*ribo*-hexitol with a higher retention time than 1,2,4,5-tetra-*O*-acetyl-3,6-dideoxy-α-D-*arabino*-hexitol, but with the same mass spectrum, apart from minor differences in peak intensities. Another part of the deacetylated VII was methylated [13] to yield the methyl 3-*O*-(3,6-dideoxy-α-D-*ribo*-hexopyranosyl)-α-D-mannopyranoside pentamethyl ether VIII which was pure by GLC on an XE-60 (3 % on Gas chrom Q) column. The MS showed, *inter alia*, the following peaks (relative intensities in brackets): 45 (16), 71 (18), 72 (100), 73 (9), 85 (12), 88 (5), 95 (5), 99 (8), 101 (12), 127 (12), 145 (24), 159 (17), 219 (5), 233 (9), 265 (8).

Acknowledgements. The authors are indebted to Professor Bengt Lindberg for his interest, to Dr. Jörgen Lönngren for valuable discussion and to *Statens Naturvetenskapliga Forskningsråd* for financial support.

REFERENCES

1. Hellerqvist, C. G., Lindberg, B., Samuelsson, K. and Lindberg, A. A. *Acta Chem. Scand.* **25** (1971) 955.
2. Borén, H., Garegg, P. J. and Wallin, N. H. *Acta Chem. Scand.* **26** (1972) 1082.
3. Garegg, P. J. and Wallin, N. H. *Acta Chem. Scand.* **26** (1972) 3892.
4. Kochetkov, N. K., Khorlin, A. J. and Bochkov, A. F. *Tetrahedron* **23** (1967) 693.
5. Lemieux, R. U., Suemitsu, R. and Gunner, S. W. *Can. J. Chem.* **46** (1968) 1040.
6. Ferrier, R. J., Prasad, N. and Sankey, G. H. *J. Chem. Soc.* **C 1969** 587.
7. Kochetkov, N. K. and Chizhov, O. S. *Advan. Carbohydrate Chem.* **21** (1966) 39.
8. Johnson, G. S., Ruliffson, W. S. and Cooks, R. G. *Chem. Commun.* **1970** 587.
9. Ferrier, R. J. and Sankey, G. H. *J. Chem. Soc.* **C 1966** 2339.
10. Sawardeker, J. S., Sloneker, J. H. and Jeanes, A. *Anal. Chem.* **37** (1965) 1602.
11. Björndal, H., Lindberg, B. and Svensson, S. *Acta Chem. Scand.* **21** (1967) 1801.
12. Björndal, H., Lindberg, B. and Svensson, S. *Carbohyd. Res.* **5** (1967) 433.
13. Hakomori, S. *J. Biochem. (Tokyo)* **55** (1964) 205.

Received August 22, 1972.

ACTA CHEMICA SCANDINAVICA 27 (1973) 561–572

Multiple Forms of a Cholinesterase from Body Muscle of Plaice (*Pleuronectes platessa*) and Possible Role of Sialic Acid in Cholinesterase Reaction Specificity

U. BRODBECK,[a] R. GENTINETTA[a] and S. J. LUNDIN[b]

[a] *Medizinisch-chemisches Institut, University of Bern, 3009 Bern 9, Switzerland.* [b] *Research Institute of National Defence, Dept. 1, S-172 04 Sundbyberg 4, Sweden*

Solubilized and partially purified cholinesterase from the body muscle of plaice (*Pleuronectes platessa*) exists as a mixture of multiple forms that could be separated by isoelectric focusing into 2 – 3 species with isoelectric points of pH 5.3, 6.9, and 7.5. These species did not differ, however, with respect to their catalytic properties when assayed with acetyl-, butyryl-, and benzoylcholine as substrates. Upon incubation of the enzyme with neuraminidase a new form with an isoelectric point of pH 8.0 was obtained. The catalytic properties of this desialylated enzyme was the same as that of the untreated one. When the new species was reincubated with neuraminidase an acetylcholinesterase with an isoelectric point of pH about 10 was obtained that had lost the ability to hydrolyse butyryl- and benzoylcholine. These data suggest that removing one or more sialic acids gives raise to an enzyme form specific for acetylcholine only.

As shown previously [1] a butyrylcholine splitting cholinesterase * was found in body muscle of plaice (*Pleuronectes platessa*) and a method of purifying the enzyme [2] has been described and also some of the enzyme properties.[3] The enzyme shows some characteristics typical for an acetylcholinesterase and some others typical for a butyrylcholinesterase. An acetylcholinesterase splits acetylcholine faster than propionyl- and butyrylcholine, the latter being hydrolyzed very slowly or not at all. A butyrylcholinesterase splits butyrylcholine faster than propionylcholine and acetylcholine. It is more sensitive toward certain inhibitors of the organophosphorus type; butyrylcholinesterases are inactivated at a much lower level of inhibitor than acetylcholinesterases. The two enzymes differ also in other respects. Acetylcholinesterase displays

* Enzymes: Acetylcholinesterase (EC 3.1.1.7), butyrylcholinesterase (EC 3.1.1.8), benzoylcholinesterase (EC 3.1.1.9). Acylcholine acylhydrolase (EC 3.1.1.8) is not called cholinesterase as recommended by IUPAC but butyrylcholinesterase in order to facilitate the representation. The cholinesterase investigated is called plaice cholinesterase. Neuraminidase (EC 3.2.1.18).

the phenomenon of substrate inhibition with the cholinesters split. This is not the case with butyrylcholinesterase.

For plaice cholinesterase the turnover number is highest for acetylcholine; thus this enzyme resembles an acetylcholinesterase.[3] Other substrates such as propionyl-, butyryl-, valeryl-, and benzoylcholine are hydrolyzed at a rate much higher than expected for an acetylcholinesterase. With these substrates the enzyme from plaice body muscle resembles more a butyrylcholinesterase. With respect to inhibition by organophosphorus compounds plaice cholinesterase differs from both acetylcholine- and butyrylcholinesterase showing even greater sensitivity towards this type of inhibitor than the other cholinesterases.[3] In addition, at high substrate levels an abnormal kinetic behaviour was observed [4] giving raise to the phenomenon of "bumpy curves" described by Teipel and Koshland [5] for a number of enzymes other than acetylcholinesterase.

Since such differences in catalytic properties could arise from a mixture of kinetically distinguishable multiple forms of an enzyme [6] plaice cholinesterase was subjected to isoelectric focusing on analytical and preparative scales. By these methods possible heterogeneities would be detected and it would be possible to isolate the forms obtained on a preparative scale. The present investigation describes the resolution of plaice cholinesterase into several species with different isoelectric points. It gives a characterization of the obtained forms with respect to their substrate specificity and their sensitivity towards diisopropylfluorophosphate. Evidence is presented that upon incubation of the enzyme with neuraminidase the isoelectric points are shifted towards higher pH values. A preliminary account of this work has been presented.[7]

MATERIALS AND METHODS

Enzymes. Lyophilized plaice cholinesterase, purified to a specific activity of 8 IU/mg of protein was obtained as described earlier.[2] The enzyme (10 mg of lyophilized powder) was dissolved in 5 ml of 5 mM Na-phosphate buffer, pH 7.0 and centrifuged at 4°C for 10 min at 2500 *g*. The clear supernatant containing 90 % or more of the total plaice cholinesterase activity was routinely used. Depending on the experiments the enzyme was stored in solution at 4°C or kept frozen at −10°C. Neuraminidase, type VI purified from *Cl. perfringens* was purchased from Sigma Chem. Comp., St. Louis, Mo., USA.

Chemicals. Acetylthiocholine iodide, butyrylthiocholine iodide, diisopropylfluorophosphate, and 5,5′-dithiobis-2-nitrobenzoic acid were obtained from Fluka AG, Buchs, Switzerland. Benzoylcholine chloride was from F. Hoffmann-La Roche AG, Basel, Switzerland, and carrier ampholine (pH 3 − 10) was purchased from LKB, Stockholm, Sweden.

All other chemicals employed were standard commercial products. Deionized water was used for the preparative work and double distilled water for the analytical procedures.

Enzyme assays. Acetylcholinesterase activity was determined at 30°C either by following the production of thiocholine (assay 1) according to the method of Ellman *et al.*[8] or by measuring the amount of benzoate produced [9] (assay 2). Enzyme activity was expressed in international units (IU = μmol of product produced per minute).

Assay 1. In a total volume of 3.0 ml the standard assay mixture contained 0.1 M Na-phosphate, pH 7.4, 0.125 mM 5,5′-dithiobis-2-nitrobenzoic acid and 1 mM acetylthiocholine or butyrylthiocholine. The reaction was started by adding varying amounts of plaice cholinesterase and was followed spectrophotometrically by measuring the increase in absorbance at 412 nm (on a Beckman DB-G Spectrophotometer equipped with a W+W Recorder 3002).

Assay 2. The incubation mixture contained the same components described in assay 1 except that 80 μM benzoylcholine was used instead of acetylthiocholine. The reaction was followed spectrophotometrically by measuring the decrease in absorbance at 240 nm.

Treatment of plaice cholinesterase with neuraminidase. Sialic acid residues were removed from plaice cholinesterase essentially according to the procedure of Carlsen and Svensmark.[10] Cholinesterase (20 IU in 2.5 ml of buffer) was diluted with an equal volume of 0.1 M Na-acetate buffer, pH 5.5, containing 0.2 M NaCl and 20 mM $CaCl_2$. To this mixture 10 μg of purified neuraminidase were added. The solution was incubated at 30°C for different amounts of time. Before isoelectric focusing the mixture was dialyzed against 3 × 1 l of a solution of 1 % glycine, pH 7.4.

Treatment of plaice cholinesterase with purified solubilizing factor from Cytophaga sp. Cholinesterase was treated with the purified cholinesterase solubilizing factor isolated from *Cytophaga sp.* as described earlier.[11] Two ml of cholinesterase (5.6 IU/ml) in 5 mM Na-phosphate buffer, pH 7.4, were added to 2 ml of a solution of 0.1 M Na-acetate buffer, pH 5.5, containing 0.1 M NaCl and 20 mM $CaCl_2$. To this mixture 80 μl of a solution of 1 mg of purified Cytophaga factor in 10 ml of 5 mM Na-phosphate buffer, pH 7.4, were added. The incubation and dialysis were carried out as desrcibed above.

Analytical isoelectric focusing. Analytical isoelectric focusing was carried out essentially as described by Godson [12] except that J-type tubes were used, filled with 36 – 40 ml of a gradient (0 – 45 % sucrose) containing 1 % ampholine solution. The tubes were filled to the top and the upper part was sealed by a dialysis membrane. To prevent the formation of Joule's heat the voltage was increased gradually over a period of 12 – 18 h keeping the total current to 1.5 mA or lower per tube. A maximum of four samples were focused together at one time. After reaching 1000 V the electrofocusing was continued for 3 days. The removal of the gradients from the J-type tubes was carried out according to the procedure of Godson. Fractions, 0.8 – 1.0 ml each were collected.

Preparative isoelectric focusing. The multiple forms of plaice cholinesterase were separated on a preparative scale using a 150 ml electrofocusing column (LKB 8001). Conditions similar to the one described above were employed. Fractions, 1.2 – 1.5 ml each, were collected.

RESULTS

Multiple forms of plaice cholinesterase. As shown in Fig. 1 freshly dissolved lyophilized powder of plaice cholinesterase could be resolved by preparative isoelectric focusing into two fractions with isoelectric points at pH 5.5 and 6.9. Similar results were obtained when the same enzyme preparation was subjected to analytical isoelectric focusing (Fig. 2). The total amount of cholinesterase used in the former experiment was approximately 40 – 100 times that required for an analytical isoelectric focusing.

When the solution containing plaice cholinesterase was kept at 4°C for several weeks a pronounced shift in the elution profile was observed. Generally the total amount of enzyme focusing at pH 5.5 was decreased and a third species focusing at pH 7.6 was gradually obtained (Fig. 3). In extreme cases practically all of the enzyme had converted to forms with isoelectric points higher than pH 6. The enzyme obtained from the preparative separation was pooled into three fractions with isoelectric points at pH 5.5, 7.0, and 7.6. The three enzyme forms were analyzed for possible differences in substrate specificity. As shown in Table 1 the enzyme forms of all three pools could not be distinguished from one another on kinetic basis and did not differ from the enzyme before its separation into the three species. Furthermore no differences among the three forms were found when the inhibition of the three enzyme species by diisopropylfluorophosphate was compared (Fig. 4). The common pI_{50} value of 8.7 is similar to the one reported for the unresolved enzyme.[3]

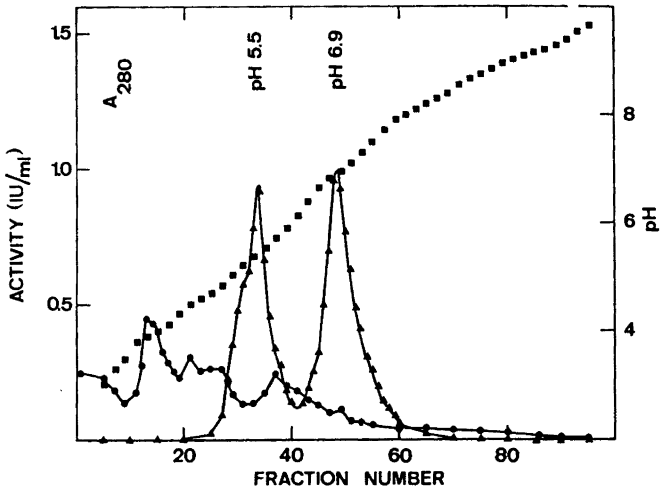

Fig. 1. Preparative isoelectric focusing of freshly dissolved plaice cholinesterase. The enzyme was dissolved and subjected to isoelectric focusing as described in METHODS. Enzyme activity: ▲, acetylthiocholine as substrate; ●, A_{280}, and ■, pH.

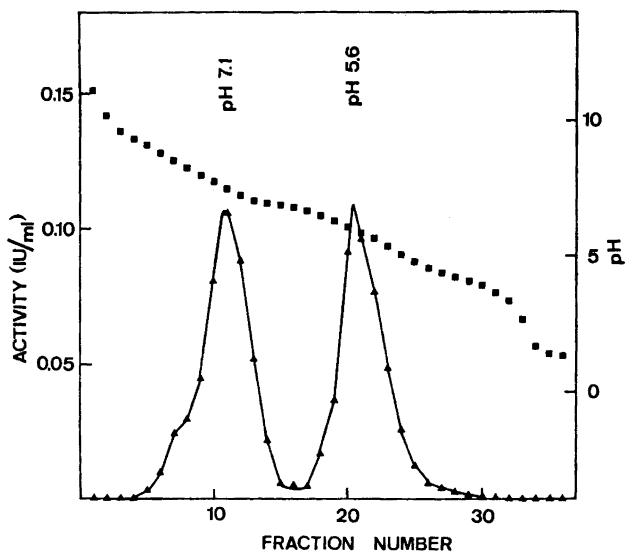

Fig. 2. Analytical isoelectric focusing of same sample as in Fig. 1. Symbols similar to Fig. 1.

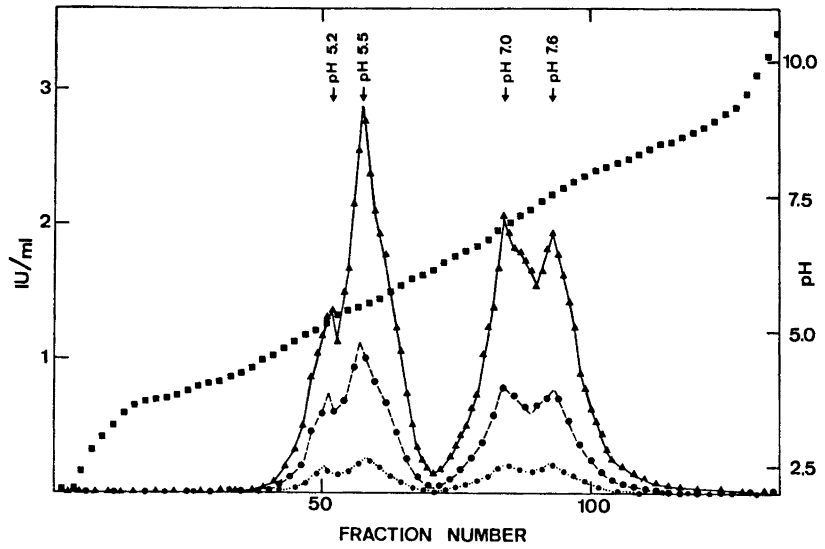

Fig. 3. Preparative isoelectric focusing of plaice cholinesterase stored at 4°C in solution for one week. Enzyme activity was assayed with acetylthiocholine (▲), butyrylthiocholine (●) and benzoylcholine (*); ■, pH.

Incubation of plaice cholinesterase with neuraminidase. The increase in the isoelectric points of plaice cholinesterase could possibly have arisen from a release of an acidic component such as sialic acid residues. Accordingly the enzyme was incubated with neuraminidase at 30°C for different periods of

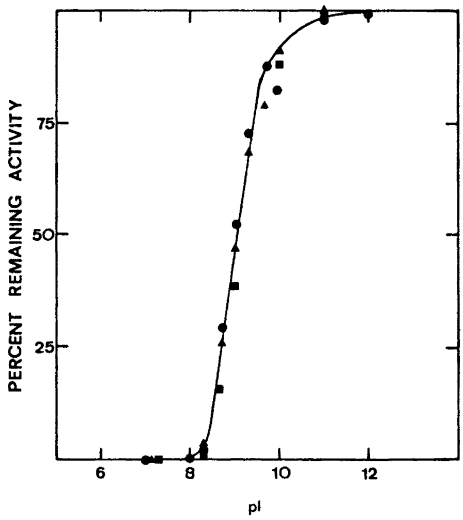

Fig. 4. Inhibition of the different forms of plaice cholinesterase by diisopropylfluorophosphate. The enzyme eluted from the preparative isoelectric focusing column (Fig. 3) was pooled as follows: pool I, fractions 55–65; pool II, fractions 80–85; pool III, fractions 92–100. The pooled fractions were incubated in 50 mM K-phosphate buffer, pH 8.2, at room temperature with increasing amounts of diisopropylfluorophosphate. After 30 min the remaining activity was determined spectrophotometrically with acetylthiocholine as substrate. pI curve of the enzyme from pool I (●); pool II (▲) and pool III (■).

Table 1. Comparison of kinetic parameters of plaice cholinesterase fractions.

Fraction	Isoelectric point	Acetylthiocholine			Butyrylthiocholine			Benzoylcholine		
	pH	K_m mM	V_{max} rel. units	Optimum activity pS	K_m mM	V_{max} rel. units	Optimum activity pS	K_m mM	V_{max} rel. units	Optimum activity pS
Enzyme before separation	–	0.19	0.33	2.47	.038	0.13	3.52	.018	.026	4.17
Pool I	5.5	0.18	0.31	2.55	.037	0.11	3.50	.018	.025	4.16
Pool II	7.0	0.18	0.36	2.55	.039	0.13	3.55	.021	.028	4.17
Pool III	7.6	0.19	0.34	2.60	.036	0.12	3.50	.020	.024	4.18

The fractions were pooled as indicated in the legend to Fig. 3 and assayed spectrophotometrically under standard conditions. The values of V_{max} and K_m were obtained from Lineweaver-Burk plots, optimal activity from plots of activity *vs.* pS. Relative units of enzyme activity are given since the exact amounts of enzyme in the different pools are unknown.

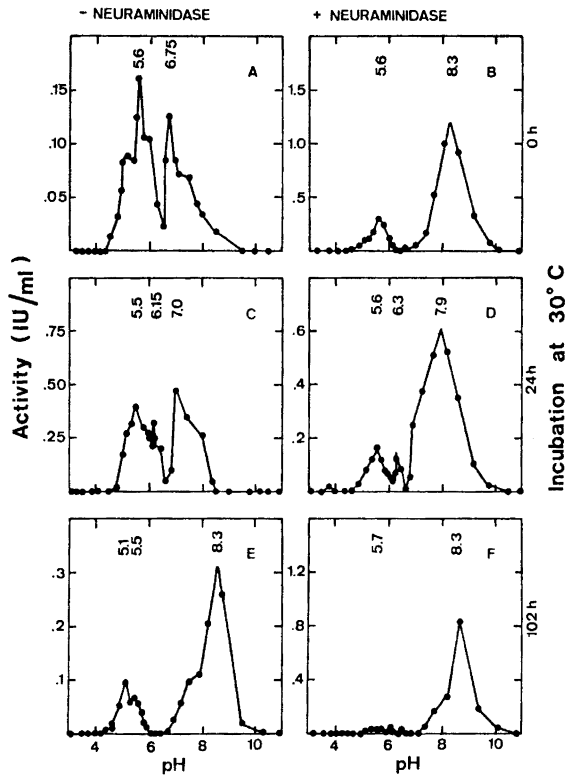

Fig. 5. Effect of neuraminidase on the isoelectric points of plaice cholinesterase. The enzyme was incubated at 30°C in presence and absence of neuraminidase for different lengths of time. Analytical isoelectric focusing was carried out on each incubation mixture after neuraminidase action. Elution patterns were drawn to a constant pH scale. Enzymatic activity assayed with acetylthiocholine as substrate (●). Enclosed numbers denominate the isoelectric points of the fractions obtained.

time. A summary of these results is shown in Fig. 5. In order to directly compare the elution patterns they were redrawn to a constant pH scale rather than to constant elution volume. As can be seen prolonged incubation with neuraminidase changes the isoelectric points of all species to a new single isoelectric point at pH 8.2 – 8.3 (Fig. 5F). In absence of neuraminidase no complete conversion to the pH 8.3 species was obtained even after a 102 h incubation period at 30°C (Fig. 5E).

To analyze each fraction for its activity towards the three substrates acetylthiocholine, butyrylthiocholine, and benzoylcholine, plaice cholinesterase was incubated with neuraminidase on a preparative scale. The elution profile obtained after isoelectric focusing of such an experiment was similar to the one in Fig. 3, and again no differences in catalytic properties could be found among the different forms of the enzyme.

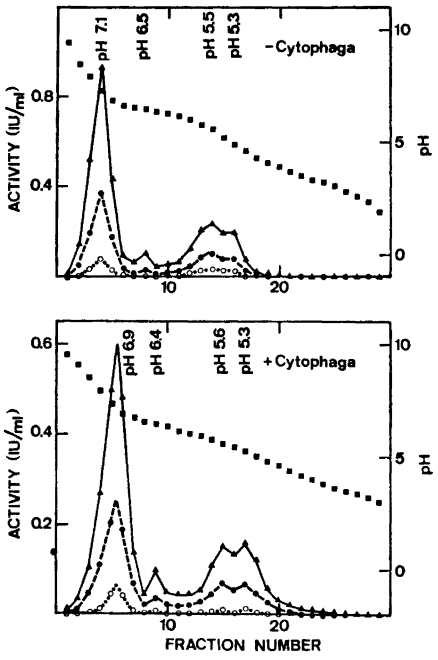

Fig. 6. Effect of enzyme solubilizing factor from Cytophaga. The enzyme was incubated at 30°C for 100 h with the purified cholinesterase solubilizing factor from Cytophaga. Analytical isoelectric focusing was carried out after completion of the incubation with the Cytophaga factor. Enzyme activities: ▲, acetylthiocholine; ●, butyrylthiocholine, and ○, benzoylcholine. ■, pH.

During these large scale incubation experiments a heavy protein precipitate was formed. After centrifugation the specific activity of plaice cholinesterase was increased 10 fold and the recovery of the enzyme was 92 – 95 %. However neuraminidase treatment on large amounts of plaice cholinesterase was less effective although the addition of neuraminidase was increased to the same extent as the total amount of cholinesterase units.

Incubation of soluble plaice cholinesterase with the enzyme solubilizing factor from Cytophaga. A unique feature in the preparation of the plaice enzyme is its solubilization from muscle tissue by a cholinesterase releasing factor obtained from *Cytophaga sp.*[11] Although the factor behaves like an enzyme its exact action on the muscle tissue remains obscure.[13] Thus it was of interest to obtain information on the possible effects of the Cytophaga enzyme on the soluble plaice cholinesterase. Plaice enzyme was incubated in presence and absence of the Cytophaga factor. After isoelectric focusing the fractions were analyzed for acetylthiocholine, butyrylthiocholine, and benzoylcholine activities. As shown in Fig. 6 the patterns obtained in presence and absence of the Cytophaga enzyme were identical.

Reincubation of plaice cholinesterase with neuraminidase. The forms of plaice cholinesterase with an isoelectric point of pH 7.0 and 7.6 isolated by isoelectric focusing were treated anew with neuraminidase and subjected to isoelectric focusing. The results of one of these experiments is shown in Fig. 7. After reincubation most of the enzyme was present in forms with isoelectric points

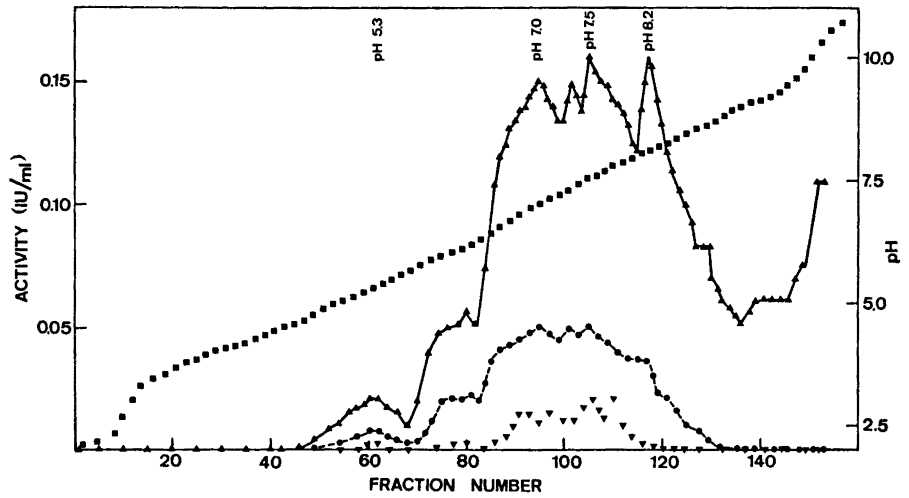

Fig. 7. Preparative isoelectric focusing pattern after reincubation of plaice cholinesterase with neuraminidase. Enzyme activities: ▲, acetylthiocholine; ●, butyrylthiocholine, and ▼, benzoylcholine. ■, pH.

at pH 7 or greater with a pronounced peak at pH 8.2. In fractions of high pH a new peak of enzyme activity was found that hydrolysed acetylthiocholine only and had no activity towards butyrylcholine and benzoylcholine. The activities of the peak fractions of this experiment together with the ratios between acetylthiocholine, butyrylthiocholine, and benzoylcholine are compared in Table 2.

Table 2. Comparison of activites of the different forms of plaice cholinesterase with acetylthiocholine, butyrylthiocholine, and benzoylcholine as substrates.

Enzyme form Isoelectric point	Activites			Ratio of activities		
	Acetyl-thio-choline	Butyryl-thio-choline	Benzoyl-choline	Acetyl-thio-choline	Butyryl-thio-choline	Benzoyl-choline
pH	IU/ml	IU/ml	IU/ml			
7.0	0.15	0.05	0.012	1.00	: 0.33	: 0.08
7.5	0.16	0.05	0.020	1.00	: 0.31	: 0.12
8.2	0.16	0.03	0.002	1.00	: 0.19	: 0.01
10.1	0.11	0.00	0.000	1.00	: 0.00	: 0.00

The peak fractions in Fig. 7 with isoelectric points at pH 7.0, 7.5, 8.2, and 10.1 were assayed spectrophotometrically for acetyl-, butyrylthiocholine, and benzoylcholine activities.

DISCUSSION

Plaice cholinesterase not only hydrolyzes acetylcholine but also choline esters of butyric, propionic, valeric, and benzoic acid. Thus this enzyme takes up a unique position between an acetylcholinesterase generally located in neuromuscular junctions and the soluble butyrylcholinesterases found in plasma and brain. Cholinesterases from a variety of sources exist as mixtures of multiple molecular forms. Differences in molecular and catalytic properties of butyrylcholinesterases were described on the basis of net charge, substrate specificity and sensitivity towards inhibition by fluorophosphate derivatives.[14,15] Multiple forms of human erythrocyte [16] and human brain acetylcholinesterase [17] have also been described. Acetylcholinesterase from the electric organ of the electric eel (*Electrophorus electricus*) exists in different oligomeric forms with apparently similar catalytic properties.[18]

The resolution of plaice cholinesterase into several enzymic species parallels the earlier observations made for acetyl- and butyrylcholinesterases. Contrary to the findings for the plasma enzyme,[14,15] no difference in catalytic properties were found for the various forms of plaice cholinesterase isolated by isoelectric focusing. Thus the unique ability of the plaice enzyme to hydrolyze acetylcholine and choline esters of aromatic and other aliphatic acids could not be explained on the basis of the presence of a mixture of kinetically distinguishable isoenzymes.

After prolonged standing an increase in the isoelectric point of plaice cholinesterase was observed which could be attributed to the spontaneous release of an acidic component from the enzyme. Treatment of this protein with neuraminidase yielded forms of the enzyme with isoelectric points up to pH 8.3 without any apparent change in catalytic reaction specificity. Similar observations were made by Svensmark and coworkers for human serum,[19,20] horse serum,[21] and human brain [10] butyrylcholinesterases. The results of Heilbronn [22] showed that there are 34 molecules of *N*-acetylneuraminic acid associated with each molecule of horse serum cholinesterase. Haupt *et al.*[23] reported figures for sialic acid content of human serum cholinesterase that would suggest that there are 80 molecules of this aminosugar in each molecule of the enzyme.

Besides cholinesterase a number of other enzymes are known to be glycoproteins in nature. In some cases it is possible to remove most of the carbohydrate from these glycoenzymes without impairment of enzymic function. Examples of this type of glycoprotein are thrombin,[24] glycoamylase,[25] and chloroperoxidase.[26] On the other hand there is a group of carbohydrate containing hormones of the anterior pituitary where even small changes in the carbohydrate moiety abolishes the specific interaction of the hormone with the target organ.[27] Similar observations were made with a number of blood group specific glycoproteins.[28]

According to a suggestion by Eylar [29] the attachement of sugars to a specific protein serves as the chemical passport for export from the synthesizing cell into the extracellular space. This hypothesis was rejected by Winterburn and Phelps [30] in favour of the idea that the attached carbohydrate determines the extracellular fate of a protein molecule in the sense that sugars serve as code

for the topographical location of the protein within an organism. Furthermore in some proteins the oligosaccharide structure attached may serve as signal for destruction of these proteins by catabolic enzymes. This effect is neutralized by the terminal sialic acid residues.[29]

Prolonged incubation of plaice cholinesterase with neuraminidase resulted in an enzyme preparation specific for acetylcholine only. Butyrylthiocholine and benzoylcholine were not hydrolyzed by this new form of the enzyme. The isoelectric point of the new species was at or around pH 10 and could not be determined accurately because the enzyme focused at the end of the ampholine gradient. In view of these results a new role for sialic acid residues might be described. In plaice cholinesterase, sialic acid residues could possibly be responsible for maintaining a specific ternary structure in this enzyme allowing the accomodation not only of acetylcholine but also of choline esters of aliphatic acids such as propionic, butyric, and valeric acid together with esters of aromatic carboxylic acids such as benzoylcholine. Upon removal of one or more sialic acid residues possibly near or at the active site the structure around the active site might become more closed up thus accomodating the smallest substrate molecule, acetylcholine, only. More detailed investigations on a pure enzyme preparation are, however, necessary to warrant this hypothesis.

Acknowledgements. The authors are indebted to Professor H. Aebi for providing financial assistance and for his continuous interest in this work.

REFERENCES

1. Lundin, S. J. *J. Cellular Comp. Physiol.* **59** (1962) 93.
2. Lundin, S. J. *Acta Chem. Scand.* **21** (1967) 2663.
3. Lundin, S. J. *Acta Chem. Scand.* **22** (1968) 2183.
4. Lundin, S. J., Gentinetta, R. and Brodbeck, U. *Unpublished observations.*
5. Teipel, D. and Koshland, Jr., D. E. *Biochemistry* **8** (1969) 4656.
6. Cleland, W. W. In Boyer, P. D. *The Enzyme*, Academic, New York 1970, Vol. II, p. 1.
7. Brodbeck, U., Gentinetta, R. and Lundin, S. J. *Abstr. Commun. 8th Meet. Fed. Eur. Biochem. Soc.* 1972, Abs. 439.
8. Ellman, G. L., Courtney, K. D., Andres, V. and Featherstone, R. M. *Biochem. Pharmacol.* **7** (1961) 88.
9. Kalow, W. and Lindsay, A. *Can. J. Biochem. Physiol.* **33** (1955) 568.
10. Carlsen, J. B. and Svensmark, O. *Biochim. Biophys. Acta* **207** (1970) 477.
11. Lundin, S. J. and Bovallius, Å. *Acta Chem. Scand.* **20** (1966) 395.
12. Godson, G. N. *Anal. Biochem.* **35** (1970) 66.
13. Lundin, S. J. *Acta Chem. Scand.* **22** (1968) 2519.
14. Augustinsson, K.-B. *Bull. World Health Organ.* **44** (1971) 81.
15. Chiu, Y. C., Tripathi, R. K. and O'Brien, R. D. *Biochem. Biophys. Res. Commun* **46** (1972) 35.
16. Shafai, T. and Cortner, J. A. *Biochim. Biophys. Acta* **236** (1971) 612.
17. Eldefrawi, M. E., Tripathi, R. K. and O'Brien, R. D. *Biochim. Biophys. Acta* **212** (1970) 308.
18. Wermuth, B. and Brodbeck, U. *Experientia* **28** (1972) 740.
19. Svensmark, O. *Acta Physiol. Scand.* **64** (1965) 23.
20. Svensmark, O. and Kristensen, P. *Biochim. Biophys. Acta* **67** (1963) 441.
21. Svensmark, O. and Heilbronn, E. *Biochim. Biophys. Acta* **92** (1964) 400.
22. Heilbronn, E. *Biochim. Biophys. Acta* **58** (1962) 222.
23. Haupt, H., Heide, K., Zwisler, O. and Schwick, H. G. *Blut* **14** (1966) 65.
24. Skaug, K. and Christensen, T. B. *Biochim. Biophys. Acta* **230** (1971) 627.
25. Pazur, J. H., Knull, K. R. and Simpson, D. L. *Biochem. Biophys. Res. Commun.* **40** (1970) 110.

26. Lee, T. and Hager, L. P. *Fed. Proc. Fed. Amer. Soc. Exp. Biol.* **29** (1970) 599.
27. Spiro, R. G. *Ann. Rev. Biochem.* **39** (1970) 599.
28. Morgan, W. T. J. In Rossi, E. and Stoll, E., Eds., *Modern Problems in Pediatrics 10, Fourth Intern. Cystic Fibrosis Symp.*, Karger Libri, Basel 1967.
29. Eylar, E. H. *J. Theor. Biol.* **10** (1966) 89.
30. Winterburn, P. J. and Phelps, C. F. *Nature* **236** (1972) 147.

Received August 10, 1972.

ACTA CHEMICA SCANDINAVICA 27 (1973) 573–581

Main-chain Sorption of Water by Serum Albumin

R. BRODERSEN, B. J. HAUGAARD, C. JACOBSEN and A. O. PEDERSEN

Institute of Medical Biochemistry, University of Aarhus, DK-8000 Aarhus C, Denmark

Infrared spectra were recorded of human serum albumin and of extensively acetylated and methylated derivatives as films. Each specimen was examined after drying as well as after equilibration with water vapour at 80 % relative humidity. After hydration an OH-stretching band of sorbed water is observed as well as changes in the Amide I and II bands and the Amide V region of the protein. These changes were similar to those reported by previous investigators for hydration of collagen and keratin. The observations seem to indicate that water, in these proteins, is sorbed to the peptide groups of the main chain rather than to polar side chains.

Pauling [1] in 1945 summarized evidence in favour of binding of water to polar side chains in several proteins, including serum albumin, and expressed the opinion that peptide carbonyl and imido groups usually have little attraction for water, due to the NH ··· O=C hydrogen bonding. Several observations have been interpreted accordingly, including those of Brey *et al.* in 1968 [2,3] who studied the nuclear magnetic resonance of water sorbed on serum albumin. On the other hand, keratin and collagen seem to bind water to the main chain, as evidenced from infrared spectroscopy by Bendit [4] and by Susi *et al.*,[5] respectively. Malcolm [6] has examined the infrared spectrum and dichroism of water adsorbed on poly-alanine, in which polar side chains are absent, and has found that the water molecules are situated in specific orientation with respect to the helical polymer, probably with a weak hydrogen bond to peptide oxygen and with a strong dipole interaction between water and peptide. Water sorbed on γ-ethyl and γ-methyl esters of poly-glutamate, according to Malcolm, likewise gives a dichroic OH-stretching band. The water is bound to the main chain and possibly to sidechain carbonyl as well.

In the present paper infrared spectra of hydration are reported for human serum albumin and for two derivatives, one of which is extensively methylated in the carboxyl side chains, and another which is acetylated in lysyl amino groups. The aim is an investigation of the binding sites of water.

EXPERIMENTAL

Human serum albumin (Kabi) was deionized in a mixed bed ion exchange column and lyophilized. The natural content of fatty acids, about 0.5 mol per mol protein, was not removed. The preparation contains about 7 % dimer and trimer albumin. The mol weight was taken as 66 000. The number of aminoacyl residues is about 570, and Stoke's radius of the monomer is 3.6 nm.[7]

Methylated albumin was prepared by reacting albumin (1 g) with 60 ml methanol, 0.1 M with respect to hydrochloric acid, for two days at room temperature. The mixture was then neutralized, dialysed, and lyophilized. Titration showed that 70 carboxyl groups per mol albumin corresponding to 73 % were esterified. The Stoke's radius could not be estimated due to low solubility. The peptide chain is largely unfolded, according to Sun.[8]

Acetylated albumin was prepared as described previously.[9] 56 amino groups per mol albumin corresponding to 96 % were acetylated. The Stoke's radius was 4.9 nm, determined by Sephadex gel-filtration in a 0.1 M phosphate buffer pH 7.4 at 5°C. This radius is significantly higher than that of the native protein, indicating unfolding of the acetylated molecule.

Films of protein were prepared by spreading 15 μl of a 1 % solution in water over each of four thallium bromide iodide (KRS-5) slabs until spontaneous drying, whereby a film of 0.16 mg/cm^2 was formed on each slab. Two of these were placed over strong sulphuric acid (93 – 94 %) at atmospheric pressure and room temperature (23°C) overnight. These moderately dried films were placed in the reference beam, as described below. Two slabs were placed over diluted sulphuric acid overnight for equilibration at a predetermined relative humidity.[10] Before opening the container, each pair of slabs were placed on either side of a rubber spacer, with the protein carrying aspects facing each other. The thickness of the spacer, 1 mm, was chosen large enough to avoid interference fringes in the spectrum, and small enough to prevent evaporation of appreciable amounts of water from the films when the temperature rose during recording. The temperature in the sample compartment was around 35°C. Each set of films, sample and reference, was moved perpendicularly to the beam by means of adjustment screws until equal protein film thickness was obtained, as judged from the spectrum. It was presumed that the CH_3 and CH_2 stretching bands at 2900 – 3000 cm^{-1} were not influenced by hydration. Neutralization of these bands were taken to indicate proper positioning. The choice of these bands for equalizing the sample and reference protein thickness was to some extent arbitrary. It was found, however, as seen from Figs. 1 – 2, that the Amide A band was neutralized as well, and the spectrum in the Amide I and II region could be interpreted as due to changes on hydration, thus confirming the constancy of the bands at 2900 – 3000 cm^{-1}.

Cracking of the dry films, signalled by discontinuities of the record, sometimes necessitated repeated experiments.

Spectra were recorded on a Beckman IR 20A infrared spectrophotometer from 4000 to 250 cm^{-1}. Slow scanning with carefully balanced gain, damping, and slit width was necessary to obtain reproducible details in the difference spectra. The time taken for each record was 4 to 16 h.

The amount of water sorbed was determined on a Cahn Gram Electrobalance. About 15 mg of the lyophilized protein were placed on one pan and a known relative humidity (r.h.) was produced by a dish of diluted sulphuric acid placed in the chamber. Constant weight was obtained in 24 h at relative humidities between 10 and 70 %. Measurements were begun at 10 % r.h., each day shifting to a higher value. The original weight at 10 % r.h. could be reproduced at the end. 10 % r.h. was chosen as a basis since it is difficult to obtain reproducible weights by more exhaustive drying. The temperature was 23°C ± 1°C.

RESULTS

Fig. 1 shows the infrared spectrum of a dried albumin film, the difference spectrum of hydration at 80 % r.h., the calculated spectrum of the wet film, obtained by adding these, and finally, the spectrum of liquid water, approximately in the same amount as found in the wet film. Equilibration at 20 % r.h.

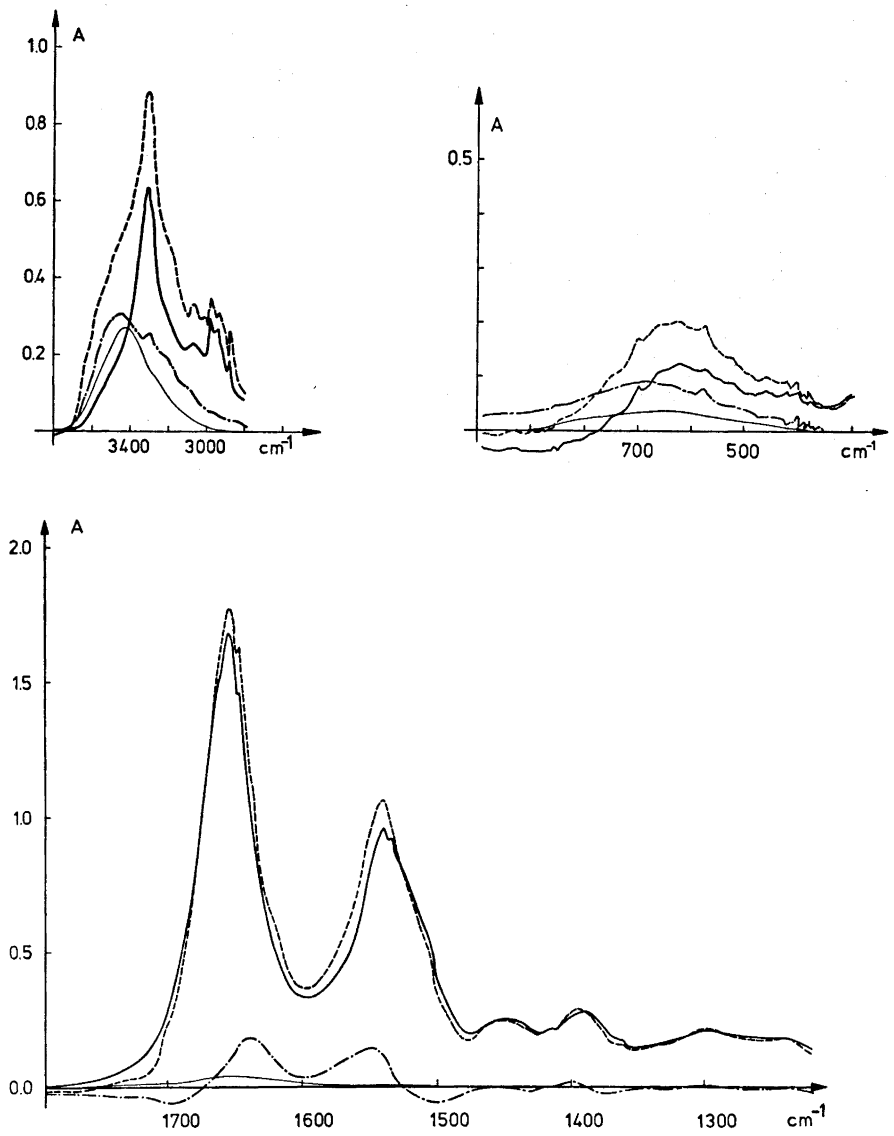

Fig. 1 a–c. ——— Infrared spectrum of human serum albumin (HSA) film, moderately dried over concentrated sulphuric acid. — · — Difference spectrum of moist HSA, 80 % r.h., against dried HSA. - - - Spectrum of moist albumin, obtained as the sum of the above spectra. ——— Spectrum of water, approximately same amount as in the moist albumin films. Ordinates, absorbance.

resulted in a difference spectrum (not shown) qualitatively similar to that of 80 % r.h. but with proportionately lower amplitudes. In repeated experiments the following spectral changes on hydration were reproducible:

In the 3 μ region the difference spectrum is rather similar to that of liquid water, except that two separate maxima are seen, at 3460 and 3300 cm^{-1}, while the principal maxima of liquid water at 3490 and 3280 [11] are registered as one skew peak.

In the 6 μ region the Amide I band is shifted slightly towards lower frequencies and the Amide II frequency is increased; both bands show higher intensities after hydration. The band at 1400 cm^{-1} (side chain carboxylate) is shifted towards higher frequencies.

In the 15 μ region is seen a shift of the Amide V band to higher frequencies and an increase of intensity. The spectral changes are larger than those which could be caused by a similar amount of liquid water alone.

Difference spectra of hydration of two albumin derivatives are shown in Fig. 2. These display the same main features as does the spectrum of native albumin, namely the double water peak and the changes of Amide I, II, and V bands. After extensive methylation of side-chain carboxyl groups no hydra-

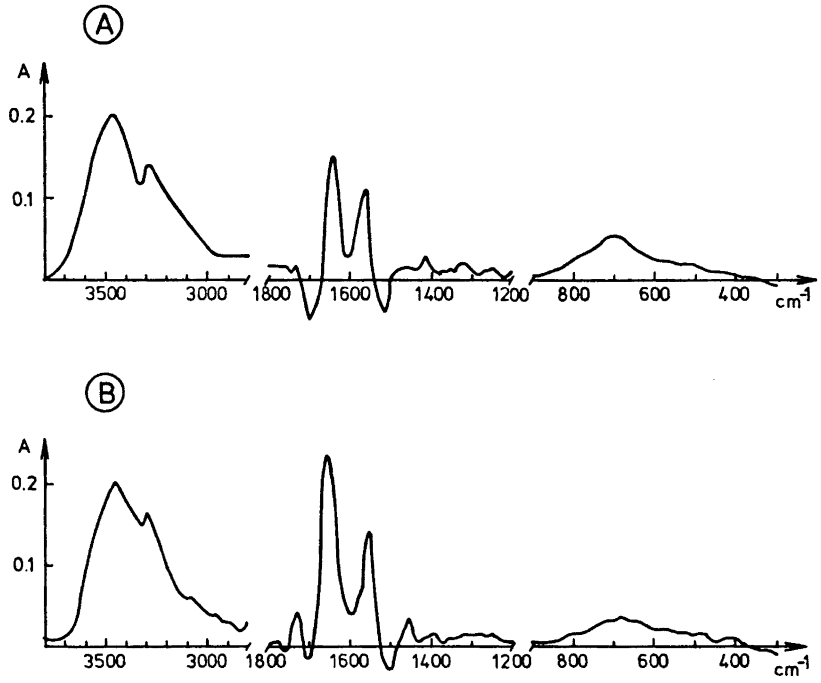

Fig. 2. Infrared difference spectra of hydration of albumin derivatives. A film of each derivative was equilibrated at 80 % r.h., and measured against a dried film of the same substance. A, all ε-amino groups acetylated. B, most carboxyl groups methylated. Ordinates, absorbance.

tion shift is observed at 1400 cm^{-1} while a change is seen at 1750 cm^{-1}, presumably a decrease of the non-hydrogen-bonded C=O absorption.

Albumin acetylated in lysyl NH_2 groups shows a hydration difference spectrum almost identical with the difference spectrum of hydration of native albumin. The shift observed at 1400 cm^{-1} for native albumin has almost disappeared in the acetylated sample in agreement with the fact that side-chain carboxyl groups are protonized in the isoelectric state.

The amounts of water sorbed to human serum albumin and to the two derivatives are depicted in Fig. 3. Approximately 100 mol H_2O could be removed

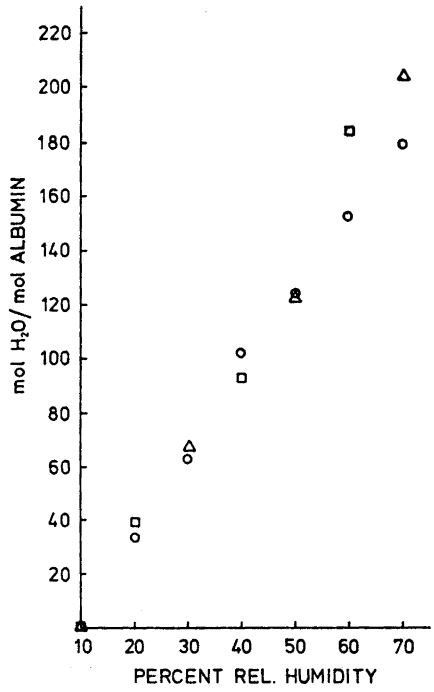

Fig. 3. Amount of sorbed water as a function of relative humidity. O, human serum albumin. △, HSA, most carboxyl groups methylated. □, HSA, all ε-amino groups acetylated.

from each mol protein, equilibrated at 10 % r.h., by drying over conc. sulphuric acid. This amount is similar in the native albumin and the two derivatives. It is noted from Fig. 3 that the amounts of water sorbed in the range 10 – 70 % r.h. are equal in the three substances. Extensive methylation of carboxyl groups or acetylation of amino groups, which are the main polar groups of the side chains, does not influence binding of water to a measurable extent.

DISCUSSION

The main infrared spectral changes due to water sorption to human serum albumin involve the principal main-chain frequencies, Amide I, II, and V. This seems to indicate that water is bound to the peptide groups of the main chain.

Binding of water exclusively to polar side-chain residues on the surface of the protein molecule could not explain the shifts observed of the main-chain bands.

After extensive chemical alterations of the polar side chains the main features of the hydration difference spectra remain unchanged. This is found after esterification of most of the carboxyl groups as well as after acetylation of all amino groups. This supports the above conclusion, that water is sorbed to the main chain.

The amount of water sorbed to the protein is not changed by these chemical modifications of the polar side-chain residues. This adds further evidence against binding of water solely to these groups.

On the other hand, it seems that carboxylate groups, besides the main chain, are involved in the binding of water molecules, as evidenced by the shift of the band at 1400 cm^{-1} by hydration of native albumin. This shift is not observed on hydration of albumin in which the carboxyl groups are esterified. In the albumin with acetylated amino groups the hydration shift at 1400 cm^{-1} is nearly absent. In this derived protein most of the carboxyl groups are protonized since 56 ammonium groups of the native albumin have lost their positive charge. Twenty-three quanidinium groups remain positively charged and a corresponding number of COO^- are unprotonized. This agrees well with the finding of a slight hydration shift of the carboxylate band at 1400 cm^{-1} if it is presumed that water may bind to these groups.

The albumin derivative with methylated carboxyl groups shows a decrease of infrared absorption at 1750 cm^{-1} on hydration. A number of non-hydrogen-bonded CO groups are probably present in this substance and contributes to a peak at 1750 cm^{-1} seen in the infrared spectrum. On hydration hydrogen bonds are probably established to these groups and the peak at 1750 cm^{-1} disappears into the large Amide I band. This probably explains the negative peak in the difference spectrum of hydration and indicates a role of the ester carbonyl in binding of water.

The carboxylate groups of the native albumin and the ester groups of the methylated derivative may contribute to binding of water by establishing additional bonds to water molecules already sorbed to the main chain or may bind water which is not bonded to peptide groups. In the latter event the amount of water sorbed would be influenced by the chemical modification if the binding affinity is changed. As seen from Fig. 3 the changes expected would hardly be perceptible and it is thus not possible to conclude whether water molecules may be bound to carboxylate and ester residues independently or with bonds to peptide groups as well. At any rate sorption of water to the main chain quantitatively out-weighs binding to polar side chains to a considerable extent.

The peptide chain is largely unfolded in both of the derived albumin preparations. Acetylation thus caused an increase of the Stoke's radius from 3.6 to 4.9 nm. The viscosity of methylated albumin has been measured by Sun [8] and likewise indicates unfolding to a considerable extent. It is interesting to note that the unfolded peptide chain shows the same changes of infrared spectrum on hydration as seen in the native protein. Also the amount of water sorbed remains the same after unfolding of the peptide chain. Loosely bound water molecules would thus appear to form an integral part of the native peptide structure of the albumin molecule.

Bendit [4] has recorded hydration difference spectra for keratin. These show the same main features, as reported above for serum albumin, *i.e.* a double maximum in the OH stretching region, similar to that of liquid water, lowering of Amide I and increase of Amide II frequencies with increased intensities. These changes are seen in α-keratin, in supercontracted "randomized" α-keratin and in β-keratin. The spectra reported by Bendit do not include the Amide III and V bands.

Susi *et al.*[5] have examined infrared spectra of collagen with varying amounts of bound water and have found similar changes in the OH-stretching and Amide I and II regions, as for albumin and keratin. The Amide V bond of collagen is shifted to higher frequencies with increased intensity, as in albumin. In addition the authors report a shift of CH-bending frequency at 1450, ascribed to hydrogen bonding to CH. This is not seen in keratin,[4] nor in albumin. The Amide III band of collagen at 1232 cm^{-1} is increased in frequency and intensity on hydration. A similar change is not seen in the albumin spectra. The Amide III band of an albumin, however, has a low intensity, and relative changes, similar to those in collagen, would not be perceptible.

The infrared spectrum of procollagen [12] shows similar changes on hydration.

Poly-lysine hydrochloride [13] and sodium poly-glutamate [14] exhibit patterns of infrared spectral changes on hydration, different from those of albumin, keratin, and collagen. These changes are due to $\alpha \rightarrow \beta$ transitions, caused by the electric charges of the side chains. Similar transitions are not seen in the proteins mentioned.

Buontempo *et al.*[15] recently reported that the difference spectrum of water bound to lysozyme and to bovine serum albumin shows two maxima, one at 3450 cm^{-1} and another somewhat below 3300 cm^{-1}. These are due to rather loosely bound water, similarly to the water dealt with in the present paper. Buontempo *et al.* have found that, in addition to this, some more tightly bound water may be removed by prolonged evacuation. This water shows a single, broad maximum at 3260 cm^{-1} when examined near liquid nitrogen temperature. Infrared spectral changes at Amide I, II, and V frequencies have not been reported for sorption of this tightly bound water.

In conclusion, a common pattern of changes of infrared spectra on hydration appears to exist in several very different proteins so far examined, *viz.* keratin in α-, β-, and amorphous conformation, collagen (triple helix), and in serum albumin (globular with partial α-helix structure) in the native state as well as after chemical modifications of polar side chains causing unfolding. This pattern can be described as follows:

(1) The OH stretching band of sorbed water shows two separate peaks, in the vicinity of those of fluid water (3490 and 3280 cm^{-1}), the former with the higher intensity.

(2) The Amide A band near 3300 cm^{-1} is unchanged. (Bendit [4] interprets the two OH stretching bands as one, modulated by a slight decrease of the Amide A frequency.)

(3) A small decrease of the Amide I frequency and an increase of the Amide II frequency. The ratio of these shifts is approximately 1:4. Increased intensity of both bands.

(4) Increased frequency and intensity of the Amide V band.

These changes are seen on sorption of relatively loosely bound water from a few per cent relative humidity to about 60 – 90 %. The amount of water bound is less than one molecule per peptide group in albumin and collagen, and less than two in keratin.

The main peptide chain seems to be involved in the binding of water in all these cases. Hydrogen bonding to peptide C = O groups may explain the changes of the Amide I, II and V bands.[4–6] The appearance of two separate peaks in the OH stretching region indicates that a water molecule is bound in a specific position in relation to the carbonyl group. This is supported by the findings of Malcolm [6] who studied infrared spectra and dichroism of water sorbed on α-helical synthetic polypeptides. The findings are consistent with binding of a water molecule through a hydrogen bond to peptide oxygen together with a strong interaction between the dipoles of water and peptide. The water molecule is thus located in a specific position which is tentatively described by Malcolm.

Brey *et al.*[2,3] have measured spin-spin relaxation times of protons of water sorbed on bovine serum albumin as a function of water coverage and temperature. They found results which are in agreement with binding of water to polar side chains. These authors emphasize a discontinuity of the NMR line width at 160 mg H_2O per gram protein. This corresponds precisely to one water molecule per peptide unit of the main chain. It may be possible to reinterpret the findings of Brey *et al.* in the light of water sorption to the peptide backbone.

Other residues, including those of side chains, take part in the binding of water, either by establishing additional hydrogen bonds to the H_2O molecules already bound to C = O, or by binding more water. This explains the variable amount sorbed to different proteins (Bull [16]). Polymers containing amide groups but without polar side chains, such as poly-alanine [6] and nylon,[16] have a low affinity for water. Even nylon may, however, bind nearly one molecule of H_2O per amide bond by exposure to saturated water vapour.[16]

Since proteins are synthetized in an aqueous surrounding it is likely that water forms an integral part of the basic peptide structure.

REFERENCES

1. Pauling, L. *J. Am. Chem. Soc.* **67** (1945) 555.
2. Fuller, M. E. and Brey, W. S. *J. Biol. Chem.* **243** (1968) 274.
3. Brey, W. S., Evans, T. E. and Hilzrot, L. H. *J. Colloid Interface Sci.* **26** (1968) 306.
4. Bendit, E. G. *Biopolymers* **4** (1966) 539.
5. Susi, H., Ard, J. S. and Carroll, R. J. *Biopolymers* **10** (1971) 1597.
6. Malcolm, B. R. *Nature* **227** (1970) 1358.
7. Ackers, G. K. *Biochemistry* **3** (1964) 723.
8. Sun, S. F. *Arch. Biochem. Biophys.* **129** (1969) 411.
9. Jacobsen, C. *Eur. J. Biochem.* **27** (1972) 513.
10. *Handbook of Chemistry and Physics*, 44th Ed., Chemical Rubber Publishing Co., Cleveland 1962, p. 2596.
11. Eisenberg, D. and Kauzman, W. *The Structure and Properties of Water*, Oxford Univ. Press, London 1969, pp. 228 – 229.
12. Chirgadze, Yu. N., Venyaminov, S. Yu. and Zimont, S. L. In Kayushin, L. P., Ed., *Water in Biological Systems*, Consultants Bureau, New York 1969, p. 51.

13. Blout, E. R. and Lenormant, H. *Nature* **179** (1957) 960.
14. Lenormant, H., Baudras, A. and Blout, E. R. *J. Am. Chem. Soc.* **80** (1958) 6191.
15. Buontempo, U., Careri, G. and Fasella, P. *Biopolymers* **11** (1972) 519.
16. Bull, H. B. *J. Am. Chem. Soc.* **66** (1944) 1499.

Received July 7, 1972.

ACTA CHEMICA SCANDINAVICA 27 (1973) 582–588

On the Crystal Structure of Ni_5As_2

ARNE KJEKSHUS and KJELL ERIK SKAUG

Kjemisk Institutt, Universitetet i Oslo, Blindern, Oslo 3, Norway

The Ni_5As_2 phase has a slight range of homogeneity extending on both sides of the stoichiometric 5 : 2 ratio. The structure is determined from three-dimensional single crystal X-ray data. The phase exhibits a temperature dependent paramagnetic susceptibility which does not obey the Curie-Weiss Law over the temperature interval 80 to 1000 K.

Although a phase of approximate composition Ni_5As_2 was described [1] as early as 1857, some one hundred years elapsed before its existence was confirmed by Hellner.[2] When the present investigation was started the Ni_5As_2 phase was known to exhibit hexagonal symmetry and a slightly temperature dependent range of homogeneity on the Ni-poor side of the stoichiometric composition.[2–4] Since no structure determination had been carried out it was considered of interest to undertake this study. However, at the time when the first draft to a report on our findings was completed, we became aware of a paper by El-Boragy *et al.*[5] which describes the crystal structure of Ni_5As_2.

EXPERIMENTAL

Materials. Samples were prepared from 99.999 + % As (Johnson, Matthey & Co.) and 99.99 + % Ni (The British Drug Houses). (The nickel powder was obtained by hydrogen reduction (600°C) of NiO.)

Preparations. Weighed quantities of the components were heated in evacuated, sealed silica tubes for 4 days at 600°C. The sintered powders were ground and reannealed at temperatures between 700 and 900°C for 15 day periods and, finally, quenched in ice water. Several samples with different initial compositions were prepared on both sides of the 5 : 2 stoichiometric ratio. Single crystals of Ni_5As_2 of rather irregular, flaky shape were found in the sintered samples heated at 750°C.

X-Ray diffraction. X-Ray powder photographs of all samples were taken in a Guinier type camera of 80 mm diameter with monochromatized Cu$K\alpha_1$-radiation using KCl as internal standard.

Three-dimensional single crystal data from the layers $hk0$ to $hk6$ were collected in an integrating Weissenberg camera of 57.3 mm diameter with Zr-filtered Mo$K\alpha$-radiation using the multiple-film technique. The intensities were measured microphotometrically except for the weakest reflections which were estimated visually by comparison with a standard scale. The intensities were corrected for the combined Lorentz and polarization factors, and for absorption. Additional intensity data from the layers $0kl$ to $3kl$ were obtained by the precession technique.

Computations. The computational work, including least squares refinements of the unit cell dimensions, corrections, data reductions, scalings, Patterson- and Fourier-syntheses, full matrix least squares refinements of the structure factors, and evaluations of interatomic distances, was carried out on a CDC 3300 computer using, in most cases, the programmes of Dahl *et al.*[6]

The atomic scattering factors were taken from Hanson *et al.*[7] The extent of the agreement between the observed and calculated structure factor data was judged from the reliability factor:

$$R = \sum||F_o| - |F_c||/\sum|F_o|$$

The unobserved reflections were not included in the calculations of R, and were omitted from the least squares refinements.

Magnetic susceptibilities were measured between 80 and 1000 K by the Faraday method (maximum field ~ 8 kØ) using $70-100$ mg samples.

RESULTS AND DISCUSSION

(i) Composition and homogeneity range. Polycrystalline samples of Ni_5As_2 are easily synthesized by direct reactions of the elements at $700-900$°C. In order to obtain thermodynamic equilibrium it is necessary to crush the samples during the annealing process.

The unit cell dimensions of the Ni_5As_2 phase decrease as the As content increases over the homogeneity range (extending from 28.09 ± 0.16 to 28.74 ± 0.16 atomic % As). It is thus inferred, in contrast with earlier findings,[3,4] that the homogeneity range extends on both sides of the stoichiometric formula Ni_5As_2.

(ii) Unit cell dimensions and space group. The unit cell dimensions range between $a = 6.815(1)$ Å, $c = 12.512(2)$ Å, $c/a = 1.8360(6)$ at 28.09 atomic % As and $a = 6.813(1)$ Å; $c = 12.502(2)$ Å; $c/a = 1.8350(6)$ at 28.74 atomic % As; $a = 6.815(1)$ Å; $c = 12.506(2)$; $c/a = 1.8351(6)$ being obtained at the stoichiometric composition. These values are reasonably consistent with those reported in the literature.[2,3,5,8]

Although all previous studies agree on the hexagonal symmetry of the Ni_5As_2 phase, there is considerable uncertainty as to the correct choice of space group. According to the X-ray powder diffraction data of Heyding and Calvert [3] indices of the type $h0l$ were found to be systematically absent for $l = 2n+1$. A later single crystal study by Saini *et al.*[8] could not confirm this, and $P6_322$ was proposed as the space group for Ni_5As_2.

On the basis of the present Weissenberg data it was very difficult to decide whether indices of the type $h0l$ for $l = 2n+1$ were absent or of low intensity, and because of this uncertainty, space group $P6_322$ was assumed in the preliminary structure analysis.

Numerous trial structures based on the (001) Patterson-synthesis were tested, but all were unfruitful. However, the precession data which were subsequently collected unequivocally showed that reflections of the type $h0l$ for $l = 2n+1$ are extinguished, hereby eliminating space group $P6_322$. A $N(z)$,z-plot demonstrated that the (001) projection is centro-symmetric. The most probable space group is thus $P6_3cm$.

(iii) Refinement of the structure. On account of the Patterson-synthesis a set of positional parameters were deduced according to space group $P6_3cm$. Apart from some problems associated with absorption corrections the least

squares refinements proceeded fairly normally and were terminated at $R = 0.095$. The final positional and thermal parameters are listed in Table 1. The value of one temperature factor is negative and another one takes a rather high positive value, indicating that the applied absorption correction is still somewhat unsatisfactory.

Table 1. Positional and thermal parameters for Ni_5As_2 according to $P6_3cm$.

Atom	Position	x	y	z	B(Å^2)
Ni(I)	2*a*	0	0	0.9478(38)	−0.15(18)
Ni(II)	4*b*	1/3	2/3	0.0768(56)	0.58(28)
Ni(III)	6*c*	0.2460(15)	0	0.0891(44)	0.43(16)
Ni(IV)	6*c*	0.6228(17)	0	0.1942(40)	0.22(14)
Ni(V)	6*c*	0.3043(20)	0	0.3057(36)	0.66(19)
Ni(VI)	6*c*	0.6212(37)	0	0.4027(59)	1.68(39)
As(I)	6*c*	0.6669(19)	0	0.9931(31)	0.60(12)
As(II)	4*b*	1/3	2/3	0.2745(35)	0.47(18)
As(III)	2*a*	0	0	0.2260(29)	0.46(26)

A similar solution for the structure of Ni_5As_2 is obtained in the independent study by El-Boragy *et al.*[5] The two investigations concur on $P6_3cm$ being the correct space group. However, considerable discrepancy is to be found between some of the values for the positional parameters. The determination of El-Boragy *et al.*[5] was based on Weissenberg data from the layers 0*kl*, 1*kl*, and 2*kl* and their refinements were terminated at $R = 0.15$. Due to the relatively high R-value we subjected their structure factor data to further least squares refinements. However, regardless of the choice of input parameters their original values for the variable parameters were obtained. There is accordingly a real discrepancy between the two studies and although the origin of this remains unknown the following considerations appear to be relevant:

(1) The two structure determinations of Ni_5As_2 are carried out at room temperature, which thus excludes temperature variation as a cause for the different values of the positional parameters.

(2) Both studies utilized crystals prepared from elements of high purity. This excludes any hypothetical difference in impurity content as the origin of the different positional parameters.

(3) Structural parameters will generally vary within a homogeneity range. If the crystals of the two studies are of different composition, this will cause a variation in the positional parameters.

(4) Another and perhaps more likely explanation may be to connect the discrepancy with the fact that El-Boragy *et al.* did not correct their intensity data for absorption.

(iv) Discussion of the structure. The atomic arrangement of the Ni_5As_2 structure is shown in Fig. 1 and using the same projection axis, the immediate environment of the different atoms is illustrated in Fig. 2. Interatomic distances (< 4 Å) are listed in Table 2, and the coordination numbers together with the average values of the Ni – Ni and Ni – As distances around each kind of atoms

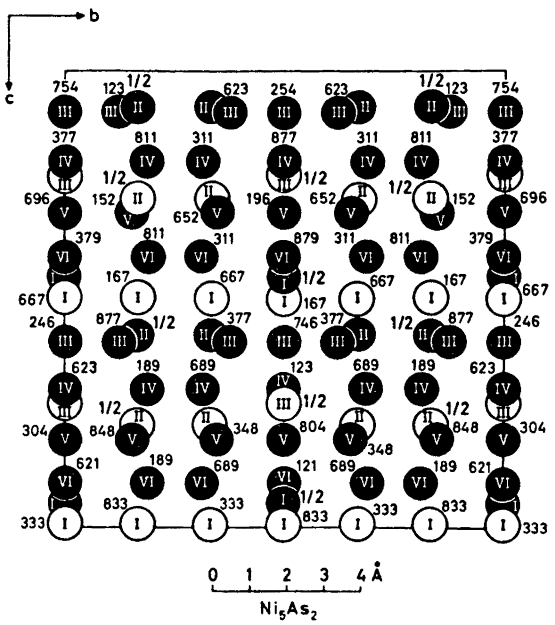

Fig. 1. The structure of Ni_5As_2 projected along [100] of the ortho-hexagonal unit cell. The filled and open circles represent Ni and As, respectively.

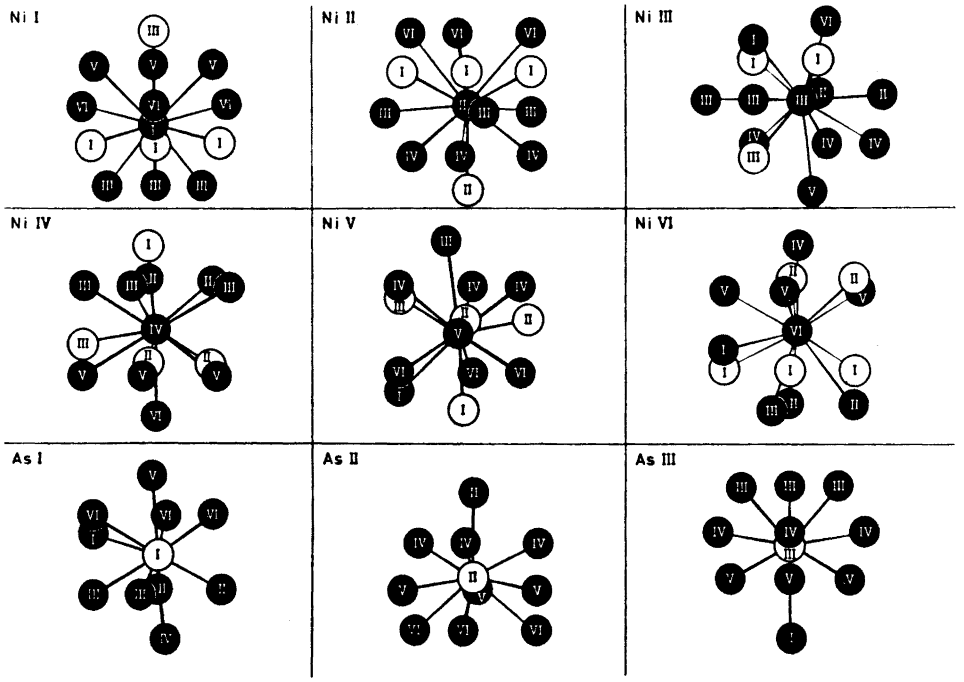

Fig. 2. The coordination polyhedra of the Ni_5As_2 structure projected along [100] of the ortho-hexagonal unit cell. The filled and open circles represent Ni and As, respectively.

Table 2. Interatomic distances (< 4 Å) in Ni_5As_2.

Type		Distance (Å)	Type		Distance (Å)
Ni(I)	– 3 Ni(III)	2.436(55)	Ni(I)	– 3 As(I)	2.341(20)
	– 3 Ni(V)	2.733(43)		– As(III)	2.777(53)
	– 3 Ni(VI)	2.643(33)		– As(III)	3.480(53)
Ni(II)	– 3 Ni(III)	2.626(8)	Ni(II)	– 3 As(I)	2.502(17)
	– 3 Ni(IV)	2.595(27)		– As(II)	2.477(44)
	– 3 Ni(VI)	3.047(51)		– As(II)	3.779(44)
	– 3 Ni(II)	3.936			
	– 3 Ni(V)	3.724(36)			
Ni(III)	– Ni(I)	2.436(55)	Ni(III)	– 2 As(I)	2.366(23)
	– 2 Ni(II)	2.626(8)		– As(III)	2.398(44)
	– 2 Ni(III)	2.905(19)		– As(I)	3.110(28)
	– 2 Ni(IV)	2.616(22)		– 2 As(II)	3.503(33)
	– Ni(IV)	2.887(24)			
	– Ni(V)	2.740(37)			
	– Ni(VI)	2.498(51)			
Ni(IV)	– 2 Ni(II)	2.596(27)	Ni(IV)	– As(I)	2.532(44)
	– 2 Ni(III)	2.616(23)		– 2 As(II)	2.364(21)
	– Ni(III)	2.887(24)		– As(III)	2.602(15)
	– Ni(V)	2.581(28)			
	– 2 Ni(V)	2.744(21)			
	– Ni(VI)	2.613(61)			
	– 4 Ni(IV)	3.705(9)			
Ni(V)	– Ni(I)	2.733(43)	Ni(V)	– As(I)	2.354(39)
	– Ni(III)	2.740(37)		– 2 As(II)	2.409(11)
	– Ni(IV)	2.581(28)		– As(III)	2.302(13)
	– 2 Ni(IV)	2.744(21)			
	– Ni(VI)	2.480(39)			
	– 2 Ni(VI)	2.664(32)			
	– 2 Ni(II)	3.724(36)			
	– 2 Ni(V)	3.593(27)			
Ni(VI)	– Ni(I)	2.643(33)	Ni(VI)	– As(I)	2.265(36)
	– 2 Ni(II)	3.047(51)		– 2 As(I)	2.691(29)
	– Ni(III)	2.498(51)		– 2 As(II)	2.671(43)
	– Ni(IV)	2.613(61)		– As(III)	3.402(54)
	– Ni(V)	2.480(39)			
	– 2 Ni(V)	2.664(32)			
	– 4 Ni(VI)	3.697(18)			
As(I)	– Ni(I)	2.341(20)	As(I)	– 2 As(I)	3.934(26)
	– 2 Ni(II)	2.502(17)		– 4 As(I)	3.937(13)
	– 2 Ni(III)	2.366(23)		– 2 As(II)	3.556(27)
	– Ni(IV)	2.532(44)		– As(III)	3.693(34)
	– Ni(V)	2.354(39)			
	– Ni(VI)	2.265(36)			
	– 2 Ni(VI)	2.691(29)			
	– Ni(III)	3.110(28)			
As(II)	– Ni(II)	2.477(44)	As(II)	– 3 As(I)	3.556(27)
	– 3 Ni(IV)	2.364(21)		– 3 As(II)	3.936
	– 3 Ni(V)	2.409(11)		– 3 As(III)	3.983(6)

Table 2. Continued.

As(II)	−3 Ni(VI)	2.671(43)			
	− Ni(II)	3.779(44)			
	−3 Ni(III)	3.503(33)			
As(III)	− Ni(I)	2.777(53)	As(III)	−3 As(I)	3.693(34)
	−3 Ni(III)	2.398(45)		−6 As(II)	3.983(6)
	−3 Ni(IV)	2.602(15)			
	−3 Ni(V)	2.302(27)			
	− Ni(I)	3.480(53)			
	−3 Ni(VI)	3.402(54)			

Table 3. The coordination numbers together with the average values of the Ni−Ni and Ni−As distances around the different atoms in Ni_5As_2. (CN(Ni) is the number of nearest Ni neighbours, CN(As) the number of nearest As neighbours, d_m the average distance in Å, R_{Ni} Goldschmidt Ni radius CN12, and r_{As} is the covalent (CN = 4) radius for As.)

Central atom	CN(Ni)	d_m(Å)	$d_m/2R_{Ni}$	CN(As)	d_m(Å)	$d_m - (R_{Ni}+r_{As})$(Å)
Ni(I)	9	2.604	1.05	4	2.449	+0.03
Ni(II)	9	2.756	1.11	4	2.496	+0.08
Ni(III)	10	2.686	1.08	3	2.377	−0.04
Ni(IV)	9	2.666	1.08	4	2.466	+0.05
Ni(V)	8	2.669	1.08	4	2.369	−0.05
Ni(VI)	8	2.707	1.09	5	2.598	+0.18
As(I)	10	2.461				+0.04
As(II)	10	2.481				+0.06
As(III)	10	2.468				+0.05

are summarized in Table 3. Each of the six different kinds of Ni atoms is surrounded by 8−10 other Ni atoms at distances ranging from 2.44 to 3.05 Å, and 3−5 As atoms at distances between 2.27 and 2.78 Å, so that each Ni atom has a total of 12−13 close neighbours. The coordination numbers of the three different kinds of As atoms are constant and equal to 10 Ni. The Ni−Ni distances which are classified as non-bonding exceed 3.59 Å, while the corresponding non-bonding Ni−As distances are greater than 3.11 Å. As seen from Table 3 the average Ni−Ni distance is smallest around Ni(I) and largest around Ni(II), the two averages differing only 5.8 %. A considerable larger degree of individual variation is found for the average Ni−As distance. The average Ni(VI)−As distance is 9.7 % greater than the average Ni(V)−As distance which represents the extremes in this case. The weighted average Ni−Ni distance in Ni_5As_2 is 2.67 Å which exceeds Goldschmidts[9] value for the Ni diameter (2.48 Å for CN = 12) by 7.7 %. The mean Ni−As distance is 2.456 Å which is 0.04 Å larger than the sum of the metal radius for nickel (1.24 Å[9]) and the tetrahedral covalent radius for arsenic (1.18 Å[9]). There are no As−As distances shorter than 3.55 Å, and As has accordingly only Ni as nearest neighbours.

The structure of Ni_5As_2 is rather complicated and the coordination polyhedra are so irregular (Fig. 2) that it is difficult to describe them in normal

terms. The structure is in fact among the most complicated for the metal rich pnictides. Apart from the isostructural Pd_5Sb_2 it is difficult to find any relationship connecting it with other structures.

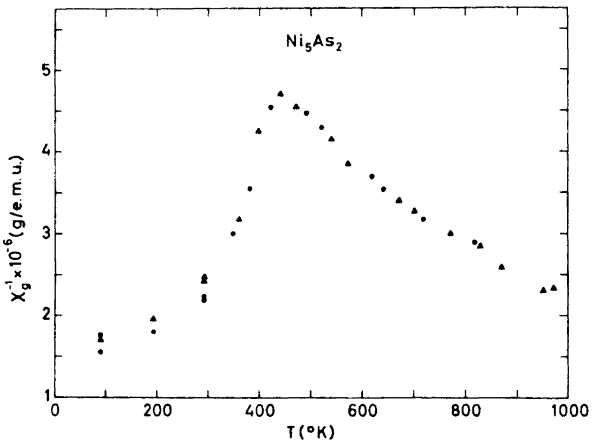

Fig. 3. Reciprocal of the magnetic susceptibility of Ni_5As_2 as function of increasing (▲) and decreasing (●) temperature.

Magnetic properties. Magnetic susceptibility measurements of Ni_5As_2 were made on samples quenched from 900°C. The results (Fig. 3) exhibit excellent reproducibility between a number of different samples. Field strength dependent susceptibilities were not observed and the results shown in Fig. 3 represent mean values obtained at several different field strengths. (The data are uncorrected for induced diamagnetism since reliable corrections are not easily estimated.) The $\chi^{-1}(T)$-curve does not follow the Curie-Weiss Law in any temperature range. Apart from a gross classification as paramagnetic it is impossible on account of the present data to establish the detailed magnetic behaviour of Ni_5As_2. In order to rectify this situation a neutron diffraction study of Ni_5As_2 is currently being undertaken.

REFERENCES

1. Gurlt *Über pyrogene künstliche Mineralien*, Freiburg 1857, p. 35; quoted from Friedrich, K. *Metallurgie* **4** (1907) 200.
2. Hellner, E. *Fortschr. Mineral.* **29–30** (1951) 58.
3. Heyding, R. D. and Calvert, L. D. *Can. J. Chem.* **35** (1957) 1205.
4. Yund, R. A. *Econ. Geol.* **56** (1961) 1273.
5. El-Boragy, M., Bhan, S. and Schubert, K. *J. Less-Common Metals* **22** (1970) 445.
6. Dahl, T., Gram, F., Groth, P., Klewe, B. and Rømming, C. *Acta Chem. Scand.* **24** (1970) 2232.
7. Hanson, H. P., Herman, F., Lea, J. D. and Skillman, S. *Acta Cryst.* **17** (1964) 1040.
8. Saini, G. S., Calvert, L. D. and Taylor, J. B. *Can. J. Chem.* **42** (1964) 150.
9. Pauling, L. *The Nature of the Chemical Bond*, Cornell University Press, Ithaca 1960.

Received August 21, 1972.

ACTA CHEMICA SCANDINAVICA 27 (1973) 589–594

Mass Spectrometry of Onium Compounds

Part XVI.[1] Pyrolytic Fragmentation of Amino Acid Betaines

KJELL UNDHEIM and TORE LÆRUM

Department of Chemistry, University of Oslo, Oslo 3, Norway

The pyrolytic behaviour in the mass spectrometer of a series of *N*-quaternary amino acid homologues has been investigated. The pyrolysis process is dependent on the number of methylene carbons separating the functional groups.

Electron induced fragmentations are discussed in relevant cases.

The salt like characteristics of *N*-quaternary amino acids and the frequent lack of a readily accessible chromophore for absorption spectroscopy complicates identification and estimation in low concentration in natural sources. The pyrolytic behaviour of such compounds in the mass spectrometer should therefore be of both theoretical and analytical interest. Recently we reported the mass spectrometry behaviour of the liver component carnitine and fatty acid esters thereof.[2] This work concerns simple aliphatic *N*-quaternary amino acids where the functional groups are separated by series of methylene groups. High resolution has been used in the determination of the composition of major fragments discussed.

$$(CH_3)_3N^+-(CH_2)_n-CO_2^-$$

I $n=1$, II $n=2$, III $n=3$, IV $n=4$, V $n=5$

The spectra recorded are formed through superimposition of the fragmentation spectra from the pyrolysis products present in the gas phase. The relative peak intensities will vary with conditions and with time in accordance with relative volatilities of the components.

The base peak in the spectrum of trimethylamine is at *m/e* 58 [M−H], the molecular ion intensity being 45 %.[3] Some *m/e* 58 species are also formed by α-cleavage from dimethylaminomethylene derivatives after electron impact and when present with trimethylamine will increase the relative intensity of the *m/e* 58 signal.

For the glycine betaine (I), which is an α-amino acid derivative, esterification is the most important pyrolytic process. With two or three methylene carbons between the functional groups (II, III) no ester formation is seen. Esterification reappears again with four methylene groups (IV), however, and is the only important process for $n = 5$ and probably also for higher homologues. The near absence of the corresponding acid in the spectra is ascribed to low volatility with high probability for esterification.

A decision between intra- or the more likely inter-alkylation process was made in each case where ester is formed by allowing homogeneous mixtures of the amino acid, quaternized with trideuteriomethyl iodide and with methyl iodide, to evaporate in the mass spectrometer. Invariably, when the spectra were recorded after a short time, four equally intense peaks were found which correspond to the molecular ion. For the glycyl betaine these were at *m/e* 117 ($(CH_3)_2NCH_2CO_2CH_3$), *m/e* 120 ($(CH_3)_2NCH_2CO_2CD_3$), *m/e* 123 ($(CD_3)_2NCH_2CO_2CH_3$), and *m/e* 126 ($(CD_3)_2NCH_2CO_2CD_3$). Therefore the transalkylation is an intermolecular process. When the spectra were recorded after the sample had been kept for some time in the instrument, the intermediate molecular ion peaks showed increased intensities. This is due to transfer of a methyl group from the quaternary nitrogen to a tertiary nitrogen which thereby is requaternized and can take part in the esterification reactions.

The spectrum of the β-alanine (II) shows that liberation of trimethylamine is the only important process with concomitant formation of acrylic acid or its isomeric β-lactone (*m/e* 72). In deuterium oxide atmosphere two peaks were found at *m/e* 72 and *m/e* 73. The intensity of the latter was about half that of the former. Deuterium exchange is in accordance with acrylic acid formation, the exchange being incomplete under these experimental conditions.* The reason for complete dominance of the Hofmann elimination lies in carboxyl group activation of the hydrogens on the β-carbon relative to the quaternary nitrogen. Trimethylamine and acrylic acid are also the products from preparative pyrolysis.[4]

With three methylenes (III) the carboxylate group is in position for γ-lactone formation and Hofmann elimination is competitively excluded, partly because the β-carbon is no longer activated. Coformation of the isomeric β,γ-unsaturated acid could be excluded since no deuterium was incorporated in the molecular ion at *m/e* 86 when the spectrum was recorded in deuterium oxide atmosphere. Preparative pyrolysis takes the same course.[4]

For $n = 4$, δ-lactone (*m/e* 100) and its fragments account for part of the ion current, but the more important pyrolytic pathway seems to go through the ester (*m/e* 159) (Fig. 2). These results agree with pyrolytic observations.[5] With five methylene groups, as discussed above, ester formation is the only important pyrolytic process (Fig. 3).

The behaviour of the hydroiodide salts of I – V was also investigated. The Hofmann elimination in II, or γ-lactone formation in III, were not affected. For the other acids (I, IV, V) the intensity of the ester molecular ion was more than halved. The relative intensity (*m/e* 58) of the methyl iodide signal (*m/e* 142) was 40 – 50 %.

* Unpublished observations.

The spectrum of II is due to superimposition of the fragmentation spectra from acrylic acid [6] and trimethylamine [3] and that of III is due to γ-lactone [7] and trimethylamine.

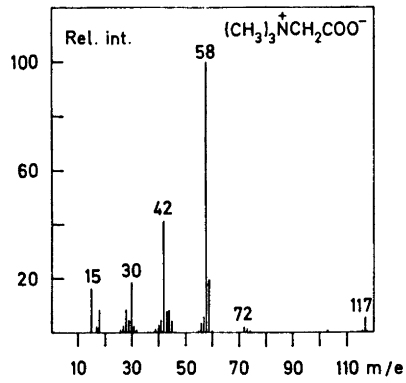

Fig. 1.

The glycine spectrum (Fig. 1) shows the gas phase molecules to be the transalkylated ester (*m/e* 117) and trimethylamine. The major peaks in the spectrum of trimethylamine [3] are at *m/e* 59 (45 %), *m/e* 58 (100 %), *m/e* 42 (42 %), *m/e* 30 (35 %), *m/e* 28 (18 %), and *m/e* 15 (20 %). The relative intensity of the base peak (*m/e* 58) in the spectrum of I is more than twice that in trimethylamine and its main origin is therefore the ester at *m/e* 117 (Scheme 1). α-Cleavage to nitrogen so strongly directs the fragmentation that other pathways are of little importance. The intensities of the *m/e* 42, 30, and 15 species are much reduced compared to the same fragments from trimethylamine. The increase in relative stability of the *m/e* 58 species is even more evident from the spectrum of V (Fig. 3) where the relative intensities of the

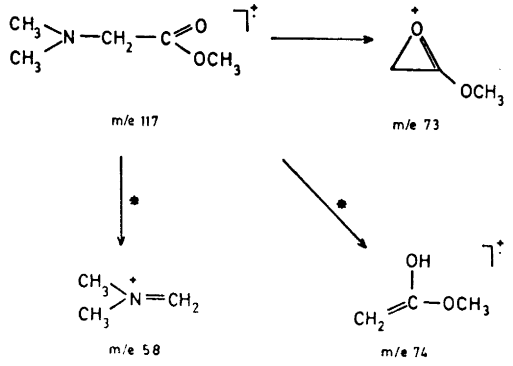

Scheme 1.

m/e 42, 30, and 15 species are below 10 %. Two energetically different structures of the *m/e* 58 species therefore exist. The weak signal at *m/e* 74 is due to

McLafferty rearrangement with transfer of a hydrogen from one of the *N*-methyl groups. Methoxyl expulsion (*m/e* 86), which is important for the esters discussed below, is hardly seen.

In the higher esters the fragmentation is also dominated by the amino function in such a way that the amino nitrogen is present in most of the important fragments. This is not unexpected since the fragmentation process will be determined by charge distribution and relative rates. The charge will largely reside on the amino group since this has much the lower ionization potential but its direction of fragmentation will be modified by interaction with the ester group.[9–11] Thus McLafferty rearrangement gives a weak signal at *m/e* 74 while methoxyl group expulsion is relatively strong. The latter mode of fragmentation is probably favoured by stabilization through the amino group (Scheme 2, Figs. 2 and 3).

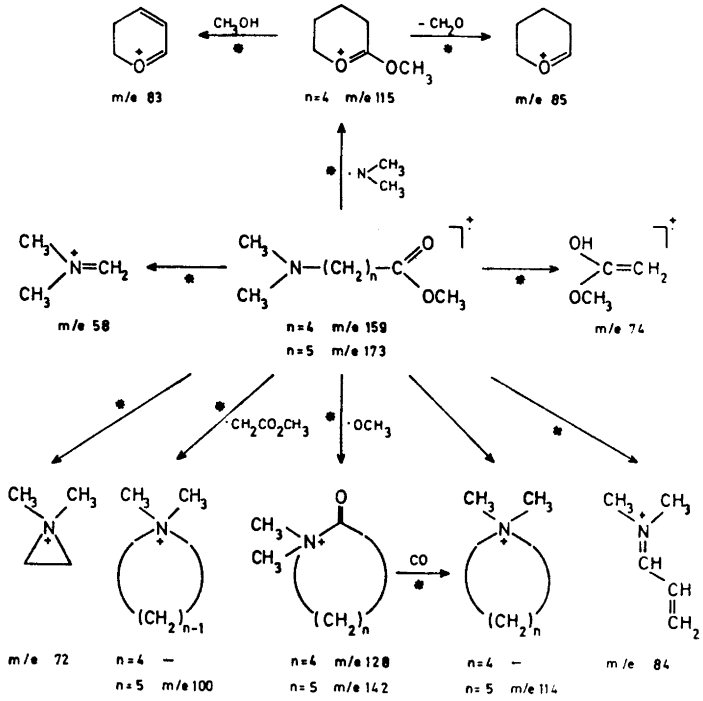

Scheme 2.

An important fragment in both spectra is found at *m/e* 84. In Scheme 2 its genesis is indicated directly from the molecular ion. Metastable defocusing shows that these species also originate from primary fragments. The base peak at *m/e* 58 is formed directly from the molecular ion but metastable defocusing shows that it is also formed from several precursor ions. IV gives

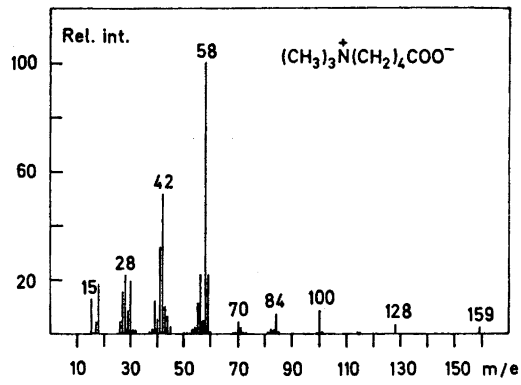

Fig. 2.

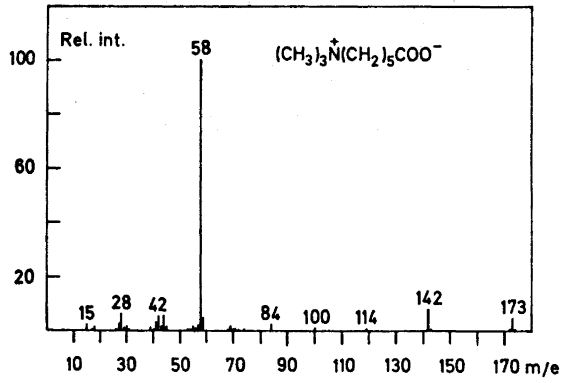

Fig. 3.

a relatively strong ion at *m/e* 115. The corresponding fragment in V is not important. On the other hand, V gives an ion at *m/e* 100 by δ-cleavage which can be formulated as a pyrrolidinium ion.

The low energy spectrum (16 eV) of V increases the molecular ion and the *m/e* 100 intensity by a few per cent. The low and high energy spectra are very similar since in both cases the major ion current is carried by the *m/e* 58 species. The low energy spectrum of IV also shows a slight increase in the molecular ion intensity but the major increase, from about 20 to 40 %, is in the *m/e* 59 species, showing the presence of trimethylamine.

The spectrum of IV also contains the fragmentation of δ-lactone. The major fragments from the latter are at *m/e* 42 (base peak in the spectrum of pure δ-lactone) and at *m/e* 56 ($M-CO_2$, 45 %). The other peaks of 10 – 20 % relative intensity are at *m/e* 100 (M), *m/e* 71 ($M-CHO$), *m/e* 55 ($M-HCO_2$), and *m/e* 41 ($M-CH_2CO_2H$).[8]

The spectra of the hydroiodides show the additional weak molecular ions (*m/e* 143 and *m/e* 159) of the respective acids. These will fragment very much in the same way as the esters.

EXPERIMENTAL

The spectra were recorded on an AEI MS-902 mass spectrometer by direct insertion. The source temperature was kept at 210 – 220°, the electron energy and trap current at 70 eV and 100 μA respectively.

The hydroiodides were prepared by quaternization of the corresponding primary amines with methyl iodide.[12] The trideuteriomethyl derivatives were similarly prepared. The zwitterions were generated by passage of an aqueous solution of the hydroiodides through DEAE – Sephadex. The evaporation temperature of the eluates should be low to avoid decomposition.

REFERENCES

1. Grønnberg, T. and Undheim, K. *Tetrahedron Letters* **1972** 3193 (Part XV).
2. Hvistendahl, G., Undheim, K. and Bremer, J. *Org. Mass. Spectrom.* **3** (1970) 1433.
3. Hvistendahl, G. and Undheim, K. *Org. Mass Spectrom.* **3** (1970) 821.
4. Willstätter, R. *Ber.* **35** (1902) 584.
5. Willstätter, R. and Kahn, N. *Ber.* **37** (1904) 1853.
6. Happ, G. P. and Stewart, D. W. *J. Am. Chem. Soc.* **74** (1952) 4404.
7. Friedman, L. and Long, F. A. *J. Am. Chem. Soc.* **75** (1953) 2832.
8. Honkanen, E., Moisio, T. and Karvonen, P. *Acta Chem. Scand.* **19** (1965) 370.
9. Wagner, P. J. *Org. Mass Spectrom.* **3** (1970) 1307.
10. Caspar, A., Teller, G. and Wolff, R. E. *Org. Mass Spectrom.* **3** (1970) 1351.
11. Wolff, R. E. and Caspar, A. *Tetrahedron Letters* **1970** 1807.
12. Griess, P. *Ber.* **8** (1875) 406.

Received June 28, 1972.

ACTA CHEMICA SCANDINAVICA 27 (1973) 595–599

Benzo[b]thiophene Formation by Thiophenol Addition to Activated Triple Bonds

KJELL UNDHEIM and REIDAR LIE

Department of Chemistry, University of Oslo, Oslo 3, Norway

Adduct formation between thiophenols and acetylenedicarboxylic acid and its methyl ester has been studied. Benzo[b]thiophenes were formed in several solvents. In methanol a vinyl thioether was formed either alone or together with the corresponding benzo[b]thiophene depending on the thiophenol substituents. The reaction mechanism has been investigated.

Michael additions of thiophenols to activated triple bonds have been reported to give the corresponding vinyl ethers.[1,2] The rate depends on the electron releasing properties of the substituents.[3] Benzo[b]thiophene is formed in the reaction between acetylene and thiophenol at 500 – 600°C.[4,5] Photochemical cyclisation of a vinyl thioether is possible.[6] Pentafluorothiophenolate will add to acetylenedicarboxylic acid ethyl ester with concomitant cyclisation which involves nucleophilic displacement of a fluorine.[7] On the other hand, thiophenolate and 2-nitrothiophenolate additions to the ethyl ester of acetylenedicarboxylic acid have been reported to yield the respective vinyl thioethers.[2,8] Addition of thiophenol to propiolic acid also gave the vinyl thioether.[1] As an extension of our interest in thiolactam addition to triple bonds [9] we have reinvestigated the reaction between thiophenols and acetylenedicarboxylic acid and its methyl ester. In ethyl acetate the methyl ester of acetylenedicarboxylic acid would add thiophenol and its methyl (Ib) and chloro (Ic) derivatives but not the nitro derivative (Id). Acetylenedicarboxylic acid reacted similarly. The reaction gave the cleanest product when run in the cold over several days. The product was identified as a benzo[b]thiophene (V) as discussed below. In methanol, however, no reaction took place in the cold. On reflux *p*-chloro- and *p*-nitrothiophenol gave the vinyl thioethers III while thiophenol and its *p*-methyl homologue yielded a mixture of the vinyl thioether III and the bicylic product V. The structure of the latter was evident from its spectroscopic properties; only aromatic protons in the NMR spectra and UV maxima in ethanol at about 290 nm, at 245 nm, and at 230 nm. For comparison the UV maxima for the vinyl ether are at about 265 nm and 225

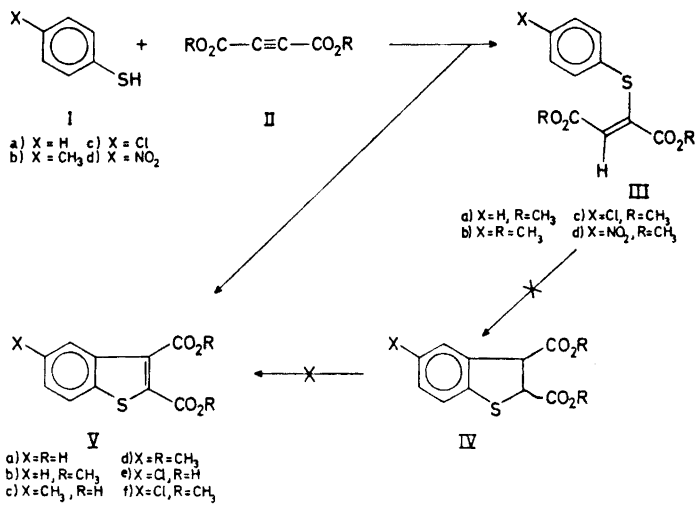

Scheme 1.

nm. In the NMR spectrum of III ($CDCl_3$) the vinyl proton appears as a sharp singlet at 3.5 τ which suggests that only one stereoisomer is present. If the usual *trans* addition is assumed, the carboxy groups in the vinyl thioether have the *trans* configuration.

In a further study of the solvent effect on the reaction between thiophenol and the methyl ester of acetylenedicarboxylic acid, the reaction was run at 35°C for 14 days in the solvents ethyl acetate, dioxane, toluene, and acetic acid. The respective yields of Vb were 29, 14, 18, and 36 %.

In the initial addition step the mechanism appears to be ionic as the rates and the product yields in ethyl acetate were not noticeably affected when the reaction was run in the presence of benzoyl peroxide or hydroquinone. The direct formation of the benzo[b]thiophene could possibly take place *via* the vinyl thioethers III involving rapid dehydrogenation of an intermediate 1,2-dihydrobenzo[b]thiophene (IV). Both gas chromatographic analysis and slow evaporation in the mass spectrometer of the crude reaction mixture from the reaction in ethyl acetate, showed that methyl acetylenedicarboxylate had been reduced to maleate/fumarate, but no succinate was seen. This establishes the acetylene to be the dehydrogenator. Attemps failed to cyclize IIIb by heating in ethyl acetate or methanol with and without the presence of methyl acetylenedicarboxylate. Neither did any cyclisation of IIIb take place when it was added to the reaction mixture of thiophenol and acetylenedicarboxylate ester, the bicyclic product formed being Vb. The above results exclude the vinyl thioether as an intermediate in the reaction.

A concerted reaction mechanism (Scheme 2) would also involve a 1,2-dihydro derivative (IV). Such a derivative was therefore synthesized by sodium amalgam reduction of Va. The reaction conditions should give the thermodynamically more stable *trans* isomer in good agreement with NMR ($J_{2,3} = 8.0$

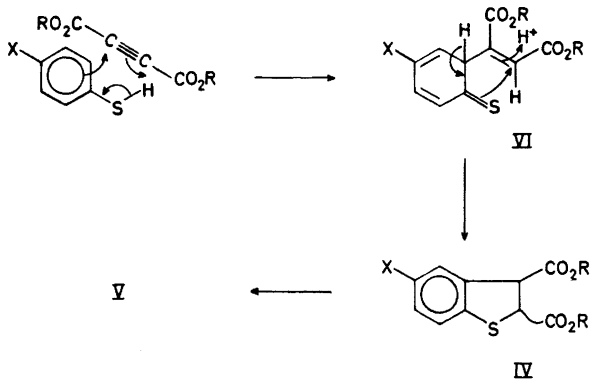

Scheme 2.

cps). Our attempts failed to dehydrogenate IV by means of acetylenedicarboxylate ester under the above reaction conditions. With the assumption that also the *cis* isomer of IV behaves similarly, a dihydro intermediate is excluded. Involvement of an intermediate carbanion type structure is an alternative possibility, at least in the formation of the bicyclic product (V). Such an anion (VII) with suggested reaction path is indicated in Scheme 3. According to this mechanism both the rate of addition and hydride abstraction are dependent on the electron releasing properties of the *para* substituent.

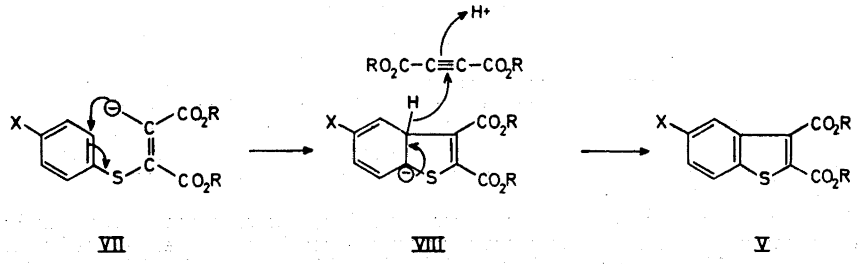

Scheme 3.

Thus the nitrothiophenol did not react in ethyl acetate and when forced in methanol gave the vinyl ether. On the other hand both thiophenol and its *p*-methyl analogue in methanol yield both products (III and V). These results could be interpreted to mean that hydride abstraction is the rate determining step in the overall reaction. A carbanion intermediate has also been suggested for the addition of pentafluorothiophenolate to ethyl acetylenedicarboxylate where the cyclisation involves nucleophilic displacement of a fluoride ion.[7]

The IR spectra in KBr of the benzo[b]thiophene-2,3-dicarboxylic acids show relatively weak hydroxyl bands around 3500 cm^{-1} and carboxyl bands at 1680 – 1700 cm^{-1}. Similar observations have been made for vicinal di-

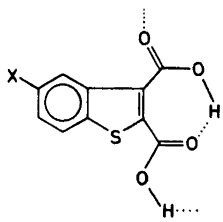

Scheme 4.

carboxylic acids of thiophene and furan and are explained by strong inter- and intra-molecular hydrogen bonding.[10,11] Strong carboxyl bands at 1705–1710 cm^{-1} are present in the spectrum recorded in chloroform solution. The dimethyl ester bands are at 1705–1735 cm^{-1}. The dihydro compound IV in KBr has two close carbonyl bands at about 1700 cm^{-1}. These results confirm strong hydrogen bonding as the cause of the relatively weak carbonyl bands in the case of the benzothiophene dicarboxylic acids.

EXPERIMENTAL

Benzo[b]thiophene-2,3-dimethylcarboxylate (Vb). A solution of thiophenol (1.10 g, 0.01 mol) and dimethyl acetylenedicarboxylate (1.42 g, 0.01 mol) in ethyl acetate was left at room temperature for 5 days. The solvent was then evaporated and the oily residue on crystallisation from methanol gave yellow needles (0.40 g, 16 %), m.p. 91°C. (Found: C 57.28; H 4.19; S 12.96. Calc. for $C_{12}H_{10}O_4S$: C 57.58; H 4.03; S 12.76.) UV maxima in 0.1 N HCl (EtOH) at 291 nm (log ε 4.10), 245 nm (4.03) and 229 nm (4.15). NMR in $CDCl_3$: 6.05 τ and 5.97 τ (OCH_3), 1.9–2.7 τ (phenyl H).

5-Methylbenzo[b]thiophene-2,3-dimethylcarboxylate (Vd). The title compound was prepared as above in 44 % yield after leaving the solution for 22 days at room temperature; yellow needles from methanol, m.p. 91°C. (Found: C 58.86; H 4.64; S 12.01. Calc. for $C_{13}H_{12}O_4S$: C 59.06; H 4.58; S 12.13.) UV maxima in 0.1 N HCl (EtOH) at 295 nm (log ε 4.17), 245 nm sh. (4.06) and 234 nm (4.18). NMR in $CDCl_3$: 6.05 and 5.97 τ (OCH_3), 7.52 τ (CH_3), 2.1–2.8 τ (phenyl H).

5-Chlorobenzo[b]thiophene-2,3-dimethylcarboxylate (Vf) was prepared as above in 36 % yield after leaving the solution at room temperature for 17 days; yellow needles from methanol, m.p. 123°C. (Found: C 50.34; H 3.25; S 11.39. Calc. for $C_{12}H_9ClO_4S$: C 50.62; H 3.18; S 11.26.) UV maxima in 0.1 N HCl (EtOH) at 292 nm (log ε 3.96), 245 nm sh. (4.06) and 233 nm (4.18). NMR in $CDCl_3$: 6.05 τ and 5.97 τ (OCH_3), 1.9–2.5 τ (phenyl H).

Benzo[b]thiophene-2,3-dicarboxylic acid (Va) was prepared as above from acetylenedicarboxylic acid. The yellow title compound crystallized out from the solution. After 14 days at room temperature the yield was 32 %; recrystallization from dilute ethanol gave m.p. 245°C. (Found: C 54.09; H 2.91; S 14.14. Calc. for $C_{10}H_6O_4S$: C 54.05; H 2.72; S 14.43.) UV maxima in 0.1 N HCl at 289 nm (log ε 3.94), 245 nm (3.97) and 229 nm (4.07).

5-Methylbenzo[b]thiophene-2,3-dicarboxylic acid (Vc) was prepared as above. The yield after leaving the solution at room temperature for 22 days was 36 %; recrystallization from ethanol gave m.p. 266–267°C. (Found: C 51.98; H 3.94; S 12.59. Calc. for $C_{11}H_8O_4S.H_2O$: C 51.95; H 3.96; S 12.61.) UV maxima in 0.1 N HCl (EtOH) at 292 nm (log ε 3.87), 245 nm sh. (3.87) and 232 nm (4.03).

5-Chlorobenzo[b]thiophene-2,3-dicarboxylic acid (Ve) was prepared as above by heating the solution at 60°C for 1 day. The product crystallized from the cold solution in 54 % yield; m.p. 270–271°C after recrystallization from dilute ethanol. (Found: C 43.85; H 2.59; S 11.89. Calc. for $C_{10}H_5ClO_4S.H_2O$: C 43.71; H 2.57; S 11.67.)

2-(4-Chlorothiophenyl)butenedioic acid dimethyl ester (IIIc). A solution of 4-chlorothiophenol (1.42 g, 0.01 mol) and dimethyl acetylenedicarboxylate (1.42 g, 0.01 mol) in methanol (50 ml) was heated under reflux for 2 h. The product crystallized from the solution on standing in the cold; yield 59 % (1.67 g). Recrystallization from methanol gave yellowish white material, m.p. 88°C. (Found: C 50.51; H 3.87; S 11.05. Calc. for $C_{12}H_{11}ClO_4S$: C 50.25; H 3.87; S 11.18.) UV maxima in 0.1 N HCl (EtOH) at 263 nm (log ε 4.06) and 223 nm (4.20). NMR in TFA: 6.40 τ and 6.05 τ (singlets, OCH_3); 3.47 τ (singlet due to vinyl H); 2.68 τ and 2.59 τ (phenyl H).

2-(4-Nitrothiophenyl)butenedioic acid dimethyl ester (IIId) was prepared as above in 47 % yield by heating the methanol solution for 3 h. Recrystallization from methanol gave yellowish-white material, m.p. 99°C. (Found: C 48.46; H 3.71; S 4.97. Calc. for $C_{12}H_{11}NO_6S$: C 48.48; H 3.73; S 4.73.) UV maxima in 0.1 N HCl (EtOH) at 331 nm (log ε 4.10) and 223 nm (4.20). NMR in TFA: 6.25 τ and 6.00 τ (singlets, OCH_3), 2.95 τ (singlet, vinyl H), 2.35 τ and 1.68 τ (phenyl H).

trans-*2,3-Dihydrobenzo[b]thiophene-2,3-dicarboxylic acid (IV).* 2 % Sodium amalgam (10.7 g) was added gradually over 30 min under vigorous stirring to a solution of benzo[b]-thiophene-2,3-dicarboxylic acid (0.89 g, 0.004 mol) in 1.5 N NaOH (16 ml). The reaction mixture was stirred overnight, the mixture acidified and the precipitated solid recrystallized from water. The yield of a white crystalline material was 79 % (0.70 g), m.p. 193–194°C. (Found: C 53.50; H 3.69; S 14.28. Calc. for $C_{10}H_8O_4S$: C 53.56; H 3.59; S 14.30.) NMR in acetone-d_6: AB-quartet at 5.00 τ and 5.17 τ (H^2, H^3, $J_{2,3}=8.0$ cps). Aromatic H at 2.4–3.0 τ.

REFERENCES

1. Montanari, F. *Tetrahedron Letters* **1960**, No. 4, 18.
2. Kalbag, S. M., Nair, M. D., Rajagopalan, P. and Talaty, C. N. *Tetrahedron* **23** (1964) 1911.
3. Krishnamurthy, G. S. and Miller, S. I. *J. Am. Chem. Soc.* **83** (1961) 3961.
4. Sakan, T., Kotake, H., Fujino, A. and Matsuura, T. *Chem. Abstr.* **46** (1952) 2047b.
5. Lesnaik, T. *Rocz. Chem.* **38** (1964) 1923.
6. Groen, S. H., Kellogg, R. M., Buter, I. and Wynberg, H. *J. Org. Chem.* **33** (1968) 2218.
7. Brooke, G. M. and Quasem, M. A. *J. Chem. Soc.* **C 1967** 865.
8. Ruheman, S. and Stapleton, H. E. *J. Chem. Soc.* **77** (1900) 1179.
9. Lie, R. and Undheim, K. *Acta Chem. Scand. In press.*
10. Oae, S., Furukawa, N., Watanabe, T., Otsuji, Y. and Hamanda, M. *Bull. Chem. Soc. Japan* **38** (1965) 1247.
11. Williams, D. and Rundle, R. E. *J. Am. Chem. Soc.* **86** (1964) 1660.

Received August 18, 1972.

ACTA CHEMICA SCANDINAVICA 27 (1973) 600–604

Polychlorinated Biphenyls

II.* Synthesis of Some Tetra- and Pentachlorobiphenyls

GÖRAN SUNDSTRÖM

Wallenberglaboratoriet, Stockholms Universitet, Lilla Frescati, S-104 05 Stockholm, Sweden

The syntheses of eighteen tetra- and pentachlorobiphenyls, most of which are unsymmetrically substituted, are described. Their physical characteristics, including relative retention times in gas-liquid chromatography and their occurrence in commerical PCB-mixtures, as previously reported, are recorded in Table 1.

The occurrence of polychlorinated biphenyls (PCB) in fish and birds from coastal waters was first reported by Jensen [1] and comprehensive reviews dealing with various aspects of the present widespread environmental pollution through PCB have recently been published.[2,3]

Commercial PCB-mixtures used, *e.g.*, in the electrical industry, contain a number of related compounds with one to ten chlorine atoms in the molecule.[4,5] Only a restricted number of these constituents have so far been prepared by unambiguous synthetic routes.[6–8]

The present paper describes the simple synthesis of 3 symmetrically and 15 unsymmetrically substituted tetra- and pentachlorobiphenyls, of interest as reference compounds in analytical work on environmental pollutants. Recently, a synthesis of ^{14}C-labelled tetrachlorobiphenyls *via* a Gomberg-Bachmann reaction between diazotised 2,4-dichloroaniline-^{14}C and 1,2-dichlorobenzene was described.[9] However, this method is not applicable in coupling reactions where the chlorobenzene component is a solid at temperatures close to 0°.[10]

In the syntheses of the biphenyls described in Table 1 we have, with two exceptions (*cf.* below), used the method described by Cadogan,[11] in which arylation of an aromatic compound is achieved through its reaction at elevated temperatures with a mixture of an aniline and isoamyl nitrite. The six isomeric dichloroanilines and 2,4,5-trichloroaniline were thus coupled with 1,4-di- and 1,2-dichlorobenzene. In the reactions with 1,2-dichlorobenzene, two isomeric biphenyls were formed in a ratio of *ca.* 2:1 as determined by GLC. The coupling

* Part I, *cf.* Ref. 9.

of 3,5-dichloroaniline with 1,2-dichlorobenzene gave substantial amounts of by-products and the Gomberg-Bachmann reaction was chosen as more suitable for that particular coupling. The structure for each individual, isolated component was assigned on the basis of the UV spectrum which in each case revealed the number of substituents in the *ortho*-position to the biphenyl linkage.[12] For pairs of related biphenyls derived from 1,2-dichlorobenzene, the one with the higher number of chlorine atoms *ortho* to the biphenyl linkage had the shortest retention time, in agreement with previous observations.[4] As expected, this isomer was the one formed in minor amounts in the coupling reaction. It is noteworthy, that throughout the series, all the minor components, on thin layer chromatography on silica gel using hexane as solvent, had slightly lower R_F-values than the major ones.

2,3′,5,5′-Tetrachlorobiphenyl is erroneously described in an encyclopaedic work[13] as having m.p. 162°. The reference given,[14] however, contains no information about this compound, but describes, instead, the synthesis of the isomeric 3,3′,5,5′-tetrachlorobiphenyl, m.p. 162°. In the same encyclopaedic work,[13] 2,3′,4,4′,5-pentachlorobiphenyl is reported as having m.p. 179°. However, the references cited [15,16] give no conclusive evidence for this structure.

Saeki *et al.*[8] recently described a compound erroneously formulated as 2,3′,4,4′,5-pentachlorobiphenyl, m.p. 82°. The two main products formed in the coupling of 2,4,5-trichloroaniline with 1,2-dichlorobenzene, from reasons given above, must be formulated as 2,3′,4,4′,5-pentachlorobiphenyl, m.p. 112–113°, and 2,2′,3′,4,5-pentachlorobiphenyl (minor component), m.p. 81.5–82.5°, respectively (*cf.* Table 1). The NMR-spectrum (100 MHz) of the compound with m.p. 112–113° was also in all parts consistent with the published 220 MHz spectrum of 2,3′,4,4′,5-pentachlorobiphenyl.[5]

EXPERIMENTAL

Melting points were determined on a Kofler micro hot stage. UV spectra were measured in 99.5 % ethanol on a Perkin-Elmer 124 spectrophotometer. 2,3-, 2,5-, 3,4-Dichloroaniline and 2,4,5-trichloroaniline (Koch-Light), 2,6- and 3,5-dichloroaniline (Fluka), and 2,4-dichloroaniline (Schuchardt) were of reagent grade and were purified by crystallization before use. 1,4-Dichlorobenzene (Kebo AB, *purum*), 1,2-dichlorobenzene (Koch-Light, ≥ 99 %), and isoamyl nitrite (Riedel-de Haën, pure, DAB. 6) were used without further purification.

Gas chromatography. The biphenyls were characterized by GLC using a Varian 1400 instrument fitted with an electron capture detector. Glass columns (0.18 × 160 cm) containing 4 % (w/w) SF 96 on Chromosorb W A/W DMCS (100–120 mesh) were used. The retention time of the standard compound, 1,1-dichloro-2,2-bis(*p*-chlorophenyl)-ethylene (*p,p′*-DDE), was kept as close to 24 min as possible. This condition was obtained with a gas flow (nitrogen) of *ca.* 25 ml/min and an oven temperature of *ca.* 160°.

Coupling of di- or trichloroanilines with 1,4-dichlorobenzene. The chloroaniline (0.5 g) was mixed with 1,4-dichlorobenzene (12 g) and the mixture was heated to *ca.* 60°. Isoamyl nitrite (1 ml) was added to the melt with stirring. The reaction mixture was slowly heated to *ca.* 130° and kept at this temperature for 1.5 h. Excess dichlorobenzene was removed by evaporation at 140–150° under a flow of nitrogen. The residue was dissolved in a small amount of hexane : chloroform (1:1) and added to the top of a silica gel (Merck, 0.05–0.2 mm) column (1.5 × 19 cm). Hexane was used as eluant. Evaporation of solvent gave oils which crystallized upon the addition of methanol or ethanol. The yields were in the range of 20–30 %. Recrystallization followed by sublimation *in vacuo* gave the analytical samples (Table 1).

Table 1.

Di- or trichloro-aniline	Dichloro-benzene	Chloro-biphenyl formed	m.p. °C	λ_{max} nm log ε	Analyses [a] % C	% H	Occurrence in Aroclors ® [b] 1242	1254	Relative retention time [c]
2,3-	1,4-	2,2′,3,5′-	49–50 (aqMeOH)	266.5 (sh) 275.5 283 2.97 3.07 3.00	49.3	2.2	(+)	++	0.46
2,4-	1,4-	2,2′,4,5′-	65–66.5 (MeOH)	274 281.5 3.08 2.99	49.2	2.2	(++)	–	0.41
2,5-	1,4-	2,2′,5,5′-	85–86.5 (MeOH) [d]	268 (sh) 275.5 283.5 3.06 3.21 3.16	–		++	++	0.39
2,6-	1,4-	2,2′,5,6′-	103–104.5 (MeOH)	268 (sh) 275.5 283.5 2.91 3.00 2.91	49.4	2.2	–	–	0.33
3,4-	1,4-	2,3′,4′,5-	104–105 (MeOH) [e]	247 285 (sh) 4.21 3.40	–		++	++	0.63
3,5-	1,4-	2,3′,5,5′-	105.5–106.5 (EtOH)	245 (sh) 283.5 (sh) 3.98 3.25	49.4	2.1	(+)	(+)	0.51
2,3-	1,2-	2,3,3′,4′-	96–97 (MeOH) [f]	251 4.18	49.5	2.1	+	+	0.74
		2,2′,3,3′-	121–122 (EtOH)	271.5 279.5 (sh) 2.88 2.80	49.6	2.1	(+)	+	0.54

		2,3′,4,4′-	127–128 (EtOH) [g]	251 4.22	–	–	+	0.65
2,4-	1,2-	2,2′,3,4′-	68.5–70 (EtOH)	272.5 280.5 2.95 2.81	49.4 2.2	+	+	0.47
		2′,3,4,6′-	Oil	272.5 (sh) 281 (sh) 3.10 2.98	49.6 1.9	–	+	0.50
2,6-	1,2-	2,2′,3,6′-	125.5–127 (MeOH)	267.5 274.5 2.89 2.85	49.5 2.2	–	–	0.38
3,4-	1,2-	3,3′,4,4′-	177–178 (EtOH) [h]	261 4.17	–	(+)	(+)	0.99
		3,3′,4,5′-	119–120 (EtOH)	258.5 4.26	49.4 2.1	–	–	0.82
3,5-	1,2-	2,3,3′,5′-	127.5–129 (MeOH)	243.5 280 (sh) 4.00 3.09	49.4 2.1	(+)	–	0.58
2,4,5-	1,4-	2,2′,4,5,5′-	76–77 (EtOH)	275.5 (sh) 281 289 3.11 3.24 3.12	44.0 1.7	+	++	0.80
		2,3′,4,4′,5-	112–113 (EtOH) [i]	251.5 4.21	44.3 1.6	–	++	1.27
2,4,5-	1,2-	2,2′,3′,4,5-	81.5–82.5 (subl.) [i]	272 281 289.5 2.64 2.70 2.62	44.3 1.7	+	++	0.92

[a] Required for $C_{12}H_6Cl_4$: C 49.4, H 2.1; $C_{12}H_5Cl_5$: C 44.2, H 1.5. [b] From Ref. 4. Commercial products manufactured by Monsanto Chemicals, containing 42 and 54 % w/w chlorine, respectively. ++: major component, +: minor component, –: not detected. Uncertain results are bracketed. [c] *p,p′*-DDE = 1.00. For conditions, see Experimental. [d] Ref. 7, 86.5–87°; Ref. 17, 84–85°. [e] Ref. 18, 103°; Ref. 19, 104°. [f] Also obtained as a minor component in the coupling of 3,4-dichloroaniline with 1,2-dichlorobenzene. [g] Ref. 8, 124°; Ref. 9, 127–128°. [h] Ref. 6, 173°; Refs. 8, 14, 172°. [i] See text.

Coupling of di- or trichloroanilines with 1,2-dichlorobenzene. The chloroaniline (1.5 g) was dissolved in 1,2-dichlorobenzene (15 ml) and isoamyl nitrite (2 ml) was added dropwise with stirring at *ca.* 40°. The mixture was heated to *ca.* 130° and kept at this temperature for 1.5 h. The work-up was performed as described above, total yield 20 – 30 %. The major products formed in the reaction from 2,3-, 2,4-, 3,4-dichloroaniline and 2,4,5-trichloroaniline, respectively, crystallized upon the addition of methanol or ethanol to the oily crude products. The analytical samples were purified by recrystallization followed by sublimation *in vacuo*.

The biphenyl fractions (*ca.* 150 mg portions) obtained from the above alcoholic mother liquors were subjected to chromatography on columns (2 × 25 cm) containing silica gel (Merck, < 0.08 mm) with hexane as eluent. The course of the separations was followed by GLC and TLC (Merck, Kieselgel HF_{254}, hexane). In all cases the minor components were eluted after the major ones. The analytical samples were purified as above.

The two tetrachlorobiphenyls formed from 2,6-dichloroaniline were obtained in a pure state only through column chromatography of the crude reaction product as described above.

Gomberg-Bachmann coupling of 3,5-dichloroaniline with 1,2-dichlorobenzene. 3,5-Dichloroaniline hydrochloride (1.5 g) was suspended in 1,2-dichlorobenzene (50 ml) and cooled to 0°. A solution of sodium nitrite (6 M, 1.5 ml) was added dropwise with vigorous stirring during 15 min. After another 15 min, a solution of sodium hydroxide (5 M, 9 ml) was added in small portions during 30 min. Stirring was continued for 1.5 h while the reaction mixture was allowed to attain room temperature. After removal of the aqueous phase the dichlorobenzene was evaporated and the residue purified as described above.

The two tetrachlorobiphenyls formed were isolated through column chromatography as described above using hexane:ether (9:1) as eluent. The analytical samples were purified as described above.

Acknowledgements. I am indebted to Dr. C. A. Wachtmeister for his interest and advice. Financial support was given by the *Research Committee at the Swedish Environmental Protection Board* and by *Carl-Bertel Nathhorst Foundation.*

REFERENCES

1. Jensen, S. *New Sci.* **32** (1966) 612.
2. Edwards, R. *Chem. Ind. (London)* **1971** 1340.
3. Fishbein, L. *J. Chromatog.* **68** (1972) 345.
4. Sissons, D. and Welti, D. *J. Chromatog.* **60** (1971) 15.
5. Welti, D. and Sissons, D. *Org. Magn. Resonance* **4** (1972) 309.
6. Hutzinger, O., Safe, S. and Zitko, V. *Bull. Environ. Contam. Toxicol.* **6** (1971) 209.
7. Safe, S. and Hutzinger, O. *J. Chem. Soc. Perkin Trans. 1* **1972** 686.
8. Saeki, S., Tsutsui, A., Oguri, K., Yoshimura, H. and Hamana, M. *Fukuoka Igaku Zassi* **62** (1971) 20. (*Chem. Abstr.* **74** (1971) 146,294y.)
9. Moron, M., Sundström, G. and Wachtmeister, C. A. *Acta Chem. Scand.* **26** (1972) 830.
10. Bachmann, W. E. and Hoffmann, R. A. *Org. Reactions* **2** (1944) 225.
11. Cadogan, J. I. G. *J. Chem. Soc.* **1962** 4257.
12. Beaven, G. H. In Gray, G. W., Ed., *Steric Effects in Conjugated Systems*, Butterworths, London 1958, p. 22.
13. Hubbard, H. L. *Encyclopedia of Chemical Technology*, Interscience – Wiley, New York 1964, Vol. 5, p. 289.
14. van Roosmalen, F. L. W. *Rec. Trav. Chim.* **53** (1934) 359.
15. Schmidt, H. and Schultz, G. *Liebigs Ann. Chem.* **207** (1881) 340.
16. Zalkind, Y. S. and Belikova, M. V. *J. Gen. Chem. USSR (Eng. Transl.)* **8** (1939) 1918.
17. Meyer, H. and Hofmann, A. *Monatsh.* **38** (1917) 145.
18. Bellavita, V. *Gazz. Chim. Ital.* **65** (1935) 632.
19. German Patent 870, 106, March 9, 1953. (*Chem. Abstr.* **50** (1956) 16,863h.)

Received September 7, 1972.

ACTA CHEMICA SCANDINAVICA 27 (1973) 605–612

The Inhibition of a *p*-Nitrophenylphosphatase of *Streptococcus mutans* by Fluoride Ions

MATTI L. E. KNUUTTILA and KAUKO K. MÄKINEN

Institute of Dentistry, University of Turku, SF-20520 Turku 52, Finland

The effect of fluoride ions on the rate of the hydrolysis of *p*-nitrophenylphosphate, catalyzed by a purified *p*-nitrophenylphosphatase of *Streptococcus mutans*, was studied in the presence and absence of Mg^{2+} ions. The affinity of *p*-nitrophenyl phosphate for the enzyme was dependent on the concentration of Mg^{2+} ions. The kinetic data supported the formation of a Mg^{2+} – *p*-nitrophenyl phosphate complex in certain conditions. Fluoride ions had most likely reacted with the substrate, when tested at 0.67 – 1.67 mM NaF. The fluoride ions inhibited the growth of the cells but they had no repressive or inducive effect on the synthesis of the *p*-nitrophenylphosphatase.

Only few authors have reported detailed studies on the mode of action of fluoride ions on metal-requiring enzyme reactions. The inhibition of enolase by fluoride ions is one of the best known.[1–5] Phosphatases, which are often activated by Mg^{2+} ions, have been studied by several authors [6–12] as to mode of fluoride inhibition. Hewitt and Nicholas [13] have listed a number of reasons to explain why anions may exert an inhibitory influence on enzymes.

This paper will provide information about the inhibition by fluoride ions of the hydrolysis of *p*-nitrophenyl phosphate, specifically catalyzed by a purified phosphatase of *Streptococcus mutans*. The effect of fluoride ions on the synthesis of *p*-nitrophenylphosphatase was also studied. The purification and characterization of this enzyme has been described earlier.[14]

MATERIALS AND METHODS

1. *Effect of fluoride ions on the enzyme reaction.* The enzyme hydrolyzing specifically *p*-nitrophenyl phosphate was purified from the cells of *Streptococcus mutans* (strain Ingbritt) using DEAE cellulose chromatography and isoelectric focusing as the main steps.[14] The effect of different fluoride ion concentrations on the rate of the hydrolysis of *p*-nitrophenyl phosphate was studied at four substrate concentrations, varying also the amount of Mg^{2+} ions, which were found to activate the enzyme. The following fluorides were used: NaF and LiF, obtained from Merck A G (Darmstadt, Germany), and KF, from Baker Chemical Co (Phillipsburg, N.J., USA). The respective chlorides were used as controls.

The determination of the enzyme activity was based on the method of Bessey *et al.*,[15] which was performed in 0.025 M borate buffer, pH 8.0, as presented earlier.[14] If not otherwise stated, the reagents and their sources were the same as mentioned earlier.[14]

2. *Effect of fluoride ions on the synthesis of the enzyme.* The maintaining of the cells, the preparation of the inoculum medium and the cultivation procedures were the same as earlier.[14] The growth medium, which was used in the cultivations of the cells for preparing the purified enzyme, was also used in studying the effect of NaF and KF on the synthesis of the *p*-nitrophenylphosphatase. This medium was composed as follows: Trypticase ™ (1.7 g/100 ml), Phytone ™ (0.3 g/100 ml), glucose (0.25 g/100 ml), K_2HPO_4 (0.25 g/100 ml) and NaCl (0.5 g/100 ml). Fluorides were added before autoclaving to the final concentrations of 0.5, 2.1, 4.2, 8.4, and 16.8 mM.

The rate of the hydrolysis of *p*-nitrophenyl phosphate was determined during the growth of the bacteria in crude preparations resulting from ultrasonic treatments. These crude enzyme preparations were obtained from the cells of 5 ml aliquots of the growth media. The cells were harvested by centrifugation and the pellets, suspended in 0.5 ml of cold (+4°C) 0.05 M borate buffer, pH 8.0, were in principle sonicated as earlier.[14] After sonication the mixtures were centrifuged (10 min at 12 000 *g*, at +4°C, using a Sorwall Superspeed RC-2B centrifuge with rotor SS-34), and the supernatant fluids were used for the determination of the enzyme activity as mentioned above. In two cases where fluoride concentrations were 2.1 and 16.8 mM the crude enzyme preparations were dialyzed against water before the measuring of the rate of the hydrolysis. Thus a possible effect of fluoride ions in the crude enzyme preparations themselves on the enzyme reaction could be ruled out.

RESULTS

I. Effect of fluoride ions on the reaction velocity

Before the effect of fluoride was studied, it was necessary to obtain information about the role of Mg^{2+} ions in the reaction mechanism. The plots described below were constructed:

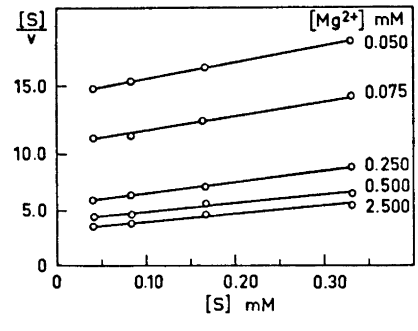

Fig. 1. Hanes' plots of the substrate concentration divided by the velocity ([S])/*v* in $10^3 \times$ min) *versus* the substrate concentration ([S]; in mM) of the hydrolysis of *p*-nitrophenyl phosphate, catalyzed by the *p*-nitrophenylphosphatase from *Streptococcus mutans*. The values of K_s obtained are: 0.43 mM for 2.50 mM $MgCl_2$, 0.53 mM for 0.50 mM $MgCl_2$, 0.55 mM for 0.25 mM $MgCl_2$, 0.85 mM for 0.075 mM $MgCl_2$, and 1.06 mM for 0.050 mM $MgCl_2$.

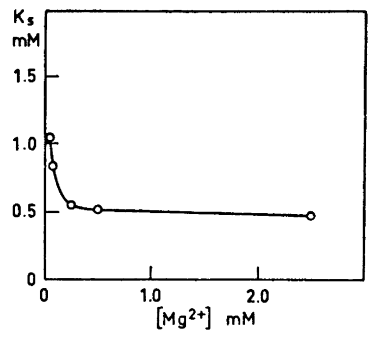

Fig. 2. Dependence of the value of the substrate constants, K_s, obtained from Fig. 1, on the concentration of Mg^{2+} ions in the hydrolysis of *p*-nitrophenyl phosphate, catalyzed by the purified *p*-nitrophenylphosphatase.

(1) A plot of [S]/*v versus* [S] at different Mg^{2+} ion concentrations is shown in Fig. 1. The results indicate that Mg^{2+} ions slightly affect the substrate constant, K_s. This is also shown in Fig. 2, where the same data were plotted using the values of K_s obtained from Fig. 1. These figures show that at low concentrations of Mg^{2+} ions the affinity between the enzyme and substrate is less than that obtained at high Mg^{2+} concentrations.

(2) A plot of $1/v$ *versus* $1/[Mg^{2+}]$ at varying *p*-nitrophenyl phosphate concentrations is shown in Fig. 3. Because there was no detectable change in the value of K_s, it was concluded that there is no competition between *p*-nitrophenyl phosphate and Mg^{2+} ions for the same site of the enzyme. Mg^{2+} ions were considered to have most likely a separate binding site at the enzyme surface. The concentration of *p*-nitrophenyl phosphate did not affect the affinity of Mg^{2+} ions for its binding site.

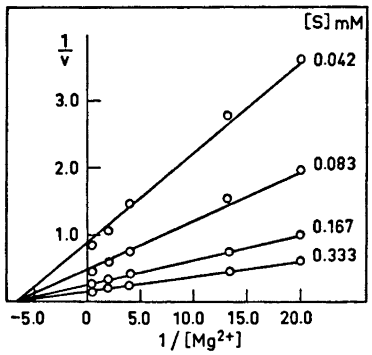

Fig. 3. The plot of the inverse value of the initial velocity ($1/v$; in $M^{-1} \times min \times 10^8$) *versus* the inverse value of $MgCl_2$ concentration ($1/[Mg^{2+}]$; in mM^{-1} in the hydrolysis of *p*-nitrophenyl phosphate catalyzed by the purified *p*-nitrophenylphosphatase. Tested at the following *p*-nitrophenyl phosphate concentrations: 0.333 mM, 0.167 mM, 0.083 mM and 0.042 mM.

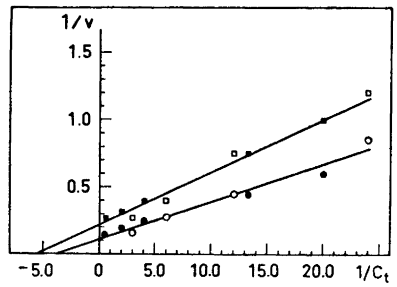

Fig. 4. Equivalence of apparent affinities of *p*-nitrophenylphosphatase for activating Mg^{2+} ions and substrate. Reciprocal plots for the hydrolysis of *p*-nitrophenyl phosphate catalyzed by the phosphatase ($1/v$ in $M^{-1} \times min \times 10^8$). C_t denotes the total molar concentrations of *p*-nitrophenyl phosphate: 0.333 mM (○) (with 2.50 mM Mg^{2+}), 0.167 mM (□) (with 0.25 mM Mg^{2+}); and of Mg^{2+} ions: 2.50 mM (●) (with 0.333 mM *p*-nitrophenyl phosphate), 0.25 mM (■) (with 0.167 mM *p*-nitrophenyl phosphate).

The apparent affinities of the enzyme for Mg^{2+} ions in the presence of 0.167 mM and 0.333 mM *p*-nitrophenyl phosphate were approximately the same as those for *p*-nitrophenyl phosphate in the presence of 0.25 mM and 2.50 mM Mg^{2+} ions, respectively (Fig. 4). Consequently, only those concentrations of activator and substrate mentioned above yielded almost the same value for both K_A (the dissociation constant of the Mg-enzyme complex) and K_s. The values of K_A and K_s in the conditions indicated above were approximately 0.17 mM and 0.25 mM, respectively.

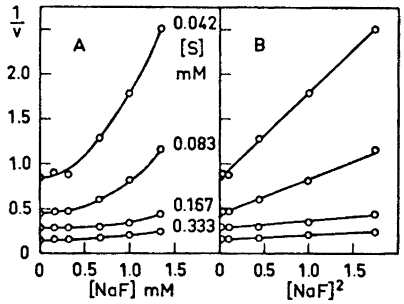

Fig. 5. The Dixon plots of the inverse value of the initial velocity ($1/v_i$; in $M^{-1} \times min \times 10^8$) *versus* the concentration of NaF (in mM), (A), and the plot of the inverse value of the initial velocity *versus* the second power of the concentration of NaF, (B). Tested at the following *p*-nitrophenyl phosphate concentrations: 0.333 mM 0.167 mM, 0.083 mM and 0.042 mM. The used Mg^{2+} ion concentration was 2.50 mM.

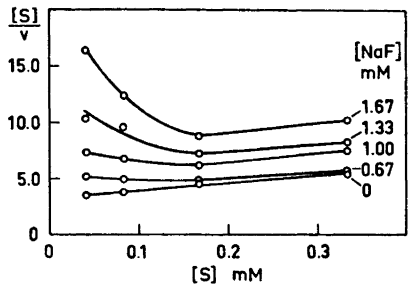

Fig. 6. Hanes' plot of the substrate concentration divided by the velocity ([S]/*v* in $10^3 \times min$) *versus* the substrate concentration ([S]; in mM) of the enzymic hydrolysis of *p*-nitrophenyl phosphate, inhibited by the following NaF concentrations: 0 mM, 0.67 mM, 1.0 mM, 1.33 mM and 1.67 mM. The used Mg^{2+} ion concentration was 2.50 mM.

The effect of fluoride ions on the reaction velocity in the presence of varying *p*-nitrophenyl phosphate concentrations is presented in Figs. 5, 6, 7, and 8. The figures present the effect of sodium fluoride, but identical results were

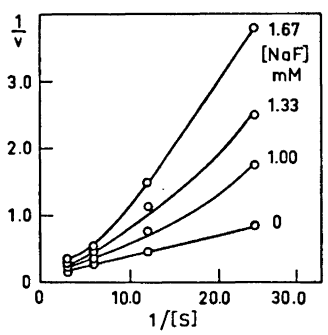

Fig. 7. The data of Fig. 6 plotted according to Lineweaver and Burk (the plot of the inverse value of the initial velocity ($1/v$; in $M^{-1} \times min \times 10^8$) *versus* the inverse value of the substrate concentration (1/[S]; in mM^{-1}).

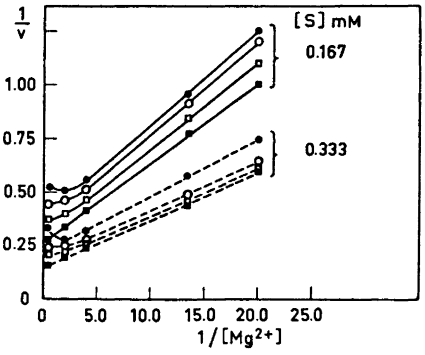

Fig. 8. The plot of the inverse value of the initial velocity ($1/v$; in $M^{-1} \times min \times 10^8$) *versus* the inverse value of $MgCl_2$ concentration ($1/[Mg^{2+}]$: in mM^{-1}) of the enzymatic hydrolysis of *p*-nitrophenyl phosphate, inhibited by the following NaF concentrations: 0 mM (■), 1.0 mM (□), 1.33 mM (○) and 1.67 mM (●). Tested at the following *p*-nitrophenyl phosphate concentrations: 0.167 mM (———) and 0.333 mM (– – –).

obtained with potassium and lithium fluorides. The corresponding chlorides had no effect on the reaction velocity. The Dixon plots (Fig. 5 A) revealed noticeable curvature at 2.50 mM $MgCl_2$ concentration, which leads to the highest rate of the hydrolysis of *p*-nitrophenyl phosphate at 0.167 mM concentration.[14]

The curvature in the plot of Fig. 5 A indicates that the inhibition may take place in one or both of the following ways: (a) the inhibitor reacts with the substrate, or (b) two or more inhibitor molecules participate in the reaction with the enzyme site. To differentiate between these possibilities, the following plots were constructed:

(1) $1/v$ *versus* the second power of the inhibitor concentration (Fig. 5 B). This showed that straight lines are obtained for all *p*-nitrophenyl phosphate concentrations used. However, this does not differentiate between the two possibilities.

(2) A plot of [S]/v *versus* [S] is presented in Fig. 6. From the same data also a plot of $1/v$ *versus* 1/[S] was made (Fig. 7). The results in Figs. 5 B, 6, and 7 were obtained in the presence of 2.50 mM $MgCl_2$ in the reaction mixture. The curvature of the plots of Figs. 6 and 7 suggests that most likely no binding of free fluoride ions to the active site of the enzyme has taken place, but rather a reaction between the substrate and the inhibitor. Consequently, the curvature of plot $1/v$ *versus* [I] (Fig. 5 A) is most likely due to reason (a) mentioned above.

Fig. 8 presents a plot of $1/v$ *versus* $1/[Mg^{2+}]$ at two *p*-nitrophenyl phosphate concentrations. When the concentration of fluoride ions was increased, there was an increasing curvature at the highest Mg^{2+} ion concentrations. The results of Fig. 8 support the earlier finding (Fig. 3) that the affinity of Mg^{2+} ions for the enzyme even in the presence of fluoride ions is not dependent on the con-

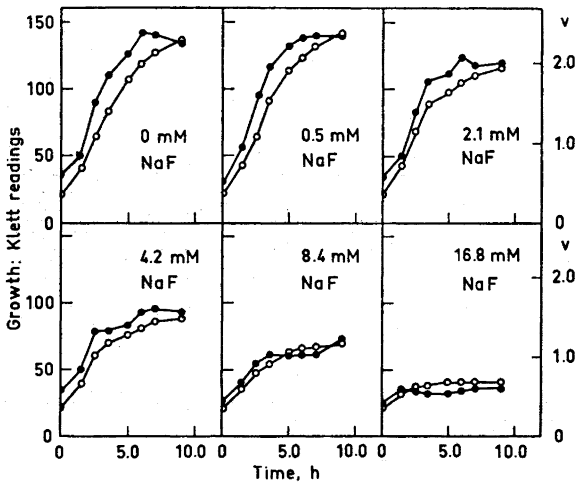

Fig. 9. The effect of NaF on the growth of *Streptococcus mutans* and on the synthesis of *p*-nitrophenylphosphatase. The enzyme preparations were obtained from sonicated cells of *Streptococcus mutans*, harvested from 5 ml cell suspensions as described in Materials and Methods, and in earlier studies.[14] ○, growth of *Str. mutans* ●, hydrolysis of *p*-nitrophenyl phosphate (v, in $M \times min^{-1} \times 10^6$).

centration of *p*-nitrophenyl phosphate. Fluoride ions very slightly increased the affinity of Mg^{2+} ions for the enzyme, if the highest $MgCl_2$ concentrations are not taken into consideration. The curvature at low values of $1/[Mg^{2+}]$ indicate that there is a type of substrate inhibition, if mere Mg^{2+} ions were also considered to represent the substrate (as a part of a complex between *p*-nitrophenyl phosphate and Mg^{2+} ions). This inhibition appeared as a result of the highest fluoride concentration (1.67 mM) used.

II. Effect of fluoride ions on the growth of the cells and the synthesis of the *p*-nitrophenylphosphatase

The fluoride ion concentration needed for effective inhibition of the growth of the cells is rather high (Fig. 9). The synthesis of *p*-nitrophenylphosphatase followed the growth pattern. The likely constitutive nature of the present enzyme was thus proved. The decrease of the synthesis of *p*-nitrophenylphosphatase is most likely a consequence of the general inhibition of cell growth, the fluoride ions affecting some vital reactions of the cells.[16]

DISCUSSION

The results show that (1) the apparent affinity of Mg^{2+} ions for the enzyme is not dependent on the concentration of *p*-nitrophenyl phosphate, and that (2) the apparent affinity of *p*-nitrophenyl phosphate is dependent on the concentration of Mg^{2+} ions.

These findings indicate that there are at least two different ways in which the substrate may be bound to the enzyme. (I) In the first alternative Mg^{2+} ions were separately bound close to the enzyme active site at a location where they do not compete with free *p*-nitrophenyl phosphate for the same enzyme site. Mg^{2+} ions would modify enzyme groups involved in the accomodation of the substrate, without reacting with the latter. (II) In the second alternative Mg^{2+} ions are combined with the enzyme, but the reacting substrate species is now represented by a *p*-nitrophenyl phosphate – Mg complex. In effect, there is a third possibility (III) which involves that Mg^{2+} ions do not combine with the enzyme at all but only with *p*-nitrophenyl phosphate. Alternatives (I) and (III) are perhaps more unlikely than (II), but the present kinetic methods are insufficient to completely rule out these possibilities.

In general, the electrophilic function of metal ions in enzyme catalysis is due to the formation of a complex between the enzyme and metal cation, in which case alternative (III) can only be considered as being theoretical. No references supporting alternative I are available; however, the following findings, *e.g.* also support the idea of a *p*-nitrophenyl phosphate – Mg^{2+} complex in the present case: (a) In nonenzymatic hydrolysis of acetyl phosphate in the presence of 0.05 M Mg^{2+} ions the cleavage is predominantly at the P – O bond. This is attributed to the formation of a chelate complex of dianionic species and Mg^{2+}.[17] (b) ATP forms complexes with Mg^{2+} and Ca^{2+} ions, which are necessary for the enzymatic action of adenosinetriphosphatase.[18,19] (c) The substrate for the inorganic pyrophosphatase from bakers' yeast is a pyrophosphate – Mg complex.[20] (d) Fig. 4 shows that the apparent affinity of both

the substrate and the activator for the enzyme is the same, when tested at certain concentrations of the substrate (0.167 mM and 0.333 mM) and the activator (0.25 mM and 2.50 mM, respectively)). The double reciprocal plots indicate that in the conditions used the following reactions can be considered: (1) Mg^{2+} + *p*-nitrophenyl phosphate ⇌ Mg – *p*-nitrophenyl phosphate complex, (2) E + Mg – *p*-nitrophenyl phosphate complex ⇌ E – Mg – *p*-nitrophenyl phosphate complex. Consequently, there are at least certain conditions where the above two reactions were likely. If there is a *p*-nitrophenyl phosphate – Mg complex, its formation could take place before its binding to the enzyme or at the enzyme surface between separately bonded *p*-nitrophenyl phosphate and Mg^{2+} ions.

The results also show that: (1) Fluoride has most likely reacted with the substrate (Figs. 5 A, 6, and 7). However, the possibility that two or more fluoride ions have reacted per each substrate molecule cannot be ruled out. (2) The apparent affinity of the substrate for the enzyme is decreased at increasing fluoride concentrations (Fig. 7). (3) Increasing fluoride concentrations slightly increase the apparent affinity of Mg^{2+} ions for the enzyme. Also the effect of fluoride most likely supports the earlier finding (Fig. 3) that the affinity of Mg^{2+} ions for the enzyme is not dependent on the concentrations of *p*-nitrophenyl phosphate (Fig. 8). (4) At high $MgCl_2$ concentrations fluoride yielded slight curvature in the plots constructed (Fig. 8).

The different effects of fluoride on the affinity of both *p*-nitrophenyl phosphate (Fig. 7) and Mg^{2+} ions (Fig. 8) evidently support the assumption of independent binding sites for them. Elliot [10] has shown that the inhibitory effect of fluoride ions on an alkaline pyrophosphatase can be explained in terms of a competition between a fluoromagnesium complex and Mg^{2+} ions for the enzyme. This would also be possible in the present case. However, it is known that the inhibitor most likely reacts with the substrate and affects its affinity for the enzyme. This may indicate that fluoride or a fluoromagnesium complex prevents the complex formation between Mg^{2+} ions and *p*-nitrophenyl phosphate. Such a complex would be necessary in the hydrolysis of *p*-nitrophenyl phosphate by the enzyme as previous suggested.

Another possibility would be based on the formation of a fluorophosphate complex, capable of forming a further complex with magnesium, as described in the case of enolase.[1] Peters *et al.*[4] have demonstrated, however, that fluorophosphate does not inhibit enolase, but is capable of forming a complex with magnesium, and also that the formation of a Mg – fluorophosphate complex can not be the real mechanism of enolase inhibition by fluoride ions. The present results are insufficient to rule out the possibility of the complex between all three reactants: Fluorine, phosphate and Mg^{2+} ions. This has been shown to be true in the case of fluoride inhibition of DNA polymerase reaction.[21]

As to the possibility that two fluorine atoms could be bound per substrate molecule it should be noticed that inorganic fluoride exists in ionized form in the pH range 6 – 9.[22] At progressively lower pH values both HF (the free acid) and $(HF_2)^-$ (the associated form) are present in increasing quantities. The present studies were carried out at pH 8.0, when the involvement of forms F^-, $2F^-$, and F_2^{2-} could be evident.

Acknowledgements. Thanks are due to the *National Research Council for Medical Sciences*, Finland, for financial support (to M.L.E.K.). The technical assistance of Miss Rauni Suominen is gratefully acknowledged.

REFERENCES

1. Warburg, O. and Christian, W. *Naturwiss.* **29** (1941) 590.
2. Warburg, O. and Christian, W. *Biochem. Z.* **310** (1942) 384.
3. Boser, H. *Naturwiss.* **44** (1957) 586.
4. Peters, E. A., Shorthouse, M. and Murray, L. R. *Nature* **202** (1964) 1331.
5. Cimasoni, G. *Abstr. XVII Orca Congr.* Debrecen, Hungary 1970.
6. Roche, J. and Thoai, N. V. *Advan. Enzymol.* **10** (1950) 83.
7. Belfanti, S., Contardia, A. and Ercoli, A. *Biochem. J.* **29** (1935) 842.
8. Reiner, J. M., Tsubol, K. K. and Hudson, P. B. *Arch. Biochem. Biophys.* **56** (1955) 165.
9. Meyers, D. K. and Slater, E. C. *Biochem. J.* **65** (1967) 572.
10. Elliot, W. H. *Biochem. J.* **65** (1957) 315.
11. Smith, Q. T., Armstrong, W. D. and Singer, L. *Proc. Soc. Exp. Biol. Med.* **102** (1959) 170.
12. Mircevova, L. and Simonova, A. *Collection Czech. Chem. Commun.* **35** (1970) 2996.
13. Hewitt, E. J. and Nicholas, J. D. In Hochester R. M. and Quastel, J. H., Eds., *Metabolic Inhibitors*, Academic, New York 1963, Vol. 2, p. 311.
14. Knuuttila, M. L. E. and Mäkinen, K. K. *Arch. Biochem. Biophys.* **152** (1972) 685. *publication.*
15. Bessey, O. A., Lowry, O. H. and Brock, M. J. *J. Biol. Chem.* **164** (1946) 321.
16. Kanapka, J. A., Khandelwal, R. L., and Hamilton, I. R. *Arch. Biochem. Biophys.* **144** (1971) 596.
17. Morton, R. K. In Florkin, M. and Stotz, E. H., Eds., *Comprehensive Biochemistry*, Elsevier, Amsterdam 1965, Vol. 16, p. 55.
18. Williams, R. J. P. In Boyer, P. D., Lardy, H. and Myrbäck, K., Eds., *The Enzymes*, Academic, New York 1959, Vol. 1, p. 391.
19. Kosower, E. M. *Molecular Biochemistry*, McGraw, New York 1962, p. 227.
20. Rapoport, T. A., Höhne, W. E., Reich, J. G., Heitman, P. and Rapoport, S. M. *Europ. J. Biochem.* **26** (1972) 237.
21. Hellung-Larsen, R. P. and Klenow, H. *Biochim. Biophys. Acta* **190** (1969) 434.
22. Wieseman, A. In Smith, F. A., Ed., *Handbook of Experimental Pharmacology*, Springer, Berlin 1970, Vol. XX/2, p. 48.

Received June 27, 1972.

ACTA CHEMICA SCANDINAVICA 27 (1973) 613–620

Conformation and Vibrational Spectra of 1,1,2,2-Tetracyanoethane and 1,2-Dichlorotetracyanoethane

D. L. POWELL,[a] T. R. DYKE,[a] C. HEBREW,[a]* C. T. VAN BUREN[a] and P. KLÆBOE[b]

[a]*Department of Chemistry, College of Wooster, Wooster, Ohio, USA.* [b]*Department of Chemistry, University of Oslo, Oslo 3, Norway*

1,1,2,2-Tetracyanoethane and 1,2-dichlorotetracyanoethane have been studied by IR and Raman spectroscopy. Both have been shown to possess C_{2h} symmetry in the crystal and evidence is presented for their retention of this conformation in solution. Partial vibrational assignments have been made.

Many halogenated ethanes have been studied by vibrational spectroscopy. It is well known that in the liquid and vapour states ethanes of the type CX_2Y-CX_2Y exist in general as a mixture of *trans* (C_{2h}) and gauche conformers (C_2), but that in the solid state the ethane will usually crystallize preferentially in only one conformation.

In 1,1,2,2-tetrafluoroethane, this more favoured conformation in the crystal is the C_{2h},[1] in 1,1,2,2-tetrachloroethane it is the C_2,[2] and in 1,1,2,2-tetrabromoethane it may be either, depending upon the conditions during crystallization.[2] The situation is more straightforward in the 1,2-dihaloethanes as three of the four crytallize in the C_{2h} conformation,[3] the data are not conclusive for difluoroethane [4] which may crystallize in both forms, although the samples may have been amorphous rather than truly crystalline. Warning against the easy assumption that a cyano group will behave as a pseudo halogen is provided by the observation that 1,2-dicyanoethane crystallizes in the C_2 conformation.[5,6] The cyano group is much more polar, with its lone pair of electrons directed outward, and, with its cylindrical shape, very different sterically. Furthermore, in the halocyanoethanes [7,8] and in 1,1,2-trichloropropionitrile,[9] the favoured conformations are those in which the cyano group is gauche to a halogen atom. Thus it is not at all clear which form of these compounds one could expect to be present in the crystal.

* National Science Foundation Research Participation for High School Teachers participant 1965 and 1966.

In solution, these compounds present an interesting test of the "gauche effect",[10] the tendency of a compound "to adopt that structure which has the maximum number of gauche interactions between the adjacent electron pairs and/or polar bonds". The gauche form (C_2) could be predicted to predominate in the case of tetracyanoethane. The case of dichlorotetracyanoethane, with its six polar substituents, is less obvious. In any case, use of a polar solvent would be expected to favour the form having the higher dipole moment, in these cases, the gauche forms.[11]

It is of interest to see how well these expectations are fulfilled. Neither of these compounds has been studied spectroscopically before nor has to our knowledge any study been made of their conformational behaviour.

EXPERIMENTAL

Tetracyanoethylene served as a starting material for both compounds. Tetracyanoethane is the less stable of the two, the solid darkening in a few days time after preparation.[12] Accordingly the spectral work, especially the Raman, was done as soon as possible after preparation and purification by recrystallization.

No evidence of decomposition was observed for dichlorotetracyanoethane even after several months standing at room temperature after preparation [13] and purification by sublimation under reduced pressure,

IR spectra in the region $5000-200$ cm^{-1} were recorded of mulls, KBr pellets, and of CH_3CN solutions on a Perkin-Elmer Model 225 and of adamantane disks in the region $400-40$ cm^{-1} on a Hitachi Perkin-Elmer Model FIS-3. Raman spectra of the solids and of CH_3CN solutions in standard Cary capillary cells or in melting point capillaries with polished ends were recorded on a Cary Model 81 equipped with a Spectra-Physics Model 125A He-Ne laser.

The solution work was restricted to the use of CH_3CN since both compounds are completely insoluble in non-polar solvents such as CCl_4 or CS_2 and in such slightly polar solvents as $CHCl_3$ or CH_2Cl_2 and are either insoluble or react with such other polar solvents as dimethyl sulfoxide or dimethylformamide. Even in CH_3CN the solubility was not very great.

The cavity cells were employed because of an apparent reaction of these compounds of the normal IR cells presumably caused by contact with metal. Even then, the solution of tetracyanoethane rapidly darkened and the solution of dichlorotetracyanoethane turned yellow during the recording of the spectra. Although the dichlorotetracyanoethane was more stable, it obviously reacted quickly with CsI and somewhat more slowly with KBr.

Neither compound was stable enough to be run as a melt (although an attempt was made to do so with dichlorotetracyanoethane) or stable and volatile enough to be run as a vapour.

In both compounds, the possibility of reversion to the very stable tetracyanoethylene had to be kept in mind. A rather pure sample of tetracyanoethane, when sublimed under reduced pressur in an attempt to remove some objectionable fluorescent impurities, gave a fine white crystalline sample which was, from the Raman spectrum, 25 to 50 % tetracyanoethylene. The solid phase IR spectra of dichlorotetracyanoethane show traces of tetracyanoethylene; in the solution spectra contamination has progressed so far that tetracyanoethylene is responsible for one of the strongest bands in the spectrum.

RESULTS AND DISCUSSION

The results in the IR and Raman for tetracyanoethane are shown in Tables 1 and 2. Similarly, the results for dichlorotetracyanoethane are shown in Tables 3 and 4. For purposes of illustration, the IR spectrum of tetracyanoethane and the Raman spectrum and far IR spectrum of dichlorotetracyanoethane are shown in Figs. 1 and 2.

Taple 1. Infrared spectral data for 1,1,2,2-tetracyanoethane.[a]

Mull	CH_3CN solution	Interpretation
4096 w[b]		1302 + 2859 = 4161
~2960, w, sh		115 + 2859 = 2974
2918 vs	2911 s	C–H str
	~2900 m, sh	
~2856 m, sh		
2604 m		1302 + 1302 = 2604
	2508 w, br	
2484 m		224 + 2273 = 2497
2360 w		
2273 m		C≡N str
2210 m		911 + 1302 = 2213
2186 w		911 + 1282 = 2193
1971 w		889 + 911 = 1800
1718 w	1722 m	437 + 1282 = 1719
~1660 vw	1678 w	362 + 1302 = 1664
1602 w	1595 mw	719 + 889 = 1608
	1372 s, sh	
1302 w		CH bend
1278 vw		575 + 719 = 1294
1260 vw	1256 m	355 + 911 = 1266
1197 vs	1203 s	CH bend
1168 vw		
1159 w	1153 vw	136 + 1034 = 1170
~1142 vw		115 + 1034 = 1149
1075 w		195 + 889 = 1084
1011 m		136 + 889 = 1025
997 s	998 vs	C–C str.
936 m	~935 m	437 + 513 = 950
911 s	906 vs	C–C str
905 m, sh		416 + 491 = 907
850 vw		362 + 491 = 853
797 w		
	780 m	
754 vw		355 + 416 = 771
719 m	728 s	160 + 575 = 735
	686 w	
600 vw		115 + 491 = 606
570 m		155 + 416 = 571
562 s	568 w	skeletal bend
	558 mw	
438 w	445 mw	skeletal bend
364 m		skeletal bend
314 w[c]		155 + 160 = 315
254 w[c]		skeletal bend
~195 m sh[c]		skeletal bend
183 m[c]		skeletal bend
160 m[c]		skeletal bend
136 w[c]		
115 w[c]		torsion

[a] Weaker infrared bands in regions where there can be no fundamentals have been omitted. [b] The following abbreviations have been used: s, strong; m, medium; w, weak; sh, shoulder and v, very. [c] Bands are from an adamantane pellet.

Table 2. Raman spectral data for 1,1,2,2-tetracyanoethane.

Solid	CH_3CN solution	Interpretation
	3002 m	
2943 w[a]		680 + 2271 = 2951
2859 m	2845 w	C–H str
2672 w		416 + 2273 = 2689
2271 vs		C≡N str
1302 s		CH bend
1282 w		CH bend
	1210 m	
	1084 m	
	1070 m	
1034 s		C–C str
889 s		C–C str
680 w		C–C str
	660 w	
575 m	573 m	skeletal bend
513 m		skeletal bend
491 s	493 m	skeletal bend
	472 w	
	~443 m	
355 vs		skeletal bend
233 m		skeletal bend
224 m		skeletal bend
155 m		skeletal bend

[a] Abbreviations as in Table 1.

The first question to be answered is which staggered conformation exists in the crystal, the *trans* with a centre of symmetry (C_{2h}) in which 15 fundamentals would be active in the IR and 15 in the Raman, or the *gauche* with symmetry C_2 in which all 30 fundamentals would be active in both effects. In both cases, the results are definite; both have a centre of symmetry. The IR and Raman spectra of both are quite simple, considering the size of these

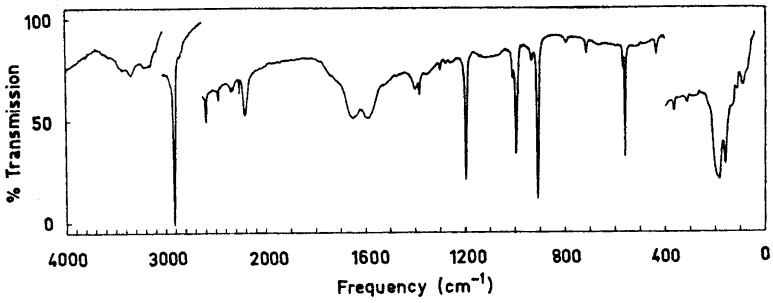

Fig. 1. IR spectrum of 1,1,2,2-tetracyanoethane, KBr pellet (4000 – 400), adamantane pellet (400 – 40 cm^{-1}).

Table 3. Infrared spectral data for 1,2-dichlorotetracyanoethane.[a]

Mull	CH_3CN solution	Interpretation
2710 w[b]		455 + 2262 = 2717
2673 w		416 + 2265 = 2681
2502 w		245 + 2262 = 2507
2471 w		225 + 2256 = 2481
2458 w		197 + 2265 = 2462
2400 w		154 + 2256 = 2410
2262 s		C≡N str
2235 vw		
2219 w		
1706 w		
1407 w		478 + 935 = 1413
1382 vw		455 + 935 = 1390
1352 w		283 + 1067 = 1350
1312 vw		416 + 902 = 1318
~1215 vw		455 + 768 = 1223
1168 vw		245 + 935 = 1180
1154 mw	1153 s	imp.[c]
1146 vw		88 + 1062 = 1150
1113 w	~1110 m	imp.
1067 m		C–C str
1048 mw		
1004 w		
1000 m		
972 w		500 + 501 = 1001
958 vw	957 m	imp.
935 m	~935 m	C–C str
915 w		imp.
904 m		
867 w		416 + 500 = 916
832 w	832 vw	283 + 552 = 835
	802 mw	imp.
785 mw		245 + 552 = 797
~768 m		C–Cl str
724 w	~720 w, sh	225 + 500 = 725
703 vw	700 w	154 + 560 = 714
	~690 w	
660 w		245 + 416 = 661
618 vw		154 + 478 = 632
587 vw		88 + 500 = 588
579 vw	574 mw	imp.
552 m	553 m	skeletal bend
501 m		skeletal bend
~490 w sh		225 + 283 = 508
455 w		225 + 245 = 470
416 mw		skeletal bend
225 m[d]		skeletal bend
197 w[d]		skeletal bend
154 ms[d]		skeletal bend
132 ms[d]		skeletal bend
88 w br[d]		torsion

[a] Weaker infrared bands in regions where there can be no fundamentals have been omitted. [b] Abbreviations as in Table 1. [c] Impurity is tetracyanoethylene. [d] Bands are from an adamantane pellet.

Table 4. Raman spectral data for 1,2-dichlorotetracyanoethane.

Solid	CH_3CN solution	Interpretation
~2945 vw[a]		
~2675 vvw		455 + 2256 = 2711
~2635 vvw		416 + 2262 = 2678
2315 vw		
2265 m		C≡N str
2256 vs		C≡N str
~1283 vw		245 + 1052 = 1297
1062 w		C–C str
1052 mw	~1050 w	C–C str
~995 vw?		2 × 500 = 1000
902 vs		C–C str
560 m	560 w	skeletal bend
	540 w?	
500 vs	500 m	C–Cl str
478 w		
455 w		skeletal bend
283 m	285 w	skeletal bend
245 m	250 w	skeletal bend
172 s		skeletal bend
164 s		skeletal bend
140 m		skeletal bend
137 s		skeletal bend
78 w		

[a] Abbreviations as in Table 1.

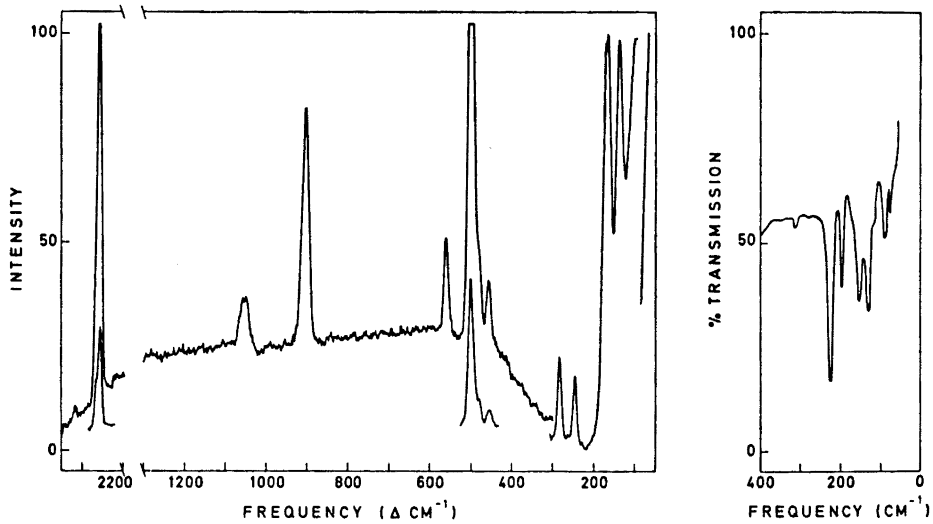

Fig. 2. Raman and far IR spectra of 1,2-dichlorotetracyanoethane.

molecules. Although coincidences may be easily pointed out, many bands, especially in the low frequency regions, may be noted which have no counterpart in the other effect.

The next question is which form predominates in solution. Here our answer is more surprising as we find no convincing evidence for any form but the *trans* in solution. Our unwillingness to make a stronger statment is closely connected with the various experimental difficulties mentioned earlier. The effect of these difficulties on our experiments can be summarized in this way. In the Raman, even though fairly wide "windows" are present, the limited solubility and availability only of a He-Ne laser make us reluctant to say that we could detect less than 10 or 20 % of the *gauche* conformer. In the IR, not only does CH_3CN have a more complex spectrum with extremely strong absorption bands than in the Raman, thus limiting our region of observation considerably, but reaction with CsI and the unsuitability of CH_3CN as a solvent in the far IR restricted us to the region above 400 cm^{-1}. This was especially unfortunate because the more interesting fundamentals (those which would be expected to be more sensitive to a change in conformation) lie in the low frequency region.

Tetracyanoethane does show some new bands in solution. However, its obvious decomposition during the course of our experiments made us very hesitant to assign these to a *gauche* conformer. We become even more cautious when we note that those new bands appearing in IR have no counterparts in Raman and *vice versa*. Since the *gauche* conformer would have no centre of symmetry, it is difficult to ascribe these sets of bands to it.

With dichlorotetracyanoethane we are a little more confident. Only one new weak, questionable band appears in solution in the Raman and no new bands appear in the IR with the exception of a set of bands which can be shown to be due to tetracyanoethylene.

To summarize, then, unless the energy difference is unusually large, at least small amounts of the C_2 conformers must exist in solution for each compound. We have no confidence that we have detected them, but we do feel that we can assert confidently that it is the *trans* form which predominates in solution. This must be looked upon as somewhat surprising. Statistically the C_2 conformer should predominate 2 : 1. The presence of the very polar solvent CH_3CN should stabilize the C_2 form to the extent of $1-2$ kcal/mol compared to nonpolar solvents. Finally, at least in the case of tetracyanoethane, one would predict [10] that the preferred conformation would be *gauche*.

VIBRATIONAL ASSIGNMENTS

For various reasons, only a partial assignment can be attempted, in spite of the fact that for each compound we are able rather easily to pick out about 15 bands in both the IR and Raman and to designate them as fundamentals. Neither compound was soluble enough in CH_3CN for us to be able to determine polarization in the Raman and hence distinguish the A_g from the B_g modes. Nor was either compound stable enough at elevated temperatures for us to obtain a vapour phase spectrum in the IR and distinguish the A_u from the B_u modes. In the higher frequency region this is not too great a handicap and we can, guided by some group frequency correlations, assign with some con-

fidence. In the lower frequency region these relationships are not as helpful and we have also richer spectra forcing us to designate many bands as skeletal bends. The unsuitability of CH_3CN as a solvent in the far IR hindered us in attempting to distinguish unequivocally the torsional frequencies from the lattice modes. We will only note those details of the assignment which gave us especial difficulty or where we have been arbitrary.

Tetracyanoethane. The strong IR band at 2917 cm^{-1} is the only possibility for the IR-active C–H stretch. In the Raman, because the peak at 2859 cm^{-1} is twice as intense at that at 2943 cm^{-1}, we choose the former as the C–H stretch. In the C≡N region, we find only one strong peak in each effect and conclude that both the A_g and B_g and the A_u and B_u modes are accidentally degenerate.

In the C_{2h} form of dicyanoethane the C–C stretches were assigned at 1023 cm^{-1} and 809 cm^{-1} in the Raman and 917 cm^{-1} in the IR.[5] Thus our choices seem quite reasonable.

Dichlorotetracyanoethane. Although the two IR-active C≡N stretches are accidentally degenerate, two bands do appear in the Raman. Picking out the C–C stretches is fairly easy. The C–Cl stretches are also fairly obvious, in particular the very strong Raman band at 500 cm^{-1}.

In the Raman we have two bands too few to assign as skeletal bands. Our assumption is not that the missing bands are too weak to be observed but that our resolution is inadequate to show which peaks actually possess two components.

Acknowledgement. We take pleasure in thanking Dr. D. H. Christensen and other members of the spectroscopy group at the H. C. Ørsted Institute for their help in obtaining the far IR spectra, and in thanking K. Ruzicka for synthesizing and purifying the compounds. Financial support from *Research Corporation* is gratefully acknowledged.

REFERENCES

1. Klæboe, P. and Nielsen, J. R. *J. Chem. Phys.* **32** (1960) 899.
2. Kagarise, R. E. *J. Chem. Phys.* **24** (1956) 300.
3. Mizushima, S. *Structure of Molecules and Internal Rotation*, Academic, New York 1954.
4. Klæboe, P. and Nielsen, J. R. *J. Chem. Phys.* **33** (1960) 1764.
5. Fitzgerald, W. E. and Janz, G. J. *J. Mol. Spectry.* **1** (1947) 49.
6. Fujiyama, T., Tokumaru, K. and Shinanouchi, T. *Spectrochim. Acta* **20** (1964) 415.
7. Wyn-Jones, E. and Orville-Thomas, W. J. *J. Chem. Soc.* **A 1966** 101.
8. Klæboe, P. and Grundnes, J. *Spectrochim. Acta* **A 24** (1968) 1905.
9. Torgrimsen, T. and Klæboe, P. *Acta Chem. Scand.* **25** (1971) 1476.
10. Wolfe, S. *Accounts. Chem. Res.* **5** (1972) 102.
11. Abraham, R. J. and Cooper, M. A. *J. Chem. Soc.* **B 1967** 202.
12. Middleton, M. J., Heckert, R. E., Little, E. L. and Krespan, C. G. *J. Am. Chem. Soc.* **80** (1958) 2783.
13. Dickinson, C. L. and McKusick, B. C. *J. Org. Chem.* **29** (1964) 3087.
14. Miller, F. A., Sala, O., Devlin, P., Overend, J., Lippert, E., Lüder, W., Moser, H. and Varchmin, J. *Spectrochim. Acta* **A 20** (1964) 1233.

Received August 7, 1972.

ACTA CHEMICA SCANDINAVICA 27 (1973) 621–642

Conformational Analysis of Coordination Compounds

Tris-diamine Cobalt(III) Complexes with Three Six-membered Chelate Rings*

S. R. NIKETIĆ** and F. WOLDBYE

Chemistry Department A, The Technical University of Denmark, DTH 207, DK-2800 Lyngby, Denmark

The method for strain energy minimization due to Wiberg has been elaborated and applied to the conformational analysis of transition metal octahedral complex ions: Tris(1,3-diaminopropane)cobalt-(III), Co tn_3, and tris(*R*,*R*-2,4-diaminopentane)cobalt(III), Co ptn_3. Energy contributions from bond length and angle deformations, non-bonded interactions and torsional strain have been considered, the required force constants being taken from the available literature data. Equilibrium geometry parameters and relative conformational energies for three symmetrical conformations ($chair_3$, lel_3, and ob_3) and ten "mixed" conformations of Co tn_3, and two conformations (lel_3 and ob_3) of Co ptn_3 were calculated and the stereochemistry of these systems was described in detail. The order of conformational energies and the comparison between calculated and X-ray conformations are presented.

The first general scheme for strain energy minimization was developed by Wiberg [1] who wrote a computer program capable of searching the minimum energy conformation by the method of steepest descent. This method has been successfully applied to the conformational analysis of cyclooctane, cyclodecane and cyclododecane,[1] some oxygen substituted carbocyclic molecules,[2] and cyclic carbonium ions.[3] The method was further developed by Allinger and co-workers [4] who have used it for a wide range of conformational calculations.

In the present study Wiberg's program has been elaborated, modified and applied to the conformational analysis of tris(chelate) octahedral coordination

* Preliminary results of this work were presented at the XVI Annual Meeting of the Serbian Chemical Society, Beograd, January 1971, and published in S. R. Niketić and F. Woldbye, *Glas. Hem. Drust. Beograd* **36** (1971) 82.

** On leave of absence from Department of Chemistry, University of Beograd, P.O. Box 550, 11001 Beograd, Yugoslavia.

compounds. Here we report our results from a study of the tris(trimethylenediamine)cobalt(III) and tris(*R*,*R*-2,4-diaminopentane)cobalt(III) complexes.*

We have chosen to carry out the detailed conformational analysis of the Co tn_3 system ** because it represents a prototype of a tris(bidentate) complex with three saturated six-membered chelate rings. The detailed stereochemistry of this system is of particular importance in connection with the interpretation of its CD spectra [5] and the relation of the N – Co – N angle to the sign of Cotton effect in T_{1g} region.[5] This is revealed by considerable recent interest in the stereochemistry of trimethylenediamine complexes and particularly Co tn_3 and by appearance of several papers [5d–f] on this issue during the progress of our work.

STEREOCHEMISTRY

One single metal-trimethylenediamine chelate ring has basically the same conformational possibilities as the cyclohexane ring. Three of the conformations of the Co-tn ring are characterized by their energy minima: one rigid chair form with C_s symmetry (Fig. 1(a)), and two enantiomeric twist-boat forms with C_2 symmetry (Fig. 1(b) and (c)) belonging to the family of flexible boat forms. For each of the twist-boat conformations of the Co-tn ring two skew lines could be defined: one connecting N-atoms and the other connecting terminal C-atoms (Fig. 1(d) and (e)). According to the helicity associated with these lines [7] the twist forms are labelled as λ and δ.

When entering a tris(chelate) a Co-tn ring in its chair conformation may adopt one of two orientations which give rise to two conformers if – and only if – the two other rings are not connected by a C_2 operation (Fig. 1(f) and (g)). Now to calculate the total number of theoretically possible conformations of Co tn_3, combinations of all four forms of chelate rings (λ, δ, and chair

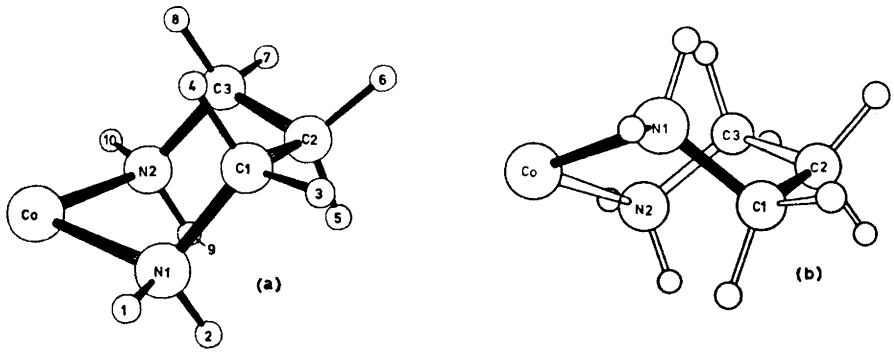

* We have also analyzed the series of tris-diamine metal complexes with ethylenediamine, propylenediamine, and 2,3-diaminobutane. These results will be described elsewhere.[6]

** Abbreviations: tn = trimethylenediamine, ptn = 2,4-diaminopentane. Ionic charges are omitted.

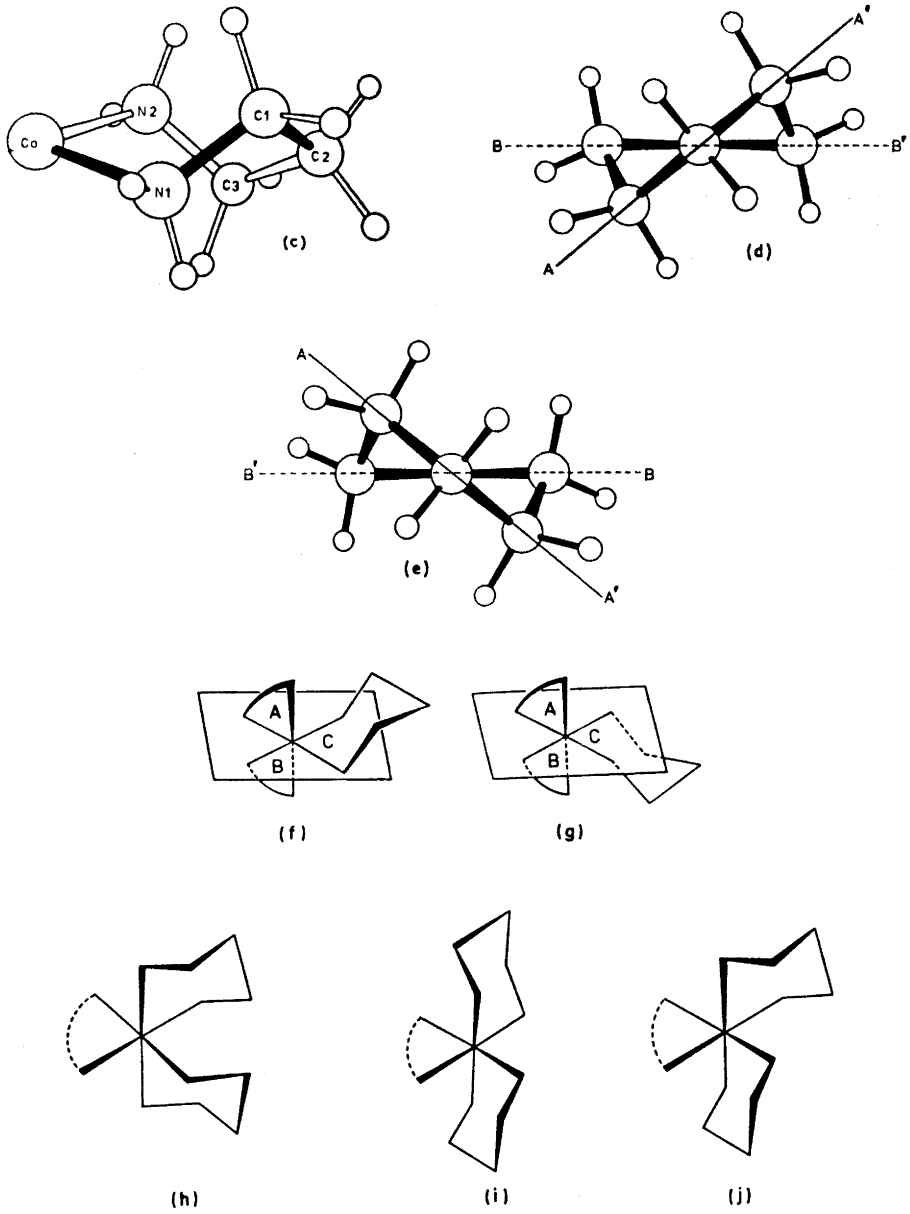

Fig. 1. Stereochemistry of a single Co-tn chelate ring. Chair conformation (a); two enantiomeric twist-boat conformations (b) and (c); skew lines AA′ and BB′ defining left-handed helix of λ-twist-boat (d) or right-handed helix of δ-twist-boat (e) conformation; provided the two rings A and B are not C_2-symmetry connected the two different orientations of a chair, C, give rise to two conformers, $cis_{(A,C)} \equiv trans_{(B,C)}$ (f), and $cis_{(B,C)} \equiv trans_{(A,C)}$ (g); *syn-*, *anti-*, and (C_1)-constellation of a pair of chairs (h), (i), and (j).

in two orientations) have to be considered. This leads to a total of 16 different conformations (Table 1)* for each of the absolute configurations, Δ, and Λ.

The lel-ob nomenclature lends itself for a convenient designation of the conformers but because of the above mentioned possibility for the chair to adopt two orientations – in some cases leading to different conformers – there is need for an additional nomenclature.** In conformers with only one chair the plane defined by the central atom and the two nitrogen atoms of that chair could form a basis for a *cis-trans* nomenclature (*vide* Fig. 1(f) and (g)). In conformers with two chairs these can adopt two conformations designated *syn* and *anti* in Fig. 1(h) and (i) in which they are connected by a C_2 operation and one conformation of symmetry C_1. In Table 1 *syn*, *anti*, and C_1 are used to distinguish conformers with two chairs. With three chairs Co tn_3 may adopt two conformations, one of symmetry C_3 and one of symmetry C_1. Three "symmetrical" conformations: (C_3)-$chair_3$, lel_3, and ob_3, together with 10 of the "mixed" conformations were subjected to the minimization procedure. Conformers 9, 11, and 14 from Table 1, all having a pair of *syn*-$chair_2$ rings, were not analysed since they appear to be sterically impossible on molecular models.

The molecular structure of $[Co(tn)_3]Br_3.H_2O$ as determined by the X-ray diffraction method [9] shows that Co tn_3 has $chair_3$ conformation in the crystalline state. Preliminary results of the X-ray analysis of $[Co(R,R\text{-}2,4\text{-}ptn)_3]Cl_3.H_2O$ show [10] that the crystalline state conformation of this complex ion is ob_3 with all the methyl groups in equatorial positions.

The chair conformation of tn rings was also found in crystal structures of $[Co\,en_2tn]Br_3$,[11] *trans*-$[Co(NO_3)_2tn_2]NO_3$,[12a] *trans*-$[Co\,Cl_2tn_2]Cl.HCl.2H_2O$,[12b] and *cis*-$[Co(NCS)_2tn_2][Sb\ tart].2H_2O$,[12c] as well as in some bis(chelate) copper(II) and nickel(II) complexes of tn.[13]

METHOD

The conformational calculations described in the present study were carried out with a single computer program *** which represents an extended and modified version of Wiberg's energy minimization program.[1,2]

* Total number of conformers was calculated using the formula: $\binom{n+i-1}{i}+\binom{n}{i}$ for the combinations with repetition of i-th order with n elements augmented by a number of sequential isomers (equal to the number of combinations without repetition). In general, for the cyclic systems of three rings with four possible ring conformations $n=4$ and $i=3$, and the total number of conformations is 24. However, due to the above-mentioned fact that among the Co tn_3 conformers containing chairs some (actually 16 of the conformers counted by this formula) are pairwise identical, as shown in the last column of Table 1, we are left with a total of 16 different conformers.

** *Note added in proof:* An ambiguity in the nomenclature used in the first version of our paper was kindly drawn to our attention by Professor K. N. Raymond whom we thank for making his results available to us prior to publication. Jurnak and Raymond [32] in an X-ray investigation of $[Cr\ tn_3][Ni(CN)_5].2H_2O$ have found that the conformation of the $[Cr\ tn_3]^{3+}$ ion corresponds to our *anti*-$chair_2$lel (No. 9 in Table 1), the conformer predicted by our calculations (using FF-2) to have the lowest energy (*vide* Fig. 8).

*** The program that treats 64 atoms (currently) and about 2240 interactions requires 104 K of storage on an IBM 360/75. One cycle of minimization including calculation of derivatives and energy contributions takes approx. 36 sec on an IBM 360/75.

Table 1. Conformations of M tn_3 system.[a]

No.	Conformation	Symmetry	Ring conformations (exemplified for *Λ* absolute configuration using Jurnak & Raymond's [32] nomenclature [b]
1	(C_3)-chair$_3$	C_3	ppp≡aaa
2	lel$_3$	D_3	$\delta\delta\delta$
3	ob$_3$	D_3	$\lambda\lambda\lambda$
4	lel$_2$ob	C_2	$\delta\delta\lambda$
5	ob$_2$lel	C_2	$\lambda\lambda\delta$
6	(C_1)-chair$_2$ob	C_1	ppλ≡aaλ
7	(C_1)-chair$_2$lel	C_1	ppδ≡aaδ
8	*anti*-chair$_2$lel	C_2	apδ
9	*syn*-chair$_2$lel	C_2	paδ
10	*anti*-chair$_2$ob	C_2	apλ
11	*syn*-chair$_2$ob	C_2	paλ
12	lel$_2$chair	C_1	$\delta\delta$p≡$\delta\delta$a
13	ob$_2$chair	C_1	$\lambda\lambda$p≡$\lambda\lambda$a
14	(C_1)-chair$_3$	C_1	ppa≡aap
15	*cis*$_{(\text{lel,chair})}$-lel ob chair	C_1	$\delta\lambda$p≡$\lambda\delta$a
16	*trans*$_{(\text{lel,chair})}$-lel ob chair	C_1	$\delta\lambda$a≡$\lambda\delta$p

[a] ob and lel refer to diastereoisomerism between *e.g.* $\Lambda(\lambda\lambda\lambda)$ and $\Lambda(\delta\delta\delta)$; $\Lambda(\lambda\lambda\lambda)$ [and $\Lambda(\delta\delta\delta)$] being lel, in analogy to the tris(ethylenediamine) complexes.[8]
[b] Added in proof after the appearance of Ref. 32.

The search for a minimum of strain energy is performed by the method of steepest descent which is described in detail elsewhere.[14] It consists of the calculation of the gradient (that is, direction of steepest descent) on an energy surface of a N-atomic molecule in $3N+1$ dimensional space.

The basic ideas and the advantages of the steepest descent minimization procedure have been discussed already by Wiberg[1] and others.[3,4,15] Therefore, we shall describe only briefly some of our modifications and refinements.

The subprograms of Wiberg's conformational program could be divided into four main groups. The first group consists of a series of subroutines which build the geometry of a molecule and effects various transformations of coordinates. These routines were modified in order to account for the sexaligacy and for the symmetry operations in D_3. Routines were added to generate methyl groups on the specified positions of the molecular framework. In addition, the program automatically places the hydrogens on primary, secondary, or tertiary carbon and nitrogen atoms maintaining tetrahedral angles. In order to decrease the computational time attached hydrogens were moved together with nonhydrogen atoms in the initial stages of minimization. This was done by recalculating the positions of hydrogens each time any one of the nonhydrogen atoms is moved, that is, both in the gradient calculation and in movement along the gradient. In this way both rotation and translation of tetrahedra were achieved. The second group of subroutines calculates the internal coordinates from the Cartesian atomic coordinates (supplied as

input or generated by the program itself) which are then used in the calculation of energy contributions. Here also the necessary changes for sexaligacy were made. The third group of subroutines calculates the various energy contributions and their sum for the conformation under consideration. These routines were rewritten in order to allow the use of individual expressions for each type of interaction (*e.g.*, in the present study five different bond-stretching types, 10 different angle-bending types, and six different non-bonded interaction types). Different subroutines were used for the characterization of different force fields (*vide infra*). The fourth group of subroutines computes the gradient.

In our program it was possible to select the size of increments to be used in the calculation of partial derivatives. The choice of increments has already been discussed by Allinger and co-workers.[4] Our program starts with increments of 0.01 Å, but it switches to smaller increments (down to 0.002 Å) when desired, either after a predetermined number of iterations or when the energy fails to decrease. In practice we have used the following simple convergence criterion:

$$|E_i - E_{i+1}| \leq \delta_E$$

where i = iteration number, and δ_E = accuracy which was numerically equal to the current increment. When this condition is satisfied the program changes to smaller increments or, if the increments are already 0.002 Å, it terminates the search. The resulting root-mean-square deviation of atomic coordinates in the final cycle of iterations proved less than 10^{-4} Å.

CALCULATIONS

Initial coordinates for Co tn_3 and Co ptn_3. The conformational program starts with an assumed initial geometry of a molecule expressed in terms of Cartesian atomic coordinates.

Initial coordinates for the tris(trimethylenediamine)cobalt(III) ion were derived in two ways. The idealized initial conformations were obtained from two sets of Cartesian coordinates calculated by the vector method [16] for two principal forms (*chair* and *twist-boat*) of a single Co-tn chelate ring.[17] Given the Cartesians for one Co-tn ring placed with its two Co–N bonds along the $+X$ and $+Y$ axes, the program calculates the atomic coordinates for the remaining two chelate rings and defines the new coordinate system in which the C_3 or quasi C_3 molecular axis is coincident with the Z-axis. In this way the entire molecule is generated with the minimum of input data (for example: coordinates of five chelate ring atoms for the Co tn_3 system). By specifying the absolute configuration and the sequence of conformations of individual chelate rings the idealized forms of the tris(chair) and the tris(twist-boat) forms were built (Table 1).

Secondly, the Cartesians for the crystalline state conformation of Co tn_3 were calculated from the available fractional crystal coordinates [9,*] using a

* The z-coordinate of Co (in Table 2 of Ref. 9) should read 4393(5), also the y-coordinate of Br(2) (*ibid.*) should read −0730(6); (Personal communication from Professor Y. Saito, 1971).

computer program which also effects the reorientation of the molecule in the same way as for the idealized initial conformations.

Coordinates for the Co ptn_3 were obtained by the generation of methyl groups on terminal carbon atoms in a Co-tn ring creating either *R* or *S* absolute configurations.

Minimization. In general minimizations have been carried out under the following conditions:

(a) All the geminal nonbonded interactions (1,3-interactions) were excluded but were accounted for in the corresponding angle-bending terms. In this way all the non-bonded interactions between ligating atoms (N···N) were omitted.

(b) Non-bonded interactions involving the cobalt atom were excluded from the present calculations.

(c) Only three chelate angles (N – Co – N) were included. These were the angles between ligating atoms belonging to a common chelate ring. The equilibrium value of 90° was assigned to these angles.

(d) All of the six possible bond angles on each tetrahedral atom were included in the calculation of angle-bending strain.

(e) All of the nine possible torsional angles formed by a pair of tetrahedra were included in the calculation of torsional strain, whereas the rotational barriers along the coordinate bonds (Co – N) were neglected (*vide infra* "Torsional Strain").

Furthermore, a series of calculations was carried out in which the chelate angle-bending terms were omitted but with the inclusion of all the 12 non-bonded interactions between nitrogen atoms.

All the calculations on idealized "symmetrical" forms ($chair_3$, lel_3, and ob_3) were carried out in two ways: with and without the C_3-symmetry constraint.

The effects of different minimization conditions will be discussed in the section "Conformational Results".

POTENTIAL FUNCTIONS

Bond-stretching and angle-bending strain. Potential energy due to the bond stretching and angle bending is described by simple harmonic functions:

$$E^{l}_{ij} = \tfrac{1}{2}K^{l}_{ij}\ (l_{ij} - l^{\circ}_{ij})^2$$

$$E^{\theta}_{ijk} = \tfrac{1}{2}\ K^{\theta}_{ijk}\ (\theta_{ijk} - \theta^{\circ}_{ijk})^2$$

Standard values [18] were used as equilibrium values for bond lengths. Equilibrium bond lengths and angles with the corresponding stretching and bending force constants are given in Table 2.

Bending force constants for different angles at carbon atoms (*i.e.*, X – C – Y, where X, Y = H, N, and C) were taken from the computer program of Wiberg and Harris.[1,2] Force constants for H – N – H and H – N – C angles were set equal to the constants for H – C – H and H – C – C angles, respectively.

Table 2. Equilibrium bond lengths and stretching force constants.

Bond	$l°$ (Å)	K^l(kcal mol^{-1} Å^{-2})	Ref.
Co – N	2.00	288	19
N – C	1.47	864	1
C – C	1.54	720	1
C – H	1.093	720	1
N – H	1.011	812	19

Equilibrium bond angles and bending force constants

Angle	$\theta°$(deg)	K^θ(kcal mol^{-1} deg^{-2})	Ref.
N – Co – N	90.0	47.3	20
Co – N – H	109.5	13.9	20
Co – N – C	109.5	27.8	20
N – C – C	109.5	77.5	1, 2
N – C – H	109.5	45.6	1, 2
H – N – H	109.5	38.3	[a]
C – N – H	109.5	45.6	[a]
H – C – H	109.5	38.3	1, 2
H – C – C	109.5	45.6	1, 2
C – C – C	109.5	77.5	1, 2

[a] Estimate (see text).

Angle-bending terms involving the cobalt(III) atom were calculated with the force constants of Snow.[20,*]

Torsional strain. Torsional strain is represented by the simple cosine function:[21]

$$E^\phi = \tfrac{1}{2}V^\phi\ (1 + \cos 3\phi)$$

Following Wiberg's concept [1,3a] of "bond torsional energy" (contrary to "group torsional energy") we took all nine possible torsional interactions for a pair of tetrahedral atoms into account by adding their contributions as follows:

$$E^\phi = \sum_{i=1}^{9} \tfrac{1}{2} \times 0.330 \times (1 + \cos 3\phi_i)$$

where 0.330 represents 1/9 of the rotational barrier in ethane. The torsional barrier around the C – N bonds was assumed to be the same as the barrier around the C – C bonds. This is supported by the fact that the rotational barrier is (to a first approximation) independent of the nature of the atoms

* While our work was still in progress Dr. M. R. Snow published [20] his results on the conformational analysis of the α,α-chlorotetraethylenepentaminecobalt(III) ion. We have adopted some of the values for bending force constants chosen by Dr. Snow for his "second set" of parameters in preference to the various estimates which we used before.

involved.[3a] Torsional contributions from rotations about coordinate bonds (Co–N) were omitted assuming that they should be negligibly small,[3a,22] owing to the 12-fold symmetry of the rotational barrier in this case.

Non-bonded interactions. Strain energy contributions due to the non-bonded interactions were calculated using a modified Buckingham-type potential function:

$$E_{ij} = A_{ij} \exp(-B_{ij} r_{ij}) - C_{ij}/r^6_{ij}$$

where i, and j = N, C, and H atoms.

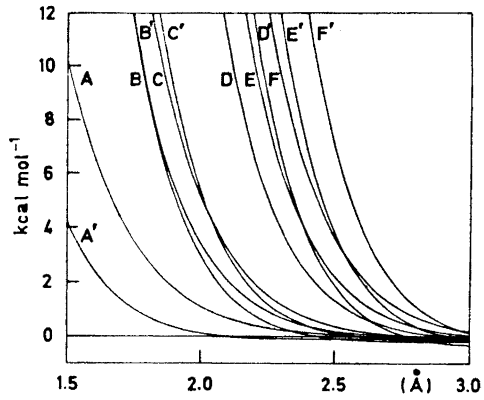

Fig. 2. Potential functions for non-bonded interactions. First set: H···H (A), H···C (B), H···N (C), C···C (D), C···N (E), N···N (F). Second set: H···H (A′), H···C (B′), H···N (C′), C···C (D′), C···N (E′), and N···N (F′).

Two sets of coefficients were used in the present study (Fig. 2 and Table 3). The first set given by Liquori and co-workers [23] is derived from the experimental data of De Coen and co-workers.[24] The function for H···H non-bonded interactions in this set is of "medium" type and is similar to Bartell's H···H function.[25] The second set given by Ramachandran and co-workers [26] yields a rather "soft" H···H function comparable to Hill's function.[27] However, the functions for non-bonded interactions between non-hydrogen atoms are "harder" than in the first set.

Table 3. Parameters for non-bonded potential functions (in kcal/atom pair).

Interaction	First set [23]			Second set [26]		
	$A_{ij} \times 10^{-4}$	B_{ij}	C_{ij}	$A_{ij} \times 10^{-4}$	B_{ij}	C_{ij}
H···H	0.66	4.08	49.2	0.829	4.6	46.8
H···C	3.14	4.32	99.2	7.79	4.6	165.8
H···N	2.81	4.20	121.1	5.34	4.6	156.0
C···C	21.21	4.32	244.0	92.4	4.6	599.9
C···N	23.70	4.44	297.8	60.5	4.6	571.2
N···N	18.64	4.55	200.0	40.4	4.6	546.9

CONFORMATIONAL RESULTS

In the following discussion FF-1 and FF-2 refer to the sets of functions with Liquori's and Ramachandran's non-bonded parameters, respectively. The FF-3 force field was the same as FF-1 with regard to the coefficients used for the different strain energy functions, except that the N–Co–N angle bending terms were omitted and the N···N non-bonded interactions included instead.

The single Co-tn chelate ring

The hypothetical system of one Co-tn chelate ring was first examined. Two principal conformations were minimized: symmetrical *chair* form and symmetrical *twist-boat* form for which the initial Cartesian atomic coordinates have been calculated by the vector method.[28,29] Table 4 summarizes the final minimized geometry of the single Co-tn ring. The main energy differences between initial chair and initial twist-boat conformations were found in the torsional and non-bonded terms. Minimization of the single ring conformations with FF-1 gave equilibrium conformations with the energy difference

Table 4.[a,b] Minimized geometry of the hypothetical single Co-tn ring system.

	FF-1		FF-2		FF-3	
Bond lengths (in Å)	C	TB	C	TB	C	TB
Co–N(1)	2.000	2.060	2.001	2.008	2.000	2.005
N(1)–C(1)	1.475	1.476	1.477	1.476	1.471	1.473
C(1)–C(2)	1.548	1.548	1.549	1.549	1.540	1.546
C(2)–C(3)	1.548	1.548	1.549	1.549	1.540	1.546
C(3)–N(2)	1.475	1.476	1.477	1.476	1.471	1.473
N(2)–Co	2.000	2.060	2.001	2.008	2.000	2.005
Bond angles (in deg.)						
N(2)–Co–N(1)	91.23	92.18	91.40	92.72	90.35	91.74
Co–N(1)–C(1)	110.37	109.80	110.10	109.50	110.20	109.50
N(1)–C(1)–C(2)	111.24	111.30	111.20	111.70	110.60	110.80
C(1)–C(2)–C(3)	111.64	111.90	111.30	111.96	111.10	111.60
C(2)–C(3)–N(2)	111.24	111.30	111.20	111.70	110.60	110.80
C(3)–N(2)–Co	110.37	109.80	110.10	109.50	110.20	109.50
Dihedral angles (in deg.)						
Co–N(1)–C(1)–C(2)	67.98	76.38	68.20	75.93	69.22	77.42
N(1)–C(1)–C(2)–C(3)	67.71	40.20	68.17	40.28	69.10	40.65
C(1)–C(2)–C(3)–N(2)	67.71	40.20	68.17	40.28	69.10	40.65
C(2)–C(3)–N(2)–Co	67.98	76.38	68.20	75.93	69.22	77.42

[a] C = chair conformation, TB = twist-boat conformation.
[b] Numbering scheme for the atoms is given in Fig. 1.

of 2.9 kcal/mol in favour of the chair form. The twist-boat was destabilized over the chair due almost entirely to the torsional strain. Similar calculations using FF-2 and FF-3 yielded energy differences of 2.6 and 2.9 kcal/mol, respectively, in favour of the chair conformation. Comparison of energy differences and geometry parameters obtained with all three force fields (Table 4) indicates that the final equilibrium conformation of a single Co-tn ring is relatively independent of the force field. Torsional angles were evenly distributed in the minimized chair form of the chelate ring, all being $68° \pm 1$. In the minimized twist-boat form dihedral angles of N – C – C – C and Co – N – C – C type were $40° \pm 1$ and $76° \pm 1$, respectively. The torsional strain, therefore, remained much higher in the latter. In addition to the torsional strain, which contributes mostly to the energy difference between chair and twist-boat conformations, the H···H non-bonded and other 1,4 non-bonded interactions although relieved to approximately the same extent in both conformations are slightly more pronounced in the twist-boat form. The chelate angle (N – Co – N) is increased by $1 - 2°$ in both chair and twist-boat minimized conformations, which does not necessarily mean that similar widening should be expected in Co tn_3. Although in the treatment of the single Co-tn ring ligands other than the two nitrogens were ignored it is to be expected that the chair conformation of the ring should be preferred over the twist-boat conformation in complexes of the type $[Co(tn)(X_4)]$ at least for relatively small ligands, X. Minimization was carried out without any symmetry constraint. Nevertheless the initial symmetries of the chelate rings (C_2 for twist-boat and C_s for chair) were preserved whereas the endocyclic bonds were slightly stretched and the endocyclic angles were widened (Table 4).

Tris-chair conformations of Co tn_3

Next we have examined the idealized and the X-ray conformations of Co tn_3. The $chair_3$ form was of special interest since it was the conformation found by X-ray diffraction studies.[9] The strain energy of the initial idealized $chair_3$ form was extremely high due to the inter-annular non-bonded H···H repulsions between amino-groups and terminal methylene groups, *i.e.*, three distances of 1.109 Å between H(8)···H(19), H(18)···H(29), and H(28)···H(9), and three distances of 1.417 Å between H(3)···H(20), H(13)···H(30), and H(23)···H(10). By minimization these distances were increased to 2.071 Å and 2.022 Å, respectively. These interactions involve only the hydrogen atoms from amino groups occupying one of the octahedral faces perpendicular to the C_3 axis, whereas inter-annular non-bonded H···H interactions involving the other three amino groups are of the same order of magnitude as the intra-annular (axial-axial) interactions. The inequality of the two sets of NH_2 groups in $chair_3$ is a corollary of its lower symmetry (C_3) as compared to the symmetry of the $twist\text{-}boat_3$ (D_3).

During the minimization of the idealized $chair_3$ either with inclusion of the N – Co – N bending terms (FF-1), or with inclusion of the non-bonded terms for N···N interactions instead (FF-3), it was observed that the chelate angles contract considerably in order to relieve the non-bonded inter-annular H···H

interactions. However, carrying out the minimization with the X-ray structure as the initial conformation we arrived at a conformation with a considerably lower energy in which the three chelate angles remained larger than or equal to 90°. We therefore suspected that the minimized idealized $chair_3$ had been trapped in a local minimum far from the extreme minimum for that system. In order to overcome this situation we chose a different route for the minimization, *i.e.*, starting with the idealized $chair_3$ we carried out the usual minimization under the constraint that the nitrogens remain fixed at their initial positions at the apices of the octahedron. The conformation thus produced served subsequently as the starting point for the complete minimization. In this way we arrived at a lower minimum with a much better correlation between the geometry parameters in the minimized $chair_3$ and X-ray $chair_3$ conformation (Figs. 3(a), 4, and 5).

Minimization of the X-ray $chair_3$ conformation causes the structure to approach slowly the C_3 symmetry and the chelate angles to decrease. Although the minimization of the X-ray structure does not lead to a conformation which is identical to that obtained from the idealized $chair_3$ when terminated ac-

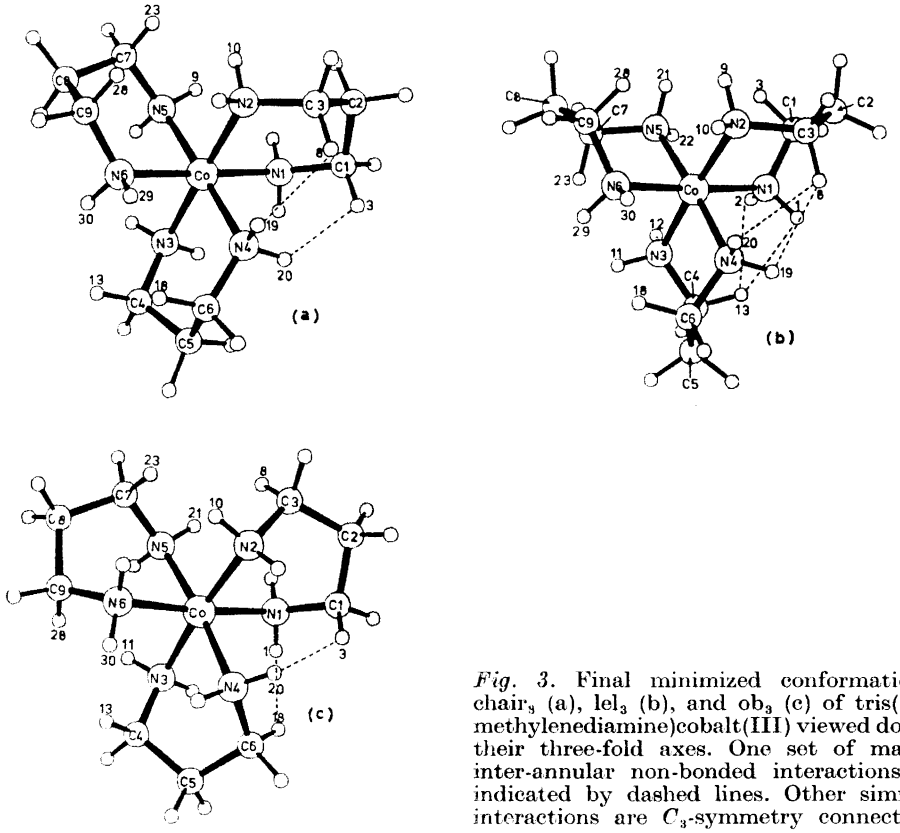

Fig. 3. Final minimized conformations $chair_3$ (a), lel_3 (b), and ob_3 (c) of tris(trimethylenediamine)cobalt(III) viewed down their three-fold axes. One set of major inter-annular non-bonded interactions is indicated by dashed lines. Other similar interactions are C_3-symmetry connected.

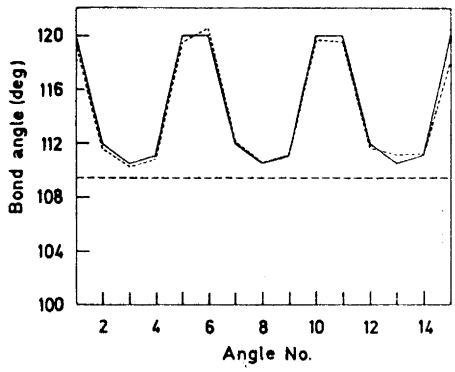

Fig. 4. Endocyclic bond angles in minimized idealized chair$_3$ (——), and in minimized X-ray chair$_3$ (- - - -) conformations of Co tn$_3$. Angle numbers: 1. Co–N(1)–C(1), 2. N(1)–C(1)–C(2), 3. C(1)–C(2)–C(3), 4. C(2)–C(3)–N(2), 5. C(3)–N(2)–Co, 6. Co–N(3)–C(4), 7. N(3)–C(4)–C(5), 8. C(4)–C(5)–C(6), 9. C(5)–C(6)–N(4), 10. C(6)–N(4)–Co, 11. Co–N(5)–C(7), 12. N(5)–C(7)–C(8), 13. C(7)–C(8)–C(9), 14. C(8)–C(9)–N(6), and 15. C(9)–N(6)–Co (*cf.* Fig. 3 (a)).

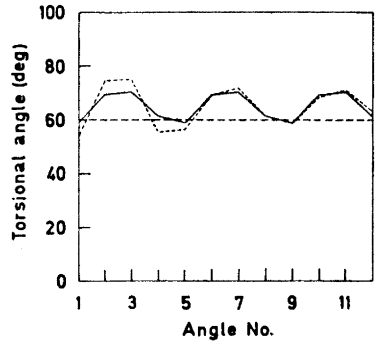

Fig. 5. Torsional angles in minimized idealized chair$_3$ (——), and in minimized X-ray chair$_3$ (- - - -) conformations of Co tn$_3$. Angle numbers: 1. Co–N(1)–C(1)–C(2), 2. N(1)–C(1)–C(2)–C(3), 3. C(1)–C(2)–C(3)–N(2), 4. C(2)–C(3)–N(2)–Co, 5. Co–N(3)–C(4)–C(5), 6. N(3)–C(4)–C(5)–C(6), 7. C(4)–C(5)–C(6)–N(4), 8. C(5)–C(6)–N(4)–Co, 9. Co–N(5)–C(7)–C(8), 10. N(5)–C(7)–C(8)–C(9), 11. C(7)–C(8)–C(9)–N(6), and 12. C(8)–C(9)–N(6)–Co (*cf.* Fig. 3 (a)).

cording to the above-mentioned criterion ($\delta_E \leq 0.002$ kcal mol^{-1}) it is reasonable to suppose that they represent points in the same shallow minimum of the potential energy surface. In order to check – if not prove – this assumption we have constructed an "average conformation" from the two minimized conformations, *i.e.* one in which the Cartesian atomic coordinates for each atom were taken as the mean values of the corresponding coordinates in the minimized conformations. As expected, the energy of this average conformation was intermediate between the two minimized energies and it remained unchanged when the conformation was subjected to the minimization procedure. In particular this minimum or "valley" seems to be flat with respect to the variations of the N–Co–N angles in either direction from the "zero-strain" value of 90°. If so, the differences between X-ray and minimized chair$_3$ conformations may be attributed to specific crystal forces. In fact the chelate angle in the Co-tn ring is known to vary considerably in varying environment, *e.g.*, ∠N–Co–N = 87.7° in Co tn$_2$(NO$_3$)$_2$,[12a] 95.4° in Co tn$_2$Cl$_2$,[12b] 90.2° in Co en$_2$tn.[11]

Bond lengths were slightly stretched in the minimized idealized chair$_3$ (Table 5) but are still within the ranges of the values found by the X-ray diffraction study.[9] Endocyclic bond angles were opened out from their assumed tetrahedral "zero-strain" values (Fig. 4 and Table 5). The N–C–C and C–C–C angles were in the range 119.5 to 120.5°, and 110.0 to 111.5°, respectively. Similar widening was also observed in the X-ray structure.[9] Dihedral angles of the type Co–N–C–C are lower than those of the type

Table 5.[a,b] Minimized conformations of tris(trimethylenediamine)-cobalt(III).

	$chair_3$		lel_3		ob_3	
	FF-1	FF-2	FF-1	FF-2	FF-1	FF-2
Bond lengths (in Å)						
Co – N(1)	2.060	2.035	2.035	2.015	2.054	2.025
N(1) – C(1)	1.480	1.475	1.474	1.470	1.476	1.472
C(1) – C(2)	1.542	1.538	1.547	1.544	1.549	1.545
C(2) – C(3)	1.542	1.538	1.547	1.544	1.548	1.546
C(3) – N(2)	1.477	1.473	1.474	1.469	1.476	1.472
N(2) – Co	2.049	2.030	2.035	2.012	2.053	2.025
Bond angles (in deg.)						
N(2) – Co – N(1)	89.35	89.79	89.14	90.98	88.02	90.14
Co – N(1) – C(1)	120.03	119.36	113.78	111.79	113.85	111.77
N(1) – C(1) – C(2)	111.98	111.60	112.08	111.61	111.83	111.40
C(1) – C(2) – C(3)	110.49	109.95	113.28	113.01	112.71	112.71
C(2) – C(3) – N(2)	111.11	110.94	112.06	111.73	111.96	111.33
C(3) – N(2) – Co	120.08	118.68	113.80	111.76	113.72	111.86
Dihedral angles (in deg.)						
Co – N(1) – C(1) – C(2)	58.73	60.02	73.86	74.70	75.06	75.70
N(1) – C(1) – C(2) – C(3)	69.52	69.73	37.58	38.84	37.76	38.77
C(1) – C(2) – C(3) – N(2)	70.48	71.26	37.65	38.80	38.39	39.42
C(2) – C(3) – N(2) – Co	61.20	62.90	73.87	74.74	75.16	75.60

[a] Numbering scheme for the atoms is given in Fig. 3.
[b] Corresponding geometry parameters for the other two chelate rings are C_3-symmetry connected and therefore identical to the values presented in the table.

N – C – C – C in the minimized idealized chair ($59 \pm 2°$ against $70 \pm 2°$) as well as in the crystal structure (56.7° against 67.1° *). This indicates a similar mode of puckering of the chelate rings which are flattened out in the "inner" moiety (*i.e.*, C – N – Co – N – C fragment) and puckered in the outer one (*i.e.*, N – C – C – C – N fragment).

Symmetrical twist-$boat_3$ conformations of Co tn_3

Next we have examined two symmetrical twist-$boat_3$ conformations: lel_3 and ob_3. As the bond lengths and angles of the initial idealized forms are at their equilibrium values the only sources of steric energy are non-bonded interactions and torsional strain.

However, the diastereoisomeric conformations lel_3 and ob_3 differed only in the non-bonded interactions. Dominant non-bonded repulsions in lel_3 conformation arise from interactions within the following six symmetry con-

* Mean value for all three rings.

nected pairs: H(8)···H(19), H(18)···H(29), H(28)···H(9), H(2)···H(13), H(12)···H(23), and H(22)···H(3), in which the initial interatomic distance of 1.98 Å increased to 2.28 Å during the minimization. There were six more contacts of 2.08 Å (increased to 2.23 Å) between H(8)···H(20), H(18)···H(30), H(28)···H(10), H(1)···H(13), H(11)···H(23), and H(21)···H(3). Corresponding dominant inter-annular H···H distances in the ob_3 conformation were: H(1)···H(18), H(11)···H(28), H(21)···H(8), H(3)···H(20), H(13)···H(30), and H(23)···H(10), all of 1.64 Å, which were increased to 2.14 Å in the minimized conformations. Other H···H non-bonded distances were of the same order of magnitude as intra-annular non-bonded distances. Calculated geometry parameters for lel_3 and ob_3 conformations obtained with different force fields are presented in Table 5. There is a slight difference between the equilibrium geometry parameters calculated using the two force fields FF-1 and FF-2. The distortions of the initial idealized structures were smaller when the minimization was carried out with FF-2 in lel_3 as well as in ob_3 conformation. This is due to the nature of the potential function for non-bonded H···H interactions chosen for FF-2 which is of the "soft" type. On the other hand differences in final geometry parameters between lel_3 and ob_3 might be regarded as a consequence of inter-annular non-bonded interactions which were more pronounced in the ob_3 conformation. With FF-1 (and FF-3) the chelate angles in lel_3 and ob_3 minimized conformations were $\sim 89.1°$ and $\sim 88.0°$, respectively. However, with the FF-2 ("soft" H···H non-bonded potential function) the final equilibrium angles were 90.98° for lel_3 and 90.14° for the ob_3 form (recall the widening of N–Co–N angles in the minimized single Co-tn chelate rings). The range of torsional angles were: 73.2° to 75.5° for Co–N–C–C type, and 37.4° to 39.4° for N–C–C–C type, both in lel_3 and ob_3 conformations of Co tn_3. The difference between the two types of dihedral angles indicates a considerably twisted shape of chelate rings in these conformations. Final minimized geometries are shown in Figs. 3(b) and (c).

Mixed conformations of Co tn_3

Next we have examined the ten sterically possible mixed conformations of Co tn_3 (see Table 1). It was found that whenever both lel and ob rings are present as in lel_2ob and ob_2lel there exist strong inter-annular H···H repulsions between, *e.g.*, H(1)···H(18) and H(7)···H(19), where the distances are 1.64 and 1.44 Å, respectively (Fig. 6). Furthermore, it was found that $E_{lel_2ob} < E_{ob_2lel}$. Because of the strong inter-annular repulsions the energies of these two conformers exceed those of the pure lel_3 and ob_3 and of any of the remaining eight mixed conformers. This is contrary to the order of conformational energies in the Co en_3 species.[6,30]

Three mixed forms consisting of chair and ob ring conformations: ob_2chair, (C_1)-$chair_2$ob, and *anti*-$chair_2$ob, were found to have nearly the same energies slightly below that of the pure ob_3 form. Similarly, three mixed forms consisting of chair and lel ring conformations: (C_1)-$chair_2$lel, lel_2chair, and *anti*-$chair_2$lel, were lower in energy than (or comparable to) the pure (C_3)-$chair_3$ form.

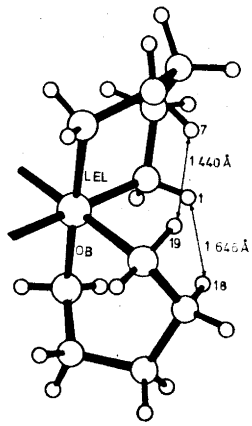

Fig. 6. The lel-ob interactions in "mixed" conformations of Co tn_3.

Finally there were two mixed forms with three different ring conformations: *cis*$_{(lel, chair)}$-lel ob chair, and *trans*$_{(lel, chair)}$-lel ob chair. The high energy of these conformations was due to the lel-ob inter-annular interactions.

Tris(*R*,*R*-2,4-diaminopentane)cobalt(III)

The most favourable conformation of a single Co(*R*,*R*-2,4-ptn) ring is undoubtedly the λ-twist-boat which permits both of the methyl groups to become equatorial. (The chair and the δ-twist-boat have one and two axial substituents, respectively.) Furthermore, molecular models show very convincingly that the presence of chair and δ-twist-boat rings in a tris complex may be excluded, whereas the tris (λ-twist-boat) appears very favourable. Therefore, Co(*R*,*R*-2,4-ptn)$_3$ complex ion is expected to have lel_3 conformation for Δ absolute configuration, and ob_3 conformation for Λ absolute configuration. This was indeed found by the X-ray diffraction study[10] of $(+)_{546}$-[Co(*R*,*R*-2,4-ptn)$_3$]Cl_3.H_2O for which the Λ absolute configuration and ob_3 chelate ring conformation were established. A preliminary examination of Δ-lel_3 and Λ-ob_3 conformations of Co(*R*,*R*-2,4-ptn)$_3$ was carried out. Minimized geometries are summarized in Table 6 and Fig. 7.

Table 6.[a,b] Minimized conformations of tris(*R*,*R*-2,4-diaminopentane)cobalt(III).

Bond lengths (in Å)	ob_3	lel_3
Co – N(1)	2.07	2.04
Co – N(2)	2.07	2.04
N(1) – C(1)	1.48	1.48
N(2) – C(3)	1.48	1.48
C(1) – C(2)	1.55	1.55
C(2) – C(3)	1.55	1.55
C(1) – C(4)	1.55	1.55
C(3) – C(5)	1.55	1.55

Table 6. Continued.

Bond angles (in deg.)		
N(1) – Co – N(2)	87.36	89.14_5
Co – N(1) – C(1)	112.41	113.50
Co – N(2) – C(3)	112.48	113.42
N(1) – C(1) – C(2)	110.63	111.51
N(2) – C(3) – C(2)	110.69	111.47
N(1) – C(1) – C(4)	110.57_5	109.89
N(2) – C(3) – C(5)	110.69	109.89
C(1) – C(2) – C(3)	112.36	113.39
C(4) – C(1) – C(2)	109.45	109.96
C(5) – C(3) – C(2)	109.52	109.95
Dihedral angles (in deg.)		
Co – N(1) – C(1) – C(2)	77.81	74.42
Co – N(1) – C(1) – C(4)	160.76	163.39
N(1) – C(1) – C(2) – C(3)	39.62	37.72
C(4) – C(1) – C(2) – C(3)	161.71	159.87
C(1) – C(2) – C(3) – N(2)	39.37	38.13
C(1) – C(2) – C(3) – C(5)	161.69	160.24
Co – N(2) – C(3) – C(2)	77.62	74.60
Co – N(2) – C(3) – C(5)	160.75_5	163.26

[a] Numbering scheme for the atoms is given in Fig. 7.
[b] Corresponding geometry parameters for the other two chelate rings are C_3-symmetry connected and therefore identical to the values presented in the table.

Short of fractional crystal coordinates we were unable to compare the calculated and observed [10] structures except for the value of chelate angles. Observed [10] N – Co – N angles are all less than 90°, the average being 87.9 ± 1.3°, which is in very good agreement with the calculated value of 87.36° for ob_3 conformer. Calculated chelate angles in the lel_3 form are also less than 90° (Table 6). The contraction of the N – Co – N angles may be considered as a consequence of inter-annular non-bonded repulsions which are relieved in the similar way as in the Co tn_3.

CONCLUDING REMARKS

Relative minimized energies of Co tn_3 conformations are given in Fig. 8 together with earlier results of similar calculations by Gollogly and Hawkins [31] and by Geue and Snow.[5f] The energy terms for "pure" tris conformations of Co tn_3 are specified in Table 7 and the energy terms for two twist-$boat_3$ conformations of Co ptn_3 in Table 8.*

* Numerical values for the energies of conformations not included in Table 7 and Cartesian atomic coordinates of conformations studied in this work may be obtained from the authors upon request.

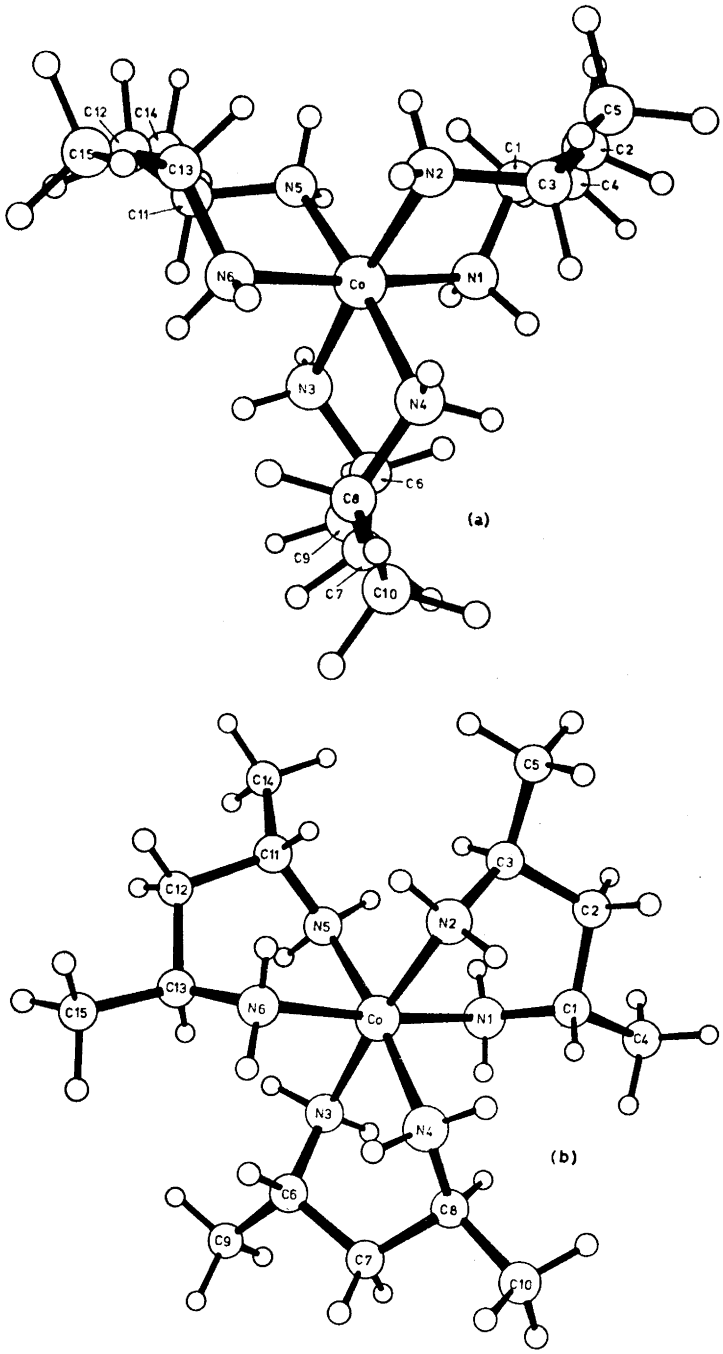

Fig. 7. Final minimized lel_3 (a) and ob_3 (b) conformations of tris(2,4-diaminopentane)-cobalt(III).

Table 7. Energy contributions for the "pure" tris conformations of Co tn_3 (kcal mol^{-1}).

FF-1	lel_3 minimized X-ray	$chair_3$	ob_3	X-ray
Bond stretching	1.11 2.84	2.57	2.55	0.63
H···H non-bonded	7.47 9.45	10.13	10.38	16.80
Other non-bonded	−6.13 −7.47	−7.38	−6.67	−5.91
N−Co−N bending	0.03 0.18	0.02	0.17	1.03
Endocyclic bend.	2.77 5.85	6.49	2.40	5.71
Exocyclic bend.	0.88 2.16	2.38	1.62	4.84
Torsional	7.36 1.62	0.94	7.72	0.98
Total energy	13.49 14.63	15.15	18.19	24.08
Conformational energy	0.00 1.14	1.66	4.70	10.59
FF-2				
Bond stretching	0.19 0.80	0.93	0.63	0.51
H···H non-bonded	−9.38 −6.17	−7.03	−7.21	−5.14
Other non-bonded	−20.99 −23.07	−23.15	−22.36	−23.10
N−Co−N bending	0.04 0.39	0.00	0.00	1.03
Endocyclic bend.	1.70 3.30	5.20	1.42	5.71
Exocyclic bend.	0.35 1.25	1.42	0.54	1.92
Torsional	7.25 1.66	1.07	7.46	0.88
Total energy	−20.84 −21.84	−21.56	−19.52	−18.19
Conformational energy	1.00 0.00	0.28	2.32	3.65

Table 8. Energy contributions for the Co(*R*,*R*-2,4-ptn)$_3$ conformations (kcal mol^{-1}).

FF-1	Λ-ob_3 (C_3)	Λ-lel_3 (C_3)
Bond stretching	4.78	2.06
H···H non-bonded	10.95	5.89
Other non-bonded	−6.55	−6.27
N−Co−N bending	0.31	0.03
Endocyclic bending	1.34	2.38
Exocyclic bending	0.56	0.83
Torsional	8.04	7.70
Total energy	19.44	12.63
Conformational energy	6.81	0.00

One of the questions originally raised in this context was whether the most stable conformation could be predicted with some degree of certainty by conformational analysis. In the first primitive calculations,[5b,17,29] in which only

"pure" tris conformations were considered, the lel_3 was found to be lowest in energy. Calculations by Gollogly and Hawkins,[31] already at a considerably higher level of sophistication in which they attempt a partial mapping of the energy surface for "pure" tris conformations, led to the result that the $chair_3$ is the most stable conformation. Snow's calculations [5f] which involve a complete minimization procedure, not very different from ours, and which are based on a force field very similar to our FF-1 again place lel_3 below $chair_3$. We have extended the calculations to include "mixed" conformations, as well as the unsymmetrical "pure" tris conformations (*e.g.* the X-ray conformation), and we have studied the effect of replacing a force field with relatively "hard" non-bonded H···H interactions and "soft" skeleton interactions (FF-1) by one with relatively "hard" skeleton but "soft" H···H non-bonded interactions (FF-2). The results are evident from Fig. 8.

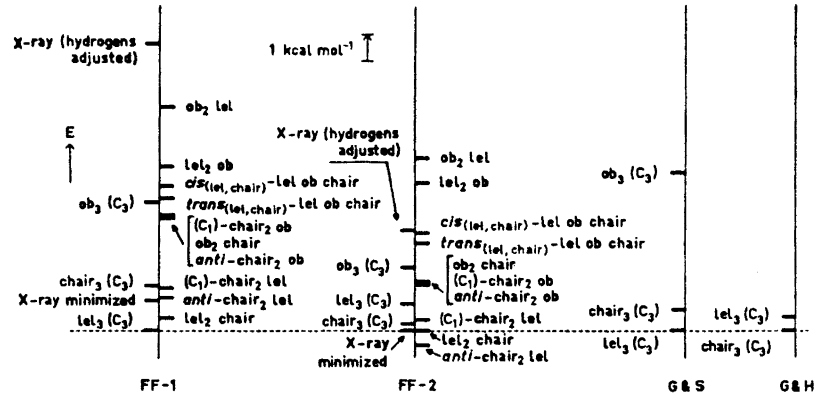

Fig. 8. Comparison of minimized energies of Co tn_3 conformations. Symbols are explained in Table 1. G & S = results by Geue and Snow,[5f] G & H = results by Gollogly and Hawkins.[31] X-ray (hydrogens adjusted) indicates the energy of a conformation obtained by supplementing the skeleton obtained from the X-ray structure [9] with hydrogens, and minimizing with respect to the positions of the hydrogens but keeping the non-hydrogen atoms fixed. (Subsequent minimization of this conformation with respect to all the atoms led to the same result as a minimization carried directly on the supplemented X-ray conformation.)

We conclude that at the present state of the art one can not by conformational analysis definitively identify the most stable conformation – not even of the gaseous ion, let alone the ion in solution. However, we think it is a safe conclusion that in solution at room temperature a conformational equilibrium involving significant amounts of two or more conformers – probably including "mixed" forms – prevails. This is in good agreement with considerations by Mason and co-workers [5e] although they did not take "mixed" conformations into account.

A further point should be kept in mind when one considers results as those given in Fig. 8. As indicated in our discussion of the minimization of the tris-chair conformation the potential energy surface of the system is complicated

enough to make the minimum actually reached by the program dependent not only on the starting conformation but also on the initial route of minimization. Therefore there is reason to believe that by further exploration of the energy surface conformations of even lower energy than those indicated in Fig. 8 may be found. *E.g.*, it seems likely that the removal of the C_3 symmetry constraint from a minimized conformation generally will make a further small but significant minimization possible. Although by further investigation lower conformational energy minima than those indicated in Fig. 8 may be located, we have at present no indication that the above conclusions or the general features of the conformational distribution as presented in Fig. 8 will be invalidated.

Acknowledgements. We wish to express our gratitude and indebtedness to Professor K. B. Wiberg for providing us with a copy of his minimization program. In addition, special thanks are due to Dr. Gunner Borch for valuable programming advice and help in the initial stages of this work. We also thank Professor I. Krstanović for making available to us a computer program for the transformation of fractional crystal coordinates, and Mr. M. P. Roy for help in preparing the computer produced drawings. Finally, we thank Professor M. B. Ćelap for promoting the contact between us. One of us (SRN) gratefully acknowledges the financial support from *The Danish Ministry of Education* and *The Technical University of Denmark*. Computer time and services were provided by *The Northern Europe University Computing Center* (NEUCC) at The Technical University of Denmark in Lyngby.

REFERENCES

1. Wiberg, K. B. *J. Am. Chem. Soc.* **87** (1965) 1070.
2. Harris, H. A. *Ph. D. Thesis*, Yale University 1966.
3. a. Gleicher, G. J. and Schleyer, P. v. R. *J. Am. Chem. Soc.* **89** (1967) 582; b. Schleyer, P. v. R. In Chiurdoglu, G., Ed., *Conformational Analysis, Scope and Present Limitations*, Academic, New York 1971, p. 241.
4. Allinger, N. L., Miller, M. A., VanCatledge, F. A. and Hirsch, J. A. *J. Am. Chem. Soc.* **89** (1967) 4345; Allinger, N. L., Hirsch, J. A., Miller, M. A., Tyminski, I. J. and VanCatledge, F. A. *J. Am. Chem. Soc.* **90** (1968) 1199; Allinger, N. L., Tribble, M. T., Miller, M. A. and Werz, D. H. *J. Am. Chem. Soc.* **93** (1971) 1637.
5. a. Woldbye, F. *Rec. Chem. Progr.* **24** (1963) 197; b. Woldbye, F. *Proc. Roy. Soc.* **A 297** (1967) 79; c. Beddoe, P. G. and Mason, S. F. *Inorg. Nucl. Chem. Lett.* **4** (1968) 433; Gollogly, J. R. and Hawkins, C. J. *Chem. Commun.* **1968** 689; d. Judkins, R. R. and Royer, D. J. *Inorg. Nucl. Chem. Lett.* **6** (1970) 305; Gollogly, J. R. *Ph. D. Thesis*, University of Queensland 1970; Butler, K. R. and Snow, M. R. *Inorg. Chem.* **10** (1971) 1838; Hawkins, C. J. *Absolute Configuration of Metal Complexes*, Wiley-Interscience, New York 1971, pp. 86–94, 131, 176; e. Beddoe, P. G., Harding, M. J., Mason, S. F. and Peart, B. J. *Chem. Commun.* **1971** 1283; f. Geue, R. J. and Snow, M. R. *J. Chem. Soc.* **A 1971** 2981.
6. Niketić, S. R. and Woldbye, F. *Conformational Analysis of Coordination Compounds*, submitted to XV ICCC, Moscow 1973; further to be published in *Acta Chem. Scand.*
7. *IUPAC Nomenclature of Inorganic Chemistry*, 2nd Ed., Butterworths, London 1971.
8. Corey, E. J. and Bailar, Jr., J. C. *J. Am. Chem. Soc.* **81** (1959) 2620.
9. Nomura, T., Marumo, F. and Saito, Y. *Bull. Chem. Soc. Japan* **42** (1969) 1016.
10. Kobayashi, A., Marumo, F., Saito, Y., Fujita, J. and Mizukami, F. *Inorg. Nucl. Chem. Lett.* **7** (1971) 777.
11. Schousboe-Jensen, H. V. F. *Acta Chem. Scand.* **26** (1972) 3413.
12. a. Yasaki, E., Oonishi, I., Kawaguchi, H., Kawaguchi, S. and Komiyama, Y. *Bull. Chem. Soc. Japan* **43** (1970) 1354; b. Matsumoto, K., Ooi, S. and Kuroya, H. *Bull. Chem. Soc. Japan* **43** (1970) 1903; c. Matsumoto, K., Yonezawa, M., Kuroya, H., Kawaguchi, H. and Kawaguchi, S. *Bull. Chem. Soc. Japan* **43** (1970) 1269.

13. Morosin, B. and Howatson, J. *Acta Cryst.* **B 26** (1970) 2062; Pajunen, A. *Suomen Kemistilehti* **B 41** (1968) 232; **B 42** (1969) 15, 44, 397; **B 43** (1970) 70.
14. Beveridge, G. S. and Schechter, R. S. *Optimization: Theory and Practice*, McGraw, New York 1970, p. 408 ff.
15. Williams, J. E., Stang, P. J. and Schleyer, P. v. R. *Ann. Rev. Phys. Chem.* **19** (1968) 531.
16. Corey, E. J. and Sneen, R. A. *J. Am. Chem. Soc.* **77** (1955) 2505.
17. Woldbye, F. *Studier over Optisk Aktivitet*, Polyteknisk Forlag, København 1969, pp. 198–211.
18. Sutton, L. E., Ed., *Tables of Interatomic Distances*, Spec. Publ. No. 11 (1958), and *Suppl.* Spec. Publ. No. 18 (1965), The Chemical Society, London.
19. Nakagawa, I. and Shimanouchi, T. *Spectrochim. Acta* **22** (1966) 1707.
20. Snow, M. R. *J. Am. Chem. Soc.* **92** (1970) 3610.
21. Millen, D. J. *Progr. Stereochem.* **3** (1962) 138.
22. Wilson, Jr., E. B. *Advan. Chem. Phys.* **2** (1959) 367.
23. Liquori, A. M., Damiani, A. and Elefante, G. *J. Mol. Biol.* **33** (1968) 439.
24. De Coen, J. L., Elefante, G., Liquori, A. M. and Damiani, A. *Nature (London)* **216** (1967) 910.
25. Bartell, L. S. *J. Chem. Phys.* **32** (1960) 827.
26. Ramachandran, G. N., Venkatachalam, C. M. and Krimm, S. *Biophysical J.* **6** (1966) 849.
27. Hill, T. L. *J. Chem. Phys.* **16** (1948) 399.
28. Woldbye, F. Ref. 17, p. 203.
29. Bagger, S. *Optisk Aktivitet og Konformationsanalyse i Koordinationskemi, Thesis*, The Technical University of Denmark 1964.
30. Sudmeier, J. L. and Blackmer, G. L. *Inorg. Chem.* **10** (1971) 2010.
31. Gollogly, J. R. and Hawkins, C. J. *Inorg. Chem.* **11** (1972) 156.
32. Jurnak, F. A. and Raymond, K. N. *Inorg. Chem.* **11** (1972) 3149.

Received June 28, 1972.

ACTA CHEMICA SCANDINAVICA 27 (1973) 643–660

An X-Ray Investigation of the Hydrolysis Products of Tin(II) in Solution

GEORG JOHANSSON and HITOSHI OHTAKI*

Department of Inorganic Chemistry, Royal Institute of Technology, S-100 44 Stockholm 70, Sweden

The X-ray scattering from hydrolyzed and acid water solutions of 3 M tin(II) perchlorate has been measured. In its inner coordination sphere the tin(II) ion has between two and three water molecules at distances of 2.3 Å. In the hydrolyzed solutions polynuclear complexes are formed with Sn – Sn distances between 3.6 Å and 4 Å. In the most hydrolyzed of the solutions investigated the average number of Sn atoms bonded to each other Sn atom is about 1.5. Possible structures for the complexes are discussed.

The hydrolytic reactions of the tin(II) ion have been investigated by several workers.[1–7] The emf measurements by Tobias,[7] which were made in a 3 M $(Na)ClO_4$ medium with tin concentrations varying from 2.50 mM to 40 mM, led to the conclusion that the main hydrolysis product is the tri-nuclear $Sn_3(OH)_4^{2+}$ with some minor products, $Sn_2(OH)_2^{2+}$ and $SnOH^+$, also formed. It is interesting to compare this with results reported for lead(II), where the tetra-nuclear $Pb_4(OH)_4^{4+}$ or the hexa-nuclear $Pb_6(OH)_8^{4+}$ are predominant in the whole accessible concentration range, with the complexes $Pb_3(OH)_4^{2+}$ and Pb_2OH^{3+} formed in lower concentrations.[8–10]

In the solid state tin(II) and lead(II) seem to form closely related hydrolysis complexes, which can be pictured as based on a group of three metal atoms arranged in a triangle with an oxygen atom slightly above the center of the triangle. By the sharing of edges these triangles combine into tetrahedra or octahedra of metal atoms. Crystals of the basic tin(II) sulfate, Sn_2OSO_4, have been reported to be built up from discrete complexes with eight tin atoms.[11] They can be described as a basic tetrahedron of tin atoms sharing its faces with four similar tetrahedra. A related structure has been found for the basic lead(II) perchlorate, $Pb_6O(OH)_6(ClO_4)_4.H_2O$, in which a tetrahedron of lead atoms shares two of its faces with other tetrahedra leading to hexa-nuclear complexes, $Pb_6O(OH)_6^{4+}$.[12] In recent structure determinations of $Sn_6O_4(OH)_4$

* Present address: Tokyo Institute of Technology, O-okayama, Meguro-ku, Tokyo, Japan.

and the isomorphous lead(II) compound, octahedra of metal atoms have been found to occur.[13,14]

An X-ray investigation of hydrolyzed lead(II) perchlorate solutions [15] has shown that the hexa-nuclear complex $Pb_6O(OH)_6^{4+}$ retains its structure in solution and that the tetra-nuclear complex has a tetrahedral arrangement of lead atoms. In view of the closely related structures of tin(II) and lead(II) in the solid state it was of interest to make a similar X-ray investigation of hydrolyzed tin(II) solutions, although tin, because of its lower atomic number, is far less suitable than lead for such an investigation.

As in previous investigations of this kind [15–18] a series of solutions with constant metal ion concentration but with varying degrees of hydrolysis has been investigated. Variations in the X-ray scattering between the different solutions are then mainly due to the formation of hydrolysis complexes and can be interpreted in terms of interatomic distances within the complexes and frequencies of these distances.

EXPERIMENTAL

Preparation of solutions. Partially hydrolyzed tin(II) perchlorate solutions were prepared by addition of $NaHCO_3$ to tin(II) perchlorate solutions which were prepared by a modification of the method described by Noyes and Toabe.[19] A schematic diagram of the apparatus used for the preparation of the solutions is shown in Fig. 1.

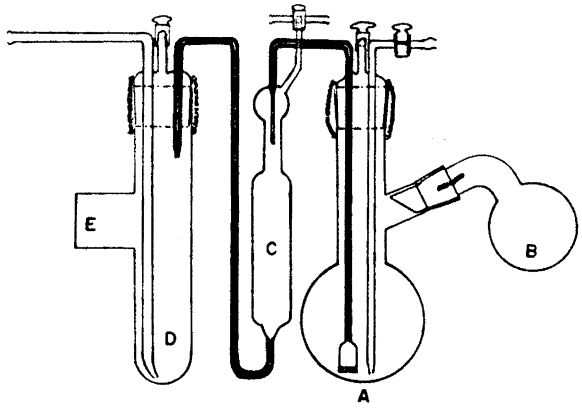

Fig. 1. The apparatus used for the preparation of the tin(II) perchlorate solution.

Granular metallic tin (*p.a.* grade of a purity better than 99.5 %) was washed three times with dilute hydrochloric acid, then with water, and finally with alcohol. The granules were dried by pressing them between sheets of filter paper and were then transferred to the bulb A (Fig. 1). The apparatus was evacuated until the metal granules were completely dried. A slightly acid copper perchlorate solution was placed in the bulb B. The air initially in the apparatus was completely replaced with argon by repeated evacuation and back-filling with pure argon. By turning the bulb B the copper perchlorate solution was then transferred to the bulb A. The displacement of the copper ions by tin was completed within a few hours. Occasional shaking of the apparatus was effective in speeding up the exchange reaction and in preventing the granules sticking. The resulting solu-

tion was clear with a pale greenish yellow color. It was transferred through a tube with a glass filter into a calibrated buret (C). About 30 ml of the solution was then transferred by means of argon gas into the tube D in which a weighed amount of $NaHCO_3$ powder had been placed at E. The resulting solution was transferred through a glass tube into a glass vessel which was placed in the X-ray diffractometer. During the preparation and the transfer of the solution it was not in contact with any stop-cock or with air. Tests for copper and for chloride in the solution were negative.

Copper perchlorate was prepared by dissolving copper(II) oxide (Merck, *p.a.*) in reagent grade perchloric acid. The crystals obtained were recrystallized three times from water.

Analysis of solutions. The determination of tin(II) was made according to Jamieson.[20] An aliquot of the tin perchlorate solution was transferred to an Erlenmeyer flask in which 30 ml of hydrochloric acid, 20 ml of water, and 2 – 4 ml of chloroform were contained. The solution was titrated with a standard potassium iodate solution. The titration was continued with thorough shaking of the stoppered flask after each addition of potassium iodate solution until the end point was reached.

A Gran plot [21] of the emf values measured when acidifying the hydrolyzed solution was used for the evaluation of the analytical hydrogen ion excess in the solution.

The total amount of perchlorate was determined with a cation exchange resin. The titration of the free acid was made with a standard sodium hydroxide solution.

The concentration of sodium ions was determined from the material balance of ions in the solution. The density of a solution was determined pycnometrically.

The compositions of the solutions investigated are given in Table 1. The values $\bar{n}$, given in the table, represent the number of OH groups per Sn atom as estimated from

Table 1. Concentrations of solutions. The volume of a stoichiometric unit of solution = V Å^3.

Solution No.	I (V = 503.5 Å^3)		II (V = 533.4 Å^3)		III (V = 555.3 Å^3)	
Concentration	g atoms/l	atoms/unit volume	g atoms/l	atoms/unit volume	g atoms/l	atoms/unit volume
Sn	3.298	1	3.113	1	2.990	1
Cl	6.825	2.070	6.431	2.067	6.422	2.148
O	67.07	20.34	65.20	20.95	65.34	21.85
H	77.77	24.19	77.34	24.85	76.97	25.74
Na			1.788	0.574	2.789	0.933
$\bar{n}$	0		0.507		0.785	

the hydrogen ion excess. Precipitates were formed in a 3 M solution when the value of $\bar{n}$ exceeded 0.8. Increase of the Sn(II) concentrations led to lower maximum $\bar{n}$ values. In chloride solutions the maximum values of $\bar{n}$ that could be obtained were lower than those in perchlorate solutions.

Measurements of the X-ray scattering. The diffractometer was the same as described in previous papers.[17,22] A glass vessel with a diameter of 40 mm and a depth of 10 mm was used to hold the solution. It was enclosed in an airtight sample holder through which a slow stream of argon gas was passed.

Mo$K\alpha$ radiation (λ = 0.7108 Å) was used for all the measurements. A focusing LiF monochromator was placed between the sample and the scintillation counter. Further monochromatization was performed by means of a pulse height discriminator. The opening slits used were 1/12°, 1/4°, and 1°. Scaling factors to convert all measured data to the same opening slit were obtained from measurements in overlapping regions. Points were measured at intervals of 0.1° in θ up to θ = 6°, and 0.25° to θ = 70°, the largest angle obtainable. Usually 40 000 counts were taken for each point, which corresponds to a statistical error of 0.5 %. A number of points were measured repeatedly in order to detect and to correct for any long time variations in the equipment. A Philips PW-1130 X-ray unit was employed for the measurements. Background radiation was determined by covering the receiving slit with a lead plate.

Table 2. Observed intensity values as a function of $s = 4\pi \sin\theta/\lambda$ for the three solutions investigated. I is the observed intensity after correction for polarization, scaling, and subtraction of incoherent radiation. The reduced intensity values $i(s)$ are also given.

	I		II		III	
s	I	i	I	i	I	i
0.420	1534	-2809.1	2457	-1939.3	2724	-1877.6
0.451	1587	-2742.6	2460	-1922.5	2784	-1802.5
0.481	1637	-2677.6	2466	-1900.3	2780	-1730.1
0.512	1771	-2527.1	2507	-1843.8	2736	-1816.8
0.543	1800	-2481.4			2769	-1765.0
0.574	1865	-2399.5	2620	-1695.9	2816	-1699.2
0.605	1925	-2321.1			2764	-1731.7
0.636	1997	-2230.1	2656	-1621.8	2717	-1757.3
0.666	2120	-2087.4			2701	-1752.1
0.682			2611	-1636.9		
0.697	2222	-1966.1	2569	-1668.4	2697	-1733.6
0.728	2273	-1893.8	2561	-1654.4	2615	-1793.3
0.759	2369	-1776.7	2549	-1644.1	2572	-1812.3
0.790	2362	-1760.6	2540	-1631.1	2511	-1849.3
0.821	2419	-1681.4	2495	-1652.6	2445	-1889.8
0.836			2451	-1684.3		
0.851	2484	-1593.2			2445	-1864.9
0.882	2475	-1578.0	2460	-1639.5	2394	-1890.1
0.913	2529	-1499.5	2445	-1629.2	2384	-1873.1
0.944	2558	-1445.8	2431	-1618.6	2359	-1870.9
0.975	2612	-1367.0	2442	-1581.3	2377	-1826.0
0.990			2458	-1553.2		
1.006	2636	-1316.5	2502	-1495.5	2345	-1830.3
1.036	2660	-1266.8	2533	-1438.8	2362	-1784.9
1.067	2774	-1126.5	2550	-1395.0	2373	-1745.5
1.098	2776	-1097.5	2565	-1352.4	2396	-1694.0
1.129	2811	-1035.7	2610	-1280.0	2403	-1657.6
1.160	2895	- 924.4	2624	-1238.4	2448	-1582.5
1.190	2932	- 858.8	2677	-1156.7	2498	-1503.3
1.221	2991	- 771.8	2718	-1087.7	2510	-1461.3
1.252	3039	- 696.1	2747	-1030.2	2551	-1389.7
1.283	3078	- 628.3	2807	- 941.6	2617	-1293.5
1.298			2808	- 925.7		
1.313	3124	- 553.7			2663	-1216.5
1.344	3213	- 436.0	2888	- 802.0	2713	-1135.7
1.375	3240	- 379.6	2954	- 706.8	2734	-1082.6
1.406	3295	- 295.9	2996	- 635.7	2854	- 931.7
1.437	3345	- 216.4	3083	- 519.2	2926	- 828.3
1.452			3100	- 487.5		
1.467	3441	-91.4	3185	- 387.5	3027	- 696.4
1.498	3431	-71.3	3724	- 268.5	3119	- 573.3
1.529	3474	1.0	3346	- 166.8	3220	- 439.9
1.560			3520	36.1		
1.590			3543	89.6	3381	- 216.1
1.606	3657	258.7				
1.621			3602	178.1	3531	-34.9
1.652			3665	271.7		
1.682	3678	354.6	3752	388.9	3831	327.9
1.713			3818	483.9	3859	388.4
1.744			3834	530.6		
1.759	3655	406.4	3883	593.7		
1.775			3862	588.1	3951	544.1
1.805			3825	581.7		
1.836	3517	342.4	3762	548.2	3997	652.8
1.913	3348	247.7	3625	485.7	3938	673.4
1.989	3128	100.8	3415	349.7	3704	518.2
2.066	2869	-85.5	3120	128.6	3416	307.5
2.143	2658	-224.5	2886	-33.5	3102	70.7
2.219	2531	-281.6	2670	-178.1	2849	-107.0
2.296	2410	-333.5	2533	-245.4	2656	-225.3
2.372	2328	-347.9	2387	-322.8	2520	-289.0
2.449	2287	-322.4	2304	-338.9	2450	-287.8
2.525	2268	-277.3	2241	-336.7	2347	-321.1
2.601	2288	-193.8	2208	-305.6	2275	-325.7
2.678	2273	-147.1	2188	-263.2	2507	
2.754	2279	-80.4	2166	-225.3	2207	-262.6
2.830	2253	-47.6	2146	-184.3	2180	-226.7
2.906	2232	-11.2	2143	-129.4	2162	-182.7
2.982	2202	14.3	2128	-88.2	2131	-154.4
3.058	2169	35.9	2105	-56.2	2124	-103.3
3.134	2132	51.6	2074	-34.3	2098	-73.1
3.210	2086	56.5	2052	-3.7	2077	-39.2
3.286			2018	12.2	2048	-14.7
3.362	1958	26.1	1984	26.8	2032	20.1
3.437	1891	6.7	1933	23.0	1997	35.7
3.513	1834	-5.1	1877	13.5	1955	42.3
3.589	1756	-39.9	1821	1.4	1905	39.0
3.664	1701	-52.3	1778	1.7	1858	37.0
3.740	1636	-75.8	1725	-9.3	1816	38.7
3.815	1575	-96.8	1679	-15.4	1774	39.4
3.890	1531	- 103.2	1627	-28.2	1692	-0.9
3.965	1488	- 108.7	1568	-49.0	1633	-20.3
4.041	1451	- 109.3	1519	-61.4	1577	-37.1
4.116	1421	- 104.7	1478	-67.0	1519	-57.9
4.191	1385	- 107.3	1438	-72.5	1472	-69.5
4.266	1352	- 107.1	1383	-94.5	1414	-92.2
4.340	1338	-90.3	1351	-93.9	1369	-103.9
4.415	1336	-61.6	1326	-88.5	1340	-100.5
4.490	1316	-52.5	1296	-88.2	1300	-108.2
4.564	1307	-35.9	1282	-73.0	1275	-102.8
4.639	1289	-23.3	1266	-60.6	1259	-89.5
4.713	1272	-13.4	1250	-49.5	1247	-72.9
4.788	1256	-3.4	1239	-35.8	1240	-53.0
4.862	1246	11.6	1224	-23.9	1225	-41.1
4.936	1237	27.3	1219	-5.8	1225	-15.3
5.010	1219	32.1	1206	7.6	1209	-6.4
5.084	1195	30.9	1193	17.0	1195	2.8
5.158	1176	34.5	1187	33.5	1198	29.8
5.232	1160	39.8	1179	47.9	1191	44.9
5.305	1140	39.9	1172	62.0	1177	52.7
5.379	1117	37.0	1147	57.3	1157	54.0
5.452	1096	35.3	1126	55.3	1134	51.1
5.526	1086	44.2	1110	59.5	1121	57.5
5.599	1072	47.6	1081	48.7	1102	58.1
5.672	1046	39.8	1063	48.4	1084	58.5
5.745	1025	36.1	1046	48.7	1072	63.9
5.818	1018	45.1	1026	45.5	1044	54.1
5.891	999	42.5	1012	47.7	1029	55.8
5.963	977	36.0	989	40.9	1001	43.8
6.036	968	33.4	966	33.1	975	33.1
6.108	946	34.4	948	29.7	956	29.5
6.181	940	42.7	929	25.2	936	24.9
6.253	921	37.2	912	22.1	918	20.3
6.325	901	29.9	894	18.3	893	9.8
6.397	882	24.1	880	16.6	881	10.6
6.469	860	14.6	859	8.9	852	
6.541	844	10.0	843	5.2	844	-0.8
6.612	829	6.9	829	2.9	838	5.7
6.684	808	-2.8	812	-1.9	816	-4.7
6.755	789	-10.5	797	-6.2	802	-6.9
6.826	774	-14.3	787	-4.9	785	-13.2
6.897	771	-7.4	775	-6.3	777	-9.6
6.968	747	-20.8	768		768	-8.6
7.039	742	-15.7	749	-11.9	756	-10.0
7.110	729	-19.0	737	-13.6	742	-14.6
7.180	711	-27.5	725	-18.1	732	-14.1
7.251	705	-24.0	706	-25.7	722	-14.3
7.321			700	-23.0	707	-20.3
7.391	682	-28.8	687	-26.5	692	-26.5
7.461	672	-30.2	681		685	-25.7
7.531	661	-33.0	669	-27.1	674	-26.7
7.601	654	-31.1	655	-32.6	663	-28.4
7.671	644	-33.3	646	-32.7	652	-30.7
7.740	639	-29.6	642	-28.5	648	-26.3
7.809	635	-25.8	630	-31.9	637	-28.8
7.878	626	-26.6	627	-27.8	633	-25.6
7.947	620	-25.0	621	-25.5	623	-27.5
8.016	614	-22.9	612	-27.2	613	-29.5
8.085	613	-16.9	604	-27.2	602	-32.5
8.154	603	-19.0	602	-22.0	601	-26.6
8.222	601	-14.2	599	-17.3	595	-24.8
8.290	606	-2.5	593	-15.8	593	-19.5
8.358	596	-5.3	591	-11.4	592	-13.7
8.426	583	-11.5	586	-9.0	587	-11.2
8.494	585	-2.2	581	-7.7	584	-7.3
8.561	577	-3.8	579	-2.9	583	-1.9
8.629	578	3.2	575	-0.4	575	-3.4
8.696	566	-1.5	572	2.6	574	1.8
8.763	569	7.4	567	4.8	570	4.7
8.830	560	4.8	563	6.3	564	5.0
8.897	558	8.1	560	9.8	560	6.3
8.963	550	5.8	556	11.0	561	13.7
9.030	552	14.1	549	10.0	552	10.8
9.096	535	3.0	542	8.7	544	7.6
9.162	541	13.6	539	10.7	543	12.9
9.228	529	7.2	532	9.5	538	12.7
9.294	529	13.0	528	10.5	535	14.9
9.359	519	7.7	526	13.8	525	10.4
9.425	510	4.4	519	12.2	527	18.1
9.490	507	6.6	505		516	12.0
9.555	500	3.8	506	9.1	510	10.8
9.620	501	9.7	496	3.3	501	6.4
9.684	494	8.0	489	1.3	498	8.7
9.749	488	6.1	489	5.9	486	1.2
9.813	481	3.7	480	1.7	483	3.0
9.877	475	2.7	478	4.2	480	3.9
9.941	469	0.8	470	1.0	477	5.7
10.005	467	3.4	462	-2.5	463	-4.2
10.068	460	0.6	460	-0.4	461	-2.0
10.132	452	-2.7	455	-1.6	458	-1.1
10.195	451	0.0	452	0.0	451	-3.4
10.258	448	1.1	449	0.9	445	-5.2
10.320	445	2.5	443	-0.8	439	-6.9
10.383	443	4.5	439	-0.9	442	-0.8
10.445	434	0.0	436	-0.2	437	-1.9
10.508	428	-3.1	430	-1.9	435	0.8
10.569	428	1.2	427	-1.8	429	-1.4
10.631	426	2.8	429	4.1	425	-1.9
10.693	420	0.5	423	2.6	424	0.7
10.754	413	-2.5	416	-1.5	422	1.6
10.815	412	-0.4	416	2.2	414	-2.8
10.876	410	2.1	410	-0.4	413	0.4
10.937	402	-3.2	409	2.7	412	2.6
10.997	403	1.6	403	-0.5	409	3.2
11.058	404	6.1	402	1.8	404	0.8
11.118	397	2.2	398	2.0	401	2.0
11.178	393	1.9	395	2.2	401	4.8
11.237	394	6.2	391	0.7	395	0.1
11.297			388	1.3	393	2.7
11.356	384	2.3	385	1.2	387	0.0

Table 2. Continued.

	I		II		III			I		II		III	
s	I	i	I	i	I	i	s	I	i	I	i	I	i
11.415	383	5.0	383	2.4	383	-0.6	14.293	263	3.2	258	4.9	273	4.5
11.474	376	0.6	378	0.3	376	-4.6	14.343	265	6.1	266	4.4	271	4.5
11.533	370	-2.2	376	1.3	374	-3.5	14.388	263	5.4	267	6.3	269	5.9
11.591	372	2.5	371	-0.9	367	-7.7	14.432	251	5.6	265	6.0	258	3.8
11.649	367	0.8	367	-1.5	367	-4.9	14.477	253	4.9	263	5.7	263	6.0
11.707	363	-0.1	365	-0.5	366	-3.2	14.521	256	3.2	261	5.3	259	7.9
11.765	363	2.4	362	-0.9	363	-3.7	14.565	257	5.0	258	3.5	266	6.6
11.822	356	-1.4	364	-5.6	362	-1.6	14.609	255	4.7	258	4.4	263	5.0
11.879	350	-4.6	355	-2.9	359	-1.9	14.652	253	4.0	258	5.6	263	6.3
11.936	349	-3.5	349	-5.5	355	-5.3	14.695	254	6.8	256	5.5	262	6.3
11.993	346	-3.7	348	-4.4	349	-6.9	14.738	248	1.6	253	4.2	258	3.7
12.050	339	-7.8	344	-5.5	349	-4.6	14.780	252	6.8	252	3.6	260	6.6
12.106	340	-4.4	340	-7.0	342	-9.0	14.821			251	3.8		
12.162	337	-4.6	339	-3.6			14.822	248	4.3			256	4.8
12.218	332	-6.9	337	-4.4	339	-8.5	14.864	247	4.9	248	2.8	258	7.3
12.274	331	-5.8	333	-6.5	337	-7.0	14.906	245	3.7	249	4.8	252	3.2
12.329	329	-5.3	329	-7.3	335	-7.9	14.947	242	2.0	246	3.2	254	6.2
12.384	322	-9.4	326	-7.9	330	-8.8	14.988	243	4.9	245	3.1	249	3.1
12.439	321	-8.7	325	-6.8	330	-6.5	15.029	241	3.4	244	3.7	248	2.8
12.494	316	-11.0	325	-4.4	326	-8.0	15.070	238	2.1	242	2.7	247	3.6
12.549	313	-11.1	322	-5.1	325	-3.0	15.110	239	4.2	239	1.5	246	3.5
12.603	310	-12.1	318	-6.9	325	-4.9	15.150	236	1.9	238	1.2	245	3.7
12.657	312	-8.4	317	-5.7	321	-4.5	15.189	235	2.7	236	0.9	242	1.8
12.711	305	-12.8	316	-4.4	323	-2.5	15.229	234	2.6	236	1.9	240	1.4
12.764	308	-7.8	314	-4.1	321	-2.1	15.268	233	2.7	235	1.6	238	0.4
12.817	305	-8.2	312	-4.5	316	-4.9	15.307	232	2.4	233	0.9	238	2.1
12.870	302	-9.1	311	-2.9	318	-1.5	15.345	230	1.9	232	1.0	235	-0.5
12.923	301	-8.5	305	-7.0	315	-0.9	15.383	228	1.4	230	0.4	234	0.5
12.976	301	-6.3			312	-2.7	15.421	230	4.0	228	0.0	233	-0.1
13.028	298	-6.8	303	-5.0	305		15.459	227	2.8	226	-1.0	231	0.0
13.080	296	-7.2	302	-4.4	307	-3.3	15.495	225	1.8	226	-0.5	229	-1.0
13.132	296	-4.5	302	-2.0	307	-2.3	15.533	224	1.4	225	0.1	229	0.1
13.183	295	-4.3	298	-4.5	305	-4.3	15.570	222	0.5	223	-1.1	227	-0.7
13.235	291	-6.2	296	-4.1	303	-2.5	15.606	220	-0.1	223	0.3	225	-1.5
13.286	292	-2.8			300	-3.1	15.642	220	1.0	221	-1.3	225	-0.7
13.336	292	-1.3	293	-3.8	293	-2.5	15.678	217	-1.4	217	-3.5	224	-0.3
13.387	287	-4.2	291	-3.2	300	-0.2	15.714	217	-0.2	218	-2.0	222	-1.2
13.437	287	-2.1	291	-1.9	298	-2.3	15.749	217	0.6	217	-1.6	221	-1.6
13.487	288	0.0	289	-2.0	294	-2.5	15.784	216	0.4	215	-2.7	221	-0.3
13.537	285	-0.5	289	-0.5	293	-1.8	15.818	213	-1.0	214	-2.5	218	-3.0
13.586	283	-0.8	285	-1.9	291	-1.7	15.853	212	-1.9	212	-3.5	217	-2.7
13.636	285	2.9	284	-1.4	290	-0.5	15.887	210	-2.2	212	-2.9	215	-3.7
13.685	285	4.9	284	0.4	291	2.2	15.920	208	-3.7	211	-2.3	213	-4.1
13.733	281	2.3	283	0.5	291	3.5	15.954	208	-2.7	210	-3.3	213	-3.9
13.782	279	2.3	280	0.0	285	-2.9	15.987	207	-3.1	208	-3.5	211	-4.9
13.830	279	4.0	279	0.6	286	1.5	16.020	207	-2.2	207	-3.6	208	-6.2
13.878	277	3.0	280	2.3	285	2.3	16.052	203	-5.3	205	-4.3	207	-6.2
13.926	275	3.1	277	1.4	284	3.0	16.085	202	-5.3	205	-4.3	207	-5.8
13.973	277	6.2	275	1.3	280	0.8	16.116	204	-2.1			206	-5.2
14.020	274	4.9	278	5.7	280	2.9	16.148	204	-1.7	202	-5.1	204	-5.7
14.067	272	5.0	274	3.4	281	4.5	16.179	200	-4.9	201	-5.8	205	-4.4
14.114	271	5.2	274	4.4	278	3.3	16.210	200	-3.6	200	-5.9	202	-7.1
14.160	270	5.7	273	2.5	279	4.6	16.241	198	-4.9	200	-4.3	201	-6.8
14.206	269	5.6	273	4.2	275	4.9	16.271	199	-5.2	198	-5.7	201	-8.5
14.252	268	4.7	267	2.0	276	5.9	16.301	196	-5.8	196	-5.5	197	-9.7

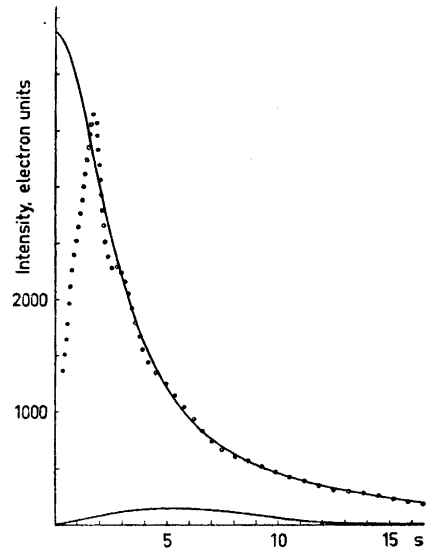

Fig. 2. Observed intensity values for the acid solution as a function of $s = 4\pi \sin\theta/\lambda$. About one fourth of the observed values are marked. The full curve represents the independent coherent scattering ($\sum n_i f_i^2$). The estimated amount of incoherent radiation reaching the counter is shown by the lower curve.

Treatment of the data. The data were treated in the same way as described in a previous paper.[17] The scattering factors used were those given by Cromer and Waber [23] for the neutral atoms. Anomalous dispersion corrections ($\Delta f'$ and $\Delta f''$) were applied according to Cromer [24] for Sn, Cl, and Na. The incoherent scattering was estimated from the values given in the International Tables [25] for Cl, O, and Na, from the values given by Compton and Allison [26] for H, and from the formula given by Bewilogua [27] for Sn. The amount of incoherent radiation passing through the monochromator was estimated from the spectrum of the X-ray tube as described previously.[17,22] At the largest scattering angles it was determined by measurements with a zirconium filter. After correction for polarization in the solution and in the monochromator the outermost part of the measured intensity curve ($\theta > 35°$) was used for the scaling, which was done by comparing observed intensity values with the sum of the independent coherent scattering ($\sum n_i f_i^2$) and the incoherent scattering. The scaled intensity values were corrected for the incoherent radiation and reduced intensities were then obtained by subtracting the independent coherent scattering. All calculations were referred to a stoichiometric unit of solution corresponding to the volume containing one Sn atom (Table 1).

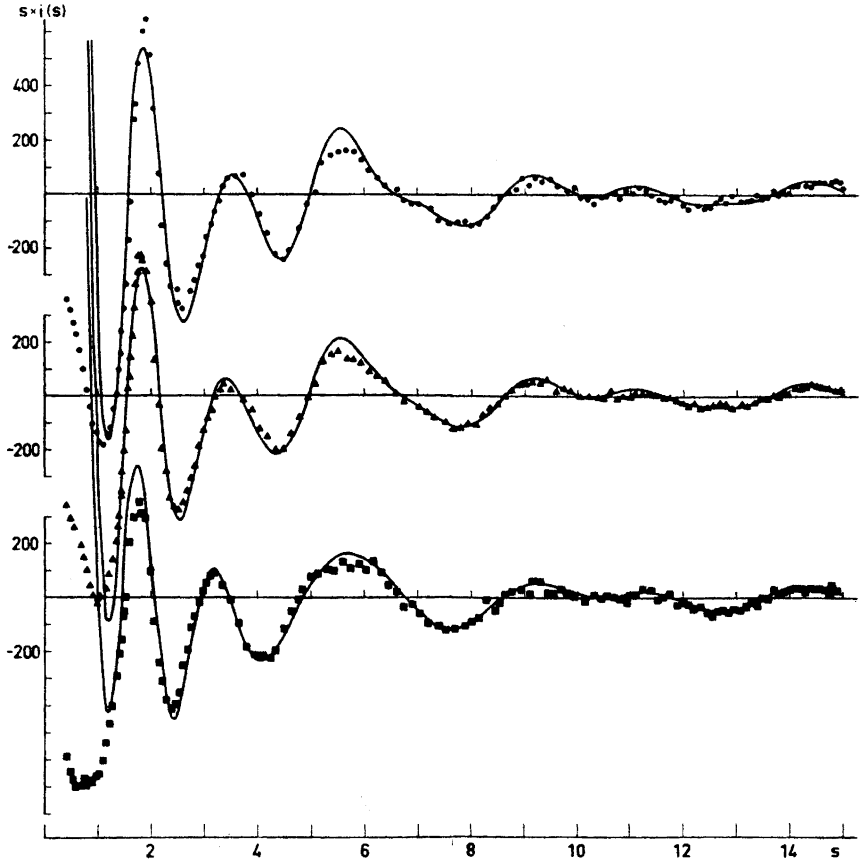

Fig. 3. Values $s \cdot i(s)$ for the three solutions investigated. Every second point has been marked. The full curves are calculated values obtained with the use of the parameters from the least squares refinements (Table 3) and the analysis of the difference curves (last column in Table 4). The lower curve represents the acid solution (I) and the upper curve the most hydrolyzed of the solutions (III).

The measured intensity values after corrections for polarization, scaling, and subtraction of incoherent radiation are given in Table 2 and in Fig. 2, as a function of $s = 4\pi \sin\theta/\lambda$. The corresponding values of the reduced intensities $i(s)$ are given in Table 2 and the $s \cdot i(s)$ values in Fig. 3 after correction for spurious peaks below 1 Å in the radial distribution curves as described in previous papers.[17,18]

The radial distribution curves were calculated from the reduced intensity values according to the expression:

$$D(r) = 4\pi r^2 \varrho_0 + 2r\pi^{-1} \int_0^{s_{max}} s \cdot i(s) [f_{Sn}(0)/f_{Sn}(s)]^2 \exp(-ks^2) \sin(rs)\, ds$$

In the sharpening factor, $[f_{Sn}(0)/f_{Sn}(s)]^2 \exp(-ks^2)$, the $f_{Sn}(s)$ represents the scattering factor of Sn for a value s ($= 4\pi \sin\theta/\lambda$). The value of k was chosen to be 0.01.

All calculations were carried out on an IBM 360/75 computer with a Fortran version of the programs previously used.[28]

ANALYSIS OF THE RADIAL DISTRIBUTION CURVES

The radial distribution curves, $D(r)$, for the solutions investigated are given in Fig. 4 and the functions $D(r) - 4\pi r^2 \varrho_0$ in Fig. 5.

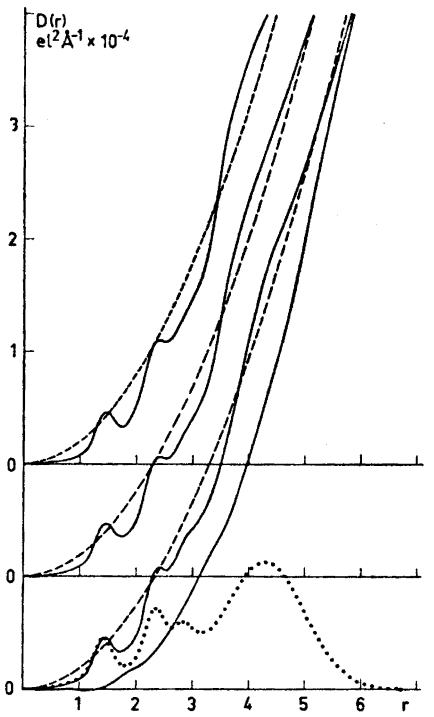

Fig. 4. Radial distribution curves, $D(r)$. Dashed lines are the corresponding $4\pi r^2 \varrho_0$ functions. The dotted curve is the sum of the peak shapes calculated with the use of the parameters obtained in the least squares refinement of the acid solution (Table 3). The difference between the $D(r)$ curve and the calculated peaks for the acid solution (lower curve) is also shown.

The Cl – O interaction at 1.4 Å in the perchlorate groups is clearly seen in all the curves. The Sn – O distances within the first coordination sphere of the Sn atom are not well resolved in the $D(r)$ curves (Fig. 4). In Fig. 5 two peaks, one at 2.3 Å and one at 2.8 Å, are indicated. The O – O interactions in the

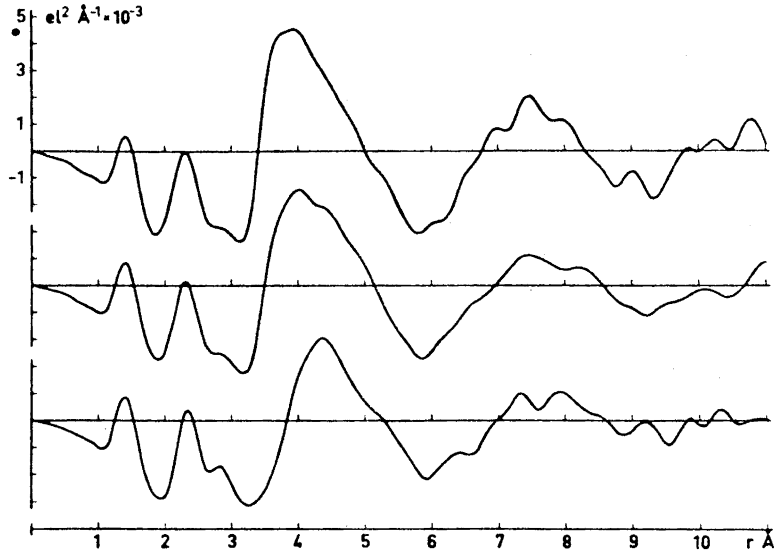

Fig. 5. $D(r) - 4\pi r^2 \varrho_0$ functions for the three solutions investigated. The lower curve represents the acid solution (I) and the upper curve the most hydrolyzed of the solutions (III).

perchlorate groups will contribute to the 2.3 Å peak, but cannot alone explain the full size of the peak. In crystals the tin(II) atom often forms three short bonds of about 2.3 Å to oxygen atoms with two or three other oxygens at distances about 0.5 Å longer.[29] These two peaks appear in approximately the same way in all the distribution curves and the corresponding interactions are thus largely unaffected by hydrolysis.

A broad peak at about 4.3 Å for the acid solution probably contains contributions from distances within a second coordination sphere around the tin atoms. It seems to be the only peak in the $D(r)$ function which changes significantly when the solution is hydrolyzed. In the following treatment of the data the 2.8 Å peak and the 4.3 Å peak will both be treated as resulting from Sn – O interactions only, although they probably contain significant contributions from light-atom interactions. Remaining parts of the water structure and hydration of the perchlorate groups may be expected to give contributions in the corresponding regions.

The changes in the distribution curves with hydrolysis are more clearly brought out by the difference curves in Fig. 6. They have been obtained by subtracting from each of the $D(r)$ functions the corresponding $4\pi r^2 \varrho_0$ function calculated for the light atoms only and then taking the differences between the resulting curves. If changes in the light atom interactions on hydrolysis are negligible, the peaks in the difference curves should be solely determined by changes in the surroundings of the tin atoms.

According to Fig. 6 only minor changes seem to occur within the first coordination sphere of the tin atoms. The peak at about 3.6 Å can probably

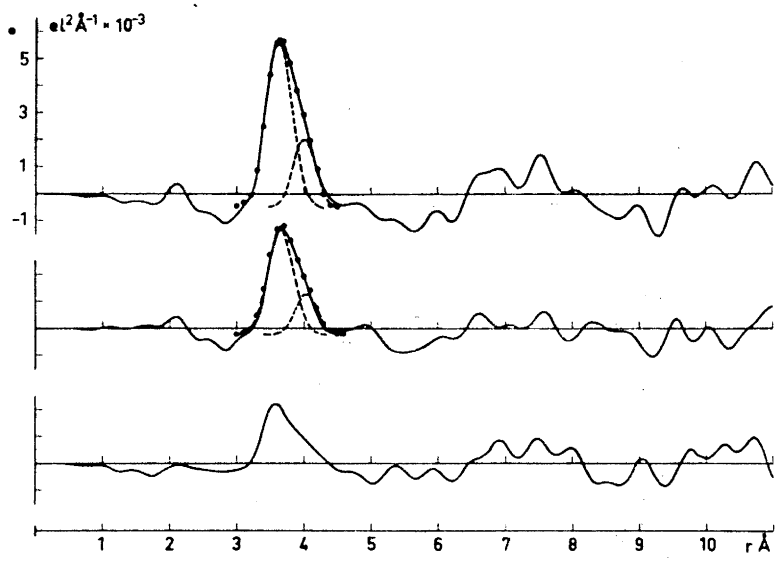

Fig. 6. Differences between the radial distribution curves. The upper curve gives the difference between the solutions with $\bar{n} = 0.8$ (III) and $\bar{n} = 0$ (I), the middle curve between the solutions with $\bar{n} = 0.5$ (II) and $\bar{n} = 0$ (I), and the lower curve gives the difference between the two hydrolyzed solutions (III – II). The dashed curves are calculated from the parameters given in the last column in Table 4. The sum of the two curves, which closely reproduces the observed peak, is marked by dots.

be correlated with Sn – Sn distances within polynuclear hydrolysis complexes. Distances between the oxygen-bridged Sn atoms within the octa-nuclear complexes in the crystals of Sn_2OSO_4 range from 3.49 Å to 3.77 Å with an average value of 3.65 Å.[11] In $Sn_6O_4(OH)_4$ the short Sn – Sn distances within the octahedra have been reported to be 3.59 Å.[13,14]

The 3.6 Å peak is not symmetric but is extended towards longer distances. Non-equal Sn – Sn distances, well-defined long Sn – O distances within the hydrolysis complexes, or a general shortening of distances within the second coordination sphere when a solution is hydrolyzed, may cause this asymmetry. Comparison with calculated peak shapes for Sn – Sn interactions shows that the left side of the peak agrees well with that calculated for an Sn – Sn interaction of 3.62 Å with a temperature factor $b = 0.0083$. If we assume that this represents a well-defined Sn – Sn distance within the complexes, its frequency in the most hydrolyzed of the solutions would correspond to an average number of about 1.2 Sn atoms bonded to each other Sn atom in the solution.

If the calculated peak shape, obtained by the best fit to the left side of the 3.6 Å peak, is subtracted from the difference curves in Fig. 6, small peaks remain at about 4 Å. The area of each of these peaks corresponds to approximately one third of that of the corresponding main peak (Table 4). If it is assumed to correspond to Sn – Sn interactions, the total number of Sn atoms bonded to each other Sn atom in the most hydrolyzed of the solutions would

Table 3. Results from the least squares refinement for the acid solution. The final values are given for the distance, d (in $Å$), the frequency of the distance (per Sn atom), n, and the temperature factor, b, obtained for each interaction in the different s ranges. The calculated standard deviations are given in brackets. The values in the columns b were obtained when the values of n and d for the perchlorate group with d representing the Cl–O distance, were kept constant during the refinement.

		$2.8<s<15$		$5.0<s<15$		$7.0<s<15$		$9.0<s<15$	
		a	b	a	b	a	b	a	b
ClO_4	d	1.410 [4]	1.406	1.410 [4]	1.406	1.405 [4]	1.406	1.406[4]	1.406
	n	0.88 [2]	1	0.90 [3]	1	0.92 [3]	1	0.99 [2]	1
	b	0.000 [1]	0.0010 [3]	0.000 [2]	0.0004 [3]	0.000[1]	0.0004 [2]	0.000[1]	0.0004 [3]
Sn–O	d	2.33 [1]	2.33 [1]	2.32 [1]	2.33 [1]	2.33 [1]	2.34 [1]		2.32 [1]
	n	2.00 [10]	2.40 [15]	1.8 [2]	1.6 [3]	2.0 [2]	2.4 [4]		2.8 [15]
	b	0.000 [3]	0.002 [1]	0.000 [2]	0.000 [2]	0.000[2]	0.0009[15]		0.003 [3]
Sn–O	d	2.81 [1]	2.83 [1]	2.86 [2]	2.87 [2]	2.79 [3]			
	n	3.1 [2]	3.0 [1]	10.0 [10]	3.2 [16]	2.0 [8]			
	b	0.017 [4]	0.015 [4]	0.055 [7]	0.018 [9]	0.02 [1]			

Table 4. Results from the least squares refinements for the hydrolyzed solutions (II and III in Table 1). For each interaction the final values obtained for each s range for the distance, d, the frequency, n (=the number of interactions per Sn atom), and the temperature factor, b, are given. Contributions from the perchlorate groups and the Sn—O interactions within the first coordination sphere were assumed to be the same as for the acid solution. In the last column are given the parameters for the two Sn—Sn interactions, which were used to calculate the peak shapes in Fig. 6.

Solution No.	Type of refinement	Type of interaction	Parameter	$1.4<s<10.2$	$2.6<s<10.2$	$4.2<s<10.2$	$6.2<s<10.2$	Values obtained from the diff. curves in Fig. 6
			d	3.672[13]	3.673[10]	3.651[10]	3.601[12]	3.62 4.00
		Sn—Sn	n	0.96 [4]	0.79 [5]	0.99 [23]	1.0 [4]	0.586 and 0.214
			b	0.036 [5]	0.024 [4]	0.035 [8]	0.027 [7]	0.0083 0.0039
	A							
			d	4.17				
		Sn—O	n	24.5 const.				
			b	0.22				
III								
			d	3.681[23]	3.701[17]	3.659[11]	3.601[12]	
		Sn—Sn	n	0.60 [9]	1.31 [19]	0.98 [23]	1.0 [3]	
			b	0.017 [6]	0.041 [7]	0.036 [9]	0.027 [6]	
	B							
			d	4.09 [2]	4.42 [8]			
		Sn—O	n	29.0 [20]	18.7 [64]	0	0	
			b	0.24 [2]	0.18 [4]			
			d	3.691[12]	3.684[10]	3.697[11]	3.615[18]	3.64 4.03
		Sn—Sn	n	0.51 [2]	0.53 [4]	0.78 [19]	1.3 [7]	0.386 and 0.128
			b	0.027 [4]	0.027 [4]	0.047 [9]	0.046[11]	0.0083 0.0039
	A							
			d	4.17				
		Sn—O	n	24.5 const.				
			b	0.22				
II								
			d	3.694[20]	3.729[16]	3.696 [9]	3.61 [2]	
		Sn—Sn	n	0.48 [6]	1.2 [2]	0.8 [2]	1.4 [7]	
			b	0.025 [6]	0.054 [8]	0.05 [1]	0.05 [1]	
	B							
			d	4.17 [2]	4.47 [7]			
		Sn—O	n	25.4 [10]	18.1 [22]	0	0	
			b	0.23 [1]	0.18 [4]			

then be about 1.6 rather than 1.2. If it is assumed to represent Sn – O interactions each Sn atom would have about two oxygens at this distance.

The ratio of the sizes of the 3.6 and 4 Å peaks is approximately constant – within the rather limited precision – for all the difference curves in Fig. 6. Thus the asymmetry of the 3.6 Å peak is independent of the degree of hydrolysis, which perhaps can be taken to indicate that it is a characteristic of one single type of complex.

The curves in Fig. 6 do not show significant features, which can be interpreted as longer Sn – Sn distances than those occurring in the 3.6 to 4 Å region. However, interactions, which have frequencies much lower than that of the primary Sn – Sn distance, may well escape detection among the spurious background peaks present in the curves.

ANALYSIS OF THE REDUCED INTENSITY FUNCTIONS

A further analysis of the predominant interactions in the solutions was made by means of a least squares procedure applied directly to the measured intensity data.

Theoretical intensity values were calculated according to the expression

$$i(s) = \sum_{n} \sum_{\substack{m \\ n \neq m}} f_n f_m \sin r_{nm}s/(r_{nm}s) \exp(-b_{nm}s^2)$$

Here r_{nm} is the distance between two atoms n and m, f_n and f_m are the scattering factors, and b is a temperature factor. For each pair interaction the distance, a temperature factor, and a frequency factor were introduced as parameters and were refined by a least squares procedure which minimized the function $\sum s^2[i_{obs}(s) - i_{calc}(s)]^2$.

Because of the low atomic number of Sn the perchlorate groups contribute relatively more to the scattering than in the solutions investigated previously.[15,17] For this reason, the corresponding parameters were also refined with the single restriction that the tetrahedral symmetry of the ClO_4^- group was preserved. Sn – O interactions corresponding to the first coordination sphere of the tin atom and a similar interaction approximating the many distances around 4.3 Å, were also introduced, as were Sn – Sn interactions for the hydrolyzed solutions.

Results from the refinement of the scattering curve of the acid solution are given in Table 3. The broad peak at about 4.3 Å in the radial distribution curve, which was interpreted as indicating a second coordination sphere around the Sn atom, corresponds to significant contributions to the scattering curves only in the low-angle region. The corresponding interaction parameters were determined in a separate refinement, which included this region, and were then kept constant in the following refinements.

The frequencies representing the interactions within the perchlorate group and the first coordination sphere of the tin atom were refined simultaneously. In order to check the constancy of the refined parameters the lower s limit was increased continuously, as shown in Table 3. For the highest s limit only the ClO_4 interactions still showed significant contributions to the observed intensity values.

The parameters obtained for the ClO_4 group (columns "a" in Table 3) are interesting as a check on the experimental data and on the refinement procedure. The Cl – O distance, which was found to be 1.41 Å ($\sigma = 0.01$ Å), is independent of the s range used and is consistent with values found in crystals, which are usually around 1.43 Å.[30] The frequency factor does not differ significantly from the expected value of one, but comes out slightly lower than this value, particularly for the lower s limits. Here, on the other hand, the temperature factor, which was assumed to be the same for the Cl – O and the O – O interactions, comes out slightly negative (about the magnitude of the standard deviation), when not restricted to positive values only.

In a second series of refinements the frequency factor of the ClO_4 interactions was assumed to have the expected value of one, and only the temperature factor was refined. These results are also given in Table 2 (columns "b").

Both the 2.3 Å and the 2.8 Å Sn – O interactions seem to represent well-defined frequencies in the scattering curves. The first gives significant contributions up to somewhat higher s values than does the second. Each of them corresponds to between two and three oxygens bonded to each tin atom. However, the precision of these determinations, as shown by the standard deviations, is low.

The comparison between the radial distribution curves (Fig. 6) shows only minor changes to occur within the first coordination sphere of the tin atom when a solution is hydrolyzed. For the refinements of the scattering curves from the hydrolyzed solutions, therefore, the same parameters were used as those found for the acid solution and only the parameters for a single Sn – Sn interaction at about 3.6 Å were refined.

Although the 3.6 Å interaction and the interactions from the second coordination sphere at about 4.2 Å are not resolved in the distribution curves (Fig. 5), they can be resolved by the least squares procedure. Two series of refinements were made for which the results are given in Table 4. In the first series (A) only the three parameters for an Sn – Sn interaction at about 3.6 Å were refined, keeping the other parameters constant at the values found for the acid solution. In the second series (B) the three parameters corresponding to Sn – O interactions from the second coordination sphere were refined in addition to those of the Sn – Sn interactions. In the first series values for the number of Sn – Sn interactions are obtained which, as expected, do not differ significantly from those estimated from the areas under the peaks in Fig. 6. Also in the second series these values come out with about the same magnitude. The precision is low, however, as shown by the standard deviations.

The results from the least squares refinements thus support the conclusions that the peaks in the difference curves in Fig. 6 are of a different character than those of the second coordination sphere and thus probably result from well-defined interactions within polynuclear complexes and not from changes in light atom positions in the second coordination sphere.

DISCUSSION OF THE RESULTS

The agreement between observed and calculated $s \cdot i(s)$ values are shown in Fig. 3. The contributions of each interaction to the $s \cdot i(s)$ curve and the $D(r)$ curve are shown in Fig. 7 for the most hydrolyzed of the solutions.

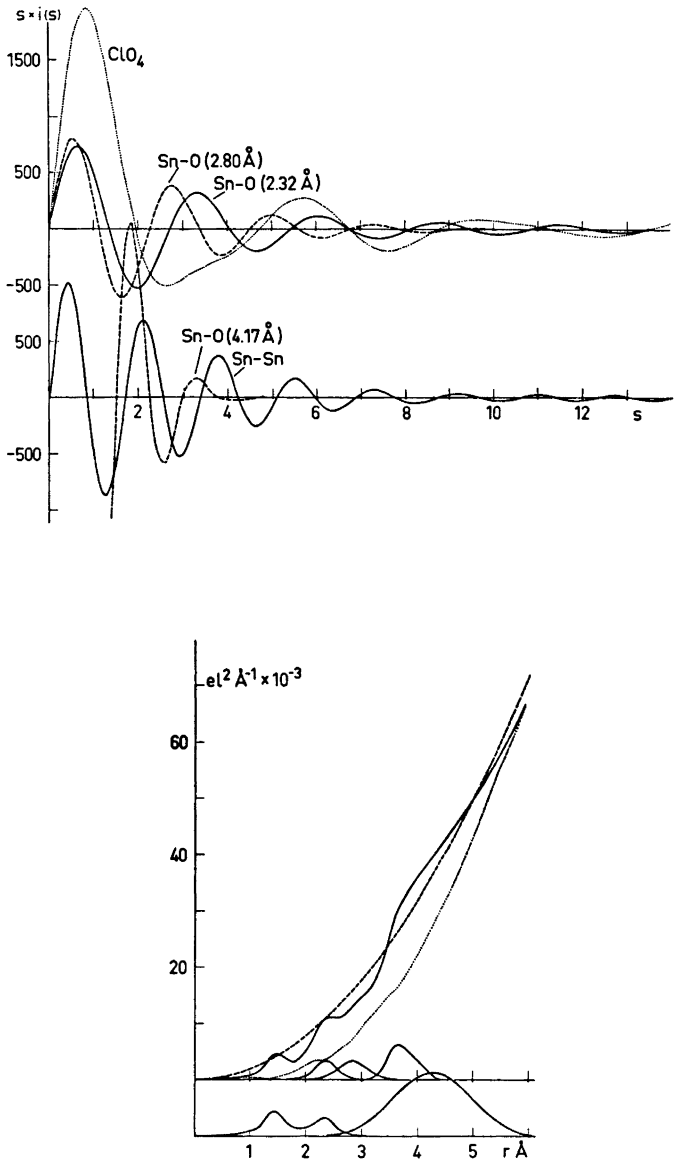

Fig. 7. The contributions of the different interactions to the $s \cdot i(s)$ and the $D(r)$ curves for the most hydrolyzed of the solutions (III). The following parameter values (distance, frequency factor, temp. factor) have been used: ClO_4: 1.406 (Cl – O), 1, 0.0008; Sn – O: 2.32, 2.3, 0.0013; 2.80, 3.0, 0.015; 4.17, 24.5, 0.22; Sn – Sn: 3.62, 0.59 × 2, 0.0083 and 4.00, 0.21 × 2, 0.0039. The experimental $D(r)$ curve, the corresponding $4\pi r^2 \varrho_0$ function, and the difference curve obtained by subtracting the calculated peak shapes from the $D(r)$ function are also shown.

At the larger scattering angles only the perchlorate groups make significant contributions to the reduced intensities. Interactions involving the tin atoms have a relatively minor influence. Two well-defined peaks, at 2.3 Å and at 2.8 Å in the radial distribution curves can, however, be related to Sn – O interactions within the first coordination sphere. The least squares analysis of the intensity curves (Table 3) show them to correspond to well-defined frequencies, each with an amplitude of a magnitude expected for two to three Sn – O contacts per Sn atom. The tin atom, therefore, may have two groups of coordinated water molecules, one of which is more strongly bonded than the other.

The less strongly bonded oxygens occur at a distance where light-atom contacts begin to dominate, such as O – O and, in the hydrolyzed solutions, Na – O contacts, and these may contribute to, or even fully explain, the 2.8 Å peak. The conclusion that the tin atom may have two groups of neighbouring water molecules is, however, in agreement with results from crystal structure determinations, where the tin atom is often found to have about three oxygens at approximately 2.3 Å with some other oxygens at longer distances. The same coordination of the Sn atom is found for all the three solutions investigated and thus it is not noticeably dependent on the degree of hydrolysis.

The Sn – Sn distances within the expected polynuclear hydrolysis complexes are less well-defined. The detailed analysis of the distribution curves and the reduced intensity functions shows, however, that such interactions are present in the 3.6 to 4 Å region. In crystals Sn – Sn distances within polynuclear complexes have also been found to be of this magnitude.[11,13,14]

The analysis of the experimental data indicates that the Sn – Sn distances may be slightly different, varying between 3.6 and 4 Å, which makes the estimate of the frequency of the distances more difficult and less accurate. For the most hydrolyzed of the solutions, however, the analysis of the results shows conclusively, that the average number of Sn atoms bound to each other

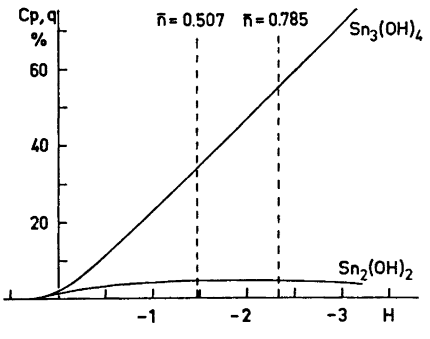

Fig. 8. Fraction of tin(II) bound in the different hydrolysis complexes, $Sn_q(OH)_p^{(2q-p)+}$, as calculated from the equilibrium constants given by Tobias.[7]

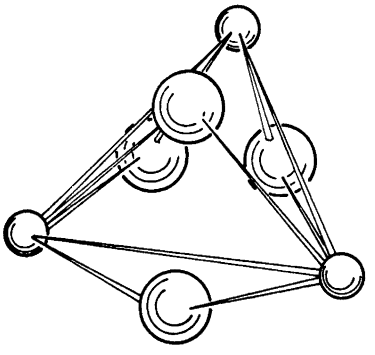

Fig. 9. Possible structure for a tri-nuclear hydrolysis complex. Small circles denote Sn(II) atoms and large circles oxygen atoms.

Sn atom in the solution is larger than one. Thus complexes containing more than two Sn atoms must be formed.

Expected concentrations of hydrolysis complexes as calculated from the stability constants given by Tobias [7] are shown in Fig. 8. The tri-nuclear complex $Sn_3(OH)_4^{2+}$ is seen to be predominant, but as the maximum concentration used by Tobias was 0.04 M compared to the 3 M concentrations used here, the constants used may not even approximately be valid for the present solutions.

Several authors have suggested a triangular structure for an $Sn_3(OH)_4^{2+}$ complex as shown in Fig. 9.[7,29] The Sn – Sn distances expected for this structure are consistent with those found from the X-ray scattering and so is – within the very limited accuracy – the expected degree of condensation, as is the absence of longer Sn – Sn distances in the distribution curves. Although Sn – O distances in such a structure would fall in the region around 4 Å and would thus, at least in part, explain the asymmetry of the peaks in the difference curves in Fig. 6, it seems that the Sn – Sn distances would still have to be slightly different in order to explain the experimental data. For a simple triangular complex, equal Sn – Sn distances would seem more likely and a well-defined frequency in the scattering curves with significant Sn – Sn contributions up to much higher s values than those now found would rather be expected for a predominant triangular complex.*

The octa-nuclear complexes found in crystals of Sn_2OSO_4 and built up from tetrahedra of Sn atoms sharing faces have been shown to have non-equal Sn – Sn distances ranging from 3.486 Å to 3.772 Å.[11] Non-equal metal-metal distances have also been found in the similarly constructed hexa-nuclear $Pb_6O(OH)_6^{4+}$ complex, where the Pb – Pb distances range from 3.45 Å to 4.09 Å.[12] In complexes of this type longer metal-metal distances would also occur, but would have a much lower frequency than the primary distance and may therefore, if such complexes occur in the solutions, escape detection in the radial distribution curves. An alternative explanation to non-equal Sn – Sn distances would, of course, be the occurrence of several complexes in the solutions, having different structures and therefore slightly different Sn – Sn distances.

CONCLUSIONS

We can conclude from the X-ray scattering data that hydrolysis of tin(II) perchlorate solutions leads to the formation of polynuclear complexes with Sn – Sn distances around 3.6 Å. This condensation of the hydrated tin(II) ions, when protons are dissociated, does not stop at dinuclear complexes since in the most hydrolyzed of the solutions investigated (Table 1), the average number of Sn atoms bonded to each other Sn atom is larger than one. These polynuclear complexes probably contain the same type of OSn_3 groups, with a triangular arrangement of the Sn atoms, which has been found in crystals

* In a preliminary note [31] on the crystal structure of $Sn_3O(OH)_2SO_4$ it has been reported that this structure contains discrete $Sn_3O(OH)_2^{2+}$ units with non-equal Sn – Sn distances. The distances found were 4.063 Å, 4.209 Å, and 4.605 Å and thus differ considerably from those in the present work and in crystal structures of other basic Sn(II) salts.[11,13,14]

of Sn_2OSO_4 [11] and $Sn_6O_4(OH)_4$.[13,14] This is indicated by the close similarity of the Sn – Sn distances in the crystals and in the solutions and by the absence of clearly marked longer Sn – Sn distances in the radial distribution curves. We can also conclude, from the absence of clearly marked longer Sn – Sn distances, that if larger complexes than trinuclear ones would be predominant in the solutions, the OSn_3 groups are probably joined into tetrahedra of the type found in Sn_2OSO_4 [11] and not into octahedra as found in $Sn_6O_4(OH)_4$.[13,14]

The X-ray data cannot distinguish between triangular and tetrahedral complexes, and even larger complexes with low-frequency longer Sn – Sn distances cannot be definitely excluded. Although the emf measurements by Tobias [7] make a trinuclear complex with the structure shown in Fig. 9 the most likely one, equilibrium measurements on more concentrated solutions than those used by Tobias [7] are needed before definite conclusions about the structures can be made.

Acknowledgements. The work has been supported by *Statens Naturvetenskapliga Forskningsråd (Swedish Natural Science Research Council)*. Computer time has been made available by the *Computer Division of the National Swedish Office for Administrative Rationalization and Economy*.

We thank Miss Anita Johansson for assistance in the work and Dr. Derek Lewis for linguistic corrections.

REFERENCES

1. Prytz, M. *Z. anorg. Chem.* **174** (1928) 355.
2. Randall, M. and Murakami, S. *J. Am. Chem. Soc.* **52** (1930) 3967.
3. Gorman, M. *J. Am. Chem. Soc.* **61** (1939) 3342.
4. Garrett, A. B. and Heiks, R. E. *J. Am. Chem. Soc.* **63** (1941) 562.
5. Vanderzee, C. E. and Rhodes, D. E. *J. Am. Chem. Soc.* **74** (1952) 3552.
6. Vanderzee, C. E. and Rhodes, D. E. *J. Am. Chem. Soc.* **74** (1952) 4806.
7. Tobias, R. S. *Acta Chem. Scand.* **12** (1958) 198.
8. Olin, Å. *Acta Chem. Scand.* **14** (1960) 126.
9. Olin, Å. *Acta Chem. Scand.* **14** (1960) 814.
10. Pajdowski, L. and Olin, Å. *Acta Chem. Scand.* **16** (1962) 983.
11. Wernfors, G. *Acta Chem. Scand.* **15** (1961) 1007.
12. Spiro, T. G., Templeton, D. H. and Zalkin, A. *Inorg. Chem.* **8** (1969) 856.
13. Howie, R. A. and Moser, W. *Nature* **219** (1968) 372.
14. Söderqvist, R. *Personal communication.*
15. Johansson, G. and Olin, Å. *Acta Chem. Scand.* **22** (1968) 3197.
16. Johansson, G. *Acta Chem. Scand.* **22** (1968) 399.
17. Johansson, G. *Acta Chem. Scand.* **25** (1971) 2787.
18. Åberg, M. *Acta Chem. Scand.* **24** (1970) 2901.
19. Noyes, A. and Toabe, R. *J. Am. Chem. Soc.* **39** (1917) 1537.
20. Jamieson, G. S. *Volumetric Iodate Methods*, The Chemical Catalog Co., New York 1926, p. 75.
21. Gran, G. *Analyst* **77** (1952) 661.
22. Johansson, G. *Acta Chem. Scand.* **20** (1966) 553.
23. Cromer, D. T. and Waber, J. T. *Acta Cryst.* **18** (1965) 104.
24. Cromer, D. T. *Acta Cryst.* **18** (1965) 17.
25. *International Tables for X-Ray Crystallography*, Kynoch Press, Birmingham 1962, Vol. III.
26. Compton, A. H. and Allison, S. K. *X-Rays in Theory and Experiment*, Van Nostrand, New York 1935.
27. Bewilogua, L. *Phys. Z.* **32** (1931) 740.

28. Johansson, G. Programs with Accession Nos. 6037 and 6038 in *IUCr World List of Crystallographic Computer Programs*, 2nd Ed., London 1966.
29. Donaldson, J. D. *Progr. Inorg. Chem.* **8** (1967) 287.
30. *Tables for Interatomic Distances and Bond Angles*, Special Publication No. 18, The Chemical Society, London 1965, p. 58.
31. Davies, C. G. and Donaldson, J. D. *Acta Cryst.* **A 25** (1969) 122, 8th IUCr. Suppl.

Received July 17, 1972.

ACTA CHEMICA SCANDINAVICA 27 (1973) 661–669

The Crystal Structures of 2-Bromo-1-methyl-benzo[c]-pyrazolo[1:2-a]pyrazole-3:9-dione and 3-Bromo-2-methyl-pyrazolo[a][3,1]benzoxazin-5-one

INGER SØTOFTE

Chemical Laboratory B, Technical University of Denmark, DK-2800 Lyngby, Denmark

The structures of monobromo-derivatives of the so-called α- and β-pyrazoisocoumarazone isomers, $C_{11}H_7N_2O_2Br$, have been confirmed by three-dimensional X-ray diffraction crystal structure analyses as being 2-bromo-1-methyl-benzo[c]pyrazolo[1:2-a]pyrazole-3:9-dione and 3-bromo-2-methyl-pyrazolo[a][3,1]benzoxazin-5-one, respectively.

Crystals of the α-derivative are monoclinic, with unit cell dimensions $a = 19.51 \pm 0.05$ Å, $b = 9.13 \pm 0.05$ Å, $c = 13.96 \pm 0.05$ Å, $\beta = 118.0 \pm 0.5°$ and space group $C2/c$, while β-derivative crystals, also monoclinic, have $a = 5.45 \pm 0.01$ Å, $b = 14.78 \pm 0.01$ Å, $c = 12.73 \pm 0.01$ Å, $\beta = 90.7 \pm 0.1°$ and space group $P2_1/n$.

Because crystals of the α-compound were extremely small and difficult to prepare, the diffraction data set consisted of only 261 photographically-determined, independent, non-zero reflections ($2\theta_{max} = 37°$ for Cu$K\alpha$). However, 1112 diffractometer-measured intensities were used in the analysis of the β-isomer. Both crystal structures were solved from successive three-dimensional Fourier maps following the initial placement of the bromine atoms from Patterson syntheses. Full matrix least squares refinement of the complete structure postulates reduced the usual R to 0.175 for the α-derivative and 0.074 for the β-compound.

Molecules of both derivatives are approximately planar and their packing in both crystal structures is determined by van der Waals forces, the shortest contact distances being from bromine atoms to oxygens of neighbouring molecules.

This paper describes the crystal structures of monobromo-derivatives of Michaelis's methyl-pyrazoisocoumarazones, and their analyses from three-dimensional X-ray diffraction data.

After condensation of *o*-carboxyphenylhydrazine with ethylacetoacetate and then distillation of the resulting *o*-carboxyphenylhydrazone, Michaelis *et al.*[1,2] isolated what were reported to be three isomeric heterocyclic products, which were called α,- β-, and γ-methyl-pyrazoisocoumarazone, respectively.

Much later Veibel *et al.*[3–6] showed that Michaelis's γ-isomer was actually a 1:2 mixture of the α- and β-compounds, and also proved that both the α- and the β-modifications yield the same pyrazolone ester when titrated in ethanol with standard base. From the method of preparation, the titration results and the dipole moments of the compounds they concluded that, of the formulae proposed by Michaelis, the β-modification might have structure II, but that there was some doubt that the α-modification had structure I. However, Mosby [7] found nothing inconsistent with this assignment of structures in the results of an infrared spectral investigation.

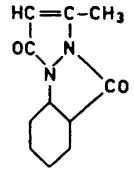

I

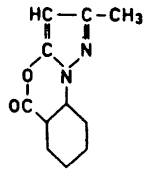

II

Further study of these and analogous compounds is being pursued by Else Plejl, Department of Organic Chemistry, Technical University of Denmark, who suggested the X-ray crystallographic analyses to resolve the structural ambiguities and who kindly provided crystals of the monobromo-derivatives of α- and β-"methyl-pyrazoisocoumarazone".

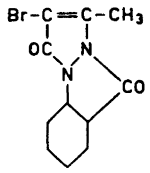

α-Compound

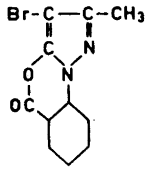

β-Compound

EXPERIMENTAL

Recrystallization. Single crystals of the *α-derivative* were obtained by evaporation of a 96 % ethanol solution at 1°C. Their melting point was 187 ± 1°C. They were very small, poorly-formed, colourless plates. None could be grown with characteristics suitable for diffractometer data measurement.

This was not the case for the *β-derivative*, however, suitable crystals being deposited by slowly decreasing the temperature of a 96 % ethanol solution from 10°C to 2°C. These formed as somewhat elongated, colourless prisms with melting point 148 ± 1°C.

X-Ray diffraction data collection and measurement. (1) *The α-derivative.* A single crystal of dimensions 0.15 × 0.05 × 0.005 mm³ was mounted on a Weissenberg goniometer with its *b* axis (see Crystal Data) parallel to the rotation axis. Space group and approximate unit cell dimensions were determined from preliminary oscillation and Weissenberg photographs. More accurate unit cell dimensions were later determined from a powder diagram taken with Cu$K\alpha$ radiation. Three-dimensional, multiple-film, equi-inclination Weissenberg photographs were taken for layers 0 to 4, inclusive, with

rotation axis b, using Cu$K\alpha$ radiation. The diffracted intensities for each layer were measured visually, scaled together and then corrected for Lorentz and polarization effects. The size and shape of the crystal did not allow data collection about a second axis, and so the layers of b-axis data were scaled together on the basis of their relative exposure times. Absorption corrections were not applied. Intensities above background were observed only to a 2θ of 37° so that the final data set consisted of 261 independent, non-zero structure amplitudes.

(2) *The β-derivative.* Unit cell dimensions were measured from precession photographs taken with Mo$K\alpha$ radiation of a single crystal of dimensions $0.10 \times 0.11 \times 0.14$ mm³ which had its a axis (see Crystal Data) parallel to the goniometer head axis. This crystal was also used to measure and collect a three-dimensional set of diffracted intensities, being mounted for the purpose on a Stoe automatic Weissenberg-geometry diffractometer. Setting angles ω and Y were read for each reflection from a punched paper tape produced as output from the FORTRAN programme PAULUS 67 supplied by the manufacturer. All reflections in a hemisphere of the reciprocal lattice with $\sin\theta/\lambda \leqslant 0.64$ were measured using graphite-monochromated Mo$K\alpha$ radiation and the ω-scan technique. The crystal scan range was 2° for layers 0 to 3, inclusive, and 3° for the remaining higher layers. Background counts were made at both ends of each ω scan range, the individual counts each being for half of the scan count time.

The measured data recorded on punched paper tape were reduced to structure amplitudes using a FORTRAN programme written locally. The tape was checked for punching errors, pairs of background counts were evaluated and compared to ensure that each reflection had been completely scanned, and then were subtracted from the appropriate scan counts, and the estimated standard deviations of the observations were calculated. It was not necessary to correct for apparent crystal decomposition or movement (as indicated by the intensities of repeated measurements of standard reflections). Finally, Lorentz and polarization, but not absorption, corrections were applied. Reflections having net intensities less than twice their corresponding estimated standard deviation were designated as "unobserved" and were omitted from the data set, thereby leaving 1112 independent, non-zero observations to be used in the structure determination.

All the crystal structure analysis computations described below were performed on an IBM 7094 computer using the X-RAY 63 crystallographic programme system of Stewart *et al.*[8] and the drawing programme ORTEP written by Johnson.[9] The X-ray atomic scattering factors used in the calculation of structure factors were those listed in the *International Tables for X-Ray Crystallography*, Volume III.[10]

CRYSTAL DATA

The α-derivative. $C_{11}H_7N_2O_2Br$; M = 279.1. Monoclinic (b unique), $a = 19.51 \pm 0.05$ Å, $b = 9.13 \pm 0.05$ Å, $c = 13.96 \pm 0.05$ Å, $\beta = 118.0 \pm 0.5°$, $V = 2195 \pm 30$ Å³, $D_m = 1.69 \pm 0.03$ g cm^{-3}, $Z = 8$, $D_c = 1.72 \pm 0.03$ g cm^{-3}. Linear absorption coefficient for X-rays [λ(Cu$K\alpha$) = 1.5418 Å], $\mu = 55.00$ cm^{-1}.[11] Number of electrons per unit cell, $F(000) = 1104$. Systematically absent reflections: hkl when $h + k$ odd, $h0l$ when h and l odd, $0k0$ when k odd; space group Cc or $C2/c$.

The β-derivative. $C_{11}H_7N_2O_2Br$; M = 279.1. Monoclinic (b unique), $a = 5.45 \pm 0.01$ Å, $b = 14.78 \pm 0.01$ Å, $c = 12.73 \pm 0.01$ Å, $\beta = 90.7 \pm 0.1°$, $V = 1025 \pm 3$ Å³. $D_m = 1.80 \pm 0.02$ g cm^{-3},[1] $Z = 4$, $D_c = 1.80 \pm 0.02$ g cm^{-3}. Linear absorption coefficient for X-rays [λ(Mo$K\alpha$) = 0.71069 Å], $\mu = 42.05$ cm^{-1}.[11] Number of electrons per unit cell, $F(000) = 552$. Systematically absent reflections: $h0l$ when $h + l$ odd, $0k0$ when k odd; space group $P2_1/n$.

DETERMINATION OF STRUCTURES

The coordinates of the bromine atom in each of the crystal structures were deduced from the respective three-dimensional Patterson maps. Structure factor contributions from each bromine atom were calculated using these coordinates, and appropriate isotropic temperature factors and corresponding heavy-atom electron density maps were plotted. The positions of atoms corresponding to parts of each structure could be located on the maps. Successive cycles of structure factor calculations from partial structure postulates followed by Fourier syntheses led eventually to the two complete structure solutions.

For the α-compound all the computations were made assuming the space group to be $C2/c$ (with one molecule per asymmetric unit). The successful solution and subsequent refinement (see below) confirm that this choice is correct.

REFINEMENT

α-Derivative. Full matrix least squares refinement minimizing $\sum\omega(|F_o| - G|F_c|)^2$, where ω is the weight accorded each observation, G is a variable overall scalefactor, $|F_o|$ and $|F_c|$ are corresponding observed and calculated structure amplitudes, respectively, and where the summation is over all the non-zero observations, gave an R factor [12] of 0.175. In this operation the scalefactor and atomic coordinates were varied but the isotropic temperature factor for bromine of 5.0 Å^2 and those for the other atoms of 8.0 Å^2 were held constant. A Wilson plot had indicated that the overall temperature factor was approximately 8 Å^2. Equal weights were given to all observations.

Some further cycles of refinement, in which individual atomic isotropic temperature factors were also varied with the scalefactor and coordinates,

Table 1. α-Compound. Atomic coordinates. The general equivalent positions are $\pm(x, y, z)$; $\pm(\frac{1}{2}+x, \frac{1}{2}+y, z)$; $\pm(x, -y, \frac{1}{2}+z)$; $\pm(\frac{1}{2}+x, \frac{1}{2}-y, \frac{1}{2}+z)$. The estimated standard deviations ($\times 10^3$) of the coordinates are given in parentheses.

Atom	x/a	y/b	z/c
Br	0.196(1)	−0.152(2)	0.074(1)
O1	0.293(4)	0.177(12)	0.182(6)
O2	0.529(5)	−0.278(11)	0.396(6)
N1	0.423(6)	−0.142(15)	0.308(7)
N2	0.410(6)	0.009(14)	0.296(8)
C1	0.317(7)	0.016(20)	0.198(10)
C2	0.294(7)	−0.132(19)	0.191(9)
C3	0.354(8)	−0.258(18)	0.221(11)
C4	0.345(7)	−0.426(18)	0.216(10)
C5	0.506(7)	−0.126(22)	0.384(10)
C6	0.534(10)	0.031(18)	0.412(12)
C7	0.618(9)	0.080(18)	0.480(11)
C8	0.618(8)	0.217(19)	0.490(10)
C9	0.551(8)	0.346(17)	0.435(9)
C10	0.481(8)	0.268(17)	0.361(11)
C11	0.475(8)	0.128(21)	0.363(10)

were computed. Unit weights were again used. Although the resulting R factor was lower, the reduction was not significant in relation to the additional parameters introduced.[13] Hence no further attempts to refine the structure were made, and the coordinates given in Table 1 and the interatomic distances and angles in Table 3 are those corresponding to the end of the first stage of refinement (thermal parameters not varied).

β-Derivative. The scalefactor, atomic coordinates, and individual isotropic temperature factors were varied in the initial stage of the full matrix least squares refinement, which used the same procedure as that mentioned for the α-compound. Observations were weighted according to the function $\omega = 1/\sigma(|F_o|^2)$, where $\sigma(|F_o|^2)$ is the estimated standard deviation of the square of an observed structure amplitude calculated from counting statistics only. The R factor dropped to 0.127. Refinement continued with variable anisotropic thermal parameters replacing the corresponding isotropic values and with a weighting scheme $\omega = 1/[0.02\ F_o + \sigma(|F_o|)]^2$. The resulting R factor was 0.075. The approximate positions of all the hydrogen atoms of the structure were calculated so that they were 1.00 Å from the carbon atoms to which they were bonded, and they were all given isotropic temperature factors of 4 Å^2. None of the hydrogen atom parameters was refined in the final cycles of anisotropic least squares refinement which followed. The final R factor of 0.074 (weighted $R = 0.068$) was obtained with the parameters given in Table 2. Table 3 presents the corresponding interatomic distances and angles.

Table 2a. β-Compound. Atomic coordinates. The general equivalent positions are $\pm(x, y, z)$; $\pm(\frac{1}{2}-x, \frac{1}{2}+y, \frac{1}{2}-z)$. The estimated standard deviations ($\times 10^4$) of the coordinates are given in parentheses.

Atom	x/a	y/b	z/c
Br	1.0865(2)	0.1461(1)	−0.0320(1)
O1	0.6408(12)	0.0430(5)	0.1029(6)
O2	0.4578(14)	−0.0792(6)	0.1613(7)
N1	0.6061(15)	0.2776(7)	0.1588(8)
N2	0.5289(16)	0.1879(6)	0.1674(8)
C1	0.6744(17)	0.1352(8)	0.1071(9)
C2	0.8394(17)	0.1868(8)	0.0580(8)
C3	0.7926(19)	0.2751(9)	0.0929(9)
C4	0.9326(23)	0.3611(9)	0.0648(10)
C5	0.4662(19)	0.0015(9)	0.1657(9)
C6	0.3060(17)	0.0619(9)	0.2286(8)
C7	0.1153(18)	0.0207(9)	0.2860(10)
C8	−0.0346(22)	0.0793(10)	0.3452(11)
C9	0.0086(21)	0.1735(9)	0.3476(11)
C10	0.1927(21)	0.2156(9)	0.2887(9)
C11	0.3403(18)	0.1570(8)	0.2287(9)
H1	0.899	0.424	0.090
H2	0.903	0.387	0.061
H3	1.125	0.326	0.013
H4	0.088	−0.046	0.285
H5	−0.174	0.054	0.386
H6	−0.097	0.212	0.393
H7	0.218	0.283	0.289

Table 2b. Mean square vibration tensors, U_{ij}, ($\times 10^4$) in Å^2. The estimated standard deviations ($\times 10^4$) of the U_{ij} are given in parentheses.

Atom	U_{11}	U_{22}	U_{33}	U_{12}	U_{23}	U_{31}
Br	422(5)	412(3)	459(7)	5(3)	−18(4)	52(2)
O1	408(40)	186(43)	431(51)	8(17)	−27(20)	97(17)
O2	622(50)	241(53)	682(67)	−5(22)	−18(24)	101(22)
N1	347(45)	341(62)	464(65)	7(23)	−31(26)	9(22)
N2	376(44)	250(56)	358(59)	8(20)	−61(23)	17(20)
C1	337(49)	295(73)	391(69)	−30(28)	−41(32)	2(24)
C2	267(46)	351(70)	268(55)	1(23)	−30(26)	28(21)
C3	432(58)	285(70)	368(74)	−44(28)	−11(30)	34(26)
C4	889(88)	182(64)	849(111)	−43(38)	−83(40)	92(38)
C5	340(55)	314(76)	281(71)	11(28)	23(30)	4(24)
C6	302(50)	390(78)	280(70)	48(26)	−4(30)	22(22)
C7	287(51)	396(79)	500(86)	9(25)	−15(32)	77(26)
C8	516(65)	540(99)	467(86)	13(33)	7(37)	51(30)
C9	449(64)	393(87)	561(91)	43(28)	−16(33)	44(30)
C10	586(69)	350(77)	366(76)	92(31)	−55(32)	62(29)
C11	376(48)	177(69)	324(64)	−42(26)	2(28)	−41(22)

Lists of the observed structure amplitudes and calculated structure factors for both structure analyses may be obtained upon request from the author.

Table 3a. Some interatomic distances. The estimated standard deviations ($\times 10^2$ for the α-compound, $\times 10^3$ for the β-compound) of the distances are given in parentheses (in Ångströms).

α-Compound		β-Compound	
Br−C2	1.85(10)	Br−C2	1.877(11)
O1−C1	1.53(21)	O1−C1	1.375(14)
		O1−C5	1.392(14)
O2−C5	1.44(22)	O2−C5	1.195(16)
N1−N2	1.40(18)	N1−N2	1.396(14)
N1−C3	1.70(17)	N1−C3	1.326(14)
N1−C5	1.46(14)		
N2−C1	1.68(14)	N2−C1	1.357(14)
N2−C11	1.60(19)	N2−C11	1.376(14)
C1−C2	1.41(25)	C1−C2	1.340(15)
C2−C3	1.56(22)	C2−C3	1.403(17)
C3−C4	1.54(23)	C3−C4	1.527(18)
C5−C6	1.52(26)	C5−C6	1.489(16)
C6−C7	1.53(21)	C6−C7	1.415(16)
C6−C11	1.36(23)	C6−C11	1.419(17)
C7−C8	1.26(24)	C7−C8	1.414(18)
C8−C9	1.66(21)	C8−C9	1.412(20)
C9−C10	1.45(18)	C9−C10	1.406(18)
C10−C11	1.28(25)	C10−C11	1.412(17)

Table 3b. Some interatomic angles. The estimated standard deviations ($\times 10$ for the β-compound) of the angles are given in parentheses (in degrees).

α-Compound		β-Compound	
		C1 – O1 – C5	120.4(9)
N2 – N1 – C3	120(8)	N2 – N1 – C3	104.9(9)
N2 – N1 – C5	94(11)		
C3 – N1 – C5	145(13)		
N1 – N2 – C1	102(10)	N1 – N2 – C1	108.8(9)
N1 – N2 – C11	123(9)	N1 – N2 – C11	126.0(9)
C1 – N2 – C11	135(12)	C1 – N2 – C11	125.2(10)
O1 – C1 – N2	107(10)	O1 – C1 – N2	120.8(9)
O1 – C1 – C2	147(11)	O1 – C1 – C2	129.5(10)
N2 – C1 – C2	102(11)	N2 – C1 – C2	109.7(10)
Br – C2 – C1	109(9)	Br – C2 – C1	126.4(9)
Br – C2 – C3	120(10)	Br – C2 – C3	128.7(8)
C1 – C2 – C3	121(12)	C1 – C2 – C3	104.8(9)
N1 – C3 – C2	88(10)	N1 – C3 – C2	111.7(10)
N1 – C3 – C4	134(10)	N1 – C3 – C4	120.9(11)
C2 – C3 – C4	132(12)	C2 – C3 – C4	127.3(10)
		O1 – C5 – O2	116.0(10)
		O1 – C5 – C6	117.0(10)
O2 – C5 – N1	99(12)		
O2 – C5 – C6	145(11)	O2 – C5 – C6	126.9(11)
N1 – C5 – C6	115(14)		
C5 – C6 – C7	126(14)	C5 – C6 – C7	117.3(11)
C5 – C6 – C11	112(13)	C5 – C6 – C11	121.1(9)
C7 – C6 – C11	122(15)	C7 – C6 – C11	121.6(10)
C6 – C7 – C8	107(13)	C6 – C7 – C8	116.4(12)
C7 – C8 – C9	135(12)	C7 – C8 – C9	121.2(12)
C8 – C9 – C10	104(12)	C8 – C9 – C10	123.0(12)
C9 – C10 – C11	122(12)	C9 – C10 – C11	115.6(12)
N2 – C11 – C6	96(14)	N2 – C11 – C6	115.3(9)
N2 – C11 – C10	136(11)	N2 – C11 – C10	122.5(10)
C6 – C11 – C10	127(14)	C6 – C11 – C10	122.2(10)

DESCRIPTION OF THE STRUCTURES

Fig. 1 shows molecules of the two derivatives as viewed along the *c*-axes of the crystals, while Table 4 gives the out-of-plane distances of all the atoms of each molecule from least squares planes calculated through the appropriate benzene ring atoms. It is clear that the molecules of both derivatives are approximately planar. From this geometry and by comparison with the known hydrogen atom positions in the β-derivative, the locations of the hydrogen atoms and the double bond in the α-compound may be confidently postulated, even though the accuracy of the crystal structure analysis itself does not permit this. The results therefore confirm that the parent compounds have the structures suggested by Veibel *et al.*[3–6] and accepted by Mosby.[7]

In both crystal structures the molecules are arranged with their shortest dimensions parallel to the *b*-axes. The directions of the longer dimensions of the molecules make angles with the respective *a*-axes of about 45° and 40° for the α- and β-derivatives, respectively. All short intermolecular distances

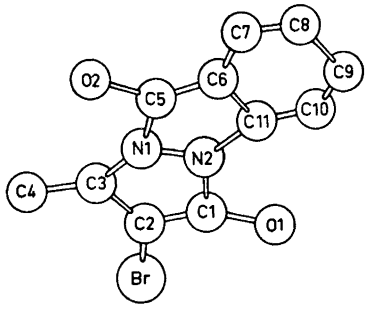

Fig. 1a. A molecule of the α-compound, as viewed along the *c* crystallographic axis.

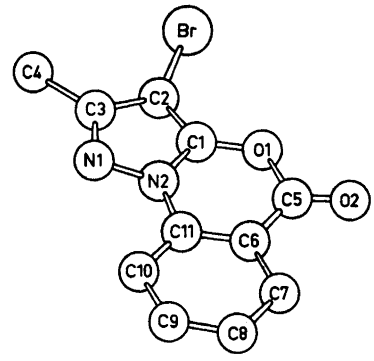

Fig. 1b. A molecule of the β-compound, as viewed along the *c* crystallographic axis.

correspond to those expected for van der Waals packing forces. In the α-compound the shortest of 3.10 Å is in the molecular plane, between the oxygen atom, O2, and the bromine of the neighbouring molecule at $(\frac{1}{2}+x, \frac{1}{2}-y, \frac{1}{2}+z)$ relative to the first. From one side of each molecule there is a contact of 3.40 Å between Cl and the carbon atom, C7, of the molecule at $(1-x, y, \frac{1}{2}-z)$. On the other side there are also carbon-carbon contacts of 3.40 Å,

Table 4. Distances (in Ångströms) of atoms from the least squares planes calculated through the benzene rings. The planes are given by the equations

$$-1.22x+3.58y+1.38z=-9.08 \text{ (α-compound)}$$

and

$$3.369x-1.485y+9.831z=3.172 \text{ (β-compound)}$$

in direct space. The estimated standard deviations of the distances are approximately 0.06 Å for the α-compound and 0.012 Å for the β-compound.

Atom	α-Compound	β-Compound
C6	−0.03	−0.014
C7	0.06	0.003
C8	−0.03	0.013
C9	−0.05	−0.017
C10	0.09	0.005
C11	−0.05	0.010
Br	0.40	0.042
O1	0.23	0.065
O2	0.01	−0.074
N1	−0.02	−0.019
N2	0.03	0.024
C1	0.24	0.048
C2	0.01	0.051
C3	0.28	−0.004
C4	0.16	−0.072
C5	−0.06	−0.025

between C5 and C6, C5 and C11, and C6 and C6 of one molecule and its neighbour at $(1-x, -y, 1-z)$. In crystals of the β-compound there is an in-plane intermolecular contact of 3.207 Å between O2 of one molecule and C10 of the molecule at $(\frac{1}{2}-x, -\frac{1}{2}+y, \frac{1}{2}-z)$ relative to it. Between the molecular planes there are Br···O and C···C contacts. The shortest, of 3.155 Å, is between Br of a reference molecule and O2 of the molecule at $(1-x, -y, -z)$. There is also a Br···O1 contact of 3.297 Å between these same molecules. Finally, between C3 of a molecule and C10 of that at $(1+x, y, z)$ there is a distance of 3.407 Å.

Unfortunately, the very limited accuracy of the structure analysis of the α-derivative does not permit a meaningful comparison of the interatomic distances and angles of the two compounds. The geometry of the β-compound, however, conforms to that which might have been expected for this structure.

Acknowledgements. The head of the laboratory, Professor, Dr. phil. R. W. Asmussen, thanks the *Danish National Science Research Council* for a grant from which the diffractometer used in this work was purchased. The author is grateful for the assistance of Mrs Ulla Lund Christensen in recrystallizing the compounds investigated and to Dr. Kenneth J. Watson for his help in preparing this manuscript.

REFERENCES

1. Michaelis, A. and Eisenschmidt, C. *Ber.* **37** (1904) 2228.
2. Michaelis, A. *Ann.* **373** (1910) 129.
3. Veibel, S. and Arnfred, N. H. *Acta Chem. Scand.* **2** (1948) 914.
4. Veibel, S. and Arnfred, N. H. *Acta Chem. Scand.* **2** (1948) 921.
5. Veibel, S., Refn, I. and Friediger, A. *Acta Chem. Scand.* **2** (1948) 927.
6. Veibel, S., Plejl, E. and Lillelund, H. *Résumés des Communications, XIV^e Congrès International de Chimie pure et appliquée*, Zürich 1955, p. 274.
7. Mosby, W. L. *Chem. Ind. (London)* **1956** 1524.
8. Stewart, J. M. *et al.* In Stewart, J. M. and High, D. F., Eds., *Crystal Structure Calculations System; X-RAY 63*, Technical Report TR-64-6 (NS 6-398), Computer Science Center, University of Maryland and Research Computer, Laboratory, University of Washington 1964.
9. Johnson, C. K. *ORTEP: A Fortran Thermal-Ellipsoid Plot Program for Crystal Structure Illustrations*, Report ORNL-3794 (revised), Oak Ridge National Laboratory, Oak Ridge, Tenn. 1965.
10. MacGillavry, C. H. and Rieck, G. R., Eds., *International Tables for X-Ray Crystallography*, Kynoch Press, Birmingham 1962, Vol. III, pp. 201–212.
11. MacGillary, C. H. and Rieck, G. R., Eds., *International Tables for X-Ray Crystallography*, Kynoch Press, Birmingham 1962, Vol. III, pp. 162–165.
12. Defined, as usual, as $R = \sum||F_o| - |F_c||/\sum|F_o|$, where $|F_o|$ and $|F_c|$ are the observed and calculated structure amplitudes.
13. Hamilton, W. C. *Statistics in Physical Science*, The Ronald Press Company, New York 1964, p. 157.

Received August 22, 1972.

ACTA CHEMICA SCANDINAVICA 27 (1973) 670–676

Extrapolation of Kinetic Data for Reactions Involving Weak Electrolytes

PER BERONIUS, ALLAN HOLMGREN and ANN-MARGRET NILSSON

Division of Physical Chemistry, University of Umeå, S-901 87 Umeå, Sweden

To enable direct comparison of rate constants for bimolecular reactions in which one of the reactants is a weak electrolyte, extrapolation to infinite dilution has to be performed. One method of accomplishing this extrapolation is to apply the Acree equation to the kinetic data. This procedure requires a predetermined association constant of the ionizable reactant, *e.g.* from electrical conductance data. In this article a method of extrapolation, requiring no independently determined association constant, is outlined. Rate constants extrapolated by this method for 23 different systems involving alkali halides and two systems involving tetraalkyl ammonium halides are compared with the corresponding rate constants derived from the Acree equation. The values extrapolated by means of the two different methods agree very well, the relative deviations being usually less than 2 %.

In analyzing kinetic data for second-order displacement reactions of the type

$$RY + AY^* \rightleftharpoons RY^* + AY \quad (1)$$

where RY denotes a nonionizable reactant and AY is a weak electrolyte, we may employ the Acree equation

$$k = k_i\alpha + k_m(1-\alpha) \quad (2)$$

in which k is the overall rate constant, k_i the rate constant for the reaction between RY and free ions

$$RY + Y^{*-} \rightleftharpoons RY^* + Y^- \quad (3)$$

k_m the rate constant for the reaction between RY and ion-pairs

$$RY + A^+Y^{*-} \rightleftharpoons RY^* + A^+Y^- \quad (4)$$

and α the degree of dissociation of the ionic reactant.

Several examples of the analysis of kinetic data by this means for displacement reactions involving organic halides and alkali halides may be found in the literature, *e.g.* Refs. 1–3.

According to eqn. (2) the association constant, K_A, of the ionizable reactant is required for calculation of α.

The purpose of the present paper is to describe a method, which permits evaluation of k_i without *a priori* knowledge of the association constant and to compare the values of k_i obtained by this means with values calculated from eqn. (2) using values of α derived from electrical conductance data.

DERIVATION

For several reactions of type (1) it has been found that the rate constant for reaction (4) involving RY and paired ions is much less than the rate constant for reaction (3) involving RY and free ions, *i.e.* $k_m \ll k_i$; see for instance Ref. 1. In fact, several reactions may be quoted in which k_m has been found to be zero within experimental errors. In such cases, and/or if the reaction is studied at sufficient dilution for α to be close to unity, we may neglect the second term on the right-hand side of eqn. (2) *i.e.*

$$k = k_i\alpha \tag{5}$$

If the ionic reactant forms ion-pairs, but no higher aggregates, we have to consider the equilibrium

$$A^+ + Y^- \rightleftharpoons A^+Y^- \tag{6}$$

Application of the law of mass action to this equilibrium yields

$$K_A = \frac{1-\alpha}{c\gamma^2\alpha^2} \tag{7}$$

where c is the analytical concentration of the ionic reactant and γ the mean molar activity coefficient.

Eliminating α between eqns. (5) and (7) yields the following equation:

$$\frac{1}{k} = \frac{1}{k_i} + \frac{K_A c\gamma^2 k}{k_i^2} \tag{8}$$

according to which k_i may be obtained from the intercept of the straight line which should result upon plotting $1/k$ *vs.* $c\gamma^2 k$; *cf.* Ref. 4.

From eqns. (5) and (8) it may be seen that the method of calculation outlined implicitly involves the use of an ion-pair association constant based on the kinetic data.

RESULTS AND DISCUSSION

In comparing extrapolated rate constants, k_i, according to the two different expressions, eqns. (2) and (8), we shall restrict ourselves to kinetic data [4–10] for isotopic exchange reactions between organic and inorganic halides obtained at this institute during the last few years.

A compilation of these reactions with pertinent references to the papers containing primary kinetic data is shown in Table 1. These reactions, which all appear to be of S_N2-type, were investigated by means of ^{131}I, ^{82}Br, or ^{36}Cl

Table 1. Compilation of reactions analyzed by means of eqns. (2) and (8).

Reactants	Solvent	Ref.
$CH_3I + NaI$, KI, RbI, or CsI	Methanol	5
$CH_3I + NaI$, KI, RbI, or CsI	Ethanol, 6.3 wt. % aq.	6
$CH_3I + NaI$, KI, RbI, or CsI	Ethanol	7
$CH_3I + NaI$, KI, RbI, or CsI	Propanol	8
$C_4H_9Br + LiBr$	Acetone, 1.5 wt. % aq.	9
$C_4H_9Br + LiBr$	Acetone, 1.0 wt. % aq.	9
$C_4H_9Br + LiBr$	Acetone, 0.6 wt. % aq.	9
$C_4H_9Br + LiBr$	Acetone, 0.3 wt. % aq.	9
$C_4H_9Br + LiBr$	Acetone, 0.1 wt. % aq.	9
$C_4H_9Br + LiBr$	Acetone	9
$p\text{-}NO_2C_6H_4CH_2Cl + LiCl$	Acetone	4
$C_4H_9Br + (C_4H_9)_4NBr$	Acetone	10
$p\text{-}NO_2C_6H_4CH_2Cl + (C_4H_9)_4NCl$	Acetone	10

as radioactive indicators. The primary kinetic data consist of overall second-order rate constants, k, according to the McKay equation for several concentrations below 0.01 M of the ionic reactant.

Mean molar activity coefficients were estimated by means of the Debye-Hückel equation in the form given in Ref. 4 using the permittivities of pure solvents and solvent mixtures listed in Table 2. Because of the dilute solutions used the difference between molar and rational activity coefficients was ignored.

In calculating k_i from eqn. (2) the association constants and ion-size parameters listed in Table 3 were used. The method employed to calculate k_i has been described.[4] With one exception (lithium chloride in acetone) the values of K_A and $\mathring{a}$ in Table 3 were derived from electrical conductance data by means of the Fuoss-Onsager equation [15] of 1957. The association constant for lithium chloride in pure acetone was obtained from the dissociation constant, $K_D = 2.8 \times 10^{-6}$ M, reported in a recent paper by Brookes *et al.*[14] who

Table 2. Permittivities of anhydrous and aqueous solvents at 25.0°C.

Solvent	ε	Ref.
Methanol	32.6	11
Ethanol, 6.3 wt. % aq.	27.1	6
Ethanol	24.3	11
Propanol	20.4	8
Acetone, 1.5 wt. % aq.	21.3	12
Acetone, 1.0 wt. % aq.	21.2	13
Acetone, 0.6 wt. % aq.	20.9	13
Acetone, 0.3 wt. % aq.	20.8	13
Acetone, 0.1 wt. % aq.	20.8	13
Acetone	20.7	13

Table 3. Ion-pair association constants and ion-size parameters at 25.0°C.

Solvent	Salt	K_A M^{-1}	$\mathring{a} \times 10^8$ cm	Ref.
Methanol	NaI	2.2	4.3	11
Methanol	KI	2.3	4.0	11
Methanol	RbI	6.0	4.0	11
Methanol	CsI	9.4	3.8	11
Ethanol, 6.3 wt. % aq.	NaI	13.2	4.7	6
Ethanol, 6.3 wt. % aq.	KI	18.9	4.0	6
Ethanol, 6.3 wt. % aq.	RbI	34.4	4.4	6
Ethanol, 6.3 wt. % aq.	CsI	52.2	4.3	6
Ethanol	NaI	8.5	3.9	11
Ethanol	KI	39.1	4.2	11
Ethanol	RbI	63.6	4.2	11
Ethanol	CsI	98.9	4.2	11
Propanol	NaI	112	4.7	8
Propanol	KI	279	5.3	8
Propanol	RbI	431	6.8	8
Propanol	CsI	622	8.0	8
Acetone, 1.5 wt. % aq.	LiBr	1 640	3.9	12
Acetone, 1.0 wt. % aq.	LiBr	2 073	5.4	13
Acetone, 0.6 wt. % aq.	LiBr	2 383	5.2	13
Acetone, 0.3 wt. % aq.	LiBr	2 786	6.4	13
Acetone, 0.1 wt. % aq.	LiBr	3 360	6.6	13
Acetone	LiBr	4 202	9.3	13
Acetone	LiCl	357 000	2.4 [a]	14
Acetone	$(C_4H_9)_4NBr$	349	7.2	10
Acetone	$(C_4H_9)_4NCl$	481	6.3	10

[a] Crystal radii sum.

evaluated K_D from conductance data according to the method of Fuoss.[16] An attempt to fit the Fuoss-Onsager equation [15] to the latter data by means of a computer programme in Ref. 11 was unsuccessful.

Extrapolation of kinetic data to infinite dilution by means of eqn. (8) was performed by fitting this equation to experimental data by means of the

Table 4. Dependence of k_i according to eqn. (8) on the ion-size parameter, $\mathring{a}$.

Reactants	Solvent	$\mathring{a} \times 10^8$ cm	$k_i \times 10^3$ M^{-1} s^{-1}
$CH_3I + CsI$	Propanol	4.0	13.99
		8.0 [a]	13.98
$C_4H_9Br + LiBr$	Acetone	4.0	7.857
		9.3 [a]	7.588
$p\text{-}NO_2C_6H_4CH_2Cl + LiCl$	Acetone	4.0	43.24
		2.4 [a]	43.41

[a] Value derived from electrical conductance data using the Fuoss-Onsager equation.[15]

Table 5. Comparison of k_i according to eqns. (2) and (8) for the exchange of iodine between methyl iodide and alkali iodides in different solvents at 25.0°C.

Solvent	$k_i \times 10^3$ M^{-1} s^{-1} Eqn. (2)	$k_i \times 10^3$ M^{-1} s^{-1} Eqn. (8)	$\frac{k_i, \text{ eqn. (8)}}{k_i, \text{ eqn. (2)}}$
		NaI	
Methanol	3.320	3.320	1.000
Ethanol, 6.3 wt. % aq.	10.72	10.73	1.001
Ethanol	10.39	10.40	1.001
Propanol	13.68	13.71	1.002
		KI	
Methanol	3.332	3.335	1.001
Ethanol, 6.3 wt. % aq.	10.70	10.71	1.001
Ethanol	10.36	10.36	1.000
Propanol	13.98	13.93	0.996
		RbI	
Methanol	3.309	3.309	1.000
Ethanol, 6.3 wt. % aq.	10.69	10.70	1.001
Ethanol	10.36	10.36	1.000
Propanol	13.92	13.76	0.989
		CsI	
Methanol	3.301	3.301	1.000
Ethanol, 6.3 wt. % aq.	10.75	10.75	1.000
Ethanol	10.42	10.42	1.000
Propanol	13.99	13.99	1.000

relative deviation least squares method since the relative error in $1/k$ appears to be independent of $c\gamma^2 k$ for the range of concentrations investigated; *cf.* Ref. 4. Activity coefficients, γ, were calculated as reported above with the exception that the value, $\mathring{a} = 4$ Å, for the ion-size parameter was used throughout. The exact choice of $\mathring{a}$-value in evaluating k_i from eqn. (8) appears not to be very critical as may be seen from the data in Table 4.

The results of these calculations are shown in Tables 5 – 7 in which values of k_i according to eqns. (2) and (8) have been listed in the second and third columns, respectively.

Table 6. Comparison of k_i according to eqns. (2) and (8) for the exchange of bromine between butyl bromide and lithium bromide in aqueous acetone at 25.0°C.

Wt. % water in solvent mixture	$k_i \times 10^3$ M^{-1} s^{-1} Eqn. (2)	$k_i \times 10^3$ M^{-1} s^{-1} Eqn. (8)	$\frac{k_i, \text{ eqn. (8)}}{k_i, \text{ eqn. (2)}}$
1.5	1.656	1.697	1.025
1.0	2.533	2.602	1.027
0.6	3.370	3.337	0.990
0.3	4.067	4.046	0.995
0.1	6.805	7.003	1.029

Table 7. Comparison of k_i according to eqns. (2) and (8) for halogen exchange reactions in "dry" acetone at 25.0°C.

Reactants	$k_i \times 10^3$ M^{-1} s^{-1} Eqn. (2)	$k_i \times 10^3$ M^{-1} s^{-1} Eqn. (8)	$\frac{k_i, \text{ eqn. (8)}}{k_i, \text{ eqn. (2)}}$
$C_4H_9Br + LiBr$	7.850	7.857	1.001
$p\text{-}NO_2C_6H_4CH_2Cl + LiCl$	43.68	43.24	0.990
$C_4H_9Br + (C_4H_9)_4NBr$	7.067	6.997	0.990
$p\text{-}NO_2C_6H_4CH_2Cl + (C_4H_9)_4NCl$	34.25	34.12	0.996

For alkali iodides in methanol and in anhydrous and aqueous ethanol, where these salts are only slightly associated under the conditions used, there is excellent agreement between the values of k_i according to the two different methods of calculation, the discrepancies being 0.1 % or less; see the last column in Table 5.

For the other systems investigated, where association to ion-pairs is more extensive, which implies longer extrapolations, the agreement between the two methods of calculation is very satisfactory. For these systems the values of k_i according to eqns. (2) and (8) deviate by only 1 or 2 %, see Tables 5 – 7.

The *p*-nitrobenzyl chloride-lithium chloride exchange reaction in acetone [4] represents an extreme example of a system for which the determination of the rate constant at infinite dilution involves a very long extrapolation. This may be seen in Fig. 1 in which the overall second-order rate constant has been

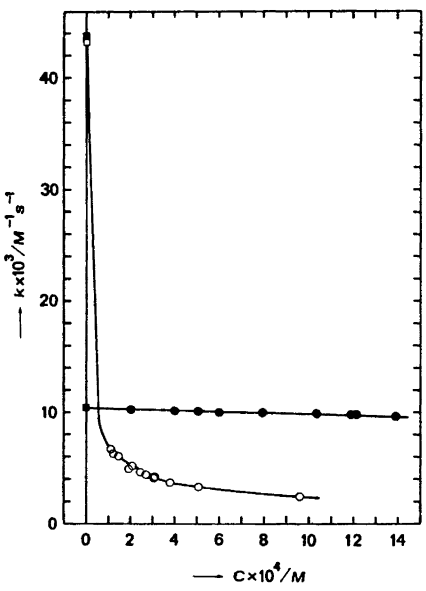

Fig. 1. Dependence of the overall second-order rate constant at 25.0°C on the analytical concentration of the ionic reactant for exchange of ^{36}Cl between *p*-nitrobenzyl chloride and lithium chloride in acetone (open circles) and for exchange of ^{131}I between methyl iodide and cesium iodide in ethanol (full circles) according to Refs. 4 and 7, respectively. The points denoted by squares at zero concentration were calculated from eqns. (2) and (8). Full squares, eqn. (2). Open square, eqn. (8). (The points at $c = 0$ according to these two equations coincide for the iodine exchange reaction.)

plotted (open circles) against the analytical concentration of lithium chloride. Under the experimental conditions [4] the concentration of lithium chloride ion-pairs greatly exceeds the concentration of unpaired chloride ions ($0.06 < \alpha < 0.17$). Nevertheless, the rate constants extrapolated to zero concentration by means of eqns. (2) and (8) agree within 1 %.

In comparison, a much shorter extrapolation is needed when association to ion-pairs is relatively unimportant as demonstrated by the rate constant *vs.* concentration curve in Fig. 1 (full circles) for the methyl iodide-cesium iodide exchange reaction in ethanol.[7] For this system the concentration of free ions is in great excess over the concentration of paired ions ($0.92 < \alpha < 0.99$). The points calculated at zero concentration by means of eqns. (2) and (8) coincide.

Acknowledgement. The authors thank the *Swedish Natural Science Research Council* for financial support.

REFERENCES

1. Evans, C. C. and Sugden, S. *J. Chem. Soc.* **1949** 270.
2. Bowers, S. D. and Sturtevant, J. M. *J. Am. Chem. Soc.* **77** (1955) 4903.
3. Lichtin, N. N. and Rao, K. N. *J. Am. Chem. Soc.* **83** (1961) 2417.
4. Beronius, P. *Acta Chem. Scand.* **23** (1969) 1175.
5. Beronius, P. and Pataki, L. *J. Am. Chem. Soc.* **92** (1970) 4518.
6. Beronius, P. and Pataki, L. *Acta Chem. Scand.* **25** (1971) 3705.
7. Beronius, P., Pataki, L., Nilsson, A.-M. and Wikander, G. *Radiochem. Radioanal. Lett.* **6** (1971) 333.
8. Holmgren, A., Nilsson, A.-M. and Beronius, P. *Radiochem. Radioanal. Lett.* **6** (1971) 339.
9. Holmgren, A. and Beronius, P. *Acta Chem. Scand.* **26** (1972) 3881.
10. Beronius, P., Nilsson, A.-M. and Wikander, G. *Acta Chem. Scand.* **24** (1970) 2826.
11. Beronius, P., Wikander, G. and Nilsson, A.-M. *Z. physik. Chem. (Frankfurt)* **70** (1970) 52.
12. Nilsson, A.-M. and Beronius, P. *Unpublished.*
13. Nilsson, A.-M. and Beronius, P. *Z. physik. Chem. (Frankfurt)* **79** (1972) 83.
14. Brookes, H. C., Hotz, M. C. B. and Spong, A. H. *J. Chem. Soc.* **A 1971** 2410.
15. Fuoss, R. M. and Onsager, L. *J. Phys. Chem.* **61** (1957) 668.
16. Fuoss, R. M. and Accascina, F. *Electrolytic Conductance*, Interscience, New York 1959.

Received September 14, 1972.

ACTA CHEMICA SCANDINAVICA 27 (1973) 677–704

Penicillin Transformations

II.* Properties and Structural Determinations of 2,2-Dimethyl-3(*S*)-methoxycarbonyl-6-acylamino-7-oxo-2,3,4,7-tetrahydro-1,4-thiazepines

ÖDÖN K. J. KOVACS, BERTIL EKSTRÖM and BERNDT SJÖBERG

Research and Development Laboratories, Astra Läkemedel AB, S-151 85 Södertälje, Sweden

In the epimerisation reaction of methyl 6β-phthalimidopenicillanate (I) to the 6α-isomer (II) in methylene chloride in the presence of triethylamine, an additional compound, the 2,2-dimethyl-3(*S*)-methoxycarbonyl-6-phthalimido-7-oxo-2,3,4,7-tetrahydro-1,4-thiazepine (III) was isolated. After transformation into its phenylacetyl derivative (VI) the non-identity of VI with the known 5-oxo-1,4-thiazepine derivative XI was shown in a parallel experiment. The structure of III was established by spectral data and degradation into the authentic 2,4-dinitrophenylhydrazones of methyl 2-oxoisovalerate (XXIII) and *O*-methyl (XVI) and *S*-benzyl 2-phthalimido-2-formylacetate (XXIVa), respectively.

III was also predominantly produced together with a small amount of the 6α-epimer (II) from I by the action of $POCl_3$ in benzene under conditions which were used in an early penicillin synthesis. It was possible to convert the 6α-epimer (II) into the 7-oxo-1,4-thiazepine derivative (III) under similar conditions as used with I. The interpretation of the formation of the 7-oxo-1,4-thiazepine derivative (III) and of the general mechanism of the epimerisation at C(6) of the penicillin structure is discussed.

The penicillin molecule is known to undergo a great number of degradation and rearrangement reactions. On the whole, the reactions appear to be initiated by an attack on the amide bond of the strained β-lactam ring which generally is considered to be the most reactive part of the molecule. Recently, however, reactions have been found which occur as a result of the special reactivity imparted to the molecule by the sulphur of the thiazolidine ring. In the penicillin structure several hydrogen atoms, at C(3), C(6) and in the dimethyl group, are situated in β-position with regard to the sulphur and may participate in β-elimination reactions leading to formation of an intermediate thiol structure. Such reactions generally require rather vigorous conditions,[1,2] but may proceed under relatively mild ones in the case of the penicillin mole-

* Part I, *Tetrahedron Letters* **1969** 1863.

cule owing to additional activation of the hydrogen atoms by the side chain, the carboxyl group or by the oxidised sulphur. Examples of such reactions are anhydropenicillin formation,[3] the rearrangement of penicillin sulphoxides into Δ^3-cephems [4] and Raney-nickel desulphurization.[5]

Some penicillin structures have been found to undergo facile C(6) epimerisation under basic conditions, and Wolfe *et al.*[6,7] have proposed a β-elimination mechanism for the epimerisation of methyl 6β-phthalimidopenicillanate involving the hydrogen at C(6). Recently we have found [8] that an additional compound is obtained in this reaction. The formation of this compound requires the occurrence of such a β-elimination. The purpose of this paper is to describe the structure and properties of this compound and to discuss its possible role in the epimerisation reaction.*

On preparing methyl 6α-phthalimidopenicillanate (II) according to Wolfe and Lee [6] by treatment of I with triethylamine in methylene chloride at room temperature, TLC showed the formation of an additional product (III), which could be isolated in a 25 % yield.[8] The same substance was also obtained in a lower yield (12 %) from the 6α-isomer (II) on prolonged treatment (10 days) under similar conditions.[8] Similarly III was produced in good yield (57 %) if the 6β-isomer (I) was treated with phosphorus oxychloride [9] under the conditions used by Sheehan and Cruickshank [10] in the total synthesis of the penicillin ring system from the racemic α-isomer of 4-methoxycarbonyl-5,5-dimethyl-α-phthalimidothiazolidine-2-acetic acid (XXVIIIb). From this reaction we have also isolated the 6α-isomer (yield 4.1 %), but no substance identical with the starting material (I) could be detected (over 1 %).**

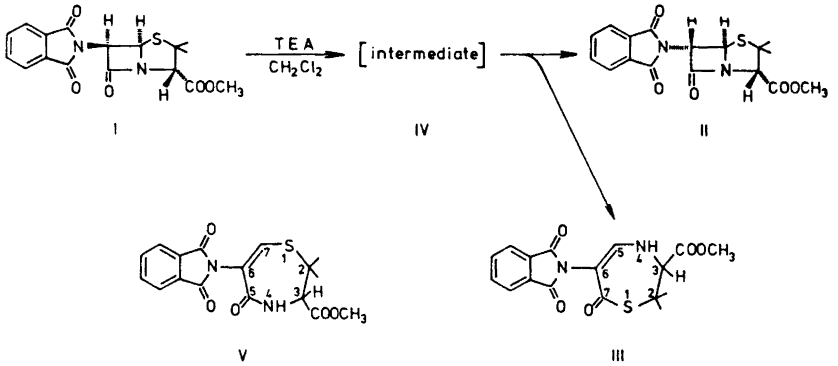

Scheme 1.

Elemental analysis and molecular weight determination of III showed it to be isomeric with I and II. Its UV and IR spectra were found to be strikingly similar to those reported by Sheehan and Cruickshank [10] for a compound (see

* Main results and conclusions were briefly reported at the 10th European Peptide Symposium.[9]

** The observation of Clayton *et al.*[11] that I is recovered unchanged after the treatment with phosphorus oxychloride has not been confirmed.[12]

Table 1. Physical and chemical properties of 7-oxo-1,4-thiazepine (III) and 5-oxo-1,4-thiazepine (V)[10] derivatives.

	III	V[10]
Formula	$C_{17}H_{16}N_2O_5S$	$C_{17}H_{16}N_2O_5S$
M.p.	217 – 218°C	237 – 237.5°C
$[\alpha]_D^{20}$	– 215° (*c* 0.5; CH_3OH)	–
UV_{CH_3OH} λ_{max}	304 mμ, ε = 11 800	304 mμ, ε = 12 000
	256 mμ, ε = 8 350	250 mμ, ε = 7 700
	238 mμ, ε = 13 000	238 mμ, ε = 13 000
	217 mμ, ε = 42 900	218 mμ, ε = 46 000
After desulphurization and acid hydrolysis	No alanine	–

Table 1) isolated as a by-product in a total synthesis of the penicillin ring system and assigned the structure of a 2,2-dimethyl-3-methoxycarbonyl-6-phthalimido-5-oxo-2,3,4,5-tetrahydro-1,4-thiazepine (V). In the IR spectrum of III the characteristic β-lactam absorption of the penicillins around 1770 cm^{-1} was missing but a broad absorption band with peaks at 1772, 1740, and 1710 cm^{-1} showed the presence of the phthaloyl and methyl ester group. It further contained a sharp band at 3440 cm^{-1}, indicating an NH-group and an absorption at 1652 cm^{-1} and a further one with double peaks at 1752 and 1550 cm^{-1} which Sheehan and Cruickshank had attributed to the vinyl sulphide and the amide bonds, respectively, in their 5-oxo-1,4-thiazepine structure. The NMR spectrum of III showed peaks corresponding to the phthaloyl, methyl ester, and the dimethyl groups in the expected position and contained in addition three multiplets coupling with each other. The appearance of the multiplets was, however, found to be solvent dependent. In deuterated dimethyl sulphoxide they consisted of two triplets each with an integral corresponding to one proton ($\tau = 5.44$ and 2.70 ppm) and a quartet ($\tau = 1.28$ ppm) with an integral corresponding to about one half of a proton. On addition of a drop of water to the test solution the triplets were converted into doublets ($\tau = 5.44$ ppm, $J = 6$ cps, $\tau = 2.70$ ppm, $J = 9$ cps) and the quartet, now with an integral corresponding to a full proton, could be recognised to consist of two doublets with $J = 6$ and 9 cps, respectively.* By spin-decoupling it was found that the two doublets coupled with the quartet, but not with each other. That the three protons were thus forming an AMX-system was further confirmed by taking a spectrum in deuterated dimethyl sulphoxide after addition of deuterium oxide, whereby the triplets collapsed into singlets corresponding to the central peaks and the quartet disappeared. In dimethylacetamide the pure AMX-system was obtained whereas triplets were found when spectrum was run in deuterated pyridine or acetone.

* In the spectrum originally published [8] the central peaks of the triplets were barely recognisable and were overlooked. The chemical shifts recorded were also slightly different from the ones now reported.

The coupling pattern found can be accommodated to the structure V only by assuming a long range coupling between the protons at N(4) and C(7). The NMR-spectrum of V has not been described, but in the spectrum of the corresponding phenylacetamido compound no such coupling is observed, the proton at C(7) appearing as a sharp singlet at $\tau = 2.34$ ppm [14] (Table 2). The spectrum instead suggested that our compound should have the 2,2-dimethyl-3-methoxycarbonyl-7-oxo-2,3,4,7-tetrahydro-1,4-thiazepine structure (III), the AMX-system being formed by the protons at C(3), C(5), and N(4), respectively. The observed solvent dependence of the spectrum could be explained by a partial dissociation of the proton at N(4). In agreement with this the compound III was found to be about as acidic as *m*-nitrophenol.

The other spectral data observed for the compound would appear to be in accordance with structure III. In IR the thiolester absorption, expected at 1660 – 1700 cm^{-1}, could be represented by a shoulder at 1680 cm^{-1} of the broad absorption band corresponding to the phthaloyl and the methyl ester; absorptions at 1630, 1570, and 1550 could be attributed to the double bond and the NH-group. The UV-spectrum would appear consistent with the chromophoric system of III as well as with that of V. Further evidence for the thiol ester group in III was obtained from the mass spectrum which contained two peaks at $m/e = 300$ (relative intensity 10 %) and 60 (relative intensity 35 %) indicating the loss of COS from the molecular ion. The mass of the first one could be estimated by high resolution mass spectrometry and was found to correspond well to that of the expected ion (found $m/e = 300.1121$; calc. for $C_{16}H_{16}N_2O_4^+$, $m/e = 300.1110$). Both ions were absent or of very low intensity in the spectra of I and II.

The spectral data obtained thus indicated that the structure of III was different from that of V. On the other hand III was found to react with the same readiness with sodium methoxide as has been reported for 2,2-dimethyl-3-methoxycarbonyl-6-phenylacetamido-5-oxo-2,3,4,5-tetrahydro-1,4-thiazepine (XI),[13] which contains the same ring structure as V. In both cases the optical activity of the compound is rapidly lost and the reaction product reacts with benzyl bromide to give a benzyl derivative, which in the case of XI was identified as the dehydrovalinate structure XIII. In order to verify that III contained a ring structure different from that of V and XI it was found necessary to prepare the phenylacetyl analogue (VI) of our compound in order to directly compare its properties with those reported for XI. Treatment of III with hydrazine hydrate in aqueous dioxane for three days at +4°C removed the phthaloyl group completely to give the corresponding derivative with a free amino group, which was not isolated but directly converted into the phenylacetyl derivative VI by treatment of the reaction mixture with phenylacetyl chloride. VI was found to have physical properties clearly differing from those reported for XI [13,14] proving that the two compounds were not identical (Table 2). In the NMR-spectrum of VI an AMX-coupling system was found corresponding to the one found for III indicating that the ring system of III had been preserved during the reactions. The compound (VI) was found to be hydrolyzed with sodium hydroxide in aqueous ethanol at about the same rate as XI (Fig. 1), and on treatment with methanolic sodium methoxide it lost its optical activity rapidly in the same manner as XI. Addition of

Table 2. Physical and chemical properties of the two 6-phenylacetamido thiazepine compounds (VI and XI [14]), the benzylthiocarbonyl derivative of VI (VIII), and the benzylthiovinyl derivative of XI (XIII).[13]

	7-Oxo VI	5-Oxo XI [14]	Benzylthiocarbonyl VIII	Benzylthiovinyl XIII [13]
Formula	$C_{17}H_{20}N_2O_4S$	$C_{17}H_{20}N_2O_4S$	$C_{24}H_{26}O_4N_2S$	$C_{24}H_{26}O_4N_2S$
M.p.	150–151°	142.8–143°	110–112°	154–155°
$[\alpha]_D$	−195° (20°, *c* 1, chloroform)	−135° (25°, *c* 3.5, chloroform)	–	–
UV λ_{max}	204 mμ, ε=14 500 258 mμ, ε= 6 400 315 mμ, ε= 9 600 (in MeOH)	235 mμ, ε=9 650 305 mμ, ε=5 250 (in EtOH)	–	299 mμ, ε=15 700 (in EtOH)
$IR_{(KBr)}$ ν_{max}	1710 1620	1745 1660	1670, 1655 1590, 1495	1662, 1635 1512, 1325
NMR τ	2.06d (*J*=8.5), 2.33–2.78, 5.40d (*J*=5.5), 6.14, 6.33, 8.37, 8.40 (in C_5D_5N)	2.34, 2.72, 2.86d (*J*=7) 5.82d (*J*=7) 6.21, 6.37, 8.48, 8.72 (in $CDCl_3$)	2.10, 2.66, 2.74, 2.80, 5.87, 6.23 6.32, 7.88, 8.10 (in $CDCl_3$)	1.85, 2.03, 2.73 6.02, 6.34, 6.41 7.89, 8.25 (in $CDCl_3$)
After desulphurization and acid hydrolysis	No alanine	Alanine	–	–

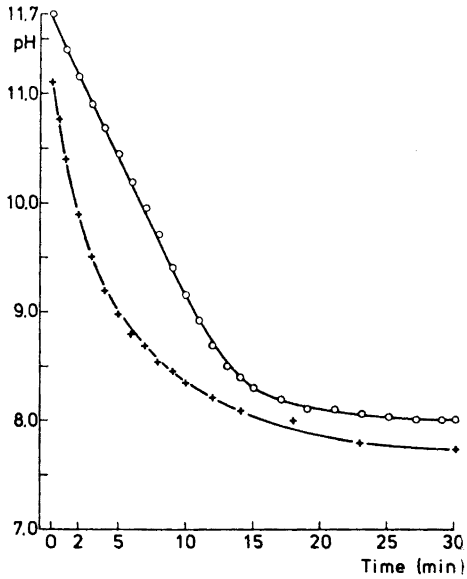

Fig. 1. Change of pH of reaction solution after treatment of 2,2-dimethyl-3(*S*)-methoxycarbonyl-6-phenylacetamido-7-oxo-2,3,4,7-tetrahydro-1,4-thiazepine (VI; O) with half-equivalent amount of NaOH. The values for 2,2-dimethyl-3(*S*)methoxycarbonyl-6-phenylacetamido-5-oxo-2,3,4,5,-tetrahydro-1,4-thiazepine (XI; +) were taken from Leonard and Ning.[13]

benzyl bromide to the reaction solution containing VII readily gave a benzyl derivative (VIII) with properties clearly differing from those reported for XIII [13] (Table 2). In the case of XI, the reaction with sodium methoxide has been found to be a β-elimination over the C(2) – C(3) bond, starting with removal of the proton at C(3) and leading to the formation of an enethiolate-dehydrovalinate structure XII, which has been isolated as its sodium salt. The facility of the elimination has been explained by the stability of the enethiolate moiety in XII.[13] In the structure VI the corresponding reaction would lead to a carbothiolate-dehydrovalinate structure VII in which the carbothiolate group would appear to be at least as stabilized as the enethiolate in XII allowing the elimination reaction to proceed as readily as in the case of XI. The reaction of the carbothiolate (VII) with benzyl bromide would then lead to a thiobenzyl ester (VIII). All spectral and other properties of the reaction product were also found to be in accordance with such a structure. Whereas the elimination reaction proceeds with the same readiness in the two ring systems the consecutive reactions of the carbothiolate and the enethiolate with alkylating agents would proceed with different rates depending on differences in nucleophilicity of the two anions. With benzyl bromide no difference was noted, but whereas XII has been found to react very rapidly with 2,4-dinitrochlorobenzene in ethanolic solution at room temperature, VII was found to be virtually unreactive under these conditions.

The 5-oxo-2,3,4,5-tetrahydro-1,4-thiazepine structure in XI is readily broken down into two amino acids, alanine and valine, by Raney-nickel desulphurisation followed by acidic hydrolysis.[14] However, under the same conditions III and VI do not give any alanine at all and only trace amounts of

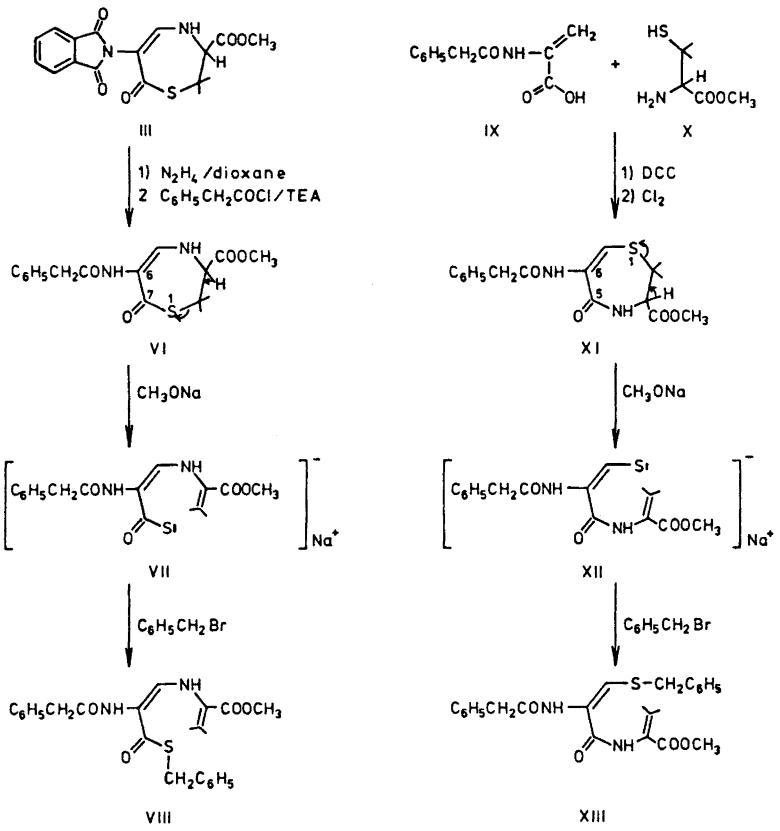

Scheme 2.

valine according to TLC in five different systems (Table 3). This is in good agreement with the 7-oxo-2,3,4,7-tetrahydro-1,4-thiazepine structure adopted for III and VI where the reductive desulphurisation step would be expected to remove the thiolester group and give an *N*-alkylated valine structure which on hydrolysis cannot form any alanine, and valine only with difficulty. In the IR spectrum of the product of the desulphurisation step, the absorption bands corresponding to the double bond (1630 cm^{-1}) and the thiolester group of III (shoulder at 1680 cm^{-1}) were absent.

Whereas the previous described reactions only give evidence that III cannot have the ring structure adopted by Sheehan and Cruickshank [10] for their compound, direct proof for the 7-oxo-2,3,4,7-tetrahydro-1,4-thiazepine ring was obtained in a study of the reactions and properties of the compounds originating from the methyl dehydrovalinate derivative formed in the reaction of III with sodium methoxide. The reactions and compounds are summarized in Scheme 3.

Table 3. TLC analysis of the degradation products of III and VI after desulphurization and hydrolysis.

Mobile phases	hR_F Values On Silica gel G			On Cellulose F	
	M	*K*	*J*	*N*	*K*
DL-Alanine	11	23	48	22	20
D-Valine	17	36	56	40	43
Main spot from III	15	18	14	43	28
Other spots from III	–	40*	55*	–	40*
Main spot from VI	14	18	13	42	28
Other spots from VI	61 34 19 16*	36* 27 8	65 55* 47 34	50 36*	42* 23

III was found to react in the same manner with sodium methoxide as the corresponding phenylacetamido derivative (VI). The elimination reaction proceeded very rapidly with complete loss of the optical activity of the reaction solution. The carbothiolate-dehydrovalinate compound (XIV) was not isolated but treated directly with two equiv. of hydrogen chloride in dry methanol at room tempreature for four days to give a mixture of the methyl ester XVII and the thiomethyl ester XVb. This is in accordance with the findings that carbothiolic acids on esterification with low molecular weight primary alcohols give mixtures of *O*- and *S*-alkyl esters, the former predominating. [15] Hydrolysis of the reaction product in 97.5 % methanol containing hydrogen chloride and 2,4-dinitrophenylhydrazine gave a mixture of three 2,4-dinitrophenylhydrazones, two of which, XVI and XXIII, could be isolated in pure form by chromatography on a silica gel column, the third one probably being the thiomethyl compound XXIVb. By comparison with authentic samples prepared according to the literature, XVI and XXIII were identified as the 2,4-dinitrophenylhydrazones of methyl 2-phthalimido-2-formylacetate [16] and methyl 2-oxoisovalerate, respectively.[17] This showed that the bis-enamine structure in XVII could be hydrolysed with release of the two oxo derivatives forming it.

The ambiguity of the esterification reaction could be avoided by going *via* the thiobenzyl ester (XVa) prepared by reaction of III with sodium methoxide in dry methanol followed by benzyl bromide. The compound was found to exist in at least two isomeric forms (see below), but after recrystallization from 75 % dioxane containing hydrogen chloride it was obtained as a homogeneous compound with analytical and spectral data in accordance with the adopted structure (XVa). The presence of an NH group was shown by a medium absorption at 3320 cm^{-1} in the IR spectrum and in the NMR spectrum (in deuteriochloroform) by a doublet at $\tau = -0.12$ ppm coupling with the adjacent vinylic proton ($\tau = 3.24$ ppm). The isopropylidene group was indicated by two singlets at $\tau = 7.98$ and 7.87 ppm. Hydrolysis of XVa in 97.5 % methanol containing hydrogen chloride and 2,4-dinitrophenylhydrazine for two days at room temperature gave a high yield of two 2,4-dinitrophenylhydrazones, which

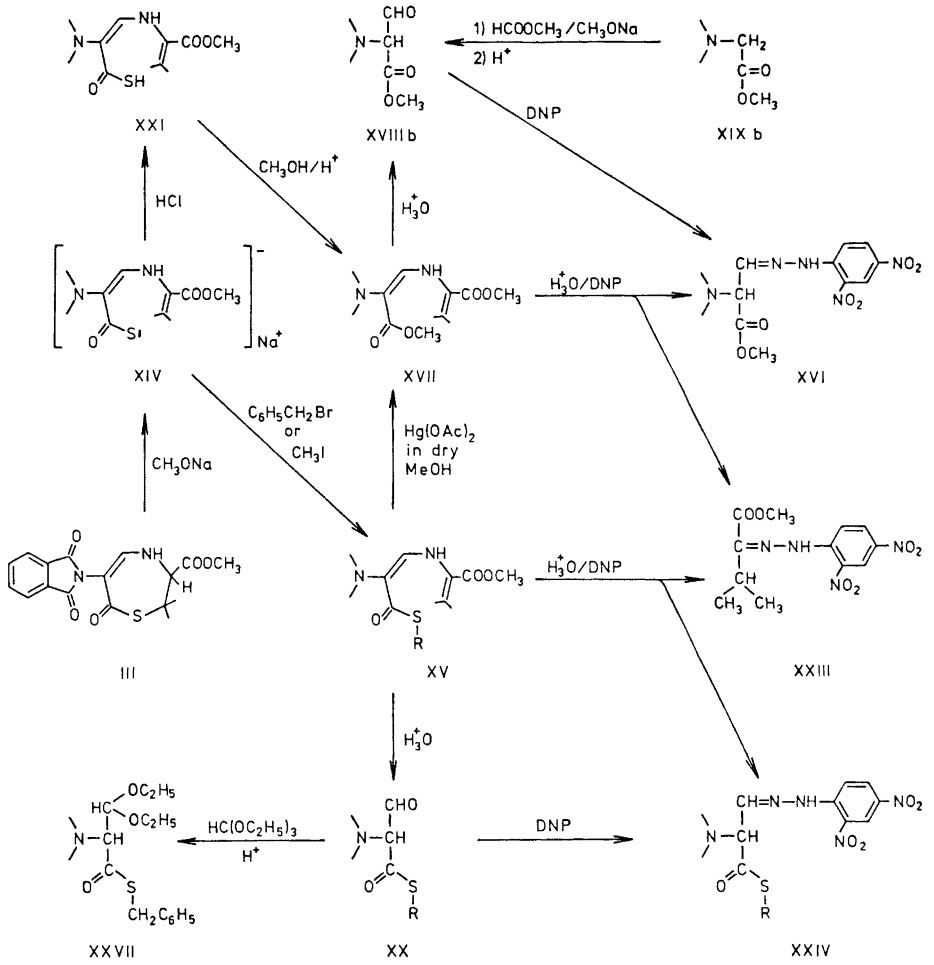

Scheme 3.

were separated and isolated by chromatography on a silica gel column. One was identical to XXIII whereas analytical and spectral data of the other one suggested that it was the 2,4-dinitrophenylhydrazone of *S*-benzyl-2-phthalimido-2-formylthioacetate (XXIVa). This was verified by preparing the compound in an independent way (Scheme 4) starting from *O*-benzyl 2-phthalimido-2-formylacetate (XVIII).[18] The latter was converted into its diethyl acetal

(XXV) and hydrogenated to give the free acid XXVI, which *via* the acid chloride or the mixed anhydride gave the thiobenzyl ester which then on hydrolysis in 97.5 % methanol containing hydrogen chloride and 2,4-dinitrophenylhydrazine gave a 2,4-dinitrophenylhydrazone in all respects identical to the compound originating from the thiazepine (III).

The methylthiocarbonyl derivative (XVb) was obtained by treatment of XIV with methyl iodide under conditions analogous to those used for the preparation of the benzyl thiocarbonyl derivative (XVa). The NMR spectrum showed that it was a mixture of two forms (see below) but on hydrolysis in the presence of 2,4-dinitrophenylhydrazine it was converted in good yield into the two 2,4-dinitrophenylhydrazones XXIII and XXIVb. If the hydrolysis of XVa was carried out in the absence of 2,4-dinitrophenylhydrazine the *S*-benzyl 2-phthalimido-2-formylthioacetate (XXa) was formed. The latter could not be isolated in crystalline form but was directly converted by treatment with 2,4-dinitrophenylhydrazine into XXIVa identical to the compound previously obtained, and into its diethyl acetal (XXVII), which also was obtained from XVIIIa [18] (Scheme 4).

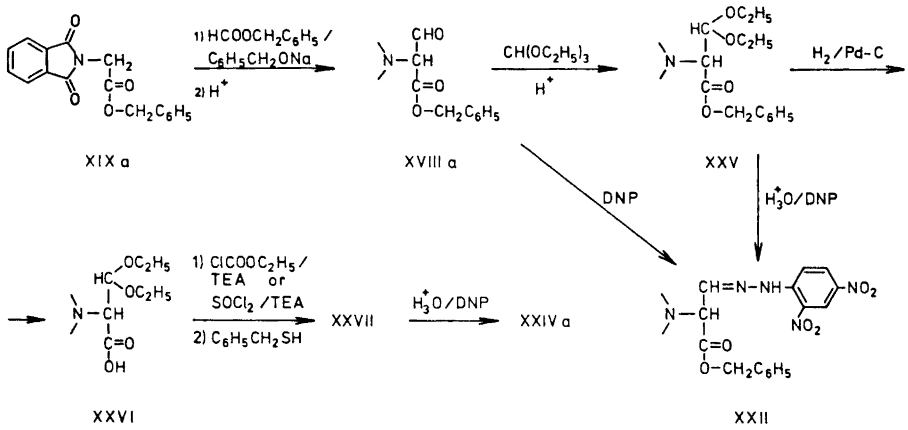

Scheme 4.

Esters of thiolcarboxylic acids are readily desulphurised by treatment with mercury salts. [19] When XVa was treated at room temperature with an equivalent amount of mercuric acetate in dry methanol it was converted in good yield into methyl *N*-(2′-phthalimido-2′-methoxycarbonyl)vinyl-2,3-dehydrovalinate (XVII) under concomitant formation of benzylthiomercuric acetate. XVII showed spectral properties similar to those of XVa with, *e.g.*, the same AX-system in the NMR spectrum, and chromatographic properties identical to those previously found for the product obtained by esterification of the carbothiolic acid XXI, but not isolated. Upon acid hydrolysis of compound XVII, methyl 2-phthalimido-2-formyl acetate (XVIIIb) was formed, identical in every respect to an authentic sample prepared from methyl

phthalimidoacetate (XIXb).[18] XVIIIb gave the 2,4-dinitrophenylhydrazone XVI identical to the product previously isolated in the preliminary hydrolysis experiment done with XVII in the presence of 2,4-dinitrophenylhydrazine.

The reactions of Scheme 3 thus show that the carbon atoms in III are arranged in one methyl isovalerate and one α-phthalimidoacrylate structure, which are linked to each other both through a thiolester bond and through an amino group in an enamine structure as required by the structure adopted for III. That III also can be obtained by treatment of I with phosphorus oxychloride, the cyclizing reagent used by Sheehan and Cruikcshank [10] in their penicillin synthesis, suggests that the by-product they regarded as a 5-oxo-1,4-thiazepine (V) rather should have the 7-oxo-1,4-thiazepine structure (III). That this really is so was recently verified by Clayton *et al.*[11] in the repetition of the original experiment. Furthermore, as the methyl 6α-phthalimidopenicillanate (II) is formed and the 6β-isomer (I) is completely consumed when the latter is treated with phosphorus oxychloride under the conditions used by Sheehan and Cruickshank, it is possible that the penicillin compound they isolated actually had the 6α-structure.[9]

Very recently further examples of the formation of 7-oxo-1,4-thiazepine derivatives have been published.[11,20–22]

The double bond system of the methyl *N*-[(2′-phthalimido-2′-carbonyl)-vinyl]-2,3-dehydrovalinate structures XV and XVII may exist in isomeric forms. Although the products obtained gave analytical figures in excellent agreement with the adopted structures, they gave two spots on TLC on inactive, buffered (pH 6.6) plates. By column chromatography or by recrystallization in the presence of hydrogen chloride it was possible in the case of XVa and XVb to isolate the main components which according to spectral data had a bis-enamine structure as shown in Scheme 5.* If the homogeneous com-

XVa XVa^{i}

Scheme 5.

pounds were chromatographed on active, unbuffered silica gel plates they appeared, however, as the same mixtures of two well separated components (Table 4) previously obtained. The phenomenon was studied more closely in the case of the thiobenzyl compound (XVa). The reaction solution obtained after treatment of III with sodium methoxide followed by benzyl bromide was investigated by TLC on buffered (pH 6.6) plates and found to contain in addition to XVa a second compound, XVa^{i}, present in a larger amount than

* In the formulae of XV and its analogues (VII, XIV, XVII, and XIII, resp.) only one of the possible geometrical isomers is given.

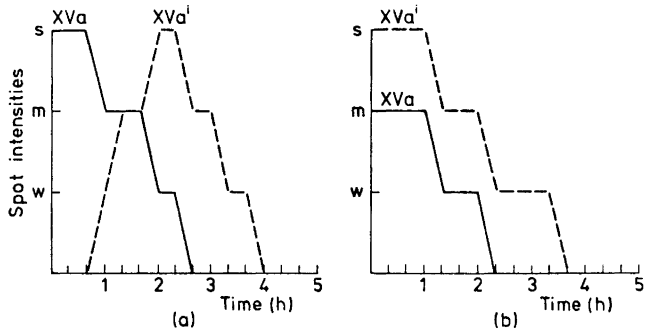

Fig. 2. Change of TLC* spot intensities on acidic hydrolysis of (a) pure XVa and (b) a mixture of XVa and XVa^i, resp.

the former. However, evaporation of the solution caused a change in the relative amounts of the two compounds so that XVa was now the main product in the residue. If, however, the reaction solution was *not* evaporated but treated with methylene chloride, washed with water and dried, the ratio of the amounts of the two compounds was preserved and they could be separated by chromatography on a silica gel column. XVa^i was found to be stable in solution at +5°C for several days, but all operations at +20°C led to partial conversion into XVa and to formation of decomposition products. That the two compounds were interconvertible and thus were isomers could be demonstrated by thin layer chromatography in several experiments and the transformation was found to be catalyzed by the active silica gel surface of the chromatographic plates and by sodium methoxide. Some information about the structure of XVa could be gained from the IR and NMR spectra taken on solutions of the compound in chloroform and deuteriochloroform, respectively, prepared from the chromatographic eluates by exchange of solvents at low temperature. It appeared from the NMR spectrum that the isopropylidene group of XVa ($\tau = 7.98$ and 7.89 ppm) was present in XVa^i too ($t = 8.02$ and 7.88 ppm) and that instead the acrylate part of the molecule had been changed, as the doublets ($J = 13$ cps) corresponding to the vinylic proton ($t = 3.24$ ppm) and the amino proton ($\tau = 0.12$ ppm) of XVa were missing. In the IR spectrum of XVa the band at 1650 cm^{-1}, probably corresponding to the unsaturated benzyl carbothiolate moiety, had disappeared. Acidic hydrolysis of XVa appears to proceed through XVa^i as shown by a comparison of the relative intensities of the TLC spots given by XVa and XVa^i during the hydrolysis (Fig. 2). We tentatively suggest XVa^i to have the methyl *N*-(2′-phthalimido-2′-benzylthiocarbonyl)ethylidene-2,3-dehydrovalinate structure.

Methyl 6α-phthalimidopenicillanate (II), on treatment with triethylamine under conditions identical to those employed with I, was also found to give III, although at a considerably slower rate and to a lesser extent. In this reaction compound I could not be detected. Treatment of III in a similar way gave neither I nor II. This suggests, however, that the two reactions, the epimerisation and the thiazepine formation, should have a common inter-

Table 4. hR_F values of methyl *N*-[(2′-phthalimido-2′-carbonyl)vinyl]-2,3-dehydrovalinate derivatives on pre-coated unbuffered and inactive buffered plates.[a]

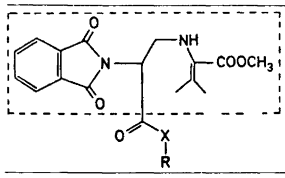 = DV		Solvent systems	Silica gel plates F_{254} pre-coated (Merck)	Silica gel plates $HF_{254+266}$ (Merck) 0.5 mm, made with McIlvaine's pH 6.6 buffer solution
DV–C(=O)–S–CH_2–C_6H_5	XVa	*E*	43 and 23	51
		N	37 and 11	30
DV–C(=O)–S–CH_3	XVb	*E*	40 and 21	44
		N	33 and 10	24
DV–C(=O)–O–CH_3	XVII	*E*	36 and 16	40
		N	30 and 6	15

[a] Plates were stored for 2 h after applying sample at room temperature and atmosphere, then developed.

mediate which is also supported by an analysis of the thermodynamics of the reaction.[7] The considerable difference in the specific rotation of I ($[\alpha]_D^{20}$ +280°) and its rearrangement product II ($[\alpha]_D^{20}$ +207°) and III ($[\alpha]_D^{20}$ −129.5°) provides a means of following the reaction in methylene chloride at 20° with varying ratios of I to triethylamine (Fig. 3). It can be seen that in all reactions, the rotations tend to reach the same end value suggesting that the product composition from the reaction is largely independent of the concentration of the base. On the other hand, it is evident that although triethylamine only acts as a catalyst, the rate of the reaction increases with increasing base concentration (Fig. 3), indicating that the reaction involves the formation of a complex between the penicillin ester and the base, the formation or decomposition of which is rate-determining. Furthermore Wolfe and Lee [6] have shown that when the reaction is carried out in the presence of *t*-BuOD, no deuterium is incorporated into the epi-compound II. In our view the experimental facts are best accommodated in a reaction mechanism according to Scheme 6 involving the formation of an intimate ion-pair between I and triethylamine (IV-A) which subsequently undergoes rearrangements leading to the epi-ester and the thiazepine.

The thiazepine (III) can arise only by internal acylation of the thiazolidine sulphur by the β-lactam carbonyl and this reaction can occur only after the C(5)–S bond has been broken. The formation of III is thus good evidence for

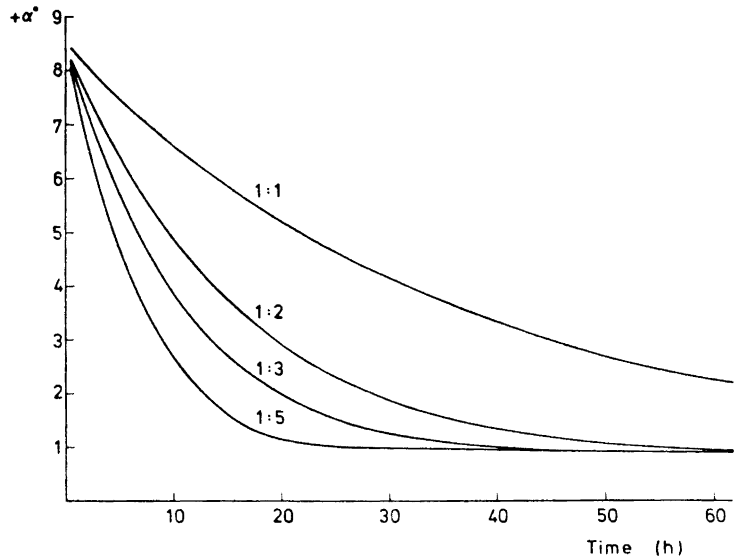

Fig. 3. Change of optical rotation (α) on treatment of methyl 6β-phthalimidopenicillanate (I) with different amounts of triethylamine in methylene chloride. (I: TEA ratios = 1:1, 1:2, 1:3 and 1:5.)

the existence of the ene-thiolate structure (IV-C) as a secondary intermediate, which would be obtained from IV-A in a β-elimination reaction, more particularly in accordance with an (E1cB)ip reaction.[23–26]

For the epimerisation several mechanistic pathways appear possible. One goes *via* the enolized structure (IV-D) which would be obtained from IV-A in a "conducted tour" mechanism where the negative and positive charges are not separated but displaced together. This type of mechanism, which also could apply to the ene-thiolate (IV-C) path, has been proposed for other isomerization reactions [27] and very recently Mayers and Kovacs suggested it for the racemization of protected cysteine esters in non-polar solvents.[28] A trialkylsilyl derivative of IV-D has been suggested as an intermediate in the epimerisation of esters of phenoxymethyl penicillin-(*S*)-sulphoxide by treatment with *N*,*O*-bis(trimethylsilyl)acetamide (BSA).[29] Very recently Vlietinck *et al.*[22] were further able to convert phenoxymethylpenicillin benzylester, which had been silylated with BSA into a 1:1 mixture of the 6α-isomer and the corresponding 7-oxo-1,4-thiazepine derivative under conditions similar to those used by Wolfe and Lee.[6] The mechanistic explanation of this experiment would be in good agreement with Scheme 6. In the epimerisation reaction IV-C and IV-D could be converted into the ion-pair IV-B where the carbanion has a C(6)-configuration opposite to that found in the penicillins and in IV-A. This configuration would be thermodynamically favoured depending on relief of the steric compression between the 6(β)-side chain and the C(2) geminal dimethyl group in the penicillin structure.[30,31] This relief of

compression may, however, also be the driving force for the third possible pathway of the epimerisation, the direct transformation of IV-A into IV-B. The carbanions of the two ion-pairs probably having pyramidal configurations with sp^3-character should well be capable of undergoing inversion.[27] The rapid and quantitative transformation of methoxymethyl 6-*p*-nitrobenzylidenimino-penicillinate into the corresponding 7-oxo-1,4-thiazepine derivative without formation of the 6α-epimer [20] shows the important role of the 6β-substituent in the establishment of the equilibrium between the intermediates; *i.e.* the azomethine linkage promotes the ene-thiolate structure (IV-C) through conjugation.

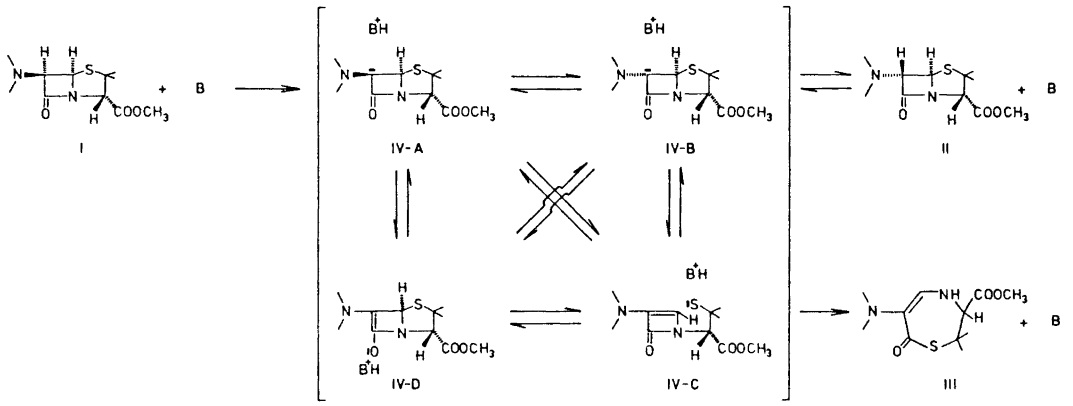

Scheme 6.

The experimental data so far available for the reaction do not allow any distinction between the various mechanistic possibilities.[32] From other closely related reactions some facts may, however, be gained which seem to disfavour the ene-thiolate as a dominating intermediate in the epimerisation. It has thus been found that an isolated β-lactam structure, *cis*-1,2-diphenyl-3-phthalimido-azetidinone, where a β-elimination reaction mechanism would appear to be excluded, is irreversibly converted into the *trans*-isomer when treated under conditions similar to those used in the present case.[33] Further, it has been shown by means of deuteration experiments that in the presence of aqueous base, simple de- and reprotonation of an intermediate carbanion explains the experimental results without any need for assuming a β-elimination step.[30,34] For this and other epimerisation reactions where bases stronger than triethylamine (OH^-, NaH, $NaNH_2$, Bu^tO^-) are used, an analogous mechanism may apply, involving not ion-pairs but solvated carbanions, which in principle could undergo the same rearrangements as the ion-pairs in Scheme 6. However, thiazepines (III) are not obtained in these reactions, indicating that structures corresponding to IV-C resulting from β-eliminations are not formed and thus that they are not necessarily intermediates in the epimerisation reaction under basic conditions.

More recently Ramsay and Stoodley have also proposed on very good experimental grounds the E1cB mechanism for the epimerisation reaction *via* an "anionic" intermediate.[21] It was postulated that the conversion of this intermediate into the ene-thiolate (IV-C) is the rate determining step of the 7-oxo-1,4-thiazepine formation, but that the ion-pairs (IV-A and IV-B, resp.) are more appropriate models for the epimerisation itself in the presence of weak bases. In apparent contrast to the results of Wolfe *et al.*[7] they found that the epimerisation of I with 1-methylpiperidine in CD_3SOCD_3 containing 5 % D_2O proceeded with deuterium exchange in the 6-position. This fact strongly supports the E1cB mechanism in that particular case, but in a solvent with less ionizing power like the dichloromethane used by Wolfe and Lee and by us the (E1cB)ip mechanism would still seem to be preferable.

A mechanism similar to that discussed above can account for the I→II + III transformation catalyzed by phosphorus oxychloride. In this case a bipolar complex ($POCl_2^+ \rightleftharpoons POCl_4^-$) originating from auto-ionization of the oxyhalide [35] may function as an acceptor of the proton at C(6) and at the same time make the sulphur involved in the β-elimination more electron attracting. This could explain the predominant formation of III (57.3 %) over II (4.1 %) in our experiment. The reactions catalyzed by antimony pentachloride can be interpreted in a similar way. However, other mechanisms are possible and for the latter reactions an attack of the inorganic halide on the amide bond of the β-lactam ring has been suggested [11] to form an acid chloride which could give III by acylation of the thiazolidine sulphur.

EXPERIMENTAL

All melting points were determined on a melting point apparatus according to Tottoli (W. Büchi Glasapparatefabrik, Flawil, Switzerland) and are uncorrected. All evaporations were carried out using a rotary evaporator at a pressure of 10 – 12 mm and a bath temperature of 24° except where stated otherwise. The symbol "→←" represents a two-component solvent system, the composition of which changes in the direction of the arrow during the recrystallisation (continuous addition of the second solvent and slow simultaneous distillation in a rotary evaporator at 24° and 10 – 100 mm pressure). Whatman Phase Separating Paper No. 1 PS was used for predrying of organic extracts.

Mobile phases used in thin layer and column chromatography:

A = benzene-acetone (9:1)
B = chloroform-benzene (1:1)
C = chloroform-benzene (7:3)
D = chloroform containing 0.7 % ethanol
E = isopropyl ether-chloroform (7:3)
F = acetone-carbon tetrachloride-ethanol (5:4:1)
G = butanone-acetic acid-water (8.5:0.5:1)
H = chloroform-benzene-acetone (6:2:2)
I = carbon tetrachloride-isopropyl ether-acetone (5:4.5:0.5)
J = 96 % ethanol-water (7:3)
K = butanol-acetic acid-water (4:1:1)
M = chloroform-methanol-17 % ammonium hydroxide (2:1:1)
N = butanol-acetone-diethylamine-water (10:10:2:5)

Analytical thin layer chromatography was carried out on Silica Gel_{254} F precoated TLC plates (Merck) except where stated otherwise. The symbol "TLC*" represents analysis on self-prepared 0.5 mm Silica Gel $HF_{254+366}$ (Merck) plates on glass with

McIlvaine's pH 6.6 buffer solution. Detection was made under UV light except where stated otherwise. The intensity of the spots are noted as strong (s), medium (m), weak (w), or very weak (vw); this symbol supplemented with a formula-number, if the spot was identified by running standard compounds along with it. hR_F values [36] of non-identical standards are mentioned *after* the data for the investigated samples. For column chromatography Silica Gel 0.05 – 0.2 mm (Merck) was used and packed by the suspension technique in dry benzene except where stated otherwise. "Two component" gradient elutions were achieved by the concave mixing of the first solvent (usually benzene) with the second solvent or with a solvent mixture. Subsequently there are also noted the total volume of the gradient period and the fraction volume. The fractions collected were checked by TLC.

The infrared spectra were recorded on a Unicam SP 200 or a Perkin-Elmer Model 21 recording spectrophotometer with potassium bromide discs or with solutions and the positions of the absorption maxima are expressed in wave numbers (cm^{-1}). The UV absorption spectra were recorded on a Unicam SP 800 recording and a Carl Zeiss PMQII spectrophotometer, respectively, and the positions of the absorption maxima or shoulder are expressed in nanometers (nm) followed by the corresponding extinction coefficient. The NMR spectra were recorded on a Varian A-60A spectrometer equipped with a V-6040 variable temperature controller and a spin decoupler Model V-6058A. The chemical shifts are given in τ-units using TMS or DDS as internal standards. Mass spectra recorded on an LKB 9000 instrument were obtained from the Mass Spectrometry Laboratory, Karolinska Institutet, Stockholm, Sweden. The most abundant ions are tabulated, followed by the relative abundance in per cent of the base peak. The specific rotations were measured on a Perkin-Elmer polarimeter 141 at 589 nm and the changes of the $[\alpha]_D$ values in the time were recorded with a coupled Servogor RE511 compensation recorder. The elemental analyses were performed by Alfred Bernhardt Microanalytical Laboratory, Elbach, Germany.

Methyl 6β-phthalimidopenicillanate (I). The compound was prepared according to Sheehan and Henery-Logan,[18] m.p. 174 – 175°, $[\alpha]_D^{20}$ +288.5° (*c* 2, chloroform), +275.3° (*c* 2, acetone), +279.7° (*c* 2, methylene chloride); (lit.[6] $[\alpha]_D$ +279°, chloroform; lit.[18] $[\alpha]_D^{23}$ +288°, butyl acetate).

IR (KBr): strong broad absorption band with peaks at 1784, 1764, 1736, 1718. NMR ($CDCl_3$): 8.49, 8.16 (2 s, 2 × 3H, $C(CH_3)_2$), 6.17 (s 3H, $COOCH_3$), 5.30 (s, 1H, CH), 4.38, 4.27 (2 d, $J = 4$, 2H, CH – CH), 2.15 (m 4H, phthaloyl). MS: 187 (18), 174 (35), 132 (98), 114 (24), 104 (100), 99 (20), 76 (50), 59 (22). Molecular ion: 360.

Treatment of methyl 6β-phthalimidopenicillanate (I) with triethylamine in dichloromethane.[6] *Isolation of methyl 6α-phthalimidopenicillanate (II) and 2,2-dimethyl-3(S)-methoxycarbonyl-6-phthalimido-7-oxo-2,3,4,7-tetrahydro-1,4-thiazepine (III).* Methyl 6β-phthalimidopenicillanate (36.04 g, 0.1 mol) was treated in dry methylene chloride (720 ml) with dry triethylamine (30.3 g, 0.3 mol) for 12 h at 20°. The yellow solution obtained was evaporated *in vacuo* (20°) to a volume of about 200 ml, dry benzene (200 ml) was added and the mixture evaporated to dryness. Repeated evaporation with several portions of benzene afforded a yellow foamy residue which was dissolved in acetone (720 ml), treated with charcoal in the cold (1 h), filtered and concentrated *in vacuo* with continuous addition of methanol to give a crystalline precipitate which was filtered and washed with cold methanol. The white product (25.22 g, 71.1 %), m.p. 161 – 167°, showed two spots on TLC (in system *H*): hR_F 52 (II) and 22 (III). Careful washing with cold methylene chloride (2 × 50 ml) gave a residue (10.1 g, 27.7 %; m.p. 217 – 218°) which after recrystallization from acetone → methanol yielded the pure 2,2-dimethyl-3(*S*)-methoxycarbonyl-6-phthalimido-7-oxo-2,3,4,7-tetrahydro-1,4-thiazepine (III) (8.9 g, 24.7 %; m.p. 218 – 219°). Analytical samples were obtained by recrystallization from methanol or from dry acetone-ether,[10] m.p. 220 – 221°, $[\alpha]_D^{20}$ −217.4° (*c* 0.5, methanol); $[\alpha]_D^{20}$ −198.9° (*c* 2, acetone); $[\alpha]_D^{20}$ −201.8° (*c* 2, pyridine); $[\alpha]_D^{20}$ −129.5° (*c* 0.2, methylene chloride). The compound dissolved in pyridine was titrated potentiometrically with tetrabutylammonium hydroxide using a Radiometer R titrigraph SBR 2d connected through a TTT11 automatic titrator.

UV (methanol): 304(11 800), 256(8 350), 238(13 000), 218(42 900). IR (KBr): 3440m, 1780m, 1740s, 1710s, 1680sh, 1630s, 1570s, 1550s. *NMR* $(CD_3)_2SO$: 8.36, 3.82 (2 s, 2 × 3 H, $C(CH_3)_2$), 6.20 (s 3H, $COOCH_3$), 5.42 (d, $J = 6.14$, CH), 2.68 (d, $J = 9$, 1H, CH), 2.03 (s, 4H, phthaloyl), 1.32 (2 d, $J = 6$ and 9, 1H, NH). MS: 360 (20, molecular ion),

332 (17), 187 (37), 174 (100), 160 (17), 140 (40), 132 (20), 114 (22), 112 (22), 104 (41), 76 (28), 60 (32). (Found: C 56.83; H 4.47; N 7.92; O 22.42; S 8.81. Equiv. weight: 354. Calc. for $C_{17}H_{16}N_2O_5S$ (360.41): C 56.65; H 4.47; N 7.77; O 22.20; S 8.90.)

The filtrate, obtained on washing the mixture of the two isomers with methylene chloride, contained the 6α-ester (II) and a little of the thiazepine compound (III) according to TLC analysis (in *H*). After evaporation of the solvent (15.8 g, 43.8 %) and subsequent recrystallization of the residue from methylene chloride →← methanol, pure methyl 6α-phthalimidopenicillanate (II; 14.1 g, 39.2 %) was obtained, m.p. 182 – 183° (lit.[6] 183°), $[\alpha]_D^{20}$ + 211.2° (*c* 2, chloroform), + 207.6° (*c* 2, acetone), + 207.4° (*c* 2, methylene chloride); (lit.[6] $[\alpha]_D^{20}$ + 228°, chloroform).

IR (KBr): strong absorption band with peaks at 1760, 1735, 1720. NMR ($CDCl_3$): 8.50, 8.32 (2 s, 2 × 3H, $C(CH_3)_2$), 6.18 (s, 3H, $COOCH_3$), 5.33 (s, 1H, CH), 4.50, 4.39 (2 d, $J = 2$, CH – CH), 2.14 (m, 4H, phthaloyl). MS: 246 (17), 187 (70), 174 (100), 172 (17), 161 (16), 160 (28), 132 (95), 114 (53), 104 (90), 99 (33), 87 (22), 76 (50), 75 (33), 53 (17), 50 (17), 46 (18), 41 (15), 28 (31). Molecular ion: 360.

In a repeated experiment with the same concentrations of I and triethylamine as above and carried out at 20 ± 0.1° the isomerization was followed by semiquantitative TLC analysis. Aliquot samples (0.1 ml) were taken every 30 min, diluted with isopropyl ether (15 ml) and washed with 0.025 N hydrogen chloride (2 ml) and water (2 × 2 ml). The organic phase was filtered and evaporated to dryness. The residue was dissolved in methylene chloride (1 ml) and samples (5 μl ~ 25 μg) were applied to 20 × 20 cm silica gel plates together with standards of II or III in increasing amounts. The standards were applied in between the test spots on a line 1 cm below (III) or above (II) the start line. For detection, the plates were sprayed with concentrated ammonia, stored over this reagent in a chamber for 2 h, dried, exposed to iodine vapor for 10 min and finally sprayed with aqueous starch-potassium iodide solution (1 %).[37] In mobile phase *H* (III as standard): hR_F 52 (I + II) and 21 (III), and in *I* (II as standard) after 4 consecutive developments: hR_F 52 (I), 47.0 (II) and 2 (III) were recorded.

The 6β-ester (I; sensitivity 2μg) could not be detected after 9 h, whereas the 6α-ester (II; sensitivity 2 μg) began to appear after 3.5 h and the thiazepine compound (III; sensitivity 0.6 μg) after 1 h. After 10 h further products could be detected. TLC analysis after 12 h: hR_F 38 (w) and 0 (w); after 36 h: hR_F 44 (w), 38 (w) and 0 (s); after 96 h: hR_F 44 (s), 38 (w) and 0 (s).

The isomerization of I was also followed polarimetrically at 20° ± 0.1° varying the ratio I:triethylamine from 1:1 to 1:2, 1:3, and 1:5, respectively (Fig. 3).

Treatment of methyl 6α-phthalimidopenicillanate (II) with triethylamine in methylene chloride. Isolation of 2,2-dimethyl-3(S)-methoxycarbonyl-6-phthalimido-7-oxo-2,3,4,7-tetrahydro-1,4-thiazepine (III). Methyl 6α-phthalimidopenicillanate (3.6 g, 0.01 mol, recrystallized three times from methylene chloride →← methanol) was treated with dry triethylamine (3.03 g, 0.03 mol) in dry methylene chloride (72 ml) at 20° for 240 h. After 19 h the thiazepine compound (III) was detectable on TLC (in *H*): samples (1 μl ~ 50μg) were applied directly from the reaction mixture: hR_F 53 (II) and 22 (III). Semiquantitative TLC analysis using a two-dimensional technique (first direction in *H*; second direction in *I* (twice); standard solutions were applied *after* development in *H*) showed the following conversions into III (%/h): 1.2/24; 2.5/48; 4/72; 7/120; 10/168; 14/240. Formation of the 6β-ester (I) could not be demonstrated by TLC. During the 10 days the $[\alpha]_D^{20}$ value of the reaction mixture changed from + 212° to + 131.6°.

Working up as described for the isomerization of I gave an acetone-insoluble white crystalline material (660 mg), m.p. 172 – 175°, after recrystallization from ethanol-ether, 184 – 186°. On the basis of m.p. and microanalytical data, the substance is most probably identical to chloromethyltriethylammonium chloride.[38] (Found: C 45.35; H 9.42; N 7.88; Cl 37.57. Calc. for $C_7H_{17}NCl_2$ (186.14): C 45.17; H 9.21; N 7.53; Cl 38.09.) IR (KBr): 3000m, 2640m, 2500w, 1630w, 1475 m.

The acetone solution was evaporated with continuous addition of methanol, finally reduced to a small volume, filtered and washed with cold methanol to give 2.25 g (68.3 %) of unchanged starting material (II), m.p. 182 – 183°, $[\alpha]_D^{20}$ + 210.8° (*c* 2, chloroform), containing a small amount of III (< 0.5 % according to TLC in *H*). The mother liquor contained five substances readily detectable by TLC (in *H*): hR_F 63 (w), 54 (m, II), 48 (m), 24 (s, III) and 0 (m). The last compound was identical to the acetone insoluble substance above according to TLC (in *G*, hR_F 7). The mother liquor was evaporated,

dissolved in mobile phase *H* (5 ml) and chromatographed on a silica gel column (40 g; gradient elution: benzene → mobile phase *H*; 400/10 ml). Fractions 29 – 35 contained the thiazepine compound (III; 430 mg, 11.9 %) after recrystallization (acetone →– methanol, 190 mg), m.p. 218 – 219°, identical to authentic III by mixed m.p. and IR.

Attempted isomerisation of the thiazepine compound (III) with triethylamine in methylene chloride. 2,2-Dimethyl-3(*S*)-methoxycarbonyl-6-phthalimido-7-oxo-2,3,4,7-tetrahydro-1,4-thiazepine (III, 90 mg, 0.25 mmol) was stirred in dry methylene chloride (1.75 ml) containing dry triethylamine (0.075 g, 0.75 mmol) at 20° for 360 h. The reaction mixture which became clear after 48 h was checked periodically by TLC (two-dimensional, first direction: mobile phase *A*; second direction: mobile phase *I*; standard solutions of III were applied at the start and of I, II, and phthalimide *after* development in *H*). Two products were detected after 2 days and five products after 15 days, none being identical with I, II, or with phthalimide. About 40 % of the starting material remained unchanged. The reaction mixture was evaporated, freed of triethylamine by several evaporations with benzene and drying *in vacuo*; the residue on PC (in butanol – ethanol – water (4:1:5) to layer) with microbiological development [39] showed no antibiotic activity.

Treatment of methyl 6β-phthalimidopenicillanate (I) with phosphorus oxychloride in dry benzene. Isolation of methyl 6α-phthalimidopenicillanate (II) and 2,2-dimethyl-3(S)-methoxycarbonyl-6-phthalimido-7-oxo-2,3,4,7-tetrahydro-1,4-thiazepine (III). To a previously prepared mixture of pure phosphorus oxychloride (100 ml) and dry benzene (460 ml) was added methyl 6-phthalimidopenicillanate (I; 7.2 g, 0.02 mol). The reaction mixture was heated under reflux for 60 min. Concentration under reduced pressure, followed by repeated evaporation with several portions of benzene, afforded a brown residue, which was dissolved in acetone (250 ml) and treated with charcoal in the cold (1 h). The filtered solution was evaporated with continuous addition of methanol and simultaneous distillation to give a crystalline mass. The crystals were filtered off and washed with cold methanol and finally with a small amount of methylene chloride. The product (3.54 g, 49.2 %) had a m.p. of 217 – 219° and gave no m.p. depression with III prepared from I with triethylamine in methylene chloride (see above). Recrystallization from acetone-dry ether gave pure 2,2-dimethyl-3(*S*)-methoxycarbonyl-6-phthalimido-7-oxo-2,3,4,7-tetrahydro-1,4-thiazepine (III; 2.95 g, 40.9 %), m.p. 220 – 221°, $[\alpha]_D^{20}$ −215.4° (*c* 0.5, methanol); $[\alpha]_D^{20}$ −202.2° (*c* 1, pyridine).

The residue (4.45 g) from the combined mother liquors was dissolved in a minimum amount of methylene chloride and chromatographed on a silica gel column (300 g; gradient elution: benzene → mobile phase *I*; 40 ml). Fractions 24 – 36 yielded a further quantity of III (1.18 g, 16.4 % total yield of III 4.13 g, 57.3 %). On evaporation of fractions 6 – 10, 682 mg material remained which was recrystallized from methylene chloride →– methanol to give 295 mg (4.1 %) of methyl 6α-phthalimidopenicillanate (II), m.p. 181.5 – 183° (lit.[6] 183°) $[\alpha]_D^{20}$ +210.6° (*c* 1, chloroform). According to mixed m.p., chromatographic behaviour and IR- and NMR-spectra, the compound was identical with the methyl 6α-phthalimidopenicillanate obtained by treatment of methyl 6β-phthalimidopenicillanate (I) with triethylamine (see above). TLC analysis (in *I*, four consecutive developments): hR_F 47; compared to hR_F 53 for methyl 6β-phthalimidopenicillanate (I).

IR (KBr): 3000w, 1765s, 1740sh, 1720s. NMR ($CDCl_3$): 8.15 (s, CH_3), 8.34 (s, CH_3), 6.18 (s, $COOCH_3$), 5.34 (s, CH), 460 (d, $J = 2$, CH), 4.42 (d, $J = 2$, CH), 2.16 (phthaloyl).

No compound identical with the starting material, the methyl 6β-phthalimidopenicillanate (I), could be isolated or detected before or after the column chromatography from the mother liquors (over 1 %).

2,2-Dimethyl-3(S)-methoxycarbonyl-6-phenylacetamido-7-oxo-2,3,4,7-tetrahydro-1,4-thiazepine (VI). To a solution of 2,2-dimethyl-3(*S*)-methoxycarbonyl-6-phthalimido-7-oxo-2,3,4,7-tetrahydro-1,4-thiazepine (III, 360 mg, 1 mmol) in dioxane, (8 ml) hydrazine hydrate (100 mg, 2 mmol) in water (2 ml) was added and the light yellow solution was stored at +4°C for three days. TLC (in *G*): hR_F 79 (m), 65 (m), 49 (m) and 21 (s; ninhydrin positive). The clear solution was treated simultaneously with 0.5 N phenylacetyl chloride solution in dry acetone (4 ml, 2 mmol) and 1 N potassium hydrogen carbonate (*ca.* 2 ml, 2 mmol) while stirring in an ice-bath at pH 6. TLC (in *G*): hR_F 80 (w), 72 (s; VI) and 45 (w); (in *H*): hR_F 52 (w), 25 (w), 13 (s; VI) and 0 (m). The solution was acidified with 2 N hydrogen chloride to pH 2 and evaporated to dryness. The residue was triturated with mobile phase *H* (10 ml), filtered and washed with *H* (3 × 5 ml). The combined filtrates concentrated to 5 ml were chromatographed on a silica gel column (35 g in mobile phase

B, elution directly with *H*, fraction volume 20 ml). Fractions 6 – 10 contained starting material (III, 15 mg, 4.1 %) and fractions 12 – 30 the title compound (VI, 310 mg, 89 %), m.p. 140 – 142°. Recrystallization from dry ethanol gave the pure compound (218 mg, 62.5 %), m.p. 150 – 151°, $[\alpha]_D^{20}$ – 195° (*c* 1, chloroform).

UV (methanol): 315(9 600), 258(6 400), 204(14 500). IR (KBr): 3180s, 1710s, 1620s, 1550s, 1515s. NMR (C_5D_5N): 8.40, 8.37 (d, 6H, $C(CH_3)_2$), 6.33 (3H, $COOCH_3$), 6.14 (2H, CH_2), 5.40 (d, $J = 5.5$, CH), 2.78 – 2.33 (m, 5H, C_6H_5), 2.06 (d, $J = 8.5$, CH), 0.83 (br, 2H, 2 NH). (Found: C 58.72; H 5.88; N 8.01; O 18.48; S 9.12. Calc. for $C_{17}H_{20}N_2O_4S$ (348.44): C 58.60; H 5.78; N 8.04; O 18.37; S 9.20.)

Sensitivity of VI toward sodium hydroxide in 50 % aqueous ethanol.[13] To a stirred solution of VI (10 mg, 0.0287 mmol) in 50 % aqueous ethanol (10 ml), kept at 25 ± 0.5°, 0.5 equiv. of sodium hydroxide (0.15 ml, 0.094 N) was added all at once. The change of pH was followed with a glass-calomel combination electrode (Titrator TTT1c, Radiometer, Copenhagen, Denmark) over a period of 30 min and plotted against time (Fig. 1).

Raney-nickel desulphurization and acid hydrolysis[14] *of the two thiazepine derivatives III and VI.* (a). The phthalimido derivate (III, 360 mg, 1 mmol) was heated under reflux with carefully washed (dry ethanol), pyrophoric Raney-nickel (10 ml) in dry ethanol (35 ml) for 7 h. After removal of the Raney-nickel by filtration (TLC in *H*: hR_F 62 (w), 55 (s), 36 (w), 30 (m, III) and 12 (w); detection: treatment with iodine vapor) the filtrate was evaporated (260 mg), dissolved in mobile phase *H* (3 ml) and chromatographed on a silica gel column (35 g in dry mobile phase *B*: gradient elution: mobile phase *B* → *H*; 450/20 ml). Fractions 16 – 21 contained the main, chromatographically pure product (110 mg) as an oil which could not be brought to crystallize. $[\alpha]_D^{24}$ + 18° (*c* 1, carbon tetrachloride).

IR (CCl_4): 2920m, 1755m, 1718s, 1700s, 1462m, 1468m, 1390s. NMR (CCl_4): 9.21 (s, 3H), 9.10 (s, 3H), 6.33 (s, 3H), 2.20 (m, 4H), 8.40 – 8.20 (m, 2H), 7.45 – 6.92 (m, 3H), 6.35 – 6.18 (m, 2H).

The compound (40 mg) was heated under reflux in 8 N sulphuric acid (4 ml) for 4 h. After standing in a refrigerator overnight, phthalic acid was isolated (14 mg, 70 %, m.p. 205 – 208°) by filtration. The filtrate was adjusted to pH 6 with barium hydroxide and filtered. The precipitate was washed with hot water, and the filtrate and washings were combined and concentrated *in vacuo* to a volume of 2 ml. This solution was used for TLC.

(b). In the same manner, the phenylacetamido-thiazepine derivative (VI, 70 mg, 0.2 mmol) was desulphurized with Raney-nickel (2 ml) in abs. ethanol (7 ml). The Raney-nickel free filtrate (TLC in *H*: hR_F 70 (s), 55 (w), 32 (w) and 14 (w); detection: treatment with iodine vapor) was evaporated to dryness, dissolved and refluxed in 8 N sulphuric acid (4 ml) for 4 h, neutralized to pH 6 with barium hydroxide, filtered, washed, evaporated and dissolved in 2 ml water. This solution was used for TLC.

The results of the TLC analysis, using pre-coated Silica gel G and Cellulose F TLC-plates (Merck) in five various solvent systems are summarized in Table 3. Spots, marked with an asterisk, were very faint and seem to be identical with D-valine (D-, L-, and DL-valine have similar hR_F values in these systems). Detection: ninhydrin spray-reagent (Merck).

Methyl N-[*(2'-phenylacetamido-2'-benzylthiocarbonyl)vinyl*]*2,3-dehydrovalinate (VIII).* The reaction was carried out under the same conditions used by Leonard and Ning.[13] A solution of 2,2-dimethyl-3(*S*)-methoxycarbonyl-6-phenylacetamido-7-oxo-2,3,4,7-tetrahydro-1,4-thiazepine (VI, 348 mg, 1 mmol) in dry methanol (5.2 ml) was treated at room temperature with 0.2 N methanolic sodium methoxide (5 ml, 1 mmol), followed after 20 min by a solution of benzyl bromide (180 mg, 1.05 mmol) in dry methanol (8.5 ml). After a further 10 min the TLC analysis (in *H*) showed complete reaction: hR_F 59 (s), 18 (w) and 2 (w); starting material (VI): hR_F 35. The mixture was evaporated to dryness and the organic products were separated from sodium bromide by extraction with chloroform (15 ml). Filtration and evaporation of the chloroform solution followed by recrystallization of the residue from benzene (1.8 ml) gave pure VIII (286 mg, 65.5 %), m.p. 110 – 112°. TLC and TLC* in *A*: hR_F 26 and 24, resp.; in chloroform: hR_F 19 and 10, resp.

IR (KBr): 3420m, 3340m, 1715s, 1670s, 1655s, 1590s, 1495s. NMR ($CDCl_3$): 8.10, 7.88 (2 s, 2 × 3H, $C(CH_3)_2$), 6.32 (s, 2H, CH_2), 6.23 (3H, $COOCH_3$), 5.87 (s, 2H, CH_2), 2.74 (s, 5H, C_6H_5), 2.66 (s, 5H, C_6H_5), 2.10 – 2.80 (m, 2 – 3H, CH, NH). (Found: C 65.86;

H 5.99; N 6.22; O 14.62; S 7.29. Calc. for $C_{24}H_{26}N_2O_4S$ (438.56): C 65.73; H 5.98; N 6.39; O 14.59; S 7.31.)

On using 1-chloro-2,4-dinitrobenzene instead of benzyl bromide in the above mentioned experiment (*cf.* Leonard and Ning [13]) no reaction was observed on the basis of TLC analysis (in *H*) even after 120 min at room temperature (lit.[13]: after 5 min reaction time 81 % conversion into the corresponding *S*-(2,4-dinitrophenyl)dehydrocysteinyl derivative; see XIII).

Methyl N-[(2'-phthalimido-2'-benzylthiocarbonyl)vinyl]-2,3-dehydrovalinate (XVa). 2,2-Dimethyl-3(*S*)-methoxycarbonyl-6-phthalimido-7-oxo-2,3,4,7-tetrahydro-1,4-thiazepine (III; 2.88 g, 8 mmol) was suspended in dry methanol (450 ml) and treated at room temperature with 0.2 N sodium methoxide solution (40 ml, 8 mmol). After 20 min 0.2 N methanolic benzyl bromide (42 ml, 8.4 mmol) was added in one portion to the bright yellow solution ($[\alpha]_D^{20}$ 0°) and the reaction mixture was kept at room temperature for one h. TLC* analysis (in *A*) showed two main spots: hR_F 47 (m; XVa) and 24 (s; denoted as XVa^i). The methanolic reaction mixture was divided into two aliquots and worked up in two different ways:

(a). The first aliquot (267 ml) was *evaporated to dryness* and the residue was dissolved in methylene chloride (200 ml) and filtered from the sodium bromide. The TLC* analysis in *A* showed a marked change in the ratio of the two isomers: hR_F 49 (s; XVa) and 23 (m; XVa^i). The clear solution was evaporated to a small volume (15 ml), treated with dry methanol (30 ml) and evaporated again slowly to a small volume. The separating crystals were filtered off and washed with cold methylene chloride – methanol (1:3). The product (1.52 g, 84.5 %, m.p. 144 – 148°) was recrystallized from methylene chloride →← methanol (1.28 g, 71.2 %, m.p. 150 – 152°). According to the TLC* analysis in *A* this product was not entirely pure: hR_F 50 (s; XVa) and 24 (w; XVa^i), mother liquor: hR_F 50 (w; XVa) and 23 (m; XVa^i). Chromatographically pure XVa was obtained, when the raw product (1.59 g) was suspended in 0.2 M hydrogen chloride in 75 % dioxane (43 ml). The substance first formed an oil, which dissolved (within 5 – 6 min) and then suddenly crystallised in long needles (945 mg, 59.5 %), m.p. 152.5 – 153°. TLC* in *A*: hR_F 50.

UV (methanol): 312(23 400), 219(46 600). IR (KBr): 3320m, 1760m, 1720s, 1710sh, 1650s, 1585m. ($CDCl_3$): 1780m, 1725s, 1650m. NMR ($CDCl_3$): 7.98, 7.87 (2 s, 2 × 3H, $C(CH_3)_2$), 6.14 (s, 3H, $COOCH_3$), 5.82 (s, 2H, CH_2), 3.24 (d, $J = 13$, 1H, CH), 2.72 (s, 5H, C_6H_5), 2.15 (m, 4H, phthaloyl), −0.12 (d, $J = 13$, 1H, NH). (Found: C 63.94; H 4.81; N 6.28; O 17.82; S 7.19; MV (Rast) 465. Calc. for $C_{24}H_{22}N_2O_5S$ (450.53): C 63.98; H 4.92; N 6.22; O 17.76; S 7.12.)

After 4 months storing at room temperature in the dark, the pure compound gave the following TLC* pattern (in *A*): hR_F 61 (w), 50 (s; XVa), 24 (m; XVa^i), 10 (w) and 0 (w).

The aqueous dioxane-hydrogen chloride mother liquor, containing the two isomers, TLC* in *A*: hR_F 50 (w; XVa) and 24 (m; XVa^i), was evaporated to dryness and this amorphous residue (580 mg, 36.5 %) was used, parallel with the pure XVa, for acidic hydrolysis in 75 % aqueous dioxane containing 2.0 M hydrogen chlororide/l at room temperature (see later).

(b). The second aliquot (267 ml) of the methanolic reaction mixture was *concentrated to one third of its volume*, diluted with methylene chloride (400 ml), washed with water (1 × 400 ml, 4 × 150 ml) and dried ($MgSO_4$). TLC* in *A*: hR_F 47 (m; XVa) and 24 (s; XVa^i). After evaporation the residue (1.89 g) was chromatographed on a silica gel column (200 g; the column had been prewashed with benzene containing 1 % acetone (200 ml), the residue was applied dissolved in a minimum amount of the same solvent and eluted by gradient techniques: benzene with 1 % acetone → mobile phase *A*: 1000/20 ml). Fractions 45 – 51 contained XVa (420 mg, 23.3 %; TLC* in *A*: hR_F 50), which after recrystallization from methylene chloride →← methanol (364 mg, 16.4 %) showed a m.p. of 152 – 153° and by mixed m.p. and spectroscopical evidence was identical with the product obtained by route *a*. The XVa^i was contained in fractions 59 – 80 (TLC* in *A*: hR_F 24). It was stable in the eluting solvent below +5° for several days. Evaporation of an aliquot of the solution gave a yellow, non-crystalline, semisolid material, which could not be brought to crystallize. Furthermore all operations even at 20° resulted in a mixture of XVa and its isomer together with decomposition products (strong benzylthiol odour). For IR and NMR analysis two aliquots could, however, be transferred without

isomerisation or decomposition into chloroform and deuteriochloroform solution by careful evaporation in the cold with continuous addition of chloroform and deuteriochloroform, respectively.

IR ($CHCl_3$): 1780w, 1720s, 1665w, 1600w. NMR ($CDCl_3$): 8.02 (s), 7.88 (s), 6.28 (s), 5.86 (s), 2.75 (m), 2.18 (m).

Methyl N-[(2'-phthalimido-2'-methylthiocarbonyl)vinyl]-2,3-dehydrovalinate (XVb). This compound was prepared in the same manner as the benzylthiocarbonyl derivative (XVa, route *a*) from III (720 mg, 2 mmol) using methyl iodide as alkylating agent. Recrystallisation from benzene-hexane gave XVb (465 mg, 62.2 %), m.p. 158 – 160°. An analytical sample was obtained by two further recrystallizations from the above solvents, m.p. 160 – 161° (hR_F values, see Table 4).

IR (KBr): 3390m, 1785m, 1750m, 1718s, 1695sh, 1650s, 1620s, 1595s. NMR ($CDCl_3$): 8.0, 7.96, 7.88, 7.84 ($C(CH_3)_2$), 7.76, 7.72 ($COOSCH_3$), 6.25, 6.16 ($COOCH_3$), 3.26 (d, $J = 13$, CH), 2.44 (d, $J = 11$, CH), 2.04 (m, phthaloyl), – 0.02 (d, $J = 13$, NH). (Found: C 57.69; H 4.80; N 7.39; O 21.50; S 8.51. Calc. for $C_{18}H_{18}N_2O_5S$ (374.43): C 57.74; H 4.85; N 7.48; O 21.37; S 8.56.)

Esterification of methyl N-[(2'-phthalimido-2'-carbothiolic)vinyl]-2,3-dehydrovalinate (XXI) with methanol and subsequent acid hydrolysis in the presence of 2,4-dinitrophenylhydrazine. Isolation of the 2,4-dinitrophenylhydrazones XVI and XXIII. 2,2-Dimethyl-3(*S*)-methoxycarbonyl-6-phthalimido-7-oxo-2,3,4,7-tetrahydro-1,4-thiazepine (III; 720 mg, 2 mmol) was suspended in dry methanol (120 ml) and 0.2 N sodium methoxide (10 ml, 2 mmol) added at room temperature. After 20 min 0.2 N methanolic hydrogen chloride (20 ml, 4 mmol) was added to the bright yellow solution, which was left for 4 days at room temperature and finally heated under reflux for 1 h. TLC* analysis (in *A*): hR_F 42 (m, elongated), 18 (m, elongated) and 0 (s). After cooling, 0.2 N methanolic (97.5 %) hydrogen chloride solution (400 ml) containing 2,4-dinitrophenylhydrazone (790 mg, 4 mmol) was added. After standing at room temperature for 24 h, the reaction mixture showed the following TLC pattern (in chloroform): hR_F 51 (s, yellow; XXIII), 39 (s, red), 13 (m, 2,4-dinitrophenylhydrazine) and 0 (w); detection: spraying with 2 N sodium hydroxide. The solution was concentrated to one tenth of its volume (*ca.* 50 ml) and left overnight. After evaporation to dryness the residue (1.15 g; 78 %) was triturated several times with benzene and filtered. The combined filtrates were concentrated to a small volume and chromatographed on a silica gel column (250 g; gradient elution: benzene → mobile phase *D*; 1600/40 ml). Fractions 24 – 31 contained a yellow crystalline substance (338 mg, 62 %), which after recrystallization from methanol melted at 180 – 181° and was by mixed m.p. and IR spectra identical with an authentic sample of 2,4-dinitrophenylhydrazone of methyl 2-oxoisovalerate (see below).

IR (KBr): 3240w, 3160w, 3020w, 1695s, 1625s, 1595s, 1575s, 1525sh, 1510s. (Found: C 46.37; H 4.76; N 17.88; O 30.88. Calc. for $C_{12}H_{14}N_4O_6$ (310.27): C 46.45; H 4.55; N 18.06; O 30.94.)

Evaporation of fractions 63 – 91 containing two substances with very similar chromatographic properties gave a reddish-brown residue (653 mg, 76.5 %). Several recrystallizations from methanol-water containing 1 mmol of hydrogen chloride per 200 mg of substance gave the pure 2,4-dinitrophenylhydrazone of methyl 2-phthalimido-2-formylacetate (XVI), m.p. 210 – 214° (157 mg, 18.4 %).

IR (KBr): 3330m, 3140w, 1760w, 1705s, 1615s, 1590s, 1515s. (Found: C 50.82; H 3.14; N 16.75; O 29.64; S 0.00. Calc. for $C_{18}H_{13}N_5O_8$: C 50.59; H 3.07; N 16.39; O 29.95.)

The product was by mixed m.p., TLC, and IR-spectrum identical to an authentic sample of XVI prepared according to Sheehan and Johnson.[16]

Methyl N-[(2'-phthalimido-2'-carbomethoxy)vinyl]-2,3-dehydrovalinate (XVII). The benzylthiocarbonyl derivative (XVa; 225 mg, 0.5 mmol) was dissolved in dry dioxane (5 ml) and methanol (10 ml), and 0.05 M dry methanolic mercuric acetate (10 ml, 0.5 mmol) was added at room temperature. After 2 h the reaction mixture contained no more starting material according to TLC (hR_F values, see Table 5). The clear solution was evaporated with continuous addition of benzene to a small volume yielding a white crystalline precipitate (155 mg, 81 %), m.p. 168 – 170° (decomp.), which analysed as benzylthiomercuric acetate.

IR (KBr): 3050w, 1580m-s, 1540m-s, 1500m, 1460m, 1405s. (Found. C 28.31; H 2.76; O 8.39; S 8.31; Hg 52.24. Calc. for $C_9H_{10}O_2SHg$: C 28.23; H 2.63; O 8.36; S 8.38; Hg 52.40.)

The filtrate was evaporated to dryness and the residue dissolved in benzene and chromatographed on a silica gel column (20 g; gradient elution: benzene →— mobile phase *A*; 200 ml/20 ml). Fractions 10 – 17 contained the title compound (XVII; 157 mg, 87 %, m.p. 142 – 143°), which was recrystallized from methylene chloride – methanol (1:1; 125 mg, 69.5 %), m.p. 143 – 145° (hR_F values, see Table 4).

IR (KBr): 3360w, 1780m, 1720s, 1680s, 1640s, 1620s, 1455s, 1410s. NMR ($CDCl_3$): 7.98 (s, 3H, CH_3), 7.84 (s, 3H, CH_3), 6.32 (s, 3H, $COOCH_3$), 6.18 (s, 3H, $COOCH_3$), 3.14 d, $J = 13$, 1H, CH), 2.16 (m, 4H, phthaloyl), 0.96 (d, $J = 13$, 1H, NH). (Found: C 60.28; H 5.14; N 7.76; O 26.67. Calc. for $C_{18}H_{16}N_2O_6$: C 60.33; H 5.06; N 7.82; O 26.79.)

Hydrolysis of XVII, isolation of O-methyl 2-phthalimido-2-formylacetate (XVIIIb). The carbomethoxy-2,3-dehydrovalinate derivative (XVII; 180 mg, 0.5 mmol) was dissolved and stirred at room temperature in 2 M hydrogen chloride in 75 % aqueous dioxane (5 ml; two phases). After 4.5 h the hydrolysis was complete: TLC analysis (in *F*): hR_F 48 (w), 33 (s; XVIIIb), 6 (m) and 0 (m): starting material (XVII) hR_F 60; visualisation: 2,4-dinitrophenylhydrazine-potassium ferricyanide reagent.[40] Then the reaction mixture was taken up in methylene chloride (150 ml), washed with water (5 × 40 ml), dried, evaporated to dryness (175 mg) and crystallized from dry benzene (1.1 ml). The *O*-methyl 2-phthalimido-2-formylacetate (XVIIIb), m.p. 138 – 140° (79 mg; 64.0 %) was recrystallized from benzene (39 mg; 31.4 %), m.p. 140 – 142°. The substance was according to mixed m.p., analytical and spectral data identical to a sample of authentic *O*-methyl 2-phthalimido-2-formylacetate (XVIIIa) prepared according to the literature.[16]

IR (KBr): 3200m, 1782m, 1720s, 1680s, 1650sh, 1625m. NMR (C_5D_5N): 6.30 (s, 3H, $COOCH_3$), 2.24 (m, 4H, phthaloyl), 193 (1H, CH), – 2.97 (1H, COH). (Found: C 58.42; H 3.74; N 5.60; O 32.18. Calc. for $C_{12}H_9NO_5$: C 58.30; H 3.67; N 5.67; O 32.36.)

XVIIIb gave a 2,4-dinitrophenylhydrazone (XVI), m.p. 214 – 215.5°, recrystallized from dioxane – water. This substance was identical with the product previously obtained *via* the route III → XIV → XXI → XVII → XVI (see above).

Acidic hydrolysis of XV a and b in the presence of 2,4-dinitrophenylhydrazine. Isolation of the 2,4-dinitrophenylhydrazones XXIV a and b and XXIII. Methyl *N*-[(2′-phthalimido-2′-benzylthiocarbonyl)vinyl]-2,3-dehydrovalinate (XIa; 450 mg, 1 mmol) was dissolved in 0.1 N methanolic (97.5 %) hydrogen chloride solution (400 ml) containing 2 mmol of 2,4-dinitrophenylhydrazine. After standing overnight at room temperature the reaction mixture was evaporated to a volume of 40 ml and left for two days. The separated crystals (625 mg) were filtered off and the mother liquor was concentrated to a small volume and diluted with water to precipitate a further crop of crystals (133 mg) corresponding to a total yield of XXIII and XXIVa of 91.4 %. TLC analysis (in *C*): hR_F 67 (s, yellow; XXIII) and 47 (s, red; XXIVa); detection: spraying with 2 N sodium hydroxide.

The mixture was chromatographed on a silica gel column (120 g; elution: first 400 ml benzene, then gradient elution: benzene → mobile phase *C*; 800/40 ml). Fractions 14 – 19 contained pure XXIII (281 mg, 90.4 %), which was recrystallized from methanol (254 mg, 81.6 %), m.p. 180 – 181°. This substance was by mixed m.p., IR, and NMR spectra identical with an authentic sample of the 2,4-dinitrophenylhydrazone of methyl 2-oxo-isovalerate and with the product previously obtained from XXI.

The second 2,4-dinitrophenylhydrazone was obtained in fractions 44 – 52 in pure form (451 mg, 87 %). Recrystallization from benzene →— 98 % ethanol containing 1 mmol hydrogen chloride per 250 mg substance gave the pure 2,4-dinitriphenylhydrazone of the *S*-benzyl-2-phthalimido-2-formylthioacetate (XXIVa; 405 mg, 77.8 %) m.p. 110 – 114° (decomp.).

IR (KBr): 3350s, 3100w, 1775m, 1715s, 1650s, 1615s, 1530s, 1500s. NMR ($(CD_3)_2SO$: 5.80 (s, CH_2), 2.57 (s, C_6H_5), 2.58 (d, $J = 10$, 1H), 1.88 (s, phthaloyl) 1.37 (q, $J = 10$, 3, 1H), 1.00 (d, $J = 3$, 1H). (Found: C 55.46; H 3.41; N 13.34; O 21.73; S 6.01. Calc. for $C_{24}H_{17}NO_7S$ (519.51): C 55.49; H 3.30; N 13.48; O 21.56; S 6.17.)

The 2,4-dinitrophenylhydrazone of phenyl 2-phthalimido-2-formylacetate[16] (see Scheme 4; XXII), *O*-benzyl analogue of XXIVa, showed very similar TLC and spectral properties. TLC in *D*: hR_F 45 (red; XXII) and 47 (red; XXIVa), in chloroform: hR_F 36 (red; XXII) and 37 (red; XXIVa); detection: spraying with 2 N sodium hydroxide.

IR (KBr): 3350m, 3120m, 1750s, 1718s, 1615s, 1540s, 1520s, 1510s. NMR ($(CD_3)_2SO$: 6.63 (s, CH_2), 2.65 (s, C_6H_5), 2.63 (d, $J = 19$, 1H), 2.05 (s, phthaloyl), 1.55 (q, $J = 10$, 3 1H), 1.17 (d, $J = 3$, 1H), – 0.24 (br, NH).

In an analogous experiment methyl *N*-[(2′-phthalimido-2′-methylthiocarbonyl)-

vinyl]-2,3-dehydrovalinate (XVb; 375 mg, 1 mmol) was treated with 2,4-dinitrophenylhydrazine in acidic medium. The two 2,4-dinitrophenylhydrazones formed (total 614 mg, 82.5 %; TLC analysis (in *C*): hR_F 66 (yellow; XXIII) and 43 (red; XXIVb); detection: spraying with 2 N sodium hydroxide) were separated by column chromatography and purified by crystallization as before. In addition to the 2,4-dinitrophenylhydrazone of methyl 2-oxoisovalerate (XXIII; 218 mg, 70.5 %), m.p. 179 – 180°, identical with the previously obtained product, the 2,4-dinitrophenylhydrazone of the *S*-methyl 2-phthalimido-2-formylthioacetate (XXIVb; 292 mg, 65.8 %) was isolated, which after recrystallization from benzene →← 98 % methanol containing 1 mmol hydrogen chloride per 200 mg of substance had m.p. 112 – 113° (dec.).

IR (KBr): 3340m, 3120w, 1775m, 1715s, 1665m, 1640sh, 1615s, 1585s, 1540sh, 1525s, 1505s. NMR $(CD_3)_2SO$: 7.72 (s, CH_3), 2.54 (d, $J = 10$, 1H), 1.86 (s, phthalimido), 1.37 (q, $J = 10$, 3, 1H), 1.00 (d, $J = 3$, CH). (Found: C 48.59; H 3.03; N 15.67; O 25.36; S 7.04. Calc. for $C_{18}H_{13}N_5O_7S$ (443.41): C 46.76; H 2.95; N 15.79; O 25.26; S 7.23.)

Hydrolysis of XVa and isolation of the S*-benzyl 2-phthalimido-2-formylthioacetate (XXa): 2,4-dinitrophenylhydrazone (XXIVa) and diethylacetal (XXVII).* Methyl *N*-[(2′-phthalimido-2′-benzylthiocarbonyl)vinyl]-2,3-dehydrovalinate (XVa; 900 mg) was hydrolyzed in the same manner as XVII for 3.5 h in 2 M hydrogen chloride in 75 % dioxane (20 ml). TLC analysis (in *F*): hR_F 29 (s, XXa), 6 (m) and 0 (m); the two lower spots disappeared after washing; starting material (XVa): hR_F 59; visualisation: 2,4-dinitrophenylhydrazine-potassium ferricyanide reagent.[40] The crude reaction product (765 mg) was separated from unchanged starting material (53 mg, 5.9 %) by trituration with dry ethanol and the filtered ethanolic solution was evaporated to dryness to give an amorphous residue (XXa; 663 mg), which was used directly for the preparation of XXIVa and XXVII.

Half of the residue (XVa; 330 mg) was converted into the 2,4-dinitrophenylhydrazone in the usual way. Recrystallization from benzene →← 98 % ethanol containing 0.5 mmol hydrogen chloride per 125 mg substance gave the pure 2,4-dinitrophenylhydrazone of *S*-benzyl 2-phthalimido-2-formylthioacetate (XXIVa; 265 mg, 51.0 %), m.p. 111 – 114° (dec.), by mixed m.p. and IR identical with the compound previously obtained *via* the route XVa→XXIII + XXIVa (see above).

The other half of the residue (XXa; 332 mg) was treated with triethyl orthoformate (163 mg, 1.1 mmol), dry ethanol (0.2 ml, 151 mg, 3.3 mmol) and one crystal of *p*-toluenesulfonic acid and stirred at room temperature overnight. Benzene (10 ml) was added to dissolve the crystals formed and the mixture was washed (2 × 2 ml sat. sodium hydrogen carbonate soln., 2 × 2 ml brine) and dried ($MgSO_4$). The TLC analysis (in isopropyl ether) showed a complete reaction: hR_F 39 (s; XXVIII), 17 (w), 13 (w) and 3 (w); starting material (XXa): hR_F 12 (w) and 1 (s). After evaporation of the solvent the residue (295 mg) was chromatographed on a silica gel column (35 g in dry isopropyl ether; elution: isopropyl ether; 20 ml). The fractions 9 – 13 gave after evaporation the *S*-benzyl 2-phthalimido-2-formylthioacetate diethylacetal (XXVII) as an oil (182 mg; 44.0 %) which rapidly solidified, m.p. 51 – 52°. The product was identical in all respects with an authentic sample (see below).

IR (KBr): 3000m, 2940m, 1765m, 1715s, 1700sh, 1670sh. (Found: C 64.08; H 5.64; N 3.45; O 19.40; S 7.62. Calc. for $C_{22}H_{23}NO_5S$ (413.50): C 63.90; H 5.61; N 3.39; O 19.35; S 7.75.)

2,4-Dinitrophenylhydrazone of methyl 2-oxoisovalerate (XXIII). The 2,4-dinitrophenylhydrazone of the 2-oxoisovaleric acid was prepared from 2-phenyl-4-isopropylideneoxazolone according to Ramage and Simonsen [41] (m.p. 195 – 196°; lit.[17] m.p. 196 – 197°). Treatment with ethereal diazomethane [42] in dioxane gave the methyl ester XXIII, which was recrystallized from methanol: m.p. 180 – 181° (lit.[17] m.p. 178 – 180°).

IR (KBr): 3240w, 3160w, 3000w, 1695m, 1626s, 1598s, 1580m, 1530sh, 1510s. NMR (C_6D_6): 8.85 (d, $J = 7$, $2CH_3$), 7.06 (q, $J = 7$, CH), 6.55 (s, $COOCH_3$), 2.34 (d, $J = 10$, CH), 2.04 (q, $J = 10$, 3, CH), 1.06 (d, $J = 3$), −4.04 (br, NH).

O-Benzyl 2-phthalimido-2-formylacetate diethylacetal (XXV). *O*-Benzyl 2-phthalimido-2-formylacetate [16] (XVIIIa; 6.46 g, 0.02 mol) was treated with triethyl orthoformate (3.26 g, 0.022 mol), dry ethanol (4 ml, 3.02 g, 0.066 mol) and *p*-toluenesulfonic acid (12 mg) and the reaction mixture which first became a clear solution and then deposited crystals was stirred at room temperature overnight. Benzene (100 ml) was added to give a clear solution, which was washed (2 × 40 ml sat. sodium hydrogen carbonate, 2 × 20 ml

brine) and dried ($MgSO_4$). TLC analysis (in isopropyl ether): hR_F 40 (s; XXV), 26 (w), 11 (w) and 0 (w; XVIIIa). After evaporation the residue was recrystallized from methylene chloride → isopropyl ether giving the pure acetal XXV (6.15 g, 77.5 %) m.p. 72–74°. An analytical sample was recrystallized from warm isopropyl ether, m.p. 75–76°.

IR (KBr): 2980m, 2940m, 1775m, 1745s, 1718s. NMR ($CDCl_3$): 9.04 (t, $J=7$, CH_3), 8.82 (t, $J=7$, CH_3), 6.60–6.04 (m, 2 CH_2), 4.98 (d, $J=7$, CH), 4.80 (s, CH_2), 4.52 (d, $J=7$, CH), 2.72 (s, C_6H_5), 2.20 (m, phthaloyl). (Found: C 66.40; H 5.95; N 3.63; O 24.19. Calc. for $C_{22}H_{23}NO_6$ (397.43): C 66.49; H 5.83; N 3.52; O 24.15.)

This diethylacetal (XXV; 40 mg, 0.1 mmol) was treated at 70° for 2 h with 0.4 N hydrogen chloride in 60 % dioxane (5 ml) containing 0.1 mmol 2,4-dinitrophenylhydrazine. TLC analysis (in *E*): hR_F 48 (w, XXV), 18 (s, red; XXII), 12 (w; DNP) and 0 (w; XVIIIa); detection: spraying with 2 N sodium hydroxide. The reaction mixture was evaporated to a small volume, treated with a few drops of water and kept in the refrigerator to give the 2,4-dinitrophenylhydrazone of *O*-benzyl 2-phthalimido-2-formylacetate (XXII), m.p. 195–196°.

IR (KBr): 3340m, 3100m, 1745s, 1715s, 1610s, 1590sh, 1520s, 1505s.

The product was by mixed m.p. and IR-spectra identical with the 2,4-dinitrophenylhydrazone prepared directly from XVIIIa.[16]

2-Phthalimido-2-formylacetic acid diethylacetal (XXVI). *O*-Benzyl 2-phthalimido-2-formylacetate diethylacetal (XXV; 4.8 g, 0.012 mol) was hydrogenated in dry ethanol (90 ml) over palladium charcoal catalyst (0.8 g; Pd cont. 5 %) at room temperature in a Parr hydrogenation apparatus. After 25 min the hydrogenation was complete (0.012 mol of hydrogen taken up) and the catalyst was filtered off. TLC analysis (in isopropyl ether): hR_F 10 (s; XXVI). After evaporation the crystalline residue was triturated with isopropyl ether, filtered and washed to give XXVI (3.65 g; 99 %), m.p. 99–101°.

IR (KBr): 2980s, 2920s, 2650w, 2550w, 1765m, 1720s, 1705sh, 1610w, 1470m, 1395s. NMR ($CDCl_3$): 9.0 (t, $J=7$, CH_3), 8.72 (t, $J=7$, CH_3), 6.58–5.96 (m, 2 CH_2), 4.98 (d, $J=7$, CH), 4.52 (d, $J=7$, CH), 2.20 (m, phthaloyl), −0.06 (s, COOH). (Found. C 58.59; H 5.75; N 4.59; O 30.96. Calc. for $C_{15}H_{17}NO_6$ (307.32): C 58.63; H 5.58; N 4.56; O 31.24.)

S-Benzyl 2-phthalimido-2-formylthioacetate diethylacetal (XXVII). (a). 2-Phthalimido-2-formylacetic acid diethylacetal (XXVI; 3.08 g, 10 mmol) and dry triethylamine (1.01 g, 10 mmol) were dissolved in methylene chloride (15 ml), the solution was cooled to −10° and ethyl chloroformate (1.08 g, 10 mmol) in methylene chloride (8 ml) was added with rapid stirring. After 10 min benzyl mercaptan (1.24 g, 1 mmol) in methylene chloride (8 ml) was added and the reaction mixture was stirred for 30 min at −10° and then at 0° overnight. The reaction mixture was diluted with methylene chloride (100 ml), washed (1 × 50 ml brine, 2 × 20 ml sat. sodium hydrogen carbonate, 2 × 20 ml brine) and dried ($MgSO_4$).

TLC analysis (in isopropyl ether): hR_F 62 (w), 41 (s; XXVII), 17 (w) and 8 (w). After evaporation the residue was chromatographed on a silica gel column (35 g in dry isopropyl ether; elution: isopropyl ether; 20 ml). The *S*-benzyl 2-phthalimido-2-formylthioacetate diethylacetal (XXVII) was contained in fractions 23–25 and after evaporation of the solvent was obtained as an oil (1.06 g, 25.6 %), which slowly crystallized, m.p. 52°.

IR (KBr): 3000m, 2940m, 1765m, 1715s, 1700sh, 1670sh. NMR ($CDCl_3$): 9.04 (t, $J=7$, CH_3), 8.75 (t, $J=7$), 6.64–6.00 (m, 2 CH_2), 5.85 (s, CH_2), 4.92 (d, $J=8$, CH), 4.45 (d, $J=8$, CH), 2.75 (s, C_6H_5), 2.20 (m, phthaloyl). (Found: C 64.02; H 5.68; N 3.49; O 19.44; S 7.69. Calc. for $C_{22}H_{23}NO_5S$ (413.50): C 63.90; H 5.61; N 3.39; O 19.35; S 7.75.)

(b). The diethylacetal acid derivative (XXVI; 616 mg, 2 mmol) was refluxed with thionyl chloride (1.2 g, 10 mmol) in dry methylene chloride (10 ml) for 2 h. The reaction mixture was evaporated to dryness, dissolved and evaporated twice with benzene (2 × 20 ml) and finally taken up in dry methylene chloride (10 ml). The chilled solution was added over a 10 min period to a stirred solution of benzyl mercaptan (248 mg, 2 mmol) and triethylamine (222 mg, 2.2 mmol) in dry methylene chloride (3 ml) at 0°. The reaction mixture was stirred overnight, treated with methylene chloride (40 ml), and in portions with water (5 ml) containing 3 mmol of sodium hydrogen carbonate at 0°. The organic phase was separated, washed (1 × 5 ml sat. sodium hydrogen carbonate, 2 × 5 ml brine) and dried ($MgSO_4$). TLC analysis (in isopropyl ether): hR_F 60 (w), 42 (s; XXVII), 19 (w) and 9 (w). After evaporation the residue was chromatographed on a silica gel column as described in route *a*. Fractions 17–21 contained the title compound which after

evaporation (272 mg, 32.8 %) gave an oil, which crystallized slowly on standing, m.p. 51 – 52°. According to analytical and spectral data, this substance was identical in all respects with the *S*-benzyl 2-phthalimido-2-formylthioacetate diethylacetal (XXVII) obtained in *a* above and furthermore with the compound isolated after degradation of III (*via* the route III → XVa → XXa → XXVII).

S-*Benzyl 2-phthalimido-2-formylthioacetate 2,4-dinitrophenylhydrazone (XXIVa).* *S*-Benzyl 2-phthalimido-2-formylthioacetate diethylacetal (XXVII; 413 mg, 1 mmol) was treated at 70° for 2 h with 0.4 N hydrogen chloride in 60 % dioxane (50 ml) containing 1 mmol 2,4-dinitrophenylhydrazine. TLC analysis (in *C*): hR_F 72 (w; XXVII), 55 (w), 48 (s; XXIVa), 36 (w) and 0 (w); detection: spraying with 2 N sodium hydroxide. Benzene (400 ml) was added and the solution was washed (8 × 20 ml brine), dried ($MgSO_4$), evaporated to a small volume and chromatographed on a silica gel column (40 g, gradient elution: benzene → mobile phase *C*; 800/40 ml). Fractions 28 – 31 contained pure XXIVa, which was isolated by evaporation. The residue (310 mg, 59.8 %) was recrystallized from benzene →← 98 % ethanol containing 1 mmol hydrogen chloride per 250 mg substance. The obtained compound (188 mg; 36.2 %) had a m.p. of 111 – 114° and was according to mixed m.p. and IR-spectrum identical in all respects with the 2,4-dinitrophenylhydrazone of *S*-benzyl 2-phthalimido-2-formylthioacetate (XXIVa) isolated from the acidic hydrolysis of XVa (XVa → XXIII + XXIVa).

IR (KBr): 3360m, 3100w, 1775m, 1718s, 1660s, 1620s, 1590s, 1530s, 1510sh.

The mutual reversible transformations of XVa and XVa^i. (a). Pure XVa (100 μg, in methylene chloride) was applied to a Silica gel F_{254} pre-coated plate (Merck) stored at room temperature for 2 h and developed in mobile phase *A*: hR_F 42 (s; XVa) and 23 (s; XVa^i). After 24 h storing hR_F 48 (w), 43 (m; XVa), 24 (s; XVa^i) and 0 (w).

A similar experiment with the XVa^i (100 μg; see preparation of XVa, route *b*, fractions 59 – 80) gave after storing for 2 h an identical chromatogram to that obtained for XVa after 24 h storing: hR_F 48 (w), 43 (m; XVa), 24 (s; XVa^i and 0 (w)).

The reversibility of this transformation was furthermore demonstrated using two-dimensional, "diagonale" [43] and "direct spot transfer" techniques [44] with similar stationary and mobile phases.

(b). XVa (50 mg, in methylene chloride) was applied with a Desaga "Autoliner" to Silica gel F_{254} pre-coated preparative plates (Merck; 8 plates), stored at room temperature in the dark for 24 h and then developed with chloroform containing 2 % ethanol. The *lower* broader band – corresponding to XVa^i – was scraped off, extracted with chloroform, evaporated, dissolved in methylene chloride, applied to preparative Silica gel plates (6 plates) again, stored 4 h at room temperature and developed with chloroform. Two bands appeared again on the chromatogram, now the *upper* band was scraped off, extracted and evaporated. The residue (9.2 mg) was crystallized from benzene-petroleum ether to give a compound, m.p. 148 – 150°, which according to mixed m.p. and IR-data was identical with the starting XVa.

(c). Pure XVa^i (about 45 mg; an aliquot from the fractions 59 – 80 obtained in the preparation of XVa, route *b*) was dissolved in dry methanol (5.5 ml), a catalytic amount of 0.2 N sodium methoxide solution (0.05 ml; 0.01 mmol) was added and the solution was left for 5 h at room temperature. TLC* analysis (in *A*): hR_F 69 (w), 62 (m), 50 (s; XVa), 24 (s; XVa^i) and 0 (w). After evaporation, the residue was chromatographed on a silica gel column (25 g) as in the original experiment (preparation of XVa, route *b*). From the fractions which contained the XVa (according to TLC* in *A*) the crystalline compound was isolated (7.8 mg). After recrystallization from methylene chloride →← methanol it had m.p. 149 – 151° and according to mixed m.p. and IR, it was identical with an authentic sample of XVa. The fractions, which contained the unchanged XVa^i, were carefully evaporated with simultaneous addition of pure chloroform and the solution, now free of benzene and acetone, was evaporated to give a *ca.* 5 % solution of XVa^i. TLC* of the solution (in *A*) indicated practically pure XVa^i and IR showed the characteristic lines of the compound.

IR ($CHCl_3$): 3060, 1775w, 1725s, 1665w, 1605w.

(d). A similar experiment to c starting from pure XVa resulted in two main spots on TLC* (in *A*): hR_F 68 (w), 61 (w), 51 (s; XVa), 24 (s; XVa^i) and 0 (w). These experiments proved the reversible mutual transformation of the two isomers (XVa and XVa^i) into each other under the catalytic action of an active silica gel surface (*a* and *b*) and of sodium methoxide (*c* and *d*).

(e). Chromatographically pure XVa and the residue from its mother liquor (see preparation XVa, route *a*), containing a mixture of the two isomers, were in parallel experiments hydrolysed (225 mg each, 0.5 mmol) with 2 M hydrogen chloride in 75 % dioxane (10 ml) as described before. The reactions were checked by TLC* (in *A*), samples being taken every 20 min (see Fig. 2): average hR_F 50 (XVa), 24 (XVa^i), 6 and 0 (hydrolytic products). After 5 h both reaction mixtures were transformed into their 2,4-dinitrophenylhydrazones and isolated by column chromatography (with TLC control) as described before. Yields (without recrystallization) of the 2,4-dinitrophenylhydrazone-derivatives of methyl 2-oxoisovalerate and of *S*-benzyl-2-phthalimido-2-formylthioacetate, XXIII and XXIVa, resp., were: (1) from pure XVa, 81.3 % XXIII and 72.5 % XXIVa; and (2) from the mixture of XVa and XVa^i, 76.5 % XXIII and 53.2 % XXIVa.

These experiments showed the existence of the XVa→XVa^i→oxo-compounds pathway on acidic hydrolysis.

Acknowledgements. We are grateful to Dr. B. Pring for discussion of the mass spectra and for linguistic corrections in the manuscript, and to B.-G. Ramsay for assistance with the polarimetric measurements. The authors are indebted to Mrs. Susanna Kovacs for excellent experimental assistance.

REFERENCES

1. Clarke, H. T. and Inouye, J. M. *J. Biol. Chem.* **94** (1932) 541.
2. Stoll, A. and Seebeck, E. *Helv. Chim. Acta* **31** (1948) 189.
3. Wolfe, S., Godfrey, J. C., Holdrege, C. T. and Perron, Y. G. *J. Am. Chem. Soc.* **85** (1963) 643.
4. Morin, R. B., Jackson, B. G., Mueller, R. A., Lavagnino, E. R., Scanlon, W. B. and Andrews, S. L. *J. Am. Chem. Soc.* **91** (1969) 1401.
5. Wolfe, S. and Hasan, S. K. *Chem. Commun.* **1970** 833.
6. Wolfe, S. and Lee, W. S. *Chem. Commun.* **1968** 242.
7. Wolfe, S., Lee, W. S. and Misra, R. *Chem. Commun.* **1970** 1067.
8. Kovacs, Ö. K. J., Ekström, B. and Sjöberg, B. *Tetrahedron Letters* **1969** 1863.
9. Kovacs, Ö. K. J., Ekström, B. and Sjöberg, B. *10th European Peptide Symposium*, Abano-Terme, Italy, September 7 – 13, 1969.
10. Sheehan, J. C. and Cruickshank, P. A. *J. Am. Chem. Soc.* **78** (1956) 3680.
11. Clayton, J. P., Southgate, R., Ramsay, B. G. and Stoodley, R. J. *J. Chem. Soc.* **C 1970** 2089.
12. *Private communication*, Beecham Research Laboratories.
13. Leonard, N. J. and Ning, R. Y. *J. Org. Chem.* **32** (1967) 677.
14. Leonard, N. J. and Wilson, G. E. *J. Am. Chem. Soc.* **86** (1964) 5307.
15. Stewart, F. B. and McKinney, P. V. *J. Am. Chem. Soc.* **53** (1931) 1482.
16. Sheehan, J. C. and Johnson, D. A. *J. Am. Chem. Soc.* **76** (1954) 158.
17. Birkinshaw, J. H., Oxford, A. E. and Raistrick, H. *Biochem. J.* **30** (1936) 394.
18. Sheehan, J. C. and Henery-Logan, K. R. *J. Am. Chem. Soc.* **84** (1962) 2983.
19. Houben, J. and Weyl, T. *Methoden der organischen Chemie*, Georg Thieme, Stuttgart 1955, Vol. 9, p. 758.
20. Jackson, J. R. and Stoodley, R. J. *Chem. Commun.* **1970** 14.
21. Ramsay, B. G. and Stoodley, R. J. *Chem. Commun.* **1971** 450.
22. Vlietinck, A., Roets, E., Claes, P. and Vanderhaeghe, H. *Tetrahedron Letters* **1972** 285.
23. Capon, B. and Rees, C. W. *Organic Reaction Mechanisms 1969*, Interscience, London – New York 1960, p. 164.
24. Kwok, W. K., Lee, W. G. and Miller, I. *J. Am. Chem. Soc.* **91** (1969) 468.
25. Lord, E., Naan, M. P. and Hall, C. D. *J. Chem. Soc.* **B 1971** 220.
26. Fiandanese, V. Marchese, G. and Maso, F. *Chem. Commun.* **1972** 250.
27. Cram, D. J. *Fundamentals of Carbanion Chemistry*, Academic, New York 1965, Chapter III.
28. Mayers, G. L. and Kovacs, J. *Chem. Commun.* **1970** 1145.
29. Gutowski, G. E. *Tetrahedron Letters* **1970** 1779.
30. Clayton, J. P., Nayler, J. H. C., Southgate, R. and Stove, E. R. *Chem. Commun.* **1969** 129.
31. Jackson, J. R. and Stoodley, R. J. *Chem. Commun.* **1971** 647.

32. Luche, J. L. and Balavoine, G. *Bull. Soc. Chim. France* **1971** 2733.
33. Bose, A. K., Narayanan, C. S. and Manhas, M. S. *Chem. Commun.* **1970** 975.
34. Johnson, D. A., Mania, D., Panetta, C. A. and Silvestri, N. H. *Tetrahedron Letters* **1968** 1903.
35. Hudson, R. F. *Structure and Mechanism in Organo-Phosphorus Chemistry*, Academic, New York 1965, p. 269.
36. Stahl, E. *Chromatographia* **1** (1968) 342.
37. Goldman, M. and Day, R. A. *Ohio J. Sci.* **67** (1967) 190.
38. Wright, D. A. and Wulff, C. A. *J. Org. Chem.* **35** (1970) 4252.
39. Batchelor, F. R., Doyle, F. P., Nayler, J. H. C. and Rolinson, G. N. *Nature* **183** (1959) 257.
40. Stahl, E. *Dünnschicht-Chromatographie*, Springer, Berlin 1967, p. 827.
41. Ramage, G. R. and Simonsen, J. L. *J. Chem. Soc.* **1935** 532.
42. Ronkainen, P. a. *Suomen Kemistilehti* **B 37** (1964) 209; b. *J. Chromatog.* **20** (1965) 403.
43. Stahl, E. *Dünnschicht-Chromatographie*, Springer, Berlin 1967, p. 89.
44. Székely, G. *J. Chromatog.* **42** (1969) 543.

Received August 9, 1972.

ACTA CHEMICA SCANDINAVICA 27 (1973) 705–731

Short Communications

Standard Potential for the System $S_2O_4^{2-}/HSO_3^-$ in Aqueous Solution

ANTS TEDER

Swedish Forest Products Research Laboratory (STFI), Box 5604, S-114 86 Stockholm, Sweden

Aqueous dithionite is extensively used in the pulping industry as a reducing bleaching agent for pulp. No direct measurements of the redox potential of dithionite solutions are, however, reported in the literature.[1] The values available for the standard potential dithionite/sulfite are obtained indirectly *via* thermodynamic calculations in which it is assumed that all components are in equilibrium with each other.[2] These data are limited to 25°C and the effect of ionic strength of the solutions has not been taken into consideration.

In the present investigation the redox potential of aqueous solutions containing dithionite, sulfite, and thiosulfate of different temperatures and ionic strengths was measured and transformed into the standard potential for the system $S_2O_4^{2-}/HSO_3^-$ using the acidity equilibrium constant for HSO_3^- previously reported.[3] NaCl was used as the inert ionic medium.

In the experiments a smooth Pt-electrode, an Ag,AgCl reference electrode (Metrohm EA 420+EA 698), a glass electrode (Metrohm EA 109 U or EA 109 H), and a millivoltmeter (ORION 801) were used. The reference electrode was calibrated against a hydrogen electrode in solutions of low and known hydrogen ion concentrations. The glass electrode was calibrated with solutions of known concentrations of H^+ or OH^- ions at the same ionic strength as the dithionite solution to be studied. The solutions were prepared from *p.a.* chemicals and analyzed according to previously described methods.[4,5]

Thiosulfate ions do not seem to have any significant effect on the redox potential of dithionite solutions. The redox potential of neutral and slightly alkaline dithionite solutions can be described with a redox equilibrium between dithionite and hydrogen sulfite ions

$$S_2O_4^{2-} + 2H_2O \rightleftharpoons 2HSO_3^- + 2H^+ + 2e^-$$

The standard potentials found at various temperatures and ionic strengths are given in Table 1. (The redox reaction can formally be expressed in other ions by using the ionic product of water and the acidity constant for the reaction $HSO_3^- \rightleftharpoons SO_3^{2-} + H^+$ determined at the corresponding conditions.[3])

Table 1. The standard potential in mV for the system $S_2O_4^{2-}/HSO_3^-$ at different temperatures and ionic strengths.

$[Na^+]$ M	25°C	40°C	60°C
0.05	17	7	−7
0.1	35	26	8
0.5	35	16	10
3.0	54	44	38

Above a certain level of alkalinity of the dithionite solutions, the redox potential was, however, higher than that expected from the standard potentials determined (Fig. 1). This level was found to be correlated with too low a concentration of HSO_3^- ions (which was found to be about 1 mM irrespective of sulfite concentration, temperature and ionic strength). This unexpectedly indicates a rapid redox equilibrium between $S_2O_4^{2-}$ and HSO_3^- but not one between $S_2O_4^{2-}$ and SO_3^{2-}. Another explanation for the phenomenon would be a mixed potential in-

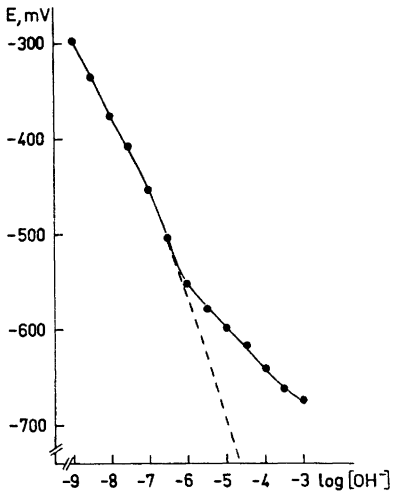

Fig. 1. An example of the deviation of the measured redox potential of dithionite-sulfite solutions from the theoretical one (broken line), calculated using the corresponding standard potential in Table 1. $[S_2O_4^{2-}] = 0.01$ M; $[HSO_3^-] + [SO_3^{2-}] = 0.01$ M. Temperature = 60°C.

volving also the H_2/H^+ potential. This is, however, improbable as the redox potential was dependent on the sulfite concentration also in the alkaline region.

Acknowledgement. I thank Miss Disa Tormund for skilful experimental work and Prof. Nils Hartler, head of the pulping department of STFI, for his interest.

1. Sillén, L. G. *Stability Constants*, Chem. Soc. Spec. Publ. No. 17, London 1964, and Supplement No. 1 Chem. Soc. Spec. Publ. No. 25, London 1971.
2. Latimer, W. M. *Oxidation Potentials*, 2nd Ed., Prentice-Hall, New York 1952.
3. Teder, A. *Svensk Papperstid.* **75** (1972) 704.
4. Ingruber, O. V. and Kopandis, I. *Pulp. Pap. Mag. Can.* **68** (1967) T-258.
5. Teder, A. and Tormund, D. *STFI Report No. 48* (1970).

Received November 29, 1972.

The Crystal Structure of an Eight-Coordinated Tellurium(IV) Complex

STEINAR ESPERÅS and STEINAR HUSEBYE

Chemical Institute, University of Bergen, N-5000 Bergen, Norway

During the study of compounds of divalent selenium and tellurium with bidentate dithio- and related ligands, it was found that the ligand 4-morpholinecarbodithioate (previously termed, morpholyl dithiocarbamate) upon reaction with Te(IV) gave a remarkably stable complex.[1] Unlike the corresponding diethyldithiocarbamate complex, it was only very slowly converted to the Te(II) dithiocarbamate and the corresponding disulphide, when heated in solution.[2,3]

Crystals of tetrakis (4-morpholinecarbodithioato)tellurium(IV) including three benzene molecules of crystallization, $[Te(OC_4H_8NCS_2)_4].3C_6H_6$, were prepared by adding an aqueous solution of sodium 4-morpholinecarbodithioate to a solution of tellurium dioxide dissolved in dilute hydrochloric acid, in the molar ratio 4:1. The resulting precipitate was then recrystallized from a mixture of benzene and ethanol. The following unit cell data were found: $a = 15.445$ (4) Å, $b = 13.565$ (4) Å, $c = 26.591$ (10) Å, $\beta = 122.23$ (4)° and $Z = 4$. The observed and calculated densities are 1.45 and 1.43 g/cm³, respectively, and the space group is $P2_1/c$.

Based on 2721 reflections above background obtained with a Siemens paper-tape controlled AED-1 diffractometer, the structure was solved by Patterson and Fourier syntheses and refined by a full-matrix least-squares program to an R-value of 0.094.

The dodecahedral D_{2d} coordination found around the central tellurium atom is shown on Fig. 1, while some bond lengths and angles are listed in Table 1. The dodecahedral TeS_8 group has a structure similar to that found for the corresponding group in tetrakis(diethyldithiocarbamato) tellurium(IV).[3,4] Thus the lone pair of electrons in the valency shell of the central tellurium atom is essentially stereochemically inert. Each ligand spans an edge m between one corner of type A and one of

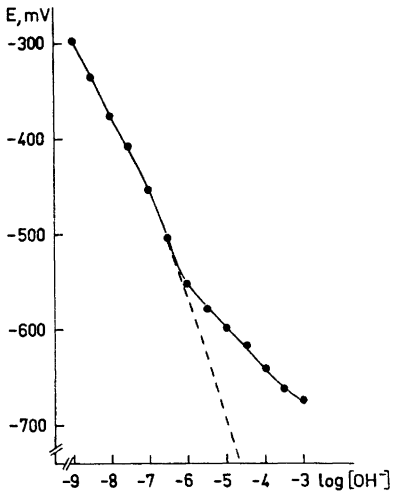

Fig. 1. An example of the deviation of the measured redox potential of dithionite-sulfite solutions from the theoretical one (broken line), calculated using the corresponding standard potential in Table 1. $[S_2O_4^{2-}] = 0.01$ M; $[HSO_3^-] + [SO_3^{2-}] = 0.01$ M. Temperature = 60°C.

volving also the H_2/H^+ potential. This is, however, improbable as the redox potential was dependent on the sulfite concentration also in the alkaline region.

Acknowledgement. I thank Miss Disa Tormund for skilful experimental work and Prof. Nils Hartler, head of the pulping department of STFI, for his interest.

1. Sillén, L. G. *Stability Constants*, Chem. Soc. Spec. Publ. No. 17, London 1964, and Supplement No. 1 Chem. Soc. Spec. Publ. No. 25, London 1971.
2. Latimer, W. M. *Oxidation Potentials*, 2nd Ed., Prentice-Hall, New York 1952.
3. Teder, A. *Svensk Papperstid.* **75** (1972) 704.
4. Ingruber, O. V. and Kopandis, I. *Pulp. Pap. Mag. Can.* **68** (1967) T-258.
5. Teder, A. and Tormund, D. *STFI Report No. 48* (1970).

Received November 29, 1972.

The Crystal Structure of an Eight-Coordinated Tellurium(IV) Complex

STEINAR ESPERÅS and STEINAR HUSEBYE

Chemical Institute, University of Bergen, N-5000 Bergen, Norway

During the study of compounds of divalent selenium and tellurium with bidentate dithio- and related ligands, it was found that the ligand 4-morpholinecarbodithioate (previously termed, morpholyl dithiocarbamate) upon reaction with Te(IV) gave a remarkably stable complex.[1] Unlike the corresponding diethyldithiocarbamate complex, it was only very slowly converted to the Te(II) dithiocarbamate and the corresponding disulphide, when heated in solution.[2,3]

Crystals of tetrakis (4-morpholinecarbodithioato)tellurium(IV) including three benzene molecules of crystallization, $[Te(OC_4H_8NCS_2)_4].3C_6H_6$, were prepared by adding an aqueous solution of sodium 4-morpholinecarbodithioate to a solution of tellurium dioxide dissolved in dilute hydrochloric acid, in the molar ratio 4:1. The resulting precipitate was then recrystallized from a mixture of benzene and ethanol. The following unit cell data were found: $a = 15.445$ (4) Å, $b = 13.565$ (4) Å, $c = 26.591$ (10) Å, $\beta = 122.23$ (4)° and $Z = 4$. The observed and calculated densities are 1.45 and 1.43 g/cm³, respectively, and the space group is $P2_1/c$.

Based on 2721 reflections above background obtained with a Siemens paper-tape controlled AED-1 diffractometer, the structure was solved by Patterson and Fourier syntheses and refined by a full-matrix least-squares program to an R-value of 0.094.

The dodecahedral D_{2d} coordination found around the central tellurium atom is shown on Fig. 1, while some bond lengths and angles are listed in Table 1. The dodecahedral TeS_8 group has a structure similar to that found for the corresponding group in tetrakis(diethyldithiocarbamato) tellurium(IV).[3,4] Thus the lone pair of electrons in the valency shell of the central tellurium atom is essentially stereochemically inert. Each ligand spans an edge m between one corner of type A and one of

Table 1. Some bond lengths and angles with standard deviations in brackets.

Te–S1	2.824 (6) Å	∠S1–Te–S2	64.4 (2)°
Te–S2	2.694 (8)	∠S3–Te–S4	65.3 (2)
Te–S3	2.684 (5)	∠S5–Te–S6	64.6 (2)
Te–S4	2.752 (7)	∠S7–Te–S8	65.2 (2)
Te–S5	2.672 (6)	∠S1–Te–S6	75.8 (2)
Te–S6	2.824 (8)	∠S4–Te–S7	73.8 (2)
Te–S7	2.744 (6)		
Te–S8	2.702 (5)		

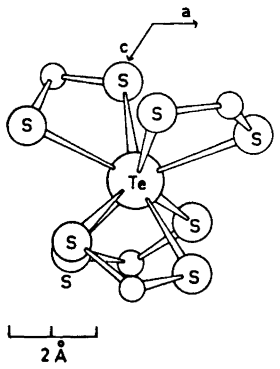

Fig. 1. The tetrakis (4-morpholinecarbodithioato) tellurium(IV) molecule seen along *b*. Unlabelled spheres represent carbon atoms. The nitrogen atoms and the ethyl groups are omitted.

type B in the dodecahedron.[5] The corresponding bond length ratio Te–S_A/Te–S_B is 1.04, with the Te–S_A and Te–S_B bond lengths ranging from 2.74 to 2.82 Å and from 2.67 to 2.70 Å, respectively. The average bite, *b*, as defined by Blight and Kepert,[6] is 1.07, and the angles θ_A and θ_B are 37.4 and 77.8° respectively, as compared to 35.2 and 73.5° given for Hoard and Silvertons "most favourable" dodecahedron.[5] The corresponding average values for tetrakis(diethyldithiocarbamato)tellurium(IV) are 35.1 and 79.9°, respectively.

The two interlocking TeS_4 trapezoids are both nearly planar, and their interplanar angle is 89.8°. As in the analogous diethyldithiocarbamate of tetravalent tellurium, the average Te–S bond length found in the present investigation, is 2.74 Å. This may be compared to 2.59 Å, the sum of the octahedral radius of tellurium and the covalent radius of sulphur. The large bond lengths may be due to increasing use of high energy *d* orbitals, the antibonding nature of the lone pair, and steric crowding.[3,4] However, in light of nuclear quadrupole measurements on octahedral tellurium(IV) complexes and MO calculations on IF_7, BrF_5, AsF_5, and PF_5,[7–9] it is possible that the *d*-orbitals on the tellurium atom are only slightly involved in the bonding.[10,11]

1. Husebye, S., Diss., University of Bergen 1969.
2. Foss, O. *Acta Chem. Scand.* **7** (1953) 226.
3. Husebye, S. and Sværen, S. E. *Acta Chem. Scand.* **27** (1973). *In press.*
4. Esperås, S., Husebye, S. and Sværen, S. E. *Acta Chem. Scand.* **25** (1971) 3539.
5. Hoard, J. L. and Silverton, J. V. *Inorg. Chem.* **2** (1963) 235.
6. Blight, D. G. and Kepert, D. L. *Inorg. Chem.* **11** (1972) 1556.
7. Nakamura, D., Ito, K. and Kubo, M. *J. Am. Chem. Soc.* **84** (1962) 163.
8. Oakland, R. L. and Duffey, G. H. *J. Chem. Phys.* **46** (1967) 19.
9. Berry, R. S., Tamres, M. T., Ballhausen, C. J. and Johansen, H. *Acta Chem. Scand.* **22** (1968) 231.
10. Coulson, C. A. *Nature* **221** (1969) 1106.
11. Cotton, F. A. and Wilkinson, G. *Advanced Inorganic Chemistry*, 3rd. Ed., Interscience, London 1972, p. 142.

Received January 24, 1973.

Sur les Réactions des Quinones avec les Anhydrides d'Acides Carboxyliques. Partie IX.*

MAURI LOUNASMAA

Centre National de la Recherche Technique, Laboratoire de Chimie, SF-02150 Otaniemi, Finlande

En continuation de nos travaux sur les réactions des quinones avec les anhydrides d'acides carboxyliques en présence du sel de sodium de l'acide correspondant,[1-8] nous avons étudié le comportement de la diméthoxy-2,6 benzoquinone-1,4 avec l'anhydride propionique.

Après avoir chauffé le mélange réactionnel plusieurs heures, nous avons ajouté de l'eau et extrait par le chloroforme un mélange à partir duquel nous avons identifié trois produits.

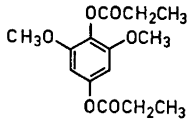

(I)

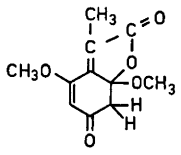

(II)

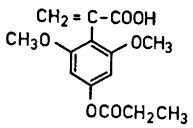

(III)

Le premier produit, obtenu en faible rendement, est identique au dipropionate de diméthoxy-2,6 hydroquinone (I).

Pour le deuxième produit, qui, après une recristallisation dans le tétrachlorure de carbone, fond à 127,5°C, nous proposons la structure (II).

Le spectre de masse montre un pic moléculaire à *m/e* 224 correspondant à la formule $C_{11}H_{12}O_5$. Le pic de base à *m/e* 193 est attribué à l'ion $(M-31)^+$ provenant de la perte du groupement méthoxy sous forme de $CH_3O\cdot$ et le pic à *m/e* 196 à l'ion $(M-CO)^{+\cdot}$. En plus, on note des pics d'intensité assez grande à *m/e* 165, 137, 136, 123 et 109.

Dans le spectre de RMN ($CDCl_3$) apparaissent des singulets à τ 4,30 (1H) (proton vinylique), τ 6,06 (3H) ($-OCH_3$), τ 6,84 (3H) ($-OCH_3$) et τ 7,80 (3H) ($CH_3-C=$), ainsi que deux doublets d'un proton à τ 6,76 (*J* 16 cps) et τ 7,36 (*J* 16 cps) (les deux protons non équivalent du $-CH_2-$ couplés entre eux). La valeur de la constante de couplage trouvée pour les deux protons est bien en accord avec un couplage géminal.

Dans le spectre IR (KBr) on observe des bandes, dues aux ν C=O et ν C=C, à 1762, 1690, 1660 et 1570 cm^{-1}.

Pour le troisième produit, qui, après une recristallisation dans le tétrachlorure de carbone, fond à 140,5°C, nous proposons la structure (III).*

Le spectre de masse montre, outre le pic moléculaire à *m/e* 280 ($C_{14}H_{16}O_6$), des pics importants à *m/e* 224 et 179, qui peuvent être attribués à la perte du groupement propionyloxy sous forme de $CH_3-CH=C=O$ à partir de l'ion moléculaire suivie de la perte de COOH. Les pics métastables à *m/e* 179,3 et 143,1 confirment ces éliminations successives.

Le spectre de RMN ($CDCl_3$) est caractérisé par des singulets à τ −0,54 (1H) (−COOH), τ 3,66 (2H) (protons aromatiques) et τ 6,24 (6H) ($-OCH_3$), ainsi que par deux doublets d'un proton à τ 3,38 (*J* 1 cps) et τ 4,16 (*J* 1 cps) ($CH_2=C-$, *cis* et *trans*, couplés entre eux). En plus, on observe un quadruplet de deux protons à τ 7,42 (*J* 7 cps) et un triplet de trois protons à τ 8,74 (*J* 7 cps) ($-O-CO-CH_2-CH_3$).

Le spectre IR (KBr) montre quatre bandes, dues aux ν C=O et ν C=C, à 1760, 1682, 1620 et 1596 cm^{-1}. Dans la région de 2500−2800 cm^{-1} plusieurs faibles bandes sont caractéristiques d'un acide carboxylique.[9]

Quoique la formation des produits (II) et (III) puisse s'expliquer par un mécanisme à six-centres, les résultats récents [8] sont en faveur d'un intermédiaire *β*-

* Partie VIII, voir Réf. 8.

* Par analogie avec la réaction entre la diméthoxy-2,6 benzoquinone-1,4 et l'anhydride acétique,[3,5] nous avons supposé que c'est le groupement carbonyle en position 1 de la diméthoxy-2,6 benzoquinone-1,4 qui réagira en préférence. Pourtant, les données analytiques présentées pour le troisième produit, n'excluent pas l'autre possibilité.

lactonique. Ainsi peut-on postuler le schéma suivant pour la formation de ces produits.

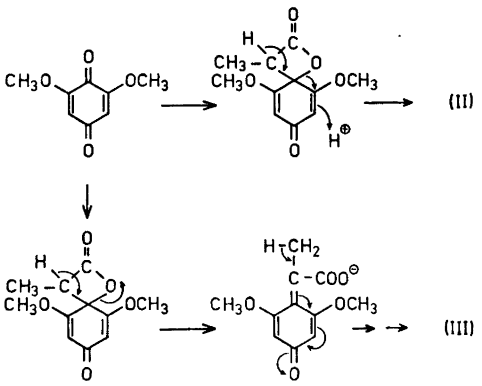

Partie expérimentale.

Les points de fusion ont été mesurés avec un appareil Mettler FP1. Les spectres de masse ont été exécutés sur un spectrographe A.E.I. MS-9. Les spectres de RMN ont été réalisés avec un appareil Varian T-60 en utilisant le tétraméthylsilane (TMS) comme référence interne. Les spectres IR ont été effectués sur spectrographe Perkin-Elmer 237.

Dipropionate de diméthoxy-2,6 hydroquinone (I). Estérifier réductivement la diméthoxy-2,6 benzoquinone-1,4 à l'aide de l'anhydride propionique, de la poudre de zinc et du propionate de sodium, p.f. 85°C (CCl_4). RMN (CCl_4) τ 3,60 (2H, s), τ 6,24 (6H, s), τ 7,40 (2H, quart., J 8 cps), τ 7,44 (2H, quart., J 8 cps), τ 8,74 (3H, t, J 8 cps), et τ 8,76 (3H, t. J 8 cps).

Réaction entre la diméthoxy-2,6 benzoquinone-1,4 et l'anhydride propionique. Maintenir le mélange de la diméthoxy-2,6 benzoquinone-1,4 (0,01 mol; 1,68 g), du propionate de sodium (3 g) et de l'anhydride propionique (50 ml) à 100°C pendant 20 heures. Ajouter de l'eau et extraire à plusieurs reprises par du chloroforme. Laver la solution chloroformique avec de l'eau, sécher sur sulfate de sodium et distiller le solvant sous vide. Fractionner le mélange obtenu par chromatographie sur colonne (gel de silice/chloroforme).

Fraction 1 (éluée par du chloroforme) (40 mg). Le produit est identifié par son point de fusion (85°C) et par son spectre de RMN au dipropionate de diméthoxy-2,6 hydroquinone (I).

Fraction 2 (éluée par du chloroforme) (1,6 g). Recristalliser dans le tétrachlorure de carbone. P.f. 127,5°C. Les résultats analytiques, donnés dans la partie théorique, indiquent qu'il s'agit du composé de structure (II).

Fraction 3 (éluée par du chloroforme/méthanol; 90/10) (100 mg). Recristalliser dans le tétrachlorure de carbone. P.f. 140,5°C. Les résultats analytiques, donnés dans la partie théorique, indiquent qu'il s'agit du composé de structure (III). La proportion entre les rendements des produits (II) et (III) varie beaucoup selon la température. Une température plus élevée augmente le rendement en produit (III).

Les spectres de masse ont été effectués au service de spectrométrie de masse de l'Institut de Chimie des Substances Naturelles à Gif-sur-Yvette par M. J.-P. Cosson que nous remercions vivement.

1. Gripenberg, J. et Lounasmaa, M. *Acta Chem. Scand.* **20** (1966) 2202.
2. Lounasmaa, M. *Acta Chem. Scand.* **20** (1966) 2304.
3. Lounasmaa, M. *Tetrahedron Letters* **1968** 91.
4. Lounasmaa, M. *Acta Chem. Scand.* **21** (1967) 2807.
5. Lounasmaa, M. *Acta Chem. Scand.* **22** (1968) 70.
6. Lounasmaa, M. *Acta Chem. Scand.* **22** (1968) 3191.
7. Lounasmaa, M. *Acta Chem. Scand.* **25** (1971) 1849.
8. Lounasmaa, M. *Acta Chem. Scand.* **26** (1972) 2703.
9. Nakanishi, K. *Infrared Absorption Spectroscopy*, Holden-Day, San Francisco 1962, p. 43.

Reçu le 22 décembre 1972.

Studies on Orchidaceae Alkaloids

XXXIV.* The Absolute Configuration of Cryptostyline I, II, and III, three 1-Phenyl-1,2,3,4-tetrahydroisoquinolines from *Cryptostylis fulva* Schlr.

KURT LEANDER,[a] BJÖRN LÜNING[a] and LEIF WESTIN[b]

[a]*Department of Organic Chemistry, University of Stockholm, Sandåsgatan 2, S-113 27 Stockholm, Sweden and* [b]*Institute of Inorganic and Physical Chemistry, University of Stockholm, S-104 05 Stockholm, Sweden*

The occurrence of three optically active 1-phenyl-1,2,3,4-tetrahydroisoquinolines in *Cryptostylis fulva* Schlr. has been reported.[2] Two papers have appeared dealing with the absolute configuration of these alkaloids. Kametani *et al.*[3] compared the CD curve of cryptostyline III with that of 1*R*-phenyl-2-methyl-6-methoxy-1,2,3,4-tetrahydroisoquinoline, and concluded that the alkaloid has the *R*-configuration. Brossi and Teitel[4] have recently determined the absolute configuration of cryptostyline I,

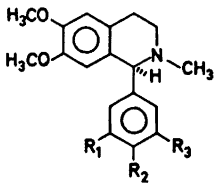

I: R_1 = H, R_2R_3 = O—CH_2—O

II: R_1 = H, R_2 = R_3 = OCH_3

III: R_1 = R_2 = R_3 = OCH_3

II, and III by CD and an X-ray investigation of the hydrobromide of the enantiomer of cryptostyline II. Their studies indicated that the alkaloids have the *S*-configuration.

In this communication an X-ray diffraction investigation of the methiodide of cryptostyline I (IV) is reported.

The crystal structure of IV was determined by the X-ray single crystal technique using an automatic Siemens diffractometer. The methiodide[2] (IV) crystallises from ethanol in the orthorhombic space group $P2_12_12_1$ with four molecules per asymmetric unit. The cell dimensions are $a = 18.093 \pm 1$ Å, $b = 11.940 \pm 1$ Å, and $c = 9.227 \pm 1$ Å. The absolute configuration of IV was established by studying the anomalous dispersion effect of Cu$K\alpha$ radiation by the iodine atoms, including an examination of the Bijvoet pairs. The difference in the *R*-values for the two enantiomers was 2 %. This analysis indicates that the cryptostylines have the *S*-configuration. This assignment is in accordance with that of Brossi and Teitel[4] but in conflict with that of Kametani *et al.*[3] Full details of the X-ray diffraction investigation has been published.[5]

It appears from the work on cherylline[6,7] and the cryptostylines[4] that a β-(*S*)-configuration is connected with two negative Cotton effects at $\simeq$290 nm and 210 nm, respectively. This is also consistent with the results from studies on some lignans[8] (4-aryltetralins) where, however, only the long wavelength band was recorded.

Acknowledgements. This work was supported by the *Swedish Natural Science Research Council.*

1. Ekevåg, U., Elander, M., Gawell, L., Leander, K. and Lüning, B. *Acta Chem. Scand.* **27** (1973). *In press.*
2. Leander, K., Lüning, B. and Ruusa, E. *Acta Chem. Scand.* **23** (1969) 244.
3. Kametani, T., Sugi, H. and Shibuya, S. *Tetrahedron* **27** (1971) 2409.
4. Brossi, A. and Teitel, S. *Helv. Chim. Acta* **54** (1971) 1564.
5. Westin, L. *Acta Chem. Scand.* **26** (1972) 2305.
6. Toome, V., Blount, J. F., Grethe, G. and Uskoković, M. *Tetrahedron Letters* **1970** 49.
7. Brossi, A., Grethe, G. and Teitel, S. *J. Org. Chem.* **35** (1970) 1100.
8. Crabbé, P. In Allinger, M. J. and Eliel, E. L., Eds., *Advances in Stereochemistry* 1967, Vol. 1, p. 144, and references therein.

Received January 9, 1973.

* For number XXXIII of this series, see Ref. 1.

Alginate Lyase in the Brown Alga *Laminaria digitata* (Huds.) Lamour

JOHN MADGWICK, ARNE HAUG and BJØRN LARSEN

Institutt for Marin Biokjemi, N-7034 Trondheim-NTH, Norway

Recent studies on alginic acid's block-like [1] structure have been directed towards the use of enzymes [2-4] which may show specificity for the different linkages of uronic acid residues in this polysaccharide. Although a decade has elapsed since the demonstration of alginate lyases,[5-8] they have only been prepared from non-algal sources.[2-8]

In this communication evidence is presented for the occurrence of an alginate-degrading enzyme system in the peripheral tissues of *Laminaria digitata*. A partially purified extract of this brown algae effected rapid reduction in the viscosity of sodium alginate with a concomitant rise in thiobarbituric acid reactive material. Preparation of the active fraction was facilitated by pretreatment of tissues with acetone at subzero temperatures.

Material and methods. L. digitata stipes were freshly harvested from Trondheimsfjord (Flakk), at low tide on 23.10.72, packed in dry ice and stored at −15°C until used. Epiphyte free outer layers, (*ca.* 0.1 mm thick; 7.96 g dry wt.), were scraped directly into a dry ice acetone bath (400 ml) in a mortar, and ground to small particles. The temperature of the solution was allowed to rise, (*ca.* −10°C), and the acetone filtered off under vacuum. The disintegrated tissues were then rinsed with diethyl ether, (10 sec) and dried in an air draft (20°C, 10 min). The pale green residue was reground as finely as possible and extracted with water for 18 h at 7°C. This brei was centrifuged in the cold and the supernatant freeze-dried (260 mg). The off-white powder was resuspended (2.4 mg/ml) in phosphate buffer, (pH 7.8, 0.05 M), and treated with ammonium sulphate, (85 % saturation at 0°C). Resulting flocculate, collected by centrifugation, (4°C), was dissolved in tap water, dialysed, (18 h, 7°C), with stirring, and freeze-dried (102 mg). Enzyme assays were carried out in collidine buffer (pH 7.1) at 21°C. The incubate contained calcium chloride (0.025 M), freeze-dried dialysate (1 mg/ml), and sodium alginate (ex. *Ascophyllum nodosum*, 93 % mannuronic acid) (0.83 mg/ml). The thiobarbituric acid reaction, TBA, was according to Weissbach and Hurwitz [9] and viscosity was measured with a pipette viscometer.

Results. Fig. 1 shows the time course of alginate degradation in terms of decreasing relative viscosity, η_r, and increasing TBA reactivity. Boiled extracts gave no increase in TBA, but had a small decrease in viscosity. A further control with no added alginate also gave no increase in TBA over the incubation period.

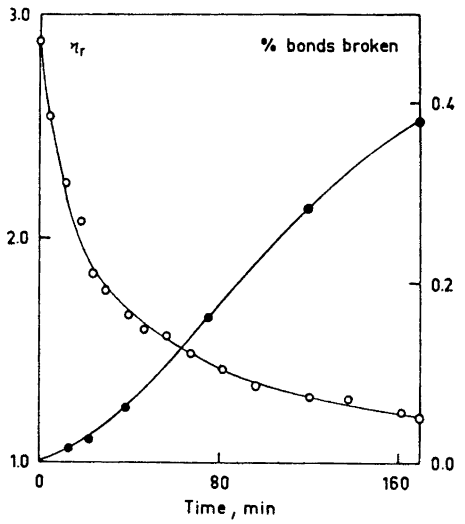

Fig. 1. Time course of enzymic degradation of alginate, (93 % mannuronic acid). ○: Relative viscosity, η_r. ●: Bonds broken, TBA.

Fig. 2 shows the viscosity drop, as function of time, expressed as the change in reciprocal intrinsic viscosity, $[\Delta(1/[\eta])]$, which is proportional to the number of bonds broken during depolymerisation. Straight lines were obtained which showed that the reaction occurred at a constant rate in the time interval studied. The slight decrease in viscosity in the boiled enzyme preparation was probably caused by the presence of small amounts of phenols.[10]

Fig. 3 shows the linear correlation between the simultaneous viscosity drop, [expressed as $\Delta(1/[\eta])$], and the rise in un-

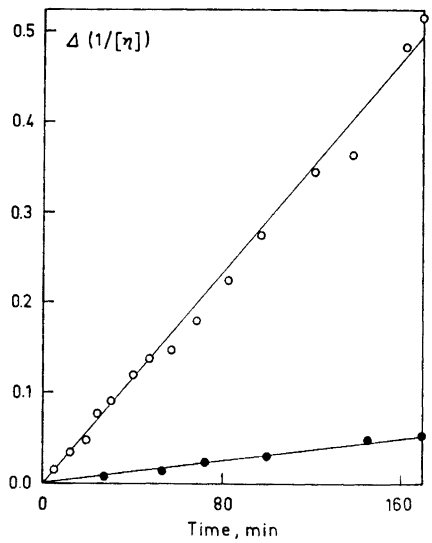

Fig. 2. Change in reciprocal intrinsic viscosity, $\Delta(1/[\eta])$, as a function of time for the enzymic breakdown of alginate by a *L. digitata* lyase preparation. ○: Enzymic degradation. ●: Boiled enzyme extract.

saturated uronic acid derivatives, (% bonds broken), and was interpreted as the result of a random scission of alginic acid by an alginate lyase [EC 4.2. 99].

A lyase was also prepared from a particulate fraction, (5 % total stipe protein), of the interior layers in *L. digitata*. Enzymic activity, per protein content, was similar for this preparation and for that from peripheral tissue described above. Demonstration of a lyase inside the plant was important because it indicated enzymic acitivity was a property of the algae and not that of microorganisms on the surface of the plants. Moreover, during enzyme preparations, care was taken to avoid the possibility of bacterial growth which might lead to formation of non-algal lyases. Studies on the characteristics and possible functions of this algal alginate lyase are in progress.

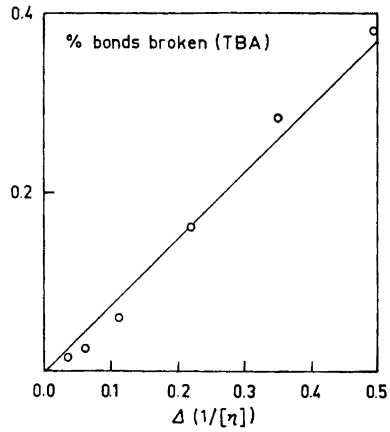

Fig. 3. Correlation between % bonds broken (as calculated from TBA reactivity), and decrease in intrinsic viscosity, $\Delta(1/[\eta])$, during degradation of alginate by an enzymic extract from *L. digitata*.

1. Haug, A., Larsen, B. and Smidsrød, O. *Acta Chem. Scand.* **20** (1966) 183.
2. Nisizawa, K., Fujibayashi, S. and Kashiwabara, Y. *J. Biochem. (Tokyo)* **64** (1968) 25.
3. Kashiwabara, Y., Suzuki, H. and Nisizawa, K. *J. Biochem. (Tokyo)* **66** (1969) 503.
4. Fujibayashi, S., Habe, H. and Nisizawa, K. *J. Biochem. (Tokyo)* **67** (1970) 37.
5. Preiss, J. and Ashwell, G. *J. Biol. Chem.* **237** (1962) 309.
6. Yoshikawa, M. and Kiyohara, T. *Sci. Rep. Hyogo Univ. Agr. Ser. Agr. Chem.* **6** (1964) 51.
7. Meland, S. M. *Nytt Magasin for Botanikk* **10** (1962) 53.
8. Eimhjellen, K. E., Rosness, P. A. and Hegge, E. *Acta Chem. Scand.* **17** (1963) 901.
9. Weissbach, A. and Hurwitz, J. *J. Biol. Chem.* **234** (1959) 705.
10. Smidsrød, O., Haug, A. and Larsen, B. *Acta Chem. Scand.* **17** (1963) 2628.

Received January 8, 1973.

The Crystal Structures of the Methylxanthates of Divalent Sulphur, Selenium, and Tellurium

NILS JOHAN BRØNDMO, STEINAR ESPERÅS, HALVOR GRAVER and STEINAR HUSEBYE

Chemical Institute, University of Bergen, N-5000 Bergen, Norway

A study of compounds of bidentate dithio- and related ligands with divalent group VI central atoms [1] has been extended to the following three compounds: Sulphur di(methylxanthate), $S(MeOCS_2)_2$ (I), selenium di(methylxanthate), $Se(MeOCS_2)_2$ (II), and tellurium di(methylxanthate), $Te(MeOCS_2)_2$ (III). Crystals of compounds II and III were obtained by a procedure similar to that used to prepare tellurium bis(dimethyldithiophosphate),[2,3] while I was prepared by nucleophilic substitution on the central sulphur atom in the pentathionate ion. Their structures have been solved by means of three-dimensional X-ray crystallographic methods. Data relevant to the solution of the structures are found in Table 1, while the structures of the molecules are shown in Fig. 1.

The configuration around the central atoms in the three compounds is trapezoid planar, as can be seen from Fig. 1. This is the characteristic configuration found earlier for compounds of divalent selenium and tellurium with bidentate dithio ligands.[1] The four-coordination in tellurium di(methylxanthate) is obtained through the formation of four intramolecular Te–S bonds, with average length 2.687 Å (sum cov. radii = 2.41 Å). This configuration is quite similar to that found in tellurium di(ethylxanthate) [4] and in divalent selenium and tellurium dithiocarbamates.[5–8] In addition, there is a tendency towards five-coordination in this type of tellurium compound, as can be seen from Fig. 1c. In the selenium and sulphur methylxanthates, the four-coordination arises through the formation of two strong intramolecular, and two extremely weak intermolecular, central atom to sulphur bonds, similar to the situation found in selenium bis(diethyldiselenophosphinate).[9] These weak bonds

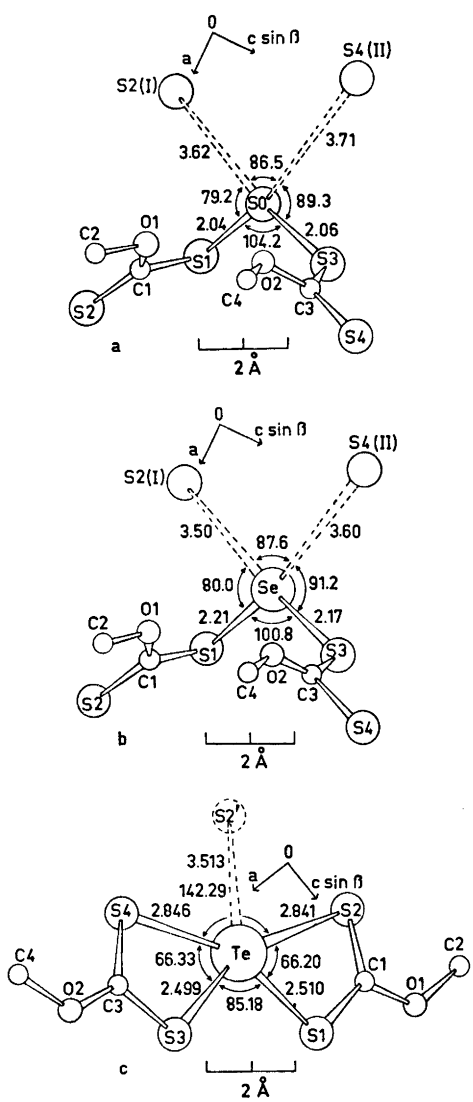

Fig. 1. a. The structure of $S(MeOCS_2)_2$ as seen along *a*. (E.s.d.: S–S = 0.007 Å, ∠S–S–S = 0.2°). b. The structure of $Se(MeOCS_2)_2$ as seen along *a*. (E.s.d.: Se–S = 0.008 Å, ∠S–Se–S = 0.2°). c. The structure of $Te(MeOCS_2)_2$ as seen along *a*. (E.s.d.: Te–S = 0.001 Å, ∠S–Te–S = 0.04°). Atom S2′ lies 1.10 Å above the TeS_4 plane and belongs to a neighbour molecule across a center of symmetry.

The standard deviations quoted above, are average values.

Table 1. a. Unit cell and space group data.

Compound	Crystal colour	Space group	a (Å)	b (Å)	c (Å)	β (°)	Z	Density (g/cm³): Calc	Found
I $S(MeOCS_2)_2$	Col. less	$I2/c$	13.580(5)	8.243(3)	18.429(4)	92.80(4)	8	1.59	1.57
II $Se(MeOCS_2)_2$	Yellow	$I2/c$	13.640(6)	8.299(3)	18.409(14)	93.56(6)	8	1.87	1.86
III $Te(MeOCS_2)_2$	Red	$P2_1/c$	4.2341(5)	14.202(2)	17.299(2)	92.99(2)	4	2.19	2.18

b. Intensity data *etc.*

	Compound I	Compound II	Compound III
No. of intensities collected above background	712 [a]	386 [a]	2124
Type of intensity data	Film	Diffractometer	Diffractometer
Radiation used	CuKα	MoKα	MoKα
Absorption correction undertaken	No	Yes	Yes
Anisotropic temp. factors used (atom type)	S	Se and S	Te, S, O and C
R-value	0.109	0.052	0.029
Method used to solve structure	Isomorphism with II	Direct methods	Patterson
Types of atoms included in full-matrix, least squares refinement	S, O, and C	Se, S, O, and C	Te, S, O and C[b]

[a] Relatively poor data due to instability of crystals.
[b] H atoms included in structure factor calculation, but their parameters were not refined.

are for I of the order of magnitude of a van der Waals contact, 3.70 Å, being 3.62 and 3.71 Å respectively. In II they are 3.51 and 3.60 Å, respectively, as compared to a Se···S van der Waals distance of 4.00 Å. However, the direction of the bonds and their coplanarity in the trapezoid planar configuration, indicate a secondary bonding interaction.[10] The structure of a dithiocarbamate of divalent sulphur shows no tendency towards planar four-coordination.[11]

The C–S–S–S–C and C–S–Se–S–C sequences of I and II have the *cis* configuration, while the *trans* configuration is found for the corresponding sequence in selenium bis(diethyldiselenophosphinate) [9] and related compounds. In the three xanthates studied here, the bonding in the S–M···S sequence, where M···S represents the weaker sulphur to central atom bond, *trans* to the stronger S–M bond, probably is of the three-center four-electron type.[1,12]

Divalent tellurium in such four-coordinate complexes is a better acceptor than selenium. It therefore has a greater tendency to form trapezoid planar complexes with the shortest average bonds, *i.e.* the type based on four intramolecular Te–S bonds. Thus with excellent donors as dithiocarbamates, both tellurium and selenium give this type complex. With the slightly poorer donor, the methylxanthate ion, only tellurium yields this type complex, while selenium gives a complex where the four-coordination is based on two intra- and two intermolecular Se–S bonds. For tellurium, this change in complex type occurs at the dimethyldithiophosphate ion,[3] which with divalent tellurium gives a complex similar to that of selenium di(methylxanthate). In tellurium bis(dimethyldithiophosphate) the intermolecular Te···S bonds are relatively strong, both being 3.31 Å.

1. Husebye, S. *Compounds of Divalent Selenium and Tellurium with Bidentate Ligands, Their Preparation, Structure and Bonding*, Diss., University of Bergen 1969.

2. Husebye, S. *Acta Chem. Scand.* **19** (1965) 1045.
3. Husebye, S. *Acta Chem. Scand.* **20** (1966) 24.
4. Husebye, S. *Acta Chem. Scand.* **21** (1967) 42.
5. Husebye, S. and Helland-Madsen, G. *Acta Chem. Scand.* **24** (1970) 2273.
6. Anderson, O. P. and Husebye, S. *Acta Chem. Scand.* **24** (1970) 3141.
7. Fabiani, C., Spagna, R., Vaciago, A. and Zambonelli, L. *Acta Cryst.* **B 27** (1971) 1499.
8. Husebye, S. *Acta Chem. Scand.* **24** (1970) 2198.
9. Husebye, S. and Helland-Madsen, G. *Acta Chem. Scand.* **23** (1969) 1398.
10. Alcock, N. W. *Advan. Inorg. Chem. Radiochem. In press.*
11. Husebye, S. *Acta Chem. Scand.* **27** (1973). *In press.*
12. Foss, O. *Acta Chem. Scand.* **16** (1962) 779.

Received January 5, 1973.

β-Lactones in the Perkin Reaction*

MAURI LOUNASMAA

Technical Research Centre, Chemical Laboratory, SF-02150 Otaniemi, Finland

It is now well established that the Perkin reaction, which is generally applied for aromatic aldehydes,[1] readily takes place, utilizing a great variety of quinones.[2-10] Due to the instability of the products formed, the reaction generally goes further, leading mostly to aromatic compounds. In the case of 2,6-dimethoxy-*p*-benzoquinone it has been shown [4,6,8,10] that with acetic, propionic, and isobutyric acid anhydrides the products (*1a*), (*1b*), (*2a*), (*2b*) and (*3a*),** respectively, are formed. Moreover, small amounts of corresponding diesters of 2,6-dimethoxy-hydroquinone are produced.

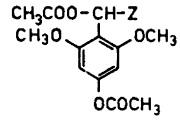

(1a) Z = H
(1b) Z = COOH

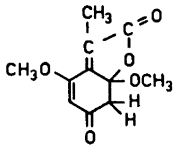

(2a)

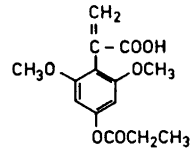

(2b)

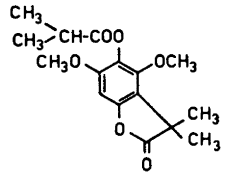

(3a)

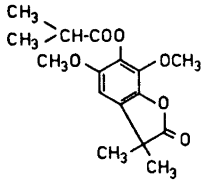

(3b)

By analogy with commonly accepted schemes, the mechanisms outlined in Refs. 2 to 8 can be presented for the formation of these compounds. However, as has been pointed out recently,[9,10] at least some of these compounds may be formed through a β-lactone.

When the standard reaction procedure [2-8] is modified by utilizing shorter reaction times and lower temperatures, it is possible in the cases of propionic and isobutyric acid anhydrides to isolate β-lactones from the reaction mixtures. For

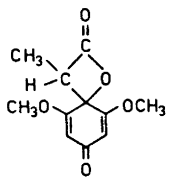

(2c)

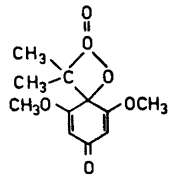

(3c)

* Part X. Sur les Réactions des Quinones. For Part IX, see Ref. 10.

** Analytical data presented for product (*3a*)[8] do not exclude the structure (*3b*).

2. Husebye, S. *Acta Chem. Scand.* **19** (1965) 1045.
3. Husebye, S. *Acta Chem. Scand.* **20** (1966) 24.
4. Husebye, S. *Acta Chem. Scand.* **21** (1967) 42.
5. Husebye, S. and Helland-Madsen, G. *Acta Chem. Scand.* **24** (1970) 2273.
6. Anderson, O. P. and Husebye, S. *Acta Chem. Scand.* **24** (1970) 3141.
7. Fabiani, C., Spagna, R., Vaciago, A. and Zambonelli, L. *Acta Cryst.* **B 27** (1971) 1499.
8. Husebye, S. *Acta Chem. Scand.* **24** (1970) 2198.
9. Husebye, S. and Helland-Madsen, G. *Acta Chem. Scand.* **23** (1969) 1398.
10. Alcock, N. W. *Advan. Inorg. Chem. Radiochem. In press.*
11. Husebye, S. *Acta Chem. Scand.* **27** (1973). *In press.*
12. Foss, O. *Acta Chem. Scand.* **16** (1962) 779.

Received January 5, 1973.

β-Lactones in the Perkin Reaction*

MAURI LOUNASMAA

Technical Research Centre, Chemical Laboratory, SF-02150 Otaniemi, Finland

It is now well established that the Perkin reaction, which is generally applied for aromatic aldehydes,[1] readily takes place, utilizing a great variety of quinones.[2-10] Due to the instability of the products formed, the reaction generally goes further, leading mostly to aromatic compounds. In the case of 2,6-dimethoxy-*p*-benzoquinone it has been shown [4,6,8,10] that with acetic, propionic, and isobutyric acid anhydrides the products (*1a*), (*1b*), (*2a*), (*2b*) and (*3a*),** respectively, are formed. Moreover, small amounts of corresponding diesters of 2,6-dimethoxy-hydroquinone are produced.

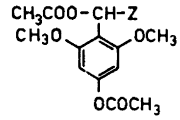

(1a) Z = H
(1b) Z = COOH

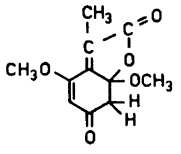

(2a)

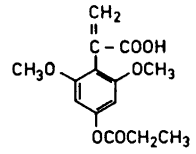

(2b)

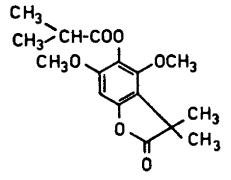

(3a)

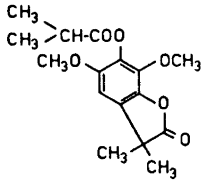

(3b)

By analogy with commonly accepted schemes, the mechanisms outlined in Refs. 2 to 8 can be presented for the formation of these compounds. However, as has been pointed out recently,[9,10] at least some of these compounds may be formed through a β-lactone.

When the standard reaction procedure [2-8] is modified by utilizing shorter reaction times and lower temperatures, it is possible in the cases of propionic and isobutyric acid anhydrides to isolate β-lactones from the reaction mixtures. For

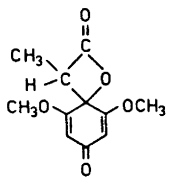

(2c)

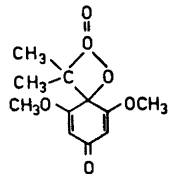

(3c)

* Part X. Sur les Réactions des Quinones. For Part IX, see Ref. 10.

** Analytical data presented for product (*3a*)[8] do not exclude the structure (*3b*).

these β-lactones, characterized here by letters A and B, the structures (*2c*) and (*3c*), respectively, are proposed.

The following physical data were obtained for the isolated β-lactones:

β-Lactone A ($C_{11}H_{12}O_5$), m.p. 134–135°C d., IR. ν_{max} 1840, 1665, 1635, and 1600 cm^{-1}, ^1H NMR ($CDCl_3$) τ 4.36 (1H, d, *J* 1 cps), τ 4.46 (1H, d, *J* 1 cps), τ 5.76 (1H, quart., *J* 7 cps), τ 6.18 (6H, s), and τ 8.70 (3H, d, *J* 7 cps), mass. *m/e* 224 (M^+), 196, 180, 169, 165, 152, and 137.

β-Lactone B ($C_{12}H_{14}O_5$), m.p. 154.5°C, IR. ν_{max} 1840, 1660, 1650, 1635, and 1602 cm^{-1}, ^1H NMR ($CDCl_3$) τ 4.46 (2H, s), τ 6.18 (6H, s), and τ 8.60 (6H, s), mass. *m/e* 238 (M^+), 210, 194, 179, 169, 166, and 151.

Transformation of β-lactone A to product (*2a*) and similarities in the ^1H NMR spectra of β-lactones A and B favour the fact that the β-lactone ring in both cases is in the position 1. Moreover, the fact that β-lactone B is not transformed to a γ-lactone by an acidic treatment according to Chitwood *et al.*,[11] supports the position 1.

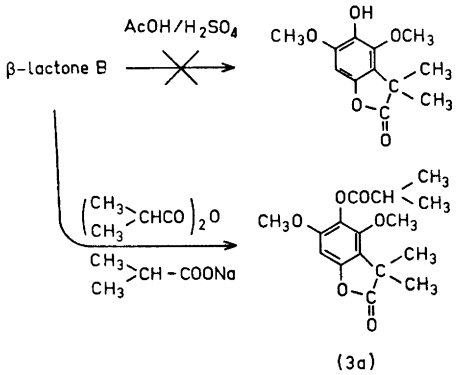

On the other hand, transformation of the β-lactone B to product (*3a*) by prolonged heating with isobutyric acid anhydride in the presence of sodium isobutyrate seems to support the position 4. However, this transformation can be explained by the equilibria between the β-lactones and the original quinone, presented below, followed by a rearrangement and an esterification.

The existence of an equilibrium between a β-lactone and the original quinone in the reaction mixture is supported by the fact

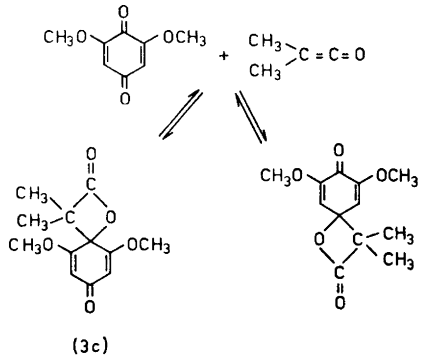

that the treatment of β-lactone B with propionic acid anhydride and sodium propionate leads to products (*2a*) and (*2b*). Due to the existence of this equilibrium, the isolation of β-lactones A and B does not prove with certainty that these β-lactones are intermediates in the formation of products (*2a*), (*2b*), and (*3a*). However, it proves that β-lactones can be formed in the Perkin reaction conditions.

The most plausible way for the formation of β-lactones A and B is presented in Scheme 1. It consists of the formation of a ketene from the corresponding carboxylic acid anhydride, followed by the addition of the ketene to the carbonyl group of the quinone.

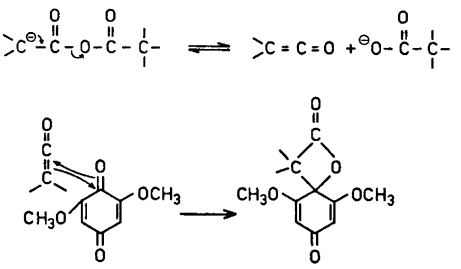

Scheme 1.

By analogy, and taking into account the general reactivity of ketenes with aldehydes,[12] it seems reasonable to suppose that at least in some favourable cases, the normal Perkin reaction of aromatic aldehydes goes through a β-lactone. A more detailed discussion on this subject has been published recently.[9]

The long known failure of aliphatic aldehydes to undergo the Perkin reaction,[13] and the fact that the reaction of ketene with aromatic aldehydes in the presence of anhydrous potassium acetate to produce α,β-unsaturated carboxylic acid anhydrides is not applicable to aliphatic aldehydes,[14] are in agreement with the above presented conclusions.

Experimental. The IR spectra have been obtained from KBr-discs on a Perkin Elmer 237 instrument. The NMR spectra have been taken with a Varian T-60 instrument in $CDCl_3$ using TMS as internal standard, and the mass spectra with an A.E.I. MS-9 instrument. The melting points have been determined on a Reichert micro hot stage and are uncorrected.

*Reaction between 2,6-dimethoxy-*p*-benzoquinone and propionic acid anhydride.* A mixture of 2,6-dimethoxy-*p*-benzoquinone (0.001 mol; 168 mg), sodium propionate (300 mg) and propionic acid anhydride (5 ml) was stirred at 95°C for 2 h. The crude mixture was separated in the normal way and successively fractionated by column and preparative layer chromatography (silica gel/chloroform). Among the fractions obtained two were analyzed more in details.

Fraction 1 (10 mg) (β-lactone A). Recrystallized from CCl_4. M.p. 134–135°C d. Analytical data, given in the theoretical part, indicate that it is a compound of structure (*2c*).

Fraction 2 (130 mg). Recrystallized from CCl_4. M.p. 127.5°C. Identified by m.p., IR and NMR as product (*2a*).

*Reaction between 2,6-dimethoxy-*p*-benzoquinone and isobutyric acid anhydride.* A mixture of 2,6-dimethoxy-*p*-benzoquinone (0.01 mol; 1.68 g), sodium isobutyrate (3 g), and isobutyric acid anhydride (50 ml) was stirred at 95°C for 6 h. The crude mixture was separated in the normal way and purified by column chromatography (silica gel/chloroform). Yield 1.5 g (β-lactone B). Recrystallized from CCl_4. M.p. 154.5°C. Analytical data, given in the theoretical part, indicate, that it is a compound of structure (*3c*).

Reaction between β-lactone A and propionic acid anhydride. A mixture of β-lactone A (5 mg), sodium propionate (5 mg), and propionic acid anhydride (0.5 ml) was stirred at 100°C for 48 h. The reaction mixture worked up in the normal way contained *inter alia* compounds (*2a*) and (*2b*).

Reaction between β-lactone B and isobutyric acid anhydride. A mixture of β-lactone B (100 mg), sodium isobutyrate (100 mg), and isobutyric acid anhydride (10 ml), was stirred at 150°C for 60 h. The reaction mixture worked up in the normal way consisted mainly of compound (*3a*).

Reaction between β-lactone B and propionic acid anhydride. A mixture of β-lactone B (100 mg), sodium propionate (100 mg), and propionic acid anhydride (10 ml) was stirred at 100°C for 72 h. The reaction mixture worked up in the normal way contained *inter alia* compounds (*2a*) and (*2b*).

Attempt to transpose the β-lactone B to a γ-lactone. To a stirred mixture of 200 mg of β-lactone B in 5 ml of glacial acetic acid was added 4 drops of conc. H_2SO_4. The mixture was stirred for 18 h at room temperature After work-up more than 80 % of β-lactone B was recovered. No γ-lactone could be detected.

The author's thanks are due to M. J.-P. Cosson, Institut de Chimie des Substances Naturelles, Gif-sur-Yvette, France, for the mass spectra.

1. House, H. O. *Modern Synthetic Reactions*, Benjamin, New York 1965, p. 235.
2. Gripenberg, J. and Lounasmaa, M. *Acta Chem. Scand.* **20** (1966) 2202.
3. Lounasmaa, M. *Acta Chem. Scand.* **20** (1966) 2304.
4. Lounasmaa, M. *Tetrahedron Letters* **1968** 91.
5. Lounasmaa, M. *Acta Chem. Scand.* **21** (1967) 2807.
6. Lounasmaa, M. *Acta Chem. Scand.* **22** (1968) 70.
7. Lounasmaa, M. *Acta Chem. Scand.* **22** (1968) 3191.
8. Lounasmaa, M. *Acta Chem. Scand.* **25** (1971) 1849.
9. Lounasmaa, M. *Acta Chem. Scand.* **26** (1972) 2703.
10. Lounasmaa, M. *Acta Chem. Scand.* **27** (1973) 708.
11. Chitwood, J. L., Gott, P. G., Krutak, Sr., J. J. and Martin, J. C. *J. Org. Chem.* **36** (1971) 2216.
12. Borrmann, D. In Houben-Weyl, *Methoden der organischen Chemie*, Thieme, Stuttgart 1968, 7/4, pp. 165–168, and references therein.
13. Johnson, J. R. *Org. Reactions* **1** (1942) 217–223, and references therein. See also, Crawford, M. and Little, W. T. *J. Chem. Soc.* **1959** 722.
14. Hurd, C. D. and Williams, J. W. *J. Am. Chem. Soc.* **58** (1936) 962.

Received January 10, 1973.

Regulation of Valine Degradation in *Pseudomonas fluorescens* UK-1. Induction of Enoyl Coenzyme A Hydratase

MATTI PUUKKA

Department of Biochemistry, University of Turku, SF-20500 Turku 50, Finland

Recent studies concerning regulation of valine catabolism in *Pseudomonas* have shown that D-amino acid dehydrogenase, branched chain 2-oxo acid dehydrogenase, 3-hydroxyisobutyryl CoA hydrolase, 3-hydroxyisobutyrate dehydrogenase, and methylmalonate semialdehyde dehydrogenase are inducible enzymes.[1-5] In *P. fluorescens* branched chain amino acid transaminase is induced by branched chain amino acids and by branched chain 2-oxo acids,[1] but in *P. putida* and *P. aeruginosa* this transaminase seems to be a constitutive enzyme.[5] Furthermore, Marshall and Sokatch [5] have established that the catabolic pathway for valine in *P. putida* and *P. aeruginosa* is induced in three separate segments: (1) D-amino acid dehydrogenase, (2) branched chain 2-oxo acid dehydrogenase, and (3) 3-hydroxyisobutyrate dehydrogenase and methylmalonate semialdehyde dehydrogenase. The regulation of enoyl CoA hydratase (EC 4. 2. 1. 17) has not yet been studied.

The data presented in this paper demonstrate that enoyl CoA hydratase in *P. fluorescens* UK-1 is induced by growth on branched chain amino acids, branched chain 2-oxo acids, and branched short chain fatty acids.

Materials. Methacrylyl coenzyme A was synthesized by the method of Simon and Shemin as described by Stadtman,[6] and sodium DL-3-hydroxyisobutyrate was prepared as described elsewhere.[7] All other reagents were commercial preparations.

Organism and cultural conditions. Pseudomonas fluorescens strain UK-1 was grown in a mineral medium containing (per litre) KH_2PO_4, 0.82 g; $MgSO_4.7H_2O$, 0.25 g; $FeSO_4.7H_2O$, 2.8 mg. The pH was adjusted to pH 6.8 with potassium hydroxide. The concentration of the carbon source was 10 mM, and ammonium sulphate (10 mM) was used as nitrogen source. The organism was precultivated in a glutamate (20 mM) medium. The cultures were aerated with an aquarium pump and incubated at 30°. Growth was estimated from turbidity measurements in a Klett-Summerson colorimeter fitted with filter 62.

Preparation and assay of the enzyme. The samples (about 4 mg dry weight) were withdrawn and cell extracts were prepared as described earlier.[1] The enzyme activity was assayed in freshly prepared cell extracts. The rate of enzymatic hydration of methacrylyl CoA to 3-hydroxyisobutyryl CoA at 30° was determined spectrophotometrically at 268 nm according to Stern *et al.*[8] The reaction system contained 70 μmol of Tris-HCl buffer, pH 7.5, 0.06 μmol of methacrylyl CoA, and a cell extract containing 12.5–125 μg dry weight. The reaction was started by adding the cell extract. The total volume of the reaction mixture was 1.00 ml. An enzyme unit is defined as the amount of enzyme which catalyzes the hydration of 1 μmol/min of methacrylyl CoA to 3-hydroxyisobutyryl CoA at 30°.

Results and discussion. The level of enoyl CoA hydratase was low, about 0.02 unit per mg dry weight, when *P. fluorescens* UK-1 was precultured for two generations in glutamate medium. If the cells were then transferred to a medium containing valine or isoleucine, the specific activity of the enzyme began to increase at the same time as the growth of the bacteria. The enzyme was formed in the presence of 2-oxoisovalerate and 2-oxoisocaproate, too. In addition, branched short chain fatty acids isobutyrate and isovalerate caused a marked increase in the enzyme activity. Maximal specific activity was reached in the middle of the exponential phase (Table 1). Glucose, lactate, propionate, and 3-hydroxyisobutyrate have no inducing ability.

The specific activity of enoyl CoA hydratase in the cells of *P. fluorescens* UK-1 grown on several carbon sources is shown in Table 1. The specific activity of the enzyme increased 23-fold on isoleucine and 2-oxoisocaproate, and almost 18-fold on isovalerate. The increase in specific activity on valine, 2-oxoisovalerate, and isobutyrate was 7-, 9-, and 13-fold, respectively.

Fig. 1 shows the kinetics of induction of enoyl CoA hydratase in response to the different growth substrates. Isoleucine and isovalerate were the most powerful inducers among the carbon sources studied. Once induction had begun the differential rate of synthesis of enoyl CoA hydratase

Table 1. Level of enoyl CoA hydratase in *P. fluorescens* UK-1 grown on different carbon sources. Crude extracts were prepared from the cells of the exponential phase and enzyme activities were determined as described under *Preparation and assay of the enzyme.*

Carbon source for growth (10 mM)	Specific activity of enoyl CoA hydratase (mU/mg dry weight)
Isoleucine	450
2-Oxoisocaproate	450
Isovalerate	350
Isobutyrate	250
2-Oxoisovalerate	170
Valine	140
3-Hydroxyisobutyrate	60
Propionate	50
Glucose	40
Lactate	40
Glutamate	30

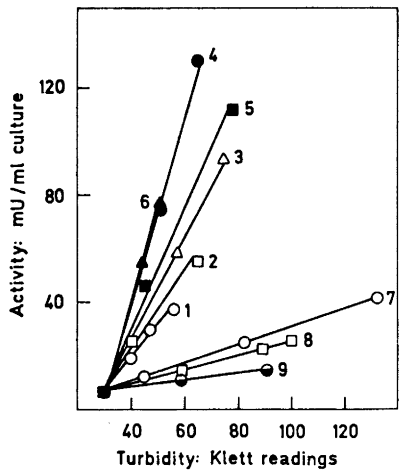

Fig. 1. Differential rate of formation of enoyl CoA hydratase during growth of *P. fluorescens* UK-1 on different carbon sources. The cells had been precultured in a glutamate medium. Samples were withdrawn from the cultures at intervals of 2–6 h, cell extracts were prepared and enzyme activities were determined as described under *Preparation and assay of the enzyme.*

1, Valine. 2, 2-Oxoisovalerate. 3, Isobutyrate. 4, Isoleucine. 5, 2-Oxoisocaproate. 6, Isovalerate. 7, 3-Hydroxyisobutyrate. 8, Propionate. 9, Glucose.

in response to the inducer remained constant.

These data indicate that in *P. fluorescens* UK-1 enoyl CoA hydratase is subject to regulatory control, and the results shown in Table 1 and Fig. 1 suggest that the enoyl CoA hydratase is induced by (growth on) branched chain amino acids, branched chain 2-oxo acids, and branched short chain fatty acids derived from branched chain amino acids, but in *Escherichia coli* enoyl CoA hydratase, which participates in β-oxidation of fatty acids, is induced only by long chain fatty acids.[9,10]

Acknowledgements. I express my sincere gratitude to Professor Veikko Nurmikko, Head of the Department of Biochemistry, for his continued interest in this work and critical reading of the manuscript.

1. Puukka, M., Lönnberg, H. and Nurmikko, V. *Acta Chem. Scand.* **26** (1972) 1271.
2. Puukka, M., Mäntsälä, P., Lönnberg, H., Pajula, R. and Nurmikko, V. *Acta Chem. Scand.* **26** (1972) 1299.
3. Nurmikko, V., Puukka, M. and Puukka, R. *Suomen Kemistilehti* **B 45** (1972) 193.
4. Puukka, M. and Nurmikko, V. *Suomen Kemistilehti* **B 45** (1972) 196.
5. Marshall, V. deP. and Sokatch, J. R. *J. Bacteriol.* **110** (1972) 1073.
6. Stadtman, E. R. In Colowick, S. P. and Kaplan, N. O. *Methods in Enzymology*, Academic, New York and London, 1957, Vol. III, p. 931.
7. Robinson, W. G. and Coon, M. J. In Colowick, S. P. and Kaplan. N. O. *Methods in Enzymology*, Academic, New York and London 1963, Vol. VI, p. 552.
8. Stern, J. R., del Campillo, A. and Raw, I. *J. Biol. Chem.* **218** (1956) 971.
9. Overath, P., Raufuss, E.-M., Stoffel, W. and Ecker, W. *Biochem. Biophys. Res. Commun.* **29** (1967) 28.
10. Weeks, G., Shapiro, M., Burns, R. O. and Wakil, S. J. *J. Bacteriol.* **97** (1969) 827.

Received January 15, 1973.

Regulation of Valine Degradation in *Pseudomonas fluorescens* UK-1. Induction of Methylmalonate Semialdehyde Dehydrogenase

MATTI PUUKKA, SIMO LAAKSO and VEIKKO NURMIKKO

Department of Biochemistry, University of Turku, SF-20500 Turku 50, Finland

Methylmalonate semialdehyde dehydrogenase catalyzes the oxidation of methylmalonate semialdehyde and propionaldehyde to propionyl CoA in the presence of NAD and CoA. It is active when mercaptoethanol replaces CoA and an active propionyl derivative is then formed as well.[1] Methylmalonate semialdehyde dehydrogenase from *Pseudomonas aeruginosa* has been purified to a form homogeneous by the criterion of disc gel electrophoresis.[1]

The object of the present study was to investigate the induction of methylmalonate semialdehyde dehydrogenase during the growth of *P. fluorescens* UK-1. We have shown earlier that *P. fluorescens* UK-1, when grown with valine as the sole source of carbon and nitrogen, produces inducible branched chain amino acid transaminase,[2] branched chain 2-oxo acid dehydrogenase,[3] enoyl CoA hydratase,[4] 3-hydroxyisobutyryl CoA hydrolase,[5] and 3-hydroxyisobutyrate dehydrogenase.[6] This report shows that methylmalonate semialdehyde dehydrogenase is induced in the presence of valine, 2-oxoisovalerate, isobutyrate, and 3-hydroxyisobutyrate, but not in the presence of glucose or propionate.

Materials. The micro-organism and chemicals used were as described in the preceding paper,[4] in which the culture methods were also described.

Cell extract and enzyme assay. The samples (about 4 mg dry weight) were withdrawn and cell extracts prepared as described earlier.[2] The activity of the enzyme was assayed with freshly prepared cell extracts. The rate of reduction of NAD at 30° was determined spectrophotometrically at 340 nm according to Sokatch *et al.*[7] In 1 ml the reaction system contained 100 μmol of Tris-HCl buffer, pH 9.2, 40 μmol of 2-mercaptoethanol, 160 μmol of propionaldehyde, 1 μmol of NAD and a cell extract with a dry weight of 0.25 mg. The reaction was started by adding the cell extract. A unit of the enzyme is defined as the amount of enzyme which catalyzes the reduction of 1 μmol/min of NAD at 30°.

Results and discussion. The data in Table 1 show the specific activity of methylmalonate semialdehyde dehydrogenase obtained when *P. fluorescens* UK-1 was grown on various single-carbon sources. The enzyme was formed in the presence of valine or its degradation products, 2-oxoisovalerate, isobutyrate or 3-hydroxyisobutyrate, but only slightly in the presence of propionate. In addition, isoleucine, leucine, 2-oxoisocaproate, and isovalerate markedly increased the specific activity of methylmalonate semialdehyde dehydrogenase. The enzyme was produced during all active growth phases, but the maximum level of activity was not reached until the culture approached the stationary phase. This indicates that the formation of methylmalonate semialdehyde dehydrogenase is

Table 1. Effect of growth substrates on the formation of methylmalonate semialdehyde dehydrogenase in *P. fluorescens* UK-1. Bacteria were grown on basal mineral medium supplemented with growth substrates as indicated. Crude extracts were prepared from the cells at the end of the exponential phase and enzyme activities were determined as described in the section *Cell extract and enzyme assay.*

Carbon source for growth	Specific activity of methylmalonate semialdehyde dehydrogenase (mU/mg dry weight)
3-Hydroxyisobutyrate	17.1
Isobutyrate	13.9
2-Oxoisovalerate	12.1
Valine	12.3
Isoleucine	6.9
Leucine	6.8
2-Oxoisocaproate	6.5
Isovalerate	6.2
Propionate	3.4
Acetate	1.1
Glucose	0.5

closely linked with cell multiplication when the inducer is the only source of carbon and energy. It should be noted that very low specific activities of the enzyme were detected when *P. fluorescens* UK-1 was cultured on glucose or acetate (Table 1). Methylmalonate semialdehyde dehydrogenase, like 3-hydroxyisobutyryl CoA hydrolase [5] and 3-hydroxyisobutyrate dehydrogenase,[6] was induced to the maximum level when *P. fluorescens* UK-1 was cultured on 3-hydroxyisobutyrate. This shows that the really effective inducer of methylmalonate semialdehyde dehydrogenase is 3-hydroxyisobutyrate. On the other hand, Marshall and Sokatch [8] have reported that in *P. putida* isobutyrate is about twice as effective as an inducer of methylmalonate semialdehyde dehydrogenase as 3-hydroxyisobutyrate.

Fig. 1 shows the results of experiments in which the deinduction and stability of the induced methylmalonate semialdehyde dehydrogenase were studied. Cells were precultured in a medium containing isobutyrate as inducer and then transferred to a glutamate medium. The cells exhibited a continuous decline in specific activity; the total activity, however, remained practically constant (Fig. 1). This indicates that the induced methylmalonate semialdehyde dehydrogenase is stable *in vivo*, the decreasing specific activity being due solely to reduction of the enzyme concentration during the growth of the bacteria.

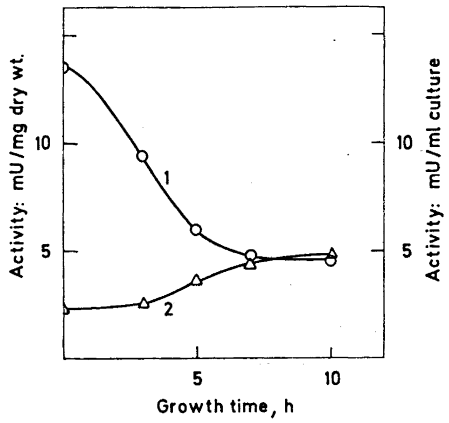

Fig. 1. The stability of induced methylmalonate semialdehyde dehydrogenase during deinduction. Cells were precultured in an isobutyrate medium, and when growth reached the late exponential phase the cells were centrifuged and transferred to a medium containing glutamate as the sole carbon source. Samples were withdrawn from the culture at intervals. Crude extracts were prepared and enzyme activities determined as described under *Cell extract and enzyme assay*.

1. Specific activity of methylmalonate semialdehyde dehydrogenase. 2. Total activity of methylmalonate semialdehyde dehydrogenase.

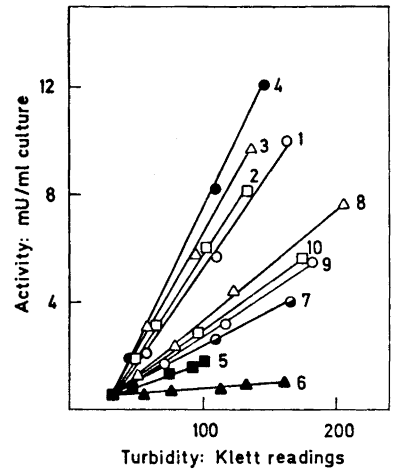

Fig. 2. Differential rate of formation of methylmalonate semialdehyde dehydrogenase during growth of *P. fluorescens* UK-1 on different growth substrates. The cells were precultured in a glutamate medium and transferred to a basal mineral medium supplemented with growth substrates as indicated. The experimental details were the same as described in the legend to Fig. 1.

1, Valine. 2, 2-Oxoisovalerate. 3, Isobutyrate. 4, 3-Hydroxyisobutyrate. 5, Propionate. 6, Glucose. 7, Leucine. 8, Isoleucine. 9, 2-Oxoisocaproate. 10, Isovalerate.

As can be seen from Fig. 2, the differential rate of synthesis of methylmalonate semialdehyde dehydrogenase remained constant to all the inducers studied. The maximal increase in total activity (about 0.02 unit per mg increase in cell mass) was obtained when *P. fluorescens* UK-1 was grown on 3-hydroxyisobutyrate.

These experimental results provide strong evidence that 3-hydroxyisobutyrate

may be the natural inducer for methylmalonate semialdehyde dehydrogenase in *P. fluorescens* UK-1. However, the possibility that methylmalonate semialdehyde, isobutyrate, 2-oxoisovalerate, or valine are also the inducers of the enzyme is not excluded.

1. Bannerjee, D., Sanders, L. E. and Sokatch, J. R. *J. Biol. Chem.* **245** (1970) 1828.
2. Puukka, M., Lönnberg, H. and Nurmikko, V. *Acta Chem. Scand.* **26** (1972) 1271.
3. Puukka, M., Mäntsälä, P., Lönnberg, H., Pajula, R. and Nurmikko, V. *Acta Chem. Scand.* **26** (1972) 1299.
4. Puukka, M. *Acta Chem. Scand.* **27** (1973) 718.
5. Nurmikko, V., Puukka, M. and Puukka, R. *Suomen Kemistilehti* **B 45** (1972) 193.
6. Puukka, M. and Nurmikko, V. *Suomen Kemistilehti* **B 45** (1972) 196.
7. Sokatch, J. R., Sanders, L. E. and Marshall, V. P. *J. Biol. Chem.* **243** (1968) 2500.
8. Marshall, V. de P. and Sokatch, J. R. *J. Bacteriol.* **110** (1972) 1073.

Received January 15, 1973.

Low-temperature Transitions of Chlorinated Polyethylenes

VÄINÖ A. ERÄ[a] and
L. LAWRENCE CHAPOY[b]

[a]*Department of Wood and Polymer Chemistry, University of Helsinki, Malminkatu 20, SF-00100 Helsinki 10, Finland, and* [b]*Institut for Kemiindustri, The Technical University of Denmark, DTH, Bygning 227, DK-2800 Lyngby, Denmark*

Several studies have been made regarding the low-temperature relaxation behavior of solution chlorinated polyethylenes.[1-4] It has been found by dynamic-mechanical studies that the γ-relaxation process occurs below -100°C in amorphous CPE-polymers. Using dielectric relaxation measurements on CPE with low chlorine content the temperature of maximum loss at a frequency of 1 kHz was about -90°C. The γ-transition of commercial polyethylenes has been reported to occur in two temperature regions, -120 to -130°C and -80 to -90°C.[5] In this study, suspension chlorinated low-density polyethylenes were investigated by differential thermal analysis measurements, DTA, in the temperature range -120° to 0°C.

Experimental. The samples were commercial suspension-chlorinated low-density polyethylenes (CPE) of varying chlorine content. The source of all CPE samples, the parent polymer, was a low-density polyethylene which was also used in these studies. The characteristics of the samples are given elsewhere.[6] The Du Pont 900 DTA apparatus was used for these measurements. The instrument was equipped with a low-temperature chamber made of polypropylene which allowed the measurements to be carried out in the temperature range -120° to 0°C. Liquid nitrogen was used as a cooling medium. The procedure employed in the runs was as follows: A macro sample tube was filled with the powdered polymer as received to depth of 5 mm. The sample was melted, pressed with the ceramic sleeve and the thermocouple was inserted in the softened mass. The reference tube consisted of a thermocouple inserted midway into 5 mm of glass beads. The tubes were placed into the low-temperature chamber. The samples were heated above melting points of the polymers, $+120$°C, to remove internal stresses and then cooled to liquid nitrogen temperature. The heating rate was 20°C/min.

Results and discussion. Thermograms of LDPE and CPE are seen in Fig. 1. The composition and transition points of the polymers are given in Table 1.

It can be seen that the transitions of CPE occur in the temperature intervals -38° to -39°C and -104° to -110°C. The latter range is seemingly related to the γ-transition of CPE. It has been found that the mechanical loss maximum at 2.7 Hz of solution chlorinated CPE with a chlorine content 20–45 % lies in the temperature range immediately below -100°C.[1,2] It has been shown that the γ-transition of semi-crystalline PE arises principally from contributions of the non-crystalline regions of the polymer.[8] On the basis of structural studies suspension chlorinated polyethylene, CPE, can be visualized as containing definite amounts of ethylene ($-CH_2-CH_2-$) and vinyl chloride ($-CH_2-CHCl-$) units when the chlorine content of the polymer varies between 0– and 56 %.[9,10] The distribu-

may be the natural inducer for methylmalonate semialdehyde dehydrogenase in *P. fluorescens* UK-1. However, the possibility that methylmalonate semialdehyde, isobutyrate, 2-oxoisovalerate, or valine are also the inducers of the enzyme is not excluded.

1. Bannerjee, D., Sanders, L. E. and Sokatch, J. R. *J. Biol. Chem.* **245** (1970) 1828.
2. Puukka, M., Lönnberg, H. and Nurmikko, V. *Acta Chem. Scand.* **26** (1972) 1271.
3. Puukka, M., Mäntsälä, P., Lönnberg, H., Pajula, R. and Nurmikko, V. *Acta Chem. Scand.* **26** (1972) 1299.
4. Puukka, M. *Acta Chem. Scand.* **27** (1973) 718.
5. Nurmikko, V., Puukka, M. and Puukka, R. *Suomen Kemistilehti* **B 45** (1972) 193.
6. Puukka, M. and Nurmikko, V. *Suomen Kemistilehti* **B 45** (1972) 196.
7. Sokatch, J. R., Sanders, L. E. and Marshall, V. P. *J. Biol. Chem.* **243** (1968) 2500.
8. Marshall, V. de P. and Sokatch, J. R. *J. Bacteriol.* **110** (1972) 1073.

Received January 15, 1973.

Low-temperature Transitions of Chlorinated Polyethylenes

VÄINÖ A. ERÄ[a] and
L. LAWRENCE CHAPOY[b]

[a]*Department of Wood and Polymer Chemistry, University of Helsinki, Malminkatu 20, SF-00100 Helsinki 10, Finland, and* [b]*Institut for Kemiindustri, The Technical University of Denmark, DTH, Bygning 227, DK-2800 Lyngby, Denmark*

Several studies have been made regarding the low-temperature relaxation behavior of solution chlorinated polyethylenes.[1-4] It has been found by dynamic-mechanical studies that the γ-relaxation process occurs below -100°C in amorphous CPE-polymers. Using dielectric relaxation measurements on CPE with low chlorine content the temperature of maximum loss at a frequency of 1 kHz was about -90°C. The γ-transition of commercial polyethylenes has been reported to occur in two temperature regions, -120 to -130°C and -80 to -90°C.[5] In this study, suspension chlorinated low-density polyethylenes were investigated by differential thermal analysis measurements, DTA, in the temperature range -120° to 0°C.

Experimental. The samples were commercial suspension-chlorinated low-density polyethylenes (CPE) of varying chlorine content. The source of all CPE samples, the parent polymer, was a low-density polyethylene which was also used in these studies. The characteristics of the samples are given elsewhere.[6] The Du Pont 900 DTA apparatus was used for these measurements. The instrument was equipped with a low-temperature chamber made of polypropylene which allowed the measurements to be carried out in the temperature range -120° to 0°C. Liquid nitrogen was used as a cooling medium. The procedure employed in the runs was as follows: A macro sample tube was filled with the powdered polymer as received to depth of 5 mm. The sample was melted, pressed with the ceramic sleeve and the thermocouple was inserted in the softened mass. The reference tube consisted of a thermocouple inserted midway into 5 mm of glass beads. The tubes were placed into the low-temperature chamber. The samples were heated above melting points of the polymers, $+120$°C, to remove internal stresses and then cooled to liquid nitrogen temperature. The heating rate was 20°C/min.

Results and discussion. Thermograms of LDPE and CPE are seen in Fig. 1. The composition and transition points of the polymers are given in Table 1.

It can be seen that the transitions of CPE occur in the temperature intervals -38° to -39°C and -104° to -110°C. The latter range is seemingly related to the γ-transition of CPE. It has been found that the mechanical loss maximum at 2.7 Hz of solution chlorinated CPE with a chlorine content 20–45 % lies in the temperature range immediately below -100°C.[1,2] It has been shown that the γ-transition of semi-crystalline PE arises principally from contributions of the non-crystalline regions of the polymer.[8] On the basis of structural studies suspension chlorinated polyethylene, CPE, can be visualized as containing definite amounts of ethylene ($-CH_2-CH_2-$) and vinyl chloride ($-CH_2-CHCl-$) units when the chlorine content of the polymer varies between 0– and 56 %.[9,10] The distribu-

Table 1. Composition and transition temperatures of polymers.

Sample	Composition [a]	Transition temperature, °C Tg	γ-transition
LDPE		−39	−90
CPE (27.8 % Cl)	$(CH_2CH_2)_{0.697}(CH_2CHCl)_{0.303}$	−39	−110
CPE (35.0 % Cl)	$(CH_2CH_2)_{0.585}(CH_2CHCl)_{0.415}$	−38	−104
CPE (42.8 % Cl)	$(CH_2CH_2)_{0.422}(CH_2CHCl)_{0.578}$	−38	−106

[a] Calculated on the basis of chlorine content.[7]

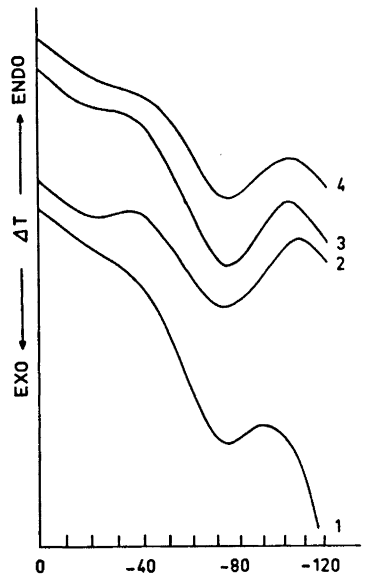

Fig. 1. Thermograms of powdery polymers. 1. LDPE; 2. CPE (27.8 % Cl); 3. CPE (35.0 % Cl); 4. CPE (42.8 % Cl).

tion of chlorines in the CPE chain can be considered as a rather statistically random distribution especially in the early steps of chlorination both in solution and suspension chlorinated polymers.[11] In CPE there are unchlorinated $-CH_2-$ groups and chlorinated segments $-CHCl-$ in amorphous regions which probably take part in thermal motions of γ-process.

The transition of the parent PE corresponds to the glass temperature of low-density polyethylene, -38 ± 5°C, found in adiabatic calorimetric studies [12] and from the extrapolation of Tg data on chlorosulfonated polyethylenes.[13] The occurrence of a transition for suspension chlorinated CPE at the same temperature as for LDPE at low chlorine contents has been demonstrated experimentally. This phenomenon has also been described by considering the Tg of the chlorinated material to be a linear function of the mol fraction of hypothetical homopolymers weighted by their respective Tg's.[14]

Thermograms have also been run on material which had been compression molded into discs between polished steel plates at 160°C at 84 kg/cm². These results were quite different and difficult to reproduce, confirming that properties if these semicrystalline polymers are sensitive to temperature and pressure history.[14]

Acknowledgement. One of the authors (V.E.) expresses his gratitude to NORDFORSK for a travel grant.

1. Schmieder, K. and Wolf, K. *Kolloid-Z.* **134** (1953) 157.
2. Wolf, K. *Z. Elektrochem.* **65** (1961) 604.
3. Kilian, H. G., Linz, H., Müller, F. H. and Ringsdorf, H. *Kolloid-Z. Z. Polym.* **202** (1965) 108.
4. Illers, K. H. *Kolloid-Z. Z. Polym.* **250** (1972) 426.
5. Boyer, R. F. *Rubber Chem. Technol.* **36** (1963) 1303.
6. Erä, V. A. and Lindberg, J. J. *J. Polym. Sci. Part. A-2* **10** (1972) 937.
7. Erä, V. A. *Makromol. Chem.* (1973). *In press.*
8. Stechling, F. H. and Mandelkern, L. *Macromolecules* **3** (1970) 242.
9. Nambu, K. J. *J. Appl. Polym. Sci.* **4** (1960) 69.

10. Tsuge, S., Okumoto, T. and Takenchi, T. *Macromolecules* **2** (1969) 200.
11. Saito, T., Matsumura, Y. and Hayashi, S. *Polym. J.* **6** (1970) 639.
12. Chang, S. A. *Polym. Prepr. Am. Chem. Soc.* **13** (1972) 322.
13. Erä, V. A. and Siren, P. *Suomen Kemistilehti* **B 45** (1972) 374.
14. Oswald, H. J. and Kubu, E. T. *SPE Trans.* **1963** 168.

Received January 30, 1973.

The Benzoylation of Some Glycosides with a Mixture of Benzoic Acid, Triphenylphosphine, and Diethyl Azodicarboxylate

GUNNEL ALFREDSSON AND PER J. GAREGG

Institutionen för organisk kemi, Stockholms universitet, S-104 05 Stockholm 50, Sweden

Mitsunobu and Eguchi have described the substitution of alchohols using nucleophiles such as benzoic acid, dibenzyl hydrogen phosphate, and phthalimide in the presence of triphenylphosphine and diethyl azodicarboxylate.[1,2] The reactions lead to products with inverted configuration and are of potential interest in carbohydrate chemistry for the synthesis of phosphorylated sugars, amino sugars, and for the inversion of the configuration at specific positions *via* benzoylation. A preliminary report by Jones and co-workers on the synthesis of some amino sugars using phthalimide,[3] following the procedures outlined by Mitsunobu and Eguchi [1,2] prompts us to report our experiences in attempted inversion reactions using benzoic acid as the nucleophile.

In connection with the synthesis of disaccharide derivatives containing 3,6-dideoxyhexopyranosyl moieties [4–6] it would be of interest to be able to effect the simultaneous inversion of two hydroxyl groups at the 2- and 4-positions in 3-deoxy-D-*arabino*-hexosides. This would give access to 3,6-dideoxy-D-*xylo*-hexosides from the previously synthesized D-*arabino* stereoisomers.[4] As a model for this conversion, methyl 3-deoxy-α-D-*arabino*-hexopyranoside (I) [4,7] was treated with benzoic acid,

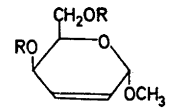

II

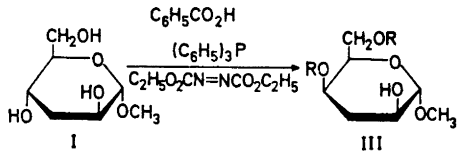

I III

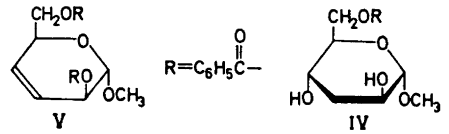

V IV

triphenylphosphine, and diethyl azodicarboxylate. The reaction mixture was fractionated on silica gel to give methyl 4,6-di-*O*-benzoyl-2,3-dideoxy-α-D-*threo*-hex-2-enopyranoside (II, 23 %) in crystalline form and with physical constants in agreement with literature values,[8] methyl 4,6-di-*O*-benzoyl-3-deoxy-α-D-*lyxo*-hexopyranoside (III, 47 %) and methyl 6-*O*-benzoyl-3-deoxy-α-D-*arabino*-hexopyranoside (IV, 12 %). The dibenzoate III was identified as follows. The NMR indicated the presence of two benzoyl groups. Acetylation afforded a monoacetate (NMR) and debenzoylation of III afforded syrupy methyl 3-deoxy-α-D-*lyxo*-hexopyranoside $[\alpha]_D$ +84° (methanol) (lit.[9] $[\alpha]_D$ +98°). Hydrolysis, conversion into the corresponding 3-deoxy-D-hexitol acetate and examination by GLC-MS showed that the derivative had the MS expected, but retention

10. Tsuge, S., Okumoto, T. and Takenchi, T. *Macromolecules* **2** (1969) 200.
11. Saito, T., Matsumura, Y. and Hayashi, S. *Polym. J.* **6** (1970) 639.
12. Chang, S. A. *Polym. Prepr. Am. Chem. Soc.* **13** (1972) 322.
13. Erä, V. A. and Siren, P. *Suomen Kemistilehti* **B 45** (1972) 374.
14. Oswald, H. J. and Kubu, E. T. *SPE Trans.* **1963** 168.

Received January 30, 1973.

The Benzoylation of Some Glycosides with a Mixture of Benzoic Acid, Triphenylphosphine, and Diethyl Azodicarboxylate

GUNNEL ALFREDSSON AND PER J. GAREGG

Institutionen för organisk kemi, Stockholms universitet, S-104 05 Stockholm 50, Sweden

Mitsunobu and Eguchi have described the substitution of alchohols using nucleophiles such as benzoic acid, dibenzyl hydrogen phosphate, and phthalimide in the presence of triphenylphosphine and diethyl azodicarboxylate.[1,2] The reactions lead to products with inverted configuration and are of potential interest in carbohydrate chemistry for the synthesis of phosphorylated sugars, amino sugars, and for the inversion of the configuration at specific positions *via* benzoylation. A preliminary report by Jones and co-workers on the synthesis of some amino sugars using phthalimide,[3] following the procedures outlined by Mitsunobu and Eguchi [1,2] prompts us to report our experiences in attempted inversion reactions using benzoic acid as the nucleophile.

In connection with the synthesis of disaccharide derivatives containing 3,6-dideoxyhexopyranosyl moieties [4–6] it would be of interest to be able to effect the simultaneous inversion of two hydroxyl groups at the 2- and 4-positions in 3-deoxy-D-*arabino*-hexosides. This would give access to 3,6-dideoxy-D-*xylo*-hexosides from the previously synthesized D-*arabino* stereoisomers.[4] As a model for this conversion, methyl 3-deoxy-α-D-*arabino*-hexopyranoside (I) [4,7] was treated with benzoic acid,

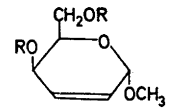

II

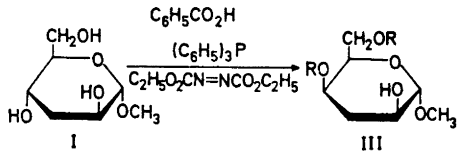

I III

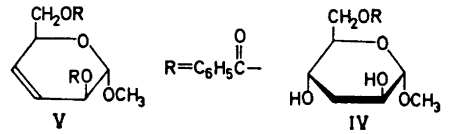

V IV

triphenylphosphine, and diethyl azodicarboxylate. The reaction mixture was fractionated on silica gel to give methyl 4,6-di-*O*-benzoyl-2,3-dideoxy-α-D-*threo*-hex-2-enopyranoside (II, 23 %) in crystalline form and with physical constants in agreement with literature values,[8] methyl 4,6-di-*O*-benzoyl-3-deoxy-α-D-*lyxo*-hexopyranoside (III, 47 %) and methyl 6-*O*-benzoyl-3-deoxy-α-D-*arabino*-hexopyranoside (IV, 12 %). The dibenzoate III was identified as follows. The NMR indicated the presence of two benzoyl groups. Acetylation afforded a monoacetate (NMR) and debenzoylation of III afforded syrupy methyl 3-deoxy-α-D-*lyxo*-hexopyranoside $[\alpha]_D$ +84° (methanol) (lit.[9] $[\alpha]_D$ +98°). Hydrolysis, conversion into the corresponding 3-deoxy-D-hexitol acetate and examination by GLC-MS showed that the derivative had the MS expected, but retention

time different to the corresponding *arabino*-, *ribo*-, and *xylo*-stereoisomers. These findings, together with the known inversion at chiral carbinol carbons in the reaction [1,2] show that the dibenzoate is III. The monobenzoate IV upon debenzoylation gave crystalline starting material (I). The assignment of the benzoate group to position 6 is based upon the expected higher reactivity at primary carbon and upon the fact that IV had the same configuration as I.

In the reaction of I with the above reagents, facile nucleophilic attack with inversion at the 4- and 6-positions therefore takes place. No inversion at C-2 was observed, presumably due to hindrance from the anomeric position. The olefin II presumably is produced from III substituted in the 2-position by a phosphonium ion intermediate, which undergoes elimination more rapidly than bimolecular nucleophilic substitution.

The sensitivity of the reaction to steric interference from neighbouring groups is indicated from the following. Methyl 2,3-di-*O*-acetyl-α-D-glucopyranoside was treated as described for I above. The only product isolated, in 77 % yield, was methyl 2,3-di-*O*-acetyl-6-*O*-benzoyl-α-D-glucopyranoside with physical properties corresponding to those described in the literature.[10] On the other hand, similar treatment of methyl 3-deoxy-α-D-*ribo*-hexopyranoside produced an olefinic sugar in 41 % yield, tentatively suggested from NMR evidence to be a 3,4-dideoxy-hex-3-enopyranoside.

The steric requirements of the reaction thus are similar to those observed by Jones and co-workers for phthalimide as nucleophile.[3] Substitution at the 6-position is much more readily effected than ring substitution. The latter process is subject to interference from vicinal groups. Provided the geometry is *trans*-1,2-diaxial, an intermediate phosphonium ion may well give rise to elimination instead of substitution.

Experimental. General methods were the same as those described in a previous paper.[6] NMR spectra on the various compounds were in accordance with the presumed structures.

Methyl 3-deoxy-α-D-*arabino*-hexopyranoside [7] (I, 900 mg), triphenylphosphine (4.014 g) and benzoic acid (1.881 g) were dissolved in tetrahydrofuran (10 ml). A solution of diethyl azodicarboxylate (2.688 g) in tetrahydrofuran (4 ml) was added with stirring at room temperature. The reaction was followed by TLC (toluene-ethyl acetate 4:1). No further reaction took place after 1 h. The solvent was removed and the residue taken up in ether. Undissolved material was filtered off and the filtrate was fractionated on silica gel (toluene-ethyl acetate 4:1). The following products (in the order of decreasing R_F value) were obtained: *Methyl 4,6-di-O-benzoyl-2,3-dideoxy*-α-D-threo-*hex-2-eno-pyranoside* (II, 425 mg) m.p. 101–102°, $[\alpha]_D$ −191° (*c*, 0.2, chloroform) (lit.[8] m.p. 101.5–102°, $[\alpha]_D$ −197°). *Methyl 4,6-di-O-benzoyl-3-deoxy*-α-D-lyxo-*hexopyranside* (III, 891 mg). Debenzoylation of part of the material (77 mg) with barium oxide in methanol afforded syrupy methyl 3-deoxy-α-D-*lyxo*-hexopyranoside (31 mg) $[\alpha]_D$ + 84° (*c*, 0.2, methanol) (lit.[9] $[\alpha]_D$ + 98°). The hexoside was converted into the corresponding 3-deoxyhexitol pentaacetate which was examined by GLC-MS. The MS corresponded to those given by the pentaacetates of 3-deoxy-D-*arabino*-, D-*ribo*- and D-*xylo*-hexitols, the GLC retention time, however, differed. Retention times on an XE-60, 3 % on Gas-Chrom Q, relative to 1,5-di-*O*-acetyl-2, 3, 4, 6-tetra-*O*-methyl-D-glucitol were 6.06, 7.08, 6.28, and 7.12 for the *arabino*-, *lyxo*, *ribo*-, and *xylo*-isomers, respectively. *Methyl 3-deoxy-6-O-benzoyl*-α-D-arabino-*hexopyranoside* (IV, 170 mg) upon debenzoylation with barium oxide in methanol afforded starting material (I).

Methyl 2,3-di-*O*-acetyl-α-D-glucopyranoside (76 mg) was treated with benzoic acid (69 mg), triphenylphosphine (147 mg), and diethyl azodicarboxylate (99 mg) in tetrahydrofuran (1 ml) as described above. The reaction was followed by TLC (diethyl ether-light petroleum (40–60°) 3:1). No further reaction was observed after 30 min. Work-up as described above and fractionation on silica gel (diethyl ether-light petroleum (40–60°) 3:1) afforded *methyl 2,3-di-O-acetyl-6-O-benzoyl*-α-D-*glucopyranoside* $[\alpha]_D$ + 97° (*c*, 0.2, chloroform) (lit.[10] $[\alpha]_D$ + 102°). Debenzoylation of an aliquot followed by acetylation with excess acetic anhydride in pyridine afforded methyl 2,3,4, 6-tetra-*O*-acetyl-α-D-glucopyranoside indistinguishable from reference material (TLC, GLC, NMR).

Methyl 3-deoxy-α-D-*ribo*-hexopyranoside (47 mg) was treated with 2.5 molar equivalents of each of benzoic acid, triphenylphosphine and diethyl azodicarboxylate in tetrahydrofuran overnight and worked up as described above. The major product (40 mg) $[\alpha]_D$ + 44° (*c*, 0.1, chloroform) was obtained chromatographically pure by TLC (diethyl ether-petroleum ether (40–60°) 3:1). NMR (deuteriochloroform): δ 3.55 (3H), singlet, methoxyl protons;

δ 4.6 (3H), multiplets, H-5, H-6, H-6'; δ 5.00 (1H), $J < 1$ Hz, H-1; δ 5.25 (1H), multiplet, H-2; δ 6.12 (2H), multiplets, H-3 and H-4; δ 7.3 – 7.6 and 8.0 – 8.2 (10H) aromatic protons. These tentative NMR assignments are based on shift considerations (aromatic protons, H3- and H-4 olefinic protons, low-field signal for H-2 on benzoxylated carbon) and upon the observation of the lanthanide induced shifts[11] caused by the successive addition of tris(dipivaloylmethanato) europium, which *inter alia* caused substantial down-field shift changes of the presumed H-2, H-6, and H-6' signals. The latter two signals became clearly differentiated. The down-field shift change of H-6 and H-6' clearly revealed H-5 as a multiplet at higher field; its coupling pattern showed coupling to three protons, excluding the possibility of the compound being a 4,5-hexenopyranoside. The small coupling constant of H-1 precludes the presence of a 2,3-hexenopyranoside, which for an α-D-glycoside would have $J_{1,2} = 2 - 3.5$ Hz[12] as displayed by III. The small coupling constant for H-2 and the above considerations indicate instead, the presence of a 3,4-hexenopyranoside, tentatively identified as methyl 2,6-di-*O*-benzoyl-3,4-dideoxy-α-D-*threo*-hex-3-enopyranoside V.

Acknowledgements. The authors are indebted to Professor Bengt Lindberg for his interest, to *Hierta-Retzius Stipendiefond* and to *Statens Naturvetenskapliga Forskningsråd* for financial support.

1. Mitsunobu, O. and Eguchi, M. *Bull. Chem. Soc. Japan* **44** (1971) 3427.
2. Mitsunobu, O., Wada, M. and Sano, T. *J. Am. Chem. Soc.* **94** (1972) 679.
3. Zamojski, A., Szarek, W. A. and Jones, J. K. N. *Carbohyd. Res.* **23** (1972) 460.
4. Borén, H. B., Garegg, P. J. and Wallin, N.-H. *Acta Chem. Scand.* **26** (1972) 1082.
5. Garegg, P. J. and Wallin, N.-H. *Acta Chem. Scand.* **26** (1972) 3895.
6. Alfredsson, G. and Garegg, P. J. *Acta Chem. Scand.* **27** (1973) 556.
7. Richards, G. N. *J. Chem. Soc.* **1954** 4511.
8. Ciment, D. M., Ferrier, R. J. and Overend, W. G. *J. Chem. Soc.* **C 1966** 446.
9. Huber, H. and Reichstein, T. *Helv. Chim. Acta* **31** (1948) 1645.
10. Navatowski, A. and Mroczkerwski, *Compt. Rend.* **218** (1944) 461.
11. Hinckley, C. C. *J. Am. Chem. Soc.* **91** (1969) 5160.
12. Ferrier, R. J. *Advan. Carbohyd. Chem.* **24** (1969) 199.

Received January 31, 1973.

The Reaction between Bis(2-bromoethyl)selenide and Potassium Selenocyanate

BJÖRN LINDGREN

Institute of Chemistry, University of Uppsala, Box 531, S-751 21 Uppsala 1, Sweden

Aliphatic selenocyanates are most conveniently synthesized by reacting the corresponding alkyl halide with potassium selenocyanate in acetone or ethanol.[1] The reaction between bis(2-bromoethyl) selenide (I) and potassium selenocyanate, however, did not give the expected bis-(2-selenocyanatoethyl) selenide (II). The main product consisted of diselenocyanatoethane (III). Elemental selenium was also isolated from the reaction mixture.

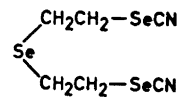

II

Bis(2-bromoethyl) selenide (I) has been subjected to some decomposition reactions and has been found to be a rather unstable compound. In several cases one of the decomposition products has been ethylene.[2] In order to investigate whether ethylene is produced also in this case, the gas evolved during the reaction was allowed to pass through a solution of selenium tetra-

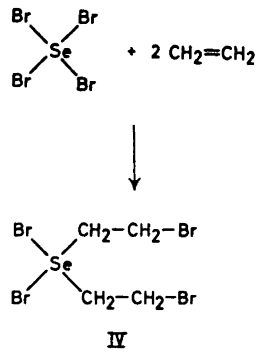

IV

Scheme 1.

δ 4.6 (3H), multiplets, H-5, H-6, H-6'; δ 5.00 (1H), $J < 1$ Hz, H-1; δ 5.25 (1H), multiplet, H-2; δ 6.12 (2H), multiplets, H-3 and H-4; δ 7.3 – 7.6 and 8.0 – 8.2 (10H) aromatic protons. These tentative NMR assignments are based on shift considerations (aromatic protons, H3- and H-4 olefinic protons, low-field signal for H-2 on benzoxylated carbon) and upon the observation of the lanthanide induced shifts[11] caused by the successive addition of tris(dipivaloylmethanato) europium, which *inter alia* caused substantial down-field shift changes of the presumed H-2, H-6, and H-6' signals. The latter two signals became clearly differentiated. The down-field shift change of H-6 and H-6' clearly revealed H-5 as a multiplet at higher field; its coupling pattern showed coupling to three protons, excluding the possibility of the compound being a 4,5-hexenopyranoside. The small coupling constant of H-1 precludes the presence of a 2,3-hexenopyranoside, which for an α-D-glycoside would have $J_{1,2} = 2 - 3.5$ Hz[12] as displayed by III. The small coupling constant for H-2 and the above considerations indicate instead, the presence of a 3,4-hexenopyranoside, tentatively identified as methyl 2,6-di-*O*-benzoyl-3,4-dideoxy-α-D-*threo*-hex-3-enopyranoside V.

Acknowledgements. The authors are indebted to Professor Bengt Lindberg for his interest, to *Hierta-Retzius Stipendiefond* and to *Statens Naturvetenskapliga Forskningsråd* for financial support.

1. Mitsunobu, O. and Eguchi, M. *Bull. Chem. Soc. Japan* **44** (1971) 3427.
2. Mitsunobu, O., Wada, M. and Sano, T. *J. Am. Chem. Soc.* **94** (1972) 679.
3. Zamojski, A., Szarek, W. A. and Jones, J. K. N. *Carbohyd. Res.* **23** (1972) 460.
4. Borén, H. B., Garegg, P. J. and Wallin, N.-H. *Acta Chem. Scand.* **26** (1972) 1082.
5. Garegg, P. J. and Wallin, N.-H. *Acta Chem. Scand.* **26** (1972) 3895.
6. Alfredsson, G. and Garegg, P. J. *Acta Chem. Scand.* **27** (1973) 556.
7. Richards, G. N. *J. Chem. Soc.* **1954** 4511.
8. Ciment, D. M., Ferrier, R. J. and Overend, W. G. *J. Chem. Soc.* **C 1966** 446.
9. Huber, H. and Reichstein, T. *Helv. Chim. Acta* **31** (1948) 1645.
10. Navatowski, A. and Mroczkerwski, *Compt. Rend.* **218** (1944) 461.
11. Hinckley, C. C. *J. Am. Chem. Soc.* **91** (1969) 5160.
12. Ferrier, R. J. *Advan. Carbohyd. Chem.* **24** (1969) 199.

Received January 31, 1973.

The Reaction between Bis(2-bromoethyl)selenide and Potassium Selenocyanate

BJÖRN LINDGREN

Institute of Chemistry, University of Uppsala, Box 531, S-751 21 Uppsala 1, Sweden

Aliphatic selenocyanates are most conveniently synthesized by reacting the corresponding alkyl halide with potassium selenocyanate in acetone or ethanol.[1] The reaction between bis(2-bromoethyl) selenide (I) and potassium selenocyanate, however, did not give the expected bis-(2-selenocyanatoethyl) selenide (II). The main product consisted of diselenocyanatoethane (III). Elemental selenium was also isolated from the reaction mixture.

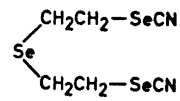

II

Bis(2-bromoethyl) selenide (I) has been subjected to some decomposition reactions and has been found to be a rather unstable compound. In several cases one of the decomposition products has been ethylene.[2] In order to investigate whether ethylene is produced also in this case, the gas evolved during the reaction was allowed to pass through a solution of selenium tetra-

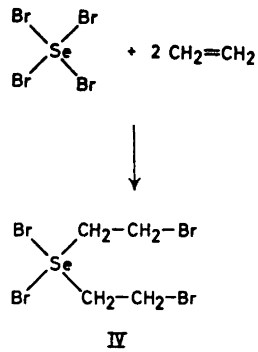

IV

Scheme 1.

bromide in benzene. After termination of the reaction it was possible to isolate yellow crystals of bis (2-bromoethyl) selenide dibromide (IV) from the benzene solution of selenium tetrabromide (Scheme 1).[3]

The stoichiometry of the reaction agreed well with that of Scheme 2. No quantitative estimation of the amount of ethylene evolved has been made.

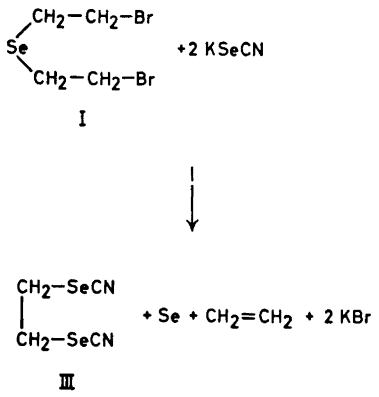

Scheme 2.

When repeating the reaction between bis(2-bromoethyl) selenide (I) and potassium selenocyanate using equimolar amounts of the starting materials, it was possible to isolate 1-bromo-2-selenocyanatoethane (V) from the reaction mixture.

With support from the above experiments and from investigations made on mustard gas (bis(2-chloroethyl) sulfide),[4,5] the following reaction mechanism is proposed (Scheme 3).

The first step in this proposed reaction mechanism consists, quite analogously with the mustard gas case, of an intramolecular attack of the selenium atom on the 2-carbon atom producing a three-membered cyclic selenonium ion. This ion is attacked by a selenocyanate ion giving 1-bromo-2-selenocyanatoethane (V) and ethylene selenide. The intermediate V will undergo further reaction with selenocyanate ion giving diselenocyanatoethane (III). Ethylene selenide being unstable

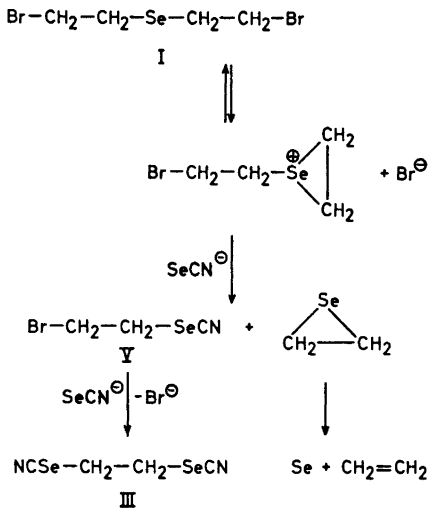

Scheme 3.

decomposes to give selenium and ethylene.[6]

A more detailed investigation of this reaction is now being made and will be published later.

Acknowledgements. I thank Prof. Göran Bergson and Dr. Lars-Börge Agenäs for valuable discussions and for their interest in this project.

1. Rheinboldt, H. In Houben-Weyl, *Methoden der organischen Chemie*, G. Thieme, Stuttgart 1955, Vol. 9, p. 939.
2. Smedslund, T. *Undersökningar över dietylselenidderivat*, Diss., University of Helsinki 1932, p. 31.
3. Smedslund, T. *Undersökningar över dietylselenidderivat*, Diss., University of Helsinki 1932, p. 45.
4. Bartlett, P. D. and Swain, C. G. *J. Am. Chem. Soc.* **71** (1949) 1406.
5. Ray, F. E. and Levine, I. *J. Org. Chem.* **2** (1937) 271.
6. Callear, A. B. and Tyerman, W. J. R. *Proc. Chem. Soc.* **1964** 296.

Received February 10, 1973.

(Trichloromethyl)cyclopentadiene from π-Cyclopentadienyl-[(trichloromethyl)cyclopentadiene]cobalt

THOMAS DAHL and CHRISTINA MOBERG

Department of Organic Chemistry, Royal Institute of Technology, S-100 44 Stockholm 70, Sweden

We have previously found that nickelocene reacts with tetrachloromethane in the presence of triphenylphosphine to give, besides π-cyclopentadienyl(triphenylphosphine)nickel chloride,[1] (trichloromethyl)cyclopentadiene, which can be dehydrohalogenated to 6,6-dichlorofulvene.[2]

Cobaltocene is known to react with tetrachloromethane to give π-cyclopentadienyl[(trichloromethyl)cyclopentadiene]-cobalt (*1*) and cobalticinium chloride.[3] We have now found that (trichloromethyl)-cyclopentadiene also can be formed from the complex (*1*).

It has been reported that ligands having acceptor properties, *e.g.* tetracyanoethylene sulphur dioxide, iodine, Ag(I),[4] and trifluorophosphine[5] displace ethylene from π-cyclopentadienyldiethylenerhodium. The rhodium complex is inert to nucleophilic ligands, *e.g.* triphenylphosphine and carbon monoxide.[3]

The cobalt complex (*1*), which has an electron configuration analogous to that of the rhodium complex, shows a similar reactivity. On reaction with one mol of iodine it gives, after distillation, a 62 % yield of (trichloromethyl)cyclopentadiene (after 1 h at 0° in diethyl ether, nitrogen atmosphere). The product is identical to (trichloromethyl)cyclopentadiene obtained earlier (GLC, MS NMR). A cobalt complex which probably has the composition (*3*) precipitates from the reaction mixture. Purification of this complex was unsuccessful.

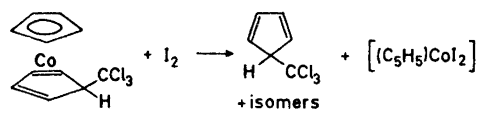

1 2 3

Silver nitrate and tetracyanoethylene react with complex (*1*) to (trichloromethyl)-cyclopentadiene in yields of 49 % (after 16 h at 20°) and 50 % (after 1 h at 0°), respectively. In the latter case *ca.* 5 % of a Diels Alder adduct from (trichloromethyl)-cyclopentadiene and tetracyanoethylene, apparently 2,2,3,3-tetracyano-7-(trichloromethyl)bicyclo[2.2.1]hept-5-ene, is also formed. (Found: C 46.2; H 1.6; N 17.9. Calc. for $C_{12}H_5N_4Cl_3$: C 46.3; H 1.6; N 18.0). Its NMR spectrum in DMSO-d_6 shows multiplets centered at $\delta = 3.50$ (1H), 4.68 (2H) and 6.65 (2H, triplet) and its mass spectrum shows the highest *m/e* values at 274/276/278 ($M^+ - HCl$). Sulphur dioxide reacts more slowly with the complex (*1*). The yield of (trichloromethyl)cyclopentadiene after 24 h at 20° is merely 5 %.

(Trichloromethyl)cyclopentadiene is displaced slowly and in a poor yield by tributylphosphine or triphenylphosphine (the estimated yield after several days is less than 8 %, GLC). Surprisingly a few per cent of chlorobenzene is formed in these reactions (MS evidence).

Acknowledgements. We thank Professor M. Nilsson for his interest in this work and for valuable discussions. The work has been supported by the *Swedish Natural Science Research Council.*

1. Ustynyuk, Yu. A., Voevodskaya, T. I., Zharikova, N. A. and Ustynyuk, N. A. *Dokl. Akad. Nauk. SSSR* **181** (1968) 372.
2. Moberg, C. and Nilsson, M. *J. Organometal. Chem.* **49** (1973) 243.
3. Green, M. L. H., Pratt, L. and Wilkinson, G. *J. Chem. Soc.* **1959** 3753.
4. Cramer, R. *J. Am. Chem. Soc.* **89** (1967) 5377.
5. Nixon, J. F. and Pinkerton, A. A. *J. Organometal. Chem.* **37** (1972) C47.

Received February 10, 1973.

A Potentiometric Investigation of Sodium Ion Activity in Micellar Sodium Dodecyl Sulphate Solutions

TIBOR GILÁNYI*

Department of Physical Chemistry, Åbo Akademi, SF-20500 Åbo 50, Finland

Determinations of counter ion binding to micelles by the use of cation-responsive glass electrodes have yielded results which are less reproducible than would be justified by the claimed experimental uncertainties. A renewed investigation of sodium ion activities and the different factors affecting their determination in sodium dodecyl sulphate (SDS) solutions has been made.

In previous investigations the binding of sodium ions to the micelles was estimated from a simple model.[1,2] Botré *et al.* formally separated the different contributions to the counter ion activity, a_{Na}, in micellar solution above the critical micelle concentration (c.m.c.) in the following way:

$$a_{Na} = f_1\ c_0 + f_2\ \alpha(c - c_0)$$

where f_1 = the activity coefficient of Na^+ in the solution surrounding the micelles, f_2 = the activity coefficient of the Na^+ in the ionic atmosphere around the micelles, α = the degree of dissociation of the micelles, c_0 = the c.m.c. and c = the total concentration of surfactant. It is found experimentally that a_{Na} changes linearly with c above the c.m.c., which suggests that f_1, f_2, and α are constant. The usual method of calculating an apparent degree of dissociation, α'', is to set f_2 = the activity coefficient of single counter ions at the c.m.c., (f_0). This assumption is probably far from realistic. The activity coefficient of the ions in the ionic atmosphere of a large colloidal ion is probably much lower than in a simple salt solution.

It is therefore proposed that an apparent degree of dissociation should be defined in the following way:

$$\alpha' = f_2\alpha$$

This quantity will represent the contribution of the micelles in the solution to the total sodium ion activity, without any assumptions being made concerning the nature of the ion-ion interactions which causes the contribution to be of this magnitude. Setting $f_2 = f_0$, ($\alpha'' = \alpha f_2/f_1$) implies a definition of f_2 on an arbitrary scale. f_0 will be quite different for different surfactants. Any abnormal changes in f_1 at low surfactant concentrations (which may be expected for long-chain compounds especially) or with the concentration of neutral salt will be indirectly reflected in α'', variations in which will thus not be exclusively dependent on real changes in the degree of dissociation. α'' does not seem to be a suitable quantity for comparing results from different surfactants, or even for the same surfactant at different ionic strengths.

α', on the other hand, can be determined directly as the slope of the straight line obtained in a plot of a_{Na} against c above c_0. There is no need to use a correct c_0 nor a correct f_0. α' may also be calculated from a combination of the slope and the intercept at $c = c_0$.

Experimental. Materials. The sodium dodecyl sulphate (SDS) was prepared by recrystallizing Merck *p.a.* SDS twice from a hot benzene-ethanol mixture. A plot of the surface tension of this substance as a function of log c (drop-weight method) showed no minimum below the c.m.c. Subsequent foam fractionation of the SDS caused the absolute value of the surface tension to rise significantly (~ 2 dyn/cm at $c = 0.004$ mol/kg). This could be due to the removal of a trace contamination (dodecanol?).

The water was distilled and passed through an ion exchange resin shortly before measurements. The sodium chloride was Merck *suprapur* quality.

Apparatus. The sodium-responsive glass electrode was an E.I.L. type GEA 33B electrode. The calomel electrode was a Radiometer type K 401 with a porous pin as liquid junction. The silver-silver chloride electrode was prepared by a procedure slightly modified from that of Brown.[3] The emf of the cell was partly compensated on a Beckman Research pH-meter, the remaining few millivolts being recorded as a function of time on a Metrohm Labograph E 478 plotter. In this way, all emf values could be extrapolated to zero time after establishing the liquid junction between the

* Permanent address: Department of Colloid Chemistry, Loránd Eötvös University, Budapest, Hungary.

electrodes. This is necessary because there is a slow precipitation at the junction after it has been formed.

All experiments were carried out in a water bath at 25±0.05°C.

The liquid junction. To check the influence of precipitation at the liquid junction measurements were performed (a) with a four-way stopcock assembly in the bridge, which permitted a fresh junction to be formed immediately before starting to record the emf values, (b) by recording the emf as a function of the time after plunging the calomel electrode with its porous pin into the solution. The calomel electrode was stored in saturated KCl solution between emf readings; prior to immersion, it was carefully washed and lightly wiped with a tissue paper. The electrode was kept in the solution for about 20 sec only. The reproducibility was found to be better with the latter method, and this was used in all subsequent measurements with the calomel electrode. The reproducibility was ±0.5 mV. No corrections for pH were made (neutral solution).

Any change in the porous pin due to precipitation in the SDS solution was checked by measuring the emf of the calomel electrode against an Ag/AgCl electrode in KCl solution saturated with AgCl. The calomel electrode always returned to its original emf value within 10 min after a prolonged storage in a SDS solution.

Contamination by potassium ions. Potassium ions may influence the measurements not only because the glass electrode is sensitive to them, but also because they are adsorbed at the micellar surface. In order to check whether KCl from the porous pin did diffuse into the solution, 0.001 mol/kg NaCl was added to a number of SDS solutions which were saturated with AgCl. The emf between an Ag/AgCl electrode in these solutions and the calomel electrode was then recorded in a way which was exactly similar to that used in the a_{Na} measurements. The change in Cl^- concentration was never more than 2×10^{-5} mol/kg, and thus seems to be insignificant.

Cell without transference. The NaCl/SDS solutions were also used to measure a_{Na} with an Ag/AgCl electrode in the SDS solution as reference electrode. From this cell, a_{Na} can be estimated if the Debye-Hückel theory is used to estimate a_{Cl}. The error of such a calculation in this concentration range is probably less than 3 %.

Reference solution. To convert emf values to sodium ion activities the electrode system was calibrated in a 0.05 mol/kg NaCl solution with known mean activity.[4] The sodium ion activity was calculated assuming that $a_{Na} + a_{Cl} = a_{Na,Cl}$ (the mean activity of Na,Cl) in the reference solution, and that the diffusion potential is the same in the reference and sample solutions. All emf readings for the reference solution were performed in the same way as those in the SDS solutions. The performance of the electrode system was checked by measuring the change in the emf with $a_{Na,Cl}$ in the reference solution. This yielded values which were within 0.5 % of those predicted by the Nernst equation.

Results. The sodium ion activity in SDS solutions were measured by changing the SDS solution after each measurement as well as by changing the SDS concentration by titration, with a maximum of 10 steps in a series. Both methods yielded the same results.

The measured sodium ion activities as a function of the SDS concentration are plotted in Fig. 1. The break in the curve is sharp enough to define the c.m.c. as $(8.1 \pm 0.1) \times 10^{-3}$ mol/kg. Below the c.m.c. there is a significant decrease in activity as compared to NaCl. The activity coefficient for SDS at the c.m.c. is about 0.75 which is 15 % below the value for NaCl at the same concentration. Shedlovsky *et al.*[2] found $f_0 = 0.81$ at c.m.c. = 0.00755 mol/kg and Botré *et al.*[1] $f_0 = 0.76$ at c.m.c = 0.00800 mol/kg.

a_{Na}, however, is the same at the break point of the curve in all investigations. The difference in f_0 is probably due to the use of different values for c_0.

Measurements with the cell without transference (also plotted in Fig. 1) show that the anomalously low sodium ion activity cannot be due to diffusion potentials; the two different methods give results that coincide remarkably well at least up to the c.m.c. Above the c.m.c., the Ag/AgCl electrode cannot be used as a reference because the solubility of AgCl increases. This is seen from the fact that the emf reaches equilibrium much slower at SDS concentrations higher than 0.007 – 0.008 mol/kg.

The possibility that the activity decrease might be due to a change in the glass electrode potential caused by the adsorption of dodecanol was also examined. Intense foam fractionation (the SDS concentration was determined after the fractionation) did not change the activities.

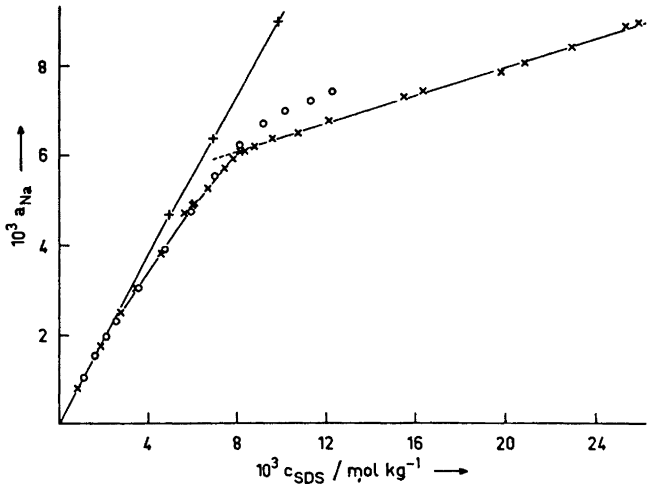

Fig. 1.

The slope of the curve above the c.m.c. and a combination of slope and intercept both yield the same value for α': 0.151 ± 0.002. Using the Botré method, α'' becomes 0.202. Shedlovsky *et al.*[2] found $\alpha'' = 0.22$ and Botré *et al.*[4] 0.16. In solutions with added NaCl, Feinstein and Rosano [5] found the value 0.16 for α''. In their experiments, however, the NaCl/SDS ratio was kept constant, and so there is probably a significant decrease in α'' since the c.m.c. changes with the NaCl concentration.

Okubo *et al.*[6] found that the single ion activity coefficient of counter ions in aqueous sodium polyacrylate solutions was 0.3, almost independently of polymer concentration over a wide concentration range. If it is assumed that in the present case the micelle can be compared to this macro molecule, *i.e.* $f_2 = 0.3$, the value 0.5 is obtained for α, which is probably closer to the real degree of dissociation than the low values for α''.

Acknowledgements. I wish to thank Professor I. Danielsson for his interest in this work and Dr. P. Stenius for many helpful discussions and for revising the English text.

Thanks are due to the whole staff of the Department of Physical Chemistry, Åbo Akademi, for all the facilities placed at my disposal.

1. Botré, C., Crescenzi, V. L. and Mele, A. *J. Phys. Chem.* **63** (1959) 650.
2. Shedlovsky, L., Jakob, C. W. and Epstein, M. B. *J. Phys. Chem.* **67** (1963) 2075.
3. Brown, A. S. *J. Am. Chem. Soc.* **56** (1934) 646.
4. Robinson, R. A. and Stokes, R. H. *Electrolyte Solutions*, Butterworths, London 1959.
5. Feinstein, M. E. and Rosano, H. I. *J. Colloid Interface Sci.* **24** (1967) 73.
6. Okubo, T., Nishizaki, Y. and Ise, N. *J. Phys. Chem.* **69** (1965) 3690.

Received January 15, 1973.

ACTA CHEMICA SCANDINAVICA 27 (1973) 733–742

Thermodynamic Properties of Rare Earth Complexes

XIV. Free Energy, Enthalpy and Entropy Changes for the Formation of Lanthanoid Malonate and Hydrogen Malonate Complexes

INGEMAR DELLIEN

Division of Physical Chemistry 1, Chemical Center, University of Lund, P.O.B. 740, S-220 07 Lund 7, Sweden

The changes in free energy, enthalpy and entropy for the formation of lanthanoid (III) malonate and hydrogen malonate complexes have been determined. The free energy changes were computed from the previously determined stability constants. The enthalpy changes were obtained from a direct calorimetric determination of the heats of complex formation. All data refer to a temperature of 25.0°C and a sodium perchlorate medium with the sodium ion concentration equal to 1.00 M.

Earlier in this series of investigations on the thermodynamic properties of lanthanoid (III) carboxylate complexes, the stability constants for the formation of malonate and hydrogen malonate complexes have been determined.[1] This paper describes a calorimetric determination of the corresponding enthalpy changes.

Values of the changes in free energy, entropy and enthalpy for the formation of the first malonate complex with lanthanum (3+), gadolinium (3+), and lutetium (3+) have been reported by Gelles and Nancollas.[2] The enthalpy changes were determined from the temperature dependence of the stability constants; a method which will give enthalpy values with low precision.

Grenthe and Hansson have determined ΔG_i°, ΔH_i° and ΔS_i° for the formation of scandium (III) malonate, diglycolate and dipicolinate complexes.[3] The values of the enthalpy change (ΔH_1°) and entropy change (ΔS_1°) for the formation of the first scandium diglycolate and dipicolinate complexes are of the expected magnitude, as estimated from the general trends in the variation of ΔH_1° and ΔS_1° with respect to the ionic radius within the lanthanoid series. This is not the case for the entropy change for the formation of the second scandium diglycolate (and dipicolinate) complex.

The formation of the diglycolate and dipicolinate complexes is exothermic, while the formation of the malonate complexes is endothermic. The values of ΔS_1° is about the same for the formation of the malonate, diglycolate and dipi-

colinate complexes, whereas ΔS_2° for the malonate complex is much larger than for the other two complexes. With data for the corresponding lanthanoid complexes available, it might be possible to decide whether this "anomalous" behaviour is due to the small radius of the scandium ion or to some property of the ligand.

The calorimeter described by Grenthe *et al.*[4] has been used in this work. The measurements were performed at 25.00°C in an aqueous sodium perchlorate medium with the total sodium ion concentration equal to 1.00 M.

NOTATIONS AND CALCULATIONS

The notations used here have been defined in Refs. 1 and 5. The enthalpy changes have been calculated from the experimental data by the least-squares method LETAGROP KALLE, developed by Arnek and Sillén.[6] Only the heats of the malonate ion have been calculated by standard graphical methods.[7]

EXPERIMENTAL

Chemicals used. Stock solutions of the various rare earth perchlorates, malonic acid, disodium malonate and sodium perchlorate were prepared and analyzed as described before.[1]

Procedure. The titration calorimeter developed by Grenthe *et al.* was used for these measurements. Two different inner vessels have been used, one containing about 120 ml and the other about 103 ml. The inner vessel is filled with a solution S with an initial volume V_0 equal to 100.0 ml or 80.0 ml. When the S solution has the same temperature as the outer thermostat bath, a portion (at most 3 ml) of the titrant solution T is added from a piston burette. Additions were made at a constant rate, 1 ml/min. When the inner vessel is filled, a suitable volume is withdrawn through the outlet tube, which is connected to a second piston burette.

The system was electrically calibrated and in general two calibrations were made during each run.

The heats of dilution of the T solutions were determined by successive additions of T solution to an S solution consisting of 1.00 M $NaClO_4$. It was assumed that the heats of dilution of the metal ions and the various complexes could be neglected.[8]

The compositions of the S and T solutions have been chosen in order to cover a wide concentration range during the titrations. The different compositions are mainly of the following three types: The S solution contains only metal ion, while T is a solution with the ratio C_H/C_A approximately equal to 1/1 (type I) or 1/3 (type II).

For type III, the S solution contains metal ion and perchloric acid (or malonic acid) and T is a buffer with the ratio C_H/C_A less than 1/3.

Fig. 1 a and b show the concentrations of the various species during titrations of types II and III in the lutetium system. Titrations of type I give concentrations of the acid complexes intermediate to those in titrations of types II and III.

The formation of a slightly soluble compound of the composition $M_2A_3.nH_2O$ complicates the measurements. Thus, for the lighter elements (La – Tb), $\Delta H^\circ_{1,0,3}$ could not be determined and the precision in the determinations of $\Delta H^\circ_{1,0,1}$ and $\Delta H^\circ_{1,0,2}$ is low. In the potentiometric measurements some information on $\beta_{1,0,3}$ could be obtained by making titration series "backwards", using an S solution with a high free ligand concentration and an acid titrator solution. This method cannot be used in the calorimetric measurements, which are considerably more time-consuming than the potentiometric ones. A precipitate is formed in the S solution before the titration series is started.

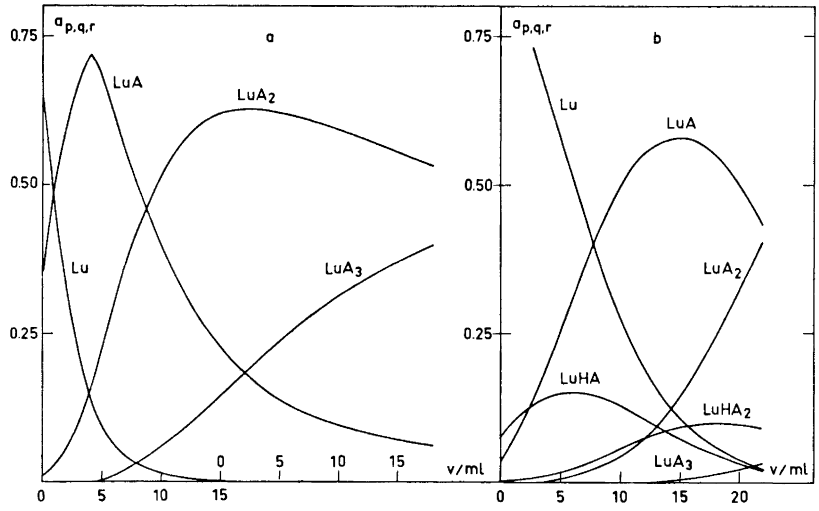

Fig. 1. The relative amounts of the different complexes in the lutetium malonate system during two titration series. *a.* Titration series of type II. Data refer to series 5a (lower volume scale) and 5b (upper volume scale) in Table 1. *b.* Titration series of type III, series 2 in Table 1.

RESULTS

The heat equivalent ε_V was the same for all experiments with the rare earths, and a linear relationship was established between ε_V and the total volume V of the system. The estimated maximum error in ε_V is ± 0.3 %.

a. The proton-malonate system. The titrations were performed by adding perchloric acid to a solution of disodium malonate. The initial total concentrations of malonate ion were 50 mM and 100 mM, respectively.

Graphical calculation of the overall entropy changes for the formation of the two proton-malonate complexes gave the values:

$$\Delta H^\circ_{0,1,1} = (2.00 \pm 0.02) \text{ kJ/mol}$$
$$\Delta H^\circ_{0,2,1} = (0.46 \pm 0.02) \text{ kJ/mol}$$

(The errors are estimated maximum errors.) These values agree with those given in Ref. 3.

Using the stability constants in Ref. 1, the following values are obtained for the changes in free energy and enthalpy for the formation of proton-malonate complexes at 25°C:

$$\Delta G^\circ_{0,1,1} = (-28.90 \pm 0.02) \text{ kJ/mol}$$
$$\Delta G^\circ_{0,2,1} = (-43.68 \pm 0.04) \text{ kJ/mol}$$
$$\Delta S^\circ_{0,1,1} = (103.6 \pm 0.2) \text{ J K}^{-1} \text{ mol}^{-1}$$
$$\Delta S^\circ_{0,2,1} = (148.0 \pm 0.2) \text{ J K}^{-1} \text{ mol}^{-1}$$

Table 1. Experimental results for the lutetium malonate system. Corresponding values of v/ml, $Q_{corr,\,exp}$/J and $(Q_{corr,\,calc} - Q_{corr,\,exp})$/J are given. The withdrawal of solution from the inner vessel during a titration series is indicated by small letters, *e.g.* Series 1a, . . . Series 1b.

Series 1a. S: $C_H = 0.05543$ M, $C_M = 0.01963$ M, $C_A = 0.02737$ M, $C_{NaClO_4} = 1.000$ M;
T: $C_H = 0.1056$ M, $C_M = 0$, $C_A = 0.3018$ M, $C_{NaClO_4} = 0.502$ M;
$V_0 = 99.95$ ml;

3.000, 4.050, −0.054; 6.000, 5.586, −0.264;

Series 1b. S: $C_H = 0.05827$ M, $C_M = 0.01852$ M, $C_A = 0.04291$ M, $C_{NaClO_4} = 0.972$ M;
T: $C_H = 0.1056$ M, $C_M = 0$, $C_A = 0.3018$ M, $C_{NaClO_4} = 0.502$ M;
$V_0 = 97.95$ ml;

2.000, 3.799 −0.029; 4.000, 3.753, 0.004;
6.000, 3.607, 0.046; 8.000, 3.514, −0.021;
11.00, 4.975, −0.059; 14.00, 4.527, −0.004;
17.00, 4.146, 0.012;

Series 2. S: $C_H = 0.05543$ M, $C_M = 0.01963$ M, $C_A = 0.02737$ M, $C_{NaClO_4} = 1.000$ M;
T: $C_H = 0.1037$ M, $C_M = 0$, $C_A = 0.3016$ M, $C_{NaClO_4} = 0.500$ M;
$V_0 = 79.93$ ml;

2.000, 2.531, 0.046; 4.000, 3.473, −0.033;
6.000, 3.807, −0.046; 8.000, 3.778, 0.017;
10.00, 3.686, −0.004; 12.00, 3.498, 0.004;
14.00, 3.289, 0.008; 16.00, 3.054, 0.038;
18.00, 2.866, 0.033; 20.00, 2.690, 0.021;
22.00, 2.468, 0.046;

Series 3. S: $C_H = 0.000479$ M, $C_M = 0.01475$ M, $C_A = 0$, $C_{NaClO_4} = 1.000$ M;
T: $C_H = 0.05723$ M, $C_M = 0$, $C_A = 0.1953$ M, $C_{NaClO_4} = 0.667$ M;
$V_0 = 100.00$ ml;

3.000, 6.054, −0.079; 6.000, 5.887, −0.046;
9.000, 5.443, −0.046; 12.00, 4.678, 0.004;
15.00, 3.849, 0.025; 18.00, 3.117, 0.067;

Series 4. S: $C_H = 0.000479$ M, $C_M = 0.01475$ M, $C_A = 0$ M, $C_{NaClO_4} = 1.000$ M;
T: $C_H = 0.05723$ M, $C_M = 0$, $C_A = 0.1953$ M, $C_{NaClO_4} = 0.667$ M;
$V_0 = 100.00$ ml;

2.000, 3.958, 0.004; 5.000, 6.008, −0.067;
8.000, 5.623, −0.046; 11.00, 4.803, 0.142;
14.00, 4.071, 0.063; 17.00, 3.330, 0.071;

Series 5a. S: $C_H = 0.001357$ M, $C_M = 0.007230$ M, $C_A = 0.003829$ M, $C_{NaClO_4} = 0.994$ M;
T: $C_H = 0.05723$ M, $C_M = 0$, $C_A = 0.1953$ M, $C_{NaClO_4} = 0.667$ M;
$V_0 = 102.00$ ml;

3.000, 4.996, 0.251; 6.000, 4.012, −0.322;
9.000, 2.577, −0.197; 12.00, 1.669, −0.071;
15.00, 1.142, −0.025;

Table 1. Continued.

Series 5b. S: $C_H = 0.00852$ M, $C_M = 0.006303$ M, $C_A = 0.02838$ M, $C_{NaClO_4} = 0.952$ M;
T: $C_H = 0.05723$ M, $C_M = 0$, $C_A = 0.1953$ M, $C_{NaClO} = 0.667$ M;
$V_0 = 100.00$ ml;

3.000, 0.766, 0.038;	6.000, 0.548, 0.046;
9.000, 0.422, 0.038;	12.00, 0.402, −0.033;
15.00, 0.293, 0.008;	18.00, 0.213, 0.038;

Series 6. S: $C_H = 0.000691$ M, $C_M = 0.01963$ M, $C_A = 0$, $C_{NaClO_4} = 1.000$ M;
T: $C_H = 0.3033$ M, $C_M = 0$, $C_A = 0.3024$ M, $C_{NaClO_4} = 0.698$ M;
$V_0 = 79.93$ ml;

2.000, 2.456, 0.117;	4.000, 1.966, 0.050;
6.000, 1.791, 0.042;	8.000, 1.607, 0.054;
10.00, 1.452, 0.067;	12.00, 1.289, 0.088;
14.00, 1.180, 0.067;	16.00, 1.063, 0.067;
18.00, 0.937, 0.084;	

Series 7. S: $C_H = 0.000691$ M, $C_M = 0.01963$ M, $C_A = 0$, $C_{NaClO_4} = 1.000$ M;
T: $C_H = 0.3033$ M, $C_M = 0$, $C_A = 0.3024$ M, $C_{NaClO_4} = 0.698$ M;
$V_0 = 79.93$ ml;

2.000, 2.456, 0.117;	4.000, 1.996, 0.021;
6.000, 1.807, 0.025;	8.000, 1.640, 0.022;
10.00, 1.477, 0.042;	

Table 2. The overall enthalpy values for the formation of lanthanoid malonate complexes. The errors are equal to three standard deviations.

Metal ion	Number of experimental points	Standard deviation in Q_{corr}/J	$\Delta H^\circ_{1,0,1}$ kJ mol^{-1}	$\Delta H^\circ_{1,0,2}$ kJ mol^{-1}	$\Delta H^\circ_{1,0,3}$ kJ mol^{-1}	$\Delta H^\circ_{1,1,1}$ kJ mol^{-1}	$\Delta H^\circ_{1,1,2}$ kJ mol^{-1}
La	29	0.082	12.1 ±0.7	20.4±2.6	–	5.2±0.7	17.8±1.7
Ce	31	0.082	12.2 ±0.8	19 ±10	–	5.3±0.8	20.0±2.5
Pr	39	0.111	12.7 ±0.7	21.5±1.8	–	5.3±0.9	19.0±4.2
Nd	33	0.086	13.1 ±0.7	21.1±3.3	–	5.0±0.7	19.2±2.2
Sm	43	0.094	12.5 ±0.5	21.3±2.0	–	5.6±0.7	18.3±1.4
Eu	42	0.085	12.8 ±0.5	20.0±3.8	–	5.9±0.8	16.8±1.0
Gd	47	0.087	12.6 ±0.5	20.1±2.1	–	6.5±0.8	18.1±1.5
Tb	42	0.072	12.61±0.33	22.0±0.7	–	7.6±0.7	17.2±0.8
Dy	49	0.086	12.83±0.36	22.3±0.9	23 ±11	8.2±1.2	18.0±1.7
Ho	53	0.080	13.51±0.32	22.1±0.6	30 ± 4	6.9±1.2	18.0±1.2
Er	49	0.110	13.4 ±0.5	22.5±1.0	28 ±11	6.3±1.5	20.5±2.0
Tm	52	0.077	14.46±0.34	23.2±0.5	33.9±2.5	5.8±1.8	17.0±2.2
Yb	74	0.061	14.24±0.20	24.40±0.24	33.1±0.9	7.9±1.0	21.6±1.6
Lu	57	0.091	14.59±0.37	25.4±0.6	35.2±3.3	8.0±1.5	24.6±3.9

b. The lanthanoid-malonate systems. The data for the lutetium malonate system are given in Table 1. The corrections for the dilution of the various titrator solutions have not been tabulated. These corrections are small and do not exceed 0.03 J/per ml added T solution.

Table 3. — $\Delta G°$ and $\Delta S°$ for the formation of lanthanoid malonate complexes at 25.0°C. (The entropy unit, J K^{-1} mol^{-1}, is written e.u.)

Metal ion	$-\Delta G°_{1,0,1}$ kJ mol^{-1}	$-\Delta G°_{1,0,2}$ kJ mol^{-1}	$-\Delta G°_{1,0,3}$ kJ mol^{-1}	$-\Delta G°_{1,1,1}$ kJ mol^{-1}	$-\Delta G°_{1,1,2}$ kJ mol^{-1}	$\Delta S°_{1,0,1}$ e.u.	$\Delta S°_{1,0,2}$ e.u.	$\Delta S°_{1,0,3}$ e.u.	$\Delta S°_{1,1,1}$ e.u.	$\Delta S°_{1,1,2}$ e.u.
La	17.51	29.4	–	36.0	52.4	99	167	–	138	235
Ce	18.6	29.9	–	36.4	53.1	103	170	–	140	245
Pr	18.8	32	–	36.9	53	106	179	–	142	240
Nd	19.29	33.8	–	37.0	53.9	109	184	–	141	245
Sm	20.98	34.7	–	37.6	56.3	112	188	–	145	250
Eu	21.24	35.6	–	37.0	57.0	114	186	–	144	248
Gd	21.30	35.6	–	37.1	55.8	114	187	–	146	248
Tb	21.78	36.4	–	36.3	57.6	115	196	–	147	251
Dy	21.97	36.2	43	36.0	56.0	117	196	220	148	248
Ho	21.87	36.4	43.8	36.0	56.8	119	196	250	144	251
Er	21.98	36.5	43.5	36.2	56.7	119	198	240	143	259
Tm	21.95	36.7	43.5	35.8	57.0	122	201	260	140	248
Yb	22.09	36.6	44.4	35.5	55.7	122	205	260	146	259
Lu	22.14	36.6	45.0	35.7	54	123	208	269	147	260

The overall enthalpy changes for the formation of the various complexes are given in Table 2. All values have been calculated by the least-squares procedure. Table 3 gives the corresponding free energy and entropy changes.

Table 2 also gives the standard deviation in the individual measurements. There are several sources for these errors and some of them will be discussed.

(i) An error of about 0.04 J in Q_{corr} can be attributed to errors in the calorimetric procedure, *e.g.* uncertainties in the graphical evaluation of the thermistor resistance change at the addition of titrant, and to temperature changes in the thermostat bath or in the calorimeter room during the measurements.

(ii) The data in Table 1 show the presence of systematic errors in some titration series. If the enthalpy values are calculated for some of these series separately, results which differ slightly will be obtained. This is exemplified in Table 4, where data from Table 1 have been used.

Table 4. Enthalpy values for the lutetium malonate system, calculated from different titration series in Table 1.

Series used	Standard deviation in Q_{corr}/J	$\Delta H°_{1,0,1}$ kJ mol^{-1}	$\Delta H°_{1,0,2}$ kJ mol^{-1}	$\Delta H°_{1,0,3}$ kJ mol^{-1}	$\Delta H°_{1,1,1}$ kJ mol^{-1}	$\Delta H°_{1,1,2}$ kJ mol^{-1}
1 – 7	0.0913	14.59 ± 0.37	25.4 ± 0.6	35.2 ± 3.3	8.0 ± 1.5	24.6 ± 3.9
1 – 5	0.0933	14.56 ± 0.38	25.5 ± 0.6	35.3 ± 3.4	8.9 ± 1.9	26.2 ± 4.5
3 – 7	0.0937	14.67 ± 0.40	25.6 ± 0.7	35.2 ± 3.4	7.1 ± 2.8	19.6 ± 8.7

The effects of concentration errors vary with the different types of compositions. The order of magnitude of these errors has been estimated for the various types of titrations. The figures given below refer to titrations performed with $(C_M)_S = 20$ mM and $(C_A)_T = 300$ mM, which corresponds to the conditions for the lutetium and most of the other systems. Only concentration errors which cause a large error in the measured heat are discussed.

Type I. An error of 1 % in the ratio $(C_H/C_A)_T$ gives a corresponding change on Q_{corr} of 0.05 J/3 ml addition.

Type II. An error of 1 % in $(C_M)_S$ or $(C_A)_T$ each gives a change in Q_{corr} of about 0.04 J/3 ml addition.

Type III. An error of 1 % in $(C_A)_T$ gives a change in Q_{corr} of $0.10 - 0.04$ J/3 ml addition.

(iii) The heats of formation of the malonate complexes, which were determined in separate measurements, could be regarded as two additional unknown parameters to be determined from the measurements on the metal systems. When this was done in the ytterbium system, the following values were calculated

$$\Delta H^\circ_{0,1,1} = (1.80 \pm 0.25) \text{ kJ/mol}$$
$$\Delta H^\circ_{0,2,1} = (0.3 \pm 0.6) \text{ kJ/mol}$$

The other enthalpy values and the standard deviation in Q_{corr} remained the same. Thus, reasonable errors in $\Delta H^\circ_{0,1,1}$ and $\Delta H^\circ_{0,2,1}$ do not influence the other enthalpy values.

(iv) The complexes of the type MA_j are rather strong and the enthalpy values are thus not sensitive to errors in $\beta_{1,0,j}$. For the equilibrium $M + HA \rightleftharpoons MHA$ the equilibrium constant has a value of about 20 M^{-1}, and the concentration of MHA thus strongly depends on the value of $\beta_{1,1,1}$. Table 5 shows values of the error square sum U and $\Delta H^\circ_{1,1,1}$, calculated for three different values of $\beta_{1,1,1}$, with data from the ytterbium system.

Table 5. The error square sum U and $\Delta H_{1,1,1}$ calculated for three different values of $\beta_{1,1,1}$. The calculation refers to the ytterbium system with 74 experimental points.

$\beta_{1,1,1} \times 10^6$ / M^{-2}	$\Delta H^\circ_{1,1,1}$ / KJ mol^{-1}	U / J^2
1.41	8.4 ± 1.0	0.2715
1.63	8.1 ± 0.9	0.2678
1.85	7.8 ± 0.8	0.2666

The shifts in $\beta_{1,1,1}$, which correspond to three standard deviations, have a very small effect on the error square sum. Only Q_{corr}-values from titration series of types I and III are affected, and this with 0.025 J at most. The changes in the concentration of the complex MHA are compensated by opposite concentration changes in MA, and as all the enthalpy values are of the same order or magnitude, the resulting change in Q_{corr} is small.

Calorimetric measurements on solutions with a low C_H/C_A ratio can be described by the same set of "false" equilibrium constants that described the potentiometric measurements on this type of solutions, and a set of enthalpy values, which are nearly the same as the correct enthalpy values. The discussion in Ref. 1 showed that in these systems the erroneously calculated value of the concentration of free ligand, a^*, is greatly in error, whereas the error in $\bar{n}^*$ is small. This means that the error in the concentration of MA is small. Thus, if the measurements had been performed by using only solution with the ratio C_H/C_A less than ½, neither the potentiometric nor the calorimetric measurements would have shown the existence of acid complexes in these solutions.

The calorimetric measurements do not give any check on the stability constants in these systems.

DISCUSSION

The enthalpy and entropy changes of the complex formation reactions of lanthanoid ions with charged bases as ligands are often described by using a simple electrostatic model in connection with the Frank and Evans "iceberg" concept. Species in water solution are surrounded by a cloud of water molecules with a geometry different from that of the bulk water. The extension of this cloud depends on the size and charge of the central ion. As the complex formed has a greater radius and reduced charge as compared to the reactants, water molecules will be released in the association reaction. Thus, as regards the stepwise reactions, the entropy changes are expected to decrease in the order $\Delta S_1^\circ > \Delta S_2^\circ > \Delta S_3^\circ$. This is in acordance with experiments for the malonates and a number of other complexes.[9] The values in Table 3 also permit a calculation of the entropy changes for the reactions

$$MA^+ + A^{2-} \rightarrow MA_2^- \qquad \text{I}$$

$$MHA^{2+} + A^{2-} \rightarrow MHA_2 \qquad \text{II}$$

and the expected relationship $\Delta S^\circ_{II} > \Delta S^\circ_{I}$ is found.

Also, a ligand forming a chelate is expected to give a more positive entropy change than a unidentate ligand. The results for the reactions

$$MA^+ + A^{2-} \rightarrow MA_2^- \qquad \text{I}$$

$$M^{3+} + HA^- \rightarrow MHA^{2+} \qquad \text{IV}$$

for which $\Delta S^\circ_{I} > \Delta S^\circ_{IV}$, are in accordance with this. As arguments based on radius and charge would have given the opposite relationship, this result indicates that malonate ion acts as a bidentate ligand. However, the model cannot be used to make any quantitative estimates of the thermodynamic properties.

This same model also predicts that the function ΔH° *vs.* $1/r$ (or ΔH° *vs.* Z, as $1/r$ is an approximately linear function of Z for the lanthanoid ions), where r is the radius of the lanthanoid ion, should be linear. This is not the case, as is shown in Fig. 2a. The similar shape of ΔH° *vs.* Z plots (and also ΔS° *vs.* Z) for the complex formation with many different ligands is an in-

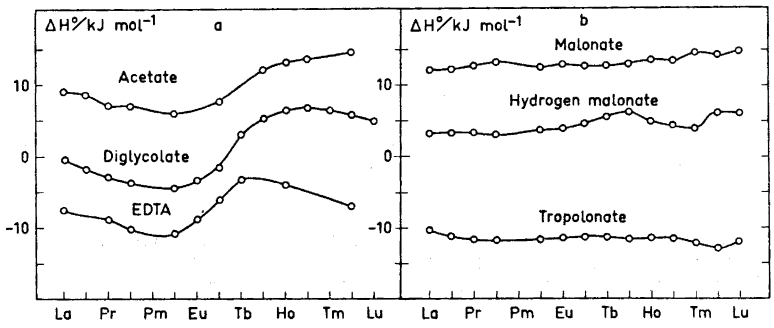

Fig. 2. The enthalpy changes for the formation of (*a*) the first acetate,[16] diglycolate,[8] and EDTA [18] lanthanoid complexes, and (*b*) for the formation of the first malonate, hydrogen malonate, and tropolonate [17] complexes.

dication that the variation is due to some property of the metal ions, *i.e.* there is in the lanthanoid series a change of the structure of the solvation sphere or of the coordination number. A host of thermodynamic and other data have as yet not given any clear picture regarding these structural changes.[10–13] However, the thermodynamic investigation on diglycolate complexes by Grenthe and Ots [14] gave evidence for the presence of a hydration equilibrium

$$M(diglyc)_2(H_2O)_x \rightleftharpoons M(diglyc)_2(H_2O)_y + (x-y)H_2O$$

for the second complex.

For the malonate complexes, the variation in $\Delta H^\circ_{1,0,1}$ is small (Fig. 2b) and a plot of $\Delta S^\circ_{1,0,1}$ *vs.* Z is approximately linear, increasing with decreasing metal ion size. The value of $\Delta H^\circ_{1,0,1}$ for the formation of the scandium complex is the same as for the heavy lanthanoids, whereas $\Delta S^\circ_{1,0,1}$ is about 30 J K^{-1} mol^{-1} more positive than one might expect from the value of the ionic radius of scandium. This behaviour might be compared with that of some other ligands of bidentate character, with oxygen as donor atoms.

Choppin and Friedman have determined the changes in free energy, enthalpy and entropy for the formation of lanthanoid lactate and α-hydroxyisobutyrate complexes.[15] The ΔH_1° -values are negative and vary little across the lanthanoid series and the ΔS_1°-values have a small positive value, 15 to 40 J K^{-1} mol^{-1} throughout the series. For the corresponding complexes with propionate and isobutyrate, respectively, the enthalpy changes are positive and the entropy changes are greater, 60 to 100 J K^{-1} mol^{-1}. An interpretation of this behaviour has been discussed by Grenthe.[16]

For the tropolonate systems,[17] a plot of ΔH°_1 *vs.* Z is given in Fig. 2b. The behaviour of ΔS_1° *vs.* Z is similar to that of the malonate systems. Campbell and Moeller propose that a change in the hydration structure of the metal ions is compensated by a parallel structural change in the hydration spheres of the 1:1 complexes. This suggestion has as yet no experimental basis. In this connection, precise values of the thermodynamic parameters for the higher tropolonato complexes would be of interest. Due to experimental difficulties, such data have not been determined, neither for the malonate nor for the tropolonate systems.

Entropy data for bidentate dicarboxylate complexes are scarce. One reason for this is the formation of sparingly soluble solids with this type of ligand. However, measurements on some maleate systems are in progress at this laboratory and will be reported in a following publication.

Note added in proof. Degischer and Choppin have recently reported (*J. Inorg. Nucl. Chem.* **34** (1972) 2823) the changes in free energy, enthalpy and entropy for the formation of the 1:1 lanthanoid-malonate complexes at ionic strength 0.10 M.

Acknowledgements. The author wishes to thank Dr. Ingmar Grenthe for his interest and encouragement and Professor Ido Leden for helpful criticism of the manuscript. This work has been sponsored by a grant from the *Swedish Natural Science Research Council.*

REFERENCES

1. Dellien, I. and Grenthe, I. *Acta Chem. Scand.* **25** (1971) 1387.
2. Gelles, E. and Nancollas, G. H. *Trans. Faraday Soc.* **52** (1956) 680.
3. Grenthe, I. and Hansson, E. *Acta Chem. Scand.* **23** (1969) 611.
4. Grenthe, I., Ots, H. and Ginstrup, O. *Acta Chem. Scand.* **24** (1970) 1067.
5. Grenthe, I. and Gårdhammar, G. *Acta Chem. Scand.* **26** (1972) 3207.
6. Arnek, R. *Arkiv Kemi* **32** (1970) 81.
7. Gerding, P. *Acta Chem. Scand.* **20** (1966) 79.
8. Grenthe, I. *Acta Chem. Scand.* **17** (1963) 2487.
9. Grenthe, I. *Acta Chem. Scand.* **18** (1964) 293.
10. Geier, G., Karlen, U. and v. Zelewsky, A. *Helv. Chim. Acta* **52** (1969) 1967.
11. Geier, G. and Karlen, U. *Helv. Chim. Acta* **54** (1971) 135.
12. Izatt, R. M., Eatough, D., Christensen, J. J. and Bartholomew, C. H. *J. Chem. Soc.* **A 1969** 47.
13. Padova, J. *J. Phys. Chem.* **71** (1967) 2347.
14. Grenthe, I. and Ots, H. *Acta Chem. Scand.* **26** (1972) 1217.
15. Choppin, G. R. and Friedman, Jr., H. G. *Inorg. Chem.* **5** (1966) 1599.
16. Grenthe, I. *Acta Chem. Scand.* **18** (1964) 283.
17. Campbell, D. J. and Moeller, T. *J. Inorg. Nucl. Chem.* **32** (1970) 945.
18. Ots, H. *Personal communication.*

Received September 1, 1972.

ACTA CHEMICA SCANDINAVICA 27 (1973) 743–746

Reaction Rates of Optically Active Tris(1,10-phenanthroline)* and Tris(2,2′-bipyridyl)* Complexes of Iron(II) in Aqueous Hydroxide and Cyanide Solutions

GWYNETH NORD

Chemistry Department I, Inorganic Chemistry, H. C. Ørsted Institute, University of Copenhagen, Universitetsparken 5, DK-2100 Copenhagen Ø, Denmark

At 25°C, total loss of optical activity accompanies the rate-determining second order reaction of $Fe(phen)_3^{2+}$ and $Fe(bipy)_3^{2+}$ with OH^- and with CN^-. Intramolecular (solvent) racemisation also occurs. Air oxidation of the complexes in alkaline solutions is preceded by the rapidly reversible dissociation of the three chelate ligands.

In our earlier work,[1] we showed that oxygen, although not involved in the rate-determining step, is necessary for the decomposition of $Fe(phen)_3^{2+}$ and $Fe(bipy)_3^{2+}$ in sodium hydroxide solutions. We further suggested that racemisation rates might provide a useful mechanistic probe for these systems. These rates are presented here for hydroxide, and also for some cyanide solutions, together with the spectrophotometrically determined reaction rates of the complexes in the same media.

EXPERIMENTAL

The complexes were resolved through the antimonyl tartrate and converted to the perchlorate as described in the literature.[2] Reactants and products were identified by their visible absorption spectra.[3,4] Changes in optical rotation of both isomers were measured with a Perkin Elmer, Model 141, polarimeter at 436 nm and at 546 nm, and of optical density with a Cary 14 Recording Spectrophotometer at the maximum of the visible absorption bands of the reactants and (cyanide) products. All measurements were made at 25°C and with three series of solutions with salt concentration adjusted with NaCl or KCl to (0.1 or 1.0) M. These contained (a) NaOH, (b) KCN, and (c) KCN + NaOH ($[OH^-] \geq [CN^-]$) (see tables and legends to the figures). The concentrations of OH^- and CN^- were always much greater than that of the complex, which varied from 10^{-5} M to 10^{-4} M. $Na_2S_2O_4$ (see Ref. 1) was added in most cases to the polarimeter cells. Optical rotation rates were also measured in the pure chloride media (see Table 2).

* Referred to in this article as *phen* and *bipy*, respectively.

Table 1.

Complex	Medium M	$10^4 k_r$ s^{-1} (25°C)	$10^4 k_d$ s^{-1} (25°C)	$10^4 k_1$ s^{-1} mol^{-1} (25°C)	$10^4 k_2$ s^{-1} mol^{-1} (25°C)
$Fe(bipy)_3^{2+}$	0.1 KCl	6.6	2.0	70	80
	1.0 NaCl	5.9	(~1) [a]	28.8	60
$Fe(phen)_3^{2+}$	1.0 NaCl	5.3	0.3 (0.69) [b]	61	110

[a] Estimated. [b] Ref. 6.

Table 2.

Complex	Medium M	10^4 k_r s^{-1} (25°C)	Reference
$Fe(bipy)_3^{2+}$	0.1 KCl	6.5	This work
	1.0 NaCl	6.0	This work
	Water	6.0	6
$Fe(phen)_3^{2+}$	0.1 KCl	6.5	This work
	1.0 NaCl	5.8	This work
	0.1 HCl	5.7	6
	1.0 HCl	6.7	6 (24.8°C)

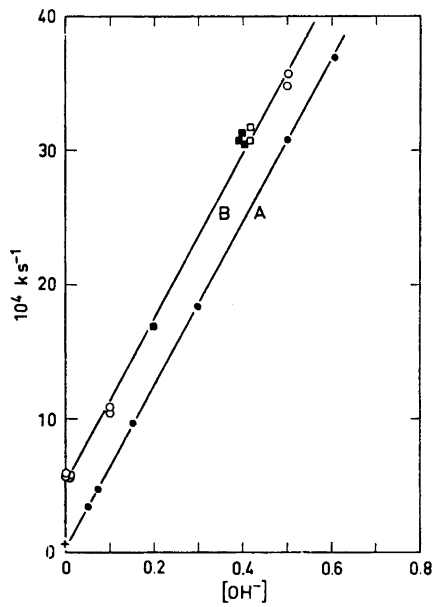

Fig. 1. $Fe(phen)_3^{2+}$ in NaOH-NaCl, 1 M. A. Spectrophotometrically determined $k = k_{sp}$. ● perchlorate, present work, + perchlorate in 1 M KCl, Ref. 6. B. Polarimetrically determined $k = k_{pol}$. ○ antimonyltartrate, ■ perchlorate, □ without $Na_2S_2O_4$ (all others with).

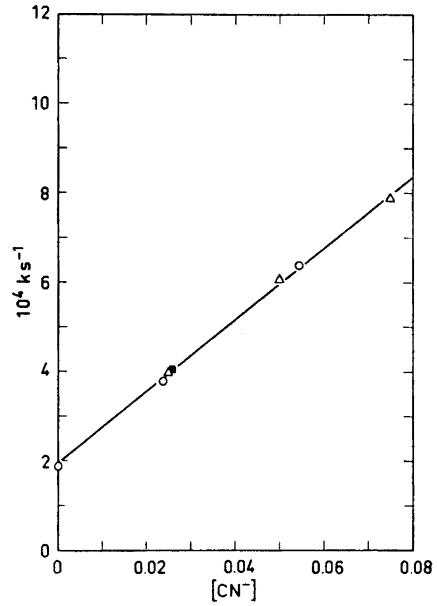

Fig. 2. $Fe(bipy)_2(ClO_4)_2.2H_2O$ in KCN-KCl, 0.1 M. ○ $k_{pol} - 4.6 = k_{pol} - (k_r - k_d)$ (see Table 1), △ k_{sp}, Ref. 7, 25.3°C, ■ k_{sp}, this work.

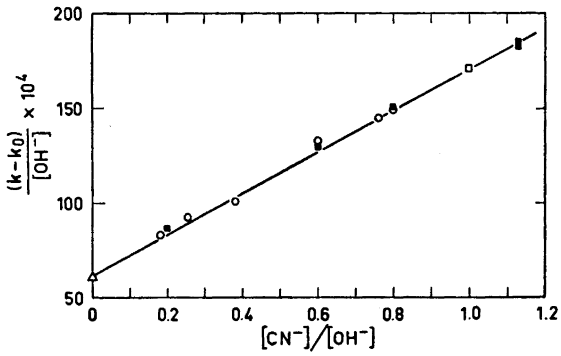

Fig. 3. $Fe(phen)_3(ClO_4)_2.2H_2O$ in KCN-NaOH-NaCl, 1 M. ■ $k-k_0=k_{pol}-k_r=k_{pol}-$ intercept B, Fig. 1, $[OH^-]=0.5$ M, ○ $k-k_0=k_{sp}-k_d=k_{sp}-$intercept A, Fig. 1, $[OH^-]=(0.1-0.4)$ M, □ k_1+k_2 (see Table 1), △ k_1 (see Table 1).

The rates were all strictly first order in complex and were followed for at least four half lives. All kinetic runs were made in duplicate. The rate constants were calculated from the half lives read from the usual logarithmic plots.

In no case was a product optically active. We did not find the small product activity which has been reported [5] to accompany the reaction of *more concentrated* cyanide solutions (up to 2 M) with $\Delta Fe(phen)_3^{2+}$ at 0.5°. Because of this report we also investigated series (b) and (c) at 0°C but obtained only racemic products.

The addition of $Na_2S_2O_4$ did not affect the polarimetrically determined rates although under these conditions no change in optical density was observed in hydroxide solutions of the complex (series (a)). In the presence of O_2 for (a), and both in the presence and absence of O_2 for (b) and (c), the stoichiometry is given below (*biL* is used for *phen* and *bipy*):

(a) $4\ Fe(biL)_3^{2+} + 8\ OH^- + 2\ H_2O + O_2 \rightarrow 4\ Fe(OH)_3 + 12\ biL$

(b) $Fe(biL)_3^{2+} + 2\ CN^- \rightarrow Fe(biL)_3(CN)_2 + biL$

(c) $Fe(biL)_3^{2+} + 4\ CN^- \xrightarrow{(OH^-)} Fe(biL)\ (CN)_4^{2-} + 2\ biL.$

RESULTS AND DISCUSSION

The general rate law in all three sets of solutions (see figures) is:

$$-d[Fe(biL)_3^{2+}]/dt = \{constant + k_1[OH^-] + k_2[CN^-]\}[Fe(biL)_3^{2+}]$$

The two cyanide products thus do not reflect a change in rate determining step. The spectrophotometric and the polarimetric methods give the same second order constants (k_1 and k_2), which are larger for $Fe(phen)_3^{2+}$ than for $Fe(bipy)_3^{2+}$. The first order constants for racemisation (k_r) are larger than for dissociation (k_d) and are similar to those for the pure salt media and to those published for hydrochloric acid (see Tables 1 and 2).

(k_r-k_d) is the rate constant for the intramolecular racemisation as defined and discussed in Ref. 6.

We agree with earlier workers that the rate-determining step produces a bis-chelate probably as in eqns. 1 and 2:

$$Fe(biL)_3^{2+}{}_{aq} + OH^- \xrightarrow{k_1} Fe(biL)_2OHH_2O^+ + biL \qquad (1)$$

$$Fe(biL)_3^{2+}{}_{aq} + CN^- \xrightarrow{k_2} Fe(biL)_2CNH_2O^+ + biL \quad (2)$$

The decomposition of $Fe(bipy)_2(CN)_2$ is independent of $[OH^-]$ and slow ($k = 2.0 \times 10^{-6}\ s^{-1}$ at 35°C; Ref. 7). The corresponding reaction for $Fe(phen)_2(CN)_2$ would be expected to be even slower. $Fe(biL)_2(CN)_2$ thus cannot be formed as an intermediate in the presence of comparable concentrations of OH^- and CN^- (series c).

In order to explain the complete conversion to $Fe(biL)(CN)_4$ it is necessary for OH^- to complete successfully with CN^- for the intermediate species $Fe(biL)_2CNH_2O^+$. This seems sensible as it only requires a proton shift. The product of this reaction must rapidly form the monochelate. The dissociation of the product of reaction of $Fe(biL)_2OHH_2O^+$ with OH^- is also required to be rapid. This, unlike $Fe(biL)_2(CN)_2$ and $Fe(biL)(CN)_4$ which are spin-paired and robust, would be expected to be spin-free and labile.

The capture and stabilisation of the monochelate iron(II) species by cyanide shows that complete loss of chelate ligand in a series of rapidly reversible steps precedes air oxidation.

Earlier workers [6] have suggested that the mechanism of the intramolecular racemisation may involve an expanded high-spin reactive intermediate. This intermediate does not lead to dissociation of a biL ligand but could well be formed by attack on the complex by a solvent molecule. It therefore could be analogous to the seven-coordinated reactive intermediates which can explain the rate law for the CN^- and OH^- dependent paths. Since loss of optical activity accompanies ligand loss, this common mechanism can adequately accommodate our experimental results.

Acknowledgement. Thanks are due to Hans Matthes for preparing the optically active salts and for making many of the measurements.

REFERENCES

1. Nord, G. and Pizzino, T. *Chem. Commun.* **1970** 1633.
2. Davies, N. R. and Dwyer, F. P. *Trans. Faraday Soc.* **48** (1952) 244.
3. Schilt, A. A. *J. Am. Chem. Soc.* **82** (1960) 3000.
4. Burgess, J. *Spectrochim. Acta* **A 26** (1970) 1369.
5. Archer, R. D., Snydam, L. J. and Dollberg, D. D. *J. Am. Chem. Soc.* **93** (1971) 6837.
6. Basolo, F. and Pearson, R. G. *Mechanisms of Inorganic Reactions*, 2nd Ed., Wiley, New York 1967, Chapter 4. This also contains full references to earlier work.
7. Burgess, J. *J. Chem. Soc. Dalton* **1972** 1061.

Received September 18, 1972.

ACTA CHEMICA SCANDINAVICA 27 (1973) 747–755

Mass Spectra of Thioamides

F. C. V. LARSSON,[a] S.-O. LAWESSON,[a] JØRGEN MØLLER[b] and GUSTAV SCHROLL[c]

[a]*Department of Organic Chemistry, Aarhus University, DK-8000 Aarhus C,* [b]*Physical Laboratory II, University of Copenhagen, The H. C. Ørsted Institute, DK-2100 Copenhagen Ø and* [c]*Department of General and Organic Chemistry, University of Copenhagen, The H. C. Ørsted Institute, DK-2100 Copenhagen Ø, Denmark*

The mass spectra of various thioamides have been recorded and interpreted with the aid of exact mass measurements and metastable defocussing technique. Loss of a sulfhydryl radical from the molecular ions is generally an important process and may in some cases be taken as evidence for a strong enethiolization of the molecular ion.

Thiocarbonyl compounds investigated by mass spectrometry include thionoesters,[1,2] thiocarbonates,[1,3] thiocarbamates,[1,3] thioureas,[1,4–6] thiohydrazides, thiourethanes,[7] a few thioamides,[8,9] and various heterocyclic compounds.[10]

From our study of the mass spectra of various thioamides we here want to discuss the mass spectra of the following compounds:

I. Thioacetamide. II. Thiobenzamide. III. *o*-Methoxythiobenzamide. IV. *N*-Methylthiobenzamide. V. *N*,*N*-Dimethylthiobenzamide. VI. Thioacetanilide. VIII. *p*-Methylthioacetanilide. IX. *o*-Methyoxythioacetanilide.

RESULTS AND DISCUSSION

The mass spectrum (Fig. 1) of thioacetamide (I) displays an abundant molecular ion peak as expected for a small molecule. From the reported mass spectrum of acetamide [4,11] (Table 1) thioacetamide is expected to undergo α-cleavages upon electron impact.

This was also the case, as abundant peaks at *m/e* 60 and 59, corresponding to the loss of $\cdot CH_3$ and $\cdot NH_2$ from the molecular ion, are found, but in addition the mass spectrum of thioacetamide contains a 50 % peak at *m/e* 42 due to an M − ·SH ion. This decomposition can best be rationalized with the assumption of an initial "enethiolization" of the molecular ion prior to α-cleavage,[8] as depicted in Scheme 1.

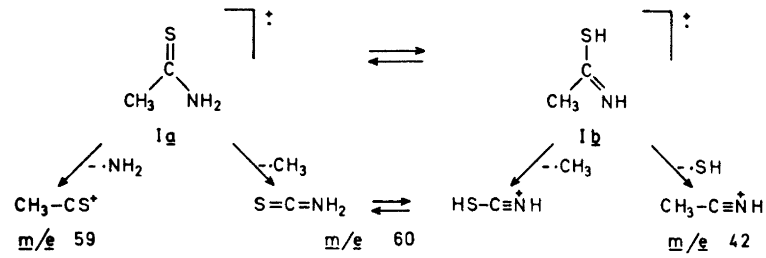

Scheme 1.

Table 1. Comparison of the mass spectra of CH_3CONH_2 and CH_3CSNH_2.

Ion	CH_3CONH_2 %	CH_3CSNH_2 %
M	100	100
$M-CH_3$ (α_1)	76	71
$M-NH_2$ (α_2)	57	28
α_1/α_2	1.33	2.53

Whereas the abundance of the $M-\cdot CH_3$ ion is 1.33 times that of the $M-\cdot NH_2$ ion in the case of acetamide, the ratio is 2.53 in the case of thioacetamide, as seen from Table 1. This fact can be taken as evidence for an initial "enethiolization", as the ion I*b* is unable to undergo loss of $\cdot NH_2$, but it might also

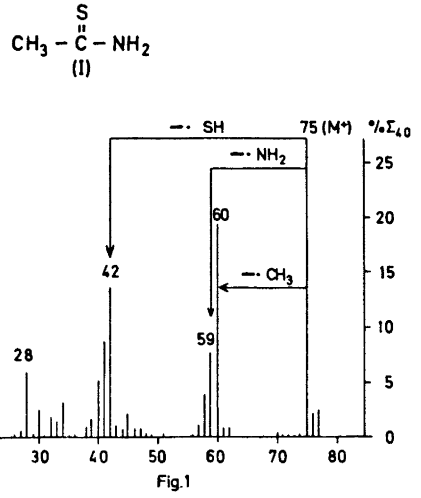

Fig.1

indicate a more pronounced interaction between the lone pair on the nitrogen atom and the double bond in the thioamide than in the amide. This interaction will lead to a delocalization of the charge as well as the unpaired electron, as described with the resonance structures:

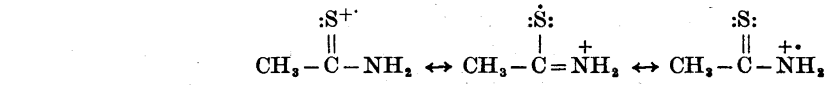

The mass spectrum (Fig. 2) of thiobenzamide (II) has recently been published and discussed.[9] The more important fragmentation and rearrangement processes of thiobenzamide are depicted in Fig. 2. In connection with the discussion of the abundance of $M^{+\cdot} - \cdot CH_3$ ion *versus* that of the $M^{+\cdot} - \cdot NH_2$ ion from thioacetamide it should be noted that in the case of thiobenzamide loss of $\cdot NH_2$ is twice as important as the expulsion of $\cdot C_6H_5$, indicating the mesomeric interaction between the aromatic moiety and the CS group.

It has been suggested in the discussion of the mass spectrum of thiobenzamide by Holmes and Benoit [9] that the ion of mass 103 (corresponding in

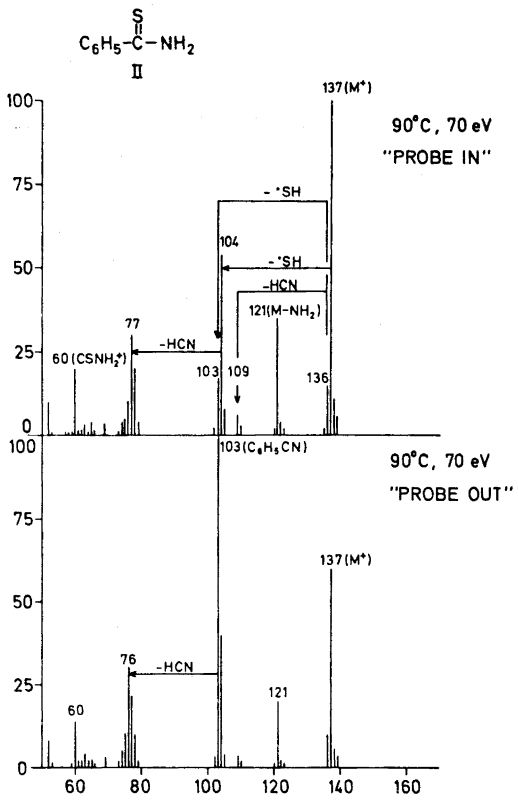

Fig. 2

composition – and most likely also in structure – to ionized benzonitrile) might be formed by the decomposition of $M^{+\cdot}$ by loss of H_2S and/or by the loss of a hydrogen atom from 104^+ ($M^{+\cdot} - \cdot SH$). We have, however, found certain indications for a thermal as well as an electron impact induced origin of this ion as stressed in the following paragraph.

The mass spectrum (Fig. 2) of thiobenzamide was recorded at two different sets of conditions. In both cases the direct insertion technique was applied. The mass spectrum marked "Probe in" was obtained with the probe right in the ionization chamber, whereas that marked "Probe out" was recorded with the probe pulled a distance back. In the first case the sample evaporized direct into the electron beam, in the latter the sample passes along the heated walls of the ion source increasing the possibility for thermal decomposition.

The formation of 104^+ from the molecular ion gives rise to a metastable peak at *m/e* 79.0, and this peak is retained even at 12 eV, whereas no metastable peaks indicating the formation of $103^{+\cdot}$ have been observed, neither at 70 eV nor at low voltages (20 – 12 eV). Application of the defocussing technique, however, revealed that the M – 1 ion is a precursor for $103^{+\cdot}$, clearly demonstrating the electron impact induced origin of the $M - H_2S$ ion.

That the ionized benzonitrile can also be due to a thermal degradation prior to ionization is clearly evidenced by the mass spectrum recorded with the probe a short distance apart from the electron beam. This spectrum is a superposition of the mass spectra of thiobenzamide and benzonitrile.

Introduction of substituents into the aromatic ring did surprisingly not lead to new electron impact induced processes. Out of the compounds investigated we here want to report our findings dealing with the mass spectrum of *o*-methoxythiobenzamide (III), as the methoxy group is known often to conduct the fragmentation pattern of aromatic compounds, and when situated in the 2-position to participate in "ortho-effect" reactions.

Skeletal rearrangements as those reported for 2-ethoxy benzamide [12] were not observed and the α-cleavages have become unimportant. The fragment

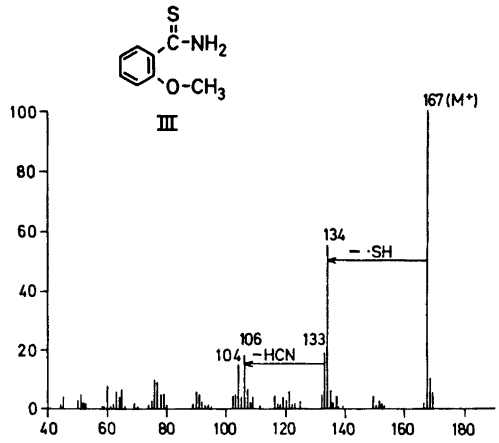

Fig. 3

ion peak of highest abundance is due to the loss of ·SH from the molecular ion.

In the mass spectrum (Fig. 4) of *N*-methylthiobenzamide (IV) the peak due to M − ·SH (*m/e* 118) is of less importance than in the preceding spectra. Two abundant peaks are found at *m/e* 150 (M − 1) and 121 ($C_6H_5CS^+$). The

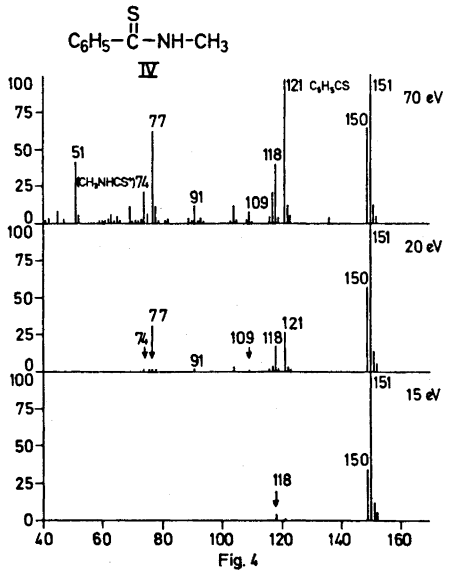

Fig. 4

mass spectrum of thiobenzamide contained an M − 1 peak, but it was only 17 % of the molecular ion peak, and the abundance decreased rapidly with the electron energy. In the mass spectrum of IV the M − 1 peak is 64 % of the molecular ion peak and it remains important at low voltage.[13] This mass spec-

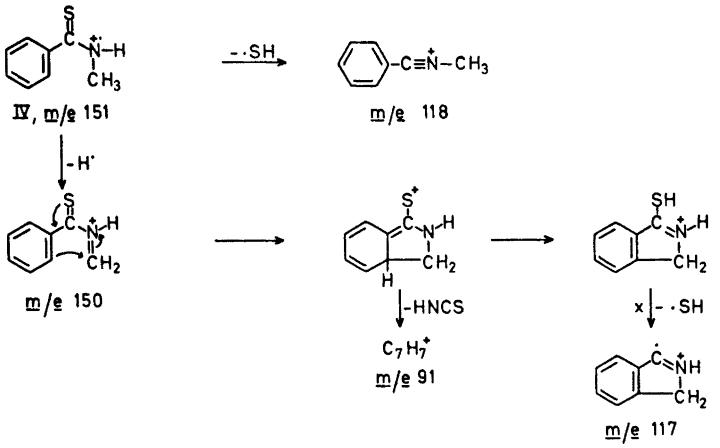

Scheme 2.

trum also contains metastable peaks, corresponding to the loss of ·H from $M^{+\cdot}$ and the loss of ·SH from the M − 1 ion. Further, this spectrum as well as that of *N*,*N*-dimethylthiobenzamide (V, Fig. 5) contain peaks at *m/e* 91 corresponding to $C_7H_7^+$, whereas no such peak was found in the mass spectrum of thiobenzamide (II).

Assuming the formation of a bond between the *N*-methyl and the aromatic ring, the formation of 150^+, 117^+, and 91^+ can be rationalized as depicted in Scheme 2.

The mechanism suggested in Scheme 2 is based upon the assumption that the M − 1 ion is formed by the abstraction of a hydrogen atom from one of the methyl groups. However, it has been shown [13] that the M − 1 peak in the mass spectrum of *N*,*N*-dimethylbenzamide is due to the loss of a hydrogen from the phenyl group, thus questioning our assumption, but whereas the M − 1 ion from the *N*,*N*-dimethylbenzamide has not been observed to decompose further, the loss of ·SH from the M − 1 ions from IV and V as well as the formation of $C_7H_7^+$ ions are best interpreted by the mechanism above.

The mass spectrum of *N*,*N*-dimethylthiobenzamide (V, Fig. 5) contains peaks corresponding to some of the processes observed for the monomethyl analogue. It should be noted, however, that whereas the loss of ·SH took place from the molecular ion as well as from the M − 1 ion of IV, the dimethyl derivative primarily undergoes ·SH abstraction from the M − 1 ion. This difference can be taken as evidence for a thiolization of IV prior to the loss of ·SH. Due to the absence of a hydrogen bonded to nitrogen in V, this compound is unable to undergo enethiolization.

Walter *et al.*[8] have discussed the mass spectra of various thioformanilides. A dominating feature of the mass spectra of these compounds is the presence of abundant M − 1 peaks. These peaks are due to ions formed by the abstraction of an *ortho*-hydrogen from the phenyl group. In the mass spectrum (Fig. 6) of thioacetanilide (VI) an abundant M − 1 peak at *m/e* 150 is found, and this

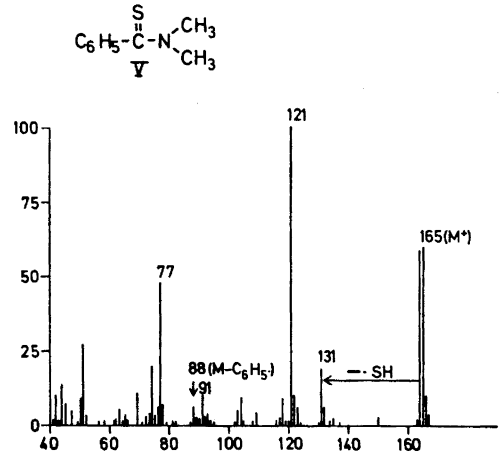

Fig. 5

peak is also prominent at low voltage. If it is assumed that an *o*-hydrogen is abstracted from the aromatic ring in connection with bond formation, the structure of the M − 1 ion can be depicted as *a* (Scheme 3). A metastable peak at *m/e* 79.2 indicates the loss of CH_3CN from *a*. In order to investigate the structure of the M − 1 ion further, the mass spectrum of 2,2-dimethyl-2,3-dihydrobenzthiazole (VII) was recorded, as the same 150^+ ion was expected to be formed by the loss of $\cdot CH_3$ from the molecular ion. The mass spectrum of VII displays only three prominent peaks corresponding to M, M − $\cdot CH_3$, and M − $\cdot CH_3$ − CH_3CN. The metastable peak at 79.2 ($150^+ \rightarrow 109^+$) mentioned above was also found in the mass spectrum of VII, supporting the assumed mechanism (Scheme 3).

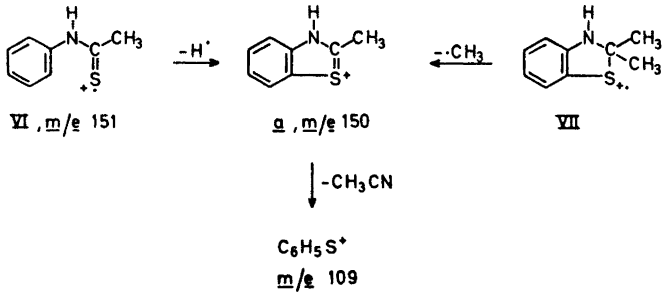

Scheme 3.

Loss of acetonitrile not only takes place from the M − 1 ion, but also from the molecular ion, leading to ionized thiophenol (*m/e* 110). Loss of ·SH from the molecular ion is also observed. The abundant peak at *m/e* 93 corresponds to ionized aniline.

In the mass spectrum (Fig. 7) of *p*-methylthioacetanilide (VIII) the features of thioacetanilide (VI) are found. The presence of an abundant M − 2 doubly charged ion peak at *m/e* 81.5 (15 %) can be assigned to the formation of *b*.

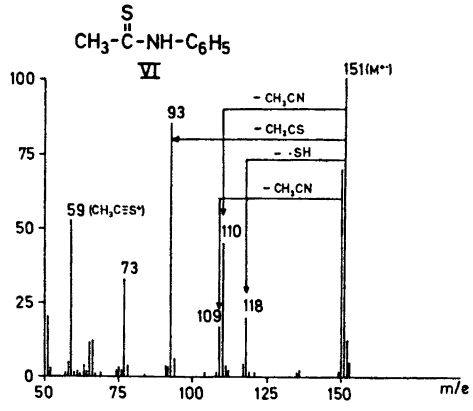

Fig. 6

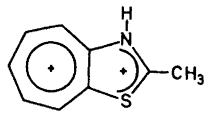

b, m/e 81.5

As it was not possible to obtain a sample of *o*-thioacetotoluid completely free of the oxygen analogue, the mass spectrum is not reported here. As in the case of the *p*-isomer an abundant peak is observed at *m/e* 81.5, but whereas

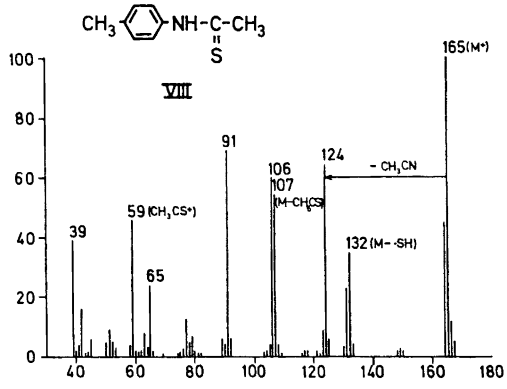

Fig. 7

the *p*-isomer eliminates a hydrogen atom from the molecular ion, this compound undergoes the loss of a methyl radical.

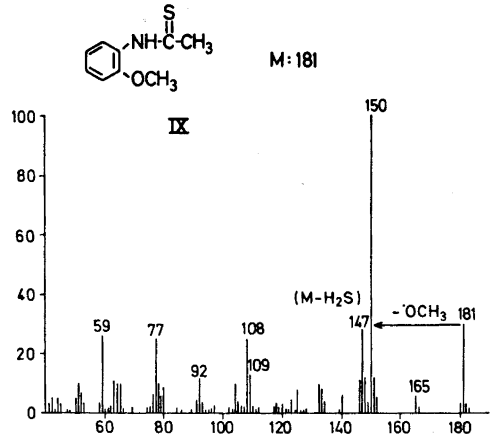

Fig. 8

Corresponding to this process *o*-methoxythioacetanilide (IX) undergoes the loss of a methoxy group leading to the formation of *a*, whereas the mass spectrum of the *p*-isomer (not reported here) only displays a minor M − 31 peak.

EXPERIMENTAL

The mass spectra were recorded with an AEI MS 902 doubly focussing mass spectrometer, using the direct inlet with a source temperature of 100 − 135°C.

All thioamides were either commercially or synthesized in known ways.[14]

REFERENCES

1. Bowie, J. H., Simons, B. K. and Lawesson, S.-O. *Rev. Pure Appl. Chem.* **19** (1969) 61.
2. Ohno, A., Koizumi, T., Ohnishi, Y. and Tsuchihashi, G. *Org. Mass. Spectrom.* **3** (1970) 261.
3. Thomson, J. B., Brown, P. and Djerassi, C. *J. Am. Chem. Soc.* **88** (1966) 4049.
4. Budzikiewicz, H., Djerassi, C. and Williams, D. H. *Mass Spectrometry of Organic Compounds*, Holden-Day, San Francisco 1967.
5. Duffield, A. M., Djerassi, C., Neidlein, R. and Henkelbach, E. *Org. Mass Spectrom.* **2** (1969) 641.
6. Shapiro, R. H., Serum, J. W. and Duffield, A. M. *J. Org. Chem.* **33** (1968) 243.
7. Duffield, A. M., Djerassi, C. and Sandström, J. *Acta Chem. Scand.* **21** (1967) 2167.
8. Walter, W., Becker, R. F. and Grützmacher, H. F. *Tetrahedron Letters* **1968** 3515.
9. Holmes, J. L. and Benoit, F. *Org. Mass Spectrom.* **5** (1971) 525.
10. Porter, Q. N. and Baldas, J. *Mass Spectrometry of Heterocyclic Compounds*, Wiley-Interscience, New York 1971.
11. Gilpin, J. A. *Anal. Chem.* **31** (1959) 935.
12. Spiteller, G. *Monatsh.* **92** (1961) 1147.
13. Biellmann, J. F. and Hirth, C. G. *Org. Mass Spectrom.* **2** (1969) 723.
14. Reid, E. E. *Organic Chemistry of Divalent Sulfur*, Chemical Publishing Co., New York 1962, Vol. IV, pp. 81 and 82.

Received August 29, 1972.

ACTA CHEMICA SCANDINAVICA 27 (1973) 756–762

The Crystal Structure of Bis(4-morpholinethiocarbonyl) Trisulphide

STEINAR HUSEBYE

Chemical Institute, University of Bergen, N-5000 Bergen, Norway

The structure of bis(4-morpholinethiocarbonyl) trisulphide has been determined by three-dimensional X-ray methods. The yellow crystals are orthorhombic with $a = 22.284(6)$ Å, $b = 8.840(3)$ Å, $c = 15.937(4)$ Å, and $Z = 8$. The space group is *Pbca*, and the density is: calc. 1.51, found 1.50 g/cm³.

Using multiple-film Weissenberg techniques and Cu$K\alpha$ radiation, 724 reflections above background were estimated visually. The structure was solved by means of the symbolic addition procedure, and refined by full-matrix least squares methods to a conventional R-value of 9.2 %.

The bond lengths and angles involving the trisulphide group are: S0–S1 = 2.011(9) Å, S0–S3 = 2.016(8) Å, ∠S1S0S3 = 108.8(4)°, ∠S0S1C1 = 104.6(8)°, and ∠S0S3C6 = 103.7(6)°. For the dihedral angles C1S1S0/S1S0S3 and C6S3S0/S3S0S1, the values 92.4 and 101.5°, respectively, were found.

During the investigation of structures of compounds of divalent selenium and tellurium with dithio and related ligands, a strong tendency to planar four-coordination around the central atoms were found.[1–4] Of the ligands used, dithiocarbamates seemed to form the stronger Te–S and Se–S bonds. Examples of such dithiocarbamate complexes are the isomorphous tellurium and selenium bis(4-morpholinecarbodithioates).[3,4] (These compounds were earlier [3,4] termed morpholyldithiocarbamates.) Their structures are trapezoid-planar with two short and two long M–S bonds, each short bond roughly *trans* to a long one, with the bonding probably being of the three-center four electron type.

The present structure investigation of the analogous sulphur compound was undertaken to see if the tendency to planar four-coordination found for divalent tellurium and selenium could be observed for divalent sulphur also.

EXPERIMENTAL

Bis(4-morpholinethiocarbonyl) trisulphide was synthesized following the procedure of Blake.[5] In the first step, 4-morpholine monosulphide was made by the reaction between morpholine and sulphur dichloride in petrol ether:

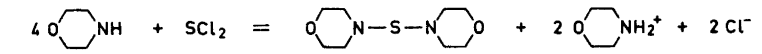

In the next step, the sulphide was dissolved in excess carbon disulphide and the mixture refluxed for 30 h:

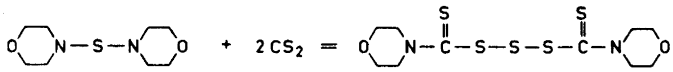

Upon cooling, small yellow prisms of the trisulphide crystallized out, m.p. 146 – 147°C. Recrystallization from benzene gave crystals with m.p. 152°C, while the m.p. reported by Blake [5] is 152 – 153°C. The bis(4-morpholinethiocarbonyl) trisulphide is very stable and does not break down into mixtures of mono- and polysulphides like its non-cyclic aliphatic analogs.[3]

Unit cell data were computed from 57 high-order reflections, read from NaCl-calibrated Weissenberg films, using a least squares program. The orthorhombic crystals are elongated along *c*, with $a = 22.284(6)$ Å, $b = 8.840(3)$ Å, $c = 15.937(4)$ Å, and $Z = 8$. The density is: calc. 1.51, found 1.50 g/cm³. From systematic extinctions, the space group is D_{2h}^{15}-*Pbca*.

Integrated Weissenberg equi-inclination photographs were taken of the *h*0*l*, *h*1*l*, *h*2*l*, *hk*0, and *hk*1 layers, using the multiple-film technique and Cu$K\alpha$ radiation. Reflection intensities were estimated visually, and 724 out of 1385 independent reflections with $\sin\theta \leq 0.985$ were observed and measured. During exposure, the reflections had a tendency to split in two with increasing exposure time, thus the crystals had to be changed several times. Only small crystals were obtained during preparation and recrystallization, the average size of the crystals used for obtaining intensities was: cross-section 0.03×0.09 mm², length 0.15 mm. The small size is probably the reason why so many reflections were not observed. The intensities were corrected for secondary extinction effects, but not for absorption ($\mu = 43$ cm^{-1}).

STRUCTURE ANALYSIS

After the usual corrections had been made, the intensities were put on the same relative scale by comparison of reflections common to two layers. Overall scale and temperature factors were then computed from a Wilson plot [6] and used in calculation of normalized structure factors for all reflections, using a program written by Shiono.[7]

Phase determination for the 144 reflections with $|E| > 1.50$ was then carried out by the symbolic addition procedure, using a program written by Long.[8] Origin of the unit cell was specified by arbitrarily assigning positive phases to three reflections with high E-values; and three other reflections with high E-values were given variable signs.

Of the resulting eight sign sets, the one with the highest consistency index was chosen as basis for computing an E map.

The five sulphur atoms and most light atoms showed up in this map and the rest of the atoms were found from successive Fourier syntheses. Full-matrix least squares methods were then employed to refine the structure. The program used minimizes the expression $r = \sum W[|F_o| - |KF_c|]^2 / \sum W|F_o|^2$, where K is a variable scale factor and W, the relative weight assigned to a reflection, is equal to $1/\sigma^2(F)$. $\sigma^2(F)$ is evaluated as $(Ka_1)^2 + (a_2F_o)^2/4W_o$, where W_o is a weight factor related to the reliability with which the intensity of a given reflection is measured, and a_1 and a_2 are constants, here put equal to 2.0 and 1.0, respectively.

With anisotropic temperature factors for the sulphur atoms, the reliability index $R = \sum||F_o| - |F_c||/\sum|F_o|$ converged to the final value of 0.092. A three-dimensional difference synthesis after the refinement showed no spurious peaks.

The final observed and calculated structure factors can be obtained from the author upon request. Atomic scattering factors for sulphur, nitrogen, and carbon were taken from *International Tables*,[9] those for sulphur were corrected for anomalous dispersion according to Cromer.[10] Atomic parameters are listed in Tables 1 and 2, while interatomic distances and angles based on the coordinates from Table 1 are listed in Tables 3 and 4.

Table 1. Final atomic coordinates in fractions of cell edges, with standard deviations.

	x	y	z
S0	0.0112(2)	0.1420(9)	0.3370(4)
S1	0.0509(2)	0.3000(8)	0.2651(3)
S2	0.1587(2)	0.1501(8)	0.3426(4)
S3	0.0035(2)	0.2226(9)	0.4548(3)
S4	−0.0804(2)	0.4289(9)	0.3611(3)
O1	0.2269(6)	0.4511(21)	0.0783(9)
O2	−0.1617(6)	0.3736(19)	0.6660(9)
N1	0.1602(6)	0.3305(24)	0.2097(10)
N2	−0.0868(6)	0.3762(25)	0.5239(9)
C1	0.1296(7)	0.2556(28)	0.2700(11)
C2	0.1363(9)	0.4490(36)	0.1507(14)
C3	0.1609(10)	0.4315(37)	0.0692(15)
C4	0.2506(11)	0.3247(36)	0.1305(14)
C5	0.2295(9)	0.3372(33)	0.2136(13)
C6	−0.0604(7)	0.3474(29)	0.4491(10)
C7	−0.0665(8)	0.3102(31)	0.6057(12)
C8	−0.1210(9)	0.2507(34)	0.6529(14)
C9	−0.1857(8)	0.4294(27)	0.5874(12)
C10	−0.1350(7)	0.4876(29)	0.5338(11)

Table 2. Components of atomic vibration tensors, $U \times 10^3$, in Å^2 with standard deviations, referred to crystallographic axes. For Te and S, the expression is $\exp\{-2\pi^2 [h^2a^{-2}U_{11} + k^2b^{-2}U_{22} + l^2c^{-2}U_{33} + 2\ hka^{-1}b^{-1}U_{12} + 2\ klb^{-1}c^{-1}U_{13} + 2\ hla^{-1}c^{-1}U_{13}]\}$. For the other atoms, the expression is $\exp[-8\pi^2U(\sin^2\theta/\lambda^2)]$.

	U_{11}	U_{22}	U_{33}	U_{12}	U_{23}	U_{13}
S0	72.1(3.0)	67.6(6.2)	96.6(4.2)	−12.7(4.1)	−18.3(6.9)	17.5(3.2)
S1	52.5(2.2)	75.5(5.0)	64.4(2.9)	4.2(3.7)	3.4(6.0)	2.3(2.4)
S2	73.5(2.9)	64.8(4.7)	77.6(3.6)	9.3(4.0)	30.6(6.6)	−0.6(2.9)
S3	66.5(2.7)	80.2(7.1)	69.3(3.1)	8.7(4.2)	9.7(6.5)	7.4(2.7)
S4	73.2(3.0)	95.3(7.1)	49.5(2.5)	11.9(4.3)	8.7(5.6)	2.3(2.7)

	U		U		U		U
O1	83.6(4.8)	C1	54.7(5.1)	C5	83.9(7.1)	C9	58.0(5.5)
O2	74.9(4.4)	C2	87.0(7.6)	C6	47.9(5.0)	C10	54.7(5.3)
N1	69.1(5.0)	C3	98.8(8.5)	C7	69.2(6.2)		
N2	59.5(4.5)	C4	110.1(8.0)	C8	85.3(7.4)		

Table 3. Bond lengths and angles in the trisulphide molecule, with standard deviations.

Distance		Angle	
S0–S1	2.011(9) Å	∠ S1–S0–S3	108.8(4)°
S0–S3	2.016(8)	∠ S0–S1–C1	104.6(8)
S1–C1	1.800(16)	∠ S0–S3–C6	103.7(6)
S2–C1	1.621(21)	∠ S1–C1–S2	123.1(11)
S3–C6	1.803(21)	∠ S1–C1–N1	110.8(14)
S4–C6	1.638(19)	∠ S2–C1–N1	126.0(13)
C1–N1	1.35(3)	∠ S3–C6–S4	121.8(10)
C6–N2	1.35(2)	∠ S3–C6–N2	114.5(14)
N1–C2	1.51(3)	∠ S4–C6–N2	123.5(16)
C2–C3	1.42(3)	∠ C1–N1–C2	127.3(16)
C3–O1	1.49(3)	∠ C1–N1–C5	119.7(16)
O1–C4	1.49(3)	∠ C2–N1–C5	110.6(17)
C4–C5	1.41(3)	∠ N1–C2–C3	111.1(22)
C5–N1	1.55(3)	∠ C2–C3–O1	106.2(19)
N2–C7	1.50(3)	∠ C3–O1–C4	108.6(19)
C7–C8	1.52(3)	∠ O1–C4–C5	110.3(22)
C8–O2	1.43(3)	∠ C4–C5–N1	107.0(17)
O2–C9	1.45(2)	∠ C6–N2–C7	124.1(17)
C9–C10	1.51(3)	∠ C6–N2–C10	122.8(16)
C10–N2	1.47(3)	∠ C7–N2–C10	112.9(15)
		∠ N2–C7–C8	108.9(15)
		∠ C7–C8–O2	108.4(22)
		∠ C8–O2–C9	111.5(16)
		∠ O2–C9–C10	109.3(14)
		∠ C9–C10–N2	112.4(19)

Table 4. Some intramolecular distances and angles.

Distance		Angle	
S0–S2	3.288(5) Å	∠ S1–S0–S2	64.0(2)°
S0–S4	3.278(9)	∠ S1–S0–S4	78.6(3)
S1–S2	3.009(8)	∠ S2–S0–S3	93.0(2)
S3–S4	3.008(9)	∠ S2–S0–S4	127.0(3)
S2–S4	5.877(8)	∠ S3–S0–S4	64.2(3)
S1–S3	3.275(7)	∠ S0–S2–C1	66.0(6)
S2–S3	3.946(7)	∠ S0–S4–C6	65.8(8)
S1–S4	3.492(7)		

THE STRUCTURE OF THE BIS(4-MORPHOLINETHIOCARBONYL) TRISULPHIDE

In Fig. 1, the molecule is seen in projection along *b*, with bond lengths and angles indicated. The molecules are monomeric and non-planar, thus there is no tendency to planar four-coordination around the central sulphur atom, as was found for the central tellurium and selenium atoms in analogous molecules. The two dithiocarbamate groups S1S2C1N1C2C5 and S3S4C6N2C7C10 are nearly planar, no atom deviating more than 0.12 and 0.15 Å, respectively, from the least squares planes through those groups. If one includes S0 in both

Table 5. Intermolecular distances. The left column represents distances from an atom in the original molecule to an atom in a molecule whose transformation from the original one is listed in the next column.

S4 – C4	$-\frac{1}{2}+x,\ y,\ \frac{1}{2}-z$	3.88 Å
O2 – C5	$-\frac{1}{2}+x,\ \frac{1}{2}-y,\ 1-z$	3.61
S0 – S1	$-x,-\frac{1}{2}+y,\ \frac{1}{2}-z$	3.70
S0 – C2	$-x,-\frac{1}{2}+y,\ \frac{1}{2}-z$	3.71
S1 – C7	$x,\ \frac{1}{2}-y,-\frac{1}{2}+z$	3.78
S4 – C8	$x,\ \frac{1}{2}-y,-\frac{1}{2}+z$	3.79
C1 – C4	$\frac{1}{2}-x,\ \frac{1}{2}+y,\ z$	3.44
S4 – C1	$-x,\ \frac{1}{2}+y,\ \frac{1}{2}-z$	3.73
S2 – C3	$x,\ \frac{1}{2}-y,\ \frac{1}{2}+z$	3.68
O1 – C9	$\frac{1}{2}+x,\ y,\ \frac{1}{2}-z$	3.29
O1 – C10	$\frac{1}{2}+x,\ y,\ \frac{1}{2}-z$	3.57
C4 – C9	$\frac{1}{2}+x,\ y,\ \frac{1}{2}-z$	3.86
C4 – C10	$\frac{1}{2}+x,\ y,\ \frac{1}{2}-z$	3.93
S2 – C8	$-x,\ -y,\ 1-z$	3.64
S2 – C9	$\frac{1}{2}+x,\ \frac{1}{2}-y,\ 1-z$	3.71
S2 – C10	$-x,\ 1-y,\ 1-z$	3.80
S3 – C10	$-x,\ 1-y,\ 1-z$	3.90
O2 – N1	$-x,\ 1-y,\ 1-z$	3.28
O2 – C1	$-x,\ 1-y,\ 1-z$	3.51
O2 – C2	$-x,\ 1-y,\ 1-z$	3.36
O2 – C5	$-x,\ 1-y,\ 1-z$	3.54
C1 – C9	$-x,\ 1-y,\ 1-z$	3.81
C1 – C10	$-x,\ 1-y,\ 1-z$	3.86
C5 – C9	$-x,\ 1-y,\ 1-z$	3.91

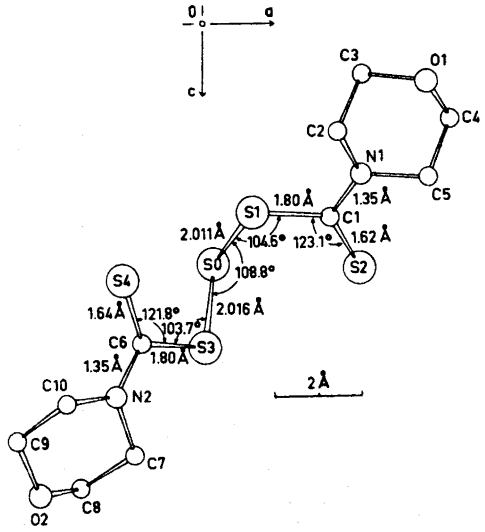

Fig. 1. The structure of the bis(4-morpholinethiocarbonyl) trisulphide molecule seen along the *b*-axis.

groups above, they are still roughly planar, the maximum deviation of any atom from the plane to which it belongs, now being 0.26 Å. The interplanar angle S0S1S2C1N1C2C5/S0S3S4C6N2C7C10 is 52.0°. This angle represents the twisting of the two halves of the molecule relative to a planar configuration.

The central part of the molecule, represented by the C6S3S0S1C1 chain, has the *trans* configuration often found in pentathionates,[11] thus C6 is 1.7 Å above the S1S0S3 plane while C1 is 1.7 Å below. The dihedral angles C1S1S0/S1S0S3 and C6S3S0/S3S0S1 are 92.4 and 101.5°, respectively. The S – S bond lengths in the trisulphide group are S1 – S0 = 2.011(9) Å, and S3 – S0 = 2.016(8) Å. These values are not significantly different from the corresponding values, 2.03 Å and 2.04 Å, estimated on the basis of Hordvik's single bond length-dihedral angle relationship for sulphur-sulphur bonds.[12] Although the S0 – S2 and S0 – S4 distances are only 3.28 Å and 3.29 Å, they cannot be regarded as bonds. They are both significantly longer than the S – S "bites" in the dithiocarbamate groups, which are both 3.01 Å, and they are about equal to the S1 – S3 distance of 3.28 Å. The central sulphur atom has a valency angle of 108.8(4)°. This value is higher than those usually found for sulphur,[13] but is not significantly different from the average value of 107°54′ found in orthorhombic sulfur.[14] Other compounds in which sulphur has large valency angles are 3,3′-trithiobis(2,4-pentanedione) with 106.7°,[15] 1,2,3,6,7,8-hexathiecan with 109.5°,[16] cyclodecasulphur with 107.8°,[17] and potassium pentathionate with 107.4°.[18]

The other two sulphur valency angles, ∠S0 – S1 – C1 and S0 – S3 – C6, are 104.6 and 103.7°, which is quite normal.

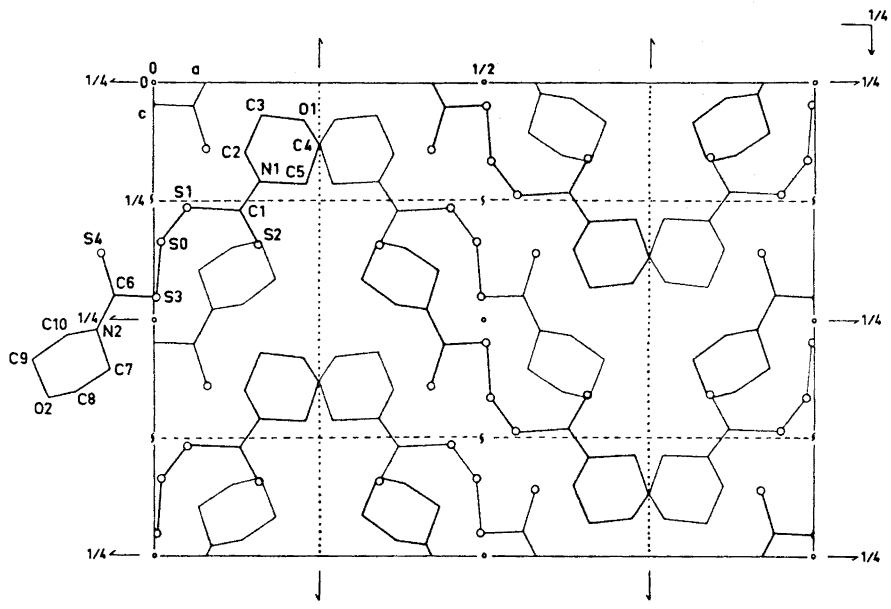

Fig. 2. The molecular arrangement seen along the *b*-axis.

In each dithiocarbamate group there is a short and a long C–S bond. The lengths correspond within the error limit to double and single bonds, respectively, and agree well with the values found for corresponding bonds in tetramethylthiuram disulfide where the short and long bonds are 1.634 and 1.829 Å, respectively.[19] Similar values are also found in tetraethylthiuram disulphide.[20] In complexes where both sulphur atoms in a dithiocarbamate ligand are bonded to the central atom, the two C–S bonds are more equal, a short M–S bond corresponding to a long C–S bond and *vice versa*.[3,4]

The two C–N bonds are both 1.35 Å, which is normal for such a bond. Bond lengths and angles in the morpholine rings are similar to those found in the (4-morpholine)-carbodithioates of divalent selenium and tellurium.[3,4]

No unusually short intermolecular contacts were found.

REFERENCES

1. Husebye, S. *Acta Chem. Scand.* **20** (1966) 24.
2. Husebye, S. *Acta Chem. Scand.* **21** (1967) 47.
3. Husebye, S. *Acta Chem. Scand.* **23** (1969) 1389.
4. Husebye, S. and Helland-Madsen, G. *Acta Chem. Scand.* **23** (1969) 1398.
5. Blake, E. S. *J. Am. Chem. Soc.* **65** (1943) 1267.
6. Wilson, A. J. C. *Nature* **150** (1942) 151.
7. Shiono, R. *Normalized Structure Factors Program*, The Crystallography Laboratory, University of Pittsburgh, Pittsburgh 1966.
8. Long, R. E. *Ph. D. Dissertation*, University of California at Los Angeles 1965.
9. *International Tables for X-Ray Crystallography*, Kynoch Press, Birmingham 1962, Vol. III, p. 204.
10. Cromer, D. T. *Acta Cryst.* **18** (1965) 17.
11. Foss. O. *Advan. Inorg. Chem. Radiochem.* **2** (1960) 237.
12. Hordvik, A. *Acta Chem. Scand.* **20** (1966) 1885.
13. Abrahams, *Quart. Rev.* **10** (1956) 407.
14. Caron, A. and Donohue, J. *Acta Cryst.* **14** (1961) 548.
15. Power, L. F. and Jones, R. D. G. *Inorg. Nucl. Chem. Lett.* **7** (1971) 33.
16. Lemmer, F., Feher, F., Gieren, A., Hechtfischer, S. and Hoppe, W. *Angew. Chem.* **82** (1970) 319.
17. Kutoglu, A. and Hellner, E. *Angew. Chem.* **78** (1966) 1020.
18. Marøy, K. *Acta Chem. Scand.* **25** (1971) 2580.
19. Marøy, K. *Acta Chem. Scand.* **19** (1965) 1509. *Private communication.*
20. Karle, I. L., Estlin, J. A. and Britts, K. *Acta Cryst.* **22** (1967) 273.

Received September 11, 1972.

ACTA CHEMICA SCANDINAVICA 27 (1973) 763–778

The Crystal and Molecular Structure of Tetrakis-(diethyldithiocarbamato)tellurium(IV)

STEINAR HUSEBYE and STEIN EGIL SVÆREN

Chemical Institute, University of Bergen, N-5000 Bergen, Norway

Tetrakis(diethyldithiocarbamato)tellurium(IV), $[Te(Et_2NCS_2)_4]$, forms flat, prismatic, orange crystals belonging to the orthorhombic space group $C_{2v}^9-Pn2_1a$. The unit cell dimensions are $a=19.805(2)$ Å, $b=35.178(4)$ Å, and $c=9.371(2)$ Å. There are eight formula units per cell; the density, found and calculated, is 1.46 g/cm³.

The structure is based on 4477 intensities above background, collected on a Siemens AED-1 diffractometer using Cu$K\alpha$ radiation. The structure was solved by conventional heavy atom methods, and full-matrix least squares refinement has given a conventional R-value of 0.05.

There are two crystallographically independent but very similar molecules in the asymmetric unit. The central tellurium atom is bonded to all eight sulphur atoms in each molecule in a slightly distorted dodecahedral configuration. The Te–S bond lengths vary between 2.631 and 2.845 Å with an average of 2.744 Å.

The solution of this structure is part of a study of the configuration in complexes with central atoms[1–3] possessing an $(n-1)\ d^{10}\ ns^2$ electronic configuration. Earlier work on Te(IV) complexes shows that the ns^2 lone pair is sometimes stereochemically inert[1,4–6] and sometimes active.[7–11]

For Te(IV), most of the known structures are of complexes with monodentate ligands. The solution of the structure of tetrakis(diethyldithiocarbamato)tellurium(IV) represents the first structural work on a Te(IV) complex with bidentate ligands only.

IR, UV, and NMR spectra have been obtained for tetrakis(diethyldithiocarbamato)tellurium(IV), $Te(dtc)_4$, by Nikolov *et al.*[12] In the NMR spectrum, two types of CH_2 quartets were found: one centered almost at the position of the CH_2 quartet of tetraethylthiuram disulphide and the other shifted 0.2 ppm to lower magnetic fields. The first quartet should then be due to monodentate ligands, the latter to bidentate. In the latter the electron shift from nitrogen to the sp^2 carbon atom is expected to be greatest, hence the deshielding of the CH_2 protons should be greater in bidentate than in unidentate (and asymmetric) ligands.[12–14] Both CH_2 quartets have the same area, thus an

octahedral Te(dtc), complex with two monodentate and two bidentate ligands is expected.[12] The recent structure determination of tetrakis(diethyldithiocarbamato)tin(IV) represents an example of an octahedral complex with two monodentate and two bidentate diethyldithiocarbamate ligands.[15]

The NMR spectrum is obtained in solution, and the structures in solution and in the crystalline phase may be different.

In the complex, tris(diethyldithiocarbamato)phenyltellurium(IV), $Te(dtc)_3Ph$, the coordination number of Te(IV) is seven.[2,3] It was therefore felt that tellurium in the present structure might have as high a coordination number as eight in the solid state.

The IR spectrum of $Te(dtc)_4$ in $CHCl_3$ solution is also interpreted in terms of both mono- and bidentate ligands.[12] An IR spectrum based on KBr mulls was reported to give the same information as the corresponding spectrum in solution.[17]

EXPERIMENTAL

The crystals used in this investigation were made by Nikolov *et al.*[12] They were prepared by adding a 10 % solution of sodium diethyldithiocarbamate to a 0.1 M solution of K_2TeO_3, buffered to pH 8.4 by a phosphate-borate buffer. The precipitate was dried in vacuum and recrystallized from benzene. The crystals used in the structural work were flat orange prisms.

For recording of data, a Siemens automatic off-line single crystal diffractometer (AED-1) was used. The diffractometer was operated as a three-circle instrument using Cu$K\alpha$ radiation. A crystal, elongated along c, with dimensions $0.21 \times 0.04 \times 0.17$ mm^3 was mounted along the c axis. The crystal orientation and rough cell dimensions were first determined by measuring θ, χ, and ϕ for three non-coplanar reciprocal vectors. The rough setting angles for all reflections were then calculated.

For determination of accurate unit cell dimensions by least squares methods, the θ angles of 16 reflections with high values of θ were measured. The cell dimensions are $a = 19.805(2)$ Å, $b = 35.178(4)$ Å, and $c = 9.371(2)$ Å. There are eight formula units per cell, with density, calculated and found, 1.46 g/cm^3. The systematic absences are $hk0$ for $h = 2n+1$, and $0kl$ for $k+l = 2n+1$ in the orthorhombic crystals. Thus the space group is either $Pnma$ or $Pna2_1$.

Intensity data were collected using a scintillation counter and $\theta - 2\theta$ scan technique. The scan speed was 0.5°/min, with automatic setting of greater speed for strong reflections. Attenuation filters were used to avoid counting losses, and the correct filter was automatically inserted in the primary beam. The reflections were scanned between $\theta_1 = \theta - 0.40°$, and $\theta_2 = \theta + 0.32 + 0.19$ tg θ, where θ is the Bragg angle for the α_1 peak. The scanning was performed by going from θ to θ_1, then from θ_1 to θ_2, and finally from θ_2 to θ. The intensities for all three scans, and their sum I_t were recorded. Likewise the background was measured for half the total scan time at both θ_1 and θ_2, and the respective intensities and their sum I_b were also recorded. The net intensity for a reflection I_N was put equal to $I_t - I_b$. This scan procedure also checks the setting angles.

Two reference reflections were measured at intervals of 100 reflections. The intensity variations for these reflections were used to scale the net intensities of the recorded reflections. The lower intensity limit for an observed reflection was put equal to twice the standard deviation in net intensity. This standard deviation was defined as the square root of the sum of the total intensity and the background intensity. Unobserved reflections were assigned intensities equal to the lower intensity limit.

Of 5 378 reflections with $\sin\theta \leq 0.891$, 4477 were observed and measured. The data were corrected for Lorentz, polarization, absorption [16] ($\mu = 122.3$ cm^{-1}) and secondary extinction effects. The University of Bergen's IBM 360/50H computer was used in all computations.

STRUCTURE ANALYSIS

The structure analysis was started with the assumption that the space group was *Pnma*. This space group would result in a Te–Te vector giving a maximum in the Patterson function at $0,\frac{1}{2}-2y,0$. In the three-dimensional Patterson map no such peak could be found, unless it coincided with the origin peak. Assuming the latter to be the case, this in turn leads to a y-coordinate of 1/4 for tellurium, *i.e.* that tellurium is located on a mirror plane in four-fold special positions. Since there are eight formula units in a cell, it follows that there is either a binuclear complex present or there are two crystallographically non-equivalent molecules in the asymmetric unit. Since the tellurium atoms in the y-direction then must be $b/2$, or 17.6 Å apart, packing considerations seem to rule out *Pnma* as the correct space group. Also two prominent peaks in the map could not be explained on the basis of this space group.

Attention was therefore shifted to the other possible space group, the non-centric $Pna2_1$. In order to preserve the labeling of axes and the reflection indices based on *Pnma*, the setting $Pn2_1a$ was chosen. This is then equivalent to an interchange of b and c axes relative to $Pna2_1$. Since this space group has four equivalent positions, there must be two tellurium atoms in the asymmetric unit.

Both tellurium positions were then found from the map. Their x-coordinates were close to 0.0 and 0.25 in agreement with semi-extinctions found from films. In the *y-direction*, Te1 was arbitrarily assigned the coordinate 0.000, which was kept constant throughout the later refinements. Successive Fourier syntheses revealed the positions of all atoms, except hydrogen, in the two crystallographically non-equivalent molecules in the asymmetric unit.

Full-matrix least squares refinement was then started using a program (BDLS) which minimizes the expression $r=\sum W(|F_o|-K|F_c|)^2$. Here K is a scale factor and W, the weight of a reflection, is the inverse of the variance of F_o. The variance of F_o is $\sigma^2(F_o)=F_o^2[I_t+I_b+k^2(I_t-I_b)^2]/4(I_t-I_b)^2$, where k may be interpreted as the relative standard deviation in the scaling curve based on the variation in the intensities of the reference reflections. Non-observed reflections with $K|F_c|$ larger than the observable limit are included in the refinement with F_o put equal to the limit.

After a few cycles of refinement, based on isotropic temperature factors for all atoms except tellurium (anisotropic), the factor $R=\sum(||F_o|-|F_c||)/\sum|F_o|$ reached a value of 0.14. After corrections for absorption, the R-value was reduced to 0.08. After introducing anisotropic temperature factors for the sulphur atoms and correcting the intensities for secondary extinction effects, the R-value reached its final value of 0.050.

Observed and calculated structure factors following the last refinement cycle can be obtained from the author St. H. upon request. Atomic scattering factors were taken from the *International Tables*.[7] The atomic scattering factors for tellurium and sulphur were corrected for anomalous dispersion, using f' and f'' values calculated by Cromer.[18] Final atomic parameters are listed in Table 1, and components of atomic vibration tensors in Tables 2 and 3. Inter-atomic distances and angles are listed in Tables 4–7, while least squares planes through groups of atoms are listed in Tables 8–10.

Table 1. Final atomic coordinates in fractions of cell edges, with standard deviations in brackets.

	x	*y*	*z*
Te1	0.00516(7)	0	0.17889(19)
Te2	0.25219(7)	0.28604(5)	0.17501(17)
S11	−0.0487(3)	−0.0597(2)	0.0451(8)
S12	0.0873(3)	−0.0623(2)	0.1669(9)
S13	−0.0688(3)	0.0350(2)	−0.0303(8)
S14	0.0748(3)	0.0153(2)	−0.0549(8)
S15	0.0300(5)	0.0750(4)	0.2537(8)
S16	0.1323(4)	0.0163(3)	0.2995(10)
S17	−0.0259(3)	−0.0298(2)	0.4478(8)
S18	−0.1253(5)	0.0128(4)	0.2781(9)
S21	0.1990(3)	0.3444(2)	0.0403(9)
S22	0.3347(3)	0.3466(2)	0.1612(9)
S23	0.1779(3)	0.2500(2)	−0.0364(8)
S24	0.3224(3)	0.2672(2)	−0.0552(8)
S25	0.2728(5)	0.2092(4)	0.2588(7)
S26	0.3790(4)	0.2679(3)	0.2940(10)
S27	0.2205(3)	0.3150(2)	0.4417(8)
S28	0.1229(5)	0.2711(4)	0.2703(8)
N11	0.0342(6)	−0.1200(4)	0.0187(13)
N12	0.0019(9)	0.0489(6)	−0.2609(14)
N13	0.1590(6)	0.0905(4)	0.2834(14)
N14	−0.1539(6)	−0.0166(4)	0.5309(14)
N21	0.2811(6)	0.4036(4)	0.0181(14)
N22	0.2564(9)	0.2326(6)	−0.2622(14)
N23	0.4050(6)	0.1939(4)	0.3061(16)
N24	0.0933(6)	0.3019(4)	0.5226(14)
C11	0.0256(7)	−0.0855(4)	0.0700(16)
C111	−0.0191(8)	−0.1398(5)	−0.0589(18)
C112	−0.0128(13)	−0.1333(9)	−0.2254(23)
C113	0.1003(7)	−0.1400(5)	0.0355(18)
C114	0.1036(10)	−0.1623(6)	0.1722(25)
C12	0.0047(6)	0.0352(4)	−0.1296(17)
C121	−0.0563(8)	0.0651(5)	−0.3315(21)
C122	−0.0798(10)	0.1053(7)	−0.2829(23)
C123	0.0704(9)	0.0517(5)	−0.3400(21)
C124	0.1071(12)	0.0901(8)	−0.3043(29)
C13	0.1107(8)	0.0642(5)	0.2830(19)
C131	0.1446(9)	0.1304(6)	0.2638(19)
C132	0.1511(11)	0.1412(7)	0.1084(26)
C133	0.2318(8)	0.0792(5)	0.2909(20)
C134	0.2566(10)	0.0795(6)	0.4479(22)
C14	−0.1055(7)	−0.0125(4)	0.4271(16)
C141	−0.1369(8)	−0.0376(6)	0.6680(22)
C142	−0.1673(10)	−0.0771(6)	0.6624(24)
C143	−0.2253(8)	−0.0043(5)	0.5075(17)
C144	−0.2327(9)	0.0356(6)	0.5727(21)
C21	0.2727(7)	0.3685(4)	0.0696(16)
C211	0.2267(9)	0.4231(5)	−0.0706(20)
C212	0.2301(12)	0.4144(8)	−0.2303(20)
C213	0.3475(8)	0.4245(5)	0.0342(19)
C214	0.3478(10)	0.4480(7)	0.1753(27)
C22	0.2514(7)	0.2479(5)	−0.1276(18)
C221	0.1909(9)	0.2215(6)	−0.3377(22)

Table 1. Continued.

C222	0.1809(10)	0.1789(7)	−0.3119(27)
C223	0.3203(9)	0.2294(5)	−0.3400(21)
C224	0.3480(12)	0.1885(8)	−0.2978(29)
C23	0.3575(7)	0.2227(5)	0.2827(17)
C231	0.4802(9)	0.2025(6)	0.3160(23)
C232	0.4980(10)	0.2109(6)	0.4757(22)
C233	0.3871(8)	0.1516(6)	0.3034(22)
C234	0.3884(8)	0.1386(5)	0.1426(20)
C24	0.1405(6)	0.2967(4)	0.4236(15)
C241	0.1053(8)	0.3194(5)	0.6619(21)
C242	0.0753(9)	0.3617(6)	0.6564(24)
C243	0.0237(7)	0.2847(5)	0.5040(17)
C244	0.0160(10)	0.2438(6)	0.5644(20)

Table 2. Components of atomic vibration tensors for Te and S, $U \times 10^3$, in Å^2 with standard deviations, referred to crystallographic axes. The expression used is $\exp\{-2\pi^2[h^2a^{-2}U_{11}+k^2b^{-2}U_{22}+l^2c^{-2}U_{33}+2hka^{-1}b^{-1}U_{12}+2klb^{-1}c^{-1}U_{23}+2hla^{-1}c^{-1}U_{13})\}$.

Te1	33.6(0.8)	36.9(0.7)	42.8(1.0)	(U_{11}, U_{22}, U_{33})
	2.8(0.7)	3.6(1.3)	0.1(0.8)	(U_{12}, U_{23}, U_{13})
Te2	33.5(0.8)	37.5(0.7)	41.4(1.0)	
	−3.8(0.7)	−1.7(1.3)	0.6(0.9)	
S11	39.4(3.8)	46.8(4.3)	69.3(5.8)	
	0.5(3.4)	−5.7(4.1)	−7.7(3.7)	
S12	48.9(4.0)	48.5(4.1)	71.6(5.7)	
	9.3(3.5)	−10.5(4.4)	−21.8(4.1)	
S13	41.0(3.9)	66.5(5.0)	50.5(5.1)	
	11.3(3.6)	14.3(4.3)	4.0(3.5)	
S14	38.7(3.6)	69.4(5.0)	50.1(4.7)	
	6.6(3.6)	7.3(4.3)	7.4(3.4)	
S15	39.3(5.5)	35.1(6.0)	85.3(9.7)	
	3.5(4.9)	−0.4(3.4)	−2.9(3.3)	
S16	47.3(4.1)	43.0(4.1)	67.1(5.2)	
	5.0(3.4)	4.6(5.7)	−9.6(4.7)	
S17	52.5(4.5)	62.4(5.0)	58.1(5.4)	
	11.9(4.0)	16.0(4.4)	−0.6(3.7)	
S18	46.5(4.8)	77.6(7.7)	55.6(5.1)	
	13.9(4.9)	28.4(5.7)	13.1(3.9)	
S21	35.5(3.6)	48.2(4.4)	75.1(6.0)	
	2.0(3.4)	5.0(4.2)	−9.4(3.7)	
S22	46.7(3.7)	50.2(4.2)	68.9(6.0)	
	−15.0(3.3)	11.3(4.5)	−15.7(3.9)	
S23	37.9(3.5)	60.0(4.6)	54.3(5.1)	
	−8.2(3.5)	−12.7(4.2)	4.8(3.2)	
S24	38.0(3.5)	75.2(5.3)	53.6(5.0)	
	−9.6(3.8)	−3.7(4.4)	6.6(3.3)	
S25	32.9(5.2)	51.3(7.5)	59.3(7.5)	
	−10.0(5.2)	1.5(3.5)	−2.9(3.0)	
S26	41.3(3.9)	43.1(3.9)	72.6(5.5)	
	−8.1(3.3)	7.5(5.5)	−8.2(4.4)	
S27	49.5(4.4)	68.7(5.2)	52.6(5.2)	
	−9.4(4.0)	−19.3(4.4)	2.8(3.7)	
S28	37.2(4.4)	63.3(6.8)	55.6(5.5)	
	−7.4(4.5)	−12.4(4.7)	3.0(3.4)	

Table 3. Final isotropic vibration tensors ($\times 10^2$) in Å^2 for N and C. The expression used is exp $[-8\pi^2 U(\sin^2\theta/\lambda)]$.

	U		U
N11	46.1(3.2)	N21	52.8(3.5)
N12	53.3(5.7)	N22	51.5(5.7)
N13	49.8(3.6)	N23	51.8(3.3)
N14	57.1(3.6)	N24	54.4(3.5)
C11	41.0(3.6)	C21	47.3(4.0)
C111	60.6(4.8)	C211	68.7(5.4)
C112	90.8(8.6)	C212	73.0(7.4)
C113	54.7(4.4)	C213	60.7(4.8)
C114	87.5(6.2)	C214	93.8(6.6)
C12	43.0(3.8)	C22	49.6(4.2)
C121	69.3(5.0)	C221	74.1(5.4)
C122	86.0(6.7)	C222	101.7(7.0)
C123	72.8(5.3)	C223	70.9(5.2)
C124	109.3(7.9)	C224	114.7(8.4)
C13	49.8(4.7)	C23	37.1(3.9)
C131	65.6(5.8)	C231	71.8(5.1)
C132	107.9(7.7)	C232	83.1(6.0)
C133	60.2(4.8)	C233	61.7(4.7)
C134	88.2(6.3)	C234	69.2(5.3)
C14	48.9(4.1)	C24	42.2(3.7)
C141	73.1(5.3)	C241	67.4(5.0)
C142	87.8(6.3)	C242	90.2(6.5)
C143	60.0(4.4)	C243	56.2(4.1)
C144	79.0(5.5)	C244	88.8(6.4)

Table 4. Bond lengths with standard deviations, in Å.

Te1–S11	2.669(7)	Te2–S21	2.631(8)
Te1–S12	2.732(7)	Te2–S22	2.689(7)
Te1–S13	2.740(7)	Te2–S23	2.774(7)
Te1–S14	2.644(7)	Te2–S24	2.651(7)
Te1–S15	2.774(13)	Te2–S25	2.845(14)
Te1–S16	2.819(8)	Te2–S26	2.821(8)
Te1–S17	2.797(8)	Te2–S27	2.771(8)
Te1–S18	2.782(9)	Te2–S28	2.763(9)
S11–C11	1.74(2)	S21–C21	1.71(2)
S12–C11	1.73(2)	S22–C21	1.68(2)
S13–C12	1.73(2)	S23–C22	1.69(2)
S14–C12	1.70(2)	S24–C22	1.70(2)
S15–C13	1.67(2)	S25–C23	1.76(2)
S16–C13	1.75(2)	S26–C23	1.65(2)
S17–C14	1.70(2)	S27–C24	1.72(1)
S18–C14	1.70(2)	S28–C24	1.73(2)
C11–N11	1.32(2)	C21–N21	1.34(2)
C12–N12	1.32(2)	C22–N22	1.37(2)
C13–N13	1.33(2)	C23–N23	1.40(2)
C14–N14	1.37(2)	C24–N24	1.33(2)
N11–C111	1.46(2)	N21–C211	1.53(2)
N11–C113	1.49(2)	N21–C213	1.51(2)
N12–C121	1.45(2)	N22–C221	1.53(2)

Table 4. Continued.

N12–C123	1.55(2)	N22–C223	1.47(2)
N13–C131	1.44(2)	N23–C231	1.52(2)
N13–C133	1.50(2)	N23–C233	1.53(2)
N14–C141	1.52(2)	N24–C241	1.46(2)
N14–C143	1.49(2)	N24–C243	1.51(2)
C111–C112	1.58(3)	C211–C212	1.53(3)
C113–C114	1.50(3)	C213–C214	1.56(3)
C121–C122	1.56(3)	C221–C222	1.53(3)
C123–C124	1.57(3)	C223–C224	1.59(3)
C131–C132	1.51(3)	C231–C232	1.57(3)
C133–C134	1.55(3)	C233–C234	1.58(3)
C141–C142	1.52(3)	C241–C242	1.60(3)
C143–C144	1.54(3)	C243–C244	1.55(3)

Table 5. Non-bonded S–S distances in the $Te(dtc)_4$ molecules, in Å.

S11–S12	2.928(10)	S21–S22	2.917(9)
S13–S14	2.936(9)	S23–S24	2.930(9)
S15–S16	2.925(14)	S25–S26	2.967(15)
S17–S18	2.939(13)	S27–S28	2.950(13)
S12–S16	3.158(11)	S22–S26	3.160(12)
S13–S18	3.200(12)	S23–S28	3.163(11)
S11–S15	5.358(15)	S21–S25	5.381(15)
S14–S17	5.356(11)	S24–S27	5.346(11)
S11–S13	3.431(11)	S21–S23	3.423(12)
S11–S14	3.719(10)	S21–S24	3.762(10)
S11–S17	3.944(11)	S21–S27	3.924(11)
S11–S18	3.684(14)	S21–S28	3.684(14)
S12–S13	4.970(10)	S22–S23	4.961(10)
S12–S14	3.441(11)	S22–S24	3.460(11)
S12–S17	3.642(11)	S22–S27	3.641(11)
S12–S18	5.078(13)	S22–S28	5.070(12)
S15–S13	3.590(12)	S25–S23	3.640(12)
S15–S14	3.682(12)	S25–S24	3.713(13)
S15–S17	4.256(15)	S25–S27	4.228(16)
S15–S18	3.781(16)	S25–S28	3.684(16)
S16–S13	5.084(11)	S26–S23	5.083(10)
S16–S14	3.512(12)	S26–S24	3.458(12)
S16–S17	3.791(11)	S26–S27	3.811(11)
S16–S18	5.107(12)	S26–S28	5.079(12)

Table 6. Bond angles with standard deviations, in degrees.

S11–Te1–S12	65.6(0.2)	S21–Te2–S22	66.5(0.2)
S13–Te1–S14	66.1(0.2)	S23–Te2–S24	65.3(0.2)
S15–Te1–S16	63.1(0.3)	S25–Te2–S26	63.2(0.3)
S17–Te1–S18	63.6(0.3)	S27–Te2–S28	64.4(0.3)
S12–Te1–S16	69.3(0.2)	S22–Te2–S26	70.0(0.2)
S13–Te1–S18	70.8(0.3)	S23–Te2–S28	69.7(0.2)
S11–Te1–S15	159.8(0.3)	S21–Te2–S25	158.7(0.3)
S14–Te1–S17	159.6(0.2)	S24–Te2–S27	160.9(0.2)
Te1–S11–C11	90.5(0.5)	Te2–S21–C21	88.2(0.6)

Table 6. Continued.

Te1 – S12 – C11	88.8(0.5)	Te2 – S22 – C21	86.7(0.6)
Te1 – S13 – C12	86.3(0.6)	Te2 – S23 – C22	85.7(0.6)
Te1 – S14 – C12	90.0(0.6)	Te2 – S24 – C22	89.5(0.6)
Te1 – S15 – C13	89.7(0.8)	Te2 – S25 – C23	85.2(0.7)
Te1 – S16 – C13	86.6(0.6)	Te2 – S26 – C23	87.9(0.6)
Te1 – S17 – C14	88.1(0.6)	Te2 – S27 – C24	88.9(0.6)
Te1 – S18 – C14	88.7(0.6)	Te2 – S28 – C24	89.0(0.6)
S11 – C11 – N11	122.6(0.9)	S21 – C21 – N21	120.5(1.0)
S12 – C11 – N11	122.4(0.9)	S22 – C21 – N21	120.9(1.0)
S13 – C12 – N12	117.8(1.1)	S23 – C22 – N22	122.9(1.1)
S14 – C12 – N12	124.5(1.1)	S24 – C22 – N22	117.6(1.1)
S15 – C13 – N13	122.1(1.2)	S25 – C23 – N23	117.8(1.1)
S16 – C13 – N13	119.6(1.1)	S26 – C23 – N23	120.9(1.0)
S17 – C14 – N14	121.9(1.0)	S27 – C24 – N24	121.8(1.0)
S18 – C14 – N14	118.5(1.0)	S28 – C24 – N24	120.5(0.9)
S11 – C11 – S12	114.9(0.7)	S21 – C21 – S22	118.6(0.8)
S13 – C12 – S14	117.7(0.8)	S23 – C22 – S24	119.4(0.8)
S15 – C13 – S16	118.1(1.0)	S25 – C23 – S26	121.0(0.9)
S17 – C14 – S18	119.5(0.8)	S27 – C24 – S28	117.6(0.7)
C11 – N11 – C111	121.9(1.1)	C21 – N21 – C211	121.6(1.1)
C11 – N11 – C113	120.5(1.1)	C21 – N21 – C213	121.5(1.1)
C12 – N12 – C121	127.1(1.3)	C22 – N22 – C221	117.7(1.3)
C12 – N12 – C123	115.6(1.3)	C22 – N22 – C223	123.2(1.3)
C13 – N13 – C131	122.3(1.3)	C23 – N23 – C231	121.5(1.2)
C13 – N13 – C133	120.6(1.3)	C23 – N23 – C233	123.0(1.1)
C14 – N14 – C141	119.7(1.1)	C24 – N24 – C241	124.4(1.1)
C14 – N14 – C143	121.7(1.1)	C24 – N24 – C243	120.3(1.1)
C111 – N11 – C113	117.6(1.1)	C211 – N21 – C213	116.7(1.2)
C121 – N12 – C123	117.0(1.3)	C221 – N22 – C223	119.0(1.3)
C131 – N13 – C133	116.9(1.3)	C231 – N23 – C233	115.0(1.2)
C141 – N14 – C143	118.4(1.1)	C241 – N24 – C243	114.7(1.1)
N11 – C111 – C112	111.5(1.4)	N21 – C211 – C212	114.4(1.4)
N11 – C113 – C114	111.9(1.2)	N21 – C213 – C214	110.3(1.3)
N12 – C121 – C122	117.5(1.5)	N22 – C221 – C222	106.7(1.5)
N12 – C123 – C124	111.0(1.5)	N22 – C223 – C224	104.1(1.5)
N13 – C131 – C132	110.5(1.5)	N23 – C231 – C232	108.4(1.4)
N13 – C133 – C134	110.4(1.3)	N23 – C233 – C234	107.2(1.4)
N14 – C141 – C142	109.2(1.4)	N24 – C241 – C242	107.6(1.4)
N14 – C143 – C144	107.2(1.2)	N24 – C243 – C244	114.6(1.2)

Table 7. Some short, intermolecular interatomic separations, in Å. The left column represents distances from an atom in one of the two original molecules (Table 1), to an atom in a molecule whose transformation from one of the two original ones is listed in the next column.

S11 – C211	$-x, y-\frac{1}{2}, -z$	3.58(2)
S12 – C213	$\frac{1}{2}-x, y-\frac{1}{2}, \frac{1}{2}+z$	3.71(2)
S14 – C214	$\frac{1}{2}-x, y-\frac{1}{2}, z-\frac{1}{2}$	3.79(2)
S15 – C234	$x-\frac{1}{2}, y, \frac{1}{2}-z$	3.72(2)
S18 – C133	»	3.73(2)
S21 – C111	$-x, \frac{1}{2}+y, -z$	3.61(2)
S22 – C113	$\frac{1}{2}-x, \frac{1}{2}+y, \frac{1}{2}-z$	3.77(2)
S22 – C112	»	3.75(3)
S25 – C131	x, y, z	3.76(2)
S25 – C132	»	3.68(3)

Table 7. Continued.

N11 – C242	$-x, y-\frac{1}{2}, 1-z$	3.79(2)
N14 – C121	$x, y, 1+z$	3.70(2)
N24 – C221	»	3.67(2)
C11 – C242	$-x, y-\frac{1}{2}, 1-z$	3.74(3)
C121 – C14	$x, y, z-1$	3.68(2)
C121 – C144	»	3.75(2)
C123 – C13	»	3.65(3)
C112 – C142	»	3.79(3)
C122 – C224	$x-\frac{1}{2}, y, -z-\frac{1}{2}$	3.34(3)
C122 – C234	»	3.62(3)
C124 – C222	x, y, z	3.45(4)
C124 – C134	$x, y, z-1$	3.78(3)
C142 – C21	$-x, y-\frac{1}{2}, 1-z$	3.79(3)
C221 – C24	$x, y, z-1$	3.60(2)
C221 – C244	»	3.67(3)
C223 – C23	»	3.62(2)
C224 – C232	»	3.74(3)
C212 – C242	»	3.74(3)

Table 8. Least squares planes. The following planes were calculated:

Plane 1	Te1,	S11,	S12,	S15,	S16	
Plane 2	Te1,	S13,	S14,	S17,	S18	
Plane 3	Te2,	S21,	S22,	S25,	S26	
Plane 4	Te2,	S23,	S24,	S27,	S28	
Plane 5	S11,	S12,	C11,	N11,	C111,	C113
Plane 6	S13,	S14,	C12,	N12,	C121,	C123
Plane 7	S15,	S16,	C13,	N13,	C131,	C133
Plane 8	S17,	S18,	C14,	N14,	C141,	C143
Plane 9	S21,	S22,	C21,	N21,	C211,	C213
Plane 10	S23,	S24,	C22,	N22,	C221,	C223
Plane 11	S25,	S26,	C23,	N23,	C231,	C233
Plane 12	S27,	S28,	C24,	N24,	C241,	C243

Equation of planes, based on the cell axes and coordinates in fractions of cell edges.

Plane 1	$-7.661x - 8.690y + 8.325z - 1.310 = 0$
Plane 2	$5.579x + 30.723y + 3.723z - 0.659 = 0$
Plane 3	$-7.399x + 9.472y + 8.318z - 2.174 = 0$
Plane 4	$5.401x - 30.632y + 3.834z + 6.718 = 0$
Plane 5	$-6.932x - 13.746y + 7.978z - 1.553 = 0$
Plane 6	$4.345x + 31.528y + 3.612z - 0.648 = 0$
Plane 7	$-1.802x + 3.116y + 9.295z - 2.588 = 0$
Plane 8	$5.179x + 30.303y + 4.080z - 0.833 = 0$
Plane 9	$-7.174x + 13.831y + 7.919z - 3.674 = 0$
Plane 10	$3.259x - 31.754y + 3.726z + 7.561 = 0$
Plane 11	$-2.646x + 0.659y + 9.285z - 1.856 = 0$
Plane 12	$5.886x - 30.001y + 4.023z + 6.358 = 0$

RESULTS AND DISCUSSION

The two molecules in the asymmetric unit with atoms labeled are shown in Fig. 1, as seen along the *c* axis. From the figure it may be seen that the molecules are near to being mirror images of each other, the direction of the

Table 9. Distances in Å from atoms listed to least squares planes. (Input coordinates in fractions of cell edges give distances in Å.)

Plane 1		Plane 2		Plane 3	
Te1	0.1400	Te1	0.0356	Te2	0.1258
S11	−0.0418	S13	−0.0791	S21	−0.0482
S12	−0.0477	S14	0.0243	S22	−0.0253
S15	−0.0791	S17	−0.0507	S25	−0.0579
S16	0.0286	S18	0.0698	S26	0.0056
Plane 4		**Plane 5**		**Plane 6**	
Te2	−0.0105	Te1	−0.1614	Te1	0.0203
S23	−0.1189	S11	−0.0340	S13	0.0483
S24	0.0630	S12	0.0299	S14	−0.0387
S27	−0.0479	C11	0.0038	C12	0.0126
S28	0.1142	N11	0.0097	N12	−0.0420
		C111	0.0314	C121	−0.0383
		C113	−0.0408	C123	0.0581
		C112	−1.4297	C122	1.3041
		C114	1.3341	C124	1.5574
Plane 7		**Plane 8**		**Plane 9**	
Te1	−0.9341	Te1	−0.0768	Te2	−0.1406
S15	−0.0498	S17	−0.0423	S21	−0.0183
S16	0.0087	S18	0.0397	S22	−0.0034
C13	0.0434	C14	−0.0148	C21	0.0181
N13	0.0418	N14	0.0328	N21	0.0350
C131	0.0101	C141	0.0442	C211	−0.0075
C133	−0.0542	C143	−0.0595	C213	−0.0238
C132	−1.4128	C142	−1.3334	C212	−1.4170
C134	1.3608	C144	1.3782	C214	1.4159
Plane 10		**Plane 11**		**Plane 12**	
Te2	−0.0475	Te2	−0.7097	Te2	−0.0349
S23	0.0663	S25	−0.0370	S27	−0.0187
S24	−0.0786	S26	0.0475	S28	0.0358
C22	0.0344	C23	−0.0306	C24	−0.0109
N23	0.0339	N23	0.0423	N24	−0.0473
C221	−0.1093	C231	−0.0592	C241	0.0575
C223	0.0533	C233	0.0369	C243	−0.0165
C222	1.3078	C232	1.3826	C242	−1.4082
C224	1.5993	C234	−1.4686	C244	1.4090

Table 10. Interplanar angles.

Plane 1 − Plane 2	88.4°
Plane 3 − Plane 4	88.5°

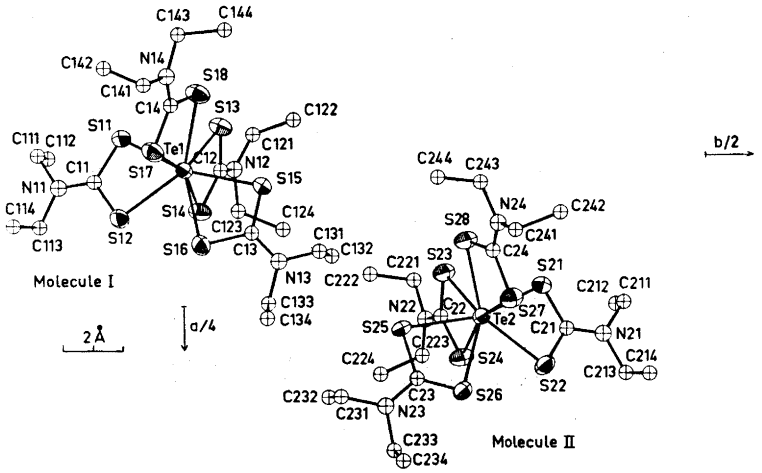

Fig. 1. The two molecules in the asymmetric unit seen along *c*.

"mirror plane" being roughly parallel to the *ac* plane. Thus in both molecules only one ligand has both methyl groups pointing to the same side relative to the ligand plane. Most corresponding bond lengths and angles are also nearly equal in the two molecules; only a few are significantly different. As can be seen from the figure, and Table 4, all eight sulphur atoms in each molecule are bonded to the central tellurium atom. This is presumably the first time tellurium has been shown to have as high a coordination number as eight. For a better view of the configuration around tellurium, a stereoscopic pair of one of the crystallographically independent molecules is shown in Fig. 2.

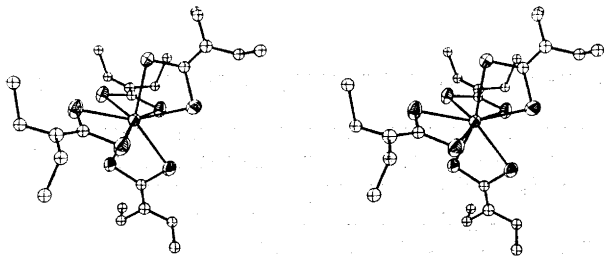

Fig. 2. Stereo drawing of molecule I.

The configurations around the central atoms in the molecules are distorted dodecahedral. In the tellurium valency shell there are eight bonded electron pairs plus the 5*s* lone pair. Assuming that the lone pair does not occupy a position in the coordination polyhedron, being essentially inert, as in the hexahalotellurate(IV) complex ions,[4–6] the configuration should be based on the most energetically favourable distribution of the eight bonding pairs.[19,20]

This is either at the vertices of a dodecahedron as found here, or a square antiprism.[21] Several metal complexes of the type $M(dtc)_4$ where M = Th, Np, and Ti, show both types of configuration.[22–24]

A regular dodecahedron can be visualized as two interleaving planar trapezoids at right angles to each other.[25,26] In $Te(dtc)_4$ such trapezoids are defined by S11, S12, S15, S16 and S13, S14, S17, S18 for molecule I, and by S21, S22, S25, S26 and S23, S24, S27, S28 for molecule II. The average coordination within such a trapezoid is shown in Fig. 3. Least squares planes through

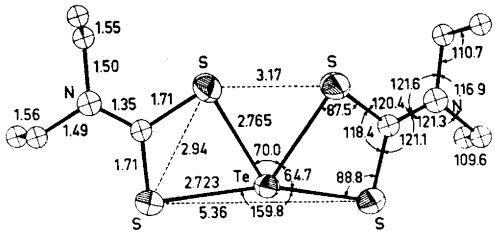

Fig. 3. Average bond lengths and angles. The figure is based on the Te1, S11, S12, S15, and S16 trapezoid.

the TeS_4 groups in such trapezoids show that the groups are nearly planar, the maximum deviation of atoms from planes being 0.14 Å. The average interplanar angle between the two trapezoids in a $Te(dtc)_4$ molecule is 88.5°, leading to some distortion from D_{2d} symmetry, in the TeS_8 group.

Such a $Te^{IV}S_4$ group as mentioned above is not very different from the $Te^{II}S_4$ group found in trapezoid planar tellurium bis(dialkyldithiocarbamates).[27,28] On heating $Te(dtc)_4$ in solution, an equi-molecular mixture of $Te(dtc)_2$ and the corresponding disulphide is produced.[29]

$$Te^{IV}(Et_2NCS_2)_4 \xrightarrow{\Delta} Te^{II}(Et_2NCS_2)_2 + Et_2NC(=S)-S-S-C(=S)NEt_2$$

Thus the formation of disulphide may result when two of the ligand sulphur atoms lying closest to each other in one trapezoid form an S–S bond, while the four Te–S bonds in the same trapezoid are broken.

The remaining two ligands then presumably form $Te(dtc)_2$ with relatively small rearrangement of bond lengths and angles.

Hoard and Silverton have studied both dodecahedral and square antiprismatic configurations in some detail.[26] In a dodecahedron, the eight corners are not equivalent. In $Te(dtc)_4$ the chelation is along edges *m*; S12, S13, S16, and S18 in molecule I, and S22, S23, S26, and S28 in molecule II are at dodecahedral corners of type A. The other sulphur atoms, then, are at corners of type B, which are not equivalent with those of type A.

A dodecahedral complex can be described by several parameters, among which are θ_A, θ_B and MA/MB.[26] $\theta_A(\theta_B)$ represents the angle between bonds from the central atom, M, to ligand atoms of type A(B) and the unique axis

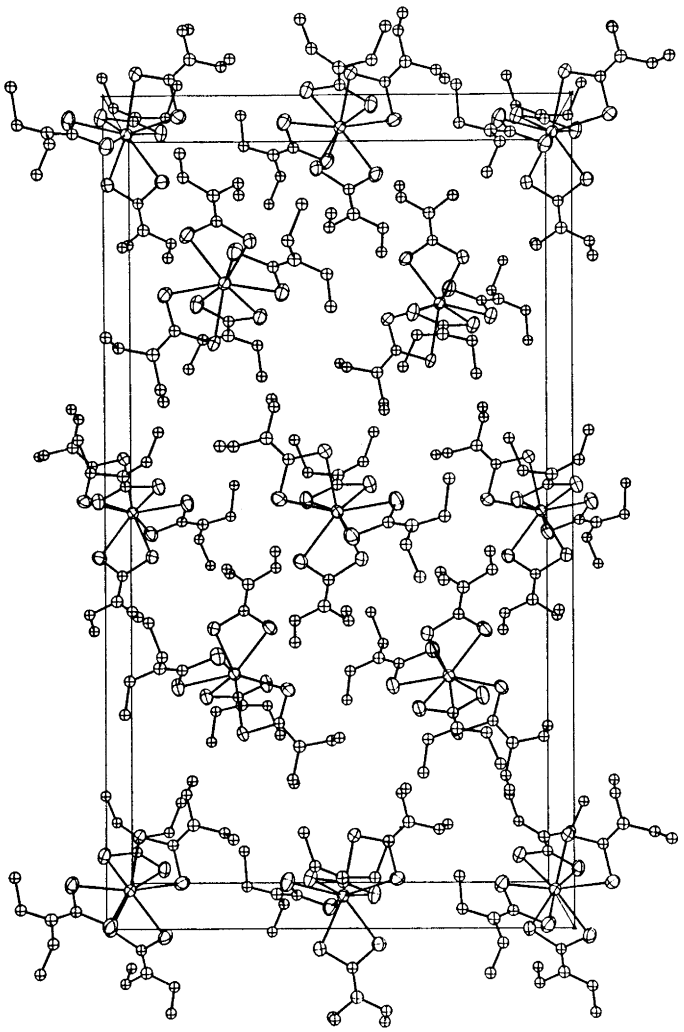

Fig. 4. The contents of the unit cell, seen parallel to *c* towards the center of the cell.

passing through the midpoints of the A–A(B–B) contacts in the two trapezoids. MA and MB are the bond lengths MA and MB. The "most favourable" D_{2d} dodecahedron is characterized by the following values:[26]

$\theta_A = 35.2°$ $\theta_B = 73.5°$ MA/MB = 1.03

For $Te(dtc)_4$, the values are

$\theta_A = 35.1°$ $\theta_B = 79.9°$ MA/MB = 1.016 for molecule I,

and $\theta_A = 34.9°$ $\theta_B = 79.8°$ MA/MB = 1.014 for molecule II.

For comparison, the values for a square antiprism, where A and B are equivalent, are $\theta_A = \theta_B = 57.3°$, MA/MB = 1.

From the above, it is clear that the configurations for the $Te(dtc)_4$ molecules are distorted dodecahedral. From inspection of Tables 4 – 6, there appears to be no systematic distortion toward nine-coordination with the lone pair playing a stereochemically active role in the two molecules. Such a stereochemically inert pair is found in several complexes with central atoms from the lower right hand corner of the periodic table. Examples are the well known octahedral $[TeCl_6]^{2-}$,[4] $[SeCl_6]^{2-}$,[4] $[SeCl_6]^{2-}$,[30] $[SbCl_6]^{3-}$,[31] $[BiCl_6]^{3-}$,[32] and hexathiourealead(II)[33] complex ions. For such complexes, according to Urch,[34] the lone pair of electrons may go into a low lying antibonding a^*_{1g} molecular orbital, mostly localized on the ligands, thus being stereochemically inert. According to Gillespie, the *ns* lone pair is forced inside the valency shell because of ligand-ligand repulsions, when ligand size and coordination numbers are large.[20]

In the solid phase, the configuration around the tellurium atoms in $TeCl_4$ (tetramers) is distorted octahedral, with three short Te – Cl bonds *trans* to and nearly collinear with three long Te···Cl bonds with average lengths of 2.311 Å and 2.929 Å, respectively.[7] A corresponding configuration is found for the addition compound $TeCl_3^+AlCl_4^-$.[8] In these compounds, the lone pair is presumably located between the long Te···Cl bonds. Such distortions are also found in complexes of Pb(II) and Tl(I) and are probably due to mixing of *s* and *p* orbitals.[35]

The Te – S bond lengths in $Te(dtc)_4$ vary from 2.63 to 2.85 Å, with an average of 2.744 Å. The average standard deviation is 0.008 Å. These bond lengths are much larger than 2.37 Å, the sum of the covalent radii corrected for bond polarity. They are also significantly larger than 2.59 Å, the sum of the octahedral radius of tellurium and the covalent radius of sulphur.

However, for $TeX_4(tmtu)_2$ (X = Cl or Br, tmtu = tetramethylthiourea) the average Te – S bond length is 2.71 Å.[1] For $Te(dtc)_3Ph$ the average Te – S bond length, excluding a long Te – S bond weakened by the *trans*-effect of the phenyl group, is 2.714 Å.[2,3] These latter values are more in agreement with the value 2.744 Å found in the present investigation. The increase in bond length going from $TeX_4(tmtu)_2$ to $Te(dtc)_4$ is probably due to the stronger ligand-ligand repulsion following the increase in coordination number, and to increasing use of high energy *d*-orbitals. From the theory of Urch,[34] one should expect such bonds to be relatively weak in the hexahalotellurates, because of the weak bonding capacity of the electrons in the a_{1g} bonding orbital, and the antibonding nature of the lone pair in the a^*_{1g} orbital. This line of reasoning must also be valid for $Te(dtc)_3Ph$ and $Te(dtc)_4$.

The structure of another dithiocarbamate of tetravalent tellurium, tetrakis-(4-morpholinecarbodithioato)tellurium(IV), has just been solved in this laboratory. At the present stage of refinement ($R = 0.09$) the average Te – S bond length is 2.74 Å, the same as found in the present investigation. The configuration around the central tellurium atom is again dodecahedral, but the distortion from D_{2d} symmetry is probably smaller than that found for the diethyldithiocarbamate.

In hexahydroxotellurium(VI), $Te(OH)_6$, tellurium has no 5*s* lone pair of electrons. The average Te – O bond length in this octahedral complex is 1.916 Å as compared to 1.91 Å, the sum of the covalent radii of tellurium and

oxygen corrected for bond polarity. This seems to indicate that the stereochemically inert lone pair above has a bond lengthening effect. However, the possibility of π-bonding in $Te(OH)_6$,[36] and also the smaller size of oxygen as compared to the heavier halogens and sulphur, and the smaller radius and larger charge of Te(VI) as compared to Te(IV), may all be important factors contributing to a strong tellurium-oxygen bond.

In the dithiocarbamate complexes of divalent tellurium,[27,28] the average Te – S bond length is close to 2.68 Å, but the weak average bonds found in such compounds are probably due to three-center four-electron bonding.[27,28]

Since there are many heavy atoms in the tetrakis(diethyldithiocarbamato) tellurium(IV) molecules, the bond lengths involving light atoms are determined with relatively small accuracy.

In the ligands, the C – S bond lengths vary between 1.65 and 1.76 Å, the average being 1.71 Å corresponding to a π-bond order[3] close to 0.25. In $Te(dtc)_3Ph$, the average is 1.713 Å.[2,3] These values agree well with values found in other dithiocarbamates.

For the C···N bonds, the average bond length is 1.35 Å, corresponding to a π-bond order[3] of 0.27, which seems to be normal for dithiocarbamate complexes. The other interatomic bonds are normal within the error limits.

The average S – Te – S angle, where both sulphur atoms come from the same ligand, is 64.7°, which seems to be normal for intraligand S – Te – S angles. The two S – Te – S angles, where the sulphur atoms come from different ligands in one trapezoid, are 70.0 and 159.8° respectively. These may be compared to 80.1(1) and 147.8(1)° found for the corresponding angles in $Te(dtc)_2$.[28] This difference in angles may be due to steric factors. In $Te(dtc)_4$, where two TeS_4 trapezoids are interleaved at almost right angles, the large interligand S – Te – S angles in a trapezoid has to open up in order to accommodate atoms from the other trapezoid. As the trapezoids remain planar and the intraligand S – Te – S angles are nearly constant, the other interligand S – Te – S angle in a trapezoid must decrease relative to that found in $Te(dtc)_2$. As this bond angle is reduced, the corresponding Te – S bond lengths increase relative to those in $Te(dtc)_2$ in order to minimize S···S repulsion.

The Te – S – C angles vary from 85.2 to 90.5°, indicating that *p*-orbitals on the sulphur atoms are used for bonding to tellurium. The angles on sp^2 hybridized carbon and nitrogen are near 120°, the variation mostly following the pattern predicted from VSEPR theory;[20] *i.e.* that the electron density in a double bond has a greater repulsion effect than that in a single bond.

Least squares planes through various parts of the molecules are shown in Tables 8 – 10. The ligands, except for methyl carbon atoms and hydrogen atoms, are nearly planar.

The intermolecular distances are normal except for two C – C distances of 3.34 and 3.45 Å. The other C – C distances are all above 3.60 Å. The short interactions may in this case, where such large molecules are involved, be due to packing effects.

Acknowledgement. A gift of a sample of $Te(dtc)_4$ from Dr. G. St. Nikolov, Bulgarian Academy of Sciences (Sofia), is greatly appreciated.

REFERENCES

1. Husebye, S. and George, J. G. *Inorg. Chem.* **8** (1969) 313.
2. Esperås, S., Husebye, S. and Sværen, S. E. *Acta Chem. Scand.* **25** (1971) 3539.
3. Esperås, S. and Husebye, S. *Acta Chem. Scand.* **26** (1972) 3293.
4. Hazell, A. C. *Acta Chem. Scand.* **20** (1966) 165.
5. Das, A. K. and Brown, I. D. *Can. J. Chem.* **44** (1966) 939.
6. Soyama, S., Osaki, K. and Kusanagi, S. *Inorg. Nucl. Chem. Lett.* **8** (1972) 181.
7. Buss, B. and Krebs, B. *Inorg. Chem.* **10** (1971) 2795.
8. Krebs, B., Buss, B. and Altena, D. *Z. anorg. allgem. Chem.* **386** (1971) 257.
9. Maslin, S. H., Ryan, R. R. and Asprey, L. B. *Inorg. Chem.* **9** (1970) 2100.
10. Knobler, C., McCullough, J. D. and Hope, H. *Inorg. Chem.* **9** (1970) 797.
11. Weiss, J. and Pupp, M. *Angew. Chem.* **82** (1970) 447.
12. Nikolov, G., St., Jordanov, N. and Havezov, I. *J. Inorg. Nucl. Chem.* **33** (1970) 1059.
13. Nikolov, G., St. and Tyutyulkov, N. *Inorg. Nucl. Chem. Lett.* **7** (1971) 1209.
14. Nikolov, G., St. *Inorg. Nucl. Chem. Lett.* **7** (1971) 1213.
15. Harreld, C. S. and Schlemper, E. O. *Acta Cryst.* **B 27** (1971) 1964.
16. Coppens, P., Leiserowitz, L. and Rabinovich, D. *Acta Cryst.* **18** (1965) 1035.
17. *International Tables for X-Ray Crystallography*, Kynoch Press, Birmingham 1962, Vol. III, p. 204.
18. Cromer, D. T. *Acta Cryst.* **18** (1965) 17.
19. Gillespie, R. J. and Nyholm, Q. *Quart. Rev. (London)* **11** (1957) 339.
20. Gillespie, R. J. *J. Chem. Educ.* **47** (1970) 18.
21. Cotton, F. A. and Wilkinson, G. *Advanced Inorganic Chemistry*, 2nd Ed., Interscience – Wiley, London 1967, p. 135.
22. Brown, D., Holah, D. G. and Richard, C. E. F. *J. Chem. Soc.* **A 1970** 423.
23. Brown, D., Holah, D. G. and Richard, C. E. F. *J. Chem. Soc.* **A 1970** 786.
24. Colapietro, M., Vaciago, A., Bradley, D. C., Hursthouse, M. B. and Rendall, I. F. *Chem. Commun.* **1970** 743.
25. Kettle, S. F. A. *Studies in Modern Coordination Chemistry*, T. Nelson and Sons, London 1969, p. 18.
26. Hoard, J. L. and Silverton, J. V. *Inorg. Chem.* **2** (1963) 235.
27. Husebye, S. *Acta Chem. Scand.* **24** (1970) 2198.
28. Fabiani, C., Spagna, R., Vaciago, A. and Zambonelli, L. *Acta Cryst.* **B 27** (1971) 1499.
29. Foss, O. *Acta Chem. Scand.* **7** (1953) 226.
30. Engel, G. *Z. Krist.* **90** (1935) 341.
31. Vonk, C. G. and Wiebenga, E. H. *Acta Cryst.* **12** (1959) 859.
32. Morss, L. R. and Robinson, W. R. *Acta Cryst.* **B 28** (1972) 653.
33. Goldberg, I. and Herbstein, F. H. *Acta Cryst.* **B 28** (1972) 400.
34. Urch, D. S. *J. Chem. Soc.* **1964** 5775.
35. Orgel, L. E. *J. Chem. Soc.* **1959** 3815.
36. Lindquist, O. *Acta Chem. Scand.* **24** (1970) 3178.

Received September 11, 1972.

ACTA CHEMICA SCANDINAVICA 27 (1973) 779–796

The Chemistry of Hexahydro-1,2,4,5-tetrazines

IV. The Reactions of Alkylhydrazines with Formaldehyde*

STEEN HAMMERUM

Department of General and Organic Chemistry, University of Copenhagen, The H. C. Ørsted Institute, Universitetsparken 5, DK-2100 Copenhagen Ø, Denmark

The condensation reactions of alkylhydrazines with formaldehyde are shown to lead to formaldehyde alkylhydrazones. These dimerize in an acid-catalyzed reaction to yield 1,4-dialkylhexahydro-1,2,4,5-tetrazines. With straight-chain alkyl groups the dimerization process is too rapid to allow isolation of the hydrazones in a pure state. A stepwise ionic mechanism for the dimerization process rather than dimerization of 1,3-dipolar azomethine imines is suggested. Condensations with alcoholic formaldehyde in excess lead to formaldehyde *N*-alkyl-*N*-alkoxymethylhydrazones. The reaction course is not significantly influenced by the inclusion of functional groups in the alkyl moieties of the hydrazines. The hexahydro-1,2,4,5-tetrazines are characterized as diacyl and bis(thiocarbamoyl)derivatives. NMR spectra of 1,4-dialkylhexahydro-1,2,4,5-tetrazines give evidence of hindered nitrogen inversion, the barrier to which is increased upon acyl substitution.

In a recent communication [1] we reviewed the formation of 1,4-dimethyl and 1,4-diphenyl hexahydro-1,2,4,5-tetrazines by condensation of formaldehyde and formaldehyde derivatives with methyl- and phenylhydrazine. Only a very few reactions of alkylhydrazines with formaldehyde have been reported in the literature: Müller and Rundel [2] prepared 1,4-dimethylhexahydro-1,2,4,5-tetrazine (III*a*) from methylhydrazine and aqueous formaldehyde, and Schmitz and Ohme [3] further described the isolation of the 3:2 and 4:2 condensation products VI and IX from methylhydrazine with excess formaldehyde. Dorn and Dilcher [4] have reported the preparation of hexahydro-1,2,4,5-tetrazines (III) by reaction of substituted benzylhydrazines with weakly alkaline aqueous formaldehyde, and Zurini and Rosicky [5] reported the formation of 1,4-bis(2-phenylethyl)hexahydro-1,2,4,5-tetrazine (III*o*) from aqueous formaldehyde and phenethylhydrazine. None of these authors mention the intermediate formation of formaldehyde alkylhydrazones. Ioffe,[6] however,

* A preliminary account of part of this work has appeared in *Tetrahedron Letters* **1972** 949.

has isolated the isopropylhydrazone of formaldehyde (II*f*), which dimerized upon standing. The only other formaldehyde monoalkylhydrazone that has been reported in the literature is the methylhydrazone (II*a*), which was detected by Hutton and Steel [7] in solution after base-catalyzed isomerization of azomethane. In a preliminary report Block and Young [8] recently noted the apparent failure of β-hydroxyethylhydrazine to react with formaldehyde.

We now report the results of an investigation of the reaction of formaldehyde with a series of alkylhydrazines (*cf.* Fig. 1) in various media. The product distribution has been found to be dependent on the molar ratio of the reactants, since the initial reaction products, formaldehyde alkylhydrazones, may react further with formaldehyde, and on the nature of the alkyl group, since the reactivity of the hydrazones has been found to depend upon chain length and branching.

RESULTS

The addition of aqueous formaldehyde to an equimolar amount of an alkylhydrazine produces an alkylhydroxymethylhydrazine (I), which subsequently eliminates water with formation of a formaldehyde alkylhydrazone (II).

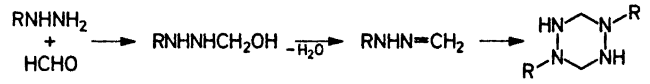

I II III

a: R = CH_3 g: R = C_4H_9 n: R = $CH_2C_6H_5$

b: R = C_2H_5 h: R = i-C_4H_9 o: R = $CH_2CH_2C_6H_5$

c: R = C_2H_4OH i: R = sec.-C_4H_9 p: R = CHC_6H_5 (CH_3)

d: R = C_2H_4CN j: R = $C_2H_4OC_2H_5$

e: R = $CH_2CH{=}CH_2$ k: R = cyclo-C_6H_{11} q: R = $CH_2CH_2CH_2C_6H_5$

f: R = i-C_3H_7 l: R = C_6H_{13} r: R = $CH_2CHC_6H_5$ (CH_3)

m: R = C_8H_{17}

Fig. 1

Only hydrazones derived from hydrazines with branched alkyl groups or from aralkylhydrazines have been isolated in a pure state, whereas straight-chain aliphatic formaldehyde hydrazones dimerize *in situ* or upon attempted purification (distillation) to give 1,4-dialkylhexahydro-1,2,4,5-tetrazines (III). The rate of dimerization varies inversely with the length of the n-alkyl group. Lower alkylhydrazones have been detected (by NMR spectroscopy) only in chloroform extracts of the reaction mixtures, since dimerization takes place upon evaporation of solvent. Hydrazones with higher alkyl substituents (*e.g.* octyl) may be distilled in vacuum after removal of solvent, but the distillates

Table 1. 1,4-Dialkylhexahydro-1,2,4,5-tetrazines (III).

	Alkyl	M.p.	Yield %	Formula		Analyses (C, H, N)		
a	CH_3	123–125[a]	70	$C_4H_{12}N_4$	Found	41.07	10.18	48.10
					Calc.	41.33	10.42	48.25
b	C_2H_5	139–140	25	$C_6H_{16}N_4$	Found	49.64	11.11	38.61
					Calc.	49.97	11.18	38.85
c	C_2H_4OH	146½–148	70	$C_6H_{16}N_4O_2$	Found	41.02	9.14	31.78
					Calc.	40.89	9.15	31.80
d	C_2H_4CN	122–123	40	$C_8H_{14}N_6$	Found	49.20	7.30	43.28
					Calc.	49.46	7.27	43.27
e	$CH_2CH=CH_2$	103–104	40	$C_8H_{16}N_4$	Found	57.00	9.61	33.48
					Calc.	57.11	9.59	33.30
g	C_4H_9	135–135½	70	$C_{10}H_{24}N_4$	Found	59.80	12.05	27.88
					Calc.	59.95	12.08	27.97
h	*i*-C_4H_9	109–110	65	$C_{10}H_{24}N_4$	Found	60.34	12.24	28.22
					Calc.	59.95	12.08	27.97
j	$C_2H_4OC_2H_5$	93–101[b]	20	$C_{10}H_{24}N_4O_2$	Found	51.65	10.25	24.02
					Calc.	51.70	10.41	24.12
l	C_6H_{13}	128½–130	45	$C_{14}H_{32}N_4$	Found	65.60	12.62	21.50
					Calc.	65.57	12.58	21.85
m	C_8H_{17}	125–127	70	$C_{18}H_{40}N_4$	Found	69.30	12.82	17.98
					Calc.	69.17	12.90	17.93
n	$C_6H_5CH_2$	165–167[c]	90	$C_{16}H_{20}N_4$	Found	71.65	7.80	20.72
					Calc.	71.61	7.51	20.88
o	$C_6H_5CH_2CH_2$	151–153[d]	40	$C_{18}H_{24}N_4$	Found	73.08	8.20	18.73
					Calc.	72.94	8.16	18.90
p	$C_6H_5CH(CH_3)$	102–107[b]	–[e]	$C_{18}H_{24}N_4$	Found	72.84	8.22	18.98
					Calc.	72.94	8.16	18.90
q	$C_6H_5CH_2CH_2CH_2$	75–77½	25	$C_{20}H_{28}N_4$	Found	74.10	8.72	17.26
					Calc.	74.03	8.70	17.27
r	$C_6H_5CHCH_2(CH_3)$	137–138	45	$C_{20}H_{28}N_4$	Found	73.75	8.82	16.97
					Calc.	74.03	8.70	17.27

[a] Lit.[2] 121–123°C. [b] Possibly accompanied by dissociation. [c] Lit.[4] 158–160°C. [d] Lit.[5] 143–145°C. [e] Not determined.

partially solidify in the receiver as the dimers. The dimerization of these hydrazones has been monitored by NMR spectroscopy and is essentially complete in nonaqueous solvents within a few hours. Addition of water to the samples causes weak signals (< 10 %) corresponding to the methylene protons of the hydrazones to reappear, indicating that the dimerization process is reversible and to some degree solvent-dependent.

The reactions of aralkylhydrazines are sufficiently slow to allow the various steps of the reaction sequence to be observed separately. Addition of aqueous formaldehyde to benzylhydrazine in the presence of Na_2CO_3 produces II*n* as a clear viscous liquid. This can be vacuum-distilled without significant dimerization, and can be stored unchanged in a closed vessel at low temperatures for periods of up to a week. The dimerization process is, however, fairly rapid in

solution, especially in the presence of acid. Addition of acetate buffer (pH 5.5) in aqueous methanol to the liquid hydrazone causes almost instantaneous solidification. Likewise, addition of formaldehyde to benzylhydrazine in acetate buffer (pH 5.5) causes the hexahydro-1,2,4,5-tetrazine III*n* to precipitate immediately from the reaction mixture.

Formaldehyde alkylhydrazones with secondary alkyl groups (II*f*, II*i*, II*p*) are stable compounds that dimerize only slowly in solution or neat, an extreme example being II*p*, where the dimerization process is only 75 % complete after 24 months at +4°C. Hydrazones where the chain branching is once removed from the nitrogen atom (*e.g.* isobutyl, II*h*) also undergo dimerization at a slower rate than the corresponding hydrazones with unbranched alkyl groups and may be distilled without appreciable dimer formation. This stability is assumed to reflect steric hindrance in the transition state leading to the hexahydro-1,2,4,5-tetrazine.

The inclusion of unsaturation or of functional groups such as C–C double bonds or hydroxyl, alkoxyl, or cyano groups in the alkyl moieties (*cf.* Fig. 1) does not appreciably influence the reaction course, since hexahydro-1,2,4,5-tetrazines have been isolated in all cases in fair to good yields. It is of interest to note that tetrahydro-1,3,4-oxadiazine is not formed in detectable amounts in the condensation of formaldehyde with β-hydroxyethylhydrazine, in contrast to what has been reported for the reactions of other aldehydes with hydrazines of this kind.[8–12]

The condensation reactions have been carried out with aqueous formaldehyde or paraformaldehyde, neat or in aqueous or alcoholic solutions, at temperatures ranging from −10°C to reflux, with no significant variation in product distribution. Hexahydro-1,2,4,5-tetrazines are likewise formed in fair to good yields in reactions of alkylhydrazines with methylene bromide in the presence of Na_2CO_3. Formaldehyde hydrazones are assumed to be intermediates in this reaction also.

The earlier proposal by Ioffe [6] that the dimer of formaldehyde isopropylhydrazone should have an open-chain structure (deprotonated XIII) is believed to be erroneous in view of these results. The assignment was made on the basis of signals in the NMR spectrum corresponding to an equal number of $CH_2{=}N$ and $N{-}CH_2{-}N$ protons. These probably arise from an approx-

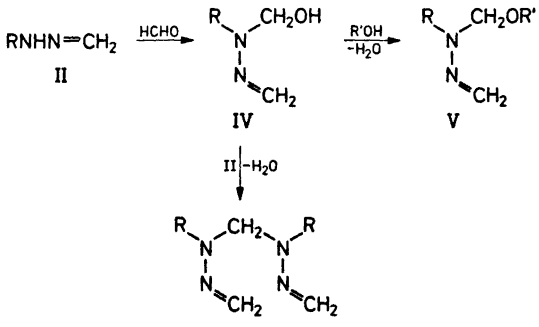

Fig. 2

imately 2:1 mixture of II*f* and III*f*; the τ-value quoted for the $N-CH_2-N$ protons (6.37) agrees well with the average value found in this study for the ring methylene protons of the 1,4-dialkylhexahydro-1,2,4,5-tetrazines (*cf.* Table 5). We have obtained similar misleading results from the NMR spectra of, *e.g.*, III*p*, which also dissociates very easily in solution to give the hydrazone II*p*.

Condensations with formaldehyde in excess produce formaldehyde *N*-alkyl-*N*-alkoxymethylhydrazones (V) when performed in alcoholic solution, probably *via* IV. Similar compounds have been isolated by Howard *et al.*[13] and by Dorn *et al.*[14] from acid-catalysed reactions of aromatic aldehydes with alkylhydrazines in methanol. The reaction of cyclohexylhydrazine and excess formaldehyde is an exception, producing 1,4-dicyclohexyl-1,2,4,5-tetraazabicyclo[2,2,1]heptane (VII*k*), as has also been reported by Schmitz and Ohme.[3] Their identification was based mainly on elemental analysis and infrared evidence. We have examined the NMR and mass spectra of this compound, and found excellent agreement with the proposed structure. Bicyclic compounds of this nature have been observed by Schmitz and Ohme[15] and by Karabatsos and Taller[16] to arise from condensations of phenylhydrazine with excess formaldehyde; their formation appears to be quite general for arylhydrazines.[17,18] We have, however, not found definitive evidence for the formation of VII in reactions of other alkylhydrazines with formaldehyde. Recently, Nelsen and Hintz[19] reported that compounds of this kind may be formed in reactions of 1,4-dialkylhexahydro-1,2,4,5-tetrazines with formaldehyde, but experimental conditions were not given.

Reactions with excess formaldehyde carried out in aqueous solutions give rise to complicated reaction mixtures, apparently arising from condensation in a variety of molar ratios. In a few instances, 3:2 condensation products, methylene-*bis*-alkylhydrazones of formaldehyde (VI), have been isolated in agreement with the report by Schmitz and Ohme.[3] Rabjohn and Sloan[20] have shown that condensations of methylhydrazine with aliphatic aldehydes also lead to compounds of this nature. We have found that reactions of other alkylhydrazines with acetaldehyde proceed in a similar manner.[21]

A 4:2 condensation product has been isolated from the reaction of methylhydrazine with formaldehyde. The structure suggested earlier[3] for this compound (IX) is probably incorrect, since NMR spectra obtained at several temperatures indicate that the two methyl groups are situated permanently in magnetically different positions. A possible structure is VIII. Johns *et al.*[18] have shown that the reactions of phenylhydrazine and *p*-nitrophenylhydrazine with excess formaldehyde also produce compounds similar to VIII and IX.

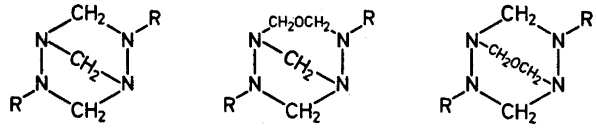

VII VIII IX

Fig. 3

DISCUSSION

Dorn and Dilcher [4] have suggested that the formation of hexahydro-1,2,4,5-tetrazines by condensation of aliphatic hydrazines with formaldehyde occurs *via* azomethine imines (X or XI), which were assumed to undergo 1,3-dipolar cyclodimerization.

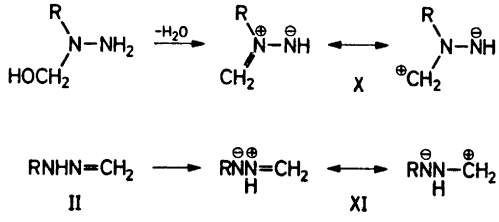

Fig. 4

Similar 1,3-dipolar species have been suggested by Grashey and coworkers [22] to be intermediates in the formation of 3,6-diarylhexahydro-1,2,4,5-tetrazines from aromatic aldehydes and 1,2-dialkylhydrazines, and by Zinner and collaborators [23] in the condensations of di- and trisubstituted hydrazines with aldehydes. However, Zwanenburg *et al.*,[24] have argued that the formation of 1,3-dipolar intermediates will be unfavourable in purely aliphatic systems of this kind. The evidence presented here strongly suggests that 1,3-dipolar intermediates are not important in the formation of 1,4-dialkylhexahydro-1,2,4,5-tetrazines. It should also be noted that a concerted dimerization of 1,3-dipolar species such as these would be a disallowed reaction under the Woodward-Hoffman rules.

The formation of species such as X would require formaldehyde to add to the substituted nitrogen atom of the hydrazine, with subsequent elimination of water. The polarographic evidence presented by Dorn and Dilcher [4] appears, however, to establish that the attack takes place at the unsubstituted nitrogen atom. Possible 1,3-dipolar species involved in the dimerization process will consequently be of structure XI. This molecule is a tautomer of the hydrazone II, but the equilibrium concentration of XI will probably be exceedingly small, which then requires that the subsequent dimerization should occur very rapidly. This, in turn, demands that XI be very reactive, but attempts to "trap it" have proved unsuccessful. It would be expected to add to the CN double bond of formaldehyde hydrazones, forming *N*-aminotriazolidines,[25] but these have not been observed to be formed in the reactions examined, nor were they observed by Schmitz [26] in condensations of formaldehyde with mixtures of 1,1- and 1,2-dialkylhydrazines. Furthermore, the condensations of butyl- and benzylhydrazine with formaldehyde are unaffected by added dipolarophiles such as diphenylacetylene or norbornene, and no adducts are observed. 1,3-Dipolar cycloadditions are usually reversible, but 1,4-dialkylhexahydro-1,2,4,5-tetrazines are not observed to react with dipolarophiles at elevated temperatures (*e.g.* reflux in xylene for 24 h). Similar

results have been reported by Oppolzer,[27] who has shown that 1,3-dipolar species are not present in significant amounts in the formation of 1,2,4,5-tetraalkylhexahydro-1,2,4,5-tetrazines from formaldehyde, in contrast to what was observed [27] in the reactions of 1-acyl-2-alkylhydrazines and 1-alkyl-2-arylhydrazines with formaldehyde.

The catalytic effect of acid on the dimerization of the formaldehyde hydrazones described above indicates that a protonated hydrazone (XII) is involved in the dimer formation. Addition of XII to the hydrazone produces XIII, which by deprotonation would yield the open-chain dimer claimed by Ioffe [6] to be formed from formaldehyde isopropylhydrazone. Intramolecular addition in XIII across the CN double bond produces the hexahydro-1,2,4,5-tetrazine.

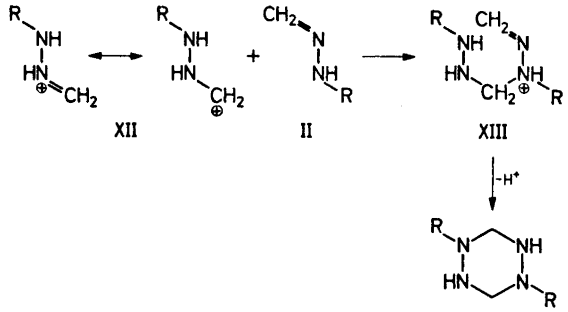

XII II XIII III

Fig. 5

Skorianetz and Kováts [28] have found that the dimerization of acetaldehyde hydrazone also is subject to acid catalysis; they suggest a mechanism of dimerization similar to ours. The acid-catalyzed reductive dimerization of formaldehyde dialkylhydrazones has likewise been suggested to occur *via* protonated hydrazone intermediates.[29,30]

CHEMICAL PROPERTIES

The alkylhydrazine derivatives of formaldehyde described in the present study are all hydrolyzed rapidly by aqueous mineral acid with regeneration of the starting materials. The (alkoxyalkyl)alkylhydrazones, V, and methylenebis(alkylhydrazones), VI, should be kept in closed vessels, since even atmospheric moisture causes partial hydrolysis with liberation of formaldehyde, which in some cases recondenses to give other products. The formaldehyde hydrazones, II, are quite stable compounds but for the dimerization reactions described above. Compounds II, V, and VI are mostly colourless liquids that rapidly acquire a slight yellow tint upon contact with air, probably due to oxidation.[28]

1,4-Dialkylhexahydro-1,2,4,5-tetrazines are likewise stable compounds, though the lower members of the series examined are somewhat sensitive to hydrolysis and oxidation. They may form yellow, oily substances upon

prolonged standing in open vessels and should be stored at low temperatures, preferably under nitrogen.

1,4-Dialkylhexahydro-1,2,4,5-tetrazines dissociate slowly to formaldehyde alkylhydrazones upon heating. They undergo reactions typical of substituted hydrazines, and have been characterized as diacyl derivatives (XIV) by the action of acetic or propionic anhydride (*cf.* Table 3) and as bis-thiosemicarbazides (XV) by addition of isothiocyanates (*cf.* Table 4).

Table 2. Formaldehyde alkylhydrazones (II).

	Alkyl	B.p. (°C/mmHg)	Yield (%)	Formula	Analyses (C, H, N)			
h	i-C_4H_9	35 – 38/12	75	$C_5H_{12}N_2$	Found	60.21	11.91	27.69
					Calc.	59.95	12.08	27.97
i	*sec*-C_4H_9	42 – 45/12	55	$C_5H_{12}N_2$	Found	60.21	11.89	27.89
					Calc.	59.95	12.08	27.97
m	C_8H_{17}	70 – 74/0.5	[a]		Found [a]			
					Calc.			
n	$CH_2C_6H_5$	53 – 56/0.5	40	$C_8H_{10}N_2$	Found	71.65	7.54	21.13
					Calc.	71.61	7.51	20.86
p	CHC_6H_5 | CH_3	*ca.* 60/0.4	45	$C_9H_{12}N_2$	Found	73.50	8.37	18.02
					Calc.	72.94	8.16	18.90
q	$CH_2CH_2CH_2C_6H_5$	80 – 85/0.5	45	$C_{10}H_{14}N_2$	Found	74.25	8.68	16.75
					Calc.	74.03	8.70	17.27

[a] Dimerizes; *cf.* Table 1 for yield and analysis of dimer.

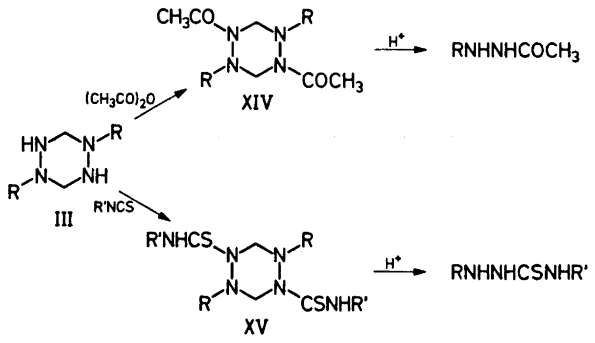

Fig. 6

These derivatives are thermally very stable, for they may be recovered unchanged in more than 80 % yield after 4 h reflux in inert solvents at 200°C. Hydrolysis in dilute mineral acids proceeds only slowly and takes place at the aminal bonds (ring cleavage) with formation of formaldehyde and hydrazides or 1,4-disubstituted thiosemicarbazides.

Table 3. 1,4-Dialkyl-2,5-diacylhexahydro-1,2,4,5-tetrazines (XIV).

	Alkyl	Acyl	M.p.	Yield %	Formula	Analyses (C, H, N)			
b	C_2H_5	CH_3CO	169–171	55	$C_{10}H_{20}N_4O_2$	Found	52.37	8.82	24.46
						Calc.	52.61	8.83	24.54
d	C_2H_4CN	CH_3CO	286–289	75	$C_{12}H_{18}N_6O_2$	Found	51.62	6.54	30.04
						Calc.	51.78	6.52	30.20
g	$CH_2CH=CH_2$	CH_3CO	184–185	95	$C_{12}H_{20}N_4O_2$	Found	57.20	8.08	22.15
						Calc.	57.10	7.99	22.22
j	C_4H_9	CH_3CO	103–105	60	$C_{14}H_{28}N_4O_2$	Found	59.10	9.96	19.64
						Calc.	59.12	9.92	19.70
j[1]	C_4H_9	C_2H_5CO	83–85	65	$C_{16}H_{32}N_4O_2$	Found	61.62	10.32	18.09
						Calc.	61.50	10.32	17.93
i	i-C_4H_9	CH_3CO	139–140	40	$C_{14}H_{28}N_4O_2$	Found	59.25	10.02	19.69
						Calc.	59.12	9.92	19.70
k	$C_2H_4OOCCH_3$	CH_3CO	164–168	80	$C_{14}H_{24}N_4O_6$	Found	48.88	7.32	16.28
						Calc.	48.83	7.03	16.27
	$C_2H_4OC_2H_5$	CH_3CO	128–131	85	$C_{14}H_{28}N_4O_4$	Found	53.20	8.96	17.42
						Calc.	53.14	8.92	17.71
	C_6H_{13}	CH_3CO	91–93	70	$C_{18}H_{36}N_4O_2$	Found	63.50	10.65	16.44
						Calc.	63.49	10.65	16.46
n	C_8H_{17}	CH_3CO	97–99	70	$C_{22}H_{44}N_4O_2$	Found	66.35	11.07	14.05
						Calc.	66.62	11.18	14.13
a	$C_6H_5CH_2$	CH_3CO	221–222[a]	95	$C_{20}H_{24}N_4O_2$	Found	68.38	6.92	15.92
						Calc.	68.16	6.86	15.90
l	$C_6H_5CH_2$	C_2H_5CO	207–211	65	$C_{22}H_{28}N_4O_2$	Found	69.20	7.61	14.48
						Calc.	69.44	7.42	14.73
	$C_6H_5CH_2CH_2$	CH_3CO	152–154	45	$C_{22}H_{28}N_4O_2$	Found	69.21	7.45	14.78
						Calc.	69.44	7.42	14.73
	$C_6H_5CH(CH_3)$	CH_3CO	267–268[b]	45	$C_{22}H_{28}N_4O_2$	Found	69.50	7.47	14.68
						Calc.	69.44	7.42	14.73
	$C_6H_5CH_2CH_2CH_2$	CH_3CO	110½–111½	50	$C_{24}H_{32}N_4O_2$	Found	70.40	7.84	13.62
						Calc.	70.56	7.90	13.72
	$C_6H_5CHCH_2(CH_3)$	CH_3CO	160–162	60	$C_{24}H_{32}N_4O_2$	Found	70.40	7.94	13.67
						Calc.	70.56	7.90	13.72

[a] Lit.[4] 222–223°C. [b] With concurrent sublimation.

SPECTROSCOPIC PROPERTIES

Infrared and ^1H nuclear magnetic resonance (NMR) spectra of all compounds described have been recorded and found to be in agreement with the proposed structures. The mass spectra of the 1,4-dialkylhexahydro-1,2,4,5-tetrazines and their acyl derivatives have been published elsewhere.[31]

The NMR spectra of 1,4-dialkylhexahydro-1,2,4,5-tetrazines formed in the condensation reactions described above confirm that these compounds are all centrosymmetrically substituted. The alkyl substituents give rise to one set of lines, and the ring methylene protons give rise to a broad singlet at τ 6.37 ± 0.10 (*cf.* Table 5), which splits upon cooling to give a multiplet. This becomes

Table 4. 1,4-Dialkyl-2,5-bis(thiocarbamoyl)-1,2,4,5-tetrazines (XV).

	R	R¹	M.p.[a]	Yield %	Formula	Analyses (C, H, N, S)				
b	C_2H_5	CH_3NHCS	225–226	65	$C_{10}H_{22}N_6S_2$	Found	41.57	7.79	29.15	22.17
						Calc.	41.37	7.64	28.95	22.04
c	C_2H_4OH	CH_3NHCS	247–248½	75	$C_{10}H_{22}N_6O_2S_2$	Found	37.55	6.97	26.05	19.98
						Calc.	37.25	6.88	26.06	19.89
e	$CH_2CH=CH_2$	CH_3NHCS	195–210[b]	85	$C_{12}H_{22}N_6S_2$	Found	45.80	7.06	26.65	20.13
						Calc.	45.85	7.05	26.74	20.36
g	C_4H_9	CH_3NHCS	178–180	95	$C_{14}H_{30}N_6S_2$	Found	48.75	8.76	24.48	18.75
						Calc.	48.54	8.73	24.26	18.47
*g*¹	C_4H_9	C_6H_5NHCS	215–217	95	$C_{24}N_{34}N_6S_2$	Found	61.10	7.22	17.81	13.79
						Calc.	61.24	7.28	17.85	13.62
h	i-C_4H_9	CH_3NHCS	255–257	40	$C_{14}H_{30}N_6S_2$	Found	48.64	8.71	24.12	18.47
						Calc.	48.54	8.73	24.26	18.47
j	$C_2H_4OC_2H_5$	CH_3NHCS	200–203[b]	80	$C_{14}H_{30}N_6O_2S_2$	Found	44.49	8.11	22.13	–[c]
						Calc.	44.43	7.99	22.21	–
n	$C_6H_5CH_2$	CH_3NHCS	291–292[b]	80	$C_{20}H_{26}N_6S_2$	Found	57.90	6.47	20.20	15.71
						Calc.	57.96	6.32	20.28	15.44
o	$C_6H_5CH_2CH_2$	CH_3NHCS	261–263	20	$C_{22}H_{30}N_6S_2$	Found	59.59	6.85	18.70	14.56
						Calc.	59.71	6.83	18.99	14.46

[a] Several compounds give off liquid before melting; the figure listed is the apparent m.p. of the main portion. [b] Strongly dependent upon rate of heating. [c] Analytical figures for S not reproducible.

Table 5. Chemical shifts of ring methylene protons in 1,4-dialkylhexahydro-1,2,4,5-tetrazines (III).

Alkyl	Chemical shift[c]	Solvent	Coalescence[e] temp., °C
CH_3[a]	6.37	$CDCl_3$	10[f,g]
–[a]	6.57	CCl_4	–
C_2H_5	6.35	$CDCl_3$	–
C_2H_4OH	6.44	DMSO-d_6	–[h]
C_2H_4CN[b]	6.30	$CDCl_3$	–[i]
$CH_2CH=CH_2$	6.35	$CDCl_3$	20[f]
C_4H_9	6.38	$CDCl_3$	25[f]
i-C_4H_9	6.45	$CDCl_3$	15[f]
$C_2H_4OC_2H_5$	6.27	$CDCl_3$	–
C_6H_{13}	6.38	$CDCl_3$	–[h]
C_8H_{17}	6.39	$CDCl_3$	–
$CH_2C_6H_5$	6.32	$CDCl_3$	15[f]
$C_2H_4C_6H_5$	6.30	$CDCl_3$	10[f]
$CH(CH_3)C_6H_5$	6.42	$CDCl_3$	–
$C_3H_6C_6H_5$	6.40	$CDCl_3$	15[f]
$CH_2CH(CH_3)C_6H_5$	6.40[d] 6.52[d]	$CDCl_3$	–

[a] Taken from Ref. 1. [b] The chemical shifts of all exocyclic protons coincide. [c] τ-values. [d] AB-quartet at 40°C, J_{HH} = 11 Hz; doublet centers given. [e] Approximate, ±5°C. [f] J_{HH} = 11 Hz. [g] *Cf.* Ref. 31. [h] Above 0°C. [i] Below 0°C.

one AB pair of doublets when the amino hydrogen atoms are replaced by deuterium, showing that the two CH_2-groups are magnetically equivalent. Also, the ring methylene protons of the acyl and thiocarbamoyl derivatives (XIV and XV) give rise to only one AB system, and the acyl (thioacyl) groups appear as one set of lines at all temperatures examined.

Dorn and Dilcher [4] have previously employed similar NMR data for acyl derivatives of III*a* and III*n* to show the centrosymmetric nature of these compounds; the structure of III*a* has since been conclusively confirmed by an X-ray examination.[32]

Table 6. Chemical shift of ring methylene protons in 1,4-dialkyl-2,5-diacylhexahydro-1,2,4,5-tetrazines (XIV).

Alkyl	Acyl	Chemical shift [h]		J_{HH}(Hz)	Solvent	Temp. °C
CH_3	CH_3CO	5.02	5.58	13½	$CDCl_3$	40
–	–	4.87	5.42	13½	$CDCl_3$	−50
–	–	5.22	5.53	13½	DMSO-d_6	40
–	–	5.32		–	DMSO-d_6	80
C_2H_5	CH_3CO	4.85	5.70	13½	$CDCl_3$	40
– [a]	–	4.80	5.60	13½	$CDCl_3$	−50
$CH_2CH=CH_2$	CH_3CO	4.88	5.77	13½	$CDCl_3$	40
C_4H_9 [a]	CH_3CO	4.94	5.77	13½	$CDCl_3$	40
C_4H_9 [a]	CH_3CH_2CO [g]	4.90	5.75	13½	$CDCl_3$	40
– [a]	– [g]	5.12	5.67	13½	DMSO-d_6	40
– [a]	– [g]	5.12	5.70	13½	DMSO-d_6	100
i-C_4H_9 [b,c]	CH_3CO	4.93	5.74	13½	$CDCl_3$	40
– [a,c]	–	5.17	5.62	13½	DMSO-d_6	40
– [a]	–	5.15	5.67	13½	DMSO-d_6	100
–	–	5.25 [i]	5.57 [j]	–	DMSO-d_6	120
–	–	5.42 [k]		–	DMSO-d_6	140
$C_2H_4OC_2H_5$ [d]	CH_3CO	4.90	5.72	13½	$CDCl_3$	40
$C_2H_4OOCCH_3$ [d]	CH_3CO	4.81	5.73	13½	$CDCl_3$	40
C_6H_{13} [a]	CH_3CO	4.95	5.78	13½	$CDCl_3$	40
C_8H_{17} [a]	CH_3CO	4.93	5.75	13½	$CDCl_3$	40
$CH_2C_6H_5$ [e]	CH_3CO	4.85	5.63	13½	$CDCl_3$	40
– [a]	–	4.79	5.56	13½	DMSO-d_6	40
$CH_2C_6H_5$ [f]	CH_3CH_2CO [g]	4.80	5.60	13½	$CDCl_3$	40
$C_2H_4C_6H_5$ [d]	CH_3CO	4.80	5.73	13½	$CDCl_3$	40
$CH(CH_3)C_6H_5$	CH_3CO	5.02	6.00	13½	$CDCl_3$	40
$C_3H_6C_6H_5$ [d]	CH_3CO	4.92	5.78	13½	$CDCl_3$	40
$CH_2CH(CH_3)C_6H_5$ [d]	CH_3CO	4.85	5.78 [i] 5.85	13½	$CDCl_3$	40
– [d]	–	5.04	5.62 [i] 5.74	13½	DMSO-d_6	40

[a] α-Methylene protons magnetically non-equivalent. [b] α-Methylene protons magnetically non-equivalent; ABC-system observed. [c] Methyl groups also magnetically non-equivalent. [d] α-Methylene protons appear as part of multiplet due also to other protons. [e] α-Methylene protons magnetically non-equivalent; AB-system observed with $\Delta\nu_{AB}=0.25$ ppm, $J_{AB}=12\frac{1}{2}$ Hz. [f] α-Methylene protons magnetically non-equivalent; AB-system observed with $\Delta\nu_{AB}=0.28$ ppm, $J_{AB}=12\frac{1}{2}$ Hz. [g] CH_2-protons magnetically non-equivalent. [h] AB pair of doublets; doublet centers given in τ-values, calculated according to $\delta_A-\delta_B=\sqrt{(\nu_1-\nu_4)(\nu_2-\nu_3)}$. [i] High-field doublet appears as pair of doublets, both given. [j] Two broad singlets. [k] Very broad singlet.

Table 7. Chemical shifts of ring methylene protons in 1,4-dialkyl-2,5-bis(thiocarbamoyl)-hexahydro-1,2,4,5-tetrazines (XV).

Alkyl	Thiocarbamoyl	Chemical shift		J_{HH}(Hz)	Solvent
CH_3 [a]	CH_3NHCS	4.04	5.42	14	$CDCl_3$
CH_3 [a]	t-C_4H_9NHCS	3.76	5.52	13½	$CDCl_3$
C_2H_5 [b]	CH_3NHCS	3.92	5.60	13½	$CDCl_3$
C_2H_4OH [c]	CH_3NHCS	4.05	5.42	14	DMSO-d_6
$CH_2CH=CH_2$	CH_3NHCS	4.15	5.50	13½	DMSO-d_6
C_4H_9 [b]	CH_3NHCS	3.96	5.60	13½	$CDCl_3$
C_4H_9 [b]	C_6H_5NHCS	3.70	5.43	13½	$CDCl_3$
i-C_4H_9 [d,e]	CH_3NHCS	3.93	5.55	13½	$CDCl_3$
$C_2H_4OC_2H_5$ [c]	CH_3NHCS	3.95	5.62	13½	$CDCl_3$
$CH_2C_6H_5$ [f]	CH_3NHCS	3.71	5.38	13½	DMSO-d_6
$C_2H_4C_6H_5$ [c]	CH_3NHCS	3.74	5.61	13½	DMSO-d_6

[a] Taken from Ref. 1. [b] α-Methylene protons magnetically non-equivalent; pattern and coupling constants obscured by overlapping CH_3NH signal. [c] α-Methylene protons resonance lines appear as part of multiplet due to other protons. [d] α-Methylene protons magnetically non-equivalent; ABC-system observed. [e] Methyl groups magnetically non-equivalent. [f] α-Methylene protons magnetically non-equivalent; AB-system observed with $\Delta\nu_{AB}=0.39$ ppm, $J_{AB}=12\frac{1}{2}$ Hz.

The appearance of an AB pair of doublets in the NMR spectra of III upon cooling must be due to the onset either of slow ring inversion or slow nitrogen inversion. Anderson and Roberts [33] have shown that in 1,2,4,5-tetramethyl-hexahydro-1,2,4,5-tetrazine the barrier to nitrogen-inversion, though here unobservable by the NMR method, is at least as high as the observable barrier to ring inversion. By analogy we assume that the AB systems observed in the spectra of III are due to a relatively high barrier to inversion at the nitrogen atoms. The approximate coalescence temperatures have been determined for a number of compounds and are usually slightly below room temperature (*cf.* Table 5). In spectra of several of the compounds below the coalescence temperature the protons of the α-methylene groups of the alkyl substituents also are magnetically nonequivalent. This effect is another consequence of slow inversion; the resulting multiplets coalesce at approximately the same temperature as the AB-system of the endocyclic methylene protons.

Introduction of acyl or thiocarbamoyl substituents causes a considerably increase in the difference in chemical shift between the axial and equatorial protons of the ring methylene groups (*cf.* Tables 6 and 7), and raises the coalescence temperatures of the AB-system. In general, introduction of *N*-acyl substituents in saturated nitrogen heterocycles of cyclohexane-like structure such as these is expected to lower the barrier to ring inversion by making the nitrogen atom nearly planar.[34] At the same time the acyl (or thioacyl) groups will exert an electron-withdrawing effect, which will increase the electronegativity of the amide nitrogen atoms and in consequence raise the barrier to inversion at the adjacent nitrogen. The increase in energy barrier to inversion observed in XIV and XV relative to III is therefore consistent with the assumption that restricted inversion of the nitrogen atoms is responsible

for the magnetic non-equivalence of the ring methylene protons in III as well as in XIV and XV. The coalescence temperatures of the AB-systems due to the endocyclic CH_2-groups of XIV and XV are very dependent upon the nature of the alkyl substituents. The two doublets in the spectrum of the diacetyl derivative of III*a* collapse to give a singlet between 60 and 80°C, whereas the non-equivalence for most of the other compounds persists above 120°C. Magnetic non-equivalence is also observed for exocyclic groups; the α-methylene protons of the alkyl substituents generally give rise to multiplets (*cf.* Tables 6 and 7), and also groups further removed from the ring may exhibit nonequivalence, *e.g.* the CH_2-groups of propionyl substituents and the CH_3-groups in derivatives of III*h*. These may, however, collapse to identical peaks at temperatures lower than those required for coalescence of the AB-system due to the ring methylene groups.

The preferred conformation of the acyl and thiocarbamoyl derivatives is belived to be as shown in Fig. 7 for the diacetyl derivative of III*a*, with the

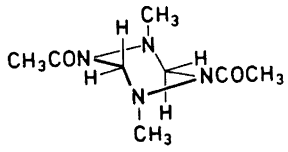

Fig. 7

alkyl substituents axial. This conformation will minimize the steric repulsion of the alkyl and acyl substituents in the same manner as has been found for *N*-acetyl piperidines, in which alkyl substituents at the 2-carbon atoms have been shown to be axial.[35] Simultaneously, this conformation will reduce the interaction of lone-pairs on neighbouring nitrogen atoms.

It is evident from this model that the equatorial proton of the ring CH_2-group will be much more strongly influenced by the anisotropy of the neighbouring carbonyl group than the axial proton. This is borne out by the difference between the chemical shifts of H_a and H_e, which in XIV is 0.8 ppm (average value for $CDCl_3$ solution, slightly less in DMSO-d_6). The corresponding difference in XV is 1.8 ppm, in good agreement with the results obtained by Walter and coworkers [36] for the relative anisotropy of C=O and C=S groups. The average chemical shift of the axial protons in XIV is nearly the same as in XV (τ 5.71 ± 0.15 and 5.52 ± 0.11), confirming that these protons are not subjected very much to the deshielding effects of the acyl or thioacyl groups. Similar values have been found [1] for the axial protons of the ring methylene groups in acyl and thiocarbamoyl 1,4-diphenylhexahydro-1,2,4,5-tetrazines (τ 5.60 ± 0.16), which indicates that the magnetic environment of these protons in acylated hexahydro-1,2,4,5-tetrazines is not affected very much by the substituents on the 1 and 4 nitrogen atoms.

EXPERIMENTAL

Elemental analyses were carried out in the microanalytical department of this laboratory. The NMR spectra were recorded on a Varian A-60A spectrometer, and the mass spectra on an AEI MS-902 mass spectrometer.

Starting materials. The alkylhydrazines employed in the present study were commercial products where available (methylhydrazine, β-hydroxyethylhydrazine, ethylhydrazine oxalate, butylhydrazine oxalate, cyclohexylhydrazine hydrogenoxalate, benzylhydrazine oxalate) or prepared by modified versions of reported procedurs.[37,38] The formaldehyde, unless otherwise noted, was used as a *ca.* 40 % aqueous solution, the formaldehyde content of which was determined before use by titration according to Walker.[39]

Reaction between equimolar amounts of alkylhydrazine and formaldehyde

The 1,4-dialkylhexahydro-1,2,4,5-tetrazines and formaldehyde alkylhydrazones described were prepared by one or more of the procedures *a* – *e*. Physical constants for these compounds are found in Tables 1 and 2; the yields given were not optimized. The identities of the reaction products were ascertained by mass spectrometry,[31] NMR spectroscopy, and elemental analyses.

a. Formaldehyde (0.1 mol) was added slowly with stirring to the alkylhydrazine (0.1 mol), care being taken to keep the temperature of the reaction mixture below 5°C. After 2 h, Na_2CO_3 (2 g) was added and the mixture extracted with 3 × 25 ml chloroform. The organic phase was dried over Na_2SO_4 and the solvent removed *in vacuo*. The residue, which was an oil (formaldehyde alkylhydrazone) or a solid (1,4-dialkylhexahydro-1,2,4,5-tetrazine), was purified by vacuum distillation or recrystallization.

b. Methylene bromide (0.1 mol) was added dropwise to a stirred suspension of Na_2CO_3 (0.1 mol) in alkylhydrazine (0.1 mol). After 8 h the reaction mixture was extracted several times with warm diethyl ether, which was subsequently evaporated to dryness, leaving the solid hexahydrotetrazine.

c. Paraformaldehyde (0.1 mol) was added slowly to a stirred and cooled solution of alkylhydrazine (0.1 mol) in methanol (10 ml). After 2 h at room temperature the reaction mixture was warmed gently for 15 min and Na_2CO_3 (2 g) was added. The solution was extracted with 3 × 25 ml chloroform and worked up as in *a*.

d. To a stirred and cooled suspension of alkylhydrazine oxalate (0.1 mol) and NaOH (0.2 mol) in methanol (100 ml) was added formaldehyde (0.1 mol). The mixture was left overnight, decanted from solid material and the solvent evaporated *in vacuo*; the residue was purified as given under *a*.

e. Formaldehyde (0.1 mol) was added dropwise to a refluxing solution of alkylhydrazine (0.1 mol) in methanol or ethanol (50 ml). After 1 h the reaction mixture was cooled to −30°C, and the precipitated material (III) collected by filtration. The mother liquor was evaporated to half the original volume and extracted with chloroform after addition of Na_2CO_3 (2 g). The organic phase was then worked up as given under *a* to give a second crop of III.

1,4-Dimethylhexahydro-1,2,4,5-tetrazine (III*a*) was prepared as described in the literature and by procedure *c* in 40 % yield. It is best purified by vacuum sublimation (60°C/12 mmHg).

1,4-Diethylhexahydro-1,2,4,5-tetrazine (III*b*) was prepared by procedure *d* and recrystallized from diethyl ether.

1,4-Bis(β-hydroxyethyl)hexahydro-1,2,4,5-tetrazine (III*c*) was prepared by procedure *e* and recrystallized from 2-propanol.

1,4-Bis(β-cyanoethyl)hexahydro-1,2,4,5-tetrazine (III*d*) was prepared by procedure *a*; the precipitated crystals were sufficiently pure after washing with ice cold methanol and diethyl ether.

1,4-Diallylhexahydro-1,2,4,5-tetrazine (III*e*) was prepared according to procedure *a* and recrystallized from diethyl ether. The NMR spectrum of a chloroform extract shows that this contains II*e* as well as III*e*. The relative concentration of these was not determined due to interference from overlapping peaks.

1,4-Dibutylhexahydro-1,2,4,5-tetrazine (III*g*) was prepared by procedure *a* (yields 45–70 %), *b* (yield 40 %), *c* (yield 55 %), *d* (yield 25 %), and *e* (yield 60 %). Preparation according to procedure *e* but run at room temperature gave similar results, as did preparation with 1 ml 4 M aqueous HCl added (procedure *e*). NMR spectra of extracts of the reaction mixture (procedure *a*) after 2 h showed II*g* and III*g* to be present in a ratio of *ca.* 1:3.

Formaldehyde isobutylhydrazone (II*h*) and *1,4-diisobutylhexahydro-1,2,4,5-tetrazine* (III*h*). Procedure *a* was followed, and the reaction mixture was extracted with 4 × 25 ml ether. Removal of the ether and distillation gave II*h* in 75 % yield. This dimerized with formation of III*h* upon standing in a closed vessel at room temperature for a week. Yield 65 % (based on isobutylhydrazine), recrystallized from hexane.

Formaldehyde sec-*butylhydrazone* (II*i*) was prepared as was II*h*, in 55 % yield. Dimerization was not observed but may take place under suitable conditions.

1,4-Bis(β-ethoxyethyl)hexahydro-1,2,4,5-tetrazine (III*j*) was prepared according to procedure *a* and recrystallized from ether.

1,4-Dihexylhexahydro-1,2,4,5-tetrazine (III*l*) was prepared according to procedure *a*. Extraction with chloroform was unnecessary, since III*l* precipitated from the reaction mixture after two days at 4°C. Recrystallized from ether.

Formaldehyde octylhydrazone (II*m*) *and 1,4-dioctylhexahydro-1,2,4,5-tetrazine* (III*m*). Procedure *a* was employed, with methanol (5 ml) added to the reaction mixture to break the emulsion formed. Distillation of the residue after removal of chloroform afforded II*m*, which partly solidified in the receiver as III*m*. NMR spectra of the distillate immediately after distillation showed the ratio II*m*:III*m* to be 1:2; after 2 h at room temperature the ratio was found to be 1:7. III*m* was recrystallized from hexane.

Formaldehyde benzylhydrazone (II*n*) *and 1,4-dibenzylhexahydro-1,2,4,5-tetrazine* (III*n*). Reaction of benzylhydrazine with formaldehyde according to procedure *a* yielded an oil from which crystalline material slowly deposited at room temperature (III*n* in 25 % yield). The liquid was filtered and distilled to give II*n* in 40 % yield. This compound is fairly stable towards dimerization when kept at −30°C (no precipitation of III*n*; NMR spectra taken at frequent intervals showed only slight appearance of III*n* after a week).

Procedure *b*, *c*, and *d* afforded III*n* in yields of 10 %, 45 %, and 10 %, respectively.

An improved procedure for the preparation of III*n* based on the observation that the dimerization of formaldehyde alkylhydrazones is promoted by acid is given below. It is expected that similar procedures for the preparation of other water-insoluble hexahydro-1,2,4,5-tetrazines (C_4 and up) will lead to improved yields.

Benzylhydrazine (0.1 mol) was dissolved in methanol (20 ml) and added to 150 ml aqueous acetic acid/acetate buffer (pH = 5.5, 0.5 mol CH_3COOH per l). Formaldehyde (0.1 mol) was added slowly, with almost instantaneous precipitation of solid material. This was collected by filtration after an hour, dissolved in chloroform and dried over Na_2SO_4. The solvent was removed *in vacuo* and the solid residue was washed with cold ether to give III*n* in 90 % yield.

Acid catalyzed dimerization of II*n*. A methanolic solution of II*n* in methanol (1g in 2 ml) was added slowly to 5 ml aqueous acetic acid/acetate buffer (pH = 5.5), which caused immediate solidification (precipitation) of the organic material. The NMR-spectrum of the solid showed this to be III*n*. Similar addition of II*n* in methanol to water or 0.5 M NaCl was without effect, and the hydrazone was recovered almost quantitatively.

Preparation of III*n in the presence of dipolarophiles*. Benzylhydrazine (0.1 mol) and norbornene (0.1 mol) were dissolved in methanol (20 ml) and cooled to 0°C. Formaldehyde (0.1 mol) was then added slowly and the reaction mixture was left for 4 h, and extracted with chloroform. The solvent was removed *in vacuo* after drying over Na_2SO_4 and the residue taken up in ether. III*n* precipitated overnight at 4°C in 55 % yield.

Similar results were obtained with diphenylacetylene added instead of norbornene.

1,4-Bis(2-phenylethyl)hexahydro-1,2,4,5-tetrazine (III*o*) was prepared by procedure *a*; the reaction mixture was not extracted but left at 4°C for a week. The precipitated material (III*o*) was collected and recrystallized from 2-propanol. NMR spectra of CCl_4 extracts of the mother liquor showed the presence of II*o*, which was not isolated.

Formaldehyde (1-phenylethyl)hydrazone (II*p*) and *1,4-bis-(1-phenylethyl)hexahydro-1,2,4,5-tetrazine* (III*p*). Reaction of (1-phenylethyl)hydrazine with aqueous formaldehyde according to procedure *a* yielded a clear oil, which was distilled to give II*p* in 45 % yield.

NMR spectra of the reaction mixture and of the distillate did not show any III*p* to be present. After one year at 4°C no solid material had precipitated, while after two years nearly complete crystallization had occurred. NMR spectra of the solid showed this to consist of at least 75 % III*p* (the rest being unchanged II*p*). An exact determination of the degree of dimerization was rendered impossible by dissociation III*p*→2II*p* taking place in solution.

Formaldehyde (3-phenylpropyl)hydrazone (II*q*) and *1,4-bis-(3-phenylpropyl)-hexahydro-1,2,4,5-tetrazine* (III*q*). Formaldehyde and (3-phenylpropyl)hydrazine were reacted according to procedure *a*. The reaction mixture was extracted with ether. The extracts were dried over Na_2SO_4 and distilled to give II*q*. This dimerized within five days nearly completely (> 85 % on NMR) when left at 4°C; the resulting III*q* was recrystallized from hexane.

1,4-Bis(2-phenylpropyl)hexahydro-1,2,4,5-tetrazine (III*r*) was prepared according to procedure *a*. III*r* precipitated from the reaction mixture when kept at 4°C for four days. Recrystallized from hexane.

2,5-Diacyl-1,4-dialkylhexahydro-1,2,4,5-tetrazines (XIV*a*–*r*) were prepared by treating an ethereal solution of the appropriate 1,4-dialkylhexahydro-1,2,4,5-tetrazine with excess acetic anhydride and recrystallized from methanol or ethanol. Physical constants for these derivatives are listed in Table 3.

According to Dorn and Dilcher [4] XIV may also be prepared from the crude dialkylhexahydro-1,2,4,5-tetrazine without prior purification. We have found this to be generally true, even though the yields are lower and the purity of the diacylated derivative less satisfactory. In a few instances we have found acetylation with acetic anhydride of the mother liquors from the preparation of III (procedure *a*) to result in formation of isomers of the desired diacyl derivatives (XIV). The identity of these products is not yet clear.

Isomer of XIV*h*. The mother liquor from the preparation of III*h* (procedure *a*, reaction mixture not extracted with chloroform but left at 4°C for a week, when the precipitated III*h* was removed by filtration) was treated with excess acetic anhydride and a catalytic amount of pyridine. The precipitated material was removed after a day and recrystallized from methanol. M.p. 115–116°C. (Found: C 59.30; H 9.90; N 19.78. Calc. for $C_{14}H_{28}N_4O_2$: C 59.12; H 9.92; N 19.70.) The mass spectrum was quite similar to that of XIV*h*,[31] showing the molecular ion at *m/e* 284(4 %) and major fragment ions at *m/e* 241(23 %), *m/e* 143(100 %), *m/e* 142(33 %), *m/e* 141(17 %), *m/e* 113(72 %), *m/e* 99(48 %), *m/e* 87(23 %), *m/e* 86(17 %), *m/e* 85(10 %), *m/e* 84(28 %), *m/e* 57(60 %). The NMR-spectrum ($CDCl_3$) showed four broad peaks at τ 5.6, 5.9, 6.1, 6.3 (total 4H), and peaks at 7.1 (broad d, $J = 7$ Hz, 4H), 7.9 (s, 6H), 8.1–8.7 (m, 2H), 9.0 (d, $J = 6$ Hz, 6H), 9.1 (d, $J = 6$ Hz, 6H).

Isomer of XIV*c*. This compound was prepared in a similar manner. M.p. 133–134°C. (Found: C 48.81; H 7.28; N 16.36. Calc. for $C_{14}H_{24}N_4O_6$: C 48.83; H 7.03; N 16.27.) The NMR-spectrum ($CDCl_3$) showed peaks at τ 5.5–6.1 (broad, 6H), 6.4–6.8 (broad, 4H), 7.8 (s, 6H), 7.9 (s, 6H).

Isomer of XIV*n*. This compound was prepared in a similar manner. M.p. 180–181°C. (Found: C 68.15; H 7.04; N 15.97. Calc. for $C_{20}H_{24}N_4O_2$: C 68.16; H 6.86; N 15.98.) The NMR-spectrum ($CDCl_3$) showed peaks at τ 2.6 (s, 10H), 5.6, 5.8, 6.0 (three broad peaks, total 8H), 8.2 (broad s, 6H).

1,4-Dialkyl-2,5-bis(thiocarbamoyl)hexahydro-1,2,4,5-tetrazines (XV) were prepared by treating the appropriate 1,4-dialkylhexahydro-1,2,4,5-tetrazine in ether or pyridine with an excess of methyl or phenyl isothiocyanate and recrystallized from ethanol. Physical constants for these compounds are given in Table 4.

Thermal stability of XIV and XV. Benzonitrile solutions of the derivatives XIV*a*, *g*, and *n*, or XV*g* and *n* (0.5 g in 10 ml) were heated under reflux for 4 h. Cooling and removal of solvent left unchanged starting material in 80–90 % yield. Similar results were obtained in refluxing nitrobenzene and ethylene glycol.

Reaction between alkylhydrazines and excess formaldehyde

Formaldehyde N-*ethoxymethyl*-N-*methylhydrazone* (V, $R = CH_3$, $R' = C_2H_5$). Formaldehyde (0.3 mol) was added dropwise and with stirring to a solution of methylhydrazine

(0.1 mol) in ethanol (50 ml). After 1 h the reaction mixture was saturated with Na_2CO_3 and extracted with $CHCl_3$. The resulting solution was dried over Na_2SO_4 and distilled to give a clear liquid, b.p. 42–45°C/15 mmHg. (Found: C 51.68; H 10.27; N 23.16. Calc. for $C_5H_{12}N_2O$: C 51.70; H 10.41; N 24.12.) NMR spectrum ($CDCl_3$): τ 3.9 (d, $J=11$ Hz, 1H), 4.1 (d, $J=11$ Hz, 1 H), 5.3 (s, 2H), 6.6 (q, $J=7$ Hz, 2H), 7.2 (s, 3H), 8.9 (t, $J=7$ Hz, 3H).

Formaldehyde N-*methoxymethyl*-N-*benzylhydrazone* (V, $R=C_6H_5CH_2$, $R'=CH_3$) was prepared in a similar manner from formaldehyde (0.3 mol) and benzylhydrazine (0.1 mol) in methanol. B.p. 70–72°C/0.5 mmHg. (Found: C 67.54; H 8.11; N 15.44. Calc. for $C_{10}H_{14}N_2O$: C 67.39; H 7.92; N 15.72.) NMR spectrum ($CDCl_3$): τ 2.8 (s, 5H), 3.9 (d, $J=11$ Hz, 1H), 4.1 (d, $J=11$ Hz, 1H), 5.3 (s, 2 H), 5.6 (s, 2H), 6.8 (s, 3H).

Formaldehyde N-*ethoxymethyl*-N-*benzylhydrazone* (V, $R=C_6H_5CH_2$, $R'=C_2H_5$) was prepared from formaldehyde (0.3 mol) and benzylhydrazine (0.1 mol) in ethanol, as given for the methyl analog (above). B.p. 72–75°C/0.5 mmHg. (Found: C 68.59; H 8.60; N 14.47. Calc. for $C_{11}H_{16}N_2O$: C 68.72; H 8.39; N 14.57.) NMR spectrum ($CDCl_3$): τ 2.9 (s, 5H), 4.0 (d, $J=11$ Hz, 1H), 4.2 (d, $J=11$ Hz, 1H), 5.3 (s, 2H), 5.7 (s, 2H), 6.6 (q, $J=7$ Hz, 2H), 8.9 (t, $J=7$ Hz, 3H). In addition small peaks were observed corresponding to the methoxy analog (see above), which was formed from traces of methanol in the aqueous formaldehyde.

Formaldehyde N-*methoxymethyl*-N-*(2-phenylethyl)hydrazone* (V, $R=C_6H_5CH_2CH_2$, $R'=CH_3$) was formed from (2-phenylethyl)hydrazine (0.1 mol) and formaldehyde (0.3 mol) in methanol. B.p. 77–78°C/0.4 mmHg. (Found: C 69.02; H 8.40; N 14.04. Calc. for $C_{11}H_{16}N_2O$: C 68.72; H 8.39; N 14.57.) NMR spectrum ($CDCl_3$): τ 2.8 (s, 5H), 3.7 (d, $J=11$ Hz, 1H), 4.0 (d, $J=11$ Hz, 1H), 5.5 (s, 2H), 6.4–6.7 (m, 2H), 7.0–7.4 (m, 2H).

*Methylene bis(*N-*methyl*-N′-*methylenehydrazine)* (VI, $R=CH_3$). Methylhydrazine (0.1 mol) was mixed with solid paraformaldehyde (0.2 mol) without a solvent; the reaction mixture was kept at room temperature after the initial exothermic reaction for 10 h, and then made strongly basic with NaOH (pH = 11), saturated with NaCl and extracted several times with ether. The ethereal solution was dried over Na_2SO_4 and distilled. The fraction boiling 60–70°C/11 mmHg was taken and redistilled to produce a clear, slightly yellow liquid, b.p. 65–68°C/11 mmHg (lit.[3] 68–69°C/13 mmHg). (Found: C 46.52; H 9.36; N 43.57. Calc. for $C_5H_{12}N_4$: C 46.85; H 9.44; N 43.71.) NMR spectrum ($CDCl_3$): τ 4.0 (d, $J=11$ Hz, 2H), 4.1 (d, $J=11$ Hz, 2H), 5.3 (s, 2H), 7.3 (s, 6H.)

A higher boiling fraction was collected at 85–90°C/12 mmHg and redistilled to give a clear liquid, b.p. 95–97°C/16 mmHg (lit.[3] 79–80°C/13 mmHg). (Found: C 45.75; H 9.08; N 35.66. Calc. for $C_{16}H_{14}N_4O$: C 45.55; H 8.92; N 35.41.) The NMR spectrum ($CDCl_3$) showed a series of multiplets in the region τ 5.1–6.7 (total 8H), and two sharp singlets at τ 7.4 and 7.6 (each 3H). The latter do not coalesce upon heating to 100°C (in DMSO-d_6). These results are compatible with the structure *5,8-dimethyl-3-oxa-1,5,6,8-tetraazabicyclo[4,2,1]nonane*, (VIII, $R=CH_3$).

Reaction of benzylhydrazine and excess aqueous formaldehyde. Formaldehyde (0.15 mol) was added slowly with stirring and cooling to a mixture of benzylhydrazine (0.1 mol), acetic acid (0.11 mol), and sodium acetate (0.01 mol) in water (10 ml). During the addition III*n* separated as a white solid, which liquefied as more formaldehyde was added. The reaction mixture was left overnight, extracted with chloroform, dried over Na_2SO_4, and evaporated *in vacuo*. The remainder was then taken up in ether, filtered from solid III*n*, and, after removal of solvent, distilled at 190–210°C/2 mmHg. The product became semi-solid when kept at 4°C. (Found: C 72.82; H 7.33; N 19.70. Calc. for $C_{17}H_{20}N_4$: C 72.83; H 7.19; N 19.98.) The NMR spectrum ($CDCl_3$) suggests the product to be a mixture of *methylene bis(*N-*benzyl*-N′-*methylenehydrazine)*, (VI, $R=C_6H_5CH_2$) and *1,4-dibenzyl-1,2,4,5-tetraazabicyclo[2,2,1]heptane*, (VII, $R=C_6H_5CH_2$).

1,4-Dicyclohexyl-1,2,4,5-tetraazabicyclo[2,2,1]heptane, (VII, R = cyclo-C_6H_{11}). Cyclohexyl hydrogenoxalate (0.1 mol) was mixed with formaldehyde (0.16 mol) in 10 ml 50 % methanol. The stirred reaction mixture became nearly homogeneous over 5 min, when a slightly yellow solid precipitated. The reaction mixture was made slightly basic with Na_2CO_3 and then extracted with chloroform. Evaporation of the solvent after drying over Na_2SO_4 left a colorless product, m.p. 138–139°C in 70 % yield. (Found: C 68.20; H 10.65; N 21.13. Calc. for $C_{15}H_{28}N_4$: C 68.13; H 10.67; N 21.19.) NMR spectrum ($CDCl_3$):

τ 6.4 (d, $J = 7.5$ Hz, 2H), 6.7 (s, 2H), 6.8 (d, $J = 7.5$ Hz, 2H), 7.5 – 9.2 (m, 22H). Mass spectrum: *m/e* 264 (3 %, M^+), *m/e* 153 (11 %), *m/e* 139 (92 %), *m/e* 126 (27 %), *m/e* 97 (11 %), *m/e* 83 (100 %), *m/e* 70 (25 %), *m/e* 69 (13 %), *m/e* 68 (25 %), *m/e* 67 (31 %).

REFERENCES

1. Jensen, K. A. and Hammerum, S. *Acta Chem. Scand.* **26** (1972) 1258.
2. Müller, E. and Rundel, W. *Chem. Ber.* **90** (1957) 1299.
3. Schmitz, E. and Ohme, R. *Monatsber. Deut. Akad. Wiss. Berlin* **6** (1964) 425.
4. Dorn, H. and Dilcher, H. *Ann.* **717** (1968) 104.
5. Zurini, M. and Rosicky, J. *Swiss Pat.* 403.784 (1962).
6. Ioffe, B. V., Stopskii, V. S. and Sergeeva, Z. I. *Zh. Org. Khim.* **4** (1968) 986.
7. Hutton, R. F. and Steel, C. *J. Am. Chem. Soc.* **86** (1964) 745.
8. Block, M. J. and Young, D. C. *Nature – New Biology* **231** (1971) 288.
9. Kalm, M. J. *U. S. Pat,* 3,351,838 (1966).
10. Dorman, L. C. *J. Org. Chem.* **32** (1967) 255.
11. Ioffe, B. V. and Potekhin, A. A. *Tetrahedron Letters* **1967** 3505.
12. Potekhin, A. A. *Zh. Org. Khim.* **7** (1971) 16.
13. Howard, J. C., Gever, G. and Wei, P. H. L. *J. Org. Chem.* **28** (1963) 868.
14. Dorn, H., Walter, K. and Arndt, D. *Z. Chem.* **11** (1971) 145.
15. Schmitz, E. and Ohme, R. *Ann.* **635** (1960) 82.
16. Karabatsos, G. J. and Taller, R. A. *Tetrahedron* **24** (1968) 3557.
17. Hammerum, S. *To be published.*
18. Johns, S. R., Lamberton, J. A. and Nelson, E. R. *Aust. J. Chem.* **24** (1971) 1859.
19. Nelsen, S. F. and Hintz, P. J. *J. Am. Chem. Soc.* **94** (1972) 3138.
20. Rabjohn, N. and Sloan, K. B. *J. Heterocycl. Chem.* **6** (1969) 187.
21. Hammerum, S. *Unpublished.*
22. Grashey, R., Huisgen, R., Sun, K. K. and Moriarty, R. M. *J. Org. Chem.* **30** (1965) 74.
23. Zinner, G., Kliegel, W., Ritter, W. and Böhlke, H. *Chem. Ber.* **99** (1966) 1678.
24. Zwanenburg, B., Weening, W. E. and Strating, J. *Rec. Trav. Chim.* **83** (1964) 877.
25. Grashey, R., Leitermann, H., Schmidt, R. and Adelsberger, K. *Angew. Chem. Int. Ed. Engl.* **1** (1962) 406.
26. Schmitz, E. *Ann.* **635** (1960) 73.
27. Oppolzer, W. *Tetrahedron Letters* **1970** 2199.
28. Skorianetz, W. and Kováts, E. sz. *Helv. Chim. Acta* **53** (1970) 251.
29. Condon, F. E. and Farcasiu, D. *J. Am. Chem. Soc.* **92** (1970) 6625.
30. Gafarov, A. N. *Zh. Org. Khim.* **6** (1970) 1552.
31. Hammerum, S. and Møller, J. *Org. Mass Spectrom.* **5** (1971) 1209.
32. Ansell, G. B., Erickson, J. L. and Moore, D. W. *Chem. Commun.* **1970** 446.
33. Anderson, J. E. and Roberts, J. D. *J. Am. Chem. Soc.* **90** (1968) 4186.
34. LeCam, P. and Sandström, J. *Chemica Scripta* **1** (1971) 65.
35. Paulsen, H., Todt, K. and Ripperger, H. *Chem. Ber.* **101** (1968) 3365.
36. Walter, W., Schaumann, E. and Paulsen, H. *Ann.* **727** (1969) 61.
37. Stroh, H.-H. and Scharnow, H.-G. *Chem. Ber.* **98** (1965) 1588.
38. Ohme, R., Schmitz, E. and Sterk, L. *J. prakt. Chem.* [4] **37** (1968) 257.
39. Walker, J. F. *Formaldehyde,* Reinhold, New York 1944, pp. 25 – 27.

Received September 11, 1972.

ACTA CHEMICA SCANDINAVICA 27 (1973) 797–813

The Crystal and Molecular Structure of 4,5-Dichloro-3,6-pyridazinedione

T. OTTERSEN

Department of Chemistry, University of Oslo, Oslo 3, Norway

The crystal and molecular structure of 4,5-dichloro-3,6-pyridazinedione (dichloromaleic hydrazide) has been determined by X-ray methods using 2429 reflections above background level collected by counter methods. The crystals are orthorhombic, space group *Iba*2, with cell dimensions $a = 10.89_3$ Å, $b = 17.05_1$ Å, $c = 13.63_5$ Å. The structure model has been refined on the basis of a low-angle data set (1341 reflections with $\sin\theta/\lambda < 0.71$) and a high-angle data set (1317 reflections with $\sin\theta/\lambda > 0.61$). A comparison between the results of the two refinements is given. The nitrogen-nitrogen bond length is found significantly different in the two cases. Estimated standard deviations in bond lengths are about 0.004 – 0.006 Å, and in angles 0.3 – 0.4°. The molecule is found to be in the monolactim form, but the bond lengths indicate considerable resonance stabilization of the heterocycle. The hydrogen bond system is discussed.

Reactions of maleic hydrazids have been extensively studied (Ref. 1 and references therein). These compounds are interesting as starting materials for the synthesis of a number of drugs. It has also been found that maleic hydrazide is a powerful plant growth inhibitor.[2]

Maleic hydrazide has three possible tautomeric forms (I, II, and III):

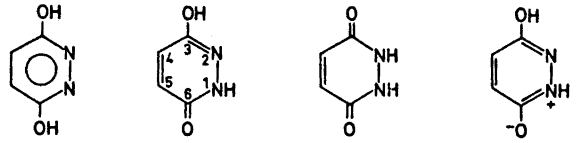

From spectral evidence Druey *et al.*[3,4] concluded that the structure in the solid state corresponds to the monolactim (II). Further evidence for this structure is found in the reaction of maleic hydrazide with diazomethane,[5] in which a methoxy compound is rapidly formed, whereas the 1-methyl-3-methoxy

derivative forms more slowly. Reaction with dimethyl sulphate seems to yield 1-methyl-3-methoxy-6-pyridazone as the kinetic product, while 1,2-dimethyl-3,6-pyridazinedione is the end product.[1]

It has been pointed out that the monolactim permits resonance stabilization of the heterocycle.[5] The unshared pair of electrons on the single bonded nitrogen may be utilized to fill a molecular orbital, giving the resonance structure IV with an sp^2-hybridized N1-atom.

Both 6-amido-3-pyridazone [6,7] and 3-pyridazthione [8] are found to exist in the monolactim form in the crystal.

The main reason for the present structural work was to establish which of the tautomers exist in the solid state.

Errors in parameters connected with the asphericity of the electron density have been discussed.[9–11] Shifts in positional parameters for nitrogen atoms [9] and terminal oxygen atoms [10] may be significant. A refinement based on high-angle data would therefore be of interest.

EXPERIMENTAL

Dichloromaleic hydrazide was synthesized from dichloromaleic anhydride and hydrazine hydrochloride by the method of Mizzoni and Spoerri.[12] The product was recrystallized by slow evaporation of a 70 % ethyl alcohol solution. Rectangular, colourless plate-shaped crystals were formed.

Oscillation, Weissenberg and precession photographs indicated orthorhombic symmetry; reflections (hkl): $h+k+l$ odd, ($0kl$): k odd, and ($h0l$): h odd were systematically absent. Wilsons statistical method later applied on the intensity data indicated a non-centrosymmetric space group. It was therefore concluded that the space group was $Iba2$ with two molecules, called I and II, in the asymmetric unit.

Unit cell parameters were determined with the use of a Picker manual diffractometer using Cu$K\beta$ radiation ($\lambda = 1.3922$ Å) and a take off angle of 1.0°. 37 reflections and their Friedel equivalents were measured. The computer program used in least-squares calculations of cell parameters and programs employed in all subsequent calculations are part of an assembly of programs for CDC-3300 computer.[13]

Three-dimensional intensity data were recorded using an automatic Syntex-P$\bar{1}$ four-circle diffractometer with graphite monochromated Mo$K\alpha$ radiation. The take-off angle was 4°, and the temperature was kept constant within 1° at 18°C.

Intensity data were first recorded for reflections with 2θ less than 60°, and then for reflections with 2θ between 52° and 110°. A crystal of dimensions $0.9 \times 0.42 \times 0.14$ mm^3 was used for the data collection. The $w - 2\theta$ scanning mode was utilized with scan speed variable from 1° to 12° min^{-1} depending on the peak intensity of the reflection. Background counting time was equal to the scan time. Reflections for which the counts exceeded 10^5 cps were remeasured with reduced primary beam intensity. Intensities of six standard reflections were measured for every 50 reflections, and the data were adjusted according to the variations in the test reflection intensity.

Reflections for which the peak counts were less than 50 cps were not measured in the low-angle data set. All reflections with 2θ between 52° and 110°, which had calculated structure factors (based on the structure model found for the low-angle data set) higher than 5.0, were measured in the high-angle data set. The estimated standard deviations were taken as the square root of the total counts with a 2 % addition for adjustment uncertainty. All 1341 reflections measured in the low-angle data set had intensities higher than six times the standard deviation. 1601 reflections were measured in the high-angle data set. Of these, 1317 had intensities larger than twice the standard deviation. These were regarded as "observed" whereas the remaining reflections were excluded from further calculations.

The intensity data were corrected for Lorentz, polarization, and absorption effects.

Atomic form factors used were those of Doyle and Turner [14] for chlorine, oxygen, nitrogen, and carbon, and of Stewart *et al.*[15] for hydrogen. Anomalous scattering factors were obtained from Cromer and Liberman.[16]

CRYSTAL DATA

4,5-Dichloro-3,6-pyridazinedione (dichloromaleic hydrazide) $C_4H_2Cl_2N_2O_2$; m.p. 303 – 305°C; orthorhombic.

$a = 10.892$ (0.002) Å, $b = 17.051$ (0.003) Å, $c = 13.635$ (0.003) Å.

Figures in parentheses are estimated standard deviations. $V = 2532.3$ Å^3; $M = 181.0$, D_{obs} (flotation) $= 1.89$ g/cm^3; $Z = 16$; $D_{calc} = 1.899$ g/cm^3, $F(000) = 1472$; $\mu = 0.95$ cm^{-1}.

Absent reflections: (hkl) for $h+k+l$ odd, $(0kl)$ for k odd, $(h0l)$ for h odd. Space group $Iba2$.

STRUCTURE DETERMINATION AND REFINEMENTS

The structure was solved using the low-angle data. Positions for two of the four chlorine atoms were derived from the Patterson map. The positions for all other non-hydrogen atoms were found in a Fourier map based on these two positions. The structure model was refined to an R of 0.15. Introduction of anisotropic temperature factors for all non-hydrogen atoms and least-squares refinement lowered R to 0.043. Positions of all hydrogen atoms were localized in a difference Fourier map. Least-squares refinements of all positional parameters, anisotropic thermal parameters for non-hydrogen atoms, and isotropic thermal parameters for hydrogen yielded a conventional R of 0.032 and a weighted R_w of 0.019 (refinement A). The overdetermination ratio was 6.8.

The final parameters for non-hydrogen atoms are listed in Table 2 and for hydrogen in Table 3.

Magnitudes and directions of the principal axes of the ellipsoids of vibration are given in Table 4. The total discrepancy between the atomic vibration tensor components and those calculated from the rigid-body parameters found by analysis of the librational, translational, and screw motion of the molecules is 0.016 Å^2 for both molecules. The atomic positions were accordingly corrected for the librational motion.

At this stage the high-angle data were introduced. Refinement of positional and anisotropic thermal parameters for non-hydrogen atoms resulted in a conventional R of 0.066, and a weighted R_w of 0.025 (refinement B). The overdetermination ratio was 7.3. The final parameters are listed in Table 2. This structure model yielded a conventional R of 0.051 for the low-angle data.

A comparison of observed and calculated structure factors is given in Table 1.

Magnitudes and directions of the principal axes of the ellipsoids of vibration are given in Table 4. The total discrepancy between the atomic vibration tensor components and those calculated from the rigid-body parameters found by analysis of the librational, translational, and screw motion of the molecules is 0.019 Å^2 for molecule I and 0.014 Å^2 for molecule II. This indicates that the molecules may be regarded as rigid bodies. The atomic positions were accord-

Table 1. Observed and calculated structure factors. Data based on refinement B. The columns are h, k, l, $10|F_o|$, $|10F_c|$.

0	0	2	168	158
0	0	4	1351	1290
0	0	6	1717	1700
0	0	8	1916	1952
0	0	10	1301	1352
0	0	12	1027	1033
0	0	14	1235	1246
0	0	16	220	219
0	2	0	418	446
0	2	2	1097	1095
0	2	4	1595	1471
0	2	6	1245	1080
0	2	8	1465	1384
0	2	10	461	453
0	2	12	709	707
0	2	14	258	259
0	2	16	158	173
0	2	18	303	296
0	4	0	216	206
0	4	2	74	50
0	4	4	1997	2053
0	4	6	285	265
0	4	8	306	252
0	4	10	1877	1624
0	4	12	662	609
0	4	14	105	81
0	4	16	167	151
0	4	18	199	188
0	6	0	652	711
0	6	2	1485	1556
0	6	4	1577	1604
0	6	6	661	649
0	6	8	359	366
0	6	10	187	143
0	6	12	643	617
0	6	14	430	409
0	6	16	214	190
0	6	18	256	231
0	8	0	1027	1093
0	8	2	44	64
0	8	4	614	626
0	8	6	400	382
0	8	8	257	257
0	8	10	359	384
0	8	12	691	735
0	8	14	275	265
0	8	18	154	156
0	10	0	1084	1133
0	10	2	1299	1362
0	10	4	503	512
0	10	6	92	81
0	10	8	233	241
0	10	10	615	644
0	10	12	803	816
0	10	14	182	160
0	10	16	417	405
0	12	0	80	63
0	12	2	273	270
0	12	4	233	263
0	12	6	653	698
0	12	8	298	301
0	12	12	297	305
0	12	14	143	138
0	12	16	194	194
0	14	0	246	257
0	14	2	509	538
0	14	4	137	142
0	14	6	52	538
0	14	8	256	256
0	14	10	211	231
0	14	14	121	125
0	16	0	126	113
0	16	2	460	496
0	16	4	199	221
0	16	8	303	314
0	16	10	171	170
0	16	12	194	188
0	16	14	173	161
0	18	0	177	171
0	18	2	159	166
0	18	4	517	522
0	18	6	291	300
0	18	8	116	139
0	18	10	188	177
0	18	12	211	195
0	20	2	135	146
0	20	8	259	272
0	22	0	201	200
0	22	4	288	292
1	1	0	191	176
1	1	2	765	706
1	1	4	1226	1104
1	1	6	954	840
1	1	8	1064	944
1	1	10	262	241
1	1	12	444	441
1	1	14	288	264
1	1	18	214	209
1	2	1	870	814
1	2	3	450	426
1	2	5	450	393
1	2	7	163	158
1	2	9	264	192
1	2	11	569	557
1	2	19	191	184
1	3	0	1180	1195
1	3	2	1015	954
1	3	4	1294	1170
1	3	6	603	511
1	3	8	442	388
1	3	10	493	473
1	3	12	112	89
1	3	14	127	110
1	3	18	247	232
1	4	1	1357	1317
1	4	3	1486	1428
1	4	5	630	560
1	4	7	809	731
1	4	9	167	158
1	4	11	961	879
1	4	13	158	151
1	4	15	226	203
1	5	2	530	577
1	5	4	1413	1401
1	5	6	1094	1025
1	5	8	947	867
1	5	10	462	437
1	5	12	127	126
1	5	14	405	356
1	5	18	215	204
1	6	1	941	953
1	6	3	822	859
1	6	5	252	270
1	6	7	489	443
1	6	9	194	181
1	6	11	671	651
1	6	13	270	236
1	6	15	211	195
1	6	17	266	252
1	7	0	174	190
1	7	2	712	743
1	7	4	519	494
1	7	6	1218	1211
1	7	8	483	483
1	7	10	345	348
1	7	12	462	463
1	7	14	149	135
1	7	16	376	339
1	8	1	621	691
1	8	3	722	775
1	8	5	1030	1058
1	8	7	860	882
1	8	9	310	305
1	8	11	388	377
1	8	13	125	129
1	8	15	337	319
1	8	17	185	167
1	9	0	617	614
1	9	2	43	62
1	9	4	935	980
1	9	6	533	539
1	9	8	326	328
1	9	10	311	312
1	9	12	211	236
1	9	16	115	111
1	10	1	986	1060
1	10	3	488	532
1	10	5	291	278
1	10	7	685	695
1	10	9	112	106
1	10	11	324	348*
1	10	13	189	193
1	10	15	197	189
1	10	17	194	190
1	11	0	423	415
1	11	2	841	909
1	11	4	393	434
1	11	6	724	749
1	11	8	341	353
1	11	10	252	242
1	11	12	415	434
1	11	16	372	363
1	12	1	270	304
1	12	3	417	435
1	12	5	104	102
1	12	7	486	514
1	12	9	147	141
1	12	11	172	155
1	12	13	206	204
1	12	15	255	243
1	13	0	436	460
1	13	4	154	157
1	13	6	157	156
1	13	8	272	278
1	13	10	189	215
1	14	1	462	486
1	14	3	269	285
1	14	5	278	290
1	14	7	244	270
1	14	9	300	323
1	14	11	151	150
1	14	13	129	130
1	14	15	110	108
1	15	0	224	227
1	15	2	470	501
1	15	4	253	266
1	15	6	450	479
1	15	8	394	414
1	15	10	155	145
1	15	12	189	198
1	16	1	247	257
1	16	3	252	267
1	16	5	256	256
1	16	7	335	344
1	17	0	320	348
1	17	4	299	303
1	17	6	263	272
1	17	8	124	124
1	17	10	172	175
1	17	12	122	112
1	18	1	107	111
1	18	3	283	299
1	18	5	316	324
1	18	7	173	186
1	18	9	184	191
1	19	0	102	107
1	19	2	207	216
1	19	4	115	118
1	19	6	258	270
1	19	8	166	183
1	20	1	155	155
1	20	3	155	160
1	20	5	154	158
1	21	0	160	165
1	21	4	184	188
1	21	6	129	136
1	22	5	155	152
2	0	0	324	299
2	0	2	195	153
2	0	6	318	300
2	0	8	322	274
2	0	10	1947	1841
2	0	12	689	654
2	0	16	111	106
2	0	18	217	207
2	1	5	313	286
2	1	7	366	313
2	1	9	225	230
2	1	11	957	916
2	1	15	209	187
2	1	17	146	145
2	2	0	309	287
2	2	2	1382	1262
2	2	6	964	836
2	2	8	854	790
2	2	10	371	342
2	2	14	390	364
2	2	18	339	318
2	3	1	1120	1053
2	3	3	528	501
2	3	5	1396	1257
2	3	7	701	651
2	3	9	383	326
2	3	11	684	654
2	3	15	171	171
2	3	17	155	138
2	4	2	101	93
2	4	4	1092	998
2	4	6	910	857
2	4	8	1009	962
2	4	10	422	369
2	4	12	941	888
2	4	14	814	739
2	4	16	187	168
2	5	3	233	236
2	5	5	154	127
2	5	7	594	542
2	5	9	95	95
2	5	11	364	364
2	5	13	108	118
2	5	15	233	211
2	6	0	691	712
2	6	2	1337	1314
2	6	4	918	909
2	6	6	560	513
2	6	8	720	691
2	6	10	594	556
2	6	12	771	712
2	6	16	322	295
2	7	1	377	395
2	7	3	395	368
2	7	5	577	554
2	7	7	259	258
2	7	9	447	412
2	7	11	243	226
2	7	13	299	277
2	7	15	259	232
2	7	17	203	177
2	8	0	251	256
2	8	2	251	242
2	8	4	391	386
2	8	6	413	436
2	8	8	333	315
2	8	10	582	554
2	8	12	429	403
2	8	14	156	133
2	9	1	510	542
2	9	3	185	201
2	9	5	164	168
2	9	7	186	192
2	9	9	339	351
2	9	11	182	201
2	10	0	50	70
2	10	2	747	804
2	10	4	399	397
2	10	6	370	389
2	10	8	183	178
2	10	10	114	126
2	10	12	279	273
2	10	14	162	172
2	11	1	483	478
2	11	3	107	102
2	11	5	261	275
2	11	7	497	515
2	11	9	231	236
2	11	11	179	182
2	11	13	258	249
2	12	0	377	385
2	12	2	452	485
2	12	4	248	264
2	12	6	241	239
2	12	8	367	374
2	12	10	278	289
2	13	1	189	208
2	13	3	229	237
2	13	5	659	674
2	13	7	319	338
2	13	9	183	181
2	14	0	486	522
2	14	2	498	541
2	14	4	458	481
2	14	6	223	238
2	14	8	120	137
2	14	10	294	302
2	14	12	396	407
2	15	1	251	279
2	15	3	219	238
2	15	5	176	188
2	15	7	219	234
2	15	9	169	166
2	15	13	151	151
2	16	2	182	193
2	16	4	110	125
2	16	6	146	154
2	16	8	288	311
2	16	12	177	192
2	17	1	104	100
2	17	5	261	258
2	17	7	115	131
2	18	0	266	282
2	18	2	180	186
2	18	4	191	209
2	18	6	195	200
2	18	8	184	183
2	19	3	189	197
2	19	7	202	206
2	20	2	182	195
2	22	4	159	155
3	1	0	107	78
3	1	2	993	960
3	1	4	1792	1648
3	1	6	762	682
3	1	8	336	322
3	1	10	311	305
3	1	12	290	265
3	1	14	258	239
3	1	18	260	246
3	2	1	1278	1189
3	2	3	800	747
3	2	5	363	361
3	2	7	465	405
3	2	9	317	275
3	2	11	622	600
3	2	13	391	316
3	2	15	249	222
3	2	17	265	244
3	3	0	1008	973
3	3	2	753	725
3	3	4	323	275
3	3	6	1333	1202
3	3	8	892	811
3	3	10	152	132
3	3	12	553	553
3	3	14	297	266
3	3	16	311	281
3	4	1	1193	1148
3	4	3	377	383
3	4	5	946	872
3	4	7	783	734
3	4	9	442	399
3	4	11	412	378
3	4	13	112	115
3	4	15	259	242
3	4	17	129	124
3	5	2	487	479
3	5	4	966	943
3	5	6	333	341
3	5	8	496	483
3	5	10	725	704
3	5	12	487	473
3	5	18	221	212
3	6	1	1147	1129
3	6	3	359	348
3	6	5	124	119
3	6	7	970	936
3	6	11	173	149
3	6	13	199	190
3	6	15	202	189
3	7	0	577	514
3	7	2	1037	1063
3	7	4	924	921
3	7	6	279	269
3	7	8	293	272
3	7	10	328	293
3	7	12	359	341
3	7	16	341	313
3	7	18	158	136
3	8	1	921	948
3	8	3	906	887
3	8	5	354	349
3	8	7	452	449
3	8	9	325	305
3	8	11	704	654
3	8	13	309	277
3	8	15	403	359
3	8	17	140	133
3	9	0	692	720
3	9	2	254	267
3	9	4	307	305
3	9	6	270	276
3	9	8	393	385
3	9	10	404	405
3	9	12	313	305
3	9	14	262	250
3	10	1	247	235
3	10	3	659	673
3	10	5	334	346
3	10	7	170	188
3	10	9	388	406
3	10	11	425	435
3	11	2	343	364
3	11	4	348	358
3	11	6	747	775
3	11	8	573	596
3	11	10	169	168
3	11	12	212	213
3	11	14	166	154
3	12	1	450	493
3	12	3	475	510
3	12	5	486	500
3	12	7	529	554
3	12	9	240	236
3	12	11	251	252
3	12	13	294	290
3	12	15	161	149
3	13	0	399	413
3	13	4	335	337
3	13	6	139	142
3	13	8	127	144
3	13	12	274	286
3	13	14	118	129
3	14	1	346	377
3	14	3	462	503
3	14	5	387	400
3	14	7	212	234
3	14	9	240	239
3	14	11	200	210
3	14	13	153	145
3	15	0	173	175
3	15	2	268	302
3	15	4	273	295
3	15	6	380	408
3	15	12	196	204
3	16	1	166	173
3	16	3	283	301
3	16	5	125	144
3	16	7	131	142
3	16	9	187	198
3	17	0	209	218
3	17	4	128	145
3	17	10	150	159
3	18	1	367	382
3	18	5	187	191
3	18	7	178	179
3	18	9	165	157
3	19	0	143	157
3	19	2	166	172
3	21	0	143	144
3	21	6	185	185
4	0	2	128	98
4	0	4	1211	1117
4	0	6	675	636
4	0	8	468	452
4	0	10	373	394
4	0	12	787	803
4	0	14	505	484
4	0	16	236	225
4	0	18	233	223
4	1	1	1143	1137
4	1	3	317	309
4	1	5	1145	1080
4	1	7	1280	1203
4	1	9	335	313
4	1	11	337	312
4	1	13	179	176
4	1	15	359	352
4	1	17	161	154
4	2	2	621	614
4	2	4	1291	1217
4	2	6	713	665
4	2	8	436	409
4	2	10	541	505
4	2	12	395	397
4	2	14	265	258
4	2	16	240	227
4	2	18	176	159
4	3	1	926	929
4	3	3	1273	1227
4	3	5	519	457
4	3	7	271	258
4	3	9	637	604
4	3	11	542	517
4	3	13	328	300
4	3	15	484	451
4	3	17	342	316
4	4	0	90	52
4	4	2	494	445
4	4	4	675	676
4	4	6	456	439
4	4	8	364	320
4	4	10	857	814
4	4	12	474	440
4	4	14	241	209
4	4	16	154	146
4	4	18	154	147
4	5	1	431	404
4	5	3	862	858
4	5	5	338	352
4	5	7	241	227
4	5	9	262	255
4	5	11	616	577
4	5	15	204	183
4	6	2	790	748
4	6	4	568	559
4	6	6	207	202
4	6	8	304	293
4	6	10	263	253
4	6	12	184	186
4	6	16	144	123
4	7	1	617	623
4	7	3	416	419
4	7	5	424	447
4	7	7	996	1008
4	7	9	321	306
4	7	11	346	323
4	7	13	274	245
4	7	15	179	170
4	8	2	590	598
4	8	4	135	134
4	8	6	537	537
4	8	8	918	896
4	8	10	212	225
4	8	14	229	219
4	9	1	485	503
4	9	3	303	332
4	9	5	666	680
4	9	7	235	243
4	9	9	237	245
4	9	11	159	155
4	9	15	115	116
4	9	17	183	168
4	10	0	204	207

Table 1. Continued.

4	10	2	455	473
4	10	4	635	651
4	10	6	552	568
4	10	8	339	345
4	10	10	231	215
4	10	12	423	420
4	10	14	88	96
4	10	16	158	147
4	11	1	392	393
4	11	3	548	564
4	11	5	314	320
4	11	7	216	219
4	11	9	240	228
4	11	11	172	156
4	12	0	280	295
4	12	2	235	263
4	12	4	255	256
4	12	6	134	129
4	12	8	398	422
4	12	10	223	227
4	12	12	268	266
4	13	1	415	441
4	13	3	135	159
4	13	5	421	444
4	13	7	237	249
4	13	9	267	260
4	13	11	139	156
4	13	15	238	235
4	14	0	217	241
4	14	2	230	247
4	14	4	525	564
4	14	6	93	87
4	14	8	174	193
4	14	12	213	226
4	14	14	163	155
4	15	1	183	184
4	15	3	263	288
4	15	5	136	142
4	15	9	153	174
4	15	11	131	137
4	15	13	178	176
4	16	2	126	158
4	16	4	224	223
4	16	6	157	177
4	17	5	[illegible]	382
4	17	9	[illegible]	259
4	19	1	[illegible]	[illegible]
4	19	7	[illegible]	178
4	22	6	[illegible]	125
5	1		1314	1242
5	1	2	957	[illegible]
5	1	4	[illegible]	323
5	1	6	625	590
5	1	8	147	129
5	1	10	463	463
5	1	12	716	740
5	1	16	338	318
5	2	1	1395	1353
5	2	3	389	355
5	2	5	214	268
5	2	7	879	861
5	2	9	79	79
5	2	11	263	252
5	2	13	292	268
5	2	15	195	177
5	3	0	804	753
5	3	2	1019	1038
5	3	4	1370	1368
5	3	6	544	511
5	3	8	283	278
5	3	10	408	385
5	3	12	353	328
5	3	16	256	237
5	3	18	165	151
5	4	1	292	306
5	4	3	204	198
5	4	5	521	524
5	4	7	282	275
5	4	9	252	266
5	4	13	363	343
5	4	15	317	303
5	5	0	163	116
5	5	2	459	457
5	5	4	284	287
5	5	6	409	418
5	5	8	181	180
5	5	10	557	546
5	5	12	168	180
5	5	14	242	252
5	6	1	387	361
5	6	3	804	795
5	6	5	332	352
5	6	7	198	189
5	6	9	430	448
5	6	11	424	435
5	6	13	119	127
5	7	0	664	652
5	7	2	409	399
5	7	4	283	293
5	7	6	811	800
5	7	8	788	786
5	7	10	165	158
5	7	12	198	199
5	7	14	320	304
5	8	1	790	813
5	8	3	405	427

5	8	5	404	410
5	8	7	517	523
5	8	9	372	374
5	8	11	277	271
5	8	13	263	247
5	8	15	192	185
5	9	0	1556	1586
5	9	2	240	253
5	9	4	572	575
5	9	6	115	122
5	9	8	221	240
5	9	10	429	419
5	9	12	522	519
5	9	14	302	288
5	9	16	172	168
5	10	1	218	250
5	10	3	501	533
5	10	5	341	350
5	10	7	81	99
5	10	9	218	218
5	10	11	153	179
5	10	13	193	190
5	11	0	252	249
5	11	2	316	328
5	11	4	668	698
5	11	8	296	298
5	11	10	191	187
5	12	1	448	447
5	12	3	505	540
5	12	5	243	254
5	12	7	178	182
5	12	9	313	311
5	12	11	399	399
5	13	0	298	314
5	13	2	123	129
5	13	4	112	135
5	13	6	141	149
5	13	8	110	110
5	13	10	232	243
5	13	12	146	136
5	13	14	174	174
5	14	1	399	427
5	14	3	78	90
5	14	5	271	266
5	14	7	181	190
5	14	9	204	202
5	14	11	182	188
5	14	13	310	296
5	15	0	187	211
5	15	4	119	128
5	15	6	275	288
5	15	8	221	240
5	16	1	152	175
5	16	5	167	163
5	16	11	140	134
5	17		117	121
5	17	2	173	187
5	17	10	146	151
5	18	1	170	171
5	18	3	144	171
5	18	5	187	188
5	18	9	311	322
5	19	0	145	150
5	19	2	154	165
5	19	4	108	115
5	19	6	183	196
5	19	8	111	116
5	21	2	173	180
6	0	0	271	318
6	0	2	600	599
6	0	4	432	407
6	0	6	824	834
6	0	8	303	298
6	0	10	153	145
6	0	12	258	236
6	0	14	354	339
6	0	16	345	338
6	1	1	554	555
6	1	3	1012	1010
6	1	5	116	92
6	1	7	285	295
6	1	11	369	355
6	1	13	245	238
6	1	15	444	427
6	1	17	196	190
6	2	0	222	239
6	2	2	696	717
6	2	4	600	573
6	2	6	400	407
6	2	8	102	91
6	2	10	408	395
6	2	12	283	301
6	2	16	276	265
6	3	1	938	928
6	3	3	362	377
6	3	5	449	452
6	3	7	1454	1438
6	3	9	84	88
6	3	11	192	184
6	3	13	323	313
6	3	15	166	158
6	4	0	1054	1034
6	4	2	531	549
6	4	4	322	331
6	4	6	582	574
6	4	8	653	656

6	4	10	340	328
6	4	16	142	132
6	5	1	354	381
6	5	3	235	229
6	5	5	85	94
6	5	7	249	258
6	5	11	306	303
6	5	13	148	144
6	5	15	183	180
6	6	2	158	160
6	6	4	601	611
6	6	6	765	791
6	6	8	337	336
6	6	10	146	137
6	6	14	239	233
6	7	1	129	114
6	7	3	963	995
6	7	5	402	372
6	7	7	289	268
6	7	9	213	208
6	7	11	280	287
6	7	13	115	114
6	8	2	430	452
6	8	4	474	491
6	8	6	92	115
6	8	8	495	506
6	8	10	433	444
6	8	12	387	379
6	9	1	76	94
6	9	3	271	283
6	9	5	567	598
6	9	7	164	186
6	9	9	190	175
6	9	11	351	342
6	9	13	245	254
6	9	15	181	173
6	10	0	355	368
6	10	2	288	287
6	10	4	697	731
6	10	8	329	344
6	10	10	187	181
6	10	14	249	248
6	11	1	369	381
6	11	3	324	342
6	11	5	114	134
6	11	7	82	99
6	11	9	233	242
6	11	11	183	183
6	11	13	193	187
6	12	0	731	765
6	12	2	182	214
6	12	4	277	291
6	12	8	169	169
6	12	10	288	290
6	12	12	123	112
6	13	1	340	358
6	13	3	108	100
6	13	5	399	415
6	13	9	375	387
6	13	11	154	169
6	14	0	142	154
6	14	4	165	171
6	14	6	181	187
6	14	8	212	216
6	14	10	175	187
6	15	1	291	305
6	15	3	193	223
6	15	9	129	111
6	15	11	147	162
6	15	13	192	199
6	16	0	218	236
6	16	2	149	137
6	16	6	259	272
6	16	8	132	124
6	17	1	151	161
6	17	5	185	208
6	17	7	102	108
6	18	2	162	171
6	20	2	118	128
7	1	0	417	419
7	1	2	634	624
7	1	4	183	190
7	1	6	299	305
7	1	8	111	124
7	1	10	256	251
7	1	12	233	239
7	1	16	182	167
7	2	1	601	608
7	2	3	549	546
7	2	5	414	421
7	2	7	254	262
7	2	9	549	568
7	2	11	291	288
7	2	13	118	123
7	3	0	437	451
7	3	2	438	440
7	3	4	198	182
7	3	6	475	465
7	3	8	546	540
7	3	10	187	201
7	3	12	291	300
7	3	14	167	160
7	4	1	249	266
7	4	3	242	243
7	4	5	510	535
7	4	9	104	100

7	4	11	185	187
7	4	13	205	204
7	4	15	224	223
7	5	0	1038	1070
7	5	2	587	599
7	5	4	728	734
7	5	6	375	376
7	5	10	295	281
7	5	12	714	725
7	5	14	339	333
7	5	16	352	344
7	6	1	534	538
7	6	3	448	478
7	6	5	358	374
7	6	7	187	199
7	6	9	201	207
7	6	11	127	133
7	6	13	249	252
7	7	0	190	186
7	7	2	281	301
7	7	4	1025	1029
7	7	6	204	193
7	7	8	389	403
7	7	10	352	351
7	7	12	147	143
7	8	1	140	134
7	8	3	296	308
7	8	5	256	272
7	8	7	257	263
7	8	9	378	392
7	8	13	161	150
7	9	0	84	87
7	9	2	186	190
7	9	4	118	135
7	9	6	227	230
7	9	10	423	428
7	9	14	192	186
7	10	1	397	415
7	10	3	77	86
7	10	5	268	262
7	10	7	217	225
7	10	9	216	212
7	10	11	130	136
7	10	13	326	326
7	11	0	592	640
7	11	2	149	163
7	11	6	358	377
7	11	8	429	434
7	11	14	281	291
7	12	1	353	363
7	12	3	107	103
7	12	5	173	169
7	12	13	139	137
7	13	0	695	717
7	13	2	167	173
7	13	4	158	188
7	13	6	150	155
7	13	8	193	199
7	14	1	100	95
7	14	3	174	186
7	14	5	211	216
7	14	7	185	181
7	14	9	387	399
7	15	0	263	268
7	15	2	236	297
7	15	4	280	312
7	15	6	105	103
7	15	8	186	189
7	15	10	147	150
7	15	12	151	152
7	16	1	263	265
7	16	7	136	139
7	16	11	148	154
7	17	0	142	139
7	17	2	182	203
7	17	4	126	139
7	17	8	223	237
7	18	1	197	208
7	18	3	174	167
7	18	5	152	149
7	19	6	138	142
7	20	3	150	159
8	0	0	686	646
8	0	2	655	681
8	0	4	316	328
8	0	6	531	537
8	0	8	820	841
8	0	10	265	259
8	0	12	392	395
8	0	14	149	140
8	0	16	185	181
8	1	1	474	424
8	1	3	210	193
8	1	5	137	155
8	1	7	691	698
8	1	9	113	134
8	1	11	279	273
8	1	13	24	243
8	2	0	226	234
8	2	2	411	423
8	2	4	486	519
8	2	6	581	629
8	2	8	306	345
8	2	1	165	170
8	2	12	141	146
8	2	14	170	162

8	2	16	170	163
8	3	1	464	461
8	3	3	991	1007
8	3	5	301	309
8	3	7	167	174
8	3	9	262	254
8	3	11	259	251
8	3	13	106	94
8	4	0	244	269
8	4	2	543	575
8	4	4	154	136
8	4	6	245	235
8	4	8	467	485
8	4	12	234	231
8	4	16	155	150
8	5	3	478	483
8	5	5	302	320
8	5	7	307	328
8	5	9	100	95
8	5	11	213	218
8	5	15	139	137
8	6	0	199	201
8	6	2	303	313
8	6	4	657	663
8	6	6	149	157
8	6	8	264	271
8	6	10	262	263
8	6	12	190	195
8	6	14	209	194
8	7	1	373	383
8	7	3	292	285
8	7	5	169	176
8	7	7	379	382
8	7	9	145	139
8	7	13	235	233
8	8	0	117	136
8	8	2	224	252
8	8	4	320	341
8	8	6	207	206
8	8	8	101	111
8	9	1	367	379
8	9	3	77	75
8	9	5	162	146
8	9	7	252	254
8	9	9	305	310
8	9	11	125	126
8	10	0	173	262
8	10	2	161	175
8	10	4	183	194
8	10	6	324	349
8	10	8	241	256
8	10	10	175	185
8	10	12	107	104
8	10	14	174	176
8	11	1	196	221
8	11	3	88	96
8	11	5	149	147
8	11	7	132	138
8	11	9	133	138
8	11	13	253	264
8	12	2	149	149
8	12	6	303	322
8	12	10	201	197
8	13	1	130	138
8	13	3	175	171
8	13	5	295	316
8	13	9	137	153
8	13	11	291	305
8	14	0	143	164
8	14	2	164	177
8	14	4	123	148
8	14	8	152	173
8	15	1	163	177
8	15	9	147	166
8	16	0	289	307
8	16	4	159	173
8	16	10	162	171
8	17	1	215	231
8	18	2	147	158
8	18	4	165	182
9	1	0	616	628
9	1	2	272	281
9	1	4	507	525
9	1	6	256	251
9	1	8	319	321
9	1	1	137	137
9	1	12	325	332
9	1	14	131	137
9	2	1	281	299
9	2	3	506	536
9	2	5	436	454
9	2	7	280	297
9	2	9	353	373
9	2	11	183	196
9	2	13	179	172
9	3	2	224	229
9	3	4	283	287
9	3	6	139	161
9	3	8	324	332
9	4	1	130	148
9	4	3	118	124
9	4	5	296	311
9	4	7	164	158
9	4	9	172	189
9	4	15	259	266
9	5	0	194	187

9	5	2	324	315
9	5	4	239	278
9	5	6	190	190
9	5	8	148	151
9	5	10	214	211
9	5	12	107	110
9	5	14	274	277
9	6	1	485	529
9	6	3	157	165
9	6	5	302	302
9	6	7	253	265
9	6	9	343	367
9	6	13	346	350
9	7	0	232	253
9	7	4	86	63
9	7	6	249	259
9	7	8	224	228
9	7	14	268	267
9	8	1	106	122
9	8	5	376	422
9	8	7	145	159
9	8	9	161	165
9	8	11	128	130
9	9	0	454	474
9	9	4	248	271
9	9	6	221	228
9	9	8	111	119
9	9	12	215	219
9	10	1	290	305
9	10	3	167	186
9	10	5	243	256
9	10	7	214	209
9	10	9	391	407
9	11	0	181	176
9	11	2	206	216
9	11	4	443	471
9	11	8	207	218
9	11	10	220	244
9	11	12	115	114
9	12	1	165	161
9	12	3	154	189
9	12	7	201	209
9	12	9	151	157
9	13	2	263	276
9	13	4	193	217
9	13	8	221	229
9	13	10	209	212
9	14	1	215	220
9	14	3	234	238
9	14	5	185	196
9	15	0	215	225
9	15	6	190	213
9	16	3	203	210
9	17	0	277	292
9	17	2	210	225
10	0	0	203	240
10	0	2	538	568
10	0	4	246	286
10	0	8	545	581
10	0	12	271	298
10	1	1	217	240
10	1	3	573	596
10	1	5	380	410
10	1	7	118	136
10	1	9	155	156
10	1	11	191	196
10	1	13	147	157
10	2	0	91	110
10	2	2	254	280
10	2	4	268	292
10	2	6	345	373
10	2	8	247	276
10	2	10	120	130
10	3	1	250	266
10	3	3	348	357
10	3	5	108	120
10	3	7	177	178
10	3	9	195	203
10	3	11	190	290
10	3	13	225	228
10	4	0	113	123
10	4	2	311	351
10	4	4	125	149
10	4	6	122	120
10	4	8	306	321
10	4	12	178	182
10	5	1	320	329
10	5	5	210	234
10	5	7	522	539
10	5	9	266	288
10	6	0	248	275
10	6	4	135	139
10	6	6	262	278
10	6	8	229	258
10	6	10	163	174
10	7	1	367	385
10	7	7	112	124
10	7	9	165	158
10	7	13	260	263
10	8	0	193	215
10	9	3	321	339
10	9	5	214	241
10	9	7	116	121
10	9	9	162	165
10	9	11	192	198
10	10	2	141	155

Table 1. Continued.

10	10	4	146	151	13	10	3	138	161	12	3	13	245	249	8	3	17	141	140	2	4	24	119	133	7	10	21	91	104
10	10	6	115	129	13	11	2	120	133	13	5	8	234	240	8	1	19	158	155	2	1	25	80	89	7	5	22	137	125
10	10	8	135	140	14	0	4	157	164	13	2	9	277	277	8	4	20	181	170	2	4	26	108	102	7	9	22	117	118
10	11	1	182	184	14	6	4	156	162	0	22	0	198	200	9	17	2	223	225	3	21	0	143	144	7	5	24	119	121
10	11	7	124	118	14	7	3	135	151	0	18	10	180	177	9	16	3	214	210	3	22	5	146	141	7	7	24	87	117
10	11	9	122	123	14	7	5	159	180	0	16	12	190	188	9	15	6	201	213	3	21	8	133	140	7	5	26	82	96
10	12	2	120	132	14	9	3	213	228	0	18	12	199	195	9	2	13	172	172	3	18	9	159	157	8	20	0	120	120
10	12	4	153	171	2	4	0	5706	5971	0	16	14	157	161	9	1	16	179	177	3	17	10	155	159	8	18	2	156	158
10	13	1	262	277	3	5	0	2735	2532	0	12	16	179	194	9	9	16	180	192	3	14	13	146	145	8	17	3	123	119
10	14	2	172	183	2	5	1	1817	1787	0	16	18	188	195	9	2	17	179	181	3	13	14	130	129	8	20	6	152	147
10	14	4	227	238	4	8	0	2480	2633	0	2	20	162	170	9	8	17	150	159	3	17	14	126	127	8	14	8	171	173
10	15	3	145	133	4	0	0	2059	1961	1	19	8	176	183	10	14	2	181	183	3	12	15	154	149	8	16	8	134	131
10	16	2	136	131	2	2	4	1903	1713	1	18	9	188	191	10	16	6	181	187	3	5	16	105	115	8	17	11	121	119
10	16	6	175	187	2	1	3	1625	1498	1	17	10	169	175	10	3	11	203	200	3	15	16	115	110	8	12	12	117	136
11	1	2	141	142	2	1	1	1506	1428	1	15	12	197	198	10	9	11	192	198	3	19	16	150	133	8	13	9	154	153
11	1	4	358	397	2	0	4	2533	2400	1	10	15	186	189	10	17	11	198	192	3	4	17	110	124	8	14	12	139	137
11	1	8	136	153	1	5	0	1648	1686	1	15	16	191	192	10	4	12	178	182	3	8	17	133	133	8	0	14	144	140
11	2	1	306	336	0	22	4	292	292	1	8	17	162	167	10	1	13	158	157	3	9	18	95	106	8	1	15	124	126
11	2	3	240	258	0	10	16	391	405	1	10	17	173	190	11	13	0	163	169	3	4	19	110	108	8	3	15	124	132
11	2	5	269	282	0	2	18	286	296	1	15	18	162	173	11	21	0	159	169	3	10	19	149	131	8	5	15	139	137
11	2	7	209	216	0	0	20	217	219	1	8	19	174	158	11	12	3	190	204	3	5	20	127	124	8	8	16	125	123
11	2	9	241	258	0	12	20	241	244	1	5	20	120	136	11	15	4	174	184	3	2	21	98	111	8	12	16	124	133
11	2	13	255	266	0	0	22	295	307	1	11	20	180	175	11	12	5	192	198	3	6	21	95	107	8	5	17	144	151
11	3	2	97	103	1	7	16	346	339	1	8	21	170	164	11	12	7	187	194	3	1	22	134	139	8	10	18	126	108
11	3	4	282	321	1	11	16	346	363	2	19	7	214	206	11	7	8	219	215	3	5	22	114	110	8	2	20	109	108
11	3	6	233	262	1	6	17	255	252	2	16	12	178	192	11	10	9	175	173	3	5	24	113	112	8	10	22	109	110
11	3	8	173	168	1	3	18	225	232	2	17	15	160	164	11	6	11	165	168	4	22	[illegible]	113	117	9	16	1	117	121
11	4	5	124	129	0	6	16	196	190	2	1	17	138	145	12	11	3	200	199	4	22	6	125	125	9	20	1	154	148
11	4	9	194	196	2	2	18	320	317	2	3	17	145	138	12	13	3	224	225	4	18	[illegible]	134	132	9	19	2	149	147
11	5	[illegible]	331	313	2	3	19	320	312	2	7	17	179	177	12	10	4	200	199	4	15	11	129	137	9	19	4	119	130
11	5	4	224	247	3	7	16	323	313	2	4	20	121	129	12	2	8	199	189	4	16	12	106	124	9	16	5	134	138
11	5	8	181	184	3	2	17	250	244	2	8	21	166	159	12	8	8	228	229	4	13	13	113	128	9	20	7	112	120
11	6	1	182	193	3	1	19	259	246	2	3	21	163	159	12	7	9	177	172	4	9	15	113	116	9	17	8	154	134
11	6	3	294	331	4	3	17	322	316	2	0	22	162	168	13	6	1	232	[illegible]	4	6	16	134	123	9	12	9	154	157
11	6	5	365	333	5	18	9	323	322	2	6	24	152	147	13	2	5	233	223	4	7	17	153	[illegible]	9	6	11	136	[illegible]
11	6	9	349	371	5	14	13	292	297	3	21	6	183	185	13	6	5	205	203	4	4	18	145	147	9	10	11	[illegible]	111
11	6	11	156	168	5	9	14	287	288	3	22	9	182	187	13	7	6	198	206	4	9	19	164	166	9	16	11	107	105
11	7	2	175	183	5	1	16	323	318	3	15	12	196	214	13	8	7	177	183	4	11	19	119	117	9	5	12	95	[illegible]
11	7	4	161	175	6	0	16	342	338	3	11	14	154	154	13	9	8	182	182	4	6	2	121	126	9	7	12	93	102
11	7	6	131	155	6	2	16	266	265	3	14	17	172	182	14	9	2	232	226	4	8	2	[illegible]	82	9	11	12	125	114
11	7	8	198	216	6	0	20	320	314	3	7	18	152	136	14	7	5	178	179	4	8	22	[illegible]	[illegible]	9	8	13	124	136
11	8	1	139	153	7	14	9	399	399	3	2	19	137	137	15	5	2	179	184	4	0	24	113	115	9	10	13	164	153
11	8	3	211	232	7	10	13	321	326	3	12	19	171	173	0	20	6	97	97	5	20	1	127	[illegible]	9	1	14	131	137
11	8	7	164	163	7	5	14	336	333	3	3	20	148	143	0	22	8	139	139	5	22	1	133	143	9	9	14	110	119
11	9	2	216	237	7	11	14	285	291	3	7	2	163	157	0	20	12	113	117	5	19	9	121	116	9	11	14	131	126
11	9	4	154	156	7	5	16	343	344	3	4	21	174	171	0	12	14	137	138	5	21	8	144	132	9	10	17	104	115
11	9	8	129	143	8	13	11	304	305	3	1	24	154	158	0	14	14	13	125	5	15	1	109	119	9	1	18	114	[illegible]
11	10	1	284	303	8	9	15	291	288	4	15	13	179	176	0	22	14	164	155	5	17	1	147	151	9	3	18	99	105
11	10	3	235	238	9	17	[illegible]	284	292	4	19	13	166	172	0	16	16	124	125	5	16	11	135	135	9	7	18	116	111
11	10	5	223	235	9	6	13	339	350	4	14	14	152	156	0	0	18	119	120	5	18	11	126	131	9	2	19	97	112
11	10	7	141	137	9	5	14	274	277	4	4	16	152	146	0	8	18	153	156	5	13	12	135	136	9	8	19	119	143
11	10	9	175	173	9	7	14	268	267	4	10	16	151	147	0	12	18	119	121	5	19	12	135	145	9	16	19	104	118
11	11	2	109	115	10	0	12	292	298	4	1	17	162	154	0	0	24	151	153	5	5	16	123	119	9	4	21	96	104
11	11	6	146	152	11	6	9	364	371	4	9	17	169	168	0	8	24	125	128	5	2	17	143	139	9	5	22	114	109
11	12	3	183	204	11	1	14	285	279	4	2	18	167	159	0	0	26	103	127	5	4	17	112	110	10	17	1	135	131
11	12	5	176	198	13	5	2	289	287	4	6	18	176	174	1	21	[illegible]	161	165	5	6	17	161	161	10	16	2	14	131
11	12	7	171	194	13	3	4	279	281	4	10	18	173	163	1	22	1	136	135	5	10	17	153	165	10	18	2	[illegible]	[illegible]
11	13		166	169	0	20	8	267	272	4	1	19	184	186	1	22	5	158	152	5	6	19	132	131	10	15	3	147	133
11	13	2	141	143	0	4	18	187	188	4	0	20	139	134	1	21	6	135	136	5	8	19	133	129	10	17	3	145	152
11	15	4	172	184	0	6	18	239	231	4	4	20	165	162	1	21	10	109	111	5	1	20	122	113	10	15	5	155	162
12	0	2	254	269	0	2	22	225	238	4	0	22	156	160	1	17	12	124	112	5	2	21	93	111	10	12	6	134	129
12	0	4	212	223	0	6	22	202	218	4	2	24	169	163	1	14	13	131	130	5	6	21	103	100	10	11	7	138	118
12	1	1	202	214	1	12	15	241	243	5	21	2	174	180	1	16	13	134	127	5	8	21	115	102	10	10	8	142	140
12	1	3	135	143	1	1	18	201	209	5	19	6	188	196	1	14	15	112	108	5	9	22	133	143	10	9	9	167	164
12	1	5	119	128	1	5	18	203	204	5	14	11	186	188	1	9	16	117	111	5	4	23	141	137	10	11	9	114	123
12	1	7	236	247	1	2	19	176	184	5	16	13	171	169	1	4	17	138	138	5	1	24	147	145	10	10	10	120	137
12	1	9	236	262	1	7	21	199	194	5	13	14	172	174	1	9	18	134	136	5	3	24	[illegible]	[illegible]	10	13	11	146	438
12	2	2	132	151	2	14	16	203	195	5	15	14	167	166	1	13	18	114	122	6	20	2	122	128	10	12	12	127	118
12	2	4	122	136	2	0	18	208	206	5	8	15	185	185	2	6	16	304	295	6	22	2	112	119	10	5	13	108	106
12	2	6	195	218	2	4	22	219	226	5	9	16	177	168	0	4	22	184	187	6	20	4	131	134	10	2	14	154	145
12	2	8	174	189	3	18	13	220	219	5	3	18	146	151	0	8	22	173	168	6	21	5	111	120	10	6	14	149	150
12	3	1	241	262	3	5	18	213	212	5	5	18	170	167	0	6	24	139	160	6	16	8	137	124	10	3	15	96	99
12	3	5	153	153	3	11	19	216	214	5	11	18	151	153	0	10	24	180	181	6	12	12	108	112	10	5	15	145	146
12	3	7	159	175	4	17	9	260	259	5	4	19	164	158	1	21	4	195	188	6	14	12	92	95	10	7	15	112	116
12	4		151	184	4	14	12	220	226	6	13	11	168	169	1	4	19	103	112	6	4	16	134	132	10	13	15	144	139
12	4	6	124	152	4	13	15	229	235	6	15	11	166	162	1	6	19	137	135	6	6	16	116	120	10	6	16	132	128
12	5	3	399	423	4	2	16	230	227	6	11	13	182	187	1	1	20	121	128	6	16	16	131	128	10	1	17	126	141
12	5	5	261	289	4	0	18	215	223	6	15	13	199	199	1	9	20	129	117	6	3	17	103	115	10	2	18	127	121
12	5	9	142	148	4	8	18	216	206	6	14	14	162	162	1	4	21	98	107	6	13	17	148	150	10	4	18	151	151
12	6	6	143	158	4	7	19	212	206	6	3	15	161	158	1	6	21	98	105	6	0	18	148	145	10	6	18	98	109
12	7	1	136	139	4	1	21	216	208	6	5	15	166	180	1	1	22	144	141	6	4	18	101	111	10	6	20	157	155
12	7	3	144	153	5	3	16	241	237	6	9	15	165	173	1	7	22	99	110	6	12	18	110	109	10	0	22	139	135
12	7	9	163	172	5	7	18	217	223	6	13	15	188	188	1	4	23	100	115	6	4	20	103	109	11	14	1	150	134
12	8	8	212	230	5	3	20	196	193	6	1	17	186	190	1	5	24	99	101	6	3	21	126	114	11	13	2	139	140
12	9	1	225	240	6	10	14	247	248	6	7	17	194	192	1	9	24	105	103	6	1	23	106	105	11	11	6	158	152
12	9	7	234	242	6	6	18	243	240	6	10	18	172	166	2	23	3	157	152	6	2	24	113	101	11	13	6	154	158
12	10	4	189	199	7	17	8	237	237	6	3	19	159	155	2	22	4	160	155	7	21	2	164	170	11	10	7	133	137
12	11	1	136	156	7	4	15	226	223	6	5	19	179	168	2	23	7	146	134	7	18	3	172	167	11	14	7	150	147
12	11	3	177	196	7	3	18	208	206	6	13	19	157	159	2	15	13	149	151	7	20	3	155	159	11	16	7	133	137
12	11	5	161	167	7	7	18	198	197	6	2	20	167	169	2	18	14	120	127	7	18	5	149	148	11	9	8	140	143
12	13	3	206	225	8	17	1	235	230	7	18	1	204	207	2	11	15	114	108	7	20	5	121	130	11	13	8	141	139
13	1	2	161	185	8	7	13	240	233	7	15	8	191	189	2	13	15	143	141	7	19	6	145	142	11	7	10	129	119
13	1	4	155	187	8	11	13	256	264	7	9	14	189	186	2	15	15	104	112	7	16	7	131	139	11	12	11	117	122
13	2	1	136	148	8	0	18	248	246	7	1	16	170	167	2	9	17	128	114	7	15	10	149	150	11	3	12	122	121
13	2	5	211	223	8	2	18	258	253	7	6	17	185	187	2	13	17	115	123	7	16	11	155	154	11	7	12	99	103
13	2	9	259	277	9	13	8	233	229	8	18	4	177	181	2	6	18	90	89	7	15	12	158	152	11	10	13	115	120
13	3	4	247	281	9	11	10	240	244	8	15	9	159	166	2	8	18	121	124	7	17	12	139	140	11	11	14	113	116
13	4	3	169	172	9	13	10	212	212	8	12	10	195	197	2	12	18	132	137	7	8	13	148	150	11	8	15	123	116
13	5	2	265	287	9	9	12	219	219	8	16	10	170	171	2	14	18	118	118	7	12	13	126	137	11	10	15	104	112
13	5	8	216	240	9	4	15	260	266	8	2	14	178	162	2	1	19	117	117	7	15	14	91	111	11	3	16	141	139
13	6	1	214	230	10	14	4	222	238	8	6	14	207	194	2	5	19	103	110	7	9	16	95	101	11	5	16	120	127
13	6	5	183	204	10	3	13	225	228	8	10	14	178	176	2	7	19	146	132	7	8	17	102	118	11	9	16	158	164
13	7	4	127	144	10	7	13	264	263	8	0	16	181	181	2	9	19	147	141	7	2	19	141	147	11	6	17	126	129
13	7	6	181	206	11	2	13	269	265	8	2	16	161	163	2	8	22	103	106	7	4	19	109	119	11	4	19	151	143
13	8	3	154	166	12	9	7	250	242	8	4	16	139	150	2	10	22	121	121	7	1	20	128	137	11	6	19	112	115
13	8	7	163	184	12	1	9	262	262	8	6	16	157	153	2	7	23	113	126	7	8	21	100	113	11	9	20	136	122

Table 1. Continued.

12	11	1	135	150	1	11	22	74	78	4	19	11	83	89	6	12	16	113	103	8	4	14	95	88	10	0	16	98	96
12	10	2	104	112	1	12	23	89	93	4	18	12	76	74	6	14	16	87	88	8	14	14	64	53	10	2	16	108	97
12	14	4	118	130	1	11	24	81	64	4	10	14	97	96	6	11	17	76	67	8	11	15	66	74	10	12	16	89	94
12	11	5	169	167	1	4	25	69	84	4	12	14	62	69	6	17	17	67	71	8	17	15	101	79	10	10	16	76	68
12	6	6	138	158	2	26	0	93	81	4	16	14	91	64	6	2	18	82	76	8	19	15	91	83	10	3	17	78	103
12	14	6	110	117	2	22	2	81	96	4	18	14	75	81	6	14	18	72	72	8	10	16	104	100	10	5	17	79	75
12	4	8	129	119	2	20	6	116	98	4	11	15	84	90	6	16	18	84	82	8	9	17	88	84	10	9	17	66	70
12	6	8	132	133	2	22	6	78	88	4	8	16	85	82	6	1	19	77	83	8	13	17	88	94	10	8	18	106	106
12	16	8	129	125	2	24	6	87	105	4	12	16	79	74	6	7	19	94	89	8	4	18	62	59	10	10	18	71	65
12	3	9	129	122	2	22	8	97	65	4	16	16	72	89	6	9	19	107	102	8	6	18	82	81	10	14	18	70	64
12	5	9	135	148	2	26	8	91	77	4	18	16	100	102	6	11	19	66	67	8	12	18	96	118	10	3	19	85	75
12	2	10	122	124	2	21	9	86	93	4	11	17	67	79	6	15	19	85	60	8	14	18	79	70	10	9	19	88	82
12	3	11	113	120	2	22	10	97	102	4	17	17	123	110	6	6	21	69	82	8	5	19	87	68	10	0	20	86	99
12	5	11	149	154	2	13	13	69	72	4	19	17	75	73	6	10	20	73	64	8	11	19	75	53	11	11	7	67	68
12	7	11	129	119	2	17	13	73	91	4	14	18	69	87	6	12	20	91	66	8	13	19	90	92	11	10	1	69	92
12	13	11	132	131	2	14	14	87	106	4	16	18	77	65	6	5	21	85	78	8	8	20	103	80	11	15	2	94	112
12	4	12	123	139	2	20	14	90	93	4	20	18	93	85	6	0	22	88	84	8	12	20	81	73	11	17	2	74	87
12	1	13	121	124	2	9	15	77	71	4	3	19	85	95	6	4	22	75	62	8	14	20	109	83	11	21	2	123	122
12	0	14	101	114	2	19	15	74	66	4	5	19	64	57	6	10	22	77	78	8	9	21	77	71	11	14	3	75	76
13	9	0	149	134	2	21	15	77	89	4	17	19	82	84	6	12	22	79	88	8	13	21	77	67	11	20	3	79	76
13	9	2	145	136	2	8	16	84	71	4	2	20	74	79	6	7	23	92	72	8	0	22	68	68	11	11	4	104	91
13	11	2	143	133	2	10	16	84	70	4	10	20	94	77	6	13	25	80	61	8	4	22	78	44	11	19	4	70	71
13	4	3	164	172	2	12	16	79	99	4	16	20	81	82	6	1	29	79	68	8	8	22	75	86	11	20	5	74	65
13	6	3	133	139	2	11	17	96	97	4	13	21	69	82	7	22	1	82	75	8	14	22	73	54	11	15	6	81	65
13	8	3	172	166	2	15	17	70	67	4	2	22	85	84	7	19	2	97	96	8	1	23	78	62	11	19	6	96	98
13	10	3	162	161	2	10	18	97	84	4	4	22	91	93	7	22	3	74	69	8	6	24	71	64	11	15	8	100	84
13	7	4	138	144	2	20	18	80	79	4	6	22	97	94	7	19	4	73	71	8	1	25	93	72	11	17	8	82	91
13	10	5	169	121	2	17	19	74	80	4	14	22	95	94	7	17	6	83	95	9	21	0	75	65	11	19	8	67	100
13	9	6	125	118	2	16	20	88	92	4	3	23	76	89	7	21	6	88	59	9	22	1	71	73	11	14	9	64	62
13	12	7	139	142	2	1	21	74	91	4	7	23	69	69	7	23	6	70	86	9	25	2	71	72	11	1	10	83	91
13	3	8	117	126	2	7	21	72	68	4	15	23	78	50	7	19	8	78	59	9	18	3	79	80	11	3	10	78	57
13	6	9	118	113	2	13	21	82	61	4	5	25	85	52	7	21	8	60	61	9	23	4	87	57	11	5	10	107	103
13	3	14	164	163	2	2	22	85	75	4	17	25	73	51	7	23	8	72	63	9	17	6	108	95	11	9	10	88	81
13	1	16	137	130	2	6	22	89	83	4	0	26	80	85	7	17	10	105	95	9	19	6	103	94	11	11	10	67	58
13	5	16	163	111	2	1	23	72	84	4	6	30	72	64	7	19	10	71	58	9	16	7	71	96	11	13	10	67	94
14	1	1	132	131	2	3	23	76	73	5	21	0	60	74	7	21	10	103	98	9	18	7	120	105	11	15	10	83	81
14	3	1	114	116	2	9	23	70	77	5	23	0	76	55	7	12	11	74	86	9	15	8	84	91	11	17	10	92	94
14	5	1	165	170	2	2	24	93	90	5	25	0	71	52	7	18	11	76	83	9	19	8	78	71	11	2	11	63	55
14	7	3	144	151	2	8	24	83	58	5	23	2	92	106	7	20	11	112	104	9	21	8	80	81	11	4	11	76	75
14	0	4	164	164	2	14	24	85	63	5	25	2	91	86	7	11	12	80	88	9	16	9	89	88	11	9	12	83	57
14	6	4	162	162	3	23	0	75	73	5	20	3	76	83	7	13	12	62	74	9	14	11	87	78	11	11	12	93	85
14	10	4	136	146	3	24	1	95	85	5	24	3	101	95	7	14	13	63	82	9	20	11	86	94	11	15	12	66	70
14	1	5	126	130	3	21	2	97	89	5	19	4	110	115	7	18	13	88	89	9	13	12	71	86	11	17	12	75	94
14	0	6	126	134	3	23	2	104	95	5	21	4	77	66	7	13	14	71	78	9	21	12	82	96	11	6	13	90	84
14	3	7	101	114	3	25	2	91	79	5	22	5	84	87	7	2	15	64	69	9	4	13	76	82	11	8	13	92	92
14	5	7	112	122	3	22	3	98	99	5	21	6	103	94	7	6	15	83	90	9	14	13	94	90	11	16	13	96	89
14	13	7	174	164	3	28	3	74	70	5	18	7	99	98	7	8	15	97	99	9	3	14	61	53	11	7	14	63	71
14	2	8	137	147	3	21	4	87	72	5	20	7	110	113	7	10	15	65	61	9	15	14	82	93	11	9	14	74	74
14	2	8	131	121	3	20	4	91	109	5	17	8	104	98	7	12	15	84	85	9	2	15	102	103	11	4	15	71	69
14	3	9	164	155	3	20	5	92	108	5	25	8	69	69	7	18	15	90	80	9	6	15	75	74	11	15	16	119	112
14	1	13	125	121	3	23	6	104	106	5	16	9	57	54	7	3	16	112	105	9	10	15	77	49	11	2	17	105	93
15	9	2	112	120	3	20	7	81	69	5	24	11	76	61	7	17	16	89	93	9	12	15	89	69	11	4	17	101	104
15	2	3	136	150	3	24	7	94	74	5	15	12	88	83	7	2	17	70	84	9	14	15	78	80	11	8	17	87	69
15	7	4	117	119	3	19	8	115	108	5	12	13	91	93	7	4	17	85	83	9	5	16	96	88	11	3	18	79	80
15	2	5	169	158	3	23	8	98	96	5	22	13	64	65	7	10	17	91	59	9	7	16	111	94	11	7	18	84	86
15	1	8	132	126	3	20	9	106	102	5	11	14	77	62	7	12	17	70	76	9	13	16	107	99	11	11	18	91	92
16	3	3	132	142	3	19	10	107	95	5	19	14	75	83	7	14	17	69	84	9	19	16	101	87	11	2	19	91	95
16	3	5	141	139	3	21	10	114	99	5	6	15	98	81	7	1	18	63	54	9	9	18	85	69	11	10	19	71	64
17	9	2	131	136	3	18	11	64	74	5	10	15	89	87	7	5	18	104	85	9	4	19	70	66	11	2	21	75	94
0	20	0	77	64	3	19	12	84	72	5	12	15	109	77	7	9	18	87	102	9	12	19	85	73	11	9	26	83	64
0	24	2	104	99	3	16	13	99	76	5	16	15	96	98	7	11	18	82	72	9	14	19	90	99	12	0	0	99	99
0	26	2	106	99	3	20	13	74	72	5	7	16	75	72	7	6	19	88	91	9	1	20	83	90	12	12	0	57	54
0	24	4	72	86	3	14	15	78	79	5	15	16	89	85	7	8	19	71	93	9	7	20	85	91	12	16	0	62	96
0	20	10	62	55	3	16	15	73	90	5	21	16	93	84	7	14	19	76	66	9	9	20	86	85	12	13	1	96	101
0	26	10	71	65	3	18	15	82	88	5	2	17	135	139	7	18	19	87	76	9	13	20	70	63	12	15	1	67	57
0	8	16	92	79	3	20	15	74	58	5	18	17	97	87	7	3	20	66	63	9	2	21	80	71	12	17	1	100	102
0	14	16	87	93	3	9	16	71	67	5	15	18	77	57	7	12	19	86	82	9	6	21	95	92	12	19	1	68	59
0	24	16	73	72	3	11	16	93	102	5	14	19	80	84	7	18	19	77	76	9	1	22	90	80	12	12	2	87	103
0	18	18	99	101	3	13	16	69	82	5	18	19	71	86	7	3	21	76	63	9	4	23	75	79	12	14	2	85	85
0	20	18	91	97	3	17	16	71	62	5	5	20	74	88	7	5	20	92	96	9	8	23	87	72	12	20	2	71	84
0	6	20	80	83	3	6	17	78	72	5	9	20	71	75	7	7	23	91	82	9	11	24	98	81	12	9	3	92	89
0	10	22	78	66	3	12	17	63	65	5	4	21	79	80	7	9	23	85	64	9	5	24	85	63	12	15	4	107	99
0	2	24	96	91	3	12	17	103	93	5	14	21	69	66	7	17	23	87	88	10	18	0	81	79	12	18	4	91	84
0	8	26	69	71	3	22	17	83	70	5	1	22	76	73	7	2	21	78	92	10	19	1	66	78	12	20	4	82	93
0	10	26	83	71	3	1	23	84	72	5	5	22	67	74	7	6	21	77	65	10	21	1	76	75	12	9	5	101	102
0	0	28	71	65	3	11	20	79	88	5	11	22	75	79	7	2	23	68	72	10	19	3	90	95	12	17	5	63	79
1	25	0	75	59	3	15	20	104	90	5	2	23	69	79	7	4	23	102	90	10	18	4	105	115	12	12	6	103	100
1	23	2	90	74	3	8	21	76	61	5	8	23	77	75	7	6	23	72	63	10	17	5	76	94	12	18	6	89	89
1	22	3	83	85	3	10	21	78	84	5	9	24	71	84	7	8	23	90	58	10	14	6	92	91	12	11	7	79	76
1	23	4	89	71	3	12	21	107	80	5	9	26	71	66	7	6	25	84	63	10	18	6	102	103	12	13	7	101	107
1	25	4	64	65	3	7	22	87	66	5	2	27	71	55	8	24	0	70	71	10	13	7	91	96	12	15	7	99	94
1	23	6	63	80	3	11	22	73	57	8	21	1	83	73	7	19	1	58	67	10	17	7	97	111	12	17	7	107	118
1	20	7	102	97	3	13	22	85	79	8	24	2	59	70	8	21	1	83	81	10	21	7	74	69	12	0	8	97	94
1	22	7	112	116	3	2	23	68	85	8	19	3	76	90	8	20	2	94	88	10	12	8	110	97	12	10	8	105	96
1	20	9	117	104	3	4	23	86	80	8	21	3	67	69	8	22	2	68	68	10	16	8	92	77	12	12	8	69	71
1	26	9	64	69	3	12	23	76	93	8	22	4	99	109	8	19	3	82	81	10	18	8	80	96	12	14	8	87	84
1	18	11	84	93	3	3	24	97	92	8	19	5	60	72	8	21	3	94	97	10	20	8	95	85	12	0	10	65	79
1	19	12	72	61	3	2	25	87	54	8	23	5	83	82	8	17	5	108	102	10	15	9	61	70	12	6	10	104	104
1	21	12	87	72	3	8	25	93	80	8	18	6	118	111	8	19	5	101	99	10	14	10	81	96	12	10	10	73	85
1	18	13	63	55	4	20	2	93	99	8	20	6	78	88	8	21	5	71	64	10	16	10	104	106	12	14	10	66	72
1	22	13	91	80	4	22	2	72	88	8	22	6	99	85	8	16	6	57	57	10	5	11	69	74	12	9	11	106	124
1	17	14	104	93	4	26	2	64	69	8	17	7	102	108	8	18	6	103	93	10	11	11	67	86	12	11	11	83	76
1	21	14	92	71	4	23	3	80	96	8	19	7	94	94	8	21	7	73	73	10	15	11	60	69	12	0	12	114	108
1	20	15	88	87	4	24	4	91	72	8	23	7	63	64	8	18	8	72	74	10	2	12	87	98	12	2	12	85	82
1	17	16	65	73	4	26	4	99	89	8	18	8	86	90	8	20	8	87	72	10	6	12	80	69	12	12	12	71	75
1	12	17	103	97	4	21	5	97	93	8	20	8	98	75	8	24	8	93	65	10	10	12	90	69	12	14	12	75	79
1	14	17	81	79	4	20	6	97	88	8	22	8	92	74	8	14	10	100	105	10	18	12	101	96	12	9	13	79	69
1	18	17	114	109	4	24	6	59	55	8	24	8	66	67	8	18	10	74	81	10	9	13	69	58	12	0	14	92	87
1	7	18	101	80	4	26	6	88	65	8	17	9	128	119	8	11	11	72	70	10	13	13	73	76	12	2	14	93	90
1	11	18	78	88	4	23	7	61	75	8	19	9	92	100	8	8	12	90	93	10	0	14	77	86	12	1	15	95	102
1	10	19	84	84	4	18	8	59	75	8	16	10	84	84	8	10	12	103	104	10	4	14	71	81	12	11	15	94	95
1	14	19	91	101	4	20	8	100	87	8	18	10	73	78	8	16	12	111	112	10	8	14	117	102	12	13	15	91	97
1	16	19	103	92	4	22	8	111	93	8	19	11	65	85	8	18	12	82	77	10	12	14	74	70	12	2	16	114	99
1	15	20	88	77	4	19	9	88	76	8	18	12	100	99	8	9	13	76	74	10	1	15	89	91	12	4	16	98	85
1	2	21	98	98	4	23	9	64	67	8	20	12	129	112	8	13	13	73	84	10	11	15	91	76	12	14	16	99	88
1	9	22	76	55	4	16	10	100	86	8	13	13	84	85	8	17	13	69	55	10	17	15	72	75	12	16	16	72	71

Table 1. Continued.

12	1	17	76	102	13	14	9	90	80	14	6	2	94	101	14	10	10	90	80	15	6	5	114	112	16	12	4	83	77
12	6	18	103	103	13	3	10	61	49	14	8	2	108	108	14	1	11	74	71	15	3	6	91	103	16	7	5	97	79
12	5	19	63	86	13	9	10	84	101	14	12	2	75	72	14	9	11	86	98	15	7	6	95	90	16	13	5	75	77
12	9	19	69	72	13	21	10	79	81	14	16	2	89	94	14	0	12	87	86	15	11	6	121	116	16	0	6	83	67
12	0	20	69	89	13	2	11	75	69	14	1	3	91	91	14	4	14	83	65	15	2	7	69	61	16	4	6	77	75
12	2	20	103	103	13	8	11	89	90	14	5	3	99	92	14	8	14	96	85	15	4	7	113	113	16	6	6	66	68
12	10	20	81	65	13	10	11	99	84	14	13	3	71	68	14	12	14	87	64	15	8	7	125	117	16	10	6	82	85
12	0	22	76	70	13	1	12	72	58	14	17	3	84	70	14	3	15	66	73	15	9	8	91	99	16	7	7	101	97
13	11	0	80	73	13	7	12	67	84	14	4	4	103	110	14	7	15	87	89	15	11	8	69	75	16	9	7	95	101
13	17	0	118	112	13	13	12	78	71	14	8	4	75	103	14	0	16	127	115	15	13	8	94	81	16	0	8	90	85
13	25	0	101	94	13	15	12	72	61	14	12	4	85	101	14	8	16	70	69	15	2	9	82	91	16	8	8	87	90
13	10	1	129	124	13	2	13	94	75	14	16	4	119	119	14	10	16	69	97	15	6	9	107	94	16	10	8	75	69
13	12	1	91	99	13	6	13	104	102	14	3	5	85	84	15	13	0	81	102	15	16	9	75	76	16	16	8	74	71
13	14	1	103	103	13	8	13	67	69	14	9	5	123	114	15	2	1	123	109	15	5	10	91	74	17	17	0	97	86
13	17	2	94	106	13	1	14	86	83	14	11	5	61	71	15	6	1	93	89	15	5	12	91	88	17	5	4	74	69
13	16	3	98	102	13	5	14	115	103	14	13	5	66	68	15	10	1	74	86	15	10	13	70	63	17	2	5	68	63
13	9	4	75	73	13	6	15	124	111	14	2	6	110	97	15	20	1	69	78	15	9	14	107	94	17	7	6	73	68
13	15	4	103	109	13	11	16	109	92	14	4	6	73	71	15	1	2	111	118	15	2	15	99	96	17	1	8	107	101
13	19	4	64	67	13	2	17	67	79	14	8	6	113	108	15	7	2	67	71	15	1	20	82	61	17	5	14	83	70
13	21	4	71	69	13	4	17	86	77	14	10	6	86	99	15	13	2	82	98	16	1	1	112	118	18	4	2	77	66
13	8	5	65	69	13	2	19	86	98	14	14	6	94	108	15	15	2	78	59	16	9	1	63	68	18	2	4	66	81
13	3	6	127	125	13	5	20	93	81	14	1	7	75	59	15	4	3	95	94	16	0	2	101	112	18	8	4	88	87
13	11	6	123	119	14	0	0	117	113	14	0	8	125	111	15	10	3	72	73	16	12	2	94	95	18	0	16	91	76
13	15	6	92	81	14	12	0	77	71	14	4	8	115	100	15	12	3	61	86	16	13	3	92	88	20	0	4	89	79
13	14	7	83	74	14	7	1	101	121	14	6	8	118	116	15	14	3	97	101	16	2	4	104	97	0	28	6	71	58
13	15	8	75	78	14	13	1	82	97	14	10	8	101	114	15	3	4	76	77	16	4	4	84	70	0	30	8	72	45
13	4	9	84	64	14	0	2	93	99	14	1	9	105	104	15	11	4	95	77	16	6	4	93	129	0	24	2	105	99
13	10	9	104	87	14	2	2	73	65	14	5	9	64	64	15	17	4	64	67	16	8	4	107	120	0	20	14	65	31

Table 2. Fractional atomic coordinates and thermal parameters with estimated standard deviations ($\times 10^5$) for non-hydrogen atoms. The first two lines are for low-angle data refinement, the next two lines for high-angle data refinement. The temperature factor is given by $\exp -(B_{11}h^2+B_{22}k^2+B_{33}l^2+B_{12}hk+B_{13}hl+B_{23}kl)$.

Atom	x	y	z	B_{11}	B_{22}	B_{33}	B_{12}	B_{13}	B_{23}
Cl2	−6506	9670	174	1163	380	284	−41	536	58
	10	5	8	9	3	4	10	11	7
	−6481	9641	176	1100	342	315	−50	560	54
	19	10	9	15	4	3	13	11	7
Cl1	1682	13579	22057	818	402	457	−439	182	−108
	9	6	8	8	3	5	9	11	80
	1707	13554	22099	726	370	493	−401	187	−112
	17	12	12	9	5	5	11	12	8
O1	−28424	−671	66	752	517	189	107	−70	−142
	23	19	19	22	11	10	27	28	20
	−28520	−729	68	688	491	204	116	−129	−135
	41	36	20	29	19	7	34	23	20
O2	−14374	6509	36370	802	416	185	−286	−170	19
	25	15	17	22	10	10	24	24	17
	−14409	6442	36463	714	393	201	−313	−166	27
	41	30	17	28	13	7	30	21	15
N1	−30296	−1402	16502	597	370	207	−74	−64	−84
	26	18	19	24	12	13	27	28	19
	−30355	−1354	16569	482	330	217	−94	−83	−34
	35	26	20	22	14	7	25	22	16
N2	−27254	151	26004	555	335	188	−9	1	6
	23	19	20	21	10	11	25	29	18
	−27283	105	25939	478	327	207	−73	2	13
	34	30	18	22	11	7	28	20	16

Table 2. Continued.

C3	−17823	4648	27410	554	253	198	59	−48	26
	28	18	21	26	10	13	26	29	19
	−17833	4637	27429	420	266	210	29	−25	5
	34	27	20	21	10	8	25	21	15
C4	−10739	7903	19510	574	238	247	23	10	17
	28	18	23	24	9	15	26	31	20
	−10688	7909	19448	544	208	237	15	−8	−27
	38	22	22	24	16	8	24	23	15
C5	−14212	6238	10200	663	277	205	110	144	30
	31	20	22	28	12	14	28	30	20
	−14258	6257	10132	532	283	209	51	124	−21
	41	28	20	26	12	7	28	22	16
C6	−24710	1198	8416	628	336	208	151	−61	−35
	29	21	23	24	13	15	30	36	22
	−24802	1197	8430	525	325	204	73	−39	−7
	44	32	21	24	13	8	27	23	17
Cl12	26860	23483	35416	850	414	493	501	−91	−37
	9	6	9	8	3	5	9	11	8
	26865	23467	35404	786	384	505	460	−120	−60
	18	12	13	10	5	5	12	13	9
Cl22	20381	28360	57575	1317	453	319	164	−619	103
	10	6	8	11	4	5	11	13	8
	20303	28334	57595	1216	404	340	151	−600	94
	22	13	10	16	5	3	15	13	7
O12	−674	39422	57973	970	397	223	−178	234	−70
	28	16	20	24	16	11	27	30	19
	−596	39394	57968	900	371	213	−109	165	−90
	50	31	20	35	15	7	35	29	17
O22	11757	31391	21444	765	371	198	258	102	−53
	22	14	17	22	9	10	24	26	17
	11750	31391	21425	723	328	218	205	78	−60
	40	27	18	28	12	7	30	23	15
N12	−3111	39941	41531	582	303	241	2	144	−60
	25	16	20	24	10	14	25	27	18
	−3127	39887	41500	497	248	253	55	103	−68
	34	25	21	21	10	8	23	22	16
N22	−481	38159	31931	607	292	195	20	6	−28
	23	17	20	21	9	12	26	26	19
	−558	38139	32038	449	217	228	43	−16	−39
	35	24	18	22	9	8	24	21	15
C32	8375	33283	30563	522	254	197	−77	−10	−22
	27	18	21	26	10	13	26	30	19
	8444	33307	30483	472	224	213	10	−4	3
	36	24	20	22	9	8	23	22	15
C42	15355	29766	38380	622	268	273	60	−66	−18
	29	19	23	26	11	16	28	33	21
	15342	29817	38373	560	243	249	136	−85	−34
	41	26	23	26	10	9	27	26	17

Table 2. Continued.

C52	12560	31811	47700	715	294	241	−103	−196	88
	31	20	24	30	11	15	31	34	22
	12434	31773	47727	719	255	236	109	−183	12
	52	29	23	35	11	9	35	28	18
C62	2615	37187	49558	660	304	224	−184	−8	−41
	30	21	25	29	11	15	28	36	21
	2569	37166	49567	610	272	209	−94	−1	−51
	44	28	23	26	12	8	28	25	17

Table 3. Fractional atomic coordinates ($\times 10^4$) and isotropic thermal parameters with estimated standard deviation for hydrogen atoms.

Atom	x	y	z	B
HN1	−3703	−522	1436	6.32
	40	27	41	1.37
HO2	−1859	346	4044	4.82
	37	25	37	1.13
HN12	−1006	4377	4302	3.07
	29	19	31	.79
HO22	635	3362	1747	4.30
	36	23	34	1.04

Table 4. R.m.s. amplitudes of vibration $(\overline{u^2})^{\frac{1}{2}}$ (Å) and B-values (Å^2) along the principal axes of vibration given by the components of a unit vector **e** in fractional coordinates ($\times 10^3$). Results from the low-angle data refinement are given in parentheses.

Atom	$(\overline{u^2})^{\frac{1}{2}}$	B	e_x	e_y	e_z
Cl12	.274(.284)	5.94(6.36)	57(58)	44(45)	−14(−8)
	.216(.215)	3.67(3.64)	6(0)	12(8)	72(72)
	.172(.178)	2.34(2.51)	72(71)	−36(−36)	5(6)
Cl22	.290(.299)	6.62(7.07)	83(84)	11(13)	−28(−24)
	.246(.259)	4.77(5.30)	−8(−13)	56(56)	19(17)
	.143(.139)	1.62(1.52)	37(34)	−12(−10)	65(66)
O12	.247(.262)	4.83(5.41)	63(65)	−41(−39)	14(14)
	.222(.224)	3.89(3.98)	66(61)	41(43)	2(7)
	.136(.138)	1.46(1.50)	−14(−19)	7(3)	72(71)
O22	.236(.251)	4.41(4.99)	56(53)	46(48)	−2(0)
	.193(.197)	2.93(3.05)	71(73)	−34(−32)	19(17)
	.139(.132)	1.52(1.37)	−17(−17)	11(8)	71(71)
N12	.195(.213)	3.00(3.57)	19(7)	56(57)	−16(−12)
	.178(.192)	2.50(2.91)	81(86)	−5(8)	34(23)
	.143(.142)	1.62(1.60)	−40(−31)	17(8)	63(68)

Table 4. Continued.

N22	.198(.208)	3.10(3.42)	15(12)	57(58)	−10(−4)
	.163(.192)	2.11(2.87)	−90(−91)	10(−8)	3(5)
	.145(.135)	1.67(1.44)	5(−1)	7(4)	73(73)
C32	.182(.200)	2.61(3.17)	9(53)	58(47)	1(2)
	.168(.180)	2.24(2.56)	−91(−75)	6(33)	2(−5)
	.142(.136)	1.58(1.45)	2(3)	−1(4)	73(73)
C42	.205(.204)	3.31(3.30)	59(54)	43(46)	14(−10)
	.169(.189)	2.24(2.81)	−66(−72)	39(36)	14(9)
	.150(.159)	1.78(1.99)	24(17)	1(2)	71(72)
C52	.218(.225)	2.76(4.01)	80(63)	25(38)	−17(−22)
	.189(.196)	2.81(3.03)	−35(−61)	52(43)	18(5)
	.141(.141)	1.57(1.57)	28(24)	−7(−9)	69(69)
C62	.208(.227)	3.42(4.06)	50(54)	−49(−47)	8(4)
	.184(.183)	2.67(2.64)	77(76)	31(34)	−8(−9)
	.139(.144)	1.52(1.64)	4(6)	9(7)	72(72)
Cl2	.275(.279)	5.98(6.15)	83(85)	−2(−1)	30(26)
	.226(.237)	4.02(4.45)	−2(−1)	58(58)	9(7)
	.140(.136)	1.54(1.45)	38(33)	7(6)	−66(−67)
Cl1	.269(.279)	5.70(6.15)	53(55)	−43(−44)	25(18)
	.208(.202)	3.41(3.22)	−11(−2)	20(18)	68(69)
	.171(.181)	2.31(2.58)	74(73)	34(34)	−8(−12)
O1	.273(.280)	5.90(6.17)	17(15)	57(57)	−11(−10)
	.202(.211)	3.23(3.51)	−89(90)	12(10)	10(3)
	.132(.129)	1.37(1.30)	16(6)	7(7)	72(72)
O2	.260(.265)	5.32(5.53)	−49(−49)	49(49)	7(6)
	.187(.202)	2.77(3.22)	74(75)	31(32)	−19(−14)
	.131(.127)	1.36(1.27)	25(19)	4(2)	71(71)
N1	.223(.236)	3.91(4.39)	19(14)	−57(−57)	3(9)
	.171(.189)	2.32(2.83)	84(89)	10(8)	−27(−13)
	.138(.135)	1.50(1.44)	32(15)	7(8)	68(71)
N2	.221(.222)	3.85(3.90)	16(−2)	58(58)	2(0)
	.168(.183)	2.22(2.63)	90(91)	10(1)	−1(0)
	.139(.133)	1.54(1.40)	0(0)	2(0)	73(73)
C3	.198(.197)	3.10(3.06)	9(41)	58(52)	1(2)
	.159(.180)	2.00(2.55)	−90(−81)	6(25)	13(12)
	.140(.135)	1.55(1.44)	16(12)	−2(−6)	72(73)
C4	.182(.190)	2.61(2.84)	86(54)	19(46)	−6(6)
	.175(.184)	2.42(2.66)	31(35)	−54(−74)	12(2)
	.148(.152)	1.74(1.83)	2(2)	11(5)	72(73)
C5	.206(.215)	3.34(3.66)	20(64)	57(40)	−1(13)
	.182(.189)	2.62(2.81)	84(62)	−12(−42)	25(10)
	.134(.134)	1.42(1.42)	−30(−21)	5(1)	69(71)
C6	.220(.230)	3.83(4.19)	18(39)	57(53)	−2(−6)
	.176(.186)	2.45(2.72)	−89(−82)	12(25)	8(5)
	.138(.139)	1.50(1.52)	11(10)	0(2)	73(72)

ingly corrected for the librational motion. The eigenvalues of **T** are 0.19, 0.17, and 0.14 Å,^{2} and 0.19, 0.18, and 0.14 Å^2 for molecules I and II, respectively. The r.m.s. librational amplitudes are 4.5, 3.7, and 2.5°, and 4.0, 3.2, and 2.8°, respectively. The major axes of libration are nearly parallel to a line through O1 – O2 and a line through O12 – O22 for the two molecules.

For both data sets it was found that effects caused by secondary extinction and anomalous scattering were insignificant.

Standard deviations were calculated from the correlation matrix ignoring standard deviations in cell parameters.

Differences between the results from the two refinements are significant. The thermal parameters are generally smaller in refinement B (see Table 4). This is in agreement with what is usually found.[11]

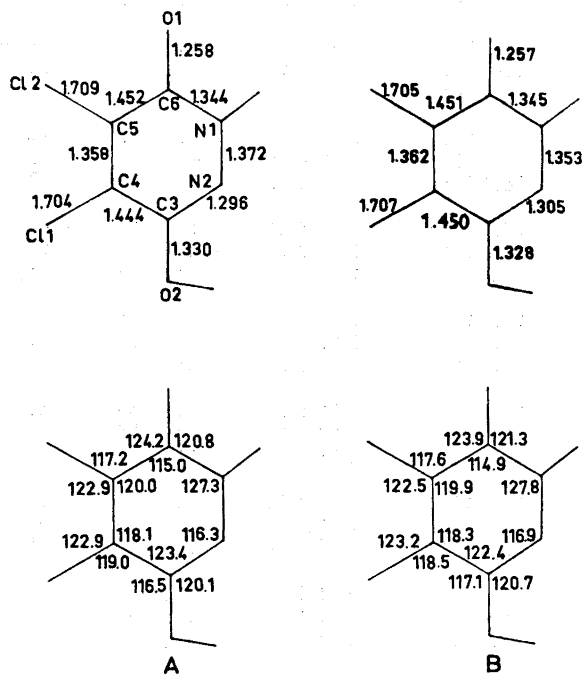

Fig. 1. Mean bond lengths (Å) (corrected for thermal vibration effects), and mean bond angles (°). A, results from low-angle data. B, results from high-angle data.

Mean bond lengths found in the two refinements are listed in Fig. 1. The O2 – C3 bond length, which was found significantly different in the two molecules after refinement A, is found less than one σ different after refinement B. The nitrogen bond length is found 0.019 Å shorter. In molecule II the nitrogen atoms are moved in towards the center of the ring in refinement B as compared with refinement A. This was also found in *s*-triazine.[17] But in molecule I the nitrogen atoms have only moved towards each other. This

is not as expected.[9] Further it was found that the thermal motion in the molecular plane had increased for some of the atoms. It has been noted earlier that parameter shifts attributed to valence electron influence is not a function of the electron density only, but rather of the total crystallographic-experimental environment.[18]

In the discussion only results from the refinement based on high-angle data will be used.

DISCUSSION

Bond lengths and bond angles are listed in Tables 5 and 6 and also in Fig. 1, where the numbering of the atoms is indicated.

The monolactim nature of the molecule is revealed not only by the different carbon-nitrogen and carbon-oxygen bond lengths, but also by the location of the hydrogen atoms on O2 and N1.

Table 5. Bond lengths (Å). Estimated standard deviations in parentheses. Results from the low-angle data refinement are given on the second line for each bond. The first three columns are for molecule I, the next three for molecule II.

	Bond length	E.s.d. ($\times 10^4$)	Corrected bond length	Bond length	E.s.d. ($\times 10^4$)	Corrected bond length
Cl1 – C4	1.697	(37)	1.702	1.706	(48)	1.711
	1.699	(32)	1.705	1.698	(33)	1.703
Cl2 – C5	1.701	(46)	1.706	1.700	(40)	1.704
	1.708	(31)	1.713	1.699	(32)	1.704
O1 – C6	1.254	(40)	1.256	1.255	(41)	1.257
	1.250	(41)	1.252	1.261	(44)	1.263
O2 – C3	1.323	(36)	1.326	1.327	(38)	1.330
	1.317	(36)	1.320	1.336	(35)	1.339
N1 – N2	1.344	(36)	1.348	1.353	(38)	1.357
	1.363	(37)	1.367	1.374	(37)	1.377
N2 – C3	1.303	(54)	1.307	1.298	(53)	1.302
	1.296	(43)	1.301	1.278	(42)	1.291
C3 – C4	1.449	(48)	1.454	1.441	(49)	1.445
	1.437	(42)	1.442	1.440	(42)	1.445
C4 – C5	1.358	(44)	1.363	1.356	(48)	1.360
	1.357	(44)	1.359	1.352	(45)	1.357
C5 – C6	1.455	(74)	1.460	1.436	(76)	1.441
	1.451	(57)	1.456	1.442	(59)	1.447
N1 – C6	1.337	(47)	1.341	1.345	(42)	1.349
	1.335	(42)	1.339	1.344	(43)	1.349
O2 – HO2	0.87			0.88		
	0.89			0.89		
N1 – HN1	1.03			1.03		
	1.02			1.02		

Table 5. Continued.

Hydrogen bond lengths	
O2 – O1 $(x, -y, \frac{1}{2}+z)$	2.598 2.611
N1 – O12 $(x-\frac{1}{2}, y-\frac{1}{2}, z-\frac{1}{2})$	2.953 2.954
O22 – O12 $(-x, y, -\frac{1}{2}+z)$	2.589 2.590
N12 – O1 $(-\frac{1}{2}-x, \frac{1}{2}-y, \frac{1}{2}+z)$	2.963 2.957

Table 6. Bond angles (°). Estimated standard deviations in parentheses. Results from low-angle data refinement are given on the second line. The first columns are for molecule I, the last columns for molecule II.

Atom	Bond angle	E.s.d.	Bond angle	E.s.d.
Cl1 – C4 – C5	123.0	(.31)	123.4	(.31)
	122.2	(.25)	123.5	(.26)
Cl1 – C4 – C3	119.1	(.25)	117.9	(.27)
	119.6	(.23)	118.4	(.24)
Cl2 – C5 – C6	117.8	(.24)	117.4	(.29)
	117.1	(.23)	117.2	(.26)
Cl2 – C5 – C4	122.2	(.37)	122.8	(.39)
	122.8	(.27)	122.9	(.29)
O1 – C6 – C5	123.7	(.40)	124.0	(.40)
	124.0	(.30)	124.4	(.33)
O1 – C6 – N1	121.6	(.49)	121.0	(.45)
	121.4	(.31)	120.2	(.31)
O2 – C3 – N2	120.4	(.31)	120.9	(.31)
	120.4	(.28)	119.8	(.27)
O2 – C3 – C4	117.4	(.36)	116.8	(.38)
	116.7	(.28)	116.3	(.27)
N1 – N2 – C3	117.0	(.30)	116.8	(.31)
	116.6	(.27)	115.9	(.27)
N2 – C3 – C4	122.4	(.27)	122.3	(.28)
	122.9	(.27)	123.9	(.27)
C3 – C4 – C5	117.9	(.37)	118.6	(.29)
	118.1	(.29)	118.0	(.30)

Table 6. Continued.

C4–C5–C6	119.9	(.32)	119.8	(.33)
	120.1	(.28)	119.9	(.30)
C5–C6–N1	114.7	(.30)	115.0	(.29)
	114.7	(.28)	115.3	(.29)
C6–N1–N2	128.1	(.39)	127.5	(.35)
	127.6	(.28)	127.0	(.27)

The mean nitrogen-nitrogen bond length of 1.353 Å is significantly longer and the mean C4–C5 bond length of 1.362 Å significantly shorter than the corresponding bond lengths of 1.330 Å and 1.395 Å, respectively, found in pyridazine.[19] The nitrogen-nitrogen bond and both of the nitrogen-carbon bonds (mean lengths 1.305 Å and 1.345 Å) are significantly shorter than in diacetylhydrazine.[20] The nitrogen-nitrogen bond length is also shorter than those reported for phenylhydrazine [21] and phenylhydrazine hydrochloride.[22]

The double bonds are more localized in dichloromaleic hydrazine than in pyridazine, but resonance stabilization of the heterocycle is still evident.

On the basis of these results it may be concluded that both the nitrogen atoms in the ring are sp^2-hybridized.

The heterocycle is planar, the atoms being displaced from a least-squares plane through the six ring atoms by less than 0.006 Å for both molecules. The oxygen and the chlorine atoms deviate significantly from the plane (see Table 7).

Table 7. Deviations from a least-squares plane through the six ring atoms. The first column is for molecule I, the second for molecule II. (Molecule I: Eqn.: $(-0.0547\,X + 0.0471\,Y - 0.0003\,Z)\,R - 1.771 = 0$. (Molecule II: Eqn.: $(0.0591\,X + 0.0448\,Y - 0.0027\,Z)\,R - 4.777 = 0$.)

Atom	Deviation (Å)	Deviation (Å)
Cl1	−0.030	−0.010
Cl2	−0.038	0.055
O1	−0.021	0.030
O2	0.024	0.033
N1	0.002	−0.002
N2	−0.003	−0.003
C3	0.005	0.006
C4	−0.006	−0.004
C5	0.005	0.000
C6	−0.004	0.003

The chlorine-carbon bond lengths are as expected for bonds between chlorine and an sp^2-hydridized carbon atom. The distortion of the external angles from 120° at C4 and C5 is possibly caused by repulsion between the chlorine atoms in the molecule.

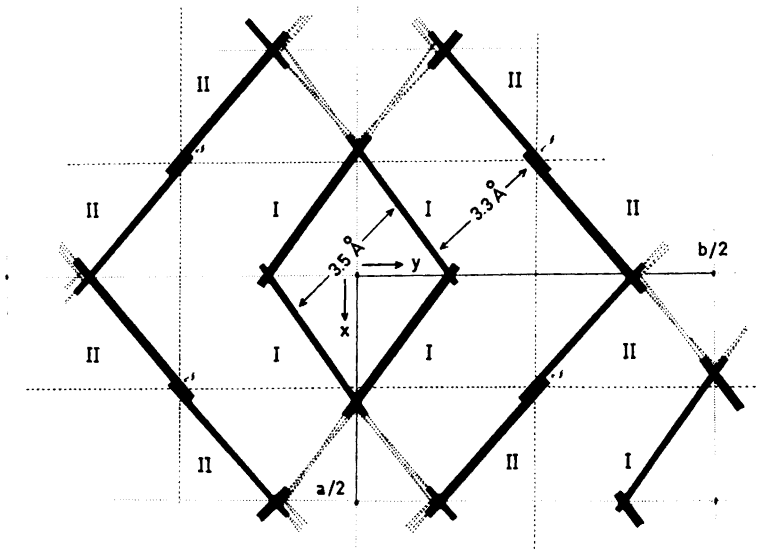

Fig. 2. The crystal structure as seen along the *c*-axis. The figure indicates the numbering of the molecules and the mean distances between the molecular planes. Hydrogen bonds are indicated by dotted lines.

The molecular arrangement in the crystal is visualized in Figs. 2 and 3 and may be described as layers parallel to (110). Within these layers the molecules are hydrogen bonded from O2(O22) to O1(O12).

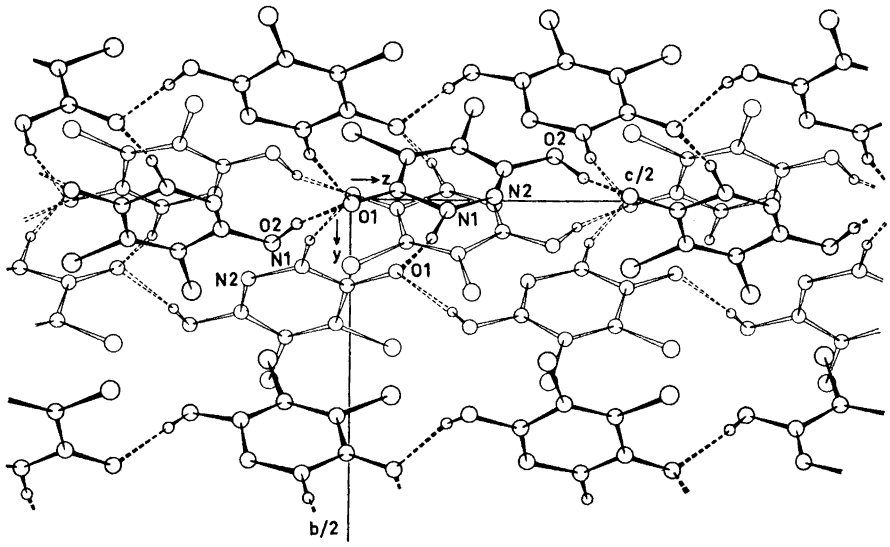

Fig. 3. The crystal structure as seen along the *a*-axis.

Each molecule of type I (II) is bonded to two molecules of type II (I) by hydrogen bonds parallel to (420) from N1 to O12 and from N12 to O1. The N1 – O12 hydrogen bond is close to the plane through molecule I and the N12 – O1 hydrogen bond to the plane through molecule II.

Between the layers the bonding seems to be dominated by van der Waals forces with many short contacts (3.2 – 3.6 Å) (see Fig. 3).

Acknowledgement. The author thanks Professor H. Hope for helpful discussions.

REFERENCES

1. Eichenberger, K., Staehelin, A. and Druey, J. *Helv. Chim. Acta* **37** (1954) 837.
2. Schoene, D. L. and Hoffmann, D. L. *Science* **109** (1949) 588.
3. Druey, J., Meier, K. and Eichenberger, K. *Helv. Chim. Acta* **37** (1954) 121.
4. Eichenberger, K., Rometsch, R. and Druey, J. *Helv. Chim. Acta* **37** (1954) 1299.
5. Arndt, F. *Angew. Chem.* **61** (1949) 397.
6. Cucka, P. and Small, R. W. H. *Acta Cryst.* **7** (1954) 199.
7. Cucka, P. *Acta Cryst.* **16** (1963) 318.
8. Carlisle, C. H. and Hossain, M. B. *Acta Cryst.* **21** (1966) 249.
9. Dawson, B. *Acta Cryst.* **17** (1964) 990.
10. Coppens, P. and Coulson, C. A. *Acta Cryst.* **23** (1967) 718.
11. Coppens, P. *Acta Cryst.* **B 24** (1968) 1272.
12. Mizzoni, R. H. and Spoerri, P. E. *J. Am. Chem. Soc.* **76** (1954) 2201.
13. Dahl, T., Gram, F., Groth, P., Klewe, B. and Rømming, C. *Acta Chem. Scand.* **24** (1970) 2232.
14. Doyle, P. A. and Turner, P. S. *Acta Cryst.* **A 24** (1968) 390.
15. Stewart, R. F., Davidson, E. R. and Simpson, W. T. *J. Chem. Phys.* **42** (1965) 3175.
16. Cromer, D. T. and Liberman, D. *Private communication.*
17. Coppens, P. *Science* **158** (1967) 1577.
18. Stevens, E. D. and Hope, H. *Abstr. Am. Cryst. Ass. Summer Meeting*, 1971.
19. Werner, W., Dreizler, D. and Rudolph, H. D. *Z. Naturforsch.* **22a** (1967) 531.
20. Shintani, R. *Acta Cryst.* **13** (1960) 609.
21. Srinivasan, S. and Swaminathan, S. *Z. Krist.* **127** (1968) 442.
22. Koo, H. C. *Bull. Chem. Soc. Japan* **38** (1965) 286.

Received September 11, 1972.

ACTA CHEMICA SCANDINAVICA 27 (1973) 814–822

Refinement of the Crystal Structure of Thenardite, Na_2SO_4(V)

ANDERS G. NORD

Institute of Inorganic and Physical Chemistry, University of Stockholm, Box 6801, S-113 86 Stockholm, Sweden

The crystal structure of thenardite, Na_2SO_4(V), has been analysed and refined by the method of least squares on the basis of three-dimensional X-ray diffractometer data down to a final R value of 3.6% for about 800 independent reflections. At 25°C the orthorhombic (*Fddd*) unit cell has the dimensions $a = 5.8596$, $b = 12.3044$, $c = 9.8170$ Å. The investigation has confirmed the general features of the atomic arrangement reported in 1932 by Zachariasen and Ziegler. The crystal structure may be described in terms of distorted NaO_6 octahedra and nearly regular SO_4 tetrahedra. All S–O distances in these are 1.476 ± 0.001 Å.

This investigation was performed in order to elucidate the size and configuration of the sulphate ion as precisely as possible. For this reason the thenardite phase is convenient since all S–O distances are equal due to the space group (*Fddd*) where the sulphur atom is fixed in a special point position with 222 point symmetry. Moreover, it is interesting to compare the regularity and dimensions of the sulphate ion in different sulphates.

The phase diagram of sodium sulphate shows some very interesting features. According to Gmelin [1] there are eight different anhydrous phases of sodium sulphate. The crystallographic data of most of these phases are quite unsatisfactory and insufficient. The phase Na_2SO_4(V) is usually called thenardite after the mineral. It is reported to be stable between 32°C and about 180°C.[1] It seems that the presence of traces of H_2O in inclusions changes the conditions for the stability of thenardite.[2]

The present results have confirmed the general features of the atomic arrangement reported in 1932 by Zachariasen and Ziegler.[3]

EXPERIMENTAL

Preparation of the crystals. When a water solution of sodium sulphate is evaporated above 32°C, crystals of thenardite are formed (but below 32°C $Na_2SO_4.10H_2O$ crystals are obtained). There are several contradictory recommendations in the literature as to

proper conditions for the evaporation process.[1,2] A fairly quick evaporation overnight at 70°C gave the most well-developed crystals. This was the best result from a series of experiments. These crystals also gave the most distinct powder diffraction pattern. The sample contained small amounts of moisture; on ignition the loss of H_2O was 0.14 %.

X-Ray powder diffraction data. The powder pattern of the sample was found to be in good accordance with the data given by Swanson and Fuyat.[4] Values for the cell dimensions were calculated from a photograph taken with strictly monochromatized Cu$K\alpha_1$ radiation ($\lambda = 1.54050$ Å) in a Guinier-Hägg type focusing camera. Potassium chloride ($a = 6.29228$ Å) [5] was used as an internal standard. The lattice parameters were

Table 1. X-Ray powder data for Na_2SO_4(V) at 25°C. Cu$K\alpha_1$ radiation ($\lambda = 1.54050$ Å).

hkl	$\sin^2\theta$ obs	$\sin^2\theta$ calc	I_{obs}	*d* (Å) obs	*d* (Å) calc
111	0.02736	0.02735	60	4.6567	4.6572
022	0.04028	0.04030	16	3.8378	3.8369
131	0.05873	0.05870	47	3.1784	3.1791
040	0.06278	0.06270	41	3.0742	3.0761
113	0.07660	0.07660	100	2.7830	2.7830
220	0.08478	0.08479	45	2.6453	2.6452
202	0.09370	0.09374	1	2.5163	2.5158
004	0.09859	0.09850	1	2.4531	2.4542
133	0.10799	0.10795	5	2.3439	2.3443
222	0.10931	0.10940	22	2.3297	2.3287
151	0.12142	0.12140	4	2.2105	2.2106
044	0.16124	0.16120	4	1.9182	1.9185
311	0.16562	0.16559	2	1.8927	1.8929
153	0.17070	0.17065	47	1.8643	1.8646
115	0.17508	0.17510	6	1.8408	1.8407
224	0.18336	0.18330	6	1.7988	1.7991
260	0.21026	0.21019	21	1.6798	1.6801
313	0.21490	0.21484	12	1.6616	1.6618
244	0.23030	0.23031	6	1.6050	1.6050
262	0.23472	0.23481	3	1.5898	1.5895
026	0.23732	0.23730	3	1.5811	1.5812
333	0.24618	0.24619	20	1.5524	1.5524
351	0.25967	0.25964	3	1.5116	1.5116
173	0.26471	0.26470	10	1.4971	1.4971
400	0.27651	0.27647	1	1.4648	1.4649
206	0.29073	0.29074	11	1.4285	1.4285
371	0.35370	0.35369	4	1.2951	1.2951

refined from 27 reflections (Table 1) by the method of linear regression using the program POWDER.[6] The dimensions of the orthorhombic unit cell (with standard deviations) at 25°C are:

$$\left.\begin{array}{lll} a = & 5.8596 \pm 5 \text{ Å} & (5.863) \\ b = & 12.3044 \pm 12 \text{ Å} & (12.304) \\ c = & 9.8170 \pm 10 \text{ Å} & (9.821) \end{array}\right\} \text{ Ref. 4.}$$

From X-ray photographic methods (oscillations and Weissenberg photographs around the *a* and *c* axes) the space group was, from the reflections systematically absent, uniquely determined as No. 70, $Fddd$ [7] in agreement with Zachariasen and Ziegler. The crystal selected for collection of X-ray data had the dimensions 0.15 mm (in the direction of the *c* axis) × 0.06 mm × 0.03 mm and was mounted along the *c* axis. The X-ray intensity data were collected with $\theta - 2\theta$ scan technique on an automatic single-

crystal diffractometer Siemens AED (Automatischer Einkristall-Diffraktometer) equipped with a graphite monochromator and a scintillation detector. Mo$K\alpha$ radiation was used. All independent reflections with $\theta \lesssim 50°$ were measured at a temperature of 22°C. Punched paper tape was used as input/output medium for the diffractometer. The computer programs used for the calculations involved in the present work are summarized in Table 9. A survey of the IBM 360/75 programs used at this institute is also given in a paper by Brandt and Nord.[8]

All reflections with $\sigma(I_{net})/I_{net} < 0.50$ were accepted leaving 812 reflections from about 900 measured ones. The net intensities were corrected for Lorentz, polarization and absorption ($\mu = 10.3$ cm^{-1}) effects.

REFINEMENT OF THE CRYSTAL STRUCTURE

All atom position parameters were readily determined from peaks in a three-dimensional Patterson function $P(uvw)$. These parameters agreed within a few per cent with those given by Zachariasen and Ziegler. The crystal structure was then refined by the full-matrix least-squares program LALS minimizing $\sum w(|F_{obs}| - |F_{calc}|)^2$. Hughes' weighting function [9] with $h = 4$ was used in the final refinements. The atomic scattering curves applied were those for S^0, Na^+, and O^-. Correction was made for the real part of the anomalous dispersion. After a few cycles with isotropic temperature factors the reliability index $R = \sum||F_{obs}| - |F_{calc}||/\sum|F_{obs}|$ dropped to 5.0 %. When all atoms in the model were allowed to vibrate anisotropically (within the restrictions fixed by the space group symmetry) the final R was reduced to 3.6 % for all 812 reflections. This large drop in weighted and unweighted R values from the isotropically to the anisotropically refined model enables the Hamilton test [10] to show, that the model with anisotropically vibrating atoms is the more realistic one. The weighting scheme obtained in the final cycle of the anistropic refinement is shown in Table 2. Reflections with $1.20 < |F_{obs}/F_{calc}| < 0.70$ were given zero weight in the refinement.

A list of the observed and calculated structure factors is presented in Table 3. The atomic parameters arrived at in the last cycle of anisotropic refinement are listed in Table 4. The temperature factors obtained in the

Table 2. Weight analysis obtained in the final cycle of the anisotropic least-squares refinement of thenardite. w = weighting factor, $\Delta = ||F_{obs}| - |F_{calc}||$.

Interval F_{obs}	$\overline{w\Delta^2}$	Number of independent reflections	Interval sin θ	$\overline{w\Delta^2}$	Number of independent reflections
0.0 – 7.4	1.08	75	0.000 – 0.362	1.35	84
7.4 – 9.3	1.15	76	0.362 – 0.456	1.31	93
9.3 – 11.5	1.08	76	0.456 – 0.522	1.11	81
11.5 – 13.6	0.91	75	0.522 – 0.575	0.96	85
13.6 – 16.5	0.88	77	0.575 – 0.619	0.88	81
16.5 – 20.3	0.90	75	0.619 – 0.658	0.77	82
20.3 – 26.4	0.86	75	0.658 – 0.693	0.85	70
26.4 – 35.9	1.31	74	0.693 – 0.724	0.97	66
35.9 – 51.8	0.97	75	0.724 – 0.753	0.81	68
51.8 – 206.1	0.87	76	0.753 – 0.780	0.72	44

Table 3. Observed and calculated structure factors of thenardite, Na_2SO_4(V).

h	k	l	F_o	F_c
2	26	0	19.9	-20.7
4	24	0	27.8	-27.4
0	24	0	17.6	16.4
6	22	0	13.4	-13.7
2	22	0	35.9	35.3
8	20	0	13.0	-12.9
4	20	0	45.8	45.2
0	20	0	28.2	-28.1
6	18	0	39.0	38.5
2	18	0	46.1	-45.8
8	16	0	32.4	32.0
4	16	0	33.2	-32.7
0	16	0	95.5	95.4
10	14	0	11.4	11.7
6	14	0	62.4	-61.7
2	14	0	68.6	68.5
8	12	0	46.7	-45.7
4	12	0	60.4	60.5
0	12	0	124.5	-125.3
6	10	0	50.9	50.7
2	10	0	127.3	-127.7
12	8	0	17.5	-17.8
8	8	0	37.4	36.6
4	8	0	153.5	-156.0
0	8	0	55.1	57.1
10	6	0	45.0	44.2
6	6	0	59.1	-59.3
2	6	0	190.5	191.9
12	4	0	22.0	21.6
8	4	0	51.7	-51.5
4	4	0	145.0	148.5
0	4	0	206.0	-208.3
10	2	0	24.2	-24.2
6	2	0	116.0	116.5
2	2	0	187.3	-189.3
12	0	0	20.9	-20.7
8	0	0	74.1	73.6
4	0	0	64.3	-66.6
3	25	1	8.1	-7.7
1	25	1	8.0	-9.5
5	23	1	9.3	-8.8
3	23	1	16.8	-17.3
5	21	1	14.4	-13.6
3	21	1	17.5	19.1
7	19	1	5.6	-4.9
5	19	1	7.6	7.5
3	19	1	10.8	11.3
1	19	1	16.3	-17.6
7	17	1	16.0	14.4
5	17	1	18.5	19.9
3	17	1	10.1	-9.6
1	17	1	13.1	-14.2
9	15	1	6.6	6.4
7	15	1	23.4	24.2
5	15	1	13.2	-12.3
3	15	1	6.8	3.9
1	15	1	30.8	31.7
11	13	1	6.1	4.5
9	13	1	10.7	11.6
7	13	1	21.4	-21.2
5	13	1	5.6	-3.3
1	13	1	41.5	42.2
11	11	1	5.5	3.7
9	11	1	7.6	-7.5
7	11	1	15.1	-14.5
5	11	1	26.6	27.8
3	11	1	27.5	28.2
11	9	1	10.4	-11.8
9	9	1	19.5	-20.2
7	9	1	5.3	4.3
5	9	1	8.4	8.8
3	9	1	40.1	-40.4
1	9	1	9.8	-11.7
11	7	1	13.4	-15.0
9	7	1	17.1	17.2
7	7	1	4.9	-4.0
5	7	1	19.8	-20.7
3	7	1	61.9	-63.3
1	7	1	15.8	-15.4
11	5	1	8.3	10.1
9	5	1	8.0	7.8
7	5	1	7.9	-7.9
5	5	1	40.8	-41.9
3	5	1	61.0	61.5
1	5	1	50.9	-48.1
11	3	1	9.8	9.9
9	3	1	19.4	-18.6
7	3	1	21.4	-22.8
5	3	1	3.2	-2.3
3	3	1	19.0	-17.3
1	3	1	103.1	-107.8
9	1	1	6.1	-5.7
7	1	1	37.4	38.1
5	1	1	24.2	24.9
3	1	1	38.3	37.1
1	1	1	83.4	-83.2
2	26	2	8.7	8.6
0	26	2	8.0	-8.2
2	24	2	9.4	-10.4
4	22	2	14.3	-14.9
8	20	2	7.1	-7.3
6	20	2	6.3	-7.5
4	20	2	7.6	-8.2
2	20	2	14.0	13.4
8	18	2	7.7	-7.0
6	18	2	10.7	-12.0
4	18	2	12.6	13.1
2	18	2	21.0	-21.5
0	18	2	16.2	-16.2
8	16	2	4.2	2.9
6	16	2	19.8	19.2
4	16	2	4.0	2.6
2	16	2	10.8	-11.6
8	14	2	14.0	15.0
4	14	2	5.4	-3.8
2	14	2	9.7	-10.4
0	14	2	32.7	33.2
10	12	2	6.8	7.2
8	12	2	15.1	14.6
6	12	2	16.7	-17.5
4	12	2	17.0	16.4
2	12	2	13.5	13.2
10	10	2	3.4	5.1
8	10	2	12.8	-13.8
6	10	2	19.0	20.0
4	10	2	20.8	20.9
2	10	2	47.6	50.6
10	8	2	16.8	-17.0
8	8	2	3.8	-2.8
6	8	2	5.1	4.0
4	8	2	3.3	-1.7
2	8	2	17.9	-17.6
12	6	2	8.2	-7.8
8	6	2	11.1	10.2
6	6	2	11.4	13.0
4	6	2	32.4	-32.6

h	k	l	F_o	F_c
2	6	2	52.2	51.6
0	6	2	49.5	-49.0
12	4	2	8.8	-8.2
10	4	2	12.5	12.8
8	4	2	19.3	-19.9
6	4	2	13.4	-14.1
4	4	2	32.7	-34.1
12	2	2	8.8	8.8
10	2	2	5.8	-4.0
8	2	2	18.0	-18.9
6	2	2	22.6	-24.2
4	2	2	13.7	-14.3
2	2	2	105.2	-107.4
0	2	2	67.6	-70.3
10	0	2	4.9	-4.9
6	0	2	29.2	30.7
2	0	2	22.0	19.6
3	25	3	16.4	16.5
1	25	3	9.8	-9.6
5	23	3	11.7	11.6
3	23	3	12.4	-13.5
1	23	3	22.9	-22.5
7	21	3	10.5	11.3
5	21	3	12.8	-12.4
3	21	3	20.9	-21.1
1	21	3	29.6	29.9
7	19	3	18.2	-18.3
5	19	3	33.5	-33.7
3	19	3	31.9	32.6
1	19	3	16.9	17.8
9	17	3	19.8	-20.6
7	17	3	19.7	-20.2
5	17	3	15.5	15.8
3	17	3	27.7	28.2
1	17	3	49.1	-49.6
9	15	3	13.2	-13.9
7	15	3	18.4	18.7
5	15	3	35.5	35.6
3	15	3	46.9	-47.1
1	15	3	43.4	-44.0
7	13	3	30.8	31.5
9	13	3	12.4	12.6
5	13	3	54.3	-54.8
3	13	3	56.0	-57.0
1	13	3	38.9	39.6
11	11	3	17.6	17.3
9	11	3	31.7	31.4
7	11	3	30.0	-31.1
5	11	3	22.0	-22.7
3	11	3	47.9	47.3
1	11	3	103.3	104.8
11	9	3	12.3	12.5
9	9	3	15.4	-15.8
7	9	3	36.8	-37.5
5	9	3	70.3	70.3
3	9	3	81.3	83.0
1	9	3	64.9	-64.3
11	7	3	11.6	-12.8
9	7	3	25.3	-25.8
7	7	3	46.0	46.3
5	7	3	64.1	65.0
3	7	3	82.6	-81.8
1	7	3	101.0	-100.5
11	5	3	21.5	-21.3
9	5	3	39.1	39.2
7	5	3	41.3	42.1
5	5	3	35.3	-35.1
3	5	3	76.8	-76.5
1	5	3	190.6	190.3
11	3	3	13.3	13.5
9	3	3	15.8	16.1
7	3	3	47.5	-48.2
5	3	3	110.4	-112.8
3	3	3	140.1	138.4
1	3	3	55.1	51.5
11	1	3	20.7	21.2
9	1	3	35.1	-35.3
7	1	3	44.4	-45.3
5	1	3	60.2	60.8
3	1	3	107.2	106.7
1	1	3	182.8	-188.7
4	24	4	8.5	8.0
2	24	4	5.8	7.0
0	24	4	18.8	-19.9
6	22	4	15.9	15.9
2	22	4	15.3	-14.8
8	20	4	15.2	15.0
4	20	4	11.2	-11.8
2	20	4	10.2	11.0
0	20	4	28.3	28.4
8	18	4	8.7	-8.4
6	18	4	13.5	-13.5
4	18	4	8.4	-7.6
2	18	4	27.2	27.0
8	16	4	10.1	-11.5
6	16	4	5.5	-7.8
4	16	4	35.9	37.3
2	16	4	12.8	-12.7
0	16	4	13.9	-13.8
10	14	4	16.6	-17.1
8	14	4	4.9	-4.5
6	14	4	16.2	16.7
4	14	4	7.9	-7.2
2	14	4	37.3	-38.1
8	12	4	14.1	15.0
6	12	4	12.0	-12.0
4	12	4	41.8	-42.4
2	12	4	29.9	-30.7
0	12	4	29.2	30.3
10	10	4	10.3	10.8
8	10	4	10.6	11.8
6	10	4	37.3	-38.0
4	10	4	15.3	15.2
2	10	4	38.2	38.5
8	8	4	31.4	-32.1
6	8	4	7.9	8.3
4	8	4	14.8	14.9
2	8	4	15.0	15.6
0	8	4	102.5	-100.3
10	6	4	11.2	-11.1
8	6	4	11.5	10.5
6	6	4	45.2	46.4
4	6	4	13.5	15.4
2	6	4	46.5	-44.2
12	4	4	10.3	-10.7
8	4	4	29.2	29.7
6	4	4	20.8	21.2
4	4	4	42.7	-42.3
2	4	4	85.1	83.2
0	4	4	73.6	74.2
12	2	4	4.7	-5.4
10	2	4	24.4	24.9
8	2	4	13.0	-13.7
6	2	4	26.3	-27.4
4	2	4	23.0	-22.2
2	2	4	72.8	73.8

h	k	l	F_o	F_c
12	0	4	13.5	13.3
8	0	4	17.3	-18.3
4	0	4	94.4	92.5
0	0	4	31.0	31.6
1	25	5	8.4	7.8
5	23	5	6.8	5.4
1	23	5	8.8	-8.9
7	21	5	12.4	11.6
5	21	5	5.1	3.6
3	21	5	3.6	2.6
1	21	5	10.9	-11.5
7	19	5	5.5	5.5
3	19	5	4.4	-4.2
1	19	5	13.7	13.5
9	17	5	5.6	5.8
5	17	5	10.1	-10.1
3	17	5	19.4	18.4
9	15	5	10.1	-8.9
7	15	5	5.0	3.7
5	15	5	9.4	8.1
3	15	5	23.7	23.7
1	15	5	4.2	4.5
9	13	5	7.2	-6.6
7	13	5	6.6	-5.1
5	13	5	8.5	8.5
3	13	5	22.5	-21.0
11	11	5	4.5	-3.2
7	11	5	9.8	10.3
5	11	5	20.0	-18.7
3	11	5	6.2	-6.7
1	11	5	4.8	-6.3
11	9	5	3.1	2.2
9	9	5	6.0	5.3
7	9	5	20.4	-19.5
3	9	5	23.9	-24.2
1	9	5	30.7	28.7
9	7	5	4.8	-3.3
7	7	5	25.3	-24.7
3	7	5	35.6	-34.9
1	7	5	31.7	-30.2
7	5	5	22.0	21.1
5	5	5	10.1	9.9
3	5	5	20.7	20.9
1	5	5	4.0	2.7
11	3	5	9.4	-9.6
9	3	5	14.3	13.2
5	3	5	8.4	8.0
3	3	5	6.3	-5.2
11	1	5	10.3	10.4
9	1	5	9.8	9.5
7	1	5	10.7	10.5
5	1	5	16.1	-14.3
3	1	5	44.1	45.7
1	1	5	72.8	-71.8
2	24	6	16.8	16.4
4	22	6	10.3	10.6
0	22	6	40.1	-40.0
6	20	6	24.4	24.1
2	20	6	30.3	-29.1
8	18	6	21.9	21.4
4	18	6	33.7	-32.9
0	18	6	35.4	35.8
6	16	6	18.3	-17.8
2	16	6	54.0	53.0
8	14	6	17.9	-17.2
4	14	6	71.1	69.3
2	14	6	5.7	-3.4
0	14	6	26.9	-27.2
10	12	6	21.3	-22.4
6	12	6	38.9	38.1
2	12	6	71.3	-68.5
8	10	6	34.2	33.1
6	10	6	7.6	5.5
4	10	6	55.8	-52.9
2	10	6	9.0	7.7
0	10	6	107.7	107.4
10	8	6	10.8	11.4
6	8	6	76.2	-74.5
2	8	6	76.7	77.4
8	6	6	49.5	-49.6
6	6	6	6.5	4.1
4	6	6	49.6	46.2
2	6	6	8.2	9.2
0	6	6	178.2	-181.0
10	4	6	25.1	-25.0
8	4	6	4.4	-2.3
6	4	6	67.0	64.6
2	4	6	113.9	-115.6
12	2	6	16.5	-16.1
8	2	6	37.2	36.3
6	2	6	6.4	-6.0
4	2	6	126.3	-127.6
2	2	6	14.7	-13.4
0	2	6	68.9	69.5
10	0	6	42.9	41.5
6	0	6	41.5	-40.4
2	0	6	149.8	151.5
1	25	7	12.3	12.9
3	23	7	7.4	7.3
1	23	7	13.7	13.7
5	21	7	14.5	13.7
3	21	7	5.7	7.4
1	21	7	15.7	-15.4
7	19	7	13.3	12.8
3	19	7	11.6	-10.3
1	19	7	27.4	-27.0
7	17	7	8.4	7.2
5	17	7	19.8	-20.4
3	17	7	29.8	-29.4
1	17	7	12.2	11.4
9	15	7	14.0	13.7
7	15	7	9.4	-9.3
5	15	7	19.7	-18.8
3	15	7	34.5	33.7
1	15	7	17.5	16.7
9	13	7	18.1	-17.2
7	13	7	6.8	-7.4
5	13	7	16.3	15.4
3	13	7	35.3	33.9
1	13	7	33.0	-31.1
9	11	7	6.5	-4.2
7	11	7	17.0	17.3
5	11	7	42.1	40.4
3	11	7	41.0	-39.1
1	11	7	19.6	-17.9
11	9	7	7.8	-7.4
9	9	7	13.7	15.0
7	9	7	31.8	30.6
5	9	7	21.2	-20.7
3	9	7	12.6	-12.1
1	9	7	62.7	61.9
11	7	7	7.9	8.0
9	7	7	12.0	12.3
7	7	7	34.2	-33.4
5	7	7	28.0	-25.9
3	7	7	14.7	14.7

h	k	l	F_o	F_c
1	7	7	68.1	67.5
11	5	7	4.9	5.9
9	5	7	7.0	-7.8
7	5	7	32.5	-31.7
5	5	7	48.0	47.8
3	5	7	37.1	37.7
1	5	7	37.9	-37.6
11	3	7	12.9	-13.3
9	3	7	27.2	-27.2
7	3	7	23.2	22.8
5	3	7	16.5	15.4
3	3	7	41.0	-40.3
1	3	7	74.3	-74.5
11	1	7	13.8	-13.9
9	1	7	18.7	18.4
7	1	7	13.8	12.5
5	1	7	45.7	-45.1
3	1	7	82.1	-81.5
1	1	7	16.2	16.4
2	24	8	7.7	6.7
0	24	8	4.4	6.5
6	22	8	4.6	6.5
6	20	8	6.2	4.8
4	20	8	5.7	3.9
2	20	8	12.3	11.5
0	20	8	11.6	-11.4
8	18	8	7.9	-7.3
6	18	8	5.9	6.4
4	18	8	6.9	-6.6
2	18	8	8.4	-8.7
8	16	8	8.2	7.7
6	16	8	9.3	-8.1
4	16	8	12.0	-10.2
2	16	8	12.0	-11.2
0	16	8	4.3	4.5
8	14	8	4.6	-5.7
6	14	8	4.8	-3.0
4	14	8	9.2	-6.8
2	14	8	12.7	12.0
8	12	8	7.5	-6.1
6	12	8	13.3	-13.1
4	12	8	14.6	13.0
2	12	8	30.8	-28.5
10	10	8	6.3	-5.7
8	10	8	11.4	10.7
6	10	8	13.3	11.8
4	10	8	11.6	11.3
2	10	8	5.4	-4.5
8	8	8	9.2	7.5
6	8	8	8.5	7.3
2	8	8	14.3	11.3
0	8	8	13.8	13.8
10	6	8	3.8	3.4
8	6	8	9.8	9.9
6	6	8	16.5	-16.2
4	6	8	12.2	12.2
2	6	8	3.8	-3.8
10	4	8	6.0	4.1
8	4	8	9.5	-9.9
6	4	8	23.3	21.6
2	4	8	55.2	55.0
10	2	8	11.3	-10.0
8	2	8	13.6	-12.2
4	2	8	15.3	-15.0
8	0	8	10.8	10.0
4	0	8	11.5	-11.5
0	0	8	26.0	-26.6
3	23	9	11.8	-10.8
1	23	9	12.5	12.3
5	21	9	7.6	-9.9
3	21	9	15.2	14.7
1	21	9	16.5	16.7
7	19	9	11.4	-13.2
5	19	9	22.5	23.0
3	19	9	18.9	19.0
1	19	9	8.7	-9.3
7	17	9	16.0	15.3
5	17	9	8.1	7.3
3	17	9	11.7	-11.8
1	17	9	33.0	-33.1
9	15	9	10.2	9.2
7	15	9	13.9	15.4
5	15	9	18.3	-18.1
3	15	9	22.5	-22.6
1	15	9	28.5	28.5
9	13	9	9.6	10.0
7	13	9	21.7	-21.8
5	13	9	28.5	-29.8
3	13	9	28.5	28.3
1	13	9	23.3	23.1
9	11	9	21.7	-21.6
7	11	9	16.5	-16.0
5	11	9	9.2	9.0
3	11	9	27.8	26.7
1	11	9	54.8	-53.7
9	9	9	7.6	-8.5
7	9	9	16.5	16.6
5	9	9	44.3	43.3
3	9	9	51.1	-49.0
1	9	9	23.3	-23.2
9	7	9	15.0	13.8
7	7	9	22.5	21.4
5	7	9	39.8	-39.1
3	7	9	48.8	-47.2
1	7	9	37.5	36.1
11	5	9	16.5	15.9
9	5	9	23.3	23.1
7	5	9	20.2	-19.7
5	5	9	18.7	-19.0
3	5	9	39.8	39.1
1	5	9	73.6	71.3
11	3	9	6.7	6.5
9	3	9	8.2	-8.3
7	3	9	31.5	-30.4
5	3	9	60.8	57.5
3	3	9	57.1	55.7
1	3	9	28.5	-28.0
11	1	9	10.8	-10.5
9	1	9	24.8	-23.2
7	1	9	32.3	30.9
5	1	9	24.8	23.9
3	1	9	37.5	-35.8
1	1	9	79.6	-77.5
0	22	10	7.4	8.6
2	20	10	19.9	19.9
6	18	10	7.3	4.8
4	18	10	19.5	19.2
2	18	10	11.3	10.1
0	18	10	30.2	-29.0
6	16	10	26.0	26.5
4	16	10	7.0	-2.8
2	16	10	26.0	-25.6
8	14	10	23.5	23.6
4	14	10	15.5	-15.9
0	14	10	52.6	53.2
8	12	10	8.9	-8.2

h	k	l	F_o	F_c
6	12	10	27.4	-26.6
4	12	10	9.4	-8.9
2	12	10	40.3	40.0
8	10	10	19.6	-19.5
6	10	10	7.2	-7.6
4	10	10	46.9	46.7
2	10	10	18.8	-18.4
0	10	10	35.8	-35.9
10	8	10	22.6	-22.6
6	8	10	23.0	23.0
4	8	10	6.0	1.9
2	8	10	56.5	-56.8
8	6	10	16.7	17.1
6	6	10	6.4	-3.4
4	6	10	65.4	-65.9
2	6	10	11.7	-12.2
0	6	10	33.1	33.3
10	4	10	18.3	17.9
8	4	10	10.9	11.2
6	4	10	37.9	-37.9
4	4	10	13.6	14.0
2	4	10	59.3	60.2
8	2	10	33.8	-33.4
6	2	10	9.0	7.9
4	2	10	35.7	35.5
2	2	10	21.1	21.8
0	2	10	88.4	-92.9
10	0	10	11.2	-10.6
6	0	10	51.8	51.3
2	0	10	55.7	-56.9
3	21	11	9.7	-9.0
5	19	11	4.6	-5.6
3	19	11	7.6	6.7
1	19	11	4.2	4.5
7	17	11	8.7	-9.6
5	17	11	8.9	8.1
1	17	11	8.0	-7.6
7	15	11	13.5	12.7
5	15	11	4.8	2.1
3	15	11	5.5	6.4
1	15	11	17.0	-16.3
7	13	11	11.0	10.0
1	13	11	15.3	15.3
9	11	11	5.5	6.2
7	11	11	7.3	-8.2
5	11	11	7.3	-6.6
3	11	11	8.4	7.4
1	11	11	4.6	4.1
9	9	11	8.4	-8.8
7	9	11	3.6	4.6
5	9	11	4.7	4.7
3	9	11	20.3	20.9
9	7	11	7.2	-6.4
7	7	11	5.2	-6.7
5	7	11	11.7	10.7
3	7	11	26.7	-26.8
1	7	11	9.7	9.0
9	5	11	5.0	5.7
7	5	11	4.0	2.3
5	5	11	12.3	-12.3
3	5	11	17.3	-16.2
1	5	11	6.4	-6.2
9	3	11	4.5	4.2
7	3	11	7.5	-7.2
5	3	11	4.4	-3.5
1	3	11	13.7	14.0
9	1	11	4.5	-2.3
7	1	11	20.7	-20.9
5	1	11	5.6	5.7
3	1	11	15.3	-15.4
1	1	11	18.1	-19.3
4	20	12	20.2	-19.5
2	20	12	6.2	4.3
0	20	12	8.4	8.5
2	18	12	16.2	16.1
6	14	12	25.1	25.7
4	14	12	4.6	-2.0
2	14	12	20.4	-20.5
8	12	12	18.9	18.9
6	12	12	5.7	-6.0
4	12	12	17.5	-17.1
2	12	12	8.6	-8.8
0	12	12	39.1	39.1
6	10	12	15.3	-15.3
2	10	12	36.4	36.2
8	8	12	13.0	-13.4
4	8	12	46.8	47.8
0	8	12	11.1	-11.7
10	6	12	19.8	-19.8
6	6	12	15.4	15.0
4	6	12	2.9	2.2
2	6	12	44.2	-45.0
10	4	12	4.8	4.0
8	4	12	17.0	17.6
6	4	12	9.9	8.9
4	4	12	38.3	-38.9
2	4	12	12.3	12.8
0	4	12	37.6	38.8
10	2	12	7.3	7.8
8	2	12	3.5	-1.7
6	2	12	38.2	-38.4
2	2	12	35.9	36.6
8	0	12	27.3	-26.3
4	0	12	14.1	14.8
0	0	12	77.0	-79.5
3	19	13	10.3	-10.9
1	19	13	17.1	16.8
5	17	13	18.3	-17.8
3	17	13	15.6	15.4
1	17	13	12.0	12.1
7	15	13	15.8	-16.3
5	15	13	15.3	15.5
3	15	13	10.0	9.4
1	15	13	21.9	-21.8
7	13	13	15.4	15.4
5	13	13	9.0	9.4
3	13	13	11.3	-11.1
1	13	13	31.8	-31.7
7	11	13	14.2	14.0
5	11	13	25.5	-25.9
3	11	13	27.0	-26.9
1	11	13	15.7	15.7
9	9	13	17.1	17.1
7	9	13	13.7	-13.8
5	9	13	12.7	-12.8
3	9	13	26.1	26.7
1	9	13	29.5	30.1
9	7	13	15.6	-16.0
7	7	13	9.4	-9.4
5	7	13	19.1	18.6
3	7	13	34.7	36.3
1	7	13	26.4	-26.8
9	5	13	8.4	-8.4
7	5	13	13.4	13.7
5	5	13	33.7	33.8
3	5	13	40.3	-40.9

h	k	l	F_o	F_c
1	5	13	17.2	-17.4
9	3	13	17.9	17.7
7	3	13	20.8	20.6
5	3	13	13.5	-14.0
3	3	13	20.3	-20.6
1	3	13	47.8	49.0
9	1	13	6.7	6.8
7	1	13	23.4	-23.8
5	1	13	30.5	-31.5
3	1	13	24.8	24.6
1	1	13	33.8	36.1
4	18	14	8.2	-8.2
2	18	14	10.5	10.5
2	16	14	7.1	7.0
4	14	14	7.4	8.2
2	14	14	6.1	4.3
0	14	14	10.3	-10.8
6	12	14	9.3	10.0
4	12	14	7.0	-7.5
2	12	14	9.2	-8.8
8	10	14	9.0	8.7
6	10	14	9.2	-9.7
4	10	14	7.6	-8.0
2	10	14	17.3	-17.1
0	10	14	12.8	12.2
6	8	14	7.5	-5.9
2	8	14	13.4	13.5
8	6	14	10.3	-9.6
6	6	14	7.0	-5.2
4	6	14	11.4	11.0
2	6	14	12.2	-12.4
0	6	14	8.5	-10.2
8	4	14	8.1	10.0
6	4	14	9.8	8.8
4	4	14	9.6	10.1
2	4	14	13.5	-12.7
8	2	14	5.9	5.7
6	2	14	9.6	9.6
4	2	14	12.6	-12.5
2	2	14	18.2	18.7
0	2	14	12.0	13.2
6	0	14	14.0	-14.0
2	0	14	10.3	9.8
3	17	15	8.6	-8.6
1	17	15	11.7	11.6
5	15	15	11.2	-11.3
3	15	15	15.1	14.3
1	15	15	6.1	6.3
5	13	15	15.6	15.8
3	13	15	13.9	13.5
1	13	15	4.0	-4.7
7	11	15	9.3	7.2
3	11	15	7.5	-7.6
1	11	15	22.0	-22.3
7	9	15	13.3	12.6
5	9	15	14.5	-15.2
3	9	15	11.3	-12.0
1	9	15	11.7	12.0
7	7	15	15.8	-14.8
5	7	15	10.4	-10.3
3	7	15	8.4	9.0
1	7	15	18.6	19.0
7	5	15	9.8	-9.5
5	5	15	3.4	2.2
3	5	15	8.3	10.1
1	5	15	27.7	-28.4
7	3	15	10.1	10.6
5	3	15	23.7	24.3
3	3	15	21.8	-22.1
1	3	15	5.3	-4.8
5	1	15	12.0	-12.1
3	1	15	19.6	-19.8
1	1	15	16.1	17.7
0	16	16	10.4	9.2
2	14	16	21.4	20.8
4	12	16	23.3	23.0
2	12	16	4.5	4.8
0	12	16	19.6	-19.1
6	10	16	21.6	21.2
4	10	16	3.9	-4.7
2	10	16	22.6	-22.5
4	8	16	11.9	-12.2
2	8	16	5.0	-3.2
0	8	16	43.3	43.1
6	6	16	24.5	-24.4
4	6	16	4.2	-3.3
2	6	16	28.3	27.1
8	4	16	17.5	-16.9
4	4	16	25.5	24.8
2	4	16	9.1	-8.2
0	4	16	34.1	-34.3
8	2	16	5.0	4.4
6	2	16	17.3	17.0
4	2	16	5.0	4.9
2	2	16	34.0	-34.3
8	0	16	9.4	10.1
4	0	16	41.2	-41.4
3	13	17	12.1	11.7
5	11	17	7.3	6.8
3	11	17	4.5	4.3
1	11	17	6.6	-6.6
5	9	17	4.2	5.1
1	9	17	12.8	-12.5
5	7	17	5.8	-6.0
1	7	17	14.2	13.8
7	5	17	11.0	-11.1
5	5	17	4.1	-5.0
3	5	17	2.7	1.2
1	5	17	13.3	12.6
5	3	17	7.9	6.8
3	3	17	12.8	12.8
1	3	17	6.7	-6.7
5	1	17	8.5	8.2
3	1	17	16.8	-16.9
1	1	17	2.8	-1.9
2	12	18	9.7	10.6
4	10	18	6.1	8.1
2	10	18	5.0	-5.3
0	10	18	15.0	-15.0
2	8	18	8.5	-8.6
6	6	18	3.9	-3.1
4	6	18	5.5	-4.5
2	6	18	4.0	-4.7
0	6	18	22.1	23.0
6	4	18	10.0	-10.4
4	4	18	3.4	1.4
2	4	18	12.6	13.0
6	2	18	5.9	4.4
4	2	18	16.4	17.3
2	2	18	5.2	6.0
0	2	18	5.4	-6.3

Table 4. The crystal structure of Na_2SO_4(V), thenardite.

Space group: (No. 70) *Fddd.*

Unit cell dimensions: $a = 5.8596 \pm 5$ Å
$b = 12.3044 \pm 12$ Å
$c = 9.8170 \pm 10$ Å
$V = 707.8$ Å^3. $D_{calc} = 2.666$ g/cm^3, $D_{obs} = 2.65$ g/cm^3.

Cell content: $8Na_2SO_4$.

Arrangement of atoms (f denotes translations characteristic of a face centered lattice):
8 S in 8(*a*): $\pm(\frac{1}{8}, \frac{1}{8}, \frac{1}{8})_f$
16 Na in 16(*g*): $\pm(\frac{1}{8}, \frac{1}{8}, z)_f$, $\pm(\frac{1}{8}, \frac{1}{8}, \frac{1}{4}-z)_f$
32 O in 32(*h*): $\pm(x, y, z)_f$, $\pm(x, \frac{1}{4}-y, \frac{1}{4}-z)_f$, $\pm(\frac{1}{4}-x, y, \frac{1}{4}-z)_f$ $\pm(\frac{1}{4}-x, \frac{1}{4}-y, z)_f$

Fractional atomic coordinates

Atom	$x \pm \sigma(x)$	$y \pm \sigma(y)$	$z \pm \sigma(z)$
S	$\frac{1}{8}$	$\frac{1}{8}$	$\frac{1}{8}$
Na	$\frac{1}{8}$	$\frac{1}{8}$	0.4414 ± 1
O	-0.0203 ± 2	0.0572 ± 1	0.2137 ± 1

Anisotropic thermal parameters ($\times 10^5$).
$T = \exp[-(B_{11}h^2 + B_{22}k^2 + B_{33}l^2 + B_{12}hk + B_{13}hl + B_{23}kl)]$.

Atom	B_{11}	B_{22}	B_{33}	B_{12}	B_{13}	B_{23}
S	518 ± 6	113 ± 2	206 ± 3	0	0	0
Na	926 ± 11	192 ± 3	432 ± 5	35 ± 8	0	0
O	1041 ± 12	207 ± 3	345 ± 5	-297 ± 10	319 ± 12	65 ± 5

isotropic refinement were $B_S = 0.74 \pm 0.01$, $B_{Na} = 1.30 \pm 0.02$, $B_O = 1.29 \pm 0.02$ Å^2. A three-dimensional ΔF Fourier synthesis was then computed with the anisotropic model. This showed no peak or hole greater than 0.6 eÅ^{-3}. A close inspection of Table 3 shows that the extinction effects are so small that they are negligible.

DESCRIPTION AND DISCUSSION OF THE CRYSTAL STRUCTURE

The crystal structure may be described in terms of nearly regular SO_4 tetrahedra and distorted NaO_6 octahedra. In fact, the NaO_6 octahedra are more distorted than Zachariasen and Ziegler reported. The interatomic distances and standard deviations (σ) and some angles of interest are listed in Table 5. No corrections have been made for the thermal vibration.

The sodium atoms are each surrounded by 6 oxygen atoms, two at 2.334 Å, two at 2.426 Å, and two at 2.534 Å, forming distorted NaO_6 octahedra with a 2-fold axis parallel to the *c* axis. These Na – O distances are quite in accordance with those reported in other compounds, *e.g.* $Na_2SO_4\ 10H_2O$.[11] All the sulphate ions are separated from each other by distances > 3 Å for two oxygen

Table 5. Interatomic distances (Å) with standard deviations and some angles in Na_2SO_4(V). All angles have standard deviations of $\pm 0.05°$ or less. No corrections have been made for thermal vibration. Atom denotations used in Table 5, Table 7, and Fig. 2: S, Na, and O(1) in (x, y, z), O(2): $(x, \frac{1}{2}-y, \frac{1}{2}-z)$, O(3): $(\frac{1}{2}-x, y, \frac{1}{2}-z)$, O(4): $(\frac{1}{2}-x, \frac{1}{2}-y, z)$, O(5): $(\frac{1}{2}+x, \frac{1}{2}-y, \frac{3}{2}-z)$, O(6): $(\frac{1}{2}+x, -y, \frac{1}{2}+z)$, O(7): $(-\frac{1}{2}-x, y, \frac{3}{2}-z)$, O(8): $(-x, \frac{1}{2}+y, \frac{1}{2}+z)$. Oxygen-oxygen edges shared by SO_4 and NaO_6 are marked (*).

SO_4 group	S – O(1,2,3,4)	1.476 ± 1	O(1) – S – O(2)	109.55°
	O(1) – O(2)	2.412 ± 2	O(1) – S – O(3)	111.15°
	O(1) – O(3)	2.435 ± 2	O(1) – S – O(4)	107.74°
	O(1) – O(4)*	2.384 ± 2	Average:	109.48°
NaO_6 group	Na – O(1,4)	2.534 ± 1	O(1) – Na – O(4)	56.13°
	Na – O(5,7)	2.426 ± 1	O(1) – Na – O(6)	81.64°
	Na – O(6,8)	2.334 ± 1	O(6) – Na – O(7)	81.89°
			O(1) – Na – O(7)	86.43°
	O(1) – O(4)*	2.384 ± 2	O(7) – Na – O(8)	93.97°
	O(6) – O(7)	3.120 ± 2	O(1) – Na – O(8)	108.09°
	O(1) – O(6)	3.186 ± 2	O(5) – Na – O(7)	134.82°
	O(1) – O(7)	3.397 ± 2	O(1) – Na – O(5)	137.74°
	O(7) – O(8)	3.481 ± 2	O(6) – Na – O(8)	169.27°
	O(1) – O(8)	3.942 ± 2		
	O(5) – O(7)	4.479 ± 2		
	O(1) – O(5)	4.626 ± 2		
	O(6) – O(8)	4.648 ± 2		

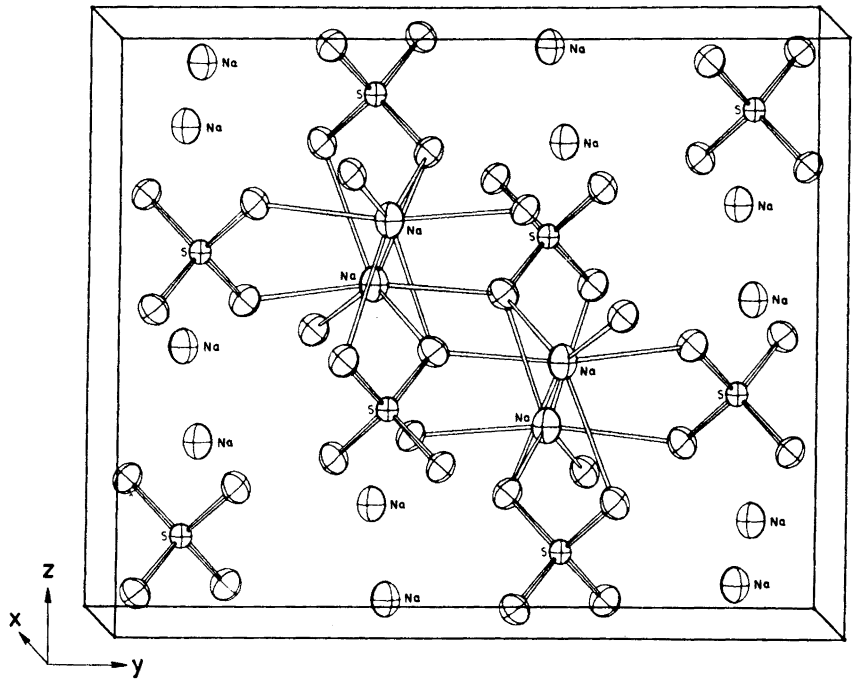

Fig. 1. The crystal structure of thenardite. One unit cell with eight sulphate ions and four NaO_6 octahedra is shown.

atoms belonging to different sulphate groups (Table 5). The SO_4 tetrahedra are nearly regular. All S – O distances are equal, 1.476 ± 0.001 Å, due to the space group since the sulphur atom is fixed in a special point position with 222 point symmetry. Each SO_4 tetrahedron shares two of its edges with two different NaO_6 octahedra. The longest Na – O distance of 2.534 Å represents the distances to oxygens forming the shared tetrahedral edge. The remaining corners of the NaO_6 octahedron are shared with another four SO_4 tetrahedra thus giving a three-dimensional framework. Fig. 1 shows a three-dimensional model of the crystal structure. It has been produced by the plot program ORTEP.[12] Fig. 2 is an ORTEP plot picture showing one NaO_6 octahedron.

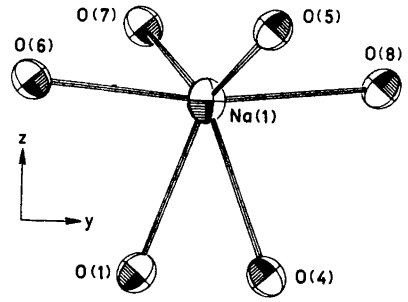

Fig. 2. One NaO_6 octahedron showing the coordination of oxygen atoms around a sodium atom in thenardite. The atoms have been numbered as in Tables 5 and 7.

Table 6. Analysis of anisotropic thermal parameters.

Atom	Axis	Root of mean square amplitude (Å)	R.m.s. radial thermal displacement (Å)
S	1	0.093	0.167
	2	0.095	
	3	0.100	
Na	1	0.120	0.228
	2	0.128	
	3	0.145	
O	1	0.094	0.226
	2	0.136	
	3	0.154	

Table 7. Some interatomic distances (Å) in thenardite.

	Uncorrected	"Independent"
S – O(1,2,3,4)	1.476	1.497
O(1) – O(2), O(3) – O(4)	2.412	2.427
O(1) – O(3), O(2) – O(4)	2.435	2.451
O(1) – O(4), O(2) – O(3)	2.384	2.401
Na – O(1)	2.534	2.546
Na – O(5)	2.426	2.440
Na – O(6)	2.334	2.350

Table 8. Data for sulphate groups. Uncorrected and corrected S–O bond distances (in Å) are given for six carefully determined sulphate structures. The corrected distances have all been calculated in the same manner, *i.e.* assuming the riding motion model.

Compound: Ref.:	Na_2SO_4(V) This work	$Li_2SO_4.H_2O$ Larson [14]	$MgSO_4.4H_2O$ Baur [15]	$MgSO_4.7H_2O$ Baur [16]	$FeSO_4.7H_2O$ Baur [17]	β-K_2SO_4 McGinnety [18]
Uncorr. bond dist.						
Shortest	1.476±1	1.462±2	1.466±5	1.460±4	1.462±4	1.459±4
Longest	1.476±1	1.482±2	1.480±4	1.482±4	1.488±4	1.473±4
Average	1.476	1.472	1.473	1.471	1.474	1.469
Corrected bond dist.						
Average	1.484	1.480	1.479	1.486	1.486	1.486

Table 9. Computer programs used for the crystallographic calculations. All programs are written in FORTRAN IV for an IBM 360/75 computer except program SIMSA.

Program name and function	Authors
1. LAZY. Calculation of $\sin^2\theta$- and d-values from a Guinier powder photograph after internal standard correction.	A. G. Nord, Stockholm, Sweden.
2. POWDER. Refinement of cell constants. Ref. 6.	O. Lindqvist and F. Wengelin, Göteborg. Modified by A. G. Nord and B. G. Brandt, Stockholm, Sweden.
3. SIP. Generation of steering paper tape for Siemens AED.	R. Norrestam, Stockholm, Sweden.
4. SIMSA. Interpretation and evaluation of paper tape output from Siemens AED. IBM 1800.	R. Norrestam, Stockholm, Sweden.
5. DATAP2. Lp- and absorption correction.	P. Coppens, L. Leiserowitz and D. Rabinovich, Rehovath, Israel. Modified by O. Olofsson and M. Elfström, Uppsala. Further modifications by S. Åsbrink, B. G. Brandt and A. G. Nord, Stockholm, Sweden.
6. DRF. Fourier summations and structure factor calculations.	A. Zalkin, Berkeley, USA. Local modification.
7. LALS. Full matrix least squares refinement of positional and thermal parameters.	P. K. Gantzel, R. A. Sparks, and K. N. Trueblood, Los Angeles, USA. Modified by A. Zalkin, J. O. Lundgren, R. Liminga, C. I. Brändén, A. G. Nord and B. G.Brandt.
8. DISTAN. Calculation of interatomic distances and bond angles with e.s.d.	A. Zalkin, Berkeley, USA. Local modification.
9. ORFFE. Crystallographic function and error program. Ref. 13.	W. R. Busing, K. O. Martin, and H. A. Levy, Oak Ridge, USA. Modified by L. Kihlborg, Stockholm, Sweden.
10. ORTEP. Thermal ellipsoid plot program for crystal structure illustrations. Ref. 12.	C. K. Johnsson, Oak Ridge, USA.

The anisotropic thermal parameters were analysed to find the axes of the ellipsoids. Some results from program ORFFE are presented in Table 6. The character of thermal vibration may also be studied in Figs. 1 – 2. Table 7 contains some bond lengths in thenardite corrected due to thermal motion. The effect of thermal motion on the distances is calculated assuming the "independent motion" model.[13]

Pertinent data relating to the sulphate group in some compounds are given in Table 8. All "corrected" S – O distances have been calculated in the same manner, *i.e.* assuming the "riding motion" model.[13] Although the ligand atoms of the different sulphate groups vary, all uncorrected S – O distances as well as all corrected ones are nearly identical. The S – O distances within each sulphate group are also very similar, but the differences exceed the reported standard deviations. However, all these facts show that the sulphate ion in the compounds discussed is fairly stable and it also possesses a high degree of regularity.

Acknowledgements. The author thanks Professors Peder Kierkegaard and Arne Magnéli for their active and stimulating interest in this work. Thanks are also due to Dr. B. G. Gäfvert for revising the English of this paper. The work has been supported by the *Swedish Natural Science Research Council.*

REFERENCES

1. Gmelin, *Handbuch der anorganischen Chemie* **21:3** (1966) 1091.
2. Kracek, F. C. *J. Phys. Chem.* **33** (1929) 1281.
3. Zachariasen, W. H. and Ziegler, G. E. *Z. Krist.* **81** (1932) 92.
4. Swanson, H. E. and Fuyat, R. K. *Natl. Bur. Std. U.S. Circ.* **539:2** (1953) 59.
5. Hambling, P. G. *Acta Cryst.* **6** (1953) 98.
6. Lindqvist, O. and Wengelin, F. *Arkiv Kemi* **28** (1967) 179.
7. *International Tables for X-Ray Crystallography*, Kynoch Press, Birmingham 1962, Vol. I.
8. Brandt, B. G. and Nord, A. G. *Chem. Commun. Univ. Stockholm* (1970) No. V.
9. Hughes, E. W. *J. Am. Chem. Soc.* **63** (1941) 1737.
10. Hamilton, W. C. *Acta Cryst.* **18** (1965) 502.
11. Ruben, H. W., Templeton, D. H., Rosenstein, R. D. and Olovsson, I. *J. Am. Chem. Soc.* **83** (1961) 820.
12. Johnson, C. K. AEC Accession No. 33516, ORNL-3794, Oak Ridge National Laboratory, U.S.A. 1965.
13. Busing, W. R. and Levy, H. A. *Acta Cryst.* **17** (1964) 142.
14. Larson, A. C. *Acta Cryst.* **18** (1965) 717.
15. Baur, W. H. *Acta Cryst.* **17** (1964) 863.
16. Baur, W. H. *Acta Cryst.* **17** (1964) 1361.
17. Baur, W. H. *Acta Cryst.* **17** (1964) 1167.
18. McGinnety, J. A. *Acta Cryst.* **B 28** (1972) 2845.

Received October 10, 1972.

ACTA CHEMICA SCANDINAVICA 27 (1973) 823–834

Structural Studies on the Rare Earth Carboxylates

16. The Crystal and Molecular Structure of Tetra-aquo Tris-oxalato Diytterbium(III) Dihydrate

EVA HANSSON

Physical Chemistry 1, Chemical Center, University of Lund, P.O. Box 740, S-220 07 Lund 7, Sweden

The crystal and molecular structure of the triclinic compound $Yb_2(C_2O_4)_3.6H_2O$ has been determined from three-dimensional, photographic X-ray intensity data. The space group used is $A\bar{1}$. The lattice parameters are $a=9.611(2)$ Å, $b=8.457(2)$ Å, $c=9.778(2)$ Å, $\alpha=93.39(1)°$, $\beta=106.24(1)°$, and $\gamma=85.29(2)°$, and $Z=4$.

The structure is isotypic with that of $Sc_2(C_2O_4)_3.6H_2O$. A comparison of the two structures reveals that the change in size of the metal ion is accompanied by a distortion of the metal-oxalate network resulting in an almost unchanged hydrogen bond system in the two compounds.

The structure of the lanthanoid oxalate hexahydrates is closely related to that of the lanthanoid oxalate decahydrates. The variation of the unit cell dimensions through the lanthanoid series has been determined for the two types of hydrates. The lattice parameters of the various compounds have been calculated from powder data obtained with a Guinier-Hägg focusing camera.

Isomorphous rare earth oxalates of the composition $M_2(C_2O_4)_3.6H_2O$ are formed for M = Ho – Lu, Y, and Sc. The structure of $Sc_2(C_2O_4)_3.6H_2O$ (SCOX) has been determined previously.[1] The present investigation of the structure of $Yb_2(C_2O_4)_3.6H_2O$ (YBOX) has been undertaken in order to study the alterations of the structure that may be induced by an increase in size of the metal ion.

Similar investigations of the lanthanoid oxydiacetate [2] and hydroxyacetate [3] structures have revealed that the change in the metal-oxygen bond distances, caused by the change of metal ionic radius, is accompanied by distortions of the coordination polyhedron and of the ligands. Very small changes were found in the hydrogen bond distances shorter than 2.8 Å, indicating that the preservation of a favourable hydrogen bond system plays an important role in deciding the detailed geometry of hydrogen bonded lanthanoid carboxylate structures. In SCOX all hydrogen bond distances but one

are longer than 2.8 Å. Seven of them are in the range 2.8 – 3.1 Å. Hydrogen bonds in this range were not represented in the structures cited, and the present study may thus give more information about the importance of the hydrogen bonds in structures of this type.

The lighter elements of the lanthanoid series form isomorphous oxalates of the composition $M_2(C_2O_4)_3.10H_2O$. The crystal structure of these decahydrates is closely related to that of the hexahydrates as shown by a structural study of the neodymium compound (NDOX).[4–6] The unit cell dimensions of the compounds of the two series have been determined and are included in this paper.

EXPERIMENTAL

Preparation. The mixing of dilute solutions of oxalic acid and lanthanoid chloride at room temperature results in the precipitation of the decahydrate, $M_2(C_2O_4)_3.10H_2O$, for M = La – Ho while oxalates with a variety of hydration numbers are formed for M = Er – Lu. Increasing the temperature of precipitation above 90°C results in the formation of the hexahydrate, $M_2(C_2O_4)_3.6H_2O$ for M = Er – Lu and in a mixture of the deca- and hexahydrates for M = Ho. The lighter elements form the decahydrate also at this temperature. The pure hexahydrate with M = Ho is not obtained even from boiling solutions. The pure decahydrate with M = Er is precipitated at 50°C. The decahydrate with M = Tm is not formed at any temperature between 20 and 100°C.

The oxalates prepared in this way were all fine powders. They were identified by their X-ray powder patterns.

Large crystals of YBOX were prepared according to Weigel *et al.*[8] by saturating a boiling solution of 5 g oxalic acid in 100 ml 3 M sulphuric acid with the lanthanoid oxide and slowly cooling it to 0°C. With M = La – Ho this method results in large crystals of the decahydrate while the elements Er and Tm form the acid oxalate $MC_2O_4.HC_2O_4.3H_2O$. The structure of the latter solid has been determined by Steinfink and Brunton.[9]

The ranges of existence for the deca- and hexahydrates, respectively, indicated by the results of the preparations first described, agree with those found by Watanabe and Nagashima [10] in a recent study of the hydration number of $M_2(C_2O_4)_3.nH_2O$ as a function of the temperature of formation and the metal ionic radius for M = Dy – Lu, Y, and Sc.

Powder work. The powder photographs were taken at room temperature with a Guinier-Hägg focusing camera, using Cu$K\alpha$ radiation ($\lambda = 1.5418$ Å). Lead nitrate (cubic, $a = 7.8568$ Å) was used as internal standard.

The preliminary unit cell parameters for NDOX and SCOX obtained from Weissenberg and oscillation photographs were used for indexing the powder lines of the deca- and hexahydrates, respectively. The unit cell dimensions were least squares refined. The function minimized was $\sum w(\sin^2\theta_o - \sin^2\theta_c)^2$ with weights, $w = 1/\sin^2 2\theta_o$. The final unit cell dimensions with estimated standard deviations are given in Table 1. Tables of the observed powder patterns may be obtained from Department of Physical Chemistry, University of Lund, Sweden.

The lattice parameters of the decahydrates with M = La – Dy have been determined by several authors (see Ref. 6) and the values obtained in the present work agree with those previously reported, within the limits of errors.

Watanabe and Nagashima [10] give lattice parameters of $Er_2(C_2O_4)_3.10H_2O$ and $Sc_2(C_2O_4)_3.6H_2O$. For both compounds their values are significantly different from those obtained in the present work (see Table 1). Since no details are given of their method of recording the powder patterns or of the refinement of the parameters, it seems difficult to find a reason for the deviations.

Weissenberg work. The crystals of YBOX large enough for single crystal work are invariably twinned. The *b*-axis is common for the two parts and the Weissenberg photographs of a crystal mounted along this axis show two reciprocal lattices related to each other by a rotation 180° around *b*.

A tabular crystal of the approximate dimensions 0.05 × 0.05 × 0.02 mm³ mounted along an 0.05 mm edge was used in recording the layers *h0l* – *h5l*. Non-integrated Weissen-

Table 1. Unit cell parameters (in Å and °) and volumes (in Å^3) for the rare earth oxalates $M_2(C_2O_4)_3.nH_2O$.

M	*a*	*b*	*c*	*α*	*β*	*γ*	*V*
A. The monolinic decahydrates							
Ce	11.780(3)	9.625(3)	10.401(3)		119.07(2)		1029.7
Nd	11.678(3)	9.652(3)	10.277(2)		118.92(2)		1013.9
Sm	11.577(2)	9.643(2)	10.169(2)		118.87(2)		994.2
Gd	11.516(2)	9.631(3)	10.081(3)		118.82(2)		979.6
Dy	11.433(2)	9.615(3)	9.988(3)		118.76(2)		962.5
Ho	11.393(3)	9.607(3)	9.955(3)		118.75(2)		955.2
Er [a]	11.359(2)	9.616(2)	9.940(2)		118.72(1)		952.1
B. The triclinic hexahydrates.							
Er	9.644(3)	8.457(3)	9.836(3)	93.54(1)	105.99(1)	85.05(3)	767.7
Tm	9.620(3)	8.458(3)	9.808(3)	93.44(1)	106.12(1)	85.13(3)	763.3
Yb	9.611(2)	8.457(2)	9.778(2)	93.39(1)	106.24(1)	85.29(2)	760.0
Lu	9.597(3)	8.455(2)	9.758(3)	93.42(1)	106.27(1)	85.41(2)	757.1
Sc[b]	9.317(2)	8.468(2)	9.489(2)	93.04(1)	106.50(1)	86.27(2)	715.9

[a] The values given by Watanabe and Nagashima[10] are $a=11.07(4)$ Å, $b=9.52(2)$ Å, $c=9.63(4)$ Å, and $\beta=118.6(2)°$.

[b] The values given by Watanabe and Nagashima, recalculated to the A-centered cell used in the present paper, are $a=9.252(5)$ Å, $b=8.418(5)$ Å, $c=9.446(5)$ Å, $\alpha=92.7(2)°$, $\beta=107.7(2)°$, and $\gamma=86.3(2)°$. The indexes of the two cells are related by $(h,k,l)=(1,0,0/0,-\frac{1}{2},\frac{1}{2}/0,\frac{1}{2},\frac{1}{2})$ $(h,'k',l')$ where h',k',l' refer to the A-centered cell.

berg photographs were taken with Cu$K\alpha$ radiation. The intensities of 828 independent reflexions, representing about 75 % of the possible number in the region investigated, were measured visually by comparison with a calibrated scale. Reflexions from both parts of the crystal were used and in this way all reflexions of a layer could be measured on the same half of the photograph.

The linear absorption coefficient is 238 cm^{-1}, but because of the twinning the intensities could not be corrected for absorption effects. Transmission factors calculated assuming the crystal to be a single crystal range from 0.25 to 0.57 and are for 97 % of the reflexions in the interval 0.35 – 0.55. Too long exposure to X-rays results in disintegration of the crystals and the use of Mo$K\alpha$ radiation was impossible.

REFINEMENT OF THE STRUCTURE

The space group used for the refinement and description of YBOX is $A\bar{1}$ with the general fourfold position $(0,\frac{1}{2},\frac{1}{2}) \pm (x,y,z,)$. The approximate positions of the 13 non-hydrogen atoms of the structure were known from the investigation of the isostructural compound SCOX.[1]

The preliminary atomic coordinates and isotropic temperature factors were improved together with the inter-layer scale factors by full matrix least squares refinement. The function minimized was $\sum w(|F_o|-|F_c|)^2$ with weights w chosen according to Cruickshank.[11] In addition, reflexions not obeying the condition $0.80 \leq |F_o|/|F_c| \leq 1.25$ were given zero weight. The value of $w\Delta^2$ is approximately constant between different $|F_o|$ and sin θ intervals (Table 2),

Table 2. Analysis of the weighting scheme $w = 1/(30 + |F_o| + 0.01|F_o|^2 + 0.001|F_o|^3)$. The averages, $\overline{w\Delta^2}$, where $\Delta = |F_o| - |F_c|$, are normalized.

Interval $\|F_o\|$	Number of reflexions	$\overline{w\Delta^2}$	Interval $\sin\theta$	Number of reflexions	$\overline{w\Delta^2}$
0 – 50	72	1.16	0.00 – 0.37	61	1.16
50 – 59	75	1.10	0.37 – 0.47	61	1.02
59 – 68	74	1.04	0.47 – 0.54	67	0.90
68 – 79	78	1.11	0.54 – 0.59	54	0.69
79 – 92	77	0.99	0.59 – 0.64	46	1.09
92 – 104	74	1.10	0.64 – 0.68	49	1.15
104 – 119	75	0.87	0.68 – 0.71	33	0.97
119 – 140	74	1.05	0.71 – 0.74	37	1.19
140 – 170	67	0.88	0.74 – 0.77	43	0.85
170 – 374	60	0.71	0.77 – 0.80	39	0.99

indicating that the weighting scheme used is reasonable. The atomic scattering factors for the neutral atoms were taken from *International Tables* [12] for O, and C and from Cromer *et al.*[13] for Yb.

After six cycles of refinement the R-factors $R = \sum||F_o| - |F_c||/\sum|F_o|$ and $wR = [\sum w(|F_o| - |F_c|)^2/\sum w|F_o|]^{\frac{1}{2}}$ had converged to 0.118 and 0.103, respectively. Further refinement using anisotropic thermal parameters for Yb and an over-all scale factor resulted in $R = 0.114$ and $wR = 0.097$. In the last cycle of refinement the shifts in all parameters were less than 1 % of their

Table 3. Atomic parameters with estimated standard deviations for the compound $Yb_2(C_2O_4)_3.6H_2O$. The space group is $A\bar{1}$. The transformation of the positional parameters from the A-centered cell to the primitve cell is given by the matrix $(0,-1,-1/-1,-1,1/-1,0,0)$.

Atom	Group	$x \times 10^4$	$y \times 10^4$	$z \times 10^4$	B/Å^2
Yb	$-COO^-$	3072(1)	43(2)	1945(1)	(1.815)[a]
O(1)	$-COO^-$	1076(17)	−307(22)	−430(16)	1.6(2)
O(2)	$-COO^-$	638(13)	303(21)	1865(14)	1.0(2)
O(3)	$-COO^-$	4109(18)	1523(23)	662(17)	2.1(3)
O(4)	$-COO^-$	4561(14)	−1569(22)	833(14)	1.2(2)
O(5)	$-COO^-$	5517(19)	106(26)	3343(19)	2.4(3)
O(6)	$-COO^-$	3110(19)	71(25)	4424(18)	2.4(3)
O(7)	H_2O	2631(16)	2765(23)	2465(16)	1.8(3)
O(8)	H_2O	251(34)	−1520(41)	4312(33)	5.7(6)
O(9)	H_2O	2429(16)	−2525(23)	2100(16)	1.8(3)
C(1)		315(17)	−107(28)	−674(17)	0.6(3)
C(2)		4867(20)	839(29)	−50(17)	1.0(3)
C(3)		5662(17)	36(29)	4758(18)	0.8(3)

[a] The anisotropic thermal parameters for ytterbium, calculated from the expression $\exp[-(h^2\beta_{11} + hk\beta_{12} + \ldots)]$, are $\beta_{11} = 0.0058(1)$, $\beta_{22} = 0.0066(4)$, $\beta_{33} = 0.0045(1)$, $\beta_{12} = -0.0000(2)$, $\beta_{13} = 0.0029(1)$, and $\beta_{23} = 0.0001(2)$, resulting in root mean square displacements along the principal axis of the thermal ellipsoid, $R_1 = 0.163$ (Å), $R_2 = 0.141$ (Å), and $R_3 = 0.152$ (Å).

estimated standard deviations, and 102 reflexions did not obey the condition $0.80 \leq |F_o|/|F_c| \leq 1.25$.

The final atomic parameters with their estimated standard deviations are given in Table 3. Tables of the observed and calculated structure factors may be obtained from Department of Physical Chemistry, University of Lund, Sweden.

The electron density maps of a difference synthesis based upon the parameters given in Table 3 showed, except for a peak of about 4 $e/Å^3$ at the position of Yb, only spurious peaks $1-2$ $e/Å^3$ above a slightly varying background.

Programmes used. All computations were performed on the UNIVAC 1108 computer at Lund Sweden, using the programmes CELSIUS, DRF, LALS, DISTAN, PLANE, and ORTEP.[14]

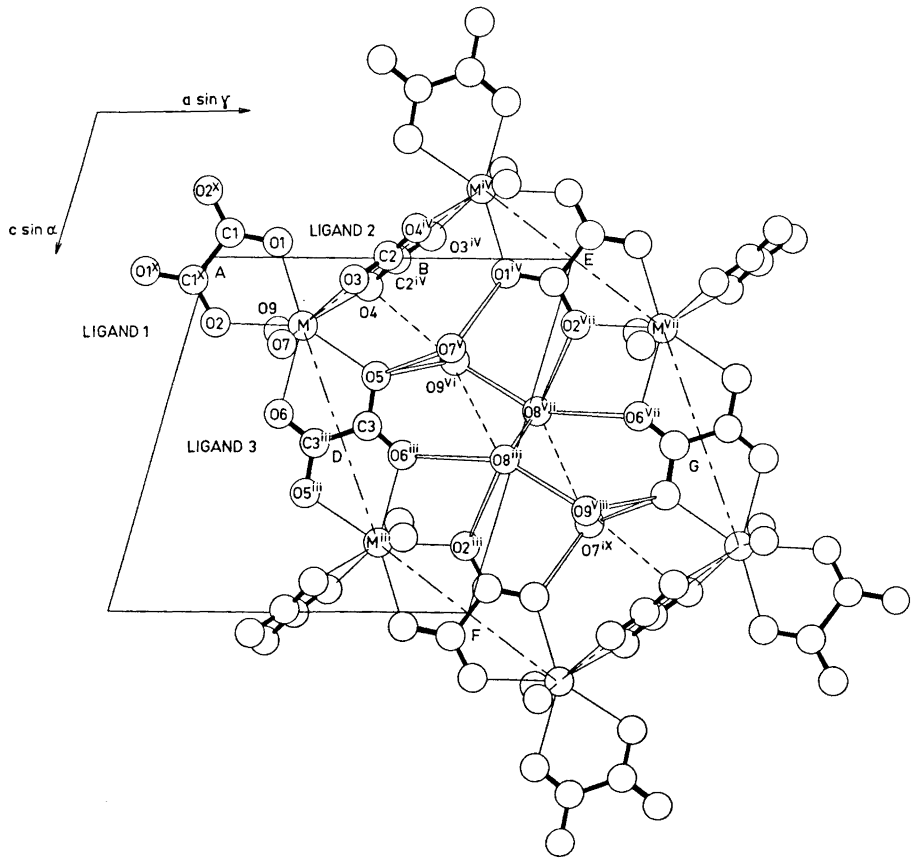

Fig. 1. Part of the metal-oxalate network around $y = 0$ in YBOX and SCOX. It is projected along the b-axis, with $-0.30 \leq y \leq 0.30$, *i.e.* the water oxygens immediately above and below the network are included. Metal-oxygen bonds are drawn as single lines and covalent bonds are filled. The hydrogen bonds probable in both structures are open while the additional possible hydrogen bond distances in SCOX are marked with dashes.

Table 4. Selected distances (Å) and angles (°) with their estimated standard deviations in YBOX and SCOX.

		Yb	Sc			Yb	Sc
A. The metal-oxalate network							
$M^{iv}-M^{vii}$		6.070(4)	5.844(3)	A–M–B		105.53(9)	106.14(5)
M–M^{iv}		6.000(3)	5.814(3)	A–M–D		146.45(4)	145.95(6)
M–M^{iii}		6.090(4)	5.928(3)	B–M–D		107.97(9)	107.84(5)
B. The coordination polyhedron							
M–O(1)		2.341(15)	2.259(6)	O(1)–O(2)	*m*	2.73(2)	2.648(8)
M–O(2)		2.313(13)	2.206(6)	O(1)–O(3)	*g*	2.80(2)	2.739(8)
M–O(3)		2.281(17)	2.184(6)	O(1)–O(4)	*g*	2.83(2)	2.716(1)
M–O(4)		2.342(15)	2.257(6)	O(1)–O(7)	*b*	3.69(2)	3.590(8)
M–O(5)		2.368(18)	2.251(6)	O(1)–O(9)	*b*	3.08(2)	2.924(9)
M–O(6)		2.413(17)	2.258(6)	O(2)–O(6)	*a*	2.94(2)	2.708(8)
M–O(7)		2.359(20)	2.233(6)	O(2)–O(7)	*g*	2.86(2)	2.685(8)
M–O(9)		2.325(19)	2.205(6)	O(2)–O(9)	*g*	2.82(2)	2.782(8)
O(3)–O(4)	*a*	2.62(3)	2.604(8)	O(3)–M–O(4)	$2\theta_A$	69.1(6)	72.9(2)
O(3)–O(5)	*g*	2.88(3)	2.850(8)	O(2)–M–O(6)	$2\theta_A$	76.8(5)	74.7(2)
O(3)–O(7)	*m*	2.68(3)	2.471(8)	O(1)–M–O(5)	$2\theta_B$	140.5(6)	142.4(2)
O(4)–O(5)	*g*	2.72(2)	2.634(7)	O(7)–M–O(9)	$2\theta_B$	145.9(5)	147.4(2)
O(4)–O(9)	*m*	2.86(2)	2.658(9)	A–M–O(7)		88.8(4)	89.3(2)
O(5)–O(6)	*m*	2.80(3)	2.625(8)	B–M–O(7)		104.3(4)	103.6(2)
O(5)–O(7)	*b*	3.38(3)	3.198(8)	D–M–O(7)		84.8(4)	84.8(2)
O(5)–O(9)	*b*	3.73(3)	3.457(8)	A–M–O(9)		76.5(4)	78.9(2)
O(6)–O(7)	*g*	2.99(3)	2.845(9)	B–M–O(9)		109.3(4)	108.8(2)
O(6)–O(9)	*g*	3.03(3)	2.782(8)	D–M–O(9)		90.8(4)	88.3(2)
C. Ligand 1.							
C(1)–$C(1^x)$		1.59(3)	1.537(15)	O(1)–C(1)–O(2)		127(2)	127.5(8)
C(1)–O(1)		1.29(2)	1.244(10)	O(1)–C(1)–$C(1^x)$		117(2)	115.2(9)
C(1)–O(2)		1.28(2)	1.256(10)	O(2)–C(1)–$C(1^x)$		115(2)	117.3(9)
D. Ligand 2.							
C(2)–$C(2^{iv})$		1.43(5)	1.527(15)	O(3)–C(2)–O(4)		123(2)	127.1(7)
C(2)–O(3)		1.23(3)	1.272(10)	O(3)–C(2)–$C(2^{iv})$		118(2)	113.8(8)
C(2)–O(4)		1.27(2)	1.233(10)	O(4)–C(2)–$C(2^{iv})$		119(2)	119.1(9)
E. Ligand 3.							
C(3)–$C(3^{iii})$		1.48(3)	1.513(15)	O(5)–C(3)–O(6)		119(2)	127.6(7)
C(3)–O(5)		1.36(3)	1.279(9)	O(5)–C(3)–$C(3^{iii})$		119(2)	115.3(8)
C(3)–O(6)		1.23(2)	1.243(9)	O(6)–C(3)–$C(3^{iii})$		123(2)	117.1(8)
F. Possible hydrogen bonds.							
$O(7^v)$–$O(1^{iv})$		2.85(2)	2.905(8)	$O(8^{vii})$–$O(9^{vi})$		2.72(4)	2.734(12)
$O(7^v)$–O(5)		2.91(3)	2.931(8)	$O(8^{vii})$–$O(8^{iii})$		2.90(7)	2.932(23)
				$O(8^{vii})$–$O(2^{vii})$		3.04(4)	3.065(12)
$O(9^{vi})$–O(5)		2.93(3)	2.977(8)	$O(8^{vii})$–$O(6^{ii})$		3.12(4)	3.070(12)
$O(9^{vi})$–O(4)		3.10(2)	2.982(9)	$O(8^{vii})$–$O(7^{ix})$		3.34(4)	3.205(12)

DISCUSSION OF THE STRUCTURE

YBOX is isotypic with SCOX the structure of which has been described in detail in Ref. 1. In the present paper the numbering of the atoms and oxalate ions (see Table 3 and Fig. 1) is the same as that used in Ref. 1, as in the significance of the superscripts (i)–(x),* used to indicate equivalent sites in the structure.

The ratio $\sum Z^2_{\text{heavy}}/\sum Z^2_{\text{light}}$ is equal to 7 in YBOX. As a result of this high value the accuracy in the coordinates of the light atoms is fairly low. Fortunately the oxalate ions all have a centre of symmetry whose position may sometimes be used when comparing YBOX with SCOX. Some of these symmetry centres are denoted in the following way:

A: 0,0,0 B: $\frac{1}{2}$,0,0 D: $\frac{1}{2}$,0,$\frac{1}{2}$ E: 1,0,0
F: 1,0,1 G: $\frac{3}{2}$,0,$\frac{1}{2}$

The structure is composed from almost planar metal-oxalate networks parallel to (010). Fig. 1 shows one of these networks projected along b and it is seen that the oxalate ions join the metal ions in a ring centered at (1,0$\frac{1}{2}$). The metal ions are situated at $\pm$ 0.04 Å from the plane $y = 0$. and the intra-ring M–M connecting lines form a hexagon, indicated by dash-dotted lines in Fig. 1, and with the dimensions given in Table 4A. Ligands 1 and 3 are almost in the plane $y = 0$ while ligand 2 is approximately perpendicular to that plane.

Adjacent networks are related by the translation (0,$\frac{1}{2}$,$\frac{1}{2}$) and are held together by hydrogen bonds formed by the three independent water molecules, which are situated between the networks. Two water molecules, O(7) and O(9), are coordinated to the metal ion while the third one, O(8), is hydrogen bonded in the structure. A stereoscopic view of the structure is given in Fig. 2.

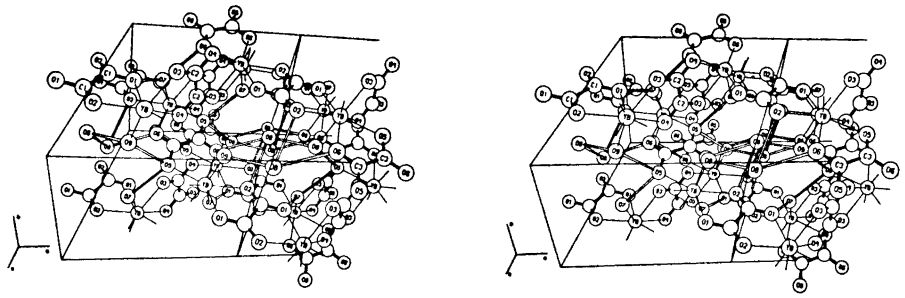

Fig. 2. A stereoscopic view of the YBOX structure drawn by using the program ORTEP. The bonds are indicated as in Fig. 1.

*	x,y,z	(iii)	$1-x,\bar{y},1-z$	(vii)	$1+x,y,z$
(i)	$x,\frac{1}{2}+y,\frac{1}{2}+z$	(iv)	$1-x,\bar{y},\bar{z}$	(viii)	$1+x,\frac{1}{2}+y,\frac{1}{2}+z$
(ii)	$x,-\frac{1}{2}+y,\frac{1}{2}+z$	(v)	$1-x,\frac{1}{2}-y,\frac{1}{2}-z$	(ix)	$1+x,-\frac{1}{2}+y,\frac{1}{2}+z$
		(vi)	$1-x,-\frac{1}{2}-y,\frac{1}{2}-z$	(x)	$\bar{x},\bar{y},\bar{z}$

x,y,z are the atomic coordinates given in Table 3.

The coordination polyhedron. Each ytterbium ion is coordinated by three oxalate ions bonded as chelates and by two water molecules. The Yb – O bond distance is in average 2.34 Å, in agreement with the value 2.23 Å found in SCOX if the difference in metal ionic radius, 0.11 Å,[15] is taken into account.

The eight coordinated oxygens form a distorted $\bar{4}2m$ dodecahedron. The metal ion is approximately in the mean trapezoidal planes of this polyhedron (Table 5) and is also situated very near the planes of the oxalate ions (Table 6). In this respect, the situation is the same in YBOX and SCOX.

Table 5. The deviations in Å from the mean trapezoidal planes, of the central ion and the ligand atoms defining the respective planes.

	Yb	Sc		Yb	Sc
O(1)	−0.10	−0.126	O(7)	−0.12	−0.132
O(2)	0.15	0.201	O(3)	0.21	0.211
O(6)	−0.15	−0.202	O(4)	−0.20	−0.196
O(5)	0.10	0.127	O(9)	0.11	0.117
M	0.05	0.094	M	−0.08	−0.046

Table 6. The deviations in Å of the metal ion and ligand atoms from the respective least squares planes through the ligands. The lower signs refer to the superscripted atoms.

	Ligand 1			Ligand 2			Ligand 3	
	Yb	Sc		Yb	Sc		Yb	Sc
C(1),C(1^{x})	∓0.05	±0.015	C(2),C(2^{iv})	∓0.01	±0.002	C(3),C(3^{iii})	±0.02	±0.000
O(1),O(1^{x})	±0.02	∓0.004	O(3),O(3^{iv})	±0.00	∓0.001	O(5),O(5^{iii})	±0.01	∓0.001
O(2),O(2^{x})	∓0.02	±0.004	O(4),O(4^{iv})	∓0.00	±0.001	O(6),O(6^{iii})	∓0.01	∓0.000
M	−0.03	−0.107	M	−0.11	−0.013	M	−0.17	−0.088

The dimensions of the dodecahedron are given in Table 4B, where the notation of the edges (a, m, g, b) and angles (θ_A, θ_B) are those used by Hoard and Silverton [16] in describing a dodecahedron. The mean distance between coordinated oxygens not belonging to the same oxalate ion is 2.97 Å. The corresponding value for SCOX is 2.82 Å. The number of O – O contacts shorter than 2.80 Å is two in YBOX and nine in SCOX. Thus, not surprisingly, the O – O repulsive forces seem to be less around Yb than around Sc.

In Table 7 the dimensions of the hard sphere model, HSM, of a dodecahedron around Yb(III) and Sc(III), respectively, are given and compared to the dimensions found in the structure determinations. In both structures the polyhedra show deviations in the average edge lengths and angles from the HSM, which are of the magnitude and sign theoretically predicted to minimize the ligand-ligand repulsive forces in a dodecahedron.[17] The ranges of the edge

Table 7. Mean dimensions of the dodecahedra formed by the eight coordinated oxygens in YBOX and SCOX. The corresponding hard sphere models, HSM, have been calculated using the mean M – O bond distance in the respective structures, *viz.* for YBOX 2.34 Å and for SCOX 2.23 Å.

	YBOX			SCOX		
	HSM	Mean	Range	HSM	Mean	Range
Edge (Å)						
a, *m*, *g*	2.81	2.83	2.62 – 3.03	2.68	2.70	2.47 – 2.85
b	3.51	3.47	3.08 – 3.73	3.35	3.29	2.92 – 3.59
Angle (°)						
θ_A	36.9	36.5	34.6 – 38.4	36.9	36.9	36.5 – 37.4
θ_B	69.5	71.6	70.3 – 73.0	69.5	72.5	71.2 – 73.4

lengths found are approximately equal in the two polyhedra. The variation in the angles θ_A and θ_B is larger in YBOX than in SCOX indicating that the YBOX-polyhedron may be somewhat less regular than that of SCOX.

The positions of the coordinated water molecules relative to the oxalate ions are illustrated by the angles formed by the bonds M – O(water) and the lines connecting M with the symmetry centre of the oxalate ions. These angles are included in Table 4B and it is seen that when going from SCOX to YBOX the position of O(9) is changed in a direction towards ligand 1 while that of O(7) is almost unchanged.

The oxalate ions. The three independent oxalate ions are planar within the limits of errors (*cf.* Table 6). The bond distances and angles are given in Table 4, C, D, and E. They do not differ significantly from those commonly found for oxalate ions (see, *e.g.*, Ref. 18). These features were also found in SCOX.

Nevertheless a comparison of the corresponding ligands in the two structures shows a significant decrease in the angle O(5) – C(3) – O(6^{iii}) by $9.1 \pm 1.7°$ in going from SCOX to YBOX and also significant changes in the "bites" of ligands 1 and 3; the distance O(1) – O(2) increases by 0.08 ± 0.02 Å and O(5) – O(6) by 0.17 ± 0.03 Å. A slight increase in this distance might have been expected as a result of the decreased van der Waals repulsions between the coordinated oxygens, but the value 2.80 Å found for O(5) – O(6) must be regarded with some suspicion in view of the values found in other oxalate structures. Thus in $K_2C_2O_4.H_2O$ [18] and $Li_2C_2O_4$ [19] where the oxalate ion is expected to interact relatively weakly with the metal ion, the "bites" are 2.707 and 2.675 Å, respectively. The values found in metal complexes are always smaller. The decrease seems to be more pronounced for oxalate ions in mononuclear complexes than for bridging oxalate ions, *i.e.* those forming two chelates, as judged from the values available in the literature, *viz.* for mononuclear complexes, $Zr(C_2O_4)_4^{4-}$: 2.55 – 2.58 Å,[20] $Pt(C_2O_4)_2^{2-}$: 2.61 – 2.65 Å,[21] $Pd(C_2O_4)_2^{2-}$: 2.63 Å,[21] $NbO(C_2O_4)_3^{3-}$: 2.51 – 2.58 Å,[22] and $Nb(O_2)_2(C_2O_4)_2^{3-}$: 2.59 – 2.60 Å,[23] and for bridges, SCOX: 2.63 – 2.65 Å,[1] NDOX: 2.65 – 2.67 Å,[6] and $NH_4Y(C_2O_4)_2.H_2O$: 2.67 – 2.70 Å.[24] An increase in this distance is found only for the non-chelating part of the oxalate ions in mononuclear complexes; 2.75 – 2.90 Å for the compounds mentioned above.

Hydrogen bonds. The possible hydrogen bond distances are given in Table 4 F. The hydrogen bonds form links between the metal oxalate layers, as is seen in Fig. 2 where the probable hydrogen bonds are indicated by open lines.

The hydrogen bond scheme outlined is very probable also in SCOX. An expected result of the expansion of the structure caused by the increased M – O bond distances in going from SCOX to YBOX might have been increased hydrogen bond distances, but they all remain constant within the limits of errors (Table 6F). Two distances included in Table 6F increase significantly, *viz.* $O(8^{vii}) - O(7^{ix})$ and $O(9^{vi}) - O(4)$. These are the least probable as hydrogen bonds in SCOX: $O(8^{vii}) - O(7^{ix})$ because of its length, 3.20 Å, and $O(9^{vi}) - O(4)$ because of the unfavourable angle $C(2^{iv}) - O(4) - O(9^{vi})$, which is 90°. Hydrogen bonds between these oxygens are still more improbable in YBOX and thus excluded from the hydrogen bond scheme.

The unit cell dimensions and the metal-oxalate network. In Fig. 3 the least squares refined values of *a*, *b*, and *c* for the various lanthanoid oxalate hexahydrates are plotted *versus* the crystal radius, *r*, of the lanthanoid ion.

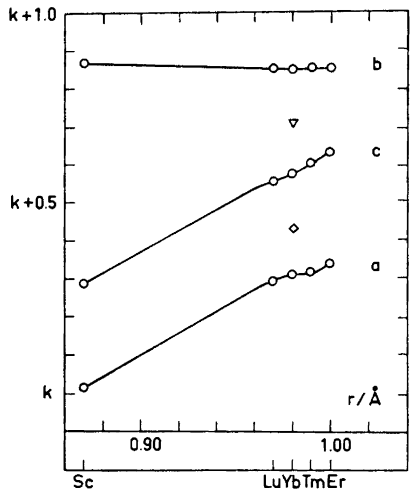

Fig. 3. The lattice parameters *a*, *b*, and *c* of the triclinic compounds $M_2(C_2O_4)_3.6H_2O$ with M = Er – Lu and Sc, plotted *versus* the crystal radius, *r*, of the trivalent metal ions in eight coordination. The values of *k* are, respectively, 9.3, 7.6, and 9.2. The values of *a* and *c* calculated for YBOX by using the model described in the text are denoted by ◇ and ▽, respectively.

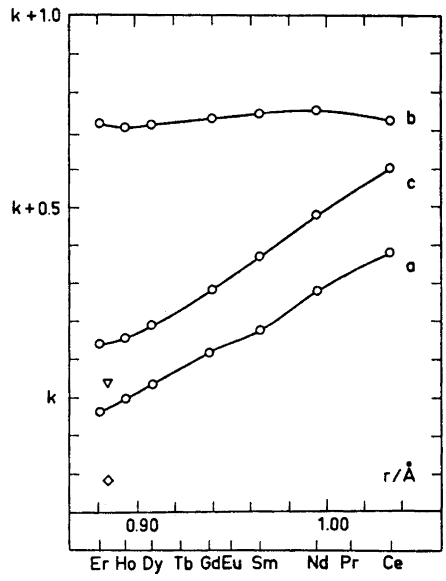

Fig. 4. The lattice parameters *a*, *b* and *c* of the monoclinic compounds $M_2(C_2O_4)_3.10H_2O$ with M = Ce – Er plotted *versus* the crystal radius, *r*, of the trivalent metal ions in six coordination. The values of *k* are, respectively, 11.4, 9.1, and 9.8. The values of *a* and *c* calculated for *r* = 0.885 Å by using the model described in the text and starting with NDOX are denoted by ◇ and ▽, respectively.

Expected changes in a and c in going from SCOX to YBOX may be calculated geometrically assuming the only change of the metal-oxalate network to be the increase in the M–O bond distances by 0.11 Å. Under this assumption the increase in the distance between adjacent metal ions in the ring is found to be 0.26 Å or 4.4 % of the mean value found for this distance in SCOX which is 5.86 Å. This means that all edges of the hexagon will increase by 4.4 % as will all distances between points on the hexagon. Especially the distances D–G and E–F (see Fig. 1), *i.e.* the cell edge lengths a and c, will increase by 4.4 %. The values of a and c calculated for YBOX in this way are included in Fig. 3 and it is obvious that the real values of these parameters are less than expected. This fact shows that the increase in the M–O bond distances is accompanied by changes of the metal-oxalate network that counteract its expansion.

The main features of this distortion of the network may be described by the dimensions of the metal-oxalate hexagon given in Table 4A. The changes in the M–M distances are all less than 0.26 Å. They are 0.23, 0.19, and 0.16 Å and correspond to increases in the M–O bond distances of 0.10, 0.08, and 0.07 Å for the ligands Nos. 1, 2, and 3, respectively. These values are within the limits of errors for those found for ligands 1 and 2 but not for ligand 3 (*cf.* Table 4B), a fact that indicates that the distortion of ligand 3 discussed on p. 831 may be real. There are also small changes in the hexagon angles resulting in a compression of the polygon along [10$\bar{1}$].

The distortions observed result in almost unchanged hydrogen bond distances between SCOX and YBOX. This indicates that the preservation of even this rather weak hydrogen bond system is of great importance for the stability of the structure.

The values of a, b, and c found for the lanthanoid oxalate decahydrates are plotted *versus* r in Fig. 4. The decahydrate structure is composed from metal-oxalate networks very similar to those of the hexahydrates. They are parallel to the ac-plane and joined together by hydrogen bonds. Values of a and c calculated for a 0.11 Å decrease of the M–O bond distances in NDOX, in the way described above, are included in Fig. 4. It is obvious that the change of metal ion even in this structure leads to distortions of the metal-oxalate network. In view of the findings for the hexahydrates and the structures mentioned in the introduction it seems reasonable to assume that also these distortions occur with preserved hydrogen bonds.

In both lanthanoid oxalate series the distance between adjacent metal-oxalate layers, *i.e.* the value of b, is almost independent of the size of the lanthanoid ion (Figs. 3 and 4). For the hexahydrates this distance seems to be determined by the close contact between ligands 2 and 3 of adjacent layers; the shortest nonbonded distance between the layers, $O(3^{I})-O(5)$, is 2.97 Å in YBOX and 3.00 Å in SCOX. No such close contacts were found in NDOX and since only 20 % of the uncoordinated water molecules of that structure have been located it seems meaningless to try to find a reason for the constant inter-layer distance for the decahydrates.

Acknowledgement. I thank Professor Ido Leden and Drs. Jörgen Albertsson and Ingmar Grenthe for useful discussions and helpful comments on the manuscript. This work is part of a research project supported by the *Swedish Natural Sience Research Council.*

REFERENCES

1. Hansson, E. *Acta Chem. Scand.* **26** (1972) 1337.
2. Albertsson, J. *Acta Chem. Scand.* **24** (1970) 3527.
3. Grenthe, I. *Acta Chem. Scand.* **26** (1972) 1479.
4. Hansson, E. and Albertsson, J. *Acta Chem. Scand.* **22** (1968) 1682.
5. Ollendorff, W. and Weigel, F. *Inorg. Nucl. Chem. Lett.* **5** (1969) 263.
6. Hansson, E. *Acta Chem. Scand.* **24** (1970) 2969.
7. Ivanov, V. J. *Russ. J. Inorg. Chem.* **15** (1970) 16.
8. Weigel, F., Ollendorff, W., Sherer, V. and Hagenbruch, R. *Z. anorg. allgem. Chem.* **345** (1966) 119.
9. Steinfink, H. and Brunton, G. D. *Inorg. Chem.* **9** (1970) 2112.
10. Watanabe, M. and Nagashima, K. *J. Inorg. Nucl. Chem.* **33** (1971) 3604.
11. Cruickshank, D. W. J. In Rollet, J. S., Ed., *Computing Methods in Crystallography*, Pergamon, Glasgow 1965, pp. 99–116.
12. *International Tables for X-Ray Crystallography*, Kynoch Press, Birmingham 1962, Vol. III.
13. Cromer, D. T., Larsson, A. C. and Waber, J. T. *Acta Cryst.* **17** (1964) 1044.
14. Liminga, R. *Acta Chem. Scand.* **21** (1967) 1206.
15. Shannon, R. D. and Prewitt, C. T. *Acta Cryst.* **B 25** (1969) 925.
16. Hoard, J. L. and Silverton, J. V. *Inorg. Chem.* **2** (1963) 235.
17. Kepert, D. L. *J. Chem. Soc.* **1965** 4736.
18. Hodgson, D. J. and Ibers, J. A. *Acta Cryst.* **25** (1969) 469.
19. Beagly, B. and Small, R. W. H. *Acta Cryst.* **17** (1964) 783.
20. Glen, G. L., Silverton, J. V. and Hoard, J. L. *Inorg. Chem.* **2** (1963) 250.
21. Krogmann, K. *Z. anorg. allgem. Chem.* **364** (1966) 188.
22. Mathern, G. and Weiss, R. *Acta Cryst.* **B 27** (1971) 1610.
23. Mathern, G. and Weiss, R. *Acta Cryst.* **B 27** (1971) 1572.
24. McDonald, T. R. R. and Spink, J. M. *Acta Cryst.* **23** (1967) 944.

Received September 25, 1972.

ACTA CHEMICA SCANDINAVICA 27 (1973) 835–845

The Crystal and Molecular Structure of 1,2-Dimethyl-3,6-pyridazinedione

T. OTTERSEN

Department of Chemistry, University of Oslo, Oslo 3, Norway

The crystal and molecular structure of 1,2-dimethyl-3,6-pyridazinedione (*N*,*N*-dimethylmaleic hydrazide) has been determined by X-ray methods using 2113 reflections above background level collected by counter methods. The crystals are monoclinic, space group $P2_1/c$, with cell dimensions $a = 8.82_7$ Å; $b = 5.72_3$ Å; $c = 13.25_4$ Å; $\beta = 100.5_8°$. Estimated standard deviations in bond lengths are about 0.0016 Å, and in angles 0.1°. The molecule is found to be non-planar with a C4–C5-bond length of 1.33$_7$ Å. The dihedral angle around the N–N-bond is 29.$_6$°, but the bond lengths indicate a resonance stabilization of the O–C–N-system.

The structure determination of 1,2-dimethyl-3,6-pyridazinedione was carried out as part of a series of structure investigations of 3,6-pyridazinediones.

N,*N*-Dimethylmaleic hydrazide may be resonance stabilized by structures II and III. These resonance structures would give a nearly planar molecule, but resonance structures involving charge separation are not usually favoured.

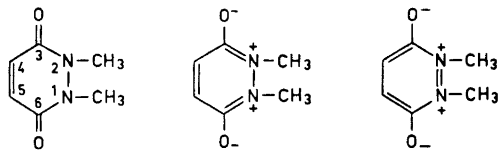

I II III

The molecule is easily hydrogenated to give 1,2-dimethylhexahydro-3,6-pyridazinedione, and also undergoes bromine addition.[1] On this basis Eichenberger *et al.*[1] conclude that *N*,*N*-dimethylmaleic hydrazide is not aromatic.

The structure of 4,5-dichloro-3,6-pyridazinedione has been published.[2] The present structural work was carried out to determine the effect of *N*,*N*-disubstitution on the heterocyclic system.

EXPERIMENTAL

1,2-Dimethyl-3,6-pyridazinedione was synthesized from 3,6-pyridazinedione by the method of Eichenberger *et al.*[1]

The product was recrystallized by slow evaporation of a chloroform/ethyl ether solution. Large rectangular, slightly yellow crystals were formed.

Oscillation, Weissenberg and precession photographs indicated monoclinic symmetry; all reflections ($h0l$) for l odd, and ($0k0$) for k odd, were systematically absent. This uniquely defines the space group as $P2_1/c$.

Unit cell parameters were determined on a Picker manual diffractometer using Cu$K\beta$ ($\lambda = 1.3922$ Å) and Cu$K\alpha$ ($\lambda = 1.5418$ Å) radiation. 24 reflections and their Friedel equivalents were measured. The computer program used in the least square calculations of cell parameters, and programs employed in all subsequent calculations are part of an assembly of programs for CDC-3300 computer.[3]

Three-dimensional intensity data were recorded on an automatic Picker four-circle diffractometer with graphite monochromated Mo$K\alpha$ radiation. The take off angle was 4°, and the temperature during the data collection was 18 ± 1°C.

A crystal of dimensions $0.4 \times 0.35 \times 0.25$ mm was used for the data collection. The $w - 2\theta$ scanning mode with a 2θ scan speed of 1° min^{-1} was utilized. Background counts were taken for 30 sec at each of the scan range limits. Intensities of three standard reflections were measured for every 100 reflections, and the data were adjusted according to the variations in the test reflection intensity. The estimated standard deviations were taken as the square root of the total count with a 2 % addition for experimental uncertainty.

Out of the 2841 unique reflections measured ($2\theta_{max} = 70$°), 2113 had intensities larger than twice the standard deviation. These were regarded as "observed" reflections whereas the remaining reflections were excluded from further calculations.

The intensity data were corrected for Lorentz and polarization effects.

Atomic form factors used were those of Doyle and Turner [4] for oxygen, nitrogen, and carbon, and of Stewart *et al.*[5] for hydrogen.

CRYSTAL DATA

1,2-(N,N')-Dimethyl-3,6-pyridazinedione, $C_6H_8N_2O_2$, monoclinic. $a = 8.827(0.001)$ Å; $b = 5.722(0.001)$ Å; $c = 13.254(0.002)$ Å; $\beta = 100.58°(0.01°)$. Figures in parentheses are estimated standard deviations.

$V = 658.0$ Å^3, $M = 140.1$; D_{obs} (flotation) $= 1.41$ g/cm^3; $Z = 4$; $D_{calc} = 1.413$ g/cm^3; $F(000) = 296$.

Absent reflections: ($h0l$) for l odd; ($0k0$) for k odd; space group $P2_1/c$.

STRUCTURE DETERMINATION

The phase problem was solved by a computer procedure based on direct methods, using symbolic addition [6] and tangent refinement.[7]

The structure model was refined to an R of 0.17. Introduction of anisotropic thermal parameters and least squares refinement resulted in an R of 0.093.

Attempts to locate the hydrogen atoms were not successful, and they were placed in calculated positions (Table 3). A difference Fourier map indicated that the methyl hydrogen atoms were disordered and six hydrogen atoms with half weight were therefore placed around each methyl carbon atom.

In order to reduce valence electron influence it was decided to use only structure factors with sin θ/λ greater than 0.46 in the refinement.

Table 1. Observed and calculated structure factors. The columns are h,k,l, $10|F_o|$, $10\ F_c$.

-12	0	6	57	61	2	0	4	146	- 147	5	1	1	37	36	0	1	13	35	36	-6	1	12	43	40
-12	0	4	25	25	2	0	2	530	- 494	6	1	2	24	- 16	0	1	17	8	- 7	-6	1	13	16	- 14
-12	0	2	15	- 15	2	0	0	599	- 601	6	1	3	45	46	-1	1	18	18	- 18	-6	1	15	44	- 42
-11	0	2	48	50	3	0	0	235	222	5	1	4	10	- 15	-1	1	16	19	- 18	-6	1	16	30	- 29
-11	0	4	40	- 38	3	0	2	24	- 29	5	1	5	87	76	-1	1	15	22	22	-6	1	17	29	- 28
-11	0	6	31	- 30	3	0	4	155	- 161	5	1	6	46	- 43	-1	1	13	49	56	-7	1	16	25	- 23
-11	0	8	20	- 22	3	0	6	150	- 149	5	1	8	19	- 17	-1	1	12	54	56	-7	1	14	25	- 25
-11	0	10	9	- 15	3	0	8	121	121	5	1	9	52	- 53	-1	1	11	21	- 19	-7	1	13	18	17
-10	0	10	26	- 27	3	0	10	100	95	5	1	11	78	- 77	-1	1	10	11	- 10	-7	1	11	19	18
-10	0	6	70	- 70	3	0	14	23	26	5	1	12	14	11	-1	1	9	42	- 36	-7	1	10	85	84
-10	0	4	44	- 44	4	0	14	10	- 8	5	1	12	32	33	-1	1	8	73	63	-7	1	9	86	79
-10	0	2	8	6	4	0	12	32	32	5	1	11	43	45	-1	1	7	201	186	-7	1	8	91	90
-9	0	2	41	40	4	0	10	138	137	5	1	10	108	107	-1	1	6	472	436	-7	1	7	79	80
-9	0	4	8	- 9	4	0	8	8	15	5	1	8	47	46	-1	1	5	13	15	-7	1	6	42	- 39
-9	0	6	47	- 45	4	0	6	24	- 27	5	1	7	24	22	-1	1	4	115	93	-7	1	5	32	- 32
-9	0	10	48	49	4	0	4	210	- 186	5	1	6	68	- 68	-1	1	3	233	216	-7	1	4	89	- 83
-9	0	12	26	- 22	4	0	2	172	- 173	5	1	5	10	13	-1	1	2	189	- 162	-7	1	3	70	- 59
-9	0	14	9	- 9	4	0	0	243	- 226	5	1	4	86	- 83	-1	1	1	167	- 155	-7	1	2	50	- 41
-8	0	14	18	17	5	0	0	121	- 137	5	1	3	101	92	-1	1	0	157	- 145	-7	1	1	56	- 53
-8	0	12	28	29	5	0	2	100	109	5	1	2	115	102	-2	1	0	894	- 977	-7	1	0	9	13
-8	0	10	50	- 52	5	0	4	89	78	5	1	1	66	- 61	-2	1	1	348	- 300	-8	1	0	59	62
-8	0	8	106	- 100	5	0	6	14	14	5	1	0	23	26	-2	1	2	294	- 267	-8	1	1	47	- 46
-8	0	4	12	6	5	0	8	81	76	4	1	0	41	30	-2	1	3	112	109	-8	1	3	19	- 20
-7	0	2	170	- 154	5	0	10	79	83	4	1	1	235	221	-2	1	4	455	413	-8	1	4	41	- 44
-7	0	4	181	- 169	5	0	12	52	55	4	1	2	383	- 343	-2	1	5	259	237	-8	1	5	25	28
-7	0	6	11	- 8	5	0	14	41	- 41	4	1	3	147	- 143	-2	1	6	181	161	-8	1	6	24	- 23
-7	0	8	239	230	6	0	12	37	- 37	4	1	4	320	- 291	-2	1	7	7	- 8	-8	1	7	42	44
-7	0	10	79	82	6	0	10	113	- 112	4	1	5	147	- 130	-2	1	8	26	- 22	-8	1	8	95	- 97
-7	0	12	14	13	6	0	8	100	- 93	4	1	6	9	14	-2	1	11	131	128	-9	1	9	58	- 54
-7	0	16	33	30	6	0	6	78	71	4	1	7	39	31	-2	1	12	114	- 111	-9	1	10	93	- 93
-6	0	16	104	- 105	6	0	4	306	296	4	1	8	156	149	-2	1	14	46	- 49	-9	1	11	15	- 15
-6	0	14	87	- 89	6	0	2	71	56	4	1	9	100	99	-2	1	15	18	- 17	-8	1	12	31	- 29
-6	0	12	73	72	6	0	0	39	- 47	4	1	10	94	90	-2	1	16	20	18	-8	1	13	15	15
-5	0	10	312	304	7	0	0	43	- 41	4	1	11	63	61	-2	1	17	14	- 14	-8	1	14	57	57
-5	0	8	94	96	7	0	2	47	- 52	4	1	12	8	- 7	-2	1	18	76	75	-9	1	15	45	44
-5	0	6	62	- 56	7	0	4	27	- 23	4	1	15	19	19	-3	1	18	11	- 10	-9	1	10	36	- 38
-5	0	4	71	69	7	0	6	56	58	3	1	16	15	13	-3	1	17	24	26	-9	1	9	28	- 28
-5	0	2	14	16	7	0	8	43	- 44	3	1	15	28	29	-3	1	16	26	- 22	-9	1	8	68	- 68
-5	0	2	47	51	7	0	10	65	- 65	3	1	13	52	52	-3	1	15	9	- 9	-9	1	7	48	- 47
-5	0	4	178	159	7	0	12	55	- 60	3	1	12	19	- 20	-3	1	14	37	- 40	-9	1	6	76	- 74
-5	0	6	203	180	8	0	10	45	45	3	1	11	48	- 45	-3	1	13	28	- 31	-9	1	5	40	43
-5	0	8	235	- 222	8	0	8	26	26	3	1	10	107	- 107	-3	1	12	69	- 72	-9	1	4	31	31
-5	0	10	207	- 207	8	0	6	16	- 15	3	1	9	18	11	-3	1	11	7	4	-9	1	2	94	88
-5	0	12	34	- 32	8	0	4	37	- 37	3	1	8	132	- 128	-3	1	10	158	- 159	-9	1	1	41	- 41
-5	0	16	26	- 22	8	0	2	23	- 25	3	1	7	70	66	-3	1	9	186	180	-9	1	0	114	116
-4	0	18	43	43	8	0	0	83	- 84	3	1	6	186	- 185	-3	1	8	6	- 4	-10	1	6	9	8
-4	0	16	82	81	9	0	0	17	18	3	1	5	95	77	-3	1	7	129	- 110	-10	1	1	25	25
-4	0	14	13	- 17	9	0	2	40	- 43	3	1	4	5	- 4	-3	1	6	28	- 11	-10	1	2	17	- 19
-4	0	12	86	- 82	9	0	4	31	34	3	1	3	312	- 278	-3	1	5	247	- 234	-10	1	3	10	11
-4	0	10	187	- 177	9	0	6	14	14	3	1	2	7	6	-3	1	4	109	81	-10	1	4	10	- 6
-4	0	8	38	33	10	0	6	18	20	3	1	1	198	- 183	-3	1	3	146	- 116	-10	1	5	54	- 54
-4	0	6	16	27	10	0	4	12	- 12	3	1	0	13	5	-3	1	2	68	- 50	-10	1	6	67	69
-4	0	4	187	159	10	0	2	13	10	2	1	6	873	977	-3	1	1	231	203	-10	1	7	34	- 35
-4	0	2	22	- 14	10	0	0	52	55	2	1	1	640	- 669	-3	1	0	13	- 5	-10	1	8	65	67
-3	0	2	319	- 296	11	0	0	83	84	2	1	2	703	710	-4	1	0	42	- 30	-10	1	9	18	18
-3	0	4	239	213	11	0	2	60	59	2	1	3	95	93	-4	1	1	21	19	-10	1	10	9	9
-3	0	6	159	143	11	0	4	12	- 12	2	1	4	97	- 91	-4	1	2	51	38	-11	1	9	15	- 15
-3	0	8	6	4	11	1	3	24	25	2	1	5	97	82	-4	1	3	41	- 20	-11	1	7	9	8
-3	0	10	12	9	11	1	2	26	26	2	1	6	73	- 64	-4	1	4	16	- 12	-11	1	6	36	35
-3	0	16	52	- 55	11	1	1	50	50	2	1	7	49	36	-4	1	6	50	- 35	-11	1	5	18	- 17
-3	0	18	26	26	11	1	0	47	48	2	1	8	79	- 75	-4	1	7	89	77	-11	1	4	18	18
-2	0	16	16	17	12	1	0	11	- 8	2	1	9	71	- 65	-4	1	8	11	19	-11	1	3	9	- 5
-2	0	14	13	- 13	12	1	1	28	27	2	1	10	82	- 80	-4	1	9	152	- 144	-11	1	2	33	- 35
-2	0	12	57	- 60	12	1	2	32	- 33	2	1	11	11	- 11	-4	1	10	206	202	-11	1	1	34	33
-2	0	8	85	- 69	12	1	5	27	28	2	1	12	22	- 22	-4	1	11	159	- 155	-11	1	0	48	- 48
-2	0	6	185	161	12	1	7	10	8	2	1	13	14	- 12	-4	1	12	135	133	-12	1	1	14	- 14
-2	0	4	103	- 84	3	1	9	9	9	2	1	14	36	36	-4	1	14	51	- 53	-12	1	3	11	10
-2	0	2	125	91	3	1	7	8	- 6	2	1	15	30	- 30	-4	1	15	40	40	-12	1	4	12	13
-1	0	2	292	- 265	3	1	6	18	17	2	1	16	26	25	-4	1	16	50	50	-12	1	5	34	35
-1	0	4	337	298	3	1	5	20	22	1	1	17	12	- 13	-4	1	17	34	33	-11	2	0	14	- 12
-1	0	6	268	236	3	1	4	17	18	1	1	16	11	9	-5	1	17	17	- 15	-11	2	2	26	- 29
-1	0	10	93	- 95	3	1	3	14	15	1	1	15	17	- 18	-5	1	16	23	21	-11	2	3	11	- 9
-1	0	12	127	133	3	1	2	45	- 42	1	1	14	51	51	-5	1	14	30	28	-11	2	4	8	- 0
-1	0	14	64	66	3	1	1	52	- 52	1	1	13	53	- 55	-5	1	13	27	- 27	-11	2	6	42	42
-1	0	16	37	38	3	1	0	114	- 116	1	1	11	26	22	-5	1	12	19	- 17	-11	2	7	21	22
0	0	18	52	- 49	4	1	0	59	- 62	1	1	10	52	51	-5	1	11	12	- 14	-11	2	8	25	25
0	0	14	114	118	4	1	1	36	- 35	1	1	9	66	- 63	-5	1	10	120	116	-11	2	9	30	32
0	0	12	27	- 24	4	1	2	27	25	1	1	8	87	- 81	-5	1	9	146	- 133	-10	2	12	18	- 16
0	0	10	53	- 44	4	1	3	18	- 14	1	1	7	121	- 107	-5	1	8	104	100	-10	2	11	33	31
0	0	8	8	8	4	1	4	65	66	1	1	6	201	190	-5	1	7	46	- 49	-10	2	10	27	28
0	0	6	379	- 341	4	1	5	64	- 64	1	1	5	29	- 31	-5	1	6	94	- 77	-10	2	9	21	21
0	0	4	453	- 429	4	1	6	37	38	1	1	4	243	231	-5	1	5	135	116	-10	2	8	33	35
0	0	2	608	605	4	1	8	21	- 21	1	1	3	18	2	-5	1	4	245	- 230	-10	2	7	29	31
1	0	0	113	- 108	5	1	9	27	27	1	1	2	363	- 343	-5	1	3	206	170	-10	2	6	18	- 19
1	0	2	583	594	5	1	10	10	- 8	1	1	1	273	250	-5	1	2	79	- 65	-10	2	3	16	15
1	0	4	318	- 290	5	1	11	34	35	1	1	0	156	145	-5	1	1	21	26	-10	2	2	19	20
1	0	6	411	- 383	7	1	11	31	- 33	0	1	1	560	584	-5	1	0	23	- 26	-10	2	1	15	- 17
1	0	8	311	- 285	7	1	10	34	35	0	1	2	59	36	-6	1	1	69	68	-10	2	0	22	21
1	0	10	39	38	7	1	9	9	- 7	0	1	3	95	89	-6	1	2	51	- 49	-9	2	4	36	- 36
1	0	12	59	- 62	7	1	8	26	26	0	1	4	132	131	-6	1	3	60	- 65	-9	2	1	89	87
1	0	14	53	- 53	7	1	6	11	- 13	0	1	5	114	- 99	-6	1	4	12	5	-9	2	2	43	- 45
1	0	16	9	8	7	1	5	21	- 22	0	1	6	154	- 139	-6	1	5	18	- 19	-9	2	3	53	50
2	0	14	40	- 38	7	1	4	15	18	0	1	7	225	- 208	-6	1	6	56	- 50	-9	2	4	51	54
2	0	12	25	22	7	1	3	27	- 29	0	1	8	10	- 3	-6	1	7	10	14	-9	2	5	28	- 31
2	0	10	30	- 30	7	1	2	8	9	0	1	9	31	33	-6	1	8	11	- 17	-9	2	6	17	14
2	0	8	153	148	7	1	1	55	57	0	1	10	56	- 60	-6	1	9	134	128	-9	2	7	65	- 64
2	0	6	148	141	7	1	0	9	- 13	0	1	11	13	- 10	-6	1	11	45	43	-9	2	8	66	- 64

Table 1. Continued.

-9	2	9	37	-	36	-2	2	0	338	-	302	5	2	12	9		5	4	3	8	8	-	7	-3	3	3	87	-	71
-9	2	10	27	-	29	-1	2	0	49	-	52	5	2	13	20		19	4	3	11	9	-	10	-3	3	2	14	-	2
-9	2	11	27	-	27	-2	2	1	10	-	10	5	2	14	12	-	10	4	3	12	22	-	19	-3	3	1	57	-	42
-9	2	13	34		33	-1	2	1	90		84	6	2	13	30		31	4	3	13	28	-	28	-3	3	0	58		52
-8	2	15	16		18	-1	2	2	17		9	6	2	10	19	-	20	4	3	14	10	-	11	-4	3	0	90		88
-8	2	14	40		38	-1	2	3	37		20	5	2	9	18	-	18	3	3	15	26		25	-4	3	2	105		101
-8	2	10	35	-	31	-1	2	4	65		52	6	2	11	8		7	3	3	14	18	-	17	-4	3	3	106	-	92
-8	2	9	54	-	57	-1	2	5	224	-	206	5	2	8	31		30	3	3	13	23	-	22	-4	3	4	69	-	60
-8	2	8	44		45	-1	2	6	127		109	5	2	6	9		10	3	3	12	28		29	-4	3	5	105	-	98
-8	2	7	126	-	126	-1	2	7	10		17	5	2	5	24	-	23	3	3	11	39	-	39	-4	3	6	7	-	8
-8	2	6	105		110	-1	2	8	30		30	6	2	4	77	-	69	3	3	8	51		50	-4	3	7	23	-	15
-8	2	5	18	-	15	-1	2	9	76		69	5	2	3	74		63	3	3	7	16		11	-4	3	8	86	-	96
-8	2	3	41		40	-1	2	10	79	-	79	5	2	2	119	-	112	3	3	6	29	-	26	-4	3	9	73		76
-8	2	2	60	-	58	-1	2	11	105		107	5	2	1	70		75	3	3	5	31	-	31	-4	3	10	89	-	91
-8	2	1	57		56	-1	2	12	21	-	19	6	2	0	33		35	3	3	4	12	-	2	-4	3	11	67		65
-8	2	0	24	-	23	-1	2	13	29	-	29	7	2	0	151		145	3	3	3	100		97	-4	3	12	17	-	16
-7	2	0	153		145	-1	2	14	11	-	7	7	2	1	34		31	3	3	2	15	-	18	-4	3	13	23		22
-7	2	1	141	-	137	-1	2	15	23		22	7	2	2	40		38	3	3	1	152		132	-4	3	15	11		11
-7	2	2	99		97	-1	2	16	15	-	14	7	2	3	36	-	35	3	3	0	59	-	52	-4	3	16	11		11
-7	2	3	86	-	82	0	2	16	8		6	7	2	4	76	-	75	2	3	2	55		61	-5	3	16	15	-	17
-7	2	4	20		22	0	2	14	39	-	37	7	2	5	24		20	2	3	3	53		33	-5	3	15	27	-	27
-7	2	5	7	-	0	0	2	13	79		76	7	2	6	39	-	39	2	3	5	54		55	-5	3	14	31		31
-7	2	6	31	-	35	0	2	12	61	-	61	7	2	8	22		19	2	3	6	27		21	-5	3	13	48		50
-7	2	7	66		65	0	2	11	70		65	7	2	10	27		27	2	3	7	63	-	55	-5	3	11	21		22
-7	2	8	9	-	5	0	2	10	11		14	7	2	11	19	-	19	2	3	8	102	-	102	-5	3	10	22		26
-7	2	9	22	-	23	0	2	9	50		47	8	2	7	19		17	2	3	9	91	-	90	-5	3	9	10	-	13
-7	2	10	21	-	20	0	2	8	90		77	8	2	6	48	-	49	2	3	10	62	-	61	-5	3	8	43	-	38
-7	2	11	30		30	0	2	7	57		56	8	2	5	9		0	2	3	11	8		8	-5	3	7	47		47
-7	2	12	9	-	8	0	2	6	51		54	8	2	4	38	-	38	2	3	12	47	-	44	-5	3	6	68		68
-7	2	13	9	-	4	0	2	5	16	-	5	8	2	3	13	-	12	2	3	13	56		54	-5	3	5	75		73
-7	2	15	19	-	20	0	2	4	75		60	8	2	2	24		21	2	3	14	22	-	22	-5	3	4	113		117
-6	2	16	14		14	0	2	3	41		37	8	2	1	25		25	2	3	15	29		29	-5	3	3	108	-	110
-6	2	15	11	-	14	0	2	2	306	-	257	8	2	0	23	-	23	1	3	16	41	-	40	-5	3	2	155		150
-6	2	14	10		10	0	2	1	246	-	227	9	2	0	97	-	98	1	3	15	36	-	38	-5	3	1	180	-	168
-6	2	13	17		14	0	2	0	439	-	415	9	2	1	76	-	74	1	3	14	23	-	24	-5	3	0	154		144
-6	2	10	64	-	62	1	2	0	49	-	52	9	2	2	41	-	41	1	3	13	27	-	28	-6	3	0	91	-	90
-6	2	12	46	-	46	1	2	1	391		383	9	2	4	24		22	1	3	12	45	-	48	-6	3	1	19		31
-6	2	9	95		95	1	2	2	91		72	9	2	6	13		16	1	3	11	78		76	-6	3	2	107	-	98
-6	2	8	53	-	55	1	2	3	170		135	9	2	7	18		19	1	3	10	54		56	-6	3	3	215		202
-6	2	7	41		49	1	2	4	43		43	9	2	8	18		18	1	3	9	144		140	-6	3	4	64		67
-6	2	6	18	-	32	1	2	7	63	-	55	10	2	6	23		23	1	3	8	46		48	-5	3	5	24		22
-5	2	2	70		52	1	2	8	79		81	10	2	5	22	-	24	1	3	7	59	-	49	-6	3	6	103		99
-6	2	1	99	-	95	1	2	9	98		95	10	2	4	13		12	1	3	6	22		21	-6	3	7	133	-	137
-5	2	0	32		35	1	2	10	104		97	10	2	3	29	-	30	1	3	5	134	-	117	-5	3	8	127		134
-5	2	0	22	-	28	1	2	11	23	-	24	10	2	0	22		21	1	3	4	85		88	-5	3	9	59	-	61
-5	2	1	49	-	44	1	2	12	15		12	11	2	0	14	-	12	1	3	3	101		87	-6	3	11	22		21
-5	2	2	83		73	1	2	13	28	-	25	11	2	1	30		31	1	3	2	75		77	-5	3	13	26	-	25
-5	2	3	93	-	77	1	2	14	41	-	40	11	2	2	16		14	1	3	1	17		8	-5	3	15	11	-	14
-5	2	4	61		46	1	2	16	34	-	32	11	2	3	9		12	1	3	0	169		140	-7	3	15	47		44
-5	2	5	144		135	2	2	16	11	-	10	11	3	0	12	-	13	0	3	1	84	-	75	-7	3	14	37	-	36
-5	2	6	14		17	2	2	15	15		13	10	3	0	13		13	0	3	2	223	-	199	-7	3	13	8	-	10
-5	2	7	10		10	2	2	13	13	-	13	10	3	1	13	-	10	0	3	3	306	-	279	-7	3	11	42	-	41
-5	2	8	8	-	9	2	2	12	11		8	10	3	2	18	-	18	0	3	4	118	-	106	-7	3	10	29	-	27
-5	2	9	21		16	2	2	11	11		7	10	3	3	36	-	34	0	3	5	22	-	17	-7	3	9	12	-	10
-5	2	10	36		41	2	2	10	118	-	112	10	3	4	21	-	22	0	3	6	10	-	10	-7	3	8	20	-	19
-5	2	11	46		47	2	2	9	195	-	188	9	3	7	24		23	0	3	7	317		309	-7	3	7	35	-	34
-5	2	12	25		27	2	2	8	172	-	170	9	3	5	35		36	0	3	8	207		205	-7	3	6	26		28
-5	2	13	46		49	2	2	7	198	-	179	9	3	3	11	-	13	0	3	9	101		96	-7	3	5	79	-	79
-5	2	17	27	-	28	2	2	6	7		0	9	3	1	42	-	41	0	3	10	142		135	-7	3	4	27	-	28
-4	2	17	47	-	48	2	2	5	74		51	8	3	0	41	-	40	0	3	11	123	-	118	-7	3	3	32		31
-4	2	14	44		45	2	2	4	313		291	8	3	1	30		31	0	3	12	110		114	-7	3	2	99	-	91
-4	2	13	9	-	7	2	2	3	406		369	8	3	2	27	-	30	0	3	13	82	-	84	-7	3	1	177		166
-4	2	12	14		18	2	2	2	151		123	8	3	3	48		49	0	3	15	17		16	-7	3	0	153	-	149
-4	2	11	50		48	2	2	1	330		296	8	3	4	37	-	37	0	3	16	13	-	11	-8	3	0	39		40
-4	2	10	81	-	76	2	2	0	337	-	302	8	3	5	13		12	-1	3	16	41		39	-8	3	1	35	-	34
-4	2	9	23		29	3	2	0	14		24	8	3	7	27	-	28	-1	3	15	8		4	-8	3	2	19		21
-4	2	8	35	-	43	3	2	1	26	-	16	9	3	8	13	-	13	-1	3	14	33		31	-8	3	3	18	-	12
-4	2	7	87		87	3	2	2	248	-	225	8	3	9	20		19	-1	3	13	13		11	-8	3	4	22	-	23
-4	2	6	70	-	62	3	2	3	53		43	7	3	11	10		13	-1	3	12	43		43	-8	3	5	29		31
-4	2	5	229	-	204	3	2	4	35		37	7	3	10	25	-	28	-1	3	11	52	-	49	-8	3	6	20	-	22
-4	2	4	184	-	165	3	2	5	65	-	58	7	3	9	13		13	-1	3	10	30		24	-8	3	8	21	-	23
-4	2	3	144	-	154	3	2	6	134		123	7	3	8	31	-	34	-1	3	9	129	-	121	-8	3	9	18	-	17
-4	2	2	29	-	30	3	2	7	55	-	54	7	3	6	28	-	27	-1	3	8	76	-	74	-8	3	10	31		29
-4	2	1	196		183	3	2	8	11	-	10	7	3	5	52	-	53	-1	3	7	28		17	-8	3	13	23		22
-4	2	0	325		290	3	2	9	92	-	88	7	3	4	10		7	-1	3	6	134	-	122	-9	3	11	9		12
-3	2	0	10		24	3	2	10	115	-	114	7	3	3	64	-	66	-1	3	5	240		232	-9	3	10	17	-	19
-3	2	1	120	-	107	3	2	11	50	-	50	7	3	2	23		23	-1	3	4	266	-	241	-9	3	9	14		13
-3	2	2	24	-	5	3	2	13	15		14	7	3	1	62		64	-1	3	3	13	-	24	-9	3	7	12	-	13
-3	2	3	222		203	3	2	14	56		55	7	3	0	152		149	-1	3	2	7		9	-9	3	5	14	-	13
-3	2	4	383	-	331	3	2	16	33		34	5	3	0	91		90	-1	3	1	233	-	210	-9	3	4	27		26
-3	2	5	78		53	4	2	15	29	-	29	6	3	1	163	-	157	-1	3	0	169	-	140	-9	3	3	39		38
-3	2	6	354	-	311	4	2	14	13		9	6	3	2	113		109	-2	3	0	188		178	-9	3	2	19	-	17
-3	2	7	77	-	66	4	2	11	36		37	6	3	3	64	-	63	-2	3	1	139		118	-9	3	1	15		12
-3	2	9	75	-	68	4	2	10	55		53	5	3	4	79		80	-2	3	4	15	-	4	-10	3	0	12	-	13
-3	2	11	81	-	85	4	2	9	102		99	5	3	5	25		26	-2	3	5	106	-	98	-10	3	1	13		16
-3	2	12	23	-	30	4	2	8	38		40	5	3	7	11		14	-2	3	6	51	-	53	-10	3	2	13		14
-3	2	13	28	-	32	4	2	7	10		9	6	3	11	39		38	-2	3	7	45	-	37	-10	3	3	16	-	14
-3	2	15	43	-	44	4	2	6	33	-	32	5	3	12	43		41	-2	3	8	95	-	95	-10	3	5	12	-	9
-3	2	16	36		34	4	2	5	34		26	5	3	13	11	-	4	-2	3	9	44	-	41	-10	3	7	25		25
-3	2	17	24		26	4	2	4	29	-	19	5	3	11	13		11	-2	3	10	47	-	42	-10	3	9	28		29
-2	2	17	35		35	4	2	3	204	-	188	5	3	9	26	-	26	-2	3	11	9		11	-11	3	5	17		18
-2	2	16	39	-	41	4	2	2	272		261	5	3	8	8	-	5	-2	3	12	53	-	53	-11	3	4	13	-	13
-2	2	15	39		37	4	2	1	356	-	330	5	3	7	65	-	59	-2	3	14	38		39	-11	3	3	19	-	19
-2	2	14	21	-	22	4	2	0	326		290	5	3	6	70		68	-2	3	15	21	-	21	-11	3	1	21	-	20
-2	2	13	65	-	64	5	2	0	20	-	28	5	3	5	14		17	-3	3	16	12		13	-11	3	0	13		13
-2	2	12	117		119	5	2	1	52	-	43	5	3	3	95		90	-3	3	14	20	-	19	-10	4	7	30		29
-2	2	11	200	-	195	5	2	2	46		47	5	3	2	16	-	11	-3	3	13	26		24	-10	4	6	12	-	11
-2	2	10	198		186	5	2	3	123	-	114	5	3	1	15		11	-3	3	12	13	-	13	-10	4	5	19		16
-2	2	9	43	-	42	5	2	4	60		56	5	3	0	153	-	144	-3	3	11	28		27	-10	4	2	10		10
-2	2	8	12		10	5	2	5	17		13	4	3	0	98	-	88	-3	3	10	46	-	44	-10	4	1	9		10
-2	2	7	124		114	5	2	6	30	-	23	4	3	1	87	-	80	-3	3	9	23	-	25	-10	4	0	29	-	28
-2	2	6	16		22	5	2	7	61		58	4	3	2	95	-	88	-3	3	8	50		44	-9	4	0	11		15
-2	2	5	276		240	5	2	8	72	-	73	4	3	3	131		106	-3	3	7	29		24	-9	4	1	29	-	28
-2	2	4	112		92	5	2	9	10		10	4	3	4	56		52	-3	3	6	52	-	50	-9	4	2	28		29
-2	2	3	193	-	170	5	2	10	38	-	38	4	3	6	16		13	-3	3	5	11	-	4	-9	4	4	13		14
-2	2	2	56	-	57	5	2	11	48		48	4	3	7	56	-	55	-3	3	4	49		37	-9	4	5	26		27

Table 1. Continued.

-9	4	7	29		28	-1	4	12	28	-	26	9	4	2	42		39	-2	5	10	23		26	-3	6	2	9		8
-9	4	9	12		14	-1	4	13	59		58	9	4	3	13		14	-2	5	11	19	-	23	-3	6	6	14		17
-9	4	10	37		35	-1	4	14	38		37	9	4	4	29		29	-2	5	12	25		25	-3	6	7	9		5
-8	4	10	12	-	14	-1	4	15	45		45	9	4	5	17	-	17	-2	5	13	25		28	-3	6	9	13		8
-8	4	9	16		17	0	4	15	28	-	28	10	4	2	52	-	53	-2	5	14	28		27	-3	6	10	26	-	25
-8	4	8	20	-	21	0	4	14	28	-	28	10	4	1	22	-	22	-3	5	14	36	-	34	-3	6	11	11		13
-8	4	7	19		17	0	4	12	27	-	28	10	4	0	27	-	28	-3	5	13	57	-	58	-2	6	9	28		29
-8	4	6	33	-	34	0	4	11	30		30	9	5	1	30		30	-3	5	10	21		20	-2	6	8	11		7
-8	4	5	19	-	18	0	4	9	98		97	8	5	0	44		44	-3	5	9	33		36	-2	6	7	57		58
-8	4	3	74	-	74	0	4	8	77		77	8	5	1	70		70	-3	5	8	21		20	-2	6	6	30	-	27
-8	4	2	18	-	18	0	4	7	89		81	8	5	2	21		19	-3	5	7	17		18	-2	6	4	42		42
-8	4	0	39		39	0	4	6	58		53	8	5	3	34		31	-3	5	6	11	-	6	-2	6	3	29	-	29
-7	4	1	11		7	0	4	5	59	-	48	8	5	4	15	-	17	-3	5	5	77	-	74	-2	6	2	29		29
-7	4	2	18	-	18	0	4	4	52	-	51	7	5	7	55		53	-3	5	4	36	-	36	-2	6	1	25	-	24
-7	4	3	14		13	0	4	3	43	-	44	7	5	6	17		18	-3	5	3	147		140	-2	6	0	20		17
-7	4	4	38	-	39	0	4	2	7		10	7	5	5	13		14	-3	5	2	99	-	98	-1	6	1	68		67
-7	4	5	53	-	53	0	4	1	68	-	62	7	5	4	12	-	10	-3	5	1	181		177	-1	6	2	117	-	119
-7	4	6	10		5	0	4	0	18	-	16	7	5	2	46	-	43	-3	5	0	57	-	59	-1	6	3	46		46
-7	4	8	21	-	19	1	4	0	25	-	5	7	5	1	29	-	27	-4	5	0	10	-	9	-1	6	4	57	-	57
-7	4	9	12		9	1	4	1	73	-	75	7	5	0	34	-	35	-4	5	1	46	-	48	-1	6	6	11		10
-7	4	10	15	-	13	1	4	2	21	-	23	6	5	0	39	-	41	-4	5	2	14		11	-1	6	7	13	-	15
-7	4	12	31	-	31	1	4	3	55	-	59	6	5	2	22	-	20	-4	5	3	97	-	96	-1	6	8	29	-	28
-7	4	13	21	-	20	1	4	4	47	-	43	6	5	3	35	-	34	-4	5	4	9		7	-1	6	9	18		19
-6	4	14	26	-	28	1	4	5	147		141	6	5	4	24	-	24	-4	5	5	92		92	0	6	11	44	-	47
-6	4	12	9		7	1	4	6	119	-	115	6	5	5	20	-	19	-4	5	6	49		49	0	6	9	66	-	66
-6	4	11	25	-	24	1	4	7	44		40	6	5	7	23		24	-4	5	7	127		129	0	6	8	32		35
-6	4	10	12		13	1	4	8	13	-	9	6	5	10	16	-	15	-4	5	8	57		56	0	6	7	31	-	31
-6	4	9	9		2	1	4	9	11	-	7	5	5	7	18	-	18	-4	5	9	41		44	0	6	6	19	-	19
-6	4	8	9		10	1	4	10	16		14	5	5	6	45		48	-4	5	10	18		18	0	6	5	36		34
-6	4	7	32		37	1	4	11	33	-	33	5	5	5	17		21	-4	5	11	31	-	29	0	6	4	135	-	135
-6	4	6	26	-	27	1	4	12	28		28	5	5	4	39		40	-4	5	13	24	-	23	0	6	3	64		65
-6	4	5	60		57	1	4	15	23	-	24	5	5	3	43	-	43	-5	5	13	34		36	0	6	2	24	-	24
-6	4	4	21		14	2	4	14	53		56	5	5	2	15		12	-5	5	12	11		8	0	6	1	46		48
-6	4	3	19		17	2	4	13	38	-	41	5	5	1	39	-	38	-5	5	10	24	-	25	0	6	0	28		28
-6	4	2	79		80	2	4	12	72		71	5	5	0	29		29	-5	5	9	13		12	1	6	0	11	-	11
-6	4	1	48	-	50	2	4	11	44	-	45	4	5	0	8		9	-5	5	8	45	-	46	1	6	1	21	-	19
-6	4	0	18	-	16	2	4	10	73		71	4	5	1	29	-	32	-5	5	7	34	-	32	1	6	2	115		116
-5	4	0	134	-	133	2	4	8	23	-	23	4	5	2	16		15	-5	5	6	8		3	1	6	3	12		17
-5	4	1	211		205	2	4	7	98		99	4	5	3	9		4	-5	5	4	14		15	1	6	4	113		115
-5	4	2	158	-	151	2	4	6	19	-	12	4	5	5	22	-	21	-5	5	3	17		17	1	6	5	19	-	18
-5	4	3	104		91	2	4	5	12	-	5	4	5	6	28	-	28	-5	5	2	23	-	22	1	6	6	17	-	16
-5	4	4	36		33	2	4	4	15	-	19	4	5	7	22		22	-5	5	1	27	-	28	1	6	8	23		22
-5	4	5	26	-	21	2	4	3	90	-	77	4	5	8	17	-	17	-5	5	0	30	-	29	1	6	9	17		12
-5	4	7	51	-	50	2	4	2	25	-	15	4	5	11	52	-	51	-6	5	0	39		41	1	6	10	22		19
-5	4	8	12	-	11	2	4	1	9		8	3	5	12	17		18	-6	5	2	46		44	2	6	9	22		24
-5	4	9	16		17	2	4	0	71		73	3	5	10	15	-	12	-6	5	3	32	-	31	2	6	8	18	-	11
-5	4	11	17	-	16	3	4	0	129		119	3	5	9	32	-	35	-6	5	4	12		10	2	6	7	32	-	33
-5	4	12	27		27	3	4	1	78	-	75	3	5	8	28	-	29	-6	5	5	64	-	62	2	6	6	39		39
-5	4	14	13	-	11	3	4	2	24		20	3	5	7	56		57	-6	5	6	44	-	47	2	6	5	21	-	21
-5	4	15	28		27	3	4	3	51	-	52	3	5	6	50	-	53	-6	5	7	19		21	2	6	4	34		32
-4	4	14	25		23	3	4	4	27	-	34	3	5	4	80	-	84	-6	5	8	33	-	34	2	6	2	15	-	15
-4	4	13	14	-	13	3	4	5	78	-	75	3	5	3	91	-	93	-6	5	10	17	-	17	2	6	0	18		17
-4	4	12	12	-	10	3	4	6	59		50	3	5	2	47	-	48	-6	5	11	12		13	3	6	0	19	-	21
-4	4	11	24		23	3	4	8	14		14	3	5	0	56		59	-7	5	11	37	-	38	3	6	1	18		21
-4	4	10	54		57	3	4	9	22		20	2	5	0	33	-	31	-7	5	10	12		8	3	6	3	16		13
-4	4	9	84	-	85	3	4	10	27	-	24	2	5	1	27	-	25	-7	5	9	11		9	3	6	4	53	-	54
-4	4	8	116		119	3	4	11	21		20	2	5	3	23	-	19	-7	5	7	35		35	3	6	5	9		2
-4	4	7	74	-	79	3	4	14	10	-	9	2	5	4	42		45	-7	5	5	19		18	3	6	7	20	-	21
-4	4	6	150		146	4	4	12	65	-	63	2	5	5	58		63	-7	5	3	49	-	48	3	6	8	21		22
-4	4	5	59		54	4	4	11	38	-	37	2	5	6	28		25	-7	5	2	11		11	3	6	9	10	-	7
-4	4	4	93	-	86	4	4	10	45	-	43	2	5	7	19	-	21	-7	5	1	25	-	23	4	6	6	14	-	17
-4	4	3	175		167	4	4	8	21		17	2	5	9	28		27	-7	5	0	35		35	4	6	5	11		6
-4	4	2	163	-	166	4	4	7	9	-	10	2	5	10	34		32	-8	5	0	45	-	44	4	6	4	26		25
-4	4	1	11	-	3	4	4	6	44	-	48	2	5	11	59		56	-8	5	2	16	-	15	4	6	3	20		21
-4	4	0	42	-	37	4	4	5	21	-	25	2	5	12	18		15	-8	5	3	25	-	26	4	6	2	12		10
-3	4	0	129		119	4	4	4	28	-	28	2	5	13	30		31	-8	5	4	14	-	13	4	6	0	12		8
-3	4	1	86	-	86	4	4	3	33	-	35	1	5	13	38		39	-8	5	5	22		19	5	6	0	23		21
-3	4	2	227		222	4	4	1	84		75	1	5	12	25	-	25	-8	5	6	32	-	28	5	6	1	35		31
-3	4	3	108	-	104	4	4	0	42	-	37	1	5	11	9		7	-8	5	7	18		14	5	6	2	12		12
-3	4	4	63		54	5	4	0	133	-	133	1	5	8	27		26	-8	5	8	13	-	14	5	6	4	11	-	9
-3	4	5	52	-	50	5	4	2	18	-	11	1	5	7	33	-	33	-9	5	6	19		19	5	6	5	15	-	14
-3	4	6	10		1	5	4	3	89		89	1	5	6	12		11	-9	5	4	10		11	5	6	6	57	-	57
-3	4	7	52		52	5	4	4	49		52	1	5	5	18		19	-9	5	3	16		14	5	6	7	30	-	29
-3	4	8	52		51	5	4	5	49		55	1	5	3	74		76	-9	5	2	12		8	6	6	6	20		18
-3	4	9	36		36	5	4	6	10		14	1	5	1	10	-	7	-9	5	1	14	-	13	6	6	5	23		27
-3	4	10	25		27	5	4	7	22		23	1	5	0	42	-	42	-7	6	2	10		10	6	6	4	14		11
-3	4	11	15	-	18	5	4	8	8	-	6	0	5	1	9	-	13	-7	6	4	25	-	23	6	6	3	19	-	17
-3	4	12	9	-	10	5	4	9	11		11	0	5	3	13		15	-7	6	6	27		30	6	6	2	23	-	22
-3	4	13	10	-	5	5	4	10	35		35	0	5	4	58		53	-7	6	7	21	-	19	6	6	1	59	-	58
-3	4	14	37	-	38	5	4	11	11	-	9	0	5	5	74	-	74	-6	6	9	20	-	24	6	6	0	57	-	54
-3	4	15	32	-	29	5	4	12	9		5	0	5	6	27		23	-6	6	8	42	-	42	7	6	1	48	-	46
-2	4	13	40		38	6	4	11	15		14	0	5	7	30	-	29	-6	6	7	18	-	21	7	6	2	24	-	22
-2	4	12	10	-	9	6	4	10	15		13	0	5	8	35	-	34	-6	6	6	76	-	76	7	6	3	44	-	43
-2	4	11	64		64	6	4	8	13		13	0	5	9	12	-	9	-6	6	5	21	-	22	5	7	2	19		16
-2	4	10	111	-	111	6	4	6	32		32	0	5	10	65	-	64	-6	6	4	20	-	15	5	7	1	29		27
-2	4	9	13	-	9	6	4	4	32	-	27	0	5	11	43		46	-6	6	3	10	-	5	5	7	0	15		16
-2	4	8	163	-	162	6	4	3	51		47	0	5	12	35	-	36	-6	6	1	55		58	4	7	0	44		44
-2	4	7	206	-	196	6	4	2	42	-	40	-1	5	11	9	-	11	-6	6	0	57	-	54	4	7	1	42		42
-2	4	6	103	-	101	6	4	1	33		30	-1	5	10	24		25	-5	6	0	22		21	4	7	2	25		26
-2	4	5	71	-	71	6	4	0	17	-	16	-1	5	7	13	-	11	-5	6	1	60	-	58	4	7	4	17	-	18
-2	4	4	145		135	7	4	1	42		39	-1	5	5	11	-	10	-5	6	3	14	-	10	3	7	6	50		51
-2	4	3	41		45	7	4	3	34		34	-1	5	4	70		68	-5	6	4	36		37	3	7	5	15		13
-2	4	2	107		100	7	4	4	21	-	21	-1	5	3	128	-	118	-5	6	5	16		13	3	7	4	45		46
-2	4	1	77		66	7	4	5	18	-	18	-1	5	2	138		131	-5	6	7	18		15	3	7	3	30	-	23
-2	4	0	71		73	7	4	6	22	-	23	-1	5	1	29	-	31	-5	6	8	20	-	23	3	7	2	28		25
-1	4	0	26	-	5	7	4	7	39	-	40	-1	5	0	43		42	-5	6	10	10	-	9	3	7	1	36	-	34
-1	4	1	62	-	60	7	4	8	26		25	-2	5	0	32		31	-4	6	9	33		35	3	7	0	20	-	20
-1	4	2	86	-	81	8	4	7	13	-	13	-2	5	1	30		30	-4	6	7	45		46	2	7	0	19		19
-1	4	3	79	-	70	8	4	5	9		5	-2	5	2	69	-	74	-4	6	6	47		44	2	7	2	32	-	32
-1	4	4	12	-	17	8	4	4	57		59	-2	5	3	186		186	-4	6	5	8		4	2	7	3	31		31
-1	4	5	32		35	8	4	3	9	-	12	-2	5	4	98	-	96	-4	6	3	67	-	67	2	7	4	47	-	47
-1	4	6	76		71	8	4	2	70		70	-2	5	5	51		47	-4	6	2	24		23	2	7	5	38		39
-1	4	8	45	-	45	8	4	1	25	-	27	-2	5	6	26	-	21	-4	6	1	44	-	42	2	7	6	31	-	33
-1	4	9	103	-	103	8	4	0	39		39	-2	5	7	153	-	152	-4	6	0	9		8	2	7	7	12	-	5
-1	4	10	47	-	45	9	4	0	11		15	-2	5	8	23		26	-3	6	0	21	-	21	1	7	4	24	-	25
-1	4	11	27		29	9	4	1	19		18	-2	5	9	94	-	95	-3	6	1	12		17	1	7	3	50		51

Table 1. Continued.

1	7	2	31	-	32	-9	1	18	13	-	9	2	3	17	14	-	13	7	5	10	17		14	7	6	5	10		8		
1	7	1	33		34	-10	1	17	15		15	2	3	16	13		12	6	5	13	19		12	7	6	4	10		12		
0	7	3	24	-	26	-10	1	15	16	-	18	1	3	19	9		8	6	5	12	14	-	15	8	6	1	19		19		
0	7	4	9		8	-10	1	13	17	-	17	0	3	18	15	-	15	5	5	10	9	-	10	8	6	5	14	-	13		
0	7	5	18	-	15	-11	1	12	9	-	6	0	3	17	26		28	5	5	12	14	-	12	9	6	5	9		7		
0	7	6	10		8	-11	1	13	15		15	-1	3	17	21	-	22	4	5	14	21		24	3	6	0	12	-	1		
0	7	7	30		31	-11	1	15	18		19	-1	3	18	9	-	8	4	5	13	27	-	28	10	6	0	18		19		
-1	7	8	12	-	11	-12	1	11	12		12	-2	3	18	12		12	4	5	12	16		18	10	6	1	12		14		
-1	7	7	9	-	8	-13	1	0	17	-	17	-3	3	18	23		24	3	5	14	10		10	8	7	1	16	-	17		
-1	7	5	12	-	12	-13	1	1	13	-	10	-4	3	19	28	-	27	2	5	16	14	-	14	9	7	0	11	-	11		
-1	7	3	53	-	55	-13	1	3	12		10	-4	3	18	29	-	29	2	5	15	13	-	13	7	7	6	18	-	18		
-1	7	2	59	-	59	-13	1	4	13		11	-4	3	17	26	-	26	1	5	16	11		7	5	7	8	11	-	6		
-1	7	1	12	-	12	-13	1	6	20		16	-5	3	17	37	-	37	0	5	14	26	-	26	6	7	6	12		10		
-2	7	0	18	-	19	-13	1	9	12		15	-5	3	19	14		11	-1	5	16	11		10	5	7	5	21		22		
-2	7	1	42	-	41	-13	1	10	10	-	7	-6	3	19	20		22	-1	5	17	10	-	15	6	7	4	9		8		
-2	7	2	37		37	-13	2	9	14	-	14	-6	3	18	35		34	-2	5	17	10		11	5	7	2	10	-	8		
-2	7	3	25	-	25	-13	2	6	15	-	18	-6	3	17	42		41	-2	5	15	16	-	14	5	7	1	17	-	16		
-2	7	4	48		49	-13	2	2	10		10	-6	3	16	19		21	-3	5	16	24	-	24	6	7	0	18	-	14		
-2	7	6	14		14	-12	2	0	19	-	20	-7	3	17	12		11	-3	5	17	16		20	5	7	3	35		37		
-2	7	8	10		12	-12	2	4	18		18	-8	3	17	10	-	9	-4	5	15	19		21	5	7	4	17	-	15		
-3	7	7	19		20	-12	2	6	9	-	7	-8	3	16	21	-	22	-5	5	14	10		11	5	7	5	17	-	18		
-3	7	6	17		17	-12	2	8	29	-	31	-10	3	14	24	-	19	-6	5	15	15	-	14	5	7	6	56	-	59		
-3	7	3	10		12	-12	2	9	9	-	1	-10	3	13	15	-	16	-7	5	12	40		42	5	7	7	61	-	59		
-3	7	2	37		37	-12	2	13	12		12	-11	3	7	38		39	-7	5	13	59	-	60	5	7	8	19	-	17		
-3	7	1	16	-	12	-10	2	13	14	-	14	-11	3	8	21		20	-7	5	14	38		38	5	7	9	18	-	16		
-3	7	0	21		20	-10	2	14	34	-	35	-11	3	10	47		47	-8	5	13	25		25	4	7	9	20		19		
-4	7	0	44	-	44	-10	2	15	19	-	21	-11	3	11	42	-	40	-8	5	12	10		8	4	7	8	17		21		
-4	7	1	42		41	-10	2	16	10	-	12	-11	3	12	25		27	-8	5	11	27	-	27	4	7	6	10		8		
-4	7	2	38	-	37	-9	2	16	22	-	20	-11	3	13	29	-	31	-9	5	10	22		24	4	7	5	47	-	50		
-4	7	5	11		10	-9	2	15	12		13	-12	3	9	32	-	34	-9	5	7	16	-	15	3	7	7	42		42		
-4	7	6	34	-	32	-9	2	14	16	-	13	-12	3	6	20	-	18	-9	5	8	17		16	3	7	8	17		17		
-4	7	7	9		7	-8	2	16	22		23	-12	3	5	16		13	-9	5	10	25	-	25	3	7	9	14		13		
-5	7	5	14		9	-7	2	19	18		17	-12	3	2	11	-	7	-9	5	11	63		63	3	7	10	10		12		
-5	7	2	12		9	-7	2	18	13	-	11	-12	3	4	14	-	13	-9	5	12	42	-	40	2	7	12	11		8		
-5	7	1	17	-	16	-7	2	17	14	-	13	-13	3	5	16	-	16	-9	5	13	34		33	2	7	11	19	-	19		
-5	7	0	17	-	15	-7	2	16	13		14	-13	3	6	11	-	11	-10	5	9	12		12	2	7	10	14		11		
-14	0	4	17	-	14	-5	2	17	19		19	-13	3	7	15	-	16	-10	5	6	21		20	2	7	9	17	-	18		
-13	0	6	9		11	-5	2	18	22		23	-12	4	1	13	-	11	-10	5	4	29		30	2	7	8	17		19		
-13	0	4	22		24	-5	2	20	17		16	-12	4	2	9		8	-10	5	2	16		17	1	7	9	10		6		
-13	0	2	14	-	13	-4	2	18	48	-	48	-12	4	3	14	-	13	-10	5	1	10		5	1	7	10	14	-	17		
-12	0	8	24		25	-4	2	19	37	-	36	-12	4	4	16		15	-11	5	1	10	-	11	0	7	12	12	-	8		
-12	0	12	12		7	-4	2	20	28	-	26	-12	4	5	10	-	7	-11	5	3	12	-	12	0	7	11	14	-	11		
-12	0	14	16		16	-3	2	20	14	-	16	-12	4	8	10	-	16	-11	5	4	13	-	11	-1	7	10	21	-	20		
-11	0	14	16		16	-3	2	18	25		26	-11	4	12	37	-	37	-11	5	6	13	-	12	-1	7	12	11	-	6		
-10	0	16	13		12	-2	2	19	44		44	-11	4	11	41		39	-11	5	9	11	-	11	-1	7	13	19		22		
-9	0	18	20		20	-2	2	20	20		21	-11	4	10	39	-	37	-10	6	0	20		19	-2	7	11	26		26		
-9	0	16	11		11	-1	2	20	9	-	10	-11	4	9	20		16	-10	6	1	10	-	8	-2	7	9	24		24		
-9	0	18	17	-	17	-1	2	19	9		1	-11	4	7	10	-	7	-10	6	2	16		16	-3	7	10	10		5		
-5	0	20	16		18	-1	2	18	33	-	36	-11	4	6	10		11	-10	6	4	12	-	5	-3	7	12	17		18		
-5	0	18	38	-	35	0	2	18	27		25	-11	4	3	18	-	17	-10	6	6	11		9	-3	7	13	29	-	29		
-3	0	20	9		8	0	2	19	24	-	23	-10	4	9	17	-	20	-10	6	7	10	-	8	-4	7	11	19	-	20		
-2	0	20	32		32	1	2	18	9		7	-10	4	10	27		27	-9	6	6	19	-	21	-4	7	10	11		5		
-1	0	20	9	-	1	3	2	18	13		12	-10	4	11	20	-	20	-9	6	2	19		21	-4	7	9	12	-	15		
2	0	18	19		19	3	2	17	12		12	-10	4	12	11	-	7	-8	6	1	15	-	15	-4	7	8	24	-	22		
4	0	16	13	-	3	5	2	17	13	-	12	-9	4	15	21	-	19	-8	6	2	15	-	15	-5	7	7	29	-	29		
5	0	16	20	-	18	5	2	15	10		11	-9	4	14	14		15	-8	6	3	10		11	-5	7	8	34		35		
6	0	16	9	-	12	6	2	14	20		19	-9	4	13	38	-	37	-8	6	4	31		33	-5	7	9	16	-	16		
7	0	16	15		13	6	2	15	15		16	-9	4	12	63		65	-8	6	5	10	-	1	-5	7	11	25		25		
9	0	12	34		34	6	2	16	9		4	-9	4	11	35	-	35	-8	6	6	35		33	-5	7	12	28	-	27		
8	0	14	9	-	9	7	2	15	10	-	6	-8	4	14	10		12	-8	6	8	11		10	-6	7	11	14		14		
9	0	12	24		22	7	2	14	9		10	-8	4	15	11	-	9	-7	6	13	30		29	-6	7	10	10		7		
9	0	10	10	-	9	8	2	11	31	-	31	-8	4	16	20	-	19	-7	6	12	67	-	67	-6	7	7	30	-	30		
11	0	6	14	-	14	8	2	13	33	-	32	-7	4	17	17		17	-7	6	11	33		31	-6	7	5	28	-	28		
13	0	4	16	-	16	8	2	14	12	-	10	-7	4	16	18		17	-7	6	8	36		36	-6	7	4	11	-	11		
13	0	2	39	-	41	9	2	11	9	-	13	-7	4	15	21		20	-6	6	10	18		20	-6	7	3	18		18		
13	0	0	39	-	40	9	2	10	13		15	-6	4	17	28		27	-5	6	12	23		22	-6	7	2	11		7		
13	1	0	16		17	10	2	8	13		13	-5	4	16	44	-	44	-5	6	13	11		12	-6	7	0	17		14		
13	1	1	23	-	27	10	2	9	25		25	-3	4	16	19		19	-5	6	14	23	-	23	-7	7	0	19		18		
13	1	3	19	-	19	10	2	11	17		16	-2	4	16	18	-	17	-5	6	15	16	-	17	-7	7	3	12	-	13		
12	1	7	13	-	9	11	2	7	12	-	10	-1	4	18	9		6	-5	6	14	52		54	-7	7	6	18	-	14		
12	1	1	18	-	18	11	2	6	9	-	12	0	4	16	22		20	-5	6	13	17	-	19	-7	7	8	10		9		
11	1	5	16	-	15	12	2	8	18	-	20	1	4	17	19	-	19	-5	6	12	54		55	-7	7	10	11		6		
11	1	8	11	-	11	12	2	1	11		9	2	4	15	13		14	-5	6	11	17	-	15	-8	7	8	14		16		
10	1	10	16		17	12	2	3	29		30	3	4	15	10	-	11	-4	6	12	37	-	37	-8	7	7	10		12		
9	1	10	22	-	24	12	2	4	12		12	4	4	14	33	-	34	-4	6	13	10	-	6	-8	7	6	22		24		
9	1	11	14		15	12	2	5	15		15	4	4	15	17		18	-4	6	15	14	-	14	-8	7	5	15		19		
9	1	12	11	-	12	13	2	0	10		6	5	4	15	13		14	-3	6	15	10		11	-8	7	4	13		14		
9	1	13	16		15	12	3	4	13		13	5	4	13	28	-	27	-3	6	14	19	-	19	-8	7	1	21	-	22		
8	1	14	19	-	21	12	3	3	11		5	6	4	12	22		22	-2	6	12	22		21	-6	8	0	14		17		
8	1	13	9	-	5	12	3	2	25		25	8	4	8	17	-	15	-2	6	14	10		5	-6	8	2	12		15		
8	1	12	17	-	18	12	3	1	18		12	8	4	10	10		7	-1	6	13	13	-	14	-6	8	4	12		8		
7	1	13	25	-	25	12	3	0	14		13	9	4	10	23	-	25	0	6	12	9	-	7	-5	8	5	12	-	14		
7	1	14	9	-	9	11	3	1	13	-	11	9	4	9	20	-	19	0	6	13	18	-	18	-5	8	3	11	-	10		
7	1	15	13		13	11	3	2	15	-	16	9	4	8	40	-	40	0	6	14	12		14	-5	8	1	16	-	18		
5	1	15	27	-	27	11	3	3	22	-	22	9	4	7	24	-	25	0	6	15	16		17	-4	8	6	21		22		
5	1	17	10	-	10	11	3	4	20	-	18	10	4	4	19	-	20	1	6	13	15	-	17	-4	8	4	14	-	15		
4	1	18	9		10	11	3	5	11	-	12	10	4	5	14		15	1	6	12	10		10	-4	8	7	20	-	21		
2	1	19	21		19	11	3	6	11		8	10	4	7	9	-	8	2	6	11	34		35	-3	8	9	12	-	10		
2	1	18	23	-	21	11	3	7	13		12	11	4	5	12		11	2	6	13	21		16	-3	8	8	28		27		
1	1	18	17		19	10	3	7	24		22	11	4	4	18	-	18	2	6	14	9	-	8	-3	8	5	14		14		
1	1	19	17		19	10	3	8	19	-	18	11	4	3	26	-	25	3	6	14	11	-	13	-3	8	2	29		30		
0	1	20	15	-	15	9	3	9	16	-	17	11	4	2	19	-	20	3	6	13	11		11	-3	8	1	16		16		
0	1	19	31	-	30	9	3	10	9	-	6	11	4	1	21	-	21	3	6	12	10	-	13	-2	8	0	38	-	40		
-1	1	19	30	-	28	9	3	11	10	-	10	10	5	4	13	-	17	3	6	11	14		15	-2	8	1	20		21		
-1	1	20	22		20	8	3	12	18	-	20	10	5	3	16	-	16	4	6	11	9		13	-2	8	2	21	-	23		
-2	1	19	35		36	8	3	10	12	-	12	10	5	1	25	-	26	4	6	13	10		7	-2	8	3	22		21		
-3	1	19	13		13	7	3	12	11	-	10	9	5	2	28		27	5	6	12	12		9	-2	8	6	20	-	18		
-4	1	19	19	-	20	7	3	13	19		19	9	5	3	42		41	5	6	9	15	-	15	-2	8	7	11		14		
-4	1	18	32	-	32	6	3	14	16		14	9	5	6	26	-	27	5	6	8	53	-	54	-2	8	8	13	-	11		
-5	1	18	8		3	6	3	13	28		25	9	5	7	36	-	38	5	6	8	25	-	25	-1	8	5	14		12		
-5	1	20	11	-	12	5	3	15	11	-	10	9	5	8	26	-	24	6	6	9	14	-	14	-1	8	1	25	-	26		
-6	1	18	14	-	12	5	3	16	13		16	8	5	10	12		12	5	6	11	10	-	7	0	8	2	14		16		
-7	1	17	18		15	4	3	17	11		12	8	5	9	18		19	7	6	9	21		15	0	8	3	31	-	34		
-7	1	19	18	-	19	4	3	16	15	-	19	8	5	7	11	-	8	7	6	8	48		47	0	8	4	23		23		
-8	1	16	29		31	4	3	15	18	-	18	7	5	8	34		33	7	6	7	42		42	0	8	5	12	-	5		
-9	1	15	24	-	23	3	3	17	21		20	7	5	9	35		34	7	6	6	51		51	0	8	6	16		16		

Table 1. Continued.

0	8	8	10		5	2	8	0	38	-	40	3	8	5	41		45	5	8	1	10	-	9	-1	9	1	14	-	12
1	8	8	14	-	15	2	8	1	23	-	25	3	8	2	40	-	40	6	8	0	19		17	-2	9	1	11	-	9
1	8	7	21	-	21	2	8	4	36		40	4	8	0	22		22	5	8	1	13		15	-2	9	0	13		10
1	8	6	23	-	23	2	8	5	13		14	4	8	1	10		10	1	9	0	10		10	1	2	6	99		89
1	8	5	45	-	46	2	8	8	18	-	20	4	8	4	36	-	39	1	9	2	12		18	-3	2	8	73		68
1	8	4	13	-	15	3	8	0	17		16	4	8	6	23	-	26	0	9	2	18	-	21	2	3	0	189	-	178
1	8	3	11	-	10	3	8	7	35		35	5	8	4	17		19	0	9	1	24		25	2	3	1	100		87
1	8	1	17		14	3	8	6	42		42	5	8	2	13		10														

Table 2. Fractional atomic coordinates and thermal parameters with estimated standard deviations ($\times 10^5$) for non-hydrogen atoms. The temperature factor is given by $\exp-(B_{11}h^2+B_{22}k^2+B_{33}l^2+B_{12}hk+B_{13}hl+B_{23}kl)$.

Atom	x	y	z	B_{11}	B_{22}	B_{33}	B_{12}	B_{13}	B_{23}
O1	42603	17762	36483	2081	2688	681	1927	1178	117
	18	22	10	20	32	7	40	20	23
O2	9878	71535	57226	1459	3663	562	1348	505	−824
	14	25	9	14	41	6	35	14	23
N1	19929	64726	42923	977	1881	444	644	210	−120
	11	18	7	11	25	5	25	11	16
N2	28472	50364	37516	1034	1904	408	429	400	70
	11	17	7	11	25	5	26	11	17
C3	35509	30490	41568	1119	1816	490	578	530	64
	14	19	9	12	29	6	29	13	20
C4	34786	35756	52303	1224	2262	483	727	425	399
	15	24	9	14	32	6	32	15	22
C5	27482	40274	57627	1208	2733	406	499	343	118
	15	25	9	14	36	5	34	14	22
C6	18504	59992	52817	985	2372	425	355	215	−469
	13	22	9	12	31	6	29	13	21
C7	9190	81033	36837	1286	2676	665	1393	153	371
	17	27	13	16	39	8	40	18	28
C8	32060	59518	27923	1669	2941	414	497	533	388
	19	27	10	19	40	6	43	17	24

Table 3. Fractional atomic coordinates ($\times 10^4$) and isotropic thermal parameters for hydrogen atoms.

Atom	x	y	z	Weight	B
H41	3988	1152	5566	1.0	3.0
H51	2798	3742	6513	1.0	3.0
H71	1033	9830	3614	0.5	3.0
H711	−61	7906	3951	0.5	3.0
H712	791	7493	2967	0.5	3.0
H72	−102	7580	3295	0.5	3.0
H721	699	9336	4171	0.5	3.0
H722	1482	8798	3167	0.5	3.0
H81	2772	5669	2053	0.5	3.0
H811	3089	7676	2868	0.5	3.0
H812	4321	5544	2846	0.5	3.0
H82	4104	7043	2861	0.5	3.0
H821	3432	4587	2373	0.5	3.0
H822	2278	6805	2431	0.5	3.0

Least squares refinement of positional and anisotropic thermal parameters for non-hydrogen atoms yielded a conventional R of 0.057 and a weighted R of 0.052. The overdetermination ratio was 17.3, 91 parameters being refined on the basis of 1577 reflections with sin θ/λ between 0.46 and 0.81. This structure model yielded a conventional R of 0.075 for the whole data-set. A total difference Fourier map showed no electron density above 0.3 e/Å^3.

A comparison of observed and calculated structure factors is given in Table 1, and the final parameters for non-hydrogen atoms are listed in Table 2.

Table 4. R.m.s. amplitudes of vibration $(\overline{u^2})^{\frac{1}{2}}$ (Å) and B-values (Å^2) along the principal axes of vibration given by the components of a unit vector **e** in fractional coordinates ($\times 10^3$).

Atom	$(u^2)^{\frac{1}{2}}$	B	e_x	e_y	e_z
O1	.313	7.71	99	66	38
	.225	3.99	8	101	−60
	.162	2.07	−58	126	28
O2	.283	6.33	55	138	−22
	.237	4.42	87	−26	59
	.163	2.11	−51	104	44
N1	.211	3.50	79	97	−25
	.194	2.97	57	19	72
	.158	1.98	−61	144	8
N2	.209	3.45	98	68	39
	.180	2.56	16	87	−62
	.168	2.22	−59	135	21
C3	.224	3.97	92	49	52
	.190	2.84	42	83	−55
	.161	2.04	−55	145	14
C4	.235	4.34	87	92	40
	.197	3.05	−61	23	56
	.175	2.41	45	−147	34
C5	.228	4.12	84	119	17
	.199	3.11	79	−128	12
	.184	2.67	10	8	−74
C6	.222	3.89	37	128	−41
	.192	2.91	105	−13	43
	.166	2.18	−29	118	49
C7	.254	5.10	87	107	−6
	.245	4.75	6	50	73
	.167	2.20	75	−129	23
C8	.259	5.28	105	65	26
	.219	3.78	−47	152	15
	.176	2.45	5	56	−71

Magnitudes and directions of the principal axes of the ellipsoids of vibration are given in Table 4. The total discrepancy between the atomic vibration tensor components and those calculated from the rigid-body parameters found by analysis of the librational, translational, and screw motion of the molecule, is 0.0017 Å^2. This indicates that the molecule may be regarded as a rigid body.

The atomic positions were accordingly corrected for the librational motion. The eigenvalues of **T** are 0.19, 0.18, and 0.16 Å. The r.m.s. librational amplitudes are 4.7, 4.2, and 3.4°.

Standard deviations were calculated from the correlation matrix ignoring standard deviations in cell parameters.

DISCUSSION

Bond lengths and bond angles are listed in Table 5 and also in Fig. 1, where the numbering of the atoms is indicated. Dihedral angles around the N1–N2, N1–C6, and N2–C3 bonds are listed in Table 7.

The non-aromatic nature of the molecule is revealed not only by the non-planarity of the molecule (see Table 6), but also by the bond lengths. The C4–

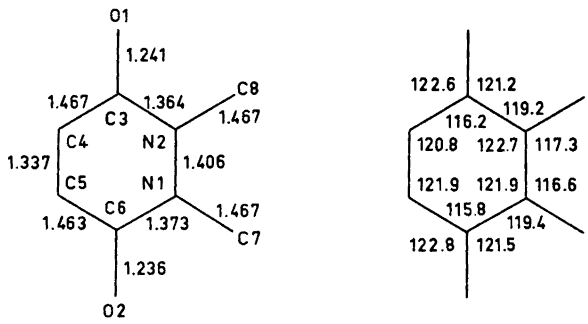

Fig. 1. Bond lengths (Å) (corrected for thermal vibration effects) and bond angles (°) in *N,N*-dimethylmaleic hydrazide.

Table 5. Bond lengths (Å) and bond angles (°). Estimated standard deviations in parentheses.

	Bond length	E.s.d. ($\times 10^4$)	Corrected bond length		Bond angle	E.s.d.
C3–O1	1.238	(16)	1.241	O1–C3–N2	121.2	(.11)
C6–O2	1.233	(16)	1.236	O1–C3–C4	122.6	(.12)
N1–N2	1.399	(13)	1.406	O2–C6–N1	121.5	(.12)
N1–C6	1.367	(16)	1.373	O2–C6–C5	122.8	(.12)
N2–C3	1.358	(14)	1.364	C3–N2–N1	122.7	(.09)
C3–C4	1.461	(16)	1.467	C4–C3–N2	116.2	(.10)
C4–C5	1.331	(19)	1.337	C5–C4–C3	120.8	(.11)
C5–C6	1.457	(17)	1.463	C6–C5–C4	121.9	(.11)
N1–C7	1.463	(15)	1.467	N1–C6–C5	115.8	(.10)
N2–C8	1.463	(15)	1.467	N2–N1–C6	121.9	(.09)
				C8–N2–C3	119.2	(.10)
				C8–N2–N1	117.3	(.10)
				C7–N1–N2	116.6	(.10)
				C7–N1–C6	119.4	(.10)

Table 6. Deviations from a least squares plane through: O1, O2, C3, C4, C5, and C6. (Eqn.: $(0.0908X + 0.1062Y + 0.0188Z)R - 3.967 = 0$.)

Atom	Deviation (Å)	Atom	Deviation (Å)
O1	−0.015	C6	0.065
O2	−0.049	N1	0.192
C3	0.023	N2	0.189
C4	−0.045	C7	−0.040
C5	0.044	C8	0.617

Table 7. Dihedral angles (°) with estimated standard deviations in parentheses.

Planes	Angle	E.s.d.
C6–N1–N2–C3	2.0	(0.17)
C7–N1–N2–C8	29.6	(0.17)
C5–C6–N1–N2	5.0	(0.17)
O2–C6–N1–C7	10.6	(0.19)
N1–N2–C3–C4	4.9	(0.17)
C8–N2–C3–O1	13.4	(0.17)

C5 bond length of 1.337 Å indicates a pure double bond,[9] and is significantly shorter than the corresponding bond lengths, 1.395 Å and 1.362 Å, reported for pyridazine [8] and 4,5-dichloro-3,6-pyridazinedione.[2]

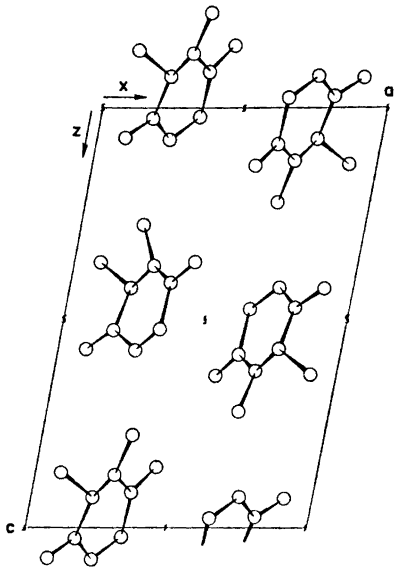

Fig. 2. The crystal structure as seen along the *b* axis.

The C–O bonds (mean length 1.238 Å) are slightly longer than those found for C–O double bonds in similar structures.[10–12] This may indicate a resonance stabilization of the O–C–N system. Further the C–N bonds (mean length 1.369 Å) are considerably shorter than those reported for phenylhydrazine [13] and phenylhydrazine hydrochloride.[14]

The N1–N2 bond length of 1.406 Å is significantly longer than the nitrogen-nitrogen bond lengths of 1.330 Å and 1.353 Å reported for pyridazine [8] and 4,5-dichloro-3,6-pyridazinedione,[2] suggesting only a small contribution from resonance structures II and III. This is also indicated by the dihedral angle C7–N1–N2–C8 of 29.6°.

The molecular arrangement in the crystal is visualized in Fig. 2 and may be described as layers parallel to (100).

REFERENCES

1. Eichenberger, K., Staehelin, A. and Druey, J. *Helv. Chim. Acta* **37** (1954) 837.
2. Ottersen, T. *To be published.*
3. Dahl, T., Gram, F., Groth, P., Klewe, B. and Rømming, C. *Acta Chem. Scand.* **24** (1970) 2232.
4. Doyle, P. A. and Turner, P. S. *Acta Cryst.* **A 24** (1968) 390.
5. Stewart, R. F., Davidson, E. R. and Simpson, W. T. *J. Chem. Phys.* **42** (1965) 3175.
6. Zachariasen, W. H. *Acta Cryst.* **5** (1952) 68.
7. Hughes, E. W. *Acta Cryst.* **6** (1953) 871.
8. Werner, W., Dreizler, D. and Rudolph, H. D. *Z. Naturforsch.* **22a** (1967) 531.
9. Bastiansen, O. and Trætteberg, M. *Tetrahedron* **18** (1962) 147.
10. Shintani, R. *Acta Cryst.* **13** (1960) 609.
11. Tomiie, Y., Koo, C. H. and Nitta, I. *Acta Cryst.* **11** (1958) 774.
12. Sabelli, C. and Zanazzi, P. F. *Acta Cryst.* **B 28** (1972) 1173.
13. Srinivasan, S. and Swaminathan, S. *Z. Krist.* **127** (1968) 442.
14. Koo, H. C. *Bull. Chem. Soc. Japan* **38** (1965) 286.

Received September 20, 1972.

ACTA CHEMICA SCANDINAVICA 27 (1973) 846–850

Current-Potential Effects of Trace Impurities in Zinc Sulfate Electrolyte

ØYSTEIN VENNESLAND, HANS HOLTAN and SVEIN SOLHJELL

Division of Industrial Electrochemistry, Norwegian Institute of Technology, The University of Trondheim, N-7034 Trondheim-NTH, Norway

The influence of combinations of impurities on the current-potential curves for electrolysis of zinc has been studied by a method described by Mantell and Ferment. The experiments show that for the single impurities antimony and β-naphthol there is a quantitative relationship between transition current and impurity concentration. For mixtures of the impurities cobalt, antimony, and β-naphthol the effects upon the current-potential curves show no law of additivity related to the effect of the single impurities. For mixtures the hydrogen overvoltage is reduced to a considerable degree.

Some of the trace impurities in the zinc sulfate electrolyte studied most extentisely are cobalt, antimony, and β-naphthol. Investigations concerning the relationship between cathode potential, current efficiency with respect to zinc and the amount of impurities in the electrolyte have been reported[1–5].

We have studied the effect of said impurities – single and in combinations – upon the current-potential curve. The method – described by Mantell and Ferment[6] for the manganese electrolyte – is based upon the curve produced by continuously changing the cathode potential at a programmed rate. Starting with a clean aluminium cathode the initial cathode potential is adjusted to yield zero current. The potential drive is then started and the current is recorded as a function of the cathode potential.

EXPERIMENTAL

The electrolytic cell consisted of a 400 ml Pyrex beaker and a cover of polyethylene plastic.

The cathode was a commercial aluminium alloy (analysis: 3.8 % Cu, 0.3 % Fe, 0.3 % Mg, 0.6 % Mn, 1.0 % Pb, 0.6 % Si, and 0.2 % Zn) and the anode a lead-silver (1 % Ag) alloy. Both electrodes were moulded in plastic.

The potential applied was measured by means of a saturated calomel electrode and a Luggin capillary and transformed to the Normal Hydrogen Scale. The distance between the cathode and the capillary tip was constant, 1 mm.

The potentiostat used was a Beckman Electroscan 30. The voltage variation was −60 mV/min.

Between each run the cathode surface was polished with different grades of suspended alumina of which the finest had a particle size of 0.05 μ.

The reagents used was of *p.a.* quality. The standard electrolyte contained 125 g/l Zn and 80 g/l H_2SO_4. Cell temperature 30°C.

RESULTS

The standard curve is shown in Fig. 1. Its particular form depends on the alloying metals of the cathode. This was demonstrated by a test with pure (99.998 %) Al-cathode. No current was then observed before the cathode

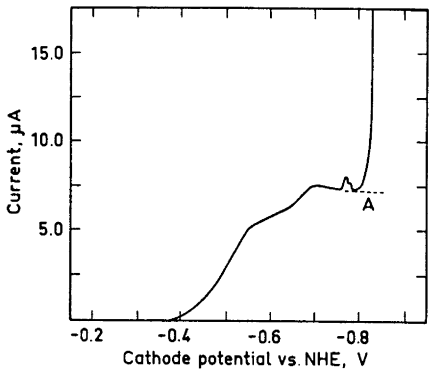

Fig. 1. Standard current-potential curve.

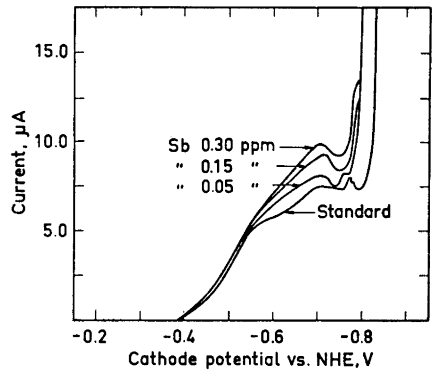

Fig. 2. Effect of antimony concentration.

potential was close to the reversible potential for zinc-deposition. From then it rose sharply and followed the form of the standard curve. The current at the point A at the standard curve is called the transition current.

Single impurities. Figs. 2 – 4 show the effect of the single impurities cobalt, antimony, and β-naphthol. Following the argument of Mantell and Ferment

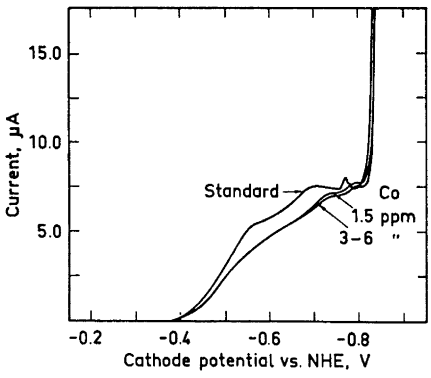

Fig. 3. Effect of cobalt concentration.

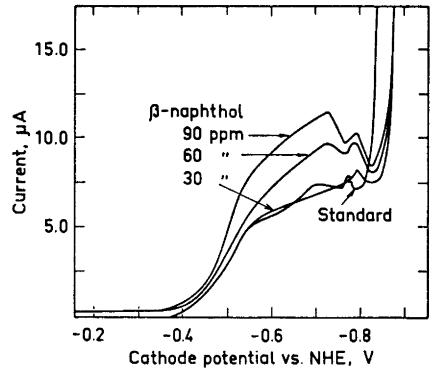

Fig. 4. Effect of β-naphthol concentration.

antimony and β-naphthol decrease the hydrogen overpotential of the base metal, while cobalt surprisingly under the existing conditions seems to increase it.

Antimony and β-naphthol show a correlation between transition current and impurity concentration. Cobalt has little effect. Antimony shifts the deposition potential in the positive direction while β-naphthol has the opposite effect.

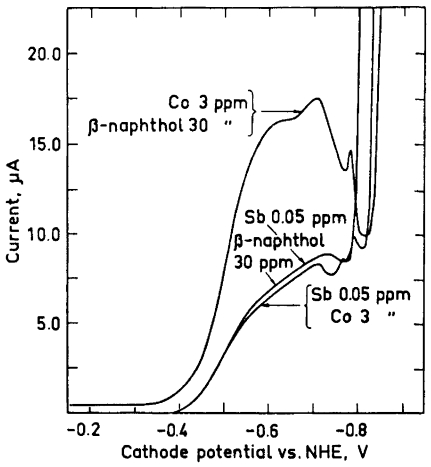

Fig. 5. Effect of combination of impurities.

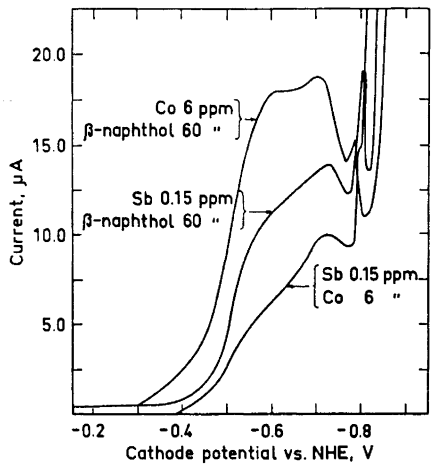

Fig. 6. Effect of combination of impurities.

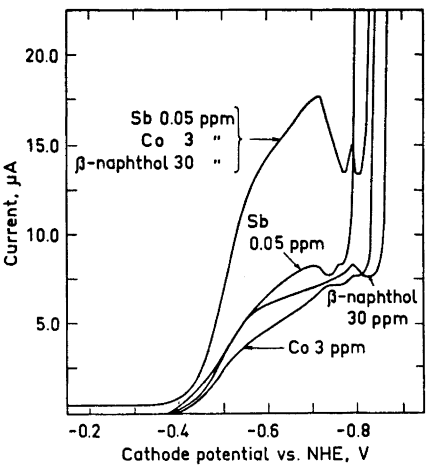

Fig. 7. Effect of combination of impurities.

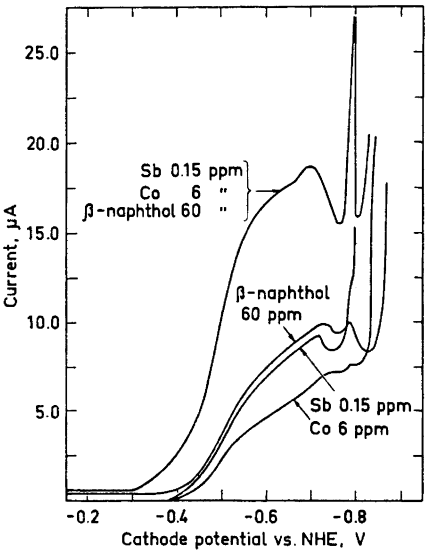

Fig. 8. Effect of combination of impurities.

Binary mixtures of impurities. Current-potential curves for pairs of impurities are shown in Figs. 5 and 6. The effect upon the curves does not follow an additive law related to the effect of single impurities.

Ternary mixtures of impurities. With all three impurities present (Figs. 7 and 8), this effect is even more marked. This is in agreement with reports for electrolysis of zinc. According to Turomshina and Stender[2] and Steintveit and Holtan[4] presence of only one impurity may not reduce the current efficiency at all, but when to or three are present simultaneously they may be very harmful.

The effect of binary and ternary mixtures upon the transition current is shown in Table 1.

Table 1. Effect of combinations of impurities upon the transition current.

Impurity, ppm	Transition current, μA
Standard	7.4
a. 0.05 Sb	7.7
b. 3 Co	7.6
c. 30 β-naphthol	7.7
a+b	7.7
a+c	9.2
b+c	9.9
a+b+c	13.4
d. 0.15 Sb	8.5
e. 6 Co	7.6
f. 60 β-naphthol	8.5
d+e	9.5
d+f	13.7
e+f	11.1
d+e+f	16.0

CONCLUSIONS

1. For the single impurities antimony and β-naphthol there is a quantitative relationship between transition current and impurity concentration.

2. For mixtures of the impurities cobalt, antimony, and β-naphthol the effects upon the current-potential curves show no law of additivity related to the effect of the single impurities.

3. Presence of the three impurities cobalt, antimony, and β-naphthol simultaneously reduces the hydrogen overvoltage to a considerable degree.

REFERENCES

1. Turomshina, U. F. and Stender, V. V. *J. Appl. Chem. USSR (English Transl.)* **28** (1955) 347.
2. Turomshina, U. F. and Stender, V. V. *J. Appl. Chem. USSR (English Transl.)* **28** (1955) 447.

3. Levin, A. J., Pomosov, A. V., Krymakova, E. E. and Falicheva, V. J. *J. Appl. Chem. USSR (English Transl.)* **31** (1958) 569.
4. Steintveit, G. and Holtan, Jr., H. *J. Electrochem. Soc.* **107** (1960) 247.
5. Znamenskii, G. N. and Stender, V. V. *J. Appl. Chem. USSR (English Transl.)* **33** (1960) 2692.
6. Mantell, C. H. and Ferment, G. *Trans. Met. Soc. AIME* **236** (1966) 718.

Received October 13, 1972.

ACTA CHEMICA SCANDINAVICA 27 (1973) 851–858

Phthalic Acid as a Reagent in Inorganic Qualitative Analysis of Metal Ions. Part I. A New System for Qualitative Analysis

PAAVO LUMME and JOUNI TUMMAVUORI

Department of Chemistry, University of Jyväskylä, Jyväskylä, Finland

A new scheme for the qualitative chemical analysis of metal ions that is based on the use of phthalate ion as a precipitating reagent is outlined. Sulphide ion is not employed as a precipitating reagent. Evaporations of solutions are minimized and mineral acid and hydrogen sulphide vapours in the laboratory atmosphere are avoided. The analysis scheme has worked well during twelve semesters (from June, 1968) when several hundreds of students have used it in our laboratory.

The value of classical qualitative analysis in the teaching of chemistry has been discussed in, for example, the columns of the Swedish journal Svensk Kemisk Tidskrift in recent years.[1] Opinions that stress the importance of the subject have been expressed but also derogatory ones. The fact remains that at least at present inorganic qualitative analysis offers the cheapest and most effective method for teaching and learning laboratory procedures and reactions of inorganic chemistry.[2]

The greatest changes and improvements in qualitative analysis have resulted from the introduction of semimicro and micro methods and the replacement of precipitation with hydrogen sulphide by homogeneous precipitation with thioacetamide.[3] A further step towards a more systematic analytical scheme was the introduction by West and Vick [4] of precipitation with hydroxide and benzoate ions to replace precipitation with sulphide ions.

We have here in the Department of Chemistry at the University of Jyväskylä investigated this last-mentioned analytical scheme and its application as a method of instruction in inorganic qualitative analyses to freshmen and sophomore students and have come to the conclusion that phthalate ion (*e.g.*, potassium biphthalate) is a better reagent than benzoate ion in combination with hydroxide ion as a precipitant.[5–6] The alkaline earth metals calcium, magnesium, strontium, and barium are precipitated as their fluorides and certain divalent metal ions as their hydroxides with sodium hydroxide as in the scheme of West and Vick.[4] In other respects the analytical scheme follows

the classical scheme and the reactions of individual ions are the generally known customary ones.[4,7]

The analytical scheme that is briefly outlined below has been devised primarily for practical laboratory work and instruction and hence only the most essential aspects of the nature and reactions of the elements and their ions are presented.[5,6] The most noteworthy advantage of the presented analytical scheme in addition to its more systematic nature is the almost complete elimination of the evil-smelling, poisonous and corrosive hydrogen sulphide and the suppression of the evaporation of ammoniacal solutions and solutions containing mineral acids to a minimum. Also the costs of chemicals consumed are lower in the new scheme than in the earlier analytical schemes. The scheme does, however, require that the student exercises care in the handling of reagents and the adjustment of the pH values of the solutions.

THE ANALYTICAL SCHEME

The various ions that can be identified by following the analytical scheme and the reagents that divide them into groups are presented in Table 1. The ions in parentheses are not included in the samples to be analysed in the early stages of instruction. The underlined ions are only rarely identified in the groups in question or they are transferred to the groups under exceptional conditions.

The sample of unknowns is examined by semimicro methods. Anions are analysed first. Preliminary tests that are extensively employed in many other analytical schemes have been omitted almost completely because the information they provide is of relatively minor significance from the point of view of systematic analysis.[5,6]

Table 1. The ions identified by the presented analytical scheme and their division into groups.[5,6]

Group	Group reagent	Ions identified
Anion group I	None	NO_3^-, HS^-, S^{2-}, HCO_3^-, CO_3^{2-}, (BO_2^-)
Anion group II	None	Cl^-, Br^-, I^-, HSO_4^-, SO_4^{2-}, $H_2PO_4^-$, HPO_4^{2-}, PO_4^{3-}, Ac^-, AsO_2^-, AsO_4^{3-}
Cation group I	HCl	Ag^+, Hg_2^{2+}, Pb^{2+}
Cation group II	Potassium biphthalate and sodium hydroxide	(Sn^{2+}), (Sn^{4+}), (Sb^{3+}), (Bi^{3+}), Fe^{2+}, Fe^{3+}, Al^{3+}, (Cr^{3+})
Cation group III	NaF	Mg^{2+}, Ca^{2+}, (Sr^{2+}), Ba^{2+}, $\underline{Pb^{2+}}$
Cation group IV	NaOH	Mn^{2+}, Hg^{2+}, Cu^{2+}, (Co^{2+}), (Ni^{2+}), (Cd^{2+})
Cation group V	NH_4OH	$\underline{AsO_2^-}$, $\underline{AsO_4^{3-}}$, Zn^{2+}, ($\underline{Sn^{2+}}$)
Cation group VI	None	Na^+, K^+, $\underline{NH_4^+}$

Identification of anions

Several systematic analytical schemes have been presented in the literature for the analysis of anions in groups, but they are mostly complicated and laborious.[7] In the scheme presented here, the anions are not grouped on the basis of their analyticl properties but are mainly listed in the order in which they are effectively identified. This has been made possible by the relatively small numbers of anions that has been selected for identification by the scheme.[5,6]

The anions of group I give gaseous products when they are treated with acid reagents and they are identified directly in the original sample in a simple gas detection unit. Also the presence of ammonium ion in the sample can be detected at this stage. Anions of group II are identified by means of the customary reactions in a solution of the sample from which heavy metals have been replaced by an alkali metal.[7]

Identification of cations

Investigation of the cations is begun directly on the original sample of unknowns if it is a solution or as a solution obtained by dissolving the sample in dilute mineral acid or base. If the sample contains a phase that dissolves with difficulty or if such a phase is formed when the sample is dissolved in dilute acid or base, it is separated from the other components of the sample, dissolved and examined separately.

Scheme 1. Precipitation and identification of group I cations.

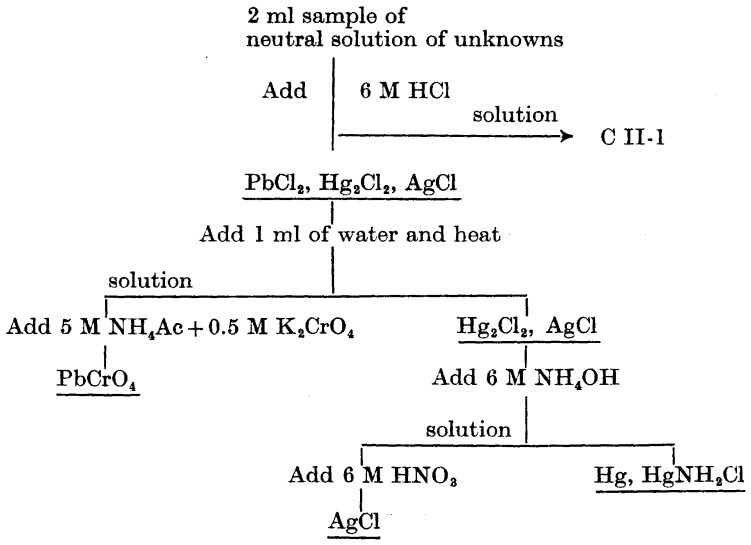

Customary tests are applied to identify the ions.[4,7]

Examination of cation group I. The tests are carried out on a practically neutral solution of the sample of unknowns. If the solution must be neutralized, this is done either with 6 M nitric acid or with 6 M sodium hydroxide.

The actual analysis is begun by taking a sample of the solution that is about 2 ml in volume and adding 6 M hydrochloric acid. If care is taken to avoid adding an excess of the reagent and the solution is cooled near 0°C before the precipitate is collected by filtration, the metals of the first group and lead are precipitated almost completely as chlorides. In the analytical schemes presented below, the precipitated compounds are underlined.

Examination of cation group II. Tests for the presence of cations of this group are done on the filtrate (C II – 1) collected after the cations of group I have been precipitated from the solution of the sample of unknowns which

Scheme 2. Precipitation and identification of group II cations.

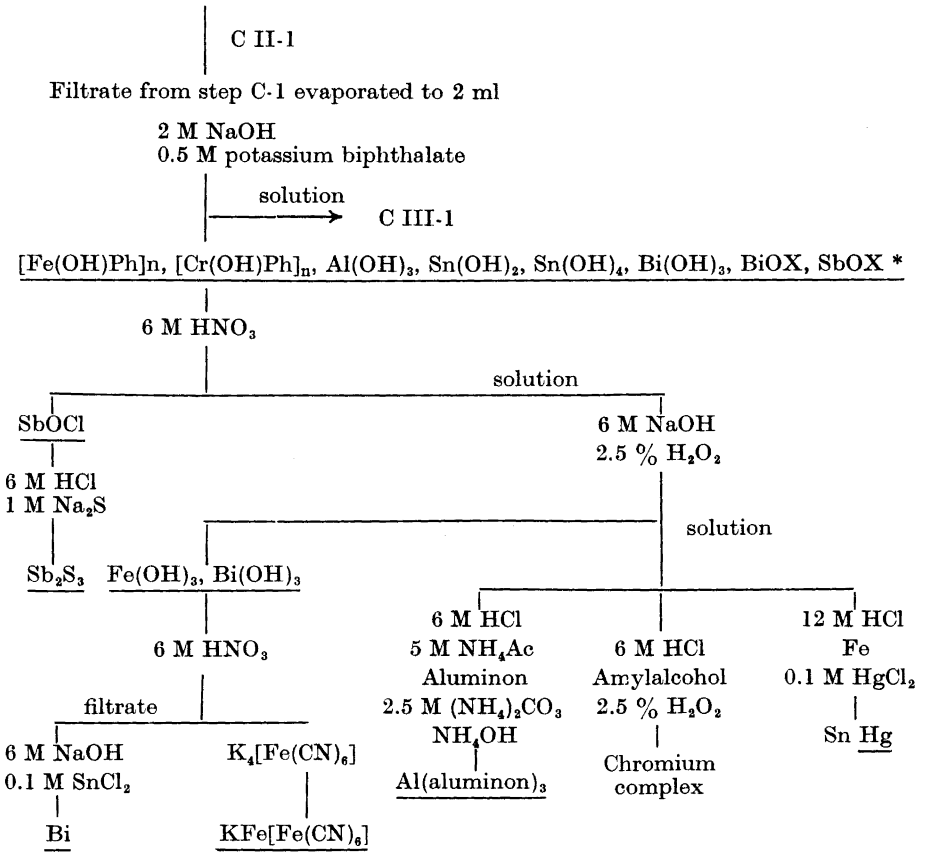

* Where $X = Cl^-$, NO_3^-, or some other anion depending on the composition of the solution. The presented evaporations are the most probable ones.

The metals are identified by customary tests.[4,7]

must be free from phosphate and borate ions. (If the sample solution contains phosphate or borate ions, these are removed with an ion exchange resin.) The pH of the filtrate is adjusted to 2, several drops of 0.5 M potassium biphthalate solution are added and the pH of the solution is adjusted to 4 – 5 with sodium hydroxide solution. The solution is heated on a water bath for about 10 min during which the pH is checked to ensure that it remains between 4 and 5;

Scheme 3. Precipitation and identification of cations of group III.

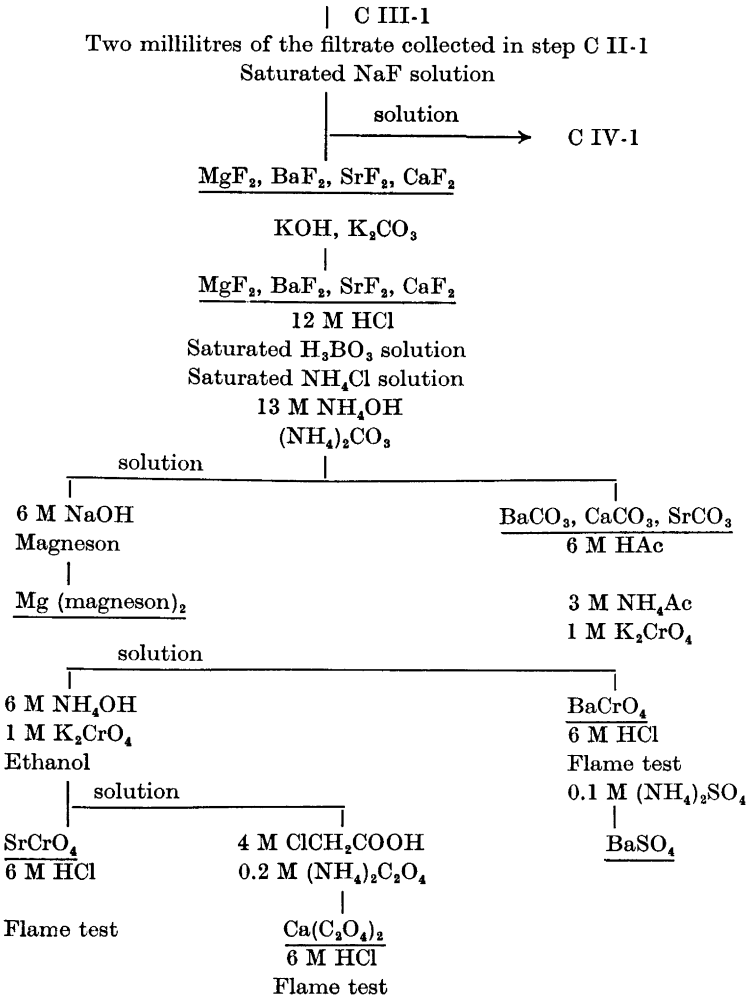

The group precipitate is examined further according to West and Vick [4] and the metals are identified by means of customary reactions.[4,9]

any adjustments that are required are made with the precipitating reagents. It is essential that the solution is heated for 10 min, because metals of other groups may otherwise coprecipitate, primarily as hydroxides. The solution and precipitate are cooled to room temperature and the precipitate is removed immediately by filtration. The cations precipitate as hydroxides, basic phthalates, and oxides of variable composition depending on the conditions. The composition of the group precipitate is discussed in part II.[8]

An excess of biphthalate must be avoided when this cation group is precipitated because some cations, particularly chromium, iron, and copper, readily form complex ions with phthalate ions and also because phthalic acid is sparingly soluble in water and may easily precipitate from acid solutions and thus interfere in later stages of the analysis.

Scheme 4. Precipitation and identification of cations of group IV.

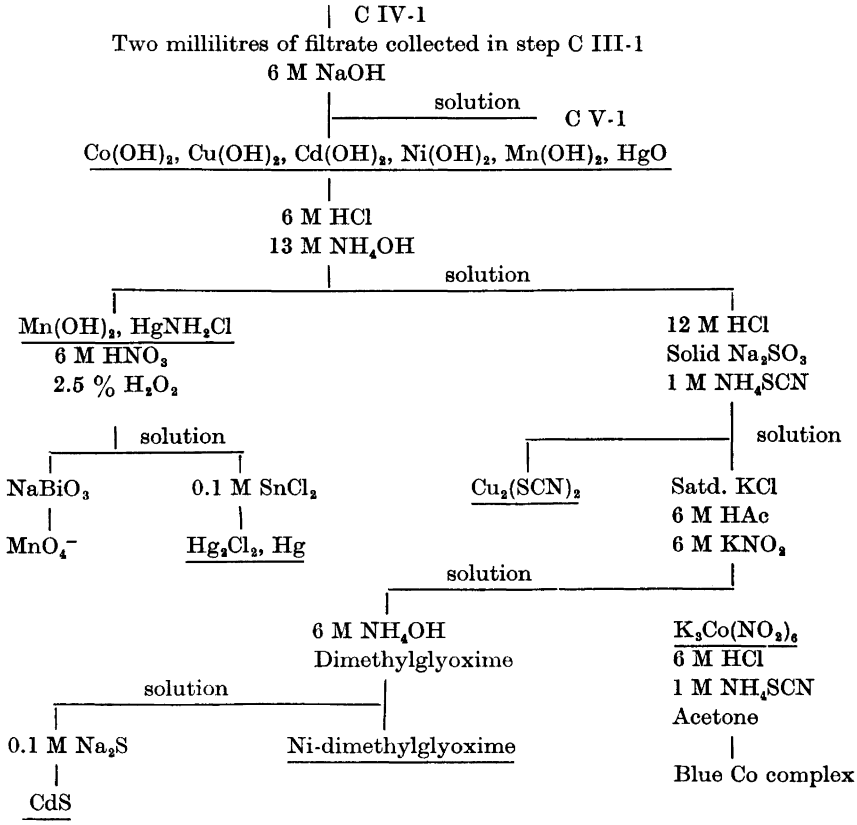

The metals are identified by customary tests.

Examination of cation group III. A saturated sodium fluoride solution is added to the filtrate collected after the precipitation of cations of group II and the solution is allowed to stand for at least 5 min with occasional stirring. The solution and precipitate are cooled near 0°C before the precipitate is collected by filtration.

Identification of group IV cations. The filtrate remaining after the cations of group III were precipitated is made clearly alkaline and the solution is evaporated until its volume is 2 ml, during which any ammonia present volatilizes. The cations of group IV precipitate mainly as hydroxides or oxides.

Examination of cation group V. The filtrate collected after precipitating group IV is evaporated to a volume of 2 ml and acidified with hydrochloric acid. (Phthalic acid may precipitate at this stage, but is removed by filtration.) Ammonia is then added; in rare cases tin that has been transferred from cation group II may precipitate as stannous hydroxide. The solution is tested for the presence of arsenic and zinc.[4,7]

Scheme 5. The examination of cation group V.

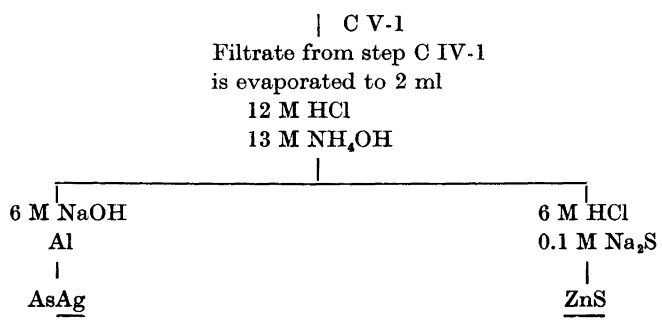

Examination of cation group VI. Tests for cations of this group are carried out on the original sample of unknowns in the order given in Scheme VI.

SUMMARY

The main advantages of the described analytical system involving the use of phthalate ion as a precipitating agent may be summarized as follows.

1. No difficulties are encountered in precipitating copper(II) and tin(II)-ions as when benzoic acid is used as precipitating agent.[4]
2. Dibasic phthalic acid has a wider buffer range than monobasic benzoic acid and therefore the precipitation conditions are more easily controlled.
3. The formed heavy metal precipitates settle rapidly and are easily collected. In these respects the precipitates are at least as good as the precipitates obtained with benzoic acid.

4. The formation of soluble phthalate or hydroxo complexes is avoided by immediate separation.

5. Phthalic acid is only about half as expensive as benzoic acid and ten times cheaper than thioacetamide.

Scheme 6. The examination of cation group VI.

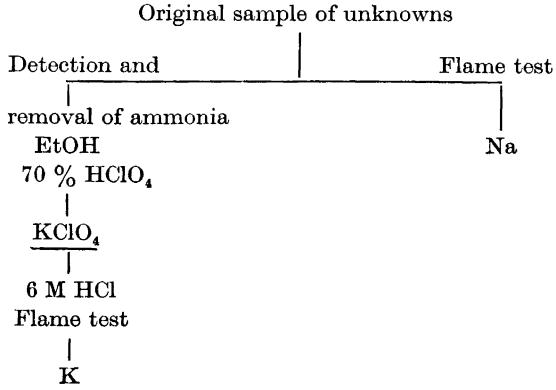

Acknowledgement. The authors are indebted to Mr. R. Korte, Ph.D. (h.c.) for the English translation of the manuscript.

REFERENCES

1. Mäcs, M. and Sundström, Y. *Svensk Kem. Tidskr.* **79** (1967) 192, and literature cited therein.
2. Stephen, W. I. *Educ. Chem.* **6** (1969) 221; Hovey, N. W. *J. Chem. Educ.* **40** (1963) 410.
3. Barber, H. H. and Grzeskowiak, E. *Anal. Chem.* **21** (1949) 192.
4. West, P. W. and Vick, M. M. *Qualitative Analysis and Analytical Chemical Separations*, 2nd Ed., MacMillan, New York 1959.
5. Lumme, P. O. and Tummavuori, J. *Kemia II, Kvalitatiivinen analyysi approbatur-arvosanaa varten*, Jyväskylän yliopiston kemian laitos, Jyväskylä 1968. (In Finnish.)
6. Lumme, P. O. and Tummavuori, J. *Kemia IV, Kvalitatiivinen analyysi approbatur- ja cum laude-arvosanaa varten*, Jyväskylän yliopiston kemian laitos, Jyväskylä 1968. (In Finnish.)
7. Treadwell, F. P. and Hall, W. T. *Analytical Chemistry*, Vol. I, *Qualitative Analysis*, 9th Ed., Wiley, New York 1963.
8. Lumme, P. and Tummavuori, J. *Acta Chem. Scand. To be published.*

Received September 1, 1972.

ACTA CHEMICA SCANDINAVICA 27 (1973) 859–867

The Crystal Structure of Ammonium Hexasulphitoferrate(III), $(NH_4)_9[Fe(SO_3)_6]$

LARS OLOF LARSSON and LAURI NIINISTÖ*

Institute of Inorganic and Physical Chemistry, University of Stockholm, S-10405 Stockholm, Sweden

The crystal structure of ammonium hexasulphitoferrate(III) $(NH_4)_9[Fe(SO_3)_6]$ has been determined from three-dimensional X-ray data measured on an automatic diffractometer. The crystals are hexagonal, space group $P\bar{3}$ (No. 147); $a = 10.2226(33)$ Å, $c = 7.2055(14)$ Å, and $Z = 1$. The final R index is 0.053 for 359 independent reflections. The structure consists of FeO_6 octahedra whose oxygen atoms belong to six different sulphite groups. The $Fe(SO_3)_6$ groups are linked together by ammonium ions. The Fe–O distance is 2.028(6) Å and the average dimensions of the sulphite ion are: S–O distance 1.517 Å, O–O distance 2.399 Å, and O–S–O angle 104.5°.

The crystal structures of several metal sulphites have been studied over a period of some years at this institute by means of X-ray methods. A survey of the results obtained has recently been given by Kierkegaard *et al.*[1] In all the sulphites studied except in sodium sulphite, the sulphite group is coordinated to a metal atom through the sulphur atom. Because iron has a lower affinity for sulphur than for oxygen it could be expected that in iron sulphites the ferric ion would be bonded to oxygen atoms. In $(NH_4)_9[Fe(SO_3)_6]$ the dimensions of the sulphite group would be affected by (a) hydrogen bonds between ammonium ions and sulphite oxygen atoms and (b) the lone electron pair of sulphur. Thus, the crystal structure investigation of this compound was started in order to obtain additional information on these effects.

Ammonium hexasulphitoferrate(III) was first synthesized by Erämetsä [2] who found, by microscopic investigation, that the crystals were hexagonal. This conclusion was later confirmed by X-ray powder diffractometric studies.[3,4] This article describes the determination and refinement of the crystal structure of $(NH_4)_9[Fe(SO_3)_6]$ from three-dimensional X-ray single crystal data.

* Present address: Department of Chemistry, Helsinki University of Technology, SF-02150 Otaniemi, Finland.

EXPERIMENTAL

Preparation of crystals. The crystals were prepared according to Erämetsä.[2] In order to avoid oxidation all preparations were carried out in nitrogen atmosphere. The obtained crystals were orange brown hexagonal prisms which had a tendency to form cross shaped twins.

Data collection and reduction. The accurate unit cell dimensions were calculated, by a least squares program, from a powder photograph obtained in a Guinier-Hägg focusing camera of 80 mm diameter with strictly monochromatized Cu$K\alpha_1$ radiation

Table 1. X-ray powder data of $(NH_4)_9[Fe(SO_3)_6]$. Cu$K\alpha_1$ radiation ($\lambda = 1.54050$ Å).

$h\ k\ l$	d_{obs} (Å)	$10^5 \times \sin^2\theta_{obs}$	$10^5 \times \sin^2\theta_{calc}$	I_{obs}
1 0 0	8.900	749	756	s
0 0 1	7.294	1115	1123	s
1 0 1	5.627	1874	1880	m
1 1 0	5.126	2258	2270	m
1 1 1	4.183	3391	3394	s
2 0 1	3.783	4146	4151	w
0 0 2	3.632	4497	4495	w
2 1 0	3.347	5297	5298	s
2 1 1	3.039	6424	6422	m
1 1 2	2.961	6766	6766	s
3 0 0	2.949	6823	6812	s
2 0 2	2.806	7537	7523	w
3 0 1	2.735	7931	7936	w
2 1 2 3 1 0	2.458	9819	9794 9840	w
0 0 3	2.452	9868	10115	w
2 2 1	2.421	10123	10207	vw
1 0 3	2.338	10852	10872	vw
3 1 1	2.324	10981	10964	w
3 0 2	2.289	11324	11308	w
4 0 0	2.225	11989	12111	s
1 1 3	2.187	12404	12386	m
4 0 1	2.115	13258	13235	w
2 2 2	2.090	13578	13579	m
3 1 2 3 2 0	2.033	14359	14336 14382	m
2 1 3	1.960	15438	15414	w
3 2 1	1.953	15560	15506	vw
4 1 0	1.930	15934	15896	w
4 0 2	1.888	16637	16607	w
4 1 1	1.863	17091	17020	w
0 0 4	1.816	17984	17982	w
3 2 2	1.770	18938	18878	w
2 2 3	1.755	19273	19198	w

($\lambda = 1.54050$ Å). Potassium chloride ($a = 6.29228$ Å)[5] was used as internal standard. The powder photograph was measured and interpreted to $\sin^2\theta = 0.48$. The cell dimensions (see Table 1) at 25°C are:

$$a = 10.2226 \pm 33 \text{ Å}; \quad c = 7.2055 \pm 14 \text{ Å}; \quad \gamma = 120°.$$

The powder data are in agreement with the results obtained by Erämetsä [3] ($a = 10.15$, $c = 7.24$ Å) and by Erämetsä and Valkonen [4] ($a = 10.177$, $c = 7.247$ Å).

The observed density 1.77 g cm^{-3} determined by loss of weight in benzene corresponds to one formula unit in the unit cell (calculated density 1.78 g cm^{-3}).

During the collection of the single crystal data it was found that the crystals are very unstable under the influence of X-rays and usually decompose within 30 min. Even if the crystals were coated with three layers of shellac they lasted a maximum of two days. Therefore a new crystal was used for each layer line during the collection of film data with a Weissenberg camera. Complete data were collected but in the course of the structure determination and refinement it became evident that the quality of the film data obtained was unsatisfactory because of decomposition of the crystals. New intensity data were therefore collected on a diffractometer.

Three crystals, with dimensions $0.076 \times 0.040 \times 0.040$ mm^3, $0.066 \times 0.026 \times 0.026$ mm^3, and $0.118 \times 0.017 \times 0.017$ mm^3, respectively, were used in the data collection. The crystals were coated with shellac and three test reflections were used to check for possible decomposition during the data collection.

The X-ray intensity data were measured on a Philips PW 1100 computer controlled four circle diffractometer. Graphite monochromatized CuK radiation and a scintillation counter with pulse height discrimination were used. The $\theta - 2\theta$ scan technique was employed with a scan range of 1°. The background intensities were calculated as averages of the intensities at each end of the scan interval. All 1805 reflections with $\theta < 55°$ were measured, but only the 1238 reflections with $\sigma(I_{net})/I_{net} < 0.25$ were used for further data reduction. The net intensity, I_{net}, was calculated as $I_{tot} - I_{back}$ and its standard deviation, $\sigma(I_{net})$, was estimated as $(I_{tot} + I_{back})^{1/2}$ where I_{tot} and I_{back} are the number of counts for the total intensity and background intensity, respectively.

The data were corrected by application of Lorenz and polarization factors. Absorption correction was made by the method of Coppens *et al.*[6] The crystals were defined by eight faces, and the linear absorption coefficient, $\mu = 98.4$ cm^{-1}, was calculated from the mass absorption values given in the International Tables.[7]

After averaging of the intensities of symmetry related reflections the data were reduced to 404 independent reflections. However, a comparison of intensities measured on the three crystals revealed that a partial decomposition of the second crystal had taken place rather rapidly. This decomposition was not apparent from the test reflections chosen. The unreliable data obtained from crystal two were discarded, and the remaining 390 independent reflections measured on crystals one and three were used in the subsequent calculations.

Computer programs. All calculations were performed on the IBM 1800 and IBM 360/75 computers using the following programs:

PIRUM. Indexing of powder photographs and least squares refinement of unit cell parameters. Written by P.-E. Werner, Stockholm, Sweden.

DATAP1/DATAP2. Lp- and absorption corrections. Originally written by P. Coppens, L. Leiserowitz and D. Rabinovich, Rehovoth, Israel. Modified by O. Olofsson and M. Elfström, Uppsala, Sweden, and by B. G. Brandt, S. Åsbrink and A. G. Nord, Stockholm, Sweden.

DRF. Fourier summations and structure factor calculations. Originally written by A. Zalkin, Berkeley, USA. Modified by R. Liminga and J.-O. Lundgren, Uppsala, Sweden. Further modified by O. Lindgren, Gothenburg, Sweden, and by A. G. Nord and B. G. Brandt, Stockholm, Sweden.

DISTAN. Calculation of interatomic distances and bond angles with estimated standard deviations. Originally written by A. Zalkin, Berkeley, USA, and modified by A. G. Nord and B. G. Brandt, Stockholm, Sweden.

LALS. Full matrix least squares refinement. Originally written by P. K. Gentzel, R. A. Sparks and K. N. Trueblood, Los Angeles, USA. Modified by A. Zalkin, Berkeley, USA, and by J.-O. Lundgren, R. Liminga and C. I. Brändén, Uppsala, Sweden. Further modified by A. G. Nord and B. G. Brandt, Stockholm, Sweden.

ORTEP. Crystal structure illustrations. Originally written by C. K. Johnson, Oak Ridge, USA. Modified by I. Carlbom and A. G. Nord, Stockholm, Sweden.

THE STRUCTURE DETERMINATION

The X-ray photographs showed trigonal symmetry and no systematically absent reflections were found. Among the several possible space groups, $P\bar{3}$ (No. 147) was chosen as a starting point for the structure determination. The position of the iron atom was chosen to be (0,0,0). A three-dimensional Patterson synthesis gave the position of the sulphur atom. The oxygen and nitrogen positions were found from a three-dimensional Fourier synthesis phased on the iron and sulphur atoms.

The structure was refined by the full matrix least squares technique. Atomic scattering factors [7] for neutral atoms were used except for iron which was taken as Fe^{3+}. With isotropic temperature factors the discrepancy index $R = \sum||F_o| - |F_c||/\sum|F_o|$ was 10.2 %. At this stage the temperature factors were allowed to change anisotropically and the R-value was further reduced to 7.5 %. An inspection of the intensity data revealed that for about 31 weak reflections, F_o was several times higher than F_c. For these reflections a strong independent reflection with the same $\sin^2\theta$ value could be found. It was therefore assumed that diffraction from crystalline powder on the crystals had caused the higher observed intensities for these reflections. An inspection of the Weissenberg photographs also showed the existence of faint powder lines. A least squares refinement with these reflections excluded gave a final R-value of 5.3 %. A weighting scheme $1/w = (A + B|F_o| + C|F_o|^2 + D|F_o|^3)$

Table 2. Fractional atomic coordinates with estimated standard deviations.

Atom	Position	x	y	z
Fe	1(*a*)	0	0	0
S	6(*g*)	0.7140(3)	0.6820(3)	0.1386(3)
O(1)	6(*g*)	0.5704(6)	0.6740(7)	0.2070(10)
O(2)	6(*g*)	0.7507(7)	0.5972(7)	0.2774(9)
O(3)	6(*g*)	0.8352(6)	0.8499(7)	0.1702(8)
N(1)	6(*g*)	0.6131(10)	0.9570(10)	0.3488(11)
N(2)	2(*d*)	1/3	2/3	−0.0117(20)
N(3)	1(*b*)	0	0	1/2

Table 3. Anisotropic thermal parameters and their standard deviations. The temperature factor is given by $\exp\{-[\beta_{11}h^2 + \beta_{22}k^2 + \beta_{33}l^2 + \beta_{12}hk + \beta_{13}hl + \beta_{23}kl]\}$.

Atom	β_{11}	β_{22}	β_{33}	β_{12}	β_{13}	β_{23}
Fe	0.0056(3)	0.0056(3)	0.0086(10)	0.0055(3)	0	0
S	0.0042(3)	0.0060(4)	0.0089(7)	0.0038(6)	0.009(7)	−0.0004(7)
O(1)	0.0040(9)	0.0079(10)	0.0259(22)	0.0062(16)	0.0040(21)	0.0038(22)
O(2)	0.0099(11)	0.0097(10)	0.0208(19)	0.0121(18)	0.0043(22)	0.0087(23)
O(3)	0.0069(9)	0.0071(14)	0.0073(14)	0.0040(15)	0.0029(18)	0.0013(18)
N(1)	0.0103(14)	0.0165(16)	0.0129(19)	0.0196(27)	0.0039(27)	−0.0034(29)
N(2)	0.0039(10)	0.0039(10)	0.0214(41)	0.0048(20)	0	0
N(3)	0.0223(30)	0.0323(30)	0.0135(64)	0.0312(30)	0	0

Table 4. Observed and calculated structure factors of $(NH_4)_9[Fe(SO_3)_6]$. The reflections marked with one asterisk were rejected by the least squares refinement program and reflections marked with two asterisks were rejected before the refinement due to the decomposition of crystal two. F_o and F_c values listed in the table have been multiplied by 10.0.

H	K	L	FO	FC	H	K	L	FO	FC	H	K	L	FO	FC	H	K	L	FO	FC
1	1	-7	-	-52	6	3	-3	191	193	1	7	-1	-	79	2	4	1	305	281
2	1	-7	-	145**	1	4	-3	328	335	2	7	-1	167	174	3	4	1	509	507
1	2	-7	-	7	2	4	-3	164	-83*	3	7	-1	287	277	4	4	1	-	76
2	2	-7	120	120	3	4	-3	186	-167	1	8	-1	144	133	5	4	1	-	44
1	1	-6	204	-188**	4	4	-3	116	112	2	8	-1	126	134	6	4	1	220	223
2	1	-6	-	-33	5	4	-3	135	43*	1	0	0	456	456	0	5	1	325	-331
3	1	-6	212	131**	1	5	-3	169	157	2	0	0	-	56	1	5	1	174	-177
4	1	-6	-	-31	2	5	-3	-	-38	3	0	0	981	1001	2	5	1	277	284
5	1	-6	-	23	3	5	-3	184	205	4	0	0	-	65	3	5	1	131	-89
1	2	-6	-	-44	4	5	-3	377	377	5	0	0	-	75	4	5	1	138	-149
2	2	-6	215	189**	1	6	-3	139	-37*	6	0	0	389	392	5	5	1	244	237
3	2	-6	-	-40	2	6	-3	-	65	7	0	0	391	400	0	6	1	280	284
4	2	-6	170	-163**	3	6	-3	203	209	8	0	0	-	-34	1	6	1	254	271
1	3	-6	158	185**	1	7	-3	127	101	9	0	0	-	53	2	6	1	174	137
2	3	-6	-	219**	2	7	-3	148	-123	1	1	0	259	-263	3	6	1	-	16
3	3	-6	-	83	1	8	-3	187	191	2	1	0	530	538	4	6	1	111	69*
1	4	-6	-	-95	1	1	-2	1457	1489	3	1	0	378	376	0	7	1	281	280
2	4	-6	191	148**	2	1	-2	195	190	4	1	0	152	122	1	7	1	-	103
1	5	-6	-	-23	3	1	-2	393	392	5	1	0	178	158	2	7	1	256	236
1	1	-5	-	14	4	1	-2	645	653	6	1	0	566	581	3	7	1	-	58
2	1	-5	-	-261**	5	1	-2	253	249	7	1	0	309	307	0	8	1	274	-278
3	1	-5	-	-90	6	1	-2	-	-65	8	1	0	-	-25	1	8	1	-	-54
4	1	-5	-	3	7	1	-2	-	88	1	2	0	217	122*	2	8	1	192	185
5	1	-5	-	5	8	1	-2	190	193	2	2	0	176	-181	0	9	1	-	-4
6	1	-5	137	109	1	2	-2	216	249	3	2	0	148	-116	0	0	2	752	-720
1	2	-5	-	-31	2	2	-2	143	154	4	2	0	176	-24*	1	0	2	152	166
2	2	-5	190	168**	3	2	-2	406	429	5	2	0	-	18	2	0	2	281	300
3	2	-5	-	94	4	2	-2	386	388	6	2	0	117	-87	3	0	2	288	271
4	2	-5	-	-182**	5	2	-2	140	141	7	2	0	165	-159	4	0	2	353	360
5	2	-5	216	167**	6	2	-2	157	122	8	2	0	-	18	5	0	2	392	391
1	3	-5	141	142**	7	2	-2	368	380	1	3	0	306	-257	6	0	2	236	235
2	3	-5	130	270**	1	3	-2	249	239	2	3	0	109	-108	7	0	2	-	15
3	3	-5	-	-69	2	3	-2	205	140	3	3	0	338	344	8	0	2	278	288
4	3	-5	-	97	3	3	-2	187	185	4	3	0	169	146	9	0	2	160	162
5	3	-5	337	350	4	3	-2	186	-160	5	3	0	114	-81	0	1	2	136	130
1	4	-5	-	20	5	3	-2	215	-239	6	3	0	-	74	1	1	2	367	-370
2	4	-5	-	-9	6	3	-2	-	66	7	3	0	122	120	2	1	2	150	-142
3	4	-5	-	32	7	3	-2	-	23	1	4	0	325	338	3	1	2	172	-45*
4	4	-5	235	221	1	4	-2	375	333	2	4	0	500	515	4	1	2	215	-196
1	5	-5	-	-24	2	4	-2	146	66*	3	4	0	304	304	5	1	2	117	61*
2	5	-5	191	199**	3	4	-2	222	221	4	4	0	126	119	6	1	2	159	-34*
3	5	-5	123	-20*	4	4	-2	-	63	5	4	0	117	78	7	1	2	-	-40
1	6	-5	293	315	5	4	-2	143	55*	6	4	0	352	348	8	1	2	-	15
1	1	-4	101	113	6	4	-2	-	12	1	5	0	224	196	0	2	2	203	194
2	1	-4	143	83*	1	5	-2	112	84	2	5	0	166	151	1	2	2	151	-149
3	1	-4	198	-190	2	5	-2	136	100	3	5	0	-	-4	2	2	2	655	662
4	1	-4	-	55	3	5	-2	213	214	4	5	0	176	-196	3	2	2	165	-50*
5	1	-4	-	-14	4	5	-2	295	305	5	5	0	147	142	4	2	2	222	-217
6	1	-4	139	-136	5	5	-2	140	139	1	6	0	202	-35*	5	2	2	282	294
7	1	-4	-	60	1	6	-2	155	-156	2	6	0	192	185	6	2	2	211	217
1	2	-4	282	289	2	6	-2	206	-226	3	6	0	147	168	7	2	2	-	75
2	2	-4	379	368	3	6	-2	146	138	4	6	0	134	-42*	0	3	2	246	221
3	2	-4	-	130**	4	6	-2	-	58	1	7	0	130	58*	1	3	2	463	485
4	2	-4	218	216	1	7	-2	-	128	2	7	0	285	288	2	3	2	461	457
5	2	-4	168	170	2	7	-2	138	40*	3	7	0	151	145	3	3	2	286	288
6	2	-4	123	118	3	7	-2	169	173	1	8	0	-	-76	4	3	2	255	267
1	3	-4	113	96	1	8	-2	230	246	2	8	0	196	190	5	3	2	500	488
2	3	-4	136	108**	1	1	-1	841	851	0	0	1	805	834	6	3	2	196	203
3	3	-4	-	23	2	1	-1	145	48*	1	0	1	305	311	7	3	2	-	-12
4	3	-4	233	232	3	1	-1	181	171	2	0	1	139	129	0	4	2	230	211
5	3	-4	338	355	4	1	-1	190	209	3	0	1	268	227	1	4	2	249	-244
6	3	-4	186	172	5	1	-1	215	240	4	0	1	203	-32*	2	4	2	110	-44*
1	4	-4	-	276**	6	1	-1	395	406	5	0	1	251	252	3	4	2	115	60*
2	4	-4	160	-129	7	1	-1	179	186	6	0	1	306	307	4	4	2	195	192
3	4	-4	219	-221	8	1	-1	121	111	7	0	1	220	225	5	4	2	156	152
4	4	-4	255	250	1	2	-1	401	410	8	0	1	227	213	6	4	2	-	-24
5	4	-4	126	54*	2	2	-1	199	215	9	0	1	152	158	0	5	2	253	-207
1	5	-4	239	239	3	2	-1	144	162	0	1	1	265	244	1	5	2	142	-128
2	5	-4	-	62	4	2	-1	335	341	1	1	1	488	-463	2	5	2	268	282
3	5	-4	170	123	5	2	-1	-	72	2	1	1	220	-192	3	5	2	175	-25*
4	5	-4	205	205	6	2	-1	218	-222	3	1	1	363	385	4	5	2	-	50
1	6	-4	252	240	7	2	-1	226	239	4	1	1	-	134	5	5	2	-	82
2	6	-4	195	219	8	2	-1	147	168	5	1	1	146	-131	0	6	2	-	52
3	6	-4	142	126	1	3	-1	181	-177	6	1	1	379	383	1	6	2	464	475
1	7	-4	129	125	2	3	-1	-	93	7	1	1	-	86	2	6	2	182	181
1	1	-3	278	287	3	3	-1	199	201	8	1	1	147	-166	3	6	2	-	-3
2	1	-3	496	491	4	3	-1	117	-31*	0	2	1	190	-193	4	6	2	120	134
3	1	-3	-	21	5	3	-1	453	-442	1	2	1	315	-315	0	7	2	-	-104
4	1	-3	348	350	6	3	-1	-	30	2	2	1	161	-116	1	7	2	141	161
5	1	-3	165	137	7	3	-1	165	127	3	2	1	184	-155	2	7	2	-	-15
6	1	-3	358	-376	1	4	-1	230	245	4	2	1	431	-425	3	7	2	-	32
7	1	-3	-	98	2	4	-1	255	272	5	2	1	169	147	0	8	2	147	-126
8	1	-3	176	151	3	4	-1	181	161	6	2	1	328	317	1	8	2	-	13
1	2	-3	283	253	4	4	-1	-	86	7	2	1	320	-340	0	0	3	396	-412
2	2	-3	214	223	5	4	-1	-	80	8	2	1	-	7	1	0	3	191	-177
3	2	-3	-	130**	6	4	-1	222	223	0	3	1	601	634	2	0	3	126	125
4	2	-3	421	413	1	5	-1	373	365	1	3	1	271	296	3	0	3	103	108
5	2	-3	122	107	2	5	-1	118	138	2	3	1	325	-319	4	0	3	-	74
6	2	-3	134	155	3	5	-1	175	99*	3	3	1	272	287	5	0	3	316	321
7	2	-3	275	282	4	5	-1	-	82	4	3	1	223	193	6	0	3	-	-18
1	3	-3	-	121**	5	5	-1	-	97	5	3	1	281	289	7	0	3	190	-185
2	3	-3	-	48	1	6	-1	197	-162	6	3	1	141	147	8	0	3	253	262
3	3	-3	193	190	2	6	-1	171	-162	7	3	1	-	32	0	1	3	179	-164
4	3	-3	-	68	3	6	-1	185	172	0	4	1	547	541	1	1	3	263	283
5	3	-3	173	163	4	6	-1	110	-65*	1	4	1	-	0	2	1	3	181	191

Table 4. Continued.

H	K	L	FO	FC	H	K	L	FO	FC	H	K	L	FO	FC	H	K	L	FO	FC
3	1	3	169	-146	2	0	4	237	239	3	5	4	206	199	1	5	5	313	315
4	1	3	-	-39	3	0	4	244	-237	3	5	4	191	199	2	5	5	-	20
5	1	3	120	104	4	0	4	-	31	4	5	4	144	132	3	5	5	131	108
6	1	3	313	-318	5	0	4	121	87	0	6	4	-	-1	3	5	5	123	108
7	1	3	113	88	6	0	4	-	-116	1	6	4	-	-65	0	6	5	136	139
8	1	3	205	193	7	0	4	-	-32	2	6	4	-	75	1	6	5	-	-58
0	2	3	177	211	8	0	4	120	73*	3	6	4	159	150	0	0	6	467	457
1	2	3	98	-27*	0	1	4	-	-62	0	7	4	-	0	1	0	6	116	128
2	2	3	674	663	1	1	4	718	698	1	7	4	142	136	2	0	6	-	-45
3	2	3	301	258	2	1	4	225	190	0	8	4	228	229	3	0	6	274	279
4	2	3	140	133	3	1	4	-	49	0	0	5	-	106**	4	0	6	-	-3
5	2	3	267	272	4	1	4	446	454	1	0	5	139	155	5	0	6	-	-60
6	2	3	-	46	5	1	4	-	-17	2	0	5	138	132	0	1	6	282	282
7	2	3	130	117	6	1	4	195	-190	3	0	5	-	-6	1	1	6	291	301
0	3	3	107	-90	6	1	4	195	-190	4	0	5	-	8	2	1	6	167	177
1	3	3	213	203	7	1	4	119	118	5	0	5	-	-83	3	1	6	134	120
2	3	3	633	652	0	2	4	109	111	6	0	5	-	66	4	1	6	149	159
3	3	3	-	25	0	2	4	117	111	0	1	5	114	111	5	1	6	239	248
4	3	3	187	170	1	2	4	439	450	0	1	5	117	111	0	2	6	235	242
5	3	3	370	368	2	2	4	415	417	1	1	5	417	415	1	2	6	-	44
6	3	3	-	100	2	2	4	404	417	2	1	5	159	128	2	2	6	207	-227
0	4	3	167	-165	3	2	4	400	422	3	1	5	-	29	3	2	6	-	30
1	4	3	135	148	4	2	4	421	415	4	1	5	403	400	4	2	6	-	82
2	4	3	239	-226	5	2	4	162	174	5	1	5	183	169	0	3	6	242	217
2	4	3	231	-226	5	2	4	165	174	6	1	5	-	21	1	3	6	142	-139
3	4	3	265	-254	6	2	4	-	72	0	2	5	174	186	2	3	6	-	-84
4	4	3	212	217	0	3	4	181	-170	1	2	5	392	380	3	3	6	176	177
5	4	3	146	123	0	3	4	181	-170	2	2	5	-	-27	0	4	6	198	202
0	5	3	196	195	1	3	4	222	233	3	2	5	219	192	1	4	6	158	163
1	5	3	-	-51	2	3	4	146	105	4	2	5	297	317	2	4	6	189	192
2	5	3	155	112	3	3	4	129	-95	5	2	5	-	-20	0	5	6	169	183
3	5	3	157	143	4	3	4	-	63	0	3	5	-	34	1	5	6	167	147
4	5	3	-	18	5	3	4	-	19	1	3	5	-	2	0	0	7	333	341
0	6	3	131	-98	0	4	4	128	-84*	2	3	5	127	-109	1	0	7	174	111**
1	6	3	236	205	1	4	4	460	450	3	3	5	-	64	2	0	7	-	-61
2	6	3	242	250	2	4	4	-	-57	4	3	5	-	-78	3	0	7	189	207
3	6	3	-	67	3	4	4	133	-125	5	3	5	152	-157	0	1	7	-	141**
0	7	3	146	-141	3	4	4	143	-125	5	3	5	156	-157	1	1	7	-	16
1	7	3	152	132	4	4	4	-	77	0	4	5	-	-13	2	1	7	-	91**
2	7	3	125	-136	5	4	4	-	-15	1	4	5	282	269	0	2	7	-	10
0	8	3	142	126	0	5	4	349	333	2	4	5	143	161	1	2	7	-	-82
1	8	3	119	-35*	1	5	4	222	236	3	4	5	-	-60	0	3	7	-	217**
0	0	4	236	-240	1	5	4	235	236	4	4	5	-	59					
1	0	4	108	108	2	5	4	131	76*	0	5	5	256	258					

was used in the refinement, with coefficients A = 3667.9, B = − 140.45, C = 2.095 and D = − 0.00558.

Attempts were also made to refine the structure in space group $P3$ (No. 143). No improvement in R-value was obtained and the isotropic temperature factor for one of the nitrogen atoms became negative. Space group $P\bar{3}$ was therefore considered to be correct for the nonhydrogen atoms. Attempts to locate the hydrogen atoms from the difference Fourier maps were not successful, revealing definitely only the hydrogen atoms around the nitrogen atom at the 2(d) position (1/3, 2/3, $\pm z$). The relatively high errors in F_o for the weak reflections may explain why it was not possible to locate the rest of the hydrogen atoms.

The final values of the atomic parameters and their standard deviations are presented in Tables 2 and 3. These values are based on a least squares refinement using atomic scattering factors for ammonium ion.[8] The observed and calculated structure factors are listed in Table 4.

DESCRIPTION AND DISCUSSION OF THE STRUCTURE

The structure of $(NH_4)_9[Fe(SO_3)_6]$ can be described as being built of $Fe(SO_3)_6$ groups linked together by ammonium ions (*cf.* Fig. 1). The iron atom is octahedrally surrounded by six oxygen atoms, O(3), belonging to six different sulphite groups. The FeO_6 octahedron thus formed is rather regular

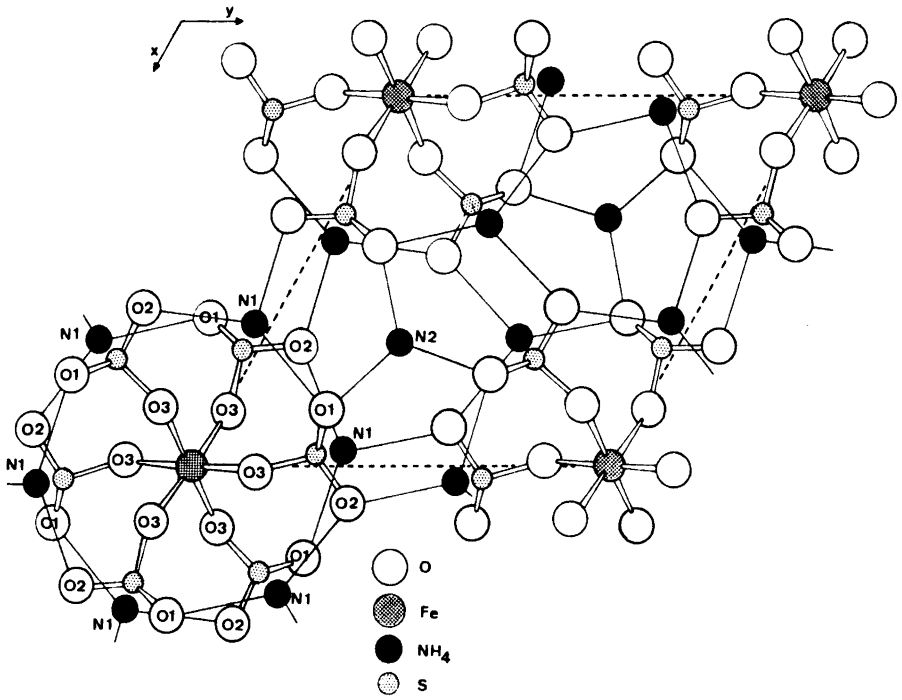

Fig. 1. The structure of $(NH_4)_9[Fe(SO_3)_6]$. The ammonium ions N(3) at position $(0,0,\frac{1}{2})$ are not shown in the figure. A possible hydrogen bond scheme is indicated by solid lines.

(*cf.* Table 5 for interatomic distances and angles), and the Fe–O distance is 2.028 Å. This value is in good agreement with Fe–O distances of 1.993 Å, 2.00 Å and 2.02 Å found for six-coordinated iron in $FeNH_4(SO_4)_3.3H_2O$,[9] $FeOHSO_4$,[10] and in $Na_3Fe_5O_9$,[11] as well as with the sum, 2.04 Å,[12] of the ionic radii of Fe^{3+} (0.64 Å) and O^{2-} (1.40 Å).

Table 5. Interatomic distances (Å) and angles (°) with their standard deviations. The distances are uncorrected for thermal motion.

Fe –O(3)	2.028(6)	N(1)–O(2)	2.786(11)
–S	3.257(2)	–O(1)	2.868(11)
S –O(2)	1.488(7)	–O(1)	2.888(11)
–O(1)	1.512(6)	–O(2)	2.893(11)
–O(3)	1.551(6)	–O(3)	3.240(10)
O(1)–O(2)	2.391(9)	N(2)–O(1)	2.860(10)
–O(3)	2.401(8)	–O(2)	3.060(11)
O(2)–O(3)	2.404(9)	N(3)–O(3)	2.873(6)
O(1)–S–O(2)	105.7(4)		
O(1)–S–O(3)	103.2(3)		
O(2)–S–O(3)	104.5(4)		
O(3)–Fe–O(3)	87.2(2)		
O(3)–Fe–O(3)	92.8(2)		

The sulphite group coordinates to the iron atom through O(3) only. The difference between the length of the S – O(3) bond 1.551 ± 0.006 Å and the average value, 1.500 Å, of the two other S – O bond lengths (1.512(6) and 1.488(7) Å, respectively) is 0.051 Å, or eight times the standard deviation. If the sulphite oxygen atoms have metal ions as ligands, the S – O bond will be longer than it is in the free anion. The O(1) and O(2) atoms have no metal ligands, and the corresponding average S – O bond distance of 1.500 Å is in good agreement with the value of 1.504 Å found for the free anion.[13]

The effect exerted by the Fe^{3+} ion on the S – O(3) bond is very pronounced due to the high polarizing power of the ferric ion. The same effect has been observed in $ZnSO_3.2\frac{1}{2}H_2O$ where the sulphite oxygen atoms have zinc ions as ligands and the S – O mean distance is 1.54 Å.[14] In $Tl[Cu(SO_3)_2]$ [15] close contacts exist between copper and two of the sulphite oxygen atoms. The Cu – O distance is 1.99 Å, and the corresponding S – O bond length is 1.550 ± 0.005 Å. The third S – O bond length is 1.515 ± 0.006 Å, so that there is a difference between the two bonds lengths of 6σ.

The ammonium ions may form hydrogen bonds between the $Fe(SO_3)_6$ groups as well as within the groups. A possible hydrogen bond scheme is indicated in Fig. 1. The ammonium ion N(3) in position $(0,0,\frac{1}{2})$ is situated inside a distorted octahedron. There are six N – O distances of equal length, and thus the ammonium ion might have several equivalent orientations.

The average distances in the sulphite group, *i.e.* the S – O distance (1.517 Å) and the O – O distance (2.399 Å) are approximately the same as in other sulphites of type $SO_3^{2-}\cdots X$, where X is nitrogen, oxygen, and/or metal ion. In $(NH_4)_2SO_3.2H_2O$ the S – O and O – O distances are 1.524 Å and 2.408 Å.[16] The average O···(H) – N distances in $(NH_4)_9[Fe(SO_3)_6]$ are 2.872 Å, 2.913 Å, and 3.057 Å for O(1), O(2), and O(3), respectively; and in $(NH_4)_2SO_3.2H_2O$, the corresponding values are 2.85 Å, 2.83 Å, and 2.84 Å.

Acknowledgements. The authors are indebted to Professor Peder Kierkegaard and Professor Arne Magnéli for their encouraging interest in this work, for advice and many stimulating discussions. Thanks are also due to Dr. Anne-Marie Pilotti for her help during the data collecting with diffractometer and to Dr. Sven Westman for his correction of the English of this paper. This investigation has been performed with financial support from the *Tri-Centennial Fund of the Bank of Sweden* and from the *Swedish Natural Science Research Council*. A scholarship from the *Finnish Swedish Cultural Foundation* to one of us (L.N.) is gratefully acknowledged.

REFERENCES

1. Kierkegaard, P., Larsson, L. O. and Nyberg, B. *Acta Chem. Scand.* **26** (1972) 218.
2. Erämetsä, O. *Ann. Acad. Sci. Fenn. Ser. A.* **59** (1943) No. 11.
3. Erämetsä, O. *Suomen Kemistilehti* **B 37** (1964) 56.
4. Erämetsä, O. and Valkonen, J. *Suomen Kemistilehti* **B 45** (1972) 91.
5. Hambling, P. G. *Acta Cryst.* **6** (1953) 98.
6. Coppens, P., Leiserowitz, L. and Rabinovich, D. *Acta Cryst.* **18** (1965) 1035.
7. *International Tables for X-Ray Crystallography*, Kynoch Press, Birmingham 1962, Vol. III.
8. Davis, M. F. *Acta Cryst.* **21** (1966) 822.
9. Palmer, K. J., Wong, R. Y. and Lee, K. S. *Acta Cryst.* **B 28** (1972) 236.
10. Johansson, G. *Acta Chem. Scand.* **16** (1962) 1234.

11. Romers, C., Rooymans, C. J. M. and DeGraaf, R. A. G. *Acta Cryst.* **22** (1967) 766.
12. Pauling, L. *The Nature of the Chemical Bond*, 3rd Ed., Cornell University Press, Ithaca 1960.
13. Larsson, L. O. and Kierkegaard, P. *Acta Chem. Scand.* **23** (1969) 2253.
14. Nyberg, B. *Acta Chem. Scand.* **26** (1972) 857.
15. Hjertén, I. and Nyberg, B. *Acta Chem. Scand.* **27** (1973) 345.
16. Batelle, L. F. and Trueblood, K. N. *Acta Cryst.* **19** (1965) 531.

Received October 10, 1972.

ACTA CHEMICA SCANDINAVICA 27 (1973) 868–874

Acid-Base Properties of Atropine, Scopolamine and Some Glycolic Acid Esters

ANITA MEYERHÖFFER[a] and OLOF WAHLBERG[b]*

[a]*The Research Institute of National Defence (FOA), S-172 04 Sundbyberg 4, Sweden.* [b]*Department of Inorganic Chemistry, Royal Institute of Technology (KTH), S-100 44 Stockholm 70 and Institute of Inorganic and Physical Chemistry, University of Stockholm, S-104 05 Stockholm 50, Sweden*

The dissociation constants of atropine and ten related anticholinergic compounds have been obtained from emf titrations in 0.1 M NaCl medium at 25°C using glass electrodes. All the compounds studied were tertiary amines and the acids corresponding to them had a $pK_a = 8-10$. One compound has been studied at different concentrations of Na^+, Ca^{2+}, and Cl^-. No association with these ions could be detected. The data were treated by graphical as well as computer methods such as the least squares program LETAGROP ETITR, allowing for small acid impurities.

This investigation is part of a research program with the intention to investigate possible relationships between structure and activity of anticholinergic drugs.

The degree of ionization and the lipophilic character of a drug influence the passage of the drug through cell membranes. There are experimental results, which indicate that glycolates affect membrane processes in the central nervous system.[1] In connection with this problem it has been questioned whether these drugs can form complexes with calcium.[2]

This investigation has been undertaken in order to determine dissociation constants of atropine, scopolamine, and some glycolic acid esters, and the possible formation of calcium complexes with such compounds.

EXPERIMENTAL

Chemicals and analysis. The compounds studied in this paper are listed in Table 1. *Atropine* and *scopolamine hydrobromide* were commercial products from Vitrum AB, Stockholm. All the other drugs were synthetized and analysed for C, H, N at the Research Institute of National Defence, Sweden (Table 1, Nos. 1–7 analysed by Flormark and

* The measurements have been made by A.M. at FOA and the calculations have been performed by A.M. and O.W.

Table 1. Name, code number, formulae and melting points of the compounds studied.

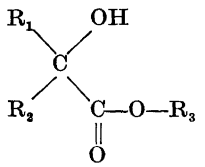

Code number	Name	R_1	R_2	R_3	M.p. (°C)	Notes
1	1-Methyl-4-piperidyl benzilate				166	
2	3-Tropyl benzilate	-"-	-"-		237 – 241	Melting point of the hydrochloride
3	3-Quinuclidinyl benzilate	-"-	-"-		166 – 168	
4	3-Quinuclidinyl cyclopentyl phenylglycolate	-"-		-"-	98 – 102	
5	3-Quinuclidinyl phenyl 2-thienylglycolate	-"-		-"-	237 – 240	
6	3-Quinuclidinyl 9-hydroxy 9-fluorenecarboxylate	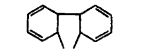		-"-	213 – 216	
7	3-Tropyl 9-hydroxy 9-fluorenecarboxylate	-"-			225	Melting point of the hydrochloride
8	3-Quinuclidinyl di-2,2'-thienylglycolate				154 – 155	
9	3-Quinuclidinyl di-3,3'-thienylglycolate			-"-	139	
10	Atropine	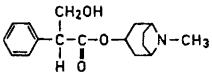			115 – 116	
11	Scopolamine	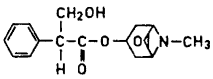			55	Melting point of the hydrobromide

Larsson [3] and Nos. 8 – 9 by Nyberg *et al.*[4]). Melting points of the substances are tabulated in Table 1. *Sodium hydroxide.* A 50 % stock solution was prepared from the EKA Bohus AB, analytical grade product. From this stock solution portions were taken and diluted with de-aerated water. NaOH solutions were standardized by titration with potassium hydrogen phthalate, using phenolphthalein as an indicator.[5] *Hydrochloric acid.* Merck AG (Darmstadt) Titrisol stock solutions were used. The concentration of HCl was determined from the first acid points in each titration using the Gran method of extrapolations to the equivalence point.[6] *Sodium chloride* and *calcium chloride.* Merck's analytical grade products were used.

Apparatus. Potentiometer: Radiometer, Copenhagen, *PHM 26c* and Autoburet *AMU 1b.* The emf values could be read to a precision of ±0.2 mV. *Electrodes:* Glass electrode *202C* from Radiometer. Ag,AgCl electrode prepared according to Brown.[7] *Thermostat:* A water mantle at 25.00±0.02°C. The equilibrium solution was stirred with a magnet and commercial nitrogen gas was bubbled through.

Emf measurements and titration procedure. The emf of the following cell was measured:

$$-\text{Ag,AgCl/S/glass electrode}+$$

The solution S contained A mol/l of a weak acid and the analytical (total excess) concentration of H^+ over A and $H_2O = H$ mol/l. The concentrations in the starting solution, before the addition of buret solution, are called A_0 and H_0 mol/l, respectively. In order to keep the activity coefficients approximately constant, NaCl was added so that $[Cl^-] = 0.1$ M (except for one acid, *cf.* Table (2b)).

The emf of the cell can be written:

$$E = E_0 + 59.155 \log h \quad (1)$$

where $h = [H^+]$. Usually we started with 30 ml of an acid solution containing HCl + A and then 2 – 3 ml of NaOH solution was added in small portions from a buret to change H. A solution of 0.2 M NaCl was added from a second buret. The acids studied were very slightly soluble in water (≈ 1 mM of A). At the end of the titrations a precipitate was often formed causing a drift in the emf values.

Each titration was carried out within 30 min in order to avoid decomposition by hydrolysis. The emf usually reached a stable value ($\pm$ 0.2 mV) within 1 min. The alkaline hydrolysis of some of the glycolates has recently been studied.[8] By separate experiments, it was checked that the decomposition during the titrations did not exceed 2 %. For 3-quinuclidinyl di-3,3′-thienylglycolate forward and back titrations agreed within the limits of experimental error (*cf.* Fig. 1, a and b). Thus the reversibility of the equilibria was confirmed.

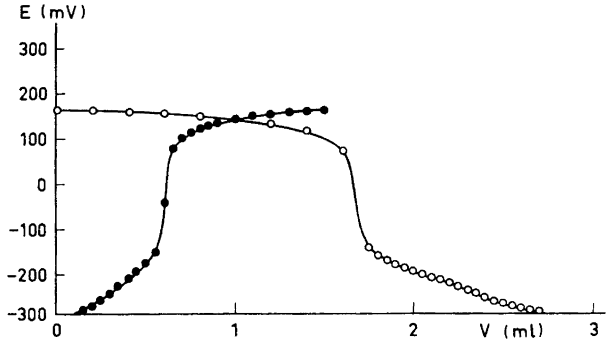

Fig. 1a. Titration curves for 3-quinuclidinyl di-3,3′-thienylglycolate. The filled symbols represent a back titration. E = the measured emf. V = the volume added from a buret to V_0 ml of a solution S_0. The buret contained 0.0457 M NaOH for the forward titration and 0.1004 M HCl for the back titration. The solution S_0 for the forward titration contained the total concentration 0.993 mM weak acid ($= A_0$) and the analytical concentration of $H^+ = 3.46$ mM ($= H_0$). $E_0 = 320.4$ mV.

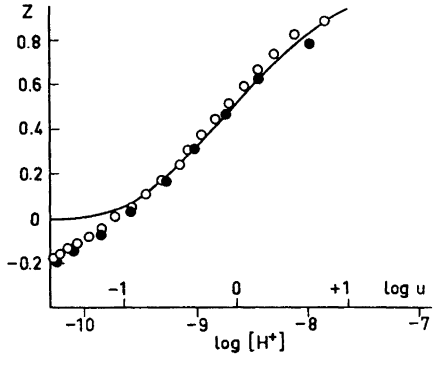

Fig. 1b. The data in Fig. 1a transformed to $Z(\log h)$ with $pK_w = 13.8$ (*cf.* eqn. (3c)). Z = the average number of H^+ bound per A. The line corresponds to $pK_{a1} = 8.6$.

Hydrogen electrodes could not be used in these experiments due to the rather rapid hydrolysis of the esters studied. The glass electrodes used were checked against hydrogen electrodes.

By using a coulometer one can avoid possible impurities of the sodium hydroxide solution. The accuracy of a coulometric titration is usually very high.[9] However, in the present case, it was not possible to get reproducible results by the coulometric technique, possibly due to decomposition of the compounds studied during the electrolysis.

TREATMENT OF DATA

The reaction studied can be written

$$HA^+ + H_2O \rightleftharpoons H_3O^+ + A \quad (2)$$

The law of mass action gives for this equilibrium $[HA^+] = \beta_1 h[A]$, where $h = [H^+]$. The total concentration of the weak acid ($= A$) and the concentration of H^+ bound to the weak acid ($= ZA$) can be written as

$$A = [A] + \beta_1 h[A] \quad (3a)$$

$$ZA = \beta_1 h[A] \quad (3b)$$

The experimental values of Z were calculated from

$$ZA = H - h + K_w h^{-1} \quad (3c)$$

Note that Z = the average number of H^+ bound per A. For the ionic product of water in 0.1 M NaCl at 25°C we have used the value of $\log K_w = -13.80$.[10]

The primary data are values of volume and emf (V,E) at different total concentrations H and A (*cf.* Fig. 1a). Experimental points in the range $-2.5 \geq \log h \geq -3.5$ were used in a Gran [6] plot to correct H_0 and for calculation of E_0. The primary data (V,E) were then transformed to $Z(\log h)$ using eqns. (1) and (3c) (*cf.* Fig. 1b).

Graphical determination of the dissociation constants. If it is assumed that HA^+ and A are the only A-species present in the solution, then from eqns. 3 (a–b)

$$Z = \beta_1 h/(1 + \beta_1 h) \quad (4a)$$

By introducing the substitution $u = \beta_1 h$ one obtains

$$Z = u/(1 + u) \quad (4b)$$

$Z(\log u)$ is a normalized function,[11] which could be very well fitted to the experimental curves $Z(\log h)$ for $\log h > -10$. The last points of each titrations revealed a small additional buffer capacity (*cf.* Fig. 1b). This can be due to (i) imperfections of the glass electrodes; (ii) acid-base impurities, such as carbonic acid or silicic acid, with pK_a values of ~ 10 (*cf.* Ref. 12); (iii) decomposition of the compound studied; or (iv) a second dissociation step of the acids. Since the equilibria were found to be reversible a decomposition can be ruled out.

For 3-quinuclidinyl di-3,3′-thienylglycolate the graphical method gave the best fit with

$$pK_a = \log \beta_1 = 8.6 \pm 0.1 \quad (4c)$$

Since all the compounds studied have very similar titration curves, the graphical treatment was carried out only for a few acids. Instead all equilibrium constants were obtained using the generalized least squares program LETAGROP.[13,14]

Computer refinement of the dissociation constants. In the computer treatment the error squares sum $U = \sum(H_{calc} - H_{exp})^2$ was minimized.[13,14] For each titration we have assumed small errors δH and δE_0 in H and E_0, respectively. These errors correspond to small shifts in the curve $Z(\log h)$.

In order to correct for the extra buffer capacity at high pH values (see above), we have adjusted one parameter together with pK_{a1} and the systematic errors δH and δE_0. The same values of pK_{a1} were obtained either a second dissociation constant pK_{a2}, or the ionic product of water, pK_w, was adjusted, or if an acid impurity with a concentration of 0.5 – 1.0 mM was assumed. Such a large amount of impurities is rather unlikely. Values of pK_w ranging from 12.6 to 13.6 were necessary to explain the extra buffer capacities in all the titrations.

Table 2a. Results of the least squares calculations (LETAGROP). $pK_{a1} = \log \beta_1$. The standard deviations of $H = \sigma(H)$, and the total concentrations of the weak acids in the starting solutions, A_0 are in mM.

Substance	Number of points	log ($\beta_1 \pm 3\,\sigma$)	$\sigma(H)$	A_0
1	19	8.37 ± 0.17	0.021	0.517
2	25	9.39 ± 0.08	0.013	0.488
3	34	8.72 ± 0.05	0.020	1.200
4	30	8.81 ± 0.07	0.031	1.031
5	24	8.48 ± 0.11	0.012	0.511
6	34	8.62 ± 0.08	0.010	0.469
7	36	9.73 ± 0.08	0.020	0.527
8	27	8.64 ± 0.04	0.008	1.111
9	36	8.63 ± 0.08	0.022	0.993
10	32	9.76 ± 0.07	0.023	0.906
11	39	7.81 ± 0.02	0.009	1.253

Table 2b. Calculations of $pK_{a1} = \log \beta_1$ for 3-quinuclidinyl benzilate for various total concentrations and media. The standard deviations of $H = \sigma(H)$, and the total concentrations of the weak acid in the starting solutions, A_0 are in mM. The extra buffer capacity may be explained with $pK_{a2} = 10.0 \pm 0.1$ (and $pK_w = 13.8$) or $pK_w = 13.3 \pm 0.1$ (assuming one dissociation step). No correction for the varying ionic medium has been introduced.

Medium	Number of points	A_0	log ($\beta_1 \pm 3\,\sigma$)	$\sigma(H)$
0.1 M NaCl	34	1.200	8.72 ± 0.05	0.020
»	29	0.770	8.79 ± 0.07	0.014
»	43	0.536	8.88 ± 0.10	0.024
»	27	0.230	8.67 ± 0.22	0.015
0.3 M NaCl	30	1.132	8.82 ± 0.06	0.021
0.5 M NaCl	30	1.076	8.88 ± 0.08	0.028
0.25 M $CaCl_2$	32	0.978	8.90 ± 0.10	0.031

The analytical errors in H are very small, ~ 0.02 mM, and so is the standard deviation of H, *viz.* $\sigma(H) \sim 0.02$ mM (*cf.* Table 2, a and b).

RESULTS AND DISCUSSION

The final equilibrium constants given in Table 2a are valid in 0.1 M NaCl solution at 25°C. Most of the quinuclidinyl glycolates have $pK_a = 8.6 \pm 0.1$, while the pK_a of the tropyl derivates are 9.4 – 9.8. For atropine $pK_a = 9.8 \pm 0.1$, and for scopolamine $pK_a = 7.81 \pm 0.05$. These values are consistent with previously determined values, *viz.* 9.85 (18°C) [15,16] and 10.20 (16.5°C) [17] for atropine, 7.62 (21 ± 2°C) [18] and 7.55 (23°C) [19] for scopolamine. Abood [1] has found $pK_a = 7.8$ for 1-methyl-4-piperidyl benzilate (our value is 8.4 ± 0.2). The rather different media and temperatures used in the investigations make a direct comparison difficult.

No association of 3-quinuclidinyl benzilate with the medium ions Na^+, Cl^+, or Ca^{2+} could be detected (*cf.* Table 2b). The change of pK_a is so small that complex formation to Cl^- and Ca^{2+} can be neglected. Since charges cancel in reaction (2), the variation of $\log \beta_1$ with ionic strength can be expected to be due mainly to the salting out of the base form. The salting out coefficient can be estimated to 0.12, which is not unreasonable.[20]

In fact, the "best" fit to the data was obtained by assuming a second dissociation step. This may be due to the proton in the hydroxyl group (see Table 1). The values of pK_{a2} varied from 9.6 ± 0.5 for the 2-substituted thienylglycolates (5, 8 in Table 2a) to ~ 11 for atropine and scopolamine (10, 11 in Table 2a). However, pK_{a2} needs further documentation before it can be established with certainty. It deserves to be mentioned that a value of $pK_{a2} = 11$ seems very low for the primary alcohols atropine and scopolamine. Spectrophotometric studies might give the elucidations on this point.

Acknowledgements. Thanks are due to Dr. Erik Ekedahl for valuable comments and suggestions. We are indebted to Arne Flormark and Gun Wallerberg for supplying the substances. Dr. Don Koenig has kindly revised the English text.

This investigation has been financially supported by the *Tricentennial Fund of the Bank of Sweden* and by the *Swedish Natural Science Research Council.*

REFERENCES

1. Abood, L. G. In Burger, A., Ed., *Drugs Affecting the Central Nervous System*, Dekker, New York 1968, Vol. 2, p. 127.
2. Rogeness, G. A., Krugman, L. G. and Abood, L. G. *Biochim. Biophys. Acta* **125** (1966) 319.
3. Flormark, A. and Larsson, L. *Unpublished results.*
4. Nyberg, K., Östman, B. and Wallerberg, G. *Acta Chem. Scand.* **24** (1970) 1590.
5. Kolthoff, I. M. and Sandell, E. B. *Textbook of Quantitative Inorganic Analysis*, Macmillan, New York 1952, p. 528.
6. Gran, G. *Analyst* **77** (1952) 661.
7. Brown, A. S. *J. Am. Chem. Soc.* **56** (1934) 646.
8. Wallerberg, G. *To be published.*
9. Högfeldt, E., Wallin, T., Fredlund, F. and Zabicky, J. *Acta Chem. Scand.* **24** (1970) 369.
10. Harned, H. S. and Mannweiler, G. E. *J. Am. Chem. Soc.* **57** (1935) 1873.

11. Sillén, L. G. *Acta Chem. Scand.* **10** (1956) 187; 803.
12. Sillén, L. G. and Martell, A. E. *Stability Constants of Metal-ion Complexes, Chem. Soc. (London) Spec. Publ.* **17** (1964).
13. Arnek, R., Sillén, L. G. and Wahlberg, O. *Arkiv Kemi* **31** (1969) 353.
14. Brauner, P., Sillén, L. G. and Whiteker, R. *Arkiv Kemi* **31** (1969) 377.
15. Kolthoff, I. M. *Biochem. Z.* **162** (1925) 289.
16. Perrin, D. D. *Dissociation Constants of Organic Bases in Aqueous Solution*, Butterworths, London 1965, p. 343; 351.
17. Müller, F. *Z. Elektrochem.* **30** (1924) 587.
18. Bottomley, W. and Mortimer, P. I. *Austr. J. Chem.* **7** (1954) 189.
19. Schoorl, N. *Pharm. Weekblad* **76** (1939) 1497.
20. von Halban, H., Kortüm, G. and Seiler, M. *Z. phys. Chem. Abt. A* **172 – 3** (1935) 449.

Received September 20, 1972.

ACTA CHEMICA SCANDINAVICA 27 (1973) 875–887

Complex Formation between Silver and Iodide Ions in Fused Potassium — Sodium Nitrate. I. A Potentiometric Investigation of the Complex Formation at High Iodide Concentrations

BERTIL HOLMBERG

Division of Physical Chemistry, Lund University, Chemical Center, P.O.B. 740, S-220 07 Lund 7, Sweden

The stepwise formation of complexes $Ag_mI_n^{(n-m)-}$ in fused equimolar (K,Na)NO_3 at 280°C has been followed by means of potentiometric determination of the free silver ion concentration at varied concentrations of (K,Na)I, *viz.* in the range 0.3 mol $kg^{-1} \leq C_I \leq 1.5$ mol kg^{-1}. From separate potentiometric measurements in melts saturated with (K,Na)I it has been shown, that only mono- and dinuclear species are present in significant amounts. In the concentration range investigated the complexes AgI_2^-, AgI_3^{2-}, and $Ag_2I_6^{4-}$ have been proved to exist, and the corresponding stability constants have been calculated. Evidence has also been found for the existence of a fourth mononuclear complex, AgI_4^{3-}, and an approximate value of the stability constant β_{41} has been estimated.

The complex formation between Ag^+ and I^- in fused salt media has lately been studied by solubility [1] and electromotive force [1–5] measurements. As compared to the silver chloride and bromide systems our knowledge of the iodide system is rather scarce. This may to some extent be due to the small solubility of AgI in most ionic melts, causing the concentration range available for thermodynamic measurements to be narrow and unfavourably situated. In most works carried out hitherto no higher complexes than AgI_2^- have been reported. Elding and Leden,[1] however, recently proved the existence of AgI_3^{2-} in fused equimolar (K,Na)NO_3 at 280°C by solubility measurements.

As for the bromide system no higher mononuclear complex than $AgBr_3^{2-}$ could be detected in the same medium by Cigén and Mannerstrand,[6] employing both solubility and emf measurements.

One aim of the present investigation has been to make clear what higher complexes are formed in the iodide system. It is of particular interest to determine whether silver co-ordinates at most three halide ions or the complex

formation proceeds to AgI_4^{3-} in the iodide system as is the case in aqueous solution.[7]

This paper reports results from emf measurements with cells of the following three types:

I:	Ag	C_{Ag} $AgNO_3$	asbestos fibre	$C_{Ag}°$ $AgNO_3$	Ag
II:	Ag	C_{Ag} $AgNO_3$ (K,Na)I, saturated	asbestos fibre	$C_{Ag}°$ $AgNO_3$ (K,Na)I, saturated	Ag
III:	Ag	C_{Ag} $AgNO_3$ C_I (K,Na)I	asbestos fibre	$C_{Ag}°$ $AgNO_3$ $C_I°$ (K,Na)I	Ag

In order to avoid the experimental difficulties in the emf measurements, reported by Elding and Leden,[1] a different kind of high-temperature thermostat for potentiometric work has been constructed and tested. The elimination of temperature gradients in the test melt has been of major concern.

EXPERIMENTAL

Chemicals used. Potassium nitrate and sodium nitrate (Merck, *p.a.*) were powdered and dried at 120°C for two weeks. Silver nitrate (Engelhard, *p.a.*) was used without further treatment. Potassium iodide (Merck, *p.a.*) and sodium iodide (Mallinckrodt, *p.a.*) were dried at 140°C before use.

Apparatus. The thermostated cell compartment is shown schematically in Fig. 1. The aluminium block is furnished with two tubes for temperature measurement with Pt-resistance thermometers and two tubes for occasional illumination and observation of the melt. The block is thermostated by a proportional temperature regulator (SWEMA,

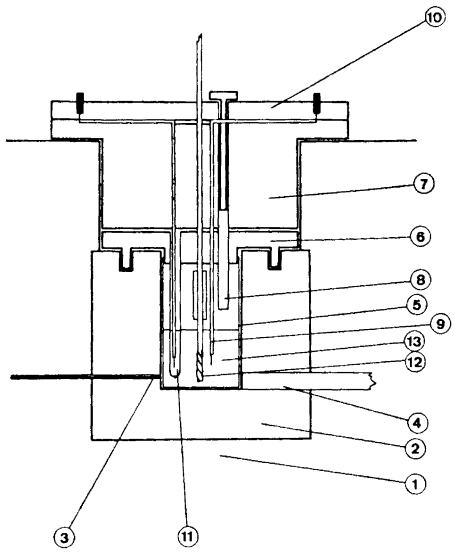

Fig. 1. Schematic view of the thermostated cell. 1. Insulation. 2. Aluminium block. 3. Platinum resistance thermometer. 4. Observation tube. 5. Pyrex vessel. 6. Aluminium lid. 7. Asbestos plug. 8. Immersed teflon-plugged addition funnel. 9. Bent electrode. 10. Top asbestos lid. 11. Reference half-cell. 12. Stirrer. 13. Test melt.

TK 65). In order to effect heating of the melt from above, a removable aluminium lid is resting at the top of the block. The electrodes and the upper part of the reference half-cell vessels are closely fixed to this hot lid.

Four electrodes and the stirrer run through narrow apertures in an 80 mm thick asbestos plug over the hot lid. The screw-formed Pyrex glass stirrer has two parallel wings along the axis, making the air circulate over the melt. At their upper end the electrodes are bent at right angles, and the horizontal part is fixed in tracks under the insulating top asbestos lid. This construction provides a well closed system with good temperature uniformity.

The temperature is measured by a Pt-resistance thermometer connected to a bridge (KNAUER), which is furnished with an external variable comparison arm. Since the working Pt-sensor is located in the aluminium block at a distance of ca 4 mm from the melt, it has been calibrated against a standard Pt-resistance thermometer (calibrated by National Physical Laboratory, Teddington) immersed in the test melt. By the same procedure the maximum temperature differences in the bulk melt were recorded. At constant temperature in the aluminium block the maximum differences amounted to 0.04°C. The temperature was maintained at 280.0°C with maximal over-all variations of ± 0.1°C during the emf measurements. Work at further modifications of the furnace construction is in progress.

Two reference electrodes and two indicator electrodes have been used simultaneously. The electrodes were made from spectrographically pure silver wire of 1 mm diameter (Johnson, Matthey & Co., London). They were spotwelded to a platinum wire (0.3 mm diameter) which was sealed into the end of a glass tubing. The electrodes were bent at right angles about 50 mm from their upper end, where the platinum wire ran freely out of the glass tubing. The ends of the platinum wires were connected to plugs in the top asbestos lid. The electrodes were silver-plated before use. Reference electrode vessels were of the same kind as described by Cigén and Mannerstrand.[6]

For the emf measurements a valve potentiometer, PHM4d from Radiometer, Copenhagen, was used. The accuracy of the emf measurements was ± 0.1 mV.

Procedure. In all series of measurements the test melt contained 250.0 g of equimolar $(K,Na)NO_3$. Successive weighed amounts of solidified stock melts of $AgNO_3$ in $(K,Na)NO_3$ (cells of type I), of pure $AgNO_3$ (type I and II), or equimolar (K,Na)I (type III) were added through a Pyrex glass addition funnel, which was temporarily immersed through the asbestos plug and the hot aluminium lid.

For cells containing unsaturated solutions stable emf's were obtained within 10 min after each addition. For saturated solutions (cells of type II) stabilization times of about 1 h were required, probably due to slow attainment of equilibrium between solid phase and solution. Occasional checks showed, that the measured emf was stable to ± 0.3 mV for at least 24 h. The measurements could as a rule be reproduced to within 0.5 mV (or better for cells of type I).

Cells of type I. These cells were used to elucidate the validity of the Nernst equation in the form

$$E = E_0 - RTF^{-1} \ln 10 \log C_{Ag} \quad (1)$$

Reference half-cells with $C_{Ag}^{\circ} = 6.03 \times 10^{-3}$ mol kg^{-1} (*i.e.* mol per kg solvent, $(K,Na)NO_3$) and $C_{Ag}^{\circ} = 6.02 \times 10^{-4}$ mol kg^{-1} were used. Repeated series of measurements were performed in the range 10^{-5} mol kg$^{-1} < C_{Ag} < 3 \times 10^{-1}$ mol kg^{-1}.

Cells of type II. The number of silver atoms in polynuclear species has been directly determined from measurements of the emf of cells of type II. In the reference half-cell C_{Ag}° was kept at 8.19×10^{-2} mol kg^{-1}. Melts, saturated with (K,Na)I, have been investigated in the range 1×10^{-2} mol kg$^{-1} \leqslant C_{Ag} \leqslant 12 \times 10^{-2}$ mol kg^{-1}.

Cells of type III. Unsaturated solutions have been investigated by emf measurements with cells of type III. The composition of the reference half-cell solution was 0.0300 mol kg^{-1} $AgNO_3$ and 1.300 mol kg^{-1} (K,Na)I. In the test melt C_{Ag} was kept constant and C_I was varied in each series of measurements. The following values of C_{Ag} were used: (1, 3, 10, 20, 40 and 80) $\times 10^{-3}$ mol kg^{-1}. For each C_{Ag} the maximal possible range of C_I was utilized. Thus, most of the concentration range available [8] has been studied.

VALIDITY OF THE NERNST EQUATION

The measurements of the emf for concentration cells of type I indicate, that eqn. (1) is applicable in the range $C_{Ag} > 10^{-4}$ mol kg^{-1}. Fig. 2 shows the results from a typical series of measurements. The total amount of experimental data yields a value 109.2 ± 0.2 mV for the factor RTF^{-1} ln 10. This value has been used in the further calculations from the emf data. The temperature 280.0°C, however, should give a somewhat higher value, 109.7 mV.

The approximate validity of the Nernst equation for silver concentration cells in different fused nitrate media and at different temperatures has been verified by several authors.[4,6,9-18] For those cases, where the experimental value of the coefficient RTF^{-1} ln 10 has been given explicitly, this value is lower than the theoretical one at the actual temperature. This remarkable feature has been paid attention to by Cigén and Mannerstrand [6] and by Elding and Leden.[1] They assume, that their low experimental value, 108.1 mV, is caused by a local cooling of the electrode metal surface due to heat leakage through the connection wires. This assumption is strongly supported by the result from this work, where a more thorough care for the thermostating of the system has effected a decrease of the distance from the theoretical value 109.7 mV with 2/3 as compared to the experimental value of Cigén and Mannerstrand.

The linear dependence of E on log C_{Ag}, indicating constant activity factors and negligible liquid junction potentials in these systems, ceases at $C_{Ag} < 10^{-4}$ mol kg^{-1} (*vide* Fig. 2). Similar deflections at such low silver nitrate concentrations have been observed before by different authors.[4,6] This may be due in part to the appearance of a mixed electrode function caused by the presence of additional redox systems in minor concentrations. Furthermore, corrosion of the silver electrodes would give a too high concentration of silver ions close to the electrode. This might influence the results to some extent in the most dilute solutions (*cf.* Ref. 15).

Obviously concentrations on the molality scale may be used for activities in the range where eqn. (1) holds, and these melts may – in this respect – be regarded as ideal solutions. On the other hand, no conclusions about solvation phenomena (*cf.* Ref. 19) can be drawn, since measurements of this kind do not give any information on, *e.g.*, species $Ag(NO_3)_n^{(n-1)-}$. As a matter of fact evidence for Ag – O bonds of covalent character in fused nitrate medium has emerged from data on excess volumes of mixtures,[20] enthalpies of mixing,[21,22] and Raman spectroscopy.[23]

SOLUTIONS SATURATED WITH ALKALI METAL IODIDE

The rather limited solubility of alkali metal iodide in fused (K,Na)NO_3 offers a unique opportunity of studying the formation of polynuclear silver-iodide complexes under in many respects optimal conditions. In principle one is enabled to determine the number of central atoms in the complexes present by measuring the emf of cells of type II at different C_{Ag}. There are at least three obvious advantages associated with this method:

a. The reference half-cell solution and the test solution can be made rather similar in composition. Thus, the effects of junction potentials of unknown magnitude may be minimized.

b. At maximum concentration of free ligand the total central ion concentration may be varied over the largest range. This is of course a favourable situation when polynuclear complexes are studied.

c. There is no need for calculations of the free ligand concentration, based on assumptions about the existence of certain complexes and their stability, since the free ligand concentration has a known constant value, 1.577 ± 0.004 mol kg^{-1}, independent of C_{Ag}. This is important when solutions with high total central ion concentrations are used.

Calculations and results

The complex formation between the central ion M and the ligand L is described by the equilibria

$$m\mathrm{M} + n\mathrm{L} \rightleftharpoons \mathrm{M}_m\mathrm{L}_n$$

The stability constants, β_{nm}, are defined by

$$\beta_{nm} = [\mathrm{M}_m\mathrm{L}_n]/([\mathrm{M}]^m[\mathrm{L}]^n) \qquad (2)$$

The total concentration of central ion may be written

$$C_\mathrm{M} = [\mathrm{M}] + \sum_m \sum_n m\ [\mathrm{M}_m\mathrm{L}_n] \qquad (3)$$

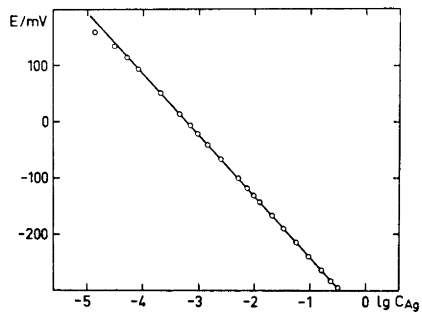

Fig. 2. Test of the Nernst equation. The equation of the full-drawn line is $E/\mathrm{mV} = -351.8 - 109.2 \log C_{Ag}$. In the reference half-cell $C_{Ag}^\circ = 6.02 \times 10^{-4}$ mol kg^{-1}, yielding $109.2 \log C_{Ag}^\circ = -351.7$.

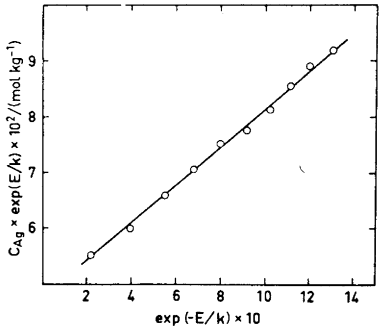

Fig. 3. Relation between C_{Ag} exp (E/k) and exp $(-E/k)$ for melts saturated with (K,Na)I.

Introducing the symbols

$$X = 1 + \sum_n \beta_{n1}[\mathrm{L}]^n$$

$$Y = \sum_n \beta_{n2}[\mathrm{L}]^n$$

$$Z = \sum_n \beta_{n3}[\mathrm{L}]^n$$

etc.

eqn. (3) may be rewritten as

$$C_\mathrm{M}/[\mathrm{M}] = X + [\mathrm{M}]\,2Y + [\mathrm{M}]^2\,3Z + \ldots \quad (4)$$

Since [L] is constant, the polynomials X, Y, Z, . . . take constant values. As C_M and [M] are known from the measurements, it is, in principle, possible to determine the order of the polynomial function of [M] in the right member of eqn. (4).

The emf, E, of cell II is

$$E = k \ln [\mathrm{Ag}^+]_0/[\mathrm{Ag}^+] \quad (5)$$

where $k = 109.2$ mV/ln 10. $[\mathrm{Ag}^+]$ and $[\mathrm{Ag}^+]_0$ stand for the silver ion concentration in the test melt and in the reference melt, respectively. Combination of eqns. (4) and (5) gives

$$C_\mathrm{Ag} \exp(E/k) = [\mathrm{Ag}^+]_0\,X + [\mathrm{Ag}^+]_0^2\,2Y \exp(-E/k) + [\mathrm{Ag}^+]_0^3\,3Z\,[\exp(-E/k)]^2 + \ldots \quad (6)$$

Table 1 gives data from a typical series of measurements. A plot of $C_\mathrm{Ag} \exp(E/k)$ *versus* $\exp(-E/k)$ reveals which terms are important in the right member of eqn. (6) (see Fig. 3). It is obvious that there is a linear relationship between these quantities. Consequently the only significant terms in the right member of eqn. (6) are the X and Y terms, *i.e.* only mono- and dinuclear species are present in observable amounts. The treatment of data from measurements in unsaturated solutions has been partly based upon this fact.

From eqns. (4) and (6) it is obvious that the sum of the intercept and the slope of the straight line in Fig. 3 should be equal to the total silver ion concentration in the reference half cell, C_Ag°. The sum of the slope and the intercept amounts to 0.081 mol kg^{-1} whereas C_Ag° was 0.0819 mol kg^{-1}. This good agreement indicates that these measurements are self-consistent. A further discussion of the values of the intercept, $[\mathrm{Ag}^+]_0\,X$, and the slope, $[\mathrm{Ag}^+]_0^2\,2Y$, in relation to the results from the measurements in unsaturated melts will appear below.

Table 1. Potentiometric measurements in solutions, saturated with (K,Na)I. Data from a typical series.

$C_\mathrm{Ag} \times 10^2/(\mathrm{mol\ kg^{-1}})$, E/mV, $\exp(-E/k) \times 10$, $C_\mathrm{Ag} \exp(E/k) \times 10^2/(\mathrm{mol\ kg^{-1}})$;

1.206, 72.1, *2.185*, *5.52;* 2.375, 43.9, *3.96*, *5.99;* 3.63, 28.3, *5.51*, *6.59;* 4.80, 18.4, *6.78*, *7.07;* 6.00, 10.7, *7.97*, *7.53;* 7.14, 4.0, *9.19*, *7.76;* 8.34, −1.1, *10.24*, *8.13;* 9.53, −5.1, *11.13*, *8.56;* 10.69, −8.7, *12.00*, *8.91;* 11.83, −12.6, *13.05*, *9.09;*

EMF MEASUREMENTS IN UNSATURATED MELTS

The measurements have been performed with cells of type III. If the emf of the cell is E_1 for $C_{L'}=0$ and E_2 for $C_{L'}>0$, eqn. (7) is valid for the difference $E_M=E_1-E_2$.

$$E_M = 109.2 \text{ mV} \log C_M/[M] \tag{7}$$

For a system containing dinuclear and four mononuclear species eqn. (4) may be rewritten as

$$\frac{C_M/[M]-1-\beta_{11}[L]-\beta_{21}[L]^2}{[L]^4} = \beta_{41}+\beta_{31}[L]^{-1}+2[M]\sum_n \beta_{n2}[L]^{n-4} \tag{8}$$

The left hand member of eqn. (8) is denoted f_4. In f_4 the term $C_M/[M]$ is known from eqn. (7) and the last term in the denominator is a small correction term in the pertinent range of [L]. A preliminary value of this term is obtained from Ref. 1. The two remaining terms of the denominator are negligible. Hence f_4 is known as a function of [L], which is obtained from the equation

$$[L] = C_{L'} - \bar{n}\, C_M \tag{9}$$

where $\bar{n}=3$ is a good starting value in the first step of an iterative procedure to determine the stability constants from eqn. (10)

$$f_4 = \beta_{41} + \beta_{31}[L]^{-1} + 2[M]\sum_n \beta_{n2}[L]^{n-4} \tag{10}$$

More accurate values of $\bar{n}$ can then be calculated from eqn. (11)

$$\bar{n} = \frac{\sum_n n\ \beta_{n1}[L]^n + [M]\sum_n n\ \beta_{n2}[L]^n}{1+\sum_n \beta_{n1}[L]^n + 2[M]\sum_n \beta_{n2}[L]^n} \tag{11}$$

From eqn. (9) better values of [L] are obtained to be used in eqn. (10), *etc.*

Calculations

The data from the measurements are given in Table 2. A plot of f_4 against $[I^-]^{-1}$ for each series of measurements, in which C_{Ag} is kept constant, gives a family of curves similar to the one in Fig. 5. For various fixed $[I^-]$ the limiting values

$$\lim_{[Ag^+]\to 0} f_4 = f_4^\circ$$

have been determined by means of linear least squares extrapolations to $[Ag^+]=0$ (*cf.* eqn. (10)). The requisite values of $[Ag^+]$ have been obtained by graphical interpolations between the measured values of $[Ag^+]$ (from eqn. (7)) as a function of calculated $[I^-]$ for each series.

A plot of f_4° *vs.* $[I^-]^{-1}$ yields a straight line (*cf.* Fig. 6) represented by the equation

$$f_4^\circ = \beta_{41} + \beta_{31}[L]^{-1}$$

Table 2. Potentiometric measurements in unsaturated solutions. The values of f_4 and $[I^-]$ are those calculated in the last cycle.

C_I/(mol kg^{-1}), E_M/mV, $[I^-]$/(mol kg^{-1}), $f_4 \times 10^{-7}$/(mol kg^{-1})$^{-4}$;

$C_{Ag} = 0.916 \times 10^{-3}$ mol kg^{-1}

0.348, 670.0, *0.346*, *6.95;* 0.394, 686.9, *0.392*, *6.28;* 0.437, 701.1, *0.434*, *5.77;* 0.484, 715.2, *0.481*, *5.25;* 0.535, 729.1, *0.532*, *4.83;* 0.579, 739.2, *0.576*, *4.40;* 0.623, 749.3, *0.620*, *4.12;* 0.662, 757.6, *0.660*, *3.86;* 0.712, 768.0, *0.709*, *3.65;* 0.758, 776.7, *0.756*, *3.43;* 0.805, 785.2, *0.802*, *3.26;* 0.857, 794.9, *0.854*, *3.15;* 0.904, 802.3, *0.901*, *2.986;* 0.950, 809.3, *0.947*, *2.855;* 0.999, 816.5, *0.997*, *2.728;* 1.046, 823.2, *1.043*, *2.630;* 1.095, 829.5, *1.092*, *2.509;* 1.142, 835.3, *1.139*, *2.408;* 1.186, 841.0, *1.183*, *2.343;* 1.234, 846.7, *1.231*, *2.263;* 1.279, 852.3, *1.276*, *2.214;* 1.324, 857.3, *1.321*, *2.152;* 1.370, 862.1, *1.367*, *2.081;* 1.414, 866.5, *1.411*, *2.015;* 1.465, 871.3, *1.462*, *1.942;*

$C_{Ag} = 0.980 \times 10^{-3}$ mol kg^{-1}

0.339, 666.9, *0.336*, *7.24;* 0.396, 687.6, *0.393*, *6.28;* 0.463, 709.2, *0.460*, *5.51;* 0.500, 719.3, *0.498*, *5.04;* 0.553, 733.5, *0.550*, *4.66;* 0.616, 747.7, *0.613*, *4.14;* 0.667, 758.1, *0.664*, *3.80;* 0.724, 770.0, *0.721*, *3.56;* 0.780, 780.9, *0.777*, *3.37;* 0.837, 791.0, *0.834*, *3.18;* 0.891, 800.3, *0.888*, *3.03;* 0.943, 807.9, *0.940*, *2.848;* 0.991, 815.2, *0.988*, *2.743;* 1.059, 824.0, *1.056*, *2.548;* 1.133, 833.9, *1.130*, *2.408;* 1.197, 842.4, *1.194*, *2.333;* 1.251, 849.5, *1.248*, *2.280;* 1.310, 856.2, *1.307*, *2.196;* 1.371, 863.1, *1.368*, *2.120;* 1.426, 868.8, *1.422*, *2.054;*

$C_{Ag} = 3.22 \times 10^{-3}$ mol kg^{-1}

0.405, 692.7, *0.396*, *6.99;* 0.452, 707.0, *0.443*, *6.15;* 0.501, 721.0, *0.492*, *5.56;* 0.549, 734.0, *0.539*, *5.15;* 0.597, 745.5, *0.587*, *4.74;* 0.645, 756.2, *0.635*, *4.40;* 0.694, 767.1, *0.685*, *4.15;* 0.740, 776.3, *0.731*, *3.93;* 0.789, 785.6, *0.780*, *3.72;* 0.835, 793.7, *0.826*, *3.54;* 0.886, 802.1, *0.877*, *3.34;* 0.937, 810.2, *0.927*, *3.19;* 0.991, 818.0, *0.981*, *3.02;* 1.045, 825.9, *1.035*, *2.894;* 1.093, 832.4, *1.083*, *2.780;* 1.146, 839.0, *1.136*, *2.656;* 1.197, 845.3, *1.187*, *2.552;* 1.247, 851.3, *1.237*, *2.461;* 1.295, 857.0, *1.285*, *2.393;* 1.343, 862.4, *1.333*, *2.327;* 1.390, 867.2, *1.380*, *2.244;* 1.439, 872.2, *1.429*, *2.173;* 1.491, 877.0, *1.481*, *2.090;*

$C_{Ag} = 9.89 \times 10^{-3}$ mol kg^{-1}

0.605, 751.2, *0.577*, *5.91;* 0.659, 762.7, *0.630*, *5.36;* 0.711, 773.5, *0.682*, *4.93;* 0.770, 784.6, *0.741*, *4.51;* 0.826, 794.7, *0.797*, *4.21;* 0.887, 805.1, *0.857*, *3.95;* 0.944, 814.2, *0.914*, *3.72;* 1.002, 822.9, *0.972*, *3.51;* 1.064, 831.5, *1.034*, *3.31;* 1.122, 839.4, *1.092*, *3.16;* 1.181, 846.7, *1.151*, *2.993;* 1.241, 854.1, *1.211*, *2.869;* 1.298, 860.8, *1.267*, *2.767;* 1.354, 867.0, *1.323*, *2.660;* 1.409, 872.8, *1.378*, *2.562;* 1.464, 878.9, *1.434*, *2.495;*

$C_{Ag} = 20.08 \times 10^{-3}$ mol kg^{-1}

0.860, 807.9, *0.801*, *5.61;* 0.914, 816.6, *0.855*, *5.21;* 0.968, 824.7, *0.908*, *4.86;* 1.026, 832.6, *0.965*, *4.52;* 1.082, 840.3, *1.022*, *4.24;* 1.137, 846.6, *1.076*, *3.95;* 1.190, 852.9, *1.129*, *3.73;* 1.242, 858.9, *1.181*, *3.55;* 1.298, 864.9, *1.237*, *3.35;* 1.351, 871.0, *1.290*, *3.23;* 1.403, 876.1, *1.342*, *3.08;* 1.460, 882.1, *1.400*, *2.959;* 1.513, 887.9, *1.451*, *2.899;* 1.567, 894.3, *1.506*, *2.873;*

$C_{Ag} = 39.7 \times 10^{-3}$ mol kg^{-1}

1.087, 843.4, *0.968*, *5.69;* 1.138, 851.1, *1.019*, *5.47;* 1.192, 857.8, *1.072*, *5.15;* 1.247, 864.4, *1.127*, *4.86;* 1.303, 871.1, *1.183*, *4.61;* 1.356, 876.3, *1.236*, *4.33;* 1.414, 882.6, *1.294*, *4.13;* 1.467, 887.6, *1.347*, *3.91;* 1.525, 893.3, *1.405*, *3.73;* 1.578, 898.4, *1.457*, *3.60;* 1.633, 904.0, *1.512*, *3.50;*

Table 2. Continued.

$C_{Ag} = 39.9 \times 10^{-3}$ mol kg^{-1}

1.091, 845.0, *0.971*, *5.82;* 1.142, 851.1, *1.022*, *5.40;* 1.192, 856.8, *1.072*, *5.04;* 1.250, 863.5, *1.130*, *4.72;* 1.308, 870.1, *1.187*, *4.45;* 1.363, 876.0, *1.243*, *4.21;* 1.416, 881.4, *1.295*, *4.00;* 1.473, 886.9, *1.352*, *3.79;* 1.531, 892.8, *1.410*, *3.64;*

$C_{Ag} = 79.3 \times 10^{-3}$ mol kg^{-1}

1.541, 899.7, *1.301*, *5.86;* 1.596, 904.2, *1.356*, *5.47;* 1.652, 908.8, *1.412*, *5.13;* 1.706, 913.6, *1.466*, *4.89;* 1.760, 917.8, *1.519*, *4.64;*

The constants β_{31} and β_{41} have been determined from the $f_4°$-data, employing least squares calculations.

The number of ligands in dinuclear species has been determined as follows. Introduce

$$D_4 = f_4 - \beta_{41} - \beta_{31}[L]^{-1}$$

Hence, from eqn. (10)

$$D_4\,[Ag^+]^{-1} = 2 \sum_n \beta_{n2}\,[I^-]^{n-4} \qquad (12)$$

$D_4\ [Ag^+]^{-1}$ has been computed for each pair ($[I^-]$; f_4) in series with $C_{Ag} \geqslant 3 \times 10^{-3}$ mol kg^{-1}. In Fig. 4 log ($D_4\ [Ag^+]^{-1}$) is plotted *vs.* log $[I^-]$. Points from

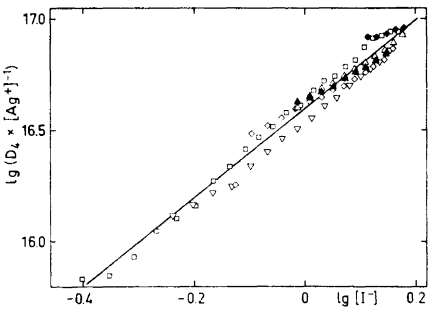

Fig. 4. A plot of log ($D_4[Ag^+]^{-1}$) *vs.* log $[I^-]$. Symbols used: $C_{Ag} \times 10^3$/mol kg^{-1} = 3.22 (□), 9.89 (▽), 20.08 (◇), 39.7 (△), 39.9 (▲), 79.3 (◆).

different series fall on the same straight line. (The weak tendency to systematic deviation from the line at the highest C_{Ag}-values will be discussed below.) The equation of the straight line is

$$\log (D_4\,[Ag^+]^{-1}) = A + B \log [I^-]$$

with the parameter values:

$$A = 16.59 \pm 0.06$$
$$B = 1.99 \pm 0.05$$

The linearity and the fact that B assumes the integer value 2 would be the expected result, if only one dinuclear complex, $Ag_2I_6^{4-}$ (with $n-4=2$), is formed (*cf.* eqn. (12)). Hence, β_{62} may be computed from the relationship $A = \log 2\beta_{62}$.

Table 3. The equilibrium constants determined from emf measurements in unsaturated melts. For comparison the stability constants of Elding and Leden[1] are included. The errors quoted for the constants β_{n1} from this work are equal to three standard deviations. For β_{62} an estimated maximum error is given. Because of systematic errors the uncertainty of β_{41} is probably much higher than the error given here.

	AgI	AgI_2^-	AgI_3^{2-}	AgI_4^{3-}	$Ag_2I_6^{4-}$
$\beta_{nm}/(\text{mol kg}^{-1})^{(1-n-m)}$ Ref. 1. Solubility data.	$(4.2 \pm 0.3) \times 10^3$	$(3.6 \pm 0.2) \times 10^6$	$(2.9 \pm 0.3) \times 10^7$	–	–
$\beta_{nm}/(\text{mol kg}^{-1})^{(1-n-m)}$ This work.	–	$(3.1 \pm 0.3) \times 10^6$	$(2.27 \pm 0.06) \times 10^7$	$(2.8 \pm 0.6) \times 10^6$	$(1.9 \pm 0.7) \times 10^{16}$
$K_n/(\text{mol kg}^{-1})^{-1}$ K_1 from Ref. 1, others from this work.	4.2×10^3	7.4×10^2	7.3	0.12	–

Finally a refined value of β_{21} has been derived from eqn. (8). The computation was performed with data from series with $C_{Ag} = 1 \times 10^{-3}$ and 3×10^{-3} mol kg^{-1} in the concentration range where $\bar{n} < 3$.

The final values of β_{nm} were obtained after four iterations. Table 2 gives all experimental data and the values of f_4 and $[I^-]$, calculated in the last cycle.

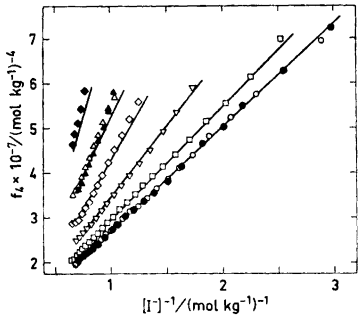

Fig. 5. f_4 as a function of $[I^-]^{-1}$. Final values. Symbols used: $C_{Ag} \times 10^3$/mol kg^{-1} = 0.916 (○), 0.980 (●), 3.22 (□), 9.89 (▽), 20.08 (◇), 39.7 (△), 39.9 (▲), 79.3 (◆). The full-drawn lines are calculated from the set of constants in Table 3.

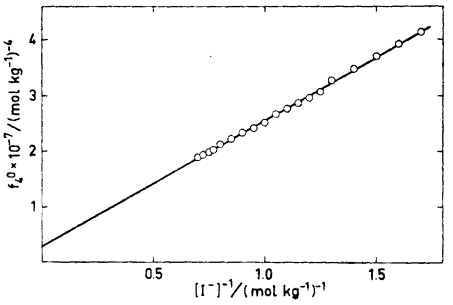

Fig. 6. f_4° as a function of $[I^-]^{-1}$. The circles represent the extrapolated values.

Fig. 6 shows f_4° as a function of $[I^-]^{-1}$. The final set of stability constants is given in Table 3 together with the values determined by Elding and Leden.[1]

In Fig. 5 f_4 is plotted *vs.* $[I^-]^{-1}$ for all series of measurements. The full-drawn curves have been calculated from eqns. (4) and (10) using the final set of stability constants.

Possible systematic errors

The results from the measurements with cells of type III may be directly compared with those from cells of type II. In principle, the experimental values of $[Ag^+]_0\ X$ and $[Ag^+]_0^2\ 2Y$ at $[I^-] = 1.577$ mol kg^{-1} permit an estimation of *one* stability constant, provided the others are known. Since the values of β_{21} and β_{31} on the whole agree with those from previous solubility measurements (*vide* Table 3), the main interest will be focused to β_{41} and β_{62}. With the values of β_{21}, β_{31}, and β_{62} obtained from the measurements with cells of type III, the data from cell II yield $\beta_{41} = 1.6 \times 10^7$ (mol kg^{-1})$^{-4}$. If, on the other hand, β_{21}, β_{31}, and β_{41} are fixed, the value 0.64×10^{16} (mol kg^{-1})$^{-7}$ is obtained for β_{62}.

Even if the estimates of β_{41} and β_{62} refer to one single value of the free ligand concentration, the disagreements with the values of Table 3 are too pronounced to be completely neglected.

It is highly probable that the emf data from cells of type II are on the whole unaffected by liquid junction potentials. On the other hand, the E_M-values are in principle obtained from the cell

Ag	C_{Ag} $AgNO_3$	asbestos fibre	C_{Ag} $AgNO_3$ C_I (K,Na)I	Ag

The rather high values of C_I in these cells might undoubtedly have given rise to a liquid junction potential of unknown magnitude, causing a systematic error in the E_M-values. Hence, the observed discrepancies in the β-values might be due to the junction potentials.

The magnitude of the liquid junction potential for this cell should most probably depend on C_I alone. A simple calculation shows that this would cause an error in β_{41} rather than β_{62}. An error in β_{62} alone can only be explained by assuming a liquid junction potential depending on C_{Ag} but rather independent of C_I. Since the latter behaviour seems rather improbable for a cell of this kind, the errors are mostly likely to appear in β_{41}. This might be the explanation of the disagreement between the results from the emf data of cells of type II and III.

DISCUSSION

On the whole there is a good fit between the calculated curves of Fig. 5 and the experimental data. At the highest C_{Ag}, however, a small deviation is found. A somewhat better fit at these high C_{Ag}-values might be obtained by adding one or more terms to the right hand member of eqn. (10). This procedure has been tried, yielding a better, although not perfect fit to the experimental data. Furthermore, there is no unique set of additional terms, giving this small improvement, but the choice may be made rather arbitrarily within certain limits. Thus, one or more additional terms would probably be of questionable physical meaning and it seems, especially in the light of the previous discussion of systematic errors, advisable to refrain from postulating further polynuclear species. It is also possible that the small discrepancies might in part be due to increasing deviations from ideality as the concentration of big complex ions increases.

The values of β_{21} and β_{31} obtained by Elding and Leden [1] from solubility measurements are slightly higher than those from this work (*vide* Table 3). The main reason for this is that the stability constants from the solubility data were calculated without taking into consideration the fraction of silver present as AgI_4^{3-} and $Ag_2I_6^{4-}$.

In the major part of the concentration range investigated, AgI_3^{2-} is the predominating species. The existence of a fourth complex, AgI_4^{3-}, is probable although a precise value of β_{41} is difficult to obtain, presumably because of the unknown liquid junction potentials. From the discussion of possible systematic errors above it may be concluded that $\beta_{41} \approx 10^7$ (mol kg^{-1})$^{-4}$ is a fair estimate.

The complex $Ag_2I_6^{4-}$ is the only polynuclear species found. A possible structure of this ion would be the one of two tetrahedral AgI_4-links, sharing an edge like in solid $[Ni(en)_2][AgI_2]_2$.[26]

For the dimerization reaction

$$2\ AgI_3^{2-} \rightleftharpoons Ag_2I_6^{4-}$$

the equilibrium constant $k_{3/6} = \beta_{62}/\beta_{31}^2$ is $(4 \pm 1) \times 10$ (mol kg^{-1})$^{-1}$.

Acknowledgement. My thanks are due to Professor Ido Leden. His support and stimulating interest has strongly promoted this work.

REFERENCES

1. Elding, I. and Leden, I. *Acta Chem. Scand.* **23** (1969) 2430.
2. White, S. H., Inman, D. and Jones, B. *Trans. Faraday Soc.* **64** (1968) 2841.
3. Guion, J. *Inorg. Chem.* **6** (1967) 1882.
4. Alvarez-Funes, A., Braunstein, J. and Blander, M. *J. Am. Chem. Soc.* **84** (1962) 1538.
5. Braunstein, J. and Hagman, R. E. *J. Phys. Chem.* **67** (1963) 2881.
6. Cigén, R. and Mannerstrand, N. *Acta Chem. Scand.* **18** (1964) 1755.
7. Leden, I. *Acta Chem. Scand.* **10** (1956) 540; 812.
8. Holmberg, B. *To be published.*
9. Blander, M., Blankenship, F. F. and Newton, R. F. *J. Phys. Chem.* **63** (1959) 1259.
10. Hill, D. G., Braunstein, J. and Blander, M. *J. Phys. Chem.* **64** (1960) 1038.
11. Flengas, S. N. and Rideal, E. *Proc. Roy. Soc. (London)* **A 233** (1956) 443.
12. Duke, F. R. and Garfinkel, H. M. *J. Phys. Chem.* **65** (1961) 461.
13. Sacchetto, G. A., Mazzocchin, G. A. and Bombi, G. G. *J. Electroanal. Chem.* **20** (1969) 435.
14. Gaur, H. C. and Sethi, R. S. *Trans. Faraday Soc.* **64** (1968) 445.
15. Boxall, L. G. and Johnson, K. E. *Trans. Faraday Soc.* **67** (1971) 1433.
16. Peleg, M. *J. Phys. Chem.* **75** (1971) 3711.
17. Gaur, H. C. and Bansal, N. P. *Indian J. Chem.* **9** (1971) 1273.
18. Sacchetto, G. A., Bombi, G. G. and Maccà, C. *J. Electroanal. Chem.* **36** (1972) 47.
19. Arnikar, H. J. and Sharma, D. K. *J. Electroanal. Chem.* **5** (1963) 481.
20. Cleaver, B. and Neil, B. C. J. *Trans. Faraday Soc.* **65** (1969) 2860.
21. Kleppa, O. J., Clarke, R. B. and Hersh, L. S. *J. Chem. Phys.* **35** (1961) 175.
22. Meschel, S. V. and Kleppa, O. J. *J. Chem. Phys.* **48** (1968) 5146.
23. Vallier, J. *J. Chim. Phys.* **65** (1968) 1762.
24. Leden, I. *Potentiometrisk undersökning av några kadmiumsalters komplexitet, Diss.*, Lund 1943.
25. Lieser, K. H. *Z. anorg. Chem.* **292** (1957) 97.
26. Stomberg, R. *Acta Chem. Scand.* **23** (1969) 3498.

Received October 11, 1972.

ACTA CHEMICA SCANDINAVICA 27 (1973) 888–890

Preparation of Carboxylic Acids from Aldehydes (Including Hydroxylated Benzaldehydes) by Oxidation with Chlorite

BENGT O. LINDGREN and TORSTEN NILSSON

Swedish Forest Products Research Laboratory, Box 5604, S-114 86 Stockholm, Sweden

During the oxidation of aldehydes to acids with sodium chlorite, chlorine dioxide is simultaneously formed and may react with starting material and products in undesirable side-reactions. By performing the reaction in the presence of a chlorine scavenger, *e.g.* sulphamic acid, the formation of chlorine dioxide is avoided, and high yields of the acids from the corresponding aldehydes (even hydroxylated benzaldehydes) are obtained.

The oxidation of vanillin (3-methoxy-4-hydroxybenzaldehyde) with chlorite and with chlorine dioxide has previously been studied by Purves and co-workers,[1] Sarkanen *et al.*,[2] and Ishikawa *et al.*[3] They obtained complicated oxidation mixtures from which a few compounds could be isolated in low yields. Neither chlorine dioxide nor chlorite oxidation yielded any vanillic acid.

We reported recently that the chlorite oxidation of vanillin [4] (as well as of some other phenolic lignin model compounds and some lignin materials [5]) is retarded when a chlorine scavenger is added. Further, the reaction is accelerated by chlorine addition. From these observations we concluded that the oxidation proceeds by a chain mechanism with the following propagation reactions:

$$Cl_2 + 2\ ClO_2^- \rightarrow 2\ ClO_2 + 2\ Cl^-$$

$$\text{vanillin} + 2\ ClO_2 \rightarrow \text{products} + ClO_2^- + {}^1/_2Cl_2 + H^+$$

(The reaction can also be formulated with hypochlorous acid instead of chlorine.)

The way in which the chain process is initiated was not elucidated, but was suggested to be caused by the chlorine formed by a slow reaction between chlorite and vanillin. This proposal is confirmed in this paper.

RESULTS AND DISCUSSIONS

According to the proposed mechanism, the chlorite oxidation of vanillin in the presence of a chlorine scavenger should give the reaction products of

the initial reaction. When such an oxidation was performed with sulphamic acid or resorcinol as scavenger under proper conditions (room temperature, pH 3.5), vanillic acid was obtained in good yield (81 – 84 %). In the experiment with resorcinol addition, 4-chloro-1,3-dihydroxybenzene was formed in almost theoretical amounts. When phenol was used as scavenger, the vanillic acid formed was difficult to isolate from the reaction mixture.

These results indicate that the initiating reaction between chlorite and vanillin gives hypochlorite and vanillic acid. The oxidation probably starts with an attack by a chlorite ion on the protonized aldehyde group:

$$R-CHO \xrightarrow{H^+} R-C^+H(OH) \xrightarrow{+ClO_2^-} R-CH(OH)(OClO) \xrightarrow{-HOCl} R-COOH$$

This assumption is supported by the relative reaction rates between different aldehydes (see below) and by the fact that the reaction is catalysed by acids.

Chlorite seems to be a rather selective agent for oxidation of aldehydes to carboxylic acids and it has been used repeatedly for this purpose in the carbohydrate field.[6,7] Its use is hampered, however, by the formation of chlorine dioxide. This gas is unpleasant and may cause side reactions which by the above mentioned chain mechanism may predominate as in the oxidation of vanillin. These complications may be avoided by adding a chlorine scavenger.

The synthesis of vanillic acid from vanillin has earlier been carried out by oxidation with silver oxide and by dehydrogenation in alkali hydroxide solution, but no *convenient* method has been published for the oxidation of hydroxylated benzaldehydes (such as vanillin and *o*-vanillin) to their corresponding acids. Chlorite oxidation in the presence of a scavenger now seems to be a suitable and inexpensive method.

The disagreeable formation of chlorine dioxide was avoided also when the chlorite oxidations of benzaldehyde, cinnamic aldehyde, *p*-nitrobenzaldehyde and cyclohex-3-ene aldehyde were performed in the presence of a scavenger. The corresponding acids were obtained in good yields.

The reaction rate (determined by the chlorite consumption) increased in the order vanillin, benzaldehyde, and *p*-nitrobenzaldehyde, as should be expected for a reaction involving a nucleophilic attack by chlorite, as postulated above.

EXPERIMENTAL

The sodium chlorite used was technical grade (about 80% pure). The chlorite concentrations were determined iodometrically. Besides the m.p. determination, all products were identified by their IR and/or NMR spectra.

2-Hydroxy-3-methoxybenzoic acid. To a solution of *o*-vanillin (10 mmol) and sulphamic acid (13 mmol) in water (500 ml), sodium chlorite (13.4 mmol) in water (20 ml) was added. After 30 min the solution was extracted with ether. Evaporation of the ether and recrystallisation of the residue from water gave 2-hydroxy-3-methoxy-benzoic acid monohydrate (1.30 g, yield 80%, m.p. 151 – 152°C, lit. 151°C).

Vanillic acid. (a) Sulphamic acid as scavenger. To a solution of vanillin (98.6 mmol) and sulphamic acid (134 mmol) in water (2 l) a solution (150 ml) of sodium chlorite (102 mmol) was added. The precipitate of vanillic acid (13.9 g, 84 %; m.p. 208 – 211°C, lit. 211°C) was filtered off after 1 h.

Resorcinol (b) as scavenger. Vanillin (10 mmol) in *t*-butanol (19 ml) and resorcinol (13 mmol) in an acetate buffer (pH 3.93) and aqueous sodium chlorite solution (12 mmol, 13 ml) were mixed. The precipitate of vanillic acid (yield 50 %) was filtered off. From the

filtrate, a further amount (31 %, total yield 81 %) of vanillic acid was obtained: the filtrate was extracted with methylene chloride and from the extract the fraction soluble in a sodium hydrogen carbonate solution was isolated. The extract fraction soluble in a sodium hydroxide solution contained 4-chloro-1,3-dihydroxybenzene; the yield estimated by NMR was 87 %.

Cyclohex-3-ene carboxylic acid. To a mixture of cyclohex-3-ene aldehyde (100 mmol) in a phosphate buffer (pH 3.5, 100 ml) sodium chlorite (120 mmol) in water (40 ml) was slowly added at −5°C. The temperature rose rapidly to 20°C. After 15 min the main part of the dioxane was removed by evaporation. The residue was then acidified and extracted with ether from which the acidic product (13.1 g) was collected as above.

An aliquot (5 g) of the residue was distilled under nitrogen. The main fraction (138–140°C, 3 mmHg) consisted of cyclohex-3-ene carboxylic acid (4.0 g, yield 80 %) indistinguishable by IR and NMR from an authentic sample.

Cinnamic acid. To a mixture of cinnamic aldehyde (10 mmol) in *t*-butanol (25 ml) and resorcinol (13 mmol) in an acetate buffer (20 ml, pH 3.92), sodium chlorite (12.4 mmol) in water (18 ml) was added. After 45 min the mixture was evaporated in order to remove most of the *t*-butanol and was then extracted with ethyl ether. From the ether solution the acidic fraction (1.15 g) was collected as above. It consisted of cinnamic acid contaminated with 4-chloro-1,3-dihydroxybenzene. Sublimation of an aliquot (202 mg) of the mixture gave cinnamic acid (171 mg), m.p. 136–137°C, which corresponds to an over all yield of 72 %.

p-Nitrobenzoic acid. To a mixture of *p*-nitrobenzaldehyde (10 mmol) in *t*-butanol (60 ml) and resorcinol (13 mmol) in an acetate buffer (50 ml, pH 4) an aqueous solution of sodium chlorite (12 mmol, 13 ml) was added. After 30 min the mixture was extracted with ether. Evaporation of the ether gave *p*-nitrobenzoic acid, m.p. 241–243°C, lit. 242°C, (yield 76 %).

Benzoic acid. To a mixture of benzaldehyde (10 mmol) in *t*-butanol (10 ml) and resorcinol (13 mmol) in an acetate buffer (20 ml, pH 3.93) a solution of sodium chlorite (12 mmol) in water (13 ml) was added. After 18 h the reaction mixture was extracted with methylene chloride, from which the acid fraction (0.955 g, m.p. 85–110°C) was collected as above. Fractionated sublimation of an aliquot (100 mg) gave benzoic acid (84.3 mg, over-all yield 88 %), m.p. 124–125°C.

Acknowledgements. We are grateful to Miss Annette Grünewald and Mr. Örjan Eriksson for valuable experimental assistance and one of us (Torsten Nilsson) thanks *Cellulosaindustriens stiftelse för teknisk och skoglig forskning samt utbildning* for a scholarship. We also are indebted to Dr. Stan Froehner for linguistic revision of this manuscript.

REFERENCES

1. Husband, R. M., Logan, C. D. and Purves, C. B. *Can. J. Chem.* **33** (1955) 68.
2. Sarkanen, K. V., Kakehi, K., Murphy, R. A. and White, H. *Tappi* **45** (1962) 24.
3. Ishikawa, T., Sumimoto, M. and Kondo, T. *J. Jap. Tappi* **23** (1969) 117.
4. Lindgren, B. O. *Svensk Papperstid.* **74** (1971) 57.
5. Lindgren, B. O. and Nilsson, T. *Svensk Papperstid.* **75** (1972) 161.
6. Jeanes, A. and Isbell, H. S. *J. Res. Natl. Bur. Std.* **27** (1941) 125.
7. Nevell, T. P. *Methods Carbohyd. Chem.* **3** (1963) 182.

Received October 11, 1972.

ACTA CHEMICA SCANDINAVICA 27 (1973) 891–902

Lipid Biosynthesis in Human Thoracic Duct Lymphocytes and Thymocytes

LARS LILJEQVIST

The Department of Clinical Chemistry and the Department of Surgery, Huddinge sjukhus, and Serafimerlasarettet, Karolinska Institutet, Stockholm, Sweden

The biosynthesis of lipids in human thymocytes (thymus lymphocytes) and thoracic duct lymphocytes *in vitro* was studied by incubation of the cells with acetate-1-^{14}C.

The label was mainly incorporated into cholesterol and the fatty acids of glycerides and phospholipids. Among the phospholipids, radioactivity was found mainly incorporated into lecithin. In glycerides, phospholipids and individual phospholipids, the main radioactivity was confined to fatty acids with 18 – 24 carbon atoms, indicating that the label was incorporated mainly by chain elongation. An exception, however, was thymocyte lecithin where 50 % of the radioactivity was confined to palmitic acid.

Although there are slight differences between the synthesis of different lipid fractions of human thymocytes and thoracic duct lymphocytes, the principal impression is the striking similarity indicating a similar biochemical mechanism for synthetizing lipids.

Although the lymphocytes in blood, lymph, spleen, bone marrow, lymph nodes, and thymus are morphologically almost identical, variations in their functional capacity, responses to antigens, life span, cellular and/or tissue origin and their pathway of circulation are generally recognized. In view of the previous finding that there is an efficient biosynthesis of various lipids by human thoracic duct lymphocytes,[1] it appeared to be of interest to study the possibility that there are differences in the biosynthesis of the lipids by human thymocytes (thymus lymphocytes) and thoracic duct lymphocytes. In the present work, the lipid composition and incorporation of ^{14}C-acetate into different lipid fractions, inclusive individual fatty acids in human thoracic duct lymphocytes and thymocytes have been studied. In previous work there is limited information concerning composition of different fatty acids in the different lipid fractions in human lymphocytes and nothing has been previously reported concerning lipid composition in human thymocytes.

EXPERIMENTAL

The biological material, *i.e.* lymph and thymi, used for the study were obtained from patients operated on for diagnostic and/or therapeutic reasons. The material had otherwise not been used.

Patient codes are given as a number and the letter L if lymph was obtained, T if thymus was obtained. The experiment codes are the same as the patient codes or if many experiments were done with lymph from the same patient a number is added after the letter.

Clinical. Thoracic duct lymph for 10 experiments was obtained from 7 patients. More important clinical data on the patients is found in Table 1a.

Table 1a. Patients from whom thoracic duct lymph was obtained.

Patient	Sex	Age	Diagnosis
3/L	♂	69	Suspicion of gastric carcinoma [a]
23/L	♀	52	Mammary carcinoma
45/L	♀	48	Adispositas dolorosa
46/L	♀	31	Glomerulonephritis and uraemia. In hemodialysis.
48/L	♂	70	Thyroid carcinoma
54/L	♂	25	Glomerulonephritis and uraemia. In hemodialysis.
55/L	♂	28	Uraemia. Nephrectomized. In hemodialysis.

[a] Was not verified by gastric resection.

In patient 3/L, 23/L, and 48/L the thoracic duct was cannulated in order to detect and drain cancer cells.[2] Patient 45/L was cannulated in order to investigate the possibility of a metabolic disorder. It was shown that the fatty acid synthesis was affected in the pathologic but not in the healthy fat tissue.[3] In patients 46/L, 54/L, and 55/L thoracic duct lymph was drained as immunosuppressive therapy prior to kidney transplantation[4,5].

Thymi were removed for surgical reasons in search for metastasis and/or the parathyroids.[6] The more important clinical data on these patients are found in Table 1b.

Table 1b. Patients from whom thymi were obtained.

Patient	Sex	Age	Diagnosis
33/T	♀	26	Thyroid carcinoma
34/T	♀	29	Thyroid carcinoma
36/T	♀	23	Toxic goitre
52/T	♀	21	Thyroid carcinoma

Cell culture procedure. Lymph was collected and incubated with acetate-1-^{14}C as earlier.[1] In experiments 3/L, 23/L, 45/L, and 55/L/4 2 IU heparin (Heparin, Vitrum) per ml lymph were used as anticoagulant instead of ACD-solution. The present results and those obtained earlier [1] did not indicate that the lipid composition and the synthesis

is different when lymphocytes are incubated in ACD-lymph in comparison with lymphocytes incubated with heparin. Lymph was collected during the first two days of drainage except in experiments 46/L/1 and 46/L/2, where the lymph was collected on the 10th and 12th day, respectively. The lymph was usually incubated directly. In experiments 46/L/1, 46/L/2, and 48/L/3 the lymph was, however, centrifuged and the main part of the lymphocytepoor supernatant was removed by suction. In experiments 54/L/3 and 54/L/6 the lymphocytes were isolated by centrifugation, washed and then incubated in Krebs balanced saline solution, medium 1 [7] (Krebs medium) and lymph, respectively. The lymphocyte viability was 90 – 100 % as judged by trypan blue exclusion.[8] The incubates contained 4 – 67 × 10^3 lymphocytes per μl and 0 – 10 erythrocytes per lymphocyte but practically no other cells as determined by microscopic investigations.[9] Acetate-1-^{14}C (specific radioactivity 53 – 57 mCi/mmol, The Radiochemical Centre, Amersham, England) was added in a concentration of 1 – 10 μC/ml incubate and the incubation time varied between 2 and 6 h. The results did not indicate that the different radioactivity dosage or incubation time influenced the results.

The thymi were, immediately after removal, minced in precooled Krebs medium. The obtained thymus suspension was filtered through gauze compresses. The filtered suspension contained 30 – 340 × 10^3 thymus lymphocytes and 1 – 18 × 10^3 erythrocytes per μl and very few other cells. The thymocyte viability was 80 – 95 %. The thymus suspensions were incubated for 2 – 5 h with acetate-1-^{14}C in a concentration of 5 – 25 μC/ml media.

All incubations took place at +37°C in a shaking water bath and the media were continuously flushed with 5 % CO_2 + 95 % O_2. After incubation lymphocytes and thymocytes were immediately isolated at +4°C.[10]

Lipid analysis. The lipids were extracted and then separated by silicic acid chromatography into three fractions, (1) hydrocarbons + cholesterol esters, (2) glycerides, free cholesterol and free fatty acids, (3) phospholipids and other polar lipids as described earlier.[10,11] The radioactivity and weights of the lipid fractions were determined.[10]

The lipid fractions were then analyzed by thin-layer chromatography (TLC).[10,12] Silica gel G plates were developed in pentane:ether, 9:1, to separate the neutral lipids and in chloroform:methanol:13 N ammonia, 14:6:1, to separate the phospholipids. The mass distribution among lipids separated by TLC was determined by transmission densitometry in a Vitatron TLD 100 densitometer (Vitatron, Dieren, Holland). A representative recording is shown in Fig. 1. The radioactivity distribution among the lipids

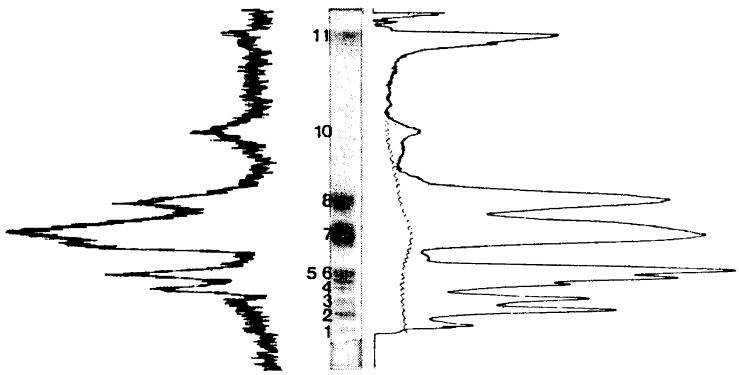

Fig. 1. Photo, radioscan (left) and densitometric recording (right) of thin-layer chromatogram with separated phospholipids from lymphocytes incubated with acetate-1-^{14}C. 1. Start fraction. 2. Fraction with the chromatographic behaviour of phosphatidic acid. 3. Fraction with the chromatographic behaviour of phosphatidyl serine. 4. Fraction with the chromatographic behaviour of phosphatidyl inositol. 5 – 6. Sphingomyelin separated into two portions. 7. Lecithin. 8. Phosphatidyl ethanolamine. 10. Fraction with the chromatographic behaviour of cerebrosides. 11. Front fraction, mainly contaminants.

separated by TLC was measured in two ways: (1) The charred lipid bands were scraped off the plates, emulsified in 15 ml Insta Gel emulsifier (Packard Instrument Co., Ill., USA) to which 1 ml distilled water had been added and counted in a liquid scintillation spectrometer (Packard Tri Carb Counter, Model 3003) with an external standard. This procedure was applied for all neutral lipids in the study. (2) The radioactivity of the separated phospholipids was measured on the plate with a Berthold thin-layer scanner II (Berthold Laboratories, Wildbad, W. Germany) equipped with a 2 π detector and connected to a ratemeter (LB 242 K). The output of the ratemeter was monitored on a Methrohm Labograph E 478 (Methrohm AG, Herisau, Switzerland). A representative recording is shown in Fig. 1.

The percentage distribution of mass and radioactivity was calculated by cutting out the peaks from copies of the densitometric and radioactivity scanning recorder charts and weighing the paper. The reproducibility of the techniques for determining mass and radioactivity distribution was found reasonably reliable.[12]

The lipids were identified by comparing their retention times on TLC with those of the purified references (see below). In some cases for further identification the lipids were isolated from the gel and rerun in another TLC system or the eluted lipids were analyzed for phosphorus content and fatty acid composition.

Fatty acid analysis. The fatty acid composition and the distribution of radioactivity among the fatty acids of different lipid fractions were analyzed by radio gas chromatography mainly in accordance with Blomstrand [1] and Blomstrand and Gürtler.[13] A Perkin-Elmer 801 gas chromatograph with flame ionization detector was used. The glass column (2.20 m long and 10 mm ID) was packed with 14 % PEGS on acid-washed and siliconized Chromosorb W (100 – 120 mesh). The fatty acid methyl esters were identified by comparing their retention times to those of reference fatty acid methyl esters (Supelco Inc., Pa., USA, or The Hormel Institute, USA). Fatty acids of the different phospholipids from thoracic duct lymphocytes of one experiment (48/L/3) have been analyzed with an improved radio gas chromatographic method using hydrocracking as described recently.[14]

Fatty acid methyl esters, which did not separate on the PEGS column, were trapped from the effluent with glass tubes (5 cm), packed with 3 % Se 30 on Chromosorb W (100 – 120 mesh). The trapped methyl esters were eluted with chloroform and identified by GLC-mass spectrometry (LKB 9000) using an Se 30 column. The conditions for the mass spectrometer were: molecular separator temperature 240°C; electron energy 70 eV; column temperature 150 – 200° with a program rate of 3°/min.

Lipid standards. Phospholipids from human brain tissue were separated according to Svennerholm.[15] The individual phospholipids were isolated from the thin-layer plates and checked on different thin-layer systems. The fatty acids of these phospholipids were also analyzed and agreed with the results published by Svennerholm.[15,16] These phospholipids were used as phospholipid standards. Individual phospholipids from bull testis were also prepared in the same way and used as reference phospholipids.

The following lipids were purchased: cholesteryl oleate, triolein, oleic acid, and methyl oleate (Mixture No. 1); cholesterol, cholesteryl oleate, triolein, oleic acid, and hydrogenated lecithin (Mixture No. 2); monopalmitin, dipalmitin, and tripalmitin (Mixture No. 3); all obtained from the Hormel Institute. Lysolecithin, sphingomyelin B-grade, phosphatidyl ethanolamine A-grade, synthetic dipalmitoyl lecithin A-grade from Calbiochem, Los Angeles, Calif., USA. Phosphatidyl serine, cerebrosides, cardiolipin, sulphatides, phosphatidyl inositol from Applied Science Laboratories, Pa., USA. Phosphatidyl choline-1,2-^{14}C (spec. radioactivity 117 mCi/mmol) and phosphatidyl ethanolamine-1,2-^{14}C (44 mCi/mmol) were purchased from Tracerlab., Mass., USA. All these lipids have been used as reference compounds after purification in appropriate TLC-systems.

RESULTS

Incorporation of acetate-1-^{14}C into lipids. The lipid composition of the lymphocytes varied slightly among the experiments but in all lymphocytes the phospholipids were consistently the largest fraction (Table 2a). The thymocytes contained a lower percentage of phospholipids than the lympho-

Table 2. In 6 experiments with lymphocytes (3/L, 45/L, 46/L/1, 48/L/1, 54/L/6, and 55/L/4) and 2 experiments with thymocytes (33/T, 52/T), the cells were incubated with acetate-1-^{14}C at 37°C. Total lipids were extracted and separated by silicic acid chromatography into three fractions: (1) hydrocarbons+cholesterolesters, (2) other neutral lipids, and (3) phospholipids. The weights and the radioactivity of the fractions were determined. Fraction 2 was further analyzed by TLC. The lipids were visualized by charring. The mass distribution among the separated lipids was estimated by densitometry. The lipid bands were then scraped off and the radioactivity determined. The distribution of mass among the lipids is given in Table 2a and the distribution of radioactivity in Table 2b.

Table 2a. Distribution of mass among lipids from lymphocytes and thymocytes. Values are expressed as relative percentages of total lipids.

Fraction [a]	Lipid	Lymphocytes						Thymocytes	
		3/L	45/L	46/L/1	48/L/1	54/L/6	55/L/4	33/T	52/T
1	Hydrocarbons+ cholesterolesters	6.2	21.4	12.9	7.4	13.0	13.0	4.0	11.2
2 a	Monoglycerides	9.6	3.0	4.0	3.5	3.6	4.5	6.5	4.4
2 b	Cholesterol [b]	12.6	4.8	6.1	5.2	7.0	6.7	6.0	6.8
2 c	Free fatty acids	3.9	1.6	1.0	3.5	1.9	2.1	Tr	0.7
2 d	Triglycerides	7.6	10.4	15.4	7.7	12.7	6.4	57.8	20.1
2 e	Unknown neutral lipids	2.0	4.0	—	0.8	1.2	2.7	—	3.0
3	Phospholipids	58.1	54.8	60.6	71.9	60.6	64.6	25.7	53.8
	Total lipids	100.0	100.0	100.0	100.0	100.0	100.0	100.0	100.0

[a] Numbers refer to the silicic acid and letters to the thin-layer separation.
[b] Contained also small amounts of mass and radioactivity confined to free fatty acids and diglycerides.

cytes. In the biosynthesis of lipids from acetate there was no difference between thymocytes and lymphocytes (Table 2b). Considerable differences among the experiments have been observed, however, which may depend on the different cell sources and conditions. Experiment 46/L/1 demonstrated the

'able 2b. Distribution of radioactivity among lipids from lymphocytes and thymocytes. Values are expressed as relative percentages of radioactivity in total lipids.

Fraction [a]	Lipid	Lymphocytes						Thymocytes	
		3/L	45/L	46/L/1	48/L/1	54/L/6	55/L/4	33/T	52/T
1	Hydrocarbons+ cholesterolesters	0.0	2.2	1.1	6.7	2.0	3.7	15.7	0.8
2 a	Monoglycerides [c]	14.8	12.8	18.3	8.5	12.4	14.8	14.5	22.8
2 b	Cholesterol [b]	5.4	7.1	26.3	4.6	11.7	8.0	3.0	9.5
2 c	Free fatty acids	1.3	4.8	8.3	6.2	4.3	5.8	2.9	5.2
2 d	Triglycerides	2.7	9.4	14.2	18.8	26.6	8.0	12.7	21.7
2 e	Unknown neutral lipids	1.5	3.0	1.6	2.1	1.1	3.6	1.7	4.0
3	Phospholipids	74.3	60.7	30.2	53.1	41.9	56.1	49.5	36.0
	Total lipids	100.0	100.0	100.0	100.0	100.0	100.0	100.0	100.0

[a] See note [a] in Table 2a. [b] See note [b] in Table 2a. [c] Part of the radioactivity is confined to an unknown ›mpound.

Table 3. In four experiments with lymphocytes (3/L, 48/L/1, 54/L/3, and 54/L/6) and in two experiments with thymocytes (33/T and 52/T), the cells were incubated at +37°C. The lymphocytes were, with one exception (54/L/3), incubated in lymph. The thymocytes and lymphocytes of experiment 54/L/3 were incubated in Krebs-medium. Acetate-1-^{14}C was added at start of incubation. The phospholipids were isolated by silicic acid chromatography. The phospholipids were further separated by thin-layer chromatography. The radioactivity distribution among the separated phospholipids were determined by radioactivity scanning and, after charring, the mass distribution was estimated by transmission densitometry. The distribution of mass among the phospholipids is given in Table 3a, and the distribution of radioactivity in Table 3b.

Table 3a. Mass distribution among phospholipids of lymphocytes and thymocytes. Values are expressed as percentages of total mass of phospholipids.

TLC fraction	Phospholipid	Lymphocytes 3/L	48/L/1	54/L/3	54/L/6	Thymocytes 33/T	52/T
1	Start fraction [a]	4.9	1.3	2.1	1.6	6.2	2.0
2	Phosphatidic acid	3.7	2.2	7.6	7.5		3.9
3	Phosphatidyl serine	2.5	7.8	6.6	4.1	6.4	5.3
4	Phosphatidyl inositol	9.0	8.6	4.9	4.1	6.9	8.1
5–6	Sphingomyelin	13.6	12.4	20.2	25.2	7.4	9.9
7	Lecithin	51.0	39.3	30.0	30.9	42.2	41.4
8	Phosphatidyl ethanolamine	14.3	23.7	22.3	20.9	10.5	22.1
9	Cardiolipin		2.6	1.3	1.0	3.9	3.4
10	Cerebrosides		1.4	2.0	2.5	4.3	1.1
12	Unknown other	1.0	0.7	3.0	2.2	12.2	2.8
	Total phospholipids	100.0	100.0	100.0	100.0	100.0	100.0

[a] Containing phosphorus and fatty acids.

Table 3b. Distribution of radioactivity among phospholipids of lymphocytes and thymocytes. Values expressed as percentages of radioactivity of total phospholipids.

TLC fraction	Phospholipid	Lymphocytes 3/L	48/L/1	54/L/3	54/L/6	Thymocytes 33/T	52/T
1	Start	5.1	0.1	0.7	0.9	5.3	0.8
2	Phosphatidic acid	5.1	1.0	1.1	1.0		0.9
3	Phosphatidyl serine	2.3	2.8	1.9	1.3	6.8	1.1
4	Phosphatidyl inositol	8.1	5.6	5.8	5.0	7.9	8.6
5–6	Sphingomyelin	15.5	8.1	10.6	12.3	6.0	2.2
7	Lecithin	48.8	55.3	47.7	49.7	39.8	58.4
8	Phosphatidyl ethanolamine	13.1	13.3	14.7	12.8	12.9	19.2
9	Cardiolipin			1.7	1.5	2.2	2.3
10	Cerebrosides		9.9	7.2	9.2	6.1	2.1
12	Unknown other	2.0	3.9	8.6	6.3	13.0	4.4
	Total phospholipids	100.0	100.0	100.0	100.0	100.0	100.0

Table 4. Distribution of mass and radioactivity among fatty acids in neutral lipids of human lymphocytes (3/L, 23/L, 48/L/3) and human thymocytes (33/T, 34/T, 36/T) incubated at +37°C with acetate-1-^{14}C. Glycerides and free fatty acids were isolated by silicic acid chromatography. After hydrolysis the fatty acids obtained were methylated and subjected to radio gas chromatography. Values are expressed as relative percentages of fatty acid methyl esters and of their radioactivity. The study does not include fatty acids with longer retention time than 24:2. Tr= Traces.

GLC peaks No.	Fatty acids [a]	3/L		23/L		48/L/3		33/T		34/T		36/T	
		Mass %	Act. %	Mass %	Act. %	Mass %	Act. %	Mass %	Act. %	Mass %	Act. %	Mass %	Act. %
1	12:0	0.8		2.3		1.9		1.7		1.3		1.2	
2	12:1					1.7							
3	14:0	1.9		2.9		2.5	1.4	3.6	4.4	3.9	2.1	2.3	3.2
4	14:1					2.6							
5	15:0			1.8		3.6							
6	16:0	25.0	2.9	24.8	5.3	14.4	4.5	22.1	10.9	24.5	6.7	19.1	8.7
7	16:1	1.0		4.3		7.2	1.3	4.4	2.1	4.3	0.8	2.5	1.5
8	18:0	25.1	34.8	16.5	20.3	10.2	9.5	9.0	3.6	9.4	7.6	30.3	8.5
9	18:1	17.5	17.1	11.6	23.8	17.0	12.3	39.8		40.4	3.5	25.4	6.5
10	18:2	8.9	3.1	3.1		6.5	1.4	14.3		8.8		4.5	3.2
11	20:0	Tr		1.4		1.7	1.2					1.4	
12	20:1	0.9	12.8	0.4	7.5	0.5	8.6	2.7		2.0	5.4	1.5	7.8
13	20:2		6.0	Tr	16.1	3.5	7.0				6.0	Tr	Tr
14	22:0 and 20:3 [b]	1.0	3.3	3.4	8.7	2.4	4.7	Tr	23.2		17.0	0.7	19.8
15	20:4, 22:0 and 22:1	13.7	5.5	10.4		8.6	4.5	2.4	6.0	2.5	7.5	1.7	Tr
16	22:2 and 23:0 [c]	4.2		13.7		12.1				2.1		5.6	
17	22:4 and 24:0			3.4	4.9	1.4				0.5		1.8	
18	22:4 and 24:1 [b]		14.5	Tr	13.4	1.1	31.5		49.8	0.3	43.4		40.8
19	22:5 and 24:2 [e]					1.1	12.1						
		100.0	100.0	100.0	100.0	100.0	100.0	100.0	100.0	100.0	100.0	100.0	100.0

[a] Denoted by chain length: number of double bonds.
[b] The radioactivity mainly confined to 20:3 (see also Ref. 19).
[c] It cannot be excluded that part of the peak was derived from ghost compounds, because experience in this laboratory with GLC-mass spectrometry indicates that in this region we sometimes have peaks as contaminants.
[d] The radioactivity mainly confined to 22:4 (see Ref. 19).
[e] The radioactivity confined to 22:5 (see Ref. 19).

most pronounced deviation in the incorporation of label into lipids, the relative incorporation into cholesterol being increased with a concomitant relative decrease in phospholipid radioactivity. This lymph portion (46/L/1) was obtained on the 10th day of drainage and it is known [5,17,18] that the proportion of larger lymphocytes in lymph increases with prolonged drainage.

Incorporation of acetate-1-^{14}C into phospholipids. The phospholipid composition (Table 3a) of lymphocytes and thymocytes varied among the experiments, but lecithin was consistently the largest fraction. The thymocytes contained a lower percentage of sphingomyelin than the lymphocytes.

Table 3b shows that the biosynthetic activity in the different experiments varied, but that most radioactivity was consistently incorporated into lecithin. In the experiments performed on thymocytes, a lower percentage of label was incorporated into sphingomyelin.

Incorporation of acetate-1-^{14}C into fatty acids of neutral lipids. Considerable quantitative differences have been obtained in the fatty acid composition of glycerides (Fraction 2 from the silicic acid column) among the experiments (Table 4). The main fatty acids were 16:0, 18:0, 18:1, and 18:2. In comparison with the lymphocytes the glycerides of the thymocytes contained more oleic acid and less erucic and/or arachidonic acid, but otherwise the fatty acid composition of glycerides from lymphocytes and thymocytes was similar.

The radioactivity distribution pattern among fatty acids of glycerides also exhibited considerable quantitative differences among the experiments. In thymocytes there were less radioactivity incorporated into stearic and oleic acids and more into the peaks corresponding to 20:3 + 22:0 and 22:4.

Incorporation of acetate-1-^{14}C into fatty acids of phospholipids. Large percentages of mass but comparatively small percentages of radioactivity were found in 16:0 in all experiments (Table 5).

Considerable quantities of mass and radioactivity were confined to 18:0 and 18:1. In 20:1 and 20:2 small percentages of mass and comparatively large percentages of radioactivity were found. In all cases a large percentage of radioactivity was found in peak 18, in which 24:1 and 22:4 were identified by mass spectrometry.

Qualitatively the fatty acid composition of phospholipids from lymphocytes and thymocytes showed great similarity. Quantitatively, the mass distribution among the fatty acids differed in all the experiments, but the differences were not specially pronounced between thymocytes and lymphocytes. Quantitative differences in the distribution of radioactivity among the fatty acids was found among all the cases. A difference between thymocytes and lymphocytes was found for 20:3 and/or 22:0.

Incorporation of acetate-1-^{14}C into fatty acids of individual phospholipids. The distribution of mass and radioactivity among the fatty acids of the individual phospholipids was quite different (Figs. 2a and 2b).

The fatty acid composition of lecithin was similar in lymphocytes and thymocytes (Table 6). The radioactivity distribution shows that in lymphocytes most radioactivity was found in 18:0 and in 18:1, and in 48/L/3 also fatty acids with 20 carbon atoms, while a low percentage of radioactivity was found in 16:0. In the thymocytes almost equal amounts of radioactivity were found in 16:0 and 18:0.

Table 5. Distribution of mass and radioactivity among the fatty acids in phospholipids of lymphocytes (45/L, 46/L/2, 48/L/3) and thymocytes (36/T) incubated at +37°C with acetate-1-^{14}C. The phospholipids isolated by silicic acid chromatography were hydrolyzed and the fatty acids obtained were methylated and subjected to radio gas chromatography. Values are expressed as relative percentages of fatty acid methylesters and their radioactivity. The study does not include fatty acids with longer retention times than 24:2. Tr=Traces.

GLC peaks No.	Fatty acids	45/L		46/L/2		48/L/3		36/T	
		Mass %	Act. %	Mass %	Act. %	Mass %	Act. %	Mass %	Act. %
1	12:0	1.3		0.3		0.2		0.2	0.6
2	12:1	1.6				0.2		Tr	
3	14:0	0.4		0.8		0.3		0.5	2.2
4	14:1	2.1				0.3		Tr	
5	15:0	2.7		0.7		2.9		2.5	1.2
6	16:0	26.2	5.6	28.7	11.3	21.7	4.9	16.2	8.5
7	16:1	4.3		1.3		1.2	1.6	1.1	
8	18:0	22.8	39.9	20.3	37.5	19.1	21.9	21.5	21.8
9	18:1	15.8	18.3	24.4	27.3	16.9	18.7	21.3	11.7
10	18:2	6.8	3.5	5.9	3.4	10.5	3.3	6.9	3.4
11	20:0	1.1		Tr		Tr		Tr	
12	20:1	Tr	9.6	1.0	8.3	0.7	7.5	1.9	4.9
13	20:2	1.6	9.8	Tr		1.1	16.6	0.2	3.0
14	20:3 and 22:0 [a]	1.5	2.6	2.0		2.3	5.1	4.4	16.1
15	20:4, 22:0 and 22:1 [b]	9.2	Tr	9.4		17.8	3.5	20.1	8.8
16	23:0 and 22:2	Tr		Tr		0.5		1.8	
17	22:4 and 24:0	0.1		0.6		0.6			
18	22:4 and 24:1 [c]	1.6	10.7	3.4	12.2	1.6	10.8	1.4	17.8
19	22:5 and 24:2 [d]	0.9	Tr	1.2		2.1	6.1	Tr	
		100.0	100.0	100.0	100.0	100.0	100.0	100.0	100.0

[a] Mass and radioactivity mainly confined to 20:3 (see also Ref. 19).
[b] Mass mainly confined to 20:4 (see also Ref. 19).
[c] Radioactivity mainly confined to 24:1 (see also Ref. 19).
[d] Radioactivity confined to 24:2 (see also Ref. 19).

Table 6. Mass and radioactivity distribution among the fatty acids of lecithin from lymphocytes (3/L, 48/L/3) and thymocytes (36/T) incubated with acetate-1-^{14}C. Values are expressed as percentages of total mass and radioactivity of fatty acids in lecithin.

	Lymphocytes				Thymocytes	
	3/L		48/L/3		36/T	
	Mass %	Radio-activity %	Mass %	Radio-activity %	Mass %	Radio-activity %
14:0	0.3		0.8			
15:0	0.4		0.4			
16:0	41.0	5.6	51.9	11.1	51.4	46.3
16:1	Tr		3.9		1.4	
18:0	19.8	52.1	15.9	31.2	16.9	53.7
18:1	16.9	29.4	21.0	24.1	17.0	
18:2	7.6	5.0	4.1	3.9	3.8	
20:0						
20:1	1.3	7.9	2.0	15.2	1.3	
20:2	0.6			11.7		
20:3	1.2			2.8	2.2	
20:4	10.9				6.0	
	100.0	100.0	100.0	100.0	100.0	100.0

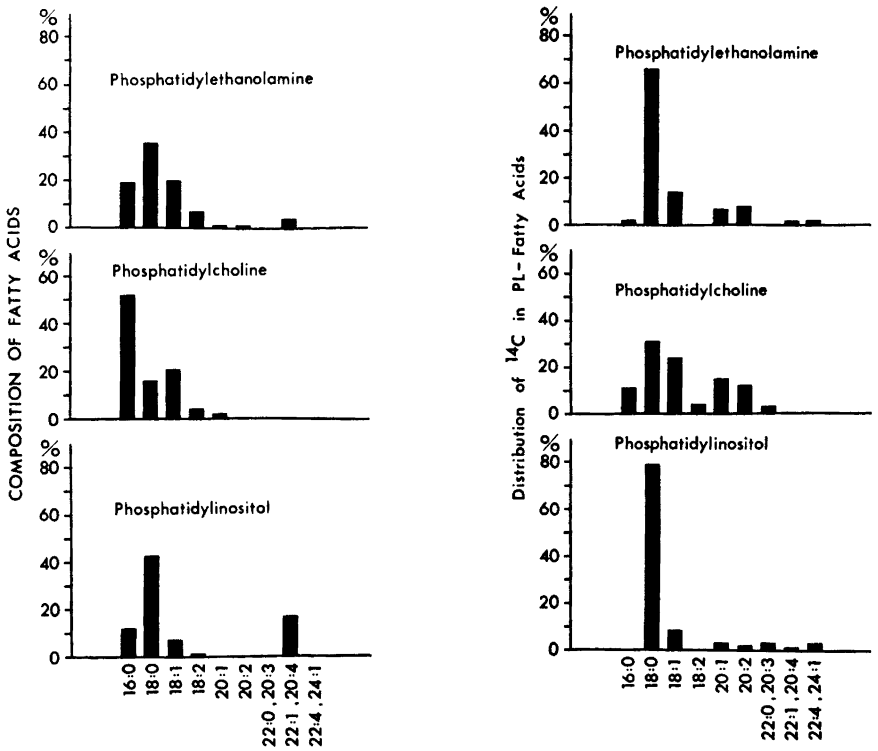

Fig. 2a–b. Composition of the main fatty acids and distribution of ^{14}C, in the main fatty acids of phosphatidyl ethanolamine, phosphatidyl chloline, and phosphatidyl inositol from human lymphocytes incubated with acetate-1-^{14}C.

DISCUSSION

This study indicates that lipid composition and biosynthesis is similar for lymphocytes and thymocytes. Among the different experiments with lymphocytes and thymocytes there were, however, some quantitative differences both in lipid composition and lipid synthesis.

Except for experiment 33/T, the phospholipids constituted the main part of the total lipids. This finding is in accordance with earlier results obtained for human lymphocytes,[1] leucocytes,[20] and erythrocytes.[21] Gottfried,[22] however, found lower values for the phospholipid content in his studies on human lymphocytes and leucocytes.

In 5 out of 7 experiments with lymphocytes the main part of label was incorporated into the phospholipids. In one experiment (46/L/1) where the lymphocytes were obtained late during the drainage only 30 % of the label of total lipids was recovered from the phospholipids. In the experiments with thymocytes, 49 and 36 % of the total radioactivity were recovered in the phospholipids.

Malamos *et al.*[23] and Kidson[24] found that in normal leucocytes more acetate-1-^{14}C was incorporated into neutral lipids than into phospholipids, while in leucemic leucocytes the main part of radioactivity was recovered from the phospholipids.

The diverging results may be explained by differences in cell clones and cell condition, but type and composition of media may also influence the results.[25,26]

The composition of phospholipids in lymphocytes and thymocytes was similar and mainly in agreement with values obtained by Gottfried[22] and Huber *et al.*[27] Sphingomyelin, which is most extensively found in plasma membranes,[28] seemed to make up a larger part of the phospholipids in the lymphocytes than in the thymocytes. Phosphatidyl ethanolamine, on account of the high content of polyunsaturated acids, is one of the most easily oxidized lipids[29] and in spite of precautions it cannot be excluded that the low content of this lipid in experiment 3/L and 33/T may be due to auto-oxidation.

Proportionately less radioactivity was incorporated into sphingomyelin in the thymocytes than in the lymphocytes, but otherwise the radioactivity distribution among the phospholipids was similar and in accordance with the results of Huber *et al.*[27]

The variability in the mass and radioactivity pattern of the fatty acids obtained for the phospholipids and the glycerides both among the lymphocyte and thymocyte experiments may reflect different proportions of subfractions of the lipids analyzed but may also be due to the different living conditions of cells before and during incubation.[26]

The mass and radioactivity distribution among the fatty acids of glycerides and phospholipids was mainly similar for thymocytes and lymphocytes and in accordance with earlier results obtained for lymphocytes.[1] In thymocytes, however, a larger amount of radioactivity was confined to 20:3 of glycerides and phospholipids and to 16:0 of lecithin.

The radioactivity distribution among fatty acids indicates that the label is incorporated into fatty acids mainly by chain elongation. This assumption is in accordance with earlier studies on lymphocytes[1] and leucocytes.[30,31] Majerus *et al.*[31] reported that the human leucocytes were unable to synthetize fatty acids *de novo*. The leucocytes lacked acetyl CoA carboxylase which, however, was detected in leucemic blast cells. The high percentage of radioactivity incorporated into the palmitic acid of thymocyte lecithin may suggest that a fatty acid synthesis *de novo* also is possible. Because of the small amounts of material available it was not possible to further elucidate this problem.

Acknowledgements. This work was supported by grants from the *Swedish Cancer Society*, the *Swedish Society of Medical Science*, and *Reservationsanslaget*, Karolinska Institutet.

The skilled technical assistance of Mr. Paul Aronsson and Mr. Göran Nyborg is gratefully acknowledged.

REFERENCES

1. Blomstrand, R. *Acta Chem. Scand.* **20** (1966) 1122.
2. Blomstrand, R., Franksson, C. and Werner, B. In *The Transport of Lymph in Man*, Appelbergs Boktryckeri AB, Uppsala 1965.

3. Blomstrand, R., Juhlin, L., Nordenstam, H., Ohlsson, R., Werner, B. and Engström, J. *Acta Dermato-Venereol.* **51** (1971) 243.
4. Franksson, C. and Blomstrand, R. *Scand. J. Urol. Nephrol.* **1** (1967) 123.
5. Sarles, H. E., Remmers, A. R., Fish, J. C., Lindley, J. D., Beathard, G. A. and Ritzman, S. E. *3rd Int. Congr. Lymphology*, Brussels 1970.
6. Alveryd, A. *Acta Chir. Scand. Suppl.* **389** (1968).
7. Paul, J. In *Cell and Tissue Culture*, Livingstone, London 1961.
8. Ling, N. R. *Lymphocyte Stimulation*, North-Holland, Amsterdam 1968.
9. Ernström, U. and Larsson, B. *Acta Pathol. Microbiol. Scand.* **67** (1966) 267.
10. Liljeqvist, L., Gürtler, J. and Blomstrand, R. *Acta Chem. Scand.* **27** (1973) 197.
11. Blomstrand, R., Gürtler, J. and Werner, B. *J. Clin. Invest.* **44** (1965) 1766.
12. Liljeqvist, L., Aronsson, P. and Nyborg, G. *To be published.*
13. Blomstrand, R. and Gürtler, J. *Acta Chem. Scand.* **19** (1965) 249.
14. Blomstrand, R., Gürtler, J., Liljeqvist, L. and Nyborg, G. *Anal. Chem.* **44** (1972) 277.
15. Svennerholm, L. *J. Lipid Res.* **9** (1968) 570.
16. Ställberg-Stenhagen, S. I. and Svennerholm, L. *J. Lipid. Res.* **6** (1965) 146.
17. Beathard, G. A., Ritzman, S. E., Fish, J. E., Townsend, C. M. and Sarles, H. E. *3rd Int. Congr. Lymphology*, Brussels 1970.
18. McGregor, D. D. *Proc. 50th Annual Meeting of the Federation of American Societies for Experimental Biology* **25** (1966) 1713.
19. Liljeqvist, L. *Ann. Clin. Res.* **5** (1973) 7.
20. Kim, H., Suzuki, M. and O'Neal, R. M. *Amer. J. Clin. Pathol.* **48** (1967) 314.
21. Nelson, G. J. *Biochim. Biophys. Acta* **144** (1967) 221.
22. Gottfried, E. L. *J. Lipid Res.* **8** (1967) 321.
23. Malamos, B., Miras, C., Levis, G. and Mantzos, J. *J. Lipid Res.* **3** (1962) 222.
24. Kidson, C. *Australasian Ann. Med.* **10** (1961) 282.
25. Miras, C. J. In Frazer, A. C., Ed., *Biochemical Problems of Lipids*, Elsevier, Amsterdam 1963.
26. Rothblat, C. H. *Advan. Lipid Res.* **7** (1969) 135.
27. Huber, H., Strieder, N., Winnler, H., Reiser, G. and Koppelstaetter, K. *Brit. J. Haematol.* **15** (1968) 203.
28. Stoffel, W. *Arzneimittel-Forsch.* **19** (1969) 253.
29. Dodge, J. T. and Philips, G. B. *J. Lipid Res.* **7** (1966) 387.
30. Miras, C. J., Mantozos, J. D. and Levis, G. M. *Biochem. Biophys. Res. Commun.* **19** (1965) 79.
31. Majerus, P. W. and Lastra, R. R. *J. Clin. Invest.* **46** (1967) 1596.

Received October 2, 1972.

ACTA CHEMICA SCANDINAVICA 27 (1973) 903–914

Gaschromatographische Analyse von Ligninoxydationsprodukten. VIII.* Zur Struktur des Lignins der Fichte

MAGNUS ERICKSON, SAM LARSSON und GERHARD E. MIKSCHE

Institutionen för organisk kemi, Chalmers Tekniska Högskola och Göteborgs Universitet, Fack, S-402 20 Göteborg 5, Schweden

Björkman-Lignin aus Fichtenholz (*Picea abies*) wurde methyliert und in zwei Stufen ($KMnO_4$–$NaJO_4$ in verdünnter NaOH und H_2O_2 bei pH 9–10) oxydativ abgebaut. Ebenso wurde mit einem Björkman-Lignin verfahren, das vor der Methylierung mit CuO-NaOH aufgeschlossen worden war. Die resultierenden Gemische an Carbonsäuren wurden mit Diazomethan verestert. Die Methylester der 7 wichtigsten Abbausäuren (*1*–*7*) konnten gaschromatographisch getrennt und quantitativ bestimmt werden. Aus den Ausbeuten an diesen Estern in den beiden Abbauversuchen wurde die Frequenz der wichtigsten Verknüpfungstypen von Phenylpropaneinheiten im Fichtenlignin ermittelt. Weiters werden Ergebnisse von Versuchen mitgeteilt, die den Vergleich des Björkman-Lignins mit dem gesamten Lignin des Fichtenholzes zum Gegenstand haben.

In einer vorangehenden Mitteilung wurde über die Frequenz der wichtigsten Verknüpfungstypen von Phenylpropaneinheiten im Birkenlignin berichtet.[1a] Der Frequenzbestimmung liegen die Ergebnisse des zweistufigen Abbaus ($KMnO_4$ bei pH 11–12 und H_2O_2 bei pH 9–10)[1b] von methyliertem Björkman-Lignin und von Björkman-Lignin, das vor der Methylierung mit CuO-NaOH aufgeschlossen worden war, zugrunde. Inzwischen ist der oxydative Abbau weiter verbessert worden; der Abbauschritt mit $KMnO_4$ wurde durch eine Behandlung mit $KMnO_4$-$NaJO_4$ in 15 % *tert.*-Butanol enthaltender, verdünnter Natronlauge ersetzt.[2] Auch die Methylierung der phenolischen Hydroxylgruppen des Lignins mit Dimethylsulfat wurde weiter entwickelt.[2]

In der vorliegenden Arbeit soll über die Bestimmung der Frequenz der wichtigsten Verknüpfungstypen von Phenylpropaneinheiten im Fichtenlignin (*Picea abies* (L.) Karst.) unter Verwendung des verbesserten Abbauverfahrens[2] berichtet werden. Ausserdem sollen Versuche mitgeteilt werden, die den Vergleich des nach Björkman[3b] erhaltenen Ligninpräparates mit dem Lignin der Fichte zum Gegenstand haben.

* VII. Mitteilung siehe Lit. 2.

FREQUENZ DER IN DEN STRUKTURTYPEN 1b – 7b VORLIEGENDEN PHENYLPROPANEINHEITEN

Bisher sind insgesamt 40 Abbausäuren aus methyliertem Björkman-Lignin der Fichte nachgewiesen worden.[1b–e] Die Mehrzahl dieser Säuren wurde nur in sehr geringen Mengen erhalten; den ihnen entsprechenden Strukturtypen des Fichtenlignins kommt daher in quantitativer Hinsicht geringe Bedeutung zu. Es überwogen die Abbausäuren *1 – 7* («wichtigste Abbausäuren«).[1c] Sie konnten als Methylester (*1a – 7a*) gaschromatographisch getrennt und quantitativ bestimmt werden; ihre Ausbeuten liegen der Frequenzbestimmung der wichtigsten Strukturtypen zugrunde. Das gleiche gilt für die Abbausäuren von Björkman-Lignin, das vor der Methylierung und dem oxydativen Abbau unter alkalischen Bedingungen aufgeschlossen wurde (s.u.). Die Abbausäuren *1 – 3* sind aus den «nicht kondensierten« Substrukturen vom Typ *1b – 3b*, die übrigen Säuren (*4 – 7*, sowie die Mehrzahl der Spurenkomponenten) aus «C-kondensierten« und «O-kondensierten« Substrukturen (Typ *4b – 7b*, die Spurenkomponenten aus entsprechenden Substrukturen) entstanden.

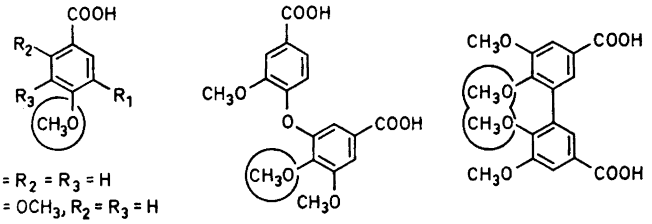

1 $R_1 = R_2 = R_3 = H$
2 $R_1 = OCH_3, R_2 = R_3 = H$
3 $R_1 = R_3 = OCH_3, R_2 = H$
4 $R_1 = OCH_3, R_2 = H, R_3 = COOH$
5 $R_1 = OCH_3, R_2 = COOH, R_3 = H$

6 *7*

1a-7a Methylester der Abbausäuren *1-7*
1b-7b den Abbausäuren *1-7* entsprechende Strukturtypen des Lignins; Carboxylgruppen sind durch die ursprünglichen Seitenketten, durch Kreise hervorgehobene Methoxylgruppen durch OH oder OR zu ersetzen

Die beim Abbau von methyliertem Björkman-Lignin erhaltenen Säuren stammen aus Einheiten, deren phenolische Hydroxylgruppe im Lignin nicht verätherт war (Versuche 1 – 3, Tab. 1).

Im Björkman-Lignin der Fichte enthält allerdings nur etwa ein Viertel der aromatischen Ringe unverätherтes Phenolhydroxyl (0,26 Phenol-OH per OCH_3),[4] der Rest liegt in der Hauptsache in Form von Aroxylresten in Arylglycerin-β-aryläther-strukturen und in Arylglycerin-α,β-diaryläther-strukturen, sowie in cyclischen Benzyl-aryläther-strukturen (Phenylcumaranstrukturen) vor. Dieses verätherte Phenolhydroxyl kann durch eine entsprechende Behandlung des Ligninpräparats freigelegt werden. Dafür im vorliegenden Fall am besten geeignet ist der Aufschluss mit CuO-NaOH,[5] bei dem gleichzeitig die Seitenketten des Lignins bereits «voroxydiert« und so dem späteren oxydativen Abbau leichter zugänglich gemacht werden. Die nach Aufschluss mit

Tab. 1. Ausbeuten an Methylestern (in mg per 100 mg Lignin) beim oxydativen Abbau von methyliertem Fichtenlignin.[a]

Versuch	Ligninpräparat [b]	Methylester						
		1a	*2a*	*3a*	*4a*	*5a*	*6a*	*7a*
	Björkman-Lignin							
1	Lignin A	0,7	11,2	0,25	2,0	0,75	1,1	1,55
2	»	0,65	10,7	0,25	2,0	0,85	1,1	1,55
3	Lignin B	0,55	9,8	0,2	1,7	0,65	1,1	1,5
	Björkman-Lignin nach Sulfatkochung							
4	Lignin A	0,5	21,4	0,15	6,1	0,55	1,75	3,6
5	»	0,5	20,6	0,15	6,0	0,55	1,75	3,9
6	»	0,5	21,1	0,15	5,8	0,55	1,6	4,0
7	Lignin B	0,45	21,4	0,3	5,8	0,7	1,65	4,6
8	Lignin C	0,45	19,4	0,15	5,8	0,6	1,6	4,5
9	Lignin D	0,4	20,3	0,1	5,6	0,7	1,45	3,5
10	*Holzmehl (40–60 mesh) nach Sulfatkochung* [c]	0,5	21,3	0,45	5,9	0,6	1,65	3,4
	Björkman-Lignin nach Sodakochung in Gegenwart von CuO							
11	Lignin A	0,7	29,8	0,5	5,0	1,1	2,1	6,0
12	Lignin E	0,7	29,3	0,6	5,0	0,9	1,9	6,7

[a] Methylierung und Abbauverfahren siehe Lit. 2.
[b] Methoxylgehalt der Björkman-Ligninpräparate (in %), Mittelwerte aus 2 Bestimmungen: A 15,73; B 15,23; C 15,27; D 15,38; E 15.31.
[c] mg Ester per 400 mg Holzmehl.

CuO-NaOH, Methylierung und Oxydation erhaltenen Abbausäuren stammen also sowohl aus den ursprünglich phenolischen wie aus den ursprünglich verätherten Einheiten des Lignins (Versuche 11 und 12, Tab. 1).

Auch beim sogenannten Sulfataufschluss des Lignins (Erhitzen mit natriumsulfidhaltiger Natronlauge) wird das verätherte Phenolhydroxyl freigelegt. Die Ausbeuten an den wichtigsten Abbausäuren blieben allerdings hinter denen eines Lignins, das mit CuO-NaOH aufgeschlossen wurde, zurück (Versuche 4–10, Tab. 1). Dies ist in der Hauptsache auf die erschwerte Angreifbarkeit der Seitenketten eines Sulfatlignins beim oxydativen Abbau zurückzuführen (siehe auch die Modellversuche in Lit. 2); sie ist das Ergebnis von Kondensationsreaktionen beim Sulfataufschluss des Lignins. Nichtsdestoweniger ist der Sulfataufschluss in Verbindung mit dem oxydativen Abbau zur Charakterisierung von Ligninen vorzüglich geeignet, da sich hierbei eine Isolierung des Lignins als Björkman-Lignin erübrigt.[2]

Die Vorgangsweise bei der Berechnung der Frequenz der den Strukturtypen *1b–7b* angehörenden Phenylpropaneinheiten (Tab. 2) aus den Ausbeuten an den Methylestern der Abbausäuren wurde in einer vorangehenden Arbeit aus-

führlich erläutert.[1a] Sie geht von der Annahme aus, dass die Seitenketten der verschiedenen Substrukturen eines Ligninpräparats in etwa den gleichen Ausbeuten zu aromatischen Carboxylgruppen abgebaut werden.

Tab. 2. Frequenz der den Strukturtypen *1b* – *7b* angehörenden Phenylpropaneinheiten des Fichtenlignins.

	Frequenz (Mol-%)							
	1b	*2b*	*3b*	*4b*	*5b*	*6b*	*7b*	*1b* – *7b*
Gesamtes Lignin [a]	1,55	56,6	0,85	12,2	2,7	6,9	19,1	99,9
Strukturtypen mit freier phenolischer Hydroxylgruppe [b]	1,25	16,7	0,35	3,1	1,25	2,3	3,2	28,2

[a] Versuch 11, Tab. 1. Berechnet für eine 60-proz. Ausbeute per C-Substituent. Der Anteil der Spurenkomponenten der Abbausäuren wurde auf 3 – 5 % geschätzt.
[b] Mittelwerte aus Versuch 1 und 2, Tab. 1. Der analytisch gefundene Wert für Phenol-OH (0,26 per C_9-Einheit) [4] diente als Kriterium für die Wahl der Ausbeute per C-Substituent (75 %) beim Abbau des methylierten Björkman-Lignins. Aus den tabellierten Frequenzwerten ergibt sich ein Wert von 0,27 Phenol-OH per C_9-Einheit, wenn man berücksichtigt, dass in Diarylätherstrukturen (*6b*) nur der eine Kern eine phenolische Hydroxylgruppe trägt.

Eine Ausnahme von dieser Regel bildet die C_1-Kernverknüpfung in Diphenylmethanstrukturen; sie kann nur durch oxydativen Abbau eines der beiden aromatischen Kerne gespaltet werden.[2] Experimentelle Befunde weisen jedoch darauf hin, dass die Frequenz von Diphenylmethanstrukturen im Fichtenlignin gering sein dürfte. Beim Abbau von Modellverbindungen dieses Strukturtyps wurden nämlich die erwarteten Abbausäuren *2* und *4* bzw. *2* und *5* in ähnlichen Ausbeuten (zwischen 4,5 und 13 % d. Th.) und ausserdem die Benzophenoncarbonsäuren *8* und *9* (Ausbeute je *ca.* 5 % d. Th.) erhalten. Unter den Produkten des oxydativen Abbaus von methyliertem Björkman-Lignin (Fichte) wurde die Ketosäure *8* nur in Spuren (Ausbeute < 0,01 % vom Gewicht des Lignins), Metahemipinsäure (*5*) hingegen in einer Ausbeute von 0,8 % vom Gewicht des Lignins aufgefunden;[1c] 5-Veratroyl-veratrumsäure (*9*) konnte nicht nachgewiesen werden.

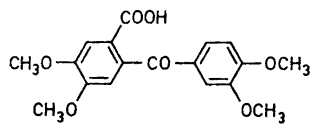

8

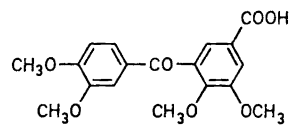

9

ZUR BILDUNG DES FICHTENLIGNINS

Die früher über die Bildung des Birkenlignins gemachten Aussagen gelten sinngemäss auch für das Fichtenlignin. Inzwischen wurden Modellversuche über die gekreuzte Kopplung der Phenoxylradikale von Coniferyl und Sinapylalkohol mit Phenoxylradikalen von in der Seitenkette abgesättigten Phenolen vom Guajacyl- und Syringylpropantyp mitgeteilt.[6] Sie bilden, zusammen mit noch zu veröffentlichenden Versuchen an künstlichen Dehydrierungspolymerisaten, eine wesentliche Stütze für die Auffassung, dass die Bildung des Fichten-

lignins ein vorwiegend «kontinuierlicher« Dehydrierungsprozess [6] ist. Der sehr geringe Gehalt des Fichtenlignins an Zimtalkoholgruppierungen (0,03 per C_9-Einheit)[7] ist ebenfalls ein wichtiger Hinweis auf die Art des Dehydrierungsvorgangs.[1a,8a]

Das Wasserstoffdefizit des Fichtenlignins beträgt im ersten Dehydrierungsschritt [1a] 1,0. Das aus den Frequenzwerten in Tab. 2 für den zweiten Dehydrierungsschritt [1a] berechnete Wasserstoffdefizit (Tab. 3) ergab sich zu 0,95 per C_9-Einheit, das Gesamtwasserstoffdefizit beträgt demnach 1,95 per C_9-Einheit. Die hier nicht berücksichtigten Spurenkomponenten sind vorwiegend aus Strukturen hervorgegangen, deren Dehydrierungsgrad über dem des Gesamtlignins lag. Auch andere Faktoren [1a] üben einen Einfluss auf das Wasserstoffdefizit aus; die hierdurch verursachte Abweichung des gefundenen Wertes für das H-Defizit vom wirklichen Wert dürfte allerdings gering sein.[1a] In guter Übereinstimmung mit dem gefundenen Wert (1,95 per C_9-Einheit) ist das von Freudenberg aus Elementar- und Methoxylanalysen von Björkman-Lignin (Fichte) berechnete Wasserstoffdefizit von 1,96;[9a] die von Björkman angegebenen Werte für H aus Elementaranalysen von Björkman-Lignin (Fichte)[3a] dürften demnach zu hoch sein.

Tab. 3. Wasserstoffdefizit des Fichtenlignins als Folge des zweiten Dehydrierungsschritts (Mol-%).

Strukturtyp	H-Defizit	
1b	(1,55 – 1,25)	0,3
2b	(56,6 – 16,7)	39,9
3b	(0,85 – 0,35)	0,5
4b	12,2 [a]	12,2
5b	(2,7 – 1,25)	1,45
6b	$\left(6{,}9 + \frac{6{,}9 - 2{,}3}{2}\right)$	9,2
7b	(19,1 + 19,1 – 3,2 – 3,2)	31,8
$\sum$ *1b – 7b*		95,35

[a] Die beim Abbau von methyliertem Björkman-Lignin (Tab. 1) aufgefundene Isohemipinsäure (*4*) stammt zum überwiegenden Teil aus Biphenylstrukturen, von denen nur der eine Kern eine freie phenolische Hydroxylgruppe besass. Etwa vorhandene, ebenfalls *4* liefernde Strukturen, die durch «postmortale« Alkyl-arylkondensation in 5-Stellung entstanden sind, wurden hier vernachlässigt (siehe auch Tab. 4).

Am untersuchten Björkman-Lignin (Präparat A) wurde bei der Methoxylbestimmung ein Wert für 15,7 % OCH_3 erhalten. Für ein ausschliesslich aus Guajacylpropaneinheiten bestehendes, fiktives Fichtenlignin der Zusammensetzung $C_9H_{7,05}O_2(H_2O)_{0,40}(OCH_3)_{1,0}$ (der Wert für formal geschriebenes Wasser nach Freudenberg) [9a] berechnet sich der Methoxylwert zu 16,7 %. Diese Differenz ist zum Teil auf den Kohlehydratgehalt von Björkman-Lignin (Fichte)[3a] zurückzuführen. Weiters ist zu beachten, dass das Fichtenlignin neben Guajacylpropaneinheiten geringe Anteile von *p*-Hydroxyphenylpropaneinheiten und

Syringylpropaneinheiten enthält. Berücksichtigt man die Zusammensetzung der Spurenkomponenten des oxydativen Abbaus,[1b–e] so findet man, dass das Fichtenlignin etwa 5 % *p*-Hydroxyphenylpropaneinheiten und 1 % Syringylpropaneinheiten enthält. Diese Werte sind erheblich niedriger als die von Freudenberg angenommenen.[9c]

FREQUENZ DER WICHTIGSTEN VERKNÜPFUNGSTYPEN VON PHENYLPROPANEINHEITEN IM FICHTENLIGNIN

Auf gleiche Weise wie in der Mitteilung über Birkenlignin [1a] wurde nun aus den Frequenzwerten in der Tab. 2 unter Zuhilfenahme anderer gesicherter Befunde über die Struktur des Lignins die Frequenz der wichtigsten Verknüpfungstypen der Phenylpropaneinheiten des Fichtenlignins hergeleitet (Tab. 4).

Tab. 4. Frequenz der wichtigsten Verknüpfungstypen von Phenylpropaneinheiten im Fichtenlignin.

Verknüpfungstyp	Frequenz per 100 C_9-Einneiten	Berechnet aus
Arylpropan-β-aryläther-strukturen [a] (A)	49 – 51	Freilegung von phenolischem Hydroxyl [b] abzüglich nicht cyclischer Benzyl-aryläther-strukturen
Nicht-cyclische Benzyl-aryläthers trukturen (B)	6 – 8	Lit. 4
Phenylcumaranstrukturen (C)	9 – 12	Oberer Grenzwert aus *4* (Tab. 2), unterer Grenzwert Lit. 16
In 2- oder 6-Stellung kondensierte Strukturen (D)	2,5 – 3 [c]	*5* (Tab. 2); Hemipinsäure wird nur in Spuren gebildet;[1c] oberer Grenzwert durch Einbeziehung der Spurenkomponenten geschätzt
In 5-Stellung kondensierte Strukturen (E)	0 – 3	Differenz zwischen oberem und unterem Grenzwert für Phenylcumaranstrukturen
Biphenylstrukturen (F)	9,5 – 11	Unterer Grenzwert aus *7* (Tab. 2), oberer Grenzwert durch Einbeziehung der Spurenkomponenten geschätzt
Diphenylätherstrukturen (G)	3,5 – 4	Unterer Grenzwert aus *6* (Tab. 2), oberer Grenzwert durch Einbeziehung der Spurenkomponenten geschätzt
1,2-Diarylpropanstrukturen (H) [d]	2	Unterer Grenzwert, Lit. 17
β,β-Verknüpfte Strukturen (J)	2	[e]
Chinonketalstrukturen (K)	Spuren	Lit. 1e

[a] Einschliesslich Glyceraldehyd-2-arylätherstrukturen.
[b] Vergleiche Lit. 1a.
[c] Oberer Grenzwert unsicher, da zum Teil Diphenylmethanstrukturen.
[d] Entsprechend einer ebenso hohen Frequenz von Glyceraldehyd-2-arylätherstrukturen.
[e] Aus Ergebnissen der Acidolyse von Björkman-Lignin (Fichte).[18] Pinoresinol wurde nicht aufgefunden, hingegen aber das β,β-verknüpfte (±)-3,4-Bis-vanillyl-tetrahydrofuran, dessen Entstehung noch nicht geklärt ist.

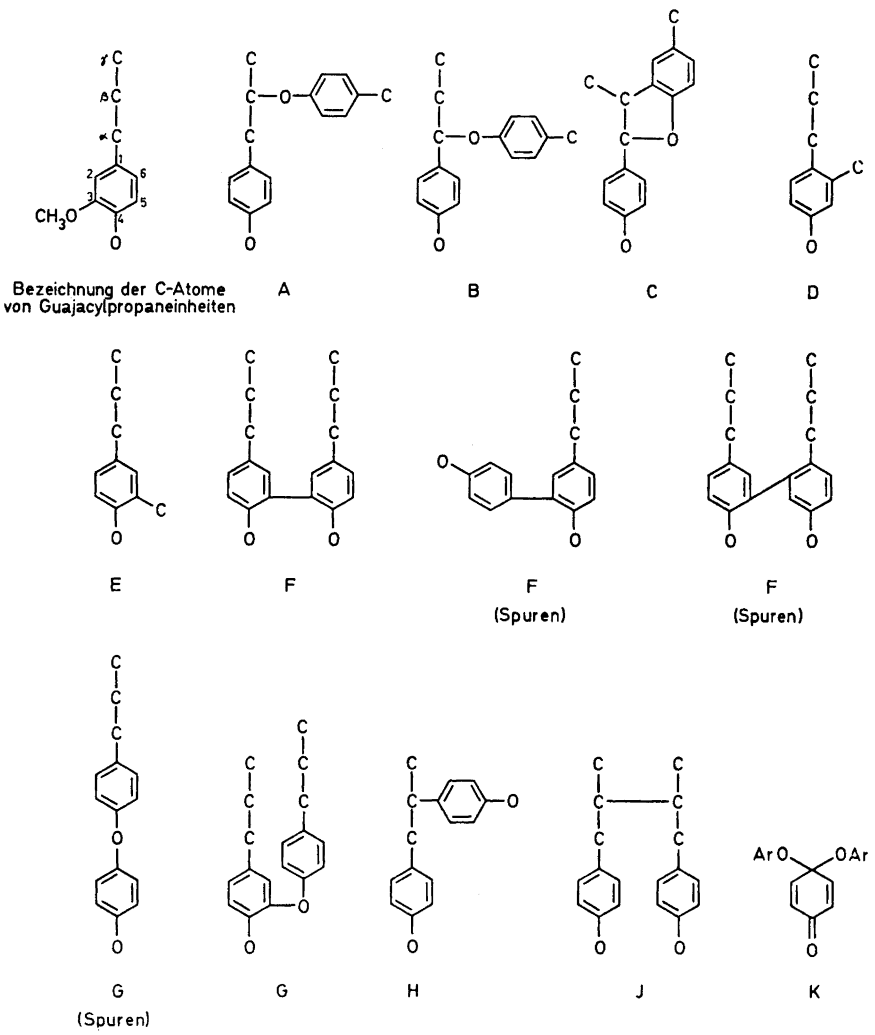

Die meisten in Tab. 4 angegebenen Frequenzwerte zeigen gute Übereinstimmung mit entsprechenden Werten einer neueren Übersicht,[8c] die zum Teil auf einem von Freudenberg angegebenen Strukturschema [9b] fusst. Diese beiden Zusammenfassungen sind durch kritische Wertung und Einordnung einer grösseren Anzahl von analytischen Befunden am Fichtenlignin zustande gekommen; hinsichtlich der Frequenz einiger wichtiger Verknüpfungstypen von Phenylpropaneinheiten (Biphenyl- und Diphenylätherstrukturen) war jedoch nur eine grobe Schätzung möglich gewesen.

Die hier beschriebene Methode ermöglicht in Verbindung mit einer Bestimmung des Phenolhydroxyls eine verhältnismässig einfache Ermittlung der wichtigsten Verknüpfungstypen von Phenylpropaneinheiten in Ligninen

verschiedenen Ursprungs. Sie ist auf alle Pflanzenmaterialien anwendbar, aus denen ein lösliches Lignin nach dem Verfahren von Björkman dargestellt werden kann.

LIGNIN IM HOLZ UND BJÖRKMAN-LIGNIN (FICHTE). EINWIRKUNG DES MAHLVORGANGS AUF DIE STRUKTUR DES LIGNINS

Das nach Björkman [3b] durch Feinmahlung von in Toluol suspendiertem, grobgemahlenem Fichtenholzmehl in einer Kugelschwingmühle, Extraktion des erhaltenen Mahlguts und Umfällung des so gewonnenen Lignins dargestellte Björkman-Lignin ist das heute wohl am häufigsten für ligninchemische Studien verwendete lösliche Ligninpräparat. Wir ziehen diese Bezeichnung der vom Autor vorgeschlagenen «Lignin aus feingemahlenem Holz« (engl. Bezeichnung «milled wood lignin«) vor, da so eine Verwechslung von Björkman-Lignin mit ähnlichen, nach Arbeitsvorschriften anderer Autoren dargestellten, Ligninpräparaten vermieden wird. Da mittels dieses Verfahrens maximal 50 % des Fichtenlignins löslich gemacht werden können, ist wiederholt die Frage aufgeworfen worden, in welchem Grad das Björkman-Lignin für das gesamte Lignin des Fichtenholzes repräsentativ sei. Wir haben unsere Untersuchungen vorwiegend an Björkman-Lignin ausgeführt; es war also naheliegend, unter Heranziehung des oxydativen Abbaus dieses mit dem Gesamtlignin der Fichte zu vergleichen.

Die weitgehende strukturelle Übereinstimmung des Björkman-Lignins aus Fichtenholz mit dem gesamten Lignin desselben Holzes (28,3 % Klason-Lignin) geht schon aus dem Befund hervor, dass beim oxydativen Abbau der durch Sulfatkochung von Björkman-Lignin und von grobgemahlenem Fichtenholzmehl erhaltenen Sulfatlignine die wichtigsten Abbausäuren (*1* – *7*) in etwa den gleichen Ausbeuten entstehen (Tab. 1, Versuche 4 – 9 und 10). Entsprechende Ergebnisse wurden bereits früher beim oxydativen Abbau der aus Björkman-Lignin von Birke (*Betula verrucosa*) und Birkenholzmehl dargestellten Sulfatlignine erhalten.[1a]

In weiteren Versuchen wurde nun die Einwirkung der Dauer der Feinmahlung auf die Ausbeuten an Abbausäuren aus methyliertem Fichtenholz untersucht (Tab. 5). Bei diesen und den in Tab. 6 (s.u.) angeführten Versuchen wurde noch das in der 2. Mitteilung dieser Reihe [1b] beschriebene Abbauverfahren verwendet; die mit diesem bei einer Reaktionstemperatur von 100° im ersten Abbauschritt erzielten Ausbeuten liegen durchwegs etwas niedriger als die mit dem verbesserten Verfahren [1a] erhaltenen.

Die Summe der aus methyliertem, grobgemahlenem Holzmehl erhaltenen Ausbeuten an den Methylestern der Abbausäuren *2*, *4*, *5*, *6* und *7* (die Abbausäuren *1* und *3* wurden nicht beachtet) war etwa halb so gross (Versuche 1 und 2, Tab. 5) wie die aus methyliertem Björkman-Lignin (Versuche 6 und 7, Tab. 5). Mit Zunahme der Mahldauer in der Kugelschwingmühle stieg die Gesamtausbeute an, bis sie nach sehr langer Mahldauer (336 Stunden) der durch Abbau von methyliertem Björkman-Lignin erhaltenen nahekam (Versuche 3, 4 und 5, Tab. 5). Der Mahleffekt von Kugelschwingmühlen verschiedener Fabrikate kann sehr unterschiedlich sein; die hier erhaltenen Ergebnisse sind bezüglich Mahldauer nur innerhalb der Versuchsreihe ver-

Tab. 5. Ausbeuten an Methylestern (in mg per 100 mg Lignin) beim oxydativen Abbau von methyliertem Fichtenholz.[a]

Versuch	Präparat	methyliert mit	Methylester					
			2a	*4a*	*5a*	*6a*	*7a*	Gesamt
	Holzmehl [b]							
1	100 – 200 mesh	CH_2N_2	4,3	0,4	0,3	0,1	0,2	5,3
2	»	Me_2SO_4 [c]	4,8	1,0	0,3	0,2	0,2	6,5
3	Kugelmühle 6 Stunden	Me_2SO_4	5,4	1,1	0,4	0,3	0,4	7,6
4	Kugelmühle 48 Stunden	Me_2SO_4	7,7	1,8	0,6	0,7	1,0	11,8
5	Kugelmühle 336 Stunden	Me_2SO_4	7,6	2,2	0,5	1,0	1,3	12,6
6	*Björkman-Lignin*	CH_2N_2	8,3	1,6	0,9	1,2	1,5	13,5
7	»	Me_2SO_4	8,3	2,0	0,8	1,0	1,4	13,5
8	*Lignin-Kohlehydrat-komplex* [d]	Me_2SO_4	8,3	2,2	0,9	1,1	1,4	13,9
9	*Extraktions-rückstand*	Me_2SO_4	7,1	2,2	0,8	0,7	1,1	11,9

[a] Methylierung und Abbauverfahren siehe Lit. 1b. [b] Ligningehalt 28,3 % (Klason-Lignin). [c] Dimethylsulfat. [d] Ligningehalt 32,2 %. [e] Ligningehalt 20 %, Rückstand der Gewinnung des Lignin-Kohlehydratkomplexes.

gleichbar. Die Steigerung der Ausbeuten durch den Mahlvorgang dürfte vorwiegend auf eine erhöhte Zugänglichkeit des Lignins für die Methylierung zurückzuführen sein; daneben ist vielleicht eine bei der Feinmahlung in geringem Ausmass erfolgende Spaltung von Alkyl-arylätherbindungen inbetracht zu ziehen.[10]

Die Ausbeuten an den Methylestern der Abbausäuren *2* und *4 – 7* aus Björkman-Lignin und aus grobgemahlenem Fichtenholz, die mit Diazomethan, bzw. mit Dimethylsulfat methyliert worden waren, unterscheiden sich nur wenig (Versuche 1, 2 und 6, 7; Tab. 5). Der grösste Unterschied besteht hinsichtlich der Isohemipinsäure (*4*), die aus mit Dimethylsulfat methylierten Proben in höherer Ausbeute entstand. Dies ist auf eine teilweise Öffnung von *p*-Hydroxy-phenylcumaranstrukturen in der alkalischen Methylierungslösung zurückzuführen (vergl. Lit. 11). Mit dem neuen Methylierungsverfahren [2] wird diese Ringöffnung vermieden.

Aus dem nach der Extraktion des Lignins aus feingemahlenem Holz verbleibenden Rückstand stellte Björkman [3c] einen Lignin-Kohlehydratkomplex her. Dieser gab beim oxydativen Abbau die in Tab. 5 angeführten Abbausäuren in ähnlichen Mengen (Versuch 8, bezogen auf den Ligningehalt des Komplexes) wie das Björkman-Lignin. Der oxydative Abbau des methylier-

ten Extraktionsrückstands aus der Darstellung des Lignin-Kohlehydratkomplexes gab die Abbausäuren in etwa denselben Ausbeuten (Versuch 9, Tab. 5) wie Fichtenholz, das längere Zeit in der Kugelschwingmühle gemahlt worden war (Versuche 4 und 5, Tab. 5).

Auch die Ergebnisse der Sodakochung von grobgemahlenem Holzmehl, von in der Kugelmühle 3 Stunden gemahlenem Holzmehl und von Björkman-Lignin (Versuche 1 – 3, Tab. 6) bestätigen die bereits durch die voranstehend beschriebenen Versuche sowie durch die Ergebnisse des oxydativen Abbaus von Sulfatligninen (s.o.) gewonnene Ansicht, dass Björkman-Lignin mit dem gesamten Lignin des Fichtenholzes weitgehend übereinstimmt. Der Vergleich von Björkman-Lignin und von Cellulase-Lignin aus Fichte führt zum gleichen Ergebnis.[10]

Tab. 6. Ausbeuten an Methylestern (in mg per 100 mg Lignin) beim oxydativen Abbau von methyliertem, durch Erhitzen mit Natronlauge aufgeschlossenem Fichtenlignin.[a]

Versuch	Sodalignin aus	Methylester					
		2a	*4a*	*5a*	*6a*	*7a*	Gesamt
1	*Holzmehl*, 60 – 100 mesh	19,1	5,4	0,6	1,6	2,7	29,4
2	*Holzmehl*, 3 Stunden in der Kugelmühle gemahlen	19,1	4,8	0,8	1,9	3,5	30,1
3	*Björkman*-Lignin	22,1	6,2	0,7	2,0	3,7	34,7

[a] Aufschluss: 3-stündiges Erhitzen in 2 M NaOH auf 170° (1-proz. Lösung von Björkman-Lignin oder 3-proz. Suspension von Holzmehl. Methylierung und Abbauverfahren siehe Lit. 1b. Ligningehalt des Holzmehls 28,3 % (Klason-Lignin).

Die eben beschriebenen Versuche haben zwar eine weitgehende Übereinstimmung von Björkman-Lignin (Fichte) mit dem Lignin des Fichtenholzes ergeben, diese ist aber nicht vollkommen. Das zeigt der Nachweis von Spurenmengen von *5*-Benzoyl-veratrumsäure (*11*) unter den Produkten des oxydativen Abbaus von Björkman-Lignin.[1c] Der 5-Benzoylrest von *11* kann nicht aus den aromatischen Kernen des Lignins hervorgegangen sein, er dürfte vielmehr aus dem bei der Feinmahlung des Holzmehls in der Kugelschwingmühle als Suspensionsmittel verwendeten Toluol stammen. Ein Versuch zur Erklärung der Bildung von *11* soll anschliessend gegeben werden.

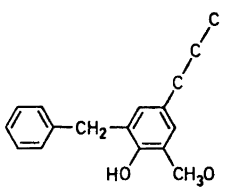

10

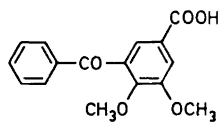

11

Die Fragmentierung des Holzes beim Mahlvorgang in der Schwingmühle ist von einer homolytischen Spaltung von C–C und C–O Bindungen im Lignin und im Kohlehydratanteil [12] des Holzes begleitet (zur Theorie des Mahlvorgangs siehe Lit. 8b). Die Konzentration von Radikalen im Holzmehl, das durch Feinmahlung in einer Kugelmühle erhalten worden war, ist nach ESR-Messungen bedeutend höher als der sehr geringe Radikalgehalt des Holzes.[13] Es ist allerdings fraglich, ob dies das Ergebnis des Mahlvorgangs ist (vergl. Lit. 14).

Die an der Oberfläche der Fragmente fixierten Radikale reagieren zunächst unter H-Abstraktion mit Toluol zu Benzylradikalen. Letztere geben in einer weiteren H-Übertragungsreaktion mit phenolischen Kernen an der Oberfläche der Teilchen Phenoxylradikale unter Rückbildung von Toluol; durch die Fixierung dieser Phenoxylradikale in der festen Phase ist deren Dimerisierung ausgeschlossen. Ihre Stabilisierung erfolgt durch Kopplung mit Benzylradikalen. Beim hier aufgefundenen Kopplungstyp koppelt das Benzylradikal über das C_α, das Phenoxylradikal über das C-Atom in *o*-Stellung zum Phenoxylsauerstoff. Der so gebildete Strukturtyp *10* kommt mit geringer Frequenz im Björkman-Lignin vor; beim oxdativen Abbau von methylierten Strukturen des Typs *10* wird *5*-Benzoyl-veratrumsäure gebildet.

Eine analoge Kopplungsreaktion, bei der ein Benzylradikal in 4-Stellung koppelt, sollte zum Strukturtyp *12* führen; die aus diesem nach Methylierung und oxydativem Abbau zu erwartende Säure *13* wurde jedoch nicht unter den Abbauprodukten von methyliertem Björkman-Lignin (Fichte) aufgefunden.

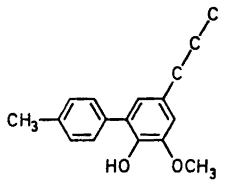

12

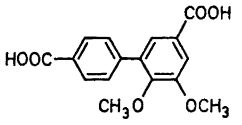

13

Es war naheliegend, auch nach Produkten der Dimerisierung von Benzylradikalen zu suchen. Tatsächlich wurden im Destillationsrückstand des bei der Mahlung in der Kugelschwingmühle verwendeten Toluols geringe Mengen von Bibenzyl und 4-Methyldiphenylmethan aufgefunden. Eine nachträgliche Kontrolle des käuflichen Produktes zeigte jedoch, dass auch in diesem Spuren der beiden Verbindungen vorhanden waren.

EXPERIMENTELLER TEIL

Methylierung und oxydativer Abbau. Siehe Literaturangaben bei den entsprechenden Tabellen.

Sulfatkochung. Siehe Lit. 1a.

Sodakochung. Ausführung wie bei Sulfatkochung, aber in 2 M NaOH anstelle von Weisslauge. Bei Kochungen von Holzmehl wurde der Autoklaveninhalt durch Pendelbewegung des Autoklaven durchmischt.

Feinmahlung. Siehe Lit. 3a.

5,6-Dimethoxy-biphenyl-3,4'-dicarbonsäure-dimethylester (Dimethylester von *11*). Ein Gemisch, bestehend aus 2,15 g 4-Brom-benzoesäure-methylester, 3,22 g 5-Jod-veratrumsäure-methylester [15] und 7 g Cu-Bronze wurde 2 Stunden auf 225° erhitzt. Darauf wurde

das erkaltete Reaktionsgemisch mit Essigester ausgelaugt und der nach Verdampfen des Lösungsmittels verbleibende Rückstand im Kugelrohr destilliert. Bei 160 – 180° und 0,01 Torr ging der Dimethylester von *11* zusammen mit 5,5′-Dehydro-diveratrumsäure-dimethylester über; letzterer konnte durch Kristallisation aus Methanol zum grössten Teil abgeschieden werden. Aus Essigester-Hexan kristallisierte der Dimethylester von *11* in Form farbloser Nadeln vom Schmp. 87 – 88°. Für das Molekülion wurde massenspektroskopisch eine Masse von 330,1112 gefunden (ber. für $C_{18}H_{18}O_6$: 330,1103). *Bedingungen für die Gaschromatographie:* siehe Lit. 1b. Retentionszeit (relativ zu 5,5′-Dehydro-diveratrumsäure-dimethylester): 0,58.

5,6-Dimethoxy-biphenyl-3,4′-dicarbonsäure (11). Aus dem Dimethylester durch Verseifen mit methanolischer KOH. Farblose, feine Nadeln aus wässr. Essigsäure, Schmp. 271 – 274°.

Herrn Prof. Dr. Adler danken wir für wertvolle Diskussionen, Ing. Ilona Somfai für die Darstellung der Björkman-Ligninpräparate. Das in dieser und früheren Arbeiten zur Herstellung von Björkman-Lignin verwendete Holzmehl wurde von Dr. Brita Swan, Forschungsinstitut, Billeruds AB, Säffle, zur Verfügung gestellt. Hierfür möchten wir unseren besten Dank aussprechen. Diese Arbeit wurde von der Westvaco Corp., New York, sowie durch ein Stipendium (G. E. M.) von *Cellulosaindustriens Stiftelse för teknisk och skoglig forskning samt utbildning* unterstützt.

LITERATUR

1. a. Larsson, S. und Miksche, G. E. *Acta Chem. Scand.* **25** (1971) 647; b. *Ibid.* **23** (1969) 917; c. *Ibid.* **23** (1969) 3337; d. *Ibid.* **25** (1971) 673; e. *Ibid.* **26** (1972) 2031.
2. Erickson, M., Larsson, S. und Miksche, G. E. *Acta Chem. Scand.* **27** (1973) 127.
3. a. Björkman, A. und Person, B. *Svensk Papperstid.* **60** (1957) 158; b. Björkman, A. *Ibid.* **59** (1956) 477; c. *Ibid.* **60** (1957) 243.
4. Adler, E., Miksche, G. E. und Johansson, B. *Holzforschung* **22** (1968) 171.
5. Pearl, I. A. *J. Am. Chem. Soc.* **64** (1942) 1429.
6. Erickson, M. und Miksche, G. E. *Acta Chem. Scand.* **26** (1972) 3085.
7. Lindgren, B. O. und Mikawa, H. *Acta Chem. Scand.* **11** (1957) 826; Marton, J. und Adler, E. *Ibid.* **15** (1961) 370.
8. a. Sarkanen, K. V. In Sarkanen, K. V. und Ludwig, C. H. *Lignins*, Wiley-Interscience, New York 1971, S. 150 – 155; Lai, Y. Z. und Sarkanen, K. V. *Ibid.* S. 197 – 198; b. *Ibid.* S. 170 – 175; c. *Ibid.* S. 227.
9. a. Freudenberg, K. In Freudenberg, K. und Neish, A. C. *Constitution and Biosynthesis of Lignin*, Springer, Berlin 1968, S. 113; b. *Ibid.* S. 102 – 108; c. *Ibid.* S. 81.
10. Cowling, E. B. *et al. Unveröffentlicht.*
11. Miksche, G. E. *Acta Chem. Scand.* **27** (1973) 3269.
12. Assarsson, A., Lindberg, B. und Theander, O. *Acta Chem. Scand.* **13** (1959) 1231.
13. Kleinert, T. N. und Marton, J. R. *Nature* **196** (1962) 334.
14. Rånby, B., Kringstad, K., Cowling, E. B. und Lin, S. Y. *Acta Chem. Scand.* **23** (1969) 3257.
15. Erdtman, H. *Svensk Kem. Tidskr.* **47** (1935) 223.
16. Adler, E., Delin, S. und Lundquist, K. *Acta Chem. Scand.* **13** (1959) 2149; Adler, E. und Lundquist, K. *Ibid.* **17** (1963) 13.
17. Lundquist, K., Miksche, G. E., Ericsson, L. und Berndtson, L. *Tetrahedron Letters* **1967** 4587.
18. Lundquist, K. *Acta Chem. Scand.* **24** (1970) 889.

Eingegangen am 20. September 1972.

ACTA CHEMICA SCANDINAVICA 27 (1973) 915–923

A Dependence of Transition Properties of the Univalent Nitrates upon Structural Entities

J. H. FERMOR and A. KJEKSHUS

Kjemisk Institutt, Universitetet i Oslo, Blindern, Oslo 3, Norway

Low temperature dielectric transitions occurring in $LiNO_3$, $NaNO_3$, KNO_3, $RbNO_3$, $CsNO_3$, $AgNO_3$, $TlNO_3$, and NH_4NO_3 are shown to have characteristic temperatures which depend on the degree of packing of ions in the crystal lattice. The same factor is also shown to influence the melting points of the compounds. As an example of transformations at intermediate temperatures, observed values of dielectric constant in KNO_3 at 1 kHz are considered in relation to the phase II to I transition at ~402 K. The range of existence of phase IIIm (m = metastable) appears to be connected with a region of increased dielectric constant in phase II.

Changes in the physical properties of univalent nitrates with temperature form a rather extensive topic; much of the literature dealing with the structural and order-disorder transformations occurring above room temperature. The present work is concerned primarily with the low temperature, and melting transitions, since these are found to have features in common. Between these temperature extremes, the phase II to I transformation in KNO_3 is taken as an example of a first order structural transition.

TRANSFORMATIONS BELOW ROOM TEMPERATURE

As reported earlier,[1] dielectric transitions occur below room temperature in $LiNO_3$(263 K), $NaNO_3$(243 K), KNO_3(213 K), $RbNO_3$(228 K), $CsNO_3$(238 K), $AgNO_3$(238 K), $TlNO_3$(238 K), and NH_4NO_3(241 K); the temperatures in parentheses being characteristic of the transitions on cooling in each case. In general, the transitions are detected by a peak in the dielectric constant ϵ on cooling, with a discontinuity in slope at the maximum value. On heating, there is a considerably larger and more rounded maximum at a somewhat higher temperature. Corresponding minima are found in the a.c. resistivities. In the case of KNO_3, a determination of unit cell dimensions showed there to be an anomalous variation in cell volume in the region of the transition.[2] That lattice expansion can have an important bearing on dielectric transitions has been shown on

theoretical grounds by Simpson[3] for cases where there is a change in the freedom of orientation of electric dipoles.

The transitions in the univalent nitrates appear to involve only small changes in energy, since no corresponding anomalies are noted in the specific heat curves of $NaNO_3$ and KNO_3,[4] or by means of differential thermal analysis in $RbNO_3$ and $CsNO_3$.[5] In $TlNO_3$, on the other hand, a discontinuity in slope has been noted[6] in previously published specific heat data.

The dielectric anomalies are in themselves insufficient to enable the nature of the transitions to be determined in detail, but some progress in interpretation may be made, pending the use of supplementary experimental techniques. The values of the electrical parameters obtained below room temperature for $LiNO_3$,[7] $NaNO_3$,[8] KNO_3,[2] $RbNO_3$,[9] $CsNO_3$,[9] $AgNO_3$,[6] $TlNO_3$,[6] and NH_4NO_3[6] suggest that the anomalies reflect considerable alterations in lattice forces. The form of the curves does not, for example, appear to be consistent with an impurity relaxation effect, or to result from the reorientation of dipoles constituted by interstitial ions closely associated with vacancies in the corresponding sublattice. These phenomena would be expected to result in more symmetrical maxima and minima, smaller variations in ϵ, and an absence of hysteresis, as may be seen for example in Ref. 10.

Although the exclusion of water from the nitrate samples was given a high priority, at the cost of obtaining non-standard values of dielectric parameters, the complete absence of water is unlikely. The dielectric transitions do not reflect a freezing and remelting of solutions of the salts, however, the eutectic temperatures being in most cases much higher. If additional impurities were included in solution, thus reducing the operative eutectic temperatures, the anomalous increases in dielectric constant on heating which were found for KNO_3 ($\Delta\epsilon = 9.2$), $RbNO_3$ ($\Delta\epsilon = 2.5$), $CsNO_3$ ($\Delta\epsilon = 4.0$), and $AgNO_3$ ($\Delta\epsilon = 2.8$) would indicate extremely high impurity contents, and therefore this cannot be regarded as a reasonable explanation of the anomalies.

The dielectric anomalies may, however, reflect structural or order-disorder transformations; and it is natural to suppose that the nitrate groups play an important role by reason of internal changes, modifications in ordering, or a combination of such effects. A noticeable feature of the transitions is that on heating the samples, an increasing value of ϵ is continued into the region of the normal room temperature phase to form a maximum. Such high values of ϵ as those recorded, in combination with low a.c. resistivities, can be most simply accounted for by the rotation of electric dipoles through restricted angles, by large ionic displacements, or a combination of the two. Dipoles could, for example, arise from distortions from planarity of the nitrate groups, and the transitions involve the ordering of these dipoles. The symmetrical out of plane mode of oscillation of the group, of frequency $\nu_2 \approx 830$ cm^{-1},[11] is largely restricted to the ground state within the temperature range of the anomalies (210 to 265 K), and this favours a locking of distorted groups into an ordered structure.

The possibility that the dielectric transitions reflect structural order-disorder transformations is supported by the similarity of the experimental data with those obtained by Guillien[12] for the lambda transitions in ammonium halides at comparable temperatures. The first of these transformations was

discovered calorimetrically by Simon [13] in NH_4Cl, and the results of a large number of investigations including those using neutron diffraction [14,15] show that whereas the orientations of the NH_4^+ tetrahedra are ordered in the low temperature phases, at room temperature they are randomly distributed between two alternative orientations. Some aspects of the order-disorder process itself are still uncertain, however, in spite of the large number of studies on the subject. By analogy, it may be suggested as a possibility that the low temperature dielectric transitions in the univalent nitrates correspond to the onset of orientational disorder of the nitrate group. Only very small amounts of energy are involved in reorientations between equivalent positions at low frequencies. If the nitrate group is regarded as planar, as claimed by Walsh [16] on quantum mechanical grounds, the most probable reorientations are those through angles of 120° about the threefold axis of the group. These reorientations would be consistent with the suggestion by Schroeder *et al.*,[17] on the basis of infrared measurements, that the barrier opposing reorientation is surmounted at room temperature in several nitrates.

An additional possibility which cannot be definitely excluded at present, however, is that small departures from planarity of the nitrate groups are involved in the transitions. In this case, additional crystallographic parameters are introduced in the structural model, with corresponding possibilities for disordering. Whichever form the disorder takes, it is interesting to consider the variation of the transition temperature T_a within the family of compounds. It is reasonable to suppose that anion-cation and anion-anion interactions influence this parameter, and therefore the lattice volume V_l associated with each anion is selected as an independent variable. Thus V_l is the unit cell volume per formula unit less that of the cation. The latter is assumed to be spherical, and of radius r_c appropriate to sixfold coordination.

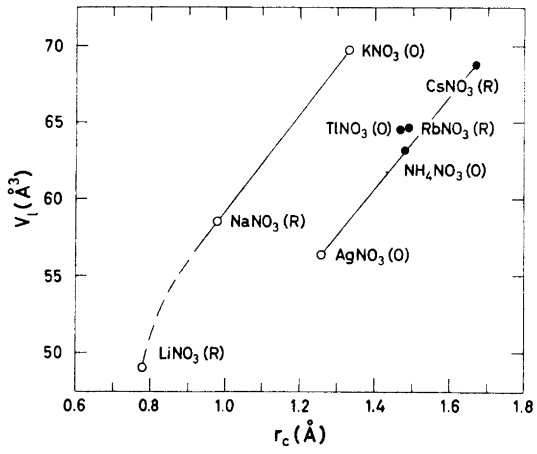

Fig. 1. Lattice volume per anion V_l *versus* cation radius r_c for univalent nitrates. The crystal structures of the room temperature phases are (R) rhombohedral, and (O) orthorhombic. Filled circles represent compounds adopting a cubic phase I structure ($r_c > 1.4$ Å).

INFLUENCE OF CATION RADIUS UPON PACKING

Before examining the dependence of T_a upon V_l, it is interesting to see from Fig.1 that the connection between V_l and r_c is such that the compounds fall into two, approximately linear groups. The values of r_c employed in this diagram may be regarded as having been well established, except possibly in the case of Li^+, for which Goldschmidt's value of 0.78 Å [18] has been selected, consistent with its use in related work.[6] The values of V_l are calculated for the room temperature phase in each case. There is seen to be a degree of correlation between the data for $LiNO_3$,[19] $NaNO_3$,[20] and KNO_3,[21] despite differences in structure, which may be obtained from the references given. The overall symmetries only are indicated in the figure, like symbols not necessarily indicating like structures. The data for $RbNO_3$,[22] $CsNO_3$,[23] $TlNO_3$,[24] and NH_4NO_3,[25] form a separate group, the members of which have cubic high temperature phase I structures,[26] while $LiNO_3$, $NaNO_3$, KNO_3, and $AgNO_3$ are rhombohedral, at least in their high temperature phases.[27] Thus, independent of the structure type at room temperature, that of the highest temperature phase depends on whether $r_c \gtrless 1.4$ Å. The separation of the room temperature data of Fig. 1 into two linear sets suggests two types of lattice bonding, independent of the crystal structures involved.

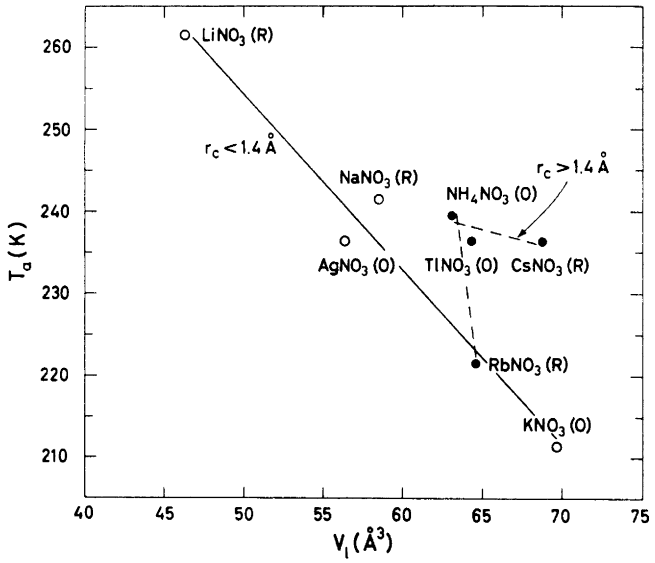

Fig. 2. The low temperature dielectric transition temperatures T_a *versus* the lattice volume per anion V_l for univalent nitrates. The crystal structures of the room temperature phases are (R) rhombohedral and (O) orthorhombic. Filled circles denote compounds with $r_c > 1.4$ Å.

DEPENDENCE OF DIELECTRIC TRANSITION TEMPERATURE ON PACKING

No consistent trend including all of the compounds is to be found on plotting T_a *versus* r_c, but overall correlations between T_a and V_l may be seen in Fig. 2. The results suggest that in general the lesser the ionic interaction (*i.e.* the greater V_l), the lower the transition temperature. As in Fig. 1, the influence of cation radius also appears to be in evidence in Fig. 2, since the points fall into two groups according to whether $r_c \gtrless 1.4$ Å. In order of increasing r_c, the group comprising $LiNO_3$, $NaNO_3$, $AgNO_3$, and KNO_3 is approximately linear, while $TlNO_3$, NH_4NO_3, $RbNO_3$, and $CsNO_3$ may also form a related group if $RbNO_3$ or $CsNO_3$ are excepted. It should be noted that the probable error limits in the values of T_a are not well defined, but may provisionally be set at ± 5 K. It may be relevant that $RbNO_3$ is unusual among these compounds in undergoing a small contraction on melting,[28] suggesting peculiar bonding properties. The indicated correlations, which imply T_a to be a monotonic function of V_l for each group of compounds, are of course to be regarded as suggestive rather than conclusive. It is not supposed that proximity effects alone determine the value of T_a, but the results do tend to confirm the fundamental or intrinsic nature of the anomalies, and may assist in the choice of methods suitable for their further investigation. The correlations are consistent with the order-disorder models considered above in selecting V_l as independent parameter.

The influence of packing upon the internal characteristics of nitrate groups has been demonstrated by Bues,[29] who showed a dependence of the symmetrical in-plane oscillation frequency ν_1 upon the free lattice volume per anion V_f (*i.e.* $V_f = V_l - V_a$, where V_a is the volume of the anion). Bues considered $LiNO_3$, $NaNO_3$, KNO_3, and $AgNO_3$, in solid and liquid states; finding no evidence of variation in the strength of the internal binding forces of the nitrate groups in these compounds, with the exception of $AgNO_3$.

INFLUENCE OF PACKING ON THE MELTING TRANSFORMATION

It was proposed earlier [30] that the thermal response of the anion sublattice is primarily responsible for the anomalously low melting points T_f of the univalent nitrates, whose values are some 200 to 400 K lower than for the alkali halides. The relationship between T_f and V_l for the univalent nitrates is shown in Fig. 3, where it is seen that, with the exception of $CsNO_3$, the alkali metal nitrates show an approximately linear correlation. It is important to note that KNO_3 provides an exception to the ordering of points according to cation radius. The influence of ionic radius upon T_f for the alkali halides, which provide a convenient class of compounds for comparison, has been noted earlier.[30] The deviation of $CsNO_3$ may perhaps be due to its limiting value of cation radius, possibly resulting from a screening effect. The influence of V_l upon T_f for the alkali metal nitrates is consistent with both a variation in lattice energy and a modification of the nitrate groups, on the assumption that the modes of oscillation or disorder of the latter, over and above those of spherical ions, control the melting process.

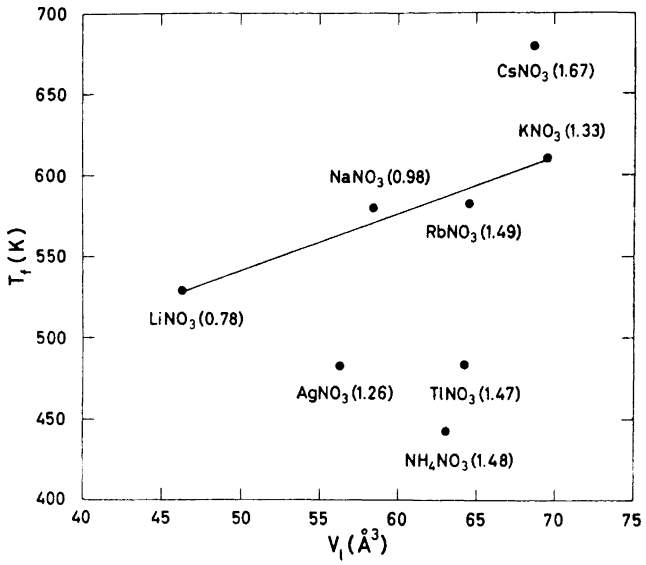

Fig. 3. Melting points T_f *versus* lattice volume per anion V_f for univalent nitrates. Values of cation radii are shown in parentheses.

The positions of $AgNO_3$, $TlNO_3$, and NH_4NO_3, relative to the other compounds in Fig. 3, clearly result from the operation of factors additional to those considered above. The electronic polarizabilities of the ions might be one such factor, but while the value for Tl^+ (90.1 Å^3) exceeds even that of Cs^+ (71.3 Å^3), that for Ag^+ (39.4 Å^3) is less than for K^+ (47.3 Å^3), according to the data reported by Roberts.[31] Additional evidence for the uniformity of anion-cation bonding in univalent nitrates is presented elsewhere.[6]

In regarding ionic interactions as the controlling factor in determining T_f for $LiNO_3$, $NaNO_3$, KNO_3, $RbNO_3$, and $CsNO_3$, variations in the internal mode frequencies of the anion have not been mentioned. According to the concept of the "Lockerungseffekt" introduced by Theimer,[32] however, deformation of the anion by the electrostatic field generated between it and the surrounding cations can diminish the internal binding forces of the anion, with a consequent reduction in internal mode frequencies. This has been shown by Bues [29] to occur in $AgNO_3$, but not in $LiNO_3$, $NaNO_3$, and KNO_3, and it is possible therefore that the low value of T_f for $AgNO_3$, and probably also for $TlNO_3$, reflects a displacement to lower temperatures of the activation of internal modes.

Also important in an understanding of the melting process is the exceptionally high self diffusion rate of cations in the vicinity of the melting point, which has been clearly shown to exist in the high temperature disordered state of $NaNO_3$ by means of NMR, [33,34] d.c. conductivity,[8] and low frequency dispersion [35] experiments. These results show an instability of the cation sublattice which makes cooperative anion vibrations particularly effective in producing the disorder of melting.

In this connection, values of the partition functions for simple harmonic oscillators of the frequencies of internal oscillation of the nitrate group show that appreciable activation occurs in the temperature range of the thermal transformations above room temperature, and of the melting points.[36] These vibrations tend to increase the effective degree of sphericity of the group, and to cause fluctuations in the lattice barrier potentials opposing positional and orientational disorder of the ions. On increasing the temperature of a crystal, both of the above consequences of vibration tend to favour transformations into structures of a higher degree of symmetry and disorder, and lead eventually to the melt.

THE FIRST ORDER STRUCTURAL TRANSFORMATION IN KNO_3

The most common type of solid-state transformation occurring in the univalent nitrates is the discontinuous, or first order structural transition. As an example of this type of transformation, that between phases II and I in KNO_3 at ~402 K is extremely sharp, as may be seen from the temperature variation of the electrical resistivity.[37] If the characteristic modes of anion vibration are of importance in causing this and other transformations in the nitrates, the sharpness of the transition seems paradoxical in view of the gradual thermal activation of the vibrational modes. Experimental evidence of changes premonitory to the II to I transformation in KNO_3 is, however, shown in Fig. 4, where there is seen to be a gradual increase in the dielectric constant, beginning at ~350 K. These data were obtained for a polycrystalline *p.a.* grade (Merck) sample, according to the method described in Ref. 8. The measuring frequency used was 1 kHz, compared with the higher values ($\geq$10 kHz) employed in previous determinations,[38–42] with which the present results are consistent. No other premon-

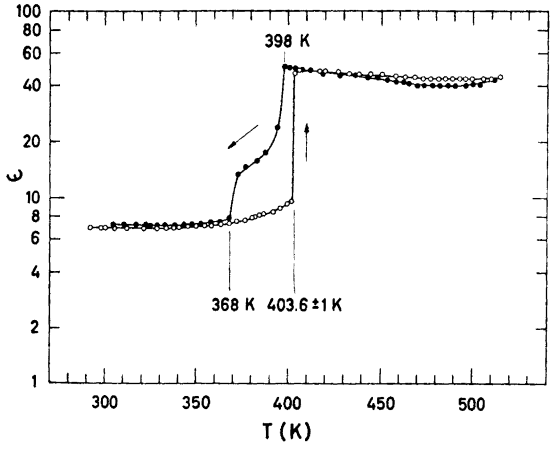

Fig. 4. Dielectric constant ϵ *versus* absolute temperature T for polycrystalline *p.a.* grade KNO_3 at 1 kHz. Arrows indicate the direction of temperature change.

itory effects are known to have been found in connection with this transformation. Also to be seen in the diagram is a high value of ϵ of ~ 50 in phase I ($T > 403.6$ K), where there is known to be orientational disorder of the nitrate groups,[43] leading to a reduction in mean energy barriers. The formation of the intermediate phase IIIm (m = metastable; $368 < T < 398$ K, approximately) on cooling is also apparent.

The observed increase in ϵ prior to the phase II to I transformation is also relevant to the soft mode interpretation of phase transitions. According to this model, the lattice modes directly associated with the displacement of atoms to new structural positions become unstable as the transition is approached. Thus, diminished values of force constants cause the frequencies of certain lattice modes to fall to zero at the transition temperature; and the reduced force constants result in increased displacements in the presence of an externally applied electric field, thus causing the observed increase in ϵ. The stability of the phase IIIm on cooling is no doubt related to the increased value of ϵ of phase II over the temperature range of existence of the phase IIIm recorded here. The transitional quality of phase IIIm is apparent from its values of ϵ.

Treatments of internal and librational modes of oscillation of molecules or ionic groups on the one hand, and of soft lattice modes on the other, provide complementary aspects of transformations in crystals. Whereas soft mode studies lead to insight into the transitional mechanism connecting initial and final lattice structures, consideration of spatial factors, molecular or ionic group disorder, and of internal modes and their interactions have been found of value in suggesting how solid state and melting transformations originate in the compounds considered.

Acknowledgements. This work was made possible by the financial support of *Norges almenvitenskapelige forskningsråd.*

REFERENCES

1. Fermor, J. H. and Kjekshus, A. *Acta Chem. Scand.* **22** (1968) 2054.
2. Fermor, J. H. and Kjekshus, A. *Acta Chem. Scand.* **22** (1968) 836.
3. Simpson, J. H. *Can. J. Phys.* **29** (1951) 163.
4. Southard, J. C. and Nelson, R. A. *J. Am. Chem. Soc.* **55** (1933) 4865.
5. Owen, R. W. and Kennard, C. H. L. *Aust. J. Chem.* **24** (1971) 1295.
6. Fermor, J. H. and Kjekshus, A. *To be published.*
7. Fermor, J. H. and Kjekshus, A. *Acta Chem. Scand.* **23** (1969) 1581.
8. Fermor, J. H. and Kjekshus, A. *Acta Chem. Scand.* **22** (1968) 1628.
9. Fermor, J. H. and Kjekshus, A. *Acta Chem. Scand.* **26** (1972) 2645.
10. Breckenridge, R. G. *J. Chem. Phys.* **18** (1950) 913.
11. Herzberg, G. *Infrared and Raman Spectra of Polyatomic Molecules*, Van Nostrand, New York 1945.
12. Guillien, R. *Compt. Rend.* **208** (1939) 1561.
13. Simon, F. *Ann. Physik* **68** (1922) 241.
14. Levy, H. A. and Peterson, S. W. *J. Am. Chem. Soc.* **75** (1953) 1536.
15. Goldschmidt, G. H. and Hurst, G. D. *Phys. Rev.* **86** (1952) 797.
16. Walsh, A. D. *J. Chem. Soc.* **1953** 2301.
17. Schroeder, R. A., Weir, C. E. and Lippincott, E. R. *J. Res. Natl. Bur. Std.* **A 66** (1962) 407.

18. Goldschmidt, V. M. *Skrifter Norske Videnskaps-Akad. Oslo, I: Mat.-Naturv. Kl.* **1926**. No. 1.
19. Zachariasen, W. H. *Skrifter Norske Videnskaps-Akad. Oslo, I: Mat.-Naturv. Kl.* **1928** No. 4.
20. Cherin, P., Hamilton, W. C. and Post, B. *Acta Cryst.* **23** (1967) 455.
21. Edwards, D. A. *Z. Krist.* **80** (1931) 154.
22. Brown, R. N. and McLaren, A. C. *Acta Cryst.* **15** (1962) 974.
23. Delacy, T. P. and Kennard, C. H. L. *Aust. J. Chem.* **24** (1971) 165.
24. Brown, R. N. and McLaren, A. C. *Acta Cryst.* **15** (1962) 977.
25. West, C. D. *J. Am. Chem. Soc.* **54** (1932) 2256.
26. Finbak, C. and Hassel, O. *Z. physik. Chem.* **B 35** (1937) 25.
27. Fischmeister, H. F. *J. Inorg. Nucl. Chem.* **3** (1956) 182.
28. Schinke, H. and Sauerwald, F. *Z. anorg. allgem. Chem.* **304** (1960) 25.
29. Bues, W. *Z. physik. Chem. (Frankfurt)* **10** (1957) 1.
30. Fermor, J. H. and Kjekshus, A. *Acta Chem. Scand.* **24** (1970) 1015.
31. Roberts, S. *Phys. Rev.* **76** (1949) 1215.
32. Theimer, O. *Monatsh.* **81** (1950) 424.
33. Eades, R. G., Hughes, D. G. and Andrew, E. R. *Proc. Phys. Soc. (London)* **71** (1958) 1019.
34. Andrew, E. R., Eades, R. G., Hennel, J. W. and Hughes, D. G. *Proc. Phys. Soc. (London)* **79** (1962) 954.
35. Fermor, J. H. and Kjekshus, A. *Acta Chem. Scand.* **26** (1972) 3235.
36. Bjørseth, O., Fermor, J. H. and Kjekshus, A. *Acta Chem. Scand.* **25** (1971) 3791.
37. Fermor, J. H. and Kjekshus, A. *Acta Chem. Scand.* **21** (1967) 1265.
38. Sawada, S., Nomura, S. and Fujii, S. *J. Phys. Soc. Japan* **13** (1958) 1549.
39. Sawada, S., Nomura, S. and Asao, Y. *J. Phys. Soc. Japan* **16** (1961) 2486.
40. Khodakov, A. L. and Mirskaya, E. Z. *Soviet Phys.-Cryst. (English Transl.)* **7** (1962) 382.
41. Chen, A. and Chernow, F. *Phys. Rev.* **154** (1967) 493.
42. Leong, J. T. and Emrick, R. M. *J. Phys. Chem. Solids* **32** (1971) 2593.
43. Strømme, K. O. *Acta Chem. Scand.* **23** (1969) 1625.

Received September 22, 1972.

ACTA CHEMICA SCANDINAVICA 27 (1973) 924–930

Determination of the Acidity Constant of Boric Acid in Synthetic Sea Water Media

INGEMAR HANSSON

Department of Analytical Chemistry, University of Göteborg, Fack, S-402 20 Göteborg 5, Sweden

The acidity constant of boric acid has been determined by potentiometric titrations in synthetic sea water covering a salinity range of 20 – 40 ‰ and a temperature range of 5 – 30°C. The activity scale is chosen so that the activity coefficient approaches unity when the concentrations of H^+, OH^-, $B(OH)_3$ and $B(OH)_4^-$ approach zero in synthetic sea water of a certain salinity. The concentration unit is M_w, mol per kg solution.

This work is a determination of the acidity constant of boric acid (the stability constant for hydrolysis of boric acid) as defined by

$$K_B = [H^+][B(OH)_4^-]/[B(OH)_3] \quad (1)$$

in activity scales based on sea water of different salinities. These values should be used when correcting measured total alkalinity to carbonate alkalinity if the pH-alkalinity method is used for determination of the concentrations of the carbonate species in a sea water sample with our pH-scale [1] and dissociation constants of carbonic acid.[2,3]

The total alkalinity of a sea water sample, not being polluted or anoxic, and neglecting trace phosphate and organic carboxylates, can be expressed in equilibrium concentrations by

$$A_t = [B(OH)_4^-] + 2[CO_3^{2-}] + [HCO_3^-] + [OH^-] - [H^+] \quad (2)$$

The carbonate alkalinity, denoted A_C and used in the expressions for calculation of the concentrations of the carbonate species, is defined by

$$A_C = 2[CO_3^{2-}] + [HCO_3^-] \quad (3)$$

Thus $[B(OH)_4^-]$ and $([OH^-]-[H^+])$ must be subtracted from A_t to evaluate A_C for a sample. The term $([OH^-]-[H^+])$ can be neglected for most sea water samples. The term $[B(OH)_4^-]$ can be expressed in K_B and B_t, defined by

$$B_t = [B(OH)_3] + [B(OH)_4^-] \quad (4)$$

by the equation

$$[B(OH)_4^-] = B_t K_B/(K_B + [H^+]) \quad (5)$$

B_t can usually be calculated from the chlorinity by the constant ratio $B_t(\text{mol/kg})/Cl\ (‰) = 2.13 \times 10^{-5}$.

The activity scales based on sea water used in our definitions of constants and pH are treated in detail by Sillén [4] and discussed by the present author in papers on the carbonate system.[2,3]

Previously, Buch [5] and Lyman [6] have determined the acidity constant of boric acid in sea water at various salinities and temperatures. However, they used different activity scales for H^+ and the borate species. This is discussed in detail elsewhere.[3]

SYMBOLS AND UNITS

The concentration unit used in the present work is M_w = mol per kg solution, a pressure and temperature independent concentration unit suggested by Dyrssen and Sillén.[7] Concentrations of buret solutions are given in M = mol per litre of solution.

Most of the notations used in the text are listed below:

A_C carbonate alkalinity defined by eqn. (3).
A_t total alkalinity defined by eqn. (2).
B total concentration of boric acid in equilibrium solutions.
B_0 value of B in starting equilibrium solutions.
B_t total concentration of boric acid defined by eqn. (4).
C_{Na}, C_{Mg}, C_{Ca}, C_{Cl}, C_{SO4}, total concentrations of Na^+, Mg^{2+}, Ca^{2+}, Cl^-, and SO_4^{2-} in equilibrium solutions.
E measured emf.
E_0 a constant in $E = E_0 + (RT \ln 10/F) \log h$.
H excess hydrogen ion concentration.
H_0 value of H in starting equilibrium solution.
H_T excess hydrogen ion concentration over H_2O in buret solutions ($-H_T$ is the titre of sodium hydroxide).
h free concentration of H^+, $h = [H^+]$.
K_B acidity constant of boric acid defined by eqn. (1).
K_w the ionic product of water.
S equilibrium solution.
S_0 starting equilibrium solution.
T_1, T_2 buret solutions.
β_{-10}, β_{-11}, β_{-13}, stability constants defined under Calculations.
σ,σ(H) standard deviations defined in Ref. 18.

EXPERIMENTAL

Chemicals and solutions. The *synthetic sea-water media* were prepared (mainly following Sillén [4,8]) with composition of Na^+, Mg^{2+}, Ca^{2+}, Cl^-, and SO_4^{2-} as previously described.[2] Stock solutions of *boric acid* in synthetic sea water were prepared by weighing in sodium chloride, sodium sulphate, and stock solutions of magnesium- and calcium

chlorides, and adding distilled water to about 95 % of the final weight of the solution. After deaeration to remove carbon dioxide, a weighed amount of dried boric acid (Merck Suprapur ®) was added followed by deaerated distilled water to the final weight of the solution.

Hydrochloric acid (Merck Titrisol ®) was added to each weighed amount of equilibrium solution before titration started.

The *sodium hydroxide* was prepared from 50 % NaOH and standardized against potassium hydrogen phthalate.

Solutions of synthetic sea water with the double concentrations of all ions (except sodium ions; see T_2 below) were prepared and added from a second buret to keep the ionic strength and main composition of the equilibrium solutions constant. The *hydrogen gas* was purified in a Deoxo ® (Engelhard Ind. AB) cartridge.

Apparatus. The *titration vessel* was a five-necked glass vessel. The *voltmeter* for measuring the emf of the cell was a Solartron digital voltmeter, model 1867, with 10 μV resolution and free from measurable drift.

The *hydrogen electrodes* were prepared according to Bates.[9] The *reference electrodes* were Ag,AgCl-electrodes (prepared according to Brown [10]) in a saltbridge solution of synthetic sea water saturated with AgCl. The design of the *saltbridge* has been described previously by the author.[2]

A paraffin oil bath *thermostat* was used which could be adjusted to the temperature desired within 0.05°C.

The equilibrium solution was stirred by a stream of hydrogen gas. The hydrogen gas from the tank was washed in three bottles containing H_2SO_4, NaOH, and synthetic sea water, and the stream was divided into two; one for the hydrogen electrode and one for stirring the solution.

THE EMF MEASUREMENTS

The experimental investigation of the hydrolysis of boric acid in sea water was carried out as potentiometric titrations. In each titration the analytical hydrogen excess H in the equilibrium solution S was varied by adding sodium hydroxide (solution T_1) from a buret. The concentrations of the medium ions in S were kept practically constant by adding equal volumes from T_1 and a buret solution T_2 described below. The total boron concentration was altered by dilution from 10 mM_w in the starting solution S_0 to about 8.8 mM_w in the final solution. The compositions of the solutions can be represented by the following equations:

$$S = H\ M_w\ H^+,\ C_{Na}\ M_w\ Na^+,\ C_{Mg}\ M_w\ Mg^{2+},\ C_{Ca}\ M_w\ Ca^{2+},\ C_{Cl}\ M_w\ Cl^-,\ C_{SO_4}\ M_w\ SO_4^{2-},\ B\ M_w\ B(OH)_3$$

$$T_1 = -H_T\ M\ NaOH$$

$$T_2 = (2C_{Na} + H_T)\ M_w\ Na^+,\ 2C_{Mg}\ M_w\ Mg^{2+},\ 2C_{Ca}\ M_w\ Ca^{2+},\ 2C_{Cl}\ M_w\ Cl^-,\ 2C_{SO_4}\ M_w\ SO_4^{2-}$$

The starting solution contained an excess of H^+ (over H_2O and $B(OH)_3$). Gran [11] extrapolation can be performed using titration points with excess of H^+ to give preliminary values of E_0, the constant in Nernst's equation (6).

The titrations were followed by measuring the emf, E, of the cell

$$-\ RE\ |\ \text{solutions S}\ |\ H_2(1\ \text{atm}),\ Pt\ +$$

where RE is a reference half cell of the composition

$$RE = \text{synthetic sea water saturated with AgCl}\ |\ AgCl,Ag$$

The emf of this cell, in the range of log h investigated, can be written

$$E = E_0 + (RT \ln 10/F) \log h \quad (6)$$

since the liquid junction potential is negligible if the test and reference solutions are based on the same ionic medium and the junction is well defined.[12] Thus the hydrogen ion concentration at equilibrium, h, can be evaluated from eqn. (6). After an addition of the buret solutions, the emf values became constant in 10 to 20 min. Back titrations were not performed since the reversibility of the borate equilibria has been previously demonstrated by Ingri.[13]

CALCULATIONS AND RESULTS

For each titration, about 30 (V_T,E)-values ("titration points") were collected in the log h range $-2.7 > \log h > -9.5$. These primary data were processed with an IBM 360/65 computer, using a Fortran version of the generalised least squares program LETAGROP, with procedures ETITR written by Sillén *et al.*[14,15] In the LETAGROP calculations no other species were assumed to be present in the solution than H^+, OH^-, $B(OH)_3$, $B(OH)_4^-$, and $B_3O_3(OH)_4^-$. Each titration was executed separately. With H^+ and $B(OH)_3$ as components, the stability constants can be written

$$\beta_{-10} = K_w = [H^+][OH^-] \quad (7)$$

$$\beta_{-11} = K_B = [B(OH)_4^-]/h^{-1}[B(OH)_3] \quad (8)$$

and

$$\beta_{-13} = [B_3O_3(OH)_4^-]/h^{-1}[B(OH)_3]^3 \quad (9)$$

(Adding $3H_2O$, the species $B_3O_3(OH)_4^-$ can be written $(B(OH)_3)_3OH^-$; the $-1,3$-complex of $B(OH)_3$ with H^+.) In the executions the constant β_{-11}, and the "analytical parameters" E_0, H_0, and B_0 were adjusted. The values of K_w and β_{-13} were held fixed. Values for K_w were taken from Ref. 2 and the value of β_{-13} was chosen as 10^{-6} in all titrations. This was based on a rough mean obtained from preliminary calculations. The reasons for including the $-1,3$-complex in the calculations is discussed elsewhere.[16]

Changes in the liquid junction potential have been neglected because of the low values of h and $[OH^-]$ in the titrations. Experiments described in a previous paper [2] gave evidence for protolytic impurities present in all solutions on the concentration level 2×10^{-5} M_w. However, their inclusion in the LETAGROP calculations only very slightly influenced the error squares sum and pK_B; they were therefore omitted.

During the titration the concentration of $MgOH^+$ increases, but no correction was made because $Mg(OH)_2$ is not precipitated and $[Mg^{2+}]$ and thus $[OH^-]/[MgOH^+]$ will be pratically constant. $MgOH^+$ may therefore be included as a medium effect in K_w and is considered in the choice of activity scale. This is fully discussed in a subsequent paper.[17] The error squares sum minimized was $U = \sum(H_{calc} - H_{tot})^2$, defined in Ref. 15. The quantity $(H_{calc} - H_{tot})/B_{tot}$, the "error" in H_{tot} divided by B_{tot} in each titration point, showed a random scattering of numerically small values around zero.

Table 1. Values from the output of LETAGROP executions of $-\log \beta_{-11}$, the standard deviation given as 3σ (as defined in Ref. 18), and the standard deviation in H, $\sigma(H)$ (defined in Ref. 18), for the titrations performed in this work.

Temperature °C	Salinity ‰	$-\log \beta_{-11} = pK_B$	3σ	$\sigma(H) \times 10^3$(mM)
25	35	8.611 [a]	0.003	5.15
25	35	8.611 [a]	0.002	4.25
15	35	8.728	0.008	14.7
15	35	8.731	0.004	8.3
5	35	8.857 [b]	0.003	6.91
5	35	8.862 [b]	0.004	5.97
25	30	8.638	0.003	4.20
25	20	8.716	0.004	6.89

[a] Frydman *et al.*[19] found $pK_B = 8.63 \pm 0.03$ in a synthetic sea water medium similar to that used in this work.
[b] Frydman *et al.*[19] found $pK_B = 8.86 \pm 0.02$.

In Table 1 values of $\log \beta_{-11} = pK_B$ with standard deviation (given as 3σ) and the standard deviation in H, $\sigma(H)$, as defined in Ref. 18, are listed for eight titrations. The values for 35 ‰ were plotted against $1/T$ and a linear regression of the pK_B-values against $1/T$ was performed assuming that $\Delta H°$ for the hydrolysis of boric acid is constant over the temperature range studied. The equation for the regression line is

$$pK_B = 1026/T + 5.170 \quad (10)$$

A procedure to interpolate values of pK_B in the temperature range 5° to 30°C and salinity range 20 to 40 ‰ is described in Ref. 16.

DISCUSSION

The values of pK_B for 35 ‰ given in tables of Buch,[5] Lyman,[6] and this work are listed in Table 2 for temperatures between 5 and 30°C. Larger differences between the values for 5 and 30°C are observed for the constants determined in this work than for the constants from the other authors. The

Table 2. Values of pK_B in sea water as tabulated by Buch,[5] Lyman,[6] and this work form for 35 ‰ salinity.

Author	Temp. °C 5	10	15	20	25	30	pK_B (5°) − pK_B (30°)
Buch	8.85	8.81	8.75	8.72	8.68	8.65	0.20
Lyman	8.89	8.84	8.79	8.75	8.70	8.66	0.23
This work	8.86	8.79	8.73	8.67	8.61	8.55	0.31

different pH-scales used may explain this observation. The differences between values of pH in the scales according to Sørensen (used by Buch) and NBS (used by Lyman) are approximately constant with temperature. The pH scale used in this work is in very close agreement with an activity scale for H^+ where activity can be replaced by the total concentration of H^+, both free and bound to sulfate in the sea water medium. On this scale the variation of pH with temperature seems to be greater than the temperature variation of pH on other scales. The difference of pK-values between high and low salinities is greater for boric acid than for carbonic acid. This indicates that the medium ions form somewhat stronger complexes with $B(OH)_4^-$ than with HCO_3^-. In Ref. 17 comparisons are made between values of the acidity constant of boric acid determined in synthetic sea water and sodium chloride media of corresponding ionic strength. A special investigation of the weak complexing between Ca^{2+} and $B(OH)_4^-$ in 3 M $NaClO_4$ has been carried out by Frydman *et al.*[19]

A calculation of the distribution of boron between the different species proposed by Ingri using HALTAFALL [20,21] was performed for the total boron concentration of 0.00042 M found in sea water of 35 ‰ salinity. The stability constants valid for 3 M $NaClO_4$ were used. The polynuclear species contributed to less than 0.001 % of the total boron content. It might be safe to state that no other species are formed in the hydrolysis of boric acid in sea water than the borate ion $B(OH)_4^-$ and its complexes with the medium ions.

Acknowledgements. I thank the head of this department, Professor David Dyrssen, for valuable discussions and Mrs. Agneta Edlund, fil. kand., for careful experimental work. Thanks are also due to Dr. Louis Henderson who revised the English text of this article.

Grants from *the Swedish Natural Science Research Council* and from *Chalmers Technical University*, the latter to cover the costs of the computer work, are gratefully acknowledged.

REFERENCES

1. Hansson, I. *Deep-Sea Res. In press.*
2. Hansson, I. *Acta Chem. Scand.* **27** (1973) 931.
3. Hansson, I. *Deep-Sea Res. In press.*
4. Sillén, L. G. In *Equilibrium Concepts in Natural Water System, Advan. Chem. Ser.* **67** (1967).
5. Buch, K. *J. Conseil Conseil Perm. Intern. Exploration Mer* **8** (1933) 309.
6. Lyman, J. *Buffer Mechanism of Sea Water, Ph.D. Thesis*, University of California, Los Angeles 1957.
7. Dyrssen, D. and Sillén, L. G. *Tellus* **19** (1967) 113.
8. Sillén, L. G. *Lecture Manuscript*, University of California, Los Angeles, La Jolla 1966.
9. Bates, R. G. *Determination of pH*, Wiley, New York 1964, p. 241.
10. Brown, A. S. *J. Am. Chem. Soc.* **56** (1934) 56.
11. Gran, G. *Analyst* **77** (1952) 661.
12. Biedermann, G. and Sillén, L. G. *Arkiv Kemi* **5** (1952) 425.
13. Ingri, N. *Equilibrium Studies of Polyanions Containing B^{III}, Si^{IV}, Ge^{IV} and V^V, Thesis*, Stockholm 1963; *Svensk Kem. Tidskr.* **75** (1963) 3.
14. Sillén, L. G. and Warnqvist, B. *Arkiv Kemi* **31** (1969) 315.
15. Brauner, P., Sillén, L. G. and Whiteker, R. *Arkiv Kemi* **31** (1969) 365.
16. Hansson, I. *An Analytical Approach to the Carbonate System in Sea Water, Thesis*, Göteborg 1972.

17. Dyrssen, D. and Hansson, I. *Mar. Chem. In press.*
18. Sillén, L. G. *Acta Chem. Scand.* **16** (1963) 159.
19. Frydman, M., Sillén, L. G. and Högfeldt, E. *Preliminary results.*
20. Ingri, N., Kakolowicz, W., Sillén, L. G. and Warnqvist, B. *Talanta* **14** (1967) 1261.
21. Dyrssen, D., Jagner, D. and Wengelin, F. *Computer Calculations of Ionic Equilibria and Titration Procedures*, Almqvist & Wiksell, Stockholm 1968.

Received September 26, 1972.

ACTA CHEMICA SCANDINAVICA 27 (1973) 931–944

The Determination of Dissociation Constants of Carbonic Acid in Synthetic Sea Water in the Salinity Range of 20—40 $^0/_{00}$ and Temperature Range of 5—30°C

INGEMAR HANSSON

Department of Analytical Chemistry, University of Göteborg, Fack, S-402 20 Göteborg 5, Sweden

The dissociation constants of carbonic acid have been determined by potentiometric titrations in synthetic sea water covering a salinity range of 20—40 ‰ and a temperature range of 5—30°C. Corresponding values of pK_w have also been determined. The activity scale is chosen so that the activity coefficient approaches unity when the concentrations of H^+, OH^-, $H_2CO_3+CO_2$, HCO_3^-, and CO_3^{2-} approach zero in synthetic sea water of a certain salinity. The concentration unit is M_w, mol per kg solution.

Chemical analysis of the carbonate system in sea water involves the determination of the total concentrations of CO_3^{2-}, HCO_3^-, and dissolved CO_2 including such species as ion-pairs with the major cations (*e.g.* $MgCO_3$ and $MgHCO_3^+$) and hydrated forms (*e.g.* H_2CO_3). No methods are available for direct determination of all these concentrations in a sample of sea water. However, with knowledge of the dissociation constants of carbonic acid, they may be computed from values of two or three of the parameters pH, alkalinity, total carbonate content or equilibrium pressure of carbon dioxide of a sample. Methods have been reported for measurement of these parameters with good accuracy and precision (Refs. 1—4). An evaluation of different methods for chemical analysis of the carbonate system in sea water is given in a review by Park.[5] Tables of dissociation constants of carbonic acid determined for the purpose of analysis of the carbonate system in sea water have been published by Buch [6–8] and Lyman.[9] They used different activity scales for H^+ (both based on infinite diluted water solutions) and for H_2O, H_2CO_3, and CO_2. Therefore a direct comparison between the values of both sets of constants is difficult, and, for a certain pH (corrected to the proper scale) and alkalinity, each set of constants will not give the same calculated concentrations of the carbonate species. A redetermination therefore seemed to be desirable.

Dyrssen and Sillén suggested [10] that the dissociation constants of carbonic acid should be determined with the activity of all the species defined in the same activity scale. The logical choice is then to define the activity scale for $X = H^+$, OH^-, $H_2CO_3 + CO_2$, HCO_3^-, and CO_3^{2-} so that the activity coefficient $f_X = \{X\}/[X]$ approaches unity as [X] approaches zero in sea water of a given salinity. This means that the activity of H_2O at each salinity is unity and that every salt solution is treated as an independent solvent. However, for most oceanographic measurements of the carbonate system the salinity will be in the range of 35 ‰, and the corrections for the salinity will then be quite small. The choice of activity scale is further elucidated in Ref. 11.

This article describes the fairly elaborate technique that was used to produce a new set of dissociation constants of carbonic acid together with values of the ionic product of water. These constants are both thermodynamically well defined and applicable without corrections to practical analytical work. The technique can be used for the determination of acidity constants in media that differ considerably from dilute aqueous solutions, *e.g.* body fluids and mixed electrolyte-organic solutions.

SYMBOLS AND UNITS

The concentration unit used in the present work is M_w = mol per kg solution, a temperature and pressure independent concentration unit suggested by Dyrssen and Sillén.[10] The concentrations of solutions added from burets are, however, given in M = mol per litre of solution. Emf values are given in millivolts. H_2CO_3 *denotes the sum of hydrated and unhydrated carbon dioxide in solution.*

LETAGROP stands for "finding the pit", a computer program used for the calculation of the titration data (see below).

Notations used in the text are listed below.

B	total concentration of $B = H_2CO_3$ given in the input to LETAGROP.
B_0	B in the starting solutions.
B_{tot}	total concentration of B adjusted for systematic error by $B_{tot} = f_B B$.
f_B	adjustable parameter in LETAGROP defined by $B_{tot} = f_B B$.
b	free concentration of B, $b = [H_2CO_3]$.
C_{HX}	concentration of monobasic weak acid HX given in the input to LETAGROP.
E	measured emf.
E_0	a constant in $E = E_0 + (RT \ln 10/F) \log h + E_j$.
E_j	liquid junction potential.
H_{calc}	excess concentration of H^+ over H_2O and H_2CO_3 calculated by eqn. (10).
H_{tot}	excess analytical concentration of H^+ over H_2O and H_2CO_3.
H_0	H_{tot} in the starting solutions.
H_T	excess analytical concentration of H^+ over H_2O in buret solutions (= titre of hydrochloric acid, given in M).
δH_0	adjustable parameter in LETAGROP defined in eqn. (9).
h	free concentration of H^+, $h = [H^+]$.

K_{1C} first dissociation constant of carbonic acid, $K_{1C}=[H^+][HCO_3^-]/[H_2CO_3]$.
K_{2C} second dissociation constant of carbonic acid, $K_{2C}=[H^+][CO_3^{2-}]/[HCO_3^-]$.
K_{HX} acidity constant of monobasic weak acid HX given in the input to LETAGROP.
K_w ionic product of water, $K_w=[H^+][OH^-]$.
m_0 weight of starting solutions.
n_{CO_2} number of mol of carbon dioxide.
P_{CO_2} equilibrium partial pressure of carbon dioxide.
t_{HCl} titre of hydrochloric acid in buret solutions (in M).
t_{OH} titre of sodium hydroxide in buret solutions (in M).
T temperature in K.
v_e equivalence volume of buret solution (in ml).
V volume of equilibrium solutions.
v_T volume of buret solutions.
σ standard deviation of parameters as defined in Ref. 24 obtained in the output from LETAGROP.
$\sigma(H)$ standard deviation of H_{tot} as defined in Ref. 24 obtained in the output from LETAGROP.

CHOICE OF EXPERIMENTAL CONDITIONS

The experiments for determination of the dissociation constants of carbonic acid were carried out as potentiometric titrations. The total carbonate concentration (0.002 M_w) was held approximately constant during the titration and the total hydrogen concentration (analytical excess of H^+ over H_2O) was varied by adding hydrochloric acid from a buret. Since carbon dioxide can leave the solution at high total hydrogen concentrations the titrations were performed in a closed titration vessel filled to 99 – 99.5 % of its volume with equilibrium solution. Acid was added from a microburet, the total volume added being 0.2 % of the total volume of the titration vessel. With this arrangement the amount of carbon dioxide leaving the solution during a titration was very small and the total carbonate concentration was nearly constant. The effect of possible escape of carbon dioxide is treated below. Ionic strengths of the synthetic sea water media used varied in the range 0.4 M_w to 0.8 M_w (corresponding to salinities from 20 to 40 ‰) and titrations were performed at temperatures from 5 to 30°C. The cell used for measuring h is conveniently written as

RE | solution | GE

where GE denotes a glass electrode and RE a reference half cell; RE = ionic medium titrated saturated with AgCl|AgCl, Ag.

Emf of this cell can, in the log h-range studied, be written

$$E = E_0 + (RT \ln 10/F) \log h \quad (1)$$

where E_0 is a constant characteristic of the electrodes used. The validity of this equation will be discussed below. The initial value of $-\log h$ was 9 and

the final value was about 3, the excess acid being used to evaluate E_0 in eqn. (1).

EXPERIMENTAL

Chemicals and solutions. The *synthetic sea water media* were prepared (mainly following Sillén [12,13]) with compositions similar to the main composition of sea water of corresponding salinity. Compositions of "normal sea water" and synthetic sea-water used in this work are listed in Table 1. As seen from this table K^+ of "normal" sea water has been

Table 1. Main ionic composition [10] in mol per kg sea water of "normal" sea water distributed from I.A.P.S.O., Standard Sea Water Service, Charlottenlund Slot, Denmark, with chlorinity 19.374 ‰ corresponding to a salinity of 35.000 ‰ and the synthetic sea water medium of 35 ‰ salinity used in this work.

Cation	"Normal" sea water	Synthetic sea water	Anion	"Normal" sea water	Synthetic sea water
Na^+	468.04	478.0	Cl^-	545.88	550.0
Mg^{2+}	53.27	54.0	SO_4^{2-}	28.20	28.0
Ca^{2+}	10.33	10.0	Br^-	0.83	–
K^+	10.00	–	F^-	0.07	–
Sr^{2+}	0.10	–	HCO_3^-	2.40	–
Equivalent sum of cations	605.44	606.0	$B(OH)_3 + B(OH)_4^-$	0.43	–
			Equivalent sum of anions	605.62	606.0

replaced by Na^+. Furthermore, minor constituents like Sr^{2+}, Br^-, F^- and $B(OH)_3 + B(OH)_4^-$ have also been excluded. For the salinities 20, 25, 30, and 40 ‰ the listed concentrations were reduced by 4/7, 5/7 and 6/7 or increased by 8/7. The solutions were prepared from weighed amounts of dried NaCl, Na_2SO_4, and stock solutions of magnesium and calcium chlorides. Chloride concentrations in the stock solutions were checked by a chlorinity titration technique developed by Jagner and Årén.[14]

Carbonate was added to the ionic medium from a stock solution of sodium carbonate and hydrogen carbonate. In the starting equilibrium solution the total carbonate content was about 2.0 mM_w and the analytical excess hydrogen concentration over H_2O about 1.3 mM_w (corresponding to 1.3 mM_w HCO_3^- and 0.7 mM_w CO_3^{2-}). The carbonate was added very carefully to the ionic medium to avoid a sudden pH-change that may disturb the glass electrode function. The initial titration solution becomes supersaturated with regard to calcium carbonate. To avoid precipitation of calcium carbonate the addition of carbonate was carried out with vigorous stirring within 2 h before the titration started. The hydrochloric acid (Merck Titrisol ®) was 2 M and standardized against Tl_2CO_3 using the same microburet as that used in the carbonate titrations. All reagents were Merck *p.a.* grade and the water used to prepare the solutions was doubly distilled deionized water.

Purity of the medium. To estimate the amount of weak protolytic impurities present in the ionic media used a procedure was followed similar to the titration method described by Ciavatta.[15] A solution of 250 ml ionic medium containing about 0.125 mmol HCl was deaerated for 2 h with a CO_2-free nitrogen stream and transferred to the argon-filled titration vessel described under Apparatus. The solution was then titrated with 0.2 M NaOH and back-titrated with 0.2 M HCl. For each titration Gran [16] functions were plotted against v ml titrant. The intersections of these functions with the v-axis (Fig. 1 in Part I of Ref. 11) corresponded to an impurity of weak protolytes of 15 – 25 μmol per

kg solution. A full discussion of the medium purity is given in Ref. 11. One reason for careful investigation of the impurity concentration in the salt media is that in the LETAGROP calculation (see below) a better fit of experimental data from carbonate titrations was achieved when introducing $C_{HX} = 2.0 \times 10^{-5}$ M_w. With this parameter fixed in the calculations and the parameter K_{HX} varied the program came out with $K_{HX} \simeq 10^{-5}$ M_w for most titrations treated.

APPARATUS

The titration vessel is illustrated in Fig. 1. The volume of the reaction vessel (Quickfit FV 250) is 250 ml. The titration vessel was placed in a paraffin oil thermostat bath, which held temperatures between 5 and 30°C within 0.05°C.

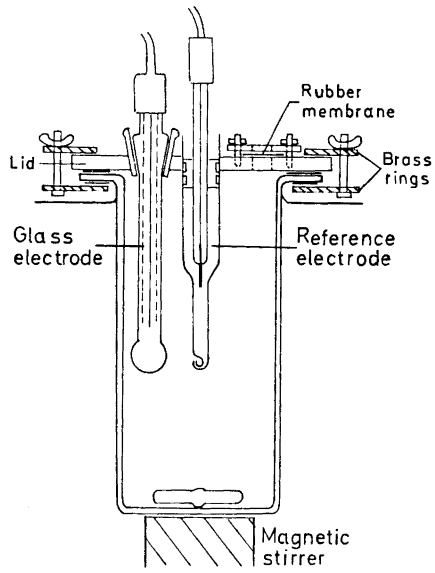

Fig. 1. Titration vessel.

The *buret* was an Agla syringe microburet of 0.5 ml capacity with a micrometer screw. It was mounted in a stand which permitted vertical motion. The buret tip was a platinum needle which was run through the flexible rubber membrane during titration. The tip was allowed to dip into the solution when adding reagent but was pulled out of the solution (but not the membrane) after each addition to avoid leakage of reagent from the tip during the emf measurements.

The *circuit for measuring the emf* of the glass-reference electrode cell used included a digital voltmeter (Solartron LM 1867) with 10 μV resolution and a voltage follower circuit connected to the input of the voltmeter. The follower circuit including a high quality operational amplifier (Philbrick SP2A) serves as a current amplifier (or impedance transformer) with a voltage amplification equal to 1.0000. This circuit allowed for rapid glass electrode measurements, which are impossible without a current amplifier because of the necessity of using the input RC-filter of this type of digital voltmeter.

EMF MEASUREMENTS

A more detailed diagram of the cell used is

IR	Inner ref. soln.	Glass membrane	Test soln.	Outer ref. soln.	OR
E_1	E_2	E_3	$E_4 = E_j$	E_5	

IR and OR denotes the solid phases of the two reference half cells, which in the experiments were

IR = Ag,AgCl(s) or IR = Tl(Hg),TlCl(s) (Thalamid ®)
OR = Ag,AgCl(s)

The measured emf, E, is the algebraic sum of the potential differences $E_1 - E_5$ existing at the phase boundaries in the cell, and we assume the equation

$$E = E_0 + (RT \ln 10/F) \log h + E_j \quad (2)$$

to be valid. For precise measurements of h with the cell three conditions must be fulfilled: (a) E_1, E_2, and E_5 must remain constant during the experiment, (b) for E_3 the equation

$$E_3 = \text{const} + (RT \ln 10/F) \log h \quad (3)$$

must be valid, (c) the liquid junction potential E_j must be known. E_0 is the sum of E_1, E_2, E_5, and the constant term of the equation for E_3. In a well designed cell one can normally trust the constancy of E_0. E_j can, except in very acid or alkaline solutions, be neglected if the test and reference cell solutions as here are based on the same ionic medium.[17] The dependence of E_3 on log h, *i.e.* the validity of eqn. (3), must be tested for each glass electrode if precise values of h are to be measured.

The *saltbridge* designed for this investigation is illustrated in Fig. 1. The upper part is an internally drilled glass tube with 13.0 mm inner diameter. Teflon flanges glued to the Ag,AgCl-electrode glass stem fit into this tube. The end of the lower part is J-shaped and forms the liquid junction. This junction may be renewed by pressing the stem with the flanges down. The Ag,AgCl-electrodes used in the reference electrodes were prepared according to Brown.[18]

Glass electrodes for use in the equilibrium titrations were checked for "Nernstian behaviour" according to eqn. (3) and long term stability. A test procedure with the hydrogen electrode as described by Olin [19] was adopted. The hydrogen electrodes were prepared according to Bates.[20] The extensive work in selecting good glass electrodes is fully described in Ref. 11. For the electrodes finally chosen (Jena type U, Schott & Genossen, Mainz, W. Germany) it was found that the emf against the hydrogen electrode was constant to within ± 0.1 mV in the range $-2.1 < \log h < 8.5$ and the sodium error was about 0.3 mV (0.005 log h-units) for log $h = -9.0$ at 25°C increasing slightly at lower temperatures.

It is important that log h is not changed more than about 0.3 units on each addition of strong acid or base in the test procedure, as for large rapid changes in log h there is a risk that the electrode function is disturbed. In spite of the capriciousness of the glass electrodes it would appear that more difficulties would be encountered in using a hydrogen electrode that removes carbon dioxide continuously. Buch,[7,8] using the hydrogen electrode, tried to cancel this effect with a system of wash bottles, whereas Lyman [9] used the glass electrode.

Precise potentiometric measurements with cells involving high resistance glass electrodes in solution chemistry work have not been reported in literature until recently.[21] The time-consuming check procedures for testing of long term stability and Nernstian behaviour, often with disappointing results and rejection of several electrodes, may explain the preference of the hydrogen electrode over the glass electrode although the latter has several advantages. The increased use of computer processed measuring systems in many laboratories making these check procedures more convenient may change this attitude.

TITRATIONS FOR DETERMINATION OF K_w

The experiments for purity control of ionic media could be designed for the determination of K_w, the ionic product of water, in the medium investigated. Such experiments were performed as three successive potentiometric titrations in an initially deaerated "pure" ionic medium solution in a closed titration vessel:

(1) Titration with 0.2 M HCl to $h \approx 2 \times 10^{-4}$ M_w.
(2) Titration with 0.2 M NaOH to $[OH^-] \approx 2 \times 10^{-4}$ M_w.
(3) Backtitration with 0.2 M HCl to $h \approx 2 \times 10^{-4}$ M_w.

The equivalence points were evaluated with Gran [16] diagrams; in all, five equivalence points were determined in each experiment (three with excess H^+, two with excess OH^-). The following equations are then used for the calculation of E_0 and pK_w.

$$E = E_0 + (RT \ln 10/F) \log h = E_0 + (RT \ln 10/F) \log K_w - (RT \ln 10/F) \log [OH^-] \quad (4)$$

In the regions with excess of H^+

$$[H^+] = h = (v_T - v_e) t_{HCl}/(m_0 + v_T) \quad (5)$$

In regions with excess of OH^-

$$[OH^-] = (v_T - v_e) t_{OH}/(m_0 + v_T) \quad (6)$$

The concentration of OH^- cannot be raised to more than about 2×10^{-4} M_w in a sea water medium because of the low solubility of $Mg(OH)_2$. Furthermore the sodium error of the glass electrode makes it unsuitable for measurements at higher OH^--concentrations. These pK_w-determinations were performed to obtain chemically reasonable values for K_w to be used in the LETAGROP computer program as will be discussed in the next section. The choice of value of the parameter C_{HX} in LETAGROP is also based on values obtained in these experiments.

Values of K_w were determined for 35 ‰ synthetic sea water of six temperatures from 5 to 30°C and at five salinities from 20 to 40 ‰ at 25°C. Ex-

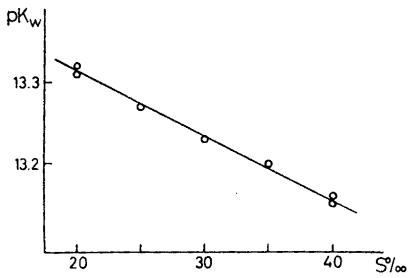

Fig. 2a. Plot of experimental values of pKw at 25°C against salinity.

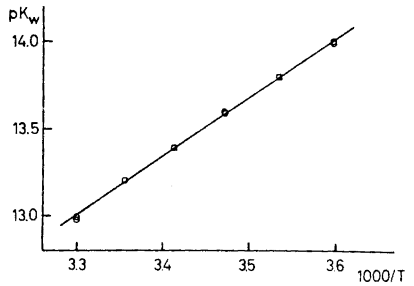

Fig. 2b. Plot of experimental values of pK_w at 35 ‰ salinity against $1/T$.

perimental values of pK_w are plotted in Figs. 2a and 2b. Details of the calculation of pK_w as well as tables with experimental and interpolated values of pK_w are given in Ref. 11.

CALCULATIONS AND RESULTS

For each titration 30–40 (v_T, E)-values ("titration points") were collected in the log h range $-9 < \log h < -3$. These primary data were processed with an IBM 360/65 computer using the generalized least squares program LETAGROP written by Sillén *et al.* in the recent Fortran-version ETITR.[22,23] With known experimental parameters and a certain model chosen for the chemical system investigated by potentiometric titrations this program finds "best" values of the stability constants for the most reasonable species in this system. The program can also be used to adjust and refine experimental parameters like E_0 and the total concentrations of the chemical system studied.[23]

In this case the species formed between carbonate ions and protons are quite well established, and a fixed model can therefore be used. This increases the possibility of refining both the stability constants and some experimental parameters.

Titrations were performed so that H_0, B_0, and E_0 could be refined with a LETAGROP treatment. Therefore these parameters only had to be approximately known for each experiment (in principle the treatment constitutes an analytical determination of alkalinity, total carbonate, and pH of the initial solution). Thus it was not necessary to prepare equilibrium solutions from deaerated carbon dioxide free ionic medium solutions since carbon dioxide is one of the components of the chemical system studied. Approximate values of H_0, B_0, and E_0 for each experiment were determined using a Gran method designed for determination of alkalinity and total carbonate by Dyrssen and Sillén.[10]

The final LETAGROP calculation for each titration was carried out assuming no other species present in the solutions than H^+, OH^-, CO_3^{2-}, HCO_3^-, and H_2CO_3. This may be justified as long as the free concentrations of sulphate, magnesium, and calcium ions remain constant in the solution titrated and no carbon dioxide leaves the solution. The experimental conditions are so chosen that these conditions are very closely fulfilled. H^+ and H_2CO_3 have been chosen as components which may seem strange at first. H_2CO_3 is, however, a predominating species over a large range of the titration whereas CO_3^{2-} is not predominating in any region of the titration. The equilibria and stability constants can be written with the notations $[H^+] = h$, and $[H_2CO_3] = b$

$$H_2CO_3 - H^+ \rightleftharpoons HCO_3^- \qquad \beta_{-11} = [HCO_3^-]/h^{-1}b \tag{7}$$

$$H_2CO_3 - 2H^+ \rightleftharpoons CO_3^{2-} \qquad \beta_{-21} = [CO_3^{2-}]/h^{-2}b \tag{8}$$

The relations between the dissociation constants of carbonic acid and these constants are

$$pK_{1C} = -\log \beta_{-11} \text{ and } pK_{2C} = \log \beta_{-11} - \log \beta_{-21}$$

The equations used by the program in these calculations are eqn. (1) and

$$H_{tot} = v_T H_T/(m_0 + v_T) + m_0(H_0 + \delta H_0)/(m_0 + v_T) \quad (9)$$

$$H_{calc} = h - K_w h^{-1} - \beta_{-11} h^{-1} b - 2\beta_{-21} h^{-2} b - \\ - K_{HX} C_{HX} m_0/[(m_0 + v_T)(K_{HX} + h)] \quad (10)$$

$$B_{tot} = f_B B = b + \beta_{-11} h^{-1} b + \beta_{-21} h^{-2} b \quad (11)$$

Each titration was treated separately and the error squares sum $U = \sum(H_{calc} - H_{tot})^2$ was minimized. The equilibrium constants K_{HX}, β_{-11}, and β_{-21} were adjusted in the calculations and K_w was held constant. The adjustable parameters are E_0, δH_0, f_B, and C_{HX}; however, C_{HX} (see purity of medium above) was not adjusted during the calculation.

Changes in the liquid junction potential have been neglected because of the low values of h and $[OH^-]$ in the titrations. The ionic product of water, K_w, was independently determined as described above.

The values of log β_{-11}, log β_{-21}, and pK_{2c} with their standard deviations (given as 3σ) and the standard deviation in H, σ(H), defined as in Ref. 24, are given in Ref. 11. Experimental data and some calculated values for a representative titration are listed in Table 2. In this example and for most

Table 2. Experimental data (computer output from LETAGROP) for a titration at 20°C and 35 ‰ salinity. For each titration point are given V_T = the volume of buret solution with $H_T = 1.990$ M added to 248.1 g solution, E = measured emf in millivolts, H_{tot} as calculated from eqn. (9) in mM_w, log h calculated from eqn. (1), $Z = (H_{tot} - h + [OH^-])/B_{tot}$ and $\Delta Z = 10^3(H_{calc} - H_{tot})/B_{tot}$. H_{calc} and B_{tot} are calculated from eqns. (10) and (11).

V_T	E	H_{tot}	log h	Z	ΔZ
0.000	−954.50	−2.61	−8.716	−1.347	−0.12
0.016	−946.83	−2.49	−8.584	−1.281	0.26
0.032	−937.99	−2.36	−8.432	−1.215	−0.31
0.048	−926.71	−2.23	−8.238	−1.148	−0.08
0.060	−915.34	−2.13	−8.043	−1.099	0.09
0.068	−905.28	−2.07	−7.870	−1.066	0.11
0.076	−892.05	−2.00	−7.642	−1.033	0.48
0.084	−876.72	−1.94	−7.379	−1.000	0.20
0.092	−862.52	−1.88	−7.135	−0.967	0.27
0.104	−846.90	−1.78	−6.866	−0.917	0.33
0.116	−835.98	−1.68	−6.678	−0.868	−0.39
0.128	−827.43	−1.59	−6.531	−0.818	−0.94
0.144	−817.98	−1.46	−6.369	−0.752	−0.56
0.164	−808.17	−1.30	−6.200	−0.670	−0.94
0.188	−797.53	−1.11	−6.017	−0.571	0.82
0.212	−787.57	−0.91	−5.846	−0.472	0.94
0.232	−779.14	−0.75	−5.701	−0.389	0.47
0.248	−771.92	−0.62	−5.577	−0.323	0.09
0.264	−763.85	−0.50	−5.438	−0.258	−0.05
0.276	−756.93	−0.40	−5.319	−0.209	−0.38
0.288	−748.67	−0.30	−5.177	−0.160	−0.28
0.300	−738.20	−0.21	−4.997	−0.112	−0.03
0.308	−729.24	−0.14	−4.843	−0.082	−0.22
0.316	−717.41	−0.08	−4.640	−0.053	−0.02
0.324	−701.96	−0.02	−4.374	−0.030	0.34

Table 2. Continued.

0.332	−685.99	0.05	−4.100	−0.016	0.09
0.344	−668.28	0.14	−3.795	−0.008	0.14
0.356	−657.04	0.24	−3.602	−0.005	−0.25
0.368	−649.03	0.34	−3.464	−0.003	−0.30
0.380	−642.84	0.43	−3.358	−0.003	0.13
0.392	−637.91	0.53	−3.273	−0.002	−0.14
0.408	−632.48	0.66	−3.180	−0.002	0.23

$U=\sum(H_{calc}-H_{tot})^2=2.00\times10^{-5}$ mM^2.
$\sigma(H)=0.00088$ mM.
"Best values" calculated: $K_{HX}=(6.8\pm1.4)\times10^6$, $\beta_{-11}=(1.222\pm0.003)\times10^{-6}$, $\beta_{-21}=(1.142\pm0.007)\times10^{-15}$.
$H_0=-2.615$ mM_w, $B_0=1.941$ mM_w, $E_0=(-447.54\pm0.03)$ mV.
Values of $K_w=4.1\times10^{-14}$ and $C_{HX}=0.02$ mM_w were not adjusted.

titrations a random scattering of numerically small values around zero was found for the quantity $(H_{calc}-H_{tot})/B_{tot}$, which is the "error" in H_{tot} divided by B_{tot} in each titration point. The low values of this quantity and thereby of $\sigma(H)$ in each titration indicates good internal precision in each titration. Double determinations for each salinity and temperature generally gave values for each constant differing in the order of 3σ for each constant.

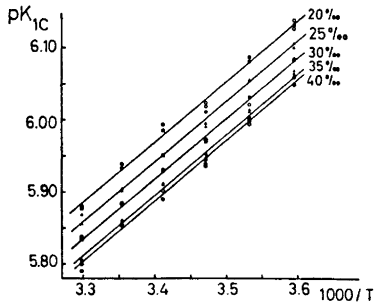

Fig. 3a. Plot of experimental values of pK_{1C} at various salinities against $1/T$. The fitting of the lines is described in Ref. 11.

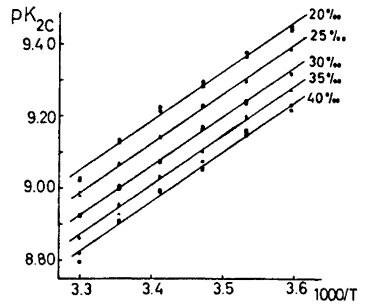

Fig. 3b. Plot of experimental values of pK_{2C} at various salinities against $1/T$. The fitting of the lines is described in Ref. 11.

In Figs. 3a and 3b values of pK_{1C} and pK_{2C} are plotted against $1/T$. In Figs. 4a and 4b the values are plotted against salinity. The fitting of the lines in Figs. 3 and 4 is described in Ref. 11 where also tables of interpolated values are given.

The accuracy of the equilibrium constants may be lower than the precision in each determination. Errors in the emf measurements and consequently in $\log h$ are likely to be very small and errors caused by drift are relatively easy to detect with the high resolution of the emf measuring circuit used in this work. Errors in H_{tot} are not as easy to detect during experiments. Two sources of error will be indicated. Small volumes of hydrochloric acid may by capillary

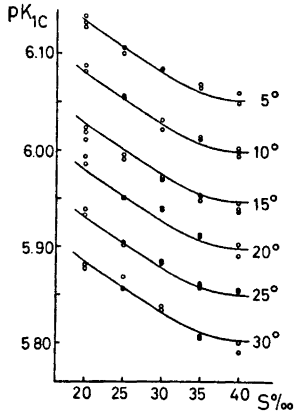

Fig. 4a. Plot of experimental values of pK_{1C} at various temperatures against salinity. Curves correspond to values obtained from the lines in Fig. 3a.

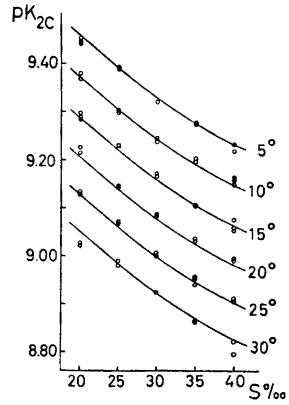

Fig. 4b. Plot of experimental values of pK_{2C} at various temperatures against salinity. Curves correspond to values obtained from the lines in Fig. 3b.

forces have leaked out of the microburet syringe. Since additions are almost equal and performed with equal time intervals this leaking may give an error corresponding to a too low value of H_T, the titre of the hydrochloric acid used. The values of pK_{1C} and pK_{2C} computed may have decreased by $0.002-0.005$ log units as a consequence of this error in H_T. The presence of a small gas volume in contact with the solution may introduce an error in H_{tot}, discussed in the next section, since some carbon dioxide (equal to H_2CO_3 in the calculations) may leave the solution into the gas phase.

Note on the use of HALTAFALL and LETAGROP for estimation of the effect of systematic errors. The computer program HALTAFALL [25,26] calculates free concentrations of all species assumed in a certain model of a chemical system when total concentrations of the components and stability constants are given as data input to the program. Thus it can be used to simulate titration curves by increase or decrease of total concentrations in each new titration point. In this work titration curves corresponding to experimental carbonate titrations were simulated using the total concentrations used in the experiments and suitable constants. Values of log h for each titration point were transformed to emf-values E according to eqn. (1) with certain values chosen for E_0 and T. The (v_T, E) values obtained for a simulated titration curve may now be treated with LETAGROP to find best values of pK_{1C} and pK_{2C}. The effect of a small change in some experimental condition on the values of pK_{1C} and pK_{2C} found in a LETAGROP treatment of experimental data can be estimated as follows. Input data to a HALTAFALL calculation are given so that they correspond to the actual change in experimental parameters. The (v_T, E) values obtained in this HALTAFALL calculation are subsequently treated in LETAGROP to obtain "best" values of pK_{1C} and pK_{2C}. The procedure will be exemplified in three examples where a simulated curve including some "error" is compared to an "error-free" curve, referred to as the original titration.

Example 1. An acid impurity HX with $[HX]_{tot} = 2 \times 10^{-5}$ M and $K_{HX} = 1.0 \times 10^{-5}$ is added to the original input to HALTAFALL. In the subsequent LETAGROP treatment no acid impurity is assumed. The "best" fit gives a pK_1-value 0.009 log units lower and an unchanged pK_2-value as compared to the original titration. The value of B_0 is also changed. When $C_{HX} = 2 \times 10^{-5}$ M was given in the input data to LETAGROP the original values of pK_{1C}, pK_{2C}, and B_0 were obtained and K_{HX} came out with the value 1.02×10^{-5}. The values are of course dependent on the choice of range of H_{tot} and the number of points, but in this case a H_{tot}-range and number of points corresponding to experimental titrations were used.

Example 2. There is a "drift" in E_0, constantly decreasing during the titration, to a value 0.3 mV lower than the original value. From each E-value in the original titration numbers were subtracted corresponding to the "drift". LETAGROP treatment shows very slight differences in calculated values of pK_{1C} and pK_{2C}. The values were lower than the original by 0.001 and 0.003 log units, while the value for E_0 was 0.15 mV lower than the original. Although the shifts in E_0 for the last points of the titration as compared to the original are about 0.30 mV, the value of 3σ for E_0 calculated in LETAGROP is only 0.04 mV, a somewhat optimistic value. The value of $\sigma(H)$ for this treatment was, however, considerably increased.

Example 3. In this case the assumption was made that carbon dioxide leaves the solution of 250 ml to a 2 ml gas volume, a reasonable approximation of an experimental titration. Equilibrium for distribution of carbon dioxide between solution and gas phase is assumed. The relations $[CO_2]_{aq}/P_{CO_2} = 0.03$ M_w/atm [27] and $P_{CO_2}V = n_{CO_2}RT$ are used to calculate the amount of carbon dioxide present in the gas phase assuming constant total pressure for every titration point. This amount, expressed as $[CO_2]_{aq}$ in the 250 ml solution, is subtracted from B_{tot} and twice this value from H_{tot} in each titration point where carbon dioxide (H_2CO_3 in the calculations) is present. The treatment implies some simplification but is rather reasonable. When the simulated curve, obtained by HALTAFALL, is treated with LETAGROP the "best" fit gives a pK_1-value 0.005 log units higher and an unchanged pK_2-value as compared with the original titration.

This method for estimating the quantitative effect of certain changes in experimental conditions on calculated equilibrium constants is relatively convenient and may save some time when designing experiments for equilibrium studies of chemical systems in solutions. The versatility of HALTAFALL-calculations when designing methods for quantitative analysis in solutions has been demonstrated by Jagner [28] and for testing reasonable models of chemical systems by Wahlberg.[29]

DISCUSSION

A direct comparison of the present set of constants with those of Buch [6–8] and Lyman [9] is difficult since different activity scales are used. The differences are discussed elsewhere.[30] For the precise determination of the carbonate species in a sample of sea water from pH and some other measurable parameter (*e.g.* total alkalinity or carbon dioxide pressure) it is necessary to measure pH

on a pH-scale that is consistent with the activity scale used in the determination of the present set of constants. In a separate work [31] it is shown how pH values on such a scale can be assigned to buffer solutions containing "tris" (2-amino-2-hydroxymethylpropane-1,3-diol) in synthetic sea water. It is also shown that errors due to liquid junction potentials can be kept quite small if such buffer solutions are used in the pH determination of a sea water sample. Differences in the values of the dissociation constants of carbonic acid determined in synthetic sea water and in sodium chloride media of corresponding ionic strengths are treated elsewhere.[32]

Acknowledgements. This problem was suggested by Professor David Dyrssen in cooperation with the late Professor Lars Gunnar Sillén. The author thanks Professor David Dyrssen for valuable discussions and support during the work. I am indebted to the late Professor Lars Gunnar Sillén and Dr. Björn Warnqvist for help to start the LETAGROP calculations and Mr. Ove Lindgren, fil.lic., for adapting the program to the IBM 360/65 computer in Göteborg. Part of the experimental work has been carried out by Mrs. Agneta Edlund, fil.kand. This help is gratefully acknowledged. Thanks are also due to Dr. Louis Henderson who revised the English text of this article.

The work on the chemistry of sea water is supported by the *Swedish Natural Science Research Council*. Free computer time has been available by grants from *Chalmers Technical University*.

REFERENCES

1. Takahashi, T., Weiss, R. F., Culberson, C. H., Edmond, J. M., Hammond, D. E., Wong, C. S., Li, Y. and Bainbridge, A. E. *J. Geophys. Res.* **75** (1970) 7648.
2. Edmond, J. M. *Deep-Sea Res.* **17** (1970) 737.
3. Wong, C. S. *Deep-Sea Res.* **17** (1970) 9.
4. Pytkowicz, R. M., Kester, D. R. and Burgener, B. C. *Limnol. Oceanog.* **11** (1966) 417.
5. Park, K. P. *Limnol. Oceanog.* **14** (1969) 179.
6. Buch, K., Harvey, H. W., Wattenberg, H. and Gripenberg, S. *Rapp. Cons. Explor. Mer* **79** (1932).
7. Buch, K. *Kolsyrejämvikten i Baltiska havet*, Fennia **68** (1945) No. 5.
8. Buch, K. *Havsforskningsinstitutets Skrifter*, Helsingfors 1951, No. 151.
9. Lyman, J. *Buffer Mechanism of Sea Water, Ph.D. Thesis*, University of California, Los Angeles 1957.
10. Dyrssen, D. and Sillén, L. G. *Tellus* **19** (1967) 113.
11. Hansson, I. *An Analytical Approach to the Carbonate System in Sea Water, Thesis*, Göteborg 1972.
12. Sillén, L. G. In *Equilibrium Concepts in Natural Water System. Advan. Chem. Ser.* **67** (1967).
13. Sillén, L. G. *Lecture manuscript*, University of California, Los Angeles, La Jolla 1966.
14. Jagner, D. and Årén, K. *Anal. Chim. Acta* **52** (1970) 491.
15. Ciavatta, L. *Arkiv Kemi* **20** (1963) 417.
16. Gran, G. *Analyst* **77** (1952) 661.
17. Biedermann, G. and Sillén, L. G. *Arkiv Kemi* **5** (1952) 425.
18. Brown, A. S. *J. Am. Chem. Soc.* **56** (1934) 56.
19. Olin, Å. *Acta Chem. Scand.* **14** (1960) 126.
20. Bates, R. G. *Determination of pH*, Wiley, New York 1964.
21. Henry, R. P., Prue, J. E., Rossotti, F. J. C. and Whewell, R. J. *Chem. Commun.* **1971** 868.
22. Sillén, L. G. and Warnqvist, B. *Arkiv Kemi* **31** (1969) 315.
23. Brauner, P., Sillén, L. G. and Whiteker, R. *Arkiv Kemi* **31** (1969) 365.
24. Sillén, L. G. *Acta Chem. Scand.* **16** (1963) 159.
25. Ingri, N., Kakolowicz, W., Sillén, L. G. and Warnqvist, B. *Talanta* **14** (1967) 1261.
26. Dyrssen, D., Jagner, D. and Wengelin, F. *Computer Calculations of Ionic Equilibria and Titration Procedures*, Almqvist & Wiksell, Stockholm 1968.

27. Harned, H. S. and Davis, R. *J. Am. Chem. Soc.* **65** (1943) 2030.
28. Jagner, D. *A Computer Treatment of Theoretical and Practical Aspects of Titration Procedures, Thesis*, Göteborg 1971.
29. Wahlberg, O. *Studies on Equilibria of Vitamin C in Aqueous Solution, Thesis*, Stockholm 1971. Chem. Comn. No. III, Univ. Stockholm 1971.
30. Hansson, I. *Deep-Sea Res. In press.*
31. Hansson, I. *Deep-Sea Res. In press.*
32. Dyrssen, D. and Hansson, I. *Mar. Chem. In press.*

Received September 21, 1972.

ACTA CHEMICA SCANDINAVICA 27 (1973) 945–969

Crystal Structure of Some Benzoxazoline Derivatives

P. GROTH

Department of Chemistry, University of Oslo, Oslo 3, Norway

The compounds investigated (six in all) are of the type with X = S, O, benzylimino, and Y = H, CH_3: (I) 3-methyl-benzoxazoline-2-

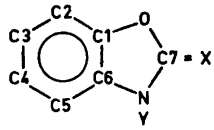

thione; (II) benzoxazoline-2-thione; (III) 3-methyl-benzoxazoline-2-one; (IV) benzoxazoline-2-one; (V) 2-benzylimino-3-methyl-benzoxazoline; and (VI) 2-benzylimino-benzoxazoline. Neither methylation nor substitution of S with O changes the geometry significantly for (I) – (IV). For the methylated compound (V) there are very small changes also on substitution with $N-CH_2-C_6H_5$. The molecules of (VI) form dimers with N···H···N bonds of length 2.933 Å. Some averaged bond distances and angles for (I) – (V) with corresponding values for (VI) in parentheses are: O – C7: 1.383(1.375) Å; N – C7: 1.349(1.310) Å; C1 – O – C7: 107.4(104.0)°; O – C7 – N: 107.8(114.2)°; C7 – N – C1: 109.9(105.1)°. The differences are probably related to the hydrogen bond formation.

The interactions of benzoxazolone, benzoxazolethione, and their derivatives with fatty, aromatic, and alkylaromatic amines have been studied by Simov *et al.*[1–4] The main features are: (1) the heteroatomic ring is opened and asymmetric di- or tri-substituted ureas or thioureas are obtained; (2) the products are derivatives of 2-aminobenzoxazole;[5] and (3) substitution of H in NH by CH_3 reduces the interaction rate in the case of benzoxazolone, while it has the opposite effect for benzoxazolethione.

Infrared stretching frequencies of C = N in iminobenzoxazolines have been determined to lie in the interval 1717 – 1745 cm^{-1}.[6] This is considerably higher than reported values (1670 – 1690 cm^{-1}) for azomethine groups in non-conjugated positions to conjugated systems.[7,8]

Hoping to elucidate these and some other characteristics, X-ray crystal structure analyses of the following benzoxazoline derivatives have been carried out:

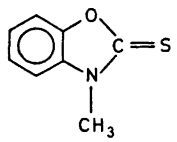
(I)

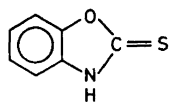
(II)

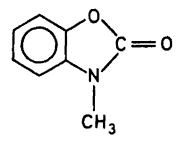
(III)

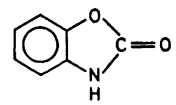
(IV)

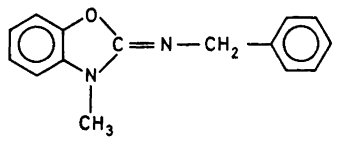
(V)

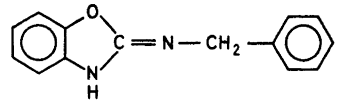
(VI)

(I) 3-methyl-benzoxazoline-2-thione, (II) benzoxazoline-2-thione, (III) 3-methyl-benzoxazoline-2-one, (IV) benzoxazoline-2-one, (V) 2-benzylimino-3-methyl-benzoxazoline, and (VI) 2-benzylimino-benzoxazoline. The crystal structure determination of (I) (based on film data) has been presented earlier.[9] For comparison some results will be included in this paper.

For the compounds (II) – (VI) the intensities have been measured on an automatic four circle diffractometer with a highly orientated graphite crystal monochromator. The radiation used was Mo$K\alpha$ and $2\theta_{max}$ ranged from 45° to 50°. No corrections for absorption or secondary extinction effects were carried out.

The phase problems for (III) – (VI) were solved by direct methods [10]* while the solution for (II) was obtained from the Patterson function. All structures have been refined by full-matrix least squares technique with weights calculated from the standard deviations in intensities, $\sigma(I)$, taken as

$$\sigma(I) = [C_T + (0.02C_N)^2]^{\frac{1}{2}}$$

where C_T is the total number of counts and C_N the net count (peak minus background). Anisotropic temperature factors were introduced for all non-hydrogen atoms, the expression for the vibration being:

$$\exp - (B_{11}h^2 + B_{22}k^2 + B_{33}l^2 + B_{12}hk + B_{13}hl + B_{23}kl)$$

Crystal data and final R-values are given in Table 1. Methyl hydrogens were localized in difference Fourier maps; other H-positions were calculated. Refinements of isotropic thermal parameters for hydrogens gave reasonable results for (II) and (IV) only. Final fractional coordinates and thermal parameters with estimated standard deviations are given in Tables 2 and 3. A comparison between observed and calculated structure factors is presented in Table 4.

The principal axes of the thermal vibration ellipsoids were calculated from the thermal parameters of Table 2.

* All programs used are included in this reference.

Table 1. Crystal data and final R-values.

Compound	Space group	Cell dimensions	Z	ϱ_{calc}	ϱ_{obs}	Observed reflections	R %	R_w %
I	$P2_1/c$	a = 9.24 Å b = 6.90 c = 12.86 β = 99.0°	4	1.35	1.34	674	7.7	11.3
II	$P2_1$	a = 8.573(3)Å b = 9.039(3) c = 4.353(2) β = 90.00 (3)°	2	1.49	1.49	545	3.2	3.7
III	$P2_1/c$	a = 5.716(1)Å b = 4.340(1) c = 29.506(4) β = 105.00 (1)°	4	1.40	1.37	912	3.3	3.8
IV	$P2_12_12_1$	a = 4.457(2)Å b = 6.654(3) c = 20.996(7)	4	1.44	1.43	506	2.7	3.0
V	$P2_1$	a = 14.267(5)Å b = 5.540(1) c = 8.946(3) β = 119.44 (3)°	2	1.28	1.25	957	5.1	5.5
VI	$P2_1/c$	a = 13.265(4)Å b = 7.556(3) c = 12.270(4) β = 111.96 (3)°	4	1.30	1.28	1016	3.8	4.6

Root mean square amplitudes, the corresponding B-values for the atomic anisotropic thermal vibration along the principal axes, as well as their components along the crystal axes are listed in Table 5.

By including all atoms in the molecules, the r.m.s. discrepancies between atomic anisotropic vibration tensor components calculated from the thermal parameters of Table 2, and those calculated from the rigid-body parameters obtained by analysis of librational, translational and screw motion [11] are:

(I)	(II)	(III)	(IV)	(V)	(VI)
0.0080	0.0031	0.0018	0.0021	0.0061	0.0051

The values for (III) and (IV) support the assumption of regarding these molecules as oscillating rigid bodies. However, the r.m.s. librational amplitudes are moderate:

(III) L1 = 5.4°, L2 = 3.7°, L3 = 3.4°
(IV) L1 = 6.0°, L2 = 4.8°, L3 = 3.7°

and no bond distance increased more than three times e.s.d. when corrected for libration. Uncorrected values for bond distances and angles are therefore presented in Table 6.

Table 2. Fractional atomic coordinates and anisotropic thermal vibration parameters with estimated standard deviations (multiplied by 10^5). For numbering of atoms, see Fig. 1.

Atom	x	y	z	B_{11}	B_{22}	B_{33}	B_{12}	B_{13}	B_{23}
					(II)				
S	−16237	50000	−08389	01583	01048	05966	−00081	−00292	−00731
	10		20	15	13	59	39	40	78
O	05887	38945	27322	01553	00663	05978	−00020	00586	−00054
	53	32	100	59	39	219	72	170	146
N	07392	63036	22841	01584	00690	05384	−00012	00596	00352
	65	45	122	70	50	249	91	205	171
C1	18584	43555	44423	01211	00879	04555	00061	01211	00025
	65	62	131	85	59	323	104	270	187
C2	28553	35168	61025	01641	01069	06811	00283	01043	00945
	77	73	152	99	73	364	153	310	269
C3	40512	42855	75835	01875	01564	05863	00666	01017	01427
	92	87	182	123	98	386	179	368	309
C4	41853	58117	73870	01309	01537	05866	−00031	−00121	00109
	87	85	175	86	87	359	146	294	291
C5	31454	66496	57007	01599	00986	06289	−00267	01136	−00372
	74	75	139	97	69	362	122	290	251
C6	19944	58849	41907	01412	00813	04438	00017	01202	−00001
	68	61	128	94	60	306	106	286	203
C7	−00869	51069	14042	01497	00832	04542	−00021	01479	−00262
	36	76	70	48	47	170	145	150	278
					(III)				
O1	23850	05901	43900	05114	09109	00216	−01027	00816	00204
	24	35	5	58	106	2	124	20	26
O2	16386	30043	36851	03374	07063	00197	−01196	00319	−00208
	19	29	4	40	85	2	97	16	22
N	51493	39313	41963	03251	06574	00156	00060	00325	−00310
	23	33	4	49	97	2	113	16	26
C1	29478	50369	34816	03236	05289	00170	00222	00345	−00355
	28	40	6	59	102	3	133	22	28
C2	22918	62688	30432	03876	06877	00183	00522	00137	−00337
	36	48	7	68	133	3	162	24	34
C3	39747	82174	29206	05089	06498	00182	01223	00531	−00108
	37	46	7	80	127	3	176	27	34

Table 2. Continued.

C4	61710	88316	32345	04609	06225	00212	−00302	00813	−00178
	37	46	7	80	126	4	161	29	25
C5	68101	75495	36789	03384	06530	00191	−00586	00427	−00498
	32	45	7	60	119	3	149	23	34
C6	51339	56207	37960	03103	05193	00158	00679	00375	−00420
	28	38	5	58	101	3	124	20	27
C7	30472	23409	41291	03767	06593	00178	00448	00522	−00302
	32	46	7	65	120	3	155	24	33
CM	70878	37979	46198	04272	09934	00168	00525	00281	−00309
	39	67	7	77	184	3	203	26	40
				(IV)					
O1	48036	38625	20099	08708	03794	00311	−03531	−00542	−00466
	36	30	10	116	57	6	144	39	30
O2	14726	31072	12387	05823	02158	00254	−00718	−00272	00108
	28	21	8	84	34	4	87	28	23
N	25352	07379	19347	05761	02560	00204	00964	−00282	00143
	39	31	10	103	49	5	121	38	28
C1	−01331	13934	10816	03983	02055	00215	00248	00120	−00007
	37	28	11	90	48	6	109	34	27
C2	−20513	11422	05757	04846	03192	00239	00247	−00250	00171
	49	47	12	111	74	6	156	44	40
C3	−33607	−07291	05194	04761	03868	00284	−01147	−00111	−00568
	50	49	15	121	88	8	169	48	46
C4	−27438	−22479	09440	05382	02672	00372	−01692	00579	−00618
	51	44	14	138	66	9	169	56	43
C5	−07933	−19796	14491	05683	02171	00310	00687	00684	00063
	47	37	14	122	57	8	141	49	41
C6	05126	−00998	15064	03841	02045	00214	00802	00260	−00032
	38	31	11	91	47	6	109	38	29
C7	31358	26487	17668	05564	02608	00215	−00526	−00104	−00151
	48	37	11	117	63	6	148	41	33
				(V)					
O	23120	71900	48112	00632	03690	01474	00836	00920	01137
	20		30	21	134	52	109	55	157
N1	19308	75930	19240	00591	04741	01551	00116	01091	−00459
	25	93	41	25	195	64	131	67	201
N2	12481	101778	32170	00522	04132	01380	00587	00868	00639
	24	106	38	25	171	63	132	65	194

Table 2. Continued.

C1	19998	85614	58089	00516	03443	01310	−00154	00919	−00151
	30	103	46	29	193	73	148	77	226
C2	22753	81456	74840	00582	04188	01405	−00125	00772	00077
	33	116	52	31	215	77	160	80	232
C3	18751	98070	82012	00763	05196	01390	−00329	01073	−00781
	35	124	57	37	266	82	196	91	280
C4	12318	116716	72510	00764	04223	01800	00017	01413	−01053
	37	120	56	35	225	91	173	94	262
C5	09464	120543	55327	00610	04449	01940	00132	01193	00283
	34	126	55	31	217	90	168	87	269
C6	13480	104029	48421	00437	03112	01342	−00049	00678	00276
	29	100	45	28	171	78	140	75	222
C7	18308	82921	31832	00453	03229	01419	00057	00701	00092
	30	99	47	30	192	74	145	78	215
C8	26260	55334	21394	00705	04533	01970	−00689	01349	−01334
	39	124	69	35	238	96	178	95	275
C9	36952	62633	22746	00562	03655	01192	00262	00811	00201
	31	101	48	32	199	71	138	82	209
C10	41465	48115	15573	00621	03548	01672	00196	00864	−00277
	33	116	51	32	210	84	162	84	234
C11	51445	54041	17245	00742	04918	02317	01096	01506	00603
	38	129	63	38	249	107	192	107	210
C12	56738	74331	25964	00624	05759	02176	00325	01216	00957
	40	132	62	38	283	105	201	111	328
C13	52195	89143	32704	00696	03780	01997	−00300	00796	−00369
	37	122	55	36	220	93	171	97	271
C14	42286	83354	31261	00704	04150	01631	−00035	00983	−01005
	36	109	56	35	220	83	174	92	247
CM	05663	116275	17160	00588	04291	01697	00538	00754	01873
	40	129	59	30	217	80	158	83	256
				(VI)					
O	80232	23283	51889	00641	01888	00714	−00478	00536	00284
	13	22	13	15	44	17	53	28	46
N1	98300	31827	60403	00632	01980	00544	−00139	00216	00541
	16	28	16	19	54	19	54	32	55
N2	87039	40006	41039	00654	01353	00743	−00272	00587	00151
	16	27	17	19	47	22	50	33	53
C1	71998	26057	40993	00559	01582	00663	−00251	00451	00049
	20	33	21	20	62	24	60	39	65

Table 2. Continued.

C2	61464	20388	37215	00670	02394	00975	−00638	00758	00019
	22	43	26	26	76	30	73	47	79
C3	54822	24949	25919	00552	02542	00909	−00092	00384	−00216
	23	42	24	22	85	30	70	45	86
C4	58865	35198	19011	00694	01961	00768	00453	00307	00072
	22	38	25	25	72	27	69	43	73
C5	69555	40994	23031	00663	01635	00721	00135	00446	00160
	21	36	22	23	63	27	65	43	65
C6	76126	36343	34354	00506	01343	00672	−00141	00443	−00251
	18	31	20	21	56	24	56	37	61
C7	88988	32220	51161	00656	01235	00707	−00202	00708	00147
	20	32	21	22	54	26	58	41	61
C8	98988	24026	71608	00705	01659	00700	−00145	00538	00349
	22	40	22	23	62	25	64	41	67
C9	110656	21027	79414	00656	01228	00671	−00131	00530	00251
	20	32	20	22	53	25	59	38	60
C10	114644	26424	91017	00812	01892	00659	−00046	00546	00164
	24	37	22	25	68	25	69	41	70
C11	125247	23244	98301	00952	02456	00685	−00318	00371	00214
	25	43	25	30	82	26	81	48	79
C12	132214	14545	94109	00739	02194	01003	00118	00240	00616
	25	42	27	26	81	33	74	48	81
C13	128414	09183	82581	00770	01949	01162	00432	00737	00170
	24	41	29	26	78	34	74	51	83
C14	117802	12269	75326	00868	01703	00754	−00071	00626	−00049
	23	37	25	28	68	27	69	46	70

The molecules (I), (II), (III), and (IV) are planar to within 0.02 Å. By excluding CM in (V), the parts of the molecules (V) and (VI) separated by the N1 – C8-bond are also planar to within 0.02 Å, with angles between the planes of 89° and 117°, respectively. CM is out of the plane through O, N1, N2, C1,..., C7 by 0.14 Å. (For numbering of atoms, see Fig. 1.)

In the reactions mentioned above the opening of the heteroatomic ring occurs at the C7 – O bond. As mentioned above, the interaction rate is larger for (I) than for (II). The C7 – O distance of (I) (1.393 Å) seems to be somewhat longer than that of (II) (1.369 Å). However, the standard deviations are large, and the difference is not significant. The opposite effect for benzoxazolone, (IV) reacting faster than (III), is not at all reflected in the C – O distances (1.379 Å for (III) and 1.368 Å for (IV)). The bonds are equal within error limits. For the iminobenzoxazolines, however, the C – O bond distance of the 2-

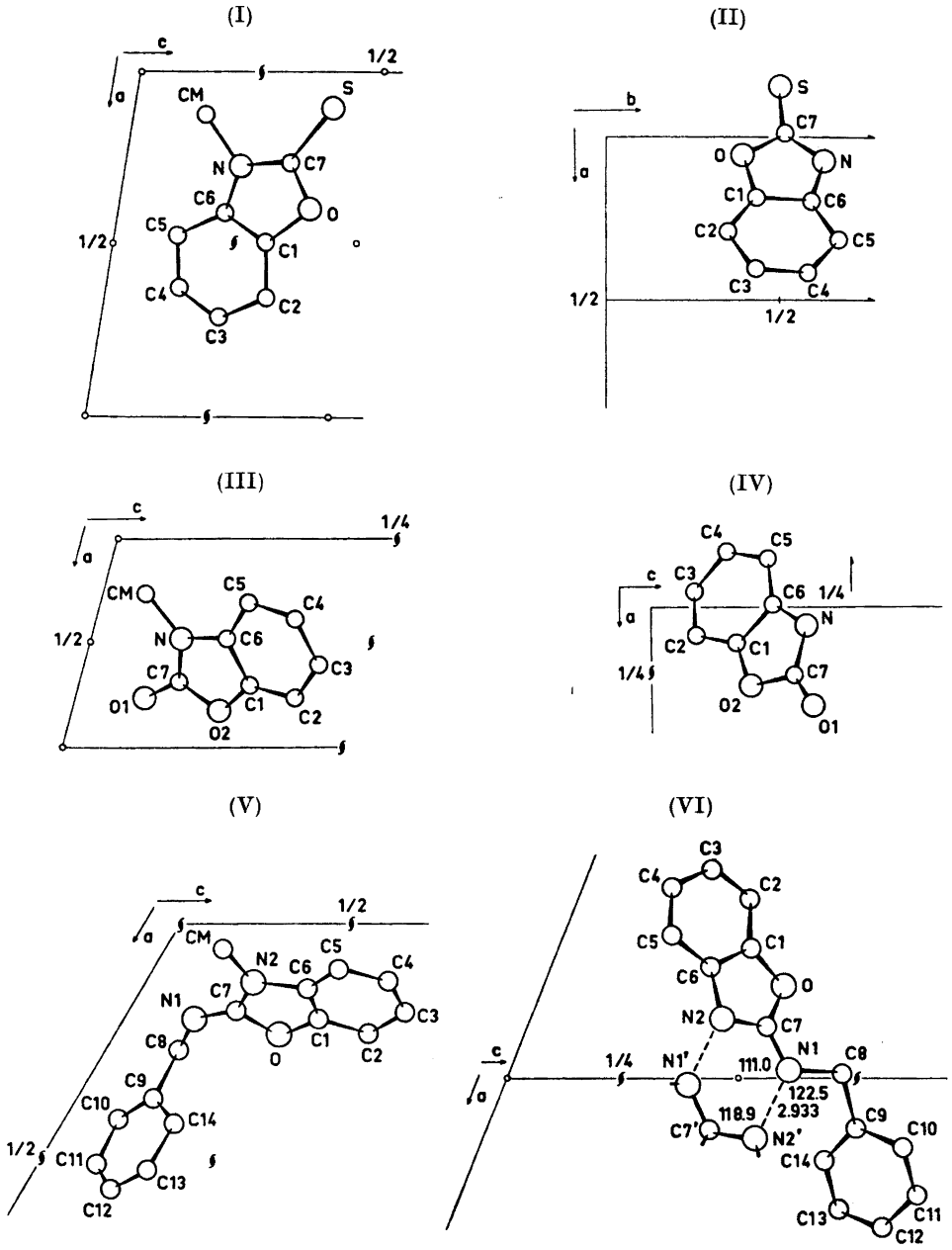

Fig. 1. (I) 3-Methyl-benzoxazoline-2-thione viewed along [010], (II) benzoxazoline-2-thione viewed along [001], (III) 3-methyl-benzoxazoline-2-one viewed along [010], (IV) benzoxazoline-2-one viewed along [010], (V) 2-benzylimino-3-methyl-benzoxazoline viewed along [010], and (VI) 2-benzylimino-benzoxazoline viewed along [010].

Table 3. Fractional atomic coordinates and isotropic thermal parameters, with estimated standard deviations, for hydrogen atoms. Hm and Hm,n are bonded to Cm, HM,n to CM and HN to N.

Atom	x	y	z	B(Å²)
		(II)		
HN	.0502	.7207	.1734	3.7
	47	54	91	1.0
H2	.2774	.2387	.6404	4.2
	50	61	99	1.0
H3	.4885	.3825	.9016	5.3
	65	67	120	1.4
H4	.5033	.6346	.8262	4.9
	70	62	131	1.4
H5	.3242	.7666	.5368	3.9
	50	65	102	1.1
		(III)		
H2	.0780	.5791	.2831	5.0
	33	40	6	
H3	.3657	.9193	.2603	5.0
	32	42	7	
H4	.7344	1.0100	.3136	5.0
	33	43	6	
H5	.8293	.7947	.3898	5.0
	34	41	6	
HM,1	.7347	.5759	.4765	5.0
	33	47	6	
HM,2	.8498	.3017	.4557	5.0
	35	44	6	
HM,3	.6671	.2370	.4851	5.0
	32	47	6	
		(IV)		
HN	.3331	.0064	.2227	4.3
	49	38	15	0.6
H2	−.2432	.2131	.0294	4.6
	52	42	14	0.7
H3	−.4630	−.0998	.0183	6.6
	60	53	19	0.6
H4	−.3686	−.3553	.0910	5.0
	52	41	14	0.5
H5	−.0317	−.3023	.1763	4.7
	45	44	14	0.6

Atom	x	y	z	B(Å²)
		(V)		
H2	.2770	.6748	.8147	5.0
	33	96	48	
H3	.2056	.9816	.9387	5.0
	32	95	53	
H4	.0958	1.2711	.7757	5.0
	34	89	50	
H5	.0495	1.3416	.4799	5.0
	32	95	49	
H8,1	.2244	.4322	.1203	5.0
	33	90	52	
H8,2	.2748	.4603	.3123	5.0
	33	92	54	
H10	.3693	.3024	.0870	5.0
	30	92	48	
H11	.5443	.4457	.1242	5.0
	34	97	49	
H12	.6335	.8028	.2654	5.0
	34	90	50	
H13	.5553	1.0399	.3914	5.0
	33	111	50	
H14	.3884	.9465	.3599	5.0
	31	90	48	
HM,1	−.0109	1.1577	.1441	5.0
	37	96	51	
HM,2	.0815	1.1345	.0888	5.0
	32	80	52	
HM,3	.0671	1.3293	.2177	5.0
	35	97	51	
		(VI)		
HN2	.9181	.5187	.4097	5.0
	18	36	20	
H2	.5875	.1424	.4193	5.0
	20	35	22	
H3	.4706	.2128	.2247	5.0
	22	35	22	

Table 3. Continued.

Atom	x	y	z	B(Å²)	Atom	x	y	z	B(Å²)
H4	.5376	.3774	.1078	5.0	H11	1.2775	.2711	1.0657	5.0
	21	34	23			21	35	24	
H5	.7243	.4860	.1834	5.0	H12	1.3925	.1200	.9941	5.0
	20	36	23			22	34	23	
H8,1	.9499	.1285	.6946	5.0	H13	1.3303	.0305	.7981	5.0
	20	36	22			20	37	22	
H8,2	.9506	.3223	.7573	5.0	H14	1.1483	.0844	.6721	5.0
	20	36	21			20	34	23	
H10	1.0896	.3221	.9363	5.0					
	20	35	21						

methyl derivative (1.408 Å) is significantly longer than that of (VI) (1.375 Å). The reaction rates of these compounds are unknown to the author.

By taking into account the estimated limits of error, it may be seen from Table 6 that none of the bond distances and angles of (I) and (III) differ significantly from the corresponding values for (II) and (VI), respectively. This means that the geometry is unchanged on methylation. By comparing the geometry of (I) with (III), and (II) with (IV) it is also clear that no significant changes occur on substitution of S with O.

The C=N bond of (V) (1.264(5) Å) corresponds to that of α-*p*-dimethylaminobenzaldoxime (1.264(5) Å).[12] The authors point out that this is slightly longer than what, according to Bayer and Häflinger,[13] is a normal C−N double bond (1.225 Å). However, in cyclohexane-1,4-dioxime [14] the two independent C=N bonds are 1.275(4) Å and 1.277(3) Å, respectively, and the C=N infrared stretching frequency is about 1670 cm^{-1}. The crystal structure determination of diiminosuccinonitrile has recently been carried out,[15] and shows C=N bond distance of 1.275(2) Å. The corresponding IR frequency for this compound is 1630 cm^{-1}. C−N double bond lengths found by microwave investigations of formaldoxime [16] and *N*-methyl-methylenimine [17] are 1.276 Å and 1.30 Å, respectively. The difference between the values above and that of (V) are not significant, and do not account for the high C=N stretching frequencies of iminobenzoxazolines.

The molecules of (VI) form dimers with strong intermolecular hydrogen bonds of length 2.933 Å (Fig. 1 (VI)). Since the hydrogen atom of this bond could not be localized in the difference Fourier map, multiplicity factors of half-hydrogens at N1 and N2 were refined. Five cycles of least squares refinement did not discriminate between the sites. The lowest *R*-factor was obtained with H at a distance of 1.09 Å from N2. However, the *R*-value differences were small, and it cannot be stated with confidence that this is the true position. The N1···H···N2′ distance of (VI) is somewhat shorter than a similar hydrogen bond in isocystine,[18] where two centrosymmetrically related molecules are

Table 4. Observed and calculated structure factors (on 10 times absolute scale).

II

h	k	l	Fo	Fc
1	0	0	299	320
2	0	0	45	43
3	0	0	79	81
4	0	0	55	57
5	0	0	93	94
6	0	0	66	67
7	0	0	45	44
8	0	0	91	90
9	0	0	61	59
1	1	0	200	209
2	1	0	137	192
3	1	0	126	129
4	1	0	102	109
5	1	0	172	180
6	1	0	63	63
7	1	0	32	32
8	1	0	44	43
9	1	0	65	64
10	1	0	16	14
0	2	0	476	477
1	2	0	210	210
2	2	0	14	16
3	2	0	224	233
4	2	0	80	83
5	2	0	172	175
6	2	0	96	97
7	2	0	57	55
8	2	0	21	22
9	2	0	44	43
1	3	0	340	344
2	3	0	190	200
3	3	0	60	53
4	3	0	77	77
5	3	0	43	45
6	3	0	29	28
7	3	0	71	73
8	3	0	55	54
0	4	0	106	103
1	4	0	58	59
2	4	0	70	73
3	4	0	141	143
4	4	0	52	52
5	4	0	93	94
6	4	0	128	130
7	4	0	75	80
8	4	0	42	40
1	5	0	238	241
2	5	0	183	180
3	5	0	113	114
4	5	0	81	86
5	5	0	29	30
6	5	0	48	51
7	5	0	52	55
8	5	0	45	46
0	6	0	66	69
1	6	0	76	78
2	6	0	55	58
3	6	0	53	54
4	6	0	33	35
5	6	0	40	42
6	6	0	84	85
7	6	0	54	56
1	7	0	87	90
2	7	0	75	76
3	7	0	21	23
4	7	0	154	163
5	7	0	54	67
6	7	0	24	26
7	7	0	34	34
0	8	0	109	109
1	8	0	112	119
2	8	0	49	52
3	8	0	41	44
5	8	0	15	20
6	8	0	26	27
1	9	0	69	72
2	9	0	21	21
3	9	0	40	42
4	9	0	57	61
5	9	0	54	57
0	10	0	57	55
1	10	0	50	54
2	10	0	17	18
3	10	0	36	37
10	0	1	67	63
-8	0	1	22	21
-7	0	1	105	108
-6	0	1	112	113
-5	0	1	32	34
-4	0	1	18	18

h	k	l	Fo	Fc
-3	0	1	51	51
-1	0	1	236	225
0	0	1	44	43
1	0	1	72	74
2	0	1	267	283
3	0	1	180	190
4	0	1	116	120
5	0	1	51	57
8	0	1	42	44
9	0	1	29	25
-8	1	1	40	40
-5	1	1	132	132
-4	1	1	24	25
-3	1	1	58	58
-2	1	1	375	354
0	1	1	55	53
1	1	1	53	50
2	1	1	84	84
3	1	1	155	158
4	1	1	220	229
5	1	1	62	64
6	1	1	31	30
7	1	1	153	154
8	1	1	55	54
9	1	1	26	24
10	1	1	26	22
-9	2	1	28	26
-8	2	1	14	15
-7	2	1	106	106
-6	2	1	70	68
-5	2	1	72	71
-4	2	1	60	63
-3	2	1	106	106
-2	2	1	128	120
-1	2	1	237	223
0	2	1	234	228
1	2	1	35	34
2	2	1	193	187
3	2	1	64	61
4	2	1	28	27
5	2	1	69	72
6	2	1	86	89
7	2	1	32	33
9	2	1	31	29
-9	3	1	48	43
-8	3	1	63	59
-7	3	1	60	58
-6	3	1	45	45
-5	3	1	78	77
-4	3	1	55	53
-3	3	1	151	157
-2	3	1	181	178
-1	3	1	70	70
0	3	1	107	108
1	3	1	190	184
2	3	1	242	228
3	3	1	54	55
4	3	1	221	220
5	3	1	70	72
7	3	1	18	18
8	3	1	18	23
-9	4	1	16	15
-8	4	1	20	23
-7	4	1	47	45
-6	4	1	37	35
-5	4	1	62	61
-4	4	1	148	143
-3	4	1	152	153
-2	4	1	169	164
-1	4	1	153	150
0	4	1	258	247
1	4	1	71	68
2	4	1	31	30
3	4	1	41	42
4	4	1	89	88
5	4	1	135	138
6	4	1	129	127
7	4	1	37	38
8	4	1	47	49
9	4	1	30	28
-8	5	1	74	70
-7	5	1	58	56
-6	5	1	50	49
-5	5	1	56	53
-4	5	1	23	23
-3	5	1	94	92
-2	5	1	96	96
-1	5	1	90	84
0	5	1	106	105
1	5	1	200	198

h	k	l	Fo	Fc
2	5	1	34	33
3	5	1	52	52
4	5	1	57	56
5	5	1	85	86
6	5	1	17	20
7	5	1	15	17
-6	6	1	55	55
-5	6	1	62	60
-4	6	1	103	100
-3	6	1	81	80
-2	6	1	36	35
-1	6	1	121	118
0	6	1	132	128
1	6	1	84	81
2	6	1	18	19
3	6	1	171	169
4	6	1	39	39
5	6	1	118	112
6	6	1	68	70
7	6	1	24	24
8	6	1	30	33
-6	7	1	83	82
-5	7	1	27	27
-4	7	1	49	48
-3	7	1	78	78
-2	7	1	117	119
-1	7	1	56	55
0	7	1	19	18
1	7	1	70	67
2	7	1	90	92
3	7	1	54	55
5	7	1	42	43
6	7	1	24	21
7	7	1	27	25
-6	8	1	55	54
-5	8	1	59	57
-4	8	1	38	38
-1	8	1	98	99
0	8	1	101	100
2	8	1	77	77
3	8	1	121	126
4	8	1	22	24
5	8	1	25	26
6	8	1	42	39
-5	9	1	36	34
-3	9	1	74	75
-2	9	1	88	90
-1	9	1	37	35
0	9	1	43	43
1	9	1	34	34
2	9	1	23	23
3	9	1	34	37
4	9	1	53	53
-3	10	1	28	25
-1	10	1	53	53
0	10	1	55	56
2	10	1	40	41
3	10	1	22	23
-8	0	2	36	34
-7	0	2	34	34
-6	0	2	52	53
-5	0	2	51	50
-4	0	2	31	29
-3	0	2	145	142
-2	0	2	244	238
-1	0	2	129	128
0	0	2	56	65
1	0	2	138	142
2	0	2	251	261
3	0	2	113	118
5	0	2	78	82
6	0	2	172	182
8	0	2	42	39
-9	1	2	35	32
-8	1	2	69	66
-7	1	2	23	22
-6	1	2	45	46
-5	1	2	26	28
-4	1	2	103	102
-3	1	2	402	393
-2	1	2	161	159
-1	1	2	23	21
0	1	2	129	126
1	1	2	148	143
2	1	2	72	68
3	1	2	56	57
4	1	2	78	84
5	1	2	74	74
6	1	2	67	66
9	1	2	41	36

h	k	l	Fo	Fc
-6	2	2	35	34
-5	2	2	53	52
-4	2	2	97	95
-3	2	2	140	138
-2	2	2	15	18
-1	2	2	120	118
0	2	2	30	26
1	2	2	60	54
2	2	2	172	165
3	2	2	140	133
4	2	2	59	60
5	2	2	85	88
6	2	2	68	71
7	2	2	25	26
8	2	2	37	35
9	2	2	29	26
-8	3	2	53	53
-6	3	2	76	76
-5	3	2	40	40
-4	3	2	32	32
-3	3	2	38	38
-2	3	2	118	116
-1	3	2	49	46
0	3	2	154	149
1	3	2	68	67
2	3	2	172	162
3	3	2	143	140
4	3	2	132	130
5	3	2	75	75
6	3	2	19	19
7	3	2	45	46
9	3	2	31	26
-7	4	2	26	25
-6	4	2	28	28
-5	4	2	69	65
-4	4	2	141	139
-3	4	2	29	30
-2	4	2	170	170
-1	4	2	161	157
0	4	2	150	142
1	4	2	26	23
2	4	2	71	70
3	4	2	44	41
4	4	2	47	47
5	4	2	60	60
6	4	2	26	26
7	4	2	36	35
8	4	2	43	39
-7	5	2	35	34
-6	5	2	25	24
-5	5	2	56	54
-4	5	2	13	14
-3	5	2	20	22
-2	5	2	90	92
-1	5	2	16	13
0	5	2	23	22
1	5	2	16	18
3	5	2	158	152
4	5	2	141	137
5	5	2	70	71
7	5	2	41	45
-7	6	2	64	61
-6	6	2	25	26
-5	6	2	59	57
-4	6	2	86	85
-3	6	2	26	28
-2	6	2	74	75
-1	6	2	108	107
0	6	2	81	78
1	6	2	140	139
2	6	2	65	64
3	6	2	37	37
5	6	2	54	52
6	6	2	14	11
-6	7	2	39	38
-5	7	2	35	33
-4	7	2	38	36
-3	7	2	59	58
-2	7	2	93	94
-1	7	2	31	31
0	7	2	21	20
1	7	2	49	49
2	7	2	87	87
3	7	2	70	69
4	7	2	57	56
6	7	2	28	27
-5	8	2	23	24
-4	8	2	67	65
-3	8	2	29	31
-2	8	2	31	31

h	k	l	Fo	Fc
-1	8	2	27	28
0	8	2	31	32
1	8	2	104	104
2	8	2	68	68
3	8	2	28	26
4	8	2	28	27
5	8	2	58	53
-4	9	2	37	37
-3	9	2	41	41
-2	9	2	76	76
-1	9	2	43	41
0	9	2	40	41
1	9	2	51	50
-8	0	3	25	25
-7	0	3	17	15
-5	0	3	112	115
-4	0	3	220	225
-3	0	3	13	13
-2	0	3	32	31
-1	0	3	57	57
0	0	3	42	40
1	0	3	114	116
2	0	3	68	70
4	0	3	173	183
5	0	3	63	66
6	0	3	27	28
7	0	3	20	21
8	0	3	38	35
-6	1	3	25	28
-5	1	3	61	64
-4	1	3	57	60
-3	1	3	18	18
-2	1	3	29	29
-1	1	3	90	91
0	1	3	68	68
1	1	3	101	102
2	1	3	18	19
3	1	3	41	47
4	1	3	47	50
5	1	3	55	61
6	1	3	44	42
-8	2	3	24	23
-6	2	3	26	24
-5	2	3	94	96
-4	2	3	104	105
-3	2	3	36	36
-2	2	3	45	45
-1	2	3	116	114
0	2	3	49	50
1	2	3	168	162
2	2	3	74	72
3	2	3	19	17
4	2	3	67	67
5	2	3	39	40
7	2	3	44	38
8	2	3	38	35
-7	3	3	23	20
-6	3	3	43	43
-5	3	3	42	43
-4	3	3	64	65
-3	3	3	100	103
-2	3	3	39	39
0	3	3	28	30
1	3	3	28	28
2	3	3	49	48
3	3	3	121	115
4	3	3	55	54
5	3	3	40	38
6	3	3	48	45
7	3	3	21	21
-6	4	3	23	23
-5	4	3	34	34
-2	4	3	68	69
-1	4	3	64	63
0	4	3	35	33
1	4	3	109	106
2	4	3	107	105
3	4	3	55	52
4	4	3	29	28
5	4	3	19	17
7	4	3	43	38
-6	5	3	44	44
-5	5	3	43	45
-4	5	3	49	49
-3	5	3	90	92
-2	5	3	70	69
-1	5	3	30	29
0	5	3	81	79
1	5	3	40	41
2	5	3	85	84
3	5	3	86	84
4	5	3	36	36

h	k	l	Fo	Fc
5	5	3	45	47
6	5	3	41	37
-6	6	3	24	25
-5	6	3	36	35
-4	6	3	15	20
-2	6	3	37	40
-1	6	3	31	30
0	6	3	22	24
1	6	3	18	20
2	6	3	90	88
3	6	3	27	26
5	6	3	30	29
-5	7	3	20	21
-4	7	3	37	35
-3	7	3	57	58
-2	7	3	36	37
-1	7	3	38	37
0	7	3	125	121
1	7	3	13	16
2	7	3	45	44
3	7	3	47	45
4	7	3	31	29
5	7	3	22	18
-3	8	3	34	34
-1	8	3	21	22
0	8	3	14	13
1	8	3	19	21
2	8	3	36	36
-6	0	4	75	78
-5	0	4	26	27
-3	0	4	25	25
-2	0	4	47	49
1	0	4	49	49
2	0	4	30	29
3	0	4	14	12
5	0	4	22	22
6	0	4	29	27
-6	1	4	52	56
-5	1	4	43	49
-4	1	4	27	28
-2	1	4	12	13
-1	1	4	80	81
0	1	4	76	75
2	1	4	51	55
3	1	4	106	110
5	1	4	33	34
6	1	4	25	24
-6	2	4	41	44
-5	2	4	47	49
-4	2	4	17	21
-3	2	4	33	33
-2	2	4	38	39
-1	2	4	31	32
0	2	4	24	25
1	2	4	58	58
2	2	4	34	34
3	2	4	20	20
-4	3	4	30	30
-3	3	4	37	39
-2	3	4	24	25
-1	3	4	53	53
0	3	4	70	68
2	3	4	35	35
5	3	4	30	28
-5	4	4	37	37
-4	4	4	27	31
-2	4	4	17	14
-1	4	4	23	24
0	4	4	63	62
1	4	4	82	79
2	4	4	71	68
4	4	4	47	48
-4	5	4	31	30
-3	5	4	38	40
-2	5	4	28	29
-1	5	4	41	43
0	5	4	21	20
1	5	4	15	17
-3	6	4	19	18
-2	6	4	25	25
-1	6	4	47	46
0	6	4	52	51
1	6	4	61	60
2	6	4	35	35
-2	0	5	38	39
1	0	5	34	37
2	0	5	46	51
-2	1	5	35	37
-1	1	5	25	27
1	1	5	43	43
2	1	5	21	20
0	2	5	28	29
1	2	5	35	39

III

h	k	l	Fo	Fc
0	0	3	7	0
0	0	4	787	-786
0	0	5	8	0
0	0	6	52	-51
0	0	7	8	0
0	0	8	236	-235
0	0	9	10	0
0	0	10	58	-56
0	0	11	11	0
0	0	12	296	-292
0	0	13	13	0
0	0	14	202	200
0	0	15	12	0
0	0	16	151	150
0	0	17	13	0
0	0	18	192	-188
0	0	19	13	0
0	0	20	85	-84
0	0	21	11	0

h	k	l	Fo	Fc
0	0	22	32	32
0	0	23	12	0
0	0	24	109	105
0	0	25	13	0
0	0	26	12	7
0	0	27	12	0
0	0	28	29	-28
0	0	30	12	-6
0	0	32	13	8
1	0	-34	24	-25
1	0	-32	37	37
1	0	-30	95	94
1	0	-28	14	15
1	0	-26	68	-67
1	0	-24	76	-76
1	0	-22	102	-97
1	0	-20	17	13
1	0	-18	101	102
1	0	-16	212	-210
1	0	-14	85	84

k	k	l	Fo	Fc
1	0	-12	208	207
1	0	-8	493	491
1	0	-4	313	320
1	0	-2	483	-473
1	0	0	801	-802
1	0	2	492	480
1	0	4	120	119
1	0	6	156	150
1	0	8	152	-155
1	0	10	294	-287
1	0	12	325	-324
1	0	14	100	-97
1	0	16	217	217
1	0	18	11	7
1	0	20	114	112
1	0	22	111	111
1	0	24	87	-88
1	0	28	12	-11
2	0	-32	75	-71
2	0	-30	50	-48

h	k	l	Fo	Fc
2	0	-28	45	47
2	0	-26	47	49
2	0	-24	12	11
2	0	-22	30	32
2	0	-20	33	-31
2	0	-18	165	-165
2	0	-16	10	-11
2	0	-14	143	147
2	0	-12	141	141
2	0	-10	173	168
2	0	-8	106	-111
2	0	-6	9	-4
2	0	-4	68	69
2	0	-2	411	-412
2	0	0	555	-551
2	0	2	187	179
2	0	6	315	-306
2	0	8	291	297
2	0	10	285	282
2	0	12	115	117

h	k	l	Fo	Fc
2	0	14	147	-150
2	0	16	26	-28
2	0	18	181	180
2	0	20	145	-146
2	0	22	73	-76
2	0	24	70	72
2	0	26	12	9
3	0	-32	19	-16
3	0	-30	33	-33
3	0	-28	46	45
3	0	-26	39	-37
3	0	-24	22	-22
3	0	-22	112	111
3	0	-20	104	105
3	0	-18	88	86
3	0	-16	182	-185
3	0	-14	66	-70
3	0	-12	39	38
3	0	-10	345	-356
3	0	-8	73	-75

h	k	l	Fo	Fc
3	0	-6	175	169
3	0	-4	204	208
3	0	-2	162	165
3	0	0	39	-36
3	0	2	248	-239
3	0	4	93	93
3	0	6	124	118
3	0	8	51	-48
3	0	10	116	114
3	0	12	72	73
3	0	14	30	-34
3	0	16	17	-114
3	0	20	42	44
4	0	-32	68	66
4	0	-28	98	-100
4	0	-26	73	73
4	0	-24	18	18
4	0	-22	69	-69
4	0	-20	12	-9
4	0	-18	34	34

Table 4. Continued.

h	k	l	Fo	Fc
4	0	-16	50	52
4	0	-14	151	-151
4	0	-12	11	6
4	0	-10	148	152
4	0	-8	19	-19
4	0	-6	112	-111
4	0	-4	74	-73
4	0	-2	163	170
4	0	0	131	133
4	0	2	78	77
4	0	4	11	5
4	0	6	108	-105
4	0	8	116	-116
4	0	10	107	-103
4	0	12	15	16
4	0	14	105	107
4	0	16	12	-2
4	0	18	39	-38
4	0	20	28	23
5	0	-28	43	40
5	0	-26	33	-36
5	0	-24	49	-49
5	0	-22	73	-78
5	0	-20	12	-16
5	0	-18	57	59
5	0	-16	83	83
5	0	-14	12	1
5	0	-12	24	-23
5	0	-10	99	99
5	0	-8	83	-82
5	0	-6	19	-20
5	0	-4	118	118
5	0	-2	75	-72
5	0	0	88	-92
5	0	2	87	-87
5	0	4	48	49
5	0	6	92	93
5	0	8	29	-30
5	0	12	17	-14
5	0	14	13	-16
5	0	16	26	22
6	0	-24	65	61
6	0	-22	48	44
6	0	-20	58	-53
6	0	-18	59	-56
6	0	-16	12	3
6	0	-14	84	80
6	0	-12	21	-17
6	0	-10	51	-51
6	0	-8	105	107
6	0	-6	52	-51
6	0	-4	120	-116
6	0	-2	13	13
6	0	0	56	56
6	0	2	28	28
6	0	4	51	-53
6	0	6	13	8
6	0	8	40	39
0	1	1	309	304
0	1	2	106	108
0	1	3	209	-200
0	1	4	02	804
0	1	5	87	-186
0	1	6	89	-84
0	1	7	295	289
0	1	8	51	49
0	1	9	190	182
0	1	10	108	-105
0	1	11	102	-100
0	1	12	146	-141
0	1	13	43	-45
0	1	14	149	141
0	1	15	12	-20
0	1	16	43	43
0	1	17	165	-170
0	1	18	12	4
0	1	19	68	-70
0	1	20	103	-104
0	1	21	12	8
0	1	22	40	-41
0	1	23	12	9
0	1	24	13	18
0	1	25	115	111
0	1	26	13	8
0	1	27	47	44
0	1	28	27	28
0	1	29	44	-45
0	1	33	13	-4
1	1	-32	13	-11
1	1	-31	13	13
1	1	-29	30	30
1	1	-28	72	72
1	1	-27	44	-47
1	1	-26	63	64
1	1	-25	43	-45
1	1	-24	51	-50
1	1	-23	18	-18
1	1	-22	80	-80
1	1	-21	46	46
1	1	-20	78	80
1	1	-19	100	100
1	1	-18	16	-14
1	1	-17	27	-29
1	1	-16	11	-110
1	1	-15	83	-80
1	1	-14	99	98
1	1	-13	44	-140
1	1	-12	29	-31
1	1	-11	37	-35
1	1	-10	80	-102
1	1	-8	85	-381
1	1	-6	29	226
1	1	-5	99	969
1	1	-4	56	936
1	1	-3	202	195
1	1	-2	325	-307
1	1	-1	431	-417
1	1	0	321	-308
1	1	3	330	-328
1	1	4	233	237
1	1	5	210	-224
1	1	6	16	-12
1	1	7	9	3
1	1	8	133	-136
1	1	10	307	301
1	1	11	24	26
1	1	12	66	-69
1	1	14	244	-239
1	1	16	113	-116
1	1	17	42	41
1	1	18	60	60

h	k	l	Fo	Fc
1	1	19	21	-22
1	1	20	113	111
1	1	21	39	39
1	1	22	91	-88
1	1	23	24	26
1	1	24	22	21
1	1	25	69	-70
1	1	26	63	63
1	1	27	12	-3
1	1	28	15	-14
1	1	29	38	31
1	1	30	13	-2
2	1	-34	26	26
2	1	-32	18	-13
2	1	-31	23	-23
2	1	-30	25	-24
2	1	-29	12	-11
2	1	-28	25	-23
2	1	-27	39	-36
2	1	-26	12	10
2	1	-25	27	-27
2	1	-24	19	18
2	1	-23	57	59
2	1	-22	24	28
2	1	-21	71	-68
2	1	-20	19	-16
2	1	-19	11	-5
2	1	-18	11	-19
2	1	-17	126	133
2	1	-16	67	-68
2	1	-15	93	95
2	1	-14	113	-111
2	1	-13	158	163
2	1	-12	149	147
2	1	-11	105	-101
2	1	-10	107	104
2	1	-9	9	-4
2	1	-7	128	-120
2	1	-5	458	-463
2	1	-4	88	85
2	1	-3	102	99
2	1	-2	90	96
2	1	-1	134	127
2	1	0	65	-63
2	1	1	172	170
2	1	2	70	-71
2	1	3	110	109
2	1	4	166	-171
2	1	5	186	-183
2	1	6	10	4
2	1	7	257	-254
2	1	8	111	-117
2	1	9	32	29
2	1	10	56	-54
2	1	11	135	139
2	1	12	133	134
2	1	13	11	-5
2	1	14	38	-42
2	1	15	59	62
2	1	16	43	46
2	1	17	113	115
2	1	18	12	18
2	1	19	47	49
2	1	21	75	75
2	1	22	45	45
2	1	23	12	3
2	1	24	29	-32
2	1	25	12	13
2	1	27	12	-4
2	1	29	19	-15
3	1	-32	21	16
3	1	-31	13	13
3	1	-29	21	24
3	1	-28	47	47
3	1	-27	61	62
3	1	-26	31	-32
3	1	-25	44	-46
3	1	-24	60	62
3	1	-23	85	-89
3	1	-22	58	-59
3	1	-21	70	70
3	1	-20	12	-12
3	1	-19	23	21
3	1	-18	96	95
3	1	-17	31	-31
3	1	-16	54	50
3	1	-15	22	23
3	1	-14	26	21
3	1	-13	54	53
3	1	-12	127	-127
3	1	-11	11	-6
3	1	-10	84	82
3	1	-9	121	-125
3	1	-8	63	62
3	1	-7	23	-29
3	1	-6	268	-264
3	1	-5	54	-57
3	1	-4	94	-93
3	1	-2	202	200
3	1	-1	38	-36
3	1	0	41	45
3	1	1	130	-130
3	1	2	117	-118
3	1	3	180	183
3	1	4	46	45
3	1	5	192	193
3	1	6	11	7
3	1	7	85	85
3	1	8	28	-30
3	1	9	52	-52
3	1	10	38	-39
3	1	11	86	-86
3	1	12	92	93
3	1	13	23	22
3	1	14	120	118
3	1	15	90	-90
3	1	16	63	-65
3	1	17	39	-42
3	1	18	44	-48
3	1	19	81	83
3	1	20	12	11
3	1	22	20	19
3	1	24	17	-14
3	1	25	13	-5
4	1	-32	25	25
4	1	-31	13	-8
4	1	-30	19	-16
4	1	-29	24	-24
4	1	-28	24	21
4	1	-27	20	18
4	1	-26	18	16

h	k	l	Fo	Fc
4	1	-25	75	74
4	1	-24	32	-31
4	1	-23	34	34
4	1	-22	12	14
4	1	-21	65	-67
4	1	-20	25	-25
4	1	-19	56	-60
4	1	-18	67	68
4	1	-17	30	-28
4	1	-16	35	36
4	1	-15	89	-93
4	1	-14	101	-102
4	1	-13	12	-8
4	1	-12	44	-42
4	1	-11	121	120
4	1	-10	17	18
4	1	-9	50	50
4	1	-8	80	84
4	1	-7	37	40
4	1	-6	33	-33
4	1	-5	53	53
4	1	-4	33	-31
4	1	-3	124	-124
4	1	-2	12	-6
4	1	-1	28	32
4	1	0	25	-24
4	1	1	92	94
4	1	2	41	41
4	1	3	64	-64
4	1	4	51	49
4	1	5	12	-16
4	1	6	103	104
4	1	7	14	-17
4	1	8	13	14
4	1	9	18	22
4	1	10	97	-101
4	1	11	12	-8
4	1	12	45	-44
4	1	13	38	-27
4	1	14	15	11
4	1	17	24	-23
4	1	21	13	10
5	1	-28	13	14
5	1	-27	31	-29
5	1	-25	13	-12
5	1	-24	13	10
5	1	-23	12	-8
5	1	-22	18	14
5	1	-21	16	17
5	1	-20	45	-45
5	1	-19	33	35
5	1	-18	99	-97
5	1	-17	13	15
5	1	-16	38	38
5	1	-15	12	-9
5	1	-14	79	81
5	1	-13	42	-41
5	1	-12	26	24
5	1	-10	79	-78
5	1	-9	29	31
5	1	-8	29	-29
5	1	-7	15	-13
5	1	-6	119	118
5	1	-5	45	46
5	1	-4	41	-42
5	1	-3	106	107
5	1	-2	12	-1
5	1	-1	58	-62
5	1	0	72	74
5	1	1	104	-101
5	1	2	30	-32
5	1	3	24	-23
5	1	4	61	-62
5	1	5	12	12
5	1	6	60	-59
5	1	7	12	2
5	1	8	53	51
5	1	9	13	3
5	1	10	48	49
5	1	11	25	24
5	1	12	43	-42
5	1	14	21	-17
5	1	15	18	12
6	1	-22	19	15
6	1	-20	28	26
6	1	-18	13	-14
6	1	-16	27	-27
6	1	-15	53	52
6	1	-14	13	13
6	1	-13	24	-18
6	1	-12	24	-25
6	1	-11	43	-40
6	1	-10	44	41
6	1	-9	26	25
6	1	-8	46	44
6	1	-6	24	-25
6	1	-5	54	-55
6	1	-4	22	-16
6	1	-3	23	-23
6	1	-2	42	-40
6	1	-1	34	34
6	1	0	21	17
6	1	1	45	43
6	1	4	23	-19
0	2	0	56	-58
0	2	1	130	131
0	2	3	57	58
0	2	4	88	85
0	2	6	21	18
0	2	7	34	37
0	2	8	161	-162
0	2	9	32	33
0	2	10	129	-124
0	2	11	35	-33
0	2	12	106	108
0	2	13	55	53
0	2	14	46	-47
0	2	15	84	81
0	2	16	11	-1
0	2	17	12	-14
0	2	18	108	108
0	2	19	44	-46
0	2	20	40	40
0	2	21	107	-111
0	2	22	67	-72
0	2	23	20	-25
0	2	24	67	-64
0	2	25	28	33
0	2	26	59	59
0	2	27	35	-32
0	2	28	13	10

h	k	l	Fo	Fc
0	2	29	45	41
0	2	30	34	-34
0	2	31	28	30
1	2	-31	24	23
1	2	-30	24	23
1	2	-29	27	26
1	2	-26	12	11
1	2	-25	17	16
1	2	-24	26	22
1	2	-23	34	-33
1	2	-22	59	-59
1	2	-21	12	6
1	2	-20	32	-36
1	2	-19	23	-23
1	2	-18	23	-24
1	2	-17	24	26
1	2	-16	13	-13
1	2	-15	58	55
1	2	-14	53	59
1	2	-13	11	8
1	2	-12	159	163
1	2	-11	11	-12
1	2	-10	65	62
1	2	-9	412	-414
1	2	-8	266	-266
1	2	-6	19	-17
1	2	-5	239	237
1	2	-4	115	110
1	2	-3	18	2
1	2	-2	64	-62
1	2	-1	299	300
1	2	0	78	-76
1	2	1	55	56
1	2	2	10	10
1	2	3	54	56
1	2	4	138	141
1	2	5	37	-37
1	2	6	12	-4
1	2	7	262	-268
1	2	8	65	67
1	2	9	20	12
1	2	10	16	18
1	2	11	128	121
1	2	12	102	-98
1	2	13	102	-101
1	2	14	17	20
1	2	15	95	-95
1	2	16	56	-55
1	2	17	12	11
1	2	18	12	-9
1	2	19	25	27
1	2	20	65	64
1	2	21	37	40
1	2	22	53	53
1	2	23	13	-2
1	2	24	21	-22
1	2	25	16	14
1	2	26	53	-50
1	2	27	27	24
1	2	28	13	11
1	2	29	24	-22
2	2	-32	16	14
2	2	-29	12	-4
2	2	-28	37	-36
2	2	-27	24	-23
2	2	-26	13	-13
2	2	-25	21	22
2	2	-24	81	86
2	2	-23	55	-55
2	2	-22	55	58
2	2	-21	57	-55
2	2	-20	105	-108
2	2	-19	84	87
2	2	-18	12	-12
2	2	-17	95	-100
2	2	-16	47	52
2	2	-15	31	-32
2	2	-14	82	-81
2	2	-13	11	-11
2	2	-12	145	-143
2	2	-11	93	88
2	2	-10	238	248
2	2	-9	351	357
2	2	-8	324	329
2	2	-7	176	-175
2	2	-6	250	-258
2	2	-5	74	-73
2	2	-4	198	-200
2	2	-3	19	22
2	2	-2	90	86
2	2	-1	167	-162
2	2	0	75	74
2	2	1	10	8
2	2	2	67	-67
2	2	3	57	61
2	2	4	77	-78
2	2	5	139	144
2	2	6	85	90
2	2	7	38	-39
2	2	8	11	12
2	2	9	136	-136
2	2	10	11	4
2	2	11	77	-77
2	2	12	25	21
2	2	13	12	1
2	2	14	18	17
2	2	15	78	77
2	2	16	12	5
2	2	17	32	35
2	2	18	73	-72
2	2	19	39	36
2	2	20	33	-33
2	2	21	18	18
2	2	22	27	27
2	2	23	30	-29
2	2	24	36	35
2	2	26	13	-4
3	2	-31	14	-14
3	2	-27	29	30
3	2	-25	16	-17
3	2	-24	51	-50
3	2	-23	25	27
3	2	-22	13	15
3	2	-21	33	-36
3	2	-20	88	84
3	2	-19	59	-59
3	2	-18	18	20
3	2	-17	77	75
3	2	-16	12	5
3	2	-15	25	26
3	2	-14	38	-43

h	k	l	Fo	Fc
3	2	-13	56	59
3	2	-12	79	-84
3	2	-11	12	11
3	2	-10	91	-97
3	2	-9	44	-41
3	2	-8	54	54
3	2	-7	12	-8
3	2	-6	116	111
3	2	-5	34	-29
3	2	-4	11	-1
3	2	-3	78	78
3	2	-2	39	38
3	2	-1	92	-94
3	2	0	48	-47
3	2	1	51	-48
3	2	2	108	-112
3	2	3	57	-58
3	2	4	26	27
3	2	5	38	-41
3	2	6	74	74
3	2	7	125	123
3	2	8	20	-18
3	2	9	12	15
3	2	10	67	-71
3	2	11	91	92
3	2	12	38	38
3	2	13	45	45
3	2	14	28	30
3	2	15	91	-93
3	2	16	17	-18
3	2	18	12	9
3	2	19	13	-13
3	2	21	13	8
3	2	23	13	13
4	2	-27	22	-21
4	2	-25	31	31
4	2	-23	39	39
4	2	-22	13	-17
4	2	-21	17	17
4	2	-20	12	-8
4	2	-19	38	38
4	2	-18	12	-5
4	2	-17	12	1
4	2	-16	12	2
4	2	-15	81	-82
4	2	-14	91	89
4	2	-13	73	-72
4	2	-12	12	4
4	2	-11	20	-16
4	2	-10	116	-120
4	2	-9	27	29
4	2	-8	60	-61
4	2	-7	81	81
4	2	-6	79	81
4	2	-5	69	-69
4	2	-4	15	13
4	2	-3	32	-33
4	2	-2	73	-72
4	2	-1	116	117
4	2	0	106	116
4	2	1	61	-65
4	2	2	84	87
4	2	3	16	15
4	2	4	107	-110
4	2	5	46	48
4	2	6	72	-70
4	2	7	12	8
4	2	8	69	68
4	2	9	13	11
4	2	10	45	46
4	2	11	79	-80
4	2	12	66	-65
4	2	13	21	17
4	2	15	30	32
4	2	16	32	34
4	2	17	22	-21
4	2	18	14	10
5	2	-25	19	-18
5	2	-22	29	27
5	2	-21	13	11
5	2	-20	23	-23
5	2	-19	45	-45
5	2	-18	26	-26
5	2	-16	12	1
5	2	-15	59	58
5	2	-14	12	2
5	2	-13	12	6
5	2	-12	53	54
5	2	-11	41	-39
5	2	-10	22	27
5	2	-9	22	-23
5	2	-8	32	-27
5	2	-7	12	-13
5	2	-6	40	-37
5	2	-5	47	48
5	2	-4	12	10
5	2	-3	26	24
5	2	-1	16	15
5	2	0	21	-26
5	2	1	44	43
5	2	2	37	34
5	2	3	25	-27
5	2	4	17	20
5	2	5	46	-44
5	2	6	28	-22
5	2	7	35	-34
5	2	11	13	10
6	2	-17	17	13
6	2	-14	25	-22
6	2	-12	17	-12
6	2	-11	29	25
6	2	-10	38	36
6	2	-9	13	11
6	2	-8	28	23
6	2	-7	13	13
6	2	-4	21	-13
0	3	1	35	-38
0	3	2	39	-42
0	3	3	86	-86
0	3	4	146	146
0	3	5	52	50
0	3	6	77	71
0	3	7	35	35
0	3	8	17	16
0	3	9	13	13
0	3	10	24	-28
0	3	11	30	31
0	3	12	102	-103
0	3	13	42	45
0	3	14	12	-4
0	3	15	55	-54

h	k	l	Fo	Fc
0	3	16	33	29
0	3	17	24	-21
0	3	18	24	-28
0	3	19	68	64
0	3	20	12	2
0	3	21	13	-15
0	3	23	13	-11
0	3	26	14	-16
0	3	27	15	9
1	3	-28	25	-20
1	3	-26	16	17
1	3	-25	18	17
1	3	-24	40	39
1	3	-23	15	20
1	3	-22	35	34
1	3	-21	13	-6
1	3	-20	36	-37
1	3	-19	13	13
1	3	-18	105	-105
1	3	-17	64	62
1	3	-16	48	47
1	3	-15	88	-88
1	3	-14	19	20
1	3	-13	13	4
1	3	-12	85	-83
1	3	-11	49	49
1	3	-10	23	19
1	3	-9	49	-49
1	3	-8	62	58
1	3	-7	52	-53
1	3	-6	21	17
1	3	-5	57	-57
1	3	-4	47	-47
1	3	-3	128	122
1	3	-2	17	-16
1	3	-1	29	-28
1	3	0	99	96
1	3	1	62	-60
1	3	2	20	-25
1	3	3	94	92
1	3	4	117	-123
1	3	5	12	-8
1	3	6	27	-27
1	3	7	18	-15
1	3	8	87	91
1	3	9	14	-13
1	3	10	38	38
1	3	11	12	10
1	3	12	12	0
1	3	13	54	52
1	3	14	12	-10
1	3	15	35	34
1	3	16	68	-68
1	3	17	48	-52
1	3	18	47	-48
1	3	19	37	-37
1	3	20	23	23
1	3	21	14	17
1	3	22	34	36
1	3	23	24	-23
1	3	24	33	27
1	3	25	13	-10
2	3	-27	13	-10
2	3	-26	22	-21
2	3	-25	13	7
2	3	-23	22	-22
2	3	-20	33	34
2	3	-19	30	-31
2	3	-18	54	53
2	3	-17	53	55
2	3	-16	35	-37
2	3	-15	75	77
2	3	-14	121	-125
2	3	-13	171	-175
2	3	-12	59	-64
2	3	-11	13	12
2	3	-10	108	115
2	3	-9	60	60
2	3	-8	67	69
2	3	-7	50	-53
2	3	-6	47	50
2	3	-5	19	14
2	3	-4	18	18
2	3	-3	18	18
2	3	-2	51	-49
2	3	-1	102	102
2	3	0	12	5
2	3	1	51	-51
2	3	2	62	-61
2	3	3	28	-28
2	3	4	12	-11
2	3	5	47	52
2	3	6	73	75
2	3	7	17	-15
2	3	8	69	-66
2	3	9	12	13
2	3	10	58	-56
2	3	11	42	-44
2	3	12	16	14
2	3	13	30	-29
2	3	14	50	51
2	3	15	13	-7
2	3	16	73	72
2	3	17	13	13
2	3	18	13	-3
2	3	19	22	18
2	3	20	35	-35
2	3	23	13	15
3	3	-26	15	-15
3	3	-24	17	-20
3	3	-23	22	20
3	3	-22	13	-11
3	3	-21	19	-17
3	3	-19	23	-22
3	3	-18	12	0
3	3	-17	57	-57
3	3	-16	18	13
3	3	-15	41	42
3	3	-14	151	159
3	3	-13	98	102
3	3	-12	25	23
3	3	-11	49	-51
3	3	-10	181	-183
3	3	-9	34	33
3	3	-8	62	-59
3	3	-7	20	21
3	3	-6	25	27
3	3	-5	54	-53
3	3	-4	74	77
3	3	-3	47	-46
3	3	-2	12	7

Table 4. Continued.

h	k	l	Fo	Fc
3	3	-1	41	44
3	3	0	48	-47
3	3	1	58	59
3	3	2	64	65
3	3	3	98	-98
3	3	4	26	-25
3	3	5	36	38
3	3	6	91	-95
3	3	7	17	17
3	3	8	40	42
3	3	9	64	-65
3	3	10	83	79
3	3	11	21	19
3	3	12	13	8
3	3	13	14	9
3	3	14	52	-54
3	3	15	31	28
3	3	17	13	-10
3	3	18	31	31
4	3	-22	21	17
4	3	-21	13	13
4	3	-20	13	5
4	3	-18	13	-9
4	3	-16	12	-3
4	3	-15	16	-17
4	3	-14	28	-32
4	3	-13	12	8
4	3	-12	24	24
4	3	-11	18	-21
4	3	-10	44	46
4	3	-9	12	-13
4	3	-8	12	-9
4	3	-7	63	61
4	3	-6	47	-49
4	3	-5	16	-10
4	3	-4	54	-58

h	k	l	Fo	Fc
4	3	-2	12	3
4	3	-1	47	-44
4	3	0	39	37
4	3	1	24	26
4	3	2	32	27
4	3	3	27	25
4	3	4	15	16
4	3	5	65	-67
4	3	6	14	15
4	3	7	56	56
4	3	8	13	12
4	3	9	36	37
4	3	10	44	-42
4	3	11	23	-26
5	3	-16	15	-13
5	3	-15	13	-12
5	3	-14	24	-20
5	3	-12	22	22
5	3	-11	14	18
5	3	-10	17	16
5	3	-9	26	-23
5	3	-8	13	-12
5	3	-7	27	-26
5	3	-6	16	16
5	3	-5	47	43
5	3	-3	14	9
5	3	-1	22	-19
5	3	0	13	-14
5	3	2	21	-22
5	3	3	32	34
5	3	4	36	32
0	4	0	13	-3
0	4	1	67	-69
0	4	2	13	14
0	4	3	31	-31
0	4	4	71	-71

h	k	l	Fo	Fc
0	4	5	34	34
0	4	6	12	-2
0	4	7	16	9
0	4	8	90	87
0	4	9	45	-45
0	4	10	36	-37
0	4	11	35	-37
0	4	12	13	-3
0	4	13	71	69
0	4	14	34	33
0	4	15	28	26
0	4	16	15	-15
0	4	17	15	-11
0	4	18	13	4
0	4	19	26	-26
0	4	20	13	15
0	4	21	14	-14
1	4	-22	13	14
1	4	-21	29	-26
1	4	-20	21	-21
1	4	-19	13	-8
1	4	-18	15	16
1	4	-17	28	27
1	4	-16	22	19
1	4	-15	43	42
1	4	-14	55	-55
1	4	-13	13	11
1	4	-12	32	33
1	4	-11	66	-65
1	4	-10	40	38
1	4	-9	19	-19
1	4	-8	64	-63
1	4	-7	13	-0
1	4	-6	12	2
1	4	-5	14	16
1	4	-4	21	-21

h	k	l	Fo	Fc
1	4	-3	13	-8
1	4	-2	39	-38
1	4	-1	22	21
1	4	0	28	26
1	4	1	48	47
1	4	2	42	41
1	4	3	35	-37
1	4	4	32	31
1	4	6	19	-19
1	4	7	18	-12
1	4	8	12	-3
1	4	9	13	-2
1	4	10	23	-20
1	4	13	29	-25
1	4	14	49	46
1	4	15	14	8
1	4	18	22	-23
2	4	-21	13	6
2	4	-20	14	10
2	4	-19	20	-19
2	4	-18	13	9
2	4	-17	13	5
2	4	-14	17	-19
2	4	-12	21	-24
2	4	-11	20	21
2	4	-10	29	-29
2	4	-9	13	8
2	4	-8	13	-8
2	4	-7	14	12
2	4	-6	48	45
2	4	-5	61	-59
2	4	-4	58	56
2	4	-3	19	-19
2	4	-2	17	18
2	4	-1	21	20
2	4	0	57	-58

h	k	l	Fo	Fc
2	4	1	13	13
2	4	2	40	-38
2	4	3	13	6
2	4	4	67	66
2	4	5	21	-21
2	4	6	13	-5
2	4	7	55	54
2	4	8	25	-26
2	4	9	13	-3
2	4	10	61	57
2	4	11	55	-52
2	4	12	44	-41
2	4	13	13	5
2	4	14	64	-61
2	4	15	21	23
2	4	16	18	17
3	4	-19	24	-25
3	4	-18	65	-65
3	4	-17	50	-51
3	4	-15	33	36
3	4	-14	66	69
3	4	-13	21	23
3	4	-11	13	-9
3	4	-10	13	16
3	4	-8	13	9
3	4	-7	13	17
3	4	-6	29	-30
3	4	-5	44	46
3	4	-4	13	-12
3	4	-3	51	-50
3	4	-1	31	-30
3	4	0	47	47
3	4	1	21	18
3	4	2	13	5
3	4	3	13	16
3	4	4	53	-54

h	k	l	Fo	Fc
3	4	6	13	-4
3	4	7	29	-31
3	4	8	13	-10
3	4	9	36	38
3	4	11	23	24
4	4	-12	13	9
4	4	-9	13	9
4	4	-7	13	4
4	4	-6	13	-3
4	4	-3	23	21
4	4	-2	17	-17
4	4	-1	21	-19
4	4	0	13	-5
4	4	1	14	-8
4	4	2	13	-4
0	5	3	25	-20
0	5	4	14	-7
0	5	5	13	3
0	5	6	40	41
0	5	7	46	46
0	5	8	18	-19
1	5	-8	14	1
1	5	-7	14	-4
1	5	-6	36	38
1	5	-5	14	-1
1	5	-4	14	-2
1	5	-3	21	-23
1	5	-2	20	-20
1	5	-1	14	14
1	5	0	43	-38
1	5	1	27	24
1	5	2	14	7
1	5	3	21	20
1	5	4	26	20
1	5	5	42	-37

IV

h	k	l	Fo	Fc
0	0	2	199	204
0	0	4	653	738
0	0	6	174	187
0	0	8	258	267
0	0	10	105	107
0	0	12	236	238
0	0	14	34	37
0	0	16	107	110
0	0	20	102	96
0	0	24	42	40
0	1	1	210	223
0	1	2	475	513
0	1	3	368	391
0	1	4	202	211
0	1	5	233	246
0	1	6	103	118
0	1	7	113	107
0	1	8	186	191
0	1	9	116	109
0	1	10	80	74
0	1	11	36	37
0	1	12	102	110
0	1	13	259	265
0	1	15	79	83
0	1	16	35	43
0	1	17	126	125
0	1	18	54	54
0	1	19	19	19
0	1	22	94	90
0	2	0	214	228
0	2	1	177	182
0	2	2	41	39
0	2	3	44	40
0	2	4	342	353
0	2	5	145	149
0	2	6	67	63
0	2	7	32	31
0	2	8	196	200
0	2	9	122	118
0	2	10	95	96
0	2	11	24	21
0	2	12	34	38
0	2	13	101	102
0	2	14	80	77
0	2	15	64	64
0	2	16	18	15
0	2	17	29	31
0	2	18	26	24
0	2	19	14	18
0	2	20	84	82
0	2	21	38	35
0	2	22	21	21
0	2	23	30	24
0	2	24	17	23
0	3	1	97	98
0	3	2	108	115
0	3	3	182	184
0	3	4	246	254
0	3	5	56	59
0	3	6	14	13
0	3	7	187	187
0	3	8	58	52
0	3	9	96	99
0	3	10	61	65
0	3	11	83	83
0	3	12	11	7
0	3	13	50	57
0	3	14	52	57
0	3	15	69	70
0	3	16	28	29
0	3	17	79	79
0	3	18	15	14
0	3	19	29	27
0	3	21	50	48
0	3	22	34	31
0	3	23	62	56
0	4	0	41	40
0	4	1	178	186
0	4	2	35	36
0	4	3	51	51
0	4	4	92	99
0	4	5	154	159
0	4	6	114	119
0	4	7	48	48

h	k	l	Fo	Fc
0	4	8	74	76
0	4	9	13	8
0	4	10	81	87
0	4	11	38	42
0	4	12	111	112
0	4	13	29	27
0	4	14	14	10
0	4	16	66	62
0	4	17	64	68
0	4	18	28	23
0	4	20	27	28
0	4	21	29	25
0	5	1	88	94
0	5	2	17	18
0	5	3	21	28
0	5	4	72	74
0	5	5	128	132
0	5	6	19	20
0	5	8	23	24
0	5	9	64	69
0	5	10	13	14
0	5	11	54	60
0	5	12	40	43
0	5	13	11	8
0	5	14	91	92
0	5	15	17	12
0	5	16	70	69
0	5	18	69	67
0	5	19	55	52
0	6	0	11	12
0	6	1	75	79
0	6	2	11	10
0	6	3	130	135
0	6	4	76	76
0	6	5	47	48
0	6	7	49	52
0	6	8	112	115
0	6	9	53	48
0	6	10	50	47
0	6	11	19	17
0	6	14	39	38
0	6	16	29	31
0	7	1	14	15
0	7	2	19	18
0	7	3	21	23
0	7	5	50	47
0	7	6	46	50
0	7	8	12	12
0	7	9	47	45
0	7	10	12	13
1	0	1	162	161
1	0	2	53	53
1	0	3	465	450
1	0	4	771	807
1	0	5	454	449
1	0	6	77	77
1	0	7	299	303
1	0	9	348	352
1	0	11	75	76
1	0	12	180	182
1	0	14	71	73
1	0	15	18	21
1	0	16	36	36
1	0	17	37	37
1	0	18	85	85
1	0	20	26	28
1	0	22	42	42
1	0	24	39	36
1	1	0	167	160
1	1	1	528	528
1	1	2	357	352
1	1	3	405	402
1	1	4	419	417
1	1	5	282	287
1	1	6	276	274
1	1	7	58	58
1	1	8	103	106
1	1	9	70	70
1	1	10	190	196
1	1	11	99	98
1	1	12	72	73
1	1	13	42	43
1	1	14	34	33
1	1	15	54	54

h	k	l	Fo	Fc
1	1	16	82	85
1	1	17	75	76
1	1	18	82	82
1	1	19	48	49
1	1	21	41	41
1	1	23	52	48
1	2	0	261	256
1	2	1	74	72
1	2	2	46	43
1	2	3	84	86
1	2	4	128	125
1	2	5	155	149
1	2	6	87	81
1	2	7	92	91
1	2	8	199	203
1	2	9	48	48
1	2	10	163	161
1	2	11	115	114
1	2	12	62	63
1	2	13	54	54
1	2	14	83	81
1	2	15	52	54
1	2	16	85	87
1	2	17	63	62
1	2	18	80	78
1	2	20	52	51
1	2	21	45	46
1	2	22	55	53
1	2	23	13	14
1	3	0	312	311
1	3	1	59	59
1	3	2	39	39
1	3	3	175	173
1	3	4	211	207
1	3	5	92	92
1	3	6	41	42
1	3	7	162	161
1	3	8	84	85
1	3	9	63	63
1	3	10	26	29
1	3	11	67	66
1	3	12	40	42
1	3	13	68	69
1	3	14	30	31
1	3	15	14	15
1	3	16	67	65
1	3	17	26	29
1	3	19	57	56
1	3	20	14	15
1	3	21	25	23
1	4	0	110	110
1	4	1	103	107
1	4	2	50	49
1	4	3	107	110
1	4	4	53	52
1	4	5	67	68
1	4	6	53	55
1	4	7	81	81
1	4	8	76	77
1	4	9	12	12
1	4	10	66	67
1	4	11	22	23
1	4	12	75	75
1	4	13	110	112
1	4	14	35	34
1	4	15	70	72
1	4	16	50	49
1	4	17	57	54
1	4	18	36	37
1	4	19	47	45
1	4	20	25	21
1	4	21	19	15
1	5	0	79	81
1	5	1	82	83
1	5	2	79	81
1	5	3	17	17
1	5	4	82	83
1	5	5	15	15
1	5	6	73	77
1	5	7	93	97
1	5	8	49	48
1	5	9	99	101
1	5	10	62	63
1	5	11	34	32

h	k	l	Fo	Fc
1	5	12	25	26
1	5	13	81	79
1	5	14	25	24
1	5	15	41	40
1	5	16	28	29
1	5	17	29	29
1	5	18	36	37
1	6	0	97	98
1	6	1	83	82
1	6	2	24	26
1	6	3	43	44
1	6	4	96	98
1	6	5	58	59
1	6	6	50	48
1	6	7	42	41
1	6	8	34	35
1	6	9	26	27
1	6	10	34	36
1	6	12	46	47
1	6	13	11	13
1	6	14	14	12
1	7	0	38	39
1	7	1	34	35
1	7	2	13	14
1	7	3	29	31
1	7	4	37	35
1	7	5	27	26
1	7	6	12	13
1	7	8	26	26
1	7	9	34	32
1	7	10	22	18
2	0	0	94	96
2	0	1	118	115
2	0	2	146	143
2	0	3	51	52
2	0	4	86	85
2	0	5	195	194
2	0	6	115	111
2	0	7	61	63
2	0	8	200	196
2	0	9	66	64
2	0	11	76	76
2	0	13	29	27
2	0	14	73	72
2	0	15	14	18
2	0	16	97	96
2	0	20	37	36
2	0	22	49	45
2	1	1	19	18
2	1	2	52	52
2	1	3	55	54
2	1	4	179	176
2	1	5	144	145
2	1	6	343	340
2	1	7	142	145
2	1	8	236	241
2	1	9	166	167
2	1	10	84	83
2	1	11	59	61
2	1	12	97	98
2	1	14	136	136
2	1	15	46	46
2	1	16	34	35
2	1	17	58	58
2	1	19	46	47
2	1	20	27	27
2	1	21	19	20
2	1	22	19	18
2	2	0	103	99
2	2	1	144	140
2	2	2	123	121
2	2	3	173	168
2	2	4	178	177
2	2	5	90	94
2	2	6	14	18
2	2	7	213	212
2	2	8	48	46
2	2	9	169	171
2	2	10	22	21
2	2	12	59	60
2	2	13	102	105
2	2	14	69	71
2	2	15	34	36
2	2	16	52	54

h	k	l	Fo	Fc
2	2	17	67	67
2	2	18	27	28
2	2	19	51	50
2	2	20	14	18
2	2	21	36	33
2	3	0	142	141
2	3	1	135	133
2	3	2	51	58
2	3	3	136	132
2	3	4	30	30
2	3	5	113	113
2	3	6	94	94
2	3	7	56	54
2	3	8	21	19
2	3	9	99	99
2	3	10	67	65
2	3	11	17	20
2	3	12	106	104
2	3	13	65	66
2	3	14	37	36
2	3	15	21	22
2	3	16	55	57
2	3	17	19	23
2	3	18	26	27
2	3	19	11	11
2	3	20	32	29
2	3	21	25	25
2	4	0	73	73
2	4	1	103	105
2	4	2	41	43
2	4	3	13	12
2	4	4	33	31
2	4	5	38	38
2	4	6	65	65
2	4	8	72	73
2	4	9	80	80
2	4	10	142	143
2	4	11	56	55
2	4	12	47	47
2	4	13	25	26
2	4	14	76	74
2	4	15	35	34
2	4	16	14	14
2	4	17	33	31
2	4	18	26	25
2	4	19	28	27
2	5	0	52	55
2	5	1	38	38
2	5	2	88	89
2	5	3	81	80
2	5	4	75	76
2	5	5	52	52
2	5	6	48	49
2	5	7	36	37
2	5	8	52	51
2	5	9	39	39
2	5	10	18	15
2	5	11	48	46
2	5	12	29	31
2	5	13	56	55
2	5	14	48	47
2	5	16	23	23
2	5	17	20	20
2	6	0	91	93
2	6	1	21	23
2	6	2	11	13
2	6	3	53	49
2	6	4	41	40
2	6	5	34	36
2	6	6	19	20
2	6	7	27	26
2	6	8	23	24
2	6	9	29	28
2	6	10	24	21
2	6	12	13	9
2	7	0	51	46
2	7	1	19	15
2	7	2	37	37
2	7	3	24	25
2	7	4	29	26
2	7	5	38	34
2	7	6	12	11
2	7	7	17	17
3	0	2	32	32
3	0	3	64	64

h	k	l	Fo	Fc
3	0	4	121	118
3	0	5	19	18
3	0	6	37	36
3	0	7	28	29
3	0	8	14	15
3	0	9	16	15
3	0	10	26	25
3	0	11	72	72
3	0	12	55	58
3	0	13	92	95
3	0	14	25	26
3	0	17	63	62
3	0	18	19	21
3	0	20	31	29
3	1	0	33	35
3	1	1	105	106
3	1	2	104	103
3	1	3	100	99
3	1	4	62	62
3	1	5	24	24
3	1	6	26	25
3	1	7	13	14
3	1	8	24	24
3	1	9	99	101
3	1	10	101	101
3	1	11	40	41
3	1	12	74	76
3	1	13	82	85
3	1	14	58	58
3	1	15	17	21
3	1	16	49	49
3	1	17	11	16
3	1	18	29	29
3	1	19	19	20
3	2	0	63	63
3	2	1	13	13
3	2	2	89	88
3	2	3	81	80
3	2	4	98	99
3	2	5	31	31
3	2	6	31	30
3	2	7	48	49
3	2	8	126	128
3	2	9	103	106
3	2	10	123	124
3	2	11	44	45
3	2	12	82	83
3	2	13	84	86
3	2	14	42	48
3	2	16	18	16
3	2	17	18	17
3	2	18	24	24
3	2	19	11	9
3	3	0	50	50
3	3	1	46	45
3	3	2	41	41
3	3	3	67	66
3	3	4	76	77
3	3	5	81	81
3	3	6	125	124
3	3	7	24	24
3	3	8	89	89
3	3	9	100	108
3	3	10	70	71
3	3	11	25	23
3	3	12	29	32
3	3	13	54	52
3	3	14	48	48
3	3	16	29	26
3	3	17	28	25
3	3	18	11	6
3	4	0	68	67
3	4	1	48	48
3	4	2	42	42
3	4	3	70	71
3	4	4	39	39
3	4	5	70	78
3	4	6	47	46
3	4	7	74	73
3	4	8	48	38
3	4	9	21	24
3	4	10	24	21
3	4	11	31	31
3	4	12	63	61

Table 4. Continued.

h	k	l	Fo	Fc
3	4	13	18	15
3	4	14	30	20
3	4	15	24	24
3	4	16	21	20
3	5	0	26	26
3	5	1	42	44
3	5	2	29	30
3	5	3	11	13
3	5	4	42	40
3	5	5	46	45
3	5	6	26	26
3	5	7	33	32
3	5	8	29	27
3	5	9	18	17
3	5	10	41	42
3	5	11	31	30
3	5	12	17	15
3	5	13	17	10
3	6	0	30	32

h	k	l	Fo	Fc
3	6	2	20	19
3	6	4	32	31
3	6	7	22	21
3	6	8	24	22
4	0	1	21	22
4	0	2	32	33
4	0	5	59	57
4	0	7	11	15
4	0	8	51	51
4	0	9	68	69
4	0	10	83	83
4	0	11	17	16
4	0	13	21	25
4	0	14	23	26
4	1	0	71	70
4	1	1	35	36
4	1	2	51	53
4	1	3	12	10
4	1	4	11	12

h	k	l	Fo	Fc
4	1	5	47	40
4	1	6	35	38
4	1	7	38	36
4	1	8	65	64
4	1	9	15	17
4	1	10	38	39
4	1	11	14	16
4	1	12	39	38
4	1	13	23	23
4	1	15	21	23
4	2	0	19	21
4	2	1	56	57
4	2	2	59	61
4	2	3	71	72
4	2	4	38	38
4	2	5	50	50
4	2	6	53	54
4	2	7	55	55
4	2	8	15	17

h	k	l	Fo	Fc
4	2	9	17	16
4	2	11	36	37
4	2	12	37	40
4	2	13	38	41
4	2	14	37	37
4	2	15	37	37
4	3	0	18	17
4	3	1	78	69
4	3	2	59	68
4	3	3	32	33
4	3	4	55	51
4	3	5	52	52
4	3	6	48	49
4	3	7	44	44
4	3	8	24	22
4	3	9	15	17
4	3	10	35	37
4	3	11	38	38

h	k	l	Fo	Fc
4	3	12	36	34
4	3	13	42	41
4	4	0	30	31
4	4	2	23	22
4	4	3	47	46
4	4	5	42	41
4	4	6	50	48
4	4	7	45	42
4	4	8	13	9
4	4	9	41	40
4	4	10	25	22
4	5	0	18	12
4	5	1	18	15
4	5	3	11	10
5	0	1	25	23
5	0	3	22	20
5	0	4	19	22
5	0	5	26	25

h	k	l	Fo	Fc
5	0	6	53	50
5	0	7	31	29
5	0	8	23	25
5	1	0	44	43
5	1	1	15	15
5	1	2	29	30
5	1	3	20	20
5	1	4	49	49
5	1	5	12	9
5	1	6	28	31
5	1	7	14	11
5	1	8	18	17
5	2	0	61	62
5	2	1	18	21
5	2	2	72	71
5	2	3	24	22
5	2	4	27	20
5	2	5	13	14

V

h	k	l	Fo	Fc
0	0	-8	53	54
0	0	-6	120	120
0	0	-5	29	34
0	0	-4	176	174
0	0	-3	302	302
0	0	-2	589	623
0	0	-1	344	335
0	0	1	344	335
0	0	2	597	623
0	0	3	308	302
0	0	4	176	174
0	0	5	30	34
0	0	6	122	120
0	0	8	55	54
1	0	-9	19	13
1	0	-8	97	99
1	0	-7	103	107
1	0	-6	20	19
1	0	-5	101	100
1	0	-4	72	70
1	0	-3	165	166
1	0	-2	305	303
1	0	-1	17	19
1	0	0	59	57
1	0	1	380	386
1	0	2	156	157
1	0	3	54	55
1	0	4	33	32
1	0	5	61	63
1	0	7	86	85
1	0	8	37	45
2	0	-8	37	44
2	0	-7	128	123
2	0	-6	27	30
2	0	-5	135	135
2	0	-4	65	67
2	0	-3	138	131
2	0	-2	119	118
2	0	-1	81	83
2	0	0	169	165
2	0	1	193	186
2	0	2	18	17
2	0	3	116	114
2	0	4	201	198
2	0	5	37	32
2	0	6	32	36
2	0	8	18	16
3	0	-8	93	96
3	0	-7	15	11
3	0	-6	94	95
3	0	-5	64	64
3	0	-4	27	28
3	0	-3	35	34
3	0	-2	241	243
3	0	-1	343	345
3	0	0	661	694
3	0	1	132	133
3	0	2	27	31
3	0	4	35	36
3	0	5	111	115
3	0	6	70	75
4	0	-8	50	52
4	0	-7	108	113
4	0	-6	85	87
4	0	-5	143	149
4	0	-4	104	109
4	0	-3	220	222
4	0	-2	131	131
4	0	-1	184	188
4	0	2	23	25
4	0	3	54	57
4	0	4	36	34
4	0	5	16	16
4	0	6	37	35
4	0	7	25	29
5	0	-9	25	26
5	0	-8	23	25
5	0	-7	30	32
5	0	-6	16	15
5	0	-5	48	50
5	0	-4	106	109
5	0	-3	59	60
5	0	-2	36	35
5	0	-1	27	32
5	0	0	196	195
5	0	1	104	101
5	0	2	149	153
5	0	3	96	97
5	0	4	63	63
5	0	5	56	58
6	0	-8	55	57
6	0	-6	61	64
6	0	-5	66	65
6	0	-4	202	204
6	0	-3	16	20
6	0	-2	118	117
6	0	-1	232	227
6	0	0	147	150
6	0	1	64	66
6	0	2	67	69

h	k	l	Fo	Fc
6	0	3	90	88
6	0	4	26	24
6	0	5	22	21
7	0	-8	47	51
7	0	-5	90	90
7	0	-4	35	34
7	0	-3	131	133
7	0	-2	57	59
7	0	-1	90	88
7	0	0	90	94
7	0	1	51	50
7	0	3	91	93
7	0	4	17	16
7	0	5	65	66
8	0	-10	17	8
8	0	-8	107	107
8	0	-7	29	35
8	0	-6	42	46
8	0	-5	135	135
8	0	-4	113	110
8	0	-3	20	18
8	0	-1	89	87
8	0	0	18	13
8	0	1	172	181
8	0	2	52	53
8	0	4	59	62
8	0	5	23	27
9	0	-9	18	14
9	0	-6	60	60
9	0	-5	23	23
9	0	-3	127	123
9	0	-1	157	154
9	0	0	53	53
9	0	1	54	56
9	0	2	58	61
9	0	4	75	80
10	0	-8	94	97
10	0	-7	197	208
10	0	-6	60	61
10	0	-5	52	54
10	0	-4	94	92
10	0	-3	138	136
10	0	-2	47	49
10	0	-1	34	34
10	0	0	45	45
10	0	2	19	17
10	0	3	43	48
10	0	4	26	29
11	0	-10	19	19
11	0	-9	77	79
11	0	-8	97	97
11	0	-7	49	52
11	0	-6	41	43
11	0	-5	138	138
11	0	-4	28	15
11	0	-3	19	21
11	0	-2	43	44
11	0	0	24	28
11	0	1	58	54
11	0	2	22	25
11	0	3	31	33
12	0	-10	24	25
12	0	-9	30	32
12	0	-8	31	29
12	0	-7	19	16
12	0	-6	77	78
12	0	-5	48	46
12	0	-4	41	39
12	0	-3	93	95
12	0	-1	62	64
12	0	0	28	30
13	0	-8	120	120
13	0	-7	108	100
13	0	-6	44	41
13	0	-5	18	13
13	0	-4	72	72
13	0	-3	30	29
13	0	-2	73	74
13	0	-1	33	32
13	0	0	66	68
14	0	-9	17	12
14	0	-8	57	54
14	0	-7	33	32
14	0	-6	17	17
14	0	-4	20	27
14	0	-1	38	40
15	0	-7	32	30
15	0	-6	24	23
15	0	-5	37	34
15	0	-4	32	34
15	0	-1	37	32
0	1	-8	50	49
0	1	-7	73	75
0	1	-6	68	67
0	1	-5	91	89
0	1	-4	261	265
0	1	-3	168	175
0	1	-2	389	395
0	1	-1	407	439
0	1	1	460	439

h	k	l	Fo	Fc
0	1	2	410	395
0	1	3	178	175
0	1	4	273	265
0	1	5	92	89
0	1	6	69	67
0	1	7	75	75
0	1	8	51	49
1	1	-9	21	20
1	1	-8	25	28
1	1	-7	40	38
1	1	-6	59	60
1	1	-4	124	128
1	1	-3	211	214
1	1	-2	210	212
1	1	-1	294	323
1	1	0	445	431
1	1	1	335	330
1	1	2	224	221
1	1	3	60	56
1	1	4	84	85
1	1	5	101	101
1	1	6	33	35
1	1	7	54	52
1	1	8	22	26
2	1	-9	19	16
2	1	-8	31	30
2	1	-7	62	59
2	1	-6	45	47
2	1	-5	63	63
2	1	-4	141	137
2	1	-3	72	73
2	1	-2	168	172
2	1	-1	268	285
2	1	0	549	556
2	1	1	135	129
2	1	2	222	215
2	1	3	89	89
2	1	4	51	47
2	1	5	49	48
2	1	6	61	58
2	1	7	51	45
2	1	8	22	25
3	1	-8	70	73
3	1	-7	68	68
3	1	-6	33	29
3	1	-5	97	93
3	1	-4	282	271
3	1	-3	174	169
3	1	-2	250	252
3	1	-1	386	400
3	1	0	580	584
3	1	1	97	93
3	1	2	157	148
3	1	3	193	188
3	1	4	133	128
3	1	5	57	60
3	1	6	41	40
3	1	7	55	55
3	1	8	23	25
4	1	-10	18	20
4	1	-9	19	14
4	1	-8	93	94
4	1	-7	92	95
4	1	-6	68	70
4	1	-5	76	69
4	1	-4	62	60
4	1	-3	27	24
4	1	-2	45	48
4	1	-1	329	325
4	1	0	384	377
4	1	1	60	59
4	1	2	91	87
4	1	3	125	124
4	1	4	21	25
4	1	5	55	55
4	1	6	32	31
4	1	7	27	28
5	1	-8	72	74
5	1	-7	80	80
5	1	-6	83	83
5	1	-5	60	54
5	1	-4	74	74
5	1	-3	124	120
5	1	-2	58	58
5	1	-1	282	275
5	1	0	160	158
5	1	1	43	39
5	1	2	115	115
5	1	3	66	66
5	1	4	58	58
5	1	5	78	77
5	1	6	32	33
5	1	7	24	28
6	1	-9	36	39
6	1	-7	26	25
6	1	-6	97	97
6	1	-5	122	114
6	1	-4	160	155
6	1	-3	54	54
6	1	-2	202	194

h	k	l	Fo	Fc
6	1	-1	180	176
6	1	0	304	290
6	1	1	149	110
6	1	2	35	35
6	1	3	45	47
6	1	4	73	76
6	1	5	62	62
6	1	6	20	23
7	1	-9	20	17
7	1	-8	115	115
7	1	-7	114	118
7	1	-6	32	31
7	1	-5	78	79
7	1	-4	137	133
7	1	-3	236	226
7	1	-2	15	9
7	1	-1	81	82
7	1	0	70	66
7	1	1	120	120
7	1	2	68	73
7	1	3	66	68
7	1	5	62	65
8	1	-10	21	17
8	1	-9	23	22
8	1	-8	60	60
8	1	-7	83	85
8	1	-6	65	60
8	1	-5	54	56
8	1	-4	16	17
8	1	-3	31	31
8	1	-2	102	100
8	1	-1	44	45
8	1	0	46	42
8	1	1	55	58
8	1	2	16	13
8	1	3	93	93
8	1	4	64	65
8	1	5	31	34
9	1	-10	21	24
9	1	-9	21	19
9	1	-8	77	79
9	1	-7	57	59
9	1	-6	25	23
9	1	-5	40	39
9	1	-4	106	106
9	1	-3	95	91
9	1	-2	62	68
9	1	-1	27	26
9	1	0	54	51
9	1	1	27	23
9	1	2	50	51
9	1	3	38	37
10	1	-9	36	37
10	1	-8	58	55
10	1	-7	60	64
10	1	-6	57	56
10	1	-5	81	80
10	1	-4	16	17
10	1	-3	138	138
10	1	-2	59	58
10	1	-1	80	78
10	1	0	52	50
10	1	1	56	57
10	1	2	59	58
10	1	3	21	19
10	1	4	55	53
11	1	-10	24	26
11	1	-9	31	27
11	1	-8	61	62
11	1	-7	44	41
11	1	-6	71	78
11	1	-5	79	77
11	1	-4	47	45
11	1	-3	40	38
11	1	-2	48	47
11	1	-1	52	52
11	1	0	47	45
11	1	1	68	69
11	1	3	42	39
12	1	-9	26	25
12	1	-8	76	76
12	1	-7	88	86
12	1	-6	89	89
12	1	-5	88	82
12	1	-4	80	78
12	1	-3	60	59
12	1	-2	27	27
12	1	-1	18	17
12	1	0	18	22
12	1	1	37	36
12	1	2	47	45
13	1	-9	46	43
13	1	-8	38	34
13	1	-6	54	56
13	1	-5	49	49
13	1	-4	73	72
13	1	-3	60	60
13	1	-2	47	44
13	1	-1	64	63
13	1	0	30	30

h	k	l	Fo	Fc
13	1	1	32	33
14	1	-9	42	37
14	1	-8	52	50
14	1	-7	17	16
14	1	-6	32	29
14	1	-5	45	46
14	1	-4	23	21
14	1	-2	18	16
14	1	-1	23	27
14	1	0	35	35
15	1	-8	39	40
15	1	-7	36	37
15	1	-6	46	44
15	1	-5	27	22
15	1	-4	19	14
15	1	-3	26	24
15	1	-2	27	27
15	1	-1	18	16
0	2	-8	21	27
0	2	-7	36	37
0	2	-6	59	64
0	2	-5	38	47
0	2	-4	159	157
0	2	-3	202	209
0	2	-2	28	28
0	2	-1	146	158
0	2	0	97	99
0	2	1	169	158
0	2	2	28	28
0	2	3	212	209
0	2	4	161	157
0	2	5	53	47
0	2	6	62	64
0	2	7	34	37
0	2	8	21	27
1	2	-9	25	26
1	2	-8	34	35
1	2	-7	67	69
1	2	-6	92	93
1	2	-5	23	24
1	2	-4	180	178
1	2	-3	111	108
1	2	-2	76	80
1	2	-1	14	16
1	2	0	188	196
1	2	1	185	167
1	2	2	113	97
1	2	3	163	159
1	2	4	83	80
1	2	5	156	150
1	2	6	25	23
1	2	7	38	39
2	2	-7	60	62
2	2	-6	48	46
2	2	-5	26	17
2	2	-4	123	123
2	2	-3	55	56
2	2	-2	134	152
2	2	-1	108	118
2	2	0	124	125
2	2	1	68	69
2	2	2	226	211
2	2	3	150	153
2	2	4	64	65
2	2	5	90	89
2	2	6	71	69
2	2	8	29	28
3	2	-9	33	34
3	2	-8	41	40
3	2	-7	63	62
3	2	-6	132	131
3	2	-5	43	46
3	2	-3	93	93
3	2	-2	74	79
3	2	-1	97	101
3	2	0	140	140
3	2	1	146	130
3	2	2	148	144
3	2	3	33	33
3	2	4	66	70
3	2	5	63	70
3	2	7	25	29
4	2	-9	33	32
4	2	-8	60	58
4	2	-7	111	111
4	2	-6	73	74
4	2	-5	64	73
4	2	-4	88	89
4	2	-3	160	155
4	2	-2	164	179
4	2	-1	241	249
4	2	0	138	134
4	2	1	43	38
4	2	2	62	61
4	2	3	26	24
4	2	4	69	69
4	2	6	48	45
4	2	7	31	25
5	2	-9	18	21
5	2	-8	56	54

h	k	l	Fo	Fc
5	2	-7	45	49
5	2	-5	69	69
5	2	-4	110	108
5	2	-2	173	179
5	2	-1	142	140
5	2	0	226	223
5	2	1	36	33
5	2	2	21	26
5	2	3	20	20
5	2	4	21	24
5	2	6	40	34
6	2	-8	70	69
6	2	-7	94	94
6	2	-6	30	28
6	2	-5	96	96
6	2	-4	149	154
6	2	-3	30	31
6	2	-2	58	57
6	2	-1	277	280
6	2	0	110	114
6	2	1	62	60
6	2	2	45	42
6	2	3	55	53
6	2	5	46	44
7	2	-9	40	40
7	2	-8	52	53
7	2	-7	100	102
7	2	-6	73	75
7	2	-5	33	39
7	2	-4	92	100
7	2	-3	116	112
7	2	-2	34	38
7	2	-1	273	271
7	2	0	120	120
7	2	1	88	87
7	2	2	54	55
7	2	3	81	81
8	2	-9	43	41
8	2	-8	51	49
8	2	-6	58	56
8	2	-5	35	36
8	2	-4	38	36
8	2	-3	35	32
8	2	-2	27	24
8	2	-1	111	107
8	2	0	154	153
8	2	1	39	37
8	2	2	101	103
8	2	4	39	40
9	2	-9	22	20
9	2	-8	78	79
9	2	-7	62	63
9	2	-6	61	64
9	2	-4	51	66
9	2	-1	83	81
9	2	0	65	63
9	2	1	94	93
9	2	2	47	46
9	2	3	69	71
9	2	4	36	38
10	2	-9	42	41
10	2	-8	50	49
10	2	-7	39	42
10	2	-6	35	32
10	2	-5	56	57
10	2	-3	84	81
10	2	-1	130	132
10	2	0	64	64
10	2	1	61	60
10	2	2	27	31
10	2	3	26	19
11	2	-9	23	20
11	2	-8	24	24
11	2	-6	91	91
11	2	-5	41	43
11	2	-4	89	92
11	2	-3	38	37
11	2	-2	99	98
11	2	-1	33	31
11	2	0	25	30
11	2	2	25	24
12	2	-7	24	25
12	2	-6	38	36
12	2	-5	99	99
12	2	-4	71	76
12	2	-3	31	30
12	2	-2	75	75
12	2	-1	56	54
12	2	0	26	28
12	2	1	35	42
13	2	-8	24	27
13	2	-6	28	26
13	2	-4	41	42
13	2	-3	57	56
13	2	-2	21	18
13	2	-1	49	50
14	2	-7	32	29
14	2	-6	50	51
14	2	-5	22	12
14	2	-4	35	37

Table 4. Continued.

h	k	l	Fo	Fc
14	2	-3	46	48
14	2	-2	43	43
15	2	-5	36	38
15	2	-4	40	40
15	2	-2	38	42
0	3	-8	25	23
0	3	-7	60	58
0	3	-6	48	50
0	3	-5	143	144
0	3	-4	43	46
0	3	-3	70	71
0	3	-2	150	155
0	3	-1	63	68
0	3	1	72	68
0	3	2	171	159
0	3	3	72	71
0	3	4	44	46
0	3	5	146	144
0	3	6	53	50
0	3	7	63	58
1	3	-8	25	25
1	3	-7	84	83
1	3	-6	116	112
1	3	-5	42	41
1	3	-4	47	49
1	3	-3	91	93
1	3	-2	179	185
1	3	-1	136	156
1	3	0	87	86
1	3	1	101	88
1	3	2	37	36
1	3	3	46	45
1	3	4	42	41
1	3	6	42	45
1	3	7	21	20
2	3	-6	46	44
2	3	-5	57	56
2	3	-4	67	70
2	3	-2	76	75
2	3	-1	57	63
2	3	0	93	89
2	3	1	78	74
2	3	2	45	48
2	3	3	59	58
2	3	4	67	61
2	3	6	70	69
2	3	7	52	54
3	3	-8	34	39
3	3	-7	51	56
3	3	-6	88	88
3	3	-5	94	88
3	3	-4	131	133
3	3	-3	98	98
3	3	-2	96	97
3	3	-1	110	111
3	3	0	72	67
3	3	1	13	10
3	3	2	25	24
3	3	3	41	38
3	3	4	34	35

h	k	l	Fo	Fc
3	3	5	31	32
4	3	-8	26	24
4	3	-7	81	75
4	3	-6	56	54
4	3	-5	43	46
4	3	-3	78	70
4	3	-2	64	68
4	3	-1	104	101
4	3	0	84	79
4	3	1	103	109
4	3	2	36	38
4	3	3	103	100
4	3	4	21	26
4	3	5	23	18
4	3	6	21	23
5	3	-9	25	23
5	3	-7	81	79
5	3	-6	64	60
5	3	-5	89	81
5	3	-3	27	20
5	3	-2	53	52
5	3	-1	95	96
5	3	0	102	99
5	3	1	86	83
5	3	2	64	74
5	3	3	48	46
5	3	4	56	55
5	3	5	31	31
6	3	-6	77	70
6	3	-5	33	34
6	3	-3	42	37
6	3	-1	51	51
6	3	0	43	42
6	3	1	17	13
6	3	2	27	28
6	3	3	17	36
6	3	4	26	23
7	3	-7	16	16
7	3	-6	31	27
7	3	-5	94	90
7	3	-4	65	58
7	3	-3	52	51
7	3	-2	72	70
7	3	-1	41	50
7	3	0	30	27
7	3	2	51	52
7	3	3	34	32
7	3	4	27	21
7	3	5	20	21
8	3	-7	51	50
8	3	-6	37	34
8	3	-4	80	72
8	3	-3	83	79
8	3	-2	80	80
8	3	-1	144	154
8	3	0	33	33
8	3	1	95	97
8	3	2	28	17
8	3	3	42	39
8	3	4	21	28

h	k	l	Fo	Fc
9	3	-9	27	25
9	3	-7	24	22
9	3	-6	73	75
9	3	-5	88	87
9	3	-4	30	31
9	3	-3	24	26
9	3	-2	64	63
9	3	1	31	36
9	3	2	19	20
10	3	-9	43	41
10	3	-7	34	36
10	3	-6	47	47
10	3	-5	52	62
10	3	-3	39	42
10	3	-2	94	92
10	3	-1	60	58
10	3	0	27	26
10	3	1	41	43
10	3	2	35	37
11	3	-8	50	47
11	3	-6	41	36
11	3	-5	17	16
11	3	-3	35	33
11	3	-2	82	80
11	3	-1	34	36
11	3	0	37	38
11	3	2	23	26
12	3	-8	33	24
12	3	-7	21	19
12	3	-6	38	37
12	3	-5	33	28
12	3	-4	32	32
12	3	-3	35	37
12	3	-2	41	42
12	3	-1	98	101
12	3	0	62	60
12	3	1	23	21
13	3	-8	31	17
13	3	-6	21	18
13	3	-5	38	38
13	3	-2	42	41
13	3	-1	33	35
14	3	-6	24	18
14	3	-5	26	9
14	3	-2	19	24
0	4	-7	19	22
0	4	-6	42	41
0	4	-5	17	10
0	4	-4	23	23
0	4	-3	88	89
0	4	-2	51	51
0	4	0	69	69
0	4	1	16	12
0	4	2	59	51
0	4	3	95	89
0	4	4	31	23
0	4	6	39	41
1	4	-5	33	37
1	4	-4	20	27
1	4	-3	63	61

h	k	l	Fo	Fc
1	4	-2	23	27
1	4	-1	18	38
1	4	0	20	29
1	4	1	85	79
1	4	2	33	32
1	4	3	38	37
1	4	4	40	42
1	4	5	20	18
1	4	6	22	21
2	4	-7	22	22
2	4	-6	42	37
2	4	-5	63	64
2	4	-3	24	25
2	4	-2	55	56
2	4	-1	65	64
2	4	0	53	61
2	4	1	54	53
2	4	2	86	80
2	4	3	62	57
2	4	4	29	29
2	4	5	28	25
2	4	6	46	42
3	4	-7	31	37
3	4	-6	80	79
3	4	-5	84	83
3	4	-4	33	43
3	4	-3	83	88
3	4	-2	71	72
3	4	-1	57	58
3	4	0	67	71
3	4	2	83	79
3	4	3	61	53
3	4	4	48	48
3	4	5	43	40
3	4	6	24	21
4	4	-8	23	18
4	4	-7	33	28
4	4	-6	54	52
4	4	-5	94	96
4	4	-4	104	112
4	4	-3	78	83
4	4	-2	53	65
4	4	0	16	12
4	4	1	64	66
4	4	2	49	53
4	4	3	29	27
4	4	4	39	33
5	4	-8	25	23
5	4	-6	44	46
5	4	-5	18	22
5	4	-3	68	77
5	4	-1	68	71
5	4	0	19	26
5	4	1	32	41
5	4	2	27	32
5	4	3	53	51
6	4	-7	25	20
6	4	-6	42	49
6	4	-5	55	63
6	4	-4	46	51

h	k	l	Fo	Fc
6	4	-3	19	42
6	4	-2	65	69
6	4	-1	70	71
6	4	0	36	48
6	4	1	60	69
6	4	3	43	40
7	4	-8	21	13
7	4	-7	24	25
7	4	-6	37	37
7	4	-5	47	47
7	4	-4	40	43
7	4	-2	41	49
7	4	-1	46	48
7	4	0	53	51
7	4	1	42	33
7	4	2	33	30
8	4	-7	24	25
8	4	-6	24	32
8	4	-5	61	62
8	4	-3	72	78
8	4	-2	78	83
8	4	-1	68	71
8	4	3	27	27
9	4	-7	26	22
9	4	-5	25	32
9	4	-4	60	69
9	4	-2	20	39
9	4	-1	18	17
9	4	0	27	26
9	4	1	25	24
9	4	2	33	30
10	4	-7	21	16
10	4	-6	19	15
10	4	-5	22	26
10	4	-4	38	31
10	4	-1	36	53
11	4	-2	26	36
11	4	-1	35	47
11	4	0	27	20
12	4	-1	38	49
13	4	-5	26	24
0	5	-5	25	18
0	5	-4	61	57
0	5	-3	17	16
0	5	-2	28	33
0	5	1	18	10
0	5	2	34	33
0	5	3	18	16
0	5	4	66	57
0	5	5	22	18
1	5	-5	46	35
1	5	-4	23	21
1	5	-3	47	45
1	5	-2	53	56
1	5	-1	25	26
1	5	0	43	47
1	5	1	45	43
1	5	2	46	45
1	5	3	33	28
1	5	4	21	18

h	k	l	Fo	Fc
1	5	5	28	28
2	5	-6	18	15
2	5	-5	46	45
2	5	-3	21	19
2	5	-2	79	69
2	5	-1	40	50
2	5	0	41	47
2	5	1	35	36
2	5	2	39	34
2	5	3	24	22
2	5	4	21	20
3	5	-5	34	35
3	5	-4	66	70
3	5	-3	38	36
3	5	-2	27	26
3	5	-1	59	66
3	5	0	52	51
3	5	1	22	30
3	5	2	25	26
3	5	3	19	21
4	5	-3	65	60
4	5	-1	68	77
4	5	0	38	49
4	5	1	58	51
4	5	2	44	45
4	5	3	24	14
4	5	4	26	19
5	5	-6	28	25
5	5	-5	19	32
5	5	-3	40	36
5	5	-2	40	46
5	5	2	24	27
6	5	-6	50	45
6	5	-3	53	50
6	5	-1	27	28
6	5	1	30	34
6	5	2	41	30
7	5	-6	32	39
7	5	-4	27	29
7	5	-3	24	18
7	5	-2	24	27
7	5	2	26	20
8	5	-5	39	48
0	6	-2	38	39
0	6	-1	44	44
0	6	0	46	51
0	6	1	54	44
0	6	2	46	39
0	6	3	19	13
1	6	-2	27	26
1	6	1	22	17
1	6	3	17	6
2	6	-3	17	17
2	6	1	29	23
2	6	2	32	28
3	6	1	44	46
4	6	-4	33	31

VI

h	k	l	Fo	Fc
0	0	2	182	-183
0	0	4	315	321
0	0	6	222	-215
0	0	8	129	126
0	0	10	171	170
0	0	12	97	96
1	0	-10	40	42
1	0	-8	39	-43
1	0	-6	683	-675
1	0	-4	120	130
1	0	-2	202	214
1	0	0	495	531
1	0	2	373	386
1	0	4	81	-78
1	0	6	384	376
1	0	8	112	109
1	0	10	259	257
1	0	12	75	69
2	0	-12	155	-155
2	0	-10	61	-60
2	0	-6	232	-224
2	0	-4	287	-271
2	0	-2	622	-621
2	0	0	562	-605
2	0	2	352	-372
2	0	6	209	-213
2	0	10	179	178
3	0	-12	122	-128
3	0	-10	106	113
3	0	-8	30	-35
3	0	-4	143	-134
3	0	-2	389	-382
3	0	0	45	37
3	0	2	78	-84
3	0	4	398	-387
3	0	6	47	-44
3	0	8	142	-141
3	0	10	71	-63
4	0	-12	113	110
4	0	-10	104	-102
4	0	-8	132	134
4	0	-6	18	15
4	0	-4	357	366
4	0	-2	386	-395
4	0	0	62	55
4	0	2	30	35
4	0	4	106	-99
4	0	6	99	100
5	0	-12	137	-139
5	0	-10	70	-66
5	0	-8	167	169
5	0	-6	193	205
5	0	-4	26	39
5	0	-2	44	-50
5	0	0	17	-32
5	0	2	36	-34
5	0	4	40	-45
5	0	6	58	57
5	0	8	88	89

h	k	l	Fo	Fc
6	0	-14	70	-72
6	0	-12	70	-69
6	0	-8	179	179
6	0	-6	413	-404
6	0	-4	254	-251
6	0	-2	17	-5
6	0	4	189	197
6	0	6	219	-229
7	0	-12	132	131
7	0	-10	151	153
7	0	-8	37	-32
7	0	-6	142	-138
7	0	-4	343	-344
7	0	-2	513	-524
7	0	0	475	468
7	0	2	88	91
7	0	4	53	46
7	0	6	234	-244
7	0	8	60	-53
8	0	-10	222	216
8	0	-6	83	88
8	0	-4	95	-96
8	0	-2	61	53
8	0	0	130	129
8	0	2	138	145
8	0	4	294	-302
8	0	6	38	33
9	0	-14	78	72
9	0	-12	57	-61
9	0	-10	56	62
9	0	-8	89	94
9	0	-6	156	155
9	0	-4	66	62
9	0	-2	130	123
9	0	0	107	109
9	0	2	60	-65
9	0	4	147	154
9	0	6	58	-64
10	0	-12	97	-93
10	0	-8	122	128
10	0	-6	51	50
10	0	-4	79	70
10	0	-2	95	-94
10	0	0	162	169
10	0	2	71	69
10	0	4	70	86
10	0	6	55	42
11	0	-10	65	-61
11	0	-8	62	59
11	0	-6	137	-143
11	0	-4	245	237
11	0	-2	84	-86
12	0	-12	84	-77
12	0	-10	122	-115
12	0	-8	127	-128
12	0	-4	72	66
12	0	-2	109	-100
12	0	0	65	-55
13	0	-12	59	-52

h	k	l	Fo	Fc
13	0	-10	104	-104
13	0	-8	146	144
13	0	-6	114	-113
13	0	-4	118	-117
13	0	-2	167	-158
14	0	-10	61	61
14	0	-8	68	65
14	0	-4	125	-121
0	1	1	480	485
0	1	2	570	588
0	1	3	17	14
0	1	4	207	209
0	1	5	142	-139
0	1	6	148	-149
0	1	8	59	-58
0	1	10	117	-118
0	1	11	59	54
0	1	12	47	-52
1	1	-10	161	157
1	1	-9	41	40
1	1	-8	152	148
1	1	-7	94	-98
1	1	-6	32	37
1	1	-5	142	-134
1	1	-4	17	9
1	1	-3	77	-70
1	1	-2	304	291
1	1	-1	302	304
1	1	0	357	351
1	1	1	229	236
1	1	2	91	-82
1	1	3	175	-168
1	1	4	228	-217
1	1	5	40	-35
1	1	6	121	116
1	1	8	86	83
1	1	9	108	104
1	1	10	77	-76
2	1	-12	63	68
2	1	-10	54	-57
2	1	-9	44	48
2	1	-8	87	-85
2	1	-7	36	-42
2	1	-6	200	204
2	1	-5	137	-136
2	1	-4	197	193
2	1	-3	717	714
2	1	-2	1485	1495
2	1	-1	246	-240
2	1	0	307	-303
2	1	1	30	-37
2	1	2	87	94
2	1	3	262	-262
2	1	4	126	122
2	1	6	232	226
2	1	8	101	99
2	1	9	136	137
3	1	-9	165	-169
3	1	-8	234	-234

h	k	l	Fo	Fc
3	1	-7	82	74
3	1	-5	17	-12
3	1	-4	51	-54
3	1	-2	220	206
3	1	-1	93	91
3	1	0	342	354
3	1	1	31	24
3	1	2	155	-154
3	1	3	25	-29
3	1	4	231	226
3	1	5	59	-54
3	1	6	46	52
3	1	8	295	293
4	1	-10	92	92
4	1	-8	255	-251
4	1	-7	52	-55
4	1	-6	332	-325
4	1	-5	159	169
4	1	-4	27	-37
4	1	-3	522	-503
4	1	-2	243	225
4	1	-1	17	-29
4	1	0	261	-259
4	1	1	17	-15
4	1	2	378	-370
4	1	4	185	-187
4	1	5	68	-66
4	1	6	134	-133
4	1	7	157	159
4	1	8	228	229
4	1	9	84	-82
5	1	-12	140	144
5	1	-11	107	-106
5	1	-10	58	-52
5	1	-9	104	111
5	1	-8	199	-197
5	1	-7	79	84
5	1	-5	103	-90
5	1	-4	30	-36
5	1	-3	100	-94
5	1	0	365	375
5	1	1	243	-261
5	1	2	543	-553
5	1	3	90	91
5	1	4	90	-89
5	1	6	294	-292
5	1	8	63	69
6	1	-12	94	-87
6	1	-10	167	171
6	1	-8	88	-85
6	1	-7	146	148
6	1	-6	255	250
6	1	-5	238	-222
6	1	-4	233	-238
6	1	-3	65	-62
6	1	-2	267	258
6	1	-1	52	-56
6	1	0	220	223
6	1	1	85	83

h	k	l	Fo	Fc
6	1	2	91	-90
6	1	3	42	40
6	1	6	105	112
6	1	7	154	-154
7	1	-14	61	-67
7	1	-12	121	-117
7	1	-11	126	120
7	1	-10	145	144
7	1	-9	49	47
7	1	-7	30	43
7	1	-5	111	-101
7	1	-3	55	-63
7	1	-2	113	-116
7	1	0	24	30
7	1	1	150	157
7	1	3	67	70
7	1	4	287	290
7	1	5	60	-64
8	1	-12	131	-132
8	1	-11	67	67
8	1	-10	66	67
8	1	-8	177	-183
8	1	-6	117	-119
8	1	-5	94	98
8	1	-4	168	-168
8	1	-3	54	-62
8	1	-2	245	-234
8	1	-1	83	78
8	1	0	58	63
8	1	1	96	96
8	1	4	90	-90
8	1	6	62	-62
9	1	-8	44	-43
9	1	-6	211	-214
9	1	-5	24	-35
9	1	-4	68	-69
9	1	-3	83	71
9	1	-2	47	-49
9	1	-1	101	96
9	1	1	70	76
9	1	2	159	-171
9	1	3	58	-49
9	1	4	128	-136
10	1	-12	83	85
10	1	-10	94	92
10	1	-8	45	47
10	1	-6	136	131
10	1	-5	31	-42
10	1	-4	96	99
10	1	-1	78	79
10	1	0	75	77
10	1	1	79	-75
10	1	2	108	-117
10	1	3	50	55
11	1	-10	100	94
11	1	-8	157	159
11	1	-7	49	-53
11	1	-6	56	-61
11	1	-5	147	146

h	k	l	Fo	Fc
11	1	-4	121	122
11	1	-3	60	-65
11	1	-2	197	196
11	1	-1	49	-47
11	1	0	175	177
11	1	2	87	87
12	1	-11	49	-47
12	1	-8	93	-87
12	1	-6	88	-87
12	1	-2	188	187
12	1	-1	93	-86
12	1	0	68	61
13	1	-8	126	-123
13	1	-7	93	86
13	1	-6	87	85
13	1	-5	72	-74
13	1	-4	106	-97
14	1	-8	54	49
14	1	-4	71	-68
14	1	-3	58	-53
14	1	-2	64	-65
15	1	-4	57	-49
0	2	0	1595	-1532
0	2	1	879	864
0	2	2	311	-306
0	2	3	260	-254
0	2	4	249	-247
0	2	5	131	125
0	2	6	65	58
0	2	7	114	115
0	2	8	128	-129
0	2	10	141	-144
0	2	11	77	-81
1	2	-12	102	99
1	2	-11	83	87
1	2	-8	111	113
1	2	-7	159	160
1	2	-6	172	158
1	2	-5	257	-252
1	2	-4	89	90
1	2	-3	183	178
1	2	-2	82	-78
1	2	-1	17	-6
1	2	0	336	-304
1	2	1	103	-105
1	2	2	80	-80
1	2	3	21	-12
1	2	4	272	-271
1	2	5	217	-217
1	2	6	212	-205
1	2	7	54	52
1	2	8	60	-58
1	2	10	162	-161
2	2	-13	63	64
2	2	-12	89	87
2	2	-10	82	80
2	2	-9	88	95
2	2	-8	93	-100
2	2	-7	93	-94

Table 4. Continued.

h	k	l	Fo	Fc
2	2	-6	225	228
2	2	-5	17	-2
2	2	-4	72	78
2	2	-3	17	2
2	2	-2	1323	1347
2	2	-1	1160	1138
2	2	0	106	-100
2	2	1	71	76
2	2	2	215	213
2	2	3	190	-181
2	2	4	80	-81
2	2	5	93	-91
2	2	6	72	73
2	2	8	98	98
2	2	9	48	-52
2	2	11	76	71
3	2	-13	73	68
3	2	-12	49	51
3	2	-11	52	51
3	2	-10	124	-126
3	2	-9	85	87
3	2	-8	140	-146
3	2	-7	226	-226
3	2	-6	180	176
3	2	-5	127	-120
3	2	-4	233	244
3	2	-3	449	437
3	2	-2	318	325
3	2	-1	241	226
3	2	0	112	112
3	2	1	17	19
3	2	2	166	-175
3	2	3	153	156
3	2	4	295	285
3	2	6	76	76
3	2	7	127	123
3	2	8	163	159
3	2	10	59	54
4	2	-12	81	-79
4	2	-11	83	88
4	2	-9	85	-81
4	2	-8	82	-90
4	2	-7	69	-65
4	2	-6	74	70
4	2	-5	116	114
4	2	-4	247	-229
4	2	-3	172	163
4	2	-2	194	-186
4	2	-1	26	21
4	2	0	151	-156
4	2	1	43	-41
4	2	3	35	27
4	2	5	104	-104
4	2	6	89	88
4	2	7	142	143
4	2	9	123	122
5	2	-11	60	-68
5	2	-10	83	82
5	2	-9	117	-121
5	2	-7	73	-67
5	2	-6	72	-65
5	2	-3	182	178
5	2	-2	106	-101
5	2	-1	164	164
5	2	0	249	-256
5	2	1	153	-147
5	2	2	133	129
5	2	3	196	-191
5	2	6	36	-32
5	2	7	133	105
5	2	8	100	-101
6	2	-9	135	-135
6	2	-8	22	27
6	2	-7	47	42
6	2	-6	194	204
6	2	-5	181	-178
6	2	-4	100	96
6	2	-3	142	-148
6	2	-1	53	-51
6	2	0	38	34
6	2	1	133	-125
6	2	3	141	-142
6	2	4	32	32
6	2	5	195	196
6	2	7	73	-65
7	2	-13	95	-91
7	2	-10	76	-86
7	2	-9	89	86
7	2	-8	55	60
7	2	-6	83	88
7	2	-5	57	-66
7	2	-4	198	200
7	2	-3	51	-48
7	2	-2	164	157
7	2	-1	281	-275
7	2	0	115	-116
7	2	3	99	-103
7	2	6	169	178
8	2	-10	90	-94
8	2	-9	140	136
8	2	-8	89	-85
8	2	-7	117	-124
8	2	-6	40	-32
8	2	-5	51	-59
8	2	-4	56	47
8	2	-2	29	13
8	2	-1	48	53
8	2	0	111	-111
8	2	1	83	-78
8	2	2	58	62
8	2	3	90	87
8	2	5	163	-167

h	k	l	Fo	Fc
9	2	-13	89	92
9	2	-9	48	51
9	2	-8	131	-127
9	2	-7	47	-47
9	2	-6	116	-118
9	2	-5	33	34
9	2	-4	154	-164
9	2	-3	195	-191
9	2	-2	183	173
9	2	-1	154	159
9	2	0	99	-102
9	2	1	136	132
9	2	4	136	-134
10	2	-12	89	84
10	2	-10	78	-82
10	2	-9	79	83
10	2	-8	96	-91
10	2	-7	76	75
10	2	-6	92	-90
10	2	-5	118	-122
10	2	-3	61	65
10	2	-2	96	88
10	2	0	67	-75
10	2	1	114	120
10	2	2	153	-150
11	2	-6	145	147
11	2	-5	82	-81
11	2	-4	98	-102
11	2	-3	172	174
11	2	-1	70	74
11	2	0	104	-107
12	2	-10	88	94
12	2	-8	75	80
12	2	-3	62	63
13	2	-6	96	90
13	2	-2	99	95
15	2	-5	67	-54
0	3	1	303	-288
0	3	3	75	-77
0	3	4	35	32
0	3	5	41	33
0	3	6	44	39
0	3	8	111	113
1	3	-9	43	-46
1	3	-7	41	-44
1	3	-6	94	-92
1	3	-5	153	149
1	3	-4	78	-78
1	3	-3	145	148
1	3	-2	229	-226
1	3	-1	215	-190
1	3	0	58	-61
1	3	1	252	-261
1	3	2	82	83
1	3	3	173	162
1	3	4	43	-43
1	3	5	126	-129
1	3	6	29	-28
1	3	8	95	-97
1	3	9	129	-127
1	3	10	86	86
1	3	11	57	-53
2	3	-9	112	-121
2	3	-8	88	95
2	3	-7	22	25
2	3	-6	175	-170
2	3	-5	142	137
2	3	-4	439	-436
2	3	-3	431	-427
2	3	-2	55	53
2	3	-1	157	169
2	3	0	260	254
2	3	1	74	-74
2	3	2	20	21
2	3	3	164	157
2	3	4	182	-183
2	3	5	54	52
2	3	6	125	-125
2	3	8	207	-205
2	3	9	68	-70
2	3	10	82	77
3	3	-10	156	156
3	3	-9	89	87
3	3	-8	85	-84
3	3	-6	103	-97
3	3	-5	96	94
3	3	-3	25	-19
3	3	-1	63	-55
3	3	0	124	119
3	3	1	189	-197
3	3	2	86	92
3	3	3	128	-133
3	3	4	213	-210
3	3	5	170	163
3	3	7	52	47
3	3	8	154	-150
4	3	-10	89	-89
4	3	-8	164	171
4	3	-7	50	55
4	3	-6	50	-55
4	3	-5	162	171
4	3	-4	688	681
4	3	-3	374	384
4	3	-2	274	-277
4	3	0	131	125
4	3	1	183	-188
4	3	3	74	71
4	3	4	81	80
4	3	5	114	114
4	3	7	111	-108
4	3	8	111	108
5	3	-11	66	68
5	3	-10	196	-196

h	k	l	Fo	Fc
5	3	-8	135	139
5	3	-7	76	-70
5	3	-6	64	65
5	3	-5	247	256
5	3	-3	91	97
5	3	-1	89	91
5	3	0	146	-141
5	3	1	269	262
5	3	2	82	86
5	3	3	38	-23
5	3	4	53	55
5	3	5	115	116
5	3	6	255	252
6	3	-10	146	-145
6	3	-7	184	-101
6	3	-6	43	-39
6	3	-5	125	128
6	3	-3	148	150
6	3	-2	187	-188
6	3	-1	26	10
6	3	0	209	-199
6	3	1	31	-39
6	3	5	88	92
6	3	6	107	104
6	3	7	159	150
6	3	8	52	-57
7	3	-11	117	-117
7	3	-9	89	-95
7	3	-7	79	-82
7	3	-5	73	77
7	3	-4	61	-68
7	3	0	251	-247
7	3	1	120	-126
7	3	3	77	-71
7	3	4	144	-149
7	3	5	52	64
8	3	-12	83	83
8	3	-11	87	-91
8	3	-8	179	175
8	3	-7	128	-127
8	3	-5	147	-141
8	3	-4	176	175
8	3	-2	60	66
8	3	-1	87	-93
8	3	0	39	-32
8	3	1	82	-84
8	3	2	87	84
9	3	-12	58	52
9	3	-8	82	79
9	3	-7	42	-33
9	3	-6	95	94
9	3	-4	142	-147
9	3	-2	73	84
9	3	-1	130	-138
9	3	0	110	117
9	3	1	111	-117
9	3	2	228	233
9	3	4	46	41
10	3	-6	101	-107
10	3	-5	75	75
10	3	-4	121	-127
10	3	-1	42	-54
10	3	0	126	130
10	3	3	77	-71
11	3	-10	80	-71
11	3	-8	53	-63
11	3	-6	117	-124
11	3	-5	83	-85
11	3	-4	81	84
11	3	-3	54	49
11	3	-2	73	-72
11	3	-1	83	80
11	3	0	81	-87
11	3	2	80	-84
12	3	-6	68	61
12	3	0	122	-120
13	3	-6	85	73
13	3	-4	52	45
14	3	-4	66	61
0	4	0	20	31
0	4	1	147	148
0	4	2	182	184
0	4	3	149	144
0	4	4	153	143
0	4	7	156	-157
0	4	8	56	57
0	4	10	97	96
1	4	-12	79	-78
1	4	-8	184	-188
1	4	-7	32	36
1	4	-6	85	79
1	4	-5	44	-41
1	4	-3	144	-145
1	4	-1	52	56
1	4	0	75	81
1	4	1	43	46
1	4	2	30	28
1	4	3	230	231
1	4	4	85	80
1	4	6	63	61
1	4	10	76	72
2	4	-10	90	-91
2	4	-8	80	82
2	4	-7	68	-62
2	4	-6	144	-151
2	4	-5	22	22
2	4	-3	297	-300
2	4	-2	796	-775
2	4	-1	53	-48
2	4	0	86	89
2	4	1	122	-125
2	4	2	76	-80
2	4	3	136	139

h	k	l	Fo	Fc
2	4	4	79	79
2	4	5	55	54
2	4	7	118	-114
2	4	8	79	-84
2	4	10	109	-106
3	4	-11	52	-59
3	4	-10	62	67
3	4	-9	61	-57
3	4	-8	198	201
3	4	-7	68	-60
3	4	-6	44	-47
3	4	-5	68	66
3	4	-4	157	-156
3	4	-3	242	-251
3	4	-2	151	-142
3	4	-1	125	-125
3	4	0	70	-68
3	4	1	101	98
3	4	2	94	-98
3	4	3	297	-297
3	4	4	36	34
3	4	5	41	-37
3	4	6	65	-66
3	4	7	113	-108
3	4	8	111	-111
4	4	-10	49	51
4	4	-8	56	56
4	4	-7	30	-22
4	4	-6	69	-70
4	4	-5	46	-36
4	4	-4	362	374
4	4	-3	164	168
4	4	-2	248	251
4	4	-1	165	-165
4	4	0	173	169
4	4	1	80	-82
4	4	2	31	-36
4	4	3	79	-75
4	4	5	52	-46
4	4	6	68	-65
4	4	9	83	-75
5	4	-8	108	-116
5	4	-7	100	108
5	4	-5	140	145
5	4	-4	159	165
5	4	-2	218	218
5	4	-1	74	-70
5	4	0	97	93
5	4	1	88	-87
5	4	2	44	39
5	4	3	141	143
5	4	5	40	37
5	4	6	46	46
5	4	8	108	104
6	4	-9	73	79
6	4	-8	132	-138
6	4	-7	154	156
6	4	-5	110	106
6	4	-4	55	-48
6	4	-3	54	43
6	4	-2	63	-60
6	4	-1	43	-35
6	4	1	132	139
6	4	4	62	-56
6	4	5	50	43
6	4	6	124	124
7	4	-7	120	127
7	4	-6	96	-92
7	4	-5	61	62
7	4	-4	70	-63
7	4	-3	96	94
7	4	-1	66	-62
7	4	1	53	62
7	4	2	90	-92
7	4	3	149	148
7	4	5	58	47
7	4	6	64	-69
8	4	-7	94	99
8	4	-6	67	-62
8	4	-5	46	38
8	4	-3	107	-113
8	4	2	124	-130
8	4	3	149	148
8	4	4	85	90
9	4	-8	80	77
9	4	-4	184	193
9	4	-3	59	-58
9	4	-2	281	-278
9	4	1	86	-81
9	4	3	45	41
9	4	4	72	78
10	4	-9	119	-121
10	4	-8	52	54
10	4	-7	58	-65
10	4	-6	86	88
10	4	-3	49	-43
10	4	-2	44	-49
10	4	2	79	85
11	4	-6	75	-76
11	4	0	129	127
12	4	-6	69	-68
12	4	-5	51	45
12	4	1	73	-66
0	5	1	59	-59
0	5	2	83	77
0	5	3	64	59
0	5	5	92	87
0	5	6	51	-50
0	5	7	35	-38
0	5	8	87	-84
0	5	9	66	72
1	5	-7	64	65
1	5	-6	69	-64

h	k	l	Fo	Fc
1	5	-3	49	-58
1	5	-2	34	37
1	5	-1	22	-17
1	5	1	102	107
1	5	2	49	46
1	5	4	196	192
1	5	6	188	-184
2	5	-9	66	71
2	5	-8	98	-93
2	5	-6	77	76
2	5	-4	70	71
2	5	-3	116	-115
2	5	-2	124	-128
2	5	-1	79	87
2	5	0	96	-94
2	5	1	102	107
2	5	6	53	54
2	5	7	60	58
2	5	8	58	55
2	5	9	88	-80
3	5	-10	82	-89
3	5	-9	90	92
3	5	-6	105	110
3	5	-5	92	-91
3	5	-2	53	-57
3	5	-1	30	-27
3	5	0	103	-104
3	5	1	202	205
3	5	2	74	-72
3	5	3	91	87
3	5	5	85	-86
3	5	7	49	-51
3	5	8	77	71
4	5	-8	100	-94
4	5	-5	355	-367
4	5	-4	233	-242
4	5	-3	108	118
4	5	-2	64	56
4	5	1	152	152
4	5	2	45	-40
4	5	3	52	-54
4	5	5	89	-98
4	5	6	65	-70
4	5	8	87	-83
5	5	-11	71	62
5	5	-10	85	87
5	5	-9	125	-128
5	5	-6	35	-38
5	5	-5	185	-190
5	5	-1	44	-39
5	5	0	38	-35
5	5	1	54	-61
5	5	2	39	-31
5	5	5	108	-104
5	5	6	100	-102
6	5	-10	82	84
6	5	-6	229	234
6	5	-5	49	57
6	5	-4	63	55
6	5	-3	143	-137
6	5	-2	120	110
6	5	1	43	-48
6	5	4	71	70
6	5	5	130	-125
7	5	-9	61	64
7	5	-7	78	77
7	5	-6	84	83
7	5	-4	84	81
7	5	-2	143	-141
7	5	-1	91	88
7	5	0	214	209
7	5	1	64	-76
7	5	2	79	82
7	5	4	137	134
8	5	-7	104	101
8	5	-5	80	87
8	5	-4	124	-127
8	5	-1	57	49
8	5	3	82	80
8	5	4	68	64
9	5	-5	60	62
9	5	-3	114	-114
9	5	0	91	-91
9	5	2	136	-129
10	5	-8	57	-59
10	5	-6	49	52
10	5	-4	73	74
10	5	0	61	-61
10	5	1	78	77
11	5	-5	86	-82
11	5	1	74	65
0	6	0	192	-189
0	6	1	130	-133
0	6	2	53	53
0	6	3	75	-75
0	6	4	71	-70
0	6	6	102	101
0	6	7	68	66
1	6	-8	114	118
1	6	-7	122	-123
1	6	-4	58	-54
1	6	-3	87	94
1	6	-1	85	-86
1	6	4	95	91
1	6	5	68	-67
2	6	-7	53	59
2	6	-5	36	-32
2	6	-3	105	107
2	6	-2	103	104
2	6	-1	110	-111
2	6	0	147	148
2	6	2	83	84
2	6	5	70	-68

h	k	l	Fo	Fc
2	6	7	59	63
3	6	-7	123	120
3	6	-6	105	-109
3	6	-3	80	84
3	6	-2	38	45
3	6	0	52	58
3	6	1	43	41
3	6	2	158	163
3	6	4	96	-96
3	6	5	59	59
4	6	-8	48	-52
4	6	-7	65	69
4	6	-6	55	-54
4	6	-5	54	-59
4	6	-4	294	-299
4	6	-1	79	71
4	6	0	88	-84
4	6	1	69	70
4	6	3	80	87
4	6	6	80	-76
5	6	-7	62	-56
5	6	-5	61	-65
5	6	-4	143	-143
5	6	-2	108	-108
5	6	-1	75	68
5	6	0	43	47
5	6	1	90	-84
5	6	2	76	-88
5	6	4	89	-91
5	6	6	77	-73
6	6	-7	124	-127
6	6	-5	83	89
6	6	-2	86	88
6	6	1	65	-58
6	6	4	81	-81
6	6	5	59	-56
7	6	-7	53	-49
7	6	-6	139	137
7	6	-3	62	-69
7	6	-2	57	59
7	6	-1	64	60
7	6	0	104	-102
7	6	3	78	-78
8	6	-8	74	78
8	6	-6	83	78
8	6	-3	43	38
8	6	-2	43	-43
8	6	3	112	-110
9	6	-4	59	-63
9	6	-3	124	118
9	6	-1	51	-57
11	6	-4	76	-71
0	7	2	106	-115
0	7	4	70	-74
0	7	6	55	56
1	7	-7	78	74
1	7	-5	86	-88
1	7	-4	86	89
1	7	-2	43	48
1	7	2	51	-54
1	7	4	54	-55
1	7	5	118	116
1	7	6	88	91
2	7	-4	86	92
2	7	-1	45	-42
3	7	-8	56	60
3	7	-7	57	-56
3	7	-5	45	38
3	7	-3	67	-66
3	7	1	56	-52
3	7	2	62	66
4	7	-5	79	77
4	7	-3	77	-76
4	7	-2	68	59
4	7	6	75	71
5	7	-4	56	-51
5	7	-1	100	98
5	7	2	61	63
6	7	-7	89	-94
6	7	-6	169	-174
6	7	-5	67	67
6	7	-3	65	62
6	7	-2	56	-56
6	7	4	55	-57
7	7	-6	89	-92
7	7	-2	61	60
7	7	-1	142	-142
7	7	2	87	-91
8	7	-4	51	54
0	8	0	87	95
0	8	1	63	-63
1	8	-5	94	94
1	8	-1	70	70
1	8	5	78	78
2	8	-5	55	55
2	8	0	80	-76
2	8	2	72	-71
2	8	5	77	84
3	8	-6	62	61
4	8	-6	54	57
4	8	-4	72	69
4	8	-3	53	-55
4	8	0	69	59
5	8	-4	108	103
5	8	1	101	102
5	8	2	70	-70
6	8	-5	91	-96
6	8	-4	58	51
6	8	-1	64	59

Table 5. The principal axes of the thermal vibration ellipsoids given by the components of a unit vector in fractional coordinates e_x, e_y, e_z; the corresponding r.m.s. amplitudes, and the B-values.

Atom	e_x	e_y	e_z	$(\overline{u^2})^{\frac{1}{2}}$ Å	B(Å^2)
		(II)			
	.069	.028	−.176	.249	4.88
S	.093	−.038	.116	.241	4.57
	.016	.100	.092	.200	3.15
	.084	−.002	.159	.251	4.99
O	.081	.001	−.166	.228	4.11
	.001	.111	.004	.166	2.16
	.102	.005	.112	.249	4.90
N	−.057	.017	.198	.222	3.88
	.004	.109	−.036	.167	2.21
	.085	.006	.157	.236	4.42
C1	.010	.109	−.038	.191	2.88
	−.079	.020	.163	.181	2.59
	.068	.035	.173	.277	6.07
C2	−.094	.012	.133	.231	4.21
	.012	−.104	.073	.201	3.20
	.075	.068	.105	.298	7.03
C3	−.089	.057	.090	.237	4.43
	.001	−.067	.184	.214	3.61
	−.006	.109	.035	.253	5.04
C4	.016	.017	−.225	.237	4.44
	.115	.003	.033	.220	3.83
	.080	−.022	.161	.268	5.68
C5	−.081	.013	.164	.222	3.90
	.026	.108	.013	.198	3.11
	.098	.001	.126	.245	4.74
C6	.063	.013	−.191	.188	2.78
	−.009	.110	.022	.183	2.65
	.097	−.006	.127	.255	5.13
C7	.050	.077	−.132	.191	2.87
	−.041	.079	.139	.180	2.56
		(III)			
	.076	.110	.030	.308	7.49
O1	.110	−.180	.011	.300	7.12
	.122	.093	−.015	.253	5.04
	.007	−.064	.003	.291	6.70
O2	−.070	.203	.006	.263	5.46
	.167	.088	.011	.221	3.87

Table 5. Continued.

	.002	.153	−.025	.272	5.86
N	.012	.172	.023	.232	4.24
	.181	−.014	.008	.224	3.96
	.002	−.096	.031	.276	6.02
C1	.174	.060	.012	.225	3.98
	−.051	.201	.011	.211	3.52
	.058	.097	−.026	.303	7.24
C2	−.072	.201	.006	.246	4.76
	.156	.057	.023	.235	4.37
	.163	.091	.002	.286	7.45
C3	.053	−.049	.034	.275	5.99
	−.059	.206	.007	.240	4.53
	.104	−.037	.033	.303	7.27
C4	.139	.106	−.008	.248	4.86
	−.054	.201	.010	.240	4.56
	.025	−.119	.030	.297	6.97
C5	−.084	.166	.013	.232	4.25
	.158	.107	.013	.226	4.02
	.001	−.119	.029	.272	5.83
C6	.162	.089	.016	.224	3.98
	−.081	.176	.012	.195	3.01
	.031	−.120	.030	.281	6.24
C7	.136	.143	.015	.250	4.92
	−.116	.135	.011	.226	4.03
	.028	.209	−.012	.316	7.90
CM	−.105	.093	.019	.267	5.62
	.145	.027	.027	.249	4.89
		(IV)			
	.159	−.106	.003	.336	8.93
O1	.106	.061	−.037	.293	6.78
	.118	.087	.030	.208	3.42
	−.162	.051	.029	.258	5.26
O2	.137	−.016	.037	.226	4.05
	.074	.140	−.006	.214	3.63
	.169	.098	−.004	.255	5.14
N	−.110	.096	.028	.238	4.47
	.099	−.060	.038	.198	3.11
	.073	.019	.045	.221	3.87
C1	.043	.145	−.009	.216	3.67
	−.208	.037	.014	.197	3.06
	.001	.144	.014	.271	5.80
C2	.140	.034	−.036	.238	4.46
	.175	−.027	.029	.209	3.46

Table 5. Continued.

	.027	−.131	.023	.315	7.82
C3	−.128	.050	.036	.238	4.46
	.182	.055	.022	.206	3.36
	.078	−.074	.038	.323	8.22
C4	−.151	.069	.028	.226	4.03
	.147	.111	.008	.209	3.43
	.129	.022	.038	.285	6.41
C5	.091	.121	−.021	.224	3.95
	−.160	.086	.019	.209	3.46
	.121	.062	.035	.227	4.08
C6	.034	.122	−.027	.219	3.77
	−.186	.063	.018	.181	2.59
	.102	−.129	.012	.249	4.90
C7	.186	.046	−.022	.236	4.41
	.072	.062	.041	.211	3.51

(V)

	.046	.145	.055	.263	5.46
O	−.037	.027	.069	.220	3.82
	.055	−.105	.094	.189	2.81
	.003	.177	−.021	.274	5.94
N1	.068	.014	.112	.222	3.89
	−.043	.035	.059	.196	3.03
	.028	.168	.033	.261	5.40
N2	.006	−.024	.116	.203	3.25
	.075	−.061	.045	.192	2.91
	.016	−.176	.019	.233	4.27
C1	.067	.037	.110	.204	3.29
	.041	.010	−.063	.187	2.76
	−.011	.177	.008	.256	5.19
C2	.050	.035	−.045	.223	3.92
	.062	.002	.120	.205	3.33
	.018	−.175	.029	.288	6.55
C3	.077	.033	.033	.244	4.70
	.017	.033	.121	.198	3.10
	.016	−.154	.067	.271	5.78
C4	.076	.053	.074	.246	4.79
	−.020	.078	.081	.197	3.05
	.013	.173	.036	.265	5.54
C5	.036	−.051	.123	.242	4.64
	.071	−.007	.002	.210	3.47
	−.004	.157	.052	.225	4.00
C6	.003	−.089	.099	.204	3.28
	.080	.011	.063	.185	2.70

Table 5. Continued.

C7	.005	.178	.021	.224	3.98
	.003	.026	−.108	.216	3.67
	.080	−.012	.066	.188	2.79
	.037	−.144	.073	.287	6.50
C8	.028	.103	.105	.224	3.96
	.066	.035	−.009	.218	3.77
	.025	.172	.016	.241	4.60
C9	.073	−.055	.027	.207	3.40
	.022	−.010	.125	.190	2.84
	.015	.119	−.057	.250	4.93
C10	.008	.125	.086	.224	3.96
	.076	−.053	.077	.217	3.71
	.044	.150	.047	.298	7.01
C11	.022	−.055	.119	.262	5.42
	.063	−.085	.005	.204	3.30
	.013	.168	.037	.306	7.39
C12	.022	−.065	.117	.252	5.02
	.076	−.011	.025	.215	3.65
	−.029	.003	.082	.276	6.01
C13	.035	−.160	.048	.248	4.87
	.067	.084	.087	.220	3.82
	.006	.152	−.055	.269	5.71
C14	.077	−.038	.039	.236	4.41
	.022	.090	.109	.209	3.46
	.010	.142	.076	.287	6.49
CM	.058	.063	−.022	.234	4.31
	.055	−.092	.101	.188	2.80
		(VI)			
	−.039	.104	.017	.259	5.30
O	.059	.013	.079	.220	3.81
	.040	.081	−.034	.185	2.71
	−.033	.097	.032	.264	5.50
N1	.065	.076	.012	.220	3.83
	.036	−.049	.081	.174	2.39
	.072	−.061	.018	.231	4.20
N2	.025	.044	.083	.223	3.93
	.030	.109	−.023	.182	2.61
	−.043	.102	.011	.227	4.06
C1	.040	−.007	.087	.208	3.43
	.056	.084	−.006	.193	2.95
	.038	−.116	.007	.279	6.15
C2	.035	.017	.087	.253	5.07
	.063	.061	−.010	.194	2.99

Table 5. Continued.

	.003	−.124	.030	.274	5.94
C3	−.012	.046	.061	.251	4.99
	.080	.011	.042	.205	3.30
	.051	.073	−.025	.267	5.63
C4	.004	.090	.062	.234	4.32
	.063	−.064	.058	.204	3.29
	.067	.025	−.017	.232	4.25
C5	.022	.094	.062	.225	4.01
	.041	−.090	.060	.207	3.40
	.026	−.071	.074	.218	3.75
C6	−.063	.043	.018	.198	3.10
	.044	.103	.043	.186	2.74
	.074	−.016	.063	.232	4.26
C7	−.019	.088	.050	.208	3.40
	.029	.098	−.036	.171	2.31
	−.047	.084	.023	.243	4.64
C8	.066	.052	.063	.227	4.08
	.007	.089	−.058	.192	2.92
	.075	−.039	.010	.226	4.05
C9	.030	.057	.079	.216	3.68
	.011	.113	−.036	.176	2.43
	.077	−.031	.011	.252	5.02
C10	.024	.123	.028	.236	4.38
	.014	−.038	.083	.204	3.27
	−.059	.071	.012	.296	6.93
C11	.044	.110	.008	.255	5.13
	.035	−.019	.087	.210	3.47
	−.026	.053	.059	.299	7.08
C12	.050	−.103	.009	.252	4.99
	.059	−.063	.064	.213	3.59
	.026	.020	.087	.277	6.07
C13	.055	.087	−.005	.258	5.27
	.054	−.098	.013	.217	3.72
	.080	−.012	.020	.259	5.30
C14	.001	−.019	.047	.223	3.92
	.014	.075	.072	.219	3.79

linked by bonds (of length 2.980 Å) between heterocyclic and amino nitrogens. This type of hydrogen bond occurs also in adenosine,[19] but is there much longer (3.133 Å). Other bond lengths reported [25] show that the value 2.933 Å corresponds to a strong hydrogen bond of this type.

The considerable change in geometry of the heterocyclic part of (VI) with respect to (V) (and the others) are probably related to the hydrogen bonds.

Table 6. Bond distances and angles with estimated standard deviations.

Distance	(Å) (I)	(II)	Distance	(Å) (I)	(II)
S – C7	1.629(7)	1.643(3)	C2 – C3	1.370(12)	1.396(11)
O – C7	1.393(9)	1.369(8)	C3 – C4	1.368(13)	1.387(6)
N – C7	1.354(8)	1.347(8)	C4 – C5	1.397(13)	1.381(10)
O – C1	1.414(8)	1.383(7)	C5 – C6	1.374(10)	1.385(10)
N – C6	1.404(9)	1.398(8)	C6 – C1	1.375(10)	1.390(5)
C1 – C2	1.390(12)	1.352(9)	N – CM	1.470(9)	–

Angle	(°) (I)	(II)	Angle	(°) (I)	(II)
S – C7 – O	123.1(5)	122.8(4)	N – C6 – C5	133.2(7)	134.1(6)
S – C7 – N	129.5(6)	129.7(5)	C1 – C2 – C3	114.1(8)	115.6(6)
O – C7 – N	107.3(6)	107.5(3)	C2 – C3 – C4	121.7(8)	121.8(9)
C7 – O – C1	108.5(5)	108.6(3)	C3 – C4 – C5	123.3(8)	121.7(9)
C7 – N – C6	109.6(6)	110.5(4)	C4 – C5 – C6	116.2(8)	116.5(7)
O – C1 – C6	106.9(6)	108.3(6)	C5 – C6 – C1	119.0(7)	120.7(7)
N – C6 – C1	107.8(6)	105.2(6)	C6 – C1 – C2	125.7(7)	123.7(7)
O – C1 – C2	127.4(7)	128.1(5)	C6 – N – CM	125.5(6)	–
			C7 – N – CM	124.9(6)	

Distance	(Å) (III)	(IV)	Distance	(Å) (III)	(IV)
O1 – C7	1.210(2)	1.211(3)	C2 – C3	1.397(3)	1.380(4)
O2 – C7	1.379(2)	1.368(3)	C3 – C4	1.380(3)	1.375(4)
N – C7	1.355(2)	1.346(3)	C4 – C5	1.384(3)	1.383(4)
O2 – C1	1.390(2)	1.386(2)	C5 – C6	1.382(3)	1.385(3)
N – C6	1.388(2)	1.390(3)	C6 – C1	1.373(2)	1.366(3)
C1 – C2	1.360(3)	1.374(3)	N – CM	1.441(2)	–

Angle	(°) (III)	(IV)	Angle	(°) (III)	(IV)
O1 – C7 – O2	122.2(2)	121.7(2)	N – C6 – C5	132.9(2)	133.7(2)
O1 – C7 – N	129.7(2)	129.9(2)	C1 – C2 – C3	116.5(2)	116.0(3)
O2 – C7 – N	108.1(2)	108.4(2)	C2 – C3 – C4	120.7(2)	121.5(2)
C7 – O2 – C1	107.2(1)	106.8(2)	C3 – C4 – C5	122.0(2)	121.9(2)
C7 – N – C6	109.5(1)	109.8(2)	C4 – C5 – C6	116.8(2)	116.6(3)
O2 – C1 – C6	108.8(2)	109.5(2)	C5 – C6 – C1	120.7(2)	120.8(2)
N – C6 – C1	106.4(1)	105.5(2)	C6 – C1 – C2	123.3(2)	123.2(2)
O2 – C1 – C2	127.9(2)	127.3(2)	C6 – N – CM	126.4(2)	–
			C7 – N – CM	124.1(2)	–

Table 6. Continued.

Distance	(Å) (V)	(VI)	Distance	(Å) (V)	(VI)
N1 – C7	1.264(5)	1.329(3)	C6 – C1	1.365(6)	1.379(3)
O – C7	1.408(4)	1.375(3)	N2 – CM	1.453(6)	–
N2 – C7	1.345(5)	1.310(3)	N1 – C8	1.461(6)	1.467(3)
O – C1	1.401(5)	1.390(3)	C8 – C9	1.524(6)	1.502(4)
N2 – C6	1.395(5)	1.399(3)	C9 – C10	1.371(6)	1.382(4)
C1 – C2	1.369(5)	1.366(4)	C10 – C11	1.396(6)	1.376(4)
C2 – C3	1.395(7)	1.379(4)	C11 – C12	1.365(8)	1.381(4)
C3 – C4	1.366(7)	1.395(4)	C12 – C13	1.357(7)	1.373(4)
C4 – C5	1.399(6)	1.387(4)	C13 – C14	1.392(6)	1.375(4)
C5 – C6	1.377(6)	1.381(3)	C14 – C9	1.381(6)	1.394(4)

Angle	(°) (V)	(VI)	Angle	(°) (V)	(VI)
N1 – C7 – O	125.3(4)	118.2(2)	C6 – C1 – C2	124.0(4)	123.9(2)
N1 – C7 – N2	126.9(4)	127.6(2)	C6 – N2 – CM	126.4(4)	–
O – C7 – N2	107.8(3)	114.2(2)	C7 – N2 – CM	123.3(4)	–
C7 – O – C1	106.1(3)	104.0(2)	C7 – N1 – C8	119.2(4)	121.4(2)
C7 – N2 – C6	110.2(3)	105.1(2)	N1 – C8 – C9	113.0(4)	110.3(2)
O – C1 – C6	109.4(3)	108.1(2)	C8 – C9 – C10	119.3(4)	121.2(2)
N2 – C6 – C1	106.4(4)	108.5(2)	C8 – C9 – C14	121.5(4)	121.3(2)
O – C1 – C2	126.6(4)	128.0(2)	C9 – C10 – C11	120.1(5)	121.5(3)
N2 – C6 – C5	132.5(4)	131.7(2)	C10 – C11 – C12	120.2(5)	120.3(3)
C1 – C2 – C3	115.5(5)	116.7(3)	C11 – C12 – C13	120.1(5)	119.0(3)
C2 – C3 – C4	121.0(4)	120.2(3)	C12 – C13 – C14	120.3(5)	120.6(3)
C3 – C4 – C5	122.8(5)	122.2(3)	C13 – C14 – C9	120.1(5)	121.1(3)
C4 – C5 – C6	115.6(5)	117.0(3)	C14 – C9 – C10	119.2(4)	117.4(3)
C5 – C6 – C1	121.1(4)	119.8(2)			

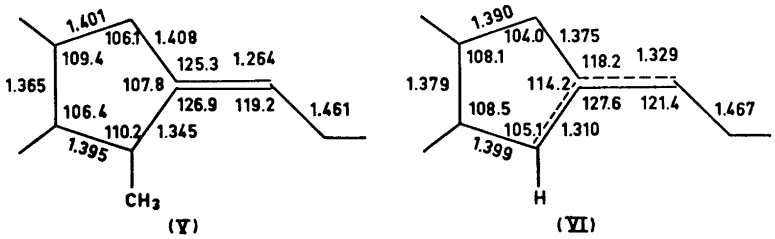

Fig. 2.

C7 – N1 is longer, in fact even longer than C7 – N2, which, on the other hand, is significantly shorter than in (V). The effect on the O – C7 bond is the same (see Fig. 2). Together with these changes in bond lengths, there are corresponding differences in angles. The angle O – C7 – N2 is opened by 6.4°, while C1 – O – C7 and C7 – N2 – C6 are 2.1° and 5.1° smaller, respectively. In agreement with the longer bond, the C7 – N1 stretching frequency of (VI) has recently been determined [26,27] to bee about 1650 cm^{-1}.

The C=S distances (1.629 Å) and (1.643 Å) agree within error limits with the value obtained for 1,3-dithiolane-2-thione (1.652 Å),[20] but is significantly shorter than that of ethylenethiourea (1.708 Å).[21] 1.210 Å and 1.211 Å for C=O bonds correspond to the value of 1.211 Å in 2-oxazolidinone,[22] which, however, has a considerably shorter N – C7 bond (1.304 Å). The O – C7 bond of 2-oxazolidinone is also shorter (1.354 Å) than in the benzoxazoline derivatives. The angles C – O – C, C – N – C and O – C – N of the heterocyclic ring resemble those of *N*-methyl-5,5-dimethyl-oxazolidine-2,5-dione,[23] and also the N – C(methyl) single bond distance of this compound (1.461 Å) agrees with the values of (I), (III), and (V). The geometry around the central bond, C1 – C6, corresponds to that of 2-acetyl-3-indazolinone.[24]

Bond distances and angles in the benzylidene parts of (V) and (VI) have normal values.

Except for the hydrogen bond in (VI), no short intermolecular contacts have been observed.

Acknowledgement. The author would like to thank Dr. K. Davidkov* for supplying the compounds and preparing the crystals.

REFERENCES

1. Simov, D. and Davidkov, K. *Compt. Rend. Acad. Bulgare Sci.* **23** (1970) 1361.
2. Simov, D. and Atanassov, K. *Compt. Rend. Acad. Bulgare Sci.* **20** (1967) 433.
3. Simov, D. and Kaltceva, V. *Annaire de l'Université de Sofia, Faculté de Chimie* **61** (1966/1967) 155.
4. Simov, D. and Kaltceva, V. *Annaire de l'Université de Sofia, Faculté de Chimie* **57** (1962/1963) 105.
5. Davidkov, K. and Simov, D. *Compt. Rend. Acad. Bulgare Sci.* **21** (1968) 1193.
6. Davidkov, K. *Personal communication.*
7. Bellamy, L. J. *The Infrared Spectra of Complex Molecules*, 2nd Ed., Wiley, New York 1958, p. 532.
8. Jones, R. N. and Sandorfy, S. *Chemical Application of Spectroscopy*, Interscience, New York 1956, p. 268.
9. Groth, P., Davidkov, K. and Simov, D. *Acta Chem. Scand.* **26** (1972) 1141.
10. Dahl, T., Gram, F., Groth, P., Klewe, B. and Rømming, C. *Acta Chem. Scand.* **24** (1970) 2232.
11. Schomaker, V. and Trueblood, K. N. *Acta Cryst.* **B 24** (1968) 63.
12. Bachechi, F. and Zambonelli, L. *Acta Cryst.* **B 28** (1972) 2489.
13. Bayer, E. and Häflinger, G. *Chem. Ber.* **99** (1966) 1689.
14. Groth, P. *Acta Chem. Scand.* **22** (1968) 142.
15. Hope, H. and Klewe, B. *Personal communication.*
16. Levine, I. *J. Chem. Phys.* **38** (1963) 2326.
17. Sastry, K. V. L. N. and Curl, Jr., R. F. *J. Chem. Phys.* **41** (1964) 77.
18. Sharma, B. D. and McConnell, J. F. *Acta Cryst.* **19** (1965) 797.

* Present address: Department of Chemistry, University of Sofia, Sofia, Bulgaria.

19. Marsh, R. and Lai, T. F. *Acta Cryst.* **B 28** (1972) 1982.
20. Klewe, B. and Seip, H. M. *Acta Chem. Scand.* **26** (1972) 1860.
21. Wheatley, P. J. *Acta Cryst.* **6** (1953) 369.
22. Turley, J. W. *Acta Cryst.* **A 25** (1969) 130.
23. Kistenmacher, T. J. and Stucky, G. D. *Acta Cryst.* **B 26** (1970) 1445.
24. Smith, D. L. and Barrett, E. K. *Acta Cryst.* **B 25** (1969) 2355.
25. Pimentel, C. G. and McClelland, A. L. *The Hydrogen Bond*, Reinhold, New York 1959, p. 288.
26. Simov, D., Galatov, B. and Davidkov, K. *Zh. Prikl. Spectrosk.* **14** (1971) 339.
27. Klæboe, P. *Personal communication.*

Received October 12, 1972.

ACTA CHEMICA SCANDINAVICA 27 (1973) 970–976

Metal Ammine Formation in Solution

XVI. Stability Constants of Some Metal(II)-Pyridine System

JANNIK BJERRUM

Chemistry Department I, Inorganic Chemistry, The H. C. Ørsted Institute, University of Copenhagen, DK-2100 Copenhagen Ø, Denmark

In the Tables of Stability Constants [1,2] the author has presented values for the stability constants for pyridine complexes of Mn^{2+}, Fe^{2+}, Co^{2+}, Ni^{2+}, Zn^{2+}, and Cd^{2+}, the measurements of which have not been published. This paper gives the experimental data, and a discussion of the slightly revised constants (see Table 2).

Metal pyridine complex formation was studied by glass electrode measurements by the author (as early as in 1941 – 45) partly in cooperation with Else Plejl. The data were used in a review article,[3] and our values for the pyridine stability constants of nine metal ions are presented in Tables of Stability Constants.[1,2] However, only the measurements with Cu^{2+}, Ag^{+}, and Hg^{2+} are published in detail.[4,5] As pointed out in these publications, an important cause of error appears when determining the stability constants of the relatively weak pyridine complexes by glass electrode measurements, an error caused by "the strong activity decreasing effect of pyridine on pyridinated ions as well as on the pyridine itself". Probably owing to this effect, some authors have found too high values for the stability constants, especially at high pyridine concentrations. Thus Atkinson and Bauman [6] by glass electrode measurements determine log K_1 in the Mn(II)-system to be as high as 1.86 compared to the author's value 0.14 (see Table 2). Owing to this and other disagreements with data in the newer literature, the author has found it appropriate to contribute to the discussion by publishing in detail also the remaining part of the old measurements. The stability constants were in all cases determined by glass electrode measurements at 25°C in 0.5 M pyridinium nitrate solutions with varying concentrations of metal(II) salt and pyridine.

EXPERIMENTAL

Solutions. The various solutions were prepared in calibrated measuring flasks by weighing or pipetting from stock solutions of metal(II) salt, pyridinium nitrate, and pyridine.

The stock solutions of manganese(II) and iron(II) were the chlorides, in all other cases the nitrates. Good quality chemicals were used, and the solutions were analyzed by conventional methods. The stock solutions of the metal(II) salts were stabilized with a small titrated excess of acid. This was especially necessary for the iron(II) chloride solution, which was prepared under air-free condition, and found to contain less than 0.5 % iron(III).

The pyridine was distilled and analyzed as previously described.[4] A 2.5 M stock solution of pyridinium nitrate was prepared by neutralizing pyridine with 5 M nitric acid. The small excess of acid or base in the pyridinium nitrate stock solution was determined by pH-measurements.[4]

The iron(II)-, manganese(II)-, and cobalt(II)-pyridine solutions were prepared under airfree conditions, and oxidation during the measurements was found to be negligible.

Glass electrode measurements. These measurements were made as previously described.[7] A Radiometer potentiometer, PHM3, was used. The glass electrodes were especially selected and proved to have a theoretical pH-dependence. The whole apparatus was placed in an air thermostat at 25 ± 0.1°C.

TREATMENT OF MEASUREMENTS

The data for all the metal ions studied are collected in Table 1. The calculations were based on the potential differences, as measured by glass electrodes, between the metal(II)-pyridine-0.5 M $pyHNO_3$ solution and a standard 0.5 M $pyHNO_3$ solution with a small known pyridine concentration in the range $0.02-0.04$ M. What is denoted as the apparent pyridine activity a_{py}' was calculated from the measured potential difference $E-E_{st}$, according to the expression

$$-\log\ a_{py}' = (E-E_{st})/0.0591 - \log\ [py]_{st} \qquad (1)$$

As discussed in the preceding papers,[4,5] the relationship between the pyridine concentration and a_{py}' is given by the expression

$$-\log\ [py] = -\log\ a_{py}' - 0.082[py] + \alpha C_M \qquad (2)$$

The experimental factor 0.082 corrects for the influence of the pyridine itself, and α is a salting-out factor found to have weak positive values for aqua ions and negative values for the pyridine complexes and increasing with the number of pyridine ligands taken up. Utilizing this knowledge, the following relationship has been assumed to be valid

$$\alpha = \tfrac{1}{7}(0.5-\bar{n}) \qquad (3)$$

The expression is made to agree with what has been found for the Cu(II) system in 0.5 M $pyHNO_3$, $\alpha \sim -0.4$ for $\bar{n} \sim 3.5$,[4] and gives a correction for the weakly salting-out effect of the aqua metal ions by estimating that $\alpha \sim 0$, when half of the aqua ions have been converted into monopyridine complex. Utilizing the expressions (2) and (3),

$$\bar{n}_{exp} = \frac{C_{py} + [H^+] - [py]}{C_M} \qquad (4)$$

is calculated from the experimental data and given in Table 1. In expression (4), for the average ligand number, C_{py} and C_M are the stoichiometrical concentrations of pyridine and metal(II) salt. The stoichiometrical pyridine con-

Table 1. Glass electrode measurements in metal(II) nitrate solutions in 0.5 M $pyHNO_3$ at 25°C.

$$-\log[py] = -\log a'_{py} - 0.082[py] - \tfrac{1}{7}(\bar{n} - 0.5)C_M$$

No.	C_M	C_{py}	$-\log a'_{py}$	$\bar{n}'$	$-\log[py]$	$[py]$	$[H^+]$	$\bar{n}_{exp.}$	$\bar{n}_{calc.}$
				Mn(II): $\log K_1$ 0.14, $\log\beta_2$ -0.4					
1	0.0963	0.1002	1.045	0.104	1.043	0.0906	0.00003	0.098	0.114
2	0.2044	0.2351	0.733	0.246	0.7255	0.1882	-	0.229	0.223
3	0.3108	0.3491	0.599	0.313	0.587	0.2588	-	0.290	0.284
4	0.3445	0.5086	0.447	0.440	0.422	0.3782	-	0.379	0.382
				Fe(II): $\log K_1$ 0.6, $\log\beta_2$ 0.9					
1	0.04125	0.03931	1.465	0.124	1.464	0.0344	0.00009	0.121	0.135
2	0.06046	0.08005	1.186	0.247	1.183	0.0656	0.00005	0.240	0.251
3	0.1040	0.09459	1.198	0.300	1.196	0.0637	0.00005	0.297	0.244
4	0.1561	0.1492	1.057	0.394	1.052	0.0887	0.00003	0.387	0.333
5	0.1013	0.1940	0.858	0.547	0.846	0.1425	-	0.508	0.503
6	0.1432	0.2932	0.715	0.702	0.696	0.202	-	0.635	0.662
7	0.2140	0.4769	0.570	0.971	0.535	0.292	-	0.865	0.854
				Co(II): $\log K_1$ 1.15, $\log\beta_2$ 1.7, $\log\beta_3$ 1.4					
1	0.0357	0.03692	1.592	0.321	1.591	0.02564	0.00012	0.319	0.305
2	0.0907	0.09623	1.306	0.517	1.302	0.0499	0.00006	0.512	0.522
3	0.03465	0.09662	1.147	0.732	1.140	0.0725	0.00004	0.698	0.681
4	0.2480	0.4008	0.876	1.079	0.845	0.1430	-	1.039	1.027
5	0.1387	0.3505	0.758	1.268	0.729	0.1868	-	1.180	1.174
6	0.2480	0.6498	0.579	1.559	0.522	0.3008	-	1.406	1.436
				Ni(II): $\log K_1$ 1.78, $\log\beta_2$ 3.0, $\log\beta_3$ 3.3, $\log\beta_4$ 3.0, $\log\beta_5$ (2.7)					
1	0.04132	0.01724	2.252	0.283	2.252	0.00560	0.00053	0.283	0.292
2	0.04416	0.03727	1.903	0.569	1.902	0.01252	0.00024	0.568	0.563
3	0.09794	0.09677	1.697	0.784	1.692	0.0203	0.00015	0.782	0.776
4	0.04336	0.09548	1.370	1.220	1.363	0.0434	0.00007	1.204	1.209
5	0.1492	0.3312	1.069	1.647	1.038	0.0915	0.00004	1.606	1.635
6	0.1519	0.3867	0.961	1.826	0.925	0.1189	0.00003	1.763	1.776
7	0.1824	0.4714	0.914	1.916	0.868	0.1355	-	1.840	1.848
8	0.2387	1.0068	0.494	2.875	0.393	0.405	-	2.522	2.450
9	0.2565	1.290	0.356	3.310	0.226	0.595	-	2.710	2.683
10	0.2550	1.481	0.273	3.717	0.122	0.755	-	2.846	2.823
				Zn(II): $\log K_1$ 0.98, $\log\beta_2$ 1.45, $\log\beta_3$ 1.6, $\log\beta_4$ 1.4					
1	0.03985	0.01806	1.866	0.117	1.867	0.01360	0.00022	0.117	0.124
2	0.02851	0.03659	1.538	0.270	1.537	0.0291	0.00010	0.266	0.249
3	0.1016	0.09606	1.291	0.442	1.288	0.0515	0.00006	0.439	0.416
4	0.02850	0.09676	1.101	0.616	1.094	0.0805	0.00004	0.572	0.596
5	0.09946	0.1946	0.971	0.882	0.957	0.1104	0.00003	0.847	0.770
6	0.1500	0.3479	0.768	1.182	0.740	0.182	-	1.106	1.100
7	0.2013	0.5835	0.589	1.619	0.538	0.290	-	1.458	1.476
8	0.1300	0.6303	0.439	2.050	0.3835	0.4135	-	1.669	1.797
9	0.2473	0.9775	0.381	2.271	0.290	0.513	-	1.879	1.998
10	0.1312	0.8604	0.327	2.962	0.248	0.565	-	2.251	2.086
				Cd(II): $\log K_1$ 1.30, $\log\beta_2$ 2.14, $\log\beta_3$ 2.5, $\log\beta_4$ 2.3					
1	0.0402	0.01702	2.008	0.187	2.009	0.00980	0.00031	0.187	0.183
2	0.03965	0.03665	1.656	0.371	1.655	0.02212	0.0014	0.370	0.386
3	0.1006	0.09530	1.448	0.594	1.444	0.0360	0.00008	0.591	0.582
4	0.03976	0.09589	1.211	0.867	1.204	0.0625	0.00005	0.842	0.887
5	0.1004	0.1943	1.081	1.110	1.066	0.0860	0.00004	1.079	1.102
6	0.1790	0.3452	0.981	1.345	0.951	0.1120	0.00003	1.302	1.299
7	0.2776	0.6021	0.858	1.670	0.802	0.1578	-	1.600	1.567
8	0.1599	0.4849	0.749	1.918	0.703	0.1981	-	1.793	1.750
9	0.2785	0.7783	0.692	2.065	0.615	0.2426	-	1.923	1.913
10	0.2228	0.6945	0.657	2.128	0.589	0.2577	-	1.960	1.961

centration is given as the added molar concentration corrected for eventual excess of acid in the metal(II) stock solutions, and for non-equivalence of acid or base in the pyridinium nitrate stock solution. The hydrogen ion concentration is in most cases very small compared with the concentration of free pyridine, but is corrected for by means of $pK_{pyH^+} = 5.21$.[4] For comparison, the 5th column of Table 1 gives the values for the ligand number $\bar{n}'$ as calculated without correction for salt effects, as most authors do, by inserting a_{py}' for [py] in (4).

The cumulative stability constants stated in Table 1 are computed using mass action expressions with concentrations inserted for the metal ions, but as discussed in the preceding papers [4,5] with the value of a_{py}' for $C_M = 0$, inserted instead of [py]. For comparison the last column of Table 1 gives the values for the ligand number, $\bar{n}_{calc}$, as calculated from the estimated stability constants for the values of $a_{py}' = [py]10^{0.082[py]}$ in question.

The agreement between the two sets of ligand numbers is on the whole satisfactory. This is also seen from Fig. 1 in which the formation curves are drawn through the calculated points. However, it must be considered that the

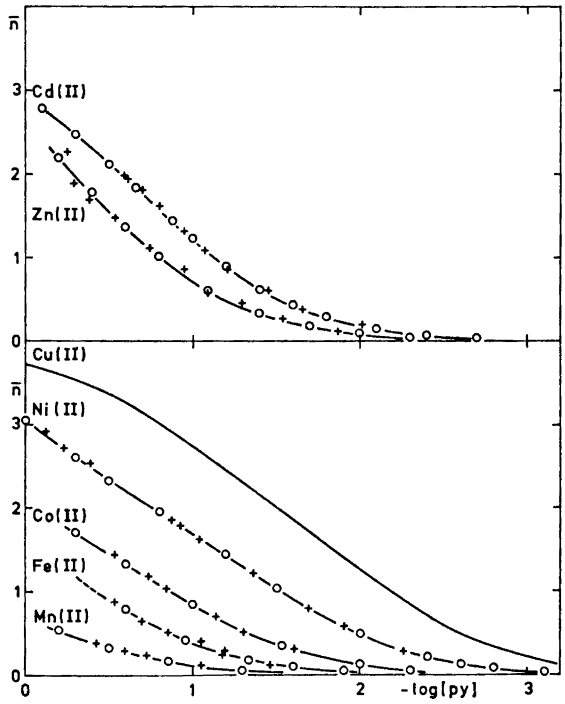

Fig. 1. Formation curves ($\bar{n}$ *vs.* $-\log$ [py]) for the metal(II) pyridine systems studied in 0.5 M $pyHNO_3$ at 25°C. The upper part of the figure is for zinc and cadmium, and the lower part is for divalent manganese iron, cobalt, and nickel. For comparison the curve for the copper(II) pyridine system [4] is also given. +, experimental points; O, calculated points.

derived concentrations of free pyridine have a relatively high uncertainty. The uncertainty on $\bar{n}_{exp}$, and consequently also on the calculated constants, are therefore rather high. The log β_n constants for the higher complexes are for this reason only shown to one decimal place.

DISCUSSION

In Table 2 the logarithm of the consecutive constants, log K_n, as calculated in this paper are compared with the previously published values [1,2] as well as with newer data from the literature. The abbreviations used in the table are the same as in the Tables of Stability Constants.[2] It will be seen that the recalculated values in this paper (73 B) agree well with the earlier published values, but that more of the consecutive constants have been estimated in this paper. Comparison with the constants of other authors [8–17] determined under similar conditions shows that log K_1 and log K_2 as a whole are in fair agreement if one does not include the much too high values found by Atkinson and Bau-

Table 2. Comparison of stepwise pyridine stability constants.

Ie²+	Method	Temp.	Medium	log K_1	log K_2	log K_3	log K_4	log K_5	Ref.
In²+	gl	25	0.5 $pyHNO_3$	0.14					50 B[1,3]
	gl	25	0.5 $pyHNO_3$	0.14	−0.5				73 B
	gl	25	1 $NaClO_4$	1.86	1.6	0.9	0.6		63 A[6]
'e²+	gl	25	0.5 $pyHNO_3$	0.71					50 B[1,3]
	gl	25	0.5 $pyHNO_3$	0.6	0.3				73 B
o²+	gl	25	0.5 $pyHNO_3$	1.14	0.4				50 B[1,3]
	gl	25	0.5 $pyHNO_3$	1.15	0.55	−0.3			73 B
	gl, dist	20	1 NH_4NO_3	1.35	0.60	0.3	0.1		66 F[8]
i²+	gl	25	0.5 $pyHNO_3$	1.78	1.05	0.3			50 B[1,3]
	gl	25	0.5 $pyHNO_3$	1.83	1.2				59 A[10]
	gl	25	0.5 $pyHNO_3$	1.78	1.22	0.3	−0.3	(−0.3)	73 B
	gl	25	0.5 $LiClO_4$	1.88	1.20				70 F[11]
	gl	25	0.6 KNO_3	1.91	1.28	0.5			67 S[12]
	gl	25	0.1 $NaClO_4$	1.85					64 K[13]
	gl, dist	20	1 NH_4NO_3	1.98	1.04	0.4	0.0		66 F[8]
	gl	25	1 $NaClO_4$	2.13	1.66	1.1	0.6		63 A[6]
n²+	gl	25	0.5 $pyHNO_3$	0.95	0.50				50 B[1,3]
	gl	25	0.5 $pyHNO_3$	0.98	0.47	0.15	−0.2		73 B
	gl	25	0.5 $LiClO_4$	0.99	0.28				70 F[11]
	gl	25	0.1 $NaClO_4$	1.07					64 K[13]
	Zn, Hg	30	0.1 $NaClO_4$	1.10	0.61	0.2			66 D[14]
	gl, dist	20	1 NH_4NO_3	1.45	0.56	−0.2	0.3		67 F[9]
	gl	25	1 $NaClO_4$	2.08	1.69	1.0	0.6		63 A[6]
d²+	gl	25	0.5 $pyHNO_3$	1.27	0.80				50 B[1,3]
	gl	25	0.5 $pyHNO_3$	1.30	0.84	0.36	−0.2		73 B
	Cd, Hg	25	0.1 KNO_3	1.28	0.74				71 B[15]
	pol	30	0.1 KNO_3	1.36	0.50	0.04			65 S[16]
	qh, Hg	30	1 $NaClO_4$	1.26	0.69	0.34			61 D[17]
	gl, dist	20	1 NH_4NO_3	1.51	0.95	log β_4 = 2.50			67 F[9]

man.[6] In the present paper in case of Ni^{2+} as much as 5, and in case of Zn^{2+} and Cd^{2+} as much as 4 consecutive constants were found necessary in order to obtain the best possible agreement with the experimental data in the accessible concentration range. Further it should be observed that the consecutive constants decrease with the number of pyridine molecules taken up as would be expected for systems of this kind.

The formation curves in Fig. 1 show that the stability of the complexes follow the natural order,[18] *i.e.* increasing stability for the series of 1st transition group metal ions from Mn^{2+} to Cu^{2+}, and thereafter decreasing from Cu^{2+} to Zn^{2+}. For many zinc systems it is characteristic that the consecutive constants follow closer after each other than in the corresponding cadmium systems. The somewhat higher steepness of the zinc formation curve shows directly that this is also the case in the pyridine system.

Pyridine adducts of the 1st transition group metals of the type MX_2, 6py have usually the constitution [M py_4 X_2] with only 4 pyridine molecules coordinated to the metal ions, and with the remaining 2 pyridine molecules bound in the lattice.[19] That this is a result of the weak coordinating properties of pyridine, and is not a steric property, is illustrated by the existence of the compound [Fe py_6][$Fe_4(CO)_{13}$], the structure of which has recently been determined.[20] Further evidence for the existence of octahedral hexapyridine complexes is given by Rosenthal and Drago,[21] who in solution of $Ni(ClO_4)_2$,6py in nitromethane have shown the existence of Ni py_6^{2+}. Herlocker and Rosenthal [22] have also postulated the existence of Co py_6^{2+}, when $Co(BF_4)_2$, 6py is dissolved in pyridine.

It is the opinion of the present author that the metal ions from Mn^{2+} to Ni^{2+} all tend to approach the formation of octahedral hexapyridine complexes. The zinc and cadmium ions similarly must be assumed to approach tetrahedrally built tetrapyridine complexes.

In conclusion it may be said that when the complex formation cannot be completed in aqueous solution, it is because of the relatively weak coordinating properties of pyridine combined with the fact that the decrease in dielectric constant with increasing pyridine concentration ($\varepsilon = 12.3$ in pure pyridine) strongly favours the tendency to inner sphere complex formation with the anions present.

Acknowledgement. My thanks are due to Mrs. Else Plejl for assistance during the measurements.

REFERENCES

1. Bjerrum, J., Schwarzenbach, G. and Sillén, L. G. *Stability Constants, Chem. Soc. Special Publ. No. 6* (1957).
2. Sillén, L. G. and Martell, A. E. *Stability Constants, Chem. Soc. Special Publ. No. 17* (1964), and *Supplement No. 25* (1970).
3. Bjerrum, J. *Chem. Rev.* **46** (1950) 381.
4. Bjerrum, J. *Acta Chem. Scand.* **18** (1964) 843.
5. Bjerrum, J. *Acta Chem. Scand.* **26** (1972) 2734.
6. Atkinson, G. and Bauman, Jr., J. E. *Inorg. Chem.* **2** (1963) 64.
7. Bjerrum, J. and Refn, S. *Suomen Kemistilehti* **B 29** (1956) 68.
8. Fridman, Ya. D., Levina, M. G. and Sorochau, R. I. *Russ. J. Inorg. Chem.* (*English Transl.*) **11** (1967) 877.

9. Fridman, Ya. D. and Levina, M. G. *Russ. J. Inorg. Chem.* (*English Transl.*) **12** (1967) 1425.
10. Schweig, A. and Sansoni, B. *Personal communication.*
11. Faraglia, G., Rossotti, F. J. C. and Rossotti, H. S. *Inorg. Chim. Acta* **4** (1970) 488.
12. Sun, M. S. and Brewer, D. G. *Can. J. Chem.* **45** (1967) 2729.
13. Kahmann, K., Sigel, H. and Erlenmeyer, H. *Helv. Chim. Acta* **47** (1964) 1754.
14. Desai, A. G. and Kabadi, M. B. *J. Inorg. Nucl. Chem.* **28** (1966) 1279.
15. Berthon, G. and Luca, C. *Chim. Anal.* (*Paris*) **53** (1971) 40.
16. Sharma, V. K. and Gaur, J. N. *Electroanal. Chem.* **9** (1965) 321.
17. Desai, A. G. and Kabadi, M. B. *J. Indian Chem. Soc.* **38** (1961) 805.
18. Irving, H. and Williams, R. J. P. *J. Chem. Soc.* **1953** 3192.
19. Nuttall, R. H., Cameron, A. F. and Taylor, D. W. *J. Chem. Soc.* **A 1971** 3104.
20. Doedens, R. I. and Dahl, L. F. *J. Am. Chem. Soc.* **88** (1966) 4847.
21. Rosenthal, M. R. and Drago, R. S. *Inorg. Chem.* **4** (1965) 840.
22. Herlocker, D. W. and Rosenthal, M. R. *Inorg. Chim. Acta* **4** (1970) 501.

Received October 9, 1972.

ACTA CHEMICA SCANDINAVICA 27 (1973) 977–984

Multicomponent Polyanions

III. A Potentiometric Study of Germanate–Mannitol Equilibria in 0.5 M Na(Cl) Medium

LAGE PETTERSSON and INGEGÄRD ANDERSSON

Department of Inorganic Chemistry, University of Umeå, S-901 87 Umeå, Sweden

Equilibria between H^+, $Ge(OH)_4$, and D-mannitol ($C_6H_{14}O_6$) have been studied in 0.5 M Na(Cl) medium at 25°C by means of potentiometric (glass electrode) measurements. The pH-range 2–9 has been covered. All data could be explained with the ternary complexes $(H)_{-1}(Ge(OH)_4)(C_6H_{14}O_6)^-$ and $(H)_{-1}(Ge(OH)_4)(C_6H_{14}O_6)_2^-$ together with a small amount of an additional complex $(H)_{-2}(Ge(OH)_4)_2(C_6H_{14}O_6)_2^{2-}$. The existence of the first two species seems to be well established whereas the existence of the third is questionable. Data have been treated using the least squares computer program LETAGROPVRID. "Best" equilibrium constants and standard deviations are collected in Table 2.

In a series of investigations in progress in this department we are studying three component polyanion equilibria:

$$pA + qB + rC \rightleftharpoons A_pB_qC_r$$

In the present report we will present an investigation of the system H^+-$Ge(OH)_4$-mannitol; thus A, B, and C stands for H^+, $Ge(OH)_4$, and mannitol, respectively. The aim is to obtain a quantitative description of the equilibria in the system. It is an experimentally rather easy system. The study may provide an evaluation of the method, and would give a basis for further studies in other similar systems, *e.g.* in systems with borate and silicate ions.

PREVIOUS WORK

Complex formation between germanic acid and mannitol was first reported by Tchakirian [1] in 1928. He observed that the solubility of GeO_2 in water was increased by the addition of mannitol and that the pH of the solution decreased by formation of acids which are much stronger than germanic acid itself. He found that the acids formed consumed one OH^- per germanium

and proposed the formula $H_2[Ge_2O_5(Ma)_n]$ with $n \geq 2$. Mannitol will in the following often be denoted Ma. The Ge–Ma acids soon found use in the analytical determination of germanium.[2–6]

Only a few investigators have studied the germanium-mannitol system thoroughly. Antikainen [7] found (from potentiometric investigations, 25°C, 0.1 M KCl), that only one singly charged complex is formed with a Ge-Ma ratio of 1:2 and with a formation constant of $10^{-4.050}$. Nazarenko and Flyantikova [8] came to the same result by means of pH measurements (a molar ratio method). Like Antikainen they used an excess of mannitol. They determined the thermodynamic ionization constant (25°C) by means of an indicator method (using a spectrophotometer) and obtained the value $(1.21 \pm 0.01) \times 10^{-5}$. Everest and Harrison [9] studied the Ge-Ma system in the pH-range 3 – 12 by using ion-exchange resins. They proposed complexes with Ge-Ma ratios of 1:1, 1:2, and 1:3 with charges −1, −2, and −2, respectively. They also found indications for an uncharged 1:1, a singly charged 1:2, and a singly or doubly charged polynuclear complex. The authors also make suggestions for the structures of the various species.

The existence of a complex with a Ge-Ma ratio of 1:2 seems to be well established when excess of mannitol is used. However, at low Ma-Ge ratios other complexes appear probable, the compositions of which are rather uncertain. It thus seems worthwhile making a more general investigation by taking all three components into consideration.

EXPERIMENTAL

Chemicals and analyses. Sodium chloride, sodium hydroxide, and germanium dioxide were prepared and analysed as described by Ingri [10] and D-mannitol as described by Pettersson.[11] Hydrochloric acid, Merck *p.a.*, was standardized against $KHCO_3$ or tris-hydroxymethylaminomethane (TRISMA-base).

Apparatus. The emf equipment and arrangement used were the same as described by Sjöberg.[12]

Coulometric (OH^-)-addition. In titrations with low B concentrations (2.5 and 5.0 mM), OH^- was added by using a coulometer with the following cell-arrangement:

Pt-gauze −	Equilibrium solution	‖	0.5 M Na(Cl)	Ag +

cathode reaction: $H^+ + e^- \rightleftharpoons 1/2\ H_2(g)$
anode reaction: $Ag(s) + Cl^- \rightleftharpoons AgCl(s) + e^-$
The coulometer used was a Metrohm type E 211.

Method

The present study has been carried out as a series of emf titrations at 25°C and in 0.5 M Na(Cl) medium. In each titration the total concentrations of germanium, B, and mannitol, C, have been kept constant and $[H^+] = h$ has been varied by the addition of OH^- or H^+. B and C have been varied within the limits $2.5\ mM \leq B \leq 30\ mM$ and $5 \leq C \leq 320$ mM. The free hydrogen ion concentration, h, has been measured with a glass electrode with an accuracy of ±0.2 mV. The range of pH ($= -\log h$) has been kept within the limits $2 < pH < 9$.

The free H^+-concentration was determined by measuring the emf of the cell

Ag, AgCl	0.500 M Na^+ 0.500 M Cl^-	‖	equilibrium solutions	glass electrode

Assuming the activity coefficients to be constant the following expression is valid for the measured emf:

$$E = E_0 + 59.157 \log h + E_j \quad (1)$$

E_0 is a constant that could be determined in every titration in the acid range where the binary and ternary reactions can be neglected. For the liquid junction potential, E_j, we have used $E_j = -83\ h + 41\ K_w h^{-1}$ (mV), where $K_w = 2.0 \times 10^{-14}$ m² (the ionic product of water in 0.5 m Na(Cl)).[13,14]

From h, calculated by using eqn. (1), and from H, the excess concentration of hydrogen ions over the zero level $Ge(OH)_4$, mannitol, and H_2O, one can calculate Z, the average number of H^+ bound per B, using the relation:

$$Z = (H - h)/B \quad (2)$$

Equilibria, the law of mass action and the conditions for the concentrations. In the present study in addition to the three component equilibria:

$$pA + qB + rC \rightleftharpoons A_pB_qC_r \quad (3)$$

we need to consider the binary equilibria:

$$pA + qB \rightleftharpoons A_pB_q \quad (4)$$

In eqns. (3) and (4) $A = H^+$, $B = Ge(OH)_4$, and C = mannitol ($C_6H_{14}O_6$). The complex $A_pB_qC_r$ will be referred to as the (p,q,r) species or complex.

In the formation of the different two and three component complexes in the present system protons are split off and consequently p will obtain negative values.

Accurate equilibrium data for H^+-$Ge(OH)_4$ (25°C and 0.5 m Na(Cl)) have already been presented by Ingri.[10] He reports the following species and formation constants (given on the molal scale):

$$GeO(OH)_3^-(\log \beta_{-1,1} = -9.03);\ GeO_2(OH)_2^{2-}(\log \beta_{-2,1} = -21.26);$$
$$(Ge(OH)_4)_8(OH)_3^{3-}(\log \beta_{-3,8} = -11.96)$$

Note that the values of the constants given by Ingri are calculated with OH^- as component and they have been recalculated with H^+ as component using the ionic product of water in 0.5 m Na(Cl) medium ($\log K_w = -13.70$).[13,14] The equilibrium constants in the 0.5 M Na(Cl) medium are assumed to have the same values as in the 0.5 m Na(Cl) medium.

We have found that within the pH-range $1 < pH < 9$ mannitol does not react either with H^+ or OH^-.

Applying the law of mass action to equilibria (3) and (4) the conditions for the concentrations give:

$$B = b + B_1 + \sum q\beta_{pqr} h^p b^q c^r \quad (5)$$

$$C = c + \sum r\beta_{pqr} h^p b^q c^r \quad (6)$$

$$H = h + B_1 Z_1 + \sum p\beta_{pqr} h^p b^q c^r \quad (7)$$

where $b = [Ge(OH)_4]$, $c = [C_6H_{14}O_6]$, $h = [H^+]$, $\beta_{pqr} = [A_pB_qC_r]\ h^{-p} b^{-q} c^{-r}$ and B_1, B_1Z_1 are the "known" quantities for the binary equilibria:

$$B_1 = \beta_{-1,1} h^{-1} b + \beta_{-2,1} h^{-2} b + 8\ \beta_{-3,8} h^{-3} b^8 \quad (8)$$

$$B_1 Z_1 = -\beta_{-1,1} h^{-1} b - 2\beta_{-2,1} h^{-2} b - 3\ \beta_{-3,8} h^{-3} b^8 \quad (9)$$

The summations are made over all ternary species present.

Data treatment. The refinement of constants and error calculations have been made with the least squares program LETAGROPVRID,[15] version ETITR.[16] The error squares sums $U = \sum (H_{calc} - H)^2$ or $U = \sum (Z_{calc} - Z)^2$ have been minimized. The standard deviations are defined and calculated according to Sillén.[17,18] The computation has been performed both on CD 3600 (Uppsala) and on CD 3200 (Umeå).

DATA, CALCULATIONS AND RESULTS

In Fig. 1 we have plotted experimental data $Z(\log h)_{BC}$ for a section at $B = 2.5$ mM and with $C = 5$, 10, 20, 40, 80, 160, and 320 mM.

Similar diagrams were obtained also for the other B sections studied $B(C)$ in mM: 5 (40, 80, 160, 320); 10 (5, 20, 80, 160, 320); 20 (5, 20, 80, 160, 320); 30 (80, 320) but for clarity these data have been omitted in the figure.

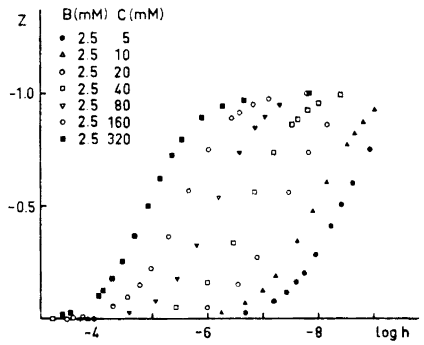

Fig. 1. Experimental data $Z(\log h)_{BC}$ for a section at $B = 2.5$ mM.

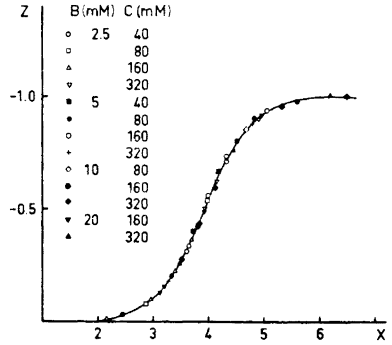

Fig. 2. Experimental data $Z(X)_{BC}$ for $C/B \geq 8$. $X = -\log h + 2 \log [C + 2(H - h)]$.

From Fig. 1 we see that in the Z-range $-1 < Z < 0$ different curves are obtained for different C-concentrations, thus clearly indicating that at least one mixed complex $A_pB_qC_r$ must be formed. The curves seem to reach a limiting value at $Z = -1$ indicating formation of complexes where one proton has been set free per complexed germanic acid ($q = -p$). Furthermore, for $C/B > 4$ the space between the curves is approximately constant and the quotients $(\Delta \log h/\Delta \log C)_{B,Z}$ are equal to two. This would indicate formation of a main complex with $r/p = -2$ and the simplest complex would be $A_{-1}BC_2$. In order to test this proposition further we constructed a diagram Z *versus* X, where $X = -\log h + 2 \log (C + 2(H - h))$.

If the hypothesis of a single complex $A_{-1}BC_2$ is correct, the plot, $Z(X)_{BC}$, would give a single curve independent of B and C. This has also been found for $C/B > 8$ (see Fig. 2), and the plot strongly confirms the complex $A_{-1}BC_2$ when an excess of mannitol is used. We also determined the formation constant and found $\log \beta_{-1,1,2} = -3.93 \pm 0.02$.

For the refinement of the graphically found $\beta_{-1,1,2}$-value the LETAGROP computer program was used. The calculation was started with the sections $B = 2.5$ and 5.0 mM.

For $C/B > 8$ the fit was rather good but for lower ratios systematic deviations were found indicating at least one additional complex. We found that addition of the complex $(-1,1,1)$ completely explained the data.

The calculations were then extended by including the other B-sections studied ($B = 10$, 20, and 30 mM). We found that the value of $\log \beta_{-1,1,1}$ changed (from -6.40 to -6.32) and we obtained small systematic deviations which were most marked for $C/B < 4$. These deviations could, however, be satisfactorily explained when adding the complex $(-2, 2, 2)$.

In order to test the influence of the dissociation constant of $Ge(OH)_4$ ($\beta_{-1,1,0}$), a final covariation of $\beta_{-1,1,0}$, $\beta_{-1,1,2}$, $\beta_{-1,1,1}$, and $\beta_{-2,2,2}$ was made which resulted in very small changes in the values of the constants (see Table 2).

Results from the different LETAGROP calculations are collected in Table 2. Data used and residuals $\Delta = (Z_{calc} - Z) \times 1000$ obtained for the "best" explanation are collected in Table 1.

Table 1. Experimental data $H(\log h)_{BC}$. For each point the quantities H (in mM), log h, and Δ are given. The quantity Δ is the residual $(Z_{calc} - Z) \times 1000$.

SATS 1
B = 0.0025 C = 0.005
.39 -3.411 .11
.30 -3.521 .32
.20 -3.697 .11
.11 -3.945 .01
-0.06 -6.681 -0.57
-0.19 -7.205 -2.28
-0.29 -7.425 -3.32
-0.40 -7.607 -4.49
-0.50 -7.741 -5.92
-0.70 -7.957 -6.55
-1.02 -8.234 -0.54
-1.26 -8.422 2.41
-1.51 -8.616 4.38
-1.88 -8.927 11.73

SATS 2
B = 0.0025 C = 0.010
.36 -3.453 -2.78
.30 -3.528 -0.02
.22 -3.656 -0.44
.15 -3.817 -0.34
.10 -3.983 .27
-0.07 -6.250 .67
-0.17 -6.684 -0.99
-0.31 -6.992 -3.41
-0.47 -7.230 -5.35
-0.86 -7.616 -2.35
-1.19 -7.898 -3.02
-1.51 -8.153 -1.39
-1.93 -8.525 4.31
-2.05 -8.659 6.88
-2.18 -8.811 10.77

SATS 3
B = 0.0025 C = 0.020
.52 -3.282 -0.11
.46 -3.338 -0.36
.40 -3.401 -0.07
.33 -3.477 -0.68
-0.12 -6.005 -0.12
-0.37 -6.551 -2.02
-0.67 -6.890 -1.96
-1.39 -7.465 -0.07
-1.84 -7.824 11.29
-2.15 -8.163 15.19

SATS 4
B = 0.0025 C = 0.040
.85 -3.070 .47
.75 -3.123 1.65
.60 -3.223 -0.41
.49 -3.314 -1.03
-0.12 -5.443 -2.77
-0.39 -5.998 -1.75
-0.84 -6.437 .95
-1.40 -6.851 6.86
-1.84 -7.195 10.86
-2.15 -7.523 15.03
-2.21 -7.631 10.61
-2.31 -7.813 11.33
-2.38 -8.009 11.27
-2.48 -8.412 15.88

SATS 5
B = 0.0025 C = 0.080
.27 -3.572 -2.91
.23 -3.636 -3.14
.19 -3.714 -3.99
-0.04 -4.591 -3.38
-0.19 -5.065 -1.77
-0.44 -5.460 -0.22
-0.81 -5.810 4.94
-1.34 -6.199 7.61
-1.84 -6.579 11.24
-2.11 -6.862 12.93
-2.24 -7.037 14.24
-2.37 -7.299 16.82

SATS 6
B = 0.0025 C = 0.160
.25 -3.578 -3.69
.20 -3.658 -3.58
.15 -3.753 -4.01
-0.08 -4.300 -2.12
-0.21 -4.557 -1.54
-0.36 -4.784 -1.51
-0.55 -4.994 -1.26
-0.90 -5.298 -2.59
-1.41 -5.663 -2.10
-1.88 -6.018 3.90
-2.23 -6.441 4.84
-2.29 -6.583 .74
-2.38 -6.821 1.52
-2.44 -7.114 2.04
-2.50 -7.800 5.41

SATS 7
B = 0.0025 C = 0.320
.35 -3.399 -9.07
.29 -3.460 -9.16
.23 -3.531 -10.73
-0.16 -4.036 -10.28
-0.24 -4.118 -7.20
-0.39 -4.276 -3.94
-0.60 -4.465 .23
-0.90 -4.692 4.68
-1.24 -4.925 6.29
-1.55 -5.148 3.92
-1.81 -5.359 1.64
-1.98 -5.537 -2.64
-2.23 -5.902 -6.94
-2.36 -6.265 -10.81
-2.42 -6.661 -12.67
-2.48 -7.839 -5.86

SATS 8
B = 0.005 C = 0.040
.39 -3.413 -0.49
.31 -3.506 -0.57
.21 -3.673 -0.89
-0.50 -5.781 -2.13
-2.00 -6.610 -0.83
-3.33 -7.124 8.83
-4.02 -7.445 13.53

SATS 9
B = 0.005 C = 0.080
.42 -3.379 -1.86
.37 -3.435 -2.21
.32 -3.497 -2.40
.27 -3.570 -2.66
-0.12 -4.642 -2.36
-1.00 -5.546 -1.96
-2.00 -5.991 -2.21
-3.12 -6.407 .85
-4.00 -6.786 7.81
-4.50 -7.117 11.04

SATS 10
B = 0.005 C = 0.160
.40 -3.377 -2.93
.35 -3.428 -3.08
.29 -3.499 -3.27
-0.43 -4.554 -2.58
-1.68 -5.257 -2.28
-2.68 -5.623 -1.42
-3.55 -5.954 1.26
-4.36 -6.390 5.42
-4.67 -6.686 7.34

SATS 11
B = 0.005 C = 0.320
.52 -3.219 -1.93
.48 -3.244 -2.42
.42 -3.292 -3.99
-0.57 -4.119 -2.63
-0.84 -4.276 -1.85
-1.70 -4.665 -2.89
-2.64 -5.000 -2.55
-4.38 -5.798 2.53
-4.77 -6.231 4.84

SATS 12
B = 0.010 C = 0.005
4.29 -2.367 -0.03
2.73 -2.564 .02
1.11 -2.963 -1.76
-0.13 -6.492 -2.62
-0.71 -7.282 -5.96
-1.61 -7.779 -8.96
-2.11 -7.975 -10.96
-2.91 -8.221 -11.32
-3.65 -8.413 -8.66
-4.47 -8.602 -3.82
-5.23 -8.766 1.55
-6.15 -8.956 9.08

SATS 13
B = 0.010 C = 0.020
4.86 -2.314 -0.57
3.62 -2.441 -0.09
1.22 -2.923 -2.24
-0.33 -5.869 -3.18
-0.80 -6.295 -4.28
-1.26 -6.541 -4.86
-2.11 -6.872 -5.40
-2.91 -7.115 -5.05
-3.29 -7.220 -4.95
-4.00 -7.409 -4.31
-4.98 -7.659 -3.76
-5.87 -7.887 -4.08
-6.94 -8.172 -3.89
-7.89 -8.457 -3.17
-8.93 -8.862 .28

SATS 14
B = 0.010 C = 0.080
4.85 -2.310 4.40
3.23 -2.490 .70
1.78 -2.754 -1.83
.47 -3.348 -3.92
-0.13 -4.454 -4.01
-0.71 -5.051 -4.12
-1.78 -5.509 -4.61
-2.75 -5.771 -4.60
-3.21 -5.875 -4.52
-4.47 -6.136 -5.33
-5.58 -6.356 -5.15
-6.58 -6.562 -4.92
-7.47 -6.771 -4.75
-8.53 -7.094 -4.64
-9.45 -7.616 -4.47
-9.72 -7.947 -3.62

SATS 15
B = 0.010 C = 0.160
4.86 -2.313 -0.02
2.85 -2.545 -1.32
1.66 -2.776 -0.72
.37 -3.370 -1.14
-0.23 -4.055 -0.49
-0.80 -4.493 .37
-1.78 -4.890 -1.10
-2.76 -5.144 -1.91
-3.65 -5.334 -2.94
-4.20 -5.441 -3.35
-5.23 -5.633 -4.14
-6.15 -5.809 -5.03
-7.19 -6.027 -5.37
-8.11 -6.266 -5.39
-9.01 -6.612 -4.90
-9.74 -7.283 -3.61

SATS 16
B = 0.010 C = 0.320
4.85 -2.314 -2.87
2.85 -2.541 -1.32
1.11 -2.927 -2.01
.06 -3.441 -1.52
-0.52 -3.798 -0.23
-1.61 -4.243 -1.08
-2.60 -4.503 -2.54
-4.34 -4.850 -5.01
-5.35 -5.032 -5.85
-5.93 -5.139 -6.50
-6.99 -5.351 -7.44
-7.93 -5.578 -7.73
-8.77 -5.862 -7.19
-9.53 -6.352 -6.24
-9.95 -7.528 -2.60

SATS 17
B = 0.020 C = 0.005
4.90 -2.305 2.86
3.48 -2.456 .85
2.14 -2.674 -1.21
1.29 -2.909 -2.70
.46 -3.414 -3.70
-0.73 -6.967 -4.30
-2.23 -7.506 -8.07
-3.46 -7.768 -8.31
-5.43 -8.141 -7.49
-7.23 -8.458 -3.12
-8.89 -8.721 4.93
-10.42 -8.937 15.08

SATS 18
B = 0.020 C = 0.020
5.31 -2.278 -2.05
3.59 -2.444 .14
1.96 -2.700 1.58
.41 -3.345 1.86
-0.58 -5.748 2.26
-1.77 -6.381 .90
-3.14 -6.770 1.03
-4.45 -7.060 1.15
-6.30 -7.412 .41
-8.03 -7.709 -1.47
-9.66 -7.972 -4.15
-11.67 -8.284 -6.26
-13.08 -8.496 -5.96
-14.41 -8.693 -3.57
-15.66 -8.885 -0.34
-16.46 -9.014 2.63

SATS 19
B = 0.020 C = 0.080
6.51 -2.184 1.26
4.16 -2.381 -0.04
3.59 -2.445 -0.55
3.04 -2.519 -0.90
-0.09 -4.138 -2.19
-1.30 -5.006 -1.56
-3.37 -5.502 -0.79
-5.29 -5.793 -0.02
-7.09 -6.016 1.20
-8.77 -6.208 2.32
-10.35 -6.383 3.52
-11.83 -6.550 5.06
-13.23 -6.715 6.10
-14.97 -6.942 7.31
-16.19 -7.129 7.65
-18.09 -7.526 6.22
-19.50 -8.145 4.00

SATS 20
B = 0.020 C = 0.160
6.39 -2.194 -0.09
4.89 -2.311 -0.71
2.80 -2.553 -0.99
.87 -3.046 -1.66
-0.34 -3.933 -1.57
-1.49 -4.468 -1.08
-3.12 -4.833 -0.95
-4.63 -5.061 -1.01
-6.50 -5.285 -1.20
-8.22 -5.465 -1.72
-9.79 -5.623 -1.75
-11.25 -5.767 -1.85
-13.24 -5.973 -1.47
-15.03 -6.181 -0.43
-16.89 -6.457 .16
-18.33 -6.774 .64
-19.14 -7.078 1.21
-19.98 -7.948 4.05

SATS 21
B = 0.020 C = 0.320
6.37 -2.195 -1.06
4.16 -2.377 -0.91
2.78 -2.547 -1.25
.85 -2.983 -1.95
-0.36 -3.493 -0.94
-2.61 -4.134 -0.05
-4.16 -4.378 -0.33
-5.13 -4.501 -0.52
-6.96 -4.699 -1.19
-8.69 -4.863 .62
-10.18 -5.008 -2.88
-11.61 -5.142 -3.57
-13.25 -5.304 -3.53
-15.23 -5.527 -3.70
-17.31 -5.844 -2.68
-18.86 -6.256 -1.22
-19.99 -7.415 2.34

SATS 22
B = 0.030 C = 0.080
5.63 -2.254 -1.90
3.48 -2.456 .34
2.14 -2.659 1.43
.26 -3.419 2.19
-0.34 -4.193 2.29
-2.04 -5.018 1.62
-4.63 -5.475 1.86
-7.37 -5.792 2.40
-9.79 -6.021 3.77
-12.59 -6.264 6.40
-15.57 -6.513 10.22
-18.54 -6.765 14.96
-21.56 -7.050 17.51
-23.93 -7.306 18.61
-25.77 -7.549 17.92
-27.64 -7.881 15.18
-29.98 -8.885 11.35

SATS 23
B = 0.030 C = 0.320
5.61 -2.244 1.02
4.87 -2.305 .47
4.15 -2.373 -0.08
2.78 -2.543 -1.16
.23 -3.166 -1.82
-0.56 -3.453 -1.46
-2.07 -3.846 -0.33
-4.16 -4.165 1.07
-6.97 -4.449 1.38
-10.19 -4.699 .37
-12.95 -4.885 -0.82
-15.33 -5.040 -2.07
-18.35 -5.241 -4.25
-20.86 -5.420 -5.16
-23.09 -5.601 -5.15
-26.11 -5.929 -4.78
-27.94 -6.255 -4.07

Table 2. Results from LETAGROP calculations minimizing $U = \sum (Z_{calc} - Z)^2$ using data given in Table 1. The value of $\log \beta_{-3,8,0} = -11.96$ was not varied and $\log \beta_{-1,1,0}$ was varied only in the two cases when 3σ is given.

B (mM)	Number of points	$U \times 10^4$	$\sigma(Z)$	$\log (\beta_{-1,1,0} \pm 3\sigma)$	$\log (\beta_{-1,1,2} \pm 3\sigma)$	$\log (\beta_{-1,1,1} \pm 3\sigma)$	$\log (\beta_{-2,2,2} \pm 3\sigma)$
2.5 and 5.0 ($C/B \geq 8$)	102	118	0.0108	−9.03	−3.917 ± 0.011	—	—
2.5 and 5.0 (all ratios)	131	767	0.0243	−9.03	−3.892 ± 0.022	—	—
»	»	49	0.0062	−9.03	−3.941 ± 0.007	−6.397 ± 0.035	—
$2.5 \leq B \leq 30$	319	202	0.0080	−9.03	−3.950 ± 0.006	−6.320 ± 0.026	—
»	»	202	0.0080	−9.034 ± 0.037	−3.950 ± 0.006	−6.317 ± 0.039	—
»	»	101	0.0057	−9.03	−3.944 ± 0.004	−6.460 ± 0.038	−10.68 ± 0.09
»	»	90	0.0053	−9.084 ± 0.027	−3.945 ± 0.004	−6.428 ± 0.037	−10.62 ± 0.08

In order to test the existence of uncharged complexes between germanic acid and mannitol we measured the optical rotation of acid solutions (pH≈2). For $B < 30$ mM we found that the optical rotation was the same as for pure mannitol at the corresponding concentration. However, for $B > 30$ mM there was a small increase in the optical activity, thus indicating the possibility of uncharged complexes.

CONCLUSIONS

The present investigation has shown that in the system H^+-$Ge(OH)_4$-mannitol the main ternary complexes are $(-1,1,2)$ and $(-1,1,1)$. For germanium concentrations greater than 5 mM with not too high mannitol excess additional complexes are indicated. The data range available favouring the formation of these additional complexes is, however, too limited to allow a meaningful data analysis (testing different *pqr*-sets). Neither can the concentration range be extended over the entire pH-range studied because of the limited solubility of $Ge(OH)_4$ (~ 40 mM in 0.5 M NaCl). However, some different *pqr*-sets were tested and the complex $(-2,2,2)$ gives a satisfactorily explanation of additional effects.

In all the three ternary complexes one proton is set free per complexed germanic acid ($p/q = -1$). However, for some *BC*-combinations we found *Z*-values < -1 (indicating complexes with $p/q < -1$) but the corresponding pH-values were $\gtrsim 9$. In this pH-range the glass electrode does not give reliable values and to be able to determine these complexes the pH-range must be extended by, for instance, using a hydrogen electrode.

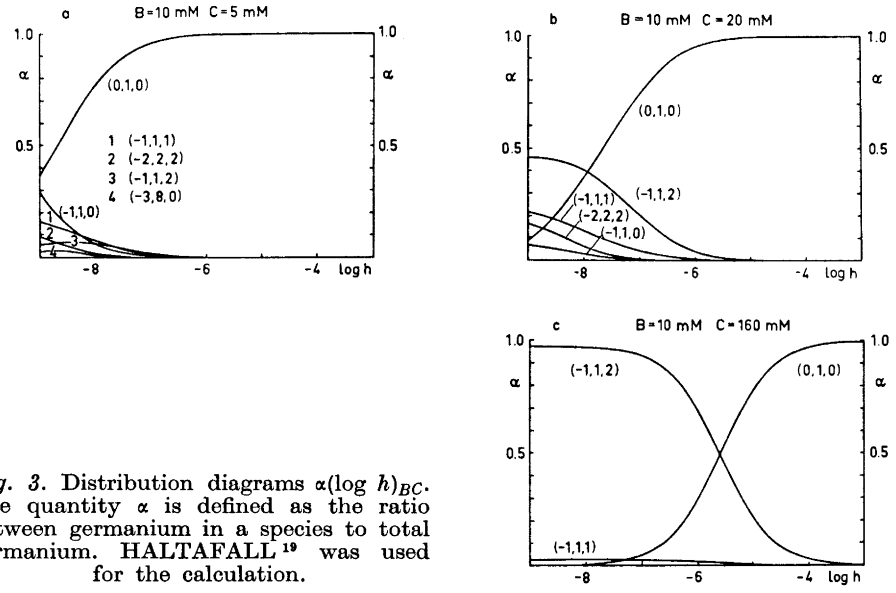

Fig. 3. Distribution diagrams $\alpha(\log h)_{BC}$. The quantity α is defined as the ratio between germanium in a species to total germanium. HALTAFALL [19] was used for the calculation.

Strengths and concentrations of the ternary complexes found in the pH-range 3 – 9 are illustrated by the distribution diagrams given in Fig. 3, a – c, for $B,C = 10,5$; 10,20; 10,160 mM, respectively. In Fig. 3, a and b, ($B/C =$ 2 and 1/2) the (–1,1,1), (–2,2,2), and (–1,1,2) complexes all are present in considerable amounts, but in Fig. 3c, ($B/C = 1/16$), the (–1,1,2)-complex is quite predominating. It is not surprising that investigators using a great excess of mannitol have been able to explain their data with solely the (–1,1,2)-complex.

Acknowledgements. We thank Professor Nils Ingri for much valuable advice, for his great interest, and for all the facilities placed at our disposal. The English of the present paper has been corrected by Dr. Michael Sharp. The work forms part of a program, financially supported by the *Swedish Natural Science Research Council.*

REFERENCES

1. Tchakirian, A. *Compt. Rend.* **187** (1928) 229.
2. Poluektov, N. S. *Microchemie* **18** (1935) 48.
3. Tchakirian, A. *Ann. Chim.* **12** (1939) 415.
4. Bradley, D. C., Kay, L. J. and Wardlaw, W. *J. Chem. Soc.* **1956** 4924.
5. Csapo, F. and Repetschnig, H. *Z. anal. Chem.* **173** (1960) 273.
6. Nazarenko, V. A. and Flyantikova, G. V. *Ukr. Khim. Zh.* **30** (1964) 762.
7. Antikainen, P. J. *Suomen Kemistilehti* **B 30** (1957) 147; **B 31** (1958) 291; *Acta Chem. Scand.* **13** (1959) 312.
8. Nazarenko, V. A. and Flyantikova, G. V. *Zh. Neorg. Khim.* **8** (1963) 1370, 2271.
9. Everest, D. A. and Harrison, J. C. *J. Chem. Soc.* **1957** 4319; **1960** 1745.
10. Ingri, N. *Acta Chem. Scand.* **17** (1963) 597.
11. Pettersson, L. *Acta Chem. Scand.* **26** (1972) 4067.
12. Sjöberg, S. *Acta Chem. Scand.* **25** (1971) 2149.
13. Ingri, N. *Acta Chem. Scand.* **13** (1959) 758.
14. Ingri, N. *Acta Chem. Scand.* **17** (1963) 597.
15. Ingri, N. and Sillén, L. G. *Arkiv Kemi* **23** (1964) 97.
16. Arnek, R., Sillén, L. G. and Wahlberg, O. *Arkiv Kemi* **31** (1969) 353; Brauner, P., Sillén, L. G. and Whiteker, R. *Arkiv Kemi* **31** (1969) 365.
17. Sillén, L. G. *Acta Chem. Scand.* **16** (1962) 159.
18. Sillén, L. G. and Warnqvist, B. *Arkiv Kemi* **31** (1969) 341.
19. Ingri, N., Kakolowicz, W., Sillén, L. G. and Warnqvist, B. *Talanta* **14** (1967) 1261.

Received October 11, 1972.

ACTA CHEMICA SCANDINAVICA 27 (1973) 985–989

Effect of 1-Hydroxymethyl- and 1-Methyl-1-aminoalkanes on Enzymatic Leucine-2-oxoglutarate Transamination

RAIMO RAUNIO, TIMO KORPELA and ANTTI MUSTRANTA

Department of Biochemistry, University of Turku, SF-20500 Turku 50, Finland

Studies were made on the effect of some 1-hydroxymethyl- and 1-methyl-1-aminoalkanes on the enzymatic leucine-2-oxoglutarate transamination reaction catalyzed by *Escherichia coli* cell extract, and on the transamination of the analogs and their effect on the growth of *E. coli*. All the analogs inhibited the enzymatic leucine-2-oxoglutarate transamination reaction and this inhibition was competitive with leucine. The analogs were not able to donate an amino group to 2-oxoglutarate when *E. coli* cell extract was used as enzyme source and they acted as growth inhibitors when *E. coli* cells were cultured in a simple glucose-mineral salt medium. It is concluded that the carboxylate group of leucine is essential for the enzymatic leucine-2-oxoglutarate transamination reaction.

In the transamination reaction between an amino acid and 2-oxoglutarate, the 2-amino group and α-carbon hydrogen play the key role in the formation of a Schiff base with amino acid and pyridoxal-5′-phosphate and in the formation of the end product, a keto acid. The role of the carboxyl group of the amino acid in the reaction is poorly understood. There is some experimental evidence to suggest that the carboxylate anion is involved in the reaction and it is supposed that this anion becomes attached to the apoenzyme part, effecting the breakage of a bond specific to the reaction.[1–3]

We selected some 1-hydroxymethyl- and 1-methylalkylamines and tested their effect on the enzymatic leucine-2-oxoglutarate transamination reaction and their ability to donate an amino group to 2-oxoglutarate catalyzed by partially purified *E. coli* leucine aminotransferase (EC 2.6.1.6).

MATERIALS AND METHODS

Organism. A wild-type *Escherichia coli* U5-41 was used in the growth inhibition studies and as source for leucine aminotransferase. The compositions of the transfer, inoculation and test media have been reported earlier.[4]

Assay methods. Chromatographic and isotopic methods were used in the leucine aminotransferase activity determinations. The isotopic method, in which the reaction

mixture contained 5 mM L-leucine, 25 mM 2-oxoglutarate and 10 μM pyridoxal-5′-phosphate in 50 mM Tris-HCl buffer, pH 8.0, has been published elsewhere.[5] Analogs were added to the reaction mixture to give 10 or 30 mM concentrations. In this assay 0.05 – 0.1 μCi of uniformly labeled L-leucine-U-C-14 (specific activity 344 mCi/mmol) was added to the reaction mixture to the volume of 1 ml. In some experiments lower leucine concentrations were used to obtain higher counts and these experiments are mentioned later. The radiocarbon was counted in a scintillation solution containing 3.92 g of PPO (2,5-diphenyloxazole) and 0.08 g of bis-MSB (*p*-bis(*o*-methylstyryl)benzene) in 1 l of toluene. The liquid scintillation counter was Decem NTL^{314} from Wallac Co., Turku, Finland.

The chromatographic method was a modification of a previously published method in which glutamate formed from 2-oxoglutarate was estimated after it had been separated by paper chromatography and sprayed with ninhydrin. The modification consisted of using lower substrate concentrations, as in the isotopic assay.

Enzyme preparation. Leucine aminotransferase (EC 2.6.1.6) was partially purified from a wild-type *E. coli* U5-41 by a method presented earlier.[4]

Analogs and their preparation. The following 2-amino compounds were purchased as follows: 2-aminoethanol, DL-2-aminobutyric acid from British Drug Houses Ltd, Poole, England, 2-aminopropanol, 2-aminobutanol, 2-aminopropane, 2-aminobutane, 2-amino-4-methylhexane from Koch-Light Laboratories Ltd, Colnbrook, England, 2-aminoethane, 2-amino-3-methylpentane, 2-amino-6-methylheptane from Fluka AG, Buchs, Switzerland, 2-aminopentane and 2-aminohexane from K & K Laboratories Inc., Hollywood, California. Leucinol, isoleucinol, valinol, norleucinol, and norvalinol were prepared from the corresponding L-amino acids by the method of Vogl and Pöhm.[6] An ascending paper chromatographic method, with butanol-acetic acid-water 4 : 1 : 1 (v/v/v) as solvent, was used to test that the preparations were free from amino acids, and the absence of a carboxylic group and the presence of the amino group were demonstrated by infrared analysis. All other reagents were chromatographically pure reagent grade compounds.

NMR spectra. The differences between chemical shifts were determined on a 60 MHz Perkin-Elmer R 10 NMR spectroscope at 33.5°.

Table 1. Effect of 1-hydroxymethyl- and 1-methyl-1-alkylamines on the enzymatic leucine-2-oxoglutarate transamination catalyzed by partially purified leucine aminotransferase from *E. coli*. Initial velocities were followed in the reaction mixture containing 5 μmol L-leucine, 3.4×10^{-4} μmol uniformly labelled L-leucine (0.1 μCi), 25 μmol 2-oxoglutarate, 0.01 μmol pyridoxal-5-phosphate in 50 mM Tris-HCl buffer, pH 8.0, plus 10 mM or 30 mM analog. The total reaction volume was 1.0 ml and the activities are compared to the activity without analog which is taken as 100.

Analog	Concentration	
	10 mM	30 mM
None	100	100
2-Aminoethanol	91	70
2-Aminopropanol	85	77
2-Aminobutanol	96	71
Norvalinol	80	–
Norleucinol	91	84
Valinol	60	–
Leucinol	90	70
Isoleucinol	89	72
2-Aminoethane	76	33
2-Aminopropane	84	30
2-Aminobutane	62	25
2-Aminopentane	57	40
2-Aminohexane	67	25
2-Amino-3-methylpentane	59	36
2-Amino-4-methylhexane	74	37
2-Amino-6-methylheptane	78	26
L-Isoleucine	51	19

RESULTS

Effect of analogs on the enzymatic transamination of leucine. When one of the analogs at a concentration of 10 mM or 30 mM was added to the reaction mixture containing 5 mM L-leucine and 25 mM 2-oxoglutarate, the reaction rate was lower than in its absence. The results are tabulated in Table 1.

With all the 1-hydroxymethyl- and 1-methyl type analogs a sixfold amount of the analog, as compared with the leucine concentration, caused marked inhibition. The inhibition was higher with 1-methyl analogs than with 1-hydroxymethyl compounds. No marked differences were found with different side chains of alkylamines.

Inhibition constants and type of inhibition. Fig. 1 shows the graphical determination of inhibitor constants K_i and they were 2.0 mM for leucinol, 1.7 mM for 2-amino-4-methylhexane and 0.6 mM for isoleucine. The Dixon plot method was used to determine the constants, and the activity assays were made with the isotopic method.[7] The type of inhibition was competitive in

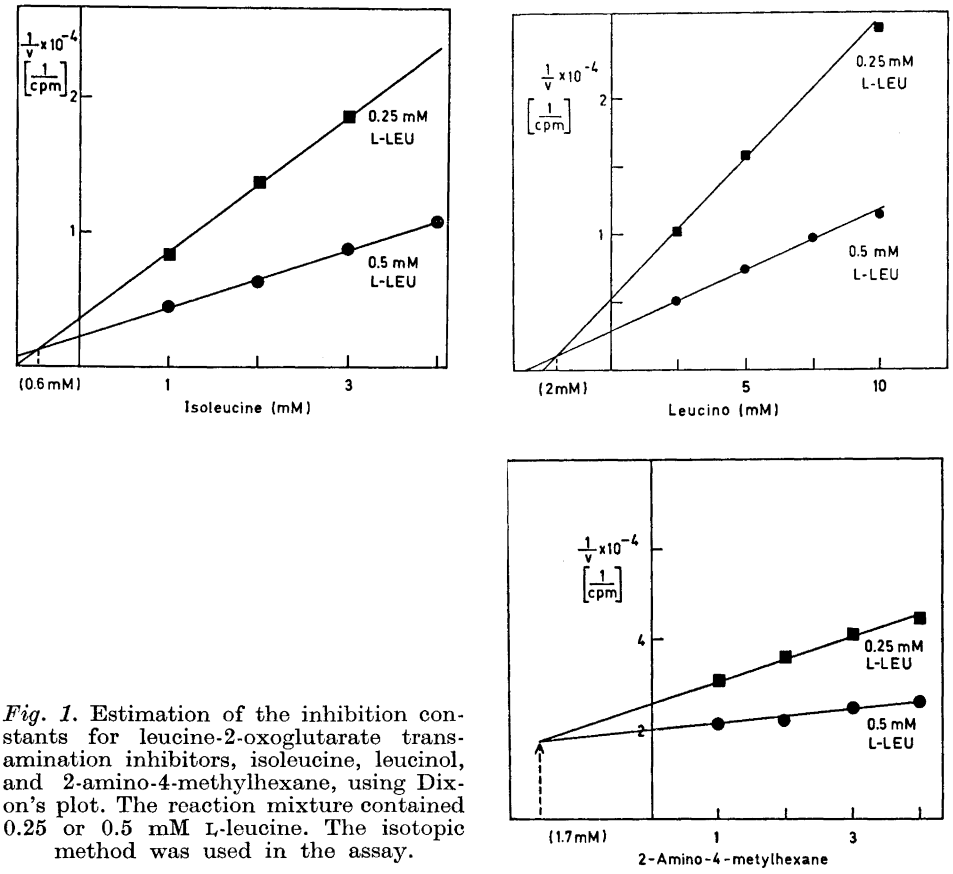

Fig. 1. Estimation of the inhibition constants for leucine-2-oxoglutarate transamination inhibitors, isoleucine, leucinol, and 2-amino-4-methylhexane, using Dixon's plot. The reaction mixture contained 0.25 or 0.5 mM L-leucine. The isotopic method was used in the assay.

all three cases studied. The K_m value for leucine was 0.3 mM with *E. coli* U5-41 enzyme.

Transamination of analogs. The deamination of the analogs used was studied by following the release of hydrogen from the α-carbon in the presence of 2-oxoglutarate by the NMR technique and also the formation of glutamate from 2-oxoglutarate. Fig. 2 shows the spectra obtained by the NMR technique when the reaction mixture contained L-leucine and isoleucinol as amino donor.

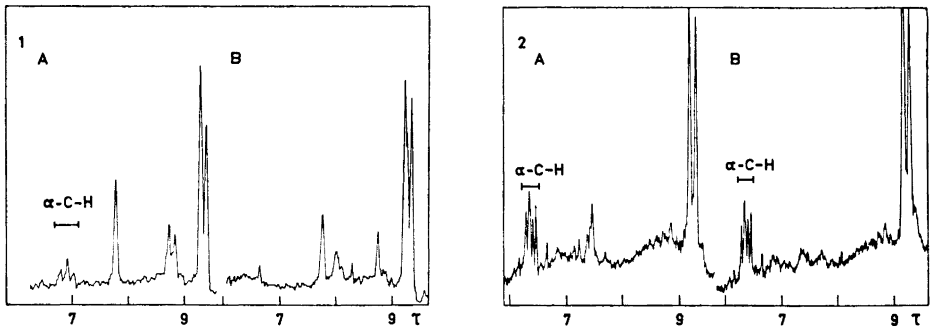

Fig. 2. NMR spectra of L-leucine (1) and isoleucinol (2) in D_2O before (A) and after (B) incubation of 30 mg of amino compound for 24 h at 37° in the presence of 30 mg 2-oxoglutarate and 30 mg of *E. coli* protein containing leucine aminotransferase per ml (pD was 8.0 and it was adjusted with NaOD). The protein was precipitated by heating and centrifuged off before NMR analysis. The position of the α-carbon hydrogen is marked as α-C-H. There was no release of hydrogen from the other analogs mentioned in Table 1.

The results showed that none of the analogs, except leucinol with an activity less than 10 % of that of leucine, acted as an amino donor to keto acid or was able to release hydrogen from the α-carbon. The concentration of the amino acid or amino compound in the reaction mixture was 30 mM in the chromatographic method, in which the formation of glutamate was followed. The composition of the reaction mixture in the NMR analysis is mentioned in Fig. 2.

Inhibition of E. coli growth by analogs. The effects of the analogs on the growth of a wild-type, branched-chain amino acid resistant *Escherichia coli* U5-41 were also studied. The additions were made at concentrations of 10^{-4} to 10^{-1} M to the medium, which contained glucose, ammonium chloride, and mineral salts.[5] The analogs were added to the medium aseptically before drop inoculation of 10 ml of the medium. The tubes were incubated overnight at 37° without shaking and the turbidities were determined with a Klett colorimeter, using filter No. 42 (400 – 450 nm). The 50 % inhibition concentrations of the analogs were as follows: 84 mM for 2-aminoethanol, 70 mM for 2-aminopropanol, 62 mM for 2-amino-1-butanol, 27 mM for leucinol, 38 mM for 2-aminobutane, 3 mM for 2-aminopentane, 21 mM for 2-aminohexane, 8 mM for 2-amino-3-methylpentane, 6 mM for 2-amino-4-methylhexane, and 2 mM for 2-amino-6-methylheptane. Isoleucinol and valinol up to the concentration of 10^{-1} M did not cause any growth inhibition. Very volatile compounds like 2-aminoethane and 2-aminopropane were not tested in the growth experiments.

The results showed again that 1-methyl type analogs are more efficient inhibitors than 1-hydroxymethyl type compounds.

DISCUSSION

It is supposed that in the present models of the transamination reaction mechanism the carboxyl group is needed to put the amino acid into the right position in the transaminase enzyme molecule, and thus that the group attachment on the enzyme determines which of the bonds in the Schiff base is broken in the reaction.

The results in Table 1 strongly support this evidence that the carboxyl group is essential for the enzymatic leucine-2-oxoglutarate transamination reaction. All the analogs tested were inhibitory and these analogs either had a 1-hydroxymethyl or a 1-methyl group instead of the carboxyl group in the amino compound. The change of the group resulted in inhibition with both types of analogs, although the 1-methyl group gave higher inhibition values than the 1-hydroxymethyl group. The study showed that the effect of the side chain was less strong. This is understandable if it is the carboxyl group, and not the side chain, that plays the key role in stabilizing the structure of the Schiff base or if the specificity of the leucine aminotransferase from *E. coli* is very low. Similar results were obtained with valyl-sRNA synthetase from *E. coli* when various amino acid analogs were studied.[8] The carboxyl group of the amino acid seems to be essential for the liberation of hydrogen from the α-carbon (Fig. 2). However, the K_i values in Fig. 1 show, that the binding of the analogs is of about the same order as the K_m values for L-leucine. This finding is consistent with the results of experiments with valyl-sRNA synthetase.[8] It is thus likely that the role of the carboxyl group in the binding process is very weak but may be important in the Schiff base structure, as suggested by Heinert and Martell [9] and by Martell.[10]

Acknowledgements. The authors wish to thank Mr. P. Koponen for skillful assistance and the *National Research Council for Sciences* for financial aid (to R. R.). Also we thank Dr. K. Pihlaja, of the Department of Chemistry, for the NMR service.

REFERENCES

1. Ivanov, V. I. and Karpeisky, M. Ya. *Advan. Enzymol.* **32** (1969) 21.
2. Jenkins, W. T. In Snell, E. E., Fasella, P. M., Braunstein, A. and Rossi Fanelli, A., Eds., *Chemical and Biological Aspects of Pyridoxal Catalysis*, Pergamon, Oxford 1963, p. 139.
3. Dunathan, H. C. *Proc. Natl. Acad. Sci. U.S.* **55** (1966) 712.
4. Raunio, R. P. *Acta Chem. Scand.* **22** (1968) 2733.
5. Raunio, R. P. *Acta Chem. Scand.* **23** (1969) 1168.
6. Vogl, O. and Pöhm, M. *Monatsh.* **83** (1952) 541.
7. Dixon, M. *Biochem. J.* **55** (1953) 170.
8. Owen, S. L. and Bell, F. E. *J. Biol. Chem.* **245** (1970) 5515.
9. Heinert, D. and Martell, A. E. *J. Am. Chem. Soc.* **84** (1962) 3257.
10. Martell, A. E. In Snell, E. E., Fasella, P. M., Braunstein, A. and Rossi Fanelli, A., Eds., *Chemical and Biological Aspects of Pyridoxal Catalysis*, Pergamon, Oxford 1963, p. 26.

Received October 16, 1972.

ACTA CHEMICA SCANDINAVICA 27 (1973) 990–994

Effect of Electron Donors and Acceptors on Alcohol Dehydrogenase Activity during the Growth of *Escherichia coli*

RAIMO RAUNIO and ESA-MATTI LILIUS

Department of Biochemistry, University of Turku, SF-20500 Turku 50, Finland

Alcohol dehydrogenase was activated by electron donors and inactivated by electron acceptors during the growth of *Escherichia coli*. A correlation was found between the k value, which expresses how much energy will be needed to remove an electron from a molecule, and the activity of this enzyme. The smaller the k value, the better the molecule in question acts as an electron donor, and the higher the alcohol dehydrogenase activity rises.

The electron donors obviously protect the enzyme molecule from the electron-catching effect of the environment. On the contrary, the electron acceptors catch electrons from the enzyme molecule, causing its inactivation.

At the turn of the 1930's and 1940's many workers were interested in the effect of the redox state on enzyme activity. They noticed that a number of different enzymes are activated by certain reducing agents (*e.g.* KCN, $Na_2S_2O_4$, H_2S, cysteine) and inactivated by oxidizing agents (*e.g.* H_2O_2, $KMnO_4$, $K_3Fe(CN)_6$). Such enzymes include amylase,[1] esterase and lipase,[2] ribonuclease,[3] and urease.[4] By contrast pepsin and pepsinogen are inactivated by reductants and reactivated by oxidants.[5] The hydrolytic activity of urease,[6] pancreatic lipase,[7] and liver esterase [8] is inactivated by oxidants and activated by reductants but their synthetic activity is affected by these agents in the opposite way. Sizer and Tytell [9] noticed that crystalline urease has a bell-shaped activity curve as a function of redox potential.

The workers referred above assumed that the effect of redox compounds on enzyme activity is due to oxidation and reduction of the sulfhydryl groups in the enzyme molecule and they studied this effect on enzyme activity *in vitro*.

In this work we have studied the effect of electron donors and acceptors on alcohol dehydrogenase activity *in vivo* during the growth of *Escherichia coli* by adding different agents to the growth medium.

MATERIALS AND METHODS

Organism. Escherichia coli U5-41, a wild type strain, details of the source and maintenance of which have previously been published.[10] The organism was precultured in one liter of medium in a 2 l Erlenmeyer flask at 37° without aeration. The composition of the medium was as described.[11] Culture was carried out at 37° in a shaker (Buhler Sm 1) in 1 l Erlenmeyer flasks containing 500 ml of minimum medium of the following composition: 0.1 % NH_4Cl, 0.7 % Na_2HPO_4, 0.3 % KH_2PO_4, 0.5 % NaCl, 0.01 % $MgSO_4.7H_2O$, 0.2 % glucose.

Redox effect experiments. Different amounts of different redox compounds were added to the test culture, usually at the early logarithmic phase. Growth was measured using a Klett-Summerson colorimeter with filter No. 62 (590 – 640 nm). Samples of 5 – 20 ml were taken from the test culture and reference culture, which did not contain any redox compound, at various time intervals for estimations of the enzyme activity. The cells of the samples were centrifuged at 4000 *g* for 10 min, washed twice with cold saline, and frozen at −25°.

Enzyme activity estimation. The cells were disintegrated for 3 min with a sonic oscillator (MSE Ultrasonic Disintegrator 60W, 20 kHz). The cell debris was centrifuged as above and the supernatant was used as enzyme preparation. The alcohol dehydrogenase activity was measured by the method of Vallee and Hoch.[12] Blank cuvettes contained all the reaction mixture components except ethanol. The protein determination for the specific activity estimations were carried out by the sulfosalicylic acid method of Heepe, Karte and Lambrecht, as modified by Heinonen.[13]

RESULTS AND DISCUSSION

Effect of a strong reductant or oxidant on the alcohol dehydrogenase activity during growth. After addition of sodium dithionite, $Na_2S_2O_4$, in a concentration of 5 mM to the growth medium of *E. coli* at the beginning of the logarithmic phase, the specific activity, which normally decreases at the end of the logarithmic phase, increased and remained at a high level. The growth of *E. coli* was slower in a dithionite-containing culture than in the normal medium.

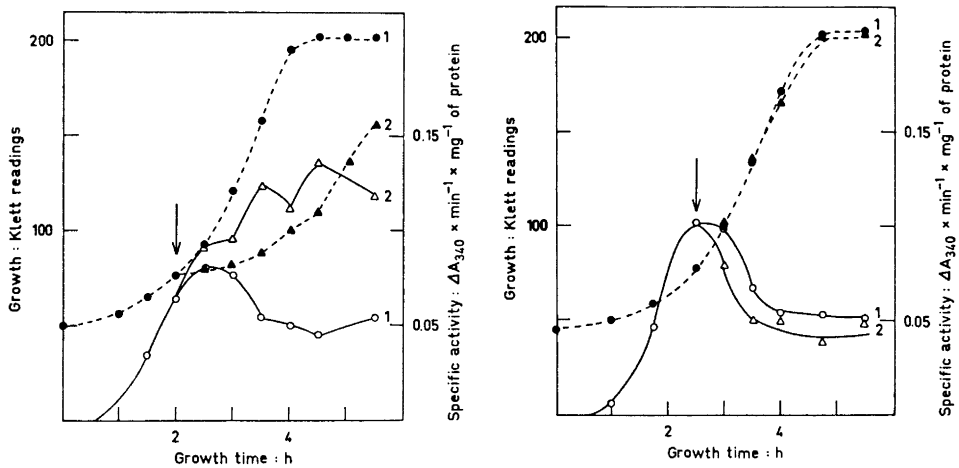

Fig. 1. Addition of $Na_2S_2O_4$ (A) and KNO_3 (B) to the concentration of 5 mM (dithionite) and 50 mM (KNO_3) to the growth medium of *E. coli* at the time indicated by the arrow. Solid symbols = growth curves; open symbols = specific activity of alcohol dehydrogenase. 1 = no addition; 2 = addition of dithionite or KNO_3 at the time indicated by the arrow.

On the contrary, when an oxidant, KNO_3, was added in a concentration of 50 mM to the growth medium, the decrease in specific activity was accelerated. There was no difference in the growth curves (Fig. 1).

Effect of different electron donors and acceptors in different concentrations on alcohol dehydrogenase activity during growth. A number of different electron donors and acceptors were also tested. They were added in various concentrations to the growth medium at the beginning of the logarithmic phase and samples were taken at the end of the logarithmic phase. The specific alcohol dehydrogenase activity of the test samples was estimated and the increase or decrease in relation to the normal specific activity was calculated and is presented as percentages in Table 1.

Table 1. Effect of different electron donors and acceptors in different concentrations on alcohol dehydrogenase activity during the growth of *E. coli*. The percentages are deviations from the initial activity which was taken as 100.

Compound	Concentration mM	Activity %	Compound	Concentration mM	Activity %
1. $KMnO_4$	0.5	−100	8. Catechol	50	−100
»	0.1	−18	»	10	20
»	0.01	31	»	1	37
2. KIO_4	25	−100	9. L-Histidine	50	13
»	10	−88	»	10	28
»	1	−29	»	1	35
3. KNO_3	50	−26	10. Cytosine	50	15
»	10	−34	»	10	64
»	1	−26	»	1	64
4. Oxidized glutathione	10	−8	11. L-Tryptophan	25	50
»	1	−8	»	10	53
»	0.1	−31	»	1	85
5. $Na_2S_2O_4$	10	46	12. Ascorbic acid	50	15
»	1	43	»	10	28
»	0.1	28	»	1	30
6. Na_2S	10	21	13. Thymine	30	93
»	1	41	»	10	93
»	0.1	14	»	1	100
7. L-Phenylalanine	50	1	14. *p*-Phenylenediamine	50	95
»	10	3	»	10	41
»	1	16	»	1	23

It is seen from Table 1 that both inorganic and biochemical electron donors in different concentrations activated alcohol dehydrogenase. Similarly, the electron acceptors inactivated the enzyme. It should be noted that the results are from separate cultures. The following experiment was made in one culture and the values are comparable to each other.

Correlation between the k value and the increase in alcohol dehydrogenase activity during growth. Szent-Györgyi [14] has listed the *k* values calculated by

A. and B. Pullman and G. Karreman for a number of molecules taking part in different biological reactions. The k value for the highest filled orbital indicates how much energy will be needed to remove an electron. The smaller its value, the more readily the molecule in question will give up this electron and act as an electron donor. We have tried to determine how the k values correlate with the increase in alcohol dehydrogenase activity during the growth of *E. coli*. The following substances (k values in brackets) were tested: *p*-hydroquinone (1.000), L-phenylalanine (0.908), L-histidine (0.660), cytosine (0.595), L-tryptophan (0.534), thymine (0.510), and *p*-phenylenediamine (0.321). Each compound was added in a concentration of 30 mM in the beginning of the logarithmic growth phase of *E. coli* and samples were taken at the end of the logarithmic phase. In Fig. 2 we can see that these is a correlation between the k value and the enzyme activity in the cells. Low k values gave the highest activities.

Addition of an electron donor at different points of the growth cycle of E. coli. We added L-tryptophan, which decreases the inactivation of the specific activity of alcohol dehydrogenase during the growth cycle, to the concentration of 30 mM at three different points during the growth cycle, *viz.* at the acceleration phase, in the beginning of the logarithmic phase and in the middle of the logarithmic phase, to the growth medium of *E. coli*. The growth of the organism and the variations in the specific alcohol dehydrogenase activity

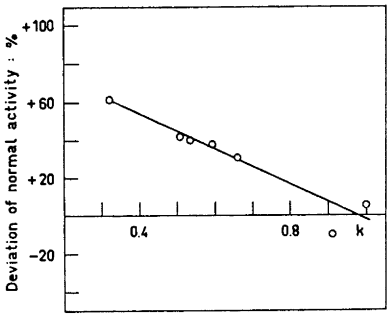

Fig. 2. Correlation between the k value and the specific alcohol dehydrogenase activity during the growth of *E. coli*. Experimental details, see Results and Discussion. Deviations from normal activity are expressed as percentages (see Table 1).

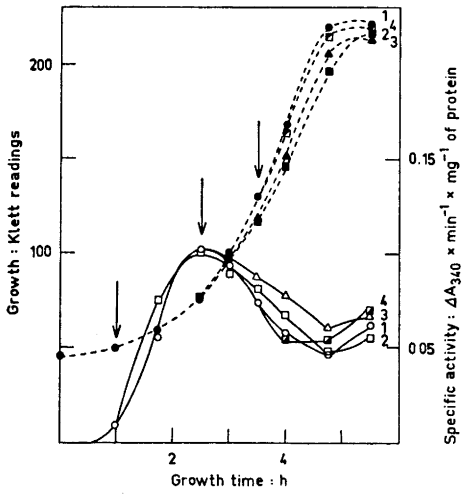

Fig. 3. Addition of L-tryptophan to the concentration of 30 mM to the growth medium of *E. coli* at three different times indicated by the arrows. Solid symbols = growth curves; open symbols = specific activity of alcohol dehydrogenase. 1 = no addition; 2 = addition at the growth time of 1 h; 3 = addition at the growth time of 2.5 h; 4 = addition at the growth time of 3.5 h.

are presented in Fig. 3. We can see that if an electron donor is added at the acceleration phase the enzyme activity will rise slightly faster and remain higher than in the normal medium. Similarly, if the addition is made in the beginning of the logarithmic phase, when the enzyme activity is highest, the fall of the activity will clearly be slower. On the other hand, when tryptophan is added in the middle of the logarithmic phase, when the enzyme activity has fallen to half the total decrease, there is not such a clear retarding effect. Only in the stationary growth phase is the activity higher than in the reference culture. We do not get total protection of alcohol dehydrogenase, as with dithionite, but on the other hand the k value of tryptophan is higher.

The explanation offered here to account for these results is that normally at the end of growth electrons are removed from the enzyme protein causing enzyme inactivation. When we add an electron donor to the medium, it donates electrons, thus leaving the enzyme protein intact. On the contrary, when we add an electron acceptor to the medium, enzyme inactivation will be faster because the acceptor will take the electrons from the enzyme protein, too.

The most usual reason for inactivation of an enzyme by oxidants and reactivation by reductants is the presence of thiol groups in the enzyme molecule. When the sulfur is in the reduced $-SH$ form the enzyme is active, whereas in the oxidized $-SS-$ form the enzyme is inactive. We assume that these are other labile groups in the enzyme molecule, too. In this work we have seen that certain free amino acids, tryptophan, histidine and phenylalanine, are rather good enzyme protectors as well as being good electron donors. It is possible that these amino acids in the enzyme molecule will also donate electrons. That might cause alteration in the enzyme protein conformation which changes the active site of the enzyme causing the enzyme inactivation. One also has to pay attention to the regulatory effect on enzyme activities of several biologically important electron donating compounds, such as the amino acids mentioned in this paper, purines and pyrimidines.

REFERENCES

1. Janicki, J. *Enzymologia* **7** (1939) 182.
2. Itoh, R., Kayashima, S. and Fujimi, K. *J. Biochem. (Tokyo)* **30** (1939) 283.
3. Ledoux, L. *Biochim. Biophys. Acta* **13** (1954) 121.
4. Pillemer, R., Ecker, E., Myers, V. and Muntwyler, E. *J. Biol. Chem.* **123** (1948) 365.
5. Nakagawa, Y. and Perlmann, E. *Federation Proc.* **29** (1970) 401.
6. Tono, M. *J. Biochem. (Tokyo)* **29** (1939) 361.
7. Itoh, R. and Nakamura, T. *J. Biochem. (Tokyo)* **26** (1937) 187.
8. Kayashima, S. *J. Biochem. (Tokyo)* **28** (1939) 175.
9. Sizer, I. and Tytell, A. *J. Biol. Chem.* **138** (1941) 631.
10. Nurmikko, V. and Laaksonen, S. *Suomen Kemistilehti* **B 34** (1961) 7.
11. Newton, W. and Snell, E. *J. Bacteriol.* **89** (1965) 355.
12. Vallee, B. and Hoch, F. *Proc. Natl. Acad. Sci.* **41** (1955) 327.
13. Heinonen, J. *Ann. Acad. Sci. Fennicae Ser. A II* **151** (1970) 17.
14. Szent-Györgyi, A. *Introduction to a Subcellular Biology*, Academic, New York and London 1960, p. 38.

Received October 16, 1972.

ACTA CHEMICA SCANDINAVICA 27 (1973) 995–1003

Crystal Structure of the Triclinic Form of the 1 : 1 Complex Between Hexamethylbenzene and Hexafluorobenzene at −40°C

TOR DAHL

*Department of Chemistry, University of Oslo, Oslo 3, Norway**

The crystal structure at −40°C of the 1 : 1 addition compound between hexamethylbenzene and hexafluorobenzene in the triclinic form, stable below 0°C, has been determined. The partner molecules are stacked alternately in infinite columns. An angle of 3.6° has been found between the molecular planes, whose mean separation within the stack is 3.43 Å. The formation of repeated twins by phase transformation from the trigonal to the triclinic form is described and the relation between the structures in these modifications is discussed. Attention is given to the relatively great differences between the structures of this complex at −40°C and that of the complex between mesitylene and hexafluorobenzene at approximately the same temperature.

The crystal structure of the 1 : 1 complex between mesitylene and hexafluorobenzene (HFB)[1] shows some features not usually found in $\pi-\pi$ complexes. The lack of traceable charge-transfer bonds in the spectra of complexes between HFB and aromatic hydrocarbons [2,3] also indicates some difference between these complexes and ordinary $\pi-\pi$ complexes.

To obtain more information about the intermolecular forces present in this type of complexes, the 1 : 1 complex between hexamethylbenzene (HMB) and HFB has been studied.[4] The crystals were found to be trigonal at room temperature and transformed into repeated twins of a triclinic modification when cooled below 0°C. The structure of the trigonal form is disordered and the model arrived at shows several orientations of the HFB-molecule. The structure of the triclinic modification at −40°C is presented in the present paper.

* Present address: Institute of Medical Biology, University of Tromsö, Box 977, N-9001 Tromsö, Norway.

DESCRIPTION OF THE TWINNING. CRYSTAL DATA

X-Ray diagrams taken when a crystal is cooled below 0°C show two or more reflections near the spot where a single reflection is present in the room-temperature diagrams. After heating above 0°C the same single crystal diagrams are obtained as before the cooling. The number of separated reflections is not the same each time the crystal is cooled down. The separation is very small just below 0°C, but increases when the temperature is lowered. This dependence on temperature is relatively small below ~ -30°C. One crystal, which was kept at -80°C, was damaged after a few days. Crystals which have not been heated above 0°C give the same separated reflection as those described.

These observations are satisfactorily explained when it is assumed that phase transformation into a triclinic, pseudo-trigonal modification occurs and repeated twins are formed. The following cell parameters were found at -40°C. $a = 8.740 \pm 0.010$ Å, $b = 8.834 \pm 0.011$ Å, $c = 7.149 \pm 0.012$ Å, $\alpha = 110.82 \pm 0.06°$, $\beta = 107.34 \pm 0.07°$, $\gamma = 111{,}14 = 0.05°$. Although the diagonal [111] is shorter (8.248 Å) than the a- and b-axes, this cell was chosen as the molecular planes turned out to be not far from parallel to (001). A cell based on the corresponding vectors $\mathbf{a}' = \frac{1}{3}\mathbf{a} + \frac{2}{3}\mathbf{b} - \frac{1}{3}\mathbf{c}$, $\mathbf{b}' = \frac{2}{3}\mathbf{a} - \frac{1}{3}\mathbf{b} - \frac{1}{3}\mathbf{c}$, $\mathbf{c}' = \mathbf{c}$ in the trigonal modification has the parameters $a' = b' = 8.755$ Å, $c' = 7.124$ Å, $\alpha' = \beta' = 105.74°$, $\gamma' = 112.94°$. Assuming one molecule of each kind in the cell the calculated density at -40°C is 1.39 g/cm^3. The corresponding value found for the trigonal modification is 1.32 g/cm^3.

Assuming the planes (100), (010), and (1$\bar{1}$0) to be possible twin planes, all the reflections could be indexed. Following Friedel's classification the twins are of the pseudo-merohedral type.[5] The obliquity is 2.1°, 5.2°, and 7.1° when the twin plane is (1$\bar{1}$0), (100), and (010), respectively. Even when the temperature is lowered very slowly through the transition point, the probability for each of these planes to be twin plane seems to be approximately equal. The corresponding planes in the trigonal modification are all mirror planes. The direction of the c-axis, which is along the needle axis, seems to be unaltered relative to the outer shape of the crystal during the phase transformation.

EXPERIMENTAL

Needle-shaped crystals were obtained from an ether solution of the two components at -30°C. The crystals are unstable on exposure to the atmosphere and were kept in sealed glass capillaries.

Cu $K\alpha$-radiation was used for all the diagrams, which were taken at -40°C after cooling the crystal slowly down from room temperature. Cell parameters were determined from Weissenberg diagrams taken about the c-axis and a direction corresponding to the a-axis in the trigonal modification. Diagrams were taken on the same films at room temperature at which accurate cell parameters were known, in order to calibrate the camera radius.

The intensity data were collected from Weissenberg diagrams taken mainly about the c-axis. One diagram taken about a direction corresponding to the a-axis in the trigonal form, and one about the c-axis which registered the zero and first layer simultaneously were taken to calculate interlayer scale factors. To avoid overlap of reflections from different individuals of the twin crystals, it was necessary to use non-integrated diagrams. All the 343 observed reflections were measured visually, and the intensities of those having important reflection spot extention were corrected for this effect.[6] Absorption correction was considered unimportant and not performed.

STRUCTURE DETERMINATION

As both the partner molecules may have centres of symmetry, the space group $P\bar{1}$ was assumed. From a three-dimensional, sharpened Patterson synthesis the orientations of the molecules, which seemed to be approximately equal, were found. The HFB- and the HMB-molecule were placed in the centres of symmetry $(0,0,\frac{1}{2})$ and (0,0,0), respectively. Structure factors based on the F- and C-atoms were calculated, giving an R-value of 28 %, and least squares refinement was started.

73 low-angle reflections, which with certainty could be classified as unobserved, were given values of $\frac{1}{4}\ I_{min}$ for I_o and included in the least squares refinement. The R-values given below are calculated from the observed reflections only. The weight factors chosen were $A(F_o)^{-0.6}$ for reflections with $F_o > \sim 3\ |F_{min}|$, while a constant weight was used for the weaker observed reflections and $\frac{1}{3}$ of this weight for the unobserved reflections. Hydrogen atoms with positions calculated assuming disorder due to rotation of the methyl groups were included in the structure factor calculations.

An R-value of 12.0 % was arrived at when positional and anisotropic thermal parameters were varied for the F-atoms and the methyl C-atoms, while positional and isotropic thermal parameters were varied for the ring C-atoms. To obtain more reasonable atomic positions and to allow introduction of anisotropic thermal parameters also for the ring C-atoms without varying too many parameters independently, some restrictions were put on the geometry of the molecules in the last four refinement cycles. Straight lines were assumed to run along the C – F bonds and the C – CH_3 bonds through the centres of the molecules. The quotient between the length of each of these bonds and the distance of the corresponding ring C-atom from the centre of the molecule was kept constant, with a value of 1.326/1.394 for the HFB-molecule [7] and 1.52/1.40 for the HMB-molecule.[8] As anisotropic thermal parameters were varied for all the F- and C-atoms, the scale factor was kept constant to avoid correlation with these parameters. 90 parameters were varied independently in these cycles which gave a conventional R-value of 8.2 %. When the unobserved reflections also are included, the conventional R-value is 10.1 %, while the weighted R-value is 11.3 %.

Difference syntheses gave no indication neither of positions of the H-atoms nor of any disorder in the structure. Rigid body analysis of the thermal vibrations was performed but the results were not good enough to justify any correction for this effect. No effect of secondary extinction has been found.

All programs used are described in Ref. 9, and the atomic form factors are given in Ref. 10.

DISCUSSION

Observed and calculated structure factors are given in Table 1, positional and thermal parameters in Table 2, bond distances and angles in Table 3, and principal axes of the vibration ellipsoids in Table 4. Fig. 1 shows sections parallel to (001) through a three-dimensional Fourier map. The orientation

and packing of the molecules and intermolecular distances are shown in Fig. 2. Considering that corrections for librational motion have not been performed, all the bond distances and angles seem reasonable.

Table 1. Observed and calculated structure factors, ten times the absolute values. The columns listed are h, k, l, F_o, and F_c. Unobserved reflections have F_o-values like $\frac{1}{2}F_{min}$ and are marked with asterisks.

0	1	0	375	398	-5	3	1	13	- 5 *	5	-3	1	26	21	1	-4	2	82	91	-4	-4	4	86	81
0	2	0	216	-242	-5	4	1	33	38	5	-2	1	41	46	1	-3	2	66	66	-4	-3	4	65	- 56
0	3	0	187	-205	-5	5	1	14	13 *	5	-1	1	28	19	1	-2	2	117	-115	-4	-2	4	99	-105
0	4	0	159	-164	-4	-2	1	14	17 *	5	0	1	16	- 21 *	1	-1	2	57	34	-4	-1	4	109	-111
0	5	0	51	51	-4	-1	1	59	59	6	-6	1	31	- 26	1	0	2	130	-138	-4	0	4	30	31
0	6	0	11	- 8 *	-4	0	1	11	- 16 *	6	-3	1	49	59	1	1	2	51	50	-4	1	4	11	- 17 *
0	7	0	29	- 34	-4	1	1	75	- 73	6	-2	1	38	21	1	2	2	51	39	-4	2	4	81	- 69
1	-7	0	46	- 47	-4	2	1	96	- 80	6	-1	1	36	- 21	1	3	2	37	- 32	-3	-6	4	66	64
1	-6	0	43	41	-4	3	1	40	- 31	6	3	2	63	65	1	4	2	45	40	-3	-5	4	98	88
1	-5	0	11	- 7 *	-4	4	1	12	4 *	7	2	2	120	117	2	-7	2	14	51 *	-3	-4	4	54	- 50
1	-4	0	190	-187	-4	5	1	31	28	7	3	2	72	75	2	-6	2	13	- 3 *	-3	-3	4	34	26
1	-3	0	8	- 17 *	-4	6	1	46	54	6	1	2	13	5 *	2	-5	2	50	- 49	-3	-2	4	9	1 *
1	-2	0	121	-128	-3	-3	1	48	55	6	2	2	13	- 8 *	2	-4	2	82	80	-3	-1	4	77	- 81
1	-1	0	369	383	-3	-2	1	12	- 28 *	6	3	2	13	- 7 *	2	-3	2	146	-146	-3	0	4	9	4 *
1	0	0	373	382	-3	-1	1	62	- 48	7	0	2	134	-131	2	-2	2	38	- 42	-3	1	4	58	- 44
1	1	0	139	-139	-3	0	1	17	10	5	-2	2	53	51	2	-1	2	18	- 13 *	-3	2	4	13	6 *
1	2	0	206	211	-3	1	1	58	62	5	-1	2	53	48	2	0	2	134	-131	-3	3	4	15	2 *
1	3	0	48	- 37	-3	2	1	18	- 14	5	0	2	106	- 97	2	1	2	47	- 44	-2	-7	4	31	- 21
1	4	0	64	- 53	-3	3	1	18	- 13 *	5	1	2	60	- 59	2	2	2	39	- 35	-2	-6	4	29	32
1	5	0	42	39	-3	4	1	44	- 48	5	2	2	54	- 47	2	3	2	50	48	-2	-5	4	37	- 24
2	-6	0	26	33	-3	5	1	31	18	5	3	2	101	- 97	2	4	2	68	62	-2	-4	4	61	- 61
2	-5	0	83	- 75	-2	-4	1	44	51	5	4	2	15	- 26 *	3	-7	2	144	138	-2	-3	4	52	63
2	-4	0	68	64	-2	-3	1	35	- 38	5	5	2	14	15 *	3	-6	2	13	24 *	-2	-2	4	39	- 49
2	-3	0	206	204	-2	-2	1	90	- 73	5	6	2	65	61	3	-5	2	85	- 87	-2	-1	4	125	142
2	-2	0	232	-244	-2	-1	1	51	54	5	7	2	44	42	3	-4	2	181	-181	-2	0	4	175	185
2	-1	0	136	-136	-2	0	1	51	57	4	-4	2	136	126	3	-3	2	112	-115	-2	1	4	11	- 2 *
2	0	0	255	-256	-2	1	1	7	24 *	4	-3	2	15	61 *	3	-2	2	121	120	-2	2	4	25	- 21
2	1	0	8	- 24 *	-2	2	1	87	98	4	-2	2	78	- 68	3	-1	2	47	- 55	-2	3	4	56	- 51
2	2	0	69	75	-2	3	1	24	- 17	4	-1	2	235	-226	3	0	2	128	-127	-1	-8	4	33	- 39
2	3	0	71	- 67	-2	4	1	45	- 45	4	0	2	108	-109	3	1	2	37	- 34	-1	-7	4	16	- 29 *
2	4	0	85	78	-2	5	1	27	13	4	1	2	180	179	3	3	2	58	58	-1	-6	4	60	58
2	5	0	65	65	-1	-2	1	73	79	4	2	2	80	- 79	4	-8	2	54	55	-1	-5	4	112	-107
3	-7	0	54	56	-1	-1	1	6	- 3 *	4	3	2	142	-156	4	-7	2	92	94	-1	-4	4	120	-129
3	-6	0	72	69	-1	1	1	62	- 58	4	4	2	59	- 58	4	-6	2	14	29 *	-1	-3	4	88	- 75
3	-5	0	66	- 62	-1	2	1	63	55	4	5	2	14	8 *	4	-5	2	14	- 7 *	-1	-2	4	82	95
3	-4	0	64	- 51	-1	3	1	53	- 50	4	6	2	65	72	4	-4	2	82	- 89	-1	-1	4	359	400
3	-3	0	203	-211	-1	4	1	31	29	3	-5	2	122	129	4	-3	2	60	53	-1	0	4	144	142
3	-2	0	7	- 19 *	-1	6	1	34	- 36	3	-4	2	111	107	4	-2	2	34	- 32	-1	1	4	51	- 44
3	-1	0	217	213	0	-6	1	54	- 45	3	-3	2	83	- 84	4	-1	2	59	- 58	-1	2	4	45	- 45
3	0	0	205	-210	0	-5	1	13	48 *	3	-2	2	99	- 95	4	0	2	16	19 *	-1	3	4	51	- 44
3	1	0	201	-208	0	-4	1	11	28 *	3	-1	2	191	-179	4	1	2	17	26 *	0	-8	4	51	- 60
3	2	0	93	- 83	0	-3	1	9	- 46 *	3	0	2	58	- 51	5	-5	2	38	43	0	-7	4	15	22 *
3	3	0	71	65	0	-2	1	38	38	3	1	2	35	- 34	6	-4	2	62	64	0	-6	4	14	8 *
3	4	0	115	118	0	0	1	139	- 99	3	2	2	126	-136	6	-3	2	95	93	0	-5	4	128	-126
4	-7	0	103	108	0	1	1	19	- 13	3	3	2	58	52	-4	1	3	44	- 47	0	-4	4	11	- 8 *
4	-6	0	82	84	0	2	1	38	48	3	4	2	14	- 15 *	-4	2	3	28	- 31	0	-3	4	22	- 18
4	-5	0	50	- 38	0	3	1	27	- 25	3	5	2	14	- 6 *	-3	-2	3	39	- 47	0	-2	4	102	109
4	-4	0	146	-148	0	4	1	34	39	2	-5	2	64	72	-3	0	3	29	40	0	-1	4	138	133
4	-3	0	182	-191	1	-5	1	38	42	2	-4	2	85	- 80	-3	1	3	28	19	0	0	4	35	- 34
4	-2	0	57	67	1	-4	1	71	- 61	2	-3	2	64	67	-3	2	3	27	36	0	1	4	14	- 4 *
4	-1	0	56	- 40	1	-3	1	44	39	2	-2	2	198	206	-2	-3	3	40	- 35	0	2	4	19	- 18 *
4	0	0	153	-160	1	-2	1	34	30	2	-1	2	188	-193	-2	-1	3	54	53	1	-7	4	45	33
4	1	0	11	- 9 *	1	-1	1	52	- 54	2	0	2	38	30	-2	1	3	38	37	1	-6	4	51	- 36
4	2	0	33	41	1	0	1	16	- 16	2	1	2	37	- 53	-2	3	3	29	- 34	1	-5	4	12	2 *
4	3	0	55	60	1	1	1	92	83	2	2	2	10	0 *	-1	-2	3	50	59	1	-4	4	52	49
5	-7	0	55	47	1	2	1	74	- 68	2	3	2	45	44	-1	0	3	73	- 77	1	-3	4	67	- 75
5	-6	0	28	31	1	3	1	13	- 18 *	2	4	2	75	- 74	0	-3	3	28	23	1	-2	4	20	- 5
5	-5	0	52	50	1	4	1	29	22	2	5	2	14	7 *	0	-2	3	36	38	1	-1	4	42	- 36
5	-4	0	11	3 *	2	-6	1	50	- 19	1	-6	2	14	12 *	0	-1	3	56	- 63	1	0	4	39	- 42
5	-3	0	82	- 73	2	-5	1	12	- 19 *	1	-5	2	14	10 *	1	-4	3	38	- 23	1	1	4	15	- 7 *
5	-2	0	67	- 65	2	-4	1	73	- 70	1	-4	2	171	-179	1	-3	3	21	21	1	3	4	29	29
5	-1	0	52	- 48	2	-3	1	9	13 *	1	-3	2	9	- 15 *	2	-4	3	38	- 46	2	-8	4	53	52
5	0	0	50	58	2	-2	1	54	43	1	-2	2	121	-129	2	-1	3	33	- 32	2	-7	4	86	80
5	1	0	37	44	2	-1	1	92	90	1	-1	2	439	424	-8	1	4	35	43	2	-6	4	14	- 19 *
6	-5	0	29	26	2	0	1	9	16 *	1	0	2	844	880	-8	2	4	78	76	2	-5	4	36	- 34
6	-4	0	27	33	2	1	1	52	- 57	1	1	2	48	52	-8	3	4	34	36	2	-4	4	91	- 91
6	-3	0	69	68	2	2	1	38	- 45	1	2	2	109	-115	-7	-2	4	42	- 46	2	-3	4	42	- 45
6	-2	0	83	80	2	3	1	58	57	1	3	2	128	-135	-7	1	4	53	51	2	-2	4	29	27
6	-1	0	27	37	3	-6	1	59	48	1	4	2	58	- 65	-7	2	4	44	37	2	-1	4	54	- 54
6	1	0	41	- 47	3	-5	1	58	- 24	0	-7	2	47	- 54	-6	-2	4	30	24	2	0	4	56	- 48
7	-6	0	38	- 42	3	-4	1	51	- 53	0	-6	2	75	85	-6	-1	4	33	33	2	3	4	30	33
7	-4	0	49	48	3	-2	1	10	- 7 *	0	-5	2	74	- 74	-6	0	4	39	- 30	3	-7	4	95	92
7	-3	0	97	113	3	-1	1	68	- 58	0	-4	2	235	-260	-6	1	4	27	- 24	3	-7	4	83	74
7	-2	0	51	57	3	0	1	35	- 32	0	-3	2	139	-152	-6	2	4	31	- 28	3	-6	4	15	- 12 *
-7	3	1	30	32	3	1	1	29	26	0	-2	2	24	- 31	-5	-4	4	79	68	3	-5	4	58	- 53
-6	0	1	44	- 34	3	2	1	28	34	0	-1	2	911	799	-5	-3	4	36	40	3	-4	4	72	- 75
-6	2	1	66	71	4	-6	1	32	42	0	0	2	429	414	-5	-1	4	109	-108	3	-3	4	14	- 4 *
-6	3	1	32	21	4	-5	1	13	23 *	0	1	2	85	- 93	-5	0	4	58	- 46	3	-2	4	29	- 17
-6	4	1	28	- 8	4	-3	1	35	- 33	0	2	2	12	- 10 *	-5	1	4	24	21	3	-1	4	49	- 40
-5	-1	1	14	- 18 *	4	-2	1	55	- 54	0	3	2	74	- 81	-5	2	4	68	- 63	4	-8	4	31	33
-5	0	1	31	35	4	-1	1	13	- 11 *	0	4	2	14	- 7 *	-5	3	4	65	- 51	4	-1	4	33	12
-5	1	1	12	19 *	4	0	1	47	51	1	-6	2	13	36 *	-5	5	4	32	29	5	-4	4	35	39
-5	2	1	12	- 12 *	5	-4	1	14	12 *	1	-5	2	124	-123	-4	-5	4	135	130	5	-3	4	48	44
																				6	-4	4	45	45

Table 2. Coordinates and anisotropic thermal parameters according to the expression: $\exp -(B_{11}h^2+B_{22}k^2+B_{33}l^2+B_{12}hk+B_{13}hl+B_{23}kl)$, with estimated standard deviations. All values multiplied by 10^4.

	x	y	z	B_{11}	B_{22}	B_{33}	B_{12}	B_{13}	B_{23}
F1	2144	−1526	5243	726	985	1119	1191	1035	1127
	15	16	17	38	49	70	81	92	91
F2	3637	2080	6324	283	860	790	82	396	622
	13	15	17	22	42	49	48	55	70
F3	1535	3654	6087	999	244	708	274	820	517
	14	11	14	45	20	48	48	74	52
C1	1099	−782	5124	380	624	565	580	647	771
	8	8	9	46	63	87	99	112	126
C2	1863	1066	5678	319	332	595	32	325	687
	7	8	9	45	44	78	79	102	100
C3	786	1872	5557	609	232	384	382	532	401
	7	6	7	57	42	72	85	104	93
C4	2336	−1639	266	513	455	940	828	725	952
	17	16	21	43	41	89	80	107	101
C5	4003	2353	1711	227	407	627	144	375	673
	14	15	19	37	37	66	61	77	82
C6	1678	4026	1419	454	321	566	343	456	494
	16	18	19	43	40	73	67	92	90
C7	1120	−786	127	340	270	382	437	383	426
	8	8	10	37	31	61	62	78	74
C8	1919	1128	821	156	344	151	183	163	161
	7	7	9	27	39	45	61	57	68
C9	805	1930	680	263	250	310	207	306	370
	8	9	9	32	35	58	60	67	75

The deviations from least squares planes through the molecules are 0.009 Å for all the methyl C-atoms, and 0.003 Å for all the ring C-atoms of the HMB-molecule, 0.003 Å for all the F-atoms, and 0.002 Å for all the ring C-atoms of the HFB-molecule. None of these deviations are significant. The angle between the *c*-axis and the plane normal of the molecular plane, "the stacking angle", is 14.4° for the HMB-molecule and 17.9° for the HFB-molecule. The angle between the molecular planes is 3.6°. The effect of this non-parallelism is to reduce the distances, 3.32 Å and 3.31 Å, from the plane of the HMB-molecule for two fluorine atoms, F2 and F3, respectively, situated approximately above the ring carbon atoms, and to increase the corresponding distances, 3.60 Å and 3.61 Å, for the two equivalent fluorine atoms situated approximately above the methyl groups. Steric hindrance may thus explain this finding. The mean separation between the molecular planes is 3.43 Å.

Table 3. Bond distances (Å) and angles (°). Estimated standard deviations are approximately 0.01 Å for the distances, and approximately 0.7° for the angles.

Distance		Angle	
C3′ – C1	1.39	∠C3′ – C1 – C2	120.3
C1 – C2	1.37	∠C1 – C2 – C3	120.9
C2 – C3	1.37	∠C2 – C3 – C1′	118.9
C1 – F1	1.30	∠F1 – C1 – C3′	119.7
C2 – F2	1.30	∠F1 – C1 – C2	120.0
C3 – F3	1.32	∠F2 – C2 – C1	119.8
C9′ – C7	1.40	∠F2 – C2 – C3	119.3
C7 – C8	1.39	∠F3 – C3 – C2	120.4
C8 – C9	1.40	∠F3 – C3 – C1′	120.7
C7 – C4	1.51	∠C9′ – C7 – C8	120.7
C8 – C5	1.51	∠C7 – C8 – C9	120.4
C9 – C6	1.53	∠C8 – C9 – C7′	118.9
		∠C4 – C7 – C9′	119.4
		∠C4 – C7 – C8	119.9
		∠C5 – C8 – C7	120.2
		∠C5 – C8 – C9	119.4
		∠C6 – C9 – C8	120.4
		∠C6 – C9 – C7′	120.7

Table 4. Principal axes of the thermal vibration ellipsoids.

	R.m.s. amplitudes Å	*B*-values Å²	Components of the r.m.s. amplitudes (Å) *U(x)*	*U(y)*	*U(z)*
F1	.508	20.4	.399	.605	.197
	.431	14.7	.189	.116	.500
	.350	9.7	−.293	.103	.032
F2	.568	25.5	−.099	.533	.033
	.383	11.6	.071	.138	.437
	.256	5.2	.308	.192	.114
F3	.572	25.8	.598	.002	.128
	.340	9.1	.123	.185	.408
	.221	3.8	.118	.250	.029
C1	.397	12.5	.195	.494	.230
	.308	7.5	.303	.048	.259
	.238	4.5	.131	.180	−.161
C2	.425	14.3	−.185	.291	.209
	.298	7.0	.279	.159	.332
	.162	2.1	.108	.147	−.023
C3	.416	13.6	.472	.090	.121
	.250	4.9	.110	.243	.277
	.204	3.3	.036	.156	−.090
C4	.406	13.1	.267	.342	.490
	.370	10.8	.349	.221	−.052
	.166	2.2	.072	−.119	.030

Table 4. Continued.

C5	.385	11.7	−.031	.364	.267
	.298	7.0	.216	.028	.302
	.202	3.2	.200	.166	.012
C6	.362	10.3	.356	−.014	.000
	.312	7.7	.192	.215	.383
	.271	5.8	.109	.284	−.012
C7	.302	7.2	.357	.261	.153
	.250	4.9	.008	.136	.269
	.194	3.0	.063	−.141	.060
C8	.334	8.8	.023	.346	.011
	.201	3.2	.242	.105	.081
	.156	1.9	.033	.075	.180
C9	.287	6.5	−.194	.150	.037
	.249	4.9	.250	.264	.245
	.190	2.8	.043	.081	−.137

As may be seen in the part of Fig. 2 showing the packing along $(1\bar{1}0)$, the plane normals of both molecules are lying approximately in this plane. The mutual displacement of centres of symmetry, relative to their positions in the trigonal form, is much greater in the neighbouring stacks shown in this figure than in the other pairs of neighbouring stacks. Molecules of different kinds belonging to this pair of stacks (*e.g.* situated in (0,0,0) and $1,1,\frac{1}{2}$)) are lying nearly in the same plane. Their interatomic distances, although shorter than between molecules belonging to other pairs of stacks, are not short enough to indicate any forces stronger than normal van der Waals interaction.

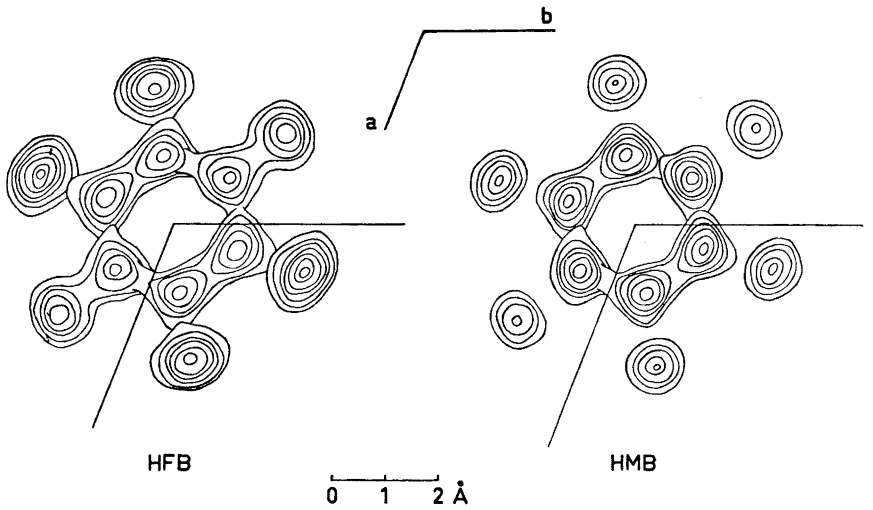

Fig. 1. Sections parallel to (001), through a three-dimensional Fourier map viewed perpendicular to this plane. Contour intervals of ½ e/Å³, and lowest contour at 2 e/Å³.

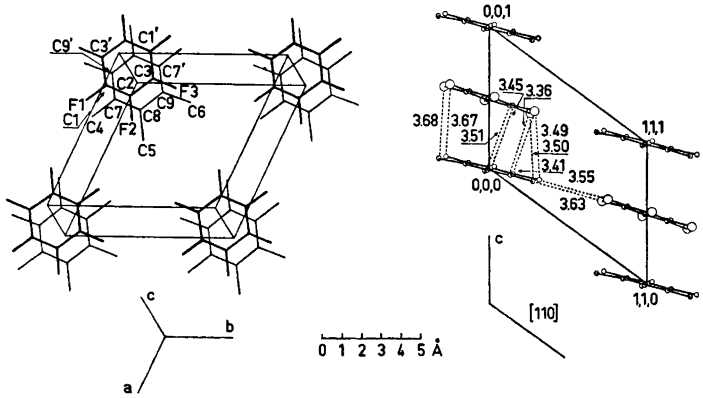

Fig. 2. The packing and the orientation of the molecules viewed perpendicular to the plane of the HMB-molecule (left) and perpendicular to $(1\bar{1}0)$ (right). Intermolecular distances within the stack and the shortest distances between different stacks are given.

The orientations of the molecules correspond very closely to that of the HMB-molecule and the most probable orientation of the HFB-molecule in the trigonal modification. Although only one orientation of the HFB-molecule is preferred, the thermal vibration ellipsoids indicate that reorientation of this molecule occurs also in the triclinic modification. The finding that the molecular planes are not parallel in the trigonal form due to tilting of the HFB-molecule is in accordance with this structure, but the stacking angle of the HMB-molecule adds weight to the suspicion that this molecule, too, is tilted in the trigonal form. Important interactions within the stack between methyl groups and fluorine atoms, whose existence was discussed in the report of the trigonal modification, are not confirmed in this work. No indications have been found of disorder in the stacking sequence like that found in the trigonal form.

A comparison of this structure with the structure of the complex between HFB and mesitylene at approximately the same temperature shows considerable differences. In spite of the greater number of methyl groups, the mean separation between the planes is 0.13 Å shorter in the HMB-complex, and the molecules, which have nearly the same orientation in this complex, are twisted 30° relative to each other in the mesitylene-complex. No short distance between a methyl group and a fluorine atom, like that found in the mesitylene-complex, is present in the HMB-complex. In general, the structure of the HMB-complex is much more similar to those of the majority of the $\pi-\pi$ complexes which have been investigated.[11] This finding may be interpreted as an indication that the dominating intermolecular forces are of the same kind as in this type of complexes.

REFERENCES

1. Dahl, T. *Acta Chem. Scand.* **25** (1971) 1031.
2. Beaumont, T. G. and Davis, K. M. C. *J. Chem. Soc.* **B 1967** 1131.
3. Hammond, P. R. *J. Chem. Soc.* **A 1968** 145.

4. Dahl, T. *Acta Chem. Scand.* **26** (1972) 1569.
5. Cahn, R. W. *Advan. Phys.* **3** (1954) 363.
6. Phillips, D. C. *Acta Cryst.* **9** (1956) 819.
7. Almenningen, A., Bastiansen, O., Seip, R. and Seip, H. M. *Acta Chem. Scand.* **18** (1964) 2115.
8. Colton, R. H. and Henn, D. E. *J. Chem. Soc.* **B 1970** 1532.
9. Dahl, T., Gram, F., Groth, P., Klewe, B. and Rømming, C. *Acta Chem. Scand.* **24** (1970) 2232.
10. Hanson, H. P., Herman, F., Lea, J. D. and Skillman, S. *Acta Cryst.* **17** (1964) 1040.
11. Herbstein, F. H. *Perspectives in Structural Chemistry*, Wiley, London 1971, Vol. 4.

Received September 29, 1972.